# *A Tracer Study on the Penetration of a Sample Solution into Carbon Electrode of Spectrographic Analysis*

By Kenjiro KIMURA and Kazuo SAITO

(Received August 28, 1956)

Quantitative spectrographic analysis of non-ferrous metals is carried out by means of spark spectra. This method is normally satisfactory to obtain accurate results, but is less desirable when applied to samples of a high purity, since its sensitivity is rather low. Non-ferrous metals of a high purity are analysed through the solution-arc method, which consists in dissolving the sample in acid, making the solution up to a definite volume, impregnating it into a porous carbon electrode and using this in an arc discharge. This method is certainly very sensitive; it requires however, a very careful procedure in accordance with precise directions.

The present authors are of the opinion that the need for precision could be, at least partly, ascribed to the different nature of the carbon electrode. They intended therefore to examine the penetration process into a carbon electrode with the aid of tracer technique[1].

**Radioactive Isotope.** — Radioactive zinc-65 was used as indicator. Its $\beta$-activity (electron capture 97.5%, $\beta^+$ 2.5%) of a half life of 245 days is satisfactory for the present purpose; since its decay product is not radioactive, the measurement of activity directly indicates the relative amount of zinc. A solution was prepared from a solution of radioactive zinc chloride and pure lead nitrate, which contained 0.24 g. of lead nitrate and 0.11 mg. of zinc (carrier) in one cc., corresponding to 0.07% of zinc in lead. This content is slightly greater than the practical content of zinc in lead ingot, but a less concentrated solution could not maintain radioactivity strong enough to be measured. This solution was used throughout this work.

**Procedure.**—Several sorts of carbon electrode were examined as shown in Table I. Each capital letter A, B etc. corresponds to a product of a different manufacturer. The preliminary treatment of an electrode may affect the penetration of the sample solution; the various treatments are also shown in Table I. After the preliminary discharge, carbon electrodes were cooled to about 60°C and the sample solution was dripped from a measuring pipette so slowly that the second drop was not added until the first one had already been absorbed. Then they were dried in an air-bath and sections cut with a saw so that several fractions of carbon powder containing salt were obtained corresponding to the definite distance from the top of the elctrode. They were weighed in a steel dish and their radioactivity measured with a counter. Some of the electrodes are of so close a texture that it takes a long time for the solution to penetrate into them, whilst that of others is less so. About 30 mg. of the powder were used for each activity measurement. The influence of geometrical distribution of the sample powder in the dish was examined and not found to be significant.

Table I shows the results. Each frame corresponds to a fraction of the carbon powder, each figure showing the average count per 10 mg. of the powder. The count should be directly proportional for any one elctrode to the amount of zinc in the sample. The error of measurement was of the order of 10%.

**Autoradiograph.** — A carbon electrode, after being submitted to impregnation of the solution, is vertically divided into two pieces and put on to a piece of photographic film. Non-screen Eastman Kodak X-ray film was used, since it is quite sensitive, though coarse grained. They were set aside for six days and developed. The results coincide well with those in Table I.

**Measurement of Density.**—The apparent density ($d$) of the carbon electrodes was found from their size and weight. The real density ($d_0$) was measured with a pyknometer and benzene. The porosity ($p$) can be calculated from the following formula. $p=(d_0-d)/d_0$. They were measured at $15\pm0.02$°C and the results are tabulated in Table II. When an electrode is heated at a high temperature for a long time, the apparent density decreases and the real density increases, resulting in a higher porosity. (Electrodes of maker B do not do this, but the quality is not uniform even in one packet so that no account was taken of these results.)

## Discussion

From Table I it can be seen that the zinc ion penetrates farther into a carbon electrode than expected, showing a marked maximum at a distance several millimeters from the top. The apparent hardness of carbon appears to bear little relation to the extent of penetration, presumably because the apparent hardness depends

1) The authors could not find any reference about such a consideration nor any such kind of application of radioactive tracers.

TABLE I

| Carbon | A | B | B | C | C | A | B | C | D | A | A |
|---|---|---|---|---|---|---|---|---|---|---|---|
| Diameter | 5.2 | 5.4 | 5.4 | 8.1 | 8.1 | 5.3 | 5.7 | 8.3 | 7.9 | 5.3 | 5.3 |
| Preliminary Discharge (sec.) | 55 V 6 A 40 | 55 V 5 A 30 | 55 V 8 A 60 | 55 V 6 A 50 | 55 V 6 A 50 | none | none | none | none | 55 V 6 A 30 | 55 V 6 A 30 |
| Solution Added, ml. | 0.2 | 0.2 | 0.2 | 0.5 | 0.2 | ca. 0.02 | ca. 0.02 | ca. 0.01 | ca. 0.01 | 0.15 | 0.15 |
| Distance from the top of the electrode, mm. 2 | 377 | 277 | 252 | 620 | 357 | 168 | 125 | 276 | 120 | 58 | 68 |
| | | | | 190 | 314 | 118 | | 0 | 8 | | |
| 4 | 205 | 172 | 243 | 152 | | | | 0 | 0 | | 113 |
| | | | | 166 | 220 | | 74 | | | 70 | |
| 6 | 187 | 153 | 231 | 231 | | 52 | | | 0 | | |
| | | | | 558 | 167 | | | | | | 127 |
| 8 | 505 | | 184 | 405 | | 6 | | | | 69 | |
| | | | | 148 | 200 | | 14 | | | | |
| 10 | 228 | 185 | 118 | 90 | | | | | | | 220 |
| | | | | 132 | 128 | | | | | 123 | |
| 12 | 87 | 201 | 128 | | | | | | | | 172 |
| | | | | 290 | 6 | | | | | 138 | |
| 14 | | 175 | 187 | | | | | | | | 198 |
| 16 | | 211 | | | | | | | | 89 | |
| 18 | | | | 125 | | | | | | | 120 |
| 20 | | 143 | | | | | | | | 44 | |
| 22 | | | 156 | | | | | | | | |
| 24 | | 5 | | | | | | | | | |
| 26 | | | | | | | | | | | |
| Note | | | | | | Without preliminary discharge, the solution soaks very slowly and with difficulty. | | | | Kerosene, 0.07 ml. | |

mainly on the nature of the binding material and not on the nature of carbon itself. The penetration should, on the contrary, be dependent on the nature of carbon, the conditions of preliminary discharge and the way the solution is put on to the electrode. Since the zinc ion extends in front of the lead ion in a chromatographic series, the formation of a maximum point of zinc content can be correlated to the chromatographic effect of capillary texture of the carbon, although the way of addition of the solution is certainly too complicated for the comparison to be made. As a matter of fact, the heterogeneous distribution of the zinc ion should be considered in connection with the relative ratio of zinc to lead, nevertheless this fact ought to be taken into account in the practice of spectrographic analysis.

Another line of argument may be introduced from the data of porosity. It should be noticed that the values of $d$, $d_0$ and $p$ are independent of the apparent hardness

TABLE II

MEASUREMENT OF DENSITY AND POROSITY

| Manufacturer | Preliminary Discharge | $d$ | $d_0$ | $p$ |
|---|---|---|---|---|
| A | Without | 1.65 | 2.20 | 0.25 |
| A | 6A, 40 sec. | 1.47 | 2.26 | 0.35 |
| B | Without | 1.43 | 1.89 | 0.24 |
| B | 5A, 30 sec. | 1.51 | 1.65 | 0.08 |
| B | 6A, 40 sec. | 1.42 | 1.70 | 0.16 |
| B | 8A, 60 sec. | 1.40 | 1.84 | 0.24 |
| C | Without | 1.28 | 1.55 | 0.17 |
| C | 6A, 50 sec. | 1.27 | 2.01 | 0.37 |
| D | Without | 1.38 | 1.64 | 0.16 |
| D | 6A, 50 sec. | 1.29 | 1.89 | 0.32 |

of the carbon, and so is the extent of penetration. This fact can be easily seen from the comparison of Tables I and II. The depth of penetration appears to increase with porosity, at least for the electrode of the same manufacturer, whilst the time taken for penetration depends on the apparent hardness of the carbon.

The authors also examined the effects of some liquids on the penetration, including liquid paraffine and other organic solvents, which may affect the surface state of carbon, only to find that these have very little effect. These liquids were dripped on to the electrode prior to the addition of the sample solution.

The authors wish to express their thanks to Chairman Professor Hidehiro Goto of Tohoku University and other members of "JIS Committee for Spectroscopic Analysis of Zinc and Lead Metal" for their interest and valuable discussion.

*Department of Chemistry*
*Faculty of Science*
*The University of Tokyo*
*Hongo, Tokyo*

# *Synthetic Studies on the Benzofuran Derivatives. II. Reactions of Aromatic o-Hydroxyaldehyde Derivatives and Ethyl Bromomalonate*

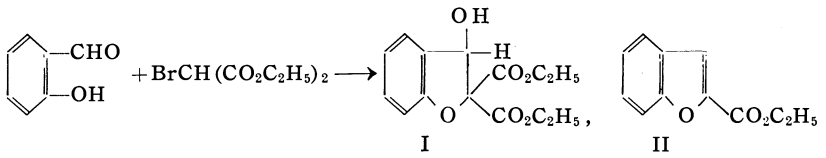
By Takashi MATSUMOTO and Kenji FUKUI

(Received June 18, 1956)

Since the discovery of the new synthetical method of coumarones by Tanaka[1] this process has been widely utilized for obtaining many sorts of benzofuran derivatives, for instance, 6-nitro- and 6-amino-coumarones[2]; 5,6-dimethoxycoumarone[3]; karanjin[4]; 3-methylcoumarilic acid[5]; coumarones[6].

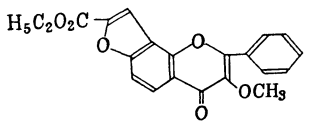
It was already noticed by Tanaka[7] that his intermediate product I of benzofuran (or its derivatives) synthesis starting from salicylic aldehyde (or its derivatives) and bromomalonic ester, was not obtained in some cases but II was procured instead. The reason for this exceptional appearance of II in the course of benzofuran synthesis was fully interpreted by the oral presentation of S. Akagi[8] who insisted that the essential point lies in the previous dehydration of the solvent (methyl ethyl ketone) applied in this reaction. When the solvent had been completely dried the reaction product was I, while II was obtained in place of I when the solvent there applied had been carelessly dried previously.

In an earlier paper[4], we and Kawase reported that 3-methoxyflavone-7,8-furan-




1) S. Tanaka, *J. Am. Chem. Soc.*, **73**, 872 (1951).
2) P. Rumpf, Ch. Gansser, *Helv. Chim. Acta.*, **37**, 435 (1954).
3) F. E. King, J. R. Housley and T. J. King, *J. Chem. Soc.* 1392 (1954).
4) Y. Kawase, T. Matsumoto and K. Fukui, This Bulletin, **28**, 273 (1955).
5) T. A. Geissmann and A. Armen, *J. Am. Chem. Soc.*, **77**, 1623 (1955).
6) Y. Odaira, This Bulletin, **29**, 470 (1956).
7) S. Tanaka, *J. Chem. Soc. Japan (Pure Chem. Sect.)* **73**, 282 (1953)
8) Presented at the Annual Meeting of Pharmaceutical Society of Japan, April 10, 1955.

$\alpha$-carboxylic acid ethyl ester (III) was obtained directly as an intermediate product from 7-hydroxy-3-methoxyflavone-8-aldehyde and ethyl bromomalonate by the method of Tanaka[1] for benzofuran synthesis. This compound III corresponds to the intermediate product II.



III

We examined the condensation products between some another aromatic o-hydroxyaldehyde derivatives and ethyl bromomalonate.

2, 6-Dihydroxy-3-carbomethoxybenzaldehyde (IV)[9,10] and ethyl bromomalonate were refluxed in methyl ethyl ketone or acetone in the presence of potassium carbonate, and 2-carbethoxy-4-hydroxy-5-carbomethoxycoumarone (V) was obtained as colorless needles of m.p. 133–4°C.

This condensation product V was hydrolysed to 4-hydroxycoumarone-2, 5-dicarboxylic acid (VI), m.p. 287–9°C (decomp.) or a mixture of VI and 2-carbethoxy-4-hydroxycoumarone-5-carboxylic acid (VII), m.p. 192–3°C by the reaction condition. Then, this dibasic acid VI was decarboxylated at 155–165°C (bath temperature) in quinoline in a stream of nitrogen gas with copper powder into karanjol (VIII), m.p. 55–6°C and karanjic acid (IX), m.p. 219–220°C (decomp.), which was identical with an authentic sample[4,11].

When the same condensation reaction was carried out with 4-benzyloxy-2-hydroxybenzaldehyde (X)[12,13], 2, 2-dicarbethoxy-3-hydroxy-6-benzyloxycoumaran (XII) was obtained as colorless crystals of m.p. 105–6°C, but ethyl 6-benzyloxycoumarone-2-carboxylate (XIV)[14] was not obtained.

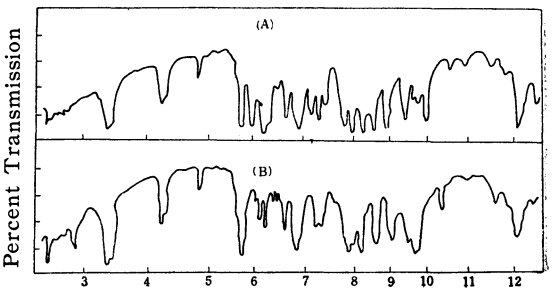
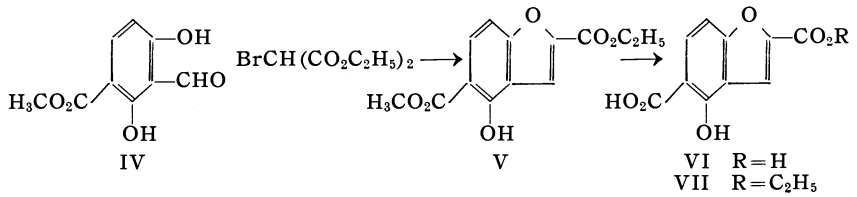
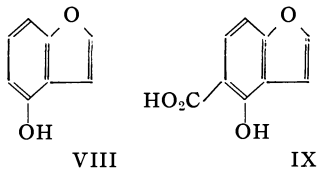
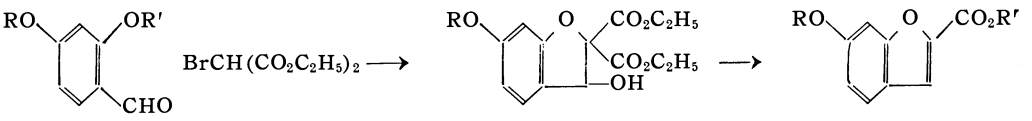



Fig. 1. Infrared Absorption Spectra (in Nujol).
A: Ethyl 5-benzyloxy-2-formylphenoxyacetate (XI)[14].
B: 2, 2-Dicarbethoxy-3-hydroxy-6-benzyloxycoumaran (XII).




X R=$CH_2C_6H_5$ R'=H
XI R=$CH_2C_6H_5$ R'=$CH_2CO_2C_2H_5$
XII R=$CH_2C_6H_5$
XIII R=$CH_2C_6H_5$ R'=H
XIV R=$CH_2C_6H_5$ R'=$C_2H_5$

9) K. Nakazawa, *J. Pharm. Soc. Japan*, **59**, 169(1939).
10) R. C. Shah and M. C. Laiwalla, *J. Chem. Soc.*, 1828 (1938).
11) R. T. Foster and A. Robertson, ibid., 115 (1948).
12) J. S. H. Davis, P. A. McCrea, W. L. Norris and G R. Ramage, ibid. 3206 (1950).
13) T. Reichstein, R. Oppenauer, A. Grussner, H. Hirt, L. Rhymer and C. Glatthaar, *Helv. Chim. Acta*, **18**, 816 (1935).
14) R. T. Foster, Alexander Robertson and Anis Bushura, *J. Chem. Soc.*, 2254 (1948).

The structure of XII was characterized by microanalytical data and infrared spectra which proved to have a hydroxyl group, as shown in the Fig. 1. This condensation product XII was hydrolysed to 6-benzyloxycoumarone-2-carboxylic acid (XIII), m.p. 199–200°C* (c.f. Reichstein et al.[13], who gave m.p. 208–9°C**) with alkaline solution or a mixture of XIII and XIV, m.p. 94°C with potassium carbonate solution.

As the result of the present investigation, 2-carbethoxy-coumarone (V) or 2,2-dicarbethoxy-3-hydroxycoumaran derivative (XII) was obtained by the condensation reaction of *o*-hydroxybenzaldehyde derivatives and ethyl bromomalonate, and it may be due to the structure of starting *o*-hydroxybenzaldehyde derivatives.

More detailed studies of this reaction are in progress.

## Experimental*

**2,6-Dihydroxy-3-carbomethoxybenzaldehyde (IV).**—This aldehyde was prepared from methyl β-resorcylate by the method of Nakazawa[9].

**2-Carbethoxy-4-hydroxy-5-carbomethoxycoumarone (V).**—A mixture of 4.7 g. of 2,6-dihydroxy-3-carbomethoxybenzaldehyde (IV), 6.0 g. of ethyl bromomalonate, 12 g. of anhydrous potassium carbonate in 200 cc. of absolute methyl ethyl ketone was refluxed eight hours in a steam bath. The precipitates were filtered off immediately and washed with methyl ethyl ketone. After distilling off the solvent, water and the excess of dilute sulfuric acid were added. The precipitates were collected, washed with water and recrystallised from aqueous acetone in colorless needles of m.p. 133–4°C, which gave a dark violet ferric reaction in alcohol and gave no 2,4-dinitrophenylhydrazone; yield 1.7 g.

*Anal.* Found: C, 58.88; H, 4.57. Calcd. for $C_{13}H_{12}O_6$: C, 59.09; H, 4.58%.

The potassium carbonate salts were dissolved in water and the solution was acidified with dilute sulfuric acid. The precipitates were collected and recrystallised from alcohol. 0.6 g. of unchanged 2,6-dihydroxy-3-carbomethoxybenzaldehyde (IV) was recovered.

The same result was obtained also with acetone.

**4-Hydroxycoumarone-2,5-dicarboxylic Acid (VI) and 2-Carbethoxy-4-hydroxycoumarone-5-carboxylic Acid (VII).**—**a)** A mixture of 5.1 g. of 2-carbethoxy-4-hydroxy-5-carbomethoxycoumarone (V) and 50 cc. of aqueous potassium hydroxide solution (10%) was heated in a steam bath with occasional shaking for thirty minutes. After cooling, the solution was acidified with dilute sulfuric acid and the precipitates thus formed were collected, washed with water and yielded obtained 4.2 g. of crude 4-hydroxycoumarone-2,5-dicarboxylic acid (VI), m.p. 278–280°C (decomp.). This crude substance was recrystallised from aqueous methanol in colorless crystals of m.p. 287–9°C (decomp.), which gave a blue ferric reaction in alcohol.

*Anal.* Found: C, 53.98; H, 3.12. Calcd. for $C_{10}H_6O_6$: C, 54.06; H, 2.72%.

**b)** A mixture of 1.7 g. of 2-carbethoxy-4-hydroxy-5-carbomethoxycoumarone (V) and 1.7 g. of potassium hydroxide in 100 cc. of methanol was refluxed for twenty minutes on a steam bath. After the solvent was acidified with dilute sulfuric acid and distilled off, the precipitates were collected, washed with water and recrystallised from methanol in colorless needles of 2-carbethoxy-4-hydroxycoumarone-5-carboxylic acid (VII), m.p. 192–3°C, having a dark violet ferric reaction in alcohol; yield 0.4 g.

*Anal.* Found: C, 57.90; H, 4.35. Calcd. for $C_{12}H_{10}O_6$: C, 57.60; H, 4.03%.

From the mother liquor of recrystallisation, 4-hydroxycoumarone-2,5-dicarboxylic acid (VI) was obtained.

**Karanjol (VIII) and Karanjic Acid (IX).**—A mixture of 3.5 g. of 4-hydroxycoumarone-2,5-dicarboxylic acid (VI), 3.5 g. of copper powder in 110 cc. of quinoline was heated under stirring in an atomosphere of nitrogen gas for about 2.5 hr. at 155–165°C (bath temperature) until evolution of carbon dioxide ceased. After being cooled and filtered from copper powder, the solution was acidified with dilute sulfuric acid and extracted with ether. The ethereal layer was extracted with an aqueous sodium bicarbonate solution and then with an aqueous sodium hydroxide solution (5%). Aqueous sodium bicarbonate extract (acid fraction) was acidified with dilute sulfuric acid and extracted with ether.

The crystals obtained on solvent removal from the dried ethereal extract were recrystallised from aqueous alcohol with the aid of charcoal in colorless needles, m.p. 219–220°C (decomp.), having a blue ferric reaction in alcohol; yield 0.43 g.

*Anal.* Found; C, 60.84; H, 3.66. Calcd. for $C_9H_6O_4$: C, 60.68; H, 3.40%.

These crystals were identical with an authentic karanjic acid prepared by the alkaline decomposition of karanjin[4] or by the method of Robertson et al.[11] Then, aqueous sodium hydroxide extract (phenol fraction) was acidified with dilute sulfuric acid and extracted with ether. The oil obtained on solvent removal from the dried ethereal extract was recrystallised from petroleum ether in colorless needles of karanjol (VIII), m.p. 55–6°C; yield 0.6 g.

*Anal.* Found: C, 71.70; H, 4.71. Calcd. for $C_8H_6O_2$; C, 71.63; H, 4.51%.

**4-Benzyloxy-2-hydroxybenzaldehyde (X).**—This aldehyde was prepared from resorcylaldehyde by the method of Davis et al.[12]

**Ethyl 5-Benzyloxy-2-formylphenoxyacetate (XI).**—This aldehyde was prepared from 4-benzyloxy-2-hydroxybenzaldehyde (X) by the method of Foster et al.[14] for the comparison of infrared spectra.

* No melting points were corrected.
** The melting point was corrected.

**2,2-Dicarbethoxy-3-hydroxy-6-benzyloxycoumaran (XII).**—A mixture of 11.4 g. of 4-benzyloxy-2-hydroxybenzaldehyde (X), 18 g. of ethyl bromomalonate, 25 g. of anhydrous potassium carbonate in 150 cc. of absolute acetone was refluxed for 7.5 hr. on a steam bath. The reaction mixture was filtered, distilled off the acetone and was mixed with water. The precipitates were collected, washed with water and recrystallised from dilute alcohol in colorless plates, m.p. 105–6°C, which gave a negative ferric reaction in alcohol and gave no 2,4-dinitrophenylhydrazone. Yield 11.7 g.

*Anal.* Found: C, 65.36; H, 5.85. Calcd. for $C_{21}H_{22}O_7$: C, 65.27; H, 5.74%.

**6-Benzyloxycoumarone-2-carboxylic Acid (XIII) and Ethyl 6-Benzyloxycoumarone-2-carboxylate (XIV).**—**a)** A mixture of 2.0 g. of 2,2-dicarbethoxy-3-hydroxy-6-benzyloxycoumaran (XII) and 50 cc. of aqueous sodium hydroxide (1 N) was heated in a steam bath with occasional shaking for twenty minutes. The cooled mixture was filtered and the filtrate was acidified with dilute sulfuric acid. The precipitates were collected, washed with water and then recrystallised from dilute alcohol. 6-Benzyloxycoumarone-2-carboxylic acid (XIII) was obtained in colorless plates, m.p. 199–200°C; yield 1.2 g.

*Anal.* Found: C, 71.92; H, 4.55. Calcd. for $C_{16}H_{12}O_4$; C, 71.63; H, 4.51%.

**b)** A mixture of 3.8 g. of 2,2-dicarbethoxy-3-hydroxy-6-benzyloxycoumaran (XII), 2.0 g. of potassium carbonate, 50 cc. of alcohol and 15 cc. of water was refluxed for 1.5 hr. on a steam bath. After distilling off the alcohol, the residue was cooled and acidified with dilute sulfuric acid. The precipitates were collected, washed with water and separated by the trituration with dilute sodium bicarbonate solution. Crystallisation of the residual solid from alcohol gave the ethyl 6-benzyloxycoumarone-2-carboxylate (XIV) in colorless plates, m.p. 94°C; yield 0.5 g. The melting point of this substance was not depressed by admixture with the sample prepared by the method of Foster et al.[14] Sodium bicarbonate solution was acidified with dilute sulfuric acid. The precipitates were collected, washed with water and recrystallised from alcohol in colorless plates, m.p. 199–200°C, yield 0.7 g., identical with the above (a).

## Summary

2-Carbethoxy-4-hydroxy-5-carbomethoxycoumarone (V) and 2,2-dicarbethoxy-3-hydroxy-6-benzyloxycoumaran (XII) were synthesized respectively from 2,6-dihydroxy-3-carbomethoxybenzaldehyde (IV) or 4-benzyloxy-2-hydroxybenzaldehyde (X) and ethyl bromomalonate by the method of Tanaka for benzofuran synthesis. 2-Carbethoxy-4-hydroxy-5-carbomethoxycoumarone (V) was hydrolysed to 4-hydroxycoumarone-2,5-dicarboxylic acid (VI).

This dibasic acid VI was decarboxylated in quinoline with copper powder into a mixture of karanjol (VIII) and karanjic acid (IX).

2,2-Dicarbethoxy-3-hydroxy-6-benzyloxycoumaran (XII) was hydrolysed to 6-benzyloxycoumarone-2-carboxylic acid (XIII).

The authors are grateful to the Institute of Organic Chemistry, Osaka City University for the measurement of infrared spectra and to the Institute of Agricultural Chemistry, Faculty of Agriculture, Kyoto University for carring out microanalyses.

*Faculty of Literature and Science*
*Toyama University, Toyama*

# *Photo-dichroism of Printed-out Silver. I. Some Experimental Evidences in Favor of the View that the Photo-dichroism of Printed-out Silver is an Anisotropic Herschel Effect*

By Isao KAMIYA

(Received June 20, 1956)

## Introduction

A film of a partially printed-out emulsion which has been isotropic becomes anisotropic in its optical nature when exposed to linear polarized red light for a considerable period. This phenomenon which was discovered by Weigert[1] in 1919, is called either the "Weigert effect" or photo-dichroism.

Many discussions on this subject have been carried out by many authors[2].

1) F. Weigert, *Ver. Phys. Ges.*, **21**, 479 (1919).

2) For example, F. Weigert, *Ann. Phys.*, **63**, 681(1920); F. Weigert and J. Shidei, *Z. Phys. Chem.*, **B9**, 344(1930); S. V. Chrdynlsev, *J. Phys. Chem.(USSR)*, **15**, 441(1941); J. Shidei, D. Yamamoto and I. Kamiya, *J. Chem. Soc. Japan*, **72**, 171 (1951); A. Narath and K. Warserroth, *Science et inds. phot.*, **23A**, 38 (1952); I. Kamiya, *J. Chem. Soc. Japan*, **76**, 576 (1955).

Weigert and Stiebel[3] postulated a theory that the colloidal particles of metallic silver in photographic emulsion (such as printed-out silver or latent image) would undergo a change to a vibrating of their structure, as they termed it "*Form-faktor*", in planes parallel to the electric vector of the light when exposed to polarized red light.

Cameron and Taylor advanced[4] the above theory and proposed a mechanism in a somewhat concrete way as follows.

Pointing out the fact that the colloidal particles such as printed-out silver are unlikely spherical but will have their long axes along planes of weakness in crystal of silver halide, they assumed that the particles which resonate to any particular wave-length would be destroyed by prolonged exposure, and that if the long axis of a particle is parallel to the electric vector of the exposed light, the destruction of this resonator would be the greatest.

These discussions are said to be unsatisfactory because of being based on such a metaphysical interpretation as *Form-faktor* or *destruction of resonator*. Moreover, it will be perhaps questionable as to whether such particles can operate in this manner.

The work reported here was undertaken in the hope that a more satisfactory theory of the phenomenon might be formulated.

The present author would prefer to propose the following explanation.

The phenomenon might be some specific effect related to Herschel effect; that is; this might be an anisotropic Herschel effect.

In the next paper, the author will discuss the mechanism, based on Herschel effect, by which the anisotropic nature is formed.

In the present paper, some experimental evidences in favor of this view are reported.

## Experimental Evidences

The first part of the work consisted in search for necessary and sufficient conditions for the production of the phenomenon.

The colloidal silver and selenium were prepared by the following method.

Adding the dilute solution of ammonium hydroxide to one per cent of a solution of silver nitrate until the white precipitation became soluble, and adding 5-6 drops of tannin solution; dark reddish colloidal silver was produced. Pouring 2 l. of warm water to 1 g. of selenium oxide, 15-16 drops of the solution of hydrazin hydrate, were added; it was then heated; dark reddish colloidal selenium was produced.

Each colloidal solution was added to gelatin emulsion to prepare the films. The absorption spectra of these films were analogous to that of the film of printed-out silver (printed-out Valenta's emulsion[5]).

These films were exposed to linear polarized red light, so that they could be examined to see if the phenomenon would be produced in them. There was found no phenomenon in the films, which means that silver chloride will be necessary to the phenomenon.

To decide this, another experiment was undertaken.

In the first place, a film of printed-out silver which had been previously fixed in the solution of alkaline hypo to avoid the dissolving silver chloride was exposed to polarized red light. In the second place, the film which had been exposed to the light for a short time was fixed, and then it was exposed again. In the third, it was never fixed. The values of dichroism observed in the three cases are shown in Table I, where, for simplicity, the angle of maximum rotation ($2\alpha$)* is directly taken to express the degree, as proposed by Weigert.

TABLE I

PHOTO-DICHROISM IN FIXED AND IN UNFIXED FILMS

| | Time of Exposure (min.) | | | | |
|---|---|---|---|---|---|
| | 1 | 5 | 10 | 20 | 30 |
| No. I | 0.00 | 0.00 | 0.01 | 0.02 | 0.03 |
| No. II | 1.52 | 4.78 | 5.88 | 5.90 | 5.90 |
| No. III | 1.00 | 2.72 | 3.12 | 4.44 | 6.76 |

It can be seen as the results of these experiments that silver chloride would be necessary to produce the phenomenon.

On the other hand, Zocher and Coper[6] have found the phenomenon in a silver mirror treated with chlorine gas to produce silver chloride on its surface (Chlorierten Silber Spiegeln) when exposed to polarized light, and Cameron and Taylor[4] have also observed it in a single crystal of blue silver chloride (containing printed-out silver).

From this point of view, it can be said that the phenomenon is to be observed in the systems in which the solid medium (such as gelatin or collodion) is absent.

Next, the author has examined the reversible effect in the partially printed-out Valenta's emulsion.

After exposure to the polarized red light for about forty minutes, the plane of polarization of the light was turned by 90°, so that the degree of dichroism began to diminish and soon had

3) F. Weigert and F. Stiebel, *Z. Phys. Chem.*, **B13**, 279 (1931).

4) A. E. Cameron and A. M. Taylor, *J. Opti. Soc. Am.*, **24**, 316 (1934).

5) Valenta in Eder, *Jahrb. Photogr.*, **76**, 960 (1898).

* $D=2\log\tan(45\pm\alpha)$, $D$ : dichroism

6) H. Zocher and M. Coper, *Z. Phys. Chem.*, **132**, 303 (1928).

entirely disappeared. Now, if the exposure was still continued, the phenomenon appeared again in the reversed direction as at first. This has been termed *reversible effect*[7]. The experimental results are shown in Fig. 1, where it can clearly be seen that the degree of dichroism tends to diminish as repeating the reversed exposure. This tendency depends on the time of pre-illumination to print out the film, i.e. when the film is pre-illuminated for a long time, it is not so remarkable even though the degree is comparatively small, while it is remarkable for a short-time pre-illumination.

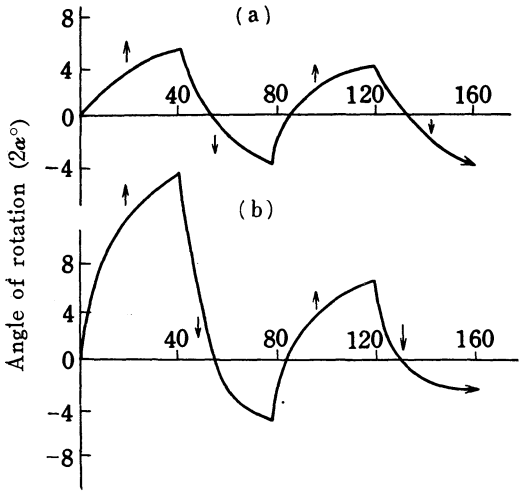



Fig. 1. Reversible effect of Photo-dichroism.
(a) and (b) show the results after 30 and 10 minutes' pre-illumination.

As the result of this, it is found that the production of photo-dichroism would be due to the partial bleaching of colloidal silver.

Finally, it is concluded that silver and silver chloride are the necessary and sufficient conditions to produce the phenomenon.

The phenomenon of photo-dichroism has been observed in the films of some gelatin-dye system as well as in the film of printed-out silver.

According to Ungar, Nikitine, and Yamamoto[8], the phenomenon observed in the films of gelatin-dye is due to an anisotropic bleaching of dye molecule; in other words, the molecules of dye-stuff of which the absorption axes orientate to the direction parallel to the electric vector of the light would be bleached, so that there remain unbleached molecules being arranged in the film after exposure to polarized light.

From this point of view, it will be emphasized that the degree of dichroism of gelatin-dye systems will decrease with increasing temperature owing to disturbance in such an arrangement.

The experimental evidence in favor of the conclusion has not been reported.

For this reason, the author has studied the temperature dependence of the phenomenon in gelatin-dye systems in just the same manner as reported by J. Shidei, M. Hosohara and D. Yamamoto[9].

The experimental results obtained in several kinds of dye-stuff are shown in Table II, where the degree of dichroism was measured with white light using 100 watt tungsten lamp, and is denoted as $2\alpha$ as before. It can be seen that the degree decreases with increasing temperature as has been expected.

TABLE II

TEMPERATURE DEPENDENCE OF DEGREE OF PHOTO-DICHROISM IN GELATIN-DYE FILMS

(a) Pinacyanol-gelatin Film (observed in white light)

| | Time of Exposure (min.) | | | | | | |
|---|---|---|---|---|---|---|---|
| | 0 | 1 | 2 | 5 | 10 | 20 | 40 |
| 6°C | 0.00 | 0.03 | 0.05 | 0.08 | 0.13 | 0.24 | 0.41 |
| Temp. 15°C | 0.00 | 0.00 | 0.02 | 0.03 | 0.04 | 0.07 | 0.15 |
| 40°C | 0.00 | 0.00 | 0.00 | 0.00 | 0.00 | 0.03 | 0.03 |

(b) Pinachrome-gelatin Film. (Observed in white light)

| | Time of Exposure (min.) | | | | | | |
|---|---|---|---|---|---|---|---|
| | 0 | 1 | 2 | 5 | 10 | 20 | 40 |
| 6°C | 0.00 | 0.01 | 0.02 | 0.04 | 0.05 | 0.11 | 0.16 |
| Temp. 15°C | 0.00 | 0.00 | 0.01 | 0.03 | 0.04 | 0.07 | 0.11 |
| 40°C | 0.00 | 0.00 | 0.00 | 0.00 | 0.01 | 0.01 | 0.02 |

On the contrary, it has been reported[9] that the degree of dichroism of printed-out silver is increased with increasing temperature. To make this sure, the decisive test was undertaken using partially printed-out Valenta's emulsion in more detail in the same manner as with the method reported by above authors[9]. These results are shown in Table III. From these evidences, it would be concluded that the mechanism of the phenomenon in printed-out silver is different essentially from that of in gelatin-dye systems.

TABLE III

TEMPERATURE DEPENDENCE OF THE DEGREE OF PHOTO-DICHROISM IN VALENTA'S FILM (OBSERVED IN RED LIGHT OF 630 mμ)

| | Time of Exposure (min.) | | | |
|---|---|---|---|---|
| | 5 | 10 | 20 | 40 |
| 10°C | 1.32 | 1.54 | 1.95 | 2.74 |
| Temp. 30°C | 2.72 | 3.12 | 4.04 | 5.86 |
| 45°C | 4.34 | 5.88 | 7.30 | 9.92 |
| 60°C | 5.36 | 6.02 | 7.06 | 8.90 |

7) S. Horiba and R. Kondo, "The Sexagint (Osaka-Fest.)" Kyoto Univ , p. 61.
8) G. Ungar, *Z. phys. Chem.*, **B38**, 427 (1938); S. Nikitine, *Ann. Phys.*, **15**, 284 (1941); D. Yamamoto, *J. Chem. Soc. Japan*, **72**, 948 (1951).
9) J. Shidei, M. Hosohara and D. Yamamoto, *J. Chem. Soc. Japan*, **73**, 184 (1952).

Now, if $D_T$ is the value of dichroism at $T$°K of temperature, and $\log D_T$ is plotted against $1/T$, then an almost approximate line is to be obtained as is shown in Fig. 2. This means that the relation between $D_T$ and $T$ must be given as,

$$\log D_T = a + b/T \qquad (1)$$

where, $a$ and $b$ are constant.

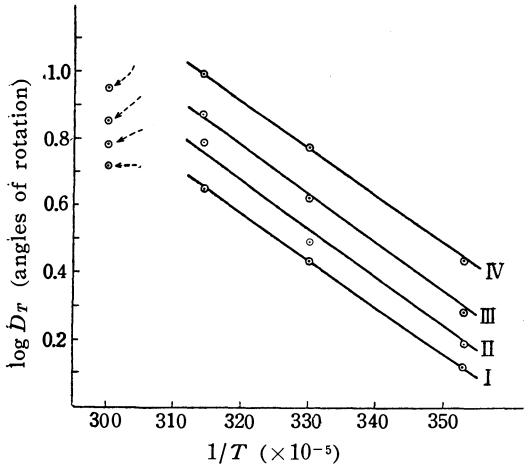



Fig. 2. Log $D_T$ vs. $1/T$.
I, II, III and IV show the results after 5, 10, 20 and 40 minutes excitation.

These results support the author's theory, which will be reported in the next paper, that the $D_T$ is to be shown as,

$$\log D_T = \log D_0 - U/2.3RT \qquad (2)$$

where, $R$ is gas constant, $D_0$ is a constant and $U$ is activation energy.

The probable value of $U$ obtained from (1), are shown in Table IV.

TABLE IV
ACTIVATION ENERGY OF PHOTO-DICHROIC CHANGE IN VALENTA'S FILM

| Time of Exposure (min.) | 5 | 10 | 20 | 40 |
|---|---|---|---|---|
| Activation energy (cal./mol.) | 6941 | 7066 | 7091 | 7120 |

Note: On this caluclation, the values observed at 60°C were neglected, probably because of deviation on account of distortion of gelatin molecules.

In the course of these experiments, the source of pre-illuminating light was a Hg-lamp, filtrated with a $UVD_1$ filter glass, (Matsuda), and that of exposing polarized red light was a five ampare carbon arc filtrated with a filter consisting of a glass tank filled with the scarlet solution transmitting the spectrum region between 630–650 m$\mu$, and a Nicol's prism. These values were measured with the 100 watt tungsten lamp, filtrated with S-63 glass filter (Shimazu).

## Discussion

It was shown in the first part of the experimental results that silver and silver chloride are the necessary and sufficient conditions to produce the phenomenon.

It has already been known that the wave length of exposed light which is the most effective is in the region between 600 m$\mu$ and 650 m$\mu$, and that the exposing for a long period is necessary to produce the phenomenon. All these facts are very similar to that in Herschel effect. Cameron and Taylor[4] have reported that the phenomenon is not produced in the film, which has been previously printed out, at the temperature of liquid nitrogen. The same behavior has also been observed by Evans and Webb[10] in the experiment on Herschel effect.

Moreover, we have just seen that the activation energy for dichroic change is obtained as about 7000 cal./mol., which is almost the same value as that of diffusion of interstitial silver ions in silver chlroride. According to the mechanism proposed by Mott and Gurney[10] the activation energy to produce the Herschel effect will be explained by the same mechanism (i.e. be diffusion energy of interstitial ions).

There is a suggestion, in opposition to the author's conclusion, that the phenomenon would be due to a solarisation. This suggestion, however, would seem not to be permissible by the following evidences.

If the solarization is, as explained by Eder[11] and Mott[10], due to the formation of a layer of silver chloride covering the metallic silver which has been attacked by the chlorine liberated in the photochemical reaction, it is not possible to explain the following fact that there is no change in the total amount of photo-silver during exposure to polarised light, which has been reported by Cameron and Taylor[4] and Weigert. Moreover, if the mechanism based on such solarization were true, the chlorine atom liberated by exposing light would be able to attack the particle of metallic silver, so that there could be found the phenomenon at liquid air temperature.

The author wishes to express his thanks to the late Prof. J. Sidei and to Dr. Yamamoto for their kind advice.

*Department of General Education*
*Nagoya University, Nagoya*

10) N. F. Mott, R. W. Gurney, "Electronic Processes in Ionic Crystals," Oxford Press(1950), p. 243; J. H. Webb and C. H. Evans, *J. Opti. Soc. Am.*, **28**, 294 (1938).
11) J. M. Eder, *Z. Phys. Chem.*, **117**, 293 (1925).

# *A Thermistor Method for the Determination of Velocity Coefficients of Vinyl Polymerization. IV*

By Hajime MIYAMA

(Received July 5, 1956)

## Introduction

In the Previous paper[1] the variation of the ratio of velocity constants of propagation and termination, $k_p/k_t$, was studied with use of a thermistor method against the conversion in vinyl acetate polymerization. In that study, however, each value of $k_p$ and $k_t$ could not be obtained. The author wishes to report, in this paper, the determination of the values of $k_p$ and $k_t$ through the study of the decomposition velocity of the sensitizer 1,1'-azo-biscyclohexanecarbonitrile, under the same conditions.

## Theoretical

Polymerization velocity $-\mathrm{d}M/\mathrm{d}t$ of vinyl acetate, as is well known, can be given as follows[2], provided that the concentration of activated molecule is constant and that the chain is long enough for the initiation velocity against the propagation to be ignored.

$$-\mathrm{d}M/\mathrm{d}t=k_p(V_{init.}/k_t)^{1/2}M \qquad (1)$$

where $V_{init.}$ represents the velocity of initiation and $M$ the concentration of the monomer. Therefore, fractional velocity $V$ can be given by

$$V=-(1/M)\mathrm{d}M/\mathrm{d}t=k_p(V_{init.}/k_t)^{1/2} \qquad (2)$$

$V$ and $k_p/k_t$ are known, as reported in the previous paper, hence $k_p$ can be calculated by the following equation when $V_{init.}$ is determined.

$$k_p=V^2\times(k_t/k_p)\times(1/V_{init.}) \qquad (3)$$

As to the mechanism of photosensitized polymerization by 1,1'-azo-biscyclohexanecarbonitrile, it is considered probable that sensitizer $S$ is decomposed by photon $h\nu$ and two activated products or radicals $R^*$ are formed from a molecule of the sensitizer,

$$S+h\nu\rightarrow 2R^* \qquad (4)$$

and this radical further activates the monomer $M$

$$R^*+M\rightarrow R+M^* \qquad (5)$$

If the following equation is taken in this mechanism, as Matheson et al.[3] assumed in the styrene polymerization with use of 2,2'-azo-bisisobutyronitrile,

$$V_{init.}=2V_s \qquad (6)$$

then equation (3) can be written as follows

$$k_p=V^2\times[2(k_p/k_t)V_s]^{-1} \qquad (7)$$

When $V$ and $k_p/k_t$ values obtained in the previous paper and $V_s$ which can be measured, are applied to the above equation (7), $k_p$ and $k_t$ values can be obtained.

## Results

Experimental apparatus and purification of samples were the same as described before[1] and the measurement was carried out at 20°C. As mentioned in the previous paper, 1,1'-azo-biscyclohexanecarbonitrile shows a big absorption band at ca. 3500 Å. Beer's law could be applied for the optical density at certain wave lengths and concentrations of the sensitizer and this relation at 3660 Å is shown in Fig. 1. D was

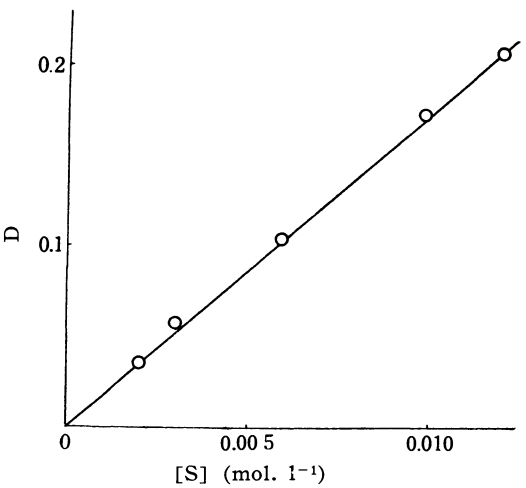



Fig. 1. Variation of the optical density with concentration of 1,1'-azo-biscyclohexanecarbonitrile.

1) H. Miyama, This Bulletin, **29**, 711, 715, 720 (1956).
2) C. E. H. Bawn, "Chemistry of High Polymers," London (1948), p. 68.
3) M. S. Matheson, E. E. Auer, E. B. Bevilacquer and E. J. Hart, *J. Am. Chem. Soc.*, **73**, 1700 (1951).

measured by use of Hitachi Spectrophotometer EPB-U in vinyl acetate and the thickness of the cell was 1 cm. Thus the decomposition velocity of the sensitizer could be determined from the optical density which, in turn, showed the concentration during the polymerization. A relation between decomposition velocity of sensitizer in vinyl acetate and initial concentration when intensity of illumination is constant, is shown in Fig. 2 and

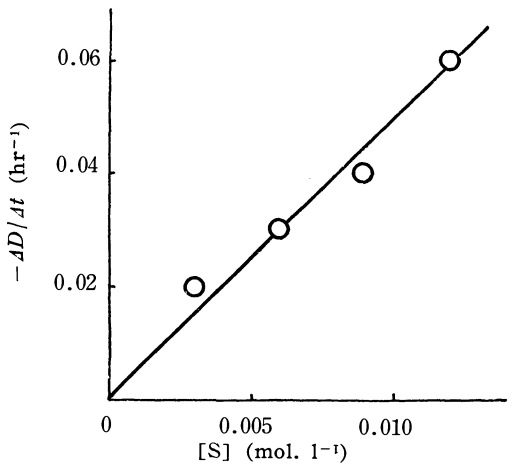



Fig. 2. The relation between decomposition velocity and concentration of 1, 1'-azo-biscyclohexanecarbonitrile.

that between intensity of light and decomposition velocity when concentration of sensitizer is constant (0.012 mol./l.), in Fig. 3. In Figs. 2 and 3, decomposition

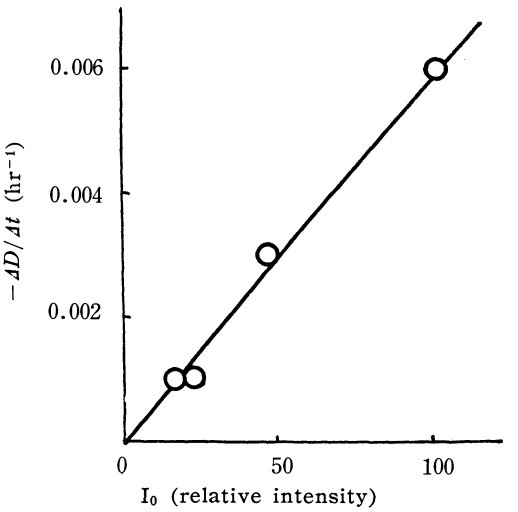



Fig. 3. The relation betweeen decomposition velocity of 1, 1'-azo-biscyclohexanecarbonitrile and intensity of illumination.

velocity $-\Delta D/\Delta t$ is a decrease of the optical density of sensitizer after one hour irradiation.

The author obtained the results shown in Fig. 4 on determination of variation of

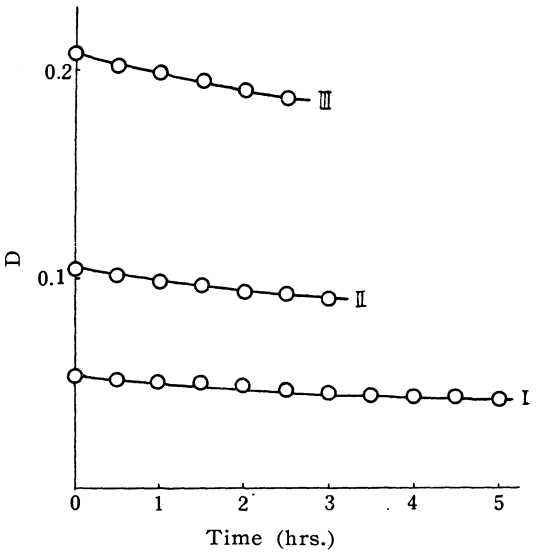



Fig. 4. Variation of the optical density of 1, 1'-azo-biscyclohexanecarbonitrile with time.
I, 0.003 mol. l$^{-1}$; II, 0.006 mol. l$^{-1}$; III, 0.012 mol. l$^{-1}$.

the optical density of sensitizer with time when continuous irradiation was applied under the same conditions as described for the vinyl acetate polymerization, which was photosensitized, in the third paper of this series. The initial concentration of the sensitizer was 0.003 mol./l., 0.006 mol./l. or 0.012 mol./l.

From the results shown in Figs. 2 and 3, it is clear that the decomposition velocity of sensitizer $V_s$ is proportional to the concentration of sensitizer $[S]$ and the intensity of light $I_0$. Absorbed light $I_{abs.}$ is shown by the next formula

$$I_{abs.}=I_0(1-e^{-\alpha[S]l}) \qquad (8)$$

where $\alpha$ is molar absorption coefficient of sensitizer (40.1) and $l$ is the thickness of the reaction vessel (8 mm.). The value of $\alpha[S]l$ is 0.096 at the concentration of sensitizer 0.003 mol./l., hence the next approximation is materialized within the error

$$I_{abs.}\fallingdotseq I_0\alpha l[S] \qquad (9)$$

thus $V_s$ is obtainable from the next equation

$$V_s=-\mathrm{d}[S]/\mathrm{d}t=kI_{abs.}=kI_0\alpha l[S] \qquad (10)$$

Since $K=kI_0\alpha l$ can be considered constant

during the measurement in Fig. 4, next equation is obtained by integrating equation (10)

$$2.303 \log [S]_0/[S] = Kt \qquad (11)$$

thus there should be a linear relation between $\log [S]_0/[S]$ and time $t$, where $[S]_0$ is the initial concentration of sensitizer. This relation can be shown in Fig. 5, in

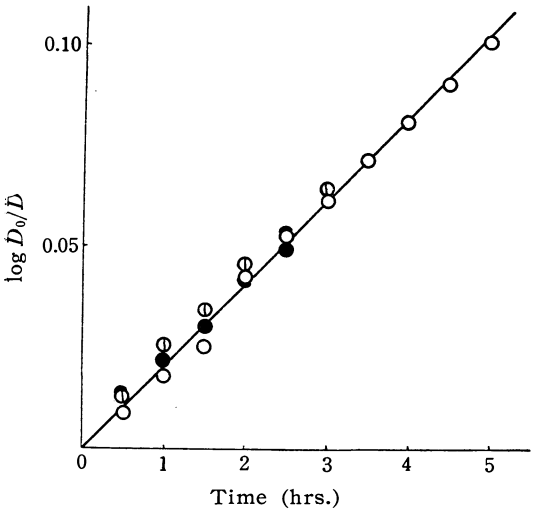



Fig. 5. Variation of $\log D_0/D$ with time. ○, 0.003 mol. $l^{-1}$; ⓘ, 0.006 mol. $l^{-1}$; ●, 0.012 mol. $l^{-1}$.

which $\log D_0/D$ is used instead of $\log [S]_0/[S]$ the former being obtained from the result of Fig. 4. The equation (11) is apparently materialized. The constant $K$ obtained from the tangent of this line is $4.66\times10^{-2}hr^{-1}$. The concentration of sensitizer in the case of determining $k_p/k_t$ of vinyl acetate polymerization was 0.003 mol./l. in the third paper of this series and thus $V_s$ at arbitrary time can be calculated by the next equation when the above value of $K$ is used.

$$V_s = K[S]_0 e^{-Kt} \qquad (12)$$

The above equation is obtained by eliminating $[S]$ from equations (10) and (11).

TABLE I

VALUES OF CONVERSION, $V_s$, $V$ AND $k_p/k_t$ AT VARIOUS IRRADIATION PERIODS

| Time (hr.) | Conversion (%) | $V_s$ (mol. $l^{-1}$. $s^{-1}$) | $V$ ($s^{-1}$) | $k_p/k_t$ |
|---|---|---|---|---|
| 0 | 0 | $3.87\times10^{-8}$ | $2.16\times10^{-5}$ | $1.08\times10^{-5}$ |
| 3 | 28.15 | $3.36\times10^{-8}$ | $2.98\times10^{-5}$ | $2.82\times10^{-5}$ |
| 4 | 39 | $3.21\times10^{-8}$ | $3.06\times10^{-5}$ | $4.13\times10^{-5}$ |
| 5 | 49.80 | $3.06\times10^{-8}$ | $2.95\times10^{-5}$ | $9.55\times10^{-5}$ |
| 6 | 59.30 | $2.92\times10^{-8}$ | $2.34\times10^{-5}$ | $32.3\times10^{-5}$ |
| 7 | 66.40 | $2.79\times10^{-8}$ | $1.61\times10^{-5}$ | $48.6\times10^{-5}$ |
| 8 | 71.10 | $2.66\times10^{-8}$ | $1.00\times10^{-5}$ | $64.2\times10^{-5}$ |

The values of $V_s$, $V$ and $k_p/k_t$, the latter two of which were obtained in the previous paper, at various times are shown in Table I. The values of $k_p$ and $k_t$, which were calculated by using equation (7) and the above values in Table I, were tabulated in Table II.

TABLE II

VALUES OF $k_p$ AND $k_t$ AT VAROUS CONVERSIONS

| Conversion (%) | $k_p$ | $k_t\times10^{-5}$ |
|---|---|---|
| 0 | 559 | 518 |
| 28.15 | 484 | 172 |
| 39 | 354 | 85.8 |
| 49.80 | 149 | 15.6 |
| 59.30 | 29.0 | 0.90 |
| 66.40 | 9.52 | 0.20 |
| 71.10 | 2.93 | 0.05 |

## Discussion

Since $k_p$ and $k_t$ values at the early stage of polymerization were obtained by many other workers, the results are shown in Table III for comparison.

TABLE III

THE VALUES OF $k_p$ AND $k_t$ OF VINYL ACETATE POLYMERIZATION AT 15°C[4]

| Reference | $k_p$ | $k_t$ |
|---|---|---|
| This work | 505 | $5.15\times10^{7}$ |
| Bengough and Melville (1955) | 574 | $2.4\times10^{7}$ |
| Bartlett et al. (1950) | 800 | $5.7\times10^{7}$ |
| Dixon-Lewis (1949) | 4180 | $2.2\times10^{8}$ |
| Matheson et al. (1949) | 630 | $4.5\times10^{7}$ |
| Burnett and Melville (1947) | 720 | $4.5\times10^{8}$ |

The value of $k_p$ obtained by the author is a little lower than the others and the $k_t$ is about the same. The methods of determination and calculation, however, are different, therefore this amount of deviation seems to be reasonable. It is doubtful whether the theory which is used for the explanation of the results at the early stage of polymerization is applicable for the later stage, but, from the results of Table II, it can be qualitatively said that $k_p$ is considered to be constant up to 40% conversion while $k_t$ gradually decreases and thus the polymerization velocity increases up to 40% conversion. As the conversion exceeds 40%, $k_p$ decreases to lower the velocity of polymerization. It is possible to consider that the velocity probably depends on the reactivity of

4) The author corrected the values at 15°C assuming that $E_p$=3.7 kcal./mole and $E_t$=0. The other values have been summarized in a literature (W. I. Bengough & H. W. Melville, *Proc. Roy. Soc.*, **230**, 429 (1955)) and corrected assuming that $E_p$=4.2 kcal./mole and $E_t$=0.

radicals or radical and monomer at the early stage of polymerization and on diffusion at the later stage, because, in the latter, viscosity increases to make diffusion very slow. From Table II, the effect of diffusion first appears in the termination process

$$M_n^* + M_m^* \rightarrow M_{n+m} \qquad (13)$$

On the other hand the propagation process shown by the next formulas is not so greatly affected by viscosity and only in conversion of more than 40% diffusion comes to have some effect on the velocity.

$$\left.\begin{aligned} &M_1^* + M \rightarrow M_2^* \\ &M_2^* + M \rightarrow M_3^* \\ &\cdots\cdots\cdots\cdots\cdots\cdots \\ &M^*_{n-1} + M \rightarrow M_n^* \end{aligned}\right\} \qquad (14)$$

This difference may be explained by the difference of mobility of monomer $M$ and radical $M_n^*$ in viscous solution.

**Summary**

Concentration change of sensitizer during vinyl acetate polymerization photosensitized by 1, 1'-azo-biscyclohexanecarbonitrile was measured with use of a spectrophotometer and the initiation velocity of polymerization was determined. Values of $k_p$ and $k_t$ at various degree of conversion were calculated from this value and the results of the previous paper. From this experiment, it was concluded that $k_p$ was nearly constant up to 40% conversion and as the conversion exceeded 40%, it decreased, while $k_t$ gradually decresed with the increase of the conversion.

The author wishes to express his hearty thanks to Dr. Momotaro Suzuki of this Academy for his helpful advice and to Mr. Shinichi Taira of Tokyo Metropolitan University for preparation of 1,1'-azobiscyclohexanecarbonitrile.

*Department of Chemistry Defense Academy Yokosuka*

# *Structures of the Erdmann's Salt, $NH_4[Co(NH_3)_2(NO_2)_4]$ and Some Other Related Nitro-ammine-cobalt (III) Complexes*

By Yoshimichi KOMIYAMA

(Received July 14, 1956)

## Introduction

Since the pioneer work of Shibata and Maruki[1], many attempts have been made to determine the configuration of tetranitro-diammine-cobaltiate ion, $[Co(NH_3)_2(NO_2)_4]^-$. As disubstituted octahedral complex has two stereoisomers, the *cis*- and the *trans*-form, there exist two possibilities in the configuration of the complex ion $[Co(NH_3)_2(NO_2)_4]^-$; i.e. the forms (A) and (A') shown in Fig. 1.

Shibata and Maruki[1] converted ammonium tetranitro-diammine-cobaltiate, $NH_4[Co(NH_3)_2(NO_2)_4]$, (Erdmann's salt) into an oxalato compound, $NH_4[Co(NH_3)_2(NO_2)_2(C_2O_4)]$. If this is derived directly from the *trans*-tetranitro-diammine (A), it can not show optical isomerism; if from the *cis*-compound (A'), two oxalato compounds should be formed, one of which, (C), has a plane of symmetry while the other (D) has no plane of symmetry so that it should be resolvable. They reported that the oxalato compound from Erdmann's salt was resolved into optical isomers ($[\alpha]_D = \pm 115°$) in the form of a potassium salt, by using brucine, strychnine and cinchonine as resolving agents and concluded that the Erdmann's salt has the *cis*-structure.

Riesenfeld and Klement[2] reported that the same attempt to resolve the oxalato compound into optical isomers was unsuccessful. Taking its chemical properties into account, they came to the conclusion that the Erdmann's salt has the *trans*-structure.

On the other hand, Thomas[3] repeated fractional crystallization of the barium

1) Y. Shibata and T. Maruki, *J. Chem. Soc. Japan*, **37**, 1142 (1916).

2) F. H. Riesenfeld and R. Klement, *Z. anorg. Chem.*, **124**, 1 (1922).

3) W. Thomas, *J. Chem. Soc.*, **123**, 617 (1923).

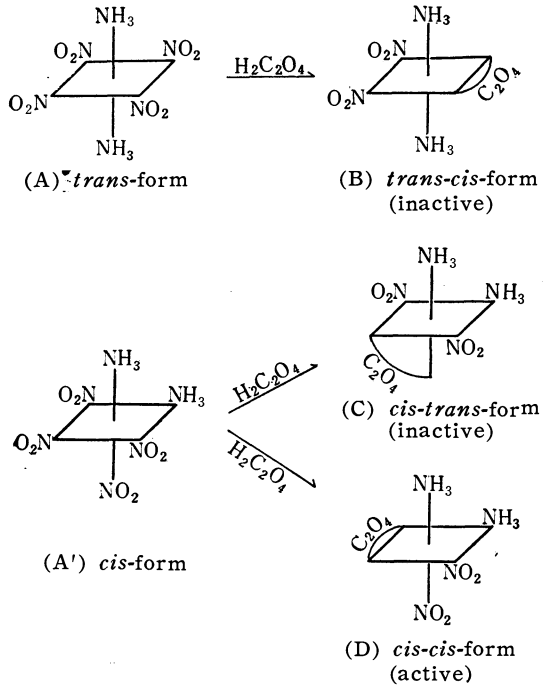



Fig. 1.

salt of the oxalato compound and obtained two different fractions; one was rhombohedral and the other was monoclinic. The rhombohedral fraction was found to be resolvable by means of strychnine and $\alpha$-phenylethylamine. The specific rotations of the optically active potassium salts measured by Na-D line were $\pm 154°$ respectively. Therefore, Thomas concluded that the two fractions had the structure (C) and (D) respectively, and assigned the *cis*-structure (A′) to the Erdmann's salt.

However, the result obtained by Ray[4] was quite contradictory. He reported that it was impossible to resolve the oxalato compound by means of salts of strychnine and *l*-$[Co\ en_3]^{3+}$. This result combined with the absorption spectrum and chemical behaviour of the compound led him to conclude that Erdmann's salt had the *trans* structure and the two fractions obtained by Thomas had been nothing but two different modifications of one compound (C).

In 1949, Kuroya and Yamasaki[5] repeated fractional crystallizations of ammonium and barium salts of the oxalato compound very carefully and concluded that the *cis*- and the *trans*-isomers of $[Co(NH_3)_2(NO_2)_4]^-$ should coexist in solution at room temperature as an equilibrium mixture.

In determining the configuration of a complex ion by various indirect means, as mentioned above, it has to be assumed that the mechanism of substitution reaction is such that they do not bring about any change of the configuration at any stage. This assumption, however, does not always seem to be valid in the case of Erdmann's salt.

Wells[6] was the first who determined the configuration of the complex anion by direct means; the crystal structure of a silver salt, $Ag[Co(NH_3)_2(NO_2)_4]$, was determined by the use of X-rays and it was shown that the complex ion possessed the *trans*-configuration. Recently, the same result was reported by E. A. Gilinskaya[7], too.

In view of the confusing results obtained by many authors, it would be of interest to determine the configuration of the complex anion in crystals of Erdmann's salt itself. As a first step, the author determined the crystal structure of a potassium salt, $K[Co(NH_3)_2(NO_2)_4]$, which was isotype to the Erdmann's salt, and the details of the work were published already in the previous report[8]. In this paper, the crystal structure of Erdmann's salt will be described, and some discussions will be given concerning the structures of various nitro-ammine-cobalt (III) complex salts, whose crystal structures[8–11] have been analyzed mainly by the author for these several years. Furthermore, the results of absorption measurements on their aqueous solutions will be reported. Since many investigators[12–14] have found interesting and important relations between the absorption spectra and the stereochemical configurations of cobalt (III) co-ordination compounds, it may be worth while to re-examine their absorption spectra.

## Experimental

Erdmann's salt, $NH_4[Co(NH_3)_2(NO_2)_4]$, has been prepared according to the method described by Jörgensen[15]. The crystals belong to the orthorhombic bipyramidal class with the axial ratio;

4) B. C. Ray, *J. Indian Chem. Soc.*, 440 (1937).
5) Read at the meeting of Chem. Soc. Japan, (1949).
6) A. F Wells, *Z. Krist.*, (A)., **95**, 74 (1936).
7) E. A. Gilinskaya, *Ser. Fiz-Mat. i Estestven. Nauk*, **3**, 133 (1953).
8) Y. Komiyama, This Bulletin, **29**, 300 (1956).
9) Y. Tanito, Y. Saito and H. Kuroya, This Bulletin, **25**, 188 (1952).
10) Y. Tanito, Y. Saito and H. Kuroya, ibid., **25**, 328 (1952).
11) Y. Tanito, Y. Saito and H. Kuroya, ibid., **26**, 420 (1953).
12) H. Sueda, *J. Chem. Soc. Japan*, **57**, 406 (1936).
13) H. Kuroya, *J. Inst. Polytech*, Osaka City Univ., Vol. 1, Ser. C, 1 (1950).
14) M. Linhard and M. Weigel, *Z. anorg. Allgem. Chem.*, **267**, 113 (1951).
15) S. M. Jörgensen, *Z. anorg. Chem.*, **17**, 477 (1898).

TABLE I

ABSORPTION MAXIMA OF NITRO-AMMINE-COBALT(III) COMPLEXES

| | $\lambda_1$(m$\mu$) | log $\varepsilon_1$ | $\lambda_2$(m$\mu$) | log $\varepsilon_2$ | $\lambda_3$(m$\mu$) | log $\varepsilon_3$ |
|---|---|---|---|---|---|---|
| *Cis*$[Co(NH_3)_4(NO_2)_2]NO_3$ | 442.0 | 2.21 | 325.0 | 3.62 | 233.5 | 4.27 |
| *Trans*$[Co(NH_3)_4(NO_2)_2]Cl$ | 429.0 | 2.49 | 341.5 | 3.83 | 251.5 | 4.37 |
| $[Co(NH_3)_3(NO_2)_3]$ | 432.0 | 2.46 | 340.0 | 3.81 | 251.0 | 4.35 |
| $[Co(NH_3)_3(NO_2)_2Cl]$ | 452.0 | 2.18 | 334.0 | 3.62 | 236.0 | 4.15 |
| $K[Co(NH_3)_2(NO_2)_4]$ | 421.0 | 2.71 | 348.0 | 4.05 | 253.5 | 4.43 |

$a : b : c = 0.8837 : 1 : 0.5226$ and are dark reddish brown in colour. They are well-formed and elongated along the *c*-crystal axis. In these respects they resemble the corresponding potassium salt.

The ammonium salt has $a = 11.39 \pm 0.02$ Å, $b = 12.97 \pm 0.02$ Å, and $c = 6.74 \pm 0.01$ Å, $Z = 4$. These values give the axial ratio $a : b : c = 0.878 : 1 : 0.520$, which are in good agreement with those obtained by crystal measurement.

From the systematic absences; ($h00$), ($0k0$) and ($00l$) for $h$, $k$ and $l$ odd, the space group was found to be $P2_12_12_1$. The calculated density 1.966 g./cc. is in agreement with that observed, 1.954 g./cc. at 25.5°C.

All the equatorial reflections around the three principal axes were recorded by using Fe K$\alpha$ radiation on a pack of three films and the intensity of the reflections were visually estimated. The usual correction factors were applied by means of Cochran's chart[16]. Observed structure amplitudes were then placed on the absolute scale by Wilson's method[17].

The measurements of absorption spectra of these nitro-ammine-complexes and two others for reference, were made over the range from 220 to 500 m$\mu$ with Beckman Model DU spectrophotometer. Concentrations of aqueous solution used for measuring absorption was ranging from $10^{-3}$ to $10^{-5}$ mol./*l*.. The absorption maxima are tabulated in Table I.

## Determination of the Structure

By comparing the general features of structure amplitudes and Patterson projections along the three principal axes of Erdmann's salt with those of the potassium salt, it was seen that they are isotype. As the first step, therefore, $F$ values were calculated by using the parameter values of the potassium salt. The agreement between the observed and calculated $F$ values was good enough to enable the usual Fourier refinement to be started. Then all the parameter values were refined successfully and the final parameters listed in Table II were obtained. A final electron density projection on a plane perpendicular to the *c*-axis is shown in Fig. 2.

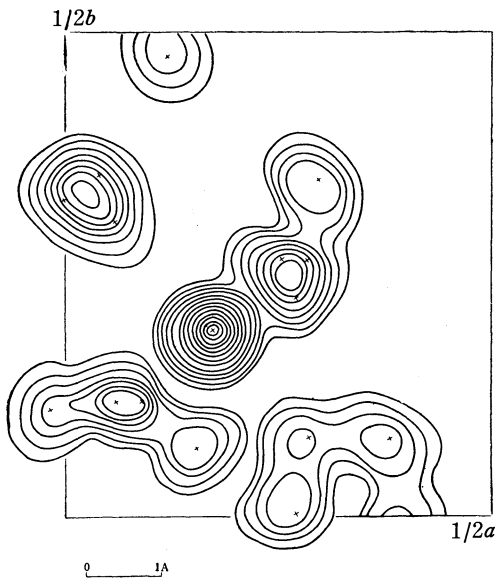



Fig. 2. Electron densities along *c*-axis of $NH_4[Co(NH_3)_2(NO_2)_4]$. Contours are at intervals of 2 e.Å$^{-2}$.

The atomic scattering factors used for the calculation of the structure factors were those listed in the International Tables. A temperature factor of the form $\exp -B(\sin\theta/\lambda)^2$ was used, where B was given the value 2.5 Å$^2$. The value of B and the scale factor were estimated by plotting the values of $\log F_c/F_o$ versus $(\sin\theta)^2$ at the final stage. The reliability factors $R = \sum||F_o| - |F_c||/\sum|F_o|$ are 0.160, 0.243 and 0.208 for ($hk0$), ($0kl$) and ($h0l$) respectively. The weighted mean value of $R$ is 0.188, for which only the observed reflections up to $\sin\theta/\lambda = 0.501$ have been used.

## Description of the Structure

The structure projected upon a plane normal to the *c*-crystal axis is shown in Fig. 3. The structure is built of ammonium ions and complex anions $[Co(NH_3)_2(NO_2)_4]^-$, thus being essentially ionic.

Interatomic distances and bond angles

16) W. Cochran, *J. Sci., Inst.*, **25**, 253 (1949).
17) A. J. C. Wilson, *Acta Cryst.*, **2**, 318 (1949).

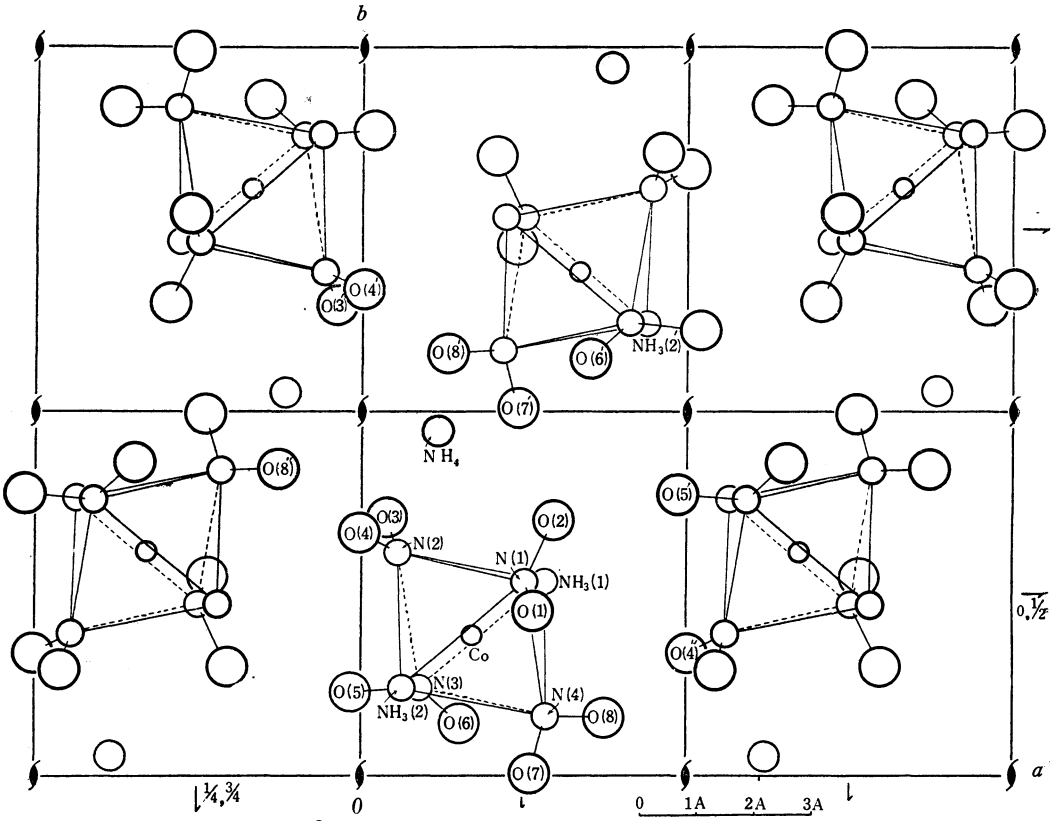



Fig. 3. Projection of the structure upon (001).

calculated on the basis of the atomic parameters in Table II are given in Table III. Two ammonia molecules are found to be co-ordinated to a cobalt atom in the *trans*-positions at the distance of 2.01 Å. Within the errors of the experiments this structure is exactly isotype to the corresponding potassium salt, and hence the detailed description of the structure will be discussed in the next section together with

TABLE II

FINAL PARAMETERS

| | *x/a* | *y/b* | *z/c* |
|---|---|---|---|
| Co | 0.1690 | 0.1915 | 0.2500 |
| $NH_4$ | 0.117 | 0.473 | 0.695 |
| $NH_3(1)$ | 0.279 | 0.265 | 0.064 |
| $NH_3(2)$ | 0.059 | 0.118 | 0.436 |
| N (1) | 0.250 | 0.264 | 0.466 |
| N (2) | 0.056 | 0.305 | 0.234 |
| N (3) | 0.088 | 0.119 | 0.034 |
| N (4) | 0.281 | 0.078 | 0.266 |
| O (1) | 0.264 | 0.226 | 0.632 |
| O (2) | 0.293 | 0.350 | 0.442 |
| O (3) | 0.040 | 0.353 | 0.077 |
| O (4) | −0.003 | 0.332 | 0.383 |
| O (5) | −0.018 | 0.112 | 0.017 |
| O (6) | 0.150 | 0.070 | −0.074 |
| O (7) | 0.260 | 0.005 | 0.376 |
| O (8) | 0.370 | 0.076 | 0.171 |

TABLE III

INTERATOMIC DISTANCES AND INTERBOND ANGLES

| | | | | |
|---|---|---|---|---|
| Co−$NH_3(1)$ | 2.01 Å | $NH_4$ | ···O(2) | 3.08 Å |
| −$NH_3(2)$ | 2.01 | | ···O(3) | 3.15 |
| −N(1) | 1.96 | | ···O(4) | 3.10 |
| −N(2) | 1.96 | | ···O(3′) | 2.99 |
| −N(3) | 1.96 | | ···O(4′) | 3.11 |
| −N(4) | 1.96 | | ···O(7′) | 3.24 |
| | | | ···O(8′) | 2.81 |
| N(1)−O(1) | 1.23 | | ···O(8″) | 3.02 |
| −O(2) | 1.23 | | | |
| ∠ONO | 116° | $NH_3(1)$ | ···O(5′) | 2.86 |
| | | $NH_3(1)$ | ···O(1) | 2.96 |
| N(2)−O(3) | 1.24 | $NH_3(2')$ | ···O(5′) | 3.07 |
| −O(4) | 1.26 | | | |
| ∠ONO | 118° | O(1) | ···O(4″) | 2.76 |
| | | O(2) | ···O(6′) | 3.06 |
| N(3)−O(5) | 1.22 | O(2) | ···O(7′) | 3.00 |
| −O(6) | 1.20 | O(3) | ···O(7′) | 3.03 |
| ∠ONO | 119° | O(3) | ···O(8″) | 2.72 |
| N(4)−O(7) | 1.23 | | | |
| −O(8) | 1.20 | | | |
| ∠ONO | 118° | | | |

those of other nitro-ammine-cobalt (III) complexes.

## Discussions on the Structure of Nitro-ammine-cobalt (III) Complexes

**General Features of Crystal Structure.** —The crystal data of various nitro-ammine-cobalt(III) complexes are listed in Table IV.

It is worth while to point out that in all these structures the cobalt atoms always occupy the sets of positions having higher symmetry than the corresponding space group. The symmetries of the arrangement of cobalt atoms, are shown in Table V.

Crystals of trinitro-triammine-cobalt(III) $[Co(NH_3)_3(NO_2)_3]$[9] and chlorodinitro-triammine-cobalt(III) $[Co(NH_3)_3(NO_2)_2Cl]$[11] are molecular, while those of potassium and ammonium tetranitro-triammine-cobaltiate(III) $K[Co(NH_3)_2(NO_2)_4]$[8], $NH_4[Co(NH_3)_2(NO_2)_4]$ are essentially ionic.

Characteristics of this structure seem to be the presence of spatial network consisting of the complex radicals. The binding force between the complex radicals is mainly due to the NH···O bonds between $NH_3$ and $NO_2$ groups.

Fig. 4 illustrates a network of complex radicals found in the structure of $[Co(NH_3)_3(NO_2)_3]$. It is perpendicular to the *a*-crystal axis. Each complex ion forms four hydrogen bonds with four neighboring complex radicals.

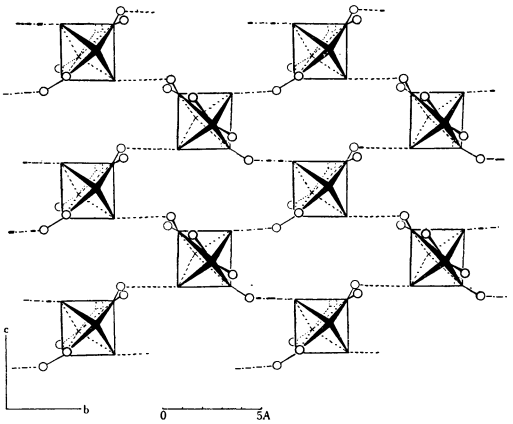



Fig. 4. Two dimensional network of complex radicals found in crystal of $[Co(NH_3)_3(NO_2)_3]$.
----: linkages of 2.74 Å.
-·-·-: linkages of 2.78 Å.

Only one of the two oxygen atoms of $NO_2$ groups which are in the *trans*-positions with respect to each other is used to form a NH···O bond of 2.74 Å and 2.78 Å with $NH_3$ of the adjacent complex radicals, and the other oxygen atom is farther from its nearest $NH_3$ groups, (3.10 Å and 3.29 Å apart).

A similar type of network was found in the structure of $[Co(NH_3)_3(NO_2)_2Cl]$, which

TABLE IV

CRYSTAL DATA OF NITRO-AMMINE-COBALT(III) COMPLEXES

| | Crystal System | Space Group | Lattice Constants | | | β | Z |
|---|---|---|---|---|---|---|---|
| | | | *a* | *b* | *c* | | |
| $[Co(NH_3)_3(NO_2)_3]$ | Orthorhombic | $D_2^4-P2_12_12_1$ | 10.20 Å | 11.77 Å | 6.99 Å | | 4 |
| $[Co(NH_3)_3(NO_2)_2Cl]$ | Tetragonal | $C_{4h}^6-I4_1/a$ | 9.87 | | 16.51 | | 8 |
| $[Co(NH_3)_3(NO_2)_2Br]$ | Monoclinic | $C_{2h}^5-P2_1/n$ | 12.24 | 10.31 | 6.85 | 103.5° | 4 |
| $K[Co(NH_3)_2(NO_2)_4]$ | Orthorhombic | $D_2^4-P2_12_12_1$ | 11.38 | 12.95 | 6.76 | | 4 |
| $NH_4[Co(NH_3)_2(NO_2)_4]$ | Orthorhombic | $D_2^4-P2_12_12_1$ | 11.38 | 12.97 | 6.74 | | 4 |

TABLE V

PSEUDO-SYMMETRIES OF THE ARRANGEMENT OF COBALT ATOMS

| | *x*/*a* | *y*/*b* | *z*/*c* | |
|---|---|---|---|---|
| $[Co(NH_3)_3(NO_2)_3]$ | 0.0686 | 1/4 | 1/4 | $D_{2h}^{17}-Bbmm$ |
| $[Co(NH_3)_3(NO_2)_2Cl]$ | 0 | 0 | 0.267 | $D_{4h}^{19}-I4_1/amd$ |
| $[Co(NH_3)_3(NO_2)_2Br]$ | 1/4 | *y* | 0 | $C_{2h}^6-A2/n$ |
| $K[Co(NH_3)_2(NO_2)_4]$ | 0.1690 | 0.1915 | 1/4 | $D_{2h}^{16}-Pbnm$ |
| $NH_4[Co(NH_3)_2(NO_2)_4]$ | 〃 | 〃 | 〃 | 〃 |

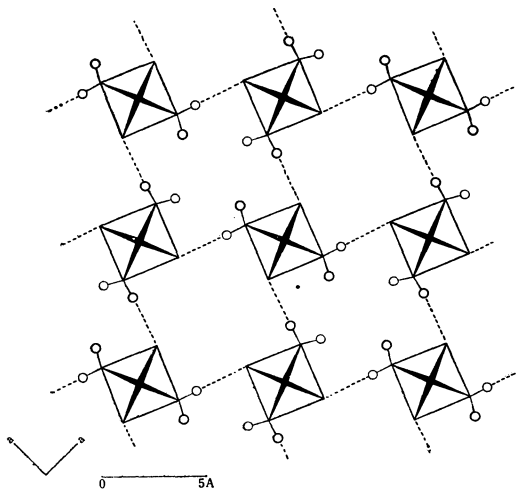



Fig. 5. Two dimensional network of complex radicals found in crystal of $[Co(NH_3)_3(NO_2)_2Cl]$.
----: linkages of 2.84 Å.

is shown in Fig. 5. The network is perpendicular to the *c*-crystal axis. Each complex ion is held together by a hydrogen bond of 2.84 Å, the mode of binding being essentially similar to that illustrated in Fig. 4. However, in the structure of $[Co(NH_3)_3(NO_2)_2Cl]$ these networks are held together by another NH···O bond between $NO_2$ and $NH_3$ of complex radical belonging to the adjacent layers, forming a three-dimensional network.

Thus, both of the oxygen atoms in the nitro-group are used to form NH···O bonds as follows:

$$N\begin{cases} O\cdots NH_3 \text{ (within a layer)} \\ O\cdots NH_3 \text{ (within an adjacent layer).} \end{cases}$$

In Fig. 6 is shown a network which is found in crystals of $K[Co(NH_3)_2(NO_2)_4]$ and $NH_4[Co(NH_3)_2(NO_2)_4]$. The plane of the network is perpendicular to the *b*-crystal axis. NH···O hydrogen bonds which are responsible for binding the complex anions with each other in a single layer are 2.87 Å and 2.97 Å.

It is interesting that the arrangement of cobalt atoms only in the network is remarkably similar to that found in the structures of $[Co(NH_3)_3(NO_2)_3]$, except that the orientation of octahedra consisting of

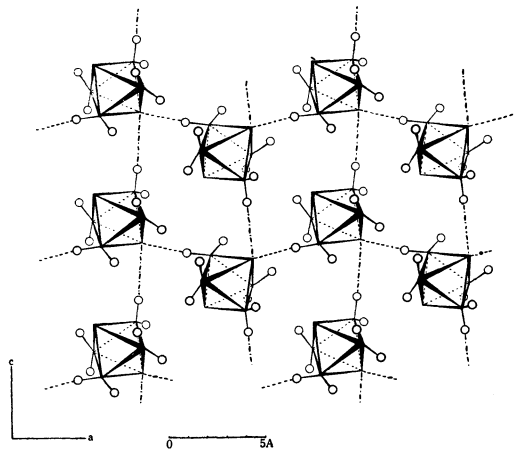



Fig. 6. Two dimensional network of complex radicals found in crystals of $K[Co(NH_3)_2(NO_2)_4]$ and $NH_4[Co(NH_3)_2(NO_2)_4]$.
----: linkages of 2.87 Å.
-·-·-: linkages of 2.97 Å.

TABLE VI

THE INTERATOMIC DISTANCES BETWEEN COBALT AND ITS LIGAND ATOMS

| | Co—$NH_3$ | In *trans*-coordination with respect to | Co—$NO_2$ | In *trans*-coordination with respect to | Co—Cl | In *trans*-coordination with respect to |
|---|---|---|---|---|---|---|
| $[Co(NH_3)_3(NO_2)_3]$ | 1.98 Å | $NH_3$ | 1.96 Å | $NH_3$ | | |
| | 1.99 | 〃 | 1.97 | $NO_2$ | | |
| | 1.97 | $NO_2$ | 1.97 | 〃 | | |
| $[Co(NH_3)_3H_2OCl_2]$ | 1.96 | $NH_3$ | | | 2.33 Å | Cl |
| $[Co(NH_3)_3(NO_2)_2Cl]$ | 1.99 | $NH_3$ | 1.99 | $NO_2$ | 2.30 | $NH_3$ |
| | 1.90 | Cl | | | | |
| $K[Co(NH_3)_2(NO_2)_4]$ | 2.00 | $NH_3$ | 1.96 | $NO_2$ | | |
| | 2.00 | 〃 | 1.96 | 〃 | | |
| | | | 1.96 | 〃 | | |
| | | | 1.96 | 〃 | | |
| $NH_4[Co(NH_3)_2(NO_2)_4]$ | 2.01 | $NH_3$ | 1.96 | $NO_2$ | | |
| | 2.01 | 〃 | 1.96 | 〃 | | |
| | | | 1.96 | 〃 | | |
| | | | 1.96 | 〃 | | |

six nitrogen atoms around each cobalt atom is slightly different from that of $[Co(NH_3)_3(NO_2)_3]$, and that the mode of binding is different. In case of $[Co(NH_3)_3(NO_2)_3]$ one ammonia group is used to form NH···O hydrogen bond with only one nitro-group, but in Erdmann's salt one ammonia group is bound to the two oxygen atoms of $NO_2$ groups belonging to different complex anions.

Potassium and ammonium ions are distributed between these networks. Hence the distances between the layers, 6.48 Å and 6.49 Å, are longer than the corresponding one, 5.10 Å, found in the crystals of $[Co(NH_3)_3(NO_2)_3]$.

Two nitro-groups which are in the *trans*-co-ordination seem to be more likely to form NH···O bonds than the case in which a nitro-group and other ligand are co-ordinated to the central cobalt atom in the *trans*-positions with respect to each other.

The interatomic distances between cobalt and its ligand atoms found in these four nitro-ammine-cobalt (III) complexes as well as dichrochloride $[Co(NH_3)_3H_2OCl_2]Cl$[10] are tabulated in Table VI.

**The Shape of Nitro-groups in Nitro-ammine-cobalt (III) Complexes.**—There have been no accurate data available for the shape and size of nitro-groups in nitro-ammine-cobalt(III) complexes. The present investigation provides the results shown in Table VII. The average of these values are: N—O=1.23$_3$Å, ∠ONO=119.3°. Such a shape and size are not very different from those found in various inorganic[6,7,19] and organic[20] compounds.

TABLE VII

THE SHAPE OF NITRO-GROUPS IN NITRO-AMMINE-COBALT(III) COMPLEXES

| | N—O | | ∠ONO |
|---|---|---|---|
| $[Co(NH_3)_3(NO_2)_3]$ | 1.24 Å | 1.25 Å | 127° |
| | 1.25 | 1.27 | 119° |
| | 1.25 | 1.27 | 121° |
| $[Co(NH_3)_3(NO_2)_2Cl]$ | 1.22 | 1.24 | 119° |
| $K[Co(NH_3)_2(NO_2)_4]$ | 1.23 | 1.24 | 115° |
| | 1.21 | 1.26 | 116° |
| | 1.20 | 1.22 | 118° |
| | 1.20 | 1.23 | 124° |
| $NH_4[Co(NH_3)_2(NO_2)_4]$ | 1.23 | 1.23 | 116° |
| | 1.24 | 1.26 | 118° |
| | 1.20 | 1.22 | 119° |
| | 1.20 | 1.23 | 118° |

18) To be published shortly.

19) Van Driel, M. and Vermeel, H. J., *Z. Krist.*, **A. 95**, 308 (1936); Gene B. Carpenter, *Acta Cryst.*, **5**, 132 (1952); Mary R. Truter, ibid., **7**, 73 (1954).

20) S. C Abrahams and J. Monteath Robertson, ibid., **1**, 252 (1948); D. June Sutor, F. J. Llewellyn and H. S. Maslen, ibid., **7**, 145 (1954); D. June Sutor, L. D. Calvert and F. J. Llewellyn, ibid., **7**, 767 (1954).

## Relation between Absorption Spectra of Aqueous Solution and Configuration of the Complex Radicals

A number of studies have been made on the relation between the structures of nitro-ammine-complexes of cobalt(III) and their absorption spectra in solution. These results are summarized as follows:

1) The special absorption band of nitro-radical appears in the region from 350 to 330 mμ ($\nu=86\sim90\times10^{13}$ sec.$^{-1}$). Since this band is extremely bathochromic, the second absorption band found in ordinary cobalt (III) complexes is strongly masked. Thus the absorption curves are usually observed which are quite different from those obtained in case of $[Co(NH_3)_6]^{+3}$, $[Co\,en_3]^{3+}$ and $[Co(NH_3)_5Cl]^{++}$.

2) When two nitro-groups enter into combination to the central cobalt atom in *trans*-positions, the third absorption band appears at approximately 250 mμ ($\nu\simeq120\times10^{13}$ sec.$^{-1}$)[21–23]. For instance see Figs.

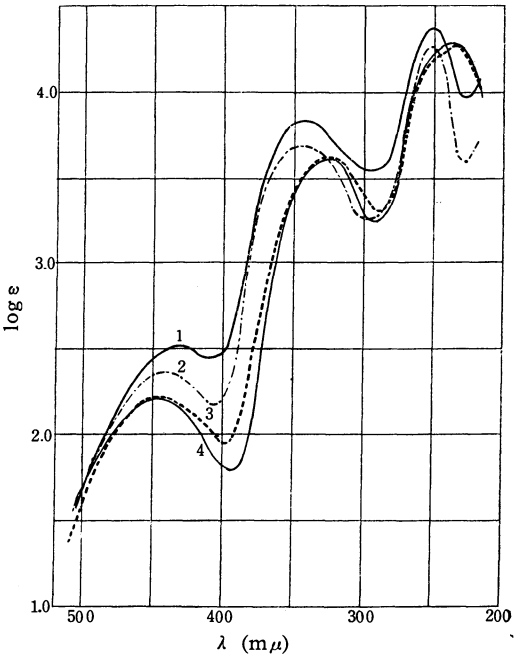



Fig. 7. Absorption spectra of *trans*- and *cis*-$[Co(NH_3)_4(NO_2)_2]^+$ in aqueous solutions.
1 and 2: *trans*-isomor, 3 and 4: *cis*-isomer,
2 and 4: obtained by M. Linhard.

21) R. Tsuchida, "Colours and Structures of the Metallic Compounds" (1944), p 96-113.

22) H. Kuroya and R. Tsuchida, This Bulletin, **15**, 427 (1940).

23) M. Linhard and M. Weigel, *Z. anorg. allgem. Chem.*, **267**, 113 (1950).

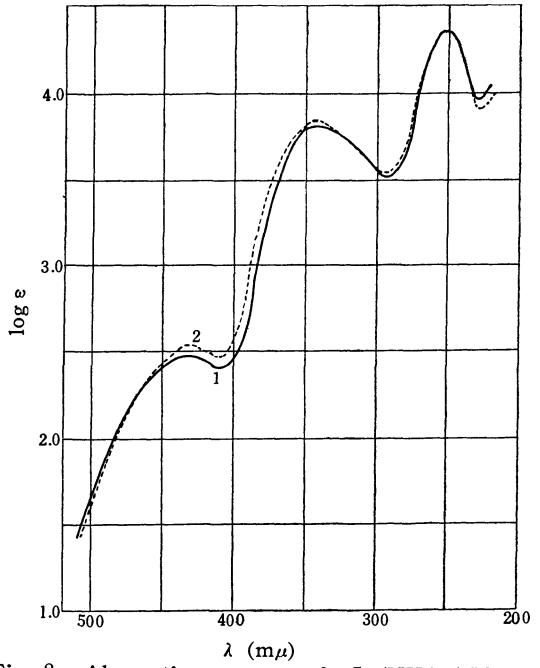



Fig. 8. Absorption spectra of $[Co(NH_3)_3(NO_2)_3]$ in aqueous solution.
2: obtained by M. Linhard.

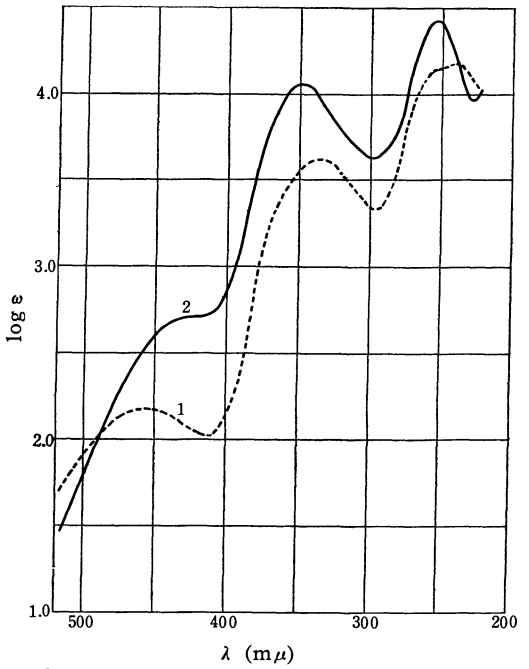



Fig. 9. Absorption spectra of $[Co(NH_3)_3(NO_2)_2Cl]$ (1) and $[Co(NH_3)_2(NO_2)_4]^-$ (2) in aqueous solutions.

7, 8 and 9. This fact has been a part of the basis of "*trans*-negative radical hypothesis". This hypothesis states that the third band appears when two negative ligands are in the *trans*-co-ordination with respect to each other. It turned out later that even when two nitro-groups or some other negative radicals are co-ordinated even in the *cis*-positions, similar third band can still be observed, but in this case the absorption maximum is very much shifted towards shorter wave lengths[24]. Therefore the "*trans*-negative radical hypothesis" should be stated as follows: the third band appears in the region near 250 mμ when two negative radicals are co-ordinated in the *trans*-positions.

The author has measured the absorption spectra of the following complex compounds: (A) $[Co(NH_3)_3(NO_2)_3]$, (B) $[Co(NH_3)_3(NO_2)_2Cl]$, (C) $K[Co(NH_3)_2(NO_2)_4]$, (D) *cis*$[Co(NH_3)_4(NO_2)_2]NO_3$ and (E) *trans* $[Co(NH_3)_4(NO_2)_2]Cl$.

Among these the crystal structures of (A), (B) and (C) have been determined by the present author. The absorption spectra of (D) and (E) were measured merely for reference. The results obtained are shown in Figs. 7, 8 and 9. All these curves were in good accord with those observed by other investigators. For comparison, the corresponding curves obtained by Linhard[23] are inserted in Figs. 7 and 8.

The X-ray evidence revealed that in (A) three nitro-groups are in the *trans-cis*-positions, and in (B) and (C) two nitro-groups are found to be in the *trans*-co-ordination. Corresponding to these configurations, the third bands appear at about 250 mμ in the absorption spectra of these compounds, as in the case of (E).

On the other hand, in (D), where two nitro-groups are in the *cis*-positions, the third band appears in the region of far shorter wave-lengths. Thus the "*trans*-negative radical hypothesis" was indeed confirmed, since the configurations of these nitro-complexes was established by the present investigation.

In view of this result a different configuration would be assigned to $[Co(NH_3)_3(NO_2)_3]$ prepared by Sueda[25], as the absorption curve is different from the one shown in Fig. 6. $[Co(NH_3)_3(NO_2)_2Br]$[26] shows similar absorption spectra to $[Co(NH_3)_3(NO_2)_2Cl]$. Since the configuration of the latter has been established, the configuration of the former is expected to be a *trans*-form with respect to two nitro-groups. The crystal structure analysis is

24) F. Basolo, *J. Am. Chem. Soc.*, **72**, 4393 (1950).
25) H. Sueda, *J. Chem. Soc. Japan*, **59**, 47 (1938).
26) M. Kobayashi, A. Hagitani and I. Mita, ibid., **58**, 391 (1937).

now being continued by the present author. The result will be published soon.


## Summary

$NH_4[Co(NH_3)_2(NO_2)_4]$ belongs to the space group $P2_12_12_1$, with four formula units per unit cell. All the atomic co-ordinates were determined by the method of two-dimensional Fourier series. The structure is found to be isotype to $K[Co(NH_3)_2(NO_2)_4]$. Two ammonia groups are co-ordinated to the central cobalt atom in the *trans*-positions.

General features of the structures of various nitro-ammine-cobalt(III) complexes were discussed. The absorption spectra of these complexes were reexamined in their aqueous solutions. Results are briefly discussed in relation to their steric configurations.


The author wishes to express his sincere thanks to Professor H. Kuroya, Dr. Y. Saito and Professor Y. Morino, who have shown keen interest during the course of this study, have critically read the manuscript, and have given the author much invaluable advice. Part of the cost of this study has been defrayed from the Grant in Aid for Fundamental Scientific Research from the Ministry of Education.

*Institute of Polytechnics*
*Osaka City University, Osaka*

# *The Separation of α-Glycerophosphoric Acid from its β-Isomer by Paper Chromatography**

By Chieko URAKAMI and Yoshiko KAKUTANI

(Received June 24, 1956)

## Introduction

Chemical configurations of naturally occurring phosphatides or phosphatidic acids have been questioned for a long time, the difficulty being due to the reversible migration or hydrolysis of the phosphoryl group during the course of isolation or hydrolytic decomposition in the determination of the structures. Recently, Baer and co-workers have shown for a number of naturally occurring phosphatides that they possess the α-structure and L-configuration[1]. The L-α-configuration of lecithins was confirmed later by Long and Maguire[2]. In addition to the reversible migration of the phosphoryl group, difficulty arises because there has been developed no simple and adequate method of direct determination or identification of β-glycerophosphoric acid (β-GPA), which is less stable than α-GPA.

For either identification or quantitative determination of the α and β-isomers, the following methods have been used: the determination of their rates of hydrolysis by enzymes[3], the isolation of barium α-glycerophosphate (GP) and the barium nitrate complex of barium β-GP[4], the periodate oxidation method[5,6], and the determination of inorganic phosphoric acid derived from oxidative and hydrolytic decomposition[7]. All of these methods are time consuming and do not afford direct identification or determination of the β-isomer. Therefore, simple methods which would give this information would have useful applications.

Although a number of papers dealing

* This work was presented, in part, before the Eighth Annual Meeting of The Chemical Society of Japan, April, 1955.

1) E. Baer and M. Kates, *J. Am. Chem. Soc.*, **70**, 1394 (1948); *J. Biol. Chem.*, **175**, 79 (1948); *J. Am. Chem. Soc.*, **72**, 942 (1950); *J. Biol. Chem.*, **185**, 615 (1950); E. Baer, H. C. Stancer and I. A. Korman, ibid., **200**, 251 (1952); E. Baer, J. Maurukas and M. Russell, *J. Am. Chem. Soc.*, **74**, 152 (1952); E. Baer and H. C. Stancer, ibid., **75**, 4510 (1953); E. Baer and J. Maurukas, *J. Biol. Chem.*, **212**, 25 (1954); ibid., **212**, 39 (1954); E. Baer, D. Buchnea and A. G. Newcombe, *J. Am. Chem. Soc.*, **78**, 232 (1956).

2) C. Long and M. F. Maguire, *Biochem. J.*, **57**, 223 (1954).

3) H. D. Kay and E. R. Lee, *J. Biol. Chem.*, **91**, 135 (1931).

4) P. Karrer and B. P. Benz, *Helv. Chim. Acta*, **10**, 87 (1927).

5) F. Rapoport, I. Reifer and H. Weinmann, *Mikrochim. Acta*, **1**, 290 (1937).

6) P. Fleury and J. Courtois, *Bull. soc. chim.*, **8**, 397 (1941).

7) C. F. Burmaster, *J. Biol. Chem.*, **164**, 233 (1946).

with the chromatographic separation of organic esters of phosphoric acid of chemical and biological interest have appeared elsewhere, none of these have applied specifically to the problem of separating the glycerophosphates. Khym[8] attained a certain degree of separation of the isomers on an anion exchanger column, but it was not quite complete.

Conditions to be used for chromatography should be selected to eliminate hydrolysis and isomerization reactions. It has been shown that alkaline rather than acidic conditions are preferable[9,10] in order to avoid the occurrence of these two reactions in the case of the glycerophosphates.

We have studied the behaviors of $\alpha$-GPA and $\beta$-GPA, and their alkaline metal and ammonium salts on alumina impregnated paper and achieved a complete separation of the two isomers as sodium salts, by using methanol-ammonia (60 : 5) as a developing solvent. Since it is known that alumina gives rise to secondary reactions in the presence of alkali during the course of chromatography[11], it would be necessary to examine if the compounds under consideration have undergone any chemical changes such as hydrolysis or migration of the phosphoryl group. It has been demonstrated that no hydrolysis or migration of the phosphoryl group takes place during the course of the chromatography. The system presented utilizes the ion exchange property of alumina and exploits differences of the ionic attractive forces which might be exhibited between a cation and anions of different acidities[12].

## Experimental

**Alumina Impregnated Paper.**—Toyo filter paper No. 50 (2×40 cm.) was used. The paper was prepared according to Bush's method[13], except that a twenty-four hour washing time and a forty-eight hour exposure time to ammonia vapor were maintained. The paper prepared in this manner showed pH 8 and had adsorbed an average of 8 per cent by weight of alumina. These conditions should be maintained in order to obtain compact spots of the glycerophosphoric acids. The paper remained sensitive for four to five days when kept in an air-tight container.

**Sample Solutions.**—The solutions of sodium $\alpha$-*, sodium $\beta$-**, barium $\alpha$-*, and barium $\beta$-glycerophosphates*** were prepared by dissolving a weighed amount of the respective salt in distilled water so that each 10 $\mu l$. of the solution contained 250 $\mu$g. of the free acid. For the preparation of a solution of a mixture of the sodium salts of the $\alpha$- and $\beta$-isomers, 104 mg. each of the salts were dissolved in 1 cc. of distilled water so that each 30 $\mu l$. of the solution contained 250 $\mu$g. of the free acids. Barium $\alpha$-GP was converted to the ammonium salt by interacting with ammonium sulfate, and sodium $\beta$-GP to the free acid by adding 1N hydrochloric acid. The solutions of these two compounds were prepared so that each 30 $\mu l$. of the solution contained 250 $\mu$g. of the free acid.

**Chromatographic Technique.**—The sample solution was applied at 3 mm. from one end of the paper (after removing 1.5 cm. from both ends of the air-dried paper) with a number of applications under air-drying at 25–30° so that the dried spot was 0.6–0.8 mm. in diameter. The temperature specified here is an important factor, and must be adhered to since the solute is strongly adsorbed at a higher temperature and the spot will not move at all. The paper was equilibrated in a closed tower containing a mixture of methanol and ammonia (60 : 5) for four hours and developed for 2.5 hr. at 11–14°C by the descending method. After airdrying, the paper was sprayed with bromothymol blue indicator, whereupon the acidic spot appeared in a distinct yellow color and a cation, when present, in a blue against a grass-green backgound. This method of identification is much easier than the one commonly used[14] for the organic phosphates. The chromatogram so obtained remained unchanged for a considerable length of time, more than a year, if kept in an air-tight container.

Although we used a sample size of 250 $\mu$g. for each spot in order to make a distinct observation of the color, the method was found to be sensitive to an amount less than 60 $\mu$g. The Rf values are not affected by varying the time of pre-exposure to the solvent vapor but are somewhat affected by varying temperature.

**Tests for Hydrolysis and Migration of the Phosphoryl Group.**—The alumina impregnated paper was cut in a length a few mm. longer than

8) Private communication.
9) M. C. Bailly, *Compt. rend.*, **206**, 1902 (1938).
10) M. C. Bailly, *Bull. soc. chim.*, **9**, 314, 340 (1942).
11) E. Lederer and M. Lederer, "Chromatography", Elsevier Publishing Co., New York, N. Y. (1954), pp. 276-9.
12) W. Kiessling, *Biochem. Z.*, **273**, 103 (1934).
13) I. E. Bush, *Nature*, **166**, 445 (1950).

* The sample was prepared from the corresponding barium salt (C. Urakami and Y. Kakutani, Repts. Sci. Living, Osaka City Univ., Series D, No. 1, 3 (1953)) by removing the barium ion as the sulfate, by adding 1N sodium hydroxide to the ammonium salt formed, by precipitating the salt with alcohol, and finally by removing any excess of alkali present by repeated washing with alcohol.

** The sample was obtained from Delta Chemical Works and was reported to be 98 per cent pure.

*** The sample was prepared from the corresponding sodium salt by converting first to the ammonium salt with ammonium oxalate and then to the barium salt with barium chloride, and by precipitating the latter salt from its concentrated aqueous solution by adding a mixture of alcohol and ether. It was purified by preparing its barium nitrate complex.

14) F. A. Isherwood and C. S. Hanes, *Nature*, **164**, 1107 (1949).

the length corresponding to the Rf value of the glycerophosphoric acids and one end was cut in a zigzag manner. Five hundred μg. each of the α and β-isomers in the free acid forms were chromatographed on a separate sheet of paper under the conditions employed previously and the solvent allowed to drip from the irregularly cut end into a small collector. Several similar runs were made with each acid so that at least 10mg. of the sample were collected. The removal of the acid from the paper took a little over 2.5 hr.; thereafter the paper showed no acid spot remaining when sprayed with the indicator. The liquid collected was concentrated at room temperature under reduced pressure and the residue converted to the barium salt in both cases. In these samples no inorganic phosphorous was detected. The barium salt of the α-compound did not give any insoluble precipitate with barium nitrate, but barium β-GP did give an insoluble precipitate. Both samples were chromatographed on fresh papers and their Rf values were found to be identical with those previously found. The sodium salt prepared from the liquid collected from the chromatogram of barium β-GP was applied on a fresh paper and developed as described above. The acid spot was detected only at the position of the application.

To test whether or not the unmoved spot of sodium β-GP had undergone any chemical changes, the salt was applied on a small piece of the paper cut in a length of about 7 mm. from the starting line and eluted for four hours to collect the sodium ion and a further three hours to collect ammonium β-GP. Within the respective time, any alkaline or acid spot disappeared from the paper. The second fraction collected was applied on a fresh paper and chromatographed. The Rf value found for this sample was identical with that observed for either its free acid or barium salt, 0.46.

**Behavior of Inorganic Phosphate, Sulfate and Chloride Ions.**—Since an inorganic phosphate ion might be formed as a product of hydrolysis during the course of the chromatography and a small amount of $(NH_4)_2SO_4$ or HCl might be present in the sample solutions prepared, it would be necessary to examine the behavior of these ions on the paper. The dilute solutions of $NaH_2PO_4$, $(NH_4)_2SO_4$, and HCl were subjected to chromatography under the conditions specified above. The phosphate and sulfate ions were found to remain unmoved (B and D in Fig. 2), whereas the chloride ion showed a strong yellow spot at the position of application and a faint one at the Rf value corresponding to that of the α-isomer (C Fig. 2). The yellow spot found at Rf 0.45 with the β-isomer was not, however, due

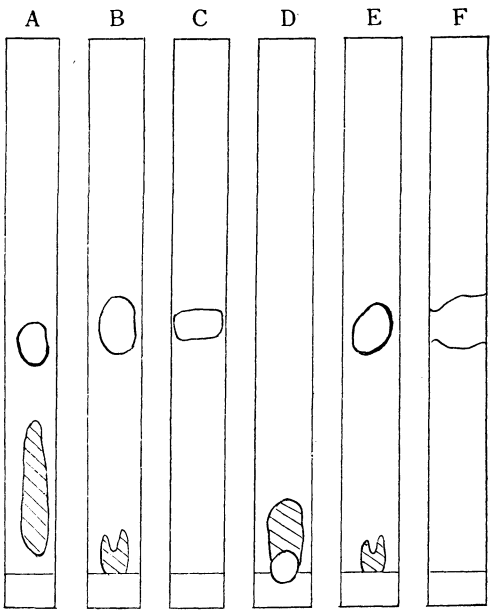



Fig. 1. Reproduction of the paper chromatograms of the glycerophosphates by the descending method. Solvent, methanol-ammonia (60 : 5); 4 hours pre-exposing to the solvent vapor; 2.5 hours developing. The shaded spots represents cations and the unshaded spots anions. A, sodium α-GP; B, barium α-GP; C, ammonium α-GP; D, sodium β-GP; E, barium β-GP; F, β-GP.

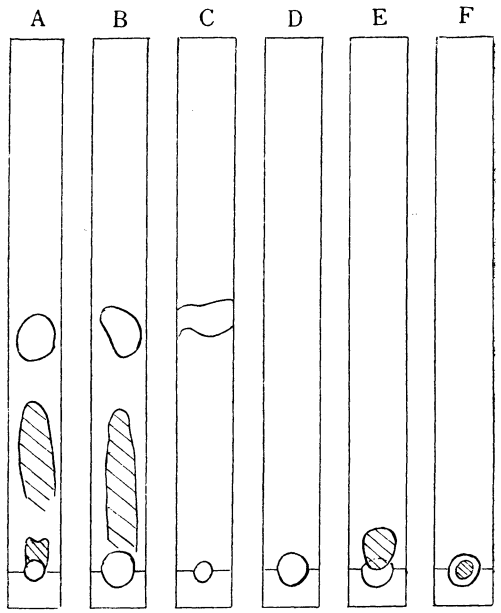



Fig. 2. Reproduction of the paper chromatograms of a mixture of sodium α- and β-GP, inorganic anions and glucose phosphates. The conditions employed are identical with those given for Fig. 1. A, a mixture of sodium α- and β-GP; B, a mixture of sodium α-GP and monosodium phosphate; C, HCl; D, ammonium sulfate; E, potassium glucose 1-phosphate*; F, barium glucose 6-phosphate*.

* We are indebted to Professor Jiro Nikuni of the Osaka University for these samples.

to this chloride ion alone since organic phosphorous was detected in the eluate.

## Results

As shown in Table 1, ammonium, barium and sodium salts of α-GPA, barium β-GP and β-GPA showed almost the same Rf value, 0.45–0.46. The Rf value of sodium α-GP was found, however, to be always somewhat lower than that of barium α-GP. Sodium β-GP, on the other hand, remained unmoved, the blue spot of the sodium ion being found just above or covering the upper half of the yellow spot of the acid (D in Fig. 1). A complete separation of α-GPA from β-GPA and from inorganic phosphoric acid was attained (A and B in Fig. 2). No hydrolysis or migration of the Phosphoryl group was found to occur during the course of the chromatography. Results of Burmaster's method on the sample collected by the column method[15] support our present observation.

The compounds which are more acidic than the glycerophosphoric acids, such as glucose 1- and 6-phosphoric acids were examined under the identical conditions. They were found to remain unmoved from the initial position of application.

## Discussion

When the behavior of the anions and cations of the sodium glycerophosphates and the glucose phosphates on the paper are examined, it is seen that dissociation of the salts becomes difficult with increase in acidity of the acid residues (A and D in Fig. 1; E and F in Fig. 2): $pKa_1$ of α-GPA, β-GPA, glucose 1- and 6-phosphoric acids are 1.40, 1.37[12], 1.10[16] and 0.94[17], respectively. This does not, however, apply to the case of the barium glycerophosphates (B and E in Fig. 1), where the Rf values of both isomers are identical (Table I). The significant difference in Rf value is observed with the sodium salts. In affording the resolution of the isomers, the effect of the sodium ion appears, therefore, to be more pronounced than that of the difference in acidity of the two isomers[18]. Analogous effects have been observed with inorganic salts[19-21]. Of course, further study on this point is indicated, but we consider that there probably exists a stronger ionic attractive force between a strongly basic cation and an anion of a salt, under the conditions specified here, than between a less basic cation and the same anion.

TABLE I

Rf VALUES OF α- AND β-GLYCEROPHOSPHATES

| Temp. °C | α | | | β | | |
|---|---|---|---|---|---|---|
| | Ba | Na | $NH_4$ | Ba | Na | Free |
| 12 | 0.46 | 0.44 | 0.46 | 0.46 | 0.00 | 0.45 |
| 14 | | 0.42 | | | | 0.46 |
| | | 0.45[a] | | | | |
| 15 | | 0.43[b] | | | | |

Each of these Rf values represents an average of those obtained from 4 or 5 chromatograms. [a] Four hours of developing time. [b] Obtained from the chromatogram of a mixture of sodium α- and β-glycerophosphates.

The movement of these acid spots is primarily facilitated by the cellulose present, since it has been observed that the acid residue of the glycerophosphates advances with wide zone formation on a plane filter paper strip at a much faster rate than on the alumina impregnated paper; and, furthermore, that it does not move at all when the concentration of alumina is increased by more than 20 per cent by weight on the paper. Thus, with respect to the apparent movement of the ions, the capillary movement through the cellulose fibers is considered to be more effective than the ion exchange mechanisms of alumina.

The compactness of the acid and base spots is perhaps brought about by such ion exchange mechanisms, exerted by the alumina adsorbed on the filter paper, since the spreading of the anions observed on the plane filter paper can be brought under control to a certain extent on the alumina impregnated paper. In the presence of a strong acid, alumina ionizes in the following manner and behaves as a base[22]:

$$Al(OH)_3 \rightarrow Al(OH)_2^+ + OH^-$$

The anion of an organic acid salt is then attracted by the cation of the alumina ionized as indicated. On the other hand, in the presence of a strong base, the alumina ionizes into the following ionic species and behaves as an acid:

$$Al(OH)_3 \rightarrow H^+ + AlO_3H_2$$
$$\rightarrow H^+ + AlO_2^- + H_2O$$

15) Presented before the 9th Annual Meeting of The Chemical Society of Japan, April, 1956.
16) C. F. Cori, S. P. Colowick and G. T. Cori, *J. Biol. Chem.*, **121**, 465 (1937).
17) O. Meyerhof and K. Lohmann, *Biochem. Z.*, **185**, 113 (1927).
18) W. D. Kumler and J. J. Eiler, *J. Am. Chem. Soc.*, **65**, 2355 (1943).
19) L. Sacconi, *Discuss. Faraday Soc.*, **7**, 173 (1949).
20) M. Shibata, Science (Japan), **19**, 570 (1949).
21) M. Tanaka and M. Shibata, *J. Chem. Soc. Japan*, **71**, 312 (1950).
22) F. P. Treadwell and W. T. Hall, "Analytical Chemistry", Vol. I, John Wiley and Sons, Inc., New York (1937), Ed. 9, pp. 189-192.

The cation dissociated from an organic phosphate is then attracted by the anion derived from the alumina as shown above.

There is, however, another factor to be taken into consideration, the solvent system. If a solvent system is of such a nature that it helps in dissociating salts into their respective ionic species, and also increases the solubilities of the anions formed, their movement may be facilitated. Such may be the case with the glucose phosphates.

When separation by electrophoretic or ion exchange methods alone fails, it may be possible to achieve a better resolution of homologoues or isomeric organic acids with somewhat different acid strengths by selecting an appropriate cation and by chromatographing on this type of adsorbent system.

## Summary

The behaviors of $\alpha$- and $\beta$-glycerophosphoric acids, their alkaline metal and ammonium salts on alumina impregnated paper, developed with a mixed solvent of methanol and ammonia (60 : 5), have been described. It has been demonstrated that a mixture of the sodium salts of the two acids may be completely separated in this way without hydrolysis or migration of the phosphoryl group. The method also affords a distinct separation of $\alpha$-glycerophosphoric acid from a mixture of the inorganic phosphates, the $\beta$-glycerophosphates, and the glucose 1- and 6-phosphates; and also of the $\beta$-glycerophosphates from a mixture of the inorganic phosphates, the glucose 1- and 6-phosphates. The mechanisms possibly involved have been discussed.

*Faculty of The Science of Living*
*Osaka City University, Osaka*

# *Studies on the Dipole Moments of Acenaphthene and its Derivatives*

By Tetsuro ISHIGURO, Takehiko CHIBA and Nobuyuki GOTOH

(Received August 1, 1956)

The dipole moment of acenaphthene was determined in 1949 by Lumbroso[1] as 0.97D, and then in 1950 by Bergmann et al.[2] as 0.85D, both measurements being made in benzene solution. Recently, Chau and Le Fèvre[3] gave the value 0.81D for this substance first determined in the gaseous phase and 0.80D in carbon tetrachloride solution.

Since there is divergence of moment values, it was thought worth while to make an exact measurement on this polar hydrocarbon using the gas-optical method at several temperatures. Measurements were carried out also in benzene solution for the sake of comparison.

Two chlorine derivatives of acenaphthene were prepared for the present work and their dipole moments were also measured in benzene solution at 25°C.

A discussion is given on the polarity of acenaphthene and on related problems.

## Experimental Procedure

**1. Materials.**—(I) *Acenaphthene.*—M.p. 95-96°C. This substance (supplied from Yawata Ironworks) was recrystallized from benzene.

(II) 5-*Chloroacenaphthene.*—M. p. 69.5-70.5°C. Acenaphthene was dissolved in chloroform, and chlorinated by sulfuryl chloride. Then the chlorinated product was distilled twice in vacuo (5 mmHg). The fraction boiling at 145-155°C was recrystallized from ethanol, and then from carbon tetrachloride.

(III) 5,6-*Dichloroacenaphthene.*—M. p. 166-168 °C. 5-Chloroacenaphthene was dissolved in 1,2-dichloroethane and chlorinated by sulfuryl chloride in the presence of $PCl_5$. The product was recrystallized from benzene.

*Solvent Benzene.*—The solvent benzene was made free from thiophene by anhydrous $AlCl_3$. It was then dried over metallic sodium and distilled.

**2. Measurement.**—The dielectric constants were measured by the heterodyne double-beat method in the gaseous state[4], and by the resonance method in solution[5].

1) H. Lumbroso, *Compt. rend.*, **228**, 1425 (1949).
2) E. D. Bergmann et al., *J. chim. phys.*, **48**, 356(1951).
3) J. Y. H. Chau and R. J. W. Le Fèvre, *Australian J. Chem.*, **8**, 562 (1955).
4) T. Chiba, This Bulletin (to be published).
5) R. J. W. Le Fèvre and P. Russel, *Trans. Faraday Soc.*, **43**, 374 (1947).

The density $d$ was measured by a pycnometer. The molar polarization of the solute extrapolated to the infinite dilution ($P_{2\infty}$) was calculated by means of the equation proposed by Halverstadt and Kumler[6].

The sum of atomic and electronic polarization ($P_E+P_A$) was assumed to be equal to $MR_D$, where $MR_D$ is the molar refraction at D-line.

$MR_D$ of (I) was calculated from refractive index and density obtained for the melted state. $MR_D$ of chlorine derivatives were taken as the sum of $MR_D$ (I) and the atomic refraction of Cl, i. e., $MR_D(\mathrm{II})=MR_D(\mathrm{I})+AR_D(\mathrm{Cl})-AR_D(\mathrm{H})$.

## Results

TABLE I

(I) Acenaphthene $MR_D=52.0$ cc.

Gaseous State

| $T$(°K) | $p$(mmHg) | $n$ | $P$(cc.) | $\Delta P$(cc.) | $\mu$(D) |
|---|---|---|---|---|---|
| 464.2 | 45—63 | 13 | 63.8 | 2.0 | 0.95 |
| 466.3 | 42—70 | 11 | 63.4 | 1.0 | 0.93 |
| 476.5 | 57—90 | 9 | 63.1 | 0.8 | 0.93 |

Mean value: 0.93D

$p$: Pressure of the observations
$n$: Number of the observations
$P$: Molecular polarization
$\Delta P$: Mean deviation of $P$

(I) Acenaphthene $MR_D=52.0$ cc.

In benzene at 25°C

| $w$(%) | ε | $d$ | $v$ | |
|---|---|---|---|---|
| 0 | 2.2720 | 0.8722 | 1.1465 | |
| 1.2096 | 2.2868 | 0.8744 | 1.1436 | $A=0.866$ |
| 2.036 | 2.2898 | 0.8759 | 1.1417 | $B=-0.232$ |
| 3.578 | 2.3034 | 0.8787 | 1.1380 | $P_{2\infty}=66.9$ cc. |
| 5.496 | 2.3187 | 0.8820 | 1.1338 | $\mu=0.85$D |
| 8.162 | 2.3421 | 0.8869 | 1.1275 | |

(II) 5-Chloroacenaphthene $MR_D=56.9$ cc.

In benzene at 25°C

| $w$(%) | ε | $d$ | $v$ | |
|---|---|---|---|---|
| 0.6078 | 2.2920 | 0.8743 | 1.1438 | $A=4.006$ |
| 1.3654 | 2.3246 | 0.8763 | 1.1412 | $B=-0.3605$ |
| 2.229 | 2.3607 | 0.8782 | 1.1387 | $P_{2\infty}=186.4$ cc. |
| 3.098 | 2.3914 | 0.8810 | 1.1351 | $\mu=2.50$D |

(III) 5,6-Dichloroacenaphthene $MR_D=61.7$ cc.

In benzene at 25°C

| $w$(%) | ε | $d$ | $v$ | |
|---|---|---|---|---|
| 0.492 | 2.3118 | 0.8741 | 1.1440 | $A=7.649$ |
| 0.996 | 2.3488 | 0.8757 | 1.1419 | $B=-0.429$ |
| 1.395 | 2.3812 | 0.8769 | 1.1404 | $P_{2\infty}=369$ cc. |
| 1.929 | 2.4243 | 0.8786 | 1.1382 | $\mu=3.85$D |

$w$: Concentration
ε: Dielectric constant
$d$: Density
$v$: Specific volume
$A, B$: Rates of change of the dielectric constant ε and specific volume $v$ with weight fraction $w/100$.

## Discussion of Results

In agreement with the results of the preceding workers, a dipole moment of acenaphthene 0.93D as vapor was found in the present measurement.

This marks high polarity as a hydrocarbon. It is to be noted in this connection that the moment of acenaphthene is approximately equal to, or slightly larger than, twice of that of toluene, that is, $0.37\mathrm{D}\times2=0.74$D.

Further, the existence of an abnormal solvent effect as suspected from the previous data*[1,2] can be definitely ruled out both from the work of Chau and Le Fèvre[3] and from the present research.

The dipole moments of acenaphthene, 5-chloroacenaphthene and 5,6-dichloroacenaphthene are compared with those of naphthalene, 1-chloronaphthalene and 1,8-dichloronaphthalene[8] (see Fig. 1). Almost equal increases in moment upon the successive substitution of Cl atoms are found both in acenaphthene and naphthalene. The increase 1.31–1.35D on the introduction of the second Cl atom is lower than the increase on the first substitution 1.51–1.65D. The apparent reduction is due to the mutual induction of the two C–Cl dipoles.

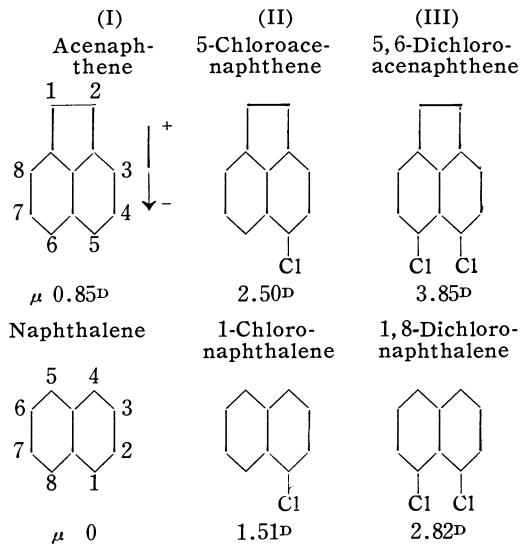



Fig. 1

From the above comparison, it will be seen that the electron displacement in an acenaphthene molecule caused by the substitution of Cl atoms is essentially not

6) I. F. Halverstadt and W. D. Kumler, *J. Am. Chem. Soc.*, **64**, 2988 (1942).
7) v. Auers and Frühling, *Ann.* **422**, 200 (1921).

* Lumbroso's value in 1947 was 1.57D.
8) G. C. Hampson and A. Weissberger, *J. Chem. Soc.*, **1936**, 393.

much different from that in naphthalene. In other words, no special change occurs which might be expected from the existence of the linkage $C_1$–$C_2$. Therefore, the dipole moments of Cl-derivatives of acenaphthene can be calculated by the simple rule of vector addition.

The moment of 5-chloroacenaphthene is larger by 0.99D than that of 1-chloronaphthalene while 5,6-dichloroacenaphthene is larger by 1.03D than 1,8-dichloronaphthalene. It can be concluded, therefore, that the dipole moment of acenaphthene of about 0.9D has the direction shown by the arrow head in Fig. 1.

This fact may deserve special attention, since it has been reported[9] that the most reactive positions of acenaphthene in the substitution reactions are its 5 and 6 positions.

## Summary

The dipole moment of acenaphthene (I) was measured in the gaseous phase as 0.93D. Measurement in benzene solution at 25°C gave the following moment values: acenaphthene (I) 0.85D; 5-chloroacenaphthene (II) 2.50D; and 5,6-dichloroacenaphthene (III) 3.85D. By the comparison with the moments of naphthalene derivatives it was shown that the moments of (II) and (III) are approximately equal to the sums of the moment of (I) and the moments arising from one and two C–Cl bonds, respectively.

The authors wish to express their sincere thanks to Prof. K. Higasi for the helpful suggestion and discussion on this subject, and to Prof. Y. Nagai, to Prof. Y. Morino, and to Dr. I. Miyagawa for the kind guidance and valuable advice through this study.

*Department of Industrial Chemistry*
*Faculty of Engineering, Chūō University*
*Department of Chemistry, Faculty of Science, The University of Tokyo*
*The Institute of Industrial Science*
*The University of Tōykō*

9) H. E. Nürsten and A. T. Peters, *J. Chem. Soc.*, **1950**, 729; N. Gotoh and Y. Nagai, *J. Chem. Soc. Japan*, (Ind. Chem. Sec.) **58**, 50 (1955).

# *Studies on the Organic Phosphorescence. II. A Revision of Lewis' Mechanism for the Phosphorescence*

By Shunji KATO and Masao KOIZUMI

(Received August 18, 1956)

## Introduction

In the previous paper[1] the decay curves (i. e. the plots of the logarithms of the phosphorescence intensities against time) of the phosphorescence of trypaflavine-filter paper were measured and found to be approximately of the first order. The concentration effect of dye was particularly studied and the conclusion was reached, on the basis of Lewis' triplet theory, that the neighbouring dye molecules chiefly affect S′ state and not T state.

Since then the apparatus has been much improved and it has now become possible to catch the features of the decay curves in the initial stage of the phosphorescence as well as to prolong the observation towards a much later stage. With this apparatus, similar experiments as reported in the previous paper were repeated, and the decay curves were found to deviate a little from a straight line, although the deviations were not so great in magnitude and moreover, only limited at the initial stage. The deviation from linearity was also observed when polyvinyl alcohol, cellophane and other substances were used as carriers, in agreement with the results reported in the literature[2], of the subject but it was most prominent in the case of trypaflavine-silica gel phosphor.

The object of the present paper is to report some experiments undertaken to

1) S. Kato and M. Koizumi, This Bulletin, **27**, 189 (1954).

2) G. N. Lewis, D. Lipkin and T. T. Magel, *J. Am. Chem. Soc.*, **63**, 3005 (1941).

elucidate the cause for this deviation, chiefly using trypaflavine-silica gel phosphor, and the conclusion obtained therefrom.

It will be found that the results obtained are interpreted by an introduction of another metastable state coupled directly with T state, the emission taking place only in S′→S transition. Furthermore, the decay curves will successfully be analysed quantitatively on the ground of the above mechanism.

## Experimental Procedures

**Materials.**—Silica gel was boiled in concentrated hydrochloric acid and was washed by hot water repeatedly until no chloride ion was detected by silver nitrate. Then the purified gel was dyed in the aqueous solution of trypaflavine in vacuum, and after decantation it was evacuated at 200°C.

To remove any trace of oxygen as completely as possible, the sample was further treated twice with water vapor, adsorption and desorption being done at room temperature and at 200°C respectively.

**Apparatus.**—The block diagram is shown in Fig. 1. At the beginning, the intensity of the

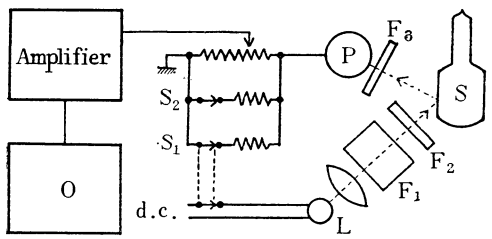



Fig. 1. Block diagram of the apparatus.
S: sample;
$F_1$: $CuSO_4$ solution;
$F_2$: Mazda V-VI filter which transmits 330-450 mμ;
$F_3$: a yellow filter which cuts off shorter than 450 mμ;
L: high pressure d. c. mercury lamp;
P: photomultiplier RCA 1P21;
O: electromagnetic oscillograph (Yokogawa, N-3).

luminescence under steady excitation (fluorescence plus phosphorescence) is recorded with switch $S_1$ and $S_2$ being closed. At the instant when the lamp is turned off, the switch $S_1$ is opened automatically, increasing the gain of the amplifier to some extent. When the photocurrent decreases under a certain value, the switch $S_2$ is opened also by an automatic device and the gain is once more increased so much that the later stage of a decay curve is accurately recorded.

In flash experiments, photoflash valves (the duration time is about 6 millisec.) are used as an exciting light. A shutter is inserted close to the window of a photomultiplier, which is opened immediately after the flashing of a valve.

## Experimental Results and Discussion

In this paper the following notations are employed.

$I_L$: The intensity of luminescence during excitation.
$I_P$: The intensity of phosphorescence.
$I_{P0}$: The intensity of phosphorescence extrapolated to $t=0$.
$I_F=I_L-I_{P0}$: The intensity of pure fluorescence.

**a) The Main Features of the Decay Curves.**—All the decay curves were found to be practically linear in the later stage but they markedly deviate upwards in the initial stage. When measurements were extended as long as ca. five minutes*, however, the later stage was also found not to be exactly linear. An example is shown in Fig. 2. The latter deviation, which may plausibly be due to non-uniformity in the state of adsorbed dye or to

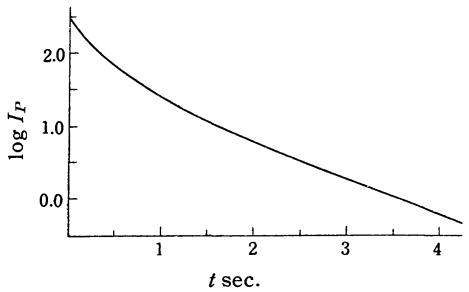



Fig. 2. An example of the decay curve.

reabsorption of phosphorescence, is so small in magnitude compared with the initial deviation, that the main points in the phosphorescence phenomenon will surely be elucidated by analysing the decay curves on the assumtion of the linearity in a later stage.

Now in order to interpret the above result, it is evidently necessary to modify more or less the scheme proposed by Lewis[2], according to which the decay is to be expressed by

$$I_P=A\exp(-\alpha t).$$

A formal amendment which occurs at once is to express $I_P$ as the sum of several exponential terms. In practice, however, it was found that the introduction of another exponential term (equation (1)) is enough to represent the experimental results satisfactorily.

* The measurements were not usually extended so long.

3) D. Yamamoto, *J. Chem. Soc. Japan*, **74**, 173 (1953).

$$I_P = A \exp(-\alpha t) + B \exp(-\beta t) \quad (1)$$

Two other mathematical formulas were also tested in view of the mechanism proposed by Yamamoto[3] (for the phosphorescence in solid solution), who assumed the existence of a conduction band and took into consideration a bimolecular process between electrons in the conduction band and dye ions, simultaneously occurring with a main unimolecular process.

One formula here attempted corresponds to the scheme in which the phosphorescent state declines as a simultaneous process consisting of unimolecular and bimolecular emitting processes, and the other refers to the case in which the unimolecular emitting process and the radiationless bimolecular process take place. Putting $N_T$ as a number of dye molecules in the phosphorescent state, the above two schemes are expressed analytically as follows:

for the former

$$I_P \propto -dN_T/dt = \alpha N_T + \beta N_T^2 \quad (2)$$

while for the latter

$$I \propto_P \alpha N_T, \quad -dN_T/dt = \alpha N_T + \beta N_T^2 \quad (3)$$

and the integrated forms for (2) and (3) are respectively

$$I_P = \frac{\alpha^2 C \exp(-\alpha t)}{\{1+\beta C \exp(-\alpha t)\}^2} \quad (4)$$

$$I_P = \frac{\alpha^2 C \exp(-\alpha t)}{1-\beta C \exp(-\alpha t)}; \quad (5)$$

(4) and (5) can represent the experimental results equally well and as satisfactorily as (1), hence it is not possible to decide which of (1), (4) and (5) is suitable from the analysis of decay curves.

**b) Effect of Exciting Light Intensity.** —The superiority of (1) against (4) and (5) was established by the examination of the effect of exciting light intensity, the results of which will be described below.

The intensity was varied with neutral filters and several decay curves were taken at various intensities down to 6 per cent of the full intensity. The result was that the shape of decay curves do not change; in other words, the curves under different intensities can be put upon one another by parallel displacement along the intensity axis, and the values of $I_L$ and $I_{P0}$ are proportional to the intensity of exciting light (Fig. 3).

The above result requires that the inclination of the curve or $d/dt \log I_P$ is a function only depending upon $t$ and is not affected by the intensity of exciting light. This requirement is consistent with (1), since according to (1)

$$\frac{d \ln I_P}{dt} = -\frac{A\alpha \exp(-\alpha t) + B\beta \exp(-\beta t)}{A \exp(-\alpha t) + B \exp(-\beta t)}$$

which is a function of only $t$, if both $A$ and $B$ are proportional to the exciting light intensity.

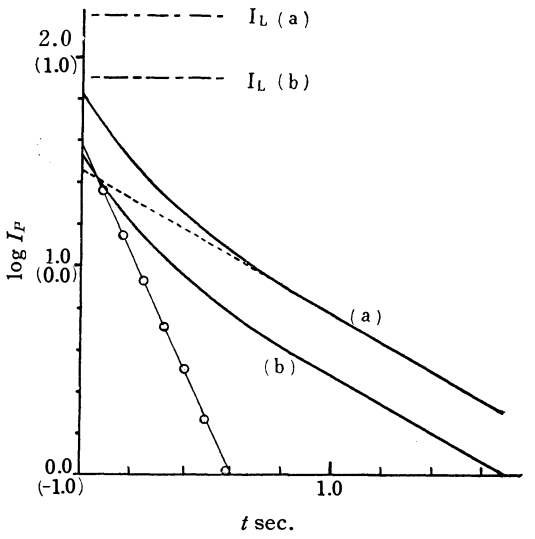



Fig. 3. Effect of exciting light intensity on the decay curve. (a) : 100, (b) : 6.0. In (b), the intensity scale takes the values in brackets.

On the contrary, for the case (2)

$$-d \ln I_P/dt = \alpha + 2\beta N_T \quad (6)$$

and for the case (3)

$$-d \ln I_P/dt = \alpha + \beta N_T \quad (7)$$

and according to these relations, $-d \ln I_P/dt$ must depend on $N_T$, the number of dyes in the phosphorescent state, which depends on the intensity of light source. Thus the schemes (2) and (3) which involve the bimolecular process can be discarded definitely.

Constants $\alpha$, $\beta$, $A$ and $B$ in (1) can easily be obtained in the following way. If $\beta$ is larger than $\alpha$, then the second term will vanish at larger $t$ values and the straight part of the decay curve corresponds to the first term. Extrapolating this straight part to the ordinate, $\alpha$ and $A$ can be decided from the inclination and the intersection respectively. Then the second term is obtained by substracting $A \exp(-\alpha t)$ from $I_P$ and putting logarithms of these values against $t$, a straight line results from which $B$ and $\beta$ can be determined. In Fig. 3, the values of

TABLE I

AT 25°C; THE TIME UNIT IS ONE SECOND

| Dye Concentration $10^{-6}$ mol./g. silica gel | $\alpha$ | $\beta$ | $A/B$ | $I_L/I_{P0}$ | $\pi_1$ | $\pi_2$ | $n_1n_2$ | $n_un_u'/\pi$ |
|---|---|---|---|---|---|---|---|---|
| 0.039 | 1.98 | 6.7 | 0.83 | 3.13 | 5.5 | 3.1 | 3.9 | 2.0 |
| 0.077 | 1.95 | 6.3 | 0.82 | 2.94 | 5.4 | 2.8 | 3.1 | 2.2 |
| 0.21 | 1.89 | 6.3 | 0.99 | 2.90 | 5.3 | 2.9 | 3.5 | 2.2 |
| 0.44 | 1.83 | 5.8 | 0.98 | 2.87 | 4.9 | 2.8 | 2.9 | 2.1 |

$\log\{I_P - A\exp(-\alpha t)\}$ are plotted against $t$ as small circles, which lie satisfactorily on a single straight line.

Some examples of the analysis are shown in Table I, which contains the results for samples of different dye concentrations. It is seen from this table that $A$, $B$, $\alpha$ and $\beta$ are almost constant, the concentration quenching being negligible in the region of dye concentration lower than 0.5 $\mu$mol./g. A slight decrease in $\alpha$ and $\beta$ with the increase of dye concentration may perhaps be due to the reabsorption of phosphorescence[4]. The last four columns will be refered to later.

From the fact that formula (1) fits the experimental results there is no doubt that another metastable state other than Lewis' T state participates in the phenomenon of phosphorescence, the life of the former being of the same order as that of the latter.

This metastable state will be denoted conventionally as "M" state in distinction from Lewis' T state.

Thus it has now become another interesting problem to characterize this M state and further to elucidate the interrelation between M and T states.

The remainder of this paper will chiefly be devoted to this problem.

**c) Absorption and Emission Spectra.** —Supposedly if M and T state were completely independent, it might happen that the emission of two different types would be observed. Hence the spectra of phosphorescence (corresponding to $I_P$) and fluorescence (plus phosphorescence in a rigorous sense—corresponding to $I_L$) were at first examined and were compared with the absorption spectra.

Absorption spectra of trypaflavine adsorbed on silica gel were measured by use of the following technique. First, the sample was ground into powder and was mixed with silica gel powder to make its optical density suitable for measurement. Then the mixture of benzene and petroleum benzine with the same refractive index as that of the sample was poured into the cell. The sample now became transparent and the absorption spectra could easily be measured by a Beckman D. U. spectrophotometer. The result was that the maximum of the extinction displaced about 10 m$\mu$ to longer wave length compared with that in an aqueous solution.

The fluorescence and phosphorescence spectra were taken by a spectrograph at 25°C using a high pressure mercury lamp as a light source. A phosphoroscope with a rotatory disc was employed for taking the phosphorescence spectrum. Both spectra were almost identical and were approximately a mirror image of the absorption spectrum as shown in Fig. 4.

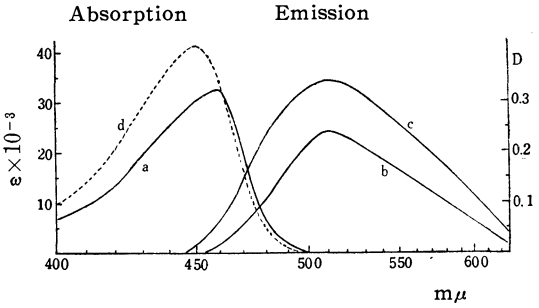



Fig. 4

a) Trypaflavine-silica gel 0.25 $\mu$mol./g.;
b) Fluorescence spectrum of the same sample;
c) Phosphorescence spectrum;
d) Trypaflavine in aqueous solution 12 $\mu$mol./l.;
ε: Extinction coefficient 1000 cm²/mol.;
D: Density of plate darkening.

Next, the decay curve for the limited wave-length region of phosphorescence was taken and compared with the result in (a); thus an orange filter cutting off shorter than 540 m$\mu$ was used in place of a yellow one, but the decay curve was exactly the same in shape.

Lastly, it was cheked by the following experiments that Lewis' $\beta$ phosphorescence is negligible for such an adsorbed phosphor at room temperature. When a film of polyvinyl alcohol dyed with trypaflavine

4) J. B. Birks and W. A. Little, Proc. Phys. Soc. (London), **66A**, 921 (1953).

($4.88\times10^{-7}$ mol./g. P. V. A.) was stretched, it showed a distinct dichroism. The extinction was about seven times larger when the electric vector of the light was perpendicular to the stretched direction than parallel. (The decay curve showed a slight deviation from linearity at the initial stage, though the order of magnitude was much smaller than in the case of trypaflavine-silica gel phosphor.) Now it was found that the green phosphorescence (and fluorescence) at room temperature had a polarization perpendicular to the stretched direction, while at liquid air temperature, the yellow phosphorescence that is Lewis' $\beta$ phosphorescence, was polarized parallel, and at dry ice temperature, the phosphorescence consisted of $\alpha$- and $\beta$-components, the former being observed only in a perpendicular direction, while the latter in a parallel direction.

At room temperature there was no $\beta$ phosphorescence observed in a parallel direction, hence $\beta$ phosphorescence can be ignored in the case of polyvinyl alcohol trypaflavine phosphor at room temperature. The situation may be the same for the case of silica gel phosphor.

From the results mentioned in this section, it is almost certain that there is only one type of emission and that it corresponds to Lewis' $\alpha$ phosphorescence.

## A Plausible Scheme for the Phosphorescence

In order to make the quantitative investigation about the decay curve, it may be desirable to put forward, at this stage, a plausible scheme which will enable us to carry out the mathematical analysis.

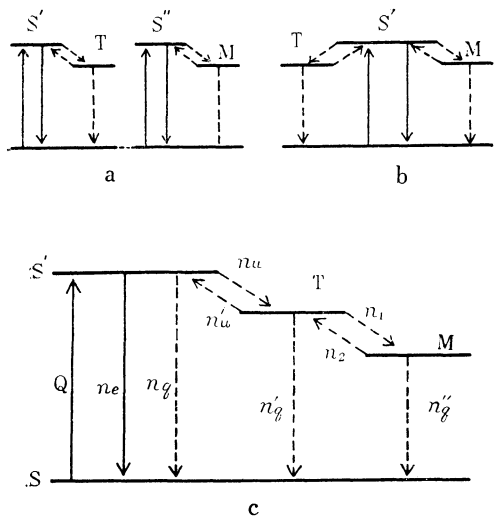



Fig. 5. Possible schemes for the phosphorescence.

Now, for the interrelation between T and M states, there are three possible schemes conceivable, which are shown in Fig. 5. In this figure, the full lines are transitions connected with radiation, while the dotted ones are radiationless transitions. The most suitable scheme will be selected by examining which of these three will fit best the following experimental results.

1) The variation of dye concentration does not affect the decay curve (at least in the small concentration range). (Table I)

2) Deviations from linearity in decay curves depend upon the nature of a carrier (the fact mentioned in introduction).

3) There is only one emitting state at ordinary temperature (the result demonstrated in (c)).

4) Even at liquid air temperature, deviations from linearity are still observed, though the magnitude becomes much smaller (preliminary observation).

Now the scheme (a) which consists of two independent processes is not compatible with the result (3), unless one supposes that the two processes are not the ones in isolated molecules but are closely related with the state of adsorption. But even if one adopts the view that there are statistically two different states of adsorption (which cause different lifetimes but do not affect the spectral behaviors), this scheme is not compatible with the result (1), since the participation of M and T states should vary in magnitude with the dye concentration.

Scheme (b) in which M and T states are separately coupled with S′ state does not fit the fact (4). Because if one assumes scheme (b) the result (4) must be interpreted to be due to the fact that M state as well as T state must emit phosphorescence at low temperature and this seems very improbable from the general view about the emission phenomena. Moreover, it seems quite strange that T and M states which have a long life don't interrelate with each other and yet they are separately coupled with an extremely short-lived S′ state.

The remaining scheme (c) in which T and M are directly coupled, is not only plausible from the general view point, but also fits the above facts well, if one assumes that M state is closely connected with the state of adsorption. Thus the result (1)

can be comprehended as due to the fact that the state of adsorption is uniform at least approximately.

There is no question about the results (2) and (3) on the basis of this scheme.

The result (4) can be comprehended if the transition between T and M takes place partially by virtue of tunneling effect.

Thus although the above discussions are not quite conclusive, the scheme (c) seems to be most suitable; hence the quantitative treatment will be given below on the basis of this scheme. One may expect that the plausibility of this scheme will be further supported by the results obtained from such an analysis. (See the following two papers)

## Quantitative Interpretation of the Decay Curve

The mathematical treatment will be given on the basis of scheme c) as shown schematically in Fig. 5c.

In this figure, S, S′ and T are ground state, excited singlet state and triplet state respectively; M is a metastable state with a life time of the same order as that of T state.

Since the spectra of phosphorescence are identical with those of fluorescence and the yellow phosphorescence is never observed at room temperature, the direct emitting transition from T or M to S can be ignored.

Furthermore

$n_e$: The rate constant of S′→S emitting transition.

$n_q$, $n_q'$, $n_q''$: The rate constant of S′→S, T→S, M→T transition respectively (without emission).

$Q$: The number of molecules excited per second by irradiation.

From the above scheme, the phosphorescence intensity $I_P$ (in number of photons), the rate of the decrease in the number of the molecules in T state and that in M state are represented respectively by the following equations

$$I_P=n_e n_u' N_T/\pi \tag{8}$$

$$-\mathrm{d}N_T/\mathrm{d}t=\pi_1 N_T-n_2 N_M \tag{9}$$

$$-\mathrm{d}N_M/\mathrm{d}t=\pi_2 N_M-n_1 N_T \tag{10}$$

where

$$\pi_1=n_u'(1-n_u/\pi)+n_q'+n_1{}^*$$

$$\pi_2=n_2+n_q''$$

$$\pi=n_e+n_q+n_u.$$

Integrating (9) and (10) one gets

$$N_T=a_1\exp(-\alpha t)+b_1\exp(-\beta t) \tag{11}$$

$$N_M=a_2\exp(-\alpha t)+b_2\exp(-\beta t) \tag{12}$$

where

$$\alpha,\beta=\frac{1}{2}\{\pi_1+\pi_2\mp\sqrt{(\pi_1-\pi_2)^2+4n_1n_2}\} \tag{13}$$

and from (9), (11) and (12)

$$a_2/a_1=(\pi_1-\alpha)/n_2,\quad b_2/b_1=(\pi_1-\beta)/n_2. \tag{14}$$

The values of $a_1$, $a_2$, $b_1$ and $b_2$ are determined by the initial condition, which corresponds to a stationary state (during the illumination) established between the exciting light and all the states involved.

The stationary state in question can be represented by the following equations,

$$-\mathrm{d}N_S/\mathrm{d}t=\pi N_{S0}-Q-n_u'N_{T0}=0 \tag{15}$$

$$-\mathrm{d}N_T/\mathrm{d}t=(\pi_1+n_u n_u'/\pi)N_{T0}-n_u N_{S0}-n_2 N_{M0}=0 \tag{16}$$

$$-\mathrm{d}N_M/\mathrm{d}t=\pi_2 N_{M0}-n_1 N_{T0}=0 \tag{17}$$

where $N_{S0}$, $N_{T0}$ and $N_{M0}$ are the values of $N_S$, $N_T$ and $N_M$ in the stationary state. From (11) and (12) on the other hand

$$N_{T0}=a_1+b_1,\quad N_{M0}=a_2+b_2 \tag{18}$$

From (14), (15), (16), (17) and (18) one gets

$$a_1=\frac{\pi_2-\alpha}{\alpha(\beta-\alpha)}\frac{n_u Q}{\pi},\quad b_1=\frac{\beta-\pi_2}{\beta(\beta-\alpha)}\frac{n_u Q}{\pi} \tag{19}$$

Substituting (11) and (19) into (8), an ultimate expression for the phosphorescence intensities is obtained as follows:

$$I_P=A\exp(-\alpha t)+B\exp(-\beta t) \tag{20}$$

where

$$A=\frac{n_e n_u n_u'(\pi_2-\alpha)Q}{\pi^2\alpha(\beta-\alpha)}$$

$$B=\frac{n_e n_u n_u'(\beta-\pi_2)Q}{\pi^2\beta(\beta-\alpha)}$$

(20) is identical with (1) and the following relations hold, as are easily verified.

$$A/B=(\pi_2-\alpha)/(\beta-\pi_2)\times\beta/\alpha \quad \text{(i)}$$

$$\alpha+\beta=\pi_1+\pi_2,\quad \alpha\beta=\pi_1\pi_2-n_1n_2 \quad \text{(ii)} \tag{21}$$

$$I_L/I_{P0}=\pi\alpha\beta/n_u n_u'\pi_2+1 \quad \text{(iii)}$$

* Since the life time of S′ is $10^7$~$10^8$ times shorter than that of T and M, it is possible to apply a stationary state method to S′ state. Hence it is easily proved that, the fraction $n_u/\pi$ of the molecules transferred from T to S′ returns to T state, leading the net decrease of the molecules in T via S′ as $n_u'(1-n_u/\pi)$.

Since $A/B$, $\alpha$, $\beta$ and $I_I/I_{P0}$ are determined experimentally, $\pi_1$, $\pi_2$, $n_1n_2$ and $n_un_u'/\pi$ can be calculated from (21). Some of the results are shown in Table I.

**Flash Excitation.**—Now it will be interesting to examine how the decay curve will change in shape when a sample is excited by a flash lamp. In this case, since the duration of a flash (several milliseconds) is much shorter than the life time of T and M state, the stationary state cannot be established except for S'. Thus the initial condition for the decay curve will approximately be such that there are no molecules in M state.

Assuming such an initial condition, (16) and (17) must be replaced by the following relations.

$$N_{M0}=0 \quad \text{hence} \quad a_2+b_2=0 \qquad (22)$$

$N_{T0}=Qn_u/\pi$ ($Q$ is a total number of photons absorbed)

From (22) and (14) one gets

$$A/B=(\pi_2-\alpha)/(\beta-\pi_2) \qquad (23)$$

Comparing (21 i) and (23) it can be expected that the values of $A/B$ in flash experiments are smaller than those in steady excitation by a factor near $\alpha/\beta$, while the values of $\alpha$ and $\beta$ must not change, since the rate constants $n_e$, $n_u$, $n_q'$ etc. are only dependent on the sample.

Now, the decay curves were taken for the same sample, using a mercury lamp on one hand and replacing it by a photo-flash valve on the other. The result was that the two decay curves markedly differ with each other. Three parameters, $A/B$, $\alpha$ and $\beta$ for the same sample are shown in Table II for flash and mercury lamps. In both excitations, $\alpha$ and $\beta$ have the same or approximately the same values (within experimental accuracy) while $A/B$ differs about two or three times.

TABLE II

0.5 $\mu$mol./g. AT 25°C

| Sample | Exciting Light | $\alpha$ | $\beta$ | $A/B$ | $A/B\times\alpha/\beta$ |
|---|---|---|---|---|---|
| a | Hg-lamp | 1.74 | 5.67 | 0.78 | 0.24 |
| | Flash | 1.74 | 6.25 | 0.31 | — |
| b | Hg-lamp | 2.18 | 7.45 | 0.91 | 0.27 |
| | Flash | 2.18 | 7.08 | 0.24 | — |

The values in column 3 and 4 conform with the above requirements quite well. The agreement between $A/B$ in flash excitation and $A/B\times\alpha/\beta$ in steady excitation is better than expected*.

Thus it can be concluded that the present mechanism not only explains the experimental results of various kinds qualitatively, but it is quite satisfactory from a quantitative standpoint.

## Summary

Decay curves of the trypaflavine-silica gel phosphor were measured accurately by means of an oscillograph and a marked deviation from linearity was found at the initial stage. From the spectroscopic studies of fluorescence and phosphorescence, and the effect of light intensity on the shape of the decay curve, it was concluded that Lewis' scheme must be modified in such a way that another state with a life time of the same order as that of T state directly couples with T state.

The quantitative analysis was performed successfully and some of the transition constants between the states involved were partially evaluated.

*Institute of Polytechnics*
*Osaka City University, Osaka*

* It is to be noted, however, that scheme (a) and (b) can interpret the result of a flash experiment equally well. Hence the above success cannot be considered as a strong support for the scheme(c).

# *Studies on the Organic Phosphorescence. III. Quenching by Some Gases and Vapors*

By Shunji KATO

(Received August 18, 1956)

## Introduction

The preceding investigation[1] on the phosphorescence of trypaflavine-silicagel phosphor has led to a plausible conclusion that there exists a metastable state (M state), which is directly coupled with a triplet state, and it has been proposed that Lewis' scheme must be replaced by the one shown schematically in Fig. 1.

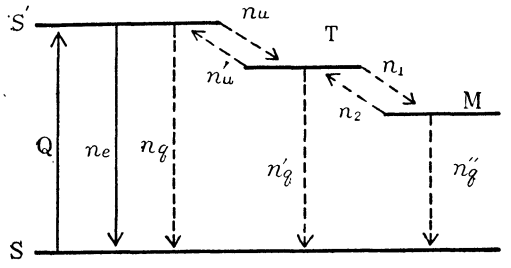



Fig. 1.

On the basis of this mechanism, decay curves are represented by the following equation,

$$I_P = A \exp(-\alpha t) + B \exp(-\beta t) \qquad (1)$$

and putting

$$\pi_1 = n_u'(1 - n_u/\pi) + n_1 + n_q'$$
$$\pi_2 = n_2 + n_q''$$
$$\pi = n_e + n_q + n_u,$$

$\pi_1, \pi_2, n_1 n_2$ and $u_u n_u'/\pi$ are calculated from four parameters ($\alpha, \beta, A/B$ and $I_L/I_{P0}$) which are obtained from the measurement of $I_L$ (the intensity of luminescence during excitation), $I_{P0}$ (the initial intensity of the phosphorescence) and the decay curve of phosphorescence.

Now, although the existence of another metastable state other than Lewis' triplet state has been established in the preceding paper, nothing as yet is known about its nature.

As a first step to study about it, the author has investigated the influence of the addition of a third substance upon the steady state emission and upon the decay curve of phosphorescence.

Such an investigation is expected, in addition, to refer to our first plan mentioned in the first paper[2] of this series, i. e. the problem whether a third substance (quencher) affects S' or T state, because the analysis of the decay curve makes it possible to evaluate some of the transition probabilities between the states involved in the phosphorescence.

In this paper the influence of some gases and vapors upon the phosphorescence of trypaflavine-silica gel phosphor will be reported. It is well known that such a phosphorescence is effectively quenched by certain gases and especially, a remarkable quenching action of oxygen has been studied from various view points[3], but the precise investigation about the variation of the decay curve caused by the addition of these gases including oxygen, has not yet been undertaken.

## Experimental

**Materials.**—*Trypaflavine-silica gel phosphors* were prepared in the same way as described in the previous paper.

*Oxygen and hydrogen* were prepared by the electrolysis of baryta water and were first passed over platinized asbestos, then through a dry ice trap.

*Nitrogen, argon and methane*: The gas from a cylinder was stored for several days, to remove oxygen, in an ampoule the inner surface of which was covered by an evaporated film of metallic sodium.

*Nitric oxide* was prepared by the reaction between potassium nitrate and ferrous sulfate in the acidified aqueous solution, and then purified by a standard method*.

Other quenchers (*n*-hexane, propylene, benzene, acetone, methanol, $SO_2$, $I_2$, ether, dioxane, cyclohexene, 2-ethyl-1-hexene, styrene and methylmethacrylate), after ordinary purification, were distilled or sublimed five times in high vacuum to remove oxygen.

**Procedure and Measurement.**—A known amount of a gas or a vapor to be investigated was taken in a space between two taps and then

1) S. Kato and M. Koizumi, This Bulletin. **30**, 27 (1957).

2) S. Kato and M. Koizumi, This Bulletin, **27**, 189 (1954).

3) J. Franck and P. Pringsheim, *J. Chem. Phys.*, **11**, 21 (1943).

* "Inorganic Synthesis", (1939), 11, P. 126.

was introduced into the ampoule containing the phosphor. If there was any fear of even a slight reaction between a gas and tap-grease, the taps were replaced by a mercury cut and a break-seal.

The apparatus used was the same one described in the preceding paper and the phosphorescence of a sample was recorded, before and after introduction of a quencher at 25°C.

In every experiment the greatest caution was paid to eliminate any trace of oxygen and to avoid contamination of a sample with it throughout all procedures. In fact, the disturbance from oxygen is so strong that a noticeable fall of the phosphorescence is observed if the connection tube of the ampoule is carelessly sealed off by fusion.

## Results and Discussion

**a) General Remarks.** — Among the materials examined, argon ($38\times10^{-5}$ mol.), nitrogen ($43\times10^{-5}$), hydrogen ($32\times10^{-5}$), methane ($42\times10^{-5}$), *n*-hexane ($6.6\times10^{-5}$), propylene ($3.3\times10^{-5}$), benzene ($1.0\times10^{-5}$), acetone ($42\times10^{-5}$), methanol ($3.2\times10^{-5}$) and water ($3.5\times10^{-5}$) had no effects on a 4 g. phosphor (contained in an ampoule of 20 ml.) of which the dye concentration is $5\times10^{-7}$ mol./g. silica gel; the intensity of the steady state emission and the shape of the decay curve were not affected at all by the introduction of these gases.

When more than $10^{-3}$ mol. of methanol or water is introduced, the life of the phosphorescence is somewhat shortened and its initial intensity decreases, though only very little. In view of a rather large quantity of a quencher in these cases, it is more plausible to attribute these effects to the variation in the property of gel, hence these cases will be omitted from the discussion given below.

The substances which show more or less positive effects are $O_2$, NO, $SO_2$, $I_2$, ether, dioxane, cyclohexene, 2-ethyl-1-hexene, styrene and methyl methacrylate.

When a suitable amount of a quencher listed above, is introduced, the phosphorescence intensity, the decay constant as well as the intensity of the steady state emission show measurable changes. Decay curves are still represented by equation (1) unless the quantity of a quencher is not too large. When it exceeds a certain value, equation (1) must be replaced by a more general one

$$I_P=\sum a_i \exp(-\alpha_i t) \qquad (2)$$

in order to represent the decay curve satisfactorily. But even in these cases, the decay curves are exactly the same in shape for different intensities of the exciting light, so it is certain that no process of higher kinetic order is involved in the phosphorescence phenomenon.

TABLE I

| Sample Dye conc. | | Quencher mol. | $I_L$ | $I_L/I_{P0}$ | $I_L^0/(I_L^0-I_L^q)$ |
|---|---|---|---|---|---|
| 0.43 μmol./g. | 4 g. | None | 100 | 2.88 | |
| | | $O_2$ : $1.26\times10^{-8}$ | 65 | — | 2.86 |
| 0.5 μmol./g. | 4.2 g. | None | 100 | 2.59 | |
| | | Styrene : $2.63\times10^{-5}$ | 62 | — | 2.63 |

TABLE II

Phosphor: 0.5 μmol./g., 4 g.; 25°C. Time unit is second.

| No. | Quencher mol. | $\alpha$ | $\beta$ | $A/B$ | $I_L/I_{P0}$ | $\pi_1$ | $\pi_2$ | $n_1n_2$ | $n_un_u'/\pi$ |
|---|---|---|---|---|---|---|---|---|---|
| 1 | None | 2.02 | 5.6 | 0.79 | 2.77 | 4.8 | 2.8 | 2.2 | 5.2 |
| | $O_2$ : $1.5\times10^{-10}$ | 4.35 | 12.3 | 0.54 | 4.3 | 11.0 | 5.6 | 8.3 | 4.1 |
| 2 | None | 1.60 | 5.2 | 0.62 | 2.59 | 4.8 | 2.2 | 1.8 | 2.4 |
| | $O_3$ : $7.5\times10^{-10}$ | 4.49 | 30 | 0.32 | 8.72 | 29 | 5.7 | 28 | 3.0 |
| 3 | None | 1.77 | 6.2 | 0.74 | 2.66 | 5.4 | 2.5 | 2.8 | 2.6 |
| | NO : $1.2\times10^{-9}$ | 4.42 | 19 | 0.45 | 13.2 | 18 | 5.8 | 18 | 1.2 |
| 4 | None | 1.68 | 6.2 | 0.57 | 2.60 | 5.5 | 2.3 | 2.4 | 2.8 |
| | Styrene : $1.2\times10^{-6}$ | 3.54 | 12.7 | 0.49 | 7.53 | 12 | 4.7 | 9.2 | 1.5 |
| 5 | None | 1.58 | 5.3 | 0.74 | 2.94 | 4.6 | 2.2 | 1.9 | 1.9 |
| | Ether : $6.9\times10^{-6}$ | 2.82 | 8.0 | 0.51 | 3.67 | 7.2 | 3.6 | 4.4 | 1.8 |
| 6 | None | 1.42 | 5.0 | 0.68 | 2.92 | 4.4 | 2.0 | 1.7 | 1.9 |
| | Dioxane : $3.0\times10^{-5}$ | 3.46 | 16 | 0.36 | 6.32 | 15 | 4.4 | 11.0 | 2.3 |
| 7 | None | 2.52 | 8.0 | 0.88 | 2.57 | 6.8 | 2.7 | 5.0 | 3.5 |
| | $SO_2$ : $2.6\times10^{-6}$ | 6.27 | 16 | 1.31 | 3.94 | 13 | 9.6 | 21 | 3.6 |

**b) Effect of Quenchers on $I_L$.** — When a suitable amount of gas depending on its quenching efficiency is introduced, the phosphorescence is completely quenched and an interesting relation in the form of (3) is found to hold. Thus, rewriting $I_L$ before and after the addition of a quencher as $I_L^0$ and $I_L^q$ respectively and denoting the initial phosphorescence intensity as $I_{P0}^0$ and $I_{P0}^q$ respectively for the corresponding case*,

$$I_L^0/(I_L^0-I_L^q)=I_L^0/I_{P0}^0. \tag{3}$$

From (3)

$$I_L^0-I_L^q=I_{P0}^0$$

or

$$I_L^q=I_L^0-I_{P0}^0=I_F^0. \tag{4}$$

Since $$I_{P0}^q=0,\quad I_F^q=I_F^0. \tag{5}$$

Equation (5) shows that in such a favorable condition, phosphorescence is completely quenched and yet a pure fluorescence is not affected at all.

$I_F$ is the luminescence emitted by molecules which after having been excited to S′ state, drop to the ground state directly without going to T or M state. Therefore, it can be concluded that in such a case S′ state is not affected at all by a quenching gas. A few examples are shown in Table I.

For other quenchers the same relation holds, hence it is quite certain in general, that under the situation that the phosphorescence is partially quenched, the quencher does never affect S′ state and the intensity of pure fluorescence remains constant.

**c) Analysis of Decay Curves.** — Decay curves were taken for the same sample with and without a quencher; usually when a quenching gas was removed by evacuation the sample regained exactly the same decay curve as that of the original one. Results of the analysis are shown in Table II, where the data for a quenched sample is paired with them for a reference. The data for each reference sample do not always coincide, probably because of some difference in the pretreatment of the sample or in the source of silica gel.

Here it is to be noted that although the values of $\alpha$ and $I_L/I_{P0}$ are rather accurately obtained, those for $\beta$, and $A/B$ are not so accurate; probable errors for the latter two quantities would usually be ±10% or so. Hence accuracy for $\pi_1$, $\pi_2$, $n_1n_2$, $n_un_u'/\pi$ is much worse than this.

It is seen from the table that $\pi_1$, $\pi_2$ and $n_1n_2$ are increased much by the introduction of a quenching gas, while $n_un_u'/\pi$ in most cases are not affected beyond probable error. From the latter result, it can be concluded that $n_u'$, the transition probability from T to S′ is not affected by a quencher, because, as already established in the preceding section, $\pi$ and $n_u$ must remain constant in the present conditions.

This result may perhaps support the view that the transition from the lower state to the higher state is in general not promoted by such a perturbation as is due to spin orbital interaction.

It is noteworthy that the quenching gases not only induce the emissionless transitions from T to S and perhaps M to S, but they also increase the transition probability between T and M.

Judging from the relation

$$\frac{I_F}{I_{P0}}=\frac{I_l-I_{P0}}{I_{P0}}=\frac{\pi\alpha\beta}{n_un_u'\pi_2}=\frac{\pi}{n_un_u'}\left(\pi_1-\frac{n_1n_2}{\pi_2}\right),$$

the decrease in the initial intensity of phosphorescence is mainly due to the increase of $\pi_1$ value, since this is usually much greater than that of $n_1n_2/\pi_2$. Thus broadly speaking, quenching action of the gaseous substances comes from their attack on T state.

Next it is worthy to note that the quantities of quenchers are, in some cases, exceedingly small compared with that of the dye. For example, the quantity of oxygen or nitric oxide which is required to cause a measurable quenching is of the order of $10^{-10}$ mol. as against $2\times10^{-6}$ mol. of dye. Consequently it is clear that one oxygen or nitric oxide molecule acts as an effective quencher towards more than one thousand molecules of dye. Hence it may safely be concluded that the quenching action of these substances is not of static type but of kinetic or collisional one.

In other quenchers, styrene etc., the quantities are comparable to that of the dye. In spite of such great differences in quantity, the general features of quenching are similar at least qualitatively, no specificity being observed in most quenchers. It seems, however, that $SO_2$ is an exception, since the increase of $n_1n_2$ and $\pi_2$ is abnormally high compared with other cases. The problem would be worthy of further study.

**d) Effect of Oxygen on the Pure**

* Throughout this paper analogous notations will be used for all the other constants. For example, $\pi_1$, which will still be used in general case, will be replaced by $\pi^0{}_1$ and $\pi_1{}^q$ when the distinction is necessary.

**Fluorescence.**—As described above, only phosphorescence is quenched by a very small amount of oxygen, but a much larger quantity of it quenches the fluorescence too to some extent. Some examples are shown in Table III.

TABLE III

| $O_2$ press. in mmHg | <0.1 | 10 | 30 | 100 | 720 |
|---|---|---|---|---|---|
| $I_L$ | 100 | 87 | 74 | 50 | 2 |

In the experiment at <0.1 mm $O_2$ press., fluorescence keeps its full intensity while phosphorescence is completely quenched, so that $I_L$ in this case is equal to the intensity of pure fluorescence $I_F$ when the quencher is absent. Other data for $I_L$, accordingly, are the values of $I^0_F$. Now the volume of the ampoule, used for the quenching experiment of phosphorescence is about 20 ml., therefore, $10^{-10}$ mol. of oxygen corresponds to $10^{-4}$ mmHg under the assumption that oxygen is not adsorbed on silica gel at all. Thus the quenching constant for the phosphorescence is estimated to be roughly of the order more than $10^6$ times greater than that for fluorescence. The lifetime of S′ state, on the other hand, being of the order $10^{-7}$–$10^{-9}$ sec., is $10^6$–$10^8$ times shorter than that of T or M state. Thus it appears that the great difference in the behavior of T state against S′ state when oxygen is introduced, is mainly due to its long lifetime and not due to its intrinsic reactivity.

**e) Another Evidence for the Present Scheme of Phosphorescence.** — Although the present scheme of phosphorescence has been supported to some extent in the preceding paper, here another evidence will be added which can be derived from the above quenching experiments.

As already described[2], if phosphorescence obeys Lewis' mechanism and a quencher only acts on T state, promoting only the emissionless transition to the ground state, then the initial intensity of phosphorescence must be exactly proportional to the lifetime.

Now, according to the present investigation, S′ state is not affected at all when the phosphorescence is partially quenched. Therefore, if the phosphorescence consisted of two independent ones, the product of the decay constant and the initial intensity should be unchanged for each independent process when a quenching gas is introduced. In other words, $A\alpha$ and $B\beta$ should be constant and accordingly the product $A/B\times\alpha/\beta$ should also be unaffected. This conflicts with the data given in Table II.

Some examples are shown in the following Table.

TABLE IV

| | Quencher | $A/B\times\alpha/\beta$ |
|---|---|---|
| No. 1 | None | 0.28 |
| | $O_2$ $1.5\times10^{-10}$ mol. | 0.19 |
| No. 2 | None | 0.19 |
| | $O_2$ $7.5\times10^{-10}$ mol. | 0.05 |
| No. 3 | None | 0.2 |
| | NO $1.2\times10^{-9}$ mol. | 0.1 |

Thus the existence of any two independent phosphorescence processes is not compatible with the above results, unless the transition probability from T to S′ is notably increased by a quenching molecule; this increase appears to be very improbable.

## Summary

The quenching action of some gases and vapors upon the phosphorescence of silica gel-trypaflavine phosphor was investigated. The gases which have more or less quenching effects are $O_2>NO>SO_2$, styrene> ether, dioxane, cyclohexene, 2-ethyl-1-hexene, methyl methacrylate, and the gases with no effects (when the quantities are not too large) are $N_2$, Ar, $H_2$, methane, *n*-hexane, propyrene, benzene, acetone, methanol and water.

The influence of quenching gases on the decay curve of phosphorescence were accurately examined and by analysing them on the basis of the scheme proposed in the preceding paper, it was established that in general S′ is not affected while both T and M state are appreciably affected. Furthermore, it was found that T→S′ transition is not promoted in general.

The quenching actions of $O_2$ and NO were interpreted to be of kinetic type.

*Institute of Polytechnics*
*Osaka City University, Osaka*

# *Studies on the Organic Phosphorescence. IV. Quenching by Inorganic Salts*

By Shunji KATO, Ko KIMURA and Masao KOIZUMI

(Received August 18, 1956)

## Introduction

As a continuation of the preceding investigation, the present paper will chiefly deal with the effects of some inorganic salts upon the phosphorescence of trypaflavine-silica gel phosphor. Although the effects of some gases upon the trypaflavine-filter paper phosphor have also been investigated, they will be reported rather briefly since they are generally very small and cannot be discussed quantitatively.

## Experimental

**Sample.**—*Trypaflavine-silica gel phosphor*—The phosphor prepared by the same method as described in part II was soaked in the aqueous solution of a salt (usually chloride) in vacuum and after standing for many hours (sometimes the sample was kept in a bath of 100°C to make the state of adsorption as uniform as possible), water was distilled off in vacuum. The sample then was once more evacuated at 200°C under as similar condition as that for a reference sample.

Salts employed are chloride of $Fe^{3+}$, $Co^{3+}$, $Fe^{2+}$, $Cr^{3+}$, $Cu^{2+}$, $Cu^{+}$, $Ag^{+}$, $Ni^{2+}$, $Mn^{2+}$, $Co^{2+}$, $Pb^{2+}$ and $Cd^{2+}$.

Among these, cobaltic- and chromic- chloride were used in the form of ammine complex and silver- and cuprous-chloride were dissolved in the ammoniacal solution; in these cases ammonia could be expelled from the sample by the above treatment. The dye concentration was usually 0.4 $\mu$mol./g. and that of a salt was chosen in most cases to be more than several times larger.

*Trypaflavine-filter paper phosphor.*—Filter paper was dyed by immersing it in the aqueous solution of trypaflavine and was evacuated at 100°C. The concentration of dye was 0.8 $\mu$ mol./g. (filter paper, ca. 0.5 g.).

**Procedures.**—The quantities measured were

1) decay curves of the phosphorescence
2) the intensity of the steady state luminescence

$$I_L = I_F + I_{P0}$$

3) absorption spectra (only for the silica gel phosphor).

The methods for measuring (1) and (2) are essentially similar to those reported in the preceding papers.

The absorption spectra were likewise taken by the same method described in Part II. Short path cells (0.1 or 0.2 cm.) for Beckman DU were used and the solvent was a mixture of benzene and *n*-hexane 1 : 0.3 in volume ratio.

## Experimental Results and Discussion

**(a) Decay Curves.**—Decay curves are little or scarcely affected by the adsorption of all the salts tested, except cupric ion, the results of which will be discussed separately. The following data show the upper limit of concentration of each salt examined in the present investigation (expressed in $\mu$mol./g.)

$Fe^{3+}(2)$, $Co^{3+}(4)$, $Fe^{2+}(4)$, $Cr^{3+}(6)$,
$Cu^{+}(8)$, $Ag^{+}(5)$, $Ni^{2+}(7)$, $Mn^{2+}(11)$,
$Co^{2+}(3)$, $Pb^{2+}(9)$, $Cd^{2+}(12)$.

Decay curves can be analyzed by the scheme proposed in part II, and the chief results of analysis are shown in Table I. For other salts not included in this table, the decay curve was practically the same as that of the reference.

**(b) The Intensity of the Steady State Luminescence $I_L$.**—From $I_L$, the intensity of pure flurorescence $I_F$ can easily be calculated from the formula $I_F = I_L - I_{P0}$.

As to the relation between $I_F$ and the concentration of a salt, it has been established that Stern-Volmer's equation holds approximately

$$I_F^0/I_F^q = 1 + K_Q C,$$

where $I_F^0$ is the fluorescence intensity of a reference sample while $I_F^q$ is that of the sample containing a salt adsorbed on silica gel*. The concentration of a salt "*C*" is expressed in $\mu$mol./g. silica gel. The results are shown in Fig. 1 (a) and (b) (which includes the one of cupric ion) where $I_F^0/I_F^q$ are plotted against *C*.

* $\pi_1$ in the preceding paper is replaced by $\pi' = \pi_1 + n_u n'_u/\pi = n_u' + n_1 + n'_e + n'_q + n'_i$, because the latter is more expedient when the value of $n_u n_u'/\pi$ changes.

$\pi''$ is the same as $\pi_2$.

$n_q$, $n_q'$ and $n_q''$ in the preceding two papers correspond to $n_i + n_q$ etc. in this paper, $n_i$ being the constant for inner quenching.

TABLE I

Dye conc., 0.4 $\mu$mol./g.; At 25°C. Time in sec.

| Quencher | | $\alpha$ | $\beta$ | $A/B$ | $I_L/I_{F0}$ | $\pi'$* | $\pi''$* | $n_1n_2$ | $n_un_u'/\pi$ | $I_F$ |
|---|---|---|---|---|---|---|---|---|---|---|
| $Fe^{3+}$ | Reference | 2.55 | 8.60 | 1.0 | 2.74 | 10.5 | 3.9 | 6.6 | 3.2 | 26 |
| | 0.4 $\mu$mol./g. | 2.55 | 8.60 | 0.8 | 2.76 | 10.9 | 3.7 | 5.9 | 3.4 | 15 |
| $Cr^{3+}$ | Reference | 2.61 | 8.49 | 1.1 | 2.81 | 10.0 | 4.1 | 6.5 | 3.0 | 36 |
| | 6.2 〃 | 2.91 | 10.0 | 1.2 | 2.91 | 11.3 | 4.8 | 9.8 | 3.2 | 18 |
| $Cu^{+}$ | Reference | 2.58 | 9.11 | 1.2 | 2.78 | 10.7 | 4.2 | 8.0 | 3.2 | 58 |
| | 2.5 〃 | 2.72 | 9.52 | 0.9 | 2.77 | 11.7 | 4.1 | 7.3 | 3.6 | 35 |
| $Pb^{2+}$ | Reference | 2.34 | 7.35 | 0.9 | 2.84 | 9.1 | 3.4 | 4.2 | 2.8 | 43 |
| | 9.1 〃 | 2.43 | 8.21 | 0.9 | 2.48 | 10.8 | 3.6 | 5.2 | 3.8 | 40 |

TABLE II

| | $Fe^{3+}$ | $Co^{3+}$ | $Cu^{2+}$ | $Fe^{2+}$ | $Cr^{3+}$ | $Cu^{+}$ | $Ag^{+}$, $Ni^{2+}$, $Mn^{2+}$ | $Co^{2+}$, $Pb^{2+}$, $Cd^{2+}$ |
|---|---|---|---|---|---|---|---|---|
| $K_Q$ | 1.54 | 0.71 | 0.62 | 0.59 | 0.40 | 0.25 | 0.1~0.05 | 0 |

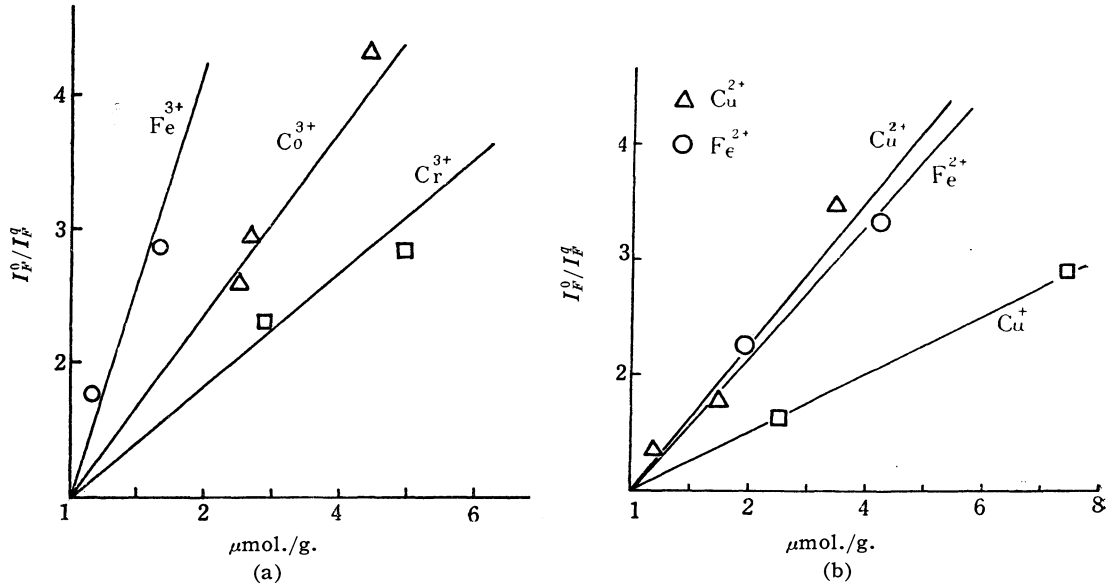



Fig. 1. Quenching of fluorescence.

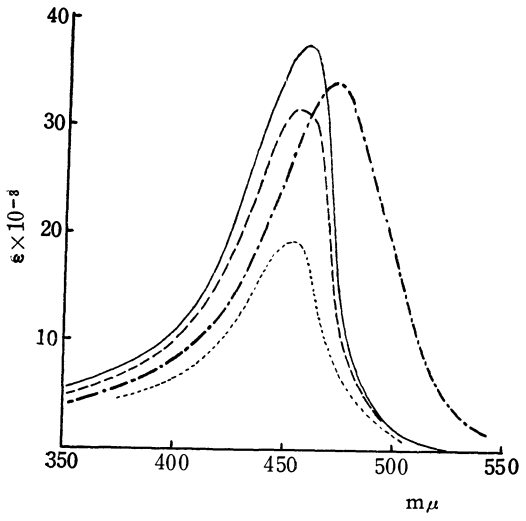
Quenching constants are evaluated from the inclinations and are tabulated in Table II.

Cobaltous-, lead- and cadmium-ion show no noticeable effects up to concentration ca. 10 $\mu$mol./g..

(c) **Absorption Spectra.**—Except cupric ion, all the salts scarcely affect the features of the original spectra of trypaflavine adsorbed on silica gel. In all cases the extinction declines more or less, but the decrease is not so large, except in the case of cobaltic- and ferrous-ion, that it may be neglected as a first approximation. Some typical examples are shown in Fig. 2. Somewhat large decreases in the cases of cobaltic- and ferrous- ion, however, are most certainly to be attributed to the partial decomposition of dye during the evacuation at elevated temperature. As for cobaltic ion, it is almost certain that it really decomposes, since it is well known that cobaltic chloride is unstable in the solid state and a part of chlorine is eliminated during the above treatment.

In view of the above results, it is true that the quenching constants shown in Table II must be corrected since they have been derived from the total decrease of fluorescence intensity which is due to a genuine quenching action on one hand and to the decomposition of dye on the other. For semiquantitative discussion, however, they may be taken as a measure of a genuine quenching action exclusive of the case of cobaltic- and ferrous-ion.

* Analogous notation will be used in general, when it is necessary to distinguish the quantity referring to the quenching experiment from that of the reference one.




——— Reference
– – – – $Fe^{3+}$ (1.7 μmol./g.),
·····  $Co^{3+}$ (3.2 〃 ),
–·–·– $Cu^{2+}$ (9.3 〃 ).

Fig. 2. Absorption spectra.

Even in the most extreme case of cobaltic ion the following data show that the fall of fluorescence intensity cannot be accounted for only by the decomposition of dye.

TABLE III

| | $\varepsilon$max. | $I_F$ |
|---|---|---|
| Reference | $37\times10^3$ | 33 |
| with $Co^{3+}$ (3.2 μmol./g.) | $20\times10^3$ | 10 |

**(d) Discussion.** — It can be concluded from the above results that except cupric chloride, the addition of a salt to the phosphor scarcely affects the absorption spectra and yet it reduces remarkably the intensity of pure fluorescence. Values of $I_F^0/I_F^q$ in Fig. 1 are considered to give the ratio $\pi^q/\pi^0$ which changes from ca. 2 to 4 in the case of ferric-, ferrous- and chromic-ion and yet the values of $\pi'^q$, $\pi''^q$, $n_1{}^q n_2{}^q$ and $n_u^q n'^q_u/\pi^q$ do not differ much from the corresponding values of a reference phosphor.

Taking the data relating to ferric ion 0.4 μmol./g., for example, the following estimation will be helpful to make the situation clear. From the 9th column of Table I,

$$n_u^0 n'^0_u/\pi^0 = 3.2/3.4\times n_u^q n'^q_u/\pi^q$$

If one assumes, as is probable, that

$$n'^q_u \simeq n'^0_u$$

then, $$n_u^0/\pi^0 = 3.2/3.4\times n_u^q/\pi^q$$

From the data of fluorescence, on the other hand,

$$\pi^q/\pi^0 = 1.7 \quad (1)$$

Hence $$n_u^q = 1.8\times n_u^0 \quad (2)$$

Combining (1) and (2) with the relations

$\pi^0 = n_i + n_e + n_u^0$, $\pi^q = n_i + n_e + n_u^q + n_q$,

one gets $$n_q = 0.7(n_i+n_e) - 0.1\times n_u^0$$

Thus it can safely be concluded that the addition of a salt quenches S′-state not only in a genuine sense, but it also promotes S′→T transition to some extent.

Here it is to be noted, however, that there is another possibility which must be taken into account. This is related to the state of adsorption of a salt. Since in general, inorganic salts are not capable of adsorbing very easily on silica gel and in view of the method of preparation of samples, it is rather likely that the state of adsorption is not uniform. There may exist on silica gel surface such a situation as that instead of a uniform distribution of positive and negative ions, a group of many ions coalesces into a tiny crystalline grain, which is located at random from place to place. If it be the case, it may occur that the dye molecule which happens to lie close to this tiny grain of a salt cannot make any contribution to the emission phenomenon and only an isolated dye molecule participates in fluorescence and phosphorescence. It is evident that in such a situation fluorescence intensity remarkably decreases and yet the decay curve remains almost unaltered. The real situation may perhaps be a superposition of the above two cases. At any rate, there is no doubt that these quenchers chiefly affect S′-state but scarcely affect T- and M-state.

**(e) Anomalous Behaviours of Cupric Ion.**—The results obtained when cupric ion was employed as a quencher are very interesting from various viewpoints. The absorption spectra of trypaflavine in this case are shown in Fig. 2. As seen from it, the maximum displaces about 15 mμ towards a longer wavelength (which corresponds to about 1.7 kcal./mol.) showing that a cupric ion affects the electronic state of dye.

From the fact that pure fluorescence is markedly quenched by cupric ion (the

TABLE IV

| Quencher | $\alpha$ | $\beta$ | $A/B$ | $I_L/I_{P0}$ | $\pi'$ | $\pi''$ | $n_1n_2$ | $n_un_u'/\pi$ | $I_F$ |
|---|---|---|---|---|---|---|---|---|---|
| Reference | 2.53 | 8.47 | 1.1 | 2.66 | 10 | 4.0 | 6.5 | 3.3 | 28 |
| 1.5 $\mu$mol./g. | 2.69 | 10.0 | 0.8 | 2.61 | 13 | 4.0 | 7.9 | 4.2 | 17 |
| 3.6 〃 | 3.92 | 20.0 | 0.4 | 1.94 | 35 | 5.1 | 18 | 16 | 8 |

quenching constant is 0.6 as listed in Table II), it is evident that S'-state is remarkably affected. But, in contrast to other salts, the change in the decay curve is rather large. The analysis is possible, at least approximately, on the basis of our scheme, and the results obtained from the analysis of the decay curves at 25°C are shown in Table IV.

A notable result in Table IV is that the value of $n_un_u'/\pi$ is increased by the addition of cupric ion. In all the other cases so far investigated including gaseous molecules, this quantity is almost constant. $\pi''$ remains practically unaltered, while $\pi'$, $n_1n_2$ and $n_un_u'/\pi$ increase remarkably. Hence it can be said that M-state is not affected and the increase of $n_1n_2$ can be attributed mainly to $n_1$.

If one assumes that the adsorption of cupric chloride is uniform, the reduction of pure fluorescence must be attributed to the increase of $\pi$. For example in the case of 3.6 $\mu$mol./g. cupric chloride,

$$\pi^q=3.5\times\pi^0$$

from the data in Fig. 1.

Combining with the data in Table IV, $n_u^qn_u'^q=18\times n_u^0n_u'^0$. Thus it is certain that the transitions between S'- and T-state are enormously promoted. If one assumes, as it seems probable, that the main part of the increase in $n_u^qn_u'^q$ is due to that of $n_u^q$, then the great value of $\pi'^q$ must partially be attributed to the participation of a genuine quenching process.

Thus it is plausible that the cupric ion not only influences S'-state but also T-state pretty markedly while it scarcely affects M-state.

The temperature effect on various constants in the range from 0°C to 50°C, throughout which $\beta$-phosphorescence is practically negligible, is shown in Table V.

In this table, apparent activation energy obtained from the Arrhenius' plot for $\pi'$, $\pi''$, $n_un_u'/\pi$ and $n_1n_2$ respectively, is also included.

The activation energy for $\pi'$, $\pi''$ and $n_un_u'/\pi$ does not change beyond probable error but it seems quite definite that the activation energy for $n_1^qn_2^q$ is about half that for $n_1^0n_2^0$. Since $n_2$ is approximately independent of the existence of cupric ion and moreover $\pi''$ has practically the same temperature dependence, the above result is mainly due to the difference in the temperature dependence of $n_1^0$ and $n_1^q$.

Thus it seems plausible to consider that T→M transition is a process accompanied with an activation energy the magnitude of which, however, is much less than that for T→S' transition; the promotion of the transition T→M by the cupric ion at least partially, is attributed to the decrease of this activation energy.

Finally the decrease of $I_L/I_{P0}$ by the addition of a cupric ion and its temperature dependence will be discussed briefly.

From the relation

$$I_F/I_{P0}=I_L/I_{P0}-1=\frac{\pi_1-(n_1n_2/\pi_2)}{n_un_u'/\pi}$$

it is evident that $I_F/I_{P0}$ decreases when $n_un_u'/\pi$ and $n_1n_2/\pi_2$ increases while it increases when $\pi_1$ increases. In the present case $\pi_2$ and $n_2$ are scarcely affected by a cupric ion and the increase of $\pi_1$ and $n_1$ partially cancels, so that the variation of the numerator on the right side becomes much less than that of $n_un_u'/\pi$. Thus the main factor which reduces $I_F/I_{P0}$ is $n_un_u'/\pi$, which in the present case is remarkably increased by the addition of cupric ion.

The result that the value of $I_F/I_{P0}$ decreases with rise of temperature, irrespective of the addition of cupric ion, is due to the fact that the temperature coefficient of $n_un_u'/\pi$ is larger than that of $\pi_1$, $\pi_2$ and $n_1n_2$ (see Table V).

**(f) Trypaflavine-filter Paper Phosphor.** —As already reported in part II, deviation from linearity in decay curves is much smaller than that of silica gel phosphor. Moreover the effect of addition of a third substance is also much smaller than that in the case of silica gel, so that the analysis on the basis of the scheme involving M-state cannot be done very accurately. Here only a few examples will be shown and the results will be discussed only qualitatively.

The Table VI shows the results of analysis of the decay curve when oxygen or water vapor is added to the phosphor.

In the case of oxygen $\pi'$ and $\pi''$ remain constant while $n_1n_2$ seems to be somewhat

TABLE V

Dye conc., 0.4 μmol./g.; $CuCl_2$, 3.6 μmol./g.; Time in sec.

| $1/T$ | $\alpha$ | $\beta$ | $A/B$ | $I_L/I_{P0}$ | $\pi'$ | $\pi''$ | $n_1n_2$ | $n_un_u'/\pi$ |
|---|---|---|---|---|---|---|---|---|
| $3.65\times10^{-3}$ | 2.08 | 15.4 | 0.48 | 2.53 | 22 | 2.9 | 10 | 7.2 |
| 3.51 | 2.65 | 16.6 | 0.48 | 2.38 | 24 | 3.7 | 12 | 8.7 |
| 3.36 | 3.92 | 20.0 | 0.40 | 1.94 | 35 | 5.1 | 17 | 16 |
| 3.24 | 4.58 | 23.6 | 0.29 | 1.87 | 44 | 5.6 | 19 | 22 |
| 3.12 | 6.5 | 27.1 | 0.24 | 1.73 | 58 | 7.6 | 22 | 32 |
| Apparent activation energy (kcal./mol.) | | | | | 1.7 | 1.6 | 1.2 | 2.6 |
| | | | | Reference Sample | | | | |
| 3.65 | 1.43 | 4.58 | 1.4 | 3.73 | 4.59 | 2.4 | 2.2 | 0.99 |
| 3.53 | 1.84 | 6.28 | 1.3 | 3.12 | 6.9 | 3.0 | 3·9 | 1.8 |
| 3.36 | 2.53 | 8.47 | 1.1 | 2.66 | 10.3 | 4.0 | 3.3 | 6.3 |
| 3.24 | 3.04 | 10.35 | 0.77 | 2.53 | 13.7 | 4.4 | 7.8 | 4.7 |
| 3.12 | 4.51 | 14.85 | 0.75 | 2.42 | 21.7 | 5.8 | 12 | 8.1 |
| Apparent activation energy (kcal./mol.) | | | | | 2.3 | 1.3 | 3.2 | 2.4 |

TABLE VI

Dye conc., 0.8 μmol./g. (filter paper, ca. 0.5 g). At 25°C. Time in sec.

| | $\alpha$ | $\beta$ | $A/B$ | $I_L/I_{P0}$ | $\pi'$ | $\pi''$ | $n_1n_2$ | $n_un_u'/\pi$ | $I_F$ |
|---|---|---|---|---|---|---|---|---|---|
| Reference | 2.15 | 6.43 | 1.5 | 4.59 | 6.0 | 3.6 | 4.2 | 1.1 | 76 |
| $O_2$, 2.4 *m*.mol. (190 mmHg) | 2.08 | 5.79 | 0.7 | 5.95 | 6.0 | 2.8 | 2.2 | 0.9 | 65 |
| $O_2$, 3.6 *m*.mol. (290 mmHg) | 2.32 | 6.30 | 0.5 | 8.31 | 6.3 | 3.0 | 2.2 | 0.7 | 60 |
| Reference | 2.28 | 7.11 | 1.4 | 4.74 | 6.7 | 3.8 | 5.0 | 1.1 | 80 |
| $H_2O$, 40 μmol. (1/4 mmHg) | 2.35 | 6.85 | 1.4 | 5.04 | 6.3 | 3.9 | 4.3 | 1.0 | 55 |
| $H_2O$, 320 μmol. (2 mmHg) | 2.52 | 6.52 | 1.9 | 7.69 | 5.4 | 4.2 | 3.7 | 0.6 | 21 |

diminished. But since the results are not so certain and moreover data are rather few, it will not be suitable to discuss further about this point. There is however no doubt that the decrease of $I_F$ is closely connected with that of $n_un_u'/\pi$. Hence broadly speeking, it can be said that only S'-state is affected and only fluorescence is quenched.

This result is in sharp contrast with that obtained for the case of trypaflavine-silica gel phosphor. It is to be noted, however, that in the present case the quantity of oxygen is very large compared with that in the case of silica gel.

The situation is quite similar for the quenching caused by water vapor; thus only S'-state is affected and the intensity of pure fluorescence decreases without any noticeable effect on the decay curve.

The influence of the addition of some organic vapors such as acrylonitrile (the quantity is 1700 times that of dye), styrene (about equal to that of dye), etc. was also tested but none of them showed any effects beyond experimental error.

## General Features of the Quenching Phenomena as Revealed from the Results so far Obtained

The main features of the quenching phenomena so far established can be summarized in Table VII.

TABLE VII

| Carrier | Quencher | S' | T | M |
|---|---|---|---|---|
| Silica gel | Gases | × ← ×O | O → °O | ° |
| | $SO_2$ | × ← ×O | O → °O | O |
| | Salts | O | × | × |
| | $CuCl_2$ | O | O → ° | × |
| Filter-paper | $O_2$, $H_2O$ | O | × | × |
| | Self-quenching | O | × | × |

In this Table O and × under S'-, T- and M-state represent respectively that the state in question is affected or not by a quencher. A small circle means that the action is somewhat small. Very little can be said whether each transition is influenced or not by a quencher, but the

results written in this Table are reliable.

The informations summarized in the above Table are still very scanty, yet some suggestive arguments will be based upon them.

From the survey of the above Table it seems permissible to classify the quenching effects into two groups; collisional quenching which attacks chiefly T- and M-state, and a static one attacking S'-state. Let us consider the results from this point of view.

That the quenching action of oxygen toward silica gel phosphor is of collisional nature has been argued already in part III. Hence it is considered that oxygen on silica gel phosphor is so weakly adsorbed that it is quite free to move.

On the contrary, filter paper is less porous than silica gel and oxygen adsorbed on it is supposed to be fixed at a definite position. The adsorbed oxygen in this case is thus remote from the adsorbed dye molecule and this is perhaps the reason why it falls into the class of a static type. There may be no question that salts act as static quenchers since they are adsorbed on fixed positions. Self quenching in the case of filter paper is also undoubtedly of static type. Thus all the results conform well with the above classification.

Now, this classification becomes more plausible and more instructive if one assumes the following molecular model of adsorbed dye. From the observations made when polyvinyl alcohol was used as a carrier (Part II), it seems probable that molecules of trypaflavine are fixed on a carrier at the positions of two amino-groups. It is very natural then, to suppose that if the two amino-groups attached on a carrier are subject to some perturbation, then T- or M-state will be affected appreciably. Such a reasoning conforms well with the general view that molecular rigidity is one of the essential conditions for the phosphorescence to be observed. Thus it is comprehended that only when a quencher molecule approaches closely to an amino-group can it affect T- or M-state. This may be the reason why only collisional quenching affects T- and M-state. In the case of a cupric ion which is a sole exception in static quenching, the field may be so intense that it is able to affect amino-groups to some extent.

To sum up, the behavior of T- and M-state probably depends on the interaction of amino and polar group of a carrier and is supposed to be perturbed only by extremely short range force.

The physical or chemical property of M-state is not yet known, but the fact that cupric chloride only affects T-state while oxygen and other gases attack both T- and M-state seems to be due to a specific nature of this state.

In order to reveal the nature of M-state, it will be most helpful to study about various combinations of dye and carrier.

## Summary

The effects of the addition of inorganic salts upon trypaflavine-silica gel phosphor were studied, and it was found that decay curves are not affected much by any of the metallic ions except cupric ion. On the contrary, the intensity of pure fluorescence ($I_L - I_{P0}$) was reduced more or less by many metallic ions. From these results, it was concluded that many metallic ions chiefly affect S'-state but not T- and M-state.

The result for cupric chloride was somewhat anomalous on the point that a cupric ion affects both S'- and T-state.

A general survey on the quenching action of various substances upon adsorbed trypaflavine phosphor was given.

The cost of the present research has been partly defrayed from the Scientific Research Grant from the Ministry of Education.

*Institute of Polytechnics*
*Osaka City University, Osaka*

# *Microcolorimetric Determination of Sulfate by Reduction to Hydrogen Sulfide with Tin(II)—Strong Phosphoric Acid*

By Toshiyasu KIBA and Ikuko KISHI*

(Received August 27, 1956)

In a previous paper[1] from the authors' laboratory it was shown that both soluble and insoluble sulfates could be quantitatively reduced to hydrogen sulfide by heating with tin(II)-strong phosphoric acid, a new powerful and stable reducing agent first described by the authors. The discovery of this reagent led the authors to the development of a new rapid and simple method for the determination of semimicro quantities of sulfate sulfur. The established method[1] consists of the following three succesive steps: (a) reduction of sulfate to hydrogen sulfide by tin(II)-strong phosphoric acid, (b) absorption of the hydrogen sulfide by zinc acetate solution, (c) iodometric titration of the resulting zinc sulfide by ordinary procedures.

The present report concerns a later investigation in which the above method has been extended to the microgram scale by adopting the sensitive methylene blue method for sulfides[2]. The rapidity and simplicity of the original method are still retained in this new colorimetric procedure, by which 1 to 35 micrograms of sulfate sulfur can be estimated.

## Apparatus

**Reduction and Absorption Apparatus.**—The apparatus for the reduction of the sulfate and the absorption of the hydrogen sulfide evolved is shown in Fig. 1. The reaction vessel (A) is of fused silica. Unexpectedly high values of sulfur were occasionally obtained when glass vessels were used, probably owing to minute amounts of sulfur in the glass. A bent glass tube (F) is attached to the outlet arm of the reaction vessel with a short piece of rubber tubing (G). A detachable delivery tube (D) is connected with another rubber tubing to the bent tube (F) and inserted into the absorbing vessel (C). Since zinc sulfide adheres to that part of the tube immersed in the solution, it must be disconnected and allowed to remain in the absorbing vessel during the development of the methylene blue color. A Kipp's apparatus is employed for the production of carbon dioxide, which is purified by six-washing bottles (not shown in Fig. 1.) and introduced into the reaction vessel through the inlet arm. Solutions used for the purification of carbon dioxide are described below.

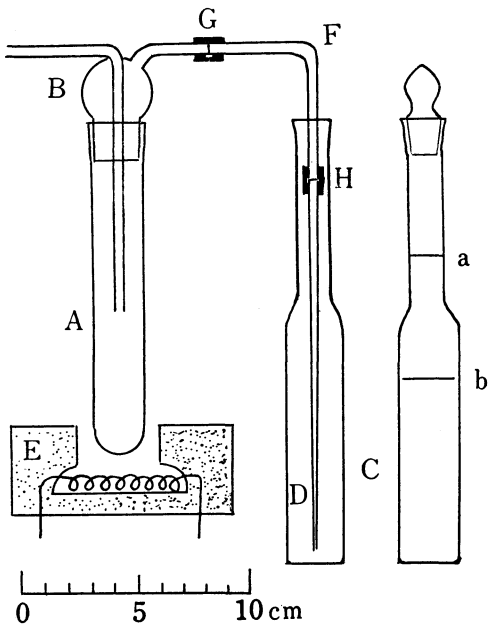



Fig. 1. Apparatus for reduction and absorption.
A: Reaction vessel of fused silica
B: Glass cap fitted to the reaction vessel
C: Absorbing vessel a: the mark of 50 ml.
b: the mark of 35 ml.
D: Detachable delivery tube (4 mm. in outside diameter)
E: Electric heater
F: Gas leading tube
G, H: Short pieces of rubber tubing

**Photoelectric Colorimeter.**—A "Hirama" photoelectric colorimeter with 1 cm. cells and a filter 655 mμ were used throughout this work.

## Reagents

**Tin(II)-Strong Phosphoric Acid.**—Prepare from 250 g. of strong phosphoric acid and 50 g. of tin(II) chloride dihydrate of extra pure grade as described in the previous paper[1].

**Carbon Dioxide.**—Purify carbon dioxide produced in the Kipp's apparatus by passing through five gas-washing bottles containing respectively

* Her present name is Mrs. Ikuko AKAZA.

1) T. Kiba et al., This Bulletin, **28**, 641 (1955).
2) J. F. Fogo and M. Popowsky, *Anal. Chem.*, **21**, 732 (1949).
3) S. Nakayama, *J. Chem. Soc. Japan*, **47**, 197 (1926).

water, 1% potassium permanganate in 10% sodium carbonate solution, vanadium (II) sulfate in sulfuric acid, 5% barium chloride, and zinc acetate absorbing solution. Place a sixth, empty bottle to equalize the flow of the gas and to intercept mist. The vanadium (II) sulfate solution is employed to remove oxygen completely from the carbon dioxide. To prepare it, dissolve 2 g. of ammonium vanadate in 200 ml. of water, add 20 ml. of 6 N sulfuric acid, and shake vigorously with 3% zinc amalgam in an atmosphere of carbon dioxide until the violet color of vanadium (II) appears. Transfer the solution quickly into a gas-washing bottle containing a small amount of the amalgam.

**Zinc Acetate Absorbing Solution.**— Dissolve 20 g. of zinc acetate dihydrate of extra pure grade in 1 l. of redistilled water. If necessary, add two or three drops of glacial acetic acid to clarify the solution, but the pH of the solution should not be below 5. The redistilled water is prepared by distilling ordinary distilled water with a small amount of sodium hydroxide in an all-glass still.

***p*-Amino Dimethyl Aniline Solution.**—Dissolve 1.4 g. of *p*-amino dimethyl aniline sulfate crystals of pure grade in 200 ml. of 1:1 sulfuric acid.

**Ferric Chloride Solution.**—Dissolve 10 g. of ferric chloride hexahydrate in 100 ml. of distilled water.

**Standard Sulfate Solution.**—Dissolve 4.4299 g. of anhydrous sodium sulfate of extra pure grade in 1 l. of sulfur-free water. Take 20 ml. of this solution with a pipet and dilute it to 1 l., so that the final solution contains 20 micrograms of sulfur in 1 ml. Pipet accurately required amounts of this stock solution for the analysis.

**Barium Chloride Solution.** — Dissolve 1 g. of barium chloride dihydrate in 100 ml. of sulfur-free water, and use 0.5 ml. of this solution in each test.

## Procedure

When the sample is a solution, pipet accurately an aliquot containing 1 to 35 micrograms of sulfur. When it is a solid, take an accurately weighed quantity containing the same range of sulfur. Put the measured sample into the reaction vessel (A) (Fig. 1.), add 0.5 ml. of the barium chloride solution to fix the sulfate as barium sulfate, and evaporate the content to dryness at the bottom of the vessel. Pour 5 ml. of tin (II)-strong phosphoric acid over the dried residue from a pipet. Fill the absorbing vessel up to the 35 ml. mark with the zinc acetate solution. Connect all the apparatus as shown in Fig. 1. Pass carbon dioxide very rapidly through the apparatus for five minutes. The passage of the gas should be rapid enough to cause strong agitation of the surface of the liquid in the absorbing vessel, and the end of the gas delivery tube should reach to the bottom of the vessel. After five minutes, reduce the flow of the gas to a rate of one bubble per second. Heat the bottom of the reaction vessel on a small etectric heater, which is regulated by a variable transformer, until white fumes of phosphoric acid appear. Continue the heating for about fifteen minutes. It is unnecessary to keep the reaction temperature strictly constant, but it should be high enough to ensure that the mixture exhibits a white turbidity near the end of the reaction. Stop the heating and continue to pass carbon dioxide for about five minutes.

Remove the absorbing vessel, leaving the gas delivery tube in it. Stopper the vessel and place it in a thermostat kept at 24°C for several minutes. Add quickly 1.5 ml. of *p*-amino dimethyl aniline solution using a rapid delivery pipet, stopper the vessel, shake it vigorously, and then quickly add 0.5 ml. of the ferric chloride solution. Stopper and shake the vessel again. After keeping the vessel in the thermostat at 24°C for fifteen minutes, add more distilled water till the liquid reaches the 50 ml. mark, while the delivery tube is hung up from the solution with washing. Stopper and shake the vessel so as to make the solution homogeneous. Read the absorbancy of the solution in the colorimeter at 655mμ within thirty minutes.

## Results and Discussion

**Standard Sulfate Calibration Curve.**— As shown in Fig. 2, the linear relationship

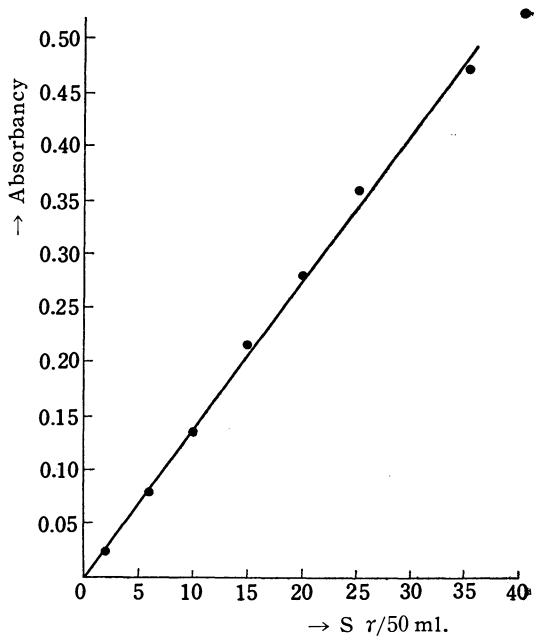



Fig. 2. Standard sulfate calibration curve.

was obtained between the amount of sulfate and the absorbancy of the resulting methylene blue solutions in the range 1 to 35 micrograms of sulfur. Measurements were made in 1-cm. cells at 655 mμ, using

a mixture of the absorbing solution and the reagent of the same amounts as reference. For more than 40 micrograms of sulfur the linearity is not held, because of mutual interaction of the light-absorbing molecules or of spectral purity of the instrument. According to the authors' experience, the main sources of error in this method seemed to be imperfect removal of oxygen from the carbon dioxide and careless delay in adding the reagents, viz., *p*-amino dimethyl aniline and ferric chloride.

A comparison of the standard curve with that drawn for sodium sulfide by direct coloration with *p*-amino dimethyl aniline, indicated that the two curves coincided with each other satisfactorily. Both curves could be expressed by the equation, $x=a+by$, where $x$ is the absorbancy measured and $y$ the amount of sulfur in micrograms. The average values of $a$ and $b$ computed from the sulfate curves were 0.00614 and 0.01084, respectively, whereas those obtained from the sulfide curves were 0.00245 and 0.01087, respectively. These numerical values were calculated by the method of the least square. It may be concluded from this fact that the sulfate was completely reduced to hydrogen sulfide under the given condition.

**Interferences and their Elimination.**— The effect of chloride was examined by the addition of various amounts of sodium chloride to sodium sulfate solutions, containing 1 to 35 micrograms of sulfur through the standard procedure. It was found that, when the amount of the sulfate sulfur was less than 20 micrograms, the presence of as much as 36.9 mg. of the chloride ion does not interfere with the determination. When the amount of coexisting chloride ions was decreased to 12 mg., the linearity of the curve was recovered for a wider range of sulfur, i. e., from 1 to 35 micrograms.

The presence of nitrate in the sample, on the other hand, was found to result in apparently low values for sulfate sulfur.

As the sulfate ion is customarily separated from other anions with barium chloride, the effect of the barium ion was examined. By the addition of 1 ml. of 1% barium chloride solution to sodium sulfate solutions containing 1 to 40 micrograms of sulfur, the determination of sulfate sulfur was carried out. Although in this case a large excess of the barium ion was always present, it did not bring about any deviation from the linear relationship as shown in the standard sulfate sulfur curve. The experiment conclusively showed that the barium ion does not affect the accuracy of the method.

The collector action of ferric hydroxide may have great importance in analytical procedures, particularly in a micro analysis. Minute amounts of the sulfate ion, coexisting with other interfering soluble ions, may also be separated by centrifugation or filtration as barium sulfate, which is occluded in the ferric hydroxide precipitate. So the effect of the ferric ion was examined as follows. To sodium sulfate solution containing 1 to 40 micrograms of sulfur were added 0.5 ml. of 1% solution of barium chloride and 3.35, 5.58, and 11.17 mg. of ferric ion as iron(III) chloride, respectively. After the drying of the mixed solutions in the reaction vessels, the entire procedure was carried out and the absorbancy of the resulting methylene blue solution was measured. As illustrated in Fig. 3, the solution containing 11.17 mg. of the ferric ion showed lower

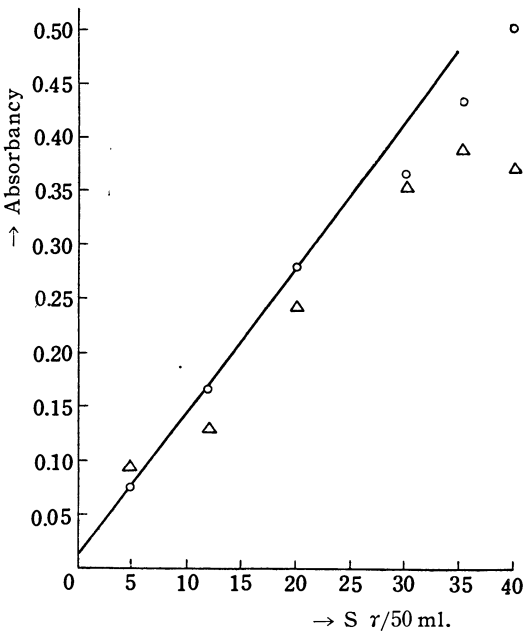



Fig. 3. Effect of ferric and chloride ions on the sulfate calibration curve.

○: $5.5_8$ mg. Fe and 12.2 mg. Cl
△: $11.1_7$ mg. Fe and $22.9_5$ mg. Cl

sulfur values. Moreover, even by the use of 5.58 mg. of ferric ions, the linearity of the curve could not be preserved for more than 20 micrograms of sulfur content. As it might be considered that the effect was caused by both ferric and chloride

ions, the following experiments were carried out to eliminate their interference. To the sulfate solution taken in the reaction vessels were added 11.2 mg. of ferric ion as ferric chloride, 0.5 ml. of 1% barium chloride solution, and 0.5 ml. of aqueous ammonia (d=0.88). The mixture was evaporated to dryness, and heated in an electric oven to 500°C. By this treatment all acidic components but sulfate would be decomposed, unless too large amounts of alkali or alkaline earth metal ions were present. The ferric chloride was eventually converted into ferric oxide. Then the reduction of the sulfate to hydrogen sulfide was carried out according to the procedure without further addition of barium chloride. The linear relationship between the amount of the sulfate and the absorbancy of the resulting methylene blue solution was obtained. So it was found that the elimination of the effects of ferric and chloride ions could be completed by this treatment.

**Determination of Sulfur in Commercial Ferric Chloride Reagent.**—The method described above can be readily applied to the determination of sulfate in various substances. For example, weigh accurately about 27 g. of ferric chloride hexahydrate, and dissolve it in 500 ml. of distilled water.

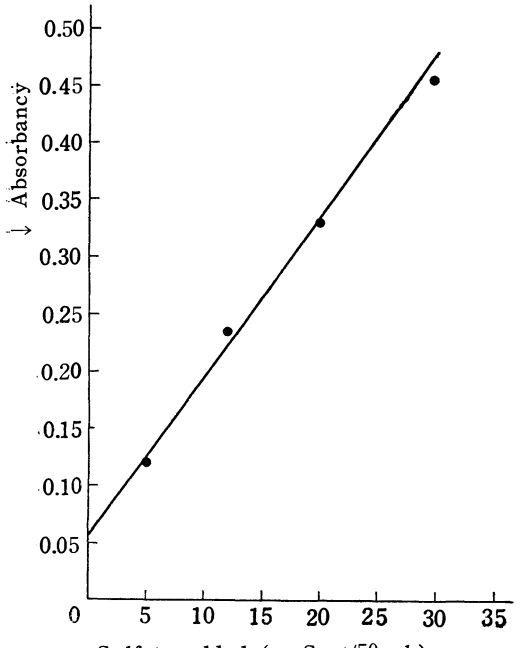



Fig. 4. Sulfate calibration curve after treatment with ammonia, in the presence of 54 mg. of ferric chloride hexahydrate.

Pipet 1 ml. of the solution into a reaction vessel, and after the treatment described above, the analysis is similarly carried out. In the course of the treatment some ferric chloride volatilizes, but barium sulfate is stable at as high as 900°C[3] and most of the ferric chloride is converted into ferric oxide at 500°C[4]. The experimental data of the analysis are given in Fig. 4 showing satisfactory recovery of the sulfate added. The absorbancy measured in the absence of sulfate was 0.052, which is the sum of the absorbancy of 0.039 for the blank of ammonia and that of 0.019 for sulfur in the ferric chloride tested. So the amount of sulfur in 54 mg. of ferric chloride hexahydrate is estimated to be as small as 1 microgram and that contained in 0.5 ml. of aqueous ammonia 2.4 micrograms.

**Determination of Sulfur in Japanese Acid Clay.**—A 0.1 to 0.5 g. portion of air-dried clay was weighed directry in a reaction vessel. The analysis was similarly carried out without any preliminary treatment. As shown in Table I, a linear relationship was obtained between the amount of the clay and that of sulfur found. Moreover, it was verified that as little as 4 micrograms of sulfur in 0.1 g. of the clay could be estimated accurately and rapidly with satisfactory reproducibility.

TABLE I

DETERMINATION OF SULFUR IN JAPANESE ACID CLAY

| Acid Clay Taken g. | Absorbancy | Sulfur Found μg. | Sulfur Content % |
|---|---|---|---|
| 0.1000 | 0.056 | 3.8 | 0.0038 |
| 0.2175 | 0.119 | 8.6 | 0.0039 |
| 0.3825 | 0.195 | 14.3 | 0.0037 |

## Summary

A new reagent, "Tin(II)-strong phosphoric acid" has been prepared to permit a rapid and simple determination of sulfate sulfur by reduction to hydrogen sulfide. The procedure for the determination of semi-micro quantities of sulfate sulfur, previously devised by the authors, has been extended to the microgram scale by adopting the sensitive methylene blue colorimetric method. The rapidity and simplicity of the original method are still retained in this new colorimetric method,

4) L. Marvin, *Ind. Eng. Chem. Anal. Ed*, **17**, 554 (1945).

by which 1 to 35 micrograms of sulfate sulfur can be estimated. The apparatus is very simple, a test-tube of fused silica being employed as the reaction vessel. The standard calibration curve for colorimetric determination of sulfate sulfur by this method coincides well with that drawn for sodium sulfide by direct coloration with *p*-amino dimethyl aniline and ferric chloride. Interference of other anions can be kept out of consideration, because the sulfate ion is easily separated by addition of barium chloride solution and coprecipitation with ferric hydroxide. Large amounts of ferric hydroxide do not affect the method. Some examples of the determination of sulfate sulfur in ferric chloride reagent and Japanese acid clay are described.

A part of the expenses for this study was defrayed from a grant given by the Ministry of Education, to which the authors' thanks are due.

*Department of Chemistry*
*Faculty of Science*
*Kanazawa University*
*Kanazawa*

# *Studies on Amino-hexoses. IV. N-Deacylation with Hydrazine and Deamination with Nitrous Acid, a Clue to the Structure of Aminopolysaccharides*[1]

By Yoshio MATSUSHIMA and Noriko FUJII

(Received August 30, 1956)

Considerable confusion is observed in the older literature concerning the nitrous deamination products of glucosamine. However, the formation of chitose, a 2, 5-anhydro-hexose[2], from glucosamine is understood in terms of intramolecular rearrangement[3,4] which accompanies the deamination, and a few years ago one of present authors demonstrated experimentally that the same mechanism operated in the nitrous deamination both of glucosaminol and 2-amino-erythro-pentitols which form 2-deoxy-glucose[3] and 2-deoxy-ribose[5] respectively.

The nitrous deamination of chitosan (deacetylated chitin or polyglucosamine) has also resulted in conflicting conclusions[6], but it is noteworthy that every worker reports the rupture of glucosaminidic linkage and the formation of highly reducing saccharides. More recently, it was reported[7] that ψ-heparin (the desulfated heparin) also produced reducing saccharides with nitrous acid. In these instances, it is not conceivable that the hydrolytic cleavage of amino-glycosidic linkages preceede the deamination, since it is known[8] that glucosaminidic linkage strongly resists to acid hydrolysis (see Fig. 1) and nitrous acid is so weak an acid. Therefore, some special mechanism must operate.

It may be expected that the cleavage of glucosaminidic linkage (or probably 2-amino-glycosidic linkages in general) with nitrous acid will provide a clue to the structure of amino-polysaccharides. However, it seems desirable to obtain more experimental evidences and to establish the theory according to which the 2-amino-glycosidic linkage cleaves.

The authors have isolated from the deamination mixture of chitosan a diphenylhydrazone which is identical with the long known diphenylhydrazone[9] which was obtained from the deamination mixture of glucosamine. Although, as we

1) A Part of this article was delivered at the 9th annual meeting of the Chemical Society of Japan, April 1956.

2) E.Fischer and F.Tiemann, *Ber.*, **27**, 138 (1894); E.Fischer and F. Andreae, ibid., **36**, 2587 (1903); W. N.Haworth, E.L.Hirst and V.S.Nicholson, *J. Chem. Soc.*, **1927**, 1513.

3) Y.Matsushima, *Bull. Chem. Soc. Japan*, **24**, 144 (1951).

4) A.B.Foster, *Chem. and Ind.*, **1955**, 627.

5) Y.Matsushima and Y.Imanaga, This Bulletin, **26**, 506 (1953).

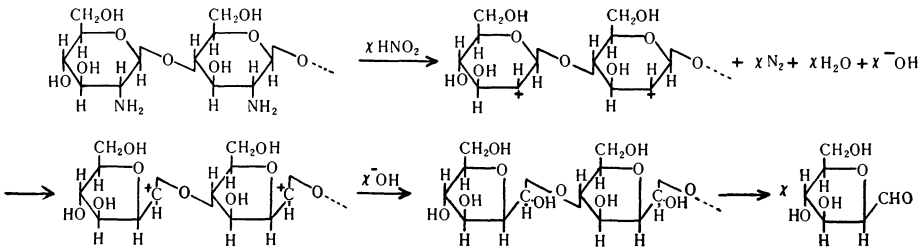
6) W.Armbrecht, *Biochem. Z.*, **95**, 108 (1919); P. Karrer and S.M.White, *Helv. Chim. Acta*, **13**, 1105 (1930); K.H.Meyer and H.Wehrli, *Helv. Chim. Acta* **20**, 353 (1937).

7) A.B.Foster, E.F.Martlew and M.Stacey, *Chem. and Ind.* **1953**, 825.

8) J.C.Irvine and A.Hynd, *J. Chem. Soc.*, **101**, 1128 (1912).

9) P.Schorigin, and N. N. Makarowa-Semljanskaya, *Ber.* **68**, 965 (1935).

lacked the structural proof, the diphenylhydrazone was not necessarily thought to be the diphenylhydrazone of chitose until recently, a report[10] proving the 2,5-anhydromannose structure of the diphenylhydrazone has appeared. Therefore, the isolation



of the diphenylhydrazone provides a proof of the existence of chitose in the deamination products of chitosan. How chitose is produced may be seen in the following scheme:

Here also the mechanism of intramolecular rearrangement operates and the formation of the intermediate half-acetal which may be highly labile explains the result. This theory has its counterparts in the anomerism of free sugars[11] and in the ease of hydrolysis of fructofuranosidic linkage[11,12]. The ease of hydrolysis of fructofuranosidic linkages, e. g. of sucrose, was attributed to the foregoing hydrolysis of the furanoid ring of fructose moiety, thus forming an intermediate half-acetal structure.

Unfortunately, since the amino residue of natural amino-polysaccharides is acylated without exception, nitrous acid can not attack it as such. Common deacylating agents, strong acid or alkali, may cause too far reaching degradation with two known exceptions of chitin and heparin. Therefore, the authors adopted the method of hydrazinolysis which was successfully introduced[13] into the protein chemistry. With anhydrous hydrazine, the amide linkage, or ester linkage if present, in polysaccharides may be cleaved, liberating free amino residue and the glycosidic or other linkages may remain intact.

To begin with, the authors applied the hydrazinolysis method to chondroitin sulfate. The ratio of amino to total nitrogen reaches about 0.9 when barium chondroitin sulfate is treated with anhydrous hydrazine for 10 hours at 100°. The hydrazine-treated specimen, only after treatment with nitrous acid, gives several spots on paper chromatograms, thus indicating the cleavage of galactosaminidic linkage with nitrous acid (see Fig. 2). Though no quantitative conclusion about the structure of chondroitin sulfate can be drawn so far, this method seems to be promising for the structural study of amino-polysaccharides. The work will be continued.

## Experimental Part

**Appearance of Reducing Power when Chitosan is treated with Nitrous Acid.**—500 mg. of chitosan was dissolved in 25 cc. of acetic acid (ca. 15%) and a solution of 230 mg. of sodium nitrite in 25 cc. of water was added. 5 cc. aliquots were pipetted off and the reducing power was determined by Bertrand's method. A comparison run with hydrochloric acid was carried out similarly.

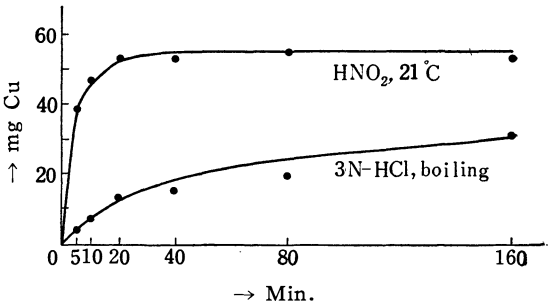



Fig. 1. The velocity of the appearance of reducing power in nitrous deamination and acid hydrolysis respectively of chitosan. Ordinate: Reducing power in mg. Cu. Abscissa: Time in minutes.

**Isolation of Chitose Diphenylhydrazone from the Nitrous Deamination Mixture of Chitosan.**—To the highly viscous solution which was prepared by dissolving 2 g. of chitosan into a mixture of 1N hydrochloric acid (13.2 cc.) and water (20 cc.), 4.6 g. of silver nitrite was added at room temperature. The evolution of gas and

10) S. Akiya and T. Osawa, *J. Pharm. Soc. Japan*, **74**, 1259 (1954).
11) S. Akabori and K. Uehara, "Discussion on Enzymes," Tokyo, (1942).
12) S. Matsumoto, *J. Chem. Soc. Japan*, **61**, 387, 395 (1940).
13) S. Akabori, K, Ohno and K. Narita, This Bulletin, **25**, 214 (1952).

the diminution of viscosity was observed immediately. After two days standing at room temperature, the silver chloride formed and the residual silver nitrite was filtered off, and the silver ion in the solution was removed by hydrochloric acid. A small amount of urea could exclude residual nitrous acid. To the solution the pH of which was adjusted to 4, were added 1.5 g. of diphenylhydrazine and a necessary amount of ethanol to obtain a clear solution. After heating at 80° for one hour the solution was concentrated in vacuo and the residue was agitated with a small amount of benzene and seed crystals. White needles began to crystallize in an hour. The crystals were washed thoroughly with water and benzene. The crude crystals thus obtained melted at 140–141° and weighed 0.97 g. Recrystallization was carried out as follows: the crude crystals were dissolved in 10 cc. of ethanol, and 40 cc. of water was added. Fine crystals came out immediately and the mixture was agitated thoroughly with a small amount of benzene-petroleum ether (1 : 1) in order to make free from coloring matter, filtered and washed with ethanol-water (1 : 4) and benzene. The recrystallized specimen weighed 0.67 g. and melted at 143.4–144.0° alone or at 145–145.5° with an authentic specimen of chitose diphenylhydrazone melting at 145.8–146.2°.

*Anal.* Found: C, 65.39; H, 6.05; N, 8.28. Calcd. for $C_{18}H_{20}O_4N_2$: C, 65.85; H, 6.09; N, 8.54%.

**Hydrazinolysis of Barium Chondroitin Sulfate.**—4.57 g. of barium chondroitin sulfate (N, 2.7%) was heated with 11.1 g of anhydrous hydrazine at 100° for ten hours. The excess hydrazine was evaporated off in vacuo and the residue was dissolved in 20 cc. of water and dialysed to running water of nineteen hours using collodion membrane. The inorganic precipitate was discarded and the solution was dried up in vacuo yielding 0.5 g. of a faintly yellow substance.

*Anal.* Found: N, 3.02 (Kjeldahl method); 2.65 % (van Slyke method).

**Deamination of the Hydrazine-treated Specimen with Nitrous Acid.**—0.4 g. of the specimen was dissolved in 4.6 cc. of water and to this solution 0.87 g. of silver nitrite and 3.4 cc. of 1N hydrochloric acid was added. A gas evolved immediately. After standing for one day at room temperature, the silver chloride formed and the residual silver nitrite was filtered off and the silver ion was removed with 1N hydrochloric acid. A small amount of urea was added in order to decompose the residual nitrous acid, and after the pH was adjusted to 5.8 the solution was concentrated in vacuo. The residue was paper-chromatographed. It is to be noted that color develops with such ketose reagents as resorcinol-hydrochloric acid or urea-hydrochloric acid[14]. These facts suggest that every spot in chromatograms contains 2,5-anhydro-hexose (Hydrofurfural) structure.

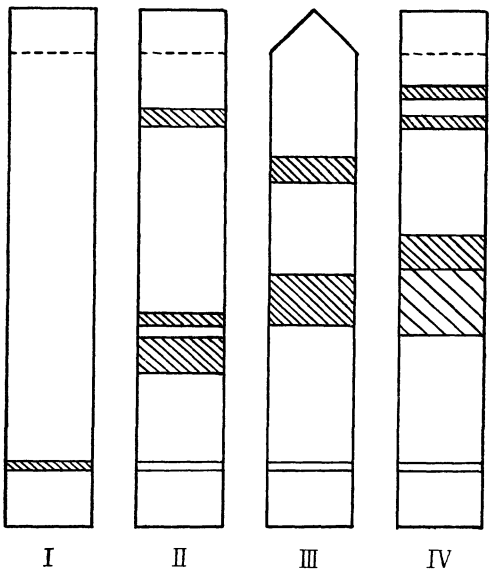



Fig. 2. Diagrammatic representation of the paper chromatograms.
I: The specimen without the treatment with nitrous acid. II: Urea-HCl development. III: Long run chromatography with urea-HCl development. IV: Resorcinol-HCl development. The moving solvent is butanol-ethanol-water-acetic acid (35 : 35 : 30 : 10) in all the run.

The authors wish to record their thanks to Professor S. Akabori of the Osaka University, for his stimulating discussions and encouragement.

*Department of Science,*
*Nara Women's University, Nara*

14) A.I. Oparin, *J. Japanese Chem.* **10**, 506 (1956).

# *Bromometric Oxidation of Red Phosphorus by Bromide Bromate Mixtures*

By M. VENUGOPALAN and K. J. GEORGE

(Received June 12, 1956)

In a previous communication, Venugopalan and George[1] suggested the utility of the instantaneous and complete reaction

$$5Br^- + BrO_3^- + 6H^+ = 3Br_2 + 3H_2O \quad \text{(i)}$$

for a quantitative oxidation of red phosphorus to phosphoric acid bromometrically. Various substances react quantitatively with an excess of bromine, and acid solutions of bromine of exactly known concentration can readily be obtained from a standard potassium bromate solution by adding acid and an excess of bromide. In this reaction one mole of bromate yields six atoms of bromine and hence the equivalent weight is identical with that of potassium bromate alone. Bromine is very volatile and hence the experiments are carried out at as low a temperature as possible and in Erlenmeyer flasks provided with ground glass stoppers. The excess of bromine is determined iodometrically and from the reacted bromine the amount of phosphorus can be calculated.

Earlier workers[2] have shown that bromine reacts with red phosphorus at a very rapid rate at the ordinary temperature; but the reaction could proceed with a measurable speed at low temperatures and hence, it was of interest to undertake a kinetic study of the oxidation process.

## Experimental

Solutions of bromide and bromate were prepared in the proportions given in equation (i) so that when mixed together in presence of an acid ($H_2SO_4$) both bromide and bromate react together instantaneously and completely to give a known amount of bromine.

Pure dry red phosphorus was weighed into a ground-glss stoppered Erlenmeyer flask. Equal volumes (40 cc.) of bromide and bromate solutions were added, followed by 20 ml. of 1 N sulphuric acid so that the overall normality of the system was maintained at or about 0.2 N $H_2SO_4$. The phosphorus dissolved in the evolved bromine in solution, thereby indicating that the initial reaction is very rapid and almost instantaneous. The system was maintained at a desired constant temperature for a few minutes prior to the addition of the oxidant and also during the course of subsequent observations in an ice-cooled water bath provided with an accurate thermometer. The contents of the flask were swirled from time to time and an aliquot portion (5 ml.) of the clear solution was pippetted out carefully at different time intervals and titrated iodometrically with standard thiosulphate[3]. Experiments were carried out at different temperatures, viz., 5, 10, 15, 20°C using the same concentration and by varying the concentration of the oxidant.

## Results and Discussion

The order of the reaction was calculated by the integration method from the initial titre value of bromide bromide-bromate mixture and that obtained at various time intervals during the course of the oxidation, applying the equation

$$K = \frac{2.303}{tC_\infty} \log_{10} \frac{C_t(C_o - C_\infty)}{C_o(C_t - C_\infty)}$$

where $C_o$—initial concentration of bromide-bromate mixture
$C_t$—concentration at time $t$
$C_\infty$—concentration at time $\infty$
and $t$—time in minutes

A representative group of results is shown in Table I. These results therefore show

TABLE I

Temperature: 20°C
Reaction Mixture: 5 ml.
Weight of P: 0.02 g.
Strength of KBr—$KBrO_3$ Mixture: N/35 solution

| Time in Minutes | N/40 Thio ml. | $\frac{C_t(C_o - C_\infty)}{C_o(C_t - C_\infty)}$ | $K \times 10^3$ |
|---|---|---|---|
| 0 | 3.40 | — | — |
| 15 | 3.05 | 0.0363 | 3.98 |
| 30 | 2.80 | 0.0706 | 3.87 |
| 45 | 2.60 | 0.1053 | 3.85 |
| 60 | 2.45 | 0.1375 | 3.86 |
| 90 | 2.20 | 0.2088 | 3.82 |
| ∞ | 1.40 | — | — |

Mean $K = 3.87 \times 10_3$

1) M. Venugopalan and K. J. George, *Bull. Chem. Soc. Japan*, **29** (3), 350-353, (1956).
2) J. W. Mellor, "A comprehensive Treatise on Inorganic and Theoretical Chemistry", Vol. VIII, Longmans Green & Co. (1928). p. 785.
3) A. I. Vogel, "Text Book of Quantitative Inorganic Analysis", Longmans Green & Co., London (1953). p. 369.

that the oxidation of red phosphorus by bromide-bromate mixture is an overall bimolecular reaction.

The influence of temperature on the velocity constant $K$, when the concentrations of the reactant are kept constant are given in Table II. The above results show

TABLE II

Weight of P Taken: 0.02 g.
Strength of Bromide-bromate Mixture: N/35
Normality of Thiosulphate: N/40

| Temperature ($t$) °C | Mean $K\times10^3$ |
|---|---|
| 5 | 2.0 |
| 10 | 2.4 |
| 15 | 3.1 |
| 20 | 3.87 |

that the velocity constant $K$ increases with a rise in temperature; the values of $\log_{10}\frac{C_t(C_o-C_\infty)}{C_o(C_t-C_\infty)}$ plotted against time $t$ for different temperatures, at which the reaction has been studied are represented graphically in Fig. 2.

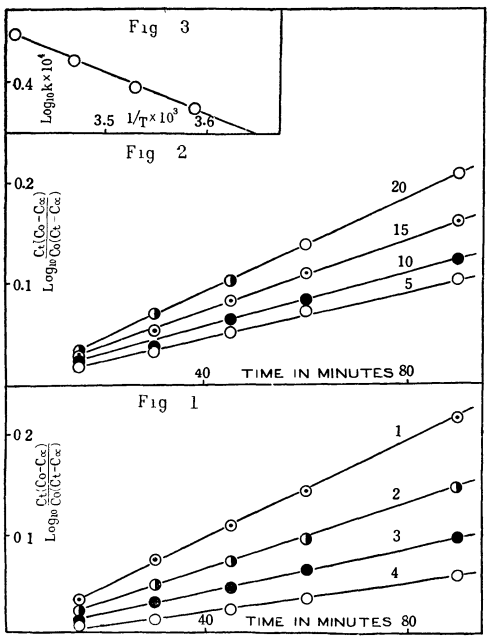



Fig. 1. Variation of $\log_{10}\frac{C_t(C_o-C_\infty)}{C_o(C_t-C_\infty)}$ with time $t$ for different initial concentrations of bromide-bromate mixture at the same temperature.

Fig. 2. Variation of $\log_{10}\frac{C_t(C_o-C_\infty)}{C_o(C_t-C_\infty)}$ with time $t$ for different temperatures.

Fig. 3. Variation of $\log_{10}K$ with $1/T$.

Variation of the velocity constant $K$ for different initial concentrations of the reactants has been studied by varying the concentration of bromide-bromate mixture and keeping the weight of phosphorus constant in all the experiments.

TABLE III

Temperature: 5°C
Weight of Phosphorus Taken: 0.02 g.
Normality of Thiosulphate: N/30

| Expt. No. | Concentration of KBr—$KBrO_3$ Mixture | Mean $K\times10^3$ |
|---|---|---|
| 1 | N/35 | 4.0 |
| 2 | N/40 | 2.9 |
| 3 | N/45 | 2.1 |
| 4 | N/50 | 1.2 |

Fig. 1 represents graphically the variation of $\log_{10}\frac{C_t(C_o-C_\infty)}{C_o(C_t-C_\infty)}$ with time for different concentrations of the oxidant (bromide-bromate mixture) at the same temperature.

The temperature coefficient and energy of activation were calculated from the values obtained for $K$ at different temperatures $T_1$ and $T_2$ and are given below:

TABLE IV

| Temp. $T_1$—$T_2$ | $K_1$ | $K_2$ | Temp. Coeff. $K_2/K_1$ | Energy of Activation/g. kcal. |
|---|---|---|---|---|
| 278-288 | 2.0 | 3.1 | 1.56 | 7.00 |
| 283-293 | 2.4 | 3.87 | 1.60 | 7.78 |

The variation of $\log_{10}K$ with $1/T$ is shown in Table V; the results are plotted in Fig. 3.

TABLE V

| Temperature Absolute $T°$ | $1/T\times10^3$ | $K\times10^3$ | $\log_{10}K\times10^3$ |
|---|---|---|---|
| 278 | 3.59 | 2.0 | 0.3010 |
| 283 | 3.53 | 2.4 | 0.3802 |
| 288 | 3.47 | 3.1 | 0.4914 |
| 293 | 3.41 | 3.87 | 0.5877 |

The linear relationship between $\log_{10}K$ and $1/T$ (Fig. 3) is in accord with the Arrhenius equation[4] which expresses the influence of temperature on reaction velocity.

## Bromometric Determination of Red Phosphorus

A series of experiments was carried out in which the difference in the quantity of bromide-bromate mixture added initially

4) S. Arrhenius, *Z. Phys. Chem.* **4**, 226 (1889); *Trans. Farad Soc.*, **33**, 72 (1937).

to a given weight of phosphorus and that left over after its complete disappearance i.e. the titre value at infinite time served as a measure of the quantity of bromide-bromate mixture required for the oxidation reaction. Hence a knowledge of the quantity of bromide-bromate mixture utilized in the reaction is useful for the direct determination of red phosphorus bromometrically. A typical set of results of such determinations are given in Table VI.

TABLE VI

| Wt. of P Taken g. | Wt. of P Calculated* g. | Difference in g. |
|---|---|---|
| 0.018 | 0.01788 | −0.00012 |
| 0.015 | 0.01488 | −0.00012 |
| 0.028 | 0.02772 | −0.00028 |
| 0.017 | 0.01693 | −0.00003 |
| 0.029 | 0.02909 | +0.00009 |
| 0.018 | 0.01788 | −0.00012 |
| 0.032 | 0.03208 | +0.00008 |
| 0.023 | 0.02272 | −0.00028 |
| 0.020 | 0.01983 | −0.00013 |

* Weight of P calculated from reacted bromine according to the equations:

$$5Br^- + BrO_3^- + 6H^+ = 3Br_2 3H_2O$$

and $$2P + 5Br_2 + 8H_2O = 12H^+ + 10Br^- + 2H_2PO_4^-$$

## Mechanism of the Reaction

Since the interaction of bromide-bromate mixture is instantaneous and complete

$$5Br^- + BrO_3^- + 6H^+ = 3Br_2 + 3H_2O$$

bromine is quantitatively liberated. This bromine oxidizes phosphorus to phosphoric acid according as

$$2P + 3Br_2 + 6H_2O = 6H^+ + 6Br^- + 2H_3PO_3$$

$$H_3PO_3 + Br_2 + H_2O = 3H^+ + 2Br^- + H_2PO_4^-$$

The former reaction is quite rapid, whereas the tatter one is slow and depends on the $H^+$ ion concentration. It appears that the oxidation of phosphorus acid by bromine (obtained from acid bromide-bromate mixture) determines the rate of reaction as a whole.

## Summary

Bromometric oxidation of red phosphorus using an acid solution of bromide-bromate mixture has been studied and applied in the volumetric determination of red phosphorus. The kinetics of the oxidation process show that the reaction is of the second order. The influence of temperature and concentration of the reactants, have been investigated and the energy of activation calculated. Further the applicability of this procedure for a bromometric determination of red phosphorus is emphasized and such determinations can be carried out over a period of three to four hours.

The grateful thanks of the authors are due to Prof. S. S. Joshi for facilities and for his kind interest in the work.

*Department of Chemistry, Banaras Hindu University, India*

# *Interaction between Surface Active Agents and Proteins. IV. Heat of Interaction of Sodium Dodecyl Sulfate and Egg Albumin*

By Koichiro AOKI* and Yasushi SUZUKI

(Received January 11, 1956)

## Introduction

As previously described[1], we studied electrophoretically the sodium dodecyl sulfate (SDS) and egg albumin system at points of higher pH's than that of the isoelectric point of egg albumin. In that study it was concluded that SDS-egg albumin complexes were formed in the following way at pH 6.8: When the weight mixing ratio albumin/SDS was between 100/0 and 80/20 the composition of the complex was $AD_n$ (n=40), and when the mixing ratio albumin/SDS was between 80/20 and 35/65 the composition of the complex changed continuously from $AD_n$ to the completion of $AD_{8n}$.

In the present study we measured the temperature change occurring when SDS

* Present temporary address: Department of Chemistry, Purdue University, Lafayette, Indiana, U. S. A.

1) K. Aoki, This bulletin **29**, 369 (1956).

and egg albumin solutions were mixed at the same condition as in the above electrophoretic study and calculated the heat of interaction.

## Experimental

The apparatus is shown in Fig. 1[2]. Experiments were carried out in a thermostat at 25± 0.001°C. Because very slight temperature changes accompanied the reaction, 10-junction of copper-constantan thermocouple and a galvanometer of high sensitivity were used to trace the temperature change[3,4]. We found that the sensitivity of the apparatus we assembled was such that a 1 mm movement of the needle on the lamp scale corresponded to 0.0006°C. The reaction vessel was unsilvered Dewar flask, the volume of which was about 120 cc. and the water equivalent 93.0 cal.*

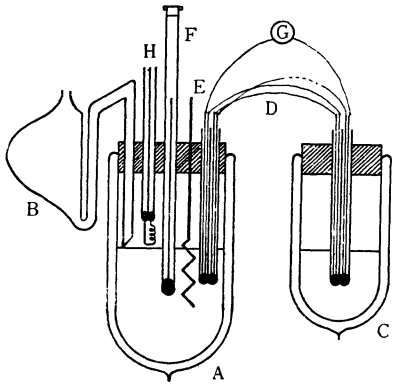



Fig. 1. Apparatus.

A. Reaction vessel.
B. Vessel for warming SDS solution.
C. Vessel for holding one end of thermocouple.
D. 10-junction of copper-constantan thermocouple.
E. Stirrer.
F. Beckmann thermometer.
G. Galvanometer.
H. Platinum wire.

The buffer solution used was pH 6.8 and ionic strength 0.10. Into a reaction vessel A, 50 cc. of 1.00% buffered albumin solution was put. Fifty cc. of buffered SDS solution varying in concentration were put into another vessel B. Then we let these two solutions stand in the thermostat for about ten hours to make them aquire the temperature of the thermostat. After that they were mixed, and at the same time we began to measure the temperature change which accompanied the reaction.

In addition, we measured the heat of dilution of albumin and of SDS. We put 50 cc. of buffered albumin solution or buffered SDS solution into reaction vessel A and put the same amount of buffer solution into vessel B. We measured the temperature change occurring when albumin or SDS solution was diluted to twice the original volume by pouring the solution in vessel B into vessel A.

## Results

Heat was generated when SDS or albumin solution was diluted with the buffer. Fig. 2 shows a typical run of the temperature change occurring when albumin and SDS solutions were diluted. Considering the maximum value of this curve to be the amount of heat generated, the following values were obtained for the heats of dilution:

| | |
|---|---|
| SDS | 1.2 cal./g. |
| egg albumin | 0.8 cal./g. |

These are the values obtained when the solutions, the concentrations of which were less than 1.00%, were diluted to twice their original volumes.

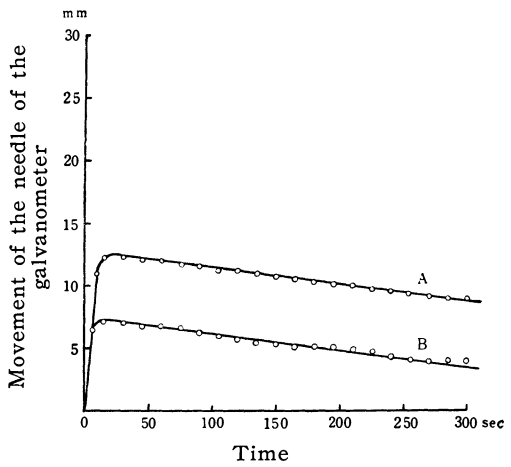



Fig. 2. Heat of dilution.

A: Heat generated when 1.00% buffered SDS solution was diluted to twice its original volume.
B: Heat generated when 1.00% buffered albumin solution was diluted to twice its original volume.

Hutchinson et. al.[5] measured accurately the heats of dissolution of sodium alkyl sulfates. Using their data, we can calculate the heat produced when 0.050M (1.30%) aqueous sodium decyl sulfate solution is diluted to 0.025 M (0.65 %) at 25.00°C. The value is found to be 1.0 cal./g. Our values of the heat of dilution are considered reasonable when compared with this value.

Heat was instantly generated when SDS and egg albumin solutions were mixed. Fig. 3 shows

2) E. Suito, *Rev. Phys. Chem. Japan*, **13**, 74 (1939).
3) N. H. Ray. *Trans. Faraday Soc.*, **48**, 809 (1952).
4) J. Osugi and K. Hiromi, *Rev. Phys. Chem. Japan.* **22**, 76 (1952).
* The experimental procedure to find this value was the same as used by E. Suito[2].

5) E. Hutchinson, K. E. Manchester and L. Winslow, *J. Phys Chem.*, **58**, 1124 (1954).

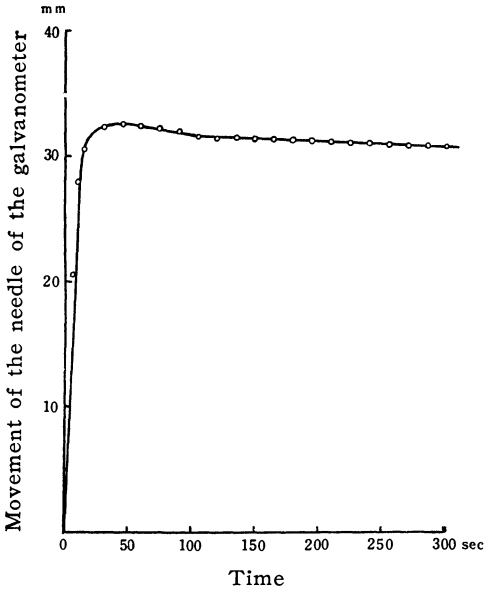



Fig. 3. Heat of reaction.
Heat produced when 1.00% SDS solution and 1.00% albumin solution were mixed.

one tracing of the temperature change with time. Taking the maximum value of this curve as the total heat produced, we deducted from this maximum value the heat of dilution of egg albumin and that of SDS, to obtain the value of the heat of the reaction itself. As the amount of SDS used was different in each experiment, the value of the heat of dilution of SDS to be deducted was calculated proportionally using the value of 1.2 cal./g.

In this study the concentration of egg albumin was kept constant at 1.00%. Each of the SDS solutions varying in concentration from 0.05% to 1.00% was mixed with this egg albumin solution. Thus we obtained the relation between the mixing ratio albumin/SDS and the heat evolved. The results are shown in Fig. 4. In these experiments any error in measuring the heat produced is within ±0.2 cal.

## Discussion

It was concluded from the electrophoretic experiment that SDS and egg albumin did not combine in the same way above and below the mixing ratio albumin/SDS=80/20, that is, the composition of the complex was constant when the mixing ratio albumin/SDS was between 100/0 and 80/20, while it changed continuously in the region from 80/20 to 35/65[1]. Referring to the result, we assume that the curve *abc* in Fig. 4 consists of two straight lines *ab* and *bc*, which change the slope near the point albumin/SDS=80/20.

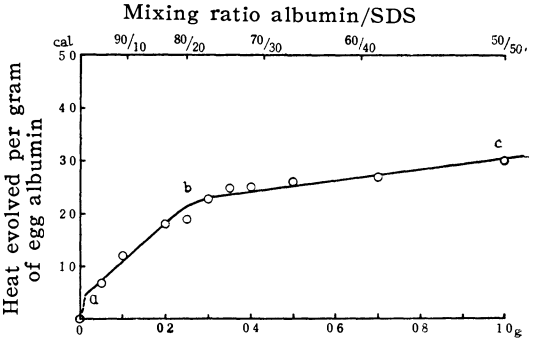



Fig. 4. Relation between mixing ratio albumin/SDS and heat of reaction.

Recently, Hill[6] observed by equilibrium dialysis that after one mole of anionic detergent* combined with one mole of egg albumin, another kind of interaction took place. Considering his results SDS and egg albumin may combine in a different way also above and below the mixing ratio albumin/SDS=99.4/0.6. Here the molecular weight of egg albumin and of SDS was assumed to be 46,000 and 288, respectively. When *ba* in Fig. 4 is extended to the left, it does not pass the origin. This may be fact which corresponds to the above Hill's observation.

In the region where the mixing ratio albumin/SDS is between 100/0, or more precisely 99.4/0.6, and 80/20, 40 molecules of SDS are bound to one egg albumin molecule. Using the molecular weights cited above, the following equation is obtained from the slope of the straight line *ab*.

$$\text{Egg albumin} + 40\,\text{SDS} = \text{Complex} + 92.1\,\text{kcal.}$$

or

$$-\Delta H = 92.1\ \text{kcal./mol. albumin} = 2.3\ \text{kcal./mol. SDS}$$

If we assume that one $NH_3^+$ radical on the egg albumin molecule reacts with one $OSO_3^-$ radical of SDS within this mixing ratio, we can rewrite the above equation as

$$\cdots NH_3^+ + \cdots OSO_3^- = \text{Complex} + 2.3\ \text{kcal.}$$

This value of heat of reaction is far smaller than that of the heat of neutralization between strong acid and strong base, 13.7 kcal./mol. (at about 30°C).

In the range where the mixing ratio albumin/SDS is between 80/20 and 35/65,

6) R. M. Hill, Ph. D. Thesis, University of Minnesota, 1955.

* He used sodium-*n*-octylbenzene-*p*-sulfonate.

the following equation is obtained from the slope of the straight line *bc*.

$$\text{Complex}+\text{SDS}=\text{Complex}'+0.3\ \text{kcal.}$$

The values of the heat of interaction obtained in this study are of the same order as those found by Goddard and Pethica[7] in the bovine serum-albumin-SDS system.

The CMC (critical micelle concentration) of SDS is 0.04% (0.0013 mol./l.) in a buffer solution of ionic strength 0.1[8]. Thus when 1.00% albumin solution and 0.05% SDS solution are mixed, the concentration of SDS is above the CMC before mixing and below it after mixing. When they are mixed, there should be an adsorption of heat owing to the decomposition of the micelle. Goddard and Benson[9] calculated the heat of micelle formation of SDS to be ca. 0.1 kcal./mol. SDS at 25°C, using their data and the assumption of Hutchinson et. al.[5] The amount of SDS used at this mixing ratio was so small, 0.05 g. (0.002 mol.), that such a small quantity of heat could not be measured.

7) E. D. Goddard and B. A. Pethica, *J. Chem. Soc.*, **1951**, 2659.
8) K. Aoki and J. Hori, This bulletin, **29**. 104 (1956).
9) E. D. Goddard and G. C. Benson, *Trans. Faraday Soc.*, **52**, 409 (1956).

## Summary

We measured the heat evolved when egg albumin and SDS solutions were mixed at pH 6.8 and at 25.00°C, and calculated the heat of interaction.

The authors wish to express their sincere thanks to Prof. R. Goto of Kyoto University for his kind encouragement throughout this work, and to Prof. J. F. Foster of Purdue University for information about Dr. Hill's thesis. The cost of this work has been partially covered by a Research Grant from the Ministry of Education.

*Chemistry Laboratory, Nagoya City University, Nagoya*

# *Studies on Azeotropic Mixtures. II. Constancy of Molecular Interchange Energies in Homologous Azeotropic Series and Calculation of Azeotrope-forming Range**

By Toshio YOSHIMOTO and Yo-ichiro MASHIKO

(Received September 25, 1956)

## Introduction

Reflecting the importance of azeotrope formation in the distillation process, a great number of experimental data have been accumulated in recent times[1]. Also, several independent correlation rules of azeotropic data have been proposed on the practical side[2]. They are, however, all empirical and it appears difficult to find out the physical basis from any of them or to derive the one from the other without any additional assumptions. The following is an attempt to correlate binarily azeotropic data by a method with explicit representation of interaction energies of component molecules.

Recently Prigogine[3] has presented a similar method of correlating azeotropic

* Partly Presented at the 9th Annual Meeting of the Chemical Society of Japan held in Kyoto, April, 1956.

1) L. H. Horsley, "Azeotropic Data", American Chemical Society (1952); F. D. Rossini, B. J. Mair and A. J. Streiff, "Hydrocarbons from Petroleum", Reinhold (1952), p. 88; L.H. Horsley, *Anal. Chem.*, **19**, 508 (1947); **21** 831 (1949); Lange, "Handbook of Chemistry", 5th ed., Handbook Publishers (1944); Ewell, Harrison and Berg, *Petroleum Engr.*, **16** 219, 255, 259 (1944); "Chemical Engineers' Handbook" 2nd ed., McGraw-Hill (1941); "International Critical Tables" Vol.3 McGraw-Hill (1928); M. Lecat, "La tension de vapeur des mélanges des liquides. L'Azéotropisme", Lamertin, Brussels (1918).

2) M. Lecat, *Z. anorg. u. allgem. Chem.*, **186**, 123 (1930); H. Skolnik, *Ind. Eng. Chem.*, **40**, 442 (1948); H. P. Meissner and S. H. Greenfeld, ibid., **40**, 438 (1948); R. L. Denyer, F. A. Fidler and R. A. Lowry, ibid., **41**, 2727 (1949); D. H. Desty and F. A. Fidler, ibid., **43**, 905 (1951); L. H. Horsley, *Anal. Chem.*, **19**, 603 (1947).

3) I. Prigogine and R. Defay, "Chemical Thermodynamics", (Translated by D. H. Everett), Longmans (1954), Chapt. XXVIII.

data that is very satisfactory also from our standpoint. As has been mentioned in part I[4], our standpoint is, however, a little different from that of Prigogine in that we are always considering the phenomenon from the molecular point of view, i. e., using the explicit form of the molecular interchange energy.

## Graphical Method of Correlating Azeotropic Data

It has been shown in part I[4] that the azeotrope-forming power of many binary solutions could be estimated by molecular interchange energies $w$ which were calculated from

$$\Delta_v S_1^0(T_1^0-T^a)=Nwx_2^2 \qquad (1)$$

and

$$\Delta_v S_2^0(T_2^0-T^a)=Nwx_1^2, \qquad (2)$$

where $T^a$ is the azeotropic point (for $p=$ 1 atm.), $N$ the Avogadro number and $\Delta_v S_i^0$ the molar entropy of vaporization at boiling point (for $p=1$ atm.) of $i$th pure component. ($i=1$ and 2).

Here, $w$ is expressed, based on the quasi-crystalline model of the solution, as

$$w=\frac{z}{2}(\varepsilon_{11}+\varepsilon_{22}-2\varepsilon_{12}),$$

where $z$ is the average coordination number of the quasi-lattice and $\varepsilon$'s are all the absolute average potential energies of molecular pairs. Equations (1) and (2) have only one unknown parameter $w$, all others being known from experiment.

Trouton proposed the celebrated rule that the entropy of vaporization is the same for all liquids[5]. A glance at the entropies of vaporization (for $p=1$ atm.) given in literature[6] shows, however, that the rule applies only roughly, and departs seriously from the truth if the liquids are "abnormal". Nevertheless, the rule appears to stand, to some degree, for members of homologous series if the liquids are not so highly associated. This condition will accordingly make it possible to apply invariably the equations (1) and (2) to the azeotropes formed by a fixed azeotropic reagent (or azeotrope former) with a series of homologues, if $w_s$ are nearly the same for the series of azeotropes. Thus, if these allowances are made, we can expect straight-line relationships between $T_i^0-T^a$ and $x_i^2$ for the series.

In the following, we have examined the relationship on a number of series by taking the known values of the thermodynamic quantities appearing in equations (1) and (2). In most cases, however, because of lack of data, an appropriate value of $\Delta_v S_1^0$ for the series is assumed from the known values for a few members of the series.

In each case two kinds of plots, that is, first $T_2^0-T^a$ against $x_1^2$ and second $T_1^0-T^a$ against $x_2^2$ are presented. For each case the second component 2 is a fixed azeotropic reagent and the first components 1 are homologous members. Examples taken are arranged into four classes according to the different types of intermolecular forces as in part I.

### (a) Dispersion Force Solutions

Examples taken are azeotropes of toluene with paraffinic and naphthenic hydrocarbons. They form always minimum type azeotropes[4] (A, Fig. 1).

### (b) Solutions Involving Addition Compounds

Examples taken are azeotropes of bromodichloromethane with "donor type" liquids such as ketones and esters. They form always maximum type azeotropes[4] (B, Fig. 2).

### (c) Solutions Involving Associations in Non-polar Solvents

This class involves most of the useful azeotropes, since they have the largest azeotrope-forming powers among four classes. The following nine series are taken as examples.

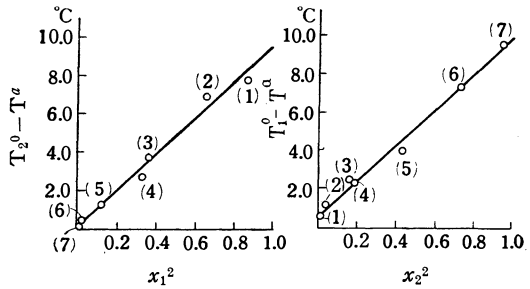



Fig. 1. The plots of toluene azeotropes with aliphatic hydrocarbons.
Aliphatic hydrocarbons (A): (1), ethylcyclopentane; (2), 1,1,3-trimethylcyclopentane; (3), 2,5-dimethylhexane; (4), *cis-trans-cis*-1,2,4-trimethylcyclopentane; (5), 2,3,4-trimethylpentane; (6), 2-methylheptane; (7), *cis*-1,3-dimethylcyclohexane.

4) T. Yoshimoto and Y. Mashiko, This Bulletin, **29**, 990 (1956).
5) F. Trouton, *Phil. Mag.* (5), **18**, 54 (1884).
6) "International Critical Table", Vol. V (1929).

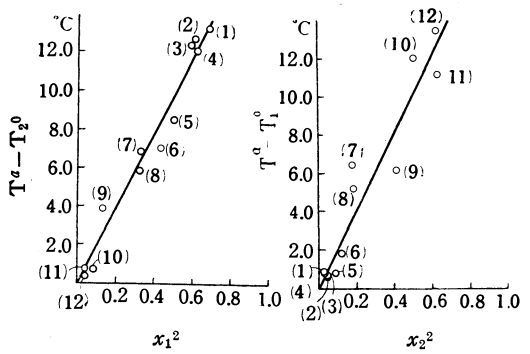



Fig. 2. The plots of bromodichloromethane azeotropes with "donor type liquids".
Donor liquids (B): (1), methyl butyrate; (2), 2-pentanone; (3), 3-pentanone; (4), propyl acetate; (5), isobutyl formate; (6), 3-methyl-2-butanone; (7), *n*-propyl ether; (8), isopropyl acetate; (9), diethoxymethane; (10), propyl formate; (11), 2-butanone; (12), ethyl acetate.

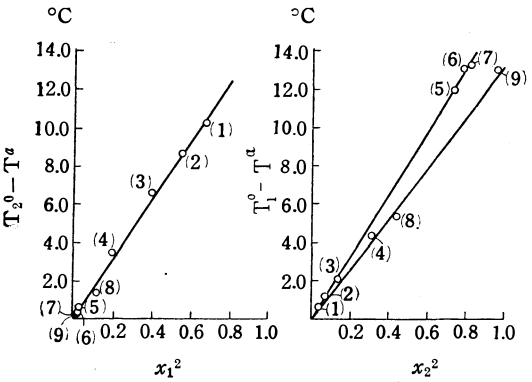



Fig. 3. The plots of 1-propanethiol azeotropes with paraffinic and naphthenic hydrocarbons.
Paraffinic hydrocarbons (C): (1), 2,3-dimethylbutane; (2), 2-methylpentane; (3), 3-methylpentane; (4), *n*-hexane; (5), 2,2-dimethylpentane; (6), 2,4-dimethylpentane; (7), 2,2,3-trimethylbutane.
Naphthenic hydrocarbons(D): (8), methylcyclopentane; (9), cyclohexane.

1-Propanethiol
—Paraffinic Hydrocarbons (C, Fig. 3)
1-Propanethiol
—Naphthenic Hydrocarbons (D, Fig. 3)
1-Butanethiol
—Paraffinic Hydrocarbons (E, Fig. 4)
1-Butanethiol
—Naphthenic Hydrocarbons (F, Fig. 4)
1,2-Benzenediol
—Aromatic Hydrocarbons (G, Fig. 5)
1,3-Benzenediol
—Aromatic Hydrocarbons (H, Fig. 6)

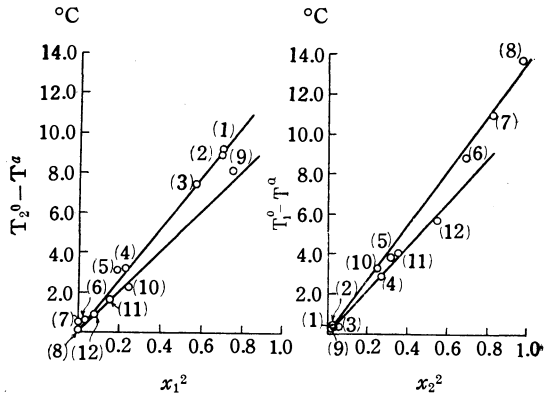



Fig. 4. The plots of 1-butanethiol azeotropes with paraffinic and naphthenic hydrocarbons.
Paraffinic hydrocarbons (E): (1), 2,3-dimethylpentane; (2), 2-methylhexane; (3), 3-methylhexane; (4), *n*-heptane; (5), 2,2,4-trimethylpentane; (6), 2,2-dimethylhexane; (7), 2,5-dimethylhexane; (8), 3,3-dimethylhexane.
Naphthenic hydrocarbones (F): (9), *trans*-1,3-dimethylcyclopentane; (10), *cis*-1,2-dimethylcyclopentane; (11), methylcyclohexane; (12), ethylcyclopentane.

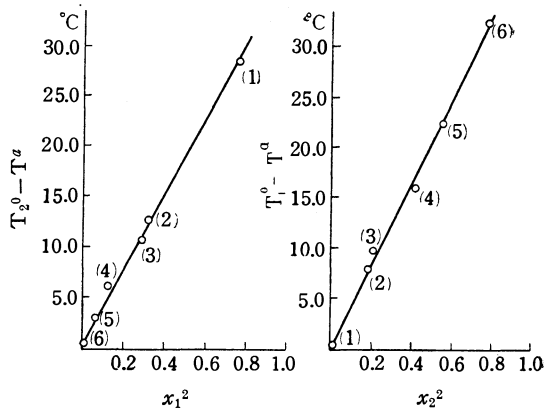



Fig. 5. The plots of 1,2-benzenediol azeotropes with aromatic hydrocarbons.
Aromatic hydrocarbons (G): (1), naphthalene; (2), 2-methylnaphthalene; (3), 1-methylnaphthalene; (4), biphenyl; (5), diphenyl methane, (6), acenaphthene.

Nitromethane
—Aliphatic Hydrocarbons (I, Fig. 7)
Nitromethane
—Aromatic Hydrocarbons (J, Fig. 7)
Methanol
—Paraffinic Hydrocarbons (K, Fig. 8)
The last involves highly associated liquid that is apparently not to be regarded as a component of regular solutions even at azeotropic points[4].

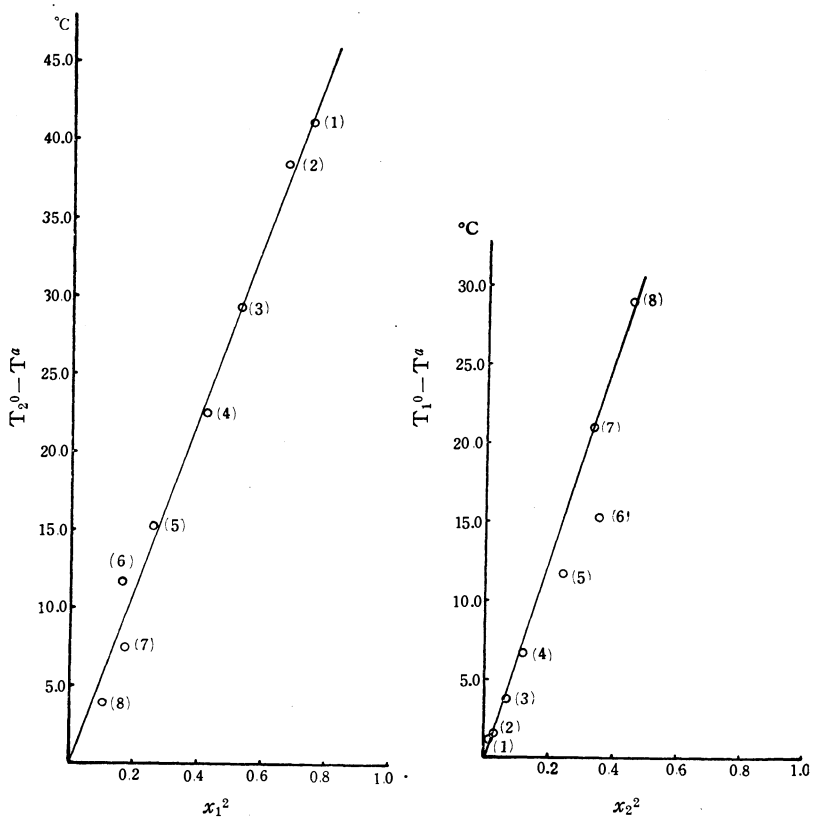



Fig. 6. The plots of 1,3-benzenediol azeotropes with aromatic hydrocarbons.
Aromatic hydrocarbons (H): (1), 2-methylnaphthalene; (2), 1-methylnaphthalene; (3), biphenyl; (4), diphenyl methane; (5), acenaphthene; (6), 1,2-diphenylethane; (7), fluorene; (8), *trans*-stilbene.

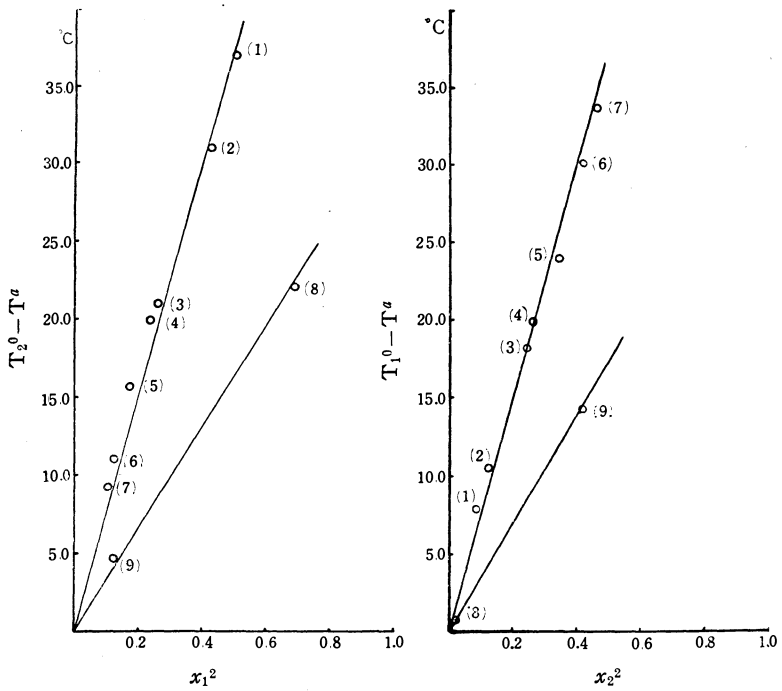



Fig. 7. The plots of nitromethane azeotropes with aliphatic and aromatic hydrocarbons.
Aliphatic hydrocarbons (I): (1), methylcyclopentane; (2), cyclohexane; (3), *n*-heptane; (4), methylcyclohexane; (5), 2,5-dimethylhexane; (6), 1,3-dimethylcyclohexane; (7), *n*-octane. Aromatic hydrocarbons (J): (8), benzene; (9), toluene.

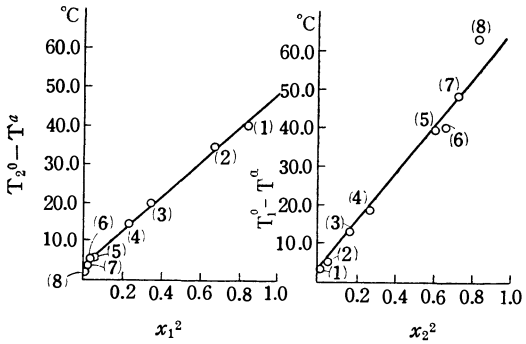



Fig. 8. The plots of methanol azeotropes with paraffinic hydrocarbons.
Paraffinic hydrocarbons (K): (1), isopentane; (2), *n*-pentane; (3), 2,3-dimethylbutane; (4), *n*-hexane; (5), *n*-heptane; (6), 2,2,4-trimethylpentane; (7), 2,5-dimethylhexane; (8), *n*-octane.

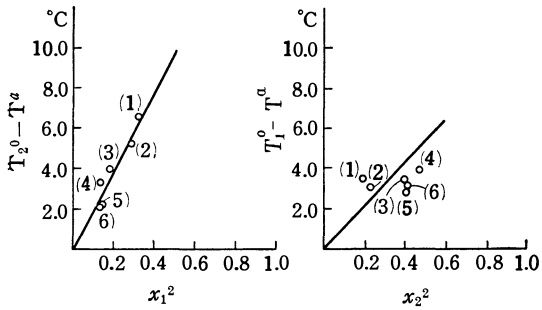



Fig. 9. The plots of nitromethane azeotropes with ketones and esters.
Ketones and esters (L): (1), butyl formate; (2), ethyl propionate; (3), propyl acetate; (4), methyl butyrate; (5), 3-pentanone; (6), 2-pentanone.

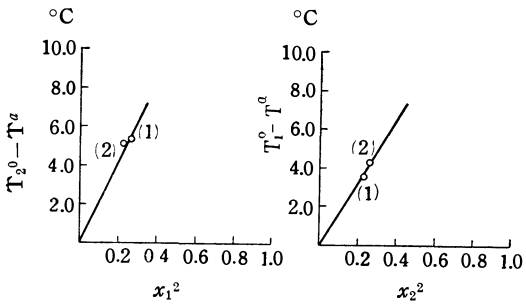



Fig. 10. The plots of acetonitrile azeotropes with esters.
Esters (M): (1), methyl propionate; (2), propyl formate.

### (d) Solutions Involving Associations in Polar Solvents

Azeotropes in this class have smaller azeotrope-forming powers and involve more complicated interaction of component molecules than those in class (c).

Examples taken are as follows.
Nitromethane
—Ketones and Esters (L, Fig. 9)
Acetonitrile—Esters (M, Fig. 10)

In general the straight-line relationship is observed satisfactorily in every plot except the series which involves special molecular interactions such as in class (b) and (d). Furthermore, as shown in Table I, the slopes of two independent plots that involve $T_1^0-T^a$ and $x_2^2$ on the one hand, and $T_2^0-T^a$ and $x_1^2$ on the other are approximately equal when devided by $\Delta_v S_1^0$ and $\Delta_v S_2^0$ respectively. This leads to a conclusion from equations (1) and (2) that the molecular interchange energy $w$ of azeotropes, which are formed between a fixed azeotropic reagent and members of a homologous series, is characteristic of the series in many cases and therefore regarded as azeotrope-forming power of a series of azeotropic mixtures. The new correlation thus introduced from equations (1) and (2) is considered to be essential to compare azeotrope-forming powers of a number of solutions.

TABLE I

MOLECULAR INTERCHANGE ENERGIES CALCULATED FROM THE SLOPES OF TWO KINDS OF PLOTS

| Azeotropic[a] Series | $N\omega_1$ $\left(\frac{\text{kcal.}}{\text{M}}\right)$ | $N\omega_2$ $\left(\frac{\text{kcal.}}{\text{M}}\right)$ | $\Delta_v S_1{}^{0}$[b] $\left(\frac{\text{cal.}}{\text{M°C}}\right)$ | $\Delta_v S_2{}^{0}$[b] $\left(\frac{\text{cal.}}{\text{M°C}}\right)$ |
|---|---|---|---|---|
| A | 190 | 200 | (20.3) | 20.8 |
| B | −450 | −430 | (22.0) | 21.0 |
| C | 340 | 340 | (20.3) | (22.0) |
| D | 270 | — | (20.4) | — |
| E | 280 | 280 | (20.3) | (22.0) |
| F | 230 | 230 | (20.3) | (22.0) |
| G | 850 | 850 | (20.3) | (22.5) |
| H | 1300 | 1300 | (20.3) | (23.5) |
| I | 1560 | 1630 | (20.3) | 22.1 |
| J | 710 | 730 | 20.8 | 22.1 |
| K | 1170 | 1140 | (20.3) | 25.0 |
| L | Diffuse | 420 | — | 22.1 |
| M | 360 | 420 | (22.0) | 20.2 |

a) Azeotropic data are all taken from Horsley's "Azeotropic Data"[1].
b) Values taken from "International Critical Table" Vol. V (1929). Values enclosed in parentheses are assumed ones.

Here, it should be mentioned from the view-point of our approximation[4] that as $x_2$ approaches to 0 in $(T_1^0-T^a)-x_2^2$ plots and $x_1$ to 0 in $(T_2^0-T^a)-x_1^2$ plots, the error of the above approximation will be considerable. In fact, the error in the plots of methanol-paraffins series is remarkable as shown in Fig. 8, while it is con-

sidered to be small in other series according to the results so far obtained. The $(T_1^0-T^a)-x_2^2$ plots in toluene-hydrocarbons series does not pass through the origin (Fig. 1). The cause of this abnormality is uncertain and will be left to the further study.

### Azeotrope-forming Range

From equations (1) and (2) we obtain maximum boiling point $T_1^{0\max}$ and minimum boiling point $T_1^{0\min}$ of pure component 1 that can form azeotropes with component 2 as follows.

If $w>0$, we have

$$T_1^{0\max}=T_2^0+\frac{Nw}{\Delta_v S_1^0} \tag{3}$$

and

$$T_1^{0\min}=T_2^0-\frac{Nw}{\Delta_v S_2^0}. \tag{4}$$

If $w<0$, we have

$$T_1^{0\max}=T_2^0+\frac{Nw}{\Delta_v S_2^0} \tag{5}$$

and

$$T_1^{0\min}=T_2^0-\frac{Nw}{\Delta_v S_1^0}. \tag{6}$$

Graphically the intercepts of the lines with the ordinate at $x_2^2=1$ in $(T_1^0-T^a)-x_2^2$ plots and at $x_1^2=1$ in $(T_2^0-T^a)-x_1^2$ plots give respectively $T_1^{0\max}$ and $T_1^{0\min}$ (see Figs. 1–10). The difference between maximum and minimum boiling points give therefore the boiling point range, over which azeotrope formation is allowable for the series. Denyer et al.[7] and Swietoslawsky[8] regarded azeotrope-forming range, $T_1^{0\max}-T_1^{0\min}$, as a measure of the azeotrope-forming powers of a given azeotropic series. We have for this range, with explicit representation of $w$, from (3) and (4) or (5) and (6),

$$T_1^{0\max}-T_1^{0\min}=Nw\left(\frac{1}{\Delta_v S_1^0}+\frac{1}{\Delta_v S_2^0}\right). \tag{7}$$

$T_1^{0\max}$ and $T_1^{0\min}$ are calculated from $w$'s which are obtained from the slopes of plots in Figs. 3 and 4, and are presented in Table II along with those obtained from Denyer's and Skolnik's[9] plots. The agreement is excellent. Denyer's and Skolnik's azeotropic ranges are considered to be slightly different in their physical meaning, though the difference will be trivial whenever $w$ is small as will be shown later.

TABLE II

COMPARISON OF $T_1^0$ max AND $T_1^0$ min CALCULATED BY THREE METHODS

| Azeotropic Series | This work | | Denyer's | | Skolnik's |
|---|---|---|---|---|---|
| | $T_1^0$ max (°C) | $T_1^0$ min (°C) | $T_1^0$ max (°C) | $T_1^0$ min (°C) | $T_1^0$ max (°C) |
| C | 85 | 52 | 84 | 52 | 83.5 |
| E | 112 | 86 | 112 | 85 | 112 |

### Conclusion

Applying Trouton's rule to a homologous series, the constancy of molecular interchange energy $w$ for azeotropes composed of a fixed component and the series is exemplified in a number of cases. The fundamental equations derived in part I is thus proved to be useful in correlating azeotropic data. Also maximum and minimum boiling points of components in a homologous azeotropic series are derived and values calculated are compared with those obtained by other methods.

*Government Chemical Industrial Research Institute, Tokyo*

7) R. L. Denyer, F. A. Fidler and R. A. Lowry, *Ind Eng. Chem.*, **41**, 2727 (1949); D. H. Desty and F. A. Fidler, ibid., **43**, 905 (1951).

8) W. Swietoslawsky, *Prezemyl. Chem.*, **1**, 363 (1951).

9) H. Skolnik, *Ind. Eng. Chem.*, **40**, 442(1948).

# *A Refinement of the Crystal Structure of Tropolone Hydrochloride*

By Yoshio SASADA and Isamu NITTA

(Received September 27, 1956)

## Introduction

Previously we have reported the crystal structure of tropolone hydrochloride as an example of successful application of the inequality method[1]. Owing to the following two reasons we had for a time to abandon further refinements of the structure: (i) The crystals are considerably hygroscopic and unstable. Even the specimens sealed in the borosilicate capillaries were decomposed in summertime, giving Debye-Scherrer patterns together with single crystal reflexions of this compound. (ii) Crystals with suitable form were rather few and much of them were twinned. Therefore it was impossible to obtain reliable data for the general (*hkl*) reflexions except for (0*kl*). Thus we had to be contented with the approximate crystal structure described in the previous paper.

On the other hand, we have investigated the crystal structure of sodium tropolonate by means of $(F_o-F_c)$ and three-dimensional Fourier techniques and obtained very accurate molecular dimensions together with approximate positions of hydrogen atoms and some knowledge of anisotropic thermal vibrations[2].

As emphasized in the previous papers[1,2], the comparative determinations of accurate structures of tropolone, its anion and cation are very interesting problems of the structural chemistry of tropolone derivatives. Moreover it will be significant in the case of cation to determine, if possible, directly the positions of hydrogen atoms attached to oxygen, which were supposed to be somewhere between O and Cl atoms. Such situations made us hope to re-investigate the crystal structure of hydrochloride. Fortunately, at this time Nozoe and his collaborators brought us suitable specimens of this compound and we have been able to find non-twinned crystals among them. This account will describe the refinement of the structure based on new sets of three-dimensional data obtained from integrated Weissenberg photographs with multiple-film technique, the main features of the structure, of course, being unchanged.

### Crystal Data and Intensity Measurement

Crystals were obtained from ethanol-ether solution saturated with hydrogen chloride gas as white needles[3], elongated in the *a* axis direction.

Crystallographic and physical data obtained are:

Tropolone hydrochloride $C_7H_7O_2Cl$ : m. p. 125–130°C, monoclinic,

$$a=4.71\pm0.02\,\text{Å},\quad b=18.01\pm0.03\,\text{Å},$$
$$c=8.56\pm0.03\,\text{Å},\quad \beta=98.2°\pm0.5°.$$

Absent spectra: (*h*0*l*) when *l* is odd, (0*k*0) when *k* is odd. Space group $P2_1/c$. Four formula units per cell. Volume of unit cell=718 Å$^3$.

Density (by floatation)=1.43,

Density (calc.)=1.47 g.cm$^{-3}$.

Linear absorption coefficient for Cu $K_\alpha$ radiation, $\mu=42.0\,\text{cm}^{-1}$. Total number of electrons per unit cell, $F(000)=328$.

These cell dimensions slightly differ from those reported in the previous paper[1]. The differences are mainly due to low accuracy of previous value of $\beta$.

In order to refine the atomic coordinates and to reveal the positions of hydrogen atoms by $(F_o-F_c)$ syntheses, it is necessary to use considerably accurate intensity data. Two complete sets of relative intensities for (0*kl*), (1*kl*), (2*kl*) and (3*kl*) were obtained by the integrated Weissenberg procedures. The specimens used have the following maximum and minimum dimensions at right angle to the axis of rotation:

Crystal 1: 0.04×0.02; Crystal 2: 0.03×0.02cm.

Intensities were estimated by visual comparison with the calibrated scale. The multiple-film technique was used to correlate strong and weak reflexions, ranging in relative intensities from 6000 to 1 for (0*kl*) zone. The corrections for absorption were made in the usual way only for (0*kl*). The values of structure factors used in the following analysis are the weighted means of the values in the above-mentioned two sets. Reflexions from 150 planes were observed out of 186 possible (0*kl*)'s and 458 out of 995 (*hkl*)'s.

## Refinement of Atomic Coordinates and Location of the Hydrogen Atoms.

Starting from the approximate structure

1) Y. Sasada, K. Osaki and I. Nitta, *Acta Cryst.* **7**, 113, (1954).

2) Y. Sasada and I. Nitta, ibid., **9**, 205 (1956).

3) T. Nozoe, S. Seto, T. Mukai. K. Yamane and A. Matsukuma, *Proc. Japan Acad.*, **27**, 224 (1951).

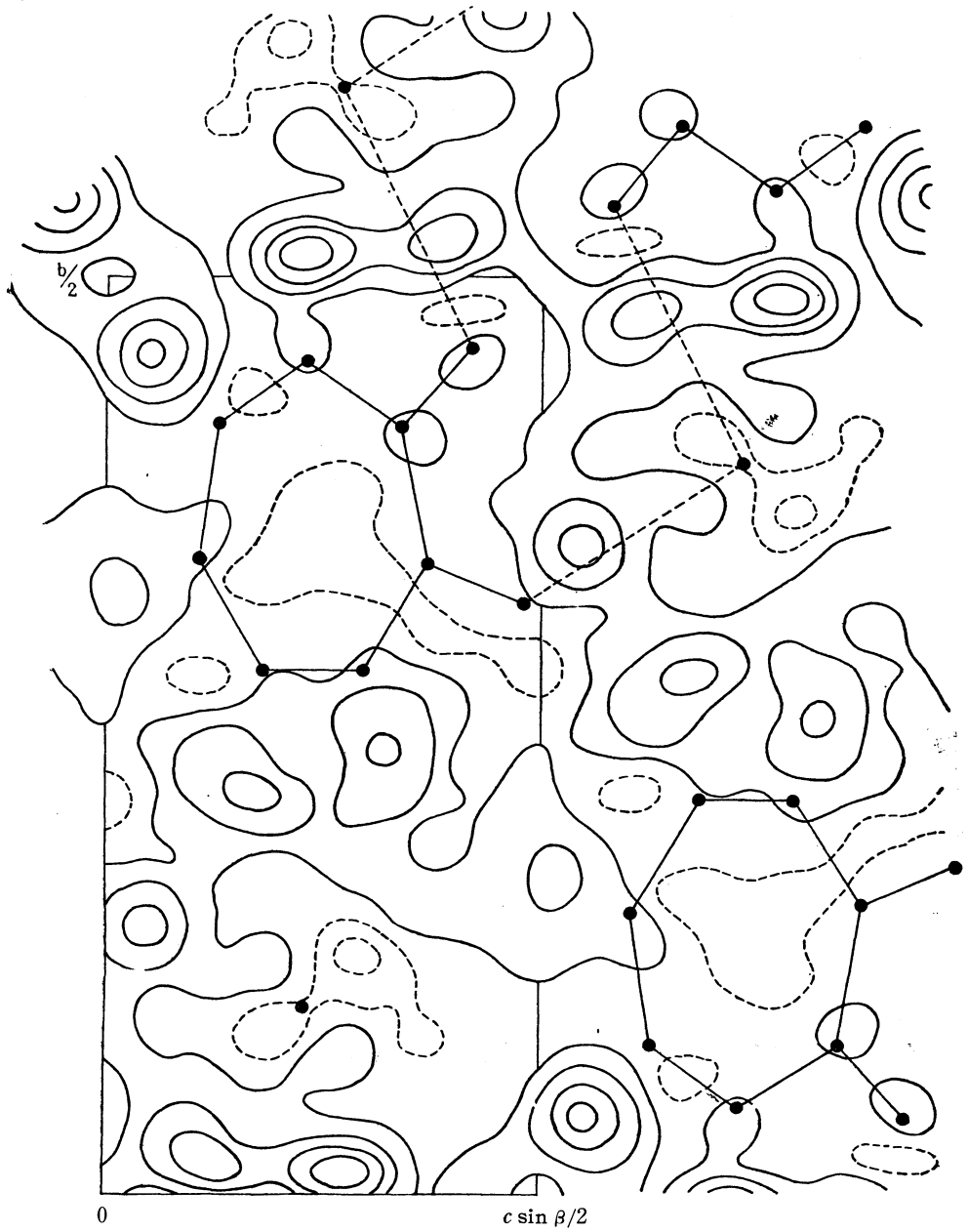



Fig. 1. The final ($Fo-Fc$) projection along the $a$ axis. Contours at intervals of 0.2 eÅ$^{-2}$ with the lowest solid contour at 0.2 eÅ$^{-2}$.

projected along the $a$ axis mentioned in the previous paper[1], (at this stage the value of $R=\sum||F_o|-|F_c||/\sum|F_o|$ was 0.168, unobserved reflexions being omitted), successive refinements by ($F_o-F_c$) syntheses were made[4]. In the structure-factor calculation, the atomic scattering factors were taken from McWeeny[5], using for oxygen $\bar{f}_0=\frac{1}{3}(f^{\parallel}+2f^{\perp})$, and for carbon the values for 'valence states'.

It was observed from the ($\rho_o-\rho_c$) maps that the thermal vibration of chlorine ion was considerably anisotropic. Consequently scattering factor of form, $f=f_0\exp[-\{\alpha+\beta\sin^2(\varphi-\psi_c)\}(\sin\theta/\lambda)^2]$ were employed[4,6] for this atom, where $\alpha$ and $\beta$

4) W. Cochran, *Acta Cryst.*, **4**, 81 (1951).
5) R. McWeeny, ibid., **4**, 513 (1951).
6) E. W. Hughes, *J. Am. Chem. Soc.*, **63**, 1737 (1941).

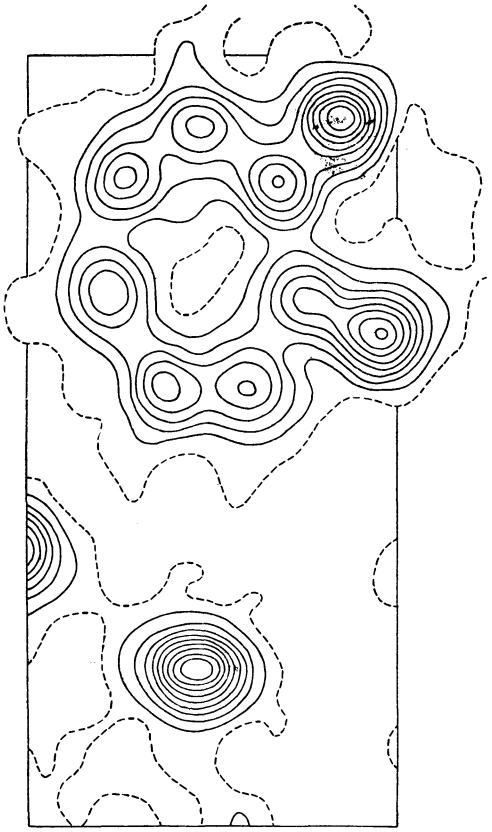



Fig. 2. The final Fourier projection of the electron density along the $a$ axis.
Contours at intervals of $2 e\text{Å}^{-2}$ for chlorine and those at intervals of $1 e\text{Å}^{-2}$ for the other atoms. Contour at $1 e\text{Å}^{-2}$ is broken.

are constants, $\psi_c$ is the angle between the direction of maximum vibration and the $c$ axis, and $(2 \sin \theta, \varphi)$ are the polar coordinates of a point in the $(0kl)$ section of the reciprocal lattice, measured from the $b^*$ axis. In the projection it should be noted that only two chlorine ions are equivalent in relation to anisotropic vibrations. As thermal motions of the other atoms were not significantly anisotropic, ordinary $B$ factors were applied. The assignments of these thermal constants proceeded simultaneously with the refinement of atomic coordinates. (The detailed procedures will be shown elswhere[7].) The best thermal factors deduced from the seventh $(\rho_o - \rho_c)$ map were:

$B=5.55$ for oxygen, 5.15 for $C_1$ and $C_2$, 5.95 for $C_3 \cdots\cdots C_7$, 5.75 for $H$ and $\{3.75 + 4.0 \sin^2 (\varphi - 25°)\}$ for chlorine.

The $R$ index for $(0kl)$ was 0.071 including the contributions from hydrogen atoms.

7) Y.Sasada and I. Nitta, Unpublished.

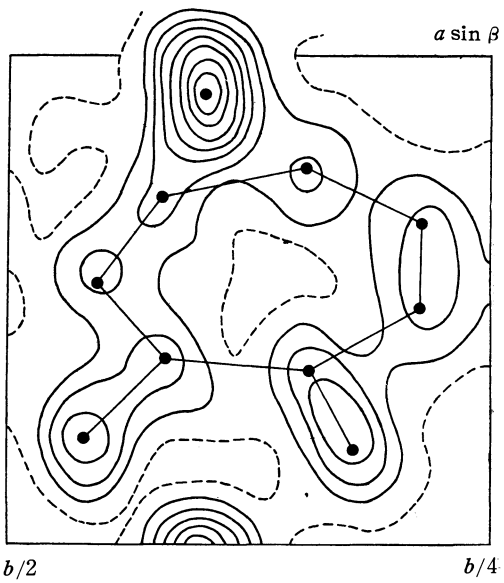



Fig. 3. The final Fourier projection of the electron density along the $c$ axis.
Contours at intervals of $2 e\text{Å}^{-2}$, that at $2 e\text{Å}^{-2}$ being broken. Black circles show the final atomic positions.

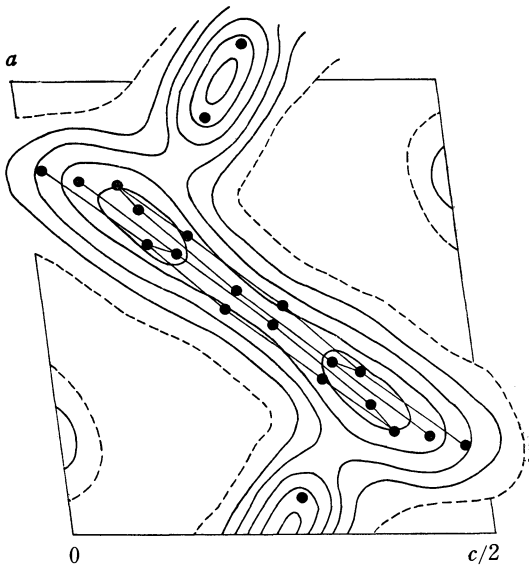



Fig. 4. The final Fourier projection of the electron density along the $b$ axis.
Contours at intervals of $4 e\text{Å}^{-2}$, that at $4 e\text{Å}^{-2}$ being broken. Black circles show the final atomic positions.

The final $(\rho_o - \rho_c)$ map (the eighth) is shown in Fig. 1. The significant peaks are evidently due to the hydrogen atoms. It should be emphasized that the positions of some hydrogen atoms, especially one attached to $O_2$, are revealed after the full correction was made for anisotropic motion of chlorine.

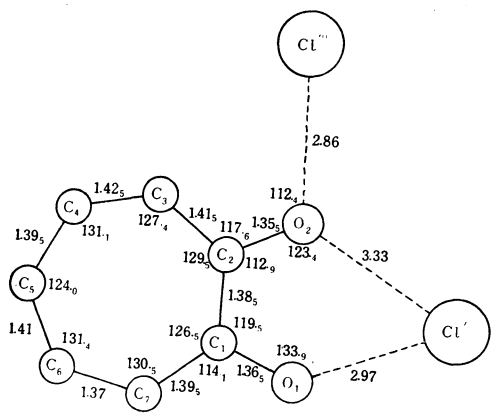



Fig. 5. Bond lengths (Å) and bond angles (°).

As the projections along the *b* and *c* axes were unsuitable for refinement owing to considerable overlapping, the *x*-coordinates of the carbon, oxygen and chlorine atoms were determined by successive three-dimensional line syntheses through atomic centres. Series termination errors were corrected by means of the back-shifts[8]. In the structure-factor calculation for (*hkl*), the mean value of *B*, 4.8, was used and the contributions from the hydrogen atoms were omitted. That the *B* for (*hkl*) came out smaller than those for (0*kl*) was mainly due to the omission of correction for absorption. The *R* index was 0.227 for (*hkl*), (0.127 unobserved reflexions being omitted).

The final electron density projections along three principal axes are shown in Figs. 2, 3 and 4.

## Coordinates, Molecular Dimensions and Estimation of Accuracy

The final values of the coordinates of carbon, oxygen and chlorine atoms are shown in Table I. The coordinates *x*, *y* and *z* are referred to the monoclinic axes, and *X'*, *Y* and *Z'* referred to orthogonal axes *a*, *b* and *c'*, *c'* being taken perpendicular to the *a* and *b* crystal axes.

TABLE I

ATOMIC COORDINATES

| Atom | *y/b* | *z/c* | *x/a* | *Y*(Å) | *Z'*(Å) | *X'*(Å) |
|---|---|---|---|---|---|---|
| Cl | 0.1015 | 0.2268 | −0.075 | 1.828 | 1.921 | −0.630 |
| $O_1$ | 0.3205 | 0.4785 | 0.191 | 5.772 | 4.053 | 0.316 |
| $O_2$ | 0.4610 | 0.4200 | 0.217 | 8.303 | 3.557 | 0.509 |
| $C_1$ | 0.3430 | 0.3680 | 0.355 | 6.177 | 3.117 | 1.223 |
| $C_2$ | 0.4180 | 0.3350 | 0.375 | 7.528 | 2.837 | 1.357 |
| $C_3$ | 0.4540 | 0.2280 | 0.533 | 8.177 | 1.931 | 2.232 |
| $C_4$ | 0.4200 | 0.1280 | 0.713 | 7.564 | 1.084 | 3.202 |
| $C_5$ | 0.3455 | 0.1030 | 0.773 | 6.222 | 0.872 | 3.515 |
| $C_6$ | 0.2860 | 0.1795 | 0.655 | 5.151 | 1.520 | 2.866 |
| $C_7$ | 0.2850 | 0.2960 | 0.483 | 5.133 | 2.507 | 1.914 |

The bond lengths and valency angles in the tropolone ring are shown in Fig. 5.

The standard deviations of the atomic coordinates, $\sigma(x)$, etc., were estimated using

$$\sigma(x)=\frac{1}{V}\frac{2\pi}{a}\{\sum h^2\sigma^2(F)\}^{\frac{1}{2}}\Big/\left|\frac{\partial^2\rho_3}{\partial x^2}\right|,$$

$$\sigma(y)=\frac{1}{A}\frac{2\pi}{b}\{\sum k^2\sigma^2(F)\}^{\frac{1}{2}}\Big/\left|\frac{\partial^2\rho_2}{\partial y^2}\right|$$

and the corresponding expression for $\sigma(z)$[9,10], where $A$ is the area of the cell projection, $V$ the volume of the cell, $\sigma(F)$ the standard deviation of $F$ values, $\frac{\partial^2\rho_3}{\partial x^2}$ the curvature of the three-dimensional electronic density at the atomic centre, and $\frac{\partial^2\rho_2}{\partial y^2}$ the curvature of two-dimensional density. In evaluating these expressions, we have taken $\sigma(F)=||F_o|-|F_c||$. The curvature was estimated by assuming that the electron density within 0.4 Å from the atomic centre can be represented by the Gaussian distribution, so that $\partial^2\rho/\partial x^2=-2p\rho(0)$. The constant $p$ was evaluated by graphical plots of $\log\rho$ against $r^2$ from the final $F_0$ synthesis.

The coordinate standard deviations obtained by these methods were:

$\sigma(y)=\sigma(z)=0.003$, $\sigma(x)=0.004$ Å for chlorine,
$\sigma(y)=\sigma(z)=0.008$, $\sigma(x)=0.010$ Å for oxygen,
$\sigma(y)=\sigma(z)=0.015$, $\sigma(x)=0.017$ Å for carbon.

From these results the standard deviation of a C–C bond comes out to be about 0.023 Å and that of a C–O bond about 0.018 Å. The average standard deviation of bond angles computed by the equation given by Ahmed and Cruickshank[11] was found to be 1.4°. The standard deviation of electron density, given by

$$\sigma(\rho)=\frac{1}{A}\{\sum(|F_o|-|F_c|)^2\}^{\frac{1}{2}},$$

was found to be 0.17 eÅ$^{-2}$ for the projection along the *a* axis.

## Discussion

**Planarity of Tropolone Ring.**—First it

8) A. D. Booth, *Proc. Roy. Soc.*, (London), **A188**, 77 (1946).

9) D. W. J. Cruickshank, *Acta Cryst.*, **2**, 65 (1949).
10) D. W. J. Cruickshank, ibid., **7**. 519 (1954).
11) F. R. Ahmed and D. W. J. Cruickshank, ibid., **6**, 385 (1953).

will be examined more in detail whether all atoms in tropolone ring lie on one plane or not. By least squares the best plane through seven carbon atoms was determined to be

$$X' = -0.0786\,Y - 1.0257\,Z' + 4.8786. \quad (1)$$

The perpendicular displacements of the carbon atoms from this plane are listed in Table II. From the standard deviations of atomic coordinates only the displacement of $C_6$ is possibly significant. However, it will be noticed that there is a systematic variation in the displacements. In order to confirm this the $\chi^2$ test was applied[12]. The value of $\chi^2$ is 8.92 and $n=4$, then $P=0.06$; that is seven-membered carbon ring is not truly planar.

If $O_1$ and $O_2$ were included in the calculation, the mean plane was

$$X' = -0.0907\,Y - 1.0246\,Z' + 4.9546, \quad (2)$$

and perpendicular displacements are also listed in Table II. In this case, the displacements of $O_1$, $O_2$, $C_4$ and $C_6$ seem to be possibly significant. But $\chi^2$ test shows that $P=0.0001$; that is, the deviation from this plane is highly significant.

TABLE II
PERPENDICULAR DISPLACEMENTS OF ATOMS FROM POSSIBLE MOLECULAR PLANES (Å)

| Atom | Plane (1) | Plane (2) |
|---|---|---|
| $O_1$ | $+0.03_2$ | $+0.02_6$ |
| $O_2$ | $-0.04_8$ | $-0.03_3$ |
| $C_1$ | $+0.01_7$ | $+0.01_7$ |
| $C_2$ | $-0.01_4$ | $-0.00_5$ |
| $C_3$ | $-0.01_7$ | $-0.00_1$ |
| $C_4$ | $+0.02_1$ | $+0.03_1$ |
| $C_5$ | $+0.01_3$ | $+0.01_3$ |
| $C_6$ | $-0.03_4$ | $-0.04_4$ |
| $C_7$ | $+0.00_6$ | $-0.00_5$ |
| Cl′ | $+0.52_9$ | |
| Cl″ | $-1.13_9$ | |
| $O_2'$ | $-0.56_2$ | |

Thus we may say only that the tropolone ring deviates slightly from a strictly planar form. It seems to be likely from the molecular packing and somewhat shorter intermolecular distances between particular atoms that such deviations may be due to some effects of crystalline field or others.

**Intramolecular Distances.**—The C–O distances are 1.355 and 1.365 Å as shown in Fig. 5. From the significant test, the two C–O bonds are of the same nature. The identical character of the two C–O bonds, which have been observed in the case of sodium tropolonate[2] (mean C–O length; 1.285 Å), is an essentially different feature from the case of neutral tropolone, in which C–O lengths are 1.26 and 1.34 Å[13]. As previously mentioned, these three compounds are isoelectronic with respect to the $\pi$-electron system. It is noted that the mean values of two C–O distances become larger when the number of added protons increases.

The mean C–O length, 1.360 Å in the present case, is in good agreement with those in the structures of resorcinol[14,15] and 1–4 dimethoxy benzene[16].

The canonical formulae of the Kekulé type with formal charges are shown in Fig. 6. In terms of the resonance theory, the bond lengths observed will imply that, in the actual ground state, the contributions from the structures of the type (B), including III–IX, should be considered to be more appreciable than those of the type (A). It agreed with the famous conclusion[17] that the seven-membered carbon ring prefers to lose one electron to form the stable $6\pi$ electron system, and with also more recent molecular orbital calculation of tropolone[18]. It can further account for the measurement of dipole moment[19] and some chemical evidences[20].

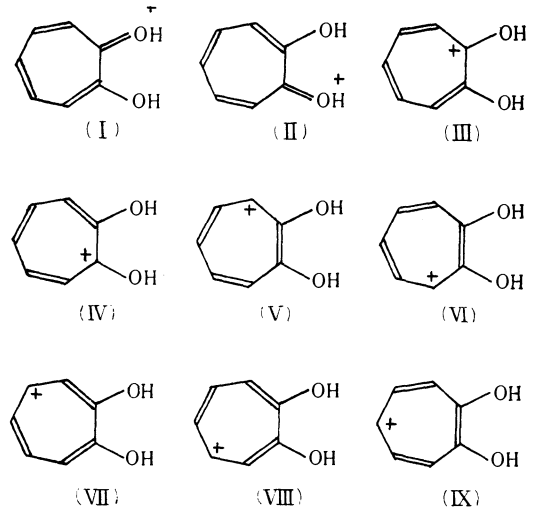



Fig. 6. Canonical formulae of tropolonium cation.

12) P. J. Wheatley, *Acta Cryst.*, **6**, 369 (1953).

13) M. Kimura and M. Kubo, This Bulletin, **26**, 250 (1953).

14) J. M. Robertson, *Proc. Roy. Soc.* (*London*)., **A 157**, 79 (1936).

15) J. M. Robertson, ibid., **A167**, 122 (1938).

16) T. H. Goodwin, M. Przybylska and J. M. Robertson. *Acta Cryst.*, **3**, 279 (1950).

17) E. Hückel, *Z. Physik*, **70**, 204 (1931).

18) Y. Kurita and M. Kubo, This Bulletin, **24**, 13 (1951).

19) Y. Kurita, T. Nozoe and M. Kubo, ibid., **24**, 10 (1951).

20) T. Nozoe, *Proc. Japan Acad.*, **26**, 30 (1950).

As the standard deviations of the C–C bonds are about 0.023 Å, the bond $C_6$–$C_7$ is shorter than the bonds $C_2$–$C_3$ and $C_3$–$C_4$ significantly, while the other fluctuations among the bonds can not be discussed seriously. The significant fluctuations among the seven C–C bonds show evidently that the contributions from the component structures of the type B are not equal. As complete interpretation of this fact is not yet given, we will only present some qualitative considerations. The first reason will be the non-equivalent orientations of the two O–H bonds with respect to the line through $C_5$ and the mid-point of $C_1$–$C_2$. In 1-4 dimethoxy benzene[16] the C–C bond in the cis-position to the methyl group is greater than that in the trans-position significantly (1.44 and 1.36 Å). The same situation is observed in the molecule of hydroquinone in the quinhydron crystal (1.42 and 1.34 Å[21]). However, it is not the case for the structure of resorcinol, although the accuracy of the analysis is rather low[14,15]. For a quantitative discussion, it will be desirable to make complete structure analysis of catechol[22,23].

The second reason is the rather closer approaches of chlorine ions to some ring atoms; that is, $C_3$, $C_5$ and $C_6$ as shown in Fig. 8. These values are smaller than those in similar cases, that is, 3.85 Å in aniline hydrochloride[24], 3.63 Å in *m*-toluidine dihydrochloride[25], 3.71 Å in adenine hydrochloride[4], 3.56 Å in guanine hydrochloride[26]. At twin boundary in the crystal of *m*-toluidine dihydrochloride[25] the nearest approaches between carbon and chlorine are 3.52 Å, but this value seems to be less significant. It will be natural to consider that these carbon atoms close to chlorine ions become more positively charged than the others. If we use the terms of the resonance theory, it corresponds to the increased contributions of the components, V, VIII and IX.

The best agreement between measured and calculated bond lengths was obtained taking the following contributions:

I–II, each 11%, III and VII–IX, each 10%, IV and VI, each 4%, V, 30%, the relation $R=R_1-(R_1-R_2)3x/(2x+1)$[27], where $x$ is double bond character, being used with $R_1=1.54$ (C–C), $R_2=1.34$ (C=C), $R_1=1.42$ (C–O) and $R_2=1.20$ Å (C=O). The calculated values are shown in Fig. 7(b), together with observed values in the present crystal (a) and in sodium tropolonate(c).

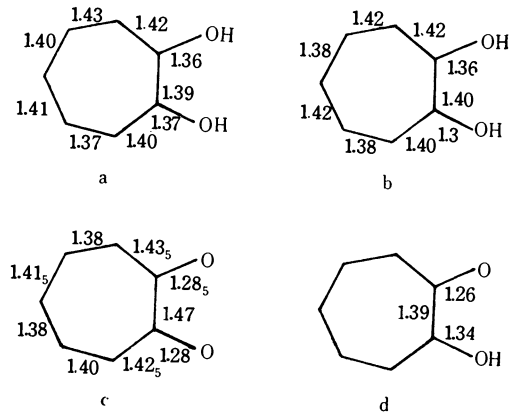



Fig. 7. (a) Observed bond lengths.
(b) Bond lengths calculated, using Pauling's relation.
(c) Bond lengths in tropolonate anion.
(d) Bond lengths in neutral tropolone.

**Hydrogen Bonding and Molecular Arrangement.**—The refined values for O···Cl are 2.97 and 2.86 Å, and are slightly shorter than those in chloral hydrate[28](3.05kX),

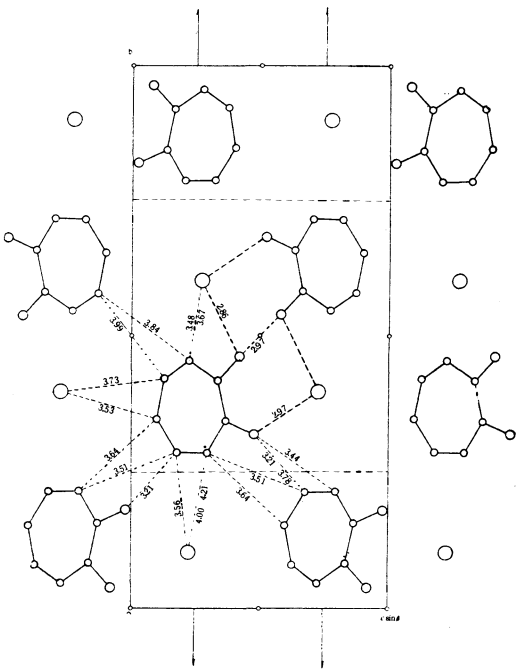


Fig. 8. Arrangement of molecules projected along the *a* axis.

21) I. Nitta, K. Osaki and H. Matsuda, To be published.
22) W. A. Caspari, *J. Chem. Soc.*, **1926**, 573.
23) A. N. Sarker, *Phil. Mag.*, **2**. 1153 (1926).
24) C. J. Brown, *Acta Cryst.*, **2**,228 (1949).
25) F. Fowweather and A. Hargreaves, ibid., **3**, 81 (1950).
26) J. M. Broomhead, ibid., **4**, 92 (1951).
27) L. Pauling, "The nature of the chemical bond" (1948).
28) S. Kondo and I. Nitta, *X-ray*, **6**, 53, (1950).

hydroxyl ammonium chloride[29] (2.99 Å), guanine hydrochloride[26] (3.16 Å), adenine hydrochloride[4] (C–H=0.95 and H···Cl=2.17 Å), ephedrine hydrochloride[30] (3.06 Å) and D(−) isoleucine hydrochloride[31](3.05, 3.07 and 3.24 Å). Although it seems to be not quite reasonable to claim the hydrogen bonding only from these distances, the angles C–O–Cl, 133.9° and 112.4°, are favourable to hydrogen bond formation. Further this conclusion is supported evidently by the direct determination of the positions of hydrogen atoms, as seen in Fig. 1. If the hydrogen bonds are operative in this crystal, the dimer formation linked by them may be concluded and it seems interesting in respect to the relation with the cystal structure of neutral tropolone, in which the presence of dimer was supposed[32]. Moreover, it is observed from the difference map that the anisotropic thermal motions of each atom seem to originate from the oscillation of the dimer, as a whole, about its centre.

Finally will be described an outline of the crystal structure ignoring, for the present, the dimer formation. Each tropolone ring was surrounded by six chlorine ions and each chlorine ion has six tropolone rings as first neighbours. The packing is closely related to ionic crystals of the NaCl type. This arrangement of chlorine ions and centres of gravities of tropolone rings also supports the above argument that the net positive charges distribute over the whole ring of the latter.

The authors wish to express their thanks to Professor T. Nozoe and his collaborators for supplying the specimens and also for continued encouragement. We are also indebted to the members of the group who have been making the cooperative physico-chemical investigations of "tropolone chemistry" for their helpful discussions. This research was supported by a grant from the Ministry of Education.

*Department of Chemistry*
*Osaka University, Osaka*

29) B. Jerslev, *Acta Cryst.* **1**, 21, (1948).
30) D. C. Phillips, ibid., **7**, 159, (1954).
31) J. Trommel and J. M. Bijvoet, ibid., **7**, 703,(1954).
32) K. Osaki and I. Nitta, Unpublished.

# *Studies on the Chemical Constitution of Agar-agar. XIX*[1]*. Pyruvic Acid as a Constituent of Agar-agar (Part 1). Identification and Estimation of Pyruvic Acid in the Hydrolysate of Agar*

By Susumu HIRASE

(Received October 8, 1956)

Agar is composed mainly of D-galactose and 3,6-anhydro-L-galactose. Partial depolymerization by means of acid hydrolysis[2], mercaptolysis[3] and methanolysis[4] gave rise to agarobiose(4-O-$\beta$-D-galactopyranosyl-3,6-anhydro-L-galactose)and its derivatives. Enzymatic hydrolysis[1] led to the isolation of neoagarobiose (3-O-3,6-anhydro-$\alpha$-L-galactopyranosyl-D-galactose). From this and other evidences, Araki[5] recently suggested that 1,3-linked $\beta$-D-galactopyranose and 1,4-linked 3,6-anhydro-$\alpha$-L-galactopyranose are alternately repeated to build up the chain of agarose, a principal polysaccharide of agar. Through further investigation, however, it has become probable that agar contains a small amount of pyruvic acid as a constituent.

A preliminary experiment involving the use of paper chromatography has indicated that pyruvic acid is produced in the hydrolysate of agar. For confirmation, agar was hydrolysed with very dilute hydrochloric acid, which caused little formation of degradation products of sugar components. Pyruvic acid liberated was easily isolated as its 2,4-dinitrophenylhydrazone though in a slight yield. The fact that pyruvic acid is set free with very dilute acid suggests that it would not

1) Part XVIII : C. Araki, and K. Arai, This Bulletin, **29**, 339 (1956).
2) C. Araki, *J. Chem. Soc. Japan*. **65**, 533, 627 (1944).
3) S. Hirase and C. Araki, This Bulletin, **27**, 105 (1954).
4) C. Araki and S. Hirase, ibid., **27**, 109 (1954).
5) C. Araki, ibid., **29**, 543 (1956).

be a secondary by-product, but an inherent constituent of agar, and also that, in the latter instance, it is engaged in the linkage susceptible to hydrolysis.

In order to examine the content of pyruvic acid, agar was subjected to hydrolysis with N-sulfuric acid. Pyruvic acid produced was completely extracted with ether, and the ether was then removed by distillation. Pyruvic acid obtained was contaminated by a large amount of formic acid, levulinic acid and hydroxymethylfurfural[6], the contaminants arising chiefly from 3,6-anhydro-L-galactose[7], and hence the 2,4-dinitrophenylhydrazine method could not be applied for the estimation of pyruvic acid. The method successfully employed in this study involves the oxidation with sodium metaperiodate at 65° followed by gravimetric determination of carbon dioxide liberated thereby:

$$CH_3COCOOH \xrightarrow{NaIO_4} CH_3COOH + CO_2$$

The content of pyruvic acid found by this method was 1.06% of agar by weight, or one residue for every fifty one hexose residues.

Since it has never been reported that pyruvic acid is present in a polysaccharide, further experiment has been made to examine any distribution of pyruvic acid in several polysaccharides other than agar. But it was detected in none of hydrolysates of mucilages of *Chondrus ocellatus Holmes* and *Gloiopeltis furcata*, gum arabic, apple pectin, konjak mannan and starch. Pyruvic acid seems to be a component peculiar to agar.

It may be of interest from the view point of biochemistry that agar contains pyruvic acid, because agar constitutes the chief cell wall structural material in several red sea weeds and pyruvic acid represents an important intermediate in the metabolism of carbohydrate, fat and protein.

## Experimental

**Isolation of Pyruvic Acid from Agar.**—Commercial agar powder (10.0 g., moisture 17.31%) was hydrolysed with 0.1N-hydrochloric acid (100 cc.) in a boiling water bath for four hours. The solution was decolorized with active carbon, and 2,4-dinitrophenylhydrazine (1 g.) dissolved in warm 4N-hydrochloric acid (150 cc.) was added, when no precipitation occurred. After being kept overnight at room temperature, the solution was extracted four times with 50 cc. portion of ethyl acetate. The extracts were combined, washed once with water, and then treated five times with 10 cc. portion of 5% sodium carbonate solution. The carbonate extracts were combined, and ethyl acetate dissolved in it was removed by evaporation under reduced pressure at 40°. Acidification with concentrated hydrochloric acid under ice cooling afforded fine yellow crystals of pyruvic acid 2,4-dinitrophenylhydrazone, which was then collected on a glass filter, washed with dilute hydrochloric acid and water, and dried at 100° until a constant weight was reached. Yields in duplicate runs were 0.157 g. and 0.162 g., which were equivalent, respectively, to 0.0514 g. and 0.0532 g. of free pyruvic acid. The crystals obtained were nearly pure as indicated by m.p. 214°. Recrystallization from ethanol-ethyl acetate gave a pure specimen melting at 218°. The m.p. was not depressed on admixture with an authentic sample (m.p. 218°).

*Anal.* Found: C, 40.43; H, 3.34; N, 20.68. Calcd. for $C_9H_8O_6N_4$: C, 40.30; H, 3.01; N, 20.89 %.

**Examination of Polysaccharides other than Agar.**—Each 10 g. of mucilages of *Chondrus ocellatus Holmes* and *Gloiopeltis furcata*, gum arabic and apple pectin was hydrolysed with 0.1N-hydrochloric acid (100 cc.) in a boiling water bath for four hours. Konjak mannan and starch (each 10 g.) was hydrolysed with N-hydrochloric acid (100 cc.) for five hours. Each hydrolysate was treated with 2,4-dinitrophenylhydrazine exactly in the same manner as that described for agar. None of them afforded 2,4-dinitrophenylhydrazone of pyruvic acid.

**Quantitative Determination of Pyruvic Acid.**—*Apparatus and Procedure.*—The quantitative determination of carbon dioxide evolved from pyruvic acid during the periodate oxidation was carried out by passing a slow current of carbon dioxide-free air through the reaction flask to sweep the evolved gas into an adsorption vessel through a train assembled as follows: (1) a washing bottle containing a 30% potassium hydroxide solution, and an U-tube filled with soda-lime, (2) the reaction flask (an 100 cc. Erlenmeyer flask) with two-holed rubber stopper carrying the inlet and outlet tubes, (3) a trap kept at −10° for the removal of most of moisture, (4) an adsorption vessel charged with concentrated sulfuric acid for the prevention of any moisture and volatile organic material from getting into the next adsorption vessel, and (5) a weighed adsorption vessel charged with a 30% potassium hydroxide solution for the quantitative determination of carbon dioxide.

A sample containing 0.05–0.3 g. of pyruvic acid was dissolved in water (20 cc.) in the reaction flask. Crystals of sodium metaperiodate (1.0 g.) were added, and the flask was immediately connected to the remainder of the apparatus. The mixture was then heated at 65°, while a slow stream of air was bubbled through the apparatus. The increase in weight of the carbon dioxide adsorption vessel was measured after two

6) C. Araki, *J. Chem. Soc. Japan*, **58**, 1214 (1937).
7) C. Araki and K. Arai, ibid., **63**, 1720 (1942).

hours, and the amount of pyruvic acid was calculated from the weight of carbon dioxide found.

*Control Analysis.* — Pyruvic acid alone and contaminated by arbitrary amounts of a mixture of formic acid, levulinic acid and hydroxymethylfurfural was analysed by the above method. These contaminants exhibited no harmful influence upon the results. Some typical results are given in Table I.

TABLE I

QUANTITATIVE DETERMINATION OF PYRUVIC ACID IN THE PRESENCE OF CONTAMINANTS

| PA, g. taken | FA, LA and HMF, g. added | PA, g. found | Error, g. |
|---|---|---|---|
| 0.1119 | — | 0.1123 | +0.0004 |
| 0.1116 | — | 0.1105 | −0.0011 |
| 0.3387 | — | 0.3377 | −0.0010 |
| 0.1211 | each 0.5 | 0.1215 | +0.0004 |
| 0.1100 | each 1.5 | 0.1145 | +0.0045 |
| 0.1048 | each 3.0 | 0.1065 | +0.0017 |

PA: Pyruvic acid. FA: Formic acid.
LA: Levulinic acid. HMF: Hydroxymethylfurfural.

**Quantitative Determination of Pyruvic Acid in the Hydrolysate of Agar.**—Each 10 g. of agar powder (moisture 17.31%) was hydrolysed with N-sulfuric acid (100 cc.) in a boiling water bath for two, four and six hours, respectively. Humus substances formed were removed by filtration through a charcoal bed, and the filtrate was extracted with ether for thirty hours in a Soxhlet's apparatus. A control experiment indicated that the extraction was complete. Water (10 cc.) was added to the extract, and ether was then removed by careful distillation. The residual solution was quantitatively transferred to the reaction flask for analysis, and the pyruvic acid present in the solution (20 cc.) was determined by the method above described. The results obtained were 0.0777 g. in a two hours hydrolysate, 0.0853 g. and 0.0877 g. in a four hours hydrolysate, and 0.0885 g. and 0.0873 g. in a six hours hydrolysate, respectively. The average value excluding the result of two hours hydrolysis is 0.0872 g. or 1.06% of moisture-free agar by weight. This figure indicates the presence of one residue of pyruvic acid for every fifty one residues of hexose.

## Summary

1. Pyruvic acid has been isolated as its 2,4-dinitrophenylhydrazone from the hydrolysate of agar for the first time.

2. Quantitative determination has indicated that the content of pyruvic acid is 1.06% of agar or one residue for every fifty one hexose residues.

3. It has been suggested that pyruvic acid would be an intrinsic constituent of agar.

4. Several polysaccharides other than agar have been examined, but none of them produced pyruvic acid on hydrolysis.

The writer wishes to express his hearty thanks to Professor S. Tanaka, Department of Science, Kyoto University, and Professor C. Araki, this University, for their great interest and discussion. Thanks are also due to Mr. K. Arai for microanalysis and to Mr. T. Ito for assistance.

*Institute of Chemistry, Faculty of Industrial Arts, Kyoto Technical University*
*Matsugasaki, Kyoto*

# *Studies on the Chemical Constitution of Agar-agar. XIX. Pyruvic Acid as a Constituent of Agar-agar (Part 2)*[1]*. Isolation of a Pyruvic Acid-linking Disaccharide Derivative from the Methanolysis Products of Agar*

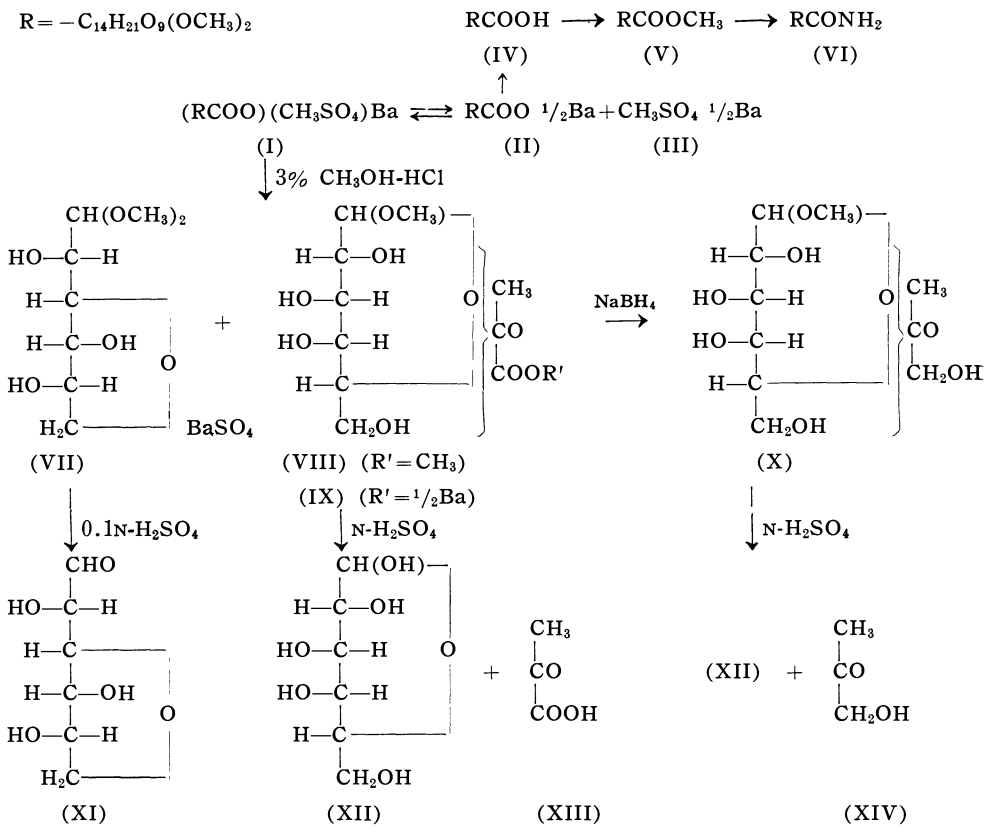
By Susumu HIRASE

(Received October 8, 1956)

In the previous communication[1], it was suggested that pyruvic acid, produced in 1.06% yield by the hydrolysis of agar, would not be secondary by-product, but an intrinsic constituent. This suggestion has been substantiated herein by the isolation of a crystalline disaccharide derivative carrying a pyruvic acid residue in the molecule from the partial methanolysis products of agar.

The partial methanolysis of agar has been carried out by heating it in 0.5%

1) Part XIX-1 : S. Hirase, This Bulletin, **30**, 68 (1957).




methanolic hydrogen chloride for two hours according to the method of Araki and the present writer[2]. The product was treated with barium hydroxide solution and passed through columns of cation and anion resins in succession. Acidic compounds, which were retained by the anion resin, were eluted by displacement with excess sulfuric acid. Neutralization with barium hydroxide followed by evaporation afforded a mixture of barium salts, from which a crystalline salt was isolated in 6.3% yield by weight.

The crystalline barium salt obtained has been proved to be monohydrates of a double salt (I) consisting of barium methylsulfate (III) and a barium salt of an organic acid (II). This follows from the fact that the double salt was separated into its two component salts II and III by means of an anion exchange resin. When II and III were separately dissolved in methanol and the solutions were mixed, the double salt was immediately regenerated. Methylsulfuric acid constituting a part of the double salt may have arisen from the sulfuric acid residues present in agar.

2) C. Araki and S. Hirase. ibid., **27**, 109 (1954).

From the barium salt (II), there has been obtained a free acid (IV) having the formula $C_{14}H_{21}O_9(OCH_3)_2COOH$ as its crystalline monohydrates. The acid was converted into the methyl ester (V) by reaction with diazomethane, and the ester was further converted into the amide (VI) by reaction with ammonia. Both derivatives were obtained in a crystalline condition.

In order to examine the components of the acid (IV), the original double salt (I) was subjected to methanolysis. There were produced barium sulfate, 3,6-anhydro-L-galactose dimethylacetal (VII) and a methyl ester methyl glycoside (VIII), the last one being separated from the second through its barium salt (IX). 3,6-Anhydro-L-galactose dimethylacetal (VII) was hydrolysed to give a free sugar (XI), which was identified as its crystalline diphenylhydrazone. The barium salt methyl glycoside (IX) yielded upon hydrolysis D-galactose (XII) and pyruvic acid (XIII). D-Galactose was isolated as crystals, and pyruvic acid was identified as its semicarbazone, phenylhydrazone and *p*-nitrophenylhydrazone. This result indicates that the acid (IV) is a disaccharide derivative composed of 3,6-anhydro-L-

galactose and D-galactose, the latter component carrying a pyruvic acid residue.

On the other hand, the ester group of VIII was reduced to a hydroxyl group with sodium borohydride. Hydrolysis of the resulting product (X) yielded D-galactose (XII) and hydroxyacetone (XIV), the latter product being identified as its semicarbazone. This result demonstrates that the pyruvic acid residue is linked through its carbonyl group with the D-galactose residue.

The isolation of the compound (IV) verifies the view that pyruvic acid is a constituent of agar, because the mild treatment in its isolation completely excludes the possibility that pyruvic acid might be a secondary product derived from some unidentified compound. For instance, oxalacetic acid would be decarboxylated to give pyruvic acid on being heated in an aqueous medium, but it undergoes no decarboxylation on being treated with methanolic hydrogen chloride.

The compound (IV) represents the first example of a carbohydrate with which pyruvic acid is linked through its carbonyl group. The structure will b elater reported.

## Experimental

Unless otherwise stated, concentration and evaporation were carried out under reduced pressure below 40°. Melting points are uncorrected.

**Partial Methanolysis of Agar.**—Commercial agar powder (50 g., dry weight 41.9 g.) was suspended in 0.5% methanolic hydrogen chloride (500 cc.) and heated under reflux for two hours. The undissolved agar (5.5 g.) was removed by filtration, and the filtrate was neutralized with silver carbonate, refiltered and concentrated to a sirup (40.7 g.). It was then saponified by heating in a 0.2N-barium hydroxide solution (500 cc.) at 60° for two hours. Excess barium hydroxide was removed by neutralization with carbon dioxide and filtration, and the filtrate was passed through a column of Amberlite IR-120 (2.8×20 cm.) to remove cations, and then through a column of Amberlite IR-4B (2.8×25 cm.), where anions of acidic compounds were adsorbed. The columns were thoroughly washed with water (5 l.), and the neutral effluent was concentrated to a sirup (32.1 g.); $[\alpha]_D^{26}$-17.7° (water, *c* 1.64). This was a mixture of neutral sugar derivatives, which were not investigated in this communication.

**Isolation of the Double Salt (I).**—The above IR-4B resin, by which acidic compounds were retained, was stirred with N-sulfuric acid (300 cc.) under ice cooling for ten minutes, poured into a glass tube (2.8 cm. diameter), and drained. The column was washed with additional 100 cc. of N-sulfuric acid and then with water (2 l.). The effluent and washings were immediately neutralized with a saturated barium hydroxide solution as soon as they percolated, barium sulfate removed by filtration, and the filtrate was concentrated to a sirup. Dissolution in boiling methanol (50 cc.) followed by cooling afforded crystals of the double salt (I), which were filtered, washed with methanol and dried; yield 2.3 g. (6.3% of the agar concerned in methanolysis); $[\alpha]_D^{26}$-29.0° (water, *c* 1.0). The filtrate and washings were concentrated to a sirup (3.0g.), $[\alpha]_D^{26}$-2.3° (water, *c* 1.75).

The crude crystals above obtained were purified by recrystallization from aqueous methanol until no more change in specific rotation and in barium content was recognized. The pure double salt forms elongated prisms, having $[\alpha]_D^{14}$-30.1° (water, *c* 1.56) and slowly decomposing over 200°C. It is soluble in water and insoluble in organic solvents.

*Anal.* Found: Ba, 19.42; $SO_4$, 13.55; $OCH_3$, 13.09; Ash, 33.01. Calcd. for $(C_{17}H_{27}O_{13})(CH_3SO_4)Ba \cdot H_2O$: Ba, 19.48; $SO_4$, 13.61; $OCH_3$, 13.20; Ash (as $BaSO_4$), 33.09%.

**Separation of the Double Salt (I) into its Component Salts.**—The double salt (I) (6.0 g.) in water (30 cc.) was passed through a column of Amberlite IR-120 (2.8×10 cm.) to remove barium ion, and the column was washed with water (100 cc.). The acidic effluent and washings were combined and immediately passed through a column of Amberlite IR-4B (sulfate form) (2.8×20 cm.), which had been prepared by the reaction of the resin (hydroxide form) with excess N-sulfuric acid and had been washed with large volumes of water (20 l.). The column was then washed with water (400 cc.). In this process, methylsulfuric acid was retained by the resin, while the carboxylic acid (IV) was passed through.

**(a) Barium Salt (II).**—The effluent from the above anion resin was immediately neutralized with a barium hydroxide solution and concentrated to dryness. The residue was dissolved in a small volume of methanol, filtered and poured into dry acetone, giving a white powder of the barium salt (II), which was collected on a glass filter, washed with acetone and dried in vacuo; yield 4.0 g. (93%); $[\alpha]_D^{20}$-40.3° (water, *c* 1.54).

*Anal.* Found: $OCH_3$, 11.95; Ba, 13.34; $SO_4$, nil. Calcd. for $(C_{17}H_{27}O_{13})_2Ba$: $OCH_3$, 12.20; Ba, 13.52%.

**(b) Barium Methyl sulfate (III).**—Methylsulfuric acid, which had been adsorbed by the IR-4B resin, was eluted from the column with N-sulfuric acid (50 cc.) and then with water (300 cc.). Effluents were immediately neutralized with a hot saturated barium hydroxide solution, filtered and evaporated to dryness. The residue was crystallized from aqueous ethanol, giving barium methylsulfate dihydrates; yield 1.4 g. (82%).

*Anal.* Found: Ba, 34.66; $SO_4$, 48.39; $OCH_3$,

15.81. Calcd. for $(CH_3SO_4)_2Ba \cdot 2H_2O$: Ba, 34.73; $SO_4$, 48.58; $OCH_3$, 15.67%.

**Regeneration of I from II and III.**—The barium salt (II) (0.51 g.) and barium methylsulfate dihydrate (III) (0.20 g.) were separately dissolved in methanol. When the solutions were combined, the double salt (I) was immediately crystallized; yield 0.71 g. (100%); $[\alpha]_D^{15}$ -30.6° (water, *c* 1.21).

*Anal.* Found: Ba, 19.33; $SO_4$, 13.40; $OCH_3$, 13.31. Calcd. for $(C_{17}H_{27}O_{13})(CH_3SO_4)Ba \cdot H_2O$: Ba, 19.48; $SO_4$, 13.61; $OCH_3$, 13.20%.

**Free Acid (IV).**—The barium salt (II) (2.0g.) in water (20 cc.) was passed through a column of Amberlite IR-120 (2.8×10 cm.) to remove barium ion, and the column was washed with water (80 cc.). The acidic effluent was partly neutralized with 1 cc. of 0.1N-barium hydroxide solution and concentrated below 30° to a sirup, which was freed from a barium compound by dissolution in dry acetone and filtration. The filtrate was concentrated to a sirup (1.7 g.), which was redissolved in ethyl acetate and kept overnight in a refrigerator. Crystals deposited were filtered, washed with ethyl acetate and dried; yield 1.4 g (78%). Recrystallization twice from ethyl acetate afforded a pure specimen of the acid (IV) in a monohydrate form melting at 118-120° and foaming at 122°; $[\alpha]_D^{20}$ -46.7° (water, *c* 1.05) and -51.6° (methanol, *c* 1.24). It is soluble in water, methanol, ethanol and acetone, and hardly soluble in cold ethyl acetate and ether. Seliwanoff's ketose reaction was strongly positive.

*Anal.* Found: C, 44.39; H, 6.83; $OCH_3$, 13.31%; Neutralization equivalent, 457. Calcd. for $C_{17}H_{28}O_{13} \cdot H_2O$: C, 44.55; H, 6.59; $OCH_3$, 13.53; Neutr. equiv., 458.

**Methyl Ester (V).**—To a solution of the acid (IV) (0.5 g.) in methanol (5 cc.) was added dropwise an ethereal solution of diazomethane, evolution of nitrogen being observed. After being kept for one hour, it was concentrated to a sirup (0.5 g.), which was then dissolved in ethyl acetate, and a small amount of ether was added to form a slight cloudiness. The solution was left in a refrigerator, when the methyl ester (V) was slowly crystallized; yield 0.32 g. An additional crop (0.10 g.) was obtained from the mother liquor. Crude crystals were purified by recrystallization twice from ethyl acetate-ether, giving prisms; m. p. 153-154°; $[\alpha]_D^{15}$ -44.4° (water, *c* 1.04), and -52.9° (methanol, *c* 1.04). It is soluble in water, methanol, ethanol and acetone, hardly soluble in cold ethyl acetate, and insoluble in ether.

*Anal.* H, Found: C, 47.51; 6.75; $OCH_3$, 20.69%; Saponification equivalent, 452. Calcd. for $C_{18}H_{30}O_{13}$: C, 47.57; H, 6.65; $OCH_3$, 20.47%; Sapon. equiv., 454.

**Amide (VI).**—A methanolic solution (5 cc.) of the methyl ester (V) (0.15 g.) was saturated with dry ammonia under ice cooling, and left overnight at room temperature. Evaporation gave a sirup, which solidified on standing. Recrystallization was carried out by dissolving it in acetone and adding ether, the amide (VI) being obtained as monohydrates; yield 0.08 g.; m. p. 102-105°; $[\alpha]_D^{25}$ -43.2° (water, *c* 0.51).

*Anal.* Found: C, 44.66; H, 6.95; N, 3.11. Calcd. for $C_{17}H_{29}O_{12}N \cdot H_2O$: C, 44.64; H, 6.82; N, 3.06%.

**Methanolysis of the Double Salt (I).**—The double salt (I) (4.0g.) in 3% methanolic hydrogen chloride (150 cc.) was heated under reflux for twenty hours. Barium sulfate precipitated was removed by filtration, and the filtrate was neutralized with silver carbonate, filtered and concentrated to a colorless sirup (2.5 g.); $[\alpha]_D^{13}$ +35.1° (water, *c* 0.74). This was proved to be a mixture of VII and VIII, the separation being effected by saponification as described below.

**(a) Barium Salt Methyl Glycoside (IX).**—The above sirup was heated in 0.3N-barium hydroxide solution (150 cc.) at 60° for two hours. The solution was neutralized with carbon dioxide, filtered and concentrated to a sirup (3.1 g.). It was then dissolved in a small volume of methanol and poured into dry acetone with stirring, the barium salt methyl glycoside (IX) being precipitated as a white powder, which was collected on a glass filter, washed with acetone and dried in vacuo; yield 2.3 g.; $[\alpha]_D^{14}$ +56.2° (water, *c* 0.89).

*Anal.* Found: $OCH_3$, 9.05; Ba, 20.66. Calcd. for $(C_{10}H_{15}O_8)_2Ba$: $OCH_3$, 9.34; Ba, 20.70%.

**(b) 3,6-Anhydro-L-galactose Dimethylacetal (VII).**—The filtrate and washings, separated from the above salt (IX), were combined and evaporated to dryness, when VII was obtained as a colorless sirup[3]; yield 0.7 g.; $[\alpha]_D^{13}$ -27.0° (water, *c* 0.74); $OCH_3$, found: 26.32% (calcd. for $C_8H_{16}O_6$: 29.81%). It migrated on a paper chromatogram at the same rate as an authentic sample ($R_f$ 0.67[2]), *n*-butanol-ethanol-water (4:1:2) being used as a solvent and *o*-aminophenol reagent[4] being sprayed.

**3,6-Anhydro-L-galactose Diphenylhydrazone.**—The dimethylacetal (0.15 g.) above obtained was hydrolysed with 0.1N-sulfuric acid at 95° for two hours in the usual manner, giving 3,6-anhydro-L-galactose (XI) (0.12 g.). It was then converted into its diphenylhydrazone in the usual manner[3]; m. p. 153-155°, not depressed on admixture with an authentic sample; $[\alpha]_D^{13}$ -34.4° → -21.5° (methanol, *c* 0.93).

**Methyl Ester Methyl Glycoside (VIII).**—The barium salt methyl glycoside (IX) (2.6 g.) above obtained was esterified by heating in 4% methanolic hydrogen chloride (100 cc.) for four hours. The solution was neutralized with silver carbonate, filtered and concentrated to a sirup, which was purified by extraction with hot acetone and evaporation. The methyl ester methyl glycoside

3) C. Araki, *J. Chem. Soc. Japan*, **65**, 725, (1944).
4) S. Hirase, C. Araki and S. Nakanishi, This Bulletin, **26**, 183 (1953).

(VIII) was obtained as a pale yellow viscous sirup; yield 1.7 g.; $[\alpha]_D^{13}$ +74.8° (water, *c* 1.27) and +69.0° (methanol, *c* 1.26).

*Anal.* Found: $OCH_3$, 21.80%; Saponification equivalent, 278. Calcd. for $C_{11}H_{18}O_8$: $OCH_3$, 22.29 %; Sapon. equiv., 278.

**Hydrolysis of IX.**—The barium salt methyl glycoside (IX) (0.8 g.) was dissolved in a small amount of water and N-sulfuric acid (15 cc.) was added with stirring. Barium sulfate precipitated was removed by filtration, and the filtrate was heated in a boiling water bath until the optical rotation of the solution reached a constant value after five hours ($[\alpha]_D$ +52° → +28°). The solution was placed in a Soxhlet's apparatus and treated with ether for seven hours to extract pyruvic acid. The residual solution was used for isolation of D-galactose.

(a) **D-Galactose (XII).**—The residual solution just mentioned was neutralized with barium carbonate, filtered and concentrated to a sirup, which gave D-galactose on dissolution in hot methanol and cooling; yield 0.30 g.; m. p. 166–168°, not depressed on admixture with an authentic sample; $[\alpha]_D^{14}$ +80.6° (after twentyfour hours, water, *c* 1.08).

(b) **Pyruvic Acid (XIII).**—The ether extract above described was distilled under atmospheric pressure to remove ether, and the residue was dissolved in water (9 cc.). The solution was used to prepare the following derivatives of pyruvic acid in the usual manner.

*Phenylhydrazone.*—Needles; m. p. and mixed m. p. 192°.

*p-Nitrophenylhydrazone.*—Yellow fine crystals; m. p. and mixed m. p. 226°.

*Semicarbazone.*—Prisms; m. p. and mixed m. p. 212°.

**Reduction of VIII and Hydrolysis.**—Sodium borohydride (0.3 g.) was added to a solution of VIII (0.9 g.) in water (10 cc.). The reaction solution was left aside with occasional shaking for five days at room temperature. Then it was neutralized with dilute sulfuric acid, deionized by passing through columns of Amberlite IR-120 and IR-4B in succession, and concentrated to a sirup, which was purified by dissolution in absolute methanol and filtration. Evaporation afforded a viscous sirup of the reduction product (X); yield 0.8 g.; $[\alpha]_D^{24}$ +74.5° (water, *c* 0.50); $OCH_3$, found: 12.15% (calcd. for $C_{10}H_{18}O_7$: 12.40%).

The product (X) (0.40 g.) obtained was heated in N-sulfuric acid (10 cc.) until the optical rotation of the solution reached a constant value after four and a half hours ($[\alpha]_D$ +74°→+40°). The solution was neutralized with barium carbonate and filtered. The filtrate, diluted with water up to 40 cc., was distilled under atmospheric pressure, the same volume of water as that of the distillate being supplied as the distillation progressed. Forty cc. of the distillate was collected to identify hydroxyacetone therein, while the residual solution was used for the isolation of D-galactose.

(a) **D-Galactose (XII).**—The residual solution of the distillation was concentrated to dryness, giving D-galactose; m. p. and mixed m. p. 166–167°; $[\alpha]_D^{25}$ +80.5° (after twentyfour hours, water, *c* 1.15).

(b) **Hydroxyacetone (XIV).**—To the distillate above obtained, semicarbazide hydrochloride (0.5 g.) and sodium acetate trihydrate (0.8 g.) were added. After being left overnight at room temperature, the solution was concentrated to a small volume, when hydroxyacetone semicarbazone was crystallized; yield 0.06 g.; m. p. 195–196°, not depressed on admixture with an authentic sample.

**Decarboxylation of Oxalacetic Acid.**—Oxalacetic acid (0.3064 g.) in water (25 cc.) was heated in a boiling water bath, the evolved gas being swept by a slow current of carbon dioxide-free air into an adsorption vessel charged with a 30% potassium hydroxide solution. Carbon dioxide found was 0.1013 g. (99.3% of theory). From the reaction solution, pyruvic acid was obtained as its phenylhydrazone melting at 192°. When oxalacetic acid (0.3106 g.) was heated under reflux in 0.5% methanolic hydrogen chloride (25 cc.), which was used for the isolation of I from agar, carbon dioxide evolved was only 0.0042 g. (4.06% of theory). From the reaction solution, methyl oxalacetate was obtained as its phenylhydrazone, melting at 116–118°.

## Summary

1. Partial methanolysis of agar has led to isolation of a crystalline double barium salt, which is separable into its components, barium methylsulfate and a barium salt of an organic acid.

2. From the last salt above mentioned, there has been obtained a free acid having the formula $C_{14}H_{21}O_9(OCH_3)_2COOH$ as its crystalline monohydrates. Its methyl ester and amide have also been prepared in a crystalline condition.

3. The acid obtained, a new compound, has been proved to be a disaccharide derivative composed of 3,6-anhydro-L-galactose, D-galactose and pyruvic acid.

4. It has also been proved that the pyruvic acid residue is linked through its carbonyl group with the D-galactose residue.

5. The isolation of the pyruvic acid-linking disaccharide derivative substantiates the view that pyruvic acid is an intrinsic constituent of agar.

The writer wishes to express his hearty thanks to Professor S. Tanaka, Department of Science, Kyoto University, and

Professor C. Araki, this University, for their great interest and discussion. Thanks are also due to Mr. K. Arai for micro-analysis and to Mr. T. Ito for assistance.

*Institute of Chemistry, Faculty of Industrial Arts, Kyoto Technical University*
*Matsugasaki, Kyoto*

# *Studies on the Chemical Constitution of Agar-agar. XIX. Pyruvic Acid as a Constituent of Agar-agar (Part 3)[1]. Structure of the Pyruvic Acid-linking Disaccharide Derivative Isolated from the Methanolysis Products of Agar*

By Susumu HIRASE

(Received Octover 8, 1956)

In the previous work[1], a crystalline acid having the formula $C_{14}H_{21}O_9(OCH_3)_2$-COOH was isolated from the partial methanolysis products of agar. The compound was shown to be a disaccharide derivative consisting of 3,6-anhydro-L-galactose, D-galactose and pyruvic acid, the pyruvic acid residue being linked through its carbonyl group with the D-galactose residue. The structure of the compound has been further investigated, and has been proved to be 4-O-4′,6′-O-1″-carboxyethylidene-β-D-galactopyranosyl-3,6-anhydro-L-galactose dimethylacetal (I).

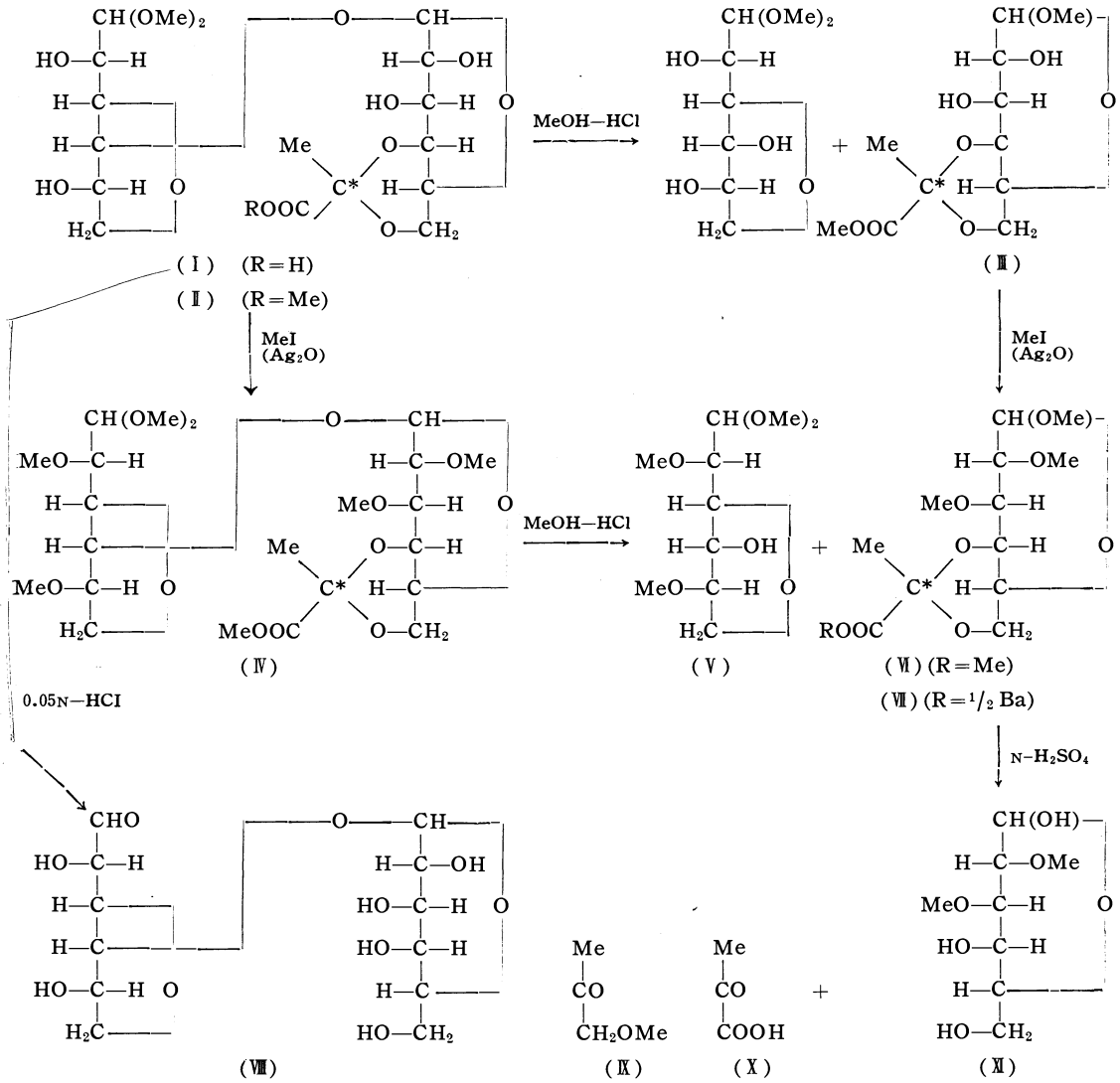
First, the manner in which the pyruvic acid is linked with the D-galactose residue has been studied by methylation of the methyl ester methyl galactoside (III), obtained by methanolysis of I in the previous work. The methylation was carried out by the use of Purdie's reagents to give a methylated methyl ester (VI), a viscous liquid purified by distillation in high vacuum. On hydrolysis it afforded pyruvic acid (X) and 2,3-di-O-methyl-D-galactose (XI). Pyruvic acid was identified as its crystalline phenylhydrazones. 2,3-Di-O-methyl-D-galactose, which had been synthetically known, was identified as follows. (1) Treatment with aniline gave a crystalline anilide, which was in good agreement with a synthetic sample. (2) Treatment with phenylhydrazine and acetic acid resulted in the formation of 3-O-methyl-D-galactosazone, a methoxyl group on the carbon atom $C_2$ being lost meanwhile. The osazone was identical with a synthetic sample. And, (3) according to the procedure of Luckett and Smith[2], the sugar was oxidized with nitric acid to give 2,3-di-O-methyl-D-galactaric acid, which was then converted to a crystalline bisamide. The identity was again established by comparison with a synthetic sample. The identification of pyruvic acid and 2,3-di-O-methyl-D-galactose as cleavage fragments of VI indicates that the pyruvic acid residue is connected through acetal linkages either with carbon atoms $C_4$ and $C_6$ of the D-galactopyranose residue or with $C_5$ and $C_6$ of the D-galactofuranose residue. The former structure, namely, methyl 4,6-O-1′-carbomethoxyethylidene-D-galactopyranoside, has been assigned to the methyl ester methyl galactoside (III), because the compound shows a positive value of optical rotation, which is in agreement only with the pyranoside structure.

On the other hand, the ester group of VI was reduced to a hydroxyl group with lithium aluminium hydride and the newly formed hydroxyl group was methylated with Purdie's reagents. The resulting product on hydrolysis yielded methoxyacetone (IX) and again 2,3-di-O-methyl-D-galactose (XI), the former product being identified as its *p*-nitrophenylhydrazone. This fact brings the same conclusion as that already brought as to the linkage between pyruvic acid and D-galactose residues.

Next, in order to study the mode of the linkage between 3,6-anhydro-L-galactose and 4,6-O-1′-carboxyethylidene-D-galactose residues, the methyl ester (II), prepared

1) Part XIX-2 : S. Hirase, This Bulletin, **30**, 70 (1957).

2) S. Luckett and F. Smith, *J. Chem. Soc.*, **1940**, 1106.




in the previous work, was methylated with Purdie's reagents. The resulting methylated compound (IV) was obtained as crystals. On methanolysis it afforded a mixture of 2,5-di-O-methyl-3,6-anhydro-L-galactose dimethylacetal (V) and methyl 2,3-di-O-methyl-4,6-O-1′-carbomethoxyethylidene-D-galactoside (VI). The latter, separated from the former through its barium salt (VII), was further hydrolysed to give pyruvic acid (X) and 2,3-di-O-methyl-D-galactose (XI) in the same manner as that already described. 2,5-Di-O-methyl-3,6-anhydro-L-galactose dimethylacetal (V) was hydrolysed to the corresponding reducing sugar, which was then oxidized with bromine water to give crystalline 2,5-di-O-methyl-3,6-anhydro-L-galactonic acid. The amide of the last compound was also prepared in a crystalline condition. These two crystalline derivatives were exactly identical with the corresponding authentic samples. The identification of V and VI as cleavage fragment of IV points to the conclusion that the D-galactopyranose residue is glycosidically joined with the carbon atom $C_4$ of the 3,6-anhydro-L-galactose residue. Furthermore, on the basis that the compound (I) and its derivatives have negative values of optical rotation, the galactoside linkage has been suggested to be of the $\beta$-configuration. Thus, it becomes now possible to assign the structure 4-O-4′, 6′-O-1″-carboxyethylidene-$\beta$-D-galactopyranosyl-3,6-anhydro-L-galactose dimethylacetal (I) to the compound under problem.

Further support for the structure is

derived by the fact that careful hydrolysis of I resulted in the formation of pyruvic acid (X) and agarobiose (4-O-β-D-galacto-pyranosyl-3, 6-anhydro-L-galactose) (VIII). Moreover, the compound (I) rapidly consumed one mole of periodate in the presence of a sodium bicarbonate buffer, indicating that the presence of a pair of adjacent hydroxyl groups. In conclusion, all the experimental results are compatible with only one structure (I) for the compound isolated from the methanolysis products of agar. However, no information has been made available as to the configuration of the carbon atom $C_1$ (starred) of the ethylidene group.

It is of interest to note that biochemically important pyruvic acid is connected with an agarobiose unit, which is a repeating unit of agarose, a principal polysaccharide of agar[3]. Moreover, it seems probable that the carboxyl group of the pyruvic acid residue may make some contribution to a gel-forming behavior of agar. But further work is needed to solve the problem whether or not pyruvic acid is connected in the same manner of the linkage in the polysaccharide molecule as that in the compound (I) isolated.

## Experimental

Unless otherwise stated evaporation and concentration were carried out under reduced pressure below 40°. All the melting points are uncorrected.

**Methyl 2,3-Di-O-methyl-4,6-O-1'-carbomethoxyethylidene-D-galactoside (VI).**— Methyl 4, 6-O-1'-carbomethoxyethylidene-D-galactoside (III) (2.0 g.), designated as a methyl ester methyl glycoside (VIII) in the previous paper[1], was directly dissolved in methyl iodide (20 g.) and methylated with silver oxide (7 g.) in the usual manner. The methylation was repeated four times, and the final product was purified by high vacuum distillation, VI being obtained as a colorless viscous liquid boiling at 110–115°/0.027 mm Hg; yield 1.7 g.; $n_D^{20}$ 1.4711; $[\alpha]_D^{10}$ +97.1° (water, *c* 1.02) and +98.5° (chloroform, *c* 0.65).

*Anal.* Found: C, 50.65; H, 7.32; $OCH_3$, 40.76%; Saponification equivalent, 300. Calcd. for $C_{13}H_{22}O_8$: C, 50.97; H, 7.24; $OCH_3$, 40.48%; Sapon. equiv., 306.

**Hydrolysis of VI.**—The methylated compound (VI) (1.25 g.) above obtained was dissolved in N-sulfuric acid (50 cc.) and heated in a boiling water bath until the optical rotation of the solution reached a constant value after five hours ($[\alpha]_D$ +96°→+54°). The solution was treated with ether in a Soxhlet's apparatus for seven hours. The ether extract was used for the identification of pyruvic acid, while the residual solution was used for the isolation of 2,3-di-O-methyl-D-galactose.

**(a) Pyruvic Acid (X).**—The ether extract was evaporated under atmospheric pressure to remove ether. The residue, which revealed no spot of a sugar derivative on a paper chromatogram, was treated in the same manner as described in the previous paper[1]. Phenylhydrazone and *p*-nitrophenylhydrazone of pyruvic acid were prepared, the identity being established by mixed m.p. determination.

**(b) 2, 3-Di-O-methyl-D-galactose (XI).**— The residual solution, separated from pyruvic acid, was neutralized with barium carbonate, filtered and concentrated to a sirup, which was redissolved in acetone, filtered and again evaporated to dryness. The sugar (XI) was obtained as a colorless sirup; yield 0.70 g.; $[\alpha]_D^{11}$ +61.5° (an initial value)→+84.6° (an equilibrium value, water, *c* 0.78); $OCH_3$, found: 30.23% (calcd. for $C_8H_{16}O_6$: 29.81%). It migrated on a paper chromatogram to the same position as that of a synthetic sample[4,5], *n*-butanol-ethanol-water (4 : 1 : 2) being used as a mobile phase.

*Anilide.*—The sugar (0.16 g.) above obtained and aniline (0.07 g.) in ethanol (3 cc.) were heated under reflux for three hours. The anilide was crystallized from acetone-petroleum ether; m.p. 152–154°; $[\alpha]_D^{13}$ −61.9° (an initial value)→+12.9° (an equilibrium value, ethanol, *c* 0.63). Reported values[5] are m.p. 154–155° and $[\alpha]_D$ −56.8°→+12.1° (ethanol). The melting point was not depressed on admixture with an synthetic sample melting at 153–154°.

*Anal.* Found: C, 59.23; H, 7.46; N, 5.37. Calcd. for $C_{14}H_{21}O_5N$: C, 59.35; H, 7.24; N, 4.95%.

*3-O-Methyl-D-galactosazone.*—A mixture of 2, 3-di-O-methyl-D-galactose (0.15 g.), phenylhydrazine (0.25 g.) and 50% aqueous acetic acid (0.5 cc.) in water (2 cc.) was heated in a boiling water bath for two hours. Reddish precipitates formed were filtered, washed with water and dried. The precipitates were chromatographed on a column of active alumina, ethyl acetate being used as a developing solvent. The fresh yellow zone at the top of the column was eluted by methanol containing pyridine, and the eluate was concentrated to a small volume. Addition of water precipitated the osazone, which was further purified by dissolution in ethyl acetate and precipitation with petroleum ether; yield 0.05 g.; yellow powder; m. p. 188–191°; $[\alpha]_D^{13}$ −13.3° (ethanol, *c* 0.30). Various values are reported: m. p. 176–179°[4], 178–194°[6] and about 200°[6]. The synthetic sample, prepared and purified exactly in the same manner as above mentioned, melted at188–191°. Mixed m.p. determination showed no depression.

*Anal.* Found: N, 15.31; $OCH_3$, 8.52. Calcd. for $C_{19}H_{24}O_4N_4$: N, 15.05; $OCH_3$, 8.38%.

*2,3-Di-O-methyl-D-galactaric Acid Bisamide.*—

3) C. Araki, This Bulletin, **29**, 543 (1956).

4) G. J. Robertson and R. A. Lamb, *J. Chem. Soc.*, **1934**, 1321.

5) D. J. Bell and G. D. Greville, ibid., **1955**, 1136.

6) F. Rebber and T. Reichstein, *Helv. Chim. Acta*, **28**, 1164 (1945).

2,3-Di-*O*-methyl-D-galactose (0.15 g.) obtained was treated by the procedure of Luckett and Smith[2], 2,3-di-*O*-methyl-D-galactaric acid bisamide was obtained as prisms; m.p. 226–228°, not depressed on admixture with a synthetic sample (m.p. 226–228°).

*Anal.* Found: C, 40.50; H, 6.90. Calcd. for $C_8H_{16}O_6N_2$: C, 40.67; H, 6.83%.

**Reduction of VI.**—A solution of VI (1.3 g.) in dry ether (20 cc.) was added dropwise to a solution of lithium aluminium hydride (0.5 g.) in dry ether (30 cc.) with stirring. After thirty minutes, an excess of water was added to the reaction mixture, which was then filtered, and the residue was washed thoroughly. Evaporation of the filtrate and washings gave a sirup, which was purified by dissolution in ether and filtration. Evaporation gave methyl 2,3-di-O-methyl-4,6-O-hydroxyisopropylidene-D-galactoside, a colorless sirup; yield 1.2 g.; $n_D^{20}$ 1.4780; $[\alpha]_D^{23}$+101.3° (water, *c* 0.78); $OCH_3$, found: 32.50% (calcd. for $C_{12}H_{22}O_7$: 33.42%).

**Methyl 2,3-Di-O-methyl-4,6-O-methoxyisopropylidene-D-galactoside and its Hydrolysis.**—The reduction product (1.1 g.) above obtained was twice methylated with methyl iodide and silver oxide in the usual manner. Methyl 2,3-di-O-methyl-4,6-O-methoxyisopropylidene-D-galactoside was obtained as a colorless sirup; yield 1.0 g.; $n_D^{20}$ 1.4681; $[\alpha]_D^{24}$+108.1° (water, *c* 0.74); $OCH_3$, found: 41.77% (calcd. for $C_{13}H_{24}O_7$: 42.42%).

The sirup (0.9 g.) above obtained was dissolved in N-sulfuric acid (20 cc.) and heated in a boiling water bath for four and a half hours, at which time the optical rotation of the solution reached a constant value ($[\alpha]_D$+107°→+66°). Methoxyacetone liberated in the hydrolysate was distilled in steam under atmospheric pressure, 60 cc. of the distillate being collected. The residual solution was used for the isolation of 2,3-di-O-methyl-D-galactose.

**(a) Methoxyacetone (IX).**—To the above distillate was added a methanolic solution of *p*-nitrophenylhydrazine, which caused an immediate precipitation of methoxyacetone *p*-nitrophenylhydrazone; golden needles; yield 0.35 g.; m.p. 112–113°, not depressed on admixture with an authentic sample (m.p. 112–113°).

**(b) 2,3-Di-O-methyl-D-galactose (XI).**—The distillation residue was neutralized, filtered and evaporated to dryness, giving 2,3-di-O-methyl-D-galactose, a colorless sirup; yield 0.55 g.; $[\alpha]_D^{24}$ +55.6° (an initial value)→+82.8° (an equilibrium value, water, *c* 0.70); $OCH_3$, found: 29.62% (calcd. for $C_8H_{16}O_6$: 29.81%). It migrated to the same position on a paper chromatogram as that of a synthetic sample. Identification was carried out by its conversion into the anilide, 3-O-methyl-D-galactosazone and 2,3-di-O-methyl-D-galactaric acid bisamide exactly in the same manner as that already described.

**4-O-2′,3′-Di-O-methyl-4′,6′-O-1″-carbomethoxyethylidene-β-D-galactopyranosyl-2,5-di-O-methyl-3,6-anhydro-L-galactose Dimethylacetal (IV).**—The methyl ester (II) (1.0 g.), prepared in the previous paper[1], was directly dissolved in methyl iodide (35 g.), and was methylated by occasional additions of silver oxide (10 g.) in the usual manner. The methylation was repeated five times. The final product, isolated by extraction with ether and evaporation, was a colorless sirup (1.0 g.), which solidified on standing for a few months. It was recrystallized by dissolving in a small amount of absolute ether, adding petroleum ether (b.p.34–45°) and keeping the solution in a refrigerator for a few weeks. Pure IV was obtained as brilliant prisms; yield 0.78 g., m. p. 78–80°; $[\alpha]_D^{20}$ −31.6° (water, *c* 1.33) and −20.9° (chloroform, *c* 1.15).

*Anal.* Found: C, 51.96; H, 7.39; $OCH_3$, 42.50%; Saponification equivalent, 508; m.w. (Rast), 510. Calcd. for $C_{22}H_{38}O_{13}$: C, 51.75; H, 7.50; $OCH_3$, 42.55%; Sapon. equiv. and m.w., 511.

**Methanolysis of IV.**—The methylated compound (IV) (2.7 g.) in 3% methanolic hydrogen chloride (30 cc.) was heated under reflux for twentyfive hours. It was neutralized with silver carbonate, filtered and concentrated to a sirup (2.7 g.), which was proved to be a mixture of V and VI. The separation was effected by saponification as described below.

**(a) Barium Salt of Methyl 2,3-Di-O-methyl-4,6-O-1′-carboxyethylidene-D-galactoside (VII).**—The above mixture (2.7 g.) was heated in a 0.3 N-barium hydroxide solution (50 cc.) at 60° for two hours. The solution was neutralized with carbon dioxide, filtered and concentrated to a sirup (3.0 g.). It was then dissolved in methanol (10 cc.) and ether (100 cc.) was added with shaking, the barium salt (VII) being precipitated as a fine powder; yield 2.1 g.; $[\alpha]_D^{19}$+48.8° (water, *c* 1.33). The filtrate was kept aside for the isolation of V.

*Anal.* Found: $OCH_3$, 25.32; Ba, 19.11. Calcd. for $(C_{12}H_{19}O_8)_2$ Ba: $OCH_3$, 25.84; Ba, 19.08%.

**Methyl Ester (VI).**—The above barium salt (2.2 g.) was converted to the methyl ester by heating in 3%methanolic hydrogen chloride (20 cc.) for five hours. The product, isolated in the usual manner, was purified by distillation in high vacuum, yielding VI as a colorless viscous liquid; yield 1.2 g.; b. p. 110–115°/0.030 mmHg; $[\alpha]_D^{21}$+67.7° (water, *c* 0.93) and +72.4° (chloroform, *c* 1.16); $n_D^{20}$ 1.4685.

*Anal.* Found: C, 50.78; H, 7.26; $OCH_3$, 40.42%; Saponification equivalent, 304. Calcd. for $C_{13}H_{22}O_8$: C, 50.97; H, 7.24; $OCH_3$, 40.48%; Sapon. equiv.; 306.

*Hydrolysis.*—The methyl ester (VI) above obtained was hydrolysed with N-sulfuric acid (30 cc.) for five hours. Pyruvic acid (X) and 2,3-di-*O*-methyl-D-galactose (XI) produced were identified in the same manner as that already described.

**(b) 2,5-Di-O-methyl-3,6-anhydro-L-galactose Dimethylacetal (V).**—The filtrate, separated from the barium salt (VII), was evaporated to dryness, V being obtained as a colorless sirup; yield 0.50 g.; $[\alpha]_D^{19}$ −6.67° (water, *c* 0.90); $n_D^{20}$ 1.4563; $OCH_3$, found: 52.15% (calcd. for $C_{10}H_{20}O_6$: 52.48%).

*2,5-Di-O-methyl-3,6-anhydro-L-galactonic Acid.*

—The above dimethylacetal (0.35 g.) was hydrolysed with 0.1N-sulfuric acid (5 cc.) in a boiling water bath for two hours, neutralized with barium carbonate, filtered and concentrated to dryness. 2,5-Di-O-methyl-3,6-anhydro-L-galactose was obtained as a slightly colored sirup; yield 0.25 g.; $[\alpha]_D^{2}$ −13.3° (water, *c* 0.75); $OCH_3$, found: 32.02% (calcd. for $C_8H_{14}O_5$: 32.60%).

The sugar (0.20 g.) obtained was oxidized by bromine water in the usual manner[7]. The product was crystallized from ethyl acetate. 2,5-Di-O-methyl-3,6-anhydro-L-galactonic acid was obtained as colorless prisms; yield 0.12 g.; m.p. 159-161°, not depressed on admixture with an authentic sample[7]; $[\alpha]_D^{21}$ −61.9° (water, *c* 0.42).

The mother liquor from the above crystals was concentrated to a sirup (0.08 g.), which was esterified by diazomethane in ether. The methyl ester obtained was converted to the amide by reaction with ammonia in the usual manner[7]; m.p. 171-172°, not depressed on admixture with an authentic sample[7]; $[\alpha]_D^{22}$ −71.7° (water, *c* 0.46).

**Partial Hydrolysis of I.**—The crystalline acid (I) (0.50 g.) in 0.05N-hydrochloric acid (10 cc.) was heated in a boiling water bath until the optical rotation of the solution reached a constant value: $[\alpha]_D$ −46.7° (initial), −30.0° (0.5 hour), −22.0° (1 hour), −18.6° (1.5 hours), −14.6° (2.0 and 2.5 hours). The solution was neutralized with silver carbonate, filtered and concentrated to a sirup. Extraction with absolute methanol separated agarobiose from insoluble silver pyruvate.

(a) **Pyruvic Acid.**—The silver pyruvate (0.20 g.) obtained was dissolved in water (2 cc.), N-hydrochloric acid (2 cc.) was added, and precipitates of silver chloride were removed by filtration. When phenylhydrazine (0.10 g.) was added to the filtrate, pyruvic acid phenylhydrazone was crystallized; yield 0.12 g.; m.p. and mixed m.p. 190-191°.

(b) **Agarobiose (VIII).**—The methanol extract, separated from silver pyruvate, gave on evaporation agarobiose as a colorless sirup, which reduced Fehling's solution at room temperature; yield 0.33 g.; $[\alpha]_D^{14}$ −13.8° (water, *c* 0.80). It was identified by conversion into its dimethylacetal.

*Agarobiose Dimethylacetal.*—The above sirup (0.30 g.) was dissolved in 0.5% methanolic hydrogen chloride (3 cc.) and heated under reflux for two hours. The solution was neutralized with silver carbonate, filtered and concentrated to a sirup (0.30 g.), which was then chromatographed on a cellulose powder column, *n*-butanol-water (6 : 1) being used as a mobile phase. Agarobiose dimethylacetal was obtained as crystals, which were further purified by recrystallization from ethanol-acetone (1 : 2); yield 0.20 g.; m.p. 163-164°, not depressed on admixture with an authentic sample[8]; $[\alpha]_D^{14}$ −29.5° (water, *c* 0.98); $OCH_3$, found; 16.39% (calcd. for $C_{14}H_{26}O_{11}$: 16.76%).

**Periodate Oxidation of I.**—The compound (I) (0.1615 g.) was dissolved in water (10 cc.), and 0.215M-solution of sodium metaperiodate (10.0 cc.) was added. The solution was immediately neutralized with sodium bicarbonate until it became slightly alkaline to a methyl redi ndicator, and then was diluted exactly to 50.0 cc. Aliquotes were withdrawn periodically for the determination of the residual oxidant in the usual manner. The sample consumed 0.63, 1.02 and 1.05 mole of the oxidant, respectively, after six, twenty-four and forty-eight hours. On standing for a longer period, up to two moles of the oxidant were consumed on account of the gradual hydrolysis of the pyruvic acid residue.

## Summary

1. The structure of the acidic compound, isolated from the partial methanolysis products of agar in the previous work, has been investigated.

2. Methylation data have indicated that the structure of the compound is 4-O-4′, 6′-O-1″-carboxyethylidene-β-D-galactopyranosyl-3,6-anhydro-L-galactose dimethylacetal, the β-linkage being suggested on the basis of the optical rotatory behavior.

3. The structure assigned is also supported by the result of partial hydrolysis and periodate oxidation of the compound.

4. No information has been obtained as to the configuration of the carbon atom $C_1$ of the ethylidene group in the molecule.

The writer wishes to express his hearty thanks to Professor S. Tanaka, Department of Science, Kyoto University, and Professor C. Araki, this University, for their great interest and discussion. Thanks are also due to Mr. K. Arai for microanalysis and to Mr. T. Ito for assistance.

*Institute of Chemistry, Faculty of Industrial Arts, Kyoto Technical University, Matsugasaki, Kyoto*

7) C. Araki, *J. Chem. Soc. Japan*, **65**, 627 (1944).

# *Studies on the Organic Reagents for the Inorganic Analysis. I. Phenylfluorone as Sensitive Reagent for Colorimetric Determination of Zirconium*

By Kenjiro KIMURA and Hirotoshi SANO

(Received September 25, 1956)

Although many reagents and procedures are available for the determination of macro amounts of zirconium, the situation is far from satisfactory with respect to the determination of microgram amounts. Alizarin (or Alizarin Reds)[1-5] is the most general reagent for the colorimetric determination of zirconium, but its reaction is not too sensitive. The procedures using *p*-dimethylaminoazophenylarsonic acid[6,7] and the method using phosphomolybdic acid[8] are both indirect. Only quercetin has been recently reported as the sensitive reagent for the colorimetric determination of zirconium[9].

The purpose of this investigation was to find a colorimetric reagent sensitive to small concentrations of zirconium. The studies on the reaction between ortho diphenol derivatives and zirconium or other metals show that the ortho diphenol derivatives, having the mesomeric group at its para position, combine with metals and cause remarkable color change, which is larger in the case of zirconium than the other metals[10]. On the other hand the phenylfluorone (abbreviation of 2,3,7-trihydroxy-9-phenylfluorone), which is one of the ortho diphenol derivatives concerned, has been recently employed as the sensitive reagent for germanium[11]. These facts lead us to the expect that this reagent might be one of the most sensitive reagents for the colorimetric determination of zirconium.

## Experimental

**Apparatus and Reagents.**—The absorbancy measurements were made with a Beckman Model DU spectrophotometer and 1 cm. glass cell. The reference cell contained distilled water for all the measurements.

The alcoholic solution of phenylfluorone (1 ml. contain 0.6 mg. of phenylfluorone) was made up in the following way: 0.6 g. phenylfluorone, which was synthesized from hydroxyhydroquinone triacetate and benzaldehyde according to Cluley's prescription[11], was dissolved into 800 ml. of ethyl alcohol and 5 ml. of 0.1N hydrochloric acid and was diluted to 1 l. with ethyl alcohol.

Zirconyl chloride stock solution was prepared from reagent grade zirconium dioxide contained less than 0.2 per cent hafnium dioxide by spectrographic tests, and standardized gravimetrically using distilled ammonium hydroxide. The working zirconium chloride solution was prepared by dilution from the stock solution every time of experiment.

*Distilled hydrochloric acid* was used for all work.

*Ethyl alcohol*: Reagent grade 100 percent ethyl-alcohol.

*Cyclohexanol*: Reagent grade.

**Fundamental Reaction.**—The treatment of slightly acidic solution of zirconyl ions with an excess of a standard phenylfluorone solution results in the color change from yellow to red, and then the precipitation after being allowed to stand. This precipitation has the composition of four phenylfluorone to a zirconium atom quantitiatively. This shows, therefore, also the possibility of micro gravimetric analysis of zirconium. Various organic solvents, such as benzene, toluene, cyclohexanol, ethyl ether, isopropyl ether, acetone, ethyl isopropyl ketone, dioxane, methyl alcohol, ethyl alcohol, isopropyl alcohol, *n*-butyl alcohol, isobutyl alcohol, *n*-amyl alcohol, acetic acid, acetic anhydride, ethyl acetate, carbon tetrachloride, chloroform, petroleum ether, quinoline, carbon disulfide, etc., were tried to dissolve the red colored complex, but it was difficult. Then, it was alternatively tried to keep the complex in the colloidal solution with the addition of a suitable stabilizer. Among gum arabic, gelatin, soluble starch, cylohexanol, etc., tested, cyclohexanol was found as the most favorable stabilizer. In the experiments all the

1) H. A. Liebhafsky and E. H. Winslow, *J. Am. Chem. Soc.*, **60**, 1776 (1938).
2) J. F. Flagg, H. A. Liebhafsky and E. H. Winslow, ibid., **71**, 3630 (1949).
3) D. E. Green, *Anal. Chem.*, **20**, 370 (1948).
4) G. B. Wengert, ibid., **24**, 1449 (1952).
5) A. Mayer and G. Bradshaw, *Analyst*, **77**, 476 (1952).
6) V. A. Nazarenko, *Zhur, Priklad, Khim*, **10**, 1666 (1937).
7) W. G. Hayes and E. W. Jones, *Ind. Eng. Chem., Anal. Ed.*, **13**, 603 (1941).
8) E. W. Kiefer and D. F. Boltz, *Anal. Chem.*, **24**, 542 (1952).
9) F. S. Grimaldi and C. E. White, ibid., **25**, 1886 (1953).
10) F. Ihmura, H. Sano and M. Asada, Symposium on complex Chemistry, Osaka City Univ., Nov. 1955 : To be published shortly.
11) H. J. Clueley, *Analyst*, **76**, 523 (1951).

solutions were made to a total volume of 50 ml. The order of addition of the reagents was always the same. The zirconium solution was added first; and acid, alcohol, cyclohexanol, and alcoholic solution of phenylfluorone were added in this order.

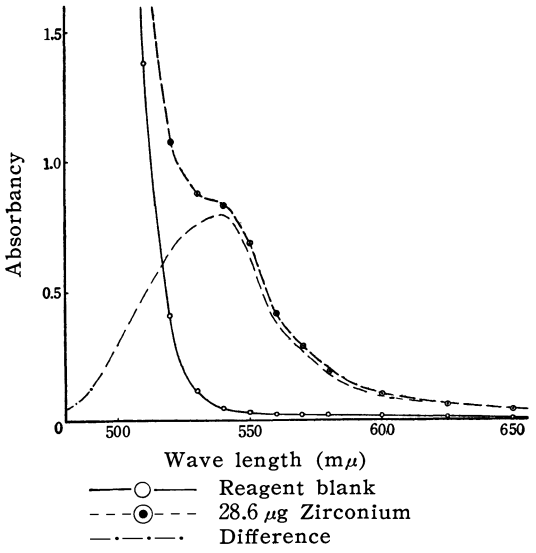



Fig. 1. Absorption spectra.

Spectral absorbancy data for the reagent blank and 28.6 μg. of zirconium (following the standard procedure mentioned later) are given in Fig. 1. The optimum wave length was taken as 530-550 mμ because at this range the absorption given by the blank is small and that by zirconium sufficiently large.

**Effect of Alcohol and Cylohexanol Concentration.**—A precipitate of zirconium phenylfluoronate is obtained after a while from solutions containing no cyclohexanol and less than 10ml. of alcohol. Although the colored solution becomes stable with increase in the amount of cyclohexanol added, cyclohexanol layer separates from alcoholic.water layer in above a certain amount of cyclohexanol to the amount of alcohol added. The solution shows no differece in its absorbancy with the variation of the amount of alcohol or cyclohexanol added. From these results 5 ml. of cyclohexanol, 10 ml. alcohol and 10ml. alcoholic solution of phenylfluorone was taken as optimum.

**Effect of Acidity and Digestion Time.**— The effect of acid concentration and digestion time on the absorbancy given by 17.2 μg. of zirconium and 3 mg. phenylfluorone is illustrated in Table I. A precipitate of zirconium phenylfluoronate is obtained after it is allowed to stand for a day, but the stable suspension is able to regenerate with short shaking by hand. The absorbancy given by this procedure was shown as the data after a day. The absorbancy in 0.05 N hydrochloric acid solution is nearly constant but that in 0.10 N hydrochloric acid solution increases slowly by time. These data show that the increase of acidity causes the decrease of its absorbancy and that it means the decrease of the velocity to reach its equilibrium.

From these results it would be expected that the increase of the amount of phenylfluorone is available for obtaining the stable absorbancy in higher acidity, because the reaction should be the competition of hydrogen ion concentration with reagent concentration. The data given by 17.2 μg. of zirconium and 6 mg. of phenylfluorone are shown in Table I, too.

The stability in this condition is more favorable particularly in 0.10N HCl, than the case of 3 mg. reagent. The reagent blank shows no variation in absorbancy at 540 mμ or more, for increasing its acidity, though the decrease in absorbancy occurs at below 530 mμ.

The stability of absorbancy for the time in the acid concentrations above 0.15 N is not so suitable as below 0.10 N for the practical procedure, probably because of its slow velocity to reach the equilibrium.

**Standard Procedure.**—The following was recommended as the optimum procedure from the results above mentined.

Transfer the sample solution (less than 20ml.) to a 50 ml. volumetric flask. If the sample is known to contain more than 40 to 50 μg. zirconium, an aliquot portion of the sample solution containing the desired amount of zirconium in a final volume is pipetted into a 50 ml. volumetric flask. Additional acid will then be required to bring the acidity up to 0.10 N hydrochloric acid used in the determination of zirconium with phenylfluorone. Adjust the volume to about 20 ml. with distilled water. Add 10 ml. of alcohol, 5 ml. of cyclohexanol, and 10 ml. of alcoholic solution containing 6 mg. of phenylfluorone in this order using pipettes. Make the solution to the mark, mix with shaking by hand, allow to stand for about two hours, and obtain the absorbancy of the solution in the spectrophotometer

TABLE I

ABSORBANCY IN DIGESTION TIME (min.)

| Amount of Phenylfluorone | 30 | 50 | 75 | 90 | 120 | 180 | 240 | 1500 | Concn. of HCl |
|---|---|---|---|---|---|---|---|---|---|
| 3 mg. | 0.410 | 0.450 | 0.448 | 0.448 | 0.447 | 0.445 | 0.444 | 0.443 | 0.05N |
| | 0.226 | 0.260 | 0.295 | 0.317 | 0.349 | 0.389 | 0.418 | 0.432 | 0.10N |
| | 0.507 | 0.520 | 0.528 | 0.535 | 0.542 | 0.557 | 0.565 | 0.574 | 0.05N |
| 6 mg. | 0.442 | 0.470 | 0.486 | 0.496 | 0.510 | 0.523 | 0.530 | 0.540 | 0.10N |
| | 0.359 | 0.400 | 0.430 | 0.445 | 0.463 | 0.492 | 0.501 | 0.518 | 0.15N |

at 540 mμ using a 1 cm. glass cells and distilled water as a control solution. Determine the amount of zirconium by reference to a standard working curve.

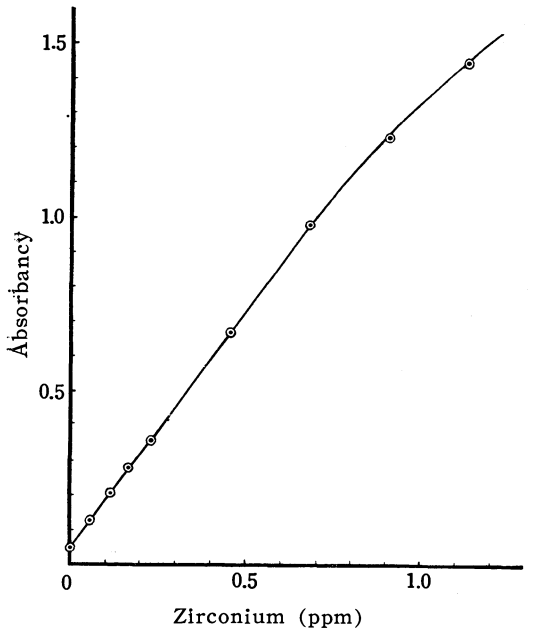



Fig. 2. Working curve

**Working Curve.**—Data for the working curve are given in Fig. 2. These data were obtained following the standard procedure. The solution was 0.10 N in hydrochloric acid and contained 10 ml. of alcohol, 5 ml. of cyclohexanol, and 10 ml. alcoholic solution of phenylfluorone in a total volume of 50 ml. The absorbancy was measured after allowing it to stand for about two hours. A straight line relationship between absorbancy and micrograms of zirconium is shown up to 0.7 p. p. m. Solutions containing from 0.7 to 1.0 p. p. m. deviate from the Beer's law but their absorbancies are reproducible.

The sensitivity of this method, given by the inclination of the working curve, is about forty or fifty times for Alizaline Red S method, and several times for quercetin method reported as the sensitive method for the determination of zirconium.

**Effect of Diverse Ions.**—The effect of various ions was studied using 0.3 p. p. m. of zirconium. The standard procedure was employed, with the exception that the desired amount of the diverse ion was added prior to the zirconium solution. In present of iron (III) or titanium (IV) a precipitation occurs, so the solution was allowed to stand for about two hours in a cell and the absorbancy was measured after they precipitated. The concentration of zirconium and diverse ion are expressed on the basis of the final volume 50 ml. The change in absorbancy was then measured at 540 mμ. Errors of less than 2 per cent of the zirconium present were considered negligible. A negligible error was obtained with the following maximum about:

2000 p. p. m. of: sodium, potassium, ammonium, magnesium, calcium, barium, strontium, zinc, cadmium, mercurous and mercuric.

500 p. p. m. of: lanthanum, neodymium, cerrous, silver and lead.

100 p. p. m. of: aluminium, thorium and uranyl. Chloride, bromide, nitrate, acetate (2000 p. p. m.) and sulfate (1000 p. p. m.) ions do not interfere.

Some elements interfere by decreasing the color intensity given by zirconium. Some elements produce colors with phenylfluorone. Table II lists the interfering ions and their effect.

TABLE II

INTERFERING DIVERS IONS

| Ion | Amount added p. p. m. | Error, % | Permissible Amount, p. p. m. |
|---|---|---|---|
| $Fe^{3+}$ | 1.5 | 10 | 0.3 |
| $Ti^{4+}$ | 0.5 | 20 | 0.05 |
| $Ge^{4+}$ | 0.1 | 10 | 0.02 |
| $Sn^{4+}$ | 0.1 | 10 | 0.02 |
| $As^{3+}$ | 10 | 2 | 10 |
| $Sb^{3+}$ | 1 | 5 | 0.4 |
| $F^-$ | 2 | 25 | 0.1 |
| $C_2O_4^{2-}$ | 55 | 20 | 0.5 |
| $HPO_4^{2-}$ | 5 | 10 | 1 |

Serious interference is given by the following ions: oxalate, fluoride, phosphate, titanium, germanium, tin, iron (III) and antimony tested.

Some additional observations are to be noted. Phenylfluorone is useful as a colorimetric reagent for fluorine (by quenching of the zirconium phenylfluoronate color)[12] and may prove effective for tin (IV) or hafnium. These color reactions are being investigated.

## Summary and Discussion

Methods reported in the literature for the determination of zirconium are generally designed for relatively large amounts of this element, in spite of the fact that a procedure using colorimetric reagent for the determination of trace amounts is desirable. The systematic studies on the organic reagents for the spectrophotometric determination of several metals led us the phenylfluorone as one of the most sensitive reagents for the colorimetric determination of zirconium. The phenylflurone method recommended here, which is carried out in 0.1 N hydrochloric acid solution, shows the about forty or fifty times sensitivity of Alizarine Red S method and the several times of Quercetin method reported later as a sensitive reagent for zirconium. The solution becomes stable enough to carry on the colorimetric determination by adding some cyclohexanol and

12) H. Sano, *Japan Analyst*, **5**, 289 (1956).

ethyl alcohol, although it is not true solution but colloidal.

On the other hand the investigation to find a phenylfluorone derivative to make a soluble complex with metals has succeeded recently[13]. The new reagent, 2,3,7-trihydroxyl-9-(4-dimethylaminophenyl)-fluorone, synthesized by the authors and Miss M. Asada give a soluble colored complex with germanium and make colorimetric procedure very convenient. This new reagent also forms a soluble intense colored complex with zirconium. This detailed investigation will be published before long.

The authors are indebted to Dr. Nobufusa Saito, Assistant Professor in this laboratory, for his encouragement to carry on this study.

*Department of Chemistry*
*Faculty of Science*
*The University of Tokyo*
*Tokyo*

13) K. Kimura, H. Sano, and M. Asada, *Bull. Chem. Soc. Japan*, **29**, 640 (1956).

# *Mikroanalyse mit Hilfe von Ionenaustauschharzen. IX. Über den Nachweis geringer Menge des Wismutes mit Thioharnstoffe*[1]

Von Masatoshi FUJIMOTO

(Eingegangen am 25. Juni, 1956)

## Einleitung

Es ist wohl bekannt, dass eine intensiv orange bzw. orangegelbe Färbung, die der Thioharnstoff mit wässeriger Lösung der Wismutsalze gibt, wegen ihrer bemerkenswerten Empfindlichkeit für den Nachweis[2] oder die Bestimmung geringer Menge des Wismutes und für die komplexometrische Titration des Wismutes häufig angewandt worden ist.

Kürzlich hat der Verfasser gefunden, dass die genannte sich färbende Verbindung in die Kationenaustauschharzphase stark adsorbiert wird und infolgedessen auf diese Phase eine gelbe bzw. orange Färbung, welche ausserordentlich stärker als die der Aussenlösung ist, liefert.

Im folgenden werden die Ergebnisse verschiedenartiger Versuche, die, um die Optimalbedingungen von einer neuen Nachweismethode für Wismut festzustellen, durchgeführt wurden, eingehend beschrieben.

## Die in der vorliegenden Untersuchung benutzten Kationenaustauschharze

Es wurden die beinahe farblosen sowie starksauren Kationenaustauschharze[3], „1proz. DVB," „2.5proz. DVB," Dowex 50 W-X8 und -X12 angewandt und zwar alle diese als NaR- oder HR- Form.

## Versuchsanordnung

Auf eine weisse Tüpfelplatte bringt man einige Körnchen der starksauren sowie farblosen Kationenaustauschharze und einen Tropfen der Probelösung, rührt sie mit einem Glasstäbchen völlig um, und lässt sie zehn Minuten lang stehen. Dann fügt man dazu einen Tropfen der wässerigen Lösung des Thioharnstoffes, und nach einigen Minuten beobachtet man mit einer Lupe eine orange bzw. orangegelbe Färbung, die in der Harzphase entsteht.

## Bestimmung der Experimentalbedingungen höchster Empfindlichkeit[4]

**(1) Massflüssigkeit.**—Man stellte eine Stammlösung der Massflüssigkeiten des Wismutes her, indem man das Wismutnitrat in die verdünnte Salpetersäure eintrug. 1 ccm dieser Lösung enthielt genau 100.0 mg von Wismut[5].

**(2) Einfluss des Vernetzungsgrades von starksauren Harzen.**—Zu diesem Zwecke wurden die obigen vier Arten der starksauren Kationenaustauschharze von verschiedenem Vernetzungs-

1) Die achte Mitteilung: M. Fujimoto, Dieses Bulletin **29**, 833 (1956).

2) Z. B., vgl. I. Mellan, „Organic Reagents in Inorganic Analysis," 1. Aufl., Philadelphia (1941), S. 278.

3) M. Fujimoto, Dieses Bulletin, **29**, 600 (1956).

4) In bezug auf die halbquantitative Darstellungsweise der scheinbaren Durchschnittsintensität der Färbung der Harzphase, vergleiche die dritte Mitteilung: M. Fujimoto, Dieses Bulletin, **29**, 567 (1956).

5) Der Wismutgehalt von der genannten Massflüssigkeit wurde durch komplexometrische Titration mit 0.01 M Massflüssigkeit des Äthylendiamintetraessigsauren Natriums und 0.1prozentiger wässeriger Lösung des Brenzkatechinsulfophthaleins als Metallindikator genau bestimmt.

grade, d. h., die Harze, in denen 1-, 2.5-, 8- und 12-prozentiges Divinylbenzol enthalten sind, angewandt. Die Resultate der mit gesättigter wässeriger Lösung des Thioharnstoffes durchgeführten Untersuchung stehen gesamt in Abb. 1.

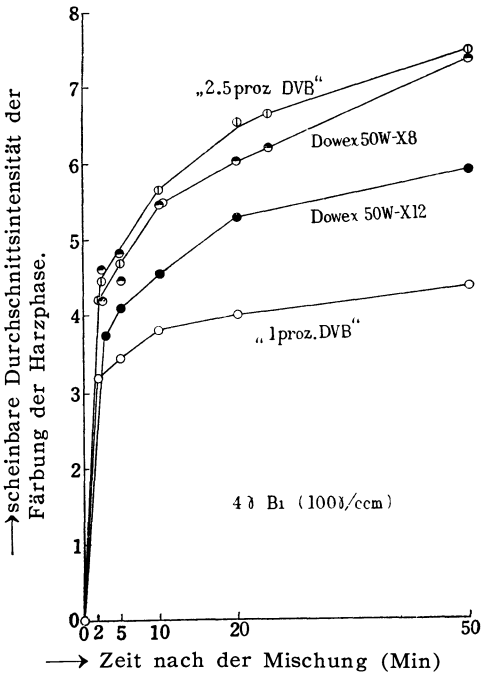



Abb. 1. Einfluss der Differenz des Vernetzungsgrades von den benutzten Harzproben (HR-Form).

Wie in dieser Abbildung zu ersehen ist, nimmt die scheinbare Intensität der Färbung von der Harzphase nach folgender Reihenfolge ab:

„2.5 proz. DVB" > Dowex 50 W-X8 > Dowex 50 W-X12 > „1 proz. DVB."

Daher wurde im folgenden lediglich „2.5proz. DVB" zur Gegenüberstellung der Experimentalbedingungen angewandt.

**(3) Einfluss der anfänglich benutzten Form von „2.5 proz. DVB."**—Die Gegenüberstellung von Abb. 2 stellt den Einfluss der HR- oder NaR-Form des Harzes, „2.5 proz. DVB," auf die scheinbare Intensität der Färbung von der Harzphase dar. Hier wurde auch die gesättigte Lösung des Thioharnstoffes angewandt. In Betracht des Verlaufes beider Kurven scheint es, dass das Harz von HR-Form dem von NaR-Form etwas überlegen ist.

**(4) Einfluss der Zeitdauer des Eintauchens der Harzkörnchen in die Probelösung.**—Abb. 3 stellt den Einfluss der Differenz von der Zeitdauer, in der die Harzkörnchen in die Probelösung eingetaucht waren, auf die Färbungsintensität der Harzphase dar; nämlich, bei der Kurve „A" wurden die Harzkörnchen zehn Minuten lang, vor dem Zusatze von Reagenslösung, in die Probelösung eingetaucht, und bei „B" wurde die Reagenslösung sofort nach dem Eintauchen der Harzkörnchen in die Probelösung hinzugefügt. Wie klar zu ersehen ist, ist es sehr wirksam, Harzkörnchen eine Weile in der Probelösung stehen zu lassen. Dies führt darauf zurück, dass die Menge des in die Harzphase adsorbierten Wismutes während etwa zehn Minuten, wegen seiner hohen Austauschaffinität

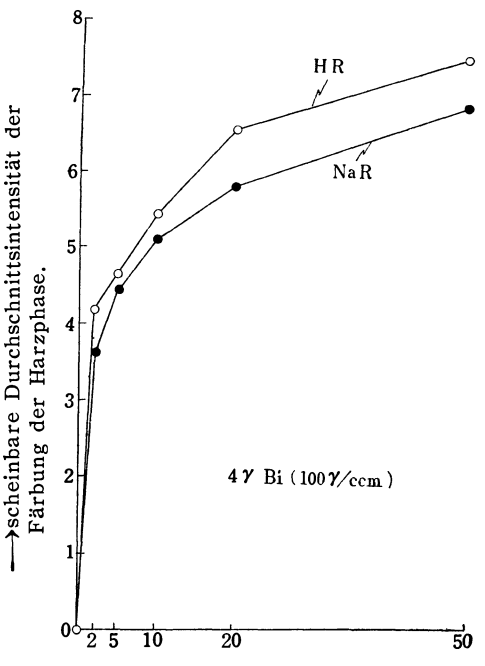



Abb. 2. Einfluss der Differenz von der Form des Harzes, „2.5 proz. DVB", auf die scheinbare Färbungsintensität.

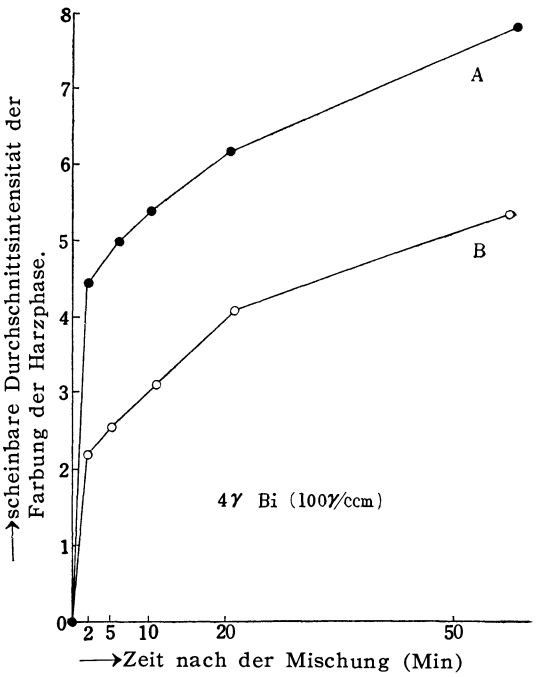



Abb. 3. Einfluss der Differenz von der Zeitdauer, in der man die Harzkörnchen in der Probelösung stehen lasst.

sowie seiner etwas kleineren Austauschgeschwindigkeit, merklich zunimmt.

**(5) Einfluss der Konzentration der Reagenslösung.**—Um die genannte Orangefärbung vollkommen zu entwickeln, sei es notwendig, hohe Konzentration an der Thioharnstofflösung anzuwenden, wie es in der genannten Literatur Mellans darauf hingewiesen wird, dass es bei der Anwendung betreffender Reaktion zur gewöhnlichen Tüpfelmethode empfehlenswert sei, einige Kristallchen des Thioharnstoffes hinzuzufügen[2]. Abb. 4 stellt die Abhängigkeit der

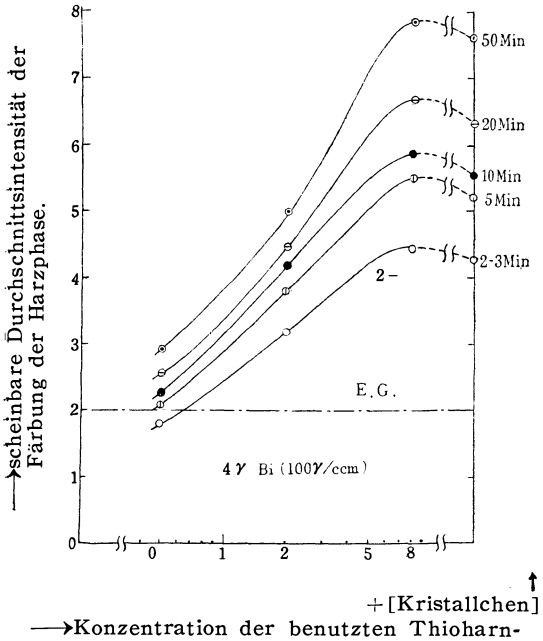



Abb. 4. Beziehung der Konzentration der benutzten Thioharnstofflösung auf die scheinbare Intensität der Färbung der Harzphase.

scheinbaren Intensität der an der Harzphase entstandenen Färbung von der Konzentration der hinzugefügten Thioharnstofflösung dar. Wie aus dem Verlauf dieser Kurvengruppe zu ersehen ist, hat die Intensität der auf die Harzphase gelieferten Färbung beim Zusatze von etwa achtprozentiger Lösung des Thioharnstoffes, d.h., von gesättigter Reagenslösung, einen Optimalwert. Zusatz von überschüssigen Kristallchen des Thioharnstoffes wirkt vielmehr nachteilig auf die Farbenentwicklung an der Harzphase ein. Über diese Tatsache könnte man aus blosser Rücksicht des später diskutierten Einflusses von der Neutralsalzkonzentration etwas erwarten.

**(6) Einfluss der Salzkonzentration.**—Abb. 5 stellt den Einfluss der Neutralsalzkonzentration an der Probelösung auf die scheinbare Intensität der Färbung der Harzphase dar. Ammoniumnitrat wurde dabei als ein Vertreter solcher

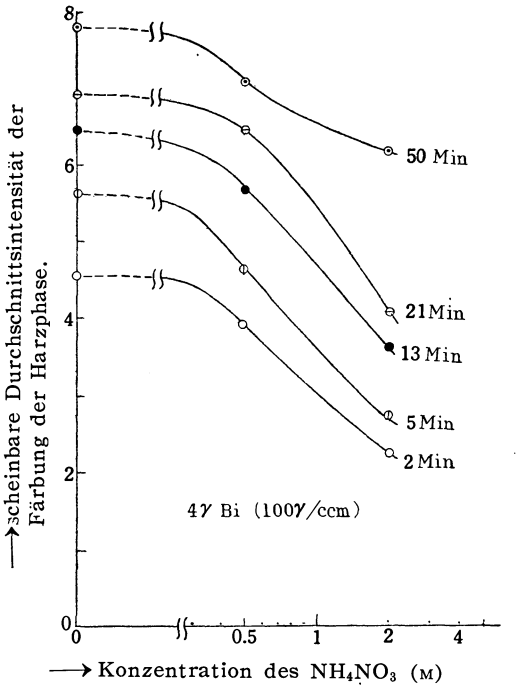



Abb. 5. Einfluss von der Neutralsalzkonzentration an der Probelösung auf die scheinbare Intensität der Färbung der Harzphase.

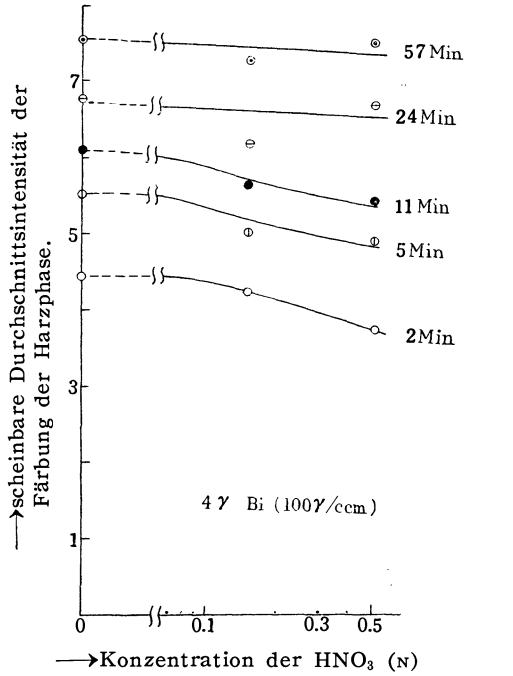



Abb. 6. Einfluss von der Säurekonzentration an der Probelösung auf die scheinbare Intensität der Färbung der Harzphase.

Neutralsalze ausgewählt. Diese Kurven zeigen, dass die in der Probelösung vorhandenen Neutralsalze bis zu etwa 0.5 M an ihrer Konzentration kaum die Färbung der Harzphase schwächen.

(7) **Einfluss der Säurekonzentration.**—Wie Abb. 5 und 6 zeigen, übt die Anwesenheit der Salpetersäure, deren Konzentration niedriger als 0.5 N liegt, auf die Färbungsintensitat der Harzphase keinen Einfluss mehr als die der letzterwähnten Neutralsalzkonzentration aus.

(8) **Experimentalbedingungen höchster Empfindlichkeit.** — Aus Rücksicht aller obenerwähnten Fa ktoren wurde das folgende Verfahren als das empfindlichste ausgewählt:

„Man bringt auf eine weisse Tüpfelplatte einige Körnchen starksauren Kationenaustauschharzes, dessen Divinylbenzolgehalt etwa 2.5 prozentig ist, einen Tropfen der Probelösung, fur welche man vorher die Neutralsalzkonzentration niedriger als 0.5 N reguliert, rührt dieses Gemisch mit einem Glasstäbchen völlig um und lässt es länger als zehn Minuten stehen. Dann fugt man einen Tropfen gesättigter wässeriger Lösung des Thioharnstoffes dazu, und nach etwa zehn Minuten beobachtet man eine in der Harzphase entstandene Orange- bzw. Gelborangefärbung gewöhnlicherweise mit einer Lupe von zwanzigfacher Vergrösserung."

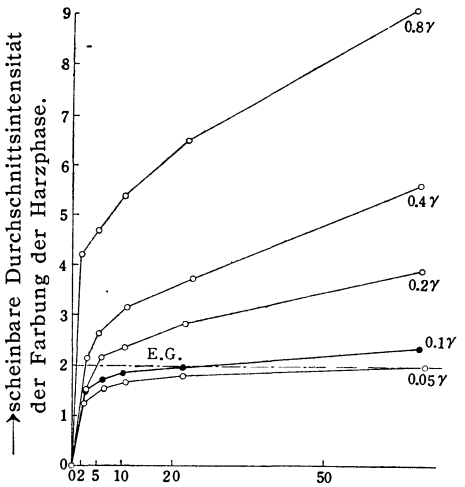



Abb. 7. Bestimmung der Erfassungsgrenze.

TABELLE I

EINFLÜSSE DER BEGLEITSTOFFE

| Begleitstoffe | benutzter Verbindungstypus | Farbung der Harzphase* | Menge der Begleitstoffe | nachweisbare Wismutmenge | Grenzverhaltnis | Bemerkungen** |
|---|---|---|---|---|---|---|
| Ti(IV) | $TiOSO_4$ | farblos | 110 γ | 0.1 γ | $1:1.1\times10^3$ | — |
| V(V) | $NH_4VO_3$ | himmelblau | 40 γ | 0.4 γ | $1:1\times10^2$ | *a*, V≦0.2 proz. |
| Cr(III) | $KCr(SO_4)_2$ | dunkelgrau-violettblau | 400 γ | 0.4 γ | $1:1\times10^3$ | *a* |
| Mn(II) | $MnSO_4$ | farblos | 1600 γ | 0.1 γ | $1:1.6\times10^4$ | — |
| Fe(III) | $Fe(NO_3)_3$ | hellviolett | 200 γ | 0.1 γ | $1:2\times10^3$ | — |
| Fe(II) | Mohrsches Salz | farblos | 510 γ | 0.1 γ | $1:5.1\times10^3$ | — |
| Co(II) | $CoSO_4$ | hellblau | 320 γ | 0.16 γ | $1:2\times10^3$ | *a* |
| Ni(II) | $Ni(NO_3)_2$ | hellblaugrün | 360 γ | 0.1 γ | $1:3.6\times10^3$ | *a* |
| Cu(II) | $CuSO_4$ | himmelblau | 160 γ | 0.16 γ | $1:1\times10^3$ | *a*, Cu≦0.4 proz. |
| Zn(II) | $ZnSO_4$ | farblos | 360 γ | 0.1 γ | $1:3.6\times10^3$ | — |
| Cd(II) | $CdSO_4$ | farblos | 1800 γ | 0.1 γ | $1:1.8\times10^4$ | — |
| Hg(II) | $Hg(NO_3)_2$ | dunkelgelb bzw. schwarz | 115 γ | 0.34 γ | $1:3.4\times10^2$ | Hg≦0.3 proz. |
| Cr(VI) | $K_2Cr_2O_7$ | grasgrün | 20 γ | 0.4 γ | $1:5\times10$ | Cr(VI)≦0.1 proz. |
| Mo(VI) | $(NH_4)_2MoO_4$ | farblos | 410 γ | 0.1 γ | $1:4.1\times10^3$ | — |
| W(VI) | $Na_2WO_4$ | farblos | 450 γ | 0.4 γ | $1:1.1\times10^3$ | — |
| U(VI) | $UO_2(CH_3COO)_2$ | sehr hell gelb | 36 γ | 0.1 γ | $1:3.6\times10^2$ | *a*, U≦0.1 proz. |
| Pb(II) | $Pb(NO_3)_2$ | blassgelb | 2200 γ | 0.1 γ | $1:2.2\times10^4$ | *a* |
| Ge(IV) | $GeO_2$ | farblos | 26 γ | 0.1 γ | $1:2.6\times10^2$ | — |
| Al(III) | $Al(NO_3)_3$ | sehr hell gelb | 1600 γ | 0.16 γ | $1:1\times10^4$ | — |
| Ag(I) | $AgNO_3$ | farblos | 180 γ | 0.1 γ | $1:1.8\times10^3$ | — |
| $F^-$ | KF | farblos | 660 γ | 0.16 γ | $1:4.1\times10^3$ | — |
| $HPO_4^{2-}$ | $Na_2HPO_4$ | farblos | 190 γ | 0.4 γ | $1:4.8\times10^2$ | — |
| $NO_2^-$ | $NaNO_2$ | farblos | 350 γ | 0.1 γ | $1:3.5\times10^3$ | — |

* Dies bedeutet die Färbung der Harzphase in dem Falle, wo nur der Begleitstoffe in der Versuchslösung vorhanden ist.

** *a*: Nur dann ist das gegebene Grenzverhältnis nutzbar, wenn der Nachweis mit einem Blindversuche miteinander ausgeführt wird.

### Bestimmung der Erfassungsgrenze

Die Resultate der für verschiedene Wismutmengen durch das obigerweise bestimmte beste Verfahren durchgeführten Untersuchung werden in Abb. 7 zusammengestellt, woraus man als Erfassungsgrenze für Wismut 0.1 $\gamma$ einfach bestimmen kann. Die Grenzkonzentration des in der Probelösung vorhandenen Wismutes beträgt $1 : 4 \times 10^5$.

### Einflüsse der Begleitstoffe

Die Resultate dafür stehen gesamt in Tabelle I.

Wie aus der genannten Tabelle zu ersehen ist, übt die grössere Menge von allen fremden Stoffen ausser Vanadate, Chromate und Uranylsalze kaum einen Einfluss auf die Nachweisreaktion aus, d. h., die vorliegende Nachweismethode ist von hoher Selektivitat.

## Zusammenfassung

1. Die Anwendung der niedriger vernetzten, farblosen und starksauren Kationenaustauschharze zur Farbenreaktion zwischen Wismutsalzen und Thioharnstoffen ist für den Nachweis des Wismutes entschieden wirksam und dadurch kann man geringe Menge des Wismutes sehr scharf und auch spezifisch nachweisen.

2. Das beste Verfahren wird durch ausführlichste Untersuchung über verschiedenartige Experimentalbedingungen vollkommen bestimmt (vgl. den Abschnitt „Bestimmung der Experimentalbedingungen"), und die Einflüsse von zahlreichen Begleitstoffen werden genau untersucht.

Zum Schluss möchte der Verfasser Herrn Prof. Dr. E. Minami für seine zahlreichen wertvollen Ratschläge bei der vorliegenden Untersuchung seinen herzlichsten Dank aussprechen.

Für die Harzproben, „1 proz. DVB" und „2.5 proz. DVB", ist der Verfasser Herrn Prof. Dr. A. Kawamura an der Landwirtschaftlichen und Technischen Universität zu Tokyo zu grossem Dank verpflichtet.

Die hier benutzte komplexometrische Titration für die Wismutmassflüssigkeit wurde von Herrn K. Mizumachi freundlich angeleitet, wofür der Verfasser ihm seinen verbindlichsten Dank sagt.

*Laboratorium der analytischen Chemie,*
*Chemisches Institut der*
*wissenschaftlichen Fakultät,*
*Tokyo Universität, Tokyo*

# *Mikroanalyse mit Hilfe von Ionenaustauschharzen. X. Über den Nachweis geringer Menge des Kupfers mit p-Phenylendiamin und Ammoniumrhodanid*[1]

Von Masatoshi FUJIMOTO

(Eingegangen am 28. Juni, 1956)

## Einleitung

Wenn eine ammoniakalische Lösung der Kupfersalze mit *p*-Phenylendiamin und Kalium- oder Ammoniumrhodanid reagiert, so fällt ein schwarzer Niederschlag, sogenanntes „Kupferrhodanid-*p*-phenylendiamin," aus. Dieser Niederschlag ist zum Nachweis geringer Menge des Kupfers anwendbar, obgleich dessen Zusammensetzung gegenwärtig nicht genau bekannt ist[2]. Bei der vorliegenden Arbeit wurden die farblosen sowie starksauren Kationenaustauschharze zur genannten Niederschlagbildungsreaktion angewandt, und eine empfindliche sowie spezifische Nachweismethode für Kupfer wurde neu festgestellt[3].

### Die in der vorliegenden Untersuchung benutzten Ionenaustauschharze

Zum gegenwärtigen Zwecke wurden hauptsächlich beinahe farblose sowie starksaure Kationenaustauschharze[4] von verschiedenem Vernetzungsgrad, „1proz. DVB," „2.5proz. DVB," Dowex 50W-X8 und „20proz. DVB,"

1) Die neunte Mitteilung: M. Fujimoto, Dieses Bulletin **30**, 83 (1957).

2) Es ist empirisch schon bekannt, dass der genannte schwarze Niederschlag 25.08prozentiges Kupfer enthält: vgl. I. Mellan, „Organic Reagents in Inorganic Analysis" 1. Aufl., Philadelphia (1941), S. 356.

3) Hinsichtlich der mikroanalytischen Anwendbarkeit der Ionenaustauschharze zur Niederschlagbildungsreaktionen, vergleiche M. Fujimoto, Dieses Bulletin **29**, 646 (1956).

angewandt. Überdies wurde ein käufliches aus Methacrylsäure und Divinylbenzol dargestelltes schwachsaures und weisses Harz von Carbonsäuretypus angewandt.

Alle diese wurden vor dem Gebrauch in gewöhnlicher Weise durch zweimaliges Durchlaufen der 2N Salzäure sowie des „entionisierten Wassers“[5] in die HR-Form völlig übergeführt.

### Versuchsanordnung

Zuerst bringt man auf eine weisse Tüpfelplatte einige Körnchen des farblosen, starksauren Kationenaustauschharzes von HR-Form und einen Tropfen verdünnter wässeriger Lösung des *p*-Phenylendiamins, rührt sie mit einem Glasstäbchen völlig um und lässt sie etwa fünf Minuten stehen. Dann fügt man nacheinander je einen Tropfen der Probelösung, verdünnten Ammoniakwassers und verdünnter wässeriger Lösung des Ammoniumrhodanids dazu. Nach etwa zehn Minuten beobachtet man mit einer Lupe eine Dunkelviolettbraun- bzw. Violettgraufärbung, die in der Harzphase entsteht.

### Massflüssigkeit und Reagenzien

**(1) Massflüssigkeit.**—Man stellte eine Stammlösung der Massflüssigkeiten des Kupfers her, indem man umkristallisiertes Kupfersulfat in 0.1N Schwefelsäure eintrug. 1 ccm dieser Stammlösung enthielt genau 1.000 mg von Kupfer[6].

### (2) Reagenzien

**(1) Entionisiertes Wasser.**—Um die Verunreinigung der Spurmenge des Kupfers, welches in dem mit einem Messingapparat destillierten Wasser häufig enthalten ist, gründlich zu beseitigen, wurde bei dieser Arbeit ausserordentlich reines Wasser, das aus gewöhnlichem destilliertem Wasser durch eine Mischharzsäule (Durchmesser von 4.5 cm und Länge von 5 cm), welche aus Äquivalentmenge des Kationenaustauschharz von HR-Form sowie des Anionenaustauschharz von ROH-Form besteht, d. h., sogenanntes „Monobed,“ dargestellt wurde, folgerichtig angewandt[7]. Nunmehr wird dieses Wasser kurz als „entionisiertes Wasser“ bezeichnet.

**(2) Einprozentige Lösung des *p*-Phenylendiamins.**—Als Stammlösung des *p*-Phenylendiamins wurde 1prozentige wässerige Reagenslösung hergestellt. Diese Stammlösung wird, wenn es nötig ist, mit entionisiertem Wasser beliebig verdünnt. Da die wässerige Lösung des *p*-Phenylendiamins nicht länger als ein paar Tage vorhält, ist es wünschenswert, dass man diese gerade vor dem Gebrauch frisch herstellt.

**(3) Zwanzigprozentige wässerige Lösung des Ammoniumrhodanids.**—Aus extrareinem Ammoniumrhodanid und entionisiertem Wasser wurde diese Stammlösung hergestellt.

**(4) Ammoniakwasser.**—Käufliches extrareines Ammoniakwasser wurde vorbereitet.

### Bestimmung der Bedingungen höchster Emfindlichkeit[8]

**(1) Vergleichung verschiedenartiger Verfahren.**—Abb. 1 zeigt den Färbungsverlauf der Harzphase an, worin die Resultate der durch verschiedenartige Verfahren durchgeführten Untersuchungen gegenübergestellt werden. In diesem Falle wurde lediglich „1proz. DVB“ von HR-Form und 6N Ammoniakwasser benutzt. Wie aus dieser Vergleichung zu erwarten ist, wurde hiernach das Verfahren „$I_c$“ als das beste Verfahren verwandt.

**(2) Einfluss der Konzentration benutzter**

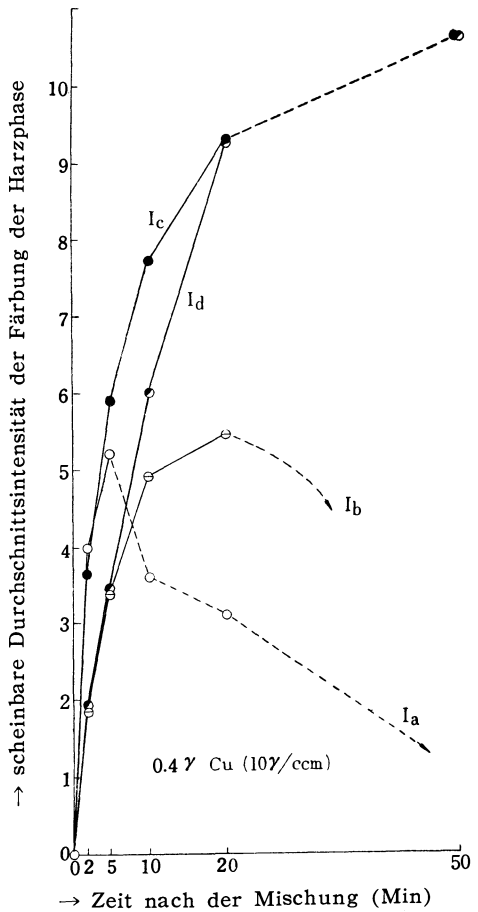



Abb. 1. Vergleichung verschiedener Verfahren

4) In bezug auf die abgekürzte Schreibweise wie „1proz. DVB“ usw., vergleiche die sechste Mitteilung: M. Fujimoto, Dieses Bulletin, **29**, 600 (1956).

5) Dieses „entionisierte Wasser“ wurde von Herrn Y. Sateau in solcher weise, wie in den Abschnitt „Massflüssigkeit und Reagenzien“ genau erwähnt, dargestellt.

6) Die Menge des in der obengenannten Stammlösung vorhandenen Kupfers wurde aus der Menge des anfänglich benutzten umkristallisierten Kupfersulfates, $CuSO_4 \cdot 5H_2O$, rückgängig berechnet.

7) Herr Y. Sateau hat kürzlich die Reinheit dieses Wassers mit Dithizon geprüft und er hat es bewiesen, dass das betreffende Wasser überhaupt kein Kupfer enthielt.

8) In bezug auf die halbquantitative Darstellungsweise der scheinbaren Durchschnittsintensität der Färbung der Harzphase, vergleiche die dritte Mitteilung: M. Fujimoto, Dieses Bulletin, **29**, 567 (1956).

TABELLE I

VERSCHIEDENE EXPERIMENTALBEDINGUNGEN VON ABB. 1

| Nr. des Expts. | Zeichen der Kurve | Ordnung der Versetzung von Harze, Reagenzien u. Probelsg. 1. | 2. | 3. | 4. | 5. | Bemerkungen* |
|---|---|---|---|---|---|---|---|
| Ia | ---○--- | HR** | 6N Ammoniakwasser | 20proz. Lsg. des Ammoniumrhodanids | Probelsg.*** | 1proz. Lsg. des *p*-Phenylendiamins | *a* |
| Ib | ---⊖--- | HR | 6N Ammoniakwasser | 20proz. Lsg. des Ammoniumrhodanids | Probelsg. | 0.1proz. Lsg. des *p*-Phenylendiamins | *b* |
| Ic | ——●—— | HR | 0.1proz. Lsg.—(5 Min)**** des *p*-Phenylendiamins | →Probelsg. | 6N Ammoniakwasser | 1proz. Lsg. des Ammoniumrhodanids | *c* |
| Id | ——◐—— | HR | Probelsg.—(5 Min) | →6N Ammoniakwasser | 1proz. Lsg. des Ammoniumrhodanids | 0.1proz. Lsg. des *p*-Phenylendiamins | *c* |

* *a*: Da die Harzkörnchen sich selbst dann schwarz bzw. grauschwarz färben, wenn kein Kupfer in der Probelösung enthalten ist, ist der Nachweis geringer Menge des Kupfers kaum ausführbar.
*b*: Die Harzkörnchen färben sich etwas schwächer violettbraun.
*c*: Die Harzkörnchen färben sich bedeutend stark braunschwarz. Enthält die Probelösung kein Kupfer, so färbt sich die Harzphase nur sehr hell bläulich grau.
** An dieser Tabelle bedeutet HR „1 proz. DVB" von HR-Form.
*** Die hier angewandte Probelösung enthielt 0.4 γ Kupfer (10 γ/ccm).
**** Zeitdauer nach dem Eintauchen der Harzkörnchen in die betreffende Lösung.

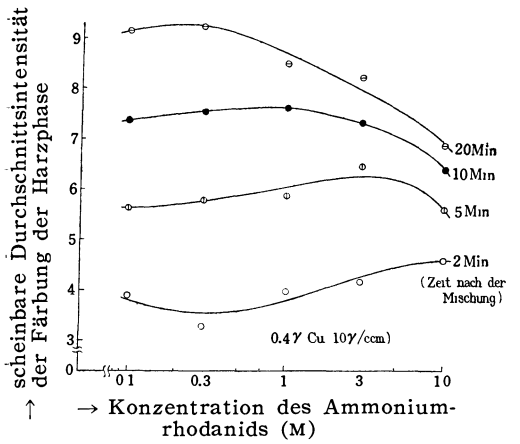



Abb. 2. Einfluss der Konzentration des Ammoniumrhodanids auf die scheinbare Intensität der Färbung.

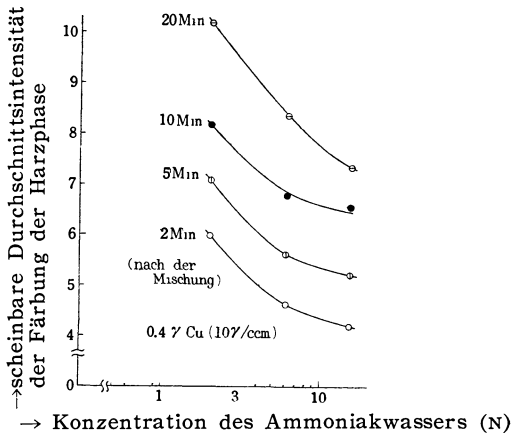
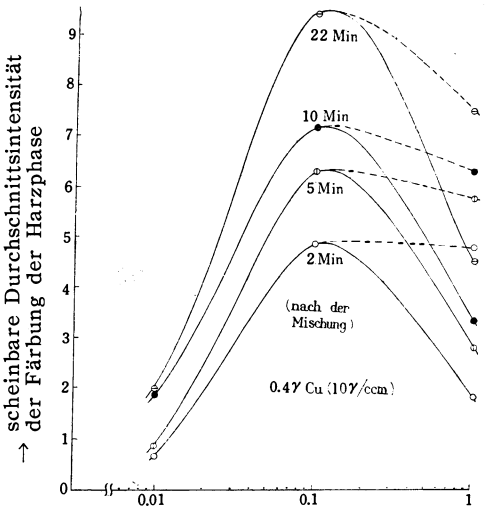



Abb. 3. Einfluss der Konzentration des Ammoniakwassers auf die scheinbare Intensität der Färbung

**Ammoniumrhodanidlösung.**—Wie in Abb. 2 zu ersehen ist, ubt die Konzentration der benutzten Ammoniumrhodanidlösung auf die Färbungsintensität der Harzphase nur geringfügigen Einfluss aus. Jedoch wurde im folgenden 0.3prozentige Lösung des Ammoniumrhodanids deshalb besser angewandt, weil bei dieser Konzentration die Färbung der Harzphase später als etwa 15 Min nach der Mischung merklicher als bei den Fällen der anderen Konzentrationen zunimmt.

**(3) Einfluss der Konzentration des Ammoniakwassers.** — Die Anwendung konzentrierten Ammoniakwassers beeinflusst die Färbung der Harzphase nachteilig. Abb. 3 zeigt die Abhängigkeit der Färbungsintensität der Harzphase von der Ammoniakwasserkonzentration. Aus der Vergleichung von 2,6 und 15N Ammoniakwasser, wurde 2N Ammoniakwasser als das geeignetste ausgewählt.

**(4) Einfluss der Konzentration der Reagenslösung.**—Mit dem Harze, „1proz. DVB", von HR-Form, 0.3prozentiger Lösung des Ammoniumrhodanids, 2N Ammoniakwasser und 1-, 0.1- und 0.01-prozentiger Lösung des *p*-Phenylendiamins wurde der Einfluss der Konzentration der *p*-Phenylendiaminlösung auf die Färbungsintensität der Harzphase gegenübergestellt. Die Resultate stehen in Abb. 4. Mit 0.01prozentiger Lösung war die Färbung sehr schwach, mit 1prozentiger Lösung färbte sich die Harzphase selbst dann stark violettbraun, auch wenn die Probelösung kein Kupfer enthielt. Daher ist hierbei die Anwendung 1prozentiger wässeriger Lösung des *p*-Phenylendiamins wünschenswert.

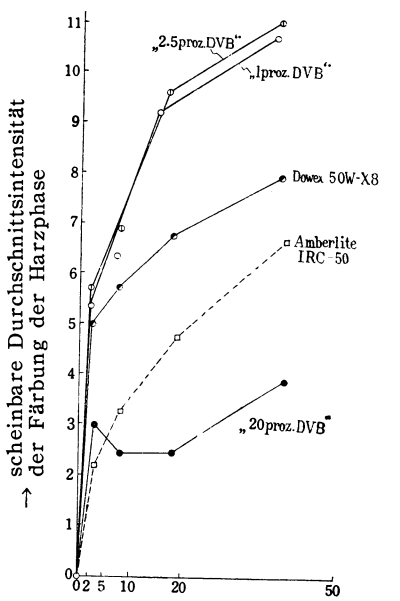



→ Konzentration der Reagenslösung (proz.)

Abb. 4. Einfluss der Konzentration benutzter Reagenslösung
--- Bruttofärbungsintensität der Harzphase
—— Nettofärbungsintensität der Harzphase verglichen mit dem Blindversuche.

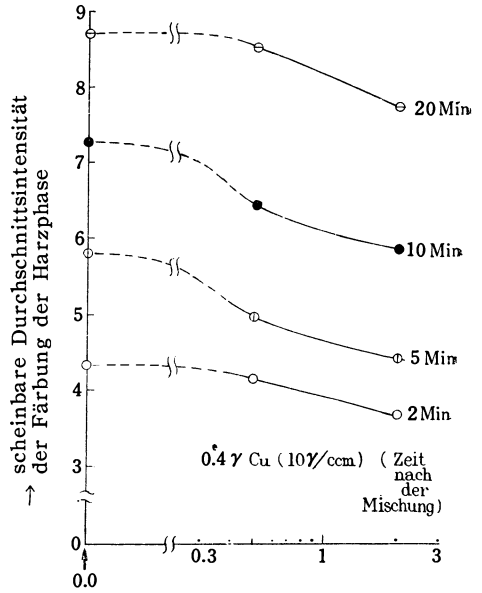
(5) **Einfluss der Harzart.**—Schliesslich wurde der Einfluss verschiedenartiger Harzproben von HR-Form auf die Färbungsintensität untersucht. Abb. 5 zeigt die Resultate solcher Versuche an, wonach die scheinbare Intensität der Färbung von der Harzphase nach folgender Reihenfolge abnimmt:

„1proz. DVB" > „2.5proz. DVB" > Dowex 50 W-X8 > Amberlite IRC-50 > „20proz. DVB."




→ Zeit nach der Mischung (Min)

Abb. 5. Einfluss der Harzart




→ Konzentration des in der Probelösung vorhandenen Natriumchlorids (N)

Abb. 6. Einfluss der Neutralsalzkonzentration auf die Färbungsintensität der Harzphase

Mit Rücksicht auf die Färbung des Blindversuches, wurde im folgenden „1proz. DVB" schlechthin angewandt.

(6) **Einfluss der Neutralsalzkonzentration.**—Wie aus dem Verlaufe in Abb. 6 beschriebenen Kurven zu ersehen ist, beeinflusst die Salzkonzentration der Probelösung die scheinbare Färbungsintensität der Harzphase sehr wenig, d. h., wenn man nur die Neutralsalzkonzentration an der Probelösung niedriger als 3N hält, so wird die Violettbraunfärbung der Harzphase kaum geschwächt.

(7) **Bedingungen höchster Empfindlichkeit.**—Alles Obenerwähnte zusammengenommen, wird das beste Verfahren wie folgt genau festgestellt:—

„Man bringt auf eine weisse Tüpfelplatte einige Körnchen des starksauren und niedrig vernetzten farblosen Kationenaustauschharzes, „1proz. DVB," von HR-Form und einen Tropfen frisch hergestellter 0.1prozentiger wässeriger Lösung des *p*-Phenylendiamins, rührt sie mit einem Glasstäbchen sorgfältig um, und lässt sie etwa fünf Minuten stehen. Dann fügt man dazu nacheinander je einen Tropfen der Probelösung, des 2N Ammoniakwassers, und 0.3prozentiger Lösung des Ammoniumrhodanids, und lässt dieses Gemisch noch etwa zehn Minuten stehen. Schliesslich beobachtet man eine in der Harzphase entstandene Dunkelviolettbraun- bzw. Violettgraufärbung unter Beleuchtung einer Tischlampe mit einer Lupe von zwanzigfacher Vergrösserung."

## Bestimmung der Erfassungsgrenze

Die Resultate der mit dem letztgenannten besten Verfahren durchgeführten Experimente,

TABELLE II

EINFLÜSSE DER BEGLEITSTOFFE

| Begleitstoffe | benutzter Verbindungstypus | Färbung der Harzphase* | Menge der Begleitstoffe | nachweisbare Kupfermenge | Grenzverhältnis | Bemerkungen** |
|---|---|---|---|---|---|---|
| Cr(III) | $KCr(SO_4)_2$ | hellgraugrün | 32 γ | 0.04 γ | $1:8\times10^2$ | *a*, Cr(III) ≦0.1proz. |
| Mn(II) | $MnSO_4$ | farblos | 360 γ | 0.04 γ | $1:9\times10^3$ | — |
| **Fe(III)** | **$FeCl_3$** | **dunkelgelbbraun** | **3.2 γ** | **0.08 γ** | **$1:4\times10$** | **Fe(III)≦0.01proz.** |
| 〃 | 〃 | grau | 32 γ | 0.08 γ | $1:4\times10^2$ | *a*, *b*, Fe(III)≦0.1proz. |
| Fe(II) | Mohrsches Salz | dunkelgrün | 46 γ | 0.08 γ | $1:5.7\times10^2$ | *a*, Fe(II)≦0.15proz. |
| **Co(II)** | **$CoCl_2$** | **olivengrün (?)** | **2.8 γ** | **0.16 γ** | **$1:1.8\times10$** | **Co(II)≦0.01proz.** |
| Ni(II) | $Ni(NO_3)_2$ | dunkelgrün | 1000 γ | 0.2 γ | $1:5\times10^3$ | — |
| Zn(II) | $ZnSO_4$ | hellviolettbraun | 320 γ | 0.08 γ | $1:4\times10^3$ | *a* |
| Cd(II) | $CdSO_4$ | dunkelgrün | 1200 γ | 0.06 γ | $1:2\times10^4$ | — |
| Hg(II) | $Hg(NO_3)_2$ | hellviolettgrau | 72 γ | 0.04 γ | $1:1.8\times10^3$ | *a* |
| **Ag(I)** | **$AgNO_3$** | **bläulich hellgrau** | **3.2 γ** | **0.04 γ** | **$1:8\times10$** | **Ag≦0.01proz.** |
| 〃 | 〃 | 〃 〃 | 270 γ | 0.13 γ | $1:2\times10^3$ | *c* |
| Pb(II) | $Pb(NO_3)_2$ | grauviolettbraun | 2300 γ | 0.02 γ | $1:1.1\times10^5$ | *a* |
| Bi(III) | $Bi(NO_3)_3$ | hellgrünbraun | 3200 γ | 0.08 γ | $1:4\times10^4$ | — |
| **Cr(VI)** | **$K_2Cr_2O_7$** | **bläulich grauviolett** | **3.6 γ** | **0.02 γ** | **$1:1.8\times10^2$** | ***a*, Cr(VI)≦0.01proz.** |
| Mo(VI) | $(NH_4)_2MoO_4$ | sehr hell violettbraun | 36 γ | 0.02 γ | $1:1.8\times10^3$ | Mo(VI)≦0.2proz. |
| 〃 | 〃 | grauviolett | 440 γ | 0.04 γ | $1:1.1\times10^4$ | *a*, *b* |
| W(VI) | $Na_2WO_4$ | dunkelviolett | 330 γ | 0.08 γ | $1:4.1\times10^3$ | *a* |
| U(VI) | $UO_2(CH_3COO)_2$ | grau | 72 γ | 0.02 γ | $1:3.6\times10^3$ | U(VI)≦0.2proz. |
| Al(III) | $Al(NO_3)_3$ | hellgraublauviolett | 160 γ | 0.08 γ | $1:2\times10^3$ | *a*, Al≦0.5proz. |
| **$NO_2^-$** | **$NaNO_2$** | **hell violettlich grau** | **7 γ** | **0.04 γ** | **$1:1.8\times10^2$** | ***a*, $NO_2^-$≦0.02proz.** |
| 〃 | 〃 | hell violettlich braun | 350 γ | 0.04 γ | $1:8.8\times10^3$ | *d* |
| $C_2O_4^{2-}$ | Oxalsaures Ammonium | hellgrauviolett | 890 γ | 0.04 γ | $1:2.2\times10^4$ | — |
| $C_4H_4O_6^{2-}$ | Seignettesalz | bläulich hellgrau | 950 γ | 0.04 γ | $1:2.4\times10^4$ | — |
| $C_6H_5O_7^{3-}$ | Zitronensaures Ammonium | bläulich grau | 1340 γ | 0.04 γ | $1:3.6\times10^4$ | — |

* Dies zeigt den Ton der Färbung, die in der Harzphase dann entsteht, wenn die genannte Probelösung nur den Begleitstoff enthält.

** *a*: Nur dann ist das obige Grenzverhältnis nutzbar, wenn der Nachweis mit einem Blindversuche miteinander ausgeführt wird.

*b*: Nach dem Zusatze eines Tropfens 5prozentiger Lösung des Ammoniumzitrates wurde der Nachweis ausgeführt.

*c*: Hier fallen alle Silberionen durch Zusatz eines Tropfens der 0.5N Lösung von Natriumchlorid als Silberchlorid aus. Danach wurde der Nachweis mit einem Tropfen von dessen Lösungsphase ausgeführt.

*d*: Nach dem Zusatze eines Tropfens der 6N Salzsäure und von etwa 5 mg festen Harnstoffes wurde der Nachweis ausgeführt.

bei denen die verschiedene Menge des Kupfers enthaltenden Probelösung angewandt wurden, stehen zusammen in Abb. 7:

Die Erfassungsgrenze von 0.02 γ Kupfer unter Grenzkonzentration $1:2\times10^6$ wurde so eindeutig bestimmt.

### Einflüsse der Begleitstoffe

Tabelle II schildert die Einflüsse fremder Stoffe auf die vorliegende Nachweismethode. Eisen(III)-, Kobalt(II)- und Silbersalze, Chromate, Bichromate und Nitrite stören den Nachweis beträchtlich. Diese werden an der genannten Tabelle mit fetten Schriften beschrieben.

### Beobachtung des an der Grenzfläche zweier Phasen sich bildenden Niederschlags

Abb. 8 stellt das vergrösserte Bild des mit einer Sicherheitsrasierklinge abgeschnittenen Querschnitts von einem der Harzkörnchen dar, „1 proz. DVB", welche sich nach dem Verfahren „$I_c$" von Abb. 1 etwa eine Stunde nach der Mischung stark färben. Dabei ist es sehr interessant, dass, wie Abb. 8c klar zeigt, nur die

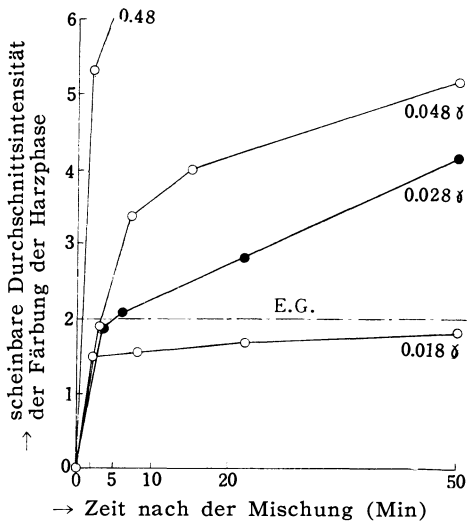



Abb. 7. Bestimmung der Erfassungsgrenze.

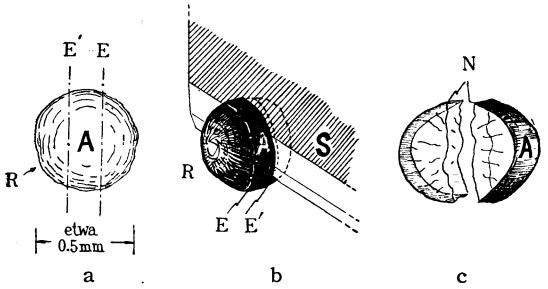



Abb. 8. Vergrössertes Bild des mit Rasierklinge abgeschnittenen Harzkörnchens

R: Harzkörnchen,
A: Abschnitt des Harzkörnchens,
E, E': Einschnitt,
S: Sicherheitsrasierklinge,
N: Niederschlagschale des Kupferrhodanid-*p*-Phenylendiamins, und
c: vergrössertes Bild vom Abschnitt des Harzkörnchens, das sich in die zwei Bruchstücke abspaltet.

Oberfläche des Harzkörnchens wie die Apfelschale sich entschieden stark färbt, während gerade die Innenseite der Oberfläche des Harzkörnchens genau wie dessen Kern sich gar nicht färbt.

Aus dieser Beobachtung wird es klar, dass die hier gewonnene ausserordentliche Erhöhung der Empfindlichkeit von der gegenwärtigen Nachweisreaktion gerade auf dem Niederschlag beruht, der sich an der dünnsten Grenzfläche zweier Phasen bildet[3].

## Zusammenfassung

1. Durch mikroanalytische Anwendung farbloser starksaurer sowie niedrig vernetzterKationenaustauschharze zurNiederschlagbildungsreaktion zwischen den Kupfersalzen und dem *p*-Phenylendiamin sowie dem Ammoniumrhodanid steigt die Empfindlichkeit genannter Reaktion ausserordentlich an, und dadurch wird eine empfindliche Nachweismethode für die geringe Menge des Kupfers neu festgestellt.

2. Das empfindlichste Nachweisverfahren wird durch genaue Vergleichung verschiedener Experimentalfaktoren, wie Ordnung der Versetzung, Konzentration des Ammoniakwassers, der Ammoniumrhodanid- oder der *p*-Phenylendiaminlösung, Harzart, Neutralsalzkonzentration der Probelösung, usw., einwandfrei genau bestimmt.

3. Die Einflüsse verschiedenartiger Begleitstoffe werden, wie in Tabelle II zu ersehen ist, ausführlich untersucht.

4. Aus der einfachen Beobachtung des mit einer Rasierklinge abgeschnittenen Querschnitts des Harzkörnchens, wird die auf die dünnste Grenzfläche zwischen Harz- und Lösungsphase eingeschränkte Niederschlagbildung deutlich gezeigt.

Herrn Prof. Dr. E. Minami sowie den jüngeren Fachgenossen an seinem Laboratorium möchte der Verfasser für ihre zahlreichen freundlichen Anregungen bei dieser Untersuchung seinen herzlichsten Dank aussprechen.

Für die Harzproben, „1 proz. DVB", „2.5 proz. DVB" und „20 proz. DVB" ist der Verfasser Herrn Prof. Dr. A. Kawamura an der Landwirtschaftlichen und Technischen Universität zu Tokyo zu verbindlichstem Dank verpflichtet.

*Laboratorium der analytischen Chemie,*
*Chemisches Institut der*
*wissenschaftlichen Fakultät,*
*Tokyo Universität, Tokyo*

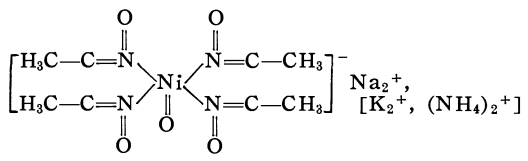
# *Mikroanalyse mit Hilfe von Ionenaustauscherharzen.*[*1] *XI. Über den Nachweis kleinster Menge des Nickels mit Dimethylglyoxim und Bromwasser*[1]

Von Masatoshi FUJIMOTO

(Eingegangen am 31. August, 1956)

## Einleitung

Es wurde hier eine Rosa- bzw. Braunfärbung, die die ammoniakalische wässerige Lösung der Nickelsalze bei Anwesenheit von verschiedenartigen Oxydationsmitteln unter Einwirkung von Dimethylglyoxim gibt[2], zur Mikroanalyse mit Ionenaustauscherharzen angewandt. Nach F. Feigl wurde vermutet, dass die genannte Färbung auf der Bildung von einer wasserlöslichen Chelatverbindung vierwertigen Nickels wie



$Na_2^+$, $[K_2^+, (NH_4)_2^+]$

beruht[3],[*2].

Lässt man in diese sich stark färbende Lösung einige Körnchen farblosen starkbasischen Anionenaustauscherharzes eintauchen, so werden derartigeChelatanionen in die Harzphase stark adsorbiert. Die Harzkörnchen werden infolgedessen entschieden stärker als die Aussenlösung gefärbt.

Bei dieser Arbeit wurde die obengenannte Ionenaustauschreaktion zum Nachweis geringer Menge des Nickels angewandt, und durch ausführliche Untersuchung über die Experimentalbedingungen wurde eine neue verbesserte Nachweismethode für Nickel festgestellt.

### Die in der gegenwärtigen Untersuchung benutzten Anionenaustauscherharze

Die wohlbekannten beinahe farblosen käuflichen Anionenaustauscherharze, Dowex 1-X1, -X2, -X4, -X8; Dowex 2-X2; Amberlite XE-114 und Amberlite IR-45, wurden alle in Chloridform angewandt[5].

### Versuchsanordnung

Auf einer weissen Tüpfelplatte versetzt man je einen Tropfen von Probelösung, Ammoniakwasser und Bromwasser miteinander, und lässt sie etwa fünf Minuten stehen. Dann fügt man dazu einen Tropfen verdünnter alkoholischer Lösung des Dimethylglyoxims und einige Körnchen starkbasischen sowie farblosen Anionenaustauscherharzes, und danach rührt man dieses Gemisch mit einem Glasstäbchen gründlich um. Einige Minuten nach der Mischung beobachtet man mit einer Lupe eine Orangerosa- bzw. Orangebraunfärbung in der Harzphase.

### Massflüssigkeit und Reagenzien

**1. Massflüssigkeit.** — Man stellt hier eine Stammlösung der Nickelmassflüssigkeit her, indem man kobalt- und eisenfreies Nickel(II)-chlorid („Scherring-Kahlbaum A. G." zur Analyse) in 0.01N Salzsäure eintrug. 1 ccm dieser Stammlösung enthielt genau 44.02 mg von Nickel[*3]. Alle folgende Untersuchungen über die beste Experimentalbedingungen werden mit einer 0.01N-salzsauren Lösung ausgeführt, deren 1 ccm 4.40 $\gamma$ von Nickel enthielt.

**2. Reagenzien.**—**(1) Bromwasser.**—Etwa 0.3-prozentige wässerige Bromlösung wurde durch Verdünnung gesättigter Bromwasser mit etwa zweifacher Menge destillierten Wassers hergestellt.

**(2) Ammoniakwasser.**—Käufliches extrareines 15N Ammoniakwasser wurde vorbereitet.

**(3) Alkoholische Lösung des Dimethylglyoxims**[*4].—Einprozentige alkoholische Lösung des extrareinen Dimethylglyoxims („Wako" zur Analyse) wurde vorbereitet.

---

*1 Von nun an wird die in den vorhergehenden Mitteilungen angewandte Terminologie „Ionenaustauscharz" durch „Ionenaustauscherharz" ersetzt, da diese gegenwärtig üblicher als jene im Gebrauch ist.

1) Die zehnte Mitteilung: M. Fujimoto, Dieses Bulletin, **30**, 87 (1957).

2) F. Feigl, *Ber.*, **57**, 758 (1924).

3) F. Feigl, „Chemistry of Specific, Selective and Sensitive Reactions," übersetzt von R. E. Oesper, 1. Aufl., New York (1949), S. 278.

*2 Es wurde kürzlich von K. Yamasaki und Ch. Matsumoto vermutet, dass in alkalischer Lösung ein Komplexanion, $[Ni^{IV}D_3]^{2-}$ sich bildet ($DH_2$ bedeutet Dimethylglyoximmolekül)[4].

4) K. Yamasaki und Ch. Matsumoto, *J. Chem. Soc. Japan* (*Pure Chem. Sect.*) **77**, 1111 (1956).

5) Vgl. die siebente Mitteilung: M. Fujimoto, Dieses Bulletin **29**, 776 (1956).

*3 Der Nickelgehalt von der obigen Massflüssigkeit wurde durch komplexometrische Titration mit 0.01 M Massflüssigkeit des Äthylendiamintetraessigsauren Natriums und Murexide als Metallindikator genau bestimmt.

*4 Eine Dimethylglyoximlösung in Aceton wurde auch angewandt, und dabei wurden gleicherweise befriedigende Ergebnisse erhalten.

### Bestimmung der Bedingungen höchster Empfindlichkeit*5

**1. Abhängigkeit der Färbungsintensität der Harzphase von der Menge des Dimethylglyoxims.**—Mit 6N Ammoniakwasser und Dowex 1-X1 wurde der nachfolgende Versuch ausgeführt. Wie aus Abb. 1 klar zu ersehen ist, übt die Menge des angewandten Dimethylglyoxims auf die Färbungsintensität der Harzphase beträchtlichen Einfluss aus. Bei allzu niedriger Konzentration des Dimethylglyoxims färbt sich die Harzphase ungenügend. Die Färbung dieser Phase verstärkt sich allmählich mit steigender Reagenskonzentration und bei etwa Einprozent zeigt sie den höchsten Wert. Die Anwendung mehrerer Tropfen dieser einprozentigen Reagenslösung wirkt auf die Farbenentwicklung der Harzphase nachteilig ein. Diese Tatsachen zusammengenommen, empfiehlt es sich, nur einen Tropfen (=0.015 ccm) der einprozentigen alkoholischen Dimethylglyoximlösung anzuwenden.

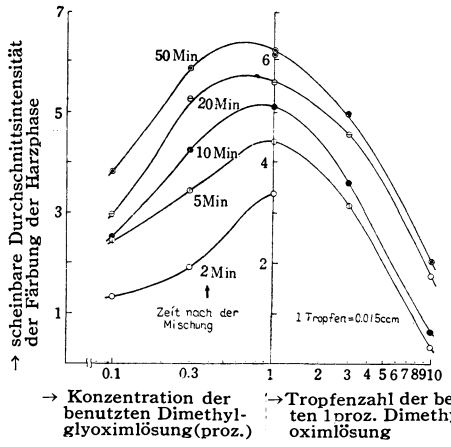



Abb. 1. Abhängigkeit der Färbungsintensität von der benutzten Dimethylglyoximmenge

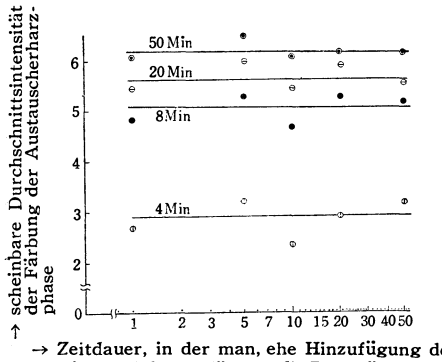



Abb. 2. Einfluss der Berührungsdauer der Probelösung mit Bromwasser.

*5 In bezug auf die halbquantitative Darstellungsweise von der scheinbaren Durchschnittsintensität der Färbung, vergleiche die dritte Mitteilung: M. Fujimoto, Dieses Bulletin, **29**, 567 (1956).

**2. Einfluss der Berührungsdauer der Probelösung mit Bromwasser.**—Abb. 2 zeigt den Einfluss der Zeitdauer, die nach der Versetzung der Probelösung und Ammoniakwasser mit Bromwasser verläuft. Aus dieser Abbildung ist es klar, dass die Nickel(II)salze in ammoniakalischer Lösung durch Einwirkung des Broms zu Nickel(IV)salze schon nach 1 Minute fast vollkommen oxydiert werden.

**3. Einfluss der Ammoiakwasserkonzentration.**—Abb. 3 stellt den Einfluss der Konzentration des Ammoniakwassers auf die Färbungsintensität der Harzphase dar. Wie man darin klar ersieht, übt der Überschuss freien Broms auf den Färbungsverlauf höchst schädlichen Einfluss aus. So ist es nötig, das Ammoniakwasser in solch einem grösseren Überschusse anzuwenden, dass die Bromfarbe von der Versuchslösung völlig verschwindet.

Wie es in dem Verlauf genannter Kurven deutlich zu ersehen ist, nimmt die Färbungsintensität der Harzphase mit steigender Konzentration des Ammoniakwassers allmählich ab (vgl. den Paragraph, „5. Einfluss der Salzkonzentration"). Im folgenden wurde lediglich 1N Ammoniakwasser angewandt.

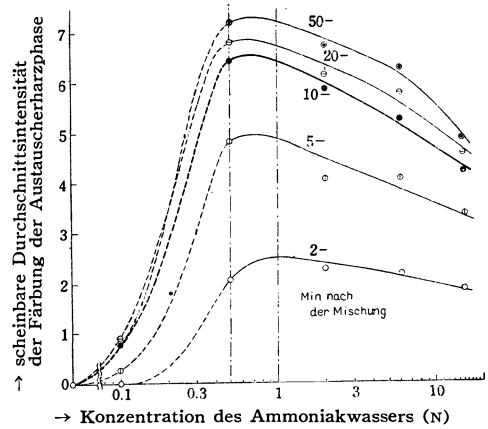



Abb. 3. Einfluss der Konzentration des benutzten Ammoniakwassers auf die scheinbare Färbungsintensität der Harzphase.

**4. Einfluss der Sorte sowie des Vernetzungsgrades der Harze.**—Aus dem in Abb. 4 dargestellten Färbungsverlauf wurde Dowex 1-X4 als das am besten geeignete Harz ausgewählt.

Dowex 2-X2 sowie Dowex 1-X2 färben sich etwas schwächer, und Dowex 1-X1 sowie -X8 beträchtlich schwächer. Schwachbasische Harze, Amberlite IR-45 sowie XE-114, waren dabei nicht zweckmässig.

**5. Einfluss der Salzkonzentration.** — Mit steigender Salzkonzentration der Probelösung wird die Rosafärbung der Harzphase bedeutend geschwächt. Wie in den Kurven in Abb. 5 klar gezeigt wird, nimmt die scheinbare Färbungsintensität der Harzphase dann rasch ab, wenn die Salzkonzentration der Probelösung höher als

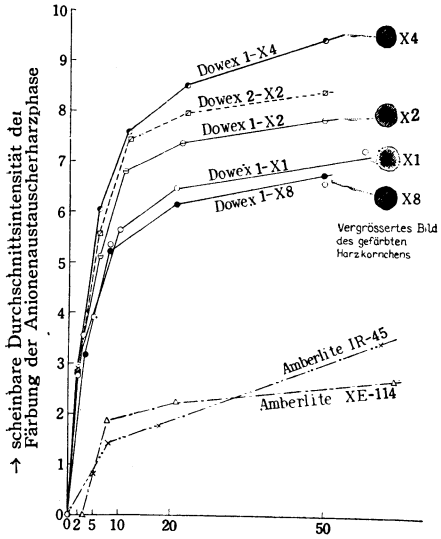



Abb. 4. Abhängigkeit der Färbungsintensität von Sorten der Harze (RCl-Form)

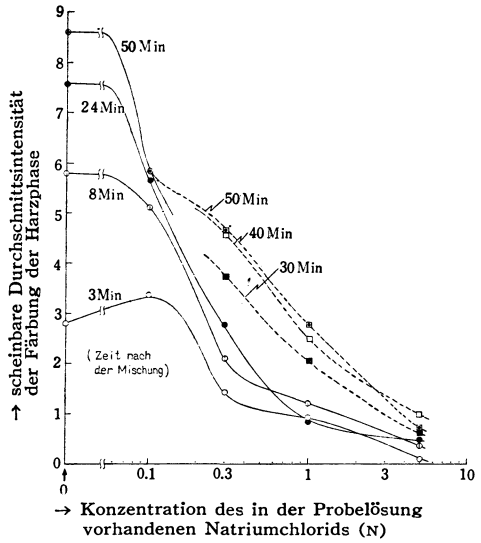



Abb. 5. Einfluss der Konzentration des in der Probelösung vorhandenen Neutralsalzes auf die scheinbare Färbungsintensität der Harzphase.

TABELLE I

EINFLÜSSE DER BEGLEITSTOFFE

| Begleitstoffe | benutzter Verbindungstypus | Farbton der Harzphase* | Menge der Begleitstoffe | nachweisbare Nickelmenge | Grenzverhältnis | Bemerkungen** |
|---|---|---|---|---|---|---|
| V(V) | $NH_4VO_3$ | farblos | 18 γ | 0.018 γ | $1:1\times10^3$ | *a*, V≦0.05proz. |
| Cr(III) | $KCr(SO_4)_2$ | grau | 64 γ | 0.035 γ | $1:1.8\times10^3$ | *b* |
| Mn(II) | $MnSO_4$ | farblos | 32 γ | 0.021 γ | $1:1.5\times10^3$ | Mn≦0.1proz. |
| **Fe(III)** | **$FeCl_3$** | **farblos** | **13 γ** | **0.12 γ** | **$1:1.1\times10^2$** | — |
| **Fe(II)** | **Mohrsches Salz** | **farblos** | **8 γ** | **0.14 γ** | **$1:5.7\times10$** | *c* |
| Co(II) | $Co(NO_3)_2$ | farblos | 118 γ | 0.053 γ | $1:2.3\times10^3$ | *a* |
| Cu(II) | $CuSO_4$ | sehr hell braun | 36 γ | 0.018 γ | $1:2\times10^3$ | Cu≦0.1proz. |
| Zn(II) | $ZnSO_4$ | farblos | 270 γ | 0.035 γ | $1:7.7\times10^3$ | *a* |
| Cd(II) | $CdSO_4$ | farblos | 18 γ | 0.021 γ | $1:8.5\times10^2$ | Cd≦0.1proz. |
| Hg(II) | $Hg(NO_3)_2$ | beinahe farblos | 34 γ | 0.016 γ | $1:2.2\times10^3$ | *a* |
| Cr(VI) | $K_2Cr_2O_7$ | zitronengelb | 32 γ | 0.035 γ | $1:9\times10^2$ | *d*, Cr≦0.1proz. |
| Mo(VI) | $(NH_4)_2MoO_4$ | farblos | 330 γ | 0.062 γ | $1:5.3\times10^3$ | — |
| W(VI) | $Na_2WO_4$ | farblos | 330 γ | 0.035 γ | $1:9.4\times10^3$ | — |
| U(VI) | $UO_2(CH_3COO)_2$ | lebhaft gelb | 270 γ | 0.062 γ | $1:4.4\times10^3$ | *b* |
| Pb(II) | $Pb(NO_3)_2$ | farblos | 170 γ | 0.035 γ | $1:4.8\times10^3$ | — |
| **Al(III)** | **$Al(NO_3)_3$** | **farblos** | **70 γ** | **0.12 γ** | **$1:5.7\times10^2$** | *a* |
| $F^-$ | KF | farblos | 170 γ | 0.021 γ | $1:8\times10^3$ | — |
| $C_6H_5O_7^{3-}$ | Zitronensaures Ammonium | farblos | 430 γ | 0.13 γ | $1:3.3\times10^3$ | — |
| $C_4H_4O_6^{2-}$ | Seignettesalz | farblos | 770 γ | 0.028 γ | $1:2.7\times10^4$ | — |
| $C_2O_4^{2-}$ | Oxalsaures Ammonium | farblos | 495 γ | 0.09 γ | $1:5.7\times10^3$ | — |

* Der Farbton hervorgerufen durch nur die Begleitstoffe:

** *a*: 6N Ammoniakwasser (1 Tropfen) wurde angewandt.
*b*: 15N Ammoniakwasser (1 Tropfen) wurde angewandt.
*c*: Hierbei wurde überschüssiges Bromwasser angewandt, um alle gebildete Eisen(II)-hydroxyd zum Eisen(III)hydroxyd völlig zu oxydieren.
*d*: Neben Blindversuche wurde der Nachweis durchgeführt.

0.1N ist. Diese Tatsache ist der einzige Fehler vorliegender Nachweismethode. Jedoch, durch Verdünnung der Probelösung mit etwa 1 ccm destillierten Wassers, ist dieser Nachteil bis zu einem gewissen Grade zu vermeiden, wie die gestrichelten Kurven der genannten Abbildung zeigen. Auf alle Fälle empfiehlt es sich, die Salzkonzentration der Versuchslösung niedriger als 0.3N zu halten.

**6. Bedingungen höchster Empfindlichkeit.**— So wurde das beste Verfahren wie folgt vollkommen festgestellt:

„Auf einer weissen Tüpfelplatte versetzt man je einen Tropfen von Probelösung, 1N Ammoniakwasser und 0.3prozentigem Bromwasser miteinander. Wenn die Salzkonzentration der Probelösung höher als 0.3N liegt, so empfiehlt es sich, noch etwa 1 ccm destillierten Wassers zuzugeben. Nach zwei bis fünf Minuten langem Stehen fügt man dazu einen Tropfen (etwa 0.015 ccm mit Kapillarpipette) einprozentiger alkoholischer Dimethylglyoximlösung und einige Körnchen starkbasischen sowie farblosen Anionenaustauscherharzes, Dowex 1-X4 (RCl-Form), und danach rührt man dieses Gemisch mit einem Glasstäbchen gründlich um. Etwa zwanzig Minuten nach der Mischung beobachtet man, mit einer Lupe, eine in der Harzphase entstandene Orangerosa- bzw. Orangebraunrosafärbung."

### Bestimmung der Erfassungsgrenze

Aus dem Verlauf der Kurven in Abb. 6 wurde die Erfassungsgrenze vorliegender Nachweisreaktion als 0.011 $\gamma$ Nickel(II) unter Grenzkonzentration $1 : 3.8 \times 10^6$ eindeutig bestimmt.

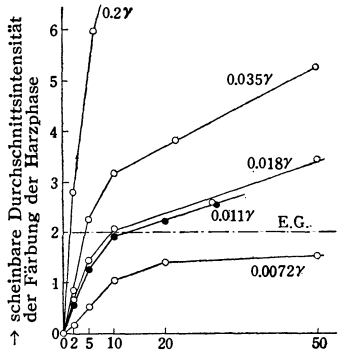



Abb. 6. Bestimmung der Erfassungsgrenze.

### Einflüsse der Begleitstoffe

Tabelle I stellt die Einflüsse verschiedenartiger fremder Ionen auf die vorliegende Nachweisreaktion zusammenfassend dar. Wie es klar zu ersehen ist, stört nur Eisen(III)- und Eisen(II)-salze beträchtlich den genannten Nachweis*6.

## Zusammenfassung

1. Durch einfache Anwendung der farblosen starkbasischen Anionenaustauscherharze zur Farbenreaktion zwischen Nickelsalzen und Dimethylglyoxim bei Anwesenheit des Bromwassers steigt die Empfindlichkeit der genannten Reaktion beträchtlich an.

2. Die besten Experimentalbedingungen werden durch gründliche Untersuchung der verschiedenen Faktoren, wie Konzentration der Reagenzien, Harzart, Salzkonzentration der Probelösung, usw., vollkommen festgestellt. Der etwas grössere Einfluss der Neutralsalzkonzentration der Probelösung zur Reaktionsempfindlichkeit ist der einzige Nachteil von der hier vorgeschlagenen Nachweismethode.

3. Die Einflüsse der verschiedenartigen Begleitstoffe werden auch ausführlich untersucht. Eisen(III)- und Eisen(II)salze stören den Nachweis.

Zum Schluss möchte der Verfasser Herrn Prof. Dr. E. Minami für seine freundlichen Anregungen zur vorliegenden Untersuchung seinen herzlichsten Dank aussprechen.

*Laboratorium der analytischen Chemie,*
*Chemisches Institut der*
*wissenschaftlichen Fakultät,*
*Tokyo Universität, Tokyo*

*6 Über das raffinierte mikrochemische Verfahren zur Trennung verschiedenartiger Übergangselemente mit einer Mikrosäule des Anionenaustauscherharzes, wird der Verfasser später in der nächsten Mitteilung genau diskutieren.

# *Electrochemical Study of Ethylene Glycol-Acetic Acid System*

By V. K. VENKATESAN and C. V. SURYANARAYANA

(Received April 21, 1956)

## Introduction

The well known effect of certain hydroxy bearing compounds in increasing the acidity of aqueous solutions of boric acid pointed to a further exploration into the possibility of such and other similar effects of ethylene glycol on anhydrous acetic acid. Hence a systematic investigation of electrical conductance, volume contraction, viscosity, dielectric constant, and refractometric measurements has been made and reported herein.

### Experimental Procedure

Purest Eastman Kodak ethylene glycol was dried over anhydrous sodium sulphate, decanted and fractionally distilled under reduced pressure and the middle fraction collected. Dielectric constant determinations showed the same value both for the original material and for the purified one. So further requirements of ethylene glycol were drawn from the Eastman Kodak supply. Purest Kahlbaum glacial acetic acid was used. Ethylene glycol and acetic acid were kept at 30°C in a thermostat for several hours and by pipetting out the required volumes of the two compounds totalling 50 cc. into 250 cc. glass stoppered pyrex bottles, different compositions of the mixtures differing by 10 per cent were made ranging from 10 to 90 per cent. Weight per cent or mole per cent composition could be computed by considering the density of the glycol (1.10800) and that of acetic acid (1.03777) and their respective molecular weights.

For measuring the dielectric constant "Dekameter type DKO3" of Wissenschaftlich-Technische Werkstatten was used at a fixed frequency of 1.8 MC/S controlling the temperature of the cell with Hoppler's ultra thermostat.

A platinized vertical cell with a cell constant value of 0.1845 was used for measuring conductance. Resistance of the solutions was measured with conductivity bridge type LBR of Wissenschaftlich-Technische Werkstatten, at 50 cycles per second (due to high resistance of the solutions). Temperature was controlled at $30\pm0.05$°C using Townson and Mercer's thermostat, S427. The same thermostat, provided with glass panels with suitable arrangements, was used for viscometric measurements, with an Ostwald viscometer. Hilger's Abbe refractometer with Hoppler's utlra thermostat was used for making refractometric measurements. pH measurements were attempted with a Cambridge pH meter using a glass electrode. But no steady reproducible pH values could be recorded. Also with quinhydrone electrode irreproducible values were obtained. Results are reported below.

The resistance of ethylene glycol could not be measured with the above set-up due to its very high value. Hence in reporting equivalent conductivity values no solvent correction could be applied.

## Discussion

Acetic acid is known, from surface tension measurements[1,2], to exist as $(C_2H_4O_2)_2$ throughout the temperature range from 15 to 150°C. From the variation of the Ramsay-Shield's constants with temperature[3] and the dispersion and absorption of polyhydric alcohols in the Hertzian region[4] molecular associations are known to exist in ethylene glycol.

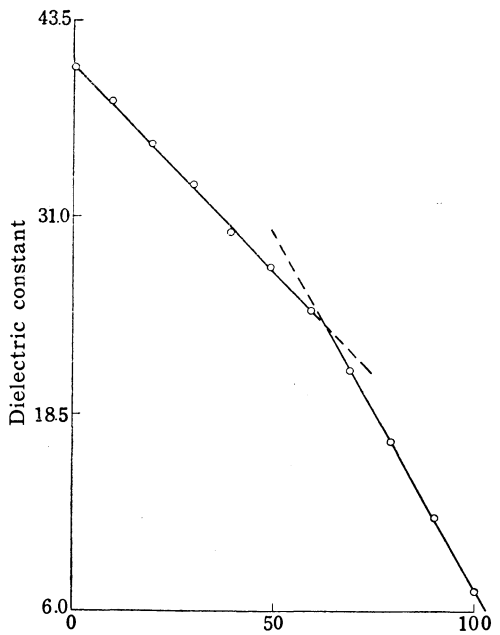



Fig. 1. Dielectric constant of ethylene-glycol-acetic acid system.

1) G. M. Bennet, *J. Chem. Soc.*, 351-360, 107 (1915).
2) Emile Band, *Bull. Soc. Chim.*, 435-438, 13 (IV) (1913).
3) G. G. Eliseef and W. A. Kurbastoff, *J. Russ. Phys. Chem. Soc.*, 1426-1427, 41 (1909).
4) Pierre Girand and P. Abadie, *Compt. rend*, 1995-1997, 196 (1933)

TABLE I

ETHYLENE GLYCOL-ACETIC ACID SYSTEM

| Vol. Percent of Acetic Acid | Mole Percent of Acetic Acid | Density | Volume Contraction in c.c. | Viscosity in Poises | Dielectric Constant | Molar Polarization | Specific Conductivity | Equivalent Conductivity | Refractive Index | Molar Refraction |
|---|---|---|---|---|---|---|---|---|---|---|
| (1) | (2) | (3) | (4) | (5) | (6) | (7) | (8) | (9) | (10) | (11) |
| 0 | 0 | 1.10800 | | 0.1346 | 40.500 | 52.08 | | | 1.4270 | 14.38 |
| 10 | 9.712 | 1.10494 | 0.49 | 0.1188 | 38.250 | 51.83 | $6.151\times10^{-6}$ | $3.548\times10^{-3}$ | 1.4243 | 14.29 |
| 20 | 19.480 | 1.10086 | 0.67 | 0.1013 | 35.625 | 51.57 | $5.741\times10^{-6}$ | $1.651\times10^{-3}$ | 1.4198 | 14.18 |
| 30 | 29.350 | 1.09722 | 0.77 | 0.08750 | 33.000 | 51.23 | $6.331\times10^{-6}$ | $1.210\times10^{-3}$ | 1.4148 | 14.03 |
| 40 | 39.220 | 1.09224 | 0.71 | 0.07350 | 30.500 | 50.94 | $6.963\times10^{-6}$ | $0.9963\times10^{-3}$ | 1.4118 | 13.97 |
| 50 | 49.180 | 1.08798 | 0.71 | 0.06127 | 27.750 | 50.35 | $6.474\times10^{-6}$ | $0.7387\times10^{-3}$ | 1.4070 | 13.81 |
| 60 | 59.210 | 1.08130 | 0.56 | 0.04976 | 24.875 | 50.05 | $6.625\times10^{-6}$ | $0.6301\times10^{-3}$ | 1.4020 | 13.71 |
| 70 | 69.330 | 1.07477 | 0·48 | 0.03829 | 21.250 | 49.17 | $7.236\times10^{-6}$ | $0.5891\times10^{-3}$ | 1.3968 | 13.61 |
| 80 | 79.490 | 1.06583 | 0.32 | 0.02775 | 16.610 | 47.58 | $6.933\times10^{-6}$ | $0.4948\times10^{-3}$ | 1.3905 | 13.48 |
| 90 | 89.710 | 1.05539 | 0.17 | 0.01819 | 12.075 | 44.94 | $4.500\times10^{-6}$ | $0.2865\times10^{-3}$ | 1.3820 | 13.29 |
| 100 | 100.000 | 1.03777 | | 0.01040 | 6.400 | 37.20 | | | 1.3700 | 13.09 |

A plot of dielectric constant values (column 6 of the Table) against mole per cent of acetic acid (Fig. 1) is made up of two straight lines intersecting at a composition of 62 mol. per cent of acetic acid. From 62 mol. per cent of acetic acid onwards the rate of fall of " D " is greater. All the mixtures have in each case a value for dielectric constant greater than to be expected if the variation is linear and at 62 mole per cent the deviation is a maximum. Likewise the plot of molar polarization against mole per cent of acetic acid (Fig. 2) is almost linear varying slightly with composition up to about 60 mole per cent of acetic acid, beyond which the fall is very rapid. All the mixtures have for each a value of molar polarization greater than to be expected if the variation is linear. The equation for molar polarization of a mixture

$$P_{1,2}=\frac{D-1}{D+2}\cdot\frac{M_1x_1+M_2x_2}{\rho_{1,2}}$$

is expected to hold[5] only for solutions of non-associated liquids. But some workers[6] applied it with success to mixtures of associated liquids. It is known[7] that the effect of association on the dielectric constant depends on the sizes and shape of the participating dipoles. As a result of a greater electrostatic moment of a polymerised molecule[8] than the simple one the dielectric constant of the solvent will be greater in its associated state. De-association in some solutions is indicated by the lowering of the dielectric constant of that component in solution. Conversely when dipole-dipole interaction occurs the forces holding the electric charge will be weakened as a result of a probable increase of the electrostatic moment of the molecule and the dielectric constant of a component becomes greater in solutions than in pure state. It has been shown[9] that when liquids are mixed there are at least two simultaneous reactions taking place, a de-association of the liquids and a combination between the two liquids. These

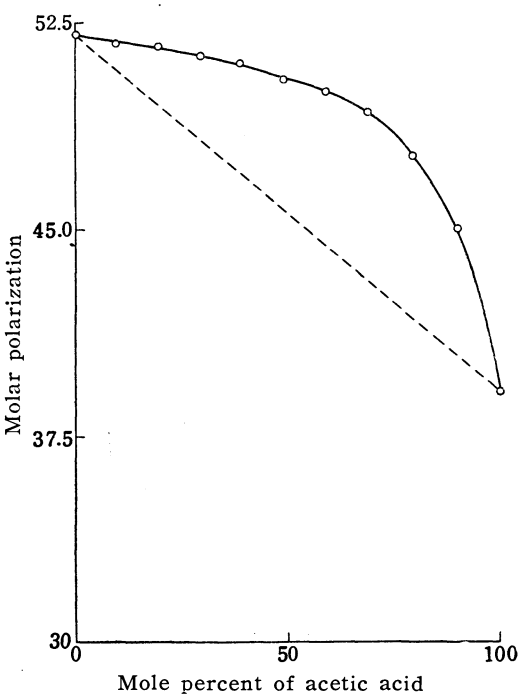



Fig. 2. Molar polarization of ethylene-glycol-acetic acid system.

5) G. Åkerlöf, *J. Am Chem. Soc.*, 4125, **54** (1932).
6) W Graffunder and Erich Heymann, *Z. Physik. Chem.*, 744, 72 (1931).
7) R. N. Kerr, *J. Chem. Soc.*, 2796-2804, 128 (1926).
8) J. W. Williams and I. J. Krchma, *J. Am. Chem. Soc.*, 1886, 48 (1926).
9) J. W. Williams and F. Daniels, ibid., 1490, 47 (1925).

factors should lead to opposing tendencies in any physical property. The only obvious conclusion is that starting from zero per cent ethylene glycol and proceeding towards per cent of it, the positive deviation of either the dielectric constant or the molecular polarization from linearity increases to a maximum at about 60 mole per cent of acetic acid and decreases from there onwards. It is probable that from zero to about 40 mole per cent of ethylene glycol dipole-dipole interaction predominates attaining its maximum at 40 mole per cent of ethylene glycol from where further increase of mole per cent of ethyleneglycol results in setting off a de-association of one or both of the components.

A plot of equivalent conductivity against mole per cent of acetic acid (Fig. 3) shows a rapid fall from 10 to 30 mole per cent of acetic acid, then a gradual fall up to about 60 mole percent round about which an inflexion occurs in the curve followed by a rapid fall towards the end. An electrochemical study of water-glycerol and water-ethylene glycol mixtures[10] showed that while it is possible to assume with ethanol the production of $EtOH_2^+$ ions, in the case of glycol or glycerol, ions of this type are formed to such a slight degree that the electrode potential remains practically unchanged. Since the equivalent conductivity, though slight, rises rapidly from 30 mole per cent of acetic acid downwards, it may be probable that in this region acetic acid starts slightly dissociating. From 60 mole per cent to 30 mole per cent the equivalent conductivity rises more rapidly than from 90 to 60 mole per cent of acetic acid, the overall increase in the former region being about double that in the latter. Hence it is probable that to anhydrous acetic acid, as more and more ethylene glycol is added, dipole-dipole interactions should occur up to about 60 mole per cent of acetic acid from where it starts de-association up to 30 mole per cent of acetic acid from where it must start slightly dissociating.

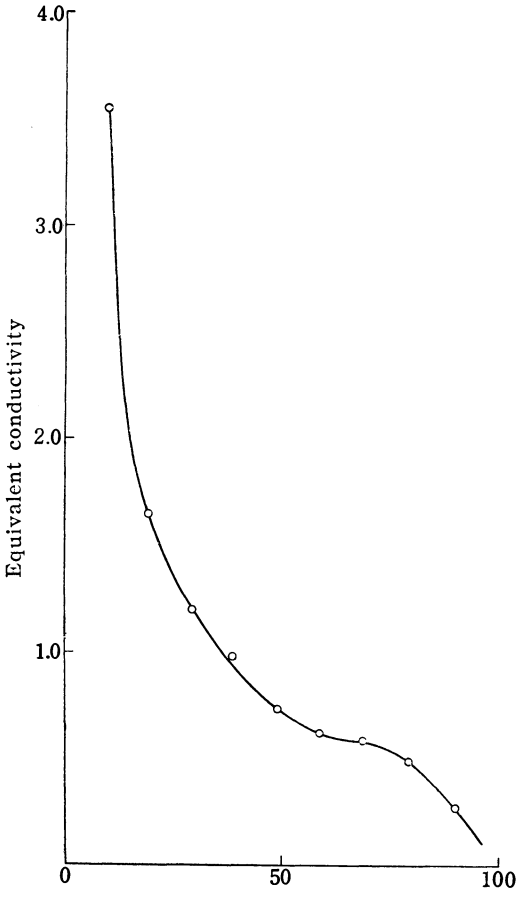



Fig. 3. Equivalent conductivity of ethylene-glycol-acetic acid system.

A plot of viscosity (column 5 of the Table) against percentage compositions (not shown) shows a gradual fall as mole per cent of acetic acid increases deviating from linearity with a convexity towards the axes.

Plots of refractive index and molar refractions (column 10 and 11) against mole per cent composition (not shown) show a gradual fall with increase in the mole per cent of acetic acid with a slight dip at 30 mole per cent of it.

A plot of volume contraction in c.c. against mole per cent composition (not given) shows an unsymmetrical parabola with a maximum at 30 mole per cent of acetic acid with a stationary value between 40 and 50 mole per cent of it.

Comparison of the behaviour of ethylene glycol-acetic acid system with those of aqueous boric acid and some polyhydric alcohols brings out a great dissimilarity. Perhaps the presence of water as an additional component and the basicity of the acid used may be among other contributing factors for the above dissimilarity.

## Summary

Equivalent conductivity, volume contraction, viscosity, dielectric constant and

10) I. I. Zhukov and I. F. Karpova, *J. Gen. Chem. (U.S.S.R.)*, 161-166, 6 (1936).

refractometric measurements of mixtures of ethylene glycol and acetic acid at different percentage compositions have been made. Probably a predominating dipole-dipole interaction occurs when ethylene glycol is added to anhydrous acetic acid up to about 60 mole per cent of the latter from where up to 30 mole per cent of acetic acid de-association seems to occur and from 30 mole per cent of acetic acid downwards slight dissociation is evidenced. This system is dissimilar in behaviour to those of aqueous boric acid and some polyhydric alcohols.

*Physico-Chemical Laboratory*
*Annamalai University*
*South India*

# *Electron Diffraction Investigation on the Molecular Structures of Some Organosilicon Compounds. I*

By Masatoki YOKOI*

(Received September 19, 1956)

## Introduction

Those organosilicon polymers, which have bonds between silicon and organic radicals, possess various properties of practical importance, i. e., low boiling points, small temperature coefficients of viscosity, high thermal stability, etc. These characteristic properties are closely related to their molecular structures. The knowledge of bond lengths and valence angles of low-molecular compounds provides the basis for consideration of the structures of polymers. The present study deals with the electron diffraction experiments on the vapors of several low-molecular organosilicon compounds. Organosilicon compounds which have so far been investigated by electron diffraction are mainly the derivatives of silane containing methyl groups and halogen atoms as substituents. In the present study, hexamethyldisiloxane, tetra-(trimethylsiloxy)-silane, octamethylcyclotetrasiloxane, and the two lowest members of dimethylcyclopolysilazanes and dimethylcyclopolysilthianes were investigated in order to determine the bond lengths of Si-O, Si-N and Si-S as well as the valence angles of O, N, S and Si atoms. In addition to the results on these compounds, data are also presented on several methyl, ethyl and phenyl derivatives of silane and halogenosilane.

## Experimental

**Method and Apparatus.**—The electron diffraction apparatus used in this study has been described by Kimura[1]. The photographs taken were studied visually. The radial distribution curves and the theoretical intensity curves were calculated accorcing to the approximate formula used by Spurr and Schomaker[2]. In the temperature factors, $\exp(-b_{ij}q^2)$, for the theoretical intensity curves, $b_{ij}$ was assumed to be equal to zero for all bonded distances, 0.0001 or 0.0002 for the atom pairs $\overset{Si}{\overset{\wedge}{O\cdots C}}$, $\overset{Si}{\overset{\wedge}{C\cdots C}}$, $\overset{Si}{\overset{\wedge}{Cl\cdots Cl}}$, $\overset{O}{\overset{\wedge}{Si\cdots Si}}$, etc., and 0.0004 or larger values for other non-bonded long distances. As the compounds used in this study constained relatively large numbers of parameters concerning their molecular structures, it was very difficult to derive unique conclusions from the observed intensity data unless some reasonable assumptions were made. Therefore the C-H distance and the valence angle of carbon in aliphatic organic radicals were assumed to be 1.09 Å and 109.5°, respectively. For particularly complicated compounds such as $((CH_3)_2SiS)_3$ and $((CH_3)_2SiO)_4$, the bond lengths well resolved in the radial distribution curves were used to evaluate the valence angles. The results thus obtained gave one of the models which could reproduce the observed intensity data, but other possibilities could not entirely be ruled out.

**Compounds Studied.**—(1) *Methylbromosilanes.*—Monomethyltribromosilane and dimethyldibromosilane were prepared by passing methyl bromide over heated silicon containing copper at 350°[3]. The product was fractionated. The boiling point of $(CH_3)SiBr_3$ was 130-134° and that of $(CH_3)_2SiBr_2$ was 112-113°. Trimethylmonobromosilane was prepared by passing the mixture of methyl bromide and dimethyldibromosilane over aluminum heated at 350°[4]. It boiled at 80°.

* Present address : Faculty of Textile and Sericulture, Shinshu University, Ueda, Nagano Prefecture.

1) M. Kimura, *Chem. Researches (Japan)*, **9**. 53 (1951).
2) R.A.Spurr and V.Schomaker, *J. Am. Chem. Soc.*, **64**, 2693 (1942).
3) E.G.Rochow, *J. Am. Chem. Soc.*, **67**, 963 (1945).
4) D.T. Hurd, ibid., **67**, 1545 (1945).

TABLE I

| Compounds | Si-Br (Å) | Si-C (Å) | ∠Br-Si-Br | ∠C-Si-C |
|---|---|---|---|---|
| $(CH_3)SiBr_3$ | 2.17±0.03 | 1.93 (assumed) | 109.5±2° | — |
| $(CH_3)_2SiBr_2$ | 2.21±0.03 | 1.92±0.06 | 109.5±2° | 109.5° (assumed) |
| $(CH_3)_3SiBr$ | 2.21±0.03 | 1.86±0.05 | — | 114±4° |

(2) *Tetramethylorthosilicate.*—This compound was prepared by the reaction of silicon tetrachloride with methanol[5]. Its boiling point and melting point were 118-120° and 1-2°, respectively.

(3) *Hexachlorodisiloxane.* — This compound was prepared by passing the mixture of oxygen and chlorine over heated silicon[6] and fractionating the product. Its boiling point was 136-138°.

(4) *Hexamethylcyclotrisilazane and Octamethylcyclotetrasilazane.*—These compounds were prepared after Brewer and Haber[7]. The solution of dimethyldichlorosilane in benzene was treated with ammonia. After ammonium chloride was separated by filtration the filtrate was subjected to fractional distillation. The boiling point of the trimer was 185-187° and that of the tetramer was 223-225°.

(5) *Tetramethylcyclodisilthiane and Hexamethylcyclotrisilthiane.*—The trimer was prepared by the method of Champetier et al. who prepared its ethyl homologue[9]. The dimer was prepared by the thermal rearrangement of the trimer at 200° in a stream of hydrogen sulfide[8]. The boiling point of the dimer was 172-173°, and that of the trimer was 151.5-153.5°/38 mmHg.

(6) *Ethyltrichlorosilane, α- and β-chloroethyltrichlorosilane, tetraphenylsilane, phenyltrichlorosilane, octamethylcyclotetrasiloxane and tetra-(trimethylsiloxy)-silane* were furnished by Mr. M. Murata of the Osaka Municipal Technical Research Institute. Hexachlorodisilmethylene and hexamethyldisiloxane were given to the present writer by Dr. M. Kumata of Osaka City University and Mr. I. Hizawa of Sumitomo Chemical Co., respectively.

## Results

**(1) Methylbromosilanes[10].**—The molecular structures of these compounds as revealed by electron diffraction experiments at 20-30° are shown in Table I. Calculations were based on the following: 1) C-H distance equal to 1.09 Å, 2) ∠H-C-Si equal to 109.5°, and 3) staggered relative positions of Br and H in a $CH_3$ radical with respect to a Si-C bond.

**(2) Ethyltrichlorosilane ($(C_2H_5)SiCl_3$), α-Chloroethyltrichlorosilane ($CH_3 \cdot CHCl \cdot SiCl_3$), β-Chloroethyltrichlorosilane ($ClCH_2 \cdot CH_2 \cdot SiCl_3$) and Hexachlorodisilmethylene ($Cl_3Si \cdot CH_2 \cdot SiCl_3$)** These compounds were studied to obtain data on the structure of $SiCl_3$ radical as well as on rotation about Si-C bond. The structure of $SiCl_3$ remains unchanged throughout these compounds, that is Si-Cl=2.00±0.02 Å, and ∠Cl-Si-Cl=109.5±2°. Ethyl, chloroethyl, and disilmethylene radicals contribute little to intensity curves and therefore it was necessary to assume the structure of these radicals, i. e., C-C 1.54 Å, C-Cl 1.76 Å, Si-C 1.88 Å, and the valence angles of carbon 109.5°. Under these assumptions, the value of about 3 kcal./mol. was deduced for the potential barrier of the hindered rotation about Si-C bond in α-chloroethyltrichlorosilane. For hexachlorodisilmethylene, almost free rotation about Si-C bond was found to exist.

**(3) Tetraphenylsilane and Phenyltrichlorosilane[12].**—Two compounds, $Si(C_6H_5)_4$ and $(C_6H_5)SiCl_3$, were studied to determine the bond lengths between silicon and aromatic carbon and to get some information on the rotation about the Si-C bond. For tetraphenylsilane, the interatomic distance Si-C=1.87±0.03Å was obtained. Rotation about the bond between the silicon atom and the phenyl group was found to be restricted. The equilibrium position of four phenyl groups was the same as that of four nitro groups of tetranitromethane studied by stosick[13]. Model B in Fig. 1 is a sketch of the equilibrium configuration of the molecule in which all groups are rotated through the same angle 30° about Si-C bond from the positions of A in Fig. 1. In phenyltrichlorosilane, the contribution of phenyl group to the total scattering curve was so small that no data could be obtained except the following structure of the $SiCl_3$ radical; Si-Cl=2.00±0.02 Å, ∠Cl-Si-Cl=109.5±2°.

5) E.G.Rochow, ibid., **70**, 2170 (1945).
6) L. Troost and P. Hautefeuille, *Bull. Soc. Chim. France*, **13**, 213 (1870), ibid., **35**, 360 (1881).
7) S.D.Brewer and C.P.Haber, *J. Am., Chem. Soc.*, **70**, 3888 (1948).
8) T.Nomura, M.Yokoi, and K.Yamasaki, *Proc. Japan Acad.*, **29**, 342 (1953).
9) T.Nomura. *J. Chem. Soc. Japan, (Pure Chem. Sect.)*, **74**, 513 (1953).
10) K.Yamasaki, A.Kotera, M.Yokoi and M.Iwasaki, *J. Chem. Soc. Japan, (Pure Chem. Sect.)*, **71**, 349 (1950); *J. Chem. Phys.*, **17**, 1355 (1949).
11) C.Iida, M Yokoi, and K.Yamasaki, *J. Chem. Soc. Japan, (Pure Chem.Sect.)*, **73**, 882 (1952).
12) M.Yokoi, *J. Chem. Soc Japan, (pure Chem. Sect.)*, **73**, 822 (1952).
13) A.J. Stosick, *J. Am. Chem. Soc.*, **61**, 1127 (1937).

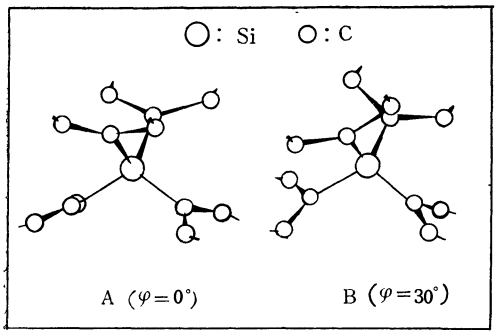



Fig. 1

**(4) Tetramethylorthosilicate Si $(OCH_3)_4$**[14].—The bond lengths and valence angles obtained were Si-O=1.64±0.03 Å, C-O=1.42±0.04 Å, and ∠Si-O-C=113±2°. A carbon atom in a methoxy group had a staggered configuration relative to the oxygen atoms in the other groups.

**(5) Hexamethyltrisilazane $((CH_3)_2SiNH)_3$ and Octamethylcyclotetrasilazane $((CH_3)_2SiNH)_4$**[15]. — Trimeric and tetrameric cyclic dimethylpolysilazane were studied for the purpose of evaluating the Si-N bond length and the Si-N-Si valence angle. For the trimer, the following data were obtained assuming ∠C-Si-C to be 110°; Si-N=1.78±0.03 Å, Si-C=1.87±0.05 Å, ∠N-Si-N=111±5° and ∠Si-N-Si=117±4°. For the tetramer, by assuming the values of Si-N, Si-C, ∠N-Si-N and ∠C-Si-C to be the same as those in the trimer, the valence angle of nitrogen was found to be 123±4°. The rings of these two compounds are puckered, although detailed shapes of the rings could not be determined.

**(6) Tetramethylcyclodisilthiane and Hexamethylcyclotrisilthiane**[16]. — Two compounds, $((CH_3)_2SiS)_2$ and $((CH_3)_2SiS)_3$, were studied to determine the Si-S bond length and the Si-S-Si valence angle. The Si-S bond length was found to be 2.18± 0.03 Å in the former compound and 2.15± 0.03 Å in the latter. Assuming ∠C-Si-C to be 110°, estimated bond agles were ∠Si-S-Si=75° and ∠S-Si-S=105° for the disilthiane, and ∠Si-S-Si=110° and ∠S-Si-S= 115° for the trisilthiane.

**(7) Hexamethyldisiloxane $(CH_3)_3SiOSi(CH_3)_3$.**—The visual curve (V) and the radial distribution curve (R) are shown in Fig. 2. In (R), two maxima at 1.63 and 1.88 Å correspond to Si-O and Si-C bond lengths. The maxima at 2.84 and 3.12 Å are supposed to correspond to Si Si
O···C and C···C respectively. As the values Si
2.84 and 3.10 Å are obtained to O···C and Si
C···C respectively by assuming Si-O 1.63Å, Si-C 1.88 Å and ∠O-Si-C 108°, this choice seems to be adequate. The distance Si···Si seems to be masked by these two maxima. If this distance overlaps on the maximum at 3.12 or 2.84 Å, the corresponding valence angle of oxygen would be about 150 or 120°.

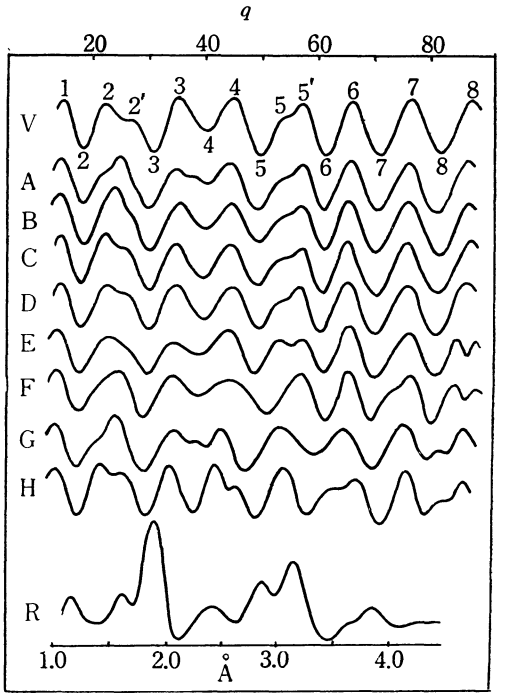



Fig. 2. Visual infensity, theoretical intensity and radial distribution curves of hexamethyldisiloxane.

To estimate Si-O-Si angle and to determine the accuracy of values of Si-O and Si-C bond lengths and O-Si-C angle, the theoretical intensity curves of several models, the bond lengths and the valence angles of which are listed in Table II, were compared with the visual curve in Fig. 2. The configuration of two trimethylsilyl groups was assumed to be the one as illustrated in Fig. 3 throughout these models. Since the relative contribution of long atomic distances to the total intensity was small, and moreover large temperature factors were adopted for the long

14) K.Yamasaki, A.Kotera, M.Yokoi and Y.Ueda. *J. Chem. Soc. Japan (Pure Chem. Sect.)*, **72**, 544 (1951); *J. Chem. Phys.*, **18**, 1414 (1950).
15) M.Yokoi and K.Yamasaki, *J. Am. Chem. Soc.*, **75**, 4139 (1953).
16) M.Yokoi, T.Nomura, and K.Yamasaki, *J. Am. Chem. Soc.*, **77**, 4484 (1955).

distances, a change in the configuration gave little change in the theoretical intensity curves. The shapes and the $q$-values

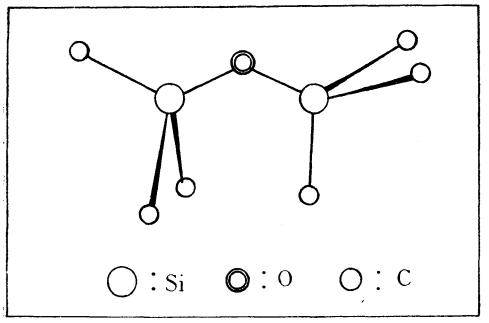



Fig. 3

TABLE II

| Model | Si-O (Å) | Si-C (Å) | ∠Si-O-Si | ∠O-Si-C |
|---|---|---|---|---|
| A | 1.63 | 1.88 | 114° | 108° |
| B | 1.63 | 1.88 | 120 | 108 |
| C | 1.63 | 1.88 | 130 | 108 |
| D | 1.63 | 1.88 | 140 | 108 |
| E | 1.59 | 1.92 | 130 | 108 |
| F | 1.69 | 1.86 | 130 | 108 |
| G | 1.63 | 1.88 | 130 | 102 |
| H | 1.63 | 1.88 | 130 | 112 |

of 2nd and 2nd′ maxima of the theoretical intensity curves vary with the change of Si–O–Si angle. The best qualitative fit was obtained by curve C, the Si–O–Si angle of the model being equal to 130°. In the range of $q$ larger than 40, theoretical curves A–D are consistent with the visual curve. The deviations of O–Si–C angle from 108° gave the change of the $q$-values of 4th and 5th maxima (G and H), while the change of Si–O/Si–C caused the disagreement in the shapes and the $q$-values of 5th and 5th′ maxima (E and F). The observed and the calculated $q$-values of curve C are compared quantitatively Table IV. The final results obtained are: Si–O=1.63±0.05 Å, Si–C=1.88±0.03 Å, ∠Si–O–Si=130±10° and ∠O–Si–C=108±4°.

(8) **Hexachlorodisiloxane ($Cl_3SiOSiCl_3$).**—In this compound the change of Si–O–Si angle had little effect on the over-all scattering intensity. Therefore the Si–O–Si angle was assumed to be 130°. Several theoretical curves are compared with the visual curve (V) in Fig. 4. The bond lengths and the valence angle ∠Cl–Si–Cl of each model are listed in Table III.

TABLE III

| Model | Si-O (Å) | Si-Cl (Å) | ∠Cl-Si-Cl |
|---|---|---|---|
| A | 1.64 | 2.02 | 109.5° |
| B | 1.64 | 2.02 | 109.5 |
| C | 1.68 | 2.01 | 109.5 |
| D | 1.58 | 2·03 | 109.5 |
| E | 1.64 | 2.02 | 112 |
| F | 1.64 | 2.02 | 107 |

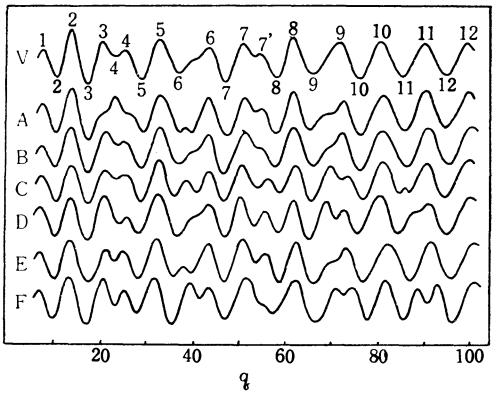



Fig. 4. Visual and theoretical intensity curves of hexachlorodisiloxane.

TABLE IV

| Max. | Min. | $((CH_3)_3Si)_2O$ $q_{obs.}$ | $((CH_3)_3Si)_2O$ $q_C/q_{obs.}$ | $(Cl_3Si)_2O$ $q_{obs.}$ | $(Cl_3Si)_2O$ $q_B/q_{obs.}$ |
|---|---|---|---|---|---|
| 1 | | 15.2 | 0.974 | 8.0 | 1.013 |
| | 2 | 18.5 | 1.030 | 10.7 | 0.973 |
| 2 | | 21.9 | 1.072 | 14.2 | 0.972 |
| 2′ | | 27.1 | 0.996 | — | — |
| | 3 | 30.5 | 1.015 | 17.3 | 1.000 |
| 3 | | 34.9 | 1.005 | 20.3 | 1.024 |
| | 4 | 40.5 | 0.970 | 23.1 | — |
| 4 | | 45.1 | 0.980 | 25.4 | 1.000 |
| | 5 | 49.5 | 0.990 | 28.8 | 0.993 |
| 5 | | 53.8 | 0.991 | 32.2 | 0.991 |
| 5′ | | 57.3 | 1.007 | — | — |
| | 6 | 61.3 | 1.000 | 36.5 | 0.982 |
| 6 | | 65.8 | 1.000 | 43.2 | 0.991 |
| | 7 | 70.9 | 0.994 | 46.7 | 1.000 |
| 7 | | 76.8 | 0.994 | 50.2 | 1.007 |
| 7′ | | — | — | 54.4 | 1.000 |
| | 8 | 82.3 | 1.000 | 57.8 | 1.011 |
| 8 | | 87.4 | 0.999 | 61.9 | 1.001 |
| | 9 | | | 66.7 | 0.988 |
| 9 | | | | 71.8 | — |
| | 10 | | | 76.2 | 1.012 |
| 10 | | | | 80.9 | 1.002 |
| | 11 | | | 86.1 | 0.994 |
| 11 | | | | 90.1 | 1.018 |
| Mean | | | 1.001 | | 0.999 |
| Mean deviation | | | 0.015 | | 0.010 |

When two $SiCl_3$ radicals were fixed in a certain relative position, the interference of long Cl···Cl had some effect on 3rd and 4th maxima as shown in the curve A of Fig. 4. The most satisfactory model (curve B) was the free rotation model. Approximate curves were calculated ignoring the effect of long distances which vary by rotation. Curves C–F were calculated also with the omission of long distances. The change of Cl–Si–Cl angle from tetrahedral angle to 112° gave a small maximum between 5th and 6th maxima, while for ∠Cl–Si–Cl equal to 107°, 7th′ maximum disappeared and the shape and the position of 6th maximum were not in accord with those of the visual curve (E and F). The shapes and the $q$-values of 7th′ and 9th maxima of the model, Si–O/Si–Cl in which is 1.58/2.03 or 1.68/2.01, were not in accord with the visual curve (C and D). With these qualitative considerations and the quantitative comparisons given in Table IV, the final results obtained are: Si–Cl=2.02±0.02 Å, Si–O=1.64±0.05 Å and ∠Cl–Si–Cl=109.5±2°.

**(9) Tetra-(trimethylsiloxy)-silane ($Si(OSi(CH_3)_3)_4$).** — The radial distribution curve calculated from the visual curve is shown in Fig. 5 together with that of octamethylcyclotetrasiloxane. Maxima at 1.63, 1.88 and 3.06 Å appear on both curves. Maxima at 1.63 and 1.88 Å are due to bonded Si–O and Si–C distances, respectively, which are consistent with values determined for hexamethyldisiloxane. In the vicinity of 3 Å in the curves, maxima corresponding to non-bonded Si–O···C and Si–O···Si distances should appear. If Si–O–Si angle is larger than O–Si–C, and the maximum at 3.06 Å is due to Si–O···Si, then Si–O–Si angle should be 140°. To clarify this point, comparisons were made of theoretical intensity curves with the visual intensity curve, for models having various valence angles, Si–O and Si–C bond lengths being assumed to be 1.63 and 1.88 Å respectively as obtained from the radial distribution curve. The valence angle of central silicon atom was assumed to be

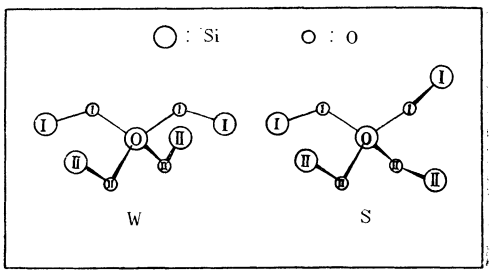



Fig. 6

W: The two Si atoms, the two O atoms designated by I (or II) and the central Si atom are coplanar, forming W-shaped chain.

S: One Si atom at the end of each chain is twisted through 60° about Si–O bond from the position of the W-form.

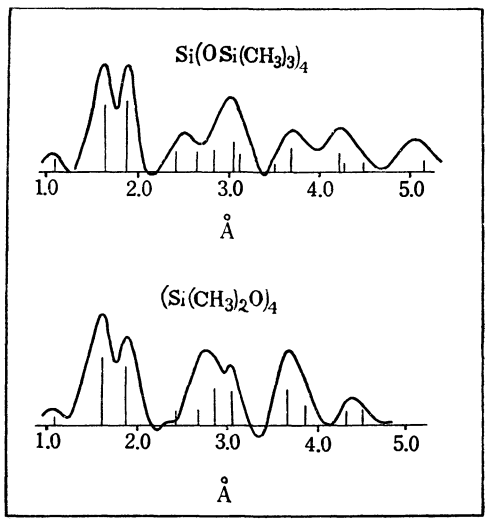



Fig. 5. Radial distribution curves of tetra-(trimethylsiloxy)-silane and octamethylcyclotetrasiloxane.

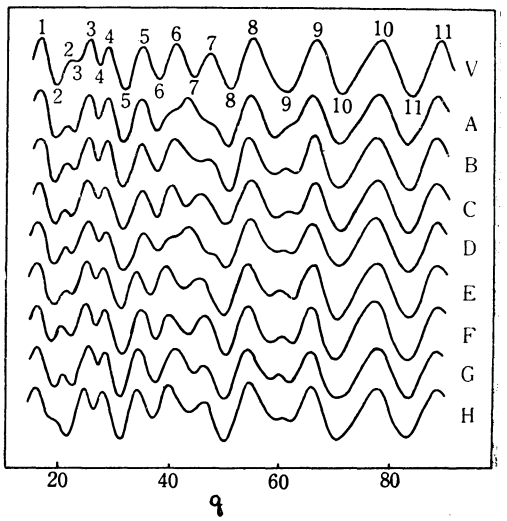



Fig. 7. Visual and theoretical intensity curves of tetra-(trimethylsiloxy)-silane.

tetrahedral. These curves are shown in Fig. 7 with the visual curve (V). The valence angles of each model are listed in Table V. The relative positions of four trimethylsiloxy groups were assumed to take either W- or S-form as shown in Fig. 6. In the theoretical curves of models of W-form (for example, curve H in Fig. 7), the second maximum was near the first maximum and was not consistent with the visual curve. Therefore models having W-form were rejected. For models of S-form (curves A-G), good agreement was obtained for the second maximum. The features of the theoretical intensity curve, which are sensitive to the change of Si-O-Si and O-Si-C angles are the shapes and the $q$-values of 5th and 6th and 7th maxima. Curve B corresponding to the model in which Si-O-Si and O-Si-C angles are 140° and 107° respectively, well reproduces the features of the visual intensity curve. The variation of $Si_0$-O and $Si_1$-O in the vicinity of 1.63 Å gave curve F and G, in which the $q$-values of 6th maxima are not consitent with the visual curve. From these considerations the values of ∠Si-O-Si and ∠O-Si-C which well reproduce the visual intensity curve, were found to be 140±5° and 107±3° respectively.

TABLE V

| Model | $Si_0$-O(Å) | $Si_1$-O(Å) | ∠Si-O-Si | ∠O-Si-C |
|---|---|---|---|---|
| A | 1.63 | 1.63 | 140° | 110° |
| B | 1.63 | 1.63 | 140 | 107 |
| C | 1.63 | 1.63 | 140 | 104 |
| D | 1.63 | 1.63 | 135 | 107 |
| E | 1.63 | 1.63 | 145 | 107 |
| F | 1.60 | 1.65 | 140 | 107 |
| G | 1.65 | 1.60 | 140 | 107 |
| H | 1.63 | 1.63 | 140 | 107 |

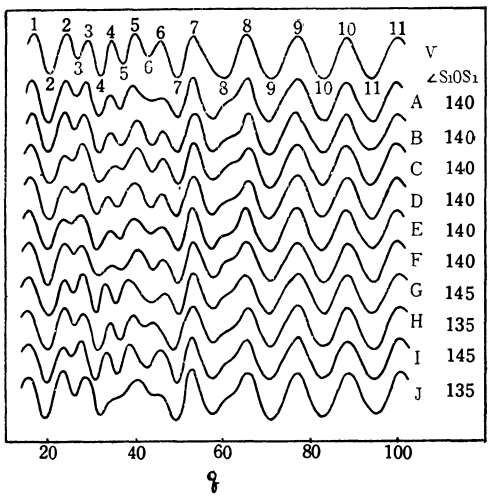



Fig. 8. Visual and theoretical intensity curves of octamethylcyclotetrasiloxane.

**(10) Octamethylcyclotetrasiloxane** $((CH_3)_2SiO)_4$.—Theoretical intensity curves for models assuming the tetrahedral angle of silicon atom are shown in Fig. 8 together with the visual curve (V). There are several conceivable forms of an eight-membered ring of $(Si-O)_4$ as shown in Fig. 9. The variation of the form caused minor changes in the shapes and the $q$-values of 2nd and 3rd maxima. This is a natural consequence of large temperaturs factors used for long distances. The

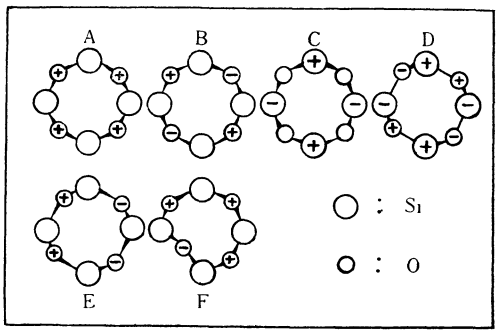



Fig. 9

TABLE VI

| Max. | Min. | $Si(OSi(CH_3)_3)_4$ $q_{obs.}$ | $Si(OSi(CH_3)_3)_4$ $q_B/q_{obs.}$ | $((CH_3)_2SiO)_4$ $q_{obs.}$ | $((CH_3)_2SiO)_4$ $q_B/q_{obs.}$ |
|---|---|---|---|---|---|
| 1 | | 16.2 | (0.950) | 16.1 | 0.975 |
| | 2 | 18.6 | 1.000 | 20.1 | 1.009 |
| 2 | | 20.8 | 0.981 | 23.4 | 1.000 |
| | 3 | 22.2 | 0.972 | 26.1 | 0.976 |
| 3 | | 24.7 | 0.979 | 28.6 | 0.973 |
| | 4 | 26.4 | 0.992 | 31.2 | 0.987 |
| 4 | | 27.9 | 0.993 | 33.8 | 0.994 |
| | 5 | 31.0 | 1.006 | 36.5 | 0.994 |
| 5 | | 34.2 | 1.002 | 39.1 | 1.006 |
| | 6 | 37.0 | 1.011 | 43.0 | 0.986 |
| 6 | | 40.2 | 0.997 | 46.1 | 0.982 |
| | 7 | 43.2 | 1.027 | 49.5 | 0.988 |
| 7 | | 46.4 | 0.991 | 52.9 | 1.012 |
| | 8 | 50.0 | 0.989 | 60.4 | — |
| 8 | | 54.0 | 0.989 | 65.4 | 1.017 |
| | 9 | 60.7 | — | 71.2 | 0.995 |
| 9 | | 65.6 | 1.011 | 77.3 | 0.993 |
| | 10 | 69.7 | 1.012 | 83.4 | 0.991 |
| 10 | | 77.7 | 0.998 | 88.8 | 1.000 |
| | 11 | 83.4 | 0.993 | 95.2 | 0.990 |
| 11 | | 88.4 | 0.982 | 100.3 | 0.998 |
| Mean | | | 0.994 | | 0.994 |
| Mean deviation | | | 0.011 | | 0.009 |

variation of the Si–O–Si angle of a symmetrical crown form considerably affects the relative positions of 4th, 5th and 6th maxima as indicated by curves G and H. The same is true for a cradle form (cf. curves I and J). In this case, too, the best agreement with the visual curve was obtained with models in which the Si–O–Si angle was 140°. The quantitative comparison of the observed $q$-values with the calculated ones for the best models of tetra-(trimethylsiloxy)-silane and octamethylcyclotetrasiloxane is shown in Table VI. For the latter compound, the curve of cradle form (B in Fig. 8) was found to be better than those of other forms. The distances appearing in the best curve are shown schematically in Fig. 5. The distances ranging from 2.4 to 2.9 Å in the distribution curve are not consistent with the distances appearing in the best model.

*Department of Chemistry*
*Faculty of Science*
*Nagoya University, Nagoya*

# *Electron Diffraction Investigation on the Molecular Structures of Some Organosilicon Compounds. II*

By Masatoki YOKOI

(Received September 19, 1956)

The results of studies on the molecular structures of several organosilicon compounds as revealed by electron diffraction experiments are described in part I of this report. The results obtained are discussed below.

**(1) Silicon-halogen Bond.**—A number of compounds containing silicon-halogen bond have been investigated by electron diffraction and by microwave spectroscopy. The data on silicon-halogen bonds which have hitherto been determined are listed in Table 1 together with those of the present study. According to our finding, the distance between silicon and halogen

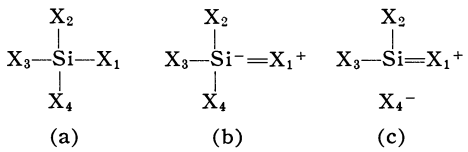
TABLE I

| Compounds | By Electron Diffraction | By Microwave Spectroscopy | Reference |
|---|---|---|---|
| | (Si-F length (Å)) | | |
| $SiF_4$ | 1.54±0.02 | | 3 |
| $HSiF_3$ | | 1.565±0.005 | 4 |
| $H_3SiF$ | | 1.593, 1.595±0.010 | 5, 4 |
| $(CH_3)_3SiF$ | 1.57±0.02 | | 6 |
| | (Si-Cl length (Å)) | | |
| $SiCl_4$ | 2.01±0.02 | | 7 |
| $HSiCl_3$ | 2.01±0.03 | 2.021±0.002 | 8, 9 |
| $H_2SiCl_2$ | 2.02±0.03 | | 10 |
| $H_3SiCl$ | 2.06±0.05 | 2.0479±0.0007, 2.048 | 10, 4, 9 |
| $(CH_3)SiCl_3$ | 2.01±0.02 | 2.021 | 11, 9 |
| $(CH_3)_2SiCl_2$ | 1.99±0.03 | | 11 |
| $(CH_3)_3SiCl$ | 2.09±0.03 | 2.03 | 12, 9 |
| $(CH_3)_2SiClF$ | 2.03±0.03 | | 6 |
| $F_3SiCl$ | 2.01±0.02 | | 10 |
| | (Si-Br length (Å)) | | |
| $SiBr_4$ | 2.15±0.02 | | 1 |
| $HSiBr_3$ | 2.16±0.03 | | 1 |
| $H_3SiBr$ | | 2.209±0.001 | 2 |
| $(CH_3)SiBr_3$ | 2.17±0.03 | | Present work |
| $(CH_3)_2SiBr_2$ | 2.21±0.03 | | Present work |
| $(CH_3)_3SiBr$ | 2.21±0.03 | | Present work |
| $F_2SiBr$ | | 2.16±0.02 | 5 |
| $F_3SiBr$ | | 2.147 | 5 |

1) R.Spitzer, W.J.Howell and V Schomaker, *J. Am. Chem. Soc.*, **64**,62 (1942).
2) A.H.Sharbaugh, J.K. Bragg, J.C. Madison and V. G. Thomas, *Phys. Rev.*, **76**, 1419 (1949).
3) L.Pauling and L.O.Brockway, *J. Am. Chem. Soc.*, **57**, 2684 (1935).
4) B.Bak J,Bruhn and J.Rastrup-Anderson, *Acta Chem. Scand.*, **8**, 367 (1954).
5) J. Sheridan and W.Gordy, *J. Chem. Phys.*, **17**, 965 (1951).
6) C.J.Wilkins and L.E.Sutton, *Trans Faraday Soc.*, **50**, 783 (1954).
7) K. Yamasaki, A. Kotera, M. Iwasaki and N. Tatematsu, *J. Chem. Soc. Japan, (Pure Chem. Sect.)*, **69**, 104 (1953).
8) L.O.Brockway and J.Y.Beach, *J. Am. Chem. Soc.*, **60**, 1836 (1938).
9) R.C.Mockler, Jep H.Bailey and W.Gordy, *J. Chem. Phys.*, **21**, 1710 (1953).
10) L.O.Brockway and I.E.Coop, *Trans. Faraday Soc.*, **34**, 1429 (1938).
11) R.L.Livingston and L.O.Brockway, *J. Am. Chem. Soc.*, **66**, 94 (1944).
12) R.L.Livingston and L.O.Brockway, ibid., **68**, 719 (1946).

is not affected when hydrogen atoms of halogenosilane are replaced by methyl radicals. For example, The Si-Br lengths of $(CH_3)SiBr_3$ and $(CH_3)_3SiBr$ agree with these of $HSiBr_3$[1] and $H_3SiBr$[2]. On the other hand, these bond lengths vary when the number of halogen atoms attached to silicon is altered.

In general, silion-halogen distance of the derivatives of monohalogenosilane is longer by 0.03–0.06 Å than that of respective tetrahalogenosilane. The sum of Pauling-Huggins atomic radii[13] is longer than the observed lengths, as is also the length calculated from Schomaker-Stevenson's rule[14]. The double bond character of silicon-halogen bond and the change of character with the number of substituents provide an explanation of these facts[13]. A reasonable representation of the ground electronic state of these molecule is a resonance hybrid of the forms a, b and c.



(a) (b) (c)

The structure b implies the double bond formation with the use of 3d orbital of silicon. When the number of halogen atoms attached to silicon is more than one, the contribution of the structure c becomes large. This may explain the change of the bond length with the number of substituents.

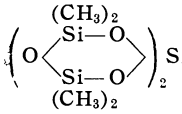
(2) **Silicon-carbon Bond.** — Available date on the bond length of Si–C are listed in Table II. These date agree with a value of 1.88 Å within an error of 0.03 Å. Bond and Brockway[15], however, they have recently shown in their electron diffraction investigation using a sector on $Si(CH_3)_nH_{4-n}$ ($n$=1, 2 and 3) that Si–C length increased by about 0.01 Å with the introduction of each successive methyl radical. The bound length between silicon and aromatic carbon agress with that of

TABLE II

| Compounds | Si-C Length (Å) | Reference |
|---|---|---|
| $Si(CH_3)_4$ | 1.888±0.02 | 16 |
| $Si_2(CH_3)_6$ | 1.90 ±0.02 | 17 |
| $HSi(CH_3)_3$ | 1.873±0.006 | 15 |
| $H_2Si(CH_3)_2$ | 1.860±0.004 | 15 |
| $H_3Si(CH_3)$ | 1.857±0·007 | 15 |
| $(CH_3)_3SiF$ | 1.89 ±0.02 | 6 |
| $(CH_3)_2SiClF$ | 1.89 ±0.02 | 6 |
| $(CH_3)_3SiCl$ | 1.89 ±0.03, 1.87 | 12,9 |
| $(CH_3)SiCl_3$ | 1.876 | 9 |
| $(CH_3)_3SiCH_2Cl$ | 1.88 ±0.04 | 18 |
| $(CH_3)_3SiBr$ | 1.86 ±0.05 | Present work |
| $((CH_3)_2SiO)_3$ | 1.86 ±0.04 | 19 |
| $((CH_3)_3Si)_2O$ | 1.88 ±0.03 | Present work |
| $Si(C_6H_5)_4$ | 1.87 ±0.03 | Present work |

TABLE III

MOLECULAR STRUCTURES OF SILOXANES

| Compounds | Si-O (Å) | Si-C (Å) | ∠Si-O-Si | ∠O-Si-O | ∠C-Si-C | Reference |
|---|---|---|---|---|---|---|
| $((CH_3)_3Si)_2O$ | 1.63±0.05 | 1.88±0.03 | 130±10° | — | 114±4° | Present work |
| $((CH_3)_2SiO)_3$ | 1.66±0.04 | 1.86±0.04 | 125±5 | 115±5° | 112±6 | 19 |
|  | 1.64±0.03 | 1.88±0.03 | 130±4 | 109±4 | 109±4 | 21* |
| $((CH_3)_2SiO)_4$ | 1.63 | 1.88 | 140±5 | 109.5 (assumed) | 109.5 (assumed) | Present work |
| $((CH_3)_2SiO)_4$ | 1.65 | 1.92 | 142.5 | 109 | 106 | 22* |
| $((CH_3)_3SiO)_4Si$ | 1.63 | 1.88 | 140±5 | 109.5 (assumed) | 112±4 | Present work |
| $(CH_3O)_4Si$ | 1.64±0.03 | — | 113±2(∠Si-O-C) | | | Present work |

* Data from X-ray crystal analysis

13) L.Pauling, "The Nature of the Chemical Bond", Cornell Univ. Press, 2nd Ed. (1940).
14) V.Schomaker and D.P.Stevenson, *J. Am. Chem. Soc.*, **63**, 37 (1941).
15) A.C.Bond and L.O.Brockway, *J. Am. Chem. Soc.*, **76**, 3312 (1954).
16) W. F. Sheehan, Jr. and V. Schomaker, *J. Am. Chem. Soc.*, **74**, 3956 (1952).
17) L.O.Brockway and N.R.Davidson, ibid., **63**, 3287 (1941).
18) J. M. Hastings and S.H.Bauer, *J. Chem. Phys.*, **18**, 13 (1950).
19) E.H.Aggarwal and S.H.Bauer, ibid., **18**, 42 (1950).

silicon and carbon in methyl radical within 0.03 Å. The bond angle of C–Si–C of trimethylsilyl group, $-Si(CH_3)_3$, is approximately tetrahedral, and somewhat larger values are obtained in certain compounds such as: $(CH_3)_3SiCl$ (113±2°), $(CH_3)_3SiBr$ (114±4°) and $Si(OSi(CH_3)_3)_4$ (112±4°).

**(3) Silicon-oxygen Bond.**—Silicon-oxygen bond is an important one which builds up the framework of both inorganic silicates and organosilicon polymers. The nolecular structures of organic compounds containing Si–O bond are summarized in Table 3. The Si–O lengths obtained for organosilicon compounds agree without exception with 1.64 Å. Smith[20] deduced a value of 1.60±0.01 Å for Si–O length by reviewing the obtainable deta on various inorganic silicates and aluminosilicates. Introduction of methyl radical may increase Si–O length somewhat.

The valence angle of the oxygen atom in Si–O–C linkage, 112±3°, obtained for $(CH_3O)_4Si$ is in agreement with that in C–O–C linkage of methyl ether[23]. On the other hand, the angle Si–O–Si has a larger value, 130±10° in $((CH_3)_3Si)_2O$, 125±5° in $((CH_3)_2SiO)_3$, and 140±5° in $((CH_3)_2SiO)_4$ and $((CH_3)_3SiO)_4Si$. Since there may be a strain causing distortion in the ring structure of $((CH_3)_2SiO_3)$, a value of about 140° seems to be normal. The values of Si–O–Si angle reported for $\alpha$-quartz and for $\alpha$-cristobalite are 142°[24] and 150°[25] respectively. These values are consistent with those of organic siloxanes. It may be said, therefore, that Si–O–Si chain in organic siloxanes has a geometrical structure similar to that in inorganic silicates.

Smyth and Holland[26] studied the dielectric properties of hexamethyldisiloxane in detail over a wide range of temperature and discussed the properties of Si–O bond. They calculated a dipole moment of 0.66 D in the vapor phase, and of 0.46 D in the pure liquid. The atomic polarization was determined to be 7.9 cc. There were large discrepancies between the values of the group moment of $(CH_3)_3SiO$. Assuming Si–O–Si angle to be 130°, calculation from the observed moment gave 0.54 D (liquid) and 0.78 D (vapor), while a group moment 1.6–2.0 D was obtained from an approximate formula relating ionic character of the bond to electronegativity difference. These data were considered to be consistent with a valence angle of oxygen greater than 130°. However silicon has the ability to expand its 3d orbital and to form a partial double bond with more electronegative elements. Kurita and Kondo[27], assuming Si–O–Si angle to be 130°, showed that there was a fairly good agreement between a bond moment 1.55 D of Si–O calculated from the dipole moment data of hexamethyldisiloxane and a value of 1.1 D obtained by the Pauling's method[28], which permitted us to calculate the degrees of the double bond character and the ionic character of bonds in oxy-acid molecules.

**(4) Cyclic Compound Containing Silicon Atoms as Ring Members.**—Dimethylcyclopolysiloxane, dimethylcyclopolysilazane and dimethylcyclopolysilthiane can be prepared by treating dimethyldichlorosilane with water, ammonia and hydrogen sulfide respectively.

As regards the trimer of cyclosiloxane, electron diffraction data[19] indicated that the six-membered ring is planar. The trimer can be prepared by the cracking of dimethylpolysiloxanes, while the hydrolysis product of dimethyldichlorosilane contains only a small amount of the trimer[29]. Scott[30] investigated the redistribution equilibrium between dimethylcyclopolysiloxanes and linear polysiloxanes catalyzed by sulfuric acid. He concluded that the ring having the smallest number of members of cyclic polysiloxane, as in the trimer in this case, had a slight strain, while the ring structures of the tetramer or the polymer of larger size were probably free from strain. He attributed this strain to the deformation of normally large Si–O–Si angle in forming a small membered ring. Actually the difference between the molecular structure of the trimer and that of the tetramer exists in the Si–O–Si angle, which is 125° for the trimer and 140° for the tetramer. It is likely that a strain free Si–O–Si angle takes a probable value of about 140° and is easily deformable by intra- and intermolecular forces.

20) J.Smith, *Acta Cryst.*, **7**, 479 (1954).
21) W.L.Roth and D.Harker, ibid., **1**, 34 (1948).
22) H.Steinfink, B.Post and I.Fankuchen, ibid., **5**, 802 (1954).
23) Cited in a paper by P.W.Allen and L. E. Sutton, *Acta Cryst.*, **3**, 46 (1950).
24) F.Machatschki, *Fortschr. Mineral. Krist. Petrog.*, **20**, 45 (1936).
25) W.Niewenkamp, *Z.Krist.*, **96**, 454 (1937).
26 R.S.Holland and C.P.Smyth, *J. Am. Chem. Soc.*, **77**, 268 (1955).
27) U.Kurita and M.Kondo, This Bulletin, **27**, 160 (1954).
28) L.Pauling, *J. Phys. Chem.*, **56**, 361 (1952).
29) W.Patenode and D.Wilcock, *J. Am, Chem. Soc.*, **68**, 358 (1946).
30) D.W.Scott, ibid., **69**, 803 (1947).

As regards the silthiane compounds, dimethylsubstituted polymers having a ring larger than that of the trimer have not yet been isolated. When the cyclic trimer is heated at about 200° under atomospheric pressure, the dimer is distilled. In this case, the valence angle of sulfur atom should have been deformed from about 110° in the trimer to about 75° in the dimer. The ring structure of the dimer is similar to that of silicon disulfide, in which successive $SiS_4$ tetrahedrons are joined with a common edge leading to a fibrous frame extending in one dimension. This structure of silicon disulfide have been interpreted as an ionic packing of $Si^{4+}$ and $S^{2-}$ whose ionic radii ratio has a certain critical value, at which the change in coordination number four to three may be expected to occur. The Si-S bond of tetramethylcyclodisilthiane is supposed to have as large ionic character as that of silicon disulfide.

Brewer and Haber[31] studied the rearrangement equilibrium between linear and cyclic dimethylpolysilazanes at high temperature under high pressure. They found that the tendency of ring formation is greater in the silazane than in the corresponding siloxane systems. The rings of both the trimer and the tetramer of dimethylcyclopolysilazane have puckered structures. The difference between the valence angles of the nitrogen atom in the trimer and the tetramer may be due to the steric repulsion of methyl radicals.

In Table IV, comparison is made of the observed bond lengths of silicon and other electronegative elements with the sums of Pauling-Huggins radii and with the values calculated from Schomaker-Stevenson's rule.

TABLE IV

| Bond | Bond Length (Å) Obs. | Calcd. after Pauling-Huggins | Calcd. after Schomaker-Stevenson | Electronegativity Difference |
|---|---|---|---|---|
| Si-C | 1.88 | 1.94 | 1.88 | 0.7 |
| Si-N | 1.73[32], 1.78 | 1.87 | 1.80 | 1.2 |
| Si-O | 1.63 | 1.83 | 1.76 | 1.7 |
| Si-F | 1.54-1.60[3,4] | 1.81 | 1.69 | 2.2 |
| Si-S | 2.15-2.18 | 2.21 | 2.15 | 0.7 |
| Si-Cl | 2.00-2.02 | 2.16 | 2.15 | 1.2 |
| Si-Br | 2.17-2.21 | 2.31 | 2.22 | 1.0 |

In general, with increasing electronegativity difference, the difference increases between the calculated bond lengths and observed ones. Among these values, the contraction is remarkable for the most polar Si-O and Si-F bonds. This may indicate the presence of either one or both of the following causes; 1) larger ionic character of the bond than is suggested by the electronegativity difference, 2) partial double bond character arising from resonance. Craig et al.[33] discussed this problem in detail, and were led to the conclusion that presumably $d\pi-p\pi$ bonding is a common one giving rise to a strong bond and that the polar character in $\sigma$-bonds can give extra stability by increasing the $d\pi-p\pi$ overlap.

## Summary

The vapors of methyl or ethyl substituted silicon compounds containing Si-Cl, Si-Br, Si-O, Si-N and Si-S bonds were studied by electron diffraction method and their molecular structures were determined. Bond lengths obtained are summarized in Table IV. The Si-Br length in methylbromosilane series changes with the number of substitutions of Br, but the length is in accord with the data of corresponding bromosilanes. The valence angles of oxygen in linear and cyclic siloxanes were estimated to be about 140° and this value is nearly the same as that in $\alpha$-quartz. The valence angles of silicon in cyclic compounds are almost tetrahedral and those of oxygen, nitrogen and sulfur vary with the size of the ring.

The author expresses his sincere gratitude to Drs. K. Yamasaki and M. Kimura for their encouragement and kind discussions throughout this work, and to Mr. H. Murata of the Osaka Municipal Technical Research Institute, Dr. M. Kumata of Osaka City University, and Mr. I. Hizawa of Sumitomo Chemical Co. for furnishing samples.

*Department of Chemistry, Faculty of Science, Nagoya University Nagoya*

31) S. D Brewer and C. P. Haber, *J. Am. Chem. Soc.*, **70**, 3888 (1948).
32) K. Hedberg. E. Goldish and M. E. Jones, *J. Am. Chem.* Soc., **77**, 5278 (1955).
33) D. P. Craig, A. Maccoll, R. S. Nyholm and L. E. Sutton, *J. Chem. Soc.*, **1954** 332.

# SHORT COMMUNICATIONS

## *An Improved Synthesis of O-Benzyl-DL-serine*

By Kenji OKAWA

(Received September 20, 1956)

In the previous paper*, it was reported that O-benzyl-DL-serine was synthesized from methyl acrylate in 51% yields. The method, however, is not profitable for a large scale preparation. In the present work, ethyl acrylate was used in place of methyl acrylate and the method was improved as follows:

**α-Bromo-β-benzyloxy-propionic Acid.**—To a solution of 115 g. of ethyl acrylate in 100 cc. of absolute ether was added 57 cc. of dry bromine dropwise at 5°C under stirring, and the mixture was allowed to stand over-night at room temperature (Solution-A).

Twenty six grams of metallic sodium was dissolved in an ether-benzylalcohol mixture (500 cc. of ether-300 cc. of benzylalcohol) under reflux-condenser (Solution-B).

Solution-B was added portionwise into the solution -A under strong stirring at −10°C for one hour, the stirring was continued at the same temperature for thirty minutes after the addition was over.

The precipitated sodium bromide was removed from the ether solution by washing with 200 cc. of water and the extract was acidified with conc. hydrochloric acid. The oily product separated was extracted with ether and both the ether solutions were combined. After removal of the ether, the mixture was shaken with 180 g. of barium hydroxide in 3 l of water for five hours at room temperature. In order to complete the hydrolysis, the residual oil was treated with 100 g. of barium hydroxide in 1.5 l of water under the same conditions. The water layers were collected and acidified with conc. of hydrochloric acid. Then the separated oily product was extracted with ether. After removal of the ether, 370 g. of crude α-bromo-β-benzyloxy-propionic acid was obtained.

**O-Benzyl-DL-serine.**—The crude product of the α-brom acid was dissolved in 5 l. of aq. ammonia (34%) containning 500 g. of ammonium carbonate and then allowed to stand for 1 week at room temperature. The reaction mixture was concentrated in vacuo until crystals of the amino acid appeared. A small amount of the crystals were obtained from the mother liquor. The fine crystals of O-benzyl-DL-serine (150 g.) were prepared in 67% yields.

*Department of Chemistry*
*Faculty of Science*
*Osaka University*
*Osaka*

* K. Okawa and H. Tani, *J. Chem. Soc. Japan.*, **75** 1197 (1950).

# *On Carotenoids of a Sponge "Reniera japonica"**

By Masaru YAMAGUCHI

(Received August 6, 1956)

The orange-colored sponge "*Reniera japonica*" which is widely distributed in the tidal zone in our shores contains a number of polyene pigments consisting of various carotenoid hydrocarbons with different types of chromophores as well as of several oxygenated carotenoids.

The six carotenoid hydrocarbons isolated in crystalline states from this sponge have already been reported in the preceding paper[1]. In the present paper are reported the results obtained by further investigations which have clarified to a considerable extent the total composition of the coloring matters of this sponge by the isolation of nine different polyene pigments in crystalline states in addition to the above six hydrocarbons.

The materials were collected near the Amakusa Marine Laboratory attached to the Faculty of Science, Kyushu University. The sponge was extracted with acetone and petroleum benzine, and after saponification the crude pigment which consisted mainly of carotenoid hydrocarbons was precipitated from the petroleum benzine solution by the addition of ethanol. The crude pigment and the mother liquor were separately subjected to chromatography. Almost all zones in the chromatograms afforded crystallized pigments. All pigments obtained are listed in Table I in the sequence of increasing adsorbability. Several of these pigments appear to be new pigments hitherto unknown.

It should be emphasized that only one species of sponge contains such numerous polyene pigments. Of course it may be possible that a few minor pigments do not belong to this sponge but, in reality, to a small quantity of algae with which the sponge is inevitably contaminated. Of these pigments listed above, renieratene predominates in quantity, the pigments which melt at 199° and $\beta$-carotene are the next, and the quantities of other pigments are much smaller.

TABLE I

PIGMENTS OBTAINED FROM "*Reniera japonica*"

| Spectral absorption maxima in $CS_2$; in m$\mu$ | Melting point | Yield from 5.7 kg. of sponge; in mg. |
|---|---|---|
| 507, 478, 447 ($\alpha$-carotene) | 185° | 2 |
| 520, 485, 452 ($\beta$-carotene) | 183° | 20 |
| 520, 484, 452 | 199° | 45 |
| 524, 488, 453 | 194° | —a) |
| 532, 496, 463 (renieratene) | 185° | 93 |
| 536, 499, 467 | 205° | 1.1 |
| 544, 504, 475 (renierapurpurin) | 230° | 4.4 |
| 531, 494, 463 | 123° | —a) |
| 558, 521, (492) (renieraxanthin) | 161° | 2.6 |
| 548, 512, (471) | | —a) |
| 495, a single maximum | | —a) |
| 507, 475, 445 | | —a) |
| 518, 483, 452b) | 153-4° | 0.4 |
| 530, 493, 461c) | 173-4° | 1.0 |
| 558, 517, (485) | | —a) |

a) As the yields of these pigments were very small, they were not weighed.
b) Not identical with cryptoxanthin.
c) Not identical with rubixanthin, nor probably with gazaniaxanthin.

The main pigment "renieratene" seems to have a molecular formula $C_{40}H_{48}$ or $C_{40}H_{50}$ on the basis of the analytical data, and it shows the highest carbon content of the carotenoid pigments hitherto reported. The study on the structure of this unique carotenoid hydrocarbon is now in progress.

The pigment of m. p. 199° is of interest, since it shows the same spectral properties as those of $\beta$-carotene. It closely resembles leprotin[2] ($C_{40}H_{54}$; abs. max. in $CS_2$, 517, 479, 447 m$\mu$; m. p. 198–200°) especially in melting point and in spectral properties. However, as the elementary analysis showed 90.91% carbon and 9.38% hydrogen, which corresponds to the formula $C_{40}H_{48}$ or $C_{40}H_{50}$, it may not be said safely that

* "Pigments of Marine Animals", III. II of this series; *J. Chem. Soc. Japan. (Pure Chem. Sect.)*, **75**. 605 (1954)

1) T. Tsumaki, M Yamaguchi and T. Tsumaki, *J. Chem. Soc Japan. (Pure Chem. Sect.)* **75**, 297 (1954).

2) C. Grundmann und Y. Takeda, *Naturwissenschaften*, **25**, 27 (1937); Y. Takeda und T. Ohta, *Z. Physiol. Chem.* **258**, 6 (1939).

the two pigments are identical with each other.

The pigment of m. p. 230° also appears to be a new carotenoid having a molecular formula $C_{40}H_{50}$. This pigment is termed renierapurpurin by the author.

These three hydrocarbons have a common feature of high carbon content, and therefore these pigments appear to be closely related to one another in their constitutions.

Although the pigment of m. p. 161° forms only a small proprotion of the total amount of all the pigments obtained, it is of importance, since it is the greatest in quantity among the oxygenated pigments isolated. This pigment resembles rhodovibrin[3] which has been isolated by Karrer and his co-workers from rhodovibrio-bacteria, but the identity is improbable. The name renieraxanthin is tentatively proposed for this pigment by the author. The elementary analysis shows that this pigment has the molecular formula $C_{40}H_{56}O_2$. Both the oxygen atom in the molecule do not appear to exist in the form of hydroxyl groups or a carboxyl group, since the pigment exhibits an almost epiphasic nature in the partition test. The possibility of the presence of epoxide groups may also be excluded on the basis of the negative result in the color test with concentrated hydrochloric acid. The solution of this pigment in petroleum benzine is orange, while the solution in ethanol is wine-red, and, though the former exhibits an absorption spectrum with three sharp maxima, the latter shows a single banded absorption spectrum. These facts indicate that renieraxanthin contains at least one carbonyl group in the molecule, since these phenomena are generally accepted as the typical properties of carotenoids containing systems of conjugated double bonds terminated by carbonyl groups. This conclusion is also in accord with the long-wavelength locations of the absorption maxima of the pigment.

Other pigments were not analysed because of the small quantities of materials.

The coloring matter of the sponge has hitherto often been studied by different investigators on various species[4]. However, more precise investigations are relatively few. Lederer[5] observed by means of chromatography that the red sponges, "*Suberites domuncula*" and "*Ficulina ficus*" contained the following pigments: epiphasic pigments with absorption maxima similar to those of $\alpha$-, $\beta$-, and $\gamma$-carotene, respectively; the corresponding oxygenated carotenoids; and a somewhat hypophasic pigment with absorption maxima similar to those of tolurin. Of these pigments, $\beta$-carotene was isolated in the crystalline state. Drumm and his co-workers[6] studied the red sponge "*Hymeniacidon sanguineum*" and isolated from its $\alpha$-, $\beta$-, $\gamma$-carotene and echinenone in crystalline states. Karrer and his co-workers[7], on the other hand, described the presence of the crustacean pigment, astacene, in the red sponge of the Mediterranean Sea, "*Axinella crysta galli*". However, no elementary analysis of the pigments were reported in these miscel laneous reports.

Being compared with these results, the sponge "*Reniera japonica*" has proved to have the following characteristic features with regard to the constituents of the coloring matter.

1. The main pigment exhibiting the same spectral properties as those of $\gamma$-carotene is not $\gamma$-carotene but is a new carotenoid hydrocarbon ($C_{40}H_{48}$ or $C_{40}H_{50}$), for which the name renieratene has been proposed in the preceding paper.

2. Two hydrocarbons which show the same absorption maxima as those of $\beta$-carotene are present in considerable quantities. One of them is $\beta$-carotene and the other is leprotin-like carotenoid hydrocarbon ($C_{40}H_{48}$ or $C_{40}H_{50}$).

3. A pigment which shows the spectral properties similar to those of torulin is isolated, but it has the nature of a carotenoid ketone ($C_{40}H_{56}O_2$). It is termed renieraxanthin.

4. In addition to the pigments above described, several hitherto unknown pigments are present in small quantities, one of which has proved to be a hydrocarbon ($C_{40}H_{50}$) and is termed renierapurpurin.

## Experimental

Solutions of the pigments were evaporated under reduced pressure in the stream of carbon dioxide. In chromatography benzene containing a little methanol was employed for elution. In the partition tests, petroleum benzine b. p. 70–80° and 90% methanol were employed unless otherwise mentioned. In the color tests with conc.

3) P. Karrer und U. Solmssen, *Helv. Chim. Acta*, **19**, 1019 (1936).
4) P. Karrer und E. Jucker, "Carotinoide", Basel (1948), P. 95.
5) E. Lederer, *Bull. soc. chim. biol.*, **20**, 567 (1938).
6) P. J. Drumm, W. F. O'Connor and L. P. Renouf. *Biochem. J.*, **39**, 208 (1945).
7) P. Karrer und U. Solmssen, *Helv. Chim. Acta*, **18**, 915 (1935).

sulfuric acid or with antimony trichloride, the pigments were dissolved in chloroform. Melting points were determined in evacuated tubes.

**Extraction and the Separation of the Crude Pigment.**—The sponge, 5.7 kg. (wett weight), was extracted with acetone and petroleum benzine by the addition of water. After the saponification with ethanolic potassium hydroxide, the solution was concentrated and the oily residue was treated with acetone to remove most of the colorless lipids which were less soluble in this solvent. The concentrate, 35 g., was dissolved in 60 cc. of petroleum ether, and by the addition of 50 cc. of ethanol, the crude pigment was precipitated. The crude pigment, which weighed 120 mg. after the recrystallization from benzene ethanol, was separated by chromatography on alumina into six pigments[8]. Sixtyseven mg. of renieratene, 29 mg. of the pigment of m. p. 199°, 4 mg. of renierapurpurin, 1 mg. of the pigment of m. p. 205°, and small quantities of the pigment of m. p. 194° and β-carotene were thus obtained.

*Anal.* (Renieratene), Found: C, 90.98, 90.62; H, 9.22, 9.34%. Molecular weight (cyclopentadecanone), 510, 579, 530.

*Anal.* (The pigment of m. p. 199°), Found: C, 90.91: H, 9.38%.

*Anal.* (Renierapurpurin), Found: C, 90.12; H, 9.36.

Calcd. for $C_{40}H_{48}$: C, 90.85; H, 9.15. Calcd. for $C_{40}H_{50}$: C, 90.51; H, 9.49%; molecular weight, 531.2.

**Separation of Pigments of the Mother Liquor.**—The mother liquor of the crude pigment and the filtrate of recrystallization were combined together, washed alcohol-free with water, dried with anhydrous sodium sulfate, and concentrated. The residue was treated with acetone and the colorless lipids were removed repeatedly as completely as possible. The concentrate was finally dissolved in petroleum ether and chromatographed on alumina (Merck, standardized according to Brockmann) (6×20 cm.). Petroleum benzine-benzene mixture with increasing percentage of the latter (finally 50% benzene) was employed for the developer. All zones observed are listed in Table II, the lower six of these, from 9 to 14, being separated by means of liquid chromatography.

*Zone* 1.—No crystalline pigment was obtained. It seems to be decomposition product.

*Zone* 2.—The pigment was only incompletely eluted. The eluted fraction contained a large quantity of colorless lipid which melted at 113° after recrystallization from methanol. Rechromatography on calcium carbonate gave seven red zones, but none of these zones afforded any crystallized pigment. The concentrates of the eluates showed blue colorations with conc. sulfuric acid or with antimony trichloride.

*Zone* 3.—This consisted of several zones, which were eluted together. The concentrate of the eluate was dissolved in hot ethanol. On cooling, colorless lipids crystallized out, which were removed by filtration. The concentrate was dissolved in a small quantity of petroleum ether and left to stand in an ice chamber. The red brown precipitates were redissolved in a small quantity of benzene, diluted with petroleum benzine and adsorbed on calcium carbonate (3×20 cm.). Petroleum benzine containing 10% of benzene was employed as the developer. The chromatogram observed is given in Table III in the sequence of decreasing adsorbability.

TABLE II

| No. of the Zones | Width of the Zones (in mm.) | Color of the Zones |
|---|---|---|
| 1 | 5 | Dark brown |
| 2 | 40 | Deep red |
| | 15 | Colorless |
| 3 | 12 | Brown (heterogeneous) |
| | 9 | Colorless |
| 4 | 3 | Purplish brown |
| | 5 | Colorless |
| 5 | 3 | Reddish brown |
| | 9 | Colorless |
| 6 | 30 | Purple |
| 7 | 26 | Faint purple |
| | 14 | Colorless |
| 8 | 18 | Pale yellow |
| 9 | Liquid chromatography | Pale pink |
| 10 | | Pale red |
| 11 | | Orange red |
| 12 | | Yellowish orange |
| 13 | | Yellow |
| 14 | | Bright yellow |

TABLE III

| | Width of the Zones (in mm.) | Color of the Zones |
|---|---|---|
| a | 2 | Purplish red |
| | 6 | Colorless |
| b | 5 | Pale yellow |
| c | 18 | Orange |
| d | 20 | Yellow |
| | 7 | Colorless |
| e | 12 | Yellow |
| f | 15 | Pale yellow |

*Zone* a.—On recrystallizing the residue of the eluate from benzene-methanol, a minute quantity of purplish glistening fine needles was obtained. Absorption maxima, in carbon disulfide, 558, 517 485 mμ. In the partition test, the pigment colored both the layers.

*Zone* c.—Recrystallization from benzene-methanol gave purplish brown plates, m. p. 173-4°, 1 mg., absorption maxima; in carbon disulfide, 530, 493, 461 mμ; in hexane, 493, 462 mμ. In the partition test, the pigment colored both the layers.

8) Operations were carried out in the way described in the previous paper[1].

*Zone* d.—Recrystallization from petroleum benzine-methanol gave fine long orange needles, m. p. 153-4°, 0.4 mg., absorption maxima; in carbon disulfide, 518, 483, 452 mμ; in hexane, 482, 454 mμ. In the partition test both the layers also become colored. The solubility of the pigment was larger than that of the pigment of the zone c.

*Zone* e.—A minute quantity of brown plates of absorption maxima, 507, 475, 445 mμ in carbon disulfide was obtained.

*Zone* 4.—No crystalline pigment was obtained. The carbon disulfide solution gave a single maximum at 480 mμ.

*Zone* 5.—A minute quantity of almost black needles with a single maximum at 495 mμ in carbon disulfide was obtained.

*Zones* 6 *and* 7.—They were eluted together and the reddish black residue of the eluate was recrystallized with a little petroleum benzine containing ethanol, and then with benzene-methanol. The crystals obtained were again adsorbed on alumina (2×20 cm.) from a petroleum benzine-benzene solution. The upper narrow purple zone afforded a minute quantity of red needles with absorption maxima 548, 512, (471) mμ in carbon disulfide. Partition test, almost epiphasic. The lower purple zone contained renieraxanthin. The residue of the eluate was recrystallized twice from a small quantity of benzene by the addition of methanol, the crystals being washed with a little cold petroleum ether and then with boiling methanol after each crystallization. Renieraxanthin, 2.6 mg., m. p. 161°, had a glistening purplish brown appearance and under microscope the crystals showed purplish red hexagonal plates. Absorption maxima; in carbon disulfide, 558, 521. (492) mμ; in hexane, 521, 487, 456 mμ; in benzene, 536, 511 mμ; in ethanol, a broad band with a single maximum at 500 mμ. The absorption curves in hexane and in ethanol are given in Fig. 1. In the partition test using 95% methanol, the pigment was almost epiphasic, but the methanol phase also somewhat colored. The pigment was very easily soluble in chloroform, easily soluble in benzene, considerably less soluble in petroleum ether, and very slightly soluble in ethanol and in methanol. In the color tests, conc. sulfuric acid gave a deep blue coloration and antimony trichloride a purple coloration which gradually changed into blue. On treating an ethereal solution with conc. hydrochloric acid no blue color was observed.

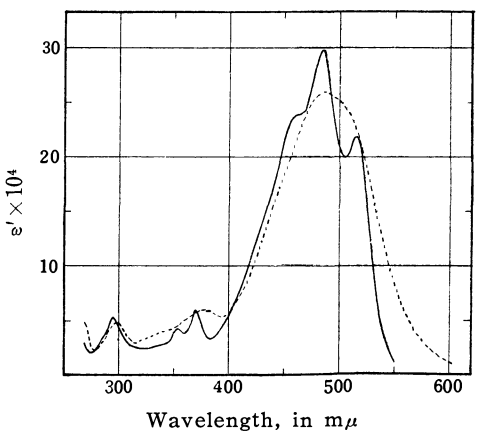



Fig. 1. Absorption spectra of renieraxanthin.
—— in hexane solution
--- in ethanol solution
ε' is given by $\varepsilon' = 2.3/cd \times \log (I_0/I)$

*Anal.* Found: C, 84.64; H, 10.08. Calcd. for $C_{40}H_{56}O_2$: C, 84.45; H, 9.92%.

*Zone* 8.—Rechromatography on alumina and recrystallization from benzene-methanol gave a minute quantity of fine glistening copper red needles which sintered at 123°, changed simultaneously somewhat pale in color but did not melt even above 200°. This sample did not seem to be in an entirely pure state. Absorption maxima: in carbon disulfide, 531, 494, 463 mμ; in hexane, 494, 463, (435) mμ. Partition test, entirely epiphasic.

*Zones* 9, 10, 11 *and* 12.—Each fraction obtained by liquid chromatography was repeatedly chromatographed on alumina when necessary. Recrystallization from benzen-ethanol or from chloroform-methanol gave the following pigments; 0.4 mg. of renierapurpurin, a minute quantity of the pigment of m. p. 205°, 26 mg. of renieratene and a small quantity of the pigment of m. p. 194°, and 16 mg. of the pigment of m. p. 199°, corresponding to the fractions 9, 10, 11 and 12, respectively. These pigments were exactly identical with those obtained by the chromatography of the crude pigment already described.

*Zones* 13 *and* 14.—Both solutions were operated together. Recrystallization from benzene-methanol gave carotene mixture, m. p. 170°, 29 mg. Chromatography on calcium hydroxide (4×30 cm 2 columns) gave α-carotene, m. p. 185°, 2 mg, absorption maxima, in carbon disulfide, 507, 478, 447 mμ; and β-carotene, m. p. 183°, 20 mg, absorption maxima in carbon disulfide, 520, 485, 452 mμ. The colorimetric determination[9] showed that the ratio of α-carotene to β-carotene was 14 : 86.

*Anal.* α-Carotene, Found: C, 89.53; H, 10.52. β-Carotene, Found: C, 89.35; H, 10.65. Calcd. for $C_{40}H_{56}$: C, 89.49; H, 10.51%.

The author wishes to thank Prof. Tokuichi Tsumaki for his exceeding kind directions throughout this work. The author is also indebted to Mr. Michio Shido[10] for microanalysis.

*The Department of Chemistry*
*Faculty of Science*
*Kyushu University*
*Fukuoka*

9) R Kuhn und H Brockmann, *Z Physiol Chem.*, **206**, 41 (1932)

10) Research member of The Service Centre of the Elementary Analysis of Organic Compounds, Faculty of Science, Kyushu Univ.

# *Note on the Donnan Membrane Equilibrium in Polymer Salt Solutions with Extraneous Salts*

By Hiroshi INAGAKI

(Received August 14, 1956)

## Introduction

It has been reported that the osmotic behavior of polymer salts in aqueous salt solutions is in qualitative agreement with that predicted from the theory of the Donnan equilibrium, which is expressed by the following equation[1,2],

$$\pi/C_p = RT\{1/M + [\beta + (r^2/4X)]C_p\}, \quad (1)$$

where $\pi$ is the osmotic pressure, $C_p$ is the polymer concentration, $R$ and $T$ are, respectively, the gas constant and the absolute temperature, $M$ is the molecular weight of the polymer salt, $\beta$ is the interaction parameter between the polymeric ions, $X$ is the salt content, and $r$ is the number of equivalents per gram of the polymer salt.

It was found, however, that the calculation in terms of Equation (1) gives too great a value for the second virial coefficient in comparison with observed data. This difference has been interpreted in several ways[2-4]. In the membrane equilibrium, if a certain fraction of the added simple ions is bound or fixed in or on the molecular domain of the polymeric ion, the number of the permeant (free) ions, which coexist with the polymeric ions, will decrease in comparison with a case where the association does not occur. This, in turn, results in a decrease in the osmotic pressure contributed by the permeant ions.

The present work deals theoretically with the osmotic equilibrium on the basis of the Donnan method, by taking *formally* the simple ion association into account. It is shown that the expression for the osmotic pressure is identical in form with Equation (1) derived by previous investigators[1,5] for the electrolyte-ideal solution, provided that the value of $r$ is replaced by a parametric factor $r^*$, which is smaller than $r$. The ratio $r^*/r$, which is evaluated from the observed data, is discussed in terms of the Oosawa-Imai-Kagawa theory for the simple ion association[6].

## Theoretical

### Derivation of the Osmotic Pressure Equation

On one side (phase I) of a semipermeant membrane we have an aqueous solution of a uni-univalent electrolyte, the concentration of which is $C_0$ (molecules/cc.). On the other side (phase II) of the membrane, impermeant anionic polymeric ions are present together with the electrolyte.

The concentrations of the electrolyte in phase II may be written in the form:

$$C_+ = J_+/(V - Nv) \quad \text{and}$$

$$C_- = J_-(V - Nv), \quad (2)$$

where $J_+$ and $J_-$ are, respectively, the numbers of *free* positive and negative ions, $V$ is the total volume of phase II, and $N$ and $v$ are, respectively, the total number and the molecular volume of the polymeric ion. $C_+$ and $C_-$ may be regarded as the actural concentrations of simple ions which may contribute to the osmotic pressure of the solution.

The requirement for the Donnan equilibrium can thus be given by

$$C_+ C_- = C_0^2, \quad (3)$$

subject to the condition for neutrality

$$C_+ = C_- + NZ^*/V', \quad (4)$$

where $V' = V - N_v$.

Here $Z^*$ is the effective charge of the polymeric ion and given by the equation:

$$Z^* = Z - n_+ + n_-, \quad (5)$$

where $Z$ is the stoichiometric valence of the polymeric ion, and $n_+$ and $n_-$ are, respectively, the numbers of positive and

1) D T. F. Pals and J. J. Hermans, *Rec. trav. chim., Bay-Bas*, **71**, 458 (1952).
2) H. Inagaki and T. Oda, "Makromolekulare Chemie", **21**, 1 (1956).
3) H. J. L. Trap and J. J. Hermans, *J. Phys. Chem.*, **58**, 757 (1954).
4) N S. Schneider and P. Doty. ibid., **58**, 762 (1954).
5) H. R. Kruyt, "Colloid Science", Vol. I, Elsevier Publ. Co., Amsterdam (1952), p. 188.
6) F. Oosawa, N. Imai and I. Kagawa, *J. Polymer Sci.*, **13**, 93 (1954).

negative ions bound in the molecular domain of the polymeric ion. It follows that the total concentrations of positive and negative ions present in phase II are given, respectively, by $(J_+ + Nn_+)/V$ and $(J_- + Nn_-)/V$. It should be noticed that activity coefficient is formally introduced in Equation (3) for the interaction between the polymeric ions and the simple ions but not for those between simple ions themselves.

Substituting Fquation (4) for $C_+$ in Equation (3), we obtain,

$$C_- = -\frac{1}{2}(Z^*N/V') + \frac{1}{2}\sqrt{(Z^*N/V')^2 + 4C_0}. \quad (6)$$

If the term $Z^*N/V'$ is small compared with $C_0$, expansion of Equation (6) yields

$$C_- = -\frac{1}{2}(Z^*N/V') + C_0 + (1/8)(Z^{*2}/8C_0)(M/V')^2 + \cdots\cdots, \quad (7)$$

so that concentration $C_+$ can be written

$$C_+ = \frac{1}{2}(Z^*N/V') + C_0 + (1/8)(Z^{*2}/8C_0)(N/V')^2 + \cdots\cdots. \quad (8)$$

We shall now assume that the observed osmotic pressure $\pi$ is formally the sum of pressures, $\pi_1$ and $\pi_2$, which are, respectively, the contributions from the permeant ions and from the polymeric ions. Thus the osmotic pressure $\pi_1$ is given approximately by

$$\pi_1 = kT(C_+ + C_- - 2C_0), \quad (9)$$

which may be put with the aid of Equations (7) and (8) in the form:

$$\pi_1 = kT\frac{Z^{*2}}{4C_0}\left(\frac{N}{V}\right)^2. \quad (10)$$

The term $(Z^{*2}/4C_0)$ in Equation (10) is the Donnan term.

If the osmotic pressure $\pi_2$ is assumed to be identical with the osmotic pressure in dilute solutions of neutral polymers and if the unit of concentration in Equation (10) is converted into the usual one, we have

$$\pi/C_p = RT\{1/M + [\beta + r^{*2}/4X)]C_p\}, \quad (11)$$

where $r^*$ is the parametric factor related with the $Z^*$-value, and the other notations are the same as those used in Equation (1). Equation (11) becomes identical with Equation (1) derived for the electrolyte-ideal solution[1,5], if $r^*$ is replaced by $r$. Thus the ratio $r^*/r$, which is equated to $Z^*/Z$, may be considered to be the degree of electrolytic dissociation of the polymer salt, and will now be interpreted in terms of the theory developed by Oosawa, Imai and Kagawa[6].

## Short Summary of the Oosawa-Imai-Kagawa Theory

As for the association of simple ions with a polymeric ion, we may refer to the theoretical work made by Oosawa, Imai and Kagawa[6]. They solved the Poisson-Boltzmann equation for the coiled polymeric ion in salt solutions without introducing the Debye-Hückel approximation. In so doing, they assumed that the fixed electric charges on the polymeric chain are continuously distributed in a volume $v$ occupied by the polymeric ion ($v = (4/3) \times \pi a^3$, where $a$ is the apparent radius of the polymeric ion) and that the dissociation of the polymeric ion is sufficiently suppressed by the simple ion association that $\langle\lambda\rangle \ll 1$, where $\langle\lambda\rangle$ is the degree of dissociation averaged over the volume $v$.

In accordance with the theory, the theoretical value of $Z^*$ is given by an equation of the form:

$$Z^* = Z\langle\lambda\rangle = \frac{DkTa}{e_0^2}\ln\left(\frac{Z}{v}\frac{V_+}{ZN+J}\frac{1+\sqrt{1+\delta^2}}{2}\right), \quad (12)$$

where

$$\delta^2 = \frac{v^2}{Z^2}\frac{J}{V_-}\frac{ZN+J}{V_+}, \quad (12')$$

and $D$ is the dielectric constant in the volume $v$, $e_0$ is the unit charge, $J$ is the total number of molecules of added salt and the other notations are the same as those used in the foregoing section. Further notations $V_+$ and $V_-$ are the normalization factors of the Boltzmann relation for the distribution of charges.

## Experimental Results and Discussion

The experimental details of osmometry and viscometry for the present data have been described in a previous paper[2]; only the results, which are necessary for the present discussion, are shown below. The molecular weight of sodium carboxymethyl cellulose used as the sample was osmometrically found to be $8.3 \times 10^4$. The slopes of the osmotic pressure plot for the system sodium carboxymethyl cellulose and sodium chloride are collected in Table I, wherein those calculated in accordance with Equation (1) are also recorded. The fourth column in the table gives the ratio of the

observed slope against the theoretical one, $S_0/S_t$; the square root of this ratio is equal to $r^*/r$ if $\beta$ is neglected (see Equations (1) and (11)), and will be discussed in terms of the degree of dissociation.

TABLE I

SLOPES OF OSMOTIC PRESSURE PLOT.

| Added Salt Concentration $X$(mole/cc.) $\times 10^3$ | Observed Slope $S_0\times 10^{-7}$ | $10^{-7}RT\times(r^2/4X)/(S_t)$ | $S_0/S_t$ | $r^*/r^*$ |
|---|---|---|---|---|
| 0.1 | 13.7 | 44 | 0.31 | 0.55 |
| 0.05 | 25 | 88 | 0.28 | 0.52 |
| 0.03 | 42 | 146 | 0.29 | 0.53 |
| 0.02 | 60 | 220 | 0.27 | 0.51 |
| 0.01 | 120 | 440 | 0.27 | 0.51 |

* The $r$-value for the sample polymer salt is $2.7\times10^{-8}$.

TABLE II

INTRINSIC VISCOSITIES AS A FUNCTION OF ADDED NaCl CONTENTS

| Added Salt Concentration (mole/l.) | $[\eta]$ |
|---|---|
| 0.004 | 11.29 |
| 0.010 | 9.20 |
| 0.020 | 7.48 |
| 0.040 | 6.40 |
| 0.100 | 5.41 |
| $\rightarrow\infty$ | $[\eta]_\infty=4.69$ |

Table II gives the intrinsic viscosity obtained for the same system as a function of the salt content. The value of intrinsic viscosity is plotted against $x^{-1/2}$ ($x$ is the salt content) according to Pals and Hermans' treatment[7], and the extrapolation of the plot to $x\rightarrow\infty$ enables us to evaluate the intrinsic viscosity $[\eta]_\infty$ for the polymer salt discharged completely.

To compare experimental data with the theory, we shall first estimate the apparent radius of the polymeric ion, $a$, which appears in Equation (12). As was suggested by Fujita et al.[8] and by Inagaki et al.[9], an approximate dimension of the polymeric ion may be estimated from the value of $[\eta]_\infty$ with the aid of the Flory-Fox viscosity equation[10]:

$$\sqrt{\langle h^2\rangle}=([\eta]M/\Phi)^{1/3}, \tag{13}$$

where $\langle h^2\rangle$ is the mean square end-to-end distance of the polymer, $M$ is the molecular weight and $\Phi$ is the Flory universal constant of the order of $2.1\times10^{-21}$. Putting $[\eta]=4.7$, $\Phi=2.1\times10^{-21}$ and $M=8.3\times10^4$ into Equation (13), we have 1200 Å for $\sqrt{\langle h^2\rangle}$. Conversion of this into the mean square distance from the center of gravity $\langle s^2\rangle$ in the terms of the following equation[11]:

$$a=\sqrt{\langle s^2\rangle}=\sqrt{\langle h^2\rangle}/6 \tag{14}$$

gives 500 Å.

Now we shall assume $V_+=V_-=V$ in Equation (12). Let us take $C=2$ g./l., $Z=230$ and $X=0.1$ mole/l. as a typical example. We then obtain

$$ZN/V\approx3\times10^{18}\ \text{molecules/cm}^3,$$

and

$$J/V\approx6\times10^{19}\ \text{molecules/cm}^3.$$

Putting the values obtained above into Equation (12), the $\langle\lambda\rangle$-value is found to be 0.006 for the condition assumed here.

It is seen from Table I that, although the $\langle\lambda\rangle$-value changes with the polymer- and salt-concentrations in accordance with Equation (12), the observed ratios $r^*/r$ are practically independent of these factors and are much higher than the $\langle\lambda\rangle$-value. This discrepancy between experimental and theoretical values may be due to the fact that the Oosawa-Imai-Kagawa theory is only applicable to solutions of high dilution: In the solutions studied in the present work, the free volume of the polymeric ion is so small that the effect of neighbouring polymeric ions can not be neglected on the distribution of the permeant ions. In order to obtain agreement between experiment and theory, one should extended the theory to solutions of higher concentrations of polymer.

The author wishes to express his thanks to Prof. Dr. M. Horio and Dr. H. Fujita for encouragement in the course of this work. He also thanks Messrs. T. Oonishi and N. Imai, Department of Physics, Nagoya University, who gave helpful suggestions to him.

*Institute for Chemical Research*
*Kyoto University, Kyoto*

7) D. T. F. Pals and J. J. Hermans, *Rec. trav. chim. Pay-Bas*, **71**, 433 (1952).
8) H. Fujita, K. Mitsuhashi and T. Homma, *J. Colloid Sci.*, **9**, 466 (1954).
9) H. Inagaki, H. Sakurai and T. Oda, *Bull. Inst. Chem. Res., Kyoto Univ.*, **33**, 257 (1955).
10) P. J. Flory and T. G. Fox, *J. Polymer Sci.*, **5**, 745 (1950).
11) See for example, P. J. Flory, "Principles of Polymer Chemistry", Chap. X. Ib. cornell Univ. Press (1955).

# *Relationships between the Photolysis and Crystallinity of Zinc Sulfide Phosphors*

By Shigeo SHIONOYA and Koh WATANABE*

(Received August 17, 1956)

## Introduction

Zinc sulfide phosphors are known to be photodecomposed and blackened under the irradiation of strong ultraviolet rays, a phenomenon usually called "blackening". The blackness is attributed to the metallic zinc formed as a result of the photolysis and deposited in the colloidal form. Previously one of the present authors, Shionoya[1], studied this phenomenon, extensively and discussed conclusively the mechanism of the process by which the blackening is caused. Here it was investigated how the blackening characteristics are influenced by the variation of the crystallinity, i. e. the degree of crystal growth, of zinc sulfide.

The results of Shionoya's previous work are briefly summarized here. (1) The spectral region efficient for causing the blackening coincides with the fundamental absorption region of zinc sulfide. (2) The adsorbed water is necessary for the occurrence of the blackening, the amount of which is less than the order of 0.0 x wt.%. (3) Under a constant humidity and temperature the blackening proceeds according to the following equation after the lapse of the induction period of several or several ten minutes,

$$D^3 = kt + l, \qquad (1)$$

where $D$ is the blackening density, $k$ the rate constant, $t$ the time, and $l$ a constant. The reciprocal of the induction period is proportional to the humidity. (4) It is suggested that the mechanism of the blackening is as follows. The adsorbed water reacts photochemically on the crystal surface and the nucleus of zinc is formed. This nucleus trapps the electron in the conduction band, attracts the interstitial zinc ion from within the host crystal, and grows to the colloidal zinc. Eq. (1) corresponds to this stage of the blackening reaction, and is explained by an assumption that the migration of the interstitial zinc ion is the rate-determining step for this stage.

## Experimental

**Sample.**—Copper-activated zinc sulfide phosphors having different crystallinities, i. e. degrees of crystal growth, were prepared by changing the time of the firing. They were fired with the flux of 4 wt.% NaCl at 1100°C for 5-90 min. Copper content was 0.003 wt.%.

The crystallinity seems to be indicated by the particle size. By means of Blaine's air permeability method[2] the specific surface area of these samples was measured, and the mean volume surface diameter, $d_{vs}$, was calculated by the following equation, assuming that all the particles are spheres,

$$d_{vs} = \sum_i n_i d_i^3 / \sum_i n_i d_i^2 = 6/\rho S_w, \qquad (2)$$

where $\rho$ is the density of the particle and $S_w$ the specific surface area per unit mass. The values of the time of the firing and $d_{vs}$'s are given in Table I.

TABLE I
THE TIME OF THE FIRING AND THE MEAN VOLUME SURFACE DIAMETER, $d_{vs}$, OF THE SAMPLES

| No. | 1 | 2 | 3 | 4 |
|---|---|---|---|---|
| Time of the firing (min.) | 5 | 20 | 30 | 90 |
| $d_{vs}$ ($\mu$) | 3.0 | 4.4 | 6.3 | 8.2 |

**Measurement of the Blackening.—(1) Method.**—A high pressure mercury discharge lamp made of quartz and having the capacity of 650W. was used to blacken the phosphors. The blackening density, $D$, was measured by means of Yamabe's type photographic densitometer using the diffuse reflected light. The dencity, $D$, is defined by

$$D = \log_{10} I_0/I, \qquad (3)$$

where $I_0$ and $I$ are the light intensities thrown on and reflected back from the sample, respectively.

The rate of the blackening was measured under several humidities and at 20°C in the way similar to that mentioned in the previous

* Present address : Nisshin Ind. Co., Ltd. Adachi-ku, Tokyo.

1) S. Shionoya, *J. Chem. Soc. Japan (Ind. Chem. Sect.)*, **52**, 79 (1949) ; **53**. 55 (1950). *J. Chem. Soc. Japan (Pure Chem. Sect.)*, **71**, 461, 584 (1950). *Bull. Fac. Eng., Yokohama Natl. Univ.*, **5**, 129 (1956).

2) R. L. Blaine, *A. S. T. M. Bull.*, No. 123, 5 (1948).

paper[1]. The samples were washed thoroughly by distilled water so as to remove completely the chlorides of sodium and zinc contained in them. Zinc chloride formed by the reaction of flux on zinc sulfide influences the blackening characteristics because of its strong tendency to absorb water, so that the removal of this is needed previous to the measurement of the blackening. Then the samples were packed in small containers after being dried by heating, and placed in closed quartz tubes in which the humidity was kept constant by means of sulfuric acid of the appropriate concentration. These tubes were sunk into the circulating water to keep the temperature in them constant, and ultraviolet light from the mercury lamp set above the water surface was thrown onto the samples through the water. Thus the curves of the blackening density vs. the time of irradiation were measured under the pressure of water vapor of 6.2-13.2 mmHg.

(2) **Results.**—Results under 7.2 and 6.2 mmHg are shown in Fig. 1 and 2 as examples. Under 6.7-13.2 mmHg all the samples were remarkably blackened, whereas under 6.2 mmHg the samples, except in the case of No. 2, could hardly be blackened at all.

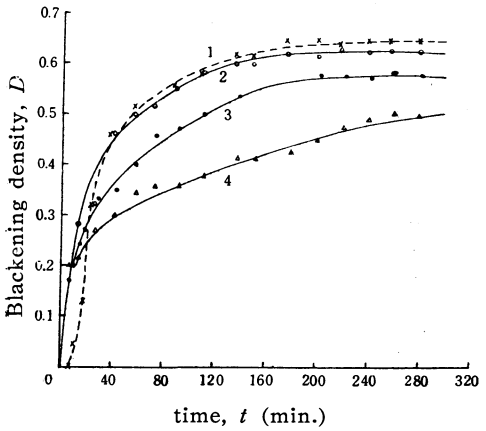



Fig. 1. Blackening curves under the pressure of water vapor of 7.2 mmHg for four samples cited in Table I.

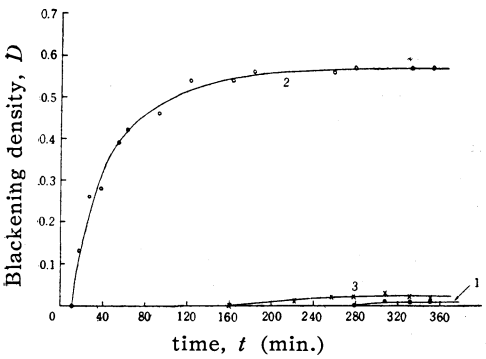



Fig. 2. Blackening curves under the pressure of water vapor of 6.2 mmHg for four samples cited in Table I. Sample No. 4 was not blackened.

The build-up parts of the blackening curves satisfy Eq. (1) and then the rate constants are calculable. After the long irradiation the blackening curves became rather flat. This effect is attributed to the simultaneous occurrence of the bleaching of blackened samples. The bleaching takes place even when the blackening is proceeding, and its rate increases with the increase of blackening density as mentioned in the previous papers[1]. Therefore, after the long irradiation, the rates of the blackening and bleaching become equal to each other, and a state of equilibrium state is reached. In Fig. 3 the rate constants for the blackening under several humidities are plotted against the particle sizes. The rate constant decreases with the growth of the particle size.

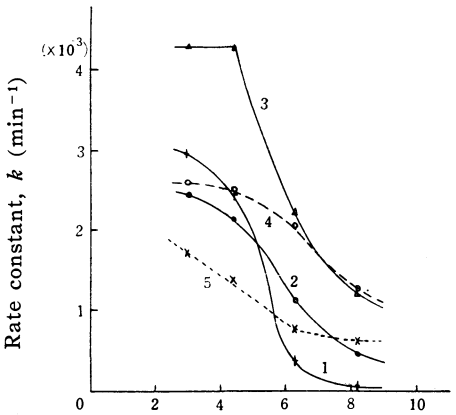



Fig. 3. Rate constants for the blackening against the particle sizes, the mean volume surface diameters, for four samples cited in Table I. The pressures of water vapor are (1) 6.7, (2) 7.2 (3) 8.1, (4) 10.0 and (5) 13.2 mmHg.

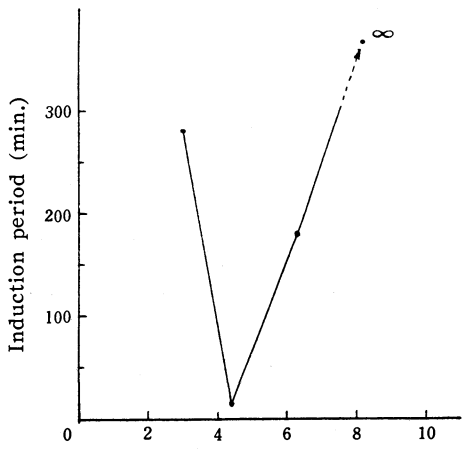



Fig. 4. Induction periods under the pressure of water vapor of 6.2 mmHg the against particle sizes, the mean volume surface diameters, for four samples cited in Table I.

Under low humidities long induction periods are observed in the beginning of the blackening reaction. In Fig. 4 the induction periods under 6.2 mmHg are plotted against the particle sizes. The induction period shows a minimum value at sample No. 2 with the diameter of 4.4 $\mu$.

**Luminescence and Blackening.**—These samples emit a yellow green luminescence due to the copper activator. The relative brightness of the copper luminescence under the excitation by a high pressure mercury discharge lamp is plotted against the particle size in Fig. 5. Sample No. 2 which shows the minimum induction period has the maximum brightness.

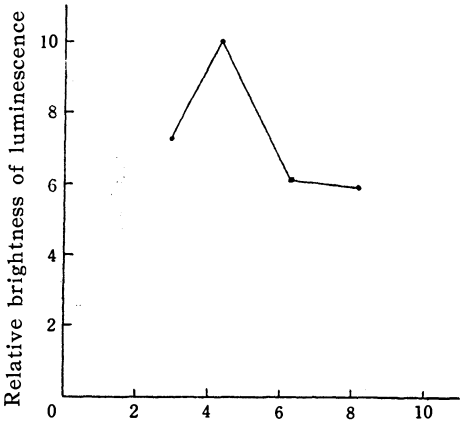



Fig. 5. Relative brightnesses of luminescence against the particle sizes, the mean volume surface diameters, for four samples cited in Table I.

## Discussion

Zinc sulfide is made luminescent by the firing, during which the particle size of crystal grows owing to the sintering of small particles, and the activating impurity is incorporated by the diffusion. The result, namely, that the luminescent brightness of sample No. 1 with the smallest diameter is lower than that of sample No. 2 may be attributed to the incompleteness not only of the activator incorporation but of the crystal growth. The lowering of the brightness in the samples with larger diameters seems to be predominantly due to the oxidation of the samples caused by the over-firing.

Comparing Fig. 4 with Fig. 5, it is seen that the sample with the minimum induction period shows the maximum luminescent brightness. Since earlier days it has been known that zinc sulfide phosphors with bright luminescences are apt to be blackened. Recently Gobrecht and Kunz[3] studied the relationship between the luminescent brightness and blackening, and found that the blackening is nearly proportional to the brightness. However, this is not exactly true according to the present results. As seen from Figs. 3, 4 and 5, the reciprocal of the induction period, i. e. the reaction rate during the induction period, is nearly proportional to the brightness, but the rate constant for the blackening is not. Therefore, as seen by comparing Fig. 1 with Fig. 5 the blackening density is not always proportional to the luminescent brightness after long irradiation. The relationship between the luminescence and blackening should be discussed using the induction period.

This relationship is explained as follows, based on the mechanism of the blackening presented in the previous papers[1]. It was found that the reciprocal of the induction period is propotional to the amount of adsorbed water. From this result it was suggested that the adsorbed water reacts on the sulfur atom formed momentarily as a result of the photoabsorption and consequently it disappears from the crystal. This is the starting reaction of blackening and determines the reaction rate during the induction period. Therefore, it is said that the rate of this surface photochemical reaction is proportional to the luminescent brightness. This photochemical reaction would be accelerated by the condition that the conduction electron produced by the photoabsorption can move freely over the wide range through the whole crystal. As understood from the fact previously found that the blackening occurs in the spectral region of the fundamental absorption of zinc sulfide, but does not in the region of the absorption of activating impurities, such as copper, the existence of activating impurities which form the luminescent center does not contribute essentially to the occurrence of the blackening. In other words, the blackening and luminescence do not essentially correlate to each other. However, the condition of free moving of the photoelectron would also intensify the luminescence, especially in the case of the excitation by host crystal absorption. Then this condition would be necessary for both the luminescence and blackening, and this fact seems to be the reason for the fact that phosphors with bright luminescences are apt to be blackened.

The result that sample No. 1 has a long induction period is attributed to the in-

3) H. Gobrecht and W. Kunz, *Z. Phys.* **136**, 21 (1953).

sufficiency of the above condition. In this sample, a photoelectron will not be able to move through the whole crystal as freely as in the other samples because of the incompleteness of the crystal growth. Sample No. 3 and 4 have long induction periods, although it appears that they have more complete lattices than sample No. 2. Then the circumstances would be different in these samples. Surface oxidation caused by the over-firing would prevent the occurrence of the surface photochemical reaction, so shat this would explain the reason for the long induction periods of these samples.

Furthermore, the variation of the water-adsorbing power with the particle size would also have influence on the induction period. It appears reasonable that the water-adsorbing power decreases with the growth of the particle size, because the crystal surface becomes flat and perfect as the crystal grows larger. Then the induction period would become longer with the growth of the particle size. This suggestion may be responsible for the results shown in the light half part of Fig. 4.

The decrease of the rate constant for the blackening with the growth of the particle size is also explained. It was inferred that the migration of the interstitial zinc ion determines this reaction rate, and further that the migration occurs, not through the perfect lattice, but along the internal imperfections in the crystal, such as internal surface, grain boundaries and dislocations. As the particle size grows larger the phosphor crystal would approach the perfect one, and the number of the internal imperfections would be decreased. This would make it difficult for the migration of the zinc ion to occur, and thus would cause the decrease of the rate constant.

*Department of Electrochemistry*
*Faculty of Engineering*
*Yokohama National University*
*Minami-ku, Yokohama*

# *Adsorption of Hydrogen on Copper-Magnesia Catalysts*

By Toyosaburo TAKEUCHI and Masakazu SAKAGUCHI

(Received August 27, 1956)

Most researches on copper-magnesia catalysts which have appeared so far in the literature are concerned with reaction kinetics[1], and little is known about the physical properties of the catalysts. In the present paper are reported the adsorption characteristics of hydrogen on the copper catalyst containing 1% magnesia. The catalyst is treated at various stages of thermal sintering. The effect of sintering upon adsorption heat is primarily investigated and a tentative suggestion is made concerning the nature of the copper-magnesia catalyst.

## Experimental

The copper-magnesia catalyst was prepared by dissolving copper oxide and magnesia in a molar ratio of 99 to 1 in extra-pure nitric acid. The mixture was dried gently on a water bath, and then ignited at 500°C in an electric furnace. The copper oxide was prepared from metallic copper supplied by Ishizu Chemical Co., in a manner as reported previously[2]. Traces of Mg, Fe, Si, Mn and Pb were found in this oxide sample by a spectroscopic analysis.

The catalyst was reduced in an atmosphere of hydrogen for three weeks at 200°C, until no more decrease in hydrogen pressure was perceptible. Before adsorption measurement, the catalyst was evacuated at the reduction temperature (or sintering temperature) for six hours under $10^{-5}$ mmHg. Adsorption measurements were made at 100° and 160°C on this reduced catalyst as well as on those sintered at 400° and 500°C in an atmosphere of hydrogen. Much care was taken in attaining adsorption equilibrium, as has been done previously*.

The magnesia was supplied by Kanto Chemical Co. The sample was treated in hydrogen at 200° and 500°C for a week before adsorption

1) R. Wynkoop and R. H. Wilhelm, *Chem. Eng. Progress*, **46**, 300 (1950) ; M. V. Sussman, *Ind. Eng. Chem.*, **46**, 457 (1954). M. Erlenbach and A. Sieglitz, *C. A.*, **48**, 2756e (1954).

2) T. Takeuchi and M. Sakaguchi, This Bulletin., To be published shortly.

* See Ref. 2) and also T. Kwan, "*Advances in Catalysis*", **6**, Academic Press, New York (1954), p. 67.

measurement. During this treatment, neither the adsorption nor any kind of consumption of hydrogen was measurable to any extent.

## Results

Surface areas determined by the B. E. T. method, using ethylene at −183°C for the freshly reduced copper-magnesia catalyst and the sintered one as well are given in Table I, in which those for pure copper, copper containing 1% nickel (copper-nickel) and magnesia powder are also listed for comparison. The Table shows that the surface area of the copper catalyst increases by six times with the addition of magnesia, far more so than with the addition of nickel. Raising the sintering temperature decreases the surface area of the catalyst, this effect being pronounced on the unpromoted copper catalyst, less pronounced on the copper-nickel and least on the copper-magnesia catalyst. On the contrary, the surface area of the magnesia powder increases about twice as much when the sintering temperature is increased from 200° to 500°C.

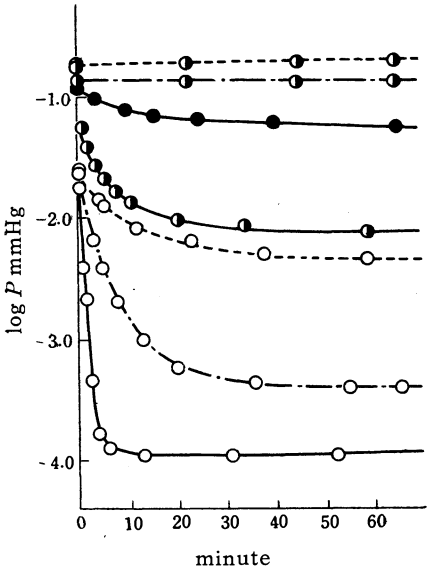



Fig. 1. Rates of adsorption of hydrogen at 160°C on Cu-MgO, Cu and Cu-Ni catalysts (5.0 g).

—○— Cu-MgO reduced at 200° (initial pressure; $1.83\times10^{-2}$ mmHg).
—◑— Cu-MgO sintered at 400° ($2.01\times10^{-1}$ mmHg).
—●— Cu-MgO sintered at 500° ($1.21\times10^{-1}$ mmHg).
- - -○- - - Cu reduced at 200° ($2.50\times10^{-2}$ mmHg).
- - -◑- - - Cu sintered at 400° ($1.87\times10^{-1}$ mmHg).
—·-○-·— Cu-Ni reduced at 200° ($2.66\times10^{-2}$ mmHg).
—·-◑-·— Cu-Ni sintered at 400° ($1.40\times10^{-1}$ mmHg).

TABLE I
SURFACE AREA OF COPPER CATALYSTS ($M^2$/g.)

| | Cu | Cu-Ni | Cu-MgO | MgO |
|---|---|---|---|---|
| Reduced at 200° | 0.69 | 0.80 | 3.90 | 13.8 |
| Sintered at 400° | 0.25 | 0.34 | 2.70 | — |
| Sintered at 500° | 0.20 | — | 1.50 | 27.0 |

Fig. 1 shows the rate of the adsorption of hydrogen at 160°C on copper-magnesia, pure copper, and copper-nickel. As shown in the figure, the rate of adsorption on copper-magnesia reduced at 200°C is markedly greater than that on the others; more than ten times as great as that on pure copper, and three times that on copper-nickel. Of particular interest is the fact that the increase in the rate of adsoption by the addition of magnesia well exceeds the corresponding increase of the surface area. Raising the temperature of heat treatment considerably decreases the rate of adsorption, but it is less effective compared with that of pure copper and copper-nickel catalysts[2]. Thus, it becomes apparent that the promoting action of magnesia involves something more than maintaing the surface area.

Fig. 2 shows the adsorption isotherms per unit area of the catalyst**. It is found that the

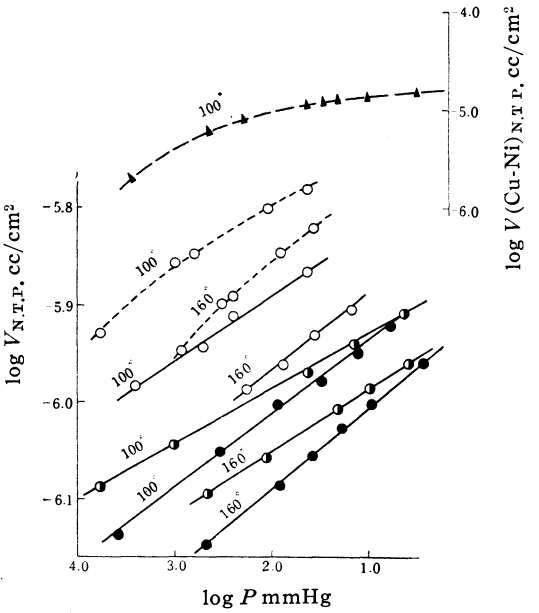



Fig. 2. Adsorption isotherms of Cu-MgO, Cu, and Cu-Ni catalysts.

—○— Cu-MgO reduced at 200°
—◑— Cu-MgO sintered at 400°
—●— Cu-MgO sintered at 500°
- - -○- - - Cu reduced at 200°
— —▲— — Cu-Ni reduced at 200°

** The saturation value, as derived from the Langmuir plot or dissociative type, is $2.07\times10^{-5}$cc. N. T. P. per sq cm. on pure copper while $1.44\times10^{-6}$cc. N. T. P. on copper-magnesia. This indicates that the abundance of active site on the latter catalyst is only 7% of that on copper alone.

addition of magnesia decreases the amount of hydrogen adsorbed, while, on the contrary, the addition of nickel increases it. The heat treatment of copper-magnesia decreases the amount of hydrogen adsorbed.

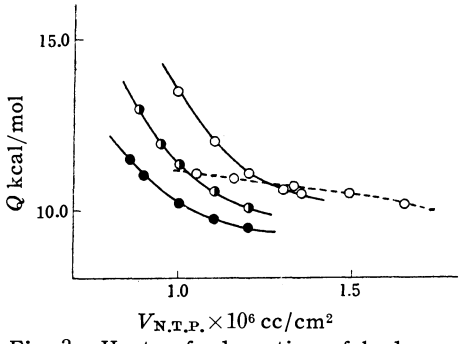



Fig. 3. Heats of adsorption of hydrogen on Cu-MgO and Cu catalysts.
—○— Cu-MgO sintered at 200°
—◑— Cu-MgO sintered at 400°
—●— Cu-MgO sintered at 500°
---○--- Cu reduced at 200°

Fig. 3 shows the relationship between the heat of adsorption and the amount adsorbed on the copper-magnesia catalyst. The broken line represents the heat of adsorption on pure copper. The heat of adsorption $q$ was calculated by using Clapayron-Clausius' equation

$$(\partial \ln P/\partial T)_v = q/RT^2$$

where $P$ is the equilibrium pressure and $V$ is the amount adsorbed.

The heat decreases gradually as the temperature of heat treatment increases, as frequently happens on most reduced catalysts. A notable thing is that the decline of the heat curve is very steep on magnesia added to copper.

Adsorption measurement was carried out on a magnesia powder at 100° and 160°C, but the adsorption was too small to detect.

## Discussion

On the basis of the fact that the amount of hydrogen adsorbed per unit area of the copper-magnesia catalyst is less than that on unpromoted copper and that hydrogen is scarcely adsorbed on the magnesia powder, it is suggested that the magnesia occupies a considerable portion of the surface. This is amplified by the study of electron diffraction as shown in Fig. 4; that is, diffraction pattern due to magnesia can be found together with that of copper, and no compound formation appears between magnesia and copper. The pattern also indicates that the magnesia exists in microcrystal particles on the surface. This was confirmed by Yamaguchi[3], who studied this sample by changing the accelerating potential of electron.

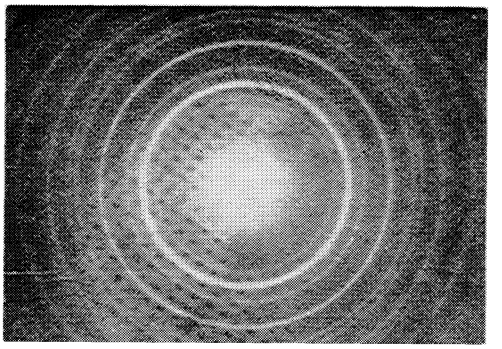


Fig. 4. Electron diffraction photograph of Cu-MgO catalyst: Wave length of electrons; 0.0306 Å, Camera length; 495 mm.

It is expected that copper in the catalyst may sinter upon heating and decrease its surface area, while magnesia, with a very high melting point, may not. Thus, the ratio of the surface area of the copper particles to those of the magnesia in the catalyst would decrease with increasing the reduction temperature of the catalyst. The B. E. T. surface area as given in Table I most probably includes the "dead area" which is inert toward hydrogen adsorption.

If the dead area is excluded for the adsorption of hydrogen, each of the three heat curves would shift parallel to the horizontal axis toward the right respectively according to the temperature of heat treatment. Thus the heat of adsorption of hydrogen on copper-magnesia catalyst well exceeds that on pure copper catalyst at a low coverage.

The greater heat value and the greater adsorption rate on the copper-magnesia catalyst would suggest that the physical property of copper in this mixed catalyst differs from that of pure copper.

How should the difference in the physical property of copper be explained? It has been proved by Willstätter[4] that the catalytic hydrogenation of phthalic anhydride and benzene over platinium or palladium is promoted by the presence of traces of oxygen, while it is often suppressed if the metallic catalyst is scrupulously freed from oxygen. Exhaustively reduced copper at 400°C, according to Kwan[5], shows an activation energy as high as 20 kcal. for

3) S. Yamaguchi, *Z. Physik. Chem.*, **7**, 115 (1956).

4) R. Willstätter and D. Jacquet. *Ber.*, **51**, 767 (1918); R. Willstätter and E. Waldschmidt-Leitz, ibid., **54**, 113 (1921).

5) T. Kwan, *J. Res. Inst. Catalysis*, **2**, 95 (1949).

the chemisorption of hydrogen. The chemisorption rate is measurable only above 300°C. In view of these observations, it is impossible that the copper in the present catalyst is entirely freed from oxygen contamination. This must be a kind of contamination that would result in an increase in adsorption heat, and probably a decrease in activation heat for the adsorption.

According to Gwathmey[6], the small amounts of a metal or a metallic oxide added to a copper single crystal modifies the rearrangement of the surface either by controlling the development of certain facets, or by promoting the formation of copper powder at different rates on the different faces. Surface irregularities caused by the presence of magnesia might promote to an extent the adsorption of hydrogen on the copper-magnesia catalyst. It is hoped, however, that the effect of oxygen can be explained on the electronic basis. Possibly the copper in the copper-magnesia would lose electrons from its filled 3d shell by the interaction with the oxygen of magnesia, and $Cu^{++}$ may act as an active site for the adsorption of hydrogen.

## Summary

(1) The adsorption of hydrogen on a copper catalyst containing 1% magnesia sintered at various temperatures has been investigated at 100° and 160°C, and compared with that on copper alone. The addition of magnesia increases markedly both the surface area and the rate of adsorption. The latter increase, however, is far beyond the increase in surface area.

(2) The hydrogen adsorption per unit area of the copper magnesia catalyst is less than that on pure copper, and decreases with increasing heat treatment. The adsorption of hydrogen on magnesia powder is immeasurably small. The heat curves on differently heated catalysts do not agree with each other, but approximately do so if the effective area for hydrogen adsorption is taken into consideration. The adsorption heat for a low coverage is certainly greater on the magnesia added copper than on copper alone.

(3) By aid of the electron diffraction study, it is concluded that the magnesia in the catalysts exists on the surface and forms microcrystal particles. Presumably, copper in the magnesia added catalyst is modified by the oxygen of the magnesia and irregular defects are formed on the surface in the presence of magnesia.

*Faculty of Literature and Science*
*Toyama University*

6) R. E. Cunningham and A. T. Gwathmey, *J. Am. Chem. Soc.*, **76**, 391 (1954).

# *The Adsorption of Non-polar Gases on Alkali Halide Crystals. I. The Low-temperature Adsorption of Non-polar Gases on Cubic Sodium Chloride**

By Teruo HAYAKAWA

(Received August 24, 1956)

## Introduction

The quantitative measurements of the low-temperature adsorption of non-polar gases (argon, oxygen, and nitrogen) on cubic potassium chloride and cesium iodide (rhombic dodecahedron) were reported by Orr[1] and Tompkins and Young[2] respectively. The adsorption of argon on two samples of octahedral potassium chloride (lead- and dye-modified) has recently been measured by Young[3].

Though the adsorption equilibrium is

* Part of this paper was read before the 8th Annual Meeting of the Chemical Society of Japan held in Tokyo, April, 1955. Other part of this papar was also read before the symposium on the surface heterogeneity of catalysis held in Kyoto, March, 1956.

1) W. J. C. Orr, *Proc. Roy, Soc.*, **A173**, 349 (1939).
2) F. C. Tompkins and D. M. Young, *Trans. Farad. Soc.*, **47**, 77 (1951).
3) D. M. Young, ibid., **48**, 548 (1952).

influenced both by the heats and the entropies of adsorption, the variation in the isosteric heats of adsorption with the surface coverage was discussed only in the investigations mentioned above. The variation in the entropies of argon with the coverage on cubic potassium chloride was given by Kemball[4] only from Orr's results[1]. Moreover, no reasonable explanation was given for the differences in the values of the initial heat of adsorption (the values extrapolated to zero coverage) with molecular species of adsorbates.

The present experiments were undertaken as a part of the systematic investigations to obtain the precise information on the following properties of the low-temperature adsorption.

(1) The surface heterogeneity of alkali halide crystals.

(2) The differences in the values of the initial heat of adsorption with molecular species of non-polar adsorbates.

(3) The characteristic behavior of each non-polar molecule on alkali halide crystals.

(4) The differences in these adsorptive properties with lattice parameters and crystal planes.

The choice of argon, oxygen, nitrogen and carbon dioxide as nonpolar adsorbates mainly depended on avoiding the complications which the presence of permanent dipoles would introduce and on the intention of examining the influence of permanent quadrupoles of these molecules.

## Experimental

**Materials.**—*Sodium Chloride* was recrystallized by cooling rapidly an aqueous solution of sodium chloride (extra pure grade) saturated at 100°C. The crystals were collected on a sintered glass filter funnel, washed with successive portions of 70% ethyl alcohol, absolute alcohol, and dry ether, and stored in a vacuum dessicator over phosphorous anhydride during about two weeks. Microscopic examination of this sample of sodium chloride revealed a large number of small cubes plus a few cubes in which the defects in the corners or edges were somewhat perceptible. The examination of this sample by an electron diffraction apparatus also revealed the regular pattern of (100) faces.

*Helium* was supplied by Teikoku Oxygen Co. as spectroscopically pure and was not further purified. *Argon* was also supplied by the Teikoku Oxygen Co. (purity was about 99.9%); this sample was purified by passing over phosphorous anhydride and then by farctionation. *Oxygen* was prepared by the thermal decomposition of silver oxide at 250°C, and was purified by passing over phosphorous anhydride and then passing through traps cooled in liquid oxygen, and finally by fractionation. *Nitrogen* was prepared by heating pure sodium azide, outgassed at 150°C for five hours, to 270°C and was purified by passing over phosphorous anhydride and then passing through traps cooled in liquid nitrogen. *Carbon dioxide* was prepared by heating magnesium carbonate (analytically pure), outgassed at 450 °C for three hours, to 650°C and was purified by passing over phosphorous anhydride, passing through traps cooled in solid carbon dioxide, and finally by several fractionations. Each sample gas was analysed using a Hitachi-RMC mass spectrometer (single focusing, 90° sector type of magnetic field, 135-mm. radius of curvature of ion path), and no impurity was detected excepting few small background peaks.

**Apparatus.** — The principal diagrams of the apparatus are shown in Figs. 1 and 2. The diagram of the adsorption apparatus is shown in Fig. 1. This consisted of a doser, whose volume

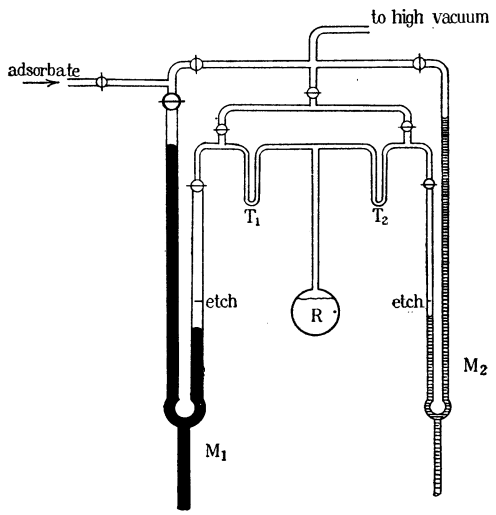



Fig. 1. Diagram of the adsorption apparatus.

was accurately determined with mercury, (18.06 cc. at 20°C), connected to an adsorption bulb R containing 32.3 g. of cubic sodium chloride crystals (passed through a 45-mesh sieve) and a manometer $M_2$ containing the oil (Apiezon B). $M_1$ shows a mercury manometer (inner diameter was about 12 mm.) by means of which the equilibrium pressure could be accurately determined to 0.05 mm. with a cathetometer. The lower equilibrium pressure could be accurately determined by an oil (Apiezon B) manometer $M_2$ to 0.05 mm. (i. e., 0.004 mmHg) with a cathetometer. $T_1$ and $T_2$ indicate traps cooled in liquid refrigerant, and the liquid level of each Dewar vessel attached to $T_1$ and $T_2$ was maintained constant throughout the measurement. In order to minimize the dead space, the adsorption system (excepting the bulb R and the doser) and

4) C. Kemball, "Advances in Catalysis" Vol. II, Acedemic Press Inc., New York (1950), p. 233.

manometer $M_2$ were of small bore tubing (3 mm.).

The diagram of the low-temperature thermostat regulator (similar to that used by Orr) is shown in Fig. 2. A closed Dewar vessel was filled with

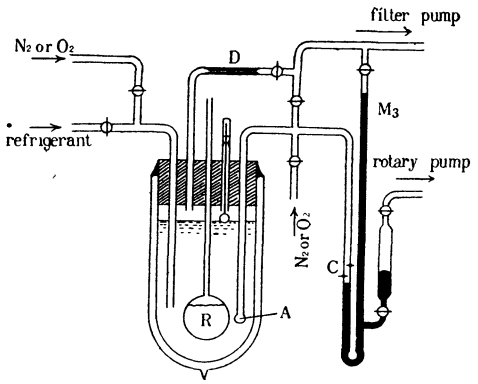



Fig. 2. Diagram of the low temperature thermostat regulator.

liquid refrigerant enclosing the small bulb (A) of a vapour pressure thermometer ($M_3$) containing oxygen or nitrogen, depending on the temperature to be measured. The vapour pressure thermometer acted both as a temperature resister and as a manostatic device. In one limb two Pt contacts were sealed at C, and at any desired pressure, depending on the temperature required, a relay circuit operated a filter pump through a fine capillaries (D) for controlling the rate of evacuation. Because of the low thermal conductivity of the liquid refrigerants, vigorous stirring was essential and attained by a regulated stream of oxygen or nitrogen. The position of the liquid level in the closed Dewar vessel was indicated by a float and maintained constant (2 mm.) throughout the measurements. The temperature variation recorded by the vapour pressure thermometer was never greater than 0.02°C. The vapour pressure data of Cath[5] for oxygen and of Giauque and Clayton[6] for nitrogen were used.

For the adsorption measurements of carbon dioxide, the enclosed Dewar vessel (c. f. Fig. 2) was filled with a mixture of each organic solvent (purified methanol, absolute alcohol, or dry ether) and solid carbon dioxide, depending on the temperature to be measured. In this case, the temperature was measured by a Copper-Constantan thermocouple inserted into the Dewar vessel.

**Procedure.**—After outgassing at 280~300°C for six hours before commencing each experiment and cooling the adsorbent to the desired temperature of adsorption, gas was admitted to the doser and the pressure at constant volume was measured by means of a mercury manometer ($M_1$ in Fig. 1). Then the gas was completely transferred to the adsorption system by admitting mercury into the doser. The adsorption was practically instantaneous and the equilibrium pressure at constant volume was measured.

The amount of gas adsorbed is given by

$$\left.\begin{aligned} v &= \frac{(\sum P_D)V_D}{RT_R} - \frac{P}{R}f \\ f &= \frac{V_0}{T_R} + \frac{V-C}{T_c} + \frac{V'-C'}{T_c'} \end{aligned}\right\} \quad (1)$$

where $\sum P_D$ is the sum of the successive doser pressures in atm., $V_D$ the volume of the doser in litres, $P$ the equilibrium pressure in atm., $V_0$ the volume in litres of the adsorption system exposed at room temperature, $V$ the volume in litres of the adsorption bulb (excluding the adsorbent) and the connecting tube up to the level of liquid refrigerant, $V'$ the volume in litres of traps ($T_1$ and $T_2$) up to the level of liquid refrigerant, $C$ the volume contraction in litres of the adsorbent and bulb on cooling, $C'$ the volume contraction in litres of traps ($T_1$ and $T_2$) on cooling, $R$ the gas constant in l·atm./degree·mol., $v$ the amount of gas adsorbed in moles, $T_R$ room temperature in °K, $T_c$ the adsorption temperature in °K, and $T_c'$ the temperature of traps ($T_1$ and $T_2$) in °K.

The value of the factor $f$ for each successive measurement was determined by carrying out a blank run with helium, using Eq. (1) and assuming $v$ to be zero. The experimental error in $v$ mainly comes from the measurement of the equilibrium pressure, but the low equilibrium pressure was accurate to 0.004 mmHg as mentioned above and the consequent error in $v$ was about ±1%. The value of $f$ was different for two series of measurements.

## Results

The isotherms obtained for the four gases on cubic sodium chloride crystals are summarized in Figs. 3, 4, 5 and 6. The adsorption was found to be reversible in this temperature range. The isosteric

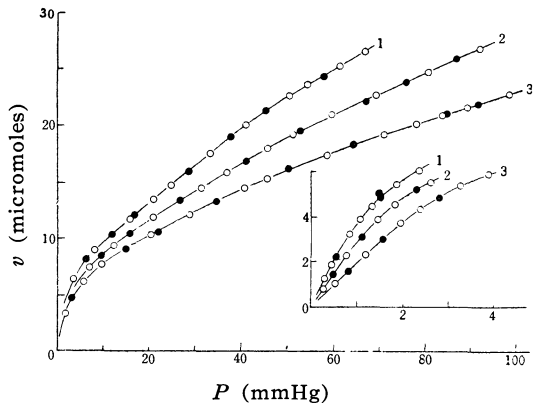



Fig. 3. Adsorption isotherms of argon on cubic sodium chloride.
1···73.69°K, 2···75.40°K, 3···77.32°K,
—○—○— adsorption, —●—●— desorption.

5) A. Cath, Comm. Phys Lab. Univ. Leiden, No. 152d (1918).
6) W. F. Giauque and J. O. Clayton, *J. Am. Chem. Soc*, **55**, 4875 (1933).

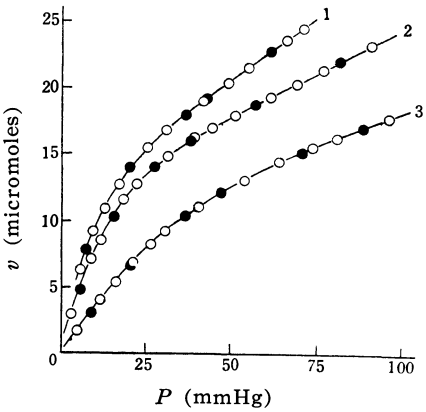



Fig. 4. Adsorption isotherms of oxygen on cubic sodium chloride.
1···75.40°K, 2···77.32°K, 3···83.08°K,
—○—○— adsorption, —●—●— desorption.

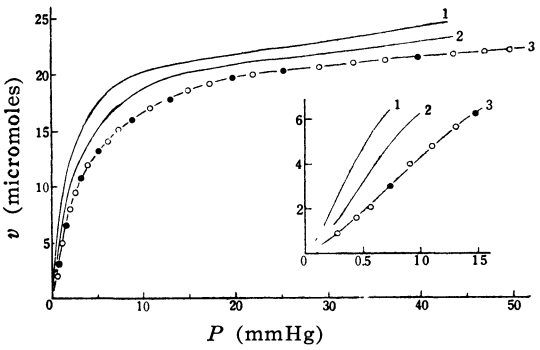



Fig. 5. Adsorption isotherms of nitrogen on cubic sodium chloride.
1···73.75°K, 2···75.41°K, 3···77.32°K,
—○—○— adsorption, —●—●— desorption.

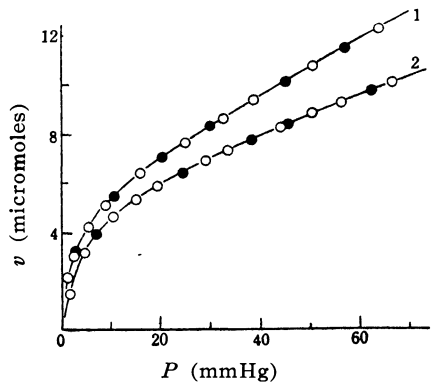



Fig. 6. Adsorption isotherms of carbon dioxide on cubic sodium chloride.
1···187.6°K, 2···194.6°K,
—○—○— adsorption, —●—●— desorption.

heats of adsorption as a function of $v$ were calculated from these isotherms using the Clausius-Clapeyron equation in the form

$$\left(\log \frac{P_1}{P_2}\right)_v = \frac{\Delta H}{2.303\,R}\left(\frac{1}{T_1}-\frac{1}{T_2}\right) \qquad (2)$$

where $P_1$ and $P_2$ are the equilibrium pressures (in mmHg) at the temperatures of $T_1$(°K) and $T_2$(°K) respectively, $-\Delta H$ the isosteric heat of adsorption in cal./mol., $R$ the gas constant (1.987 cal./degree·mol.). The isosteric heats of adsorption for argon, oxygen and nitrogen showed no definite trend with temperature within the experimental error.

The entropy decrease due to the adsorption as a function of $v$ was then calculated from the following equation

$$\left.\begin{aligned} 4.576\,T\log(P/760)_v &= \Delta H - T\cdot\Delta S \\ -\Delta S &= (S_g - S_s) \end{aligned}\right\} \qquad (3)$$

where $T$ is the temperature of each isotherm in °K, $P$ the equilibrium pressure in mmHg, $-\Delta S$ the entropy of adsorption in e. u./mol., $S_g$ the entropy of the gas phase under the standard state in e. u./mol., $S_s$ the entropy of the adsorbed phase in e. u./mol. The choice of the standard states of the gas was such that the pressure is 760 mmHg (independent of temperature) and the temperature coincides with that of each isotherm. Fig. 7, 8, 9 and 10 show the isosteric heats of adsorption averaged over the whole temperature range and the entropy of adsorption. The measurements were not extended to the high adsorption region for carbon dioxide, because the amount adsorbed was considerably small in this temperature range.

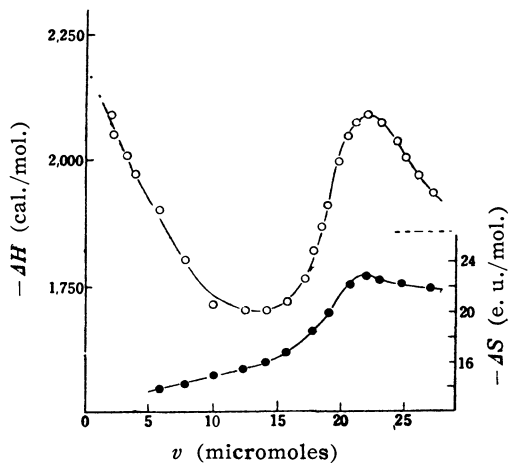



Fig. 7. Isosteric heats and entropies of adsorption for argon on cubic sodium chloride.
—○—○— isosteric heats of adsorption ($-\Delta H$),
—●—●— entropies of adsorption ($-\Delta S$),
- - - - - latent heat of sublimation.

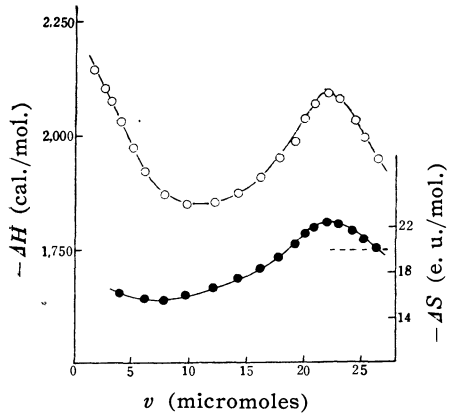



Fig. 8. Isosteric heats and entropies of adsorption for oxygen on cubic sodium chloride.
—○—○— isosteric heats of adsorption ($-\Delta H$),
—●—●— entropies of adsorption ($-\Delta S$),
----- latent heat of evaporation.

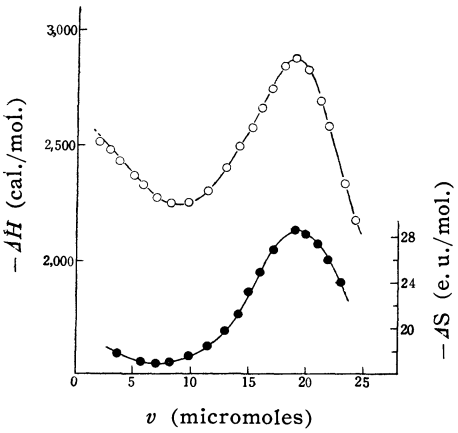



Fig. 9. Isosteric heats and entropies of adsorption for nitrogen on cubic sodium chloride.
—○—○— isosteric heats of adsorption ($-\Delta H$),
—●—●— entropies of adsorption ($-\Delta S$).

## Discussion

**Isosteric Heats of Adsorption.** — The isosteric heats of adsorption thus obtained for the three gases (argon, oxygen and nitrogen) fall initially, rise to a maximum, and then fall steadily to the value of latent heat of vaporization or sublimation with increasing amount of adsorption. These results of the present experiments for cubic sodium chloride are similar to the results obtained by Orr for cubic potassium chloride. The initial decrease in the heat of adsorption of these four non-polar gases is attributed to the non-uniformity of the surface. Since

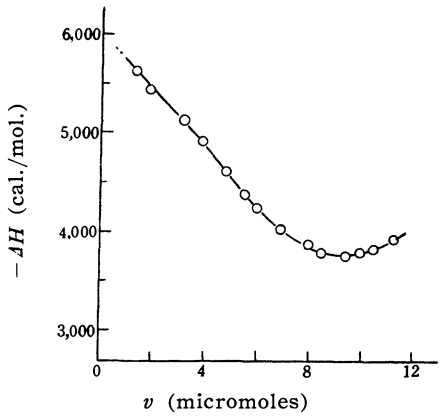



Fig. 10. Isosteric heats of adsorption for carbon dioxide on cubic sodium chloride.

mutual interaction forces of adsorbed molecules are attractive, the isosteric heats on the uniform surface in this low coverage region must be slightly increased with the increase of the amount adsorbed. The non-uniformity of alkali halide surface in the low coverage region was attributed by Tompkins and Young[2] to the defects in the corners and edges of the crystals. As it was generally observed, the crystal defects in the present sample were clearly visible under the microscope.

Though it seems reasonable to consider that the crystal defects or the lattice imperfections have some influence over the non-uniformity of alkali halide crystals, the magnitude of these influences in the present systems seems rather small compared with the present results. (The detailed discussion will be given in the succeeding paper.) The values of the initial heat of adsorption obtained for the four non-polar gases are summarized in Table I, together with the calculated values which will be given in the succeeding paper.

TABLE I

INITIAL HEAT OF ADSORPTION, $-\Delta H_0$, ON CUBIC (100) SODIUM CHLORIDE

| Adsorbate | $(-\Delta H_0)_{\text{expt.}}$ (cal./mol.) | $(-\Delta H_0)_{\text{calc.}}$ (cal./mol.) |
|---|---|---|
| Argon | 2190 | 1980 |
| Oxygen | 2240 | — |
| Nitrogen | 2670 | 2400 |
| Carbon Dioxide | 6070 | 5420 |

As seen in Table I, the experimental value of the initial heat of adsorption for argon comes closely near to that for oxygen. This is in good agreement with

the fact that there is a very close similarity between the potential energy curves for two argon atoms and two oxygen molecules[7,8]. On the other hand, the initial heat of adsorption for nitrogen is about 450 cal./mol. greater than those of argon and oxygen. This result is, however, not peculiar to the present experiment but has been similarly observed by Orr[1] with adsorption on cubic potassium chloride. In the case of nitrogen it would be expected from the lower heat of evaporation of the liquid compared with argon or oxygen and also from the similarity of the intermolecular potential energy between nitrogen and argon, that the adsorption heat of nitrogen would be somewhat smaller than that of argon or oxygen. Though the intermolecular potential energy curve for carbon dioxide is considerably different from that of argon or oxygen, the present differences in the initial heat of adsorption for these gases are considerably greater than the results anticipated from the differences in their intermolecular potential energy curves[9].

Recently, Smith and Howard[10] and Hill and Smith[11] have been able to measure the permanent quadrupole moments from line broadening of microwave spectra. Their results show that nitrogen and carbon dioxide (especially carbon dioxide) have considerably larger permanent quadrupole moments compared with argon and oxygen. Although, in general, permanent electric dipoles and quadrupoles are of minor importance in intermolecular potentials between gas molecules[12], the situation seems quite different when considering the adsorption potential of a molecule in the large electric field near the surface of an ionic crystal. The theoretical treatment of the adsorption potential between a nitrogen or a carbon dioxide molecule and the lattice ions of cubic (100) sodium chloride has been carried out by the present author. Though the details of this theoretical treatment will be reported in the succeeding paper, it is pointed out that the order of magnitude of the experimentally obtained initial heat of adsorption for argon, nitrogen and carbon dioxide is in considerably good agreement with the results of these theoretical calculations (see Table I).

**Entropies of Adsorption.**—As indicated in Figs. 7, 8 and 9, the variation of the entropies of adsorption with the amount adsorbed in the comparatively high coverage region is in the similar tendency with the variation of the isosteric heats of adsorption.

The present results on the entropy of adsorption for three non-polar gases are listed in Table II. For the reasons discussed below, the amount adsorbed corresponding to the maximum value of the heats or the entropies of adsorption was preferred as the monolayer capacity.

TABLE II
ENTROPIES OF ADSORPTION, $-\Delta S$, ON CUBIC SODIUM CHLORIDE AT 76.3°K

| Adsorbate | $-\Delta S$ (e. u./mol.) | |
|---|---|---|
| | $\theta=0.5$ | $\theta=1.0$ |
| Argon | 15.2 | 22.8 |
| Oxygen | 16.4 | 22.5 |
| Nitrogen | 18.0 | 28.7 |

As seen in Table II, Figs. 7, 8 and 9, the magnitudes of the entropies of adsorption and the variation of these with coverage for argon and oxygen resemble each other, while nitrogen shows considerably different features from those in the region of $\theta=0.5\sim1$. In order to obtain more information about the freedom of the adsorbed molecules, the entropy curves obtained in the present experiments were compared with the calculated values for these three gases. The entropy (the practical entropy) of each gas under the standard state (760 mmHg) was statistically calculated in the following manner.

The translational entropy of a perfect three-dimensional gas was calculated from the Sackur-Tetrode equation. No correction depending on deviation from ideal behavior was made, because each correction calculated from the Berthelot equation resulted in a small value and, furthermore, no correction of the same kind was made for the translational entropy (two-dimensional) of each adsorbed molecule.

The rotational entropy was calculated from an expression given by Halford[13], and the vibrational entropy was calculated from the usual statistical expression given below, which was shown to be nearly zero. Further, oxygen has an electronic entropy amounting to 2.17 e. u./mole., while the

7) J. E. Lennard-Jones, *Proc. Phys. Soc.*, **43**, 461 (1931).
8) R. H. Fowler, *Physica*, **5**, 44 (1938).
9) J. O. Hirschfelder, R. B. Bird and E. D. Spoz, *J. Chem. Phys.*, **16**, 968 (1948).
10) W. V Smith and R. Howard, *Phys. Rev.*, **79**, 132 (1950).
11) R. M. Hill and W. V. Smith, ibid, **82**, 451 (1951).
12) H. Margenau, *Rev. Mod. Phys.*, **11**, 1 (1939).
13) J. O. Halford, *J. Chem. Phys.*, **2**, 694 (1934).

nuclear spin contribution of nitrogen was omitted in the present calculations according to the common practice.

The statistical calculation of the entropy of the adsorbed material was as follows.

For non-localized adsorption the translational entropy of a perfect two-dimensional gas was calculated according to the equation derived by Kemball[14]

$$S'_T(\text{e. u./mol.}) = 4.576 \log MTa_0\left(\frac{1-\theta}{\theta}\right) \tag{4}$$

where $M$ is the molecular weight and $a_0$ the cross-sectional area of the adsorbed molecule.

The entropy associated with the vibration normal to the surface, replacing the translational motion, was calculated from an expression

$$S_v(\text{e. u./mol.}) = 1.987\left\{\frac{h\nu}{KT}(e^{h\nu/KT}-1)^{-1} - 2.303 \log (1-e^{-h\nu/KT})\right\} \tag{5}$$

where $\nu$ is the frequency of the vibration normal to the surface*, $h$ the Planck's constant and $K$ the Boltzmann's constant.

Since the surfce essentially introduces a high potential barrier restricting the turning over of the molecule, the two rotational degrees of freedom of oxygen or nitrogen will become effectively one degree of freedom of planar rotation in the plane parallel to the surface and one degree of freedom of rocking vibration as discussed by Hill[15]. In the present calculations the entropy associated with this rocking vibration was assumed to be negligible and the entropy associated with one degree of planar rotation was calculated from the above-mentioned expression given by Halford. The entropy associated with the intramolecular vibration of the adsorbed molecule was also calculated from Eq. (5), but these calculations resulted in the values of nearly zero.

For the localized adsorption there will be a configurational term associated with the number of ways of distributing the molecules over the surface. The configurational entropy on the Langmuir model, where the surface heterogeneity and the mutual interaction between the adsorbed molecules are both ignored, is given by

$$S'_c(\text{e. u./mol.}) = 4.576\left\{\frac{1}{\theta}\log\frac{1}{\theta} - \left(\frac{1-\theta}{\theta}\right)\log\left(\frac{1-\theta}{\theta}\right)\right\} \tag{6}$$

This equation (6) could not be used for the present calculations, because the heat curves indicate that the non-uniformity of the surface and the mutual interaction between the adsorbed molecules are both predominant.

Drain and Morrison[16] have recently experimentally determined the configurational entropy for the system in which the non-uniformity of the surface was taken into consideration and the mutual interaction between the adsorbed molecules was ignored. From this, we obtain approximately for the present systems

$$S_c(\text{e. u./mol.}) = 1.987 \times \frac{\pi^2}{3} \times \frac{d\ln v}{d\ln P} \tag{7}$$

where $v$ is the amount adsorbed and $P$ the equilibrium pressure.

The entropy curves determined from the present experimental results and the entropy curves calculated from the above-mentioned methods are summarized in Figs. 11, 12 and 13. The experimentally determined values in these figures are the partial molar total entropies and hence

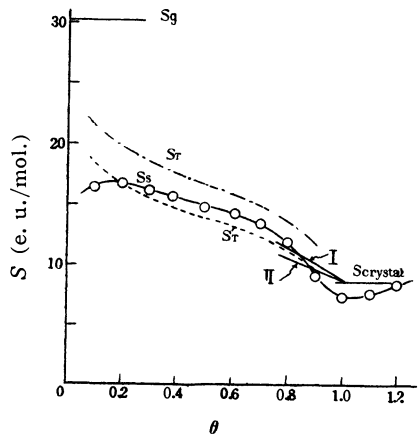



Fig. 11. Entropies of argon adsorbed on cubic sodium chloride at 76.4°K.

$S_S$···experimental values, $S_T$···calculated values (two-dimensional gas), Curve I··· (Scrystal+$S_c$) Curve II···(Scrystal+$\bar{S}_c$). (The entropy of the solid was calculated from the heat of sublimation and the value of the saturation pressure at 76.4 °K.)

14) C. Kemball, *Proc. Roy. Soc.*, A **190**, 117 (1947).

* Since each adsorption site gives a slightly different value, as will be shown in the succeeding paper, the average value was used for the present calculations.

15) T. L. Hill, *J. Chem. Phys.*, **16**, 181 (1948).

16) J. M. Drain and J. O. Morrison, *Trans. Farad. Soc.*, **48**, 316 (1952).

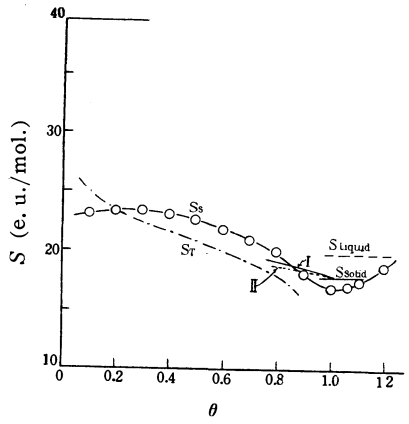



Fig. 12. Entropies of oxygen adsorbed on cubic sodium chloride at 76.4°K.

$S_S$···experimental values, $S_T$···calculated values (two-dimension gas). Curve I··· ($S_{solid}+S_c$), Curve II··· ($S_{solid}+S_c$).
(The entropies of solid and liquid oxygen were calculated from the data obtained by Giauque and Johnston[17].)

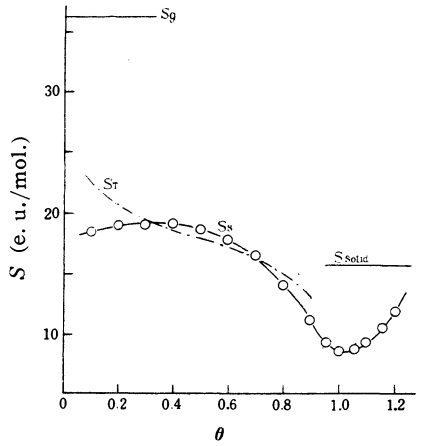



Fig. 13. Entropies of nitrogen adsorbed on cubic sodium chloride at 76.4°K.

$S_S$···experimental values, $S_T$···calculated values (two-dimensional gas).
(The entropy of solid nitrogen at 76.4°K was calculated from the data obtained by Giauque and Clayton[6].)

contain the entropy changes of the adsorbent caused by the adsorption[18]. On the other hand, the calculated values are all the integral entropies and are usually somewhat greater than the values of the partial molar total entropies. Considering the problem from this fact, the experimental entropies ($S_S$) for adsorbed argon and nitrogen are in considerably good agreement with the calculated entropies of the two-dimensional gas ($S_T$) in the region of $\theta=0.3\sim0.9$. Since the entropy for oxygen associated with the vibrational motion normal to the surface was calculated from assuming that the frequency of oxygen is identical with that of argon, the calculated entropies of the two-dimensional gas for oxygen ($S_T$) probably resulted in smaller values. Therefore, the agreement of the experimental curve for oxygen in the region of $\theta=0.2\sim0.9$ with the calculated curve of the two-dimensional gas is rather good. The discrepancy between the experimental and calculated values in the low coverage region ($\theta<0.2$) must be mainly attributed to the entropy changes of the adsorbent.

The suggestion of the phase change of argon adsorbed on cubic potassium chloride from a gaseous film to a condensed film was made by Kemball[4]. According to this, the phase change of argon on cubic potassium chloride occurred at about $\theta=0.8$, because the experimental values shifted from the curve of the two-dimensional gas to the curve of the localized adsorption obtained by adding the configurational entropy (Eq. (6)) to the entropy of the solid argon. This explanation involves considerable uncertainties, because it seems unreasonable to use Eq. (6) for the calculations of the configurational entropy on the adsorption system in which the non-uniformity of the surface and the mutual interaction between the adsorbed molecules are both predominant.

In the present work, the configurational entropy for the localized adsorption was calculated from Eq. (7) given by Drain and Morrison. From the results shown in these figures it will be seen that the phase changes of argon and oxygen occur at about $\theta=0.9$. But the mutual interaction between the adsorbed molecules was ignored in Eq. (7) ; therefore, the present results on the phase change of the adsorbed molecules from a gaseous film to a condensed film also contain considerable uncertainties as those obtained by Kemball do.

**Monolayer Capacities.** — Since the present results (Figs. 7, 8 and 9) indicate that the non-uniformity of the surface considerably predominate in the low coverage region and the mutual interaction (including the mutual interaction caused by the induced dipoles) in the succeeding region is sharply increased with the increase of

17) W. F. Giauque and H. J. Johnston, *J. Am. Chem. Soc.*, **51**, 2300 (1929).
18) T. L. Hill, *J. Chem. Phys*, **17**, 520 (1949).

the amount adsorbed, it is unreasonable to apply the B. E. T. theory to the present adsorption systems. In these figures the isosteric heats and also the entropies of adsorption in the region of the comparatively high coverage are sharply increased and there is a fairly sharp maximum for all three gases on cubic sodium chloride. Here, the values of the amount adsorbed for the maximum heat and entropy change of adsorption coincide well with each other.

The gradual decrease in each heat curve (and also in each entropy change curve) beyond the maximum may be attributed to the formation of multilayers. Thus it seems reasonable to assign this value corresponding to the maximum in the heat curve or in the entropy change curve as the monolayer capacity as Orr adopted[1].

The present results on the monolayer capacities and the surface areas are summarized in Table III. Each value of the cross-sectional area in Table III was determined from the results of the entropies of the adsorbed molecules.

TABLE III

MONOLAYER CAPACITIES ($v_m$) AND SURFACE AREAS ($A$), CUBIC SODIUM CHLORIDE (32.3 g.)

| Adsorbate | Cross-sectional Area, $a_0$(Å$^2$) | $v_m$(Micromoles) From ($-\Delta H$) | $v_m$(Micromoles) (B.E.T.) | $A$(m$^2$) From ($-\Delta H$) | $A$(m$^2$) (B.E.T.) |
|---|---|---|---|---|---|
| Argon | 12.8 | 22.1 | (19.1) | 1.70 | (1.47) |
| Oxygen | 12.1 | 21.9 | (20.4) | 1.60 | (1.49) |
| Nitrogen | 13.8 | 19.0 | (22.0) | 1.58 | (1.83) |


## Summary

The low-temperature adsorption of non-polar gases (argon, oxygen, nitrogen and carbon dioxide) on cubic sodium chloride was investigated. The present results on the isosteric heats of adsorption for these four gases indicate that the non-uniformity of the surface considerably predominate in the low coverage region and the mutual interaction between the adsorbed molecules is also distinguished in the region of the comparatively high coverage.

The entropies of the adsorbed materials (argon, oxygen and nitrogen) were experimentally determined and compared with the calculated values of the two-dimensional gas. These results show that the adsorbed molecules have the nature of the two-dimensional gas at least in the region of $\theta=0.3\sim0.9$.

The present results indicate that the phase change (a gaseous film→a condensed film) of argon or oxygen may occur at about $\theta=0.9$, but this fact is somewhat uncertain.


The author wishes to express his grateful thanks to Dr. S. Horiba and Professor O. Toyama of Osaka Prefectural University for their kind encouragement and discussions.

*Department of Chemistry*
*Faculty of Education*
*Osaka Prefectural University, Sakai*

# *The Stabilities of Metal Ammine Complexes. I. The Absorption Spectra of a Series of Hexammine Ni(II) and Tetrammine Pt(II) Complexes*

By Hayami YONEDA

(Received September 22, 1956)

## Introduction

The formation constants of numerous metal complexes have been determined using the now familiar method established by J. Bjerrum[1]. From these results it was concluded that there existed a pretty good correlation[2,3,4] between the stability of the complex and the proton affinity of the ligand. This conclusion means, in case of ammine complexes, that the stronger basicity an amine has, the more stable

1) J. Bjerrum, "Metal Ammine Formation in Aqueous Solution". P. Haase and Son, Copenhagen (1941).

2) M. Calvin and Wilson, *J. Am. Chem. Soc.*, **67**, 2003 (1945).

3) J. Bjerrum, *Chem. Revs.*, **46**, 381 (1950).

4) W. S. Fyfe, *J. Chem. Soc.*, 2018 (1952).

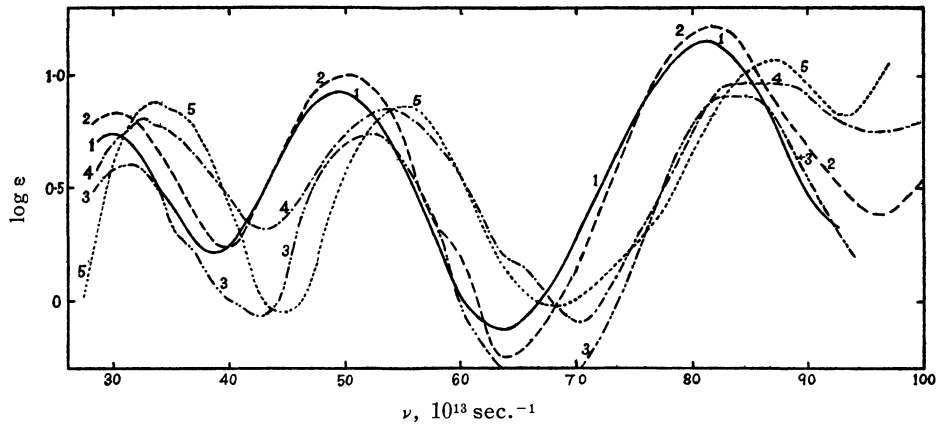



Fig. 1. The absorption spectra of hexammine Ni(II) complexes.

1 ——— $Ni(CH_3CH_2NH_2)_6^{2+}$ 4 —·—·— $Ni(NH_2OH)_6^{2+}$

2 - - - - - $Ni(OHCH_2CH_2NH_2)_6^{2+}$ 5 ---------- $Ni(NH_2CH_2CH_2NH_2)_3^{2+}$

3 —··—·· $Ni(NH_3)_6^{2+}$

complex it produces. However, we must notice that the determination of the formation constant can be made only when the complex is fairly labile and when it forms a reversible equilibrium system with its components in a solution. Accordingly, it should be carefully reexamined from another kind of data, to discover whether or not the law which governs the stability of the complex of highly covalent character coincedes with the above mentioned conclusion. The absorption spectra of complexes can give such reexamining means. The ammine complex of a transition metal ion having an unsaturated d-shell shows, in general, a definite number of absorption bands characteristic of the metal ion concerned from the near infrared to the near ultraviolet regions. For examle, Cu(II) complexes have one, Co(III) and Cr(III) complexes have two, and Ni(II) complexes have three such absorption bands. Hitherto, such absorption bands have been considered to be originated from the energy transitions between the splitting d-levels of the central metal ion[5,6]. Accordingly, when we can get knowledge about the correlation between the field strength set up by the ligands and the degree of splitting of the d-levels, we can discuss the stability of the complex from the absorption data. In the present investigation the absorption spectra of a series of hexammine Ni(II) and tetramine Pt(II) complexes were measured, and from these results a very interesting experimental rule was found between the stability of a complex and the basic strength of the coordinating amine.

## Experimental

The measured nickel ammine complexes were those of $NH_2OH$, $NH_3$, $OHCH_2CH_2NH_2$, $CH_3NH_2$, $CH_3CH_2NH_2$ and $NH_2CH_2CH_2NH_2$. As these complexes are all labile and hydrolyzed partly in a solution, the solution used in the measurement was prepared as follows: A solution containing an amine and its sulphate in the concentrations of 6 M and 2 M respectively was prepared. To such a solution, nickel sulphate was dissolved to 0.1 M. (Under these conditions, all nickel ions in a solution may be considered to exist as the form of hexammine complex ions.)

The plato ammine complexes measured were those of $NH_2OH$, $NH_3$, $CH_3NH_2$, $CH_3CH_2NH_2$, and $NH_2CH_2CH_2NH_2$. These complexes were prepared from $K_2PtCl_4$ and the corresponding amine through Magnus' salt. For the absorption measurement, 0.01 M solution of the complex was used in every case.

The absorption measurement was carried out by means of the Beckman DU spectrophotometer using tungsten and hydrogen lamps and 1 cm. quartz cells.

## Results

The absorption spectra of Ni ammine complexes are shown in Fig. 1. As the curves of both methylamine and ethylamine complexes are quite similar to each other, only that of the ethylamine complex is shown in the figure. All these curves have three absorption bands which are called the first, second and third bands from the long wavelength. The maximum positions of these three absorption bands and the pK*

5) R. Tsuchida, This Bulletin, **13**, 388 (1938).
6) M. Linhard and W. Weigel, *Z. anorg. u. allgm. Chem.*, **264**, 321 (1951).
7) "Inorganic Systheses", Mc Graw-Hill, New York (1949), Vol. II, 250.
* Negative logarithm of the ionization constant.

values of the coordinating amines are tabulated in Table I.

TABLE I

MAXIMUM POSITIONS OF THE THREE ABSORPTION BANDS OF $Ni(amine)_6^{2+}$

($\nu$, $10^{13}$ sec.$^{-1}$)

| Amine | pK | 1st Band | 2nd Band | 3rd Band |
|---|---|---|---|---|
| $CH_3CH_2NH_2$ | 3.27 | 29.70 | 49.2 | 81.5 |
| $CH_3NH_2$ | 3.37 | 30.0 | 50.0 | 81.5 |
| $OHCH_2CH_2NH_2$ undetermined | | 30.0 | 50.0 | 81.5 |
| $NH_3$ | 4.75 | 31.6 | 51.7 | 84.5 |
| $NH_2OH$ | 7.97 | 32.4 | 53.6 | 86.0 |
| $NH_2CH_2CH_2NH_2$ | 5.45* | 33.5 | 55.0 | 87.0 |

From the table it is easily seen that these three absorption bands shift to the same direction in variation of ligands. At the same time it is seen that the maximum position of the bands of the complex shifts with the basic strength of the coordinating amine.

The results obtained about Pt(II) ammine complexes are shown in Fig. 2.

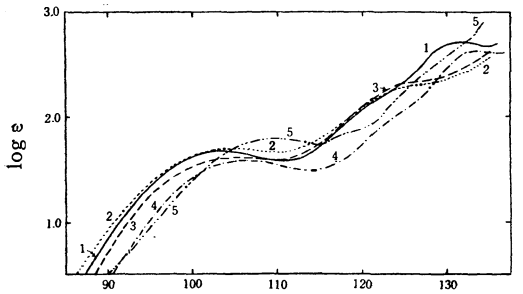



Fig. 2. The absorption spectra of tetrammine Pt(II) complexes

1 ——— $Pt(CH_3CH_2NH_2)_4^{2+}$
2 ---------- $Pt(CH_3NH_2)_4^{2+}$
3 - - - - - $Pt(NH_3)_4^{2+}$
4 —·—·— $Pt(NH_2CH_2CH_2NH_2)_2^{2+}$
5 —··—·· $Pt(NH_2OH)_4^{2+}$

TABLE II

MAXIMUM POSITIONS OF THE FIRST ABSORPTION BAND OF $Pt(amine)_4^{2+}$

($\nu$, $10^{13}$ sec.$^{-1}$)

| Amine | 1st Band |
|---|---|
| $CH_3CH_2NH_2$ | 103.4 |
| $CH_3NH_2$ | 105.0 |
| $NH_3$ | 105.0 |
| $NH_2CH_2CH_2NH_2$ | 107.0 |
| $NH_2OH$ | 110.1 |

* As ethylenediamine is a diacidic base and coordinates to the metal ion as a bidentate ligand, the mean value of $pk_1$ (4.08) and $pk^2$ (6.81) was taken as the pk for comparison. This mean pk value can give a rough estimation of the relative coordinating ability in the monoamine series.

In this case, the general feature of the absorption spectra is considerably complicated. Except the one appearing in the long wavelength region, the absorption bands in the shorter wavelengths have large values of log ε, and the discrimination from the charge transfer bands is difficult. Consequently, only the maximum position of the the absorption band in the long wavelength region is listed in Table II.

Here it is also shown that the maximum position of the absorption band shifts with the basic strength of an amine.

## Discussion

Before discussing the stability of the metal ammine complex from its absorption bands, we must consider the general relationship between the absorption bands and the electronic states of the complex radical.

The splitting of d-levels due to the influence of various outer fields was first evaluated by H. Bethe[8], and this view was further developed by J. H. Van Vleck[9] to the more general theory to account for the magnetic properties of crystals. The idea of using this crystal field theory on the complex radical is due to H. Hartmann and F. E. Ilse[10], who applied it to explain the absorption spectra of the titanium(III) and vanadium(III) complexes. Recently, C. J. Ballhausen[11] and L. E. Orgel[12] extended this theory to the spectra of many other transition metal complexes. Although various mechanisms are able to remove the degeneracy of the d-orbitals as there are various intermediates between the purely ionic and highly covalent bonds, in the crystal field theory the splitting of the degeneracy of the d-orbitals is regarded as the consequence of the electrostatic field set up by the ligands. Here the covalent character of the bond is expressed by the polarization of the ligand. Now it is easily understood that the energy intervals between the splitting d-levels increase with the increase of the electrostatic field set up by the ligands. As the energy transitions between such splitting d-levels appear as the characteristic absorption bands of the complex, it can be said that the stronger the field by the ligands is, the more the absorption bands of the complex appear in the shorter wavelength.

8) H. Bethe, *Ann. Physik.* 5 Folge, **3**, 133 (1929).
9) J. H. Van Vleck, "The Therory of Electric and Magnetic Susceptibilities", Oxford Press (1932).
10) H. Hartmann and F. E. Ilse, *Z. physik. Chem.*, **197**, 239 (1951) ; *Z. Naturforschg.*, **6A**, 751 (1951).
11) C. J. Ballhausen, *Dan. Mat. Fys. Med*, **29**, No.4 (1954) ; ibid., **29**, No. 8 (1955).
12) L. E. Orgel, *J. Chem. Phys.*, **23**, 1004 (1955).

As indicated by C. J. Ballhausen, the polarization of the ligand in case of Ni(II) complexes is pretty large and the resulting induced dipole moment of the ligand is much larger than its permanent dipole moment. Accordingly, in the ammine complex whose ligand is neutral, it is concluded that the amount of polarization chiefly determines the field strength. In other words, the blue shift of the absorption bands of the complex in variation of the ligand corresponds to the increase of the field strenth set up by the ligand, and the increase of the field strength corresponds to the increase of polarization.

The present experimental results about Ni(II) and Pt(II) ammine complexes indicate that the weaker the basic strength of an amine is, the more the absorption bands of the produced complex appear in the shorter wavelength. Therefore, when this fact is connected with the above mentioned conclusion about the relationship between the absorption bands and the field strength by the ligands, the following rule can be drawn: In the complex of a transition metal ion with an unsaturated d-shell, the weaker the basicity of an amine is, the larger its polarization by the metal ion is. The increase in the polarization indicates the increase in the interaction between the ligand and the metal ion, and the increase in the interaction can be regarded as the increase of the stability of the complex.

Here it should be noticed that this conclusion is quite reverse to that presumed by many investigators. After the view hitherto believed, the affinity of the amine toward the metal ion should be in principle parallel with that toward hydrogen ion. However, we must point out that the data which formed the basis of such a view were all those about the ammine complexes of pseudo-inert gas type ions, such as $Ag^{+}$, $Hg^{2+}$ etc. As the d-shell of the pseudo-inert gas type ion is completely closed, the contribution of the d-electrons to the coordination bond may be considered to be negligibly small. Therefore, it is quite natural that such an ion behaves in the same manner with hydrogen ion. While, in the complex of transition metal ions with an unsaturated d-shell, the contribution of d-electrons to the coordination bond must be taken into account. Consequently, it is possible that such an ion with an unsaturated d-shell shows the quite different behaviour from the pseudo-inert gas type ion.

## Summary

The absorption spectra were measured about a series of hexammine Ni(II) and tetrammine Pt(II) complexes having various amines as ligands. These amines were hydroxylamine, ammonia, ethanolamine, methylamine, ethylamine and ethylenediamine. The results of the measurement indicate that the weaker the basic strength of an amine is, the more the absorption bands of the produced complex appear in the shorter wavelength. This fact was connected with crystal field theory, and the following rule was drawn: In the complex of a transition metal ion having an unsaturated d-shell, the weaker the basic strength of an amine is, the more stable the produced complex is.

The author wishes to express his heartfelt thanks to Professor R. Tsuchida and Professor M. Kobayashi of Osaka University for their kind advice and encouragement. The author's appreciation is also expessed to Professor O. Nagai of Wakayama Medical College who gave him a chance to use the Beckman DU spectrophotometer, and to Mr. S. Kida of Wakayama University for his helpful discussions.

*Department of Chemistry*
*Wakayama Uiversity, Wakayama*

# *Photochemical Reactions between Methylene Blue and Tri-, Di- and Monomethylamine. I*

By Hiroshi OBATA and Masao KOIZUMI

(Received September 19, 1956)

## Introduction

Imamura and Koizumi[1], one of the present authors, have found that eosine is photobleached in the alcoholic solution in vacuo but not in the aqueous solution, while in the aerobic condition it bleaches in the latter case but not in the former case. The bleaching of eosine in these cases is irreversible and the reaction as a whole is quite complicated. Now in contrast to eosine, it has long been known that methylene blue in the evacuated alcoholic solution is photobleached and the reaction in this case is the formation of a leuco dye, which returns to the original dye when the solution is exposed to the atmospheric air. The aqueous solution of methylene blue is of course stable against illumination in vacuo, but a notable fact has been found by Weil[2] that the addition of some suitable oxidizable compounds causes the photobleaching to take place in the evacuated aqueous solution. The aim of his work, however, was not to study the bleaching reaction but to study the photosensitized oxidation of various organic substances from the biochemical standpoint using methylene blue as a sensitizer. He therefore measured the rate of oxygen absorption when the aqueous solution of various organic substances in the presence of oxygen and methylene blue[2,3]. In the case of trimethylamine, he particularly analyzed the reaction product and identified it to be trimethylamine oxide. Hence he considered that the overall reaction in this case is

$$MB + TA + \frac{1}{2}O_2 \xrightarrow{h\nu} MB + TAO,$$

where TA is trimethylamine.

The above mentioned experiments of Weil seem to have been done merely for a supplementary purpose, and no scheme for the reaction in vacuo was given. There seems to be no doubt that the reaction in vacuo was given. These seems to be no doubt that the reaction consists of the formation of leuco dye and TAO (trimethylamine oxide), since the coloration is regained when the solution is exposed to air. But if so, it is very natural to suppose that the hydrogen donor in this case is water itself and not trimethylamine, since it is very difficult to detach the hydrogen atom from the latter compound. Thus the bleaching reaction in this case would be interpreted as a result of the photochemical fission of water molecule. An interesting analogue to the first process of photosynthesis by chloroplast as postulated by van Niel[4] was known.

The object of the present papers is to establish the above scheme definitely and to make clear the mechanism of the reaction. It is to be added here, that a certain attempt has been made[5] recently to explain the photobleaching of methylene blue in the deoxygenated solution by dint of ethylenediamine tetraacetic acid, on the postulate that the primary process is the photosensitized decomposition of water, but no conclusive evidence has yet been reported.

## Experimental Method

**Materials.**—*Methylene Blue.*—Grübler's reagent was used without further purification.

*Trimethylamine*[6].—Trimethylamine hydrochloride was prepared by the reaction of paraformaldehyde with ammonium chloride at about 160°C. From the reaction mixture, a free base was evolved by the neutralization with NaOH and was liquified by a condenser, using dry ice as a cooling reagent.

*Dimethylamine*[7].—Dimethylamine hydrochloride was prepared by the reaction of ammonium chloride with formaldehyde. The product was reocystallized five times from absolute alcohol, m.p. 165°C. The Free base was prepared from its hydrochloride. The neutralization was done by the same method as for trimethylamine.

*Monomethylamine*[8].—Monomethylamine hydro-

1) M. Imamura and M. Koizumi, This Bulletin, **28**, 117 (1955).
2) L. Weil, *Science* **107**, 426 (1948) ; L. Weil and J. Maher, *Arch. Biochem.*, **29**, 241 (1950).
3) For example. L. Weil, W. G. Gordon and A. R. Buchert, *Arch. Biochem.*, **33**, 90 (1951).
4) Van Niel, *Advances in Enzymology*, **1**, 263 (1941).
5) J. R. Merkel and W. J. Nickerson, *Biochim. et Biophys. Acta*, **14**, 303 (1954).
6) "Organic. Syntheses" Collect. vol. **1**, p. 517, 514.
7) "Beilstein Handbuch" Erst. Ergänz. III-IV, p. 320.
8) Organic Syntheses" Collect. vol. **1**, p. 340.

chloride was prepared from ammonium chloride and formaldehyde. The product was recrystallized from absolute alcohol washed with cold chloroform and once more recrystallized from butanol, m.p. 224°C. The free base was prepared from its hydrochloride in the same way as for trimethylamine.

*Trimethylamine Oxide*[9].—It was prepared from trimethylamine and hydrogen peroxide. The product was crystallized from alcohol-ether and then recrystallized twice from methanol. $(CH_3)_3NO2H_2O$, m.p. 96°C.

Since the solutions of tri-, di-, and monomethylamine are all autoöxidized in the air, it is necessary to degass the solutions and maintain them in the evacuated ampoules. Caution had to be taken to employ the fresh solution in each experiment.

**Apparatus and Procedures for Measuring the Rate of Photobleaching.**—Fig. 1 shows the main part of the apparatus. As a light source, a tungsten lamp for automobile (6 V, 35 W./35 W.) was employed and the range of wave lengths was adequately chosen by means of a filter for photography, the transmission of which is shown in Fig. 2. A drum-shaped reaction cell had an inner diameter of 27 mm. and a thickness of 10 mm. The light intensity was measured by Se-photocell.

The aqueous solutions of methylene blue and trimethylamine which were separately degassed in a vacuum system were poured into a reaction cell. The procedure for evacuation is quite analogous to that employed by Imamura[1]. The bleaching can be pursued continuously by measuring the intensity of a purallel beam which has passed through the reaction cell. A calibration curve between methylene blue concentration and photocurrent is shown in Fig. 3. The number of photons entering the reaction cell was usually ca. $10^{16}$ when the metallic nets as shields were not employed.

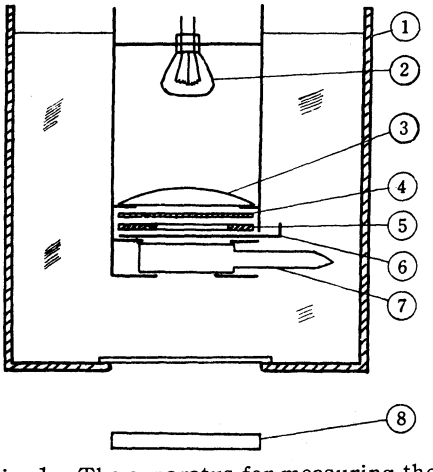



Fig. 1. The apparatus for measuring the photobleaching.
① Thermostat
② Light source (6 V, 35 W./35 W.)
③ Condensor lens
④ Metallic net to adjust the light intensity
⑤ Filter
⑥ Shutter
⑦ Reaction cell
⑧ Se-photocell

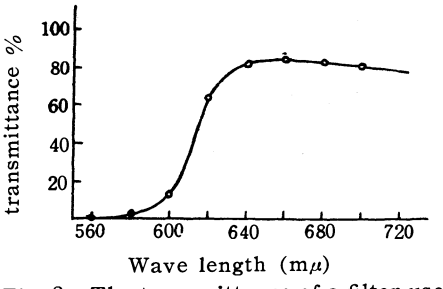



Fig. 2. The transmittance of a filter used.

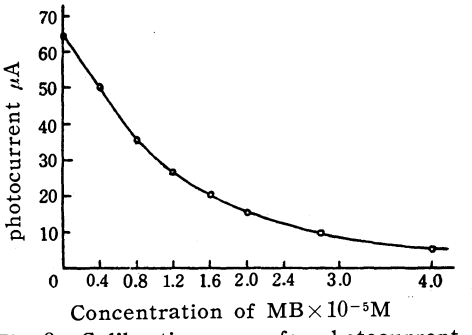



Fig. 3. Calibration curve for photocurrent.

## Experimental Results

**(A) Preliminary Observations.—(a) The Influences of Solvents.**—Photobleaching of methylene blue with trimethylamine was examined in various solvents: namely water, ethanol, isopropanol, butanol, acetone, methyl-ethyl ketone, acetic acid, and acetic anhydride. The bleaching was observed in all solvents except acetic acid and acetic anhydride, but its rate depended very much upon the kind of solvent. For example, the bleaching proceeded remarkably faster in butanol than in water and ethanol, and in acetone and methyl ethyl ketone a considerable dark reaction took place. After the photobleaching was complete, the solution was kept in dark for a long time, but the coloration of the solution was not observed in all cases. But when the solution was exposed to air, the solution regained its original color sooner or later. Similar experiments were carried out with monomethylamine and dimethylamine, and the results were the same at least qualitatively. In the aqueous solution the rate of photobleaching was the lowest in the case of monomethylamine and somewhat slower in

9) Meisenheimer, *Ann.* **397**, 286 (1913) : Dunstan, *J. Chem. Soc.*, **75**, 1004 (1899).

dimethylamine. From the above results, it is clear that the rate depends very much on solvents, and this is natural since the solvent molecule is considered to participate in the reaction.

**(b) The Reaction Products between Methylene Blue and Trimethylamine.**—The absorption spectrum of photobleached aqueous solution was examined by Beckman spectrophotometer and found to be the same as that of the aqueous solution of leuco dye which was produced by the action of sodium hydrosulfite upon the original dye (Fig. 4). Hence there is no doubt

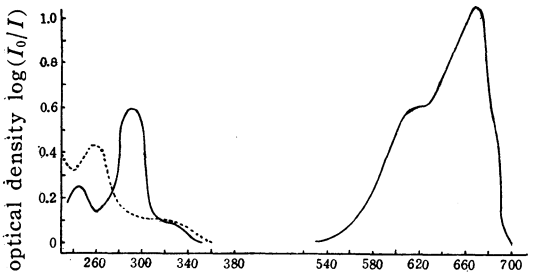



Fig. 4. Absoption spectra of methylene blue and leuco methylene blue.
full line: methylene blue
broken line: leuco methylene blue

that one product of the bleaching reaction is leuco methylene blue. Another product is most certainly supposed to be trimethylamine oxide. To confirm it definitely, one cannot rely upon a spectroscopic method, since this compound has no absorption through visible to near ultraviolet region. Hence, a chemical method was employed which is based on the fact that TAO effectively separates iodine from potassium iodide in the acidic medium; a particular experiment was done for such an analytical purpose. A large quantity of the evacuated aqueous solution of methylene blue and trimethylamine was illuminated by the sun light and after the decoloration occured almost completely, the solution was treated with Japanese acid clay in situ to remove the bleached and unbleached dye. The colorless filtered solution was concentrated to some extent under reduced pressure, and then some quantity of dilute acidic solution of KI and a drop of 1% starch solution were added. An intense blue coloration could be observed at once. The above experiment, however, had to be further checked by a blank using the aqueous solution of trimethylamine without the addition of dye, since there was some doubt that unreacted trimethylamine would be oxidized by atmospheric oxygen during the process of concentrating the solution. The blank experiment also showed an iodine-starch reaction but its extent was much smaller.

Hence one can safely conclude the formation of trimethylamine oxide. Thus the overall reaction in the aqueous solution has been determined as follows:

$$MB + H_2O + TA \longrightarrow MBH_2 + TAO$$

The formation of leuco dye was also established in the case of ethanol and butanol solution, but no further analysis was undertaken in these cases.

**(B) Kinetic Investigations.**—Since the overall reaction in the aqueous solution has now become clear, the authors investigated next some general features of the reaction from kinetic viewpoints. The concentration of dye cannot be changed so much because the change in light intensity is sensitive to that of dye concentration only in a small range of the latter, as judged from the calibration curve in Fig. 3. Almost all the experiments were carried out in the concentration of $2.0\times10^{-5}$ M of methylene blue since this concentration is suitable for the intensity measurement and moreover it is expected that the mechanism will be simpler in such a low concentration. Below will be summarized the chief results obtained by the various experiments kinetically in nature.

**(1) General Features of the Bleaching Curves.**—Fixing the pH of solution at 9.2 by using M/35 borate buffer, the effect of the trimethylamine concentration was investigated at 30°C. The results can be summarized as follows.

(a) At high concentration of trimethylamine (about 100 times as that of methylene blue), the bleaching curve is quite simple as shown in Fig. 5, and the bleaching is practically complete within about fifty minutes. The reaction can be expressed satisfactorily as a simple first order one in dye concentration.

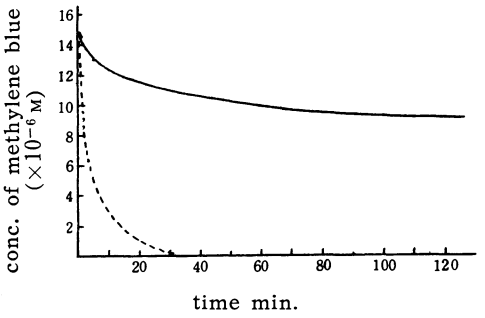



Fig. 5. The bleaching curve of methylene blue.
Methylene blue: $2.0\times10^{-5}$ M.
Temp. 30 C, Buffer was not used.
Trimethylamine:
$0.1\times10^{-3}$ M (full line)
$1.6\times10^{-3}$ M (broken line)

(b) At low concentration of trimethylamine (about several to thirty times as much as that of methylene blue) the reaction practically came to an end at a certain stage of decoloration, and the rate cannot be expressed as a simple first order one in dye concentration. The kinetics of bleaching must be complicated since plots of $\log(-dc/dt)$ against $\log c$, $c$ being the dye concentration, gives S-shaped curve. A typical example is shown in Fig. 5.

**(2) The Existence of a Reverse Reaction.**—The recovery of color was never observed under

the above experimental condition when the photobleached solution was kept in the dark for a long time. Neither could the back reaction be perceived in the partially photobleached solution obtained under the experimental condition (b). Thus the dark back reaction does not exist at least in the above experimental conditions. To determine whether a reverse reaction occurs or not in other conditions, the following experiments were undertaken. By the vacuum distillation, water and unreacted trimethylamine were eliminated from the photobleached solution and then about the same quantity of pure water was added to the residue consisting of leuco methylene blue and trimethylamine oxide. All these procedures were of course done without any contact of air. When the obtained solution was kept in the dark for a few days, the blue color of methylene blue could clearly be observed. The following experiments demonstrate more definitely the existence of such a back reaction. Adding various quantities of trimethylamine oxide to the original solution, the quantity of photobleaching in vacuo was examined. The results are summarized as follows. From the bellow table it is clear that the addition of a large amount of TAO strongly suppresses the bleaching reaction, and the photobleaching takes place only partially even after a long illumination.

When the partially photobleached solution obtained in experiment (a) (4) in Table I was kept in the dark, the blue color became more dense within a few hours. Thus it is clear that when a large quantity of TAO exists, the dark back reaction can occur and that a certain photostationary state is realized.

**(3) The Existence of an Intermediate Complex.**—Judging from the type of overall reaction it seems natural to suppose that the reaction is successive in nature. Moreover, the results in (1) suggest the existence of a long lived intermediate. Hence such a possibility was examined spectroscopically. Immediately after the illumination of the aqueous solution ($2.0\times10^{-5}$ M of dye, $6.0\times10^{-4}$ M of TA, pH 9.2) for about two minutes, the absorption spectra were carefully examined by Beckman spectrophotometer in the region from 750 to 1100 mμ, where methylene blue practically has no absorption. Repeated examinations showed that there really exist very small absorptions near 800 mμ, 850 mμ and 950 mμ as shown in Table II.

The above absorption was recognized even in the presence of oxygen. This will be discussed in the next paper.

When kept in the dark, the absorption in question slowly declines. Fig. 6 shows the optical density at 950 mμ as a function of time after two minutes illumination. That this intermediate slowly disappears in the dark was further confirmed by the recognition of a recovery in 665 mμ band of methylene blue slowly. The following data give the values of $\log(I_0/I)$ of the solution (methylene blue $2.0\times10^{-5}$ M. trimethyl-

TABLE I

THE EFFECT OF THE ADDITION OF TAO

(a) Methylene Blue Conc. $2.0\times10^{-5}$ M
M/35 Borate buffer (pH 9.2) was used.

| | Conc. of TA, M | Conc. of TAO, M | Ratio of TAO/TA | Stationary conc. of MB, M | Note |
|---|---|---|---|---|---|
| (1) | $6\times10^{-4}$ | $6\times10^{-2}$ | 100 | $0.65\times10^{-5}$ | |
| (2) | $6\times10^{-4}$ | $6\times10^{-2}$ | 100 | $0.80\times10^{-5}$ | Intensity of light was 1/2.5. |
| (3) | $4\times10^{-4}$ | $4\times10^{-2}$ | 100 | $0.6\times10^{-5}$ | |
| (4) | $4\times10^{-4}$ | $8\times10^{-3}$ | 20 | | The rate was much slower than that when no TAO was added. |

(b)* Methylene Blue Conc. $2.0\times10^{-5}$ M
Trimethylamine $1.7\times10^{-3}$ M

| | Conc. of TAO, M | Ratio of [TAO] to [TA] | Degree of bleaching |
|---|---|---|---|
| (1) | $2.0\times10^{-4}$ | 0.1 | Complete |
| (2) | $2.0\times10^{-3}$ | 1 | Almost complete |
| (3) | $2.0\times10^{-2}$ | 10 | Slight |
| (4) | $2.0\times10^{-1}$ | 100 | Not practically observed. |

* These experiments were rather preliminary in nature and were done in quite different conditions from those for kinetic purposes.

TABLE II

ABSORPTION BAND OF AN INTERMEDIATE

| Wave length (mμ) | | 750 | 800 | 850 | 900 | 950 | 1000 | 1100 |
|---|---|---|---|---|---|---|---|---|
| $\log(I_0/I)$ | initial | 0.020 | 0.018 | 0.017 | 0.017 | 0.017 | 0.017 | 0.019 |
| | after 2 min. illumination | 0.020 | 0.020 | 0.021 | 0.017 | 0.020 | 0.018 | 0.019 |

amine $1\times10^{-3}$ M, pH 9.2) at 670 mμ, as a function of time after two minutes illumination.

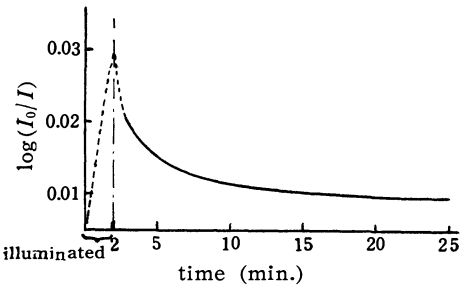



Fig. 6. Optical densities at 950 mμ after 2 min. illumination.
full line: The part experimentaly observed

TABLE III
THE RECOVERY OF 665 mμ BAND OF METHYLENE BLUE IN THE DARK AFTER 2 MIN. ILLUMINATION OF SOLUTION

| | Optical Density |
|---|---|
| Initial | 0.792 |
| Immediately after 2 min. illumination | 0.553 |
| 30 min. in the dark | 0.599 |
| 60 min. 〃 | 0.610 |
| 120 min. 〃 | 0.628 |

The analogous phenomena were also observed in the cases of di- and monomethylamine.

## Mechanism of the Reaction

From the above experiments, a probable scheme of the reaction would be

$$MB^+ \xrightarrow{h\nu} MB^{+*}$$

$$MB^{+*} + H_2O + TA \underset{II\ (k_2)}{\overset{I\ (k_1)}{\rightleftharpoons}}$$

$$\text{Intermediate} \underset{IV}{\overset{III\ (k_3)}{\rightleftharpoons}} MBH + TAO \quad (2)$$

and from the fact that the completely decolorized solution never regains its color in the dark, the process IV can be neglected practically for the photobleaching reaction. The order of the rate of the process IV can be estimated from the data given in the previous section (B) (2). From the data given in Table I (b) the apparent equilibrium constant of the photostationary state is estimated to be about 10, while from the data in Table I (a) it is to be of the order of 100. These constants, of course, depend upon the intensity of light and other experimental conditions, but the conditions in case (a) are quite similar to those employed for the bleaching experiment except the addition of TAO. Now the concentration of trimethylamine oxide in the experiments for Table I (a) is ca. $10^{-2}$ M while it is $2\times10^{-5}$ M at most when trimethylamine oxide is not particularly added. The back reaction in the former case is perceived only after several hours, hence in the latter case it will be observed only after several thousand hours if one assumes that the rate is proportional to the concentration of TAO.

The genuine equilibrium constant $K=\frac{[MBH]\,[TAO]}{[MB^+]\,[TA]}$ for the reactoin,

$$MB^+ + H_2O + TA \rightleftharpoons MBH + TAO$$

has not yet been studied but it would be much less than one, since the thermal forward reaction is negligible in the present experimental condition. In fact, a preliminary experiment showed that the bleaching is observed even in the dark after about several hours if $10^5$ times TA to MB is added. The magnitude of the rate seems to support the above estimation. Thus the bleaching reaction would be the one accompanied with the increase of free energy.

Next, a suitable rate formula will be derived. In most experiments the concentration of trimethylamine is much larger than that of the dye, hence it will be allowed to put it as a constant through the reaction. Then the concentration of dye is a sole quantity which must be expressed as a function of time.

If one assumes the scheme (2) and neglects the process IV, then the rate formula can easily be deduced as follows. Putting the concentration of dye and the intermediate as $x$ and $y$ respectively, the following differential equations can be written.

$$\begin{cases} -dx/dt = k_1x - k_2y \\ -dy/dt = (k_2+k_3)y - k_1x \end{cases}$$

The solution for $x$ is

$$x = Ae^{-(k+s)t} + Be^{-(k-s)t}$$

where $k=\frac{1}{2}(k_1+k_2+k_3)$

$$s=\frac{1}{2}\sqrt{(k_1+k_2+k_3)^2-4k_1k_3}$$

and $A=\frac{c}{2}\left(1+\frac{k_1-k}{s}\right)$ $B=\frac{c}{2}\left(1-\frac{k_1-k}{s}\right)$

($c$ is the initial concentration of dye.)

One can decide, by the method of trial and error, the values of $A$, $B$, $k$, and $s$ from the bleaching curves experimentally obtained. In fact, all the data can be analyzed by the above method, though the

TABLE IV

pH 9.2 Temp. 30°C

| | [MB] | [TA] | $k_1$ | $k_2$ | $k_3$ | |
|---|---|---|---|---|---|---|
| Expt. A | $2.0\times10^{-5}$ M | $6\times10^{-4}$ M | 0.157 | 0.0706 | 0.0604 | $x=0.6e^{-0.2t}+0.9e^{-0.03t}$ |
| Expt. B | $2.0\times10^{-5}$ M | $1\times10^{-4}$ M | 0.0224 | 0.0321 | 0.0091 | $x=0.5e^{-0.2t}+1.0e^{-0.0035t}$ |

accuracies for the four constants are not so good and some degree of arbitrariness cannot be avoided. A few examples are shown in Fig. 7 and Table IV.

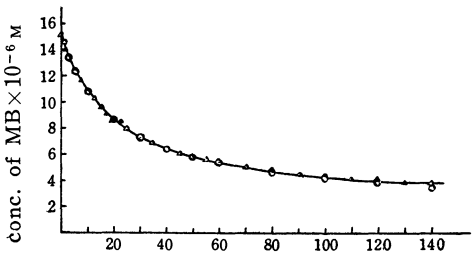



Fig. 7

MB $2.0\times10^{-5}$ M TA $2.0\times10^{-4}$ M
pH 9.2, Metallic net was not used, Temp. 30°C
△: observed
○: calculated

When the concentration of TA is in large excess, the relation $(k+s) \gg (k-s)$ holds, and the first term becomes negligible after a short time, and almost the whole bleaching curve can be expressed only by the second term. This is the reason why the rate formula is a simple first order type when the concentration of TA is in large excess. In contrast to a very small rate for the disappearance of the intermediate in the dark, $k_2$ and $k_3$ are in fact not so small compared with $k_1$. This fact and the fact that the intermediate has very small absorption, suggest that the main process II and III are also photochemical.

In the next paper, systematic investigations under various experimental conditions will be reported and the above suggestion will be found to be true.

## Summary

The photobleaching of the evacuated aqueous solution of methylene blue by dint of tri-, di- or monomethylamine was studied. The reaction products were identified to be leuco dye and amine oxide, the former by a spectroscopic method and the latter by a chemical one.

It was found that a long lived metastable intermediate is produced and this intermediate slowly returns to the original dye even in the dark. Furthermore it was found that this intermediate has its own absorption near infrared region. On the basis of the above observations, the following scheme was proposed for the reaction.

$$MB^+ + H_2O + TA \underset{II\ (k_2)}{\overset{I\ (k_1)}{\rightleftharpoons}}$$

$$\text{Intermediate} \underset{IV}{\overset{III\ (k_3)}{\rightleftharpoons}} MBH + TAO$$

in which the process IV can be neglected in the present experimental conditions.

From the above scheme, ths following rate formula was derived which can represent all the experimental results satisfactorily.

$$x=Ae^{-(k+s)t}+Be^{-(k-s)t}$$

where $x$ is the concentration of methylene blue.

*Institute of Polytechnics, Osaka City University, Osaka*

# *Photochemical Reactions between Methylene Blue and Tri-, Di- and Monomethylamine. II*

By Hiroshi OBATA and Masao KOIZUMI

(Received September 19, 1956)

## Introduction

In the preceding paper[1] the scheme for the reaction was established and a satisfactory rate formula was proposed. Now there will be reported in this paper some quantitative investigations upon the effects of various factors such as amine concentration, pH, light intensity, temperature upon the rate of the reaction. How the rate depends upon three kinds of amines will also be reported, analysing the bleaching curve by the proposed rate formula. Further, the influence of the addition of some metallic ions will be described. Though these experiments are still somewhat preliminary, the results obtained are very interesting and are considered to give further support for the reaction scheme. Lastly, there will be some discussion about the connection between the vacuum photobleaching reaction and the process of oxygen absorption in aerobic condition.

## Experimental Results

**1. Quantitative Investigations upon the Rate of Photochemical Reaction between Methylene Blue and Trimethylamine.—a. The Effect of pH.**—pH was controlled between 7.7 and 9.2 by the use of M/35 borate buffer. Table I gives one series of typical results.

TABLE I

THE EFFECT OF pH

Methylene blue $2.0\times10^{-5}$ M
Trimethylamine $1.0\times10^{-3}$ M
Temperature 30°C

| pH | [OH⁻] | ratio of [OH⁻] | $k_1$ | $k_2$ | $k_3$ |
|---|---|---|---|---|---|
| 7.7 | $5\times10^{-7}$ M | 1 | 0.014 | 0.023 | 0.04 |
| 8.0 | $1\times10^{-6}$ M | 2 | 0.056 | 0.066 | 0.014 |
| 8.55 | $3.57\times10^{-6}$ M | 7.1 | 0.156 | 0.126 | 0.039 |
| 9.2 | $1.59\times10^{-5}$ M | 32 | 0.69 | 0.64 | 0.141 |

It can be said that all the constants are approximately proportional to the hydroxyl ion concentration.

**b. The Effect of Light Intensity $I_0$.**—The intensity of light was varied by successively inserting metallic nets between the filter and the condenser lens (See Fig. 1 of the preceding paper[1]). Table II shows two series of typical results.

TABLE II

THE EFFECT OF LIGHT INTENSITY

Methylene blue $2.0\times10^{-5}$ M
pH 9.2
Temperature 30°C

| [TA] | Number of metallic nets | Relative intensity | $k_1$ | $k_2$ | $k_3$ |
|---|---|---|---|---|---|
| $0.1\times10^{-3}$ M | 0 | 15.6 | 0.048 | 0.037 | 0.013 |
| $0.1\times10^{-3}$ M | 1 | 6.2 | 0.019 | 0.024 | 0.009 |
| $0.1\times10^{-3}$ M | 2 | 2.5 | 0.008 | 0.014 | 0.004 |
| $0.6\times10^{-3}$ M | 0 | 15.6 | 0.157 | 0.125 | 0.104 |
| $0.6\times10^{-3}$ M | 1 | 6.2 | 0.066 | 0.071 | 0.013 |
| $0.6\times10^{-3}$ M | 2 | 2.5 | 0.023 | 0.020 | 0.011 |
| $0.6\times10^{-3}$ M | 3 | 1 | 0.009 | 0.013 | 0.004 |

As is expected, $k_1$ is almost exactly proportional to the light intensity, but a remarkable result is that $k_2$ and $k_3$ also increase with the light intensity. Though the exact relationship cannot be given, the extrapolated $k_2$ value to zero light intensity is evidently not zero. The values of $k_3$ are so randomly located that nothing can be said as to whether it has a finite value at zero intensity or not.

As already suggested in the preceding paper[1], it can be concluded that all the steps are photochemical in nature, though there exists a small contribution of the dark back reaction from the intermediate complex. It is to be added here that the absorption of the intermediate is so small, as already established in the preceding paper, that it will never disturb the method of measurement employed in the present investigation.

**c. The Effect of Amine Concentration.**—

TABLE III

Methylene blue $2.0\times10^{-5}$ M
Temperature 30°C
pH 9.2
Metallic net None

| [TA] | Ratio of [TA] to [MB] | $k_1$ | $k_2$ | $k_3$ |
|---|---|---|---|---|
| $6\times10^{-4}$ M | 30 | 0.157 | 0.071 | 0.060 |
| $4\times10^{-4}$ M | 20 | 0.107 | 0.076 | 0.037 |
| $2\times10^{-4}$ M | 10 | 0.048 | 0.037 | 0.012 |
| $1\times10^{-4}$ M | 5 | 0.022 | 0.032 | 0.01 |

1) H. Obata and M. Koizumi, This Bulletin, **30**, 136 (1957).

As seen from the above table, $k_1$ is satisfactorily proportional to the concentration of trimethylamine. $k_2$ and $k_3$ also increase with the rise of amine concentration.

**d. The Effect of Temperature.**—The results are summarized in Table IV.

TABLE IV

Methylene blue $2.0\times^{-5}$ M
Buffer Not used

| Expt. No. | [TA] | Metallic net | Temp. | $k_1$ | $k_2$ | $k_3$ |
|---|---|---|---|---|---|---|
| 1 | $2.0\times10^{-3}$ M | 3 | 45°C | 0.178 | 0.084 | 0.094 |
| | | | 30°C | 0.166 | 0.067 | 0.077 |
| | | | 20°C | 0.114 | 0.064 | 0.049 |
| 2 | $2.0\times10^{-4}$ M | 0 | 45°C | 0.031 | 0.048 | 0.018 |
| | | | 40°C | 0.030 | 0.046 | 0.014 |
| | | | 35°C | 0.025 | 0.043 | 0.016 |
| | | | 25°C | 0.018 | 0.040 | 0.022 |

$k_1$ evidently increases with the rise of temperature and the activation energies calculated from the above data are ca. 3.4 kcal. and 4.9 kcal. for case 1 and 2 respectively. Both $k_2$ and $k_3$ also seem to increase a little when the temperature is raised, but the data are not accurate enough to enable an estimation of the activation energy to be made. At any rate the temperature coefficients for $k_2$ and $k_3$ are about the same as or less than that of $k_1$.

**e. Quantum yield for the Initial Step.**—Quantum yield for the initial step (Process I) can easily be calculated from the value of $k_1$, the number of dye molecules ($1.2\times10^{16}$ per ml.) and the number of photons absorbed by the solution at the initial stage. The last quantity was measured and found to be $3.1\times10^{15}$/sec. ml. when no metallic nets were inserted. Table V shows the results of two series of various calculations.

TABLE V

QUANTUM YIELD $\gamma$

a) Methylene blue $2.0\times10^{-5}$ M
pH 9.2
Temperature 30°C
Metallic net was not used

| [TA] | $\gamma$ |
|---|---|
| $6\times10^{-4}$ M | $1.0\times10^{-2}$ |
| $4\times10^{-4}$ M | $6.9\times10^{-3}$ |
| $2\times10^{-4}$ M | $3.1\times10^{-3}$ |
| $1\times10^{-4}$ M | $1.4\times10^{-3}$ |

b) Methylene blue $2.0\times10^{-5}$ M
Trimethylamine $6.0\times10^{-4}$ M
pH 9.2
Temperature 30°C

| Metallic net | $\gamma$ |
|---|---|
| 0 | $1.0\times10^{-2}$ |
| 1 | $1.1\times10^{-2}$ |
| 2 | $1.1\times10^{-2}$ |
| 3 | $1.0\times10^{-2}$ |

**f. Resumé for the Photobleaching of Methylene Blue by means of TA.**—

(1) $k_1$ can be expressed as follows,

$$k_1=k_{1_0}[OH^-][TA]I_0$$

(2) $k_2$ is proportional to $[OH^-]$ and increases steadily with the light intensity and the amine concentration.

(3) Roughly speaking, $k_3$ behaves similarly as $k_2$.

**2. The Photobleaching of Methylene Blue by means of Dimethylamine (DA) and Monomethylamine (MA).**—The efficiency for the photobleaching of methylene blue in the evacuated aqueous solution was found to be in the order tri > di > mono. These results conform with those of Weil. In order to make clear which of the three processes-I, II and III is most affected by an amine of any kind, similar experiments as those for trimethyl amine were performed and the results were analyzed in the same way.

**a. The Effect of Amine Concentration**—The results are summarized in Table VI. They can be compared with the data in Table III, because the experimental conditions are quite similar.

TABLE VI

THE EFFECT OF THE CONCENTRATIONS OF DI-, AND MONOMETHYLAMINE

Methylene blue $2.0\times10^{-5}$ M
M/35 Borate buffer pH 9.2
Temperature 30°C

| Species | Amine conc. | Ratio of conc. of amine to [MB] | $k_1$ | $k_2$ | $k_3$ |
|---|---|---|---|---|---|
| DA | $2.0\times10^{-2}$ M | 1000 | 0.035 | 0.036 | 0.016 |
| DA | $1.4\times10^{-2}$ M | 700 | 0.026 | 0.022 | 0.009 |
| DA | $1.0\times10^{-2}$ M | 500 | 0.017 | 0.019 | 0.008 |
| DA | $0.6\times10^{-2}$ M | 300 | 0.013 | 0.017 | 0.007 |
| DA | $0.2\times10^{-2}$ M | 100 | 0.005 | 0.016 | 0.004 |
| MA | $4.0\times10^{-2}$ M | 2000 | 0.046 | 0.046 | 0.029 |
| MA | $2.8\times10^{-2}$ M | 1400 | 0.026 | 0.021 | 0.022 |
| MA | $2.0\times10^{-2}$ M | 1000 | 0.019 | 0.011 | 0.015 |
| MA | $1.2\times10^{-2}$ M | 600 | 0.011 | 0.009 | 0.007 |
| MA | $0.8\times10^{-2}$ M | 400 | 0.008 | 0.010 | 0.006 |

The values of $k_1$, $k_2$ and $k_3$ are much smaller than those for trimethylamine. They are of the same order of magnitude for $4.0\times10^{-2}$ M of monomethylamine, $2.0\times1.0^{-2}$ M of dimethylamine and $2.0\times10^{-4}$ M of trimethylamine. $k_1$ is approximately proportional to the amine concentration in the above two cases and the dependency of $k_2$ and that of $k_3$ upon the amine concentration resemble that in case of trimethylamine.

**b. The Effect of Light Intensity.**—The results are summarized in Table VII.

The results are quite analogous to those of trimethylamine. Thus $k_1$ is proportional to the light intensity; $k_2$ and $k_3$ also increase with the light intensity, indicating the participation of the photochemical process in processes II and III.

TABLE VII

THE EFFECT OF LIGHT INTENSITY

Methylene blue $2.0\times10^{-5}$ M
pH 9.2
Temperature 30°C

| | Metallic net | Relative light intensity | $k_1$ | $k_2$ | $k_3$ |
|---|---|---|---|---|---|
| Dimethyl- | 0 | 15.6 | 0.053 | 0.045 | 0.023 |
| amine | 1 | 6.2 | 0.019 | 0.026 | 0.015 |
| ($2.0\times10^{-2}$ M) | 2 | 2.5 | 0.007 | 0.014 | 0.011 |
| | 3 | 1 | 0.004 | 0.012 | 0.008 |
| Monomethyl- | 0 | 15.6 | 0.074 | 0.043 | 0.049 |
| amine | 1 | 6.2 | 0.031 | 0.016 | 0.017 |
| ($4.0\times10^{-2}$ M) | 2 | 2.5 | 0.015 | 0.015 | 0.015 |
| | 3 | 1 | 0.005 | 0.004 | 0.006 |

**c. The Effect of Hydrogen Ion Concentration.**—The rate constants in the low pH values could not be measured because it was impossible to adjusted pH values by the use of borate buffer at the high concentration of amine. Though the data in Table VIII are scanty, it will be possible to say that $k_1$, $k_2$ and $k_3$ are all proportional to $[OH^-]$, the results being the same as that for trimethylamine.

TABLE VIII

THE EFFECT OF HYDROGEN ION CONCENTRATION

Methylene blue $2.0\times10^{-5}$ M
Dimethylamine $2.0\times10^{-2}$ M
1/35 M Borate buffer
Temperature 30°C

| pH | Relative conc. of $[OH^-]$ | $k_1$ | $k_2$ | $k_3$ |
|---|---|---|---|---|
| 10.1 | 7.94 | 0.26 | 0.24 | 0.227 |
| 9.2 | 1 | 0.039 | 0.044 | 0.040 |

The data for monomethylamine are similar to the above.

**d. The Effect of Temperature.**—This was investigated only for the case of dimethylamine.

TABLE IX

THE EFFECT OF TEMPERATURE

Methylene blue $2.0\times10^{-5}$ M
Dimethylamine $2.0\times10^{-2}$ M
pH 9.2

| Temp. °C | $k_1$ | $k_2$ | $k_3$ |
|---|---|---|---|
| 40 | 0.078 | 0.052 | 0.047 |
| 30 | 0.039 | 0.043 | 0.041 |
| 20 | 0.025 | 0.030 | 0.022 |
| 10 | 0.012 | 0.013 | 0.010 |

The activation energy for process I was calculated as 8.6 kcal./mol. This is evidently much greater than that for trimethylamine. The temperature coefficients for $k_2$ and $k_3$ are somewhat smaller than that for $k_1$, but they are conspicuously greater than the corresponding ones for trimethylamine. (compare with Table IV.)

**3. The Influence of the Addition of $Cu^{++}$ and $Fe^{+++}$.**—For the further elucidation of the reaction mechanism and of the nature of the intermediate, the investigation about the influence of some metallic ions upon the reaction seems to be very helpful, because perhaps some of the ions may selectively act on three processes-I, II and III. Taking into account the data of oxidation-reduction potential, $Fe^{+++}$ ($E^0_h=0.772$ V.) and $Cu^{++}$ ($E^0_h=0.167$ V.) were selected and the bleaching reaction was examined in the presence of these ions.

a. The photobleaching reaction can be examined without any difficulty in the case of $Fe^{+++}$, so long as the concentration is not very large. Apparently the bleaching proceeds in the same way as when no metallic ion is added. The results of the analysis of the bleaching curve are given in Table X.

TABLE X

THE EFFECTS OF THE VARIOUS CONCENTRATIONS OF $Fe^{+++}$

Methylene blue $2.0\times10^{-5}$ M
Trimethylamine $6.0\times10^{-4}$ M
pH 9.2
Temperature 30°C

| $[Fe^{+++}]$ | Ratio of $[Fe^{+++}]$ to [MB] | $k_1$ | $k_2$ | $k_3$ |
|---|---|---|---|---|
| $4.5\times10^{-4}$ M | 22.5 | 0.085 | 0.046 | 0.006 |
| $3\times10^{-4}$ M | 15 | 0.084 | 0.045 | 0.007 |
| $0.75\times10^{-4}$ M | 3.75 | 0.100 | 0.045 | 0.027 |
| 0 | 0 | 0.099 | 0.041 | 0.075 |

From the above data it is clear that $k_1$ and $k_2$ are scarcely affected, while $k_3$ is decreased by the addition of $Fe^{+++}$. Corresponding to this result, the absorption of the intermediate at 950 mμ could be observed more prominently. Table XI (a) gives the value of $\log(I_0/I)$ of

TABLE XI

Methylene blue $2.0\times10^{-5}$ M
Trimethylamine $6.0\times10^{-4}$ M
$FeCl_3$ $6.0\times10^{-4}$ M
pH 9.2

(a) The absorption spectra of the intermediate at 950 mμ.

| | Initial | Directly after 2 min. exposure | After 10 min. in the dark |
|---|---|---|---|
| $\log(I_0/I)$ | 0.008 | 0.025 | 0.011 |

(b) Dark back reaction in the presence of $Fe^{+++}$. (The increase of the optical density at 665 mμ)

| | After 5 min. illumination | After 10 min. illumination | After 20 min. illumination |
|---|---|---|---|
| Initial | 0.760 | 0.754 | 0.750 |
| Immediately after exposure | 0.298 | 0.095 | 0.027 |
| 10 min. in the dark | 0.380 | 0.120 | 0.038 |
| 24 hr. in the dark | 0.618 | 0.296 | 0.137 |

the intermediate at 950 mμ immediately after two minutes exposure and Table XI (b) gives the variation of $\log(I_0/I)$ at 665 mμ of methylene blue in the dark after a certain time of illumination.

If one compares Table XI (a) with Table II in the preceding paper, it is clear that the quantity of the intermediate is larger in the present case. Table XI (b) shows that the recovery of dye takes place in the dark.

Since the recovery of the color can never be observed if the bleaching is made to proceed completely, the above data are only related with process II in which the intermediate goes back to the original dye. It is noteworthy that ferric ion only affects the intermediate, namely stabilizes the intermediate, and only reduces the value of $k_3$.

b. When cupric chloride was added to the system the induction period appeared, after which the photobleaching began to take place, and during the induction period, cuprous chloride was precipitated. The existence of this precipitate made it very difficult to pursue the photobleaching quantitatively. Taking into account the light dispersion by the precipitate of $Cu^+$, it seemed that the rate of photobleaching does not differ so markedly compared with the rate obtained in the absence of $Cu^{++}$. A typical example for the variation of photocurrent is shown in Fig. 1. The induction period was found to be proportional to the added $Cu^{++}$ ion concentration as shown in Table XII.

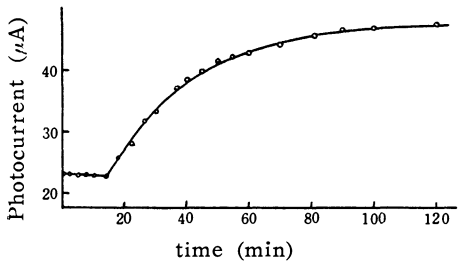



Fig. 1. The variation of photocurrent in the presence of $Cu^{++}$.
MB $2.0\times10^{-5}$ M, TA $6.0\times10^{-4}$ M,
$CuCl_2$ $6.0\times10^{-5}$ M, pH 9.2,
Metallic net was not used, Temp. 30°C

TABLE XII

INDUCTION PERIOD IN THE PRESENCE OF $Cu^{++}$

| | | | | | |
|---|---|---|---|---|---|
| Methylene blue | $2.0\times10^{-5}$ M | | | | |
| Trimethylamine | $6.0\times10^{-4}$ M | | | | |
| Temperature | 30°C | | | | |
| pH | 9.2 | | | | |
| Ratio of $[Cu^{++}]$ to [MB] | 1.5 | 3 | 7.5 | 10 | 15 |
| Induction period (min.) | 7 | 14 | 25 | 48 | 65 |

## Discussion

The photobleaching of methylene blue by means of mono-, di- and trimethylamine takes place via the common scheme with only different specific rates. There is no doubt that an intermediate having quite a long life participates in the reaction and a probable scheme can be written as follows:

$$MB^+ + H_2O + TA \underset{II\ (k_2)}{\overset{I\ (k_1)}{\rightleftharpoons}} \text{Intermediate} \underset{IV}{\overset{III\ (k_3)}{\rightleftharpoons}} MBH + TAO \quad (1)$$

Recently Kutsaya and Dain[2] reported that methylene blue in alcohol was decolorized under degassed condition on exposure to light. They explained the reaction according to the following two-step's. The first step is the formation of a colored photoproduct between dye and alcohol, and the further action of light reduces this product to the colorless leuco dye. Their scheme seems to conform well with our present one.

The nature of the intermediate is not yet certain, but it is conceivable that the intermediate may have a structure such as $MBH\cdot\cdots O^-\cdots TA$ which is produced by the following process.

$$MB^+ + OH^- + TA \longrightarrow MB^+\cdots HO^-\cdots TA$$

The fact that $k_1$ can be expressed as $k_1=k_{1_0}[OH^-][TA]I_0$ is consistent with the above picture of the intermediate. Although the scheme (1) cannot be said to have been definitely established, most of the experimental results can be interpreted well by the rate formula derived on the ground of scheme (1). Some of the results will be discussed along this line.

**(1) The Life of an Intermediate.**— Putting the concentration of methylene blue and the intermediate as $x$ and $y$ at time $t$, and the initial concentration of the former as $c$ differential equations for the rate process are

$$\begin{cases} -\dfrac{dx}{dt} = k_1x - k_2y \\ -\dfrac{dy}{dt} = (k_2+k_3)y - k_1x \end{cases}$$

and the solution for $x$ is

$$x = Ae^{-(k+s)t} + Be^{-(k-s)t}$$

as shown in the previous paper.

On the other hand, $y$ can be expressed as follows.

$$y = \frac{c}{2}\frac{k_1}{s}\left\{e^{-(k-s)t} - e^{-(k+s)t}\right\} \quad (2)$$

2) B. F. Kutsaya and B. Ya. Dain, *Ukrain. Khim. Zhur*, **17**, 820 (1951) ; *C. A.* **49**, 13789c (1955).

Time relations of $x$ and $y$, for one example, are shown in Fig. 2. The analytical formula for this case are

$$\begin{cases} x = 0.6e^{-0.2t} + 0.9e^{-0.03t} \\ y = 0.87(e^{-0.03t} - e^{-0.2t}) \end{cases}$$

As shown in Fig. 2, the concentration of the intermediate must reach its maximum value a few minutes after the start. This conforms well with the observed magnitude of the absorption of the intermediate.

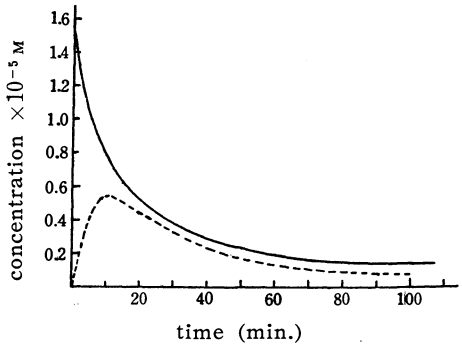



Fig. 2. Concentration curves of MB and the intermediate.
Full line: MB (x)
Broken line: intermediate (y)
MB $2.0\times10^{-5}$ M, TA $6.0\times10^{-4}$ M,
pH 9.2, Temp. 30°C.
Metallic not was not used

In the case of the addition of $Fe^{+++}$ ion where $k_3$ is reduced remarkably while $k_2$ and $k_3$ are scarcely affected, equation (2) requires that $y$ gets quite a large value. This was clearly demonstrated experimentally. Perhaps the discovery of such a unique effect of $Fe^{+++}$ will be considered to be the strongest support for the scheme (1).

(2) **The Effect of $Cu^{++}$ Ion.**—The data in Table XII can be interpreted as follows. From the fact that the induction period is proportional to the concentration of $Cu^{++}$, it can be said that the rate of its disappearance is of the zeroth order in $[Cu^{++}]$. Hence $Cu^{++}$ must attack the intermediate or the leuco dye as soon as it is produced. The following calculation shows that the first alternative is favorable. If the $Cu^{++}$ ion destroys the intermediate as soon as it is formed, the rate of the reaction, $Cu^{++} \rightarrow Cu^{+}$, is written as

$$-\frac{d[Cu^{++}]}{dt} = k_1[MB], \qquad (3)$$

while in case $Cu^{++}$ attacks the leuco dye, the rate of the reaction, $Cu^{++} \rightarrow Cu^{+}$, must be represented as

$$-\frac{d[Cu^{++}]}{dt} = \frac{k_1k_3}{k_1+k_2+k_3}[MB]. \qquad (4)$$

Using the values of $k_1$, $k_2$ and $k_3$ in the corresponding experimental conditions which are 0.157, 0.071 and 0.063 respectively, equations (2) and (3) can be written in the forms of (5) and (6) respectively.

$$\begin{cases} -\frac{d[Cu^{++}]}{dt} = 0.157[MB] = 3.14\times10^{-6} & (5) \\ -\frac{d[Cu^{++}]}{dt} = 0.034[MB] = 6.8\times10^{-7} & (7) \end{cases}$$

In the following Table XIII, the induction period as calculated from (5) and (6) assuming that it comes to an end when $Cu^{++}$ is eliminated, are compared with the experimental one (Table XII).

TABLE XIII

THE COMPARISON OF THE INDUCTION PERIOD

| Ratio of $[Cu^{++}]$ to [MB] | 1.5 | 3 | 7.5 | 10 | 15 |
|---|---|---|---|---|---|
| Induction period (min.) calc. from (5) | 9.5 | 19 | 48 | 63 | 95 |
| 〃 calc. from (6) | 44 | 88 | 220 | 290 | 440 |
| 〃 obs. (Table 12) | 7 | 14 | 25 | 48 | 65 |

From the above results it seems highly probable that $Cu^{++}$ attacks the intermediate as soon as it is produced. It is to be noted, however, that the absorption spectra of the intermediate are still observed in the presence of $Cu^{++}$, hence further study seems to be necessary.

(3) **The Relation between the Vacuum Photobleaching and the Experiment of Weil.**—The fact that the absorption of the reaction intermediate is still observed in the presence of oxygen strongly supports the view that oxygen attacks only leuco dye. If this attack takes place very rapidly, the rate of the oxygen uptake must be expressed by the following equation after the arrival of the stationary state.

$$\frac{d[O_2]}{dt} = \frac{1}{2}\frac{k_1k_3}{k_1+k_2+k_3}[MB]$$

Hence the rate of the oxygen uptake must be independent of the pressure after a certain induction period. According to Kihara's unpublished experiments using ethanol as a solvent, oxygen absorption really takes place with the same rate irrespective of the pressure of oxygen, and some induction period really exists.

The above scheme is noteworthy since it differs greatly much from the postulate, as proposed by Schenck and other investigators, that oxygen attacks directly the

triplet state of dye molecules in general[3]. The question will be further studied in future.

To sum up, it can be concluded that the proposed scheme is very satisfactory. Yet there still remain many things to be solved in future. Above all, each of the processes I, II and III are considered to be complex of itself, since all the apparent reaction constants, $k_1$, $k_2$, $k_3$ depend upon various factors. Another thing which seems to be very curious is that all these rate constants decrease in about the same manner when trimethylamine is replaced by dimethylamine and monomethylamine. When the detailed mechanism of each step is clarified, the reason for this will also be clear.

## Summary

The effects of various factors upon the photobleaching of methylene blue in the evacuated aqueous solution by means of mono-, di- and trimethylamine, were studied experimentally, and the result were analyzed by the rate formula presented in the preceding paper on the basis of the following scheme;

$$MB^+ + H_2O + TA \underset{II\ (k_2)}{\overset{I\ (k_1)}{\rightleftharpoons}}$$

$$\text{Intermediate} \underset{IV}{\overset{III\ (k_3)}{\rightleftharpoons}} \text{Product}$$

The results obtained can be summarized as follows: $k_1$ is written in the form; $k_1 = k_{1_0}[OH^-][TA]I_0$. $k_2$ and $k_3$ are also proportional to $[OH^-]$ and they both increase monotonously with the light intensity and amine concentration.

In addition, the photobleaching was examined in the presence of $Fe^{+++}$ and $Cu^{++}$. It was found that in the case of $Fe^{+++}$, $k_3$ is much decreased while $k_1$ and $k_2$ are scarcely affected. The absorption spectra of the intermediate were observed more prominently than when no $Fe^{+++}$ was present. From these results it was concluded that $Fe^{+++}$ stabilizes the intermediate. In case of $Cu^{++}$ some induction period was observed during which Cu precipitates, and its duration was found to be proportional to the concentration of $Cu^{++}$. From these results it was tentatively concluded that $Cu^{++}$ attacks the intermediate.

The cost of this research has been partially defrayed from the Scientific Research Grant from the Ministry of Education.

*Institute of Polytechnics, Osaka City University, Osaka*

3) For example. G. O. Schenck, *Naturwiss.*, **40**, 205, 229 (1953); M. Pestemer, *Z. Elektrochem.* **59**, 121 (1954).

# *Correlation between Two Molecular Orbital Theories on Organic Reactions. I.* Ionic Substitutions*

By Hiroaki BABA

(Received October 26, 1956)

## Introduction

Among the theories which treat the reactivity of organic molecules on the basis of the method of molecular orbitals, the static and localization theories are extensively used. As was pointed out by Wheland[1], the basic assumptions of the two theories are entirely different and run to two opposite extremes. That is, in the static theory[2-5] the measure of the activity in substitution reactions is the $\pi$-electron density, the self-polarizability, or the free valence of the atom to be attacked. All these quantities refer to the normal state of the molecule. On the other hand, the corresponding measure in the localization theory[1,5] is the localization energy. The

* Read at the Symposium on $\pi$-Electron Problems held by the Chem. Soc. Japan, Oct. 1954 (See Abstract of the Meeting, p. 60). A part of this paper, in Japanese, is to be found in K. Higasi and H. Baba, "Quantum Organic Chemistry", Asakura Publishing Company, Tokyo (1956), p. 314.

1) G. W. Wheland, *J. Am. Chem. Soc.*, **64**, 900 (1942).

2) G. W. Wheland and L. Pauling, *J. Am. Chem. Soc.*, **57**, 2086 (1935).

3) C. A. Coulson and H. C. Longuet-Higgins, *Proc. Roy. Soc.*, **A191**, 39 (1947); **A192**, 16 (1947).

4) C. A. Coulson, *Faraday Soc. Discussion*, No. **2**, 9 (1947).

5) R. D. Brown, *Quart. Rev.*, **6**, 63 (1952).

latter quantity has been presumed by the authors of the theory to be associated with the actual " transition state ".

Notwithstanding the above situation, the same conclusions were reached by the route of each of the two theories. Both of them were found in good accord with known experimental results. Astonishing agreement was obtained for alternant hydrocarbons. Several authors[5-11] have paid attention to this peculiar fact, and tried to see if there may be any correlations between the two antagonistic theories. It seems, however, that there are available no successful attempts that have made clear under what condition the two theories should become equivalent to each other. In the present paper a mathematical proof will be given for this problem. It will be shown that the static theory becomes equivalent to the localization theory, in case a certain condition is fulfilled. In fact, the latter condition is satisfied in many alternant hydrocarbons.

## Terminology and Basic Relations

The LCAO molecular orbital (MO) method[3] in its simplest form is employed. Resonance integrals between non-adjacent atomic orbitals (AO) and overlap integrals are not considered here.

Symbols used in the present and subsequent papers in this series are given below.

$n$=number of AO's.
$r, s, t, v, w$=atoms of a conjugated system.
$\chi_r$=AO for atom $r$.
$\phi_j$=$j$th MO.
$c_{jr}$=coefficient of $\chi_r$ in $\phi_j$.
$\varepsilon$=energy of a MO.
$\beta_{rs}$=resonance integral between atoms $r$, $s$.
$\alpha_r$=coulomb integral of atom $r$.
$E$=total energy of $\pi$-electrons.
$q_r$=$\pi$-electron density at atom $r$.
$p_{rs}$=$\pi$-bond order of bond $rs$.
$N_r$=bond number at atom $r$.
$F_r$=free valence at carbon atom $r$.
$\pi_{r,r}$=self-polarizability of atom $r$.
$D(\varepsilon)$=secular determinant for a conjugated molecule, regarded as a function of $\varepsilon$.
$D_{r,s}(\varepsilon)$=determinant obtained by striking out the $r$th row and $s$th column of $D(\varepsilon)$.
$E_N^{(r)}$, $E_E^{(r)}$, $E_R^{(r)}$=total $\pi$-electron energies of the residual molecules[5] in nucleophilic, electrophilic and radical substitutions at carbon atom $r$.
$L_N^{(r)}$, $L_E^{(r)}$, $L_R^{(r)}$=localization energies in nucleophilic, electrophilic and radical substitutions at carbon atom $r$.

The prime after the symbol of summation denotes that the sum is taken only for the atoms adjacent to a given atom; e.g. for $\sum_s' p_{rs}$ the sum refers to atoms $s$ adjacent to atom $r$.

The symbol to which a small zero is affixed, e.g. $p_{rs}^0$, $E_0$, refers to the initial state of a molecule, unless otherwise stated.

Every determinant occurring in an integral with respect to $y$ is to be taken as a function of $iy$, where $i$ is the imaginary unit, $\sqrt{-1}$.

The resonance integral between two adjacent carbon atoms of any molecule in its initial state is assumed to have a constant value $\beta$, which is negative. The energy of a MO and the coulomb integral of any atom are measured relative to the coulomb integral for carbon atom.

The general theory of molecular orbitals includes the following basic relations.

$$\int \phi_j \phi_k d\tau = \sum_{r=1}^{n} c_{jr} c_{kr} = \delta_{jk}, \tag{1}$$

$$N_r = \sum_s' p_{rs}, \tag{2}$$

$$F_r = \sqrt{3} - N_r, \tag{3}$$

$$E = \sum_{r=1}^{n} q_r \alpha_r + 2 \sum_{r>s} \sum p_{rs} \beta_{rs}, \tag{4}$$

$$q_r = \frac{\partial E}{\partial \alpha_r}, \tag{5}$$

$$2p_{rs} = \frac{\partial E}{\partial \beta_{rs}}, \tag{6}$$

$$\pi_{r,r} = \frac{\partial q_r}{\partial \alpha_r} = \frac{\partial^2 E}{\partial \alpha_r^2} < 0, \tag{7}$$

$$0 \leqq q_r \leqq 2, \tag{8}$$

$$L_N^{(r)} = E_N^{(r)} - E_0, \quad L_E^{(r)} = E_E^{(r)} - E_0,$$

$$L_R^{(r)} = E_R^{(r)} - E_0. \tag{9}$$

All compounds treated in this study are even alternant hydrocarbons (AH). For

6) R. Daudel, C. Sandorfy, C. Vroelant, P. Yvan and O. Chalvet, *Bull. Soc. Chim. France*, **17**, 66 (1950).
7) F. H. Burkitt, C. A. Coulson and H. C. Longuet-Higgins, *Trans. Faraday Soc.*, **47**, 553 (1951).
8) H. H. Greenwood, *Trans. Faraday Soc.*, **48**, 585 (1952).
9) M. J. S. Dewar, *J. Am. Chem. Soc.*, **74**, 3355 (1952).
10) B. Pullman and A. Pullman, " Les théorie électroniques de la chimie organique ", Masson et Cie (1952), chapitre X.
11) K. Higasi, *Monogr. Res. Inst. Appl. Elec.*, **4**, 27 (1954).

such molecules the additional equations (10)-(12) hold:

$$q_r^0=1, \tag{10}$$

$$E_N^{(r)}=E_E^{(r)}=E_R^{(r)}, \tag{11}$$

$$L_N^{(r)}=L_E^{(r)}=L_R^{(r)}=L^{(r)}. \tag{12}$$

The quantities associated with the static and localization theories will be termed "static" and "dynamic", respectively.

## Change in Total Energy of $\pi$-Electrons with Variation of Coulomb Integral

The fundamental equation[3] in the treatment of ionic substitutions by the static theory is as follows:

$$\delta E=q_r^0\delta\alpha_r+\frac{1}{2}\pi_{r,r}^0\delta\alpha_r^2+\cdots\cdots, \tag{13}$$

where $\delta\alpha_r$ is assumed to be small in magnitude. Its sign is positive for a nucleophilic reagent and negative for an electrophilic one. Since in an AH, with which we are concerned, the initial electron density $q_r^0$ is 1 irrespective of $r$ (see Eq. (10)), the difference in reactivity at its various positions is determined by the second term $\frac{1}{2}\pi_{r,r}^0\delta\alpha_r^2$.

Now, suppose that the coulomb integral of atom $r$ changes from its initial value $\alpha_r^0=0$ to $\alpha_r$ which can be of any value from $-\infty$ to $+\infty$, and that the other coulomb and resonance integrals are throughout kept constant at their initial values. Then, instead of Eq. (13), the change in total energy will be given by

$$\Delta E_r(\alpha_r)=E_r(\alpha_r)-E_0=\int_0^{\alpha_r}\frac{dE_r(\alpha_r)}{d\alpha_r}\,d\alpha_r, \tag{14}$$

which, from Eq. (5), may be written as

$$\Delta E_r(\alpha_r)=\int_0^{\alpha_r}q_r(\alpha_r)\,d\alpha_r. \tag{15}$$

In the following some relations between $\alpha_r$ and $q_r(\alpha_r)$ will be described. First, it is easily seen that

$$\lim_{\alpha r\to+\infty}q_r(\alpha_r)=0, \tag{16}$$

$$\lim_{\alpha r\to-\infty}q_r(\alpha_r)=2. \tag{17}$$

From relation (7) it follows that, when $\alpha_r$ changes from $-\infty$ to $+\infty$, $q_r(\alpha_r)$ decreases monotonously from 2 to 0. According to the integral expression given by Coulson and Longuet-Higgins[3]

$$q_r(\alpha_r)=1-\frac{1}{\pi}\int_{-\infty}^{\infty}\frac{D_{r,r}(iy)}{D(iy)}\,dy. \tag{18}$$

This reduces to

$$q_r(\alpha_r)=1-\frac{\alpha_r}{\pi}\int_{-\infty}^{\infty}\frac{-(D_{r,r}^0)^2}{(D^0)^2-\alpha_r^2(D_{r,r}^0)^2}\,dy, \tag{19}$$

since $D_{r,r}=D_{r,r}^0$, $D=D^0+\alpha_rD_{r,r}^0$, and $D^0$ and $D_{r,r}^0$ are even and odd functions of $y$, respectively[3]. Therefore

$$q_r(-\alpha_r)-1=-\{q_r(\alpha_r)-1\}; \tag{20}$$

namely, the point, where $\alpha_r=0$ and $q_r=1$ is situated at the center of symmetry of the $q_r(\alpha_r)$ curve. This will be clear at a glance at the curve of Fig. 1, which was obtained by numerical calculations for benzene.

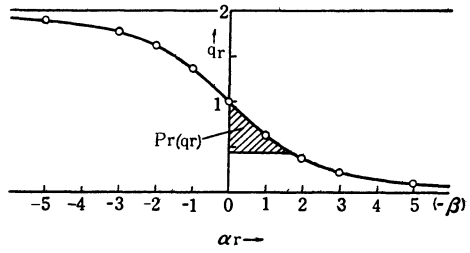



Fig. 1. $q_r(\alpha_r)$ for benzene.

Returning to Eq. (15), it will be seen that $\Delta E_r(\alpha_r)$ is equal to the area under the curve between $\alpha_r=0$ and $\alpha_r=\alpha_r$. Consequently, from Eq. (20)

$$\Delta E_r(\alpha_r)=\Delta E_r(-\alpha_r)+2\alpha_r. \tag{21}$$

Since $D=D^0+\alpha D_{r,r}^0$ it is easily seen that, when $\alpha_r\to+\infty$ or $-\infty$, one of the solutions of the secular equation $D=0$ reduces to $\alpha_r$, and the others to the solutions of $D_{r,r}^0=0$. $D_{r,}^0=0$ is identical with the secular equation for the residual molecule. Hence it is verified that

$$\lim_{\alpha r\to+\infty}\Delta E_r(\alpha_r)=L_N^{(r)} \tag{22}$$

and

$$\lim_{\alpha r\to-\infty}\{\Delta E_r(\alpha_r)-2\alpha_r\}=L_E^{(r)}. \tag{23}$$

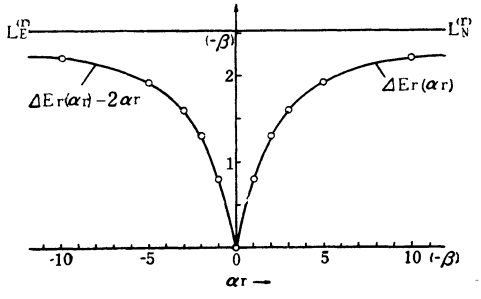



Fig. 2. $\Delta E_r(\alpha_r)$ and $\Delta E_r(\alpha_r)-2\alpha_r$ for benzene.

From Eqs. (21), (22) and (23) it follows that $L_N^{(r)}=L_E^{(r)}$. This is a well-known relation already cited as Eq. (12). Eqs. (21), (22) and (23) will be illustrated by an example shown in Fig. 2, where $\Delta E_r(\alpha_r)$ and $\Delta E_r(\alpha_r)-2\alpha_r$ for benzene are given.

## Definition of Partial Polarization Energy

To begin with, a new quantity will be introduced. In the previous section the $\pi$-electron density at atom $r$ was defined as a function of $\alpha_r$, which was expressed as $q_r(\alpha_r)$. Conversely let $\alpha_r$ be regarded as a function of $q_r$ and be written $\alpha_r(q_r)$. Since $q_r(\alpha_r)$ is a single-valued, continuous and monotonous function of $\alpha_r$, $\alpha_r(q_r)$ is also such a function of $q_r$.

Consider a function of $q_r$ as follows:

$$P_r(q_r)=\Delta E_r(\alpha_r(q_r))-q_r\alpha_r(q_r). \quad (24)$$

Taking into account the definition of $\Delta E_r(\alpha_r)$ it is easily seen that $P_r(q_r)$ is equal to the area hatched in Fig. 1. Then $P_r(q_r)$ is expressed in an alternative form:

$$P_r(q_r)=-\int_{q_r^0}^{q_r}\alpha_r(q_r)\,dq_r. \quad (25)$$

From Eqs. (14) and (24) it follows that

$$P_r(q_r)=E_r^*(q_r)-E_0, \quad (26)$$

where

$$E_r^*(q_r)=E_r(\alpha_r(q_r))-q_r\alpha_r(q_r). \quad (27)$$

Since it has been assumed that coulomb integrals except for $\alpha_r$ and resonance integrals are all kept at their initial values,

$$E_r(\alpha_r(q_r))=q_r\alpha_r(q_r)+2\sum_{v}\sum_{w}p_{vw}\beta \quad (28)$$

(cf. Eq. (4)), where $p_{vw}$ is the $\pi$-bond order of bond $vw$ corresponding to $\alpha_r(q_r)$. So

$$E_r^*(q_r)=2\sum_{v}\sum_{w}p_{vw}\beta. \quad (29)$$

Consider now the following conditions: (1) all the coulomb and resonance integrals, including $\alpha_r$, should be invariant, i.e. they have the same values with those at the initial state of the molecule; (2) the coefficients of AO's should satisfy Eq. (1). Under these two conditions, the lowest value of the total energy of $\pi$-electrons is, of course, $E_0$, and the $\pi$-electron density at atom $r$ is $q_r^0$ (=1). On the other hand, if the former value were calculated under the same conditions with an additional one, i.e. (3) the $\pi$-electron density at atom $r$ should be of a given value $q_r(\neq q_r^0)$, then it would become identical with $E_r^*(q_r)$. Consequently it is seen that

$$\left.\begin{aligned} &E_r^*(q_r)=E_0 \text{ and } P_r(q_r)=0 \quad (q_r=q_r^0),\\ &E_r^*(q_r)>E_0 \text{ and } P_r(q_r)>0 \quad (q_r\neq q_r^0). \end{aligned}\right\} \quad (30)$$

In short, $P_r(q_r)$ corresponds to the increment of the total energy due to the variation of $\pi$-electron density of atom $r$ from its normal value $q_r^0=1$ to an imaginary one $q_r\neq q_r^0$. Then $P_r(q_r)$ might be called the partial polarization energy for atom $r$.

It follows from Eq. (20) that

$$P_r(q_r)=P_r(2-q_r), \quad (31)$$

and by considering Eqs. (16) and (17) it is verified that

$$\lim_{q_r\to 0}E_r^*(q_r)=E_N^{(r)},\quad \lim_{q_r\to 0}P_r(q_r)=L_N^{(r)}, \quad (32)$$

$$\lim_{q_r\to 2}E_r^*(q_r)=E_E^{(r)},\quad \lim_{q_r\to 2}P_r(q_r)=L_E^{(r)}. \quad (33)$$

Therefore

$$L_N^{(r)}=P_r(0)=P_r(2)=L_E^{(r)}. \quad (34)$$

This is again in accord with Eq. (12).

By differentiating Eq. (25)

$$\frac{dP_r(q_r)}{dq_r}=-\alpha_r(q_r), \quad (35)$$

$$\frac{d^2P_r(q_r)}{dq_r^2}=-\frac{1}{\pi_{r,r}}>0. \quad (36)$$

In Fig. 3 the relation between $q_r$ and $P_r$ is shown for benzene. It is to be noted that $dP_r(q_r)/dq_r=0$ at $q_r=q_r^0$ and that $|\pi_{r,r}^0|$ is equal to the radius of the curvature of the curve at $q_r=q_r^0$.

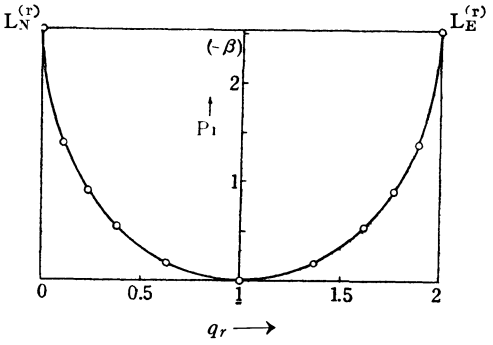



Fig. 3. $P_r(q_r)$ for benzene.

## Correlation between the Two Sets of Quantities

Let us now consider the correlation between the static and dynamic quantities. It is well known that for an even AH

$D^0(\varepsilon)$ and $D^0_{r,r}(\varepsilon)$ are of the forms[3]:

$$D^0(\varepsilon)=\varepsilon^n-a_{n-2}\beta^2\varepsilon^{n-2}+a_{n-4}\beta^4\varepsilon^{n-4}-\cdots\cdots+(-1)^{n/2}a_0\beta^n, \quad (37)$$

$$D^0_{r,r}(\varepsilon)=-\varepsilon^{n-1}+a^{(r)}_{n-3}\beta^2\varepsilon^{n-3}-a^{(r)}_{n-5}\beta^4\varepsilon^{n-5}+\cdots\cdots+(-1)^{n/2}a^{(r)}_1\beta^{n-2}\varepsilon, \quad (38)$$

where

$$a_l\geqq 0 \quad (l=0,2,\cdots\cdots,n-2), \quad (37')$$

$$a^{(r)}_l\geqq 0 \quad (l=1,3,\cdots\cdots,n-3). \quad (38')$$

That is, the signs are alternately positive and negative, and $D^0(\varepsilon)$ has only even powers of $\varepsilon$, while $D^0_{r,r}(\varepsilon)$ only odd powers. From Eqs. (37) and (38) it follows that

$$D^0(iy)=(-1)^{n/2}(y^n+a_{n-2}\beta^2y^{n-2}+a_{n-4}\beta^4y^{n-4}+\cdots\cdots+a_0\beta^n), \quad (39)$$

$$D^0_{r,r}(iy)=(-1)^{n/2}iy\,(y^{n-2}+a^{(r)}_{n-3}\beta^2y^{n-4}+a^{(r)}_{n-5}\beta^4y^{n-6}+\cdots\cdots+a^{(r)}_1\beta^{n-2}). \quad (40)$$

Now consider two positions $r$ and $s$ in an even AH, and suppose that

$$a^{(r)}_l\geqq a^{(s)}_l \text{ for } l=1,3,\cdots\cdots,n-3, \quad (41)$$

where $a^{(r)}_l$, $a^{(s)}_l$ are the coefficients of $\varepsilon^l$ appearing in the expansions of $D^0_{r,r}$ and $D^0_{s,s}$, respectively. Throughout the following discussions it is assumed that for at least one value of $l$ the inequality in (41) holds. Then, from Eq. (40), we have

$$\frac{D^0_{r,r}(iy)}{(-1)^{n/2}iy}>\frac{D^0_{s,s}(iy)}{(-1)^{n/2}iy}>0 \text{ for } -\infty<y<+\infty. \quad (42)^*$$

As will be shown later, the relation (41) is valid in many conjugated molecules, e.g., for positions 1 and 2 in naphthalene:

$$\left.\begin{aligned}D^0_{1,1}(\varepsilon)&=-\varepsilon^9+9\beta^2\varepsilon^7-26\beta^4\varepsilon^5+29\beta^6\varepsilon^3-11\beta^8\varepsilon,\\ D^0_{2,2}(\varepsilon)&=-\varepsilon^9+9\beta^2\varepsilon^7-25\beta^4\varepsilon^5+26\beta^6\varepsilon^3-8\beta^8\varepsilon.\end{aligned}\right\} \quad (43)$$

The integral expression given by Coulson and Longuet-Higgins[3] for the self-polarizability of atom $r$ is

$$\pi^0_{r,r}=\frac{1}{\pi}\int_{-\infty}^{\infty}\left\{\frac{D^0_{r,r}(iy)}{D^0(iy)}\right\}^2dy, \quad (44)$$

* If $a^{(r)}_1=a^{(s)}_1=0$, both the first and second symbols of inequality, and if $a^{(r)}_1=a^{(s)}_1>0$, the first symbol should be replaced by symbols of equality at $y=0$. But these corrections will cause no change to occur in the later results.

and the integral expression for $q_r(\alpha_r)$ has been already indicated as Eq. (19). If relation (41) is valid, then relation (42) will hold, so that

$$\{D^0_{r,r}(iy)\}^2<\{D^0_{s,s}(iy)\}^2<0 \quad (-\infty<y<\infty), \quad (45)$$

except for $y=0$, where both terms are equal to zero. Then, considering the fact that $D^0(iy)$ is real for any value of $y$ (cf. Eq. (39)), it follows that

$$\left.\begin{aligned}&\pi^0_{r,r}<\pi^0_{s,s}<0,\\ \text{or}\quad&|\pi^0_{r,r}|>|\pi^0_{s,s}|>0.\end{aligned}\right\} \quad (46)$$

Further, under the above condition, it is evident that, when $\alpha_r=\alpha_s$,

$$\frac{-\{D^0_{r,r}(iy)\}^2}{\{D^0(iy)\}^2-\alpha_r^2\{D^0_{r,r}(iy)\}^2}>\frac{-\{D^0_{s,s}(iy)\}^2}{\{D^0(iy)\}^2-\alpha_s^2\{D^0_{ss,}(iy)\}^2}>0 \quad (-\infty<y<\infty,\ y\neq 0). \quad (47)$$

Consequently, we have

$$\left.\begin{aligned}&q_r(\alpha_r)<q_s(\alpha_s)<1 \quad (\alpha_r=\alpha_s>0),\\ &q_r(\alpha_r)>q_s(\alpha_s)>1 \quad (\alpha_r=\alpha_s<0),\end{aligned}\right\} \quad (48)$$

which are illustrated in Fig. 4. Hence, according to the definitions of $\Delta E_r(\alpha_r)$ and $P_r(q_r)$, it can be easily shown that

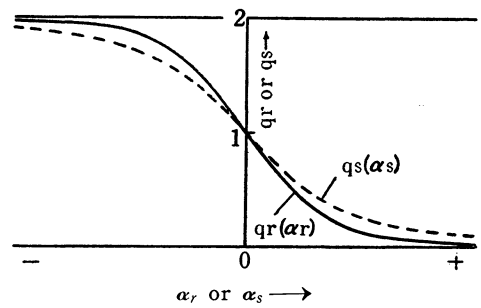



Fig. 4

$$\left.\begin{aligned}&\Delta E_r(\alpha_r)<\Delta E_s(\alpha_s) \quad (\alpha_r=\alpha_s>0),\\ &\Delta E_r(\alpha_r)-2\alpha_r<\Delta E_s(\alpha_s)-2\alpha_s \quad (\alpha_r=\alpha_s<0),\end{aligned}\right\} \quad (49)$$

and

$$P_r(q_r)<P_s(q_s) \quad (q_r=q_s\neq 1). \quad (50)$$

Therefore, from Eqs. (21), (22) and (23) or from Eq. (34)

$$L^{(r)}_N=L^{(r)}_E<L^{(s)}_N=L^{(s)}_E. \quad (51)$$

These situations are explained by Figs. 5 and 6. From Eqs. (36) and (46), it is seen that at $q_r=q_s=1$ the curvature of the curve $P_r(q_r)$ in Fig. 6 is smaller than that of the curve $P_s(q_s)$.

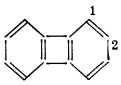
TABLE I

| Compound | Position* $r$ | $a_l^{(r)}$ $l$=11 | 9 | 7 | 5 | 3 | 1 | $\pi_{r,r}^0$ (1/$\beta$) | $F_r^0$ | $L^{(r)}$ ($-\beta$) |
|---|---|---|---|---|---|---|---|---|---|---|
| Butadiene | 1 | | | | | | 2 | 0.626(a) | 0.838(e) | 1.644(k) |
| | 2 | | | | | | 1 | 0.402(a) | 0.391(e) | 2.472(k) |
| Hexatriene | 1 | | | | | 4 | 3 | 0.685(a) | 0.861(e) | 1.524(k) |
| | 3 | | | | | 3 | 2 | 0.470(a) | 0.464(e) | 2.160(k) |
| | 2 | | | | | 3 | 1 | 0.389(a) | 0.378(e) | 2.516(k) |
| Octatetraene | 1 | | | | 6 | 10 | 4 | | 0.870(e) | 1.463(k) |
| | 3 | | | | 5 | 7 | 3 | | 0.479(e) | 2.080(k) |
| | 4 | | | | 5 | 7 | 2 | | 0.445(e) | 2.217(k) |
| | 2 | | | | 5 | 6 | 1 | | 0.375(e) | 2.530(k) |
| Decapentaene | 1 | | | 8 | 21 | 20 | 5 | | 0.874(e) | 1.426(k) |
| | 3 | | | 7 | 16 | 14 | 4 | | 0.485(e) | 1.999(k) |
| | 5 | | | 7 | 16 | 13 | 3 | | 0.458(e) | 2.117(k) |
| | 4 | | | 7 | 16 | 13 | 2 | | 0.441(e) | 2.237(k) |
| | 2 | | | 7 | 15 | 10 | 1 | | 0.374(e) | 2.536(k) |
| Benzene | | | | | | 4 | 3 | 0.398(a) | 0.399(e) | 2.536(k) |
| Naphthalene | 1 | | | 9 | 26 | 29 | 11 | 0.443(a) | 0.452(f) | 2.299 |
| | 2 | | | 9 | 25 | 26 | 8 | 0.405(a) | 0.404(f) | 2.480 |
| | 9 | | | 8 | 21 | 20 | 5 | 0.330(a) | 0.104(f) | 3.056 |
| Anthracene | 9 | 14 | 74 | 188 | 245 | 158 | 40 | 0.526(b) | 0.520(g) | 2.01 (k) |
| | 1 | 14 | 73 | 181 | 224 | 129 | 26 | 0.454(b) | 0.459(g) | 2.25 (k) |
| | 2 | 14 | 72 | 173 | 203 | 107 | 18 | 0.411(b) | 0.408(g) | 2.40 (k) |
| Phenanthrene | 1 | 14 | 73 | 182 | 228 | 135 | 29 | 0.439(b) | 0.452(g) | 2.30 (k) |
| | 9 | 14 | 73 | 181 | 227 | 137 | 31 | 0.442(b) | 0.451(g) | 2.30 (k) |
| | 4 | 14 | 73 | 181 | 224 | 129 | 26 | 0.429(b) | 0.440(g) | 2.39 (k) |
| | 3 | 14 | 72 | 174 | 208 | 116 | 24 | 0.407(b) | 0.407(g) | 2.41 (k) |
| | 2 | 14 | 72 | 174 | 207 | 113 | 21 | 0·403(b) | 0.404(g) | 2.50 (k) |
| Diphenyl | 2 | | 11 | 43 | 74 | 56 | 15 | 0.423(c) | 0.436(g) | 2.400(c) |
| | 4 | | 11 | 42 | 70 | 53 | 15 | 0.411(c) | 0.412(g) | 2.447(c) |
| | 3 | | 11 | 42 | 69 | 49 | 12 | 0.396(c) | 0.395(g) | 2.544(c) |
| | 1 | | 10 | 36 | 58 | 43 | 12 | | 0.124(g) | 2.919(k) |
| Styrene | $\beta$ | | | | 7 | 13 | 7 | | 0.821(h) | 1.704(h) |
| | 2 | | | | 6 | 10 | 4 | | 0.443(h) | 2.370(h) |
| | $\alpha$ | | | | 6 | 9 | 4 | | 0.415(h) | 2.424(h) |
| | 4 | | | | 6 | 9 | 4 | | 0.415(h) | 2.424(h) |
| | 3 | | | | 6 | 9 | 3 | | 0.395(h) | 2.546(h) |
| | 1 | | | | 5 | 7 | 3 | | 0.106(g) | 2.960(k) |
| *o*-Quinodimethane | 1′ | | | | 7 | 13 | 7 | | 0.957(i) | 1.23 (k) |
| | 1 | | | | 5 | 6 | 1 | | 0.094(i) | 2.96 (k) |
| *p*-Quinodimethane | 1′ | | | | 7 | 13 | 7 | | 0.974(i) | 1.21 (k) |
| | 2 | | | | 6 | 9 | 2 | | 0.462(i) | 2.21 (k) |
| | 1 | | | | 5 | 5 | 1 | | 0.070(i) | 3.02 (k) |
| Diphenylene | 1 | | 12 | 48 | 80 | 53 | 9 | 0.419(d) | 0.428(j) | 2.408(d) |
| | 2 | | 12 | 47 | 77 | 53 | 12 | 0.443(d) | 0.421(j) | 2.352(d) |

* The numbering of positions is given as follows:



for *o*-quinodimethane,


for *p*-quinodimethane,


for diphenylene.

For the other molecules the numbering system of Chemical Abstracts has been employed.

(a) From reference 3.
(b) H. C. Longuet-Higgins and C. A. Coulson, *J. Chem. Soc.*, **1949**, 971.
(c) R. D. Brown, *Experientia*, **6**, 376 (1950).
(d) R. D. Brown, *Trans. Faraday Soc.*, **46**, 146 (1950).
(e) C. A. Coulson, *Proc. Roy, Soc.*, **A169**, 413 (1939).
(f) J. E. Lennard-Jones and C. A. Coulson, *Trans. Faraday Soc.*, **35**, 811 (1939).
(g) R. D. Brown, *Aust. J. Sci. Res.*, A, **2**, 564 (1949).
(h) R. D. Brown, *J. Am. Chem. Soc.*, **75**, 4077 (1953).
(i) A. Pullman, G. Berthier and B. Pullman, *Bull. Soc. Chim. France*, **15**, 450 (1948).
(j) R. D. Brown, *Trans. Faraday Soc.*, **45**, 296 (1949).
(k) From Table I of reference 7.

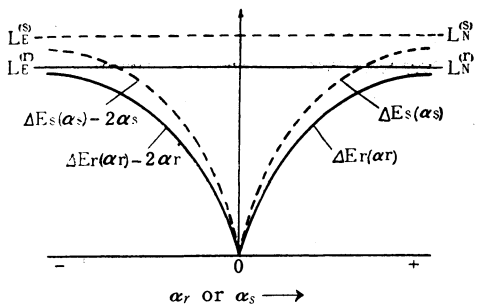



Fig. 5

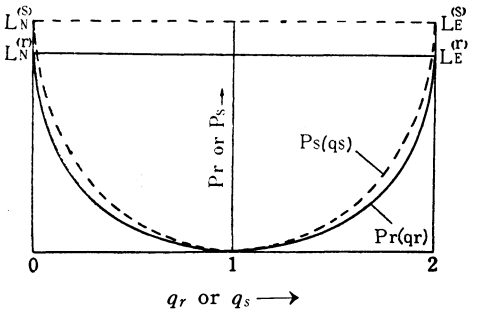



Fig. 6

Thus it has been strictly proved that, when the condition of inequalities (41) holds, the self-polarizability of atom $r$ becomes larger in magnitude than that of atom $s$, and the localization energy for atom $r$ becomes smaller than that of atom $s$. That is, if the relation (41) can be found for any two atoms $r$ and $s$ in a given molecule, whether we employ the static theory or the localization one, we necessarily reach the same conclusion that atom $r$ is more reactive than atom $s$ in both electrophilic and nucleophilic substitutions. Regarding naphthalene, for instance, the static and localization theories should give the same prediction that the position 1 is more reactive than position 2 (cf. Eqs. (43)). The values of $a_i^{(r)}$, $\pi_{r,r}^0$, $F_r^0$ and $L^{(r)}$ for various even AH's are summarized in Table I.

## Discussion

In studying the relationship between the static and dynamic quantities, it is highly important to note that the self-polarizability $\pi_{r,r}^0$ for atom $r$, which is a static quantity, is closely related to the determinant $D_{r,r}^0$ (cf. Eq. (44)), which is the very secular determinant for the residual molecule at the transition state. This fact may suggest that some correlation between the two sets of quantities, $\pi_{r,r}^0$ and $L^{(r)}$ ($=L_N^{(r)}=L_E^{(r)}$), should be found in the property of the determinant $D_{r,r}^0$ itself. It is not unnatural, if we be led to the inequalities (41).

For every pair of positions in molecules treated in Table I this condition of inequalities is satisfied. There are only a few cases of exception, viz. positions 1 and 9 in phenanthrene and 1 and 2 in diphenylene. The sequences found in the magnitudes of both the static and dynamic quantities are also in accord with what should be expected from our preceding arguments. However, for positions 1 and 9 in phenanthrene the results of the two theories do not agree with each other. It is to be noted here that inequalities (41) are a sufficient but not necessary condition, and therefore even if the inequalities do not hold, it should not always lead to the conclusion that the static and localization theories give contradictory predictions concerning the reactivity of positions $r$ and $s$. This is the reason why the predictions of the two theories for positions 1 and 2 in diphenylene do not contradict each other.

Next, we shall proceed to the discussion of the quantity $P_r(q_r)$ that has been defined as the partial polarization energy. In the localization theory it is assumed that, in the transition state, 0 or 2 $\pi$-electrons are held fixed on the carbon atom attacked according as the reagent is nucleophilic or electrophilic, respectively. As described previously this assumption of complete localization (or polarization) is obviously an extreme one, and it might be more plausible to consider that there should occur partial localization (or polarization) of $\pi$-electrons at the transition state. Remember that we have defined the partial polarization energy $P_r$ as a function of $q_r$ which can take any value between 0 and 2. Then we may preferably employ $P_r(q_r)$, instead of the localization energy $L_N^{(r)}$ or $L_E^{(r)}$, as the measure of the reactivity in the ionic substitutions.

In general, it is difficult to estimate to what extent the polarization of the electrons will take place at the transition state. Fortunately, however, when inequalities (41) hold for two positions $r$ and $s$ in an alternant hydrocarbon, $P_r(q_r)$ will be less than $P_s(q_s)$ for any value of $q_r=q_s$ (see Eq. (50)). In such a case, therefore, from the viewpoint of partial polarization the conclusion will be reached that atom $r$ is more reactive than atom $s$ both in

nucleophilic and electrophilic substitutions.

As is seen from Eq. (36) the quantity $P_r(q_r)$ is also related to static quantity $\pi^0_{r,r}$ at $q_r=q^0_r$. We can thus say that the partial polarization energy $P_r(q_r)$ is a quantity of a more general nature which can represent the static and dynamic quantities at some special values of $q_r$.

A similar situation will arise with the quantity $\Delta E_r(\alpha_r)$ or $\Delta E_r(\alpha_r)-2\alpha_r$. Indeed, $\Delta E_r(\alpha_r)$ defined by Eq. (14) is more general than $\delta E$ of Eq. (13), since the latter is the same as $\Delta E_r(\delta\alpha_r)$.

In the discussion of the relationship between the static and dynamic quantities, Brown[5] has derived a rule of chemical non-crossing which is in good agreement with the trends in curves of Fig. 6 or Fig. 5.

Only alternant hydrocarbons have been treated in this study. In a non-alternant hydrocarbon or a molecule containing hetero atoms, such a relation as inequalities (48) does not necessarily hold, because the $\pi$-electron densities $q^0_r$ and $q^0_s$ are in general not equal to each other. Therefore it cannot be expected that the two theories should always give the identical prediction for the reactivity of positions $r$ and $s$, either for nucleophilic or electrophilic reagents.

## Summary

A mathematical proof is given that under a certain condition the static and localization theories become completely equivalent to each other in predicting the reactivities in ionic substitutions of the positions in a given even alternant hydrocarbon. The said condition is concerned with the coefficients of the powers in the expansions of the secular determinants for the residual molecules. It is shown by numerical calculations that the condition is fulfilled by almost all positions in 12 molecules treated. The change in total energy of $\pi$-electrons is given as a function of a coulomb integral, and a new quantity called partial polarization energy is introduced which is defined as a function of the $\pi$-electron density at a given position. Both are useful for relating the static quantity to the dynamic one. The latter is a new measure of a general nature for the reactivity of the position towards the ionic reagents.

The author wishes to express his sincere thanks to Professor K. Higasi for his guidance and encouragement throughout the present work. Thanks are also due to Professor K. Fukui and Dr. S. Nagakura for valuable criticism. He is indebted to the Ministry of Education for a grant-in-aid.

*Research Institute of Applied Electricity*
*Hokkaido University, Sapporo*

# *Correlation between Two Molecular Orbital Theories on Organic Reactions. II*. Radical Substitution*

By Hiroaki BABA

(Received October 26, 1956)

## Introduction

It has been pointed out in the previous paper[1] (hereafter referred to as I) that in ionic substitutions the static measures of chemical reactivity are closely associated with the corresponding dynamic quantities. That is, they become equivalent to each other, if a certain condition is fulfilled. That condition refers to the coefficients of the powers appearing in the expansions of the secular determinants for the residual molecules appropriate to the substitutions concerned. In the present paper it will be shown that under the same conditions the two sets of quantities used as the measures of the reactivity in radical substitution become also mutually correlated. Further, it will be proved that in the same relation, Dewar's approximate values[2,3] of localization energy become

* Read in part at the Symposium on $\pi$-Electron Problems held by the Chem. Soc. Japan, in October 1954.

1) H. Baba, This Bulletin, **30**, 147 (1957).

2) M. J. S. Dewar, *J. Am. Chem. Soc.*, **74**, 3355 (1952).

3) M. J. S. Dewar, *J. Am. Chem. Soc.*, **74** 3357 (1952).

completely parallel with the accurate ones.

### Change in Total Energy of $\pi$-Electrons with Variation of Resonance Integrals

Before entering into the subject of this article we shall briefly refer to the role of the free valence in radical substitution[4]. Consider an even AH, and let the positions adjacent to position $r$ be denoted by $t$, $t'$……. Suppose that a radical reagent attacking at position $r$ brings about the same amount of change, $\beta\delta$, in the resonance integrals $\beta_{rt}$ $\beta_{rt'}$,……. Then the energy change will be expressed as a Taylor series:

$$\delta E=\sum_t{}' \frac{\partial E}{\partial \beta_{rt}}\delta\beta+\cdots\cdots, \tag{1}$$

where $\delta\beta$ is assumed to be small and positive. By the use of Eqs. (2), (3) and (6) of I, this may be rewritten as

$$\delta E=2N_r^0\delta\beta+\cdots\cdots=2(\sqrt{3}-F_r^0)\delta\beta+\cdots\cdots. \tag{2}$$

Eq. (2) shows that the samllest increase in energy will occur for the largest value of free valence $F_r^0$ or the smallest value of bond number $N_r^0$, and hence the most reactive position is the one with the highest free valence or the lowest bond number in the initial state of the molecule.

Now, for the purpose of relating the above-mentioned static quantities $F_r^0$ and $N_r^0$ to the dynamic one $L_R^{(r)}$, let it be assumed that the resonance integrals $\beta_{rt}$, $\beta_{rt'}$,…… change simultaneously from their initial value $\beta$ to a certain value between $\beta$ and 0. Further it is assumed that the other resonance integrals and coulomb integrals are all kept at their initial values. Then the total energy of $\pi$-electrons $E_r$, bond order $p_{rt}$ and bond number $N_r$ may be regarded as continuous functions of $\beta_r$, where $\beta\leqq\beta_r=\beta_{rt}=\beta_{rt'}=\cdots\cdots\leqq 0$. These functions will be denoted by $E_r(\beta_r)$, $p_{rt}(\beta_r)$ and $N_r(\beta_r)$, respectively. Then, instead of Eq. (1), the following expression will be otained as the energy change[5]:

$$\Delta E_r(\beta_r)=E_r(\beta_r)-E_0=\int_\beta^{\beta_r}\frac{dE_r(\beta_r)}{d\beta_r}d\beta_r$$

$$=\sum_t{}'\int_\beta^{\beta_r}\frac{\partial E_r}{\partial\beta_{rt}}d\beta_r. \tag{3}$$

Again this may be rewritten as

$$\Delta E_r(\beta_r)=\sum_t{}'\int_\beta^{\beta_r}2p_{rt}(\beta_r)d\beta_r$$

$$=\int_\beta^{\beta_r}2N_r(\beta_r)d\beta_r. \tag{4}$$

Thus the bond number $N_r$ as a function of $\beta_r$ has come to be important, so that some remarks on it will be given.

First, from the definition of $N_r^0$

$$N_r(\beta)=N_r^0. \tag{5}$$

Next, let us consider what happens to the value of $N_r(\beta_r)$ when $\beta_r$ approaches to zero. Consider a system consisting of carbon atom $r$ and odd AH obtained when atom $r$ is excluded from the even AH in question, and suppose that in this system there is no interaction between atom $r$ and the odd AH; then we may regard $\beta_r=\beta_{rt}=\beta_{rt'}\cdots\cdots$ as zero.

An odd AH has always a non-bonding molecular orbital (NBMO), so that there exists a degenerate level of zero energy in the system. The NBMO of the odd AH will be expressed as

$$\phi_{\text{zero}}^{(r)}=\sum_v b_{0v}\chi_v. \tag{6}$$

The coefficients $b_{0v}$'s can be easily calculated on account of the characteristic property of NBMO[6].

Now consider such a perturbation for this system under which $\beta_r$ changes from zero to negative. The correct zeroth order MO's for this perturbation will be linear combinations of $\chi_r$ and $\phi_{\text{zero}}^{(r)}$[7]:

$$\phi_{\text{zero}}^{\pm}=\frac{1}{\sqrt{2}}(\chi_r\pm\phi_{\text{zero}}^{(r)}). \tag{7}$$

It may be assumed without loss of generality that it is $\phi_{\text{zero}}^{+}$ which becomes a bonding orbital under the influence of the perturbation. Conversely, when $\beta_r$ for the even AH tends to zero, one of the MO's will reduce to $\phi_{\text{zero}}^{+}$ and the others to the bonding orbitals of the odd AH. Therefore it follows from Eqs. (6) and (7) that

$$p_{rt}(0)\equiv\lim_{\beta_r\to 0}p_{rt}(\beta_r)=2\cdot\frac{1}{\sqrt{2}}\cdot\frac{1}{\sqrt{2}}b_{0t}=b_{0t}, \tag{8}$$

$$N_r(0)\equiv\lim_{\beta_r\to 0}N_r(\beta_r)=\sum_t{}'b_{0t}. \tag{9}$$

It should be noticed that $p_{rt}(\beta_r)$ and hence $N_r(\beta_r)$ do not vanish even if $\beta_r$ tends to

4) R. D. Brown, *Quart. Rev.*, **6**, 63 (1952).
5) F. H. Burkitt, C. A. Coulson and H. C. Longuet-Higgins, *Trans. Faraday Soc.*, **47**, 553 (1951).
6) H. C. Longuet-Higgins, *J. Chem. Phys.*, **18**, 265, 275 (1950).
7) M. J. S. Dewar, *J. Am. Chem. Soc.*, **74**, 3341 (1952).

zero. On the basis of these considerations the relation between $2N_r$ and $\beta_r$ may be represented schematically by the curve shown in Fig. 1.

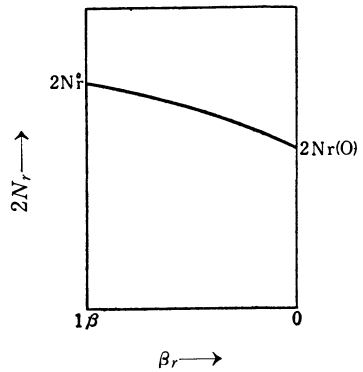



Fig. 1

According to the foregoing arguments, it follows at once that

$$\lim_{\beta r \to 0} E_r(\beta_r) = E_R^{(r)} \tag{10}$$

and

$$\lim_{\beta r \to 0} \Delta E_r(\beta_r) = L_R^{(r)}. \tag{11}$$

On the other hand the approximate values of $L_R^{(r)}$, given by Dewar[2,3] based on the treatment of perturbation theory, are $-2\beta\sum_t{}' p_{rt}^0$ and $-2\beta\sum_t{}' b_{0t}$. If these values be designated as $L_R^{(r)\prime}$ and $L_R^{(r)\prime\prime}$, then we have

$$L_R^{(r)\prime} = -2N_r^0\beta, \tag{12}$$

$$L_R^{(r)\prime\prime} = -2N_r(0)\beta. \tag{13}$$

Now Eq. (4) shows that the value of $\Delta E_r(\beta_r)$ is equal to the area under the curve of Fig. 1 between $\beta_r=\beta$ and $\beta_r=\beta_r$. Hence, $L_R^{(r)}$ is equal to the area under the curve between $\beta_r=\beta$ and $\beta_r=0$, while $L_R^{(r)\prime}$ is equal to the area of the reactangle whose adjacent sides are $-\beta$ and $2N_r^0$, and $L_R^{(r)\prime\prime}$ to that of the rectangle whose adjacent sides are $-\beta$ and $2N_r(0)$ (see Fig. 1).

As an example, the relation between $N_r$ and $\beta_r$ for benzene is shown in Fig. 2. In this example,

$$p_{rt}(0) = p_{rt'}(0) = \frac{1}{\sqrt{3}},$$

and

$$N_r(0) = \frac{2}{\sqrt{3}},$$

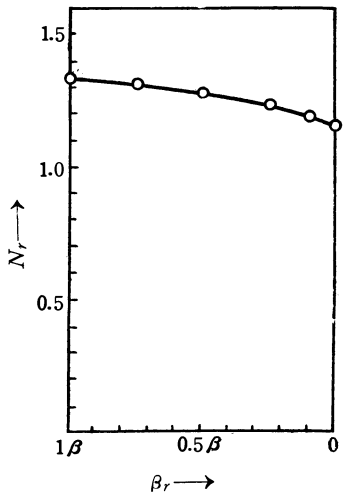



Fig. 2. $N_r(\beta_r)$ for benzene.

since the coefficients of the AO's in the NBMO of pentadienyl are calculated as shown in Fig. 3. It may be worthy of note that there exists the following relation among the magnitudes of $N_r^0$, $L_R^{(r)}$ and $N_r(0)$:

$$2N_r^0 > \frac{L_R^{(r)}}{-\beta} > 2N_r(0).$$

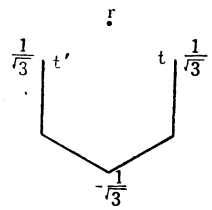



Fig. 3

This is easily seen from Fig. 2; in fact the calculated values of the three terms are 2.667, 2.536 and 2.309, respectively. The above relation means that $2N_r^0$ is the upper limit of $L_R^{(r)}/-\beta$, while $2N_r(0)$ is the lower one.

## Correlation between the Static and Dynamic Quantities

Consider two positions $r$ and $s$ in an even AH. According to the integral expression given by Coulson and Longuet-Higgins[8] for $\pi$-bond order

$$p_{rt}(\beta_r) = (-1)^{r+t+1}\frac{1}{\pi}\int_{-\infty}^{\infty}\frac{D_{r,t}}{D}\,dy. \tag{14}$$

8) C. A. Coulson and H. C. Longuet-Higgins, *Proc. Roy. Soc.*, **A191**, 39 (1947); **A192**, 16 (1947).

When $D$ is expanded with respect to the $r$th row,

$$D=\sum_t{}'(-1)^{r+t}\beta_r D_{r,t}-\varepsilon D_{r,r}. \tag{15}$$

Therefore it can be shown that

$$N_r(\beta_r)=\frac{-1}{\pi\beta_r}\int_{-\infty}^{\infty}\frac{D(iy)+iyD_{r,r}(iy)}{D(iy)}dy, \tag{16}$$

which reduces to

$$N_r(\beta_r)=\frac{-\beta_r}{\pi\beta^2}\times\int_{-\infty}^{\infty}\frac{D^0(iy)+iyD^0_{r,r}(iy)}{(\beta_r/\beta)^2D^0(iy)+\{(\beta_r/\beta)^2-1\}iyD^0_{r,r}(iy)}\times dy. \tag{17}$$

A similar expression may be obtained for $N_s(\beta_s)$. Now, if inequalities (41) and hence inequality (42) of I hold, then it follows

$$\frac{iyD^0_{r,r}(iy)}{(-1)^{n/2}}<\frac{iyD^0_{s,s}(iy)}{(-1)^{n/2}}<0 \qquad (-\infty<y<\infty,\ y\neq 0). \tag{18}$$

Consequently, using Eq. (39) of I, it is easily verified that

$$N_r(\beta_r)<N_s(\beta_s) \text{ for } \beta\leqq\beta_r=\beta_s\leqq 0. \tag{19}*$$

In particular cases where $\beta_r=\beta_s=\beta$ and $\beta_r=\beta_s=0$, we have

$$N^0_r<N^0_s, \tag{20}$$

and

$$N_r(0)<N_s(0), \tag{21}$$

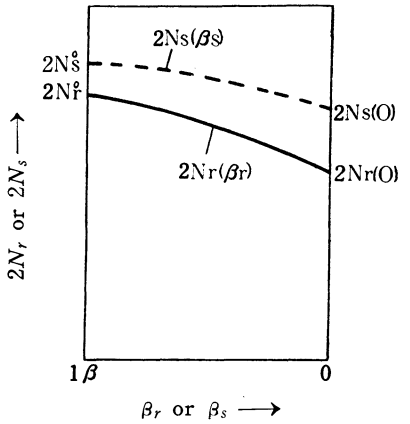


Fig. 4

respectively. These relations are explained by Fig. 4.

Thus, the conclusions derived from inequalities (41) of I are summarized as follows:

(1) The bond number $N^0_r$ is smaller than $N^0_s$, and hence the free valence $F^0_r$ is larger than $F^0_s$;
(2) The localization energy $L_R^{(r)}$ is smaller than $L_R^{(s)}$;
(3) Dewar's approximate values of localization energy $L_R^{(r)\prime}$ and $L_R^{(r)\prime\prime}$ are smaller than $L_R^{(s)\prime}$ and $L_R^{(s)\prime\prime}$, respectively;
(4) The bond number $N_r(\beta_r)$ is smaller than $N_s(\beta_s)$ for $\beta\leqq\beta_r=\beta_s\leqq 0$;
(5) The change in total energy of $\pi$-electrons $\Delta E_r(\beta_r)$ is smaller than $\Delta E_s(\beta_s)$ for $\beta<\beta_r=\beta_s\leqq 0$.

From (2) and (3) it follows that the two approximate values of $L_R^{(r)}$, i.e. $-2N^0_r\beta$ and $-2N_r(0)\beta$ will run parallel to the accurate one. Conclusion (5) is in accord with the concept of chemical non-crossing rule.

All the correlations stated above may be found for any pair of positions in those molecules shown in Table I of the previous paper except for positions 1 and 9 in phenanthrene, and 1 and 2 in diphenylene.

Lastly, it should be added that the method used in the present paper in dealing with the radical substitution is essentially the same as that used previously in treating the ionic substitutions. This situation may be understood by inspection of Table I where the correspondence among the used variables is recorded*.

TABLE I

| Ionic substitutions | | Radical substitution |
|---|---|---|
| Nucleophilic | Electrophilic | |
| $0\leqq\alpha_r<+\infty$ | $-\infty<\alpha_r\leqq 0$ | $\beta\leqq\beta_r\leqq 0$ |
| $q_r(\alpha_r)$ | $q_r(\alpha_r)$ | $N_r(\beta_r)$ |
| $\Delta E_r(\alpha_r)$ | $\Delta E_r(\alpha_r)-2\alpha_r$ | $\Delta E_r(\beta_r)$ |

* For $\beta_r=\beta_s=0$ it is assumed that $a_1^{(r)}>a_1^{(s)}$ in inequalities (41) of I. If $a_1^{(r)}=a_1^{(s)}$, then $\lim_{\beta_r\to 0}N_r(\beta_r)=\lim_{\beta_r\to 0}N_s(\beta_s)$.

* A quantity corresponding to the partial polarization energy $P_r(q_r)$ in ionic substitutions may be defined as

$$L_r(N_r)=\Delta E_r(\beta_r(N_r))-2N_r\{\beta_r(N_r)-\beta\},$$

which might be called partial localization energy. $L_r(N_r)$ appears to be not so useful as $P_r(q_r)$. This is partly due to the fact that, so far as the $\pi$-bond order is calculated according to its usual definition, $N_r(\beta_r)$ does not reduce to zero when $\beta_r$ tends to zero.

## Conclusion

Both the argument of the present paper and that of the previous one have made clear that: When the condition of inequalities (41) of I hold for two positions in an even alternant hydrocarbon, the same conclusion follows for the relative reactivities of the positions both in ionic and radical substitutions, and it does not matter which quantity be employed as a measure of the reactivity from among self-polarizability, free valence and locarization energy (accurate or approximate). This condition of inequalities (41) is satisfied in many alternant hydrocarbons. Therefore, it is not peculiar that the two theories usually give the same prediction concerning the reactivity of this sort of molecules, notwithstanding the fact that there is a striking difference in fundamental assumptions involved in them.

The author wishes to express his sincere thanks to Professor K. Higasi for reading the manuscript and for valuable criticism.

*Research Institute of Applied Electricity*
*Hokkaido University, Sapporo*

# *Studies on Crystals of Metallic Tris-ethylenediamine-complexes. II. The Crystal Structure of Sodium* D-*Tris-ethylenediamine-cobalt (III) Chloride Hexahydrate,* 2D-[Co $en_3$]$Cl_3$·NaCl·$6H_2O$

By Kazumi NAKATSU, Motoo SHIRO*, Yoshihiko SAITO and Hisao KUROYA

(Received October 27, 1956)

## Introduction

Meisenheimer et al.[1] described a mixed salt having the composition 2[Co $en_3$]$Cl_3$·NaCl·$6H_2O$. It was prepared from an aqueous solution containing racemic [Co $en_3$]$Cl_3$ and NaCl.

Hitherto unrecorded double salt having the same chemical composition has been prepared from a solution containing optically active D-[Co $en_3$]$Cl_3$ and NaCl. This double salt was chosen for confirming the "*gauche*" configuration of the ethylenediamine ligands in the complex ion [Co $en_3$]$^{3+}$, found in crystals of D,L-[Co $en_3$]$Cl_3$·$3H_2O$ by X-ray method[2]. Since the *c*-axis is as short as 8.06 Å, it should be possible to obtain a clear projection of a single complex ion with less overlapping of atom.

The determination of the absolute configuration of the optically active complex ion, [Co $en_3$]$^{3+}$ was also made successfully in regard to this compound by using absorption edge technique[3] and a brief account has already been published[4]. In the present paper details of the structure analysis will be described.

## Preliminary Investigation

The crystals were grown from a solution of D-[Co $en_3$]$Cl_3$ and NaCl in proportion of 5 : 3 by weight by slow evaporation in a desiccator containing calcium chloride. They form hexagonal prisma, belonging to the hexagonal pyramidal class. Crystals are orange, optically uniaxial and possess optical activity. The form exhibited by the salt is shown in Fig. 1. Assuming the pyramidal planes to be $(10\bar{1}1)$ an axial ratio, $a : c = 1 : 0.704$, was obtained, in agreement with the

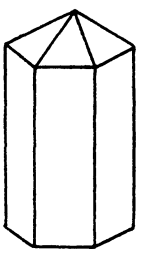


Fig. 1. A crystal of 2D-[Co $en_3$]$Cl_3$·NaCl·$6H_2O$.

1) J. Meisenheimer. L. Angermann and H. Holsten. *Ann.*, **438**, 269 (1924).
2) K. Nakatsu, Y. Saito and H. Kuroya, This Bulletin, **29**, 428, (1956).
3) J. M. Bijvoet, *Proc. Roy. Soc. Amsterdam*, B **52**, 313 (1949) ; A. F. Peerdemann and A. J. van Bommel, ibid., B **54**, 16 (1951) ; J. M. Bijvoet. A. F. Peerdemann and A. J. van Bommel, *Nature*, **168**, 271 (1951).
4) Y. Saito, K. Nakatsu, M, Shiro and H. Kuroya, *Acta. Cryst.*, **8**. 729 (1955).
* Present adress ; Momotani Juntenkan Co., Ltd., Osaka.

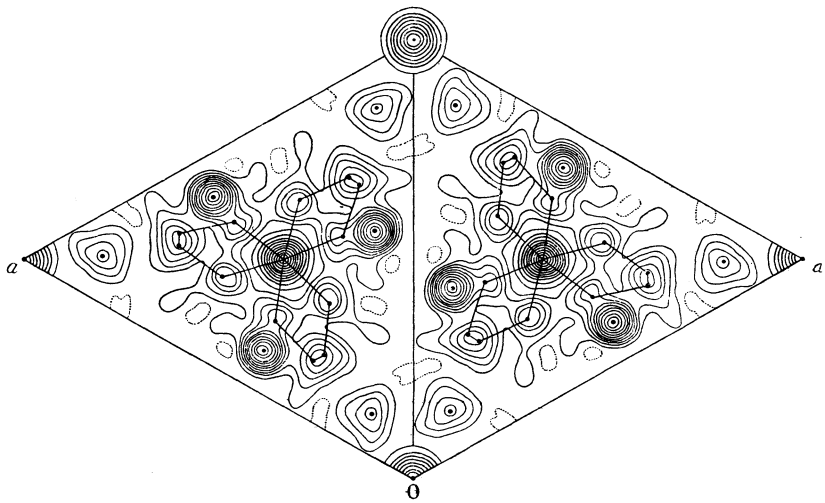



Fig. 2. Electron density projection of 2D-[Co en$_3$]Cl$_3$·NaCl·6H$_2$O along the *c*-axis. Contours are drawn at intervals of 4 e. Å$^{-2}$ for peaks at (0, 0), (1/3, 2/3), and (2/3, 1/3), and of 2 e. Å$^{-2}$ for other peaks, zero-electron contour being broken. The atomic positions are indicated by dots, outlines of the complex ions being shown.

value $a : c = 1 : 0.703$ subsequently obtained from diffraction photographs. The density determined by the pyknometer method using organic liquid was 1.559 g./cc. at 20°C.

The results of chemical analysis and the values of specific rotation measured at wave lengths of the Na-D line in aqueous solution are shown below:

| Found | Calcd. as $C_{12}H_{48}N_{12}Cl_7Co_2Na\cdot 6H_2O$ |
|---|---|
| Cl 29.0% | 29.0% |
| $H_2O$ 11.8% | 12.6% |
| Specific rotation of | |
| D-compound | $[\alpha]_D = +138°$ |
| L-compound* | $[\alpha]_D = -133°$. |

## Determination of the Structure

Laue photographs taken with X-ray beam parallel to the *c*-crystal axis showed hexagonal symmetry. Oscillation photgraphs around the *c*-axis indicated the presence of a symmetry plane perpendicular to the *c*-axis. Hence the Laue symmetry was found to be $C_{6h}$-6/*m*.

The unit cell dimensions were found from higher order reflections observed on equatorial lines of oscillation photographs. They are

$$a = 11.47 \pm 0.03 \text{ Å and } c = 8{\cdot}06 \pm 0.02 \text{ Å}.$$

Iron K$\alpha$ radiation was used throughout ($\lambda$ = 1.937 Å). The unit cell contains one formula unit. The calculated density is 1.552 g./cc., in good agreement with the observed value.

Two cylindrical specimens of about 0.2 mm. in diameter were cut one parallel to each principal axis. All the equatorial reflections were recorded on Weissenberg triple film photographs. The intensities of the observed reflections were estimated by visual comparison procedure and were corrected for Lorentz and polarisation factors using Cochran's chart[5]. No absorption corrections were made. The resulting *F*-values were correlated so that all the observed data were on the same relative intensity scale, and they were later converted into an absolute scale by comparison with the calculated values.

No systematic extinctions were observed, hence the space lattice must be primitive. However, it was found that odd order reflections of (000*l*) are always very weak, contributing only two per cent of total (000*l*) intensity. The corresponding space group should have no center of symmetry, since the crystal is optically active as well as piezoelectric active. The facts indicate that the symmetry is very near but not exactly to that of the space group $P6_3$. Accordingly it was decided to adopt the space group $P6_3$ during the preliminary treatment of the structure. The space group $P6_3$ affords sixfold general positions and two sets of twofold positions. Since there is one formula unit in the unit cell, cobalt atoms must occupy special positions and all other atoms except one sodium and one chlorine atom must occupy sets of general positions leading 21 parameters. In the space group $P6_3$ there exists no singlefold special position for a sodium or a chlorine atom, so they must lie on some position belonging to lower symmetry class.

In attempting to fix the positions of the cobalt and chlorine atoms in the (000*l*) projection, the Patterson function $P(UV)$ was evaluated. This projection fixed the positions of these atoms with certainty. At the outset of Fourier syntheses only the cobalt and chlorine atoms were used for calculating the signs of the observed structure factors

* L-compound can be prepared in the same way from L-[Co en$_3$]Cl$_3$ and NaCl.

5) W. Cochran, *J. Sci. Instruments*, **25**, 253 (1949).

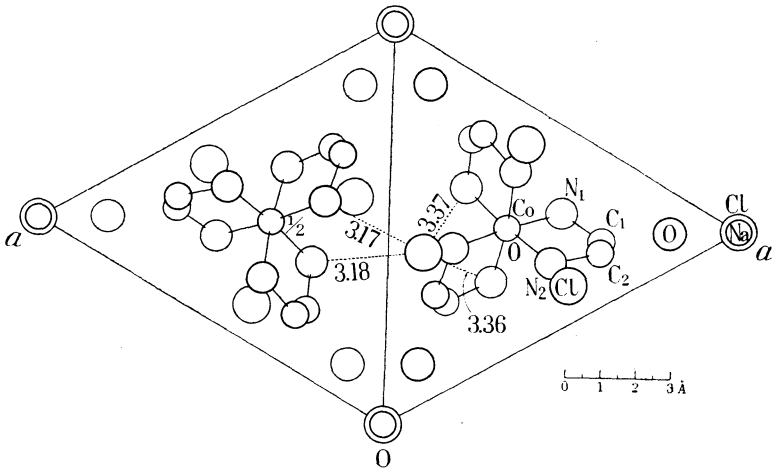



Fig. 3. Projection of the structure along the $c$-axis.
Important N···Cl distances are given.

and the series $\dot{\rho}\,(XY)$ was evaluated. Successive refinements with $(F_o-F_c)$ syntheses were successful and the atoms were mostly resolved. It was found that the odd sodium and chlorine atoms lie on $(00z)$. The projection finally obtained is shown in Fig. 2, which can be interpreted with the aid of Fig. 3. Although some knowledge about the position of hydrogen atoms were obtained from $\{\rho_0(XY)-\rho_c(XY)\}$ as well as $\rho_0\,(XY)$, it does not seem to be significant because the analysis was less accurate.

Since the size and shape of five membered cobalt-ethylenediamine ring and other interatomic distances were known by our previous investigation, $z$-parameters of all the atoms could be fixed approximately from packing considerations, assuming that all the atoms except $Na^+$ and $Cl^-$ of NaCl component are arranged according to the symmetry of $P6_3$. The positions of $Na^+$ and $Cl^-$ were also deduced by packing considerations. They are: $z_{Na}\approx 0.77$ and $z_{Cl}\approx 0.27$. Thus the assumed structure is based on the space group $P3$. It was easily shown that such an

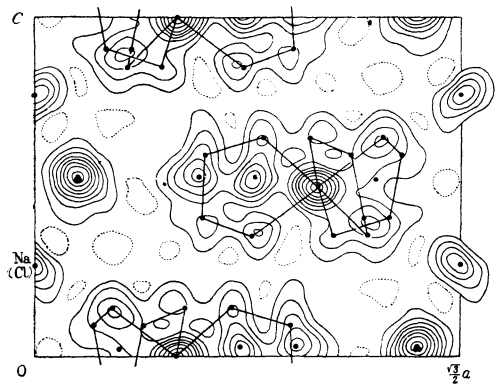



Fig. 4. Electron density projection along the $a$-axis.
Contours are drawn at intervals of 4 e. Å$^{-2}$, zero-electron contour being broken.

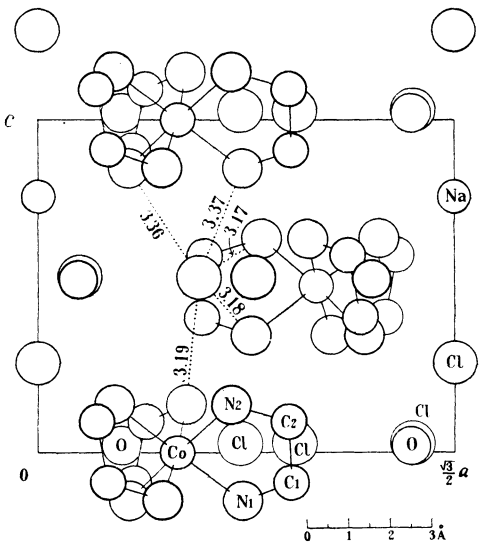



Fig. 5. Projection of the structure along the $a$-axis.

arrangement of atoms may well account for the charactersitic features of Laue and osciallation photographs. The assumed structure was then confirmed by evaluating the Patterson projection $(P)VW$. The real and imaginary parts of $F(0k\bar{k}l)$ were then calculated. The agreement between the observed and calculated values was sufficiently good to start Fourier refinements. $\rho\,(YZ)$ was then evaluated and refinements were repeated as usual. Final projection shown in Fig. 4 lead the structure illustrated in Fig. 5, which corresponds to an elevation of the structure shown in Fig. 3. The $z$-parameter of oxygen atoms is less reliable because of the poor resolution of the projection $\rho\,(YZ)$. Parameter values thus obtained are listed in Table I. These parameters gave the reliability index $(R=\sum||F_o|-|F_c||/\sum|F_o|)$ of 0.144 and 0.221 for $(hki0)$ and $(0k\bar{k}l)$ respectively.

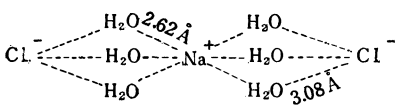
TABLE I
FRACTIONAL ATOMIC COORDINATES

| Atom | $x$ | $y$ | $z$ |
|---|---|---|---|
| Co | 2/3 | 1/3 | 0 |
| $N_1$ | 0.783 | 0.295 | 0.854 |
| $N_2$ | 0.647 | 0.183 | 0.146 |
| $C_1$ | 0.773 | 0.167 | 0.907 |
| $C_2$ | 0.742 | 0.140 | 0.093 |
| $Cl_1$ | 0.617 | 0.100 | 0.528 |
| O | 0.897 | 0.098 | 0.520 |
| Na | 0 | 0 | 0.770 |
| $Cl_2$ | 0 | 0 | 0.270 |

All the atoms except Na and $Cl_2$ are arranged on the basis of $P6_3$

In the calculation of the structure factors the atomic scattering curves given in International Tables were employed. The structure amplitudes were adjusted in the usual way by multiplication by a temperature factor $\exp -B(\sin\theta/\lambda)^2$. $B$ was evaluated graphically from the slope of a plot of $\log F_0/F_c$ against $(\sin\theta/\lambda)^2$. $B$ was found to be 3.5 Å$^2$.

Though it is certain that the structure thus deduced gives a clear picture of the essential features of the structure, the intensities of the odd order reflections of $(000l)$ cannot be satisfactorily explained by the present model. The higher $R$-value for $(0k\bar{k}l)$ zone compared with that for $(hki0)$ zone may indicate a presence of errors in $z$-parameters. Namely, the intensities of the odd order reflections of $(000l)$, especially strong intensity of (0003), cannot be quantitatively explained. Calculation of interatomic distances on the basis of the parameters listed in Table I reveals that both $Na^+$ and $Cl^-$ ions on a line $(00z)$ are surrounded octahedrally by six water molecules at a distance of 2.84 Å. This would be a rather unlikely occurrence. It is well established that $Na^+$ has a smaller ionic radius than $Cl^-$. If we change the $z$-parameters of oxygen atoms slightly and assume a following sequence of $Na^+$, $H_2O$ and $Cl^-$:




the symmetry of the arrangement of oxygen atoms becomes that of the space group $P\bar{3}$. The calculated $F(000l)$ values based on this model indeed gave a better agreement with the observed values, however, the distribution of calculated intensities $I(hkil)$ did not show the presence of a plane of symmetry perpendicular to the $c^*$-axis in the reciprocal space. This fact is not in conformity with the observed Laue symmetry. In order to account for the observed diffraction symmetry we have to assume a random arrangement of $Na^+$ and $Cl^-$ ions on $2(a)$ of $P6_3$. But, if we assume complete randomness, then the odd order reflections of $(000l)$ should disappear. However, it may not be impossible to overcome this difficulty, if we assume a kind of polycrystalline twinning. Let us denote as P and Q the two structures where the relative positions in the $z$-direction of $Na^+$-$(H_2O)_3$-$Cl^-$-sequence are different with respect to the rest of the structure;

| | P | Q | |
|---|---|---|---|
| $z_{Na}$ | $z$ | $\bar{z}$ | |
| $z_{Cl}$ | $z+\frac{1}{2}$ | $\bar{z}+\frac{1}{2}$ | with $z=0.770$ |

If these two structures occur in a given single crystal with the same frequency and the size of each crystallites are larger than the coherent region of X-rays, the intensities of $(hkil)$ reflection will be given as sum of contributions from P and Q, for in a polycrystalline twin there will be no phase relation between two structures. So that we have;

$$I(hkil) = L.p \quad 1/2\{F_P^2(hkil) + F_Q^2(hkil)\} \qquad (1)$$

$$I(hki\bar{l}) = L.p \quad 1/2\{F_P^2(hki\bar{l}) + F_Q^2(hki\bar{l})\} \qquad (2)$$

where $L.p$ denotes Lorentz and polarisation factors.

It is possible to show that the difference between $I(hkil)$ and $I(hkil)$ becomes smaller by considering such a twinned structure, thus resulting better agreement with the observed diffraction symmetry.

On the other hand, the odd order reflections of $(000l)$ can be given as;

$$I(000l) = L.p\, 1/2\{F_P^2(000l) + F_Q^2(000l)\} \fallingdotseq 0 \qquad (3)$$

The calculation of intensities based on this model led to improved agreement with the observed values. $z$-parameters of oxygen atoms were adjusted so as to give the best fit with the observed intensities. This time the value of $R$ reduced to 0.173 for $(0k\bar{k}l)$ zone, giving the weighted mean value of 0.161 for all the observed reflections around the two principal axis. In Table II the parameters of O, Na and Cl atoms are listed.

TABLE II
ATOMIC COORDINATES OF O, Na AND $Cl_2$ ATOMS IN THE STRUCTURE P AND Q

| | Model P | | | Model Q | | |
|---|---|---|---|---|---|---|
| | $x$ | $y$ | $z$ | $x$ | $y$ | $z$ |
| $O_1$ | 0.897 | 0.098 | 0.560 | 0.897 | 0.098 | 0.440 |
| $O_2$ | 0.098 | 0.201 | 0.980 | 0.098 | 0.201 | 0.020 |
| Na | 0 | 0 | 0.770 | 0 | 0 | 0.230 |
| $Cl_2$ | 0 | 0 | 0.270 | 0 | 0 | 0.730 |

Observed and calculated structure amplitudes based on the parameter values shown in Tables I and II are shown in Table III.

With the parameters given in Tables I, and II the interatomic distances and interbond angles tabulated in Table IV were calculated. The accuracy of the determination was estimated using the equation given by Cruickshank[6]. The standard deviation in electron density is $\sigma(\rho) = 0.68$

6) D. W. J. Cruickshank, *Acta Cryst.*, **2**, 65 (1949).

TABLE III

OBSERVED AND CALCULATED STRUCTURE AMPLITUDES

| $1k.0$ | $F_o$ | $F_c$ | $3k.0$ | $F_o$ | $F_c$ | $5k.0$ | $F_o$ | $F_c$ | $7k.0$ | $F_o$ | $F_c$ |
|---|---|---|---|---|---|---|---|---|---|---|---|
| 0 | 31 | −35 | 0 | 7 | 4 | 0 | 12 | 17 | 0 | 29 | −27 |
| 1 | 78 | 77 | 1 | 22 | 21 | 1 | 38 | 35 | 1 | 15 | 18 |
| 2 | 75 | 70 | 2 | 18 | 23 | 2 | 7 | 13 | 2 | 5 | −7 |
| 3 | 10 | −21 | 3 | 53 | 50 | 3 | <9 | 0 | 3 | 12 | −14 |
| 4 | 81 | 83 | 4 | 42 | 38 | 4 | 10 | −10 | 4 | 10 | 0 |
| 5 | 25 | −28 | 5 | 24 | −22 | 5 | 12 | 11 | $8k.0$ | | |
| 6 | <9 | −3 | 6 | 28 | 24 | 6 | 13 | −11 | 0 | 18 | 21 |
| 7 | 41 | 37 | 7 | 11 | −12 | $6k.0$ | | | 1 | <8 | 1 |
| 8 | 11 | −6 | 8 | 11 | −13 | 0 | 32 | 30 | 2 | 14 | 15 |
| 9 | 11 | −5 | $4k.0$ | | | 1 | 3 | −1 | 3 | 3 | 6 |
| $2k.0$ | | | 0 | 28 | −23 | 2 | 8 | −4 | $9k.0$ | | |
| 0 | 7 | 12 | 1 | 30 | 34 | 3 | 47 | 49 | 0 | 10 | 14 |
| 1 | 40 | −43 | 2 | 13 | −10 | 4 | 13 | −15 | 1 | 5 | 5 |
| 2 | 35 | 31 | 3 | 27 | 33 | 5 | 13 | 13 | $10k.0$ | | |
| 3 | 6 | −7 | 4 | 21 | 22 | | | | 0 | 18 | 18 |
| 4 | 7 | 3 | 5 | 10 | 12 | | | | | | |
| 5 | 67 | 58 | 6 | 9 | 13 | | | | | | |
| 6 | 5 | −3 | 7 | 12 | 10 | | | | | | |
| 7 | 12 | −21 | | | | | | | | | |
| 8 | 46 | 37 | | | | | | | | | |
| 9 | 6 | 2 | | | | | | | | | |

| $0k.2$ | $F_o$ | $F_c$ | $F_c$(P, Q)* | $0k.8$ | $F_o$ | $F_c$ | $F_c$(P, Q) | $0k.5$ | $F_o$ | $F_c$ | $F_c$(P, Q) |
|---|---|---|---|---|---|---|---|---|---|---|---|
| 0 | 138 | 140 | 135 | 0 | 38 | 33 | 27 | 0 | 9 | 2 | 14 |
| 1 | 35 | 39 | 42 | 1 | 15 | 4 | 9 | 1 | 16 | 9 | 17 |
| 2 | 17 | 20 | 24 | $0k.1$ | | | | 2 | 32 | 35 | 41 |
| 3 | 15 | 12 | 15 | 0 | 5 | 6 | 5 | 3 | 17 | 27 | 17 |
| 4 | 62 | 65 | 63 | 1 | 47 | 58 | 53 | 4 | 20 | 9 | 12 |
| 5 | 40 | 40 | 40 | 2 | 26 | 36 | 40 | 5 | 10 | 14 | 17 |
| 6 | 5 | 5 | 7 | 3 | 84 | 78 | 82 | 6 | 7 | 5 | 4 |
| 7 | 31 | 34 | 33 | 4 | 22 | 12 | 14 | 7 | 23 | 28 | 24 |
| 8 | 4 | 6 | 8 | 5 | 9 | 6 | 8 | $0k.7$ | | | |
| 9 | 4 | 5 | 4 | 6 | 5 | 8 | 11 | 0 | 5 | 2 | 10 |
| $0k.4$ | | | | 7 | 60 | 65 | 63 | 1 | 18 | 17 | 21 |
| 0 | 41 | 71 | 54 | 8 | 19 | 15 | 20 | 2 | 16 | 22 | 18 |
| 1 | 4 | 12 | 14 | 9 | 17 | 15 | 8 | 3 | 8 | 17 | 9 |
| 2 | 34 | 29 | 27 | $0k.3$ | | | | 4 | 12 | 12 | 9 |
| 3 | 41 | 31 | 39 | 0 | 26 | 3 | 24 | 5 | 8 | 8 | 8 |
| 4 | 20 | 19 | 25 | 1 | 38 | 29 | 32 | | | | |
| 5 | 12 | 20 | 21 | 2 | 42 | 43 | 37 | | | | |
| 6 | 20 | 14 | 17 | 3 | 31 | 39 | 30 | | | | |
| 7 | 10 | 12 | 11 | 4 | 18 | 10 | 12 | | | | |
| 8 | 17 | 15 | 13 | 5 | 13 | 12 | 11 | | | | |
| $0k.6$ | | | | 6 | 5 | 8 | 11 | | | | |
| 0 | 28 | 45 | 38 | 7 | 35 | 34 | 34 | | | | |
| 1 | 37 | 21 | 26 | 8 | 5 | 6 | 5 | | | | |
| 2 | 8 | 7 | 12 | | | | | | | | |
| 3 | 11 | 15 | 16 | | | | | | | | |
| 4 | 14 | 16 | 17 | | | | | | | | |
| 5 | 29 | 25 | 22 | | | | | | | | |
| 6 | 14 | 13 | 13 | | | | | | | | |

* Calculated on the basis of twinned structure.

e. Å$^{-2}$ on the (0001) projection. The standard deviation $\sigma(x)$ of some atoms are 0.014 Å for $Cl_1$, 0.031 Å for $N_1$, 0.048 Å for $N_2$ and 0.051 Å for O, respectively.

TABLE IV
CALCULATED INTERATOMIC DISTANCES AND BOND ANGLES

| | | | |
|---|---|---|---|
| Co—$N_1$ | 1.98 Å | ∠Co—$N_1$—$C_1$ | 109.6° |
| Co—$N_2$ | 2.00 | ∠Co—$N_2$—$C_2$ | 109.4° |
| $N_1$—$C_1$ | 1.48 | ∠$N_1$—$C_1$—$C_2$ | 109.0° |
| $N_2$—$C_2$ | 1.47 | ∠$N_2$—$C_2$—$C_1$ | 110.2° |
| $C_1$—$C_2$ | 1.54 | ∠$N_1$—Co—$N_2$ | 87.4° |
| $Cl_1$···$N_1$ | 3.18, 3.36, 3.37 Å | | |
| $Cl_1$···$N_2$ | 3.17, 3.19 Å | | |
| $Cl_1$···$C_1$ | 3.43, 3.82, 4.07 Å | | |
| $Cl_1$···$C_2$ | 3.73, 4.06, 3.66 Å | | |

| | | Model P | Model Q |
|---|---|---|---|
| $O_1$···$Cl_1$ | 3.22 Å | 3.23 Å | 3.30 Å |
| $O_2$···$Cl_1$ | 3.22 | 3.25 | 3.22 |
| $O_1$···$C_1$ | 3.38 | 3.48 | 3.26 |
| | 3.67 | 3.76 | 3.56 |
| | 3.68 | 3.41 | 4.24 |
| $O_2$···$C_1$ | 3.38 | 3.31 | 3.38 |
| | 3.67 | 3.58 | 3.67 |
| | 3.68 | 3.95 | 3.68 |
| $O_1$···$C_2$ | 3.37 | 3.17 | 3.40 |
| | 3.83 | 3.79 | 3.98 |
| | 4.08 | 4.36 | 3.56 |
| $O_2$···$C_2$ | 3.37 | 3.29 | 3.37 |
| | 3.83 | 3.89 | 3.83 |
| | 4.08 | 3.81 | 4.08 |
| Na···$O_1$ & $O_2$ | 2.84 | 2.62 | 2.62 |
| $Cl_2$···$O_1$ & $O_2$ | 2.84 | 3.08 | 3.08 |
| $O_1$···$O_1$ ($O_2$···$O_2$) | 3.46 | 3.46 | 3.46 |

## Description of the Structure

The arrangements of the atoms in the unit cell can be most clearly seen in the projection on the plane (0001), which is shown in Fig. 3. The size and shape of the complex ion are in good agreement with those previously described by us. The ethlyenediamine molecules take "*gauche*" forms and six nitrogen atoms form a slightly distorted octahedron around the central cobalt atom.

The azimuthal angle between planes containing the C—N bond and the C—C bond is found to be 48°. A complex ion is surrounded by nine $Cl^-$ ions, six being at the corners of a trigonal prism and the other three at the apexes of an equilateral triangle. The closest approach of the complex ions and $Cl^-$ occurs between $NH_2$ group and $Cl^-$, suggesting hydrogen bond of type N—H···$Cl^-$. The $Cl^-$···N distances are 3.17, 3.18 and 3.19 Å, which are comparable to the values obtained by various authors. The way in which a complex ion forms ionic bonds is very similar to that of racemic [Co en$_3$] $Cl_3 \cdot 3H_2O$.

If we adopt the above mentioned model having a twinned structure, a sodium ion is surrounded nearly octahedrally by six water molecules at a distance of 2.62 Å. forming $[Na(H_2O)_6]^+$ group. The packing of the complex ions and $Cl^-$ ions brings about a structure having hollow tunnels parallel to the *c*-axis, in which the above mentioned sequence of $[Na(H_2O)_6]^+$ and $Cl^-$ ions is held.

This structure was worked out without assuming any other relationship to the racemic [Co en$_3$]$Cl_3 \cdot 3H_2O$, except the initial assumption of the interatomic distances and bond angles. The unit cell dimensions of both substances show interesting relations; namely, both unit cells have nearly the same *a*-axis, and the *c*-axis of the racemic chloride is about twice that of the optically active double salt. Moreover, the above mentioned surroundings of the complex ion $[Co\ en_3]^{3+}$ are very similar in both structures, so that one may expect to find some common building units of which both structures are made up. In an effort along this line we pick out from the two substances, neglecting the minor differences, the groups, having the composition [Co en$_3$]$Cl_3 \cdot 3H_2O$. This group is marked A in Fig. 3 in the previous report. If we double this group by the operation of a digonal screw axis, the structure, having the space group $P6_3$, would be obtained. This is the structure of this double salt without NaCl component. In the structure of D,L-[Co en$_3$]$Cl_3 \cdot 3H_2O$, whose corresponding space group is $P\bar{3}cl$, the group [Co en$_3$] $Cl_3 \cdot 3H_2O$ is repeated four times by the operation of a glide plane *c* and *a* center of symmetry. Thus the concept of the polysynthetic structure developed by Ito[7] is applicable to the broad structural principles and is shown to be useful in discussing the structure of related complex compounds as illustrated by the present example. It enables us to describe the complicated structure in a straightforward and simple way.

## Summary

The preparation of two mixed salts, 2D-[Co en$_3$]$Cl_3 \cdot NaCl \cdot 6H_2O$ and 2L-[Co en$_3$] $Cl_3 \cdot NaCl \cdot 6H_2O$ is described. The space group is P3, with one formula unit in

7) T. Ito, "X-ray Studies on Polymorphism", Maruzen, Tokyo (1950).

a cell of dimensions: $a=11.47\pm0.03$ Å, $c=8.06\pm0.02$ Å. However, the structure has the pseudo space group $P6_3$. By evaluating the functions $\rho(XY)$ and $\rho(YZ)$, projections of the structure on two crystallographic planes were obtained. A kind of twinned structure was proposed to get a better agreement between the observed and calculated intensities. The structure shows very close resemblance to that of D,L-[Co $en_3$]$Cl_3 \cdot 3H_2O$. A sodium ion is octahedrally surrounded by six water molecules, with Na $\cdots$O distances of 2.62 Å. The whole structure is ionic consisting of the ions $[Co\ en_3]^{3+}$, $[Na(H_2O)_6]^{+}$ and $Cl^-$.

The authors are grateful to Professors I. Nitta and T. Watanabé of the Osaka University for their kind advice and encouragement throughout this work. Helpful discussions were given by Mr. K. Osaki of the Osaka University. Thanks are also due to Mr. Y. Iidaka of the Mineralogical Institute, University of Tokyo for piezoelectric test of the cystals. The authors are indebted to the Ministry of Education for financial assistance.

*Institute of Polytechnics, Osaka City University, Osaka*

# *Studies on the Intramolecular Hydrogen Bond in Conjugated Systems by the Measurements of Dipole Moments. II. Salicylaldehyde and o-Hydroxyacetophenone*

By Bunzo EDA and Kazuo ITO

(Received November 9, 1956)

## Introduction

It is well known from infrared absorption spectra that salicylaldehyde and *o*-hydroxyacetophenone have no free hydroxyl groups and hence all the molecules form intramolecular hydrogen bonds[1]. In the previous paper[2], the present authors discussed the magnitudes and the directions of charge migrations caused by the hydrogen bonding in an *o*-nitrophenol molecule. Since a similar charge migration due to the intramolecular hydrogen bonding is also expected in the case of salicylaldehyde and *o*-hydroxyacetophenone molecules, it would be of interest to determine its magnitude and direction. The same treatment as that of *o*-nitrophenol can be applied to these two compounds.

## Experimental

**Materials.**—All the materials were prepared in the present authors' laboratory except *p*-chloroacetophenone, *p*-nitroacetophenone and 5-chloro-2-hydroxybenzaldehyde which were purchased. 5-Chloro-2-hydroxybenzaldehyde, 5-methyl-2-hydroxybenzaldehyde and *p*-nitroacetophenone were purified by recrystallization, while

1) L. Pauling, "The Nature of the Chemical Bond", Cornell University Press, Ithaca, New York (1940), pp. 318, 319.

TABLE I

DIELECTRIC CONSTANTS AND DENSITIES OF THE DERIVATIVES OF SALICYLALDEHYDE AND ACETOPHENONE IN BENZENE SOLUTIONS

| Compounds | $w \times 10^5$ | $\varepsilon$ | $d$ |
|---|---|---|---|
| 4-Chloro-2-hydroxybenzaldehyde (m. p. 52°) | 130 | 2.2693 | 0.86692 |
| | 240 | 2.2726 | 0.86723 |
| | 597 | 2.2869 | 0.86839 |
| | 690 | 2.2905 | — |
| 5-Chloro-2-hydroxybenzaldehyde (m. p. 100°) | 395 | 2.2677 | 0.86771 |
| | 616 | 2.2710 | 0.86837 |
| | 1198 | 2.2793 | 0.87017 |
| | 1748 | 2.2867 | 0.87188 |
| 5-Methyl-2-hydroxybenzaldehyde (m. p. 55°) | 124 | 2.2850 | 0.87202 |
| | 207 | 2.2924 | 0.87248 |
| | 298 | 2.3014 | 0.87283 |
| *p*-Chloroacetophenone (b. p. 232°) | 366 | 2.2791 | 0.86817 |
| | 1137 | 2.3074 | 0.86987 |
| | 2568 | 2.3659 | 0.87321 |
| | 4460 | 2.4432 | 0.87774 |
| *p*-Nitroacetophenone (m. p. 80°) | 215 | 2.2785 | 0.86716 |
| | 485 | 2.2972 | — |
| | 870 | 2.3252 | 0.86888 |
| | 1876 | 2.3953 | 0.87185 |
| 5-Chloro-2-hydroxyacetophenone (m. p. 54°) | 271 | 2.2693 | 0.86753 |
| | 574 | 2.2754 | 0.86841 |
| | 1813 | 2.3004 | 0.87195 |
| | 3750 | 2.3410 | 0.87741 |

TABLE II

MOLECULAR POLARIZATIONS AND DIPOLE MOMENTS OF THE DERIVATIVES OF SALICYLALDEHYDE AND ACETOPHENONE IN BENZENE SOLUTIONS

| Compounds | $t$(°C) | $\varepsilon_1$ | $d_1$ | $\alpha$ | $\beta$ | $P_{2\infty}$ | $MR_D$ | $\mu$(D) |
|---|---|---|---|---|---|---|---|---|
| 4-Chloro-2-hydroxybenzaldehyde | 30 | 2.2639 | 0.86649 | 3.85 | 0.317 | 148.6 | 38.5 | 2.31 |
| 5-Chloro-2-hydroxybenzaldehyde | 30 | 2.2623 | 0.86648 | 1.40 | 0.309 | 76.3 | 38.5 | 1.37 |
| 5-Methyl-2-hydroxybenzaldehyde | 25 | 2.2732 | 0.87147 | 9.43 | 0.464 | 263.9 | 38.1 | 3.32 |
| *p*-Chloroacetophenone | 30 | 2.2630 | 0.86725 | 4.03 | 0.234 | 157.1 | 40.4 | 2.40 |
| *p*-Nitroacetophenone | 30 | 2.2634 | 0.86650 | 7.04 | 0.283 | 259.4 | 42.2 | 3.29 |
| 5-Chloro-2-hydroxyacetophenone | 30 | 2.2635 | 0.86678 | 2.06 | 0.284 | 106.2 | 41.9 | 1.79 |

4-chloro-2-hydroxybenzaldehyde and 5-chloro-2-hydroxyacetophenone were purified by steam distillation followed by recrystallization. *p*-Chloroacetophenone was purified by distillation.

**Measurements.**—All the measurements were made in benzene solutions at 30°C or 25°C. The apparatus and the method of measurements were the same as those used in the previous study[2]. Halverstadt-Kumler's method was employed throughout.

**Results.**—The results are shown in Table I and Table II, in which notations have the same significance as those used in the previous paper.

## Results and Discussions

It was shown in the previous paper[2] that unless there is hydrogen bonding or a special steric effect between the substituents the dipole moments of benzene derivatives having certain substituents can be expressed by the vector sum of the group moments of the respective substituents within 0.1 D. In order to discuss the dipole moments of salicylaldehyde and *o*-hydroxyacetophenone, therefore, it is necessary to obtain the moments of aldehyde and acetyl groups which are required for calculating the dipole moments of the hypothetical salicylaldehyde and *o*-hydroxyacetophenone molecules having no intramolecular hydrogen bonds.

Since it is known that benzaldehyde and acetophenone molecules are planar[3], let the molecules be placed in a coordinate system as in Fig. 1. The $x$- and $y$-components of the dipole moment of benzaldehyde are denoted by $\mu_{x1}$ and $\mu_{y1}$ and

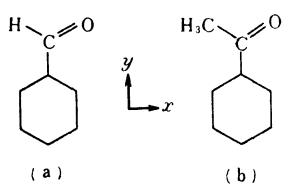



Fig. 1

2) B. Eda and K. Ito, This Bulletin, **29**, 524 (1956).
3) W. Klyne, "Progress in Stereochemistry", Butterworths Scientific Publications, London (1954), p. 148.

TABLE III

DIPOLE MOMENTS OF BENZALDEHYDE, ACETOPHENONE AND THEIR DERIVATIVES IN BENZENE SOLUTIONS

| Compounds | $\mu$obs.(D) | $\mu$calcd.(D) | $\Delta\mu$(D) |
|---|---|---|---|
| Benzaldehyde | 2.96[4] | 3.00 | +0.04 |
| *p*-Fluorobenzaldehyde | 1.96[5] | 2.02 | +0.06 |
| *p*-Chlorobenzaldehyde | 2.03[4] | 1.97 | −0.06 |
| *p*-Methylbenzaldehyde | 3.30[6] | 3.33 | +0.03 |
| *p*-Nitrobenzaldehyde | 2.41[4] | 2.41 | 0.00 |
| Acetophenone | 2.96[7] | 2.96 | 0.00 |
| *p*-Chloroacetophenone | 2.40 | 2.37 | −0.03 |
| *p*-Methylacetophenone | 3.23[7] | 3.22 | −0.01 |
| *p*-Nitroacetophenone | 3.29 | 3.22 | −0.07 |

those of *o*-hydroxyacetophenone by $\mu_{x2}$ and $\mu_{y2}$, respectively. The second column of Table III shows the observed moments, $\mu_{obs.}$, of benzaldehyde, acetophenone and their derivatives in benzene solutions. The two components of the moment of benzaldehyde, $\mu_{x1}$ and $\mu_{y1}$, must satisfy the following five equations, since the dipole moment of fluorobenzene is 1.48 D, that of chlorobenzene 1.60 D, that of toluene 0.4 D, and that of nitrobenzene 4.0 D in benzene solutions.

$$\mu_{x1}^2+\mu_{y1}^2=(2.96)^2 \quad \text{(for benzaldehyde)} \tag{1}$$

$$\mu_{x1}^2+(\mu_{y1}-1.48)^2=(1.96)^2 \quad \text{(for } p\text{-fluorobenzaldehyde)} \tag{2}$$

$$\mu_{x1}^2+(\mu_{y1}-1.6)^2=(2.03)^2 \quad \text{(for } p\text{-chlorobenzaldehyde)} \tag{3}$$

$$\mu_{x1}^2+(\mu_{y1}+0.4)^2=(3.30)^2 \quad \text{(for } p\text{-methylbenzaldehyde)} \tag{4}$$

$$\mu_{x1}^2+(\mu_{y1}-4.0)^2=(2.41)^2 \quad \text{(for } p\text{-nitrobenzaldehyde)} \tag{5}$$

The two components of acetophenone, $\mu_{x2}$

4) D. I. Coomber and J. R. Partington, *J. Chem. Soc.*, **1938**, 1444.
5) N. J. Leonard and L. E. Sutton, *J. Am. Chem. Soc.*, **70**, 1564 (1948).
6) J. N. Pearce and L.F. Berhenke, *J. Phys. Chem.*, **39**, 1005 (1935).
7) J. B. Bentley, K. B. Everard, R. J. B. Marsden and L. E. Sutton, *J. Chem. Soc.*, **1949**, 2963.

end $\mu_{y2}$, have to satisfy the following four aquations.

$$\mu_{x2}^2+\mu_{y2}^2=(2.96)^2 \quad \text{(for acetophenone)} \tag{6}$$

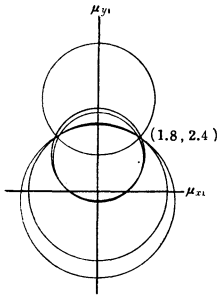
$$\mu_{x2}^2+(\mu_{y2}-1.6)^2=(2.40)^2 \quad \text{(for } p\text{-chloroacetophenone)} \tag{7}$$

$$\mu_{x2}^2+(\mu_{y2}+0.4)^2=(3.23)^2 \quad \text{(for } p\text{-methylacetophenone)} \tag{8}$$

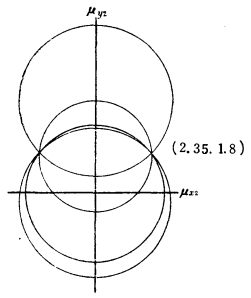
$$\mu_{x2}^2+(\mu_{y2}-4.0)^2=(3.29)^2 \quad \text{(for } p\text{-nitroacetophenone)} \tag{9}$$

It is known that the nitro group is not suitable for the treatment of vector summation because it has a large mesomeric interaction with other substituents. But in this case, *p*-nitrobenzaldehyde was chosen because the interaction of the nitro group with the aldehyde group is smaller than those of halogens[5].

When these equations were solved graphically it was found that the circles intersect each other almost at a point as illustrated in Fig. 2 and Fig. 3. Thus $\mu_{x1}$, $\mu_{y1}$, $\mu_{x2}$ and $\mu_{y2}$ were determined as ±1.8D, 2.4 D, ±2.35 D and 1.8 D, respectively. Of



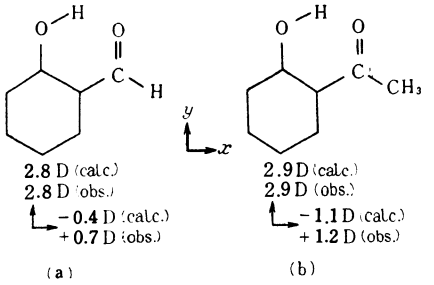

benzaldehyde
Fig. 2




acetophenone
Fig. 3

the double sign of these values, the plus sign is reasonable. When these values were used for calculating the dipole moments of benzaldehyde, acetophenone and their derivatives, good agreements were found between the observed and calculated moments as shown in the third and fourth columns of Table III.

The *x*- and *y*-components, $\mu_{xI(calcd.)}$ and $\mu_{yI(calcd.)}$*, of a hypothetical salicylaldehyde molecule having no intramolecular hydrogen bond were calculated by the use of the components of the moment of benzaldehyde and those of the moment of phenol[2]. The values of $\mu_{xI(calcd.)}$ and $\mu_{yI(calcd.)}$ were calculated to be −0.4 D and +2.8 D, respectively. (See Fig. 4a). For the purpose of obtaining the *x*- and *y*-components of the dipole moment of a real salicylaldehyde molecule which has the intramolecular hydrogen bond, it is required to determine the components which satisfy the observed moments of salicylaldehyde, 4-chloro-2-hydroxybenzaldehyde, 5-chloro-2-hydroxybenzaldehyde and 5-methyl-2-hydroxybenzaldehyde. These values, $\mu_{xI(obs.)}$ and $\mu_{yI(obs.)}$, were determined to be +0.7 D and +2.8 D, respectively. As shown in Table IV, these two components give good agreement between the observed and calculated moments of the derivatives of salicylaldehyde.




(a) (b)

Fig. 4

TABLE IV
DIPOLE MOMENTS OF SALICYLALDEHYDE AND ITS DERIVATIVES IN BENZENE SOLUTIONS

| Compounds | $\mu$obs.(D) | $\mu$calcd.(D) | $\Delta\mu$(D) |
|---|---|---|---|
| Salicylaldehyde | 2.88[8] | 2.89 | +0.01 |
| 4-Chloro-2-hydroxybenzaldehyde | 2.31 | 2.20 | −0.11 |
| 5-Chloro-2-hydroxybenzaldehyde | 1.37 | 1.39 | +0.02 |
| 5-Methyl-2-hydroxybenzaldehyde | 3.32 | 3.28 | −0.04 |

When the two components of salicylaldehyde, $\mu_{xI(obs.)}$ and $\mu_{yI(obs.)}$, are compared with the calculated components, $\mu_{xI(calcd.)}$ and $\mu_{xI(calcd.)}$, it is found that the difference is 1.1 D in the *x*-direction and 0.0 D in the *y*-direction. Presumably this difference is due mainly to the intramolecular hydrogen bond between the hydroxyl group and the carbonyl group, because it is greater than the errors inherent to the vector summation, the errror being estimated to be within 0.1 D for such molecules as given in Table III and Table IV of the previous paper[2] and in Table III of the present paper. If it is assumed from the consideration of the inaccuracy of the present method of approximation that $\mu_{x1}$ is 1.75～1.9 D and $\mu_{y1}$ is 2.3～2.5 D instead of $\mu_{x1}$=

* In this paper, the suffixes I and II attached to $\mu$ refer to salicylaldehyde and *o*-hydroxyacetophenone, respectively.

8) B. C. Curran, *J. Am. Chem. Soc.*, **67**, 1835 (1945).

1.8D and $\mu_{y1}=2.4$D, it is found that $\mu_{xI(calcd.)}$ and $\mu_{yI(calcd.)}$ are $-0.3\sim-0.5$ D and $2.7\sim2.8$ D, respectively. The difference turns out to be $1.0\sim1.2$ D in the $x$-direction and $0.0\sim0.1$ D in the $y$-direction. The conclusion is unaltered that the difference is great in the $x$-direction whereas there is little difference in the $y$-direction.

The dipole moment of *o*-hydroxyacetophenone can be discussed in a similar way. The calculated components of *o*-hydroxyacetophenone, which were assumed to be those of a hypothetical molecule having no hydrogen bond, were obtained from the components of phenol and the aforementioned $x$- and $y$-components of acetophenone, $\mu_{x2}$ and $\mu_{y2}$. They are $-1.1$ D for $\mu_{xII(calcd.)}$ and $+2.9$ D for $\mu_{yII(calcd.)}$. (See Fig. 4b). The components of the dipole moment of a real *o*-hydroxyacetophenone molecule are those satisfying the observed moments 3.16 D[8] of *o*-hydroxyacetophenone and 1.79 D of 5-chloro-2-hydroxyacetophenone. They are determined to be $\pm1.2$ D for $\mu_{xII(obs.)}$ and 2.9 D for $\mu_{yII(obs.)}$ as shown in Fig. 4(b). The sign of $\mu_{xII(obs.)}$ can be determined to be plus in analogy to salicylaldehyde. When these components, $\mu_{xII(obs.)}$ and $\mu_{yII(obs.)}$, are compared with $\mu_{xII(calcd.)}$ and $\mu_{yII(calcd.)}$ respectively, the difference is 2.3 D in the $x$-direction and 0.0 D in the $y$-direction. That is to say, there is a large difference only in the $x$-direction, which is definitely beyond the errors attributable to the vector summation. In the same manner as in salicylaldehyde, it will be necessary to make allowance for the degree of inaccuracy in $\mu_{x2}$ and $\mu_{y2}$. If it is assumed that $\mu_{x2}$ is $2.35\sim2.4$ D and $\mu_{y2}$ is $1.75\sim1.8$ D, the calculated components of the hypothetical molecule having no hydrogen bond are $-1.1\sim-1.2$ D for $\mu_{xII(calcd.)}$ and $2.9\sim3.0$ D for $\mu_{yII(calcd.)}$. Therefore, the difference is $2.3\sim2.4$ D in the $x$-direction and $0.0\sim0.1$ D in the $y$-direction. Again the difference is great only in the $x$-direction.

The results mentioned above show that the charge migrations caused by the intramolecular hydrogen bond are from the hydroxyl oxygen to the carbonyl oxygen and their magnitudes are about 1.1 D in salicylaldehyde and about 2.3 D in *o*-hydroxyacetophenone. On the basis of the fact that the charge migration is caused mainly in the $x$-direction and is almost zero in the $y$-direction for the compounds in question, it is concluded that the contribution of the resonance structure shown in Fig. 5 is increased greatly and that its degree is about 10 to 20%. It is

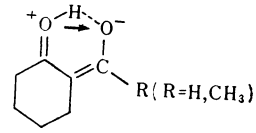



Fig. 5

very interesting that there is a remarkable difference between the magnitude of salicylaldehyde and that of *o*-hydroxyacetophenone. Anyway, it should be emphasized that the charge migration in the $x$-direction is great, or in other words, that the contribution of the resonance structure as shown in Fig. 5 due to the intramolecular hydrogen bond is indubitable.

## Summary

Dipole moments of 4-chloro-2-hydroxybenzaldehyde, 5-chloro-2-hydroxybenzaldehyde, 5-methyl-2-hydroxybenzaldehyde, *p*-chloroacetophenone, *p*-nitroacetophenone and 5-chloro-2-hydroxyacetophenone were measured in benzene solutions. Their values are 2.31 D, 1.37 D, 3.32 D, 2.40 D, 3.29 D and 1.79 D, respectively. The components of the dipole moments of salicylaldehyde and *o*-hydroxyacetophenone, which were evaluated from the components of the moments of phenol, benzaldehyde and acetophenone, do not agree at all with the components that satisfy the observed moments of salicylaldehyde and *o*-hydroxyacetophenone and their derivatives. The magnitudes of the discrepancies are about 1.1 D in the $x$-direction for salicylaldehyde, about 2.3 D in the $x$-direction for *o*-hydroxyacetophenone, and almost 0.0 D in the $y$-direction for both compounds. It was concluded that the charge migration was caused from the hydroxyl oxygen to the carbonyl oxygen by the intramolecular hydrogen bonding.

The authors wish to express their sincere thanks to Prof. M. Kubo and Dr. Y. Kurita for their kindness in participating in discussions. A part of the expense for the experiment has been defrayed from a grant given by the Ministry of Education, to which the authors' thanks are due.

*Department of Chemistry, Faculty of Science, Nagoya University*
*Nagoya*

# *Electronic States of para-Benzoquinone. I. Calculation of the Energy Levels by a Semi-empirical Molecular Orbital Method Neglecting Configuration Interaction*

By Tosinobu ANNO*, Ikuo MATUBARA** and Akira SADÔ

(Received October 15, 1956)

## Introduction

The electronic structure and the spectrum of *p*-benzoquinone have been studied by many workers. Evans et al.[1] as well as Basu[2] have discussed the oxidation-reduction potential of this molecule with reference to $\pi$-electron structure. Absorption spectrum in vapor phase was studied by Light[3] and Seshan[4] and solution-spectrum data are also available[5]. Fixl and Schauenstein, whose paper we can see in only a brief abstract form[6], studied the absorption spectrum of the *p*-benzoquinone crystal using the polarized light and showed that in the region of 23,000-$cm^{-1}$ (ca. 4,500 Å) absorption band this molecule absorbs the light polarized along the long axis more intensely than the light polarized along the short axis. Recently, Sidman[7] has also investigated the *p*-benzoquinone crystal in wider wavelength region than Fixl and Schauenstein and arrived at the conclusion concerning the direction of polarization opposed to that of Fixl and Schauenstein. From the solvent effect of the absorption spectrum, McConnell[8] as well as Nagakura and Kuboyama[9] concluded that the absorption near 4,500 Å was due to an $n$-$\pi$ transition while the absorption around 3,000 Å was due to a $\pi$-$\pi$ transition. Nagakura and Kuboyama[9] have also calculated the electonic structure of this molecule using the naive empirical molecular orbital(MO) method based on the one-electron approximation.

On the other hand the semi-empirical MO method proposed by Pariser and Parr[10] has been applied by various authors[11-13] to the elucidation of the $\pi$-electronic structures and spectra of conjugated hydrocarbons and heteromolecules and has proved to be very useful. Kon[13] has calculated the electronic states of *p*-benzoquinone combining this method with the self-consistent field method of Roothaan[14]. In these previous works only the $\pi$-electrons have been taken explicitly into the electronic interaction term in the Hamiltonian and the so-called non-bonding electrons ($n$-electrons) localized at the heteroatoms, in the case of the heteromolecules, have been considered implicitly in the core. Therefore, no information about the excited states of the heteromolecules due to the excitation of $n$-electrons have been obtained. Thus, in spite of the usefulness of Pariser and Parr's method in explaining the $\pi$-electronic structure of conjugated molecules, there has been no attempt to apply this method to the problems of the excitation of $n$-electrons.

In the present series of papers, both the theoretical and the experimental studies in the electronic states of *p*-benzoquinone will be reported. As the first part of this series, the calculation of energy levels of this molecule by the semi-empirical MO method due to Pariser and Parr will be

* Department of Chemistry, College of General Education, Ootsubo-machi, Fukuoka.
T. A. is greatly indebted to the Dean of the Faculty of Science and Professor S. Imanishi for permitting him to continue his work at the Faculty.
** Present adress : The Central Research Laboratory, Tôyô Rayon Co., Ltd., Ootsu.

1) M. G. Evans. *Trans. Faraday Soc.*, **42**, 113 (1946); M. G. Evans, J. Gergely and J. de Heer, *ibid.*, **45**, 312 (1949).
2) S. Basu, ibid., **52**, 6 (1956).
3) L. Light, *Z. physik. Chem.*, **122**, 414 (1926).
4) P. K. Seshan, *Proc. Indian Acad. Sci.*, **3A**, 172 (1936). For earlier works see reference cited there.
5) Collected in Landolt-Börnstein, "Zahlenwerte und Funktionen" Springer, Berlin, (1951), Vol. I, Part 3, Molekeln II . See especially Fig. 263 on p. 307.
6) J. O. Fixl and E. Schauenstein, *Monatsh.*, **81**, 598 (1950) ; C A., **45**, 4136f (1951).
7) J. W. Sidman, *J. Am. Chem. Soc.*, **78**, 2363 (1956).
8) H. McConnell, *J. Chem. Phys.*, **20**, 700 (1952).
9) S. Nagakura and A. Kuboyama, *J. Chem. Soc. Japan* (Pure Chem. Sect.), **74**, 499 (1953), and *J. Am. Chem. Soc.*, **76**, 1003 (1954).
10) (a) R. Pariser and R. G. Parr, *J. Chem. Phys.*, **21**, 466 (1953).
(b) R. Pariser and R. G. Parr, *J. Chem. Phys.*, **21**, 767 (1953).
11) R. Pariser, *J. Chem. Phys.*, **24**, 250 (1956).
12) C. M. Moser, *J. Chem. Soc.*, **1954**, 3455.
13) H. Kon, This Bulletin, **28**, 275 (1955).
14) C. C. J. Roothaan, *Rev. Modern Phys.*, **23**, 69 (1951).

given taking account of the $n$-electrons explicitly as well as $\pi$-electrons into the electronic interaction term in the Hamiltonian.

## Outline of the Theory[14a)]

In our approximation the Hamiltonian operator will be expressed in the form

$$H=H_{\text{core}}+(1/2)\sum_{i\neq j}(e^2/r_{ij}), \tag{1}$$

where $e^2/r_{ij}$ is the electrostatic repulsion between electrons $i$ and $j$, and

$$H_{\text{core}}=\sum_i H_{\text{core}}(i), \tag{2}$$

where

$$H_{\text{core}}(i)=T(i)+U_{\text{core}}(i), \tag{3}$$

in which $T(i)$ is the kinetic energy operator for electron $i$ and $U_{\text{core}}(i)$ is the potential energy operator for this electron in the field of the core. It should be noted that the $n$-electrons are considered explicitly apart from the core; i. e., $i$ and $j$ denote any one of $\pi$- or $n$-electrons.

The MO $\phi_i$ will be taken to be the orthonormal linear combination of atomic orbitals $\chi_p$ on the several nuclei:

$$\phi_i=\sum_p C_{ip}\chi_p. \tag{4}$$

As we are considering $n$-electrons as well as $\pi$-electrons it will be convenient to distinguish between $\pi$-atomic orbital (AO) and the so-called non-bonding orbital ($n$-orbital). The former is one of $2p$-AO's and has its node in the molecular plane and is represented by $\chi_p$ without superscript. In the case of the $p$-benzoquinone molecule each $n$-orbital is the $2p$-orbital of the oxygen atom, the node of which is in a plane perpendicular to the molecular plane and containing the C–O axis. These $n$-orbitals will be represented by $\chi_p^n$ with a superscript $n$. Subscript $p$ denotes the atom to which the AO $\chi_p$ refers. Neglecting formally the differential overlap, the configurational energies and the interaction matrix elements among different configurations are expressible in terms of the core integrals over AO's and the coulomb interaction integrals over AO's of the following form:

$$(pp\mid qq)=\iint\chi_p^*(1)\chi_p(1)(e^2/r_{12})\chi_q^*(2)\chi_q(2)\,dv_1dv_2, \tag{5}$$

and

$$(pp\mid q^nq^n)=\iint\chi_p^*(1)\chi_p(1)(e^2/r_{12})\chi_q^{n*}(2)\chi_q^n(2)\,dv_1dv_2. \tag{6}$$

The evaluation of the integral of the type (5) has been discussed by Pariser and Parr[10]. We shall describe the method for evaluation of the latter type of integrals. If the distance between $p$ and $q$ is fairly great, $(pp\mid q^nq^n)$ will be evaluated fairly correctly using the Slater AO's as $\chi$'s. If $p$ and $q$ are close to each other,

14a) Note added in proof — In the case of $p$-benzoquinone for which the application of the theory is intended in the present paper, descriptions concerning the integral of the type $(pp\mid q^nq^n)$ in the present and the following sections are correct only when both $p$ and $q$ lie on the $y$-axis (Fig. 1). When $p$ refers to a carbon atom which is not on the $y$-axis and $q$ refers to an oxygen atom $(pp\mid q^nq^n)$ may be expressed as

$$(pp\mid q^nq^n)=\cos^2\theta(pp\mid q^{\pi}q^{\pi})+\sin^2\theta(pp\mid q^{\sigma}q^{\sigma}), \tag{P1}$$

where $p$ is the $2p\pi$ AO of atom $p$ and $q^n$ is the $2p$ AO of atom $q$ nodal plane of which is perpendicular to the molecular plane and containing the $y$-axis. $q^{\pi}$ and $q^{\sigma}$ represent $2p$ AO's of atom $q$ whose nodal planes are perpendicular to the molecular plane and containing and perpendicular to the $pq$-direction, respectively. $\theta$ is an angle between $pq$-direction and the $y$-axis. It may be clear that it is for $(pp\mid q^{\pi}q^{\pi})$ in Eq. (P1) that the extrapolation formula presented in this paper (see especially Eq. (17)) applies. For $(pp\mid q^{\sigma}q^{\sigma})$ it can be shown that following extrapolation formula applies from a similar reasoning as that used by Pariser and Parr (ref. 10b) for $(pp\mid qq)$:

$$(pp\mid q^{\sigma}q^{\sigma})-(1/2)\{(pp\mid p^{\sigma}p^{\sigma})+(qq\mid q^{\sigma}q^{\sigma})\}=a''r^2+b''r. \tag{P2}$$

One-center integrals $(pp\mid p^{\sigma}p^{\sigma})$ and $(qq\mid q^{\sigma}q^{\sigma})$ are identical with $(pp\mid p^{\pi}p^{\pi})$ and $(qq\mid q^{\pi}q^{\pi})$, respectively. If $a''$ and $b''$ are determined from values of one-center integrals derived from atomic spectral data and the theoretical values of $(pp\mid q^{\sigma}q^{\sigma})$ at 2.80 and 4.14 Å Eq. (P2) becomes

$$(pp\mid q^{\sigma}q^{\sigma})\text{ (in ev)}=11.23-2.81589r+0.227815r^2, \tag{P3}$$

where $r$ is in Å. We use Eq. (P3) in obtaining $(pp\mid q'q')$ when $r_{pq}<2.80$ Å and when $r_{pq}>2.80$ Å we use theoretical value for $(pp\mid q^{\sigma}q^{\sigma})$. Thus, using the molecular dimension shown in Fig. 2, it follows that

$$(C'_1C'_1\mid O^n{}_1O^n{}_1)=5.691\text{ ev},$$
$$(C'_2C'_2\mid O^n{}_1O^n{}_1)=3.958\text{ ev}.$$

These values should be used instead of those included in Table III. Fortunately, the changes in the value of these integrals over AO's are small. Moreover, it can be shown that such a change does not affect the energies of those configurations which are produced by "pure $\pi-\pi$ transitions" from the ground configuration when the energy of the ground configuration is taken as the reference. Even in the other cases changes of the configurational energies amount only to a few thousandths which are within the computational errors. Therefore, corrections of Fig. 3 may be unnecessary.

15) The following abbreviations are used:

$$(4!)^{-\frac{1}{2}}\,\mathrm{Det}\{(\chi_p\alpha)^1(\chi_q\beta)^2(\chi_p^n\alpha)^3(\chi_q^n\beta)^4\}$$
$$=(1/4!)^{\frac{1}{2}}\begin{vmatrix}(\chi_p\alpha)^1(\chi_q\beta)^1(\chi_p^n\alpha)^1(\chi_q^n\beta)^1\\(\chi_p\alpha)^2(\chi_q\beta)^2(\chi_p^n\alpha)^2(\chi_q^n\beta)^2\\(\chi_p\alpha)^3(\chi_q\beta)^3(\chi_p^n\alpha)^3(\chi_q^n\beta)^3\\(\chi_p\alpha)^4(\chi_q\beta)^4(\chi_p^n\alpha)^4(\chi_q^n\beta)^4\end{vmatrix},\text{ etc.},$$

where $\alpha$ and $\beta$ are the usual spin functions and should not be confused with the similar symbols for the core integrals. Superscript $i$ ($i$=1,2,3,4) indicates that the variable in the spin orbital function to which $i$ refers is the coordinate of the $i$-th electron.

$(pp \mid q^n q^n)$ must be extrapolated using atomic data just as for $(pp \mid qq)$.

Let us consider a four-electron double $\pi$-bond between atoms $p$ and $q$. The covalent structure with two good bonds is expressed as a superposition of the following wave functions[15]:

$$\left.\begin{aligned}\Phi_1 &= (4!)^{-\frac{1}{2}}\mathrm{Det}\{(\chi_p\alpha)^1(\chi_q\beta)^2(\chi_p^n\alpha)^3(\chi_q^n\beta)^4\}\\ \Phi_2 &= (4!)^{-\frac{1}{2}}\mathrm{Det}\{(\chi_p\alpha)^1(\chi_q\beta)^2(\chi_p^n\beta)^3(\chi_q^n\alpha)^4\}\\ \Phi_3 &= (4!)^{-\frac{1}{2}}\mathrm{Det}\{(\chi_p\beta)^1(\chi_q\alpha)^2(\chi_p^n\alpha)^3(\chi_q^n\beta)^4\}\\ \Phi_4 &= (4!)^{-\frac{1}{2}}\mathrm{Det}\{(\chi_p\beta)^1(\chi_q\alpha)^2(\chi_p^n\beta)^3(\chi_q^n\alpha)^4\}\end{aligned}\right\} \quad (7)$$

While the singly ionic structure with unit positive charge on atom $q$ and with a single covalent bond is described in terms of the following functions:

$$\left.\begin{aligned}\Phi_5 &= (4!)^{-\frac{1}{2}}\mathrm{Det}\{(\chi_p\alpha)^1(\chi_q\beta)^2(\chi_p^n\alpha)^3(\chi_p^n\beta)^4\}\\ \Phi_6 &= (4!)^{-\frac{1}{2}}\mathrm{Det}\{(\chi_p\beta)^1(\chi_q\alpha)^2(\chi_p^n\alpha)^3(\chi_p^n\beta)^4\}\\ \Phi_7 &= (4!)^{-\frac{1}{2}}\mathrm{Det}\{(\chi_p\alpha)^1(\chi_p\beta)^2(\chi_p^n\alpha)^3(\chi_q^n\beta)^4\}\\ \Phi_8 &= (4!)^{-\frac{1}{2}}\mathrm{Det}\{(\chi_p\alpha)^1(\chi_p\beta)^2(\chi_p^n\beta)^3(\chi_q^n\alpha)^4\}\end{aligned}\right\} \quad (8)$$

the reversed singly ionic structure with unit positive charge on atom $p$ and not on $q$ is described by the following functions:

$$\left.\begin{aligned}\Phi_9 &= (4!)^{-\frac{1}{2}}\mathrm{Det}\{(\chi_p\alpha)^1(\chi_q\beta)^2(\chi_q^n\alpha)^3(\chi_q^n\beta)^4\}\\ \Phi_{10} &= (4!)^{-\frac{1}{2}}\mathrm{Det}\{(\chi_p\beta)^1(\chi_q\alpha)^2(\chi_q^n\alpha)^3(\chi_q^n\beta)^4\}\\ \Phi_{11} &= (4!)^{-\frac{1}{2}}\mathrm{Det}\{(\chi_q\alpha)^1(\chi_q\beta)^2(\chi_p^n\alpha)^3(\chi_q^n\beta)^4\}\\ \Phi_{12} &= (4!)^{-\frac{1}{2}}\mathrm{Det}\{(\chi_q\alpha)^1(\chi_q\beta)^2(\chi_p^n\beta)^3(\chi_q^n\alpha)^4\}\end{aligned}\right\} \quad (9)$$

On the other hand

$$\left.\begin{aligned}\Phi_{13} &= (4!)^{-\frac{1}{2}}\mathrm{Det}\{(\chi_p\alpha)^1(\chi_p\beta)^2(\chi_p^n\alpha)^3(\chi_p^n\beta)^4\}\\ &\text{and}\\ \Phi_{14} &= (4!)^{-\frac{1}{2}}\mathrm{Det}\{(\chi_q\alpha)^1(\chi_q\beta)^2(\chi_q^n\alpha)^3(\chi_q^n\beta)^4\}\end{aligned}\right\} \quad (10)$$

represent doubly ionic structures $p^{--}q^{++}$ and $p^{++}q^{--}$, respectively.

In Eqs. (7)—(10) $\chi_p$, $\chi_q$, $\chi_p^n$ and $\chi_q^n$ are "$\pi$-orbitals" of atoms $p$ and $q$, the nodal planes of $\chi_p$ and $\chi_q$ being perpendicular to those of $\chi_p^n$ and $\chi_q^n$. Since in this system

$$H = \sum_{i=1}^{4} H_{\mathrm{core}}(i) + (1/2)\sum_{i\neq j=1}^{4}(e^2/r_{ij}),$$

$$\int \chi_p^*(1)\,H_{\mathrm{core}}(1)\,\chi_p(1)\,\mathrm{d}v_1 = \int \chi_p^{n*}(1)\,H_{\mathrm{core}}(1)\,\chi_p^n(1)\,\mathrm{d}v_1 \equiv \alpha_p,$$

and

$$\int \chi_q^*(1)\,H_{\mathrm{core}}(1)\,\chi_q(1)\,\mathrm{d}v_1 = \int \chi_q^{n*}(1)\,H_{\mathrm{core}}(1)\,\chi_q^n(1)\,\mathrm{d}v_1 \equiv \alpha_q,$$

the matrix elements for the determination of the energy are

$$\left.\begin{aligned}H_{1,1} &= H_{2,2} = H_{3,3} = H_{4,4} = 2\alpha_p + 2\alpha_q\\ &\quad + 2(pp \mid qq) + 2(pp \mid q^nq^n)\\ &\quad + (pp \mid p^np^n) + (qq \mid q^nq^n)\\ &\quad - (1/2)(pp^n \mid pp^n) - (1/2)(qq^n \mid qq^n)\\ &\quad - (pq^n \mid pq^n)\\ H_{5,5} &= H_{6,6} = H_{7,7} = H_{8,8} = 3\alpha_p + \alpha_q\\ &\quad + (pp \mid qq) + (pp \mid pp) + 2(pp \mid p^np^n)\\ &\quad + 2(pp \mid q^nq^n) - (pp^n \mid pp^n)\\ &\quad - (pq^n \mid pq^n)\\ H_{9,9} &= H_{10,10} = H_{11,11} = H_{12,12} = \alpha_p + 3\alpha_q\\ &\quad + (pp \mid qq) + (qq \mid qq) + 2(pp \mid q^nq^n)\\ &\quad + 2(qq \mid q^nq^n) - (pq^n \mid pq^n)\\ &\quad - (qq^n \mid qq^n)\\ H_{13,13} &= 4\alpha_p + 2(pp \mid pp) + 4(pp \mid p^np^n)\\ &\quad - 2(pp^n \mid pp^n)\\ H_{14,14} &= 4\alpha_q + 2(qq \mid qq) + 4(qq \mid q^nq^n)\\ &\quad - 2(qq^n \mid qq^n)\end{aligned}\right\} \quad (11)$$

where $H_{i,i} = \int \Phi_i^* H \Phi_i \mathrm{d}v$.

From these equations one obtains

$$(1/2)(H_{5,5} + H_{9,9}) - H_{1,1} = (1/2)\{(pp \mid pp) + (qq \mid qq)\} - (pp \mid qq). \quad (12)$$

The left-hand side of this equation should become zero when $r_{pq}\to 0$. Therefore, the right-hand side of (12) may be represented as follows:

$$(pp \mid qq) - (1/2)\{(pp \mid pp) + (qq \mid qq)\} = ar^2 + br. \quad (13)$$

This equation is identical with that obtained by Pariser and Parr[10] and may be used for the determination of $(pp \mid qq)$ at moderate internuclear distances using the values of one-center integrals obtained from atomic data and $(pp \mid qq)$-values at

large internuclear distances calculated theoretically.

Moreover, one obtains from (11)

$$(H_{13,13}+H_{14,14})-2H_{1,1}=\{2(pp \mid pp)+2(qq \mid qq)-4(pp \mid qq)\}+\{2(pp \mid p^np^n)+2(qq \mid q^nq^n)-4(pp \mid q^nq^n)\}+\{2(pq^n \mid pq^n)-(pp^n \mid pp^n)-(qq^n \mid qq^n)\}. \quad (14)$$

Let us consider the case where $r_{pq}=0$. In this case, it holds that[15a]

$$(pq^n \mid pq^n)=(pp^n \mid qq^n). \quad (14')$$

Therefore the right-hand side of (14) becomes

$$-(3/2)\{2(pp \mid qq)-(pp \mid pp)-(qq \mid qq)\}-(5/2)\{2(pp \mid q^nq^n)-(pp \mid p^np^n)-(qq \mid q^nq^n)\}, \quad (15)$$

where the following relation which holds among integrals over Slater AO's was used:

$$2(pp^n \mid qq^n)=(pp \mid qq)-(pp \mid q^nq^n). \quad (16)$$

Since from (12) the first term of (15) becomes zero when $r_{pq}=0$, the second term of (15) should also be zero in this case, because the left-hand side of (14) becomes zero. Therefore, the approximate analytical expression of the following form may apply for the expression in the second bracket of (15):

$$(pp \mid q^nq^n)-(1/2)\{(pp \mid p^np^n)+(qq \mid q^nq^n)\}=a'r^2+b'r. \quad (17)$$

15a) Using Slater AO's it can be shown that this equality holds accurately only when $Z_p$ and $Z_q$ (the effective nuclear charges) are equal to each other. More generally we obtain when $r_{pq}=0$

$$\frac{(pq^n \mid pq^n)-(pp^n \mid qq^n)}{(pq^n \mid pq^n)}=1-\left\{\frac{4}{9}+\frac{1}{4}\left(\frac{Z_p}{Z_q}+\frac{Z_q}{Z_p}\right)+\frac{1}{36}\left(\frac{Z_p^2}{Z_q^2}+\frac{Z_q^2}{Z_p^2}\right)\right\}, \quad (N\,1)$$

if we use Slater AO's and we assume that the effective nuclear charge for $\chi_p$ is equal to that for $\chi_p^n$ and the same applies to $\chi_q$ and $\chi_q^n$. If $Z_p=Z_q$ the right-hand side of (N 1) becomes zero, therefore $(pq^n \mid pq^n)$ is exactly equal to $(pp^n \mid qq^n)$ as stated above. It is true that in the heteropolar case ($Z_p \neq Z_q$) the right-hand side of (N 1) is not equal to zero, but it is nearly equal to zero. For example, if we take the carbon and fluorine atoms as $p$ and $q$, respectively, the right-hand side of (N 1) becomes $-0.0827$, using $Z_C=3.25$ and $Z_F=5.20$. This is an extremely heteropolar case and the right-hand side of (N 1) is usually much smaller. Moreover, in the right-hand side of (14) $(pp^n \mid pp^n)$ is much smaller than either $(pp \mid pp)$ or $(pp \mid p^np^n)$, $(qq^n \mid qq^n)$ is much smaller than either $(qq \mid qq)$ or $(qq \mid q^nq^n)$ and $(pq^n \mid pq^n) \simeq (pp^n \mid qq^n)$ is much smaller than either $(pp \mid qq)$ or $(pp \mid q^nq^n)$. Therefore the use of (14') does not bring any serious errors in the arguments for the validity of (17).

Equation (17) may be used to determine $(pp \mid q^nq^n)$ in just the same way as (13) was used for $(pp \mid qq)$.

## Evaluation of the Coulomb Integrals Over AO's

In order to calculate the integrals which are needed in the calculation of the energy levels of $p$-benzoquinone from Eqs. (13) and (17), one-center integrals of the type $(pp \mid pp)$ and $(pp \mid p^np^n)$ must be evaluated, where $p$ denotes the carbon or the oxygen atoms. The values of these integrals for the oxygen atom were taken from Fumi and Parr's paper[16], where these were obtained from the analysis of the atomic spectral data.

One-center integrals over carbon atomic orbitals were determined from an analysis of the valence states of C, $C^+$ and $C^-$. The energies of these valence states were obtained by Skinner and Pritchard[17] from the Mulliken-type treatment of the atomic spectral data. The location of these valence states in energy is given in Table I, taking the ground state of the neutral carbon atom as reference.

TABLE I
ENERGIES OF SOME OF THE SPECTROSCOPIC AND VALENCE STATES OF C, $C^+$ AND $C^-$ (eV.)

| State | Energy[a] |
|---|---|
| $C^+(syz,\ V_3)$ | 19.68 |
| $C^+(s^2p,\ ^2P)$ | 11.26 |
| $C(sxyz,\ V_4)$ | 8.14 |
| $C^-(sx^2yz,\ V_3)$ | 7.68 |
| $C(s^2p^2,\ ^3P)$ | 0.00 |
| $C^-(s^2p^3,\ ^4S)$ | −1.7 |

a) The figures in this column were obtained from energies of valence states, ionization potentials and electron affinities listed in reference 17 in text taking the ground state of the neutral carbon atom as zero.

Let us consider the following equation relating the theoretical and the experimental energy change for the dissociation process:

$$2C(sxyz,\ V_4) \rightarrow C^+(syz,\ V_3)+C^-(sx^2yz,\ V_3)$$
$$\Delta E=(pp \mid pp)=11.08\ \text{eV}., \quad (18)$$

where the "experimental side" was taken from Table I. On the other hand, the following equation holds:

$$(pp^n \mid pp^n)=3G_2,$$

where $G_2$ is the Slater-Condon parameter,

16) F. G. Fumi and R. G. Parr, *J. Chem. Phys.*, **21**, 1864 (1953).
17) H. A. Skinner and H. O. Pritchard, *Trans. Faraday Soc.*, **49**, 1254 (1953).

TABLE II

MOLECULAR ORBITALS AND ORBITAL ENERGIES OF *p*-BENZOQUINONE

(Orbital energies are in units of $\beta_{CC\ benzene}$)

| | |
|---|---|
| $\phi_1(B_{1u}) = 0.47584(\chi_{O_1}+\chi_{O_2}) + 0.38010(\chi_{C_1}+\chi_{C_2}) + 0.25406(\chi_{C_1'}+\chi_{C_2'}+\chi_{C_1''}+\chi_{C_2''})$ | $\varepsilon_1 = 6.259$ |
| $\phi_2(B_{3g}) = 0.60166(\chi_{O_1}-\chi_{O_2}) + 0.34963(\chi_{C_1}-\chi_{C_2}) + 0.08877(\chi_{C_1'}-\chi_{C_2'}+\chi_{C_1''}-\chi_{C_2''})$ | $\varepsilon_2 = 6.041$ |
| $\phi_3(B_{1u}) = 0.47112(\chi_{O_1}+\chi_{O_2}) - 0.10035(\chi_{C_1}+\chi_{C_2}) - 0.36604(\chi_{C_1'}+\chi_{C_2'}+\chi_{C_1''}+\chi_{C_2''})$ | $\varepsilon_3 = 5.247$ |
| $\phi_4(B_{2g}) = 0.50000(\chi_{C_1'}+\chi_{C_2'}-\chi_{C_1''}-\chi_{C_2''})$ | $\varepsilon_4 = 5.02$ |
| $\phi_5(B_{3g}) = 0.35339(\chi_{O_1}-\chi_{O_2}) - 0.46481(\chi_{C_1}-\chi_{C_2}) - 0.28202(\chi_{C_1'}-\chi_{C_2'}+\chi_{C_1''}-\chi_{C_2''})$ | $\varepsilon_5 = 4.145$ |
| $\phi_6(B_{1u}) = 0.22730(\chi_{O_1}+\chi_{O_2}) - 0.58775(\chi_{C_1}+\chi_{C_2}) + 0.22680(\chi_{C_1'}+\chi_{C_2'}+\chi_{C_1''}+\chi_{C_2''})$ | $\varepsilon_6 = 2.874$ |
| $\phi_7(A_u) = 0.50000(\chi_{C_1'}-\chi_{C_2'}-\chi_{C_1''}+\chi_{C_2''})$ | $\varepsilon_7 = 2.78$ |
| $\phi_8(B_{3g}) = 0.11470(\chi_{O_1}-\chi_{O_2}) - 0.40212(\chi_{C_1}-\chi_{C_2}) + 0.40320(\chi_{C_1'}-\chi_{C_2'}+\chi_{C_1''}-\chi_{C_2''})$ | $\varepsilon_8 = 1.954$ |
| $\phi_{n1}(B_{3u}) = (1/\sqrt{2})(\chi_{O_1}^n+\chi_{O_2}^n)$ | $\varepsilon_{n1} = 5.46$[a] |
| $\phi_{n2}(B_{1g}) = (1/\sqrt{2})(\chi_{O_1}^n-\chi_{O_2}^n)$ | $\varepsilon_{n2} = 5.46$[a] |

a) The electronegativities of the carbon and the oxygen atoms are 2.5 and 3.5, respectively (L. Pauling, "The Nature of the Chemical Bond", Corronell University Press, Ithaca, New York (1940), p. 64). From this the coulomb integral at the oxygen atom is found to be 5.46 $\beta_{CC\ benzene}$ (see ref. 22 in text), which is taken as the value of the orbital energy of $\phi_{n1}$ and $\phi_{n2}$ since the resonance integrals between two oxygen atoms is expected to be small.

the value of which is determined to be 1,665 $cm^{-1}$ by Skinner and Pritchard[17] from the least square treatment of the energy levels of the carbon atom. Thus, one obtains

$$(pp^n \mid pp^n) = 0.619\ \text{eV}. \tag{19}$$

From (18) and (19) and using (16) one obtains

$$(pp \mid p^np^n) = 9.84\ \text{eV}.$$

All the coulomb integrals over AO's were calculated for $r_{pq} > 2.80$ Å from Roothaan's formula[18,19] using the effective nuclear charge of 3.25 and 4.55 for the carbon and oxygen atoms, respectively. For $r_{pq} < 2.80$ Å, they were obtained from Eqs. (13) and (17) in which the coefficients $a$, $b$, $a'$ and $b'$ were obtained from the one-center integral values obtained above and theoretically-calculated $(pp \mid qq)$- and $(pp \mid q^nq^n)$- values at $r_{pq} = 2.80$ and 4.14 Å. Thus the following formulas were obtained:

$$\begin{aligned}
&(\text{CC} \mid \text{OO}) = 12.80 - 3.8837\,r + 0.39142\,r^2 \\
&(\text{CC} \mid \text{O}^n\text{O}^n) = 11.23 - 2.9506\,r + 0.25760\,r^2 \\
&(\text{CC} \mid \text{C}'\text{C}')^{20} = 11.08 - 2.9226\,r + 0.26203\,r^2
\end{aligned} \tag{20}$$

where $r$ is the internuclear distance in Å and the values of the integrals may be obtained in eV.

18) C. C. J. Roothaan, *J. Chem. Phys.*, **19**, 1445 (1951).

19) See Appendix I.

20) C′ denotes the carbon atom different from that which is represented by C.

## Application to Para-benzoquinone

In order to apply the present method to a particular molecule, MO's must be expressed linearly in terms of AO's. As we are neglecting the configuration interaction, the choice of the MO's may be important. From the results of previous works on hydrocarbons the recommended MO to be used is that which is self-consistent for the ground state or that which is derived from the naive Hückel-type treatment[11,12]. For simplicity we use the latter type of MO. Of course, in contrast with the case of hydrocarbons, in the case of heteromolecules such as *p*-benzoquinone these MO's will be dependent on the assumed values of $\alpha$'s and $\beta$'s[21]. The calculation of the orbital coefficient was made using the assumptions described elsewhere[22]. The MO's thus obtained are shown in Table II where the designation of the atoms given in Fig. 1 are used. The designation of the coordinate axes is also given in the figure. Then, the symmetry notations are the same as those given by Herzberg[23]. In Table II the orbital energies are also listed in units of $\beta_{CC\ benzene}$[21].

Coulomb integrals over AO's were determined as described above and are shown in Table III, the values of the internuclear distances used being shown in Fig. 2.

21) $\alpha$'s and $\beta$'s mentioned here are the coulomb and the resonance integrals used in the naive MO method and should not be confused with the core integrals in Pariser and Parr's scheme.

22) T. Anno and A. Sadô, This Bulletin, **28**, 350 (1955).

23) G. Herzberg, "Infrared and Raman Spectra of Polyatomic Molecules", D. Van Nostrand Co., New York (1945), p. 108.

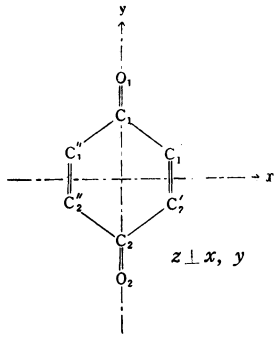



Fig. 1. Designation of the atoms and the coordinate axes in *p*-benzoquinone.

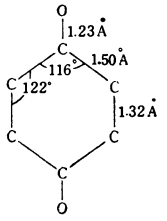



Fig. 2. Internuclear distances and bond angles in *p*-benzoquinone[a].

a) S. M. Swingle, *J. Am. Chem. Soc.*, **76**, 1409 (1954).

TABLE III

THE VALUES OF THE VALENCE-STATE IONIZATION POTENTIAL[a] AND THE COULOMB INTERACTION INTEGRALS OVER AO'S[b] (eV).

| | | | |
|---|---|---|---|
| $W^{C}_{2p\pi}$ | 11.54 | (CC \| $O^{n}O^{n}$)[c] | |
| $W^{O}_{2p\pi}$ | 17.21 | $r_{CO}$=1.23 Å | 7.991 |
| $W^{O}_{2pn}$ | 14.75 | 2.391 | 5.648 |
| (CC \| C'C') | | 3.5785 | 3.949 |
| $r_{CC'}$=0 Å | 11.08 | (OO \| O'O') | |
| 1.32 | 7.679 | $r_{OO'}$=0 Å | 14.52 |
| 1.50 | 7.286 | 5.370 | 2.667 |
| 2.468 | 5.463 | (OO \| O'$^{n}$O'$^{n}$) | |
| 2.544 | 5.341 | $r_{OO'}$=0 Å | 12.62 |
| 2.866 | 4.846 | 5.370 | 2.666 |
| (CC \| OO) | | | |
| $r_{CO}$=1.23 Å | 8.615 | | |
| 2.391 | 5.752 | | |
| 3.5785 | 3.951 | | |
| 4.140 | 3.430 | | |

a) Taken from reference 17 in text.
b) For $r<2.80$ Å the values are obtained from Eq. (20). For $r>2.80$ Å calculated values using Slater AO's with $Z_C=3.25$ and $Z_O=4.55$ are given. One-center integrals are obtained from the analysis of atomic spectral data.
c) Note added in proof—See footnote 14a.

The values of the core integrals $\alpha$'s were calculated from the following equation:

$$\alpha_{C_1}=\int\chi^{*}_{C_1}(1)H_{core}(1)\chi_{C_1}(1)\,dv_1$$
$$=-W^{C_1}_{2p\pi}-2(C_1C_1\mid O_1{}^{n}O_1{}^{n})$$
$$-2(C_1C_1\mid O_2{}^{n}O_2{}^{n})-(C_1C_1\mid O_1O_1)$$
$$-(C_1C_1\mid O_2O_2)-2(C_1C_1\mid C_1'C_1')$$
$$-2(C_1C_1\mid C_2'C_2')-(C_1C_1\mid C_2C_2)$$
$$-(O_1:C_1C_1)-(O_2:C_1C_1)$$
$$-2(C_1':C_1C_1)-2(C_2':C_1C_1)$$
$$-(C_2:C_1C_1),$$

$$\alpha_{C_1'}=\int\chi^{*}_{C_1'}(1)H_{core}(1)\chi_{C_1'}(1)\,dv_1$$
$$=-W^{C_1'}_{2p\pi}-2(C_1'C_1'\mid O_1{}^{n}O_1{}^{n})$$
$$-2(C_1'C_1'\mid O_2{}^{n}O_2{}^{n})-(C_1'C_1'\mid O_1O_1)$$
$$-(C_1'C_1'\mid O_2O_2)-(C_1'C_1'\mid C_1C_1)$$
$$-(C_1'C_1'\mid C_2'C_2')-(C_1'C_1'\mid C_2C_2)$$
$$-(C_1'C_1'\mid C_1''C_1'')-(C_1'C_1'\mid C_2''C_2'')$$
$$-(O_1:C_1'C_1')-(O_2:C_1'C_1')$$
$$-(C_1:C_1'C_1')-(C_2':C_1'C_1')$$
$$-(C_2:C_1'C_1')-(C_1'':C_1'C_1')$$
$$-(C_2'':C_1'C_1'),$$

$$\alpha_{O_1}=\int\chi^{*}_{O_1}(1)H_{core}(1)\chi_{O_1}(1)\,dv_1$$
$$=-W^{O_1}_{2p\pi}-2(O_1O_1\mid O_1{}^{n}O_1{}^{n})$$
$$-2(O_1O_1\mid O_2{}^{n}O_2{}^{n})-(O_1O_1\mid O_2O_2)$$
$$-(O_1O_1\mid C_1C_1)-(O_1O_1\mid C_2C_2)$$
$$-2(O_1O_1\mid C_1'C_1')-2(O_1O_1\mid C_2'C_2')$$
$$-(O_2:O_1O_1)-(C_1:O_1O_1)$$
$$-(C_2:O_1O_1)-2(C_1':O_1O_1)$$
$$-2(C_2':O_1O_1),$$

$$\alpha^{n}_{O_1}=\int\chi^{n*}_{O_1}(1)H_{core}(1)\chi^{n}_{O_1}(1)\,dv_1$$
$$=-W^{O_1}_{2pn}-(O_1{}^{n}O_1{}^{n}\mid O_1{}^{n}O_1{}^{n})$$
$$-2(O_1{}^{n}O_1{}^{n}\mid O_2{}^{n}O_2{}^{n})-(O_1{}^{n}O_1{}^{n}\mid O_1O_1)$$
$$-(O_1{}^{n}O_1{}^{n}\mid O_2O_2)-(O_1{}^{n}O_1{}^{n}\mid C_1C_1)$$
$$-(O_1{}^{n}O_1{}^{n}\mid C_2C_2)-2(O_1{}^{n}O_1{}^{n}\mid C_1'C_1')$$
$$-2(O_1{}^{n}O_1{}^{n}\mid C_2'C_2')-(O_2:O_1{}^{n}O_1{}^{n})$$
$$-(C_1:O_1{}^{n}O_1{}^{n})-(C_2:O_1{}^{n}O_1{}^{n})$$
$$-2(C_1':O_1{}^{n}O_1{}^{n})-2(C_2':O_1{}^{n}O_1{}^{n}),$$

where $W^{q}_{2p\pi}$ and $W^{q}_{2pn}$ are the valence state ionization potentials of a $\pi$-electron and $n$-electron at atom $q$, respectively. These values of ionization potentials were obtained from Skinner and Pritchard's paper[17] and are also listed in Table III. $(q:pp)$ is the coulomb penetration integral and is defined by

$$(q:pp) = -\int U_q(1)\chi_p^*(1)\chi_p(1)\,d\nu_1,$$

where $U_q(1)$ is the potential due to neutral atom $q$. Penetration integrals were neglected throughout except when $p$ and $q$ refer to the nearest neighbors with each other. When $p$ and $q$ are the nearest neighbors, the values of this type of integrals were calculated theoretically[24].

$\beta_{pq}$ was neglected except in the case where $p$ refers to the nearest neighbor with $q$. When $p$ and $q$ refer to the nearest neighbors with each other, $\beta_{pq}$ may be determined semi-empirically. Kon[13] gave a functional form for $\beta_{CC}$ and $\beta_{CO}$ with respect to the internuclear distance defined in such a way as to fit the calculated energy levels with experiment. Although the theoretical representation of $\beta$[25] is slightly different depending on whether the $\pi$-electrons are considered explicitly or not, in our calculation $\beta$'s were calculated from this formula, because it can be shown that $\beta$ is approximately the same in both cases using Mulliken's approximation[26] for integrals.

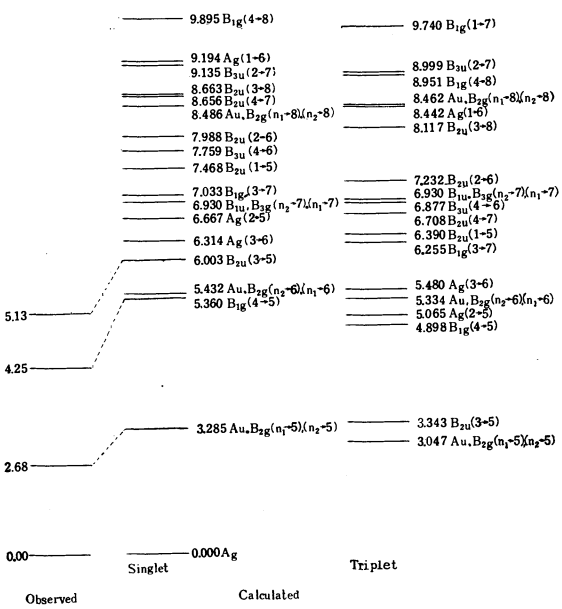



Fig. 3. Calculated and observed energy levels of $p$-benzoquinone.

The figure on the right of each level is the energy interval (in eV.) above the ground state and is followed by species notation of the state. On the right of the species notation the difference of the electron configuration from the ground state is indicated; e. g., ($n_1 \rightarrow 5$) indicates that the participating configuration is produced from the ground configuration with the excitation of an electron from $\phi_{n_1}$ (see Table II) to $\phi_5$.

Using the coulomb and core integrals over AO's the integrals over MO's are obtained from the MO's in LCAO form enbodied in Table II as described above. Energies of various electronic states may be obtained in the usual manner. The state energies thus obtained are shown in Fig. 3 diagramatically, the energy of the ground configuration being taken as reference. Only the singly-excited states which lie within 10 eV. above the ground state are given and the effect of the configuration interaction was neglected. Two singlets which result from doubly-excited configurations lie within this energy region, i. e., at 8.506 eV. ($A_u$, $B_{2g}$) and 7.495 eV. ($B_{1u}$, $B_{3g}$) above the ground state. It is to be noted that any one of $A_u$ states is found to be degenerate with one of $B_{2g}$ states. The same applies to $B_{1u}$ and $B_{3g}$ states. These degeneracies are accidental, so they are not exact but only approximate degeneracy. However, it can be shown that they persist even after the effect of the configuration interaction is taken into account.

## Discussion

The hexane solution of $p$-benzoquinone has three absorption regions in visible or the near ultraviolet; these are $\lambda_{max}=2400$ Å (5.13 eV., $\log \varepsilon_{max}=4.2$), $\lambda_{max}=2900$Å (4.25 eV., $\log \varepsilon_{max}=2.5$) and $\lambda_{max}=4600$Å (2.68 eV., $\log \varepsilon_{max}=1.2$[5]). The longest-wavelenth absorption band was assigned to an $n-\pi$ transition by McConnell[8] and Nagakura and Kuboyama[9] from the solvent effect on this band. From the MO point of view and from the comparison of the spectral data of various molecules containing CO group, McMurry[27] has also suggested this assignment. The shortest-wavelength one of the above mentioned absorptions has the extinction coefficient of 20,000, which shows that this absorption may be due to an allowed electronic transition. The remaining one is assigned to a $\pi-\pi$ transition from the solvent effect[8,9]. The extinction coefficient might suggest that this absorption would be due to an allowed electronic transition. The alternative

24) See Appendix II.

25) See footnote 11 in reference 10a and references cited there.

26) R. S. Mulliken, "Report on Molecular Orbital Theory", 1947-8 and 1948-9 ONR Reports of the Physics Department Spectroscopic Laboratory of the University of Chicago, Eqs. (63) and (154b).

27) H. L. McMurry, *J. Chem. Phys.*, **9**, 241 (1941).

assignment for this absorption is that it may be due to a forbidden transition and the fairly large extinction coefficient of it might be due to the proximity of this absorption to an allowed electronic transition. We prefer the latter assignment with some reservations.

From the above argument the observed bands at 2.68 eV. and 5.13 eV. may be assigned to the $^1A_g \rightarrow {}^1A_u$, $^1B_{2g}$ (nearly degenerate) and $^1A_g \rightarrow {}^1B_{2u}$ transitions, respectively. It is to be noted that the theory indicates that two electronic transitions are involved in 2.68-eV. absorption. The remaining absorption band at 4.25 eV. may be correlated with the calculated values of 5.432 eV. or 5.360 eV., both of which are predicted to correspond to forbidden transitions. As mentioned previously the solvent effect shows that this absorption may be due to a $\pi-\pi$ transition, so we correlate this absorption with the calculated value of 5.360 eV. rather than 5.432 eV.

One thing should be mentioned concerning the absorption spectrum of the *p*-benzoquinone crystal. If the assignment proposed above is correct the electronic transition corresponding to the band at 5.13 eV. is produced with the transition moment lying in the long-axis (axis connecting two oxygen atoms) of the *p*-benzoquinone molecule and it is interpreted that electronic transitions corresponding to 2.68- and 4.25-eV. bands are made allowed through the vibrational-electronic interaction with 5.13-eV. transition. This is consistent with the result of Fixl and Schauenstein[6] on the *p*-benzoquinone crystal, since they concluded that 2.68-eV. absorption is polarized along the long axis. However, recently Sidman[7] has also investigated the *p*-benzoquinone crystal in a wider wavelength region than Fixl and Schauenstein and arrived at the opposite conclusion. Although, Sidman could not investigate the region around 5.13 eV., he inferred that this absorption is polarized along the short axis of the molecule and the excited state of this absorption has the symmetry of $B_{3u}$ (in our notation) from the polarization experiment at 2.68- and 4.25-eV. absorption regions. Then, our assignment concerning the symmetry of the first allowed electronic transition of the *p*-benzoquinone molecule is apparently inconsistent with Sidman's result.

As for the absorptions appearing in the visible region Sidman[7] reported that at least three electronic transitions exist in this region, all of which are $n-\pi$ transitions. He assigned two of these transitions to singlet-singlet absorptions. These assignments are in agreement with the present theory in the fact that there exists a pair of nearly degenerate electronic states, transitions to which from the ground state lie in the visible region. The third absorption region found by Sidman[7] was very weak and lay in the longer wavelength region than the above-mentioned two absorptions, although the separation from these two absorptions was small. Sidman[7] assigned it to a singlet-triplet $n-\pi$ transition. This is also consistent with the present calculation.

In conclusion, although there are some inconsistencies between the theory and the experiments, the results of the present calculation are encouraging. The reason for the inconsistencies is not clear at present, since the configuration interaction is neglected on the theoretical side and the vibrational analysis and the polarization experiments have not been completed on the experimental side. The oriented gas model as applied to the pure *p*-benzoquinone crystal may lead us to false conclusions[28].

## Summary

A semi-empirical MO method proposed by Pariser and Parr was extended, taking account of the non-bonding electrons at the heteroatoms explicitly as well as $\pi$-electrons. The electronic states of *p*-benzoquinone were calculated neglecting configuration interactions.

The authors express their sincere thanks to Professor S. Imanishi for his encouragement throughout this work and for his helpful suggestions. Discussions with the members of authors' laboratory are also acknowledged.

T. A. and A. S. are also indebted to the Ministry of Education for the grant-in-aid given to them.

## Appendix I: Calculation of Coulomb Integrals over AO's

In the course of calculations reported in this paper we have calculated several coulomb integrals over Slater AO's using Roothaan's formula[18]. In Roothaan's method coulomb integrals over AO's are expressed in terms of "basic integrals".

28) D. S. McClure, *J. Chem. Phys.*, **22**, 1668 (1954); **24**, 1 (1956).

TABLE IV

THE VALUES OF BASIC COULOMB INTEGRALS (ATOMIC UNIT[a])

(IV A) $a$: Carbon with effective nuclear charge of 3.25.
$b$: Oxygen with effective nuclear charge of 4.55.

| $r$(Å) | $[3S_a \mid 3S_b]$ | $[3S_a \mid 3D\Sigma_b]$ | $[3D\Sigma_a \mid 3S_b]$ | $[3D\Sigma_a \mid 3D\Sigma_b]$ | $[3D\Delta_a \mid 3D\Delta_b]$ |
|---|---|---|---|---|---|
| 1.1615 | $4.2535^{-1}$[b] | $7.8303^{-3}$ | $1.7041^{-2}$ | $6.6494^{-4}$ | $7.5582^{-4}$ |
| 1.230 | $4.0761^{-1}$ | $7.5598^{-3}$ | $1.6203^{-2}$ | $7.2766^{-4}$ | $6.3216^{-4}$ |
| 2.391 | $2.2127^{-1}$ | $2.0572^{-3}$ | $4.0449^{-3}$ | $2.0847^{-4}$ | $3.8425^{-5}$ |
| 2.800 | $1.8902^{-1}$ | $1.3002^{-3}$ | $2.5501^{-3}$ | $1.0276^{-4}$ | $1.7620^{-5}$ |
| 3.5785 | $1.4791^{-1}$ | $6.2514^{-4}$ | $1.2253^{-3}$ | $3.1025^{-5}$ | $5.1797^{-6}$ |
| 4.140 | $1.2785^{-1}$ | $4.0377^{-4}$ | $7.9141^{-4}$ | $1.4994^{-5}$ | $2.4994^{-6}$ |

(IV B) $a$, $b$: Carbon with effective nuclear charge of 3.25.

| $r$(Å) | $[3S_a \mid 3S_b]$ | $[3S_a \mid 3D\Sigma_b]$ | $[3D\Sigma_a \mid 3D\Sigma_b]$ | $[3D\Delta_a \mid 3D\Delta_b]$ |
|---|---|---|---|---|
| 1.320 | $3.7291^{-1}$ | $1.0619^{-2}$ | $5.7500^{-4}$ | $7.5658^{-4}$ |
| 1.500 | $3.3848^{-1}$ | $9.5678^{-3}$ | $7.0566^{-4}$ | $5.0462^{-4}$ |
| 2.468 | $2.1418^{-1}$ | $3.5880^{-3}$ | $3.1092^{-4}$ | $6.3199^{-5}$ |
| 2.544 | $2.0786^{-1}$ | $3.3044^{-3}$ | $2.7790^{-4}$ | $5.4652^{-5}$ |
| 2.800[c] | $1.8898^{-1}$ | $2.5246^{-3}$ | $1.8879^{-4}$ | $3.4379^{-5}$ |
| 2.866 | $1.8463^{-1}$ | $2.3594^{-3}$ | $1.7060^{-4}$ | $3.0576^{-5}$ |
| 2.910 | $1.8185^{-1}$ | $2.2574^{-3}$ | $1.5956^{-4}$ | $2.8365^{-5}$ |
| 4.140 | $1.2785^{-1}$ | $7.9133^{-4}$ | $2.9354^{-5}$ | $4.8986^{-6}$ |

(IV C) $a$, $b$: Oxygen with effective nuclear charge of 4.55.

| $r$(Å) | $[3S_a \mid 3S_b]$ | $[3S_a \mid 3D\Sigma_b]$ | $[3D\Sigma_a \mid 3D\Sigma_b]$ | $[3D\Delta_a \mid 3D\Delta_b]$ |
|---|---|---|---|---|
| 5.370 | $9.8566^{-2}$ | $1.8502^{-4}$ | $2.0838^{-6}$ | $3.4730^{-7}$ |

a) Atomic unit: energy in $e^2/a_H = 27.204$ eV.
b) $4.2535^{-1}$ is the abbreviation of $4.2535 \times 10^{-1}$.
c) Interpolated.

We shall give here the values of these basic integrals rather than the integrals over AO's. These basic integrals give quickly the values of coulomb integrals over $2s$ or $2p$ AO's of respective atoms using Roothaan's formula. The results are shown in Table IV, the notations being the same as those used by Roothaan.

## Appendix II: Calculation of Coulomb Penetration Integrals

The potential of electron 1 due to a neutral carbon atom Uc(1) is represented by

$$\begin{aligned} U_C(1) = U_C^{4+}(1) &+ \int \mid 2s_C(2) \mid^2 (e^2/r_{12})\,dv_2 \\ &+ \int \mid 2p\sigma_C(3) \mid^2 (e^2/r_{13})\,dv_3 \\ &+ \int \mid 2p\pi_C(4) \mid^2 (e^2/r_{14})\,dv_4 \\ &+ \int \mid 2p\bar{\pi}_C(5) \mid^2 (e^2/r_{15})\,dv_5, \end{aligned} \qquad (A\,1)$$

where $U_C^{4+}(1)$ is the potential due to carbon nucleus plus two $1s$ electrons and is approximated by

$$U_C^{4+}(1) = -(4e^2/r_{C1}),$$

in which $r_{C1}$ is the distance between the carbon nucleus and the electron 1. $2s_C$, $2p\sigma_C$, $2p\pi_C$ and $2p\bar{\pi}_C$ are the carbon AO's 2p$\pi$ and $2p\bar{\pi}$ are $\pi$-orbitals whose nodal planes are perpendicular to each other.

On the other hand, the potential of electron 1 due to neutral oxygen atom $U_O(1)$ is represented by

$$\begin{aligned} U_O(1) = U_O^{6+}(1) &+ 2\int \mid 2s_O(2) \mid^2 (e^2/r_{12})\,dv_2 \\ &+ \int \mid 2p\sigma_O(3) \mid^2 (e^2/r_{13})\,dv_3 \\ &+ \int \mid 2p\pi_O(4) \mid^2 (e^2/r_{14})\,dv_4 \\ &+ 2\int \mid 2p\bar{\pi}_O(5) \mid^2 (e^2/r_{15})\,dv_5, \end{aligned} \qquad (A2)$$

where $U_O^{6+}(1)$ is the potential due to oxygen nucleus plus $1s$ electrons and is approximated by

$$U_O^{6+}(1) = -(6e^2/r_{O1}),$$

the notations being analogous to those in (A 1).

Therefore, coulomb pentration integrals are expressed as

$$\begin{aligned}
&\int U_C(1)\chi_q^*(1)\chi_q(1)\,dv_1 \equiv -(C : qq)\\
&= -4(C \mid qq) + (2s_C 2s_C \mid qq)\\
&\quad + (2p\sigma_C 2p\sigma_C \mid qq) + (2p\pi_C 2p\pi_C \mid qq)\\
&\quad + (2p\bar{\pi}_C 2p\bar{\pi}_C \mid qq)\\
&\int U_O(1)\chi_q^*(1)\chi_q(1)\,dv_1 \equiv -(O : qq)\\
&= -6(O \mid qq) + 2(2s_O 2s_O \mid qq)\\
&\quad + 2(2p\sigma_O 2p\sigma_O \mid qq) + (2p\pi_O 2p\pi_O \mid qq)\\
&\quad + 2(2p\bar{\pi}_O 2p\bar{\pi}_O \mid qq)
\end{aligned} \quad , \qquad \text{(A3)}$$

where $\chi_q$ is one of $2p$-orbitals and

$$(C \mid qq) \equiv \int (e^2/r_{C1})\chi_q^*(1)\chi_q(1)\,dv_1,$$

$$(O \mid qq) \equiv \int (e^2/r_{O1})\chi_q^*(1)\chi_q(1)\,dv_1,$$

which may be obtained from literatures[29]. The remaining terms in the right-hand side of Eq. (A3) are coulomb integrals over $2s$- or $2p$-AO's which may be obtained from the basic integrals as described in Appendix I. It is to be noted that in calculating the penetration integrals we have used theoretical values of these coulomb integrals in contrast with the case of the calculation of the electron interaction energy. This is because we have not obtained the values of coulomb integrals referring $2s$- or $2p\sigma$-AO's by the extrapolation using atomic spectral data.

*Department of Chemisty*
*Faculty of Science, Kyushu*
*University, Fukuoka*

29) H. J. Kopineck, *Z. Naturforsch.*, **5A**, 420 (1950).

# *The Surface of Copper-Nickel Catalyst. I. The Reaction between Hydrogen Chloride and the Catalyst*

By Toyosaburo TAKEUCHI and Masakazu SAKAGUCHI

(Received December 28, 1955)

Much work has been done by many researchers on the structure of copper catalysts containing a small amount of nickel as a component of the catalyst, prepared from copper and nickel salts, but much remains unexplored. Emmett and Skau[1], as the result of a study on hydrogenation of hydrocarbons, suggested that the nickel which was added to a copper catalyst might alter the crystal habit of copper, or collect preferentially on the surface of the powdery catalyst. From the results of measurements by Morris and Ross on magnetic susceptibility, Selwood[2] assumed that the surface of copper catalyst containing a small amount of nickel consists of microcrystals of pure nickel or of a nickel rich alloy. Recently, from a study by means of X-ray diffraction, Best and Russel[3] proposed that the catalyst should be an alloy.

The present investigation was undertaken to determine the state of the nickel which is contained in the catalyst — whether it exists as an alloy, or as microcrystals of pure nickel or as some other special form — by studying the reaction between hydrogen chloride and the catalyst, and also by the use of an electron microscope.

It is well known that hydrogen chloride reacts readily with copper and nickel, producing their chlorides, which are soluble in water. When hydrogen chloride is brought into contact with the copper-nickel catalyst, the reaction can be expected to start from the surface and extend to the interior of the catalyst. Two kinds of cations, $Cu^{++}$ and $Ni^{++}$, will be found in the solution obtained by washing the catalyst with water; and from this solution the amount of nickel on the surface of the catalyst can be estimated. With this view in mind, the experiments were carried out on a copper catalyst containing 1% nickel (copper-nickel), and also both on copper and on nickel, for the purpose of comparison of their reaction rates.

1) P. H. Emmett and N. Skau, *J. Am. Chem. Soc.*, **65**, 1029 (1943).
2) P. W. Selwood, "Magnetochemistry," Interscience Publishers, Inc., N. Y. (1943), p. 257.
3) J. Best and W. W. Russel, *J. Am. Chem. Soc.*, **76**, 838 (1954).

## Experimental

The copper catalyst was prepared from metallic copper supplied by Ishizu Chemical Co. by dissolving it in extra pure nitric acid, recrystallizing the copper nitrate thus obtained, drying the nitrate gently on the water bath, and finally igniting it at 500°C in air. The nickel catalyst was prepared from metallic nickel supplied by Kanto Chemical Co. in the same way as the copper catalyst. The copper catalyst containing 1% nickel was prepared by dissolving both nitrates in distilled water, then gently drying the mixture on a water bath, and igniting it at the same temperature as in the cases of the copper and nickel catalysts. The spectroscopic observation of the copper purified by recrystallization showed traces of Mg, Fe, Si, Mn, and Pb.

The hydrogen used for reduction was prepared by electrolysis of water, and purified by diffusion through a palladium thimble, preceded and succeeded by liquid oxygen traps. The ethylene used for the measurement of surface area was prepared by the dehydration of ethyl alcohol with sulfuric acid, and purified by vacuum distillation.

Hydrogen chloride was prepared from hydrochloric acid by heating it in a flask. The gas evolved by heating was condensed in a trap cooled by liquid oxygen, distilled in vacuum, and then dried by putting it in contact with phosphoric pentoxide for about two weeks.

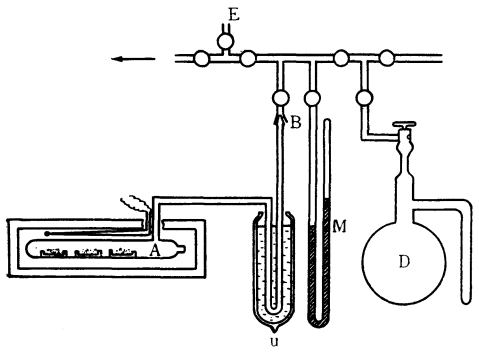



Fig. 1. Apparatus for the reaction between hydrogen chloride and catalysts.

Fig. 1 shows the main parts of the apparatus for examining the reaction between hydrogen chloride and the catalyst. In this figure, A is a reaction vessel of about 100 cc. in volume, and is made of pyrex glass. De Khotinsky cement was used to connect the reaction vessel and the part of the apparatus which is made of ordinary glass. U is a U-tube cooled by liquid oxygen or ice for the purpose of protecting the samples from being contaminated with vapors of grease and mercury. M is a mercury manometer, D a gas reservoir, and E a MacLeod gauge. 0.5 g. of nickel oxide, and 1.0 g. of their mixture were taken, and placed in pyrex boats side by side. The reduction of these oxides to corresponding catalysts with hydrogen was carried out at a constant temperature of 200°C for three weeks. After the reduction was completed, these samples were degassed at $10^{-5}$ mmHg at 200°C for three hours. Then the temperature was lowered to the reaction temperature of 150°C, the liquid oxygen bath of the U-tube was replaced with an ice bath, and a known quantity of hydrogen chloride was admitted into the reaction vessel. After a certain number of hours, the reaction was stopped by replacing the ice bath of the U-tube with the liquid oxygen bath to condense the residual hydrogen chloride.

The hydrogen chloride consumed by the reaction was determined by the measurement of the quantity of gas which was not condensed by the cooling with liquid oxygen, on the assumption that the gas was only hydrogen produced by the reaction.

After the reaction had been stopped, the vessel was cut open, and the samples were drawn out and were washed with distilled water until no chloride ion could be detected. To facilitate the analysis each solution was concentrated by heating on a water bath. Both metallic ions were analysed by means of the polarographic method, using ammonium chloride, ammonia, and tylose as supporting electrolytes. The suface areas of the catalysts were determined at −183°C by the B.E.T. method with ethylene using 17.6 Å$^2$/molec. as the cross-sectional area.

## Results

Table I shows the results of the measurements of the surface area of the catalysts. In this table, the amount of sample is represented by the weight of each original oxide. In Table II are shown the conditions and the results of the experiment on the reaction between hydrogen chloride and the catalyst. In this table runs (8) and (9) represent the results of the experiments which were carried out to observe the effect of reduction temperature on the reaction. $\Delta P$ denotes the pressure decrease of hydrogen chloride in the reaction, and S and M denote respectively the single component catalyst (copper and nickel) and the mixed catalyst (copper-nickel).

Column 6 shows the number of ions produced by the reaction of one g. of each catalyst. Column

TABLE I

SURFACE AREAS OF COPPER, COPPER-NICKEL, AND NICKEL CATALYST, OBTAINED BY THE B. E. T. METHOD, USING ETHYLENE

| Catalyst | Reduction temp. C° | Area $\times 10^4$ cm$^2$/g. |
|---|---|---|
| Cu | 200 | 0.69 |
| | 400 | 0.25 |
| Cu-Ni | 200 | 0.80 |
| | 400 | 0.34 |
| Ni | 200 | 49.2 |
| | 400 | 16.4 |

TABLE II

DATA ON THE REACTIONS BETWEEN HYDROGEN CHLORIDE AND CATALYSTS

| No. | Reduction temp. °C | Initial press. mmHg | Reaction time hr. | $\Delta P$ mmHg | Sample | No. of ion produced/g. | No. of ion produced/ No. of site | $N_{Cu}/N_{Ni}$ |
|---|---|---|---|---|---|---|---|---|
| 1 | 200 | 162.0 | 88 | 14.4 | S Cu | $1.1\times10^{20}$ | 15.6 | 14.2 |
| | | | | | S Ni | $7.1\times10^{20}$ | 1.1 | 1 |
| | | | | | M Cu | $1.5\times10^{21}$ | | |
| | | | | | M Ni | $2.3\times10^{19}$ | | |
| 2 | 〃 | 162.0 | 20 | 14.2 | S Cu | $2.4\times10^{20}$ | 33.6 | 15.3 |
| | | | | | S Ni | $1.4\times10^{21}$ | 2.2 | 1 |
| | | | | | M Cu | $8.0\times10^{20}$ | | |
| | | | | | M Ni | $2.7\times10^{19}$ | | |
| 3 | 〃 | 115.0 | 18 | 9.6 | S Cu | $5.8\times10^{19}$ | 8.0 | 13.3 |
| | | | | | S Ni | $3.6\times10^{20}$ | 0.6 | 1 |
| | | | | | M Cu | $5.3\times10^{19}$ | | |
| | | | | | M Ni | $5.6\times10^{19}$ | | |
| 4 | 〃 | 97.5 | 64 | 7.8 | S Cu | $4.4\times10^{19}$ | 6.0 | 12.0 |
| | | | | | S Ni | $3.5\times10^{20}$ | 0.5 | 1 |
| | | | | | M Cu | $2.7\times10^{19}$ | | |
| | | | | | M Ni | $1.2\times10^{19}$ | | |
| 5 | 〃 | 164.0 | 16 | 3.0 | S Cu | $7.0\times10^{18}$ | 1.0 | 16.6 |
| | | | | | S Ni | $3.9\times10^{19}$ | 0.06 | 1 |
| | | | | | M Cu | $1.2\times10^{19}$ | | |
| | | | | | M Ni | $1.2\times10^{19}$ | | |
| 6 | 〃 | 98.5 | 4 | 3.0 | S Cu | $1.3\times10^{19}$ | 1.8 | 20.0 |
| | | | | | S Ni | $5.4\times10^{19}$ | 0.09 | 1 |
| | | | | | M Cu | $2.3\times10^{20}$ | | |
| | | | | | M Ni | $4.8\times10^{19}$ | | |
| 7 | 〃 | 21.5 | 0.1 | 0.3 | S Cu | $2.2\times10^{17}$ | 0.03 | 15.0 |
| | | | | | S Ni | $1.4\times10^{18}$ | 0.002 | 1 |
| | | | | | M Cu | $2.3\times10^{18}$ | | |
| | | | | | M Ni | $1.6\times10^{19}$ | | |
| 8 | 400 | 81.0 | 15 | 1.0 | S Cu | $6.8\times10^{18}$ | 1.0 | 50.0 |
| | | | | | S Ni | $9.4\times10^{18}$ | 0.02 | 1 |
| | | | | | M Cu | $5.0\times10^{19}$ | | |
| | | | | | M Ni | $6.3\times10^{19}$ | | |
| 9 | 500 | 70.0 | 50 | 2.5 | S Cu | $4.0\times10^{18}$ | 0.5 | 50.0 |
| | | | | | S Ni | $7.1\times10^{18}$ | 0.01 | 1 |
| | | | | | M Cu | $5.1\times10^{19}$ | | |
| | | | | | M Ni | $1.9\times10^{19}$ | | |

7 shows the ratio of ions to the number of atoms existing on the surface of the catalyst. In these calculations the numbers of atoms on the surface of the catalysts were determined by using the assumption proposed by Yamaguchi[4], that the surface of the copper catalyst is composed of (100) faces, and that of the nickel catalyst (100) and (110) faces in the ratio of 2 to 1. The lattice constants used in these calculations were 3.608 Å for copper, and 2.49 and 3.52 Å for nickel respectively.

This shows that the number of ions produced per unit site is conspicuously larger for copper than for nickel, irrespective of the reaction time, in the ratio of about 15 to 1 in the case of every run except runs (8) and (9), where the catalysts were reduced at 400° and 500°C, and the ratio is far greater (about 50 to 1)*.

Fig. 2 shows the plot of the logarithm of the number of the ions attacked per g. of the catalysts against $\Delta P$. It is found that the amounts of the ions given by copper and nickel catalysts increase with $\Delta P$. Of particuler note is the fact that the number of nickel ions gained from the copper-nickel catalyst is in the range of $10^{19}$ to $10^{20}$, practically constant, independent of $\Delta P$, while the number of copper ion increases with increasing $\Delta P$ as in the case of the copper catalyst. The experiment on the catalysts reduced at 400° and 500°C gives the same results.

Plate 1 contains the electron micrographs of copper and copper-nickel catalysts. It is found that the copper-nickel catalyst has a conspicuously rough surface, especially after being reduced at 200°C; and many small particles of several hundred Å in diameter adhere to it. The surface of the copper catalyst is not so rough as that of copper-nickel; and the small particles which are found in the copper-nickel catalysts can scarcely be found on the copper. The surfaces of both the copper and copper-nickel catalysts are less rough when reduced at 400°C.

## Discussion

The results of the experiment on the reaction with hydrogen chloride show that

4) S. Yamaguchi, *Japan Chem. Meeting*, April (1949).

* The values of the surface area used in the calculation of the ratio on the samples reduced at 500°C were those reduced at 400°C, because the measurement of the area reduced at 500°C had not been carried out.

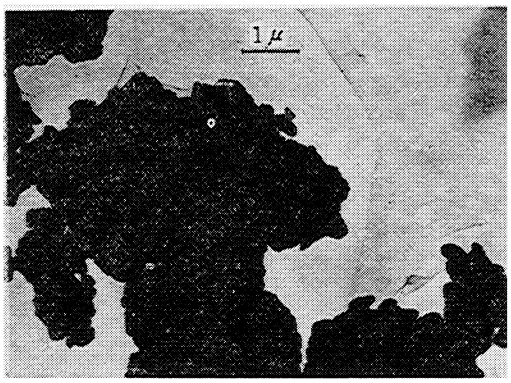



Photo. 1. Copper reduced at 200°C.

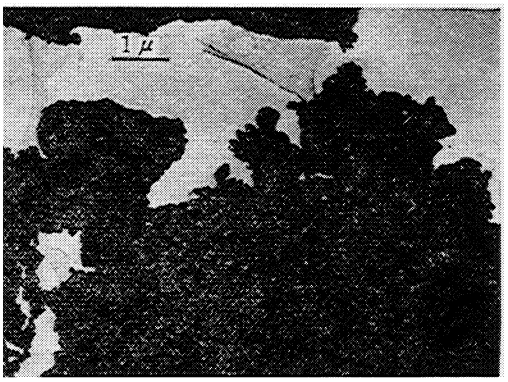



Photo. 3. Copper-nickel reduced at 200°C.

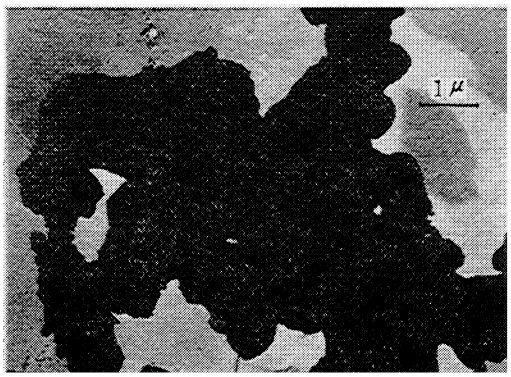



Photo. 2. Copper reduced at 400°C.

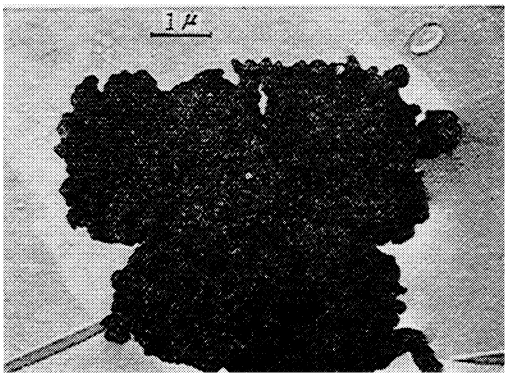



Photo. 4. Copper-nickel reduced at 400°C.

Plate 1. Electron micrographs of copper and copper-nickel catalyst.

the amount of copper ion obtained from the copper-nickel catalyst increases with the consumption of hydrogen chloride, whereas that of nickel ion remains roughly constant within the range $10^{19}$—$10^{20}$ ions, the average being $2.8\times10^{19}$ ions/g., which is 3% of the total amount of nickel contained in the catalyst. This amount may be considered as that existing on the surface of the catalyst.

Masing[5] has recently reported that the copper does not dissolve so easily when combined with nickel, as has generally been believed. Kuczynski[6] has found that a particle of nickel of about 0.3 mm. in diameter placed on a copper plate sinters to the plate, forming a very deep groove in the copper around the place of contact, when heated in hydrogen. According to these facts and our study[7] on this catalyst by means of electron diffraction by changing the accelerating potential of electron, it can be said that the nickel in the copper-nickel catalyst does not compose an alloy.

In plate 1 the electron micrograph of a copper-nickel catalyst reduced at 200°C shows many indentations and small particles, similar in appearance to that observed by Kuczynski. Accordingly, the small particles seem to be composed of nickel, being sintered to the copper surface at the place of contact.

The ratio of the total surface area of nickel particles to that of the copper-nickel catalyst can be obtained by the following procedure, based on the assumption that the amount of nickel obtained by the reaction with hydrogen chloride is all that exists on the surface of the catalyst, and that the size of nickel particles is the same as that of the particles of a pure nickel catalyst. The average diameter $\bar{D}$ of the particles of nickel can be obtained as follows, when they are assumed to be spherical:

$$\bar{D}=6/\rho S \qquad (1)$$

where $\rho$ is the density, and $S$ the surface area of nickel powder per g.

5) C. Masing, "Grundlagen der Metallkunde," Springer-Verlag.. Göttingen (1951), p. 57.
6) Kuczynski, *J. Metals*, **185**, 813 (1949), Kuczynski, *J. Metals*, **187**, 169 (1949).
7) S. Yamaguchi and T. Takeuchi, in *Kolloid Zeit.*, accepted for publication.

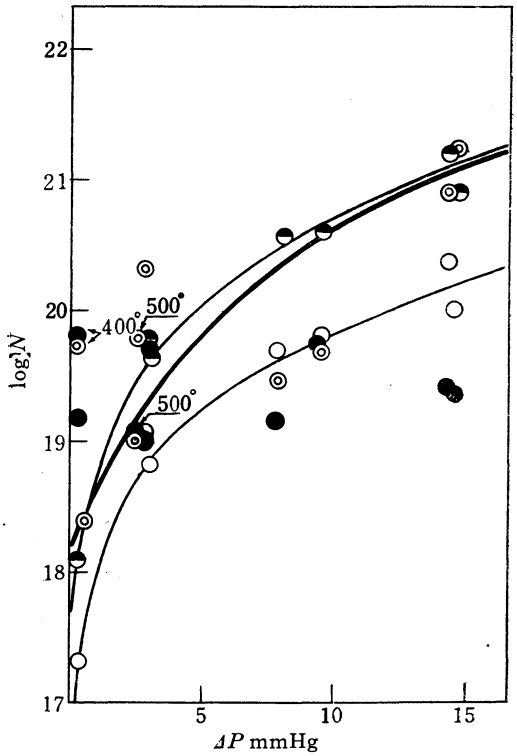



Fig. 2. Numbers of copper and nickel ions given by the reaction of hydrogen chloride with copper, nickel, and copper-nickel (per g.) as a function of $\Delta P$.
○ Cu-ion from Cu Catalyst.
◎ Cu-ion from Cu-Ni Catalyst.
◓ Ni-ion from Ni Catalyst.
● Ni-ion from Cu-Ni Catalyst.

The number of nickel atoms $\bar{n}$ in one particle is given as

$$\bar{n}=\pi\rho\bar{D}^3N/6M \qquad (2)$$

where $N$ is Avogadro's number, and $M$ the atomic weight of nickel.

The number, $A$, of particles of nickel on a surface per g. of the catalyst is given as

$$A=n/\bar{n} \qquad (3)$$

where $n$ is the total number of nickel atoms on a surface per g. of the catalyst.

The ratio $\gamma$ of the total surface area of nickel particles to the total of the catalyst is given as

$$\gamma=A\pi\bar{D}^2/S' \qquad (4)$$

where $S'$ is the specific surface area of copper-nickel catalyst. Assuming the value $62.4\times10^4$ cm.$^2$/g. to $S$, 8.85 to $\rho$, $\bar{D}$ is given as $1.1\times10^{-6}$ cm. from equation (1). Assigning the value $2.8\times10^{19}$ to $n$, and $1.0\times10^4$ cm.$^2$/g. to $S'$, $\gamma$ is given as 0.17 from (4)**.

According to the electron micrograph, the diameter of the particles on the catalyst can be estimated as $5\times10^{-6}$ cm. or less. This size is roughly in accord with the calculated value $\bar{D}$ mentoined above. This corroborates the supposition we have made on the structure of the copper-nickel catalyst.

The amount of nickel obtained from the catalyst remains constant, independent of the reduction temperature. This suggests that the nickel on the surface of the catalyst has already settled on the surface before the reduction of the catalyst set in ; and the amount of nickel on the surface might depend mainly on the way in which the mixture of copper and nickel nitrates is prepared.

## Summary

(1) The reactions of hydrogen chloride with copper, nickel and copper containing 1% nickel, and the observation by means of an electron microscope were carried out to determine the state of the nickel contained in the copper-nickel catalyst.

(2) The numbers of copper ion gained from the copper-nickel catalyst per g., after the reaction with hydrogen chloride, increase with the amount of consumption of hydrogen chloride used, whereas that of nickel ion is in the range of $10^{19}$—$10^{20}$/g., practically constant, independent of the amount of the consumption of hydrogen chloride.

(3) The electron micrograph shows that the copper-nickel catalyst has a conspicuously rough surface, and many particles of several hundred angstroms in diameter are scattered on the surface of the catalyst.

(4) The results of the hydrogen chloride reaction experiment suggest that about 3% of the total amount of nickel contained in the catalyst exists adhering to the surface of the catalyst, in the state of metallic nickel particles.

(5) The ratio of the total surface area of nickel particles on the surface of the catalyst to the total surface area of the copper-nickel catalyst is given as 17%, by the calculation using the assumption that the size of the nickel particle is the same as that of the pure nickel catalyst prepared in the same way.

*Faculty of Literature and Science*
*Toyama University, Toyama*

** The values of $S$ and $S'$ used in the calculation were obtained as follows, from Table 1 ;
$S=49\times10^4 M_{NiO}/M_{Ni}$ cm$^2$, $S'=8.0\times10^3 M_{CuO\cdot NiO}/M_{Cu\text{-}Ni}$ cm$^2$, where $M$ denotes atomic or molecular weight of material represented by the suffix.

# *The Surface of Copper-Nickel Catalyst. II. Adsorption of Hydrogen on Copper, Nickel, and Copper-Nickel Catalysts*

By Toyosaburo TAKEUCHI and Masakazu SAKAGUCHI

(Received January 17, 1956)

In the previous paper[1] the authors reported their study of the surface of copper catalyst containing 1% nickel, a study carried out by means of the reaction of hydrogen chloride with the catalyst and through the use of an electron microscope; and they proposed that a small percentage of the total amount of nickel contained in the catalyst occupies a comparatively large proportion of the surface area of the catalyst, existing in the metallic nickel state.

The present work was undertaken to determine the heat of adsorption of hydrogen on copper, nickel, and copper-nickel catalyst at high temperature in order to obtain further knowledge of the structure of copper-nickel catalysts.

It is well known that the heat of adsorption of a gas on a metal at high temperature (heat of chemisorption) is greatly dependent upon the kind of metal as well as upon the gas adsorbed on it. If the metallic nickel particles supposed to exist in a large proportion on the surface of the catalyst is in an exposed state, it is expected that the heat of adsorption of the gas on the catalyst (copper-nickel) may be the same or nearly the same as that for a pure nickel catalyst. If the nickel particles are covered with copper, the heat of adsorption can be expected to be the same as that of a pure copper catalyst. If copper-nickel alloy is formed (contradictory to the conclusion of the previous paper), and is in an exposed state, the heat of adsorption can be expected to differ from both that for nickel catalyst and that of copper catalyst.

With a view to ascertain whether the surface of the copper-nickel catalyst is composed of nickel, copper, or alloy, the adsorptions of hydrogen on copper, nickel, and copper-nickel (copper containing 1% nickel) catalysts have been investigated, and the heats of adsorption given by the adsorption isotherms for these three catalysts have been compared with one another. Further, the effects of reduction temperatures upon the surface area and upon the adsorption velocity of hydrogen have also been investigated.

## Experimental

The copper, nickel, copper-nickel, hydrogen, and ethylene which were used in this experiment were prepared in the same ways as in the experiment described in the previous report[1].

The apparatus used is shown in Fig. 1. In this figure, A is the reaction vessel of about 30 cc. volume. B is the U-tube which is cooled by liquid oxygen throughout the whole process of the reduction of the catalyst and the adsorption experiment, for the purpose of protecting the catalyst from being contaminated by grease or mercury vapor. C is the MacLeod gauge which can measure pressures as low as $10^{-6}$ mmHg. D is a 40 cc. messburette calibrated to 0.1 cc. E is the mercury reservoir connected to the burette and gas reservoirs. F and G are reservoirs for hydrogen and ethylene, respectively.

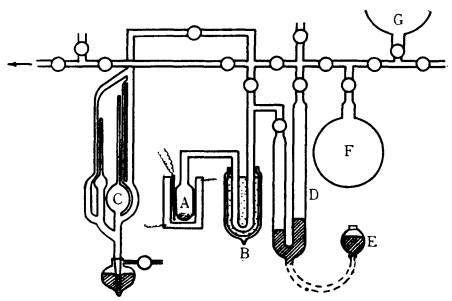



Fig. 1. Apparatus for adsorption of hydrogen on copper, copper-nickel, and nickel catalysts.

In the Knudsen pressure range, the relationship between the pressure $P_1$ of the reaction vessel A at the room temperature $T_1$ and $P_2$ at the reaction temperature $T_2$ is given as

$$P_1/P_2=\sqrt{T_1}/\sqrt{T_2}$$

In this experiment the corrected value of pressure $P_2$ was obtained empirically according to the method used by Kwan[2], because of the complexity of the temperature distribution of the apparatus, which was heated partially in the furnace and cooled partially by liquid oxygen.

1) Part I, preceding paper.

2) T. Kwan, *J. Research Inst. Catalysis*, Hokkaido Univ., **1**, 81 (1949).

The quantities of the samples which were admitted into the reaction vessel were 2.0 g. for copper oxide and copper-nickel oxide, and 0.5 g. for nickel oxide. Reduction in hydrogen gas at a pressure of several cmHg was continued for three weeks at 200°C. In no case was there any decrease of hydrogen after about two weeks. Previous to the experiment of adsorption, the samples had been degassed at $10^{-5}$ mmHg for three hours at a constant temperature of 200°C.

The equilibrium pressure on each catalyst was determined as follows: After the admission of hydrogen into the reaction vessel, rapid decrease in pressure was observed with every catalyst. With nickel catalyst the pressure, after the first ten minutes of rapid decrease, was found to be constant for several hours, suggesting that the adsorption equilibrium had been rapidly attained; whereas with copper and copper-nickel catalysts, it took one or two days until the pressure became apparently constant.

In the cases of nickel and copper catalysts each equilibrium pressure was determined by the procedure used by Kwan[2]. That is, when the pressure attained a constant value, the temperature was lowered or raised, then was kept constant until the pressure attained a constant value; then the initial temperature was restored. At this initial temperature the initial equilibrium pressure was reached rapidly on nickel and could easily be determined, but it took about one or two hours on copper.

In the case of copper-nickel catalyst, changing the pressure by raising the temperature was not so simple as in the cases of copper and nickel catalysts. When the temperature was raised from 100° to 130°C, it was found that the pressure increased for a time, then decreased gradually to a constant value; and when the temperature change was repeated, the pressure which had apparently become stable at each temperature, attained a constant value lower than the former one. The difference in pressures between the system immediately after the attainment of the temperature and that in the steady state was found to diminish gradually until it became hardly recognizable, as shown in Fig. 2. The authors define the equilibrium pressure with reference to this final state.

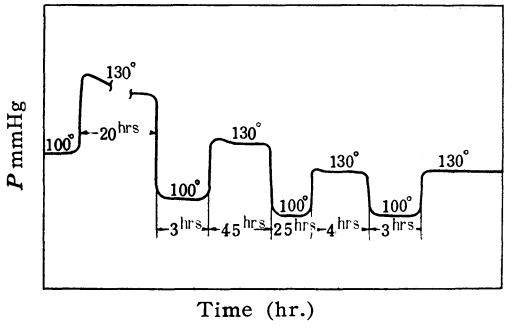



Fig. 2. Pressure change of hydrogen on copper-nickel catalyst on raising and lowering temperature.

After the adsorption experiment had been carried out, the surface area was determined from the adsorption isotherm deta of ethylene at −183 °C by the B. E. T. method. In the cases of copper and of copper-nickel catalysts, after the surface areas were determined, the temperature of the reaction vessel was raised to 400°C, and the catalysts were treated in hydrogen for a week. Then the same observations as those mentioned above were reported.

## Results

The relationship between surface area and reduction temperature in the three catalysts is shown in the previous report[1]. From the result it is found that the surface area of nickel is remarkably larger than those of the others at every reduction temperature, and that of copper-nickel catalyst is a little larger than that of copper catalyst. On raising the reduction temperature from 200° to 400°C, each catalyst decreased its surface area, to about 30% of its original value for nickel catalyst, to 35% for copper catalyst, and to 45% for copper-nickel catalyst. This shows that the addition of nickel increases the surface area of the catalyst, and prevents the surface from shrinking with the increasing reduction temperature.

Fig. 3 gives the hydrogen adsorption isotherms on the catalysts, namely that on nickel catalyst determined at 100° and 120°C, that on copper catalyst at 100° and 130°C, and 160°C and that on copper-nickel catalyst at 100° and 130°C. The results are shown by a plot of the logarithm of the adsorbed quantity $V$ in cc. N. T. P. per g. against the logarithm of the equilibrium pressure $P_e$ in mmHg. The curves show that Freundlich's adsorption formula is not applicable to any of these catalysts, and that the amount of hydrogen adsorbed on nickel catalyst is by far the largest of the three, about ten times that of copper-nickel catalyst, while that of copper-nickel catalyst is about five times that of copper catalyst at 100°C. But when the adsorption amounts are represented as those per unit area, that of nickel catalyst is not larger than that of copper catalyst. Thus, the adsorption amount of copper catalyst is about 1.6 times larger, and that of copper-nickel catalyst is about five times larger than that of nickel catalyst, at the same equilibrium pressure of $10^{-2}$ mmHg.

From these isotherms, the differential heats of adsorption $\Delta q$ were determined according to the usual equation

$$\Delta q = RT^2(\partial \ln P_e/\partial T)_v,$$

where $P_e$ denotes the equilibrium pressure, $T$ the absolute temperature, $V$ the amount adsorbed.

The results are shown in Fig. 4. These results show that the heat of adsorption of hydrogen on copper is remarkably smaller than that of nickel catalyst at the same coverage, that of copper catalyst being 10.6 kcal./mol., and that of nickel catalyst 24.2 kcal./mol. on each sparsely covered surface. The heat of copper-nickel catalyst may be the same as that of copper catalyst as presumed

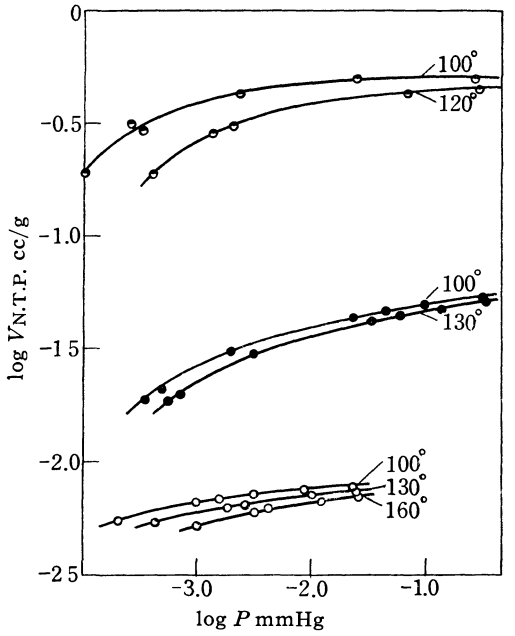



Fig. 3. Adsorption isotherms of hydrogen on copper, copper-nickel, and nickel catalysts reduced at 200°C.
○ Copper, ● Copper-nickel, ◓ Nickel.

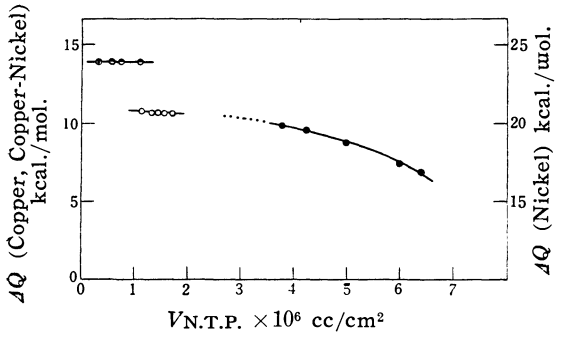



Fig. 4. Adsorption heats of hydrogen on copper, copper-nickel, and nickel catalysts reduced at 200°C.
○ Copper, ● Copper-nickel, ◓ Nickel.

by extrapolating the heat curve of copper-nickel catalyst up to its sparse coverage.

Fig. 5 shows the rate of adsorption of hydrogen on copper and copper-nickel catalysts, represented by a plot of the logarithm of the pressure $P$ against time. The results show that the first-order equation can not be applicable to the rates contrary to the results of Kwan[3]. The dotted line in the figure indicates the results obtained by Kwan, which are represented by a straight line. It is found that the rate of adsorption on copper catalyst in our experiment is far greater than that given by Kwan.

In the case of the copper and copper-nickel catalysts reduced at 400°C, the rates of adsorption decrease markedly when compared with those reduced at 200°C; and the pressure de-

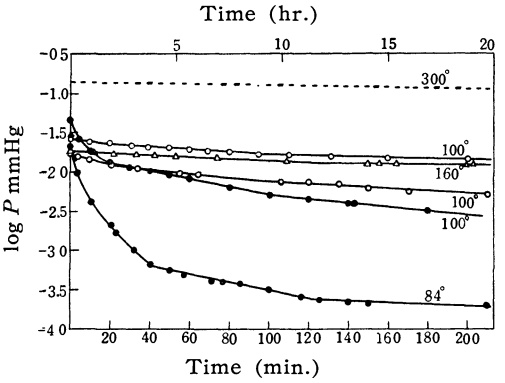



Fig. 5. Changes of hydrogen pressure with time on copper and copper-nickel catalysts.
● Copper-nickel reduced at 200°C,
○ Copper reduced at 200°C, △ Copper reduced at 400°C (time unit is hr.),
---- Copper reduced at 450°C (time unit is hr.), reproduced from Kwan[5].

crease of hydrogen still continues after a week. Therefore, the isotherms of those reduced at 400 °C could not be obtained.

## Discussion

The heat of adsorption of hydrogen on nickel has already been measured by many reseachers[4]. However, the results of these measurements do not agree among themselves, and the value (26 kcal.) given by Kwan[3], who carried out his experiment very carefully, is nearest to the authors' value of 24.2 kcal. for a sparsely covered surface.

The reports on the heat of adsorption of hydrogen on copper are not so numerous as those on nickel. Kistiakowski et al[5] measured it by means of a glass vacuum calorimeter, and found a rise in the curve of heat of adsorption when plotted against the amount adsorbed; about 4 kcal. for a sparsely covered surface, 18 kcal. for a more densely covered surface, and 12 kcal. for a fully covered surface. The unusually low value and the sudden rise to the maximum value are unacceptable in the light of recent researches on the heat of adsorption on other metals, which invariably shows that the heat of adsorption gradually decreases as the amount adsorbed increases.

3) T. Kwan, *J. Research Inst. Catalysis*, Hokkaido Univ., **1**, 95 (1949).
4) P. A. Beebe and H. S. Taylor, *J. Am. Chem. Soc.*, **46**, 43 (1924). C. F. Fryiing, *J. Phys. Chem.*, **30**, 818 (1926). O. Beeck, "Advances in Catalysis," Academic press. Inc., N. Y. (1950). p, 173.
5) Kistiakowski and Taylor, *Z. Physik. Chem.*, **125**, 341 (1929).

Ward[6] reported that the heat of adsorption on copper is within the wide range of about 80—9.8 kcal. In his report there is no detailed description of the process of reduction of the sample. It seems that the irreproducibility of adsorption, as well as the large value of the heat found after the initial treatment of baking of the sample, might be due to the reaction between hydrogen and the oxygen remaining on the surface of the sample. The value of 9.8 kcal. which was obtained after the last treatment of baking sample seems to be most reliable in his experiments, which agrees approximately with the value obtained in our experiment. Therefore, it is most probable to estimate the heat of adsorption on copper to be approximately 10 kcal. Thus, the heats of adsorption on copper and on copper-nickel coincide with each other, but they are both vastly different from the heat of adsorption on nickel. This suggests that the surface of copper-nickel catalyst is mainly composed of copper.

The error of the heat of adsorption is about 0.5 kcal. in this experiment. Using the heats of adsorption of hydrogen on pure copper and nickel catalysts at near zero coverage (24.2 and 10.6 kcal.), and the ratio of adsorption amounts per unit area at zero coverage $X_{Cu}/X_{Ni}$ (2.0), the proportion of the area of the exposed nickel on the copper-nickel catalyst to the total surface area—even if the exposed nickel particles exist on the surface of the catalyst—can be estimated as about 6% or less. This value is far smaller than that value of 17% estimated by the study reported previously[1]; and therefore, it is suggested that the nickel particles, which have been supposed to exist on the surface of the catalyst, are covered with films of copper which has a far lower melting point than nickel. It was found that the wall of the reaction vessel was colored by copper during the reduction of the copper-nickel catalyst. This facts shows that the copper vaporizes easily from the surface of the copper-nickel catalyst which is covered with copper atoms during the reduction.

It is quite plausible that the orientation of the copper films formed by the evaporation of the copper atoms was affected by the structure of the underlying metal face, and that the great activity of the copper-nickel catalyst was due to a special orientation of the copper atoms on the nickel particles of the surface of the catalyst, and to the electronic effect of nickel on copper. This is supported by Beeck[7], who pointed out that copper films prepared by the evaporation in hydrogen are far more active than ordinary copper films; and by Dowden[8], who electronically described the catalytic activity of copper-nickel alloy catalyst.

The decrease of the hydrogen adsorption activity of the copper-nickel catalyst with increase in reduction temperature may be due to the growth of the thick copper layer on the nickel particles, and consequently to the decrease of the electronic effect of the nickel on copper.

According to Kwan[3] the adsorption rate on copper is represented by a first-order expression throughout the adsorption process, while the results obtained in this experiment do not, and are far greater in value. Kwan carried out the reduction of the sample at high temperature (450°C), and measured a comparatively initial part of adsorption. We have found that the rates of adsorption on copper and copper-nickel catalysts decrease as the reduction temperature rises. It is doubtful whether his results could be represented by a first-order expression, if the pressure change due to adsorption had been measured until adsorption had practically ceased.

## Summary

(1) The adsorption of hydrogen on copper, nickel and copper-nickel (containing 1% nickel) catalysts, prepared from the nitrates of copper and nickel were observed in the range of 100° to 130° or 120°C.

(2) The shrinkage of surface with increase of reduction temperature was smaller for copper-nickel catalyst than for pure copper catalyst.

(3) The rates of adsorption of hydrogen on copper and copper-nickel catalysts were far smaller than that of nickel; and the adsorption amount per unit area was the greatest for copper-nickel catalyst, while that of nickel catalyst was the smallest among the three.

(4) The differential heats of adsorption of hydrogen at near zero coverage were given as 10.6 kcal. both for copper and copper-nickel catalysts, and 24.2 kcal. for nickel catalyst.

6) A. F. H. Ward, *Proc. Roy. Soc.*, **A133**, 506 (1935).

7) O. Beeck, *Discussion Faraday Soc.*, No. 8. 118(1950).

8) D. A. Dowden, and P. W. Reynolds, ibid., No. 8. 184 (1950).

(5) On the basis of the coincidence of the adsorption heats of copper and copper-nickel catalysts, it is suggested that the nickel particles supposed to exist on the surface of the copper-nickel catalyst may be covered with copper atoms.

*Faculty of Literature and Science*
*Toyama University, Toyama*

# *The Studies on Micelles. II. The Relation between Surfactant Concentration and Micellar Concentration in Aqueous Surfactant Solutions*

By Hiroji SASAKI, Shūji SAITO and Haruhiko OKUYAMA

(Received June 17, 1956)

## Introduction

The very important and interesting problem about micelles in aq. surfactant solutions is the relation between micellar concentration and surfactant concentration. Hartley[1] said that in dilute soap solution, the aggregate of paraffin chain salt has a well-marked optimum size and that no picture has given any satisfactory explanation for limitation of the size of aggregates. If this assumption could be applied to the rather concentrated range of surfactants, we should reach the curious conclusion, e. g., of 0.48 molecules of dimethyl amino azobenzene being solubilized in one micelle of dodecyl amine hydrochloride, which consists of 39 surfactant molecules[2], namely, notwithstanding the fact that the surfactant solution was completely saturated with dye, there would be about half of all micelles which were free from the dye molecule. It is generally believed that at about CMC there are small micelles and at high concentration of surfactants there exist large micelles, which consist of several double layers or have branching form in large dimension. But there is no satisfactory explanation about the relation between both kinds of micelles. In order to obtain some information on the relation between the surfactant concentration $C_s$ and the micellar concentration $C_m$, we have used the following fact on spectroscopy; "in some cases the absorption spectra of associable molecules in solutions change by the effect of association". When such an absorber, whose spectral change by association is great, and which is water-insoluble, is solubilized in an aq. surfactant solution and its spectrum is measured, we should observe some influences of association in the absorption band, so long as there are some micelles which contain more than two absorber molecules in them. Now keeping the concentration of surfactant $C_s$ constant, i. e., the micellar concentration $C_m$ constant, and increasing the concentration of absorber $C_a$, the number of absorber molecules in solution should exceed at last that of micelles. If we can detect the absorber concentration $C_a$, upon which the influence of association appears first, this absorber concentration $C_a$ should be equal to the concentration of micelles $C_m$, i. e., $C_m=C_a$, and further the number of molecules forming every micelle, $N_m$, is given by the equation

$$N_m=(C_s-C)/C_m \qquad (1)$$

where C is the CMC and the unit of $C_s$, C and $C_m$ are given by moles per liter; if the surfactant concentration is given by weight percent, $C'_s$, as is in usual cases, the molar concentration $C_s$ is obtained by $10\times C'_s/M$, where $M$ is the molecular weight of the surfactant.

## Materials and Methods

**Samples.**—*Trans*-azobenzene (AB) is used as a water-insoluble dye. As surfactants we have used sodium dodecyl sulfate (SDS), sodium oleate (SO), trimethyl dodecyl ammonium chloride (TMD), cetyl pyridinium chloride (CPC) and dodecyl polyethylene glycol ether (E120, average molecular weight is 1066). About the purification

1) G. S. Hartley, *Quarterly Reviews* (London), II, 179, (1948).
2) M. E. L. McBain and E. Hutchinson "Solubilization," Academic Press Inc., Publishers, New York (1955), p. 95.

of AB, SDS, TMD and E120 we have already reported[3]. CPC, manufactured by the L. Light and Co., Ltd. (England), was purified by ether. SO, from the E. Merck Co., is the purest grade and used without special purification.

**Methods.**—$10^{-3}M/L$ of AB were solubilized in aq. surfactant solutions of certain concentrations and these solutions were used as stock solutions. Every stock solution was diluted in turn by the aq. surfactant solution of the same concentration respectively, and their absorption intensities at certain wave length were measured by the Beckman DU spectrophotometer immediately after dilution.

## Results

Fig. 1 is the relation between the absorption intensity of $\pi$ band and the concentration of AB

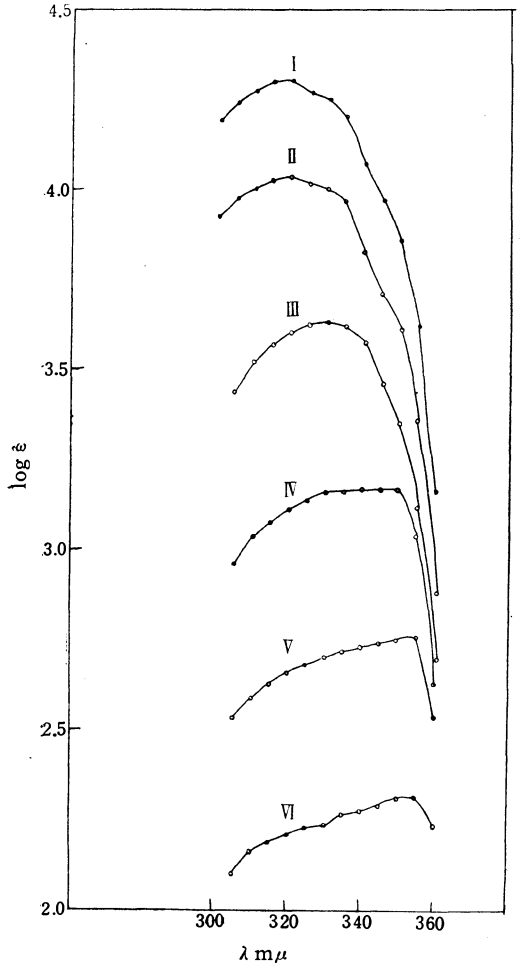



Fig. 1. The $\pi$ band of azobenzene in $CCl_4$. Concentration of azobenzene; I : $10^{-4}$ M, II : $4\times10^{-4}$ M, III : $10^{-3}$ M, IV : $3.2\times10^{-3}$ M, V : $10^{-2}$ M, VI : $3.2\times10^{-2}$ M.

3) H. Sasaki, H. Okuyama and S. Saito, This Bull., **29**, 752 (1956).

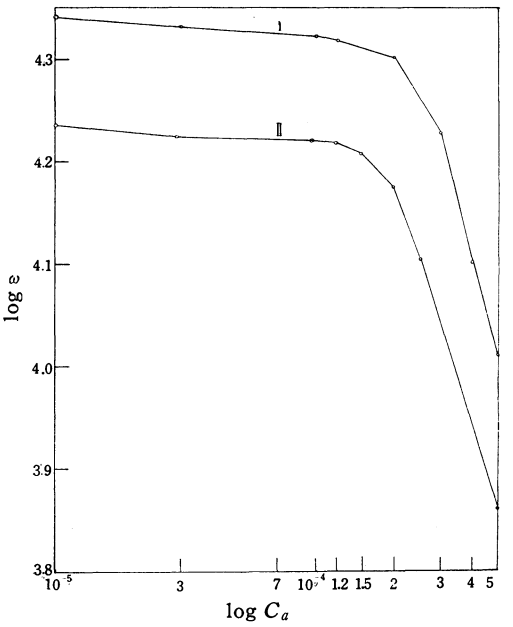



Fig. 2. The absorption intensity of azobenzene at 320 mμ. $C_a$ is the molar concentration of azobenzene. Solvents; I. hexane, II. 10% aq. SDS.

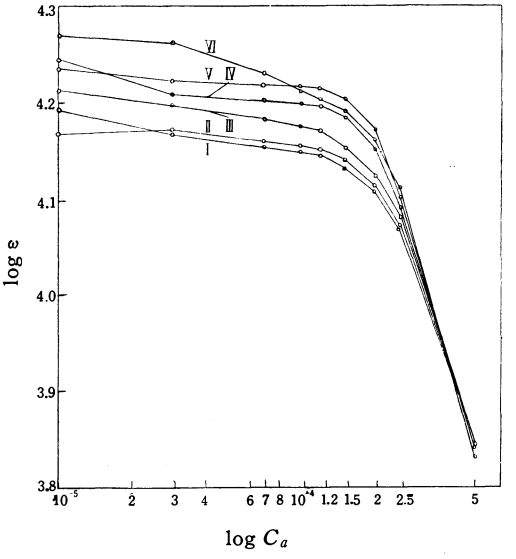



Fig. 3. The absorption intensity of azobenzene at 320 mμ in the aq. SDS solutions. Concentration of SDS; I : 0.5%, II : 1%, III : 2.5%, IV : 5%, V : 10%, VI : 20%.

in $CCl_4$. Fig. 2 is the relation between absorption intensity at 320 mμ and the concentration of AB in hexane and 10% aq. SDS solution. Figs. 3—7 are the relations between the absorption intensity at a certain wave length and the concentration of AB in various kinds of aq. surfactant solutions of various cocentrations.

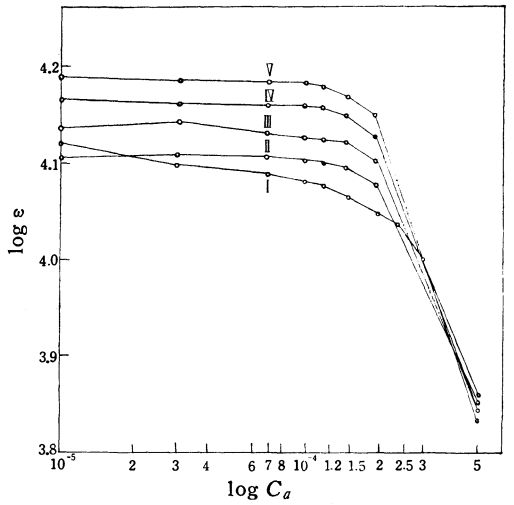



Fig. 4. The absorption intensity of azobenzene at 320 mμ in the aq. TMD solutions. The concentration of TMD; I : 0.3%, II : 0.5%, III : 1%, IV : 2.5%, V : 5%.

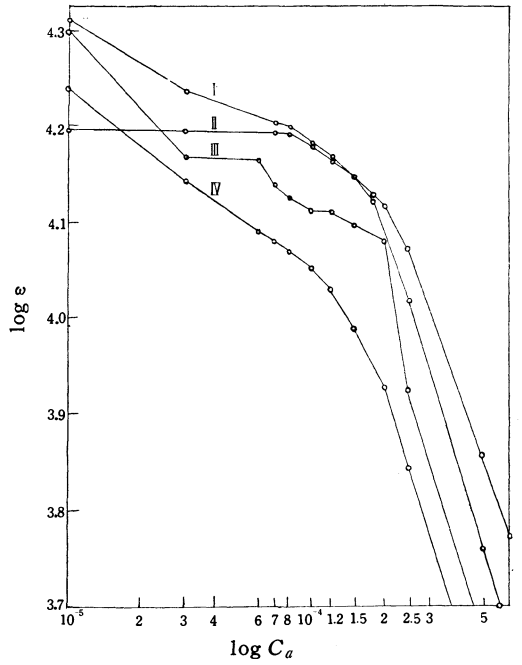



Fig. 5. The absorption intensity of azobenzene at 335 mμ in the aq. SO solutions. The concentration of SO; I : 0.05%, II : 0.5%, III : 1%, IV : 5%.

## Discussion

As is shown in Fig. 1, the $\pi$ band of AB in $CCl_4$ depends remarkably on its concentration $C_a$. It is reasonable to think that the cause of this dependence of absorption intensity upon the concentration is association, because AB is a neutral

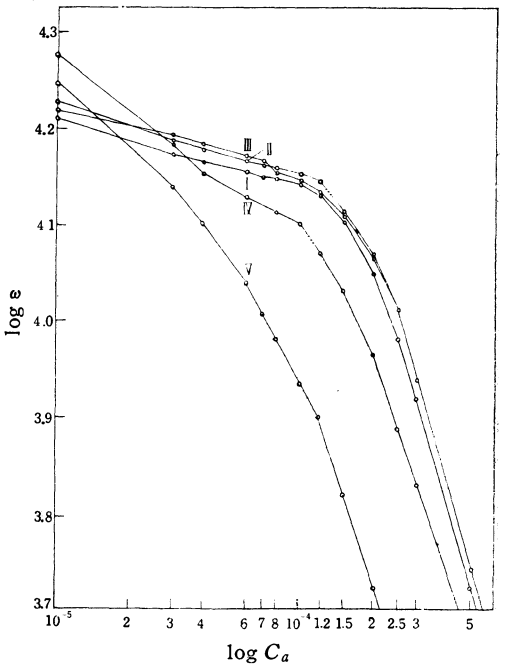



Fig. 6. The absorption intensity of azobenzene at 325 mμ in the aq. E120 solutions. The concentration of E120; I : 0.5%, II : 2.5%, III : 5%, IV : 10%, V : 20%.

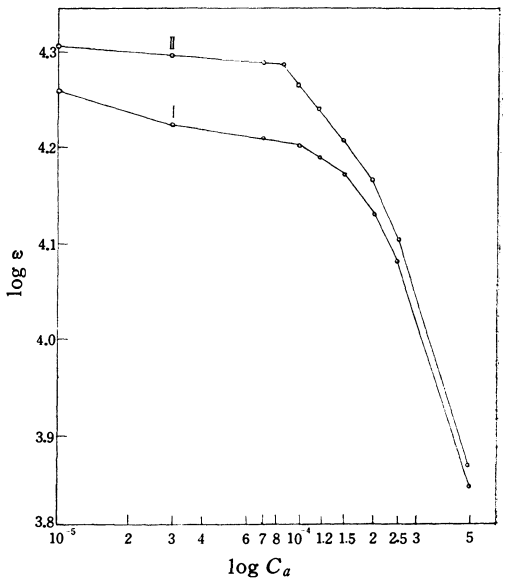



Fig. 7. The absorption intensity of azobenzene at 320 mμ in the aq. CPC solutions. The concentration of CPC; I:0.5%, II:1%.

molecule and no dissociation occurs, and in $CCl_4$ no pH effect occurs, moreover *trans*- and *cis*-azobenzene have no absorption maximum at 355 mμ[4]. From the curve

4) W. R. Brode, J. H. Gould and G. M. Wyman, *J. Am. Chem. Soc.*, **75**, 1856 (1953).

I in Fig. 2 we can observe the relation between the concentration and the absorption intensity of AB at 320 m$\mu$ in hexane. The curve is approximately parallel to the abscissa in the range of $C_a \leq 1.2\times10^{-4}M$, which shows that AB molecules are almost in the unassociated state. In the range of $C_a > 1.2\times10^{-4}M$, the absorption intensity decreases with increasing $C_a$, which shows AB molecules are in the associated state. The curve II in Fig. 2 shows the relation between the absorption intensity at 320 m$\mu$ and the concentration of AB in aq. SDS solution. As $C_s$, the surfactant concentration, is kept constant, the micellar concentration $C_m$ is also constant. If we follow the curve II from the left to the right, the number of AB molecules increases and at about $C_a=1.2\times10^{-4}M$ both the micellar concentration and the concentration of AB are equal, i. e., $C_m=C_a$, for at this point the curve begins to bend markedly. We will explain this reason again; as the lowering of the absorption intensity of AB in hexane or in $CCl_4$ is caused by the association, as mentioned above, then from resemblance of curves I and II, this lowering of the absorption intensity of AB solubilized in aq. SDS solution must be also caused by the association of AB molecules in micelles, and in order to cause AB molecules to associate in a micelle, the micelle must contain more than two AB molecules. Therefore the $C_a$, at this AB concentration where the intensity curve begins to bend markedly, must be equal to the micellar concentration $C_m$. Beyond this value of $C_a$, every micelle solubilizes 2, 3, and more AB molecules, therefore, paying the attention to AB molecules, the associate concentration of AB is constant, i. e., equal to $C_m$, and only the association number of AB increases with increasing $C_a$. All the curves in Fig. 3 show similar behavior; that is, in the range of $1.2\times10^{-4}M \leq C_a \leq 2.5\times10^{-4}M$ the curves bend remarkably, and the concentration of SDS, $C_s$, is concerned little with this general behavior of the intensity curves. Therefore it is concluded that the micellar concentration of SDS is about $1.2\times10^{-4}M/L$ in the range of $0.5\% < C_s < 20\%$, that is, $C_m$ is constant irrespective of $C_s$ in this range*. Accordingly, the association number of molecules forming every micelle, $N_m$, of SDS increases with the increase of $C_s$ in the range of $C_s$ being at least above 0.5%, and can be given by equation (1), inserting the value $C=8.12\times10^{-3}M$ (0.234%)[5] and $C_m=1.2\times10^{-4}M$. In the case of $C_s=20\%$ in Fig. 3, the curve differs a little from the others. We shall explain the reason for this afterwards. TMD gives also the similar curves as SDS as observed in Fig. 4, $C_m$ is about $1.2\times10^{-4}M$ in the range of $C_s \geq 0.5\%$. At $C_s=0.3\%$, AB is in suspension state (not perfectly solubilized) and this curve is not reliable. The association number of a micelle of TMD is given by equation (1), inserting the value $C=0.016M$[6]. In the case of SO, as shown in Fig. 5, the values of $C_m$ is smaller than those of SDS or TMD, that is, $C_m$ is about $8\times10^{-5}M$ in the range of 0.05%—0.5%, and that, with increasing $C_s$, the bending part of the curves shifts towards the left, i. e., at 1% of $C_s$, $C_m$ is about $6\times10^{-5}M$ and at 5% we can no longer detect the clear bending part on the curve where AB molecules are in the transitional state from the unassociated to the associated state. The value of association number of every micelle is given by the equation (1), in-

* In these discussions, we take the assumption of approximately monodispersed state of AB molecules solubilized in every micelle, as all micelles are also in the approximately monodispersed state. The reasons to take this assumption are as follows; (1) The facts that the approximately parallel part of the absorption intensity curve of AB in an aq. surfactant solution often shows irregular knicks and decreases with increasing $C_a$ prove that AB molecules in micelles are in some degree in a polydispersed state. But the degree of polydispersity of AB molecules in this range, e. g. in aq. SDS solutions $C_a \leq 10^{-4}M$, is very little. On the other hand, in the range of $C_a > 10^{-4}M$ in SDS, the intensity curves decrease steeply, and this fact shows that when micelles containing more than two AB molecules appear largely, the absorption intensity of solutions decreases markedly. Because this great lowering of the intensity is not observed in the range of $C_a \leq 10^{-4}M$, we can safely say that AB molecules are mainly in a monomer state in the range of $C_a \leq 10^{-4}M$ in SDS. Moreover, it is thought that our assumption is justified, because the values of $N_m$ tabulated in Table 1, which are obtained by the assumption of approximately monodispersed state of AB molecules in micelles, are in good agreement with those obtained by other authors, at least in low values of $C_s$. (2) If we assume, on the contrary, that at a certain $C_s$, the micelles were in a polydispersed state (P. A, Thiessen in Zsigmondy, "Lehrbuch der Kolloidchemie." 2, Leipzig (1927), p. 167), instead of approximately monodispersed state, whose solubilizing powers must be different after a different association number, then some possibility would occur that AB molecules might be solubilized also in a polydispersed state. But if so, the degree of polydispersity of AB must be subject to $C_s$, and the regular form of intensity curves irrespective of $C_s$, as is observed in Fig. 3, could not be observed. From these reasons mentioned above in (1) and (2), it is understandable that the assumption of the monodispersed state of AB molecules solubilized in micelles as well as surfactant micelles in aq. phase may be allowed in practical meaning, though it can not be admitted in strict meaning.

5) P. Mukerjee and K. J. Mysels, *J. Am. Chem. Soc.*, **77**, 2937 (1955).

6) H. B. Klevens, *J. Phys. Chem.*, **52**, 130 (1948). $0.016M/L$ is the CMC of dodecyl trimethyl ammonium bromide and we assume that the CMC of TMD does not differ so much from this value.

serting the value $C=6\times10^{-4}M$[7]. In Fig. 6, it is shown the case of E120, $C_m$ decreases also with increasing $C_s$, i. e., in the range of $0.5\%\leq C_s\leq 2.5\%$, $C_m$ is about $1.2\times10^{-4}M$; at 5%, $C_m$ is about $10^{-4}M$; at 10%, $C_m$ is about $6\times10^{-5}M$; and at 20%, there can not be observed the clear bending point. The number of micellar molecules is given by equation (1), inserting the value C= 0.1%* and values of $C_m$ given above. In Fig. 7 shown the experiment on CPC, $C_m$ is about $10^{-4}M$ at $C_s=0.5\%$, and about $8\times10^{-5}M$ at $C_s=1\%$. $N_m$s are given by equation (1), inserting the value $C=9\times10^{-4}M$ and these values of $C_m$ given above. In Table 1 these calculated values of $N_m$ are tabulated.

The fact that when $C_s$ increases largely, $C_m$ decreases, and that at last the clear bending point disappears seems to be due to the general phenomenon about surfactant micelles. The values of $N_m$, given in Table I, at the low values of $C_s$, are in good agreement with what are obtained by other methods, for example, 75 for aq. SDS solution by the light scattering[8]. The range of $C_s$, where $C_m$ is kept constant, seems to be subject to the volume of surfactant molecules, and to whether the unsaturated part exists or not in surfactant molecules; this upper limiting concentration seems to be 20%** in SDS, 5% in SO and 10% in E120.

TABLE I

THE VALUES OF MICELLAR CONCENTRATION, $C_m$, AND THE NUMBER OF SURFACTANT MOLECULES, $N_m$, IN THE CERTAIN CONCENTRATION OF SURFACTANTS, SUCH AS SODIUM DODECYL SULFATE (SDS), TRIMETHYL DODECYL AMMONIUM CHLORIDE (TMD), SODIUM OLEATE (SO), LAURYL POLYETHYLENE OXIDE ETHER (E120) AND CETYL PYRIDINIUM CHLORIDE (CPC)

| Surfactants | | $C_m M/L$ | $N_m$ |
|---|---|---|---|
| SDS | 0.5% | $1.2\times10^{-4}$ | 77 |
| | 1.0 | 〃 | 220 |
| | 2.5 | 〃 | 650 |
| | 5.0 | 〃 | 1380 |
| | 10.0 | 〃 | 2800 |
| TMD | 0.5% | $1.2\times10^{-4}$ | 50 |
| | 1.0 | 〃 | 230 |
| | 2.5 | 〃 | 800 |
| | 5.0 | 〃 | 1740 |
| SO | 0.05% | $8\times10^{-5}$ | 13 |
| | 0.5 | 〃 | 198 |
| | 1.0 | $6\times10^{-5}$ | 550 |
| E120 | 0.5% | $1.2\times10^{-4}$ | 32 |
| | 1.0 | 〃 | 70 |
| | 2.5 | 〃 | 188 |
| | 5.0 | $1.0\times10^{-4}$ | 460 |
| | 10.0 | $6\times10^{-5}$ | 1550 |
| CPC | 0.5% | $10^{-4}$ | 138 |
| | 1.0 | $8\times10^{-5}$ | 358 |

7) I. M. Kolthoff and W. Stricks, ibid., **53**, 424 (1949).
* This value is estimated from the solubilization of AB and not the precise value.

## Summary

From the spectral change of $\pi$ band, caused by the association of azobenzene solubilized in aq. surfactant solutions, we have reached the conclusion that in a certain wide range of surfactant concentration, the micellar concentration is constant and only the number of surfactant molecules forming every micelle increases with increasing surfactant concentration. These values of the number of micellar molecules, obtained by spectral method, are in good agreement with those reported previously, in low concentration of surfactants.

The authors wish to express their sincere thanks to Prof. N. Sata for his encouragement.

*Department of Chemistry, Faculty of Science, Osaka University, Osaka*

8) E. Hutchinson and J. G. Melrose, *Z. physik. Chem., Neue Folge* **2**, 363 (1954).
** Suppose that $C_m=1.2\times10^{-4}M/L$ and volume of 1000 cm³ is divided by the sphere of $NC_m$ ($N$ is the Avogadro's Number), the radius of this sphere is given by the equation $(4/3)\pi r^3NC=(10^{27})$ Å³, i. e., $r=150$ Å. According to Debye's opinion (P. Debye and E. W Anaker, *J. Phys. Chem.*, **55**, 644 (1951)). the size of micelle does not exceed 300 Å, and Hess et. al. (K. Hess and H. Kiessig, *Ber.*, **81**, 327 (1948)). reported that the shape of large micelles is blade-like. A micelle which consists of less than one hundred surfactant molecules might be spherical, but a large micelle consisting of some hundreds of molecules can not be spherical, so we assume that this large micelle is a disk-like shape, which consists of one double layers. As one surfactant molecule occupies 25 Å², (J. W. McBain, in R. E. Burk and O. Grumitt "Frontiers in Colloid Chemistry," New York (1950), p. 133). the radius of this disk, $r$, at 10% of SDS is given be the equation $\pi r^2=25\times(2800/2)$, i. e., $r=105$ Å, where 2800 is $N_m$ tabulated in Table I. If this micelle continues its growth until 20% of SDS concentration, then $N_m=5720$, which is obtained by the equation (1), and $r=151$ Å. It is understandable easily that the micelles, even if they have a different shape, will combine wrth each other and form larger micelles when $C_s$ exceeds some limiting value, given above.

# SHORT COMMUNICATIONS

## *Dependence of the Characteristics of Calcium Halophosphate Phosphors on the Condition for Preparing Secondary Calcium Hydrogen Orthophosphate*

By Yoshihide KOTERA, Michiko YONEMURA and Tadao SEKINE

(Received October 5, 1956)

The development of calcium halophosphate phosphors has been described by Jenkins, McKeag and Ranby[1] and Nagy, Wollentin and Lui[2]. Two main stages are involved in the preparation of calcium halophosphates: the first is the preparation of calcium phosphate of suitable purity and physical condition, the second being a thermal treatment in which the mixture of raw materials is fired in a suitable atmosphere at a temperature of 1050~1200°C. Doherty and Harrison[3] gave a detailed description of dry and wet syntheses, while Wanmaker, Hoekstra and Tak[4] and Wanmaker and Verheyke[5] investigated the second stage (thermal treatment) of the preparation. We have investigated the first stage and found the dependence of the characteristics of calcium halophosphates on the conditions for preparing secondary calcium hydrogen phosphate.

Three samples of calcium phosphate were prepared as follows:

Sample $I_a$·····Pure phosphoric acid, which was prepared by the reaction of the purified diammonium hydrogen orthophosphate with distilled nitric acid, was reacted with purified calcium carbonate at pH 3.6 and about 30°C.

Sample $I_b$·····The same as $I_a$ except that the reaction between phosphoric acid and calcium carbonate proceeded under water cooling (about 10°C).

Sample II·····Purified diammonium hydrogen orthophosphate solution was added to purified calcium nitrate solution at pH 3.6 and boiling temperature.

All raw materials were purified by the process described in a previous paper[6] and their purity was established spectrographically. The results of chemical analyses fos these samples are shown in Table I, where values in the forth column were calculated from those in the second one, while those in the fifth column were calculated from those in the second and fourth ones. Employing them as one of the starting materials for the preparation of calcium halophosphate, phosphors were prepared as follows:

$CaHPO_4$ 27.0 $CaCO_3$ 8.8(I) or 8.6(II)
$CaCl_2 \cdot 2H_2O$ 1.8 $CaF_2$ 1.7 Mn phosphate 1.0 $Sb_2O_3$ 1.1 (g.).

They are mixed by ball mill and fired at 1175°C for one hour (40 g. for one batch). The brightness of fired samples before and after grinding is shown in Table II, where the value of 100 is given for American commercial phosphor (Westinghouse 4500°K white). Their emission spectra illustrated in Figure 1 were obtained by means of spectroradiometer[7]. The residual amounts of activators after firing were determined polarographically[8] and the results are given in Table III.

Jenkins, McKeag and Ranby[2] found that the precipitate obtained from aqueous solutions of calcium chloride and diammonium hydrogen phosphate consists of

TABLE I
ANALYSIS OF SECONDARY CALCIUM HYDROGEN ORTHOPHOSPHATE

| Sample No. | CaO | $H_2O$ | $P_2O_5$ (calcd.) | CaO/$P_2O_5$ (calcd.) | Density of Bulk |
|---|---|---|---|---|---|
| $I_a$ | 40.30 | 7.78 | 51.92 | 0.776 | 0.71 |
| $I_b$ | 40.32 | 7.73 | 51.95 | 0.776 | 0.65 |
| II | 40.63 | 7.55 | 51.82 | 0.784 | 0.44 |
| Theor. | 41.21 | 6.62 | 52.17 | 0.790 | |

TABLE II
THE BRIGHTNESS OF CALCIUM HALOPHOSPHATE PHOSPHORS

| Sample No. | Before Grinding | After Grinding |
|---|---|---|
| $I_a$ | 90 | 88 |
| $I_b$ | 96 | 91 |
| II | 91 | 91 |

1) H. G. Jenkins, A. H. McKeag and P. W. Ranby, *Trans. Electrochem. Soc.*, **96**, 1 (1949) ; A. H. McKeag and P. W. Ranby, Brit. Pat., 578,192 (1942).
2) R. Nagy, R. W. Wollentin and C. K. Lui, *Trans. Electrochem. Soc.*, **95**, 187 (1949).
3) M. Doherty and W. Harrison, *British J. Applied Phys.*, Supplement No. 4, p. 11 (1955).
4) W. L. Wanmaker, A. H. Hoekstra and M. G. A. Tak, *Philips Res. Repts.*, **10**, 11 (1955).
5) W. L. Wanmaker and M. L. Verheyke, *Philips Res. Repts.*, **11**, 1 (1956).
6) Y. Kotera and T. Sekine, This Bulletin, **27**, 13 (1954).
7) Y. Kotera, *Rept. Govt. Chem. Ind. Research Institute, Tokyo*, **50**, 398 (1955).
8) Y. Kotera, M. Yonemura and T. Sekine, This Bulletin, **28**, 132 (1955).

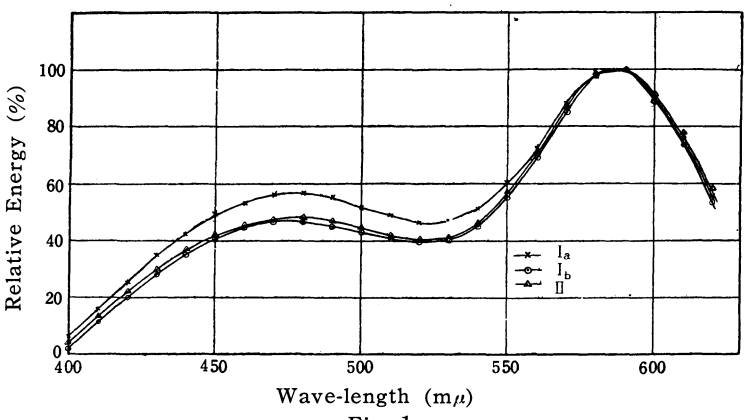



Fig. 1

TABLE III

ANALYSIS OF RESIDUAL AMOUNT OF ANTIMONY AND MANGANESE IN CALCIUM HALOPHOSPHATE PHOSPHORS

| Sample No. | Antimony (g./g.) | Manganese (g./g.) |
|---|---|---|
| $I_a$ | 0.0056 | 0.0086 |
| $I_b$ | 0.0057 | 0.0081 |
| $I_b$ (before grinding) | 0.0059 | 0.0078 |
| II | 0.0049 | 0.0086 |
| Westinghouse 4500°K white | 0.0070 | 0.0069 |
| Westinghouse 3500°K white | 0.0040 | 0.0095 |

$CaHPO_4 \cdot 2H_2O$ when precipitated cold and $CaHPO_4$ when precipitated from boiling solutions. We found that, although calcium phosphate was prepared by almost the same processes, the ratio CaO : $P_2O_5$ changes according to small differences of the preparing conditions and chemical analysis is necessary for the determination of the mixing ratio for resulting phosphor (Table I). The characteristics of phosphors with the same mixing ratio ($I_a$ and $I_b$) are however affected by the conditions for preparing calcium phosphate. In particular, the initial brightness and its decrease during grinding shown in Table II depend on these conditions, indicating that the imperfections of the phosphor crystal, which might be related to the brightness and its decrease, would be affected by the physicochemical properties of raw materials. This idea is supported from the analytical result for the residual activator amount as given in Table III. Whether the migration of antimony and manganese in the apatite lattice and the formation of active centers are easy or not, might depend upon the properties of integrants. The spectral energy distribution curves illustrated in Fig. 1 show a little difference between phosphor samples and this fact might be explained by the idea described above.

A detailed account of this work will be published elsewhere.

*Government Chemical Industrial Research Institute, Tokyo*

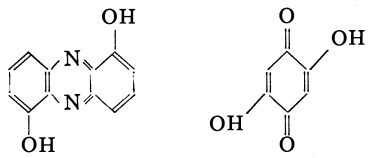
## *Synthesis of Co-ordination Compounds of High Molecular Weight*

By Seiichi KANDA and Yoshihiko SAITO

(Received November 19, 1956)

An attempt has been made to synthesize polymers through co-ordination with metals. When bifunctional co-ordinating units enter into combination with a certain metal, linear polymers of the type -A-M-A-M-A- would be formed. Very little is known about the physico-chemical properties of such co-ordination polymers. The linear shape of the compounds would make them interesting subjects for various physico-chemical studies.

Along this line, two groups of compounds were synthesized: metal complexes of 1,6-dihydroxyphenazine (A) and those of 2,5-dihydroxybenzoquinone (B),




(A) (B)

It was found that (A) gives stable co-ordination compounds with Cu (II), Ag (I), Fe (III) and Hg (II). For instance, when an alcoholic solution of (A) was

added to an aqueous solution of Cu (II) sulfate or acetate, a black precipitate formed at once, which was so fine that it was necessary to use a centrifugal machine to separate it from the solution (Found: Cu, 22; C, 52.22; N, 10.58; H, 2.35. Calcd. for $CuC_{12}H_6O_2N_2$: Cu, 23; C, 52.65; N, 10.28; H, 2.95%). Electron micrograph of the precipitate showed circular image of diameter ranging from 0.1 $\mu$ to 1 $\mu$. Correspondingly x-ray diffraction pattern obtained by using Norelco x-ray diffractometer showed two diffuse haloes.

Cu (II), Ni (II) and Cd (II) form complex compounds with (B) by simply mixing aqueous solutions of these metal salts and an aqueous solution of sodium salt of (B) or an alcoholic solution of (B). Elementary analyses showed that all these compounds are 1:1 complexes. For example, Cu (II) compound was obtained as dark green precipitate (Found. Cu, 30; C, 35.5; H, 1.52. Calcd. for $CuC_6H_2O_4$: Cu, 31.6; C, 35.8; H, 1.0%). Under certain conditions, it suspends in water, forming colloidal solution, which can be kept unchanged over two months. The solution exhibited streaming double refration. Electron micrographs of the compound revealed that it consists of small rodlike crystals of dimensions 100 500 m$\mu$ in length and 50 m$\mu$ in width. P. V. A. film containing the colloidal particles of this compound shows, on stretching, marked dichroism: by plane polarized light whose electric vector is parallel to the direction of stretching the film seems to be brown, while it is almost colorless when the electric vector is perpendicular to the direction of stretching. This anisotropy in absorption was measured by means of a Beckman Model DU spectrophotometer. A strong absorption band was found at $25\times 10^3$ $cm^{-1}$ (400 m$\mu$).

The results of elementary analyses indicate that all these compounds are coordination polymers. Moreover, the observations on Cu(II)-(B) complex appear to suggest that this compound is a linear polymer. Various physico-chemical studies including structure analyses are now going on. The details of the work will be published later. The authors express their sincere thanks to Dr. M. L. Huggins* for suggesting this problem.

*Institute of Polytechnics Osaka City University, Osaka*

* Fulbright Exchange Professor, Osaka and Kyoto Universities, 1955-1956, on leave from the Research Laboratories of the Eastman Kodak Company, Rochester 4, New York, U. S. A.

## *Relation between Foaming Properties and the Structure of Surfactant Solution*

### (Determination of Critical Micelle Concentration of Sodium Dodecyl Sulfate by Foaming Power Measurement)

By Maresuke KASHIWAGI

(Received November 12, 1956)

Because of the difficulty to make accurate reproducible measurement and accordingly to interpret experimental data quantitatively, the foaming power measurement has been applied largely to find only relative foaming power of a detergent solution. The author, however, found a very useful technique in the forming power measurement concerning the study of the structure of detergent solution. The method applied here is that of Ross-Miles[1] since this gives the most reproducible results among other methods.

**Experimental**

The apparatus used has somewhat different size from the standard Ross-Miles apparatus which is shown in Fig. 1. The diameter of a

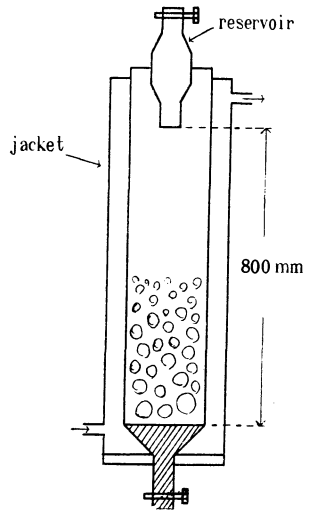



Fig. 1. Ross-Miles apparatus.

receiver containing the sample is 55 mm. instead of usual 50 mm. and the height from the orifice of a pipette reservoir to the level of the bottom solution is 800 mm. instead of 900mm. The other parts are the same. The temperature is kept at $40\pm0.1$°C. The height of the foam part is measured from the water level to the top of the foam part by the mm. scale marked on the re-

1) J. Ross, G. D. Miles, *Oil and Soap*, **18**, 99 (1941).

ceiver. The analysis of sodium dodecyl sulfate shows that 98.72% is an active substance in which unreacted alcohol amounts 0.74% and very small quantity of alkali is also present.

The data are averaged over three measurements and reproducibility was found to be very good.

This is plotted on a graph as shown in Fig. 2.

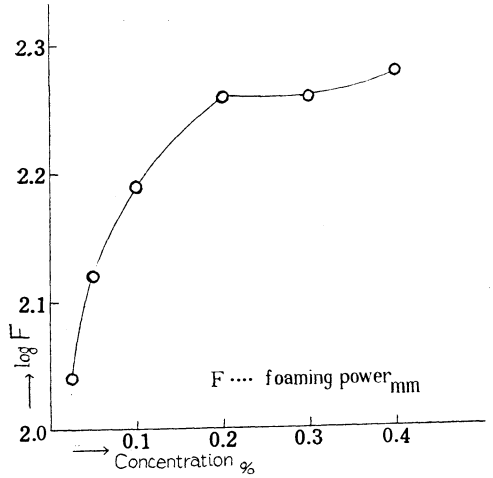



Fig. 2. Foaming power of sodium dodecyl sulfate.

From the curve it is very clear that there is a marked singular point (i.e. critical micelle concentration) at around the concentration of $7\times10^{-3}$ M. This is in good agreement with surface tension ($7.2\times10^{-3}$ M)[2], conductivity ($7.2\times10^{-3}$ M)[3] and viscosity ($9\times10^{-3}$ M)[4] data.

2) J. Powney and C. C. Addison, *Trans. Faraday Soc.*, **33**, 1243 (1937).
3) H. F. Ward, *Rroc. Roy. Soc. London*, **176 A**, 412 (1940).
4) K. Hess, W. Philippoff and H. Kiessig, *Kolloid Z.*, **88**, 40 (1939).

## Conclusion

The application of Ross-Miles method measuring foaming properties of detergent solution is found to be useful for the study of the structure of surfactant solution, and critical micelle concentration of aqueous sodium dodecyl sulfate is determined, which shows a good agreement with the values from other methods.

The same method is being applied to many other surfactants including soaps and the detail of the work will be published elsewhere.

The author expresses deep thanks to Mr. H. Ezaki and Dr. I. Odaira for their constant encouragement throughout this research project.

*Mitsuwa Chemical Laboratory*
*Marumiya Co. Ltd., Tokyo*

## *Syntheses of Kinetin-analogs. I**

By F. Shigeo OKUMURA, Mitsuo MASUMURA, Toshiyuki MOTOKI, Tadashi TAKAHASHI and Susumu KURAISHI**

(Received November 2, 1956)

The discovery of kinetin[1], 6-(2-furfuryl)-aminopurine (isolated from autoclaved

* Presented at the meeting of the Chugoku-shikoku Branch of the Chemical Society of Japan, Niihama, Oct. 18 th. 1956.

** Botanical Institute, Faculty of Science, Univ. of Tokyo.

1) C. O. Miller, F. Skoog, F. S. Okumura, M. H. Von Saltza and F. M. Strong, *J. Am. Chem. Soc.*, **77**, 1392, 2662 (1955) ; **78**, 1375 (1956).

TABLE I

SYNTHESES OF 6-SUBSTITUTED PURINES

| Purine | Temp. (°C) and time (hr.) of run | Yield (%) | M. p. (°C) | Analysis C Calcd | C Found | H Calcd | H Found | N Calcd | N Found |
|---|---|---|---|---|---|---|---|---|---|
| 6-(2-Thenyl)-amino[a] | 120–30[e], 12 hr. | 19.3 | 247–7.5[i] | 52.17 | 51.94 | 3.48 | 3.70 | 30.43 | 30.18 |
| | 120–5[f], 10. | 39.9 | | | | | | | |
| 6-Benzylamino-[b] | 120–5[f], 10. | 44.3 | 229–30[i] | 64.29 | 64.01 | 4.46 | 4.76 | 31.25 | 31.00 |
| 6-(α-Phenylethyl)-amino-[c] | 120–30[e], 8. | 54.2 | 240–1[i] | 65.55 | 65.29 | 5.04 | 5.27 | 29.41 | 29.19 |
| 6-(*n*-Amyl)-amino- | 90–100[e], 15. | 36.7 | 164–5[j] | 58.82 | 58.50 | 6.86 | 7.03 | 34.31 | 34.15 |
| 6-(*n*-Hexyl)-Amino- | 130–5, 9. | 31.0 | 177–8[k] | 60.23 | 60.13 | 7.82 | 7.70 | | |
| 6-(*p*-Methoxybenzyl)-amino- | 120–30[e], 8. | 48.2 | 233–4[i] | 61.42 | 61.15 | 4.72 | 5.00 | 27.56 | 27.28 |
| 6-(3,4-Dimethoxy-benzyl)-amino | 120–5[f], 10. | 48.1 | 240.5–1[i] | 59.16 | 59.41 | 4.93 | 5.10 | 24.65 | 24.58 |
| 6-(3,4-Methylenedioxy-benzyl)-amino- | 120–30[g], 12. | 40.3 | 259–60[i] | 58.21 | 57.95 | 3.73 | 4.02 | 26.12 | 25.90 |
| 6-Furfurylthio-[d] | [h] | 26.2 | 174–5[k] | 51.72 | 52.56 | 3.47 | 3.70 | | |

TABLE II
SYNTHESES OF 6-SUBSTITUTED 3-METHYLPYRIDAZINES

| 3-Methylpyridazine | Temp. (°C) and time (hr.) of run | Yield (%) | M. p. (°C) | Analysis C Calcd | C Found | H Calcd | H Found | N Calcd | N Found |
|---|---|---|---|---|---|---|---|---|---|
| 6-(2-Furfuryl)-amino- | 125[f], 24 hr. | 66.0 | 161-2[j] | 63.49 | 63.68 | 5.82 | 6.06 | 22.22 | 22.05 |
| 6-Benzylamino- | 100-30[f], 18. | 59.0 | 138.5-9[j] | 72.36 | 72.10 | 6.53 | 6.68 | 21.11 | 21.01 |
| 6-Anilino- | 100[f], 1. | 56.0 | 167.5-8[l] | 71.35 | 71.51 | 5.95 | 6.14 | 22.70 | 22.82 |
| 6-(2-Thenyl)-amino- | 130[f], 20. | 81.0 | 178-9[m] | | | | | 20.49 | 20.21 |
| 6-(*p*-Methoxybenzyl)-amino- | 125[f], 18. | 79.5 | 142-3[j] | | | | | 18.34 | 18.25 |
| 6-(3,4-Dimethoxybenzyl)-amino- | 135-40[f], 16. | 49.6 | 127-8[l] | | | | | 16.22 | 16.01 |

a) M. p., 241.5-2°C[3], M. p., 250°C[4]. b) M. p. 231°C[3], M. p. 229°C[4], M. p. 216-8°C[2].
c) M. p., 199-202°C[3]. d) M. p., 178-8.5°C[3]. e) In $H_2$-Stream. f) In sealed tube.
g) In air without $CO_2$. h) Prepared with 6-mercaptopurine and furfurylchloride in air.
(Solvents of recrystallization) i) Absolute alcohol j) Benzene
k) 60% alcohol l) Water m) Alcohol

sperm deoxyribonucleic acid as a cell division factor for tobacco callus tissue), has stimulated an interest in preparing various 6-substituted purines through the use of 6-chloropurine[2,3] or 6-methylmercaptopurine[4] as possible cytokinetic agents.

Recently Kuraishi and Okumura[5] found that kinetin is the leaf-growth factor for Raphanus sativus L.

In Tokushima we have synthesized various kinetin-analogs such as 6-substituted purines and 6-substituted 3-methylpyridazines by condensing 6-methylmercaptopurine[6] and 6-chloro-3-methylpyridazine[7] respectively with various amines. The results are shown in Tables I and II.

The biological test on 6-(2-thenyl)-amino-, 6-benzylamino- and 6-*n*-hexylamino-purines prove to have the same effect on the growth of Raphanus leaf as kinetin. It is very interesting that 6-benzylaminopurine shows leaf-growth activity but 6-phenylethylaminopurine does not.

The authors are indebted to the research institute of Tanabe Parm. Co. in Tokyo for the microanalyses.

*Department of Applied Chemistry*
*Faculty of Engineering Tokushima*
*University, Tokushima*

2) J. W. Daly and B. E. Christensen, *J. Org. Chem.*, **21**, 177 (1956).
3) M. W. Bullock, J. J. Hand and E. L. R. Stokstad, *J. Am. Chem. Soc.*, **78**, 3693 (1956).
4) C. G. Skinner and W. Shive, ibid., **77**, 6692 (1955).
5) S. Kuraishi and F. S. Okumura, *Bot. Mag.* (Tokyo), **69**, 300 (1956).
6) G. B. Elion, E. Burgi and G. H. Hitchings, *J. Am. Chem. Soc.*, **74**, 411 (1952).
7) W. G. Overend and L. F. Wiggins, *J. Chem. Soc.*, **1947**, 239.

## *Chemical Structure of Deoxynupharidine, the Alkaloid Obtained from Nuphar Japonicum*

By Munio KOTAKE, Shiro KUSUMOTO and Takashi OHARA

(Received December 18, 1956)

Hofmann degradation and subsequent ozonolysis of deoxynupharidine, $C_{15}H_{23}NO$ (I), the alkaloid obtained from the roots of *Nupher Japonicum* afforded 3-furaldehyde (Dimedone derivative, m. p. 167–170°, Found : C, 70.35 ; H, 7.18. Calcd. for $C_{21}H_{26}O_5$ : C, 70.39 ; H, 7.26), which was identified by silver oxide oxidation to 3-furoic acid (m. p. 122–123°. Found : C, 53.89 ; H, 3.47. Calcd. for $C_5H_4O_3$ : C, 53.57 ; H, 3.57), and characterization of the latter by means of mixed melting point and infrared spectrum. Compound I which gives an orange colored Ehrlich reaction, has a $\lambda_{max}$ at 213 m$\mu$ ($\log \varepsilon = 3.9$), and shows infrared absorptions at 873, 1500, and 3120 $cm^{-1}$ corresponding to a furan ring ; these absorption maxima and coloration dissappear upon conversion into tetrahydrodeoxynupharidine by catalytic reduction of I.

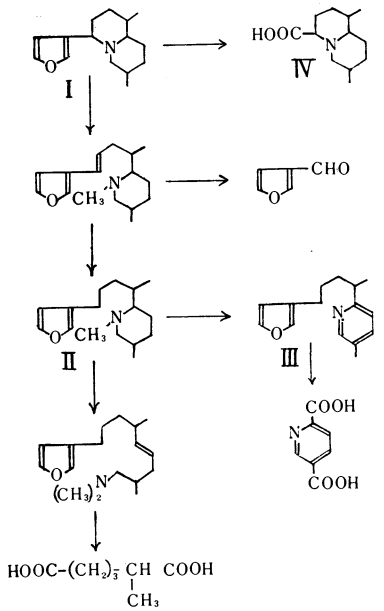
Palladium dehydrogenation of I, or dehydrogenation of $C_{15}H_{24}NO \cdot CH_3$, (II) (Perchlorate, m. p. 97–98°) resulting from Hofmann degradation and catalytic reduction of (I), afforded $C_{15}H_{19}ON$ (III) (Platinum chloride complex, m. p. 155–160°) ; potassium permanganate oxidation of (III) yielded pyridine 2, 5-dicarboxylic acid (Dimethylester, m. p. 163–164°. Found : C, 55.36 ; H, 4.39 ; N, 7.24. Calcd. for $C_9H_9NO_4$ : C, 55.33 ;

H, 4.56; N, 7.11), which was identified through a mixed melting point test and infrared absorption comparison with an authentic sample.

Further Hofmann degradation and ozonolysis of II gave a dicarboxylic acid, m. p. 84.5–85° (Found: C, 52.78: N, 7.22. Calcd. for $C_7H_{12}O_4$: C, 52.50; H, 7.50.), which was shown to be $\alpha$-methyladipic acid from the infrared spectra of its dimethyl ester and *p*-bromophenancyl ester (measured in chloroform).

An acid, m. p. 181–183° (Found: C, 68.07; H, 9.85; N, 6.53. Calcd. for $C_{12}H_{21}NO_2$: C, 68.25; H, 10.02; N, 6.64.), resulting from the nitric and chromic acid oxidation of I, and the two $pK_a'$ values at 2.0 and 10.8 suggested that it is presumably an $\alpha$-amino acid of formula IV.

The mentioned facts point to the proposed structure I, and the reactions involved may be represented by the following scheme:




*Faculty of Science, Osaka University*
*Kita-ku, Osaka*

## *The Competitive Nitration of Biphenyl and Benzene by Nitric Acid in Acetide Anhydride*

By Osamu SIMAMURA and Yoshiyuki MIZUNO

(Received December 10, 1956)

Biphenyl is known to undergo electrophilic substitutions at positions 2 and 4[1], and the chlorination in acetic acid[2] and the Friedel-Crafts acetylation[3] have been shown to take place more rapidly than benzene. In accord with these observations, a theoretical consideration by means of the molecular orbital method[4] predicts more facile substitutions at positions 2 and 4 of biphenyl than at one nuclear position of benzene. The relative rate of nitration of biphenyl appeared, however, to have not yet been studied experimentally, and we have been carrying out experiments on this subject and also on the nitration of substituted biphenyls to elucidate the nature of the polar effect of substituents in the biphenyl system in general. In view of the recent announcement in the Current Chemical Papers, 1956, No. 9, that Dewar and his collaborators have published several papers concerning the nitration of aromatic hydrocarbons including biphenyl, which are not yet available to us, we wish to publish here part of the results of our study on the nitration of biphenyls.

The experimental conditions and the results are listed in Tables I and II.

TABLE I

COMPETITIVE NITRATION OF BIPHENYL AND BENZENE

| Expt. No. | 1 | 2 | 3 |
|---|---|---|---|
| Benzene (millimol.) | 125 | 125 | 177 |
| Biphenyl (millimol.) | 12.5 | 12.5 | 12.5 |
| Acetic Anhydride (millimol.) | 200 | 200 | 200 |
| Nitric Acid (millimol.) | 10 | 7.5 | 9 |
| Reaction Time (hrs.) | 3 | 3.5 | 3.5 |
| Nitrobenzene formed (millimol.) | 2.37 | 1.62 | 2.14 |
| Nitrobiphenyls formed (millimol.) | 6.99 | 5.11 | 4.76 |
| Relative Rate | 42 | 40 | 39 |

TABLE II

THE ISOMERIC RATIO OF NITROBIPHENYLS FORMED AND THE PARTIAL RATE FACTORS FOR THE NITRATION OF BIPHENYL

| Nuclear Position | 2- | 3- | 4- |
|---|---|---|---|
| Isomer Formed (%) | 68 | <1 | 32 |
| Partial Rate Factor | 41 | <0.6 | 38 |

A mixture of biphenyl and benzene was nitrated with nitric acid in acetic anhydride at 0°C. The reaction mixture was added to 400 cc. of ice water, left to stand over-night, neutralized with

1) For a review of the literature see Y. Mizuno, *J. Soc. Org. Synthet. Chem., Japan*, **14**, 479 (1956).
2) P. W. Robertson, cited by P. B. D. de la Mare, *J. Chem. Soc.*. **1954**, 4450.
3) Y. Ogata and R. Oda, *Bull. Inst. Phys. Chem. Research* (Tokyo), **21**, 728 (1942).
4) F. Seel, *Z. Naturforsch.*, **3a**, 35 (1948) : R. D. Brown, *J. Am. Chem. Soc.*, **75**, 4077 (1953).

sodium hydrogen carbonate and extracted thoroughly with ether. The ethereal solution was washed with water and dried over anhydrous calcium chloride, and the ether and part of benzene were removed through a Vigreux column. The residue was analyzed for the nitro group by titrating an aliquot with 0.1 N titanium trichloride to determine the total amount of the nitration products. The remainder of the residue was distilled at 20 mmHg, with occasional addition of a little aniline as a carrier for nitrobenzene, until removal of nitrobenzene was complete. Analysis for the nitro group of an aliquot portion of the residue from this distillation gave the amount of isomeric nitrobiphenyls formed and hence that of the nitrobenzene by difference. These analytical results gave the relative rate of nitration of biphenyl with respect to benzene (Table I) according to the method of Ingold and Shaw[5]. The remaining mixture of nitrobiphenyls and unreacted biphenyl was dissolved in petroleum ether and chromatographed through a column of alumina, yielding a mixture of isomeric nitrobiphenyls, the composition of which was estimated spectrophotometrically (Table II), absorptions at 245, 250, 262.5, 300 and 310 m$\mu$ being used. In a separate experiment, nitration of biphenyl without benzene under otherwise the same experimental conditions as above gave a mixture of nitrobiphenyls of the same isomeric composition. The ratio of the isomers formed and the relative rate (the mean value of 40) gave the partial rate factors for the nitration of biphenyl, the rate constants of separate nuclear positions of biphenyl relative to one nuclear position of benzene as unity.

The present results show that positions 2 and 4 of biphenyl are very much activated towards nitration by the electromeric effect of the phenyl group, whereas position 3 is deactivated, probably owing to the electron attracting inductive effect of the phenyl group. The possibility can not be excluded that the deactivation is attributable to a destabilizing conjugation, in the transition state, of the substituent phenyl group with the nucleus undergoing substitution at position 3.

*Department of Chemistry*
*Faculty of Science*
*Tokyo University*
*Tokyo*

5) C. K. Ingold and F. R. Shaw, *J. Chem. Soc.*, **1927**, 2918.

## *Nuclear Magnetic Resonance of Deuterated P. V. A. Films*

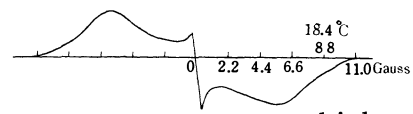
By Masako YOSHIDA, Minoru ODAJIMA, Kōji TANAKA and Kyōzō YAMAGATA

(Received November 20, 1956)

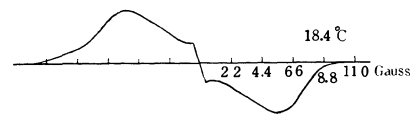
In our previous communication[1], it was described that the derivative curve of the nuclear magnetic resonance absorption of P. V. A. fiber was composed of two parts; one is at the center and very narrow in width and the other very broad. In order to investigate what kinds of hydrogen atoms these two parts were based on, we measured the proton reaonance in the deuterated P. V. A.[2]

The films used for this experiment were cast from about 2.5% aqueous solution of the purified and fractionated P. V. A., on a glass plate placed horizontally in an air thermostat at 50°C. The films were about 0.1 mm. thick, and were cut in pieces with the size of about 5 mm.×20 mm.

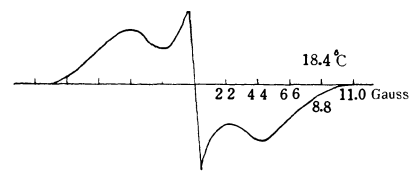
The heavy water vapour was passed for about one hour through the glass tubes mounted by P. V. A. films. One deuterated sample was sealed in an evacuated glass tube, and the other was sealed in a glass tube with the atmosphere of heavy water. As shown in Fig. 1, the derivative curves of nondeuterated P. V. A. film was almost




Non deuterated and vacuum-dried sample




Deuterated and vacuum-dried sample




The sample deuterated and adsorbed with heavy water

Mod.

Fig. 1. Derivative curves of P. V. A. films.

1) Kōji Tanaka, Kyōzō Yamagata and Shigeyoshi Kittaka, This Bulletin, **29**, 843 (1956).

2) Hiroyuki Tadokoro, Syuzo Seki and Isamu Nitta, ibid., **28**, 559 (1955).

similar to that of P. V. A. fiber previously communicated. In deuterated and dried film, the broad component became narrow slightly. In the sample deuterated and adsorbed with the heavy water, the center peak became stronger and the width of the broad component became narrower than those of the dried sample, respectively.

The above result may be interpreted as follows. That is, some parts of the hydrogen atoms in O—H groups in P. V. A. molecules were exchanged by deuterium and partly swelled by heavy water so that the hydrogen atoms of the deuterated molecules became less rigid than those of nondeuterated molecules.

The authors wish to express their appreciation to Prof. Masatami Takeda for his kind discussion on our works.

*Tokyo College of Science, Tokyo*

## *On the Crystal Structure of 2, 2-Dichloro-3, 3-dimethylbutane*

By Tsutomu KOIDE, Tsutomu ODA and Isamu NITTA*

(Received December 4, 1956)

Hexachloroethane and hexamethylethane are characterized by relatively high melting points, 185°C and 100.6°C, respectively; by polymorphism in the solid state, the transition points being 43°C and 71°C for hexachloroethane[1] and −125°C for hexamethylethane[2]; and by high symmetry of the high temperature modifications, as shown by optical isotropy and confirmed by x-ray studies[3,4]. Recently, it has been confirmed[5] that hexabromoethane is also isotrimorphous[6] with hexachloroethane. It seems of interest to examine what will occur in the phase just below the melting point of a hexa-substituted ethane of the type of $(CH_3)_xCl_{3-x}CC(CH_3)_{x'}Cl_{3-x'}$. We have carried out an x-ray diffraction study of 2,2-dichloro-3,3-dimethylbutane, which was reported[7] to have high volatility and a relatively high melting point such as 151–152°C.

This compound was prepared by the method of P. D. Bartlett and L. J. Rosen[7]. Pinacolone was added to powdered phosphorus pentachloride with mechanical stirring, the reaction being maintained at about 5°C. The time of addition was about three hours, after which stirring was continued for ten hours. This mixture was poured on ice. The solid was removed by filtration, washed with water, and air-dried. It was recrystallized twice from ether and then subjected to sublimation twice under abuot 20 mmHg. The solid is volatile and plastic, its vapour having a camphoric odour. A melting point of 151°C was observed in sealed tubes. The crystals were found to be optically isotropic.

Using Cu $K_\alpha$ radiation and materials sealed in thin-walled capillary tubes, we prepared x-ray powder photographs, in which seven lines appeared. The reflections were indexed with a body-centered cubic lattice, the edge length being 7.58 Å. By suspension in a solution of sodium chloride in water, the density of the solid was measured as 1.17 g./cc. at 23°C. Hence it was found that the unit cell contains two molecules, yielding the calculated density as 1.18 g./cc.

Since the lattice is body-centered and the unit contains two molecules, we may place them at the lattice points 0, 0, 0 and 1/2, 1/2, 1/2, of which the symmetry should be at least $T$-23. On the other hand, as the rigid molecule of $(CH_3)_3C\text{-}C(CH_3)Cl_2$ can have at the highest only one plane of symmetry which contains the central C-C bond axis, it becomes necessary to consider some statistical explanation of the structure, as is always so in plastic crystals[3,4,5,8]. In order that the statistical symmetry of the molecule be higher than $T$-23 at 0, 0, 0 and 1/2, 1/2, 1/2, the molecule of the symmetry $C_s$-$m$ should orientate its central axis C-C parallel to each one of the four body-diagonals statistically equally and at

* Faculty of Science, Osaka University.

1) I. Nitta and S. Seki, *J. Chem. Soc. Japan*, **62**, 581 (1941); K. J. Ivin and F. S. Dainton, *Trans. Faraday Soc.*, **43**, 32 (1947); S. Seki and M. Momotani, This Bulletin, **23**, 30 (1950). See also O. Lehman, *Z. Krist.*, **1**, 106 (1877); ibid., **6**, 584 (1882).

2) G. S. Parks, H. M. Huffman and B. Thomas, *J. Am. Chem. Soc.*, **52**, 1032 (1930).

3) C. D. West, *Z. Krist.*, **88**, 195 (1934).

4) C. Finbak, *Tids. Kjem. Bergv.* **17**, No. 9, 2 (1937). M. Atoji, T. Oda and T. Watanabé, *Acta Cryst.*, **6**, 868 (1953).

5) G. J. Snaauw and E. H. Wiebenga, *Rec. Trav. Chim. Pay-Bas.*, **61**, 3 (1942).

6) B. Goszner, *Z. Krist.*, **38**, 151 (1904).

7) P. D. Bartlett and L. J. Rosen, *J. Am. Chem. Soc.*, **64**, 543 (1942).

8) J. Timmermans, *J. Chim. Phys.*, **35**, 331 (1938); I. Nitta and T. Watanabé, This Bulletin, **13**, 28 (1938); T. Oda and T. Watanabé, *J. Chem. Soc. Japan.* **65**, 154 (1944); T. Oda and I. Nitta, ibid., **65**, 621 (1944); R. S. Schwartz, B. Post and I. Fankuchen, *J. Am Chem. Soc.*, **73**, 4490, 5113 (1951); T. B. Reed and W. N. Lipscomb, *Acta Cryst.*, **6**, 108 (1953).

the same time laterally so that the C-C axis acquires a statistical symmetry of 3 at least. It is also conceivable that the observed feature of x-ray diffraction can be explained by molecules in free rotation about the central C-C axis. Which one is the case of the present statistical structure seems almost entirely indiscriminable from consideration of intensity data, since the lines are so few as mentioned above. However, it may be said that this structure is statistically isomorphous with cubic hexamethylethane at room temperatures and hexachloroethane above 71°C. The edge length 7.58 Å is between those[3] of 7.69 Å for $C_2(CH_3)_6$ and 7.43 Å for $C_2Cl_6$ at 80°C. In the diffraction of x-rays by the present crystal, we have observed, similarly to those hexa-substituted ethanes stated above, very rapid decrease of intensity with increasing angles of scattering, which is evidently in close relationship with the disordered orientation of the molecule in intense thermal motion.

It will be expected that such "rotational" mode of the molecule in the crystal will change at lower temperatures. We have undertaken a differential thermal analysis and observed, on its heating curve from liquid air temperature, anomalous heat effect at about −94.9°C and a small effect at −75.1°C. As a result, x-ray studies of single crystals of probably ordered phase below the transition point must await techniques for the growth of the single crystals below this temperature.

In conclusion, we should express our hearty appreciation to Doctor S. Seki, Faculty of Science, Osaka University for his gracious interest during this work. We also wish to thank Mr. H. Chihara for his kind aid. The cost of this research was defrayed from the Scientific Research Grant from Ministry of Education, to which the thanks of the present authors are due.

*Chemical Laboratory, Osaka University of Liberal Arts and Education*
*Tennoji, Osaka*

## *A Method for the Preparation of the Raney Nickel Catalyst with a Greater Activity*[1]

By Shigeo NISHIMURA and
Yoshiyuki URUSHIBARA

(Received November 20, 1956)

The authors have found that the Raney nickel catalyst loses partly its activity during the development from the alloy with a strong caustic alkali, and that, by adding the alkali in portions to the alloy instead of adding the alloy in portions to the alkali, a greater activity is obtained. The procedure is described by an example as follows:

Two grams of a Raney alloy, consisting of 40% of nickel and 60% of aluminium, and 6 cc. of water are placed in a conical flask of 25 cc. capacity and warmed on a waterbath of 50°C, and 0.1 cc. of 40% caustic soda is added with vigorous stirring. The mixture is stirred vigorously at the temperature until the violent reaction subsides and the alloy is covered with grey films. Then 6 cc. of 40% caustic soda is added in portions slowly at the beginning but at a growing speed as long as the reaction does not become too violent, which needs about five minutes. The mixture is stirred at the same temperature just until the grey precipitate in the liquid becomes nearly white. The time needed for the digestion depends on the nature of the alloy used. The upper liquid is removed and the metal is washed three times with 10 cc. of distilled water and twice with 10 cc. of ethanol by decantation.

The catalyst prepared in this way reduces 3.926 g. (0.04 mole) of cyclohexanone, dissolved in 20 cc. of ethanol, to cyclohexanol in twenty-two minutes at 25°C and under the ordinary pressure. The reduction with a catalyst of W 7 type prepared by the procedure described by Adkins and Billica[2] from the same amount of the same alloy needs forty to fifty minutes under the same conditions. Similar results are obtained with other specimens of the Raney alloy, for instance an alloy containing 50% of nickel and 50% of aluminium.

*Department of Chemistry, Faculty of Science, The University of Tokyo, Tokyo*

1) Cf. Jiro Yasumura, "Kagaku-no-Ryoiki", Vol. 6, p. 733 (1952).
2) H. Adkins and H. R. Billica, *J. Am. Chem. Soc.*, **70**, 695 (1948).

# *Chemical Studies on Wood Hemicelluloses. I. On the Hemicellulose of Japanese Beech Wood. I**

By Seishi MACHIDA, Mitsumasa INANO and Yasuo MATSUMURA

(Received September 8, 1956)

## Introduction

Concurrently with the development of an improved type of chemical pulp has appeared the need for still more minute knowledge of the carbohydrates associated with wood cellulose[1].

Generally speaking, more hemicelluloses, which are said to have undesirable influences upon the manufacture and qualities of viscose or acetate rayon[2], are contained in the chemical pulp from deciduous wood than from coniferous. But the chemical structure of wood hemicellulose is not yet clear. The deciduous woods, for all that, have recently appeared to be used increasingly for the dissolving pulp in Japan, owing to unavoidable circumstances of natural sources.

This research was designed to find out a suitable method of analysing wood hemicellulose by paper chromatography; and the behaviour of hemicelluloses in Japanese beech wood (*Fagus crenata* Blume) during the pulping processes was analysed. The state of hemicelluloses in wood pulp was also investigated.

## Experimental Results and Discussion

(1) **Preparation of Samples.**—Beech wood grown in Hokkaido was employed in the present study. The normal analysis is shown in Table I.

TABLE I
THE COMPOSITION OF THE JAPANESE BEECH WOOD

| | (%) |
|---|---|
| Ash | 0.55 |
| Extract with alcohol-benzene | 1.50 |
| Lignin | 22.76 |
| Pentosan | 19.86 |
| Uronic acid | 0.76 |
| Total cellulose | 54.80 |
| $\alpha$-cellulose | 40.61 |
| $\beta$-cellulose | 6.74 |
| $\gamma$-cellulose | 7.45 |

**a. Wood.**—Sawdust (40 mesh) of the wood was air-dried.

**b. Unbleached Pulp.**—Chips of the wood were cooked by sulfite pulping process using calcium base.

Cooking liquor: total $SO_2$ 7%, combined $SO_2$ 0.8%, liquor ratio 1 : 5. Time to 100°C, 2; time from 100°C to 110°C, 2; time from 110°C to 140°C, three hours. Maximum temperature, 140°C; maximum pressure, 7 atm. Cooking time at maximum temperature, five hours.

The pulp resulting from the procedure was washed and air-dried. Cuprammonium viscosity:** 4.20.

**c. Bleached Pulp at the First Step.**—Fifty grams of the unbleached pulp were treated with 1665 ml. of water containing 5.65 g. of chlorine for an hour. After the bleaching, the sample was washed with water until the filtrate indicated no reaction with potassium iodide-starch test paper, and air-dried.

**d. Bleached Pulp at the Second Step.**—Thirty grams of the said pulp were secondly treated with 600 ml. of NaOH solution at 90-95°C for an hour. The amount of NaOH used was 7% of that of the pulp. The pulp was washed and dried. Cuprammonium viscosity, 4.24.

**e. Bleached Pulp at the Third Step.**—Sixteen gram of the pulp were subsequently bleached with 300 ml. of water containing 1 g. of NaClO and 0.1 g. NaOH at 50°C for four hours. Cuprammonium viscosity, 4.06.

(2) **Analytical Procedure of Hemicellulose.**—As the hemicellulose was not satisfactorily extracted with alkali directly from the wood[3], holocellulose was prepared from each sample by Wise's method[4].

About 4 g. of the holocellulose was mixed with 72% sulfuric acid at room temperature. After 17.5 hours, the solution was diluted with water to a concentration of 4% sulfuric acid, heated in a bath of boiling water, neutralized with barium carbonate using congo-red test paper and filtered. The filtrate was evaporated to 50 ml.

The component sugars in each hydrolysate of the sample were detected by paper chromatography.

As much work has been done on the paper

* Read before the 9th Annual Meeting of the Chemical Society of Japan on April 5, 1956 at Kyoto.

1) W. J. Polglase; "Advances in Carbohydrate Chemistry," Vol **10**, (1955), p. 283.

2) G. Jayme and U. Schench *Mell. Textilber.*, **31**, 153 (1950).

** Cuprammonium viscosity means the specific viscosity of the solution of 50 mg. sample in 100 ml. Schweizer's reagent at 20°C.

3) H. Sobue and A. Hatano, *J. Chem. Soc. Japan. Ind. Chem. Sec.*) **55**, 131 (1952).

4) L. E. Wise and E. K. Ratliff, *Anal. Chem.*, **19**, 459 (1947).

chromatography of carbohydrates[5], various solvents were tested to find the most suitable method for the present research. After many preliminary experiments, it became clear that the use of circular chromatograms which were reported by Buurman[6] would have certain advantages. $R_f$ values of reference-sugars obtained are shown in Table II.

TABLE II

$R_f$ VALUE OF REFERENCE-SUGARS

| Solvent / Sugars | Butanol-acetic acid-water (4 : 5 : 1) | Butanol saturated with water | Phenol saturated with water | Butanol-pyridine-water (4 : 1 : 2) |
|---|---|---|---|---|
| Arabinose | 0.46 | 0.15 | 0.58 | 0.41 |
| Xylose | 0.47 | 0.17 | 0.49 | 0.46 |
| Glucose | 0.38 | 0.10 | 0.40 | 0.36 |
| Galactose | 0.35 | 0.09 | 0.45 | 0.33 |
| Mannose | 0.44 | 0.15 | 0.47 | 0.40 |

**(3) Composition of Beech Pulp Hemicellulose.**—Referring to the results mentioned above, the chromatographic separations were carried out on a sheet of Toyo-Roshi No. 2 filter-paper with the solvent mixture of *n*-butanol-pyridine-water (4 : 1 : 2).

Aniline hydrogen phthalate in *n*-butanol was used as a spray to reveal the sugars[7]. In every case where a sugar was indicated by $R_f$ value, the identity was established by running further chromatograms with reference-sugar spots. And each component sugar was analysed quantitatively according to Buurman[6]. The results obtained are shown in Table III.

TABLE III

COMPOSITION OF HEMICELLULOSE OF BEECH WOOD

| | Xylan | Araban | Mannan | Uronic acid |
|---|---|---|---|---|
| Wood | 19.7 | 1.0 | 0.1 | 0.76 |
| Unbleached pulp | 5.7 | trace | trace | 0.26 |
| Bleached pulp at the 1st step | 5.0 | — | trace | 0.44 |
| Bleached pulp at the 2nd step | 3.1 | — | trace | 0.49 |
| Bleached pulp at the 3rd step | 2.8 | — | trace | 0.58 |

Uronic acid is perhaps 4-O-methyl-D-glucuronic acid. Rhamnose was not found in the hemicellulose, which differs from that of European beech wood (*Fagus sylvatica*) reported by Aspinall et al[8].

It is found, as is shown in Table III, that the greater part of xylan is removed from the wood during the sulfite cooking. Oxidative bleaching is less effective for the removal of the remaining xylan than the alkali treatment. About 3% of xylan still remains in the final pulp, which is so-called resistant xylan.

Mannan is contained in the original wood in small amount, but a trace of it is found to remain still in the final pulp without being removed in each step of the pulping process.

Both xylan and mannan, having similar chemical structure to cellulose, are considered to exist not only in the amorphous but also in the crystalline region of cellulose.

Araban contained originally in small quantity in the wood is almost completely removed during the sulfite cooking and chlorine-bleaching.

Uronic acid, which is probably 4-O-methyl-D-glucuronic acid, is found to be ruptured during the sulfite cooking, but D-glucuronic acid is formed again in the subsequent oxidative treatments of the pulp. Koike[9] found that most of the carboxyl group is distributed in the outer secondary lamellae. The fact that two-thirds of the carboxyl group is removed during the sulfite cooking indicates that the cooking liquor penetrates tolerably into the cell walls.

It was found by electron microscopy that these bleaching reactions proceed topochemically***. At any rate, the hemicellulose consisting mainly of xylan, mannan and uronic acid was found to be contained in the beech wood pulp for all the bleaching reactions; further treatment is needed to remove the residual xylan and mannan from the wood cellulose.

It is a characteristic of wood hemicellulose that it is very firmly associated with cellulose. The studies of the molecular structure of the Japanese beech wood hemicellulose will be published in subsequent papers.

## Summary

1. A suitable method of analysing wood hemicelluloses by paper chromatography was studied.

2. The behavior of hemicellulose in Japanese beech wood (*Fagus crenata* Blume) during the chemical pulping processes was studied; the state of the hemicelluloses in wood pulp was investigated.

The beech wood used in this work was generously provided by Dr. H. Okada of Kokusaku Pulp Ind. & Co. Ltd.

*Chemical Laboratory of Textile Fibers*
*Kyoto University of Industrial*
*Arts and Textile Fibers, Kyoto*

5) G. N. Kowkabany, "Advances in Carbohydrate Chemistry," Vol. 9, 303 (1954).
6) A. Buurman, *Text. Res. J.*, **23**, 888 (1953).
7) S. M. Partridge, *Nature*, **164**, 443 (1949); S. Machida, M. Inano, This Bulletin, **28**, 630 (1955).
8) G. O. Aspinall, E. L. Hirst and R. S. Mahomed, *J. Chem. Soc.*, **1954**, 1734.
9) R. Koike and S. Nagatomo, *J. Tappi*, **9**, 375 (1955).
*** The results will be published elsewhere.

# *Molecular Rotations of Glucides in Relation to their Structures. I. The Absolute Configuration of γ-Lactones*

By Shukichi YAMANA

(Received September 29, 1956)

## Introduction

About the problem of the absolute configuration of an optically active molecule, several studies were undertaken from the standpoint of X-ray analysis of a substance[1], or by calculation of the signs of optical rotatory powers of appropriate molecules[2].

Referring to the hypothesis that the sign of the optical rotatory power of a molecule under investigation is determined by Kirkwood's term $g^{(0)}$, Wood, Fickett and Kirkwood presumed the absolute configuration of the enantiomorph of 2,3-epoxybutane[2]. They first divided the molecule of 2,3-epoxybutane into the following unit groups; a three-membered ring with attached hydrogen atoms and two methyl groups which combine with the ring. Next, by using experimental data, they calculated the partial rotations caused by dynamical coupling effects between these unit groups. However, for lack of experimental data in relation to the three-membered ring, they could not calculate the partial rotations caused by the dynamical coupling effects with which the three-membered ring is concerned. Therefore, they resorted to a quasi-empirical evaluation of them, by using the experimental datum of the optical rotatory power of configurationally related 1,2-epoxypropane. Formerly, Kirkwood proposed a convenient method of calculation of the partial rotation caused by the dynamical coupling effect of OH group, in calculating the optical rotatory power of secondary butyl alcohol[3],*1. To evaluate the optical rotatory powers of polypeptides of alanine, Murakami used a concept of bond-interaction in place of the idea of group-interaction and proposed a method of calculation of the partial rotation caused by the dynamical coupling effect of C=O bond. He demonstrated also that the observed values of optical rotatory power were proportional to the values calculated by Kirkwood's polarizability theory[4]. It was explained that the contribution of the one-electron effect[5] is much smaller than that of the dynamical coupling effect[6].

The author presumed the absolute configuration of γ lactones of a five-membered ring, by using a method*2 which was devised by adopting the conception of Freudenberg's Verschiebungssatz[7] on the basis of Kirkwood's group-interaction method[3] and Murakami's bond-interaction method[4]. In order to avoid the difficulty caused by the impossibility of calculation of the terms with which the five-membered ring is concerned, a new method, different from Kirkwood's, was proposed*3.

## Theoretical Formulae

The molecular rotation of plane polarized light of wave-length $\lambda$ by an optically active substance is given as follows[3],

$$[\mathrm{M}]=\frac{288\pi^2 N}{\lambda^2}\cdot\frac{n^2+2}{3}g. \qquad (1)$$

where $N$ is Avogadro's number and $n$ is the refractive index of the medium (solution or pure liquid). If every one of the substituent groups of the molecule—strictly speaking, unit groups made by division of the molecule—has its own optical axis of cylindrical symmetry,

$$g\fallingdotseq g^{(0)}=\frac{1}{6}\sum_{i>k=1}^{N}\alpha_i\alpha_k\beta_i\beta_k G_{ik}\vec{R}_{ik}(\vec{b}_i\times\vec{b}_k)\text{*4}$$

1) A. F. Peerdeman, A. J. van Bommel and J. M. Bijvoet, *Koninkl. Ned. Akad. Wetenschap. Proc.*, B. **54**, 16 (1951).

2) W. W. Wood, W. Fickett and J. G. Kirkwood, *J. Chem. Phys.*, **20**, 561 (1952).

3) J. G. Kirkwood, *J. Chem. Phys.*, **5**, 479 (1937).

*1 Ref. "Molecular Model and Data Used" in this article.

4) H. Murakami, This Bulletin, **27**, 246 (1954), **28**, 583 (1955).

In these papers, the author presumed that the proportional constant depends upon the quantitative ratio between various isomers in the equilibrium state.

5) W. J. Kauzmann, J. E. Walter and H. Eyring, *Chem. Rev.*, **26**, 339 (1940).

6) W. Kuhn, *Z. Electrochem.*, **56**, 506 (1952).

*2 The idea of this method had already been demonstrated in the previous paper, (S. Yamana, This Bulletin, **23**, 259 (1950)).

7) K. Freudenberg und W. Kuhn, *Ber.*, **64**, 726 (1931).

*3 Ref. "Method Proposed" in this paper.

*4 The error of signs in reference (3) is corrected in reference 2).

$$G_{ik}=\frac{1}{R^3_{ik}}\left[\vec{b}_i\cdot\vec{b}_k-3\frac{(\vec{b}_i\cdot\vec{R}_{ik})(\vec{b}_k\cdot\vec{R}_{ik})}{R^2_{ik}}\right]$$

$$\vec{R}_{ik}=\vec{R}_k-\vec{R}_i$$

where $\alpha_i$ (mean polarizability of group or bond $i$) $=(3/4\pi N)\cdot\sum_s^{(i)} A_s$, but $A_s$ is atomic refraction; $\beta_i$ (anisotropy ratio of the polarizability of group or bond $i$) $=\alpha_{11}^{(i)}-\alpha_{22}^{(i)}/\alpha_i$, but $\alpha_{11}^{(i)}$ and $\alpha_{22}^{(i)}$ are components of $\alpha_i$ parallel and perpendicular to $\vec{b}_i$ and $\beta_i$ can be calculated from the depolarization-degree $\Delta$ of light, scattered by vapor; $\vec{b}_i$ (unit vector along the optical symmetry axis of group or bond $i$) and $\vec{R}_i$ (vector distance from the center of mass of the molecule to the center of mass of group or bond $i$) are determined from the geometry of the molecule.

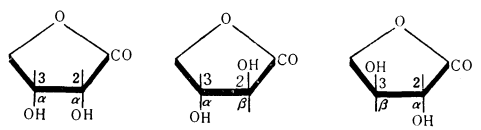
## Molecular Model and Data Used

$\gamma$-Lactones to which the calculations were applied and their corresponding molecular rotations, are as follows,

| Name | Unit Groups | $[M]_D^{20}$(W) | Lit. |
|---|---|---|---|
| D-erythronic $\gamma$-lactone | [CO, $(OH)^{2\alpha}$,*5, $(OH)^{3\alpha}$, Ring]*6 | $-86.5^0$ | (a) |
| D-threonic $\gamma$-lactone | [CO, $(OH)^{2\beta}$, $(OH)^{3\alpha}$, Ring] | $-36.6^0$ | (b) |
| L-threonic $\gamma$-lactone | [CO, $(OH)^{2\alpha}$, $(OH)^{3\beta}$, Ring] | $36.6^0$ | (b) |

Square brackets [ ], written on the right side of these names imply unit groups of the corresponding $\gamma$-lactone molecules, and any two members of these unit groups in the same square bracket couple together to produce their own partial molecular rotation. (ref. Fig. 1). Haworth's perspective formulae of these $\gamma$-lactones are shown in Fig. 1.

It was concluded that all of four carbon atoms and one oxygen atom of the aldofuranose ring lie on one plane — namely, the $\gamma$-lactone ring plane — from the results of investigations measuring the dipole moment[8] of an aldofuranose molecule and examining its crystal with X ray[9].




D-Erythronic-$\gamma$-lactone D-Threonic-$\gamma$-lactone L-Threonic $\gamma$-lactone

Fig. 1. Haworth's perspective formulae

In order to simplify the calculations, the values of bond lengths and valency angles were assumed as follows*7,

(1) The lengths of C—C and C—O bonds in the $\gamma$-lactone ring are all 1.54Å, that is to say, the $\gamma$-lactone ring plane is a regular pentagon and the length of its side is 1.54Å.

(2) C=O bond (its length is 1.24Å)[c] projects out from $C^1$-atom*8, in the direction of the extension line from the center of the ring to $C^1$-atom.

(3) The hydroxyl oxygen atom (represented by $O^h$) and H atom combine with C atom of the $\gamma$-lactone ring and the angle $\angle O^hCH$ (tetrahedral angle = 109°28′) is bisected by the $\gamma$-lactone ring plane. The length of C-$O^h$ bond is 1.42 Å*9. The refractive indices of aqueous solutions of three $\gamma$-lactones given in Fig. 1, whose concentrations are suitable for measurement of the optical rotatory power, can be considered equal*10.

Concerning the experimental data and the manner of treatment of OH groups and of C=O bond, the following two methods of treatment were employed.

Kirkwood's Treatment[3].— It is supposed that OH group has its optical axis of cylindrical symmetry directed along its bond to C atom, and the optical center of OH group is located at O atom*11. Values of mean polarizability $\alpha$ and of anisotropy

*5 $(OH)^{2\alpha}$ means OH group, which combines with 2-position of the ring in $\alpha$-orientation. (ref. L. F. Fieser, *J. Am. Chem. Soc.*, **72**, 623 (1950)).

*6 Because of the small polarizabilities of H atom and C-H bond, they can be neglected.

a) Ruff, *Ber.*, **32**, 3679 (1899).

b) K. Gätzi and T. Reichstein, *Helv. Chim. Acta.*, **20**, 1298 (1937).

8) H. Hilbert and J. S. Allen, *J. Am. Chem. Soc.*, **54**, 4115 (1932).

9) E. G. Cox and T. H. Goodwin, *J. Chem. Soc.*, **1932**, 1844.

*7 In the calculation of the optical rotatory power by Kirkwood's polarizability theory, a small deviation in atomic distance or in valency angle causes only a small deviation in the calculated value of optical rotatory power. Concerning a concrete example of the magnitude of this deviation, refer to the next paper "Molecular Rotations of Glucides in Relation to their Structures. II."

c) M. Kimura and Y. Kurita, *J. Chem. Soc. Japan*, **72**, 396 (1951).

*8 $C^1$-atom means the C atom at 1-position of the ring.

*9 The mean value of lengths of C-O bonds in $\alpha$-D-glucose. (ref. T. R. R. Mc Donald and C. A. Beevers, *Acta Cryst.*, **5**, 654 (1952)).

*10 For determination of optical rotatory power of a sugar-group substance, about 2% aqueous solution is used in general, and the value of $n$ of it is about 1.34.

*11 This manner of treatment was rejected by Gorin, J. Walter and H. Eyring (*J. Chem. Phys.*, **6**, 824 (1938)), because it regards a single OH group as isotropic. The author of this paper, however, thought that this was very convenient and useful for approximate estimation of partial rotation of the OH group, especially when optical rotatory power of such a substance which has many OH groups in its molecule as a sugar was the subject. Besides, for lack of data for C-O and O-H bonds, OH group cannot be divided into its component bonds.

ratio $\beta$ of OH group are $1.04\times10^{-24}$ (cc)[d] and 0.35[e] respectively.

Murakami's Treatment.[4]—It is supposed that C=O bond has its optical axis of cylindrical symmetry directed along itself. The optical center of C=O bond is located at its center of mass. Value of $\alpha\beta$ of C=O bond is $(19.4-8.0)\times10^{-25}=1.14\times10^{-24}$ (cc)[f].

## Method Proposed

Partial molecular rotations of the plane polarized light of wave-length of D line at 20°C, represented by the notation $[\mu]^{20}_{D}$, caused by the dynamical coupling effect between any two members of unit groups in the molecular model of $\gamma$-lactone, were calculated by using Eq. (1). Of course, the molecular rotation is the sum of the partial molecular rotations, namely

$$[M]^{20}_{D}=\Sigma[\mu]^{20}_{D}$$

where $\Sigma$ means the summation over all $[\mu]^{20}_{D}$s possible. Therefore, for the calculated values, the following equation can be obtained.

$$[M]^{20}_{Dcalcd}=\Sigma[\mu]^{20}_{Dcalcd} \quad (2)$$

where the suffix calcd means the calculated value. For the observed values,

$$[M]^{20}_{Dobs}=\Sigma[\mu]^{20}_{Dobs}{}^{*12} \quad (3)$$

The results of calculation are given in Table I.

TABLE I

$[\mu]^{20}_{Dcalcd}\ (3/n^2+2)$, CAUSED BY THE DYNAMICAL COUPLING EFFECT BETWEEN ANY TWO MEMBERS OF UNIT GROUPS (EXCEPT RING), WITH REGARD TO HAWORTH'S PERSPECTIVE FORMULAE

| | $3\beta$ | $3\alpha$ | $2\beta$ | $2\alpha$ |
|---|---|---|---|---|
| CO | 4.9 | −4.9 | 21.0 | −21.0 |
| $2\alpha$ | 4.4 | 0 | | |
| $2\beta$ | 0 | −4.4 | | |

Note: $2\alpha$ is an abbreviated symbol of $(OH)^{2\alpha}$, and so on.

If the theory used for the calculation of optical rotatory power is perfect and data which are used in calculation are satisfactory, the calculated value, $[M]^{20}_{Dcalcd}$, must be equal to the observed value, $[M]^{20}_{Dobs}$, in sign and magnitude. However, in fact, they are not equal, owing to the imperfectness of the theory, and of assumptions and to the errors of data used. Generally, $[M]^{20}_{Dcalcd}$ by Kirkwood's polarizability theory is equal to $[M]^{20}_{Dobs}$ in sign, and the magnitude of the former can be made equal to that of the latter by multiplying by a proportionality-constant[4],*13. Therefore,

$$[M]^{20}_{Dobs}=\kappa[M]^{20}_{Dcalcd} \quad (4)$$

where $\kappa$ is always positive. If the orientation of one unit group in a molecular model changes, $[M]^{20}_{Dobs}$ and $[M]^{20}_{Dcalcd}$ change to $[M']^{20}_{Dobs}$ and $[M']^{20}_{Dcalcd}$ respectively. By the change of the orientation of a unit group, a new molecule appears. For this new molecule,

$$[M']^{20}_{Dobs}=\kappa[M']^{20}_{Dcalcd} \quad (5)$$

where $[M']^{20}_{D}$ means the molecular rotation of a new substance. From Eq. (5) minus Eq. (4),

$$[M']^{20}_{Dobs}-[M]^{20}_{Dobs}=\kappa([M']^{20}_{Dcalcd}-[M]^{20}_{Dcalcd})$$

or $$\Delta[M]^{20}_{Dobs}=\kappa\Delta[M]^{20}_{Dcalcd} \quad (6)$$

In (6), as $\kappa$ is always positive, if, concretely speaking, the orientation of a unit group changes in a molecule, the observed value of its optical rotatory power changes toward the same direction as the calculated value. Accordingly, in calculation, with regards to a definite molecular model, of $\Delta[M]^{20}_{D}$ due to the orientation-change of a unit group, if $\Delta[M]^{20}_{Dcalcd}$ has the same sign as $\Delta[M]^{20}_{Dobs}$ this molecular model must be a structurally correct representation of the absolute configuration. On the other hand, if they are different in sign, the model used must be incorrect. In short, the problem of the absolute configuration becomes the problem of the sign of $\kappa$ of Eq. (6) or (4). The author will illustrate the above-described principle, by using concrete examples. As is seen in Fig. 1, if the ori-

d) Landolt-Börnstein, Physikalisch-Chemische Tabellen, Hw. 2. p. 985.

e) Values obtained by Ramakrishna-Rao; see Landolt-Börnstein, Physikalisch-Chemische Tabellen, 5th Ed., Eg. 2. p 90, 91.

f) Sheng-Nien Wang, *J. Chem. Phys.*, **7**, 1012 (1939).

*12 In the actual experiments, $[\mu]$ can not be observed. Then strictly speaking, $[\mu]^{20}_{Dobs}$ is of hypothetical character.

*13 In this case, the value of the proportionality-constant depends upon various factors, chiefly owing to the effect of solvation.

entation of OH group which combines with 2-position of the ring in the molecular model of D-erythronic $\gamma$-lactone changes from $\alpha$ to $\beta$, the molecular model of D-threonic $\gamma$-lactone can be obtained, and if the orientation of OH group, which combines with 3-position of the ring in the molecular model of D-erythronic $\gamma$-lactone changes from $\alpha$ to $\beta$, the molecular model of L-threonic $\gamma$-lactone can be obtained. Therefore, by calculation, with regards to Haworth's perspective formulae, of $\Delta[M]_D^{20}$ caused by the above-described two orientation-changes we can presume the absolute configuration of $\gamma$-lactones. That is to say, if $\Delta[M]_{Dcalcd}^{20}$ is in the same direction as that of $\Delta[M]_{Dobs}^{20}$, Haworth's perspective formula (accordingly, Fischer convention)[10] is presumed to be a structurally correct representation of absolute configuration, and if the change is in the opposite direction, the formula is presumed to be incorrect. This method of presumption of the absolute configuration can be easily subjected to calculation with regards to D-erythronic- and D-threonic-$\gamma$-lactones, as follows; $[\mu]_{Dcalcd}^{20}(3/n^2+2)$, caused by the dynamical coupling effects between OH group which combines with 2-position of the ring and the other unit groups in these molecules are given below. (ref. Table I)

| | CO | $3\alpha$ | Ring | Sum |
|---|---|---|---|---|
| $2\alpha$ | $-21.0$ | 0 | $(2\alpha)\times$Ring*14 | $-21.0+(2\alpha)\times$Ring |
| $2\beta$ | 21.0 | $-4.4$ | $(2\beta)\times$Ring | $16.6+(2\beta)\times$Ring |

From Eq. (2), $\Delta[M]_{Dcalcd}^{20}=\sum\Delta[\mu]_{Dcalcd}^{20}$

Therefore, $\Delta[M]_{Dcalcd}^{20}$ (namely, $\sum\Delta[\mu]_{Dcalcd}^{20}$) due to the orientation-change of OH group which combines with 2-position from $\alpha$ to $\beta$ in this case is $\{(16.6+(2\beta)\times\text{Ring})-(-21.0+(2\alpha)\times\text{Ring})\}(n^2+2)/3=\{37.6+(2\beta)\times\text{Ring}-(2\alpha)\times\text{Ring}\}(n^2+2)/3$

The corresponding $\Delta[M]_{Dobs}^{20}$ is given by ($[M]_{Dobs}^{20}$ of D-Threonic $\gamma$-lactone) minus ($[M]_{Dobs}^{20}$ of D-Erythronic $\gamma$-lactone). This is, $-36.6-(-86.5)=49.9$

By using these values, Eq. (6) becomes as below,

$$49.9=\kappa\{37.6+(2\beta)\times\text{Ring}-(2\alpha)\times\text{Ring}\}(n^2+2)/3. \quad (7)$$

The author's purpose was to know the sign of $\kappa$, but to his regret, he was unable to calculate $(2\alpha)\times$Ring and $(2\beta)\times$Ring, owing to lack of data for $\alpha$, $\beta$ and $\vec{b}$ etc. of Ring. Kirkwood used a quasi-empirical method in order to avoid the difficulty of calculating $[\mu]_D$ due to a three-membered ring*15, but the author devised a new quasi-empirical method, different from that of Kirkwood, as follows.

The same treatment was tried at 3-position of the ring, in the molecular model of D-erythronic $\gamma$-lactone as that which was carried out at 2-position, above, and the following equation was obtained.

$$123.1=\kappa\{14.2+(3\beta)\times\text{Ring}-(3\alpha)\times\text{Ring}\}(n^2+2)/3 \quad (8)$$

On the other hand, owing to the symmetry of the $\gamma$-lactone ring plane

$$(2\alpha)\times\text{Ring}=(3\beta)\times\text{Ring}$$

and $$(2\beta)\times\text{Ring}=(3\alpha)\times\text{Ring}$$

Combining these two conditional equations with Eqs. (7) and Eq. (8)

$$\kappa=10.02/n^2+2$$

where $n^2$ is always positive, then $\kappa>0$*16. This result indicates that the Fischer convention is a structurally correct representation of absolute configuration, and this is consistent with those of Bijvoet[15] and Kirkwood[2].

## Summary

The changes in optical rotatory power of $\gamma$-lactone due to orientation-changes of a unit group in the molecule were calculated by using the Kirkwood's polarizability theory with regard to molecular model, derived from Haworth's perspective formula. The Fischer convention was presumed to be the structurally correct representation of absolute configuration.

10) Wohl and Freudenberg, *Ber.*, **56**, 309 (1923).

*14 $(2\alpha)\times$Ring means $[\mu]_{Dcalcd}^{20}(3/n^2+2)$, caused by the dynamical coupling effect between $(OH)^{2\alpha}$ group and ring.

*15 Ref. "Introduction" of this paper.

*16 By using n=1.34 (ref. *10). $\kappa\fallingdotseq 2.64$. That is to say, $[M]_{Dobs}^{20}$ is about 2.64 times as large as $[M]_{Dcalcd}^{20}$. The value of $\kappa(2.64)$ happens to be very consistent with the value of $\kappa=3.97/1.43=2.78$, obtained by T. C. Kwoh and H. Eyring (*J. Chem. Phys.*, **18**, 1186 (1950)) for the optical rotatory power of the acetone solution of benzoin.

The author wishes to express his sincere gratitude to Professor S. Tanaka (Kyoto University) for his valuable advice and kind encouragement throughout the course of this study.

*Department of Chemistry*
*Kyoto Gakugei University*
*Fushimi-ku, Kyoto*

# *Molecular Rotations of Glucides in Relation to their Structures. II. The Conformation and the Absolute Configuration of Aldopyranoses. Physical Meaning of Hudson's Isorotation Rule*

By Shukichi YAMANA

(Received October 1, 1956)

## Introduction

The problem of stereochemical structure of the aldopyranose-ring in its aqueous solution is not yet solved. By x-ray analysis of the crystals of aldopyranoses, Cox, Goodwin and Wagstaff concluded that the aldopyranose-ring is composed of five coplanar C atoms and one O atom (the ring-O-atom) situated outside the plane. Such a ring is called Cox's flat ring. They presumed, moreover, that aldopyranose molecules retain Cox's flat ring even in aqueous solutions[1].

From the results of the studies on cuprammonium-glycoside complexes, Reeves concluded that an aldopyranose molecule has a slightly distorted hexagonal structure oriented in one of the Sachse strainless ring[2] conformations, and that all of D-galactose, D-glucose and D-mannose have a chair-form ring of special type (according to Reeves' symbol, C 1 conformation[3],*1.

On the other hand, Hudson reported of the quantitative relation between the structure of pyranoses and the value of their molecular rotations, and found Hudson's isorotation rule, but he could not explain the fact that the magnitude of the anomeric difference*2 of mannose is smaller than those of other pyranoses[4]. Freudenberg explained the above-described fact, paying attention to the orientation of the OH group, which combines with $C^2$-atom, but his explanation did not imply any physical or mathematical equations[5]. Kauzmann, Walter and Eyring discussed this rule from the standpoint of the one-electron theory, but they insisted upon the fact that the OH group is not isotropic and the orientations of O—H bonds are complex, and they did not give any decisive explanation for this rule[6]. In short, the physical meaning of Hudson's isorotation rule and of the deviation of mannose from this is not yet determined. The author discussed in the preceding article[7] the absolute configuration of $\gamma$ lactones by using Kirkwood's treatment of OH group, regarding it as nearly isotropic. By using this treatment, the absolute configuration of aldopyranoses was examined as follows*3; The method of investigation was quite similar to that used for the study of $\gamma$-lactones. It was, first, to assume a molecular model, and next, to calculate the variation of the molecular rotation of the plane polarized light of the wave-length of D line at 20°C, $(\Delta[M]_D^{20})$, caused by the orientation-change of one unit group in the molecule by using Kirkwood's polarizability theory[8]; lastly, to examine the sign of the proportionality-constant $\kappa$, by making the

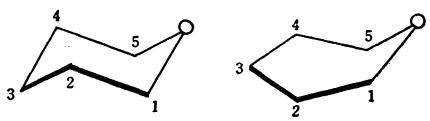
1) E. G. Cox, T. H. Goodwin and (Miss) A. I. Wagstaff, *J. Chem. Soc.*, **1953**, 1495, part 2.
2) U. Sachse, *Z. Phys. Chem.*, **10**, 203 (1892).
3) R. E. Reeves, *J. Am. Chem. Soc.*, **72**, 1499 (1950).
*1 By X-ray analysis, T. R. R. McDonald and C. A. Beevers came to the conclusion that the structure of $\alpha$-D-glucose molecule in crystalline state is almost the same as that of Reeves' C 1 conformation, but its bond lengths and valency angles are not simple (ref. T. R. R. Mc Donald and C. A. Beevers, *Acta. Cryst.*, **5**, 654 (1952)).
*2 This is the difference in optical rotation of $\alpha$ and $\beta$ aldoses.
4) C. S. Hudson and K. P. Monroe, *J. Am. Chem. Soc.*, **41**, 1141 (1919).
5) K. Freudenberg and W. Kuhn, *Ber.*, **64**, 703 (1931).
6) W. J. Kauzmann, J. E. Walter and H. Eyring, *Chem. Rev.*, **26**, 339 (1940).
7) S. Yamana, This Bulletin, **30**. 203 (1957).
*3 Then, unexpectedly, it became possible to presume the conformation of the aldopyranose-ring, and moreover, to understand the physical meaning of Hudson's isorotation rule.
8) J. G. Kirkwood, *J. Chem. Phys.*, **5**, 479 (1937).

| Name | Unit Groups | $[M]_D^{20}$(w) | Lit. |
|---|---|---|---|
| α-D-Galactose | $[(OH)^{1\alpha}, (OH)^{2\alpha}, (OH)^{3\beta}, (OH)^{4\beta}, (CH_2OH)^{5\beta}$, Ring] | 261.0° | (a) |
| β-D-Galactose | $[(OH)^{1\beta}, (OH)^{2\alpha}, (OH)^{3\beta}, (OH)^{4\beta}, (CH_2OH)^{5\beta}$, Ring] | 97.6° | (a) |
| α-D-Glucose | $[(OH)^{1\alpha}, (OH)^{2\alpha}, (OH)^{3\beta}, (OH)^{4\alpha}, (CH_2OH)^{5\beta}$, Ring] | 198.2° | (a) |
| β-D-Glucose | $[(OH)^{1\beta}, (OH)^{2\alpha}, (OH)^{3\beta}, (OH)^{4\alpha}, (CH_2OH)^{5\beta}$, Ring] | 34.7° | (a) |
| α-D-Mannose | $[(OH)^{1\alpha}, (OH)^{2\beta}, (OH)^{3\beta}, (OH)^{4\alpha}, (CH_2OH)^{5\beta}$, Ring] | 53.8° | (b) |
| β-D-Mannose | $[(OH)^{1\beta}, (OH)^{2\beta}, (OH)^{3\beta}, (OH)^{4\alpha}, (CH_2OH)^{5\beta}$, Ring] | −29.3° | (b) |

calculated value of $\Delta[M]_D^{20}$ proportional to its observed value. However, as it was impossible to calculate the terms concerning the aldopyranose-ring, a new method was applied*4.

## Molecular Model and Data Used

Reeves' C 1 conformation and Cox's flat ring were used as the molecular model of the aldopyranose-ring for calculation. These are shown in Fig. 1.




Reeves' C 1 conformation  Cox's flat ring

Fig. 1. Aldopyranose-ring
○, ring-O-atoms.

In order to simplify the calculations, the values of bond lengths and valency angles are assumed as follows, by referring to the data in the original papers. That is to say, as for Reeves' C 1 conformation[3], the lengths of C—C and C—O bonds in the ring are assumed to be all 1.54 Å, and that of C—O bond which projects out of the ring to be 1.42 Å*5. The valency angles of C and O atoms are assumed to be a tetrahedral angle (109° 28′). According to Cox's investigations, the geometry of Cox's flat ring is as follows[1]. The lengths of C—C and C—O bonds in the molecule are 1.54 Å and 1.46 Å respectively. As for the corner-angles of the ring, the valency angles of C atoms lie between 113° and 116°, the corresponding limits of the valency angle of O atom being 90° and 106°. Then the author used 114° as the valency angle of C atom which is the mean value of 113° and 116°, therefore the valency angle of O atom became 92°*6. If the hydroxyl oxygen is symbolized by $O^h$, $O^h$ atom and H atom combine with the same C atom of the ring and the angle $\angle HCO^h$ which is tetrahedral angle, 109° 28′, must be bisected by the plane which is determined by three atoms, namely, C atom and the two atoms besides H- and $O^h$- atoms attached to this C atom. The unit groups of the aldopyranose molecules were given in square brackets, as shown on the top of this page*7.

It is assumed that the orientation of OH group in $(CH_2OH)^{5\beta}$ as regards the aldopyranose-ring is definite and similar in all of the above-described aldopyranoses. The values of the optical properties of OH group and H atom, used in the preceding article[7] were used without any correction. The refractive indices of aqueous solutions of D-galactose, of D-glucose and of D-mannose, whose concentrations are suitable for measurement of the optical rotatory power, are nearly equal (1.34)*8.

## Method Proposed

Partial molecular rotations of the plane polarized light of wave-length of D line at 20°C, represented by $[\mu]_D^{20}$, caused by the dynamical coupling effect between any two members of unit groups (except $(CH_2OH)^{5\beta}$ and Ring) in the aldopyranose molecule, were calculated according to Kirkwood's polarizability theory[8]. The results of the calculation with regard to Reeves' C 1 conformation are given in Table I.

*4 Concerning this method, refer to "Method Proposed" in this article.

*5 This is the mean value of lengths of C-O bonds in α-D-glucose. (ref. *1).

*6 In order to see the magnitude of deviation of $[\mu]_{D\,\mathrm{calcd}}^{20}(3/n^2+2)$, caused by a small deviation in bond length or in valency angle, the author tried the other type of Cox's flat ring. In this ring, the valency angle of C atom and of O atom is 116° and 101.5° respectively, and lengths of C-C and C-O bonds in the molecule are 1.54 Å and 1.48 Å (ref. M. Kimura, *J. Chem. Soc. Japan.* **71**, 18 (1950)), respectively. $[\mu]_{D\,\mathrm{calcd}}^{20}(3/n^2+2)$, caused by the dynamical coupling effect of the unit groups in this molecular model is given in each parenthesis in Table II.

*7 $(OH)^{1\alpha}$ means OH group which combines with 1-position of the aldopyranose-ring, in α orientation. (ref. L. F. Fieser, *J. Am. Chem. Soc.*, **72**, 623 (1950).)

a) C. N. Riiber, J. Minsaas and R. T. Lyche, *J. Chem. Soc.*, **1929**, 2173.

b) C. N. Riiber und J. Minsaas, *Ber.*, **60**, 2402 (1927).

*8 ref. *10 in the preceding paper (7) cf. "International Critical Tables of Numerical Data," Vol. 2, p 351,347.

| | $2\alpha$ | $3\beta$ | $4\beta$ | $(CH_2OH)^{5\beta}$ | Ring | Sum |
|---|---|---|---|---|---|---|
| $1\alpha$ | 6.5 | 1.7 | 0 | $(1\alpha)\times(CH_2OH)^{5\beta}$,*10 | $(1\alpha)\times$Ring | $8.2+(1\alpha)\times(CH_2OH)^{5\beta}+(1\alpha)\times$Ring |
| $1\beta$ | −6.5 | 0 | 0 | $(1\beta)\times(CH_2OH)^{5\beta}$ | $(1\beta)\times$Ring | $-6.5+(1\beta)\times(CH_2OH)^{5\beta}+(1\beta)\times$Ring |

TABLE I

$[\mu]^{20}_{D\,calcd}(3/n^2+2,)$ CAUSED BY THE DYNAMICAL COUPLING EFFECT BETWEEN ANY TWO MEMBERS OF UNIT GROUPS (EXCEPT $(CH_2OH)^{5\beta}$ AND RING), WITH REGARD TO REEVES' C 1 conformation*9

| | $4\beta$ | $4\alpha$ | $3\beta$ | $3\alpha$ | $2\beta$ | $2\alpha$ |
|---|---|---|---|---|---|---|
| $1\alpha$ | 0 | 0 | 1.7 | 0 | 0 | 6.5 |
| $1\beta$ | 0 | 0 | 0 | −1.7 | 6.5 | −6.5 |
| $2\alpha$ | 1.7 | 0 | 6.5 | −6.5 | | |
| $2\beta$ | 0 | −1.7 | −6.5 | 0 | | |
| $3\alpha$ | 0 | 6.5 | | | | |
| $3\beta$ | 6.5 | −6.5 | | | | |

Note: $1\alpha$ is an abbreviated symbol of $(OH)^{1\alpha}$, and so on.

Then, $[\mu]^{20}_{D\,calcd}(3/n^2+2)$, caused by the dynamical coupling effects between OH group situated in the 1-position of D-galactose molecule and the other unit groups in this molecule are as shown on the top of this page.

If the orientation of $(OH)^1$ group of D-galactose molecule changes from $\beta$ to $\alpha$, then the calculated value of the optical rotatory power of this molecule changes and the value of this change is as follows,

$$\Delta[M]^{20}_{D\,calcd}=\sum\Delta[\mu]^{20}_{D\,calcd}=[\{8.2+(1\alpha)\times(CH_2OH)^{5\beta}+(1\alpha)\times Ring\}\ \text{minus}\ \{-6.5+(1\beta)\times(CH_2OH)^{5\beta}+(1\beta)\times Ring\}]\ (n^2+2)/3,$$
$$=(14.7+L)\ (n^2+2)/3$$

where

$$L\equiv(1\alpha)\times(CH_2OH)^{5\beta}-(1\beta)\times(CH_2OH)^{5\beta}+(1\alpha)\times Ring-(1\beta)\times Ring.$$

The corresponding $\Delta[M]^{20}_{D\,obs}$ is given by, $\{[M]^{20}_{D\,obs}$ of $\alpha$-D-galactose$\}$ minus $\{[M]^{20}_{D\,obs}$ of $\beta$-D-galactose$\}$. This is (261.0—97.6) =163.4. These two values must be made equal to each other by using a proportionality-constant $\kappa$. Then

$$163.4=\kappa(14.7+L)\ (n^2+2)/3. \qquad (1)$$

Of course, the left side and the right side of Eq. (1) show the observed value and the calculated value of the anomeric difference of D-galactose, respectively. By using the method like that mentioned above, two other equations are obtained.

From D-glucose,

$$163.5=\kappa(14.7+L)\ (n^2+2)/3 \qquad (2)$$

and from D-mannose,

$$83.1=\kappa(-4.8+L)\ (n^2+2)/3 \qquad (3)$$

The left side of (1) is nearly equal to that of (2), and this fact is well known as Hudson's isorotation rule[9]. The right side of (1) is equal to that of (2). In other words, the calculated value of the anomeric difference of D-galactose and that of D-glucose is equal. Now, the above-described calculation can be said to bear satisfactory results to explain Hudson's isorotation rule. On the other hand, the anomeric difference of D-mannose is given by Eq. (3), but it is apparent that these values are different from those in Eqs. (1) and (2). Namely, the anomeric difference of D-mannose is different from those of D-galactose and D-glucose. From Eq. (2) minus Eq. (3), $\kappa=12.37/n^2+2$, where $n^2$ is always positive, then $\kappa>0$. This result means that the Fischer convention from which Reeves' C 1 conformation is derived, is a structurally correct representation of the absolute configuration.

Next, the author applied the method which is analogous to that used in the case of Reeves' C 1 conformation above, to the

TABLE II

$[\mu]^{20}_{D\,calcd}(3/n^2+2)$, CAUSED BY THE DYNAMICAL COUPLING EFFECT BETWEEN ANY TWO MEMBERS OF UNIT GROUPS (EXCEPT $(CH_2OH)^{5\beta}$ AND RING), WITH REGARD TO COX'S FLAT RING*11

| | $4\beta$ | $4\alpha$ | $3\beta$ | $3\alpha$ | $2\beta$ | $2\alpha$ |
|---|---|---|---|---|---|---|
| $1\alpha$ | −1.1 (−0.9) | 1.3 (1.0) | −0.2 (0.2) | 2.9 (2.4) | 1.4 (2.0) | 6.0 (5.5) |
| $1\beta$ | 0.3 (0.4) | −0.1 (−0.2) | 1.8 (1.6) | −2.1 (−2.1) | 6.0 (5.5) | −6.4 (−6.2) |
| $2\alpha$ | 1.4 (1.4) | 0 (0) | 4.5 (4.5) | 0 (0) | | |
| $2\beta$ | 0 (0) | −1.4 (−1.4) | 0 (0) | −4.5 (−4.5) | | |
| $3\alpha$ | 4.5 (4.5) | 0 (0) | | | | |
| $3\beta$ | 0 (0) | −4.5 (−4.5) | | | | |

*9 When 1.48 Å (ref. *6) is used as the value of length of C·O bond, the values 6.1 and 1.6 appears in Table 1, instead of 6.5 and 1.7 respectively.

*10 $(1\alpha)\times(CH_2OH)^{5\beta}$ means $[\mu]^{20}_{D\,calcd}(3/n^2+2)$, caused by the dynamical coupling effect between $(OH)^{1\alpha}$ and $(CH_2OH)^{5\beta}$.

9) C. S. Hudson, *J. Am. Chem. Soc.*, **31**, 66 (1909).

*11 Concerning the values in parentheses, refer to *6.

case of Cox's flat ring. The results of calculation of $[\mu]_D^{20}(3/n^2+2)$ are given in Table II.

By using these values three equations are obtained.

From D-galactose,

$$163.4=\kappa'(9.0+L')(n^2+2)/3 \quad (4)$$

from D-glucouse,

$$163.5=\kappa'(11.8+L')(n^2+2)/3 \quad (5)$$

and from D-mannose,

$$83.1=\kappa'(-5.2+L')(n^2+2)/3 \quad (6)$$

where $\kappa'$ is a proportionality-constant and

$$L' \equiv (1\alpha)\times(CH_2OH)^{5\beta}-(1\beta)\times(CH_2OH)^{5\beta}+(1\alpha)\times\text{Ring}-(1\beta)\times\text{Ring}$$

in this case. From Eq. (5) minus Eq. (6),

$$\kappa'=14.19/n^2+2^{*12}$$

where $n^2$ is always positive; then $\kappa'>0$. That is to say, it is concluded from the result of calculation with regard to Cox's flat ring that the Fischer convention is a structurally correct representation of the absolute configuration. But the right side of Eq. (4) is different from that of Eq. (5). In other words, the calculated value of the anomeric difference of D-galactose is different from that of D-glucose, and this is not consistent with the fact that the observed value of the anomeric difference of D-galactose is equal to that of D-glucose. In short, Hudson's isorotation rule can not be explained by using Cox's flat ring.

*12 By using the values given in the parentheses in Table II, $\kappa''=15.87/n^2+2$, where $\kappa''$ is a proportionality-constant for this case.

## Conclusion

The results of calculation and presumption in this paper are as follows,

(1) The Fischer convention is a structurally correct representation of the absolute configuration.

(2) If D-galactose, D-glucose and D-mannose are of the same type of ring structure in aqueous solution, and this type should be either Reeves' C 1 conformation or Cox's flat ring, then this common type must be the former and not the latter.

(3) Hudson's isorotation rule can be explained easily, by calculation of the anomeric difference adoption Kirkwood's polarizability theory of optical rotatory power with regard to Reeves' C 1 conformation of an aldopyranose molecule.

The author wishes to express his deepest gratitude to Professor S. Tanaka (Kyoto University) for his valuable advice and kind encouragement throughout this work.

*Department of Chemistry*
*Kyoto Gakugei University*
*Fushimi-ku, Kyoto*

# *Studies on Meso-ionic Compounds. III*[1]. *Reactions of 3-Phenyl-4-bromosydnone*

By Hiroshi KATO and Masaki OHTA

(Received August 28, 1956)

In the first paper of this series[1], the conditions for preparing 3-phenyl-4-bromosydnone (I) from 3-phenylsydnone (II) have been reported in detail, and it has been shown that an excellent result was obtained by treating an ether suspension of II with bromine in the presence of sodium bicarbonate, or by refluxing a chloroform solution of II with N-bromosuccinimide, but an attempt to prepare I by the method described by Baker et al.[2] was unsuccessful. The present investigation was undertaken to study the reactions of I, since previous communications[3] on sydnones have dealt almost exclusively with their unusual structure, and little attention has been paid to their reactions.

1) Part I, II. H. Kato. K. Nakahara and M. Ohta, *J. Chem. Soc. Japan (Pure Chem. Sect.)*, **77**, 1304 (1956).

2) W. Baker, W D Ollis and V. D. Poole, *J. Chem. Soc.*, **1949**, 307

3) Works on this subject are reviewed by M. Ohta in *Chemistry and Chemical Industry Japan*, **9**, 311 (1956).

For instance, what are reported so far about I, are only its methods of preparation[1,2,4] and its decomposition reactions[4,5] by the action of acid or alkali.

When I was treated with sodium salt of *p*-thiocresol, it did not afford the expected 4-*p*-tolyl sulfide of II, but I was reduced to II and *p*-thiocresol was oxidized to form di-*p*-tolyl disulfide (III). The reaction of I with sodium hydrosulfide was then tried, and this procedure gave, quite unexpectedly, II and sulfur as reaction products. The same reaction products were obtained when I was treated with sodium sulfide. Considering the above reactions, it seems reasonable to conclude that I has a marked oxidative property. This consideration is further supported by the observation that iodine was liberated when an ethanolic solution of I and potassium iodide was kept standing at room temperature in the presence of diluted hydrogen chloride.

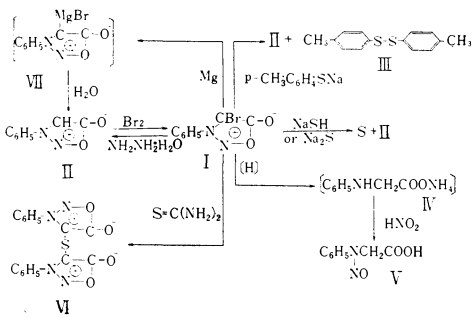
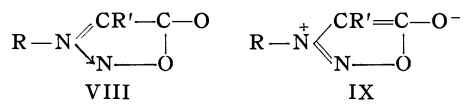


Fig. Reactions of 3-Phenyl-4-bromosydnone.

When warmed with an exess amount of hydrazine hydrate, I was reduced to II, but when an equimolecular amount of hydrazine hydrate in ethanol was used, I was recovered unchanged even after refluxing for prolonged hours. An attempt to remove the bromine atom by the action of diethylamine and Raney nickel was unsuccessful. When I was subjected to reduction with zinc dust in aqueous acetic acid, the bromine atom was removed but was accompanied by a reductive fission of the sydnone ring at the N–N bond, thus affording the ammonium salt of N-phenylglycine (IV), which was identified by conversion to N-nitroso-N-phenylglycine (V). It was not possible to determine which one of the two reactions, viz. the removal of the bromine atom or the cleavage of the sydnone ring, precedes the other. This mode of ring cleavage at the N–N bond is in accord with that reported by Earl[6] in the case of II. Considering this mode of ring cleavage, Earl concluded that, of the structures VIII and IX formerly proposed for the sydnones[7], structure VIII is more favoured. But the fact that



VIII IX

II is considerably soluble in highly polarized solvent e. g., chloroform, acetic acid or pyridine, and only sparingly soluble in carbon tetrachloride, benzine or ether favors rather the betaine type structure IX.

It seems inappropriate to conclude from these data alone reported by Earl, which structure of the two should be more favoured. Moreover, now that the structures of sydnones are best explained by molecular orbital theory[8], a trial to show their structures by conventional covalent formulae seems to have little significance.

When I was treated with thiourea, pale yellow needles (VI) melting at 164—165°C. were obtained. This substance was proved to contain sulfur, and had an empirical formula of $C_{16}H_{10}O_4N_4S$ and was insoluble in 10% sodium hydroxide solution and 10% hydrochloric acid. Woodbridge et al.[9] have reported that the reactions of 4-substituted-2-aminothiazoles with thiourea and iodine or bromine give di-5-thiazolyl sulfides. Considering the properties of VI and the above reactions on thiazoles it is evident that I reacted with thiourea to afford 4-bis (3-phenylsydnonyl) sulfide (VI) by an analogous reaction, though the mechanism of this is not known.

As for the reaction of I with magnesium metal, I did not react even at an elevated temperature when magnesium alone was used, but on adding methyl iodide I began to react smoothly with magnesium metal and went into solution. On decomposing the reaction product with water, II was obtained. From this fact, it is evident that in the presence of methyl iodide, I is capable of forming the corresponding Grignard reagent (VII).

4) J. Kenner and K. Mackay, *Nature*. **158**, 909 (1946).
5) R. A. Eade and J. C. Earl, *J. Chem. Soc.*, **1948**, 2307.
6) J. C. Earl, *Rec. trav. chim. Pay-Bas*, **75**, 346(1956).
7) J. C. Earl, *Chemistry and Industry*, **1953**, 746, W. Baker and W. D. Ollis, *Nature*, **158**, 703 (1936).
8) H. C. Longuet-Higgins, *J. chim. phys.*, **46**, 244 (1949); L. E. Orgel, T. L. Cottrel, W. Dick and L. E. Sutton, *Trans. Faraday Soc.*, **47**, 113 (1951).
9) R. G. Woodbridge and G. Dougherty, *J. Am. Chem. Soc.*, **71**, 1744 (1949).

No reaction occurred except a partial decomposition when I was treated with silver nitrate, sodium nitrite, sodium phenolate, acetyl nitrate, guanidine or sodium iodide.

In conclusion, the sydnone ring is highly aromatic in character, and I is inert to usual anionoid reagents. Most reactions reported here can be interpreted only when the oxidative effect of I is taken into consideration. Further studies on the reactions of I and VII are now under experiment.

## Experimental

**3-Phenyl-4-bromosydnone (I).**—Into a suspension of lg. of II and 2g. of sodium bicarbonate in 30 cc. of ether was added lg. of bromine under stirring. After a few minutes, the reaction mixture was filtered and washed with water, and was recrystallized from ethanol giving 1.15 g. (yield 78%) of white needles, m. p. 141°C. (decomp.). Baker et al.[2] reports its m. p. 140°C. (decomp.). I turns to a red color on prolonged exposure to sunlight.

**Reaction of I with *p*-Thiocresol.**—To a solution of 0.5 g. of *p*-thiocresol in 20 cc. of anhydrous methanol containing 0.1 g. of metallic sodium was added 1g. of I under stirring at room temperature. After standing overnight, the solvent was evaporated under reduced pressure and the residue was first washed with water and then extracted with ether. The ether extract was evaporated to dryness and the residue was crystallized from methanol giving 0.4 g. of colorless leaflets, m. p. 47—48°C.. The melting point of this substance was not depressed by admixture with authentic di-*p*-tolyl disulfide. The residue (0.4 g.) left after the extraction with ether was recrystallized twice from ethanol giving 0.15 g. of white needles melting at 134—135°C. with slight decomposition, undepressed by admixture with authentic II.

**Reaction of I with Sodium Hydrosulfide.**—A solution of 0.09 g. of sodium hydroxide in 15cc. of methanol was saturated with dry hydrogen sulfide gas. To this solution were added 0.5 g. of I and a small amount of potassium iodide, both of which soon went into solution and pale yellow precipitate began to separate out. Stirring was continued for three hours at room temperature and then allowed to stand overnight. The pale yellow precipitate which separated out was filtered and was extracted with a small amount of carbon disulfide. On evaporating the carbon disulfide 0.1 g. of pale yellow amorphous powder (m. p. 120°C.) was obtained, which was identified as sulfur. The filtrate was evaporated under reduced pressure and the orange colored residue was washed with water and recrystallized from ethanol giving 0.23 g. of slightly brown colored long needles, m. p. 133—134°C. with slight decomposition, undepressed by admixture with authentic II.

**Reaction of I with Sodium Sulfide.**—To a methanol solution (15 cc.) of sodium hydrosulfide, prepared from 0.09 g. of sodium hydroxide by the same way as is described above, was added 0.09 g. of sodium hydroxide. One gram of I was added to this solution and was treated by essentially the same method as in the preceeding experiment. This also gave II and sulfur, both of which were identified by their melting points and mixed melting points with authentic samples.

**Hydrogenolysis of I with Zinc Dust.**—Into a solution of 0.5 g. of I in 20 cc. of 80% aqueous acetic acid was added portionwise 2 g. of zinc dust during two hours under stirring and cooling by water. Stirring was continued for six hours and allowed to stand overnight. This was filtered and the residue was washed with water. This filtrate was negative to Liebermann's nitroso test. A part (1/5) of this filtrate was made alkaline with sodium hydroxide, which evolved ammonia on heating. The residue was decomposed by hydrochloric acid and was added to the other part (4/5) of the filtrate. This solution was concentrated to 10 cc. under reduced pressure and the remaining acetic acid was extracted with ether. After evaporating the ether which was dissolved in water under reduced pressure, this solution was acidified with hydrogen chloride. To this solution was added dropwise a solution of 0.15 g. of sodium nitrite under stirring and ice cooling. The pale yellow precipitate (0.16 g.) which separated out was dissolved in 5% sodium bicarbonate solution, which on acidification with hydrogen chloride afforded pale yellow needles, m. p. 101—102°C. (decomp.). This substance was negative to Beilstein's halogen test and gave a strong Liebermann's nitroso test. A mixed m. p. with authentic N-nitroso-N-phenylglycine was 102—103°C. (decomp.).

**Reaction of I with Thiourea.**—To 20 cc. of ethanol were added 1 g. each of I and thiourea and was refluxed for six hours. After standing overnight, the pale yellow needles which separated out were collected by filtration (0.2 g. m. p. 157° C.), and recrystallized first from acetone and then from ethanol giving pale yellow needles, m. p. 164—165°C.. This substance was negative to Beilstein's halogen test, insoluble in 10% sodium hydroxide solution and in 10% hydrochloric acid, and gave a positive sulfur test.

*Anal.* Found: C, 54.47; H, 3.22; N, 15.83. Calcd. for $C_{16}H_{10}O_4N_4S$: C, 54.24; H, 2.85; N, 15.81%.

The same result was obtained when an equimolecular amount of thiourea was used, but the yield in this case was poorer and a considerable amount of I was recovered unchanged, accompanied by a small amount of sulfur.

**Reaction of I with Magnesium Metal.**—To a suspension of 0.5 g. of I and 0.22 g. of magnesium ribbons in 10 cc. of anhydrous ether, was added 1.0 g. of methyl iodide under stirring. After three hours the reaction was nearly completed. Water was added and was evaporated to dryness under reduced pressure, and the residue was extracted with ethanol. On evaporating the solvent under

reduced pressure, a small amount of oily substance was obtained, which became solidified on adding water; recrystallization of this substance (0.17 g.) from ethanol gave 0.1 g. of white needles, m. p. 134—135°C. with slight decomposition. The melting point of this substance was not depressed by admixture with authentic II. In the absence of methyl iodide, no reaction occurred even when *n*-butyl ether was used as the solvent and the reaction was conducted at 100°C..

**Reaction of I with Hydrazine Hydrate.**—To 1 cc. of 80% hydrazine hydrate were added 0.5 g. of I and a few drops of ethanol and this mixture was gently refluxed on a water bath for four hours, and was kept standing overnight. On adding water, 0.1 g. of pale brown needles melting at 132—135°C. were separated out, recrystallization of which from dilute ethanol gave pale yellow needles, m. p. 134°C. with slight decomposition. A mixed m. p. with authentic II was 135°C.. When I was refluxed in ethanol with equimolecular amount of hydrazine hydrate, no reaction occurred and I was recovered unchanged.

The authors are indebted to Mr. Asaji Kondo for carrying out the microanalyses.

*Laboratory of Organic Chemistry*
*Tokyo Institute of Technology*
*Meguro, Tokyo*

# *On the Distribution and Behavior of Water in Cation-Exchange Resin Membranes*

By Yoshio Oda and Tadashi Yawataya

(Received October 9, 1956)

## Introduction

In the preceding two papers[1,2], we reported on the electro-osmotic phenomena in cation-exchange resin membranes, and discussed to some extent on the distribution of water within the resin. Therein, the water in the resin phase was classified into two groups, i.e., "mobile- and fixed waters". The former was considered to consist of the hydration water of the exchangeable and non-exchangeable ions and the solvent water in the resin, whilst the latter to consist mainly of the hydration water of the structurally bound ions, e. g., sulfonate ions in the cation-exchange resin.

Hitherto several workers have studied the water in the ion-exchange resins basing their studies on different principles.

D. Reichenberg[3], discussing on the exchange rate of sodium- and hydrogen ions in cation-exchange resins of different cross-linkings, calculated the amount of water unavailable as a diffusion medium to find five molecules per equivalent of the resin, and assumed that the ions in the resin were hydrated to this extent.

G. E. Boyd and B. A. Soldano[4], from the study on the water adsorption isotherms for cation- and anion-exchange resins, ascribed one molecule of $H_2O$ to the amount of water which is required by a structurally bond sulfonate ion.

E. Glueckauf[5] has recently determined the hydration number of sulfonate ions as 0.9 in cation exchanger of sulfonated polystyrene type. It was derived on the basis of the thermodynamical concept of electrolyte solution, modified so as to include the effect of co-volume.

According to G. H. Osborn[6], the recent work on the absorption of non-electrolyte by the hydrogen forms of the exchangers has confirmed that there are about four molecules of hydration water per equivalent of sulfonic group.

Referring to these published data, most of which are indicated with numbers of hydration water of total ionic species in the resin, including both fixed and mobile ions, our results[1], about ten molecules water for a sulfonate ion, seems far separated from them.

The difference may be explained that "the fixed water" which does not take part in electro-osmosis would involve not only the hydration water of the fixed ions but a part of water which is hindered to

1) Y. Oda and T. Yawataya, This Bulletin, **28**, 263 (1955).
2) Idem. ibid., **29**, 673 (1956).
3) D. Reichenberg, *J. Am. Chem. Soc.*, **75**, 589 (1953).
4) G. E. Boyd and B. A. Soldano, *Z. Elektrochem.*, **57**, 162 (1953).
5) E. Glueckauf, *Trans. Faraday Soc.*, **51**, 1235 (1955).
6) G. H. Osborn, "Synthetic Ion-Exchangers," Arrowsmith, London (1955), p. 7.

move due to the network structure of the resin. Thus, the determination of the number of fixed water molecules from the electro-osmotic measurements seems to deserve further discussion. The present paper deals with this problem.

## Theoretical

In the first paper of this series[1], we assumed that the free water in the resin moves with mobility equal to that of the migrating ions.

It would be more reasonable, however, to suppose that in the electro-osmosing solution the mobility of ions differs from that of the solvent water, since the water moves with velocity depending on the balance between the driving force due to ionic migration and the retardation due to the network of resin.

Thus, it will be assumed in this paper that the electro-osmosing water within ion-exchange membrane consists of two sorts with different mobilities: (1) primary shell hydration water of the mobile ions with a mobility equal to that of the ions, and (2) solvent water with smaller mobility than (1). Naturally the transferring velocity of the solvent water would not be uniform over a whole resin pore section, but would have a distribution governed by the hydrodynamic principle. For simplicity, however, it is assumed to have a certain average mobility, $u_s$.

As was stated previously[2], the fixed ion concentration $A_w$ based on the total water content in the resin is expressed as follows,

$$\frac{1}{A_w}=h_+\cdot(1+s)+h_-\cdot s+f+\alpha \qquad (1)$$

where, from the definition of $A_w$, $1/A_w$ means the amount of total water per equivalent of fixed ion. $h_+$ and $h_-$ are the amount of hydration of mobile cation and anion respectively. And $s$, $f$ and $\alpha$ are respectively the amount of Donnan absorption, solvent water and fixed water, all these being indicated basing on an equivalent of fixed ion.

When an electric field is applied on a cation-exchange membrane interposed between two solutions of equal concentration, $n_+'$ moles cations enter the cathode cell through the membrane and $n_-'$ moles anions migrate out of the cathode cell into the anode cell for each faraday of electricity. Here, $n_+'$ and $n_-'$ denote* the ture transport numbers of the cation and the anion within the membrane. In this case, the water transference may be considered to take place as illustrated schematically in Fig. 1. The hydration water of cations

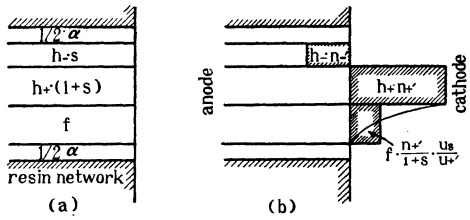



Fig. 1. (a) Distribution of water inside resin-pore
(b) Water transference for passage of one faraday (Shaded areas express the transfered water.)

or anions moves toward cathode or anode with the same mobilities as the respective ions. Whilst, the solvent water, whose amount is $f$ moles per equivalent of fixed ion, or $f\cdot\frac{n_+'}{1+s}$ moles per $n_+'$ moles of the migrating cation, transfers with a mobility $u_s/u_+'$ times as small as that of the cation. Here, $u_+'$ is the mobility of the cation in resin phase.

Therefore, the amount of electro-osmotic water transference, $\beta_w$, is correlated with the transport numbers of cation and anion as follows,

$$\begin{aligned}\beta_w\cdot F&=h_+\cdot n'_+-h_-\cdot n'_-\\&\quad+f\cdot\frac{n'_+}{1+s}\cdot\frac{u_s}{u'_+} \qquad (2)\\&=\left(h_++f\cdot\frac{u_s}{u'_+}\right)\cdot n'_+\\&\quad-\left(h_-+f\cdot\frac{u_s}{u'_-}\right)\cdot n'_-. \qquad (2')\end{aligned}$$

Cancelling $f$ from (1) and (2), and noting the fact that $n'_++n'_-=1$,

$$\begin{aligned}\frac{1}{A_w}&=\alpha+\frac{\beta_w\cdot F}{u_s/u'_+}\cdot\frac{1+s}{n'_+}\\&\quad+h_+\cdot(1+s)\cdot\left(1-\frac{1}{u_s/u'_+}\right)\\&\quad+h_-\cdot s\cdot\left(1+\frac{1}{u_s/u'_+}\right)\\&=\alpha+\frac{\beta_w\cdot F}{u_s/u'_+}\cdot\frac{1+s}{n'_+}+h, \qquad (3)\end{aligned}$$

where

$$h=h_+\cdot(1+s)\left(1-\frac{1}{u_s/u'_+}\right)$$

* The mobility notation with or without a prime refers to the quantity relative to the solution or the resin.

$$+h_-\cdot s\cdot\left(1+\frac{1}{u_s/u'_-}\right).$$

On the other hand from equations (7), (9) and (12) in the preceding paper[2],

$$\frac{n'_+-n_+}{n_-+s}=\frac{k'-k}{k'}=\frac{u_s}{u'_+\cdot(1+s)+u'_-\cdot s}$$
$$=\frac{u_s}{u_+'}\cdot\frac{1}{1+s}\cdot\frac{u'_+\cdot(1+s)}{u'_+\cdot(1+s)+u'_-\cdot s}.$$

Then, considering the relations of equations (10) and (15) in the previous paper,

$$\frac{n'_+-n_+}{n_-+s}=\frac{u_s}{u_+'}\cdot\frac{n'_+}{1+s}=A'_w\cdot\beta_w\cdot F. \quad (4)$$

Therefore, the ratio of the mobility of solvent water to that of cation is,

$$\frac{u_s}{u'_+}=\frac{1+s}{n'_+}\cdot\frac{n'_+-n_+}{n_-+s}. \quad (5)$$

By the similar way,

$$\frac{u_s}{u'_-}=\frac{s}{n'_-}\cdot\frac{n'_+-n_+}{n_-+s}. \quad (5')$$

Further, from equation (11) in the preceding of paper, the ratio anion's mobility to cation's within the moving solution is obtained as,

$$\frac{u_-}{u_+}=\frac{n_-}{n_+}\cdot\frac{1+s}{s}. \quad (6)$$

The concentration of fixed ion basing on "the mobile water", $A'_w$, is given, by use of the equation (4), as follows,

$$\frac{1}{A'_w}=\frac{\beta_w\cdot F}{u_s/u'_+}\cdot\frac{1+s}{n'_+}. \quad (7)$$

Hence,

$$\frac{1}{A'_w}=\frac{1}{A_w}-\alpha-h. \quad (8)$$

By means of equations (5) and (5') values of $u_s/u'_+$ and $u_s/u'_-$ may be estimated for each membrane from the observed values of $n'_+$, $n_+$ and $s$. These values of $u_s/u'_+$ and $u_s/u'_-$, combined with the observed value of $\beta_w$, permit an estimation of $\alpha$ by use of equation (3).

## Experimental

**Membranes.**—Two cation-exchange resin membranes were used in the present work. One is of sulfonated polystyrene type (CMA-24), and the other of sulfonated phenol resin type (P-13). The latter is one of the same series as those used previously[2]. Their exchange capacities and water contents are given in Table I.

**Measurement.**—Of the CMA-24 membrane, measurements were made for true transport numbers ($n'_+$, $n'_-$), Hittorf transport numbers ($n_+$, $n_-$), electro-osmotic water transference ($\beta_w$), Donnan absorption (s), and the fixed ions concentration ($A_w$) in the chloride solutions of 1:1 valency type such as LiCl, NaCl, $NH_4Cl$, KCl, CsCl, and HCl of varied concentration. Temperature was regulated at 25±0.2°C. The procedures of the measurements were quite the same as those described previously[2].

Of the P-13 membrane, such measurements were carried out solely in sodium chloride solution.

TABLE I

THE EXCHANGE CHARACTERISTICS OF SAMPLE MEMBRANES (Na-TYPE)

| Sample No. | Thickness (mm.) | $A°_w$ m.eq./g. $H_2O$ | $A_R$ m.eq./g. | Water content % |
|---|---|---|---|---|
| CMA-24 | 0.3 | 3.90 | 1.86 | 32.3 |
| P-13 | 0.9 | 2.02 | 3.04 | 60.1 |

$A°_w$ is the concentration of fixed ions basing on the total water content of the resin equilibrated with distilled water.
$A_R$ is the exchange capacity per one gram of dry resin.

## Results

The results are given for CMA-24 membrane unless specified.

The empirically determined true and Hittorf transport numbers of cation ($n'_-$, $n_-$) through the membrane are plotted in Fig. 2 over the concentration range of equilibrating solution from 0 to 4 N. The Hittorf transport number is highest in HCl-solution and decreases in the order, $H^+>Cs^+>K^+>NH_4^+>Na^+>Li^+$. The order is in good accord with that in free aqueous solutions. Such a situation cannot be seen so clearly regarding the true transport number curves, since in this case they

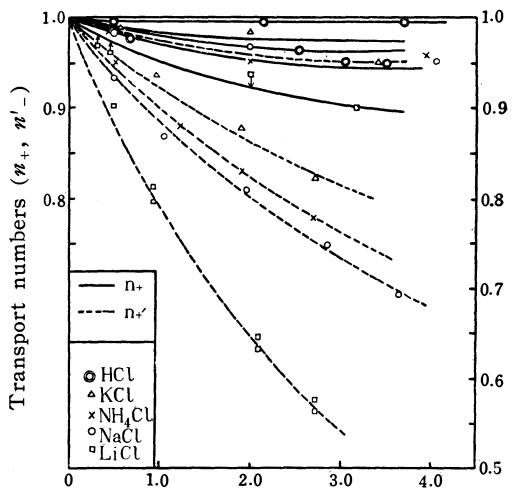



Fig. 2. Transport numbers in cation-exchange resin membrane (CMA-24).

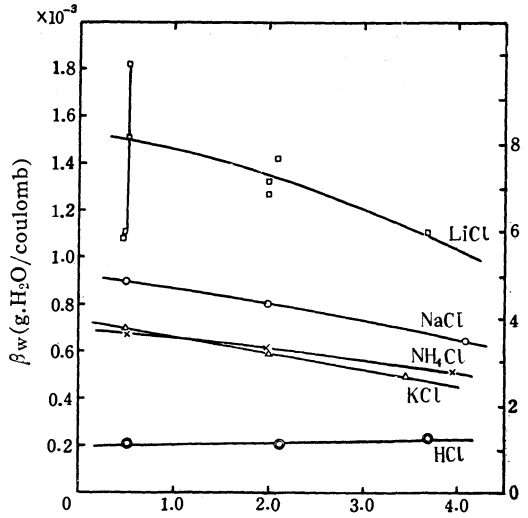



Fig. 3. Electro-osmotic water transference through cation-exchange resin membrane (CMA-24).

come together closely to approach the upper limit line: $n'_{-}=1$.

In Fig. 3 are plotted the electro-osmotic water transference, $\beta_w$, through the membrane against the concentration of outer solutions. It appears to become large as the hydration of the cation increases, except for the case of HCl-solution. The hydration numbers of the ions concerned are listed below in Table II according to E. Glueckauf. The $\beta_w$ in HCl-solution is notably and small stays nearly constant over a wide concentration range.

With LiCl-solution the observed values of $\beta_w$, particularly in dilute solution region, showed remarkable large fluctuation, and appeared to rise gradually as the duration of electrolysis increased.

The Donnan absorptions are given in Fig. 4. They increase with the rise in the concentration of equilibrating solution, and little significant variation can be seen with the difference of cation species.

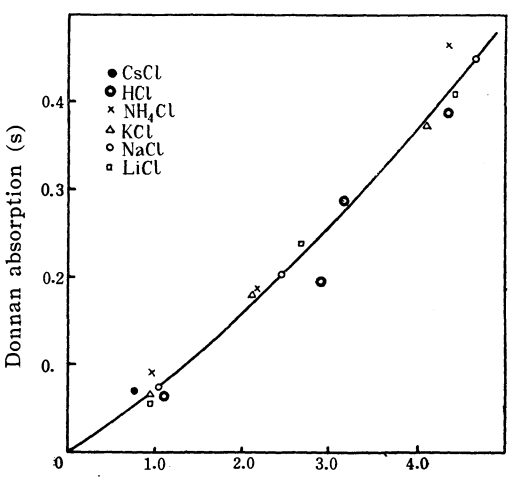



Fig. 4. Donnan absorption (CMA-24).

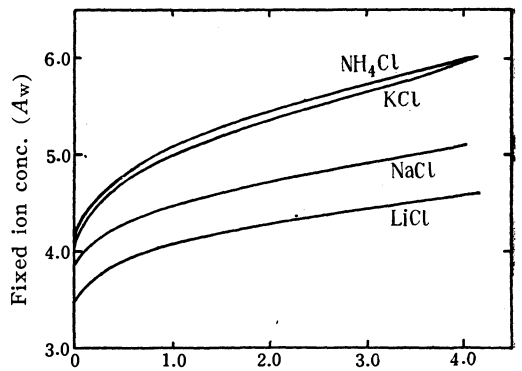



Fig. 5. Fixed ion concentration ($A_w$) (CMA-24).

Fig. 5 shows the curves of fixed ion concentrations, $A_w$, plotted against the concentration, of outer solution. As the outer solutions become concentrated, the shrinkage of the resin seems to cause the increase of $A_w$.

## Discussion

The ratios of the mobility of solvent water to that of cation, $u_s/u'_+$, were cal-

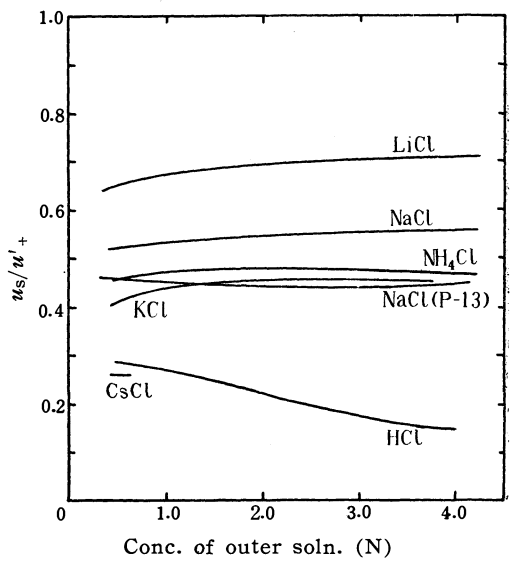



Fig. 6. Mobilities of water relative to cations.

culated by substituting the experimental data obtained above in equation (5). The results are plotted in Fig. 6 against the concentration of outer solution. In this calculation, accuracy decreases as the outer solutions become too diluted, because then the terms $(n'_+ - n_-)$ and $(n_- + s)$ in equation (5) approach zero.

It may be noted that the mobility ratio $u_s/u'_+$ appears to be almost constant over a wide concentration range of each solution, and that it becomes high to approach the limit line of $u_s/u'_+ = 1$ as the hydration degree of the cation increases, the data for HCl-solution being one exception.

As was seen in Fig. 3, in HCl-solution the electro-osmotic water transference is merely about one mole $H_2O$ per faraday through a membrane, being even smaller than the hydration number of hydrogen ion. These apparently anomalous results with HCl-solution are presumably attributable to the special conduction mechanism of hydrogen ion.

By the similar way, the ratios of anion's mobility to cation's, $u_-/u_+$, within the electro-osmosing solution were calculated using equation (6), and were shown in Fig. 7. For the sake of comparison, the ratios $u_-/u_+$ in aqueous solutions were plotted with broken lines in the same figure. It is seen that the $u_-/u_+$ ratios in electro-osmosing solution tend to approach those in free solutions as the concentration of equilibrating solution rises. This result seems reasonable, for the mobile cations and mobile anions are present in marked unbalance within the resin when the outer solution is dilute, and they tend to approach a balance, which is the case in free solution, as the outer solution, becomes concentrated.

Finally, the values of $\alpha$, the amount of hydration of sulfonic group, were estimated using equation (3) and plotted in Fig. 8. In this calculation, Glueckauf's data of hydration number of ions were applied for $h_+$ and $h_-$. They are given in Table II.

From the result, we are tempted to reach a conclusion that the hydration of a sulfonic group decreases as the effective concentration rises in resin. But the derivation of the values of $\alpha$ is not so precise as to allow it. Though it has been assumed in the above calculation that the hydration degrees of mobile ions are constant irrespective of the concentration of solutions in resin, this seems oversimplified. Also, the determinations of $\alpha$ for the case of very dilute equilibrating solutions are

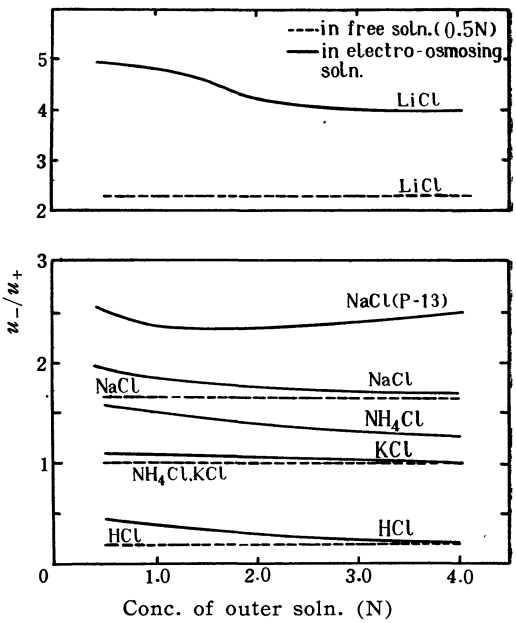



Fig. 7. Mobility ratio of anion's to cation's in electro-osmosing and free aqueous solutions.

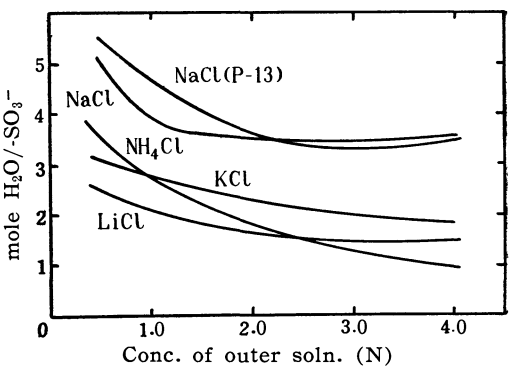



Fig. 8. Amount of hydration of sulfonic group.

TABLE II

| | $H^+$ | $Li^+$ | $Na^+$ | $K^+$ | $NH_4^+$ | $Cl^-$ |
|---|---|---|---|---|---|---|
| Primary hydration number | 4.0 | 3.4 | 2.0 | 0.6 | 0.2 | 0.9 |

not completely reliable, because as the solutions are diluted both the numerator $(n' - n_-)$ and the denominator $(n_- + s)$ in equation (4) approach zero, resulting in inaccurate values of $u_s/u'_+$.

Thus, if we take the data around 2N as the comparatively reliable values $\alpha$ may be estimated as 1.5 to 3.5 moles per equivalent. These values of $\alpha$, though still slightly higher than those found in the literature of the subject, seem much more reasonable as the hydration number of the fixed

sulfonic group than that reported previously by us.

When the circuitous process of calculation and rather drastic assumptions basing on a simple model in our treatment are considered, the concordance appears comparatively good. But more precise experiments would be desirable for membranes of wide varieties in order to make more strict discussion.

## Conclusion

It was assumed for a mechanism of electro-osmosis through ion-exchange resin membranes that (1) the primary shell hydration water of mobile ions transfers with the same mobility as the ions, and (2) the solvent water within the resin phase is dragged by the migrating cations or anions toward anode or cathode, the net result being observed as electro-osmosis. On this view, the mobilities of solvent water relative to those of cations were calculated from the measurements of electro-osmotic properties of cation exchange resin membranes equilibrated with varied concentration of LiCl, NaCl, KCl, $NH_4Cl$, CsCl and HCl solution. In addition, from these experimental data the amount of hydration of the fixed sulfonate ion was estimated as 1.5 to 3.5 moles per equivalent.

We are grateful to Dr. M. Sekino and other members in the Organic Laboratory, Asahi Glass Co. Ltd., for the kind supply of the sample membranes, and to Mr. H. Ukihashi for his valuable discussion.

*Research Laboratory of Asahi Glass Co. Ltd. 2, Benten-cho Tsurumi-ku, Yokohama*

# *Dipole Moments and Internal Rotation of Some Halogenated Hydrocarbons in the Vapor State*

By Ichiro MIYAGAWA, Takehiko CHIBA, Shoichi IKEDA and Yonezo MORINO

(Received November 11, 1956)

In the previous papers[1,2] one of the present authors (I. M.) discussed the energy differences in the rotational isomers of some halogenated hydrocarbons. By use of the experimental data two relations were pointed out[1e]. The first one is that the energy difference in these molecules depends mainly upon the configuration of the halogen atoms: that is, 1,2-dichloro-compounds have the energy difference of about 1 kcal./mole, and 1,1,2-trichloro-compounds have very large ones (ca. 2 kcal./mole), while 1,1,2,2-tetrachloro-compounds have vanishingly small ones (<0.4 kcal./mole). (See Table II). This striking result was explained qualitatively by some empirical interatomic potentials[2c].

The second interesting relation was found in the change of energy difference in 1,2-dichloro-compounds by successive substitution of the hydrogen atoms by methyl groups. By assuming that the intramolecular potential is the sum of contributions of the potentials between non-bonded atoms or groups, the observed $\Delta E$'s of dichloro-compounds are successfully reproduced. In tri- and tetrachloro-compounds, however, $\Delta E$ cannot be re produced so well as in the case of dichloro-compounds, and the qualitative explanation of these $\Delta E$'s are made in terms of the change in valence angles and of appropriate interatomic potentials. On the other hand it was inferred by Szasz[3] in his recent paper that the energy difference in *n*-propyl chlorides is very small. The second relation described above, gives 0.3 kcal./mole as the energy difference in this molecule. It is clear, therefore, that the second relation cannot be applied without any modification to such a molecule as *n*-propyl chloride. It is one of the purposes of this report to propose a possible explanation for this situation.

1) I. Miyagawa, (a) *J. Chem. Soc. Japan*, **75**, 970 (1954); (b) ibid., 1057; (c) ibid., 1061; (d) ibid., 1162; (e) ibid., 1165.

2) I. Miyagawa, (a) *J. Chem. Soc. Japan*, **75**, 1169 (1954); (b) ibid., 1173 (c) ibid., 1177.

3) G. I. Szasz, *J. Chem. Phys.*, **23**, 2449 (1955).

TABLE I

OBSERVED POLARIZATIONS, DIPOLE MOMENTS AND $\Delta E$ OF SOME HALOGENATED HYDROCARBONS*

1,2-Dichloro-2-methylpropane

$MR_D = 30.5$ cc. $P_E + P_A = 32.0$ cc.

| Temp. °K | No. of obs. | Press. range mmHg | Molar polarizn. cc. | Mean deviatn. of polarizn. cc. | Dipole moment $D$. |
|---|---|---|---|---|---|
| 339 | 6 | 68- 82 | 74.0 | 0.40 | $1.52_9$ |
| 353 | 6 | 61- 84 | 73.0 | 0.35 | $1.54_1$ |
| 384 | 7 | 82-144 | 72.2 | 0.45 | $1.63_1$ |
| 411 | 6 | 78-138 | 71.1 | 0.41 | $1.62_4$ |
| 467 | 8 | 106-205 | 66.6 | 0.80 | $1.62_3$ |

$(\mu_g)_{obs.} = 2.5$ (assuming $\mu_t = 0.49$) $\Delta E = 0.9$ kcal.
$(\mu_g)_{calcd.} = 3.01$

1,1,2,2-Tetrachloropropane

$MR_D = 35.6$ cc. $P_E + P_A = 37.4$ cc.

| | | | | | |
|---|---|---|---|---|---|
| 371.6 | 7 | 51- 77 | 75.7 | 0.50 | $1.52_8$ |
| 412.7 | 6 | 71- 97 | 72.4 | 0.49 | $1.54_0$ |
| 467 | 7 | 82-111 | 68.5 | 0.43 | $1.54_4$ |

$(\mu_g)_{obs.} = 2.0$ (assuming $\mu_t = 0.84$) $\Delta E = 0.3 - 0.4$ kcal.
$(\mu_g)_{calcd.} = 2.24$

1,2,2-Trichloropropane

$MR_D = 30.8$ cc. $P_E + P_A = 32.3$ cc.

| | | | | | |
|---|---|---|---|---|---|
| 353.5 | 8 | 61-101 | 76.4 | 0.52 | $1.59_9$ |
| 383.2 | 8 | 74- 99 | 73.0 | 0.37 | $1.60_0$ |
| 411.5 | 6 | 61-110 | 71.2 | 0.12 | $1.62_1$ |
| 467.5 | 7 | 80-131 | 67.0 | 0.19 | $1.61_9$ |

$(\mu_g)_{obs.} = 2.8$ (assuming $\mu_t = 1.55$) $E \geqq 2.0$ kcal.
$(\mu_g)_{calcd.} = 2.97$

1,1,2-Trichloro-2-methylpropane

$MR_D = 35.5$ cc. $P_E + P_A = 37.3$ cc.

| | | | | | |
|---|---|---|---|---|---|
| 382.5 | 6 | 72- 88 | 90.6 | 0.41 | $1.82_9$ |
| 413·2 | 8 | 76-103 | 87.5 | 0.52 | $1.84_5$ |
| 429.6 | 7 | 69-102 | 84.3 | 0.43 | $1.82_0$ |
| 467.4 | 7 | 78-110 | 80.7 | 0.59 | $1.82_5$ |

$(\mu_{asym.})_{obs.} = 1.83$ $\Delta E \geqq 1.5$ kcal. ($P_A \leqq 2$ cc.)
$(\mu_{asym.})_{calcd.} = 1.76$
$(\mu_{sym.})_{calcd.} = 3.09$

1,2-Dibromopropane

$MR_D = 30.6$ cc. $P_E + P_A = 32.1$ cc.

| | | | | | |
|---|---|---|---|---|---|
| 353.6 | 5 | 61- 82 | 54.2 | 0.12 | $1.13_2$ |
| 371.1 | 6 | 65- 95 | $54.4_5$ | 0.28 | $1.16_7$ |
| 412.4 | 9 | 79-108 | 55.0 | 0.35 | $1.24_5$ |
| 467.2 | 6 | 68-109 | 56.4 | 0.27 | $1.36_5$ |

$(\mu_g)_{obs.} = 2.48$ (assuming $\mu_t = 0$) $\Delta E = 1.25$ kcal.
$(\mu_g)_{calcd.} = 2.41$

1,2-Dibromo-2-methylpropane

$MR_D = 35.2$ cc. $P_E + P_A = 37.0$ cc.

| | | | | | |
|---|---|---|---|---|---|
| 353.6 | 6 | 47- 67 | 60.0 | 0.42 | $1.16_5$ |
| 370.4 | 13 | 65- 98 | 61.0-61.8 | | 1.21-1.23** |
| 411.5 | 8 | 70- 91 | 60.2-62.6 | | 1.25-1.31** |

* $P_E + P_A = 1.05\, MR_D$ is assumed throughout.
** Slight decomposition of the sample is noticed in these runs.

## Experimental

All substances used were prepared by the methods described in Beilstein's Handbooks except those with special indication.

*1,2-Dichloro-2-methylpropane and 1,1,2-trichloro-2-methylpropane.*—Isobutyl alcohol saturated with hydrogen chloride on cooling, was heated to 120°C in a sealed tube for several hours. Isobutyl chloride thus obtained was chlorinated with chlorine gas in the presence of aluminum chloride. The product was fractionated into 1,2-dichloro-2-methylpropane (b. p. 107.0–108.0°C) and 1,1,2-trichloro-2-methylpropane (162.0–163.0°C).

*1,2,2-Trichloropropane and 1,1,2,2-tetrachloropropane.*—Monochloroacetone and dichloroacetone were prepared by the method described by S. Mizushima et al[4]. Monochloroacetone was added slowly to phosphorus pentachloride in a flask and the mixture was boiled for an hour. Then 1,2,2-trichloropropane was distilled: b. p. 121–123°C.

*1,1,2,2-Tetrachloropropane* was obtained by boiling a mixture of dichloroacetone and phosphorous pentachloride for fourteen hours: b. p. 153–154°C.

*1,2-Dibromo-2-methylpropane.*—A mixture of isobutyl alcohol, sulfuric acid in the weight ratio of 5 : 1, containing sea sand as a catalyser, was boiled and isobutylene thus produced was introduced into a vessel containing bromine: b. p. 148–149°/60 mmHg.

*1,2-Dibromopropane.*—A mixture of propyl alcohol, concentrated sulfuric acid, and sea sand was boiled. Propylene gas thus produced was introduced into a vessel containing bromine: b. p. 141–142°C.

The apparatus and the procedure for measuring the dielectric constant in the vapor state are described elsewhere[5].

## Results

The results of the measurement of dipole moments in the gaseous state are given in Table I. In case when there exist two rigid rotational isomers, the *trans* and the *gauche* forms, the average moment $\mu$ at temperature $T$ is given by

$$\mu^2 = \frac{\mu_g^2 s e^{-\Delta E/RT}}{1+s e^{-\Delta E/RT}} \qquad (1)$$

where $\mu_g$ denotes the moment of the *gauche* form and $s$ the weight factor ratio of the *gauche* form to the *trans* one. When $\log \mu^2$ is plotted against $\log (1/T)$, the curve is parallel to that of $\log (se^{-x}/1+se^{-x})$ vs. $\log x$, since,

$$\log \mu^2 = \log \mu_g^2 + \log(se^{-x}/1+se^{-x}),$$

and

$$\log (1/T) = -\log(\Delta E/R) + \log x.$$

Hence the coordinate of the abscissa and that of the ordinate shifted in order to fit the experimental curve $\log \mu^2$ vs. $\log (1/T)$ to the curve $\log (se^{-x}/1+se^{-x})$ vs. $\log x$, must be equal to $\log \Delta E/R$ and $\log \mu_g^2$ respectively*.

Eq. (1) was derived from the assumption of the coexistence of the two separate isomers. Actually molecules are distributed among the whole range of internal rotational angle, depending on the shape of the potential curve, so that it may be more rigorous to take into account all positions of rotation. However, the above treatment assuming Eq. (1) is proved to be valid usually within the error in $\Delta E$ of 0.15 kcal./mole[1b].

In Table I are also given the values of $\Delta E$ and $\mu_g$ obtained from the experimental data by the above treatment. The values of $\mu_g$ are compared

TABLE II
ENERGY DIFFERENCE IN ROTATIONAL ISOMERS IN HALOGENATED HYDROCARBONS

| Compound | Energy difference (kcal./mole) Observed | Calculated |
|---|---|---|
| $H_2ClC\text{-}CClH_2$ | 1.10[a] | 1.2 |
| $H_2ClC\text{-}CClHCH_3$* | 1.0[b] | |
| $g_1$ | | 0.9 |
| $g_2$ | | 1.2 |
| $H_2ClC\text{-}CCl(CH_3)_2$ | 0.90[c] | 0.9 |
| $(CH_3)_2ClC\text{-}CCl(CH_3)_2$ | 1.30[d] | 1.3 |
| $HCl_2C\text{-}CClH_2$ | ≧2.4[e], 2.9[f] | |
| $CH_3Cl_2C\text{-}CClH_3)_2$ | ≧2.0[c] | |
| $HCl_2C\text{-}CCl(CH_3)_2$ | ≧1.5[c] | |
| $HCl_2C\text{-}CCl_2H$ | 0[e] | |
| $CH_3Cl_2C\text{-}CCl_2H$ | 0.4[c] | |
| $H_2BrC\text{-}CBrH_2$ | 1.54[a] | 1.5 |
| $H_2BrC\text{-}CBrHCH_3$* | 1.25[c] | |
| $g_1$ | | 1.2 |
| $g_2$ | | 1.5 |
| $H_2BrC\text{-}CBr(CH_3)_2$ | 1.1[g] | 1.2 |
| $(CH_3)_2BrC\text{-}CBr(CH_3)_2$ | 1.6[d] | 1.6 |
| $HBr_2C\text{-}CBrH_2$ | ≧1.5[g] | |
| $HBr_2C\text{-}CBr_2H$ | 0, or $-\infty$[g] | |
| $H_2ClC\text{-}CCH_3H_2$ | 0[h] | 0.3 |
| $H_2BrC\text{-}CCH_3H_2$ | 0[h] | 0.3 |

* This molecule has two *gauche* forms, $g_1$ and $g_2$.

a) K. Kuratani, T. Miyazawa and S. Mizushima, *J. Chem. Phys.*, **21**, 1411 (1953).
b) Y. Morino, I. Miyagawa and T. Haga, *ibid.*, **19**, 791 (1951).
c) Present results.
d) Y. Morino, I. Miyagawa, T. Haga and S. Mizushima, This Bulletin, **28**, 165 (1955).
e) J. R. Thomas and W. D. Gwinn, *J. Am. Chem. Soc.*, **71**, 2785 (1949).
f) K. Kuratani and S. Mizushima, *J. Chem. Phys.*, **22**, 1403 (1954).
g) I. Miyagawa, *J. Chem. Soc. Japan*, **75**, 1162 (1954).
h) Ref. (10).

4) S. Mizushima et al., *J. Chem. Phys.*, **21**, 815 (1953).
5) T. Chiba, This Bulletin, **28**, 19 (1955).

* In case when the moment of trans ($\mu_t$) has a non-zero value, the same relation can hold by taking $\mu^2-\mu_t^2$, and $\mu_g^2-\mu_t^2$ in place of $\mu^2$ and $\mu_g^2$. Therefore, assuming a finite $\mu_t$, the same procedure can be applied. $\mu_t$ is always small and it produces no serious error.

with those calculated by taking empirical induction moments[1c] into account. It is seen that the agreement between them is fairly good. A little discrepancy in a few cases may be due to the ambiguity of the *s*-values used. In fact, the change of the *s*-values exerts sensitive influence on $\mu_g$ but not on $\Delta E$.

## Discussion

In Table II are summarized the $\Delta E'$s obtained both by the present work and by the measurements[1d] made in solution for the compounds on which the measurement in the gaseous state is difficult owing to the small vapor pressure or thermal decomposition. It is proved that there is practically no difference between the energy difference found in the gaseous state and that in the heptane solution[1e], so that the energy difference obtained in heptane solution can be compared with those in the gaseous state without any precaution. Table II includes also the results of the related halogenated hydrocarbons which were measured by other authors.

From Table II it is easily seen that $\Delta E'$s are grouped into three classes depending on the configuration of chlorine atoms, just as Miyagawa pointed out[1e].

| | configuration | $\Delta E$ |
|---|---|---|
| 1 | $\rangle ClC—CCl\langle$ | ca. 1 kcal./mole |
| 2 | $—Cl_2C—CCl\langle$ | ca. 2 kcal./mole |
| 3 | $—Cl_2C—CCl_2—$ | ca. 0 kcal./mole |

In dichloro-compounds small differences are found from one compound to another depending on the various types of methyl substitution. If the intramolecular potential is given by the sum of these potentials between non-bonded atoms or groups and, further, if it is assumed that the following relations hold between these potentials, the energy differences of many dichloro- and dibromo-compounds calculated are in excellent agreement with the observed:

$$(Cl\cdot Cl)-2(H\cdot Cl)+(H\cdot H)=1.2\,\text{kcal./mole} \quad (2)$$

$$(Cl\cdot CH_3)-(H\cdot Cl)-(H\cdot CH_3)+(H\cdot H)=0.3\,\text{kcal./mole} \quad (3)$$

$$(CH_3\cdot CH_3)-2(H\cdot CH_3)+(H\cdot H)=0.7\,\text{kcal./mole} \quad (4)$$

$$(Br\cdot Br)-2(H\cdot Br)+(H\cdot H)=1.5\,\text{kcal./mole} \quad (5)$$

$$(Br\cdot CH_3)-(H\cdot Br)-(H\cdot CH_3)+(H\cdot H)=0.3\,\text{kcal./mole} \quad (6)$$

where (A·B) denotes a potential difference due to the change of the relative position of the atom pair A and B from the *trans* to the *gauche*.

When the above relation is applied to the case of trichloro and tetrachloro-compounds, the discrepancy between the observed and the calculated becomes apparent. In fact, if the above relation holds, the energy differences of tri- and tetrachloroethane should be just as large as that of dichloroethane. A possible explanation of this discrepancy was presented qualitatively by Mizushima et al. for tetrachloroethane[6]. The two chlorine atoms attached to the same carbon atom have the ∠ClCCl angle larger than the tetrahedral value and non-adjacent Cl···Cl atoms come closer in the *trans* form. It is expected, therefore, that the *trans* form becomes much less than that in the case when the tetrahedral angle is maintained. If it is assumed that the angle of ∠ClCCl is reduced to the tetrahedral one by the substitution of a methyl group in place of a hydrogen atom of $CHCl_2$— group then the energy difference will be expected to be between those of dichloro- and tetrachloro-ethane. This is what is found in the experiment. The observed valence angles, 111° for ∠ClCCl in methylene chloride[7], 111.5° for ∠CCC in propane[8], and 109.5° for ∠ClCCl and 109.2° for ∠CCCl in 2,2-dichloropropane[9] from the electron diffraction investigation, seem to support the above hypothesis.

Eqs. (3), (6), and (4) correspond respectively to the $\Delta E'$s of chloropropane, bromopropane, and *n*-butane. The energy difference in chloropropane obtained by spectroscopy[10] is nearly equal to zero, which was confirmed recently by electron diffraction investigation[11]. Therefore, the energy relation assumed by these equations cannot be applied accurately to *n*-propyl halide molecules. Recently Szasz[3] proposed an interesting assumption that between a halogen atom and a methyl group there must be some attractive force, large enough to cancel the so-called steric repulsion. This assumption can explain the

6) S. Mizushima, Y. Morino and K. Kozima, *Sci. Papers Inst. Phys. Chem. Research* (Tokyo), **29**, 111 (1936).
7) L. E. Sutton and L. O. Brockway, *J. Am. Chem. Soc.*, **57**, 473 (1935).
8) L. Pauling and L. O. Brockway, ibid., **59**, 1223 (1937).
9) J. W. Coutts and R. L. Livingston, ibid., **75**, 1542 (1953).
10) C. Komaki et al., This Bulletin, **28**, 330 (1955).
11) Y. Morino and K. Kuchitsu, to be published in *J. Chem. Phys.*

extremely small energy difference in *n*-propyl chloride and the related hydrocarbons but it conflicts with the energy relation found in dichloro-isobutane; that is, the observed energy difference in this molecule is considerably lower than that in 1,2-dichloroethane, contrary to what is expected from Szasz's hypothesis. It should be assumed, therefore, that the methyl groups in *n*-propyl halides are quite different from the $CH_3$ groups in 1,2-dichloro-compounds. It may be probable to assume that the methyl group in *n*-propyl chloride rotates slightly about its symmetry axis to minimize the repulsion between the halogen atom and the methyl group and to make the energy difference small.

According to this assumption the two methyl groups in isobutyl chloride rotate around their axis, keeping some liaison to each other like gears, and this fact also makes the energy difference small. In dichloro-isobutane, on the contrary, the rotation of a methyl group is hindered, probably to a considerable extent, by the chlorine atom attached to the carbon atom. Therefore, the energy difference due to this effect will make the *trans* forms unstable, and, accordingly, decrease the net energy difference from that in 1,2-dichloroethane.

The situation may be the same for the methyl-methyl interaction when a halogen atom is attached to the carbon atom to which one of the methyl groups is attached. The degrees of rigidness of methyl groups in dichloropropane, dichloro-isobutane and 2,3-dichloro-2,3-dimethylbutane may not be perfectly equal to each other. The difference of this effect in the above three molecules, however, is supposed to be small, though it may be one of the origins of a small disagreement between the observed energy difference and the calculated one given in Table II. The energy difference 0.77 kcal./mole of *n*-butane may be a result of the fact that methyl-methyl repulsion cannot be cancelled out perpectly by such a rotation of the methyl group, because van der Waals' distance between the methyl groups, 4.33 Å, is larger than the distance of the methyl groups at the *gauche* position, 3.02 Å.

The authors are grateful for aid from the Scientific Research Grant given by the Department of Education of Japan in support of this research.

*Department of Chemistry*
*Faculty of Science*
*The University of Tokyo*
*Hongo, Tokyo*

12) G. J. Szasz, N. Sheppard, and D. H. Rank, *J. Chem. Phys.*, **16**, 704 (1948).

# *Dipole Moment and Internal Rotation of 1,4-Dichloro-2-butyne in the gaseous State*

By Yonezo MORINO, Ichiro MIYAGAWA, Takehiko CHIBA and Takashi SHIMOZAWA

(Received November 24, 1956)

The dipole moment of 1,4-dichloro-2-butyne in carbon tetrachloride and benzene solutions was previously reported by us[1], and the report showed a slight increase with temperature, causing the hindering potential of 700 cal./mole. Since the solvent exerts considerable influence upon the hindering potential of the internal rotation[2], it is desirable to measure the dipole moment in the vapor state to evaluate the hindering potential of the free molecule. The sample was prepared from 2-butyne-1,4-diol according to the method of Johnson[3], b. p., 66–68°C/17 mmHg. The apparatus used is the one described already[4]. The result of the measurement is given in Table I. The moment is found to be constant through the whole range of temperature of the measurement, contrary to the

1) Y. Morino, I. Miyagawa and A. Wada, *J. Chem. Phys.*, **20**, 1976 (1952).
2) S. Mizushima, Y. Morino and K. Higasi, *Sci. Pap. Inst. Phys. Chem. Res. Tokyo*, **25**, 159 (1934).
3) A. W. Johnson, *J. Chem. Soc.*, **1946**, 1009.
4) T. Chiba, This Bulletin. **28**, 19 (1955).

TABLE I

THE OBSERVED POLARIZATIONS AND DIPOLE MOMENT OF 1,4-DICHLORO-2-BUTYNE

$P_E + P_A = 1.05\,MR_D$ (assumed) = 29.8 cc.

| Temperature °K | No. of observations | Pressure range mmHg | Polarization cc. | Mean deviation of polarization | Dipole moment $D$. |
|---|---|---|---|---|---|
| 364.8 | 9 | 34- 56 | 102.9 | 0.9 cc. | $2.09_1$ |
| 372.3 | 14 | 32- 73 | 100.5 | 2.1 | $2.07_9$ |
| 392.3 | 10 | 43- 92 | 97.9 | 0.9 | $2.09_3$ |
| 414.1 | 10 | 45- 81 | 93.7 | 1.0 | $2.08_2$ |
| 433.3 | 9 | 51-161 | 90.8 | 1.2 | $2.08_1$ |

previous results in solutions. If we assume the hindering potential of the form of $V=(V_0/2)(1-\cos\theta)$, $V_0$ is found to be less than 0.1 kcal./mole. This result confirms the results of the electron diffraction investigation on this molecule recently made by Morino and Kuchitsu[5] that in the gaseous state this molecule has no preferred position for the internal rotation.

It should be noted that the component of the $CH_2Cl$ group moment perpendicular to the C—C≡C—C axis is found to be 1.47 $D$. If we assume the C—C—Cl angle of 111°[5], this corresponds to the C-Cl moment of 1.57 $D$, which is appreciably smaller than the normal C—Cl moment, 1.86 $D$. Pauling, Gordy and Saylor[6] suggested that propargyl chloride $CH{\equiv}C-CH_2Cl$ resonates between the two formulas $CH{\equiv}C-CH_2Cl$ and $C^+H=C=CH_2\ Cl^-$, and this resonance brings about the elongation of the C—Cl bond and the contraction of the adjacent C—C bond. If the resonance of this type takes place also in dichlorobutyne, it would produce an increase of the dipole moment of the $CH_2Cl$ group, but not its decrease. Therefore, the observed decrease of the said group moment denies Pauling's resonance scheme, or at least, it indicates that the predominant form is not Pauling's one.

*Department of Chemistry*
*Faculty of Science*
*The University of Tokyo*
*Hongo, Tokyo*

5) Y. Morino and K. Kuchitsu. This Bulletin, (to be published).

6) L. Pauling, W. Gordy and J. H. Saylor. *J. Am. Chem. Soc.* **64**, 1753 (1942).

# *Dipole Moment and Bond Character of Propargyl Halides and Mono- and Di-chlorobutynes*

By Takehiko CHIBA, Takashi SHIMOZAWA, Ichiro MIYAGAWA and Yonezo MORINO

(Received November 24, 1956)

In the preceding paper[1] it was shown that the C—Cl bond moment of 1,4-dichlorobutyne was abnormally small. This is an unexpected result from the current resonance theory. In order to elucidate this circumstance, a measurement was made on the dipole moments of propargyl chloride and bromide, and monochlorobutyne in the gaseous state. Quite recently Rogers and Panish[2] made a study on the dipole moments of similar compounds including propargyl bromide and iodide. Although their measurement was made in solution, the results agreed substantially with the present one.

## Experimental

*Propargyl chloride* was prepared by the chlorination[3] of propargyl alcohol with phosphorus trichloride in the presence of pyridine at about 0°C. The raw product was washed with ice-

1) Y. Morino et al., This Bulletin, **30**, 222 (1957).
2) M. T. Rogers and M. B. Panish, *J. Am. Chem. Soc.*, **77**, 3684 (1955).
3) L. F. Hatch and V. Chiola, ibid., **73**, 360 (1951).

water and fractionated: b. p. 56-57°C.

*Propargyl bromide* was fractionated from a commercial product of General Anilin and Film Corps.: b. p. 83-84°C.

*1-Chloro-2-butyne* was prepared from an isomeride of 1,3-dichloro-2-butene (b. p. 66-67°C/95 mmHg) by the following procedure[4]: first dichlorobutene was hydrated to 1-chloro-2-butene-3-ol (b. p. 93-94°C/50 mmHg) by boiling with sodium carbonate solution. This alcohol was dehydrochlorinated to 2-butene-1-ol (b. p. 90-96°C/95 mmHg) by boiling with a concentrated solution of potassium hydroxide. 2-Butyne-1-ol was chlorinated to 1-chloro-2-butyne by the method used for propargyl chloride. The fractionated product had the boiling point of 104-107°C.

The apparatus and the procedure of the measurement of the dipole moments is described elsewhere[5].

## Results and Discussions

The results of the measurement of the dipole moments are given in Table I.

As regards propargyl chloride, Pauling et al.[6] proposed the following resonance structure for the explanation of the longer C—Cl distance;

(A) $HC\equiv C-CH_2Cl$

and (B) $H-C^+=C=CH_2\ Cl^-$.

If it is true, the dipole moment of propargyl chloride will be large, because the form (B) has a large moment (ca. 18 *D*) due to the positive charge at the carbon atom and the negative charge at the chlorine atom. The observed values 1.65 *D* of chloride and 1.52 *D* of bromide do not show any trace of this tendency. Therefore, it is impossible to take this resonance formula for the main structure of propargyl chloride.

This anomalous feature is more distinct when propargyl halides are compared with the corresponding compounds having a double bond. The moment of allyl chloride, 1.98 *D*[7], is somewhat less than that of propyl chloride, 2.10 *D*[8]. As Smyth has pointed out[7], the difference between them can be explained by taking into account a hyperconjugation of

(C) $C^1H_2=C^2H-C^3H_2Cl$

and (D) $H_2C^-—CH=CHCl\ H^+$.

According to this opinion, the observed moment 0.35 *D* of propylene molecule itself may be ascribed to this hyperconjugation, and, if this hyperconjugation is not disturbed by the substitution of a chlorine atom, the moment of allyl chloride will be calculated by taking a resultant of the two dipoles, one in the C–Cl bond direction,

TABLE I

RESULTS OF THE MEASUREMENT OF THE DIPOLE MOMENT IN THE GASEOUS STATE

| Temp. K | No. of obs. | Press. range mmHg | Molar polarizn. cc. | Mean deviatn. of polarizn. cc. | Dipole moment *D* |
|---|---|---|---|---|---|
| Propargyl chloride | | | | | |
| $MR_D$=18.8 cc.[a] | $P_E+P_A$=19.7 cc. | | | | |
| 294.3 | 7 | 26-56 | 76.2 | 0.1 | $1.65_2$ |
| 326.3 | 9 | 54-79 | 70.8 | 0.4 | $1.65_3$ |
| | | | | | av. $1.65_3$ |
| Propargyl bromide | | | | | |
| $MR_D$=22.1 cc[b] | $P_{E+A}$=23.2 cc. | | | | |
| 306.3 | 8 | 45-77 | 69.2 | 0.3 | $1.52_1$ |
| 349.8 | 9 | 54-93 | 63.6 | 0.7 | $1.52_3$ |
| 373.3 | 8 | 67-95 | 60.6 | 0.3 | $1.51_4$ |
| | | | | | av. $1.51_9$ |
| 1-Chloro-2-butyne | | | | | |
| $MR_D$=23.7 cc.[a] | $P_E+P_A$=24.9 cc. | | | | |
| 328.4 | 8 | 51-59 | 113.1 | 0.6 | $2.18_0$ |
| 354.4 | 10 | 57-85 | 105.5 | 1.0 | $2.16_5$ |
| 385.6 | 9 | 61-91 | 99.6 | 0.8 | $2.17_4$ |
| | | | | | av. $2.17_3$ |

a) Ref. (3)
b) Ref. (2)
$P_E+P_A=1.05\ MR_D$ is assumed throughout.

4) M. S. Schechter et al., idid., **74**, 4903 (1952).
5) T. Chiba, This Bulletin, **28**, 19 (1955), refer also to the forthcoming paper on the dipole moment of cyclohexadione.
6) L. Pauling, W. Gordy and J. H. Saylor, *J. Am. Chem. Soc.*, **64**, 1753 (1942).
7) N. B. Hanney and C. P. Smyth, ibid., **68**, 1005 (1946).
8) Groves and Sugden, *J. Chem. Soc.*, **1937**, 158.

and the other, that of the propylene skeleton, in the direction of the $C^2$—$C^3$ bond*. Thus, by substrating 0.35 *D* vectorially from the observed moment of allyl chloride, 1.98 *D*, the apparent C—Cl moment is calculated to be 2.08 *D*, which can be compared with the moment of the propyl chloride, 2.10 D. It will be permissible to consider that this is the moment which the form (C) has when the effect of the form (D) is eliminated.

Now, in case of propargyl halides, in order to obtain the apparent C—Cl moment eliminating the contribution from the C≡C—C skeleton, the same kind of correction should be made by taking the moment of methyl acetylene, 0.75 *D*, as the moment of the C≡C—C skeleton on the molecular axis. The observed moments of propargyl chloride, 1.65 *D*, and bromide, 1.52 *D*, yield 1.76 *D* and 1.62 *D*, which are less than those of the corresponding saturated chloride and bromide by 0.28 *D* and 0.40 *D* respectively. According to Rogers[2], this tendency is much more prominent in the case of propargyl iodide, the difference being −0.60 *D***. Thus we have no evidence for the increase of the moments of propargyl halides, so that it is difficult to regard Pauling's resonance structure as a significant contribution to these compounds.

As described in the preceding paper, the component of the $CH_2Cl$-group moment perpendicular to the C—C axis in dichlorobutyne was found to be 1.47 *D*, assuming free internal rotation, which is definitely smaller than the value 1.74 *D* calculated on the basis of the usual C-Cl bond moment, 1.86 *D*, and of the C—C—Cl angle of 111°[9]. This cannot be accounted for by the mutual induction of the two C—Cl bonds as found in case of 1,2-dichloroethane, since the C—Cl dipoles are far apart in this compound (ca. 5A). Now, if the resonance scheme proposed by Pauling takes place in this molecule too, the following structures are to be taken into account, both of which would bring about the increase of the perpendicular component of the C—C bond moment:

(E) $Cl—CH_2—C^+=C=CH_2Cl^-$

and (F) $Cl^-H_2C=C=C^+—CH_2Cl$.

Hence there is another evidence against Pauling's resonance structure.

For monochlorobutyne the measurement of the dipole moment is promising because this molecule has a symmetrical structure of carbon skeleton with no dipole moment, so that it will provide a direct estimation of the C—Cl bond moment in these molecules. The observed moment, 2.17 *D*, is unexpectedly large and really almost equal to that of the corresponding saturated compound***. Rogers attributed the small dipole moments and the long C—X bond distances of propargyl halides to the contribution of the following resonance formulas:

(G) $H—C\equiv C—CH_2^-\ X^+$

and (H) $H—C^-=C=CH_2\ X^+$

The dipole moments of propargyl halides are explained by this resonance, but the C—I bond should have larger increase than does the C—Cl bond, because the moment decrease was found to be pronounced in propargyl iodide compared with the chloride. The C—Br and C—I distances observed by Pauling et al.[6] seem to be practically normal. In addition,the large moment of monochlorobutyne described above cannot be explained by this resonance scheme alone.

If the valence angles and bond moments are assumed to be the same in the three compounds: propargyl chloride, mono- and di-chlorobutynes, the most plausible way to make all moments of these compounds consistent is to take the group moments and their directions as follows:

1. The C—Cl bond moment is 1.58 *D* along the bond direction.
2. The methyl acetylene skeleton of propargyl chloride has a moment 0.75 *D* along the axis of C≡C—C.
3. A moment of 0.93 *D* is induced in the direction of the C≡C—C bond in propargyl chloride, and a moment of 1.04 *D* is induced in monochlorobutyne.

The moment of C—Cl bond, 1.58 *D*, is obtained by use of the perpendicular component of dichlorobutyne, 1.47 *D*, and of the C—C—Cl angle of 111° (see Fig. 1(a)). If this value is kept in the molecule of monochlorobutyne and of propargyl chloride, the vector addition will not hold unless an induced moment is taken into

* Strictly speaking, the moment induced by the hyperconjugation is not in the direction of $C^2$-$C^3$ bond, but, considering the possible positions of the $C^1$-$H_2$-group, the above assumption on the direction of this moment may be justified.

** Rogers took 0.80 *D* for methyl acetylene moment.

9) Y. Morino and K. Kuchitsu, This Bulletin, (to be published).

*** If the sample we prepared were 3-chloro-1-butyne, it could be expected to give a dipole moment as high as 2 *D*. However, the boiling point and the refractive index of our sample agreed with those in the literature, and the configuration 1-chloro-2-butyne was already verified in organic chemical process (Ref. 3. p. 362).

consideration. If we assume that this induced moment is along the direction of the molecular axis, the value of 1.04 $D$ will be obtained for monochlorobutyne (see Fig. 1(b)). Similar consideration gives

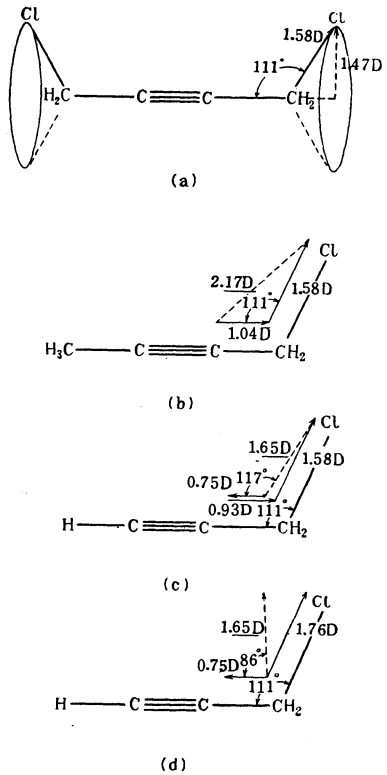



Fig. 1. Dipole moment components and their directions in mono- and di-chlorobutyne and propargyl chloride.

the value of 0.93 $D$ for the induced moment in propargyl chloride in the direction of the molecular axis, using 0.75 $D$ as the moment of the skeleton of C≡C—C (see Fig. 1(c)). Thus it must be concluded that the moment of the C—Cl bond attached to the $\alpha$ position of a C≡C bond is 0.3 $D$ smaller than the usual value and is accompanied with a fairly large moment lying on the axial direction.

Of course this is a tentative conclusion, ignoring a possible difference of the bond moments from one compound to another, as well as the difference in the direction of the induced moments. At first sight, this result may look untrustworthy and peculiar, but a similar phenomenon was found recently by microwave spectroscopy in case of propiolic aldehyde H—C≡C—CHO[10]. It was concluded that the total moment of 2.46 $D$ does not lie along the direction of the C=O bond, but in the direction close to the C≡C—C axis, making an angle of 25–30° with the carbonyl bond direction. This situation is just similar to the case of the chlorine compounds described above.

If the above argument is the case, the resultant moment of propargyl chloride lies along the direction making an angle of 117° with the molecular axis (Fig. 1(c)). On the contrary, if the moment of this compound is composed only of a moment of the C—Cl bond and of methyl acetylene skeleton, as shown in the Fig. 1(d), the resultant should lie in the direction of 86° with the axis. Therefore, it is desirable to determine the direction of the total moment of propargyl chloride by means of microwave spectroscopy, which will make a choice between the alternatives stated above.

Recently Mr. I'Haya calculated the dipole moment of propargyl chloride by the method of MO theory[11]. His result is in excellent agreement with the observed value reported here. The same calculation, however, cannot be applied to dichlorobutyne, because it does not give the dipole moment found by the measurement.

I'Haya suggested us that the induction moment along the C≡C—C axis given in Fig. 1(b) and (c) can reasonably be made smaller from the following reason. The hyperconjugation which takes place in methyl acetylene is twice as large as that in propargyl halide, since the —$CH_3$ group forms two mutually perpendicular "$\pi$-type orbitals", each of which is equivalent to that formed by —$CH_2$ group. Therefore, if the moment of methyl acetylene is entirely due to hyperconjugation, 0.38 $D$ must be assumed for the moment of the C≡C—C skeleton in propargyl chloride instead of 0.75 $D$. This enables one to reduce the inductive moment in propargyl chloride to a more reasonable value 0.56 $D$. Similarly, in monochlorobutyne one can expect that skeletal moment does not vanish but has a value 0.38 $D$. This reduces an induction moment to 0.67 $D$ in this compound.

## Summary

The dipole moments of propargyl chloride, bromide and monochlorobutyne in the gaseous state are measured to be 1.65 $D$,

10) J. A. Howe and J. H. Goldstein, *J. Chem. Phys.*, **23**, 1223 (1955).

11) I'Haya, presented at the Discussion Meeting of Structural Chemistry held in Tokyo by the Chemical Society of Japan on October, 1955.

1.52 *D* and 2.17 *D* respectively. The moment of propargyl chloride and bromide are considerably smaller than the saturated one even though the correction of C≡C—C skeletal moment is taken into account. This is consistent with the $-CH_2Cl$ group moment of dichlorobutyne obtained in the preceding work. These results are inconsistent with the resonance scheme presented by Pauling et al. for propargyl halide. The anomaly is considered as a characteristic feature of the molecules having triple bonds of this kind. By taking all of the moments of dichloro- and monochlorobutynes and propargyl chloride into account, the bond moments, the induction moments and the direction of the resultants are predicted as shown in Fig. 1.

The authors wish to express their sincere gratitude to Mr. Y. I'Haya for his valuable suggestion concerning hyperconjugation. They are also indebted to the Ministry of Education of Japan for the research grant.

*Department of Chemistry*
*Faculty of Science*
*The University of Tokyo*
*Hongo, Tokyo*

# *Magnetochemical Study of Sydnones*

By Yoshio MATSUNAGA

(Received November 26, 1956)

## Introduction

The problem of providing an adequate structural formula for sydnones has engaged the minds of chemists, since Earl and Mackney[1] obtained N-phenylsydnone by dehydration of N-nitroso-N-phenylglycine about twenty years ago. The bicylic structure proposed by the discoverers was considered to be unacceptable, and the hybrid structure derived from a number of contributing ionic forms suggested by Baker[2] seems to be consistent with the known properties of the compounds, i. e. general stability of aromatic type, dipole moment [3,4] and ultra-violet absorption spectra[2,5]. The non-localized electrons in the sydnone ring will bring about the large diamagnetic contribution, so that the exaltation of molar susceptibility may be expected against the calculated values for any of the contributing ionic forms, and its magnitude may be considered as a measure of its aromatic character. With the intention of ascertaining the aromatic character of sydnone ring, we examined the diamagnetic susceptibilities of some derivatives of sydnone.

1) J C Earl and A. W. Mackney, *J. Chem Soc.*, **1935**, 899
2) W Baker, W. D Ollis and V. D. Poole, ibid., **1949**, 307
3) J. C. Earl, E. M. W. Leake and R. J. W. Le Fèvre ibid , **1948**, 2269
4) R A. W. Hill and L. E. Sutton, ibid., **1949**, 746; **1953**, 1482
5) J. C. Earl,R. J. W. Le Fèvre and I. R. Wilson, ibid., **1949**, S. 103.

## Experimental

**Materials.**— They were prepared by the methods described in the references cited. N-phenylsydnone[1], recrystallized from boiling water and sublimed in vacuum. m. p. 132-3°C. (all of m. p. are not corrected.) N-*p*-tolylsydnone[2], sublimed in vacuum. m. p. 140-1°C. N-*p*-methoxyphenylsydnone[6], sublimed in vacuum. m. p. 123-4°C. N-*p*-chlorophenylsydnone[2], recrystallized from the mixture of benzene and light petroleum. m. p. 113°C. N-*m*-nitrophenylsydnone. The mixture of nitrosoglycine and acetic anhydride was warmed on a steam bath for six hours and concentrated under reduced pressure. The precipitated crystals were washed and recrystallized from ethanol. m. p. 137-8°C. Eade and Earl[6] obtained the same material by the reaction at room temperature for two months; the above procedure was in imitation of that for *p*-analogue given by Baker. N-*p*-nitrophenylsydnone[2], recrystallized from the mixture of benzene and light petroleum. m. p. 180-2°C. N-β-naphthylsydnone[6], recrystallized from ethanol and sublimed in vacuum. m. p. 157°C. N-benzylsydnone[2], recrystallized from the mixture of benzene and light petroleum. m. p. 67-9°C. N-phenyl-C-bromosydnone[2], recrystallized from ethanol repeatedly. m. p. 133-4°C. N-phenyl-C-iodosydnone[7], recrystallized from methanol. m. p. 157-8°C. N-phenyl-C-chloromercurysydnone[7], recrystallized from methanol. m. p. 196-8°C. bis(N-phenylsyd-

6) R. A. Eade and J. C. Earl, ibid., **1946**, 591.
7) K. Nakahara and M. Ohta, *J. Chem Soc. Japan (Pure Chem. Sect.)*, **77**, 1306 (1956).

nonyl-C-)mercury[7], precipitated crystals were washed with methanol and used without further purification.

**Magnetic Measurement.** — The susceptibility was measured using a Gouy balance as previously described[8].

## Results and Discussion

The results are shown in Table I[9] for N-arylsydnones which have no substituent in the sydnone ring. If we assume that the effect of conjugation between aryl and sydnonyl groups on the molar susceptibility is small, we may approximate their susceptibilities by the sum of those of constitutional fragments of the molecule, namely aryl and sydnonyl groups. For example, from the molar susceptibility of N-phenylsydnone the value of benzene is subtracted and twice the amount of Pascal's constant for hydrogen is added; the remainder may be considered as the molar susceptibility of the unsubstituted sydnone $C_2H_2N_2O_2$. The evaluated values by the similar method from the data of the other seven compounds are also given in column four of Table I. The following values were used for the calculations, benzene 55.2[10], toluene 65.8[11], anisol 72.6[12], chlorobenzene 70.0[13], nitrobenzene 61.8[11] and naphthalene 92.2[14]. Including the value derived from the molar susceptibility of N-benzylsydnone in which the conjugation between two constitutional fragments does not exist, their agreements are satisfactorily good, and the assumption made in the above evaluations is supported by this fact. The mean value 38.7 will be used in the discussion hereafter.

TABLE I

MOLAR SUSCEPTIBILITIES OF N-ARYLSYDNONES

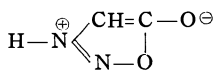
| Substance | Suscept. ($\chi$) | Molar Suscept. ($\chi_M$) ArSy.* | HSy.* |
|---|---|---|---|
| N-Phenylsydnone | 0.540 | 87.6 | 38.3 |
| N-*p*-Tolylsydnone | 0.556 | 98.0 | 38.1 |
| N-*p*-Methoxyphenylsydnone | 0.542 | 104.2 | 38.0 |
| N-*p*-Chlorophenylsydnone | 0.518 | 101.8 | 37.7 |
| N-*m*-Nitrophenylsydnone | 0.458 | 94.9 | 39.0 |
| N-*p*-Nitrophenylsydnone | 0.458 | 94.9 | 39.0 |
| N-$\beta$-Naphthylsydnone | 0.593 | 125.8 | 39.5 |
| N-Benzylsydnone | 0.568 | 100.1 | 40.2 |

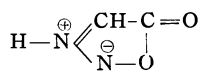
* Sy is the abbreviation of sydnonyl group.

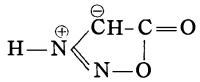
Generally the diamagnetic anisotropy of a molecule is expressed as

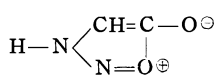
$$\Delta K = 3(\chi_M - K_t)$$

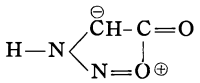
where $\chi_M$ and $K_t$ are the observed molar susceptibility for powdered specimen and its isotropic part respectively. The isotropic part of an ordinary aromatic compound is usually assumed to be equal to the principal molar susceptibility in the plane of a molecule, and approximated by the calculated value for its Kekulé form[15]. It seems to be acceptable that the isotropic part of molar susceptibility of meso-ionic compound can be approximated by the calculated value for the contributing ionic form; and the anisotropic part corresponds to the diamagnetic contribution of non-localized electrons in the meso-ionic ring. Although a regular pentagon was assigned by many chemists for the simplest model of sydnone ring, it must be noted that the application of the above formula is not restricted by the non-coplanarity of the ring[16]. In the case of aromatic compounds, the magnitude of the isotropic part does not depend on the forms in so far as we choose the Kekulé form for the purpose of evaluating it. But in the present case, the calculated values for the contributing ionic forms are not necessarily equal to each other, and it is incorrect to pick out one of them as the representative for which the isotropic part must be calculated. The following five forms (I—V) were considered by Baker[2] to make important contributions to the hybrid, and Hill and Sutton[4] suggested that there is a major contribution from form (I) and a lesser from (II) and (IV).

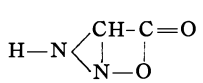

(I)


(II)


(III)


(IV)


(V)


(VI)

8) H. Akamatu and Y. Matsunaga, This Bulletin, **26**, 364 (1953).
9) All susceptibility values in this paper are recorded in $10^{-6}$ c. g. s. units and the negative signs are omitted.
10) B. C. Eggleston et al., *J. Chem. Soc.*, **1954**, 941.
11) F. G. Baddar and S. Sugden, ibid., **1950**, 308.
12) P. Rumpf snd M. Séguin, *Bull. soc. chim. France*, **1949**, D 366.
13) C. M. French and V. C. G. Trew, *Trans. Faraday Soc.*, **41**, 439 (1945).
14) H. Akamatu and Y. Matsunaga, This Bulletin, **29**, 800 (1956).
15) H. Shiba and G. Hazato, ibid., **22**, 92 (1949)
16) A. Pacault, *Bull. soc. chim. France*, **1949**, D 371.

Therefore, by means of Gray-Cruickshank's system[17] we calculated the values for these forms as the isotropic part of molar susceptibility of unsubstituted sydnone. For example, the value for form (I) was calculated based on the model shown in Fig. 1 using the constants presented in Table II.

TABLE II

CALCULATION OF MOLAR SUSCEPTIBILITY OF IONIC FORM (I) OF SYDNONE

| Atom (Charge) | Ionic Diamagnetism | Bond | Bond Depression |
|---|---|---|---|
| H (+0.04) | 2.28 | C—H | 0.53 |
| H (+0.29) | 1.68 | C=C | 9.50 |
| C (+0.02) | 9.89 | C—N | 1.78 |
| C (+0.26) | 9.10 | C—O | 1.92 |
| N (+0.08) | 8.09 | C—O | 1.92 |
| N (+0.65) | 6.74 | N—H | 0.57 |
| O (−0.21) | 7.58 | N=N | 13.3* |
| O (−1.13) | 9.82 | N—O | 2.06 |
| Total Diamagnetism | 55.18 | | 31.58 |
| Total Bond Depression | 31.58 | | |
| Resultant Molar Suscept. | 23.60 | | |

* Estimated from the constant for azo group determined previously[18].

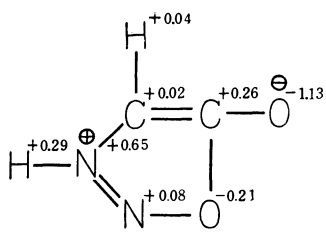



Fig. 1. Model of ionic form (I) of sydnone.

Table III illustrates the calculated values for the five forms, including also the value for bicyclic structure (VI) calculated using Pascal's constants, and the latter which must be compared directly with the experimental value appears to be unacceptable again from this standpoint. Fortunately the calculated values for (I—V) are so close to each other that we estimate the isotropic part of molar susceptibility of sydnone at the mean value 24.57. By the comparison between the value derived from the experimental data shown in Table I and the estimated one, we obtain 14.1 as the exaltation of molar susceptibility i. e. $\Delta K/3$ which must be due to the contribution of non-localized electrons in the sydnone ring. The estimated exaltation is nearly equal to those of furan 13.4 and pyrrole 14.4 and slightly less than that of thiophene 17.9 given by Pacault[19]. According to Dewar[20], an aromatic compound is defined as a cyclic compound with a large resonance energy. The relation between resonance energy and diamagnetic anisotropy is uncertain and not simple. It is not correct to affirm that the molecule which shows the larger diamagnetic anisotropy has always the larger resonance energy. As an example of the extremely conflicting cases, perylene shows the diamagnetic anisotropy less than twice as large as that of naphthalene, but its resonance energy is larger than twice the latter's[21]. As to sydnone, however, the nearly isoelectronic structure with furan and pyrrole results from a large fractional negative charge borne by the oxygen atom in carbonyl group, so it seems to be probable that sydnone ring has the aromatic character in the same order with furan and pyrrole rings.

TABLE III

CALCULATED MOLAR SUSCEPTIBILITIES OF IONIC AND BICYCLIC FORMS OF SYDNONE

| Form | Molar Suscept. ($\chi_M$ or $K_i$) |
|---|---|
| Ionic (I) | 23.60 |
| Ionic (II) | 24.69 |
| Ionic (III) | 24.74 |
| Ionic (IV) | 24.08 |
| Ionic (V) | 25.22 |
| Bicyclic (VI) | 25.46 |

Next we examined the molar susceptibilities of four derivatives of N-phenylsydnone in which the substituent is linked to the carbon atom of the sydnone ring, and compared them with the calculated values based on the constant for sydnone 38.7 derived from eight N-arylsydnone by the aid of the additivity rule. The results are presented in Table IV. Kadomtzeff[22] showed that the magnetic contribution of mercury depends markedly on the nature of the rest of the molecule and gave the values from 23.8 to 43.0 for the mercury in RHgX, and from 28.5 to 46.0 for the same atom in $R_2Hg$. We used in our cal-

17) F. W. Gray and J. H. Cruickshank, *Trans. Faraday Soc.*, **31**, 1491 (1935).
18) Y. Matsunaga, This Bulletin, **29**, 308 (1956).
19) A. Pacault, *Rev. sci.*, **86**, 38 (1948).
20) M. J. S. Dewar, "The Electronic Theory of Organic Chemistry", Oxford Univ. Press, Oxford, (1949) p. 160.
21) F. Klages, *Ber.*, **82**, 358 (1949).
22) I. Kadomtzeff, *Bull. soc. chim. France*, **1949**, D 394.

culations the constants of mercury in the most similar compounds which have ever been measured, namely the derivatives of thiophene.

TABLE IV

MOLAR SUSCEPTIBILITIES OF DERIVATIVES OF N-PHENYLSYDNONE

| Substance | Suscept. ($\chi$) | Molar Suscept. ($\chi_M$) Obs. | Calcd. | Diff. (%) |
|---|---|---|---|---|
| N-Phenyl-C-bromosydnone | 0.461 | 111.1 | 111.5 | −0.3 |
| N-Phenyl-C-iodosydnone | 0.429 | 123.6 | 125.5 | −1.4 |
| N-Phenyl-C-chloromercury-sydnone | 0.378 | 150.1 | 144.0* | +4.3 |
| Bis (N-phenyl-sydnonyl-C-) mercury | 0.383 | 200.3 | 198.5** | +1.0 |

* The constant of mercury 38.9 was used.
** The constant of mercury 28.5 was used.

The calculated molar susceptibilities agree well with the observed ones, except the case of N-phenyl-C-chloromercury-sydnone. At the present, we cannot decide conclusively between the incorrect estimation of the constant of mercury used in the calculation and the remarkable change of the contribution of non-localized electrons in a sydnone ring as the cause of this disagreement. The latter case was found by Hazato[23] in the derivatives of tropolone which some investigators regard as one type of meso-ionic compounds. However, the author is inclined to the former cause, as such a large influence of substituent on diamagnetism is not common in a number of aromatic compounds, besides such a disagreement is not found in the other three cases presented here.

23) G. Hazato et al, *Sci. Repts. Research Insts. Tohoku Univ., Ser.* A, **5**, 278 (1953); **6**, 193 (1954).

## Summary

The molar susceptibilities of eight N-arylsydnones were measured by the Gouy method. Assuming that the influence of the conjugation between aryl and sydnonyl groups on diamagnetism is practically negligible, the molar susceptibility of unsubstituted sydnone was estimated as 38.7. Its isotropic part 24.57 was evaluated from the values for five of the contributing ionic forms calculated by the Gray-Cruickshank's method. From the magnitude of the exaltation of molar susceptibility which is equal to one third of an anisotropic part, the author suggested that the aromatic character of a sydnone ring is in the same order with those of furan and pyrrole rings. Four derivatives of N-phenylsydnone which have a substituent in meso-ionic ring were also measured, and the agreements between the observed and the calculated molar susceptibilities were found to be good within the limit of the latter's estimation.

The author wishes to express his hearty thanks to Prof. H. Akamatu for his kind direction. The cost of this study has been defrayed by the Grant in Aid for Fundamental Scientific Research from the Ministry of Education, to which the author's thanks are also due.

*Department of Chemistry*
*Faculty of Science*
*The University of Tokyo*
*Hongo, Tokyo*

# *The Molecular Structure of 1,2-Difluoro-1,1,2,2-tetrachloroethane*

By Machio IWASAKI, Shunji NAGASE and Rimpei KOJIMA

(Received October 8, 1956)

## Introduction

The molecular structure of 1,2-difluorotetrachloroethane offers two interesting problems. One is concerned with rotational isomerism while the other with the effect of the neighbouring halogen atoms on the C—F and C—Cl bond distances.

The phenomenon of the rotational isomerism in halogenated ethanes has been the subject of a great number of investigations during the past two decades. However, most of these works have been carried out by measuring the change of dipole moments or infrared absorptions with temperature compared with the

results of which measurements by electron diffraction are meagre. Furthermore, the general applicability and the merits of various potential functions[1,2] that have recently been proposed cannot be criticized until comprehensive data on the structure of related molecules are available. Therefore it is desirable to carry out a study by electron diffraction side by side with studies by spectroscopy and dipole moment measurement.

Having such points in mind, the present writers have undertaken the herein described work in order to determine the molecular structure and the energy difference between two isomers by means of electron diffraction.

## Experimental

### Sample

The sample was prepared by the fluorination of hexachloroethane with $SbF_3$ in the presence of $SbCl_5$ as a catalyst. The product distilled at 92.5°C. The purity of this sample was tested with an infrared absorption spectrum. It was confirmed that the amount of $CCl_3$—$CF_2Cl$, which could not be removed by fractionation, was less than about one per cent. Hence the amount was not great enough to affect the electron diffraction pattern.

### Procedure

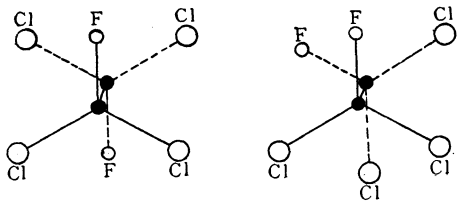
The diffraction patterns of 40 KV. electrons were obtained at a temperature of about 15°C using a rotating sector apparatus, which will be described in detail elsewhere. Two camera distances of 28 cm. and 12 cm. were used with an $s^2$ sector. The photographic density was measured up to $q=90$ by a recording microphotometer. In this measurment, the photographic plate was rotated rapidly about the center of the diffraction pattern in order to smooth out the inevitable irregularities. The traces thus obtained were measured by a coordinate comparator as a function of $q$. A procedure[3] similar to that employed by J. Karle was used for deriving an experimental intensity curve from the microphotometer record.

The experimental intensity curve, $I_m$, was obtained from the curve of the total scattered intensity, $I_t$, by drawing a smooth background, $I_b$, then

$$I_m=(I_t/I_b)-1. \qquad (1)$$

The curve A shown in Fig. 4 is $I_m$ multiplied by $q$, where the dotted portion is drawn by use of a theoretical intensity curve described below.

1) W. D. Gwinn and K. S. Pitzer, *J. Chem. Phys.*, **16**, 303 (1948).
2) H. J. Bernstein, ibid., **17**, 262 (1949).
3) I. L. Karle and J. Karle, ibid., **17**, 1052 (1949) ; **18**, 957 (1950).




*trans* form *gauche* form

Fig. 1. Stable configurations of $CFCl_2$-$CFCl_2$.

### Analysis

The radial distribution curve shown in Fig. 2 was calculated by the following equation:

$$f(r)=\sum_{q=0}^{q_{max}} qI_m \exp(-aq^2)\sin(\pi qr/10), \qquad (2)$$

where $a=0.00288$.

The curve has maxima at 1.38, 1.76, 2.5—3.3, 3.92 and 4.33Å. The first two peaks at 1.38 and 1.76 Å correspond to C—F and C—Cl bond distances, respectively. The peak at 2.5—3.3 Å is due to various non-bonded distances, while that at 4.33 Å to the *trans* Cl···Cl distance. The peak at 3.92 Å corresponds to the *trans* F···Cl distance, which is characteristic of *gauche* configuration (see Fig. 1). This peak evidently shows the existence of the *gauche* form. If only the *gauche* form exists, the ratio of the area of the peak at 4.33 Å to that at 3.92 Å must have the value of 0.86. The fact that the observed ratio has the value of 2.43, indicates that the *trans* form, having no *trans* F···Cl distance, coexists with the *gauche* form (see Fig. 1). The ratio of the two forms, $N_t/N_g$, can be calculated from the areas of the two peaks noted above by means of the following formula:

$$\frac{N_t}{N_g}=\frac{Z_F\, r_{Cl\cdots Cl}A_{Cl\cdots Cl}}{Z_{Cl}r_{F\cdots Cl}A_{F\cdots Cl}}-\frac{1}{2}, \qquad (3)$$

where $A_{Cl\cdots Cl}$ and $A_{F\cdots Cl}$ are the areas of the peaks and $r_{Cl\cdots Cl}$ and $r_{F\cdots Cl}$ are the equilibrium distances for the *trans* Cl···Cl and *trans* F···Cl, respectively. The application of this formula leads to a value of 52 per cent. for the amount of the *gauche* form.

In the calculation of the radial distribution curve, in place of the intensity curve below $q=17$ the theoretical intensity was substituted. The ratio of the areas was affected by the value of the abundance ratio of the two isomers assumed in the calculation of the theoretical part of the intensity. Therefore, the method of successive approximation was taken. If the theoretical part is calculated for 100 per cent. *gauche* form, formula 3 above leads to a value of 78 per cent. for the amount of the *gauche* form. Next, assuming the amount of the *gauche* form to be equal to 78 per cent. a value of 71 per cent. was obtained. The successive approximation being carried out as given above, a self-consistent value of 52 per cent. was obtained. This value was scarcely affected by the values of molecular parameters assumed in the calculation. The radial distribution curve shown in Fig. 2 was

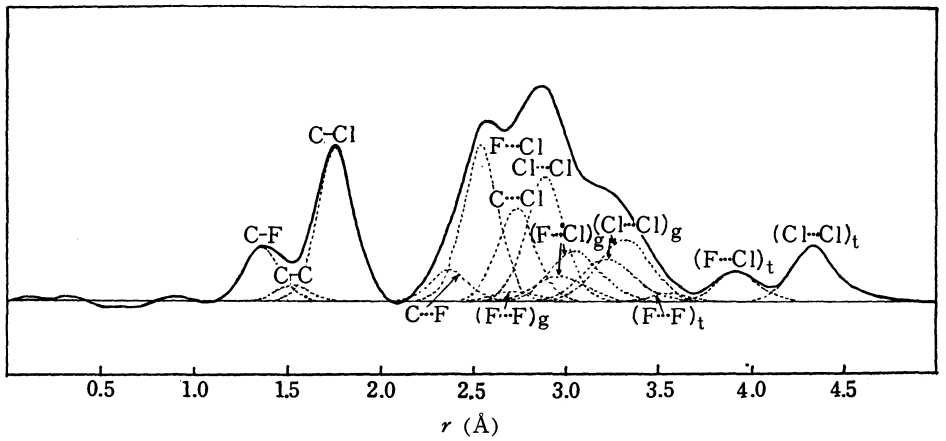



Fig. 2. Radial distribution curve of $CFCl_2$—$CFCl_2$.

obtained by the procedure described above using the values of molecular parameters listed in Table III.

The part from 2.5 to 3.3 Å of the radial distribution curve corresponds to the superposition of the contributions of 10 interatomic distances in the *trans* as well as in the *gauche* form. This part of the radial distribution curve calculated as the sum of Gaussian curves, each corresponding to the contribution of an interatomic distance, was in good agreement with the experimental curve, when the amount of the *gauche* form was assumed to be about 50 per cent. The assumed values of the mean amplitudes used in this calculation are listed in Table I. The dotted curves shown in Fig. 2 depict the contributions of various interatomic distances. Although the assumed values were used for the mean amplitudes, the result from this part of the radial distribution curve serves to confirm the percentage of the *gauche* form derived from the ratio of the peak areas at 4.33 and 3.92 Å.

The shelf at 3.2 Å corresponds to the *gauche* Cl···Cl distance in the *gauche* form*. Therefore, from this portion of the radial distribution curve, the value of 55—63° was obtained for the azimuthal angle of F—C—C—F of the *gauche* form.

The analysis of the over-all feature of the radial distribution curve gave the values listed in Table III for the interatomic distances and the valency angles. Other items of information obtained from the radial distribution curve are the values of the mean amplitudes of the bonded C—F, bonded C—Cl, *trans* F···Cl, and *trans* Cl···Cl distances. The mean amplitudes of other distances could not be determined because of the superposition of many interatomic distances in the radial distribution curve. If the observed peaks are made to fit Gaussian curves, the values listed in Table I are obtained for the mean amplitudes of these distances, which agree with the values calculated by Morino et al.[4]

TABLE I

OBSERVED AND ASSUMED MEAN AMPLITUDES IN Å

| Distance | Obs. | Calcd. | Distance | Obs. | Calcd. |
|---|---|---|---|---|---|
| C—F | 0.064 | 0.045 | $(F\cdots F)_g$ | | 0.114 |
| C—C | | 0.050 | $(F\cdots Cl)_g$ | | 0.120 |
| C—Cl | 0.062 | 0.050 | $(Cl\cdots Cl)_g$ | | 0.125 |
| C···F | | 0.059 | $(F\cdots F)_t$ | | 0.061 |
| F···Cl | | 0.065 | $(F\cdots Cl)_t$ | 0.070 | 0.070 |
| C···Cl | | 0.073 | $(Cl\cdots Cl)_t$ | 0.081 | 0.074 |
| Cl···Cl | | 0.070 | | | |

* The *gauche* Cl·····Cl distance of the *trans* form is somewhat smaller than this value.

The theoretical intensity curves were calculated by use of the following equation:

$$qI(q) = \sum_{i>j}\sum \frac{Z_i Z_j}{r_{ij}} \exp(-b_{ij}q^2)\sin(\pi q r_{ij}/10) \quad .(4)$$

In this equation, notations have their usual significances. The constant $b_{ij}$ was calculated from the mean amplitudes listed in Table I. Though the majority of these values are calculated by Morino et al.[4] from spectroscopic data, the values for the non-bonded F···Cl and the *trans* F···Cl distances were assumed appropriately from other data. The values for the *gauche* F···F and the *gauche* Cl···Cl distances were taken from Karle's experimental data on $C_2Cl_6$[5] and $C_2F_6$[6] by ascribing the contribution of the torsional oscillation to the over-all vibration. For the *gauche* F···Cl distance, use was also made of Karle's data.

The curve A in Fig. 3 is of 100 per cent. *trans* form and the curve E of 100 per cent. *gauche* form for the model obtained from the radial distribution curve on the assumption that the structural frame of the molecule does not change with rotation. The curves B, C and D are of the isomeric mixture, in which the amount of the *gauche* form is 30, 50 and 70 per cent. respectively. The curve for the *trans* form as well as the *gauche* does not agree with the experi-

4) Y. Morino, K. Kuchitsu, A. Takahashi and K. Maeda, *J. Chem. Phys.*, **21**, 1927 (1953).
5) D. A. Swick, I. L. Karle and J. Karle, ibid., **22**, 1242 (1954).
6) D. A. Swick and I. L. Karle, ibid., **23**, 1499 (1955).

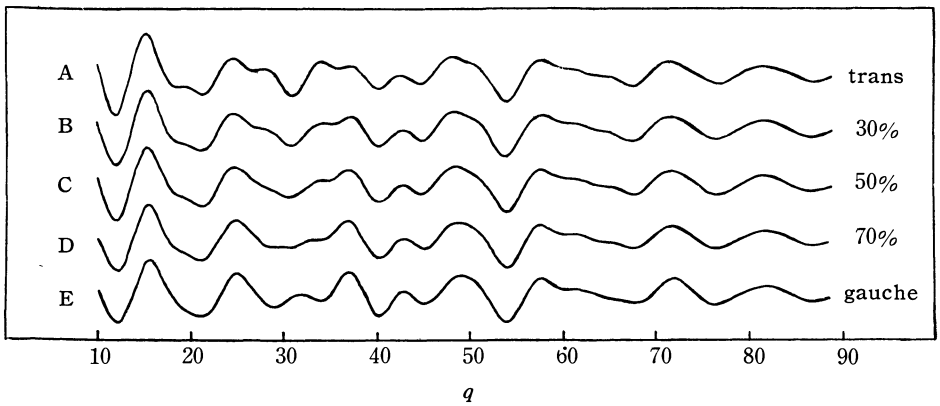



Fig. 3. Theoretical intensity curves of $CFCl_2$—$CFCl_2$.

TABLE II
MOLECULAR PARAMETERS FOR $CFCl_2$—$CFCl_2$

| Model | C—F | C—C | C—Cl | ∠CCCl | ∠ClCCl | ∠FCCl |
|---|---|---|---|---|---|---|
| B | 1.38 Å | 1.54 Å | 1.76 Å | 112° | 110°30′ | 107°30′ |
| C | 〃 | 〃 | 〃 | 110° | 〃 | 107° |
| D | 〃 | 〃 | 〃 | 114° | 〃 | 〃 |
| E | 〃 | 〃 | 〃 | 112° | 109°30′ | 〃 |
| F | 〃 | 〃 | 〃 | 〃 | 110°30′ | 〃 |
| G | 〃 | 〃 | 〃 | 〃 | 111°30′ | 〃 |
| H | 〃 | 〃 | 〃 | 〃 | 110°30′ | 106° |
| I | 〃 | 〃 | 〃 | 〃 | 〃 | 108° |
| J | 〃 | 〃 | 1.73 | 〃 | 〃 | 107° |
| K | 〃 | 〃 | 1.79 | 〃 | 〃 | 〃 |
| L | 1.34 | 〃 | 1.76 | 〃 | 〃 | 〃 |
| M | 1.42 | 〃 | 〃 | 〃 | 〃 | 〃 |
| N | 1.38 | 1.48 | 〃 | 〃 | 〃 | 〃 |
| O | 〃 | 1.60 | 〃 | 〃 | 〃 | 〃 |
| P | 〃 | 1.54 | 〃 | 〃 | 〃 | 〃 |
| Q | 〃 | 〃 | 〃 | 〃 | 〃 | 〃 |
| R | 〃 | 〃 | 〃 | 〃 | 〃 | 〃 |

ment. The curve for the mixture is in satisfactory agreement with the experiment, if the *gauche* form is present in an amount nearly equal to 50 per cent. The result confirms definitely the amount of the *gauche* form already derived from the radial distribution curve.

Moreover, the limits of errors in the percentage of the *gauche* form as well as the values of the interatomic distances, the valency angles, and the azimuthal angle of the *gauche* form were determined by the analysis of 100 theroretical intensity curves for models having a C—F distance ranging from 1.30 to 1.42 Å, a C—Cl distance from 1.73 to 1.79 Å, a C—C distance from 1.45 to 1.60 Å, ∠CCCl from 109°28′ to 115°, ∠ClCCl from 109°28′ to 111°30′ and ∠FCCl from 109°28′ to 105°30′. Some of them are shown in Fig. 3 in order to illustrate the dependence of the relative positions and intensities of maxima and minima upon the parameters. The values of the parameters used are listed in Table II. Curve B in Fig. 4 gives the best model. It reproduces the feature of the experimental curve in a satisfactory manner. The mean value of $q/q_0$ for the maximum and minimum positions is 1.000 with an average deviation of 0.002.

The variation in the parameter ∠CCCl causes changes mainly in the regions $18<q<23$ and $30<q<40$, that of ∠ClCCl mainly in the region $39<q<47$, that of ∠FCCl mainly in the region $47<q<52$, that of C—Cl mainly in the positions of the maxima and minima, and those of C—F and C—C mainly in the regions $30<q<40$ and $47<q<52$ as shown in curves C, F and D, curves E, F and G, curves H, F and I, curves J, F and K, curves L, F and M, and curves N, F and O, respectively. It was assumed for the sake of comparison that the three *gauche* Cl···Cl distances in the *gauche* form were equal and the amount of the *gauche* form was 50 per cent. in all of the models described above, although the change in the azimuthal angle or the amount of the *gauche* form may improve the agreement with the experimental curve. The changes due to the variation of these two parameters are illustrated in curves P, Q and R of Fig. 4 and curves B, C and D of Fig. 3. The curves P, Q and R depict the theoretical intensity for the models of the azimuthal

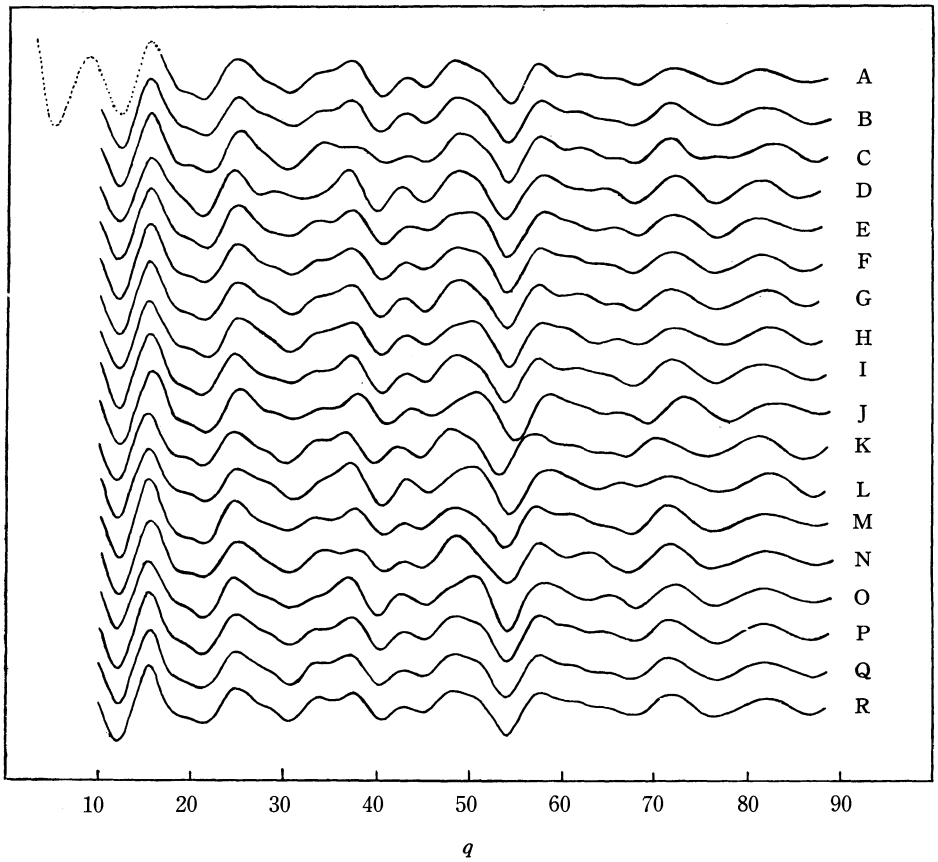



Fig. 4. Theoretical intensity curves of $CFCl_2$—$CFCl_2$

angles of 60°00′, 57°36′ and 55°12′, respectively.

As the parameter C—Cl gave large shifts for the positions of maxima and minima, the value of 1.76±0.01 Å was determined for the C—Cl distance. The relation between the depths of minima at $q=40.3$ and $q=45.0$ is very sensitive to the parameter ∠ClCCl. The feature of this region leads to the value of 110°30′±1° for the ∠ClCCl. The feature of the region $30<q<40$ is sensitive to the parameter ∠CCCl, C—F and C—C, while the feature of the region $47<q<52$ is sensitive to the parameter ∠FCCl, C—F and C—C. As the effects of these parameters appear in the same region, the limits of errors become somewhat larger for these parameters, especially for C—C. The values of C—F, C—C, ∠CCCl and ∠FCCl were determined as 1.38±0.02 Å, 1.54±0.06 Å, 112°±2° and 107°30′±1°30′, respectively. And the azimuthal angle and the amount of the *gauche* form were determined as 59°±4° and 55±10 per cent., respectively.

TABLE III

RESULTS OF ANALYSIS OF RADIAL DISTRIBUTION CURVE AND FINAL RESULTS FROM ADDITIONAL STUDY OF THEORETICAL INTENSITY CURVES

| | From radial distribution curve | Final results |
|---|---|---|
| Bond distance in Å | | |
| C—F | 1.37 | 1.38±0.02 |
| C—C | 1.54 | 1.54±0.06 |
| C—Cl | 1.76 | 1.76±0.01 |
| Valency angle | | |
| ∠CCCl | 112° | 112°±2° |
| ∠ClCCl | 110°30′ | 110°30′±1° |
| ∠FCCl | 107° | 107°30′±1°30′ |
| Azimuthal angle of *gauche* form | 55—63° | 59°±4° |
| Amount of *gauche* form | 52% at 15°C | 55±10% at 15°C |

## Discussion of Results

Using infrared and Raman spectra, Kagarise and Daasch[7] investigated the energy difference between the isomers of the molecule under investigation. On the basis of the invariance of the spectrum with respect to temperature, they proposed two possible explanations of the spectroscopic data, neither of which is completely satisfactory. One is based on the assumption of a single molecular species corresponding to a largey energ difference, while

7) R. E. Kagarise and L. W. Daasch, *J. Chem. Phys.*, **23**, 113 (1955).

the other is based on the presence of two forms having an almost equal energy ($\Delta E$ <300 cal./mol.). Although a definite conclusion could not be obtained from the spectroscopic data, the existence of two isomeric forms was concluded from the result of the electron diffraction. The energy difference of the two isomers was calculated approximately from the obtained diffraction data by use of the following formula:

$$N_g/N_t = 2\exp(-\Delta E/RT). \quad (5)$$

The application of this formula leads to a value of 0—500 cal./mol. for the energy difference of the two isomers, the *trans* form being somewhat more stable than the *gauche* form. The result of the use of the electron diffraction method favors the second explanation proposed by Kagarise and Daasch.

A number of investigations on the molecular structures of organic fluorides indicated that the C—F and C—Cl bond lengths decrease with the number of fluorine atoms bonded with a carbon atom. The data on the molecular structures of some related compounds are listed in Table IV. Although $CFCl_2$—$CFCl_2$ is a difluoride, there is only one fluorine atom bonded with a carbon atom, and therefore C—F bond distance has almost the same value as that of a monofluoride. This fact indicates that the effect of substitution by fluorine atoms on the adjacent carbon atom is very small. The C—Cl bond distance in this molecule is affected scarcely at all by the fluorine atom, but it seems to be slightly shorter than the C—Cl bond in $CH_2Cl_2$ or $CHCl_3$, although this fact can not definitely be confirmed because of the uncertainty in the value of this distance.

TABLE IV
MOLECULAR STRUCTURES OF SOME RELATED COMPOUNDS

| Compound | C—F (Å) | C—Cl(Å) | Method |
|---|---|---|---|
| $CH_3F$[a] | 1.385 | | M. W.* |
| $CH_2ClF$[b] | 1.378±0.006 | 1.759±0.003 | 〃 |
| $CHCl_2F$[c] | 1.41 ±0.03 | 1.73 ±0.04 | V. E. D.** |
| $CCl_3F$[c] | 1.40 ±0.04 | 1.76 ±0.02 | 〃 |
| $C(CH_3)_3F$[d] | 1.38 ±0.02 | | V. E. D. & M. W. |
| $CH_3CH_2F$[e] | 1.375±0.02 | | M. W. |
| $CCl_2F$—$CCl_2F$[f] | 1.38 ±0.02 | 1.76 ±0.01 | S. E. D.*** |
| $CH_2F_2$[g] | 1.358 | | M. W. |
| $CHClF_2$[c] | 1.36 ±0.03 | 1.73 ±0.03 | V. E. D. |
| $CCl_2F_2$[c] | 1.35 ±0.03 | 1.74 ±0.03 | 〃 |
| $CHF_3$[h] | 1.332±0.008 | | M. W. |
| $CClF_3$[i] | 1.328±0.002 | 1.751±0.004 | S. E. D. |
| $CF_4$[j] | 1.323±0.005 | | S. E. D. |
| $C_2F_6$[k] | 1.32 ±0.01 | | 〃 |
| $CH_3Cl$[i] | | 1.783 ±0.003 | S. E. D. |
| $C(CH_3)_3Cl$[l] | | 1.80 ±0.01 | 〃 |
| $CH_2Cl_2$[m] | | 1.7724±0.0005 | M. W. |
| $CHCl_3$[h] | | 1.767 | 〃 |

* Microwave ** Visual electron diffraction *** Sector electron diffraction.


a) O. R. Gillam, H. D. Edwards and W. Gordy, *Phys. Rev.*, **75**, 1014 (1949).
b) N. Muller, *J. Am. Chem. Soc.*, **75**, 860 (1953).
c) L. O. Brockway, *J. Phys. Chem.*, **40**, 747 (1936).
d) F. Andersen, J. R. Andersen, B. Bak, O. Bastiansen, E. Risberg and L. Smedvik, *J. Chem. Phys.*, **21**, 373 (1953).
e) J. Kraitchman and B. P. Dailey, ibid., **23**, 184 (1955).
f) The present work.
g) D. R. Lide, *J. Am. Chem. Soc.*, **74**, 3548 (1952).
h) S. N. Ghosh, R. Trambarulo and W. Gordy, *J. Chem. Phys.*, **20**, 605 (1952).
i) L. S. Bartell and L. O. Brockway, ibid., **23**, 1860 (1955).
j) L. O. Brockway, C. G. Thornton and L. S. Bartell, *Am. Chem. Soc.*, Meeting, Los Angeles, California, March 1953.
k) See ref. 6.
l) O. Bastiansen and L. Smedvik, *Acta. Chem. Scand.*, **7**, 652 (1953).
m) R. J. Myers and W. D. Gwinn, *J. Chem. Phys.*, **20**, 1420 (1952).

**Summary**

The molecular structure of 1,2-difluorotetrachloroethane was studied by the electron diffraction method. The existence of the two isomeric forms, *trans* and *gauche*, was ascertained and the amount of the *gauche* form was found to be 55±10 per cent. This corresponds to the energy difference of 0—500 cal./mol. the *trans* form being more stable. The interatomic distances and the valency angles were determind as follows:

C—F=1.38±0.02 Å, C—Cl=1.76±0.01 Å, C—C=1.54±0.06 Å, ∠CCCl=112°±2°, ∠ClCCl=110°30′±1°, ∠FCCl=107°30′±1°30′, and the azimuthal angle of the *gauche* form=59°±4°.

The C—F bond distance in this molecule is greater than those distances of compounds having more than one fluorine atom bonded with a carbon atom. On the other hand, the C—Cl bond distance seems to be slightly shorter than those of chloroalkanes having no substituted fluorine atom.

The diffraction patterns and the microphotometer records were taken by using an apparatus in Nagoya University. The writers wish to express sincere gratitude to Professor M. Kubo, Professor R. Uyeda and Dr. M. Kimura for giving permission to use the apparatus and for their valuable advice. Thanks are also due to Mr. S. Shibata, Mr. H. Morimoto and Mr. K. Kimura of Nagoya University for their friendly assistance and to Mr. K. Kuchitsu and Mr. E. Hirota of Tokyo University for their help concerning a part of the calculations of the theoretical intensity by means of a punched card machine in the Division of Health and Welfare Statistics, Welfare Minister's Secretariat.

The writers are further greatly indebted to Professor Y. Morino of Tokyo University for his helpful criticisms on this investigation.

*Government Industrial Research Institute, Chigusa-ku, Nagoya*

# *The Adsorption of Non-Polar Gases on Alkali Halide Crystals. II*[1]. *Calculations of The Adsorption Behaviour of Non-Polar Gases on Cubic Sodium Chloride**

By Teruo HAYAKAWA

(Received September 15, 1956)

## Introduction

The refined calculations of the adsorption energy of an isolated argon atom on cubic (100) potassium chloride crystal were carried out by Orr[2]. There is some discordance, however, between theory and experiment which may be attributed to the fact that the repulsive constant of Herzfeld for argon has been used in his theoretical calculations. The theoretical treatment of the quadrupole interaction of an isolated nitrogen molecule with cubic (100) potassium chloride crystal has recently been carried out by Drain[3]. His treatment, however, contains some incorrectness due to careless mistake. Moreover, his results on the total adsorption potential of an isolated nitrogen molecule on cubic (100) potassium chloride also contain considerable uncertainty.

The approximate calculation of the heat curve for argon on cubic (100) potassium chloride was carried out by Orr[2] and also by Young[4]. However, the discrepancy between the experimental and calculated heat curves is fairly remakable. It was, therefore, of interest in the present work to obtain the theoretical values for the heats of adsorption of non-polar gases.

1) Part I of this series, T. Hayakawa, This Bulletin, **30**, 124 (1957).

* Part of this paper was read before the 8 th Annual Meeting of the Chemical Society of Japan held in Tokyo. April, 1955. Other part of this paper was also read before the symposium on the surface heterogeneity of catalysis held in Kyoto, March, 1956.

2) W. J. C. Orr, *Trans. Faraday Soc.*, **35**, 1247 (1939).

3) L. E. Drain, ibid., **49**, 650 (1953).

4) D. M. Young, ibid., **48**, 548 (1952).

(argon, nitrogen and carbon dioxide) on the (100) plane of sodium chloride crystal and to compare these values with the experimental results given in the preceding paper.

In the present work, the total repulsive potential between an isolated atom or molecule and the lattice ions was calculated using the repulsive constants of the modified Buckingham-Corner (6-exp) potential for these non-polar gases. In the case of nitrogen or carbon dioxide, the total quadrupole potential was calculated, using a method similar to that adopted by Drain and the correction due to the potential barrier hindering the turning over of the molecular axis was made.

## Outline of Calculation

**Theoretical Calculation of the Adsorption Potential of an Isolated Atom or Molecule on the (100) Face of an Alkali Halide Crystal.**—The calculation of the adsorption potential may be divided into four sections,

(A) the Van der Waals' (dispersion) potential, (B) the electrostatic potential, (C) the repulsive potential, (D) the quadrupole potential and the correction due to the potential barrier hindering the turning over of the molecular axis.

Calculations were made of these quantities for the following representative positions on the (100) plane of an alkali halide crystal: (i) above the centre of a lattice cell (sites type A), (ii) above the mid-point of a lattice edge (sites type B), (iii) above an alkali ion (sites type C) and (iv) above a halogen ion (sites type D).

**A. The Van der Waals' (Dispersion) Potential.**—The total Van der Waals' potential between an adsorbate atom or molecule and a crystal is given by the Kirkwood-Müller formula[5] as

$$\left.\begin{aligned}\Phi_D = \frac{6m_e c^2}{a^6}\left[\frac{\alpha_0\alpha_+}{\alpha_0/\chi_0+\alpha_+/\chi_+}S_+(\rho)\right.\\ \left.+\frac{\alpha_0\alpha_-}{\alpha_0/\chi_0+\alpha_-/\chi_-}S_-(\rho)\right]\\ \rho=z/a\end{aligned}\right\} \quad (1)$$

where $S_+(\rho)$ and $S_-(\rho)$ are summations involving inverse sixth powers of $\rho$, $z$ the perpendicular distance from the centre of gravity of the adsorbate atom or molecule to the (100) plane, $a$ the lattice parameter of the crystal, $m_e$ the mass of the electron, $C$ the velocity of light, $\alpha$ the polarizability, $\chi$ the magnetic susceptibility. The subscripts $o$, $+$ and $-$ refer to the absorbate, alkali ions and halogen ions respectively. For the present systems the required values of $\alpha$ for the crystal ions have been derived by Mayer[6], and of $\chi$ by Brindley and Hoare[7]. The values of the ionic radii of alkali halide crystals have been given by Goldschmidt[8]. The values of $\alpha$ for these adsorbates* have been given by Landolt-Börnstein[9], and of $\chi$ by Mann[10], Havens[11] and Stoner[12].

The quantities of $S_+(\rho)$ and $S_-(\rho)$ as a function of $\rho$ for four representative positions mentioned above were evaluated by summation over the nearest 280 ions using expressions derived by Orr, and the remaining contributions were found by integration. The results are in good agreement with those obtained by Orr[2].

**B. The Electrostatic Potential.**—The resultant electrostatic potential in any given position of a non-polar molecule is given by

$$\Phi_E = -\frac{1}{2}\alpha_0 F_z^2 \quad (2)$$

where $\alpha_0$ is the polarizability of a non-polar molecule, $F_z$ the resultant electrostatic field along a line perpendicular to the surface,

The calculation of the resultant electrostatic field, $F_z$, as a function of $\rho$ was carried out following closely the method used by Lennard-Jones and Dent[13] for the (100) plane of alkali halide crystals. It is easily shown that the resultant electrostatic field is zero along a line perpendicular to the centre of a lattice cell and also along lines perpendicular to the mid-point of a lattice edge. The resultant electrostatic field, as functions of $\rho$, above an alkali ion in the lattice plane was evaluated by summation over the nearest 40 ions. The present results are in good agreement with those obtained by Lennard-Jones and Dent[13].

**C. The Repulsive Potential.**—The theoretical calculations of the total repulsive

5) A. Müller, *Proc. Roy. Soc. London*, **A154**, 624 (1936).

6) J. E. Mayer, *J. Chem. Phys.*, **1**, 270 (1933).

7) G. W. Brindley and F. E. Hoare, *Proc. Roy. Soc. London*, **A152**, 342 (1935).

8) V. M. Goldschmidt, *Trans. Faraday Soc.*, **25**, 253 (1929).

9) Landolt-Börnstein. "Zahlenwerte und Funktionen", Band 1, Part 3, Springer (1951), p. 510.

* In the case of the nitrogen or carbon dioxide molecule, the average value of $\alpha$ in the three directions was adopted.

10) K. E. Mann, *Z. Physik*, **98**, 548 (1936).

11) G. G. Havens, *Phys. Rev.*, **43**, 992 (1932).

12) E. C. Stoner, "Magnetism and Matter", Methuen and Co. Ltd., London (1934), p. 460.

13) J. E. Lennard-Jones and B. M. Dent, *Trans. Faraday Soc.*, **24**, 92 (1928); **28**, 333 (1932).

potential between an isolated argon atom and the lattice ions of potassium chloride crystal were carried out by Orr[2] and Young[4]. Their results, however, seem to be insufficiently accurate because the repulsive constant of Herzfeld for argon has been used.

In the present work, therefore, the total repulsive potential was calculated using an exponential expression derived from the Born-Mayer repulsive potential formula[14] for the lattice ions and the modified Buckingham-Corner repulsive potential formula for these non-polar molecules. The modified Buckingham-Corner (6-exp) intermolecular potential[15] is given by

$$\left.\begin{aligned}\phi(r) &= \frac{\varepsilon}{1-6/\alpha}\left\{6/\alpha \exp(\alpha-\alpha r/r_m) - (r_m/r)^6\right\} = -Ar^{-6} \\ &\quad + B\exp(-\alpha r/r_m) \\ A &= \left(\frac{\varepsilon}{1-6/\alpha}\right) r_m^6, \\ B &= b_0^2 = \left(\frac{6\varepsilon}{\alpha-6}\right)\exp(\alpha)\end{aligned}\right\} \quad (3)$$

where $\varepsilon$ is the maximum energy of attraction, $r$ the intermolecular separation, $r_m$ the separation at the minimum potential, $\alpha$ the parameter measuring the steepness of the repulsive potential, $b_0$ the repulsive constant of a molecule.

The values of the force constants are summarized in Table I. In this table the force constants for argon and nitrogen were evaluated by Mason and Rice[16] and those for oxygen and carbon dioxide were evaluated by the present author.

TABLE I
FORCE CONSTANTS OF THE MODIFIED BUCKINGHAM-CORNER INTERMOLECULAR POTENTIAL

| Molecule | $\alpha$ | $\varepsilon/k$ (°K) | $r_m$(Å) | $b_0$ ($.10^{-6}$ erg$^{1/2}$) |
|---|---|---|---|---|
| Argon | 14.0 | 123.2 | $3.86_6$ | 123.6 |
| Oxygen | 15.2 | 120.1 | $3.79_5$ | 207.5 |
| Nitrogen | 16.2 | 113.5 | $4.04_0$ | 315.6 |
| Carbon dioxide | 15.1 | 266.1 | $4.11_8$ | 287.5 |

In the present calculations the repulsive constants of Huggins and Mayer[17] for the crystal ions were used. For four representative positions considered, the total repulsive potential was calculated, for various values of $\rho$, by direct summation over the 14 to 20 nearest ions. Contributions from the remaining ions are entirely negligible.

Since these results are not of general applicability, no further details need be given.

**D. The Quadrupole Potential.**—Although, in general, permanent electric quadrupoles are of minor importance in the intermolecular potential between gas molecules[18], the situation is quite different when considering the adsorption potential of a molecule in the large electric fields near the surface of an ionic crystal. The permanent quadrupole moments of several molecules have been measured by Smith and Howard[19] and Hill and Smith[20] from line broadening of microwave spectra. Molecular orbital calculations of the permanent quadrupole moments of nitrogen and oxygen have been made by Greenhow and Smith[21]. Although many of these microwave values are somewhat uncertain, the order of magnitude is probably correct.

The total interaction potential of a linear quadrupole, $Q$, with an inhomogeneous electric field whose potential is $\phi$ is given by

$$\Phi_Q = \frac{1}{2} Q \cdot \partial^2\phi/\partial t^2 \quad (4)$$

where the axis $t$ is taken along the axis of symmetry of the quadrupole. The expression for the resultant Coulomb potential at any position near the surface of an alkali halide crystal has been derived by Lennard-Jones and Dent[13]. The non-zero second derivatives of the resultant Coulomb potential for three representative positions on the (100) plane of potassium chloride were evaluated by Drain[3]. However, since his results contain some uncertainties due to a careless mistake, the evaluation of the electric field gradient near the surface was carried out by the present author.

The maximum quadrupole interaction of the nitrogen or carbon dioxide molecule for four representative positions on the (100) plane of an alkali halide crystal are obtained from the following orientations:

(i) above the centre of a lattice cell (sites type A),

$$\partial^2\phi/\partial x\partial y = e/a^3 \cdot \sigma_A;$$

14) M. Born and J. E. Mayer, *Z. Physik*, **75**, 1 (1932).
15) W. E. Rice and J. O. Hirschfelder, *J. Chem. Phys.*, **22**, 187 (1954).
16) E. A. Mason and W. E. Rice, *J. Chem. Phys.*, **22**, 522 (1954).
17) M. L. Huggins and J. E. Mayer, ibid., **1**, 643 (1933).
18) H. Margenau, *Rev. Modern Phys.*, **11**, 1 (1939).
19) W. V. Smith and R. Howard, *Phys. Rev.*, **79**, 132 (1950).
20) R. M. Hill and W. V. Smith, ibid., **82**, 451 (1951).
21) C. Greenhow and W. V. Smith, *J. Chem. Phys.*, **19**, 1298 (1951).

(ii) above the mid-point of a lattice edge (sites type B),

$$\partial^2\phi/\partial x\partial z=\partial^2\phi/\partial y\partial z=e/a^3\cdot\sigma_B;$$

(iii) above an alkali ion (sites type C),

$$\partial^2\phi/\partial z^2=-2\partial^2\phi/\partial x^2=-2\partial^2\phi/\partial y^2=e/a^3\cdot\sigma_C;$$

(iv) above a halogen ion (sites type D),

$$\partial^2\phi/\partial x^2=\partial^2\phi/\partial y^2=e/a^3\cdot\sigma_D.$$

The cartecian axes $x$, $y$, $z$ are along the sides of a unit cell, $z$ is normal to the surface and $a$ is the lattice parameter and $e$ the electronic charge. The quantities $\sigma$ which represent summations over the lattice ions depend on the distance $a\rho$ of the point under consideration from the surface. The present results on the evaluations of these quantities $\sigma$ are summarized in Table II.

TABLE II

VALUES OF $\sigma$, ON THE (100) PLANE OF AN ALKALI HALIDE CRYSTAL

| $\rho$ | $\sigma_A$ | $\sigma_B$ | $\sigma_C$ | $\sigma_D$ |
|---|---|---|---|---|
| 0.8 | 1.5310 | 2.1739 | 3.3463 | 1.6732 |
| 0.9 | 0.9942 | 1.4102 | 2.0933 | 1.0467 |
| 1.0 | 0.6424 | 0.9105 | 1.3238 | 0.6619 |
| 1.1 | 0.4142 | 0.5865 | 0.8426 | 0.4213 |
| 1.2 | 0.2662 | 0.3768 | 0.5377 | 0.2688 |
| 1.3 | 0.1711 | 0.2420 | 0.3439 | 0.1719 |
| 1.4 | 0.1098 | 0.1553 | 0.2203 | 0.1101 |
| 1.5 | 0.0704 | 0.0996 | 0.1411 | 0.0705 |
| 1.6 | 0.0452 | 0.0639 | 0.0905 | 0.0452 |
| 2.0 | 0.0076 | 0.0108 | 0.0153 | 0.0076 |

As is easily seen in these relations, at the positon of sites type A (above the centre of a lattice cell) or sites type D (above a halogen ion), the orientation for maximum quadrupole interaction is with the molecular axis parallel to the surface. Consequently, no correction due to the potential barrier hindering the turning over of the molecule is required in these positions. On the other hand, at the positions of sites type B (above the mid-point of a lattice edge) and sites type C (above an alkali ion), the maximum quadrupole energies are obtained from the orientations in which the molecular axis makes an angle of $\pi/4$ and $\pi/2$ with the surface respectively. In these positions, then the corrections due to the potential barrier hindering the rotation must be made.

In the present calculations, the approximate estimation of this potential barrier was carried out following closely the method used by Hill[22]. Although this method seems rather inadequate for the present calculations*, unfortunately, no other reliable method has been found.

**The Total Adsorption Potential.**—The total adsorption potential is then given by

$$\Phi=\Phi_D+\Phi_E+\Phi_Q+\Phi_R-\Phi_{H.R.} \qquad (5)$$

where $\Phi_R$ is the total repulsive potential,

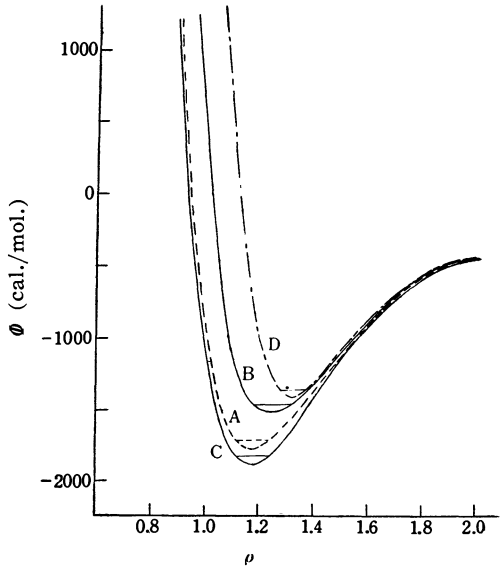



Fig. 1. Potential energy curves of argon on cubic (100) NaCl. Each symbol denotes the type of sites.

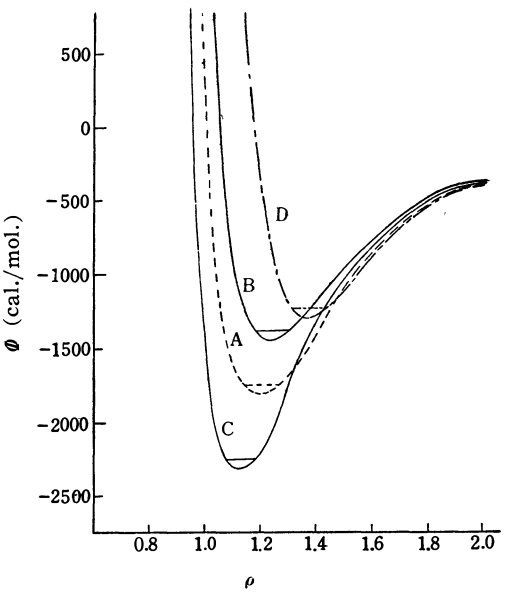



Fig. 2. Potential energy curves of nitrogen on cubic (100) NaCl. Each symbol denotes the type of sites.

22) T. L. Hill, *J. Chem. Phys.*, **17**, 762 (1949).

* In the estimations made by Hill, the adsorption potential was given by the Lennard-Jones (6-12) potential formula.

and $\Phi_{H.R.}$ the potential barrier hindering the turning over of the molecular axis. In the case of argon, both values of $\Phi_Q$ and $\Phi_{H.R.}$ are surely zero.

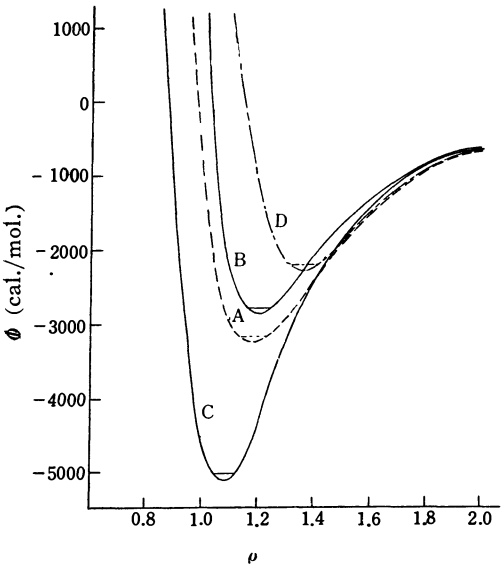



Fig. 3. Potential energy curves of carbon dioxide on cubic (100) NaCl. Each symbol denotes the type of sites.

The calculated potential energy curves for the four types of sites considered are shown in Figs. 1, 2 and 3. By plotting the region around the minimum potential on a large scale, the restoring force per unit displacement, $f'$, of the molecule (i. e. the centre of gravity) normal to the surface in this region was calculated from the following equation**

$$(\Phi-\Phi_m)=\frac{1}{2}f'(z-z_e)^2 \qquad (6)$$

where $\Phi_m$ is the minimum potential, $z$ the perpendicular distance from the surface, $z_e$ the equilibrium distance given by the position of the minimum potential.

The vibrational frequency normal to the surface, $\nu_z$ (sec.$^{-1}$), was then calculated from the relation

$$\nu_z=\frac{1}{2\pi}\sqrt{f'N/M} \qquad (7)$$

where $M$ is the molecular (or atomic) weight, $N$ the Avogadro's constant.

Then, the zero-point energy, $\varepsilon_0$ (cal./mol.), was calculated from the relation

$$\varepsilon_0=Nh\nu_z\times10^{-7}/2\times4.186 \qquad (8)$$

TABLE III

RESULTS OBTAINED FROM THE POTENTIAL ENERGY CURVE, ARGON ON CUBIC (100) NaCl

| Sites type | $Z_e$ (Å) | $r_{eff}$ (Å) | $-\Phi_m$ (cal./mol.) | $\nu_z\times10^{-12}$ (sec.$^{-1}$.) | $\varepsilon_0$ (cal./mol.) | $-\Delta H_0$ at 76°K (ca./mol.) |
|---|---|---|---|---|---|---|
| A, above the centre of a lattice cell | 3.30 | 2.04 | 1768 | 0.95 | 44.8 | 1875 |
| B, above the mid-point of a lattice edge | 3.47 | 1.94 | 1514 | 0.88 | 41.5 | 1624 |
| C, above an $Na^+$ | 3.29 | 2.31 | 1876 | 1.05 | 49.7 | 1978 |
| D, above a $Cl^-$ | 3.72 | 1.91 | 1401 | 0.92 | 43.4 | 1510 |

TABLE IV

RESULTS OBTAINED FROM THE POTENTIAL ENERGY CURVE, NITROGEN ON CUBIC (100) NaCl

| Sites type | $Z_e$ (Å) | $-\Phi_m$ (cal./mol.) | $-\Phi_Q$ at $Z_e$ (cal./mol.) | $\nu_z\times10^{-12}$ (sec.$^{-1}$) | $\varepsilon_0$ (cal./mol.) | $-\Delta H_0$ at 76°K (cal./mol.) |
|---|---|---|---|---|---|---|
| A, above the centre of a lattice cell | 3.38 | 1807 | 550 | 1.23 | 58.1 | 1901 |
| B, above the mid-point of a lattice edge | 3.42 | 1432 | 774 | 1.10 | 51.9 | 1532 |
| C, above an $Na^+$ | 3.12 | 2308 | 1738 | 1.32 | 62.3 | 2398 |
| D, above a $Cl^-$ | 3.84 | 1277 | 232 | 1.12 | 52.9 | 1376 |

TABLE V

RESULTS OBTAINED FROM THE POTENTIAL ENERGY CURVE, CARBON DIOXIDE ON CUBIC (100) NaCl

| Sites type | $Z_e$ (Å) | $-\Phi_m$ (cal./mol.) | $-\Phi_Q$ at $Z_e$ (cal./mol.) | $\nu_z\times10^{-12}$ (sec.$^{-1}$) | $\varepsilon_0$ (cal./mol.) | $-\Delta H_0$ at 190°K (cal./mol.) |
|---|---|---|---|---|---|---|
| A, above the centre of a lattice cell | 3.28 | 3245 | 1328 | 1.12 | 52.9 | 3572 |
| B, above the mid-point of an lattice edge | 3.36 | 2852 | 1869 | 1.07 | 50.6 | 3181 |
| C, above an $Na^+$ | 3.03 | 5102 | 4184 | 1.33 | 62.7 | 5419 |
| D, above a $Cl^-$ | 3.77 | 2237 | 554 | 1.06 | 50.2 | 2567 |

** In Equ. (6), $\Phi$ and $\Phi_m$ must be expressed in erg/molecule.

where $h$ is the Planck's constant.

Consequently, the initial heat of adsorption (i. e. the isosteric heat of adsorption at zero coverage), $-\Delta H_0$ (cal./mol.), is given by the expression

$$-\Delta H_0 = (-\Phi_m - \varepsilon_0) + RT = -U_0 + RT \quad (9)$$

where $U_0$ is the potential energy of the lowest vibrational state of the molecule on the bare surface.

The calculated values of these quantities for these non-polar gases are summarized in Table III, IV and V. The values of the effective radius of argon, $r_{eff.}$, were calculated from the equilibrium distances, and the results are given in column 3 of Table III.

**Approximate Calculation of the Heat Curve for Argon on the (100) Plane of Cubic Sodium Chloride.**—The approximate calculation of the heat curve for argon was carried out following similar method used by Young[4] for the (100) plane of cubic potassium chloride. In the present calculations, as well as in those made by Young, the following assumptions were made:

(1) In the formation of a primary monolayer, argon atoms are exclusively adsorbed from $\theta=0$ to about 0.4* above sodium ions (c.f. Table III), but as $\theta$ tends to unity there will be a phase transition from localized square arrays to a hexagonally closed-packed layer.
(2) The non-uniformity of the surface is negligible.
(3) The heat of adsorption of the second-layer atoms is close to the heat of sublimation of argon (i. e. 1860 cal./mol. at 76°K).
(4) In the range restricted to $\theta$ values near unity, the adsorption in the third and higher layers is negligible.

The variation of the heats of adsorption in the primary monolayer with coverage, due to Van der Waals' mutual interaction between the adsorbed atoms, was calculated using the equation statistically derived by Wang[23]. The intermolecular potential energy of a pair of argon atoms was calculated using the modified Buckingham-Corner (6-exp) potential formula, and the effect of the electrostatic repulsion between the adsorbed atoms was taken into consideration.

The effect of the second-layer formation was evaluated using the equations developed by Tompkins and Young[24].

The calculated heat curve is shown in Fig. 4, together with the experimental values reported in the preceding paper.

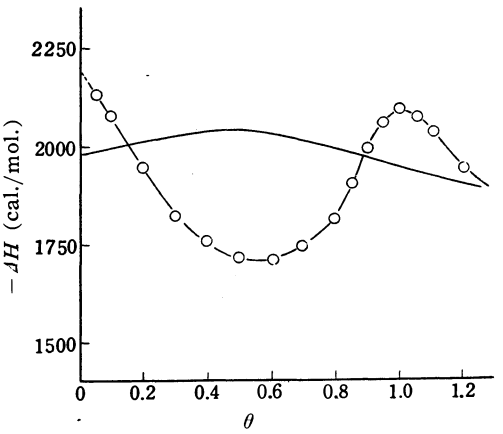



Fig. 4. Heats of adsorption of argon on cubic (100) NaCl.
———, approximately calculated curve;
-○-○-, observed curve.

## Discussion

**The Initial Heat of Adsorption.**—As seen in Table III, IV and V, the most energetic positions for these non-polar gases (argon, nitrogen and carbon dioxide) on the (100) plane of cubic sodium chloride are all sites type C (above an $Na^+$ in the lattice plane). These results are peculiar to the (100) plane of cubic sodium chloride. As will be shown in the succeeding paper, the most energetic positions for argon and nitrogen on cubic (100) KCl and cubic (100) KBr are sites type A* (above the centre of a lattice cell). This particular nature of the (100) plane of sodium chloride crystal may be attributed to the fact that the ionic radius and the repulsive constant of $Na^+$ are both considerably smaller than those of $K^+$.

The values of the initial heats of adsorption obtained from the present theoretical calculations are listed in Table VI, together with the experimental values reported in the preceding paper.

As seen in Table VI, the calculated values for these non-polar gases are in rather good agreement with the experimental values. It is quite reasonable,

* The diameter of an argon atom derived from the liquid density was taken at 4.05 Å.

23) J. S. Wang, *Proc. Roy. Soc. London*, **A161**, 127 (1937).

24) F. C. Tompkins and D. M. Young, *Trans. Faraday Soc.*, **47**, 77 (1951).

* According to the theoretical calculations made by Orr[2], the most energetic position for argon on cubic (100) KCl is also sites type A.

TABLE VI
INITIAL HEATS OF ADSORPTION ON CUBIC (100) NaCl

| Adsorbate | $(-\Delta H_0)$expt. (cal./mol.) | $(-\Delta H_0)$calc. (cal./mol.) | $(-\Delta H_0)$expt. $-(-\Delta H_0)$calc. (cal./mol.) |
|---|---|---|---|
| Argon | 2190 | 1980 | 210 |
| Nitrogen | 2670 | 2400 | 270 |
| Carbon dioxide | 6070 | 5420 | 650 |

therefore, to consider that the high initial heats of adsorption experimentally found for nitrogen and carbon dioxide are mainly attributed to the quadrupole interactions of these molecules with the surface of cubic sodium chloride.

**The Non-Uniformity of the Adsorbent Surface.**—Table III indicates that the maximum difference of the initial heat of adsorption for argon between these sites grouped in patches amounts to about 500 cal./mol. The corresponding values for nitrogen and carbon dioxide amount, as seen in Table IV and V, to about 1000 cal./mol. and about 2850 cal./mol. respectively. Since the mutual interaction between the adsorbed atoms or molecules in the low coverage region is slightly attractive and gives no marked influence upon the heats of adsorption, the surface heterogeneity of this type may be maintained, especially in the non-localized adsorption, in this low coverage region.

The difference between the experimental and theoretical values of the initial heat of adsorption shown in Table VI gives a crude measure of the surface heterogeneity of the other type due to the lattice imperfection or the defects of the crystals. An argon atom has no permanent quadrupole moment; then the value of 210 cal./mol. shown in Table VI may be attributed to the surface heterogeneity of this type. On the other hand, the theoretical values of the initial heats of adsorption for nitrogen and carbon dioxide are somewhat inaccurate, and this uncertainty is attributed to two causes:

(a) The values of the quadrupole moment of these molecules cannot yet be considered as definitely proved.

(b) The estimation of the potential barrier hindering the turning over of the molecule was carried out following the method used by Hill, but this method is rather inadequate for the present calculations.

Nevertheless, Table VI shows that the difference between the experimental and theoretical values of the initial heat of adsorption for each adsorbate is of the right magnitude to explain the difference of the intermolecular potential energy betwen these non-polar gases.

For the reasons discussed above, it is reasonable to consider that the surface heterogeneity due to the distribution of sites grouped in patches is more distinguished than that due to the lattice imperfection or crystal defects. Both types of the surface heterogeneity discussed above give rise to the decrease of the heat of adsorption as more molecules are adsorbed in the low coverage region. This is qualitatively in good agreement with the experimental heat curves.

**Surface Migration of the Adsorbed Atoms or Molecules.**—In order to enable the adsorbed atom or molecule to move along the surface from one site to the next site, where it is bounded in exactly the same manner as in the first one, this atom or molecule must pick up such an amount of energy that it may overcome the potential energy barrier separating the atoms and molecules. Owing to the high symmetry of the (100) plane of an alkali halide crystal and the small distance from one site to the adjacent site of another type, it is not unreasonable to consider that the height of this potential energy barrier is roughly equal to the difference of the heat of adsorption between them[25]. Since the mutual interaction between the adsorbed atoms or molecules in the low coverage region gives no marked influence, the heat of adsorption at each site in the low coverage region may be replaced by the initial heat of adsorption in the present discussion.

As seen in Table III, the difference of the initial heat of adsorption between two adjacent sites (i.e. the height of the potential energy barrier mentioned above) for argon amounts to about $0.7 \sim 2RT$. In the case of nitrogen, as seen in Table IV, the height of this potential energy barrier roughly amounts to about $1 \sim 3\ RT$ (excepting the value corresponding to the difference between site B and C). Since the mean kinetic energy of thermal movement of the adsorbed atom or molecule is $RT$ per mole, it is reasonable to consider that the adsorbed argon atom or nitrogen molecule easily picks up the energy corresponding to each potential energy barrier from the thermal energy fluctuations. The present results on the surface migration of the adsorbed argon atom or nitrogen molecule

25) J. H. de Boer, "The Dynamical Character of Adsorption", Clarendon Press, Oxford (1953), p. 96.

in the low coverage region are qualitatively in good agreement with the nature of the experimental entropy curves for argon and nitrogen already reported in the preceding paper.

**The Heat Curve for Argon.**—As seen in Fig. 4, the discrepancy between the experimental and approximately calculated heat curves in the region of $\theta=0.2\sim0.8$ is considerably remakable. This is mainly attributed to the fact that in the present approximate calculations, as well as in those made by Orr and Young, the uniform surface and the localized model have been assumed. These two assumptions are inconsistent not only with the results of the present theoretical calculations but with the experimental results reported in the preceding paper.

## Summary

The potential energy of each isolated atom or non-polar molecule (argon, nitrogen, or carbon dioxide) adsorbed on the (100) plane of cubic sodium chloride has been theoretically calculated at four different positions on the crystal surface. In the present calculations, the repulsive constants of the modified Buckingham-Corner (6-exp) intermolecular potential for these non-polar gases have been used. The quadrupole interaction of the nitrogen or carbon dioxide molecule with a crystal has been taken into consideration. The good agreement between the theoretical and experimental values of the initial heat of adsorption for each adsorbate has been obtained.

The present theoretical calculations suggest that the surface heterogeneity caused by the lattice imperfection or crystal defects is of minor importance compared with other types of surface heterogeneity due to the distribution of sites grouped in patches. The present results also suggest that the adsorbed argon atoms or nitrogen molecules easily migrate two-dimensionally along the surface in the low coverage region. These results on the surface migration are in good agreement with the entropy curves of adsorbed argon and nitrogen experimentally determined.

The approximate calculation of the heat curve for argon on the (100) plane of cubic sodium chloride has been carried out following a similar method used by Young. The discordance between the experimental and approximately calculated heat curves is considerable, and this is attributed to the fact that the unreliable model (i.e. the uniform surface and the localized adsorption) has been assumed in these approximate calculations.

The author wishes to express his grateful thanks to Dr. S. Horiba and Professor O. Toyama of Osaka Prefectural University for their kind encouragement and discussion. The author's sincere thanks are also due to Professor R. Kiyama of Kyoto University for his kind discussion.

*Department of Chemistry, Faculty of Education, Osaka Prefectural University, Sakai*

# *The Adsorption of Non-Polar Gases on Alkali Halide Crystals. III. The Low-Temperature Adsorption of Non-Polar Gases on Cubic Potassium Chloride**

By Teruo HAYAKAWA

(Received November 2, 1956)

## Introduction

In the former papers of this series[1,2] the author studied the adsorptive properties of non-polar gases (argon, oxygen, nitrogen and carbon dioxide) on cubic

* Part of this paper was read before the 6 th Annual Meeting of the Chemical Society of Japan held in Kyoto, April, 1953. Another part of this paper was also read before the symposium on the surface heterogeneity of catalysis held in Kyoto, March, 1956.

1) Part I of this series, T. Hayakawa, This Bulletin, **30**, 124 (1957).

2) Part II of this series, T. Hayakawa, This Bulletin, **30**, 236 (1957).

sodium chloride. Considerably good agreement between the theoretical and experimental values of the initial heat of adsorption for argon, nitrogen, or carbon dioxide was obtained. The experimental results also indicated that the adsorbed molecules of argon, oxygen, or nitrogen on cubic sodium chloride have the nature of two-dimensional gas at least in the range of $\theta=0.3\sim0.9$. The measurements of the low-temperature adsorption of non-polar gases (argon, oxygen and nitrogen) on cubic potassium chloride were already reported by Orr[3]. However, since his results were limited to the variation in the isosteric heats of adsorption with coverage, no definite information on the non-uniformity of the surface and on the freedom of the adsorbed molecules was obtained. Moreover, no reasonable explanation was given for the differences in the values of the initial heat of adsorption with molecular species of adsorbates.

It was therefore of interest in the present work to re-examine the adsorptive properties of non-polar gases on cubic potassium chloride and to compare the results with those obtained for cubic sodium chloride.

## Experimental

**Materials.**—*Potassium chloride* was recrystallized by rapidly cooling an aqueous solution of potassium chloride (Merck reagent) saturated at 100°C. The crystals were collected on a sintered glass filter funnel, washed with successive portions of 70% ethyl alcohol, absolute alcohol, and dry ether, and stored in vacuum desiccator over phosphorous anhydride during about two weeks. Microscopic examination of this sample revealed a large number of small cubes plus a few cubes in which the defects in the corners or edges were somewhat perceptible. The examination of this sample by an electron diffraction apparatus also revealed the regular pattern of (100) faces. 24.9 g. of this sample which passed through a 45-mesh sieve was used in the subsequent experiments. *Helium* was supplied by the Teikoku Oxygen Co. as spectroscopically pure and was not further purified. The method of preparation of argon, oxygen, nitrogen and carbon dioxide has already been described[1].

**Apparatus and Procedure.**—The apparatus and the procedure were already described in a previous communication[1]. The salt was outgassed by heating in vacuo at 300°C for a minimum period of 6 hr. prior to each experiment.

## Results

The isotherms obtained for the four gases on cubic potassium chloride are summarized in Fig.

3) W. J. C. Orr, *Proc. Roy. Soc.*, **A173**, 349 (1939).

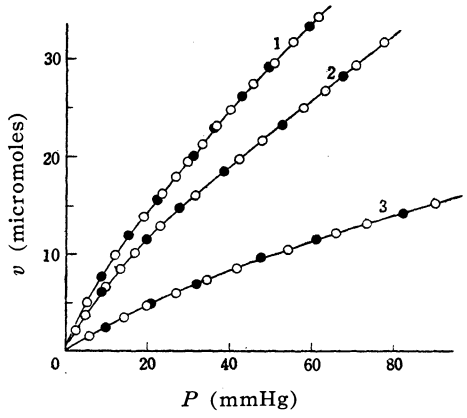



Fig. 1. Adsorption of argon on cubic potassium chloride.
curve 1……75.29°K, curve 2……77.32°K, curve 3……85.42°K; ○……adsorption, ●……desorption.

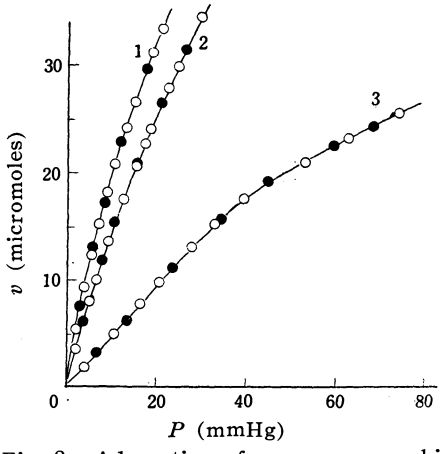



Fig. 2. Adsorption of oxygen on cubic potassium chloride.
curve 1……75.29°K, curve 2……77.32°K, curve 3……85.42°K; ○……adsorption, ●……desorption.

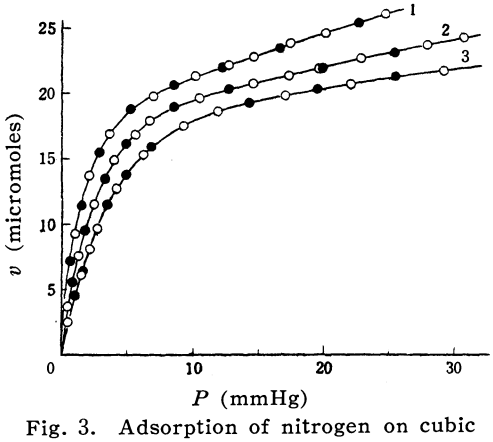



Fig. 3. Adsorption of nitrogen on cubic potassium chloride.
curve 1……73.74°K, curve 2……75.69°K, curve 3……77.32°K; ○……adsorption, ●……desorption.

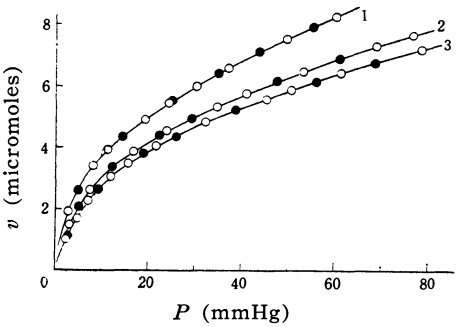



Fig. 4. Adsorption of carbon dioxide on cubic potassium chloride.
curve 1……187.66°K, curve 2……192.63°K, curve 3……194.64°K; ○……adsorption, ●……desorption.

1, 2, 3 and 4. The adsorption was found to be reversible in this temperature range. The isosteric heats of adsorption were calculated from these isotherms using the Clausius-Clapeyron equation, and these showed no definite trend with temperature within the experimental error. For the calculations of the entropy decrease due to the adsorption, the choice of the standard states of the gas phase was such that the pressure is 760 mmHg and the temperature coincides with that of each isotherm.

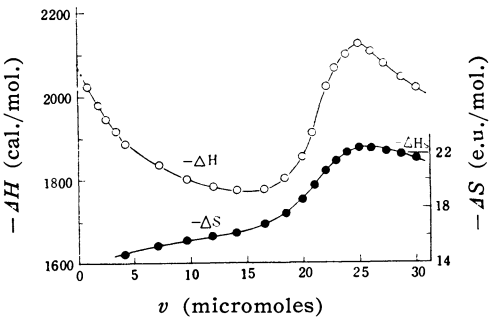



Fig. 5. Isosteric heats and entropies of adsorption for argon on cubic potassium chloride.
$-\Delta H_s$……heat of sublimation.

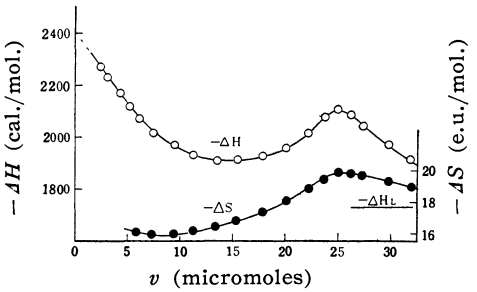



Fig. 6. Isosteric heats and entropies of adsorption for oxygen on cubic potassium chloride.
$-\Delta H_L$……heat of vaporization.

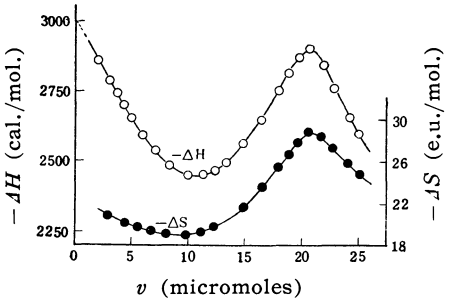



Fig. 7. Isosteric heats and entropies of adsorption for nitrogen on cubic potassium chloride.

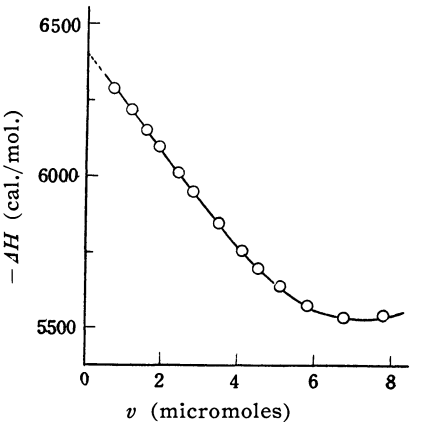



Fig. 8. Isosteric heats of adsorption for carbon dioxide on cubic potassium chloride.

The present results on the isosteric heats of adsorption and the entropy decrease due to the adsorption are shown in Fig. 5, 6, 7 and 8. The measurements were not extended to the high coverage region for carbon dioxide, since the amount adsorbed was fairly small in this temperature range.

## Discussion

**The Isosteric Heats of Adsorption.**— The magnitudes of the isosteric heats of adsorption and the variation of these with coverage for the three gases (argon, oxygen and nitrogen) are in fairly good agreement with the experimental values of Orr[3]. The experimental values of the initial heat of adsorption (i. e. the isosteric heat of adsorption extrapolated to zero coverage) obtained for the four gases are summarized in Table I, together with the experimental values of Orr[3] and Lenel[4], and the theoretical values of the present author.

4) F. V. Lenel, *Z. physik. Chem.*, **B23**, 379 (1933).

TABLE I
INITIAL HEAT OF ADSORPTION, $-\Delta H_0$, ON CUBIC POTASSIUM CHLORIDE

| Adsorbate | $(-H_0)$expt. (cal./mol.) Present author | (Literature) | $(-\Delta H_0)$calc. (cal./mol.) |
|---|---|---|---|
| Argon | 2080 | (2140*) | 1900 |
| Oxygen | 2410 | (2350*) | — |
| Nitrogen | 3010 | (3200*) | 2120 |
| Carbon dioxide | 6400 | (6500**) | 4970 |

* Obtained by Orr.
** Obtained by Lenel.

In the theoretical calculations, as will be reported in the succeeding paper, the crystal lattice was assumed to be an ideal (i. e. the surface heterogeneity due to the defects or the lattice imperfection was ignored) and the quadrupole interaction of the molecule (nitrogen or carbon dioxide) with the surface was taken into consideration. Table I indicates that the present experimental values of the initial heat of adsorption are in good agreement with those of other investigators. Although the discrepancies between the experimental and theoretical values for nitrogen and carbon dioxide are quite remarkable, as seen in Table I, the order of magnitude of the experimental values for these non-polar gases is similar to that of the theoretical values. Considering the matter from this fact, it seems reasonable to consider that the high initial heats of adsorption experimentally found for nitrogen and carbon dioxide are mainly attributed to the quadrupole interactions of these molecules with the surface of cubic potassium chloride.

The initial decrease in each heat curve is attributed to the non-uniformity of the surface, since mutual interaction forces of adsorbed molecules, being attactive, would result in an increase in the heat. The difference between the experimental and theoretical values of the initial heat of adsorption shown in Table I gives a crude measure of the surface heterogeneity due to the lattice imperfection or the defects of the crystals. Then, the value of 180 cal./mol. for argon (i. e. the difference between the experimental and theoretical values of the initial heat of adsorption) may be attributed to the surface hetrogeneity of this type, while Fig. 5 indicates that the initial decrease in the heat curve for argon roughly amounts to about 300 cal./mol.* Consequently, it is reasonable to consider that the surface may be influenced by the non-uniformity of the other type.

In the case of nitrogen or carbon dioxide, however, the situation seems quite different, since the difference between the experimental and theoretical values of the initial heat of adsorption is considerably greater than the initial decrease in the heat curve shown in Figs. 7 or Fig. 8. Although these results obtained for nitrogen and carbon dioxide are inconsistent with those for argon, it may be pointed out that the theoretical calculations of the initial heat of adsorption for nitrogen and carbon dioxide are less correct than those for argon. This incorrectness in the theoretical calculations is mainly attributed to the fact that the values of the quadrupole moment of these molecules (nitrogen and carbon dioxide) cannot yet be considered as definitely proved.

**The Monolayer Capacities and the Surface Areas.**—Since the heat curves (Figs. 5, 6 and 7) indicate that the non-uniformity of the surface considerably predominates in the low coverage region and that the mutual interaction between the adsorbed molecules in the succeeding region is sharply increased with the increase of the amount adsorbed, it is quite unreasonable to apply the B. E. T. theory to the present systems. As seen in Figs. 5, 6 and 7, there are fairly sharp maxima in the isosteric heat and the entropy decrease curves for all these gases. The gradual decrease in each heat or entropy decrease curve beyond the maximum may be attributed to the formation of multilayers. Considering these facts, it seems reasonable to assign the value corresponding to the maximum in the heat or entropy decrease curve as the monolayer capacity.

The present results on the monolayer capacities and the surface areas are summarized in Table II. Each value of the cross-sectional area in this table was determined from the results on the entropies of the adsorbed molecules.

TABLE II
MONOLAYER CAPACITIES ($v_m$) AND SURFACE AREAS ($A$), CUBIC POTASSIUM CHLORIDE (24.9 g.)

| Adsorbate | Cross-sectional area $a_0$(Å²) | $v_m$ (micromoles) from $(-\Delta H)$ | (B.E.T.) | $A$ ($m^2$) from $(-\Delta H)$ | (B.E.T.) |
|---|---|---|---|---|---|
| Argon | 12.8 | 25.1 | (24.0) | 1.93 | (1.85) |
| Oxygen | 14.1 | 25.0 | (23.6) | 2.12 | (2.00) |
| Nitrogen | 13.8 | 20.7 | (23.2) | 1.73 | (1.93) |

* Since the value of 300 cal./mol. includes the effect of the intermolecular attraction between adsorbed atoms, the true effect of the surface heterogeneity may amount to a considerably greater value than 300 cal./mol.

**The Entropies of Adsorption.**—As seen in Figs. 5, 6 and 7, the entropy decrease curve for each non-polar gas in the comparatively high coverage region has a tendency similar to the respective heat curve. The present results on the entropy of adsorption for the three gases are listed in Table III.

TABLE III
ENTROPY OF ADSORPTION, $-\Delta S$, ON CUBIC POTASSIUM CHLORIDE

| Adsorbate | Temperature (°K) | $-\Delta S$ (e. u./mol.) $\theta=0.5$ | $\theta=1.0$ |
|---|---|---|---|
| Argon | 76.3 | 15.9 | 22.2 |
| Oxygen | 76.3 | 16.9 | 19.8 |
| Nitrogen | 76.5 | 19.0 | 28.7 |

As seen in Table III, Figs. 5, 6 and 7, the magnitudes of the entropies of adsorption and the variation of these with coverage for argon and oxygen resemble each other, while nitrogen shows a considerably different feature from other gases in the region of $\theta=0.5\sim1$. In order to obtain more information about the freedom of the adsorbed molecules, the entropies of the adsorbed molecules obtained from the present experiments were compared with those statistically calculated. The methods of the statistical calculations of the entropy for each gas under the standard states and of the entropy of each adsorbed phase were already given in the preceding paper[1].

The entropy curves of the adsorbed molecules obtained from the present experiments are summarized in Figs. 9, 10 and 11, together with the calculated curves. For the sake of comparison, Kemball's values[5] obtained from Orr's results[3] are also shown in Fig. 9. The experimentally determined values in these figures are the partial molar total entropies and hence contain the entropy changes of the adsorbent[6], while the calculated values are all the integral entropies and are usually somewhat greater than the values of the partial molar total entropies. Considering this fact, the experimental values ($S_S$) for adsorbed argon and nitrogen are in fairly good agreement with the calculated values of the two-dimensional gas ($S_T$) in the range of $\theta=0.3\sim0.9$. Since the entropy for oxygen associated with the vibrational

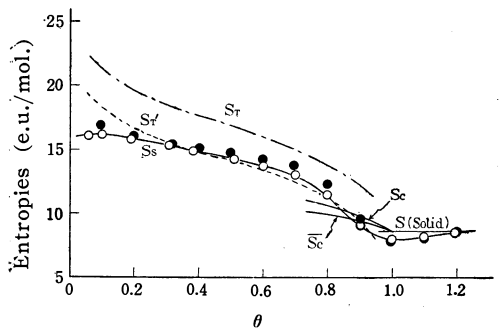



Fig. 9. Entropies of adsorbed argon on cubic potassium chloride at 76.3°K.
$S_S$……Experimental values;
○……Present values,
●……Kemball's values (79°K).
$S_T$……Entropies of the two-dimensional gas.
$S_T'$……Translational entropies of the two-dimensional gas.
$S_C$……Configurational entropies.
$\overline{S_C}$……Differential configurational entropies.

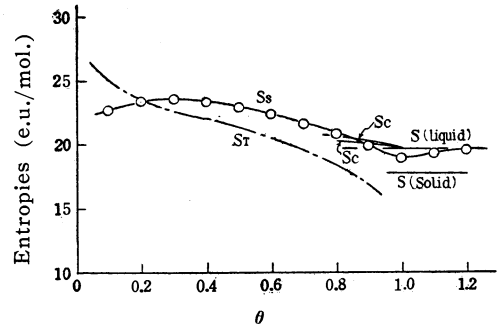



Fig. 10. Entropies of adsorbed oxygen on cubic potassium chloride at 76.3°K.
$S_S$……Experimental values.
$S_T$……Entropies of the two-dimensional gas.
$S_C$……Configurational entropies.
$\overline{S_C}$……Differential configurational entropies.

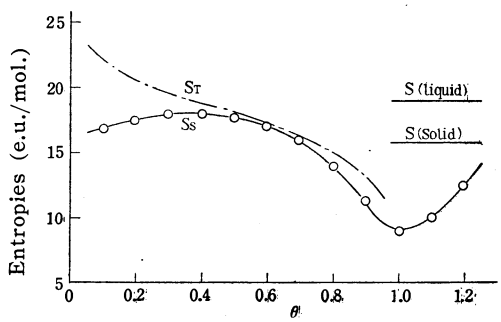



Fig. 11. Entropies of adsorbed nitrogen on cubic potassium chloride at 76.5°K.
$S_S$……Experimental values.
$S_T$……Entropies of the two-dimentional gas.

5) C. Kemball, "Advances in Catalysis", Vol. II, Academic Press Inc., New York (1950), p. 233.
6) T. L. Hill, *J. Chem. Phys.*, **17**, 520 (1949).

motion normal to the surface was calculated from assuming that the vibrational frequency of oxygen is identical with that of argon, the present calculations of the two-dimensional gas for oxygen ($S_T$ in Fig. 10) probably resulted in smaller values. Therefore, the agreement of the experimental curve ($S_S$) for oxygen with the calculated curve ($S_T$) of the two-dimensional gas in the region of $\theta=0.2\sim0.9$ is satisfied to a great extent.

The discrepancy between the experimental and calculated values at lower coverage ($\theta<0.2$) in each entropy curve would imply the entropy changes of the adsorbent. When $\theta$ approaches to unity, as seen in these figures, the restriction on the freedom of the adsorbed molecules is further increased and each entropy curve ($S_S$) falls below the calculated curve of the two-dimensional gas ($S_T$). In the range of $\theta>1$, the entropy of adsorbed argon remains close to the entropy of solid argon*, while the entropy of adsorbed oxygen closely approaches to the entropy of liquid oxygen**. This is in accord with the fact that the heat of sublimation of argon is similar to that of vaporization of oxygen. On the other hand, the entropy of adsorbed nitrogen in this same range is considerably smaller than that of solid nitrogen***.

According to the suggestion given by Kemball[5], the phase change of argon on cubic potassium chloride occurred at about $\theta=0.8$, since the experimental values shifted from the entropy curve of the two-dimensional gas to the entropy curve of the localized adsorption obtained by adding the configurational entropy on the Langmuir model to the entropy of solid argon. This explanation, however, contains considerable uncertainties, since it is unreasonable to adopt the Langmuir model for the systems in which the non-uniformity of the surface in the low coverage region and the mutual interaction in the succeeding region are both predominant. In the present work, the configurational entropy for the localized adsorption was calculated from the expression given by Drain and Morrison[7]. The results shown in Fig. 9 or Fig. 10 indicate that the phase change of argon or oxygen from a gaseous film to a condensed film occurs at about $\theta=0.9$. However, since the mutual interaction between the adsorbed molecules was ignored in the present calculations of the configurational entropy, the present results on the phase change are also somewhat inaccurate.

* The entropy of solid argon was calculated from the heat of sublimation and the value of the saturation pressure at 76.3° K.

** The entropy of liquid oxygen was calculated from the work of Giauque and Johnston( *J. Am. Chem. Soc.*, **51**, 2300 (1929)).

*** The entropy of solid nitrogen was calculated from the work of Kingston, et al (*J. Am. Chem. Soc.*, **72**, 1780 (1950)).

## Summary

The low-temperature adsorption of non-polar gases (argon, oxygen, nitrogen and carbon dioxide) on cubic potassium chloride was investigated. The present results on the isosteric heats of adsorption for these four gases indicate that the non-uniformity of the surface considerably predominates in the low coverage region and this is partly attributed to the lattice imperfection or the defects of the crystals.

The entropies of the adsorbed molecules were experimentally determined and compared with the calculated values of the perfect two-dimensional gas. These results show that the adsorbed molecules of argon, oxygen and nitrogen have the nature of the two-dimensional gas at least in the range of $\theta=0.3\sim0.9$. The present results also suggest that the phase change of adsorbed argon or oxygen from a gaseous film to a condensed film may occur at about $\theta=0.9$. These results on the freedom of the adsorbed molecules are similar with those on cubic sodium chloride previously reported.

The author wishes to express his grateful thanks to Dr. S. Horiba and Professor O. Toyama of Osaka Prefectural University for their kind encouragements and discussions. The author's sincere thanks are also due to Professor R. Kiyama of Kyoto University for his kindly discussing the problems.

*Department of Chemistly, Faculty of Education Osaka Prefectural University, Sakai*

7) J. M. Drain and J. O. Morrison, *Trans. Faraday Soc.*, **48**, 316 (1952).

# *Irreversible Photobleaching of the Solutions of Fluorescent Dyes. IV. Photoreactions in Methanol, Isopropanol and Ketones, and the General Conclusion for the Photobleaching of Eosine*

By Masashi IMAMURA

(Received November 19, 1956)

## Introduction

The present author and Koizumi have reported some investigations concerning the photoreaction of eosine in water, ethanol and water-ethanol in vacuo and in the presence of oxygen (air)[1-4]. In vacuo, no reaction occurs in water but in alcohol and in water-alcohol mixtures eosine is decolorized irreversively. In the presence of oxygen, eosine in alcohol acts as a sensitizer for the photoöxidation of alcohol, while in the aqueous solution the dye photobleaches irreversively. Our first plan was to gain some definite information on the primary processes of the photobleaching of eosine in water in the presence of oxygen, and the problem has already been partly cleared up; two possible mechanisms of the primary processes have been proposed in Part I[1] and a further discussion has been given in Part III[4].

In this paper, some results obtained in methanol, isopropanol, *n*-butanol, acetone and methyl ethyl ketone, and in their mixtures with water will be reported, and a conclusive discussion will be given of the photochemical primary process of eosine in the aqueous solution.

## Experimental

**Materials.** — Merck Co. and Grübler's Eosin Yellow were used. These two species showed almost the same absorption spectra and similar photochemical behavior. Solvents were commercial products purified by the usual methods[5]. Apparatus and procedures were exactly as described in the previous papers[1-4].

**1. Retarding Effects of Alcohols upon the Aerobic Photobleaching of the Aqueous Solution.** — As already reported[1,2], ethanol shows a very marked retardation in the aerobic photobleaching of the aqueous solution of eosine and the quantum yield, $k$, is expressed, in the low concentration region of ethanol, by the equation:

$$\frac{1}{k}=\frac{1}{k^0}+K\frac{[\mathrm{EtOH}]}{[\mathrm{H_2O}]}, \qquad (1)$$

where $k^0$ is the quantum yield in the pure aqueous solution, [EtOH] and [$H_2O$] are molar concentrations, and $K$ is a constant which gives a measure of the retarding effect of ethanol[1].

Now, it was established that other alcohols show similar behavior as ethanol[6] in the low concentration region, the rate of photobleaching

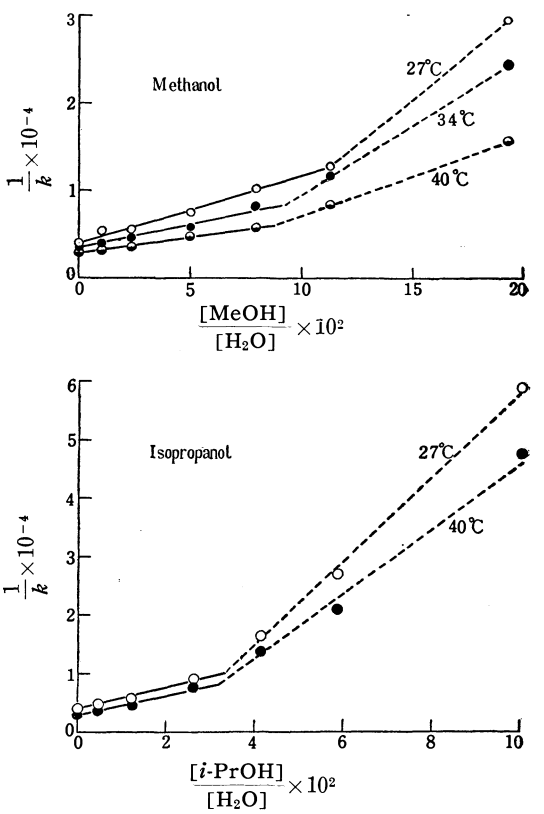



Fig. 1. Variation of the quantum yield with the mole ratio of alcohol to water. (Eq. (1))

1) M. Imamura and M. Koizumi, This Bulletin, **28**, 117 (1955).
2) M. Imamura, *J. Inst. Polytech. Osaka City Univ.*, **6**, No. 1, c, 85 (1956).
3) M. Imamura and M. Koizumi, This Bulletin, **29**, 899 (1956).
4) M. Imamura and M. Koizumi, ibid., **29**, 913 (1956).
5) A. Weissberger and E. S. Proskauer, "Organic Solvents", (Revised by J. A. Riddick and E. E. Toops, Jr.), Interscience, New York (1955).
6) Owing to the restriction of the solubility of *n*-butanol in water, experiment in a concentration higher than 8 vol. percent was impossible for it.

being expressed (Fig. 1) also by eq. (1). Values of $K$ for these alcohols are listed with those for ethanol in the third column of Table I.

TABLE I

| RH | Temp. °C | $K\times10^{-5}$ | $k^0\times10^4$ | $k^0K$ | $k^s_2/k^s_1$ |
|---|---|---|---|---|---|
| MeOH | 27 | 0.77 | 2.5 | 19 | — |
| | 34 | .58 | 2.9 | 17 | 9 |
| | 40 | .37 | 3.6 | 13 | — |
| EtOH | 20 | 1.73 | 1.9 | 33 | — |
| | 27 | 1.62 | 2.5 | 41 | 19 |
| | 34 | 1.45 | 2.9 | 42 | — |
| | 40 | 1.33 | 3.6 | 48 | — |
| *i*-PrOH | 27 | 1.94 | 2.5 | 49 | 17 |
| | 40 | 1.83 | 2.9 | 53 | — |
| *n*-BuOH | 20 | 5.18 | 1.9 | 98 | — |
| | 27 | 3.41 | 2.5 | 85 | — |
| Acetone | 27 | 2.3 | 2.5 | 58 | — |
| Methyl ethyl ketone | 27 | 4.6 | 2.5 | 115 | — |

It is evident that $K$ increases at constant temperature in the order, MeOH, EtOH, *i*-PrOH, *n*-BuOH, and the temperature coefficient is negative. As seen from Fig. 1, discontinuity appearing on each line is displaced towards the lower value of $[RH]/[H_2O]$ in the same order as above and with rising temperature.

**2. Photoreactions of Eosine in Methanol- and Isopropanol-Water Mixtures.**— As already described[4], eosine in ethanol-water mixture is converted more or less to uranine by irradiation in vacuo; the initial rate of the reaction increases with the rising concentration of ethanol and reaches a limiting value in the neighborhood of ethanol concentration of 20 vol. percent.

In expectation of similar phenomena, the experiments were made on the methanol- and isopropanol-water solutions. Experimental procedures and the calculation of the quantum yields were exactly the same as before[4].

The result with methanol at 34°C is shown in Fig. 2. Uranine production was also observed in this case but was less than with ethanol. Quantum yield reaches a limiting value in the neighborhood of concentration of 30 vol. percent methanol (in contrast to 20 vol. percent with ethanol). It is evident, from Fig. 2, that the participation of water in the primary process of the reaction can be neglected at a concentration of 30 vol. percent in vacuo, while, in the presence of oxygen (air), measurable amount of photobleaching is seen at this concentration (dotted line). The behavior is similar to that observed in the case of ethanol and this is another support in favor of the conclusion given in Part III[4] that the primary process of the photobleaching of eosine is the attack of oxygen on $D^t$.

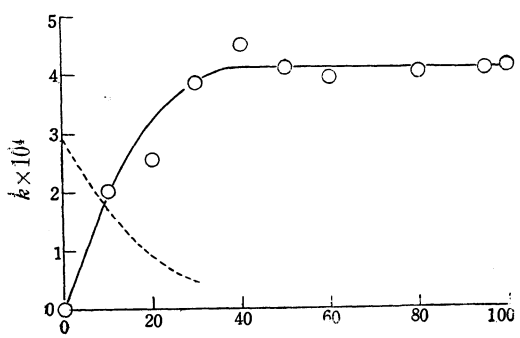



Fig. 2. Dependence of the quantum yield on methanol concentration. 34°C. Full line : in vacuo; Dotted line : aerobic.

On the other hand, quite a different result was obtained with isopropanol. In this case, uranine production was as much as with ethanol, and the difference between the quantum yields in the two pure alcohols in vacuo was not large. Nevertheless, as illustrated in Fig. 3, a prominent maximum in quantum yield was observed at a concentration of about 50 vol. percent isopropanol.

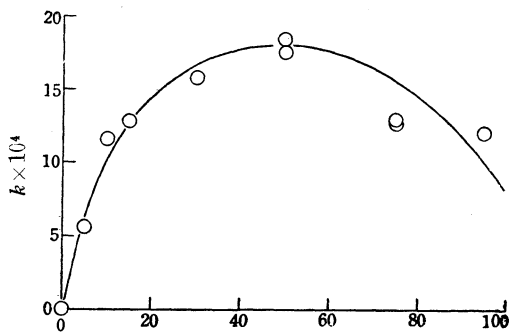



Fig. 3. Dependence of the quantum yield of the vacuum photobleaching on isopropanol concentration. 27°C.

**3. Photobleaching in Acetone and Methyl Ethyl Ketone.**— As organic solvents other than alcohols, it was attempted to use acetone and methyl ethyl ketone. Solubilities of eosine in such ketones are fairly low compared with those in alcohols. There were, in carrying out experiments with those ketones, some other difficulties since the absorption maximum gradually changes during storage in the dark. For instance, the peak at 534—536 m$\mu$ of acetone solution ($10^{-5}$ mol./l. eosine) gradually shifts to the wavelength region of 540—542 m$\mu$ and the maximum optical density increases by a small percent after several days in the dark. Though the cause for the phenomenon is not clear, it may be attributed, partially at least, to the presence of oxygen, since the evacuated solution did not show any such displacements, but its absorption maximum was fixed at 540—542 m$\mu$.

In view of the above fact, experiments were done with the solution which was maintained in the dark for a long time to attain the equilibrium condition. Rates of aerobic photobleaching of eosine both in acetone- and in methyl ethyl ketone-water mixtures were expressed well by the simple rate equation[3]:

$$-\frac{dc}{dt}=1000\,k\frac{I_0}{d}(1-e^{-acd}). \qquad (2)$$

Quantum yield, $k$, decreases markedly with increasing concentration of acetone in the low concentration region as seen for alcohols. In the higher concentration region, however, $k$ increases rapidly and reaches a high value, nearly five times that in the pure aqueous solution. This behavior is in sharp contrast with that of alcoholic solutions, in which such an increase in $k$ was not observed but $k$ was zero at 100 percent alcohols.

In methyl-ethyl-ketone, though the experiments between 20 and 95 vol. percent could not be done because of the restriction of its solubility in water, an analogous result was obtained. Though the rate at 100 percent methyl ethyl ketone does not obey eq. (2), the rate appears to be considerably large (Fig. 4).

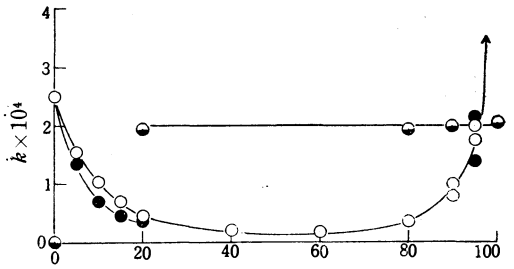



Fig. 4. Dependence of the quantum yield on the ketone concentration. 27°C.

○: acetone, aerobic
●: methyl ethyl ketone, aerobic
◒: acetone, in vacuo

Retarding effects of acetone and methyl ethyl ketone in the low concentration region can be expressed by eq. (1), values of $K$ being listed in Table I.

In the vacuum photobleaching of acetone-water solution, no such spectral displacement as in alcohol-water mixtures[4] was observed and, therefore, uranine production was not realized.

At a concentration of acetone above 20 vol. percent the rate of photobleaching is expressed by eq. (2), while below this concentration deviation from eq. (2) is remarkable. Limiting quantum yield is $2\times10^{-4}$ as illustrated in Fig. 4.

## General Discussion

From the results so far obtained, some quantitative discussions will be given of the reaction scheme for the photobleaching of eosine in various conditions. For this purpose, the rate equation for the various cases must be given. It is to be noted that the rate equations proposed in Part I must be corrected in some respects.

**1. Rate Equations.**—In Part I the following two plausible schemes were proposed for the primary processes in the aerobic photobleaching of eosine in the water-alcohol solution.

(I) First attack of oxygen on the triplet state of dye:

$$D^t+O_2\rightarrow D\cdots O_2,\quad D\cdots O_2+H_2O\cdots\rightarrow\text{products}.$$

(II) First attack of water on the triplet state of dye:

$$D^t+H_2O\rightarrow D\cdots H_2O,$$

$$D\cdots H_2O+O_2\cdots\rightarrow\text{products}.$$

The rate equations given for these two cases were, for (I)

$$k=\varphi_{S\rightarrow T}\cdot\frac{k_{O_2}}{k_{qi}+k_1[H_2O]+k_2[RH]+k_{O_2}}\times\frac{k_1'[H_2O]}{k'_{-1}+k_1'[H_2O]+k_2'[RH]} \qquad (3)$$

and for (II)

$$k=\varphi_{S\rightarrow T}\cdot\frac{k_1[H_2O]}{k_{qi}+k_1[H_2O]+k_2[RH]}\times\frac{k'_{O_2}}{k'_{-2}+k_1'[H_2O]+k_2'[RH]+k'_{O_2}} \qquad (4)$$

Both equations can be simplified into eqs. (9) and (10) to fit the experimental results, if $\varphi_{S\rightarrow T}$ is practically constant in various solvents and the following conditions are fulfilled:

for (I) $$k_{O_2}\gg k_{qi}+k_1[H_2O]+k_2[RH] \qquad (5)$$

$$k'_{-1}\approx0 \qquad (6)$$

for (II) $$k'_{O_2}\gg k'_{-2}+k_1'[H_2O]+k_2'[RH] \qquad (7)$$

$$k_{qi}\approx0 \qquad (8)$$

The conditions (5) and (7) actually hold in view of the experimental fact that the rate does not depend upon the pressure of oxygen under ordinary conditions.

Then from eq. (3)

$$k=\varphi_{S\rightarrow T}\frac{k_1'[H_2O]}{k_1'[H_2O]+k_2'[RH]} \qquad (9)$$

and from eq. (4)

$$k=\varphi_{S\rightarrow T}\frac{k_1[H_2O]}{k_1[H_2O]+k_2[RH]} \qquad (10)$$

If eqs. (9) and (10) were correct, the values of $k$ in the pure aqueous solution should be $\varphi_{S\rightarrow T}$ in both cases. The value of $\varphi_{S\rightarrow T}$ is ca. 0.1 according to Oster and Adelman[7], while $k$ is found to be of the order of $10^{-4}$. This discrepancy has arisen from the neglect of the following processes. Taking eq. (3) for example, it was assumed in Part I that the attack of oxygen on the

7) G. Oster and A. H. Adelman, *J. Am. Chem. Soc.*, **78**, 913 (1956).

triplet state leads solely to the reaction intermediate D···$O_2$, which only gives reaction products by the attack of water. But, in reality, it is very plausible that oxygen may partially deactivate $D^t$ without formation of D···$O_2$ and the similar situation can exist in the attack of water on D···$O_2$.

If one takes these deactivation processes into account, eq. (3) must be rewritten as

$$k=\varphi_{S\to T}\frac{k_{O_2}[O_2]}{k^s{}_{O_2}[O_2]}\cdot\frac{k_1'[H_2O]}{k_1'^s[H_2O]+k_2'^s[RH]} \tag{11}$$

where the superscript $s$ represents the summation of the mere deactivation and the effective process leading to the bleaching reaction.

From the similar reasoning, eq. (4) must be corrected as

$$k=\varphi_{S\to T}\frac{k_1[H_2O]}{k_1^s[H_2O]+k_2^s[RH]}\cdot\frac{k'_{O_2}[O_2]}{k'^s{}_{O_2}[O_2]} \tag{12}$$

For the vacuum photobleaching in the aqueous alcoholic solution, the primary process is

$$D^t+RH \rightarrow DH\cdot+R\cdot$$

and the specific rate of this reaction gives certainly the rate constant of the overall bleaching reaction.

$$k=\varphi_{S\to T}\frac{k_2[RH]}{k_1^s[H_2O]+k_2^s[RH]} \tag{13}$$

**2. Further Confirmation of the Primary Processes in the Aerobic Photobleaching of the Aqueous Eosine Solution.**— Though some evidences have already been presented in favor of the scheme I[4], more definite discussions will be given here analyzing the experimental data on the basis of the rate equations (11), (12) and (13).

Now all the experimental results so far obtained for the aerobic photobleaching are expressed by eq. (1) which holds in the low concentration region of alcohols or ketones. Eqs. (11) and (12) can be written in the form of eq. (1). From eq. (11),

$$\frac{1}{k}=\frac{1}{\varphi_{S\to T}}\frac{k^s{}_{O_2}}{k_{O_2}}\frac{k_1'^s}{k_1'}\left(1+\frac{k_2'^s[RH]}{k_1'^s[H_2O]}\right), \tag{14}$$

$$k^0=\varphi_{S\to T}\frac{k_{O_2}}{k^s{}_{O_2}}\frac{k_1'}{k_1'^s}$$

$$K=\frac{k_2'^s}{k_1'^s}\frac{1}{k^0}\quad\text{or}\quad\frac{k_2'^s}{k_1'^s}=k^0K \tag{15}$$

From eq. (12),

$$\frac{1}{k}=\frac{1}{\varphi_{S\to T}}\frac{k'^s{}_{O_2}}{k'_{O_2}}\frac{k_1^s}{k_1}\left(1+\frac{k_2^s[RH]}{k_1^s[H_2O]}\right) \tag{16}$$

$$k^0=\varphi_{S\to T}\frac{k'_{O_2}}{k'^s{}_{O_2}}\frac{k_1}{k_1^s}$$

$$\frac{k_2^s}{k_1^s}=k^0K \tag{17}$$

While for the vacuum photobleaching, from eq. (13).

$$\frac{1}{k}=\frac{1}{\varphi_{S\to T}}\frac{k_2^s}{k_2}+\frac{1}{\varphi_{S\to T}}\frac{k_1^s[H_2O]}{k_2[RH]}$$

or

$$\frac{1}{k}\frac{[RH]}{[H_2O]}=\frac{1}{\varphi_{S\to T}}\frac{k_1^s}{k_2}+\frac{1}{\varphi_{S\to T}}\frac{k_2^s[RH]}{k_2[H_2O]} \tag{18}$$

According to eq. (18), a plot of $[RH]/k[H_2O]$ against $[RH]/[H_2O]$ should give a straight line of slope $k_2^s/\varphi_{S\to T}k_2$ and intercept $k_1^s/\varphi_{S\to T}k_2$; from these two values $k_2^s/k_1^s$ can be evaluated. An example of such plots is shown in Fig. 5, which is satisfactory at least in the low concentration region of alcohol. In the higher

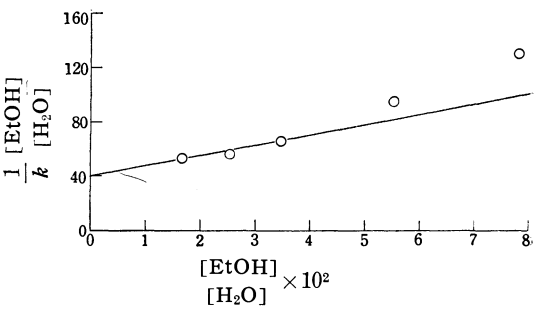



Fig. 5. Variation of the quantum yield of the vacuum photobleaching with ethanol concentration. 27°C. (Eq. (18))

region of the concentration, the deviation from the linearity becomes appreciable, and this deviation will be due to the similar situations for the aerobic photobleaching. Values of $k_2^s/k_1^s$ thus obtained for methanol, ethanol and isopropanol are summarized in the sixth column of Table I.

Now if the scheme (II) be a real one, values of $k^0K$ obtained from the aerobic photobleaching ought to be the same as those of $k_2^s/k_1^s$ obtained from the vacuum photobleaching, while this does not hold for the scheme (I) (see eqs. (15) and (17)). Values of $k^0K$ calculated from the data are listed in the fifth column of Table I.

Comparing $k^0K$ with $k_2^s/k_1^s$, it is clear that there is a large difference between them, which definitely exceeds the experimental errors. Thus it can be concluded that the primary processes of the photobleaching of eosine in the aerobic aqueous

solution proceed via the mechanism (I). The values of $k^0K$ in Table I are therefore interpreted as those of $k_2'^s/k_1'^s$ for the process (I).

Having established the reaction scheme, the values of $\varphi_{S\to T}\frac{k_2}{k_2^s}$ and $\varphi_{S\to T}\frac{k_2}{k_1^s}$ determined experimentally are tabulated in Table II.

TABLE II

| RH | Temp. °C | $\varphi_{S\to T}\frac{k_2}{k_2^s}$ | $\varphi_{S\to T}\frac{k_2}{k_1^s}$ |
|---|---|---|---|
| MeOH | 34 | $6.3\times10^{-4}$ | $5.6\times10^{-3}$ |
| EtOH | 27 | $13\times10^{-4}$ | $25\times10^{-3}$ |
| *i*-PrOH | 27 | $30\times10^{-4}$ | $53\times10^{-3}$ |

**3. Reactivities of $D^t$ and DH· with Oxygen.**— In Part I the effect of oxygen pressure on the rate of photobleaching of eosine in the aqueous solution was examined, and it was found that the rate begins to decrease below ca. $10^{-5}$ mol./l. oxygen. Though the results are not very accurate, it is possible from the data to make a rough estimation about the reactivity of $D^t$ towards oxygen and water. Since alcohol is absent in this case, the rate equation can be written as

$$k=\varphi_{S\to T}\frac{k_{O_2}[O_2]}{k^s_{O_2}[O_2]+k_1^s[H_2O]}\cdot\frac{k_1'[H_2O]}{k_1'^s[H_2O]} \qquad (19)$$

From eq. (19),

$$\frac{1}{k}\frac{[O_2]}{[H_2O]}=\frac{1}{k^0}\frac{[O_2]}{[H_2O]}+\frac{1}{k^0}\frac{k_1^s}{k^s_{O_2}}, \qquad (20)$$

where $k^0=\varphi_{S\to T}\frac{k_{O_2}}{k^s_{O_2}}\frac{k_1'}{k_1'^s}$ is the specific rate when enough oxygen is present. A plot of $[O_2]/k[H_2O]$ against $[O_2]/[H_2O]$ gives a straight line as illustrated in Fig. 6. The values of $\varphi_{S\to T}\frac{k_{O_2}}{k^s_{O_2}}\frac{k_1'}{k_1'^s}$ and $\frac{k_1^s}{k^s_{O_2}}$ at 15, 30 and 40°C are summarized in Table III.

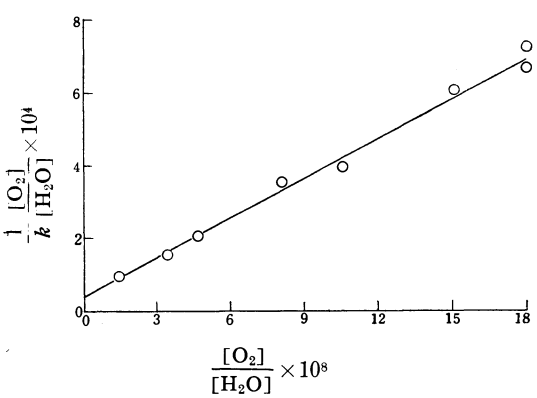



Fig. 6. Variation of the quantum yield with oxygen concentration in aqueous solution. 30°C. (Eq. (20))

TABLE III

| Temp. °C | $\varphi_{S\to T}\frac{k_{O_2}}{k^s_{O_2}}\frac{k_1'}{k_1'^s}$ | $\frac{k_1^s}{k^s_{O_2}}$ |
|---|---|---|
| 15 | $1.5\times10^{-4}$ | $2.1\times10^{-8}$ |
| 30 | $2.8\times10^{-4}$ | $1.3\times10^{-8}$ |
| 40 | $3.8\times10^{-4}$ | $3.4\times10^{-8}$ |

From the above results the ratio of the reactivity of $D^t$ with oxygen to that with ethanol can be estimated as follows. Tentatively using the values of $k^s_2/k^s_1$ at 27°C for ethanol, it may be estimated that

$$\frac{k_2^s}{k^s_{O_2}}\approx40\times10^{-8}$$

Hence, it is expected that the quantity of oxygen required for the reaction between $D^t$ and oxygen to overwhelm that between $D^t$ and alcohol, is larger than $10^{-5}$ mol./l., above which quantity the reaction between $D^t$ and water can be neglected against the reaction between $D^t$ and oxygen. In contrast to this expectation, the experimental result that $10^{-8}$ mol./l. or less oxygen is enough to inhibit the vacuum photobleaching in pure ethanol[3]. This is certainly a strong evidence that oxygen in this system acts not on $D^t$ but on DH·. The same conclusion has already been presented on the basis of different arguments in Part II.

**4. The Deviation from the Linearity between $1/k$ and $[RH]/[H_2O]$ in the Higher Region of Alcohol Concentration.** — In Part I this deviation was attributed to the change of environment around the dye ion. There is another thing, however, to be taken into account. When the concentration of alcohol is high, the term $k^s_2[RH]$ cannot be neglected against $k^s_{O_2}[O_2]$. The specific rate under this condition must be written as

$$k=\varphi_{S\to T}\frac{k_{O_2}[O_2]}{k^s_{O_2}[O_2]+k_2^s[RH]}\times\frac{k_1'[H_2O]}{k_1'^s[H_2O]+k_2'^s[RH]}$$

and eq. (14) must be replaced by

$$\frac{1}{k}=\frac{1}{\varphi_{S\to T}}\frac{k^s_{O_2}}{k_{O_2}}\frac{k_1'^s}{k_1'}\left(1+\frac{k_2'^s[RH]}{k_1'^s[H_2O]}\right)\times\left(1+\frac{k_2^s[RH]}{k^s_{O_2}[O_2]}\right) \qquad (21)$$

Though eq. (21) can qualitatively explain the above deviation, it cannot be decided at the present stage what is the principal cause for the deviation.

**5. Abnormalities Observed in Acetone and Isopropanol.**— The experimental results obtained for the aerobic photobleaching of eosine in the acetone-rich aqueous solution and those for the vacuum photobleaching in isopropanol-water mixture are somewhat anomalous as compared with the results obtained with methanol and ethanol. Generally speaking, however, there is no reason why organic substances in the aqueous solution should behave in the same way irrespective of their concentration. From the experimental results that neither aldehyde nor acid was detected in the aerobic photobleaching of eosine in the aqueous solution containing a small amount of acetone, the retarding effect of acetone might be the mere deactivation of $D\cdots O_2$ in this concentration region, while in the higher region the fate of $D\cdots O_2$ would be quite different. The result that the vacuum photobleaching of eosine in isopropanol-water mixture has its maximum rate at a concentration of about 50 vol. percent alcohol would perhaps be ascribed to the similar change of environment around the dye ion. The elucidation of these phenomena must await further studies.

## Summary

Studies on the photoreaction of eosine in the water-alcohols and -ketones have been made both in the presence and in the absence of oxygen. The corrected rate equations, giving the satisfactory explanation for the data obtained, have been presented. Analysis of the experimental results so far obtained, on the basis of these rate equations, has led to the conclusion unambigously that the primary process of the aerobic photobleaching of eosine in the aqueous solution is the attack of oxygen on the triplet state of dye.

The author indebted to Prof. M. Koizumi for many helpful discussions with respect to this research problem and to Mr. S. Ooi for carrying out a part of the experiments. The cost of this research has been partly defrayed by the Scientific Research Grant from the Ministry of Education, to which the author wishes to express his gratitude.

*Institute of Polytechnics*
*Osaka City University*
*Kita-ku, Osaka*

# *Relative Volatility of $H_2O^{16}/H_2O^{18}$ and Equilibration Time for Fractional Distillation of Water**

By Sadahiro SAKATA and Noriyoshi MORITA

(Received November 21, 1956)

## Introduction

In a previous experiment[1], fractional distillation of water was accomplished with a packed column under total reflux by continuously supplying at the top of the column the same volume of fresh normal water as that of the distillate, and the relative volatility of light- to heavy-oxygen water was calculated from the concentration of heavy oxygen in the still water by assuming the same number of theoretical plates as that determined from concentration of heavy hydrogen and by using 1.026 for the relative volatility of $H_2O/HDO$. In the kind of fractionation applied there, the equilibration time for hydrogen isotopes was about twice that for oxygen isotopes and, therefore, the apparent value of the relative volatility of light- to heavy-oxygen water diminished gradually as the fractionation proceeded toward equilibrium. Extrapolating our experimental results, we concluded that the correct value lies between 1.0043 and 1.0040.

For further confirmation of the result,

* The main part of this paper was presented at the Local Meeting of the Society of Chemical Engineers, Japan, on October 29. 1956, at Yokkaichi.

1) S. Sakata and N. Morita, This Bulletin, **29**, 284 (1956).

another kind of experiment was made with a packed column where equilibrium of fractional distillation between waters in the still and in the condenser was obtained. The effect of the concentration of $H_2O^{17}$ upon the concentration of $H_2O^{18}$ was taken into consideration. The mean value of the relative volatility of $H_2O^{16}/H_2O^{18}$ was proved to be 1.0039 with a possible error of $\pm 0.0002$.

## Experimental Procedure and Results

Distillation apparatus is shown diagramatically in Fig. 1. The column, 250 cm. in height, was

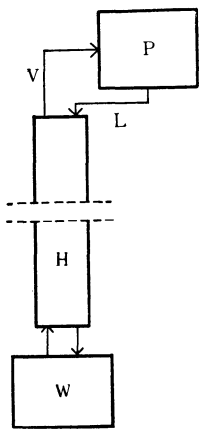



Fig. 1. Fractionation Apparatus.

made of 50 mm. copper tube with 1 mm. wall thickness. It was packed with heli-pack type packings, size $5\times5\times3$ mm., made from 0.3 mm. copper wire. The volume of the still was 2.0 l. and that of condenser was 5.0 l.

At the beginning of each series of experiments, 1.5 l. of normal water was poured into the still and 5.0 l. into the condenser. The still was heated externally with an electric furnace, and the column hold-up of water after boiling-up was judged to be about 100 cc. from the decrease of water in the still. The uncertainty of the hold-up does not seriously alter the conclusions given later. The through-put was determined from the quantity of condensate obtained during a short given interval and was calculated to be 3.3 cc./min. or 200 cc./hr.

Two series of experiments were done, the results of which are tabulated in Tables I and II. During each series of experiments, samples of about 15 cc. were taken from the still at intervals of several days and their total excess densities due to both heavy oxygen and heavy hydrogen were measured as compared with normal water. After equilibrium of fractionation was reached, two samples of water, one from the still and the other from the condenser, were taken. The total excess densities of these samples were measured first and then the heavy oxygen content of each

TABLE I
RESULTS, SERIES-1

| Duration days | Excess in Density Still $\gamma$ | Condenser $\gamma$ |
|---|---|---|
| 0.0 | 0.0 | — |
| 5.0 | 15.9 | — |
| 10.0 | 19.5 | — |
| 17.0 | 19.4 | — |
| 33.0 | 20.7 | −6.0 |
| D | 7.1 | −1.8 |
| | $n+1=19.4_1$ | |
| $O^{18}$ | 13.0 | −4.0 |
| ($O^{17}$ | 0.6 | −0.2) |
| | $\alpha=1.0038_3$ | |
| 51.0 | 21.9 | −5.0 |
| D | 7.3 | −1.5 |
| | $n+1=18.9_2$ | |
| $O^{18}$ | 13.9 | −3.3 |
| ($O^{17}$ | 0.7 | −0.2) |
| | $\alpha=1.0039_7$ | |

TABLE II
RESULTS, SERIES-2

| Duration days | Excess in Density Still $\gamma$ | Condenser $\gamma$ |
|---|---|---|
| 0.00 | 0.0 | — |
| 1.00 | 5.2 | — |
| 2.00 | 9.0 | — |
| 3.10 | 12.7 | — |
| 4.23 | 14.8 | — |
| 5.90 | 16.9 | — |
| 8.00 | 19.9 | — |
| 11.00 | 21.5 | — |
| 15.00 | 23.6 | — |
| 18.00 | 24.1 | — |
| 23.14 | 23.8 | −7.5 |
| D | 7.8 | −2.6 |
| | $n+1=22.9_2$ | |
| $O^{18}$ | 15.3 | $-4.6_9$ |
| | $\alpha=1.0038_0$ | |
| 27.00 | 24.2 | −7.1 |
| D | 7.3 | −2.6 |
| | $n+1=22.0_8$ | |
| $O^{18}$ | 16.1 | $-4.3_0$ |
| | $\alpha=1.0040_2$ | |

of these samples was determined by electrolyzing the sample and combining the evolved oxygen with standard hydrogen[2]. As will be seen from the experimental procedure, the excess density of water taken from the condenser is negative. The density due to $H_2O^{17}$ was separated from the density due to total heavy oxygen water by calculation on the assumptions that the relative volatility of $H_2O^{16}/H_2O^{18}$ was 1.0039 and of $H_2O^{16}/H_2O^{17}$ was $\sqrt{1.0039}$, and that the concentrations

2) N. Morita and T. Titani, This Bulletin, **11**, 414 (1936).

of $H_2O^{18}$ and $H_2O^{17}$ in normal water were respectively 224.7 and 21.9 in $\gamma$ unit[3,4]. The number of theoretical plates $n+1$ was calculated from the excess densities due to heavy hydrogen of the samples as determined by subtracting the densities due to heavy oxygen from the total excess densities and by using $\sqrt{1.052}$ as the relative volatility of $H_2O$/HDO and 0.000147 (15.8$\gamma$) as the atomic fraction of deuterium in normal water. Using this number of theoretical plates, the relative volatility $\alpha$ of $H_2O^{16}/H_2O^{18}$ was calculated from the excess densities due to $H_2O^{18}$ of the two samples, $\Delta s_w$ for the water from the still and $\Delta s_p$ for the water from the condenser, by the equation

$$(224.7+\Delta s_w)/(224.7+\Delta s_p)=\alpha^{n+1} \qquad (1)$$

Two sets of measurements were made for each series of experiments. Four values of $\alpha$ in Table I and II give a mean value $\alpha=1.0039_1$. If we assume an error of $\pm 0.1\gamma$ for each value of measured excess densities due to deuterium and that due to $O^{18}$, the largest possible error in $\alpha$ is $\pm 0.00014$. Although the error of each value of excess densities may be larger than $\pm 0.1\gamma$, the deviation of each calculated value of $\alpha$ from the mean value was rather small, and we concluded $\pm 0.0002$ to be the possible error of the mean value.

## Relation of Simultaneous Concentration of Heavy Oxygen and Heavy Hydrogen

Harbert[5] assumed Fenske's relation for each pair of components of a multicomponent system at equilibrium under total reflux. Normal water consists of nine components, as is shown in Table III. Mole fraction of each component in Table III was calculated by using values[3,4] of

TABLE III

COMPOSITION OF NORMAL WATER

| No. | Formula | Mole fraction |
|---|---|---|
| 1 | $HHO^{16}$ | $99.73467\cdot10^{-2}$ |
| 2 | $HHO^{18}$ | $19.80418\cdot10^{-4}$ |
| 3 | $HHO^{17}$ | $3.78889\cdot10^{-4}$ |
| 4 | $HDO^{16}$ | $29.32616\cdot10^{-5}$ |
| 5 | $HDO^{18}$ | $5.82326\cdot10^{-7}$ |
| 6 | $HDO^{17}$ | $1.11409\cdot10^{-7}$ |
| 7 | $DDO^{16}$ | $22.28229\cdot10^{-9}$ |
| 8 | $DDO^{18}$ | $4.42456\cdot10^{-11}$ |
| 9 | $DDO^{17}$ | $0.84650\cdot10^{-11}$ |

atomic fraction of isotopes, i.e. H=0.999853, D=0.000147, $O^{16}$=0.997640, $O^{18}$=0.001981 and $O^{17}$=0.000379, as well as by using the equilibrium constant for hydrogen isotopes $[HOD]^2/[HOH][DOD]=3.87$ and by assuming no isotopic effect for oxygen isotopes. As we can consider that these components in water constitute an ideal solution, we can apply Harbert's equation for equilibrium

$$x_{jw}=\alpha_{1j}^{n+1}x_{jp}/\sum_{i=1}^{9}\alpha_{1i}^{n+1}x_{ip} \qquad (2)$$

where $x$ is concentration in mole fraction, suffix i or j indicates any one component in these nine components, suffix w indicates water in still, suffix p indicates water in condenser, and $\alpha_{1j}$ is the relative volatility of the most volatile component $H_2O^{16}$ to j's component. As will be seen from Eq. (2), any two components show Fenske's relation because the denominator of the equation is common for all components and because for a pair of components j and j' there exists a relation $\alpha_{1j'}/\alpha_{1j}=\alpha_{jj'}$.

In addition to the fractionation by distillation, we must consider the following exchange reaction of hydrogen isotopes as a possible cause of change in concentration of components

$$\underset{k}{HOH}+\underset{l}{DOD}=2\underset{m}{HOD} \qquad (3)$$

From Harbert's equation we can write

$$x_{mw}/x_{kw}=\alpha_{km}^{n+1}(x_{mp}/x_{kp})$$

$$x_{mw}/x_{lw}=\alpha_{lm}^{n+1}\ (x_{mp}/x_{lp})$$

where suffixes k, l and m indicate components as shown under Eq. (3). Then

$$x_{mw}^2/x_{kw}\cdot x_{lw}=(\alpha_{km}\cdot\alpha_{lm})^{n+1}(x_{mp}^2/x_{kp}\cdot x_{lp})$$

When vapor pressures of pure components are written as $P_k$, $P_l$ and $P_m$ we have the relation

$$\alpha_{km}\cdot\alpha_{lm}=P_k\cdot P_l/P_m^2$$

Therefore when $P_m$ is geometrical mean of $P_k$ and $P_l$, $\alpha_{km}\cdot\alpha_{lm}$ becomes unity, and we have the relation

$$x_{mw}^2/x_{kw}\cdot x_{lw}=x_{mp}^2/x_{kp}\cdot x_{lp}$$

Thus we can conclude that when either the water in the still or in the condenser is in isotopic equilibrium, the other is also in isotopic equilibrium and the exchange reaction shown in Eq. (3) has no effect on change in concentration of components of water under fractional distillation.

Fig. 2 shows the calculated values of fractional concentration of each component of water which is in equilibrium with normal water versus the number of theoretical plates of a fractionation column. In this calculation we assumed the relative volatility of $H_2O^{16}$ to each component to

3) H. E. Watson, *J. appl. Chem.*, **3**, 556 (1953).
4) I. Kirshenbaum, "Physical Properties and Analysis of Heavy Water", McGraw-Hill Book Co., N. Y. (1951).
5) W. D. Harbert, *Ind. Eng. Chem.*, **37**, 1162 (1945).

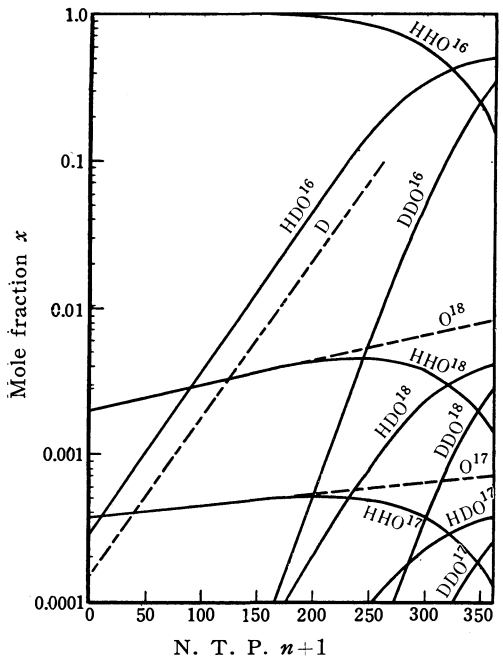



Fig. 2. Change of concentration with N. T. P.

TABLE IV

RELATIVE VOLATILITY

| | | |
|---|---|---|
| $HHO^{16}$ | $HDO^{16}$ | $DDO^{16}$ |
| 1.0000 | $\sqrt{1.052}$ | 1.052 |
| $HHO^{17}$ | $HDO^{17}$ | $DDO^{17}$ |
| $\sqrt{1.0039}$ | $\sqrt{1.0039 \cdot 1.052}$ | $1.052\sqrt{1.0039}$ |
| $HHO^{18}$ | $HDO^{18}$ | $DDO^{18}$ |
| 1.0039 | $1.0039\sqrt{1.052}$ | $1.0039 \cdot 1.052$ |

be as shown in Table IV. As are shown by dotted lines in the Fig. 2, the logarism of atomic fraction of D, $O^{18}$, and $O^{17}$ in the range as shown in the Figure each shows a linear relation with $n+1$.

## Equilibration Time

Urey and others[6,7] showed that the velocity of enrichment of a less-volatile component in a column is the greater, the nearer the plate is to the still, so that a stationary state sets in first at the lower part of the column. They, therefore, assumed that at a given moment shorter than equilibration time, the lower part of the column reaches the stationary state determined by Fenske's equation, while the upper part has the composition of the initial mixture. By applying the assumption to our experiment and assuming the upper part of the column to have the composition of the water in the condenser, the mean concentration $\bar{\eta}$ of a less-volatile component in the column is shown by

$$\bar{\eta}=\{x_w+\alpha x_p(\ln[x_w]/x_w-1)\}/n\alpha \ln \alpha \qquad (4)$$

where $x_w$ is the concentration of a less-volatile component in the still at a given moment, $x_p$ is that in the condenser, and $x$ with square brackets shows a value at equilibrium.

Additionally we assume, as was done by Urey and others, that the vapor which enters into the condenser is in one-plate equilibrium with the refluxing water, and then we have the following relation by a material balance in a short interval $dt$

$$x_pLdt-(x_p/\alpha)Vdt=Wdx_w+Hd\bar{\eta} \qquad (5)$$

where $V$ is the molar vapor velocity, $L$ is the reflux velocity, $W$ is the still hold-up, and $H$ is the column hold-up. Under total reflux $L=V$, and at any moment from material balance we have $Wx_w+Px_p=(W+P)x_0$, where $P$ is the condenser hold-up and $x_0$ is the fractional concentration of the less-volatile component in normal water. By setting $W/P=a$, $W/L=b$, and $H/L=c$, and substituting Eq. (4) into Eq. (5), we have

$$\begin{aligned} dt=&\binom{\alpha}{\alpha-1}\left[b+\frac{c\{1+\alpha a(1-\ln[x_w])\}}{n\alpha \ln \alpha}\right] \\ &\times\frac{dx_w}{\{(1+a)x_0-ax_w\}} \\ &+\binom{\alpha}{\alpha-1}\frac{ca \ln x_w dx_w}{\{(1+a)x_0-ax_w\}n \ln \alpha} \\ &-\binom{\alpha}{\alpha-1}\frac{cdx_w}{(n \ln \alpha)x_w} \end{aligned} \qquad (6)$$

Integration of Eq. (6) with a constriction that $x_w=x_0$ at $t=0$ and with the relation $(1+a)x_0-ax_w=x_p$ gives

$$\begin{aligned} t=&\binom{\alpha}{\alpha-1}\left[b+\frac{c\{1+\alpha a(1-\ln[x_w])\}}{n\alpha \ln \alpha}\right]\frac{1}{a}\ln\frac{x_0}{x_p} \\ &+\binom{\alpha}{\alpha-1}\binom{c}{n \ln \alpha}\left[-\ln\frac{x_p}{a}\ln x_w+\ln\frac{x_0}{a}\ln x_0\right. \\ &+\ln\binom{1+a}{a}x_0\ln\frac{x_w}{x_0}+\binom{a}{1+a}\left(1-\frac{x_w}{x_0}\right) \\ &\left.+\frac{1}{2^2}\binom{a}{1+a}^2\left(1-\frac{x_w^2}{x_0^2}\right)+\cdots\cdots\right] \\ &+\binom{\alpha}{\alpha-1}\binom{c}{n \ln \alpha}\ln\frac{x_0}{x_w}. \end{aligned} \qquad (7)$$

6) H. C. Urey, J. R. Huffman, H. C. Thode and M. Fox, *J. Chem. Phys.*, **5**, 856 (1937).
7) A. E. Brodsky and O. Ch. Scarre, *Acta Phys. Chim. U. R. S. S.*, **10**, 729 (1939).

Introducing in Eq. (7) the values applied in the experiments, i.e. $a=W/P=(1.5-0.1)/5.0=0.28$, $b=W/L=(1.5-0.1)/0.2=7$ hrs., and $c=H/L=0.1/0.2=0.5$ hr., and setting $n+1=20$, we obtain equilibration time 144 hrs. (6.0 days) for HDO and 147 hrs. (6.1 days) for $H_2O^{18}$. The values of $x_w$ and $x_p$ at equilibrium are calculated from the material balance relation, $Wx_w+Px_p=(W+P)x_0$, and from Fenske's equation for low concentration, $x_w/x_p=\alpha$[20]. The time necessary for equilibration for HDO is almost equal to that for $H_2O^{18}$, which is in marked contrast to the previous experiment[1]).

If we neglect the column hold-up, $c$ in Eq. (7) vanishes, and the relation reduces to a simple equation

$$t=\{\alpha/(\alpha-1)\}(b/a)\ln(x_0/x_p) \qquad (8)$$

Eq. (8) gives equilibration time 135 hrs. for HDO and 113 hrs. for $H_2O^{18}$. In this case the latter is a little shorter than the former. They are not, however, so far different from those obtained above from Eq. (7).

The assumption made in Eq. (5) becomes incorrect as the fractionation approachs equilibrium. In this respect Jackson and Pigford mentioned in their recent paper[8]) that at a range of very small concentration of a less-volatile component, such as we have treated, the time necessary to reach 90% of equilibrium from initial concentration is about twice the value of equilibration time as calculated by such an equation submitted by Urey and others. Taking this fact into consideration calculated values are nearly coincident with our experimental values.

## Discussion

As has already been mentioned, an error $\pm0.1\gamma$ each in excess densities due to deuterium in still and that in condenser combined gives, for our experimental conditions a maximum deviation of $\pm0.45$ in $n+1$, and this error combined with an error of $\pm0.1\gamma$ each in excess densities due to $O^{18}$ in still and that in condenser makes an error of $\pm0.00014$ in the relative volatility $\alpha$ of $H_2O^{16}/H_2O^{18}$. In addition to this, an error of 0.001 in the relative volatility $A$ of $H_2O$/HDO gives an error of $(\Delta n/n)=0.038$, and this error results in an error of 0.00015 in $\alpha$ (increases when $A$ increases). For example, if we apply Schutz and Zmachinsky's value[9,4]) $A=1.0295$ in place of $\sqrt{1.052}$, $\alpha$ becomes $1.0044_8$.

As concerns the relative volatility of light- to heavy-oxygen water at 100°C., Watson gave a short summary in his recent paper[3]). In his paper he introduced data from Lewis and Cornish[10]), Wahl and Urey[11]), and Riesenfeld and Chang[12]), giving values of 1.0056–1.0060, 1.003 and 1.0046, respectively, as the relative volatility. Watson also introduced the studies of Brodsky and Scarre[7]) and Hayter[13]) which gave 1.0055 and 1.0056, and he himself concluded 1.0056 as the most probable value.

Although the value 1.003 of Wahl and Urey was long accepted, it was not exact enough because it was a value which was extrapolated far from the measured values between 11.25 and 46.35°C., and this value seems much too low. Calculated values of 1.0056–1.0060 from Lewis and Cornish's data also seem inexact because their data were based on an uncertain number of the theoretical plates of their fractionation column. Increase in the assumed number of theoretical plates decreases the value of the relative volatility, and if we use a number around 50 instead of the 40 which they assumed, the value of the relative volatility of $H_2O^{16}/H_2O^{18}$ becomes 1.004. Moreover, it is uncertain whether a true equilibrium of fractionation had been reached or not within such a short time as they applied to their experiments.

Brodsky and Scarre measured ratios of concentration of heavy hydrogen and heavy oxygen of water in a still to those of normal water by using a rotating column under total reflux by continuously supplying fresh normal water at the top of the column, as was done in our previous experiment[1]). In their calculation, howerer, they used a value of $17.9\gamma$ as the concentration of heavy hydrogen in normal water and a value of $171\gamma$ as that of heavy oxygen. The resultant values of the ratio under atmospheric pressure were 2.74 for hydrogen and 1.26 for oxygen. In place of the above values for natural abundance we use $15.8\gamma$ for heavy hydrogen and $224.7\gamma$ for $O^{18}$. Then the ratios reduce to 2.97 and 1.20, respectively. The

8) R. F. Jackson and R. L. Pigford, *Ind. Eng. Chem.*, **48**, 1020 (1956), Fig. 4.

9) P. W. Schutz, SAM Report A-595, Apr. 12, 1943.

10) G. N. Lewis and R. E. Cornish, *J. Am. Chem. Soc.*, **55**, 2616 (1933).

11) M. H. Wahl and H. C. Urey, *J. Chem. Phys.*, **3**, 411 (1935).

12) E. H. Riesenfeld and T. L. Chang, *Z. physik. Chem.*, **B33**, 127 (1936).

13) A. J. Hayter, Ph. D. Thesis, London Univ., 1950.

ratio for heavy hydrogen, combined with $\sqrt{1.052}$ for the relative volatility of $H_2O$/HDO, gives $n+1=43.0$, and this value, combined with the ratio for heavy oxygen, gives 1.0042 for the relatives volatility of light- to heavy-oxygen water. If the density due to $O^{17}$ be excluded, the value of the relative volatility will reduce to about 1.0040.

Hayter's experiment, on which Watson's conclusion was based, was done with a packed column with 2500 packings which effect 0.21 theoretical plate per one packing. This number of theoretical plates was based on the fractionation of the system of benzene and carbon tetrachloride. By their fractionation of water, they obtained numbers between 250–400 from the fractionation of hydrogen isotopes, and applying these values, they concluded a value of 1.0056 as the relative volatility of $H_2O^{16}/H_2O^{18}$. The reason for the discrepancy between this value and our present value is not immediately clear. It seems probable, however, that their experiment was not based on true equilibrium of hydrogen isotopes. They used a continuous method for the fractional distillation, and the decrease of plate efficiency by such productive distillation may be more prominent for hydrogen isotopes than for oxygen isotopes, as was pointed out by Cohen[14]. In order to make applicable a value of around 1.004 for the relative volatility, the number of theoretical plates must be about 560, a value which does not seem improbable. If we use $0.12\times2500=525$ as the number of theoretical plates, we obtain 1.0043 as the relative volatility.

In conclusion, we do not find any fact which seems inconsistent to any great degree with our present result. Thus, by applying values of the natural abundance of D, $O^{18}$ and $O^{17}$ in normal water which are respectively 15.8, 224.7 and 21.9 in $\gamma$ unit and of the relative volatility of $H_2O/HDO=\sqrt{1.052}$, and by assuming that the plate efficiency of the fractionation column is identical for hydrogen and oxygen isotopes, we conclude $1.0039\pm0.0002$ as the relative volatility of $H_2O^{16}/H_2O^{18}$.

*Department of Chemical Engineering*
*Faculty of Engineering, Nagoya*
*University, Chigusa-ku, Nagoya*

14) K. Cohen, *J. Chem. Phys.*, **8**, 588 (1940).

# *Benzylation of Acetylene. I. Formation of 3,4-Diphenyl-1-butyne and 3,4-Diphenyl-1,2-butadiene*

By Teisuke ANDO and Niichiro TOKURA

(Received August 7, 1956)

Vaughn, Hennion, Vogt, and Nieuwland[1], in an attempted alkylation of acetylene by treating alkali metal acetylide (I) with various alkyl chlorides in liquid ammonia, observed that benzylacetylene (III) was not formed when benzyl chloride (II) was allowed to react with the acetylide.

The present writers carried out the same benzylation reaction and found that, instead of benzylacetylene (III), 3,4-diphenyl-1-butyne (IV) and an allenic compound, 3,4-diphenyl-1,2-butadiene (V), were formed.

To prepare the metal acetylide, lithium or sodium metal was dissolved in liquid ammonia and purified acetylene was passed through the solution until the blue color of the metal disappeared. The acetylide was allowed to react with benzyl chloride, the reaction product was taken up in ether, and the residue from the ethereal solution was fractionated under reduced pressure. The initial fraction of a small amout of unchanged benzyl chloride was followed by fractions A of b. p. 135°C (2 mmHg) and B of b. p. 190°C (2 mmHg) (total yield 10.3–34.6%), leaving a large amount of a residue which consisted of a viscous polymerized substance.

When lithium was used, the yields of A and B were 12.2% and 34.6% respectively, while sodium gave lower yields, A 0–5.2%

1) T. H. Vaughn, G. F. Hennion, R. R. Vogt and J. A. Nieuwland, *J. Org. Chem.*, **2**, 1 (1938).

and B 10.3–17.8%.

B is a yellowish, viscous liquid and forms a complex salt with silver nitrate, through which it can be purified and estimated. Thus, it has a terminal group $-C\equiv CH$ and the determination of residual silver in the complex salt and the liberated nitric acid during the complex formation gave a molecular weight 206 as a monoacetylenic compound. The structure of this substance was assumed to be

$$C_6H_5-CH_2-\underset{\displaystyle C_6H_5}{\underset{|}{CH}}-C\equiv CH. \qquad \text{(IV)}$$

Its infrared absorption spectrum exhibited a strong maximum at 3320 $cm^{-1}$ due to stretching vibration of the terminal acetylenic bond and a weak one at 2120 $cm^{-1}$ for a monosubstituted acetylene[2]. Catalytic reduction of B in the presence of palladium carbon proceeded through a rapid absorption of 1 mole of hydrogen, and then a very slow absorption of one further mole of hydrogen. The product showed physical constants in good agreement with those of 1,2-diphenylbutane (VI)[3]. The infrared absorption for the unsaturated side-chain disappeared and a new absorption appeared at 1380 $cm^{-1}$ due to methyl deformation[4]. Both the elementary analysis and the molecular refraction agreed with the theoretical values. Thus the structure of 3,4-diphenyl-1-butyne (IV) for B was concluded.

A is a colorless, clear, easily flowing liquid; it discolors bromine and potassium permanganate, but does not form a complex salt with silver nitrate. Its strong infrared absorptions at 1950, 1680, and 850 $cm^{-1}$ showed it is an allene derivative[5]. As described in the experimental part, A is formed by the isomerization of B and this may be explained by assuming a structure of 3,4-diphenyl-1,2-butadiene (V) for A, which was ascertained by the oxidation of A with ozone to desoxybenzoin (VII).

It follows, therefore, that the reaction of the metal acetylide and benzyl chloride takes the following routes:

$$\underset{\text{(II)}}{C_6H_5CH_2Cl} + \underset{\text{(I)}}{NaC\equiv CH} \xrightarrow{\text{Liq. } NH_3}$$

$$\left[\underset{\text{(III)}}{C_6H_5-CH_2-C\equiv CH}\xrightarrow{NaC\equiv CH}\right]$$

$$\left[C_6H_5-\underset{\displaystyle Na}{\underset{|}{\overset{\displaystyle H}{\overset{|}{C}}}}-C\equiv CH\right]\xrightarrow{C_6H_5CH_2Cl}$$

$$C_6H_5-CH_2-\underset{\displaystyle C_6H_5}{\underset{|}{CH}}-C\equiv CH \xrightarrow{\text{isomerization}}$$
(IV)

$$C_6H_5-CH_2-\underset{\displaystyle C_6H_5}{\underset{|}{C}}=C=CH_2$$
(V)

$$IV \xrightarrow[\text{Pd-C}]{H_2} C_6H_5-CH_2-\underset{\displaystyle C_6H_5}{\underset{|}{CH}}-CH_2-CH_3$$
(VI)

$$V \xrightarrow{O_3} C_6H_5-CH_2-\underset{\displaystyle C_6H_5}{\underset{|}{C}}=O$$
(VII)

It is known that allenic compounds are formed in general in small amounts on heating acetylenic compounds with alkali hydroxide around 170°C[6], and a phenylbenzylallene, such as V, is comparatively easily formed from the isomeric acetylene at the room temperature even in the presence of such a weak base as ammonia.

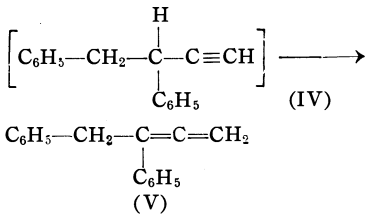
Treatment of 3,4-diphenyl-2-butanone (VIII)[7] with phosphorus pentachloride followed by dehydrochlorination with potassium hydroxide[8] did not afford the acetylenic compound (IV) but almost the whole product was the allenic compound (V), which readily polymerized during distillation to give a large amount of a distillation residue.

$$C_6H_5-CH_2-\underset{\displaystyle C_6H_5}{\underset{|}{CH}}-COCH_3 \xrightarrow{PCl_5}$$
(VIII)

$$C_6H_5-CH_2-\underset{\displaystyle C_6H_5}{\underset{|}{CH}}-\underset{\displaystyle Cl}{\underset{|}{\overset{\displaystyle Cl}{\overset{|}{C}}}}-CH_3 \xrightarrow{-HCl}$$

$$C_6H_5-CH_2-\underset{\displaystyle C_6H_5}{\underset{|}{CH}}-\underset{\displaystyle Cl}{\underset{|}{C}}=CH_2 \xrightarrow{KOH}$$

2) L. J. Bellamy, "The Infra-red Spectra of Complex Molecules" John Wiley and Sons Inc., New York (1954), p. 49.
3) A. Klages and S. Heilmann, *Ber.*, **37**, 1452 (1904).
4) R. S. Rasmussen, *J. Chem. Phys.*, **16**, 712(1948).
5) W. J. Bailey and C. R. Pfeiffer, *J. Org. Chem.*, **20**, 97 (1955).
6) E. R. H. Jones, G. H. Whitham and M. C. Whiting, *J. Chem. Soc.*, **1954**, 3201; I. L. Jacobs, R. Akawie and R. G. Cooper, *J. Am. Chem. Soc.*, **73**, 1273 (1951).
7) M. M. Tiffeneau and M. J. Levy, *Bull. soc. chim. France*, **33**, 779 (1923).
8) C. Dufraisse and J. F. Viel, ibid., **37**, 817 (1925).



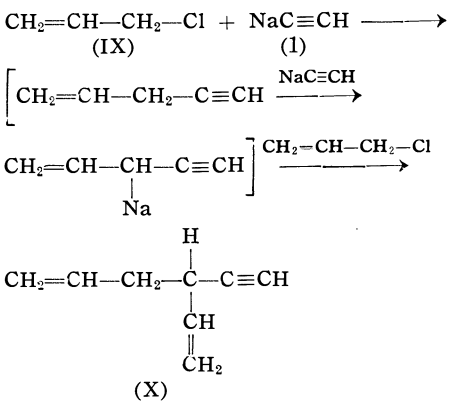
(IV)



(V)

It was observed that 3,4-diphenyl-1-butyne (IV) was changed into 3,4-diphenyl-1,2-butadiene (V) merely by dissolving it in liquid ammonia and allowing the solution to stand overnight at the room temperature.

The formation of 3,4-diphenyl-1-butyne (IV) and of no benzylacetylene (III) in the reaction of metallic compounds of acetylene and benzyl chloride is analogous to the formation of 3,4-divinyl-1-butyne (X) in the reaction of a metal acetylide and allyl chloride (IX) in liquid ammonia.

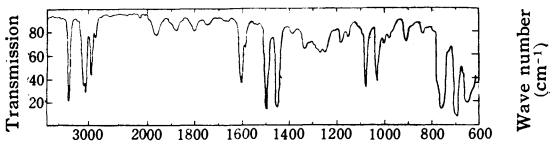


(X)

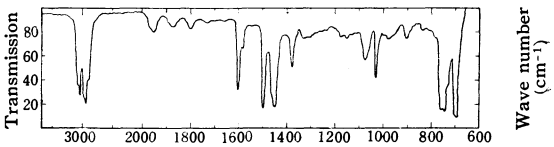
Reactions and properties of the acetylenic compound (IV) and its derivatives will be described elsewhere.

## Experimental

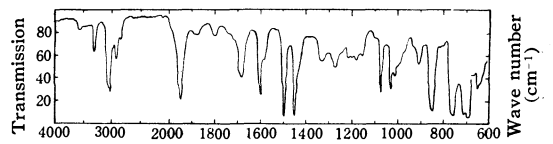
**Benzylation of Acetylene.—(1) Reaction of Lithium Acetylide and Benzyl Chloride.—** Metallic lithium (1.7 g., 1/4 mole) was dissolved in 400 cc. of liquid ammonia, contained in a three-necked flask provided with a dry-ice reflux condenser and a stirrer, and maintained at −50° ±5°C in a dry-ice-ethanol bath. Acetylene, dried and purified by passage through concentrated sulfuric acid, soda lime, and phosphorus pentoxide, successively, was introduced into the solution with stirring until the blue color faded. It required about ten minutes. After stirring the solution for further ten minutes or so, 31 g. (1/4 mole) of benzyl chloride was added from a dropping funnel during about twenty-five minutes. The solution gradually acquired a pale pink color. When the mixture was stirred for 2.5 hr., it gradually became pale pinkish orange in color with increasing amount of a white precipitate. After




3,4-Diphenyl-1-butyne




1,2-Diphenylbutane




3,4-Diphenyl-1,2-butadiene

Fig. 1. Spectra were taken by a Perkin-Elmer Model 21 Infrared Spectrophotometer.

allowing the mixture to stand in an ice bath overnight, ammonia was allowed to evaporate and 100 cc. of water was added to the residue to dissolve the greyish white solid. Then an excess of 4 N hydrochloric acid was added to transform the by-product amine into the hydrochloride insoluble in ether, and the mixture was extracted with 200 cc. of ether. After filtration, the ethereal solution was washed successively with 4 N HCl and with water and dried over anhydrous sodium sulfate overnight. A small amount of hydroquinone was added to the ethereal solution, the ether was evaporated, and the residue was submitted to a low-pressure distillation in a nitrogen stream. Besides 1 g. of recovered benzyl chloride, b. p. 39–41°C/2 mmHg, the following fractions were obtained:

(A) Pale yellow liquid, b. p. 135–143°C/2 mmHg. 3.1 g. (12.2%).

(B) Yellowish brown viscous liquid, b. p. 185–190°C/2 mmHg, 8.9 g. (34.6%).

(C) Distillation residue, ca. 15 g.

B was identified with 3,4-diphenyl-1-butyne (IV) and A with 3,4-diphenyl-1,2-butadiene (V).

**(2) Reaction of Sodium Acetylide and Benzyl Chloride.—**Metallic sodium was dissolved in liquid ammonia under the same conditions as above and benzyl chloride was allowed to react with sodium acetylide so obtained. The yields of A and B from this reaction were as follows:

| Expt. No. | Na (g.) | $PhCH_2Cl$ (g.) | Molar ratio Na/$PhCH_2Cl$ | Yield A (g.) | A (%) | B (g.) | B (%) |
|---|---|---|---|---|---|---|---|
| 1 | 46 | 253 | 1/1 | 0 | 0 | 35 | 16.9 |
| 2 | 12 | 126 | 1/2 | 5.4 | 5.2 | 10.6 | 10.3 |
| 3 | 12 | 31 | 2/1 | 0.8 | 3.1 | 4.6 | 17.8 |

**Purification of Fraction B (3, 4-Diphenyl-1-butyne (VI)**[10].—To a solution of 5.5 g. of Fraction B, b. p. 185–190°C/2 mmHg, dissolved in 20 cc. of ethanol, a solution of 10 g. of silver nitrate dissolved in a mixture of 20 cc. of water and 40 cc. of ethanol was added, and the mixture was warmed for about 40 minutes on a water bath and allowed to stand overnight. The white precipitate was collected by filtration, washed with water to remove excessive silver nitrate and then with ethanol to remove the unchanged materials, and dried in a desiccator. Yield, 12 g.

A suspension of 12 g. of the silver complex salt in a 10% potassium cyanide solution was refluxed by heating on an oil bath, when an oily layer separated as the reaction proceeded. In ten hours' refluxing, the complex salt disappeared completely. After cooling, the mixture was extracted with ether, the ethereal layer was washed with water to neutral reaction, dried over anhydrous sodium sulfate and concentrated. The residue was distilled under a reduced pressure in nitrogen stream and in the presence of hydroquinone, to give 4.5 g. of a colorless, clear, viscous liquid, b. p. 190–192°C/2 mmHg, $n_D^{25}$ 1.6040, $d_{25}^{25}$ 1.0646. Mole Ref. Found: $MR_D$, 66.78. Calcd: 66.87.

*Anal.* Found: C, 92.86; H, 6.87. Calcd. for $C_{16}H_{14}$: C, 93.16; H, 6.84%. IR $\nu_{max}$: 3320 and 2120 $cm^{-1}$. Silver determination of the complex salt: 4.350 mg. of the substance gave an ignition residue (Ag) 1.988 mg. Calcd. for $C_{16}H_{13}Ag.AgNO_3$: 1.939 mg. Mol. wt., Found 194. Calcd. for $C_{16}H_{14}$: 206. Determination of $HNO_3$ produced during formation of silver complex salt[11]: 0.1691 g., and 0.1743 g. of the substance gave nitric acid equivalent to 10.67, and 11.00 cc., respectively, of 0.1 N NaOH. (f=0.7691). Mol. wt., Found: 206,206. Calcd. for $C_{16}H_{14}$: 206.

**Catalytic Reduction of IV (Formation of 3, 4-Diphenylbutane (VI)**.—A solution of 2 g. of IV in 100 cc. of methanol with the addition of 0.3 g. of palladium-carbon was submitted to reduction at ordinary temperature and pressure in a Willstätter apparatus. One mole of hydrogen was absorbed in twenty-five minutes while another mole of hydrogen in a longer time, fifteen hours being required in total. After removal of the catalyst, the solvent was evapolated, and the residue was submitted to vacuum distillation. The fraction of b, p. 153°C/11.5 mmHg, $n_D^{17}$ 1.5882, agreed with the values of b. p. 152°C/11 mmHg and $n_D^{18}$ 1.587 given for 1, 2-diphenylbutane in the leterature[3]. Yield, 1.7 g.

**Formation of 3, 4-Diphenyl-1, 2-butadiene (V) from 3, 4-Diphenyl-2-butanone (VIII)**.—In order to change VIII, prepared by the method of Tiffeneau[7], to the acetylenic compound (IV) by the method of Dufraisse and Viel[8], VIII was treated successively with phosphorus pentachloride and with ethanolic potash. A solution of 17.4 g. of VIII dissolved in 35 cc. of petroleum ether was dropped into 25 g. of phosphorus pentachloride covered with 35 cc. of petroleum ether with stirring and the mixture was heated at 60°C for thirty hours. The mixture was then poured into ice water, extracted with ether, and ethereal layer was washed with water. After drying over anhyd. sodium sulfate, ether was evaporated and the residue was distilled under a reduced pressure, affording 10.3 g. of an oily substanc b. p. 156–158°C/5 mmHg. The oil was heated with 10% ethanolic potassium hydroxide for fifteen hours, and cooled, and ethanol was evaporated under a reduced pressure. The residue was extracted with ether, and the ethereal layer was washed with water to neutral reaction and dried over anhyd. sodium sulfate.

Distillation of the residue under a reduced pressure gave about 1 g. of V, b. p. 135–140°C/2 mmHg, and a minute amount of IV, b. p. 170–180°C 0.5 mmHg, with a distillation residue of a polymerized substance. V was identified by its infrared spectrum, exhibiting absorption maxima at 1950, 1680, and 850 $cm^{-1}$.

**Formation of 3, 4-Diphenyl-1, 2-butadiene (V) from 3, 4-Diphenyl-1-butyne (IV)**.—**(a) Allenation with Potassium hydroxide**[12].—A solution of 5 g. of IV dissolved in 100 cc. of 99% ethanol was added to a solution of 10 g. of potassium hydroxide dissolved in 10 g. of water with stirring, and the mixture was refluxed for six hours. Then, ethanol was evaporated under a reduced pressure, the residue was extracted with ether, and the ethereal layer was washed with water to neutral reaction. After drying over anhyd. sodium sulfate, the ether was evaporated and the residue was submitted to low-pressure distillation, giving 1 g. of colorless oil, b. p. 135°C/2 mmHg; I. R. $\nu_{max}$ 1950, 1680 and 850 $cm^{-1}$. The rest remained in the flask as a residue.

**(b) Allenation with Liquid Ammonia.**—A solution of 5 g. of IV dissolved in 100 cc. of liquid ammonia in a pressure bottle was allowed to stand overnight, ammonia was allowed to evaporate, and the residue was extracted with ether. After washing with water and drying over anhyd. sodium sulfate, ether was evaporated and the residue was submitted to low-pressure distillation, giving 0.6 g. (12%) of a fraction, b. p. 135°C/2 mmHg, $n_D^{18}$ 1.5992, 2.2 g. of another fraction, b. p. 140–195°C/2 mmHg, and 2 g. of a residue. The fraction b. p. 135°C/2 mmHg is the allene V, identified by its infrared absorptions at 1950, 1680 and 850 $cm^{-1}$. The fraction of b. p. 140–185°C/2 mmHg is a mixture of the allene V and the acetylene IV.

**Ozonolysis of 3, 4-Diphenyl-1, 2-butadiene (V)**.—A solution of 2 g. of V dissolved in 100 cc. of ethyl acetate was cooled to −45°C and treated with ozone (0.021 mol./hr.) for one hour. Evaporation of the solvent from the reaction mixture gave a pale yellow oil, which was decomposed with 5 cc. of water and 20 cc. of 10% aqueous

10) M. Koulkes and I. Marszak, *Bull. soc. chim. France*, **1952**, 556.

11) G. Eglinton and M. C. Whiting, *J. Chem. Soc.*, **1953**, 3055.

12) A. Favorsky, *J. Prakt. Chem.*, **37**, 382 (1888).

sodium hydroxide and further oxidized with 10 cc. of 20% hydrogen peroxide.

On standing in a refrigerator overnight, the mixture gave a pale yellow solid, melting at 54-55.5°C. Yield, 1.2 g. (64%). Recrystallized from petroleum ether, it melted at 55-56°C, and showed no depression of the melting point in admixture with an authentic specimen of desoxybenzoin (VII)[13].

## Summary

The reaction between benzyl chlorides and metal acetylides, prepared from metallic lithium and sodium in liquid ammonia resulted in the formation of new compounds, i. e. 3, 4-diphenyl-1-butyne and 3, 4-diphenyl-1, 2-butadiene. The benzylation of acetylene did not stop at benzylacetylene but another benzyl group was introduced to form 3, 4-diphenyl-1-butyne. 3, 4-Diphenyl-1, 2-butadiene was formed by the isomerisation of the butyne. This isomerisation occurred not only by the action of hot ethanolic potash but also in liquid ammonia at the room temperature. 3, 4-Diphenyl-1, 2-butadiene was readily polymerized by heat.

Infrared absorption spectra were measured by Prof. Kinumaki and his associates of this Institutes and the elementary analyses were made in the Laboratory of Shionogi Drug. Manufg. Co., Ltd. to whom the writers are deeply indebted. Thanks are also due to Miss Koko Miyaoka of this Laboratory for technical help.

*Chemical Research Institute of Non-aqueous Solutions, Tohoku University, Sendai*

13) C. F. H. Allen and W. E. Barker, *Org. Synth.*, **12**, 16 (1932).

# *Hydrogen Exchange and Isotope Effect on the Vinylation of Acetic Acid*

By Noboru YAMADA

(Received November 19, 1956)

## Introduction

As yet few investigations have been made as to the mechanism of the addition of reagent to the carbon triple bond, except that of the hydrogenation of acetylenic hydrocarbons[1]. The present investigation was undertaken to obtain some information about the mechanism of the addition to the triple bond. Vinyl acetate is synthetized by the addition of acetic acid to acetylene. By analogy with the addition of hydrogen halide to olefins it seems likely that the reaction takes place through the following process.

$$\text{(i)}\quad CH{\equiv}CH + H^+ \rightleftarrows CH_2{=}CH^+$$
$$\text{(ii)}\quad CH_2{=}CH^+ + CH_3COO^- \rightarrow CH_2{=}CH{\cdot}OCOCH_3 \qquad (1)$$

The initial step in the addition may be the donation of proton to acetylene by acetic acid to form an intermediate ion, (i), the latter then combining with acetate ion, (ii). This view suggested some ideas to the author, as follows. If (ii) is slow and rate-determining, acetylene may readily exchange its hydrogen with acetic acid in the course of reaction. However, if (i) is the slow step, the hydrogen exchange may hardly take place at all. Under this consideration the experiment of the deuterium exchange between acetylene and acetic acid-*d*, $CH_3COOD$, was undertaken. In the experiment acetylene and acetic acid-*d* were allowed to react in vapor phase with zinc acetate supported on active charcoal as catalyst at 160°C. In the course of reaction the change of deuterium concentration of acetylene was investigated. It appeared also possible to obtain some useful information about the reaction mechanism by the study of isotope effect on the reaction rate. The reaction rate was measured by a static method, and the effect of deuterium substitution on the reaction rate was studied.

## Experimental

**Materials.**—G. R. glacial acetic acid was dried by vacuum distillation over phosphor pentoxide and used without farther treatment. Acetic acid-*d*, $CH_3COOD$, was prepared with acetic anhydrate and heavy water heating at 180°C. The heavy

1) G. C. Bond, "Catalysis," III, Reinhold Publishing Corp., New York, N. Y. (1955), p. 109.

water was obtained from Osaka University by courtesy of Prof. T. Titani and Prof. K. Hirota. The deuterium concentration of acetic acid-*d* was analyzed by burning it on cupric oxide and measuring the density of the water with a pressure sensitive buoy[2]. The deuterium concentration of the acetic acid-*d* was 96.2 atom % in hydroxyl hydrogen.

Acetylene was prepared with calcium carbide and water, and purified by the usual method. Dideuteroacetylene was prepared by the distillation of heavy water over calcium carbide following Lind's method[3]. Mass spectrometric analysis of the dideuteroacetylene showed that 8.1% of $C_2HD$ was present, or 96.0 atom % in total deuterium concentration. The isotope analysis of acetylene was made in the Faculty of Science of Osaka University with the Hitachi MR-B type mass spectrometer.

**Catalysts.**—The zinc acetate catalyst supported on charcoal was prepared as follows. A proper amount of zinc acetate aqueous solution was absorbed into the active charcoal granules, Tsurumi Coal-GVAS, and they were dried at 110°C. Prior to use, the catalyst was evacuated a 170°C. Zinc acetate content of the catalyst used for the exchang experiment was 32% and that used for the isotope effect experiment was 28% in weight respectively.

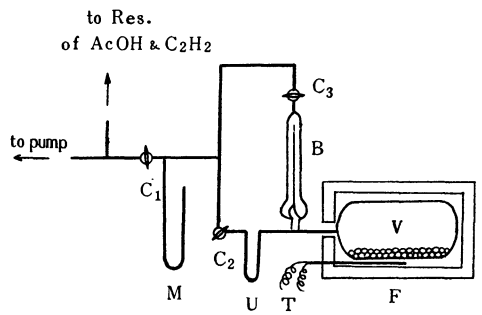



Fig. 1. Apparatus for the study of vinylation of acetic acid.

| | | | |
|---|---|---|---|
| B | Bourdon gauge | M | manometer |
| $C_1$, $C_2$, $C_3$ | stop cocks | T | thermocouple |
| | | U | U tube |
| F | heater | V | reaction vessel |

**Apparatus and Procedure.**—The main part of the apparatus is shown in Fig. 1. The glass reaction vessel, V, in which 18 g. of the catalyst had been contained, was evacuated at 160°C. A requisite amount of acetic acid-*d* was distilled into the U tube, U, in front of the reaction vessel, V, while U was cooled in liquid oxygen. Closing the stopcock, $C_2$, U was then warmed to room temperature, and the acetic acid-*d* was left to be adsorbed in the catalyst completely. Then acetylene was admitted into the reaction vessel through $C_2$. The succeeding pressure change with the reaction in the vessel was observed with the Bourdon gauge, B. The reaction temperature was kept at 160°C in the range of ±0.5°. After a definite time U was recooled in liquid oxygen, and the reaction was stopped. Acetylene was separated from the condensate in U by fractional distillation between −60° and −183°C. Prior to isotope analysis, acetylene was purified by repeated distillation through the traps at −60°C.

## Results

**I. Exchange of deuterium between acetylene and acetic acid-*d*.**—In every run 0.2 cc. of acetic aid-*d* and about half of the equivalent moles of acetylene were admitted into the reaction vessel. The acetylene were admitted into the reaction vessel. The acetic acid-*d* used in this experiment contained 24.4 atom % of deuterium at the hydroxyl hydrogen. The total pressure was about 110 mmHg. at the start of every run. The results are given in Table I. In the fourth column of the table are shown the mole ratios of $C_2HD$ and $C_2H_2$ in the acetylene samples, which were taken out in the course of vinylation by the procedure mentioned above. The formation of $C_2HD$ indicated that the hydrogen exchange between acetylene and acetic acid-*d* occurred in the course of vinylation. As to the exchange rate, however, the reproducibility of the rates was hardly sufficient to make any kinetic analysis, for the observed ratios, $C_2HD/C_2H_2$, were not parallel with reaction time. It appears that the exchange rate increased with reaction time. It appears that the exchange rate increased with repetition of experiment. Some of the runs, which were carried out at 150°C, made no marked difference in the exchange rate to the other

TABLE I
DEUTERIUM EXCHANGE BETWEEN ACETYLENE AND ACETIC ACID-*d*

| Run No. | Temp. (°C) | Reaction time (hr.) | $C_2HD/C_2H_2$ |
|---|---|---|---|
| 1 | 160 | 6 | 0.060 |
| 2 | 〃 | 12 | 0.110 |
| 3 | 〃 | 12 | 0.142 |
| 4 | 〃 | 15 | 0.191 |
| 5 | 〃 | 10.5 | 0.183 |
| 6 | 〃 | 3 | 0.170 |
| 7 | 150 | 3 | 0.182 |
| 8 | 〃 | 12 | 0.172 |
| 9 | 〃 | 6 | 0.162 |
| 10 | 〃 | 9 | 0.134 |
| 11* | 160 | 21 | 0.094 |
| 12* | 〃 | 12 | 0.108 |
| 13* | 〃 | 6 | 0.182 |

* With active charcoal only.

2) T. Okamoto and M. Shindo, *J. Chem. Soc. Japan*, **57**, 9 (1936).
3) S. C. Lind, J. C. Jungers and C. H. Schiflett, *J. Am. Chem. Soc.*, **57**, 1032 (1935).

runs, which were carried out at 160°C. The runs from No. 11 to 13 were carried out with the active charcoal only, which contained no zinc acetate. In these runs no vinyl acetate was produced, but the exchange of deuterium occurred in a rate comparable to the other runs as is shown in Table I. The value of $C_2HD/C_2H_2$ at the exchange equilibrium can be estimated experimentally as about 1.8 from the data in Table I except No. 4, which was carried out under a somewhat different condition.

**II. Deuterium isotope effect.**—The rate of vinylation of acetic acid on the zinc acetate-charcoal catalyst is of the first order with respect to acetylene pressure[4], and in the presence of a definite and larger amount of acetic acid the reaction rate is approximately given by

$$-\frac{dP_a}{dt}=k_1P_a \qquad (2)$$

where $P_a$ is the partial pressure of acetylene at any time $t$ and $k_1$ is the first order rate constant. $P_a$ is calculated approximately as the difference

$$P_a=P-P_b' \qquad (3)$$

where $P$ is the total pressure of the reaction system at the time and $P_b'$ is the adsorption equilibrium pressure of acetic acid before the admission of acetylene, or before the initiation of the reaction with acetylene. It has been assumed that in the beginning of reaction the decrease of acetic acid pressure with the reaction progress may be canceled by the increase of pressure of vinyl acetate produced. $k_1$ can be given by the slope of long $P_a$ curve plotted against time as is shown in Fig. 2, where the results for a typical run are shown. The values of $k_1$ were used as the measure of deuterium isotope effect on the reaction of rate. Under a definite condition $k_1$ of the reaction of heavy acetylene and acetic acic-*d* was compared with that of the reaction of normal acetylene and acetic acid. The results at 160°C are given in Table II. In every run 0.27 cc. of acetic acid-*d* was used, and the initial pressure of acetylene was about 100 mmHg. The

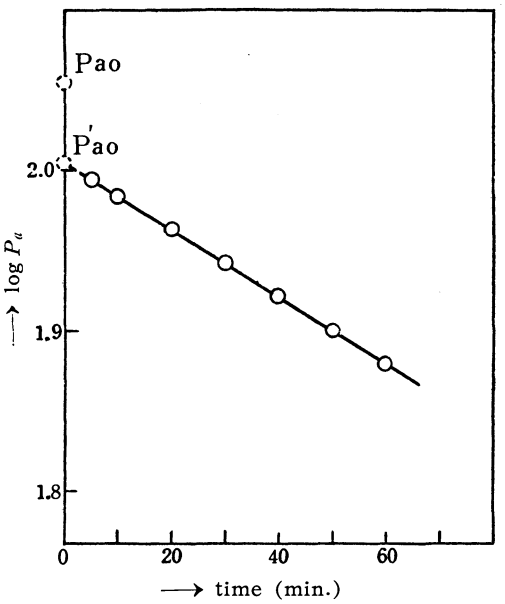



Fig. 2. The reaction rate of vinylation of acetic acid at 160°C.

runs of standard vinylation reaction with normal acetylene and acetic acid were performed before and after each run with the heavy reagents in order to confirm that the catalyst activity was not modified during this experiment. The results showed that the values of $k_1$ of the standard runs were always within $(3.6\pm0.1)\times10^{-3}$ min.$^{-1}$. In Table II the ratios, $k_D/k_H$, given in the fourth column are the ratios of $k_1$ of the reaction between the heavy reactants, of which the deuterium concentrations are given in the first and the second columns, and the $k_1$ of the reaction with the normal reactants. The ratios were always greater than unity and increased with the deuterium concentration of the reactants. The ratio was 1.6 for the reaction of almost wholly deuterated reactants, 96 atom %, at 160°C.

TABLE II

DEUTERIUM ISOTOPE EFFECT ON VINYLATION OF ACETIC ACID AT 160°C.

| Deuterium Conc. atom % | | $k_1\times10$ | $k_D/k_H$ |
|---|---|---|---|
| Acetylene | Acetic acid (in OH) | | |
| 0 | 0 | 3.6 | |
| 41 | 24 | 4.2 | 1.2 |
| 41 | 44 | 4.8 | 1.3 |
| 96 | 96 | 5.8 | 1.6 |

## Discussion

Furukawa and Kozasa[5] investigated this vapor phase synthesis of vinyl acetate at

4) In another report*, it has been shown that the rate of vinylation of acetic acid on zinc acetate-charcoal catalyst is given by

$$-\frac{dp_a}{dt}=k\frac{p_a\,p_b}{(1+Kp_b)^2}$$

where $p_a$ and $p_b$ are the partial pressure of acetylene and that of acetic acid respectively. $k$ is the rate constant and $K$ is the equilibrium constant of adsorption of acetic acid on the catalyst.

* N. Yamada, *J. Chem. Soc. Japan (Pure Chem. Sect.)*, **78**, 252 (1957).

200° to 250°C. They noticed that the reaction rate is of the first order with respect to acetylene pressure and independent of acetic acid pressure. They presumed that the rate-determining step of this reaction is the adsorption of acetylene on the catalyst, and suggested that the reaction proceeds through acetylene-zinc acetate complex as intermediate. The author also studied the kinetics of this reaction at 160°C. Then it was concluded that the rate determining step is not the adsorption of acetylene, but is the reaction on the surface of the catalyst. Now the fact of the hydrogen exchange in the course of vinylation favors the above conclusion. If the adsorption was the slowest step and determined the reaction rate, acetylene would have little chance to exchange its hydrogen with acetic acid on the catalyst.

It has been shown that acetylene exchanges its hydrogen with acetic acid in the course of vinylation. This can be explained by accepting the already proposed mechanism (1) as that of the vinylation, and the step (ii) as the slow step. The hydrogen exchange was also found to occur between acetylene and acetic acid on the active charcoal, when no vinyl acetate was produced. If we assume that the exchange reaction on the charcoal proceeds through the same mechanism as that of the exchange on the zinc acetate catalyst, which has been presumed as (1), then the fact may suggest the following. The step (i) can proceed readily both from left to right and reversely, but the step (ii) cannot proceed so readily without zinc acetate catalyst. This argument makes it more probable that the step (ii) must be the rate-determining step.

We can find a great likeness between (1) and the mechanism of specific acid-catalyzed reaction as

$$\text{(i)}\quad S + H^{\cdot} \rightleftarrows SH^{+} \qquad (4)$$
$$\text{(ii)}\quad SH^{+} \rightarrow \text{product}$$

where S is the substrate. It has been found that most acid-catalyzed reactions proceed more readily in $D_2O$ than in $H_2O$[6]. The isotope effect is caused by the pre-equilibrium (i) of (4). This means that if there is such a pre-equilibrium, the effect of the isotope mass makes the concentration of SD greater than that of SH under comparable conditions. If we find experimentally $k_D > k_H$ in an acid-catalyzed reaction, then an acid-base equilibrium must always be involved in the kinetic scheme. Now it has been found that there is such an isotope effect on vinyl acetate synthetic reaction as $k_D > k_H$.

The isotope effect obtained, $k_D/k_H = 1.6$, is of the same order as those found by other workers for acid-catalyzed reactions, $k_D/k_H = 1.3 \sim 3.0$[6]. It has not yet been fully ascertained whether vinylation reaction of organic acid with zinc acetate catalyst is an acid-catalyzed reaction[7]. However, since in the vinylation one of the reactants is an acid, it is reasonable to suppose that there exists such an acid-base equilibrium as (i) of (1). It should also be noted that usually the addition of reagents to the carbon-carbon triple bond requires a combination of a mercuric salt and a strong acid as catalyst. The fact of the hydrogen exchange between acetylene and acetic acid also favors this consideration. It may be concluded that by analogy to acid-catalyzed reaction the observed deuterium isotope effect supports the mechanism (1) as that of vinylation of acetic acid does.

In the previous papers the author reported the exchange of the acetate group between acetic acid, zinc acetate and vinyl acetate. It was shown that at 150°C acetate group exchange occurred rapidly between acetic acid and zinc acetate[8], but very slowly between acetic acid and vinyl acetate[9], and the exchange was not found between vinyl acetate and zinc acetate[10]. It is presumable that the exchange of the acetate group between acetic acid and zinc acetate proceeds through an intermediate complex as Norris[11] suggested

$$CH_3COOH + Zn(CH_3COO)_2 \rightleftarrows Zn(CH_3COO)_3 \cdot H \qquad (5)$$

In other words the proton of acetic acid may easily transfer to one of the acetate groups of zinc acetate. This may be true also in the vinylation reaction of acetic acid on zinc acetate, and possibly then the transfer of proton from acetic acid to acetylene may also readily occur on the

5) J. Furukawa, H. Kozasa and S. Yamashita, *Chem. High Polymers* (Japan), **9**, 240 (1952).

6) K. B. Wiberg, *Chem. Rev.*, **55**, 718 (1955); R. P. Bell, "Advances in Catalysis," IV. Academic Press Inc. New York, N. Y. (1952), p. 184.

7) S. Otsuka, Y. Matumoto and S. Murahashi, *J. Chem. Soc. Japan (Pure Chem. Sect.)*, **75**, 798 (1954); S. Otsuka, ibid., **75**, 1115 (1954).

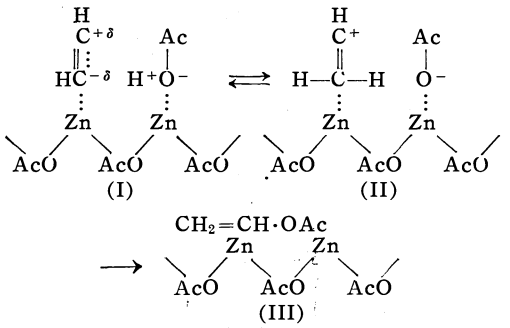
8) N. Yamada K. Suma and T. Takeuchi, ibid., **74**, 1018 (1953).

9) N. Yamada, T. Inokuchi and T. Takeuchi, ibid., **75**, 977 (1954).

10) N. Yamada, T. Inokuchi and T. Takeuchi, ibid., **75**, 1093 (1954).

11) E. A. Evance, J. L. Huston and T. H. Norris, *J. Am. Chem. Soc.*, **74**, 4985 (1952).

catalyst surface. This consideration leads to the more comprehensive picture of the reaction mechanism as shown below



The kinetic study of this reaction[4] supports the mechanism of Hinshelwood type. That is to say, the reaction takes place between the acetylene molecules and the acetic acid molecules adsorbed on adjacent active points of the catalyst, presumably on adjacent zinc atoms. Acetylene an acetic acid may be linked to a zinc atom on the catalyst surface by coordination. It may result in electronic polarization of their molecules as (I) shows. The proton transfer may occur from acetic acid to the acetate ion of zinc acetate (acetate group exchange), or to acetylene (hydrogen exchange and vinylation). The step from (II) to (III) may be irreversible, for the acetate group exchange between vinyl acetate and zinc acetate was not found. As it has been mentioned, hydrogen exchange and isotope effect on the vinylation reaction of acetic acid indicate that the step (I)-(II) should be in pre-equilibrium and the step (II)-(III) should be the rate-determining step.

## Summary

The mechanism of vinylation reaction of acetic acid was studied by the use of deuterium. The exchange of deuterium was found to occur between acetylene and acetic acid-*d* on zinc acetate-charcoal catalyst. The deuterium isotope effect of the reaction rate was also found, and the rate ratio, $k_D/k_H$, was 1.6 at 160°C. A mechanism of the reaction which contains a pre-equilibrium of intermediate ion formation, $CH{\equiv}CH + H \rightleftarrows CH_2{=}CH$ , $CH_2{=}CH + CH_3COO^- \rightarrow CH_2{=}CH{\cdot}OCOCH_3$, was proposed and discussed.

The author wishes to express his sincere gratitude to Prof. T. Titani and Prof. K. Hirota of Osaka University, and also to Prof. T. Takeuchi of Toyama University for their invaluable help and encouragement during the course of this work. The author is indebted to Mr. Y. Kobayashi of Osaka University for mass spectrometric analysis.

*Faculty of Literature and Sience*
*Toyama University, Toyama*

# *Studies on Antibiotics and Related Substances. V. Synthesis of 5-Methylenecyclopentanone-3-carboxylic Acid, an Antitumor Isomer of Sarkomycin**

By Sumio UMEZAWA and Mitsuhiro KINOSHITA

(Received December 15, 1956)

Recently, H. Umezawa and coworkers[1] obtained an antitumor substance, sarkomycin, from the fermentation broth of a *Streptomyces* similar to *S. erythrochromogenes*. Sarkomycin has not been isolated in a pure state, but Hooper et al.[2] reported that the main active principle is 2-methylenecyclopentanone-3-carboxylic acid. Therefore, it became interesting to synthesize analogues of methylenecyclopentanone-3-carboxylic acid. A brief communication[3]

* Presented before the Monthly Meeting of the Japan Antibiotic Research Association, at the Institute of Infectious Diseases, Tokyo, November 29, 1956.

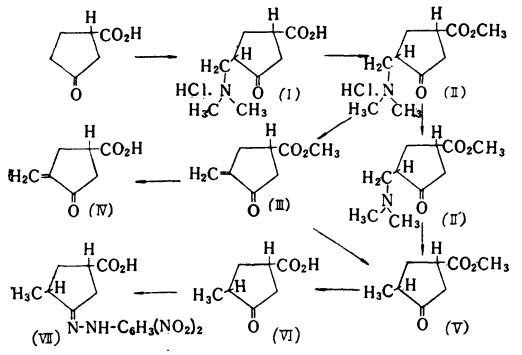
1) H. Umezawa, T. Yamamoto, T. Takeuchi, T. Osato, Y. Okami, S. Yamaoka, T. Okuda, K. Nitta, K. Yagishita, R. Utahara and S. Umezawa, *Antibiotics and Chemotherapy*, **4**, 514 (1954).

2) I. R. Hooper, L. C. Cheney, M. J. Cron, O. B. Fardig, D. A. Johnson, D. L. Johnson. F. M. Palermiti, H. Schmitz and W. B. Wheatley, ibid., **5**, 585 (1955).

3) S. Umezawa and M. Kinoshita, *J. Antibiotics, Ser. A*, **IX**, 194 (1956).

has been given of the synthesis of an isomer of sarkomycin, 5-methylene-cyclopentanone-3-carboxylic acid which showed significant antitumor and antibacterial activities.

In the present paper, we report a more detailed study of the 5-methylene derivative and related compounds.



A mixture of cyclopentanone-3-carboxylic acid[4], paraformaldehyde, and dimethylamine hydrochloride, was fused to give 23% yield of 5-(dimethylaminomethyl)cyclopentanone-3-carboxylic acid hydrochloride (I), a Mannich base hydrochloride, m. p. 147–148°C (dec.). A common procedure with aqueous formaldehyde, dimethylamine hydrochloride, and cyclopentanone-3-carboxylic acid, gave also I. Esterification of I by the Fischer-Speier method with methanol gave methyl 5-(dimethylaminomethyl)cyclopentanone-3-carboxylate hydrochloride (II), m. p. 143–143.5°C (dec.), in 89% yield.

Degradation of the ester-hydrochloride (II) by vacuum distillation afforded a 76% yield of methyl 5-methylenecyclopentanone-3-carboxylate (III), m. p. 24–27°C, which, on standing in the absence of polymerization inhibitor, polymerized gradually.

Mild hydrolysis of III with dilute sulfuric acid in the presence of hydroquinone as an inhibitor followed by extraction with ethyl acetate and evaporation of the solvent in vacuo gave a crude product of 5-methylenecyclopentanone-3-carboxylic acid (IV), an almost colorless liquid, in 83% yield. After purification, IV was obtained as colorless needles melting at 67—74°C.

Structural proof of IV was obtained by hydrogenation of III with platinum catalyst in methanol solution to give 77% yield of methyl 5-methylcyclopentanone-3-carboxylate (V), b. p. 89–95°C (3 mmHg). Hydrolysis of V with dilute sodium hydroxide solution gave 5-methylcyclopentanone-3-carboxylic acid (VI) of b. p. 125–130°C (0.3 mmHg), which, by treatment with 2,4-dinitrophenylhydrazine, gave 2,4-dinitrophenylhydrazone (VII), m. p. 141–143°C, which did not depress the melting point of the authentic sample of the 2,4-dinitrophenylhydrazone of 5-methylcyclopentanone-3-carboxylic acid which was prepared by the synthetic route of Hope and Perkin[5].

Ozonolysis of methyl 5-methylenecyclopentanone-3-carboxylate (III) and of 5-methylenecyclopentanone-3-carboxylic acid (IV) gave formaldehyde (isolated as the methone derivative) as one of the products. This established the presence of the exomethylene group in III and IV, and thus the position of the double bond which was lost when III was hydrogenated to give methyl 5-methylcyclopentanone-3-carboxylate (V).

Moreover, catalytic hydrogenolysis of methyl 5-(dimethylaminomethyl)cyclopentanone-3-carboxylate (II′), b. p. 78–85°C (0.1 mmHg), which was obtained from II by treatment with dry ammonia in chloroform followed by filtration to remove ammonium chloride and finally by vacuum distillation, afforded the methyl 5-methylcyclopentanone-3-carboxylate (V), which was again led to 2,4-dinitrophenylhydrazone (m. p. 141–143°C) of 5-methylcyclopentanone-3-carboxylic acid (VI).

The infrared absorption characteristics (Fig. 1) of 5-methylenecyclopentanone-3-carboxylic acid (IV) were those typical of sarkomycin. The absorption at 6.09 $\mu$ was the evidence of a carbon-carbon double bond. The conjugated carbonyl absorption was found at 5.84 $\mu$.

The ultraviolet absorption (Fig. 2, curve A) of IV in methanol solution showed a peak at 231 m$\mu$ suggesting an $\alpha$, $\beta$-unsaturated ketone. The ultraviolet absorption (Fig. 2, curve B) of 5-methylcyclopentanone-3-carboxylic acid (VI) in methanol was

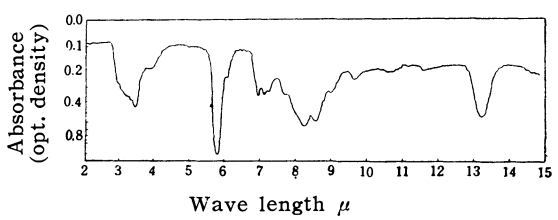



Fig. 1. Infrared absorption spectrum of 5-methylenecyclopentanone-3-carboxylic acid (Nujol)

4) F. W. Kay and W. H. Perkin, Jr., *J. Chem. Soc.*, **1906**, 1646.

5) E. Hope and W.H. Perkin, ibid., **1911**, 762.

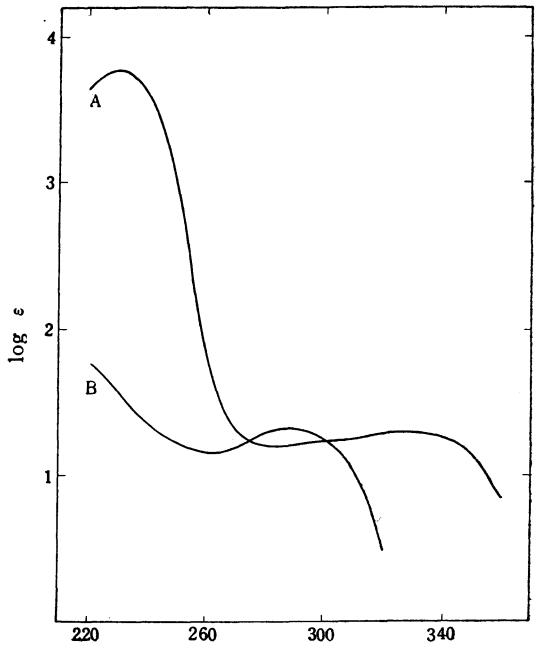



Fig. 2. Ultraviolet absorption spectra of 5-methylenecyclopentanone-3-carboxylic acid (IV, Curve A) and 5-methylcyclopentanone-3-carboxylic acid (VI, Curve B) in absolute methanol.

characterized by a carbonyl band near 285 mμ.

On treatment with methyl iodide, II' afforded in a quantitative yield a crystalline methiodide (VIII), m. p. 213°C (dec., sintered at 145°C.). However, the Hofmann degradation of VIII to obtain methylene derivative was unsuccessful.

## Experimental

**5-(Dimethylaminomethyl)cyclopentanone-3-carboxylic Acid Hydrochloride (I).**—Cyclopentanone-3-carboxylic acid prepared by the route of Kay and Perkin[4] was condensed with formaldehyde and dimethylamine hydrochloride by the Mannich reaction.

**Procedure A.**—A mixture of 5.0 g. of cyclopentanone-3-carboxylic acid and 3.2 g. of dimethylamine hydrochloride was warmed on a water bath. To the resulting melt was added 1.18 g. of paraformaldehyde and then the mixture was stirred at 75-80°C for three hours and then evaporated under reduced pressure. The resulting syrup was dissolved in 10 cc. of hot absolute ethanol and a small amount of insoluble solid was removed by filtration. The solution was allowed to stand overnight in a refrigerator to separate the crystalline hydrochloride of Mannich base, which was collected, washed with absolute ethanol, and dried. M. p. 136-138°C (dec.). Yield, 2 g. (23%). Two recrystallizations from methanol afforded an analytical sample, m. p. 147-148°C (dec.), as a colorless prisms.

*Anal.* Found: C, 48.51; H, 6.91; N, 6.14. Calcd. for $C_9H_{16}O_3NCl$: C, 48.80; H, 7.22; N, 6.32%.

**Procedure B.**—A mixture of 2.0 g. of cyclopentanone-3-carboxylic acid, 1.2 cc. of aqueous 39% formaldehyde, and 1.27 g. of dimethylamine hydrochloride, was warmed at 75°C for four hours. The initial odour of formaldehyde disappeared. The resulting clear solution was evaporated under reduced pressure to give a viscous, pale-yellow oil, which was redissolved in 10 cc. of absolute ethanol by gentle warming and allowed to crystallize overnight in a refrigerator. The yield of crude crystals was 0.8 g.. On recrystallization from absolute methanol, an analytical sample of 5-(dimethylaminomethyl)cyclopentanone-3-carboxylic acid hydrochloride of m. p. 146-147°C (dec.) was obtained. Yield, 500 mg. (14%). When mixed with a sample prepared by procedure A described above, the melting point was unchanged.

**Methyl 5-(dimethylaminomethyl)cyclopentanone-3-carboxylate Hydrochloride (II).**—A mixture of 1.7 g. of 5-(dimethylaminomethyl)cyclopentanone-3-carboxylic acid hydrochloride (I) and 80 cc. of absolute methanol was saturated with dry hydrogen chloride and allowed to stand overnight. The methanol was removed by distillation at about 40°C under reduced pressure and the residue was dried in a desiccator. The resulting crystals were dissolved in a small quantity of methanol by gentle warming and the solution was diluted with absolute ether, whereupon there separated a crystalline precipitate of methyl 5-(dimethylaminomethyl)cyclopentanone-3-carboxylate hydrochloride, m. p. 138-140°C (dec.). Yield 1.6 g.. The crude crystals were redissolved in absolute methanol containing hydrogen chloride and recrystallization by addition of absolute ether gave colorless needles melting at 143-143.5°C (dec.).

*Anal.* Found: C, 50.84; H, 7.29; N, 5.80. Calcd. for $C_{10}H_{18}O_3NCl$; C, 50.95; H, 7.64; N, 5.95%.

**Methyl 5-Methylenecyclopentanone-3-carboxylate (III).**—A sample of 0.7 g. of methyl 5-(dimethylaminomethyl)cyclopentanone-3-carboxylate hydrochloride (II) was placed in a small round-bottom flask and heated at 145-150°C in an oil bath under highly reduced pressure (0.005 mmHg). Colorless crystals of methyl 5-methylenecyclopentanone-3-carboxylate were obtained in a receiver cooled in a dry ice- acetone bath. M. p. 24-27°C. Yield, 0.35 g. (76%). On standing at room temperature in the absence of polymerization inhibitor, this compound gradually polymerized and became less soluble in methanol or ethanol. The fresh product decolorized bromine in carbon tetrachloride rapidly.

*Anal.* Found: C, 62.34; H, 6.21. Calcd. for $C_8H_{10}O_3$: C, 62.32; H, 6.54%.

**Ozonolysis of III.**—A solution of 226 mg. of freshly prepared methyl 5-methylenecyclopentanone-3-carboxylate (III) in 10 cc. of ethyl acetate was treated with an approximately 2% by weight

ozone-oxygen mixture at 0°C at a rate of 500 cc. per minute for nineteen minutes. To the resulting pale-yellow solution was added 10 cc. of water and 300 mg. of zinc dust. The mixture was refluxed on a steam bath for thirty minutes. The reaction mixture was filtered while hot into a solution of 300 mg. of methone in 10 cc. of ethanol. Dilution with 20 cc. of water afforded needles, m. p. 186–187°C. Yield, 135 mg. (31%). Recrystallization from 80% ethanol gave pure crystals melting at 187–189°C. The melting point was undepressed on admixture with an authentic sample of formaldehyde methone of m. p. 189–190°C.

**5-Methylenecyclopentanone-3-carboxylic Acid (IV).**—A mixture of 997 mg. of freshly prepared methyl 5-methylenecyclopentanone-3-carboxylate (III), 20 cc. of 1.5 N sulfuric acid, and 3 mg. of hydroquinone (as an inhibitor), was stirred at 25–27°C for three hours to give a clear solution, which was adjusted to pH 2.0 with a saturated solution of sodium bicarbonate and extracted with three 10 cc. portions of ethyl acetate. After the extract had been dried over sodium sulfate, the ethyl acetate was removed by distillation under reduced pressure at 30–35°C to yield 5-methylenecyclopentanone-3-carboxylic acid, a pale-yellow liquid. Yield, 751, mg. (83%). On standing at room temperature in the absence of an inhibitor, this compound polymerized and gradually decreased in the antibacterial activity.

A freshly prepared sample of IV was dissolved in a small quantity of water, neutralized with sodium bicarbonate, and washed with ethyl acetate. Acidification and extraction with ethyl acetate followed by evaporation of the solvent in vacuo yielded colorless needles of IV melting at 67–74°C.

*Anal.* Found: C, 59.60; H, 5.81. Calcd. for $C_7H_8O_3$: C, 59.99; H, 5.75%.

The infrared spectrum (Fig. 1) of purified 5-methylenecyclo- pentanone-3-carboxylic acid (IV) in Nujol showed a peak at 6.09$\mu$ which is characteristic of the exocyclic methylene group in sarkomycin and had a conjugated carbonyl band at 5.84$\mu$.

The ultraviolet spectrum (Fig. 2) of IV in methanol showed the presence of $\alpha$, $\beta$-unsaturated ketone at 231 m$\mu$ (log. $\varepsilon$ 3.76).

**Ozonolysis of IV.**—A solution of 200 mg. of freshly prepared 5-methylenecyclopentanone-3-carboxylic acid in 10 cc. of ethyl acetate was treated with ozone just as described in the ozonolysis of III. The yield of formaldehyde methone of m. p. 187–189°C was 113 mg. (28%). A mixed melting point determination carried out with an authentic sample of formaldehyde methone showed no change.

**Hydrogenation of Methyl 5-Methylenecyclopentanone-3-carboxylate (III) to Methyl 5-Methylcyclopentanone-3-carboxylate (V).**—A solution of 335 mg. of freshly prepared methyl 5-methylenecyclopentanone-3-carboxylate (III) in 2.5 cc. of methanol was shaken with 30 mg. of platinum oxide and hydrogen; 59 cc. (32.2°C, 754 mm.) of hydrogen was absorbed in fifteen minutes. After filtration, the filtrate was concentrated under reduced pressure to give a pale-yellow liquid. Fractional distillation in vacuo gave 260mg. (77%) of methylcyclopentanone-3-carboxylate of b. p. (bath temp.) 89–95°C (3 mm.).

**5-Methylcyclopentanone-3-carboxylic Acid (VI).**—A mixture of 558 mg. of methyl 5-methylcyclopentanone-3-carboxylate (V) in 1.5 cc. of 10% sodium hydroxide solution was stirred at room temperature for one hour. The resulting solution was acidified to pH 2.6 by addition of 1.5 N sulfuric acid, saturated with ammonium sulfate, and then extracted with ether. After the extract was dried over sodium sulfate, the ether was removed by distillation. Fractional distillation of the residue in vacuo gave a viscous liquid of 5-methylcyclopentanone-3-carboxylic acid, b. p. (bath temp.) 125–130°C (0.3 mm.). Yield, 340 mg. (66.8%). The 2,4-dinitrophenylhydrazone (VII) prepared by the general procedure melted at 141–143°C and did not depress the melting point of the authentic sample of the 2,4-dinitrophenylhydrazone of the 5-methylcyclopentanone-3-carboxylic acid which was prepared by the synthetic route of Hope and Perkin.[5]

**Methyl 5-(Dimethylaminomethyl)cyclopentanone-3-carboxylate (II').**—To a mixture of 710 mg. of methyl 5-(dimethylaminomethyl) cyclopentanone-3-carboxylate hydrochloride (II) and 5 cc. of chloroform was added 2.46 cc. of 1.23 N ammonia-chloroform solution, whereupon ammonium chloride immediately precipitated. The chloroform-layer containing the free ester-amine was separated and concentrated under reduced pressure. The oily residue was distilled in vacuo to give methyl 5-(dimethylaminomethyl)cyclopentanone-3-carboxylate, b. p. (bath temp.) 78–85°C (0.1 mmHg). Yield, 135 mg. The product had a weak smell of amine and was insoluble in water, soluble in dilute hydrochloric acid.

The reaction of II' with an excess of methyl iodide was exothermic and immediately afforded a crystalline methiodide (VIII) melting at 213°C (dec., sintered at 145°C) in a quantitative yield.

*Anal.* Found: N, 3.91 Calcd. for $C_{11}H_{20}O_3NI$: N, 4.11%.

However, the Hofmann degradation of VIII to obtain the methylene derivative was unsuccessful.

**Hydrogenolysis of Methyl 5-(Dimethylaminomethyl)cyclopentanone-3-carboxylate (II).**—A solution of 135 mg. of II' in 1.5 cc. of methanol was shaken with 15 mg. of platinum oxide and hydrogen; 25 cc. (26°C, 754.4 mmHg) of hydrogen was absorbed in twenty minutes. After filtration, the filtrate was concentrated under reduced pressure to give a crude product of methyl 5-methylcyclopentanone-3-carboxylate (IV), a fragrant, liquid. Yield, 95 mg..

The whole quantity of the crude product was hydrolyzed with 10% sodium hydroxide solution at room temperature and the after-treatment was carried out just as described above in the hydrolysis of V. A crude product of 5-methylcyclopentanone-3-carboxylic acid was obtained. Yield, 45 mg.. This was converted to the 2,4-dinitrophenylhydrazone, m. p. 139–142°C, which did not

depress the melting point of the authentic sample of 2,4-dinitrophenylhydrazone of VI.

**Bioassays.**—preliminary results have indicated that 5-methylenecyclopentanone-3-carboxylic acid (IV) possesses a potency of 12 units/mg. (in terms of sarkomycin potency) against *Staph. aureus* 209-P and about six times the potency against *Micrococcus flavus*. Methyl 5-methylenecyclopentanone-3-carboxylate (III) showed also a potency of 9.88 units/mg. (in 10% ethanol solution) against *S. aureus* 209-P and 11.2 units/mg. against *M. flavus*.

It is very interesting to find that IV possesses strong antitumor activities[6]. The minimum necessary concentration of IV for the anti-HeLa-cell effect was 5 mcg./cc.. Against cells of Ehrlich carcinoma, IV had a potency of 7.4 units/mg. (in terms of sarkomycin potency) by the cylinder plate method.[7] The daily intraperitoneal injection of 0.317 mg. of IV inhibited the ascites increase and prolonged the survival period of mice bearing ascites type of Ehrlich carcinoma by intraperitoneal route.

A detailed report on the biological activities of III and IV will be published elswhere.

6) Private communication from Prof. H. Umezawa of National Institute of Health, Tokyo.

7) S. Yamazaki, K. Nitta, T. Hikiji, M. Nogi, T.Takeuchi, T. Yamamoto and H. Umezawa, *J. Antibiotics*, **IX**, 135 (1956).

We are indebted to Prof. H. Umezawa, National Institute of Health, Tokyo, for antitumor assays.

## Summary

1) 5-(Dimethylaminomethyl)cyclopentanone-3-carboxylic acid hydrochloride (I) has been synthesized from cyclopentanone-3-carboxylic acid by means of the Mannich reaction.

2) Methyl 5-(dimethylaminomethyl) cyclopentanone-3-carboxylate hydrochloride (II) has been degraded to give methyl 5-methylenecyclopentanone-3-carboxylate (III), which has been hydrolyzed into 5-methylenecyclopentanone-3-carboxylic acid (IV), an isomer of sarkomycin.

3) The structures of III and IV have been proven.

4) It has been found that III possesses significant antitumor and antibacterial activities and IV shows also antibacterial activities.

*Department of Applied Chemistry*
*Engineering Faculty of*
*Keio University, Tokyo*

# *Effects of Mercerization on the Lateral Order Distribution of Cellulose**

By Yoshizo TSUDA and Sadataka MUKOYAMA

(Received November 24, 1956)

## Introduction

In a previous paper[1] the authors have concluded that the fractional dissolution in sodium hydroxide solutions of various concentrations after methanolysis is the best method to obtain the lateral order distribution of cellulose. It is the purpose of the present paper to study the transition phenomena in the mercerization process using this method.

A number of investigators have studied the transition behavior in the mercerization process using the x-ray diffraction measurements[2], the moisture regain measurements[2,3] and the limit D. P. measurements[4].

In the mercerization process the phase transition of cellulose I into cellulose II accompanies a considerable decrystallization, which might have induced the discrepancy in the transition intervals observed with various measurements. So it is important to know the changes in the lateral order distribution in the mercerization process. In the present study this change was investigated with cotton linters pulp which shows a considerable change in the lateral order distribution.

1) Y. Tsuda and S. Mukoyama, This Bulletin, **29**, 748 (1956).
2) B.G. Rånby and H.F. Mark, *Svensk Papperstidning*, **10**, 374 (1955).
3) B. G. Rånby, *Acta Chem. Scand.*, **6**, 101 (1952).
4) L. Jörgensen and E. Ribi, *Nature*, **166**, 148 (1950).
* The main part of this paper was presented at the 9th Annual Meeting of the Chemical Society of Japan in April, 1956, Kyoto.

### Experimental Procedure

**a. Treatment with Sodium Hydroxide Solutions.**— The pulp samples (1 g, powdered and bone-dried) were soaked at 20°C in 50 ml. of sodium hydroxide solutions for two hours. The pulps were recovered by suction on glass filter, washed with distilled water, N/2 acetic acid and distilled water again until they became acid-free. The samples were dried from alcohol.

**b. Lateral Order Distribution.**—The same method as described in the previous paper[1] was used.

**c. Cellulosic Samples.** — Cotton linters pulp and sulfite and sulfate wood pulps, the same samples as used in the previous study. BX yarn[5], a regenerated cellulose fibre of the highest lateral order among regenerated cellulose fibres[6].

## Experimental Results and Discussion

### Comparison of Lateral Order Distributions between Native and Mercerized Celluloses

In the previous paper it was shown that the lateral order distribution of cotton linters pulp is at higher order compared with wood pulps. But this difference is not observed between mercerized samples as shown in Fig. 1 and Fig. 2, at which the summative mass-order curves and lateral order distributions of both native and mercerized celluloses are shown. The distributions themselves become broad as a result of mercerization, and lower ordered portions of distributions increase. With regard to wood pulps the decrystallization accompanied by mercerization is characterized in the increase of lower ordered regions and the broadening of distributions, without appreciable changes in the lateral order of main ordered regions. However, mercerized cotton linters pulp has a similar distribution to that of wood pulp and thus the linters pulp loses its characteristic higher order after mercerization. These results mean that all of the mercerized celluloses exhibit the same lateral order distribution whatever their native origins may be. In order to compare them with regenerated cellulose fibres the lateral order distribution curve of BX yarn is also shown in Fig. 2. The lateral order of BX fibre, which is a regenerated cellulose fibre of the highest order is still lower than those of mercerized pulps, and the distribution of the former is broader than those of the latters. Therefore it will be concluded that the lateral order of regenerated cellulose is necessarily lower compared with that of native cellulose.

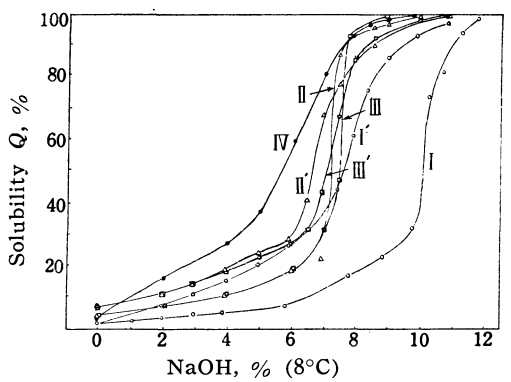



Fig. 1. Solubility curves of methanolyzed linters and sulfite and sulfate wood pulps both native and mercerized and methanolized BX yarn.
(I) native linters pulp
(I') mercerized linters pulp
(II) native sulfite wood pulp
(II') mercerized sulfite wood pulp
(III) native sulfate wood pulp
(III') mercerized sulfate wood pulp
(IV) BX yarn

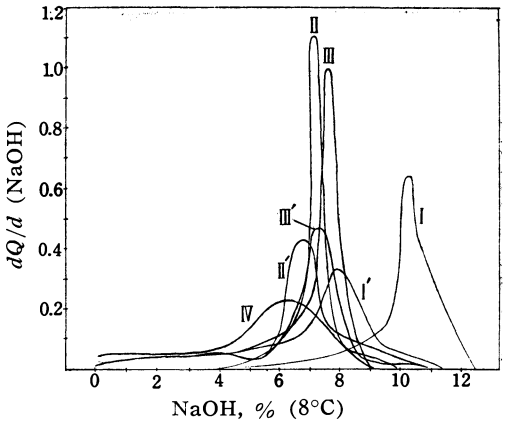



Fig. 2. Lateral order distribution curves of cotton linters and sulfite and sulfate wood pulps both native and mercerized and BX yarn.
(I) native linters pulp
(I') mercerized linters pulp
(II) native sulfite wood pulp
(II') mercerized sulfite wood pulp
(III) native sulfate wood pulp
(III') mercerized sulfate wood pulp
(IV) BX yarn

### Variation of Lateral Order Distribution in the Process of Mercerization

As shown in Fig. 1 and Fig. 2, there is a remarkable variation of lateral order in the mercerization process with regard to

5) N. Drisch and L. Soep, *Text. Res. J.*, **23**, 513 (1953).
6) S. Mukoyama, *J. Soc. Textile Cellulose Ind.*,(Japan). **12**, 772 (1955).

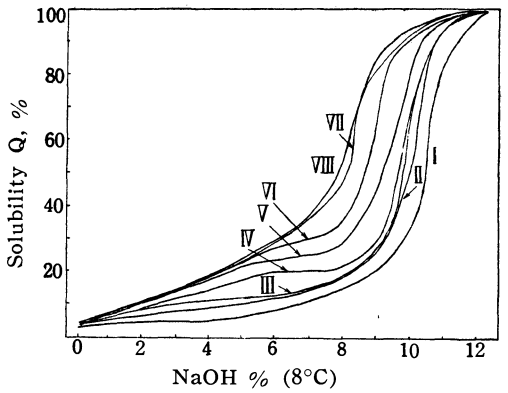



Fig. 3. Solubility curves of methanolized linters pulp pretreated with NaOH of following concentrations;
(I) original (II) 10% (III) 11% (IV) 12% (V) 13% (VI) 14% (VII) 15% (VIII) 17.5%

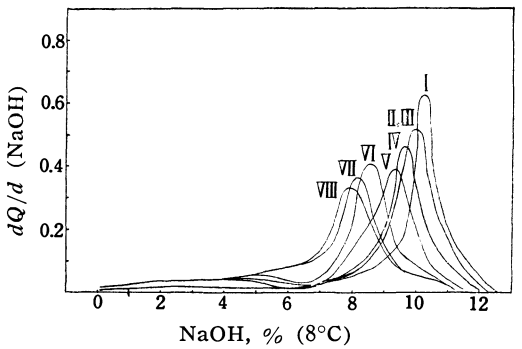



Fig. 4. Lateral order distribution curves of cotton linters pulp pretreated with NaOH of following concentrations.
(I) original (II) 10% (III) 11% (IV) 12% (V) 13% (VI) 14% (VII) 15% (VIII) 17.5%

cotton linters pulp but no appreciable variations with regard to wood pulps. Consequently as the sample for this study, cotton linters pulp was chosen. In Fig. 3 and Fig. 4 lateral order distributions of samples pretreated with sodium hydroxide solutions of various concentrations are shown. At 20°C no appreciable variation in distribution is observed up to the treatment with 10% NaOH solution. Up to the treatment with 13% NaOH solution no appreciable variations are observed in the lateral order of peak of distribution, but a successive broadening of the distribution toward the lower ordered portion can be observed with each treatment. It will be apparent in Fig. 3 and Fig. 4 that the main variation of lateral order distribution in the process of mercerization is induced by the treatment with NaOH solutions of the concentration of 13–15% at 20°C. This concentration interval of sodium hydroxide coincides with the interval which is necessary to induce phase transition. Thus the main variation of lateral order distribution is accompanied by the treatment with NaOH solutions of the concentration necessary to induce phase transition.

Here it will be possible to consider that the so-called decrystallization does not correspond to the lowering of the lateral order of the main highly ordered region but to the increase in the less highly ordered region. If these views are accepted, it will be concluded that the decrystallization is induced by the treatment with NaOH of lower concentration than that required to induce phase transition. This conclusion is consistent with the results obtained in the x-ray diffraction study as discussed in the previous paper[1].

## Summary

Lateral order distributions of native and mercerized celluloses were compared and then the variation of distribution in the process of mercerization was investigated. It was concluded that mercerization generally induces broadening of distribution, and cotton linters pulp shows almost the same lateral order distribution after mercerization as those of wood pulps. The authors are grateful to Dr. K. Hoshino for permitting this publication.

*Research Department of*
*Toyo Rayon Co., Ltd.*
*Otsu, Shiga-ken*

# *Mikroanalyse mit Hilfe von Ionenaustauscherharzen. XII. Über den Nachweis in Tausendstelgammamenge vorhandenen Nickels mit Rubeanwasserstoffsäure*[1]

Von Masatoshi FUJIMOTO

(Eingegangen am 2. November, 1956)

## Einleitung

Zur qualitativen Mikroanalyse von den Ultramikroproben wie kosmischen Stauben, ist es wünschenswert, die möglichst empfindlichen Nachweismethoden anzuwenden, mit denen man selbst Tausendstelgammastoffmengen leicht prüfen kann.

In einer Reihe nachfolgender Mitteilungen unternimmt der Verfasser, mit den wohlbekannten, empfindlichen Reaktionen noch weit empfindlichere Nachweismethoden festzustellen.

In vorliegender Arbeit wurde in erster Linie eine ausserordentlich empfindliche Nachweismethode für Spurmenge des Nickels mit der Rubeanwasserstoffsäure (Dithioxamid)[2], durch Anwendung der farblosen und starksauren Kationenaustauscherharze festgestellt. Diese Methode beruht auf der Niederschlagbildung an der Grenzflächen zwischen Harz- und Lösungsphase, wie der Verfasser schon darüber genau mitgeteilt hat[3,4]. Die in der Probelösung vorhandenen Nickelionen lassen sich vorher als komplexe Hexaminkationen in die Kationenaustauscherharzphase sehr stark adsorbieren[5], und durch Zusatz der Rubeanwasserstoffsäurelösung entsteht ein dichter intensiv blauvioletter Niederschlag von Nickelkomplexe des Reagens gerade an der Grenzfläche zweier Phasen*[1], wobei sich infolgedessen die Reaktionsempfindlichkeit bemerkenswert erhöht.

Man kann auch die Begleitionen wie Kupfer(II) oder Kobalt(II), die auch gleichfalls mit dem genannten Reagens die stark sich färbenden stabilen Chelatverbindungen bilden und infolgedessen den gegenwärtigen Nachweis stark stören, durch Anwendung der Mikrosäule[6] starkbasischen Anionenaustauscherharzes aus einer stark salzsauren Lösung als Chlorkomplexanionen[7] vollkommen beseitigen.

### Die in der gegenwärtigen Untersuchung benutzten Kationenaustauscherharze

Vier Arten farbloser und starksaurer Kationenaustauscherharze von verschiedenen Vernetzungsgraden, „1proz. DVB", „2.5proz. DVB", Dowex 50W-X8 und „20proz. DVB", und ein weisses und schwachsaures Harz, Amberlite IRC-50, wurden in der HR-Form angewandt[8].

### Versuchsanordnung

Man versetzt auf einer weissen Tüpfelplatte einige Körnchen des farblosen Kationenaustauscherharzes mit je einem Tropfen der Probelösung und des Ammoniakwassers, und lässt sie eine Weile stehen. Dann fügt man dazu einen Tropfen verdünnter alkoholischer Lösung der Rubeanwasserstoffsäure und lässt sie nochmals einige Minuten stehen. Selbst bei Anwesenheit von Spurmenge des Nickels entsteht eine deutliche Violett- bzw. Violettblaufärbung, wenn die Probelösung keine Kupfer- und Kobaltsalze enthält*[2].

### Massflüssigkeit und Reagenzien

**1. Massflüssigkeit.**—Aus derselben Stammlösung wie der in vorhergehender Mitteilung[1] wurde eine Reihe der Massflüssigkeit des Nickels durch Verdünnung mit 0.01 N Salzsäure hergestellt. Alle folgenden Untersuchungen über die besten Experimentalbedingungen wurden mit einer 0.01 N-salzsauren Lösung ausgeführt, deren 1 ccm genau 2.60 $\gamma$ von Nickel enthielt.

**2. Reagenzien.**— (1) Alkoholische Stammlösung der Rubeanwasserstoffsäure: Man zerreibt

1) Die elfte Mitteilung: M. Fujimoto, Dieses Bulletin, **30**. 93 (1954).
2) Vgl. F. Feigl, „Spot Tests. I. Inorganic Applications," übersetzt von R. E. Oesper, 4. engl. Aufl., Amsterdam (1954), S. 145.
3) M. Fujimoto, Dieses Bulletin, **29**, 646 (1956).
4) M. Fujimoto, Dieses Bulletin, **30**, 87 (1957).
5) M. Honda, *Japan Analyst*. **3**, 132 (1954).
*1 Das Reagens wird von starkbasischen Anionenaustauscherharzen stark adsorbiert, aber diese waren hier nicht gut anzuwenden, denn nicht nur die stark gelbe Färbung der das Reagens adsorbierenden Harzkörnchen macht die Unterscheidbarkeit der Reaktion sehr schwierig, sondern auch der Niederschlag entsteht, statt an der Grenzfläche, anscheinend nur in der ganzen Lösungsphase.

6) M. Fujimoto, Dieses Bulletin, **29**, 595 (1956).
7) K. A. Kraus und G. E Moore, *J. Am. Chem. Soc.*, **75**, 1460 (1953).
8) M. Fujimoto, Dieses Bulletin, **29**, 600 (1956).
*2 Über die Trennung dieser störenden Kationen, vergleiche S. 277 ff.

gründlich 0.1 g von Kristallchen der extrareinen Rubeanwasserstoffsäure („Wako" zur Analyse) mit einem Glasstab, und erwarmt sie dann mit 20ccm von 99prozentigem Äthylalkohol unter jeweiligem, lebhaftem Umrühren bei etwa 50°C. Das Reagens lost sich allmahlich und geht in eine orangerote, kolloidale Lösung uber. Nach der Abkühlung fugt man zu dieser Losung einige Menge des Alkohols bis zu genau 20 ccm. Die so erhaltene Reagenslosung halt gut, wenn man sie in einem wohl verstopselten Gefass im Dunkeln aufbewahrt.

(2) Ammoniakwasser: Käufliches extrareines 15 N Ammoniakwasser wurde vorbereitet.

## Bestimmung der Bedingungen höchster Empfindlichkeit*3

**1. Einfluss der Konzentration des angewandten Ammoniakwassers.** — Zum gegenwartigen Zwecke wurden Dowex 50W-X8 und 0.5prozentige Reagenslosung benutzt. Wie in Abb. 1 klar zu ersehen ist, sinkt die Intensitat der Farbung an den Harzkörnchen erst nur dann stark ab, wenn die Konzentration des angewandten Ammoniakwassers höher als 3 N steigt. Im folgenden wurde daher 1 N Ammoniakwasser lediglich angewandt.

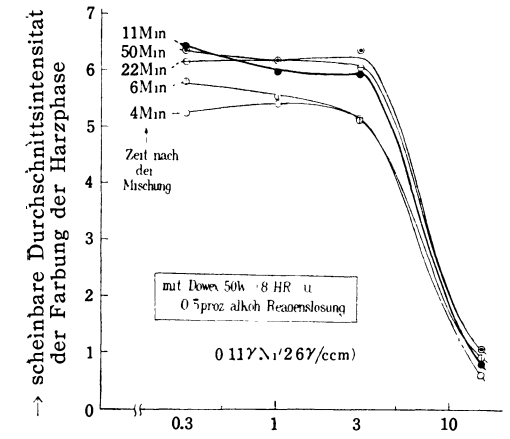



Abb. 1. Einfluss der Ammoniakwasserkonzentration.

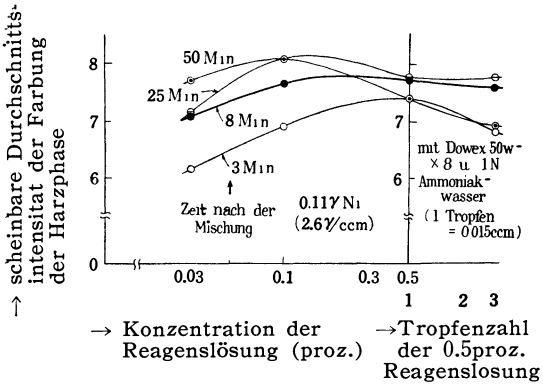



Abb. 2. Einfluss der Reagenskonzentration.

**2. Einfluss der Konzentration der Reagenslösung.**—Abb. 2 stellt den Einfluss der Reagenskonzentration auf die Farbungsintensitat der Harzkörnchen, wobei Dowex 50W-X8 und 1 N Ammoniakwasser benutzt wurden. Mit 0.03prozentiger Lösung des Reagens ist die Farbung der Harzkörnchen etwas ungenügend und mit einer starkeren als 0.5prozentigen Losung sinkt sie allmahlich mit der Zeit ab. Diese Entfarbungswirkung scheint mit dem steigenden Überschusse des Reagens zuzunehmen. So wahlt man 0.1prozentige Reagenslösung als die am besten geeignete aus.

**3. Einfluss der Harzart.**—Die Resultate dafür werden in Abb. 3 zusammengestellt:

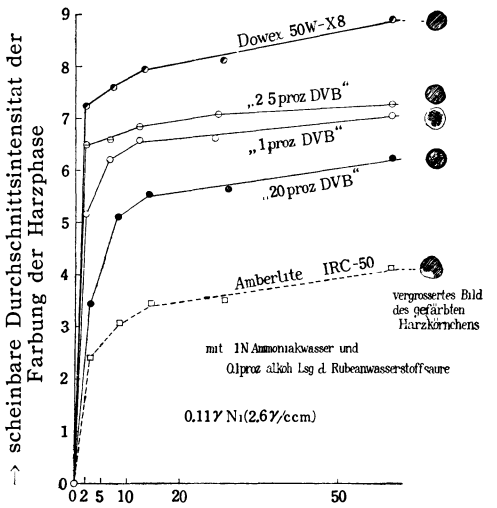



Abb. 3. Einfluss der Harzart.

Wie die genannte Abbildung uns zeigt, ubt der Vernetzungsgrad des Harzes auf die Intensität sowie auf den Zustand der Färbung der Harzkornchen einen beträchtlichen Einfluss aus. Diese Tatsache lässt sich dadurch erklären, dass die Affinität der Nickel(II)-amminkomplexkationen auf das Kationenaustauscherharz mit steigendem Vernetzungsgrade bedeutend zunimmt, und dass eine Art der Adsorption des Reagens ein wenig innerhalb der Harzkörnchen stattfindet, deren Ursachen bis jetzt nicht erklärlich ist. Man benutzt Dowex 50W-X8 (8prozentig vernetztes Harz) als die beste Harzprobe.

Es ist auch interessant, dass die Färbung der Harzphase sich hierbei schon 2 Min nach dem Zusatze des Reagens auf beinahe konstante Intensität erstreckt. Diese Tatsache bedeutet, dass das vorher in die Harzphase adsorbierte Nickel an der Grenzfläche zweier Phasen mit dem Reagens reagiert und, infolge der Entstehung der dicken Niederschlagschicht, keine Nickelionen sich weiter in die Harzphase adsorbieren lassen.

*3 In bezug auf die halbquantitative Darstellungsweise von der scheinbaren Durchschnittsintensität der Färbung, vergleiche M. Fujimoto, Dieses Bulletin, **27**, 347 (1954); **29**, 567 (1956).

**4. Einfluss der Salzkonzentration der Probelösung.** — Wegen der beträchtlich starken Affinität der komplexen Nickel(II)-amminkationen auf die Kationenaustauscherharze[5] wird die Färbungsintensität der Harzphase von der Salzkonzentration der Versuchslösung nur geringfügig beeinflusst (vgl. Abb. 4). Es ist aber wünschenswert, wenn möglich, mit der Probelösung, deren Salzkonzentration niedriger als 1 N reguliert wird, den Nachweis auszuführen.

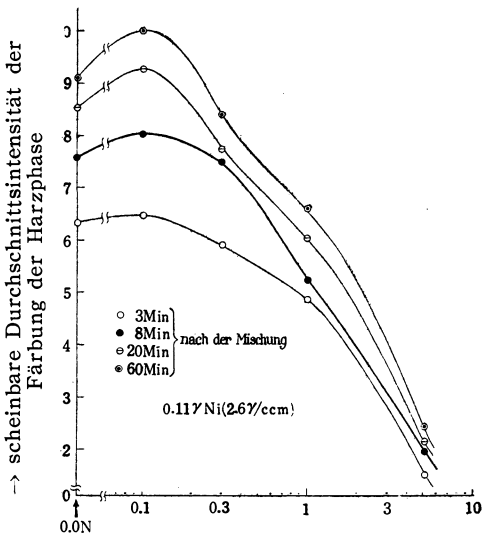



Abb. 4. Einfluss der Salzkonzentration.

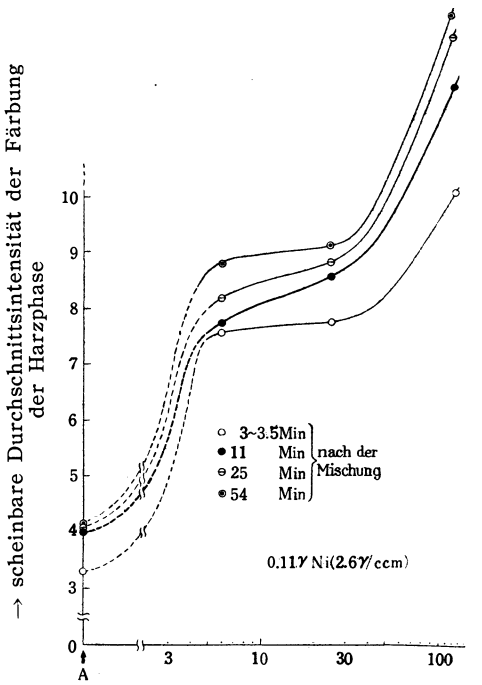



Abb. 5. Einfluss der Eintauchdauer der Harzkörnchen in der ammoniakalischen Versuchslösung auf die Färbungsintensität der Harzphase.

**5. Einfluss der Eintauchdauer der Harzkörnchen in der ammoniakalischen Probelösung.**— Versuchsweise wurde der genannte Einfluss untersucht. Wie der Verlauf der Kurven von Abb. 5 zeigt, verstärkt sich die Färbung der Harzkörnchen allmählich mit der Eintauchdauer in der ammoniakalischen Probelösung. Soweit es die Umstände erlauben, empfiehlt es sich, die Harzkörnchen möglichst lang in der ammoniakalischen Probelösung einzutauchen, aber, vom praktischen Standpunkt aus, sei das 5 Min lange Eintauchen der Harzkörnchen in die Versuchslösung genügend.

**6. Bedingungen höchster Empfindlichkeit.**— Das folgende beste Verfahren wurde aus der obigen Untersuchungen genau festgestellt:

„Man versetzt auf einer weissen Tüpfelplatte einige Körnchen des farblosen, starksauren und mittelmässig vernetzten Kationenaustascherharzes wie Dowex 50W-X8 mit je einem Tropfen der Probelösung und 1 N Ammoniakwassers, und lässt sie etwa 5 Min stehen. Wenn die Salzkonzentration der Probelösung sehr hoch ist, so empfiehlt es sich, diese durch Zusatz von destilliertem Wasser bis zu niedriger als 1 N zu verdünnen. Dann fügt man einen Tropfen 0.1prozentiger alkoholischer Lösung der Rubeanwasserstoffsäure dazu, und nach 2 oder 3 Min beobachtet man eine auf der Harzkörnchen entstandene Violett- bzw. Violettblaufärbung mit einer Lupe."

### Bestimmung der Erfassungsgrenze

Wie aus dem Verlaufe der Kurven von Abb. 6 klar zu ersehen ist, ist die hier festgestellte neue Nachweismethode ausserordentlich empfindlich; d. h. deren Erfassungsgrenze ist so klein wie 0.0021 $\gamma$ Nickel unter Grenzkonzentration $1 : 1.9 \times 10^7$. Diese Menge entspricht 0.02prozentigem Nickelgehalt in 10 $\gamma$ Probe.

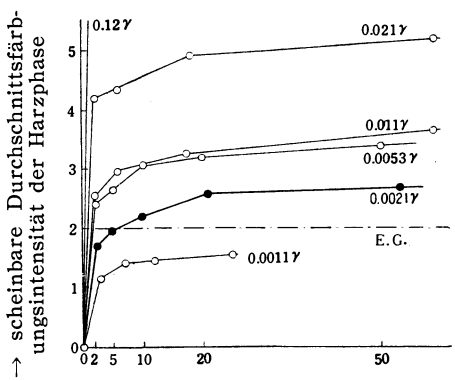



Abb. 6. Bestimmung der Erfassungsgrenze.

### Einflüsse der Begleitionen

Die Ergebnisse dafür wurden in Tabelle I gesamt dargestellt:

TABELLE I

EINFLÜSSE DER BEGLEITSTOFFE

| Begleitstoffe | benutzter Verbindungstypus | Farbton der Harzphase* | Menge der Begleitstoffe | nachweisbare Nickelmenge | Grenzverhältnis | Bemerkungen** |
|---|---|---|---|---|---|---|
| Ti(IV) | $TiOSO_4$ | bräunlich gelb | 100 γ | 0.0042 γ | $1:2.4\times10^4$ | — |
| V(V) | $NH_4VO_3$ | gräulich hellgrün | 59 γ | 0.0074 γ | $1:8\times10^3$ | — |
| Cr(III) | $KCr(SO_4)_2$ | grasgrün | 2 γ | 0.011 γ | $1:1.9\times10^2$ | Cr(III)≦0.005proz. |
| Mn(II) | $MnSO_4$ | beinahe farblos | 320 γ | 0.0042 γ | $1:7.6\times10^4$ | — |
| Fe(III) | $FeCl_3$ | farblos | 20 γ | 0.011 γ | $1:1.9\times10^3$ | *a*, *b*, Fe(III) ≦0.05proz. |
| 〃 | 〃 | farblos | 2000 γ | 0.0042 γ | $1:4.7\times10^5$ | *c* |
| Co(II) | $Co(NO_3)_2$ | gelbbraun | 0.05 γ | 0.018 γ | 1:2.8 | Co(II)≦0.0002proz. |
| 〃 | 〃 | farblos | 424 γ | 0.0044 γ | $1:9.6\times10^4$ | *c* |
| Cu(II) | $CuSO_4$ | schmutzig dunkelgrün | 0.1 γ | 0.011 γ | 1:9 | Cu(II)≦0.0005proz. |
| 〃 | 〃 | farblos | 1600 γ | 0.0042 γ | $1:3.8\times10^5$ | *c* |
| Zn(II) | $ZnSO_4$ | hellgrau | 96 γ | 0.0042 γ | $1:2.3\times10^4$ | Zn≦0.3proz. |
| Cd(II) | $CdSO_4$ | farblos | 160 γ | 0.0042 γ | $1:3.7\times10^4$ | Cd≦0.5proz. |
| Hg(II) | $Hg(NO_3)_2$ | farblos | 27 γ | 0.007 γ | $1:3.9\times10^3$ | Hg≦0.1proz. |
| Cr(VI) | $K_2Cr_2O_7$ | hellgelb | 360 γ | 0.0021 γ | $1:1.7\times10^5$ | — |
| Mo(VI) | $(NH_4)_2MoO_4$ | hellgrau | 390 γ | 0.0042 γ | $1:9.2\times10^4$ | — |
| W(VI) | $Na_2WO_4$ | farblos | 76 γ | 0.0021 γ | $1:3.6\times10^4$ | W≦0.2proz. |
| U(VI) | $(UO_2)(CH_3CO_2)_2$ | lebhaft zitronengelb | 320 γ | 0.0042 γ | $1:7.6\times10^4$ | *a* |
| Pb(II) | $Pb(NO_3)_2$ | hellbraun | 25 γ | 0.011 γ | $1:2.4\times10^3$ | Pb≦0.06proz. |
| Bi(III) | $Bi(NO_3)_3$ | hellbraun | 360 γ | 0.0021 γ | $1:1.7\times10^5$ | *a* |
| Sb(III) | $SbCl_3$ | farblos | 32 γ | 0.0048 γ | $1:6.7\times10^3$ | — |
| Sn(IV) | $SnCl_4$ | farblos | 72 γ | 0.0021 γ | $1:3.4\times10^4$ | Sn≦0.2proz. |
| Al(III) | $Al(NO_3)_3$ | farblos | 270 γ | 0.011 γ | $1:2.5\times10^4$ | — |
| $F^-$ | KF | farblos | 2800 γ | 0.0021 γ | $1:1.4\times10^6$ | — |
| $PO_4^{3-}$ | $Na_2HPO_4$ | farblos | 640 γ | 0.007 γ | $1:9\times10^4$ | — |
| $C_2O_4^{2-}$ | Oxalsaures Ammonium | farblos | 450 γ | 0.0021 γ | $1:2.2\times10^5$ | — |
| $C_4H_4O_6^{2-}$ | Seignettesalz | farblos | 840 γ | 0.0042 γ | $1:2.0\times10^5$ | — |
| $C_6H_5O_7^{3-}$ | Zitronensaures Ammonium | hellgrau? | 1100 γ | 0.007 γ | $1:1.6\times10^5$ | — |

* Farbton hervorgerufen nur durch die Begleitstoffe.

** *a*: Ein Blindversuch wurde hier nebeneinander durchgeführt.
*b*: Die Harzkörnchen wurden von orangebraunem Niederschlag bedeckt.
*c*: Nach dem Zusatze konzentrierter Salzsäure wurde die Probelösung in eine Mikrosäule starbasischen Anionenaustauscherharzes durchgelassen, um diese Begleitstoffe völlig zu beseitigen.

Chrom(III)-, Eisen(III)-, Kobalt(II)-, Kupfer(II)-, Blei(II)- und Antimon(III)-salze stören den Nachweis beträchtlich. Die Störung des Chroms(III) kann man durch Oxydation zur Chromate oder Bichromate[9] leicht beseitigen. Der höchst schädliche Einfluss der Eisen(III)-, Kobalt(II)- und Kupfer(II)-salze wurde in solcher Weise wie es im nachfolgenden Abschnitt genau beschrieben wird, leicht beseitigt.

### Trennung der Eisen(III)-, Kobalt(II)- und Kupfer(II)-salze als Chlorkomplexanionen durch Anwendung der Mikrosäule des starkbasischen Anionenaustauscherharzes

Da hier nur die Nickelsalze sich gar nicht aus der stark salzsauren Lösung von starkbasischen Anionenaustauscherharzen adsorbieren lassen, kann man die höchst schädliche Störung der Übergangselemente wie Eisen(III), Kobalt(II), oder Kupfer(II) durch chromatographische Anwendung der Mikrosäule des starkbasischen und fein pulverisierten Anionenaustauscherharzes wie folgt völlig beseitigen.

Man stellt mit geringer Menge des starkbasischen Anionenaustauscherharzes, Dowex 1-X10 (RCl-Form, 100 bis 200 Maschen), eine kleine Harzsäule (0.3 cm Durchmesser und etwa 3 cm Länge)*4 auf[6], und man reguliert vorher die Bedingungen des Harzes, indem man durch die Säule etwa zehn Tropfen 12 N Salzsäure (zur Analyse; u. dgl.) durchlaufen lässt. Man bringt

9) In bezug auf das mikrochemische Oxydationsverfahren für Chrom(III)-salze, vergleiche M. Fujimoto, Dieses Bulletin, **27**, 347 (1954).

*4 Sie entspricht der Austauschkapazität von etwa 0.4 Milliäquivalente der Anionen.

danach einige Tropfen der Probelösung auf das Ende eines Blattes Objektgläses und unter Umschütteln erhitzt sie allmählich über einem Mikrobrenner[10] bis zum beinahen Trocknen. Dann extrahiert man diesen Rückstand mit zwei oder drei Tropfen 12 N Salzsäure, und mit einer kleinen Kapillarpipette (1 Tropfen=0.02ccm) fügt man diese stark salzsaure Lösung auf die obengenannte Mikroharzsäule stückweise hinzu (etwa 0.01 ccm/Min). Man sammelt das hier erhaltene Eluat in einer Vertiefung der Tüpfelplatte an. Die in der Probelösung vorhandenen Eisen(III)-, Kobalt(II)- und Kupfer(II)-salze werden nach der genannten Reihenfolge, von dem oberen Ende der Harzsäule nach unten, als chromgelbe, grünblaue und orangegelbe Bänder adsorbiert. Schliesslich drängt man mit etwa 0.2 ccm 12 N Salzsäure nur das Nickel(II) aus der Säule heraus, dann erwärmt man eine Weile die obige Tüpfelplatte auf einem Wasserbade, um die überschüssige Salzsäure verdampfen zu lassen, und versetzt den hier erhaltenen Rückstand mit zwei Tropfen heissen destillierten Wassers. Nach der Abkühlung kann man den Nachweis des Nickels mit dieser wässerigen Lösung ohne Störung durchführen. Die gebrauchte Harzsäule wird zuerst mit 1 ccm 0.5 N Salzsäure in die RCl-Form zurückgeführt und dann mit Wasser völlig gewaschen. Man kann auch die Zinn(IV)-, Antimon(III)-, Zink- und Quecksilber(II)-salze usw. in obenerwähnter Weise völlig beseitigen.

## Zusammenfassung

1. Die farblosen, starksauren und mittelmässig vernetzten Kationenaustauscherharze werden zur wohlbekannten Niederschlagbildungsreaktion zwischen den Nickelsalzen und der Rubeanwasserstoffsäure angewandt, und eine ausserordentlich empfindliche Nachweismethode wird neu und gründlich durch Beschränkung der Fällungsstelle an der Grenzfläche zwischen Harz und Lösungsphase festgestellt.

2. Die besten Experimentalbedingungen für obengenannte Nachweismethode werden genau bestimmt durch ausführliche Untersuchung über die verschiedenen Faktoren, wie die Konzentration des Ammoniakwassers und des Reagens, Sorte und Vernetzungsgrad der Harze, Salzkonzentration an der Probelösung, Eintauchdauer der Harzkörnchen in der ammoniakalischen Probelösung, u. s. w..

3. Die Einflüsse verschiedenartiger fremder Ionen werden ausführlich untersucht und die schädliche Störung der Eisen(III)-, Kobalt(II)- und Kupfer(II)-salze wird durch chromatographische Anwendung der Mikrosäule starkbasischen Anionenaustauscherharzes raffiniert beseitigt.

Zum Schluss möchte der Verfasser Herrn Prof. Dr. E. Minami für seine zahlreichen wertvollen Ratschläge über die vorliegende Untersuchung seinen herzlichsten Dank aussprechen.

Für die Harzproben, „1proz. DVB", „2.5-proz. DVB" und „20proz. DVB" ist der Verfasser Herrn Prof. Dr. A. Kawamura an der Landwirtschaftlichen und Technischen Universität zu Tokyo zu grossem Dank verpflichtet.

*Laboratorium der analytischen Chemie,*
*Chemisches Institut der*
*wissenschaftlichen Fakultät,*
*Universität zu Tokyo, Hongo, Tokyo*

10) A. A. Benedetti-Pichler, „Introduction to the Microtechnique of Inorganic Analysis," 1. Aufl., New York (1942), S. 8.

# *Mikroanalyse mit Hilfe von Ionenaustauscherharzen. XIII. Über den Nachweis in Tausendstelgammamenge vorhandenen Kobalts mit Nitroso-R-salze*[1]

Von Masatoshi FUJIMOTO

(Eingegangen am 5. November, 1956)

## Einleitung

Bei der vorliegenden Arbeit, stellte der Verfasser über die für Kobalt ausserordentlich empfindlichen Nachweismethoden Untersuchungen an.

Es wurde das Nitroso-R-salz (1-Nitroso-2-Oxynaphthalin-3, 6-Disulfonsaures Natrium)[2] als ein Vertreter der auf Kobalt

1) Die zwölfte Mitteilung : M. Fujimoto, Dieses Bulletin, **30**, 274 (1957).

2) Vgl., z. B., I. Mellan, „Organic Reagents in Inorganic Analysis," Philadelphia, (1941), S. 332, sowie, E. B. Sandell, „Colorimetric Determination of Traces of Metals," 2. Aufl., (1950) New York, S. 274.

sehr empfindlich einwirkenden Reagenzien angewandt. Die stark sich färbenden Chelatanionen, die das Nitroso-R-salz, unter geeignetem pH-Werte der Versuchslösung, mit den Kobalt(II)-salzen bildet, werden von den farblosen und starkbasischen Anionenaustauscherharzen so stark adsorbiert, dass die Intensität der in der Harzphase entstandene intensive Rotfärbung gar nicht von der Salzkonzentration der Probelösung beeinflusst wird. Die Färbung der Harzphase ist infolgedessen entschieden stärker als die der Lösungsphase und die Reaktionsempfindlichkeit wird auffallend erhöht.

Die Reagensanionen werden dabei von den genannten Harzen gleichfalls stark adsorbiert und färben diese Phase lebhaft grünlich gelb. Wegen dieses intensiven grüngelben Hintergrundes vom Reagens wird der Nachweis besonders dann beträchtlich unsicher, wenn es sich um eine sehr geringe Menge des Kobalts handelt. Dieser Nachteil wurde jedoch dadurch leicht überwunden, dass man die Harzkörnchen, nach der Bildung betreffender Chelatanionen in der Harzphase, mit verdünnter Salpetersäure eine Weile kocht und dadurch nur das überschüssige Reagens vollständig zersetzt. Dieses Verfahren ist nicht nur zur Erhöhung der Reaktionsempfindlichkeit sehr geeignet, sondern auch zur Beseitigung der Störung von verschiedenartigen fremden Kationen wie Nickel(II), Kupfer(II) usw., die gleichfalls mit dem genannten Reagens die stark sich färbenden Chelatanionen bilden.

### Massflüssigkeit und Reagenzien

**1. Massflüssigkeit.**— Man stellte eine Stammlösung des Kobalts dar, indem man das nickel- und eisenfreie Kobalt(II)-nitrat in 0.01 N Salpetersäure eintrug. 1 ccm dieser Stammlösung enthielt genau 5.74 mg von Kobalt*[1]. Eine Reihe der Massflüssigkeiten des Kobalts wurde aus dieser Stammlösung durch Verdünnung mit 0.01N Salpetersäure hergestellt. Alle folgende Untersuchungen über das beste Verfahren wurden mit einer 0.01N-salpetersauren Lösung ausgeführt, deren 1 ccm genau 5.74 $\gamma$ von Kobalt enthielt.

**2. Anionenaustauscherharze.**—Um den Einfluss der Vernetzungsgrade der Harze auf die Färbungsintensität der Harzphase miteinander zu vergleichen, wurden hier die käuflichen, farblosen und starkbasischen Harze, Dowex 1-X1, -X2, -X4 und -X8, in der RCl-Form angewandt. Überdies wurde ein beinahe farbloses und mittelstarkbasisches Harz, Amberlite XE-114 (RCl-Form), ebenfalls angewandt.

**3. Reagenzien.** — (1) 2prozentige wässerige Stammlösung des Nitroso-R-salzes : Man löst 0.4 g des käuflichen extrareinen Nitroso-R-salzes (zur Analyse) in eine kleine Menge destillierten Wassers auf und verdünnt diese mit destilliertem Wasser genau zu 20 ccm.

(2) 4 N wässerige Lösung des Natriumacetats als Pufferlösung: Aus dem extrareinen Reagens (zur Analyse) stellt man diese Stammlösung her. Deren pH-Wert war genau 8.20.

(3) 2 N Salpetersäure.—Aus der käuflichen, extrareinen Salpetersäure bereitet man diese Lösung vor.

### Bestimmung der Experimentalbedingungen höchster Empfindlichkeit*[2]

**1. Einfluss der Ordnung der Versetzung von Reagenzien und Probelösung.** — Auf dem in Tabelle I beschriebenen Wege, wurde der Einfluss der Versetzungsordnung der Reagenzien usw. auf die Färbungsintensität der Harzphase untersucht, wobei Dowex 1-X1 (RCl-Form), 0.05prozentige Lösung des Nitroso-R-salzes und 4 N Lösung des Natriumacetats als Pufferlösung angewandt wurden.

Wie Abb. 1 uns zeigt, üben die hier ausgewählten Faktoren auf die Färbungsintensität keinen

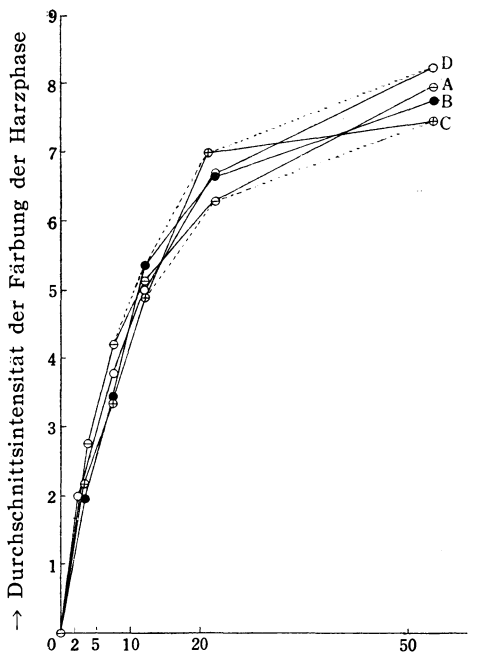



Abb. 1. Gegenüberstellung der veschiedenen Ordnung der Versetzung von Probe- und Reagenslösungen (Vgl. Tablle I).

*[1] Die Menge des in der obengenannten Stammlösung vorhandenen Kobalts wurde durch komplexometrische Titration mit 0.01 M Massflüssigkeit von Äthylendiamintetraessigsaurem Dinatrium und Murexid als Metallindikatorgenau bestimmt.

*[2] In bezug auf die schematische, halbquantitative Darstellungsweise von der scheinbaren Durchschnittsintensität der Färbung der Harzphase, vergleiche M. Fujimoto, Dieses Bulletin, **27**, 347 (1954); **29**, 567(1956).

TABELLE I

VERSCHIEDENE BEDINGUNGEN VON ABB. 1

| Verfahren | Zeichen der Kurve | Inhaltsangabe des Verfahrens |
|---|---|---|
| A | ⊖ | RCl*+Probelsg.**—(5 Min)→+0.05proz. Lsg. des Nitroso-R-salzes+4N Lsg. des $CH_3COONa$ |
| B | ● | RCl+0.05proz. Lsg. des Nitroso-R-salzes—(5 Min)→+4N Lsg. des $CH_3COONa$+Probelsg. |
| C | ⊕ | RCl+4N Lsg. des $CH_3COONa$—(5 Min)→+0.05proz. Lsg. des Nitroso-R-salzes+Probelsg. |
| D | ○ | Probelsg.+0.05proz. Lsg. des Nitroso-R-salzes—(5 Min)→+4N Lsg. des $CH_3COONa$+RCl |

* RCl bedeutet hier Dowex 1-X1 von RCl-Form.

** 1 Tropfen der obengenannten Probelösung enthält 0.21 $\gamma$ Kobalt (5.74 $\gamma$/ccm).

TABELLE II

EINFLÜSSE DER BEGLEITSTOFFE

| Begleitstoffe | benutzter Verbindungstypus | Farbton der Harzphase* | Menge der Begleitstoffe | nachweisbare Kobaltmenge | Grenzverhaltnis | Bemerkungen** |
|---|---|---|---|---|---|---|
| Ti(IV) | $TiOSO_4$ | sehr hell gelb | 100 $\gamma$ | 0.0046 $\gamma$ | $1:2.2\times10^4$ | *a* |
| V(V) | $NH_4VO_3$ | sehr hell gelb | 70 $\gamma$ | 0.0029 $\gamma$ | $1:2.4\times10^4$ | —— |
| Cr(III) | $KCr(SO_4)_2$ | farblos | 350 $\gamma$ | 0.0029 $\gamma$ | $1:1.2\times10^5$ | *b* |
| Mn(II) | $MnSO_4$ | gelb | 2600 $\gamma$ | 0.0029 $\gamma$ | $1:9\times10^5$ | —— |
| Fe(III) | $FeCl_3$ | farblos | 35 $\gamma$ | 0.0029 $\gamma$ | $1:1.2\times10^4$ | Fe(III)≦0.1proz. |
| Fe(II) | Mohrsches Salz | farblos | 350 $\gamma$ | 0.0029 $\gamma$ | $1:1.2\times10^5$ | *b* |
| Ni(II) | $NiCl_2$ | hellorangegelb | 300 $\gamma$ | 0.0057 $\gamma$ | $1:5.3\times10^4$ | *b, c, d* |
| Cu(II) | $CuSO_4$ | hellorangegelb | 320 $\gamma$ | 0.0046 $\gamma$ | $1:7.0\times10^4$ | *b, c, d* |
| Zn(II) | $ZnSO_4$ | hellbraungelb? | 270 $\gamma$ | 0.0076 $\gamma$ | $1:3.5\times10^4$ | —— |
| Cd(II) | $CdSO_4$ | hellgelb | 1600 $\gamma$ | 0.0046 $\gamma$ | $1:3.5\times10^5$ | —— |
| Hg(II) | $Hg(NO_3)_2$ | farblos | 350 $\gamma$ | 0.0029 $\gamma$ | $1:1.2\times10^5$ | —— |
| Cr(VI) | $K_2Cr_2O_7$ | gelb | 3.2 $\gamma$ | 0.0046 $\gamma$ | $1:7\times10^2$ | Cr(VI)≦0.01proz. |
| 〃 | 〃 | hellgelb | 320 $\gamma$ | 0.0046 $\gamma$ | $1:7\times10^4$ | *e* |
| Mo(VI) | $(NH_4)_2MoO_4$ | hellorange | 67 $\gamma$ | 0.0057 $\gamma$ | $1:1.2\times10^4$ | *d*, Mo≦0.2proz. |
| W(VI) | $Na_2WO_4$ | weiss*** | 330 $\gamma$ | 0.0046 $\gamma$ | $1:7.2\times10^4$ | —— |
| U(VI) | $UO_2(CH_3COO)_2$ | farblos | 350 $\gamma$ | 0.0029 $\gamma$ | $1:1.2\times10^5$ | —— |
| Pb(II) | $Pb(NO_3)_2$ | hellorangegelb | 320 $\gamma$ | 0.0046 $\gamma$ | $1:7\times10^4$ | *d* |
| Sn(IV) | $SnCl_4$ | farblos | 295 $\gamma$ | 0.0029 $\gamma$ | $1:1\times10^5$ | *f* |
| Ge(IV) | $GeO_2$ | hellgelb | 25 $\gamma$ | 0.0029 $\gamma$ | $1:8.8\times10^3$ | *d* |
| Sb(III) | $SbCl_3$ | hellorange | 320 $\gamma$ | 0.0048 $\gamma$ | $1:7\times10^4$ | *a, b* |
| Bi(III) | $Bi(NO_3)_3$ | gelb | 200 $\gamma$ | 0.011 $\gamma$ | $1:1.8\times10^4$ | Bi≦1proz. |
| Al(III) | $Al(NO_3)_3$ | farblos | 350 $\gamma$ | 0.0029 $\gamma$ | $1:1.2\times10^5$ | Al≦1proz. |
| $HPO_4^{2-}$ | $Na_2HPO_4$ | hellgelb | 1700 $\gamma$ | 0.0029 $\gamma$ | $1:6\times10^5$ | —— |
| $C_2O_4^{2-}$ | Oxalsaures Ammonium | sehr hell gelb | 720 $\gamma$ | 0.0046 $\gamma$ | $1:1.6\times10^5$ | —— |
| $C_4H_4O_6^{2-}$ | Seignettesalz | farblos | 920 $\gamma$ | 0.0029 $\gamma$ | $1:3.2\times10^5$ | —— |
| $C_6H_5O_7^{3-}$ | Zitronensaures Ammonium | farblos | 1400 $\gamma$ | 0.0029 $\gamma$ | $1:4.8\times10^5$ | —— |

* Farbton der Harzphase hervorgerufen nur durch die Begleitstoffe.

** *a*: 2 bzw. 3 Tropfen der 4N Lösung des Natriumacetats wurden angewandt.
*b*: 2 bzw. 3 Tropfen der 2N Salpetersäure wurden hinzugefügt.
*c*: 0.5proz. Reagenslösung wurde angewandt.
*d*: Erst dann, wenn man neben Blindversuche miteinander durchfuhrt, wurde die Anwesenheit des Kobalts nachgewiesen.
*e*: Durch eine Mikroharzsaule von Dowex 1-X4 (4 mm×15 mm: RCl-Form) wurde eine grosse Menge der Chromate völlig beseitigt[3].
*f*: Gibt es Kobalt in der Probelösung, so färben sich die Harzkornchen intensiv gelb.

*** Die Harzkörnchen truben sich milchweiss.

3) M. Fujimoto, Dieses Bulletin, **29**, 595 (1956).

Einfluss aus, und es scheint, dass das vorherige 5 Min lange Eintauchen der Harzkörnchen in die Reagenslösung usw. auf die Färbung der Harzphase gar nicht befördernd einwirkt. Aus diesem Grunde hat der Verfasser von nun an das Verfahen „B" als geeignetstes solcher Verfahren ausgewählt und nach diesem alle folgende Vergleichungen von verschiedenen Faktoren durchgeführt.

**2. Einfluss der Konzentration der Reagenslösung.** — Um den Einfluss des überschüssigen Reagens auf die Menge der in die Harzphase adsorbierten Chelatanionen zu erkennen, wurde eine Reihe der Versuche mit den Reagenslösungen von verschiedenen Konzentrationen durchgeführt. Wie in Abb. 2 klar zu ersehen ist, sinkt die Intensität der Färbung der Harzphase mit der steigenden Reagenskonzentration stark ab, d. h., die Menge der in die Harzphase adsorbierten Chelatanionen wird von der Reagenskonzentration beträchtlich beeinflusst. Infolgedessen wurde nur 0.05prozentige Lösung des Nitroso-R-salzes, in Betracht der Unterscheidbarkeit gegen den Blindversuch, angewandt.

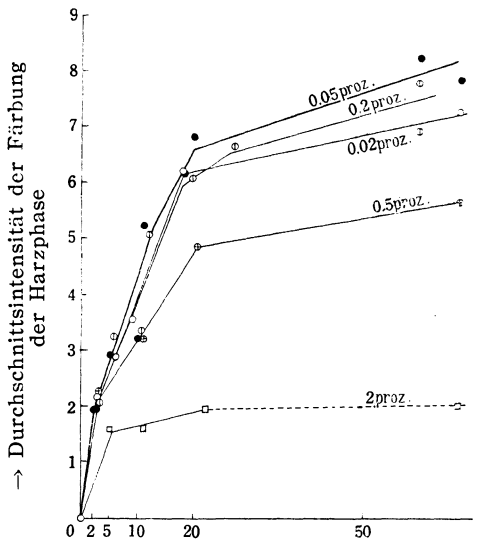



Abb. 2. Einfluss der Konzentration der Nitroso-R-salzlösung auf die Unterscheidbarkeit der Färbung der Harzphase nach dem Verfahren B von Abb. 1.

**3. Einfluss der Konzentration der Natriumacetatlösung.** — Wie Abb. 3 uns zeigt, übt die Konzentration des Natriumacetats als Pufferlösung auf die Färbungsintensität der Harzphase keinen Einfluss aus. Vom Standpunkt deren Pufferwirkung jedoch aus, empfiehlt es sich, mindestens 0.3 N Lösung des Acetats anzuwenden.

**4. Einfluss der Harzart.** — Die Färbungsintensität der Harzphase nimmt stark mit dem steigenden Vernetzungsgrade ab, wie man in Abb. 4 deutlich ersehen kann. Mittelstarkbasisches Harz, Amberlite XE-114, ist geeignet, wenn auch die Harzphase sich etwa langsam färbt. Ein

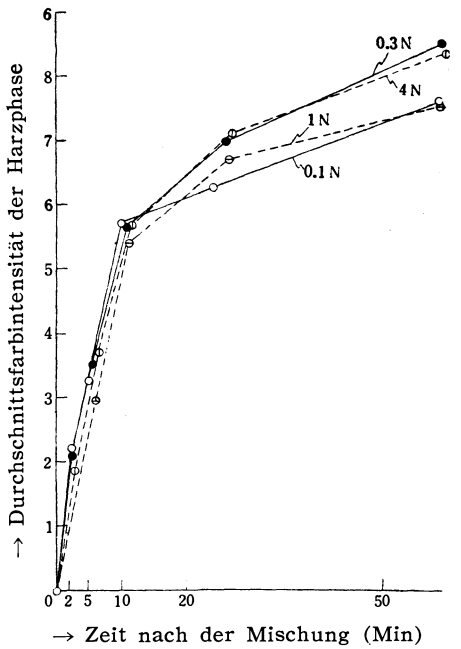



Abb. 3. Einfluss der Natriumacetatkonzentration auf die Färbungsintensität der Harzphase nach dem Verfahren „B" in Abb. 1.

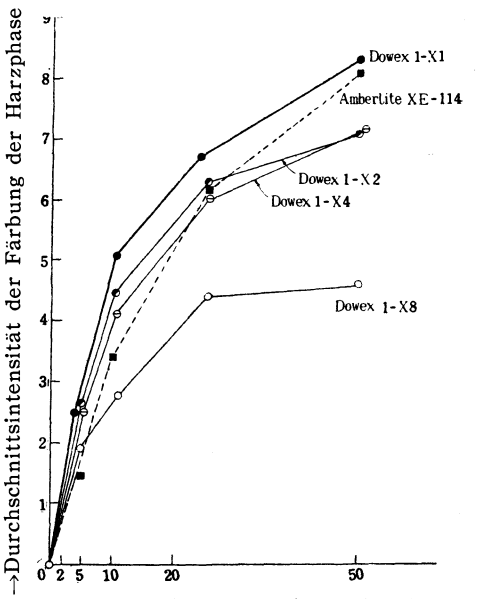



Abb. 4. Einfluss des Vernetzungsgrads der Harze auf die Färbungsintensität der Harzphase.

niedrig vernetztes Harz, Dowex 1-X1, wurde als das beste ausgewählt.

**5. Einfluss der Salzkonzentration der Probelösung.** — Wie bereits aus der Tatsache vom Abschnitt 3. leicht zu erwarten ist, wird die

Färbung der Harzphase durch Zusatz des Neutralsalzes wie Natriumchlorids gar nicht beeinflusst (vgl. die dicken, gestrichelten Linien von Abb. 5).

**6. Ausgeprägte Erhöhung der Empfindlichkeit durch Zersetzung überschüssiges, in der Harzphase vorhandenes Reagens mit Salpetersäure.**—Es wurde schon mitgeteilt, dass nur das Kobalt(II)-chelat durch Kochen mit verdünnter Salpetersäure unverändert bleibt, während die Eisen(III)-, Nickel(II)- und Kupfer(II)-chelate durch diese Behandlung leicht zersetzt werden[2]. Mit Rücksicht darauf, dass die Färbung der Harzphase von der Salzkonzentration der Probelösung kaum beeinflusst wird, untersuchte der Verfasser darüber, welchen Einfluss das genannte Verfahren auf die Färbung der Harzphase ausübt. Die Resultate werden in Abb. 6 zusammengestellt. Wenn das genannte Zersetzungsverfahren nicht angewandt wird, so färben sich die Harzkörnchen nach dem Verlauf der Kurve-A. Die Färbungsintensität der Harzphase nimmt dann merklich zu, wie in den Kurven-B und -C beschrieben, wenn man die Harzkörnchen 3 oder 8 Min nach der Bildung des Chelats in der Harzphase, mit einem Tropfen 2 N Salpetersäure auf einem Wasserbad etwa 3 Min erhitzt. Die intensive, von überschüssigem Reagens hervorgerufene Grüngelbfärbung der Harzphase verschwinden dabei vollständig. Die Kurve-D zeigt den Färbungsverlauf in dem Fall, wo man, erst nach dem Erhitzen des Gemisches der Probelösung, der Reagenslösung und der Pufferlösung mit einem Tropfen der 2 N Salpetersäure, die Harzkörnchen hinzufügt. Von diesen Resultaten aus betrachtet, ist es wünschenswert, dass man, etwa 5 Min nach der Bildung des betreffenden Chelats in der Harzphase, das Reaktionsgemisch zusammen mit 2 N Salpetersäure etwa 3 Min kocht.

**7. Das empfehlenswerteste Verfahren.**—Alles Obenerwähnte zusammengenommen, kann man wie folgt das beste Nachweisverfahren feststellen:—

„Auf einer weissen Tüpfelplatte versetzt man einige Körnchen des farblosen, starkbasischen und niedrig vernetzten Anionenaustauscherharzes wie Dowex 1-X1, mit je einem Tropfen 0.05prozentiger Lösung des Nitroso-R-salzes, 0.3N Lösung des Natriumacetats und der Probelösung. Nach 5 Min langem Stehenlassen fügt man zu diesem Gemische einen Tropfen 2 N Salpetersäure, erhitzt auf einem Wasserbad etwa 3 Min lang und lässt dieses abkühlen. Je nach dem Kobaltgehalt von der Probelösung, entsteht in der Harzphase eine mehr oder weniger intensive Rotfärbung. Wenn die Menge des Kobalts sehr gering ist, so empfiehlt es sich, einen Blindversuch daneben durchzuführen."

## Bestimmung der Erfassungsgrenze

Die Resultate der für veschiedene Kobaltmengen ausgeführten Versuche werden in Abb. 7 zusammengestellt. Die Erfassungsgrenze ist 0.0029 $\gamma$ unter Grenzkonzentration $1 : 1.4 \times 10^7$. Diese entspricht etwa 0.03prozentigem Kobaltgehalt in 10 $\gamma$ Probe.

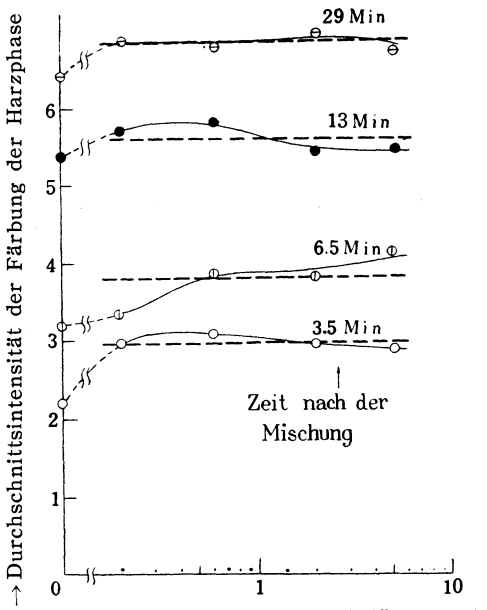



Abb. 5. Einfluss der Salzkonzentration der Probelösung auf die Färbungsintensität der Harzphase.

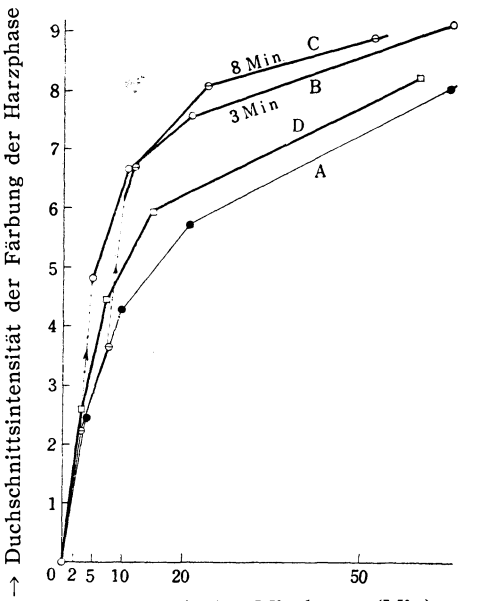



Abb. 6. Wirksamkeit des Zusatzes von Salpetersäure.

---<--- bedeutet das 3 Min lange Erhitzen des Gemisches mit 1 Tropfen der 2 N Salpetersäure bei 100°C

—— ist der Verlauf vor dem Zusatze der 2 N Salpetersäure

—— ist der Verlauf nach dem Erhitzen mit der 2 N Salpetersäure

### Einflüsse der Begleitstoffe

Die Resultate stehen in Tabelle II (S. 280). Die Störung der Nickel(II)- und Kupfer(II)-salze wurde leicht durch Erhitzen mit überschüssiger 2 N Salpetersäure beseitigt. Nur die Eisen(III)-salze beeinträchtigen etwas den Nachweis. Die hier fest gestellte Nachweismethode ist daher entschieden spezifisch.

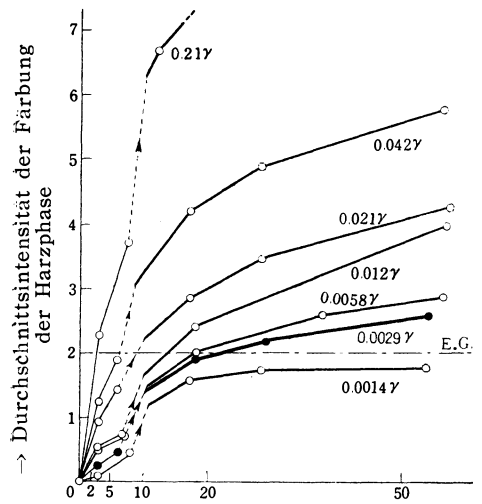



Abb. 7. Bestimmung der Erfassungsgrenze

In bezug auf die hier angewandten Zeichen, vegleiche Abb. 6.

### Zusammenfassung

1. Die Empfindlichkeit der Farbenreaktion zwischen den Kobaltsalzen und dem Nitroso-R-salze wird durch einfache Anwendung farblosen, starkbasischen und niedrig vernetzten Anionenaustauscherharzes auffallend erhöht, womit eine neue und ausserordentlich empfindliche Tüpfelmethode zum Nachweis spurweise vorhandenen Kobalts ganzlich festgestellt wird.

2. In gleicher Weise, wie in den vorhergehenden Mitteilungen genau beschrieben, wird das empfehlenswerteste Verfahren genau festgestellt. Die Anwendung verdünnter Salpetersäure ist dabei sehr geeignet, nicht nur zur Erhöhung der Reaktionsempfindlichkeit, sondern auch zur Zersetzung der den Nachweis störenden, stark sich färbenden Chelate von Nickel(II), Kupfer(II) usw.

Zum Schluss möchte der Verfasser Herrn Prof. Dr. E. Minami für seine wertvollen Ratschläge über die gegenwärtige Untersuchung seinen herzlichsten Dank aussprechen.

*Laboratorium der analytischen Chemie,*
*Chemisches Institut der*
*wissenschaftlichen Fakultät,*
*Universität zu Tokyo, Hongo, Tokyo*

# *Mikroanalyse mit Hilfe von Ionenaustauscherharzen. XIV. Über den Nachweis in Tausendstelgammamenge vorhandenen Eisens mit 2, 2'-Bipyridyl*[1]

Von Masatoshi FUJIMOTO

(Eingegangen am 5. November, 1956)

## Einleitung

Es wurde in der vorliegenden Arbeit über eine empfindliche Farbenreaktion[2] zwischen den Eisen(II)-salzen und 2, 2'-Bipyridyl untersucht. Die intensiv sich färbenden Eisen (II) - Bipyridylchelatkationen werden von den farblosen Kationenaustauscherharzen stark adsorbiert und geben dieser Phase eine entschieden deutliche Rotfärbung, mit deren Hilfe man einen ausserordentlich empfindlichen Nachweis des Eisens ausführen kann.

1) Die dreizehnte Mitteilung: M. Fujimoto, Dieses Bulletin, **30**, 278 (1957).

2) Vgl., z. B., M. L. Moss und M. G. Mellon, *Ind. Eng. Chem., Anal. Ed.*, **14**, 862 (1942).

### Versuchsanordnung

Man bringt auf eine weisse Tüpfelplatte nacheinander einige Körnchen des farblosen Kationenaustauscherharzes, und je einen Tropfen der Probelösung, verdünnter Lösung des Hydroxylaminhydrochlorids und der des Natriumacetats als Pufferlösung und verdünnter alkoholischer Lösung des 2, 2'-Bipyridyls, danach beobachtet

man eine in der Harzphase entstandene Rotfärbung mit einer Lupe.

### Massflüssigkeit und Reagenzien

**1. Massflüssigkeit.**—Aus derselben Stammlösung des Eisen(III)-chlorids wie der in der siebenten Mitteilung[3] wurde eine Reihe der Massflüssigkeit durch Verdünnung mit extrareiner 0.01N Salzsäure hergestellt. Bei den folgenden Vergleichungen verschiedener Experimentalfaktoren wurde eine 0.01N-salzsaure Lösung angewandt, deren 1 ccm genau 10 $\gamma$ von Eisen(III) enthielt.

**2. Kationenaustauscherharze.**—Die farblosen und starksauren Harze von verschiedenen Vernetzungsgraden wurden angewandt, um den Einfluss des Vernetzungsgrades zu untersuchen. Diese sind „1proz. DVB", „2.5proz. DVB", Dowex 50W-X8, Dowex 50W-X12 und „20proz. DVB"[4]. Ein käufliches Kationenaustauscherharz von Phosphonsäuretypus, Duolite C-60, wurde gleichfalls angewandt. Vor dem Gebrauch wurden alle diese Harze mit destillierter Salzsäure gründlich gewaschen, um die Spurmenge des Eisens völlig zu beseitigen, und mit destilliertem Wasser ausgewaschen.

**3. Reagenzien.**—Hierbei muss man vorher besonders sorgfältig prüfen, dass alle die hier anzuwendenden Reagenzien das Eisen nicht selbst in Spurmenge enthalten.

(1) 2prozentige alkoholische Stammlösung des 2, 2'-Bipyridyls: Man löst 0.1 g käuflichen extrareinen 2, 2'-Bipyridyls (Wakô, „zur Analyse") in 5 ccm Äthylalkohol.

(2) 10prozentige Stammlösung des Hydroxylaminhydrochlorids: Man löst 3 g eisenfreies Reagens (zur Analyse) in 30 ccm destillierten Wassers. Diese Lösung wird zur Reduktion des Eisens(III) angewand.

(3) 4N wässerige Lösung des Natriumacetats als Pufferlösung: Dieselbe Stammlösung wie die der vorhergehenden Mitteilung[1] wurde angewandt.

### Bestimmung der Experimentalbedingungen höchster Empfindlichkeit*1

**1. Einfluss des Vernetzungsgrades von den Harzen.**—Hier wurden 10prozentige Lösung des Hydroxylaminhydrochlorids, 1N Lösung des Natriumacetats und 2prozentige alkoholische Lösung des 2, 2'-Bipyridyls als die Vertreter angewandt. Die Resultate dafür stehen in Abb. 1:

Die Harzphase färbt sich dann am stärksten, wenn man „2.5proz. DVB" verwendet. Bei den hoch vernetzten Harzen wird die Färbung der Harzphase beträchtlich geschwächt. Duolite C-60 war für den vorliegenden Zweck ungeeignet.

**2. Einfluss der Reagenskonzentration.**—Hier wurde das Harz, „2.5proz. DVB" angewandt. Der Einfluss der Konzentration des benutzten

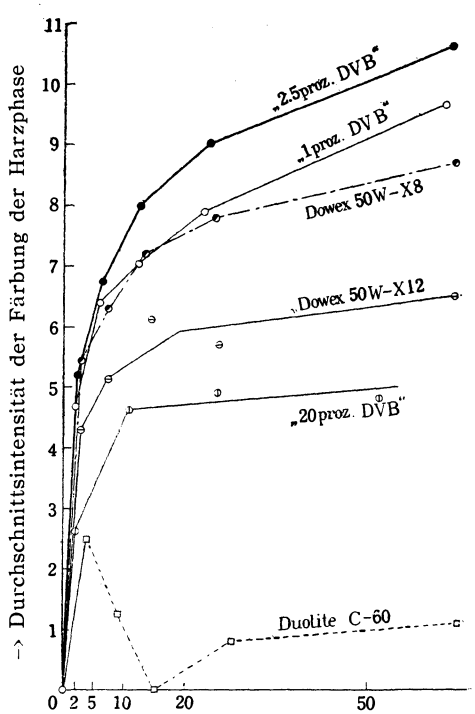



Abb. 1. Einfluss der Harzart.

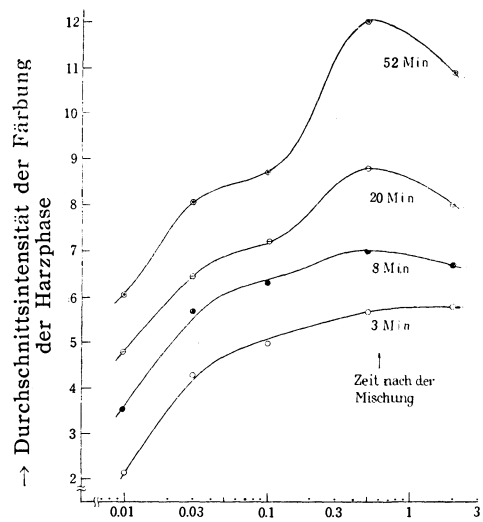



Abb. 2. Einfluss der Konzentration des 2, 2'-Bipyridyls.

2, 2'-Bipyridyls auf die Färbungsintensität der Harzphase wurde in Abb. 2 dargestellt. Wie daraus leicht zu erkennen ist, verstärkt sich die Färbung der Harzphase mit der steigenden Reagenskonzentration allmählich, bis sie bei etwa 0.5-Prozent. das Maximum beträgt, und dann wird sie etwas schwächer. Im folgenden wurde daher 0.5prozentige Reagenslösung angewandt.

3) M. Fujimoto, Dieses Bulletin, **29**, 776 (1956).
4) Vgl. M. Fujimoto, Dieses Bulletin, **29**, 600 (1956).
*1 In bezug auf die schematische, halbquantitative Darstellungsweise von der scheinbaren Durchschnittsintensität der Färbung der Harzphase, vergleiche M. Fujimoto, Dieses Bulletin, **27**, 347 (1954); **29**, 567 (1956).

**3. Einfluss der Konzentration des benutzten Hydroxylaminhydrochlorids.** — Die Resultate dafür stehen zusammengefasst in Abb. 3, aus welcher man 3prozentige Lösung als die am geeignetste auswählen kann.

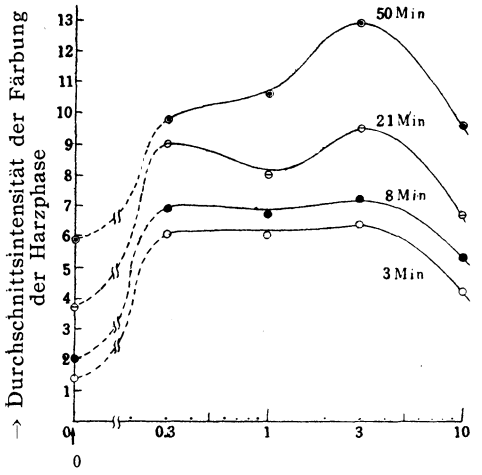



Abb. 3. Einfluss der Konzentration des Hydroxylaminhydrochlorids.

Hierbei ist sehr interessant, dass, selbst bei Abwesenheit von Hydroxylamin, die betreffende Rotfärbung in der Harzphase deutlich entsteht. Mit Rücksicht auf die Tatsache, dass die Lösungsphase sich bei Abwesenheit von Hydroxylamin dann gar nicht rot färbt, wenn man keine Harzkörnchen hinzufügt, könnte man vermuten, dass das anfangs in der Harzphase entstandene Eisen(III)-2, 2'-Bipyridyl von den häufig als die Begleiter in der Kationenaustauscherharzphase vorhandenen, ungesättigten Gruppen zum entsprechenden Eisen(II)-chelat einigermassen leicht reduziert werden.

**4. Einfluss der Konzentration der in der Probelösung vorhandenen Salze.** — Hierbei wurden die am besten geeigneten Reagenzien, d. h., „2.5proz. DVB" (HR-Form), 0.5prozentige Lösung des 2, 2'-Bipyridyls und 3prozentige Lösung des Hydroxylaminhydrochlorids angewandt. Die Färbung der Harzphase nimmt mit der steigenden Salzkonzentration der Probelösung allmählich ab, wie man in Abb. 4 ersieht, aber man kann selbst mit der Probelösung, deren Salzkonzentration so hoch wie 5N liegt, den Nachweis mit befriedigender Empfindlichkeit ausführen.

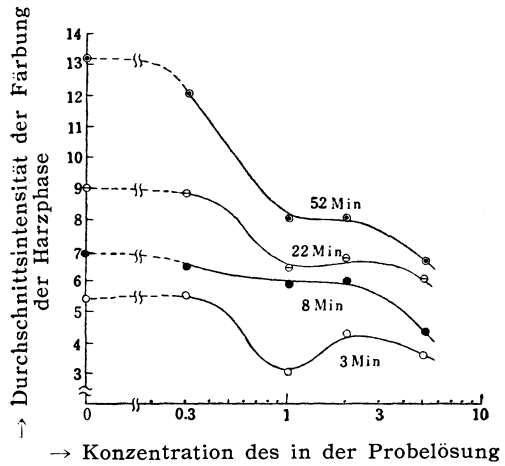



Abb. 4. Einfluss der Salzkonzentration.

**5. Das empfehlenswerteste Verfahren.**—Alles Obenerwähnte zusammengenommen, kann man das am besten geeignete Verfahren wie folgt feststellen:—

„Auf einer weissen Tüpfelplatte versetzt man einige Körnchen des farblosen, starksauren und niedrig vernetzten Kationenaustauscherharzes, mit je einem Tropfen der Probelösung, 3prozentiger Lösung des Hydroxylaminhydrochlorids, 1N Lösung des Natriumacetats als Pufferlösung und 0.5prozentiger alkoholischer Lösung des 2, 2'-Bipyridyls, und deckt dieses Gemisch mit einer Glasscheibe, um das ganze System vor dem in der Luft vorhandenen Staub zu beschützen. Einige Minuten nach der Mischung beobachtet man mit einer Lupe eine Rotfärbung, die die Harzkörnchen bei Anwesenheit von Eisen liefern. Handelt es sich um sehr geringe Menge des Eisens, empfiehlt es sich, einen Blindversuch nebenbei durchzuführen".

## Bestimmung der Erfassungsgrenze

Die Ergebnisse dafür werden in Abb. 5 dargestellt. Die Erfassungsgrenze 0.0025 $\gamma$ von Eisen unter Grenzkonzentration $1{:}1.6\times10^{7}$ wurde hier bestimmt. Diese Erfassungsgrenze entspricht 0.025prozentigem Eisengehalt in 10 $\gamma$ Probe.

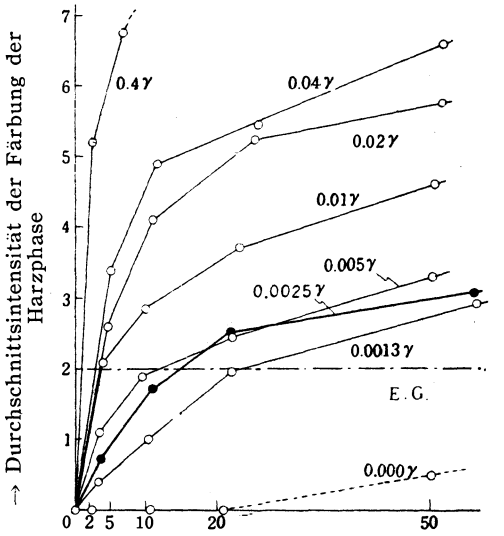



Abb. 5. Bestimmung der Erfassungsgrenze.

Wie bereits im vorhergehenden Abschnitt darauf hingewiesen, muss man hier die Tüpfelplatte

mit einer Glasscheibe fest schliessen, um keinen Staub eindringen zu lassen. Von Bedeutung ist dieses Verfahren besonders dann, wenn es sich um die Spurmenge des Eisens in der Probelösung handelt, denn selbst eine so kleine Menge Eisen, wie in dem in der Luft spurweise vorhandenen Staub enthalten ist, gibt der Harzphase eine deutliche Rotfärbung.

### Einflüsse der Begleitionen

Wie in Tabelle I zusammengestellt, ist die gegenwärtige Nachweismethode entschieden spezifisch, ausser dass Kupfer(II)- und Kobalt(II)-salze ein wenig den Nachweis stören.

TABELLE I

EINFLÜSSE DER BEGLEITSTOFFE

| Begleitstoffe | benutzter Verbindungstypus | Farbton der Harzphase* | Menge der Begleitstoffe | nachweisbare Eisenmenge | Grenzverhältnis | Bemerkungen** |
|---|---|---|---|---|---|---|
| Ti(IV) | $TiOSO_4$ | farblos | 100 γ | 0.004 γ | $1:2.5\times10^4$ | *a, b* |
| V(V) | $NH_4VO_3$ | hellgelbbraun? | 70 γ | 0.0025 γ | $1:2.8\times10^4$ | — |
| Cr(III) | $KCr(SO_4)_2$ | grauviolett | 64 γ | 0.004 γ | $1:1.6\times10^4$ | *c, d,* Cr(III)≦0.2proz. |
| Mn(II) | $MnSO_4$ | farblos | 1580 γ | 0.0025 γ | $1:6.3\times10^5$ | — |
| Co(II) | $Co(NO_3)_2$ | dunkelgelb | 11 γ | 0.007 γ | $1:1.6\times10^3$ | *c, d,* Co≦0.02proz. |
| Ni(II) | $NiCl_2$ | hellgrün | 1400 γ | 0.004 γ | $1:3.5\times10^5$ | *c, e* |
| Cu(II) | $CuSO_4$ | hellgraugrün | 17.5 γ | 0.0025 γ | $1:7\times10^3$ | *c*, Cu≦0.05proz. |
| 〃 | 〃 | weissbraun | 135 γ | 0.007 γ | $1:1.9\times10^4$ | *d, f* |
| Zn(II) | $ZnSO_4$ | farblos | 200 γ | 0.01 γ | $1:2\times10^4$ | *a* |
| Cd(II) | $CdSO_4$ | etwas milchweiss | 1400 γ | 0.0057 γ | $1:2.5\times10^5$ | *a* |
| Hg(II) | $Hg(NO_3)_2$ | farblos | 160 γ | 0.004 γ | $1:4\times10^4$ | Hg(II)≦0.5proz. |
| Cr(VI) | $K_2Cr_2O_7$ | hellbraungrau | 64 γ | 0.004 γ | $1:1.6\times10^4$ | *c, d,* Cr(VI)≦0.2proz. |
| Mo(VI) | $(NH_4)_2MoO_4$ | gelb (etwas getrübt) | 390 γ | 0.004 γ | $1:9.8\times10^4$ | *c* |
| W(VI) | $Na_2WO_4$ | farblos | 360 γ | 0.0025 γ | $1:1.4\times10^5$ | — |
| U(VI) | $UO_2(CH_3COO)_2$ | hellbraun | 350 γ | 0.0025 γ | $1:1.4\times10^5$ | — |
| Pb(II) | $Pb(NO_3)_2$ | farblos | 2200 γ | 0.0025 γ | $1:8.8\times10^5$ | — |
| Sn(IV) | $SnCl_4$ | farblos | 300 γ | 0.0025 γ | $1:1.2\times10^5$ | — |
| Ge(IV) | $GeO_2$ | farblos | 25 γ | 0.0025 γ | $1:1\times10^4$ | — |
| Sb(III) | $SbCl_3$ | farblos | 320 γ | 0.004 γ | $1:8\times10^4$ | — |
| Bi(III) | $Bi(NO_3)_3$ | farblos | 3200 γ | 0.004 γ | $1:8\times10^5$ | *c, g* |
| Al(III) | $Al(NO_3)_3$ | farblos | 1700 γ | 0.004 γ | $1:4.2\times10^5$ | — |
| Be(II) | $BeCl_2$ | farblos | 180 γ | 0.0025 γ | $1:7.2\times10^4$ | — |
| $F^-$ | KF | farblos | 650 γ | 0.01 γ | $1:6.5\times10^4$ | *h* |
| $Br^-$ | KBr | farblos | 7000 γ | 0.0025 γ | $1:2.8\times10^6$ | — |
| $J^-$ | KJ | farblos | 20000 γ | 0.004 γ | $1:5\times10^6$ | *a* |
| $PO_4^{3-}$ | $Na_2HPO_4$ | farblos | 1700 γ | 0.0025 γ | $1:6.8\times10^5$ | — |
| $NO_2^-$ | $NaNO_2$ | farblos | 340 γ | 0.0025 γ | $1:1.4\times10^5$ | — |
| $C_2O_4^{2-}$ | Oxalsaures Ammonium | farblos | 260 γ | 0.007 γ | $1:3.8\times10^4$ | — |
| $C_4H_4O_6^{2-}$ | Seignettesalz | farblos | 920 γ | 0.0025 γ | $1:3.7\times10^5$ | — |
| $C_6H_5O_7^{3-}$ | Zitronensaures Ammonium | farblos | 1400 γ | 0.0025 γ | $1:5.6\times10^5$ | — |

* Farbton der Harzphase hervorgerufen nur durch die Begleitstoffe.

** *a*: Die Probelösung wurde hier vor dem Zusatze der Reagenzien mit 3 bzw. 5 Tropfen destillierten Wassers verdünnt.

*b*: 3 Tropfen der 1N Lösung des Natriumacetats wurden beigefügt.

*c*: Erst dann, wenn der genannte Nachweis neben Blindversuche miteinander durchgeführt wurde, wurde die Anwesenheit des Eisens nachgewiesen.

*d*: Bei diesen Fällen wurden 2 Tropfen 2prozentiger Lösung des 2, 2′-Bipyridyls angewandt.

*e*: Wenn kleinste Menge des Eisens in der Probelösung enthalten ist, färben sich die Ränder der Harzkornchen hell kirschrot.

*f*: Nach dem Zusatze der 2M Kaliumjodidlösung nud 20prozentiger Natriumthiosulfatlösung zur Probelösung wurden die Reagenzien hinzugefügt.

*g*: Der hier gebildete weisse kristalline Niederschlag lieferte auch bei Anwesenheit des Eisens schöne Pfirschfarbe.

*h*: Vor dem Zusatze der Reagenzien wurde die Probelösung mit 1 Tropfen 33prozentiger Essigsäure versetzt.

**Zusammenfassung**[*2]

1. Durch einfache Anwendung von farblosen, starksauren, niedrig vernetzten und eisenfreien Kationenaustauscherharzen, nimmt die Empfindlichkeit und Selektivität der Farbenreaktion zwischen Eisen(II)-salzen und 2, 2′-Bipyridyl beträchtlich zu, und eine ausserordentlich empfindliche und spezifische Nachweismethode für Spurmenge des Eisens wird neu festgestellt.

2. Die besten Experimentalbedingungen werden genau festgestellt durch ausführliche Untersuchung über die Einflüsse von der Harzart, sowie der Konzentration des Reagens, des Hydroxylaminhydrochlorids und der in der Probelösung vorhandenen Salze. Die Einflüsse fremder Ionen werden dabei gründlich untersucht.

Zum Schluss möchte der Verfasser Herrn Prof. Dr. E. Minami für seine zahlreichen wertvollen Ratschläge über die vorliegende Untersuchung seinen herzlichsten Dank aussprechen.

Für die Harzproben, „1proz. DVB", „2.5-proz. DVB" und „20proz. DVB", ist der Verfasser Herrn Prof. Dr. A. Kawamura an der Landwirtschaftlichen und Technischen Universität zu Tokyo zu grossem Dank verpflichtet.

*Laboratorium der analytischen Chemie,*
*Chemisches Institut der*
*wissenschaftlichen Fakultät,*
*Universität zu Tokyo Hongo, Tokyo*

[*2] Der Verfasser gibt hierbei einer ganzen Reihe der neuen Nachweismethoden mit Hilfe von Ionenaustauscherharzen einen passenden Namen „Harztüpfelmethode".

# *Studies on the Chemical Constitution of Agar-agar. XX*[1]. *Isolation of a Tetrasaccharide by Enzymatic Hydrolysis of Agar-agar*[2]

By Choji ARAKI and Kiyoshi ARAI

(Received December 1, 1956)

Araki has suggested that agarose, the main polysaccharide of agar, is composed of 1, 3-linked β-D-galactopyranose and 1, 4-linked 3, 6-anhydro-α-L-galactopyranose, the residues being alternately repeated to form a chain[3]. The structure suggested has been based on the chemical composition of agar, the identification of the scission products of methylated agarose[4,5], the isolation of agarobiose (4-*O*-β-D-galactopyranosyl-3, 6-anhydro-L-galactose) and its derivatives from the products of partial acid hydrolysis[6], mercaptolysis[7] and methanolysis[8] of agar, and the isolation of neoagarobiose (3-*O*-3, 6-anhydro-α-L-galactopyranosyl-D-galactose) from the products of enzymatichydrol ysis of agar[9]. In the last-mentioned process, the extract of an agar-digesting bacterium *Pseudomonas kyotoensis* was used as an enzyme solution, and a mixture of four oligosaccharides resulted. The mixture was resolved into its components by chromatography on a charcoal column, and neoagarobiose was eluted from the column with 7.5% ethanol. This paper is concerned with a tetrasaccharide, which has been eluted from the same column with 17.5% ethanol.

The tetrasacccharide, constituting a predominant quantity (40%) among the hydrolysates, forms a crystalline tetrahydrate having the composition $C_{24}H_{38}O_{19}\cdot 4H_2O$, when crystallized from a mixture of methanol and ethanol. The fully acetylated and methylated derivatives have also been obtained as crystals having the respective compositions $C_{24}H_{28}O_{19}(COCH_3)_{10}\cdot 2H_2O$ and $C_{24}H_{28}O_9(OCH_3)_{10}$. The tetrasaccharide has been shown to be *O*-3, 6-anhydro-α-L-galactopyranosyl-(1→3)-*O*-β-D-

1) Part XIX : S. Hirase, This Bulletin, **30**. 68, 70, 75 (1957).

2) The main part of this paper was presented at the 9th Annual Meeting of the Chemical Society of Japan held in Kyoto on April 3, 1956.

3) C. Araki, This Bulletin, **29**, 543 (1956): *Memoirs of the Faculty of Industrial Arts, Kyoto Technical Univ*, **5**, 21 (1956).

4) C. Araki *J Chem. Soc. Japan*, **58**, 1362 (1937).

5) C. Araki, ibid., **61**, 775 (1940).

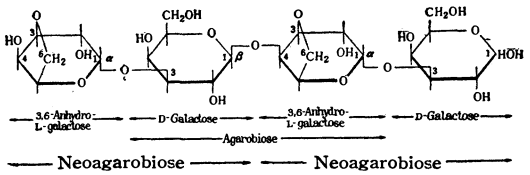
6) C. Araki, ibid., **65**, 533, 627 (1944).

7) S. Hirase and C. Araki, This Bulletin, **27**, 105 (1954).

8) C. Araki and S. Hirase, ibid., **27**, 109 (1954).

9) C. Araki and K. Arai, ibid., **29**, 339 (1956).

galactopyranosyl-(1→4)-*O*-3,6-anhydro-α-L-galactopyranosyl-(1→3)-D-galactose(I), or in a simpler expression 4'-*O*-β-neoagarobiosyl neoagarobiose. The linkages involved provide a strong evidence to support the foregoing structure of agarose suggested by one of the authors.




(I) Neoagarotetraose

The structure (I) has ben assigned for the following reasons. Complete methanolysis of the tetrasaccharide afforded 3,6-anhydro-L-galactose dimethylacetal and methyl D-galactoside in an equal molar proportion, indicating that the tetrasaccharide is composed of two moles each of 3,6-anhydro-L-galactose and D-galactose. On reduction of the tetrasaccharide with sodium borohydride, a corresponding glycitol was obtained, which on methanolysis yielded dulcitol together with 3,6-anhydro-L-galactose dimethylacetal and methyl D-galactoside, establishing thereby the reducing end of the parent tetrasaccharide as a D-galactose residue. When the tetrasaccharide was subjected to hydrolysis with the enzyme extract of *P. kyotoensis*, the sole product that could be detected and isolated was neoagarobiose. This evidence suggests that the tetrasaccharide is neoagarobiosyl-neoagarobiose involvin two 1→3 linkages. On mild hydrolysis of the tetrasaccharide with 0.04 N-oxalic acid solution, there were obtained equal molar quantities of 3,6-anhydro-L-galactose, D-galactose and agaro- biose, the separation being effected by charcoal chromatography. Identification of the last disaccharide proves the presence of the 1→4 linkage in the parent tetrasaccharide molecule. Thus it is possible to assign the structure(I) to the tetrasaccharide isolated.

The structure(I) has been supported also by the identification of the cleavage fragments of the methylated tetrasaccharide. Complete methanolysis of the fully methylated tetrasaccharide afforded a mixture of the following fragments, which were separated on a charcoal column: (a) 2-*O*-methyl-3,6-anhydro-L-galactose derivatives, identified after hydrolysis and bromine oxidation as methyl 2-*O*-methyl-3,6-anhydro-L-galactonate and also as its corresponding amide, (b) 2,4-di-*O*-methyl-3,6-anhydro-L-galactose dimethylacetal, identified after hydrolysis and bromine oxidation as 2,4-di-*O*-methyl-3,6-anhydro-L-galactonic acid and its amide, and (c) methyl 2,4,6-tri-*O*-methyl-D-galactoside, identified after hydrolysis as a crystalline sugar and its anilide.

A general nomenclature is suggested here for the oligosaccharides produced by partial break down of agarose and a similar polysaccharide. The prefix "agaro" is added to an oligosaccharide whose non-reducing end is presented by D-galactopyranose. Thus the name agarobiose was assigned to a disaccharide 4-*O*-β-D-galactopyranosyl-3,6-anhydro-L-galactose[6]. While, the prefix "neoagaro" is added to an oligosaccharide whose non-reducing end is presented by 3,6-anhydro-L-galactopyranose. Thus the name neoagarobiose was assigned to a disaccharide 3-*O*-3,6-anhydro-α-L-galactopyranosyl-D-galactose[9]. On this basis the tetrasaccharide investigated in this paper is termed neoagarotetraose.

From the fact that neoagarobiose and neoagarotetraose resulted from agar by the action of the enzymes of an agar-digesting bacterium, and also that neoagarotetraose is hydrolysed by the same enzymes to yield neoagarobiose, it may possibly be assumed that agarose is hydrolysed by the enzymes at its occasional 1→4 β-D-galactoside linkages to yield higher homologues of neoagaro-oligosaccharides, which are in turn hydrolysed at their 1→4 linkages to form neoagarobiose as the lowest fragement.

## Experimental

**General Procedure.**—Evaporation and concentration were carried out under reduced pressure below 40°. All the melting points are uncorrected. Unless otherwise stated the specific rotation was measured in the aqueous solution with a 1 dm. tube. The paper chromatograms were irrigated with *n*-butanol-acetic acid-water (4 : 1 : 2 v/v) in the ascending manner and were sprayed with an *o*-aminophenol reagent[10]. For the charcoal chromatography, there was used active carbon Shirasagi[11], which was not mixed with Celite.

**Neoagarotetraose.**—A part (2.0 g.) of the 17.5% ethanol eluate, $[\alpha]_D$+1.1°, obtained in Part XVIII[9], was dissolved in a few drops of water, and methanol was added while heating to form insoluble precipitates, which were subsequently removed by filtration. Then absolute ethanol (nearly equal in volume to that of the

10) S. Hirase, C. Araki and S. Nakanishi, ibid., **26**, 183 (1953).
11) Product of Takeda Pharmaceutical Industries, Ltd., Osaka.

methanol used) was added to the filtrate while boiling until the solution became slightly turbid, and the resulting solution was kept in a refrigerator. The crystals deposited were filtered and washed successively with ethanol-methanol (2 : 1), ethanol and ether; yield 0.8 g. The filtrate and washings were combined and evaporated, when the second crop of the crystals was obtained; yield 0.6 g.

The two crops of the recrystals were combined and recrystallized by dissolving in hot methanol, adding twice the volume of ethanol while boiling, and then keeping the solution in a refrigerator. Neoagarotetraose was deposited as colorless fine crystals, which were filtered and washed successively with ethanol-methanol (2 : 1), ethanol and ether; yield 0.50 g. It sintered at 190°, melted at 214–218° under decomposition, and had a specific rotation $[\alpha]_D^{21}$ −3.9° (after twenty four hours, *c* 1.0). It gave on a paper chromatogram a spot whose $R_{gal}$ value[9] was 0.71, and showed a reducing power 27.85% of D-galactose. The analysis of the sample dried at 100° in vacuo over phosphorus pentoxide showed that it was a tetrahydrate.

*Anal.* Found: C, 40.98; H, 6.60. Calcd. for $C_{24}H_{38}O_{19}\cdot 4H_2O$: C, 41.10; H, 6.55%.

The mother liquor of the recrystallization was diluted with methanol and again evaporated to form hygroscopic crystals, which sintered at 98°, melted at 104–107°, had a specific rotation $[\alpha]_D^{22}$ −2.8° (1.0), and which gave a spot with $R_{gal}$ value 0.71 on a paper chromatogram. The analysis of the sample dried at 65° in vacuo over phosphorus pentoxide indicated that it was a dihydrate.

*Anal.* Found: C, 43.07; H, 6.42. Calcd. for $C_{24}H_{38}O_{19}\cdot 2H_2O$: C, 43.10; H, 6.31%.

**Deca-*O*-acetylneoagarotetraose.**—Neoagarotetraose (1.0 g.) in pyridine (20 cc.) was acetylated with acetic anhydride (7.0 g), which was added dropwise under ice cooling. After being left at room temperature (18–19°) for seventy-two hours, the reaction solution was poured with stirring into ice-water (120 cc.), and crystals of the acetate formed were filtered and washed with ice-water; yield 1.0 g.; m. p. 115–116°. Recrystallization was effected first from *n*-butanol and then from methanol-ethanol; m. p. 121°; $[\alpha]_D^8$ −15.8° (chloroform, *c* 1.0) and −11.8° (methanol, *c* 1.0).

*Anal.* Found: C, 49.15; H, 5.74: $CH_3CO$, 41.58. Calcd. for $C_{24}H_{28}O_{19}(COCH_3)_{10}\cdot 2H_2O$: C, 49.10; H, 5.72; $CH_3CO$, 40.00%.

**Methyl Nona-*O*-methyl-β-neoagarotetraoside.**—A methylation of neoagarotetraose (2.0 g.) was carried out first under ice cooling and then at room temperature (24–25°) over three days in the same manner as in the case of neoagarobiose[9], using dimethylsulfate (63 cc., total) and 32% potassium hydroxide solution (150 cc., total). After completion of the reaction, the reaction mixture was filtered to remove the precipitated potassium sulfate and the filtrate was extracted four times with chloroform (200 cc., total). The extracts were combined, washed once with water, dried over sodium sulfate, and evaporated to a syrup (2.5 g.), which on dissolution in ether and evaporation afforded a semi-solid (2.28 g., $OCH_3$ 36.1%). It was then twice methylated with methyl iodide (25 g.) and silver oxide (15 g.), and the final product was obtained by extraction with ether and subsequent evaporation as a crystalline mass (2.0 g., $OCH_3$ 40.5%), which was triturated with ether. The separated crystals were then filtered; yield 0.48 g.; m.p. 164°. An additional crop was obtained from the filtrate by adding petroleum ether (45–53°) and keeping in a refrigerator; yield 0.72 g.; m. p. 163–164°. The crystals obtained were combined, recrystallized from methanol and washed with ether; m. p. 167°; $[\alpha]_D^{10}$ −87.6° (chloroform, *c* 1.0) and −85.9° (methanol, *c* 1.0). The negative values of the rotation indicate that it is a β-anomer of the methylated neoagarotetraoside.

*Anal.* Found: C, 52.90; H, 7.64; $OCH_3$, 40.37; m. w. (Rast), 768. Calcd. for $C_{24}H_{28}O_9(OCH_3)_{10}$: C, 53.12; H, 7.53; $OCH_3$, 40.27%; m. w., 770.

**Methanolysis of Neoagarotetraose.**—Neoagarotetraose (1.0 g.) in 4% methanolic hydrogen chloride (50 cc.) was heated under reflux until the optical rotation of the solution reached a constant value: $[\alpha]_D$ −25.0° (initial)→+32.0° (final). After fifteen hours the solution was neutralized with silver carbonate, filtered and evaporated to a syrup (1.15 g.). Paper chromatographic examination showed that the syrup was a mixture of 3,6-anhydro-L-galactose dimethylacetal and methyl D-galactoside. A part (1.0 g.) of the mixture was separated into its components on a powdered filter paper column in the manner previously reported from this laboratory[8,9].

*3,6-Anhydro-L-galactose Dimethylacetal.*—This substance was eluted from the column with *n*-butanol saturated with water, and was obtained as a colorless syrup on evaporation; 0.50 g.; $[\alpha]_D^{25}$ −31.1° (*c* 0.9); $OCH_3$, found: 29.62% (calcd. for $C_6H_{10}O_4(OCH_3)_2$: 29.81%). It showed a strong Seliwanoff's ketose reaction and gave on a paper chromatogram a spot corresponding to 3,6-anhydro-L-galactose dimethylacetal. Identification was carried out in the usual manner by hydrolysis to a reducing sugar, which was then converted to 3,6-anhydro-L-galactose diphenylhydrazone[12]; m. p. 153°; $[\alpha]_D^{23}$ −34.6° (initial, methanol, *c* 1.4).

*Anal.* Found: N, 8.61. Calcd. for $C_{18}H_{20}O_4N_2$: N, 8.53%.

*Methyl D-Galactoside.*—After removal of the 3,6-anhydro-L-galactose dimethylacetal from the column, methyl D-galactoside was eluted with 80% aqueous methanol, and was obtained as a syrup (0.48 g.) on evaporation. Crystallization from methanol-acetone-(1 : 2) afforded methyl α-D-galactoside monohydrate: m. p. and mixed m. p. 108–109°; $[\alpha]_D^{23}$ +180.5° (*c* 1.0); $OCH_3$, found: 14.73% (calcd. for $C_7H_{14}O_6\cdot H_2O$: 14.62%).

**Reduction and Methanolysis of Neoagarote-**

12) C. Araki, *J. Chem. Soc. Japan*, **65**, 725 (1944).

**traose.**—A solution of neoagarotetraose (1.50 g.) in water (30 cc.) was combined with a solution of sodium borohydride (0.15 g.) in water (10 cc.), and the resulting solution was left at room temperature (7°) withoccasional shaking for two and a half hours, at which time the solution showed no longer reducing power. It was then carefully neutralized with 0.25 N-aqueous acetic acid under ice cooling, and evaporated to dryness. Crude neoagarotetra-itol, obtained as an amorphous material (1.65 g.), was crystallized from methanol-ethanol (1 : 1); m. p. 60–63°; $[\alpha]_D^{11}$ −32.0° (*c* 1.3, *l* 0.5).

The above glycitol (1.60 g.) in 4% methanolic hydrogen chloride (100 cc.) was heated under reflux until the optical rotation of the solution reached a constant value ($[\alpha]_D$ −25.0° → +3.1°) After eighteen hours the solution was neutralized with silver carbonate, filtered and evaporated to give a syrupy mixture (1.45 g.) of the following three products, which were separated by chromatography.

*3,6-Anhydro-L-galactose Dimethylacetal.*—The above mixture was placed on a starch column (4.5×25 cm.) and eluted with *n*-butanol saturated with water. The eluate showing the optical rotation in the negative direction was evaporated to dryness, 3,6-anhydro-L-galactose dimethylacetal being obtained as a colorless syrup; yield 0.60 g; $[\alpha]_D^{22}$ −29.8° (*c* 0.9); $OCH_3$, found: 28.8% (calcd. for $C_6H_{10}O_4(OCH_3)_2$: 29.81%). It was identified in exactly the same manner as that above-mentioned.

*Methyl D-Galactoside.*—The chormatographic column was then eluted with *n*-butanol-ethanol-water (4 : 1 : 2), and the eluate showing the optical rotation in the positive direction was evaporated to dryness. Methyl D-galactoside was obtained as a syrup (0.40 g.) and was identified in exactly the same manner as that above-mentioned.

*Dulcitol.*—The elution with the same solvent was continued and the eluate (200 cc.) showing no optical rotation was concentrated to a syrup (0.20 g.). Then the eluant was changed to 80% aqueous methanol and the eluate (200 cc.) was concentrated to a syrup (0.20 g.). The syrups obtained were combined and subjected to crystallization from methanol, affording dulcitol; yield 0.20 g.; m. p. 186–187°, not depressed on admixture with an authenic sample; $[\alpha]_D^9 \pm 0°$ (*c* 1.0).

*Anal.* Found: C, 39.55; H, 7.42. Calcd. for $C_6H_{14}O_6$: C, 39.56; H, 7.75%.

**Hydrolysis of Neoagarotetraose with 0.04 N-Oxalic Acid.**—Neoagarotetraose (1.50 g.) in 0.04 N-oxalic acid solution (100 cc.) was heated in a boiling water bath, the progress of the hydrolysis being followed polarimetrically: $[\alpha]_D$ −1.7° (initial), −4.0° (15 min.), −3.3° (30 min.), −2.7° (1 hr.), +0.7° (1.5 hr.), +5.5° (2 hr.), +6.0 (2.5 and 3 hr., constant). After three hours the acid was removed by neutralization with calcium carbonate and filtration, the filtrate was concentrated to a syrup, which was then extracted with methanol, and the extract was again concentrated to give a light yellow syrup (1.50 g.). When chromatographed on a paper, it showed a brown spot corresponding to galactose, and two yellow with tails spots, the centres of which had the respective $R_{gal}$ values 2.07 and 3.10, corresponding to agarobiose and 3,6-anhydro-galactose, respectively. The separation of the mixture was effected by the charcoal chromatography of Whistler and Durso[13].

A 10% aqueous solution of the syrup (1.50 g.) was placed on a charcoal column (3.3×7.0 cm.) and eluted with water and with successive higher concentrations of ethanol in water. The eluate (30 cc. per fraction) was examined both polarimetrically and paper chromatographically, and the fractions containing the same material were combined and evaporated to recover the material. The result is given in Table I, and the yields cited indicate the presence of D-galactose, 3,6-anhydro-L-galactose and agarobiose in the approximate mcle ratio 1 : 1 : 1. The identification of each product was carried out in the manner described below.

*D-Galactose.*—Fraction I, which completely solidified, was recrystallized from methanol, affording D-galactose; yield 0.25 g.; m. p. 166–167°; $[\alpha]_D^6$ +96.5° (initial) → +79.5° (after twenty four hours, *c* 1.0).

*Anal.* Found: C, 40.15; H, 6.89. Calcd. for $C_6H_{12}O_6$: C, 40.00; H, 6.67%.

The filtrate of the recrystallization was concentrated to a syrup, which afforded D-galactose phenylosazone on treatment with phenylhydrazine in the presence of acetic acid; m. p. and mixed

TABLE I

CHROMATOGRAPHIC SEPARATION OF THE HYDROLYSATES OF NEOAGAROTETRAOSE WITH 0.04 N-OXALIC ACID SOLUTION

| Fraction | I | II | III | IV | V | VI | VII |
|---|---|---|---|---|---|---|---|
| Eluted by | W | W | 2.5%E | 5.0%E | 7.5%E | 10%E | 17.5%E |
| Volume (cc.) | 330 | 420 | 360 | 570 | 450 | 420 | 450 |
| $[\alpha]_D$(°) | +53.7 | −18.8 | −15.6 | −7.8 | −17.5 | −2.8 | −3.0 |
| Yield (g.) | 0.35 | 0.20 | 0.13 | 0.41 | 0.17 | 0.05 | 0.08 |
| Component identified | D-Galactose | 3,6-Anhydro-L-galactose | | Agarobiose | | Neoagarotetraose unchanged | |

W: Water, E: Ethanol

13) R. L. Whistler and D. F. Durso, *J. Am. Chem. Soc.*, **72**, 677 (1950).

m. p. 187–188°; N, found: 15.63% (calcd. for $C_{18}H_{22}O_4N_4$: 15.70%).

*3,6-Anhydro-L-galactose.*—Fractions II and III showed a distinct Seliwanoff's ketose reaction and reduced a Fehling's solution at room temperature. The phenylosazone prepared therefrom agreed with 3,6-anhydro-L-galactose phenylosazone[12]; m. p. and mixed m. p. 216–217°; $[\alpha]_D^6$ −65.3° (initial) → −37.6° (after twenty four hours, pyridine-ethanol (2 : 3), *c* 0.5, *l* 0.5).

*Anal.* Found: N, 16.62. Calcd. for $C_{18}H_{20}O_3N_4$: N, 16.46%.

*Agarobiose.*—Fractions IV and V showed a Seliwanoff's reaction and reduced a Fehling's solution at room temperature. The phenylosazone prepared therefrom agreed with agarobiose phenylosazone[6]; m. p. 218–219°; $[\alpha]_D^6$ −155.7° (initial) → −137.6° (after forty eight hours, pyridine-ethanol (2 : 3), *c* 0.6, *l* 0.5).

*Anal.* Found: N, 11.23. Calcd. for $C_{24}H_{30}O_8N_4$: N, 11.15%.

*Neoagarotetraose Recovered.*—Fractions VI and VII did not reduce a Fehling's solution at room temperature and gave on a paper chromatogram a single spot corresponding to neoagarotetraose ($R_{gal}$ 0.71), proving thereby to be an unchanged material.

**Hydrolysis of Neoagarotetraose with Enzymes.**—The enzyme solution used for the following experiments was prepared on a 100 cc. scale from *P. kyotoensis* exactly in the same manner as that reported in Part XVIII[9]. Twenty five cc. of the solution was buffered with N/15-potassium dihydrogen phosphate (10 cc.) and was diluted with water to 40 cc., and a drop of toluene was added, the pH value of the resulting solution being 5.6. Three similar batches were prepared: (A) with addition of neoagarotetraose (0.5 g.), (B) with addition of neogarotetraose (0.5 g.) after being heated to kill the enzymes, and (C) without addition of neoagarotraose. These were kept at 40° in an incubator, and aliquotes (2.0 cc.) were periodically withdrawn to determind the reducing power by Bertrand's method (table II). Only the batch A showed an increase in the reducing power, corresponding to 21.8% hydrolysis.

After forty eight hours, batches A and C were respectively heated for five minutes in a boiling water bath to stop the reaction. All the batches were separately concentrated, the residues were repeatedly extracted with hot methanol, and the extracts were again evaporated to dryness. The resulting syrups weighed (A) 0.40 g., (B) 0.40 g. and (C) 0.10g., respectively. Paper chromatographic examination indicated that syrup A was a mixture of neoagarobiose and neoagarotetraose, syrup B contained neoagarotetraose only, and the syrup C contained neither of them, proving thereby that the neoagarobiose in the syrup A was derived by the hydrolysis of neoagarotetraose with enzymes.

For the isolation of the neoagarobiose, the experiment A was repeated five times, and the combined syrups (2.4 g.) were chromatographed on a charcoal column (4.5×10 cm.) in a manner similar to the separation of the acid-hydrolysates of neoagarotetraose, the result being shown in Table III.

Fraction I was chiefly inorganic substances. Fraction II gave on a paper chromatogram a spot ($R_{gal}$ 1.15) corresponding to neoagarobiose, fraction III two spots ($R_{gal}$ 1.15 and 0.71) corresponding to neoagarobiose and neoagarotetraose, and fractions IV, V and VI a spot ($R_{gal}$ 0.71) corresponding to neoagarotetraose, respectively. The identification was carried out as follows.

*Neoagarobiose.*—Fraction II was amorphous powders, a part (0.25 g.) of which was dissolved in a few drops of water, twice its volume of methanol was added while heating, the solution was filtered, and additional methanol was added to the filtrate while heating. When the resulting solution was kept in a refrigerator, neoagarobiose

Table II

Hydrolysis of neoagarotetraose with enzymes*

| | Initial | 8 hr. | 24 hr. | 32 hr. | 48 hr. | ±** |
|---|---|---|---|---|---|---|
| A | 170.4 | 184.0 | 195.0 | 198.5 | 207.6 | +37.2 |
| B | 176.4 | 179.0 | 182.9 | 179.0 | 167.6 | −8.8 |
| C | 6.9 | 8.1 | 10.9 | 9.2 | 10.2 | +3.3 |

A: A buffered enzyme solution (40 cc.) + neoagarotetraose (0.5 g.).
B: A buffered enzyme solution (40 cc.) killed + neoagarotetraose (0.5 g.).
C: A buffered enzyme solution (40 cc.) only.
* The figures are indicated by Bertrand's copper value (mg.), calculated for the whole solution (40 cc.).
** An increase or decrease in copper value after 48 hr.

Table III

Chromatographic separation of enzymatic hydrolysates of neoagarotetraose

| Fraction | I | II | III | IV | V | VI |
|---|---|---|---|---|---|---|
| Eluted by | W | 5%E | 7.5%E | 10%E | 15%E | 17.5%E |
| Volume (cc.) | 640 | 750 | 1230 | 480 | 1050 | 720 |
| Yield (g.) | 0.1 | 0.30 | 0.25 | 0.25 | 1.20 | 0.25 |
| $[\alpha]_D$ (°) | ±0 | +16.5 | −0.9 | −1.8 | −2.9 | −3.0 |

W: Water, E: Ethanol.

was deposited; yield 0.15 g.; m. p. 202–203°, not depressed on admixture with an authentic sample[9]; $[\alpha]_D^{15}$ +25.0° → +22.5° (*c* 1.1).

*Anal.* Found: C, 44.25; H, 6.33. Calcd. for $C_{12}H_{20}O_{10}$: C, 44.44; H, 6.22%.

The filtrate from the above crystals was concentrated to a syrup, which was then treated with phenylhydrazine in the presence of acetic acid. The phenylosazone obtained had m. p. 198–199°, not depressed on admixture with neoagarobiose phenylosazone[9].

*Anal.* Found: N, 11.37. Calcd. for $C_{24}H_{30}O_8N_4$: N, 11.15%.

*Neoagarotetraose Recovered.*—All the fractions IV, V and VI were amorphous powders, which on acetylation with acetic anhydride and pyridine gave neoagarotetraose deca-acetate, m. p. 120–121°, not depressed on admixture with the sample described earlier.

**Methanolysis of Methyl Nona-*O*-methyl-β-neoagarotetraoside.**—The methylated tetraoside (1.70 g.), described earlier, was dissolved in 4% methanolic hydrogen chloride (100 cc.) and the solution was heated under reflux until the optical rotation of the solution reached a constant value ($[\alpha]_D$ −39.9° → +32.4°). After seventeen hours the solution was neutralized with silver carbonate, filtered and evaporated to a syrup, which was then dried by dissolution in ether and re-evaporation; yield 1.60 g.; $OCH_3$, found: 44.5%.

**Separation of the Methanolysates by Charcoal Chromatography.**—A 10%aqueous solution of the above methanolysates (1.60 g.) was placed on a charcoal column (3.5×10 cm.) and eluted with water and with successive higher concentrations of ethanol in water. The eluates were collected at 30 cc. intervals, and the fractions showing the same content were combined and concentrated to dryness (Table IV). The eluates with water (450 cc.) and with 2.5 % ethanol (first 750 cc.) were discarded, since they left nothing on evaporation. The compounds recovered by evaporation were identified in the manner described below.

**a) 2-*O*-Methyl-3, 6-anhydro-L-galactose Part.**—Fractions I and II, showing a distinct Seliwanoff's reaction, were proved to be derivatives of 2-*O*-methyl-3, 6-anhydro-L-galactose by the conversion into the following crystatalline compounds.

*Methyl 2-O-Methyl-3, 6-anhydro-L-galactonate.*—A part (0.27 g.) of the fraction I was hydrolysed with 3% hydrobromic acid (6 cc.) in the boilng water bath for ten minutes, and was then oxidized with bromine (0.4 cc.), which was dropped into the hydrolytic solution kept at 40° during four hours. After being left overnight room temperature, the reaction solution was aerated to remove excess bromine, neutralized with silver carbonate, filtered before and after treatment with hydrgen sulfide, and evaporated to a syrup, which solidified on dissolution in methanol and evaporation; yield 0.23 g.

The oxidation product obtained above was esterified by heating in 4% methanolic hydrogen chloride for five hours. The methyl ester, isolated in the usual manner, was separated from a syrupy contaminant by tiling; yield 0.25 g.; m. p. 85–86°. Recrystallization from benzene afforded pure methyl 2-*O*-methyl-3, 6-anhydro-L-galactonate[5]; yield 0.17 g.; m. p. 91°, not depressed on admixture with an authentic specimen; $[\alpha]_D^{24}$ −61.6° (*c* 0.8, *l* 0.5).

*Anal.* Found: C, 46.79; H, 6.68; $OCH_3$, 29.1. Calcd. for $C_6H_5O_4(OCH_3)_2$: C, 46.58; H, 6.85; $OCH_3$, 30.12%.

*2-O-Methyl-3, 6-anhydro-L-galactonamide.*—The methyl ester obtained above was converted in the usual manner into an amide[5]; m. p. 170–171°; $[\alpha]_D^{23}$ −74.3° (*c* 2.3, *l* 0.5).

*Anal.* Found: N, 7.15; $OCH_3$, 16.22. Calcd. for $C_7H_{13}O_5N$: N, 7.33; $OCH_3$, 16.23%.

**b) 2, 4, 6-Tri-*O*-methyl-D-galactose Part.**—Solid fractions III and IV were methyl 2, 4, 6-tri-*O*-methyl-D-garactoside, contaminated by a small amount of methyl 2-*O*-methyl-3, 6-anhydro-L-galactoside, which was removed as follows. The two fractions were combined and treated with N/50-sulfuric acid in a boilng water bath for two hours to hydrolyse the contaminant, and then the solution was neutralized with barium carbonate, filtered and evaporated to dryness. The resulting residue (0.70 g.), which solidified on dissolution in methanol and re-evaporation, was extrated with boiling petroleum ether (b. p. 45–55°). On cooling the extract afforded crystals of methyl 2, 4, 6-tri-*O*-methyl-D-galactoside; yield 0.40 g.; m. p. 70–72°; $[\alpha]_D^{23}$ +54.2° (*c* 1.8); $OCH_3$, found: 51.37% (calcd. for $C_6H_8O_2(OCH_3)_4$: 52.54%). Evaporation of the mother liquor afforded an additional crop (0.25 g.).

*2, 4, 6-Tri-O-methyl-D-galactose.*—The above

TABLE IV

CHROMATOGRAPHIC SEPARATION OF THE METHANOLYSATES OF METHYLATED NEOAGAROTETRAOSIDE

| Fraction | I | II | III | IV | V | VI | VII |
|---|---|---|---|---|---|---|---|
| Eluted by | 2.5%E | 5%E | 5%E | 7.5%E | 7.5%E | 10%E | 10%E |
| Volume (cc.) | 600 | 600 | 750 | 660 | 600 | 600 | 600 |
| Yield (g.) | 0.30 | 0.06 | 0.48 | 0.20 | 0.15 | 0.22 | 0.05 |
| $n_D^{25}$ | 1.4647 | 1.4655 | solid | solid | 1.4539 | 1.4526 | 1.4500 |
| $OCH_3$ (%) | 32.6 | 33.5 | 47.8 | 49.0 | 49.0 | 48.3 | 49.3 |
| $[\alpha]_D^{25}$ (°) | −29.6 | +34.2 | +73.9 | +63.2 | +50.3 | +26.1 | +54.0 |
| | | 2-*O*-Methyl-3, 6-anhydro-L-galactose part | | 2, 4, 6-Tri-*O*-methyl-D-galactose part | | 2, 4-Di-*O*-mehyl-3, 6-anhydro-L-galactose part | |

E: Ethanol

methyl glycoside (0.40 g.) was hydrolysed with N-sulfuric acid (12 cc.) in the usual manner. The resulting 2,4,6-tri-*O*-methyl-D-galactose was crystallized from ether; yield 0.25 g.; m. p. 97–98°. Recrystallization from the same solvent afforded a pure specimen; yield 0.20 g.; m. p. 113–114°, not depressed on admixture with an authentic sample[4]; $[\alpha]_D^{30}$ +111.7° (initial) → +91.3° (after twenty four hours, *c* 1.7).

*Anal.* Found: C, 48.65; H, 8.27; $OCH_3$, 41.20. Calcd. for $C_6H_9O_3(OCH_3)_3$: C, 48.65; H, 8.11; $OCH_3$, 41.89%.

*2,4,6-Tri*-O-*methyl*-L-*phenyl*-D-*galactosylamine.*—The above sugar was treated with aniline in the usual manner to give an anilide[4]; m. p. 172–173°; $[\alpha]_D^{31}$ −81.5° (initial) → +38.6° (after forty eight hours; acetone, *c* 1.4, *l* 0.5).

*Anal.* Found: N, 4.78; $OCH_3$, 31.54. Calcd. for $C_{15}H_{23}O_5N$: N, 4.71; $OCH_3$, 31.31%.

**c) 2,4-Di-*O*-methyl-3,6-anhydro-L-galactose Part.**—Fractions V, VI and VII were fairly positive to Seliwanoff's test and gave on a paper chromatogram a yellow spot corresponding to 2,4-di-*O*-methyl-3,6-anhydro-L-galactose dimethylacetal.

*2,4-Di*-O-*methyl-3,6-anhydro*-L-*galactonic Acid.*—The fractions VI and VII were combined and a part (0.25 g.) of the resulting mixture was hydrolysed and then oxidized in exactly the same manner as that described for 2-*O*-methyl-3,6-anhydro-L-galactose derivatives. The oxidation product (0.18 g.) was crystallized from ethyl acetate; m. p. 150°, not depressed on admixture with 2,4-di-*O*-methyl-3,6-anhydro-L-galactonic acid[14]; $[\alpha]_D^{17}$ −61.4° (*c* 1.2, *l* 0.5).

*Anal.* Found: C, 46.34; H, 6.86; $OCH_3$, 29.66. Calcd. for $C_6H_8O_4(OCH_3)_2$: C, 46.58; H, 6.85; $OCH_3$, 30.15%.

*2,4-Di*-O-*methyl-3,6-anhydro*-L-*galactonamide.* The above acide (0.1 g.) was esterified with boiling 4% methanolic hydrogen chloride (3 cc.) and the methyl ester obtained was further converted to the amide[14] in the usual manner; m. p. 150°; $[\alpha]_D^{24}$ −73.4° (*c* 1.3, *l* 0.5).

*Anal.* Found: N, 6.95; $OCH_3$, 29.65. Calcd. for $C_8H_{15}O_5N$: N, 6.83; $OCH_3$, 30.25%.

14) C. Araki, *J. Chem. Soc. Japan*, **61**, 503 (1940).

## Summary

1. A tetrasaccharide, forming a crystalline tetrahydrate, has been isolated from the products of enzymatic hydrolysis of agar. Its fully acetylated and methylated derivatives have also been obtained as crystals.

2. Identification of both monosaccharide and disacharide constituents has led to the assignment of the structure, *O*-3,6-anhydro-α-L-galactopyranosly-(1→3)-*O*-β-D-galactopyranosyl-(1→4)-*O*-3,6-anhydro-α-L-galactopyranosyl-(1→3)-D-garactose, to the tetrasaccharide isolated. The structure has been supported also by methylation data.

3. The tetrasaccharide has been termed neoagarotetraose, based on the general nomenclature suggested for oligosaccharides derived from agarose and a similar polysaccharide.

4. A probable course has been assumed for the enzymatic degradation of agarose.

The authors are indebted to Mr. N. Nakata for assistance in this study and to Mr. S. Hirase for help in the preparation of the manuscript. This study has been aided by the Grant for Fundamental Scientific Research from the Ministry of Education, for which our thanks are also expressed.

*Institute of Chemistry, Faculty of Industrial Arts, Kyoto Technical University, Matsugasaki, Kyoto*

# *Photo-dichroism of Printed-out Silver. II. Theoretical Consideration of the Mechanism from the point of View that the Phenomenon of Photo-dichroism would be an Anisotropic Herschel effect*

By Isao KAMIYA

(Received July 12, 1956)

In the previous paper[1], the author has reported some experimental evidences in favor of the view that the phenomenon of photo-dichroism of printed-out silver is an anisotropic Herschel effect.

In the present paper, the author carries out the theoretical consideration of the same subject and proposes the mechanism by which the films of printed out silver being exposed to polarized light become anisotroric in their optical nature.

According to the theory, the value of photo-dichroism would be given by the formula which is the function of the time of exposure, energy of exposing light, temperature and the wave length of observed light. Thus, the quantitative expression of the phenomenon, which has not been reported up to the present, can be undertaken.

## Consideration

Mott and Gurney[2] have proposed the following explanation of the mechaism of of Herschel effect.

When a previously illuminated film (in which the latent image is contained) is exposed to red light, the action of the light will remove electrons from the latent image (paticles of metallic silver) into conduction band of silver halide. The silver speck then carries a positive charge. This will cause an electrolytic current, consisting of silver ions, to flow from the latent image into the silver halide crystals. The silver speck thus will be gradually destroyed.

When a surface of metallic silver is exposed obliquely, as shown in Fig. 1, to polalized light of which the electric vector is in the plane of incidence, the number of inner-photo-electrons (say $J_{\parallel}$) is given by the following formula[3],

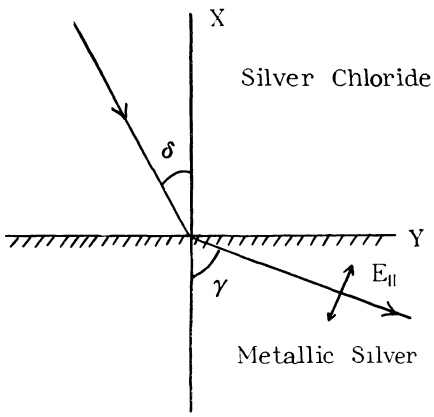



Fig. 1.

$$J_{\parallel}=\frac{R_0}{h\nu}\frac{\sin^2\gamma\sin^2\delta}{\sin^2(\gamma+\delta)\cos^2(\delta-\gamma)}\times\left(1-\sqrt{(\phi-\chi)/h\nu}\right)\left[1+\frac{3}{2}\times(2-\cos^2\gamma)\{\sqrt{(\phi-\chi)/h\nu}+(\phi-\chi)/h\nu\}\right] \quad (1)$$

by the light of which the electric vector is perpendicular to the plane ($J_{\perp}$),

$$J_{\perp}=\frac{R_0}{h\nu}\frac{\sin^2\gamma\cos^2\delta}{\sin^2(\gamma+\delta)}\left(1-\sqrt{(\phi-\chi)/h\nu}\right)\times\left[1-\frac{1}{2}\{\sqrt{(\phi-\chi)/h\nu}+(\phi-\chi)/h\nu\}\right] \quad (2)$$

where $\phi$ is the work function of metallic silver, $\chi$ is the electron affinity of silver chloride, $h\nu$ is the energy of exposiog light and $\delta$ and $\gamma$ are the angles of incidence and refraction. $R_0$ is to be given as,

$$R_0=A(\varepsilon+A)[1-\exp\{-(\varepsilon+A)d\}]$$

where $A$ is the fraction of absorbed quanta contributing to remove the electrons and $\varepsilon$ is that on other processes and $d$ is the thickness of the metal.

In fact, there would be a great many such surfaces of metallic silver in the film of printed-out silver and the normals

1) I. Kamiya, This Bulletin, **30**, 6 (1957).
2) N. F. Mott and R. F. Gurney, "Electronic. Processes in Ionic Crystals," Oxford Press (1950), p. 243.
3) I. Kamiya, *J. Chem. Soc. Japan*, **76**, 960 (1955).

of these surfaces would orientate in all directions.

The number of inner-photo-electrons for arbitrary surfaces can be calculated in the following ways.

Let $x$ be the direction of incident parallel beam of which the electric vector is in $xy$-plane ($y$ being perpendicular to $x$) and $z$ be the direction being perpendicular to $x$ and $y$.

Then, if the direction cosines of the normal to this surface are $\cos\alpha$, $\sin\alpha\cos\beta$, and $\sin\alpha\sin\beta$ with respect to $x$, $y$ and $z$, and $y$ and $z$ axes are rotated by $\beta$ on $yz$-plane, let two new axes be called to $y'$ and $z'$ axes, then the $xy'$-plane will be the plane of incidence and $xz'$-plane will be the plane being perpendicular to the plane of incidence (Fig. 2).

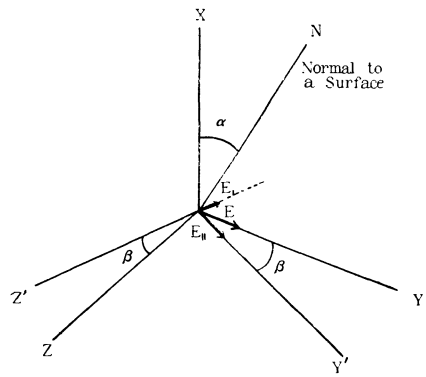



Fig. 1.

The electric vector of exposing light is divided into two components, one of which is in $xy'$plane (say $\boldsymbol{E}_{\parallel}$), and the other in $xz'$-plane (say $\boldsymbol{E}_{\perp}$).

Thus, the number of inner-photo-electrons due to $\boldsymbol{E}_{\parallel}$ can be obtained by the same method as before, that is,

$$J_{\parallel}' = \frac{R_0}{h\nu}\frac{\sin^2(\alpha+\alpha')\cos^2(\alpha-\alpha')}{\sin^2\alpha\sin^2\alpha'}\times\left(1-\sqrt{(\phi-\chi)/h\nu}\right)\times\left[1+\frac{3}{2}(2-\cos^2\alpha')\{\sqrt{(\phi-\chi)/h\nu}+(\phi-\chi)/h\nu\}\right]\boldsymbol{E}_{\parallel}^2 \quad (3)$$

and to $\boldsymbol{E}_{\perp}$,

$$J_{\perp}' = \frac{R_0}{h\nu}\frac{\sin^2\alpha\cos^2\alpha'}{\sin^2(\alpha+\alpha')}\left(1-\sqrt{(\phi-\chi)/h\nu}\right)\times\left[1-\frac{1}{2}\{\sqrt{(\phi-\chi)/h\nu}+(\phi-\chi)/h\nu\}\right]\boldsymbol{E}_{\perp}^2 \quad (4)$$

where $\alpha$ and $\alpha'$ are the angles of incidence and refraction. The relation between $\alpha$ and $\alpha'$ will be given as,

$$n_1\sin\alpha = n_2\sin\alpha'$$

in which $n_1$ is refractive index of silver chloride and $n_2$ is that of metallic silver.

Then, the total number of such electrons for all particles due to each component are given by the following formula,

To $\boldsymbol{E}_{\parallel}$,

$$J_{\parallel\,\mathrm{Tol}} = \int_0^{\pi}\int_0^{\pi/2}\frac{R_0}{h\nu}\left(1-\sqrt{(\phi-\chi)/h\nu}\right)\times\frac{\sin^2\alpha\sin^2\alpha'}{\sin^2(\alpha+\alpha')\cos^2(\alpha-\alpha')}\times\left[1+\frac{3}{2}(2-\cos^2\alpha')\{\sqrt{(\phi-\chi)/h\nu}+(\phi-\chi)/h\nu\}\right]\cos^2\beta\,d\alpha'd\beta \quad (5)$$

and to $\boldsymbol{E}_{\perp}$,

$$J_{\perp\,\mathrm{Tol}} = \int_0^{\pi}\int_0^{\pi/2}\frac{R_0}{h\nu}\left(1-\sqrt{(\phi-\chi)/h\nu}\right)\times\frac{\sin^2\alpha\cos^2\alpha'}{\sin^2(\alpha+\alpha')}\times\left[1-\frac{1}{2}\{\sqrt{(\phi-\chi)/h\nu}+(\phi-\chi)/h\nu\}\right]\sin^2\beta\,d\alpha'd\beta \quad (6)$$

where, for simplicity, the electric vector is taken to be a unit, so that $\boldsymbol{E}_{\parallel}=\cos\beta$ and $\boldsymbol{E}_{\perp}=\sin\beta$. Then, it is furthr put that $n_2$ is equal to $n_1/10$*, $R_0$ is independent on $\alpha'$.

To these approximations, $J_{\parallel\,\mathrm{Tol}}$ and $J_{\perp\,\mathrm{Tol}}$ cnn be calculated by means of approximation integration using trapezoidal rule,

$$J_{\parallel\,\mathrm{Tol}} \doteqdot \frac{1-\sqrt{(\phi-\chi)/h\nu}}{h\nu}[0.13+0.27\{\sqrt{(\phi-\chi)/h\nu}+(\phi-\chi)/h\nu\}]R_0 \quad (7)$$

$$J_{\perp\,\mathrm{Tol}} \doteqdot \frac{1-\sqrt{(\phi-\chi)/h\nu}}{h\nu}[0.09-0.05\{\sqrt{(\phi-\chi)/h\nu}+(\phi-\chi)/h\nu\}]R_0 \quad (8)$$

After the absorption process, the silver specks will be gradually destroyed by the mechaism proposed by Mott and Gurney.

* The refractive indexes of metallic silver, silver chloride and silver bromide for $\lambda=656\,m\mu$ are given as 0.25, 2.05 and 2.23 respectively. J. W. Mellor, "A Compre- hensive Trea- tise on Inorg. and Theor. Chem." Vol. III (1930), pp. 331, 396 and 421.

In order to calculated the rate of destruction of silver specks, it is assumed that the rate will depend on the concentration gradient of silver ions.

When the film in which $n_0$ particles of metallic silver have been contained is exposed to polarized red light, the number of silver ions produded in $t$ minutes is given by the following formula, since the number of such ions is equal to that of inner-photo-electrons,

$$\left.\begin{aligned} n_{\parallel}' &= n_0\{1-\exp(-J_{\parallel \mathrm{Tol}}\cdot t)\} \quad \text{to } \boldsymbol{E}_{\parallel}, \\ n_{\perp}' &= n_0\{1-\exp(-J_{\perp \mathrm{Tol}}\cdot t)\} \quad \text{to } \boldsymbol{E}_{\perp}. \end{aligned}\right\} \quad (9)$$

Now, let d$n$ be the amount of silver ions self-diffusing into silver chloride in time of dt, then this is shown as,

$$\mathrm{d}n = D\cdot S\cdot \Delta C \mathrm{d}t \quad (10)$$

where, $S$ the contact area between silver ion and silver chloride, $\Delta C$ is the concentration gradient of these ions and $D$ is diffusion constant.

In (10), it is further assumed that, $S$ is independent on exposing time and $\Delta C$ is propotional to the number of producing ions by the assumption made before, then,

$$\Delta C = k\mathrm{d}[n_0\{1-\exp(-J_{\mathrm{Tol}}\cdot t)\}]/\mathrm{d}t$$
$k$: constant.

With this consideration, the remainded number of colloidal particles of metallic silver after $t$ minutes' exposure is given,

$$n_{\parallel \mathrm{R}} = n_0 - \int_0^t DSk\mathrm{d}\{1-\exp(-J_{\parallel \mathrm{Tol}}\cdot t)\}/\mathrm{d}t\cdot \mathrm{d}t = n_0[1-DSk\{1-\exp(-J_{\parallel \mathrm{Tol}}\cdot t)\}] \quad \text{to } \boldsymbol{E}_{\parallel}, \quad (11)$$

$$n_{\perp \mathrm{R}} = n_0[1-DSk\{1-\exp(-J_{\perp \mathrm{Tol}}\cdot t)\}] \quad \text{to } \boldsymbol{E}_{\perp}. \quad (12)$$

Now, it may be taken that,

$$D = D_0\exp(-U/RT)$$

where, $U$ is the diffusion energy of silver ion at the temperature of $T^\circ$ $K$, $R$ is gas constant and $D_0$ is a constant, so that (11) and (12) will be, putting $K = D_0Sk$,

$$n_{\parallel \mathrm{R}} = n_0[1-K\{1-\exp(-J_{\parallel \mathrm{Tol}}\cdot t)\}\times\exp(-U/RT)] \quad (13)$$

$$n_{\perp \mathrm{R}} = n_0[1-K\{1-\exp(-J_{\perp \mathrm{Tol}}\cdot t)\}\times\exp(-U/RT)] \quad (14)$$

Now, if we measure the absorption of of the film, which has been exposed to polarized red light, with the light of which the electric vector is the same direction as that of exposed light, the intensity of the light after passing through the film is,

$$I_{\parallel} = I_0\exp\{-(\lambda_{\parallel} n_{\parallel \mathrm{R}} + \lambda_{\perp} n_{\perp \mathrm{R}})\} \quad (15)$$

with the light of which the electric vector is perpendicular to that of exposed light,

$$I_{\perp} = I_0\exp\{-(\lambda_{\perp} n_{\parallel \mathrm{R}} + \lambda_{\parallel} n_{\perp \mathrm{R}})\} \quad (16)$$

where, $\lambda_{\parallel}$ is the absorption coefficient when the electric vector of observed light is in the plane of incidence and $\lambda_{\perp}$ is that when the electric vector is perpendicular to the plane.

The value of photo-dichroism ($\boldsymbol{D}$) is defined[4] as,

$$\boldsymbol{D} = \ln I_{\parallel} - \ln I_{\perp} \quad (17)$$

hence, putting (15) and (16) into (17), we obtain as,

$$\boldsymbol{D} = (\lambda_{\parallel} - \lambda_{\perp})(n_{\perp \mathrm{R}} - n_{\parallel \mathrm{R}}) \quad (18)$$

Then, from (8), (9), (13) and (14), (18) is written as,

$$\boldsymbol{D} = n_0K(\lambda_{\parallel} - \lambda_{\perp}) \times [e^{-(1-\sqrt{(\phi-\chi)/h\nu})/h\nu\,[0.09-0.05\{\sqrt{(\phi-\chi)/h\nu}+(\phi-\chi)/h\nu\}]R_0t} - e^{-(1-\sqrt{(\phi-\chi)/h\nu})/h\nu\,[0.13+0.27\{\sqrt{(\phi-\chi)/h\nu}+(\phi-\chi)/h\nu\}]R_0t}] \times \exp(-U/RT) \quad (19)$$

TABLE I

THEORETICAL AND EXPERIMENTAL VALUES OF DICHROISM AGAINST THE TIME OF EXPOSURE

| Wave length of measuring light (mμ) | Time of exposure (Min.) Parameters $n_0K(\lambda_{\parallel}-\lambda_{\perp})\exp(U/RT)$. | 5 obs. | 5 calcd. | 15 obs. | 15 calcd. | 30 obs. | 30 calcd. | 60 obs. | 60 cald. |
|---|---|---|---|---|---|---|---|---|---|
| 680 | 135.4 | 18 | 15.2 | 38 | 39.7 | 62 | 65.4 | 83 | 91.4 |
| 640 | 353.5 | 45 | 39.6 | 114 | 103.7 | 159 | 170.8 | 205 | 238.4 |
| 620 | 444.9 | 62 | 65.4 | 136 | 145.2 | 227 | 239.1 | 334 | 333.9 |
| 540 | −309.8 | — | −37.8 | — | −80.8 | −152 | −148.6 | −206 | −210.7 |
| 520 | −227.2 | −26 | −25.5 | — | −66.6 | −103 | −109.7 | −162 | −153.3 |

4) F, Weigert, *Z. Phys. Chem.*, **B3**, 389 (1929).

As seen from (19), $D$ depends on the time of exposure ($t$), energy of exposing light ($h\nu$), temperature ($T$) and the wave length of measuring light. ($\lambda_{\parallel}-\lambda_{\perp}$).

With the experimental condition, we put $h\nu=1.8$ eV. and assume that $\phi-\chi$ is 1 eV[2]. and $R_0$ is equal to 1/2**, then (19) is deduced to be,

$$D=n_0K(\lambda_{\parallel}-\lambda_{\perp})\{\exp(-0.026\,t)-\exp(-0.002\,t)\}\exp(-U/RT) \quad (20)$$

In (20), if $T$ is constant, $D$ is the function of $t$ and ($\lambda_{\parallel}-\lambda_{\perp}$). Thus, by taking ($\lambda_{\parallel}-\lambda_{\perp}$) to be the suitable parameter which is the function of the wave length of observed light, $D$ can be plotted against $t$. These results are shown in Table I, where, it is found that the theoretical is in fairly good agreement with the experimental.

Furthermore, according to the author's theory, the activation energy of this dichroric change is explained as the diffusion energy of silver chloride, which has been known to be about 7000 cal/mol[5]. In the previous paper, the activation energy has been found to be of the order 7000 cal/mol[1].

From these evidences, it would be said that the author's theory might be permissible.

As has been shown, the parameter method can explain the behavior of dichroism against the time of exposure. This method, however, is not pemissible to solve the values observed with the light of which the wave lengths are in the region between 550 and 580 m$\mu$. As illustrated in Fig. 3, the continuous curves obtained by means of the parameter method are in good agreement with experimental results in the region more than 580 m$\mu$ and less than 550 m$\mu$. (being shown as triangle points). This agreement, however, is not satisfactory in the region between 550 and 580 m$\mu$ as seen in Fig. 3 (dotted lines).

This will probably be due to the fact that the values of ($\lambda_{\parallel}-\lambda_{\perp}$) are not independent to the time of exposure. This is to be discussed in the next paper.

It has been found that, when the film is exposed to the light of which the wave length is 630 m$\mu$, the value which is observed with this wave length is larger than that with any other wave length, and if exposed to green light, the value

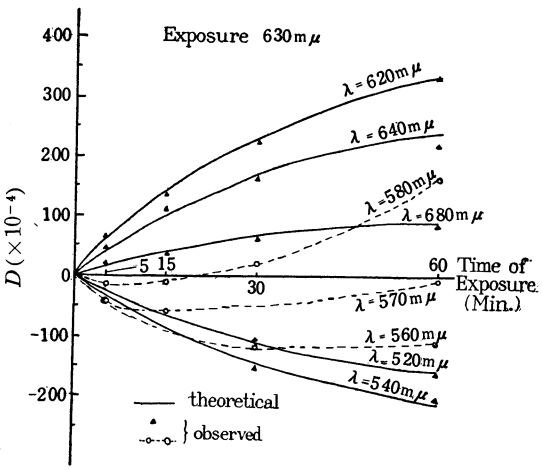



Fig. 3. The curves of theoretical and experimental values of $D$ against the time of exposure.

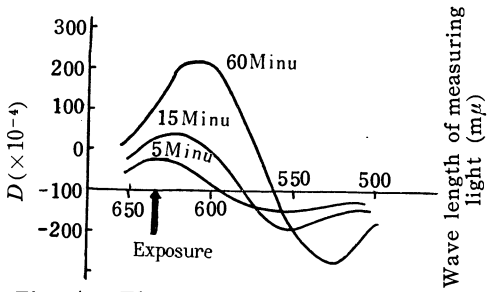



Fig. 4. The curves of $D$ against the wave length of measuring light for exposure to 630 m$\mu$.

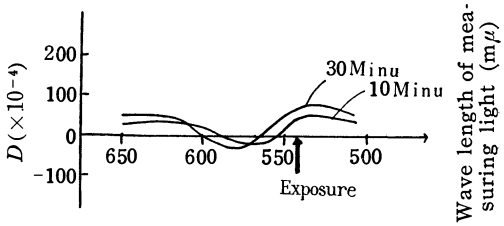



Fig. 5. The curves of $D$ against the wave length of measuring light for exposure to 540 m$\mu$.

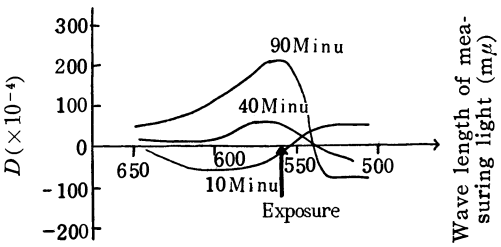



Fig. 6. The curves of $D$ against the wave length of measuring light for exposure to 560 m$\mu$.

5) Ref, (2) p. 47.

** Being $A$ equal to $\varepsilon$, $R_0$ is to be 1/2 for larger value of $\alpha$.

observed with green light is maximum and so on. In Figs. 4, 5 and 6, the observed values of dichroism with various wave lengths are shown for the films which are exposed to 630, 540 and 500 m$\mu$ respectively, in which the ordinates denote the degree of dichroism and the abscissa the wave length of observed light.

This phenomenon is termed "Color adaptation of photo-dichroism.

The phenomenon of photo-dichroism shows further peculiar behavior. The maximum point, corresponding to color adaptation, is shifted to a shorter wave length region by increasing the exposure. The values in the green region become negative for the film which is exposed to red light, whereas the values in red region become negative for one exposed to green light. These are shown in Figs. 4 and 5. This is called "Inversion effect of photo-dichroism."

Every kind of behavior can not be solved by means of the parameter method. That is, it is recessary to study the variation of $(\lambda_{\parallel}-\lambda_{\perp})$ in order to investigate these complicated kinds of behavior.

From the above point of view, the author is going to investigate the absorption spectra of the films of printed-out silver in various conditions so that these kinds of behavior may be explained by the changing of absorption coefficients.

The author wishes to express his thanks to the late Prof. J. Shidei and Dr. D. Yamamoto for their kind advice.

*Department General Education,*
*Nagoya University, Nagoya*

# *Photo-dichroism of Printed-out Silver. III. Absorption Spectra and Dichroism*

By Isao KAMIYA

(Received August 9, 1956)

According to the theory which has been developed by the author, the phenomenon of photo-dichroism is probably an anisotropic Herschel effect and when the film of printed-out silver is exposed to linear polarized red light of energy 1.8 eV. for $t$ minutes at $T°$ K, the value of dichroism is given by the following equation,

$$D=n_0K(\lambda_{\parallel}-\lambda_{\perp})\{\exp(0.002\,t)-\exp(-0.026\,t)\}\exp(-U/RT) \quad (1)$$

where $\lambda_{\parallel}$ and $\lambda_{\perp}$ are the absorption coefficients of the lightof which the electric vectors are in the plane of incidence and perpendicular to the plane. (This plane is constructed with the incident ray and the normal to the surface of colloidal silver). $U$ is activation energy, $R$ is gas constant and $n_0K$ is constant.

When $T$ is constant, with suitable values of parameter $n_0Ke^{-U/RT}(\lambda_{\parallel}-\lambda_{\perp})$, (1) gives curves of $D$ against the time of exposure closely resembling the experimental results, as has been shown in a previous paper[1]. The method of calculating $D$ with the parameter has been called the parameter method.

This parameter method, however. was not acceptable to calculate the values observed with the light of which wave lengths are in the region between 580 m$\mu$ and 550 m$\mu$.

This is probably due to the fact that $(\lambda_{\parallel}-\lambda_{\perp})$ is no longer taken to be independent of the time of exposure in this case.

Moreover, the treatment using this method did not say anything about the complicated phenomena such as *Color-adaptation* and *Inversion effect*, for, in order to explain these phenomena, the variation of $(\lambda_{\parallel}-\gamma_{\perp})$ under the action of exposing light must be considered.

From this point of view, the author has investigated the question if the variation of absorption spectrum of the film of printed-out silver is found when exposed to red or orenge light.

Actually, there appeared a new absorption spectrum in the film after prolonged exposure to red or orange light.

A possible explanation of this appearance of the new absorption spectrum could

1) I. Kamiya, This Bulletin, **30**, 294 (1957).

be given when it is assumed that the process would be an anisotropic Herschel effect.

It has been also found that the absorption difference curve by subtracting the absorption curve of an exposed film from of an unexposed one is very similar to the obsorved spectral dispersion curve of dichoroism. Then the author has been able to explain the processes of *Color-adaptation* and *Inversion effect* as well as of the peculiar behavior of the values of dichroism observed with the light of which the wave lengths are in the region between 580 mμ and 550 mμ, which is his main purpose in this paper, assuming that the phenomenon of photo-dichroism would be a results of difference in absorption of two systems, one is that before exposure and the other is that after exposure.

## Experimental

The films of Valenta's emulsion were prepared by the same method as described by Weigert[2].

One of these was washed by water so that it was almost free from all soluble silver salts (such as silver nitrate and organic silver compounds), let this plate be called "washed plate". The other was unwashed: called "unwashed plate".

Then, the absorption curves were measured by use of Beckmann-type spectrophotometer under various conditions as the following:

1. The absorption curve of washed plate of printed-out silver which had been illuminated with ultra-violet light of Hg-lamp was measured, and after that time that of the washed plate after being exposed to strong natural red light (630 mμ) was measured. The measurements are shown in Fig. 1, where the continuous line (a)

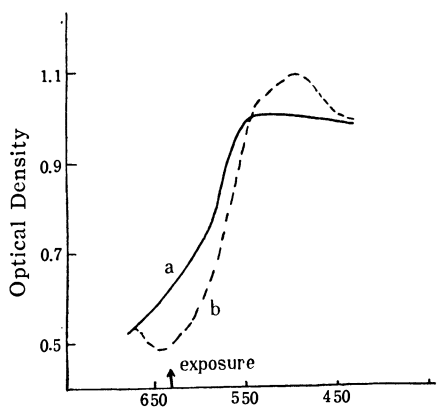



Fig. 1. Absorption curves of washed plate.
a: before exposure,
b: after exposure to 630 mμ.

2) F. Weigert, *Ann. Physik*, **63**, 685 (1920).

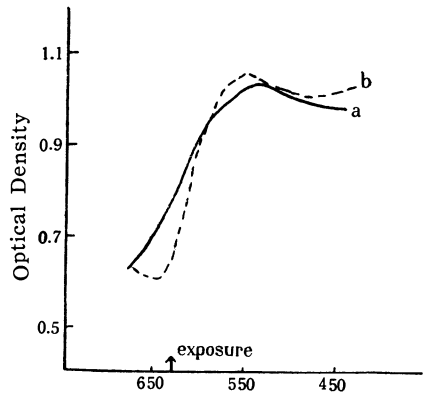



Fig. 2. Absorption curves of unwashed plate.
a: before exposure,
b: after exposure to 630 mμ.

and broken one (b) denote the absorption curves before and after exposure respectivery.

A five ampere carbon are and glass filter of 620–640 mμ spectral region (Shimazu, No. 63), were used as exposing red light source.

2. The curves of the unwashed plate were also measured under the same conditions as that of the washed plate by the same way as described above, which are shown in Fig. 2, where the descriptions are the same as those in Fig. 1. As shown in Fig. 1 and Fig. 2. there can be seen the remarkable *Color-adaptation*, that is, the plates which have been exposed to red light are transparent in red light.

The curves obtained under other conditions (such as under exposure to orange light) are to be shown in the next section.

## Discussion

After per-illumination with ultra-violet light, the film of Valenta's emulsion which bad been almost transparent turned brown at first, then became dark red.

This coloring metter, a new absorption band appearing in visible region, is attributed to the formation of colloidal particles of metallic silver[3].

According to Freundlich[4], the absorption spectra of colloidal particles of metallic siver depend on the dimensions of these particles and the maxima of the spectra shift to the shorter wave length side as the dimension become smaller. In Table I, the relation between diameters of the perticles and transmitted light is illustrated.

As seen in Fig. 1 and 2, the transparency of red light increases after exposed to red light (*Color-adaptation*).

3) R. Hilsch and R. W. Pohol, *Z. Phys.*, **77**, 42 (1933).
4) H. Freundlich, "Kapillarchemie", **I**, Leipzig (1932). P. P. 32.

TABLE I
RELATION BETWEEN DIAMETER AND TRANSMITTED LIGHT OF COLLOIDAL SILVER PARTICLES

| Diameter of colloidal silver particles in mμ | Transmitted light |
|---|---|
| 25—35 | red |
| 35—45 | red—violet |
| 50—60 | blue—violet |
| 70—80 | blue |

This may be due to the following mechanism.

When the particles of metallic silver are exposed to red light, the comparative large particles which are sensitive to red light will absorb the light and be destroyed causing Herschel effect so that the transparency in red light increases[1].

Tallert[5], in the study of Herschel effect, has concluded that colloidal particles of metallic silver do nothing but break up into smaller and more numerous parts by Herschel effect. On account of this, the opacity of the film increases in green region by such re-distributed particles which are the most sensitive to green light.

Next, if the absorption difference curve by substructing the absorption curve of exposed film from that of non-exposed one is made, i. e. the curve of (b)—(a) in Fig. 1 or 2, this is almost similar to the spectrometric dichroism curve.

In Figs. 3 and 4, the difference curves and observed dichroism curves of the washed plate and the unwashed plate are shown, where the upper curve donotes the dichroism curve and the lower the

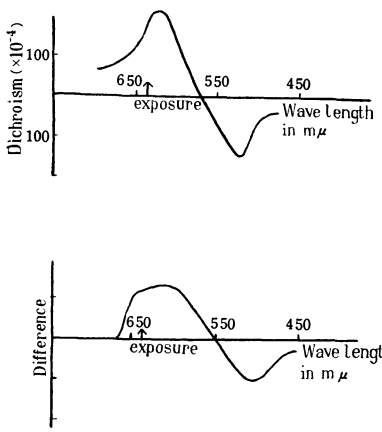



Fig. 3. Absorption difference curve and dichroism curve of washed plate when exposed to 630 mμ.

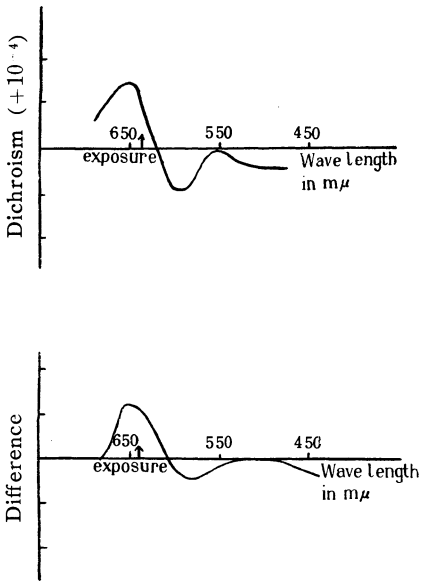



Fig. 4. Absorption difference curve and dichroism curve of unwashed plate when exposed to 630 mμ.

difference curve. The dichroism and difference curves of unwashed plate are almost similar to those of washed plate, but are displaced somewhat in the direction of the long wave length side.

This might be due to the difference of absorption spectra between washed and unwashed plates.

This similarity is also found when the film is exposed to strong orange light (580 mμ). The absorption curves after and before exposure are shown, where

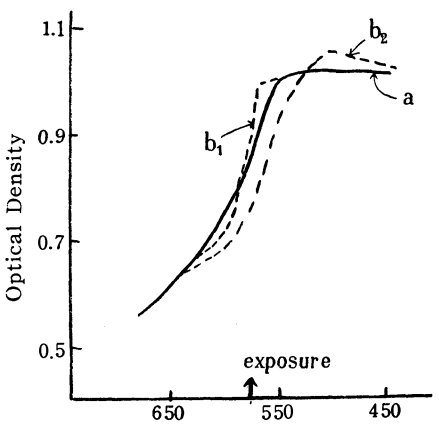



Fig. 5. Absorption curves of washed plates.
a: before exposure-
$b_1$: after 20 minutes' exposure,
$b_2$: after 90 minutes' exposure to 580 mμ.

5) H. Tallert, *Z. phys. Chem.*, **140**, 355 (1929).

(a) is the absorption curve of the washed plate before exposure, ($b_1$) and ($b_2$) are those after exposure for 20 and 90 minutes. Thus the absorption difference curves for 20 and 90 minutes' exposure were obtained as before.

In Fig. 5, these difference curves are shown. It is found that these curves are fairly analogous to dichroism curves (when exposed to linear polarized orange light), which are shown in Fig. 6.

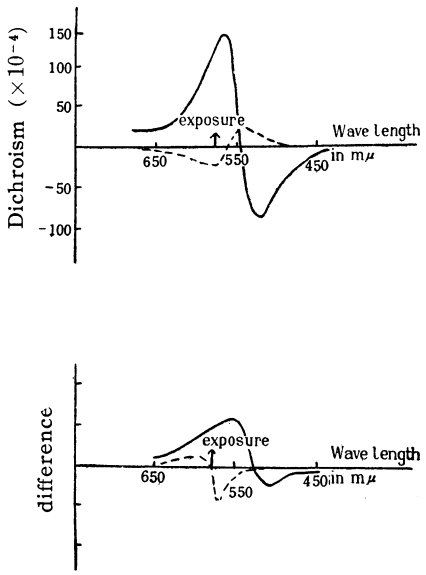



Fig. 6. Absorption difference curve and dichroism curve of washed plate when exposed to 580 mμ.
---: after 20 minutes' exposure,
——: after 90 minutes' exposure.

A five ampere carbon arc and a glass filter of 580 mμ and 600 mμ spectral region were used as orange light source.

It should be noticed here that the absorption difference curve is not color-adaptable in the beginning of exposure as the dichroism curve also is.

These results should be kept in mind for it proves to be explained that the photo-dichroism may be a results of difference in absorption between, after and before exposure.

From such a point of view, it is to be assumed that the absorption coefficients of the film before and after exposure might be similar to $a_\perp$ and $a$ respectively if the vectrial absorption coefficient having component $a_\perp$ and $a$ is perpendicular and parallel to the electric vector of exposing light.

In the previous paper[2], the author has described the phenomenon that the values of dichroism observed using the light of which the wave lengths are in the region between 580 mμ and 550 mμ can not be explained by the parameter method.

By the above assumption, the question, what causes this behavior, can be answered by considering the following mechanism.

The absorption curve of Valenta's plate is to be taken as (a) in Fig. 1 and if the same plate is exposed to red light, the colloidal perticles of metallic silver which are sensitive to red light are re-distributed causing Herschel effect; at the first step of the process the destruction would occur a little as shown as ($b_1$) in Fig. 7. By increasing exposure, the absorption will change from ($b_1$) to ($b_2$) and then to ($b_3$) in Fig. 7 owing to the fact that further destruction takes place.

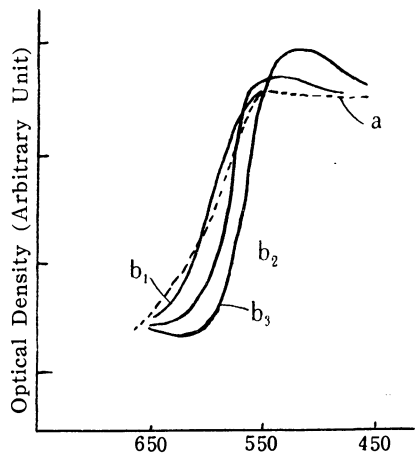



Fig. 7. Schematic changes of absorption curve by increasing exposure to red light.
a: before exposure
$b_1$, $b_2$, $b_3$: after exposure.
The curve will be changed $b_1$, $b_2$ and $b_3$ by exposing.

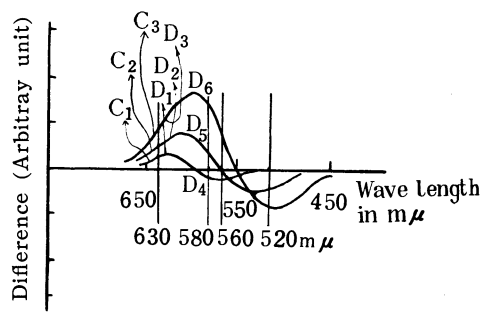



Fig. 8. Schematic absorption difference curve under various time of exposure to red light.
The curve will be changed as $c_1$, $c_2$ and $c_3$ by exposing.

From (a) and ($b_1$), ($b_2$), ($b_3$), the absorption difference curves in each case can be obtained, which are shown as ($c_1$), ($c_2$) and ($c_3$) in Fig. 8.

If the absorption difference curves are treated as dichroism curves, the theoretical values of dichroism against the time of exposure can be obtained by the following method.

When the lines perpendicular to abscissa at the points of 630 m$\mu$, 570 m$\mu$, 560 m$\mu$ and 520 m$\mu$ are drawn, and the crossing points of these lines to the absorption difference curves in Fig. 8 are denoted as $D_1$, $D_2$, $D_3$, $D_4$……, these points will be taken as the values of dichroism against the time of exposure and thus semi-quantitative curves observed with 630 m$\mu$, 570 m$\mu$, 560 m$\mu$ and 520 m$\mu$ can be obtained, which are illustrated in Fig. 9.

The experimental dichroism curves against the time of exposure measured with 630 m$\mu$, 570 m$\mu$, 560 m$\mu$ and 520 m$\mu$ are also shown in Fig. 10.

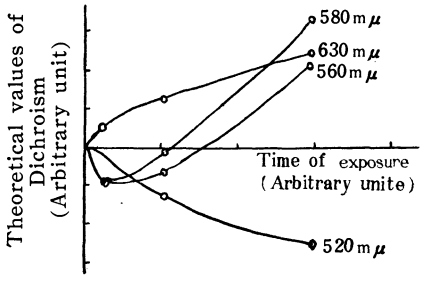



Fig. 9. Schematic change of absorption difference values against the time of exposure under various wave length of measuring light.

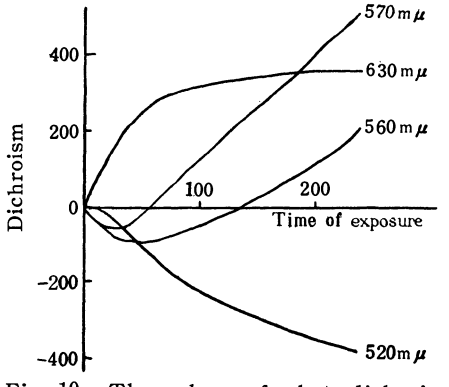



Fig. 10, The values of photo-dichroism against the time of exposure under various wave length of measuring light.

It will be seen that the experimental curves correspond to th theoretical. Thus, it can be concluded that when the film of Valenta's emulsion is exposed to 630 m$\mu$, the comparative large particles which are sensitive to the light will be destoyed and broken up into smaller particles which are sensitive to green light, so that the absorption of the film after exposure to the light will be decreased in the red and increased in the green region, and thus the parameter method is useful.

On the other hand, the amount of colloidal silver which is sensitive to orange light will be increased at the beginning of exposure to 630 m$\mu$ because some of collidal particles which are sensitive to red light will change to somewhat smaller particles, so that the values of dichroism are negative when observed with orange light at first, where-by for a long-time exposure the number of the particles which are sensitive to orange light will be descreased because these particles would be sensitive and destroyed more or less when exposed to red light, so that the values turned to positive for a long time.

This is the answer to the question why the parameter method is not useful to explain the behavior of the values observed with the light of which the wave lengths are in the region between 580 m$\mu$ and 550 m$\mu$.

From these evidences, the conclusion that the phenomenon of photo-dichoroism of printed-out silver would be produced by the same mechanism as that of Herschel effect might be permissible.

However, the question why the difference curve is analogous to that of dichroism has not been discussed.

Unfortunately, the absorption difference curve obtained by exposure with blue light was too different from the dichroism curve to make such a simple assumption.

This is probably due to the following possible events.

When the film is exposed to blue light, the photolytic process may take place to produce the colloidal particles of metallic silver or *Induced photo-dichoroism* may be caused in the system.

On this reason, the discussion has to be limited to the case when the film is exposed to red or orange light by which the photolysis or *Induced photo-dichoroism* does not occur.

The author wishes to express his thanks to the late Prof. J. Shidei and Dr. D. Yamamoto for their kind advice.

*Department of General Education, Nagoya University, Nagoya*

# SHORT COMMUNICATIONS

## *Polarographic Determinations of Minute Quantities of Lead in High-Purity Electrolytic Zinc Using the Rotated Dropping Mercury Electrode*

By Nobuyuki TANAKA and Toshiko KOIZUMI

(Received December 12, 1956)

The polarographic method with a dropping mercury electrode (DME) has been widely employed for the determination of minute quantities of lead contained in high-purity electrolytic zinc. The method, though fairly accurate, is often questioned because of its insufficient sensitivity. Recently W. Stricks and I. M. Kolthoff devised a new electrode in polarography, called rotated dropping mercury electrode (RDME), and reported an extensive fundamental work on the characteristics of the electrode and also on the polarography at the electrode[1]. Because of its high sensitivity, the RDME has been applied to the polarographic determination of minute quantities of lead contained in high-purity electrolytic zinc.

The electrode used in this study was similar to that reported by Stricks and Kolthoff[1], which was driven by means of a synchronous motor (Type A, provided with gears for speeds of 100, 150, 200, 300 r. p. m., constructed by Yanagimoto Co.), and had the characteristics of 4.957 mg./sec. for $m$ and 7.22, 5.72 and 3.54 sec. for $t$ at 100, 150 and 200 r. p. m., respectively, being measured in deaerated 0.1 M potassium chloride solution at 40.0 ± 0.1 cm. of mercury head with open circuit. A saturated calomel electrode was used for a reference electrode. Current-voltage curves were measured with Yanagimoto pen-recording polarograph Model PB-4. All measurements were carried out in a thermostat of 25° ± 0.1°C.

Current-voltage curves were obtained with various concentrations of lead in deaerated 0.1 M and 1 M sodium chloride solutions containing $5\times10^{-6}$ M polyoxyethylene lauryl ether (LEO) as a maximum suppressor. A proportionality was obtained between the concentration of lead and the limiting current. The best reproducibility was found at 100 r. p. m. as shown in Table I, although the $i_l/c$ value was the highest at 150 r. p. m.

TABLE I

LIMITING CURRENTS OF LEAD IONS IN 0.1 M KCl - $5\times10^{-6}$ M LEO

| Conc. of Pb(II), M | $i_l$, μ amp. | $i_l/c$, μ amp./$10^{-4}$ M |
|---|---|---|
| $2.94\times10^{-7}$ | $0.017_2$ | $5.8_2$ |
| $0.979\times10^{-6}$ | $0.057_5$ | $5.8_8$ |
| $2.94\times10^{-6}$ | 0.172 | $5.8_3$ |
| $0.979\times10^{-5}$ | 0.573 | 5.86 |
| $2.94\times10^{-5}$ | $1.70_4$ | 5.80 |
| $0.979\times10^{-4}$ | 5.71 | 5.83 |
| $2.94\times10^{-4}$ | 17.03 | 5.80 |

In deaerated 1 M zinc chloride solutions containing $5\times10^{-6}$ M LEO the $i_l/c$ value for lead was also found constant in the concentration range investigated, but somewhat smaller than those in 0.1 M and 1 M potassium chloride solutions. High-purity electrolytic zinc was dissolved in concentrated hydrochloric acid and the excess of the acid was removed by evaporation. The residue was dissolved into distilled water containing $5\times10^{-6}$ M LEO to make 1 M in concentration in regard to zinc chloride. The concentration of lead was determined directly from the $i_l/c$ value obtained for lead in 1 M zinc chloride and also by the standard addition method. In Table II are given some of the results obtained, which

TABLE II

LEAD CONTENT IN HIGH-PURITY ELECTROLYTIC ZINC

| Sample | Content of Lead found, % | |
|---|---|---|
| | from the $i_l/c$ value | by standard addition method |
| No. 1 | $0.0007_1$ | $0.0007_1$ |
| No. 4 | $0.0012_0$ | $0.0011_8$ |
| No. 6 | $0.0015_8$ | $0.0015_4$ |
| No. 8 | $0.0013_7$ | $0.0013_6$ |
| No. 9 | $0.0011_7$ | $0.0011_2$ |
| No. 10 | $0.0001_3$ | $0.0001_3$ |

contain the determination of lead down to 0.0001 % in content of electrolytic zinc. Further studies on the characteristics of the RDME and on other applications will be reported in subsequent publications.

The authors would like to express their gratitude to Dr. I. M. Kolthoff for his advice in this study. They also thank

1) W. Stricks and I. M. Kolthoff, *J. Am. Chem. Soc.*, **78**, 2085 (1956); See also, Nobuyuki Tanaka, *J. Japan. Chem.*, **10**, 814 (1956).

the Ministry of Education for the financial support of this research.

*Department of Chemistry*
*Faculty of Science*
*Tohoku University, Sendai*

## *Structure of Compound A, a Hydrolysis Product of Roseothricin A*

By Toshio GOTO,* Yosimasa HIRATA,* Seigo HOSOYA** and Nobuhiko KOMATSU**

(Received November 10, 1956)

Roseothricin is a streptothricin-like complex antibiotic, produced by *Streptomyces Roseochromogenus*[1] and has been separated into three components, roseothricin A, B and C, by means of ion exchange chromatography[2]. Chemical investigations have been undertaken on roseothricin A.

Acid hydrolysis of roseothricin A afforded two β-amino acids, β-lysine (I) and roseonine (II), as reported previously,[3] and a glucosamine-like sudstance (III) with properties as follows: crystalline hydrochloride, dec. p. 145–155°C, paper chromatography BuOH : AcOH : $H_2O$ (4 : 1 : 1) Rf. 0.33 (glucosamine 0.33, chondrosamine 0.25), collidine 0.44 (G. 0.43, C. 0.35), phenol : $NH_3$ 0.74 (G. 0.70, C. 0.64), AcOEt : pyridine : $H_2O$ (2 : 1 : 2) 0.86 (G. 0.87), Me COEt 0.03 (G. 0.03), Fehling, triphenyltetrazolium, ninhydrin, Elson-Morgan and Tollens reactions are positive like glucosamine; $\nu_{max.}^{KBr}$ (III. HCl) 1605 m, 1498m, 1404m, 1332 w, 1319 w, 1253 w, 1230 w, 1149 m, 1121s, 1100 s, 1070 s, 1040 s $cm^{-1}$ (s: strong, m: medium, w: weak). The infrared spectrum is slightly different from that of glucosamine, but bands at 1605 and 1498[4] due to a primary amino group are present and the shape of the absorption at 1100-1000 (alcoholic hydroxyl) is very similar to that of glucosamine. It is almost indistinguishable from glucosamine by means of paper chromatography, and these facts together with the analytical data of compound A strongly suggest that substance III is a stereoisomer of glucosamine.

Compound A, colorless needles, dec. p. 215–220°C, which consists of II and III, was obtained as one of the acid hydrolysis products of roseothricin A. Counter current distribution (CCD) (BuOH : MeOH: AcOH : $H_2O$, 18 : 2 : 1 : 19) of the partial DNP (2,4-dinitrophenyl) product of compound A afforded two peaks at K=0.16 and 9.0, as measured by the absorption at 350 mμ. From the number of the peaks it may be deduced that two amino groups capable of being DNP-ated exist in one molecule of compound A. The product of complete DNP-ation, DNP-compound A, m. p. 192–196°C (dec.), had an $E_{1\,cm.}^{1\%}$ value of 306 at 350 mμ[5] and the molecular wight calculated on the assumption of the presence of twe amino groups is ca. 682.[6] Analytical, pKa′, I. R., and other data point to 1 : 1 ratio of II and III in the compound A. Found: C, 32.65; H, 6.25; N, 16.12. Calcd. for $C_{24}H_{44}O_{13}N_{10}$. 6HCl (2 moles each of II and III minus $3H_2O$; mol. wt., 680.67[6]) : C, 32.05; H. 5.60; N, 15.57%. Compound A has eight pKa′s; to at ca. 2.4 (II-$CO_2H$), to at 6.5 (III-$NH_3^+$),[7] two at 8.9 (II β-$NH_3^+$) and two at 10.4 (II guanidinium). The mol. wt. obtained from this potentiometric curve is ca.645.[6] $\nu_{max.}^{KBr}$ (compound A. HCl) 1732 m (-$CO_2H$[8]), 1658 s (sym. trisubstituted guanidine band[9]), 1609 m, and 1490 m, br (-$NH_3^+$ of both II and III), 1405 m, 1388 m, 1220 m, br, 1075 s, and 1054 s, $cm^{-1}$ (br: broad). Since 5.96 moles of periodate are consumed by 1 mole of compound A, it is suggested that $C_2$-$NH_2$, $C_3$-and $C_4$-OH of III, and the β-$NH_2$ and OH of II in compound A may all be free.

1) S. Hosoya, M. Soeda, N. Komatsu, S. Imamura, M. Iwasaki, Y. Sonoda and K. Okada, *Jap. J. Exptl. Med.*, **20**, 121 (1949); *J. Antibiotics*, **3**, (4), 217 (1950).

2) Y. Saburi, *J. Antibiotics*, **6**, (8), 402 (1953).

3) K. Nakanishi, T. Ito, M. Ohashi, I. Morimoto and Y. Hirata. *J. Am. Chem. Soc.* **76**, 2843 (1954); This Bulletin, **27**, 539 (1954); ibid., submitted for publication.

4) K. Nakanishi, T. Goto, M. Ohashi, this Bulletin, submitted for publication.

5) Calculation was made as ε=15500 (at 350 mμ) per one mole of DNP group.

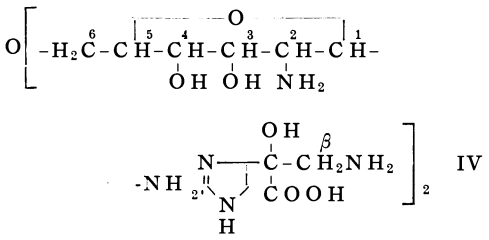
6) Molecular weight as free base.

7) The reason that these amino groups are not DNP-ated, is that rate of DNP-ation of III-$NH_2$ is much slower than that of II β-$NH_2$, and DNP-ation of III-$NH_2$is prevented by precipitation of DNP-compound A.

8) The fact that it is not an ester may be deduced from the following. When trimethylamine is added to compound A and the mixture is immediately evaporated to dryness, this band is absent and a band at ca. 1600 $cm^{-1}$ due to a carboxylate group is seen. Furthermore, this band is absent in DNP-compound A; similar to the case of DNP-roseonine, this is due to the fact that the guanidine portion cannot be DNP-ated and forms an intramolecular salt with this carboxyl group. This corresponds to the two pka′ values at 2.4.

9) N N′-Disubstituted guanidine hydrochlorides possess, two strong absorptions at 1680 and 1600 $cm^{-1}$ (roseonine-2HCl, 1682, 1581), whereas N. N′, N″-trisubstituted guanidine hydrochlorides possess only one strong absorption at ca. 1650 $cm^{-1}$. On the other hand, N, N, N′-trisubstituted guanidine hydrochlorides show three bands at 1650s, 1620s, and 1570m $cm^{-1}$. Hence the guanidine group in compound A is symmetrically trisubstituted, i. e., the 2′-amino group is linked to some other group (T. Goto, K. Nakanishi, this Bulletin, submitted for publication).

Compound A, therefore, contains a N-glucoside linkage; the Elson-Morgan reaction is positive, but the Fehling reaction is negative, and the tetrazolium reaction becomes positive after longer heating period than that of III. The strong electron attractive effect of the guanidinium ion probably accounts for the lower pKa′ of compound A (6.5) than that of III (7.8). The fact that the linkage between II and III



IV

is more stable under acidic conditions than alkaline is also explicable in terms of this effect. Compound A is extremely resistant towards acid hydrolysis; i. e., no appreciable hydrolysis occurred upon heating for 22 days with concentrated hydrochloric acid at 34°, and ca. 15% was hydrolysed upon heating for 11 days with 20% hydrochloric acid at 50°. This difficulty in hydrolysis points to the absence of an acetal linkage. Ester or amide bands were not observable in the region 1750–1500 $cm^{-1}$. These together with the amount of periodic acid consumption suggested that a primary hydroxyl group participates in an ether linkage. We wish to present IV for compound A.

We wish to thank Dr. K. Nakanishi for his advice in this research, and the Sanyo Pharmaceutical Co. for preparing a portion of roseothricin.

*Chemical Institute, Nagoya University Chikusa, Nagoya
**Institute for Infectious Diseases, Tokyo Univ., Minato. Tokyo

# *Molecular Compounds between Heterocyclic Compounds Containing Nitrogen**

By Tadashi MASAMUNE and Masato KOSHI

(Received August 30, 1956)

Although extensive researches[1-3] have been made on molecular compounds, little information[4] is found in the literature concerning those formed from heterocyclic compounds. In the present note the writers show that molecular compounds of a similar type are formed by heterocyclic compounds containing nitrogen atoms; further, interacting forces between the partner molecules are not essentially different from those acting in other molecular compounds.

## Experimental

The following compounds (I—IX, group A) and their hydrogenated compounds (group B) were prepared for the examination.

Group A; benzo-[f]-quinoline (I), 5,6-dihydrobenzo-[f]-quinoline (II), benzo-[h]-quinoline (III), acridine (IV), 1,2,3,4-tetrahydroacridine (V), 7,8,9,10-tetrahydrophenanthridine (VI), 2,3-trimethylenequinoline (VII), quinoline (VIII), and 1,2,3,4-tetrahydrocarbazole (IX).

**Preparation of Compounds.**—The following compounds were prepared by the procedure described in the literature as cited. Solid compounds were recrystallized to constant melting point from the solvents indicated and, on the other hand, oily compounds were regenerated from their solid derivatives of constant melting point and redistilled before use: (I)[5], m. p. 93-93.5°C (benzine); 1,2,3,4,7,8,9,10-octahydrobenzo-[f]-quinoline[6], m. p. 65-66°C (petroleum-ether), 1,2,3,4,5,6,4a,4b-octahydrobenzo-[f]-quinoline[6], m. p. 90-91°C (petroleum-ether), (III)[7], m. p. 51-52.5°C (petroleum-ether); 1,2,3,4-tetrahydrobenzo-[h]-quinoline[7] m. p. 46-47°C (petroleum-ether); (IV), m. p. 109-110° (benzene); (V)[8], m. p. 54-55°C (benzene); *cis*-1,2,3,4,9,10,4a,4b-octahydroacridine[9], m. p. 71-73°C (petroleum-ether); *trans*-1,2,3,4,9,10,4a,4b-octahydroacridine[10], m. p. 81-83°C (petroleum-ether); (VI)[11], m. p. 63-64°C (benzine); 5,6,7,8,9,10,6a,10a-octahydrophenanthridine[12], m. p. 70-72°C (aqueous alcohol); (VII)[13], m. p. 60-61°C (benzine); *cis*-1,2,3,4-tetrahydro-2,3-trimethylenequinoline[14], oil, benzoyl derivative[14], m. p. 159-160°C (acetone), *trans*-1,2,3,4-tetrahydro-2,3-trimethylenequinoline[14], m. p. 68-68.5°C (petroleum-ether), (VIII), m. p. about −15°C, picrate, m. p. 228-230°C (ethanol); 1,2,3,4-tetrahydroquinoline[15], m. p. about 20°C, benzoyl derivative, m. p. 73-74°C (alcohol); (IX)[16], m. p. 117-118°C (methanol); *cis*-1,2,3,4,10,11-hexahydrocarbazole[17], m.p. 98-99°C (ethanol); *trans*-1,2,3,4,10,11-hexahydrocarbazole[17], m. p. 124-126°C (ethanol).

**1, 2, 3, 4-Tetrahydrobenzo-[f]-quinoline.** — A mixture of 20 g. of benzo-[f]-quinoline and 20 g. of granulated tin was refluxed in 150 cc. of conc. hydrochloric acid for three hours until the tin was entirely consumed. The reaction mixture was made strongly alkaline with 6 N sodium hydroxide solution after cooling, and it was distilled with steam. The distillate was extracted with ether and recrystallized from ligroin after removal of ether, yielding 10 g. of pale yellow crystals[18], m. p. 93-93.5°C.

*Anal.* Found: C, 86.12, H, 6.00. Calcd. for $C_{13}H_{11}N$: C, 86.16, H, 6.12%.

This base was dissolved in 50 cc. of ether and treated with a small excess of equivalent benzoyl chloride and N sodium hydroxide solution. After the odor of benzoyl chloride had entirely disappeared, the ethereal layer was separated from

* Partly presented at the Annual Meeting of the Chemical Society of Japan, April 3, 1956. The 8 th Part on "The Condensed Polynuclear Perhydro-Compounds Containing Nitrogen." The 7th Part, T. Masamune and G. Homma, *J. Chem. Soc. Japan (Pure Chem. Sect.)*, **77**, 1766 (1956).

1) C. W. Wheland, "Advanced Organic Chemistry" John Wiley and Son's, 2nd ed., New York 1949 p. 54.

2) Ch. Shinomiya, This Bulletin, **15**, 92, 137, 259, 281, 309 (1940).

3) S. Seki and K. Suzuki. ibid., **26**, 63, 209, 372 (1953).

4) It was found by Masamune and Kubota in this laboratory that a molecular compound is formed between tetrahydro-and octahydrophenanthridine. Ref., *J. Chem. Soc. Japan. (Pure Chem. Sect.)*, **77**, 1467 (1956).

5) H. C. A. Knueppel, *Ber*, **29**, 708 (1896).

6) E. Bamberger, ibid., **24**, 2648 (1891).

7) E. Bamberger and L. Stettenheimer, ibid., **24**, 2473 (1891).

8) W. Borsche, ibid., **41**, 2203 (1908).

9) W. H. Perkin and S. G. P. Plant, *J. Chem. Soc.*, **1928**, 2583.

10) W. H. Perkin and W. G. Sedgwick. ibid., **1926**, 438.

11) B. L. Hollingsworth and L. Petrow, ibid., **1948**, 1537.

12) See Ref. (4).

13) W. Borsche, *Ann.*, **377**, 120 (1910).

14) W. H. Perkin and S. G. P. Plant, *J. Chem. Soc.*, **1928**, 638.

15) H. Rupe, M. Seiberth and W. Kussmaul, *Helv. Chim. Acta*, **3**, 75 (1920).

16) C. V. Rogers and B. B. Corson, *J. Am. Chem. Soc.*, **69**, 2910 (1947).

17) J. Gurney, W. H. Perkin and S. G. P. Plant, *J. Chem. Soc.*, **1927**, 2676.

18) This substance was shown to correspond to dihydro-derivative of benzo-[f]-quinoline from analytical value, and was proved to be a molecular compound between (I) and its pure tetrahydro-derivative in the present paper. Bamberger's "1, 2, 3, 4-tetrahydrobenzo-[f]-quinoline" would probably be the same substance as this. See Ref. (5).

the aqueous solution and was washed with 2 N hydrochloric acid to remove unreacted benzo-[f]-quinoline. A benzoylated compound obtained from the ethereal solution by removal of the solvent, had m. p. 153–4°C on recrystallization from alcohol. It was refluxed with 12 g. of potassium hydroxide in 300 cc. aqueous alcoholic solution for four hours. The product was again extracted with ether, after distillation of alcohol under reduced pressure and addition of water. The ethereal solution was treated with 2 N hydrochloric acid. After separation from the ethereal layer, the acidic solution gave 7 g. of oily tetrahydrobenzo-[f]-quinoline, b. p. 200–202°C (14mm.), on alkalification, separation from aqueous solution and distillation under diminished pressure. The hydrochloride was prepared by passing hydrogen chloride into the ethereal solution of the base.

*Anal.* Found: C, 70.95; H, 6.39. Calcd. for $C_{13}H_{13}NHCl$: C, 71.03; H, 6.42%.

Its picrate had m. p. 167–168°C, when the base was added into saturated alcoholic solution of picric acid and was recrystallized from the same solvent.

**5, 6-Dihydrobenzo-[f]-quinoline [II].**—Benzo-[f]-quinoline (10 g.) was hydrogenated with 1 g. of Raney-nickel[19] at 100°C in an autoclave, starting at 70 atmospheric pressures and the reaction was stopped when one and a half mole of hydrogen were absorbed. The products were extracted with 200 cc. of ether. When the ethereal solution was concentrated up to 50 cc. and cooled, about 4 g. of pale yellow crystals were separated. The crystals thus isolated by filtration gave m. p. 88–90°C, on recrystallization from aqueous alcohol. On the other hand, when the solvent of the filtrate was entirely removed, the residue consisting of some oil and a small amount of solid was again filtered. The filtrate thus separated was proved to be tetrahydrobenzo-[f]-quinoline as above mentioned, by derivation of the benzoyl compound and by the mixed melting point determination. The yield of the base was 6 g.

The crystals of m. p. 88–90°C were dissolved in 100 cc. of ether and subjected to benzoylation with 3.3 g. of benzoylchloride and alkaline solution. After seven hours, the ethereal solution (a) was separated from the aqueous solution and treated with 100 cc. of 2 N-hydrochloric acid. As the acidic solution was made alkaline and extracted with ether, the ethereal solution gave 1.7 g. of an oily dihydrobenzo-[f]-quinoline. Its picrate and hydrochloride had m. p. 205–206°C and m. p. 255–257°C respectively.

*Anal.* Found: C, 71.72; H, 5.73. Calcd. for

System of (I) and 1,2,3,4-tetrahydrobenzo-[f]-quinoline (Fig. 1).

| Mol % of (I) | 100 | 90 | 80 | 70 | 60 | 50 | 40 | 30 | 20 | 10 |
|---|---|---|---|---|---|---|---|---|---|---|
| Melting points | 92 | 66 | 80 | 88 | 92 | 93 | 92 | 87 | 80 | 63 |
| Thawing points | 90 | 64 | 64 | 79 | 87 | 91.5 | 88 | 78 | — | — |

System of (II) and 1,2,3,4-tetrahydrobenzo-[f]-quinoline.

| Mol % of (II) | 70 | 60 | 50 | 40 | 30 | 20 |
|---|---|---|---|---|---|---|
| Melting points | 73 | 87 | 90 | 89 | 83 | 70 |
| Thawing points | — | 80 | 88 | 84 | 75 | — |

System of (V) and *cis*-1,2,3,4,9,10,4a,9a-octahydroacridine (Fig. 2).

| Mol % of (V) | 100 | 90 | 85 | 80 | 70 | 60 | 50 | 40 | 30 | 20 | 10 | 0 |
|---|---|---|---|---|---|---|---|---|---|---|---|---|
| Melting points | 55 | 47 | 42 | 45 | 52 | 56 | 58 | 51 | 54 | 63 | 69 | 73 |
| Thawing points | 54 | 39 | 38 | 38 | 38 | 51 | 57 | 48 | 48 | 49 | 58 | 71 |

System of (VI) and 5,6,7,8,9,10,6a,10a-octahydrophenanthridine.

| Mol % of (VI) | 100 | 90 | 85 | 80 | 70 | 60 | 50 | 40 | 33 | 30 | 20 | 10 | 0 |
|---|---|---|---|---|---|---|---|---|---|---|---|---|---|
| Melting points | 64 | 60 | 54 | 60 | 63 | 69 | 73 | 75 | 76 | 75 | 73 | 66 | 72 |
| Thawing points | 63 | 52 | 52 | 52 | 52 | 53 | 66 | 73 | 75 | 74 | 66 | 64 | 70 |

System of (V) and *trans*-1,2,3,4,9,10,4a,9a-octahydroacridine.

| Mol % of (V) | 100 | 90 | 80 | 70 | 60 | 50 | 40 | 30 | 20 | 10 | 0 |
|---|---|---|---|---|---|---|---|---|---|---|---|
| Melting points | 55 | 51 | 47 | 43 | 51.5 | 57 | 63 | 68 | 75 | 80 | 83 |
| Thawing points | 54 | 43 | 42 | 42 | 43 | 43 | 44 | 45 | 51 | 64 | 81 |

System of (IV) and *cis*-1,2,3,4,9,10,4a,9a-octahydroacridine.

| Mol % of (IV) | 100 | 90 | 80 | 70 | 60 | 50 | 40 | 30 | 20 | 10 | 0 |
|---|---|---|---|---|---|---|---|---|---|---|---|
| Melting points | 110 | 105 | 102 | 98 | 95 | 90 | 80 | 55 | 65 | 71 | 73 |
| Thawing points | 109 | 99 | 94 | 89 | 83 | 73 | — | — | — | 53 | 71 |

System of (I) and 1,2,3,4,7,8,9,10-octahydrobenzo-[f]-quinoline.

| Mol % of (I) | 100 | 90 | 80 | 70 | 60 | 50 | 40 | 30 | 20 | 10 | 0 |
|---|---|---|---|---|---|---|---|---|---|---|---|
| Melting points | 93 | 91 | 85 | 78 | 69 | 55 | 42 | 40 | 50 | 61 | 66 |
| Thawing points | 92 | 80 | 66 | 47 | 36 | 34 | 33 | 33 | 35 | 43 | 65 |

System of (IX) and *cis*-1,2,3,4,10,11-hexahydrocarbazole.

| Mol % of (IX) | 100 | 90 | 80 | 70 | 60 | 50 | 40 | 30 | 20 | 10 | 0 |
|---|---|---|---|---|---|---|---|---|---|---|---|
| Melting points | 118 | 114 | 106 | 99 | 92 | 84 | 72 | 83 | 88 | 94 | 99 |
| Thawing points | 116 | 85 | 74 | 71 | 70 | 70 | 70 | 71 | 73 | 78 | 98 |

19) R. Mozingo, "Org. Syntheses" Vol. 21 (1941), p. 15.

$C_{13}H_{11}NHCl$: C, 71.72; H, 5.55%.

On the other hand, the benzoylated compound of tetrahydrobenzo-[f]-quinoline was isolated from the ethereal solution (a).

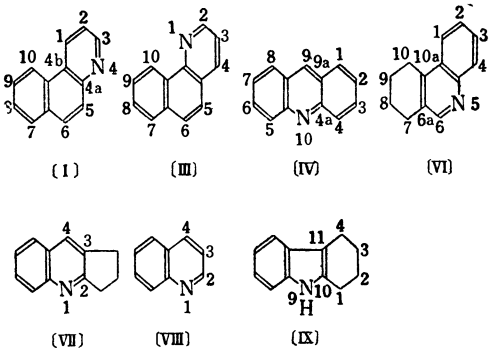
**Melting Point-Composition Diagram.** — A sample each of group (A) and group (B) was weighed (about 5 mg.) and dissolved in ether respectively. These ethereal solutions were mixed in a proper ratio, heated for a short time to remove the solvent and then poured into a capillary with a diameter 3-4 mm. The mixture was furthermore dried in a desiccator after complete removal of ether. The phase diagram was obtained by recording both the thawing and melting points of these mixtures, using the common procedures of melting point determination and sometimes using the method of Shinomiya[2].

Thawing and melting points of four combinations resulted in formation of a peak in the diagram (see below and Figs. 1 and 2). For the sake of comparison the same points of several representative cases not forming a molecular compound are also recorded in the following.

**Ultraviolet Absorption Measurements.** — The measurements were made by the use of a Beckmann quartz spectrophotometer, Model DU. Alcohol or iso-octane (dried over phosphorous pentoxide) was used as solvent. The spectrum was examined at 0.5 m$\mu$ intervals near maximum and at 3 m$\mu$ intervals at the region from 215 to 360 m$\mu$.

## Results and Discussion

The results of thermal analysis for mixtures of one of group (A) and one of group (B) were summarized in Table I and the diagrams of two representative pairs forming molecular compounds were shown in Figs. 1 and 2. Four combinations yielded a peak in the melting point diagram, viz., (I: 1,2,3,4-tetrahydrobenzo-[f]-quinoline), (II: 1,2,3,4-tetrahydrobenzo-[f]-quinoline), (V: *cis*-1,2,3,4,9,10,4a,9a-octahydroacridine) and (VI: 5,6,7,8,9,10,6a,10a-octahydrophenanthridine); but there was no peak in the others. It is to be noted that these molecular compounds are



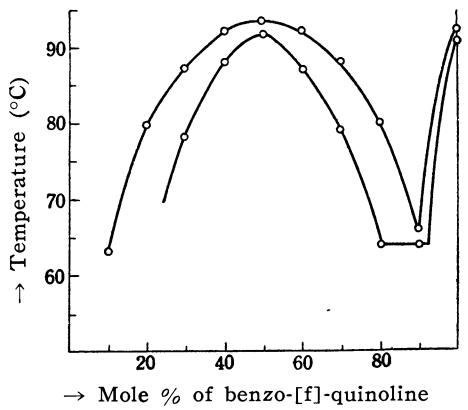




Fig. 1. Molecular compound between benzo-[f]-quinoline and 1,2,3,4-tetrahydrobenzo-[f]-quinoline.

TABLE I

ON THE FORMATION OF CRYSTALLINE MOLECULAR COMPOUNDS

| Group A | Group B | Molecular compound | |
|---|---|---|---|
| | | Molar ratio | Melting point (°C) |
| (I) | 1,2,3,4-Tetrahydrobenzo-[f]-quinoline | 1 : 1 | 93—93.5 |
| (I) | 1,2,3,4,7,8,9,10-Octahydrobenzo-[f]-quinoline | None | |
| (I) | 1,2,3,4,5,6,4a,4b-Octahydrobenzo-[f]-quinoline | None | |
| (II) | 1,2,3,4-Tetrahydrobenzo-[f]-quinoline | 1 : 1 | 88—90 |
| (III) | 1,2,3,4-Tetrahydrobenzo-[h]-quinoline | None | |
| (IV) | *cis*-1,2,3,4,9,10,4a,9a-Octahydroacridine | None | |
| (V) | 〃 | 1 : 1 | 56—58 |
| (V) | *trans*-1,2,3,4,9,10,4a,9a-Octahydroacridine | None | |
| (VI) | 5,6,7,8,9,10,6a,10a-Octahydrophenanthridine | 1 : 2 | 75—76 |
| (VII) | *cis*-1,2,3,4-Tetrahydro-2,3-trimethylenequinoline | None | |
| (VIII) | 1,2,3,4-Tetrahydroquinoline | None | |
| (IX) | *cis*-1,2,3,4,10,11-Hexahydrocarbazole | None | |
| (IX) | *trans*-1,2,3,4,10,11-Hexahydrocarbazole | None | |

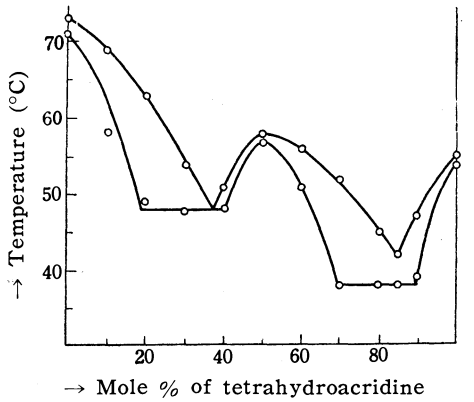



Fig. 2. Molecular compound between 1,2,3,4-tetrahydroacridine and *cis*-1,2,3,4,9,10,4a,9a-octahydroacridine.

formed between the compounds containing nitrogen of anilino-type and those of pyridino-type, but their mixture does not always result in the formation of a molecular compound.

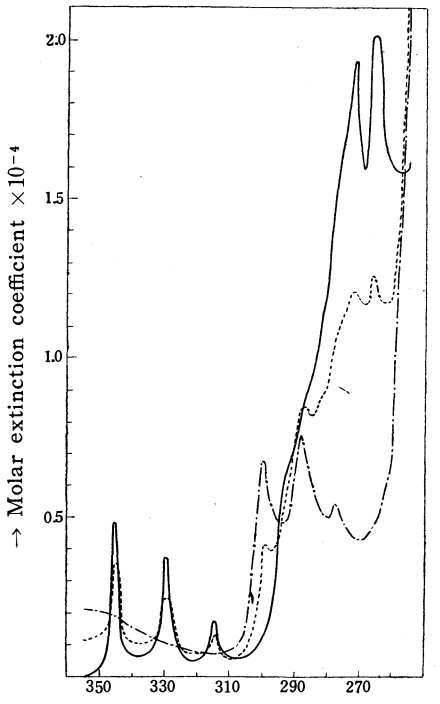



Fig. 3. Ultraviolet absorption spectrum of molecular compound between benzo-[f]-quinoline and its 1,2,3,4-tetrahydro-derivative.
Solvent: isoöctane; conc.: M×10⁻⁴
—— Benzo-[f]-quinoline
–·– 1,2,3,4-Tetrahydrobenzo-[f]-quinoline
------ Molecular compound

The ultraviolet absorption spectra of one of the molecular compounds examined are shown in Fig. 3 together with those of component molecules concerned. They refer to the measurements of the same concentration. Examination of Fig. 3 shows that the intensity of a molecular compound is half of the sum of intensity of partner molecules, indicating that the molecular compound concerned is in a state of complete dissociation. In the other three molecular compounds, a similar phenomenon is found.

There are several papers available which deal with the nature of intermolecular forces in molecular compounds[20-23]. However, no satisfactory explanation has been given even for the most familiar type of molecular compound, viz., quinhydrone formed from quinone and hydroquinone. According to Suzuki and Seki[22], the hydrogen bond is important in the same quinhydrone: they ascribed 4.6 to 1.6 kcal. of the total heat of formation (5.386 kcal.) to this cause. As the molecules of the substance in group A which form molecular compounds have one N atom and those of B have an N—H bond, a hydrogen bond of the N—H···N type may possibly be formed between the interacting molecules in the present case. But this is not the most important cause of the formation of such a molecular compound. For instance, it is to be noted that no molecular compound is formed between benzo-[f]-quinoline and 1,2,3,4,7,8,9,10-octahydrobenzo-[f]- quinoline (see Table 1).

Contrary to Suzuki and Seki, Tsubomura[23] holds a view that the effect of charge transfer is most important in quinhydrone. However, no definite support was obtained for that theory of charge transfer from the present authors' measurement of ultraviolet absorption spectra. Therefore, further measurement under different conditions is desirable.* It may, however, suffice to point out here that all the molecules concerned have $\pi$-electrons and that the formation of molecular compounds seems to be affected by such a factor as the number of unsaturated rings.

Lastly it is of interest to note that the *cis*-isomer of hydrogenated acridine is

20) K. Higasi and K. Hirota, "Riron Yuki-Kagaku," Asakura-Shoten, Tokyo (1951), p. 40.
21) H. Murakami, This Bulletin, **26**, 441 (1953).
22) S. Seki and K. Suzuki, ibid., **26**, 372 (1953).
23) H. Tsubomura, ibid., **26**, 304 (1953).
* The writers propose to study this problem in the future.

capable of participating in molecular compound formation, while the *trans*-isomer has no such capacity. Therefore, the spatial configuration seems to be one of the factors, suggesting the importance of van der Waal's force in the molecular compound formation.

The present research was conducted under the supervision of President H. Suginome of the University and the authors are especially indebted to Professor K. Higasi for his kind guidance and criticism.

*Chemistry Department, Faculty of Science*
*Hokkaido University, Sapporo*

# *Effect of Emulsifier upon the Compositions of Emulsion Copolymers of Acrylonitrile and Water-soluble Monomers*

By Moriya UCHIDA and Hideo NAGAO

(Received October 3, 1956)

## Introduction

In a previous paper[1] we reported that the compositions of emulsion copolymers of acrylonitrile and water-insoluble monomers such as vinylidene chloride or styrene depend upon the concentrations of emulsifier in aqueous solutions. In this paper, first, the relations between the compositions of emulsion copolymers of acrylonitrile and the other water-soluble monomers such as methyl methacrylate vinylacetate and methyl acrylate and the amounts of emulsifier used are given and then the deviations of monomer polymer composition curves of emulsion copolymerizations from those of bulk copolymerizations are discussed.

## Experimental

**Acrylonitrile (AN).**—Redistilled American Cyanamide Co. material was used for all experiments.

**Methyl Methacrylate (MMA).**—Redistilled Mitsubishi Rayon Co, material was used.

**Vinyl Acetate (VAc).**—Redistilled commercial material was used.

**Methyl Acrylate (MA).**—Redistilled Toa Gosei Chemical Co. material was used.

**Emulsifier (Sodium Dodecyl Sulfate).**—Recrystallized Kao soap Co. material was used.

Emulsion polymerization procedure was the same as that used in the previous report[2].

The amount of water used was 8 times as much as that of the monomer, and 0.8% by weight of the potassium persulfate as the catalyst, and 0.8% by weight of sodium bisulfate as reductant (both based on the total monomers) were employed. The polymerization temperature was 45°C. The combined acrylonitrile in copolymer was determined by the Kjeldahl method. The composition of monomer oil phase was determined by the refractive indices method as we previously reported[1].

## Results and Discussion

**(1) Effect of Emulsifier upon the Compositions of Copolymers.**—In the copolymerization 0, 0.1, 0.2, 0.4, 0.6, 1.0 and 1.5%

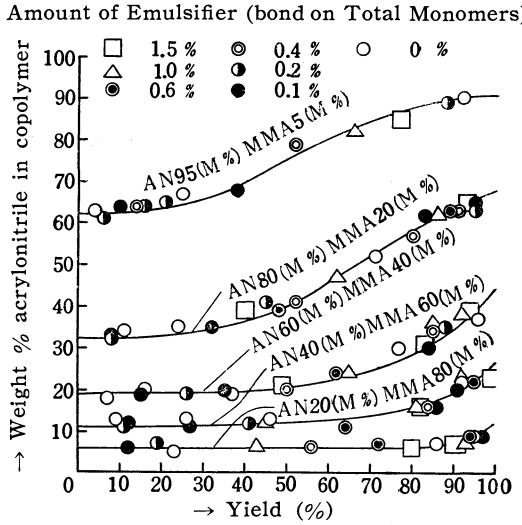



Fig. 1. Effect of emulsifier on composition of acrylonitrile methyl methacrylate copolymers.

1) M. Uchida and H. Nagao, This Bulletin, **30**, 314 (1957).
2) M. Uchida and H. Nagao This Bulletin, **29**, 928 (1956).

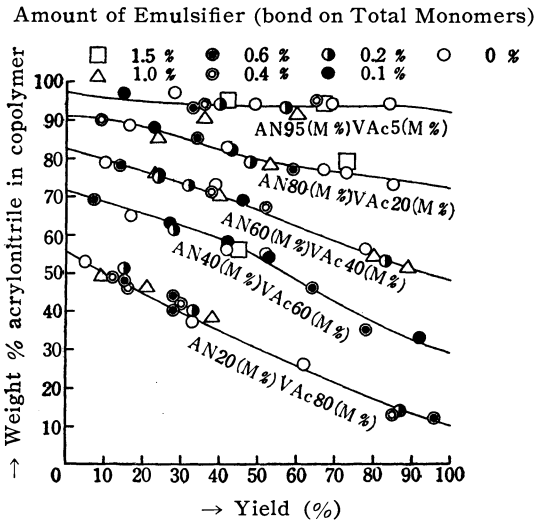



Fig. 2. Effect of emulsifier on composition of acrylonitrile vinyl acetate copolymers.

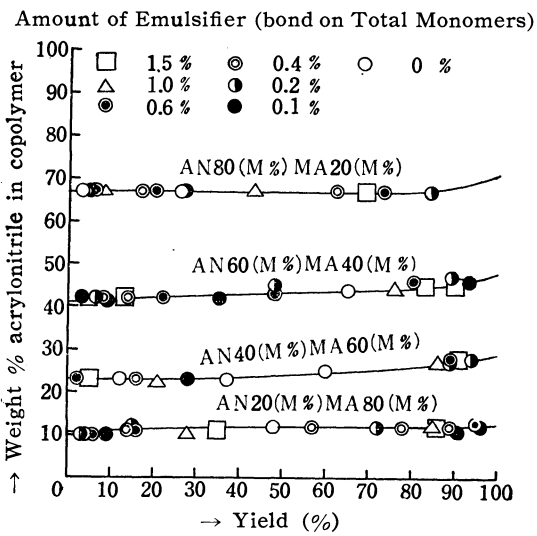



Fig. 3. Effect of emulsifier on composition of acrylonitrile methyl acrylate copolymers.

by weight of emulsifier based on total monomers were used. The compositions of copolymers thus formed in various degrees of conversion for the copolymerization of acrylonitrile and methyl methacrylate are given in Fig. 1, Fig. 2 and Fig. 3 show the corresponding results for the copolymerization of acrylonitrile and vinyl acetate and that of acrylonitrile and methyl acrylate respectively. In these copolymerizations, the compositions of copolymers are independent of the concentrations of emulsifier.

**(2) Monomer-polymer Composition Curves.**—The monomer-polymer composition curves obtained from the compositions of copolymers extrapolated to 0 conversion are given in Figs. 4, 5 and 6. As to the relative reactivities between acrylonitrile and the other monomers for the bulk copolymerization, the data hitherto known are cited as follows.

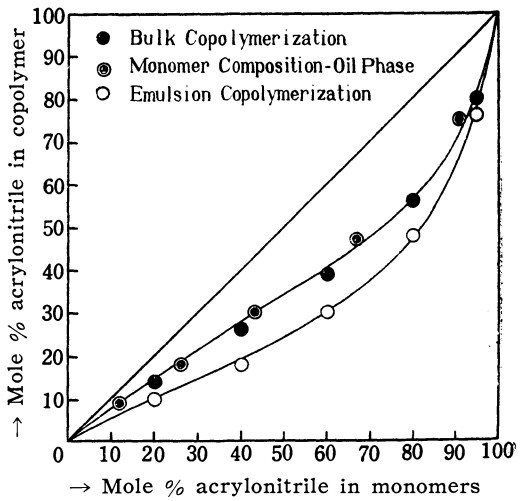



Fig. 4. Monomer-polymer composition curves for acrylonitrile methyl methacrylate copolymerization.

| Monomer | | Relative Reactivity | |
|---|---|---|---|
| $M_1$ | $M_2$ | $r_1$ | $r_2$ |
| Methyl methacrylate | Acrylonitrile | 1.35±0.1 | 0.18 ±0.1[3] |
| Acrylonitrile | Vinyl acetate | 4.05±0.3 | 0.061±0.013[4] |
| Acrylonitrile | Methyl acrylate | 0.67±0.1 | 1.26 ±0.1[5] |

From the monomer-polymer composition curves given in Figs. 4, 5 and 6, it will be seen that while the curve of acrylonitrile methyl methacrylate emulsion copolymerization is not superposed on that of the bulk copolymerization, those of the other copolymerizations fall on the latter. For the purpose of determining monomer oil phase compositions, the refractive indices of monomer mixture of known compositions saturated with water and monomer oil phases were measured. The results are given in Table I, II and III.

3) F. M. Lewis, F. R. Mayo, and W. F. Hulse, *J. Am Chem. Soc.*, **67**, 1701 (1945).
4) F. R. Mayo, C. Walling, F. M. Lewis and W. F. Hulse, ibid., **70**, 1523 (1948).
5) S. Okamura, "Outlook of High Polymer" Vol. 5, Association of High polymer Chemistry, Kyoto, Japan (1952), p. 42.

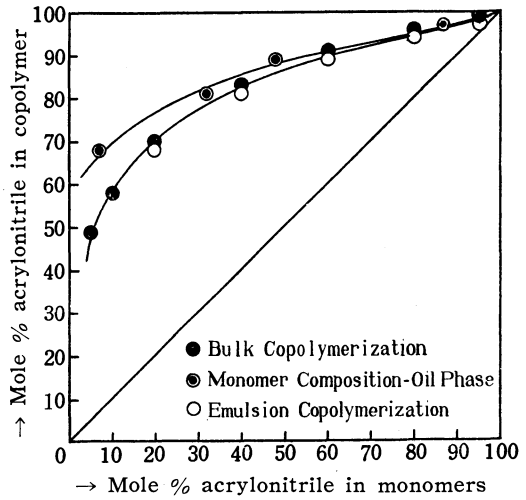



Fig. 5. Monomer-polymer composition curves for acrylonitrile vinyl acetate copolymerization.

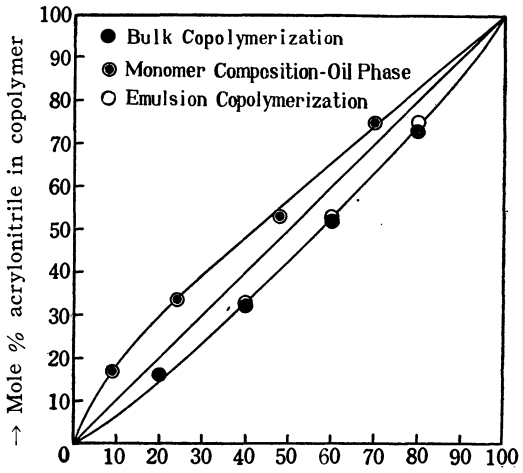



Fig. 6. Monomer-polymer composition curves for acrylonitrile methyl acrylate copolymerization.

TABLE I

REFRACTIVE INDICES OF ACRYLONITRILE-METHYL METHACRYLATE SOLUTIONS

| Composition of solution | | Monomer saturated with water | Oil phase |
|---|---|---|---|
| AN (M%) | MMA (M%) | $n_D^{45}$ | $n_D^{45}$ |
| 95 | 5 | 1.3780 | 1.3795 |
| 80 | 20 | 1.3830 | 1.3860 |
| 60 | 40 | 1.3882 | 1.3919 |
| 40 | 60 | 1.3930 | 1.3965 |
| 20 | 80 | 1.3975 | 1.3991 |
| 0 | 100 | 1.4009 | 1.4009 |

TABLE II

REFRACTIVE INDICES OF ACRYLONITRILE-VINYL ACETATE SOLUTIONS

| Composition of solution | | Monomer saturated with water | Oil phase |
|---|---|---|---|
| AN (M%) | VAc (M%) | $n_D^{45}$ | $n_D^{45}$ |
| 100 | 0 | 1.9769 | — |
| 95 | 5 | 1.3777 | 1.3779 |
| 80 | 20 | 1.3780 | 1.3787 |
| 60 | 40 | 1.3800 | 1.3804 |
| 40 | 60 | 1.3807 | 1.3808 |
| 20 | 80 | 1.3813 | 1.3814 |
| 0 | 100 | 1.3820 | 1.3820 |

TABLE III

REFRACTIVE INDICES OF ACRYLONITRILE-METHYL ACRYLATE SOLUTIONS

| Composition of solution | | Monomer saturated with water | Oil phase |
|---|---|---|---|
| AN (M%) | MA (M%) | $n_D^{45}$ | $n_D^{45}$ |
| 95 | 5 | 1.3776 | 1.3779 |
| 80 | 20 | 1.3799 | 1.3816 |
| 60 | 40 | 1.3830 | 1.3846 |
| 40 | 60 | 1.3852 | 1.3867 |
| 20 | 80 | 1.3872 | 1.3882 |
| 0 | 100 | 1.3885 | 1.3885 |

If polymerization occurs in oil phase as Fordyce, Chapin[6] and Smith[7] asserted, the monomer-polymer composition curves will be dependent upon the composition of oil phase.

The amounts of acrylonitrile in oil phase were estimated from their refractive indices. The composition of oil phase was used in place of the monomer compositions. The monomer-polymer composition curves thus represented are shown in Figs. 4, 5 and 6.

It is seen that this correction of the compositions of emulsion oil phases makes the emulsion and bulk copolymerzation composition curves identical only in the case of acrylonitrile-methyl methacrylate copolymerization. Consequently, it seems that the water solubility of the monomer affects the compositions of copolymers formed in emulsion copolymerization. The water solubility of this monomer is as follows.

6) R. G. Fordyce and E. D. Chapin, *J. Am. Chem, Soc.*, **69**, 581 (1947).
7) W. V. Smith, ibid., **70**, 2177 (1948).

TABLE IV
WATER SOLUBILITY OF THE MONOMER

| Monomer | Solubility (%) | Temperature (°C) |
|---|---|---|
| Styrene | 0.28 | 25[8] |
| Methyl methacrylate | 1.5 | 30[8] |
| Vinyl acetate | 2.5 | 20[9] |
| Methyl acrylate | 5.2 | [9] |
| Acrylonitrile | 7.4 | 25[10] |

In the emulsion copolymerizations of monomers having good water solubility, the composition curves are identical with those of the bulk copolymerizations, that is to say, such emulsion copolymerizations behave just like a solution copolymerization, even if the monomer oil phase exists.

8) F. A. Bovey, I. M. Kolthoff, A. I. Medalia and E. J. Beehan, "Emulsion polymerization," (1955) p. 157.
9) E. R. Blout, W. P. Hohenstein and H. Mark, "Monomer," Inerscience Inc. New York (1949). p. 23 in chapter on "Vinyl Acetate," p. 23 in chapter on "Esters of Acrylic Acid."
10) H. S. Davis, and O. F. Wiedeman, *Ind. Eng. Chem.* **37**, 482 (1945).


## Summary

The following facts are found from emulsion copolymerizations of acrylonitrile and water soluble monomers such as methyl methacrylate, vinyl acetate and methyl acrylate.

(1) The compositions of copolymer are independent of the concentration of the emulsifiers used.

(2) The monomer-polymer composition curve of emulsion copolymerization of acrylonitrile and methyl methacrylate is made consistent with that of bulk copolymerization, when the composition of emulsion oil phace is used in place of that of the monomer.

(3) The monomer-polymer composition curves of emulsion copolymerization of acrylonitrile and vinyl acetate or methyl acrylate fall on that of bulk copolymerization.


*Research Institute of Teikoku Rayon Co. Ltd., Iwakuni*

# *Action of Emulsifier upon Compositions of Emulsion Copolymers of Acrylonitrile and Water-insoluble Monomers*

By Moriya UCHIDA and Hideo NAGAO

(Received August 1, 1956)

## Introduction

It has been reported by several investigators[1-5] that the composition of copolymer forming in a copolymerization depends upon the monomer composition at that instant. Moreover, Alfrey and Goldfinger[6], Mayo and Lewis[7], and Walling and Briggs[8] derived independently the general equation describing monomer-polymer composition relationship, with which the experimental data determined for bulk copolymerization showed agreement. However, the water solubility of a monomer can not be neglected in the copolymerization system, in case water is used as the medium.

Fordyce and Chapin[9] compared the composition of the copolymer of styrene and acrylonitrile obtained in emulsion polymerization with that of the copolymer obtained in bulk polymerization, and found that the emulsion copolymer is consistently richer in styrene, though by a small amount, than the bulk copolymer produced from the same initial monomer composition.

They have suggested that this difference may be due solely to the decrease in the content of acrylonitrile of the oil phase, which resulted from the water solubility of acrylonitrile. Smith[10] determined the

1) F. T. Wall, *J. Am. Chem. Soc.*, **66**, 2050 (1944).
2) F. M. Lewis, F. R. Mayo and W. F. Hulse, ibid. **67**, 1701 (1945).
3) T. Alfrey, Jr., and E. Lavin., ibid., **67**, 2044 (1945).
4) T. Alfrey, Jr., E. Merz and H. Mark, *J. Polymer. Sci.*, **1**, 37 (1946).
5) T. Alfrey, Jr., and G. Goldfinger, *J. Chem. Phys.*, **14**, 115 (1946).
6) T. Alfrey, Jr., and G. Goldfinger, ibid., **12**, 202, 322 (1944).
7) F. R. May and F. M. Lewis, *J. Am. Chem. Soc.*, **66**, 1594 (1944).
8) C. Walling and E. R. Briggs, ibid., **67**, 1774 (1945).
9) R. G. Fordyce and E. C. Chapin, ibid., **69**, 581 (1947).
10) W. V. Smith, ibid., **70**, 2177 (1948).

compositions of styrene-acrylonitrile solutions in equilibrium with water-acrylonitrile solutions and showed that Fordyce and Chapins' emulsion polymerization data were indentical with their bulk polymerization data in regard to composition of copolymer produced from a given oil phase, when the equilibrium composition was used to calculate the acrylonitrile contents of the oil phases presented in their emulsion copolymerization experiments.

However, in the system of copolymerization of water soluble monomer as acrylonitrile and water-insoluble monomer such as styrene, the copolymer compositions are not always dependent upon the monomer composition in oil phase as shown by Fordyce and Smith.

As we reported, in the copolymerization of acrylonitrile-vinylidene chloride[11] and acrylonitrile-styrene[12], the compositions of emulsion copolymers depend upon the amount of emulsifier used. This paper deals with the variation of the monomer-polymer composition curve arising from the variation of the amount of emulsifier used.

## Experimental

The emulsion polymerization procedure was the same as that of previous reports[2,3]. The emulsifier is Sodium Dodecyl Sulfate.

In the case of benzoyl peroxide as a catalyst, the amount of benzoyl peroxide used was 1 weight % against total monomers and the copolymerizations were done at the temperature of 75°C. The polymerizations were allowed to proceed to low conversions (mostly <5%) and the initial polymer was isolated and purified. The amount of combined acrylonitrile in the initial copolymer was determined by the Kjeldahl analysis.

The acrylonitrile-vinylidene chloride solutions were thoroughly shaken with the given amounts of water, in a water bath maintained at 25°C and thus the solutions were separated into two phases. Then the concentrations of acrylonitrile in the partition phases were determined by the following methods.

**A. Method by Acrylonitrile Analysis.**—The acrylonitrile in a sample with-drawn from oil phase was analysed by n-dodecyl-mercaptan method[14] and the amount of acrylonitrile in oil phase was determined. In this case, vinylidene chloride did not injure the acrylonitrile analysis as shown in Fig. 1.

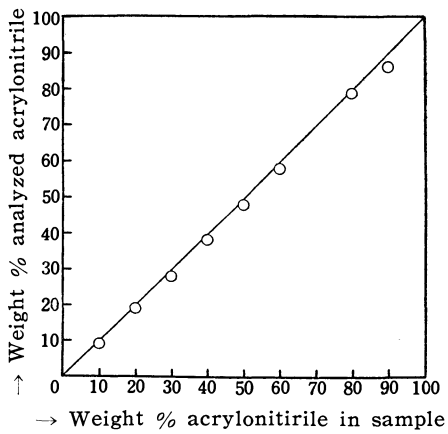



Fig. 1. Analyses of acrylonitrile in vinylidene chloride.

Then the amount of acrylonitrile in water phase was determined by the procedure.

**B. Method by Specific Gravity Measurement.**—The relationship between specific gravity and composition was established by preparing acrylonitrile-vinylidene chloride solutions of known compositions and measuring the specific gravity with pycnometer.

The results used to establish the relationship are given in Table I. All compositions were determined by linear interpolation of the data in Table I.

TABLE I

SPECIFIC GRAVITIES AND REFRACTIVE INDICES OF ACRYLONITRILE VINYLIDENE CHLORIDE SOLUTIONS

| Composition of solution | | Specific gravity | Refractive index |
|---|---|---|---|
| Acrylonitrile (weight %) | Vinylidene chloride (weight %) | 25°C | $n_D^{25}$ |
| 100.00 | 0.00 | 0.8002 | 1.3888 |
| 90.00 | 10.00 | 0.8264 | 1.3908 |
| 80.00 | 20.00 | 0.8554 | 1.3918 |
| 70.00 | 30.00 | 0.8855 | 1.3945 |
| 60.00 | 40.00 | 0.9199 | 1.3976 |
| 50.00 | 50.00 | 0.9542 | 1.3999 |
| 40.00 | 60.00 | 0·9905 | 1.4018 |
| 30.00 | 70.00 | 1.0410 | 1.4077 |
| 20.00 | 80.00 | 1.0879 | 1.4113 |
| 10.00 | 90.00 | 1.1438 | 1.4163 |
| 0.00 | 100.00 | 1.2074 | 1.4215 |

The relationship between specific gravity and acrylo-nitrile concentration in its aqueous solution was established by the same procedure as above. The results thereof are given in Table II.

11) H. Nagao, M. Uchida and T. Yamaguchi, *J. Chem. Soc. Japan*, in press "Emulsion Copolymerization of Acrylonitrile and Vinylidene chloride."

12) H. Nagao, M. Uchida and T. Yamaguchi, ibid., in press "Heat Stability of Emulsion Copolymer of Acrylonitrile and Vinylidene chloride."

13) M. Uchida and H. Nagao, This Bulletin, **29**, 928 (1956).

14) D. W. Beesing, W. P. Tyler, D. M. Kurtz and S. A. Harrison, *Anal. Chem.*, **21**, 1073 (1949).

TABLE II
SPECIFIC GRAVITIES AND REFRACTIVE INDICES OF ACRYLONITRILE AQUEOUS SOLUTION

| Composition of solution | | Specific gravity | Refractive index |
|---|---|---|---|
| $H_2O$ (weight %) | Acrylonitrile (weight %) | 25°C | $n_D^{25}$ |
| 100.00 | 0.00 | 0.9971 | 1.3325 |
| 99.00 | 1.00 | 0.9965 | 1.3329 |
| 98.00 | 2.00 | 0.9950 | 1.3337 |
| 97.00 | 3.00 | 0.9941 | 1.3341 |
| 96.00 | 4.00 | 0.9931 | 1.3348 |
| 95.00 | 5.00 | 0.9915 | 1.3363 |
| 94.00 | 6.00 | 0.9911 | 1.3375 |
| 93.00 | 7.00 | 0.9898 | 1.3376 |

Then the compositions of partition phases were determined by measuring their specific gravities, respectively.

**C. Method by Refractive Index Measurement.**—The relationship between refractive index and composition was established by preparing monomer solution and acrylonitrile aqueous solutions of known compositions and measuring the refractive index with Pulfrich refractometer. The results are given in Table I, II and III.

TABLE III
REFRACTIVE INDICES OF ACRYLONITRILE-STYRENE SOLUTIONS

| Composition of solution | | Refractive index | Refractive index of solution saturated with water |
|---|---|---|---|
| Acrylonitrile (mol. %) | Styrene (mol. %) | $n_D^{25}$ | $n_D^{25}$ |
| 100.00 | 0.00 | 1.3888 | 1.3881 |
| 95.00 | 5.00 | 1.4027 | 1.3996 |
| 80.00 | 20.00 | 1.4385 | 1.4356 |
| 60.00 | 40.00 | 1.4750 | 1.4726 |
| 40.00 | 60.00 | 1.5019 | 1.5028 |
| 20.00 | 80.00 | 1.5276 | 1.5252 |
| 0.00 | 100.00 | 1.5464 | 1.5460 |

Then the compositions of oil and water phases were determined by measuring their refractive indices.

The composition of Acrylonitrile in styrene phase was determined by refractive index measurement and by calculating from analytical value of acrylonitrile in water phase.

## Results and Discussion

**(1) Acrylonitrile-Vinylidene chloride Copolymerization.**—The various equilibrium compositions of oil and water phases were measured. The results are given in Figs. 2 and 3.

In the emulsion copolymerization of acrylonitrile-vinylidene chloride, the composition of copolymer was dependent upon

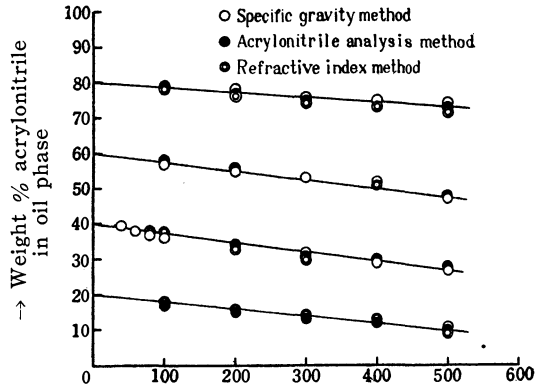



Fig. 2. Partition of acryronitrile in vinylidene chloride.

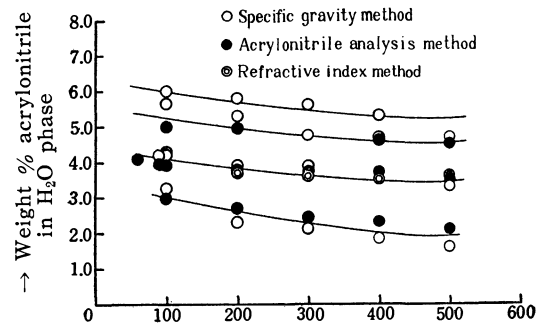



Fig. 3. Partition of acrylonitrile in water.

the amount of emulsifier used; the composition of the compolymer forming either no emulsifier or very dilute emulsifier solutions, containing much acrylonitrile. The monomer-polymer composition curves are shown in Fig. 4.

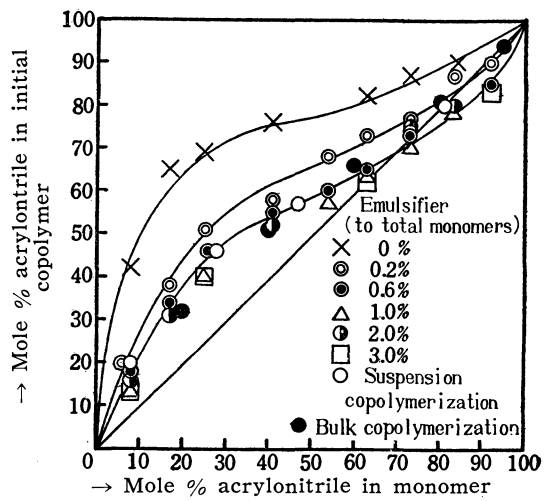



Fig. 4. Monomer-polymer composition curves for acrylonitrile-vinylidene chloride (I).

The compositions of copolymers became richer in styrene along with the increase in the amount of emulsifier used.

The relative reactivity between acrylonitrile and vinylidene chloride has been found in bulk polymerization[2].

| $r_1$ (Acrylonitrile) | $r_2$ (Vinylidene chloride) | Temperature. |
|---|---|---|
| 0.91±0.10 | 0.37±0.10 | 60°C |

When the monomer-polymer composition curve is drawn in Fig. 4 from above $r_1$, $r_2$ values, it will be seen that this curve comes between that of emulsifier-free copolymerization and that of emulsion copolymerizations. If polymerization occurs in oil phase as was asserted by Fordyce, Chapin[9] and Smith[10], the monomer-polymer composition curves will be dependent upon the composition of oil phase. The amounts of acrylonitrile in oil phase are shown in Fig. 5. As we substituted the compositions of oil phase in aqueous polymerization instead of the charged compositions, the monomer-polymer composition curves thereof are shown in Fig. 6.

It is seen that these corrections of the compositions of the emulsion oil phases make the emulsion and bulk copolymerization composition curves identical only in case of the emulsion polymerization using the emulsifier of the critical micell concentration[11]. Moreover, the monomer-polymer composition curve in aqueous suspension copolymerization using benzoyl peroxide as an oil soluble catalyst is shown in Fig. 7.

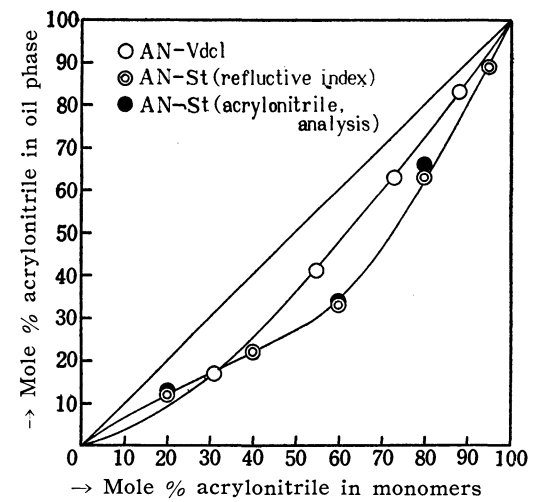



Fig. 5. Relation between composition of monomer and that of oil phase.

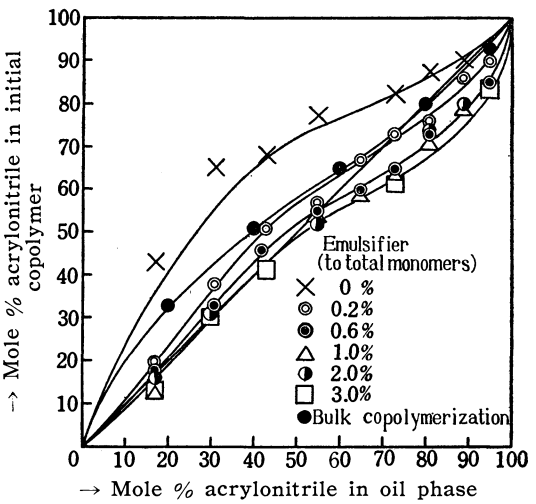



Fig. 6. Monomer-polymer composition curves for acrylonitrile vinylidene chloride (2).

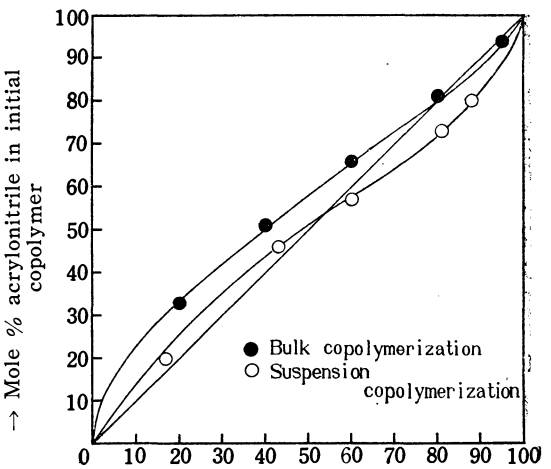



Fig. 7. Monomer-polymer composition curves for acrylonitrile-styrene (1).

It will be observed that the aqueous suspension copolymers consistently contain less combined acrylonitrile than the corresponding bulk copolymers. The copolymer composition values for suspension copolymerization were plotted on the basis of monomer concentrations charged to the reaction system, the most of the reacted monomers exist in the oil droplets of the dispersed phase.

With the oil phase compositions, the composition curve of the aqueous suspension copolymerization is identical with that of the bulk copolymerization and also with that of emulsion copolymerization using thicker emulsifier solution. Although

these identities coinside with Smith's theory of oil phase mechanism of emulsion polymerization as Fordyce and Chapin[9] reported about acrylonitrile-styrene emulsion copolymerization, it does not seem to be reasonable that the composition of emulsion copolymers is dependent only upon the oil phase composition, for the copolymer composition varies by emulsifier concentrations as showed in Fig. 6.

**(2) Acrylonitrile -Styrene Copolymerization.**—As in the case of acrylonitrile-vinylidene chloride emulsion copolymerization, the monomer-polymer composition curve in acrylonitrile-styrene emulsion copolymerization depended upon the amount of the used emulsifier. The results are shown in Fig. 8.

The relative reactivity in bulk copolymerization is shown as follows.

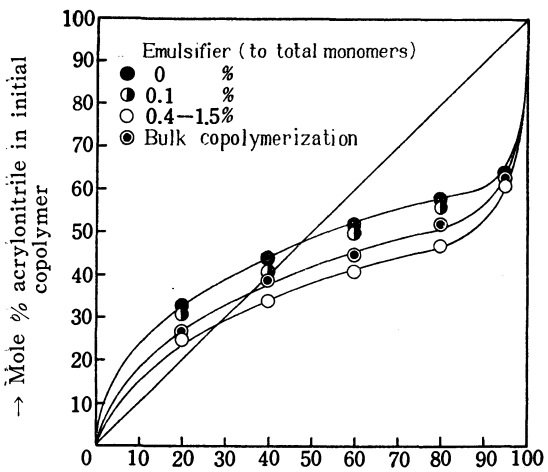



Fig. 8. Monomer-polymer composition curves for acrylonitrile-styrene. (2).

| author | $r_1$ (styrene) | $r_2$ (acrylonitrile) | Temperature °C |
|---|---|---|---|
| Lewis, Mayo and Hulse[4] | 0.41±0.08 | 0.04±0.04 | 60 |
| Fordyce and Chapin[9] | 0.41±0.08 | 0.03±0.03 | 75 |
| Simha and Wall[15] | 0.37±0.02 | 0.05±0.02 | 50 |
| Fordyce[16] | 0.52±0.04 | 0.03±0.03 | 67-80 |
| Goldfinger and Steidlitz[17] | 0.38±0.03 | 0.05±0.02 | 41.5 |
| 〃 | 0.45±0.03 | 0.02±0.02 | 65 |
| 〃 | 0.47±0.03 | 0.02±0.02 | 86.5 |

15) R. Simha and L. A. Wall., *J. Research Natl. Bur. Standards*, **41**, 521 (1948).
16) R. G. Fordyce, *J. Am. Chem. Soc.*, **69**, 1903 (1947).
17) G. Goldfinger and G. I. Carothers, *J. Polymer Sci.*, **4**, 97, (1949).

The values of $r_1$ and $r_2$ are mostly independent of the temperature of polymerization with the inrange of 40–80°C. Although our copolymerization temperature was 45°C, the monomer-polymer composition curve in bulk copolymerization was drawn from the data of Lewis, Mayo and Hulse in Fig. 8. This curve comes between the curve of emulsifier-free copolymerization and that of emulsion copolymerization. In this case, the above described emulsion oil phases make the composition curves of emulsion copolymerization using thick concentrations of emulsifier and that of bulk copolymerization identical, but emulsifier-free copolymers contain less combined styrene than the corresponding bulk copolymer.

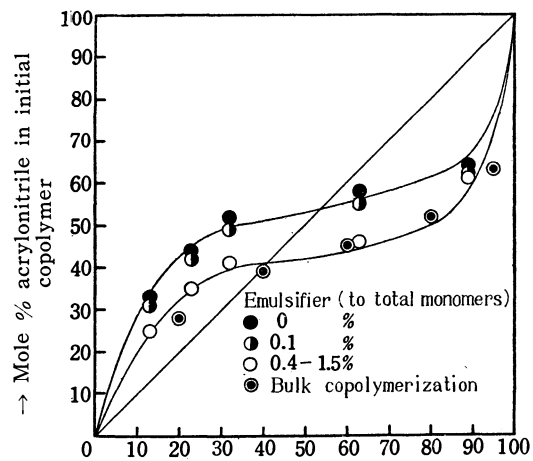



Fig. 9. Monomer-Polymer composition curves for acrylonitrile-styrene (3).

It seems that the water solubility of monomer affects the compositions of forming copolymers in aqueous copolymerizations of water soluble monomer as acrylonitrile and water insoluble monomer as styrene and vinylidene chloride using water soluble catalyst. The initiation of polymerization occurs by reaction between catalyst and monomer in water phase, since in the case of emulsifier-free copolymerization the water phase contains acrylonitrile, so the initial copolymer seems to contain much acrylonitrile. The water phase will contain more water insoluble monomer solubilized in micell, and the initial copolymer seems to contain less acrylonitrile, as the amount of emulsifier.

**Summary**

The following are the facts found from the monomer-polymer composition curves of aqueous copolymerization of the water soluble monomer as acrylonitrile and the water insoluble monomers as vinylidene chloride and styrene using the water soluble catalyst.

(1) The emulsifier-free aqueous copolymers contained consistently much more combined acrylonitrile than the corresponding bulk and emulsion copolymer.

(2) The emulsion copolymer contained less acrylonitrile as the amount of used emulsifier increased.

(3) The monomer-polymer composition curves of emulsion copolymerizations were identical with that of bulk copolymerization, only when critical micell concentration of emulsifier was in use.

*Research Institute of Teikoku Rayon Co, Ltd., Iwakuni*

# *Structure of Reineckate Complex Ion*

By Yoshio TAKÉUCHI and Yoshihiko SAITO

(Received November 30, 1956)

## Introduction

In the study of the crystal structure of Reinecke's salt, $NH_4[Cr(NCS)_4(NH_3)_2]\cdot 2/3H_2O$, it was found that the reineckate complex ion $[Cr(NCS)_4(NH_3)_2]^-$ contains linear NCS groups. The bond character of the NCS group is expressed by the structure $N\equiv C-S^-$. The reineckate complex ion with the same bond character was also found in pyridine reineckate, $C_5H_5N[Cr(NCS)_4(NH_3)_2]$. The shape and the size of the complex ion in both crystals are identical within the errors of experiment. However, a modified configuration of the complex ion has been found by the study of Patterson projections of choline reineckate, $(CH_3)_3N\cdot CH_2\cdot CH_2\cdot OH[Cr(NCS)_4(NH_3)_2]$, which was prepared from choline chloride and Reinecke's salt solution. In the case of choline reineckate, the bond distances of the complex ion are considerably different from those found in the other two cases and the bond character is no more expressed by the structure $N\equiv C-S^-$ but very close to the structure $N^-=C=S$. Although brief accounts on the crystal structures of these reineckates already appeared separately, because of the importance of understanding the nature of complex ions, a detailed description of the structure of reineckate complex ion will be given in the present paper.

## 1. The Structure of Reinecke's Salt[1]

**(i) Unit Cell and Space Group.**— The crystals of Reinecke's salt whose chemical formula had been known as $NH_4[Cr(SCN)_4(NH)_3)_2]H_2O$ crystallize from ethyl alcohol and water in well formed garnet-red rhombic dodecahedra combined with a cube (Fig. 1).

Oscillation and Weissenberg photographs taken with copper radiation ($\lambda=1.5418$ Å) gave lattice constant:

$$a=13.25\pm0.02 \text{ Å},$$

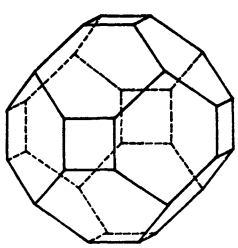


Fig. 1. The crystal habit of Reinecke's salt.

and unit cell contains six formula units. The calculated density 1.496 g./cc. was in good agreement with the observed value 1.503 g./cc. measured by the pycnometer method. The Laue symmetry is $O_h-m3m$ and $h,k,l$ reflexions are systematically absent when $h+k+l$ is odd. Hence, the possible space groups are $O_h^9-I_{m3m}$, $T_d^3-I_{43m}$

1) Y. Saito, Y. Takéuchi and R. Pepinsky, *Z. Krist.* **106**, 476, (1955).

or $O^5$—$I_{43}$. Taking account of all possibilities of these space groups, the structure analysis was started. However, by the study of Patterson projection, it became obvious that $O_h^9$ was a distinct possibility.

**(ii) Analysis.**—The multiple film technique was employed and intensities were recorded for all three dimensional reciprocal spaces which are covered by copper radiation. These intensities were measured visually using an intensity scale prepared with the same specimen as that used for intensity recording.

The following characteristics of reflexions were observed: $hkl$ is strong when $h=4n_1$, $k=4n_2$, $l=4n_3$ or $h=4n_4+2$, $k=4n_5+2$, $1=4n_6+2$, where $n_i$ are integers. These conditions immediately fixed the positions of heavy atoms as follows: 6Cr in the six-fold positions (b) $0\frac{1}{2}\frac{1}{2}$, and 24S in the twenty four-fold positions (h) $0xx$ with $x\simeq0.25$. This arrangement of heavy atoms was in good accord with conclusions drawn from the Patterson projection P($xy$). Distribution of peaks in P($xy$) also indicated that 24C and 24N atoms from the thiocyanate groups are on 12(e) $x00$. The first Fourier synthesis was calculated using the signs based on chromium and sulphur atoms. In the electron density projection $\rho(xy)$ thus obtained, two peaks were observed between chromium and sulphur. These peaks must be due to nitrogen and carbon atoms. The distances between these peaks approximately corresponded to the usual bond lengths of Cr—N, N—C and C—S. Since it seems reasonable that the majority of the signs of $F(hk0)$ reflexions are determined by the contribution of the complex ion $[Cr(NCS)_4(NH_3)_2]^-$, the further steps of refinement were made by computing $\rho(xy)$ and generalized projection $\rho(xy1)$ using the signs based on the complex ion. The atomic positions found from these refinements are:

| | $x$ | $y$ | $z$ |
|---|---|---|---|
| Cr | 0 | 0.5 | 0.5 |
| N | 0.40 | 0.40 | 0 |
| C | 0.33 | 0.33 | 0 |
| S | 0.24 | 0.24 | 0 |
| $NH_3$ | 0.34 | 0.34 | 0 |

If the empirical formula of the Reinecke's salt is correct, there should be six ammonium and six water molecules in the unit cell. However, in the space group $I_{m3m}$ and any of its subgroups, no six-fold positions are available for these atoms. Then, to find out possible positions of these atoms, the contribution of the complex ion $F_r$ was subtracted from observed structure factor $F_{hk0}$ and trial of computing $\sum\sum(F_{hk0}-F_r)\cos 2\pi(hx+ky)$ was made on X-RAC. The result showed well-defined peaks on sets of special positions 2($a$)000 and 8($c$)$\frac{1}{4}\frac{1}{4}\frac{1}{4}$ (Fig. 2.).

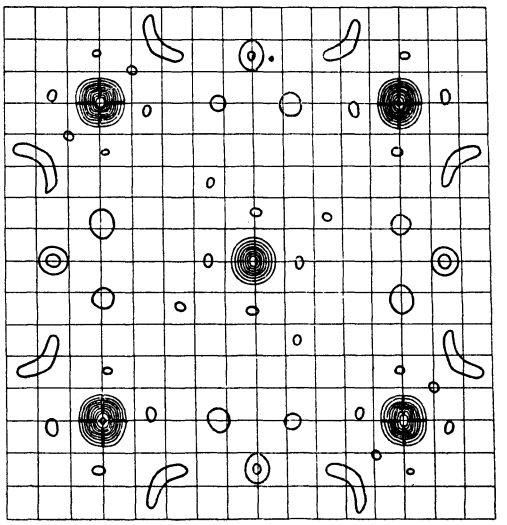


Fig. 2. Residual Fourier projection showing the positions of $NH_4$ and $H_2O$ groups. Origine is taken at the center of this projection.

In order to obtain the best agreement between observed and calculated structure factors, it was necessary to distribute $6NH_4$ and $4H_2O$ atoms random among these positions. The final refinement of the structure was made by three dimensional Fourier synthesis. The final atomic parameters are:

| | | |
|---|---|---|
| 6Cr: | 6($b$) | 0 |
| 24N: | 24($h$) | $0xx$ with $x=0.395$ |
| 24C: | 24($h$) | $0xx$ with $x=0.334$ |
| 24S: | 24($h$) | $0xx$ with $x=0.238$ |
| $12(NH_3)$: | 12($e$) | $x00$ with $x=0.338$ |
| $6(NH_4)$ and $2H_2O$: | | |
| | 8($c$) | $\frac{1}{4}\frac{1}{4}\frac{1}{4}$ |
| $2H_2O$: | 2($a$) | 000 |

With these coordinates, structure factors were calculated using the temperature factor of the form $\exp-B(\sin^2\theta/\lambda^2)$, where $B=2.0$ Å$^2$. The R-factor is 11.6% for $F(hk0)$ and 19.0% for $F(hkl)$ reflexions.

**(iii) Description of the Structure.**—Fig. 3 shows the structure of Reinecke's salt. Chromium atoms are at six corners of the one-eighth of the unit cell. The rest of the corners and the body-centered

position of the cube are occupied by ammonium ions and water molecules randomly. The ammonium ion (and water molecule) at the body-centered position is surrounded by six sulphur atoms octahedrally with the distance of 3.35 Å. The water molecules at the corners of the cube are surrounded by twelve sulphur atoms with the distance of 4.44 Å. Since the bond between ammonium ion and sulphur atoms is ionic from the stand point of atomic distances, it seems reasonable to conclude that the eight-fold position $\left[\frac{1}{4}\frac{1}{4}\frac{1}{4}\right]$ is occupied by six ammonium ions and two water molecules randomly and the two-fold position [000] is occupied by two water molecules. The correct formula of Reinecke's salt is thus $NH_4[Cr(NCS)_4(NH_3)_2]\frac{2}{3}H_2O$. A similar random distribution of atoms has also been found in the mineral analcite[2].

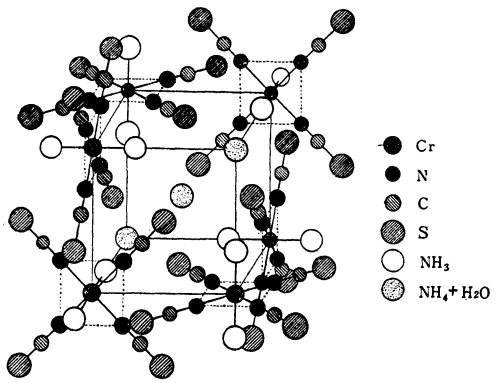



Fig. 3. 1/8 unit cell of Reinecke's salt. $NH_4[Cr(NCS)_4(NH_3)_2]\cdot 2/3\,H_2O$

The square coordination of NCS groups to chromium atoms is shown in Fig. 4 which was obtained from the zero section of the three dimensional Fourier synthesis. The supposed SCN group is actually an iso-thiocyanato group NCS, with N atoms coordinated to chromium. This iso-thiocyanato group is in contrast to $[Hg(SCN)_4][Cu(en)_2]$[3] where the thiocyanato group SCN was found. Four linear NCS groups are arranged along the diagonals of a square around the chromium atom, and $NH_3$ groups are in the remaining octahedral positions. The symmetry of the complex ion is thus $4/mmm$. Bond lengths of the complex ions are:

| | | |
|---|---|---|
| Cr—$NH_3$ | ····· | 2.15±0.03 Å |
| Cr—N | ····· | 1.97±0.03 |
| N—C | ····· | 1.14±0.03 |
| C—S | ····· | 1.80±0.03 |

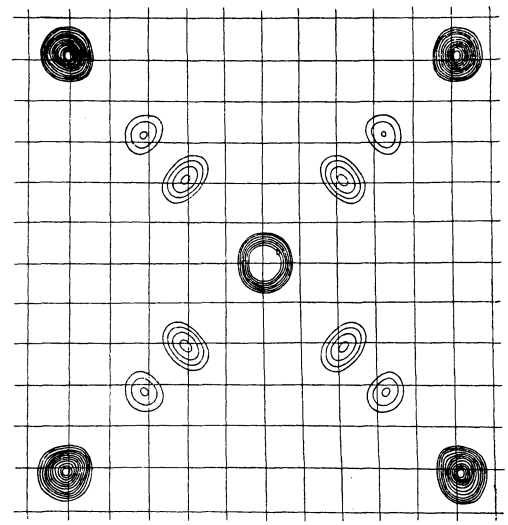


Fig. 4. Three dimensional Fourier section $\rho(xy0)$ of Reinecke's salt with origine at the center.

## 2. The Structure of Pyridine- and Choline-reineckate

Prior to the discussion on the structure of the complex ion, the crystal structures of pyridine- and choline-reineckate are described. The lattice constants and space groups of these reineckates are given in Table I.

TABLE I
THE LATTICE CONSTANTS AND SPACE GROUPS OF SOME REINECKATES

| | Lattice constants | | | | Space group |
|---|---|---|---|---|---|
| | $a$ | $b$ | $c$ | $\beta$ | |
| Reinecke's salt | 13.25 Å | | | | $O_h^9-I_{m3m}$ |
| Pyridine reineckate | 15.52 | 7.64 | 14.64 | 102°24′ | $C_{2h}^5-A_{2/a}$ |
| Choline reineckate | 12.69 | 22.80 | 6.75 | | $D_{2h}^{26}-I_{bma}$ |

**(i) Pyridine Reineckate**[4].—The crystals of pyridine reineckate were prepared by Christensen's method[5] and recrystallized in hot alchoholic solution. The measured density of the crystals 1.560 g./cc. is in agreement with the calculated

2) W. H. Taylor, *Z. Krist.*, **74**, 1 (1930); **99**, 283(1938).
3) H. Scouloudi, *Acta Cryst.*, **6**, 651 (1953).
4) Y. Takéuchi and R. Pepinsky, Presented to the Thirteenth Annual Pittsburgh Diffraction Conference, 1955.
5) O. T. Christensen, *J. Prak. Chem.*, **45**, 364 (1891).

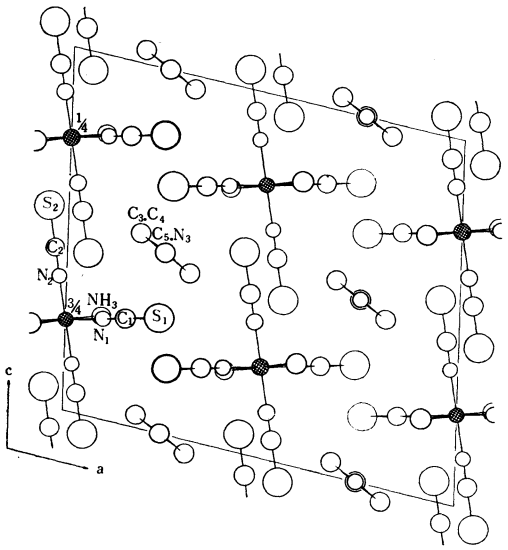



Fig. 5. Projection of the structure of pyridine reineckate aiong *b*-axis.

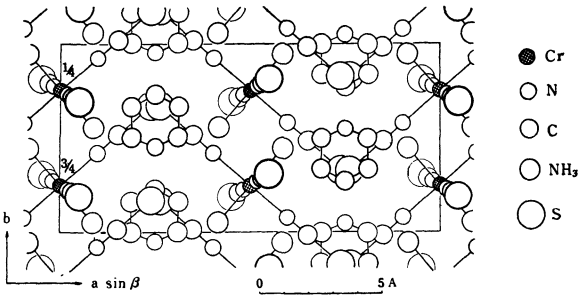



Fig. 6. Projection of the structure of pyridine reineckate along *c*-axis.

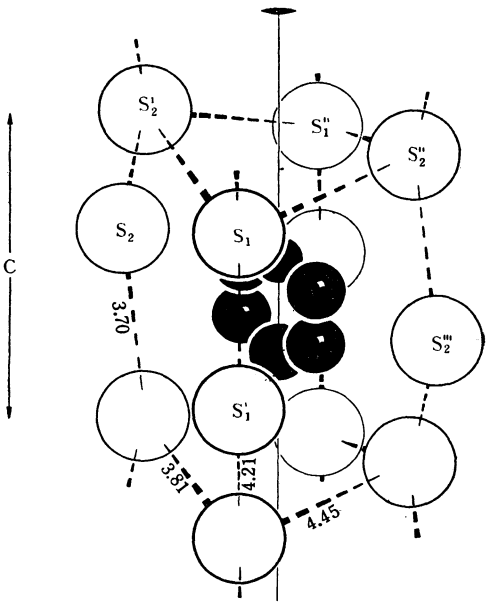



Fig. 7. Configuration of sulphur atoms about a pyridine molecule. Numbers indicate the distances between sulphur atoms in Å.

density 1.56 g./cc. The crystals obtained were found to be twinned about (101). However, it was possible to separate single crystals and they were used for X-ray work.

The structure was determined by the use of two dimensional Fourier synthesis which resulted in a final agreement factor, $R=\Sigma(|F_o|-|F_c|)/\Sigma|F_o|$, of 0.107 for the (010) projection and of 0.112 for the (001) projection. Fig. 5 and Fig. 6 show the projections of the crystal structure of pyridine reineckate on (010) and (001) respectively. Reineckate groups are arranged around a two-fold screw axis, making a frame-like structure and leaving a big hole around the two-fold axis. The pyridine molecule on the twofold axis is located in a region surrounded by twelve sulphur atoms. Four of these sulphur atoms coordinate to the nitrogen atom of the pyridine molecule with two distances of 3.36 Å and two of 3.60 Å. The configuration of sulphur atoms about a pyridine molecule is shown in Fig. 7. The mean values of the bond lengths determined for the reineckate complex ion are Cr—N= 1.95 Å, N—C=1.15 Å and C—S=1.76 Å. These values agree with those found in Reinecke's salt (p. 321). The bond lengths of pyridine molecules and non-bonded distances of atoms are given in Table III.

The estimation of the accuracy of atomic parameters was carried out especially to the atoms of pyridine molecules. Because of the special position, errors of atomic coordinates in a pyridine molecule mainly

TABLE II

COORDINATES OF ATOMS IN PYRIDINE REINECKATE

| Atom | *x/a* | *y/b* | *z/c* | No. of atoms per cell |
|---|---|---|---|---|
| Cr | 0 | 3/4 | 1/4 | 4 |
| $S_1$ | 0.237 | 0.117 | 0.306 | 8 |
| $S_2$ | −0.050 | 0.831 | 0.563 | 8 |
| $C_1$ | 0.152 | 0.021 | 0.287 | 8 |
| $C_2$ | −0.035 | 0.802 | 0.439 | 8 |
| $N_1$ | 0.095 | 0.922 | 0.273 | 8 |
| $N_2$ | −0.025 | 0.783 | 0.365 | 8 |
| $NH_3$ | 0.080 | 0.536 | 0.292 | 8 |
| $C_3$ | 0.184 | 0.489 | 0.535 | 8 |
| $C_4$ | 0.182 | 0.671 | 0.536 | 8 |
| $C_5$ | 1/4 | 0.746 | 1/2 | 4 |
| $N_3$ | 1/4 | 0.420 | 1/2 | 4 |

TABLE III
ATOMIC DISTANCES IN PYRIDINE REINECKATE

Bond lengths of pyridine molecule

| | |
|---|---|
| $C_3-C_4=1.39$ Å | $C_4-C_5=1.40$ Å |
| $C_3-N_3=1.35$ Å | |

Nonbond distances

| | |
|---|---|
| $S_1-S_1'=4.21$ Å | $S_1-S_2'=3.80$ Å |
| $S_2'-S_2=3.70$ | $S_1'-S_2''=4.45$ |
| $NH_3-N_3=3.60$ | $NH_3-C_3=3.78$ |
| $NH_3-C_3'=3.99$ | $NH_3-C_4'=4.11$ |
| $NH_3-C_4=3.90$ | $NH_3-C_5=3.84$ |
| $N_3-S_1=3.36$ | $N_3-S_2'=3.60$ |
| $C_3'-S_1=3.38$ | $C_3'-S_2''=3.47$ |
| $C_4-S_2=3.82$ | $C_4-S_1'=4.34$ |
| $C_5-S_1=4.33$ | |

distribute in their $y$-parameter. The standard deviations $\sigma(y)$ for the positions of carbon and nitrogen atoms were calculated, using Cruickshank's method[6] were found to be $1.9\times10^{-2}$ Å and $1.7\times1.0^{-2}$ Å respectively. Standard deviations $\sigma(x)$ and $\sigma(z)$ for carbon atoms of pyridine molecule were $1.2\times1.0^{-2}$ Å.

**(ii) Choline Reineckate**[7].—Choline reineckate was prepared using a diffusion method with choline chloride and Reinecke's salt solution in silica gel. The colour of the crystal is magenta as are other reineckates. A study of morphology and optical properties showed the crystal to be orthorhombic with holohedral symmetry. The crystal is tabular parallel to (010) and shows (110), (101) forms. There are four formula units of $[C_5H_{13}N(OH)][Cr(NCS)_4(NH_3)_2]$ in the cell giving a calculated specific gravity of 1.48 g./cc. which compares well with the measured value of 1.475 g./cc.

From cell dimension and space group symmetry, it is obvious that the chromium atom is located on a centre of symmetry whose point symmetry is $2/m$. On a Patterson projection $P(uv)$, a fairly well-resolved peak is observed at the point $u=0.175$, $v=0.118$. It has been known that Cr—N—C—S bond is straight and Cr—S distance is 4.9 Å, accordingly the Cr—S vector should appear on the line $y=4.9\times1/\sqrt{2}$ Å (0.153 as decimal fraction of the $b$-axis). From the packing view point, the estimated Cr—S vector position will be $u_0\simeq0.180$, $v_0\simeq0.153$. (Fig. 8) The relative peak height at $(u_0, v_0)$ seems to be unreasonable as Cr—S vector, while the peak at $(u, v)$ could not be explained from Cr—N—C—S straight configuration. However, it was found that the position $(u, v)$ is better for sulphur location to obtain better agreement between calculated and observed structure factors of several strong reflexions. Then the first Fourier based on signs of $F(hk0)$ calculated from Cr and S at $(u, v)$ position was computed on X—RAC. The result revealed that the Cr—N—C angle is not 180° as has been found in other reineckates but has a value of 158° on the (001) projection.

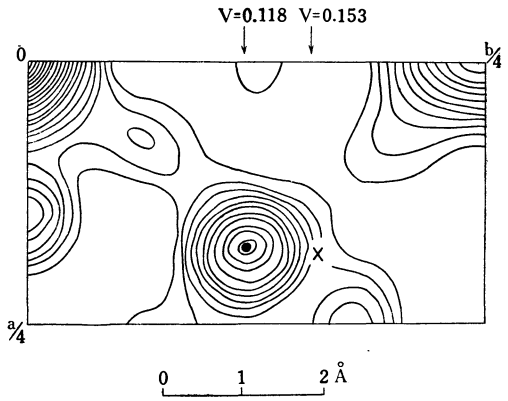



Fig. 8. Patterson projection $P(xy)$ of choline reineckate.
● Cr—S vector position in choline reineckate.
× Cr—S vector position expected from Cr—N—C—S straight configuration.

The structure was refined on the projections (100) and (001). The final refinement was made by computing a three-dimensional Fourier synthesis. The atomic parameters derived from the three-dimensional Fourier are given in Table 4. The R-factor is 11.2% for $F(hk0)$, 13.5% for $F(0kl)$ and 17.0% for $F(hkl)$.

TABLE IV
ATOMIC PARAMETERS FOUND IN CHOLINE REINECKATE

| Atom | $x/a$ | $y/b$ | $z/c$ | |
|---|---|---|---|---|
| Cr | 0 | 0 | 0 | |
| N | 0.058 | 0.057 | 0.182 | |
| C | 0.107 | 0.084 | 0.317 | |
| S | 0.173 | 0.115 | 0.493 | |
| $NH_3$ | 0.139 | 0 | −0.175 | |
| N | 0 | 0.25 | 0.03 | |
| $C_1$ | 0.07 | $0.28_3$ | 0.16 | Choline * molecule |
| $C_2$ | −0.07 | $0.28_3$ | −0.13 | |
| $C_3$ | −0.08 | $0.25_8$ | $-0.29_1$ | |
| OH | $0.01_8$ | 0.27 | $-0.29_3$ | |

6) D. W. J. Cruickshank, *Acta Cryst.*, **2**, 154 (1949).
7) Y. Takéuchi and R. Pepinsky, Presented to the ACA annual meeting (1956).

* This set of coordinates corresponds to the orientation given in Fig. 10.

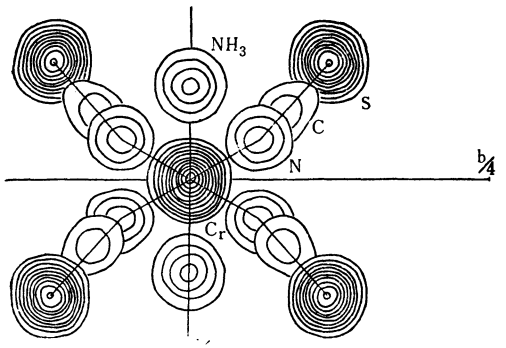



Fig. 9. Composite electron density map of the reineckate group in choline reineckate; view along *c*-axis. Even-contours only drawn for chromium.

Fig. 9 shows the composite electron density map of the complex ion found in choline reineckate. The structure projections on (001) and (100) are given in Fig. 10. The chromium atoms of the complex ions are on the mirror plane and form a layer-like structure parallel to (010). Between these layers, choline molecules are located on the two-fold axis in a region surrounded by four sulphur atoms tetrahedrally. The choline molecule is randomly oriented in four possible positions so that the two fold axis at $\left(0, \frac{1}{4}, z\right)$ has only statistical meaning. The configuration of the choline molecule was found to be close to a "gauche" configuration. Possibly, the weak interaction between the choline and the complex ion results in a significant interaction between the positive nitrogen atom and the hydroxyl group in the same molecule.

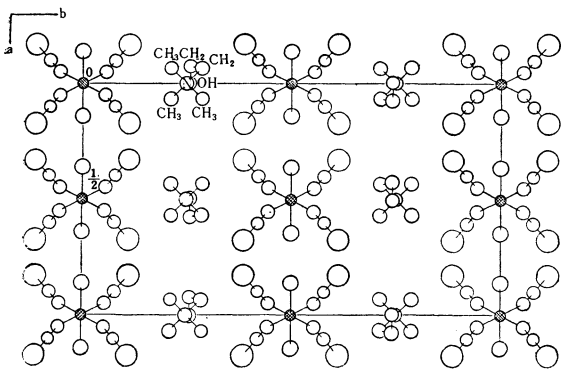



Fig. 10 (a). Structure of choline reineckate, projected on (001).

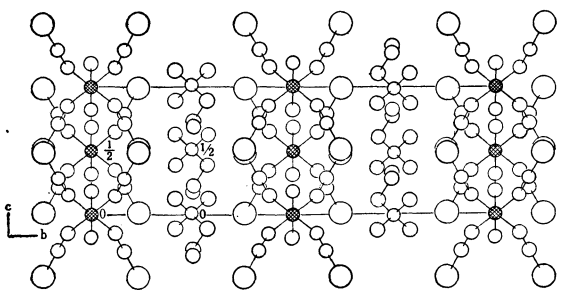



Fig. 10 (b). Structure of choline reineckate, projected on (100). Only one possible orientation is shown for choline molecule.

### 3. Structure of Reineckate Complex Ion

Fig. 11 shows two different configurations of the reineckate complex ion which we have found by the study of these three reineckates. Bond lengths and bond angles are compared in Table V.

These results suggest that in choline reineckate the contribution of the structure

$$N^{-}=C=S \qquad (1)$$

is dominant, while in ammonium and pyridine reineckates the contribution of the structure

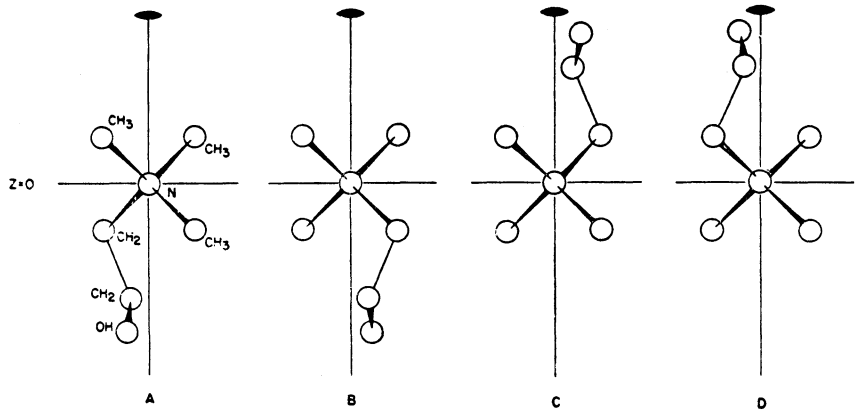
$$N\equiv C-S^{-} \qquad (2)$$

is dominant. These two different cases may be explained as follows.

TABLE V

| | Cr-S | N-C | C-S | Cr-$NH_3$ | Cr-N-C |
|---|---|---|---|---|---|
| Reinecke's salt | 1.97 | 1.14 | 1.80 | 2.15 | 180° |
| Pyridine reineckate | 1.95 | 1.15 | 1.76 | 2.11 | 180° |
| Choline reineckate | 1.94 | 1.27 | 1.64 | 2.12 | 155.5° |

In the case of ammonium and pyridine reineckates, positively charged nitrogen atoms can approach the sulphur atoms of the reineckate groups closely. The electrons are, accordingly, more shifted towards the sulphur atoms in the NCS groups due to the polarization by the nitrogen atoms. In this case, structure (2) will be more stable than structure (1). On the other hand, in the case of the choline molecule, the nitrogen atom with positive charge is surrounded by carbon atoms tetrahedrally and does not approach the sulphur atoms as closely, and the polarization effect on the NCS groups due to the nitrogen of the choline molecule will be smaller. This would result in the dominant contribution of the structure (1). Actually, the $NH_4$—S and NH—S distances in ammonium and pyridine reineckates are




Random orientation of choline molecule in choline reineckate. Four possible orientations are shown.

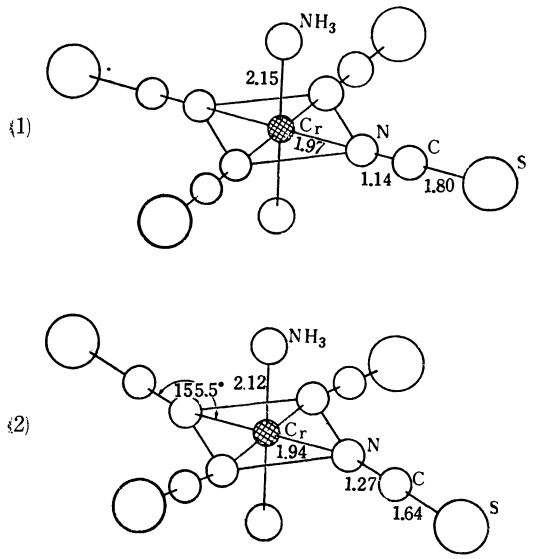



Fig. 11. Configuration of reineckate complex ion found in Reinecke's salt (1) and in choline reineckate (2). Bond distances and bond angle are shown.

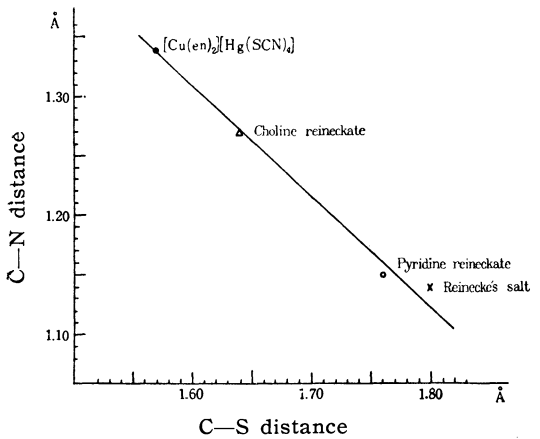



Fig. 12. Relation between the C—N and the C—S distances in various reineckates.

respectively 3.35 Å and 3.36 Å, while in choline reineckate the N—S distance is 4.9 Å. Also, it is interesting to note that in comparison with the other reineckates, the nitrogen atoms of the choline molecule are closer to the nitrogen atoms of the reineckate groups with the distance of about 4.6 Å.

An interesting relation has been found between the C—N and the C—S distances in NCS groups found in various reineckates. If C—N distances are plotted against the C—S distances, a straight line is obtained as illustrated in Fig. 12.

## Summary

The crystal structure analyses of Reinecke's salt, pyridine reineckate and choline reineckate established the configuration and bond characters of the reineckate complex ion, $[Cr(NCS)_4(NH_3)_2]^-$.

The bond character of the complex ion in Reinecke's salt and pyridine reineckate corresponds to the structure $N{\equiv}C{-}S^-$, while in choline reineckate the bond character is acounted for by the structure $N^-{=}C{=}S$. This mutation of the bond character is discussed together with crystal structures of these reineckates.

This work was done at the Pennsylvania State University in the laboratory of Prof. Ray Pepinsky, to whom we are greatly indebted for the facilities made available to us. We are also grateful to Mr. H. Yamatera of Osaka City University for helpful discussions.

*Mineralogical Institute*
*Department of Science*
*The University of Tokyo, Hongo Tokyo*

*Institute of Polytechnics*
*Osaka City University, Kita-ku, Osaka*

# *Studies on Micelles. III. A Check of the New Conclusion from the Spectral Experiments with the Well-known Experimental Facts of Other Authors*

By Hiroji SASAKI

(Received September 8, 1956)

## Introduction

From his absorption spectral experiment, the author has discovered[1] that in a certain wide concentration range of surfactants in aq. solutions the micellar concentration $C_m$ is independent of the surfactant concentration $C_s$ and that in this surfactant concentration range only the association number of micelle $N_m$ increases with increasing surfactant concentration.

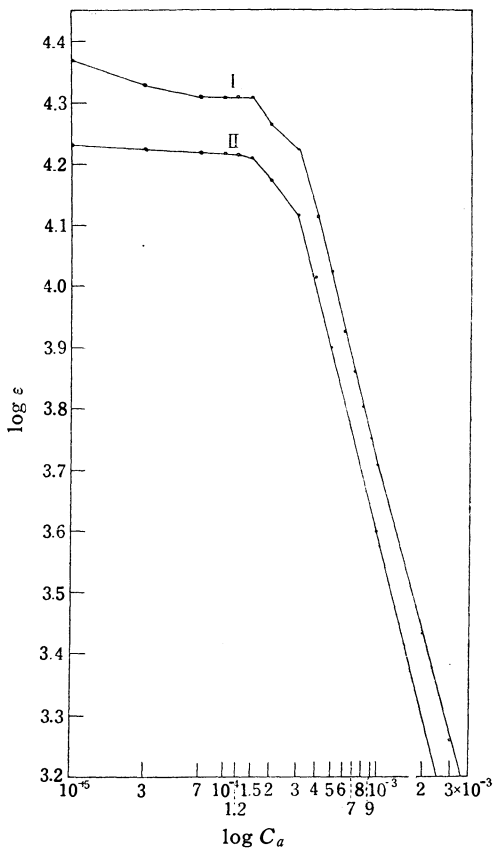



Fig. 1. Absorption intensity of azobenzene at 320 mμ. $C_a$ is the molar concentration of azobenzene. Solvents: I $C_2H_5OH$, II 10% SDS.

The facts which have led the author to this conclusion will be discussed briefly.

**(a)** The curve I in Fig. 1 is the absorption intensity of azobenzene at 320 mμ in ethanol. The curve bends remarkably at about azobenzene concentration $C_a$ being $1.2\times10^{-4}$ M. This lowering of absorption intensity is caused by the association of azobenzene. The curve II in Fig. 1 is the absorption intensity of azobenzene in aq. 10% SDS (sodium dodecyl sulfate) solution. The curve is almost parallel to the abscissa until $C_a$ reaches about $1.2\times10^{-4}$ M, which means that azobenzene molecules are mainly in the unassociated state, i. e., until $C_a$ reaches about $1.2\times10^{-4}$ M there are few micelles which contain more than two azobenzene molecules. The curve bends remarkably at about $C_a$ being $1.2\times10^{-4}$ M, which means that the micelles containing more than two azobenzene molecules appear largely at about this concentration. Therefore the micellar concentration $C_m$ can be

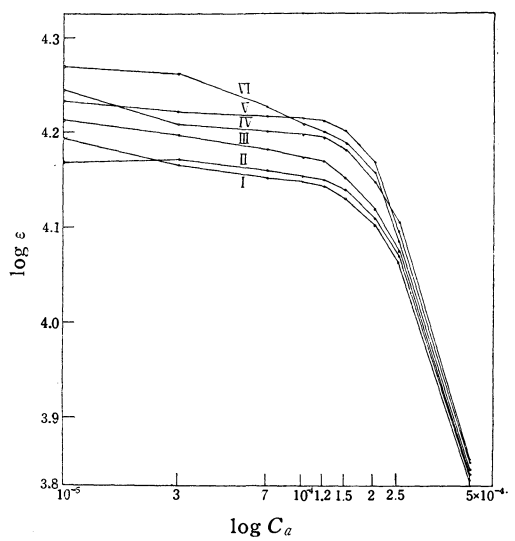



Fig. 2. Absorption intensity of azobenzene at 320 mμ. Solvents: I 0.5% SDS, II 1% SDS, III 2.5% SDS, IV 5% SDS, V 10% SDS, VI 20% SDS.

1) H. Sasaki, S. Saito and H. Okuyama, This Bulletin, **30**, 186 (1957).

estimated safely as about $1.2\times10^{-4}$ M in aqueous 10% SDS solution.

(b) Fig. 2 shows absorption intensity of azobenzene at 320 mμ in aqueous SDS solutions of various concentrations. The bending part of every curve is almost at the same azobenzene concentration, from which it is concluded that the micellar concentration of SDS is almost constant irrespec tive of SDS concentration in the range above 0.5% and below 20%.

(c) The reasonable conclusion deduced from the discussion (a) and (b) is that in a certain wide range of SDS concentration, the association number of SDS-molecules in one micelle increases with increasing SDS concentration.

The author has stated, in his previous report, how a micelle will grow*). The conclusions mentioned there and the natural inference deduced from these conclusions are as follows; (1) above the CMC, micellar concentration $C_m$ increases with increasing surfactant concentration $C_s$ but this range is very limited, meanwhile the range of $C_s$, where $C_m$ is constant, is very wide: (2) the range of surfactant concentration, where $C_m$ is constant, is dependent upon the size of surfactant molecules, especially upon whether surfactant molecules have unsaturated linkage in them or not. The author thinks that it is necessary to check the above mentioned conclusions from the absorption spectra of aqueous surfactant solutions solubilizing absorber molecules with the known experimental facts of other authors.

**The Check of the Conclusions from the Spectral Experiments with the Well-known Experimental Facts**

(1) **Solubilization.** — A curve of solubilization of water-insoluble dye in aqueous surfactant solution, i. e., (the amount of dye solubilized)/(the amount of surfactant $C_s$) vs. $C_s$ curve bends suddenly after the steep rise above CMC and becomes almost parallel to the abscissa. The curve will begin to rise again when $C_s$ becomes considerably high. Taking the conclusion of constant micellar concentration into consideration, the first rise of the curve must be due to the increase in $C_m$ with increasing $C_s$. If only $C_m$ continues to increase but $N_m$ is constant with increasing $C_s$, as are concluded by other authors, the solubilization curve would not show such a sudden bending in a very narrow surfactant concentration range; in this case there is no reason for solubilizing efficiency of micelles to change suddenly with changing surfactant concentration, so the gradient of the curve would be almost constant independent of $C_s$. An example is shown in Fig, 3, which is the result of Hartley[2] and recalculated in the form of {(the amount of dye solubilized) − (solubility of dye in aq. phase)}/($C_s$-CMC) vs. $C_s$. This curve shows that from CMC to 0.0354% of CPC (cetyl pyridinium chloride) $C_m$ increases and above 0.0354% $N_m$ increases mainly, as at this concentration of CPC the solubilization curve bends remarkably.

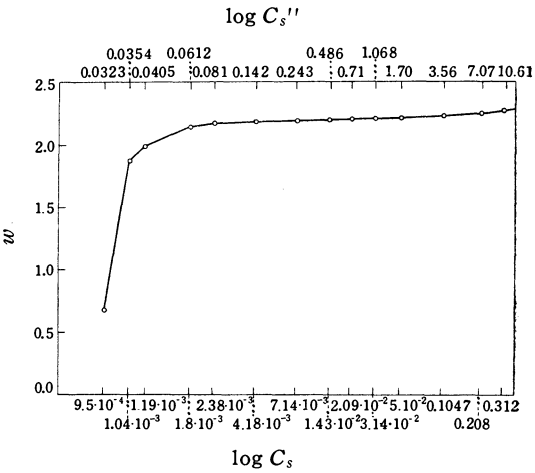



Fig. 3. Solubilization of AB (azobenzene) in aq. CPC (cetyl pyridinium chloride) solution from G. S. Hartley[2] $w=\log\{C_a'/C_s')\times10^3\}$, $C_a'=C_a-2.4\times10^{-5}$, $C_a$ is the molar concentration of AB solubilized, $2.4\times10^{-5}$ M is the solubility of AB in water. $C_s'=C_s-7.2\times10^{-4}$, $C_s$ is the molar concentration of CPC, $7.2\times10^{-4}$ M is the CMC of CPC, $C_s''$ is the weight percent. of CPC.

That the curve continues to rise slightly in the range of 0.081-3.56% shows the packing density of micelles increasing and the amount of water molecules contained in the inside of micelles[3] decreasing with increasing $C_s$. Above 3.5% the gradient of the curve begins to increase again, which shows the appearance of larger micelles with several double layers. From the solubilization curves of Green's[4] the concentrations at which the first rising finishes and the second rising begins respectively is as follows;

| Surfactant | The concentration at which the first rising finishes | The concentration at which the second rising begins |
|---|---|---|
| Na-$C_{12}$ | 0.1 M (2.3%) | |
| Na-Oleate | $5\times10^{-3}$ M (0.15%) | 0.3 M (9.12%) |
| $C_{12}NH_3Cl$ | 0.05 M (1.15%) | |
| Dodecyl sulfonic acid | 0.05 M (1.23%) | 0.727 M (16.4%) |
| Triton X-100 | 0.1% | 10% |

*) H. Sasaki et al., op. cit.

2) G. S. Hartley, *J. Chem. Soc.*, **1938**, 1968.
3) H. Sasaki, H. Okuyama and S. Saito, This Bulletin, **29**, 752 (1956).
4) S. A. A. Green, *J. Phys. Chem.*, **51**, 286 (1947).

These concentrations of various kinds of surfactant must have definite physical meaning, and the conclusion obtained by the spectral method agrees well with the behavior of these solubilization curves, as discussed above.

(2) **Diffusion.** — Hartley et. al.[5] have taken the notion that the micellar volume is independent of $C_s$, from their experimental results of diffusion of surfactants in aqueous salt or alkaline solutions. From the results of diffusion of surfactants in aqueous phase Lamm et. al.[6a] have also reached the same conclusion. M. E. L. McBain recognized that the diffusion coefficients of surfactants in aq. phase decrease with their increasing concentration, and she attributed this to the interaction among the increasing number of micelles[6b]. Stigter et. al.[6c] also accepted the interaction theory, but Abbott et. al.[6d] concluded

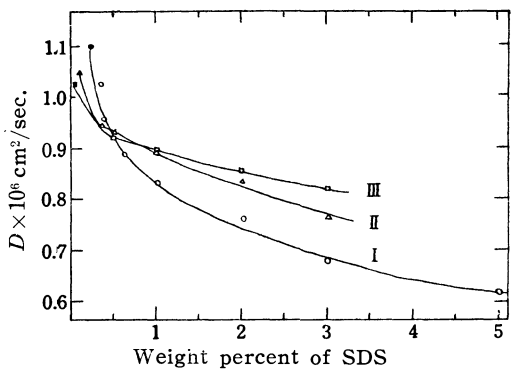



Fig. 4a. Micellar self-diffusion coefficient of SDS at 25°C from D. Stigter et. al.[6c]
Solvents; I. $H_2O$, II. 0.03 M NaCl, III. 0.1M NaCl.

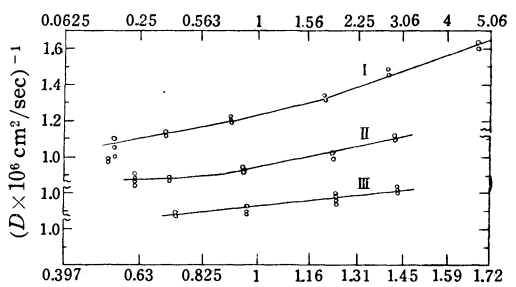



Fig. 4b. Micellar self-diffusion coefficient of SDS at 25°C.
Solvents; I. $H_2O$, II. 0.03 M NaCl, III. 0.1 M NaCl.

that the micellar radius increases with increasing concentration of the simple salt.

When simple salt is added to aqueous surfactant solution, it is thought that simple salt depresses the dissociation constant of paraffin chain salt[7] and these undissociated molecules are solubilized in the palisade of micelles; accordingly the volume of micelles increases. If so, it is natural to think that when $C_s$ is increased, the surfactant molecules newly added are solubilized in the palisade of the existing micelles, and increase their volume, also depressing their diffusion coefficient. Fig. 4a is the result of Stigter et. al.[6c]. At about 1%, the curve I bends remarkably, which shows that until $C_s$ reaches about 1%, $C_m$ increases and above 1% of SDS, $N_m$ increases mainly with increasing $C_s$. The curve $D^{-1}$ vs. $(C_s\text{-CMC})^{1/3}$ {$D$, the diffusion coefficient, is proportional to $r$, the micellar radius, and also $r$ is proportional to $(C_s\text{-CMC})^{1/3}$} must be linear in the range of $C_s \geq 1\%$, if the conclusion that above 1% of SDS, $C_m$ is constant irrespective of $C_s$ is correct. This is the case as is observed in Fig. 4b {the original paper shows that the curve $D^{-1}$ vs. $(C_s\text{-CMC})^{1/2}$ is straight, but no explanation for this was given}. It must be strictly noted that these discussions mentioned above should be applicable only to the self diffusion coefficient. In usual diffusion experiments, two aqueous surfactant solutions of different concentration, which is above CMC, are used. The diffusion coefficients obtained by such a procedure depend not only on micellar diffusion velocity but also on micellar reconstructing velocity.

(3) **Electrical Conductivity.**— Hartley et. al.[8] pointed out that the association number of micelles can not be determined by the equivalent conductivity, $\Lambda$, alone. McBain asserted that when micelles are formed from free ions, $\Lambda$ should increase[9]. But Hartley et. al. suspected McBain's theory from the consideration that after the lowering of $\Lambda$ due to the secondary effect (the inclusive and the atmospheric effects) outweighing the primary effect (McBain's effect), the equivalent conductivity $\Lambda$ should again increase owing to the occurence of the reverse case of both the effects with increasing $C_s$[8], and they presented the desorption theory[10]. McBain et. al.[11] explained the behavior of $\Lambda$ vs. $C_s^{1/2}$ curves by the hypothesis of ionic micelle and neutral colloid, but Schmid et. al.[12] were doubtful about this hypothesis from their experimental results of high frequency effect. On the other hand, in the author's opinion, when $n$ unassociated paraffin chain ions form one aggregate, $\Lambda$ would decrease owing to the secondary effect overcoming the primary effect. But if we compare a smaller micelle with a larger micelle, i. e., if we

5) G. S. Hartley and D. F. Runnicles, *Proc. Roy. Soc.*, **A168**, 420 (1938); O. Lamm, *Kolloid-Z.*, **98**, 45 (1942); G. Jander and K. F. Weitendorf, *Angew. Chem.*, **47**, 197 (1934).

6) (a) O. Lamm and H. Högberg. *Kolloid-Z.*, **91**, 10 (1940); (b) M. E. L. McBain, *J. Am. Chem. Soc.*, **55**, 545 (1933); (c) D. Stigter, R. J. Williams and K. J. Mysels, *J. Phys. Chem.*, **59**, 330 (1955); (d) A. D. Abbott and H. V. Tartar, ibid., **59**, 1193 (1955).

7) H. V. Tartar, *J. Phys. Chem.*, **59**, 1195 (1955).

8) J. L. Moilliet, B. Collie, C. Robinson and G. S. Hartley, *Trans. Faraday Soc.*, **31**, 120 (1935).

9) J. W. McBain, ibid., **9**, 99 (1913).

10) G. S. Hartley, B. Corrie and C. S. Samis ibid., **32**. 795 (1936).

11) J. W. McBain and C. S. Salmon, *J. Am. Chem. Soc.*, **42**, 426 (1920).

12) G. Schmid and E. C. Larsen, *Z. Electrochem.*, **44**, 651 (1938).

compare an aq. paraffin chain salt solution at different concentrations, the secondary effect would be almost constant for the both surfactant concentrations but the primary effect should increase with increasing micelle size. So that it is the strong evidence of constant $C_m$ irrespective of $C_s$ for $\Lambda$ to increase with $C_s$. Stigter[13] mentioned that the curve $\kappa - C_s$ ($\kappa$ is the specific conductivity) consists of, in a typical case, two straight lines in an unassociated and an associated region. But taking the conclusion of constant micellar concentration into account, the curve $\kappa - C_s$ must have, at least, three knicks, that is, at CMC, at the point where the increase of $C_m$ finishes and at the point where the larger micelle appears. Fig. 5 is the results of Ward[14] recalculated to the form $\log\kappa$ vs. $\log C_s$. At 0.25%, 0.75% and 17.5% there are definite changes in the curve. These three concentrations can be made to correspond to those points mentioned above respectively. The gradient of the curve, $\kappa'$, decreases rapidly when the curve proceeds across the CMC, which is caused by the secondary effect, but gradually recovers with increasing $C_s$, which is caused by the primary effect, and at 3.9% $\kappa'$ is 1, and still continues to increase with increasing $C_s$. In these regions $\kappa'$ is higher than even that in the unassociated region. In concordance with these changes of $\kappa'$ there appears the minimum in the curve $\Lambda$ vs. $C_s^{1/2}$ ($\Lambda = 1000\kappa/C_s$) as observed in Fig. 6. The importance is not the minimum itself but the increase of $\kappa'$ in the range from 0.75% to 17.5%. In the range of 3.9–17.5% $\kappa'$ is greater than the unit, and above 21.5% $\kappa'$ is less than the unit, therefore there appears maximum in the vs. $C_s^{1/2}$ curve, and this maximum (17.5–21.5%) is the concentration at which the larger micelle consisting of several double layers appears as mentioned above. It is easily understandable that when the larger micelle appears $\Lambda$, begins to decrease again owing to the higher viscosity. In conclusion the fact that the vs. $C_s^{1/2}$ curve has the minimum and the maximum is the proof that $C_m$ is constant and $N_m$ increases with increasing $C_s$.

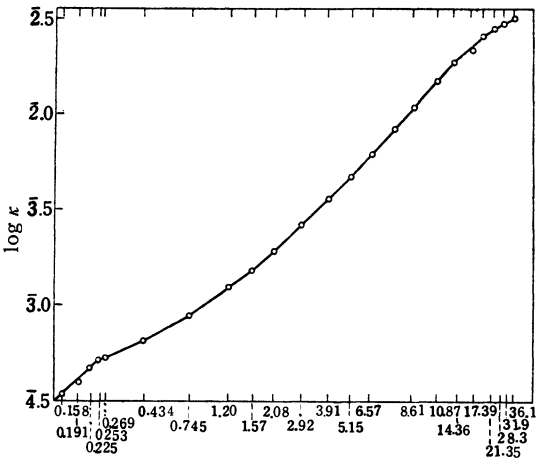



Fig. 5. Specific conductivity $\kappa$ of SDS in aq. phase from A. F. H. Ward[14].

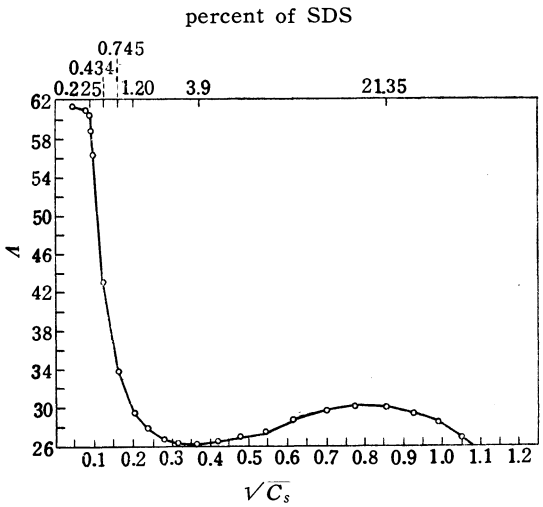



Fig. 6. Equivalent conductivity $\Lambda$ of SDS in aq. phase from A. F. H. Ward[14].
$C_s$ is the molar concentration of SDS.

13) D. Stigter, *Rec.trav. chim. Poy-Bas*, **73**, 611 (1954).
14) A. F. H. Ward, *Proc. Roy. Soc*, **A176**, 412 (1940).

**(4) Light Scattering.** — The most direct method to determine the micellar volume is light scattering, but the micellar molecular weight obtained by this method is generally at CMC[15] and there are few systematic investigations about the relation between the micellar volume and $C_s$. On the other hand, there are many studies about the charge effect[16] and different views are presented[15a,b,c]. It is desirable that some attentions are paid to nonionic surfactants (which have no charge) and also to the relation between the micellar volume and the surfactant concentration.

**(5) X-Ray.** — Corrin[17] pointed out that the micellar shape can not be determined decisively by X-Ray diffraction alone. Therefore very different micellar models have been presented by many X-Ray investigators, e. g., some authors have the idea of a larger micelle consisting of several double layers[18]. Others hold a small spherical model; especially Brady[19] has reported that the micelle of SDS is spherical even in such a high concentration as 14.71% and 29.42%, and some have explained the relation between the

15) (a) P. Debye, *Ann. N. Y. Acad. Sci.*, **51**, 575 (1949); *J. Phys. Chem.*, **53**, 1 (1949); (b) H. V. Tartar, ibid., **59**, 1185 (1955); J. N. Phillips and K. J. Mysels, ibid., **59**, 325 (1955); (c) E. Hutchinson, *Z. physik. Chem.*, neue Folge **2**, 363 (1954).
16) J. J. Hermans, *Rec. trav. chim. Poy-Bas*, **68**, 859 (1948); T. M. Doscher and K. J. Mysels, *J. Chem. Phys.*, **19**, 254 (1951); E. Hutchinson, *J. Colloid Sci.*, **9**, 191 (1954). K. J. Mysels, *J. Phys. Chem.*, **58**, 303 (1954).
17) H. L. Corrin, *J. Chem. Phys.*, **16**, 844 (1948).
18) E. W. Hughes, W. M. Swayer and J. R. Vinograd, *J. Chem. Phys.*, **13**, 131 (1945); J. Stauff, *Kolloid-Z.*, **96**, 244 (1941); H. K. Kiessig, ibid., **96**, 252 (1941).
19) G. W. Brady, *J. Chem. Phys.*, **19**, 1547 (1951).

smaller micelle and the larger micelle[20] but as yet have not ascertained it experimentally. Many authors, e. g. Philippoff[21], have discussed the X-Ray CMC. Although the values of X-Ray CMC given by these authors are not always in agreement with each other, generally X-Ray CMC is detectable in 10-20% of surfactant concentration range[21]. The concentration at which the solubilization curve for dye begins to rise again is 9.12% for sodium oleate and 16.4% for dodecyl sulfonic acid; the conductivity curve reaches its maximum at 17.5-21.5% for SDS. It is an interesting problem whether these concentrations at which larger micelles appear have any relation with the X-Ray CMC.

**(6) Density, Viscosity and Osmotic Coefficient.**—Fig. 7 is the curve of density-concentration and Fig. 8 is that of viscosity-concentration in aq. SDS solution derived from Wright et. al.[22].

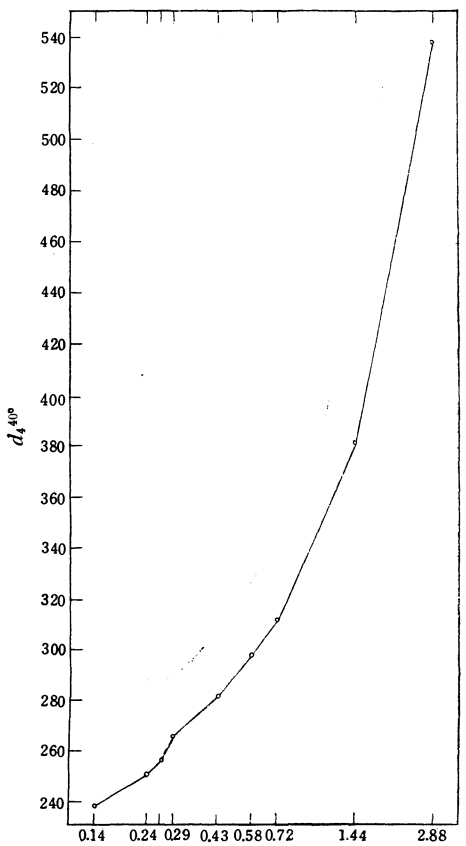



Fig. 7. Density $d_4^{40°}$ of aq. SDS solution from K. A. Wright et. al.[22].

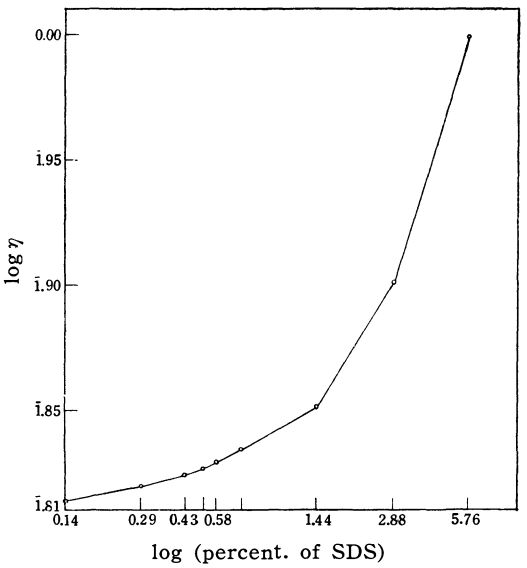



Fig. 8. Viscosity $\eta$ of aq. SDS solution from K. A. Wright et. al.[22].

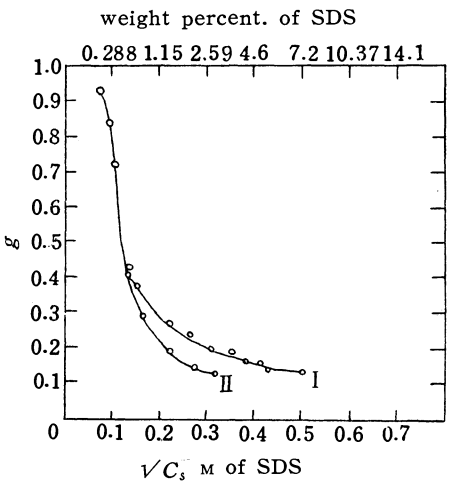



Fig. 9. Osmotic coefficient of aq. SDS solution from H. Huff et. al.[23].
Temperature; I. 30°C, II. 50°C.

At about 1.44%, the gradients of both curves increase remarkably. Huff et. al.[23] have shown that the osmotic coefficient of aqueous SDS solution vs. $C_s^{1/2}$ curve bends remarkably at about 0.023 M (0.66%) as is shown in Fig. 9. These concentrations must be those at which the increase of $C_m$ finishes. But such properties of aqueous surfactant solutions as density[24], viscosity[25], osmotic coefficient or vapor pressure depression and

20) R. W. Mattoon, R. S. Stearns and W. D. Harkins, ibid., **15**, 209 (1947); W. D. Harkins, ibid., **16**, 156 (1948); J. Stauff, *Naturwiss.*, **27**, 213 (1939); *Kolloid-Z.*, **89**, 224 (1939); J. W. McBain, *Nature*. **145**, 702 (1940).
21) W. Philippoff, *Disc. Faraday Soc.*, NO. **11**. 96 (1951).
22) K. A. Wright and H. V. Tartar, *J. Am. Chem. Soc.*, **61**, 544 (1939).
23) H. Huff, J. W. McBain and A. P. Brady, *J. Phys. Chem.*, **55**, 311 (1951).
24) R. G. Paquette, E. C. Lingafelter and H. V. Tartar, *J. Am. Chem. Soc.*, **65**, 686 (1943); A. B. Scott and H. V. Tartar, ibid., **65**, 692 (1943); C. R. Bury and G. A. Parry, *J. Chem. Soc.*, **1935**, 626.
25) W. Philippoff and K. Hess, *Ber.*, **70**, 1808 (1937).

cryoscopic behavior[26] can not sensitively reveal the relation among $C_s$, $C_m$ and $N_m$.

## Conclusion

By no experimental method other than spectral, can we obtain any intimate relationship among the surfactant concentration, the micellar concentration and association number of molecules forming every micelle; there therefore exists some space of alternative explanations for these experimental results. In the author's present paper, it is proved that the conclusion from the spectral experiments coincides well with many results obtained by various other experimental methods. Contrariwise the assumptions on the relation between micellar volume and surfactant concentration, having been presented by many authors, fail to prove any explanation of the various experimental results uniformly, especially they fail to explain the behavior of absorption intensity and solubilization curves in wide range of surfactant concentrations. For example, in aqueous SDS solution, the solute concentration, at which the micellar concentration becomes constant first, exists in the range from 0.5% to 1.5%, which is obtained by the spectral method and is not contradicted with solubilization, diffusion, conductivity, viscocity and osmotic coefficient data (here it is assumed that solubilization curve of sodium dodecyl sulfate for dye does not so much differ from that of dodecyl sulfonic acid). If we took an alternative explanation, e. g., of micellar interaction to elucidate the behavior at the minimum in the curve of equivalent conductivity or to elucidate the decrease in self diffusion coefficient at about 1% in aqueous SDS solution, there would remain some inexplicable points, e. g., why the solubilization curve bends so rapidly at about this concentration. Also the author has determined the SDS concentration at which the larger micelle appears first to be 17.5–21.5%. If we took the desorption theory of Hartley's, some doubts would remain, e. g., why the solubilization curve of SDS for dyes begins to rise again at about this concentration, where the equivalent conductivity curve reaches its maximum.

26) J. W. McBin and M. M. Barker, *Trans. Faraday Soc.*, **31**, 149 (1935); J. W. McBain and M. D. Bety, *J. Am. Chem. Soc.*, **57**, 1909 (1935); E. Gonick and J. W. McBain, ibid., **69**, 334 (1947); M. H. Norris *J. Chem. Soc.*, **121**, 2161 (1922); M. N. Fineman and J. W. McBain, *J. Phys. Chem.*, **52**, 881 (1948); A. Smits, *Z. Physik. Chem.*, **45**, 608 (1903); H. Okuyama and k. Tyuzyo, *Bull. Chem. Soc. Japan*, **27**, 259 (1954); J. W. McBain, "Colloid Science," D. C. Heath and Co., San Francisco (1950), p. 243.

## Summary

The conclusion, which is obtained by the spectral experiments on aqueous surfactant solutions, that the micellar concentration in aqueous surfactant solution is constant irrespective of surfactant concentration in the range which is from a little above the CMC to a considerably high surfactant concentration, coincides well with many other experimental results such as solubilization of dye, conductivity, self diffusion, X-Ray diffraction, density, viscosity and osmotic coefficient or cryoscopic behavior.

The author wishes to express his sincere thanks to Prof. N. Sata, Mr. H. Okuyama and Mr. S. Saito for their kind discussion and encouragement.

*Department of Chemistry,*
*Faculty of Science*
*Osaka University, Kita-ku, Osaka*

# *The Adsorption of Non-polar Gases on Alkali Halide Crystals. IV*[1] *Calculations of the Adsorption Behaviour of Non-polar Gases on Cubic Potassium Chloride and Cubic Potassium Bromide**

By Teruo HAYAKAWA

(Received November 22, 1956)

## Introduction

In the previous communication[2], the author carried out a theoretical calculations of the adsorption energy of an isolated atom or molecule (argon, nitrogen and carbon dioxide) on the (100) plane of cubic sodium chloride. In that work, the total repulsive potential between an isolated atom or molecule and the lattice ions was calculated using the repulsive constants of the modified Buckingham-Corner (6-exp) potential for these non-polar gases. The quadrupole interaction of an isolated nitrogen or carbon dioxide molecule with the lattice ions was theoretically calculated and the correction due to the potential barrier hindering the turning over of the molecular axis was made.

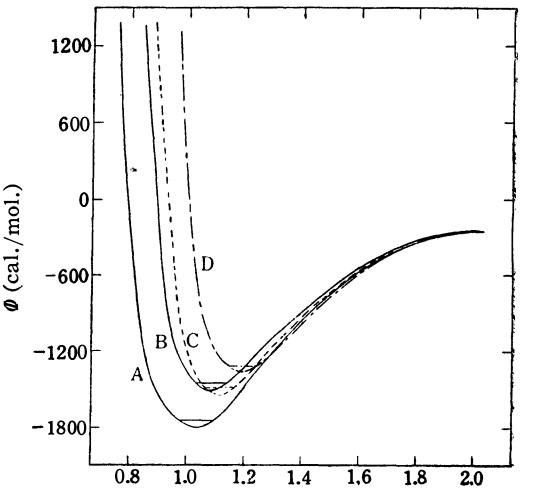
It was therefore of interest in the present work to extend a similar calculations to the (100) plane of cubic potassium chloride and cubic potassium bromide crystals and to compare the theoretical values with the experimental ones obtained by the present author.

## Outline of Calculation

The calculation of the adsorption potential was divided into four sections,

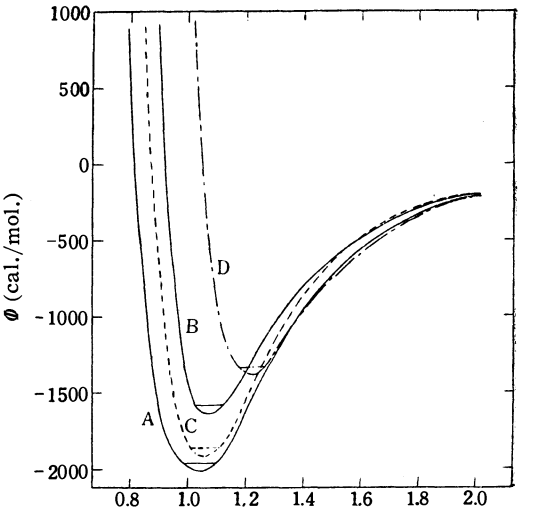
(A) the Van der Waals' (dispersion) potential, (B) the electrostatic potential, (C) the repulsive potential, (D) the quadrupole potential and the correction due to the potential barrier hindering the turning over of the molecular axis.

Calculations were made of these quantities for following four representative positions on the (100) plane of an alkali halide crystal; (i) above the center of a lattice cell (sites type A), (ii) above the




Ratio of the perpendicular distance from the surface to the lattice parameter, $\rho$

Fig. 1. Potential energy curves of argon on cubic (100) KCl. The symbols denote the type of sites.



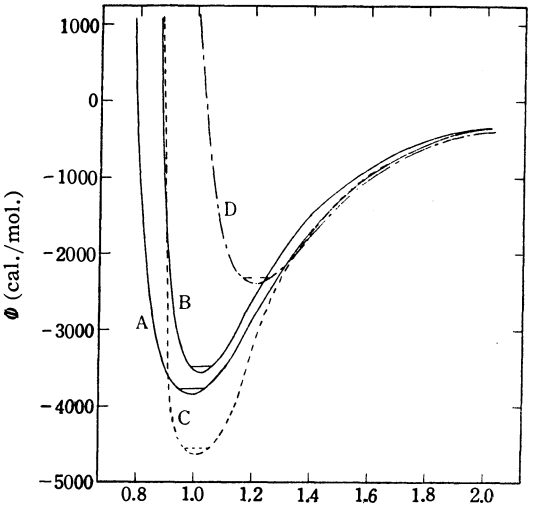

Ratio of the perpendicular distance from the surface to the lattice parameter, $\rho$

Fig. 2. Potential energy curves of nitrogen on cubic (100) KCl. The symbols denote the type of sites.

1) Part III of this series, T. Hayakawa, This Bulletin, **30**, 243 (1957).

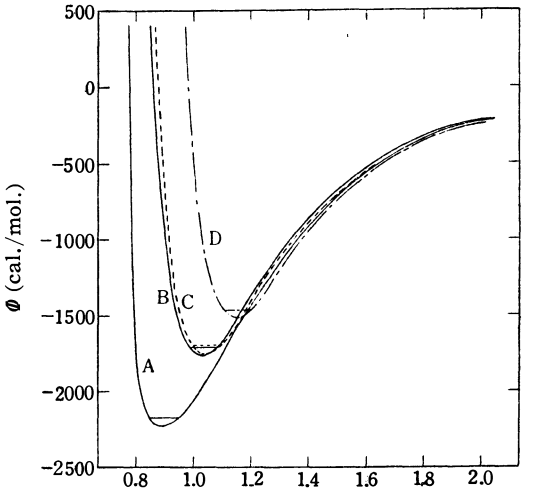
* Part of this paper was read before the 9 th Annual Meeting of the Chemical Society of Japan held in Kyoto, April, 1956. Another part of this paper was also read before the symposium on the surface heterogeneity of catalysis held in Kyoto, March, 1956.

2) Part II of this series, T. Hayakawa, This Bulletin, **30**, 236 (1957).



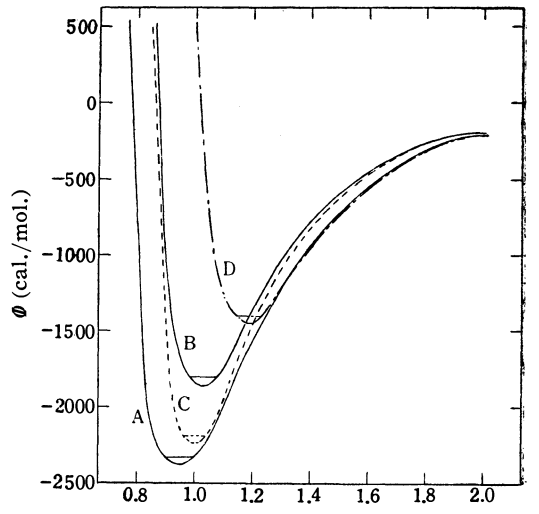

Ratio of the perpendicular distance from the surface to the lattice parameter, $\rho$

Fig. 3. Potential energy curves of carbon dioxide on cubic (100) KCl. The symbols denote the type of sites.



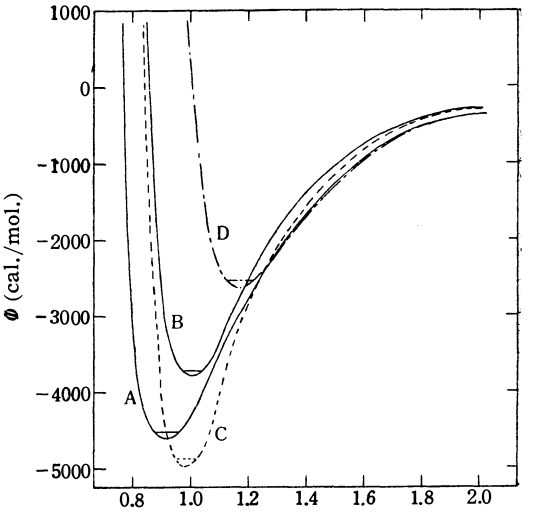

Ratio of the perpendicular distance from the surface to the lattice parameter, $\rho$

Fig. 4. Potential energy curves of argon on cubic (100) KBr. The symbols denote the type of sites.




Ratio of the perpendicular distance from the surface to the lattice parameter, $\rho$

Fig. 5. Potential energy curves of nitrogen on cubic (100) KBr. The symbols denote the type of sites.




Ratio of the perpendicular distance from the surface to the lattice parameter, $\rho$

Fig. 6. Potential energy curves of carbon dioxide on cubic (100) KBr. The symbols denote the type of sites.

mid-point of a lattice edge (sites type B), (iii) above an alkali ion (sites type C) and (iv) above a halogen ion (sites type D).

The method of calculation of each interaction potential was already described in a previous communication[2]. The calculated potential energy curves for the four types of sites considered are shown in Figs. 1, 2, 3, 4, 5 and 6. From these curves the values collected in the following tables were calculated. The position of the minimum gives the equilibrium distance $Z_e$ from the surface; the depth of the trough at $Z_e$ is $-\Phi_m$. For each curve, the region around the minimum was fitted to a parabola and the vibrational frequency normal to the surface $\nu_z$ and the zero-point energy $\varepsilon_0$ were calculated. The values of the quadrupole potential $\Phi_Q$ are also listed in these tables, from which the considerably large contribution of the quadrupole inter-

TABLE I

RESULTS OBTAINED FROM THE POTENTIAL ENERGY CURVE, ARGON ON CUBIC (100) KCl

| Sites type | $Z_e$ (Å) | $r_{eff.}$ (Å) | $-\Phi_m$ (cal./mol.) | $\nu_z \times 10^{-12}$ (sec.$^{-1}$) | $\varepsilon_0$ (cal./mol.) | $-\Delta H_0$ (at 76°K) (cal./mol.) |
|---|---|---|---|---|---|---|
| A, Above the center of a lattice cell | 3.22 | 2.10 | 1792 | 0.98 | 46.3 | 1898 |
| B, Above the mid-point of a lattice edge | 3.44 | 1.98 | 1506 | 0.90 | 42.7 | 1615 |
| C, Above a $K^+$ | 3.52 | 2.19 | 1532 | 0.99 | 46.7 | 1637 |
| D, Above a $Cl^-$ | 3.75 | 1.94 | 1365 | 0.94 | 44.2 | 1473 |

TABLE II

RESULTS OBTAINED FROM THE POTENTIAL ENERGY CURVE, NITROGEN ON CUBIC (100) KCl

| Sites type | $Z_e$ (Å) | $-\Phi_m$ (cal./mol.) | $-\Phi_Q$ at $Z_e$ (cal./mol.) | $\nu_z \times 10^{-12}$ (sec.$^{-1}$) | $\varepsilon_0$ (cal./mol.) | $-\Delta H_0$ (at 76°K) (cal./mol.) |
|---|---|---|---|---|---|---|
| A, Above the center of a lattice cell | 3.25 | 2021 | 815 | 1.19 | 56.0 | 2117 |
| B, Above the mid-point of a lattice edge | 3.34 | 1635 | 1016 | 1.06 | 50.1 | 1737 |
| C, Above a $K^+$ | 3.31 | 1915 | 1522 | 1.20 | 56.7 | 2010 |
| D, Above a $Cl^-$ | 3.85 | 1384 | 352 | 1.12 | 53.1 | 1483 |

TABLE III

RESULTS OBTAINED FROM THE POTENTIAL ENERGY CURVE, CARBON DIOXIDE ON CUBIC (100) KCl

| Sites type | $Z_e$ (Å) | $-\Phi_m$ (cal./mol.) | $-\Phi_Q$ at $Z_e$ (cal./mol.) | $\nu_z \times 10^{-12}$ (sec.$^{-1}$) | $\varepsilon_0$ (cal./mol.) | $-\Delta H_0$ (at 190°K) (cal./mol.) |
|---|---|---|---|---|---|---|
| A, Above the center of a lattice cell | 3.09 | 3826 | 2432 | 1.22 | 57.6 | 4148 |
| B, Above the mid-point of a lattice edge | 3.22 | 3548 | 2887 | 1.21 | 57.1 | 3871 |
| C, Above a $K^+$ | 3.18 | 4656 | 4390 | 1.40 | 66.0 | 4970 |
| D, Above a $Cl^-$ | 3.75 | 2483 | 968 | 1.21 | 57.1 | 2806 |

TABLE IV

RESULTS OBTAINED FROM THE POTENTIAL ENERGY CURVE, ARGON ON CUBIC (100) KBr

| Sites type | $Z_e$ (Å) | $r_{eff.}$ (Å) | $-\Phi_m$ (cal./mol.) | $\nu_z \times 10^{-12}$ (sec.$^{-1}$) | $\varepsilon_0$ (cal./mol.) | $-\Delta H_0$ (at 76°K) (cal./mol.) |
|---|---|---|---|---|---|---|
| A, Above the center of a lattice cell | 2.95 | 1.79 | 2228 | 1.17 | 55.2 | 2325 |
| B, Above the mid-point of a lattice edge | 3.39 | 1.81 | 1762 | 0.99 | 46.7 | 1867 |
| C, Above a $K^+$ | 3.42 | 2.09 | 1750 | 1.02 | 48.1 | 1854 |
| D, Above a $Br^-$ | 3.77 | 1.81 | 1507 | 0.95 | 44.8 | 1614 |

TABLE V

RESULTS OBTAINED FROM THE POTENTIAL ENERGY CURVE, NITROGEN ON CUBIC (100) KBr

| Sites type | $Z_e$ (Å) | $-\Phi_m$ (cal./mol.) | $-\Phi_Q$ at $Z_e$ (cal./mol.) | $\nu_z \times 10^{-12}$ (sec.$^{-1}$) | $\varepsilon_0$ (cal./mol.) | $-\Delta H_0$ (at 76°K) (cal./mol.) |
|---|---|---|---|---|---|---|
| A, Above the center of a lattice cell | 3.05 | 2389 | 1130 | 1.25 | 59.0 | 2482 |
| B, Above the mid-point of a lattice edge | 3.35 | 1855 | 1071 | 1.12 | 52.9 | 1954 |
| C, Above a $K^+$ | 3.29 | 2256 | 1664 | 1.26 | 59.5 | 2348 |
| D, Above a $Br^-$ | 3.92 | 1458 | 358 | 1.17 | 55.2 | 1555 |

TABLE VI

RESULTS OBTAINED FROM THE POTENTIAL ENERGY CURVE, CARBON DIOXIDE ON CUBIC (100) KBr

| Sites type | $Z_e$ (Å) | $-\Phi_m$ (cal./mol.) | $-\Phi_Q$ at $Z_e$ (cal./mol.) | $\nu_z \times 10^{-12}$ (sec.$^{-1}$) | $\varepsilon_0$ (cal./mol.) | $-\Delta H_0$ (at 190°K) (cal./mol.) |
|---|---|---|---|---|---|---|
| A, Above the center of a lattice cell | 2.99 | 4610 | 2915 | 1.33 | 62.8 | 4927 |
| B, Above the mid-point of a lattice edge | 3.32 | 3810 | 2667 | 1.25 | 59.0 | 4131 |
| C, Above a $K^+$ | 3.27 | 4982 | 3924 | 1.35 | 63.7 | 5298 |
| D, Above a $Br^-$ | 3.85 | 2601 | 952 | 1.23 | 58.1 | 2923 |

TABLE VII

INITIAL HEATS OF ADSORPTION ON CUBIC (100) KCl

| Adsorbate | $(-\Delta H_0)$ expt. (cal./mol.) | $(-\Delta H_0)$ calc. (cal./mol.) | $(\Delta H_0)$ expt. $-(-\Delta H_0)$ calc. (cal./mol.) |
|---|---|---|---|
| Argon | 2080 (2140[9]) | 1900 (1780[10]) | 180 (360[9,10]) |
| Nitrogen | 3010 (3200[9]) | 2120 | 890 |
| Carbon dioxide | 6400 | 4970 | 1430 |

TABLE VIII

INITIAL HEATS OF ADSORPTION ON CUBIC (100) KBr

| Adsorbate | $(-\Delta H_0)$ expt. (cal./mol.) | $(-\Delta H_0)$ calc. (cal./mol.) | $(-\Delta H_0)$ expt. $-(-\Delta H_0)$ calc. (cal./mol.) |
|---|---|---|---|
| Argon | 2440 | 2330 | 110 |
| Nitrogen | 3280 | 2480 | 800 |
| Carbon dioxide | 6780 | 5300 | 1480 |

action energy will be at once apparent*. The initial heat of adsorption (i. e. the isosteric heat of adsorption at zero coverage) in these tables was calculated from the relation

$$-\Delta H_0 = (-\Phi_m - \varepsilon_0) + RT.$$

The values of the effective radius of argon $r_{eff.}$ were calculated from the equilibrium distances, assuming Goldschmidt's values[3] for the radii of the ions. The results are given in column 3 of Tables I and IV.

## Discussion

**The Initial Heat of Adsorption.**—As seen in Tables I, II, IV and V, the most energetic positions for argon and nitrogen on the (100) plane of cubic potassium chloride and cubic potassium bromide are sites type A (i. e. above the center of a lattice cell), and these results are dissimilar from those obtained for the (100) plane of cubic sodium chloride. On the other hand, Tables III and VI indicate that the most energetic positions for carbon dioxide on the (100) plane of cubic potassium chloride and cubic potassium bromide are sites type C (i. e. above a $K^+$ in the lattice plane). These results may be attributed to the following causes:

(1) Although, in general, sites type C gives the greatest value of the quadrupole interaction potential for the same value of the equilibrium distance ($Z_e$) from the surface, the value of the quadrupole interaction potential at each sites type is inversely proportional to the third powers of the lattice parameter of the crystal[4].

(2) The repulsive constant of a $K^+$ is considerably greater than that of an $Na^+$ [5].

(3) The permanent quadrupole moment of the carbon dioxide molecule is considerably greater than that of the nitrogen molecule[6,7].

The values of the initial heats of adsorption obtained from the present theoretical calculations are listed in Tables VII and VIII, together with the experimental values by the present author[1,8]. For the sake of comparison, Orr's results[9,10] are also listed in Table VII.

* In the case of argon, the quadrupole potential is surely zero.

3) V. M. Goldschmidt, *Trans. Faraday Soc.*, **25**, 253 (1929).

4) L. E. Drain, *Trans. Faraday Soc.*, **49**, 650 (1953).

5) M. L. Huggins and J. E Mayer. *J. Chem. Phys.*, **1**, 643 (1933).

6) W. V. Smith and R. Howard, *Phys. Rev.*, **79**, 132 (1950).

7) R. M. Hill and W. V. Smith, ibid., **82**, 451 (1951).

8) Part V of this series, T. Hayakawa, This Bulletin, **30**, 337 (1957).

9) W. J. C. Orr, *Proc. Roy. Soc. (London)*, **A173**, 349 (1939).

10) W. J. C. Orr, *Trans. Faraday Soc.*, **35**, 1247 (1939).

As seen in Tables VII and VIII, the present theoretical values of the initial heat of adsorption for argon on the (100) plane of cubic potassium chloride and cubic potassium bromide are in considerably good agreement with the experimental values, while the discordance between the experimental and theoretical values for nitrogen or carbon dioxide is somewhat remarkable. However, since the order of magnitude of the theoretical values for these gases agrees with that of the experimental values, it seems reasonable to consider that the high initial heat of adsorption experimentally found for nitrogen or carbon dioxide is mainly attributed to the quadrupole interaction of each molecule with the surface of the crystal.

**The Non-Uniformity of the Surface.**—Tables I, II and III indicate that the differences between the highest and the weighted mean values of the initial heats of adsorption for argon, nitrogen and carbon dioxide on the (100) plane of cubic potassium chloride amount to about 230, 280 and 1030 cal./mol. respectively. In the case of cubic (100) potassium bromide, as seen in Tables IV, V and VI, the corresponding values for argon, nitrogen and carbon dioxide amount to about 380, 400 and 970 cal./mol. respectively. Since the mutual interaction between the adsorbed atoms or molecules in the low coverage region gives no marked influence upon the heats of adsorption, the surface heterogeneity of this type may be maintained especially in the non-localized adsorption.

On the other hand, the difference between the experimental and theoretical values of the initial heat of adsorption gives a crude measure of the surface heterogeneity of the other type due to the lattice imperfection or the defects of the crystals. As seen in Tables VII and VIII, the differences between the experimental and theoretical values for nitrogen or carbon dioxide are considerably greater than the values anticipated from the results for argon. Although these results are not satisfactorily explained from the difference in the intermolecular potential energy between these non-polar molecules, it may be pointed out that the accuracy of the theoretical calculations for nitrogen or carbon dioxide is somewhat inferior to that for argon. This incorrectness is mainly attributed to the facts that the values of the permanent quadrupole moment of nitrogen and carbon dioxide are somewhat uncertain and that the estimation of the potential energy barrier hindering the turning over of the molecular axis is insufficiently accurate.

**Surface Migration of the Adsorbed Atoms and Molecules.**—As already discussed in a previous communication[2], the height of the potential energy barrier separating two sites which belonged to the same type in the low coverage region is roughly equal to the difference in the initial heat of adsorption between one of them and the adjacent site separating them. In the case of the (100) plane of cubic potassium chloride, as seen in Tables I, II and III, the values of these potential energy barriers for argon, nitrogen (excepting the difference between the sites type A and D) and carbon dioxide amount to about 0.9–3.0 $RT$, 0.7–2.5 $RT$ and 0.7–3.5 $RT$ respectively. Tables IV, V and VI also indicate that the values of the potential energy barriers (excepting the difference between the sites type A and D) for argon, nitrogen and carbon dioxide on the (100) plane of cubic potassium bromide amount to about 1.5–3.0 $RT$, 0.9–3.5 $RT$ and 1.0–3.0$RT$, respectively. Since the mean kinetic energy of thermal movement of the adsorbed atoms or molecules is $RT$ per mole, it seems reasonable to consider that the adsorbed atoms or molecules easily pick up the energy corresponding to each potential energy barrier from the thermal energy fluctutaions. The present results on the surface migration of the adsorbed atoms or molecules in the low coverage region are qualitatively in good agreement with the nature of the experimental entropy curves for these non-polar gases[1,8].

## Summary

The potential energy of each isolated atom or molecule (argon, nitrogen, or carbon dioxide) adsorbed on the (100) plane of cubic potassium chloride and cubic potassium bromide has been theoretically calculated at four representative positions on the surface.

According to the present theoretical calculations, it seems reasonable to consider that the high initial heat of adsorption experimentally found for nitrogen or carbon dioxide is mainly attributed to the quadrupole interaction of each molecule with the surface of the crystals. The present results suggest that the surface may be influenced by the different types of the surface heterogeneity due to the

defects of the crystals and the distribution of sites grouped in patches. The present theoretical calculations also suggest that the adsorbed atoms or molecules of these non-polar gases easily migrate two-dimensionally along the surface in the low coverage region. These results on the surface migration are qualitatively in good agreement with the experimental entropy curves.

The author wishes to express his grateful thanks to Dr. S. Horiba and Professor O. Toyama of Osaka Prefectural University for their kind encouragement and discussion. The author's sincere thanks are also due to Professor R. Kiyama of Kyoto University for his kind discussion.

*Department of Chemistry, Faculty of Education, Osaka Prefectural University, Sakai*

# *The Adsorption of Non-polar Gases on Alkali Halide Crystals. V. The Low-temperature Adsorption of Non-polar Gases on Cubic Potassium Bromide**

By Teruo HAYAKAWA

(Received December 4, 1956)

## Introduction

In the former papers of this series[1,2,3,4], the author has described the measurements and the theoretical calculations of the low-temperature adsorption of non-polar gases (argon, oxygen, nitrogen and carbon dioxide) on cubic sodium chloride and cubic potassium chloride. The high initial heat of adsorption experimentally found for nitrogen or carbon dioxide has been considered to be mainly attributed to the quadrupole interaction of each molecule with the surface. It has also been indicated from these works that the adsorbed atoms or molecules (argon, oxygen and nitrogen) have the nature of the two-dimensional gas at least in the range of $\theta=0.3\sim0.9$ and the surface is influenced by the different types of the non-uniformity due to the defects of the crystals and the distribution of sites grouped in patches.

The present paper reports similar investigations on cubic potassium bromide and discusses these problems mentioned above on the basis of the experiments and the theoretical calculations given in the preceding paper[4].

## Experimental

**Materials.**—*Potassium bromide* was recrystallized by rapidly cooling an aqueous solution of potassium bromide (Wako Chemical Co., extra pure grade) saturated at 90°C. The crystals were collected on a sintered glass filter funnel, washed with successive portions of 70 and 99.9% ethyl alcohol, and stored in a vacuum desiccator over phosphorus pentoxide for about two weeks. Microscopic examination of this sample revealed a large number of small cubes, and in some crystals the defects in the corners or edges were somewhat perceptible. The examination of this sample by an electron diffraction apparatus also showed that the (100) was the predominant surface plane. 42.3 g. of this sample which passed through a 45-mesh sieve was used in the subsequent experiments.

*Helium* was supplied by the Teikoku Oxygen Co. as spectroscopically pure and was not further purified. The method of preparation of other gases has already been given[1].

**Apparatus and Procedure.** — The apparatus and the procedure have also been described in a previous communication[1]. The salt was outgassed by heating in vacuo at 280–300°C for a minimum period of 6 hr. prior to each experiment.

## Results

The isotherms obtained for the four gases on cubic potassium bromide crystals are summarized in Figs. 1, 2, 3 and 4. The adsorption was found

* Part of this paper was read before the 9th Annual Meeting of the Chemical Society of Japan held in Kyoto, April, 1956. Another part of this paper was also read before the symposium on the surface heterogeneity of catalysis held in Kyoto, March, 1956.

1) Part I of this series, T. Hayakawa, This Bulletin, **30**, 124 (1957).

2) Part II of this series, T. Hayakawa, This Bulletin, **30**, 236 (1957).

3) Part III of this series, T. Hayakawa, This Bulletin, **30**, 243 (1957).

4) Part IV of this series, T. Hayakawa, This Bulletin, **30**, 332 (1957).

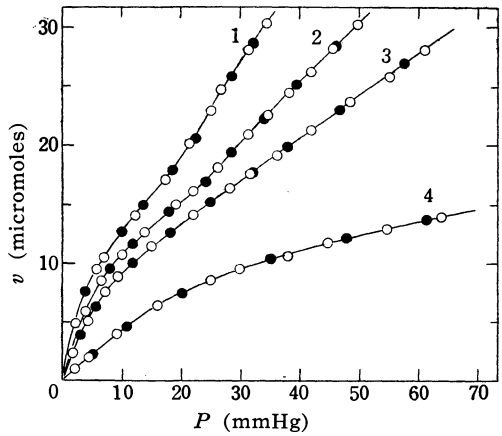



Fig. 1. Adsorption isotherms of argon on cubic potassium bromide.
curve 1……73.70°K, curve 2……75.67°K, curve 3……77.32°K, curve 4……85.01°K.
-o-o- adsorption, -•-•- desorption.

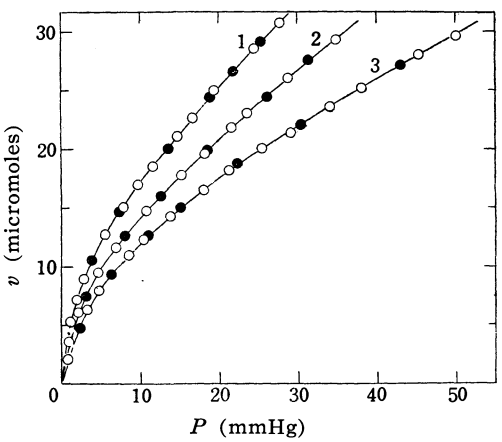



Fig. 2. Adsorption isotherms of oxygen on cubic potassium bromide.
curve 1……73.70°K, curve 2……75.44°K, curve 3……77.32°K.
-o-o- adsorption, -•-•- desorption.

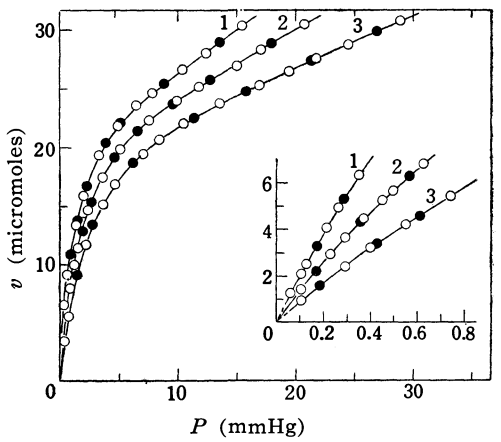



Fig. 3. Adsorption isotherms of nitrogen on cubic potassium bromide.
curve 1……73.75°K, curve 2……75.44°K, curve 3……77.32°K.
-o-o- adsorption, -•-•- desorption.

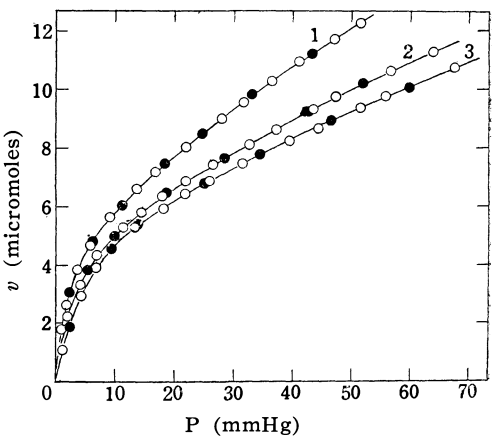



Fig. 4. Adsorption isotherms of carbon dioxide on cubic potassium bromide.
curve 1……187.66°K, curve 2……192.63°K, curve 3……194.64°K.
-o-o- adsorption, -•-•- desorption.

to be reversible in this temperature range. The isosteric heats of adsorption were calculated from these isotherms using the Clausius-Clapeyron equation and showed no definite trend with temperature within the experimental error. In the calculations of the entropy decreases due to the adsorption, the gas phase under the pressure of 760 mmHg and the temperature which coincided with that of each isotherm was chosen as the standard state.

The present results on the isosteric heats of adsorption and the entropy decreases caused by the adsorption are shown in Figs. 5, 6, 7 and 8. Since the adsorbed amount of carbon dioxide was considerably small in this temperature range, the measurements were not extended to the region of high coverage.

## Discussion

**Isosteric Heats of Adsorption.** — The heat curves shown in Figs. 5, 6 and 7 indicate that the initial decrease due to the nonuniformity of the surface and the increase in the succeeding region for these three non-polar gases are considerably predominant. The present results on cubic potassium bromide indicate, however, that the increase in the heats of adsorption for each adsorbate, which gives a measure of the mutual interaction between the adsorbed atoms or molecules, is somewhat less than that obtained for cubic sodium chloride and cubic potassium chloride[1,3].

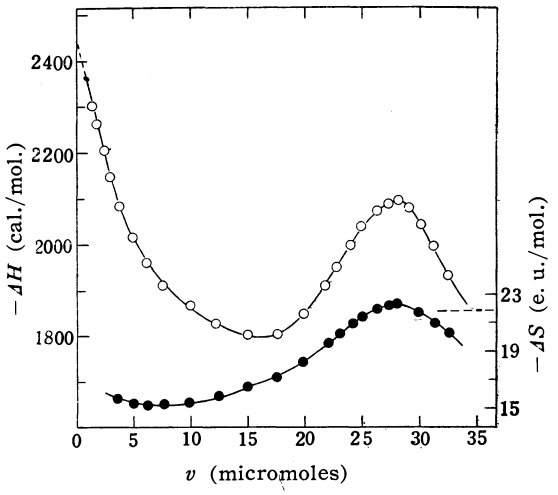



Fig. 5. Isosteric heats and entropies of adsorption for argon on cubic potassium bromide.
-o-o-, isosteric heats of adsorption ($-\Delta H$);
-•-•-, entropies of adsorption ($-\Delta S$);
-----, heat of sublimation.

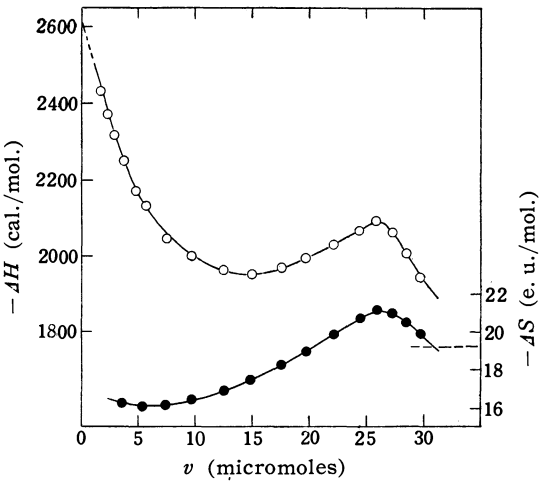



Fig. 6. Isosteric heats and entropies of adsorption for oxygen on cubic potassium bromide.
-o-o-, isosteric heats of adsorption ($-\Delta H$);
-•-•-, entropies of adsorption ($-\Delta S$);
-----, heat of evaporation.

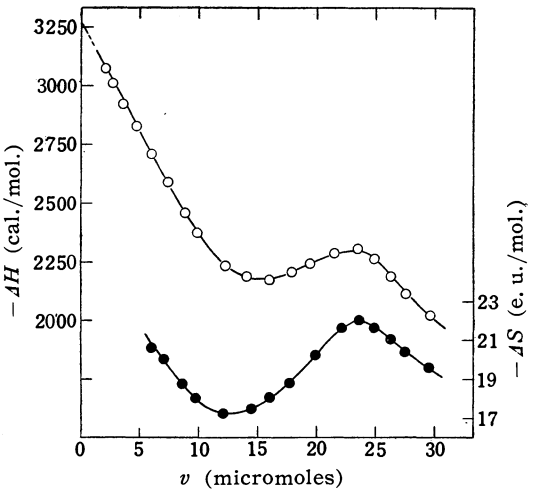



Fig. 7. Isosteric heats and entropies of adsorption for nitrogen on cubic potassium bromide.
-o-o-, isosteric heats of adsorption ($-\Delta H$);
-•-•-, entropies of adsorption.

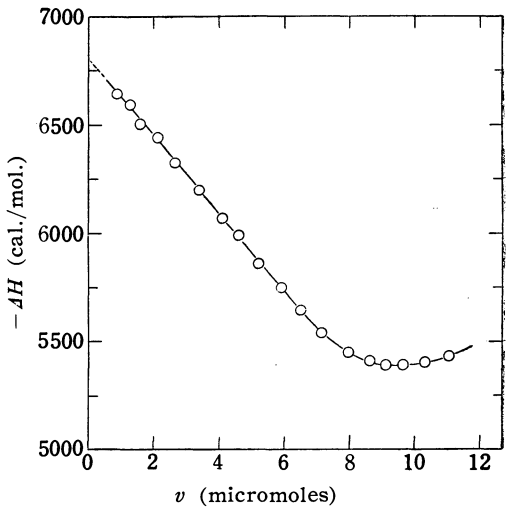



Fig. 8. Isosteric heats of adsorption for carbon dioxide on cubic potassium bromide.

TABLE I

INITIAL HEAT OF ADSORPTION, $-\Delta H_0$, ON CUBIC POTASSIUM BROMIDE

| Adsorbate | $(-\Delta H_0)$ expt. (cal./mol.) | $(-\Delta H_0)$ calcd. (cal./mol.) | $(-\Delta H_0)$ expt. $-$ $(-\Delta H_0)$ calcd. (cal./mol.) |
|---|---|---|---|
| Argon | 2440 | 2330 | 110 |
| Oxygen | 2610 | — | — |
| Nitrogen | 3280 | 2480 | 800 |
| Carbon dioxide | 6780 | 5300 | 1480 |

TABLE II

MONOLAYER CAPACITIES ($V_m$) AND SURFACE AREAS ($A$), CUBIC POTASSIUM BROMIDE (42.3 g.)

| Adsorbate | Cross-sectional area, (Å²) | $V_m$ (micromoles) from heat curve | (B. E. T.) | $A$ (m²) from heat curve | (B. E. T.) |
|---|---|---|---|---|---|
| Argon | 12.8 | 27.8 | (25.7) | 2.14 | (1.98) |
| Oxygen | 14.1 | 26.2 | (24.1) | 2.22 | (2.05) |
| Nitrogen | 13.8 | 24.1 | (28.3) | 2.00 | (2.35) |

The values of the initial heat of adsorption (i. e. the isosteric heat of adsorption extrapolated to zero coverage) obtained for the four gases are summarized in Table I, together with the theoretical values obtained by the present author[4].

As already reported in the previous paper[4], the high initial heat of adsorption theoretically obtained for nitrogen or carbon dioxide is mainly attributed to the quadrupole interaction of each molecule with the surface. Although the discordance between the experimental and theoretical values for nitrogen or carbon dioxide is somewhat remarkable (see Table I), the order of magnitude of the experimental values is similar to that of the theoretical values. Moreover, the experimental values of the initial heat of adsorption inevitably contain some uncertainty due to the extrapolation, and the theoretical values for nitrogen and carbon dioxide also contain some incorrectness due to the uncertainty of the observed values of the permanent quadrupole moment. Considering the question from these facts, it seems reasonable to consider that the high initial heat of adsorption experimentally found for nitrogen or carbon dioxide is mainly attributed to the quadrupole interaction of each molecule with the surface of cubic potassium bromide.

Since the theoretical calculations were carried out on the assumption of an ideal lattice, the difference between the experimental and theoretical values of the initial heat of adsorption gives a crude measure of the surface heterogeneity due to the lattice imperfection and the defects of the crystals. As seen in Table I, the values of this difference for argon, nitrogen and carbon dioxide amount to 110, 800 and 1480 cal./mol. respectively. On the other hand, the heat curves shown in Figs. 5, 7 and 8 indicate that the initial decreases due to the non-uniformity of the surface for argon, nitrogen and carbon dioxide roughly amount to 640, 1100 and 1400 cal./mol. respectively. Since the mutual interaction between the adsorbed atoms or molecules is included in these values of the initial decreases and the theoretical values for nitrogen and carbon dioxide are also somewhat uncertain, it is reasonable to consider that the surface is influenced not only by the non-uniformity due to the lattice imperfection and the defects of the crystals but by another type of the non-uniformity. As already discussed in the preceding paper[4], this latter type of the surface heterogeneity may be attributed to the distribution of sites on the surface.

**Monolayer Capacities.**—Since the heat curves indicate that the surface heterogeneity in the low coverage region and the mutual interaction in the succeeding region are both predominant, it is quite unreasonable to apply the B. E. T. theory to the present systems. As seen in Figs. 5, 6 and 7, there are fairly sharp maxima in the isosteric heat and entropy decrease curves for all three non-polar gases, and the gradual decrease beyond each maximum may be attributed to the formation of multilayers. Considering this fact, it is reasonable to assign the amount adsorbed corresponding to this maximum in the heat or entropy decrease curve as a monolayer capacity.

The present results on the monolayer capacities and on the surface areas which are thus obtained are summarized in Table II. The values of the cross-sectional area in this table were calculated from the results on the entropies of the adsorbed atoms and molecules using the assumption of a hexagonally close-packed layer.

**Entropies of the Adsorbed Phase.**—As seen in Figs. 5, 6 and 7, the magnitudes of the entropies of adsorption and the variation of these with the amount adsorbed for argon and oxygen are similar to each other, while nitrogen shows somewhat different features from other gases. In order to obtain more information about the freedom of the adsorbed atoms or molecules, the entropies of the adsorbed phase derived from the present results were compared with those statistically calculated. The methods of the statistical calculations of the entropies of the gas phase under the standard states and of

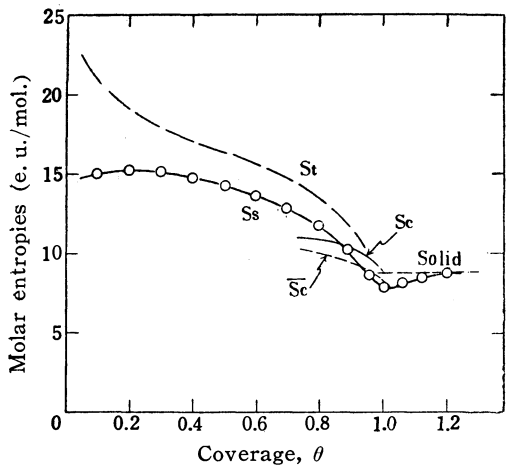



Fig. 9. Molar entropies of argon adsorbed on cubic potassium bromide at 76.5°K.
$S_s$, experimental values; $S_t$, calculated values of the two-dimensional gas; $S_c$, integral configurational entropies; $\bar{S}_c$, differential configurational entropies.

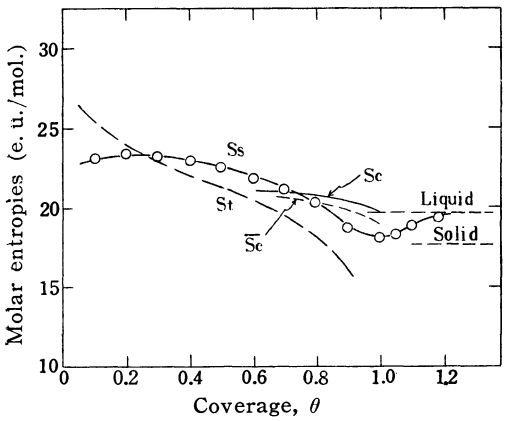



Fig. 10. Molar entropies of oxygen adsorbed on cubic potassium bromide at 76.4°K.
$S_s$, experimental values; $S_t$, calculated values of the two-dimensional gas; $S_c$, integral configurational entropies; $\bar{S}_c$, differential configurational entropies.

the entropies of the adsorbed phase were already given in a previous communication[1].

The entropy curves of the adsorbed phase obtained from the present experiments are summarized in Figs. 9, 10 and 11, together with the calculated curves. The experimental values in these figures are the partial molar total entropies and hence contain the entropy changes of the adsorbent[5], while the calculated values are all the integral entropies and are

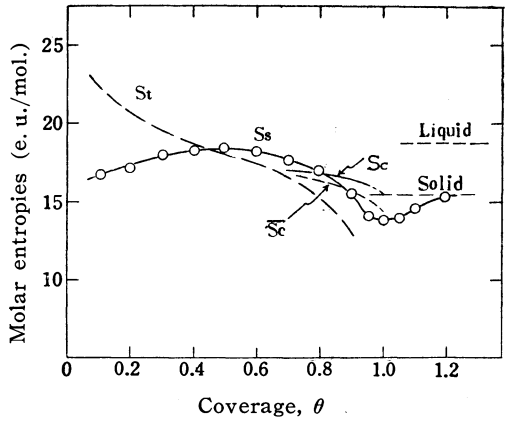



Fig. 11. Molar entropies of nitrogen adsorbed on cubic potassium bromide at 76.4°K.
$S_s$, experimental values; $S_t$, calculated values of the two-dimensional gas; $S_c$, integral configurational entropies; $\bar{S}_c$, differential configurational entropies.

usually somewhat greater than those of the partial molar total entropies. Considering this fact, the experimental curves ($S_s$) for adsorbed argon and nitrogen are comparatively in good agreement with the calculated curves ($S_t$) of the two-dimensional gas in the ranges of $\theta=0.3$–$0.9$ and $\theta=0.3$–$0.8$ respectively. In the case of oxygen, since the entropy associated with the vibrational motion normal to the surface was calculated on assuming that the vibrational frequency of the adsorbed oxygen molecule was identical with that of the adsorbed argon atom, the present calculations of the two-dimensional gas for oxygen ($S_t$ in Fig. 10) probably resulted in somewhat smaller values. Consequently, it seems reasonable to consider that the agreement of the experimental curve for oxygen with the calculated curve of the two-dimensional gas is considerably satisfied in the range of $\theta=0.2$–$0.8$.

The discrepancy between the experimental and calculated curves at lower coverage ($\theta<0.2$) in these figures would imply the entropy changes of the adsorbent. When $\theta$ approaches to unity, as seen in Fig. 9, the restriction on the freedom of adsorbed argon is further increased and the experimental curve ($S_s$) falls below the calculated curve ($S_t$) of the two-dimensional gas. At higher coverage ($\theta>1$), the entropy of adsorbed argon remains close to the entropy of solid argon*, while the entropy of adsorbed oxygen approaches

5) T. L. Hill, *J. Chem. Phys.*, **17**, 520 (1949).

* The entropy of solid argon was calculated from the heat of sublimation and the value of the saturation pressure at 76.5°K.

to the entropy of liquid oxygen**. These results obtained for cubic potassium bromide are similar to those obtained for cubic potassium chloride[3]. In the case of nitrogen, the entropy of the adsorbed phase at higher coverage approaches to the entropy of solid nitrogen***.

Kemball[6] suggested that the phase change of argon on cubic potassium chloride occurred at about $\theta=0.8$, since the experimental values shifted from the entropy curve of the two-dimensional gas to the entropy curve of the localized adsorption obtained by adding the configurational entropy on the Langmuir model to the entropy of solid argon. This explanation involves, however, considerable uncertainty, since it is quite unreasonable to apply the Langmuir model to the adsorption system in which the surface heterogeneity at lower coverage and the mutual interaction in the succeeding region are both predominant. In the present work, therefore, the configurational entropy ($S_c$) and the differential configurational entropy ($\overline{S}_c$) for the localized adsorption were calculated from the experimental results using the expressions derived by Drain and Morrison[7]. In these expressions, however, the non-uniformity of the surface was taken into consideration, while the mutual interaction between the adsorbed atoms or molecules was almost entirely ignored.

The present results on the configurational and differential configurational entropies for these three gases (argon, oxygen and nitrogen) are also summarized in Figs. 9, 10 and 11. As seen in Fig. 9, the present results suggest that the phase change of argon from a gaseous film to a condensed film has occurred at about $\theta=0.9$. On the other hand, Figs. 10 and 11 suggest that the phase changes of oxygen and nitrogen on cubic potassium bromide have occurred at about $\theta=0.8$. However, since the mutual interaction between the adsorbed atoms or molecules was almost entirely ignored in these calculations of the configurational and differential configurational entropies, the present results on the phase change of the adsorbed phase inevitably contain some uncertainty.

** The entropies of solid and liquid oxygen were calculated from the work of Giauque and Johnston (*J. Am. Chem. Soc.*, **51**, 2300 (1929)).

*** The entropies of solid and liquid nitrogen were calculated from the work of Kingston et al. (*J. Am. Chem. Soc.*, **72**, 1780 (1950)).

6) C. Kemball, "Advances in Catalysis," Vol. II, Academic Press Inc., New York (1950), p. 233.

7) J. M. Drain and J. O. Morrison, *Trans. Faraday Soc.*, **48**, 316 (1952).

## Summary

The low-temperature adsorption of non-polar gases (argon, oxygen, nitrogen and carbon dioxide) on cubic potassium bromide was investigated. According to the results of the present experiments and the theoretical calculations given in the preceding paper, the high initial heat of adsorption experimentally found for nitrogen or carbon dioxide is mainly attributed to the quadrupole interaction of each molecule with the surface of the crystal. The present results also indicate that the non-uniformity of the surface is considerably predominant at lower coverage and this is partly attributed to the lattice imperfection and the defects of the crystals.

According to the present results on the entropies of the adsorbed atoms or molecules, the adsorbed phase of argon has the nature of the two-dimensional gas at least in the range of $\theta=0.3$–$0.9$, while the adsorbed phase of oxygen or nitrogen shows a similar nature in the range of $\theta=0.3$–$0.8$. The present results suggest that the phase change of argon from a gaseous film to a condensed film has occurred at about $\theta=0.9$. In the case of oxygen or nitrogen, it is also suggested that the phase change of each adsorbed phase from a gaseous film to a condensed film has occurred at about $\theta=0.8$.

The author wishes to express his grateful thanks to Dr. S. Horiba and Professor O. Toyama of Osaka Prefectural University for their kind encouragement and discussions. The author's sincere thanks are also due to Professor R. Kiyama of Kyoto University for his kind discussions.

*Department of Chemistry*
*Faculty of Education*
*Osaka Prefectural University, Sakai*

# *The Adsorption of Non-polar Gases on Alkali Halide Crystals. VI*[1]*. The Low-temperature Adsorption of Non-polar Gases on Octahedral Potassium Chloride**

By Teruo HAYAKAWA

(Received December 15, 1956)

## Introduction

In recent years comparatively few experiments have been carried out to determine the influence of crystal face on low-temperature adsorption. Measurable differences between the heats of adsorption of nitrogen on the (100), (110) and (111) faces of copper were found by Rhodin[2]. The alkali halides lend themselves admirably to such a study, since they have certain habits in which the crystal is solely bound by one type of face. Moreover, the crystal habit of potassium chloride can easily be completely modified by both inorganic ions and by very small amounts of dyestuffs[3,4]. The low-temperature adsorption of argon on the lead-modified and dye-modified samples of octahedral potassium chloride has recently been measured by Young[5], who has found measurable difference in the heats of adsorption between the (111) and (100) faces of potassium chloride.

In the former papers of this series[1,6-9], the author has described the measurements and the theoretical calculations of the low-temperature adsorption of non-polar gases on cubic alkali halide crystals. It was therefore of interest in the present work to study the low-temperature adsorption on octahedral potassium chloride, since this permits a comparison of the adsorptive properties of the (100) and (111) faces of potassium chloride crystals.

## Experimental

**Materials.** — Lead-modified octahedral potassium chloride was prepared by rapidly cooling an aqueous solution of potassium chloride (A.R., Merck) containing enough lead chloride to provide $[Pb^{++}]/[K^+]=9/1000$. The crystals were collected on a sintered glass filter funnel, washed with successive portions of 70% ethyl alcohol, absolute alcohol and dry ether, and stored in a vacuum desiccator over phosphorous pentoxide for about two weeks. The lead content of this sample was estimated gravimetrically as lead chromate; the analysis gave $[Pb^{++}]/[K^+]=5/100$. Microscopic examination of this sample revealed a large number of very small octahedrals plus a few large cubes in which the defects in the corners or edges were somewhat perceptible; hence it was concluded that the (111) was the predominant surface plane. 25.9 g. of this sample which passed through a 48-mesh sieve was used in the subsequent experiments.

Helium was supplied by the Teikoku Oxygen Co. as spectroscopically pure and was not further purified. The method of preparation of other gases has already been given[6].

**Apparatus and Procedure.**—The apparatus and the procedure were already described in a previous communication[6]. The lead-modified salt was outgassed by heating in vacuo at 280-300°C for a minimum period of 6 hr. prior to each experiment.

## Results

The isotherms obtained for the four gases on lead-modified octahedral potassium chloride are summarized in Figs. 1, 2, 3 and 4. The adsorption was found to be reversible and practically instantaneous. The isosteric heats of adsorption were calculated from these isotherms using the Clausius-Clapeyron equation and showed no definite trend with temperature within the experimental error. In the calculations of the entropies of adsorption, the gas phase under the pressure of 760 mmHg and the temperature which coincides with that of each isotherm was chosen as the standard state.

1) Part V of this series, T. Hayakawa, This Bulletin, **30**, 337 (1957).

* Part of this paper was read before the 7th Annual Meeting of the Chemical Society of Japan held in Tokyo, April, 1954. Another part of this paper was also read before the symposium on the surface heterogeneity of catalysis held in Kyoto, March, 1956.

2) T. N. Rhodin, Jr., *J. Am. Chem. Soc.*, **72**, 5691 (1950).

3) C. Frondel, *Am. Mineral.*, **25**, 91 (1940).

4) H. E. Buckley, "Crystal Growth," Chapman and Hall Ltd., London (1951), p. 461.

5) D. M Young, *Trans. Faraday Soc*, **48**, 548 (1952).

6) Part I of this series, T. Hayakawa, This Bulletin, **30**, 124 (1957).

7) Part II of this series, T. Hayakawa, This Bulletin, **30** 236 (1957).

8) Part III of this series. T. Hayakawa, This Bulletin, **30** 243 (1957).

9) Part IV of this series, T. Hayakawa, This Bulletin, **30**, 332 (1957).

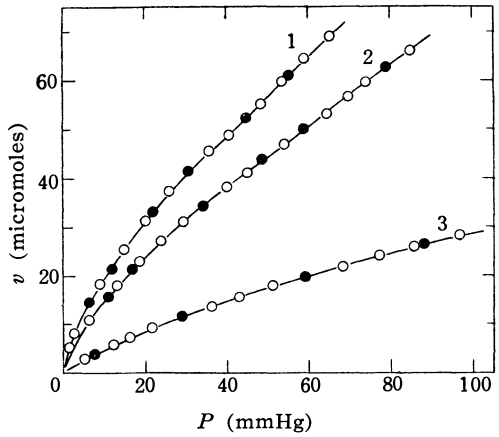



Fig. 1. Adsorption isotherms of argon on octahedral potassium chloride.
curve 1, 75.29°K; curve 2, 77.32°K;
curve 3, 85.42°K.

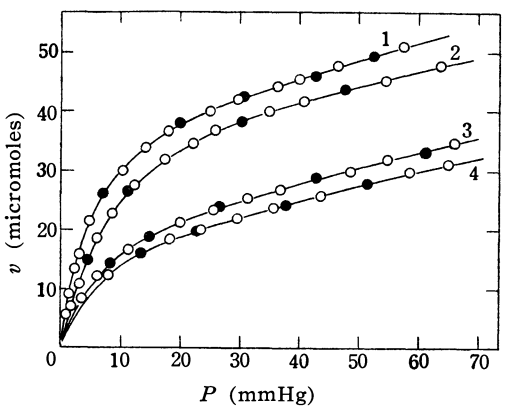



Fig. 2. Adsorption isotherms of oxygen on octahedral potassium chloride.
curve 1, 75.29°K; curve 2, 77.32°K;
curve 3, 88.41°K; curve 4, 90.20°K.

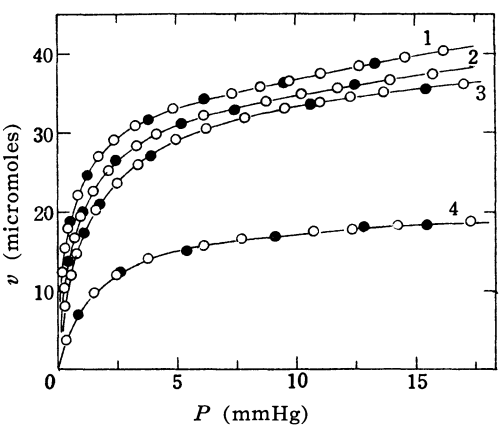



Fig. 3. Adsorption isotherms of nitrogen on octahedral potassium chloride.
curve 1, 73.69°K; curve 2, 75.79°K;
curve 3, 77.32°K; curve 4, 88.36°K.

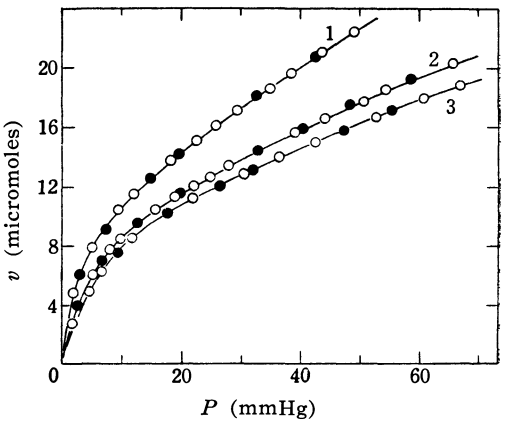



Fig. 4. Adsorption isotherms of carbon dioxide on octahedral potassium chloride.
curve 1, 187.66°K; curve 2, 192.63°K;
curve 3, 194.64°K.

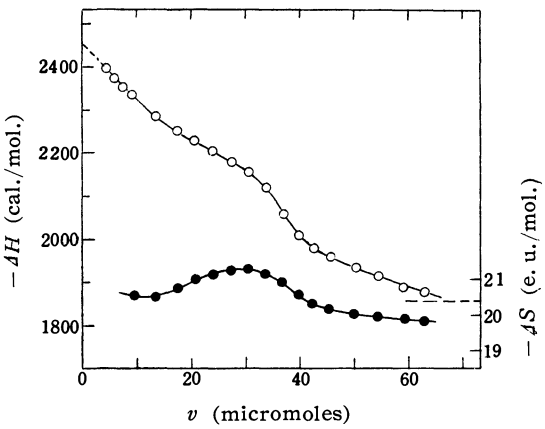



Fig. 5. Isosteric heats and entropies of adsorption of argon on octahedral potassium chloride.
-o-o-, isosteric heats of adsorption ($-\Delta H$);
-•-•-, entropies of adsorption ($-\Delta S$).

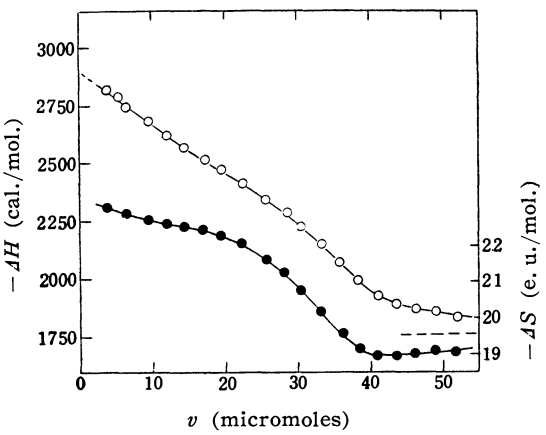



Fig. 6. Isosteric heats and entropies of adsorption of oxygen on octahedral potassium chloride.
-o-o-, isosteric heats of adsorption ($-\Delta H$);
-•-•-, entropies of adsorption ($-\Delta S$).

The present results on the isosteric heats and entropies of adsorption are summarized in Figs. 5, 6, 7 and 8. In the case of carbon dioxide, the measurements were not extended to the region of high coverage, since the amount adsorbed was considerably small in this temperature range.

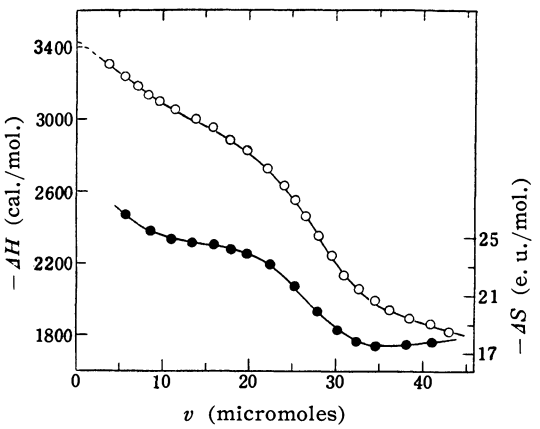



Fig. 7. Isosteric heats and entropies of adsorption of nitrogen on octahedral potassium chloride.
-o-o-, isosteric heats of adsorption ($-\Delta H$);
-•-•-, entropies of adsorption ($-\Delta S$).

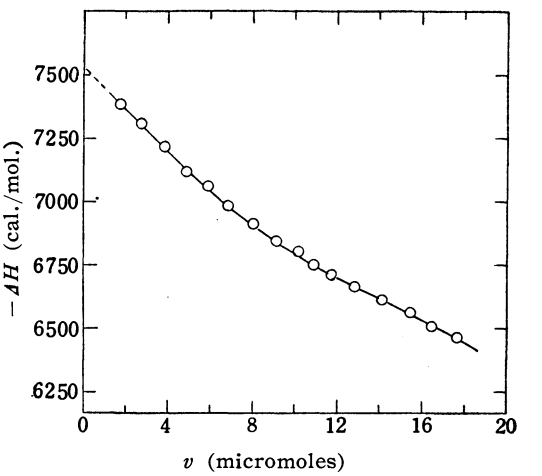



Fig. 8. Isosteric heats of adsorption of carbon dioxide on octahedral potassium chloride.

## Discussion

**Isosteric Heats of Adsorption.**—As seen in Figs. 5, 6 and 7, the isosteric heats of adsorption obtained for the three gases (argon, oxygen and nitrogen) linearly fall at low coverage, reveal a considerably well-defined loop in the succeeding region, and then fall gradually to the value of latent heat of sublimation or evaporation at higher coverage. These results are markedly distinguishable from those already obtained for cubic potassium chloride[8].

Although the technique of habit-modification is open to the criticism that the impurities incorporated into the lattice during growth may alter the properties of the crystal surface, it has been indicated from Young's results[5] that the influence of the impurities is not clearly observable in the region where the surface is sparsely covered. The situation seems, however, somewhat different in the region of moderate coverage, since octahedral potassium chloride is bound by two types of (111) plane, one composed entirely of chlorine ions and the other of potassium ions. Now the present lead-modified adsorbent contains 5 lead ions for every 100 potassium ions, so that the heats of adsorption of these non-polar gases on the potassium faces are much more likely to be somewhat increased by the presence of this impurity. In order to obtain more informations on the isosteric heats of adsorption, the theoretical calculations of the initial heat of adsorption (i. e. the isosteric heat of adsorption at zero coverage) and the approximate calculation of the heat curve for each adsorption system were

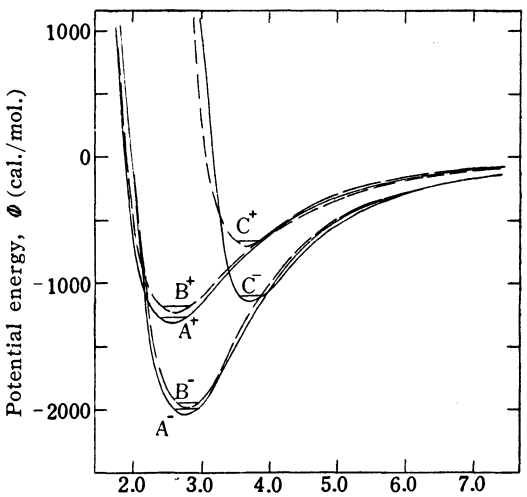



Fig. 9. Potential energy curves of argon on the (111) plane of potassium chloride. The symbols denote the type of sites and the surface layer.
A, above the center of a lattice triangle (directly above an underlying ion); B, above the centre of a lattice triangle (directly above the centre of an underlying lattice triangle); C, above a lattice point.

undertaken. In the case of nitrogen or carbon dioxide, however, owing to the low symmetry of the (111) plane and the poor covergence of the values of the quadrupole interaction potential, no satisfactory results have yet been obtained. The theoretical calculation of the adsorption potential of an isolated argon atom on the (111) plane of potassium chloride was carried out similarly following the method used by Young[10] except that the repulsive constant[7] of the modified Buckingham-Corner repulsive potential for argon was used. The calculated potential energy curves of argon for the six types of sites considered are shown in Fig. 9. From these curves the values of the equilibrium distance from the surface ($Z_e$), the minimum potential ($-\Phi_m$), the vibrational frequency normal to the surface ($\nu_z$), the zero-point energy ($\varepsilon_0$) and the initial heat of adsorption ($-\Delta H_0$) were calculated. The results are summarized in Table I, together with the theoretical values of the initial heat of adsorption by Young.

As seen in Table I, the initial heat of adsorption of argon has been evaluated theoretically as 2140 cal./mol. for the $Cl^-$ faces (sites type A) and 1420 cal./mol. for the $K^+$ faces (sites type A). Thus it may be anticipated that adsorption at low coverage proceeds exclusively on the $Cl^-$ faces and when these faces become almost covered ($\theta > 0.5$) the proportion of argon atoms being adsorbed on the $K^+$ faces greatly increases. Similar tendencies may be expected for the adsorption of other non-polar gases on octahedral potassium chloride. Since the $K^+$ faces, on which adsorption takes place predominantly between $\theta = 0.5$ and 1.0, are somewhat activated by the presence of lead ions, the loop in each experimental heat curve (see Figs. 5, 6 and 7) may be mainly attributed to this activation by lead ions. Table I also indicates that the non-localized mobile adsorption is improbable* on account of the low adsorption heat of an argon atom adsorbed above a lattice point (sites type C). The approximate calculation of the heat curve of argon was also carried out similarly following the method used by Young[10], in which a localized hexagonal arrangement and an uniform surface were assumed. In the present calculation of the heat curve in a primary monolayer, the energy of a pair of argon atoms (distance 4.44 Å) was calculated using the modified Buckingham-Corner (6-exp) intermolecular potential[11]. The calculated heat curve for argon is shown in Fig. 10, together with the corresponding experimental values. For the sake of comparison, the

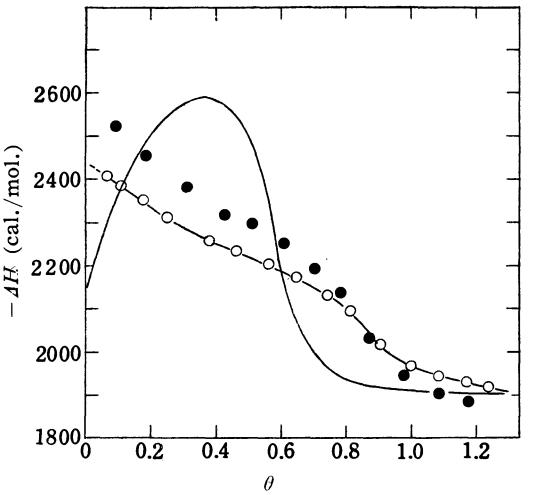



Fig. 10. Heat curves of argon on octahedral potassium chloride.
——, calculated heat curve; -o-o-, present experimental curve; •, values obtained by Young.

experimental curve obtained by Young is also shown in this figure. The values of coverage $\theta$ correlated to the present experimental values were derived from the monolayer capacity given in the subsequent discussion.

The agreement between the present experimental and calculated heat curves for argon is considerably satisfied at higher coverage, and this is probably attributed to the fact that the localized configuration has been adopted. While the discrepancy between the experimental and calculated heat curves at low coverage indicates that the surface heterogeneity is considerably predominant. Since it is of interest to compare the values of the initial heat of adsorption for the two crystal planes of potassium chloride, the experimental and theoretical values obtained in the present and preceding works[7,8] are given in Tables II and III. Since the difference between the experimental and theoretical values of the initial heat of adsorption gives a crude measure of the surface heterogeneity due to the imperfection of the crystal,

10) D. M. Young, *Trans. Faraday Soc.*, **47**, 1228 (1951).
* A partially localized arrangement seems, however, somewhat feasible on account of the similar properties of sites type A and B.
11) E. A. Mason and W. E. Rice, *J. Chem. Phys.*, **22**, 522 (1954).

TABLE I

RESULTS OBTAINED FROM THE POTENTIAL ENERGY CURVE, ARGON ON OCTAHEDRAL (111) KCl

| Sites type | Surface layer | $Z_e$ (Å) | $-\Phi_m$ (cal./mol.) | $\nu_z \times 10^{-12}$ (sec.$^{-1}$) | $\varepsilon_0$ (cal./mol.) | $-\Delta H_0$ (at 76°K) (cal./mol.) |
|---|---|---|---|---|---|---|
| Above the center of a lattice triangle (type A) | $K^+$ | 2.65 | 1307 | 0.86 | 40.7 | 1420(1610*) |
| | $Cl^-$ | 2.86 | 2030 | 0.94 | 44.6 | 2140(2220*) |
| Above the center of a lattice triangle (type B) | $K^+$ | 2.69 | 1232 | 0.82 | 38:9 | 1350(1500*) |
| | $Cl^-$ | 2.90 | 1988 | 0.96 | 45.5 | 2100(2370*) |
| Above a lattice ion (type C) | $K^+$ | 3.72 | 698 | 0.90 | 42.5 | 810( 840*) |
| | $Cl^-$ | 3.74 | 1145 | 0.90 | 42.5 | 1250(1210*) |

* values obtained by Young[10].

TABLE II

INITIAL HEAT OF ADSORPTION, $(-\Delta H_0)$, OF ARGON ON CUBIC (100) AND OCTAHEDRAL (111) KCl (in cal./mol.)

| | (111) plane | (100) plane | $(-\Delta H_0)_{(111)} - (-\Delta H_0)_{(100)}$ |
|---|---|---|---|
| $(-\Delta H_0)_{\text{expt.}}$ | 2460 | 2080 | 380 |
| $(-\Delta H_0)_{\text{calcd.}}$ | 2140 | 1900 | 240 |
| $(-\Delta H_0)_{\text{expt.}} - (-\Delta H_0)_{\text{calc.}}$ | 320 | 180 | |

TABLE III

INITIAL HEAT OF ADSORPTION, $(-\Delta H_0)_{\text{expt}}$, OF NON-POLAR GASES ON CUBIC (100) AND OCTAHEDRAL (111) KCl (in cal./mol.)

| Adsorbate | $(-\Delta H_0)_{(111)}$ | $(-\Delta H_0)_{(100)}$ | $(-\Delta H_0)_{(111)} - (-\Delta H_0)_{(100)}$ |
|---|---|---|---|
| Oxygen | 2870 | 2410 | 460 |
| Nitrogen | 3440 | 3010 | 430 |
| Carbon dioxide | 7540 | 6400 | 1140 |

TABLE IV

MONOLAYER CAPACITIES ($V_m$) AND SURFACE AREAS ($A$), OCTAHEDRAL POTASSIUM CHLORIDE (25.9 g.)

| Adsorbate | Cross-sectional area, $a$ (Å$^2$) | $V_m$ (micromoles) from $(-\Delta S)$ | (B. E. T.) | $A$ (m$^2$) from $(-\Delta S)$ | (B. E. T.) |
|---|---|---|---|---|---|
| Argon | 14.4 | 41.4 | (40.9) | 3.59 | (3.55) |
| Oxygen | 14.1 | 40.2 | (36.6) | 3.41 | (3.11) |
| Nitrogen | 17.0 | 34.4 | (37.2) | 3.52 | (3.81) |

TABLE V

NON-CONFIGURATIONAL ENTROPIES ($S_{NC}$) ON OCTAHEDRAL POTASSIUM CHLORIDE AT $\theta = 0.4$

| Adsorbate | $(S_{NC})_{\text{calcd.}}$, (e. u./mol.) | $(S_{NC})_{\text{expt.}}$, (e. u./mol.) $(S_s - S_c)$ | $(S_s - S_c)$ |
|---|---|---|---|
| Argon | 9.6(a) | 5.7 | 6.7 |
| Oxygen | 13.9(b) | 12.9 | 13.4 |
| Nitrogen | 10.9(c) | 7.8 | 8.9 |

(a) $\nu_x = \nu_y = 8.2 \times 10^{11}$ sec.,$^{-1}$ $\nu_z$ (mean value) $= 0.93 \times 10^{12}$ sec.$^{-1}$

(b) Following values were assumed: $\nu_x = \nu_y = 8 \times 10^{11}$ sec.,$^{-1}$ $\nu_z = 1.0 \times 10^{12}$ sec.$^{-1}$

(c) Following values were assumed: $\nu_x = \nu_y = 8.5 \times 10^{11}$ sec.,$^{-1}$ $\nu_z = 1.1 \times 10^{12}$ sec.$^{-1}$

Table II indicates that the surface heterogeneity of this type for octahedral potassium chloride is more predominant than that for cubic crystals. As seen in Tables II and III, the experimental values of the initial heat of adsorption for these non-polar gases on the (111) plane of potassium chloride are all considerably greater than the corresponding values on the (100) plane. As it has already been pointed out by Young[5], this is mainly attributed to the facts that the (111) plane contains fewer ions per unit area than the (100) plane and that initial adsorption on the (111) plane occurs predominantly on the $Cl^-$ faces.

**Monolayer Capacities.** — As discussed above, it is reasonable to consider that adsorption in the range between $\theta=0.5$ and 1.0 takes place predominantly on the $K^-$ faces. In this range, since the increase in the heats due to the mutual interaction may be overcome by the decrease in the heats due to the increased proportion of adsorption on the $K^+$ faces, the isosteric heats steadily decrease with the increased amounts adsorbed. At higher coverage ($\theta>1$), since the formation of multilayers proceeds on a large scale, the isosteric heats of adsorption in this range slowly decrease and approach the latent heat of sublimation or evaporation. Consequently, in the region where $\theta$ approaches unity, there will be a bend point in each heat or entropy curve (see Figs. 5, 6 and 7). Considering this fact, it seems reasonable to assign this value of the amount adsorbed as a monolayer capacity.

The present results on the monolayer capacities and thus calculated surface areas are summarized in Table IV. Each value of the cross-sectional area in this table was determined from referring to the results on the entropies of the adsorbed phase.

**Entropies of the Adsorbed Phase.** — The present results on the entropies of adsorption shown in Figs. 5, 6 and 7 are obviously distinguishable from those already obtained for cubic potassium chloride[8]. In order to obtain more information about the freedom of the adsorbed atoms or molecules, the entropies of the adsorbed phase were calculated from the experimental data and compared with those already obtained for cubic potassium chloride. The method of the statistical calculations of the entropies of the gas phase under the standard states was already given in a previous communication[6]. The integral ($S_c$) and differential ($\bar{S}_c$) configurational entropies were calculated from the present experimental data using the expressions derived by Drain and Morrison[12]. The experimental entropy curves of the adsorbed phase on octahedral potassium chloride are summarized in Figs. 11, 12 and 13, together with the experimental curves on cubic potassium chloride. As seen in these

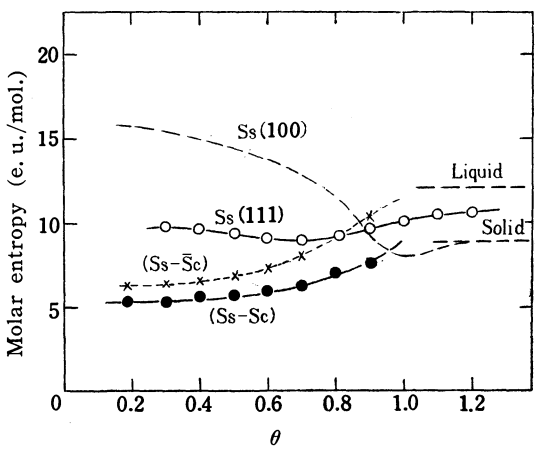



Fig. 11. Molar entropies of adsorbed argon on potassium chloride.
-o-o-, entropies on the (111) plane;
-----, entropies on the (100) plane.

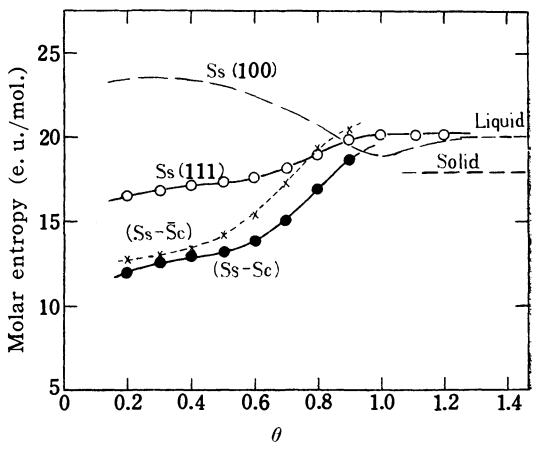



Fig. 12. Molar entropies of adsorbed oxygen on potassium chloride.
-o-o-, entropies on the (111) plane;
-----, entropies on the (100) plane.

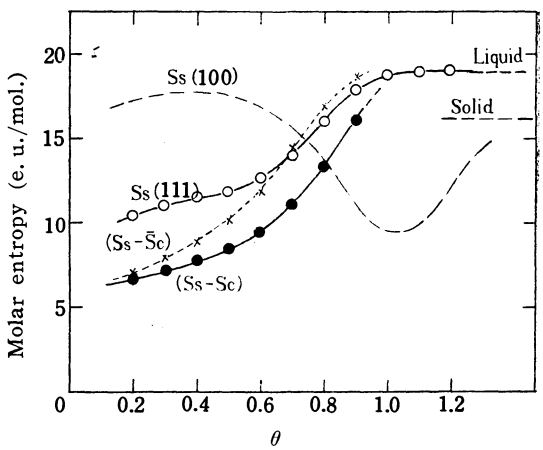



Fig. 13. Molar entropies of adsorbed nitrogen on potassium chloride.
-o-o-, entropies on the (111) plane;
-----, entropies on the (100) plane.

12) J. M. Drain and J. O. Morrison, *Trans. Faraday Soc.*, **48**, 316 (1952).

figures, the experimental curves ($S_s$) of these non-polar gases on octahedral potassium chloride show quite different features from those on cubic potassium chloride. Since the experimental curves for the (100) plane of potassium chloride well agree with the calculated curves of the two-dimensional gas at least in the range of $\theta<0.8$[8], it is reasonable to consider that the low-temperature adsorption of these non-polar gases on the (111) plane of potassium chloride is localized (or at least partially localized) in this same range. These figures also indicate that at higher coverage ($\theta>1$) the entropies of each adsorbed phase all remain close to the entropies of the liquid state.

Since the experimentally determined values ($S_s$) in these figures are the partial molar total entropies[13], the non-configurational entropies of the adsorbed phase on octahedral potassium chloride may be indicated approximately by ($S_s-\bar{S}_c$) or ($S_s-S_c$) curves shown in these figures. Now the non-configurational entropies of the adsorbed atoms or molecules are approximately calculated and compared with the experimental values at $\theta=0.4$. The reason of choosing the experimental values at $\theta=0.4$ is mainly that at this coverage adsorption proceeds exclusively on the $Cl^-$ faces and these surfaces are almost covered by the adsorbed atoms or molecules.

In the present work, the entropy associated with the vibrational motion parallel to the surface (two degree of freedom, $x$ and $y$ directions) was approximately calculated following the method used by Hill[14], in which the vibrational motion was assumed to be isotropic. In the case of oxygen or nitrogen, the entropy associated with the planar rotation in the plane parallel to the surface was calculated using an expression derived by Halford[15]. Since the surface essentially introduces a high potential barrier restricting the turning over of the molecular axis, another rotational motion may be replaced by the rocking vibration of the molecular axis[14]. In the present calculations, however, the entropy associated with this rocking vibration was assumed to be negligible. The calculations of the entropy associated with the intramolecular vibration resulted in the values of nearly zero. Further, the electronic entropy of the oxygen molecule was taken into consideration. The calculated results are summarized in Table V, together with the experimental values.

As seen in Table V, the agreement between the experimental and approximately calculated values of the non-configurational entropy for oxygen is considerably satisfied, while the experimental values of argon and nitrogen are somewhat smaller than the calculated values. However, in view of the facts that the present calculations contain considerable approximations and that the experimentally determined values ($S_s$) are all the partial molar total entropies, the agreement may be regarded as rather satisfactory.

13) T. L. Hill, *J. Chem. Phys.*, **17**, 520 (1949).
14) T. L. Hill, ibid., **16**, 181 (1948).
15) J. O. Halford, ibid., **2**, 694 (1934).

## Summary

1. The low-temperature adsorption of non-polar gases on octahedral potassium chloride was studied. The present results were compared with those already obtained for cubic potassium chloride.

2. The initial heats of adsorption of non-polar gases on the (111) plane of potassium chloride are all considerably greater than the corresponding values on the (100) plane.

3. The surface heterogeneity due to the imperfection of the crystal for octahedral potassium chloride is more predominant than that for cubic crystals.

4. The present results on the isosteric heat of adsorption and the entropies of the adsorbed phase indicate that the low-temperature adsorption of non-polar gases on the (111) plane of potassium chloride is practically localized.

The author wishes to express his grateful thanks to Dr. S. Horiba and Professor O. Toyama of Osaka Perfectural University for their kind encouragement and discussion. The author's sincere thanks are also due to Professor R. Kiyama of Kyoto University for his kind discussion.

*Department of Chemistry*
*Faculty of Education*
*Osaka Prefectural University, Sakai*

# *Photo-dichroism of Printed-out Silver. IV. An Explanation of the Relation between Dichroism Curve and Absorption Difference Curve and the Effect of After-, and Pre-illumination in Terms of the Theory of Anisotropic Herschel Effect*

By Isao KAMIYA

(Received December 4, 1956)

In the previous paper[1], the author has reported that the absorption difference curve of printed-out silver between before and after exposure to natural red (or orange) light is very analogous to spectral dispersion curve of photo-dichroism of printed-out silver which is produced after being exposed to polarized red (or orange) light, and that, if it is assumed that the absorption difference curve would be taken approximately as the dichroism curve, the author has been able to explain the mechanism of "Color adaptation" and "Inversion effect"[2], as well as of the peculiar behavior of dichroism being observed with the light of which the wave lengths are in the region between 580 and 550 m$\mu$.

However, the question why the difference curve is analogous to the dichroism curve has not been answered.

In the present paper, the author has first given a theoretical expression of this relation from the point of view that the phenomenon of photo-dichroism would be anisotropic Herschel effect.

It has been known that the values of photo-dichroism produced after being exposed to polarized red light are to be decreased by subsequent illumination with natural red light, which is called "the effect of after-illumination", and it is also known that the value of dichroism of the film which was previously illuminated with natural red light is smaller than that of non-pre-illuminated film[3].

The author has also considered the mechanism of these effects and given a quantitative explanation, which is in good agreement with experimental results, using the theory of anisotropic Herschel effect[4].

1) I. Kamiya, This Bulletin **30**, 293 (1957).
2) F. Weigert, *Z. phys. Chem.*, **B3**, 377 (1929).
3) E. Elvegård, "Über den Weigert-Effect," Univ. Leipzig (1929), p. 32.
4) I. Kamiya, This Bulletin, **30**, 294 (1957).

## Explanation of the Relation between Dichroism Curve and Absorption Difference Curve

In the previous paper, it has been shown that, if $J_{\parallel}$ and $J_{\perp}$ are the numbers of inner-photo-electrons raised from the surfaces of colloidal particles of metallic silver to conduction band of the crystals of silver chloride when exposed to polarized red light of which the electric vectors are in the plane of incidence ($L_{\parallel}$), and perpendicular to the plane ($L_{\perp}$), the plane of incidence is formed with the line of exposing ray and the normal to the surface of colloidal particle of metallic silver, and $n_0$ is the number of the colloidal particles before exposure, the number of remaining particles which have not been destroyed after $t$ minutes' exposure are given as,

$$n_{\parallel}=n_0[1-\{1-K(1-\exp(-J_{\parallel}t))\}] \text{ for } L_{\parallel} \quad (1)$$

$$n_{\perp}=n_0[1-\{1-K(1-\exp(-J_{\perp}t))\}] \text{ for } L_{\perp} \quad (2)$$

where $K$ is constant if the temperature is constant.

Then, the value of photo-dichroism ($D$) produced after $t$ minutes' exposure is given,

$$D=(n_{\perp}-n_{\parallel})(\lambda_{\parallel}-\lambda_{\perp}) \quad (3)$$

where $\lambda_{\parallel}$ and $\lambda_{\perp}$ are the absorption coefficients of observed light of which the electric vectors are in the plane of incidence and perpendicular to the plane.

In eq. (3), it may be assumed that $\lambda_{\parallel}$ is much greater than $\lambda_{\perp}$, as is probable, (3) is approximately taken as,

$$D=\lambda_{\parallel}n_{\perp}-\lambda_{\parallel}n_{\parallel} \quad (4)$$

When the above consideration is permissible, the first term in (4), $\lambda_{\parallel}n_{\perp}$, will approximately show the absorption curve analogous to that before exposure, because the value of $J_{\perp}$ might, in fact, be very small, and the second term, $\lambda_{\parallel}n_{\parallel}$, will be

shown as the absorption curve after exposure, which is shown as curve-a and curve-*c* in Fig. 1. This is the reason why the dichroism curve is analogous to absorption difference curve between, before and after exposure to natural red (or orange) light.

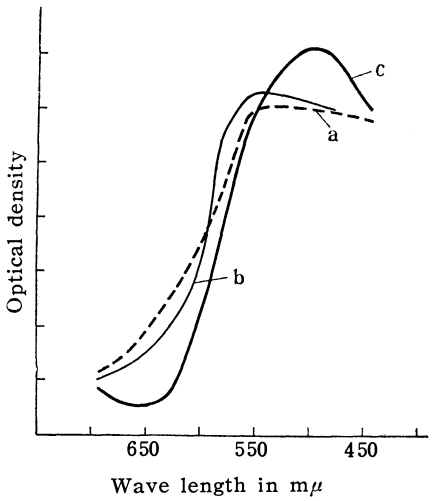



Fig. 1. Schematic representation of the absorption spectra of printed-out Valenta's film. curve-*a*: before exposure, curve-*b*: after a short exposure, curve-*c*: after a long exposure to natural red light.

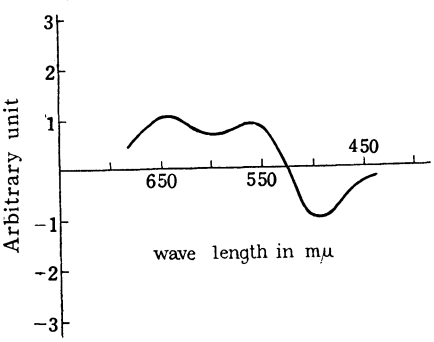



Fig. 2. Absorption difference curve between curve-*b* and curve-*c* in Fig. 1.

For long-exposure, $n_{\perp}$ will be no longer $n_0$, and hence the curve of $\lambda \parallel n_{\perp}$ will not be shown as curve-*a* but will be shown as curve-*b* in Fig. 1, since $n_{\perp}$ is decreased a little for a long-time exposure, so that the curve is to be taken as that analogous to the absorption curve after short-time exposure having been shown as curve-*b* in the previous paper[1]. Thus, the values of photo-dichroism being taken as *c*—*b*, it may be found that the spectral dispersion curve of $D$ might have two maxima in certain special cases as illustrated in Fig. 2.

In reality, these two maximum points have been observed for long-time exposure by several authors[5] (Fig. 3).

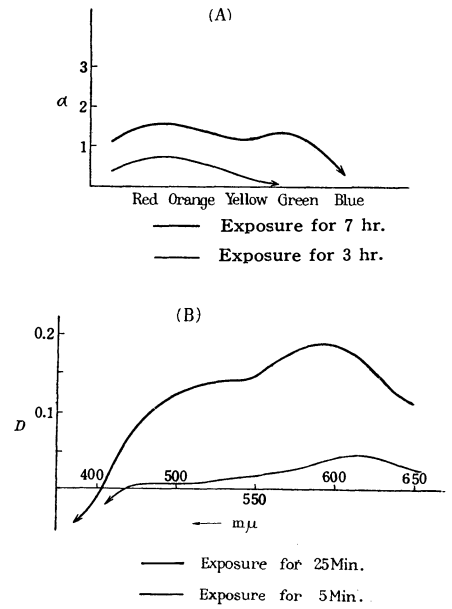



Fig. 3. Spectral dispersion curves of photo-dichroism observed by Horiba, Kondo (A), and Narath, Wasserroth (B).

## The Effect of After-illumination

It has been known that the values of photo-dichroism produced after exposure to polarized red light is to be decreased by subsequent illumination with natural red light. This is called, "The effect of after-illumination".

The author has carried out the experiments on the effect using the films of Valenta's emulsion by the way as follows.

The values of dichroism of the films which had been exposed to polarized red light for various periods were measured with red light after being illuminated for 10, 20, 30, 40 and 50 minutes with strong natural red light. The source of illuminating light was the same as described in the previous paper[6]. These results are shown in Table I.

From these, it is seen that; (i). the rate of decreasing during this after-illumination is fast in the initial stages and then becomes slower and slower, (ii). if $D$ and $D'$ are the values of dichroism before and after illumination, the values of $(D-D')/D$,

5) S. Horiba, and T. Kondo, *The Sexagint* (Osaka Fest.) Kyoto Univ., **1927**, p. 68.
A. Narath and K. Wasserroth, *Sc. et Industr. phot.*, **23A**, 39 (1952).
6) I. Kamiya, This Bulletin, **30**, 6 (1957).

TABLE I
VALUES OF DICHROISM FOR VARIOUS PERIODS OF AFTER-ILLUMINATION WITH NATURAL RED LIGHT ($D'$)

| Film No. | Time of after illumination with natural red light, (Min.) | 0 | 10 | 20 | 30 | 40 | 60 |
|---|---|---|---|---|---|---|---|
| I | $D'(2\alpha)$ | 2.31 ($=D$) | 1.61 | 1.46 | 1.30 | 1.16 | 1.12 |
| | $(D-D')/D$ | — | 0.30 | 0.37 | 0.43 | 0.50 | 0.50 |
| II | $D'(2\alpha)$ | 3.30 ($=D$) | 2.26 | 2.06 | 1.86 | 1.67 | 1.64 |
| | $(D-D')/D$ | — | 0.31 | 0.37 | 0.43 | 0.49 | 0.50 |

$D$: Values of dichroism before illuminations.

that is the percentages of decreasing values, seem to be independent of $D$. These values are also illustrated in Table I.

The author has considered the mechanism of this effect and proposed a theory, which enables him to understand why these characters described above are found, from the point of view that the phenomenon of photo-dichroism would be an anisotropic Herschel effect.

As has been shown by the author, the values of dichroism $D$ is given as,

$$D=(n_\perp-n_\parallel)(\lambda_\parallel-\lambda_\perp)$$

It is reasonable to assume that the remaining numbers of $n_\perp$ and $n_\parallel$ are destroyed by after-illumination with natural red light having the same mechanism as Herschel effect. The light of illumination being divided into two components: one is the most effective to destroy $n_\perp$ and the other $n_\parallel$ since the destruction of these colloidal particles are the most effective to be destroyed when the electric vector of illuminating light is in the plane of incidence, the numbers of destroyed particles, $\Delta n_\perp$, and $\Delta n_\parallel$ in each case are calculated from the same point of view as in the previous treatments[4].

$$\left.\begin{aligned}\Delta n_\perp &= n_\perp[1-\exp(-J_\parallel t)]ke^{-\frac{U}{RT}}\\ \Delta n_\parallel &= n_\parallel[1-\exp(-J_\parallel t)]ke^{-\frac{U}{RT}}\end{aligned}\right\} \quad (5)$$

where $J_\parallel t$ is the number of inner-photo-electrons after $t$ minutes' exposure, $k$ is constant and $U/RT$ is constant at a constant temperature. Hence, the value of dichroism after $t$ minute's illumination can be obtained,

$$D'=\{(n_\perp-\Delta n_\perp)-(n_\parallel-\Delta n_\parallel)\}(\lambda_\parallel-\lambda_\perp) \quad (6)$$

From (5), (6) becomes,

$$\begin{aligned}D' &= (n_\perp-n_\parallel)(\lambda_\parallel-\lambda_\perp)-(n_\perp-n_\parallel)\\ &\quad\times[1-\exp(-J_\parallel t)]ke^{-\frac{U}{RT}}(\lambda_\parallel-\lambda_\perp)\\ &= D-k\cdot D\cdot e^{-\frac{U}{RT}}[1-\exp(-J_\parallel t)] \quad (7a)\end{aligned}$$

where $D'$ is the value of dichroism after $t$ minutes' illumination and $D$ that before illumination.

(6) is also written as,

$$(D-D')/D=ke^{-\frac{U}{RT}}[1-\exp(-J_\parallel t)] \quad (7b)$$

In order to be in agreement with experimental results, the constants $ke^{-\frac{U}{RT}}$ and $J_\parallel$ in (7) are put to 0.5 and 0.08 respectively.

The curve of $(D-D')/D$ against $t$ using the formula of 0.5 $(1-e^{-0.08t})$ and the experimental values are illustrated in Fig. 4. These are in good agreement with each other.

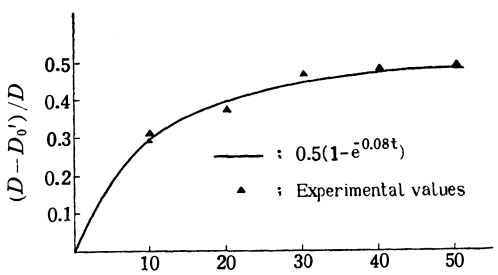



Fig. 4. Theoretical curve and experimental values of the percentages of decreasing dichroism against the time of after-illumination with natural red light.

The value of $J_\parallel$ ($=0.08$) used here is somewhat larger than that before ($=0.026$). This deviation will be probably due to the fact that the later is the value when the illuminating light was passed through a Nikol's prism whereas the former is that which was not passed through.

### The Effect of Pre-illumination

It is also known that the values of photo-dichroism of printed-out silver which had been pre-illuminated with natural red light is less than that of non-pre-illuminated silver, when exposed to polarized

TABLE II

VALUES OF DICHROISM FOR VARIOUS PERIODS OF PRE-ILLUMINATION WITH NATURAL RED LIGHT ($D'$) (Observed by Elvegård)

| Time of exposure to polarized red light (Min.) | Time of pre-illumination with natural red light (Min.) | 0 | 4 | 16 | 64 |
|---|---|---|---|---|---|
| 2 | $D'$ | 12 (=$D$) | 8.6 | 5.6 | 5.3 |
| | $(D-D')/D$ | — | 0.28 | 0.52 | 0.55 |
| 8 | $D'$ | 29 (=$D$) | 21 | 15 | 11 |
| | $(D-D')/D$ | — | 0.28 | 0.48 | 0.62 |
| 16 | $D'$ | 35 (=$D$) | 29 | 22 | 16 |
| | $(D-D')/D$ | — | 0.26 | 0.37 | 0.54 |

red light. This is called, "The effect of pre-illumination with natural red light" or "die Wirkung einer Vorbelichtung mit naturlichem lichte"[3].

Elvegård has investigated the effect. His results are shown in Table II.

The author has considered the mechanism in regard to the same points as before.

If the number of colloidal particles before being illuminated with natural red light is $n_0$, and that after $t$ minutes' pre-illumination is $n'$, $n'$ is obtained as before; that is,

$$n'=n_0[1-k'\{1-\exp(-Jt)\}e^{-\frac{U}{RT}}] \quad (8)$$

where $J$ is the number of inner-photo-electrons per minute when illuminated with natural red light.

Next, if the film is exposed to polarized red light for $t$ minutes, the number of colloidal particles of metallic silver which remained undestroyed on exposure to the light of which the electric vector is in the plane of incidence, $n_{\parallel}'$ is

$$n_{\parallel}'=n'[1-k'\{1-\exp(-J_{\parallel}t)\}e^{-\frac{U}{RT}}] \quad (9a)$$

and that to the light of which the electric vector is perpendicular to the plane, $n_{\perp}'$ is

$$n_{\perp}'=n'[1-k'\{1-\exp(-J_{\perp}t)\}e^{-\frac{U}{RT}}] \quad (9b)$$

Thus, the value of dichroism is to be taken as,

$$D'=(n_{\perp}'-n_{\parallel}')(\lambda_{\parallel}-\lambda_{\perp}) \quad (10)$$

From (8) and (9), (10) becomes

$$D'=(n_{\perp}-n_{\parallel})(\lambda_{\parallel}-\lambda_{\perp})\times[1-k'\{1-\exp(-Jt)\}e^{-\frac{U}{RT}}]$$
$$=D[1-k'\{1-\exp(-Jt)\}e^{-\frac{U}{RT}}]$$

so that

$$(D-D')/D=k'e^{-\frac{U}{RT}}\{1-\exp(-Jt)\} \quad (11)$$

where $D'$ and $D$ are the values of dichroism to be taken when the film is pre-illuminated for $t$ minutes and if the same film was not illuminated.

In reality, $D$ being unable to be determined by experiment, the following approximation is made.

$D$ obtained with a film is the same as that with another film, though these values are actually slight by different from another.

From this approximation, the author has calculated the values of $(D-D')/D$ using the values of $D$ and $D'$ obrerved by Elvegård. These results are also shown in Table II.

In order to explain the experimental results with (11), the constants $k'e^{-\frac{U}{RT}}$ and $J$ are to be taken as 0.55 and 0.16 respectively. In Fig. 5, the curve of $(D-D')/D$ against $t$ and the experimental values observed by Elvegård are illustrated. It is seen that the theoretical is in fairly good agreement with the experimental for such approximation.

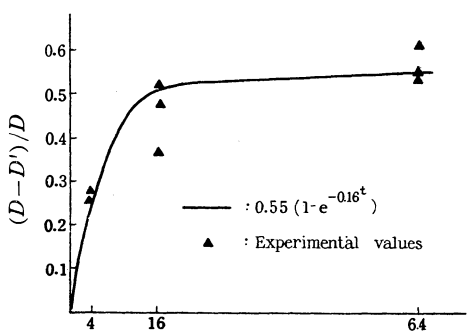



Fig. 5. Theoretical curve and experimental values of the percentages of decreasing dichroism against the time of pre-illumination with natural red light.

From these evidences described in this paper, it is also emphasized that the

phenomenon of photo-dichroism would be an anisotropic Herschel effect.

The author gives thanks to the late Prof. J. Shidei and Dr. D. Yamamoto for their kind advice.

*Department of General Education*
*Nagoya University, Nagoya*

# *Non-Newtonian Viscosity of Dilute High Polymer Solutions. III. On the Method of Measuring Zero Shear Viscosity*

By Toshiaki KUROIWA

(Received December, 4, 1956)

## Introduction

It is now recognized that, when molecular weight of a polymer is high enough, the effect of the rate of shear on the solution viscosity is by no means negligible even when working with extremely dilute solutions[1-9]. As the result, various investigators have sought to obtain a method of extrapolating the viscosity data at the finite rate of shear to zero shear rate[2-4,10,11].

Some have proposed the linear extrapolation of logarithm of viscosity vs. rate of shear plot for such a method[2,12]. E. Wada[7] and the present writer[8], however, have found that the viscosity vs. shear rate curve shows an antisigmoidal form having a horizontal tangent at the origin rather than an exponential form. This behavior is in accordance with the theories of Kuhn and Kuhn[13] and Saito[14] according to which the viscosity of a dilute polymer solution should be given by an equation of the form:

$$\eta_{sp}=\eta_{sp0}(1-aq^2+bq^4-\cdots\cdots), \qquad (1)$$

where $\eta_{sp0}$ is $\eta_{sp}$ at zero shear rate, $q$ denotes rate of shear and $a$, $b$, etc. are non-Newtonian parameters. This means that the linearity of such a semi-log plot can not be satisfied at least in low shear rate region. Fig. 1 shows log $\eta_{sp}/c$ vs. $q$ plots for several polystyrene fractions of different molecular weights in toluene by

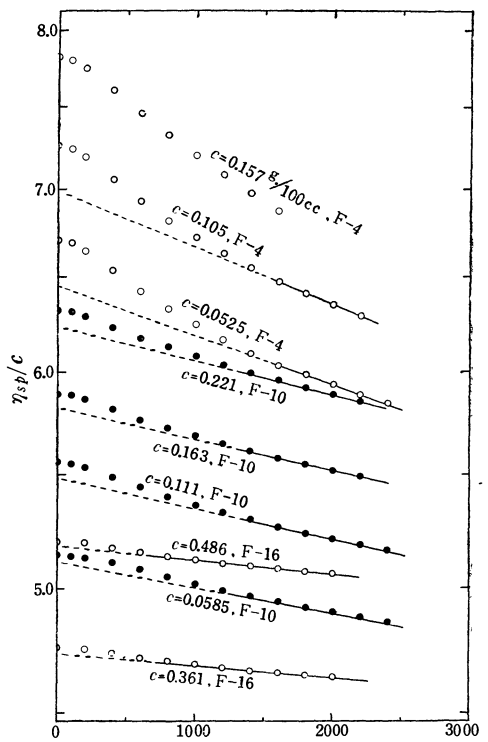



Fig. 1. log $\eta_{sp}/c$ vs. shear rate for polystyrene fractions F-4 ($M_w=4.10\times10^6$), F-10 ($M_w=3.08\times10^6$) and F-16 ($M_w=1.98\times10^6$) in toluene at 25°C.

1) C. M. Conrad, V. W. Tripp and T. Mares, *J. Phys. Colloid Chem.*, **55**, 1474 (1951).
2) T. G. Fox Jr., J. C. Fox, and P. J Flory, *J. Am. Chem. Soc.*, **73**, 1901 (1951).
3) H. T. Hall and R. M. Fuoss, ibid., **73**, 265 (1951).
4) G. De Wind and J. J. Hermans, *Rec. trav. chim.* Bay-Bas, **70**, 521, 615 (1951).
5) F. Akkerman, D. T. F. Pals and J. J. Hermans, ibid., **71**, 56 (1952).
6) L. S. Sharman, R. H. Sones and L. H. Cragg, *J. Appl. Phys.*, **24**, 703 (1953).
7) E. Wada, *J. Sci. Research Inst.*, **47**, 149, 159, 168 (1953); *J. Polymer Sci.*, **14**, 305, 307 (1954).
8) T. Kuroiwa, This Bulletin, **29**, 164, 962 (1956).
9) M. A. Golub, *J. Polymer Sci.*, **18**, 27, 156 (1955); *J. Phys. Chem*, **60**, 431 (1956).
10) J. Schurz and E. H. Immergut, *J. Polymer Sci.*, **9**, 279 (1952).
11) J. Schurz, ibid., **10**, 123 (1953).
12) W. R. Krigbaum and P. J. Flory, *J. Polymer Sci.*, **11**, 37 (1953).
13) W. Kuhn and H. Kuhn, *Helv. Chim. Acta*, **28**, 1533 (1945); ibid., **29**, 609 (1946).
14) N. Saito, *J. Phys. Soc. Japan*, **6**, 302 (1951).

the experimental data reported in the previous paper[8]*. Evidently, it is not possible to give a fully linear representation to each of these plots over the entire range of shear rate. The plots for the lower molecular weight fractions, however, may be regarded to be linear in the region of higher shear rates and the approximately linear portions of these curves appear to extend towards a low rate of shear as molecular weight of the polymer decreases. Therefore the linear extrapolation of log $\eta_{sp}/c$ in these shear ranges to zero shear will yield a fairly good approximation to the zero shear viscosity when molecular weight of the polymer is not so much high as those of the fractions shown in Fig. 1. Moreover, it seems that the tangent of the linear portion is independent of concentration for a given fraction as pointed out by Fox, Fox and Flory.[2] An upward deviation from linearity of $\ln \eta_r$ vs. $q$ curves at lower shear rates has been observed also by Cragg et al.[6] for polystyrene solutions, although the shear rate at which the deviation commences appears to be higher than in the present case.

Recently, Katchalsky[15] has suggested the method of obtaining the zero shear viscosity making use of the relationship he derived:

$$\frac{t_s}{t}=\frac{\eta_s}{\eta_0}\left(1+\frac{aP^2R^2}{3\eta_0^2L^2}\right), \qquad (2)$$

where $t$ and $t_s$ are the flow times of the solution and solvent, respectively, at pressure $P$, $\eta_s$ is the viscosity of the solvent and $\eta_0$ the viscosity of the solution at zero shear, $a$ is a non-Newtonian parameter appeared in Eq. (1), $R$ and $L$ the radius and length of the capillary, respectively. According to Eq. (2), if a series of measurements are made in viscometers of different capillary radii at the same pressure, or alternatively, at different pressures in the same viscometer, then the resulting $t_s/t$ vs. $P^2R^2$ plot should be a straight line, and the zero shear viscosity, $\eta_0$, can be determined as the reciprocal of the intercept of this line at the origin multiplied by $\eta_s$. Katchalsky derived Eq. (2) on the basis of the theoretical equation (1). For small shear rate, Eq. (1) reduces to the simpler form:

$$\eta_{sp}=\eta_{sp0}(1-aq^2), \qquad (3)$$

and this equation was used in deriving Eq. (2).

For most polymer solutions, however, the shear rate range in which Eq. (3) can adequately describe the shear dependence of solution viscosity appears to be confined to very low shear rates which the ordinary viscosity method by a capillary viscometer can deal with only with difficulty. This opinion may be borne out by the fact that such a quadratic dependence of viscosity has been observed only by a few recent investigators[7,8,16,17] who have extended the measurements down to very low shear rates by the use of a specially designed viscometer. For example, the quadratic range was found to lie below the gradients of about 200–300 sec.$^{-1}$ for those polystyrene fractions in toluene though it depends on concentration and molecular weight of the polymer to some extent (see Fig. 2). Therefore Katchalsky's equation (2) may be expected to hold when measurements are made only at small gradients to which the routine method of viscometry by a capillary viscometer is not easily accessible.

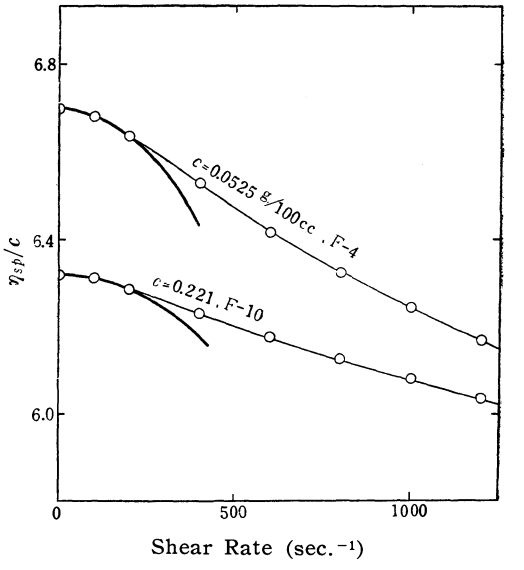



Fig. 2. $\eta_{sp}/c$ vs. shear rate. The heavier line shows the curve according to Eq. (3).

The present writer has examined these previous results on polystyrene in various ways, seeking after an available method for obtaining zero shear viscosity involving nothing more than a straight-line extrapo-

* The shear rate dealt with in the routine method of viscometry of dilute polymer solutions will usually fall in the shear rate range of 500-3000 sec$^{-1}$.

15) A. Katchalsky and N. Sternberg, *J. Polymer Sci.*, **10**, 253 (1953).

16) H. Fujita and T. Homma, *J. Polymer Sci.*, **15**, 277 (1955).

17) P. Alexander and K. A. Stacey, *Trans. Faraday Soc.*, **51**, 299 (1955).

lation, which should hold over a sufficiently wide range of shear rates. But the mathematical relationship between viscosity and shear rate was too complex to warrant generalization and none of these attempts was successful.

Another method of measuring the zero shear viscosity has been proposed by E. Wada[7] in which the use of a tilting viscometer is recommended. Taking advantage of a horizontal tangent at very small shear rates in the viscosity vs. shear curve, the apparent relative viscosities are measured at successively low pressures by tilting the viscometer until they begin to assume a constant value, which is substantially the relative viscosity at zero shear.

The present writer has measured the zero shear viscosities of polystyrene fractions in toluene according to the same principle using a multi-bulb viscometer instead of the tilting type and found that the results thus obtained are in good agreement with the zero shear viscosities previously measured by a horizontal viscometer[8]. In the following, the viscometer is briefly described and the results are compared with the previous results.

### Viscometer

A sketch of the viscometer used is shown in Fig. 3. In order to carry out measurements at sufficiently low rates of shear, the capillary was made small in radius (R=0.0131 cm.) and long (L=30.0 cm.). The upper part of each tube of the viscometer was bent as shown in Fig. 3 so as to allow the viscometer to be inclined at nearly horizontal positions without shedding the charged liquid, which procedure is necessary to fill the liquid in the capillary portions without allowing air to remain in the bent portion between the two capillaries.

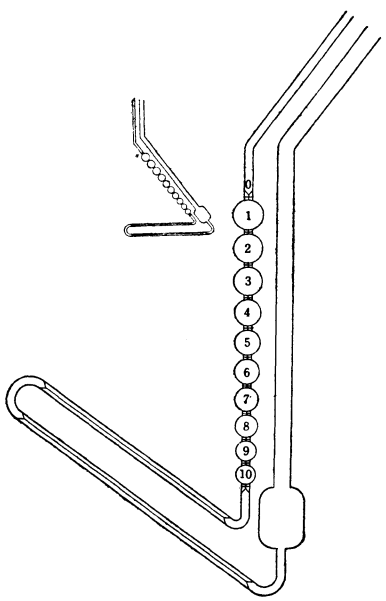



Fig. 3.

Since fairly rapid fall of the liquid in the strait portions at the etched lines (0, 1, 2, 3, etc. in Fig. 3) is desirable for the facility of flow time measurements, and since the flow velocity in this viscometer is very small owing to the long fine capillary, the straits in lower part of the viscometer were made fairly narrow (0.03 cm. in diameter for the lowest at the line 10). These narrow straits not only play a roll of capillary to some extent but also cause the surface tension error when the difference in surface tension between the solution and solvent is appreciable. But for the present case, at least, this error is considered negligible if it exists at all since the results obtained by this viscometer are in good agreement with those by a horizontal viscometer, in which the surface tension effect is almost completely absent. The measurement using the lowest efflux bulb (9-10) was found to be impossible for polystyrene solutions in toluene due to the capillary rise of the solvent in the strait at the line 10, which was absent in measurements of polymethylmethacrylate solutions in chloroform.

The viscometer was fixed on a brass frame, which in turn can be mounted on a frame in a thermostat so as to ensure the reproducibility of the viscometer position, which is very essential to the reliable measurements.

The kinetic energy correction for this viscometer was found to be negligible being consistent with the very small flow velocity in the viscometer. The drainage error was assumed to be also negligible.

### Results

The ratios of the flow times of the solution and solvent, $t/t_0$, for two polystyrene fractions in toluene, measured at 25°C are shown graphically in Figs. 4 and 5 plotted against the mean pressure head, $h$, and shearing stress, $\tau$. Here $\tau$ was calculated according to the equation:

$$\tau = \rho g h R/2L \qquad (4)$$

which is the expression for the maximum shearing stress at the capillary wall, where $\rho$ is the density of the solution. The shear rate ranges covered by these measurements are 54-201 sec.$^{-1}$ for the solution of $c=0.196$ g./100 cc. of F-4, 109-405 sec.$^{-1}$ for $c=0.0568$ of F-10.

As seen in Figs. 4 and 5, $t/t_0$ appears to attain a constant value at lower pressures and this value may be regarded as the $t/t_0$ at zero pressure. In this range of pressures, the linearity of the Katchalsky plot, $t_0/t$ vs. $h^2$, was found to be satisfied very well by these data as may be expected. Though these plots are not shown here, $t/t_0$ at zero shear rate determined from the intercept of the straight line in these plots was substantially coincident with the one provided by

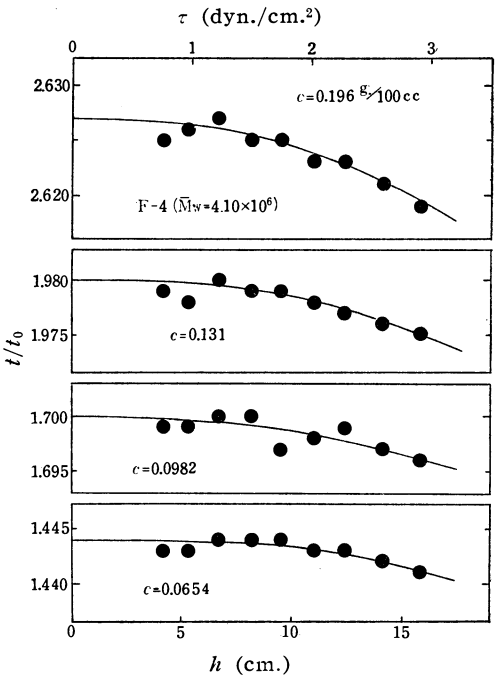



Fig. 4. The ratio of the flow times of the solution and the solvent vs. the mean pressure head, $h$, and shearing stress, $\tau$. See Eq. (4) for $\tau$.

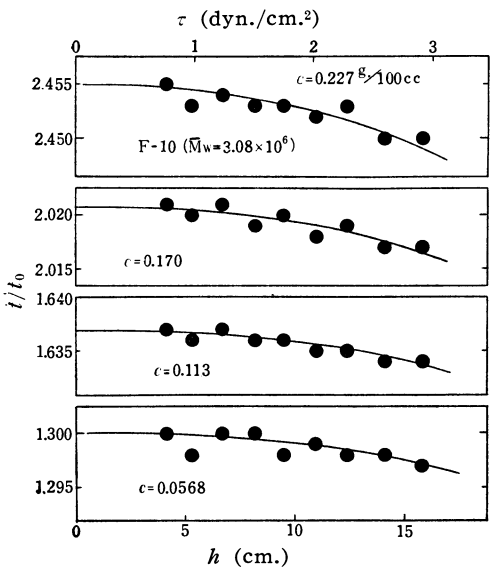



Fig. 5. The ratio of the flow times of the solution and the solvent vs. the mean pressure head, $h$, and shearing stress, $\tau$. See Eq. (4) for $\tau$.

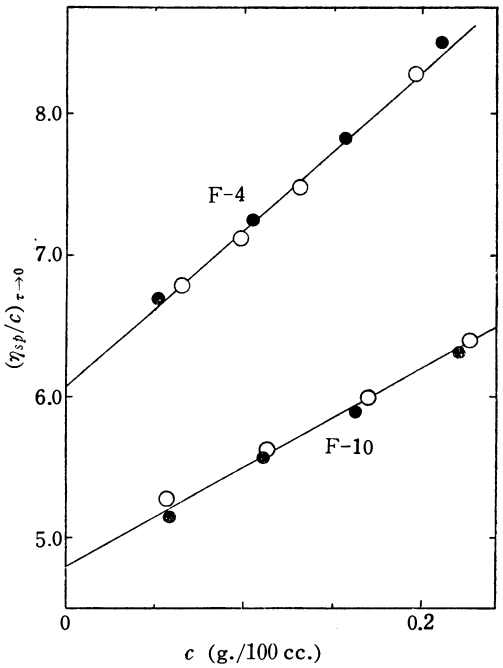



Fig. 6. $\eta_{sp}/c$ vs. $c$ relations obtained by the multi-bulb viscometer (○) and by the horizontal viscometer (●).

the conventional extrapolation such as shown in Figs. 4 and 5.

$\eta_{sp}/c$ at zero pressures, calculated from $(t/t_0)_{P\to 0}$ as $((t/t_0)_{P\to 1}-1)/c$ for each fraction is shown in Fig. 6 as a function of $c$. $\eta_{sp}/c$ vs. $c$ plots at zero pressure for these fractions obtained by a horizontal viscometer and reported previously[8], are inserted in the same figure for comparison's sake. The general agreement is not perfect but may be considered satisfactory taking account of the independence of the two methods employed.

This author would like to express his hearty thanks to Prof. S. Murahashi and Prof. S. Akabori of this university and to Mr. E. Wada of the Scientific Research Institute for their kind encouragement throughout the course of this study. The financial asistance of Tekkôsha Company is also gratefully acknowledged.

*Department of Chemistry*
*Faculty of Science*
*Osaka University, Kita-ku, Osaka*

# *Amino Acid Synthesis from Nitromalonic Ester. II*[1]. *Synthesis of Proline and Glutamic-γ-semialdehyde*

By Tôru OKUDA

(Received December 7, 1956)

Akabori, Izumi and Okuda[1] have recently reported the synthetic preparations of DL-ornithine, starting from acrylonitrile and readily available diethyl nitromalonate (I) which has a reactive methine group. A new synthesis of DL-proline and the dimethyl acetal of glutamic-γ-semialdehyde (VI) which is biochemically interesting, but has been tedious for synthetic approach, from the same nitroester (I) and acrolein is described in this communication.

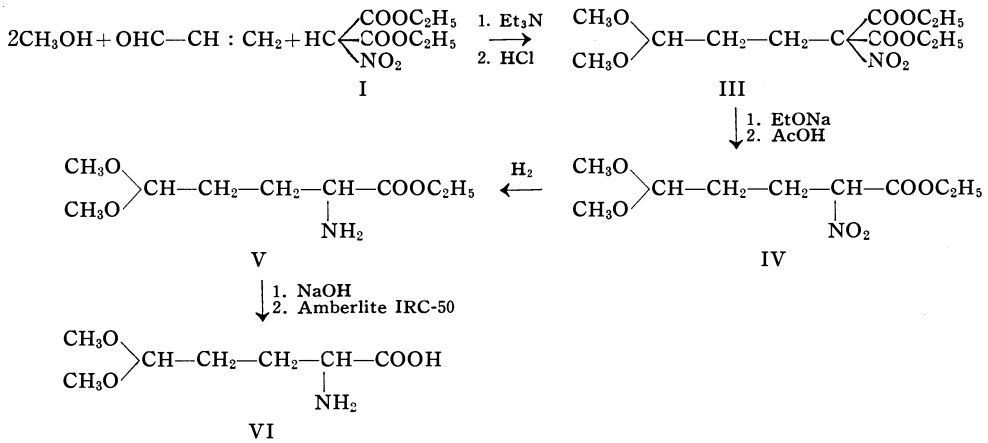
Since Albertson and Fillman[2] accomplished an excellent and practical work for the preparation of DL-proline, an amino acid that had been very difficult to synthesize, several similar or different methods[3-6] have appeared. Although inferior to their method in the yield, a simpler procedure to obtain this amino acid has been found. The addition reaction of diethyl nitromalonate (I) to acrolein proceeded very smoothly in the presence of basic catalyst such as triethylamine at lower temperature. The resulting γ,γ-dicarbethoxy-γ-nitrobutyraldehyde (II), of which the 2, 4-dinitrophenylhydrazone had already been prepared by Yamada et al[7] from the crude product for the characterization, was distilled without any decomposition in an yield of 94%. γ-Aminobutyraldehyde and the related compounds are reported to react in the cyclized form under the usual conditions[8,9]. The possibility that in the γ-aminaldehydes ring formation may be substantially complete, was proved by Vogel and Davis[10] by the fact that crude glutamic-γ-semialdehyde or $\Delta^1$-pyrroline-5-carboxylic acid prepared from γ,γ-dicarbethoxy-γ-acetamidobutyraldehyde was hydrogenated catalytically to proline.

Therefore, cyclization would be expected if γ-nitrobutyraldehyde (II) were reduced to the corresponding γ-amino compound. Accordingly, the catalytic hydrogenation of γ,γ-dicarbethoxy-γ-nitrobutyraldehyde (II) has been undertaken in glacial acetic acid containing an equimolecular amount of fused sodium acetate as condensing agent[11]. The possible intermediates, 5,5-dicarbethoxy-$\Delta^1$-pyrroline and the ethyl ester of α-carbethoxyproline were not able to be isolated. On refluxing the hydrogenated product with hydrochloric acid and on the subsequent treatment with ammonium rhodanilate, DL-proline was obtained in an yield of 12–21%.

It is well-known that glutamic-γ-semialdehyde is a common intermediate in the enzymatic interconversions of glutamic acid, proline and ornithine. Several biochemical studies are currently underway on this compound in various laboratories, but the inaccessibility in a practical amount appears to restrict the use in experiments. The Vogel's method[10] to prepare the semialdehyde itself was re-investigated in laboratory scale, but appeared inadequate from the standpoint of preparation. Good and Mitchell[12] prepared the diethyl acetal of the glutamic-γ-semialdehyde with very poor yield by alkaliere hydrolisis of the diethyl acetal of γ,γ-dicarbethoxy-γ-acetamidobutyraldehyde and paper-chromatographic separation.

The method reported here affords a simple and practical synthesis of the dimethyl acetal of the semialdehyde (VI) through the following reaction diagram:

1) Paper I in this series, S. Akabori, Y. Izumi and T. Okuda, *J. Chem. Soc. Japan*, **77**, 490 (1956).
2) N. F. Albertson and J. L. Fillman, *J. Am. Chem. Soc.*, **71**, 2818 (1949).
3) P. E. Gagnon, J. L. Boivin and P. A. Boivin, *Can. J. Research*, **28B**, 207 (1950).
4) H. Plieninger, *Chem. Ber.*, **83**, 2710 (1950).
5) J. Caprová-Jirků, J. V. Koštir and M. Vondráček, *Chem. Listy*, **44**, 19 (1950).
6) R. Gaudry and L. Berlinquet, *Can. J. Research*, **28B**, 245 (1950).
7) S. Yamada. I. Chibata and T. Tsurui, *J. Pharm. Soc. Japan*, **73**, 123 (1953).
8) C. Schöpf and F. Oechler, *Ann.*, **523**. 1 (1936).
9) C. Schöpf and H. Steuer, ibid., **558**, 124 (1947).
10) H. J. Vogel and B. D. Davis, *J. Am. Chem. Soc.*, **74**, 109 (1952).
11) "Organic Reactions", Vol. IV, John Wiley & Sons, Inc. New York, N. Y. 1948, p. 201.
12) N. Good and H. K. Mitchell, *J. Am. Chem. Soc.*, **74**, 4953 (1952).
13) Ulpiani, *Gazz. chim. ital.*, **34**, 174 (1904).
14) D. I. Weisblat and D. A. Lyttle, *J. Am. Chem. Soc.*, **71**, 3078 (1949).




When the above-described addition of diethyl nitromalonate (I) to acrolein was carried out in methanolic solution and the reaction mixture was then directly treated with a small amount of dry hydrogen chloride, the acetal diester (III) was readily obtained in one step in fairly good yield. After the decarbethoxylation of III by the Ulpiani's method[13,14,1], the resulting acetal monoester (IV) was hydrogenated catalytically under pressure in methanol. The ester of the acetal amino acid (V) was readily purified by vacuum distillation with an yield of about 80%. On treatment of the amino acid ester (V) with aqueous sodium hydroxide and then with Amberlite IRC-50 exchange resin to remove sodium ions, the dimethyl acetal of glutamic-$\gamma$-semialdehyde (VI) was obtained as white crystals. Although the diethyl acetal of the semialdehyde was reported to be very soluble in ethanol[12], the dimethyl acetal was found to be less soluble like other common amino acids.

## Experimental

**$\gamma,\gamma$-Dicarbethoxy-$\gamma$-nitrobutyraldehyde (II).**—In a three-necked flask fitted with a drying tube, a thermometer, a dropping funnel and a stirrer was placed a solution of 102.5 g. (0.50 mole) of diethyl nitromalonate (I) in 450 ml. of ethanol containing 0.2 ml. of triethylamine. A mixture of 29 g. (0.52 mole) of acrolein and 30 ml. of ethanol was added dropwise to this with vigorous stirring over the course of about one hour at such a rate that the temperature remained below 40°C. After additional stirring for two hours the solvent was removed in vacuo and the residual oil was distilled. One hundred twenty-three grams of $\gamma$, $\gamma$-dicarbethoxy-$\gamma$-nitro-butyraldehyde was obtained as yellowish oil, b. p. 134–137°C/1 mm.

*Anal.* Found: N, 5.31. Calcd. for $C_{10}H_{15}O_7N$: N, 5.36%.

2,4-Dinitrophenylhydrazone of the aldehyde (II) prepared by usual method melted at 74–76°C after recrystallization from methanol-water. (*lit.* 74–76°C[7])

*Anal.* Found: N, 15.75. Calcd. for $C_{16}H_{19}O_{10}N_5$: N, 15.87%.

**DL-Proline.**—In the pressure bottle of an apparatus for catalytic reduction were placed 26.1g. (0.10 mole) of freshly distilled $\gamma,\gamma$-dicarbethoxy-$\gamma$-nitrobutyraldehyde (II), 9 g. of fused sodium acetate, 130 ml. of glacial acetic acid and 10 g. of Raney nickel. An initial pressure of 90 atm. of hydrogen was applied. When, after about twenty-four hours, 0.4 mole of hydrogen had been absorbed, the reaction was stopped and the catalyst was removed by filtration. After removing the acetic acid in vacuo, 50 ml. of concentrated hydrochloric acid was added to the syrupy residue and the mixture was cooled overnight in an ice box. Precipitated Sodium chloride was filtered off and the filtrate was refluxed for five hours. The dark solution was concentrated to a syrup under reduced pressure, then taken up in water and charcoaled. Then the pH of the solution was adjusted to 2.6–3.0 by adding aqueous sodium hydroxide and the solution was treated with methanolic solution of 25 g. of ammonium rhodanilate by the usual method. Recrystallization of the crude product from isopropyl alcohol-ether gave 2.5 g. of white crystals of DL-proline, m. p. 206° (dec.). Yield, 21%.

*Anal.* Found: N, 11.84. Calcd. for $C_5H_9O_2N$: N, 12.17%.

**Ethyl $\delta,\delta$-Dimethoxy-$\alpha$-carbethoxy-$\alpha$-nitrovalerate (III, Dimethyl Acetal of $\gamma,\gamma$-Dicarbethoxy-$\gamma$-nitrobutyraldehyde).**—102.5 g. (0.50 mole) of diethyl nitromalonate (I), 29 g. (0.52 mole) of acrolein and 360 ml. of methanol instead of ethanol were treated in the same manner as described above. About 3 g. of dry hydrogen chloride was dissolved in the mixture and then 70 g. of anhydrous sodium sulfate was added. After standing at room temperature for forty-eight hours, the reaction mixture was neutralized with aqueous sodium bicarbonate and concentrated under reduced pressure. The residue was then poured into about 1 l. of ice water, the aqeous phase was extracted three times with ether or isopropyl ether and the extracts were combined

with the oil. The combined ether solution was washed twice with water and dried over sodium sulfate in an ice box. After removal of the ether, the residue was distilled at 0.5 mm. and the fraction boiling between 145–150°C was collected as the product. The dimethyl acetal of $\gamma,\gamma$-dicarbethoxy-$\gamma$-nitrobutyraldehyde (III) thus obtained was yellowish and weighed 130 g. Yield, 84.6%.

*Anal.* Found: N, 4.62. Calcd. for $C_{12}H_{21}O_8N$: N, 4.56%.

**Ethyl $\delta,\delta$-Dimethoxy-$\alpha$-nitrovalerate (IV, Dimethyl Acetal of $\gamma$-Carbethoxy-$\gamma$-nitrobutyraldehyde).**—Ethyl $\delta,\delta$-dimethoxy-$\alpha$-carbethoxy-$\alpha$-nitrovalerate (III), 42 g. (0.136 mole), in 400 ml. of anhydrous isopropyl ether was cooled in an ice-bath. A solution of 3.25 g. (0.141 mole) of sodium in 150 ml. of absolute alcohol was added slowly, with vigorous stirring, over a period of two hours. Precipitation of the sodium salt of IV and probably some sodium ethylate occured to form a very thick slurry. This was stirred further for five hours and allowed to stand overnight in an ice-box and then filtered. The salt was washed twice with 50 ml. portions of ether, transferred to a separatory funnel, together with the salt obtained from the mother liquor, covered with 200 ml. of isopropyl ether and acidified with 45ml. of 20% aqueous acetic acid. Vigorous shaking was continued until all the solid had disappeared. The ether layer was separated and the aqueous phase extracted with ether. The ether solutions were combined and washed with two 50 ml. of water. Drying, concentration and vacuum-distillation gave 30 g. (94%) of oily IV, which boiled at 118–123°C/2 mm.

*Anal.* Found: C, 45.94; H, 6.91; N, 5.86. Calcd. for $C_9H_{17}O_6N$: C, 45.95; H, 7.29; N, 5.96%.

Hydrolysis of the acetal group of IV and the subsequent treatment with 2, 4-dinitrophenyl hydrazine gave yellow crystals that melt at 106–108°C. (*lit.* 110–111°C[15]).

*Anal.* Found: C, 41.93; H, 4.26; N, 18.91. Calcd. for $C_{13}H_{15}O_8N_5$: C, 42.28; H, 4.07; N, 18.97%.

**Ethyl $\delta,\delta$-Dimethoxy-$\alpha$-aminovalerate (V).**—The reduction of 47 g. (0.2 mole) of IV was carried out in a stainless steel autoclave using 200 ml. of methanol and 4 g. of Raney nickel catalyst at 50–70°C for three hours. The autoclave was heated as rapidly as possible to avoid the formation of undesirable by-products. The catalyst was removed by filtration and the methanol was distilled off in vacuo. Thirty-three grams of V was obtained as colorless liquid by distillation; b. p. 105–107°C at 2 mm. Yield, 80.5%.

*Anal.* Found: C, 51.87; H, 9.23; N, 6.66. Calcd. for $C_9H_{19}O_4N$: C, 52.68; H, 9.27; N, 6.34%.

**Dimethyl Acetal of Glutamic-$\gamma$-semialdehyde (VI).**—Five grams of ethyl $\delta,\delta$-dimethoxy-$\alpha$-aminovalerate (V) was dissolved in 10 ml. of 10% aq. sodium hydroxide solution and the mixture was heated at 60°C for about one hour. The aqueous solution of the sodium salt of the dimethyl acetal of glutamic-$\gamma$-semialdehyde was treated with Amberlite IRC-50 and then evaporated to dryness in vacuo. The crude product which melts at 206–209°C was dissolved in a small volume of warm water, and then charcoaled. Addition of ethanol and ether and cooling gave 2.5 g. of white crystals of VI melting at 215–217 °C (dec.). This amino acid is very soluble in water, less soluble in ethanol and insoluble in ether and benzene.

*Anal.* Found: C, 47.08; H, 8.14; N, 7.78. Calcd. for $C_7H_{15}O_4N$: C, 47.46; H, 8.47; N, 7.91%.

15) O. A. Moe and D. T. Warner, *U. S. Patent.*, 2, 599, 653 (June 10, 1952).

## Summary

1. A synthesis of DL-proline from diethyl nitromalonate and acrolein by intramolecular reductive alkylation is described.

2. A new method for preparation of the dimethyl acetal of glutamic-$\gamma$-semialdehyde from the same starting materials in an over-all yield of 38% (based on diethyl nitromalonate) is also presented.

The author wishes to thank Professor S. Akabori for his kind guidance and also to thank Messrs. Y. Izumi and S. Sakurai for their helpful advice.

*Laboratory of Organic Chemistry*
*Faculty of Science*
*Osaka University, Kita-ku, Osaka*

# *Polymorphism of Bis-β-hydroxyethyl Terephthalate*

By Akihisa MIYAKE

(Received December 21, 1956)

In the course of a study of the infrared spectra of various derivatives of terephthalic acid, it was found that bis-β-hydroxyethyl terephthalate has several modifications. The crystal of bis-β-hydroxyethyl terephthalate prepared by the usual method, recrystallization from water or slow cooling of the melt, is obtained in the most stable form, which is called α-form in this paper. Besides this α-form, at least three other forms can be obtained by rapid cooling of the melt. These three modifications are tentatively called β-, γ- and δ-forms. The infrared spectra of these modifications are shown in Fig. 1, and the x-ray diffraction patterns in Fig. 2. There are some remarkable differences between the infrared spectra of these modifications; it seems that these differences offer some valuable information for the interpretation of the infrared spectrum of polyethylene terephthalate.

## Method of Preparation

**α-Form.**—This form is the common one. Recrystallization from water generally gives this form. It is the most stable form and cannot be changed to any other form unless remelted.

**β-Form.**—Molten mixture of bis-β-hydroxyethyl terephthalate and ethylene glycol (ca. 1:1) kept at a temperature of ca. 100°C, is quenched dropwise on the surface of an ice-cooled metal plate. Removing ethylene glycol from the solidified drops at a temperature below ca. 20°C by means of filter papers or a porous plate, β-form is obtained. It is essentially important to maintain this at a low temperature; otherwise, the δ-form is obtained. This form changes to the α-form when washed with water or alcohol. It converts to in the δ-form at ca. 40°C, and to the α-form above ca. 45°C. These transition temperatures become lower as the atmospheric humidity becomes higher.

**γ-Form.**—This form is obtained by rapid cooling of the melt. Washing with water, it changes to the α-form. It also changes gradually above ca. 60°C, to the α-form.

**δ-Form.**—Molten mixture of bis-β-hydroxyethyl terephthalate and ethylene glycol is quenched dropwise. Ethylene glycol is removed from the solidified drops by filter papers, as in the case of β-form, at a temperature of 30°C to 40°C. Once formed, this form is rather stable; it does not change when washed with water, nor when kept at 100°C for an hour.

It was ascertained that all these modifications are chemically the same. The analytical values of C and H conform to the formula $C_6H_4(CO_2CH_2CH_2OH)_2$, and determination of the ethylene glycol content by periodic acid after saponification of each modification, also agrees with the above formula.

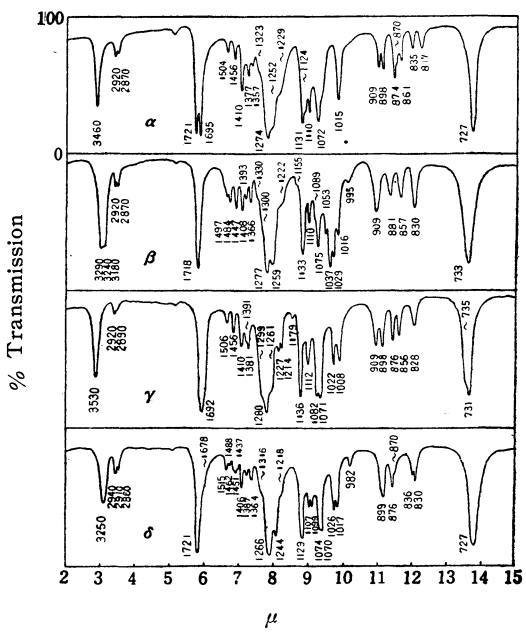



Fig. 1. Infrared spectra of four polymorphic forms.

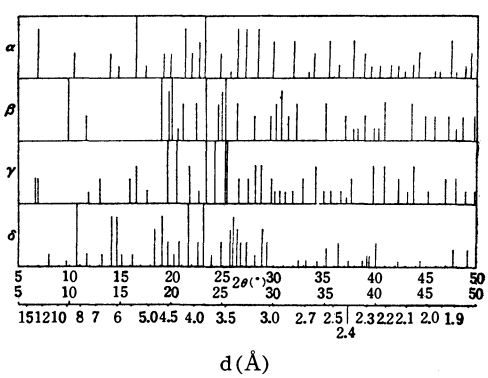



Fig. 2. X-ray diffraction patterns of four polymorphic forms.

### Infrared and X-ray Measurements

The infrared spectra were obtained with a Perkin-Elmer Model 21 Spectrometer using NaCl prism. Samples were measured as nujol mulls except in the C—H frequency region. For this region, hexachlorobutadiene or low molecular weight polytrifluorochloroethylene oil was used as the mulling agent.

X-ray diffraction patterns were obtained with a Norelco Geiger counter x-ray diffractometer. Nickel filtered radiation from a copper target was used. In the case of the $\beta$-form which is easily transformed into the $\delta$-form under the influence of atmospheric moisture, the specimen shield assembly was covered with cellophane and desiccated with phosphorous pentoxide.

### Some Remarks on the Infrared Spectra

From the differences in the infrared spectra, it might be possible to obtain some information about the molecular form or the crystal structure of the four modifications. In this respect, there are at least three characteristic points. The first of these is the absorption band at 3500-3200 $cm^{-1}$. The position of this band shows that the O—H terminal groups are all hydrogen bonded in these modifications; however the type of hydrogen bond is different between each modification. The next point is the C=O band at 1720 $cm^{-1}$ and 1695 $cm^{-1}$. The former shows the existence of free ester carbonyl groups, the latter hydrogen bonded carbonyl groups. Accordingly, $\beta$- and $\delta$-form have only free ester groups, while $\gamma$-form has hydrogen bonded carbonyls, $\alpha$-form has both of them in equal amount. The third point is concerned with the four absorption bands which appear at 910 to 850 $cm^{-1}$. The vibrations expected to appear in this region are the $CH_2$ rocking vibrations and certain vibrations of the benzene ring. For the determination of the latter, the comparison with the spectra of other terephthalic acid esters is useful. In Fig. 3, three such esters are given; comparing these spectra with that of bis-$\beta$-hydroxyethyl terephthalate, it becomes apparent that there exists only one band 875 $cm^{-1}$ which seems to be a benzene ring vibration, so long as it is assumed that the benzene ring vibrations have almost constant frequencies in such series. Thus the absorption bands chosen in Table I can be assigned to the $CH_2$ rocking vibrations.

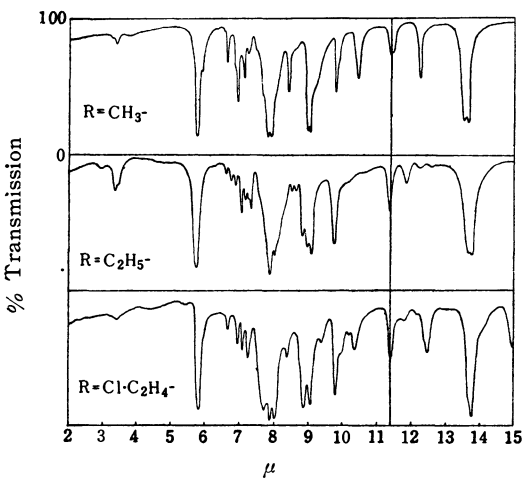



Fig. 3. Infrared spectra of ROOC·$C_6H_4$·COOR.

TABLE I
FREQUENCIES OF THE $CH_2$ ROCKING VIBRATION ($cm^{-1}$)

| | | | | |
|---|---|---|---|---|
| $\alpha$ | 909 | 898 | ~870 | 861 |
| $\beta$ | 909 | | | 857 |
| $\gamma$ | 909 | 898 | 876 | 856 |
| $\delta$ | | 899 | ~870 | |

The absorption band 876 $cm^{-1}$ of the $\gamma$-form is assumed to be composed of two components, benzene ring vibration and $CH_2$ rocking vibration. The frequencies given in Table I consist of two pairs, (909, ~857) and (899, ~870). $\beta$-Form has only the former pair, $\delta$-form only the latter, while $\alpha$-and $\gamma$-form have both.

Nakagawa[1] has shown that $CH_2$ rocking frequencies in a molecule of the type X—$CH_2$—$CH_2$—X depends profoundly on the angle of internal rotation, and their values decrease in the following order: $B_g$ (*trans*) > A (*gauche*) > B (*gauche*) > $A_u$ (*trans*). In the light of this conception, the former pair (909, ~857) can be considered as the $CH_2$ rocking frequencies arising from *trans* configuration of the O—$CH_2CH_2$—O group. The latter pair (899, ~870) represents the existence of *gauche* configuration. Thus, the configuration of the O—$CH_2CH_2$—O group in $\beta$-form is *trans*, in $\delta$-form *gauche*, in $\alpha$- and $\gamma$-form both *trans* and *gauche*.

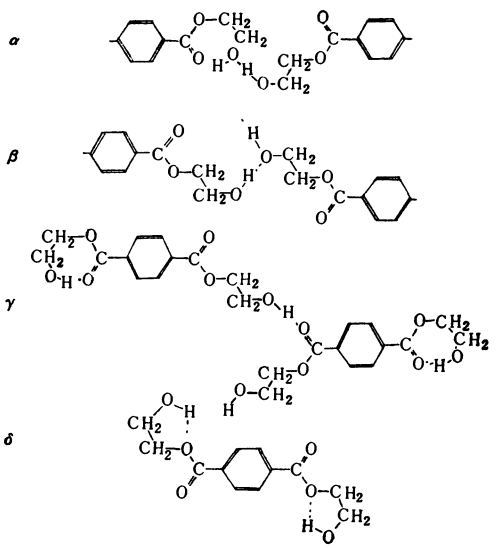



Fig. 4. Structures of four polymorphic forms.

1) I. Nakagawa. *J. Chem. Soc. Japan* (*Pure Chem. Sect.*), **76**, 813 (1955).

It might be too speculative to derive structural conceptions from only the arguments made above; the four modifications may be considered to have the structures something like those shown in Fig. 4 at the present time.

## Summary

It is found that bis-$\beta$-hydroxyethyl terephthalate shows polymorphism, and there exist at least four different modifications. From the infrared spectra of these modifications, differences between the molecular forms are elucidated to some extent. These differences occur mainly from the difference in configuration of the side chain attached to the benzene ring.

The author wishes to express his sincere thanks to Dr. K. Hoshino and Mr. Y. Numata for their encouragement and support which made the present work possible. Thanks are also due to Mr. Y. Kinoshita for the measurement of the x-ray diffraction pattern and for many discussions. The author also wishes to thank Mr. S. Tanaka for his assistance with the infrared measurements.

*Research Department, Toyo Rayon Co. Ltd., Otsu, Shiga*

# *Sorption of Monobasic Dye-acid by Nylon-6 Fibre*

By Minoru NISHIO

(Received December 27, 1956)

## Introduction

Much quantitative information has been published in regard to the mechanism accounting for the uptake of acid dyes by the polyamide fibres (wool, nylon-66). It is generally agreed that the dye molecule is held by means of a salt-type linkage between the sulphonic acid groups of the dye and the basic amine ends of the fibre in stoichiometric amounts, and that the process of formation of these linkages constitutes much of the driving force for the penetration of dyes into the fibre[1-5].

The pH isotherms obtained by dyeing nylon-6(polycapramide) fibre from baths of varying pH containing a large amount of dye salt have been described in the previous paper[6] and it was found that at moderate pH levels, adsorption was in close agreement with available end groupings. Moreover, additional evidence has been presented for this conclusion by determining the saturation adsorption of the typical monobasic acid dye onto hydrolysed nylon-6 samples which had various amounts of free amino-groups.

The objectives of the present investigation were to elucidate the mechanism of the combination of monobasic dye-acid with nylon-6 fibre under normal dyeing conditions and to calculate the magnitude of the forces involved.

## Experimental

**Materials.**—The nylon-6 sample employed for dyeing was 3 denier semidull staple fibre which had an end amino-group analysis of 0.043 milli-equivalent per g. of fibre by DNFB method*[6-9]. Before use, the fibres were scoured at 60°C for 20 min. in a bath containing 5 g. soap per 1. and then thoroughly rinsed and dried. Distilled water was used throughout.

**Dye Purification.**—The dyes used were the free acids of Orange II (β-naphthol-azo-p-benzene sulphonic acid, sodium salt, Colour Index No. 151) and Metanil Yellow YK (diphenyl-azo-m-benzene sulphonic acid, sodium salt, Colour Index No. 138).

Two dyes were first isolated as sodium salts free from inorganic electrolytes by the method

1) E. Elöd and T. Schachowsky, *Melliand Textilber.*, **23**, 437 (1942), ibid., **25**, 237 (1944).
2) R. H. Peters, *J. Soc. Dyers and Colourists*, **61**, 95 (1945).
3) P. W. Carlene, A. S. Fern and T. Vickerstaff, ibid., **63**, 388 (1947).
4) F. C. McGrew and A. K. Schneider, *J. Am. Chem. Soc.*, **72**, 2547 (1950).
5) W. R. Remington and E. K. Gladding, ibid., **72**, 2553 (1950).
6) M. Yoshida, and M. Nishio, Scientific Reports of Toyo Rayon Co. **9**, 85 (1954) (in Japanese).

* This is a simple method which is carried out chemically with the aid of dinitrofluorobenzene for the precise determination of the primary amine content of the polyamide.
7) F. Sanger, *Biochem. J.*, **39**, 507 (1945).
8) J. H. Bows and J. A. Moss, ibid., **55**, 735 (1953).
9) H. Zahn and P. Rathgeber, *Melliand Textilber.*, **34**, 239 (1953).

of Robinson and Mills[10] which involved three or fourfold salting out with sodium acetate followed by repeated extraction with ethyl alcohol until an aqueous solution containing a known amount of dye salt gave a constant optical density as shown in Fig. 1 (Orange II).

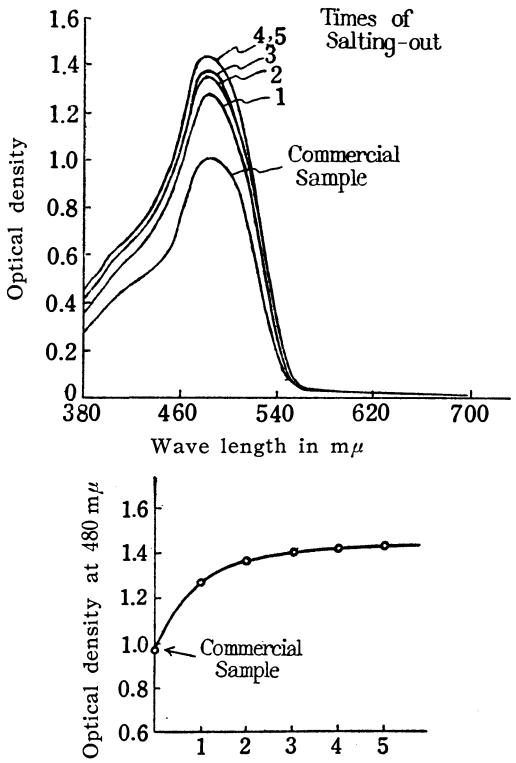



Fig. 1. Variation of absorption spectrum and optical density at 480 mμ of dye solution with time of salting-out. (Orange II, 50 mg./l.).

The free acid of Orange II was then precipitated from the concentrated solution of sodium salt of dye obtained above by means of concentrated hydrochloric acid, filtered off, washed with dilute hydrochloric acid, and finally dried in vacuo over caustic soda flakes until free from chloride ions.

In the case of Metanil Yellow YK, ion exchange resin was employed to obtain electrolyte-free dye-acid. Two % aqueous solution of the above-obtained dye-salt was allowed to run through a column of Amberlite IR-120 (strongly acidic ion exchange resin of Rohm & Hass Co.) previously washed with water and methanol and then activated by treatment with 10% hydrochloric acid.

The pure dye-acid, isolated from the effluent on evaporation and washed with water to remove any inorganic acid, was obtained as bright black sparingly soluble needles.

The ash content of both samples were almost nil and analytical values according to titanous chloride method indicated high purity of at least 98 %. They were dried to constant weight at 105°C before use.

**Procedure.**—One gram samples of nylon-6 fibre were dyed in a 200 : 1 liquor ratio at 60° (±0.1°)C for a period of 3 to 6 days (i. e. to equilibrium) in the absence of any acids. The acidity was adjusted by varying concentrations of the dye-acid and the pH values reported were those at the end of the dyeing, at room temperature. Glass electrode pH meter was used for pH determination. After dyeing the dyed sample was removed from the dye liquor, rinsed rapidly with a minimum quantity of distilled water and then air-dried.

TABLE I

ADSORPTION OF FREE DYE-ACIDS BY NYLON-6 FIBRE AT 60°C

| Dye in Solution (m.eq./l.) | Final pH of Dye-bath | Dye in Fibre (m.eq./g.) | $\theta_D$ | $-\Delta\mu°_{HD}$ (kcal./mole) |
|---|---|---|---|---|
| Orange II | | | | |
| 4.16 | 2.85 | 0.083 | — | — |
| 1.17 | 3.15 | 0.068 | — | — |
| 0.77 | 3.38 | 0.060 | — | — |
| 0.49 | 3.65 | 0.055 | — | — |
| 0.22 | 5.53 | 0.048 | 0.89 | 16.9 |
| 0.12 | 5.72 | 0.037 | 0.69 | 15.8 |
| 0.060 | 5.83 | 0.029 | 0.54 | 16.0 |
| 0.031 | 5.72 | 0.024 | 0.45 | 15.4 |
| 0.024 | 5.69 | 0.014 | 0.26 | 14.6 |
| 0.002 | 5.69 | 0.007 | 0.13 | 15.2 |
| | $[S]_F=0.054$ | | Average: | 15.7 |
| Metanil Yellow YK | | | | |
| 0.782 | 2.05 | 0.117 | — | — |
| 0.597 | 3.02 | 0.104 | — | — |
| 0.597 | 3.08 | 0.104 | — | — |
| 0.441 | 3.12 | 0.102 | — | — |
| 0.229 | 3.30 | 0.101 | — | — |
| 0.229 | 3.31 | 0.097 | — | — |
| 0.444 | 3.34 | 0.093 | — | — |
| 0.229 | 3.56 | 0.092 | — | — |
| 0.441 | 3.10 | 0.091 | — | — |
| 0.229 | 3.59 | 0.090 | — | — |
| 0.229 | 3.28 | 0.088 | — | — |
| 0.206 | 3.20 | 0.087 | — | — |
| 0.449 | 3.87 | 0.083 | — | — |
| 0.096 | 3.20 | 0.072 | — | — |
| 0.081 | 3.58 | 0.071 | — | — |
| 0.115 | 4.93 | 0.062 | — | — |
| 0.022 | 5.97 | 0.059 | — | — |
| 0.049 | 4.75 | 0.049 | 0.94 | 17.6 |
| 0.048 | 6.07 | 0.049 | 0.94 | 17.5 |
| 0.017 | 6.07 | 0.043 | 0.83 | 18.8 |
| 0.011 | 6.07 | 0.038 | 0.73 | 18.3 |
| 0.003 | 5.90 | 0.028 | 0.54 | 17.8 |
| 0.002 | 5.65 | 0.020 | 0.38 | 16.4 |
| ~0 | 6.07 | 0.015 | — | — |
| ~0 | 6.50 | 0.010 | — | — |
| | $[S]_F=0.052$ | | Average: | 17.8 |

10) C. Robinson and H. A. T. Mills, *Proc. Roy. Soc. (Lndon)*, **A131**, 576, 596 (1931).

Measurements of dye adsorbed on nylon-6 were made by dissolving the dyed fibre in 80% formic acid and determining the quantity of dye in solution by means of the photoelectric spectrophotometer (Beckman type) on the basis of the application of Beer's law.

Concentrations of dye-acid in aqueous bath were likewise measured spectrophotometrically.

## Results and Discussion

Isotherms were determined for varying concentration of the free dye-acids.

The results obtained are given in Table I, illustrated by Fig. 2.

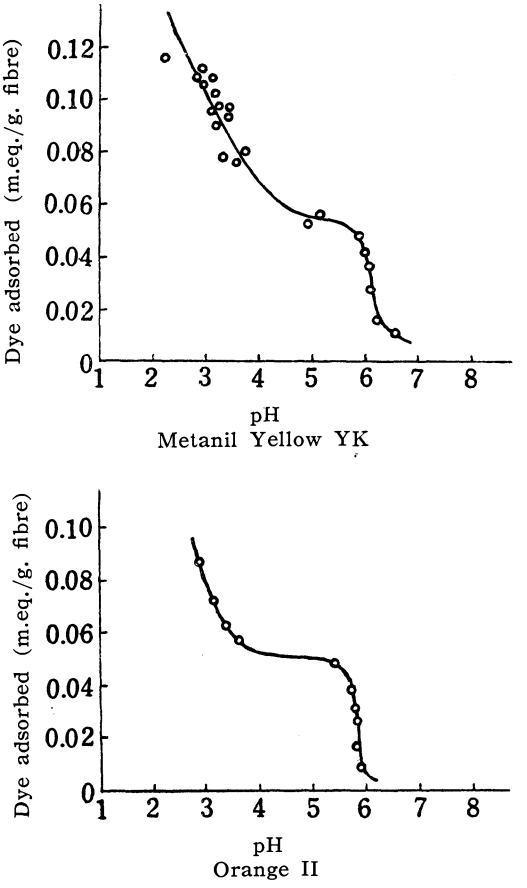



Fig. 2. Adsorption of monobasic free dye-acids on nylon-6 fibre at 60°C.

The amount of dye adsorbed at equilibrium has been plotted against the final pH of the dyebath. The curves are similar to those in the case of sodium salt of dye which was reported in the previous paper[6], being sigmoid in shape and reaching a fairly constant value (about 0.05 milliequivalent of dye-acid per g. of fibre) corresponding to saturation of the end amino-groups. Such correspondence has been found to exist generally for acid dyes[1-6].

As the pH is further decreased, there is another sharp increase in the uptake which corresponds to adsorption of the dye onto weakly basic amide-groups of the polymer chain (amide-dyeing) and new primary amine groups liberated by the occurrence of dye-catalysed hydrolysis. Such a phenomenon has been observed in the case of acid dyes and referred to as "overdyeing"[11,12].

The uptake of monobasic dye-acid by nylon may be represented schematically as

$$-OOC-N_y - NH_3^+ + H^+ + D^- \longrightarrow HOOC-N_y-NH_3^+ \cdot D^-$$

where Ny is the polyamide chain separating the end amino and carboxyl groups and $D^-$ is a dye anion. On immersion of the fibre in a dyebath containing free dye-acid, hydrogen ions are first adsorbed onto carboxyl groups and the more slowly diffusing dye anion is then able to attach itself to the positively charged amino-groups. This mechanism is now accepted as accounting for the adsorption of acid dyes by nylon.

Gilbert and Rideal[13,14] first proposed a method of analysis of the adsorption forces of acids and acid dyes on wool, which has been extended to the case with free dye-acids by Lemin and Vickerstaff[15] and later applied to nylon-66 by American workers[4,5], by the use of the equation

$$-\frac{0.434}{RT}(\Delta\mu^\circ_H+\Delta\mu^\circ_D) = 2\log\left(\frac{\theta_D}{1-\theta_D}\right)-\log[D]s+pH \qquad (1)$$

in which [D]s represents the molar concentration of the free dye-acid in solution and $\theta_D$ the fraction of the available basic sites of the fibre which are occupied by dye anion. The notations $\Delta\mu^\circ_H$ and $\Delta\mu^\circ_D$ represent the standard changes in chemical potential (partial molal free energy) for the hydrogen ion and for the monobasic dye anion involved in the sorption of the ions from the solution by the fibre, and the negative of their sum represents the

11) C. D. O'Briain and R. H. Peters, *J. Soc. Dyers and Colourists*, **69**, 435, (1950).
12) E. Atherton, D. A. Downey and R. H. Peters, *Text. Res. J.*, **25**, 977 (1955).
13) G. A. Gilbert and E. K. Rideal, *Proc. Roy. Soc.*, **A182**, 335 (1944).
14) G. A. Gilbert, ibid., **A183**, 167 (1944).
15) D. R. Lemin and T. Vickerstaff, *J. Soc. Dyers and Colourists*, **63**, 405 (1947).

standard affinity of the acid form of the dye for the fibre ($\Delta\mu^\circ_{HD}$).

This quantity gives a measure of the tendency of the dye acid to move from its standard state in solution to its standard state on the fibre. On this basis calculations were carried out by use of equation (1) and the affinity values obtained are given in the last column of Table I.

In order to evaluate $\theta_D$, the fractional saturation of the fibre sites, it is necessary to determine the saturation value $[S]_F$ which is the concentration of dye in the fibre when all the available sites, end amino-groups, are occupied.

Equation (1) may be converted into the form—

$$-\frac{0.434}{RT}\Delta\mu^\circ_{HD} = \log\left(\frac{\theta_D}{1-\theta_D}\right)^2 \cdot \frac{1}{[H]_S \cdot [D]_S} \quad (2)$$

where, $pH = \log 1/[H]_S$

$\theta_D = [D]_F/[S]_F$

Removing logarithms,

$$\left[\frac{\theta_D}{1-\theta_D}\right]^2 = \left(\frac{[D]_F}{[S]_F - [D]_F}\right)^2 = K[H]_S \cdot [D]_S \quad (3)$$

Where $K$ is a constant, $[D]_F$ and $[H]_S$ refer to the concentrations of dye in the fibre and hydrogen ions in solution respectively. Inverting both sides of the equation, and dividing by $[S]_F$,

$$\frac{1}{[D]_F} - \frac{1}{[S]_F} = \frac{1}{\sqrt{K}} \cdot \frac{1}{[S]_F} \cdot \frac{1}{[H]_S \cdot [D]_S} \quad (4)$$

A plot of the reciprocal of $[D]_F$ against the reciprocal of the mean molarity of the dye-acid in solution, $\sqrt{[H]_S \cdot [D]_S}$, should yield a straight line as is shown in Fig. 3, the intercept of which on

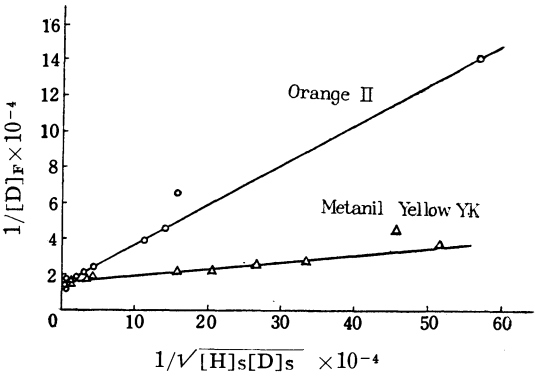



Fig. 3. $1/[D]_F$ against $1/\sqrt{[H]_S[D]_S}$ plot for adsorption of monobasic dye-acid by nylon-6 fibre at 60°C.

"$1/[D]_F$" axis gives the reciprocal of the saturation value $[S]_F$. The values obtained by extrapolation in this way are 0.054 milliequivalent per g. of nylon-6 fibre for Orange II free acid and 0.052 for Metanil Yellow YK free acid, which were used for calculation of dye affinity.

Assuming the affinity of hydrogen ion for nylon at 80°C to be −11.9 kg. cal.[16] and the heat of reaction to be negligible as temperature appears to have little effect on adsorption of hydrochloric acid by wool[15] anion affinities have been calculated for two monobasic dyes, with the results shown in the last column of Table II.

TABLE II

AFFINITY OF MONOBASIC DYE ANIONS FOR NYLON-6 FIBRE AT 60°C

| Dye-Acid | (Affinity kcal./mole) | | |
|---|---|---|---|
| | $\Delta\mu^\circ_{HD}$ | $\Delta\mu^\circ_H$ | $\Delta\mu^\circ_D$ |
| Orange II | −15.7 | −11.9 | −3.8 |
| Metanil Yellow YK | −17.8 | | −5.9 |

The value for Metanil Yellow YK anion is in good agreement with values for nylon-66 obtained by McGrew and Schneider of −6.1 and −5.9[4], by Remington and Gladding of −6.1 kcal./mole[5,16], being somewhat higher than the affinity value of this dye anion for wool of −5.0 ~ −5.3 kcal./mole[15]. The affinity of acid dye is generally known to be higher for nylon than for wool.

With Orange II, McGrew and Schneider also determined the affinity for nylon-66 of −3.3~−3.9 kcal./mole by adsorption of the sodium salt of the dye from neutral solution in presence of salt at 98°C.

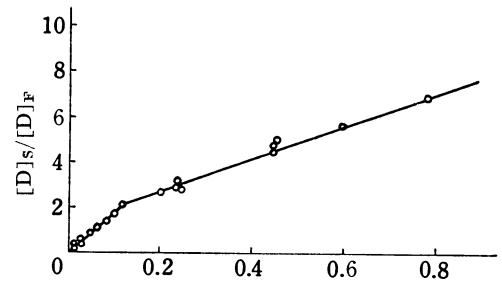
Judging from these results it seems to be possible to conclude that the affinities of two monobasic dye anions are approximately the same on two fibres, nylon-66 and nylon 6.

Thus, the fundamental energetics of dyeing process and the mode of dye attachment are the same on these two fibres and some slight differences in dyeing behavior—for instance, the rate of dyeing and levelness etc. as is often said—must be accounted for by purely physical differences due to the production process of the fibre. Under practical dyeing conditions, however, it is evident that the amine content is of course the controlling factor for building acid dyes upon nylon.

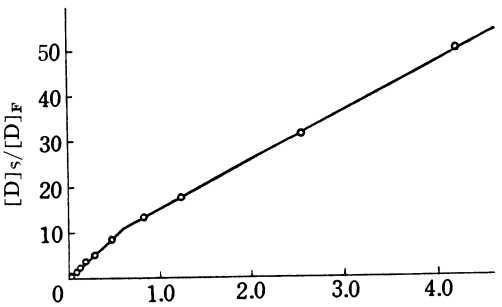
16) T. Vickerstaff, "The Physical Chemistry of Dyeing", 2nd edition, Oliver and Boyd, London (1954), p. 471.

Finally, the adsorption isotherms already determined give straight lines, when $[D]_S/[D]_F$ is plotted against $[D]_S$ according to the Langmuir's equation:

$$[D]_F = \frac{a[D]_S}{1+b[D]_S} \quad (5)$$




Free acid of Metanil Yellow YK




Free acid of Orange II

Fig. 4. $[D]_S/[D]_F$ against $[D]_S$ plot for adsorption of monobasic dye-acid by nylon-6 fibre at 60°C.

The curves of Fig. 4 consist really of two straight lines with an abrupt change of slope. It therefore appears that the type of site on which dye is adsorbed is different between these two portions. The line at higher concentration has already been discussed and can mainly be attributed to the adsorption of dye on weakly basic amide-groups of the polymer chain. The line of different slope at lower concentration must refer to the primary adsorption of dye on terminal amino-groupings which should also obey the Langmuir adsorption isotherms.

The point at which this change takes place corresponds to $[D]_F$ value of 0.054 m. eq. dye per g. of fibre for Orange II and 0.052 for Metanil Yellow YK which are in good agreement with the values obtained by extrapolation illustrated in Fig. 3 and also close to the number of free amino end groupings (0.043 m. eq./g. fibre) determined by DNFB method. The difference might be due to the substantivity of these dye-acids for nylon or attributed to the fact that overdyeing occurs to a slight extent even at moderate pH levels.

## Summary

The equilibrium uptake of two typical monobasic dye-acids by nylon-6 (polycapramide) fibre has been measured for varying concentrations and additional evidence was given to confirm the mechanism of dye attachment to nylon as consisting of (1) combination with basic amine ends at normal dye bath pH and (2) combination mainly with the weakly basic nonterminal amide groups of the polymer chain at lower pH values. The Langmuir equation can well be applied to both regions of adsorption.

It is well known that the thermodynamic affinity of a dye for the fibre represents a fundamental characteristics of the dyeing process. The anion affinities of dye-acids for nylon-6, calculated from data on the equilibrium distribution of dye-acid between bath and fibre in terms of the change in standard chemical potential of the dye sorption process using the equation for wool developed by Gilbert and Rideal, were in good agreement with values for nylon-66 obtained by other workers.

Thus, the fundamental energetics of dyeing process and the mode of dye attachment are the same on these two fibres and some slight differences in dyeing behaviour must arise solely from differences in their physical structure due to the production process.

The author wishes to express his sincere thanks to Dr. K. Hoshino and Mr. M. Yoshida for their kind encouragement and for permission to publish this paper.

*Research Department*
*Toyo Rayon Co. Ltd.*
*Otsu, Shiga*

# *Hydrogen Bonding Effect on the Fluorescence of Some Nitrogen Heterocycles. I*

By Noboru MATAGA and Shizuyo TSUNO

(Received December 19, 1956)

## 1. Introduction

It is well known that whereas the aromatic hydrocarbons such as benzene, naphthalene and anthracene fluoresce fairy well or strongly in the near ultraviolet or visible spectral region, the corresponding aza-derivatives such as pyridine, quinoline and acridine are completely non-fluorescent or emit very weakly in spite of their comparable or stronger absorption intensity compared with aromatic hydrocarbons. Some interpretations have been made for these behaviors of nitrogen heterocycles; for example according to Bowen[1], this effect has been ascribed to the increase in spin-orbital interaction by a nitrogen atom, while Förster[2], has interpreted this phenomenon in the case of pyridine as due to the predissociation of CN bond, though he has made no interpretation on the very weak fluorescence of acridine or quinoline. We will propose another interpretation, perhaps more plausible, for the phenomenon in question, on the basis of the solvent effects upon the absorption spectra and fluorescence yields of these nitrogen heterocycles. One of the present authors has previously reported[3] that, although quinoline and acridine are almost non-fluorescent in non-polar solvent such as hexane and benzene, they fluoresce fairy well in alcohols which are capable of making hydrogen bond with nitrogen atoms of these heterocycles. Moreover, the fluorescence yield has been found greatly enhanced in quinolinium and acridinium ion in the aqueous solution. He has suggested, from these facts, that the non-bonding electron pair on a nitrogen atom may play an important role in the inner quenching of fluorescence in these molecules. To elucidate the problem further, we have measured the absorption spectra and relative fluorescence yields of these molecules hydrogen bonded with various proton donors in non-polar solvent. The results obtained clearly show the parallel relation between relative fluorescence yield and proton donating power, i. e., the greater the proton donating power, the larger the increase in relative fluorescence yield. Moreover, we have found an interesting fact that the difference in the emitting $\pi$-electronic state leads to the different behavior of these nitrogen heterocycles in fluorescence quenching by a halogen atom.

The object of the present paper is to report these facts with some discussions on the role of the interaction between n- and $\pi$-electrons, and also the character of emitting $\pi$-electronic state in the fluorescence of these molecules.

## 2. Experimental

Apparatus: Absorption spectra were measured with a Beckman spectrophotometer model DU. The fluorometer was the same as described previously[4]. The fluorescence spectra were photographed with a Hilger $E_2$ type quartz spectrograph or a small type glass prism spectrograph, using a high-pressure mercury lamp with appropriate filters[3] as an exciting light source.

Reagents: Quinoline and acridine were the same samples as reported previously[3]. Chemical pure grade *n*-hexane was shaken with fuming sulfuric acid diluted with conc. sulfuric acid and distilled carefully. Extra pure grade benzene was dried over metallic sodium and distilled before use. Carbon tetrachloride and chloroform were shaken with conc. solfuric acid, washed with water, and after being dried over phosphorus pentoxide, distilled carefully. Ethanol was refluxed with silver nitrate to remove aldehyde, and after refluxing with calcium oxide, distilled carefully. Commercial $\beta$-phenylethylalcohol was fractionally distilled. Benzylalcohol was dried over potassium carbonate, and distilled under an atmosphere of dry nitrogen. Chemical pure grade mono- and trichloracetic acid were recrystallized several times from benzene, then stored over concentrated sulfuric acid in a vacuum

1) E. J. Bowen and F. Wokes, "Fluorescence of Solutions", Longmans (1953), p. 26.
2) Th. Förster, "Fluoreszenz Organischer Verbindungen", Vandenhoech and Ruprecht (1951), p. 118.
3) N. Mataga, Y. Kaifu and M. Koizumi, This Bulletin, **29**, 373 (1956).
4) N. Mataga, Y. Kaifu and M. Koizumi, ibid., **29**, 115 (1956).

desiccator. Dichloracetic acid was fractionally distilled under a pressure of 17 mm.

### 3. Experimental Results

**A. Remarks on the Electronic Spectra of Nitrogen Heterocycles.** — The $\pi$-electronic spectra of nitrogen heterocycles such as pyridine, quinoline and acridine are very similar to those of isoelectronic aromatic hydrocarbons such as benzene, naphthalene and anthracene, and their excitation energies are almost the same. A systematization of this correspondence between nitrogen heterocycles and aromatic hydrocarbons was made by Zanker[5] using Platt's perimeter model[6]. According to Platt's notation, the lowest excited singlet state ($\pi \rightarrow \pi^*$) is $^1L_b$ in pyridine and quinoline, and $^1L_a$ in acridine, and these are regarded as the emitting state of fluorescence, respectively. The second excited singlet state is $^1L_a$ in pyridine and quinoline, and $^1L_b$ in acridine.

**B. Change in Absorption Spectrum by Hydrogen Bonding.** — When various proton donors are added to the solutions of quinoline and acridine in non-polar solvent, the absorption spectra show characteristic changes due to the hydrogen bonding equilibrium. In both quinoline and acridine, hydrogen bonding strengthens the $^1L_b$ band somewhat, its wave length being not altered, but induces the red shift of $^1L_a$ band. The stronger the donating power, the larger the degree of the increase of absorption intensity of $^1L_b$ band and the red shift of $^1L_a$ band. In the case of the acid-base interaction in which trichloracetic acid was used as proton donor, the degree of the change of absorption spectrum is very close to the case of quinolinium or acridinium ion in the aqueous solution, but slightly less prominent.

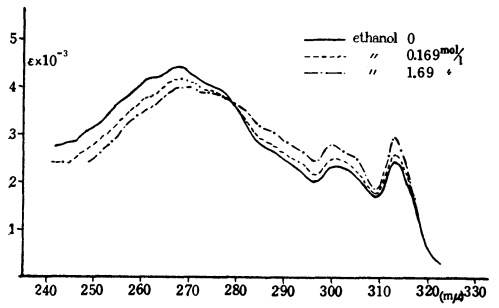



Fig. 1. Change in absorption spectrum of quinoline in *n*-hexane with addition of ethanol.
Concentration of quinoline $\sim 10^{-4}$ mol./l.

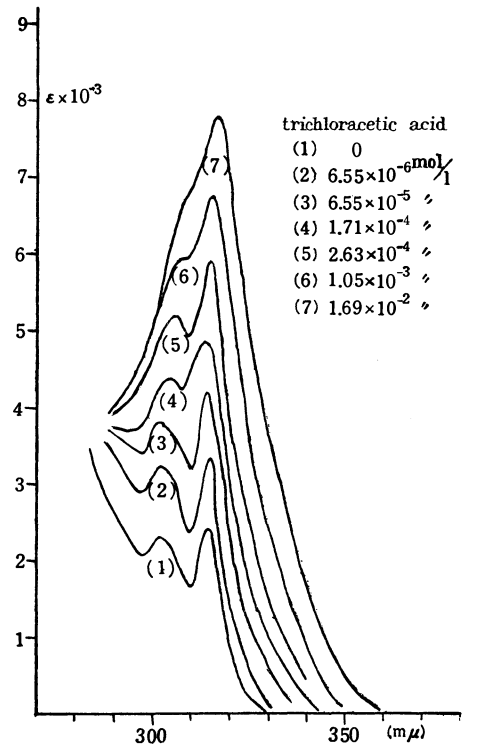



Fig. 2. Change in absorption spectrum of quinoline in benzene with addition of trichloracetic acid.
Concentration of quinoline $\sim 10^{-4}$ mol./l.

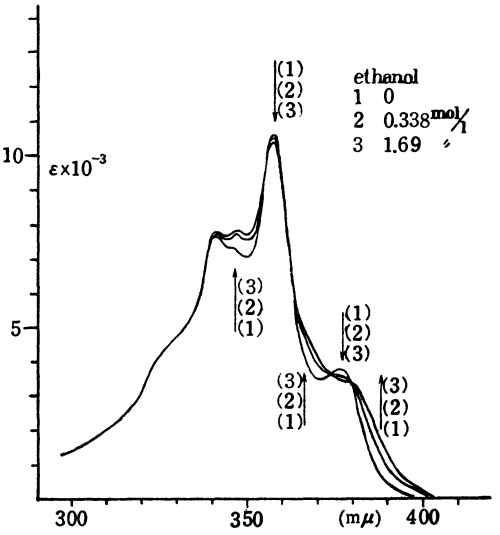



Fig. 3. Change in absorption spectrum of acridine in benzene with addition of ethanol.
Concentration of acridine: $5 \times 10^{-5}$ mol./l.

5) V. Zanker, *Z. Physikal. Chem.*, N. F., **2**, 52 (1954). see also Ref. 3).
6) J. R. Platt, *J. Chem. Phys.*, **17**, 484 (1949). H. B. Klevens and J. R. Platt, ibid., **17**, 470 (1949).

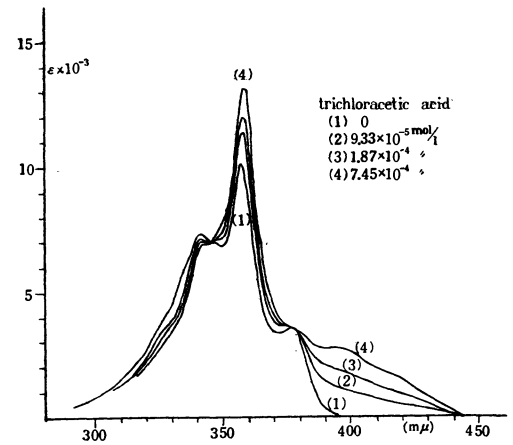



Fig. 4. Change in absorption spectrum of acridine in benzene with addition of trichloracetic acid.
Concentration of acridine: $5\times10^{-5}$ mol./l.

Some examples of these spectral changes caused by hydrogen bonding are shown in Figs. 1—4.

These spectral changes caused by the perturbation of $\pi$-electronic states by hydrogen bonding, seem to correspond definitely to the above-mentioned Zanker's assignment. The same correspondence seems to hold also in pyridine[5,7]. From these spectral changes we can obtain the equilibrium constant of hydrogen bond formation in the ground state.

**C. Method of Evaluation of Equilibrium Constant from Absorption Spectra.** —The optical density at a definite wave length, $d$, is expressed as follows, using molar extinction coefficients of a free molecule A and a hydrogen bonded one AD, $\varepsilon_a$ and $\varepsilon_c$:

$$d=\varepsilon_a[A]+\varepsilon_c[AD]=\varepsilon_a[A]+\varepsilon K[A][D]$$

The optical density of the solution without donor is:

$$d_0=\varepsilon_a[A]_0=\varepsilon_a[A](1+K[D]),$$

where $[A]_0$ is the analytical concentration of A.

From these equations we obtain:

$$\frac{1-(d_0/d)}{[D]}=-K+\left(\frac{\varepsilon_c}{\varepsilon_a}\right)K\left(\frac{d_0}{d}\right) \qquad (1)$$

For moderately weak donors, we can approximately replace [D] by $[D]_0$, the analytical concentration of D.

For a strong donor such as trichloracetic acid, however, we cannot use such an approximate method.

Instead, we put as follows:

$$K=\frac{[AD]}{([D]_0-[AD])([A]_0-[AD])},$$

$$[A]_0(\varepsilon-\varepsilon_a)=[AD](\varepsilon_c-\varepsilon_a),$$

$$[AD]=\frac{[A]_0(\varepsilon-\varepsilon_a)}{(\varepsilon_c-\varepsilon_a)}$$

where $\varepsilon$ is the apparent molar extinction coefficient. Hence,

$$K=\frac{(\varepsilon-\varepsilon_a)(\varepsilon_c-\varepsilon_a)}{[D]_0(\varepsilon_c-\varepsilon_a)(\varepsilon_c-\varepsilon)-[A]_0(\varepsilon-\varepsilon_a)(\varepsilon_c-\varepsilon)}.$$

When $\varepsilon_a=0$ at the wave length used for the calculation,

$$[D]_0\left(\frac{\varepsilon_c}{\varepsilon}-1\right)=\frac{1}{K}+[A]_0\left(1-\frac{\varepsilon}{\varepsilon_c}\right) \qquad (2)$$

By means of Tsubomura's method[8], we can obtain [AD], and from $[A]_0\varepsilon=[AD]\varepsilon_c$,

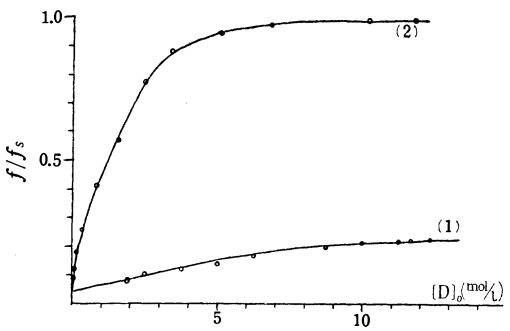



Fig. 5. Change in fluorescence intensity of acridine in benzene with addition of chloroform and ethanol.
Concentration of acridine: $5\times10^{-5}$ mol./l.
(1) chloroform, (2) ethanol.
$f_s$: fluorescence intensity of ethanol solution used as standard.

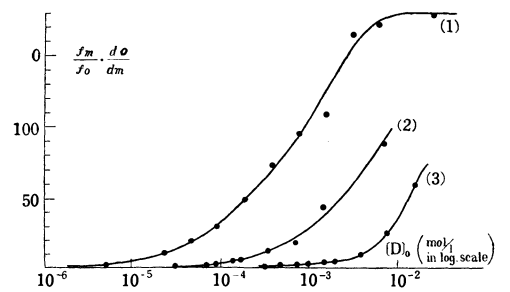



Fig. 6. Change in fluorescence intensity of acridine in benzene with addition of chloracetic acids.
Concentration of acridine: $5\times10^{-5}$ mol./l.
(1) trichloracetic acid
(2) dichloracetic acid
(3) monochloracetic acid

7) L. W. Pickett, et al., *J. Am. Chem. Soc.*, **75**, 1618 (1953).

8) H. Tsubomura, *J. Chem. Phys.*, **23**, 2130 (1955).

$\varepsilon_c$ is evaluated. Then, $K$ can be evaluated from (2).

**D. Change in Fluorescence Intensity and Its Interpretation on the Basis of Hydrogen Bonding Equilibrium.** — In all the cases of hydrogen bonding, the fluorescence intensity is increased. Moreover, the stronger the donating power, the greater the increase in fluorescence intensity. Some examples of those changes in fluorescence intensities are shown in Figs. 5 and 6.

Now it is almost certain that the observed changes in fluorescence intensity may be attributed to the fact that the free and hydrogen bonded heterocycles have different efficiency of fluorescence and that the concentration of these molecular species are determined by the association equilibrium. Hence the experimental results will be analyzed as follows.

**(i)** When the equilibrium of the ground state is maintained during the course of fluorescence, the fluorescence intensity $f_m$ with addition of D is:

$$f_m = \frac{(\varepsilon_a \Phi_a + \varepsilon_c \Phi_c K[\mathrm{D}])}{1+K[\mathrm{D}]} [\mathrm{A}]_0 I_0 \qquad (3)$$

where $\varepsilon_a$ and $\varepsilon_c$ are the molar extinction coefficient of A and AD at the wave length of the exciting light, respectively. $I_0$ is the intensity of the exciting light, and, $\Phi_a$ and $\Phi_c$ are the quantum yields of fluorescence of A and AD, respectively. It is to be noted that (3) is derived on the condition that the absorption of each molecular species is proportional to its concentration, which approximately holds in the present experiment.

From (3) we derive,

$$\frac{1-(f_0/f_m)}{[D]} = -K + \alpha\left(\frac{\varepsilon_c}{\varepsilon_a}\right)K\left(\frac{f_0}{f_m}\right) \qquad (4)$$

where $f_0$ is the fluorescence intensity of the solution without D, and $\alpha = \Phi_c/\Phi_a$.

When $\Phi_a \simeq 0$,

$$\frac{1}{f_m} = \mathrm{Const.}\left(1+\frac{1}{K}\frac{1}{[\mathrm{D}]}\right) \qquad (5)$$

**(ii)** In contradistinction to (i), when an equilibrium in the excited state is different from that of the ground state and the state of association approaches a new equilibrium state during the lifetime of the excited molecule, until a new equilibrium state is almost completely reached prior to the emission, we should use euqation (6) instead of (3):

$$f_m = \frac{(\Phi_a + K'\Phi_c[\mathrm{D}])}{1+K'[\mathrm{D}]} d_m I_0 \qquad (6)$$

$$d_m = \frac{(\varepsilon_a + \varepsilon_c K[\mathrm{D}])[\mathrm{A}]_0}{1+K[\mathrm{D}]}$$

where $K'$ is the equilibrium constant in the excited state. From equation (6) we can easily derive (7) and (8), which correspond to (4) and (5), respectively.

$$\frac{1-(f_0/f_m)(d_m/d_0)}{[\mathrm{D}]} = -K' + \alpha(d_m/d_0)K'(f_0/f_m) \qquad (7)$$

$$d_0 = \varepsilon_a[\mathrm{A}]_0, \quad d_m/f_m = \mathrm{Const.}\left(1+\frac{1}{K'}\frac{1}{[\mathrm{D}]}\right) \qquad (8)$$

For moderately weak donors such as chloroform and ethanol, we can approximate [D] with $[\mathrm{D}]_0$. Since the increase in fluorescence intensity by hydrogen bonding with those donors is not so much remarkable, we cannot neglect the fluorescence of A compared with that of AD, and we should use for these cases equations (4) or (7).

The ranges of fluorescence spectra of A and AD for these cases are practically the same.

Owing to a very small difference in extinction coefficients of A and AD at the wave length of the exciting light, (4) and (7) practically coincide in their forms and it has been established that the experimental results can be reproduced by either equations (4) or (7) satisfactorily, the equilibrium constants evaluated by (4) and (7) being practically the same.

Further, the equilibrium constant obtained in this way from fluorescence intensity measurement agrees with that evaluated from the change in the absorption spectrum.

Therefore, we can conclude that, in these cases, the association equilibrium in the excited state is practically the same as that in the ground state, in contrast to the case of naphthols[4,9].

For strong donors such as trichloracetic acid, we cannot approximate [D] with $[\mathrm{D}]_0$ and [D] should be evaluated using an equilibrium constant obtained from an absorption spectrum.

For acridine-trichloracetic acid system, the spectral range of fluorescence of AD is considerably different from that of A, but the increase of fluorescence intensity by hydrogen bonding is so remarkable, that we can neglect $\Phi_a$ compared with $\Phi_c$.

9) N. Mataga, Y. Kaifu and M. Koizumi, *Nature*, **175**, 731 (1955).

TABLE I

| Acceptor | Donor | Solvent | T°a) | $K_T$ | $\delta\tilde{\nu}$b)(cm$^{-1}$) | $\Phi_f$ |
|---|---|---|---|---|---|---|
| Acridine | Chloroform | Benzene | 286 | 0.1 | * | 0.6 |
| | Ethanol | Benzene | 290 | 1.0 | * | 1.0 |
| | | Hexane | 290 | 1.6 | * | 1.0 |
| | | $CCl_4$ | 291 | 1.8 | * | 1.0 |
| | Benzylalcohol | Benzene | 287 | 2.0 | * | 1.0 |
| | $\beta$-phenylethylalcohol | Benzene | 287 | 1.0 | * | 1.6 |
| | $CH_2ClCOOH$ | Benzene | 293 | $1.4\times10^2$ | ~600 | |
| | $CHCl_2COOH$ | Benzene | 293 | $8\times10^2$ | ~800 | 9.5 |
| | $CCl_3COOH$ | Benzene | 293 | $1.3\times10^4$ | ~900 | 11 |
| Quinoline | $CH_2ClCOOH$ | Benzene | 295 | ~$10^2$ | * | |
| | $CCl_3COOH$ | Benzene | 297 | $5\times10^3$ | * | |

a) Temperature at which measurement was made.
b) Wave number shift of $^1L_a$ band due to hydrogen bonding.
* Uncertain.

Hence it is suitable to employ equation (5) or (8) and the experimental results are really well reproduced by these equations.

In contradistinction to acridine-trichloracetic acid system, the increase in fluorescence intensity is very slight in the quinoline-trichloracetic acid system. In quinolinium ion in aqueous solution, the emitting state is $^1L_a$ in contrast to $^1L_b$ of quinoline base, and the range of fluorescence spectrum is considerably different from each other. In the quinoline-trichloracetic acid system, however, it was confirmed that the emitting state is $^1L_b$, the spectral range of fluorescence being the same as in non-polar solvent (310–360 m$\mu$).

Some examples of the analysis of fluorescence intensities are shown in Figs. 7, 8.

The concentration ranges of ethanol, benzylalcohol and $\beta$-phenylethylalcohol used for the evaluation of equilibrium constants from the results of absorption and fluorescence measurements were approximately 0.03–0.5 mol./l.

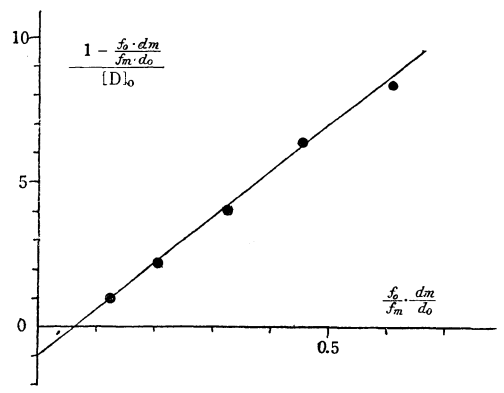



Fig. 7. $\dfrac{1-\dfrac{f_0\cdot d_m}{f_m\cdot d_0}}{[D]_0}\sim\dfrac{f_0\cdot d_m}{f_m\cdot d_0}$ relation for acridine-benzene-ethanol system.
Concentration of acridine: $5\times10^{-5}$ mol./l.

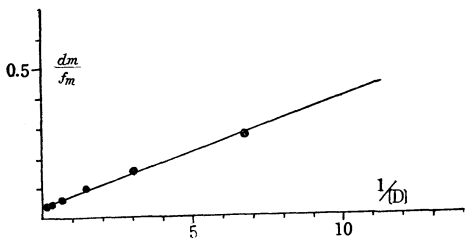



Fig. 8. $\dfrac{d_m}{f_m}\sim\dfrac{1}{[D]}$ relation for acridine-benzene-trichloracetic acid system.
Concentration of acridine: $5\times10^{-5}$ mol./l.

The results of infrared measurements[10] on the dimerization of chloracetic acids were used for the estimation of concentration ranges where the fraction of monomer is at least 80%, and the calculation of equilibrium constants was made in this concentration range.

**E. The Relative Fluorescence Yields of Hydrogen Bonded Nitrogen Heterocycles.**—It is clear from the above mentioned results, that the change in fluorescence intensity is well interpreted on the basis of hydrogen bonding equilibrium. Further, it is possible to deduce some information on the interelation between the fluorescence yields of hydrogen bonded nitrogen heterocycles and the donating powers of various proton donors.

Ethanol solution was used as a standard. The fluorescence intensity of this standard solution is expressed as follows:

$$f_s=\Phi_s\cdot d_s\cdot I_0 \qquad (10)$$

where $d_s$ is the optical density at the wave length of exciting light and $\Phi_s$ is the quantum yields of fluorescence. Then,

10) J, T. Harris, Jr. and M. E. Hobbs, *J. Am. Chem. Soc.*, **76**, 1419 (1954). H. A. Pohl. M. E. Hobbs and P. M. Gross, *J. Chem. Phys.*, **9**, 408 (1941).

from equations (10), (3) and (6), the following equations are derived.

$$f_m/f_s=\frac{\varepsilon_a(\Phi_a/\Phi_s)+\varepsilon_c(\Phi_c/\Phi_s)K[\mathrm{D}]}{1+K[\mathrm{D}]}\frac{[\mathrm{A}]_0}{d_s} \quad (11)$$

$$f_m/f_s=\frac{(\Phi_a/\Phi_s)+(\Phi_c/\Phi_s)K'[\mathrm{D}]}{1+K'[\mathrm{D}]}\frac{d_m}{d_s} \quad (12)$$

From these equations, $(\Phi_c/\Phi_s)$ can be evaluated, and the ratios of $(\Phi_c/\Phi_s)$ for various proton donors give the ratio of $\Phi_c$. The results obtained for acridine by (11) and (12) are practically the same. As shown in Table I, $\Phi_c$'s of acridine hydrogen bonded with ethanol, benzylalcohol and $\beta$-phenylethylalcohol are almost the same, and it is somewhat smaller when acridine is hydrogen bonded with chloroform.

Moreover, $\Phi_c$ for ethanol does not change irrespective of whether benzene, hexane, or carbon tetrachloride, is used as solvent. For chloracetic acids, the value of $\Phi_c$ is far greater than that for ethanol, and owing to the red shift of fluorescence spectrum, the "true value" of $\Phi_c$ may be larger than the value given in the table*.

For quinoline, since the weakness of its fluorescence intensity did not allow precise measurement, we did not attempt extensive study, and measurements were made only for monochlor- and trichloracetic acid. From the increases in fluorescence intensity, we can see, for these cases that $\Phi_c$ may be only several times of $\Phi_B$ in its order of magnitude, whereas $\Phi_s/\Phi_B\sim30$[3], therefore, $\Phi_c$ may be probably much smaller than $\Phi_s$, for these cases.

Now, $\Phi=\dfrac{k_f}{k_f+k_i}$, where $k_f$ and $k_i$ are the rate constant of fluorescent transition and that of the radiationless process. $k_f$ can be estimated using Ladenburg's formula[11],

$$k_f\simeq2.88\times10^{-9}\,n^2\tilde{\nu}^2_{\max}\int_0^\infty\varepsilon(\tilde{\nu})d\tilde{\nu}\ \mathrm{sec}^{-1}$$

Both in acridine and quinoline, the overlapping of $^1L_b$ and $^1L_a$ bands is fairy large; nevertheless, in the case of acridine, we can estimate $\int_0^\infty\varepsilon(\tilde{\nu})d\tilde{\nu}$ in its order of magnitude.

For acridine-trichloracetic acid-benzene system,

$$k_f'\sim5.5\times10^7\ \mathrm{sec}^{-1},$$

and for acridine-ethanol-benzene system,

$$k_f\sim2.5\times10^7\ \mathrm{sec}^{-1}.$$

Putting these $k_f'$ and $k_f$ value into the equation,

$$\Phi'/\Phi=\frac{k_f'}{k_f}\frac{(k_f+k_i)}{(k_f'+k_i')}\sim11,$$

the following relations are derived.

$$k_i'<\frac{1}{5}k_i,\quad \tau'\simeq5\tau$$

For quinoline, the estimation of $\int_0^\infty\varepsilon(\tilde{\nu})d\tilde{\nu}$ is more difficult. It is certain, however, that the integrated absorption is far larger in quinoline-trichloracetic acid-benzene system compared with those in benzene or ethanol solution. Therefore, it is clear that $k_i$ of quinoline hydrogen bonded with trichloracetic acid is far greater than $k_i$ in ethanol solution.

## 4. Discussion

**(a) Role of n-Electron in the Inner Quenching of Fluorescence.** — From all the facts described above, it is clear that the hydrogen bonding or proton addition plays an important role in the fluorescence of these nitrogen heterocycles. This circumstance is well comprehended by assuming that the n-electrons (non-bonding electrons) on a nitrogen atom is intimately related with the mechanism of fluorescence; the interaction between n- and $\pi$-electrons in the excited state may perhaps induce the radiationless transition to the ground state**, directly or indirectly. Such n–$\pi$ interaction may be weakened more or less owing to the acquisition of bonding character by the n-electron due to hydrogen bonding or proton addition, making the fluorescence transition possible.

In contradistinction to the case of naphthols, the equilibrium constant obtained from the fluorescence intensity is almost the same as that calculated from absorption spectrum, for these nitrogen heterocycles. This fact may be correlated with the proposed mechanism of the inner quenching by n-electron.

The possible interpretations may be as follows.

(i) Although the equilibrium in the excited state is shifted toward hydrogen bonding, the excited free molecule has such a short lifetime, due to high probability of inner quenching, that it has no time to be bonded with neighboring OH

* The phototube used is an ultraviolet sensitive one.

11) See for example, Th. Förster, loc. cit., p. 158.

** An analogous discussion was made recently by Sangster and Irvine in relation to their study of the efficiencies of organic scintillators. R. C. Sangster and J. W. Irvine, Jr., *J. Chem. Phys.*, **24**, 670 (1956).

groups during its life. Thus only the molecules which are hydrogen bonded in the ground state may be able to fluoresce.

**(ii)** Owing to the n–$\pi$ interaction the non-bonding character of n-electron may be lost more or less in the excited state, decreasing the proton accepting power, but the $\pi$-electron density on the nitrogen atom plausibly be increased in the excited state[3***], thus compensating the decrease in proton accepting power by n-electron, and the accepting power may be the same in the ground and in the excited state. In this case, even when the equilibrium state is reached during the lifetime of an excited free molecule, the equilibrium constant obtained from fluorescence intensity ought to be equal to that evaluated from absorption spectrum. In the present stage it cannot be decided definitely which of (i) and (ii) is the dominant mechanism for the phenomenon question.

**(b) Effect of $\pi$-Electronic State on the Fluorescence Quenching.** — Although the increase in fluorescence yields of quinoline and acridine by hydrogen bonding with ethanol or by proton addition in aqueous solution is almost the same, we see a distinct difference between these molecules in the effect of halogen atom on the fluorescence yields. The fluorescence yield of acridine is greatly enhanced by hydrogen bonding with trichloracetic acid, but the fluorescence yield of quinoline hydrogen bonded with trichloracetic acid is rather small compared with the fluorescence yield in ethanol solution. This distinction in these two molecules may be ascribed to the difference of emitting $\pi$-electronic state. In aromatic hydrocarbons, such as benzene, naphthalene and anthracene, there exists an $^3L_b$ state which has the same energy as $^1L_b$[12,13].

If the lowest singlet excited state is $^1L_b$, the phosphorescence transition occurs with relative ease probably by the processes, $^1L_b \cdots\rightarrow {}^3L_b \cdots\rightarrow {}^3L_a \rightarrow$ ground state. However, when the lowest singlet excited state is $^1L_a$, phosphorescence transition may be very difficult. The difference between naphthalene and anthracene in the experimental results of T→T absorption[14] may be interpreted by these mechanisms. Now, as the electronic spectra of nitrogen heterocycles are very similar to those of isoelectronic aromatic hydrocarbons, we may be allowed to assume that the analogous situation probably prevails also in these heterocyclic molecules. Thus, in the case of quinoline, the near-by existence of a halogen atom may easily accelerate $^1L_b \cdots\rightarrow {}^3L_b$ process owing to the spin-orbital perturbation, but it may be difficult to realize such a situation in acridine.

After all, the results reported in this paper, are well comprehended by assuming that the n–$\pi$ interaction is a chief cause of inner quenching and also by considering the effect of emitting $\pi$-electronic state on the quenching phenomenon. From the present results, the interpretations of the inner quenching in these molecules as due to the spin-orbital perturbation by the existence of nitrogen atom or predissociation of CN bond may not be appropriate.

*** A theoretical study using the molecular orbital method is now in progress.

12) R. Pariser, *J. Chem. Phys.*, **24**, 250 (1956).
13) J. A. Pople, *Proc. Phys. Soc.*, **68A**, 81 (1955).
14) D. P. Craig and I. G. Ross, *J. Chem. Soc.*, **1954**, 1589.

## Summary

1. The hydrogen bonding effect on the fluorescence of quinoline and acridine was studied in non-polar solvent mixed with various proton donors.

2. The equilibrium constants of hydrogen bonding calculated from the absorption and fluorescence data were the same for these molecules, in contradistinction to the case of naphthols. Possible mechanisms for this experimental fact were proposed.

3. The larger the relative fluorescence yields of hydrogen bonded nitrogen heterocycles become, the stronger the donating powers of proton donors are, and from this fact, discussions were given on the role of non-bonding electrons in the inner-quenching of these molecules.

4. The difference between quinoline and acridine in their fluorescence quenching caused by the existence of a halogen atom was ascribed to the different emitting $\pi$-electronic states in these molecules ($^1L_b$ in quinoline, $^1L_a$ in acridine), and some considerations by means of analogy to the $\pi$-electronic structures of aromatic hydrocarbons were given.

The authors express their cordial thanks to Dr. H. Baba of Hokkaido University for his discussion. Their thanks are especially due to Prof. M. Koizumi for his encouragement and discussion throughout this investigation.

*Institute of Polytechnics*
*Osaka City University*
*Kita-ku, Osaka*

# *Note on the Polymerization of Dyes in Solution*

By Noboru MATAGA

(Received December 24, 1956)

## 1. Introduction

Many investigations have been made on the aggregation of dye molecules or ions in aqueous solution, and it seems clear that some dyes form dimers and polymers in suitable conditions. For example, thionine, methylene blue, toluidine blue[1-3], rhodamine 6G[4], pyronine G[5] form dimers while acridine orange[6] forms dimer and higher polymers. Even in organic solvents dye molecules can often exist in a certain aggregated state. For example, Lewis et al.[7] reported that methylene blue in EPA at low temperature (liquid nitrogen) shows dimerization and polymerization of higher degree. Further, according to Zanker[8,9], acridine orange forms a definite polymer at low temperature in a mixed solvent of alcohol and ether.

Some qualitative discussions on the factors determining the association and also on the mechanism of spectral shift caused by association, have been made heretofore. For example, Rabinowitch and Epstein[1] have ascribed the cause of association to a large dispersion force between dye ions which have strong absorption bands in the visible spectral region.

Förster[10] has proposed a classical model for the interpretation of spectral shift caused by association. According to his theory, the dye ions in dimerized state take the plane parallel configuration, in which the dispersion force between pair of each dye ion is the largest. In this configuration, the electron oscillators of dye ions couple with each other, and there result symmetric and antisymmetric combinations, of which the former with a larger frequency than that of the original one can appear as absorption.

It is questioned, however, whether the complicated nature of the dimerization or polymerization of dyes in solution can well be comprehended by such a simplified interpretation.

As to a delicate aspect of dimerization or polymerization, some remarks were made previously by the present author in relation to the mechanism of metachromasy phenomenon[11].

Recently, Levshin has studied the effect of concentration on the optical properties of solution of acridine derivatives such as monoamino- and diamino-acridine[12-14]. He insists that the concentration effect is due to the dimerization of these molecules.

The present author has also investigated the concentration effect on the absorption spectra of 2,8-diaminoacridine (DAA) and 2,8-bisdimethylaminoacridine (BDAA) in various organic solvents. By the analysis of absorption spectrum according to the method of Zanker[8], it has been established that, contrary to Levshin's opinion, these molecules form higher polymers very easily in some organic solvents. It has also been confirmed that, the influence of solvent and of a slight difference in molecular structure between DAA and BDAA is very prominent in the phenomenon.

Levshin did not make any remarks about these points.

The object of the present paper is to report about these points with some discussions on the mechanism of dimerization or polymerization.

1) E. Rabinowitch, and L. F. Epstein, *J. Am. Chem. Soc.*, **63**, 69 (1941).
2) S. E. Sheppard, *Rev. Mod. Phys.*, **14**, 303 (1942).
3) S. E. Sheppard and A. L. Geddes, *J. Am. Chem. Soc.*, **66**, 1995, 2003 (1944).
4) V L. Levshin, *Acta Physicochim. USSR.*, **1**, 685 (1935); **4**, 221, (1936).
5) N. Mataga and M. Koizumi, *J. Inst. Polytech. Osaka City Univ.*, **4C**, 167 (1953); M. Koizumi and N. Mataga, This Bulletin, **27**, 194 (1954).
6) V. Zanker, *Z. Physikal. Chem.* **199**, 225 (1952).
7) G. N. Lewis et al., *J. Am. Chem. Soc.*, **65**, 1150 (1943).
8) V. Zanker. *Z. Physikal. Chem.*, **200**, 250 (1952).
9) G. Scheibe and V. Zanker, *Z. Physik*, **133**, 244 (1952).
10) Th. Förster, "Fluoreszenz organischer Verbindungen", Gottingen, Vandenhoech and Ruprecht (1951), p. 254.
11) N. Mataga, *J. Inst. Polytech. Osaka City Univ.*, **4C**, 189 (1953).
12) V. L. Levshin, *Doklad. Akad. Nauk SSSR*, **96**, 473 (1954).
13) V. L. Levshin, *Zhur. Eksptl. i. Teoret. Fiz.*, **28**, 201 (1954).
14) V. L. Levshin, ibid., **28**, 213 (1955).

## 2. Experimental

**Apparatus.** — Absorption spectra were measured with Beckman spectrophotometer model D. U. and the lengths of cells used were 10, 1, 0.1 and 0.007 cm. Using these cells, measurement in the concentration range from $10^{-6}$ to $10^{-2}$ mol./l. was possible.

**Reagent.**—DAA was the same sample as described elsewhere[15]. BDAA was purified by the method of Moudgill[16] and Biehringer[17]. Excess of sodium hydroxide was added to the aqueous solution of acridine orange (Zinc Salt of BDAA) which was kindly supplied by Sumitomo Chemical Co. Ltd.; BDAA was extracted with ethanol, and purified by repeated recrystallization from ethanol-water mixture.

Methanol was refluxed with calcium oxide and distilled. Ethanol was also refluxed with calcium oxide and distilled fractionally. Extra pure-grade butanol was used without further purification. Purified acrylonitrile was kindly supplied by Mr. K. Nakatsuka of this Institute.

Acetone was refluxed with potassium permanganate and, after being dried over potassium carbonate, distilled fractionally. Extra pure grade pyridine was dried over sodium hydroxide and distilled before use.

## 3. Experimental Results

Zanker[18] has systematized the electronic spectra of nitrogen heterocycles in analogy to those of aromatic hydrocarbons, using Platt's perimeter model[19]. According to his classification, the longest wave length bands of these molecules are due to the transition to $^1L_a$. Because of the light absorption by solvent, the observation of shorter wave length bands is not possible. Therefore only the effect of concentration on the $^1L_a$ band was studied. Some examples of the concentration dependence of absorption spectra are shown in Figs. 1–5.

It is clear from these spectral changes that there are only two molecular species

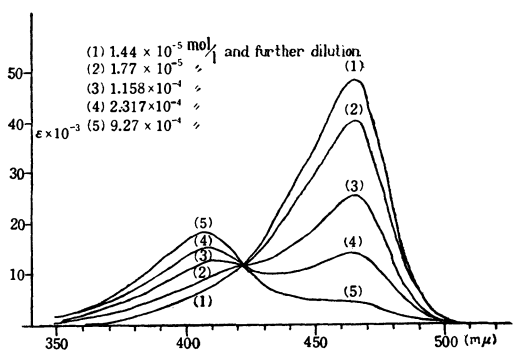



Fig. 1. DAA in pyridine

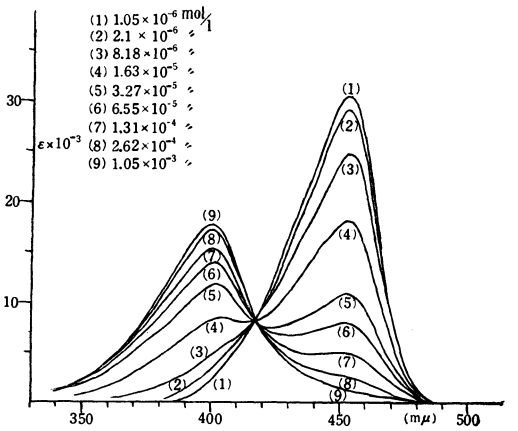



Fig. 2. DAA in acrylonitrile

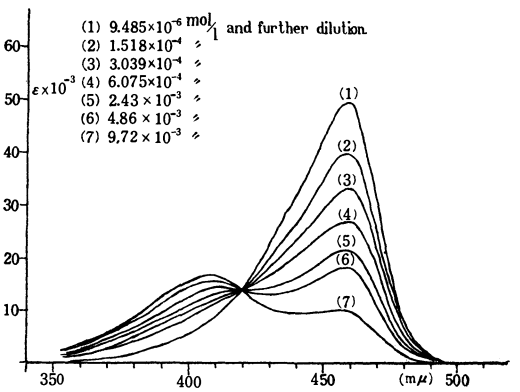



Fig. 3. DAA in ethanol

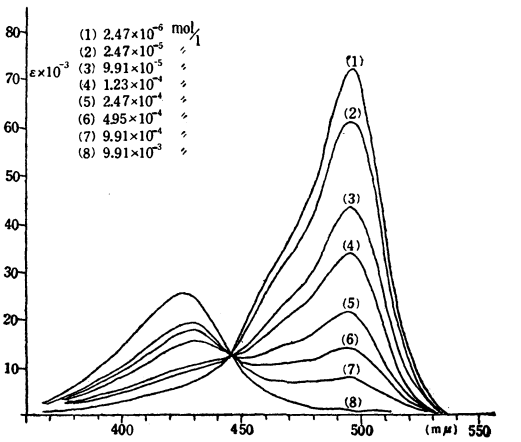



Fig. 4. BDAA in acrylonitrile

15) N. Mataga, Y. Kaifu and M. Koizumi, This Bulletin, **29**, 373 (1956).
16) K. L. Moudgill, *J. Chem. Soc.*, **1922**, 1508.
17) J. Biehringer, *J. Praktisch. Chem.*, **57**, 217 (1896).
18) V. Zanker, *Z. Physikal. Chem., N. F.*, **2**, 52 (1954).
19) J. R. Platt, *J. Chem. Phys.*, **17**, 484 (1949); H. B Klevens and J. R. Platt, ibid., **17**, 470 (1949).

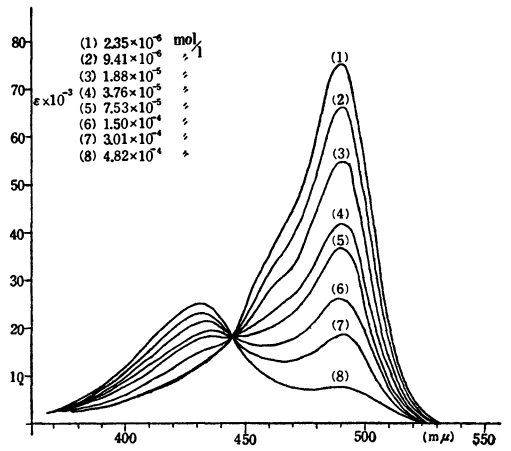



Fig. 5. BDAA in ethanol

in equilibrium, i. e., monomer and polymer. For the equilibrium between monomer and polymer of $n$th degree, the equilibrium constant of association is expressed as:

$$K=\frac{x}{nc_0^{n-1}(1-x)^n} \tag{1}$$

where, $(1-x)$ is the fraction of monomer against the total quantity as monomer and $c_0$ is the analytical concentration of dye.

The apparent extinction coefficient $\varepsilon$ at a definite wave length can be expressed by means of $\varepsilon^n$ and $\varepsilon^m$ which are the extinction coefficients of polymer and monomer, respectively, at the same wave length.

$$\varepsilon=\frac{1}{n}x\varepsilon^n+(1-x)\varepsilon^m \tag{2}$$

From (1) and (2), we obtain the following equations.

$$\log c_0\left(1-\frac{\varepsilon}{\varepsilon^m}\right)=\log(C\cdot K)+n\log c_0\left(\frac{\varepsilon}{\varepsilon^m}-\frac{\varepsilon^n}{n\varepsilon^m}\right) \tag{3}$$

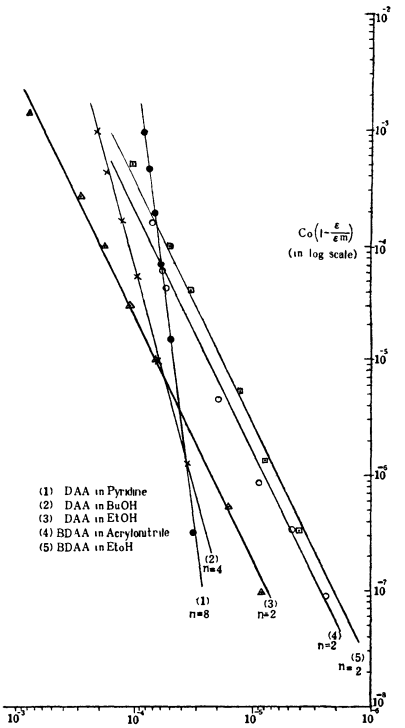
$$C=\frac{1}{n^n\left(n-\frac{\varepsilon^n}{\varepsilon^m}\right)^{n-1}}$$

In the first approximation, we can neglect $\frac{\varepsilon^n}{n\varepsilon^m}$ as compared with $\frac{\varepsilon}{\varepsilon^m}$

$$\log c_0\left(1-\frac{\varepsilon}{\varepsilon^m}\right)=\log(C\cdot K)+n\log c_0\left(\frac{\varepsilon}{\varepsilon^m}\right) \tag{4}$$

By means of (4), we can determine $n$, then using (3) we can evaluate $K$.

Some examples of $\log c_0\left(1-\frac{\varepsilon}{\varepsilon^m}\right)\sim\log c_0\left(\frac{\varepsilon}{\varepsilon^m}-\frac{\varepsilon^n}{n\varepsilon^m}\right)$ plots are shown in Fig. 6. It is clear from these plots, that there is only monomer-polymer equilibrium, in contradistinction to the case of acridine orange in aqueous solution[6] where polymerization proceeds stepwise, i. e., monomer-dimer equilibrium exists in relatively dilute solution, and dimer-tetramer equilibrium is established in a highly concentrated solution.




$C_0\left(\frac{\varepsilon}{\varepsilon^m}-\frac{\varepsilon^n}{n\varepsilon^m}\right)$ (in log scale)

Fig. 6. $\log C_0\left(1-\frac{\varepsilon}{\varepsilon^m}\right)\sim\log C_0\left(\frac{\varepsilon}{\varepsilon^m}-\frac{\varepsilon}{n\varepsilon^m}\right)$ relations for DAA and BDAA.

## 4. Discussion

The results obtained are collected in Tables I and II for DAA and BDAA, respectively.

As Levshin has pointed out[13], the dimerization or polymerization tendency has no correlation with refractive index, dielectric constant, or dipole moment of the solvent used.

TABLE I
COLLECTED DATA FOR DAA

| Solvent | Pyridine | Acrylonitrile | Acetone | BuOH | EtOH | $H_2O$ |
|---|---|---|---|---|---|---|
| Equilibrium constant | $1.2\times10^{43}$ | $1.6\times10^{19}$ | $3.0\times10^{20}$ | $9.2\times10^{15}$ | $1.7\times10^{4}$ | $2.7\times10^{3}$ |
| $K_n^T$ | $K_8^{293}$ | $K_4^{293}$ | $K_4^{293}$ | $K_4^{293}$ | $K_2^{293}$ | $K_2^{293}$ |
| $\delta\tilde{\nu}$ (kcal.) | 8.7 | 8.4 | 8.1 | 8.2 | 7.8 | 1.9 |
| $\bar{f}_{\text{monomer}}$ a) | 0.74 | 0.37 | 0.44 | 0.66 | 0.66 | 0.33 |
| $f^{v.}_{\text{monomer}}$ a) | 0.36 | 0.21 | 0.27 | 0.38 | 0.40 | 0.21 |

a) $\bar{f}_{\text{monomer}}=\dfrac{n}{N}\dfrac{c^2m}{\pi e^2}10^3\int_0^\infty \varepsilon(\tilde{\nu})\,d\tilde{\nu}=4.32\times10^{-9}\,n\int_0^\infty \varepsilon(\tilde{\nu})\,d\tilde{\nu}$

$n$: Refractive index of solvent

$\int_0^\infty \varepsilon(\tilde{\nu})\,d\tilde{\nu}$: Integrated absorption for monomeric band

$f^{v.}_{\text{monomer}}=\left(\dfrac{3}{n^2+2}\right)^2 f_{\text{monomer}}$

$\bar{f}$ and $f^{v\cdot}$ are the oscillator strengths in solution and in vapor state, respectively. N. Q. Chako, *J. Chem. Phys.*, **2**, 644 (1934).

TABLE II
COLLECTED DATA FOR BDAA

| Solvent | Acrylonitrile | Acetone | BuOH | EtOH | MeOH |
|---|---|---|---|---|---|
| Equilibrium constant | $1.2+10^5$ | $3.2\times10^6$ | $1.3\times10^5$ | $1.9\times10^5$ | $4.1\times10^4$ |
| $K_n^T$ | $K_2^{293}$ | $K_2^{295}$ | $K_2^{294}$ | $K_2^{294}$ | $K_2^{301}$ |
| $\delta\tilde{\nu}$ (kcal.) | 9.4 | 8.4 | 8.1 | 8.1 | 7.6 |
| $\bar{f}_{\text{monomer}}$ | 0.93 | 0.68 | 0.83 | 1.01 | 0.84 |
| $f^{v.}_{\text{monomer}}$ | 0.54 | 0.42 | 0.47 | 0.61 | 0.53 |

TABLE III

| Dye ions | Thionine a) | Methylene blue a) | Rhodamine 6G b) | Pyronine G c) | Acridine orange d) | Trypaflavine e) | DAA |
|---|---|---|---|---|---|---|---|
| $\delta\tilde{\nu}$ (kcal.) | 3.4 | 4.1 | 3.4 | 3.3 | 3.4 | 2.0 | 1.9 |
| $\bar{f}_{\text{monomer}}$ | 0.77 | 0.60 | 0.72 | 0.13 | 0.82 | 0.73 | 0.33 |
| $f^{v.}_{\text{monomer}}$ | 0.48 | 0.38 | 0.45 | 0.08 | 0.52 | 0.46 | 0.21 |

a) Ref. 1), b) Ref. 4), c) Ref. 5), d) Ref. 6),
e) Measured by the present writer.

An analogous idea to that of Förster[10], but in wave mechanical form was developed by Mori[20] for the case of dimerization, assuming a simplified model of dipole-dipole interaction similar to that used in the calculation of dispersion force, and the treatment was extended to the case of polymer[21].

This has its analogy in the theory of Davydov splitting or exciton migration.

According to it, the blue shift due to dimerization is expressed as follows:

$$hc\Delta\sigma=\frac{1}{R^3}(\vec{\mu}^1_{eg}\,|\,\vec{\mu}^2_{eg}) \qquad (5)$$

where $\Delta\sigma$ is the wave number shift, $R$ is the distance between dye molecules which are in plane-parallel configuration, and $\vec{\mu}_{eg}$ is the transition dipole of monomeric dye molecule, and in this configuration, $(\vec{\mu}^1_{eg}\,|\,\vec{\mu}^2_{eg})>0$. If the association is due to the dispersion force between monomers and the spectral shift is determined by equation (5), then the association tendency and the magnitude of spectral shift should depend on the oscillator strength of monomeric band.

As seen from Table III, however, the spectral shifts of various dye ions in aqueous solution have no correlation with their oscillator strengths of monomeric bands.

20) Y. Mori, Symposium on π-electronic state, *Chem. Soc. Japan*, 1955.
21) N. Mataga, Unpublished.

Moreover, it is clear from Tables I and II, that the polymerization tendencies of DAA and BDAA in organic solvents have no dependence on their oscillator strengths of monomeric bands. For the association to occur it might be necessary that the oscillator strength of monomeric band be fairy large, because, for example, the integrated absorption $\int_0^\infty \varepsilon(\tilde{\nu})d\tilde{\nu}$ of $^1L_a$ band of acridine is nearly $10^7$ in its order of magnitude, whereas it is approximately $10^8$ for DAA and BDAA, and we could not observe any concentration dependence of spectra of acridine in various solvents such as used for DAA and BDAA, in the concentration range from $10^{-5}$ to $10^{-3}$ mol./l.

It seems clear, however, that the association is very sensitive to the solvent used, and also it depends remarkably on the slight difference of molecular structures of dye molecules.

By inspection of Tables I and II, we see that the association tendency of DAA is greater than that of BDAA. Further, it is remarkable, that in pyridine, DAA forms octamer, whereas BDAA shows no associating tendency. Hydrogen bonding of solvent molecules with amino groups of DAA, might play some important role in the association.

**Summary**

The effect of concentration on the absorption spectra of DAA and BDAA in various organic solvents was studied in the concentration range from $10^{-6}$ to $10^{-2}$ mol./l. Contrary to Levshin's opinion, DAA forms polymers higher than dimer very easily in some organic solvents, and the association tendency of DAA is greater than that of BDAA.

Further, the association of these molecules is very sensitive to the solvents used. The association tendency and the spectral shift due to dimerization or polymerization have no correlation with the oscillator strengths of monomeric bands of these molecules, and this is true also for the various dye ions in aqueous solution.

The author expresses his thanks to Sumitomo Chemical Co. Ltd. for the gift of acridine orange. He is grateful to Prof. M. Koizumi for his fruitful discussion and encouragement throughout the investigation.

*Institute of Polytechnics*
*Osaka City University*
*Kita-ku, Osaka*

# *Separation of α-Glycerophosphate from Its β-Isomer by Column Chromatography**

By Chieko URAKAMI, Hiroko MURAHASHI and Yoshiko KAKUTANI

(Received January 8, 1957)

It has been reported previously from our laboratory that sodium glycerophosphates can be resolved completely into the α and β-isomers on the alumina impregnated paper with methanol-ammonia (60 : 5) as a developing solvent and that no hydrolysis or migration of the phosphoryl group seems to occur, as far as the sensitivity of the test employed is concerned[1]. The purpose of application of this method to column chromatography is twofold: firstly, to obtain pure samples of both isomers on a milligram level for biochemical interest and secondly, to give an absolute experimental evidence to support our previous results on hydrolysis and migration of the phosphoryl group. For the latter, the samples obtained by chromatography were analyzed according to Burmaster's method[2], which affords the determination of the inorganic phosphate, α and β-glycerophosphates in a mixture of the three by spectrophotometrical means on the color developed by the reduction of the phosphomolybdate with stannous chloride.

* Presented at the 10th Annual Meeting of the Chem. Soc., Japan, April, 1956.

1) C. Urakami and Y. Kakutani, This Bulletin, **30**, 21 (1957).

2) C. F. Burmaster, *J. Biol. Chem.*, **164**, 233 (1946).

## Experimental

**Apparatus.**—The chromatographic tube used was of the size 10 mm. in diameter and 150 mm. in length, provided with an inner joint connection with a sealed-in fritted glass disk and a stop-cock.

Spectrophotometric measurements were carried out with Shimazu Model DF-II with a filter No. 634. All measurements were taken within the range of its maximum sensitivity, 0.1-0.3 extinction.

**Samples and Reagents.**—The solutions for analysis of the samples, $\alpha$-1, $\alpha$-2 and $\beta$-3 as indicated in Table I, were prepared so that each ml. contained approximately 20 $\mu$g. of phosphorus. Assay of the solutions was carried out by taking one-half of this quantity.

The solutions of the following reagents were prepared according to the specifications given by Burmaster; anhydrous sodium sulfite (reagent grade of Wako Pure Chemicals Co.), ammonium molybdate (the first grade of Daito Chemical Co.), stannous chloride (special grade of Yashima Chemical Co.), and sodium periodate (Marukawa Chemical Co.).

Bromothymol blue, 0.1% solution, was used for detection of the zone of the glycerophosphoric acids.

**Adsorbent.**—One part by weight of alumina for chromatography (200 mesh, Yashima Chemical Co.) and nine parts by weight of cellulose powder (No. 50 of Toyo-filter paper Co.) were mixed thoroughly with a sufficient quantity of the mixed solvent, methanol-ammonia (60 : 5), and the mixture allowed to mercerate for ten hours. During the last two hours the mixture was stirred vigorously with a magnetic stirrer. About one gram of the slurry was poured, all at once, into the chromatographic tube and after the adsorbent had settled, the column was packed firmly with an additional quantity of the solvent, about 100 ml., by weighting at the top and applying suction at the base of the column to give 24-26 mm. in length.

**Chromatographic Technique.**—When about one ml. of the solvent was remaining over the surface of the column, a suspension of 2 mg. of the sample or the mixed sample containing one mg. each of the isomers in 5 ml. of the solvent mixture was applied and adsorption of the solute was allowed to take place for about one hour, with the stop-cock being left open and without application of suction. When a few mm. of the solvent were remaining over the surface of the column, a furthere amount of the solvent was added. Exposure of the column to air at this point should be strictly avoided, otherwise the adsorption of the solute is so strong that the zone will not move. The rate of flow was maintained at one ml. per min. by applying suction. The percolate was collected in a 100 ml. fraction up to a total volume of 1 l. The presence of the solute, the $\alpha$-glycerophosphate, was found in the fraction collected between 850 and 950 ml. of the percolate. By applying the indicator, we have observed that the glycerophosphate advanced down the column in a clean-cut narrow zone.

**Preparation of Solutions for Analysis.**—A 100 ml. fraction containing the $\alpha$-glycerophosphate was evaporated almost to dryness on a water bath at a low temperature, below 45°C, a small amount of distilled water added to the residue, any insoluble material found removed by filtration, and rinsed several times with fresh water to insure quantitative recovery of the phosphate. The filtrate and washings were combined and made up to 6 ml. in an accurately graduated tube. An aliquot of 3 ml. was used for analysis of $\alpha$-glycerophosphoric acid and 1.5 ml. each for the $\beta$-isomer and inorganic phosphate.

The $\beta$-isomer was recovered in the following manner: First, the zone of the adsorbed $\beta$-isomer was located, after about 1 l. of the percolate had been collected, by passing a solution of a few drops of bromothymol blue indicator in the solvent and by drying the column somewhat with application of vacuum. An excessive drying should be avoided, or the detection of the zone would not be possible. A distinct yellow zone was found within 5 mm. from the surface of the column, the rest being colored blue green. Therefore, after extruding the somewhat wet column from the tube, a section was cut 5 mm. from the upper end of the adsorbent. It was extracted three times with a 5 ml. portion of a weak alkaline solution, pH 8, and any insoluble material removed by centrifugation. The supernant liquid obtained was evaporated to a small volume and made up to 6 ml. with distilled water. An aliquot of 3 ml. was used for analysis of the $\alpha$- and 1.5 ml. each for the $\beta$-isomer and inorganic phosphorus.

## Results and Discussion

By applying 2 mg. of the pure sample of barium $\alpha$-glycerophosphate or sodium $\beta$-glycerophosphate to a column consisting of a mixture of alumina and cellulose (1 : 9) 25 mm. in length and by developing with methanol-ammonia (60 : 5) as a solvent, 85 % of the former was recovered in the 100 ml. fraction collected between 850 and 950 ml. of the percolate and 35 % of the latter in the extract of a section cut 5 mm. from the column surface, as shown in Table II. When a mixture of the sodium salts of the two isomers was applied, 53–56 % of the $\alpha$ and 20–30 % of the $\beta$ were recovered. No inorganic phosphorus was detected in all these samples recovered and also no $\beta$-glycerophosphoric acid was found to be present in the fraction containing the $\alpha$-isomer or the $\alpha$ in the extract containing the $\beta$-isomer, as shown in Table II.

We have also succeeded in separating the isomers by applying a 5 mg. load on the column of the same length but its retention volume was found to be less

TABLE I

ANALYSES OF GLYCEROPHOSPHATE SAMPLES

| Sample No. | Diln. factor | Extinction | | | P, μg. found | | Total P μg. found** | | Total P, μg. calcd. | Purity % | |
|---|---|---|---|---|---|---|---|---|---|---|---|
| | | Total | α | β* | α | β | α | β | | α | β |
| α—1 | 2 | 0.108 | 0.108 | 0.000 | 4.1 | 0.0 | 8.2 | 0.0 | 10 | 82 | 00 |
| | 〃 | 0.203 | 0.203 | 0.000 | 4.3 | 0.0 | 8.6 | 0.0 | 10 | 86 | 00 |
| | 〃 | 0.202 | 0.202 | 0.000 | 4.25 | 0.0 | 8.5 | 0.0 | 10 | 85 | 00 |
| α—2 | 〃 | 0.226 | 0.169 | 0.057 | 3.75 | 1.3 | 7.5 | 2.6 | 10 | 75 | 26 |
| | 〃 | 0.213 | 0.169 | 0.044 | 3.75 | 1.0 | 7.5 | 2.0 | 10 | 75 | 20 |
| | 〃 | 0.223 | 0.174 | 0.049 | 3.85 | 1.1 | 7.7 | 2.2 | 10 | 77 | 22 |
| β—3 | 〃 | 0.230 | 0.000 | 0.230 | 0.0 | 4.8 | 0.0 | 9.6 | 10 | 00 | 96 |
| | 〃 | 0.230 | 0.000 | 0.230 | 0.0 | 4.8 | 0.0 | 9.6 | 10 | 00 | 96 |
| | 〃 | 0.228 | 0.000 | 0.228 | 0.0 | 4.75 | 0.0 | 9.5 | 10 | 00 | 95 |

* Obtained by subtracting extinction of α from that of total.

** Obtained by multiplying P, μg. found directly from the extinction by the dilution factor, 2.

In all these samples no inorganic phosphorous was detected.

α-1, Barium α-glycerophosphate[3]; α-2, Disodium α-glycerophosphate. $5.5H_2O$ (Wako Pure Chemicals Co.); β-3, Disodium β-glycerophosphate. $5.5H_2O$ (Yashima Chemical Co.).

TABLE II

ANALYSES OF GLYCEROPHOSPHATES OBTAINED BY CHROMATOGRAPHIC SEPARATION

| Sample No. | Diln. factor | Extinction | | | P found μg. | | Total P found, μg. | | Total P in Sample, μg. | | Recovery % | |
|---|---|---|---|---|---|---|---|---|---|---|---|---|
| | | Total | α | β | α | β | α | β | α | β | α | β |
| α—1 | 14 | 0.234 | 0.234 | 0.000 | 10.35 | 0.00 | 144.9 | 00.0 | 171.7 | 00.0 | 84 | 00 |
| β—3 | 6 | 0.216 | 0.000 | 0.216 | 0.00 | 9.6 | 0.0 | 57.6 | 0.0 | 163.0 | | 35 |
| Mixt. of | | | | | | | | | | | | |
| α—2 | 8 | 0.103 | 0.103 | 0.000 | 4.2 | 0.0 | 33.6 | 0.0 | 63.4 | 20.3 | 53 | |
| β—2 | 4 | 0.124 | 0.000 | 0.124 | 0.0 | 5.09 | 0.0 | 20.4 | | 102.0 | | 20 |
| Mixt. of | | | | | | | | | | | | |
| α—2 | 4 | 0.109 | 0.109 | 0.000 | 8.9 | 0.0 | 35.6 | 0.0 | 63.4 | 20.3 | 56 | |
| β—3 | 4 | 0.188 | 0.000 | 0.188 | 0.0 | 7.6 | 0.0 | 30.5 | | 102.0 | | 30 |

A 2 mg. sample of the sodium salt was used for the individual run; one mg. each was used for the mixed sample. The α-sample was collected in a 100 cc. fraction taken between 850–950 ml. of the percolate: the β-sample was extracted from the adsorbent cut 5 mm. from the surface of the column. No inorganic phosphorus was detected in all these samples.

than 50 ml. and the recovery of the α less than 20%, the major portion being found in the first 100 ml. This indicates that a 5 mg. load is close to the saturation point for the capacity of the amount of the adsorbent employed. We have also attempted to increase the capacity of the column by increasing the column length but encountered some difficulty in obtaining a uniformly packed column, due to difference in density of the two components of the adsorbent used.

These results show, therefore, that a mixture of a milligram each of the sodium salts of α and β-glycerophosphoric acids can be resolved completely on the column chromatographic system of this nature and provide a conclusive evidence for our previous observation that no hydrolysis or migration of the phosphoryl group occurs during the course of the chromatography.

*Faculty of Science of Living*
*Osaka City University, Osaka*

3) C. Urakami and Y. Kakutani, *Repts. Sci. Living, Osaka City Univ., Series D*, **No. 1**, 3 (1953).

# *Primary Process in Photochemical Decomposition of $AH_N$-Type Molecules*

By Jiro HIGUCHI

(Received December 6, 1956)

## 1. Introduction

Photochemical reactions have in general been discussed in the classification of the primary process and the succeeding secondary process. The latter process is concerned in the reaction of free radicals, and is essentially a problem of chemical kinetics. On the other hand, the detailed study of the primary process requires the knowledge concerned with the electronic structures of the molecules and the free radicals produced. Above all, the full comprehension of the nature of each orbital is necessary to discuss the properties of these electronic states, and particularly of the potential energy surfaces, which are closely connected with the primary process. Unfortunately, such a knowledge has scarcely ever been obtained from experiments, except for a few simple molecules, due to the difficulty of the spectroscopic analysis for polyatomic molecules and for free radicals. Accordingly, the theoretical investigation is of great significance for such problems. Another theoretically important known fact is the adiabatic correlation rule, which has been developed by Wigner and Witmer[1], by Mulliken[2] and by Shuler[3]. The rule must be taken into consideration for the polyatomic system, although occasionally it is not so effective for intermediates of low symmetry, because there are few restrictions on the correlations of the states between reactants and products. Other theoretical considerations may be of minor importance for qualitative discussions. However, it goes without saying that the experimental facts play the conclusive part of the present discussion.

In the present paper, the primary process of photochemical decomposition in the first absorption region will be taken up for $AH_N$-type (A denotes atoms like C, N, O and others; and $N=4,3,2$) molecules from the viewpoint of the molecular orbital theory. The experimental investigations of these reactions have long been done by many authors[4], and the electronic spectra of these molecules have also been observed[4-6]. On the other hand, the theoretical investigations of some of these electronic structures have recently been done with fruitful results by several authors[7-11]. Accordingly, these reactions may be said to be one of the most suitable examples in studying the photochemical primary process.

## 2. General Consideration

**Electronic Structure.**—Before discussing the primary process, it is convenient to explain briefly the common electronic properties of the $AH_N$ molecules and the free $AH_{N-1}$ radicals. For the ground state, the electron configuration of an $AH_N$ molecule can in general be given by $K(\phi_1)^2(\phi_2)^2(\phi_3)^2(\phi_4)^2$, in which $K$ is the inner-shell of the molecule, nearly the same as that of the A atom, and $\phi_i$'s are the molecular orbitals mainly built from the valence-shell electrons of the constituent atoms in the LCAO-MO approximation. The sufficies of these MOs are chosen in the order of increasing energy. The lowest vacant orbital is $\phi_5$ with the total symmetry $A_1$ and the structure of the first excited state is $K(\phi_1)^2(\phi_2)^2(\phi_3)^2(\phi_4)(\phi_5)$. The $\phi_5$ orbital has been considered to be of a considerable $(n+1)s$ orbital character of the A atom, $n$ being the principal quantum number of the valence-shell electron.

1) E. Wigner and E. E. Witmer. *Z. Physik*, **51**, 859 (1928).
2) R. S. Mulliken, *Phys. Rev.*, **43**, 279 (1933).
3) K. E. Shuler, *J. Chem. Phys.*, **21**, 624 (1953).
4) For example, see G. K. Rollefson and M. Burton, "Photochemistry and the Mechanism of Chemical Reactions," Prentice-Hall, Inc. New York (1939), and W. A. Noyes, Jr. and P. A. Leighton, "The Photochemistry of Gases," Reinhold Publishing Corporation, New York (1941).
5) H. Sponer, "Molekülspektren und ihre Anwendung auf chemische Probleme," Verlag Julius Springer, Berlin (1935), I. Tabellen, p. 97.
6) H. Sponer and E. Teller, *Revs. Modern Phys.*, **13**, 75 (1941).
7) A. D. Walsh, *J. Chem. Soc.*, **1953**, 2260.
8) A. D. Walsh, ibid., 2296.
9) R. S. Mulliken, *J. Am. Chem. Soc.*, **77**, 887 (1955).
10) F O. Ellison and H. Shull, *J. Chem. Phys.*, **23**, 2348 (1955).
11) J. Higuchi, *J. Chem. Phys.*, **24**, 535 (1956).

TABLE I

MOLECULAR ORBITALS OF $AH_N$ MOLECULES AND THEIR BONDING POWER

| | | | | | |
|---|---|---|---|---|---|
| | | $T_d$ ($AH_4$) | | | $D_{3h}$ ($AH_3$) |
| $\phi_1$ | $1a_1$ | Strong-bonding | $\phi_1$ | $1a_1'$ | Strong-bonding |
| $\phi_2$, $\phi_3$, $\phi_4$ | $1t_2$ | Strong-bonding | $\phi_2$, $\phi_3$ | $1e'$ | Strong-bonding |
| | | | $\phi_4$ | $1a_2''$ | Non-bonding |
| $\phi_5$ | $2a_1$ | Non-bonding | $\phi_5$ | $2a_1'$ | Non-bonding |
| $\phi_r$ | $ra_1$ | Rather strong-antibonding | $\phi_r$ | $ra_1'$ | Rather strong-antibonding |
| | | $C_{3v}$ ($AH_3$) | | | $C_{2v}$ ($AH_2$) |
| $\phi_1$ | $1a_1$ | Strong-bonding | $\phi_1$ | $1a_1$ | Strong-bonding |
| $\phi_2$, $\phi_3$ | $1e$ | Strong-bonding | $\phi_2$ | $1b_2$ | Strong-bonding |
| | | | $\phi_3$ | $2a_1$ | Weak-bonding |
| $\phi_4$ | $2a_1$ | Weak-bonding | $\phi_4$ | $1b_1$ | Non-bonding |
| $\phi_5$ | $3a_1$ | Non-bonding | $\phi_5$ | $3a_1$ | Non-bonding |
| $\phi_r$ | $ra_1$ | Strong-antibonding | $\phi_r$ | $ra_1$ | Strong-antibonding |
| | | $D_{\infty h}$ ($AH_2$) | | | $C_{\infty v}$ (AH) |
| $\phi_1$ | $1\sigma_g$ | Strong-bonding | $\phi_1$ | $1\sigma$ | Strong-bonding |
| $\phi_2$ | $1\sigma_u$ | Strong-bonding | $\phi_2$ | $2\sigma$ | Weak-bonding |
| $\phi_3$, $\phi_4$ | $1\pi_u$ | Non-bonding | $\phi_3$, $\phi_4$ | $1\pi$ | Non-bonding |
| $\phi_5$ | $2\sigma_g$ | Non-bonding | $\phi_5$ | $3\sigma$ | Non-bonding |
| $\phi_r$ | $r\sigma_g$ | Rather strong-antibonding | $\phi_r$ | $r\sigma$ | Strong-antibonding |

On the other hand, the LCAO-MO calculation of the $AH_N$ molecule gives the strong-antibonding $a_1$ orbital $\phi_r$, which may correspond to the $\phi_5$ orbital, by taking the *ns* and *np* of the A atom and the 1s's of the H atoms into account. As discussed by Mulliken[12], however, the strong-antibonding orbital $\phi_r$ is not so good an approximation of the $\phi_5$ orbital as compared with the $(n+1)s$ orbital of the A atom. It is noted that one higher strong-antibonding orbital is also expected instead of the above antibonding orbital, even if the $(n+1)s$ orbital is taken into account, because of the fairly large overlap between the $(n+1)s$ orbital of the A atom and the 1*s* orbital of the H atom. In that case, a more satisfactory approximation of the $\phi_5$ orbital will be obtained with the better repulsive orbital $\phi_r$. In the present paper, however, the $\phi_i$ ($i \leqq 4$) and $\phi_r$ orbitals will be considered as linear combinations of *ns*, *np* orbitals of A atom and 1*s*'s of H atoms, and the properties on the $\phi_5$ orbital will be discussed in taking the interaction with the $\phi_r$ orbital into account[13]. In such an argument, the repulsive state with configuration $K(\phi_1)^2(\phi_2)^2(\phi_3)^2(\phi_4)(\phi_r)$ may be a rather high location near the equilibrium structure. In a similar way, the electronic structures of the ground and the first excited state of a free $AH_{N-1}$ radical can be represented by respectively $K'(\phi_1')^2(\phi_2')^2(\phi_3')^2(\phi_4')$ and $K'(\phi_1')^2(\phi_2')^2(\phi_3')(\phi_4')^2$ or $K'(\phi_1')^2(\phi_2')^2(\phi_3')^2(\phi_5')$, in which the dashes are given in order to distinguish that it is a free radical.

Actually, the stable structures of the $AH_4$, $AH_3$ and $AH_2$ molecules discussed here are respectively tetrahedral, pyramidal and isosceles triangle, the symmetry of which are $T_d$, $C_{3v}$ and $C_{2v}$ respectively. By taking the order of the increasing energy, the MOs $\phi_i$'s for each symmetry and the common bonding power near the equilibrium form can be listed as given in Table I. As can be seen from there, the bonding power of the $\phi_5$ orbital of $AH_N$ molecules can generally be shown as non-bonding and the difference is not great. But that of the $\phi_4$ is somewhat different one to the other, and decreases with decreasing number of hydrogen atoms. This is one reason why the nature of the first excited state cannot be determined simply.

**Potential Energy Surface.**—Considering the property of $\phi_5$ orbital, the first excited state $K(\phi_1)^2(\phi_2)^2(\phi_3)^2(\phi_4)(\phi_5)$ has rather less bonding property than the ground state, since the bonding power of the $\phi_4$ orbital is at least not as weak as

12) R. S. Mulliken, *J. Chem. Phys.*, **3**, 517 (1935).

13) The forms of the $\phi_i$ ($i \leqq 4$) orbitals are scarcely changed at all by including the $(n+1)s$ orbital of A atom and the higher orbitals (J. Higuchi, unpublished work).

compared with the $\phi_5$ orbital. In the approximation of single configuration, therefore, this state is not repulsive and may reach the excited doublet state $K'(\phi_1')^2(\phi_2')^2(\phi_3')(\phi_4')(\phi_5')$, or $K'(\phi_1)^2(\phi_2')^2(\phi_3')^2(\phi_5')$, of the free $AH_{N-1}$ radical and the $1s\ ^2S$ state of the H atom by increasing one of the AH internuclear distances. The above doublet state of the $AH_{N-1}$ radical, however, is in a rather high location as compared with the ground state $K(\phi_1')^2(\phi_2')^2(\phi_3')^2(\phi_4')$, since the $\phi_5'$ orbital has also a considerable $(n+1)s$ orbital character. In such a single configurational approximation, therefore, the fact that the first excited state of the $AH_N$ molecule leads to decomposition cannot be explained.

The energy of the repulsive orbital $\phi_r$ is, however, rapidly lowered with increasing one of the AH internuclear distances because of the decrease of the overlap integrals, and so the $\phi_r$ orbital becomes the fifth orbital on the energetic ground. In the present paper, however, for convenience the sufficies $i$'s are not changed at larger AH internuclear distances. Accordingly, some repulsive state $K(\phi_1)^2(\phi_2)^2(\phi_3)^2(\phi_4)(\phi_r)$ exists, which may reach the ground state $K'(\phi_1')^2(\phi_2')^2(\phi_3')^2(\phi_4')$, or the first excited state $K'(\phi_1')^2(\phi_2')^2(\phi_3')(\phi_4')^2$, of the $AH_{N-1}$ radical. However, this repulsive state has the same symmetry as that of the first excited state $K(\phi_1)^2(\phi_2)^2(\phi_3)^2(\phi_4)(\phi_5)$, and the former potential energy surface crosses that of the latter one near a somewhat larger AH internuclear distance in the single configurational approximation. In view of these facts, it is possible that the $AH_N$ molecule decomposes to give the free $AH_{N-1}$ radical and the H atom beyond the crossing curve between the above-mentioned potential energy surfaces.

**Primary Process.**—In general, no electronic spectrum of the $AH_N$ molecule exists up to comparatively short wave-lengths, occasionaly until the Schumann region[4-6]. The first absorption spectrum of the $AH_N$ molecule occurs as a continuum or as diffuse bands and is presumed to occur because of the transition from the $\phi_4$ orbital to the $\phi_5$ orbital. By absorbing the light of this region, the molecules are generally excited to the above-mentioned first excited singlet state, which is the lowest member of the Rydberg series of the molecule. The excited molecule dissociates to the ground, or the first excited, state of $AH_{N-1}$ radical and the ground state $1s\ ^2S$ of H atom due to some of the AH stretching vibrations, beyond the crossing point between the first and the repulsive excited states. In this case, the shape of the potential energy surface of the first excited state differs from one molecule to the other, and so the condition of the photochemical decomposition is not always quite the same. However, it may be noted that the following rules are valuable to discuss the types of photochemical decomposition in the first absorption region.

(1) The first absorption spectrum is continuous, if the highest occupied orbital $\phi_4$ is considerably strong-bonding.

(2) In the case of the highest occupied orbital $\phi_4$ being not so strong-bonding, the type of the first absorption spectrum is determind from the antibonding property of the first excited state due to the interaction between the lowest vacant orbital $\phi_5$ and the strong-antibonding orbital $\phi_r$. In this case, (2a) the spectrum may be diffuse, if the $\phi_r$ orbital is not so strong-antibonding; (2b) the spectrum may be continuous, if the $\phi_r$ orbital is considerably strong-antibonding.

The reason for this can be explained as follows: in the case of (1) the AH equilibrium bond distance in the first excited state is fairly lengthened, and so the crossing may take place near the equilibrium internuclear distance of this state. Since the first and the repulsive state have the same symmetry, the actual potential energy curve to this decomposing direction may not have a maximum point. Accordingly, the decomposition in the first excited state takes place very easily by some of the AH stretching vibrations and the first absorption spectrum occurs as a continuum. In the case of (2a), however, the equilibrium internuclear distance in the first excited state is not so large that the crossing may take place at a somewhat larger AH internuclear distance than the equilibrium one. Accordingly, the actual potential energy curve to this decomposing direction may have a maximum point and the first absorption spectrum occurs as diffuse.

These rules, however, are also not useful to determine the state of the decomposed free $AH_{N-1}$ radical, when its many states are lower than the first excited state of the $AH_N$ molecule. In this case, certainly the adiabatic correlation rule occasionally plays some important role, but generally is not useful because of the lowering of symmetry for the intermediate. For the determination of the states of

products, therefore, it may be safe to investigate each molecule, at least to make a distinction of the molecule according to its symmetry, as will be discussed in the following chapters.

### 3. Primary Process in Photochemical Decomposition of $AH_4$ Molecules

The photolysis of the $AH_4$ molecule, such as $CH_4$, $SiH_4$, $GeH_4$, etc., has been investigated by several authors, but the works except for the $CH_4$ molecule are very few[4]. The first absorption of the molecules occurs as continuum below about 1600 Å, but no bands have been observed[4,5]. The primary process in photochemical decomposition by this absorption has been considered as follows:

$$AH_4 + h\nu \longrightarrow AH_3 + H,$$

although the other process has also been considered in shorter wave-lengths[4].

**Electronic Structure.**—The $AH_4$ molecule has tetrahedral symmetry $T_d$ and the electron configuration of the ground state $^1A_1$ is $K(1a_1)^2(1t_2)^6$, and that of the first excited states $^{1,3}T_2$ is $K(1a_1)^2(1t_2)^5(2a_1)$. The $1a_1$ and the $1t_2$ orbitals are strong-bonding, while the $2a_1$ orbital is nearly non-bonding and has $(n+1)s$-like property of the A atom. Accordingly, the equilibrium bond distance of the $^{1,3}T_2$ states may be lengthened as compared with that of the ground state $^1A_1$, because of the excitation from the strong-bonding orbital $1t_2$ to the nearly non-bonding orbital $2a_1$. As discussed in the previous chapter, however, the molecule has a higher anti-bonding orbital $ra_1$, and so the repulsive $^3T_2$ state $K(1a_1)^2(1t_2)^5(ra_1)$ is also expected.

On the other hand, the $AH_3$ radical may be low-pyramidal with symmetry $C_{3v}$ (or may occasionally be planar with symmetry $D_{3h}$). The electron configuration of the ground state $^2A_1$ (or $^2A_2''$) is $K(1a_1)^2(1e)^4(2a_1)$ (or $K(1a_1')^2(1e')^4(1a_2'')$), and the $1a_1$ (or $1a_1'$) and the $1e$ (or $1e'$) orbitals are strong-bonding, while the $2a_1$ (or $1a_2''$) orbital is weak-bonding (or non-bonding). The excited states of the $AH_3$ radical also exist, for example, $^2E$ $K(1a_1)^2(1e)^3(2a_1)^2$ (or $^2E'$ $K(1a_1')^2(1e')^3(1a_2'')^2$) and $^2A_1$ $K(1a_1)^2(1e)^4(3a_1)$ (or $^2A_1'$ $K(1a_1')^2(1e')^4(2a_1')$), but they are rather high as compared with the first excited state of the corresponding $AH_4$ molecules as shown in Fig. 1. Accordingly, they are not responsible for this reaction and need not be discussed in detail.

TABLE II
CORRELATION BETWEEN REPRESENTATIONS OF GROUPS $T_d-C_{3v}-D_{3h}$

| $T_d$ | $C_{3v}$ | $D_{3h}$ |
|---|---|---|
| $A_1$ | $A_1$ | $A_1'$, $A_2''$ |
| $A_2$ | $A_2$ | $A_2'$, $A_1''$ |
| $E$ | $E$ | $E'$, $E''$ |
| $T_1$ | $A_2$, $E$ | $A_2'$, $A_1''$, $E'$, $E''$ |
| $T_2$ | $A_1$, $E$ | $A_1'$, $A_2''$, $E'$, $E''$ |

**Potential Energy Surface.**—The correlation between representations of groups $T_d-C_{3v}-D_{3h}$ is given in Table II. By increasing one of the AH internuclear distances, the first excited states $^{1,3}T_2$ of the $AH_4$ molecule with symmetry $T_d$ reaches the $^2A_1$ state $K(1a_1)^2(1e)^4(3a_1)$ (or $^2A_1'$ $K(1a_1')^2(1e')^4(2a_1')$) of the $AH_3$ radical with symmetry $C_{3v}$ (or $D_{3h}$) and the $^2S$ state of the H atom, passing through the $^{1,3}A_1$ state $K(1a_1)^2(1e)^4(2a_1)(3a_1)$ of the intermediate $AH_4$ with symmety $C_{3v}$, in the approximation of single configuration. But the repulsive excited state $^3T_2$ of the $AH_4$ molecule reaches the ground state $^2A_1$ (or $^2A_2''$) of the $AH_3$ radical and the $^2S$ state of the H atom[14]. The first and the repulsive excited states of the $AH_4$ molecule, however, have the same symmetry $T_2$ and so their interaction is not so weak. Furthermore, the equilibrium bond distance of the first excited state is fairly

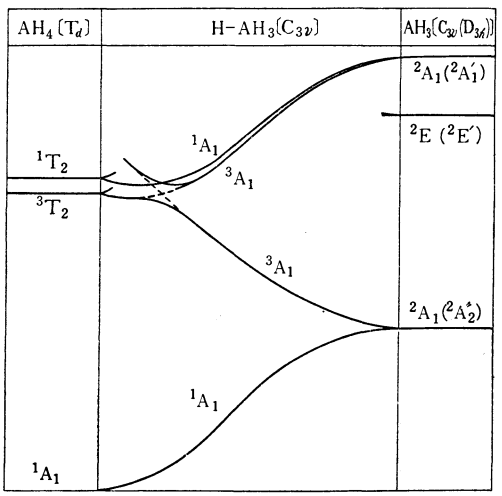



Fig. 1. Potential energy curves for photochemical decomposition of $AH_4$ molecule. The relative energy scale of the right and the left part was chosen to fit the $CH_4$ molecule and the $CH_3$ radical.

14) The instability of the $^{1,3}T_2$ states can also be supposed from the Jahn-Teller effect.

large, and the variation of energy by changing the AH internuclear distance may be small in this region. Accordingly, the actual potential energy curve of the first excited state $^3T_2$ to the $^2A_1$ state of the $AH_3$ radical may not have a maximum point as shown in Fig. 1[15]. As the result of this, the first absorption spectrum of the $AH_4$ molecule occurs as a continuum (case (1) of the rule in Chapter 2).

**Primary Process.**—In the $AH_4$ molecule, the influence of vibration is not important because the first excited states $^{1,3}T_2$ electronically correlate to the $^2A_1$ (or $^2A_2''$) state of the $AH_3$ radical and the $^2S$ state of the H atom[16]. It may, therefore, be most convenient to explain the mechanism from the electronic and energetic viewpoints. That is, the $AH_4$ molecule absorbing the wave-length of about 1600 Å is excited to the first $^1T_2$ state[17]. The excited molecule dissociates to the $^2A_1$ (or $^2A_2''$) state of the free $AH_3$ radical and the 1s $^2S$ state of the H atom due to the singlet-triplet transition and to some of the AH stretching vibration, passing through the intermediate with symmetry $C_{3v}$ as shown in Fig. 1. In the meanwhile, the bond angle of $\angle HAH'$ may gradually be increased by the action of the AH bending vibration. The electronic property of the highest singly occupied orbital also changes from $(n+1)s$-like nearly non-bonding to strong-antibonding beyond the above-mentioned crossing point. The process passing through the other structures of the intermediates can also be considered. That is, it may be probable that one of the H atoms is slightly displaced from the trigonal axis in the excited state. Certainly, the process passing through this intermediate is not contradictory to the adiabatic correlation rule, and the potential energy curve and the electronic property in such a possible process are generally similar to those in the above-mentioned case. Accordingly, such processes are not discussed here in detail.

## 4. Primary Process in Photochemical Decomposition of $AH_3$ Molecules[18]

The photolysis of the $NH_3$ molecule has long been investigated by many authors, and that of the $PH_3$, $AsH_3$ and $SbH_3$ molecules has also been studied by several authors[4]. The first absorption spectrum of the $NH_3$ and the $PH_3$ molecules begins at about 2300 Å as diffuse bands, but that of the $AsH_3$ and the $SbH_3$ molecules appears to be continuous below about 2400 Å[4,5]. The primary process in the photochemical decomposition by this absorption has generally been considered to be predissociation:

$$AH_3 + h\nu \longrightarrow AH_3^* \longrightarrow AH_2 + H.$$

**Electronic Structure.**—The $AH_3$ molecule has pyramidal symmetry $C_{3v}$ and the electron configuration of the ground state $^1A_1$ (or $^1A_1'$ for the symmetry $D_{3h}$) is $K(1a_1)^2(1e)^4(2a_1)^2$ (or $K(1a_1')^2(1e')^4(1a_2'')^2$). The $1a_1$ (or $1a_1'$) and the $1e$ (or $1e'$) orbitals are strong-bonding, while the $2a_1$ (or $1a_2''$) orbital is weak-bonding (or non-bonding) and its bonding power increases with decreasing bond angle of $\angle HAH'$. In the ground state of the $PH_3$, $AsH_3$ and $SbH_3$ molecules, the equilibrium bond angles decrease owing to the increase of the *nd*-orbital character of A atom[9,19], and the bonding power of the $2a_1$ orbital increases. As the results of this, the potential barrier of inversion increases with increasing the molecular weight of the $AH_3$ molecule[20].

The lowest vacant orbital $3a_1$ (or $2a_1'$) is nearly non-bonding and has $(n+1)s$-like property of the A atom, while the $ra_1$ (or $ra_1'$) is strong-antibonding and the antibonding power increases with decreasing the bond angle $\angle HAH'$[21]. In the first excited states $^{1,3}A_1$ $K(1a_1)^2(1e)^4(2a_1)(3a_1)$ (or $^{1,3}A_2''$ $K(1a_1')^2(1e')^4(1a_2'')(2a_1')$), the equilibrium AH bond distance is somewhat lengthened and the equilibrium bond

15) In this case, the first excited singlet state $^1T_2$ does not reach the ground state $^2A_1$ of $AH_3$ from the atomic orbital consideration in the infinite internuclear separation between the $AH_3$ and the H.

16) The $AH_4$ molecule with symmetry $T_d$ has nine fundamental vibrations: one with species $a_1$, one doubly degenerate frequencies with species $e$ and two triply degenerate ones with species $t_2$. For the electronically excited $^{1,3}T_2$ states, therefore, the corresponding vibronic states to one of the AH stretching vibrations are $^{1,3}T_2 \times A_1 = {}^{ev}1,^3T_2$ and $^{1,3}T_2 \times T_2 = {}^{ev}1,^3A_1 + {}^{ev}1,^3E + {}^{ev}1,^3T_1 + {}^{ev}1,^3T_2$ (In the present paper, only the species symbols for the vibronic states are prefixed by a left superscript $^{ev}$ to avoid confusion to the electronic states.) Accordingly, all the species come into question and therefore the vibronic correlation rule is not especially important to determine this primary process.

17) The possibility of the excitation to the first triplet state also exists, but may be fairly small as compared with that to the first excited singlet state.

18) Preliminary report on the $NH_3$ molecule was given in *Proc. Japan Acad.*, **32**, 276 (1956).

19) This decrease is also due to the considerably larger sizes of atoms, P, As and Sb, than the N atom (See, Ref. 9).

20) A. Gilchrist and L. E. Sutton, *J. Phys. Chem.*, **56**, 319 (1952).

21) This is due to the increase of $s$-$p$ hybridization in the $\phi_r$ orbital, the coefficients of which have opposite signs to those of the 1s's of H atoms. (See, Ref. (11)).

angle $\angle HAH'$ increases as compared with that of the ground state, since the one electron excitation from the weak-bonding $2a_1$ orbital decreases the power of bonding and also of pyramidalization. In fact, the first excited state of the $NH_3$ molecule is planar[11] and that of the other molecules are also expected to have a fairly large equilibrium bond angle.

On the other hand, the $AH_2$ radical is an isosceles triangle with symmetry $C_{2v}$. The ground state is the $^2B_1$ $K(1a_1)^2(1b_2)^2(2a_1)^2(1b_1)$ and the first excited state is the $^2A_1$ $K(1a_1)^2(1b_2)^2(2a_1)(1b_1)^2$. The energy separation between these states is not so large, for example, less than 2 eV for the $NH_2$ radical[22]. The $1a_1$ and the $1b_2$ orbitals are strong-bonding and the $2a_1$ orbital is weak-bonding but the $1b_1$ orbital is non-bonding, The higher excited states of the radical also exist, but they are high location as compared with the first excited states $^{1,3}A_1$ (or $^{1,3}A_2''$) of the corresponding $AH_3$ molecule. Accordingly, they are not responsible for this reaction and need not be discussed in detail.

**Potential Energy Surface.**—To discuss the potential energy surfaces, it is convenient to make a distinction between the process passing through the planar intermediate and the others, since the most stable structure of the first excited states are planar and the correlation between the planar molecules is characteristic. Accordingly, the correlations between representations of groups in Table III are separately given for $C_{3v}-D_{3h}-C_{2v}$ and $C_{3v}-C_s-C_{2v}$.

TABLE III

CORRELATION BETWEEN REPRESENTATIONS OF GROUPS $C_{3v}-D_{3h}-C_{2v}$ and $C_{3v}-C_s-C_{2v}$

| $C_{3v}$ | $D_{3h}$ | $C_{2v}$ |
|---|---|---|
| $A_1$ | $A_1'$ | $A_1$ |
| | $A_2''$ | $B_1$ |
| $A_2$ | $A_2'$ | $B_2$ |
| | $A_1''$ | $A_2$ |
| $E$ | $E'$ | $A_1$, $B_2$ |
| | $E''$ | $A_2$, $B_1$ |

| $C_{3v}$ | $C_s$ | $C_{2v}$ |
|---|---|---|
| $A_1$ | $A'$ | $A_1$, $B_1$ |
| $A_2$ | $A''$ | $A_2$, $B_2$ |
| $E$ | $A'$, $A''$ | $A_1$, $A_2$, $B_1$, $B_2$ |

For the planar $AH_3$ molecule with symmetry $D_{3h}$, the first excited states decompose to $AH_2+H$ passing through the intermediate $AH_3$ molecule with symmetry $C_{2v}$.

22) G. Herzberg and D. A. Ramsay, *Discussions Fraday Soc.*, No. **14**, 11 (1952).

As can be seen from Table III, the ground state $^1A_1'$ $K(1a_1')^2(1e')^4(1a_2'')^2$, the first excited states $^{1,3}A_2''$ $K(1a_1')^2(1e')^4(1a_2'')(2a_1')$ and the repulsive excited states $^{1,3}A_2''$ $K(1a_1'')^2(1e')^4(1a_2'')(ra_1')$ of $AH_3$ with symmetry $D_{3h}$ correspond to respectively the ground states $^1A_1$ $K(1a_1)^2(1b_2)^2(2a_1)^2(1b_1)^2$, the first excited states $^{1,3}B_1$ $K(1a_1)^2(1b_2)^2(2a_1)^2(1b_1)(3a_1)$ and the repulsive excited states $^{1,3}B_1$ $K(1a_1)^2(1b_2)^2(2a_1)^2(1b_1)(ra_1)$ of $AH_3$ with symmetry $C_{2v}$. As shown in Fig. 2, on stretching one AH bond distance, the ground state $^1A_1'$ becomes gradually unstable, and dissociates to the $^2A_1$ state of the $AH_2$ radical. Similarly, the first excited states $^{1,3}A_2''$ are also elevated and reach the second $^2B_1$ (or $^4B_1$) state $K(1a_1)^2(1b_2)^2(2a_1)(1b_1)(3a_1)$ of the $AH_2$ radical. On the other hand, the repulsive excited states $^{1,3}A_2''$ are continuously lowered with increasing one AH bond distance and dissociate to the ground state $^2B_1$. It is, however, noted that in the first excited states the difference of the equilibrium bond distance from the ground state is not much great, since the $\phi_4$ orbital is the non-bonding $1a_2''$ and the antibonding property due to the interaction between the $2a_1'$ and the $ra_1'$ orbital is rather weak because of no *p*-character in these orbitals. This makes possible the large deviation between the internuclear separation of the first excited state in equilibrium and that of the corresponding crossing point, and also makes possible the fairly large energy difference between these points. Accordingly, a maximum point exists in each actual potential energy curve of the first $^{1,3}B_1$ states as shown in Fig. 2, and the first absorption spectrum appears as diffuse in this process (case (2a) of the rule in Chapter 2, for example,

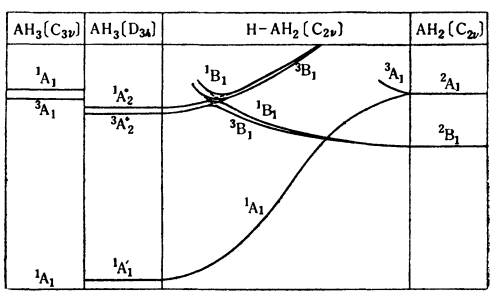



Fig. 2. Potential energy curves for photochemical decomposition of $AH_3$ molecule passing through the planar intermediate. The relative energy scale of the right and the left part was chosen to fit the $NH_3$ molecule and the $NH_2$ radical.

$NH_3$). At a fairly larger AH internuclear distance, the crossing between the $^{1,3}B_1$ states and the $^1A_1$ state also takes place, but their interactions need not be taken into consideration so greatly, because their symmetries are not the same.

For pyramidal $AH_3$ molecule with symmetry $C_{3v}$, the molecule dissociates to $AH_2$+H passing through the intermediate $AH_3$ with symmetry $C_s$. Analogous relations also exist in this case as shown in Fig. 3. The first excited states $^{1,3}A_1$, however, may be somewhat stabilized with the small increase of one AH bond distance, since the $2a_1$ orbital is weak-bonding. Furthermore, the bonding power of the $2a_1$ orbital and the antibonding power of the r$a_1$ orbital increases with decreasing the bond angle of $\angle$HAH', so that the stabilization by increasing one AH bond distance also increases[11]. Accordingly, the potential barrier in the crossing point of the first excited state $^3A'$ may be lowered and finally the potential energy curve may not have a maximum point at a bond angle smaller than a certain value. This tendency becomes strong with increasing molecular weight of the $AH_3$ molecule due to the stabilization of the $2a_1$ orbital under the influence of the *nd*-orbital character of the A atom in the molecule, and the first absorption spectrum appears as continuous (case (2b) of the rule in Chapter 2). Another difference from the planar molecule is the non-crossing between the ground state $^1A'$, which correlates with the $^1A_1$ state of $C_{2v}$, and the first excited singlet state $^1A'$, which correlates with the $^1B_1$ state of $C_{2v}$. Their symmetries are the same except for the symmetry $C_{2v}$, so

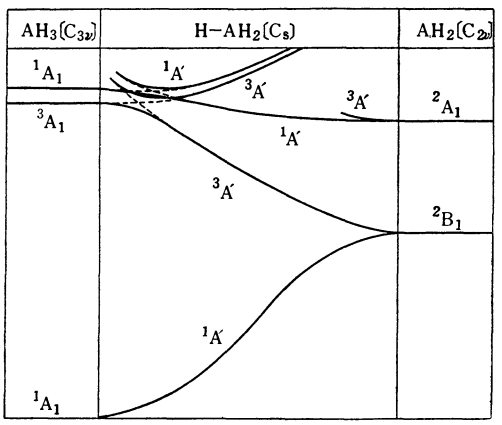



Fig. 3. Potential energy curves for photochemical decompostion of $AH_3$ molecule passing through the non-planar intermediate.

that their interaction increases with decreasing the bond angle $\angle$HAH'. Consequently, the potential energy curve of the first excited singlet state $^1A_1$ of $AH_3$ reaches the $^2A_1$ state of $AH_2$. The first excited triplet state $^3A_1$, however, reaches the $^2B_1$ state of $AH_2$ passing through the intermediate with symmetry $C_s$, because of the difference in the spin multiplicities.

**Primary Process.**—In the primary process in photochemical decomposition, the $AH_3$ molecule in the ground state $^1A_1$ (or $^1A_1'$) absorbs the wave-length of about 2200 Å, and is excited to the first excited singlet state $^1A_1$. In the first excited states $^{1,3}A_1$, the planar molecule with symmetry $D_3$ is in general most stable, so that the probability of taking this shape is very large for light $AH_3$ molecules.

Few of the excited molecules return to the ground state and most of them decompose to the free $AH_2$ radical and the H atom due to some of the AH stretching vibrations. The $AH_3$ molecule with symmetry $C_{3v}$ (or $D_{3h}$) has four fundamental vibrations: two with species $a_1$ and two doubly degenerate frequencies with species $e$ (or one with species $a_1'$, one with species $a_2''$ and two doubly degenerate frequencies with species $e'$). Accordingly, the mode of the AH stretching vibration has species $a_1$ (or $a_1'$) or preferably $e$ (or $e'$), and so the corresponding vibronic state, which arises from the excitation of such a vibrational mode, is $^1A_1\times A_1={}^{ev1}A_1$ (or $^1A_2''\times A_1'={}^{ev1}A_2''$) or preferably $^1A_1\times A_1={}^{ev1}E$ (or $^1A_2''\times E'={}^{ev1}E''$).

When the planar molecule with symmetry $D_{3h}$ has been realized, this electronically excited state correlates with the $^{ev1}B_1$ state or the $^{ev1}B_1$ and $^{ev1}A_2$ states of the intermediate $AH_3$ molecule with symmetry $C_{2v}$. On the other hand, the free $AH_2$ radical with symmetry $C_{2v}$ has three fundamental vibrations: two with species $a_1$ and one with species $b_2$. Therefore, the corresponding vibronic states are $^2B_1\times A_1={}^{ev2}B_1$ and $^2B_1\times B_2={}^{ev2}A_2$ to the electronic $^2B_1$ state and are $^2A_1\times A_1={}^{ev2}A_1$ and $^2A_1\times B_2={}^{ev2}B_2$ to the electronic $^2A_1$ state. Besides this, the electronic state of the H atom in question is 1s $^2S$. This means that in this case the restriction between these electronic states is not changed by the influence of vibration. For the excited $AH_3$ molecule with symmetry $D_{3h}$, therefore, the decomposition takes place passing through the potential energy curve shown in Fig. 2, and the products are the $^2B_1$ state of $AH_2$ and the $^2$S state of H, but

are not the $^2A_1$ state of $AH_2$ and the $^2S$ state of H. In the meanwhile, the bond angle of $\angle HAH'$ may be changed by the action of the AH bending vibration from 120° to a somewhat small angle, for example 103° for $NH_2$[23]. On the other hand, the possibility of the process passing through the triplet state may generally be very small because of the inhibition by the spin correlation rule.

Especially for the heavy $AH_3$ molecules, the planar first excited state is not necessarily realized and the decomposition may take place passing through the intermediate with symmetry $C_s$, because the equilibrium bond angle of these molecules is nearly 90° in the ground state. In this case, the influence of vibration may not be so important, since both the first excited states $^{1,3}A_1$ of $AH_3$ are possible to correlate electronically to both the $^2B_1$ and $^2A_1$ states of $AH_2$[24]. Consequently, in the case of the decomposition passing through the intermediate with symmetry $C_s$, the state of product $AH_2$ cannot be determined from the adiabatic correlation rule. It can, however, be said that the probability of the product being $^2B_1$ state may decrease with decreasing the bond angle of the $AH_3$ molecule. It is also noted that the process passing through the singlet-triplet transition mainly reaches the $^2B_1$ state of $AH_2$ from the viewpoint of potential energy surface and is of importance for heavy $AH_3$ molecules because of the rather strong spin-orbit coupling.

## 5. Primary Process in Photochemical Decomposition of $AH_2$ Molecules

The photolysis of the $AH_2$ molecules, such as $H_2O$, $H_2S$, etc., has been investigated by several authors. The first absorption of $H_2O$ and $H_2S$ occurs as a continuum below 1780 Å and 2600Å, respectively[4,5]. The primary process of photochemical decomposition in this absorption has been considered as follows:

$$AH_2 + h\nu \longrightarrow AH + H.$$

**Electronic Structure.**—The $AH_2$ molecule is an isosceles triangle with symmetry $C_{2v}$. The electron configuration of the ground state $^1A_1$ is $K(1a_1)^2(1b_2)^2(2a_1)^2(1b_1)^2$, and that of the first excited states $^{1,3}B_1$ is $K(1a_1)^2(1b_2)^2(2a_1)^2(1b_1)(3a_1)$. The $1a_1$ and $1b_2$ orbitals are strong-bonding, while the $2a_1$ is weak-bonding and its bonding power increases with decreasing bond angle of $\angle HAH'$. The highest occupied orbital $1b_1$ is non-bonding and the lowest vacant orbital $3a_1$ is also nearly non-bonding and has $(n+1)s$-like property of the A atom. The vacant orbital $ra_1$ is strong-antibonding and its antibonding power increases with decreasing bond angle of $\angle HAH'$[21] and also with increasing ordinal number of Periodic Group of the central atom A, because of the increase of $p$-character[25].

On the other hand, the AH radical is a linear form with symmetry $C_{\infty v}$. The electron configuration of the ground state $^2\Pi$ is $K(1\sigma)^2(2\sigma)^2(1\pi)^3$, in which the $1\sigma$ orbital is strong-bonding and the $2\sigma$ orbital is weak-bonding while the $1\pi$ orbital is non-bonding. The excited states of the AH radical also exist, for example $^2\Sigma^+$ $K(1\sigma)^2(2\sigma)(1\pi)^4$ and $^2\Sigma^+$, $^{2,4}\Sigma^-$ and $^2\Delta$ $K(1\sigma)^2(2\sigma)^2(1\pi)^2(3\sigma)$, but they are rather high as compared with the first excited states of the corresponding $AH_2$ molecule. Accordingly, they are not responsible for this reaction and are not discussed here in detail.

TABLE IV

CORRELATIONS BETWEEN REPRESENTATIONS OF GROUPS $C_{2v}-C_s-C_{\infty v}$ AND $C_{2v}-D_{\infty h}-C_{\infty v}$

| $C_{2v}$ | $C_s$ | $C_{\infty v}$ |
|---|---|---|
| $A_1$, $B_2$ | $A'$ | $\Sigma^+$, $\Pi$, $\Delta$,····· |
| $A_2$, $B_1$ | $A''$ | $\Sigma^-$, $\Pi$, $\Delta$,····· |

| $C_{2v}$ | $D_{\infty h}$ | $C_{\infty v}$ |
|---|---|---|
| $A_1$ | $\Sigma_g^+$, $\Pi_u$, $\Delta_g$,····· | $\Sigma^+$, $\Pi$, $\Delta$,····· |
| $A_2$ | $\Sigma_u^-$, $\Pi_g$, $\Delta_u$,····· | $\Sigma^-$, $\Pi$, $\Delta$,····· |
| $B_1$ | $\Sigma_g^-$, $\Pi_u$, $\Delta_g$,····· | $\Sigma^-$, $\Pi$, $\Delta$,····· |
| $B_2$ | $\Sigma_u^+$, $\Pi_g$, $\Delta_u$,····· | $\Sigma^+$, $\Pi$, $\Delta$,····· |

**Potential Energy Surface.**—The $AH_2$ molecule with symmetry $C_{2v}$ (or $D_{\infty h}$) dissociates to AH+H passing through the intermediate with symmetry $C_s$ (or $C_{\infty v}$). Then, Table IV gives the correlations between representations of groups $C_{2v}-C_s-C_{\infty v}$ and $C_{2v}-D_{\infty h}-C_{\infty v}$. The ground state $^1A_1$, the first excited states $^{1,3}B_1$ and the repulsive excited states $^{1,3}B_1$ of the $AH_2$ with symmetry $C_{2v}$ correspond to respectively the ground state $^1A'$, the first excited states $^{1,3}A''$ and the repulsive excited

23) D. A. Ramsay, *J. Chem. Phys.*, **25**, 188 (1956).

24) In this case, the $^{ev1,3}A_1$ state, or the $^{ev1,3}E$ states, which correlate with the first excited states $^{1,3}A_1$, correlates with the $^{ev1,3}A'$ states, or the $^{ev1,3}A'$ and $^{ev1,3}A''$ states, of the intermediate $AH_3$ molecule with symmetry $C_s$. Accordingly, all the species come into question and therefore the vibronic correlation rule is not especially important to determine this primary process.

25) This is the result of the increase of the ionization energy difference between the *ns* and the *np* orbital of the A atom.

states $^{1,3}A''$ of the $AH_2$ with symmetry $C_s$. By increasing one of the AH internuclear distances, the first excited states $^{1,3}B_1$ reach the $^{2,4}\Pi$ states $K(1\sigma)^2(2\sigma)(1\pi)^3(3\sigma)$ of the AH radical and the 1s $^2S$ state of the H atom in the approximation of single configuration, while the ground state $^1A_1$ and the repulsive excited states $^{1,3}B_1$ reach the ground state $^2\Pi$ $K(1\sigma)^2(2\sigma)^2(1\pi)^3$ of the AH radical and the 1s $^2S$ state of the H atom. Accordingly, the crossings between the first and the repulsive excited states take place. But the $ra_1$ orbital is very strong-antibonding, so that the antibonding property of the first excited states due to the interaction between the $3a_1$ and the $ra_1$ orbital is not so weak, and the elevation of the potential energy curves of these states to the crossing points may be small. As the result of this, the actual potential energy curves may not have a maximum point as shown in Fig. 4, and the first absorption spectrum of the molecule appears as continuous (case (2b) of the rule in Chapter 2)[26]. It is noted that such an argument is generally valid when the linear first excited states are realized.

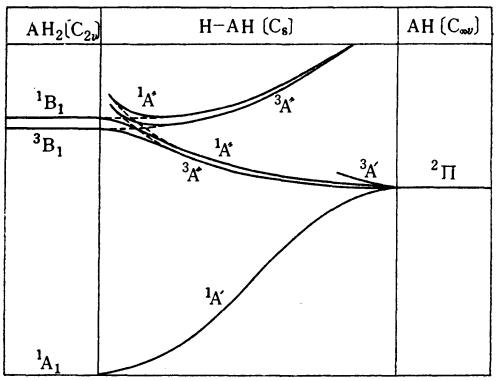



Fig. 4. Potential energy curves for photochemical decomposition of $AH_2$ molecule. The relative energy scale of the right and the left part was chosen to fit the $H_2O$ molecule and the OH radical.

**Primary Process.**—In the $AH_2$ molecule, the influence of vibration is not so important, because all the decomposition to the $^2\Pi$ state of AH are electronically allowed[27]. Accordingly, the primary process in the photochemical decomposition of the $AH_2$ molecule can be explained as follows: the $AH_2$ molecule absorbs a rather short wave-length (for example, about 1800 Å for $H_2O$ and about 2600 Å for $H_2S$) and is excited to the first excited state $^1B_1$[17]. The excited molecule dissociates to the $^2\Pi$ state of the free AH radical and the 1s $^2S$ state of the H atom due to some of the AH stretching vibration, passing through the intermediate with symmetry $C_s$. In this case, the realization of the linear intermediate with symmetry $C_{\infty v}$ may also be possible, since the equilibrium bond angle $\angle HAH'$ in the first excited states may be expected to be fairly large as compared with the ground state. Meanwhile, the electronic property of the highest singly occupied orbital changes from $(n+1)s$-like non-bonding to strong-antibonding beyond the above-mentioned crossing. The process passing through the singlet-triplet transition can also be considered, but the products are the same as in the above case and the possibility may be small from the viewpoint of spin conservation. The conclusion in the present discussion is consistent with the experimental result that the fluorescence of the OH radical has never been observed in the direct photolysis of the $H_2O$ molecule[28].

## 6. Some Remarks

The discussions in the present paper are rather similar to those of Mulliken[29] and of Walsh[7,8]. The purpose of these papers, however, was the explanation of spectra of the $AH_N$ molecules and others and not of the primary process in photochemical decomposition, so that the discussion of potential energy surface were hardly done at all. Moreover, in the former, the available data at that time were rather few so that the discussion are not necessarily complete at present. In the latter, the $(n+1)s$-like orbital $\phi_5$ and the antibonding orbital $\phi_7$ were separately treated, so that the explanations are not only ambiguous but involve some error. Accordingly, the present paper may be said to be the first one relevant to the primary process in photochemical decomposition in the approximation of the molecular orbital.

26) The difference of the potential energy surface between the cases of diffuse and continuous bands may be expected to be small by taking into consideration of the results of the free $CH_3$ and $CD_3$ radcials (G. Herzberg and J. Shoosmith, *Can. J. Phys.*, **34**, 523 (1956)).

27) The $AH_2$ molecule with symmetry $C_{2v}$ has three fundamental vibrations: two with species $a_1$ and one with species $b_2$. For the first and repulsive excited states $^{1,3}B_1$, therefore, the corresponding vibronic states are $^{1,3}B_1\times A_1=^{ev1,3}B_1$ and $^{1,3}B_1\times B_2=^{ev1,3}A_2$. As can be seen from Table IV, they evidently correlate to the $^2\Pi$ state of the AH radical, since the AH has only one stretching vibration $\sigma$.

28) L. O. Brown and N. Miller, *Trans. Faraday Soc.*, **51**, 1623 (1955).

29) R. S. Mulliken, *J. Chem. Phys.*, **3**, 506 (1935).

In the present consideration, the vacant orbitals were treated as nearly non-bonding $(n+1)s$-like and strong-antibonding. In the precise discussion, however, this consideration is not always sufficient to the present purpose, and the mixing of the $(n+1)s$ and higher orbitals, or more strictly the effect of configuration interaction, must explicitly be included. In that case, the crossing between the potential energy curves with the same symmetry and the same spin multiplicity need not be taken into consideration and more satisfactory results will be expected. For example, the potential energy curve of the first excited singlet state of $NH_3$ will be obtained so as to give an explanation of the predissociation without the crossing. However, it may be said that the present consideration based on the approximation of single configuration is also convenient to a schematic understanding of the reactions.

The author wishes to thank Professor S. Shida for his helpful advice and kind discussion. He also wishes to thank Mr. Y. Mori for his valuable suggestion and instructive discussion. This research is supported in part by the grant in aid for the miscellaneous scientific researches of the Ministry of Education.

*Laboratory of Physical Chemistry*
*Tokyo Institute of Technology*
*Ookayama, Meguro-ku, Tokyo*

# *An Electron Diffraction Investigation of the Molecular Structure of 1,4-Dichlorobutyne*. I. Determination of Bond Distances and Angles*

By Kôzo KUCHITSU

(Received January 7, 1957)

## 1. Introduction

Thermodynamic measurements have shown that the C—C≡C—C axis in dimethylacetylene has no appreciable restriction on the internal rotation of the two end groups around this axis[1-3]. One is thus led to an expectation that the hindering barriers for substituted dimethylacetylene molecules would be much lower than that for the corresponding ethane derivatives, because the distance of the groups in the former is much longer than that in the latter. This has been confirmed by the measurement of the dipole moment of 1,4-dichloro-2-butyne, $ClCH_2-C\equiv C-CH_2Cl$[4,5].

This molecule seems to stimulate an electron diffraction investigation, because a heavy chlorine atom with a relatively large scattering power is included in each rotating group, so that the diffraction pattern will give us some information of the potential barrier; in addition, there have been reported very few electron-diffraction studies on the internal rotation of the molecules whose potential barriers are relatively low[6].

It is of particular importance to determine the C—Cl bond distances of this molecule. Pauling and his coworkers[7] found, by using visual electron diffraction data, that the C—Cl bond distance in propargyl chloride, $H-C\equiv C-CH_2Cl$, is 1.82± 0.02Å. This result is very striking, for it is well known that the carbon-chlorine bond distances in most chlorinated hydrocarbon molecules[8] are about 1.77Å ("normal" C—Cl bond distance), or shorter

* Presented at the Eighth Annual Meeting of the Chemical Society of Japan, April, 1955.

1) B. L. Crawford, Jr. and W. W. Rice, *J. Chem. Phys.*, **7**, 437 (1939).

2) G. B. Kistiakowsky and W. W. Rice, ibid., **8**, 618 (1940).

3) D. W. Osborne, C. S. Garner and D. M. Yost, ibid., **8**, 131 (1940).

4) Y. Morino, I. Miyagawa, T. Chiba and T. Shimozawa, This Bulletin, **30**, 222 (1957).

5) Y. Morino, I. Miyagawa and A. Wada, *J. Chem. Phys.*, **20**, 1976 (1952).

6) For example $Si_2Cl_6$, (K. Yamasaki, et al., *J. Chem. Soc. Japan.* **69**, 104 (1948); D. A. Swick and I. L. Karle, *J. Chem. Phys.*, **23**, 1499 (1955)). See also Ref. 24.

7) L. Pauling, W. Gordy and J. H. Saylor, *J. Am. Chem. Soc.*, **64**, 1753 (1942).

8) P. W. Allen and L. E. Sutton, *Acta Cryst.*, **3**, 46 (1950).

(e. g., 1.72Å in $C_2Cl_4$)[9], and we have seldom found molecules whose C—Cl bond distances are longer than 1.80Å[10,11]. If this abnormal increase is based on a special property of $-C\equiv C-CH_2Cl$ group, then it may be of interest to decide whether the C—Cl bond in $ClCH_2-C\equiv C-CH_2Cl$ molecule is longer than the "normal" distance or not. Furthermore, various data on $C\equiv C-C$ system[12-14] show that the C—C bond distance adjacent to a triple bond is about 1.46Å, much shorter than its normal value, and is nearly constant. Therefore, it is also desirable to determine the C—C bond distance accurately and to compare it with the known results.

The subject of this article is the determination of the bond distances and angles of this molecule by the electron diffraction method with a view to apply this structural information as basic data for the study of internal rotation in this molecule, which will be discussed in the following article[15].

## 2. Experimental[16]

The electron diffraction instrument used in this investigation which incorporates a rotating sector was designed by Morino, Kimura and Iwasaki[17]. The apparatus is essentially similar to that constructed by Ino[18].

Diffraction photographs were obtained on Fuji Process Hard Plates with an $r^2$-sector, which was placed 23.7 mm. from the photographic plate and was rotated rapidly during exposure. A camera length was either 11.82 cm. or 27.91 cm., to cover the angular range of 15 to 90, and 5 to 27 in $q$ units, respectively. The accelerating voltage of the electron source was regulated to within 0.1 percent., and the electron beam was focused on the photographic plate to a point about 0.1 mm. in diameter. The wavelength of the electron was determined to be 0.0565Å by measuring the transmission patterns of gold foil.

1, 4-Dichloro-2-butyne was prepared by T. Shimozawa of our laboratory from 2-butyne-1, 4-diol and thionyl chloride[19], the boiling point being 62-64°C at 18 mmHg. The sample was introduced into the electron beam through a fine nozzle by heating to about 40°C[20]. The nozzle was surrounded by a liquid air trap to prevent the sample from diffusing through the camera. A set of two photographs were taken with consecutive exposures of 1/2 and 1 min. which were later used for density-intensity calibration[21]. The patterns were scanned by a Riken B-type recording microphotometer to measure the optical density as a function of the radius[22]. The photographic plates were rotated rapidly about the center of the diffraction pattern while being scanned by the microphotometer.

Optical densities were converted in to relative intensities by Karle's procedure[21]. The scattering intensity curve obtained with a short camera length was corrected to eliminate a small amount of extraneous scattering. A smooth background line was drawn through the intensity curve multiplied by $q$(L=11.82 cm.) or $q^{1/2}$(L=27.91 cm.), and the molecular intensity curve $M(q)$ was obtained by dividing the total intensity $I_T$ by the background intensity $I_B$: $M(q)=(I_T-I_B)/I_B$. Three sets of photographs were taken at the short camera length and two sets at the long camera length and their respective averages were taken. For comparison, a set of photographs of carbon tetrachloride taken in the same condition was analyzed by the same procedure (Section 3 B).

The molecular intensity curves obtained with the long camera length were found to agree with each other to about 0.1 percent. in a relative intensity scale; in addition, it was found possible to connect these curves smoothly with the molecular intensity curves obtained with the short camera length. However, since the molecular intensity for this molecule is small compared with that for carbon tetrachloride (less than 40 percent), considerably larger experimental errors were involved in the photographs taken with the short camera length, particularly in larger scattering angles. Although it is difficult to estimate various sources of experimental errors individually, a rough measure of their total limit may be given by the discrepancy among the three molecular intensity curves shown in Fig. 1.

The corrections for such effects as the beam size, the sample size, and double scattering were not taken into account, because they have little effect on the determination of bond distances,

9) I. L. Karle and J. Karle, *J. Chem. Phys.*, **20**, 63 (1952).

10) H. J. M. Bowen, A. Gilchrist and L. E. Sutton (*Trans. Faraday Soc.*, **51**, 1341 (1955)) reported the C-Cl bond distance in $CH_2=CH-CH_2Cl$ to be $1.82_5\pm0.025$Å.

11) P. W. Allen and L. E. Sutton (*Trans. Faraday Soc.*, **47**, 236 (1951)) also reported the C-Cl bond distance in $CH_3COCl$ to be 1.82±0.02Å. Note, however, that their conclusion was based on the data extended to a rather small scattering angle, and by our recent reinvestigation, it was found to be 1.77±0.02Å. (Y. Morino, et al., *J. Chem. Soc. Japan*, **75**, 647 (1954)).

12) See for example S. H. Bauer and P. Andersen, *Ann. Rev. Phys. Chem.*, **4**, 233 (1953).

13) G. Herzberg and B. P. Stoicheff, *Nature*, **175**, 79 (1955).

14) Recent X-ray study on solid dimethylacethylene $H_3C-C\equiv C-CH_3$ has given the following result: $C\equiv C=1.21_1$Å and $C-C=1.45_7$Å. (E. Pignataro and B. Post, *Acta Cryst.*, **8**, 672 (1955)).

15) K. Kuchitsu, This Bulletin, **30**, 399 (1957).

16) Y. Morino and K. Kuchitsu, *J. Chem. Phys.*, (to be published).

17) Y. Morino, M. Kimura and M. Iwasaki, The Sixth Annual Meeting of the Chemical Society of Japan, April 1953.

18) T. Ino, *J. Phys. Soc. Japan*, **8**, 92 (1953).

19) A. W. Johnson, *J. Chem. Soc.*, **1946**, 1009.

20) The shape of this nozzle is similar to that described by M. Kimura and M. Aoki, This Bulletin, **26**, 429 (1953),

21) J. Karle and I. L. Karle, *J. Chem. Phys.*, **18**, 957, 963 (1950).

22) The microphotometric procedure was carried out by using an apparatus at Nagoya University, collaborated by Mr. H. Morimoto and Mr. S. Shibata.

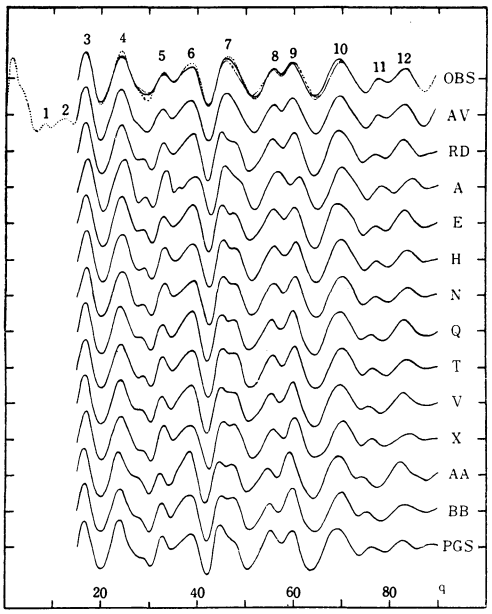



Fig. 1. Observed and calculated molecular scattering intensity curves $qM(q)$ for 1,4-dichlorobutyne.
OBS: three observed intensity curves obtained from independent experiments; AV: the averaged intensity curve, supplemented by a reasonable theoretical intensity curve in the inner region (the dotted curve). The other curves are calculated on the basis of the models indicated in the parameter chart (Fig. 5) (except the models RD and PGS, whose parameters are given in the text).

although they are quite important in the precise investigation of the mean square amplitudes[21,23].

## 3. Analysis

**A. Procedure.**—The modified radial distribution (RD) curves[24] were calculated from the molecular intensity curve according to the equation[25]

$$f(r)=\sum_{q=1}^{90} qM(q)\exp(-aq^2)\sin(\pi qr/10), \quad (1)$$

where $M(q)$ is the molecular scattering intensity, the value of $a$ (0.000284) is chosen to make the integrand of Eq. (1) converge rapidly, and $q=(40/\lambda)\sin(\theta/2)$, where $\theta$ is the angle of scattering and $\lambda$ is the wavelength of the electron beam.

The theoretical intensity curves were calculated using the equation[25,26]

$$qM_c(q)=\sum_{i>j}(c_{ij}/r_{ij})\exp(-b_{ij}q^2)\times\sin(\pi qr_{ij}/10), \quad (2)$$

where $r_{ij}$ denotes the interatomic distance between the $i$-th and the $j$-th atoms, $b_{ij}$ its temperature factor, and

$$c_{ij}=2Z_iZ_j/\{\sum_i Z_i(Z_i+1)\}, \quad (3)$$

except in the analysis of the small angle region[15], where

$$c_{ij}=2(Z_i-f_i)(Z_j-f_j)/\{\sum_i(Z_i-f_i)^2+S_i\}, \quad (4)$$

was used[27]; $Z_i$ is the atomic number (for hydrogen, an effective value 1.25 was used in place of unity), and $f_i$ and $S_i$ are the elastic and inelastic atomic scattering factors, respectively[28]. These summations were performed by use of punched cards and a Remington Rand Type-285 Model-2 tabulating machine[29,25].

**B. Carbon Tetrachloride.**—The photographs of carbon tetrachloride were analyzed in the first place, because this molecule has been frequently used as a reference molecule for the determination of atomic distances. A theoretical intensity curve was computed based on the assumption that the C—Cl distance was 1.766Å, and that the mean amplitudes[30] of the C—Cl and the Cl—Cl distance were 0.054 Å and 0.069 Å, respectively[31]. A comparison of this curve with the observed molecular intensity curve shows a good agreement as illustrated in Fig. 2. The average $q_{\text{calcd.}}/q_{\text{obs.}}$ ratio for twenty-one maxima and minima is $1.000\pm0.002$, and the average fluctuation in the $I_{\text{obs.}}/I_{\text{calcd.}}$ ratio for these maxima and minima is 5.8 percent.

The C—Cl distance obtained from this analysis, $1.76_6\pm0.01$Å, coincides with the

23) R. B. Harvey, F. A. Keidel and S. H. Bauer, *J. Appl. Phys.*, **21**, 860 (1950).
24) Y. Morino and E. Hirota, *J. Chem. Phys.*, (to be published).
25) P. A. Shaffer, Jr., V. Schomaker and L. Pauling, *J. Chem. Phys.*, **14**, 648, 659 (1946).
26) M. E. Jones and V. Schomaker, *J. Chem. Phys.*, **19**, 511 (1951).
27) The use of Eq. (3) instead of Eq. (4) causes only a small decrease (about 11 percent at $q$=17, 4 percent at $q$=20, and less than 3 percent at $q$>25) in the peak intensity of a theoretical intensity curve.
28) The $f_i$ and $S_i$ values used here were taken from the table in the following textbook: A. H. Compton and S. K. Allison, "X-Rays in Theory and Experiment", 2nd. Ed., D. Van Nostrand Co., New York, (1936) p. 780. These $f_i$ values are essentially the same as the data published recently; for example, H. Viervoll and O. Ögrim, *Acta Cryst.*, **2**, 277 (1949).
29) Y. Morino and K. Kuchitsu *X-Rays*, **8**, 37 (1954).
30) For simplicity, the term "root mean-square amplitude" will be hereafter referred to as "mean amplitude".
31) Y. Morino et al., *J. Chem. Phys.*, **21**, 1927 (1953).

TABLE I

THE RESULT OF THE ANALYSIS OF THE RADIAL DISTRIBUTION CURVE[a)]

| | | $C_1-Cl$ | $C_2—Cl$ | $C_3-Cl$ | $C_4-Cl$ | $Cl-H$ | $Cl-C_2$ | $Cl-C_3$ |
|---|---|---|---|---|---|---|---|---|
| Distance | obs. | $1.79_5$ | 2.69 | $3.71_5$ | $5.08_5$ | 2.38 | $1.47_7$ | 2.69 |
| | calcd.[b)] | — | 2.69 | 3.71 | 5.07 | 2.39 | — | 2.69 |
| Mean Amplitude | obs. | 0.055 | 0.077 | 0.080 | 0.123 | 0.086 | 0.054 | $0.051_a$ |
| | estd.[c)] | 0.054 | 0.073 | 0.080 | 0.090 | 0.114 | 0.047 | 0.051 |
| Peak Area | obs. | 197.9 | 223.3 | 171.2 | 219.7 | 53.8 | 67.8 | 77.6 |
| | calcd. | 204.0 | 204.0 | 204.0 | 204.0 | 85.0 | 72.0 | 72.0 |
| | | $C\equiv C$ | $C_1-C_4$ | $C_1-H$ | $C_2-H$ | $C_3-H$ | $C_4-H$ | $H-H$ |
| Distance | obs. | $1.21_3$ | 4.07 | $1.10_a$ | 2.10 | 3.18 | 4.63 | $1.80_a$ |
| | calcd. | — | 4.17 | — | 2.11 | 3.23 | 4.65 | 1.80 |
| Mean Amplitude | obs. | 0.061 | 0.092 | $0.077_a$ | 0.092 | — | 0.092 | $0.120_a$ |
| | estd. | 0.036 | 0.060 | 0.077 | 0.120 | 0.120 | 0.120 | 0.120 |
| Peak Area | obs. | 39.2 | 63.1 | 28.3 | 34.7 | 17.7 | 42.8 | $3.0_a$ |
| | calcd. | 36.0 | 36.0 | 30.0 | 30.0 | 30.0 | 30.0 | 3.1 |

a) Equilibrium distances and mean amplitudes are in Å unit. The subscript a denotes that the values listed were assumed in this analysis.
b) The calculated equilibrium distances are based on the four directly-bonded distances obtained from this analysis and the C-C-Cl angle of 110.5°.
c) Estimated values (see Ref. 34).

TABLE II

COMPARISON OF EXPERIMENTAL AND THEORETICAL INTENSITY CURVES[a)]

| Peak | | Peak Position | | | Peak Height | | |
|---|---|---|---|---|---|---|---|
| Max. | Min. | $q_o$ | $q_c$ | $q_c/q_o$ | $I_o$ | $I_c$ | $I_o/I_c$ |
| | 1 | 6.7 | 6.7 | 1.000 | −0.696 | −0.829 | 0.840 |
| 1 | | 8.3 | 8.3 | 1.000 | −0.440 | −0.524 | 0.840 |
| | 2 | 10.0 | 10.0 | 1.000 | −0.687 | −0.860 | 0.799 |
| 2 | | 12.4 | 12.4 | 1.000 | −0.367 | −0.360 | 1.019 |
| | 3 | 14.0 | 13.9 | 0.993 | −0.495 | −0.671 | 0.738 |
| 3 | | 16.7 | 16.7 | 1.000 | 1.140 | 1.393 | 0.818 |
| | 4 | 19.9 | 20.1 | 1.010 | −1.018 | −1.083 | 0.940 |
| 4 | | 24.2 | 24.2 | 1.000 | 1.038 | 1.262 | 0.823 |
| | 5 | 29.7 | 30.4 | (1.023) | −0.698 | −0.924 | 0.755 |
| 5 | | 33.0 | 33.0 | 1.000 | 0.222 | 0.405 | 0.548 |
| | 6 | 34.8 | 34.8 | 1.000 | −0.140 | −0.162 | 0.864 |
| 6 | | 38.8 | 38.9 | 1.003 | 0.559 | 0.877 | 0.637 |
| | 7 | 42.3 | 42.1 | 0.995 | −1.061 | −1.470 | 0.722 |
| 7 | | 45.9 | 45.2 | (0.985) | 0.780 | 0.952 | 0.819 |
| | 8 | 51.7 | 50.8 | 0.983 | −0.720 | −1.000 | 0.720 |
| 8 | | 55.7 | 55.6 | 0.998 | 0.418 | 0.619 | 0.675 |
| | 9 | 57.4 | 57.7 | 1.005 | 0.150 | 0.143 | (1.049) |
| 9 | | 59.6 | 60.0 | 1.007 | 0.682 | 0.914 | 0.746 |
| | 10 | 64.5 | 64.3 | 0.997 | −0.761 | −1.238 | 0.615 |
| 10 | | 69.6 | 69.4 | 0.997 | 0.761 | 0.986 | 0.772 |
| | 11 | 75.0 | 74.4 | (0.992) | −0.525 | −0.545 | (0.963) |
| 11 | | 77.3 | 76.7 | (0.992) | 0.016 | −0.167 | ( — ) |
| | 12 | 79.1 | 79.0 | (0.999) | −0.160 | −0.360 | (0.444) |
| 12 | | 82.9 | 82.8 | 0.999 | 0.422 | 0.600 | 0.703 |
| | 13 | 86.8 | 86.4 | (0.997) | −0.482 | −0.240 | (2.008) |
| Average[b)] | | | | 1.000 | | | 0.744 |
| Average Deviation | | | | 0.004 | | | 0.078 |

a) The theoretical intensity curve is based on the results of the RD analysis. The observed data listed above the line (min. 1∼3) are the data obtained from the long camera-length photographs, and their ratios are not included in the average.
b) The ratios enclosed in parentheses are not included in the average either (see Ref. 42).

TABLE III

DISTANCES OBTAINED FROM $q_{calcd.}/q_{obs.}$ VALUES[a)]

| Acceptable Models | Average $q_{calcd.}/q_{obs.}$ | Average deviation | ∠C-C-Cl | C−Cl | C−C | C≡C | C−H |
|---|---|---|---|---|---|---|---|
| J | 1.006 | 0.006 | 110° | $1.80_0$ | $1.47_8$ | $1.21_7$ | $1.10_6$ |
| K | 1.003 | 0.005 | 110° | $1.79_6$ | $1.48_5$ | $1.21_4$ | $1.10_5$ |
| O | 1.004 | 0.004 | 111° | $1.79_8$ | $1.46_6$ | $1.21_5$ | $1.10_5$ |
| P | 1.003 | 0.005 | 111° | $1.79_6$ | $1.47_5$ | $1.21_4$ | $1.10_3$ |
| T | 1.004 | 0.005 | 112° | $1.79_6$ | $1.45_5$ | $1.21_4$ | $1.10_4$ |
| U | 1.001 | 0.004 | 112° | $1.79_2$ | $1.46_1$ | $1.21_1$ | $1.10_1$ |
| Most probable value | | | 111° | $1.79_6$ | $1.47_0$ | $1.21_4$ | $1.10_4$ |

a) The distances are in Å unit.

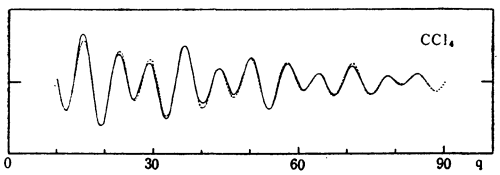



Fig. 2. Molecular intensity curves $qM(q)$ for carbon tetrachloride.
The solid and the dotted curves denote the observed and the calculated intensity curves in a relative scale, respectively.

similar sector-microphotometer data obtained by Karle and Karle[32] (1.770±0.01Å) and by Bartell and Brockway[33] (1.766 ±0.003Å).

**C. Radial Distribution Curve.**—In the calculation of the RD curve by Eq. (1) a molecular scattering curve which was computed from an assumed model (structural parameters and internal rotation) was attached to the experimental curve in the region $q=0\sim15$. A few steps of successive approximations were made in order to get a reasonable background-line which would satisfy Karle's criteria[21] as closely as possible ($q>15$), and also to make the assumed structural parameters self-consistent with the final RD curve.

In the above calculation various possible conditions of internal rotation were assumed; for instance, free rotation, a cosine-type barrier of 1 kcal./mole, and the rigid trans configuration. The RD curves show considerable difference between each other in the region $r>4.5$ Å, as shown in Fig. 3, particularly in the region of the H···Cl and Cl···Cl bond distances (5.4–6.4Å), which are dependent on the internal rotation. Therefore we cannot arrive at any confirmative conclusion about internal rotation from this RD curve alone. In order to investigate the internal rotation, it is necessary to examine the experimental molecular scattering curve in the region $q\lesssim15$.

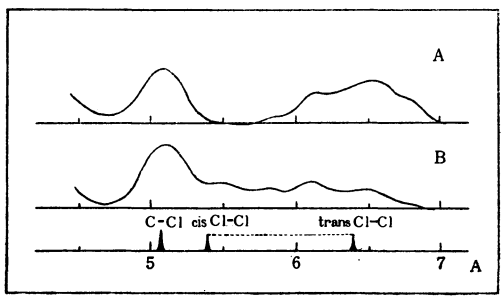



Fig. 3. A portion of a typical radial distribution curve.
(A) Rigid trans model, and (B) free rotation were assumed in the calculation of the theoretical intensity curves ($q=0-15$) which were attached to the same experimental curve. The distances under the curves indicate their approximate positions.

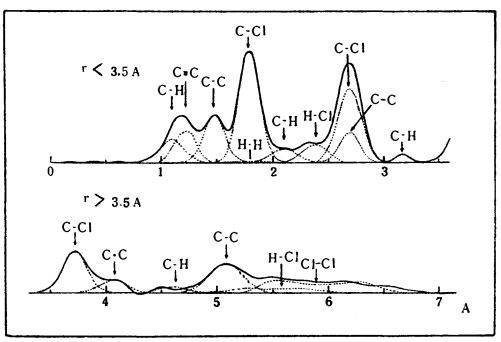



Fig. 4. A typical radial distribution curve for 1,4-dichloro-2-butyne (the solid line). Free internal rotation was assumed. The dotted line indicates the individual peak for each interatomic distance.

On the other hand, these RD curves are found to be quite identical in the region

32) I. L. Karle and J. Karle, *J. Chem. Phys.*, **17**, 1052 (1949).
33) L. S. Bartell and L. O. Brockway, ibid., **23**, 1854 (1955).

$r \lesssim 4.5$ Å; therefore, by analyzing this region, structural parameters including the mean amplitudes of vibration can be determined without any knowledge of internal rotation. The RD curve, based on the assumption of free rotation, was analyzed in detail as follows. (Fig. 4).

The first peak of the RD curve ($r \lesssim 2.0$Å) was decomposed from the right-hand side successively into the contributions from the C—Cl and C—C distances, leaving a composite peak including the C≡C and C—H distances. To obtain the C≡C distance, the equilibrium distance and the mean amplitude of the C—H bond were assumed to be 1.10 Å and 0.077 Å[34], respectively, since these distances are close together, and it is difficult to separate them unambiguously.

In order to decompose the second large peak ($r \sim 2.7$ Å) into those of the $Cl—C_3$ and $C_2—Cl$ distances, the sum of the $C_1—C_2$ and C≡C distances which had been obtained from the analysis of the first peak was used for the $C_1—C_3$ distance, and 0.051 Å was assumed for its mean amplitude[34].

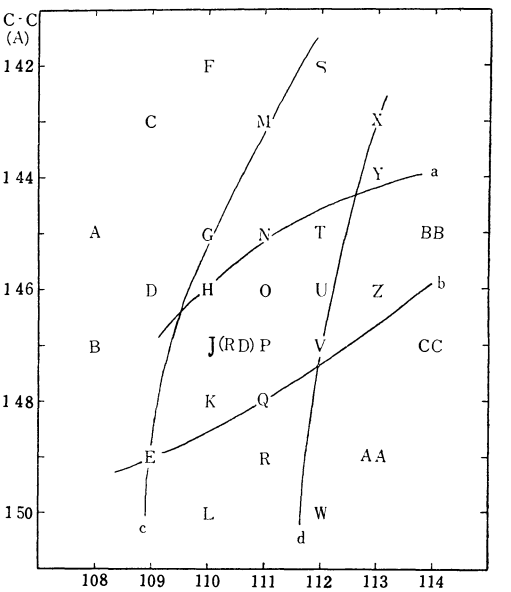
The third peak ($r \sim 3.7$ Å) is due to the $C_3—C_1$ distance overlapped by the contribution of the $C_1—C_4$ distance on the right-hand side, and the fourth peak is due to the $C_4—Cl$ distance. These peaks and other smaller peaks were analyzed in the same manner.

The area under the peak multiplied by the equilibrium distance should be proportional to the corresponding $c_{ij}$ value[21]. The areas obtained from the above analysis are in fairly good agreement with the expected values, yet there is a discrepancy of ±15 percent., which indicates that a small amount of "ghost" included in the RD curve changes the shapes of small peaks (particularly in the region $r > 3.5$Å). The most part of this ghost is probably due to the errors in the observed intensity curve. Hence, in order to estimate the uncertainty, RD curves were calculated and analyzed from various experimental intensity curves which differ within the limits of experimental error. In spite of the slight difference in the areas (about 3% for C—Cl peaks, and 10% for C—C peaks) and in the mean amplitudes (about 10% for larger peaks) among various RD curves, the centers of the larger peaks remain practically constant. The possible range of the positions of these main peaks are as follows:

C≡C: 1.20–1.22 Å; C—C: 1.46–1.48 Å;
C—Cl: 1.79–1.80 Å; Cl—H: 2.36–2.38 Å;
$C_1—C_3$: 2.67–2.70 Å; $C_2$–Cl: 2.68–2.70 Å;
$C_3$—Cl: 3.70–3.74 Å.

A typical result of the RD analysis is given in Table I. The distances listed on the second row are calculated from the model with the directly bonded distances listed in the same table, a C–C–Cl angle of 110.5°, and C–C–H and H–C–H angles of 109.5°. The mean amplitudes listed on the third row are the values directly obtained from the Gaussian-type RD peaks, without the correction for second-order effects[21,22], such as a sample size, double scattering, and the failure of Born approximation[35,36].

**D. Theoretical Intensity Curves.** — A theoretical intensity curve was computed using the values obtained from the RD curve (C—H 1.10 Å, C≡C 1.21 Å, C—C 1.475 Å, C—Cl 1.795 Å, and ∠C–C–Cl




C—Cl=1.79 Å (C≡C=1.21 Å, C—H=1.10 Å, ∠C–C–H=∠H–C–H=109.5)

Fig. 5. Parameter chart for 1,4-dichloro-2-butyne.
The positions of the letters indicate the parameters of the models for which intensity curves in Fig. 1 were computed (except RD, which does not exactly correspond to the parameters of the model RD). The lines a, b, c and d indicate the border-line of the acceptable region for certain particular features.

34) The mean amplitudes listed in the fourth row of Table I are either calculated approximately using the force constants of dimethylacetylene (B. L. Crawford, Jr., *J. Chem. Phys.*, **7**, 555 (1939)), or estimated from the Table V and VI of the Reference 31.

110.5°); these values roughly correspond to the point "RD" in Fig. 5. The $q_{calcd.}/q_{obs.}$ ratio for the maxima and minima is 1.000 ±0.004 (Table II),[37] and the average fluctuation in the $I_{obs.}/I_{calcd.}$ ratio for these maxima and minima is about 10 percent.

In order to determine the range of uncertainty in various parameters, a number of intensity curves were computed based on assumed models. Since it is not feasible to exhaust the seven independent structural parameters and the mean amplitudes, the C≡C and C–H bond distances[38] and the C–C–H and H–C–H angles[39] were kept constant at 1.21 Å, 1.10 Å, and 109.5°, respectively, only the ratio C–C/C–Cl and the angle C–C–Cl being varied systematically. The parameter chart is given in Fig. 5. Estimated mean amplitudes[34] given in Table I were used throughout. Free internal rotation was assumed, and the theoretical intensity curves computed at each rotational angle at 10° intervals were summed up; mean amplitudes of the H–Cl and Cl–Cl distances were assumed to be 0.120 Å and 0.080 Å, respectively at all rotational angles, and the contribution from the H–H distances was ignored. When a high potential barrier is assumed, the resulting intensity curve shows features which completely disagree with the observed curve even in the region $q>15$ so that such a model is definitely excluded. This disagreement is most prominent in the extreme case that the barrier is infinite (i.e., any one of *trans-*, *gauche-* and *cis-*form, similar in configuration to those of 1,2-dichloroethane[40], or one of their possible mixtures). However, when a sufficiently low barrier ($V \lesssim 1$ kcal./mole) is assumed, the variation in the barrier from zero causes little change in the features of the theoretical intensity curve, which are thus in fairly good agreement with the observed curve. As a result, the assumption of free internal rotation, in accordance with the result of the following paper[15], may be reasonable in determining the structural parameter limit.

Some of the computed curves are reproduced in Fig. 1. The computed curves have the following features which are sensitive to small changes in some parameters[41]: the relative height of maxima 5 and 6, and that of maxima 8 and 9. The curves in the parameter chart illustrated in Fig. 5 denote the limit where a particular qualitative feature in the computed curves becomes sufficiently different from the experimental curve to be considered unacceptable.

No model above the line a (A, B, C, D, F, G, M, S and X) is acceptable because the fifth maximum is higher than, or almost the same height as the sixth maximum; model H, N and Y are estimated to be on the borderline. Each model below the line b (L, R, W, AA and CC) has too high and sharp sixth maximum, E and Q being estimated to be on the borderline. The line c excludes the models A, B, C, D and F because the eighth maximum has too high and broad features in each of them. The line d excludes the models Y, Z, AA, BB and CC because the ninth maximum is too high. Acceptable models, which are in the region enclosed

35) Recently, J. A. Ibers and J. A. Hoerni (*Acta Cryst.*, **7**, 405 (1954)) calculated a scattering phase shift $\eta$, in the form applicable to any atom under any voltage not too different from 40 KeV. The percentage apparent increase in the mean amplitudes of C-Cl, H-Cl and C-H distances due to this effect was calculated by use of their tables to be about 10 %, 7 % and 1 %, respectively, the first one being in exact agreement with the corresponding value estimated be Bartell and Brockway (Ref. 36b)).

36), a) R. Glauber and V. Schomaker, *Phys. Rev.*, **89**, 667 (1953).
b) L. S. Bartell and L. O. Brockway, *Nature*. **171**, 978 (1953).

37) The ratios for some maxima and minima are not included in the average. See Ref. 42.

38) The C≡C bond distance was found to be 1.207 Å is methylacetylene (L. F. Thomas, E. I. Sheppard and J. Sheridan, *Trans. Faraday Soc.*, **51**, 619 (1955)), and as pointed out by Herzberg and Stoicheff (Ref.13) and many other authors, C≡C bond distance remains remarkably constant in various molecules independent of the atoms linked to this system through a single bond. The result of the above RD analysis is also consistent with this fact. Thus, it will be reasonable in this case to fix the C≡C bond distance at 1.21Å. See also Ref. 12

39) Recent measurement of line shapes of nuclear magnetic resonace absorption led to an H-H distance of 1.71±0.02Å in the $CH_2Cl$-group of 1,2-dichloroethane (H. S. Gutowsky, et al., *J. Chem. Phys.*, **17**, 972 (1949)). These authors pointed out that the H-C-H angle of this group is significantly smaller than the tetrahedral angle if the C-H distance of 1.10Å or 1.09Å is assumed. Since no corresponding data have yet been found in 1,4-dichlorobutyne, and since the contributions of hydrogen terms to the total intensity curve are relatively small, tetrahedral angles were assumed for both H-C-H and C-C-H angles throughout this investigation.

40) S. Mizushima, "Structure of Molecules and Internal Rotation", Academic Press Inc., New York, (1954), p. 8.

41) Although the drawing of the background line is not unique, the relative heights of adjacent maxima are little changed by the redrawing of the background line, only if the line is smooth and roughly fulfills karle's criteria. As illustrated in Fig. 1, absolute heights of the maxima 5, 6, 8 and 9 change among the measurements of different photographs; nevertheless, the relative ratios of the peaks 5 to 6, and 8 to 9 remain nearly constant. For this reason, these ratios are regarded as the essential features of the experimental intensity and are used as the criteria for the following analysis.

by these four lines, are J, K, O, P, T and U[42].

The area of this "acceptable region" cannot be further reduced by taking other features into account such as the relative depths of minima, because small differences in these features are not significant enough to exclude any of these acceptable models.

The average $q_{calcd.}/q_{obs.}$ values for these acceptable models and the C–Cl and C–C distances determined from these averages are listed in Table III; they all agree satisfactorily with the RD results. The final choice of parameters with their estimated limits of uncertainty (including the error in the determination of $q$ scale, which is estimated to be less than 0.4 percent) are as follows:

C–Cl: $1.79_6 \pm 0.01_5$ Å,
C≡C: $1.21_4$ Å (not varied),
C–C: $1.47_0 \pm 0.02_5$ Å,
(C–H: $1.10_4$ Å, assumed),
∠C-C-Cl: 111°±2°
(∠C-C-H = ∠H-C-H: 109.5°, assumed).

The C–Cl distance in this molecule is somewhat shorter than that of propargyl chloride (1.82±0.02 Å) found by Pauling et al.[7]. The theoretical intensity curve, based on the model in which all parameters were set equal to the values of propargyl chloride determined by these authors (C–Cl: 1.82 Å, C–C: 1.48 Å, C≡C: 1.20 Å, and ∠C-C-Cl: 111°), is shown as the curve PGS in Fig. 1. It shows a qualitative difficulty in the maximum 8, and its $q_{calcd.}/q_{obs.}$ average is less than unity (0.994±0.006).

## 4. Discussion

The C≡C and C–C distances obtained above agree, within the limit of experimental uncertainty, with those of similar molecules studied both by spectroscopy and by electron and X-ray diffraction[12–14]. It is a remarkable fact that the C–C distances in various molecules (1.46–1.47Å) are much shorter than the normal C–C single-bond distance (ca. 1.54Å), and that they are almost independent of the atoms or groups linked to the carbon atoms.

The C-C-Cl angle (111°±2°) is nearly the same as that in 1,2-dichloroethane (110°23′)[43] and in ethyl chloride(110°30′)[44], while the C–Cl distance ($1.79_6 \pm 0.01_5$ Å) seems to be a little longer than that in the latter molecules (1.78±0.01 Å, and 1.7770 Å, respectively). The increase in the C–Cl bond distance in this molecule compared with that in carbon tetrachloride ($1.76_6 \pm 0.01$ Å) will be real, because these data were obtained at the same condition and by the same procedure. The lengthening of the C–Cl bond is still more pronounced in propargyl chloride which was investigated by Pauling and his coworkers (1.82±0.02 Å)[7], but it is not yet clear whether there is any actual difference between the C-Cl bonds in 1,4-dichloro-2-butyne and in propargyl chloride.

Pauling and his coworkers attributed the lengthening of the C–X bond in propargyl halides to the contribution of the resonance structure (II):

(I) $H-C\equiv C-CH_2-X$,

(II) $H-\overset{+}{C}=C=CH_2 \quad X^-$.

If this were actually the case, large contribution of the similar resonance structures (III) and (IV):

(III) $Cl-H_2C-\overset{+}{C}=C=CH_2Cl^-$,

(IV) $Cl^- \; H_2C=C=\overset{+}{C}-CH_2Cl$,

would also be expected in 1,4-dichloro-2-butyne, whereas a recent measurement[45] of the dipole moments of propargyl chloride, bromide, and 1,4-dichloro-2-butyne has shown that these molecules have

42) These acceptable curves still have a slight disagreement with the experimental curve: namely, (a) the existence of the shoulders of minimum 5 and maximum 7, and (b) the feature near maximum 11. The discrepancy (b) cannot be taken so seriously because precise measurement of this region could not be made in this experiment. The discrepancy (a), however, should be noted, because it is not clear whether the main origin is in the experimental error or in the assumption of the computation.

Although the structural parameters of the acceptable models are consistent with the RD results, and the assumptions of temperature factors and of free internal rotation seems to be reasonable as stated above. there still remains some possibility that we may find a more satisfactory model by changing some of the parameters.

If, on the other hand, this discrepancy comes from the error in the experimental procedure, in other words, if these shoulders do exist, and were not resolved in this experiment, it corresponds to an error of the order of the width of the microphotometer trace (ca. 0.2 mm.). Although this is apparently larger than that of our usual measurement, existence of comparable error in these regions is suggested by the fact that the largest discrepancies among the three observed curves are found in these regions (Fig. 1). On the visual interpretation of the original diffraction pattern, no such shoulders can be clearly observed; but, of course, this visual estimation should not be conclusive.

For this reason, the $q_{calcd.}/q_{obs.}$ values of max. 7, 11, and min. 5, 11, 12 and 13 are not included in calculating their averages and average deviations.

43) J. Ainsworth and J. Karle, *J. Chem. Phys.*, **20**, 425 (1952).

44) R. S. Wagner and B. P. Dailey, ibid., **25**, 1355 (1955).

45) T. Chiba, T. Simozawa, I. Miyagawa and Y. Morino. This Bulletin, **30**, 223 (1957).

smaller C—X bond dipole moments than the normal C—X bond moments, in apparent contradiction to the above expectation. Consequently, it seems difficult to explain the lengthening of the C—Cl bond on the basis of these resonance structures.

## Summary

The structure of 1,4-dichloro-2-butyne was investigated by means of the sector-microphotometer method of electron diffraction. The following values were obtained: C≡C: $1.21_4$ Å, C—C: $1.47_0 \pm 0.02_5$ Å, C—Cl: $1.79_6 \pm 0.01_5$ Å, and ∠C-C-Cl: 111° ±2°. The C—Cl distance was found to be longer than that in carbon tetrachloride, $1.76_6 \pm 0.01$ Å.

The author wishes to express his gratiude to Professor Y. Morino, for his kind guidance and encouragement throughout the course of this work, to Professor R. Uyeda, Nagoya University, for his valuable advice for the construction of the sector apparatus, to Mr. H. Morimoto and Mr. S. Shibata, Nagoya University, for their kind help in the measurement of microphotometric tracing, and to Mr. R. Tsunoda and Mr. Y. Suzuki, Division of Health and Welfare Statistics, Welfare Minister's Secretariat, for the use of Punched Card Machine. The expenses of the work were defrayed from the Scientific Research Encouragement Grant of the Ministry of Education to which the author's thanks are also due.

*Department of Chemistry*
*Faculty of Science*
*The University of Tokyo, Hongo, Tokyo*

# *An Electron Diffraction Investigation of the Molecular Structure of 1,4-Dichlorobutyne. II. A Study of Internal Rotation by Use of Halos in Small Angle Region**

By Kôzo KUCHITSU

(Received January 7, 1957)

## 1. Introduction

The internal rotation of two methyl groups in dimethylacetylene has been investigated by several authors. The measurements of heat capacity[1,2], and the third-law entropy[3] offered a proof of practically complete absence of hindrance to the rotation of these methyl groups (less than 500 cal./mole)[2]. The analysis of the rotational structure of the perpendicular-type infrared bands[4,5] led to the conclusion that the assumption of unrestricted internal rotation is consistent with their observed data, thus giving independent support to the results of the thermal measurements.

As for the substituted dimethylacetylene[6], the complex microwave spectrum[7] of $CH_3—C\equiv C—CF_3$ was explained satisfactorily on the basis of a zero, or very low potential barrier when centrifugal distortion effects were taken into account[8], and $ClCH_2—C\equiv C—CH_2Cl$ molecule was shown, by means of temperature dependence of the dipole moment in the vapor state[9], to have a barrier of less than 0.1 kcal./mole, while in carbon tetrachloride and benzene solutions[10] the barrier was estimated to

* Presented at the Eighth Annual Meeting of the Chemical Society of Japan, April, 1955.

1) B. L. Crawford, Jr. and W. W. Rice, *J. Chem. Phys.*, **7**, 437 (1939).

2) G. B. Kistiakowsky and W. W. Rice, ibid., **8**, 618 (1940).

3) D. W. Osborne, C. S. Garner and D. M. Yost, ibid., **8**, 131 (1940).

4) D. R. J. Boyd, H. W. Thompson and R. L. Williams, *Disc. Faraday Soc.*, **9**, 154 (1950).

5) J. M. Mills and H. W. Thompson, *Proc. Roy. Soc.*, **A226**, 306 (1954).

6) A recent investigation of the vibrational spectrum of $CF_3$-C≡C-$CF_3$ by Miller and Bauman (*J. Chem. Phys.*, **22**, 1544 (1954)) has shown that this molecule follows $D_{3d}$ selection rules, so that it is in either staggered configuration or free rotation. (R. P. Bauman, *J. Chem. Phys.*, **24**, 13 (1956)). However, no definite decision has yet been given.

7) B. Bak, L. Hansen and J. Rastrup-Andersen, *J. Chem. Phys.*, **21**, 1612 (1953).

8) D. R. Lide and D. Kivelson, ibid., **23**, 2191 (1955).

9) Y. Morino, I. Miyagawa, T. Chiba and T.Shimozawa, This Bulletin, **30**, 222 (1957).

10) Y. Morino, I. Miyagawa and A. Wada, *J. Chem. Phys.*, **20**, 1976 (1952).

be 0.75±0.20 kcal./mole. It is the main purpose of this article to apply the sector-microphotometer method of electron diffraction to the study of the internal rotation of 1,4-dichloro-2-butyne, using the structural data obtained in the preceding article[11], and to confirm the results of dipole moment measurement. This method will provide one of the effective means of determining the potential barrier of such a molecule, because a heavy chlorine atom is included in each of the rotating groups so that the diffraction pattern will show essential dependence on the internal rotation of these groups.

## 2. Experimental and Results

In order to study the internal rotation of this molecule, it is necessary to examine small-angle halos ($q \lesssim 15$). The theoretical intensity curves remain almost unchanged in this range when slightly different frame parameters (distances, angles, and mean amplitudes) are assumed, so that the essential features of the curves are determined by the assumption of the potential barrier alone. In the outer $q$ region, on the other hand, the contribution from the Cl—Cl and H—Cl distances which change with the internal rotation damps rapidly, and in addition even a slight change of the frame parameters might cause a significant effect to the intensity curve enough to obscure the difference caused by the change of the potential barrier. Thus the photographs taken at the long camera length of about 27.9cm. ($q=5\sim27$) can be used as a means of estimating the potential barrier. The detail of the experimental procedure and numerical computation are given in the preceding article[11]. However, the usual technique of drawing the background line cannot be applied in this region. Karle's criterion of the non-negative Gaussian RD peaks[12a] is not applicable because the influence of $f$-factors upon the molecular intensity curve is not negligible in this region; nor can the background line be drawn through the zero-points of a reasonable theoretical curve[12b,13,14], because there is no zero-point from $q=5$ to 15. Consequently, we have to use some alternative standard for obtaining a reasonable background line. In this study a procedure similar to, but somewhat different from that of Bregman and Bauer[14] was used.

Assuming various types of potential barrier $V(\phi)$, theoretical intensity curves $M_c(q, V)$ were calculated from Eqs. (2) and (4) of Paper (I)[15]; the frame parameters were fixed at the values obtained in Paper (I), since the influence of their uncertainty was found to be negligible. To each $M_c$-curve the corresponding "background function" $I_b(q, V)$ was computed by the following formula:

$$I_b(q, V) = q^{1/2} I_o(q) / \{1 + 0.84 M_c(q, V)\} \quad (1)$$

where $I_o(q)$ is the observed total scattering intensity, which was multiplied by $q^{1/2}$ to accentuate the oscillations in the region $q=8\sim15$. The absolute molecular intensity $M_c$ was multiplied[16] by 0.84 to make it fit the experimental curve in the region $q=16.7$ to 20.0.

If the diffraction experiment were ideally performed and the assumed model were strictly correct, the $I_b$-function should have no sudden fluctuation of the frequency of the order of molecular intensity[17]; in general, the corresponding $I_b$-function will approach to a smooth curve as the assumed model becomes better. Thus the extent of its fluctuation from a smooth curve can be used as a criterion for choosing reasonable models, provided that the corrections for a non-ideal experiment are properly taken into account.

For simplicity, only the first term of the potential function

$$V(\phi) = \frac{1}{2}V_1(1-\cos\phi) + \frac{1}{2}V_2(1-\cos 2\phi) + \frac{1}{2}V_3(1-\cos 3\phi) + \cdots\cdots, \quad (2)$$

is considered first; the variable $\phi$ is the angle of rotation from the *trans* position. When free internal rotation ($V_1=0$) is assumed, the corresponding $I_b$-curve contains little fluctuation (Fig. 1A), which shows that this model is satisfactory. When the rigid *trans* structure ($V_1=\infty$) is assumed, the corresponding $I_b$-curve has much greater fluctuations, indicating that this model is definitely unacceptable (Fig. 2A). In a similar fashion, the $I_b$-curve based on the assumption that $V_1=1$ kcal./mole is also unsatisfactory because it still has some fluctuations (Fig. 3A). This implies that, so far as the cosine-type barrier is assumed, free internal rotation is the

11) K. Kuchitsu, This Bulletin, **30**, 391(1957)(hereafter referred to as paper (I)).

12a) J. Karle and I. L. Karle, *J. Chem. Phys.*, **18**, 957, 963 (1950).

12b) I. L. Karle and J. Karle, ibid., **17**, 1052 (1949).

13) J. M. Hastings and S. H. Bauer, ibid., **18**, 13(1950),

14) J. Bregman and S. H. Bauer, *J. Am. Chem. Soc.*, **77**, 1955 (1955).

15) The following formula was used:

$$qM_c(q,V) = \{\sum_{\varphi} \sum_{i>j} (c_{ij}/r_{ij}) \exp(-b_{ij}q^2) \times \sin(\pi q r_{ij}(\phi)/10) \exp(-V(\phi)/RT) \Delta\phi\} / \{\sum_{\phi} \exp(-V(\phi)/RT)\},$$

where $\Delta\phi$ is 10° and $b_{ij}$ is a constant.

16) The ratio of the observed molecular intensity to the theoretical one is always less than unity, since the background is raised by multiple and extraneous scattering. Even if the factor 0.84 is changed slightly, the conclusion given below is not altered essentially.

17) An ideal background line (atomic and inelastic scattering) is known to be a smooth function of $q$. Multiple scattering will also cause an essentially smooth background (Ref. (12a)); and extraneous scattering was found, by measuring a photograph taken without sample, to have no sudden change in intensity. Other possible sources of sudden change, such as grain irregularities, small particles of dusts on the plate, accidental error in the photometry procedure,etc., may be eliminated by rotating the plate while scanning, and by averaging among sets of plates. The smoothness of the background line is discussed more extensively in the authors' recent study on *n*-propyl chloride, (Y. Morino and K. Kuchitsu, *J. Chem. Phys.*, to be published). See also Ref. (11) of Karle's paper (Ref. (12b)).

most favorable model, $V_1$ being apparently less than 1 kcal./mole, although further quantitative estimation of its upper limit is difficult.

An alternative examination of the potential barrier is a comparison of the molecular intensity curve $qM_o(q)$, which is obtained by drawing a smooth background in such a way as to reproduce the theoretical intensity curve $qM_c$ as closely as possible, in the resulting $qM_o$-curve. The model

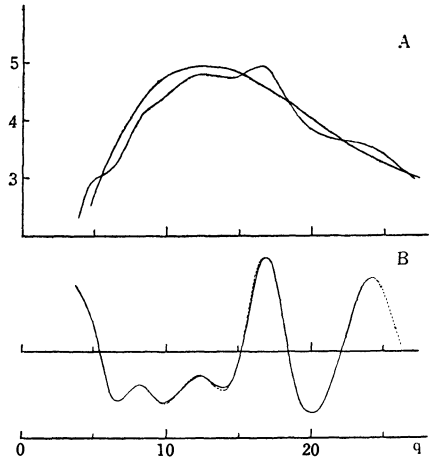



Fig. 1. (A) The observed intensity curve multiplied by $q^{1/2}$ obtained from the long camera-length photographs, and the $I_b$-curve for free internal rotation. (B) The $qM_o$-curve (solid line) which was obtained by drawing a smooth background line in such a way as to reproduce the theoretical intensity curve $qM_c$ (dotted line) for free internal rotation as closely as possible.

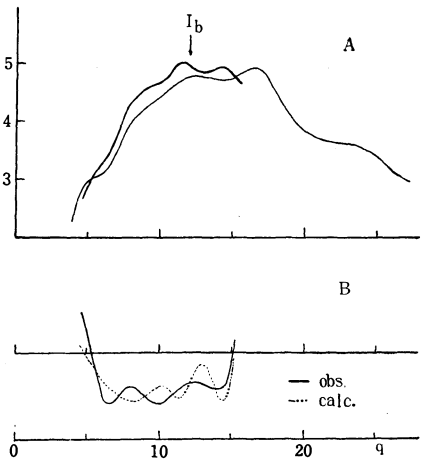



Fig. 2. (A) The $I_b$-curve for the rigid-*trans* model; the curve shows fluctuations with the frequencies of the order of molecular intensity. (B) The $qM_c$-curve (solid line) and the $qM_c$-curve (dotted line) for the rigid-*trans* model.

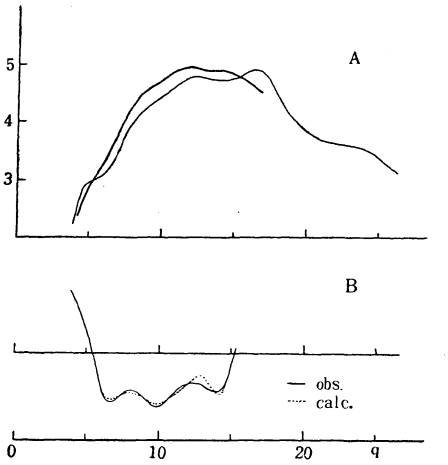



Fig. 3. (A) The $I_b$-curve for the model $V_1=1$ kcal./mole. (B) The $qM_o$-curve (solid line) and the $qM_c$-curve (dotted line) for the model $V_1=1$ kcal./mole.

$V_1=\infty$ is completely unsatisfactory because these curves disagree with each other (Fig. 2B); the $qM_c$-curve for the model $V_1=1$ kcal./mole shows features near $q=8$ and 12.5 which cannot be reproduced in the $qM_o$-curve (Fig. 3B). However, the $qM_c$-curve based on the model $V_1=0$ is reproduced satisfactorily by the corresponding $qM_o$-curve. (Fig. 1B). A factor $\sigma$ defined by the following equation may be used as a numerical measure of the overall inconsistency between the $qM_c$- and $qM_o$-curves:

$$\sigma=\sum_q\{qM_o(q)-cqM_c(q)\}^2, \qquad (3)$$

where the summation is taken over the integral $q$ values from 5 to 14, and $c$ is a numerical factor adjusted to minimize the $\sigma$-value. Table I shows that the lower the barrier, the less $\sigma$-value may be obtained, which again favors practically free internal rotation.

TABLE I

THE $\sigma$ FACTORS OF THE THEORETICAL CURVES CALCULATED BY ASSUMING VARIOUS TYPES OF POTENTIAL BARRIERS

| Assumption | $V=0$ | $V=1$ kcal. | $V=\infty$ |
|---|---|---|---|
| $V_1$ term only | 0.0070 | 0.0173 | 0.2165 |
| $V_2$ term only | 0.0070 | 0.0261 | 0.1016 |
| $V_3$ term only | 0.0070 | 0.0082 | 0.0163 |

The $\sigma$ value among the two observed curves is about 0.0002.

Similar procedure can be applied for a potential function of any shape. If, for example, the potential function is assumed to have only the second term (the *trans* and the *cis* positions being the lowest ones), a high potential barrier is found to be impossible, and the $\sigma$-factor has the lowest value when $V_2$ is zero; so too is this the case when only the third term (the *trans* and the *gauche* positions being the stable ones)

is assumed, although the fact is less prominent than in the above cases (Table I). The actual potential barrier will naturally be neither of these extreme cases but a certain combination of these terms; nevertheless, it can be inferred from the above result that the internal rotation is practically unrestricted; in other words, the barrier higher than 1 kcal./mole is improbable.

## 3. Discussion

It is to be noted, in the first place, that the electron diffraction study, particularly the analysis of small angle halos, provides one method of investigating internal rotation. By the measurement of dipole moment, only the $V_1$-term can be determined[18]; on the contrary, more than one coefficient of the potential function (2) can be estimated, at least in principle, by the electron diffraction method if sufficiently accurate scattering data are available, although its precise evaluation is limited because of the difficulty in drawing a correct background line and in estimating experimental errors.

The analysis of 1,4-dichloro-2-butyne described above indicates that free internal rotation is in good agreement with the electron diffraction data, whereas a high potential barrier is inconsistent. This conclusion is consistent with that obtained from the dipole moment measurement of this molecule in the gaseous state; Morino and his collaborators[9] observed finite and constant values of the dipole moment, 2.08–2.09 D, in the temperature range of 90–160°C., from which they concluded that the $V_1$-coefficient of the potential function (2) is less than 0.1 kcal./mole.

It is well known that the potential barriers in ethane derivatives, such as 1,2-dichloroethane, are several kcal./mole[19]. The barrier in 1,4-dichloro-2-butyne is therefore much lower. This difference in barrier height arises mainly from the fact that the distance of the two rotating groups is longer in the latter molecule. In fact, the steric repulsion between the two C—Cl bond moments is shown to be only about 0.5 kcal./mole by a simple calculation[10].

18) I. Miyagawa, *J. Chem. Soc. Japan*, **75**, 970 (1954).

19) S. Mizushima, "Structure of Molecules and Internal Rotation", Academic Press Inc., New York (1954).

## Summary

The internal rotation of 1,4-dichloro-2-butyne was investigated by the sector-microphotometer method of electron diffraction, examining the region of smaller scattering angles ($q \lesssim 15$); photographs taken at a long camera length were analyzed using a criterion that the "background function" should have no sudden fluctuation. Free internal rotation is in good agreement with the observed scattering data, and a high potential barrier is inconsistent.

The author wishes to express his gratitude to Professor Y. Morino for his kind guidance and encouragement througout the course of this work. The expenses of the work were defrayd from the Scientific Research Encouragement Grant of the Ministry of Education, to which the author's thanks are also due.

*Department of Chemistry, Faculty of Science, Tokyo University, Hongo, Tokyo*

# *Infrared Spectra of Organic Ammonium Compounds*

By Koji NAKANISHI, Toshio GOTO and Mamoru OHASHI

(Received January 7, 1957)

In connection with the structural elucidation of the natural product, roseonine[1] and roseothricin[2], the infrared spectra of about one hundred authentic amines have been compared with the spectra of their hydrochlorides[3] (potassium bromide disk). Representative results are shown in Table I, Figs. 1–4, and are summarised in Table II.

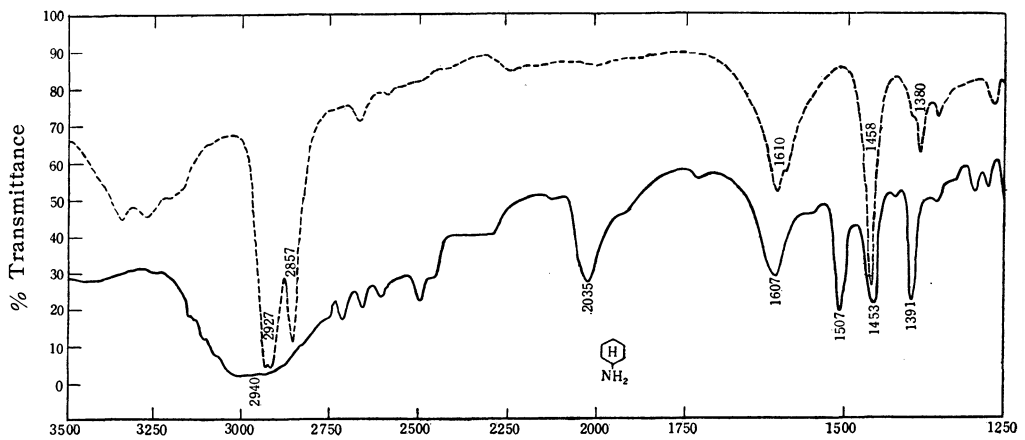



Fig. 1. Primary amine
Cyclohexylamine (No. 8, 8a): ---- free, —— hydrochloride

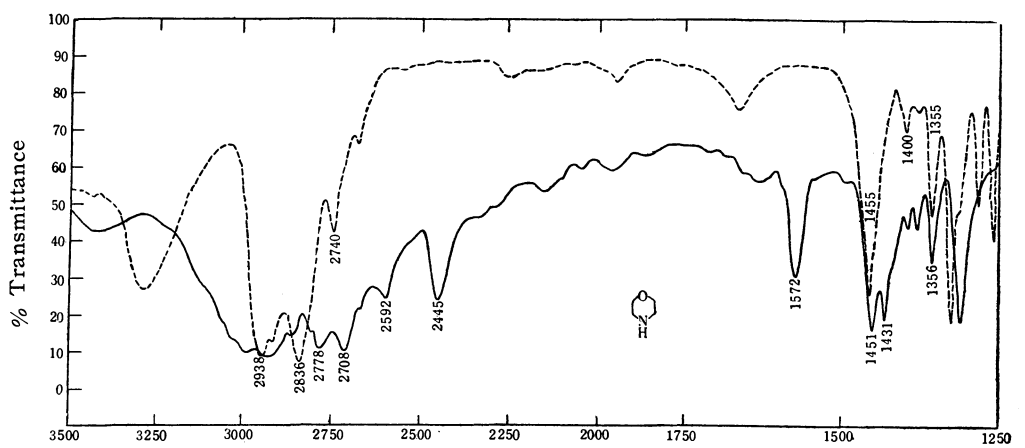



Fig. 2. Secondary amine
Morpholine (No. 18, 18a): ---- free, —— hydrochloride

1) K. Nakanishi, T. Ito, M. Ohashi, I. Morimoto and Y. Hirata, This Bulletin, **27**, 539 (1954).
K. Nakanishi, T. Ito and Y. Hirata, *J. Am. Chem. Soc.*, **76**, 2845 (1954); K. Nakanishi and M. Ohashi, This Bulletin, (in press).

2) T. Goto, Y. Hirata, S. Hosoya and N. Komatsu, ibid., **30**, 304 (1957).

3) For summaries of existing data on the ammonium group see L. J. Bellamy, "The Infrared Spectra of Complex Molecules," Methuen (1954), p. 202, and R. N. Jones and C. Sandorfy in "Chemical Applications of Spectroscopy," Interscience (1956), p. 514, 520.

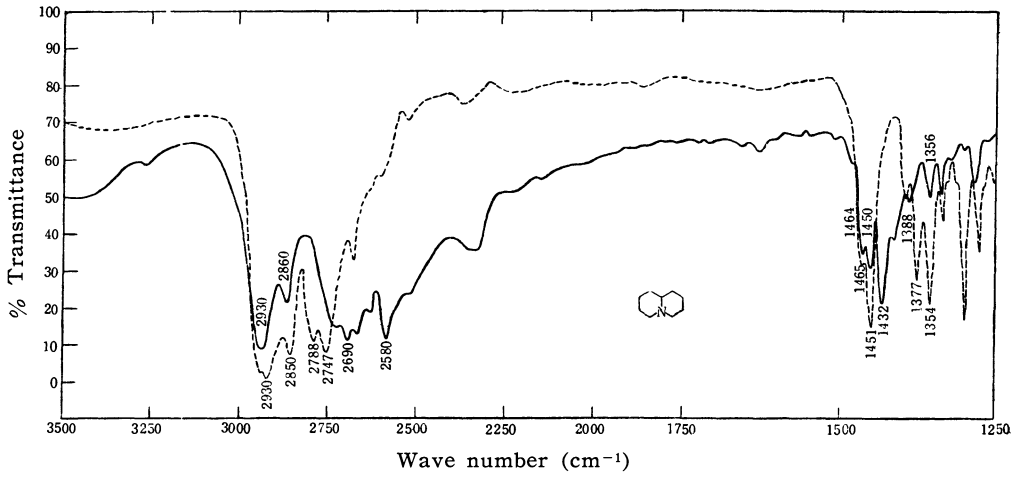



Fig. 3. Tertiary amine
Quinolizidine (No. 31, 31a): ---- free, —— hydrochloride

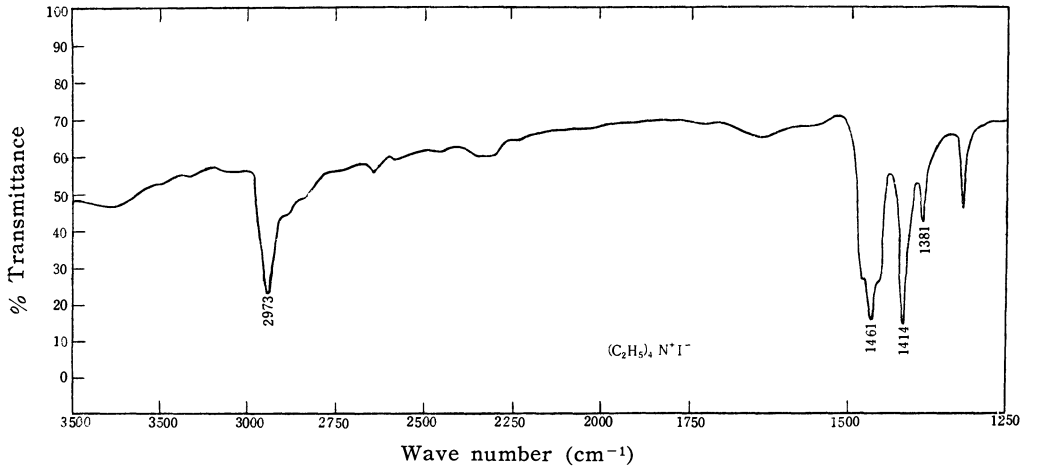


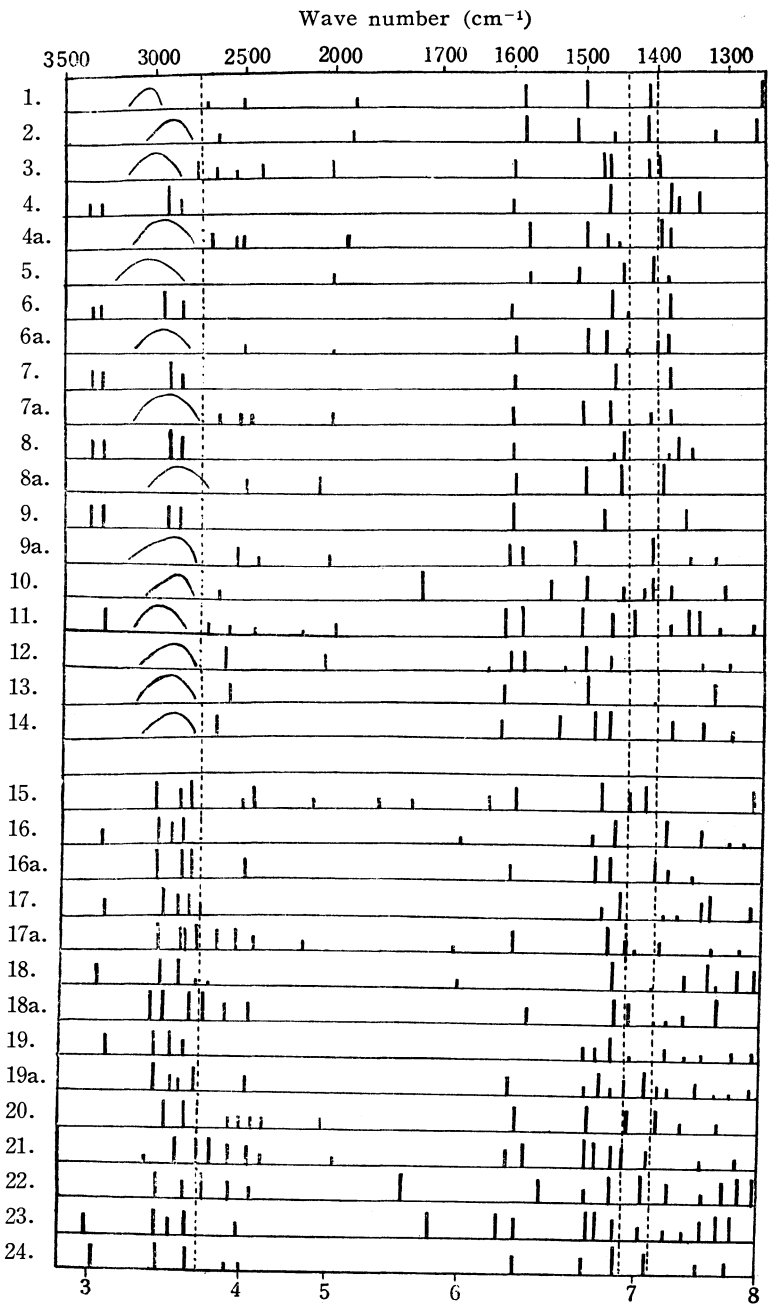

Fig. 4. Quaternary ammonium salt
Tetraethylammonium iodide (No. 50)

Thus primary, secondary, and tertiary amine hydrochlorides, and quaternary ammonium salts can be differentiated fairly accurately from the results of Table II. The characteristic shape and position of the prominent group of absorptions lying at the highest frequency usually suffice to identify primary and tertiary amine hydrochlorides. The corresponding absorption of secondary amine hydrochlorides is less characteristic and in this case absorption in the 1600–1550 $cm^{-1}$ region also has to be taken into account. Open or cyclic azomethines containing the grouping $\rangle C{=}N-$ were not included in the studies. Hydrochlorides of these compounds possess one to several absorptions in the region of 2200–1800 $cm^{-1}$ ("immonium band") in addition to the ammonium band at 2500–2300 $cm^{-1}$; furthermore the C=N stretching band is shifted 30–40 $cm^{-1}$ toward higher frequency upon attachment of a proton to the nitrogen[4]. Incidentally the region of the ammonium band of azomethine hydrochlorides is roughly similar to that of tertiary amines and seem also to be easily differentiated from normal C—H stretching absorptions (see figures in reference 4). The $\alpha$, $\beta$- and the $\beta$, $\gamma$-unsaturated tertiary amines and their salts[5] are not included in the present paper, either

4) a. B. Witkop, *Experientia*, **10**, 420 (1954)
b. *idem.*, *J. Am. Chem. Soc.*, **76**, 5597 (1954).
5) N. J. Leonard and V. W. Gash, ibid., **76**, 2681 (1954).

TABLE I

INFRARED ABSORPTION OF AMINES AND AMINE HYDROCHLORIDES



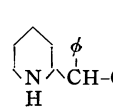

1. Methylamine HCl
   S. #6369
2. $CF_3CH_2NH_2 \cdot HCl$
   S. #7339
3. Ethylamine HCl
4. Isopropylamine
4a. Isopropylamine HCl
5. *n*-Propylamine HCl
6. *n*-Butylamine
6a. *n*-Butylamine HCl
7. *n*-Hexylamine
7a. *n*-Hexylamine HCl
8. Cyclohexylamine
8a. Cyclohexylamine HCl
9. Ethylenediamine
   S. #5319
9a. Ethylenediamine HCl
   S. #8183
10. Ethyl glycinate HCl
    S. #6702
11. Indolethylamine HCl
12. Aniline HCl
13. Benzidine 2HCl
    S. #6621
14. $H_2N$-C$_6$H$_3$(SO$_3$H)-CH=
    CH-C$_6$H$_3$(HO$_3$S)-$NH_2$
    nujol S. #5825
15. Dimethylamine HCl
16. Diethylamine
16a. Diethylamine HCl
17. Piperidine
17a. Piperidine HCl
18. Morpholine
18a. Morpholine HCl
19. *dl*-Ephedrine
19a. *dl*-Ephedrine HCl
20. 2-Me-piperidine HCl
    S. #8774
21. N-Benzylaniline HCl
    S. #8620
22. C$_6$H$_5$-CH(Cl)-CH(NHCH$_2$-$\phi$)-COOEt ·HCl S. #7911
23. C$_6$H$_3$(NH$_2$)(OC$_4$H$_9$(*n*))-COOCH$_2$CH$_2$NHCH$_2$CHMe$_2$ ·HCl
    S. #8142
24.  ·HCl S. #6687

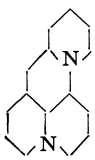
TABLE I (continued)

25. Trimethylamine HCl
S. #6377
26. Triethylamine
26a. Triethylamine HCl
27. N-Ethylpiperidine
$CCl_4$ soln.
27a. N-Ethylpiperidine HI
28. N-Ethylmorpholine HI
29. Dimethylhexylamine HCl
30. Diethylhexylamine HCl

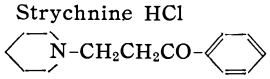
31a.  ·HCl

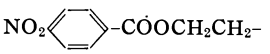
31. 

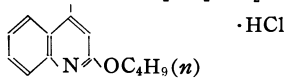
32. Dimethylbenzylamine HCl
33. Dimethylaniline HCl
34. Diethylaniline HCl

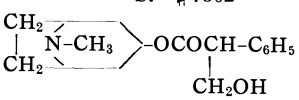
35.  ·2HCl

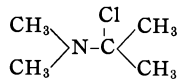
36. Morphine HCl
37. Ethylmorphine
37a. Ethylmorphine HCl
38. Strychnine
38a. Strychnine HCl

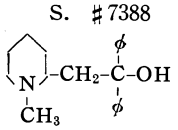
39. 
·HCl S. #8772

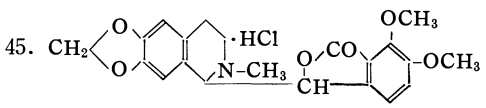
40. 
$NEt_2$·HCl S. #8419

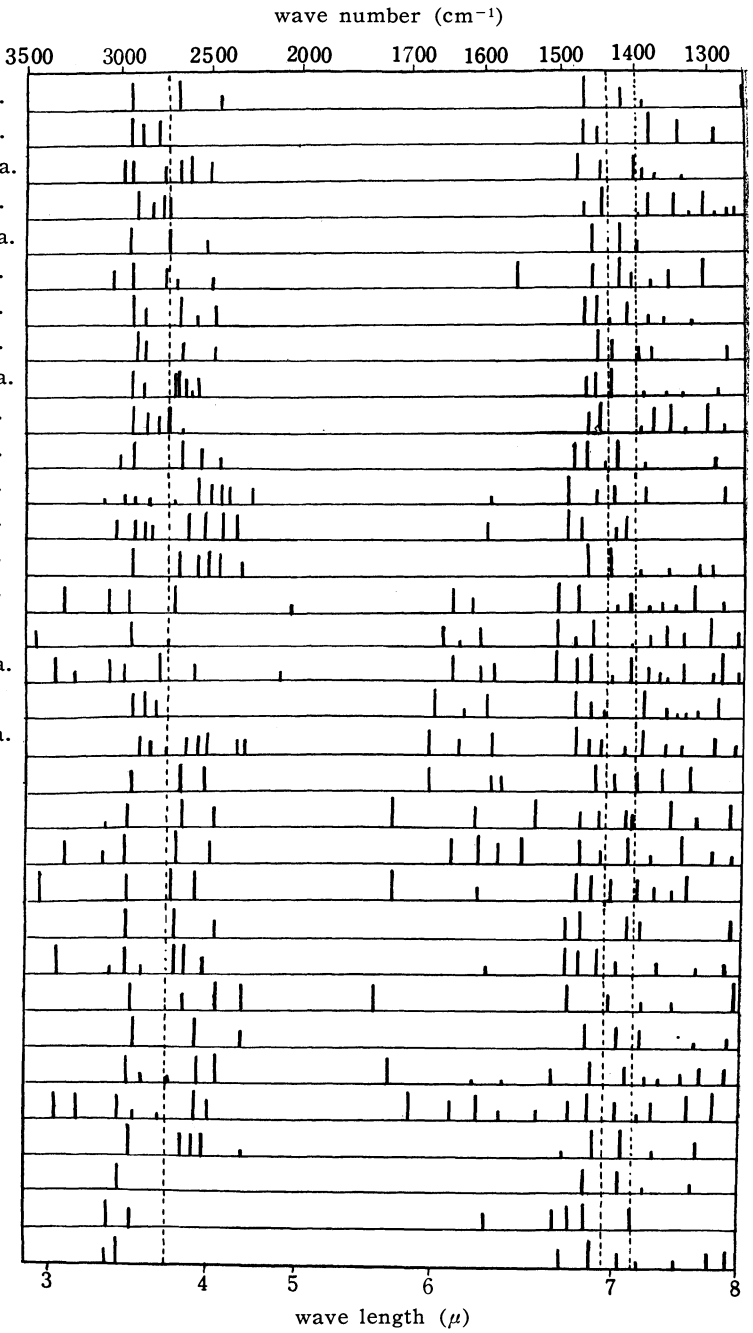
41.  ·HCl
S. #7502

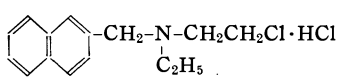
42. 
·HCl S. #7533

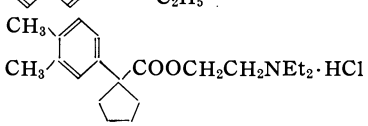
43.  ·HCl
S. #7388

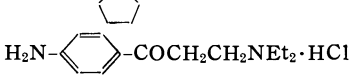
44.  ·HCl S. #6688

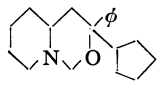
45. 
S. #7163



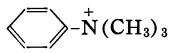

46.  S. #7444

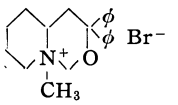
47. 

48. 

49.  ·HCl S. #6678

50. $(C_2H_5)_4N^+ I^-$

51.  S. #7333

52.  S. #6679

Dotted line at 2750 $cm^{-1}$ marks approximate differentiating line between amines and hydrochlorides.
Dotted line covering the region 1440-1400 $cm^{-1}$ shows the range of the $—CH_2—N^+—$ band.
All data were obtained with KBr disks except when specified. Data taken from the Sadtler Catalog (S. P. Sadtler and Son, Inc., 2100 Arch St., Philadelphia 3, Pa., U. S. A.) are marked with S followed by the number of the spectrum card.

TABLE II

CHARACTERISTIC ABSORPTIONS OF AMINE SALTS

Figures in parentheses show number of samples examined, samples which conformed to the generalisation (+), and samples of which differentiation by means of infrared spectroscopy was somewhat dubious (±), respectively.

**Primary amine-HCl** (19, +17, ±2)

| | |
|---|---|
| 3200-2800: | s and br, overlaps with C—H stretching bands. |
| 2800-2400: | several weak bands. |
| 2100-1900: | w, absent in some cases. |
| 1610-1550 : 1510-1480 | m, obscured in aromatic compounds by the 1600, 1580, and 1500 bands; the second band is usually the stronger. |

**Secondary amine-HCl** (18, +16, ±2)

| | |
|---|---|
| 2800-2400: | s or m, several bands; the overlap with the C—H stretching band is midway between that of primary and tertiary amine hydrochlorides. |
| 2100-1900: | w, absent in some cases. |
| 1600-1550: | m, obscured in aromatic compounds by the 1600, 1580, and 1500 bands. |

**Tertiary amine-HCl** (51, +46, ±5)

| | |
|---|---|
| 2750-2300: | s, several bands; may be clearly differentiated from C—H stretching bands. |

The intensity of the $NH^+$ bending band is too weak to be of any practical value.

**Quaternary ammonium salt** (4 samples) showed no absorption in the regions specified.

The shift to lower frequencies of the $NH^+$-stretching band of tertiary amine hydrochlorides has been attributed to a strong hydrogen bond of the type $N^+—H\cdots Cl$[6]; in connection with this, it has been found that the tetraphenyl borates of mono-, di-, and tri-methylamine, in which the hydrogen bond $N^+—H\cdots(C_6H_5)_4B^-$ is sterically hindered, all absorb around 3100 $cm^{-1}$ [7].

A peculiarity, observed in the spectra of many free secondary and tertiary amines, was the appearance of a set of medium to strong bands around 2800-2700 $cm^{-1}$, i. e., on the lower frequency side of the C—H stretching band*. For example, these are apparent in the spectra of diethylamine (Table I, No. 16), triethylamine (No. 26), piperidine (No. 17), quinolizidine (No. 31), N-dimethylbenzylamine etc. These bands, however, do not interfere with the characterization of amine types, since they disappear upon conversion into the hydrochloride. The same relation seems also to hold for solution spectra; compare the spectra of nicotine and nicotine monohydrochloride (carbon tetrachloride solution) in Fig. 1B of reference 4a, and it is seen that the band at 2809 $cm^{-1}$ in the former compound is absent in the latter.

It has also been noted that a methylene group adjacent to an ammonium nitrogen absorbed in the region 1440-1400 $cm^{-1}$ instead of the normal range around 1470 $cm^{-1}$ (Fig. 5). This is a sort of behavior similar to the well-known displacement to lower frequencies of the bands of methylene and methyl groups alpha to a carbonyl group[8]. Provided that direct comparisons of spectra of amines with their respective hydrochlorides are possible, or that absorption in the 1440-1400 $cm^{-1}$ region by other groups may safely be disregarded, the band would enable one to characterize

6) R. C. Lord and R. E. Merrifield, *J. Chem. Phys.*, **21**, 166 (1953).

7) Personal communication from Dr. K. Nakamoto, Osaka University. See also, *Kagaku-no-Ryoiki*, Extra Number, **23**, 84 (1956).

* Three communications dealing with these bands have recently been published. However, the origin is as yet not clear.
E. Wenkert, D. K. Roychaudhuri, *J. Am. Chem. Soc.*, **78**, 6417 (1965); **79** 1519 (1957).
S. Oseko, *J. Pharm. Soc. Japan*, **77**, 118 (1957).

8) S. A. Francis, *J. Chem. Phys.*, **19**, 942 (1951).
R. N. Jones and A. R. H. Cole, *J. Am. Chem. Soc.*, **74**, 5648 (1952).
R. N. Jones, A. R. H. Cole and B. Nolin, ibid., 5662.

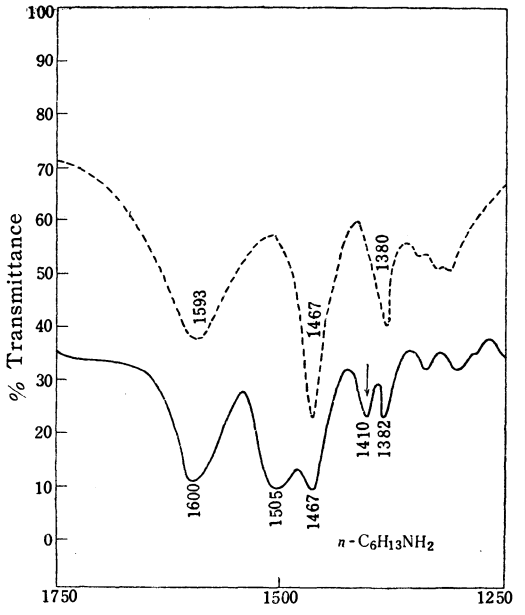



Fig. 5. $-CH_2-N^+-$ band
*n*-Hexylamine: ---- free, —— hydrochloride

the grouping $-CH_2-N^+-$. Thus the spectra of isopropylamine hydrochloride and cyclohexylamine hydrochloride (Fig. 1) which lack the adjacent methylene group show no (additional) band in this region. Amongst 74 ammonium salts devoid of groupings which could absorb around 1420 $cm^{-1}$, e. g., —COOH, —OH, $-CONH_2$, $-COOCH_3$, $-CH_2CO-$, 62 gave positive results, 5 gave somewhat dubious results, and 7 gave negative results. With amines containing the above-mentioned groups, characterization of the $-CH_2N-$ group was equally possible in most cases by comparing the spectra of the free amine and its hydrochloride.

**Infrared Absorption Measurements.**—The spectra were recorded on a Hilger H 800 double beam instrument equipped with sodium chloride optics; whenever necessary the region 1300-1750 $cm^{-1}$ was measured with a calcium fluoride prism. Potassium bromide disks were used, and the die and handpress were those supplied by the Hilger and Watts Co. Analytical grade potassium bromide was ground to pass a 200 mesh sieve and dried at 150°C for 24 hours. The samples (ca. 1 mg.) were ground evenly with 300 mg. of this potassium bromide for 5 min.

The authors wish to express their gratitude to Professor Yoshimasa Hirata for his guidance and interest in this research, to Drs. Junji Koizumi, Nihon Shinyaku Co., Shigeo Oseko, Dainihon Pharmaceutical Co., Akira Fujino and Masao Yamaguchi, Osaka City University, for the gifts of valuable amines, and to Dr. Hideo Kamio, Takeda Pharmaceutical Co. for giving them access to the Sadtler Catalog. They are also grateful for a grant from the Ministry of Education for the purchase of the spectrophotometer.

*Chemical Institute, Nagoya University*
*Chikusa, Nagoya*

# *Ionization Potentials of Some Organic Molecules. IV. Troponoid Compounds*

By Keniti HIGASI, Tetsuo NOZOE and Itiro OMURA

(Received January 16, 1957)

A considerable amount of knowledge has been accumulated concerning the physical properties of troponoid compounds. Dipole moments, electron diffraction, X-ray analysis on crystals, near-ultra violet absorption, infrared absorption, Raman effect, magnetic susceptibilities, molecular refraction and the heats of formation have been investigated. Broadly speaking these results have been found to lead to consistent conclusions[1,2].

The object of the present paper is to supply ionization potential data of some troponoid compounds. As is well-known, the energy required to remove one of the most loosely bound electrons is given by

1) P. L. Pauson, *Chem. Revs.*, **55**, 9 (1955); T. Nozoe, "Progr. Chem. Org. Nat. Prod," Bd. XIII, Springer-Verlag, Wien (1956), p. 232.

2) For a review of these studies in Japan, see M. Kubo, Y. Kurita and M. Kimura, *Monogr. Res. Inst. Appl. Elec.*, **4**, 1 (1954).

the first ionization potential of the molecule. From this energy value, an important clue is obtained to the electronic state of a molecule.

### Experimental Materials

Tropolone[1]: m. p. 50-51°C.

Tropone[1]: b. p. 84-85°C/6 mmHg, $d_4^{25}$ 1.0825, $n_D^{27}$ 1.6020.

2-Aminotropone[1]: m. p. 106-107°C.

Cyclohexanone:—this substance was kindly provided by Professor K. Kozima, Tokyo Institute of Technology—b. p. 52°C/24 mmHg.

### Experimental Method and Result

The measurements of first appearance potentials were carried out in a Hagstrum type mass-spectrometer which was constructed by the present writers[3]. Comparatively weak ion currents were observed when the troponoid compounds were treated. In order to overcome the difficulty arising from this, special attention was paid to the space-charge effects[4] in the ionization chamber and also to the sensibility of the detector of ions.

The determination of the appearance potentials has been made by a modified method of critical slope as in a previous work[3]. Besides this the linear extrapolation method was employed for the sake of comparison. Ionization efficiency curves for tropolone and tropone are shown in Fig. 1.

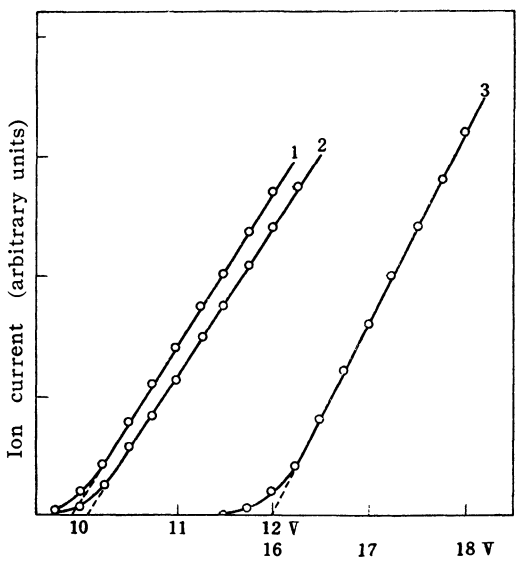



Fig. 1. Relative ionization efficiency curves for troponoids. 1 tropone; 2 tropolone; 3 argon.

The evaluation of the potential was made using the spectroscopic value for argon 15.76eV. Table I records the results thus obtained. No data for comparison exist in the literature.

TABLE I
FIRST IONIZATION POTENTIALS, eV.

| Substance | Critical slope | Linear extrapolation |
|---|---|---|
| Tropone | 9.68±0.02 | 9.69±0.02 |
| Tropolone | 9.86±0.02 | 9.83±0.02 |
| 2-Aminotropone | 9.43±0.02 | 9.50±0.02 |
| Cyclohexanone | 9.91±0.05 | 9.83±0.05 |

### Discussion

It has been concluded through the studies on dipole moment[5] and other properties[1] that the double bond of the carbonyl group

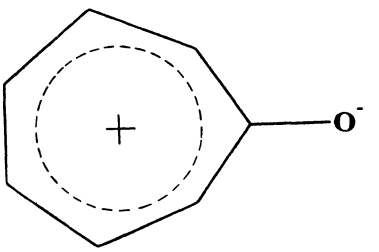



Fig. 2.

in tropone is exceptionally ionic, so that polar structure (Fig. 2) makes a large contribution to the normal state of the molecule. Concerning the structure of tropolone, it is believed that a strong hydrogen bond is formed between the two oxygen atoms of the molecule[1,5-7].

Are the above conclusions consistent with the observed ionization potentials? The answer will be affirmative, if this assumption be true: that, as in other carbonyl molecules[8-10] the first ionization energies of tropone and tropolone are largely determined by the nonbonding electrons at the O-atom of the carbonyl group.

Regarding tropone it is to be noted that both the critical slope and the linear extrapolation method gave lower ionization potential values than a related ketone, cyclohexanone by the amount 0.14-0.23 eV. The dipole moment of tropone 4.17 D[5] is

3) I. Omura, K. Higasi and H. Baba, This Bulletin, **29**, 501 (1955).
4) J. Marriott and J. D. Craggs, "Applied Mass Spectrometry," London (1954), p. 173.
5) Y. Kurita, S. Seto, T. Nozoe and M. Kubo, This Bulletin, **26**, 272 (1953).
6) K. Kuratani, M. Tsuboi and T. Simanouchi, ibid., **25**, 250 (1952).
7) S. Imanishi and M. Ito, ibid., **28**, 75 (1955).
8) C. A. Coulson, "Valence," Oxford (1952), p. 186
9) K. Higasi, I. Omura and H. Baba, *Nature*. **178**, 652 (1956).
10) I. Omura, K. Higasi and H. Baba, This Bulletin, **29**, 504 (1955).

the largest of the ketones, while cyclohexanone has a normal value of 2.75 D. Both of these facts may be interpreted as indicating that extra electric charge flows from the seven-membered ring into the oxygen. Consequently the effective electronegativity of the O-atom in tropone becomes smaller than in cyclohexanone, the ionization potential of tropone being thus decreased.

Further, by use of the same assumption the apparent rise in the potential of tropolone may be explained. Suppose that a strong hydrogen bond is formed between the two oxygen atoms in tropolone, that is, the non-bonding electrons of the oxygen atom of the carbonyl group become bound by the field of a proton. The energy for removing a loosely bound electron in tropolone will then become larger than in tropone.

The situation is more complicated in 2-aminotropone. It may be argued that only a weak hydrogen bond exists in the case of aminotropone[6]. Perhaps a decrease in ionization energy may result from this. But the observed decrease is more pronounced than is to be expected. It may be pointed out that the value 9.43 eV. for 2-aminotropone is near to that of methyl amine 9.41 eV. Generally aliphatic amines have lower potential values than corresponding ketones[10,11] e. g., ethyl amine 9.23 eV., *n*-propyl amine 9.17 eV., acetone 9.89 eV., methyl ethyl ketone 9.76 eV., etc. Therefore it may be reasonable to suppose that the most weakly bound electron in aminotropone is no longer situated at the O-atom. If it be localized at all, it will rather be near the N-atom of the $NH_2$ group.

Next, attention should be directed to the existence of pi-electrons in the seven-membered ring. Possibly these pi-electrons of the aromatic unsaturated carbon ring may be removed more easily than non-bonding electrons in the carbonyl group. But no reliable discussion can be presented on this possibility in the present stage of knowledge on this point.

Lastly a few words must be added concerning the difficulty of this sort of study. First, there are uncertainties in the interpretation of the ionization energy. For instance, against the explanation offered for tropone one may argue with good reason[8] that the measured ionization energy is very much higher than expected from the extremely ionic character of the carbonyl bond. Further one may point out that acetamide has a high ionization energy 10.39 eV.[10], so that the most loosely bound electron may not be localized at the N-atom of the molecule. In general it is questionable whether or not one can safely consider that the electron responsible for the first ionization is any one of the non-bonding electrons at a certain atom or that the ionization is due to pi-electrons of the conjugated system. Perhaps an *ad hoc* interpretation may be partly justified at the present stage, when few successful trials are known to explain the observed ionization potentials quantitatively even for the pi-electron systems containing no heteroatoms where molecular orbital calculations are relatively easy.

Second, some unknown source of error still exists in the measured potential values[12]. In the first report[3] of this series the writers tried to justify the use of argon as the standard gas and also the application of the critical slope method. The result of the examination was found satisfactory for eleven compounds. But one is not certain whether they are valid for any and every sort of molecule.

## Summary

First ionization potentials are obtained for the four substances: tropolone (a) 9.86, (b) 9.83; tropone (a) 9.68, (b) 9.69; 2-aminotropone (a) 9.43, (b) 9.50; cyclohexanone (a) 9.91, (b) 9.83 (units being eV.). Classification symbols, (a) and (b), denote that the measurement was made either by the method of critical slope or by the linear extrpolation method. These results are consistent with the conclusions from other physical data under certain conditions.

The writers' thanks are due to Asst. Prof. H. Baba for valuable suggestions.

*Research Institute of Applied Electricity Hokkaide University, Sapporo and Faculty of Science, Tohoku University, Sendai*

11) J. D. Morrison and A. J. D, Nicholson, *J. Chem. Phys.*, **20**, 1021 (1952).

12) See for instance, A. J. B. Robertson, "Mass Spectrometry," Methuen (1954), pp. 34-55. See also the subsequent paper of the writers.

# *Dielectric Studies on Colloidal Solutions. III. The Mobilities of Micelles of Long-chain Amine Hydrohalides*

By Michio SHIRAI and Bun-ichi TAMAMUSHI

(Received January 16, 1957)

In the previous paper of this series[1], the transference numbers of long-chain amine hydrochlorides were determined, and the fraction of small counter ions bound to a micelle and the mobility of a micelle were computed therefrom. In this paper, we shall present the direct measurement of the electrophoretic mobilities of the micelles of long-chain amine hydrohalides, and the relation between these mobilities and transference numbers or high-frequency effects will be discussed.

## Experimental

**Procedure.**—The measurement of electrophoretic mobility was carried out by means of the tracer electrophoresis method designed by Mysels and his collaborators[2]. The cell used is shown in Fig. 1. Silver wire is used as the

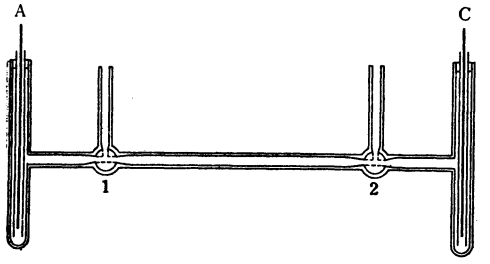



Fig. 1. The electrophoresis cell.

anode A, and silver wire coated with silver halides is used as the cathode C. These electrodes are unpolarizable. The central horizontal tube limited by three-way stopcocks 1 and 2 is filled with the solution of colloidal electrolytes tagged with orange OT, and the adjoining tubes on both sides are filled with an untagged solution. The apparatus is immersed in a thermostat. The electric current flowing through the cell is supplied by a constant current regulator. The electrophoretic mobility $u$ is expressed by the following formula:[2]

$$u=\frac{\lambda}{it}\frac{(Co-C)v}{Co} \qquad (1)$$

where $\lambda$ is the specific conductivity of the solution (mho/cm), $i$ the current flowing through the cell (amp.), $t$ the duration of the experiment (sec.), $Co$ the concentration of the tracer in the initial solution, $C$ the average concentration of the tracer after letting the current flow, and $v$ the volume of the tube between stopcocks 1 and 2.

The conductivity of the solution was measured with the impedance bridge of Yokogawa & Co., and the concentration of the tracer with the spectrophotometer of Hitachi & Co.

**Materials.**—The preparation of dodecyl-, tetradecyl-, and hexadecylamine hydrochloride has been described in the previous paper[1]. Dodecylamine hydrobromide was prepared from dodecylamine (Armour & Co., U.S.A.) by the addition of hydrobromic acid to its ethanol solution and distillation with benzene to remove the water introduced by the addition of the acid. Dodecylamine hydroiodide was prepared from dodecylamine in the same way as above by adding hydroiodic acid. All these products were recrystallized from ethanol.

Orange OT was purified from a commercial sample by solution in acetone and precipitation with water, followed by recrystallization from ethanol-benzene.

## Results and Discussion

The experimental results are shown in Table I and Fig. 2. As is shown in Fig. 2, the mobility of a micelle decreases with

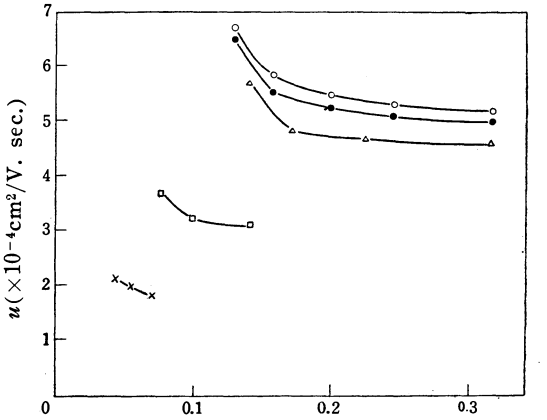



Fig. 2. The electrophoretic mobility.
○, dodecylamine hydrochloride;
●, — hydrobromide;
△, — hydroiodide;
□, tetradecylamine hydrochloride;
×, hexadecylamine hydrochloride.

1) M. Shirai and B. Tamamushi, This Bulletin, **29**, 733 (1956).
2) H. W. Hoyer, K. J. Mysels and D. Stigter, *J. Phys. Chem.*, **58**, 385 (1954).

TABLE I
ELECTROPHORETIC MOBILITY AT 30°C

| Substance | Concn. (mole/l.) | $\lambda$ ($\times 10^{-3}$mho/cm.) | $it$ (coul.) | $\frac{C_0-C}{C_0}$ | $u$ ($\times 10^{-4}$cm$^2$/v.sec.) |
|---|---|---|---|---|---|
| Dodecylamine hydrochloride | 0.017 | 1.60 | 3.30 | 0.365 | 6.7 |
| | 0.025 | 1.88 | 5.28 | 0.430 | 5.8 |
| | 0.04 | 2.24 | 8.64 | 0.559 | 5.5 |
| | 0.06 | 2.76 | 6.20 | 0.313 | 5.3 |
| | 0.1 | 4.00 | 6.30 | 0.216 | 5.2 |
| Dodecylamine hydrobromide | 0.017 | 1.46 | 2.24 | 0.262 | 6.5 |
| | 0.025 | 1.75 | 3.85 | 0.320 | 5.5 |
| | 0.04 | 2.08 | 4.62 | 0.310 | 5.3 |
| | 0.06 | 2.64 | 4.49 | 0.228 | 5.1 |
| | 0.1 | 3.60 | 7.11 | 0.260 | 5.0 |
| Dodecylamine hydroiodide | 0.02 | 1.12 | 1.86 | 0.249 | 5.7 |
| | 0.03 | 1.34 | 2.67 | 0.252 | 4.8 |
| | 0.05 | 1.65 | 2.40 | 0.180 | 4.7 |
| | 0.1 | 2.52 | 7.05 | 0.339 | 4.6 |
| Tetradecylamine hydrochloride | 0.006 | 0.558 | 1.08 | 0.187 | 3.7 |
| | 0.01 | 0.681 | 1.27 | 0.158 | 3.2 |
| | 0.02 | 0.970 | 1.37 | 0.115 | 3.1 |
| Hexadecylamine hydrochloride | 0.002 | 0.174 | 0.507 | 0.162 | 2.1 |
| | 0.003 | 0.192 | 0.648 | 0.169 | 1.9 |
| | 0.005 | 0.202 | 0.648 | 0.152 | 1.8 |

TABLE II
THE FRACTION OF BOUND IONS AND THE $\zeta$-POTENTIAL

| Substance | Concn. (mole/l.) | $\theta$ from mobility | $\theta$ from transference number | $\zeta$-Potential (mV.) |
|---|---|---|---|---|
| Dodecylamine hydrochloride | 0.017 | 0.37 | 0.42 | 119 |
| | 0.025 | 0.46 | 0.46 | 103 |
| | 0.04 | 0.59 | 0.56 | 98 |
| | 0.06 | 0.66 | 0.63 | 94 |
| | 0.1 | 0.70 | 0.66 | 92 |
| Dodecylamine hydrobromide | 0.017 | 0.44 | — | 115 |
| | 0.025 | 0.51 | — | 98 |
| | 0.04 | 0.62 | — | 94 |
| | 0.06 | 0.68 | — | 91 |
| | 0.1 | 0.73 | — | 89 |
| Dodecylamine hydroiodide | 0.02 | 0.60 | — | 101 |
| | 0.03 | 0.66 | — | 85 |
| | 0.05 | 0.75 | — | 83 |
| | 0.1 | 0.81 | — | 82 |
| Tetradecylamine hydrochloride | 0.006 | 0.22 | — | 65 |
| | 0.01 | 0.41 | 0.38 | 57 |
| | 0.02 | 0.58 | 0.60 | 55 |
| Hexadecylamine hydrochloride | 0.002 | 0.17 | 0.20 | 37 |
| | 0.003 | 0.38 | 0.46 | 34 |
| | 0.005 | 0.60 | 0.67 | 32 |

increasing concentration, the slope of the curve being considerably steep. This result is probably mainly due to the electrostatic interaction between large ionic micelles and small counter ions, as was discussed previously[3].

If we make some assumptions on the conductivity behavior of these salts, the fraction of counter ions bound to micelles can be calculated from the observed electrophoretic mobility. Those assumptions are: (1) The mobility of a free counter ion is not altered with increasing concentration, and is equal to that of a counter ion at infinite dilution; (2) beyond the critical micelle concentration there are no molecules of long-chain salts existing as single ones. Under these assumptions, if we denote the equivalent conductivity of total ions and free anions by $\Lambda$ and $\Lambda_-^0$, respectively, the relation between the fraction of bound ions $\theta$ and the electrophoretic mobility $u$ will be expressed as follows:

$$\frac{\Lambda-(1-\theta)\Lambda_-^0}{1-\theta}=Fu \qquad (2)$$

where $F$ is Faraday's constant. The solution of this equation for $\theta$ gives,

$$\theta=1-\frac{\Lambda}{\Lambda_-^0+Fu} \qquad (3)$$

On account of the second assumption, equation (2) is not valid near the critical micelle concentration. Table II shows the values of $\theta$ thus obtained, together with those computed from the transference numbers for dodecyl-, tetradecyl-, and hexadecyl- amine hydrochlorides. The difference between these two series of values may arise from the assumptions (1) and (2) above settled.

For dodecylamine hydrochloride, hydrobromide, and hydroiodide, the values of electrophoretic mobility are nearly the same, but the value for dodecylamine hydrochloride is slightly greater than that for dodecylamine hydrobromide and the latter is greater than that for dodecylamine hydroiodide. And as to the fraction of bound ions $\theta$ indicated in Table II, there is the following order: dodecylamine hydrochloride < dodecylamine hydrobromide < dodecylamine hydroiodide. On the other hand, for the critical micelle concentration the reverse order has been demonstrated, namely[4]: dodecylamine hydrochloride>dodecylamine hydrobromide>dodecylamine hydroiodide. This shows that there is a close relation between the tendency towards association of counter ions and the critical micelle concentration, that is, the stronger the tendency towards association of counter ions, the smaller the critical micelle concentration.

The electrophoretic mobility $u$ is related to the so-called $\zeta$-potential, that is, the electrokinetic potential of micelle ions. However, in order to calculate the $\zeta$-potential the knowledge concerning the thickness of the double layer, $1/\kappa$, and the radius of the micelle, $a$, is necessary. Considering that the relaxation effect is abnormally large in the range of concentration at which the measurement was a carried out, we assume $\kappa a \gg 1$. In such case, the relation between $u$ and the $\zeta$-potential has been given by Henry[5], which is shown as follows:

$$u=\varepsilon\zeta/6\pi\eta, \qquad (4)$$

where $\eta$ and $\varepsilon$ denote the viscosity and the dielectric constant of the solvent, respectively. The values of $\zeta$-potential computed from the value of $u$ by this formula are shown in Table II. Henry's formula is valid if the relaxation effect is negligible, but in our case the relaxation effect is so great that the real $\zeta$-potential is considerably greater than that indicated in Table II. Several formulas involving the relaxation effect have been proposed by Overbeek[6] and Booth[7], but to micelle ions which have abnormally high valency, these formulas are not valid, the theoretical solution of this problem being probably very difficult. But, if we can determine the high-frequency effect over a very wide range of frequency, more exact values of the $\zeta$-potential will be obtained.

## Summary

The electrophoretic mobilities of dodecylamine hydrochloride, hydrobromide and hydroiodide, as well as tetradecylamine and hexadecylamine hydrochlorides have been measured. They decrease with increasing concentration as is expected from the electrostatic point-of-view of the micelle structure.

3) M. Shirai and B. Tamamushi, This Bulletin, **28**, 545 (1955).
4) M. Shirai, *Sci. Pap. Coll. Gen. Educ., Univ. Tokyo.* **VI**, 29 (1956).
5) D. C. Henry, *Proc. Roy. Soc.* (*London*), **A133**, 106 (1931).
6) J. Th. G. Overbeek, *Koll. Beih.*, **54**, 316 (1943).
7) F. Booth, *Proc. Roy. Soc.* (*London*), **A203**, 514 (1950).

The fractions of counter ions bound to micelles are computed from the electrophoretic mobilities obtained. These values are found consistent with the result obtained by the transference number measurement.

The $\zeta$-potentials of micelle ions are calculated from the electrophoretic mobilities by Henry's formula. They must be, however, less than the real values, if we take into account the expected high-frequency effects.

*Chemistry Dept., College of General Education, and Institute of Science and Technology*
*The University of Tokyo, Meguro, Tokyo*

# *Study on the Electric Conductivity of Sodium Silicate Aqueous Solution. II*

By Hiroshi UKIHASHI

(Received August 10, 1956)

## Introduction

Few data have been reported on the dependence of the electric conductivity of sodium silicate solution on temperature. In the present paper are given the electric conductivities measured at 5°, 15°, 25°, 35°, 45° and 60°C of sodium silicate solution of silica-alkali molar ratio ranging from 1 to 3.95 over a wide range of concentration.

From the results, temperature coefficients of the specific conductivity were computed and compared with those of simple strong electrolyte solutions. The equivalent conductivity was derived in the same way as reported in the preceding paper[1]. For the dilute solutions the applicability of Walden's rule, i. e., the independency of the product of equivalent conductivity and solvent viscosity on temperature was examined, and the ionic radius of silicate ion was estimated therefrom. Theoretical treatment of the equivalent conductivity for the 3.95 molar ratio solution was extended to those at other temperatures than 25°C, and it was confirmed that they could be explained theoretically at each temperature with the same assumption as previously described.

Meanwhile, hydroxyl ion concentration was checked at these temperatures for the sodium silicate solutions of three kinds of molar ratio to examine its contribution to their conductivities.

The independence of the conductivity on the viscosity of solution in the higher concentration range was emphasized, and this problem will be discussed in the succeeding paper.

## Experimental

**Materials.** — The sodium silicate solutions were prepared by the same method as described previously[1]. The silica-alkali molar ratio of the solutions herein used were 1.00, 1.55, 2.13, 3.19, and 3.95.

**Apparatus and Measurements.**—Apparatus for the conductivity measurement was the same as previously reported. The six cells were used, the constants of which were 0.4850, 0.6568, 1.242, 1.380, 16.86 and 18.75. The measurements were made at a series of increasing temperatures from 5° to 60°C, without replacing the solution, except in the case where variation in conductivity with temperature was so much as to require the use of different cell constant. For a dilute solution having possibility of change in conductivity with time, the measurement at each temperature was made 30 minutes after preparation. However, the conductivity change with time was small as compared with the accuracy of this experiment, at most within $\pm 0.5\%$ during the first one hour after preparation. For each molar ratio solution density was measured at these temperatures over a wide range of concentration, using 25 cc. pycnometer. These values were needed for expressing concentration as normality.

Besides, pH was measured for three kinds of sodium silicate solution of molar ratio 1.00, 2.13, and 3.95, at temperatures 5°, 15°, 25°, 35 and 45°C. Beckman Model H-2 *p*H-Meter was used with Beckman type E glass electrode especially designed for the measurements in highly alkaline solution. It is questioned, however, whether the silicate solution does not give any detrimental effect on the glass electrode. To ascertain the reliability of the observed data *p*H values obtained

1) H. Ukihashi. This Bulletin, **29**, 537 (1956).

2) R. W. Harman. *J. Phys. Chem.*, **30**, 1100 (1926).

at 25°C were compared with those obtained by Harman[2] with hydrogen electrode, and those measured by Küntzel et al.[3]. They were approximately in accord with each other within ±0.1, whereas no comparison was available for the values obtained at other temperatures than 25°C[4,5]. For pH measurement, a sample solution was put in 100 cc. polyethylene beaker and covered with vinyl plate with two holes for insertion of

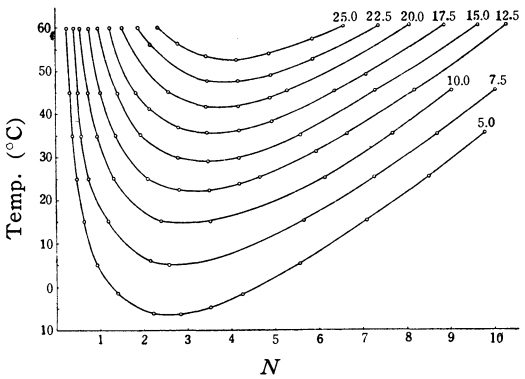



Fig. 1. Iso-conductivity curve of sodium metasilicate solution (numerals for each curve denote $\lambda \times 10^2$)

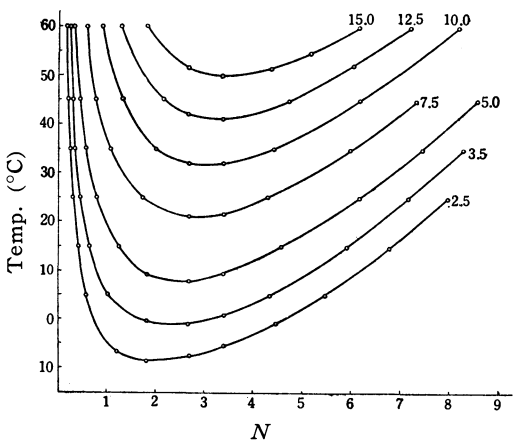



Fig. 2. Iso-conductivity curve of sodium silicate solution of molar ratio 1.55 (numerals for each curve denote $\lambda \times 10^2$)

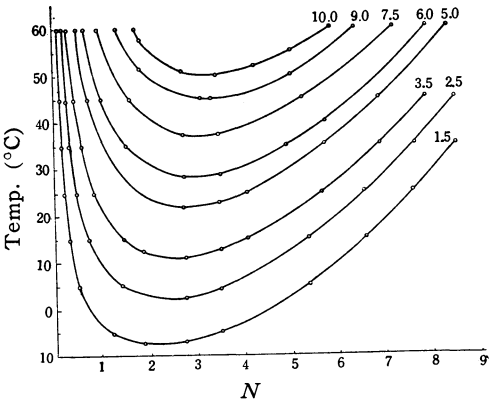



Fig. 3 Iso-conductivity curve of sodium silicate solution of molar ratio 2.13 (numerals for each curve denote $\lambda \times 10^2$)

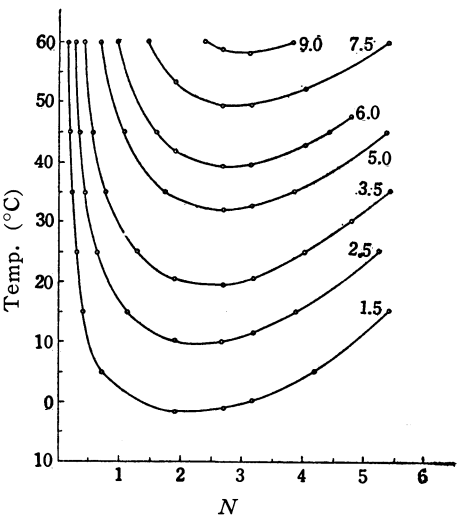



Fig. 4. Iso-conductivity curve of sodium silicate solution of molar ratio 3.19 (numerals for each curve denote $\lambda \times 10^2$)

electrodes. The meter was frequently standardized with borax and soda buffer solution at each temperature.

## Results and Discussion

In Fig. 1–5 contour maps are given, which express the specific conductivity as a function of temperature and concentration. Here points on each line have the same conductivity. These curves were drawn as follows. Points on temperature absissas of 5°, 15°, 25°, 35°, 45° and 60° were taken from the data on the curves expressing the relation between specific conductivity and concentration at respective temperatures. Other data were obtained by the inter- and extrapolation of the relation curves between conductivity and temperature at various concentrations.

3) L. E. Küntzel, J. W. Hensley and L. R. Bacon, *Ind. Eng. Chem.*, **35**, 1286 (1943).

4) Schuffelen and Hulst[6], who measured the pH of some concentrated water glass, stated that glass electrode did not produce a satisfactory result, while Sb electrode did. On the other hand, Küntzel et al. measured the pH of dilute sodium silicate solution with both hydrogen and glass electrode, and found the differences between two values to be very small at room temperature but to increase as temperature increases. The pH values obtained by Schuffelen and Hulst are 0.3—0.5 smaller than those obtained by other workers cited herein.

5) Complete data of pH hereby measured will be reported in *Reports of the Research Laboratory, Asahi Glass Co.*

6) A. C. Schuffelen and L. J. N. van der Hulst, *C. A.* **36**, 3583, 5580 (1942).

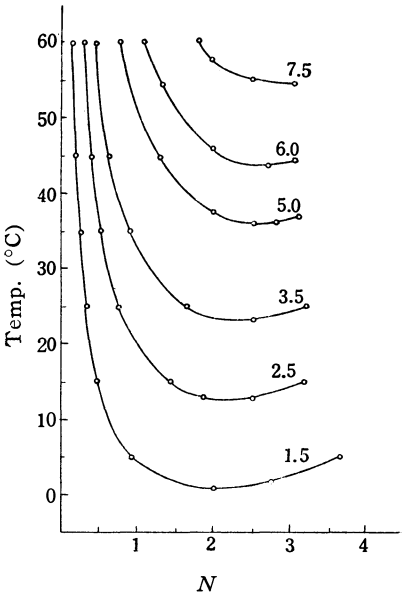



Fig. 5. Iso-conductivity curve of sodium silicate solutions of molar ratio 3.95 (numerals for each curve denote $\lambda \times 10^2$)

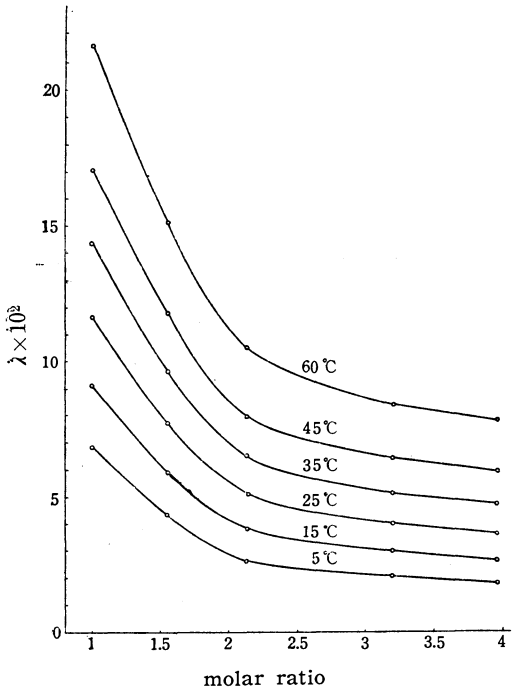



Fig. 6. Relationship between specific conductivity and molar ratio at $Na_2O$ wt. % 5.00.

Here the concentration is indicated by normality of sodium ion content. As seen in these figures the change in specific conductivity with temperature increases as concentration increases in view of wide temperature range, but at a fixed temperature it has the maximum at a moderate concentration, where maximum specific conductivity is attained. As for the concentration dependence of specific conductivity, it increases as temperature rises up, and at a fixed temperature it becomes the minimum around a moderate concentration where specific conductivity shows the maximum. This concentration moves upwards with temperature increase. Fig. 6 shows the relationship between conductivity and molar ratio of sodium silicate solution at a fixed concentration. It is seen that decrease in conductivity with molar ratio gets more remarkable as temperature goes up, and yet all the curves have an obvious bend around molar ratio 2. In Fig. 7 the concentration showing maximum conductivity is plotted against the molar ratio of the solution. In this case no bend seems to appear. This fact should be expected, because the change in conductivity with molar ratio is due primarily to the difference of hydrolysis percentage in the solutions, while the concentration giving maximum specific conductivity may be attributed to the degree of compactness of the solute molecule in the solution and dependent on the molecular volume of sodium silicate molecule in respective molar ratio solution. If the latter is admitted, intermolecular distance at that concentration may have a linear relation with cubic root of molecular weight. This was the case as seen in Fig. 8, where two curves were drawn for both 5°C and 60°C. Here molecular weight was assumed as such

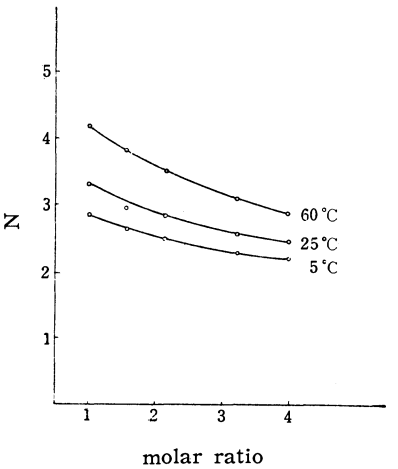



Fig. 7. Change of concentration showing maximum specific conductivity with molar ratio of sodium silicate solutions.

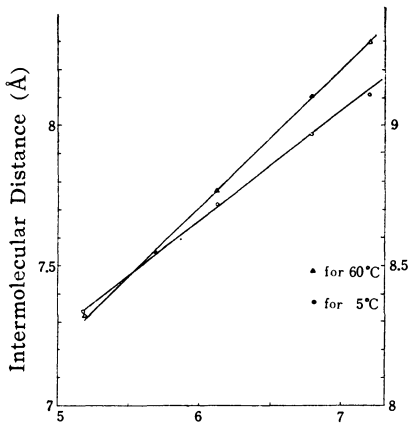



Fig. 8. Relationship between intermolecular distance at concentration showing maximum specific conductivity and cubic root of molecular weight of various sodium silicates.

expressed by the conventional formula.

The temperature coefficient of specific conductivity, as expressed by a and b in the following equation were calculated by the least square method and tabulated in Table 1.

$$\lambda=\lambda_0+aT+bT^2$$

$\lambda_0$ is the specific conductivity at 0°C. The table indicates that the first order temperature coefficient has the maximum values in a moderate concentration, while the second order temperature coefficient continues to increase with concentration. This means that the higher the temperature, the larger the temperature coefficient of the more concentrated solution becomes. In Fig. 9 $d\lambda/dT$ at 25°C was plotted against concentration of various sodium silicate solutions together with those of simple strong electrolyte solutions, the latter being quoted from "Landolt und Börnstein Tabellen" with adequate unit conversion.

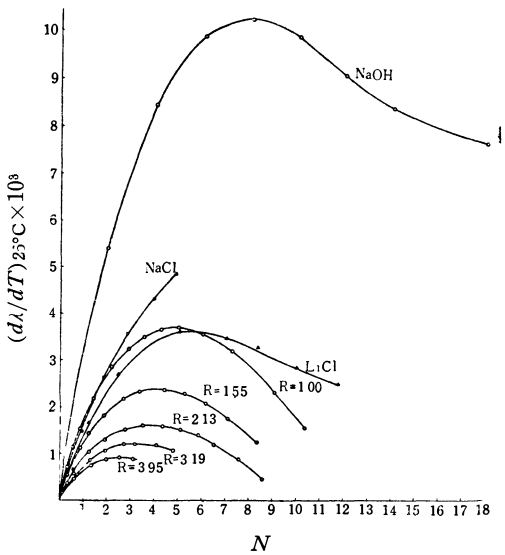



Fig. 9. The change of temperature coefficient of specific conductivity.

TABLE I

TEMPERATURE COEFFICIENT OF SPECIFIC CONDUCTIVITY OF VARIOUS MOLAR RATIO SODIUM SILICATE SOLUTIONS

| $Na_2O$ wt% / Molar Ratio | | 1.00 | 2.50 | 5.00 | 7.50 | 9.00 | 10.50 | 12.00 | 16.00 |
|---|---|---|---|---|---|---|---|---|---|
| 1.00 | $\lambda_0\times10^2$ | 1.96 | 3.93 | 5.78 | 6.20 | 5.93 | 5.31 | 4.50 | 2.03 |
| | a $\times10^4$ | 6.36 | 13.10 | 20.25 | 25.21 | 26.01 | 25.73 | 23.82 | 13.32 |
| | b $\times10^6$ | 1.74 | 4.36 | 9.18 | 14.53 | 18.29 | 22.19 | 26.77 | 37.35 |
| | | | | | | | | | (15.00) |
| 1.55 | $\lambda_0\times10^2$ | 1.35 | 2.60 | 3.57 | 3.55 | 3.21 | 2.60 | 1.97 | 0.84 |
| | a $\times10^4$ | 4.79 | 9.31 | 14.43 | 16.28 | 16.03 | 14.90 | 12.54 | 5.05 |
| | b $\times10^6$ | 1.63 | 4.14 | 7.82 | 12.15 | 15.06 | 17.78 | 20.56 | 25.25 |
| 2.13 | $\lambda_0\times10^2$ | 0.874 | 1.59 | 2.16 | 2.15 | 1.89 | 1.49 | 1.03 | 0.332 |
| | a $\times10^4$ | 3.50 | 6.77 | 9.98 | 11.10 | 10.72 | 9.06 | 6.94 | 4.72 |
| | b $\times10^6$ | 1.69 | 3.52 | 6.25 | 9.08 | 11.06 | 13.40 | 15.25 | 17.53 |
| | | | | | | | (10.13) | | |
| 3.20 | $\lambda_0\times10^2$ | 0.739 | 1.30 | 1.64 | 1.47 | 1.15 | 0.861 | | |
| | a $\times10^4$ | 2.95 | 5.71 | 8.23 | 8.34 | 7.14 | 5.58 | | |
| | b $\times10^6$ | 1.49 | 2.90 | 5.08 | 7.89 | 9.70 | 11.03 | | |
| | | | | | (6.47) | | | | |
| 3.95 | $\lambda_0\times10^2$ | 0.688 | 1.16 | 1.41 | 1.36 | | | | |
| | a $\times10^4$ | 2.93 | 5.78 | 7.86 | 8.03 | | | | |
| | b $\times10^6$ | 1.19 | 2.34 | 4.64 | 5.83 | | | | |

The figure shows that the temperature coefficient of specific conductivity of sodium silicate solution is rather small as compared with simple strong electrolyte solutions, and the decrease in temperature coefficient with concentration in the higher concentration range is more marked than that of those solutions. This might lead to a suggestion that the temperature coefficient of mobility of silicate ion is small and its trend of making a kind of configuration in the solution is greater than that with simple strong electrolyte.

The equivalent conductivity $\Lambda$ at various temperatures were plotted against the square root of concentration. Fig. 10, 11 and 12 show those obtained for the silicate solutions of molar ratio 1, 2.13 and 3.95.

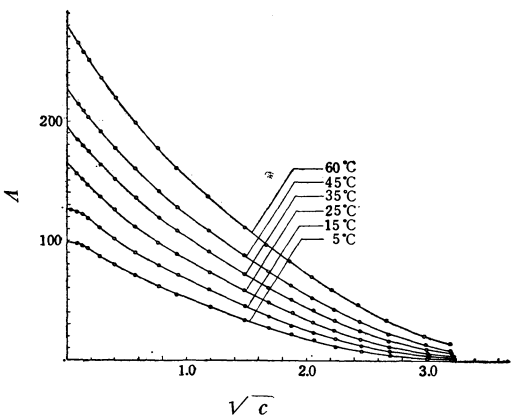



Fig. 10. Variation of the equivalent conductivity of sodium metasilicate solution with square root of concentration at various temperatures.

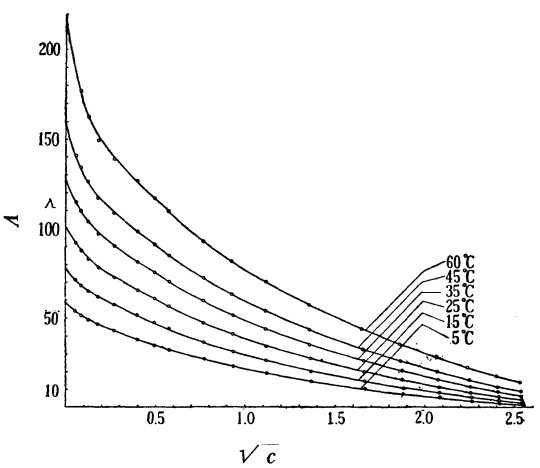



Fig. 11. Variation of the equivalent conductivity of molar ratio 2.13 sodium silicate solution with square root of concentration at various temperatures.

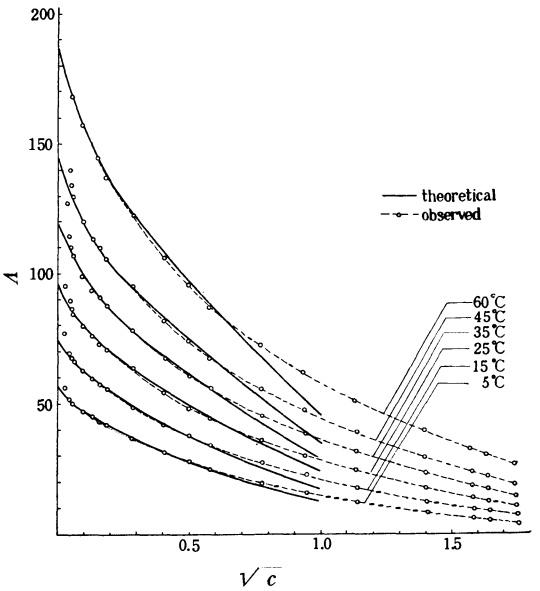



Fig. 12. Comparison of the equivalent conductivity of molar ratio 3.95 sodium silicate solution with those calculated from the theoretical equation at various temperatures.

The limiting equivalent conductivity $\Lambda_0$ was estimated by the extrapolation of curves to infinite dilute concentration. They are tabulated in Table II, together

TABLE II

LIMITING EQUIVALENT CONDUCTIVITY AND ITS PRODUCT WITH VISCOSITY OF SOLVENT

| M.R. | 1.00 | | 2.13 | | 3.95 | |
|---|---|---|---|---|---|---|
| Temp. | $\Lambda_0$ | $\Lambda_0\eta_0$ | $\Lambda_0$ | $\Lambda_0\eta_0$ | $\Lambda_0$ | $\Lambda_0\eta_0$ |
| 5°C | 98 | 149 | 59 | 90 | 56 | 85 |
| 15°C | 128 | 145 | 79 | 90 | 74 | 84.4 |
| 25°C | 165 | 148 | 102 | 91.5 | 96 | 85.8 |
| 35°C | 194 | 140 | 128 | 92.5 | 119 | 85.9 |
| 45°C | 227 | 136 | 158 | 94.6 | 144 | 86.2 |
| 60°C | 282 | 132 | 210 | 98.5 | 186 | 87.2 |

with the product of $\Lambda_0$ and solvent viscosity $\eta_0$. In Fig. 13 $\Lambda\eta$, including $\Lambda_0\eta_0$, are plotted against temperature for dilute solutions of these three kinds of molar ratio. It is seen that while Walden's rule is fully applicable to the 3.95 molar ratio solution, $\Lambda\eta$ for metasilicate solution decreases markedly with increase in temperature, and that for the 2.13 molar ratio solution increases slightly with it. These facts may be explained by considering the contribution of $OH^-$ ion in the solutions to the equivalent conductivity.

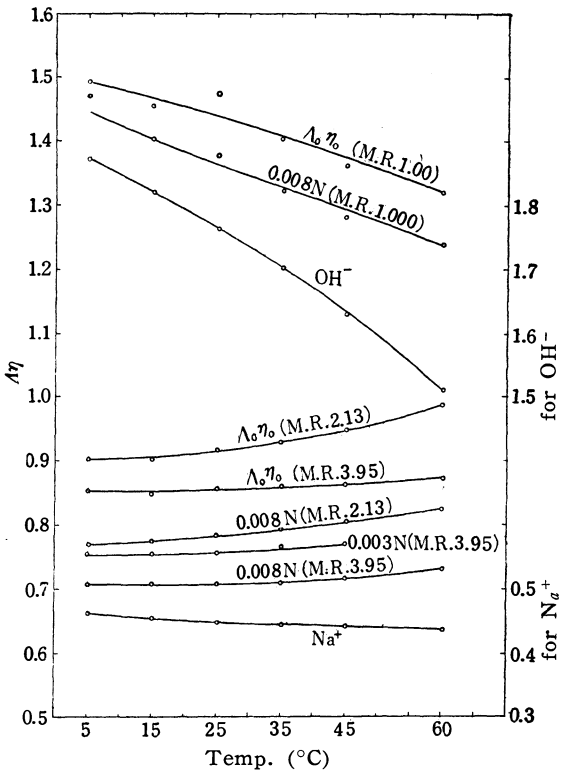



Fig. 13. Variation of $\Lambda\eta$ with temperature for extreme, and infinite dilute sodium silicate solutions and for $Na^+$ and $OH^-$ ion at infinite dilution

In order to examine this, $OH^-$ ion concentration at various temperatures was calculated from *p*H values, and hydrolysis percentages were derived from them[7]. They were 23, 26, 28, 26 and 26% at 5°, 15°, 25°, 35° and 45°C for 0.008 N metasilicate solution, 1.4, 2.8, 3.2, 3.9 and 4.2% at above respective temperatures for the 2.13 molar ratio solution. For the 3.95 molar ratio solution they were negligibly small, i. e. varies only from 0.7% to 1.9% at 0.008 N between 5° and 45°C. Thus it is well understood that for the metasilicate solution, the decreasing tendency with temperature of $\Lambda_0\eta_0$ of $OH^-$ ion, which is shown also in Fig. 13 along with that of $Na^+$ ion, appears to give a prominent effect on its $\Lambda\eta$ while the constancy of $\Lambda\eta$ of the 3.95 molar ratio solution is well satisfied. For the 2.13 molar ratio solution $\Lambda$ increase with temperature is affected by the change in $OH^-$ ion concentration with temperature, so that $\Lambda\eta$ becomes larger than in the case where the composition of the solution holds constant.

$\Lambda_0\eta_0$ for an ion is related to the ionic radius $r$ as shown by the equation $r=0.820|z|/\Lambda_0\eta_0$ where $r$ is expressed by Ångstrom and $|z|$ denotes the charge valency. Since this relation was derived from Stokes' law $r=1/(6\pi\eta u)$, where ionic mobility $u$ is related to the limiting equivalent conductivity by $6.47\times10^6\Lambda_0/|z|$, it is applicable only to the ion of symmetrical shape. Therefore, though this treatment may be merely a rough approximation, it would be of some value to estimate the radius of silicate ion by this equation. $\Lambda_0$ of silicate ion in the solution of molar ratio 1.00, 2.13 and 3.95 were computed from their limiting equivalent conductivity as follows,

$$\Lambda_{0(\text{sil.})}=(\Lambda_0-\Lambda_{0(Na^+)}-C_{OH}\Lambda_{0(OH^-)})/C_{\text{sil.}}$$

where $C_{OH}$ and $C_{\text{sil.}}$ are $OH^-$ ion and silicate ion concentration at infinite dilution. It seems difficult, however, to get the hydrolysis percentage at infinite dilution by the extrapolation of a curve plotted against concentration, and further more, unstable *p*H values observed in this dilute region do not enable one to get hydrolysis percentage. Meanwhile, the limiting equivalent conductivity was obtained by extrapolation of curve by neglecting the abruptly increased value observed in this extreme dilution. Thus replacement of the hydrolysis percentage at 0.008 N for that at infinite dilution will be tentatively justified. The concentration of silicate ion at infinite dilution was assumed to be $(1-X)$ N, where $X$ denoted degree of hydrolysis. As a result, $r$=4.0 Å was obtained for both 2.13 and 3.95 molar ratio solutions, and $r$=2.24 Å for metasilicate solution. However, it is recognized that the Stokes' law radius is known to require the correction if applied for the smaller radius than 5 Å, due to the deviation of numerical constant from $6\pi$. After the above-mentioned radii were multiplied by the correction factor[8] they become 4.56 Å and 3.63 Å. These values, despite a result of rather drastic estimation and resultant failure to distinguish between the radii of silicate ions in the 2.13 and 3.95 molar ratio solutions, their order seems quite reasonable as compared with data regarding the size of sodium silicate molecule

7) Because of lack of extreme accuracy in the measurement hereby used, pH value ±0.1 would be within the error. This led to a considerable inconsistency of data of hydrolysis percentage especially for the solution having high $OH^-$ ion concentration, such as sodium silicate solution.

8) This correction factor was cited from, R. A. Rcbinson and R. H. Stokes, "Electrolyte Solutions," Butterworths Scientific Publications, London (1955), p.119.

reported elsewhere.

In the preceding paper the change in equivalent conductivity with concentration has been computed for the 3.95 molar ratio solution at 25°C, on the basis of Falkenhagen's equation,

$$\Lambda=\left(\Lambda_0-\frac{41.25(|z_1|+|z_2|)\sqrt{I}}{\eta(\varepsilon T)^{1/2}(1+\kappa a)}\right)\times\left(1-\frac{2.801\times10^6|z_1z_2|q}{(\varepsilon T)^{3/2}(1+\sqrt{q})}\cdot\frac{e^{\kappa a(1-\sqrt{q})}-1}{\kappa a(1-\sqrt{q})}\cdot\frac{\sqrt{I}}{(1+\kappa a)}\right)$$

$$\kappa=\left(\frac{8\pi Ne^2}{1000\varepsilon kT}\right)^{1/2}\sqrt{I}$$

where notation is the same as used before.

This computation was extended for the equivalent conductivities measured at other temperatures, 7 Å for the mean ionic diameter $a$ being used as in the previous treatment. The results were corrected for the solution viscosity and plotted in Fig. 12. The accordance of observed values with those theoretically computed is quite satisfactory as far as the concentration 0.8–0.9 N is reached. This consistent agreement at any temperature of theoretical and observed data shows that the change with temperature of equivalent conductivity—square root of concentration curve is explained only in terms of temperature change and consequent change of dielectric constant and viscosity of solvent, and that the change of composition of solution need not be considered; this change may occur, if any, on the part of silicate ion or molecule therein, because $p$H measurements indicated that $OH^-$ ion concentration did not vary appreciably over the temperature range measured. Also it is recognized that the assumption, which has been set upon computing equivalent conductivity at 25°C on the basis of Falkenhagen's equation, was proved sufficient at any other temperature for the explanation of them.

Above the concentration 0.8–0.9 N, the theoretical values fall increasingly below the observed one. This was caused by the fact that the viscosity increase outgrew more and more the conductivity decrease, as concentration increased. On the other hand it has been already noticed that at the concentration where specific conductivity became maximum the viscosity of the solution varied strikingly according to the molar ratio of the solution and it appeared to have little effect on the specific conductivity at this concentration range. These facts suggest that the higher the concentration, the larger difference between the mechanisms of conductance and viscosity may appear. The correlation of conductivity and viscosity of the sodium silicate solution would be a very interesting subject, further study of which may throw some light upon the investigation of the structure of the concentrated solution. It will be dealt with in the succeeding paper.

The author would like to express his sincere thanks to Dr. T. Yawataya for his kind encouragement throughout this work.

*Research Laboratory Asahi Glass Co. Ltd. No. 2 Benten-cho Tsurumi-ku, Yokohama*

# *Relation between the Contents of Radon and Radium B in Several Radioactive Mineral Springs*

By Shunji UMEMOTO

(Received June 11, 1956)

## Introduction

The relation between the contents of radon and its decay products was first studied by K. Kimura, K. Kuroda and Y. Yokoyama[1] at Masutomi Mineral Springs. Further studies were made by Y. Yokoyama[2] at Ikeda and Misasa Springs. Their results are summerised as follows.

(1) The contents of radium A, radium B and radium C are smaller than expected from their equilibrium states with radon.

(2) The greater the radon content, the greater is the extent to which the equilibrium states between radon and its decay products decreased.

(3) In a sealed vessel the equilibrium between radon and radium A is achieved within 20 min. after the issue, and that between radon and radium B and radium C within 3 hours.

(4) In a mineral spring, the contents (expressed in Curie) of Rn, RaA, RaB and RaC decrease in this sequence.

(5) The relationship between the contents of Rn and RaA, RaB and RaC can be accounted for when it is assumed that the latter three are produced within 2 to 45 min. before the issue from Rn free from its decay products.

S. Umemoto[3] reported, however, that RaB can be present more than the equilibrium amount to the Rn, on a continuous measurement of their contents in "Hisui-no-yu" of Misasa Hot Springs. T. Ishimori and I. Hatae[4] measured the contents of Ra, Rn, RaA, RaB, RaC, RaF, ThX, Tn, ThB and ThC in Ikeda Mineral Springs and discussed the relation between the contents of Rn and RaB, showing that RaB can be present more than the equilibrium amount to the Rn*. K. Kimura, K. Nagashima, N. Ikeda and Ka. Kimura[5] also studied the contents of RaB and Rn in the mineral springs of Naegi district, Gifu Prefecture, and found that the RaB content is merely several fractions of the equilibrium amount to the Rn. S. Umemoto[6] continuously measured the contents of Rn and RaB for a year at Misasa Hot Springs. When the content of RaB was compared with that of Rn 20 min. after the issue, the ratio RaB/Rn became greater with increase in the rate of flow, with a few exceptions. It was also made clear that the ratio RaB/Rn decreases when the rate remarkably increases. In special cases, the ratio RaB/Rn is greater than unity but decreases in autumn when water is removed from the surrounding rice field.

The present author intended to determine the content of RaB and other relating components immediately after the issue in order to disclose the relationship between the contents of Rn and RaB. The measurements were made at Hamamura (Kachimi) Hot Springs, Misasa Hot Springs and Sekigane Hot Springs, Tottori Prefecture.

### Location and Methods for Experiments

These three Springs are situated in the middle of Tottori Prefecture and are found in a granite zone. Hamamura Hot Springs (I) are among sand hills along the sea side. Misasa Hot Springs (II) are found along the valley of the river Misasa. Sekigane Hot Springs (III) are found along a mountain torrent which flows into the river Ogamo (Fig. 1). Water temperature, rate of flow and the contents of chloride, sulfate, radon and radium B were measured once a month for a year at one spring in I, five springs in II and one in III. Their names are as follows:

1) K. Kimura, K. Kuroda and Y. Yokoyama, *J. Chem. Soc Japan (Pure Chem. Sect.)*, **69**, 34 (1948).
2) Y. Yokoyama, ibid., **70**, 399 (1949).
3) S. Umemoto, This Bulletin, **26**, 160 (1953).
4) T. Ishimori and I. Hatae, Read before the symposium on geochemistry of the Chemical Society of Japan, Sapporo, July, 1952,; Read before the seventh annual meeting of the Chemical Society of Japan, Tokyo, April, 1954.

* Yokoyama's report mentioned above also shows that RaB is contained more than the equivalent amount to the Rn in Ikeda Spring No.2; (he considered that this is due to escape of Rn) hence it appears certain that the amount of RaB is more than that expected from the Rn content.

5) K. Kimura, K. Nagashima, N. Ikeda and Ka. Kimura, *Radioisotopes*, **4**, 31 (1955).
6) S. Umemoto, *J. Chem. Soc. Japan (Pure Chem. Sect.)*, **75**, 352 (1954).

TABLE I

OBSERVATIONAL RESULTS IN I

| Time of sampling | Weather | Temperature °C | Rate of flow l./min. | Water temperature °C | $Cl^-$ mg./l. | Rn Mache | Rn $10^{-10}$ c./l. | RaB | RaB/Rn | $SO_4^{2-}$ mg./l. |
|---|---|---|---|---|---|---|---|---|---|---|
| 1954, 26/V a. m. 11.40 | Cloudy Fine later | 20.5 | 18.38 | 69.7 | 290.6 | 20.0 | 72.8 | 14.6 | 0.200 | 392.1 |
| 25/VI a. m. 11.40 | Cloudy | 20.2 | 17.21 | 69.7 | 289.6 | 19.5 | 70.9 | 9.08 | 0.128 | 396.1 |
| 6/VII a. m. 11.15 | Fine | 30.5 | 19.10 | 69.7 | 289.6 | 20.8 | 75.7 | 18.2 | 0.240 | 437.6 |
| 26/VIII a. m. 11.17 | Cloudy | 32.8 | 22.17 | 69.6 | 290.6 | 21.9 | 79.7 | 16.6 | 0.208 | 465.1 |
| 27/IX a. m. 11.40 | 〃 | 22.0 | 21.49 | 69.7 | 285.1 | 21.4 | 77.9 | 19.5 | 0.250 | 426.1 |
| 13/X a. m. 11.07 | 〃 | 13.8 | 17.12 | 69.7 | 287.6 | 20.1 | 73.2 | 27.5 | 0.376 | 409.1 |
| 17/XI a. m. 11.11 | Rainy | 9.3 | 17.73 | 70.0 | 281.6 | 19.8 | 72.1 | 15.3 | 0.212 | 416.4 |
| 16/XII a. m. 11.22 | Fine | 4.4 | 19.32 | 70.0 | 286.6 | 23.2 | 84.4 | 25.8 | 0.306 | 460.2 |
| 1955, 14/I a. m. 11.14 | Cloudy | 5.0 | 20.06 | 70.0 | 288.1 | 19.7 | 71.7 | 20.8 | 0.290 | 452.6 |
| 15/II a. m. 11.09 | Fine | 5.4 | 16.24 | 70.0 | 297.0 | 20.7 | 75.3 | 28.1 | 0.373 | 456.2 |
| 14/III a. m. 10.54 | Cloudy | 6.0 | 17.45 | 70.0 | 294.0 | 19.3 | 70.2 | 12.5 | 0.178 | 449.8 |
| 27/IV a. m. 11.17 | Fine | 14.0 | 21.72 | 69.9 | 293.5 | 21.5 | 78.3 | 26.8 | 0.342 | 436.5 |

TABLE II

OBSERVATIONAL RESULTS IN II-1

| Time of sampling | Weather | Temperature °C | Rate of flow l./min. | Water temperature °C | $Cl^-$ mg./l. | Rn Mache | Rn $10^{-10}$ c./l. | RaB | RaB/Rn |
|---|---|---|---|---|---|---|---|---|---|
| 1953, 1/VI a. m. 11.00 | Cloudy | 24.0 | 2.860 | 63.2 | 414.7 | 33.3 | 121 | 14.9 | 0.123 |
| 23/VI a. m. 9.10 | Cloudy Rainy later | 25.8 | 3.973 | 66.4 | 411.7 | 22.0 | 80.1 | 15.7 | 0.196 |
| 6/VII a. m. 10.18 | Cloudy | 28.6 | 4.610 | 66.6 | 390.2 | 26.6 | 96.8 | 26.4 | 0.273 |
| 11/VIII a. m. 10.20 | 〃 | 30.4 | 2.538 | 69.6 | 605.4 | 21.0 | 76.4 | 23.6 | 0.309 |
| 1/IX a. m. 10.05 | Rainy Cloudy later | 27.0 | 2.403 | 69.8 | 401.7 | 20.1 | 73.1 | 18.1 | 0.248 |
| 22/IX a. m. 10.10 | Fine Cloudy later | 22.1 | 2.750 | 69.3 | 400.2 | 18.5 | 67.3 | 18.2 | 0.271 |
| 13/X a. m. 10.07 | Cloudy Fine later | 19.0 | 1.710 | 68.2 | 396.2 | 10.7 | 38.9 | 14.5 | 0.373 |
| 9/XI a. m. 10.16 | Fine | 16.6 | 1.893 | 67.6 | 395.2 | 14.8 | 53.9 | 18.0 | 0.334 |
| 14/XII a. m. 10.10 | 〃 | 7.2 | 2.476 | 68.0 | 405.7 | 11.1 | 40.4 | 12.9 | 0.319 |
| 1954, 11/I a. m. 10.35 | Rainy | 7.8 | 2.645 | 67.0 | 400.7 | 14.4 | 52.4 | 13.5 | 0.258 |
| 15/II a. m. 10.40 | Cloudy | 6.0 | 2.091 | 66.2 | 400.2 | 13.2 | 48.0 | 15.1 | 0.314 |
| 15/III a. m. 10.22 | 〃 | 5.0 | 1.993 | 66.5 | 402.7 | 14.5 | 52.8 | 16.6 | 0.314 |
| 20/IV a. m. 10.32 | 〃 | 13.0 | 1.585 | 65.8 | 377.2 | 10.7 | 38.9 | 7.5 | 0.192 |
| 20/V a. m. 10.15 | 〃 | 21.6 | 1.673 | 67.3 | 399.2 | 13.8 | 50.2 | 12.1 | 0.240 |

TABLE III

OBSERVATIONAL RESULTS IN II-2

| Time of sampling | Weather | Temperature C° | Rate of flow l./min. | Water temperature °C | Cl⁻ mg./l. | Rn Mache | Rn $10^{-10}$ c./l. | RaB | RaB/Rn |
|---|---|---|---|---|---|---|---|---|---|
| 1953, 16/X a. m. 10.06 | Cloudy | 16.6 | 0.731 | 58.0 | 613.9 | 13.5 | 49.1 | 39.0 | 0.794 |
| 13/XI a. m. 10.06 | 〃 | 11.0 | 1.022 | 59.0 | 629.8 | 13.8 | 50.2 | 29.4 | 0.586 |
| 17/XII a. m. 10.04 | 〃 | 12.0 | 0.696 | 57.3 | 655.6 | 14.1 | 51.3 | 40.8 | 0.795 |
| 1954, 16/I a. m. 10.14 | 〃 | 7.2 | 0.745 | 58.3 | 663.3 | 16.5 | 60.1 | 41.0 | 0.682 |
| 25/II a. m. 10.30 | Fine Cloudy later | 7.0 | 1.060 | 58.0 | 657.8 | 15.7 | 57.1 | 36.0 | 0.630 |
| 18/III a. m. 10.10 | Cloudy | 8.5 | 1.063 | 59.3 | 650.8 | 19.0 | 69.2 | 42.1 | 0.608 |
| 23/IV a. m. 10.29 | Fine | 16.7 | 1.053 | 59.4 | 655.3 | 15.0 | 54.6 | 38.9 | 0.713 |
| 19/V a. m. 10.12 | Cloudy | 21.6 | 1.030 | 59.5 | 660.3 | 15.7 | 57.1 | 36.9 | 0.646 |
| 22/VI a. m. 9.54 | 〃 | 19.0 | 1.500 | 61.0 | 661.8 | 16.7 | 60.8 | 13.8 | 0.227 |
| 23/VII a. m. 10.01 | Fine | 28.5 | 1.260 | 60.4 | 620.2 | 17.1 | 62.2 | 32.8 | 0.527 |
| 23/VIII a. m. 10.06 | 〃 | 31.2 | 1.000 | 61.0 | 591.2 | 19.9 | 72.4 | 22.9 | 0.316 |
| 21/IX a. m. 9.50 | 〃 | 25.0 | 1.250 | 59.0 | 611.7 | 17.5 | 63.7 | 17.0 | 0.268 |

TABLE IV

OBSERVATIONAL RESULTS IN II-3

| Time of sampling | Weather | Temperature C° | Rate of flow l./min. | Water temperature °C | Cl⁻ mg./l. | Rn Mache | Rn $10^{-10}$ c./l. | RaB | RaB/Rn |
|---|---|---|---|---|---|---|---|---|---|
| 1953, 4/VI a. m. 10.10 | Cloudy | 22.8 | 5.06 | 41.6 | 505.6 | 268 | 976 | 248 | 0.254 |
| 24/VI a. m. 9.50 | Fine Cloudy later | 27.1 | 11.28 | 44.4 | 354.2 | 357 | 1300 | 884 | 0.680 |
| 8/VII a. m. 10.15 | Cloudy Rainy later | 28.0 | 11.59 | 44.0 | 355.2 | 372 | 1350 | 1060 | 0.788 |
| 12/VIII a. m. 10.23 | Fine | 31.3 | 9.82 | 41.3 | 188.1 | 473 | 1720 | 2100 | 1.22 |
| 2/IX a. m. 10.40 | Fine Cloudy later | 29.0 | 8.78 | 40.0 | 182.1 | 471 | 1710 | 1120 | 0.655 |
| 28/IX a. m. 10.13 | Fine | 21.2 | 7.42 | 39.2 | 216.6 | 449 | 1630 | 311 | 0.191 |
| 14/X a. m. 10.14 | 〃 | 17.2 | 2.87 | 39.4 | 375.1 | 414 | 1510 | 1450 | 0.960 |
| 10/XI a. m. 10.20 | Cloudy Rainy later | 14.7 | 2.68 | 40.0 | 505.2 | 483 | 1760 | 2650 | 1.503 |
| 15/XII a. m. 10.15 | Cloudy | 8.0 | 3.60 | 41.7 | 460.7 | 440 | 1600 | 1700 | 1.064 |
| 1954, 13/I a. m. 10.41 | Rainy | 5.0 | 4.91 | 42.0 | 495.2 | 311 | 1132 | 1260 | 1.114 |
| 24/II a. m. 10.15 | Fine | 6.3 | 6.95 | 43.0 | 392.2 | 619 | 2250 | 1660 | 0.739 |
| 16/III a. m. 10.15 | Cloudy | 7.2 | 5.90 | 42.4 | 340.1 | 610 | 2220 | 2850 | 1.285 |
| 21/IV a. m. 10.10 | Fine | 13.5 | 3.89 | 42.2 | 471.7 | 496 | 1805 | 2096 | 1.161 |
| 18/V a. m. 9.29 | 〃 | 20.9 | 3.88 | 42.6 | 492.2 | 393 | 1430 | 1270 | 0.886 |
| 24/VI a. m. 10.00 | Cloudy | 19.6 | 8.35 | 44.0 | 369.1 | 471 | 1714 | 864 | 0.504 |
| 25/VII a. m. 9.55 | Fine | 29.0 | 7.73 | 42.7 | 240.1 | 420 | 1530 | 1580 | 1.035 |
| 24/VIII a. m. 10.20 | 〃 | 30.0 | 6.50 | 42.4 | 283.6 | 568 | 2070 | 2047 | 0.989 |
| 22/IX a. m. 9.50 | 〃 | 25.0 | 4.06 | 41.3 | 272.6 | 379 | 1380 | 903 | 0.654 |

TABLE V

OBSERVATIONAL RESULTS IN II-4

| Time of sampling | Weather | Temperature C° | Rate of flow l./min. | Water temperature °C | $Cl^-$ mg./l. | Rn Mache | Rn $10^{-10}$ c./l. | RaB | RaB/Rn |
|---|---|---|---|---|---|---|---|---|---|
| 1954, 24/V a. m. 10.09 | Cloudy Rainy later | 20.5 | 2.927 | 46.7 | 580.6 | 244 | 888 | 674 | 0.759 |
| 23/VI a. m. 10.00 | Rainy | 19.7 | 4.010 | 46.3 | 505.7 | 266 | 968 | 1066 | 1.101 |
| 26/VII a. m. 9.49 | Cloudy | 29.0 | 3.000 | 50.0 | 635.5 | 237 | 863 | 803 | 0.930 |
| 25/VIII a. m. 10.08 | Fine | 30.8 | 3.150 | 50.0 | 603.8 | 240 | 873 | 947 | 1.085 |
| 24/IX a. m. 10.07 | Cloudy | 25.4 | 2.992 | 49.0 | 496.7 | 228 | 828 | 801 | 0.967 |
| 14/X a. m. 11.01 | Fine Cloudy later | 14.0 | 3.339 | 47.0 | 560.2 | 236 | 859 | 729 | 0.849 |
| 16/XI a. m. 10.30 | Cloudy Fine later | 13.0 | 3.140 | 46.0 | 522.7 | 227 | 826 | 686 | 0.830 |
| 14/XII a. m. 10.08 | Rainy | 5.2 | 2.964 | 43.0 | 522.7 | 245 | 892 | 901 | 1.01 |
| 1955, 24/I a. m. 10.33 | Fine | 5.0 | 3.258 | 39.2 | 545.2 | 231 | 841 | 717 | 0.852 |
| 14/II a. m. 10.48 | Fine Cloudy later | 3.6 | 2.719 | 40.9 | 615.2 | 213 | 775 | 721 | 0.930 |
| 11/III a. m. 10.30 | Fine | 8.3 | 0.810 | 43.2 | 634.2 | 218 | 793 | 495 | 0.624 |
| 29/IV a. m. 10.06 | Cloudy | 14.0 | 1.230 | 45.3 | 609.1 | 243 | 885 | 717 | 0.810 |

TABLE VI

OBSERVATIONAL RESULTS IN II-5

| Time of sampling | Weather | Temperature C° | Rate of flow l./min. | Water temperature °C | $Cl^-$ mg./l. | Rn Mache | Rn $10^{-10}$ c./l. | RaB | RaB/Rn |
|---|---|---|---|---|---|---|---|---|---|
| 1953, 13/VI a. m. 10.11 | Fine | 22.3 | 2.600 | 57.3 | 268.7 | 21.5 | 78.3 | 18.1 | 0.231 |
| 25/VI a. m. 9.50 | Cloudy | 28.0 | 2.892 | 57.7 | 286.2 | 22.9 | 83.4 | 22.2 | 0.266 |
| 9/VII a. m. 10.20 | 〃 | 25.5 | 3.130 | 58.0 | 273.5 | 22.0 | 80.0 | 21.9 | 0.274 |
| 13/VIII a. m. 10.15 | Fine Cloudy later | 31.0 | 2.644 | 57.6 | 280.2 | 21.4 | 77.9 | 21.4 | 0.275 |
| 3/IX a. m. 10.15 | Cloudy | 26.3 | 2.756 | 57.7 | 279.2 | 21.9 | 79.7 | 38.1 | 0.478 |
| 29/IX a. m. 10.15 | Rainy | 20.7 | 2.898 | 57.8 | 270.6 | 21.4 | 77.9 | 24.2 | 0.311 |
| 15/X a. m. 10.07 | Fine | 17.0 | 2.345 | 57.2 | 260.1 | 19.7 | 71.7 | 28.5 | 0.398 |
| 12/XI a. m. 11.25 | Cloudy | 10.3 | 3.759 | 57.6 | 275.9 | 20.2 | 73.5 | 38.7 | 0.527 |
| 16/XII a. m. 10.18 | Fine | 6.2 | 2.505 | 57.3 | 255.6 | 20.7 | 75.3 | 30.8 | 0.409 |
| 1954, 14/I a. m. 10.35 | Rainy | 7.0 | 2.904 | 57.6 | 257.6 | 21.8 | 79.4 | 29.5 | 0.371 |
| 16/II a. m. 10.31 | 〃 | 5.0 | 3.017 | 57.9 | 256.1 | 21.2 | 77.2 | 31.9 | 0.413 |
| 17/III a. m. 10.22 | Cloudy Fine later | 8.4 | 3.307 | 58.0 | 251.6 | 22.0 | 80.1 | 32.1 | 0.401 |
| 22/IV a. m. 10.13 | Cloudy | 13.5 | 3.149 | 58.0 | 232.6 | 20.7 | 75.3 | 35.1 | 0.466 |
| 17/V a. m. 10.05 | Cloudy Fine later | 17.0 | 3.178 | 58.0 | 214.1 | 19.7 | 71.7 | 14.7 | 0.201 |

TABLE VII

OBSERVATIONAL RESULTS IN III

| Time of sampling | Weather | Temperature °C | Rate of flow l./min. | Water temperature °C | $Cl^-$ mg./l. | Rn Mache | Rn $10^{-10}$ c./l. | RaB | RaB/Rn | $SO_4^{2-}$ mg./l. |
|---|---|---|---|---|---|---|---|---|---|---|
| 1954, 27/VIII a. m. 10.10 | Fine | 31.5 | 11.62 | 46.0 | 101.5 | 36.2 | 132 | 65.1 | 0.493 | 84.7 |
| 28/IX a. m. 10.05 | Rainy | — | 11.44 | 46.2 | 104.0 | 37.5 | 137 | 70.0 | 0.511 | 81.5 |
| 12/X a. m. 10.28 | Cloudy | 12.5 | 11.48 | 46.1 | 102.0 | 32.1 | 117 | 64.4 | 0.550 | 80.5 |
| 18/XI a. m. 10.29 | Fine | 12.0 | 11.44 | 46.5 | 108.5 | 33.2 | 121 | 57.2 | 0.473 | 83.6 |
| 15/XII a. m. 10.05 | 〃 | 4.5 | 10.61 | 46.4 | 108.5 | 31.9 | 116 | 64.5 | 0.556 | 87.2 |
| 1955, 12/I a. m. 10.43 | Fine Cloudy later | 2.0 | 11.76 | 46.0 | 106.0 | 31.6 | 115 | 65.3 | 0.568 | 95.4 |
| 17/II a. m. 10.04 | Cloudy | — | 11.49 | 46.0 | 110.5 | 32.6 | 119 | 67.2 | 0.565 | 94.8 |
| 15/III a. m. 10.02 | Fine | 7.3 | 11.91 | 46.0 | 109.7 | 32.1 | 117 | 36.0 | 0.308 | 95.6 |
| 26/IV a. m. 10.20 | 〃 | 13.5 | 11.91 | 45.7 | 110.5 | 26.9 | 97.9 | 36.1 | 0.369 | 91.9 |
| 19/V a. m. 10.25 | 〃 | 22.3 | 11.35 | 46.0 | 106.7 | 36.7 | 133.5 | 70.2 | 0.526 | 91.9 |
| 21/VI a. m. 10.18 | 〃 | 27.5 | 11.45 | 47.0 | 106.2 | 35.0 | 127.4 | 72.2 | 0.567 | 90.9 |
| 21/VII a. m. 10.07 | 〃 | 31.0 | 11.00 | 47.0 | 107.5 | 38.2 | 139 | 83.4 | 0.600 | 92.0 |

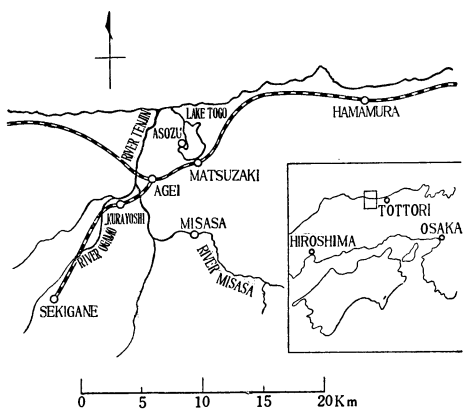



Fig. 1. Locality map

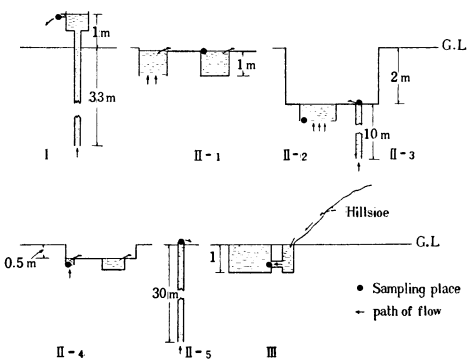



Fig. 2. Schematically states of springs

| | | |
|---|---|---|
| I | Hamamura (Kachimi) | The Institute for Live Stock. |
| II-1 | Misasa | Bun-aburaya. |
| II-2 | Misasa | Hisui-no-yu (orifice). |
| II-3 | Misasa | Hisui-no-yu (bathtub). |
| II-4 | Misasa | Gunze-shinsenryo. |
| II-5 | Misasa | Tanaka-no-yu. |
| III | Sekigane | Torikai-ryokan. |

The present states of these spings are schematically shown in Fig. 2. Chloride was determined by Mohr's method, sulfate by the barium chromate method and Rn with I. M. fontactoscope. RaB was measured by the dithyzone extraction method[7] immediately after the sampling. The same water was equally treated after three hours and the result was taken as standard*. Measurements were made by Lauritzen electroscope. Results are shown in Table I to VII.

## Discussion

Concerning the daily change in the content of various elements, some springs (I, II-2, II-5 and III) show very little fluctuation with time. Others show marked

7) S. Umemoto, *Japan Analyst*, **2**, 201 (1953).

* It is possible that RaB is adsorbed on the glass surface while kept for 3 hours. When the surface is washed with nitric acid (1:9) or acetic acid (1:9) for 3 min. after the mineral water is decanted off after 3 hours' storage, only 1 to 5 percent. of the initial activity of the original RaB is found in the extract. This value can not be regarded to be significant for the following discussion.

change in the content to different extents. (II-3 very marked; II-1, II-4 less so) This fact depends on the following factors:

(1) the depth of the well (i. e. the depth of sampling)

When water is collected at a depth of 10 m. or more, the fluctuation in the content is generally small.

(2) the location of the well.

The fluctuation is more marked when the spring is among other springs comprising water of different salt content. When the salt content of other springs in the neiborhood is similar, only a very slight fluctuation is observed with time. Springs which show marked fluctuation in the contents are about 3 m. deep on the northern beach of the river Misasa, where springs of various salt contents are found. The latter shows a marked difference between the content of the component of one compared with another, but the ratio of the components is rather similar. It is, therefore, predicted that the difference is due to the different extent to which ordinary ground water is mixed with an identical hot water which originates in a same source[8]. This also accounts for the observation that flactuation is greater for a shallower spring.

Nothing conclusive can be stated from the present data about the annual change in the content.

On the examination of the diagrams temp.—Cl, Rn—Cl, RaB—Cl, Rn—RaB and rate of flow—ratio RaB/Rn, only a few correlations are found. The correlation coefficients for rate of flow—ratio RaB/Rn in II-4, II-2 and III are respectively 0.661, −0.789 and −0.627. (Fig. 3-5) (All these coefficients are significant stochastically)

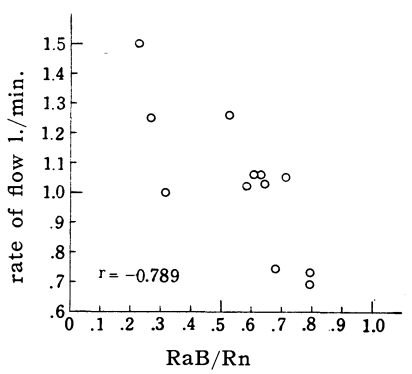



Fig. 3. Relation between rate of flow and RaB/Rn in II-2

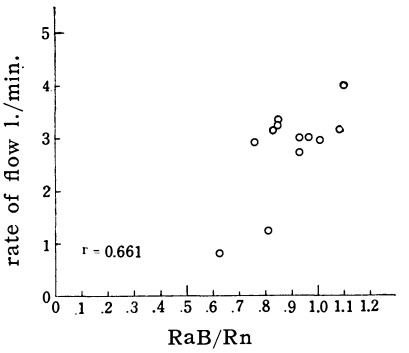



Fig. 4. Relation between rate of flow and RaB/Rn in II-4

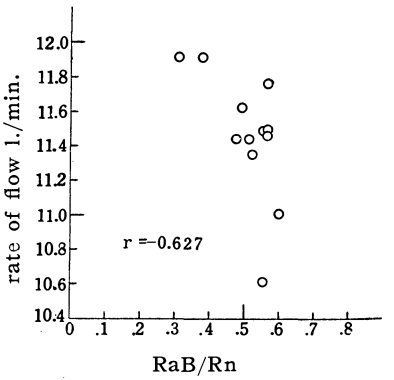



Fig. 5. Relation between rate of flow and RaB/Rn in III

The fact that the latter two have negative values of correlation coefficient provides support to the view of Kimura, Kuroda and Yokoyama about the relationship of the content of Rn and that of its decay products. They claim that radium B in the mineral spring is produced only from Rn which was supplied free from its decay products, the chemical behavior of both species being similar until they reach the surface. Since the contents of chemical constituents in II-2 and III remain almost unchanged with time, it could be reasonably assumed that a radioactive substance is supplied and springs out in a definite manner.

The correlation coefficient between the rate of flow and the ratio of RaB to Rn is positive for II-4; an inversed relationship to the above mentioned case can be predicted. Their assumption appears not to be valid in this case. Since the ratio RaB to Rn is sometimes greater than unity, there must be cases when the RaB is supplied not by the Rn only or when a part of the Rn escapes. The depth at which the mineral water of both II-4 and II-3 (sometimes both having the ratio

8) S. Umemoto, *J. Chem Soc. Japan (Pure Chem. Sect.)*, **74**, 94 (1954).

greater than unity) is taken, is less than 3 m. and both show very strong overall activity. Strongly radioactive springs are also found in their neighborhood as well as radioactive ground water[9]. They all come from shallow wells less than 3 m. in depth. It is thus possible that Rn and RaB are supplied to the mineral water near the surface or Rn escapes preferentially near the surface, resulting in unusual contents of both species as mentioned above. Another example of a mineral spring that has a greater value than unity for the ratio RaB to Rn, is provided in Ikeda Mineral Springs in Shimane Prefecture. The correlation between the rate of flow and the ratio RaB/Rn in II-4 appears to arise from a still uncertain regularity including the state of supply of both species.

No significant correlation between the rate of flow and the ratio RaB/Rn was observed in other springs. Considering the variation of the main constituents, the ratio in II-3 seems to be liable to fluctuation of influence near the surface, and also those in II-1; nothing regular can be expected for either of them. For I and II-5, the fluctuation in main constituents is less, but it is considered that the contents of minor constituents are not sufficient to fulfill the necessary assumption for Kimura et al's consideration. From the fact that more than the half of the examples are not in accord with their comments, not many mineral springs appear to satisfy the conditions suggested by them. It does not imply, however, that their examples have been rather exceptional. Their second statement appears not to be true for the present example; i. e. the extent to which the RaB content is decreased from the equilibrium amount to the Rn does not increase with increasing Rn content.

9) T. Sugihara, *Repts. Balneol. Lab. Okayama Univ.*, 9, 37 (1953).

## Conclusion

The above observed mineral springs are classified into three groups regarding the correlation between the rate of flow and the ratio RaB/Rn: (1) negatively correlating, (2) positively correlating and (3) without significant correlation. In the first group Rn appears to be free from its decay products at the point of its supply and it is the source of all other radioactive species in the mineral water, all of them showing a chemical behavior similar to one another. For the second group no appropriate explanation has been available as yet. For the third group, it could be assumed that the source, path of supply and the chemical behavior after the supply of Rn are too complicated or that these are disturbed by secondary phenomena near the surface. It appears as if the third group comprises most of mineral springs.

*Balneological Laboratory*
*Okayama University*
*Misasa Hot Springs*
*Tottori Prefecture*

# SHORT COMMUNICATIONS

## *Nuclear Magnetic Resonance of Polyvinyl-alcohol (Transition Temperature)*

By Kōji TANAKA, Kyōzō YAMAGATA, Masako YOSHIDA and Minoru ODAJIMA

(Received December 18, 1956)

In our previous communication[1], the results of the measurements of the nuclear magnetic resonance absorption of protons in polyvinyl alcohol (P. V. A.) fibers from 10°C to 170°C were reported. After that, the measurements were done for the samples of P. V. A. powder and film from −50°C to 200°C. The P. V. A. powder was purified and fractionated. The P.V.A. film was cast from about 2.5% aqueous solution of P. V. A. on a glass plate placed horizontally in an air-thermostat at 50°C and dried at 50°C and $10^{-5}$ mmHg for several days.

The apparatus used is the same as mentioned before, except that the cryostat[2] was used to cool the sample to below 20°C. The field intensity was about 3000 gauss.

The width between the points of the maximum slope of the adsorption curve is shown in Fig. 1 as the function of temperature. Below 20°C the widths are almost constant with the value of about 12 gauss, but in the range from 20°C to 50°C, the width decreases gradually with temperature and remains unchanged from

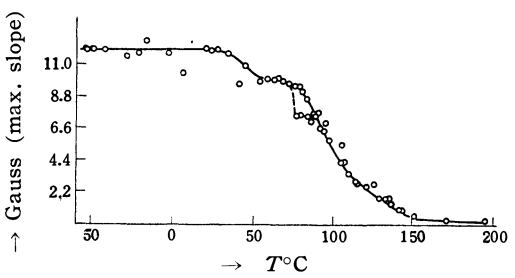



Fig. 1

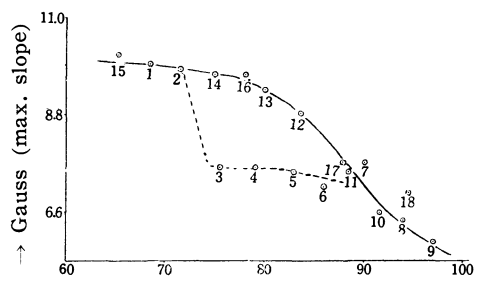



Fig. 2

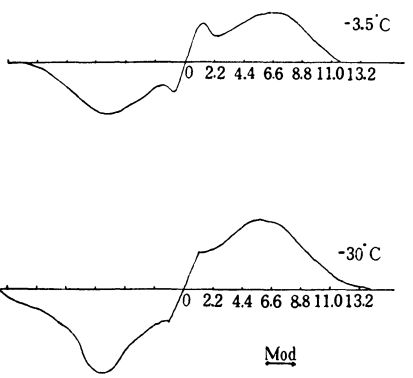



Fig. 3

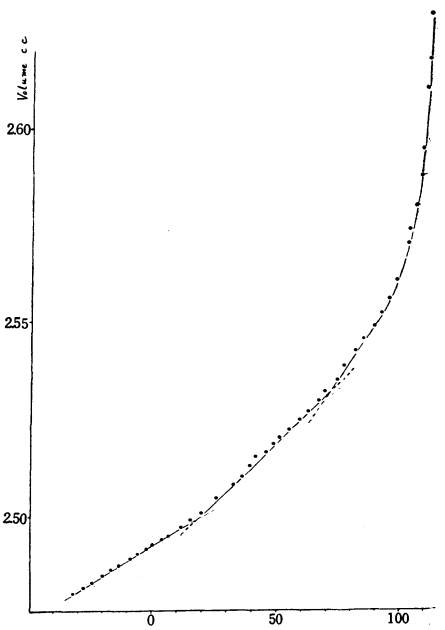



Fig. 4

1) Kōji Tanaka, Kyōzō Yamagata and Shigeyoshi Kittaka, This Bulletin, **29**, 843 (1956).
2) H. G. Gutowsky, L. H. Meyer and R. E. McClure, *Rev. Sci. Instr.* **24**, 644 (1953).

50°C to 70°C, then it decreases again in the range between 70°C and 120°C. With respect to this transition at around 70°C, an irreversible hysteresis is observed for the sample with smaller degree of crystallinity which has not been thermally pretreated. The results are shown in Fig. 2 where the numbers in the figure denote the order of the treatments of the sample. For the sample, which is thermally pretreated, this hysteresis is not observed and the decreasing of the line width occurs along the upper curve of the hysteresis curve in the figure.

The derivative curves of proton resonance at −3.5°C and −30°C are shown in Fig. 3 and at −50°C the central component is still observed though it is very weak.

In order to compare the results obtained by nuclear magnetic resonance method with those by dilatometric method, volume-temperature curve of P. V. A. film was obtained and its result is shown in Fig. 4.

It is interesting to note that the transition temperatures of about 15°C and 70°C[3] obtained by the dilatometric method coincide with the starting temperatures of the transition obtained by the nuclear magnetic resonance method.

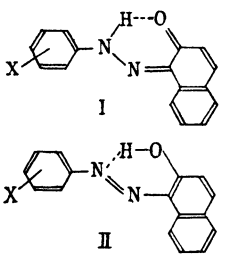
The authors wish to exress their appreciation to Prof. Masatami Takeda for his kind advice and encouragement.

*Tokyo College of Science,*
*Shinjuku-ku, Tokyo*

3) Y. Yano. *J. Chem. Soc. Japan*, **73**, 708 (1952).

found that the structure of these compounds depends on the nature and the position of the substituents.

It must be noted that our calculated values for the azophenol and the quinonehydrazone forms given by the procedure similar to that described in the previous paper, are in serious disagreement with those given by Pascal[4] and Pacault[5]. As an example, our value for the azophenol form of 1-phenylazo-2-naphthol $-146.7\times10^{-6}$ is appreciably smaller than $-154\times10^{-6}$ given by the French workers, and the value for the quinonehydrazone form $-135.8\times10^{-6}$ estimated by use of the observed value for quinone monoxime is remarkably larger than $-124.8\times10^{-6}$ given by Pascal and $-130.8\times10^{-6}$ by Pacault. However, the experimental results seem to support our estimations. The observed values of the molar susceptibility of 1-phenylazo-2-naphthol and its *o*-methyl-, *m*-nitro- and *p*-nitro-derivatives are in accordance with the calculated values for the quinonehyrazone form (I), but *p*-methyl-, *o*-methoxy-, *o*-chloro- and *p*-chloroderivatives are found to exist in the azophenol form (II) in the solid state.




The effect of substituents on the equilibria between these two tautomeric forms in various solutions was examined by Burawoy and his collaborators[6]. According to their conclusion, the concentration of the quinonehydrazone tautomers increases in the order of substituents, *p*-Me $<$H$\sim$*p*-Cl$<$*o*-Me$<$*o*-Cl$<$*m*-$NO_2$ $<$*o*-MeO $<$*p*-$NO_2$. In contrast to the above series, our results suggest that MeO, Me and Cl substituted both in the ortho- and para-positions favor the azophenol form, and methyl group in the ortho-position is not so effective as that in the para-position.

## *Diamagnetic Susceptibilities of Azo-derivatives of 2-Naphthol*

By Yoshio MATSUNAGA

(Received February 28, 1957)

In the previous paper[1], the procedure to estimate the molar susceptibilities of the azophenol and the quinonehydrazone forms of hydroxyazobenzene was presented. We applied it to twenty compounds and concluded that they are all in the azophenol form in the solid state. Continuing this study, we measured the diamagnetic susceptibilities of eight azo-derivatives of 2-naphthol. All specimens were purified finally by sublimation in vacuo. As shown in the Table, we

1) Y. Matsunaga, This Bulletin, **29**, 308 (1956).
2) Y. Matsunaga, ibid., **29**, 969 (1956).
3) P. Pascal, *Bull. soc. chim. France*, **9**, 177 (1911).
4) P. Pascal, *Ann. chim. phys.* **25**, 289 (1912).
5) A. Pacault and J. Chauvelier, *Bull. soc. chim. France*, **17**, 367 (1950).
6) A. Burawoy, A. G. Salem, and A. R. Thompson, *J. Chem. Soc.*, **1952**, 4793.

TABLE

DIAMAGNETIC SUSCEPTIBILITIES OF AZO-DERIVATIVES OF 2-NAPHTHOL

| Substance | Suscept. ($-\chi \cdot 10^6$) | Molar Suscept. ($-\chi_M \cdot 10^6$) Obs. | Calc. (I) | Calc. (II) | Lit. |
|---|---|---|---|---|---|
| β-Naphthoquinone-1-oxime | — | — | — | — | 83.9[2] |
| 2-Naphthol | — | — | — | — | 97.0[3] |
| 1-Phenylazo-2-naphthol | 0.554 | 137.6 | 135.8 | 146.7 | 140.7[4], 135.5[5] |
| 1-*o*-Tolylazo-2-naphthol | 0.567 | 148.7 | 146.4 | 157.3 | — |
| 1-*p*-Tolylazo-2-naphthol | 0.601 | 157.6 | 146.4 | 157.3 | — |
| 1-*o*-Methoxyphenylazo-2-naphthol | 0.588 | 163.6 | 152.2 | 164.1 | — |
| 1-*o*-Chlorophenylazo-2-naphthol | 0.570 | 161.0 | 150.6 | 161.5 | — |
| 1-*p*-Chlorophenylazo-2-naphthol | 0.571 | 161.4 | 150.6 | 161.5 | — |
| 1-*m*-Nitrophenylazo-2-naphthol | 0.484 | 142.0 | 142.4 | 153.3 | — |
| 1-*p*-Nitrophenylazo-2-naphthol | 0.483 | 141.7 | 142.4 | 153.3 | — |

In the solid state, the effect of substituents appears to be not necessarily similar to that observed by Burawoy on the tautomeric equilibria in the dissolved state.

The author wishes to express his hearty thanks to Professor H. Akamatu for his kind direction.

*Department of Chemistry*
*Faculty of Science*
*The University of Tokyo*
*Hongo, Tokyo*

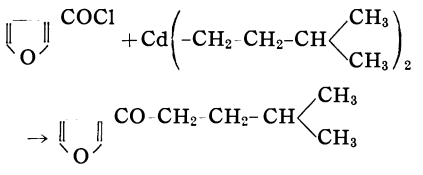
## *Natural Furan Derivatives. Part I. The Synthesis of Perillaketone*

By Teruo MATSUURA

(Received March 4, 1957)

Perillaketone was isolated from the leaves of the Manchurian *Perilla frutescens Brit.* and was given the structural formula (I) by Goto[1]. Sebe also isolated perillaketone from the Formosan Perilla frutescens form viridis Kudo and independently gave the same formula (I) to it[2]. For the purpose of the confirmation of its structure, the present synthesis of β-furyl isoamyl ketone has been furnished.

The reaction of the acid chloride of 3-furcic acid with diisoamyl cadmium gave the desired β-furyl isoamyl ketone, which was purified with the Girard reagent P. The pure ketone has the similar physical constants to natural perillaketone, as are shown in Table I, and it gives the oxime, m. p. 65–67°, and the 2,4-dinitro-phenylhydrazone, m. p. 149–150°. The latter derivative was identical with the 2,4-dinitro-phenylhydrazone of the natural substance in the infrared spectrum and the mixed melting point. From the above results, it is established that perillaketone is β-furyl isoamyl ketone.



(I)

### Experimental

**3-Furoyl chloride**[3] 3-Furoic acid (25.0 g.) and thionyl chloride (50 cc.) were heated in benzene (160 cc.) for 9 hours. The solvent and an excess of thionyl chloride were evaporated and the residual liquid was distilled *in vacuo*. The acid chloride (16.2 g.) was obtained as a colorless liquid, b. p. 73–76°/46 mm.

**β-Furyl isoamyl ketone (Perillaketone)** To the Grignard solution, prepared from isoamyl bromide (30 g.), magnesium (4.9 g.) and absolute ether (80 cc.), dried cadmium chloride (19 g.) was added in portions under ice-cooling and the mixture was refluxed until a negative Gilman-Schulz test was given. Ether was evaporated and benzene (100 cc.) was added. A solution of 3-furoyl chloride (16.2 g.) in benzene (50 cc.) was rapidly added to the above cadmium diisoamyl solution at room temperature. The mixture was refluxed for 20 minutes and was decomposed with diluted hydrochloric acid under ice-cooling. The benzene layer was separated, washed with bicarbonate solution, dried and evaporated. Distillation of the residual liquid (17.0 g.) gave the crude ketone as a pale yellow liquid (8.5 g.); b. p. 73–75°/3 mm. and $n_D^{27}$ 1.4685.

The crude product was treated with the Gigrard reagent P in the usual method. Distillation of the ketonic part gave the pure ketone as a color-

1) R. Goto. *J. Pharm. Soc. Japan*, **57**, 77 (1937).
2) Y. Sebe, *J. Chem. Soc. Japan*, **64**, 1130 (1943).
3) H. Gilman, R. Burtner, *J. Am. Chem Soc.*, **55**, 2903 (1933).

TABLE I

| | | B. P. | $n_D$ | $d$ | Oxime (m. p.) | 2,4-Dinitrophenyl-hydrazone (m. p.) |
|---|---|---|---|---|---|---|
| β-Furyl isoamyl ketone | | 72—73°/3 mm | $n_D^{17}$ 1.4741 | $d_4^{24}$ 0.9924 | 65—66° | 149—150° |
| Perillaketone | Goto[1] | 196° | $n_D^{20}$ 1.4781 | $d_{15}^{15}$ 0.9920 | 67° | — |
| | Sebe[2] | 95—97°/7 mm | $n_D^{17}$ 1.4759 | $d_4^{17}$ 0.9897 | 66—67° | 152—153° |

less liquid; b. p. 72-73°/3 mm., $n_D^{17}$ 1.4741 and $d_4^{24}$ 0.9924. The substance gives a negative test with the Ehrlich reagent and shows a pale yellow color with acetic anhydride and sulfuric acid. The ketone is sensitive to oxygen and on standing becomes a reddish orange color.

IR-absorptions: 3.18, 3.42, 3.50, 6.00, 6.41, 6.63, 6.82, 7.20, 7.30-7.34, 7.78, 8.10, 8.32, 8.66, 9.25, 9.50, 9.77, 10.02, 10.78, 11.45, 12.30, 12.90 and 13.48 μ.

**Oxime of β-furyl isoamyl ketone** The ketone (2.1 g.), hydroxylamine hydrochloride (1.3 g.) and sodium acetate (2.5 g.) were treated in the usual method in diluted alcohol. The oily product (1.9 g.) solidified on standing in the ice-chest. The oxime crystallized from petroleum ether in colorless needles, m. p. 65-66°. Anal. Found: C, 66.52; H, 8.41; N, 8.03%. Calcd. for $C_{10}H_{15}NO_2$: C, 66.27; H, 8.34; N, 7.73%.

**2,4-Dinitro-phenylhydrazone of β-furyl isoamyl ketone** The ketone (0.3 g.) and 2,4-dinitro-phenylhydrazine (0.4 g.) precipitated reddish orange needles in the presence of sulfuric acid in alcohol. Recrystallizations of the needles gave the pure 2,4-dinitro-phenylhydrazone, m. p. 149-150°, which showed no depression on admixture with 2,4-dinitro-phenylhydrazone, m. p. 151-152°, of natural perillaketone. Anal. Found: C, 55.48; H, 5.20; N, 16.08%. Calcd. for $C_{16}H_{18}N_4O_5$: C, 55.48; H, 5.24; N, 16.18%.

The author is greatly indebted to Dr. Yeigai Sebe at Kumamoto University and Dr. Yodo Rin at National Taiwan University for a gift of the authentic sample.

*Institute of Polytechnics*
*Osaka City University*
*Minamiogimachi, Kitaku, Osaka*

## *Catalytic Hydrogenation in Vapor Phase Using Urushibara Nickel as Catalyst*

By Kazuo HATA, Ken-ichi WATANABE and Shiro SATO

(Received November 20, 1956)

Urushibara nickel (U-Ni in abbreviation), a new catalyst made from nickel choride and zinc dust, has been reported to show excellent behavior in the catalytic reduction of many organic compounds[1-5].

In this paper, we introduce a new idea applying this catalyts to vapor phase hydrogenation. The procedure of the vapor phase hydrogenation with U-Ni as catalyst is not so troublesome as that with other catalysts, and efficient reduction was observed except in special cases. U-Ni-A, which was used in these experiments, was prepared by treating precipitated nickel with acetic acid as previously reported[4].

Nitrobenzene was reduced to aniline, styrene and acetophenone to ethylbenzene respectively, and benzonitrile to primary and secondary amines together with some toluene. However, benzene could not be reduced by this method. The conditions of the reaction and products are shown in Table I.

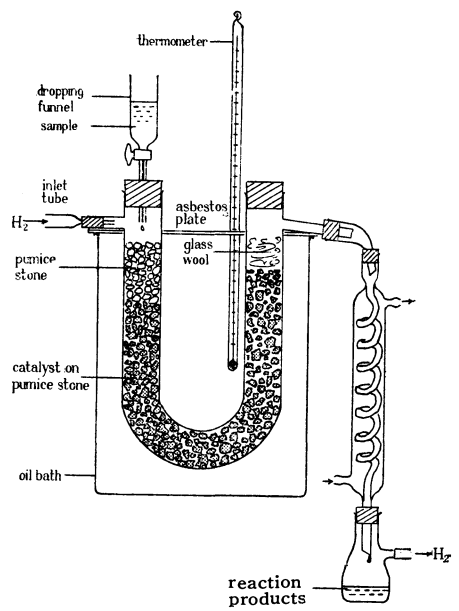



Fig. 1. Apparatus for the hydrogenation.

1) Y. Urushibara, This Bulletin, **25**, 280 (1952).
2) S. Nishimura, *J. Chem. Soc. Japan (Pure Chem. Sect.)*, **77**, 340 (1956).
3) Y. Urushibara and S. Nishimura, This Bulletin, **27**, 480 (1954).
4) Y. Urushibara, S. Nishimura and H. Uehara, ibid., **28**, 446 (1955).
5) K. Hata, K. Watanabe, S. Taira, T. Higase, I. Motoyama and T. Tamura, *J. Chem. Soc. Japan (Pure Chem. Sect.)*, **77**, 1405 (1956); T. Higase, S. Taira and K. Hata, ibid., **78**, 186 (1957).

TABLE I

VAPOR PHASE HYDROGENATION USING U-Ni-A AS CATALYST

| Compound | Weight of Sample (g.) | Nickel (g.) | Temp. (°C) | Time (hr.) | Flow Velocity of Sample (g./min.) | Weight of Product (g.) | Product and Yield (%) |
|---|---|---|---|---|---|---|---|
| Nirobenzene | 10 | 4 | 220 | 3 | 0.08 | 9.7 | Aniline (81) |
| Benzene | 10 | 4 | 180 | 4 | 0.06 | 9.0 | (Benzene recovered) |
| Styrene | 10.4 | 4 | 165 | 3 | 0.08 | 9.3 | Ethylbenzene (88) |
| Acetophenone | 9.9 | 4 | 200 | $3^1/_2$ | 0.06 | 9.1 | Ethylbenzene (90) |
| Benzonitrile | 8.0 | 4 | 250 | 3 | 0.07 | 6.5 | Toluene (14)<br>Benzylamine (29)<br>Dibenzylamine (41)<br>Ammonia (50) |

The hydrogenating apparatus used in these experiments is shown in Fig. 1. A hard glass U-tube, 3 cm. in diameter and about 50 cm. in total length, was used as a reaction tube. Small grains of pumice stone were put in the U-tube to fill about three quarters of its content. Freshly prepared U-Ni-A catalyst was washed with alcohol, and was poured on the pumice stone in the U-tube together with a small quantity of alcohol. The catalyst settled over the surface of the pumice stone when treated by this method. Then, other pieces of pumice stone were added to fill up the U-tube, and the tube was set in an oil bath after the greater part of the alcohol was decanted away. A small dropping funnel to introduce the liquid sample was fitted on the top of the U-tube over the hydrogen inlet tube. A condenser and a receiver were connected with the other branch of the U-tube. The reaction tube was heated and hydrogen was passed through the tube to expel the vapor of alcohol. Now the receiver was changed to catch the reaction products, and the temperature of the bath was suitably controlled for the hydrogenation. The liquid sample was then slowly dropped into the U-tube. The liquid was vaporized on the upper grains of pumice stone and was hydrogenated on the nickel catalyst, the reaction products being distilled into the receiver.

Each sample was hydrogenated under the suitable temperature with a large excess of hydrogen. After all the sample had been supplied, more hydrogen was passed through for 30–60 minutes to expel the hydrogenation products throughly. After the reaction was over, each product in the receiver was fractionally distilled, and then identified by preparing an appropriate solid derivative.

From these experiments, it was proved to be very convenient to use U-Ni in the vapor phase catalytic hydrogenation. For the preparation of the catalyst, it is not necessary to reduce the nickel compound at high temperature such as by Sabatier's method; all procedures are simple and quick, and the yields of the hydrogenation products are pretty good.

Different results from the hydrogenation with Sabatier's reduced nickel were obtained in the hydrogenation of benzene and benzonitrile. Benzene nucleus could not be hydrogenated with U-Ni by any way, though Sabatier's reduced nickel converts benzene into cyclohexane[6]. Benzonitrile can be hydrogenated almost perfectly to toluene and ammonia with reduced nickel catalyst at 250°C[7], but with U-Ni, the formation of toluene was largely depressed alternatively yielding primary and secondary amines.

The further investigation on the activity of Urushibara nickel in vapor phase hydrogenation is now in progress.

*Department of Chemistry, Faculty of Science, Tokyo Metropolitan University, Setagaya, Tokyo*

6) P. Sabatier and J, B. Senderens, *Compt. rend.*, **132**, 210 (1901).

7) P. Sabatier and J. B, Senderens, *Compt. rend.*, **140**, 482 (1905): K. Hata, *Sci. Papers Inst. Phys. Chem. Research* (Tokyo), **23**, 224 (1944); M. Tanaka, K. Watanabe and K. Hata, *J. Chem. Soc. Japan* (*Pure Chem. Sect.*), **76**, 1392 (1955).

# *Ultraviolet Spectrophotometric Determination of Iron(III) as Chloro-complex*

By Masayoshi ISHIBASHI, Tsunenobu SHIGEMATSU, Yuuroku YAMAMOTO, Masayuki TABUSHI and Toyokichi KITAGAWA

(Received March 6, 1956)

In order to establish a series of methods for ultraviolet spectrophotometric determination of iron(III), especially of the method based on differential absorptiometry, we have already reported the two following methods. One of them[1] is based on measurement of absorbance at 300 mμ due to the formation of ferric sulfato-complex using sulfuric acid as reagent, but in the other[2] the absorbance was measured at an isosbestic point (271 mμ) which is attributed to the equilibrium between ferric aquo ion and ferric hydroxo ion in the dilute perchloric acid solution.

Rabinowitch and Stockmeyer[3] have analyzed the absorption spectra for the ferric perchlorate solution in the presence of various amounts of $OH^-$, $Cl^-$ and $Br^-$, and Mc. Connell and Davidson[6] have investigated the nature of the absorption spectra due to the equilibrium between ferric and ferrous ion, but they almost never refered to the absorption in the ultraviolet region. Recently, Gamlen and Jordan[4] have investigated the nature of the iron chloro-complex in the concentrated hydrochloric acid solution by ultraviolet spectrophotometry, and concluded that the highest chloro-complex formed have the formula $FeCl_4^-$.

DeSesa and Rogers[5] reported a method of spectrophotometric determination of iron based upon measurement at 342.5 mμ in 6 M hydrochloric acid solution. A recent A. S. T. M. publication[7] recommends the use of constant boiling hydrochloric acid as reagent and measurment at 370 mμ for the determination of traces of iron in copper and copper alloys.

The present paper reports an investigation of the absorption of iron(III) in a hydrochloric acid solution, and also of a differential method of spectrophotometric determination for iron using this acid as reagent. Applying this method, the purity of iron alloys has been determined by means of differential spectrophotometry.

**Apparatus and Materials.** — Spectrophotometric measurements were made with a Beckman Quartz spectrophotometer Model DU with 1 cm. silica cells.

The stock solution of ferric perchlorate was prepared to the concentration of 100 p.p.m. as previously described[2]. The hydrochloric acid was purified by distillation untill it gave negative test for iron. The reagent grade perchloric acid which contains no chloride and iron ions was used.

## Experimental

**Absorption Spectra.**—The absorption spectra of ferric perchlorate in 6 M-perchloric and 6 M-hydrochloric acid solutions are shown in Fig. 1.

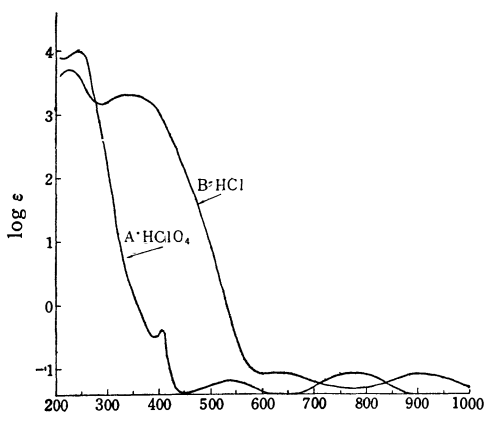



Fig. 1. Absorption Spectra of Iron(III) in 6 M Perchloric Acid and 6 M Hydrochloric Acid.

Curve A has shown good agreement with that of Rabinowitch[3], and therefore this curve may be considered as belonging exclusively to ferric aquo

1) M. Ishibashi, T. Shigematsu, Y. Yamamoto, T. Tabushi and T. Kitagawa *J. Chem. Soc. Japan (pure Chem. Sect.)* **76**, 758 (1955).
2) M. Ishibashi, T. Shigematsu, Y. Yamamoto, M. Tabushi and T. Kitagawa, This Bulletin, **29**, 57 (1956).
3) E. Rabinowitch and W. H. Stockmeyer, *J. Am. Chem. Soc.*, **64**, 335 (1942).
4) G. Gamlen and D. Jordan, *J. Chem. Soc.*, **1953**, 1435.
5) M. A. DeSesa and L. Logers, *Anal. Chim. Acta*, **6**, 534 (1952).
6) H. McConnel and N. Davidson, *J. Am. Chem. Soc.*, **72**, 5557 (1950).
7) A. S. T. M. Method for the chemical Analysis of Metals, American Society for Testing Materials. (1950).

ion. In the curve B, maxima shift to the longer region by the formation of ferric chloro-complex. As other workers have reported[3], the ordinate of curve B is the average of absorption coefficients, because the absorbing species are mixed.

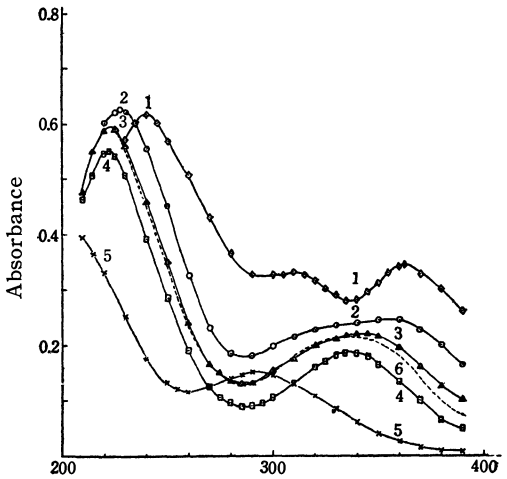



Fig. 2. Absorption Spectra of Iron(III) in the Hydrochloric Acid Solution

| | | | |
|---|---|---|---|
| $Fe^{3+}$=ca. 4.5 p.p.m. | ◈ | 1 | 9.6 N HCl |
| Temp. 12°C | ⊙ | 2 | 6.4 N 〃 |
| Ref. coresponding acid | △ | 3 | 4.8 N 〃 |
| | ⊡ | 4 | 2.4 N 〃 |
| | × | 5 | — (pH 3.4) |
| | ····· | 6 | 48 *f* NaCl (pH 2.58) |

The effect of change in the concentration of hydrochloric acid was then studied. Fig. 2 shows the spectra of ferric perchlorate in solution of various concentrations of hydrochloric acid. The absorption maximum of ferric aquo ion at 238 mμ shifts to the region of 320-360 mμ by adding hydrochloric acid. The position of maximum in the region of 320-360 mμ shifts to longer, and the absorbance in these bands also rises, with increase in the concentration of this acid. Another band appears in the region of 220-230 mμ in the solution of hydrochloric acid, and considerable changes both in absorbance and in wave length of maxima are observed with the changes in acid concentration. Curves 5 and 6 indicate the spectra of ferric perchlorate solutions, but the former is that of extreme diluted perchloric acid solution (pH 3.4) and the latter is of the solution (pH 2.6) of 4.8 M sodium chloride. As previously reported[2], curve 5 belongs to the spectrum of the ferric hydroxo-ion $Fe(OH)^{2+}$, and thus it is considered that the hydroxo-complex has transferred to iron chloro-complex in such weak acidic medium under the considerable concentration of chloride. The similarity between curve 6 and 3 indicates that the effect of hydrogen ion concentration is little in such a concentration of chloride ion as 4.8 M.

As the formation of the ferric chloro-complexes may take place stepwise according to Bjerrum's theory of complex formation, it is necessary to investigate the effects of concentration of chloride ion under the constant acidity. Fig. 3 shows the absorption spectra in the following conditions. The concentration of iron(III) was kept constant and the constancy of the concentration of hydrogen ion could be approximately held by mixing the same molar concentration of hydrochloric and perchloric acid. The variations in the absorbance and location of the absorption bands are showed in detail as follows.

(1) 1.2 and 2.4 M $H^+$ (Fig. 3-1)

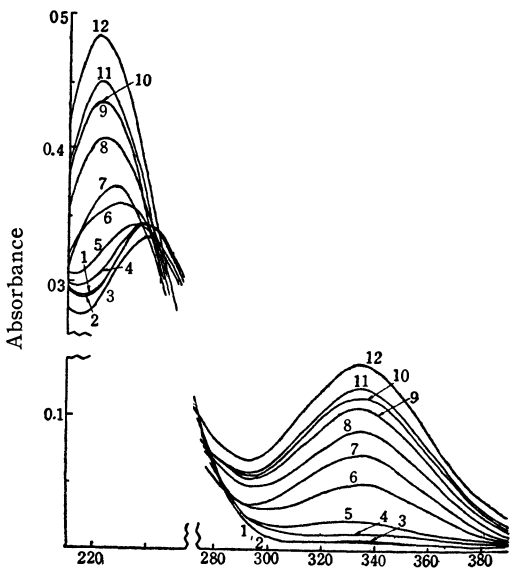



Fig. 3-1. Effect of Chloride Concn. (I) ($Fe^{3+}$=ca. 4.5 p.p.m, acidity=ca. 1.2 N)

| | Vol. of Acid in 20 ml. HCl (ml.) | Vol. of Acid in 20 ml. $HClO_4$ (ml.) | λmax. | |
|---|---|---|---|---|
| 1 | 0.05 | 18.95 | 239 mμ | — |
| 2 | 0.1 | 18.90 | 238 | — |
| 3 | 0.3 | 18.70 | 238 | — |
| 4 | 0.5 | 18.50 | 237 | — |
| 5 | 1.0 | 18.00 | 236 | — |
| 6 | 3.0 | 16.00 | 227 | 334 mμ |
| 7 | 5.0 | 14.00 | 225 | $334_5$ |
| 8 | 7.0 | 12.00 | 223 | 334 |
| 9 | 10.0 | 9.00 | 222 | $333_5$ |
| 10 | 13.0 | 6.00 | $222_5$ | $333_5$ |
| 11 | 15.0 | 4.00 | 222 | $334_5$ |
| 12 | 19.0 | — | 222 | $334_5$ |

In the region of a shorter wave length, the absorption shifts to shorter, while in the longer region the maximum is kept at constant. The absorbance increases continuously with rise of the concentration of chloride ion in both bands.

(2) 4.8 M $H^+$ (Fig. 3-2)

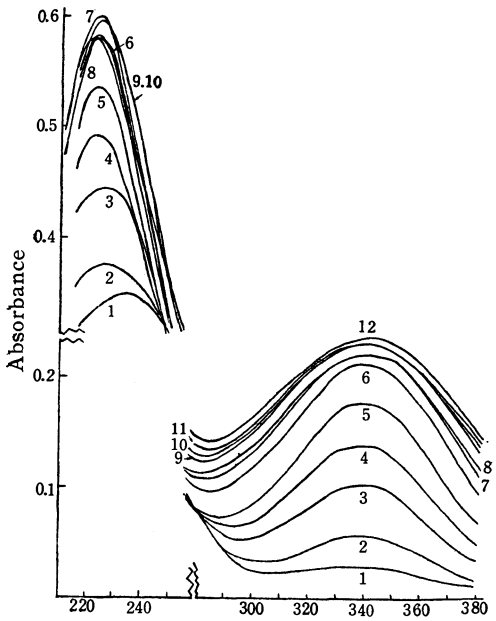



Fig. 3-2. Effected of Chloride Concentration(II) [$Fe^{3+}$=ca. 4.5 p.p.m. acidity =ca. 4.8 N]

The numbers on the curves are the same as in Fig. 3-1.

| | λmax. | |
|---|---|---|
| 1 | 234 mμ | 336 mμ |
| 2 | 227 | 334 |
| 3 | 224 | 337 |
| 4 | 223 | 338 |
| 5 | 222 | 337 |
| 6 | 222 | 340 |
| 7 | 221 | 338 |
| 8 | 223 | 341 |
| 9 | 223 | 343 |
| 10 | 223 | 343 |
| 11 | 222 | 343 |
| 12 | 222 | 343 |

The maximum at shorter wave length becomes shorter, that of longer wave length becomes longer, and the absorbance increases continuously in both bands.

(3) 6.4 M $H^+$ (Fig. 3-3)

In shorter wave length, the position of maximum is kept at constant and the absorbance rises slightly with the increase of the concentration of chloride. In the region of longer wave length, the effect of change in the concentration of chloride ion is more complicated. The position of maximum changes continuously from 342 to 354 mμ until the concentration of chloride ion grows to 1.6 M, but when the concentration becomes greater than 1.5 M, another band appears at 310 mμ. The absorbance also increases continuously while only one band is present, but when the second band appears, the change in both bands becomes very slight.

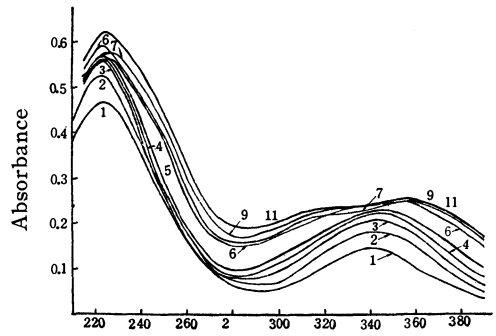



Fig. 3-3. Effect of Chloride Concn. (III) [$Fe^{3+}$=ca. 4.5 p.p.m. acidity=ca. 1.4 N] The numbers on the curves are the same as in Fig. 3-1.

| | λmax. | |
|---|---|---|
| 1 | 223 mμ | 342 mμ |
| 2 | 223 | 343 |
| 3 | 223 | 343 |
| 4 | 223 | 343 |
| 5 | 223 | 346 |
| 6 | 223 | 351 |
| 7 | 224 | 354 |
| 9 | 224 | 354.5 |
| 11 | 224 | 355 |

(4) 9.6 M $H^+$ (Fig. 3-4)

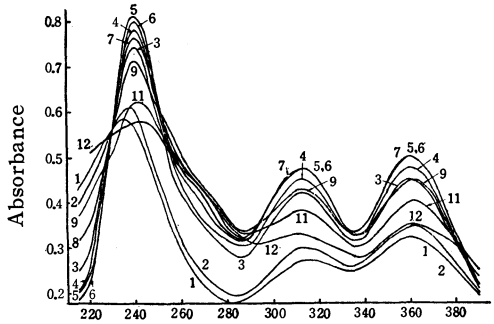
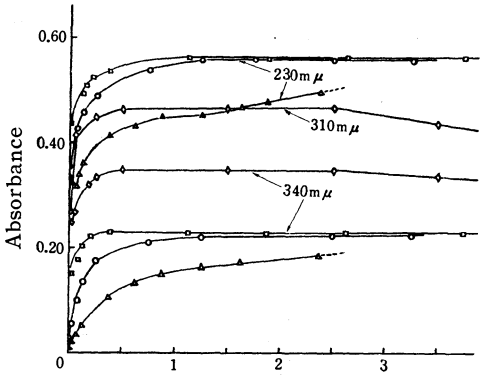



Fig. 3-4. Effect of chloride Concn. (IV) [$Fe^{3+}$=ca. 4.5 p.p.m. acidity=ca. 9.6 N] The numbers on the curves are the same as in Fig. 3-1

| | λmax. | | |
|---|---|---|---|
| 1 | 236 mμ | 315 mμ | 360 mμ |
| 2 | 237 | 313.5 | 360 |
| 3 | 240 | 312 | 360 |
| 4 | 240 | 312 | 360 |
| 5 | 240 | 312 | 360 |
| 6 | 240 | 312 | 359.5 |
| 7 | 240.5 | 312 | 260 |
| 9 | 241.5 | 312 | 361 |
| 11 | 242 | 312 | 361 |
| 12 | 242 | 310 | 363 |

In this case remarkable changes in location and absorbance of all bands occur.

The maximum in the region of shorter wave length shifts to longer. In the region of the longer wave length, two bands exist even at the small concentration of chloride ion, and the maxima of these bands shift from 315 to 310 mμ, from 360 to 363 mμ, respectively. With increase in the concentration of chloride ion, the absorbance in all bands rises at first, and then remains constant while the chloride concentration is in the range from 0.5 to 2.4 M (Curve 5, 6 and 7), and after that it begins to diminish gradually.




Chloride Concentration in Mol.

Fig. 4. Correlation of chloride concentration and Acidity.
Acidity: △ 2.4 N, ○ 4.8 N, □ 6.4 N, ◇ 9.6 N

The complicated changes in absorption spectra are due to the stepwise formation of iron(III) chloro-complex as follows.

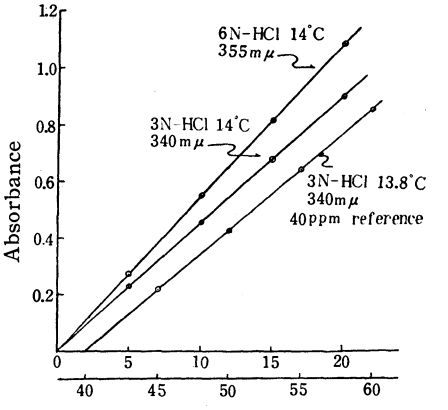
$$Fe^{3+} + Cl^- \rightleftarrows FeCl^{2+}$$
$$FeCl^{2+} + Cl^- \rightleftarrows FeCl_2^+$$
$$FeCl_2^+ + Cl^- \rightleftarrows FeCl_3$$
$$FeCl_3 + Cl^- \rightleftarrows FeCl_4^-$$

To survey the correlation of the effects of hydrogen and chloride ions, in Fig. 4 are shown the changes in absorbance at a given wave length plotted against the concentration of chloride ion at various constant acidities. From this figure, it is deduced that hydrogen ion expedites the formation of the chloro-complex when the chloride concentration is considerably low, but in the higher chloride solution, effects of acidity become small, except in the solution of 9.6 M. Since the curves in Fig. 3-4, are in accord with the spectrum of $FeCl_4^-$, calculated by Gamlen, it is found that the tetra chloro-complex is formed even at the small concentration of chloride ion when the acidity is considerably high, but it may not be formed even at higher chloride concentration if the acidity is low, as shown in Fig. 3-1, -2, and -3. The decrease in absorbance observed in Fig. 3-4, might be due to decrease of ferric ion, which may be caused by the reduction of ferric to ferrous ion in such a concentrated hydrochloric acid solution, but this assumption has not been confirmed experimentally.

## Determination of Iron(III)

From the above preliminary survey it is necessary to conduct the measurement under the constant concentration of hydrochloric acid for the determination of iron (III).

**Calibration curve.**—The preparation of the standard iron solutions was as previously reported. A 1.002 g. of electrolytic iron (purity 99.8%) was dissolved in 4 M perchloric acid and evaporated until chloride and iron(II) became absent and then diluted to 1 l.




p.p.m. Fe

Fig. 5. Calibration Curves

First, for the ordinary absorptiometry, the calibration curve was made for the ferric solution in such concentration as 5, 10, 15 and 20 p.p.m. The concentration of the acid was held at constant in 3 M and 6 M, and the absorbance was measured at 340 and 355 mμ, respectively. In both cases Beer's law is followed in the range 0.2–20 p.p.m. of iron, as shown in Fig. 5. The sensitivity in this method is considerably low compared to the other methods; however, it is more useful by means of the differential absorptiometry. For this purpose, the solution with 40 p.p.m. of iron was used as reference, and the calibration curve was made in such concentration as 45, 50, 55 and 60 p.p.m. Results are also shown in Fig. 5 and Beer's law is followed up to 60 p.p.m. As the reference, concentration higher than 40 p.p.m. of iron is not favourable, because it reduces the sensitivity of the measurement.

**Temperature.**—The effects of the temperature on absorbance were investigated and the results are shown in Table I. It is seen that the effect of the temperature is almost negligible in the range 10–25°C.

TABLE I
EFFECT OF TEMPERATURE
Concn. of Iron(III): 10 p.p.m.

| 3 M-HCl | | 6 M-HCl | |
|---|---|---|---|
| Temp. °C | As. at 340 mμ | Temp. °C | As. at 355 mμ |
| 9 | 0.440 | | |
| 10 | 0.440 | 10 | 0.543 |
| 11 | 0.441 | 12 | 0.543 |
| 13 | 0.442 | 14 | 0.544 |
| 16 | 0.442 | 18 | 0.544 |
| 17 | 0.445 | 23 | 0.543 |
| 19 | 0.448 | 30 | 0.545 |
| 20 | 0.449 | | |
| 24 | 0.451 | | |
| 28 | 0.454 | | |

TABLE II
EFFECT OF DIVERSE ION

| Diverse Ion | | Fe present | Fe found |
|---|---|---|---|
| | (p.p.m.) | (p.p.m.) | (p.p.m.) |
| $Al^{3+}$ | 200 | 10.0 | $9.9_5$ |
| $Zn^{2+}$ | 200 | 10.0 | $10.0_6$ |
| $Mn^{2+}$ | 200 | 10.0 | 10.0 |
| $Ni^{2+}$ | 200 | 10.0 | 10.1 |
| $Co^{2+}$ | 200 | 10.0 | 10.1 |
| $Ti^{4+}$ | 200 | 10.0 | 10.1 |
| $Cu^{2+}$ | 200 | 10.0 | 29.9 |
| $Cu^{2+}$ | 10 | 10.0 | 11.1 |

concn. of HCl; 6 M, wave length: 355 mμ

**Effect of diverse Ions.**—Study was made on the effect of several cations. The cations were present in solution as perchlorate. Measurements were made for the solutions containing a proper amount of foreign salt with 10 p.p.m. of iron. The results are presented in Table 2. It is found that the presence of such cations as $Na^+$, $K^+$, $NH_4^+$, $Co^{2+}$, $Zn^{2+}$, $Mn^{2+}$ and $Al^{3+}$ do not interfere in the concentration of 200 p.p.m. As DeSesa has reported, the chloride of cations such as $Cu^{2+}$, $Ti^{4+}$, $Bi^{3+}$ and $V^{5+}$ in the solution of hydrochloric acid have intense absorption in the ultraviolet region, and thus their presence will interfere with the determination of iron. For $Cu^{2+}$ and $Ti^{4+}$, it is found that the maximum allowable concentration was 2.0 p.p.m.

**Determination of Iron in Iron-base alloy.** — In order to test the reliablity of the proposed method, some iron-base alloys were shosen as samples, and the determination was done by means of differential absorptiometry.

Procedure:

A 200–150 mg of sample was dissolved in 4 M perchloric acid by warming on a sand bath. After cooling, several drops of $H_2O_2$ (30%) were added and then evaporated almost to dryness. The evaporation was repeated several times and the residue was dissolved in distilled water: then the solution was transferred to a 500 ml. volumetric flask and diluted to the volume. After being mixed thoroughly, an aliquot of 20 ml was pipetted into a 100 ml. volumetric flask and after 50 ml. of 6 M hydrochloric acid was added, diluted to the volume with water.

TABLE III
ANALYSIS OF IRON SAMPLES

| Sample | Fe (%) | | |
|---|---|---|---|
| | Present | Found | Error (%) |
| J. E. S. No. 12 (low phosphor iron) | 92.46 | 92.91 | $+0.4_9$ |
| J. E. S. No. 21 (Haematite) | 61.32 | 61.49 | $+0.2_8$ |
| J. E. S. No. 19 (Ferrovanadium) | 57.44 | 71.12 | +27.0 |
| J. E. S. No. 13 (Ferromanganese) | 15.78 | 15.71 | $-0.4_5$ |

The absorbance of the above solution was measured at 340 mμ using an iron solution (40 p.p.m.) as the reference. Results are presented in Table 3, and the error is about 0.4%. In the case of ferrovanadium alloy, the reason for the high value must be the presence of vanadium (V).

## Summary

The absorption spectra have been investigated for the solution of ferric perchlorate at various concentrations of hydrochloric acid. A method for spectrophotometric determination of iron has been studied using hydrochloric acid as reagent. Effects of temperature, acidity and diverse ions have been examined and the iron content of iron-base alloys has been determined by differential method.

*Department of Chemistry, Faculty of Science, Kyoto University, Sakyo-ku Kyoto*

# *Ultraviolet Spectrophotometric Determination of Iron with Ethylenediaminetetraacetic Acid*

By Yasumitsu UZUMASA, Masakichi NISHIMURA and Toshiko SEO

(Received August 15, 1956)

When ethylenediaminetetraacetic acid, EDTA, is added to the solution containing a considerable amount of $Fe^{3+}$ ion, a yellow color apparently akin to that produced by $Fe^{3+}$—HCl complex develops. It was already pointed out by Schwarzenbach and Heller[1] in 1951 that $Fe^{3+}$—EDTA complex shows an absorption in the near ultraviolet region. The absorption at about 400 m$\mu$ was also reported by Jones and Long[2] who used in their observation a solution of considerably high concentration. In 1954, Goto and Kobayashi[3] illustrated an end absorption similar to that reported by Jones and Long while Nielsch and Böltz[4] described the fact that the solution of $Fe^{3+}$—EDTA has an absorption maximum below 366 m$\mu$ which allows photometric estimation of the metal by EDTA. Uzumasa[5] and Nishimura[6] reported in their short communication that a dilute solution of $Fe^{3+}$—EDTA compound has a characteristic absorption peak at 260 m$\mu$ which is available for ultraviolet spectrophotometric determination of iron. The conditions under which the analysis is carried out have been investigated since and the results will be reported here.

## Experimental

An excess of disodium salt of EDTA was added to hydrochloric acid solutions containing various amounts of iron as $Fe^{3+}$. Each solution was diluted to a definite volume so that the resultant concentration should be 0.1 M with respect to hydrochloric acid and 0.001 M with respect to EDTA. The absorbance of the solutions was then measured with a Beckman DU spectrophotometer equipped with 1 cm. silica cells. Distilled water was referred to as blank throughout the present observation. In Fig. 1, curve I shows the absorption spectrum of EDTA under no iron; curves II, III and IV represent the absorption spectra of $Fe^{3+}$—EDTA solutions which contain $5\times10^{-5}$, $1.5\times10^{-4}$ and $2\times10^{-4}$ mol. $Fe^{3+}$/l. respectively. The ferric ion when combined with EDTA shows, as already reported by the authors, a remarkable absorption at 260 m$\mu$, whereas EDTA itself exhibits no absorption at this point.

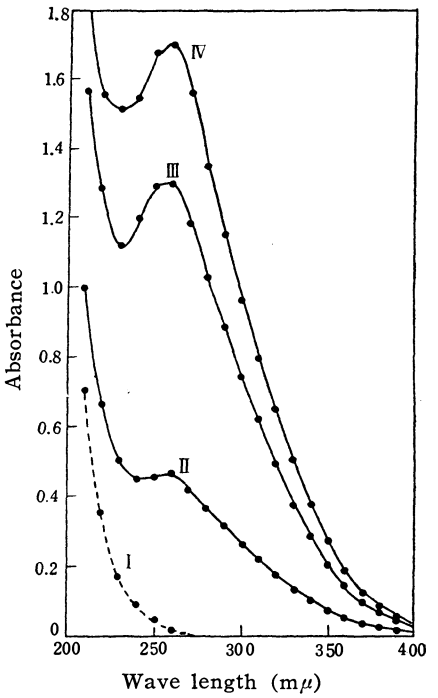



Fig. 1. Absorption of $Fe^{3+}$—EDTA complex.
I: without iron
II: $5\times10^{-5}$ M $Fe^{3+}$
III: $1.5\times10^{-4}$ M $Fe^{3+}$
IV: $2\times10^{-4}$ M $Fe^{3+}$

Fig. 2 indicates the calibration curve for iron at 260 m$\mu$ obtained by the present procedure. Conformity to Beer's law was found for concentrations up to 17 p.p.m. of iron. The sensitivity[7] of the method is 0.0065 $\gamma$ Fe/cm$^2$, a little better than that of the thiocyanate method (0.008 $\gamma$/cm$^2$; 480 m$\mu$) and nearly comparable to that of the $\alpha,\alpha'$-bipyridyl method (0.007 $\gamma$/cm$^2$; 522 m$\mu$)[7].

1) G. Schwarzenbach and J. Heller, *Helv. Chim. Acta*, **34**, 576 (1951).
2) S. S. Jones and F. A. Long, *J. Phys. Chem.*, **56**, 25 (1952).
3) H. Goto and J. Kobayashi, *J. Chem. Soc. Japan*, **75**, 964 (1954).
4) W. Nielsch and G. Böltz, *Mikrochim. Acta*, **1954**, 481.
5) Y. Uzumasa, *Japan Analyst*, **3**, 255 (1954).
6) Y. Uzumasa and M. Nishimura, This Bulletin, **28**, 88 (1955).
7) E. B. Sandell, "Colorimetric Determination of Traces of Metals", 2nd Ed. Interscience Publishers, Inc., New York, N. Y. (1950), p. 364.

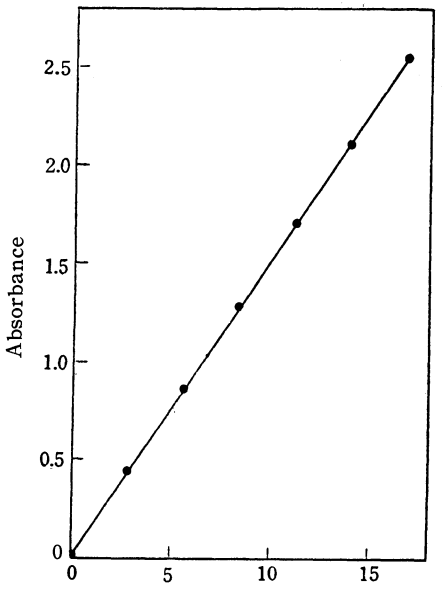



Fig. 2. Calibration curve for iron at 260 mμ.

Jones and Long[2] described in their discussion on the mechanism of the reaction that a part of $Fe^{3+}$—EDTA complex in the solution is converted into $Fe^{2+}$—EDTA complex by light, the latter returning to the former in the dark. It was also established by the present authors that the absorbance of the $Fe^{3+}$—EDTA solution decreases when irradiated by light while it recovers when placed in the dark (Fig. 3). The complex is stable in the dark, its absorbance remaining unchanged when even it is left for 13 hours.

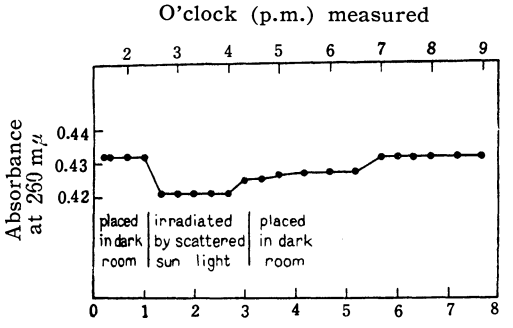



Fig. 3. Effect of light on $Fe^{3+}$—EDTA complex.

According to Schwarzenbach and Heller[1], the ratio Fe : EDTA in the complex is 1 : 1, which was ascertained by Jones and Long[2] after Job's continuous variation method. In the present study, a series of solutions was prepared by mixing 0.0002 M ferric iron solution and the EDTA solution of the same concentration in different ratios so that the acidity of the resultant liquid should be maintained to be constant, i. e., 0.1 M with respect to hydrochloric acid. Using these solutions, the absorbance at 260 mμ was observed, the result being in good accord with that of Jones and Long. Theoretically 1 mole EDTA is thus considered to react with 1 mole $Fe^{3+}$ (Fig. 4). In the practical determination of iron, however, as shown in Fig. 5, EDTA might as well be used in excess, at least one and one half times as much as iron.

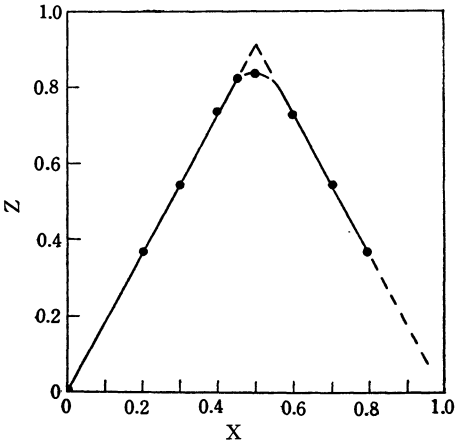



Fig. 4. Continuous variation study of the system $Fe^{3+}$ and EDTA.
X = mol. ratio of (EDTA)/($Fe^{3+}$+EDTA)
$Z = \varepsilon_2/(\varepsilon_2-\varepsilon_1)\{(As)_{obs.}-\varepsilon_1 M(1-X)\}$
Where $\varepsilon_1$ and $\varepsilon_2$ are molar extinction coeff. for $Fe^{3+}$—HCl and $Fe^{3+}$—EDTA solutions, respectively. $(As)_{obs.}$ is the absorbance observed at 260 mμ.

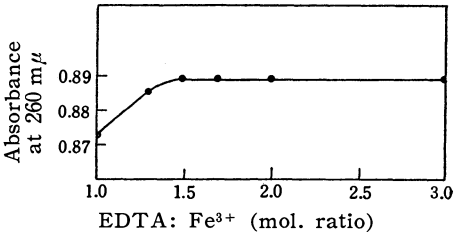



Fig. 5. Values of maximum absorbance of $1\times10^{-4}$ M $Fe^{3+}$ solutions at varying concentrations of EDTA.

**Influence of pH.**—Nielsch and Böltz[4] found the extinction of $Fe^{3+}$—EDTA complex depends upon the pH. This was further verified in the present investigation. By varying the amount of hydrochloric acid or sodium hydroxide to be

added, a series of solutions, each of which was $5\times10^{-5}$ M with respect to $Fe^{3+}$ and $1\times10^{-3}$ M with respect to EDTA, only differing in pH values, was obtained. Their absorbance was then examined at 260 m$\mu$. As shown in Fig. 6, $Fe^{3+}$-EDTA complex seems to be stable on the acid side, although its absorbance decreases rapidly below pH 0.5. In the solution containing as much as 1 M hydrochloric acid, it develops an absorption similar to that which contains no EDTA: in other words, it corresponds to the absorption of $Fe^{3+}$–HCl. The absorbance is also reduced on the alkaline side.

In place of hydrochloric acid, sulfuric, perchloric or acetic acid may be used since these acids have, like hydrochloric acid,

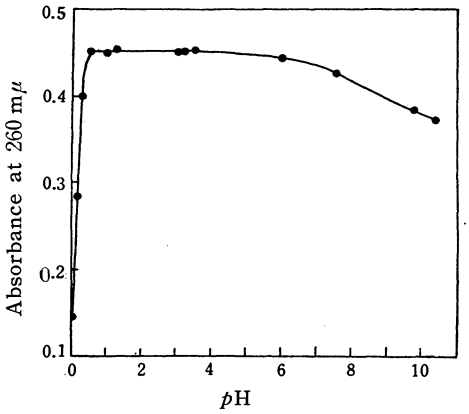



Fig. 6. Absorbance maxima for $Fe^{3+}$ –EDTA complex. Its change with *p*H.

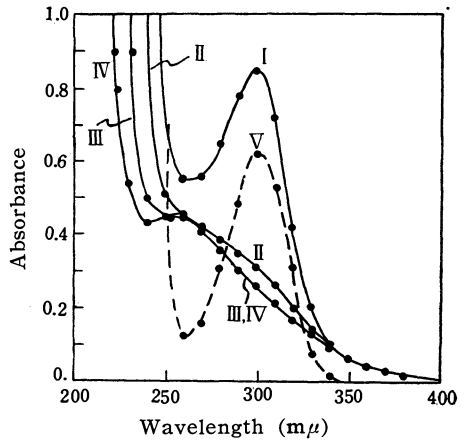



Fig. 7. Absorption of $Fe^{3+}$–EDTA complex ($5\times10^{-5}$ M) at varying concentrations of $HNO_3$.
I: in 0.1 M $HNO_3$
II: in 0.01 M $HNO_3$
III: in 0.001 M $HNO_3$
IV: in 0.0001 M $HNO_3$
V: 0.1 M $HNO_3$ itself

no characteristic absorption at 260 m$\mu$. In case of nitric acid, even though it has an absorption peak at 300 m$\mu$, its absorption is minimum at 260 m$\mu$ so that the absorbance of $Fe^{3+}$–EDTA in presence of nitric acid at 260 m$\mu$ remains unchanged provided that the concentration of the acid is kept lower than 0.01 M (Fig. 7).

**Influence of coexisting ions.**—In their study of photometric determination of iron with EDTA, Nielsch and Böltz[4] confirmed that weaker complex formers such as tartaric acid do not interfere. No observations were carried out by them on the effects of metallic ions. In order to examine the influence of the coexisting foreign substances, the absorbance measurements were carried out by the authors using the solutions with or without foreign ions. Each solution was prepared so that it was 0.1 M with respect to sulfuric or hydrochloric acid and 0.0005 M with respect to EDTA, the amount of $Fe^{3+}$ being always kept to be 2.45 p.p.m. After each solution to which the EDTA reagent had been added was placed in the dark for 30 min., the absorbance was measured. Other conditions were kept as constant as possible throughout the measurement. The results are summarized in Table I.

Among the cations examined, alkalies and alkaline earths do not interfere. $Cu^{2+}$, $Hg^{2+}$ and $Ti^{4+}$ interfere seriously when combined with EDTA. As indicated in Fig. 8 and 9, these cations unite like $Fe^{3+}$ with EDTA in the 0.1 M sulfuric acid solutions forming

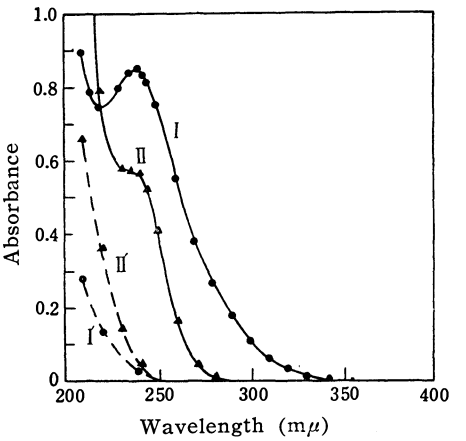



Fig. 8. Absorptions of $Cu^{2+}$— and $Hg^{2+}$— complexs in 0.1 M $H_2SO_4$.
I: 0.0002 M $Cu^{2+}$ soln. with EDTA
I′: 0.0002 M $Cu^{2+}$ soln. without EDTA
II: 0.0002 M $Hg^{2+}$ soln. with EDTA
II′: 0.0002 M $Hg^{2+}$ soln. without EDTA

TABLE I

INFLUENCE OF FOREIGN SUBSTANCES ON THE ABSORBANCE OF $Fe^{3+}$–EDTA COMPLEX

(2.45 p.p.m. $Fe^{3+}$ in 0.1 M $H_2SO_4$ solution)

| Substance added | Ion | Concentration (p.p.m.) | Absorbance at 260 mμ |
|---|---|---|---|
| None | — | 0.0 | 0.432 |
| NaCl | $Cl^-$ | 4,000 | 0.427 |
| | | 10,000 | 0.432 |
| NaF | $F^-$ | 20 | 0.431 |
| | | 60 | 0.432 |
| $NaNO_3$ | $NO_3^-$ | 248 | 0.436 |
| | | 620 | 0.442 |
| $K_2SO_4$ | $SO_4^{2-}$ | 1,200 | 0.432 |
| | | 2,500 | 0.428 |
| | | 3,700 | 0.432 |
| $H_3BO_3$ | | 570 | 0.432 |
| | | 1,140 | 0.432 |
| $NaH_2PO_4$ | | 125 | 0.434 |
| | | 250 | 0.444 |
| $Na_2C_2O_4$ | | 150 | 0.468 |
| | | 300 | 0.495 |
| Na-citrate | | 100 | 0.444 |
| | | 200 | 0.435 |
| Na-tartrate | | 130 | 0.432 |
| | | 260 | 0.432 |
| $Li_2CO_3$+HCl | $Li^+$ | 8.0 | 0.432 |
| | | 16.0 | 0.432 |
| NaCl | $Na^+$ | 2,600 | 0.427 |
| | | 6,500 | 0.432 |
| $K_2SO_4$ | $K^+$ | 1,000 | 0.432 |
| | | 2,000 | 0.428 |
| | | 3,000 | 0.432 |
| $MgSO_4$ | $Mg^{2+}$ | 960 | 0.437 |
| | | 4,800 | 0.430 |
| $CaCO_3$+HCl | $Ca^{2+}$ | 128 | 0.437 |
| | | 240 | 0.445 |
| $MnSO_4$ | $Mn^{2+}$ | 30 | 0.432 |
| | | 70 | 0.434 |
| $CuSO_4$ | $Cu^{2+}$ | 0.19 | 0.438 |
| | | 0.32 | 0.444 |
| | | 2.0 | 0.613 |
| $ZnSO_4$ | $Zn^{2+}$ | 200 | 0.432 |
| | | 400 | 0.437 |
| $CdSO_4$ | $Cd^{2+}$ | 1,140 | 0.432 |
| $HgCl_2$ | $Hg^{2+}$ | 10.3 | 0.456 |
| | | 51.4 | 0.495 |
| $SnCl_2$ | $Sn^{2+}$ | 700 | 0.437 |
| $CoCl_2$ | $Co^{2+}$ | 6 | 0.433 |
| | | 20 | 0.434 |
| $NiSO_4$ | $Ni^{2+}$ | 7 | 0.435 |
| | | 20 | 0.436 |
| | | 60 | 0.438 |
| $Cr_2(SO_4)_3$ | $Cr^{3+}$ | 10 | 0.433 |
| | | 18 | 0.446 |
| $Al_2(SO_4)_3$ | $Al^{3+}$ | 100 | 0.427 |
| | | 200 | 0.432 |
| | | 350 | 0.438 |
| $Ti(SO_4)_2$ | $Ti^{4+}$ | 0.7 | 0.438 |
| | | 20 | 1.004 |
| $Ge(SO_4)_2$ | $Ge^{4+}$ | 100 | 0.433 |

(2.45 p.p.m. $Fe^{3+}$ in 0.1 M HCl solution)

| | | | |
|---|---|---|---|
| None | — | 0.0 | 0.420 |
| $BaCl_2$ | $Ba^{2+}$ | 40 | 0.420 |
| | | 70 | 0.422 |
| $SrCO_3$+HCl | $Sr^{2+}$ | 400 | 0.436 |

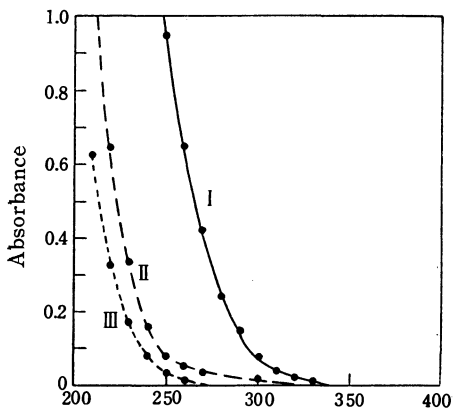



Fig. 9. Absorption of $Ti^{4+}$— complex in 0.1 M $H_2SO_4$.
I: $4\times10^{-4}$ M $Ti^{4+}$ soln. with EDTA
II: $4\times10^{-4}$ M $Ti^{4+}$ soln. without EDTA
III: EDTA only, 0.1 M $H_2SO_4$

complexes which exhibit remarkable absorption in the ultraviolet region. As expected from the curves in Fig. 1, 8 and 9, the effect of $Cu^{2+}$, $Hg^{2+}$ or $Ti^{4+}$ may be reduced to a certain extent if the measurement of $Fe^{3+}$ is carried out in the range longer than 260 mμ.

$Fe^{2+}$ can be determined by the present method if the ion is previously oxidized to $Fe^{3+}$ by adding a dilute potassium permanganate solution in acid medium until the solution develops pink color. In this case, the absorbance changes for some time after EDTA is added. It is therefore desirable that the measurement is carried out 90 min. after the addition of the reagent.

Nitrate interferes when it exists at a certain concentration. As described above, this is certainly due to the absorption of the nitrate ion itself.

## Summary

A dilute solution of $Fe^{3+}$—EDTA complex has a characteristic absorption peak at 260 m$\mu$ which is available for ultraviolet spectrophotometric determination of iron. An excess of disodium salt of EDTA was added to 0.1 M hydrochloric acid solution containing various amounts of iron as $Fe^{3+}$ and the absorbance was measured with a Beckman DU spectrophotometer. A calibration curve for iron at 260 m$\mu$ was obtained and conformity to Beer's law was found for concentrations up to 17 p.p.m. of iron. The sensitivity of the method is 0.0065 $\gamma/cm^2$.

The absorbance of $Fe^{3+}$—EDTA solution decreases when irradiated by light, while it recovers when placed in the dark.

$Fe^{3+}$—EDTA complex is stable in acidic medium, although its absorbance decreases rapidly below pH 0.5. The absorbance is also reduced on the alkaline side.

Hydrochloric, sulfuric, perchloric or acetic acid can be used in the determination. Nitric acid is used only when the concentration is kept in a certain limited value, this acid having the absorption maximum at 300 m$\mu$ and the minimum at 260 m$\mu$.

Influence of the coexisting substances on the absorption measurement of $Fe^{3+}$—EDTA complex was examined. Among the cations examined, alkalies and alkaline earths do not interfere. $Cu^{2+}$, $Hg^{2+}$ and $Ti^{4+}$ interfere seriously when combined with EDTA, because their EDTA complexes show remarkable absorption in the ultraviolet region, which may suggest a new ultraviolet spectrophotometric determination of the metals.


After the work reported herein had been completed, the authors were informed of the work of Hill-Cottingham[8], who reports a somewhat similar study on iron complexes of EDTA and other chelating agents.


*Department of Chemistry*
*Faculty of Science*
*Hokkaido University, Sapporo*


8) D. G. Hill-Cottingham, *Analyst*, **80**, 906 (1955).

# *A Simple Method of Sulfate Microdetermination*

By Fujio EGAMI and Noriko TAKAHASHI

(Received November 17, 1956)

Y. Yagi and one of the present writers (Egami)[1] devised a method to determine sulfate by dichromate titration method. Their method was modified by N. Tamiya[2]. Although the method has been shown to be sufficiently accurate and successfully applied to the microdetermination of sulfate in biochemistry, the procedure is rather complicated.

The present paper deals with the simplification of the method: sulfate is precipitated as barium sulfate, and the excess of barium is precipitated as barium chromate. Finally the excess of chromate is estimated in alkaline solution with a spectrophotometer at 375 m$\mu$. The optical density and the quantity of sulfate are in the linear relation.

1) Y. Yagi and F. Egami, *J. Chem. Soc. Japan.* **67**, 19 (1947).
2) N. Tamiya, *J. Jap. Biochem. Soc.*, **22**, 59 (1950).

## Analytical Procedure

(Reagents)

a) Barium chloride, 0.01M.

b) Potassium dichromate, a little more than 0.005 M.

c) Sodium acetate, 20% (w/v).

d) Sodium hydroxide, 1 N.

(Method of Analysis)

1) Six ml. or less of the neutralized test solution (containing sulfate sulfur in the range 10–300 $\gamma$) and 1 ml. of barium chloride are placed in a 10 ml. measuring flask, and the flask is allowed to stand for about one hour. The complete precipitation of barium sulfate takes place.

2) Two ml. of sodium acetate solution is added to the flask, and the flask is kept in an ice bath for twenty minutes.

3) One ml. of potassium dichromate is then added to the flask, the reagents are

TABLE I

DETERMINATION OF SULFATE IN RAIN WATERS AND NATURAL SULFURIC ESTERS

| Sample | Sample taken | Sulfur concn. found (γ) | Sulfur concn. found (%) | Total sulfur when 60γ of sulfur was added to the sample* (γ) | Recovery (%) |
|---|---|---|---|---|---|
| Potassium chondroitinsulfate | 2.400mg | 125 | 5.21 | 185 | |
| | | 126 | 5.25 | 187 | 99.5 |
| | | 130 | 5.42 | 186 | |
| Potassium charoninsulfate | 1.216mg | 178 | 14.6 | 237 | |
| | | 183 | 15.0 | 251 | 100.8 |
| | | 186 | 15.3 | 244 | |
| Rain water I | 100ml | 198 | — | 267 | 103.4 |
| Rain water II | 100ml | 82 | — | 136 | 95.5 |

* A small quantity of sulfate added to the test solutions was always quantitatively recovered

TABLE II

DETERMINATION OF SULFATE IN SYNTHESIZED SULFURIC ESTERS

| Sample | Sample taken (mg) | Sulfer concn. Calcd. (γ) | Calcd. (%) | Found. (γ) | Found. (%) | Relative error (%) |
|---|---|---|---|---|---|---|
| Potassium ethyl sulfate | 0.672 | 131 | 19.5 | 125 | 18.6 | 4.62 |
| | 1.058 | 206 | | 202 | 19.1 | 2.05 |
| Potassium p-nitrophenyl sulfate | 0.985 | 123 | 12.5 | 130 | 13.1 | 5.37 |
| | 1.244 | 155 | | 166 | 13.3 | 6.66 |

mixed well, the volume is brought to the 10 ml. mark with distilled water and the flask is kept cold for further twenty minutes.

4) The reaction mixture is transferred into a centrifugal tube. After being centrifuged, two ml. of the clear supernatant is mixed with 1 ml. of sodium hydroxide solution in a 10 ml. graduated test tube, and diluted to the volume with distilled water.

5) Then the extinction of this solution is measured at 375 mμ with the spectrophotometer**, and sulfate is estimated by the standard curve obtained by known sulfate solutions using the same reagent solutions.

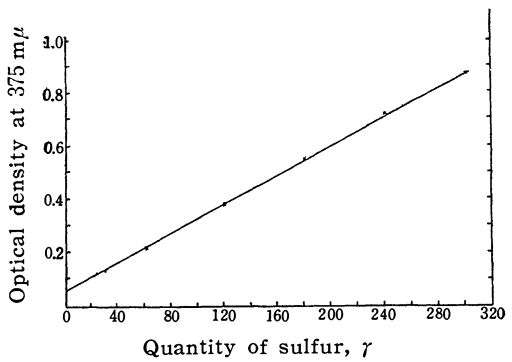



Fig. 1. A standard curve obtained by known sulfate solutions.

** We used Hitachi Type EPB-F spectrophotometer and cuvettes with a 1 cm light path.

Remarks:

1) The optical density and the quantity of sulfate are in the linear relation as shown in Fig. 1. Each time, when barium chloride or potassium dichromate solution is renewed, the standard curve must be also renewed using known sulfate solutions.

2) When a convenient spectrophotometer is not available or the test solution has an absorption band near 375 mμ, sulfate might be estimated by a spectrophotometer at a different wave length in an alkaline or an acid medium. (c.f. the absorption spectra of chromate and dichromate. Fig. 2).

3) When a large quantity of phosphate coexists with sulfate, this method can not be applied as such, unless phosphate is removed before sulfate estimation[2].

## Some Examples of Analysis

This method was successfully applied to the estimation of sulfate sulfur in some natural waters, and the natural and the synthesized sulfuric esters. (Table I and Table II).

For sulfuric esters, the analytical method was slightly modified. Each sample was hydrolyzed with 0.2 ml. of concentrated hydrochloric acid under the existence of 1 ml. of barium chloride, about 3 hours on a steam bath. The hydrochloric acid was removed by evaporation and the test solution was carefully neutralyzed.

For the rain water, one ml. of barium chloride solution was added to 100 ml. of the sample solution, and the solution was carefully concentrated to a suitable volume on a sand bath.

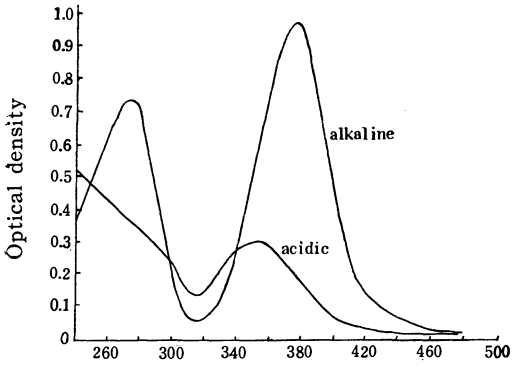



Fig. 2. The absorption spectra of chromate and dichromate ($10^{-4}$ M).

## Discussion

1) The extinction curve of the excess chromate revealed two strong absorption peaks at 273 mμ and 375 mμ in alkaline solution, and weaker one at 350 mμ in acid solution. (Fig. 2). The relationship between the amount of sulfate and the absorbance obeyed Beer's law over the range from 10γ to 320γ of sulfate sulfur. (Fig. 1).

2) Even the absorption at 375 mμ caused by the sample itself did not seriously interfere with the determination of sulfate. For example, although p-nitrophenyl sulfate (Table II) caused some absorption at 375 mμ after hydrolysis, analytical results showed it to be fairly good. In such a case, a blank without dichromate was necessary.

3) The good stability of the color of dichromate solution was also one of the advantages of this method.

## Summary

1) A simple method for sulfate microdetermination was established. Sulfate is precipitated as barium sulfate; then the excess of barium is precipitated as barium chromate. Finally the excess of chromate is estimated in alkaline solution with a spectophotometer at 375 mμ.

2) This method is able to be applied to sulfate solution containing sulfate sulfur in the range 10–300γ. (30–900γ as $SO_4^{2-}$)

3) This method was successfully applied to the estimation of inorganic sulfate such as that in rain water and organic sulfate such as chondroitinsulfate, charoninsulfate, ethyl sulfate and p-nitrophenyl sulfate.

The expense of this study was defrayed partly by a grant from Seikagaku-Kenkyusho Ltd., to which our thanks are due.

*Department of Chemistry*
*Nagoya University*
*Chikusa-ku, Nagoya*

# *On the Thermal Dissociation of Organic Compounds. XII. The Effects of the Substituents on the Thermal Dissociation of Substituted Phenylureas*

By Shoichiro OZAKI and Tsutomu NAGOYA

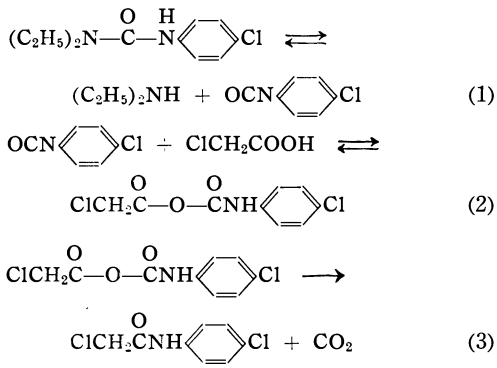
(Received August 13, 1956)

## Introduction

The kinetics of the thermal dissociation of urea, di- and tri-substituted ureas in fatty acids have been studied[1-4]. In the present work, more than ten new ureas of the types, 1,1-diethyl-3-phenylureas (I), 1-pentyl-3-phenylureas (II) and 1,3-diphenylureas (III), substituted for methoxy, methyl, chloro and nitro in ortho, meta and para positions, respectively have been synthesized, and the kinetics of the thermal dissociation of these ureas in fatty acids have been studied. The effects of the substituents on the thermal dissociation of these ureas are discussed.

1) T. Hoshino, T. Mukaiyama and H. Hoshino, *J. Am. Chem. Soc.*, **74**, 3097 (1952).
2) T. Mukaiyama and T. Matsunaga, ibid., **75**, 6209 (1953).
3) T. Mukaiyama, S. Ozaki and T. Hoshino, This Bulletin, **27**, 578 (1954).
4) T. Mukaiyama, S. Ozaki and Y. Kobayashi, ibid., **29**, 51 (1956).

The dissociation of substituted ureas, e. g., 1,1-diethyl-3-(p-chlorophenyl) ureas in chloroacetic acid, takes place according to the following equations:



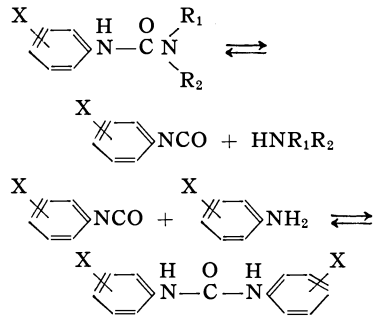
(1)

(2)

(3)

The reaction in fatty acids can be followed by measuring the rate of evolution of carbon dioxide (eq. 3), as the reaction (1) is the rate-determining step.

1,1-Diethyl-3-arylureas (I)[5] were prepared from diethylcarbamyl chloride, corresponding amines and triethylamine. 1-Pentyl-3-arylureas (II) could be obtained from pentyl isocyanate and amines. 1,3-Diarylureas (III) were obtained in the course of the syntheses of ureas (I) and (II) as mentioned below. Reactivity of aromatic amines towards isocyanate and diethylcarbamyl chloride is of a similar order to those observed by Van Opstall[6] and Linke[7] in the reaction between 1-chloro-2,4-dinitrobenzene and aromatic amines, and by C. Naegeli[8] et al. in the reaction of the amines with phenyl isocyanate. Methoxy-, methyl- and chloro- anilines react easily with pentyl isocyanate, but nitroanilines do not react at room temperature. m-Nitroaniline reacts at 80°C., and p-nitroaniline does to an extent of only 1% in 5 hours at the same temperature. The reactivity of diethylcarbamyl chloride towards amines is smaller than that of isocyanate. In the reaction of unreactive amines, such as nitro- and chloro- anilines, towards diethylcarbamyl chloride, the yields were poor, and by raising the temperature, 1,3-diarylureas were produced as byproducts. As 1,1,3-trisubstituted ureas dissociate much more easily by Eq. (4) than 1,3-diarylureas as shown in Table II and in a previous report[4], 1,3-diarylureas were obtained probably through the following mechanism.



(4)



(5)

1,3-Bis-(p-nitrophenyl) urea was produced also in the reaction of p-nitroaniline with pentyl isocyanate at 150°C.

Aniline derivatives having more than two substituents such as 2,4,5-trichloro- and 2,6-dichloro- aniline have small reactivity, and 2,4,5-trichloro- is less reactive than 2,6-dichloro-aniline.

## Experimental

**Ureas.**—The various constants of the ureas synthesized and the experimental conditions of syntheses are summarized in Table I. As an example, the synthetic procedure for 1,1-diethyl-3-(o-methoxyphenyl) urea is given: A mixture of 4.1 g. (4/100 mole) of diethylcarbamyl chloride, 4.8 g. (4/100 mole) of o-anisidine and 5 g (5/100 mole) of triethylamine are heated under a reflux condenser with a calcium chloride tube for 2 hours at 80-90°C. The triethylamine hydrochloride precipitated is filtered off, and the salt is washed with benzene. The combined filtrate and benzene washing are washed with 2 N hydrochloric acid, and then with water. After dried over anhydrous sodium sulfate, benzene was evaporated and 5.3 g. (59%) of 1,1-diethyl-3-(o-methoxyphenyl) urea was obtained by distillation, colourless liquid boiling at 143-145°C/0.40-0.45mm.

**Solvents.**—The solvents were purified by the same method as described[3] previously. The boiling point of caproic acid was 104-106°C/16-17 mm. and that of chloroacetic acid was 184-185°C.

**Rate measurement.**—The procedure for measuring the rate of dissociation of ureas in fatty acids has been described previously[1,3]. On plotting against time the logarithm of the volume of carbon dioxide, $\Delta Y$, evolved at regular intervals of time, a straight line was obtained. This indicates a first order reaction rate. The rate constant is given by the gradient of such a plot. The molar ratio of ureas to solvents was 1 : 100 in each case.

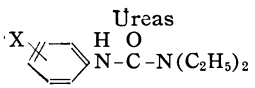
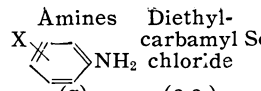
The rate constants of the thermal dissociation of these ureas in fatty acids are summarized in Table II and in part are shown in Fig. 1 and 2.

The activation energy (Ea) of the dissociation reaction of 1,1-diethyl-3-phenylurea in chloroacetic

5) Some of ureas (I) are reported to be useful as herbicides named C. M. U. (Chlorophenyl Methyl Urea). U. S. P. 2655444, 2655445, 2655446 and 2655447. Kagaku to Kogyo (Chemistry and Chemical industry) **9**, 63 (1956).
6) Van Opstall, *Rec. trav. Chim.*, **52**, 901 (1933).
7) Linke, *Ber.*, **56**, 848 (1923).
8) C. Naegeli, A. Tyabji and C. Conrad, *Helv. Chim. Acta*, **21**, 1127 (1938).

TABLE I

UREAS AND THEIR SYNTHETIC METHODS

| Ureas  | Amines  (g) | Diethyl-carbamyl chloride (c.c.) | Solvent (c.c.) benzene | Triethyl amine (c.c.) | Reaction temp. (°C.) | Reaction time. (hours) | M.P. (°C.) | Yield (%) | Analysis Nitrogen Calcd. | Found | Byproduct | M.P. (°C.) | Yield (%) | Analysis Nitrogen Calcd. | Found |
|---|---|---|---|---|---|---|---|---|---|---|---|---|---|---|---|
| X= H | 1 | 1 | 4 | 0 | 60 | 0.5 | | 0 | | | 1,3-diphenyl-urea | 235 | 16 | | |
| 〃 | 1 | 1 | 0 | 1 | room temp. (5～20) | 24 | 84.5-85 | 30 | | | | | | | |
| 〃 | 3.7 | 4.8 | 0 | 5 | 40 | 3 | 〃 | 62 | | | | | | | |
| *o*—$OCH_3$ | 4.8 | 4.12 | 0 | 4.8 | 80 | 2 | B.P.143-145/ 0.45 | 59 | 12.60 | 12.46 | | | | | |
| *p*—$OCH_3$ | 1.4 | 1.5 | 4 | 1.5 | room temp. | 24 | 61.5-62 | 33.4 | 12.60 | 12.58 | | | | | |
| *o*—$CH_3$ | 4.27 | 4.1 | 0 | 4.8 | 80-100 | 1 | 78-79 | 40 | 13.58 | 13.49 | 1,3-di-(*o*-tolyl) urea | 241-242 | 18 | 11.66 | 11.47 |
| *m*—$CH_3$ | 1 | 1 | 0 | 0 | 80-100 | 1 | | 0 | | | 1,3-di-(*m*-tolyl) urea | 221.5 | 8 | | |
| 〃 | 1.5 | 1 | 0 | 2.5 | room temp. | 24 | 101-102 | 27.1 | 13.58 | 13.52 | | | | | |
| *p*—$CH_3$ | 1 | 1 | 4 | 0 | 80 | 0.5 | | 0 | | | 1,3-di-(*p*-tolyl) urea | 265 | 25 | 11.66 | 11.89 |
| 〃 | 1.5 | 1 | 0 | 0.5 | room temp. | 24 | 67.5-68 | 32 | 13.58 | 13.60 | | | | | |
| *o*—Cl[5] | 5 | 4.1 | 0 | 4.8 | 100 | 2 | B.P.124-126/ 0.4 | 8 | Carbon 58.30 | 58.01 | 1,3-di-(*o*-chlorophe-nyl)-urea | 225-226 | 30 | 9.96 | 9.97 |
| | | | | | | | | | Hydrogen 6.65 | 6.87 | | | | | |
| 〃 | 2 | 2 | 0 | 2 | room temp. | 200 | 〃 | 42 | | | | | | | |
| *m*—Cl[5] | 1 | 1 | 0 | 1.5 | 〃 | 24 | 89-89.5 | 17 | 12.36 | 12.57 | | | | | |
| *p*—Cl[5] | 1 | 1 | 8 | 0 | 80 | 2 | | 0 | | | 1,3-di-(*o*-chlorophe-nyl) urea | 247 | 7 | | |
| 〃 | 1 | 1 | 0 | 1.5 | 50 | 1 | 118-118.5 | 17 | | | | | | | |
| *o*—$NO_2$ | 0.5 | 0.5 | 0 | 0.5 | 100 | 6 | | 0 | | | | | | | |
| *m*—$NO_2$ | 2 | 1.5 | 30 | 0 | 80 | 2 | | 0 | | | | | | | |
| 〃 | 2 | 1.5 | 0 | pyridine 5 | 100 | 2 | | 0 | | | 1,3-di-(*m*-nitrophe-nyl) urea | 244.5-245 | 17 | 18.54 | 18.44 |
| 〃 | 3 | 3 | 80 | 3 | 80 | 8 | 88-89 | 12 | | | 〃 | | 14 | | |
| *p*—$NO_2$ | 2 | 2 | 100 | 2 | 80 | 120 | | 0 | | | | | | | |
| 2,4,5-trichloro | 1.35 | 1.6 | 0 | 1.5 | 100-120 | 150 | | 0 | | | | | | | |

| X | | Pentyl isocyanate | | | | | | | | | | |
|---|---|---|---|---|---|---|---|---|---|---|---|---|
| 2,6-dichloro | 1 | 1 | 0 | 1 | 〃 | 〃 | 0 | | | | 1,3-di-(2,6-dichlorophenyl)urea | 250 sublime 275 in sealed tube |
| X= H | 2 | 2 | 2 | room temp. | 1 | 90.5-91.5 | 85 | | | | | |
| *p*—$OCH_3$ | 1 | 1 | 2 | 〃 | 1 | 120.5-121.5 | 83.5 | 11.40 | 11.69 | | | |
| *m*—$CH_3$ | 1 | 1 | 0 | 〃 | 1 | 73 | 78 | 12.72 | 13.06 | | | |
| *p*—$CH_3$ | 1 | 1 | 0 | 〃 | 1 | 105-105.5 | 82.5 | 12.72 | 12.90 | | | |
| *m*—Cl | 2 | 1.5 | 2 | 〃 | 1 | 62.5-63 | 92 | 11.64 | 11.70 | | | |
| *p*—Cl | 0.5 | 0.5 | 2 | 30 | 5 | 158-159 | 82 | 11.64 | 11.88 | | | |
| *m*—$NO_2$ | 2 | 2 | 30 | 80 | 12 | 116.5-117 | 50 | 16.73 | 16.63 | | | |
| *p*—$NO_2$ | 0.5 | 0.5 | 20 | 40 | 10 | | 0 | | | | | |
| 〃 | 0.5 | 0.5 | 20 | 80 | 5 | 121-121.5 | 1 | | | | | |
| 〃 | 0.5 | 0.5 | anisole 5 | 150 | 5 | | 0 | | | | 1,3-di-(*p*-nitrophenyl)urea | 33 |

acid was calculated from Fig. 2 to be Ea=22.7 Kcal.




Fig. 1. Thermal dissociation of phenylureas in chloroacetic acid: the plot of k against $\sigma$.
● 1,1-diethyl-3-phenylureas at 95°C.
△ 1-pentyl-3-phenylureas at 139.5°C.




Fig. 2. Thermal dissociation of 1,1-diethyl-3-phenylurea in chloroacetic acid: the plot of k against 1/T.

## Results and Discussion

Effects of the substituents on the dissociation reaction of substituted phenylureas (I), (II) and (III) are as follow: In the 1,1-diethyl-3-arylureas (I), the value of $\rho$ in the Hammett equation is $-0.196 \pm 0.028$, that is, electron donating groups, such as methoxy, accelerate the reaction. The correlation coefficient r is 0.964. In the 1,3-diarylureas (III), the value of $\rho$ is negative, and there is a large deviation from the Hammett equation in this case. Especially non-substituted diphenylurea dissociates faster than the other ureas of this type. In the 1-pentyl-3-phenylureas (II), two paths far dissociation can be considered,

TABLE II

THE RATE CONSTANTS OF THE THERMAL DISSOCIATION OF PHENYLUREAS IN FATTY ACIDS

$k \times 10^2 (min^{-1})$

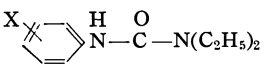
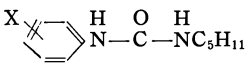
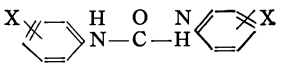
| Ureas / Fatty acids | |  | |  |  |
|---|---|---|---|---|---|
| | | chloroacetic acid | caproic acid | chloroacetic acid | chloroacetic acid |
| X | $\sigma$ | at 95°C. | at 150°C | at 139.5°C | at 139.5°C |
| *p*—$OCH_3$ | −0.268 | 3.55 | 0.81 | 3.83<br>4.69<br>5.13 | |
| *p*—$CH_3$ | −0.170 | 3.37 | 0.56 | 4.87<br>5.06<br>5.77 | 9.67<br>9.20 |
| *m*—$CH_3$ | −0.069 | 2.92 | 1.37 | 4.77<br>4.99 | |
| H | 0 | 2.82 | 1.61 | 5.46 | 10.82<br>10.58<br>10.30 |
| *p*—Cl | 0.227 | 2.77<br>2.70 | 2.92 | 5.47<br>5.75 | 6.72<br>5.61 |
| *m*—Cl | 0.373 | 2.60 | | | |
| *m*—$NO_2$ | 0.710 | 2.21 | 2.39 | 7.36<br>6.96 | 5.45<br>4.80 |
| | $\rho$ | $-0.196 \pm 0.028$ | | $0.1778 \pm 0.0025$ | |
| *o*—$OCH_3$ | | 1.16 | | | |
| *o*—$CH_3$ | | 3.3 | | | 2.1 |
| *o*—Cl | | 2.10 | | | 4.69 |

TABLE III

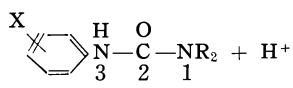
| Ureas / Products | Benzyl N-phenyl-carbamate | 1,3-diphenyl urea | Benzyl N-pentyl-carbamate | Dissociation ratio |
|---|---|---|---|---|
| (g) | (g) | (g) | (g) | (A) : (B) |
| 4 | 2.2 | 0.1 | 0.1 | 1.59 : 1 |
| 1.5 | 0.5 | 0.28 | trace | 1.57 : 1 |

$$C_5H_{11}N(H)-\overset{\overset{O}{\|}}{C}-NC_6H_5 \rightarrow \begin{cases} C_5H_{11}NH_2 + C_6H_5NCO & (A) \\ C_5H_{11}NCO + C_6H_5NH_2 & (B) \end{cases}$$

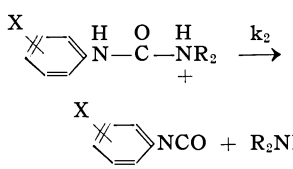
but it is impossible to determine which path is followed in the course of dissociation of the ureas in fatty acids. Therefore the dissociation ratio was determined in benzyl alcohol instead of fatty acid used in the other experiments. On heating 1-pentyl-3-phenylurea in benzyl alcohol for 4 hours at 170°C, the products shown in Table III were obtained.

From this table the ratio A/B is equal to 1.6 for 1-pentyl-3-phenylurea at 170°C. This ratio will differ in other 1-pentyl-3-arylureas. Therefore, rate constants and $\rho$ value ($0.1778 \pm 0.025$) may be insignificant in these ureas. The correlation coefficient r was low (0.895).

The dissociation mechanism of ureas in fatty acids is as follows[3]:



(6)



(7)

From Eqs. (6) and (7)

$$\frac{d(R-NCO)}{dt} = \frac{Kk_2(Ureas)(H^+)}{1+\frac{k_2}{k_{-1}}} \qquad (8)$$

where $K = \frac{k_1}{k_{-1}}$

We can consider two cases as follows:

a) When $k_{-1}$ is greater than $k_2$ or of comparable magnitude, then

$$\frac{d(R—NCO)}{dt} = CKk_2(Ureas)(H^+) \quad (9)$$

where $C$=constant

In Eq. (9), $K$ and $k_2$ will fit the Hammett equation, therefore $Kk_2$ also will agree with it. The product $\rho\sigma$ for the reaction is given by:

$$\log \frac{Kk_2}{K_0k_{2\cdot0}} = \rho\sigma \quad (10)$$

where $\log \frac{K}{K_0} = \rho_1\sigma$

$\log \frac{k_2}{k_{2\cdot0}} = \rho_2\sigma$

$\rho = \rho_1 + \rho_2$

Substituents having a positive $\sigma$-value decrease $K$ (or $k_1$), since such substituents decrease the basicity of 1 nitrogen; and they also increase $k_2$, since such substituents make the deprotonation at 3 nitrogen easier. On the other hand, substituents having a negative $\sigma$-value increase $K$ (or $k_1$) and decrease $k_2$, that is, $\rho_1$ will have a negative value and $\rho_2$ will be positive. Therefore the sign of $\rho$ will be determined by the magnitude of $\rho_1$ and $\rho_2$, and if $|\rho_1|$ is greater than $|\rho_2|$, $\rho$ will have a negative value, and *vice versa*.

The value of $\rho$ obtained in this experiment was $-0.198\pm0.028$ indicating that $|\rho_1|$ is greater than $|\rho_2|$. This seems improbable, since in reaction (6), the reaction center is 1-nitrogen, while in reaction (7), it is 3-nitrogen which is nearer the substituent[9]. Therefore the hypothesis (a) does not appear likely.

b) When $k_2$ is much greater than $k_{-1}$, then

$$\frac{d(R—NCO)}{dt} = k_1(Ureas)(H^+) \quad (11)$$

In this case, $\rho$ will have a negative value from the reason just mentioned, and the experimental data are in accord with this hypothesis.

From the above, hypothesis (b) is probable rather than hypothesis (a), that is, the rate-determining step seems to be a protonation process (Eq. 6) and not a deprotonation process (Eq. 7). This contrasts with the fact[10], that in the dissociation reaction of benzyl N-arylcarbamate in a basic medium such as an amine, the dissociation rate was proportional to the rate of the deprotonation, as indicated by the positive value of $\rho$ which was obtained.

The discussion concerning the positive $\rho$ value in the dissociation reaction of 1-pentyl-3-arylureas (II) will not be given here for the reason mentioned in the earlier part of this result and discussion.

As to the effect of ortho substituents in 1,1-diethyl-3-arylureas, 1,1-diethyl-3-(*o*-methoxyphenyl)urea dissociates one third as fast as *p*-methoxy-, *o*-chloro- slightly slower than *p*-chloro-, and *o*-methyl- at a nearly equal rate to *p*-methyl-. With 1,3-diarylureas, *o*-methyl- dissociates a quarter as fast as p-methyl-, and *o*-chloro- at a nearly equal rate to *p*-chloro-.

The activation energy of the dissociation reaction of 1,1-diethyl-3-phenylurea in chloroacetic acid was 22.4 Kcal.; this is smaller than the value obtained with 5, 6, 7 and 11 membered polymethylene ring ureas in the same solvent (24–27 Kcal.)[11], or those of 1,3-diphenylurea in propionic acid (27.9 Kcal.) and butyric acid (28.0 Kcal.)[1]. The smaller value is due to the more facile protonation on tri-substituted ureas than on 1,3-di-substituted ureas.

## Summary

Eleven new ureas of the type, 1,1-diethyl-3-arylureas and 1-pentyl-3-arylureas were synthesized. The rate constants and $\rho$ values of thermal dissociation of these ureas in fatty acids were determined. In 1,1-diethyl-3-arylureas, the $\rho$ value of the dissociation reaction at 95°C. in chloroacetic acid was $-0.196$, and it may be concluded that the protonation process seems to be the rate-determining step in the dissociation reaction of ureas in fatty acid. The activation energy was compared with those of other ureas.

The authors express their grateful thanks to Professor T. Hoshino and Mr. T. Mukaiyama for their frequent helpful advice and encouragement throughout the course of this work, and to Mr. A. Kondo for the micro analysis.

*Laboratory of Organic Chemistry*
*Tokyo Institute of Technology*
*Ookayama, Meguro-ku, Tokyo*

9) T heargument is rather weak, because $\rho_1$ and $\rho_2$ are reaction constants for reactions of different types, $\rho_1$ referring to equilibrium (6) and $\rho_2$ to reaction (7).

10) T. Mukaiyama and M. Iwanami, *J. Am. Chem. Soc.*, **79**, 75 (1957).

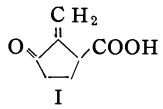
11) Unpublished data.

# *Synthesis of dl-Sarkomycin (2-Methylenecyclopentanone-3-carboxylic Acid)**

By Katsuyuki TOKI

(Received December 7, 1956)

Recently, I. R. Hooper et al.[1] reported that the effective substance contained in crude sarkomycin[2] is 2-methylenecyclopentanone-3-carboxylic acid (I).



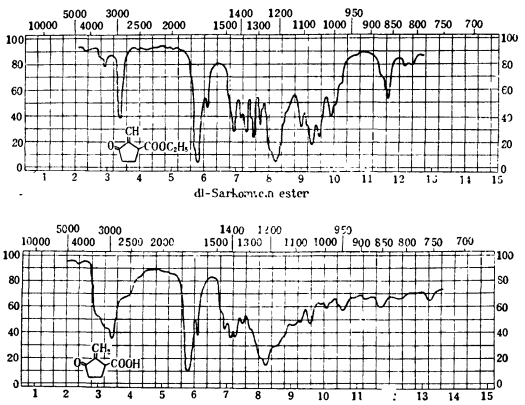
I

Though the acid is an interesting compound as an antitumor substance, nothing had been known about its synthesis when the present investigation was commenced.

The present author synthesized the acid by a four-stage process starting from ethyl cyclopentanone-3-carboxylate (II), prepared by Kay's method[3].

The Mannich reaction[4] was successfully applied to cyclopentanone-3-carboxylate to introduce a methylene group. Namely, *dl*-sarkomycin, 2-methylenecyclopentanone-3-carboxylic acid (I), was synthesized according to the scheme shown in Fig. 1.

Ethyl cyclopentanone-3-carboxylate (II) was converted into ethyl 2-(dialkylaminomethyl)-cyclopentanone-3-carboxylate hydrochloride (III) by treatment with the hydrochloride of a secondary amine (e.g. dimethylamine, diethylamine or piperidine) and formalin. Ethyl 2-methylenecyclopentanone-3-carboxylate (V) was obtained by distillation of the ethyl 2-(dialkylaminomethyl)-cyclopentanone-3-carboxylate (IV) or its hydrochloride (III) below 130°. Above 130° the substance showed a tendency to become a tarry matter. Hydrolysis of the ethyl ester (V) to the free acid, *dl*-sarkomycin, was accompanied by decomposition of the product under severe conditions while a large amount (80–90%) of the ester remained intact under mild conditions. The results of hydrolysis are summarized



*dl*-Sarkomycin

Fig. 2. Infrared absorptions of *dl*-sarkomycin and its ethyl ester.

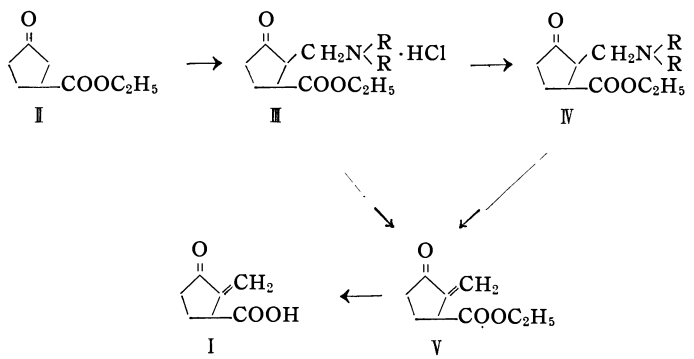


Fig. 1. Synthesis of *dl*-sarkomycin from ethyl cyclopentanone-3-carboxylate.

* Presented before the Monthly Meeting of Japan Antibiotic Research Association, at the Institute of Infectious Diseases, Tokyo, Nov. 29. (1956).

1) Hooper et al, *Antibio. & Chemo.*, **5**, 588 (1955).

2) Umezawa et al, *J. Antibio.*, Ser. A. **6**, 101, 147, 153 (1953).

3) Kay et al, *J. Chem. Soc.*, **89** 1646 (1906).

4) Mannich et al, *Arch. Pharm.*, **267**, 575 (1936).

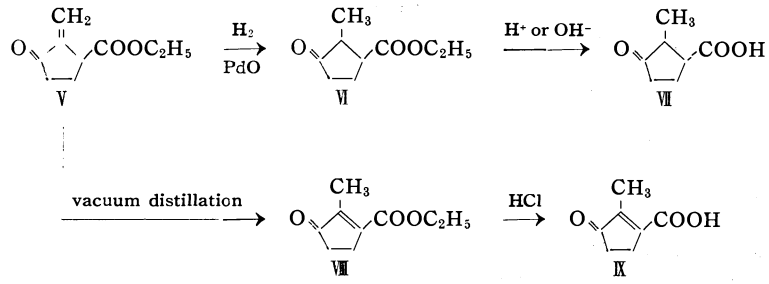



Fig. 3. Determination of the structure of V.

in Table I. Piperidine and hydroquinone had no inhibiting effect against decomposition of *dl*-sarkomycin.

The final product, *dl*-sarkomycin (I), was obtained in an oily form. The infrared spectra of the synthetic and the natural sarkomycin[1] were essentially identical and exhibited a characteristic peak at 6.1 $\mu$ (Fig. 2).

An unsuccessful attempt was made to synthesize V from IV by means of Hofmann's degradation. Treatment of the quaternary ammonium salt prepared from IV and methyl iodide or ethyl iodide with wet silver oxide or an anion exchange resin (IRA4B, IRA 400), gave no 2-methylenecyclopentanone-3-carboxylate but a tarry substance.

The present author and Hiroo Wada have also tried to prepare I by the dehydrobromination of 2-bromo-2-methylcyclopentanone-3-carboxylic acid[5], but the only product identified was 2-methyl-2-cyclopentenone-3-carboxylic acid[1,5].

Since ethyl 2-methylenecyclopentanone-3-carboxylate (V) and 2-methylenecyclopentanone-3-carboxylic acid (I) are unstable compounds, the former was transformed into stable derivatives in order to establish its structure as shown in Fig. 3.

Hydrogenation of ethyl 2-methylenecyclopentanone-3-carboxylate (V) with palladous oxide in methanolic solution followed by hydrolysis with methanolic potassium hydroxide under reflux gave a product which was identified as 2-methylcyclopentanone-3-carboxylic acid (VII) by a mixed melting point determination and a comparison of infrared absorption spectra in Nujol (in Fig. 4) with an authentic specimen prepared by Newman's[5] or Robinson's[6] procedure.

The substance (VIII) obtained by distilling the ester V under a reduced pressure was hydrolyzed with dilute hydrochloric acid to a free acid, which was identified with 2-methyl-2-cyclopentenone-3-carboxylic acid (IX) by a mixed melting point determination and a comparison of infrared spectra (Fig. 5) with an authentic specimen[1,5].

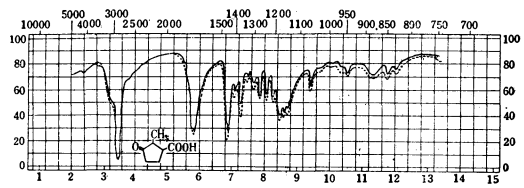



Fig. 4. Infrared absorption of 2-methylcyclopentanone-3-carboxylic acid.
····· Authentic specimen
—— Product from V

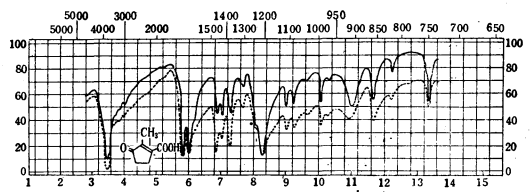



Fig. 5. Infrared absorption of 2-methyl-2-cyclopentenone-3-carboxylic acid.
····· Authentic specimen
—— Product from V

The structure of the synthetic 2-methylenecyclopentanone-3-carboxylic acid (I) was determined in the same manner (Fig. 6). Namely, 2-methylenecyclopentanone-3-carboxylic acid (I) was reduced to 2-methylcyclopentanone-3-carboxylic acid with platinum oxide in methanol at ten atmospheres, and the product was identified with the authentic specimen prepared by Newman's[5] or Robinson's[6] procedure by the melting point and the infrared absorption spectra (Fig. 5).

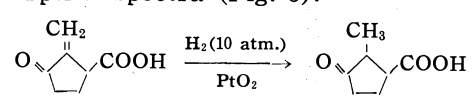



Fig. 6.

5) Newman, *J. Org. Chem.*, **19**, 1717 (1954).

6) Robinson, *J. Chem. Soc.*, **1937**, 1588.

TABLE I

| No. | Hydrolysis: Concentration of HCl and Solvent | Hydrolysis: Temp. °C | Hydrolysis: hrs. | Yield of Acid | Antibacterial Activity[2] | Anti-tumor activity[3] |
|---|---|---|---|---|---|---|
| 1 | 5% HCl-Acetone | 21 | 5 1/3 | 5-8% | 500mg.*/g | ++ |
| 2 | 10% HCl-Acetone | 21 | 5 1/3 | 10% | 800-900mg.*/g | ++ |
| 3 | 5% HCl-Acetone | 35 | 5 1/3 | 7-8% | 500mg.*/g | ++ |
| 4 | 5% HCl-Acetone | 21 | 10 | 12% | 600-700mg.*/g | ++ |
| 5 | 5% HCl-Acetone[1] | 21 | 5 1/3 | 3-5% | 800-900mg.*/g | ++ |

1) A small amount of piperidine or hydroquinone was added. The values are the average.
2) Staphylococcus aureus 209 p.
3) Ehrlich carcinoma

While the resolution of the synthetic *dl*-sarkomycin is now under investigation, the effect of the racemic sarkomycin on the growth of Ehrlich carcinoma was tested as follows[2]: The ascites of mice bearing Ehrlich ascites carcinoma was taken seven days after the transplantation of the tumor cells and diluted with isotonic saline to prepare the cell suspension containing 2.5 million tumor cells in one ml., and 0.2 ml. of the suspension was injected intraperitoneally to mice.

*dl*-Sarkomycin, and Sarkomycin "Banyu HS-94" for comparison, both dissolved in isotonic saline, were intraperitoneally injected at the dosage of 2.5mg./0.2ml./mouse at an hour after the inoculation of the tumor cells and then once daily for 12 days. The results are shown in Fig. 7 and Table I. The antistaphylococcal activity (500–1000 mg.*/g.) of the synthetic sarkomycin was lower than that of the natural one[2]. On the other hand, the synthetic sarkomycin showed a greater antitumor activity in tests on Ehrlich ascites carcinoma of mice[2] and in the agar-cell plate method[7,8]. The relatively lower antibacterial potency of the synthetic products is considered partly due to decomposition and presence of *d*-isomer.

Details of the biological studies on the synthetic sarkomycin will be published elsewhere.

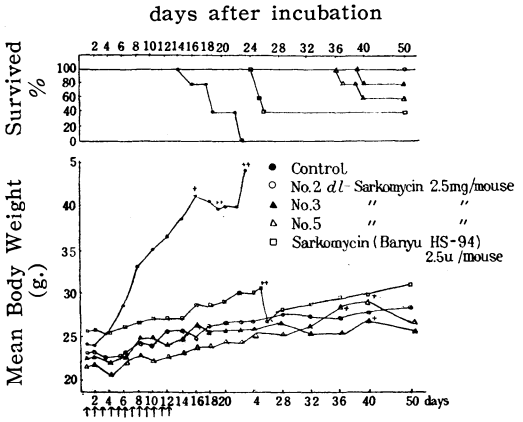



Fig. 7. The effect of synthetic Sarkomycin on Ehrlich carcinoma.

## Experimental

**Ethyl 2-(Piperidinomethyl)-cyclopentanone-3-carboxylate Hydrochloride (III, 2R=$(CH_2)_5$).**—A mixture of 10 g. (0.06 mole) of ethyl cyclopentanone-3-carboxylate (II), 7.2 g. (0.06 mole) of piperidine hydrochloride, and 4.3g. of 37% formalin was stirred on a water bath at 75–80° for thirty minutes and then at the room temperature for additional thirty minutes. The solvent was removed under a reduced pressure. The hydrochloride, colorless needles, showed m.p. 215–220° (decomposition). (Sintering at 155–156°), when recrystallized from methyl alcohol. Yield 6.2 g. (35%).

*Anal.* Found: C, 57.91; H, 8.47; N, 4.91. Calcd. for $C_{14}H_{24}O_3NCl$: C, 58.13; H, 8.30; N, 4.84%.

It was considered that the residual oil separated from crystals by filteration was one of the stereoisomeride of ethyl 2-(piperidinomethyl)-cyclopentanone-3-carboxylate hydrochloride. The oil could be used for next reaction.

**Ethyl 2-(Dimethylaminomethyl)-cyclopentanone-3-carboxylate (IV, R=$CH_3$).**—A mixture of 52 g. (0.33 mole) of ethyl cyclopentanone-3-carboxylate (II), 24 g. (0.3 mole) of dimethylamine hydrochloride and 24 g. of 37% formalin was heated at 75–80° with stirring for forty minutes. After removal of solvent from the reaction mixture, a syrupy residue was obtained, and attempts to bring it to crystallization were unsuccessful. It was used without further purification.

To a solution of ethyl 2-(dimethylaminomethyl)-cyclopentanone-3-carboxylate hydrochloride in a small amount of water was added a small excess of 5% aqueous solution of sodium

7) Umezawa et al, *J. Antibio.*, Ser. A. **9**, 135 (1956).
8) Yamamoto, *Gann*, in press.

carbonate with cooling. The reaction mixture was extracted with ether and the extract, after being washed with a saturated aqueous sodium chloride solution, was concentrated under a reduced pressure. 22 g. of IV was obtained.

**Ethyl 2-(Diethylaminomethyl)-cyclopentanone-3-carboxylate Hydrochloride (III, R=$C_2H_5$).**—A mixture of 4.7 g. (0.03 mole) of ethyl cyclopentanone-3-carboxylate (II), 3.3 g. of diethylamine hydrochloride, 2.3 g. of 40% formalin, and 1 ml. of methanol, was warmed on a water bath for twenty minutes and then allowed to stand for ten minutes with stirring at the room temperature. The hydrochloride obtained by removal of the solvent from the reaction mixture under a reduced pressure, was semisolid mass. Yeild 3.1g. (37%).

*Anal.* Found: C, 55.96; H, 8.24; N, 4.97. Calcd. for $C_{13}H_{24}O_3NCl$: C, 56.32; H. 8.66; N, 5.05%.

**Ethyl 2-Methylenecyclopentanone-3-carboxylate (V).**—(a) From ethyl 2-(piperidinomethyl)-cyclopentanone-3-carboxylate hydrochloride (III, 2R=$(CH_2)_5$). To a solution of 6.2 g. (0.02 mole) of ethyl 2-(piperidinomethyl)-cyclopentanone-3-carboxylate hydrochloride in a small amount of water was added a small excess of 5% aqueous sodium carbonate with cooling. The reaction mixture was extracted with ether and the extract, after being washed with a saturated aqueous solution of sodium chloride, was concentrated under a reduced pressure. 4.4 g. of oily ethyl 2-(piperidinomethyl)-cyclopentanone-3-carboxylate (IV, 2R=$(CH_2)_5$) was obtained.

*Anal.* Found: C, 66.19; H, 9.23. Calcd. for $C_{14}H_{23}O_3N$: C, 66.40; H, 9.09%.

Ethyl 2-(piperidinomethyl)-cyclopentanone-3-carboxylate (4.4 g.) was distilled under a reduced pressure at 90–102°/0.5 mm. and 1.6 g. of pure ethyl 2-methylenecyclopentanone-3-carboxylate (V) was obtained.

*Anal.* Found: C, 64.11; H, 7.25. Calcd. for $C_9H_{12}O_3$: C, 64.29; H, 7.14%.

The 2,4-dinitrophenylhydrazone of ethyl 2-methylenecyclopentanone-3-carboxylate melted at 176–177°C.

*Anal.* Found: C, 51.53; H, 4.61; N, 16.15. Calcd. for $C_{15}H_{16}O_6N_4$: C, 51.72; H, 4.60; N, 16.09 %.

(b) From ethyl 2-(dimethylaminomethyl)-cyclopentanone-3-carboxylate (IV, R=$CH_3$). Ethyl 2-(dimethylaminomethyl)-cyclopentanone-3-carboxylate (22 g.) was distilled under a reduced pressure. Ethyl 2-methylenecyclopentanone-3-carboxylate (V) (6.2 g.) distilled at 80–105/0.3mm.

*Anal.* Found: C, 64.25; H, 7.11. Calcd. for $C_9H_{12}O_3$: C, 64.29; H, 7.14%.

The 2,4-dinitrophenylhydrazone melted at 176–177°.

(c) From ethyl 2-(diethylaminomethyl)-cyclopentanone-3-carboxylate hydrochloride (III, R=$C_2H_5$). Ethyl 2-(diethylaminomethyl)-cyclopentanone-3-carboxylate hydrochloride (4.1 g.) was heated at 130–140° and then distilled under a reduced pressure. Ethyl 2-methylenecyclopentanone-3-carboxylate (V) (0.2 g.) distilled at 95–104°C/0.5 mm.

*Anal.* Found: C, 64.27; H, 7.21. Calcd. for $C_9H_{12}O_3$: C, 64.29; H, 7.14%.

The 2,4-dinitrophenylhydrazone melted at 176–177°C.

*Anal.* Found: C, 51.68; H, 4.48; N, 16.03. Calcd. for $C_{15}H_{16}O_6N_4$: C, 51.72; H, 4.60; N, 16.09%.

**2-Methylenecyclopentanone-3-carboxylic Acid (I).**—A mixture of 5.0 g. (0.03 mole) of ethyl 2-methylenecyclopentanone-3-carboxylate (V) and 50 ml. of 5 % HCl-acetone was allowed to stand at 21° for ten hours and then an excess of aqueous sodium carbonate was added to the mixture with cooling. After removal of acetone under a reduced pressure, the reaction mixture was shaken with ethyl acetate repeatedly. The ethyl acetate layer was washed with 5 % aqueous sodium carbonate. The combined aqueous solution was then acidified with diluted hydrochloric acid with cooling, saturated with ammonium sulfate and extracted with ether. The ether solution was concentrated under a reduced pressure. A pale yellow oil was obtained in a yield of 0.6 g, (14%), and gave a marked inhibiting effect on the growth of Ehrlich ascites carcinoma.

*Anal.* Found: C, 59.51; H, 5.29. Calcd. for $C_7H_8O_3$: C, 60.00; H, 5.71%.

The recovered ester (V) amounted to 3.8 g.

**Ethyl 2-methylcyclopentanone-3-carboxylate (VI).**—A solution of 1.35 g. of ethyl 2-methylenecyclopentanone-3-carboxylate (V) in 10 ml. of methanol was reduced with equimolecular hydrogen in the presence of palladous oxide. After removal of the solvent, the residual oil was distilled at 110–112°/28 mm. Yield 1.30 g. $n_D^{23}$ 1.4595.

The 2,4-dinitrophenylhydrazone of ethyl 2-methylcyclopentanone-3-carboxylate, when recrystallized from methanol, melted at 162–163°.

*Anal.* Found: C, 51.05; H. 5.18; N, 16.12. Calcd. for $C_{15}H_{18}O_6N_4$: C, 51.43; H, 5.14; N, 16.00%.

**2-Methylcyclopentanone-3-carboxylic Acid (VII).**—A mixture of 0.8 g. of ethyl 2-methylcyclopentanone-3-carboxylate (VI), 0.8 g. of sodium hydroxide, and 10 ml. of methanol, was heated on a water bath under reflux. After removal of methanol, the residue was poured into water and the whole mixture was extracted with ether. After removal of the solvent, the residue was allowed to stand in a refrigerator over night. The colorless plates, recrystallized from ether-petroleum ether (1 : 1), melted at 90–91°C. A mixture of the product with the authentic 2-methylcyclopentanone-3-carboxylic acid melted at 90–91°C.

*Anal.* Found: C, 58.89; H, 7.34. Calcd. for $C_7H_{10}O_3$: C, 59.15; H, 7.04%.

The 2,4-dinitrophenylhydrazone melted at 162–163°C.

**2-Methylcyclopentanone-3-carboxylic Acid from 2-Methylenecyclopentanone-3-carboxylic Acid (I).**—2-Methylenecyclopentanone-3-carboxylic acid (0.1 g.) in methanol solution,

with addition of 0.01 g. of platinum oxide, was reduced with hydrogen in an autoclave at 10 atm. at room temperature. On removal of the catalyst by filtration and of the solvent by evaporation under a reduced pressure, colorless crystals were obtained m.p. 90–91°C.

*Anal.* Found: C, 58.78; H, 7.00. Calcd. for $C_7H_{10}O_3$: C, 59.15; H, 7.04%.

The 2,4-dinitrophenylhydrazone melted at 162–163°C.

**Ethyl 2-Methyl-2-cyclopentenone-3-carboxylate (VIII).**—When ethyl 2-methylenecyclopentanone-3-carboxylate (V) was distilled at 80–92°/0.5 mm, ethyl 2-methyl-2-cyclopentenone-3-carboxylate (VIII) was obtained. $n_D^{31}$ 1.4852.

The 2,4-dinitrophenylhydrazone, recrystallized from ethanol, melted at 176°C with decomposition.

*Anal.* Found: C, 51.59; H, 4.29; N, 16.31. Calcd. for $C_{15}H_{16}O_6N_4$: C, 51.72; H, 4.60; N, 16.09%.

**2-Methyl-2-cyclopentenone-3-carboxylic Acid (IX).**—(a) Ethyl 2-methyl-2-cyclopentenone-3-carboxylate (VIII) (0.5 g.) was refluxed with 10 ml. of 5% methanolic potash on a water bath for two hours. Colorless crystals thus obtained had m.p. 175° (from benzene), and weighed 0.4g.

*Anal.* Found: C, 59.63; H, 5.31. Calcd. for $C_7H_8O_3$: C, 60.00; H, 5.71%.

The 2,4-dinitrophenylhydrazone, recrystallized from ethanol, melted at 260°C with decomposition.

*Anal.* Found: C, 48.70; H, 3.62; N, 17.41. Calcd. for $C_{13}H_{12}O_6N_4$: C, 48.75; H, 3.75; N, 17.50%.

(b) A mixture of 1 g. of ethyl 2-methyl-2-cyclopentenone-3-carboxylate (VIII) and 10 ml. of 5% HCl-acetone solution was allowed to stand at 21° for five hours. Recrystallization from benzene gave colorless crystals melting at 175°. Yield 0.5 g.

*Anal.* Found; C, 59.89; H, 5.69. Calcd. for $C_7H_8O_3$: C, 60.00; H, 5.71%.

The 2,4-dinitrophenylhydrazone, recrystallized from ethanol, melted at 260° with decomposition.

*Anal.* Found: C, 49.01; H, 3.82; N, 17.22. Calcd. for $C_{13}H_{12}O_6N_4$: C, 48.75; H, 3.75; N, 17.50%.

## Summary

*dl*-Sarkomycin (2-methylenecyclopentanone-3-carboxylic acid) was synthesized in a four-stage process starting from ethyl cyclopentanone-3-carboxylate, prepared by Kay's procedure. Namely, ethyl cyclopentanone-3-carboxylate was converted into ethyl 2-(dialkylaminomethyl)-cyclopentanone-3-carboxylate and thence to ethyl 2-methylenecyclopentanone-3-carboxylate. The ester was hydrolyzed to 2-methylenecyclopentanone-3-carboxylic acid with diluted hydrochloric acid. The final product was a pale yellow oil and was effective in inhibiting the growth of Ehrlich carcinoma of mice.

Acknowledgement is due to Prof. Shiro Akabori, Prof. Hamao Umezawa and Prof. Masanao Matsui for their continuous interest and encouragement in the present work.

The author is also indebted to Mr. Chiharu Saito et al. for biological testes, to Mr. Naofumi Ohi, Miss Kazuko Kageyama, and Mr. Keiichiro Miyazaki, for infrared analyses, to Mr. Noboru Nishimura for micro-analyses, and to Messrs. Hiroo Wada and Yoshio Suzuki for their kind collaboration.

*Sumitomo Chem. Co., Ltd.,*
*Konohanaku, Osaka*

# *Untersuchungen über die photochemischen Additionsreaktionen. IV. Die Anlagerungen von Thioessigsäure an Propargylalkohol und einige Propargylester*

Von Kazuo YAMAGISHI, Toyosuke TANAKA und Toshio HOSHINO

(Eingegangen am 20. Dezember 1956)

Im Rahmen unserer Uutersuchungen über die photochemischen Additionsreaktionen[1] haben wir festgestellt, dass bei den Anlagerungsreaktionen von Thioessigsäure an propargylalkohol, Propargylacetat und Propargylborat sich eine sehr befriedigende Ausbeute an Monoaddukten und Diaddukten der Thioessigsäure ergibt. Aus Monoaddukten und Diaddukten erhielten wir so eine gute Ausbeute an Derivat des 2-Oxypropylaldehyds bzw. an 2,3-Dithiopropanol.

Die Additionen von Thioessigsäure an Acetylenkohlenwasserstoffe sind von Bader, Cross, Heilbron und Jones[2] eingehend untersucht worden. Sie haben gefunden, dass die Addition von Thiosäure an monosubstituierte Acetylene "anormal" verläuft, entgegen der Regel von Markownikow. Als Vertreter der monosubstituierten Acetylene wurden von diesen englischen Forschern Hexin-1, Octadiin-1, 7, Phenyl-, *p*-Methoxy-phenyl-acetylen auf ihre Reaktionsweise gegenüber Thiosäure hin zumeist unter Anwendung von peroxydischen Katalysatoren wie Benzoylperoxyd, Ascaridol[3] oder mit Hilfe von ultraviolettem Licht bearbeitet und zu Mono- oder Diaddukten übergeleitet. Nahezu gleichzeitig versuchte Behringer[4] unter anderer Zielsetzung dieselben Anlagerungen mit denselben Verbindungen. Es war beabsichtigt, durch Anlagerung eines Mols Thiosäure an Acetylen oder monosubstituierte Acetylene an S-Vinyl-thiosäure-ester und durch deren Polymerisation—analog der des Vinylacetats—an einfache oder substituierte Polyvinyl-thiosäure-ester zu gelangen. Aber das wurde nur unvollständig erreicht. Gegenüber den Reaktionsbedingungen bei Jones et al. arbeitete Behringer nur mit Erhitzung der zwei Komponenten in Anwesenheit von Kaliumthioacetat oder in Abwesenheit von Katalysatoren, und erhielt dieselben Resultate wie bei Jones et al. Auch Versuche über Anlagerung von Thiosäure an Äthinylcarbinole unter den gleichen Bedingungen wie bei Jones et al. wurden 1956 von Bader[5] mitgeteilt. Bei seinen Versuchen über Äthinylcarbinole erwies sich die Anwendung von Benzoylperoxyd, welches bisher bei Anlargerung von Thiosäure an ungesättigte Verbindungen als Katalysator benutzt worden war, als unwirksam.

Durch die Ergebnisse dieser Arbeiten ist klargestellt, dass die Anlagerungen von Thiosäure besonders an Äthinylcarbinole und an die niederen Glieder der Acetylenkohlenwasserstoffe nur sehr schlechte Ausbeute ergeben.

Nach zahlreichen Anlagerungsversuchen von Thiosäure an Propargylacetat haben wir gefunden, dass die Belichtung mit ultravioletten Strahlen nach Zusatz von Azoverbindungen wie Azo-bis-isobuttersäurenitril, Azo-bis-cyclohexancarbonsäurenitril sich als beschleunigend erweist. Die 24-stündige Belichtung, mit einer 200-Watt-Quecksilberlampe[1], einer Mischung von Propargylacetat und Thiosäure im 1 : 2 Molverhältnis in Anwesenheit von Azo-bis-isobuttersäurenitril ergab Diaddukt und Monoaddukt in einer Ausbeute von 65% bzw. 10% d. Theorie.

$$\begin{aligned} &CH_2(OR)\cdot C \vdots CH \xrightarrow{HSAc} \\ &\quad CH_2(OR)\cdot CH : CH(SAc) \\ &\quad +CH_2(OR)\cdot CH(SAc)\cdot CH_2(SAc) \end{aligned} \qquad \text{(II)}$$

Bei der Untersuchung des Cyclohexenylthioacetats entdeckte Sen[6], dass, durch Einwirkung von Phenylhydrazin, für die $\cdot S\cdot CO\cdot CH_3$—Gruppe in Nachbarstellung zur Kohlenstoffdoppelbindung schliesslich die $\cdot NH\cdot NH\cdot C_6H_5$—Gruppe substituiert

1) Yamagishi, Tanaka und Hosino, dieses Bulletin, **29**, 447 (1956).
2) *J. Chem., Soc.*, **1949**, 619.
3) Cunneen, ibid., **1947**, 36; **1947**, 134.
4) *Ann.*, **564**, 219 (1949).
5) *J. Chem. Soc.*, **1956**, 116.
6) *J. Indian Chem. Soc.*, **13**, 268 (1936).

wird und sich Phenylhydrazon des Cyclohexanons ergibt. Durch die Behandlung unseres Monoaddukts mit phenylhydrazin erhielten wir phenylhydrazon des 2-Oxypropylaldehyds anstatt Phenylhydrazon des 2-Acetoxypropylaldehyds. Damit ist festgestellt, dass das Monoaddukt eine gemäss einem „anormalen" Reaktionsverlauf zu erwartende Struktur $CH_2(OR)\cdot CH:CH(SAc)$ hat. Die folgende Formel wird diesen Reaktionsverlauf zeigen.

$$CH_2(OAc)\cdot CH:CH(SAc)$$
$$[I]$$
$$+2NH_2\cdot NH\cdot C_6H_5 \longrightarrow$$
$$[CH_2(OH)\cdot CH:CH(SH)]$$
$$+2Ac\cdot NH\cdot NH\cdot C_6H_5$$
$$[CH_2(OH)\cdot CH_2\cdot CH:S]$$
$$+NH_2NH\cdot C_6H_5 \longrightarrow$$
$$CH_2(OH)\cdot CH_2\cdot CH:N\cdot NH\cdot C_6H_5+H_2S$$

Das durch Anlagerung von zwei Molekülen Thiosäuren entstehende Diaddukt erwies sich als identisch mit dem authentischen Produkt 2,3-Diacetylthio-propylacetat, das von Sjöberg[7] aus $\alpha$, $\beta$-Dibromhydrinacetat und Kaliumthioacetat hergestellt wurde. Eine Bestätigung der Konstitutionen der zwei Addukten sahen wir auch in den ultravioletten Absorptionsspektren. Der Ort des Absorptionsmaximums des Monoaddukts, welches ein Chromophor $\cdot CH:CH\cdot S\cdot CO\cdot CH_3$[8] hat, ist nm 20 m$\mu$

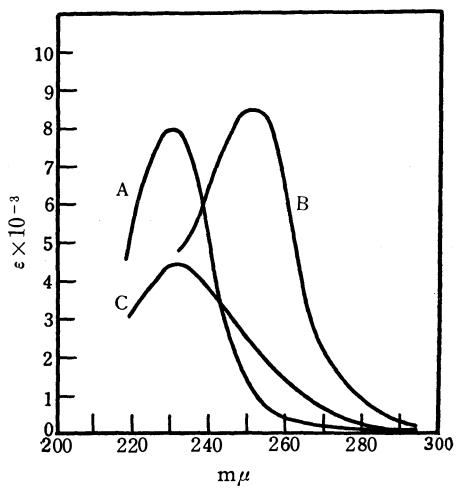



Abb. 1. Absorptionsspektren der Addukten
A: 2,3-Diacetylthio-propylacatat (II)
B: 3-Acetoxyprop-1-enylthioacetat (I)
C: Äthylthio-3-acetoxythio-propylacetat

weiter fort als der des Diaddukts verschoben:

2,3-Diacetylthio-propylacetat (II):
$\lambda_{max}$230m$\mu$, $\varepsilon_{max}$7980,

3-Acetoxyprop-1-enylthioacetat (I):
$\lambda_{max}$250m$\mu$, $\varepsilon_{max}$8500.

Das Monoaddukt polymerisiert sich, wenn man es längere Zeit in der Luft stehen lässt, allmählich zu einem braun gefärbten Harz, das elastisch ist, aber doch unter Biegekraft leicht zerbricht.

Liess man überschüssige Thiosäure auf das Monoaddukt 3-Acetoxyprop-1-enyl-thioacetat reagieren, so wurden nur 31% Ausbeute an Diaddukt isoliert. Bei Anwendung von Äthylmercaptan statt Thiosäure, das sehr glatt zu olefinischem Kohlenwasserstoff addiert[9], erhielt man eine Ausbeute von 37% an einem Addukt 2-Äthylthio-3-acetoxythio-propylacetat. Das Addukt hat ein Absorptionsmaximum an demselben Ort wie 2,3-Diacetylthiopropylacetat.

Behandelt man das Diaddukt mit 1 proz. salzsaurem Methanol und dann mit 1-N Natronlauge, so erhält man 64 proz. Ausbeute an 2,3-Dithiopropanol. 2,3-Dithiopropanol[10] ist ein wirksames Gegengift gegen Lewisit und gegen verschiedene Metallionen wie Arsen, Quecksilber, Cadmium, Gold u.a.. Im Handel führt es die Bezeichnung "BAL" (Britisch Anti-Lewisit). Andrerseits fanden wir, dass sich das Diaddukt mit Phenylhydrazin durch Erhitzung in Alkohollösung leicht in 2,3-Dithiopropanol überführen lässt, in einer Ausbeute von 75%.

$$CH_2(OAc)\cdot CH(SAc)\cdot CH_2(SAc)$$
$$+3NH_2\cdot NH\cdot C_6H_5 \longrightarrow$$
$$CH_2(OH)\cdot CH(SH)\cdot CH_2(SH)$$
$$+3Ac\cdot NH\cdot NH\cdot C_6H_5$$

Bei der Anlagerungsreaktion von Thiosäure auf propargylalkohol ergaben sich 64% Diaddukt 2,3-Diacetylthio-propanol bzw. 12% Monoaddukt, 3-Oxyprop-1-enylthioacetat. Nach Hydrolyse des Diaddukts liess sich 2,3-Dithiopropanol mit Ausbeute von 67% erhalten. Das Monoaddukt wurde durch Behandeln mit Phenylhydrazin in Phenylhydrazon des 2-Oxypropylaldehyds übergeführt.

7) *Ber.*, **75**, 13 (1942).
8) Bowden, Braude und Jones, *J. Chem. Soc.*, **1946**, 948.
9) Ipatieff und Friedmann. *J. Am. Chem. Soc.*, **61**, 71 (1939); Hoshino, Yamagishi und Ichikawa, *J. Chem. Soc. Japan*, **74**, 510 (1953).
10) Waters und Stocken, *Science*, **102**, 601 (1945); Stocken und Thompson, *Biochem. J.*, **40**, 535 (1946); Stocken, J. *Chem. Soc.*, **1947**, 592.

TAFEL I

| Katalysator | Temp. | | Zeit in Std. | Ausbeute in % | |
|---|---|---|---|---|---|
| | | | | Monoaddukt | Diaddukt |
| ABC* | Raumtemp. | UV-Licht | 24 | 9 | 64 |
| ABI* | Raumtemp. | UV-Licht | 48 | 9 | 64 |
| ABI | 60° | / | 24 | 13 | 50 |
| ABI | Raumtemp. | UV-Licht | 6 | 46 | 20 |
| Piperidin (0.1 g) | 60° | / | 24 | 16 | 13 |
| Quecksilberacetate (0.1 g) | Raumtemp. | UV-Licht | 24 | 5 | 37 |
| Keine | 60° | / | 24 | 16 | 5 |
| Keine | 100° | / | 24 | 20 | 5 |
| Keine | Raumtemp. | UV-Licht | 24 | 4 | 37 |

* ABC bedeutet: Azo-bis-cyclohexancarbonsäurenitril und ABI auf Azo-bis-isobuttersäurenitril.

Es ergab sich ferner: Bei der Anlagerung von Thiosäure an propargylborat erhielten wir ausschliesslich Monoaddukt. Dieses liess sich durch Behandln mit Wasser zu 3-Oxyprop-1-enylthioacetat verseifen, in einer Ausbeute von 61% der Theorie auf Grund von dem verwendeten Propargylborat.

Die in dieser Mitteilung beschriebenen Produkte ausser 2,3-Diacetylthio-propylacetat, 2,3-Diteiopropanol und 2-Oxypropylaldehyd[11] sind alle neue Verbindungen.

## Beschreibung der Versuche

Ultraviolette Absorptionsspektren wurden in Methanol-Lösungen bestimmt.

**Thioessigsäure**[12].—Thiosäure wurde aus Essigsäureanhydrid und Schwefelwasserstoff dargestellt und vor dem Gebrauch frisch destilliert. Sdp. 86–88° (760 mm), 29° (68 mm).

**Propargylacetat**[13].—Es wurde durch Acetylierung von Propargylalkohol mittels Essigsäureanhydrid oder Acetylchlorid dargestellt. Sdp. 122–123°.

**Propargylborat.**—Eine Mischung von 56 g Propargylalkohol, 22.7 g Borsäure und 200 ccm Benzol wurde in einem 500 ccm-Kolben mit einem Wasserfänger unter Rückfluss erhitzt, bis kein Entstehen von Wasser im Wasserfänger mehr zu erkennen war (3 stunden). Nach dem Entfernen des Benzols wurde der Rückstand im Vakuum destilliert. Sdp. 79–81° (4 mm). Ausbeute 54.3 g (71%). Rektifizierung, Sdp. 68–69° (2 mm), $n_D^{15}$ 1.4564.

*Anal.* Gef.: B, 6.20. Ber. für $C_9H_9O_3B$: B, 6.15%.

**Photochemische Anlagerung von Thioessigsäure an Propargylacetat.**—Die meisten der hier mitgeteilten photochemischen Anlagerungsreaktionen wurden auf folgende Weise herbeigeführt: Eine Mischung von 7.4 g (0.075 Mol) Propargylacetat, 11.4 g (0.15 Mol) Thiosäure und 0.1 g Azo-bis-isobuttersäurenitril wurde in einem zugeschmolzenen Reaktionsrohre von 80 ccm Inhalt 24 Stunden lang ultravioletter Belichtung mittels einer Quecksilberlampe von 200 Watt[1] ausgesetzt und anschliessend im Vakuum destilliert. Nach einem vorlauf unverbrauchter Materialien erhielt man 1.5 g Monoaddukt (10%) vom Sdp. 93–98° (2 mm) und 12.0 g Diaddukt (65%) vom Sdp. 130–135° (2 mm).

**(a) Monoaddukt, 3-acetoxyprop-1-enylthioacetat.**—Sdp. 95–97° (3 mm), $n_D^{13}$ 1.5115.

*Anal.* Gef.: C, 47.86; H, 5.88; S, 19.38. Ber. für $C_7H_{10}O_3S$: C, 48.27; H, 5.79; S, 19.37% (Absorptionsspektrum: siehe Abb. 1).

Die Substanz ist ein schwach gelbes Öl von eigenartig scharfem Geruch, färbt sich an der Luft rot-braun und polymerisiert sich allmählich zu einem elastischen Harz.

**(b) Diaddukt, 2,3-Diacetylthio-propylacetat.**—Sdp. 92–95° ($10^{-2}$mm), $n_D^{13}$ 1.5181.

*Anal.* Gef.: C, 43.01; H, 5.71; S, 25.16. Ber. für $C_9H_{14}O_4S_2$: C, 43.20; H, 5.64; S, 25.58%. Die Substanz ist identisch mit dem authentischen Produkt $\alpha,\beta,\gamma$-Triacetyl-$\alpha,\beta$-dithioglycerin, das von Sjöberg[7] aus Dibromhydrinacetat und Kaliumthioacetat dargestellt wurde (Absorptionsspektrum: siehe Abb. 1).

In Tafel I sind die unter verschiedenen anderen Bedingungen ausgeführten Versuche der Anlagerung von Thiosäure an Propargylacetat verzeichnet. Das Mol-Verhältnis der zwei Materialien ist 0.15 Mol : 0.075 Mol. Die Ausbeute wurde auf Grund der verwendeten Propargylacetats berechnet.

**2,3-Dithiopropanol aus Diaddukt (II, R=Ac).**—10 g Diaddukt wurden in 50 ccm 1proz. salzsaurem Methanol gelöst und 6 stunden lang auf 60° erhitzt. Das nach dem Entfernen des Methanols zurückgebliebene Produkt wurde mit 20 cc 1-N Natronlauge zwei Std. lang um geschüttelt. Aus der alkalischen Wasserschicht wurde der unverbrauchte Teil mit Äther entfernt und nach dem Ansäuern das 2,3-Dithiopropanol mit Äther aufgenommen. Die Ätherlösung wurde

11) *Ann.*, **335**, 219 (1904).
12) "Org. Syntheses," Vol. 31, John Wiley and Sons, Inc., New York (1951), p. 105; Clarke und Hartman, *J. Am. Chem. Soc.*, **46**, 1731 (1924).
13) U. S. Patent, 2, 340, 701 (1944); *C. A.*, **38**, 4269 (1944).

mit Magnesiumsulfat getrocknet und destilliert. Nach einem sehr geringen Vorlauf erhielt man 3.2 g eines schwach gelben Öles von Sdp. 85–90° (1 mm).

*Anal.* Gef.: S, 51.45. Ber für $C_3H_8OS_2$: S, 51.64%.

Die Substanz ist identisch mit dem aus Dibromallylalkohol und prim. Natriumsulfid dargestellten 2,3-Dithiopropanol, "BAL[10]".

**2,3-Dithiopropanol aus Diaddukt (II, R=Ac) und Phenylhydrazin.**—2.5 g Diaddukt und 3.5 g Phenylhydrazin wurden mit 20 ccm Alkohol 6 stunden lang erhitzt und dann das Lösungsmittel abdestilliert. Das gebliebene Reaktionsgemisch wurde mit Petroläther (35–70°) extrahiert. Nach dem Entfernen des Petroläthers erhielt man 1.2 g 2,3-Dithiopropanol von Sdp. 85–90° (1 mm).

*Anal.* Gef.: S, 51.40. Ber. für $C_3H_8OS_2$: S, 51.64%.

Der beim Extrahieren mit Petroläther zurückgebliebene Rückstand wurde aus Alkohol umkistallisiert. Wir erhielten 4g β-Acetylphenylhydrazin in farblosen Kristallen von Schmp. 128°. Der Mischschmelzpunkt mit dem authentischen Produkt[14] aus Phenylhydazin und überschüssigem Eisessig zeigte keine Depression.

**Überführung von 3-Acetoxyprop-1-enylthioacetat in Phenylhydrazon des 2-Oxypropylaldehyds.**—1.7 g 3-Acetoxyprop-1-enylacetat und 3.5 g phenylhydrazin wurden mit 10 ccm Alkohol 24 Stunden lang erhitzt und dann das Lösungsmittel abdestilliert. Der Rückstand wurde mit Äthers extrahiert. Nach dem Entfernen des Äthers wurde das Produkt aus Benzol-Petroläther umkristallisiert. Wir erhielten 1.3 g Phenylhydrazon des 2-Oxypropylaldehyds in gelben Nadeln von Schmp. 119–120°.

*Anal.* Gef.: N, 17.35. Ber. für $C_9H_{12}ON_2$: N, 17.06.

Der Mischschmelzpunkt von phenylhydrazon des 2-Oxypropylaldehyds mit dem authentischen Produkt zeigt keine Depression.

**2-Oxypropylaldehyd.**—Die Darstellung des Aldehyds erfolgte nach der Vorschrift von Nef[11]. 10 g Acrolein wurden mit 14 g Wasser im Einschmelzrohre auf 100° 10 Stunden lang erhitzt. Nach dem Enternen der unveränderten Materialien erhielt man 5 g 2-Oxypropylaldehyd von Sdp. 70–75° (10 mm). $n_D^{20}$ 1.4900.

**Phenylhydrazon.**—Aus Benzol-Petroläther gelbe Nadeln von Schmp. 119–120°.

**Anlagerung von Thiosäure an Monoaddukt (I, R=Ac).**—Eine Mischung von 2 g Monoaddukt, 2 g Thiosäure und 0.02 g Azo-bis-isobuttersäurenitril wurde in einem zugeschmolzenen Reaktionsrohr 24 Stunden lang UV-Licht wie vorher ausgesetzt und anschliessend im Vakuum destilliert. Nach dem Entfernen der unverbrauchten Materialien erhielt man 0.9 g Diaddukt (31%) von Sdp. 90–95° ($10^{-2}$mm).

*Anal.* Gef.: S, 25.20. Ber. für $C_9H_{14}O_4S_2$: S, 25.58%.

**Anlagerung von Äthylmercaptan an Monoaddukt (I, R=Ac).**—Eine Mischung von 2 g Monoaddukt, 2 g Äthylmercaptan und 0.02 g Azo-bis-isabuttersäurenitril wurde UV-Licht 24 Stunden lang wie vorher ausgesetzt. Man erhielt 1 g (37%) einer schwach gelben Flüssigkeit, 2-Äthylthio-3-acetoxythio-propylacetat von unangenehmen Geruch. Sdp. 110–115° (1 mm), $n_D^{20}$ 1.5091.

*Anal.* Gef.: C, 45.97; H, 7.06; S, 27.00. Ber. für $C_9H_{16}O_3S_2$: C, 45.76; H, 6.83; S, 27.09% (Absorptionsspektrum: siehe Abb. 1).

**Anlagerung von Thiosäure an Propargylalkohol.**—Eine Mischung von 5.6 g Propargylalkohol, 15.2 g Thiosäure und 0.1 g Azo-bis-isobuttersäurenitril wurde UV-Licht wie vorher ausgesetzt. Man erhielt 13 g Monoaddukt (10%) und 13 g Diaddukt (63%).

**(a) Monoadduckt, 3-Oxyprop-1-enylthioacetat (I, R=H).**—Sdp. 57° ($10^{-2}$mm) $n_D^{11}$ 1.5280.

*Anal.* Gef.: C, 45.10; H, 6.25; S, 24.22. Ber. für $C_5H_8O_2S$: C, 45.45; H, 6.10; S, 24.22%.

Die Verbindung ist ein gelbes Öl. Behandelt man 1 g Monoaddukt mit 2.5 g phenylhydrazin wie vorher, so erhält man 0.7 g phenylhydrazon des 2-Oxypropylaldehyds, dessen Schmp. 119–120° ist.

*Anal.* Gef.: N, 17.35. Ber. für $C_9H_{12}ON_2$: N, 17.30%.

**(b) Diaddukt, 2,3-Diacetylthio-propanol (II, R=H).**—Sdp. 85–90° ($10^{-2}$mm), $n_D^{25}$ 1.5159.

*Anal.* Gef.: C, 40.80; H, 5.87; S, 30.74. Ber. für $C_7H_{12}O_3S_2$: C, 40.39; H, 5.81; S, 30.74%. Die Verbindung ist ein gelbes Öl, dessen Geruch unangenehm und scharf ist.

**2,3-Dithiopropanol aus Diaddukt (II, R=H).**—15 g Diaddukt wurden mit 100 ccm 1 proz. salzsaurem Methanol 6 Stunden lang auf 60° erhitzt. Das nach dem Entfernen des salzsauren Methanols zurückgebliebene Produkt wurde der Destillation im Vakuum unterworfen. Man erhielt 6 g, 2,3-Dithiopropanol von Sdp. 57° ($10^{-2}$mm).

*Anal.* Gef.: S, 51.47. Ber. für $C_3H_8OS_2$: S, 51.64%.

**Anlagerung von Thiosäure an Propargylborat.**—Ein Gemisch von 8.6 g Propargylborat, 7.8 g Thiosäure und 0.1 g Azo-bis-isobuttersäurenitril wurde wie oben behandelt. Nach Verseifung mit 50 ccm Wasser wurde das Produkt der Destillation unterworfen. Man erhielt 8 g 3-Oxyprop-1-enylthioacetat von Sdp. 60–61° ($10^{-2}$ mm).

*Anal.* Gef: S, 24.14. Ber. für. $C_5H_8O_2S$: S, 24.22%.

Wir möchten hier dem Kultus-ministerium für die Gewährung einer Unterstützung zur Anregung wissenschaftlicher Forschung Dank sagen, ebenso Herrn A. Kondoh und N. Yamazaki für die Ausführung der Mikroanalysen.

*Institut für Organische Chemie der Technischen Hochschule, Ookayama Tokyo und Institut für Chemie der Saitama Universität, Urawa*

14) Fischer, *Ann.*, **190**, 129 (1878).

# *A Thermistor Method for the Determination of Velocity Coefficients of Vinyl Polymerization. V. The Effect of the Bulk Viscosity on the Velocity of Vinyl Polymerization*

By Hajime MIYAMA

(Received December 10, 1956)

## Introduction

It is well known that the ratio of the propagation constant to the termination constant $k_p/k_t$ for vinyl polymerization increases with the increase of the degree of conversion[1-4]. Apparently this is a result of the increasing bulk viscosity of the reaction system causing the mobility of monomer M and radical $M_n$* to slow down. However, no experiment to measure both $k_p/k_t$ and the bulk viscosity $\eta$ to obtain the relation between these values has been conducted and only M.F. Vaughan's theory[5] for the thermal polymerization of styrene is related to the subject.

The author therefore measured those two values by using a special reaction vessel, which could function as a viscosimeter, compared the results of measurements with the values of $k_p$ and $k_t$ of vinyl acetate given in the 4th paper[1] of this series, and obtained the general formula which gives the relation between $\eta$ and $k_p$ or $k_t$.

## Theoretical

The theoretical formula, postulated by E. Rabinowitch[6], expresses the effect of the bulk viscosity on the rate constant in the liquid reaction. If liquid can be assumed to possess a quasicrystalline structure, the rate constant $c$ (1.molecule$^{-1}$.sec$^{-1}$) for a second-order reaction between two molecules of the same size as the solvent molecules, is

$$c=n\nu\exp(-E/RT)/N_0\,[1+a^2Y\nu\exp(-E/RT)/2D] \quad (1)$$

where $D=D_A+D_B$, $D_A$ and $D_B$ are the diffusion constants of the two molecules, $E$ is the activation energy, $\alpha$ is the shortest distance between lattice points, $n$ is the co-ordination number of the lattice, $\nu$ is the frequency factor, $N_0$ is the number of lattice points and $Y$ is constant (ca. 2). From this equation Vaughan[5] derived the following approximate formula for the velocity constant $k$(1 mole.$^{-1}$ sec$^{-1}$) of the polymerization of styrene.

$$k=\nu\exp(-E/RT)/[1+a^2\nu\exp(-E/RT)/D]=k_0/(1+Q/D) \quad (2)$$

where $k_0=\nu\exp(-E/RT)$ and $Q=a^2k_0$.

By the application of this formula to the reaction between monomer $M$ and radical $M_n$*, the propagation process of polymerization was explained and by its application to the reaction between radicals, the termination process was explained. The equation (2) equals, the following equation

$$k_0/k=1+Q/D \quad (3)$$

If the functional relation between $D$ and $\eta$ be put as

$$1/D=f(\eta) \quad (4)$$

then

$$k_0/k=1+Qf(\eta) \quad (5)$$

Although Vaughan used the Einstein-Stokes' relation as the relation (4), it is doubtful that Einstein-Stokes' relation is applicable for a complex system such as the system of polymerization. Moreover, the validity of the application of the equation (1) seems doubtful because in the propagation and termination process of polymerization, one or both of two reacting molecules is larger in size than the solvent molecules (monomers).

When the reacting molecules are larger than the solvent molecules, the following

1) H. Miyama, This Bulletin, **29**, 711, 715, 720 (1956); **30**, 10 (1957).
2) W. I. Bengough and H. W. Melville, *Proc. Roy. Soc.*, **A230**, 429 (1955).
3) S. Fujii, This Bulletin, **27**, 216, 238 (1954).
4) M. S. Matheson, E. E. Auer, E. B. Bevilacqua and E. J. Hart, *J. Am. Chem. Soc.*, **71**, 497 (1949); **73**, 1700, 5395 (1951).
5) M. F. Vaughan, *Trans. Faraday Soc.*, **48**, 576 (1952).
6) E. Rabinowitch, *Trans. Faraday Soc.*, **33**, 1225 (1937).

relation postulated by M. von Smoluchowski[7] is applicable:

$$ {}_AZ_B = 2\pi(D_A+D_B)(r_A+r_B)N/1000 = 2\pi N(r_A+r_B)D/1000 \quad (6) $$

where ${}_AZ_B$ (1.mole$^{-1}$.sec$^{-1}$) is the collision number between two molecules A and B, when the concentrations of two molecules are a unit, $r_A$ and $r_B$ are diameters of each molecules and $N$ is Avogadro's number. If it is assumed that only the factor ${}_AZ_B$ of $k$ varies with the variation of the bulk viscosity, then the following relation can be derived

$$ k_0/k = D_0/D = D_0 f(\eta) \quad (7) $$

## Experimental

By obtaining experimentally the relation between $\eta$ and $k_p/k_t$, it is possible to ascertain whether (5) or (7) is applicable for vinyl polymerization. Details of this experiment are as follows:

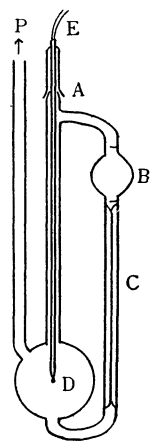



Fig. 1. Reaction vessel.
A; Joint
B, C; Viscosimeter
D; Thermistor
E; Thermistor's lead wires
P; To vacuum

The reaction vessel, shown in Fig. 1, made of soft glass and equipped with a thermistor, is ca. 19 cc. in capacity. Its inside diameter is 40 mm. and the inside depth is 15 mm. This vessel can be connected to the vacuum system at P. The lead wires of the thermistor are covered by very thin soft glass tubing which is sealed at the upper end of joint A. The glass bulb B is ca. 5 cc. in capacity. At its both ends two lines are marked. The capillary C is 10 cm in length and 2.5 mm. in diameter. Using this vessel, the values of $k_p/k_t$ can be measured by the method described in the previous papers[1], and at the same time, the bulk viscosity is obtainable by turning the vessel upside down to transfer the sample into the bulb B, then righting the vessel and measuring the time for the sample to pass between the two marks.

Other experimental procedures and the method of purification of sample and sensitizer are the same as in the previous papers[1]. But the effect of the direct irradiation of light on the thermistor was not observed, because the vessel is made of soft glass and has larger loss in transmission of light than the quartz vessel used in the first paper[1].

## Results

The measurement was accomplished on methyl

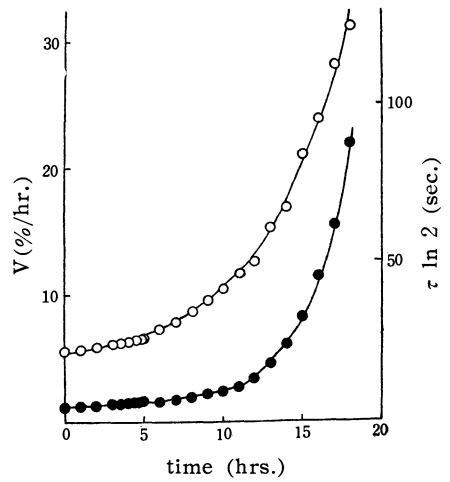



Fig. 2. The variation of rate and lifetime with time for the polymerization of methyl methacrylate.
○ V; ● $\tau$ ln 2

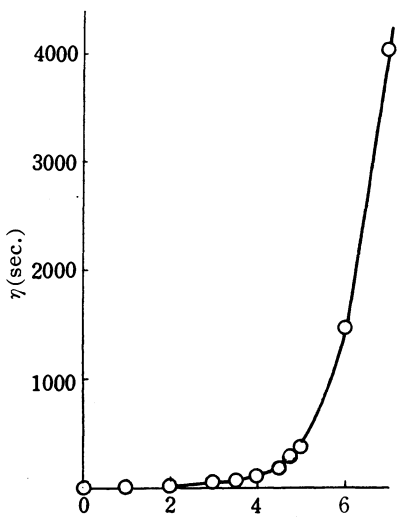



Fig. 3. The variation of bulk viscosity with time for the polymerization of methyl methacrylate.

7) M. von Smoluchowski, *Z. Physik. Chem.*, **92**, 129 (1918).

methacrylate and vinyl acetate at 30°C by using 1,1'-azo-biscyclohexanecarbonitrile as a photosensitizer, the concentration of which was 0.013 mole/l in methyl methacrylate and 0.002 mole/l in vinyl acetate.

The variation of the velocity $V$ and the lifetime $\tau$ for the polymerization of methyl methacrylate during continuous polymerization are shown in Fig. 2. The variation of the bulk viscosity $\eta$ (the time measured by viscosimeter) is shown in Fig. 3. By calculating the degree of conversion $\varphi$ (%) and the values of $k_p/k_t$ as described in the 3rd paper[1] of this series, Table I was obtained.

TABLE I
THE VARIATION OF $\eta$ AND $k_p/k_t$ WITH CONVERSION FOR THE POLYMERIZATION OF METHYL METHACRYLATE

| Conversion | $\eta$(sec.) | $(k_p/k_t)\times10^5$ |
|---|---|---|
| 0 | 1.3 | 0.99 |
| 0.6 | 4.1 | 1.01 |
| 1.1 | 11.5 | 1.12 |
| 1.7 | 33.0 | 1.23 |
| 2.0 | 53.8 | 1.30 |
| 2.3 | 99.4 | 1.38 |
| 2.7 | 185.1 | 1.40 |
| 2.8 | 286.5 | 1.48 |
| 3.0 | 365.2 | 1.54 |
| 3.7 | 1456.1 | 1.80 |
| 4.4 | 4030.0 | 2.22 |
| 5.2 | | 2.60 |
| 6.2 | | 3.34 |
| 7.2 | | 4.04 |
| 8.2 | | 5.22 |
| 9.4 | | 7.21 |
| 10.8 | | 12.1 |
| 12.4 | | 18.1 |
| 14.3 | | 32.0 |
| 16.6 | | 53.6 |
| 19.2 | | 85.5 |
| 22.1 | | 121.0 |

The value of $k_p/k_t$ over 22% conversion was not obtainable, because the lifetime was very long and the measurement was impossible. As shown in this table, the increase of $k_p/k_t$ with the degree of conversion is more remarkable than those for other monomers. This result coincides with the results obtained by other methods[3,4]. The increase in the bulk viscosity is more remarkable than the increase of $k_p/k_t$, but the measurement of the viscosity over conversion 4.4% was impossible, because it took a long time and was not reproducible.

Because details of measurements on the vinyl acetate have already been described in the third paper[1], these are omitted and only their results are shown in Table 2. The measurement of the viscosity over 16.1% was impossible.

TABLE II
THE VARIATION OF $\eta$ AND $k_p/k_t$ WITH CONVERSION FOR THE POLYMERIZATION OF VINYL ACETATE

| Conversion(%) | $\eta$(sec.) | $(k_p/k_t)\times10^5$ |
|---|---|---|
| 0 | 1.0 | 1.20 |
| 1.2 | 1.4 | 1.22 |
| 2.4 | 2.1 | 1.26 |
| 3.6 | 7.5 | 1.31 |
| 4.9 | 16.9 | 1.37 |
| 6.2 | 32.7 | 1.43 |
| 7.5 | 65.0 | 1.49 |
| 8.9 | 116.5 | 1.53 |
| 10.3 | 183.1 | 1.56 |
| 10.7 | 343.5 | 1.64 |
| 13.1 | 707.7 | 1.72 |
| 14.6 | 976.1 | 1.88 |
| 16.1 | 1734.0 | 2.10 |
| 20.8 | | 2.63 |
| 28.8 | | 3.50 |
| 37.3 | | 4.89 |
| 45.5 | | 6.15 |
| 53.2 | | 11.0 |
| 60.0 | | 18.2 |
| 68.1 | | 35.8 |

## Discussion

Let the ratio of the viscosity $\eta$ at any conversion to $\eta_0$ at 0 conversion and the same ratio of $k_p/k_t$ be $x$ and $y$ respectively, i. e.

$$\left.\begin{aligned} x&=\eta/\eta_0 \\ y&=(k_p/k_t)/(k_p/k_t)_0 \end{aligned}\right\} \quad (8)$$

Although the measurement of the viscosity was impossible at high conversion, the following relations were observed between

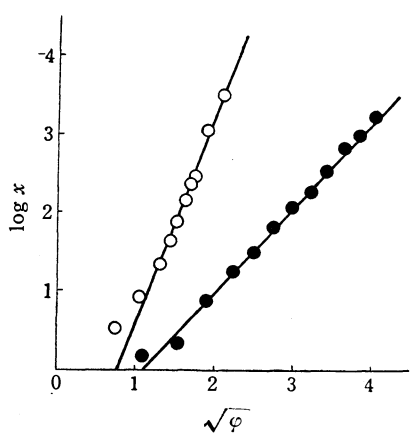



Fig. 4. The variation of $x=\eta/\eta_0$, with conversion $\varphi$.
○ Methyl Methacrylate
● Vinyl Hatate

$x$ and $\varphi$ at low conversion of polymerization as shown in Fig. 4, i. e. on methyl methacrylate,

$$\log x = 2.68\sqrt{\varphi} - 2.17 \quad (9)$$

and on vinyl acetate

$$\log x = 1.11\sqrt{\varphi} - 1.22 \quad (10)$$

These relations are in good agreement with the relation suggested by R. S. Spencer and J. L. Williams[8], in which the bulk viscosity is proportional to $\exp\sqrt{W}$, where $W$ is the weight fraction of polymer. Then the values of the bulk viscosity at high conversion, though not measurable, can be calculated by using (9) and (10). In Table 3, the values of $x$ and $y$ are tabulated.

TABLE III
THE VALUES OF $x$ AND $y$ FOR THE POLYMERIZATION OF METHYL METHACRYLATE AND VINYL ACETATE

| Methyl Methacrylate | | Vinyl Acetate | |
|---|---|---|---|
| $x^{a)}$ | $y$ | $x^{a)}$ | $y$ |
| 1.0 | 1.00 | 1.0 | 1.00 |
| 3.2 | 1.02 | 1.4 | 1.02 |
| 8.3 | 1.13 | 2.1 | 1.05 |
| 25.4 | 1.24 | 7.5 | 1.09 |
| 41.4 | 1.31 | 16.9 | 1.14 |
| 76.3 | 1.39 | 32.7 | 1.19 |
| 142.8 | 1.41 | 65.0 | 1.24 |
| 221.0 | 1.49 | 116.5 | 1.28 |
| 281.5 | 1.56 | 183.1 | 1.30 |
| 1121.0 | 1.82 | 343.5 | 1.37 |
| 3100.0 | 2.24 | 707.7 | 1.44 |
| $10^{3.96}$ | 2.62 | 976.1 | 1.57 |
| $10^{4.50}$ | 3.37 | 1734.0 | 1.75 |
| $10^{4.92}$ | 4.08 | $10^{4.05}$ | 2.19 |
| $10^{5.81}$ | 5.27 | $10^{4.74}$ | 2.92 |
| $10^{6.05}$ | 7.29 | $10^{5.57}$ | 4.07 |
| $10^{6.68}$ | 12.2 | $10^{6.28}$ | 5.12 |
| $10^{7.28}$ | 18.3 | $10^{6.90}$ | 9.17 |
| $10^{8.00}$ | 32.4 | $10^{7.42}$ | 15.2 |
| $10^{8.72}$ | 54.2 | $10^{7.94}$ | 29.2 |
| $10^{9.61}$ | 86.5 | | |
| $10^{10.45}$ | 122.2 | | |

a) In this Table exponential figures are calculated by equations (9) or (10).

Because $k_p$ is constant at the initial stage (until $\varphi$=30–40%) of polymerization and the increase of $k/k_t$ with the degree of conversion depends mainly upon the decrease of $k_t$[1-4], $y$ in equation (8) at this stage equals to $(k_t)_0/k_t$, i. e.,

$$y = (k_t)_0/k_t \quad (11)$$

8) R. S. Spencer and J. L. Williams, *J. Colloid Sci.*, **2**, 117 (1947).

As shown in Figs. 5 and 6, the following relations at the initial stage of polymerization, for methyl methacrylate may be derived:

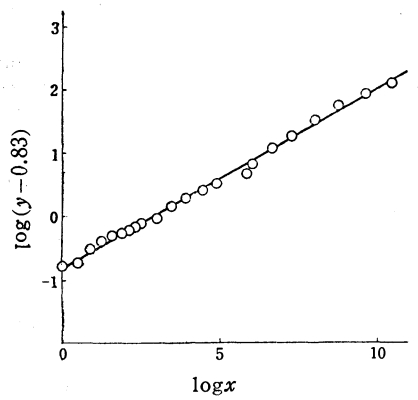



Fig. 5. The variation of $y$ with $x$ for the polymerization of methyl methacrylate.

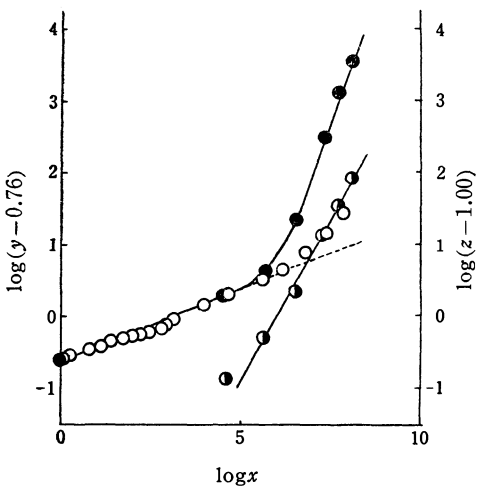



Fig. 6. The variation of $y$ and $z$ with $x$ for the polymerization of vinyl acetate.
○, $y=(k_p/k_t)/(k_p/k_t)_0$;
●, $y=(k_t)_0/k_t$
◑, $z=(k_p)_0/k_p$

$$y = 0.83 + 0.17x^{0.28} \quad (12)$$

and for vinyl acetate

$$y = 0.76 + 0.24x^{0.20} \quad (13)$$

Because $k_t$ is not constant at the later stage of polymerization and $(k_t)_0/k_t$ is not equal to $(k_p/k_t)/(k_p/k_t)_0$, it is necessary to consider $k_p$ and $k_t$ separately. Using the values of the viscosity in this report, it is possible to obtain the relation between the bulk viscosity and $k_p$ or $k_t$, which was presented on vinyl acetate in the 3rd paper[1] of this series. Since these values

of $k_p$ and $k_t$ were measured at 20°C, these were corrected to 30°C by using the values of the activation energies $E_p$ and $E_t$ given in the 4th paper[1]. Although the variation of $y$ with $x$ at the initial stage obeys the equation (13) as shown in Fig. 6, it is replaced by the relation $y \propto x^{1.5}$ at the later stage. The following equation therefore is applicable throughout the total process of polymerization.

$$y=0.76+0.24(x^{0.20}+10^{-8}x^{1.50}) \quad (14)$$

Let the ratio of $(k)_0$ to $k$, be $z$, i. e.

$$z=(k_p)_0/k_p \quad (15)$$

Then the following equation is obtainable from Fig. 6 throughout the total process of polymerization,

$$z=1+0.65\times10^{-6}x \quad (16)$$

As shown in Table IV, there is a good agreement between the calculated values of $y$ or $z$ by using equation (14) or (16) and the experimental values.

TABLE IV
THE COMPARISON OF CALCULATED VALUES WITH EXPERIMENTAL VALUES ON $y$ AND $z$ FOR THE POLYMERIZATION OF VINYL ACETATE

| Conversion (%) | $x$ | $y$(exp.) | $y$(calc.) | $z$ (exp.) | $z$ (calc.) |
|---|---|---|---|---|---|
| 0 | 1 | 1.00 | 1.00 | 1.00 | 1.00 |
| 28.15 | $10^{4.68}$ | 2.64 | 2.85 | 1.14 | 1.03 |
| 39.00 | $10^{5.71}$ | 4.82 | 4.33 | 1.50 | 1.33 |
| 49.80 | $10^{6.61}$ | 23.8 | 26.2 | 3.38 | 3.64 |
| 59.30 | $10^{7.33}$ | 337 | 248 | 14.9 | 14.9 |
| 66.40 | $10^{7.73}$ | 1250 | 966 | 35.5 | 35.9 |
| 71.10 | $10^{8.15}$ | 3780 | 3991 | 91.8 | 92.8 |

From the comparison of (14) with (7), the following equation is obtained:

$$(k_t)_0/k_t=(D_R)_0/D_R=0.76+0.24(x^{0.20}+10^{-8}x^{1.50}) \quad (17)$$

And from the comparison of (16) with (7)[9],

$$(k_p)_0/k_p=(D_M)_0/D_M=1+0.65\times10^{-6}x \quad (18)$$

where $D_M$ and $D_R$ are the diffusion constants of monomer $M$ and radical $M_n$* respectively. There is no direct measurement of the diffusion constant of monomer, but Melville et al.[2] estimated its value by measuring the diffusion velocity of $\alpha,\alpha'$-diphenylpicrylhydrazil in the various conversions of vinyl acetate. Comparison of these values of $(D_M)_0/D_M$ with the values of $\eta/\eta_0$ of this report is shown in Fig. 7. Here it is apparent that the measured values of $(D_M)_0/D_M$ obey the relation (18). This result shows that the application of (7) is reasonable. At the same time, the

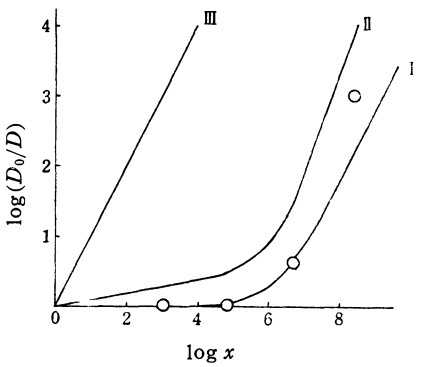



Fig. 7. The variation of $D_0/D$ with $x$
I, $D_0/D=1+0.65\times10^{-6}x$;
II, $D_0/D=0.76+0.24(x^{0.20}+10^{-8}x^{1.50})$;
III, $D_0/D=x$;
○, The measured values of $D_0/D$

relation (17) is shown in Fig. 7 and the shape of this curve is similiar to the curve (18), except that $(D_R)_0/D_R$ increases with the increase in the bulk viscosity at rather low viscosity. It seems probable that the effect of the bulk viscosity is more remarkable on the diffusion constant of the radical than on that of the monomer.

If the Einstein-stoke's relation adopted by Vaughan is applicable, $(D_M)_0/D_M$ may be expressed in a different form from (18), i.e.

$$(D_M)_0/D_M=x \quad (19)$$

The measured values of $(D_M)_0/D_M$ deviate greatly from this relation. On the other hand, if $a\fallingdotseq3\times10^{-8}$cm.[6], $k_0\fallingdotseq5\times10^{2}$ [1] and $D_0\fallingdotseq10^{-5}$ cm$^2$.sec$^{-1}$ [5] are used in the Vaughan's equation (3), the values of $Q$ becomes ca. $5\times10^{-13}$ and from the comparison of (3) with (16), $(D_M)_0/D_M$ equals ca. $10^2x$.

$$(D_M)_0/D_M=10^2x \quad (20)$$

This result (20) is more unsatisfactory than the equation (19) for the measured values of $(D_M)_0/D_M$. Therefore the application of (5), (3) and (1) is not considered reasonable. The reason why Vaughan's qualitative application of the equation (1) for the polymerization of styrene gave apparently valid results may be his rather arbitrary selection of the values of the diffusion constants and the

9) Although $D=D_M+D_R$ in the propagation process, it seems reasonable to assume $D=D_M$ because $D_M \gg D_R$.

use of an assumed relation $1/D \propto \eta$.

From the above discussion, it seems that the application of (7) and (6) is more reasonable than (5) and (1) for the propagation and termination process of polymerization, in which the reacting molecules are far larger than the solvent molecules. But to prove this conclusion absolutely, it is necessary to measure the bulk viscosity at high conversion and the diffusion constants of monomer and radicals, though they are not measurable in this study.

## Summary

The author measured the ratio of the propagation constant to the termination constant $k_p/k_t$ and the bulk viscosity $\eta$ of the reaction system for the polymerization of methyl methacrylate and vinyl acetate by using the thermistor method and a special reaction vessel, which could be used as a viscosimeter, then compared the results of these measurements with the values $k_p$ and $k_t$ of vinyl acetate presented in the previous paper[1], and thus obtained the general formula for the relation between the bulk viscosity and $k_p$ or $k$. The obtained results are summarized as follows;

1) Throughout the total procss for the polymerization of vinyl acetate the relation between the termination constant $k_t$ and $\eta$ is expressed as follows,

$$(k_t)_0/k_t = 0.76 + 0.24[(\eta/\eta_0)^{0.20} + 10^{-8}(\eta/\eta_0)^{1.50}]$$

In case of methyl methacrylate, the following formula is recommended which holds up to 22% conversion.

$$(k_t)_0/k_t = 0.83 + 0.17(\eta/\eta_0)^{0.28}$$

Where $(k_t)_0$ and $\eta_0$ are the values of $k_t$ and $\eta$ at conversion 0.

2) The propagation constant $k_p$ and $\eta$ in the polymerization of vinyl acetate are expressed as follows.

$$(k_p)_0/k_p = 1 + 0.65 \times 10^{-6}(\eta/\eta_0)$$

3) These results can be explained by the assumption that $k_t$ and $k_p$ are proportional to the diffusion constants of reacting molecules. Using the theory of Rabinowitch-Vaughan, we find some difficulties to explain our experimental results.

The author wishes to express his sincere thanks to Dr. Momotaro Suzuki of this Academy for his helpful advice and encouragement and Mr. Shinichi Taira of Tokyo Metropolitan University for his kind supply of 1,1′-azo-biscyclohexanecarbonitrile.

*Department of Chemistry,*
*Defense Academy, Yokosuka*

# *Surface Chemistry of High Polymers. VII*[1] *Polyacids and Some Vinyl Polymers*

By Hiroshi HOTTA* and Toshizo ISEMURA

(Received December 12, 1956)

As mentioned in the previous paper[2], the study of polyelectrolytes has many interesting points not only for pure physical chemistry but also as an important model of biocolloidal substances. Therefore, some investigations have been carried out along these lines. Especially, the solution of polymethacrylic acid has been studied exhaustively as a typical linear polyelectrolyte[3]. However, the surface film of polyelectrolytes has not been studied thoroughly as yet. In the present experiment, the films of poly-L-glutamic acid and of the copolymer of maleic acid and vinyl acetate were studied at the air/ and oil/water interfaces by measuring their interfacial pressure and potential in order to know the behavior of carboxyl groups as the most important component of polyelectrolytes. The interfacial

* Present address: Japan Atomic Energy Research Institute, Tokyo.

1) Part VI of this series, H. Hotta, This Bulletin, **28**, 64 (1955).

2) T. Isemura, H. Hotta and S. Otsuka, ibid., **27**, 93 (1954).

3) For example, A. Katchalsky, O. Künzel and W. Kuhn, *J. Polymer Sci.*, **5**, 283 (1950); A. Katchalsky, ibid., **7**, 393 (1951).

potential of some non-electrolytic linear polymers and di- and tri-carboxylic acids was also measured for reference in order to elucidate the behavior of the present polyacids. The obtained results were considered in the light of the knowledge of some polyacids, which had been studied previously[2,4,5].

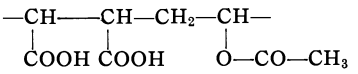
## Experimental

The films were spread at the air/and petroleum ether (b. p. 90–130°C)/aqueous phase interfaces, and their interfacial pressure and potential were measured at room temperature. The pH of aqueous phase was adjusted by hydrochloric acid. The apparutus and methods were the same as in the previous papers[2,4]

Materials and spreading solutions used in the present investigation were as follows. The copolymer of maleic acid and vinyl acetate, which was kindly supplied from Sekisui Chem. Ind. Co., Ltd., and polyvinyl alcohol, whose degree of polymerization was 2510, were dissolved in distilled water. Poly-L-glutamic acid, which was the same as that studied previously in our laboratory[6], was dissolved in N/100 sodium hydroxide solution. Isopropyl alcohol was added to all these solutions in the concentration of 20% to help the spreading. Polyvinyl acetate[7], octadecyl malonic acid[6] and hexadecane-1,1,2-tricarboxylic acid[6] were dissolved in the same solvent as in the previous studies, respectively.

## Results

We studied first the film of the copolymer of maleic acid and vinyl acetate on the aqueous phase of various pH. Since this copolymer, which is called hereafter MAVA, has



as a constitutional unit, figures for this copolymer in the present paper are plotted against the

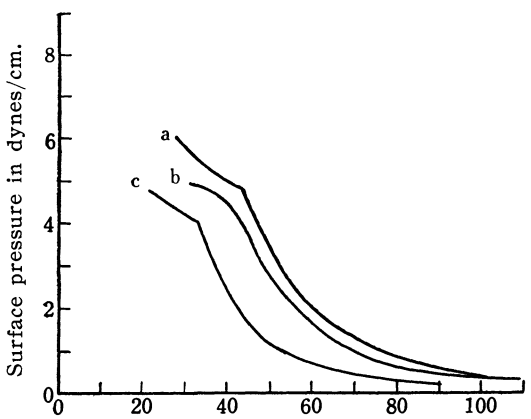



Fig. 1. The surface pressure-area curves of MAVA at the air/water interface (at about 15°C);
curve a (pH 1.6–4.0), curve b (pH 4.4), and curve c (pH 5.2).

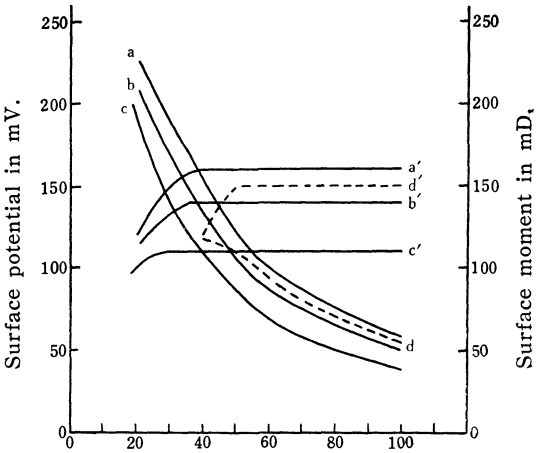



Fig. 2. The interfacial potential (moment)-area curves of MAVA at the air/water interface (curve a pH 1.6 and 2.6, curve b pH 3.2 and curve c pH 3.8), and at the petroleum ether/water interface (curve d pH 1.6 containing 2 M KCl) (at about 18°C).

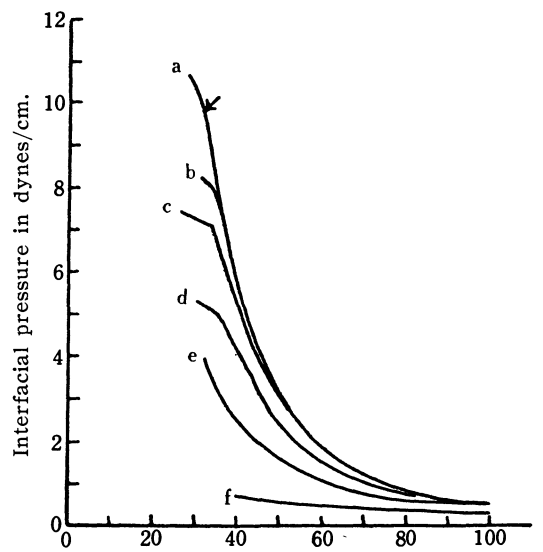



Fig. 3. The interfacial pressure--area curves of MAVA at the petroleum ether/water interface at about 20°C; curve a pH 1.6 and 2.4, curve b pH 2.8, curve c pH 3.2, curve d pH 4.0, curve e pH 4.8 and curve f pH 5.6.

4) H. Hotta, This Bulletin, **27**, 412 (1954).
5) H. Hotta and T. Isemura, ibid., **29**, 90 (1956).
6) T. Isemura and K. Hamaguchi, ibid., **27**, 339(1954).
7) T. Isemura, H. Hotta and T. Miwa, ibid., **26**, 380 (1953).

area per this unit. The surface pressure and potential at the air/water interface are shown in Figs. 1 and 2, respectively. The corresponding surface moment-area curves in the present paper are represented by prime in the same figure of surface potential. The observed value of surface potential, which will be mentioned later in Fig. 8, was somewhat various, and this tendency was considerable at pH more than 4.0.

The interfacial pressure of MAVA at the petroleum ether/water interface is shown in Fig. 3. The kink point of curve a is shown by an arrow. Curve a of this figure coincides entirely with curve a in Fig. 1 at the moderate area. It means that MAVA gives a film of expanded type like polyvinyl acetate even at the air/water interface[8]. The spreading solution dissolved partially into aqueous phase at the lower pH than at the air/water interface. (See Figs. 1 and 3.) Since the distinct interfacial potential-area curve could not be obtained in the higher pH range at the oil/water interface, only the results on the aqueous phase of pH 1.6 containing 0.2 M potassium chloride is shown with dotted line (curve d) in Fig. 2. In Fig. 2, the surface moments at both interfaces are nearly equal to each other. This is another evidence that MAVA is of expanded state even at the air/water interface, for the film could not have the same configuration, namely, the same surface moment, if it were the film of different type at both interfaces.

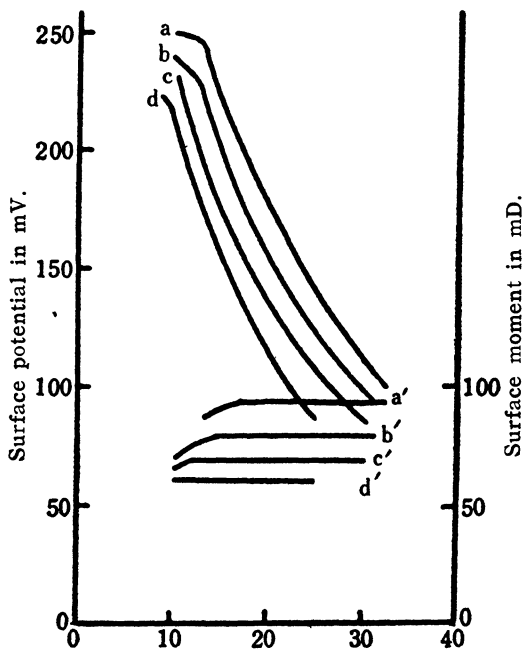



Fig. 4. The surface potential (moment)-area curves of poly-L-glutamic acid at the air/water interface at about 23°C; curve a pH 1.2 and 3.8, curve b pH 4.2, curve c pH 4..8 and curve d pH 5.2.

8) H. Hotta, *J. Colloid Sci.*, **9**, 504 (1954).

The surface potential-area curves of poly-L-glutamic acid at the air/water interface are shown in Fig. 4. The surface pressure and viscosity of this polyaminoacid had been reported previously from our laboratory[6]. The reproducible curve could not be obtained at the larger area than 30 Å² per residue. Since the interfacial potential-area curve of poly-L-glutamic acid at the oil/water interface could not be obtained due to the partial dissolution of spreading solution into aqueous phase, only the maximum interfacial potential is shown as the function of the pH of aqueous phase in Fig. 5. Nevertheless, the interfacial moment on pH 1.6 might be about 80 mD. The dependence of the maximum interfacial potential on the pH of aqueous phase is similar at both interfaces. (See Figs. 4 and 5.)

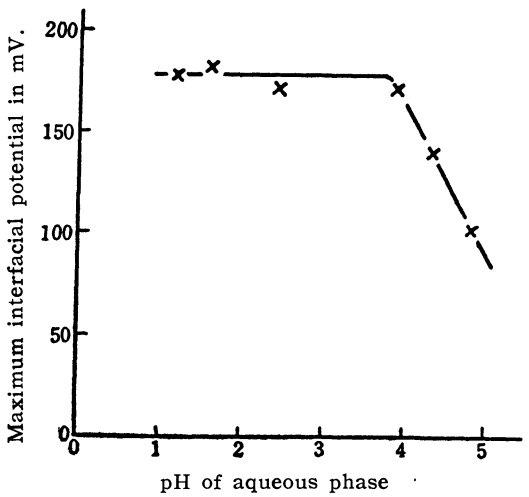



Fig. 5. The maximum interfacial potential of poly-L-glutamic acid at the petroleum ether/water interface on the various pH of aqueous phase.

As the example of simple polyacid, we measured the surface potential of octadecyl malonic acid and hexadecane-1,1,2-tricarboxylic acid at the air/water interface (pH 1.6). The surface moments obtained at the larger area are shown in Table I, although the values at the smaller area than 60 Å² per molecule show some irregularity. The surface pressure-area relation of these acids had been reported in the preceding paper[5].

On the other hand, we measured the interfacial potential of polyvinyl acetate and polyvinyl alcohol at the petroleum ether/water interface for reference. The result of polyvinyl acetate is shown in Fig. 6, together with the curve at the air/water interface in the previous paper[7]. Since the potential values at the kink point of curves a and b (422 mV.) are quite identical, the true curve at the oil/water interface may be expected as shown with dotted line, if we take imperfect spreading at the smaller area at this interface into consideration. The interfacial pressure and potential of polyvinyl alcohol at the oil water interface is shown in Fig. 7. The change of interfacial pressure with time appeared at the smaller area than

TABLE I

THE SURFACE MOMENT OF VARIOUS COMPOUNDS

| Compound | Formula | Surface Moment in mD at Air/Water Interface | Surface Moment in mD at Oil/Water Interface | Reference |
|---|---|---|---|---|
| Polyvinyl alcohol | $-CH_2-CH(OH)-$ | 40 | 45 | 12, The present |
| Polymethacrylic acid | $-CH_2-C(CH_3)(COOH)-$ | 90 | 15 | 2, 4 |
| Poly-4-vinyl benzoic acid | $-CH_2-CH(C_6H_4COOH)-$ | 100 | — | 9 |
| Poly-L-glutamic acid | $-NH-CH(CH_2CH_2COOH)-CO-$ | 95 | 80 | The present |
| Poly-ε-caproamide | $-NH-(CH_2)_5-CO-$ | 225 | — | 10 |
| Copolymer of maleic acid and vinyl acetate | $-CH(COOH)-CH(COOH)-CH_2-CH(OCOCH_3)-$ | 160 | 150 | The present |
| Octadecyl malonic acid | $CH_3-(CH_2)_{17}-CH(COOH)-COOH$ | 240 | — | The present |
| Hexadecane-1,1,2-tricarboxylic acid | $CH_3-(CH_2)_{16}-CH(COOH)-CH(COOH)-COOH$ | 200 | — | The present |
| ω-ω'-hexadecane-dicarboxylic acid | $HOOC-(CH_2)_{16}-COOH$ | 350 | — | 11 |
| Polyethylene terephthalate | $-O-CO-C_6H_4-CO-O-(CH_2)_2-$ | 350 | — | 1 |
| Polyvinyl acetate | $-CH_2CH(OCOCH_3)-$ | 340[a] / 280[b] | 280 | 7, The present |
| Polymethyl methacrylate | $-CH_2C(CH_3)(COOCH_3)-$ | 250 | — | 10 |
| Polyoctadecyl methacrylate | $-CH_2-C(CH_3)(COOC_{18}H_{37})-$ | 460 | — | 12 |
| Myristic acid | $CH_3-(CH_2)_{12}-COOH$ | 156[a] / 250[b] | — | 13 |

a) An expanded state.
b) A condensed state.

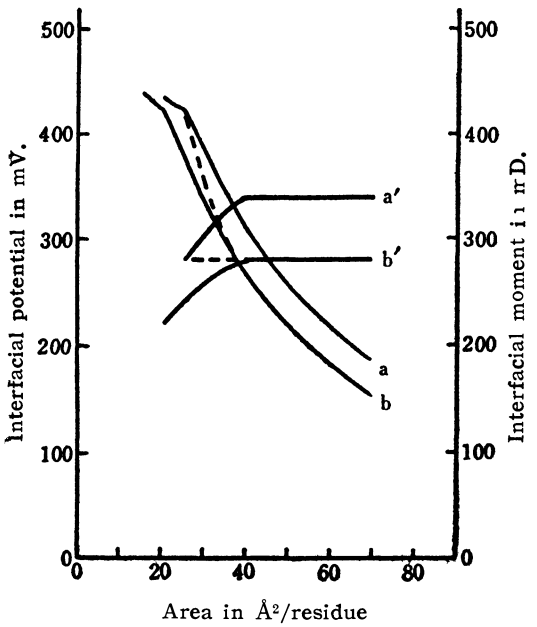



Fig. 6. The interfacial potential (moment)-area curves of polyvinyl acetate at the air/water (curve a) and petroleum ether/water (curve b) interfaces.

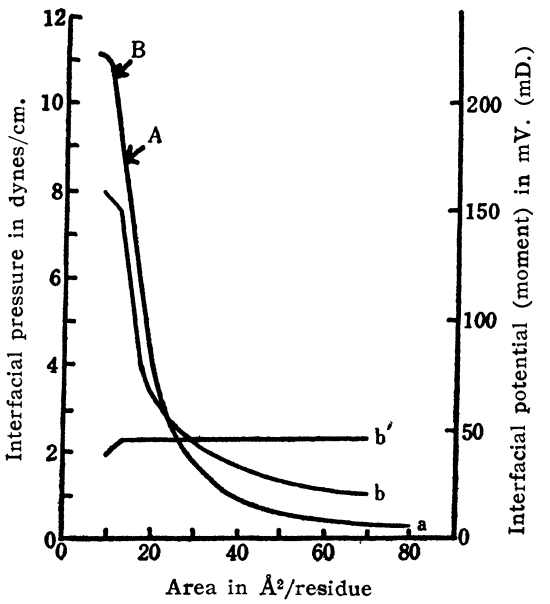



Fig. 7. The interfacial pressure-area curve a and potential (moment)-area curve b of polyvinyl alcohol at the petroleum ether/water interface.

13 Å$^2$ per monomer (arrow A), where the interfacial moment began to lower. Furthermore, the lowering of the pressure becomes more distinct in the region of the area smaller than 11 Å$^2$ per monomer (arrow B).

## Discussion

As mentioned above, the copolymer of maleic acid and vinyl acetate (MAVA) on pH 1.6 gives a film of expanded type even at the air/water interface. On the other hand, at the air/water interface, polymethacrylic acid gives a film of condensed type on the aqueous phase of pH 1.6 due to cohesion between carboxyl groups[2], and polyvinyl acetate gives a film of expanded type due to the effect of short side chains[7,8] as shown in the previous investigations. It seems that the short side chains in this copolymer still play a role of two dimensional self-plasticizer against cohesion between carboxyl groups.

In the previous paper[8] it was proposed that, when $n_{atom}$ is defined by an equation

$$n_{atom} = a\left(\frac{kT}{\pi A}\right)_{A=\infty}$$

where $a$ is the number of main atoms in the structural unit of main chain, $k$ Boltzmann's constant, $T$ absolute temperature, $\pi$ interfacial pressure, $A$ area per structural unit, $n_{atom}$ is a characteristic quantity representing the behavior at the interface. The value of $n_{atom}$ for MAVA was found to be 43, which corresponds to the mean value of 38 for polyvinyl acetate and 48 for methacrylic acid in the previous investigations[8]. The value for polyvinyl alcohol was 41.

Since the surface moment of some compounds was measured in the present investigation, we have made a list of them in the non-ionized state or of non-electrolyte with those of other related compounds[9-13] in Table I, in which the value of surface moment is for the represented formula. It may be assumed that the compounds, whose surface moment is nearly equal at both interfaces, have almost the same orientation at both interfaces. For polyvinyl acetate, the moment at the oil/water interface is identical with that at the air/water interface not at the expanded state but at the compact state. It is understood in the light of a previous model[8,10] on account of the affinity of methyl group to oil phase.

The surface moments of carboxyl groups for the polymers examined are quite different as shown in Table I. It might be due to the various orientations of C=O bond as mentioned previously[8,10]. Generally speaking, it appears that the horizontal orientation of a chain directly linking to the carbon atom of carboxyl group makes the surface moment lower, and that this tendency of lowering is more predominant for the closer approach of carboxyl groups with each other (for example, hexadecane-1,1,2-tricarboxylic acid). The surface moment of MAVA and of poly-L-glutamic acid can not be explained by the additivity of the constituent polar groups cited in Table I. (Polymethacrylic acid and polyvinyl acetate for MAVA, or polymethacrylic acid and poly-ε-caproamide for poly-L-glutamic acid) It might be attributed to the change of mutual orientation of these polar groups at the interface.

Besides, we must consider the ionization effect of carboxyl groups for polyacids with increasing pH of aqueous phase. Especially, the surface moment is most sensitive to this effect, and is lowered due to the ionization of the acid group. When the surface moment of polyacids in the range of constant value at the air/water interface are plotted against the pH of aqueous

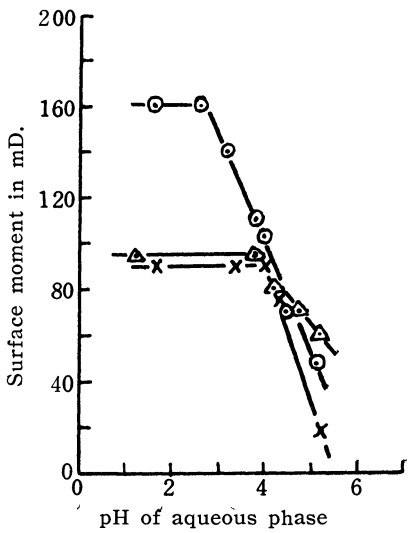



Fig. 8. The surface moment of polyacids at the constant range at the air/water interface plotted against the pH of aqueous phase; MAVA (⊙), poly-L-glutamic acid (△) and polymethacrylic acid (×).

9) I. R. Miller, *J. Colloid Sci.*, **9**, 579 (1954)
10) H. Hotta, This Bulletin, **27**, 80 (1954)
11) H. Hotta and T. Isemura, ibid., **25**, 101 (1952).
12) D. J. Crisp, *J. Colloid Sci.*, **1**, 161 (1946).
13) J. H. Schulman and E. K. Rideal, *Proc. Roy. Soc.* (London), **130A**, 270 (1931).

phase in Fig. 8, we find that the bending points of these curves correspond almost to the pK of the monomer unit of these polyacids, which is 2.85, 4.25 and 4.85 for malonic acid, glutamic acid and isobutyric acid in this case, respectively. The values of surface moment of MAVA at pH more than 4.0 in Fig. 8 are the mean values of the repeated experiments, for they were various as mentioned above. The curve for polymethacrylic acid is cited from the previous results[3].

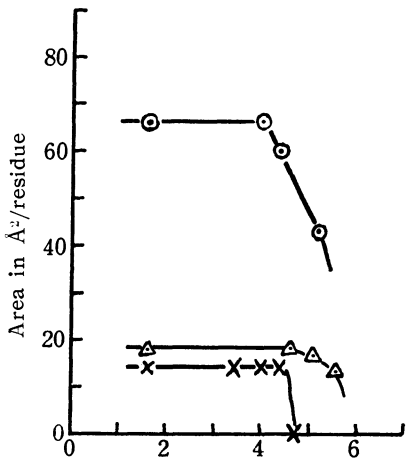



Fig. 9. The area of polyacids at the constant surface pressure (1 dyne/cm.) at the air/water interface plotted against the pH of aqueous phase (at 10–15°C); MAVA (⊙), poly-L-glutamic acid (△) and polymethacrylic acid (×).

On the other hand, the similar relationship was not found for surface pressure as shown in Fig. 9, in which the curves for poly-L-glutamic acid[6] and polymethacrylic acid[2] are cited from the previous results. In the case of surface pressure, the contribution of the non-ionizable part might be fairly effective even in the region of larger pH. Although the lowering of these curves with increasing pH is due to the partial dissolution, this would be determined not only by the degree of ionization but also the hydrophylic nature of non-ionizable part and the state of the molecule. It is necessary for complete ionization that the electrostatic repulsion between ionic groups must overcome the intramolecular cohesion (van der Waals' force or hydrogen bonding)[2,8]. All pH's at the point, where the lowering occurs, are between 4 and 5.

It is more or less difficult to obtain the distinct result not only in the ionized state, but also in the non-ionized state for polyacids studied in the present investigation except for polymethacrylic acid which gives a film of condensed type. The surface pressure changes more or less with time. The similar result is reported for polybenzoic acid[9]. It may be caused by the gelation due to hydrated carboxyl groups.

## Summary

The films of polyacids (poly-L-glutamic acid and the copolymer of maleic acid and vinyl acetate) and some related compounds were studied in order to know the behaviour of carboxyl groups in the linear polymer at the interface. The principal results obtained are as follows.

The orientation of carboxyl group is affected considerably by other accompanying groups in polymer. Hence, the surface moment of carboxylic compounds is various according to the surface orientation of respective groups in the polymer. Accordingly, the surface moment of copolymer cannot be explained by the simple additivity of the moment of constituent polar groups.

The surface moment of polyacids abruptly decreases nearly at the pH of aqueous phase equal to the pK of corresponding structural unit.

*The Institute of Scientific and Industrial Research, Osaka University, Sakai, Osaka*

# *A Study on the Electric Conductivity of Sodium Silicate Aqueous Solution. III. On the Relationship between Conductance and Viscosity*

By Hiroshi UKIHASHI

(Received November 19, 1956)

## Introduction

In the previous papers[1,2], the author has remarked that the electric conductivity of sodium silicate solution seemed independent of their viscosity at high concentration range. This has been suggested by the experimental facts that the change of viscosity with concentration varied widely among the solutions having different molar ratio around the concentration where maximum specific conductivity was shown, and that the equivalent conductivity computed theoretically, with viscosity correction, fell increasingly below the observed value above a definite concentration range.

Since conductance in electrolyte solution is a result of the movement of ions under an applied potential, and viscosity is the reciprocal of fluidity which expresses the rate of shear taking place with a definite velocity under unit force, they both can be treated as rate process. Then the comparative study of conductance and viscous flow in view of the theory of rate process is of much value on considering the structure of solution, as it gives some information concerning the bearings on the mechanisms of both phenomena.

In the present report the mechanism of conductance of concentrated sodium silicate solutions of various molar ratio has been discussed in comparison with that of viscous flow from the above mentioned standpoint, and an interpretation has been given for the structure of these solutions.

## Experimental

Preparation of sample sodium silicate solutions, apparatus and methods used for the measurement of electric conductivity were described in the preceding paper. Sample solutions for the measurement of viscosity were the same as those for that of the conductance. Viscosity was measured by the capillary method, using Ubbelohde viscometers with varied capillary constants which were originally determined by the maker and calibrated in the author's laboratory, using glycerol solutions of varied concentrations as standards. Measurements were made at a series of increasing temperatures from 5 to 60°C. The relative viscosity was calculated by the usual formula,

$$\eta_{rel} = \frac{t\ (\text{flow time of solution}) \cdot d\ (\text{density of solution})}{t_0\ (\text{flow time of water}) \cdot d_0\ (\text{density of water})}.$$

With the concentrated solutions, absolute viscosity was calculated directly by the formula $\eta/d = At$

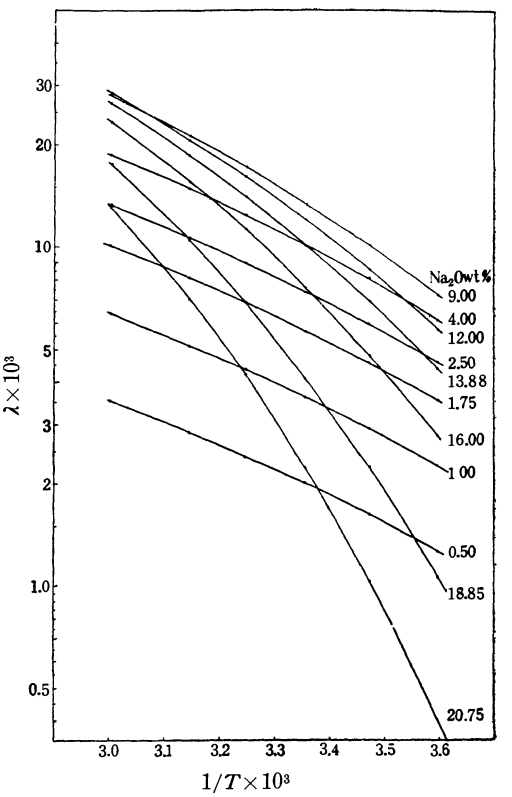



Fig. 1. Variation of the logarithm of specific conductivity with reciprocal of absolute temperature for the 1.00 molar ratio solutions.

1) H. Ukihashi, This Bulletin, **29**, 537 (1956).
2) Idem., ibid, **30**, 414 (1957).

$-B/t$, where A is constant characteristic of capillary, and B constant for kinetic energy correction. It may be conceived that as the concentrated sodium silicate solutions, especially of high molar ratio, would show structural viscosity or thixotropy, the so-called one-point method for the measurement would not be adequate. However, since the present paper has been aimed at discussing primarily the mechanism of electric conductance of sodium silicate solution in relation to that of viscous flow, it would be permissible to set aside, for the present, the problem of exact viscous behavior of the concentrated solution and to leave it for later debate.

## Results

**Activation Energy of Conductance and Viscous Flow.**—In Figs. 1 and 2, the logarithm of specific conductivity was plotted against the

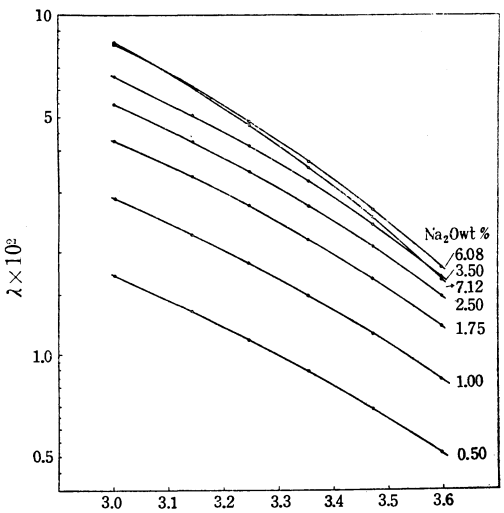



Fig. 2. Variation of the logarithm of specific conductivity with reciprocal of absolute temperature for the 3.95 molar ratio solutions.

reciprocal of absolute temperature for the sodium silicate solutions of molar ratio 1.00 and 3.95. These figures illustrate the different behavior in most marked contrast at various concentrations. The similar curves for viscosity were shown in Figs. 3 and 4 for the corresponding solutions. Although both sets of curves have slight curvature[3], they are regarded as showing approximately linear relationship over a narrow temperature range. The activation energies of conductance and viscous flow are expressed as $d\ln\lambda/d(1/T)=-E_\lambda/R$, and $d\ln\eta/d(1/T)=E_\eta/R$ respectively, where $\lambda$ is specific conductivity, $\eta$

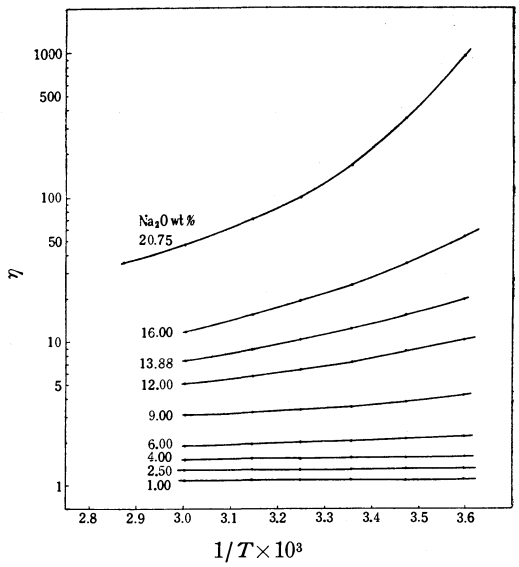



Fig. 3. Variation of the logarithm of viscosity with reciprocal of absolute temperature for the 1.00 molar ratio solutions.

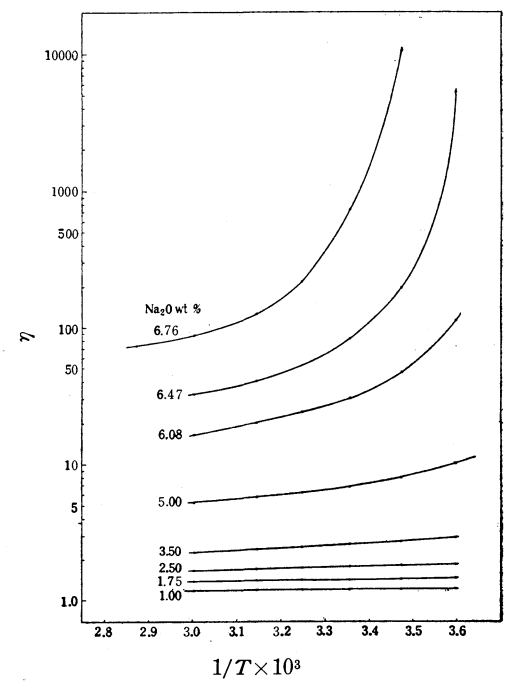



Fig. 4. Variation of the logarithm of viscosity with reciprocal of absolute temperature for the 3.95 molar ratio solutions.

viscosity, $T$ absolute temperature, $R$ gas constant, and $E_\lambda$ and $E_\eta$ activation energy of conductance and viscous flow. Their values at 25°C were calculated by the following equation, using those at 15°C and 35°C for $\lambda_1$, $\eta_1$, $T_1$ and $\lambda_2$, $\eta_2$, $T_2$ respectively.

3) Log $\eta-1/T$ curves for the highly concentrated solutions may no more be postulated as showing linearity. There must be appreciable change of structure with temperature, which results in the marked variation of $E_\eta$ with temperature.

$$\frac{R(\ln\lambda_2-\ln\lambda_1)}{(1/T_1-/1T_2)}=E_\lambda,\quad \frac{R(\ln\eta_1-\ln\eta_2)}{(1/T_1-1/T_2)}=E_\eta.$$

In Fig. 5 and 6, the results were plotted against the concentration for all systems studied. It is visualized that for the higher molar ratio solutions the increase of $E_\lambda$ with concentration is small over an entire concentration range measured, while that of $E_\eta$ appeared to become remarkably large at high concentration, and that for the lower molar ratio solutions both $E_\lambda$ and $E_\eta$ increase with similar manner up to the value several times as large as those in dilute concentration. For the convenience of discussion, the data of $E_\lambda$ and $E_\eta$ for the solutions of molar ratio 1.00 and 3.95, as extreme examples, are tabulated in Table I. It seems at first sight rather curious that for the 1.00 molar ratio solution $E_\lambda$ is smaller than $E_\eta$ even at dilute concentration range. This may be ascribed to the OH ion contribution to the conductivity as described in the previous report. Conductance by OH ion in aqueous solution requires much smaller activation energy (3.4 kcal.) as compared with usual ionic conductance owing to its special conduction mechanism, which is successfully accounted for as a prototropic process where the proton is transferred from a water molecule to an hydroxyl ion.

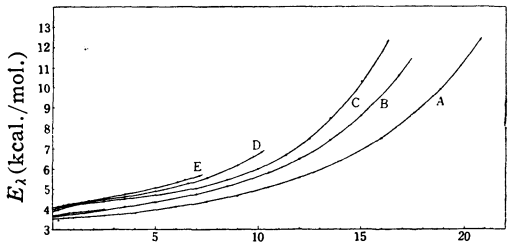



Fig. 5. Variation of the activation energy of conductance with concentration for the sodium silicate solutions of molar ratio.
A: 1.00, B: 1.55, C: 2.13, D: 3.19 and E: 3.95

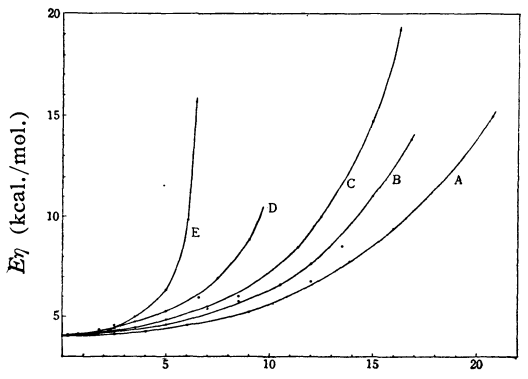



Fig. 6. Variation of the activation energy of viscous flow with concentration for the sodium silicate solutions of molar ratio.
A: 1.00, B: 1.55, C: 2.13, D: 3.19 and E: 3.95

TABLE I

| M. R.=1.00 | | | M. R.=3.95 | | |
|---|---|---|---|---|---|
| $C$(Mol./l.) | $E_\lambda$ | $E_\eta$ | $C$(Mol./l.) | $E_\lambda$ | $E_\eta$ |
| 0.08 | 3.52 | 4.04 | 0.08 | 4.14 | 4.11 |
| 0.16 | 3.57 | 4.13 | 0.16 | 4.23 | 4.11 |
| 0.42 | 3.69 | 4.11 | 0.30 | 4.40 | 4.28 |
| 0.69 | 3.84 | 4.25 | 0.44 | 4.54 | 4.40 |
| 1.09 | 4.11 | 4.56 | 0.64 | 4.74 | 4.97 |
| 1.74 | 4.68 | 5.20 | 0.98 | 5.04 | 6.31 |
| 2.47 | 5.54 | 6.70 | 1.25 | 5.32 | 9.78 |
| 2.97 | 6.31 | 7.67 | 1.35 | 5.43 | 15.61 |
| 3.58 | 7.48 | 9.37 | 1.44 | 5.55 | 179.8 |
| 5.15 | 12.37 | 14.90 | 1.53 | 5.64 | |

**The Product of Equivalent Conductivity and Solution Viscosity.**—According to Eyring[4], activation free energy of viscous flow $\Delta F_\eta$ is expressed as

$$\eta=hN/V\exp(\Delta F_\eta/RT) \qquad (1)$$

while equivalent conductivity $\Lambda$, as a result of theoretical treatment of rate process, may be expressed in terms of activation free energy of conductance $\Delta F_\lambda$ as follows[5],

$$\Lambda=\frac{V^{2/3}\Sigma Z_iF^2\cdot10^7}{hN}\exp(-\Delta F_\Lambda/RT) \qquad (2)$$

where $h$ denotes Planck's constant, $N$ Avogadro number, $V$ molal volume of moving unit, $F$ the Faraday, and $z$ charge valence.

If approximation can be made that the $\Delta F_\eta$ has the same value as $\Delta F_\Lambda$ and that volume of moving unit is similar in both cases the product $\Lambda\eta$ becomes

$$\Lambda\eta=\Sigma z_iF^2\cdot10^7/V^{1/3} \qquad (3)$$

Equation (3) implies that $\Lambda\eta$ is constant irrespective of variation of temperature and concentration, if the viscous flow and electric conduction occur by the same mechanism, and the volume of the moving unit is alike in both cases, and that its value should be the order of unity. Though this relationship has been derived only by the formal treatment of the theory of rate process basing on drastic assumption, it would be interesting to see how it can be applied for the sodium silicate solution. Fig. 7 exhibits the dependence of $\Lambda\eta$ on concentration, again for the molar ratio 1.00 and 3.95 solutions. The figure

4) S. Glasstone, K. J. Laidler and H. Eyring, "The theory of rate process", McGraw-Hill Book Co., New York, N. Y., 1941, First Edition.

5) This formula was derived for a single ion as follows, $\Lambda=uF$, $u$ is a mobility of ion under unit potential and related to diffusion coefficient $D_i$ as $u=D_ize/kT$. Then $\Lambda=D_izF^2/RT$. From the reaction rate theory $D_i=\kappa\cdot V^{2/3}/N$, where $\kappa$ is the specific rate constant, expressed as $\kappa=kT/h\exp(-\Delta F/RT)$, hence, $\Lambda$ is given as
$$\Lambda=V^{2/3}z\cdot F^2\times10^7/h\exp(-\Delta F/RT)$$
Therefore, strictly, $D_i$ should be the sum of that for each component ion, and herein the sum of averages was taken.

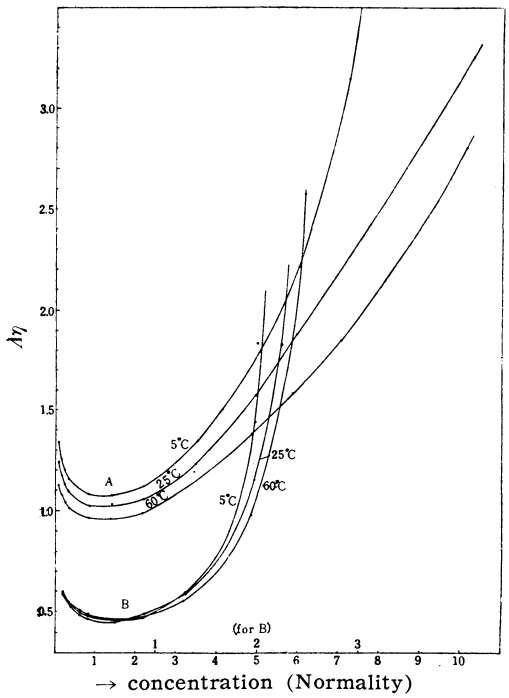



Fig. 7. Variation of the product of equivalent conductivity and viscosity with concentration for the sodium silicate solutions of molar ratio.
A: 1.00 B: 3.95

shows that $\Lambda\eta$ decreases a little in dilute concentration region and becomes constant over a certain range, then begins to increase above the value marked at start point up to a remarkably large one. The initial decreasing part of $\Lambda\eta$ curves is thought to have been brought about by the increase in molal volume with concentration as expected from the equation (3). Also, the smaller value of $\Lambda\eta$ for the high molar ratio solution may well be ascribed to the larger molal volume of the solution, as compared with the lower molar ratio ones, while the increase in $\Lambda\eta$ with concentration which takes place above a certain concentration, would predict that the change in activation free energy with concentration become different between conductance and viscous flow. All these trends seem quite similar to those found with simple strong electrolytes[6] except the fact that the degree of rise in $\Lambda\eta$ with concentration approaches a much larger value than the degree for those solutions. It is noticeable, however, that within the moderate concentration range the value of $\Lambda\eta$ spreads for all the systems only in narrow range, viz. between about 0.5 and 1.0, thus well satisfying the requirement of equation (3). As for the variation of $\Lambda\eta$ with temperature, that of the higher molar ratio solution seems independent of temperature as expected from the equation (3) except at higher concentration range. That $\Lambda\eta$ for the 1.00 molar ratio solution decreases with temperature even at low concentration range can be well attributed to the effect of OH ion, $\Lambda\eta$ of which, as stated in the previous paper, decreases with temperature rise even at infinite dilution.

Thus it may be understood that as a whole, the tendency of curves in Fig. 7 shows no speciality which distinguishes them from those for the simple electrolyte solutions. Merely the concentration above which $\Lambda\eta$ begins to increase markedly lies in lower range than with those solutions. From the comparative study on Fig. 5, 6, and Table I it is found that the concentration, where $E\eta$ exceeds $E_\lambda$ is almost the same as the above-mentioned concentration read in Fig. 7. They were about 1.45, 1.05 and 0.95 N for the solutions of molar ratio 2.13, 3.19 and 3.95 respectively. The value for the last one may be favorably compared with 0.8–0.9 N, above which the equivalent conductivities theoretically computed no longer agree with those observed experimentally and tend to fall increasingly below the latter. For the lower molar ratio solutions two curves in Fig. 5 and 6 never cross, and the similar curves to that in Fig. 7 indicate that the concerned concentration for molar ratio 1.00 and 1.55 are about 2.15 and 1.85 N respectively. It is interesting to compare these values with 5 to 6 N for $NaClO_4$, NaSCN, and NaI, which were recently reported by Miller.

## Discussion

**The Structure of Concentrated Sodium Silicate Solutions as Interpreted by the Mechanisms of Conductance and Viscous Flow.**—The foregoing results revealed that the mechanisms of conductance and viscous flow become different above a definite concentration range for all the systems studied. Herein, discussion has been made as to the actual behavior of the solutions in this concentration region.

Despite the theoretical incompleteness, it is widely accepted that the concentrated electrolyte solutions may be closely modeled after molten salts in view of the fact that they retain short range local order in component distribution, taking quasi-crystalline structure, where anion is most likely considered to play the predominant roll, due to its superiority in ion size to cation. In such a state, cation takes over progressively of the conduction. Thus, the flow of solution begins to be disturbed more and more by anion arrangement, consequently to need larger activation energy, while conductance is still performed in increasing proportion by cation so that its activation energy does not vary very much. Since the silicate ions, as already reported, are much larger than the sodium ion, particularly in the

6) M. L. Miller, *J. Phys. Chem.*, **60**, 186 (1956).

high molar ratio solutions, it would be quite reasonable to expect that this quasi-crystalline structure may be established even at lower concentration with a greater degree, as compared with simple strong electrolyte solutions. Then, with the higher molar ratio sodium silicate solution, as concentration increases above a certain limit, one silicate ion begins to get contact with another so as either to get combined by hydrogen bond or mechanically tangled, thus leading to the establishment of even rigid structure due to a kind of net work at comparatively low concentration, such as to allow the sodium ion to pass freely through its meshes. This situation is best represented in the 3.95 molar ratio solution which has at 2.88 N viscosity of 650 c.p., $E_\eta$ of 180 kcal., and yet $E_\lambda$ of only 5.5 kcal., and at 3.07 N $E_\lambda$ of 5.64 kcal. and viscosity more than 10,000 c.p.. On the other hand, a lower molar ratio solution contains rather small silicate ions together with considerable amount of OH ions, therefore it cannot afford to form net work structure,

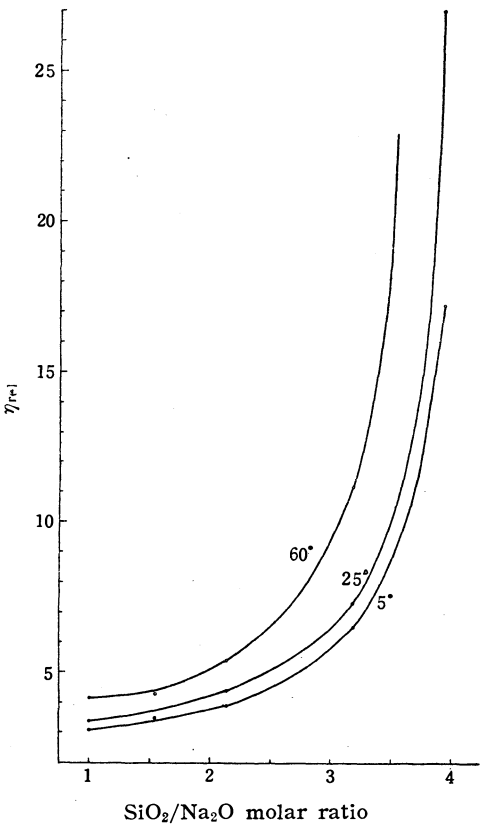



Fig. 8. Viscosity change with molar ratio of sodium silicate solutions at the concentration where maximum specific conductivity is given.

thus the rigid state as seen in the higher molar ratio one may not be yielded even at strikingly high concentration where solutions are packed so closely that sodium ion itself can no longer move with ease. Hence, $E_\lambda$ reaches much larger values than with the high molar ratio solutions, while increase of $E_\eta$ is not so great as with these ones, being parallel with that of $E_\lambda$ over a wide concentration range. For the comparison of the behavior of various molar ratio solutions, in Fig. 8, the viscosity of solutions at a concentration where maximum specific conductivity was shown, and in Fig. 9, the equivalent conductivity together with $E_\lambda$ at a concentration where the solutions exhibit the same

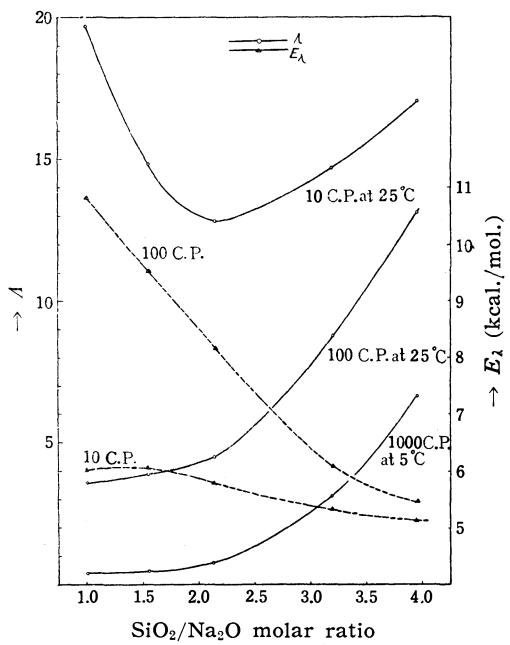



Fig. 9. Iso-viscosity curves 1. Equivalent conductivity 2. Activation energy of conductance—molar ratio relationships.

viscosity, were plotted against the molar ratio. It is recognized that the higher molar ratio solutions have the greater equivalent conductivity than with the lower molar ratio ones if compared on the same level of high viscosity.

It would be worth while to estimate the average interionic distance at the highest concentration measured of the molar ratio 1.00 and 3.95 solutions. Assuming the existence of three mole ions in one mole solution, they are calculated as 4.75 Å and 7.11 Å for 10.3 N of the 1.00 molar ratio solution and 3.07 N of the 3.95 molar ratio one.

When the values computed previously of the diameter of corresponding silicate ion, i.e., 7.2 Å and 9.2 Å, are subtracted from the values of three times the foregoing data, there remain 7 Å and 12 Å for two sodium ions in respective solutions. Since the diameter of hydrated sodium ion is supposed to be about 2.5 Å–3.0 Å it is seen that little space is left for the free passage of sodium ion in the former solution, whilst there are still available spaces for the movement of sodium ion in the latter solution. Further, this condition may well be understood if the $E_\lambda$ of the concentrated sodium silicate solution is compared with those observed for the molten alkali silicates the latter being 10–11 kcal. for all the liquid of silica-alkali weight ratio of 1.5–3.0, according to O'M Bockris et al.[7]. This value of $E_\lambda$ for molten silicates is much larger than 5.64 kcal. for the 3.95 molar ratio solution at 3.08 N, but lower than 12.4 kcal. for the 1.00 molar ratio one at 10.3 N. Considering these figures and the fact that $E_\lambda$ is about 5 kcal. for the simple strong electrolyte solutions at 10 N, water in the highly concentrated solution of lower molar ratio seems no longer to be regarded as the solvent but only as a part of kinetic entity as hydration sheath, whereas it is still available as a solvent for the higher molar ratio solution at high concentration, such as to form rigid structure.

**The Application of Absolute Reaction Rate Theory to the Conductance of the Concentrated Sodium Silicate Solutions of Molar Ratio 3.95**—Now that it seems reasonable to presume that only sodium ion carries electricity under an electric field in the concentrated sodium silicate solutions of high molar ratio, the calculation was attempted in the following of the energy barrier, namely, activation free energy of conductance $\Delta F_\Lambda$ on the basis of the absolute reaction theory. Since it is impossible to calculate the height of the energy barrier by means of quantum mechanics in such a complicated system, this height was determined from the experimental conductivity according to the method employed by Eyring in case of the proton transfer in aqueous solution.

When a field having an effective potential gradient $\Phi$ is applied, the specific reaction rate at an angle $\theta$ to the direction of the field is given by $\kappa=kT/h \exp[-(\Delta F-\delta F)/RT]$ where $\delta F$ is defined by $\delta F=\Phi\cos\theta\times d\times 23060$, $d$ being half the distance between the initial and the final state along the reaction coordinate. Since the distance travelled by an ion in the direction of the applied field is $2d\cos\theta$, the velocity of an ion in cm/sec, $v$, is:

$$v=2d\cdot\cos\theta\cdot kT/h\cdot\exp(-\Delta F/RT)\cdot \exp(a\cdot\cos\theta)$$

where $a\equiv\Phi\cdot d\times 23060/RT$.

This equation applies to motion in one direction only and to obtain the distance moved in the direction of the field it is necessary to take the average over all angles,

$$v=2d\,kT/h\,\exp(-\Delta F/RT)\times\frac{\int_0^\pi \exp(a\cdot\cos\theta)\cdot\cos\theta\cdot\sin\theta\cdot d\theta}{\int_0^\pi \sin\theta\cdot d\theta}$$

as the quantity $a$ is very small, so that it is possible to write $\exp(a\cdot\cos\theta)=1+a\cdot\cos\theta$, and hence

$$v=2d\cdot kT/h\cdot\exp(-\Delta F/RT)\cdot a/3.$$

As $\Lambda=vF$ then

$$\Lambda=2/3\cdot dF\cdot a\cdot kT/h\cdot\exp(-\Delta F/RT). \quad (4)$$

The effective potential gradient in the liquid $\Phi$ has been suggested to be placed equal to $(\varepsilon+2)/3$ for an applied potential gradient of 1 V/cm, where $\varepsilon$ is the dielectric constant of the solution. Difficulty arises, however, in knowing the dielectric constant of the solution. Hasted, Ritson and Collie[8] derived for this the equation $\varepsilon=\varepsilon_w+2\bar{\delta}C$, where $\varepsilon_w$ is the dielectric constant of solvent water, $\bar{\delta}$ half the molar depression of dielectric constant of water by electrolyte. This linear relationship is said to hold up to 2 N concentration. Though no data are available for the silicate ion, $\varepsilon$ was calculated using this equation with the assumption that $\bar{\delta}=10$ for sodium silicate, a comparable value to those for NaOH and $Na_2SO_4$, considering the extent of hydration. As to $2d$, i.e. the distance travelled by an ion in the conduction process in overcoming one potential energy barrier, it may be taken either as the average dimensions of water molecule or as that of $SiO_4$ tetrahydra, the former being 3.1 Å, the latter 3.2 Å. Therefore $d=1.6$ Å was used reasonably. The equation (4), then, is expressed as:

$$\Lambda=3.98\times10^3\times\exp(-\Delta F/RT)$$
$$=3.98\times10^3\times\exp(-\Delta H/RT)\exp(T\Delta S/R)$$

7) J. O'M. Bockris, J. A. Kitchener, S. Ignatowitcz and J. M. Tomlinson, *Trans. Farad. Soc.*, **48**, 75 (1952).

8) J. B. Hasted, D. M. Ritson and C. H. Collie, *J. Chem. Phys.*, **16**, 1 (1948).

TABLE II

| $C$ (Mol./l.) | $\Lambda$ | $\Delta F$ (kcal.) | $\Delta H$ (kcal.) | $\Delta S$ (e.u.) | $\eta$ | $\Delta F_\eta$ (kcal.) | $\Delta H_\eta$ (kcal.) | $\Delta S_\eta$ (e.u.) |
|---|---|---|---|---|---|---|---|---|
| 1.53 | 11.64 | 5.12 | 5.70 | 1.9 | | | | |
| 1.44 | 12.72 | 5.09 | 5.59 | 1.7 | 650.1 | 6.17 | 179.8 | 583 |
| 1.35 | 13.60 | 5.07 | 5.53 | 1.5 | 74.11 | 4.88 | 15.61 | 36.0 |
| 1.25 | 14.81 | 5.04 | 5.38 | 1.1 | 27.52 | 4.29 | 9.78 | 18.4 |
| 0.983 | | | | | 6.22 | 3.40 | 6.31 | 9.77 |
| 0.646 | | | | | 2.36 | 2.80 | 4.97 | 7.28 |
| 0.443 | | | | | 1.60 | 2.56 | 4.40 | 6.19 |

$\Delta H$ is heat of activation and may be taken approximately as equal to the experimental activation energy $E_\Lambda$[9], and $\Delta S$ the activation entropy. In table II the results of calculation for $\Delta F$ and $\Delta S$ are shown along with the experimentally observed $\Lambda$ and $\Delta H$ for the 3.95 molar ratio solution at several high concentrations. Also the same terms for viscous flow were computed from the equation (1), using the average molar volume over all the solute ions and solvent one, as V.

It is visualized that the activation free energy of conduction is almost the same as the activation energy which was obtained experimentally; that is, the entropy in the activated state is only slightly larger than in the equilibrium state, while the activation entropy of viscous flow increases rapidly with concentration. This implies that in order to cause the viscous flow some short range local order should be broken down; on the other hand, for the conduction process it is scarcely necessary to disrupt this structural order. Thus, the entropy behavior may be interpreted as the evidence of the occurrence of this local order which does not disturb the passage of sodium ion under electric field. Consequently this confirms the foregoing discussion.

## Conclusion

The activation energies of conductance and viscous flow, $E_\lambda$ and $E_\eta$, were computed from the experimental results of temperature dependence of conductivity and viscosity for the sodium silicate solutions of various molar ratio. And it was found that as concentration increases above a definite range, $E_\eta$ becomes progressively larger than $E_\lambda$, to the greater extent with the higher molar ratio solutions, and that the product of equivalent conductivity and viscosity may be regarded almost as independent of concentration and temperature below a definite concentration range, above which it increases rapidly. This critical concentration range for the 3.95 molar ratio solution approximately coincides with that, below which the equivalent conductivities theoretically computed agree with those experimentally observed.

These results were considered to show that in the concentrated sodium silicate solutions, short range local order comes to be established so as to make a quasi-crystalline structure in which silicate ions take a predominant role. This tendency is greater for the higher molar ratio solution, where the arrangement of silicate ions proceeds until it yields even rigid net work structure, while sodium ion can still freely pass through the meshes.

Assuming this model for the concentrated sodium silicate solution of molar ratio 3.95, the activation free energy and entropy were calculated from the conductivity at high concentration region, using the absolute reaction rate theory. The results also confirmed the above interpretation.

Thus, it may be concluded that the electric conductance behavior of the sodium silicate solutions could be explained by regarding them as a kind of strong electrolyte solution over an entire range of concentraion, since within the moderate concentration range the conductivity could be theoretically accounted for, and even at the higher concentration, as described above its behavior would not be different essentially from those seen with simple strong electrolyte solutions, if the difference of anion size and extent of hydration is considered.

The author wishes to express his sincere thanks to Dr. Tadashi Yawataya for his kind support throughout this work.

*Research Laboratory Asahi Glass Co. Ltd. Tsurumi, Yokohama*

9) $E_\Lambda$ may be related to $E_\lambda$ as follows, since $\Lambda=1000/(w\rho/M)$, where $w$ is weight of solute per 1000 g solution, $\rho$ density of solution, $M$ molecular weight of solute. Then, $d\ln\Lambda/d(1/T)=d\ln\lambda/d(1/T)-d\ln\rho/d(1/T)$, $-E_\Lambda/R=-E_\lambda/R+T^2/\rho\cdot d\rho/dT$. If $\rho$ is expressed as $\rho=\rho_0[1+\alpha(T-T_0)]^{-1}$, then, $E_\Lambda=E_\lambda+RT^2[1-\alpha(T-T_0)]$. As $\alpha$ is the order of 0.01%, the difference between $E_\Lambda$ and $E_\lambda$ is not large.

# *Effect of the Addition of Some Carbohydrates on the Decomposition Rate of Sodium Aluminate Solutions with Seeding**

By Taichi SATO

(Received December 26, 1956)

## Introduction

The Bayer process is today the most widely used method for the production of alumina. Of this process it is usually said that the precipitation of crystalline aluminum hydroxide from a sodium aluminate solution is actually performed in the presence of organic matter[1-3]. When alumina hydrate in bauxite is dissolved with a solution of caustic soda, some organic matter found in bauxite such as humus etc. dissolves too and accumulates in the alkali solution. Two methods have been proposed to avoid this phenomenon. The first is the destruction of organic matter by a calcination of bauxite at temperatures from 350° to 400°C before grinding. The second is the separation of organic matter by concentrating an alkali solution after the precipitation cycle.

Recently, however, the calcination of bauxite before grinding is not carried out in most of the alumina plants. The omission of this calcination is a debatable problem. At present, we can not answer whether this calcination will be necessary or not. From an industrial view point, the effect of the presence of organic matter on the precipitation of aluminum hydroxide from a sodium aluminate solution has an important meaning as it relates to the problem of the necessity of calcination. On the other hand this study will, beside being an academic problem, give us interesting results with regard to crystal growth and to reaction between inorganic compound, organic matter, etc. But the reports on this problem are few till now, because the phenomenon in which the presence of organic matter has influence on the precipitation of aluminum hydroxide from a sodium aluminate solution is a complicated one. Therefore this study was undertaken as the continuation of the writer's former studies[4], and it has the object of investigating fundamentally the influence of the presence of organic matter on the decomposition of sodium aluminate solution. As the first step, the investigation on the decomposition rate of sodium aluminate solution with seeding and some carbohydrates has been made.

## Experimental Methods

Various amounts (0.1, 0.3, 0.5, 1, 3, 5, 10 and 20 g./l.)*1 of glucose, sugar and starch as the representatives of carbohydrate were added to sodium aluminate solution (NaOH 140.0 g./l., $Al_2O_3$ 105.0 g./l., mol. ratio $Na_2O/Al_2O_3=1.7$). These solutions were decomposed with seeding of hydrargillite*2 (5 or 10 %*3) at a temperature of 30°C, and those decomposition rates were measured. Here the decomposition rate is given by a change of decomposition ratio expressed as follows;

$$\frac{x_1-x_2}{x_1}\times 100(\%)$$

where $x_1$ and $x_2$ are the concentrations of alumina contained in sodium alminate solutions before and after decomposition.

The carbohydrates used were as follows. Glucose of dehydrated reagent class, and cane sugar was purified by a reprecipitation of ordinary sugar obtained in the market. Starch was made by refining white potato. The contained moistures were measured with Abderhalden's drying apparatus*4. The obtained values were as follows; 0.26 % in glucose, 1.25 % in sugar and

* This paper is written as the 16 th report of Studies on the Hydrolysis of Sodium Aluminate Solutions.

A partial report was made at the Autumn Meeting of Kanto Subgroup of the Chemical Society of Japan, held in Tokyo on November 6 th, 1955.

1) "Gmelins Handbuch der anorganischen Chemie", Nr. 35,Al[B], (1933), S. 34.

2) J. D. Edwards, F. C. Frary and Z. Jeffries, "Aluminum Industry, Aluminum and its Production", Mc. Graw-Hill, New York (1930), p. 128, 160.

3) F. Ullmann, "Enzyklopädie der technischen Chemie", Bd. I, (1928), S. 306.

*1 These values designate net weight of carbohydrate exclusive of moisture.

4) T. Sato, *J. Chem. Soc. Japan (Ind. Chem. Sect.)*, **54**. 266, 755 (1951); **55**, 66, 198 (1952); **56**, 399, 478, 743, 840 (1953); **57**, 20 111, 355, 540. 805 (1954); **58**, 325, 556 (1955).

*2 This was previously precipitated by decomposition with seeding of sodium aluminate solution of NaOH 140.0 g./l., $Al_2O_3$ 105.0 g./l., mol. ratio $Na_2O/Al_2O_3=1.7$ at 30° C.

*3 This is a percentage to the amount of alumina contained in sodium aluminate solution.

*4 Aceton was used.

18.47 % in starch. These substances were added to sodium aluminate solution in the dry state.

The method of decomposition of sodium aluminate solution with seeding is as follows[5]. Sodium aluminate solution was prepared by the dissolution of aluminum (99.85 %) into a solution of caustic soda (NaOH 140.0 g./l.). 250 cc. of the solution was put in a wide-mouthed bottle of 500 cc. capacity and it was agitated with a seed charge of the prepared hydrargillite in a constant temperature water bath. The amount of alumina contained in sodium aluminate solution was determined gravimetrically.

As the viscosity of sodium aluminate solution may be influenced by the swelling of added starch particles, it was measured with Ostwald's viscosimeter at a temperature of 30°C. In this case its viscosity has to be measured after the attainment of swelling-equilibrium of starch particle. Therefore, at first, the swelling behavior of starch was investigated, and then the time within which the starch particle will attain the swelling-equilibrium was determined. Namely 1 g./l. of starch added to the caustic soda solution of prescribed concentration (NaOH 140.0 g./l.) was swollen under agitation at a temperature of 30°C. the same as in the case of decomposition with seeding of sodium aluminate solution, and the viscosity of its solution was measured after some prescribed times. Next, the sodium aluminate solutions containing 1, 3, 5 and 10 g./l. of carbohydrates were left for a prescribed time*5, and then these amounts of viscosity were measured.

## The Effect of the Addition of Carbohydrate on the Decomposition Rate

The decomposition rates, with seeding of 5 % hydrargillite, of sodium aluminate solutions containing glucose, sugar and starch are given in

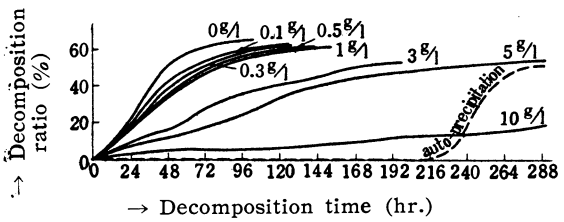



Fig. 1. Effect of addition of glucose on decomposition rate with 5% seeding.

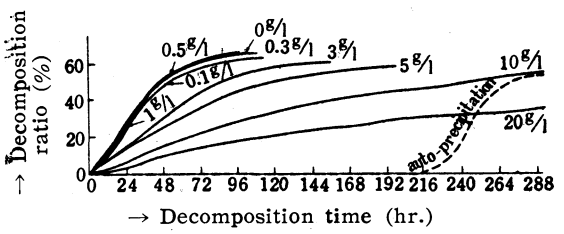



Fig. 2. Effect of addition of sugar on decomposition rate with 5 % seeding.

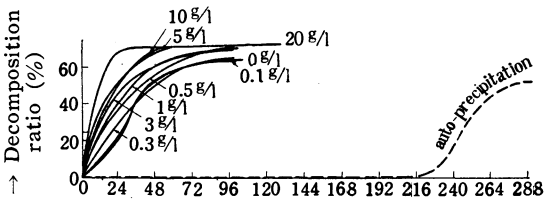



Fig. 3. Effect of addition of starch on decomposition rate with 5 % seeding.

Figs. 1, 2 and 3. Furthermore the decomposition curve of auto-precipitation is shown in these Figs.

Fig. 1 shows that the addition of glucose gives a retarding action on the decomposition with seeding, and that its action grows with the increase of the added amount. Thereafter the decomposition rate with the addition of 10g. glucose/l. is much smaller than in the case of auto-precipitation. Fig. 2 shows that the addition of sugar retards the decomposition of sodium aluminate solution as in the case of the addition of glucose. In this case we observe the tendency that the decomposition is retarded with the increase of the added amount but with the exception of the addition of 0.3, 0.5 and 1 g. sugar/l. As the addition of 0.3, 0.5 and 1 g. sugar/l. are considered the same, with no addition in the decomposition curves, the addition of 0.1 g. sugar/l. will have no influence on the decomposition. Though the tendency of Fig. 3 is different from those of Fig. 1 or 2, yet Fig. 3 suggests that the addition of starch promotes the decomposition. The decomposition is not promoted with the addition of 0.1 g. starch/l., but it begins to be promoted with the addition of 0.3 g. starch/l. Then the decomposition rate is rapidly improved with the addition of more than 0.5 g. starch/l. However, on the addition of starch to sodium aluminate solution its viscosity becomes as large as Fig. 9 indicates.

In order to investigate the actions on the decomposition of glucose, sugar and starch in all of the results of Figs. 1, 2 and 3, the comparison of decomposition rate with the addition of 1, 5 and 10 g./l, for example, is made in Fig. 4.

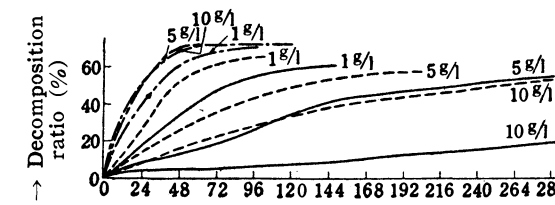



Fig. 4. Comparison of decomposition rate with 5 % seeding in presence of 1, 5 and 10 g./l. of glucose, sugar and starch respectively.
..... glucose
- - - - sugar
— - — starch

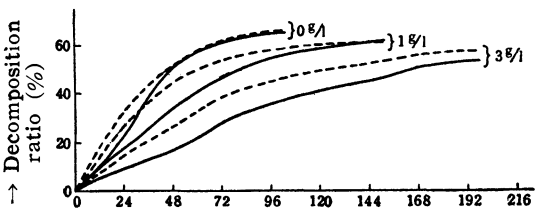
5) T. Sato, *J. Chem. Soc. Japan (Ind. Chem. Sect.)*, **58**, 325 (1955).

*5 This time is six hours in Fig. 8.

Fig. 4 shows that the retarding action of glucose is obviously larger than that of sugar. In Fig. 4 the decomposition rate with the addition of 5 g. glucose/l. coincides with those of the addition of 10 g. sugar/l. Such a result may be due to the difference in molecular formulas ($C_6H_{12}O_6$ and $C_{12}H_{22}O_{11}$) of glucose and sugar. Because the numbers of molecules of glucose contained in the same weight are about twice the number in the case of sugar.

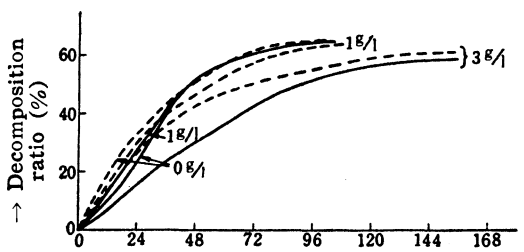
### Relation between the Amount of Seed and the Addition of Carbohydrate

As Figs. 1, 2, 3 and 4 are given with 5% seeding, the decomposition rate was next investigated with 10% seeding. Then the comparison of decomposition rate between 5 and 10% seeding was made with the addition of carbohydrate. In this experiment the added amounts of carbohydrates were 1 and 3 g./l. in the case of glucose or sugar, and 0.5, 1, 3 and 5 g./l. in starch. These results are given in Figs. 5, 6 and 7.




→ Decomposition time (hr.)

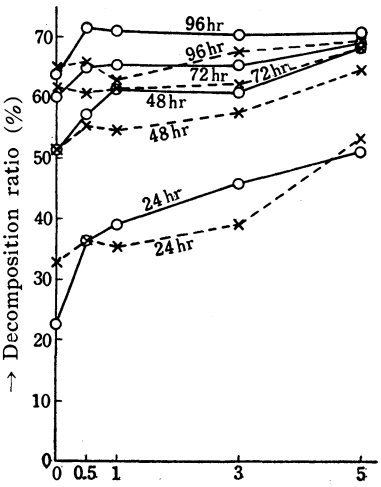
Fig. 5. Relation between amount of seed and addition of glucose.
—— 5% seeding
--- 10% seeding




→ Decomposition time (hr.)

Fig. 6. Relation between amount of seed and addition of sugar.
—— 5% seeding
--- 10% seeding

Fig. 5 shows that the decomposition rate with 10% seeding is larger than that of 5% seeding by the addition of glucose. This result suggests that the presence of seed charge acts stronger on the decomposition than glucose does. Fig. 6 shows that though with an exception of addition of 1 g. sugar/l., the decomposition rate with much seeding is larger than that with a little seeding on the addition of sugar the same as in the case of glucose. On the addition of starch




→ Added amount of starch (g./l.)

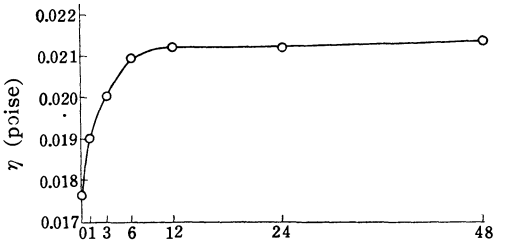
Fig. 7. Relation between amount of seed and addition of starch.
○ 5% seeding
× 10% seeding

as shown in Fig. 7, 10% seeding promotes the decomposition the same as 5% seeding, but its effect is smaller than the effect of 5% seeding.

### Discussion

From the above-mentioned results it is obviously seen that the addition of glucose or sugar retards the decomposition of sodium aluminate solution, and that the addition of starch promotes its decomposition. But the viscosity of sodium aluminate solution is improved with the addition of starch. Hence the viscosity of sodium aluminate solution containing carbohydrate was measured in order to investigate the effect of the viscosity of solution on the decomposition. On the addition of starch to sodium aluminate solution, as starch particle is steadily swollen by alkali, the viscosity of the solution in the swelling-equilibrium of starch is different from that which occurs before swelling. W. Ostwald and G. Frenkel[6] reported that the swelling of starch by alkali had taken a long time to attain the equilibrium. C. E. Mangels and C. H. Bailey[7] measured the viscosity of the solution left for three hours after the addition of alkali to starch particle, and H. Suzuki and N. Taketomi[8] measured the viscosity of solution left for from five to ten minutes after the addition of alkali. In these studies, however, the concentration of alkali solutions are below 1 N, and they are not so high as this study treats. Hence the viscosity of sodium

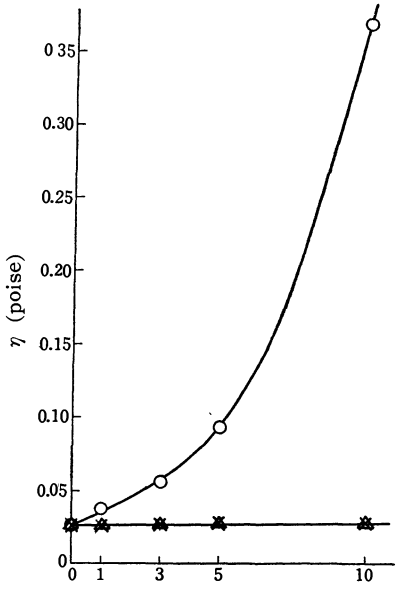
hydroxide solution (NaOH 140.0g./l.) with the addition of 1 g.starch/l. has been measured in order to investigate the swelling behavior of starch. This result is given in Fig. 8.




→ Swelling time (hr.)

Fig. 8. Swelling behavior of starch in sodium hydroxide solution at 30°C. (1 g./l. of starch in NaOH 140.0 g./l.)

Fig. 8 shows that the starch particle may attain the equilibrium of swelling within about from six to twelve hours. Therefore the viscosity of sodium aluminate solutions with the addition of carbohydrates have been measured, six hours after their addition to the solution. These results are contained in Fig. 9.




→ Added amount of carbohydrate (g./l.)

Fig. 9. Changes of viscosity of sodium aluminate solutions in presence of glucose, sugar and starch at 30°C.
△ glucose
× sugar
○ starch

Fig. 9 shows that the viscosity of sodium aluminate solution is not improved with the increase in an added amount of glucose or sugar, and that it is very much influenced by the addition of starch. However the viscosity of sodium aluminate solution with added starch may be improved by the swelling of starch at first, and then it may be rapidly lowered with the hydrolysis of starch initiated by the action of alkali, because the concentration of alkali is high. Though the viscosity of solution is almost unchanged after the swelling as shown in Fig. 8, then starch will not be influenced by alkali for the period of decomposition with seeding in this study. These results suggest the viscosity of solution is not a factor of first order for the decomposition.

On the one hand, from the results of decomposition rate, the action of starch on the decomposition is obviously different from that of glucose or sugar. Hence, the writer thinks, glucose or sugar (or their oxidation products by alkali in solution) binds with $Al^{3+}$ or $Al(OH)_3$ molecules, and they must be soluble in solution forming some compounds (for example such as saccharate). R. K. Gupta and H. E. Buckley[9] who investigated the effect of the presence of dye on the solubility of a solution considered a binding of dye and solute. The writer believes this idea may be applied to this study too. However, if the phenomena in this study should be discussed only by Gupta's thought, this decomposition has to give us such an induction period as auto-precipitation[10], because the addition of glucose or sugar makes lower the degree of supersaturation of alumina to caustic soda in solution. Auto-precipitation has an induction period and is rapidly promoted after passing that period. On the other hand, the seeding decomposition with the addition of glucose or sugar has not an induction period, and it progresses very slowly. This shows obviously the difference of decomposition mechanism between auto-precipitation and seeding decomposition with the addition of carbohydrate. In auto-precipitation, crystal nuclei are gradually formed in an induction period, and then the formation of these certain definite numbers promotes

6) W. Ostwald and G. Frenkel, *Kolloid-Z.*, **43**, 296 (1927).
7) C. E. Mangels and C. H. Bailey, *J. Am. Chem. Soc.*, **55**, 1981 (1933).
8) H. Suzuki and N. Taketomi, *J. Chem. Soc. Japan (Ind. Chem. Sect.)*, **59**, 45 (1956).
9) R. K. Gupta and H. E. Buckley, *Z. physik. Chem.*, **204**, 165, 175 (1955).
10) T. Sato, *J. Chem. Soc. Japan (Ind. Chem. Sect.)*, **54**, 755 (1951).

rapidly the precipitation of aluminum hydroxide. On the addition of glucose or sugar these bind with solutes in solution, and the degree of supersaturation of alumina to caustic soda becomes lower. Further, in this case, the activity of seed is decreased by a binding of seed charge and these carbohydrates. Therefore it seems that the formation of new crystal nuclei is retarded on the seeding decomposition with the addition of glucose or sugar. But it is obviously seen from the decomposition curves of Figs. 5 and 6 that the binding of glucose or sugar with solute is weak. In the meanwhile, it is observed from Fig. 4 that the binding between glucose and solute is stronger than that of the binding between sugar and solute.

On the other hand, the action of starch on the decomposition will be considered in relation to the facts[11] that starch is added in order to promote the separation of red mud from sodium aluminate solution. The starch added to the solution will bind with seed charge at first. E. Herrmann and others[12,13] who studied the separation of red mud in the sodium aluminate solution with the addition of starch as one of the colloid-chemical problems, pointed out that the addition of 0.25 g. starch/l. gives the optimum aggregation to red mud, and that at high starch concentration starch acts as a protective colloid for individual particles. Therefore, in this study too, more or less amounts of added starch will have a great influence on the agglomeration of particles. As the starch particle is apt to suffer hydration, it is chemisorped by $OH^-$ on the surface of seed and it causes the aggregating phenomena of individual particles by the bridge action towards other particles. When starch particles chemisorped on the surface of seed are increased, these act as a protective colloid for individual particles and disturb the aggregation of particles. However, as the active surface of seed is diminished by the absorption of starch on its surface, the decomposition with seeding of sodium aluminate solution is retarded, and the effects on the decomposition grow remarkably with the increase in the added starch. And then the decomposition is evidently promoted with the addition of starch as shown in Figs. 3 and 7. Therefore, in the opinion of the present writer the presence of starch in itself must have a promotive action*6. From the above discussion this writer believes two counter phenomena play an important role in the action of starch on the decomposition rate. First, starch is retarding in the active surface diminished by the chemisorption on the surface of seed-crystallites (negative action). Second, starch is promoting in some way on the decomposition rate (positive action). As mentioned above, Fig. 7 shows that the decomposition rate with 5 % seeding on the addition of starch is larger than that of 10 % seeding. This may owe to aggregating phenomena of seed caused by starch. It seems that the condition of this experiment with 5 % seeding and starch addition has not been necessary (for example, the dispersed concentration of seed in solution) to get the aggregation by starch-bridge. Therefore, as seed charge of 10 % seeding is aggregated by starch more than in the case of 5 % seeding, the surface area of seed under 10% seeding may be diminished by the formation of a big agglomeration of particles.

Moreover the sedimentation behavior of a particle precipitated by the decomposition of sodium aluminate solution with seeding and starch addition has been investigated. Consequently the sedimentation behavior of a particle precipitated with 5 % seeding indicates an aggregated sedimentation (that is, suspension layer settles in forming clearly a boundary from dispersed phase), and that of 10 % seeding points a tendency of free sedimentation (that is, with the state of suspension, dispersed particles settle steadily from a large particle to a small one, and a boundary of suspension layer is not clear). As these results may be closely connected with the action mechanism of starch, the writer intends to investigate these problems in his next report.

In this study the influence of temperature on carbohydrate need not be considered, because the decomposition of sodium aluminate solution has been made at the temperature of 30°C.

## Summary

In order to study the influence of the

11) W. Kerr, "Chemistry and Industry of Starch", Academic Press, Inc., New York (1950), p. 645.
12) E. Herrmann, I. Dvornik, O. Korelić and V. Matković, *Kolloid-z.*, **123**, 22 (1951).
13) I. Dvornik and E. Herrmann, ibid., **128**, 75 (1952).

*6 It seems that the effect of starch on the decomposition is owing to amylose or amylopectin. This point will be investigated in a later report.

presence of the organic matter in a sodium aluminate solution the decomposition rate was investigated by the addition of some carbohydrates as first step of study. Three kinds of carbohydrate, i. e. glucose, sugar and starch (white potato) were chosen and added to a sodium aluminate solution in verious amounts. These solutions were decomposed with seeding of hydrargillite, and these decomposition rates were compared in each case. Consequently it had been observed that the addition of glucose or sugar acts to retard the decomposition, and that the increase of an added amount of starch promotes the decomposition. But the retarding action of glucose is larger than that of sugar. On the other hand, the relation between the added amount of seed and the addition of carbohydrate was investigated. It had been seen that the presence of seed is stronger than that of glucose or sugar in the action of decomposition, and that this relation is different upon the presence of starch. Further the viscosity of sodium aluminate solution mixed with carbohydrate was measured. It has been observed from this measurement that the viscosity of sodium aluminate solution is almost unchanged with the addition of glucose or sugar, and that its viscosity is improved with the addition of starch. Then these results have been compared with the decomposition rate. From this result, it is concluded that the viscosity of solution does not always act on the decomposition as the factor of first order. Hence the action mechanism of these carbohydrates on the decomposition are discussed, and it is clearly concluded that there is a very large difference among the actions of each carbohydrate on the decomposition. In these results one must obtain some informations upon the action mechanism on the decomposition of sodium aluminate solution in the presence of organic matter.

The author wishes to express his hearty thanks to Dr. Erich Herrmann of Martinswerk G. m. b. H., Bergheim and Mr. Siniša Maričić of Institute of Physics Zagreb for their very helpful discussion.

*Government Chemical Industrial Research Institute Tokyo*
*Yoyogi p.o. Tokyo*

# *Microcolorimetric Determination of Organic Sulfur by the Tin(II)-Strong Phosphoric Acid Reduction Method*

By Toshiyasu KIBA, Ikuko AKAZA, née KISHI and Sachiko TAKI

(Received January 9, 1957)

It has long been desired by organic, biological, and medical chemists that some rapid and accurate methods for the determination of minute amounts of sulfur in organic and biological materials might be developed. The determination of organic sulfur ordinarily consists of two steps, i.e. the oxidation of the sulfur to sulfate and the estimation of the sulfate. However, oxidation of organic sulfur requires time, skill and patience even by the use of an elaborate apparatus and powerful reagents, and, furthermore, reliable estimation of the sulfate is not always easy, whether it is worked out colorimetrically or turbidimetrically. If the oxidation of organic sulfur can be completed under mild conditions with the use of an open vessel, and if the resulting sulfate can be reduced to hydrogen sulfide in some simple way, the determination of the organic sulfur will become easier and more sensitive. Although various oxidizing and reducing procedures have been proposed for this purpose[1-11], they are so

1) R. K. Siegfriedt, J. S. Wiberley and R. W. Moore, *Anal. Chem.*, **23**, 1008 (1951).
2) E. Kahane, *Oster. Chem-Ztg.*, **55**, 209 (1954).
3) E. Kahane and M. Kahane, *Bull. Soc. Chim.*, **1**, 280 (1954).
4) E. Woloensky, *Ind. Eng. Chem.*, **20**, 1234 (1928).
5) G. F. Smith and A. G. Dean, *Ind. Eng. Chem. Anal. Ed.*, **4**, 227 (1932).
6) P. O. Bethge, *Anal. Chem.*, **28**, 119 (1956).
7) I. S. Lorant, *Z. Physiol. Chem.*, **185**, 245 (1929).
8) C. L. Luke, *Ind. Eng. Chem. Anal. Ed.*, **15**, 602 (1943).
9) H. Roth, *Mikrochimie ver. Mikrochim. Acta*, **36-37**, 379 (1951).
10) C. M. Johnson and H. Nishita, *Anal. Chem.*, **24**, 736 (1952).
11) C. M. Johnson and T. H. Arkley, *Anal. Chem.*, **26**, 1525 (1954).

far too complicated to be readily applicable to routine works.

In this laboratory strong phosphoric acid has been used for the last five years for many analytical purposes with excellent results, and in a previous paper[12] the authors reported a new rapid colorimetric method for the determination of minute amounts of sulfate, in which the tin(II)-strong phosphoric acid, a new powerful reducing agent first described by the authors, was used[13]. In the present investigation, this method has been extended to the determination of organic sulfur of the order of micrograms by means of preliminary oxidation of organic sulfur with chromium(VI)-strong phosphoric acid, a new powerful oxidizing agent which is composed of potassium dichromate and strong phosphoric acid[14]. The rapidity and the simplicity of the original method are still retained in this procedure, by which 1 to 35 micrograms of organic sulfur can be estimated colorimetrically.

## Apparatus

### Apparatus for Oxidation, Reduction and Absorption.

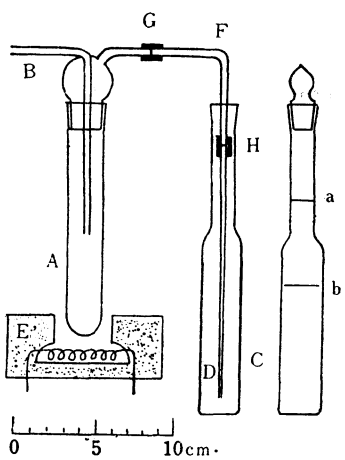



Fig. 1. Apparatus for oxidation, reduction and absorption.
A: Reaction vessel of fused silica
B: Glass cap fitted to a reaction vessel
C: Absorbing vessel
a: The 35 ml. mark
b: The 50 ml. mark
D: Detachable delivery tube (4 mm. in outside diameter)
E: Electric heater
F: Gas leading tube
G, H: A short piece of rubber tubing

12) T. Kiba and I. Kishi, This Bulletin, **30**, 53 (1957).
13) T. Kiba, T. Takagi, Y. Yoshimura and I. Kishi, ibid., **28**, 641 (1955).
14) S. Ohashi, ibid., **28**, 645 (1955).

**Reaction Vessel and Absorption.**—The vessel for the oxidation of organic sulfur to sulfate is a test-tube of fused silica, which can be used also as the reaction vessel for the reduction of the sulfate. The test-tube should be made of fused silica, since unexpectedly high values of sulfur were occasionally obtained when glass vessels were used, owing to minute amounts of sulfur in the glass.

A set-up of the apparatus for the reduction of the sulfate to hydrogen sulfide and the absorption of the hydrogen sulfide evolved is shown in Fig. 1. Six gas-washing bottles (not shown) are placed between a Kipp's apparatus for the production of carbon dioxide and the inlet arm of the reaction vessel (A). Solutions used for the purification of the carbon dioxide are described below. A bent glass tube (F) is attached to the outlet arm of the reaction vessel with a short piece of rubber tubing (G). A detachable delivery tube (D) is connected with another rubber tubing to the bent tube (F) and inserted into the absorbing vessel (C). Since some zinc sulfide adheres to that part of the tube immersed in the solution, it must be disconnected and allowed to remain in the absorbing vessel during the development of the methylene blue color.

**Photoelectric Colorimeter.**—A "Hirama" photoelectric colorimeter with 1-cm. cells and a filter of 655 mμ was used throughout this work.

## Reagents

**Tin(II)-Strong Phosphoric Acid.**—Prepare from 250 g. of strong phosphoric acid and 50 g. of tin(II) chloride dihydrate of extra pure grade as described in the previous paper[13].

**Chromium(VI)-Strong Phosphoric Acid.**—Prepare from potassium dichromate and diluted tin(II)-strong phosphoric acid by the following precaution. Even in the case of extra pure grade, potassium dichromate and phosphoric acid always contain minute amounts of sulfate as impurity, which may give occasionally too high values in the determination of sulfur by this method. In the present study, the authors used potassium dichromate of the purest reagent grade supplied by the Osaka Goverment Industrial Research Institute, which contained as little as 0.0015% of sulfate. A commercial reagent should be recrystallized twice from sulfur-free water. Sulfates contained in commercial phosphoric acid could be removed as follows: add 1 g. of tin(II) chloride dihydrate of pure grade into 100 g. of strong phosphoric acid and heat it to 300°C just as in the preparation of tin(II)-strong phosphoric acid. By this treatment, the sulfates contained in the phosphoric acid is removed as hydrogen sulfide during the heating. This will be called "Diluted Tin(II)-Strong Phosphoric Acid" in the following description. In an Erlenmyer flask, dissolve 12g. of potassium dichromate of the purest grade in 100 g. of the diluted tin(II)-strong phosphoric acid by heating on a steam bath. The chromium(VI)-strong phosphoric acid thus prepared can be stocked in a stoppered vessel without dehydrant, but it is advisable to prepare the

reagent soon before use.

**Carbon Dioxide.**—Purify the carbon dioxide produced in the Kipp's apparatus by passing it through five gas-washing bottles containing, respectively, water, 1% potassium permanganate in 10% sodium carbonate solution, vanadium(II) sulfate in sulfuric acid (see below), 5% barium chloride, and zinc acetate absorbing solution (see below). Place a sixth bottle, an empty one, for the purpose of equalizing the flow and of intercepting floating liquid droplets.

**Vanadium(II) Sulfate Solution.**—Dissolve 2g. of ammonium vanadate in 200ml. of water, add 20 ml. of 6 N sulfuric acid, and shake vigorously with 3% zinc amalgam in an atmosphere of carbon dioxide until the violet color of vanadium(II) appears. Transfer the solution quickly into a gas-washing bottle containing a small amount of the amalgam. This is employed to remove oxygen completely from the carbon dioxide.

**Zinc Acetate Absorbing Solution.**—Dissolve 20 g. of zinc acetate dihydrate of extra pure grade in 1 l. of redistilled water. If necessary, add two or three drops of glacial acetic acid to clarify the solution, but the pH of the solution should not be below 5. The redistilled water is prepared by distilling ordinary distilled water with a small amount of sodium hydroxide in an all-glass still.

***p*-Amino Dimethylaniline Solution.**—Dissolve 1.4 g. of *p*-amino dimethylaniline sulfate crystals of pure grade in 200 ml. of 1 : 1 sulfuric acid.

**Ferric Chloride Solution.**—Dissolve 10 g. of ferric chloride hexahydrate in 100 ml. of distilled water.

**Standard Sulfate Solution** —Dissolve 4.4299g. of unhydrous sodium sulfate of extra pure grade in 1 l. of sulfur-free water. Take 20 ml. of this solution with a pipet and dilute it to 1 l. so that the final solution contains 20 micrograms of sulfur in 1 ml. Pipet accurately the required volume of this solution for making the standard calibration curve for the colorimetric determination of sulfur.

**Barium Chloride Solution.**—Dissolve 1 g. of barium chloride dihydrate in 100 ml. of sulfur-free water, and use 0.5 ml. of the solution in each test.

## Procedure

When the sample is a solution, pipet accurately an aliquot containing 1 to 35 micrograms of sulfur. When it is a solid, take an accurately-weighed quantity containing the same range of sulfur. Put the measured sample into the test-tube of fused silica. Add 0.5 ml. of the barium chloride solution and evaporate the contents to dryness at the bottom of the vessel in a water-bath. Pour 1 ml. of the chromium (VI)-strong phosphoric acid over the residue from a pipet. Dip the vessel into a steam-bath till the content appears homogeneous. Place the vessel on an electric heater (E) (Fig. 1) and heat gently for about ten minutes to decompose the organic matter completely. The color change of the content from red to green shows the end of the reaction. Cool the content and pour 5 ml. of the tin(II)-strong phosphoric acid into the vessel. Fill the absorbing vessel with 35ml. of the zinc acetate solution. Connect each part of the apparatus as shown in Fig. 1., and pass carbon dioxide very rapidly for five minutes to expel the air in the reaction and the absorption vessel. The passage of the gas should be rapid enough to cause strong agitation of the surface of the liquid in the absorption vessel. The end of the gas delivery tube should reach to the bottom of the absorption vessel. At the end of five minutes, reduce the flow of the gas to a rate of one bubble per second. Heat the reaction vessel on the small electric heater (E), which is regulated by a variable transformer, till white fumes of phosphoric acid appear. Continue the heating for about fifteen minutes. It is unnecessary to keep the temperature strictly constant but it should be high enough to ensure that the content in the reaction vessel exhibits a white turbidity near the end of the fifteen minutes. Stop the heating and continue to pass carbon dioxide about five minutes.

Remove the absorption vessel and keep it in a thermostat for several minutes at 24°C. Add quickly 1.5 ml. of *p*-aminodimethylaniline solution using a rapid delivery pipet, stopper the vessel and shake it vigorously, and then quickly add 0.5 ml. of ferric chloride solution. Stopper and shake vigorously the vessel again. After keeping the vessel in the thermostat at 24°C. for fifteen minutes, remove the delivery tube from the solution, washing down the adhering solution into the vessel with distilled water. Add more distilled water till the liquid reaches the 50 ml. mark. Read the absorbancy of the solution in the colorimeter at 655 mμ within thirty minutes. According to the authors' experience, main sources of error in this method seem to be imperfect removal of oxygen from the carbon dioxide and careless delay in adding the colorization reagents viz., *p*-aminodimethylaniline and ferric chloride.

A standard calibrating curve, showing the relation between the amounts of sulfur taken and the absorbancies measured, should be prepared by carrying out the procedure with the standard sodium sulfate solution in the range 1 to 40 micrograms of sulfur. Estimate the amount of organic sulfur in the sample analyzed by comparing the absorbancy measured with this calibration curve. Use a mixture of the absorbing solution and the reagents of the definite amounts as reference for the photoelectric measurement.

## Results and Discussion

**Behavior of Chromium(VI)-Strong Phosphoric Acid.**—This oxidizing agent is so powerful that all organic compounds, even coal, are completely oxidized at a temperatures below 200°C. Moreover, it has the advantageous property that all of the chromium(VI) remaining unchanged can be decomposed to chromium(III) easily

by further heating, so that no excess of chromium(VI) will remain and consume the tin(II)-strong phosphoric acid in the succeeding reduction process. This chemical property of chromium(VI)-strong phosphoric acid is very interesting and advantageous not only for this purpose but for many other oxidizing processes.

**Results of Analysis.**—Analyses of some known organic compounds containing sulfur were carried out by this method. Each sample was first dried in an Abderhalden's apparatus at a suitable temperature for the compound, and weighed accurately. The weighed sample was dissolved in a definite volume of water, in some cases with the aid of a small amount of hydrochloric acid. An aliquot from the solution was employed for the analysis. By the measurement of the absorbancy of the methylene blue color produced in each case, the amount of sulfur in the sample tested was calculated by means of the equation:

$$x=0.047+0.01478y$$

where $x$ is the absorbancy measured and $y$ is the amount of sulfur in micrograms. The equation was derived from many experimental data obtained by carrying out the procedure with sodium sulfate as the standard. The numerical values in the equation, as a matter of course, were calculated by the method of the least square from the experimental data. The constant, 0.047 represents the sulfur contained as an impurity in the reagents used, viz., potassium dichromate and the diluted tin(II)-strong phosphoric acid. The numerical values in the equation will depend on the sulfur contained in the reagents as well as on the spectral purity of the photoelectric colorimeter employed. The results obtained with some organic compounds are listed in Tables I to VI.

TABLE I

DETERMINATION OF SULFUR IN SULFUR GUANIDINE

| Sample taken μg. | Sulfur contained μg. | Absorbancy measured | Sulfur found μg. | Recovery of sulfur % |
|---|---|---|---|---|
| 0. | 0. | 0.047 | 0. | |
| 13.4 | 2. | 0.0762 | 1.98 | 99.0 |
| 40.1 | 6. | 0.1355 | 5.99 | 99.8 |
| 66.8 | 10. | 0.1948 | 10.00 | 100.0 |
| 100.2 | 15. | 0.2688 | 15.01 | 100.1 |
| 133.6 | 20. | 0.3469 | 20.02 | 100.1 |
| 167.0 | 25. | 0.4160 | 24.97 | 99.9 |
| 200.6 | 30. | 0.4896 | 29.95 | 99.8 |
| 233.9 | 35. | 0.5630 | 34.91 | 99.7 |

TABLE II

DETERMINATION OF SULFUR IN METHYL ORANGE

| Sample taken μg. | Sulfur contained μg. | Absorbancy measured | Sulfur found μg. | Recovery of sulfur % |
|---|---|---|---|---|
| 0. | 0. | 0.047 | 0. | |
| 20.4 | 2. | 0.0760 | 1.96 | 98.0 |
| 61.3 | 6. | 0.1353 | 5.97 | 99.5 |
| 102.1 | 10. | 0.1946 | 9.97 | 99.7 |
| 153.1 | 15. | 0.2686 | 14.99 | 99.9 |
| 204.2 | 20. | 0.3545 | 19.99 | 99.9 |
| 255.2 | 25. | 0.4276 | 24.94 | 99.8 |
| 306.3 | 30. | 0.5010 | 29.91 | 99.7 |
| 357.3 | 35. | 0.5745 | 34.88 | 99.7 |

TABLE III

DETERMINATION OF SULFUR IN *l*-CYSTINE

| Sample taken μg. | Sulfur contained μg. | Absorbancy measured | Sulfur found μg. | Recovery of sulfur % |
|---|---|---|---|---|
| 0. | 0. | 0.047 | 0. | |
| 7.5 | 2. | 0.0745 | 1.86 | 93.0 |
| 22.5 | 6. | 0.1482 | 5.90 | 98.3 |
| 37.5 | 10. | 0.2078 | 9.93 | 99.3 |
| 56.2 | 15. | 0.2819 | 14.95 | 99.6 |
| 74.9 | 20. | 0.3415 | 19.93 | 99.7 |
| 93.7 | 25. | 0.4198 | 24.95 | 99.8 |
| 112.4 | 30. | 0.5030 | 29.90 | 99.7 |
| 131.1 | 35. | 0.5760 | 34.84 | 99.5 |

TABLE IV

DETERMINATION OF SULFUR IN *l*-METHIONINE

| Sample taken μg. | Sulfur contained μg. | Absorbancy measured | Sulfur found μg. | Recovery of sulfur % |
|---|---|---|---|---|
| 0. | 0. | 0.047 | 0. | |
| 9.3 | 2. | 0.0746 | 1.87 | 93.5 |
| 27.9 | 6. | 0.1350 | 5.95 | 99.2 |
| 46.5 | 10. | 0.1938 | 9.93 | 99.3 |
| 69.8 | 15. | 0.2685 | 14.99 | 99.9 |
| 93.1 | 20. | 0.3419 | 19.95 | 99.8 |
| 116.3 | 25. | 0.4150 | 24.90 | 99.6 |
| 139.6 | 30. | 0.4890 | 29.90 | 99.7 |
| 162.9 | 35. | 0.5626 | 34.88 | 99.6 |

TABLE V

DETERMINATION OF SULFUR IN THIOUREA

| Sample taken μg. | Sulfur contained μg. | Absorbancy measured | Sulfur found μg. | Recovery of sulfur % |
|---|---|---|---|---|
| 0. | 0. | 0.047 | 0. | |
| 4.7 | 2. | 0.0748 | 1.88 | 94.0 |
| 14.2 | 6. | 0.1340 | 5.89 | 98.2 |
| 23.7 | 10. | 0.1930 | 9.88 | 98.8 |
| 35.6 | 15. | 0.2670 | 14.88 | 99.2 |
| 47.5 | 20. | 0.3410 | 19.21 | 95.6 |
| 59.4 | 25. | 0.4050 | 24.22 | 96.9 |
| 71.2 | 30. | 0.4884 | 29.86 | 99.5 |
| 83.1 | 35. | 0.5284 | 34.80 | 99.4 |

TABLE VI
DETERMINATION OF SULFUR IN CRESOL RED

| Sample taken μg. | Sulfur contained μg. | Absorbancy measured | Sulfur found μg. | Recovery of sulfur % |
|---|---|---|---|---|
| 0. | 0. | 0.047 | 0. | |
| 23.9 | 2. | 0.0755 | 1.93 | 96.5 |
| 71.6 | 6. | 0.1356 | 5.99 | 99.5 |
| 119.3 | 10. | 0.1948 | 9.99 | 99.9 |
| 178.9 | 15. | 0.2690 | 15.02 | 100.1 |
| 238.5 | 20. | 0.3388 | 19.74 | 98.7 |
| 298.2 | 25. | 0.4165 | 25.00 | 100.0 |
| 357.8 | 30. | 0.4900 | 29.97 | 99.9 |
| 417.4 | 35. | 0.5635 | 34.95 | 99.9 |

In the column under "Recovery of sulfur" is given the ratio in percentage of sulfur found to the amount taken in each case.

**Preliminary Elimination of Sulfur from the Reagents.**—As described in the above section, strong phosphoric acid, prepared from commercial orthophosphoric acid (D=1.7), always contains a minute amount of sulfur as impurity. In order to eliminate the sulfur the authors have prepared the diluted tin(II)-strong phosphoric acid as described above. The amounts of sulfur contained in the untreated strong phosphoric acid and in the diluted tin(II)-strong phosphoric acid were determined by carrying out the same reduction procedure. The results are shown in Table VII, which shows that the sulfur contained in the original strong phosphoric acid was expelled almost completely by treating with as little as 1 g. of tin(II) chloride dihydrate. The contents of sulfur in potassium dichromate reagent were estimated by the same procedure, and the results are tabulated all together in Table VII.

TABLE VII
SULFUR CONTENT IN THE REAGENTS AND ITS ELIMINATION

| Reagent | Amount taken ml. | Absorbancy measured | Sulfur found in 1 ml. of the reagent μg. |
|---|---|---|---|
| Strong phosphoric acid | 1 | 0.2229 | 15.1 |
| | 1 | 0.1852 | 12.5 |
| Diluted tin(II)-strong phosphoric acid (A) | 1 | 0.011 | 0.74 |
| | 1 | 0.013 | 0.87 |
| Diluted tin(II)-strong phosphoric acid (B) | 1 | 0.013 | 0.87 |
| | 1 | 0.013 | 0.87 |
| Mixture of 100 g. of tin(II)-strong phosphoric acid (A) and 6 g. of $K_2Cr_2O_7$ (C) | 1 | 0.027 | 1.82 |
| | 1 | 0.024 | 1.62 |
| Mixture of 100 g. of tin(II)-strong phosphoric acid (B) and 12 g. of $K_2Cr_2O_7$ (C) | 1 | 0.044 | 2.98 |
| | 1 | 0.050 | 3.38 |
| Mixture of 100 g. of tin(II)-strong phosphoric acid (A) and 6 g. of $K_2Cr_2O_7$ (D) | 1 | 0.062 | 4.19 |
| | 1 | 0.051 | 3.45 |

Note:

Diluted tin(II)-strong phosphoric acid (A) was prepared from 100 g. of strong phosphoric acid and 1 g. of tin(II)-chloride dihydrate; (B) from 100 g. of the acid and 5 g. of the salt.

$K_2Cr_2O_7$ (C) was a standard reagent supplied by Osaka Goverment Industrial Research Institute; (D) was a commercial reagent recrystallized in the laboratory.


## Summary

A simple and rapid method for the determination of minute amounts of organic sulfur was established by using the oxidizing action of chromium(VI)-strong phosphoric acid and the reducing power of tin(II)-strong phosphoric acid. Organic sulfur was oxidized to sulfate by the former in a test-tube of fused silica and the sulfate was reduced to hydrogen sulfide by the latter in the same vessel. The hydrogen sulfide evolved was absorbed in zinc acetate solution and estimated colorimetrically by the ordinary methylene blue method. The absorbancy of the colored solution was measured at 655 mμ with a photoelectric colorimeter using 1-cm. cells. The sulfur content of the sample was estimated by comparing the absorbancy value with the standard curve prepared with sodium sulfate. Some organic compounds containing sulfur were analyzed by this method and satisfactory results were obtained. However, analysis of the miscellaneous organic substances such as biological specimens has not been undertaken and the problems for this purpose remain to be solved in future.


A part of the expenses for this study was defrayed by a grant by the Ministry of Education, to which the authors' thanks are due.

*Department of Chemistry, Faculty of Science, Kanazawa University*
*Kanazawa*

# *Normal Vibrations of Tetramethylmethane and Tetramethylmethane-$d_{12}$*

By Kazuhiro SHIMIZU and Hiromu MURATA

(Received January 21, 1957)

The Wilson *FG* matrix method for the tetrahedral $M(XY_3)_4$ molecules has been used by Siebert[1] But no symmetry coordinates were given and a valence force field, including only one cross term of M–X and X–M–X internal coordinates, was used. The present investigation was undertaken in an attempt to carry out a normal coordinate treatment with a Urey-Bradley potential function and to assign observed frequencies for $C(CH_3)_4$ and $C(CD_3)_4$ to fundamental modes of vibration.

## Normal Coordinate Treatment

A representation of the forty-five normal vibrational modes of the tetrahedral $M(XY_3)_4$ molecules is reduced to fourteen by $\Gamma=3a_1+4e+7f_2$. According to the well-known selection rules, all fundamentals are allowed in Raman spectrum, while only type $f_2$ fundamentals are allowed in the infrared. In the Raman spectrum, the $a_1$ vibrations correspond to polarized lines, the others to depolarized. It is possible to show that in both the $a_1$ and e species, $n^{(r)}=1$ for any sets of equivalent internal coordinates, while in the $f_2$ species, $n^{(r)}=2$ for the X–Y stretching and the Y–X–Y bending coordinates. For the latter case, it is neccesary to find *K*, which is a subgroup of *G*, and to construct the final symmetry coordinates from nondegenerate symmetry coordinates under *K*, as shown in the following manner:

| $G(T_d)$ | $K(C_{2v})$ | Symmetry coordinates | |
|---|---|---|---|
| $f_2$ | $a_1$ | $R_9$, | $R_{11}$ |
| | $b_1$ | $R_8$, | $R_{10}$ |
| | $b_2$ | None | |

From the internal coordinates (Fig. 1), the following orthonormal symmetry coordinates were formed:

for the $a_1$ vibrations,

$$R_1=\Delta(y_{11}+y_{12}+y_{13}+y_{21}+y_{22}+y_{23}+y_{31}+y_{32}+y_{33}+y_{41}+y_{42}+y_{43})/12^{1/2},$$

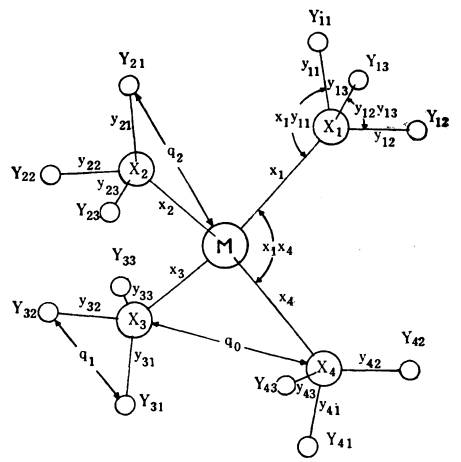



Fig. 1. Internal coordinates of $M(\times Y_3)_4$ molecule.

$$R_2=\Delta(y_{11}y_{12}+y_{11}y_{13}+y_{12}y_{13}+y_{21}y_{22}+y_{21}y_{23}+y_{22}y_{23}+y_{31}y_{32}+y_{31}y_{33}+y_{32}y_{33}+y_{41}y_{42}+y_{41}y_{43}+y_{42}y_{43}-x_1y_{11}-x_1y_{12}-x_1y_{13}-x_2y_{21}-x_2y_{22}-x_2y_{23}-x_3y_{31}-x_3y_{32}-x_3y_{33}-x_4y_{41}-x_4y_{42}-x_4y_{43})/24^{1/2},$$ and

$$R_3=\Delta(x_1+x_2+x_3+x_4)/2;$$

for the e vibrations,

$$R_{4a}=\Delta(2y_{11}-y_{12}-y_{13}+2y_{21}-y_{22}-y_{23}+2y_{31}-y_{32}-y_{33}+2y_{41}-y_{42}-y_{13})/24^{1/2},$$

$$R_{5a}=\Delta(2y_{12}y_{13}-y_{11}y_{12}-y_{11}y_{13}+2y_{22}y_{23}-y_{21}y_{22}-y_{21}y_{23}+2y_{32}y_{33}-y_{31}y_{32}-y_{31}y_{33}+2y_{42}y_{43}-y_{41}y_{42}-y_{41}y_{43})/24^{1/2},$$

$$R_{6a}=\Delta(2x_1y_{11}-x_1y_{12}-x_1y_{13}+2x_2y_{21}-x_2y_{22}-x_2y_{23}+2x_3y_{31}-x_3y_{32}-x_3y_{33}+2x_4y_{41}-x_4y_{42}-x_4y_{43})/24^{1/2},$$ and

$$R_{7a}=\Delta(2x_1x_2-x_1x_3-x_1x_4+2x_3x_4-x_2x_3-x_2x_4)/12^{1/2};$$

for the $f_2$ vibrations,

$$R_{8a}=\Delta(2y_{21}-y_{22}-y_{23}+2y_{33}-y_{31}-y_{32}+2y_{42}-y_{43}-y_{41})/18^{1/2},$$

$$R_{9a}=\Delta(3y_{11}+3y_{12}+3y_{13}-y_{21}-y_{22}-y_{23}-y_{31}-y_{32}-y_{33}-y_{41}-y_{42}-y_{43})/6,$$

$$R_{10a}=\Delta(2y_{22}y_{23}-y_{21}y_{22}-y_{21}y_{23}+2y_{31}y_{32}-y_{31}y_{33}-y_{32}y_{33}+2y_{41}y_{43}-y_{41}y_{42}-y_{42}y_{43})/18^{1/2},$$

$$R_{11a}=\Delta(3y_{11}y_{12}+3y_{11}y_{13}+3y_{12}y_{13}-y_{21}y_{22}-y_{21}y_{23}-y_{22}y_{23}-y_{31}y_{32}-y_{31}y_{33}-y_{32}y_{33}$$

1) H. Siebert, *Z. anorg. allgem. Chem.*, **268**, 177 (1952).

$$-y_{41}y_{42}-y_{41}y_{43}-y_{42}y_{43}-3x_1y_{11}-3x_1y_{12}$$
$$-3x_1y_{13}+x_2y_{21}+x_2y_{22}+x_2y_{23}+x_3y_{31}$$
$$+x_3y_{32}+x_3y_{33}+x_4y_{41}+x_4y_{42}$$
$$+x_4y_{43})/72^{1/2},$$

$R_{12a}=\Delta(3x_1-x_2-x_3-x_4)/12^{1/2}$,

$R_{13a}=\Delta(2x_2y_{21}-x_2y_{22}-x_2y_{23}+2x_3y_{33}-x_3y_{31}$
$-x_3y_{32}+2x_4y_{42}-x_4y_{41}-x_4y_{43})/18^{1/2}$, and

$R_{14a}=\Delta(x_1x_2+x_1x_3+x_1x_4-x_2x_3-x_2x_4$
$-x_3x_4)/6^{1/2}$.

The numbering of these coordinates corresponds to the numbering of the fundamentals in Table III.

From the potential constants of a Urey-Bradley force field[2] and the coefficients of the symmetry coordinates, one obtains the following $F$ matrix elements:

for the $a_1$ vibrations,

$F_{11}=K_1+4s_1^2F_1+t_2^2F_2'+s_2^2F_2$,
$F_{12}=2^{1/2}t_1s_1(F_1'+F_1)y-(t_2s_3F_2'$
$+t_3s_2F_2)x/2^{1/2}$,
$F_{13}=3^{1/2}(-t_2t_3F_2'+s_2s_3F_2)$,
$F_{22}=[(H_1-s_1^2F_1'+t_1^2F_1)y^2+(H_2-s_2s_3F_2'$
$+t_2t_3F_2)xy+3k_1/2^{1/2}]/2$,
$F_{23}=-3^{1/2}(t_3s_2F_2'+t_2s_3F_2)y/2^{1/2}$, and
$F_{33}=K_0+6s_02F_0+3t_3^2F_2'+3s_3^2F_2$;

for the e vibrations,

$F_{11}=K_1+3t_1^2F_1'+s_1^2F_1+t_2^2F_2'+s_2^2F_2$,
$F_{12}=-t_1s_1(F_1'+F_1)y$,
$F_{13}=(t_2s_3F_2'+t_3s_2F_2)x$,
$F_{22}=(H_1-s_1^2F_1+t_1^2F_1)y^2+2^{1/2}k_1/4$,
$F_{23}=k_1/2^{1/2}$,
$F_{33}=(H_2-s_2s_3F_2'+t_2t_3F_2)xy+2^{1/2}k_1/4$,
$F_{44}=(H_0-s_0^2F_0'+t_0^2F_0)x^2-2^{1/2}k_0/4$, and
$F_{14}=F_{24}=F_{34}=0$;

and for the $f_2$ vibrations,

$F_{11}=K_1+3t_1^2F_1'+s_1^2F_1+t_2^2F_2'+s_2^2F_2$,
$F_{13}=-t_1s_1(F_1'+F_1)y$,
$F_{16}=(t_2s_3F_2'+t_3s_2F_2)x$,
$F_{22}=K_1+4s_1^2F_1+t_2^2F_2'+s_2^2F_2$,
$F_{24}=2^{1/2}t_1s_1(F_1'+F_1)y-(t_2s_3F_2'$
$+t_3s_2F_2)x/2^{1/2}$,
$F_{25}=3^{1/2}(-t_2t_3F_2'+s_2s_3F_2)$,
$F_{33}=(H_1-s_1^2F_1'+t_1^2F_1)y^2+2^{1/2}k_1/4$,
$F_{36}=-k_1/2^{1/2}$,
$F_{44}=[(H_1-s_1^2F_1'+t_1^2F_1)y^2+(H_2-s_2s_3F_2'$
$+t_2t_3F_2)xy+3k_1/2^{1/2}]/2$
$F_{45}=-3^{1/2}(t_3s_2F_2'+t_2s_3F_2)y/2^{1/2}$,
$F_{55}=K_0+4t_0^2F_0'+2s_0^2F_0+3t_3^2F_2'+3s_3^2F_2$,
$F_{57}=2^{1/2}t_0s_0(F_0'+F_0)x$,
$F_{66}=(H_2-s_2s_3F_2'+t_2t_3F_2)xy+2^{1/2}k_1/4$,
$F_{77}=(H_0-s_0^2F_0'+t_0^2F_0)x^2+3k_0/8^{1/2}$, and
$F_{12}=F_{14}=F_{15}=F_{17}=F_{23}=F_{26}=F_{27}=F_{34}=F_{35}$
$=F_{37}=F_{46}=F_{47}=F_{56}=F_{67}=0$,

where the following abbreviations are adopted:

$t_0=8^{1/2}x/3q_0$, $t_1=8^{1/2}y/3q_1$, $t_2=8^{1/2}x/3q_2$,
$t_3=8^{1/2}y/3q_2$, $s_0=4x/3q_0$, $s_1=4y/3q_1$,
$s_2=(x+3y)/3q_2$, $s_3=(3x+y)/3q_2$,

and the symbols used for the equilibrium values of the interatomic distances are

$x=M-X$, $y=X-Y$, $q_0=X\cdots\cdots X$,
$q_1=Y\cdots\cdots Y$, and $q_2=M\cdots\cdots Y$.

The $G$ matrix elements, obtained by use of the table of Decius[3] and the method of Crawford[4], are as follows:

for the $a_1$ vibration,

$G_{11}=\mu_X/3+\mu_Y$,
$G_{12}=-4\mu_X/3y$,
$G_{13}=-\mu_X/3^{1/2}$,
$G_{22}=2(8\mu_X/3+\mu_Y)/y^2$,
$G_{23}=4\mu_X/3^{1/2}y$, and
$G_{33}=\mu_X$;

for the e vibrations,

$G_{11}=4\mu_X/3+\mu_Y$,
$G_{12}=32^{1/2}\mu_X/3y$,
$G_{13}=-2^{1/2}\mu_X(3/x+1/y)/3$,
$G_{14}=2\mu_X/x$,
$G_{22}=(8\mu_X/3+5\mu_Y/2)/y^2$,
$G_{23}=-2\mu_X(1/3y^2+1/xy)+\mu_Y/2y^2$,
$G_{24}=8^{1/2}\mu_X/xy$,
$G_{33}=\mu_X(3/2x^2+1/xy+1/6y^2)+\mu_Y/y^2$.
$G_{34}=-\mu_X(3/x^2+1/xy)/2^{1/2}$, and
$G_{44}=3\mu_X/x^2$;

and for the $f_2$ vibrations.

$G_{11}=4\mu_X/3+\mu y$,
$G_{13}=32^{1/2}\mu_X/3y$,
$G_{16}=-2^{1/2}\mu_X(1/x+1/3y)$,
$G_{17}=8^{1/2}\mu_X/3^{1/2}x$,
$G_{22}=\mu_X/3+\mu_Y$,
$G_{24}=-4\mu_X/3y$,
$G_{25}=-\mu_X/3^{1/2}$,
$G_{33}=8\mu_X/3_Y^2+5\mu_Y/2y^2$,
$G_{36}=-2\mu_X(1/xy+1/3y^2)+\mu_Y/2y^2$,
$G_{37}=4\mu_X/3^{1/2}xy$,
$G_{44}=16\mu_X/3y^2+2\mu_Y/y^2$,
$G_{45}=4\mu_X/3^{1/2}y$,
$G_{55}=4\mu_M/3+\mu_X$,
$G_{56}=4\mu_M/3^{1/2}x$,
$G_{57}=-8\mu_M/3x$,
$G_{66}=4\mu_M/x^2+\mu_X(3/2x^2+1/xy+1/6y^2)$
$+\mu_Y/y^2$,

2) T. Shimanouchi, *J. Chem. Phys.*, **17**, 245, 734, 848 (1949).

3) J. C. Decius, *J. Chem. Phys.*, **16**, 1025 (1948).

4) B. Crawford, Jr., *J. Chem. Phys.*, **21**, 1108 (1953).

TABLE I

RAMAN AND INFRARED SPECTRAL DATA FOR TETRAMETHYLMETHANE

| Type | Silver[a] (Raman) | YKM[b] (Infrared) | Sheppard[c] (Raman) | Siebert[d] (Raman) | SOR (Raman) | SOR (Infrared) |
|---|---|---|---|---|---|---|
| $a_1$ | 2913 | 2911 | — | 2911 | 2909 | — |
| | 1455 | 1252 | — | — | — | — |
| | — | 733 | 733 | 733 | 733 | — |
| e | 2957 | 2955 | — | 2955 | — | — |
| | 1455 | 1455 | — | 1455 | 1451 | — |
| | 925 | 925 | 925 | — | — | — |
| | — | 335 | 335 | 335 | 335 | — |
| $f_2$ | — | 2962 | — | 2962 | 2955 | 2959 |
| | — | 2876 | — | 2876 | — | 2876 |
| | — | 1455 | — | 1455 | — | 1475 |
| | — | 1370 | — | 1370 | — | 1372 |
| | — | 1280 | 1252 | 1257 | 1249 | 1256 |
| | — | 925 | 925 | 925 | 921 | 925 |
| | — | 414 | 414 | 414 | 415 | 418 |

a See reference 5; b YKM=Young, Koehler and Mckinney, reference 6; c See reference 7; d See reference 1; e SOR=Shull, Oakwood and Rank, reference 9.

$G_{67}=-8\mu_M/3^{1/2}x^2-\mu_X(3^{1/2}/x^2+1/3^{1/2}xy)$,
$G_{77}=16\mu_M/3x^2+2\mu_X/x^2$, and
$G_{12}=G_{14}=G_{15}=G_{23}=G_{26}=G_{27}=G_{34}=G_{35}=G_{46}=G_{47}=0$.

Here $\mu_M$, $\mu_X$ and $\mu_Y$ are, respectively, the reciprocals of the masses of the $M$, $X$ and $Y$ atoms.

## Normal Frequencies of Tetramethylmethane

The Raman or the infrared spectral data and the assignments of the observed frequencies for tetramethylmethane have been obtained in previous investigations[1,5-9]. A summary of the fundamentals is given in Table I. A partial normal coordinate treatment was carried out by Silver[5] and by Sheline et al.[8] for the $a_1$ and e vibrations. Recently, Siebert[1] published the normal coordinate treatment of all vibrations. The disagreement between the results of the different investigations lies in the assignment of two of type $f_2$ vibrations, i.e. C—C stretching and $CH_3$ rocking vibration. In this paper, the nature of these vibrations will be clarified. Using the $F$ and $G$ matrix elements given above, the fundamental frequencies were calculated and shown in Table III. Probable values of the observed frequencies and assignment of the Raman and the infrared bands are included in the table. The molecular and potential constants used are listed in Table II. The C—H stretching vibrations were split off by the method of Wilson. The agreement between the calculated and observed fundamentals was almost completely satisfactory. The $L$

TABLE II

MOLECULAR AND POTENTIAL CONSTANTS OF $C(CH_3)_4$ AND $C(CD_3)_4$

| Bond distance | Type | Potential constant (md/A) Set I | Set II |
|---|---|---|---|
| $x$=C—C | $K_0$(C—C) | 3.440 | 2.474 |
| =1.55A | $H_0$(C—C—C) | 0.206 | 0.105 |
| $y$=C—H | $F_0$(C·····C) | 0.333 | 0.571 |
| =C—D | $k_0$($CC_4$) | 0.040A$^2$ | 0.015A$^2$ |
| =1.09A | $K_1$(C—H) | 4.50 | 4.50 |
| | $H_1$(H—C—H) | 0.40 | 0.40 |
| | $H_2$(C—C—H) | 0.15 | 0.15 |
| | $F_1$(H·····H) | 0.10 | 0.10 |
| | $F_2$(C·····H) | 0.40 | 0.40 |
| | $k_1$($CCH_3$) | 0.05A$^2$ | 0.05A$^2$ |
| | $F'$ | $-F/10$ | $-F/10$ |

The potential constants for the skeletal vibrations were obtained from the observed frequencies of $C(CH_3)_4$:

The values of set I correspond to $\nu_1=733$, $\nu_2=335$, $\nu_3=1089$, and $\nu_4=414$ cm$^{-1}$ and those of set II, to $\nu_1=733$, $\nu_2=335$, $\nu_3=925$, and $\nu_4=414$ cm$^{-1}$ respectively.

The potential constants for the inner vibrations were obtained directly from the normal frequencies of $H_3C$—$CH_3$.

5) S. Silver, *J. Chem. Phys.*, **8**, 919 (1940).
6) C. W. Young, J. S. Koehler and D. S. Mckinney, *J. Am. Chem. Soc.*, **69**, 1410 (1947).
7) N. Sheppard, *J. Chem. Phys.*, **16**, 690 (1948).
8) R. K. Sheline and K. S. Pitzer, *J. Chem. Phys.*, **18**, 595 (1950).
9) E. R. Shull, T. S. Oakwood and D. H. Rank, *J. Chem. Phys.*, **21**, 2024 (1953).

TABLE III
PROBABLE VALUES OF THE OBSERVED FUNDAMENTALS, CALCULATED WAVE NUMBERS, AND ASSIGNMENTS FOR $C(CH_3)_4$.

| Type | Frequency | Mode of vibration | $\nu$ calc. Set I | $\nu$ calc. Set II | $\nu$ obs. |
|---|---|---|---|---|---|
| $a_1$ | $\nu_1$ | $CH_3$ sym. str. | 2932 | 2932 | 2909 |
| | $\nu_2$ | $CH_3$ sym. def. | 1395 | 1395 | — |
| | $\nu_3$ | C—C skel. str. | 791 | 790 | 733 |
| e | $\nu_4$ | $CH_3$ nonsym. str. | 2984 | 2984 | 2955 |
| | $\nu_5$ | $CH_3$ nonsym. def. | 1443 | 1442 | 1451 |
| | $\nu_6$ | $CH_3$ rocking | 905 | 905 | 925 |
| | $\nu_7$ | C—C—C skel. def. | 308 | 307 | 335 |
| $f_2$ | $\nu_8$ | $CH_3$ nonsym. str. | 2984 | 2984 | 2959 |
| | $\nu_9$ | $CH_3$ sym. str. | 2932 | 2932 | 2876 |
| | $\nu_{10}$ | $CH_3$ nonsym. def. | 1442 | 1442 | 1475 |
| | $\nu_{11}$ | $CH_3$ sym. def. | 1390 | 1377 | 1372 |
| | $\nu_{12}$ | $CH_3$ skel. str. | 1272 | 1160 | 1256 |
| | $\nu_{13}$ | $CH_3$ rocking | 873 | 852 | 925 |
| | $\nu_{14}$ | C—C—C skel. def. | 372 | 367 | 418 |

matrices, whose components give the modes of vibrations, and the potential energy distributions for the questionable two triply degenerate vibrations were calculated and shown in Tables IV and V. Judging from the values of the contribution of each symmetry coordinate to the normal coordinate $Q_{12}$ in Table IV, it is no longer accurate to designate the frequency $\nu_{12}$ as only one mode of vibration, i.e., "C—C stretching". However, it can be seen that, by taking into consideration the distribution of energy in the symmetry coordinates in Table V, the classification given in Table III is reasonable. On the contrary, it is undubitable that the frequency $\nu_{13}$, which is relatively pure, can be assigned to "$CH_3$ rocking".

TABLE IV
$L$-MATRICES OF TWO TYPE $f_2$ VIBRATIONS OF $C(CH_3)_4$.

| $f_2$ | $Q_{12}$ Set I | $Q_{12}$ Set II | $Q_{13}$ Set I | $Q_{13}$ Set II |
|---|---|---|---|---|
| $R_{10}$ | −0.09 | −0.09 | −0.07 | −0.05 |
| $R_{11}$ | −0.36 | −0.00 | 0.06 | 0.03 |
| $R_{12}$ | 0.36 | 0.34 | −0.16 | −0.22 |
| $R_{13}$ | 0.64 | 0.67 | 0.83 | 0.72 |
| $R_{14}$ | −0.41 | 0.36 | −0.04 | 0.01 |

TABLE V
POTENTIAL ENERGY DISTRIBUTION $F_{ii}L_{ia}^2/\lambda_a$ FOR $\nu_{12}$ AND $\nu_{13}$ VIBRATIONS

| $f_2$ | $\nu_{12}$ Set I | $\nu_{12}$ Set II | $\nu_{13}$ Set I | $\nu_{13}$ Set II |
|---|---|---|---|---|
| $R_{10}$ | 0.00 | 0.01 | 0.00 | 0.00 |
| $R_{11}$ | 0.13 | 0.00 | 0.01 | 0.00 |
| $R_{12}$ | 0.65 | 0.57 | 0.28 | 0.45 |
| $R_{13}$ | 0.19 | 0.25 | 0.68 | 0.53 |
| $R_{14}$ | 0.06 | 0.06 | 0.00 | 0.00 |

## Normal Frequencies of Tetramethylmethane-$d_{12}$

The Raman and the infrared spectral data and the assignments of the observed frequencies for tetramethylmethane-$d_{12}$ have been reported by Shull et al.[9], but a normal coordinate treatment has not been carried out in the literature. According to them, since the observed frequency 765 $cm^{-1}$ is analogous to the band at 921 $cm^{-1}$ in tetramethylmethane, it should be assigned to "C—C stretching" and the observed frequency 1218 $cm^{-1}$ can be assigned to "$CD_3$ rocking". In general, a normal mode of vibration in which the hydrogen atom in question oscillates with a relatively large amplitude will suffer a greater isotopic change in frequency than that of a normal mode in which this hydrogen moves with a relatively small amplitude. Since the ratio 765/921 is nearly equal to a theoretically expected value $1/2^{1/2}$, it is probably rigorous to designate the frequency observed at 765 $cm^{-1}$ as "$CD_3$ rocking". Since the frequencies observed at about 1200 $cm^{-1}$ maintain a constant value in both the ordinary and deuterated compounds, it is reasonable to assign these frequencies to "C—C stretching". Using the $F$ and $G$ matrix elements given above, the fundamental frequencies were calculated and shown in Table VI with

TABLE VI
OBSERVED AND CALCULATED FONDAMENTAL FREQUENCIES AND ASSIGNMENTS FOR $C(CD_3)_4$

| Type | Frequency | Mode of vibration | $\nu$ calc. Set I | $\nu$ calc. Set II | $\nu$ obs. |
|---|---|---|---|---|---|
| $a_1$ | $\nu_1$ | $CD_3$ sym. str. | 2110 | 2110 | 2128 |
| | $\nu_2$ | $CD_3$ sym. def. | 1130 | 1130 | 1104 |
| | $\nu_3$ | C—C skel. str. | 684 | 684 | 648 |
| e | $\nu_4$ | $CD_3$ nonsym. str. | 2221 | 2221 | — |
| | $\nu_5$ | $CD_3$ nonsym. def. | 1055 | 1055 | 1048 |
| | $\nu_6$ | $CD_3$ rocking | 695 | 694 | — |
| | $\nu_7$ | C—C—C skel. def. | 264 | 263 | 276 |
| $f_2$ | $\nu_8$ | $CD_3$ nonsym. str. | 2221 | 2221 | 2218 |
| | $\nu_9$ | $CD_3$ sym. str. | 2110 | 2110 | 2058 |
| | $\nu_{10}$ | C—C skel. str. | 1279 | 1150 | 1218 |
| | $\nu_{11}$ | $CD_3$ nonsym. def. | 1058 | 1057 | 1066 |
| | $\nu_{12}$ | $CD_3$ sym. def. | 1029 | 1020 | 1037 |
| | $\nu_{13}$ | $CD_3$ rocking | 684 | 679 | 765 |
| | $\nu_{14}$ | C—C—C skel. def. | 316 | 311 | 342 |

those observed by Shull et al. The calculation of the $L$ matrix elements (Table VII) and of the potential energy distributions (Table VIII) shows that the assignments given in Table VI are more reasonable.

TABLE VII

$L$-MATRICES OF TWO TYPE $f_2$ VIBRATIONS OF $C(CD_3)_4$

| $f_2$ | $Q_{10}$ Set I | $Q_{13}$ Set I |
|---|---|---|
| $R_{10}$ | −0.04 | 0.02 |
| $R_{11}$ | 0.51 | 0.13 |
| $R_{12}$ | 0.42 | −0.10 |
| $R_{13}$ | 0.41 | 0.62 |
| $R_{14}$ | −0.36 | −0.10 |

TABLE VIII

POTENTIAL ENERGY DISTRIBUTION $F_{ii}L_{ia}^2/\lambda_a$ FOR $\nu_{10}$ AND $\nu_{13}$ VIBRATIONS

| $f_2$ | $\nu_{10}$ Set I | $\nu_{13}$ Set I |
|---|---|---|
| $R_{10}$ | 0.00 | 0.00 |
| $R_{11}$ | 0.15 | 0.04 |
| $R_{12}$ | 0.87 | 0.17 |
| $R_{13}$ | 0.09 | 0.72 |
| $R_{14}$ | 0.11 | 0.03 |

The authors wish to express their gratitude to Drs. Y. Morino and T. Shimanouchi of Tokyo University and Dr. H. Shingu of Kyoto University for many helpful discussions.

*Osaka Municipal Technical Research Institute, Kita-ku, Osaka*

# *The Exhaustive Methylation of cis- and trans-Hexahydrocarbazoles*[1]

By Tadashi MASAMUNE

(Received January 14, 1957)

It has been established by King, Baltrop and Walley[2] that in the exhaustive methylation, *cis*-octahydroindole undergoes a fission of the N-$C_8$ bond to yield 1-(2-dimethylaminoethyl)-cyclohexene, while the corresponding *trans*-base produces no compound expected from the normal opening of the pyrrolidine ring. The methine $C_{10}H_{19}N$ (I) resulting from the *trans*-base was suggested to be II[3] and to be produced by a Wagner-Meerwein type rearrangement (a) of the carbonium ion (III) formed by ring-scission at $C_8$ (Fig. 1). However, the structure (II) was not verified experimentally. As it is desirable to investigate the behavior of similar compounds, the present author subjected *cis*- and *trans*-hexahydrocarbazoles to the exhaustive methylation. These bases may be regarded as analogs of octahydoindoles and are much more easily obtainable than *trans*-octahydroindole.

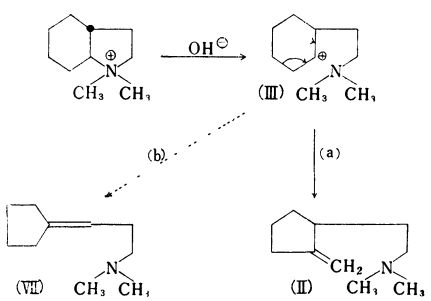
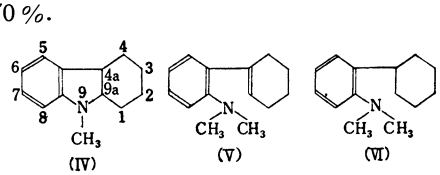



Fig. 1. The exhaustive methylation of *trans*-octahydro-N-methylindole methiodide.

Treatment of *cis*-hexahydrocarbazole and of its N-methyl-derivative (IV) with methyl iodide easily yielded the methiodide. Distillation of the compound obtained by treating an aqueous solution of the methiodide with silver oxide yielded an oily base, from which an unsaturated base $C_{14}H_{19}N$ (V) was isolated in a yield of 70%.




In order to determine its constitution the methine base (V) was subjected to

1) Part IX of "The Condensed Polynuclear Perhydro-Compounds Containing Nitrogen"; Part VIII, T. Masamune and M Koshi, This Bulletin, **30**, 307 (1957).

2) F. E. King, J. A. Baltrop and R. J. Walley, *J. Chem. Soc.*, **1945**, 277; B. Bailey, R. D. Haworth and J. McKenna, ibid., **1954**, 967.

3) F. E. King and H. Booth, ibid., **1954**, 3798.

Emde reduction. The resulting hydrocarbon gave δ-benzoylvaleric acid on oxidation and thus was found to be 1-phenylcyclohexene. Then, it follows that the product from the exhaustive methylation is 1-(*o*-dimethylaminophenyl)-cyclohexene (V). That the double bond in the cyclohexene ring is conjugated with the phenyl ring is concluded from the following fact. Comparison of the ultraviolet spectra of the methine base (V) and its dihydro-derivative (VI) with that of N-dimethyl-*o*-toluidine indicated that

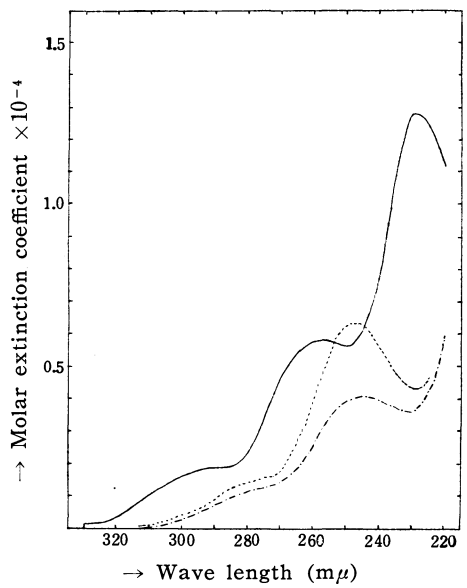



Fig. 2. Ultraviolet absorption spectra of *o*-toluidine derivatives.
Solvent: ethanol; conc. M×10⁻⁴
—— 1-(*o*-Dimethylaminophenyl)-cyclohexene (V)
- - - *o*-Dimethylaminophenylcyclohexane (VI)
-·-· N-dimethylamino-*o*-toluidine

there was no maximum in either of Doub's "secondary" bands[4] (Fig. 2). This may suggest that the bases are *o*-substituted N-dimethylanilines[5]. The absorption curves of base VI and N-dimethyl-*o*-toluidine had maxima at the almost identical wave length (247 mμ) of each "primary" band, whereas that of base V had a maximum at 259 mμ showing the existence of a double bond conjugated with the phenyl ring.

The formation of 1-(*o*-dimethylaminophenyl)-cyclohexene involves both fission of the N-$C_{9a}$ bond and attack of the hydroxide ion on the most acidic β-hydrogen atom in a *trans*-position to the bond, and may be reasonable in the light of stereochemistry[6] and of Hofmann's rule[7].

Formation and decomposition of *trans*-hexahydro-N-methyl-carbazole methohydroxide were investigated analogously to the case of the *cis*-base. Then a mixture of two bases was produced, one being 1-(*o*-dimethylaminophenyl)-cyclohexene identical with the base resulting from the exhaustive methylation of the *cis*-base, and the other *cis*-hexahydro-N-methylcarbazole (IV). This result was borne out by the mixed melting point determination of their picrates with authentic specimens, by comparison of the ultraviolet spectra, and by dehydrogenation experiment. The yield of the former was 50% of the theoretical and that of the latter 25%.

With *trans*-hexahydro-N-methylcarbazole methohydroxide, the stereochemical effect required for the usual Hofmann degradation is not satisfied. Therefore, a rearranged base was expected to appear considering the behavior of *trans*-octahydro-N-methylindole in the exhaustive methylation. But no such base could be isolated and base V was obtained instead. This is probably attributable to the ease in the elimination of the acidic β-hydrogen at $C_{4a}$ caused by the anilinium ion. Several examples of this type of elimination have already been reported[8]. On the other hand, the formation of base IV probably involves an elimination of methanol and a subsequent stereochemical rearrangement. Elimination of methanol is encountered in the exhaustive methylation of several alkaloids[9]. But no example is so far known of this type of elimination accompanied by a stereochemical rearrangment.

In the next place, the preparation of

4) L. Doub and J. M. Vandenbelt, *J. Am. Chem. Soc.*, **69**, 2714 (1947).
5) H. B. Klevens and J. R. Platt, ibid., **71**, 1714 (1949); W. R. Remington, ibid., **67**, 1838 (1945); H. E. Ungnade, ibid.. **76**. 5133 (1954).
6) For reviews see W. Klyne in "Progress in Stereochemistry" ed. W. Klyne, Vol. 1. Butterworth's Scientific Publications. London (1954), p. 64.
7) C. K. Ingold, "Structure and Mechanism in Organic Chemistry", Cornell University press, Ithaca, N. Y., (1953), p. 427.
8) J. Weinstock, R. G. Pearson and F. G. Bordwell, *J. Am. Chem. Soc.*, **78**, 3473 (1956); E. D. Hughes, C. K. Ingold and R. Pasternak, *J. Chem. Soc.*, **1953**, 3832; S. J. Cristol and N. L. Hause, *J. Am. Chem. Soc.*, **74**, 2913 (1952); S. I. Miller and R. M. Noyes,ibid., **74**, 629 (1952).
9) Cuscohygrine, lupanine, matrine, etc., do not undergo a ring fission in the exhaustive methylation, methanol being eliminated. See, for example, T. A. Henry, "The Plant Alkaloids", 4th Ed., Churchill Ltd., London (1949), p. 103, 129 and 147; J. Read and J. Walker., *J. Chem. Soc.*, **1934**, 308; N. L. McNiven and J. Read, ibid., **1952**, 153, 159.

γ-dimethylaminopropylcyclopentane was undertaken, because this compound may be produced by the Hofmann degradation of *trans*-octahydroindole, if the Wagner-Meerwein type rearrangement of III proceeds through another possible course as indicated in Fig. 1 (b), and if the methine base (VII) thus formed is hydrogenated.

A Grignard reagent from cyclopentylmethyl bromide was treated with β-chloroethyl-*p*-toluenesulfonate to yield γ-cyclopentylpropyl chloride. The latter in ethanol was heated with dimethylamine in a closed vessel. γ-Dimethylaminopropylcyclopentane thus obtained was converted into the picrate, m.p. 108–110°, and into the picrolonate, m.p. 156–158°.

King et al.[2] reported that a hydrogenation product $C_{10}H_{21}N$ from I gave a picrate of m.p. 106° and a picrolonate of m.p. 160°. The present author's substances may be identical with theirs, but a direct comparison has not yet been possible because *trans*-octahydroindole is not easily available.

## Experimental

***cis*-Hexahydro-N-methylcarbazole Methiodide.**—(a) Ten grams of *cis*-hexahydrocarbazole[10] was heated with 8.5 g. of methyl iodide in 40 cc. of ethanol for 6 hours on a water-bath. After removal of ethanol and methyl iodide under a reduced pressure, the residual oil was shaken for half an hour with 100 cc. of ether, 50 cc. of water, and 20 cc. of 6 N potassium hydroxide solution, when crystals insoluble in both layers precipitated. After separation of the ethereal solution by decantation, the precipitate was isolated from the alkaline solution by filtration. Treatment with hot acetone for half an hour on a water-bath and subsequent filtration gave the methiodide, m.p. 196–198°. Yield 3.3 g.

*Anal.* Found: C, 51.01; H, 5.95. Calcd. for $C_{14}H_{20}NI$: C, 51.07; H, 6.16%.

The ethereal solution was shaken with 3.5 g. of benzoyl chloride and N sodium hydroxide solution for 5 hours, separated from the alkali solution, treated with N hydrochloric acid, and evaporated to yield 4.2 g. of crude *cis*-hexahydro-N-benzoylcarbazole. Recrystallized from ethanol, the substance showed m. p. 103–105°.

The hydrochloric acid solution was made alkaline and the basic oil was collected with ether. On evaporation, the ethereal solution yielded 3 g. of *cis*-hexahydro-N-methylcarbazole[11], which gave a picrate melting at 144–145°.

*Anal.* Found: C, 54.99; H, 4.71. Calcd. for $C_{19}H_{20}N_4O_7$: C, 54.80; H, 4.84.%.

(b) A mixture of 3 g. of *cis*-hexahydro-N-methylcarbazole and 3 g. of methyl iodide was allowed to stand over night at the room temperature in a closed vessel. A crystalline substance thus obtained was collected by filtration. Recrystallization from acetone gave the methiodide, m.p. 196–197°. Further quantity of the methiodide, m.p. 193–195°, was obtained on concentration of the mother liquor and addition of ether. The total yield was 3.3 g.

***trans*-Hexahydro-N-methylcarbazole Methiodide.**—(a) A mixture of 2.3 g. of *trans*-hexahydrocarbazole[10] and 4.4 g. of methyl iodide in 15 cc. of ethanol was refluxed for 8 hours on a water-bath. After removal of ethanol and methyl iodide under a diminished pressure, the product was treated with 50 cc. of ether, 40 cc. of water, and 10 cc. of 6 N potassium hydroxide solution. The precipitate and the ethereal solution were separated similarly as from the *cis*-base. Treatment of the precipitate with 20 cc. of hot acetone gave 1.8 g, of *trans*-hexahydro-N-methylcarbazole methiodide, m.p. 233–234°.

*Anal.* Found: C, 51.46; H, 6.20. Calcd. for $C_{14}H_{20}NI$: C, 51.07; H, 6.16%.

The ethereal solution was shaken with benzoyl chloride and aqueous alkali and, after 4 hours, treated with N hydrochloric acid. Crude *trans*-hexahydro-N-benzoyl-carbazole (0.8 g.) from the ethereal solution was recrystallized from ethanol and showed m.p. 130–132°. The hydrochloric acid solution gave a solid base on alkalification. Recrystallization of the base from ethanol gave 0.4 g. of *trans*-hexahydro-N-methylcabazole, m.p. 59–61°.

*Anal.* Found: C, 83.57; H, 9.08. Calcd. for $C_{13}H_{17}N$: C, 83.37; H, 9.15%.

Treatment of the base with picric acid in ethanol and recrystallization of the product from the same solvent yielded a pure picrate, m.p. 122–124°.

*Anal.* Found: C, 55.13; H, 4.66. Calcd. for $C_{19}H_{20}N_4O_7$: C, 54.80; H, 4.84%.

(b) A mixture of 1 g. of *trans*-hexahydro-N-methylcarbazole and 1 g. of methyl iodide was heated on a water-bath for one hour and the methiodide, m.p. 231–233°, was obtained substantially in a quantitative yield by a method similar to that used in the case of the *cis*-base.

**Exhaustive Methylation of *cis*-Hexahydro-N-methylcarbazole Methiodide.**—A solution of 3.5 g. of *cis*-hexahydro-N-methylcarbazole methiodide in a warm mixture of 30 cc. of water and 5 cc. of ethanol was shaken for 5 hours in the dark with silver oxide, freshly prepared from 2 g. of silver nitrate. The mixture was filtered and the filtrate was evaporated under a reduced pressure at about 60°. After most of the water was removed, the temperature was gradually raised. The syrupy quaternary hydroxide decomposed violently at 140–150°. The distillate was taken with ether and subjected to redistillation, yielding 1.4 g. (70%) of 1-(*o*-dimethylaminophenyl)-cyclohexene, b.p. 144–145° (12 mm.). Its

10) J. Gurney, W. H. Perkin and S. G. P. Plant, *J. Chem. Soc.*, **1927**, 2676.

11) W. H. Perkin and S. G. P. Plant, ibid., **1924**, 1503.

12) K. V. Auwers and W. Treppmann, *Ber.*, **48**, 1207 (1915); L. F. Fieser and J. Szmuszkvicz, *J. Am. Chem. Soc.*, **70**, 3352 (1948).

picrate showed m.p. 165–167° on recrystallization from ethanol.

*Anal.* Found: C, 55.87; H, 4.98. Calcd. for $C_{20}H_{22}N_4O_7$: C, 55.81; H, 5.15%.

The methiodide of 1-(*o*-dimethylaminophenyl)-cyclohexene was prepared in the following manner. The base (5.5 g.) was refluxed with 17 g. of methyl iodide. In half an hour, a small amount (0.3 g.) of a crystalline substance was formed and collected by filtration. This salt had a formula $C_{14}H_{20}NI$, corresponding to a simple addition of methyl iodide to 1-(*o*-monomethylaminophenyl)-cyclohexene.

*Anal.* Found: C, 51.42, 51.00, 51.41; H, 5.88, 6.11, 6.14. Calcd. for $C_{14}H_{20}NI$: C, 51.07; H, 6.14%.

The solution separated from the salt was continuously refluxed for 60 hours, the precipitates thus formed being removed by filtration every 6 hours. The precipitates were combined and recrystallized from acetone. The purified methiodide decomposed at 195–196° (at 190–192° on slow heating), and amounted to 2.3 g.

*Anal.* Found: C, 52.45, 52.94: H, 6.24, 6.58. Calcd. for $C_{15}H_{22}NI$; C, 52.48; H, 6.47%.

The filtered solution gave 2 g. of unchanged 1-(*o*-dimethylaminophenyl)-cyclohexene on complete removal of methyl iodide.

1-(*o*-Dimethylaminophenyl)-cyclohexene (0.45g.) in 20 cc. of methanol was hydrogenated in the presence of 0.5g. of 10% palladium-charcoal at the room temperature under the atmospheric pressure for half an hour. After filtration, the solution was made slightly acidic with dil. hydrochloric acid and evaporated. The residue was treated with aqueous alkali and ether, and the ethereal solution gave 0.35 g. of oily dihydro-derivative. Its picrate showed m.p. 185–187° on recrystallization from ethanol.

*Anal.* Found: C, 55.20; H, 5.34. Calcd. for $C_{20}H_{24}O_4N_7$: C, 55.55; H, 5.59%.

**Emde Reduction of 1-(*o*-Dimethylaminophenyl)-cyclohexene Methochloride.** — 1-(*o*-Dimethylaminophenyl)-cyclohexene methiodide (2 g.) in 30 cc. of warm water was shaken for 45 minutes with silver chloride, freshly prepared from 10 g. of silver nitrate. The methochloride solution was filtered and heated on a water-bath with stirring, while 200 g. of sodium amalgam (5 %) was added in portions during 6 hours. The resulting hydrocarbon was extracted with ether. From the ethereal solution 0.55 g. of the hydrocarbon[12], b.p. 134–136° (22mm.), was obtained.

*Anal.* Found: C, 91.04; H, 9.60. Calcd. for $C_{12}H_{14}$: C, 91.08; H, 8.92%. Calcd. for $C_{12}H_{16}$: C, 89.94; H, 10.06%.

The hydrocarbon (0.50 g.) was dissolved in a mixture of 35 cc. of acetone and 5 cc. of water, and 1 g. of potassium permanganate was added in portions at 40–50° during 2 hours. After addition of 10 cc. of water, the solution was filtered from manganese dioxide and concentrated on a water-bath. The residue was treated with ether to remove unchanged hydrocarbon and then acidified with conc. hydrochloric acid. The oil thus separated was collected with ether and solidified after removal of ether. Upon recrystallization from benzine, δ-benzoylvaleric acid, m.p. 72–74°, was obtained in a yield of 0.18 g. An authentic specimen[12] had m.p. 75–76°, and the mixed melting point was 73–75°.

*Anal.* Found: C, 69.50; H, 6.59. Calcd. for $C_{12}H_{14}O_3$: C, 69.88; H, 6.84%.

Treatment of this acid with semicarbazide hydrochloride and sodium acetate in aqueous ethanol and subsequent recrystallization from methanol gave its semicarbazone, m.p. 184–186°, the melting point being undepressed on admixture with an authentic specimen, m.p. 185–186°.

*Anal.* Found: C, 59.46; H, 6.43. Calcd. for $C_{13}H_{17}N_3O_3$: C, 59.30; H, 6.51%.

**Exhaustive Methylation of *trans*-Hexahydro-N-methylcarbazole Methiodide.** The reaction was carried out as already described for the *cis*-isomer. The quaternary hydroxide which was obtained by treatment of 2.8 g. of *trans*-hexahydro-N-methylcarbazole methiodide with silver oxide, prepared from 1.8 g. of silver nitrate, decomposed vigorously at 160–170°, a slightly higher temperature than in the case of the *cis*-isomer, and yielded 1.25 g. of an oil, b.p. 145–149° (13 mm.). Treatment of 0.5 g. of the base with 0.6 g. of picric acid in ethanol and two recrystallizations from the same solvent yielded 0.5 g. of the pure picrate, m.p. 168–170°, of 1-(*o*-dimethylaminophenyl)-cyclohexene, the melting point being undepressed in admixture with the picrate of the base obtained by the Hofmann degradation of the *cis*-base. The base (0.1 g.), regenerated from the picrate, was dehydrogenated with 0.4 g. of palladium charcoal (10 %) at 280–300° for 30 minutes. An oil isolated by ether-extration of the reaction product was separated into a neutral and a basic fraction with 2 N hydrochloric acid, the former (0.03 g.), m.p. 68–70°, being identified as biphenyl by the mixed melting point with an authentic specimen.

The ethanolic mother liquors of the picrate were combined and evaporated. The substance, obtained when the residue was refluxed with a small amount of acetone and the mixture was cooled, was again recrystallized from ethanol containing a small amount of acetone, yielding 0.25 g. of the picrate, m.p. 141–143°, of *cis*-hexahydro-N-methylcarbazole. The melting point was undepressed in admixture with an authentic specimen. An oily base (0.01 g.), obtained by decomposition of the picrate, was dehydrogenated with 0.03 g. of 10 % palladium-charcoal at 220° for one hour to give 0.005g. of N-methylcarbazole, m.p. 84–86°, which was identified by the mixed melting point and by comparizon of ultraviolet spectra.

**δ-Dimethylaminopropylcyclopentane.** — A Grignard reagent was prepared from 10 g. of cyclopentylmethyl bromide[13], 1.5g. of magnesium, and a small amount of iodine in 15 cc. of ether, in a three-necked flask fitted with a separating funnel, a mechanical stirrer, and a reflux condenser. After addition of 5 cc. of ether, 24 g. of β-chloroethyl-*p*-toluenesulfonate[14] in 25 cc. of

13) C. R. Noller and R. Adams, ibid., **48**, 1080 (1926).
14) S. S. Rossander and C. S. Marvel, ibid., **50**, 1497 (1928).

ether was added with stirring during one hour at such a rate that the ether refluxed gently. The reaction mixture was then refluxed gently for 8 hours to give a large amount of a white precipitate. Additional ether was added from time to time in order to keep the mixture fluid enough for efficient stirring. The reaction mixture was then decomposed with cracked ice and treated with ether and enough dil. hydrochloric acid to dissolve the basic magnesium salts. The ethereal solution was subjected to distillation and a fraction, b.p. 68–80° (20 mm.), was collected, consisting mainly of γ-chloropropylcyclopentane.

Two grams of this fraction and 15 cc. of 15% ethanolic dimethylamine were heated in a sealed tube at 160–180° for 8 hours. The reaction mixture was made acidic with dil. hydrochloric acid and then ethanol was removed by evaporation. The residue was treated with ether and water. After separation of the ethereal solution, the aqueous solution was made alkaline and the oil thus formed was removed to ether. The ethereal solution gave 0.6 g. of an oil, b.p. 80–84° (20 mm.), on fractional distillation. This oil gave the picrate, m.p. 108–110°, of γ-dimethylaminopropylcyclopentane on treatment with picric acid and recrystallization from ethanol.

*Anal.* Found: C, 49.85; H, 6.00. Calcd. for $C_{16}H_{24}N_4O_7$: C, 49.99; H, 6.29%.

The picrolonate was prepared by dissolving the oil in an ethanolic solution of picrolonic acid. It showed m.p. 156–158° on recrystallization from ethanol.

*Anal.* Found: C, 57.16; H, 6.70. Calcd. for $C_{20}H_{29}N_5O_5$: C, 57.26; H, 6.97%.

The author acknowledges gratefully the supervision by Professor Harusada Suginome, President of Hokkaido University, under which the present research was carried out. Thanks are due to Mr. Minoru Inaba for his help in some of the preparations.

*Chemistry Department, Faculty of Science, Hokkaido University*
*Sapporo*

# *Sedimentation of Spheres in a Suspension of Finite Concentration*

By Haruhiko NODA

(Received January 25, 1957)

The sedimentation velocity in a centrifugal field supplies valuable information for the size and shape determination of colloidal particles and large molecules. Sedimentation velocity, however, is dependent on the concentration of particles in the suspension. Therefore, experimental values obtained by measurements performed on solutions or suspensions of finite concentration should be extrapolated to a value for infinite dilution in order to obtain information concerning the particle size and shape using the Stokes' law.

Stokes' law was calculated by using a model in which a sphere moved through a viscous fluid medium which extended infinitely in all directions, and the Reynolds' number was assumed to be very small. In cases of sedimentation experiments on molecular or colloidal suspensions the Reynolds' number is usually very small, and the latter condition is always satisfied. However, the cells used in sedimentation experiments are not infinite in size. Since the size of particles we are concerned with is so small, the volume of the sedimentation cell can be regarded as infinite when the concentration is very low. When the concentration is high, however, the distance between particles is comparable to the size of the particles, and the condition of flow around each particle is different from that in a case in which a particle is moving through an infinite medium.

When sedimentation coefficients vs. concentration curves for various substances are examined, they seem to coincide if the concentration axis is multiplied by a suitable factor. Thus if we exactly know the situation of sedimenting spheres, we can imagine a similar situation for sedimenting molecules and colloidal particles.

A number of studies on the concentration dependene of sedimentation coefficients[1-5] have appeared in the past and

1) R. E. Powell and H. Eyring, *Advances in Colloid Science*, **1**, 183 (1942).
2) J. M. Burgers, *Proc. Acad. Sci. Amsterdam*, **44**, 1045, 1177 (1941); **45**, 9, 126 (1942).
3) J. H. Fessler and A. G. Ogston, *Trans. Faraday Soc.*, **47**, 667 (1951).
4) P. G. W. Hawksley, "Some Aspects of Fluid Flow", Paper 7, Edward Arnold, London (1951).
5) S. Uchida, *Reports of the Institute of Science and Technology, University of Tokyo*, **3**, 97 (1949); An outline by J. Happel, *Ind. Eng. Chem.*, **46**, 1194 (1954).

various equations have been proposed. However, it has been difficult to verify any such equations, because of concentration ambiguity due to particle solvation or lack of particle size uniformity in the experimental cases.

Therefore an experiment was performed on polystyrene latex of uniform spherical shape. The polystyrene latex, Dow Latex 580 G, has been studied with various methods and the size and shape of particles are well established[6]. Particles are perfectly spherical and the diameter of particles is uniform within a small range. It was also shown that polystyrene particles are not hydrated to any observable amount[7], and the volume of the latex particle can be used as its hydrodynamic volume.

## Experimental

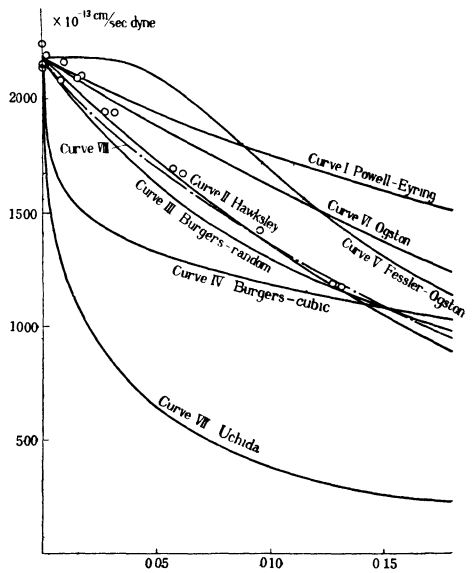
Materials and methods: By adding concentrated solution of sodium chloride, Dow Latex 580 G suspension was made 0.14 M in regard to sodium chloride, and then it was diluted to various concentrations by adding suitable amounts of 0.14 M sodium chloride solution. The solution was centrifuged in an ordinary laboratory centrifuge in a field of about $1000 \times$ g. for five minutes in order to remove aggregates.

For the determination of the concentration of latex particles, a few drops of the solution were weighed with a micro-balance, gently dried over phosphorus pentoxide and weighed again. Since the concentration of sodium chloride was known, the volume fraction concentration of latex particles was calculated using the value[7,8] for the density of polystyrene latex.

Sedimentation experiments were performed with an air-driven centrifuge of Pickels type[9] at a speed of 9000 r.p.m. The centrifugal field was about 6000 times that of gravity. The speed was controlled manually by changing the driving air pressure while observing a Lissajou's figure on a cathode ray oscillograph. The Lissajou's figure was formed by the potential caused by a magnet fixed on the air turbine, and the frequency of power supply was used as the reference. By this method the speed of rotation was readily kept within an error of 0.5%. The frequency of power supply was checked with a frequency meter.

The sedimenting boundary was observed and photographed through a schlieren optical apparatus. However, since polystyrene latex suspension was very opaque at all concentrations used in the experiment, we actually measured the absorption edge of the sedimenting boundary. The light source was a high pressure mercury discharge lamp, and was very intense. The exposure time was three seconds.

Results: sedimentation coefficients calculated and reduced for water at 20°C are shown in Fig. 1. Density and viscosity of solvent was used for the calculation. When the curve through measured points in Fig. 1 was extrapolated to zero concentration, a sedimentation coefficient of 2180 S was obtained.




Volume fraction concentration $\phi$

Fig. 1. Sedimentation coefficient for polystyrene latex particles.

## Discussion

The value of the sedimentation coefficient for Dow Latex 580 G at infinite dilution obtained above agrees well with the value obtained by Hogeboom and Kuff[10]. The work of Cheng and Schachman[11] was published after our completion of the experiment, and their value agrees well with the value obtained here when it is corrected for the temperature difference.

By using Stokes' law, the diameter of the polystyrene latex was calculated as 268 m$\mu$ from the sedimentation coefficient value extrapolated to infinite dilution. This is in good agreement with values obtained by other methods[6,12,13].

6) C. H. Gerould, *J. Appl. Phys.*, **21**, 183 (1950).
7) D. G. Sharp and J. W. Beard, *J. Biol. Chem.*, **185**, 247 (1950).
8) R. C. Williams and R. C. Backus, *J. Am. Chem. Soc.*, **71**, 4052 (1949).
9) I. Watanabe, Y. Kawade and S. Mizushima, *J. Chem. Soc. Japan (Pure Chem. Sect.)*, **73**, 828 (1952).
10) G. H. Hogeboom and E. L. Kuff. *J. Biol. Chem.*, **210**, 733 (1954).
11) P. Y. Cheng and H. K. Schachman, *J. Polymer Sci.*, **16**, 19 (1955).
12) W. B. Dandliker, *J. Am. Chem. Soc.*, **72**, 5110 (1950).
13) B. R. Leonard, Jr., J. W. Anderegg, P. Kaseberg and W. W. Beeman, *J. Appl. Phys.*, **23**, 152 (1952).

In Fig. 1, together with the experimental values, curves are shown which were calculated from formulae which have been proposed by various authors.

Curve I was calculated using the formula of Powell and Eyring[1].

$$s=s_0/(1+\nu\phi) \quad (1)$$

$\phi$: Volume fraction concentration.
$s$: Sedimentation coefficient at $\phi$.
$s_0$: Sedimentation coefficient at infinite dilution.
$\nu$: Volume fraction limiting viscosity number for solute particles.

This formula was calculated by using a model in which only one particle was assumed to be sedimenting while all the other particles were assumed not to be in motion. However, such a situation is never realized in actual cases, as all the particles sediment at the same time. The fact that curve I does not agree with experimental points shows that the model used by Powell and Eyring was not suitable. It has also been pointed out[14] that in cases in which $\nu$ was very large, the term $(1+\nu\phi)$ of formula (1) was too large to explain experimental values.

Curve II in Fig. 1 was obtained from the formula of Hawksley[4],

$$s/s_0=(1-\phi)^2\exp.(-k\phi/(1-Q\phi)) \quad (2)$$

$k$: Einstein's shape factor for viscosity. 2.5 for spheres.
$Q$: Vand's interaction constant. 39/54 for spheres.

and is quite well fitted to the experimental values. This formula was derived by considering three effects: apparent increase of the viscosity of the medium by the presence of particles, apparent increase of buoyancy due to apparent increase of the density of the medium, and the back flow of the medium. However, when we consider the fact that all the particles sediment at the same time and there is no relative velocity between particles, the first and the second effect are not likely to exist. Hawksley calculated the first effect according to Vand's modification[15] of Einstein's formula for viscosity.

$$\eta_{rel.}=\exp.(k\phi/(1-Q\phi)) \quad (3)$$

$\eta_{rel.}$: Viscosity ratio.

However, it was reported by Cheng and Schachman[11] that formula (3) does not agree with experimental values for Dow Latex 580 G. If actual values[11] of the viscosity of the suspension of Dow Latex 580 G were substituted into formula (2), the sedimentation velocity at a concentration of 8% will be about 5% lower. Thus, the excellent coincidence of the values calculated by the formula (2) with experimental values seems to be fortuitous.

Burgers derived a relation for the dependence of sedimentation velocity on concentration assuming a hypothetical function of flow[2]. Curve III and IV show results obtained by Burgers. Curve III was calculated assuming a random arrangement of sedimenting particles and curve IV was calculated by assuming a cubic arrangement of particles. Curve III follows the experimental points fairly well.

The formula of Fessler and Ogston[3] is shown in Fig. 1 as curve V. This formula was derived by considering that when the concentration is very high the resistance of sedimenting particles approaches that of a porous plug, but is unsatisfactory in two points. The equation by Sullivan ane Hertel[16] for fluid flow through a porous plug is used in the formula, and it includes the effect of back flow of the medium by the nature of the equation. The use of the Enoksson's factor[17] in the derivation of the formula was theoretically unnecessary. It is also not justifiable to add the term $1/s_0$ to the term derived from the equation by Sullivan and Hertel. Recently Ogston[18] has used a modified form, and it is shown as curve VI in Fig. 1.

Curve VII shows the result numerically calculated by Uchida[5] on a model of spheres sedimenting in a cubic arrangement. The resistance calculated by using such a model is far larger than that for actual sedimenting latex particles, and this fact suggests that the actual arrangement shows less resistance than a cubic arrangement although particles are likely to be in some kind of arrangement while sedimenting. When particles are distributed at random in space and time, the average resistance against sedimenting particles should be, as was pointed out by Hawksley[4], inversely proportional to the volume fraction of the suspending medium. The increase of resistance due to this effect is too small to explain the

14) I. Jullander, *J. Polymer Sci.*, **2**, 329 (1947).
15) V. Vand, *J. Phys. Coll. Chem.*, **52**, 277 (1948).
16) R. R. Sullivan and K. L. Hertel, *Advances in Colloid Sci.*, **1**, 37 (1942).
17) B. Enoksson, *Nature*, **161**, 934 (1948).
18) A.G. Ogston, *Trans. Faraday Soc.*, **49**, 1481 (1953).

TABLE I

APPARENT VOLUME FOR MOLECULES WITH SOLVATION CALCULATED FROM THE CONCENTRATION DEPENDENCE OF SEDIMENTATION COEFFICIENT

| Substance | $v/v_0$ | $\sqrt[3]{v/v_0}$ | $f/f_0$ | $(f/f_0)/\sqrt[3]{v/v_0}$ |
|---|---|---|---|---|
| Collagen[19] | 8.5×10 | 4.4 | 9.7* | 2.2 |
| Herring sperm deoxyribonucleic acid. (Preparation 1b)[20] | 6.4×10 | 4.0 | 5.0 | 1.25 |
| Cellulose acetate[21] (in acetone) | 4.3×10 | 3.5 | 3.5 | 1.0 |
| Cellulose nitrate (Fraction I/6)[22] (in acetone) | 3.0×10 | 3.1 | 4.6 | 1.5 |
| Sodium cellulose xanthate[23] (Preparation No. 8) | 2.0×10 | 2.7 | 3.4 | 1.3 |
| Polystyrene (Fraction PSAF)[24] (in decaline) | 1.4×10 | 2.4 | 3.3 | 1.3 |
| Bovine serum albumin[25] | 2.2 | 1.3 | 1.3 | 1.0 |
| Calf thymus histone[26] (Histone I) | 3.4 | 1.5 | 1.9 | 1.3 |
| Bovine fibrinogen[27] | | | | |
| Native | 4.9 | 1.7 | 2.2 | 1.3 |
| Denatured, at pH 5.5 | 1.2×10 | 2.3 | 3.0 | 1.3 |
| Denatured, at pH 3.5 | 2.2×10 | 2.8 | 3.0 | 1.1 |

concentration dependence of the sedimentation coefficient, and suggests that the particles are in some kind of spacial arrangement with each other.

Curve VIII was drawn according to the formula*:

$$s_0=s\{1+\phi^{2/3}/(1-\phi^{1/3})^2(1+2\phi^{1/3})\} \qquad (4)$$

Within the range of concentration in which experiments were possible with polystyrene latex, formula (4) agreed well with the experimental points. Therefore formula (4) can be used as an experimental formula for the concentration dependence of the sedimentation coefficient.

Since the relation of sedimentation coefficient to concentration was experimentally established, and can be represented by formula (4), we came to be able to find the apparent volume of particles by measuring the concentration dependence of the sedimentation coefficient. The apparent volume obtained in such a way may be different from that for the substance in dry condition. The ratio of such apparent volume to the dry volume, $v/v_0$, was calculated for various substances from available values of sedimentation experiments and the results are shown in Table I. In all cases the curves for the dependence of sedimentation coefficient were very similar to that for the polystyrene latex, when $s/s_0$ values were plotted against volume fraction concentration calculated from the apparent volume in solution. This fact seems to suggest that the particles with solvation are nearly spherical in sphape in these cases. In the fourth column of Table I, values of the frictional ratio of particles calculated from values of the sedimentation coefficient and diffusion constant are shown. The cube root of $v/v_0$ and the frictional ratio have a very close relation with each other. This suggests that values of the frictional ratio larger than unity can be explained for the most part by the increase of

* When the concentration is high and each sphere is sedimenting surrcunded by many other spheres of the same size at close distances, we may assume that at the middle point of a line which connects the center of the sphere to the center of one of the surrounding spheres, the line of flow is at a right angle to the line. Such a condition may be represented by a model in which a sphere moves at the center of a spherical shell on the surface of which the liquid slips perfectly. A simple calculation was performed on such a model using the Stokes' function of flow, and the resistance against the movement of the sphere was calculated. Then the sedimentation velocity of the sphere at the center of such a spherical shell was calculated as follows:

$$s=s_0(1-a/b)^2(1+2a/b)$$

where $a$ is the radius of the sphere and $b$ is the radius of the spherical shell. Thus $a/b$ is approximately $\phi^{1/3}$. This model was too crude, and the calculated result did not agree with experimental results.

* This value is different from the value reported in the article cited. By later experiments the diffusion constant for collagen was found to be $0.3\times10^{-7}$cm$^2$./sec.

19) H. Noda, *Biochim. Biophys. Acta*, **17**, 92 (1955).
20) Y. Kawade, ibid., **19**, 513 (1957).
21) S. J. Singer, *J. Chem. Phys.*. **15**, 341 (1947).
22) H. Mosiman, *Helv. chim. Acta*, **26**, 61 (1943).
23) N. Gralen, Inaugural Dissertation, Uppsala 1944.
24) A. F. Schick and S. J. Singer, *J. Phys. Coll. Chem.*, **54**, 1028 (1950).
25) V. L. Konig and J. D. Perrings, *Arch. Biochem. Biophys.*, **41**, 367 (1952).
26) N. Ui in Press, This Bulletin.
27) H. A. Scheraga, W. R. Carroll, L F. Nims, E. Sutton, J. K. Buckus and J. M. Saunders, *J. Polymer Sci.*, **14**. 427 (1954).

apparent volume of molecules or particles by solvation. The great amount of solvent which accompanies molecules in the cases of collagen and a preparation of deoxyribonucleic acid is surprising, but if such molecules are considered to be composed of long chains and to be in the shape of a random coil, it is possible for them to be accompanied by such an amount of solvent.

When the above method of estimating the amount of solvation was applied to the sedimentation data of fibrinogen by Scheraga et. al.[27], as is shown in Table I, the amount of solvation obtained for denatured fibrinogen was larger than that for native fibrinogen, and the increase in the frictional ratio due to denaturation was explained by the increase in the apparent volume of molecules. Scheraga et. al. reached a similar conclusion using their data on various hydrodynamic properties on the basis of the work of Scheraga and Mandelkern[28].

It should be noted that formula (4) was verified only for the case of sedimenting spheres. Therefore the above discussion is not decisive, especially in cases in which the ratio $(f/f_0)/\sqrt[3]{v/v_0}$ is far from unity. In order to determine exact contributions by the molecular shape and solvation to the increase of frictional ratio, we should know the relation between the molecular shape and the concentration dependence of the sedimentation coefficient.

28) H. A. Scheraga and L. Mandelkern, *J. Am. Chem. Soc.*, **75**, 179 (1953).


## Summary

Experiments were performed in order to find out the relation between the volume fraction concentration and the sedimentation coefficient in a suspension of spheres. The polystyrene latex suspension, Dow Latex 580 G, was used as the suspension of spheres of known hydrodynamic properties. No theoretical equation proposed in the past corresponds well with the experimental result obtained here. Therefore an experimental equation,

$$s_0=s\{1+\phi^{2\ 3}/(1-\phi^{1/3})^2(1+2\phi^{1/3})\}$$

is proposed. Using this equation the amount of solvation in solution of some proteins and other molecules was calculated. The amount of solvation found is nearly enough to explain the frictional ratio for such molecules..


We should like to express our deep gratitude to Dr. Backus of the University of California who kindly provided us with Dow Latex 580 G suspension. The author is indebted to Dr. Yoshimi Kawade of the Virus Research Institute, Kyoto University for his cooperation in performing the sedimentation experiments and for his helpful discussions.

*Institute of Science and Technology*
*The University of Tokyo, Meguro-ku, Tokyo*

# *The Stretching Vibration of N-H Link of 2-Aminopyridine*

By Reisuke SODA

(Received February 6, 1957)

## Introduction

The Watson-Crick model on the molecular structure of deoxyribonucleic acid[1] has been regarded as an excellent picture but it leaves some doubts about its certainty. One of them is concerned with the tautomerism of base. The present study is undertaken in order to provide confirmatory data for the tautomerism of 2-aminopyridine as the simplest base.

Whether 2-aminopyridine exists in the amino form or in the imino form has been discussed for years[2-4] and now many

1) J. D. Watson and F. H. C. Crick, *Nature*, **171**, 737, 964 (1953); F. H. C. Crick and J. D. Watson, *Proc Roy. Soc., London*, **A223**, 80 (1954).

2) E. A. Steck and G. W. Ewing, *J. Am. Chem. Soc.*, **70**, 3397 (1948); L. C. Anderson and N. V. Seeger, ibid., **71**, 340 (1949).

3) A. E. Tschitschibabin, R. A. Konowalowa and A. A. Konowalowa, *Chem. Ber.*, **54B**, 814 (1951).

4) S. L. Angyal and C. L. Angyal, *J. Chem. Soc.*, **1952**, 1461.

results support the amino form of this compound. Experimental results obtained from infrared absorption spectra[5,6] also support the amino form but their discussions are limited on the absorption band position of the stretching vibration and the deformation vibration of the N-H link; consequently their conclusions appear to be qualitative and unsatisfactory. In this report the observation covers not only the band frequency but also the integrated intensity; moreover a reliable conclusion for the amino form is obtained.

## Experimental

The Perkin-Elmer model 112 spectrophotometer with a lithium fluoride prism was used[7], but the measurement on toluidines was carried out with a calcium fluorite prism. The theoretically calculated slit widths were 5 $cm.^{-1}$ at 3400 $cm.^{-1}$ for the calcium fluorite and 3 $cm.^{-1}$ for the lithium fluoride. These values were about one fifth of each band width, but the actual slit widths were considered to be wider than the aforementioned values[8]. The cell thickness was about 10 mm. and the concentration of solution was taken from 0.02 moles per liter to 0.001, in order to put optical densities in the range of 0.8 to 0.2. The range of the observed wave number was from 3700 $cm.^{-1}$ to 3000 $cm^{-1}$.

The c.p. carbon tetrachloride was used as the solvent, which was distilled after drying with phosphorous pentoxide. The reagents were purified as follows. Aniline was distilled at 90°C/16 mmHg and pyrrole at 130°C. Indole[9] was recrystallized from ethanol-water solvent. 2-Aminopyridine was recrystallized from ligroine with petroleum ether, one part of which was further purified by vacuum distillation. Only c.p. toluidines were used without purification.

N-Methyl-2-pyridonimine was synthesized from methyl iodide and 2-aminopyridine by the method of Tschitschibabin et al.[3]; after recrystallization of the product, 2-aminopyridine methiodide from alcohol, its aqueous solution was treated with fresh silver oxide obtained from silver nitrate and sodium hydroxide and the filtrate was concentrated *in vacuo*. The final viscous greenish liquor was distilled at 100°C/12 mmHg. The distillate was slightly yellow and viscous, and turned to a brownish-red substance which became more viscous in the air. Therefore the distillation was carried out at every measuremnt. The purities of reagents were justified by comparison of observed spectra with those given in the literatures.

The molar extinction coefficient and the integrated intensity of the absorption band were obtained with the usual extrapolation method[5]. But in the case of a band overlapping, the following method is preferable. First, the total area of two bands is measured with planimeter. Next, the values of the products, 'the peak optical density times the half-band width' for both the absorption bands are obtained respectively and the ratio of these values is calculated. Then the total area is proportionally divided into two bands according to this ratio and the area of each band determined.

The units of those values are as follows:

$$E = (1/cl)\log_{10}(I_0/I)\ \text{cm.}^2\cdot\text{mol.}^{-1}$$

$$A = (1/cl)\int \ln(I_0/I)\,d\nu\ \text{cm.}^2\cdot\text{molecule}^{-1}\cdot\text{sec.}^{-1}$$

Where $c$ is the concentration of the solution in moles per cc. for the molar extinction coefficient $E$, and in number of molecules per cc. for the integrated intensity $A$; $l$, the thickness of the cell in cm.; $\nu$, the frequency of the infrared rays in cycles per sec,; $I_0$ and $I$, the radiation intensity transmitted through the solvent and solution respectively.

## Results

In the Table, the peak frequency (the band position) $\nu$, the molar extinction coefficient $E$, the half-band width $\Delta\nu_{1/2}$, and the integrated intensity $A$ are cited. Aniline and three isomers of toluidines, which are representatives of the compounds of the amino form, give rise to two absorption bands near 3480 $cm.^{-1}$ and 3390 $cm.^{-1}$, those bands having the intensities of the same order. The spectrum of 2-aminopyridine shows a similar tendency as the aforementioned four compounds. The heterocyclic compounds as pyrrole and indole, in which a hydrogen atom links to the ring nitrogen atom, show the spectra.

TABLE I
OBSERVED VALUES OF THE N-H STRETCHING VIBRATIONS

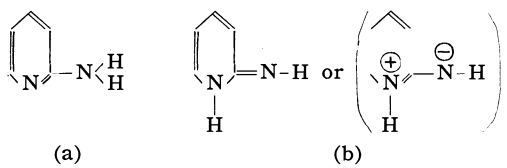
| Compounds | $\nu$ ($cm.^{-1}$) | $E\times10^{-4}$ ($cm.^2$ $mol.^{-1}$) | $\Delta\nu_{1/2}$ ($cm.^{-1}$) | $A\times10^{-8}$ ($cm.^2$ $molecule^{-1}$ $sec.^{-1}$) |
|---|---|---|---|---|
| Pyrrole | 3495 | 25 | 13 | 65 |
| Indole | 3490 | 23 | 13 | 60 |
| N-Methyl-2-pyridonimine | 3322 | 1.8 | 24 | 9 |
| 2-Aminopyridine | 3510 | 5.4 | 32 | 28 |
| | 3410 | 7.6 | 25 | 31 |
| Aniline | 3481 | 3.0 | 39 | 17 |
| | 3397 | 3.8 | 28 | 15 |
| *o*-Toluidine* | 3481 | 3.1 | 35 | 15 |
| | 3399 | 3.5 | 26 | 12 |
| *m*-Toluidine* | 3479 | 3.1 | 39 | 18 |
| | 3396 | 3.9 | 28 | 16 |
| *p*-Toluidine* | 3472 | 2.9 | 39 | 17 |
| | 3391 | 3.6 | 29 | 16 |

* The data of toluidines are obtained with a calcium fluoride prism, whilst others with a lithium fluoride prism.

5) C. L. Angyal and R. L. Werner, ibid., 2911.
6) J. D. S. Goulden, ibid., 2939.
7) The measurement was carried out in the Laboratory of Professor Kunio Kozima in Tokyo Institute of Technology, Tokyo.
8) D. A. Ramsay, *J. Am. Chem. Soc.*, **74**, 72 (1952).
9) This sample was kindly given by Mr. Takaaki Tamura, in this Institute.

with one sharp and intense absorption band attributed to the stretching vibration of the N-H link near 3490 cm.$^{-1}$. The spectrum of N-methyl-2-pyridonimine[10] which is selected as a representative of the compound of the imino form, shows a weak and broad band at 3322 cm$^{-1}$.

The above results are obtained from the measurements in a fairly dilute solution and there seems no absorption band which is ascribed to the associated molecule. From the data of the other authors[11] it can be also said that there will be no fear of the existence of the associated molecule in such a low concentration.



(a) (b)

Fig. 1. The tautomerism of 2-aminopyridine.

## Discussion

As illustrated in the Table, the compounds of the amino form generally show two absorption bands with the same order of intensities near 3480 cm.$^{-1}$ and 3390cm$^{-1}$. Of these bands, the higher frequency one is assigned to the antisymmetric and the lower to the symmetric vibration of the $NH_2$ group, and the integrated intensity of the former is somewhat larger than the latter. While in 2-aminopyridine two bands are observed at 3510 cm.$^{-1}$ and 3410 cm.$^{-1}$ respectively and the integrated intensity of the former has larger value than the latter, the values of which are considerably larger than those of aniline etc. Although there are such trivial differences from aniline etc., the facts that the bands appear at the similar positions as aniline etc. and that intensities of the two bands have the values of the same order, show the coincidence of the spectrum of 2-aminopyridine with those of the compound of the amino form[12].

If 2-aminopyridine exists in the imino form, (Fig. 1b), then the absorption spectrum will show approximately the sum of the absorption assigned to the vibrations of the N-H link of pyrrole type and that of imino type; i.e., a sharp and strong band near 3490 cm.$^{-1}$ and a broad and extraordinarily weak band near 3320 cm$^{-1}$. This feature does not even qualitatively coincide with the observed spectrum of 2-aminopyridine. In fact, in the spectrum of 2-aminopyridine, there is no band near 3320 cm.$^{-1}$ and even if for some reasons this band would shift to about 3410 cm$^{-1}$., it will be impossible to explain the fact that the value of the integrated intensity of the band of the lower frequency vibration is apparently larger.

From those facts it will be concluded that 2-aminopyridine exists mainly or decidedly in the amino form in a dilute solution of the nonpolar solvent.

In the spectrum of 2-aminopyridine, a wing of the band of 3410 cm$^{-1}$. extends to 3320 cm$^{-1}$. but no superposition of bands is observed. If the tautomerism exists between the imino and the amino form (Fig. 1), considering the experimental accuracy and the noise level of spectrum, it is possible to estimate the ratio of the number of the molecules of imino structure allowed to exist to that of the amino structure. According to the simple calculation this possibility is estimated to be less than 0.5 %, hence even if there were a tautomerism it is concluded that the amino form is decidedly predominant over the imino form. This conclusion is consistent with the measurement on the $pK_a$, in which such a possibility is estimated to be less than 0.001 %[4].

## Summary

The infrared absorption spectrum of 2-aminopyridine was observed and compared with those of other compounds and the amino form of 2-aminopyridine was confirmed. The imino form was rejected and even if this tautomeric form exists its quantity is estimated to be negligibly small.

The author wishes to express his hearty thanks to Assistant Professor Kenji Kuratani for his kind guidance and encouragement throughout this work. The author is indebted to Mr. Kiyoshi Sakashita in the Laboratory of Professor Kunio Kozima for his kind help at the time of the measurement of the infrared absorption spectra.

*Institute of Science and Technology*
*University of Tokyo, Meguro-ku, Tokyo*

10) N-Methyl-2-pyridonimine is very hygroscopic and even its dilute solution is not sufficiently transparent, but there is almost no influence of such a property on the observation.

11) N. Fuson, M-L. Josien, R. L. Powell and E. Utterback, *J. Chem. Phys.*, **20**, 145 (1952).

12) For the considerable increment of the intensity of 2-aminopyridine, the following qualitative explanation is given. Generally when the electrophilic radical or atom combines to the ring, the band shifts to the higher frequency[6] and the ionic character of NH bond is considered to increase, so that the change of the dipole moment in the vibration will become larger.

# *Absorption Spectra of Heteropolyanions. II*[1] *The Heteropolytungstates Containing Co(II), Co(III) or Mn(IV) as Central Ions*

By Yoichi SHIMURA and Ryutaro TSUCHIDA

(Received February 18, 1957)

## Introduction

In the former paper of this series[1], the absorption spectra were reported for the heteropolymolybdates containing Co(III), Cr(III), Fe(III), Al(III), Mn(IV) or Ni(IV) as central ions. X-ray investigations[2,3], magnetic measurements[4] and other physico-chemical studies[5] by many authors have revealed that the central ion M is at the center of $MO_6$ octahedron. The absorption spectra of these heteropolymolybdates were therefore regarded as the absorption spectra of $[M(O^=)_6]$-complexes.

In the present paper, absorption spectra of the heteropolytungstates containing some transition metals as central ions have been measured. Of special interest are the heteropolyanions containing Co (II) or Co(III), which were very recently discovered and thoroughly investigated by Baker and McCutcheon[6]. Our spectral studies have clearly established the fact that the Co(II) or Co(III) ion is at the center of a tetrahedron, in contrast to the conclusion of Baker et al., who offered some octahedral structures.

The present paper is probably the first one that describes the absorption spectra of $[Co^{II}(O^=)_4]$- and $[Co^{III}(O^=)_4]$-complexes.

## Experimental

The absorption measurements were made in aqueous solutions by a Beckman DU spectrophotometer at room temperature. The concentration of the solutions varied from $0.5\times10^{-2}$ to $0.2\times10^{-4}$ F/l. The formula weights were calculated from the formulae listed in Table I, on which are also tabulated the literature for preparation and the tentative structural formulae which are proposed for the anions from our spectral studies.

## Results and Discussion

(1) $3Na_2O\cdot5WO_3\cdot Mn^{IV}O_2\cdot18H_2O$—The absorption spectrum of this compound is shown in Fig. 1, in which the spectrum[1] of $[Mn^{IV}O_6Mo_9O_{26}]^{6-}$ is also plotted for

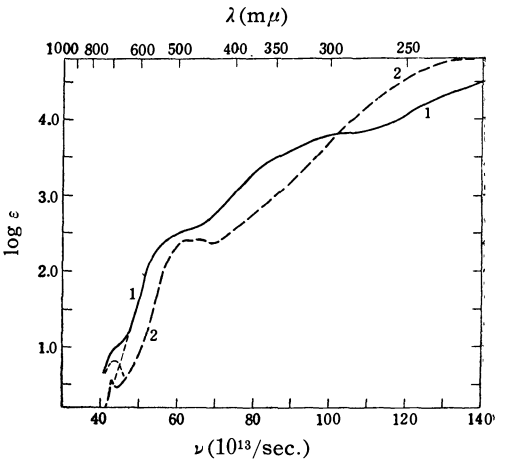



Fig. 1. Absorption spectra of:
1, $3Na_2O\cdot5WO_3\cdot Mn^{IV}O_2\cdot18H_2O$;
2, $(NH_4)_6[Mn^{IV}O_6Mo_9O_{26}]\cdot6H_2O$[1].

comparison. The structure of the latter ion was well established by an X-ray analysis[2]. Therefore, a broad band at $64.1\times10^{13}$/sec. ($\log\varepsilon_{max}=2.42$) and a narrow band at 42.9 (0.55), are equally due to the complex $[Mn^{IV}(O^=)_6]$. Recently, from the viewpoint of crystal field theory, Jørgensen[8] suggested that the narrow band is due to a spin-forbidden transition $^4\Gamma_2-^2\Gamma_3$ and the broad band to a spin-allowed transition $^4\Gamma_2-^4\Gamma_5$(F).

As to the heteropolytungstate presently studied, the narrow band is observed as an inflation of the absorption curve. A curve analysis shown in Fig. 1 as dotted lines, gives the maximum intensity log $\varepsilon$=ca. 0.8 at frequency ca. 43.5. The broad band is similar to that of the correspond-

1) Part I of this series: Y. Shimura, H. Ito and R. Tsuchida, *J. Chem. Soc. Japan*, **75**, 560 (1954).
2) J. L. T. Waugh, D. P. Shomaker and L. Pauling, *Acta Cryst.*, **7**,438 (1954).
3) C. W. Wolfe, M. L. Block and L. C. W. Baker, *J. Am. Chem. Soc.*, **77**, 2200 (1955).
4) P. Rây, A. Bhaduri and B. Sarma, *J. Indian Chem. Soc.*, **25**, 51 (1948).
5) L. C. W. Baker, G. Foster, W. Tan, F. Scholnick and T. P. McCutcheon, *J. Am. Chem. Soc.*, **77**, 2136 (1955).
6) L. C. W. Baker and T. P. McCutcheon, *J. Am. Chem. Soc.*, **78**, 4503 (1956).
7) A. Just, *Ber.*, **36**, 3619 (1903).
8) C. K. Jørgensen, *Acta Chem. Scand.*, **9**, 1362 (1955).

TABLE I

FORMULAE OF THE HETEROPOLYTUNGSTATES

| Formula previously used | Formula Weight | Color | Literature for preparation | Tentative structural formulae for the heteropoly-anions |
|---|---|---|---|---|
| $3Na_2O \cdot 5WO_3 \cdot Mn^{IV}O_2 \cdot 18H_2O$ | 1756.5 | orange red | 7) | $[(Mn^{IV}O_6W_5O_{14})_n]^{6n-}$ |
| $K_5H_5[Co^{II}(W_2O_7)_6] \cdot 16H_2O$ | 3426.1 | bluish green | 6) | $[Co^{III}O_4W_{12}O_{38}]^{10-}$ or $[Co^{III}O_4W_{12}O_{36}]^{6-}$ |
| $K_4H_5[Co^{III}(W_2O_7)_6] \cdot 18H_2O$ | 3423.0 | golden yellow | 6) | $[Co^{III}O_4W_{12}O_{38}]^{9-}$ or $[Co^{III}O_4W_{12}O_{36}]^{5-}$ |
| $(NH_4)_8[Co^{II}Co^{II}(W_{12}O_{42})] \cdot 20H_2O$ | 3501.3 | emerald green | 6) | $[Co^{II}O_4(W_{12}O_{32})O_6Co^{II}]^{8-}$ |
| $K_7[Co^{II}Co^{III}(W_{12}O_{42})] \cdot 16H_2O$ | 3558.2 | dark brown | 6) | $[Co^{III}O_4(W_{12}O_{32})O_6Co^{II}]^{7-}$ |

ing molybdenum compound, i.e., maximum at about 63 with intensity log $\varepsilon_{max}$=ca. 2.5.

Another very broad band is situated at the frequency region of 70–100. This is probably due to a polynuclear structure,

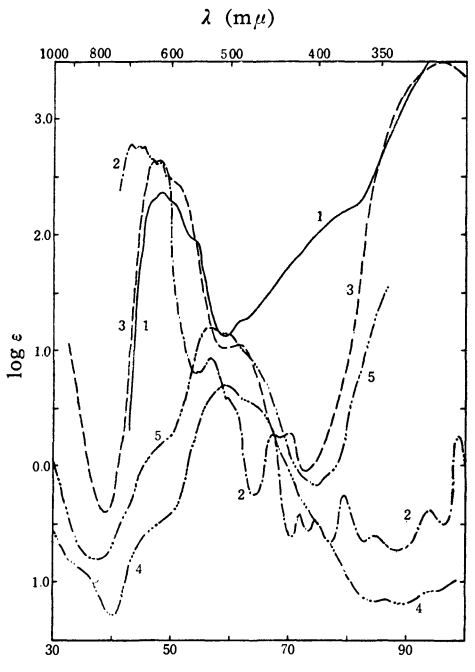



Fig. 2. Absorption spectra of:
1, $K_5H_5[Co^{II}(W_2O_7)_6] \cdot 16H_2O$;
2, $[Co\ Cl_4]^{2-}$ [11];
3, $[Co\ (NCS)_4]^{2-}$ [12];
4, $[Co\ (OH_2)_6]^{2+}$ [13];
5, $[Co\ (ox)_2\ (OH_2)_2]^{2-}$ [14].

i.e., a structure having two or more central manganese(IV) atoms with a linkage of Mn-O-Mn in the anion. A similar conclusion was previously obtained by the present authors[1] in connection with a heteropolymolybdate, $2(NH_4)_2O \cdot Co^{III}_2O_3 \cdot 10MoO_3 \cdot 12H_2O$, in which the ratio of central hetero-atom to molybdenum atom is 1 : 5. Likewise in the heteropoly tungstate concerned, the ratio of Mn : W is 1 : 5.

In conclusion, a tentative structural formula $[(Mn^{IV}O_6W_5O_{14})_n]^{6n-}$ may be assigned to the anion of this salt.

(2) $K_5H_5[Co^{II}(W_2O_7)_6] \cdot 16H_2O$—In Fig. 2, the absorption spectrum of this compound is compared with those of some cobalt (II) complexes, the structure of which was well established. $[CoCl_4]^{2-}$ and $[Co\ (NCS)_4]^{2-}$ are tetrahedral and have very different spectra in visible region as compared with those of octahedrally co-ordinated cobalt (II) complexes such as $[Co(OH_2)_6]^{2}$ etc.[12,15,16] From the figure, it is evident that the heteropolytungstate has a tetrahedrally co-ordinated cobalt (II) ion. The spectrochemical series for ligands of tetrahedrally co-ordinated cobalt (II) complexes have now been determined as follows:

$O^{=}$ (heteropolytungstate)*, $NCS^{-}$, $Cl^{-}$, $Br^{-}$ [17], $I^{-}$ [17].

The order coincides very well with that of cobalt (III) complexes[9,10]. Baker et al.[6] assigned to this heteropolyanion a structural formula $[Co^{II}O_6W_{12}O_{36}]^{10-}$. But some modifications seem necessary on the basis of the above spectral data. The anion is probably represented by the formula $[Co^{II}O_4W_{12}O_{38}]^{10-}$ or $[Co^{II}O_4W_{12}O_{36}]^{6-}$.

(3) $K_4H_5[Co^{III}(W_2O_7)_6] \cdot 18H_2O$—This is a cobalt (III) analogue of the cobalt (II)

* Maximum values: $\nu_{max}$=48.4×10¹³/sec., log $\varepsilon_{max}$=ca. 2.36.

9) R. Tsuchida, This Bulletin, **13**, 388, 436 (1938).
10) Y. Shimura and R. Tsuchida, This Bulletin, **29**, 311 (1956).
11) A. Kiss and M. Gerendás, *Z. Physik. Chem.*, **A180**, 117 (1937).
12) S. Yamada and R. Tsuchida, This Bulletin, **27**, 436 (1954).
13) H. Ito, *J. Chem. Soc. Japan*, **77**, 1383 (1956).
14) H. Ito, unpublished data.
15) C. J. Ballhausen and C. K. Jφrgensen, *Acta Chem. Scand.*, **9**, 397 (1955).
16) L. E. Orgel, *J. Chem. Phys.*, **23**, 1004 (1955).
17) W. R. Brode, *J. Am. Chem. Soc.*, **53**, 2457 (1931).

compound above mentioned. The two species can be reversibly converted into each other by oxidation and reduction[6]. This fact suggests that the central cobalt (III) atom in the oxidized species is also surrounded by four oxigen atoms. As was expected from this, the spectrum of this compound has a very unique feature and is entirely different from the spectra of hexa-coordinated Co (III) complexes (Fig. 3). A broad maximum is observed at frequency of about 77.0 with intensity $\log \varepsilon = 3.10$. This is the first example of

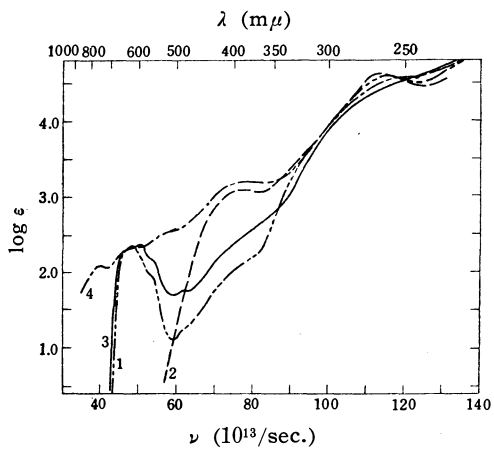



Fig. 3. Absorption spectra of:
1, $K_5H_5[Co^{II}(W_2O_7)_6]\cdot 16H_2O$;
2, $K_4H_5[Co^{III}(W_2O_7)_6]\cdot 18H_2O$;
3, $(NH_4)_8[Co^{II}Co^{II}(W_{12}O_{42})]\cdot 20H_2O$;
4, $K_7[Co^{II}Co^{III}(W_{12}O_{42})]\cdot 16H_2O$.

such a tetrahedrally co-ordinated cobalt (III) complex, of which the spectrum was measured. A heteropolymolybdate containing a hexa-coordinated Co (III) atom shows in this region two absorption bands with lower intensities[1].

(4) $(NH_4)_8[Co^{II}Co^{II}(W_{12}O_{42})]\cdot 20H_2O$ — The absorption spectrum of this compound (Fig. 3) reveals that it contains at least one cobalt(II) atom in tetrahedrally co-ordinated state. The intensity of the band characteristic of the tetrahedral cobalt(II) ion is of the same order of the uninuclear cobalt(II) heteropolytungstate above mentioned. Thus it is perhaps certain that the other cobalt(II) atom in this compound has an octahedrally co-ordinated structure. Since such an octahedrally co-ordinated cobalt(II) ion is expected to have less intense absorption than a tetrahedral cobalt(II) ion, the presence of the octahedral cobalt(II) ion has little contribution to the total form of the absorption curve. A tentative structural formula $[Co^{II}O_4(W_{12}O_{32})O_6Co^{II}]^{8-}$ seems adequate for the anion. This is in good agreement with the chemical evidence reported by Baker et al.[6] who concluded that the two cobalt atoms are structurally non-equivalent.

(5) $K_7[Co^{II}Co^{III}(W_{12}O_{42})]\cdot 16H_2O$ — This dark brown compound can be reversibly converted into the above mentioned $Co^{II}Co^{II}$ compound. The absorption curve of the compound has a complicated structure as is seen in Figs. 3 and 4. The occurrence of a broad band at about 78.0 ($\log \varepsilon_{max} = 3.20$) proves that the cobalt atom which was oxidized is the tetrahedrally co-ordinated one. Therefore the formula of this anion becomes $[Co^{III}O_4(W_{12}O_{32})O_6Co^{II}]^{7-}$.

The complicated bands in the visible region suggest the interactions between the

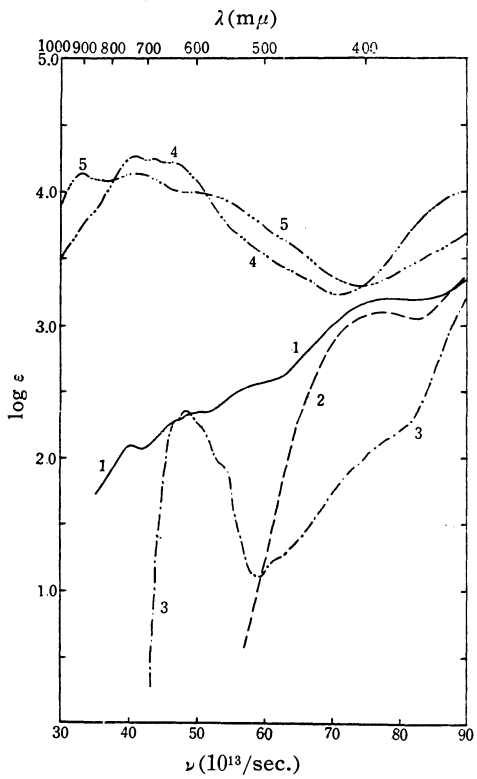



Fig. 4. Absorption spectra of:
1, $[Co^{III}O_4(W_{12}O_{32})O_6Co^{II}]^{7-}$;
2, $[Co^{III}O_4(W_{12}O_{38})]^{9-}$ or $[Co^{III}O_4(W_{12}O_{36})]^{5-}$;
3, $[Co^{II}O_4(W_{12}O_{38})]^{10-}$ or $[Co^{II}O_4(W_{12}O_{36})]^{6-}$;
4, $+4e^-$ reduction product of $H_4[SiO_4Mo_{12}O_{36}]$[18];
5, $+5e^-$ reduction product of $H_4[SiO_4Mo_{12}O_{36}]$[18].

18) J. D. H. Strickland, *J. Am Chem. Soc.*, **74**, 862 (1952).

cobalt atoms in different oxidation states. For this anion, Baker et al.[6] assigned the structure wherein given $WO_6$ octahedra are simultaneously attached to two central cobalt atoms. If this is the case, the interactions between the two cobalt atoms must occur through the bridged —O—W —O— group. If an electron-transfer-process is considered, this interaction will be represented as follows:

$$Co^{3} -O-W^{6} -O-Co^{2+} \rightleftharpoons Co^{3} -O-W^{5+} -O-Co^{3} \rightleftharpoons Co^{2} -O-W^{6+} -O-Co^{3} .$$

It is well known that the reduction products of tungstates or molybdates are colored intense deep blue. The absorption spectra of such reduction products of $H_4[SiO_4Mo_{12}O_{36}]$, which were thoroughly studied by Strickland[18], are reproduced in Fig. 4. The resemblance of these spectra with the visible spectrum of the $Co^{II}Co^{III}$ heterotungstate anion, except that the intensity of the latter compound is lower by a factor of about $10^2$, will be regarded as a proof for the interaction of the above mentioned type.

(6) Absorption band originating in tungstate skeleton.—All of the heteropolytungstates herein studied have very broad and intense absorption bands in ultraviolet region. This is certainly the absorption due to the tungstate skeleton. Similar but more diffuse molybdate bands have been observed by the present authors[1] for the heteropolymolybdates previously reported.

## Summary

The visible and ultraviolet absorption spectra have been measured for some heteropolytungstates containing cobalt(II), cobalt(III) or manganese(IV) as central ions.

It has been shown that some cobalt(II) or cobalt (III) ions in the heteropolytungstates have tetrahedral co-ordination. This is the first case of the absorption spectra of $[Co^{II}(O^{=})_4]$- and $[Co^{III}(O^{=})_4]$-complexes being measured.

This work was supported by a grant from the Ministry of Education.

*Department of Chemistry, Faculty of Science, Osaka University*
*Nakanoshima, Osaka*

# *Studies on Azeotropic Mixtures. III. Physical Basis of Azeotropic Correlation Rules**

By Toshio YOSHIMOTO

(Received February 8, 1957)

## Introduction

Though several useful correlation rules of azeotropic data have been reported, they appear to lack in a common physical basis because the theory of azeotropes is little developed. It has been exemplified in part II[1] that the molecular interchange energy $w$ for azeotropes composed of one common component (azeotropic reagent) and the members of a homologous series was constant in a number of cases, applying Trouton's rule to such a series. Also, the equations

$$\Delta_v S_1^0 (T_1^0 - T^a) = Nwx_2^2 \quad (1)$$

and

$$\Delta_v S_2^0 (T_2^0 - T^a) = Nwx_1^2 \quad (2)$$

derived in part I[2] have proved to be useful in predicting azeotropic data. Here, $T^a$ is the azeotropic point (for $p=1$ atm.), $N$, the Avogadro number, $\Delta_v S_i^0$ the molar entropy of vaporization at boiling point $T_i^0$ (for $p=1$ atm.) of pure component ($i=1$ and 2), and $x_1$, $x_2$ mole fraction of both components respectively.

It will be shown in this paper that the equations (1) and (2) may give some information about the mutual relationship between independent correlation rules as well as their physical basis.

* Partly presented at the 9th Annual Meeting of the Chemical Society of Japan held in Kyoto, April, 1956.

1) T. Yoshimoto and Y. Mashiko, This Bulletin, **30**, 56 (1957).

## Relation between Boiling Points of Homologous Members and Azeotropic Composition

Now eliminating $T^a$ between two equations (1) and (2), we have the following quadratic equation for $x_2$:

$$(S_2-S_1)x_2^2+2S_1x_2-\left\{S_1+\frac{S_1S_2}{W}(T_1^0-T_2^0)\right\}=0^{**} \quad (3)$$

This can be solved for $x_2$ to give

$$x_2=-\frac{S_1}{S_2-S_1}\pm\frac{\sqrt{S_1S_2}}{S_2-S_1}\left\{1+\frac{S_2-S_1}{W}(T_1^0-T_2^0)\right\}^{1/2}. \quad (4)$$

The necessary and sufficient condition for azeotrope existence is

$$-\frac{W}{S_2}<T_1^0-T_2^0<\frac{W}{S_1}, \quad (5)$$

as shown by us in part I and we see obviously $S_2-S_1<S_1$ in numerical values, so we can obtain readily

$$\left\{\frac{S_2-S_1}{W}(T_1^0-T_2^0)\right\}^2<1.$$

We may therefore develop (4) in convergent power series of $T_1^0-T_2^0$:

$$x_2=\frac{\sqrt{S_1S_2}-S_1}{S_2-S_1}+\frac{\sqrt{S_1S_2}}{2W}(T_1^0-T_2^0)+\frac{\sqrt{S_1S_2}(S_2-S_1)}{8W^2}(T_1^0-T_2^0)^2+\frac{3\sqrt{S_1S_2}(S_2-S_1)^2}{48W^3}(T_1^0-T_2^0)^3+\cdots\cdots. \quad (6)$$

Here, component 2 is chosen as a common azeotropic reagent, that is usually a more "associated" liquid, and must have larger entropy of vaporization than component 1. Lecat[3] obtained empirically a series of equations in the form

$$C=C_0+C_1\Delta+C_2\Delta^2$$

where $C$ is wt. % of the second component, $\Delta$ the difference between boiling points of pure component, i.e. $T_1^0-T_2^0$, and $C_0$, $C_1$ and $C_2$ are all constants for a given series of homologous azeotropes. The equation (6) will thus interpret Lecat's empirical rule despite the fact that his rule differs in composition scale of azeotrope. If for example, the numerical values given in part II[1] for the series of azeotropes between 1-butanethiol and paraffinic hydrocarbons are introduced into equation (6), i.e., $S_1=20.3$, $S_2=22.0$ and $W=280$, we obtain

$$x_2=0.49+0.038(T_1^0-T_2^0)+0.000057(T_1^0-T_2^0)^2+0.00000017(T_1^0-T_2^0)^3+\cdots\cdots. \quad (8)$$

The coincidence of calculated curve with observed values is tested and the result shown in Fig. 1.

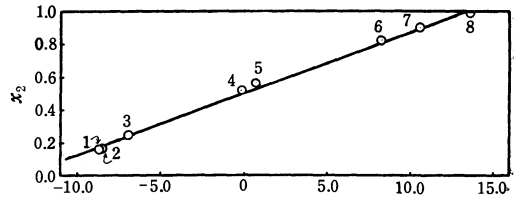



Fig. 1. Test of equation (8) for azeotropes of 1-butanethiol with paraffinic hydrocarbons: full line calculated, circles experimental. Paraffinic hydrocarbons: (1), 2, 3-Dimethylpentane; (2), 2-Methylhexane; (3) 3-Methylhexane; (4), *n*-Heptane; (5), 2,2,4-Trimethylpentane; (6), 2,2-Dimethylhexane; (7), 2,5-Dimethylhexane; (8), 3,3-Dimethylhexane.

Azeotropic data are taken from R. L. Denyer, F. A. Fidler and R. A. Lowry, *Ind. Eng. Chem.*, **41**, 2727 (1949).

Since the boiling-point difference between components in this case is less than 14°C as judged by the discussion of azeotrope-forming range presented in part II[1], we may neglect the third and higher order terms and therefore obtain approximately

$$x_2=\frac{\sqrt{S_1S_2}-S_1}{S_2-S_1}+\frac{\sqrt{S_1S_2}}{2W}(T_1^0-T_2^0). \quad (9)$$

This will thus interpret the straight-line relationship between $x_2$ and $T_1^0$ proposed by Denyer et al[4]. The straight-line relationship is true in the azeotropes of organo-sulfur compounds such as thiol, sulfone, etc. with aliphatic hydrocarbons, where the difference between $S_1$ and $S_2$ is not so great.

In the limiting case where $S_1$ is equal to $S_2$, equation (6) reduces to

$$x_2=\frac{1}{2}\left\{1+\frac{S}{W}(T_1^0-T_2^0)\right\} \quad (10)$$

and then we have

2) T. Yoshimoto and Y. Mashiko, This Bulletin, **29**, 990 (1956).

** Hereafter the $S_i$ and the $W$ refer, for brevity, to $\Delta_v S^0{}_i$ and $Nw$ respectively.

3) L. H. Horsley, *Anal. Chem.*, **19**, 603 (1947).

4) R. L. Denyer, F. A. Fidler and R. A. Lowry, *Ind. Eng. Chem.*, **41**, 2727 (1949); D. H. Desty and F. A. Fidler, ibid., **43**, 905 (1951).

$$x_1=\frac{1}{2}\left\{1-\frac{S}{W}(T_1^0-T_2^0)\right\}, \qquad (11)$$

where we write $S_1=S_2=S$ for brevity. The equations (10) and (11) are identical with those derived theoretically by Kuhn[5] for the azeotropes of dispersion force solutions where $S_1$ is approximately equal to $S_2$.

When $T_1^0$ is equal to $T_2^0$ in equation (9), we find

$$x_2=\frac{\sqrt{S_1S_2}-S_1}{S_2-S_1}<\frac{1}{2},$$

while $x_2$ is 1/2 in the limiting case where $S_1$ is equal to $S_2$.

## Relation between Boiling Points of Homologous Members and Their Azeotropes with One Common Azeotropic Reagent

Another type of correlation is noticed in azeotropic data when we plot $T^a$ against $T_1^0$. It has many advantages over the previous one especially in not needing any laborious analysis of azeotropic composition.

Eliminating $x_1$ and $x_2$ between two equations (1) and (2), we have a quadratic equation for $T_2^0-T^a$ in the form

$$\left(\frac{S_2}{W}-\frac{S_1}{W}\right)^2(T_2^0-T^a)^2+2\left\{\frac{S_1^2}{W^2}(T_1^0-T_2^0)-\left(\frac{S_1}{W}+\frac{S_2}{W}\right)-\frac{S_1S_2}{W^2}(T_1^0-T_2^0)\right\}\times(T_2^0-T^a)+\left\{\frac{S_1^2}{W^2}(T_1^0-T_2^0)-2\frac{S_1}{W}(T_1^0-T_2^0)+1\right\}=0. \qquad (12)$$

This can be solved for $T_2^0-T^a$ to give

$$T_2^0-T^a=\frac{-\left\{\frac{S_1^2}{W^2}(T_1^0-T_2^0)-\left(\frac{S_1}{W}+\frac{S_2}{W}\right)-\frac{S_1S_2}{W^2}(T_1^0-T_2^0)\right\}\pm\sqrt{4\frac{S_1S_2}{W^2}\left\{1+\left(\frac{S_2}{W}-\frac{S_1}{W}\right)(T_1^0-T_2^0)\right\}}}{\left(\frac{S_2}{W}-\frac{S_1}{W}\right)^2} \qquad (13)$$

Also noting that $\left\{\frac{S_2-S_1}{W}(T_1^0-T_2^0)\right\}^2<1$ and $S_2>S_1$, we may develop (13) in convergent power series of $T^0_1-T_2^0$:

$$T_2^0-T^a=\frac{W}{(\sqrt{S_1}+\sqrt{S_2})^2}-\frac{\sqrt{S_1S_2}-S_1}{S_2-S_1}(T_1^0-T_2^0)+\frac{\sqrt{S_1S_2}}{4W}(T_1^0-T_2^0)^2-\frac{\sqrt{S_1S_2}(S_2-S_1)}{8W^2}(T_1^0-T_2^0)^3+\cdots\cdots. \qquad (14)$$

When the numerical values for the series of 1-butanethiol-paraffinic hydrocarbon azeotropes are, as before, introduced into (14), we obtain

$$T_2^0-T^a=3.31-0.49(T_1^0-T_2^0)+0.019(T_1^0-T_2^0)^2-0.000057(T_1^0-T_2^0)^3+\cdots\cdots. \qquad (15)$$

The coincidence of calculated curve with observed values is tested and the result shown in Fig. 2.

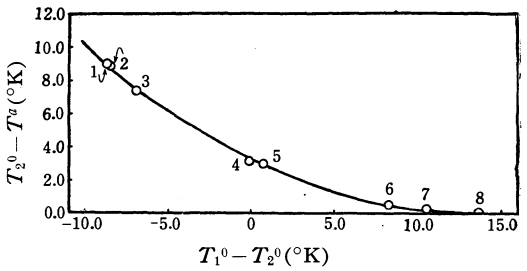



Fig. 2. Test of equation (15) for azeotropes of 1-butanethiol with paraffinic hydrocarbons: full line calculated, circles experimental.
Paraffinic hydrocarbons: see Fig. 1.

This will thus interpret Lecat's other empirical rule[6], i.e.,

$$\delta=A_0+A_1\Delta+A_2\Delta^2+A_3\Delta^3, \qquad (16)$$

where $\delta$ is the azeotropic depression $T_2^0-T^a$ and $A_0$, $A_1$, $A_2$ and $A_3$ are all constants for a given series of homologous azeotropes.†

5) W. Kuhn and P. Massini, *Helv. Chim. Acta*, **33**, 737 (1950).

†In the limiting case where $S_1$ is equal to $S_2$, we have from equation (14)

$$T_2^0-T^a=\frac{W}{4S}-\frac{1}{2}(T_1^0-T_2^0)+\frac{S}{4W}(T_1^0-T_2^0)^2. \qquad (17)$$

6) M. Lecat, *Z. anorg. allgem. Chem.*, **186**, 123 (1930); L. H. Horsley, *Anal. Chem.*, **19**, 603 (1947).
Similar explanation of this Lecat's rule was given by I. Prigogine and R. Defay, "Chemical Thermodynamics," Translated by D. H. Everett, Longmans (1954), p. 465.

This is identical with that derived by Kuhn[5] for dispersion force solutions if the third term is neglected, since it is not serious in such solutions.

The closer $T_1^0$ approaches $T_2^0$ in the equation (14), the more depression we have for azeotropic point and in the limit we have the maximum depression in the form

$$(T_2^0-T^a)^{\max}=\frac{W}{(\sqrt{S_1}+\sqrt{S_2})^2}, \qquad (18)$$

where the depression implies the difference in boiling point of azeotrope and the lower boiling component. The maximum depression is therefore regarded as a measure of azeotrope-forming power of the series.

Skolnik[7] proposed a different type of correlation between $T^a$ and $T_1^0$ in the form

$$\log (D-T^a)=E-FT_1^0, \qquad (19)$$

where $D$ is the asymptotic value and $E$ and $F$ constants. For dispersion force solutions such as azeotropes formed by toluene with naphthene homologues, $D$ is approximately $T_2^0$. The equation (19) is thus modified into

$$T_2^0-T^a=Ae^{-B(T_1^0-T_2^0)}, \qquad (20)$$

where $A$ and $B$ are constants. If we assume

$$A=\frac{W}{4S}$$

and

$$B=\frac{2S}{W},$$

then we obtain

$$\begin{aligned} T_2^0-T^a&=\frac{W}{4S}e^{-\frac{2S}{W}(T_1^0-T_2^0)} \\ &=\frac{W}{4S}\left\{1-\frac{2S}{W}(T_1^0-T_2^0)\right. \\ &\quad \left.+\frac{2S^2}{W^2}(T_1^0-T_2^0)^2-\cdots\cdots\right\} \\ &=\frac{W}{4S}-\frac{1}{2}(T_1^0-T_2^0) \\ &\quad +\frac{S}{2W}(T_1^0-T_2^0)^2-\cdots\cdots. \end{aligned} \qquad (21)$$

By comparing (21) with (17) we have an information on the physical meaning of Skolnik's constants $E$ and $F$.

7) H. Skolnik, *Ind. Eng. Chem.*, **40**, 442 (1948).

## Summary

The physical meaning of four empirical correlation rules of azeotropic data, i.e. two types of Lecat's, Denyer et al.'s and Skolnik's rules, is clarified simultaneously with their mutual relations, by using the equations derived in part I and the assumption of constancy of molecular interchange energy for homologous azeotropes found in part II of the series of this study. The theoretically derived equations by Kuhn et al. are also given as a limiting case of ours.

The author wishes to express his hearty thanks to Mr. Yo-ichiro Mashiko for his kind guidance and encouragement throughout this work.

*Government Chemical Industrial Research Institute, Yoyogi, Tokyo*

# *Estrogenic Biphenyls. I. 2,3'-Diethyl-4-methoxybiphenyl-4'-carboxylic Acid*

By Michinori ŌKI* and Takeo SATO

(Received February 11, 1957)

In connection with the hypothesis, proposed by one of the present authors (M.O.) and Y. Urushibara[1], which postulates that the estrogenic compounds should possess not only two active hydrogens at the optimum distance apart, but the optimum thickness or width of the molecule, a number of stilbene derivatives were synthesized and found to be estrogenic[2-4]. A compound is supposed to be estrogenic from the standpoint of this hypothesis if

* Present address: Department of Chemistry, Faculty of Science, The University of Tokyo, Hongo, Tokyo.

1) M. Ōki and Y. Urushibara, This Bulletin, **25**, 109 (1952).

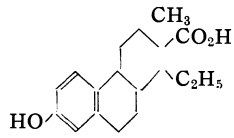
2) M. Ōki, ibid., 112.

3) idem, ibid., **26**, 66 (1953).

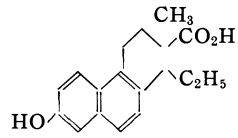
4) idem, ibid., 331.

it carries two active hydrogens at the optimum distance regardless of their nature.

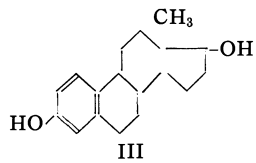
Thus, doisynolic acid (I) and bisdehydrodoisynolic acid (II) are powerful estrogens[5] in spite of the facts that their



I



II

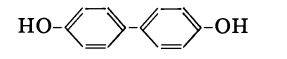


III

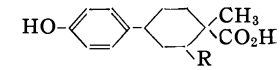
structures are different from that of the natural estrogen, estradiol (III), and that two active hydrogens are born by a hydroxyl and a carboxyl group.

Dodds et al.[6] reported that 4,4'-dihydroxybiphenyl (IV) was almost inactive. The fact seems probable, since this molecule is planar and the distance between two active hydrogens is less than the optimum. The authors postulate that even a biphenyl derivative can be a potent estrogen if it carries two active hydrogens at the optimum distance and possesses the optimum thickness of the molecule.

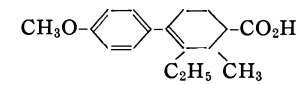
Novello et al.[7] prepared 2-alkyl-4-(*p*-hydroxyphenyl)-1-methylcyclohexanecarboxylic acids (V) and reported that they were estrogenic. Although these types of compounds are not the biphenyl derivatives, the result encouraged the authors to investigate the biphenyl series. Furthermore, while this paper was in preparation Nathan and Hogg[8] reported that 2-methyl-3-ethyl-4-(*p*-anisyl)-3-cyclohexenecarboxylic acid (VI) and its 4-unsaturated isomer (VII) were highly estrogenic.



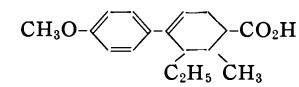
IV



V

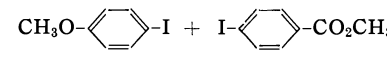


VI

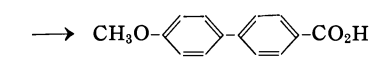


VII

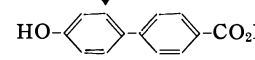
4-Hydroxybiphenyl-4'-carboxylic acid (XI) possesses, from the measurement of its scale model, two active hydrogen atoms at the suitable distance and, therefore, was supposed to be an estrogen, although the activity might be slight due to its planar structure. This substance was synthesized by the method described below and, as expected, showed estrogenic activity to 60% of the tested animals (ovariectomized mice) at the dose of 500$\gamma$.



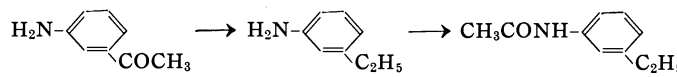
VIII IX



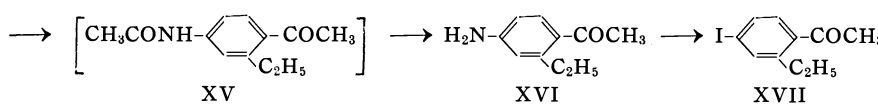
X



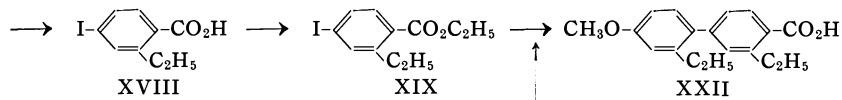
XI



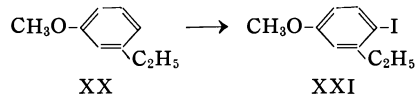
XII XIII XIV



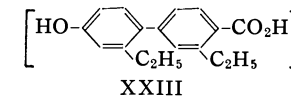
XV XVI XVII



XVIII XIX XXII



XX XXI



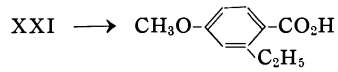
XXIII

5) K. Miescher. *Chem. Rev.*, **43**, 367 (1948).
6) E. C. Dodds and W. Lawson, *Proc. Roy. Soc. (London)*, **B125**, 222 (1938).
7) F. C. Novello, M. E. Christy and J. M. Sprague, *J. Am. Chem. Soc.*, **76**, 738 (1954).
8) A. H. Nathan and J. A. Hogg, ibid., **78**, 6163 (1956).

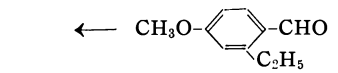
In order to give thickness and width to this molecule, the introduction of alkyl groups was attempted. Two benzene rings in biphenyl derivatives, as well known[9], cannot take coplanar structure when a substitution takes place at 2- or 2'-position. Thus thickness will be given to the molecule. As an example, 4-methoxy-2,3'-diethylbiphenyl-4'-carboxylic acid (XXII) was prepared. An ethyl group at 2-position was introduced to give steric hindrance by its bulk and to rotate benzene rings out of the coplanar structure. Another ethyl group at 3'-position was to give the optimum width of the molecule by analogy of the ethyl group next to the carboxyl group in doisynolic acid, in which, when the ethyl group is replaced by a methyl group or hydrogen, only weaker estrogenic activity is produced.

The synthesis of compound XXII is illustrated in the chart of page 509. *m*-Aminoacetophenone (XII) was reduced by modified Wolff-Kischner method[10] to *m*-ethylaniline (XIII) and the latter was acetylated. *m*-Ethylacetanilide (XIV) was treated with acetyl chloride and aluminum chloride and the product (XV) was hydrolyzed to give 2-ethyl-4-aminoacetophenone (XVI). The aminoketone (XVI) was converted into the iodo compound (XVII) through diazo reaction and the iodoketone was oxidized by sodium hypobromite to 2-ethyl-4-iodobenzoic acid (XVIII), which was esterified in the usual way. 3-Ethyl-4-iodoanisole (XXI) was prepared by direct iodination of *m*-ethylanisole (XX) in the presence of yellow mercuric oxide and submitted to the Ullmann reaction with ester XIX. Attempted demethylation of 2,3'-diethyl-4-methoxybiphenyl-4'-carboxylic acid (XXII) to 2,3'-diethyl-4-hydroxybiphenyl-4'-carboxylic acid (XXIII) with hydrogen bromide was unsuccessful.

The structural proof of 3-ethyl-4-iodoanisole was obtained in the following way. On treatment with magnesium and then with solid carbon dioxide, compound XXI yielded a carboxylic acid (XXIV). On the other hand, 2-ethyl-4-methoxybenzaldehyde (XXV)[11], prepared through modified Gattermann reaction, was oxidized by potassium permanganate to yield a carboxylic acid melting at 122–123°. These two acids were found to be identical by the mixed melting point determination.

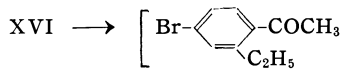


XXIV

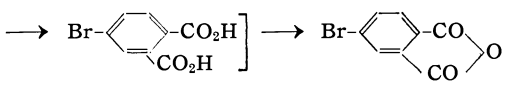


XXV

The structure of 4-amino-2-ethylacetophenone (XVI) was proven as illustrated in the following diagram. The amino group of XVI was replaced by bromine and 4-bromo-2-ethylacetophenone (XXVI) was oxidized with nitric acid and then with potassium permanganate. The dibasic acid (XXVII) was sublimed in vacuo and a produced anhydride did not depress the melting point on admixture with the authentic sample of 4-bromophthalic anhydride (XXVIII)[12].

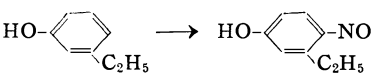


XXVI

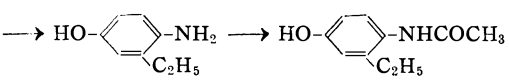


XXVII XXVIII

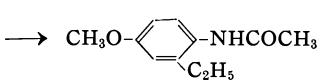
3-Ethyl-4-iodoanisole (XXI) might be synthesized through diazo reaction of 2-ethyl-4-anisidine. *m*-Ethylphenol (XXIX) was nitrosated and the product was reduced to the corresponding aminophenol (XXXI). The amino group was protected by acetylation and the hydroxyl group was methylated with dimethyl sulfate. But, before completion of this series, a more successful method than this rather lengthy one was found as described above. Therefore this method was discarded.



XXIX XXX



XXXI XXXII



XXXIII

The active dose was determined by the vaginal smear test with ovariectomized

9) R. A. Riedel, M. Orchin and L. Reggel, ibid., **70**, 199 (1948); E. A. Braude, F. Sondheimer and W. F. Forbes, *Nature*, **173**, 117 (1954).

10) Huang-Minlon, *J. Am. Chem. Soc.*, **68**, 2487 (1946); **70**, 2802 (1948); **71**, 3301 (1949).

11) B. R. Baker, ibid., **65**, 1572 (1943).

12) K. Fries and E. Hübner, *Ber.*, **39**, 435 (1906).

mice. The substance XXII was dissolved in oil and subcutaneously injected. The minimum active dose to produce estrus in 100% was found to be 100 $\gamma$.

## Experimental*

***m*-Ethylaniline (XIII).**—A solution of 135 g. (1 mole) of *m*-aminoacetophenone (XII) prepared by reduction[13] of *m*-nitroacetophenone, 280 g. of potassium hydroxide and 120 g. (2 moles) of hydrazine hydrate in 700 ml. of diethylene glycol was heated to reflux for one hour. After this period the reflux condenser was removed and the low-boiling materials were collected with a downward condenser until the reaction mixture attained the temperature of 200°. The reaction mixture was refluxed for further three hours and steam-distilled. The distillate was combined with the one obtained before heating at 200° and extracted with ether. The combined extracts were dried over potassium carbonate and distilled under reduced pressure, b.p. 75-76°/4 mm. Yield 80-90%. The melting point of the acetyl derivative was 24° (reported[14] melting point is 24°). *m*-Ethylphenol was prepared[14] through diazo reaction of this compound.

**3-Ethyl-4-nitrosophenol (XXX).**—To a well stirred solution of 43 g. (0.34 mole) of *m*-ethylphenol (XXIX) in 200 ml. of 95% alcohol and 200 ml. of concentrated hydrochloric acid, was added 35 g. (0.5 mole) of sodium nitrite in small portions, while the temperature was maintained at 0-2°. After the addition was finished, stirring was continued for ten minutes and the mixture was poured into 2 l. of water. Crystals were collected and recrystallized from benzene. Colorless needles, m.p. 135° (decomp.). Yield, 40 g. or 74% of the theoretical.

*Anal.* Found: N, 9.52. Calcd. for $C_8H_9O_2N$: N, 9.27%.

**4-Amino-3-ethylphenol (XXXI).**—To a solution of 20 g. (0.13 mole) of the compound XXX in 200 ml. of concentrated aqueous ammonia and 300 ml. of water, was introduced hydrogen sulfide. Crystals began to separate from the solution after five to ten minutes and the color of the solution changed. Hydrogen sulfide was passed through the solution for further forty-five minutes and the crystals were collected.

It was the most convenient way to use this crude material for the next reaction, since this compound was unstable and did not keep well. The analytical sample was obtaind in colorless plates by recrystallization from water, m.p. 169.5-171° (decomp.). Yield 15.5 g. or 85% of the theoretical.

*Anal.* Found: N, 10.33. Calcd. for $C_8H_{11}ON$: N, 10.20%.

**4-Acetamido-3-ethylphenol (XXXII).**—Fifteen grams (0.11 mole) of the crude aminophenol (XXXI) was treated with 25 g. of acetic anhydride. On recrystallization from water, were obtained colorless plates which melted at 137.5-139°. This compound took a molecule of water of crystallization, as analysis indicated, solidified over the first melting point and remelted at 173°. Yield 17 g. or 77% of the theoreticlal.

*Anal.* Found: N, 7.25. Calcd. for $C_{10}H_{13}O_2N \cdot H_2O$: N, 7.07%.

**4-Acetamido-3-ethylanisole (XXXIII).**—To a solution of 40 g. (0.2 mole) of the compound XXXII in 10 g. (0.25 mole) of sodium hydroxide and 200 ml. of water, was dropwise added 30 g. (0.24 mole) of dimethyl sulfate at 30-40°, while the mixture was well stirred. The crystals were collected and recrystallized from aqueous alcohol (1 : 1). Colorless needles, m.p. 118-119°. Yield 35 g. or 89% of the theoretical.

*Anal.* Found: N, 7.28. Calcd. for $C_{11}H_{16}O_2N$: N, 7.21%.

**4-Methoxybiphenyl-4'-carboxylic Acid (X).**—Methyl *p*-iodobenzoate (IX) was prepared[15] from *p*-iodobenzoic acid and methanol and *p*-iodoanisole (VIII)[16] from anisole and iodine. A mixture of 2.5 g. (0.0095 mole) of the compound IX and 5.5 g. (0.0235 mole) of VIII was preheated at 230° and 8.0 g. (0.125 atom) of copper bronze activated by Kleiderer and Adams' method[17] was added in portions with good stirring, while the temperature was maintained at 230-240°. The addition required twenty minutes. Then the temperature was raised to 280° and the reaction mixture was stirred for forty minutes at that temperature. After cooling, the mixture was extracted with acetone, the solvent was evaporated and the residue was refluxed with 10% sodium hydroxide solution in aqueous alcohol (1 : 1) for two hours. After dilution with 500 ml. of water active charcoal was added and filtered off to remove adherent oil. The filtrate was acidified with hydrochloric acid. The crystals were collected, boiled with 30 ml. of acetic acid and the mixture was filtered to remove insoluble material. The filtrate was concentrated and gave, on cooling, crystals melting at 247°. The compound gave no depression in the mixed melting point with the authentic 4-methoxybiphenyl-4'-carboxylic acid[18] prepared by oxidation of the corresponding acetyl compound. The reported melting point is 248-249°[18,19].

**4-Hydroxybiphenyl-4'-carboxylic Acid (XI).**—The compound X was demethylated according to the method of Fieser and Bradsher[18]. m.p. 259°.

**3-Ethyl-4-iodoanisole (XXI).**—To a solution of 44 g. (0.33 mole) of *m*-ethylanisole (XX),

* All boiling and melting points are uncorrected.

13) K. Buchka, *Ber.*, **10**, 1714 (1877); C. Engler, ibid., **11**, 930 (1878); L. C. King, M. McWhirter and D. M. Barton, *Ann.*, **67**, 2091 (1945).

14) Mm, A. Behal and E. Choay, *Bull. soc. chim. France*, (3), **11**, 206 (1894).

15) H. Schmidt and G. Schultz, *Ann.*, **207**, 320 (1881)

16) M. P. Brenans, *Bull. Soc. chim. France*, (3), **25**, 819 (1901).

17) E. C Kleiderer and R. Adams, *J. Am. Chem. Soc.*, **55**, 4225 (1933).

18) L. F. Fieser and C. K. Bradsher, ibid., **58**, 1738 (1936).

19) W. S. Johnson, C. D. Gutsche and R. O. Offenhauer, ibid., **68**, 1648 (1946).

prepared by methylation[20] of *m*-ethylphenol, in 70 ml. of alcohol were alternatively added 86 g. (0.4 mole) of yellow mercuric oxide and 84 g. (0.33 mole) of iodine in small portions with good swirling, while the temperature was maintained below 30°. The reaction mixture was finally heated on a water bath for ten minutes and filtered after cooling. Water was added to the filtrate and oil was extracted with ether. The combined extracts were sucessively washed with water, aqueous potassium iodide, and again with water, and dried over calcium chloride. After evaporation of the solvent, the residue was fractionated under diminished pressure. The main portion boiled at 147–150°/18 mm. and the pure compnund was obtained on redistillation, b. p. 120–120.5°/5 mm. Yield 60 g. or 76% of the theoretical.

*Anal.* Found: I, 48.63. Calcd. for $C_9H_{11}OI$: I, 48.39%.

**2-Ethyl-4-methoxybenzoic Acid (XXIV). (A) From 3-Ethyl-4-iodoanisole (XXI).**—A mixture of 5 g. (0.019 mole) of 3-ethyl-4-iodoanisole (XXI), 0.7 g. (0.029 atom) of magnesium and 50 ml. of ether was heated under reflux for one hour. To the Grignard reagent, a piece of solid carbon dioxide was added and, when the mixture attained room temperature, hydrochloric acid was added to decompose the complex. The aqueous layer was extracted with ether and the combined extracts were concentrated. The ethereal layer was extracted with 50 ml. of 10% aqueous sodium hydroxide; the aqueous layer was treated with active charcoal and acidified with hydrochloric acid. The crystals were collected and recrystallized from aqueous alcohol. Colorless plates, m.p. 120–121°. Yield 1.5 g. or 43% of the theoretical.

**(B) From 2-Ethyl-4-methoxybenzaldehyde (XXV).**—A suspension of 2-ethyl-4-methoxybenzaldehyde (XXV)[11] in excess aqueous potassium permanganate was heated on a water bath for thirty minutes. Sulfur dioxide was introduced to the suspension and crystals were collected. On recrystallization of the alkali soluble part from aqueous alcohol, there were obtained colorless plates melting at 122–123°.

*Anal.* Found: C, 66.32; H, 6.82. Calcd. for $C_{10}H_{12}O_3$: C, 66.65; H, 6.71%.

The melting point did not depress when both samples were mixed.

**4-Amino-2-ethylacetophenone (XVI).**—To a well stirred solution of 41 g. (0.25 mole) of *m*-ethylacetanilide (XIV) and 35 g. (0.45 mole) of acetyl chloride in 200 ml. of carbon disulfide, was added 116 g. (0.87 mole) of powdered aluminum chloride in portions of ca. 20 g. After the addition, the reaction mixture was heated under reflux for one hour and left to stand at room temperature for two hours. The supernatant carbon disulfide layer was decanted and the lower layer was decomposed with ice and hydrochloric acid. The aqueous layer was decanted off and the lower layer was hydrolyzed by heating with 200 ml. of dilute hydrochloric acid (1 : 1) for two hours. The cooled hydrolysate was basified with sodium hydroxide and the organic base was extracted with ether. The ethereal extracts were dried over potassium carbonate and fractionated. A fraction which boiled at 150–162°/5 mm. gave a pure sample on refractionation (b.p. 159–161°/5 mm.). The distillate solidified on cooling and the solid was recrystallized from benzene-petroleum ether. Colorless needles, m.p. 62–63°. Yield 16.5 g. or 40% of the theoretical.

*Anal.* Found: N, 8.66. Calcd. for $C_{10}H_{13}ON$: N, 8.58%.

**4-Bromophthalic Anhydride (XXVIII).**—To a diazonium solution obtained from 7.0 g. (0.043 mole) of 4-amino-2-ethylacetophenone (XVI), 20 ml. of 48% hydrobromic acid and 3.5 g. (0.051 mole) of sodium nitrite, was added a small amount of copper bronze. The mixture was heated on a water bath to complete the reaction and extracted with ether. The extracts were washed with aqueous sodium hydroxide and ether was evaporated. The residue was refluxed with dilute nitric acid, which was composed of 10 ml. of nitric acid (d; 1.38) and 40 ml. of water, for five hours. After cooling, the crystalline material was collected and further oxidized by aqueous potassium permanganate. A dicarboxylic acid, thus obtained, was sublimed under reduced pressure. Colorless plates, m.p. 105–106°. The compound did not depress the melting point on admixture with the authentic specimen of 4-bromopthalic anhydride (XXVIII) prepared through oxidation[21] of 1,6-dibromo-2-naphthol followed by sublimation[12].

**2-Ethyl-4-iodoacetophenone (XVII).**—A solution of 3-ethyl-4-acetylbenzenediazonium sulfate prepared from 33 g. (0.2 mole) of the compound XVI, 42 g. (0.4 mole) of concentrated sulfuric acid, 100 ml. of water and 14 g. (0.2 mole) of sodium nitrite in 30 ml. of water, was added to a hot solution of 50 g. (0.3 mole) of potassium iodide in 200 ml. of water. The organic material was extracted with ether and the ethereal extracts were successively washed with aqueous sodium hydroxide, aqueous sodium thiosulfate and water. After drying over calcium chloride, the solvent was evaporated and the residue was distilled under reduced pressure. Colorless oil, b.p. 166°/20 mm. Yield 33 g. or 60% of the theoretical.

*Anal.* Found: I, 46.30. Calcd. for $C_{10}H_{11}OI$: I, 46.80%.

**2,4-Dinitrophenylhydrazone** of XVII was prepared in the usual way. Scarlet needles, m.p. 152–153°.

*Anal.* Found: N, 12.61. Calcd. for $C_{16}H_{15}O_4N_4I$: 12.34.

**2-Ethyl-4-iodobenzoic Acid (XVIII).**—To a sodium hypobromite solution prepared from 79.9 g. (0.5 mole) of bromine, 63 g. (1.6 moles) of sodium hydroxide and 400 ml. of water, was dropwise added a solution of the compound XVII in 170 ml. of dioxan over a period of one hour, during which time stirring was applied and the

20) c. f. G. S. Hiers and F. D. Hager, "*Org. Synth.*," Coll. Vol. 1, (1940), p. 58.

21) c. f. A. F. Smith, *J. Chem. Soc.*, **35**, 789 (1879).

temperature was maintained below 20°. The reaction was completed by heating on a water bath for 10 minutes and the excess of hypobromite was decomposed with sodium bisulfite. Bromoform was removed by steam distillation and the remainder was acidified with hydrochloric acid. The solid was collected and recrystallized from aqueous alcohol. Colorless needles, m.p. 130–131°. Yield 25 g. or 83 % of the theoretical.

*Anal.* Found: I, 46.23. Calcd. for $C_9H_9O_2I$: I, 45.99 %.

**Ethyl 2-Ethyl-4-iodobenzoate (XIX).**—A solution of 5.0 g. of the acid (XVIII) and 5 ml. of concentrated sulfuric acid in 25 ml. of ethanol was heated under reflux for four hours. After cooling, the mixture was diluted with 100 ml. of cold water and extracted with ether. The ester boiled at 166–168°/17 mm. Yield 5.0 g. or 90 % of the theoretical.

*Anal.* Found: I, 42.03. Calcd. for $C_{11}H_{13}O_2I$: I, 41.76 %.

**2,3'-Diethyl-4-methoxybiphenyl-4'-carboxylic Acid (XXII).**—The Ullmann reaction was carried out in the same way as described in the preparation of X, using 5.0 g. (0.016 mole) of the compound XIX, 10 g. (0.038 mole) of XXI and 10.0 g. (0.157 atom) of activated copper bronze. The acidic portion was dissolved in ether and passed through an alumina column. On recrystallization from aqueous alcohol of the compound from the eluent, colorless prisms melting at 136.5–137° were obtained . Yield 0.5 g. or 10% of the theoretical based on the amount of the compound XIX.

*Anal.* Found: C, 76.34; H, 7.21. Calcd. for $C_{18}H_{20}O_3$: C, 76.03; H, 7.09%.

The authors wish to express their hearty thanks to Professor Y. Urushibara, the University of Tokyo, for his kind guidance and encouragement and to the Research Department of Teikoku Hormone Manufacturing Co., Ltd., Kawasaki, for bioassays. The authors' thanks are also due to the Ministry of Education for the Grant in Aid for Fundamental Scientific Research.

*Department of Chemistry, Faculty of Science, Tokyo Metropolitan University*
*Setagaya, Tokyo*

# *Dielectric Investigation on Coals. I. Dielectric Properties of Japanese Coals*

By Isao MIYASITA and Keniti HIGASI

(Received January 22, 1957)

## Introduction

Little information exists in the literature of the subject concerning the dielectric constant of coals. In 1948 Bond, Griffith and Maggs[1] reported a dielectric study of coals containing absorbed water. Their emphasis was then placed on the freezing mechanism of the water below 0°C and no reliable measurement was made on the dielectric constant of coal itself*.

In 1955 van Krevelen and his co-workers[2] published a report on dielectric constants of low rank and bituminous coals. The coal samples treated in their study were reduced to fine powders and the dielectric constant of the powders was indirectly estimated by the use of an immersion method. As is known with certainty, the conditions of their measurement were not free from errors of various sources. For instance, no reliable data are to be obtained in the region of the anomalous dispersion which is expected to occur from the dielectric heterogeneity of the measured system[3]. They measured apparent dielectric constants of binary mixtures composed of coal powder and an immersion liquid such as diisopropyl ether. In order to secure accuracy of measured values it is desirable that the measurements be made covering a wide range of frequencies or of temperatures. But actually their measurements were limited to a single frequency of 1 Mc/s at room temperature.

Since 1953 a dielectric investigation[4,5]

1) R. L. Bond, M. Griffith and F. A. P. Maggs, *Disc. Faraday Soc.*, **3**, 29 (1948).

2) M. P. Groenewege, J. Schuyer and D. W. van Krevelen, *Fuel*, **34**, 339 (1955).

* There are available other papers in which the dielectric method was employed to estimate the moisture content in coals. See, for example, W. Klempt, *Brennstoff-Chem.*, **34**, 294 (1953); H. Oikawa, *J. Coal Res. Inst.*, (Tokyo), **3**, 137 (1952).

3) K. W. Wagner, *Arch. Elektrotech.*, **2**, 371 (1941); R. W. Sillars, *J. Inst. Elec. Engrs.*, **80**, 378 (1937).

4) I. Miyasita, *Bull. Res. Inst. Appl. Elec.*, Hokkaido Univ., **5**, 123, (1953), **6**, 117 (1954).

5) I. Miyasita, R. Miura and K. Higasi, This Bulletin **28**, 148 (1955).

TABLE I
CHEMICAL ANALYSIS OF COALS USED FOR DIELECTRIC STUDIES*
(Composition on moisture-free basis, wt. %)

| Coal No. | Seam | Ash | Carbon | Hydrogen | Oxygen | Nitrogen | Sulfur |
|---|---|---|---|---|---|---|---|
| I | Moziri, No. 4 | 5.12 | 85.25 | 5.89 | 6.91 | 1.72 | 0.23 |
| II | Moziri, No. 3 | 11.85 | 81.71 | 5.93 | 9.78 | 2.00 | 0.58 |
| III | Moziri, No. 9 | 3.55 | 82.98 | 5.92 | 9.07 | 1.89 | 0.14 |
| IIIa | Moziri, No. 11 | 8.83 | 82.07 | 5.92 | 9.86 | 1.81 | 0.34 |
| IV | Akabira, No. 11 | 6.80 | 80.76 | 5.91 | — | — | — |
| V | Mitui-Bibai, No. 3-4 | 2.94 | 80.47 | 5.87 | — | — | — |
| Va | Mitui-Bibai, No. 4-4 | 3.87 | 80.12 | 5.78 | — | — | — |
| Vb | Mitui-Bibai, No. 1-5 | 4.12 | 78.40 | 5.78 | — | — | — |
| Vc | Mitui-Bibai, No. 1-3 | 5.00 | 80.62 | 5.71 | 11.55 | 1.88 | 0.24 |
| VI | Tempoku (brown coal) | 1.22 | 66.62 | 5.26 | — | — | — |

* The writers' thanks are due to Mr. Y. Zyomoto for providing the data of this Table.

on coals has been under way in the laboratory of the present writers. In the present article of this series detailed description will be presented of the results obtained for ten coal samples from Hokkaido mines, Japan. It may be worth while to point out that successful dielectric determination was done on coals themselves for the first time. Further, a wide range of frequencies between 50Mc/s and 300 c/s was used in the present measurement.

## Material and Method

Samples were prepared from the following ten coals (See Table I). For the sake of convenience, they have been arranged in order according to the geological age of the coal bed concerned. Coals (I)—(Vc): Hokkaido bituminous coals. Coal (VI): Tempoku brown coal, Hokkaido mine. Analyses of the coal samples are given in Table I.

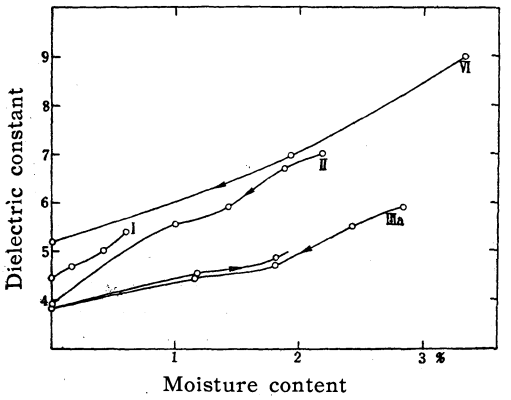



Fig. 1. Effect of dehydration on dielectric constants (at 1 Mc/s) of various coals. I, II, IIIa: Moziri bituminous coal; VI: Tempoku brown coal (cf. Table I). There is uncertainty as to the state of absolute drying.

Coal blocks which were rich in vitrain but had no cracks, were selected, carefully cut, ground, polished and finally made into the form of a circular plate of 5±0.1 mm. thick and 40 mm. in diameter. No sort of binding material such as Canada balsam was employed in the preparation of the disks.

The disks thus prepared were dried in a desiccator over phosphoric anhydride for three or four months. The presence of moisture in the sample usually results in obtaining a higher dielectric constant than expected (see Fig. 1). It is often accompanied by an anomalously large loss factor in the lower frequency region. Therefore, the complete removal of moisture was concluded to have been accomplished when the dielectric constant (especially measured in the lower frequency side) was low and became unchanged by further desiccation. Further check on this process of drying was made for one sample coal (IIIa) by making a comparison with another method of drying. The same material dried at 105°C in air for 28 hours gave little difference in dielectric constant.

The dielectric measurements were made with a Q-meter (Yokogawa QM-101) for the frequency range of 50 Mc/s to 50kc/s, and with an impedance bridge (Yokogawa BV-z-103A) for the range of 20kc/s to 300c/s. To attain a higher accuracy of the impedance bridge in the measurement of low-loss materials, a special device was necessary*. For this purpose, a combined unit of a narrow-band amplifier and a cathode-ray oscillograph was employed to detect the balance in the bridge circuit. Further, the source for the Q-meter was regulated with an automatic stabilizer.

Aluminium foils of 38 mm. diameter were pasted on the surfaces of the coal disk. They were connected with electrodes of the same 38 mm. diameter. The same electrodes were used both with the Q-meter and with the impedance bridge.

Readings of the Q-meter were taken when a resonance was established. After the test piece was removed resonace was regained by the use

* Detailed description of this device will be reported elsewhere (I. Miyasita, to be published in *Bull. Inst. Appl. Elec.*, Hokkaido University).

TABLE II

VARIATION OF DIELECTRIC CONSTANT ($\varepsilon'$) AND LOSS FACTOR ($\varepsilon''$) WITH FREQUENCY AT ROOM TEMPERATURE

| Coal No. | | 300 c | 1 kc | 3 kc | 10 kc | 20 kc | 100 kc | 300 kc | 1 Mc | 10 Mc | 50 Mc |
|---|---|---|---|---|---|---|---|---|---|---|---|
| I | $\varepsilon'$ | 4.56 | 4.55(4.54) | 4.54 | 4.52 | 4.37 | 4.49 | 4.52 | 4.47 | 4.41 | 4.49 |
| | $\varepsilon''$ | — | 0.0395 | — | — | — | 0.0346 | 0.0347 | 0.0351 | 0.0325 | 0.0318 |
| II | $\varepsilon'$ | 4.51 | 4.37(4.37) | 4.28 | 4.15 | 4.08 | 4.15 | 3.96 | 3.92 | 3.82 | 3.80 |
| | $\varepsilon''$ | — | 0.0926 | — | — | — | 0.080 | 0.076 | 0.075 | 0.070 | 0.058 |
| III | $\varepsilon'$ | 4.01 | 3.99(3.94) | 3.97 | 3.96 | 3.86 | 3.92 | 3.88 | 3.88 | 3.86 | 3.83 |
| | $\varepsilon''$ | — | 0.0334 | — | — | — | 0.0204 | 0.0173 | 0.0173 | 0.0189 | 0.021 |
| IIIa(1) | $\varepsilon'$ | 4.25 | 4.19 | 4.14 | 4.12 | 4.05 | 3.99 | 3.90 | 3.85 | 3.78 | 3.74 |
| | $\varepsilon''$ | — | — | — | — | — | 0.0585 | 0.0447 | 0.0424 | 0.0308 | 0.0278 |
| IIIa(2) | $\varepsilon'$ | 4.07 | 3.98(3.85) | 3.93 | 3.88 | 3.81 | 3.70 | 3.69 | 3.69 | 3.69 | 3.70 |
| | $\varepsilon''$ | — | 0.0404 | — | — | — | 0.032 | 0.0216 | 0.0238 | 0.0181 | 0.0228 |
| IV | $\varepsilon'$ | 3.76 | 3.75 | 3.75 | 3.66 | 3.66 | 3.66 | 3.64 | 3.66 | 3.61 | 3.46 |
| | $\varepsilon''$ | — | 0.0325 | — | — | — | 0.0206 | 0.0169 | 0.0166 | 0.0169 | 0.0204 |
| V | $\varepsilon'$ | 3.76 | 3.74 | 3.74 | 3.71 | 3.59 | 3.64 | 3.69 | 3.61 | 3.64 | 3.69 |
| | $\varepsilon''$ | — | 0.0224 | — | — | — | 0.0128 | 0.0109 | 0.0124 | 0.012 | 0.014 |
| Va | $\varepsilon'$ | 4.42 | 4.34(4.30) | 4.30 | 4.20 | 4.11 | 4.12 | 4.10 | 4.10 | 4.08 | 4.14 |
| | $\varepsilon''$ | — | (0.0316) | — | — | — | — | — | — | — | — |
| Vb | $\varepsilon'$ | 4.5 | 4.42(4.25) | 4.28 | 4.28 | 4.16 | 4.23 | 4.23 | 4.19 | 4.16 | 4.16 |
| | $\varepsilon''$ | — | (0.0442) | — | — | — | 0.030 | 0.0266 | 0.0288 | 0.0268 | 0.0337 |
| Vc | $\varepsilon'$ | 4.73 | 4.70 | 4.57 | 4.48 | 4.38 | — | — | — | — | — |
| VI | $\varepsilon'$ | 5.65 | 5.56 | 5.5 | 5.4 | 5.28 | 5.35 | 5.35 | 5.20 | 5.10 | 5.25 |
| | $\varepsilon''$ | — | — | — | — | — | 0.0815 | 0.0768 | 0.0856 | 0.101 | 0.137 |

of an auxiliary condenser when the two electrodes came to be the same distance apart. Dielectric constant and loss factor of the sample were obtained by simple calculations from the readings at the resonance points. Procedure with the impedance bridge was essentially the same as those described in the usual text book.

The range of errors in the measured quantities is largely dependent upon the frequency of the measurement. Broadly speaking the Q-meter and the impedance bridge, after the improvement above noted are believed to give errors of less than $\pm 2\%$ in dielectric constant, while the loss factors are more sensitive in respect to conditions of the measurement.

As none of the test pieces prepared from coal samples was a perfectly circular disk with two perfectly flat surfaces, error arising from the irregularity of the shape demanded special attention. Regarding edge effects, Prof. Miura of the electrical engineering dept. of this University kindly took the trouble to examine the error involved. Further, two sorts of calibration experiments were conducted: first, with a test piece of variable edge; second, comparison with Hartshorn's[6] procedure regarding this correction. Error of the edge irregularity in the dielectric constant was inferred thus to be only a small percent, or less than 5%.

Concerning the unflat surfaces, the use of aluminium foil was believed to help diminish the principal error, which arises from the possible air gap between the electrodes and the test piece. Both the inhomogeneity of the sample and the existence of ash and moisture provided other difficulties, of which the latter is more important. Every effort was made to eliminate errors arising from all these effects, but they were not always estimable. Probably one may assume that the maximum error in the absolute value in dielectric constant amounts to about 5% or near to it. Loss factors in general are more liable to errors than dielectric constants, but they are less significant in the interpretation of the results.

Measurements were carried out at room temperature. For some samples, (IIIa) (Va) and (V), measurements were also made at 100°C, but no appreciable difference was found in the dielectric constant values.

## Experimental Results

Results of the measurement are collected in Table II. Values in parentheses are those redetermined after the lapse of a few months (in a desiccator). In sample (IIIa) two test pieces prepared from the same coal specimen were examined (Compare IIIa(1) and IIIa (2) in Table II). One gave a higher value in dielectric constant than the other by the amount 0.04—0.29. The choice of the two pieces was not made at random—they were selected from blocks of entirely different appearance but the same specimen. Therefore this deviation of less than $\pm 10\%$ may suggest the range of maximum deviation in the dielectric constant which arises from any individual difference of the sample.

Perhaps the most remarkable feature in this table is that, over a wide range of frequency, observed dielectric constants show values of less than 5, while loss factors have small values below 0.1. Only one exception is found in the brown coal (VI).

There are available no refractivity data for Japanese coals. But according to our microwave measurement on Mayazi coal (83.14% carbon), its high frequency dielectric constant was 3.37[7].

6) L. Hartshorn and W. H. Ward, *Proc. Inst. Elec. Engrs.*, **79**, 597 (1936).

7) K. Higasi, I. Miyasita and Y. Ozawa, this Bulletin, **30**, 546 (1975).

Further it is reported that the refractive index for European coals amounts to 1.7-2.0[8], Therefore it may be reasonable to suppose that the observed dielectric constants should be only slightly larger than the square of the corresponding refractive index, the difference being less than 2[8]. These points will be discussed fully in subsequent papers.

## Discussion

To begin with, the dielectric constants measured at two frequencies, 1 kc/s and 1 Mc/s, are plotted against the carbon content (dry, ash- free) of the coal. For the sake of comparison the dielectric constants at 1 Mc/s given by van Krevelen[2] are plotted in the same figure. Full discussion on this problem will be given when ample data on a variety of coals are provided from the investigation on coal powders.

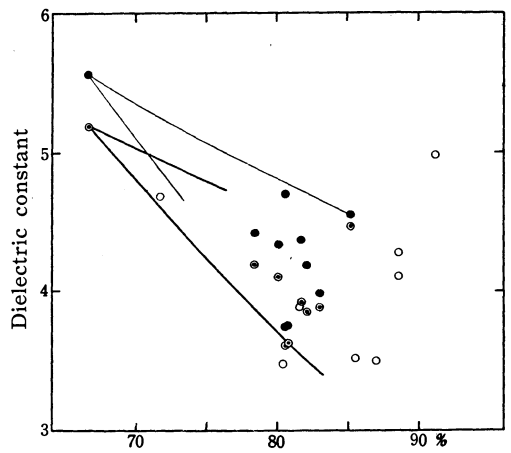



Fig. 2. Dielectric constant of coal and carbon content.
◉ 1 Mc } Present research
● 1 kc }
○ 1 Mc Krevelen's data for strongly dried coal.

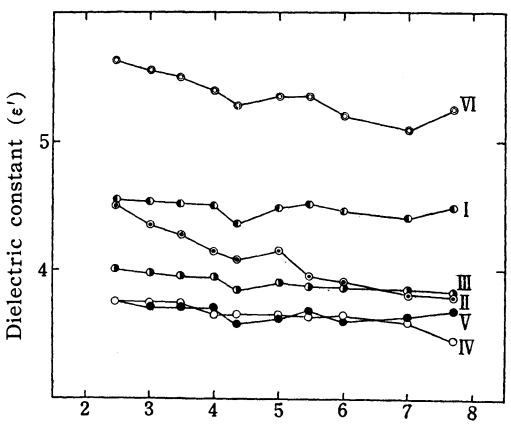



Fig. 3. Variations of dielectric constants of various coals with frequency. I, II, III: Moziri coal; IV: Akabira coal; V: Mituibibai coal; VI: Tempoku coal (cf. Table I).

In the present article attention will be focussed on the frequency dependence of dielectric constants and loss factors. These quantities, when directly obtained from coals themselves, are free from errors due to dielectric inhomogeneity. At a glance at the $\varepsilon'$ curves in Fig. 3, one is impressed by the fact that the curves for (I), (III), (IV), (V) are nearly flat and run almost parallel. That is, they are non-dispersive in the whole range of the measured frequencies 300 c/s - 50 Mc/s. Slight increases at the lower frequency side are found in the curves of (II) and (VI), but they are not very pronounced.

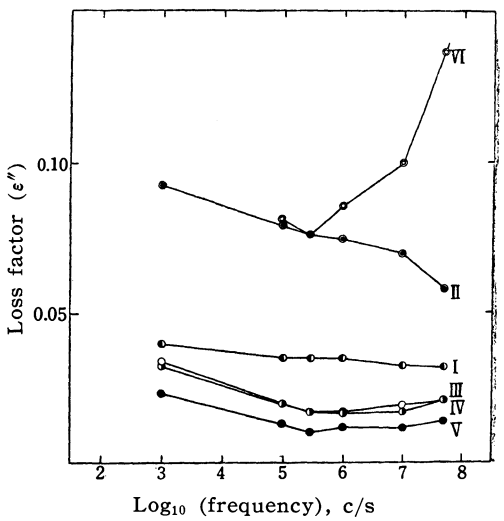



Fig. 4. Variations of loss factors of various coals with frequency. Coal No. I, II, III, etc: ditto (cf. Table I).

The curves for loss factors (Fig. 4) are of interest in this connection. It will be confirmed from loss factor that there is no anomalous dispersion in the samples of (I), (III), (IV) and (V). Samples (II) and (VI) have larger loss factors than others, but the frequency dependence is entirely different between the two. The loss factor $\varepsilon''$ of (II) gradually decreases at the higher frequency side, while that of (VI) sharply increases. This may suggest that the mechanism of dielectric absorption is different in the above two cases. From among the data not reproduced in Figs. 3 and 4, the samples of (IIIa2) and

8) D. W. van Krevelen, *Brennstoff-Chem.*, **34**, 167 (1953).

(Vb) are to be classified in the same group as (II) from the frequency dependence of the loss factor.

There are two types of causes which produce dielectric dispersion. One is the existence of movable dipoles in the system. In certain polymers and organic crystals dipoles are not completely blocked from rotation, producing distinct dispersion phenomena[9]. In Fig. 5, dielectric behavior of phenol-formaldehyde resin[10] is compared with that of Tempoku brown coal. It is generally accepted that the dielectric losses of this plastic are mainly determined by the rotation of the polar

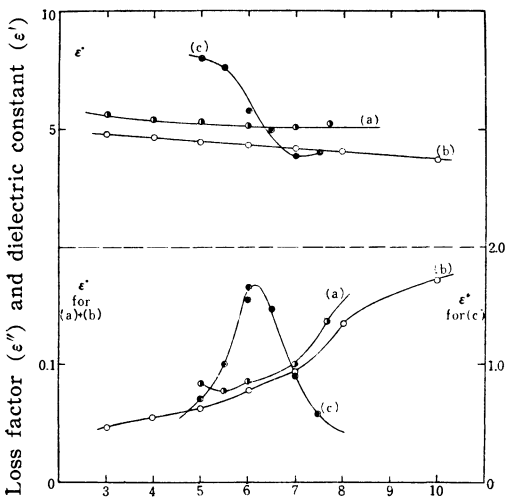



Fig. 5. Two types of dielectric dispersion.
(a) Tempoku brown coal.
(b) Phenol-formaldehyde resin.
(c) A mixture of coke-paraffin wax.

OH groups of the structure. Similarly Tempoku coal may have some polar groups such as OH group which have freedom of rotation to a certain extent. However, there is not any of the coals which exhibits dispersive charactor so clearly as Tempoku coal (Figs. 3 and 4). Most of the bituminous coals behave like non-polar substances. It seems reasonable to suppose, therefore, that in these coals the polar groups are in a state of non-rotation with the electric field applied from outside.

The other important cause of dielectric dispersion is the dielectric heterogeneity of the system. For the sake of illustration, the dielectric properties of a mixture of coke-paraffin wax[11] are shown in curves (c) in Fig. 5. A peak in the loss factor is observed at a particular frequency when a semi-conductive particle of coke is surrounded by paraffin medium with good insulating power. Indeed, the direct current conductivity of coke itself is calculable with some precision from that frequency by the use of Wagner-Sillar's theory[3,11].

It is of some interest in this connection that Ellis[12] advanced a proposition that there exist units of graphite structure in bituminous coals. If such structure corresponds to particles of semi-conductive nature, the situation may not be essentially different from that of a coke-paraffin wax system. As far as the coals treated in the present experiment are concerned, no such dispersion phenomenon was observed as would support Ellis's view on the graphite micellar structure*.

Lastly, let attention be directed to the increase of loss factor at the lower frequency region as observed in curve II in Fig. 4. There are two reasons for believing that this increase is due to the trace of water in the system. First, this sort of increase in loss factor becomes very pronounced in all the materials which are not completely dried. Second, the phenomenon itself can be theoretically accounted for by Sillar's calculation[3] on the assumption that in cracks of the coal there is some trace of water particles of elongated shape.

## Summary

In a wide frequency range covering 300 c/s to 50 Mc/s dielectric constant and loss factor of ten Japanese coals were measured at room temperature. The result provides a view that Japanese coals are almost non-polar in effect and embrace no units of graphite structure of the sort proposed by Ellis.

The writers wish to thank Prof. G. Takeya and Assit. Profs. R. Miura and M. Kugo for friendly help and stimulating discussions.

*Research Institute of Applied Electricity*
*Hokkaido University, Sapporo*

9) C. P. Smyth, "Dielectric Behavior and Structure," Chap. V, McGraw-Hill Book Co. (1955).
10) L. Hartshorn. L. V. L. Parry and E. Rushton, *Proc. Inst. Elec. Engrs.*, **100**. 23 (1953).
11) Y. Zyomoto and K. Higasi, to be published in this Bulletin. Further see Y. Zyomoto and K. Higasi, *Kagaku*, **26**, 638 (1956).
12) C. Ellis, *Proc. Roy. Soc.* (London), **212A**, 1 (1952).
* As the nature of Japanese coals is regarded to be particular as compared with European coals, this does not exclude the possibility that British bituminous coals have such graphite units.

# *Sensitization by Bismuth of the Luminescence of Manganese and Samarium in Calcium Sulfide Phosphors**

By Shigeo SHIONOYA and Koh ERA

(Received February 27, 1957)


## Abstract

Calcium sulfide phosphors doubly activated with bismuth as sensitizer and with manganese or/and samarium as activator were studied, in order to throw light on the sensitization mechanism of photoconductive phosphors. Their optical properties, reflection, excitation and emission spectra, were observed. A few estimations were done about the emission efficiency and the range of sensitization using these results. The facts directly found were that manganese is sensitized more efficiently than samarium, but the quenching takes place significantly in manganese itself, so that manganese is said to act, to some extent, as a killer. As the sensitization mechanism, the resonance transfer is considered to be more predominant than the photoelectron transfer. The contribution of the energy transport among the sensitizers is suggested. In the case of the coexistence of manganese and samarium, there will be no significant interactions between them.


## Introduction

It has been proved that the mechanism of the sensitized luminescence in the non-photoconductive phosphors is explained by the resonance transfer of absorbed energy from sensitizer to activator[1,2]. In the photoconductive phosphors, however, the sensitization by a different mechanism has been considered to take place, such that electron and positive hole, released from the sensitizer by the photoabsorption, recombine at the activator, emitting its luminescence[3-5]. Hereafter this is called "photoelectron transfer". Then, the study of the real mechanism of the sensitization in the photoconductive phosphors is very interesting. In a study on the sensitized luminescence in zinc sulfide phosphors by one of the present writers[6,7], it has been concluded tentatively that the sensitization mechanism is the resonance transfer rather than the photoelectron transfer. The present study was undertaken to throw light on the sensitization mechanism in calcium sulfide phosphors, and here will be mentioned some results obtained until now.

## Experimental

**1. Preparation of Samples.** — Bismuth as sensitizer and manganese or/and samarium as activator were selected. It has been known since earlier days that the sensitization takes place in these combinations[8,9]. The samples were prepared by mixing calcium oxide, excess sulfur, sodium sulfate as flux and the salts of activating impurities, and by firing the mixture for twenty min. at 950°C. The concentration of the sensitizer was constantly $10^{-4}$ (mole fraction relative to calcium, hereafter follow this), but that of the activator was varied from zero to $10^{-3}$.

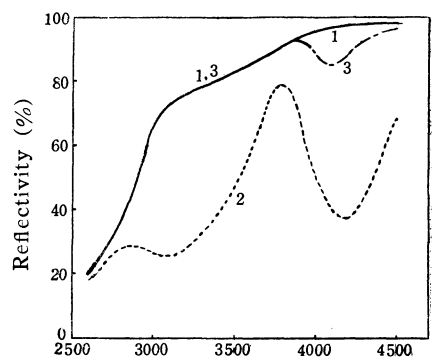



Fig. 1. Reflection spectra
(1) CaS (fired without any activating impurities)
(2) CaS:Bi($10^{-4}$)
(3) CaS:Mn($10^{-4}$)

* This work was read at the Symposium on Photochemistry held by The Chemical Society of Japan on September 29, 1956.


1) Th. P. J. Botden, *Philips Res. Rep.*, **7**, 197 (1952).
2) D. L. Dexter, *J. Chem. Phys.*, **21**, 836 (1953).
3) N. F. Mott and R. W. Gurney, "Electronic Processes in Ionic Crystals" (1940) p. 207.
4) M. Schön, *Z. Phys.*, **119**, 463 (1942).
5) H. A. Klasens, W. Ramsden and C. Quantie, *J. Opt. Soc. Am.*, **38**, 60 (1948).
6) S. Shionoya and K. Amano, *J. Chem. Phys.*, **25**, 380 (1956).
7) S. Shionoya, This Bulletin, **29**, 935 (1956).
8) S. Rothschild, *Phys. Z.*, **35**, 557 (1934); **37**, 757 (1936).
9) S. Makishima, Doctoral Thesis, University of Tokyo (1945).

**2. Reflection Spectra.**—As the samples were obtained only in the powder form, the reflection spectra were measured to learn the absorption characteristics. The measurement was done by means of "Shimazu's photoelectric spectrophotometer QB50". To eliminate the fluorescence (relatively weak in fact), a color filter, "Corning No. 9863", was inserted between the integral sphere and photomultiplier.

A part of the results is shown in Fig. 1. The long wavelength threshold of the fundamental absorption of the host crystal is located at 2500–2600Å. When bismuth is incorporated, a strong absorption appears in the long wavelength region beyond the above, the maxima of which are located at about 3100 Å and 4200 Å. The reflection spectrum due to bismuth corresponds to the spectrum of photoconduction[10]. The spectrum of the phosphor containing only manganese is very similar to that of the host crystal, but a weak absorption due to manganese appears at about 4100 Å. In the case of the phosphor containing only samarium, the spectrum is also very similar to that of the host crystal.

Reflection characteristics of doubly activated samples are very similar to that of the sample containing only bismuth; in other words their characteristics are determined only by bismuth. Small fluctuations were found in the result of each sample, but it seems to be dependent on the difference of the preparation condition, and not on the variation of the activator concentration. Then the absorption intensity in the series of samples containing a known amount of bismuth is almost constant irrespective of the activator concentrations. Therefore the emission efficiency should be in proportion to the number of emitted photons only. Then we will use the relative number of emitted photons instead of the emission efficiency, so as to compare the character of the samples with each other.

**3. Excitation Spectra.**—Since the intensity of emission excited by the light which passed through a monochromator was very weak, and further since it took a very long time to build up the emission to a saturated value, only the following method could be used. Phosphor powder was coated uniformly on a glass plate, and a photographic film was stuck on the other side of the plate sandwiching between the glass plate and film a gelatin filter which passes only the luminescence band to be measured. They were set at the focal plane of a usual quartz spectrophotometer. Then, the phosphor was irradiated for a long time (2-3 hr.) by the exciting light from a hydrogen discharge lamp. Therefore the results were not so precise and only qualitative.

A schematic figure obtained for bismuth emission of CaS:Bi is shown in Fig. 2. The excitation band for the activator, manganese or samarium, in the doubly activated phosphor is similar to that for bismuth in the singly activated phosphor. It has three peaks located at about 4200 Å (this is called $B_1$ band), 3100 Å ($B_2$ band) and 2500 Å

10) B. Gudden and R. W. Pohl, *Z. Phys.*, **3**, 98 (1920).

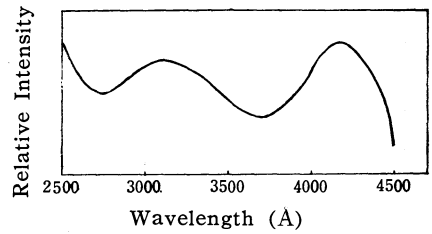



Fig. 2. Excitation spectra of CaS:Bi.

($H$ band), but the last one was not very clear.

Comparing these results with reflection spectra, it is concluded that $B_1$ and $B_2$ bands are due to the absorption of bismuth, while $H$ band is due to that of the host crystal. Then it is concluded from the above facts that the luminescence of manganese or samarium is sensitized by bismuth in the spectral region from 3000 to 4500 Å. In the present study only the luminescence sensitized by bismuth will come into question.

**4. Emission Spectra.**—The measurement was done with a glass monochromator coupled with a photomultiplier. As the excitation source the 3650Å line of a high pressure mercury discharge lamp was employed for bismuth excitation, and the 2537Å line of a low pressure mercury discharge lamp for the host excitation. Some examples of the results are shown in Figs. 3 and 4. Although it is known that samarium emission spectrum consists of six groups of line spectra[9], only two groups located in the shorter wavelength region were measured here and each group was incapable of being resolved into lines because of the limitation of the abilty of the apparatus.

As shown in Fig. 3, the emission intensity of bismuth is weakened in proportion to the increase in the activator concentration, and further the degree of the decrease of bismuth emission in

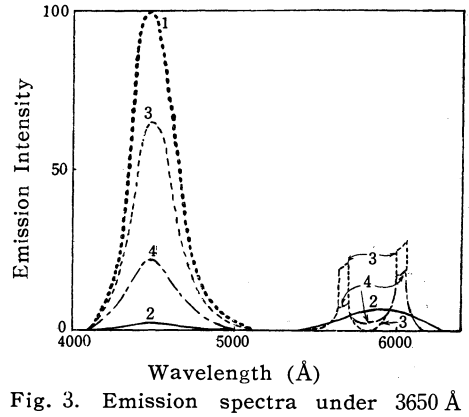



Fig. 3. Emission spectra under 3650 Å excitation. The ordinate is normalized by letting the bismuth emission peak of CaS:Bi be 100.
(1) CaS:Bi($10^{-4}$)
(2) CaS:[Bi($10^{-4}$)+Mn($10^{-3}$)]
(3) CaS:[Bi($10^{-4}$)+Sm($10^{-3}$)]
(4) CaS:[Bi($10^{-4}$)+Mn($3\times10^{-3}$)+Sm($10^{-4}$)]

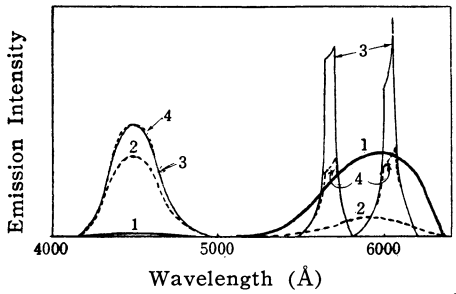



Fig. 4. Emission spectra under 2537Å excitation. The ordinate chosen arbitrarily.
(1) CaS: [Bi($10^{-4}$) + Mn($10^{-3}$)]
(2) CaS: [Bi($10^{-4}$) + Mn($10^{-5}$)]
(3) CaS: [Bi($10^{-4}$) + Sm($10^{-3}$)]
(4) CaS: [Bi($10^{-4}$) + Sm($10^{-5}$)]

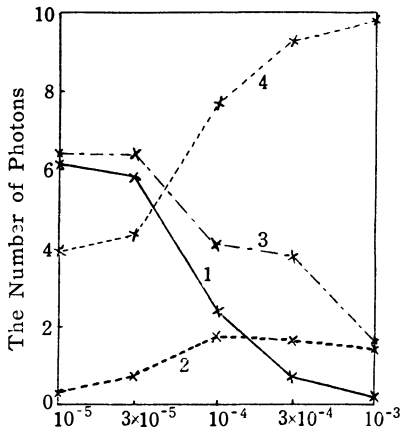



Fig. 5. The number of emitted photons for CaS: (Bi+Mn) series. The number for bimuth emission of CaS:Bi is put to be 10.
(1) Bismuth emission
(2) Manganese emission
(3) Sum of (1) and (2)
(4) The number of photons regarded to be transferred from bismuth to manganese, i.e. 10 minus (1)

Bi-Mn series is larger than in Bi-Sm series. These facts are due to the transfer of excitation energy absorbed in sensitizer to activator. In Bi-Sm series, samarium emission increases in proportion to its concentration, but in Bi-Mn series manganese emission does not become so strong in proportion to its concentration. This fact indicates that in Bi-Mn series the quenching of luminescence takes place in the manganese center after the energy transfer from bismuth to manganese.

These facts are made clearer by the estimation of the number of the emitted photons. The results of the estimation are shown in Figs. 5 and 6. The difference ($N_d$) of the numbers of photons emitted by bismuth between the case containing no activator and that containing it should be equal to the number of photons emitted by the activator. The ratio of the observed number of photons emitted by manganese to $N_d$ in Bi-Mn series, which gives the efficiency of manganese emission, is shown in Table I. The efficiency is about 10-20%, indicating that the enormous quenching takes place in manganese activator itself. This is also understood by the fact that the curve (3) in Fig. 5 showing the sum of numbers of photons emitted by bismuth and manganese decreases with the increase in the manganese concentration. Then manganese may be considered, as a matter of fact, to act, to some extent, as a killer. Moreover, in the case of the higher concentration of manganese, the concentration quenching also takes place. In Bi-Sm series the value of the ratio $N_d$ to the number of photons emitted by two groups of line spectra measured is always about 3.3, and as shown by the curve (3) in Fig. 6 the sum of the numbers of photons emitted by

TABLE I
EMISSION EFFICIENCY OF MANGANESE IN CaS: [Bi($10^{-4}$) + Mn]

| manganese | $1\times10^{-5}$ | $3\times10^{-5}$ | $1\times10^{-4}$ | $3\times10^{-3}$ | $1\times10^{-3}$ |
|---|---|---|---|---|---|
| efficiency (%) | 8.3 | 17 | 23 | 17 | 14 |

TABLE II
VALUES OF $z$

| A. CaS: [Bi($10^{-4}$) + Mn] | | | | | |
|---|---|---|---|---|---|
| manganese | $1\times10^{-5}$ | $3\times10^{-5}$ | $1\times10^{-4}$ | $3\times10^{-4}$ | $1\times10^{-3}$ |
| $z$ | $5.1\times10^{4}$ | $1.8\times10^{4}$ | $1.4\times10^{4}$ | $8.8\times10^{3}$ | $3.9\times10^{3}$ |
| B. CaS: [Bi($10^{-4}$) + Sm] | | | | | |
| samarium | $1\times10^{-5}$ | $3\times10^{-5}$ | $1\times10^{-4}$ | $3\times10^{-4}$ | $1\times10^{-3}$ |
| $z$ | $2.8\times10^{4}$ | $9.1\times10^{3}$ | $4.4\times10^{3}$ | $1.5\times10^{3}$ | $5.0\times10^{2}$ |
| C. CaS: [Bi($10^{-4}$) + Mn + Sm] | | | | | |
| manganese | $1\times10^{-4}$ | $3\times10^{-5}$ | $1\times10^{-4}$ | $1\times10^{-3}$ | $1\times10^{-4}$ |
| samarium | $3\times10^{-5}$ | $1\times10^{-4}$ | $1\times10^{-4}$ | $1\times10^{-4}$ | $1\times10^{-3}$ |
| sum of manganese and samarium | $1.3\times10^{-4}$ | $1.3\times10^{-4}$ | $2\times10^{-4}$ | $1.1\times10^{-3}$ | $1.1\times10^{-3}$ |
| $z$ | $1.2\times10^{4}$ | $6.1\times10^{3}$ | $7.6\times10^{3}$ | $3.8\times10^{3}$ | $9.5\times10^{2}$ |

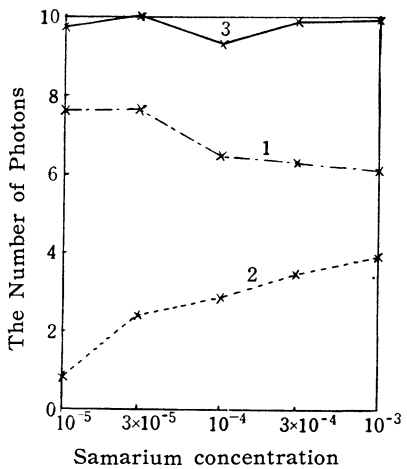



Fig. 6. The number of emitted photons for CaS:(Bi+Sm) series. The number for bismuth emission of CaS:Bi is put to be 10.
(1) Bismuth emission
(2) Samarium emission multiplied by 3.3
(3) Sum of (1) and (2)

bismuth and samarium is almost constant irrespective of the variation in the samarium concentration. Then it is considered that the quenching in the samarium activator does not take place, and that the above values of the ratio, 3.3, are really significant because only one third of the groups of the total ones of line spectra were measured. Comparing the decrease of bismuth emission in Bi-Mn series with that in Bi-Sm series, it is suggested that the ability of manganese to capture the excitation energy from bismuth is almost a hundred times that of samarium.

The emission spectra of the samples containing both manganese and samarium as activator are shown in Fig. 3. The emission intensity of bismuth is decreased with the incorporation of activators and the emissions of both activators appear.

TABLE III

THE NUMBER OF THE EMITTED PHOTONS UNDER 2537Å EXCITATION (ARBITRARY UNIT)

| | |
|---|---|
| CaS: Bi($10^{-4}$) | $4.7\times10^{2}$ |
| CaS: Mn($10^{-3}$) | $4.1\times10^{3}$ |
| CaS: Sm($10^{-3}$) | $3.0\times10^{3}$ |

The ratio of the number of photons which is regarded to be transferred from bismuth to activator to that of photons emitted as bismuth luminescence, $B$, was calculated. Using $B$ and the concentration of activator, $z$ defined below which represents the range of sensitization can be calculated. $z$ is defined as the number of lattice sites surrounding a given sensitizer, and it is assumed that if any one of these $z$ sites is occupied by an activator, the sensitization can occur always with an efficiency of 100%, but that if none of them is occupied by an activator, the emission of the sensitizer itself is caused. Moreover it should be assumed that all activators are distributed at random over all the lattice sites and the transfer of energy between sensitizers never occurs. By means of the probability calculation[7],

$$z = -\frac{\log(1+B)}{\log(1-C_a)}$$

is obtained, where $C_a$ is the mole fraction of activator. Although it is open to question whether the above assumptions are satisfied in this cases, at any rate $z$ was calculated. The results are shown in Table II.

The emitted photons of each emission band under 2537Å excitation were calculated by means of Fig. 4. The results are shown in Table III. The unit was selected arbitrarily. Those of samarium are 3.3 times the value observed.

**5. Emission under the Bismuth Excitation.** —The measurement of perfect emission spectra under the excitation by each of the two peaks of the bismuth excitation band was impossible, because the suitable excitation source which is strong enough could not be obtained. Then, only the ratio of emission intensity of activator to that of sensitizer was possibly measured by means of separating each emission band with color filters. As an excitation source a $CaWO_4$-coated fluorescent lamp was employed with filter, Matsuda UV-D2, for $B_1$ excitation, and $Ca_3(PO_4)_2$:Tl-coated fluorescent lamp with nickel sulfate solution filter for $B_2$ excitation. For the selection of bismuth emission or activator's one, filter, Schott GG3 plus Matsuda VC-1, or Matsuda VO-2 were employed, respectvely.

The calculated ratios of the emission peak intensity of an activator to that of a sensitizer are shown in Fig. 7 for the three kinds of excitation. In Bi-Sm series, the ratios under two

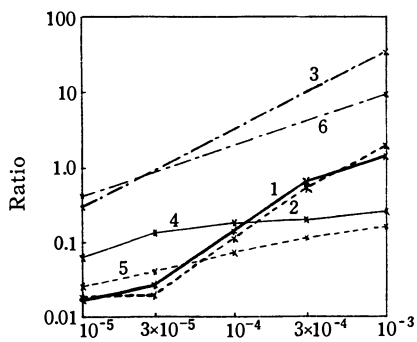



Fig. 7. The ratio of the emission peak intensity of activator to that of sensitizer under each excitation.
CaS:(Bi+Mn) series: (1) $B_1$ excitation (2) $B_2$ excitation (3) Host excitation
CaS:(Bi+Sm) series: (4) $B_1$ excitation (5) $B_2$ excitation (6) Host excitation

kinds of bismuth excitation are different from each other, and the sensitization efficiency under $B_1$ excitation is higher than under $B_2$, while in Bi-Mn series such a tendency is not found. In the case of the host excitation,the ratios in both sesies are so different from the case of bismuth excitation that it is suggested that there is a difference of luminescent mechanism between two cases.

## Discussion

**1. Sensitization Mechanism.**—If the previous two assumptions on the calculation of $z$ were realized truly, $z$ should be constant irrespective of the variation of the activator concentration. In the present case, however, $z$ decreases with the increase in the activator concentration, showing that the assumption will not be justified. Indeed, in the first place, it is considered that the assumption expressing no energy transfer between sensitizers is not realized, since the absorption spectrum of bismuth overlaps remarkably with its emission spectrum. The overlapping of an emission band with an absorption one is a necessary condition for the occurrence of resonance transfer, the probability of which is proportional to the degree of this overlapping. Then, it is considered that the sensitization in this case is caused by an energy transport, from sensitizer to activator, by which is meant a series of successive energy transfers such as sensitizer → sensitizer ⋯→ sensitizer → activator, and that the value of $z$ indicates the mean path of this transport. The higher the concentration of the activator becomes, the more frequent the chance of energy transfer from sensitizer to activator is, so that the mean path of transport becomes shorter. From this fact, the decrease of $z$ with the increase in the activator concentration previously mentioned will be explained.

Comparing $z$ of Bi-Mn series with that of Bi-Sm series, it is shown that the values of both series tend to approach each other in the lower activator concentrations, but that in the higher concentrations the values of Bi-Mn series become larger than those of Bi-Sm by about one order of magnitude. As will be mentioned below, the range of interaction between sensitizers themselves is known to be larger than that between sensitizer and activator. In the lower activator concentration, therefore, it is considered that the path of energy transport determines mainly the range of sensitization. On the other hand, in the higher concentration the direct transfer between sensitizer and activator becomes predominant. The degrees of the sensitizer-activator interaction in both series might be different from each other by one order of magnitude—this will not be improbable. If so, the above facts will be reasonable.

It may be considered that the emission of the activator under the host excitation is caused by the recombination of photoelectron with hole both created by the photoabsorption. If so, it would be deduced reasonably, at first consideration, that the emission of the activator under the bismuth excitation band, in which photoconduction is known to occur, is also caused by the same mechanism. But there are some different points to be taken into consideration between the former the and latter case as mentioned below.

Referring to the knowledge about zinc sulfide crystal[11], it is considered that calcium sulfide crystal is an $n$-type semiconductor, i.e. the majority carrier is an electron. In the case of the host excitation, hole is created at the sulfur ion, one of the constituents of the host lattice. Therefore the probability of the creation of hole in the vicinity of any activator may be high enough in order that the activator can catch hole to emit luminescence, although the mobility of hole is rather low. But in the case of bismuth excitation, hole is formed at the ground state of bismuth, which is scattered throughout the whole crystal. This hole must be released thermally into the filled band in order that the sensitization can occur. Even if the probability of this release is large, the probability of the existence of an activator in the vicinity of any bismuth is so low, and the hole mobility is considered to be so low that the hole released from bismuth will scarcely be able to reach an activator to cause its luminescence. Then, although the electron migrates the sensitization by bismuth by means of the recombination of electron and hole will seldom take place.

On account of the above consideration, in the case of the crystal in which the mobility of one of the two charge carriers, electron and hole, is much higher than that of the other, it is expected that the sensitization by an incorporated impurity by means of the recombination hardly ever

11) G F J. Garlick and A. F. Gibson, *J Opt. Soc. Am.*, **39**, 935 (1949).

takes place, although under the host excitation this can be done. As already mentioned, it has been concluded that the impurity sensitization in the non-photoconductive phosphors is caused by the resonance transfer. Also in the photoconductive phosphors the sensitization by this mechanism will be able to occur. In this case the occurrence of the photoconductivity itself is not the essential condition. In the present case, for the reason which will be mentioned below, it is considered that the resonance transfer rather than the photoelectron transfer is the predominant mechnism.

The first reason is the fact that the nature of the emission under $B_1$ and $B_2$ excitation band are different from each other in the Bi-Sm series, whereas they are not so different in the Bi-Mn series. If photoelectron transfer were predominant, the difference would be the same grade in both series since the condition for the photoelectron transfer may be the same for both series. But, if the resonance transfer is predominant, this difference may be probable, because the absorption bands of samarium and manganese may be different from each other—the absorption character is the factor of resonance probability.

The second reason is mentioned below. Comparing the number of the photons emitted by manganese with that by samarium under 2537Å excitation shown in Table III, both in the singly activated samples, it is considered that the capture cross sections of manganese and samarium for the electron and the hole are almost the same. In all cases except the sample of Bi-$10^{-3}$ Mn, bismuth emissons are almost equal irrespective of the activator concentration, but the intensities of the activator emissions are lower than those of singly activated samples. Then it is considered that free electron and hole are captured preferentially by bismuth, and that in the process of luminescence the interaction between activator and sensitizer is very weak. But in the case of Bi-$10^{-3}$ Mn this interaction seems to become fairly strong. Since, as mentioned above, the capture cross sections of manganese and samarium are not so different, it is most reasonable to consider, as the reason for this fact, that electron and hole are trapped at bismuth as the first step and then the resonance transfer occurs from bismuth to manganese. If the sensitization under bismuth excitation is due to the resonance transfer, this consideration is reasonably concluded. In all cases except Bi-$10^{-3}$Mn, because of the low activator concentration and the lower transfer probability, such a tendency scarcely appeared.

The third reason is that the estimated values of the range of sensitization, especially the relationships among them, are understood reasonably assuming the predominance of the resonance transfer. But, assuming the predominance of photoelectron transfer, these values are considered to be fortuitous. According to the theoretical treatment by Dexter[2], the sensitization range is the order of $10^4$—$10^3$ lattice sites in the case of Bi-Bi type, and the order of $10^2$ or 10 in the case of Bi-Mn or Bi-Sm. These are values for the typical cases, and considered to vary very much case by case. Now we are not speaking of the values themselves, but we are dis cussing relative tendencies. In the case of the lower activator concentration in which several successive steps of transfer may occur, the values lay in the order of $10^4$. In the higher concentration region, even though the transfer between sensitizers may yet take place, the values were the order of $10^3$—$10^2$. The difference of about one order between the Bi-Mn and Bi-Sm series will be probable on the premise that the resonance transfer is predominant and further the absorption band and the other factors are different between manganese and samarium.

So far, the distribution of activator and sensitizer has not been discussed, but implicitly assumed to be at random. The mode of distribution gives a serious influence on the sensitization efficiency. It is not fairly probable that the distribution is at random, but it is certainly considered that the activator and sensitizer form a kind of aggregate, and further that the aggregate states of Bi-Mn and Bi-Sm might be different from each other. If so, such a tendency will have the function to increase the sensitization efficiency, and true value of $z$ will be smaller than those estimated here.

**2. The Quenching in Manganese.**—It is known that in manganese several excited states are involved, and that the states from which the luminescence is emitted is the lowest one[12]. In zinc sul-

12) C. C. Klick, *Brit. J. App. Phys.*, Sup. No. 4 ("Luminescence"), p. 74 (1955).

fide phosphors the absorption of manganese from the ground state to the lowest excited one occurs at about 5100Å[13]. Since the position of the emission peak of CaS: Mn is not so different from that of ZnS: Mn, the position of manganese absorption peak to the lowest excited state in the former is probably not so different from that in the latter. The maximum of bismuth emission in calcium sulfide phosphor is located at about 4500 Å, so that the resonance transfer to manganese will take place to its higher excited state rather than to the emitting one. It is considered that there are appreciable chances to cause the radiationless transition within manganese center during the stepping down from the higher excited state to the lowest one, and then this will be the cause of the quenching mentioned in Experimental 4. Moreover, in the case of the higher manganese concentration, the concentration quenching also seems to occur simultaneously.

13) R. H. Bube, *Phys. Rev.*, **90**, 70 (1953).

**3. Interaction between Manganese and Samarium.**—The phosphors containing both somarium and manganese as activators were prepared to investigate whether the interaction between them exists. But conclusive facts were not obtained, because the separation of their emission bands was impossible. From the results of calculation of $z$ shown in Table II, it is seen in the comparison between two samples in which the sum of the concentration of two kinds of activator is the same that samples containing more manganese show larger $z$'s. This also suggests that manganese catches more energy than samarium. Since $z$'s in this case lie in the same region as in the case of singly activated ones, it may be concluded that a large interaction between manganese and samarium will not functions.

*Department of Electrochemistry, Faculty of Engineering, Yokohama National University, Minami-ku, Yokohama*

# *Size and Structure of Commercial and Graphitized Carbon Blacks by Low-angle X-Ray Scattering and Colloid-chemical Methods*

By Katsuya INOUYE*

(Received December 25, 1956)

## Introduction

The measurement of size of colloidal perticles has been one of the most extensively investigated subjects in colloid science. Among various procedures for measuring the particle size, some methods have been adopted for routine industrial assessment of the colloidal products. However, little has been known on the mutual relationships between the values obtained by different methods, and the lack of knowledge in the correlation has lead to the equivocal elucidation of properties.

It seems very desirable, therefore, that some experiments to compare results from different methods for the same sample should be carried out.

Carbon black is an industrially available colloid, the properties of which have been investigated by means of various methods including electron-microscope[1], X-ray scattering[2-5], adsorption[1,6-16], or heat of wetting[10] methods, and distinguished, in most cases, in the spherical particle shape and absence of internal surface, in other words, an example of colloid of simple structure. The general properties and industrial applications of carbon blacks are to be referred to ref. (17).

In the present work, the average particle size values obtained from low-angle X-ray scattering, electron-microscope, molecular adsorption and heat of wetting with methanol for various carbon black samples have been compared and discussed. It appears that there is no need to assert the importance of the study of this kind to the industrial uses of the samples for rubber reinforcing filter, printing ink, coloring pigment and other miscellaneous purposes.

## Description of Samples

**Carbon Blacks.**—The data characterizing fourteen carbon black samples investigated in the present work are summarized in Table I. These samples (five Japanese and nine American) appear to be representative of modern commercial carbon blacks with various general properties and uses. The designating symbols in the type of the samples are those widely adopted in the rubber industry and denote the process in manufacturing and uses: LCC, low color channel; FT, fine thermal; SRF, semi-reinforcing furnace; HAF, high abrasion furnace; HPC, hard processing channel; LFI, long flow impingement; MT, medium thermal; MAF, medium abrasion furnace; ISAF, impingement super abrasion furnace, SAF, super abrasion furnace. No pretreatment of extracting tarry matters attached to the carbon surfaces has been applied in this work.

**Graphitized Carbon Black.**—A gas thermal black, No. 1 in Table I, Tokyo Gas 300 (LCC), was subjected to heating and graphitization up to various temperatures.

To prepare the samples heated up to temperatures below 1000°C, a muffle furnace was employed. The carbon black was filled, in order to avoid oxidation by air, in a silica tube, which was thickly covered by asbestos to control the rate of heating, the temperature being measured by a thermo-couple inserted into the center of the

* The author's present address: Natural Resources Research Institute, University of Wyoming, Laramie, Wyoming, U. S. A.

1) R. B. Anderson and P. H. Emmett, *J. Appl. Phys.*, **19**, 367 (1948).
2) J. Biscoe and B. E. Warren, *J. Appl. Phys.*, **13**, 364 (1942).
3) M. H. Jellinek, E. Solomon and I. Fankuchen, *Ind. Eng. Chem., Anal. Ed.*, **18**, 172 (1946).
4) H. Brusset, *Compt. rend.*, **225**, 1002 (1947).
5) J. Turkevich and H. H. Hubbell, *J. Am. Chem. Soc.*, **73**, 1 (1951).
6) P. H. Emmett and T. DeWitt, *Ind. Eng. Chem., Anal. Ed.*, **13**, 28 (1941).
7) R. A. Beebe, J. Biscoe, W. R. Smith and C. B. Wendell, *J. Am. Chem. Soc.*, **69**, 95 (1947).
8) W. D. Schaeffer, W. R. Smith and C. B. Wendell, ibid., **71**, 863 (1949).
9) M. L. Corrin, ibid., **73**, 4061 (1951).
10) G. Kraus, *J. Phys. Chem.*, **59**, 343 (1955).
11) F. E. Bartell and E. J. Miller, *J. Am. Chem. Soc.*, **45**, 1106 (1923).
12) H. A. Smith and R. B. Hurley, *J. Phys. Colloid Chem.*, **53**, 1409 (1949).
13) C. M. Carson and L. B. Sebrell, *Ind. Eng. Chem.*, **21**, 911 (1929).
14) F. K. Shoenfeld, ibid., **27**, 571 (1935).
15) W. R. Smith, F. S. Thornkill and R. I. Bray, ibid., **33**, 1303 (1941).
16) J. Sameshima, H. Akamatu, K. Inouye, S. Kawamura, R. Matsuura and K. Tamaru, *Reviews of Modern Colloid Science*, **1**, 250 (1948).
17) W. R. Smith, "Encyclopedia of Chemical Technology," Vol. 3, The Interscience Encyclopedia, Inc., New York (1949).

TABLE I
DESCRIPTION OF CARBON BLACKS

| No. | Carbon black | Type | Process | Manufacturer |
|---|---|---|---|---|
| 1 | Tokyo Gas 300 | LCC | Gas thermal | Tokyo Gas Co. |
| 2 | Miike 20 | FT | Gas thermal | Miike-gosei Co. |
| 3 | Asahi Carbon 40 | SRF | Oil furnace | Asahi Carbon Co. |
| 4 | Seast 285 | HAF | Oil furnace | Tokai Electrode Co. |
| 5 | Shoden Acetylene black | Acetylen black | Thermal | Showa-denko Co. |
| 6 | Micronex 2 | HPC | Channel | Columbia Carbon Co. |
| 7 | Kosmos 15A | LFI | Channel | United Carbon Co. |
| 8 | Peerlees IIA | LFI | Channel | Peerless Carbon Black Co. |
| 9 | Thermax | MT | Gas thermal | Thermatomic Carbon Co. |
| 10 | Sterling S | SRF | Oil furnace | Cabot Inc. |
| 11 | Philblack A | MAF | Oil furnace | Phillips Petroleum Co. |
| 12 | Philblack O | HAF | Oil furnace | Phillips Petroleum Co. |
| 13 | Philblack I | ISAF | Oil furnace | Phillips Petroleum Co. |
| 14 | Philblack E | SAF | Oil furnace | Phillips Petroleum Co. |

tube. The samples heated up to 420, 620 and 990°C were obtained at an average heating rate of 50± 10°C/min. The graphitized carbon black samples heated at temperatures above 1000°C were prepared by means of a Tammann furnace at the Omachi Factory of Showa Denko Co. Ltd. by the average rate of temperature rise of 50±10°C/min. up to 1300, 1700, 2100, 2420, 2630 and 3170°C, maintaining at the final temeratures for further 25 minutes.

## Experimental Procedures

**Low-angle X-ray Scattering.**—Several workers[2-5] have applied the low-angle X-ray scattering method to derive the particle size of carbon blacks as a modern tool of particle size determination. Biscoe and Warren[2] employed a camera of 47.6 cm. specimen-to-film distance to record the scattering and calculated the particle size of three samples based on the Guinier's scattering intensity formula[18]. These authors showed the size in fair agreement with that obtained by the electron-microscopic method. Jellinek, Solomon and Fankuchen[3] have proposed a graphical method to obtain the particle size distribution from a single scattering recorded film and demonstrated it for a carbon black by means of a camera of specimen-to-film distance of 23.5 cm. This procedure was also applied to another sample by Turkevich and Hubbell[5] who used a camera of 70 cm. specimen-to-film distance with the Geiger counter to record the scattered X-rays. Brusset[4] also reported the size of five samples.

The calculation of particle size has been carried out by the theoretical functions relating the intensity of scattered X-ray to the scattering angles. Various functions have been proposed which differ in the treatments of the characteristics of the sample material, particle shape, particle distribution, etc. and the readers are raferred to excellent reviews by Yudowitch[19].

18) A. Guinier, *Ann. Phys.* **12**, 161 (1939).
19) K. L. Yudowitch, *Rev. Sci. Instr.*, **23**, 83 (1952); *Anal. Chem.*, **25**, 721 (1953).

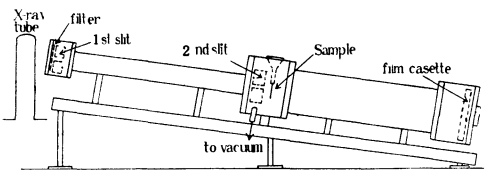



Fig. 1. A sketch of low-angle X-ray scattering camera.

The apparatus used in this work is a type of two-aperture collimating system camera. A sketch of the apparatus is drawn in Fig. 1. A first aperture of width $a_1$ and length $b_1$ is placed in metal block A. At a distence $l$ from the first aperture is the second aperture in block B with width $a_2$ and length $b_2$. The scattering specimen is placed close to the second aperture. At a distance $L$ from this specimen aperture is placed a cassette, in which the recording film is set, in the block C. The blocks A, B and C are tightly connected by means of rubber packings with two metal tubes to enable the inside of the apparatus to be evacuated. After Yudowitch[19], the intensity of the scattered rays, $I$, is considered to be

$$I \propto a_1 b_1 a_2 b_2 R^5 \rho^2 / l^2 L^2 \lambda^2 u^2, \quad (1)$$

where, $R$ is the particle radius, $\rho$ the electron density, $\lambda$ the X-ray wave length and

$$u = 2\pi \varepsilon R/\lambda, \quad (2)$$

where, $\varepsilon$ is the scattering angle. From Eqs. (1) and (2), it is noted that to give a strong intensity short length of $l$ and $L$ and a wide aperture as possible are recommended. On the other hand, Yudowitch[19] has given also the following conditions of camera geometry for the most intense usable data in the case of the slope analysis using the Guinier's equation:

$$l = L, \quad (3)$$

$$a_1 = 2 \; a_2 = \lambda L \delta u / 4\pi R \quad (4)$$

$$b_1 = b_2, \quad (5)$$

and at a tolerable error,

$$a_1 < \lambda l / 3R, \quad (6)$$

where, $\delta u$ denotes the collimation error. These relations imply that a long camera is useful to have the scattering pattern in a limited error and at the same time to employ wider apertures which are apparently easy to be made and operated. A sufficiently long specimen-to-film distance ($L$) is also necessary to assure a reasonable pattern. However, it is also clear that the long camera necessitates longer exposure time to obtain a scattering pattern on the film suitable to calculate the particle size. Fortunately, we have known that the average diameter of carbon blacks lies usually in the range of some hundreds angstrom, except very few thermal blacks with diameters of some thousands angstrom. The author has used the values of $l$ and $L$ of approximately 100 cm. (exactly, $l$ is 1013 mm. and $L$ is 993 mm.). From Eqs. (4), (5) and (6), the maximum value of $a_1$ may be calculated as shown in Table II in the case of the camera dimension described above and copper $K\alpha$ or chrome $K\alpha$ radiations. These values suggest that the exposure time may be shortened by employing a wider aperture system. In the present experiment, the dimentions of first and second appertures were taken as follows: (1) $a_1$ 1.00 mm. and $a_2$ 0.50 mm. for Cu $K\alpha$ radiation and (2) $a_1$ 1.00 mm. or 0.50 mm. and $a_2$ 0.50 mm. or 0.25 mm. for Cr $K\alpha$ radiation. In each condition, the relation (4) is applied. The height of apertures ($b_1=b_2$) is 3.00 mm. In the case of (1), the samples with the average diameter less than 1000 Å. are expected to be analyzed, while in (2) the maximum diameter to be covered would be up to nearly 4000 Å. It is thus expected that almost all carbon black samples are tested by this camera in a reasonable accuracy. Other cautions to shorten the exposure have been taken in minimizing the absorption of X-rays by air in this very long (2 m.) camera by evacuating the whole path continuously during the exposure up to $10^{-2}$ mmHg and also the absorption by foil windows and filter. As is obvious in Fig. 1, the only source of absorption by camera window is the filter (Ni for Cu ray and $V_2O_5$ on Al foil for Cr ray) which is cemented with the first aperture and at the same time constitutes the window to keet the vacuum.

TABLE II
THE MAXIMUM WIDTH OF THE FIRST APEATURE IN A FUNCTION OF PARTICLE DIAMETER

| Diameter, Å | $a_1$ maximum, mm. | |
|---|---|---|
| | Cu $K\alpha$ (1.54Å) | Cr $K\alpha$ (2.29Å) |
| 100 | 10.4 | 15.5 |
| 500 | 2.08 | 3.10 |
| 1000 | 1.04 | 1.55 |
| 2000 | 0.52 | 0.78 |
| 5000 | 0.21 | 0.31 |

To reduce spurious radiations scattered from the apertures, the apertures have been designed to have a depth of 10 mm., so that a very clear-cut slit image is obtained in blank tests. A beam-stopper was used with the width of 2.5 mm. in the case of $a_1$ width 1.00 mm. or 1.4 mm. for $a_1$ 0.50 mm.

The sample powder is extruded from a capillary in a small bar of 1 mm. diameter and set on a mount which is inserted inversely from the top of block B close to the second apperture and the sample mount is screwed in tightly to keep the vacuum.

By employing Cu radiation generated at 35 kV. and 20 mA. or Cr radiation at 35 kV. and 15 mA. Eastman-Kodak "No-screen" X-ray film, the exposure of 30 to 60 minutes was sufficient to give the suitable scattering patterns. A necessary by-earth voltage was applied to the filament of X-ray tube to reduce the focal spot width up to the same width of the first slit $a_1$; this procedure has resulted in strengthening the X-rays efficiently to pass through the camera. An example of the scattering patterns is shown in Fig. 2.

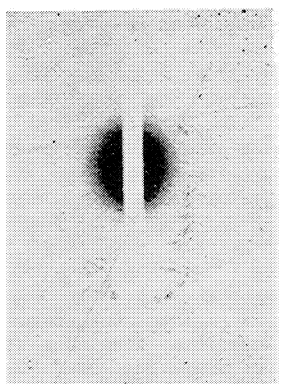


Fig. 2. An example of scattering pattern (×I). Sample: Philblack E.

The film obtained was micro-photometered by a reading photometer for each 0.25 mm. of film at a constant photometer condition. The calibration of the photographic density has been carried out by the graded-indensity scale method. The curves of the logarithm of measured (calibrated) intensity versus square of scattering angle (or of distance on film) showed a general shape as exemplified in Fig. 3. The average particle size was calculated from the straight part of the curve for each sample by use of the equation proposed by Guinier[18].

$$I=CWR^3e^{-0.221k^2R^2}, \quad (2)$$

where, $I$ is the intensity, $C$ a constant particular to the sample, $W$ the mass of scattering elements, $R$ the particle radius and $k$ is $4\pi\sin(\varepsilon/2)/\lambda$. The Eq. (7) is changed to the following form:

$$\log I=A-BR^2f^2, \quad (8)$$

where, $A$ and $B$ are constants and $f$ is the distance on film of a scattering with intensity $I$.

It has been found the reproducibility of the experiment by these procedures is approximately 10% or, in most cases, with higher accuracy for the carbon blacks of less than 1000 Å. diameter.

**X-Ray Powder Method.**—The commonly used powder method was employed, using filtered

TABLE

| No. | Carbon Black | Dia. from low-angle scattering, Å | Modal dia. by electron-microscope, Å | Iodine adsorption | |
|---|---|---|---|---|---|
| | | | | Surface area, $m^2/g$. | Dia., Å |
| 1 | Tokyo Gas 300 | 732 | 500 | 37.8 | 848 |
| 2 | Miike 20 | 1140 | 1120 | 8.77 | 3650 |
| 3 | Asahi Carbon 40 | 1390 | 1020 | 7.75 | 4580 |
| 4 | Seast 285 | 572 | 640 | 48.8 | 661 |
| 5 | Shoden Acetylene black | 1420 | 1250 | 22.3 | 1450 |
| 6 | Micronex 2 | 576 | 250 | 47.3 | 713 |
| 7 | Kosmos 15A | 686 | 460 | 83.7 | 387 |
| 8 | Peerless IIA | 608 | 370 | 76.1 | 459 |
| 9 | Thermax | 1940(Cu) 4890(Cr) | 3300 | — | — |
| 10 | Sterling S | 636 | 620 | 11.5 | 2730 |
| 11 | Philblack A | 620 | 450 | 17.4 | 1930 |
| 12 | Philblack O | 454 | 380 | 35.3 | 994 |
| 13 | Philblack I | 445 | 280 | 45.9 | 746 |
| 14 | Philblack E | 396 | 220 | 57.9 | 615 |

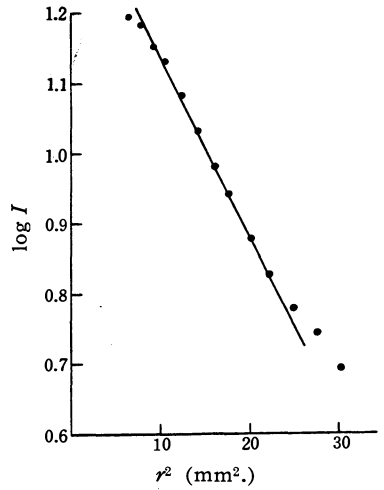



Fig. 3. An example of the relation between log $I$ and $r^2$. Sample: Philblack $E$, $I$: absolute intensity, $r$: distance on film

copper $K\alpha$ radiation at 30 kV. and 20 mA. A calibrated camera (radius 45 mm.), powder specimen of 0.5 mm. diameter and Kodak "No-screen" films were used. The patterns of (002) and (100) indices were microphotometered for each 0.5 mm. of film and the crystallite dimensions were calculated for both patterns, $Lc$ and $La$ respectively, by the Laue-Brill procedure[20]. The crystallite dimension observed in carbon blacks implies the size of fundamental structural units of which the carbon black particle (a cluster of units) is constructed.

**Electron-microscopic Method.**—The enlarged electron-micrographs obtained for the samples have varying magnifying ratios between 14000 and 79000 according to the range of particle dimension. The sizes of numerous particles on the photographs were measured with the help of a magnifying glass and transparent scale, and the diameter of the most frequent counting (called the modal diameter) was determined.

**Adsorption Measurements.**—The most accurate method to evaluate the surface area will be the low-temperature adsorption method of nitrogen at liquid-air temperature[1,6-10] but a more feasible and rapid method of determining the specific surface area by adsorption of molecules from solutions has been applied to carbon blacks is frequently adopted. The compounds used for adsorbent are organic acids[11,12], iodine[13-16], diphenylguanidine[13], methylene blue[16], etc. In this work, the iodine and the methylene blue adsorption measurements were made which had been previously applied by the author to carbon black[16], coal[21] and coke[22].

The dried sample (0.5 g.) was added to 25 cc. of 0.1 N iodine solution at 25.0°C and the mixture stirred from time to time. The change in iodine concentration was determined after 1 hour. The specific surface area value could be derived from the adsorption per unit weight of sample, it being assumed that the adsorption is monomolecular and that the cross sectional area of adsorbed iodine molecule is 16.1 Å$^2$ [23,24].

A 25 cc. portion of 0.4% methylene blue solution was added to 0.5 g. dried sample and stirred occasionally. The change in concentration after 24 hours at 25.0°C was determined with a photoelectric colorimeter. The specific surface area was again given from the adsorption data, the molecular area on solid surfaces being taken as $1.0\times10^3 m^2/g$ [25]. The surface area value was then calculated in diameter by use of real density for each sample. The density was obtained picnometrically at 25.0°C with methanol after replacing

20) K. Inouye, H. Tani and M. Abiko, *J. Fuel Soc. Japan*, **32**, 292, 386 (1953).

21) K. Inouye, ibid., **29**, 112 (1950).

22) K. Inouye and H. Tani, *Fuel* (London), **34**, 356 (1955).

23) E. J. Mack, *J. Am. Chem. Soc.*, **47**, 2468 (1925).

24) L. H. Reyerson and A. W. Wishart, *J. Phys. Chem.*, **42**, 683 (1938).

25) F. Paneth and W. Thimann, *Ber.*, **57**, 1215 (1924).

III

| Dye adsorption | | Heat of Wetting | | | Crystallite dimensions | |
|---|---|---|---|---|---|---|
| Surface area, $m^2/g.$ | Dia., Å. | Heat, cal./g. | Surface area, $m^2/g.$ | Dia., Å | La, Å | Lc, Å |
| 35.4 | 906 | 4.25 | 42.5 | 755 | 16.5 | 10.9 |
| — | — | 3.00 | 30.0 | 1070 | 15.4 | 12.0 |
| — | — | — | — | — | 17.5 | 11.4 |
| 53.3 | 606 | 2.83 | 28.3 | 1100 | 18.2 | 13.8 |
| — | — | 2.82 | 28.2 | 1150 | 43.1 | 24.8 |
| 61.0 | 553 | — | — | — | 16.5 | 14.3 |
| 189. | 172 | 12.6 | 126. | 257 | 19.5 | 10.1 |
| 120. | 291 | 11.3 | 113. | 309 | 20.9 | 12.4 |
| — | — | — | — | — | 21.5 | 11.9 |
| 17.8 | 1800 | 0.60 | 6.0 | 5350 | 17.3 | 14.2 |
| 27.1 | 1240 | 0.72 | 7.2 | 4680 | 20.7 | 13.6 |
| 50.3 | 689 | 1.95 | 19.5 | 1810 | 15.5 | 11.8 |
| 64.6 | 444 | 2.12 | 21.2 | 1660 | 18.2 | 11.1 |
| 81.7 | 365 | 3.47 | 34.7 | 1030 | 16.4 | 12.5 |

the occluded air by evacuating below 1 mmHg for several hours.

**Heat of Wetting Method.**—Kraus[10] has reported recently the heat of immersion of nine carbon black samples in water, methanol and *n*-hexane. The results was discussed in comparison with the specific surface area obtained by the nitrogen adsorption method at very low temperature and it was shown that the value of heat evolved by wetting the unit area varies with the nature of the sample, particularly the content of oxygenic radicals in carbon blacks.

In the present work, the heat-of-wetting measurements were made in order to derive the specific area on an assumption that the area per unit heat evolved is identical. The aparatus is a calorimeter comprising a Dewar flask with bakelite lid which is fixed to the flask by screws and supports all the working parts of the calorimeter: a stirrer which serves at the same time as a support of sample bulb, electrical heater and a Beckmann's thermometer to which a bulb-breaking device is attached. The Dewar vessel is immersed in a thermostat regulated at 25.0°C, which is situated in an air-bath controled at approximately 25°C. The construction and procedure are not very different from those proposed by earlier workers, in particular, by Griffith and Hirst[26]. Approximately 0.3-2.5 g. sample dried at 100-110°C for 1.5 hour and weighed in a thin-walled glass bulb, was evacuated at $10^{-4}$ mmHg for 5-6 hours at room temperature. After an equilibrium of temperature in Dewar vessel was attained, the bulb was broken in methanol (120 cc.) by a breaking device attached to the thermometer and the elevation of temperature was recorded at each 0.5 or 1 minute until when an equilibrium was again attained. The heat capacity was measured for each run by heating with known electrical energy supplied from a battery.

To derive the surface area from the heat-of-wetting, a value of area per unit heat of 10.0 $m^2$/cal. obtained by Bangham[27] and Maggs[28] for several carbonaceous substances was used.

The diameter was obtained from a specific surface area similarly as the absorption method by use of real density.

**Electrical Resistivity Measurement.**—The sample was dried at 110°C for 1 hour and the electrical conductivity of the compressed sample was then measured at various successive pressures with an apparatus constructed by Honda et at.[29]. The powder was placed in a steel tube and the pressure up to 3000 kg./$cm^2$ was exerted on it by a hydraulic system. The specific resistivity was plotted against $1/P$, $1/P^2$ or $1/\sqrt{P}$; where $P$ denotes the pressure applied. The best linearlity has been found at the relations between the specific resistance and $1/\sqrt{P}$; the value of resistivity when $P$ reaches infinity was taken as the characteristic value for each sample.

## Results and Discussions

**Carbon Blacks.**—Table III summarizes the values of particle diameter obtained from the methods explained in the preceding section. The surface area and heat of immersion as well as crystallite dimension by powder method are also tabulated for reference.

The diameters obtained by low-angle scattering method and by electron-microscope are in fairly good agreement. However, it seems important to note that the value from low-angle scattering is, in most

26) M. Griffith and W. Hirst, "Proc. of Conf. on the Ultra-fine Structure of Coals and Cokes," British Coal Utilization Research Association, London (1944), p. 80.

27) D. H. Bangham and R. I. Razouk, *Proc. Roy. Soc* (London), **A166**, 572 (1938).

28) F. A. P. Maggs, "Proc. of Conf. on the Ultra-fine Structure of Coals and Cokes," British Coal Utilization Research Association, London (1944), p. 95.

29) H. Honda, K. Ouchi and T. Toyoda, *J. Chem. Soc. Japan* (Pure Chem. Sect.), **76**, 364 (1955).

cases, larger than the value from the latter; the cause of this discrepancy may be due to some experimental errors, but it is also probable that the particles of carbon black have some connection with each other by means of bridges made of carboneceous substance with not a very different nature from the particles themselves, and the scattering dimension by X-ray is apparently larger than that expected by electron-micrographs in which all particles, even though they connect and form a skeleton or guitarshaped agglomerate, are recognized as separate particles piled up one above another. (See Fig. 4). Watson[30] has suggested that in

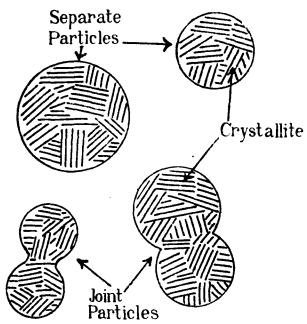



Fig. 4. Models of carbon black particles.

the electron-micrographs of shadowed carbon black particles some kinds of "essential" bridge forming between neighboring particles are observed. The possibility of the occurrence of the jointing particles as shown in Fig. 4 is also supported by the correlation between particles size and electrical resistance described in the next section. It is assumed from the results in Table III that the joining of this kind may be more noticeable in the samples with finer particle size, which showed larger discrepancy.

The particle diameter values obtained from adsoption methods and the heat-of-wetting measurement are somewhat parallel to those by X-ray and electron-microscopic method, but an exact comparison indicates that these colloid-chemical procedure, which are often employed in carbon black assessment, are by no means recognized as giving absolutely accurate results, and should be used only for a conventional qualitative comparison. As pointed out by Kraus[10], the adsorption or heat of immersion is largely affected by the chemical composition of reagents used as well as of carbon black itself, especially by the nature of surface of particles.

The crystallite size derived from line broadening of powder diffraction method gave almost similar dimensions of La (size in a-axis of hexagonal lamellae) and Lc (size in c-axis) ranging from approximately 10 to 20 Å, excluding only acetylene black which has more developed ultimate units. The concept of carbon black structure that the crystallites are piled in a very packed state so as to embrance no internal surface has been widely accepted (cf. Fig. 4). This is supported by the results of the present work (Table III) which show particle sizes from adsorption or heat of wetting methods, which will be able to measure the internal surface, are of approximately similar order as those from purely physical methods.

**Graphitized Carbon Blacks.**—The diameter revealed by low-angle method and the specific resistance method are tabulated in Table IV. The preparation of samples and measuring procedures are to be referred to the earlier descriptions.

As widely accepted, the crystallite dimensions increase with the elevation of graphitization temperature. Meanwhile, the size of particles, which are clusters of the ultimate unit crystallites, shows a very interesting change during the course of graphitization. On the other hand, the change in specific resistance is also particular. The relations between these three factors are illustrated in Fig. 5.

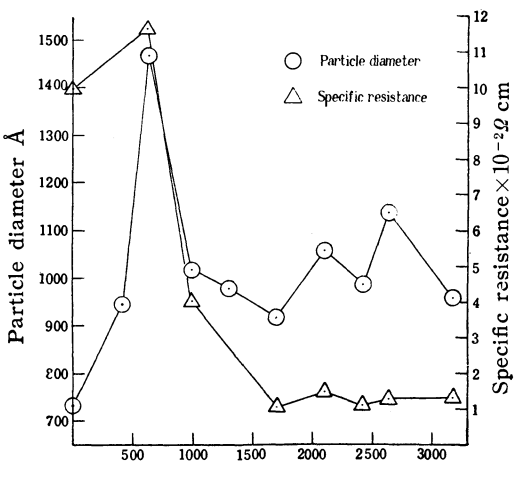



Fig. 5. Variations of particle size and specific resistance with treating temperature.

30) J. H. L. Watson, *J. Appl. Phys.*, **20**, 747 (1949).

Schaeffer et al.[31] have reported the electrical resistance variations with graphitization of some kinds of carbon black; they observed a sharp minimum of resistivity at approximately 1200°, followed by increase up to approximately 2500°C, and the second decrease at higher temperatures. An interpretation of these results was tried as the evolution of combined gaseous materials from the samples and the growth of the crystallite.

TABLE IV
PROPERTIES OF GRAPHITIZED BLACKS

| Temp., °C | Diameter, Å | Dimension Å Lc | Crystallite La | Specific resistance, Ω cm. |
|---|---|---|---|---|
| Untreated | 732 | 16.5 | 10.9 | 0.100 |
| 420 | 950 | — | — | — |
| 620 | 1470 | 21.1 | 14.1 | 0.117 |
| 990 | 1020 | 23.9 | 13.6 | 0.0410 |
| 1300 | 982 | — | — | — |
| 1700 | 920 | 50.8 | 36.9 | 0.0110 |
| 2100 | 1060 | 75.7 | 38.1 | 0.0158 |
| 2420 | 990 | 99.1 | 41.1 | 0.0119 |
| 2630 | 1140 | 47.8 | 50.0 | 0.0129 |
| 3170 | 960 | 61.9 | 40.8 | 0.0134 |

However, the present correlation between electrical resistance and particle diameter in Fig. 5 would suggest that the variation in resistivity is caused by a change in the state of agglomeration of the particles. As discussed in the earlier section, it has been indicated that the carbon black particles tend more or less to combine with each other to form conjoint particles that act as the scattering sources by X-rays and give large apparent diameter values. It is apparent that the conjoint particles shown in Fig. 4 can form only a loosely packed state and that such loose packing results in a difficulty of electrical conduction. The maxima in both electrical resistance and particle size at 620°C are most noticeable and it is expected that the carbonization of tarry substances on the surface of particles will play a part in forming a scaffolding particle system. The electron-micrographs also show somewhat agglomerated particle images for the samples treated at such temperature range. The linearity between particle size and resistance is also observed at higher temperature range in Fig. 5, but it seems that the formation of conjoint particles at higher temperature range than 1000°C is improbable. Another reason is therefore to be considered that the increase in particle size is also derived from extinction of smaller particles by heat treatment and vice versa. Based on the similar concept as suggested above, the increase in average particle size will cause a loosely packed state and have a high electrical resistance.

The author is pleased to acknowledge the helpful discussions relating to the present results by Prof. E. Suito (Kyoto Univ.) and Assis. Prof. K. Nagamatsu (Kyushu Univ.). His thanks are also due to Mr. R. Shinagawa (Resources Research Inst.) for help in designing the low-angle camera, Mr. H. Takahashi (Tokyo Univ.) for taking the electron micrographs, to Japan Carbon Black Association and Tokai Electrode Co. Ltd. for providing the samples examined and to Showa Denko Co. Ltd. for preparing the graphitized carbon black samples. The measurement of heat of wetting was carried out by A. Roppongi.

*Resources Research Institute*
*Kawaguchi, Saitama*

31) W. D. Schaeffer, W. R. Smith and M. H. Polley, *Ind. Eng. Chem.*, **45**, 172 (1953).

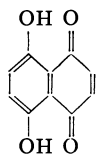
# *Crystal Structure of a Monoclinic Form of Naphthazarin**

By Hideo WATASE, Kenji OSAKI and Isamu NITTA

(Received March 6, 1957)

## Introduction

There have been reported three monoclinic modifications of naphthazarin ($C_{10}H_4O_2(OH)_2$)[1-3]. We obtained one of these, a needle crystal with metallic lustre, from acetic acid solution colored red. To this crystal Palacios and Salvia[1] have given the space group of $C_{2h}^5$ with two molecules in the unit cell**. Thus the molecule should be situated on a center of symmetry in the crystal lattice, while the usual chemical formula, 5,8-dihydroxy-1,4-naphthoquinone (I), has no center of symmetry. Thus further investigations are required to deal with the molecular structure.



(I)

Naphthazarin is similar to quinhydrone, the molecular compound of quinone and hydroquinone, in color, lustre and shape of the crystal, and has the same functional groups and planar form. From the result of X-ray analysis of quinhydrone[4], it is shown that the crystal has a very interesting structure, in which there is an anomalously short distance of 3.16 Å between the planes of successively overlying planar molecules as compared with the graphite interplanar value of 3.4 Å, and in which quinones and hydroquinones are linked linearly one after the other through the intermolecular hydrogen-bridges, these two interactions causing a layered structure to be formed. Therefore it becomes interesting to discover whether or not such special interactions are operative in the crystal structure of naphthazarin.

In this paper is given some information about the form of the molecule and the intermolecular interactions from two-dimensional X-ray analysis.

## Unit Cell and Space Group

Oscillation, Sauter and Weissenberg photographs were taken about the needle axis (*a* axis) and another axis (*b* axis), using Cu $K_\alpha$ radiation. The photographs have shown a monoclinic lattice. The dimensions of the unit cell, containing two molecules, were as follows;

$a=3.74$, $b=7.63$, $c=14.53$ Å. $\beta=97.1°$.

From the Weissenberg photographs the intensities of reflexions were estimated visually, compared with a calibrated scale, multiple-film technique being used. Structure factors were deduced from these intensity data in the usual way.

At the first stage, the space group of $C_{2h}^5-P2_1/c$ was considered to be reasonable, since it appeared that no regular absences of reflexions were observed, except for $(0k0)$ when $k$ is odd, and $(h0l)$ when $l$ is odd. However, when the Weissenberg photograph of $(h0l)$ was examined carefully once more, some of the forbidden spectra were suspected to be appearing very faintly. On the long exposed oscillation photographs of the *a* axis, very weak but definite spectra of (101), (103), (103), (105) and (105) etc. were recognized. Therefore the symmetry element of glide plane is undoubtedly missing in the crystal.

In consequence, the space group is not $C_{2h}^5-P2_1/c$, but $C_2^2-P2_1$, although it may be said that the crystal has the symmetry of $C_{2h}^5-P2_1/c$ in a rough sense.

## Application of Fourier-transform Method

It is reasonable to attempt the analysis of the structure of naphthazarin in assuming the space group of $C_{2h}^5-P2_1/c$, because the forbidden spectra are negligibly weak.

* The major part of this paper was read at the 6th Annual Meeting of the Chemical Society of Japan, April, 1953.

1) J. Palacios and R. Salvia, *Anales Soc. espan. fis. quim.*, **32**, 49 (1934).

2) M. T. Rogers, *J. Am. Chem Soc*, **69**, 1506 (1947).

3) O. Borgen, *Acta Chem. Scand.*, **10**, 867 (1956)

** According to the reports 1-3), the other two modifications have the space groups of $C_{2h}^5$, their unit cells containing two and four molecules respectively, and the volumes occupied by one molecule are nearly equal in the three modifications.

4) I. Nitta, H. Matsuda and K. Osaki, 2nd Intern. Congr. Cryst. (1951).

When the space group is $C_{2i}^5$ and the unit cell contains two planar molecules on its centres of symmetry, the best way of analysis is of application of the Fourier-transform method[5], and by this method the orientation of the reciprocal lattice to the molecule is found out easily.

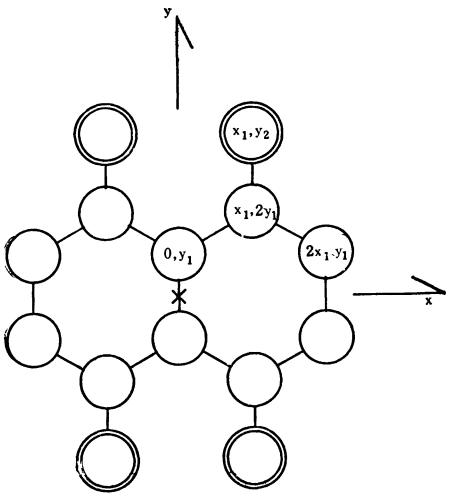



Fig. 1. Idealized molecular Model of naphthazarin for the Fourier transform. In this model $x_1=1.21$, $y_1=0.70$, $y_2=2.71$ Å, the atomic scattering factor of oxygen being assumed 3/2 of carbon. Single circles represent carbons and double circles oxygens.

An idealized molecular model was assumed as shown in Fig. 1. Then the Fourier transform of the molecule of naphthazarin was calculated, on the assumption of point-atoms, as follows ($X$, $Y$: the coordinates in reciprocal space):

$$T=2\cos 2\pi y_1 Y$$
$$+2\cos 2\pi(2x_1X+y_1Y)+2\cos 2\pi(2x_1X-y_1Y)$$
$$+2\cos 2\pi(x_1X+2y_1Y)+2\cos 2\pi(x_1X-2y_1Y)$$
$$+3\cos 2\pi(x_1X+y_2Y)+3\cos 2\pi(x_1X-y_2Y).$$

The transform map of Fig. 2 was obtained by the above calculations. From comparison between the observed structure factors and the transform map, the projection of the reciprocal lattice along the normal of the molecular plane could be determined without difficulty, as shown also in Fig. 2. The observed structure factors were fitted well with the values of the map in the following manner :***

Case ($0kl$) ;

$T_{0kl(\text{crystal})}=$

$T_{0kl(\text{molecule})}+\cos\pi(k+l)\times T_{0k\bar{l}(\text{molecule})}$.

Case ($h0l$) ;

directly on the map****.

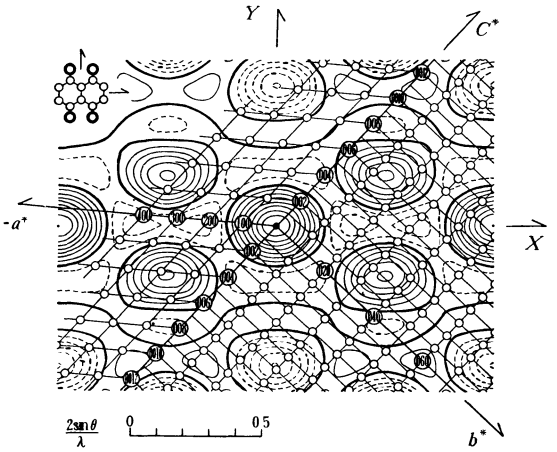



Fig. 2. The Fourier transform of naphthazarin showing the relation with the crystal reciprocal lattice. Solid, broad and broken contours are positive, zero and negative ones respectively, these intervals being of 2.

Thus the signs of the structure factors being given reliably, the Fourier summations of the electron-density projections along the $a$ and $b$ axes were then calculated, and by successive Fourier refinements the maps of Fig. 3 were derived after the signs of a few small structure factors had been changed. The atomic parameters obtained from the peaks of these maps are

(8.5/30, 9.8/60, 9.0/60),
(9.4/30, 16.2/60, 4.7/60),
(24.9/30, 29.1/60, 22.3/60),
(0.5/30, 26.3/60, 27.7/60) and
(4.3/30, 16.2/60, 29.2/60) for carbons,

and are

(25.3/30, 22.6/60. 18.3/60) and
(5.5/30, 9.5/60, 25.0/60) for oxygens.

In this stage, the reliability factors ($R=\Sigma||F_0|-|F_c||/\Sigma|F_0|$) are 0.19 and 0.22 for ($0kl$) and ($h0l$) respectively, using the value of $B=5.0$ Å$^2$ as the temperature factor. In these calculations unobserved reflexions are omitted. The observed values of $T_{hkl}$, which are the absolute values of the structure factors divided by the atomic scattering factor[6] of carbon and the temperature factor, are listed in Tables I and II for comparison in the same scale with the values of the transform map.

5) G. Knott, *Proc. Phys. Soc.*, **52**, 229 (1940).

*** Because, in the present case, two molecules are in the unit cell and the space group is $C_{2h}^5$-$P2_1/c$.

**** $T_{h0l(\text{crystal})}=2T_{h0l(\text{molecule})}\times(\cos\pi l/2)^2$.

6) R. McWeeny, *Acta Cryst.*, **4**, 513 (1951).

TABLE I

OBSERVED VALUES OF $T_{0kl}$

| $l$ \ $k$ | 0 | 1 | 2 | 3 | 4 | 5 | 6 | 7 | 8 |
|---|---|---|---|---|---|---|---|---|---|
| 0 | — | | − 5.8 | | | | + 1.9 | | + 4.0 |
| 1 | | + 6.2 | + 1.4 | + 7.0 | + 8.5 | | − 3.5 | − 7.6 | − 4.0 |
| 2 | + 6.1 | + 2.4 | − 5.0 | + 7.7 | + 9.4 | − 1.9 | − 8.2 | + 7.7 | |
| 3 | | − 5.7 | − 5.7 | + 4.9 | + 8.8 | | +16.5 | −14.7 | − 7.5 |
| 4 | − 4.6 | + 0.7 | − 0.4 | + 4.6 | + 0.9 | − 3.5 | −17.0 | + 7.8 | |
| 5 | | + 6.5 | + 4.2 | −14.9 | | | +13.3 | | − 8.3 |
| 6 | + 0.5 | + 7.6 | + 1.9 | +10.1 | | | | | |
| 7 | | + 5.0 | +10.7 | − 6.9 | + 1.8 | +12.6 | − 7.7 | | |
| 8 | − 3.4 | | + 2.9 | − 5.9 | +15.9 | +23.5 | | | |
| 9 | | − 1.2 | − 1.4 | | + 2.8 | + 3.7 | + 4.6 | | |
| 10 | | | − 4.9 | − 3.5 | | +22.4 | | | |
| 11 | | − 9.8 | +12.1 | | | | | | |
| 12 | + 8.2 | +12.0 | −11.7 | | | | | | |
| 13 | | −10.6 | | | | | | | |
| 14 | | | | | | | | | |
| 15 | | | | | | | | | |
| 16 | | | | | | | | | |

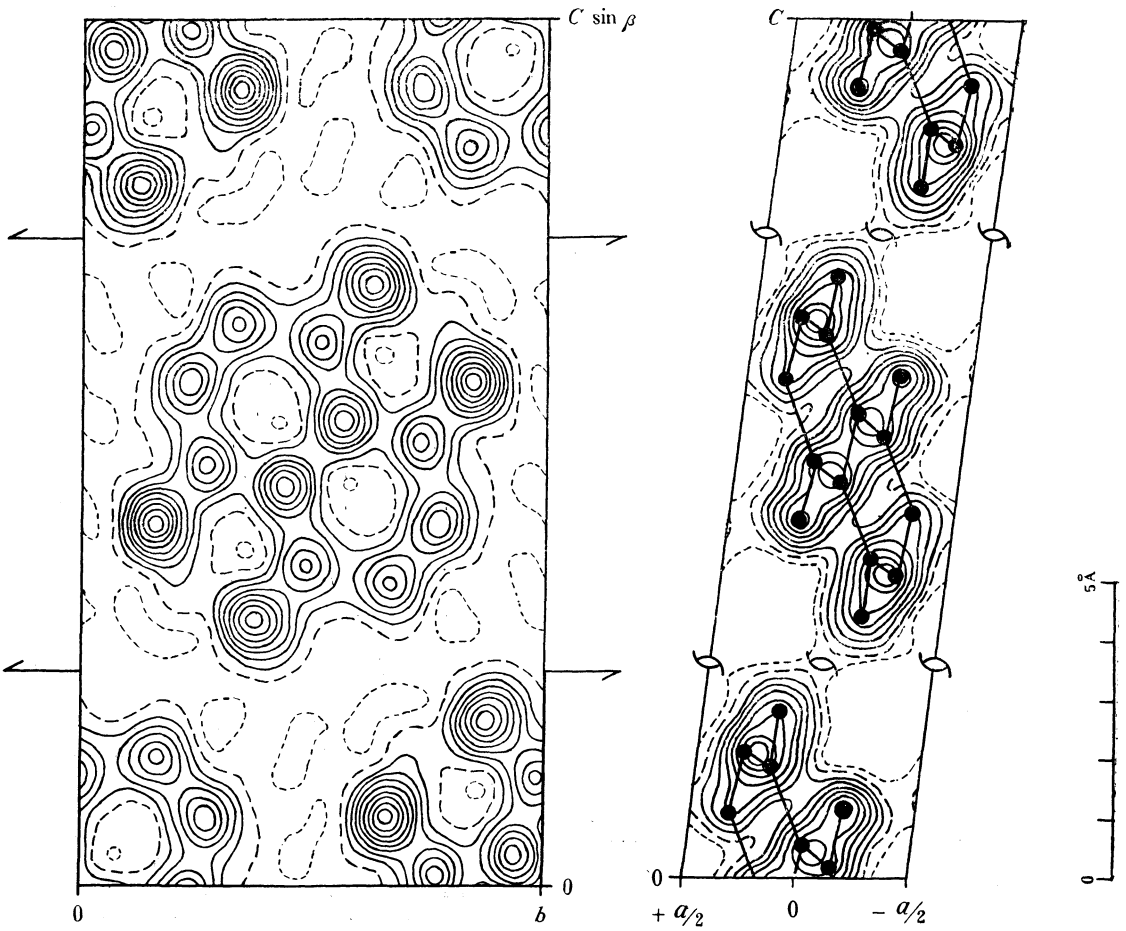



Fig 3. Electron-density projections along the $a$ and $b$ axes. Contours are drawn at equal intervals on an arbitrary scale for each map. Black circles in the $b$ axis projection indicate the atomic positions.

TABLE II

OBSERVED VALUES OF 1/2 $T_{hol}$

The odd cases of $l$ are omitted, the intensities of these reflexions being too weak to be estimated

| $l$ \ $h$ | 4 | 3 | 2 | 1 | 0 | $\bar{1}$ | $\bar{2}$ | $\bar{3}$ | $\bar{4}$ |
|---|---|---|---|---|---|---|---|---|---|
| 0 | − 0.9 | − 1.6 | − 4.6 | + 5.4 | — | + 5.4 | − 4.6 | − 1.6 | − 0.9 |
| 2 | | + 0.9 | + 1.0 | − 2.3 | + 3.2 | + 5.8 | − 1.3 | + 1.1 | + 8.0 |
| 4 | | | +10.9 | + 6.3 | − 2.4 | − 3.5 | − 2.7 | + 0.6 | + 5.3 |
| 6 | | | + 1.3 | + 3.6 | + 0.3 | + 0.2 | | | |
| 8 | | | + 0.4 | − 0.5 | − 1.5 | + 0.7 | + 2.3 | − 6.2 | − 1.6 |
| 10 | | − 8.2 | − 3.0 | | + 0.8 | + 1.7 | | − 6.9 | |
| 12 | | | − 1.9 | − 1.3 | + 3.5 | − 6.6 | − 1.9 | + 1.5 | |
| 14 | | | | | + 1.2 | − 6.9 | −12.1 | − 3.8 | |
| 16 | | | | | | + 1.2 | | | |

## Discussion

Although the electron-density projection maps, shown in Fig. 3, are not very accurate, the maps show the principal feature of the crystal structure, and the interatomic distances derived from these maps give some information, since it may be considered that the degree of approximation is fairly high. The atomic distances between the molecules are shown in Figs. 4 and 5. The crystal structure is of a type entirely different from that of quinhydrone.

In the projection along the $a$ axis, all the atoms are completely separated because of the very short period of this axis, each molecule being surrounded by six molecules two-dimensionally (Fig. 4). The molecular plane is inclined at only about 28° to the (100) plane.

The projection along the $b$ axis (Fig. 5) shows the feature of the planar molecules overlapping successively along the $a$ axis (needle axis). The perpendicular distance between the planes of the molecules is found to be about 3.4 Å, the usual contact distance. There is no especially close approach as found in the structure of quinhydrone. This fact supports the discussion based on absorption spectra[7]; special interplanar interaction will not be operative in naphthazarine, since no such particular optical dichroism as shown by quinhydrone is detected.

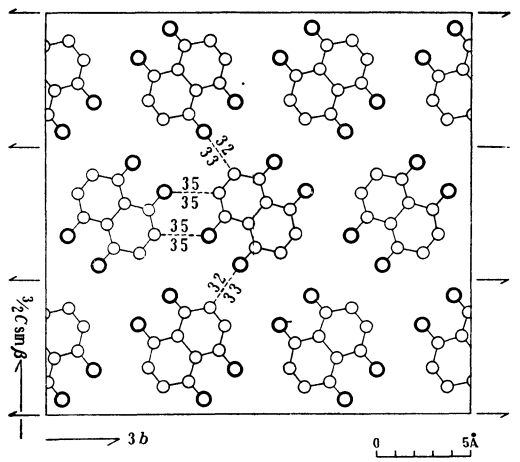



Fig. 4. Grouping of the molecules in the crystal, viewed along the $a$ axis. The intermolecular distances are shown in Å. Single circles represent carbons and double circles oxygens.

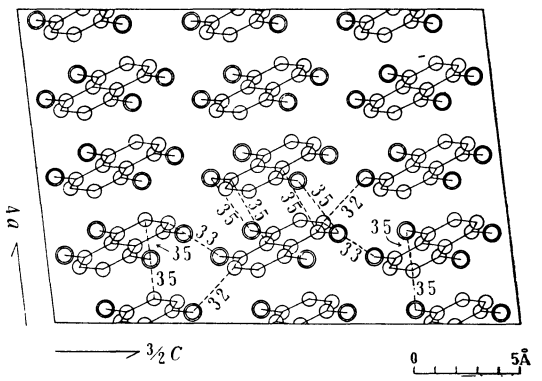



Fig. 5. Grouping of the molecules in the crystal, viewed along the $b$ axis. The intermolecular distances are shown in Å. Single circles represent carbons and double circles oxygens.

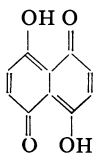
As a whole, the crystal structure resembles that of typical aromatic compounds. In an approximation, only suitable van der Waals attractive forces may be said to operate between the molecules so as to form the observed crystal structure, and each molecule is surrounded by fourteen neighbours in a manner of closest packing.

7) K. Nakamoto, *J. Am. Chem. Soc.*, **74**, 1739 (1952); This Bulletin, **26**, 172 (1953).

That there is no intermolecular hydrogen bond, is also a point which differs from the case of quinhydrone. The intramolecular O—O distance is roughly 2.5 Å and six-membered hydrogen-bonded ring is considered to be formed here. The latter point is also revealed from the missing of the free O—H stretching vibration in the infrared spectra[8].

Quite recently, Borgen[3] has analysed the crystal structure of this modification to be of the space group of $C_{2h}^5-P2_1/c$, deriving the $a$ axis electron-density projection by the use of the Patterson function, and has discussed some possible molecular models of centro-symmetry and molecular arrangements from this space group, since the usual chemical formula (I) is by itself incompatible with the space group. However, as we have pointed out above that the crystal has this symmetry only in a sense of approximation, it appears likely that those models and arrangements should be modified from this point of view, the formula (I) being not incompatible with the real crystal symmetry of $C_2^2-P2_1$.

In the classical sense the usual formula (I) and the centro-symmetric one (II) are to be considered as possible from the electron-density projection maps based upon $C_{2i}^5-P2_1/c$.




(II)

However it seems that the formula (II) is hardly suitable, since in such a manner of molecular grouping as shown by Figs. 4 and 5, it will be natural to suggest the crystal symmetry of $C_{2h}^5-P2_1/c$, if the molecule be of this formula. On the other side, from the stand point of the resonance stabilization, it may be said that the structure (II) is less stable than the formula (I).

Further, regarding the molecular structure, the spectra forbidden to the space group of $C_{2h}^5-P2_1/c$ are generally so weak that it may be supposed, as a probable explanation, that the molecule will have the structure considerably deviating from that corresponding in the classical sense to the formula (I) so as to approach the centro-symmetric form (II) to some extent. We can not of course conclude further what the real molecular structure is without more accurate determination of the atomic parameters. However, no further analysis is being attempted at present.

Finally, it is of interest to remark again that naphthazarin has at least three modifications in the region of ordinary temperatures.

We wish to express our thanks to Professor-Emeritus Chika Kuroda for supplying the specimen and to Mr. Yujiro Tomiie for continued interest.

*Department of Chemistry, Faculty of Science, Osaka University*
*Kita-ku, Osaka*

8) H. Brockmann and B. Franck, *Naturwiss.*, **42**, 45 (1955).

# *Studies on Antibiotics and Related Substances. VI. Configurations of Isomeric O-Methylphenylserines and a New Route for the Synthesis of Chloramphenicol**

By Tetsuo SUAMI and Sumio UMEZAWA

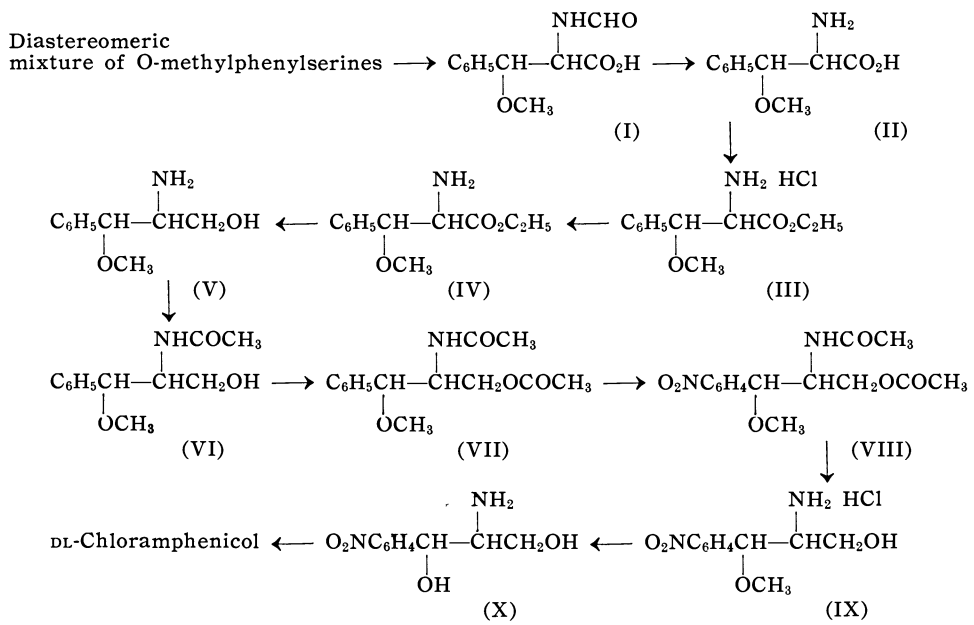
(Received February 27, 1957)

In connection with synthetic studies on chloramphenicol in this Laboratory, the two diastereomers of O-methylphenylserine which were synthesized by Carter and Van Loon[1] became attractive as possible intermediates. The synthesis involved the methoxymercuration of cinnamic acid. In another paper West, Krummel and Carter[2] obtained one racemic form of $\alpha$-bromo-$\beta$-methoxy-$\beta$-phenylpropionic acid by the reaction of methyl hypobromite with cinnamic acid in the presence of silver nitrate.

The present paper describes the studies on the configuration of diastereomeric O-methylphenylserines and the synthesis of DL-threo-2-amino-1-*p*-nitrophenyl-1,3-propanediol from one of the diastereomers.

Synthetic studies concerning the configuration of the O-methylphenylserine (II), which was synthesized through methoxymercuration, is described first and followed by the synthesis of DL-chloramphenicol from II via DL-threo-2-amino-1-*p*-nitrophenyl-1,3-propanediol. Finally, studies on the other diastereomer (XI) of O-methylphenylserines is described.

**Configuration of O-Methylphenylserine (II) Synthesized through Methoxymercuration.**—The mixture of O-methylphenylserines melting at 215–219°C (dec.) was prepared by amination of the mixture of $\alpha$-bromo-$\beta$-methoxy-$\beta$-phenylpropionic acids which was obtained by the synthetic route of Van Loon and Carter[3].




* Presented before the Division of Organic Chemistry at the Annual Meeting of the Chemical Society of Japan, at Kyoto University, April 3, 1956.

1) H. E. Carter and E. J. Van Loon, *J. Am. Chem. Soc.*, **60**, 1077 (1938).

2) H. D. West, G. S. Krummel and H. E. Carter, *J. Biol. Chem.*, **122**, 605 (1938).

3) E. J. Van Loon and H. E. Carter, *J. Am. Chem. Soc.*, **59**, 2555 (1937).

The mixture of O-methylphenylserines was formylated with concentrated formic acid to give a mixture of N-formyl derivatives, from which DL-threo-N-formyl-O-methylphenylserine (I) melting at 161–162°C was isolated as a single diastereomer by repeated recrystallization.

I was hydrolyzed with 1 N hydrochloric acid to yield DL-threo-O-methylphenylserine (II) melting at 218–220°C (dec.) in 89.3% yield. The N-benzoyl derivative of II which was obtained by benzoylation of II with benzoyl chloride in alkaline solution melted at 168–169°C.

II was treated with dry hydrogen chloride in absolute ethanol to give the ethyl ester hydrochloride (III) melting at 158–160°C. The free ethyl ester (IV) was obtained by bubbling ammonia through the ethereal suspension of III.

The ethyl DL-threo-O-methylphenylserinate (IV) was led to DL-threo-2-amino-1-*p*-nitrophenyl-1,3-propanediol and DL-chloramphenicol by the following procedure.

IV was reduced with hydrogen over Raney nickel catalyst to give DL-threo-O-methylphenylserinol (V) melting at 28–32°C in 41.9% yield. Acetylation of V with acetic anhydride at room temperature yielded N-acetyl derivative (VI) melting at 184–185°C. V was further acetylated by heating with acetic anhydride to yield N,O-diacetyl derivative (VII) melting at 120–121.5°C in 85.5% yield.

Nitration of VII with mixed acid under ice cooling yielded N,O-diacetyl-DL-threo-2-amino-1-methoxy-1-*p*-nitrophenyl-3-propanol (VIII) melting at 80–82°C, which, on hydrolysis with 10% hydrochloric acid, yielded DL-threo-2-amino-1-methoxy-1-*p*-nitrophenyl-3-propanol hydrochloride (IX) melting at 235–237°C (dec.).

Drastic hydrolysis of IX with 25% hydrochloric acid at 125–130°C in a sealed tube gave in a good yield a demethylated product (X), which did not depress the melting point of an authentic sample of DL-threo-2-amino-1-*p*-nitrophenyl-1,3-propanediol.

X was converted into N-dichloroacetyl derivative, viz. DL-chloramphenicol, which showed half the potency of the natural chloramphenicol against *Escherichia coli*. One can conclude, therefore, that a diastereomer of O-methylphenylserine which is obtained through methoxymercuration is of the threo configuration.

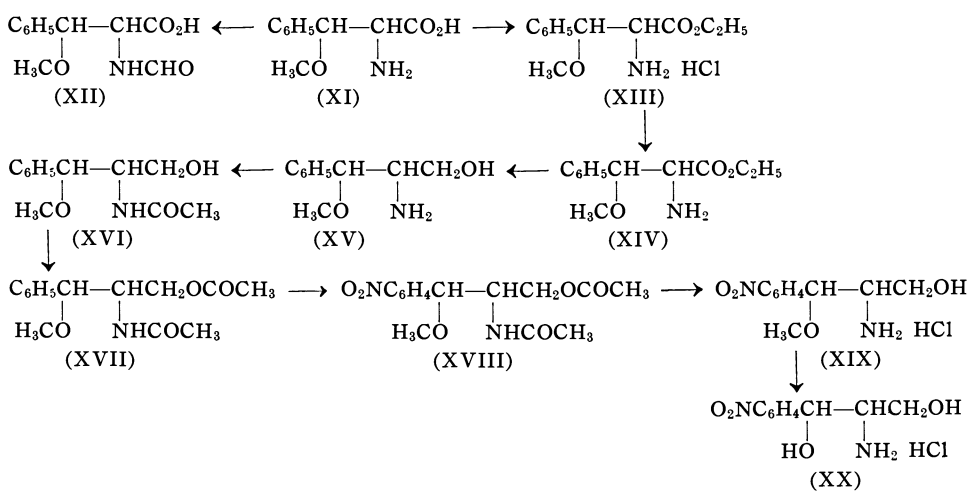
In the course of the above-mentioned investigation, we tried to demethylate the formyl derivative of O-methylphenylserine (I) by the action of concentrated hydrochloric acid. However, there was obtained 2-phenylnaphthalene, as would be expected from the report by Cater and Van Loon[1].

**Derivatives of the Other Diastereomer (XI) of O-Methylphenylserine.**—O-Methylphenylserine of m. p. 251–253°C (dec.) was prepared by the amination of α-bromo-β-methoxy-β-phenylpropionic acid by the method of Cater and co-workers[2].

The O-methylphenylserine afforded the corresponding N-formyl derivative (XII) melting at 149–150°C in a high yield by treatment with concentrated formic acid.

The O-methylphenylserine (XI) was treated with dry hydrogen chloride in absolute ethanol to yield the ethyl ester hydrochloride (XIII) melting at 179–181°C (dec.). The free ethyl ester was obtained by bubbling ammonia through an ethereal suspension of XIII.

Upon reduction of the ethyl ester (XIV)



with hydrogen over Raney nickel catalyst, the other diastereomer of O-methylphenylserinol (XV) was obtained as a syrup in 32.4% yield. When an ethereal solution of XV was saturated with dry hydrogen chloride, the crystalline hydrochoride of XV was obtained. This melted at 181–182°C. By benzoylation of XV with benzoyl chloride, N,O-dibenzoyl derivative melting at 160–161°C was obtained.

Acetylation of XV with acetic anhydride at room temperature yielded N-acetyl derivative (XVI) melting at 116–118°C. XVI was further acetylated by heating with acetic anhydride to yield N,O-diacetyl derivative (XVII) melting at 77–80°C.

Nitration of XVII with mixed acid under ice cooling yielded N,O-diacetyl-DL-erythro-2-amino-1-methoxy-1-*p*-nitrophenyl-3-propanol (XVIII) melting at 150–151°C, which, on hydrolysis with 10% hydrochloric acid, yielded DL-erythro-2-amino-1-methoxy-1-*p*-nitrophenyl-3-propanol hydrochloride (XIX) melting at 233–234°C (dec.).

Drastic hydrolysis of XIX with 25% hydrochloric acid at 125–130°C in a sealed tube gave DL-erythro-2-amino-1-*p*-nitrophenyl-1,3-propanediol hydrochloride (XX) melting at 209–210°C.

Thus, there is no contradiction in the assignment of the erythro configuration to the other O-methylphenylserine (XI).

## Experimental

**Amination of α-bromo-β-methoxy-β-phenylpropionic acid synthesized through methoxymercuration.** — The diastereomeric mixture of α-bromo-β-methoxy-β-phenylpropionic acids was prepared through methoxymercuration by the route of Van Loon and Carter[3]. Thirty-seven grams of the bromo compounds were heated with 500 cc. of concentrated ammonia water at 90–100°C for 6 hr. in an autoclave. After being kept overnight at room temperature, the content was filtered and evaporated to dryness under reduced pressure. The residue was redissolved in a small portion of water, filtered and again evaporated under reduced pressure. The residue was triturated with acetone and allowed to stand with frequent shaking. The precipitate was collected and washed with acetone. The crude product of α-amino-β-methoxy-β-phenylpropionic acid melted at 215–219°C (dec.); yield 27 g. (97.0%).

**N-Formyl-DL-threo-O-methylphenylserine (I).**—A solution of 26 g. of the crude product of α-amino-β-methoxy-β-phenylpropionic acid in 150 cc. of 83% of formic acid was warmed to 45°C and 80 cc. of acetic anhydride was added with stirring. The temperature of the reaction mixture rose to, and was maintained at, 70–80°C for about 15 min.. Then, the solution was settled at room temperature for 3 hr. and evaporated to dryness under reduced pressure to yield a crystalline residue. Recrystallization from dilute acetic acid and then twice from hot water, gave colorless plates, m. p. 158–160°C; yield 5.5 g. (18.5%). A final recrystallization from hot water yielded colorless plates having a constant m. p. of 161–162°C; yield 4.9 g. (16.5%).

Anal. Found: N, 6.21. Calcd. for $C_{11}H_{13}O_4N$: N, 6.28%. Completion of the remaining steps in the synthesis to DL-chloramphenicol proved this N-formyl derivative to be of the threo configuration.

**DL-threo-O-Methylphenylserine (II).** — Three and one-half grams of the above N-formyl derivative (I) was hydrolyzed with 40 cc. of 1 N hydrochloric acid on a boiling water bath for one hr.. The solution was neutralized with 10% sodium hydroxide solution to pH 6.5 and concentrated under reduced pressure until crystalline precipitate appeared. To the concentrate was added five volumes of absolute ethanol and the mixture was allowed to stand in a refrigerator overnight. The crystals were collected and washed with absolute ethanol; m. p. 218–220°C (dec.); yield 2.5 g. (89.3%). Recrystallization from water-ethanol gave colorless plates of O-methyl-DL-threo-phenylserine, m. p. 218–220°C (dec.).

Anal. Found: N, 7.19. Calcd. for $C_{10}H_{13}O_3N$: N, 7.18%.

**N-Benzoyl-O-methyl-DL-threo-phenylserine.**—To a solution of 0.5 g. of II in 5 cc. of 10% sodium hydroxide was added 0.5 cc. of benzoyl chloride under ice cooling with vigorous shaking. The mixture was kept at room temperature for 30 min. with occasional shaking. The solution was filtered to remove insoluble matter and then acidified with concentrated hydrochloric acid under ice cooling to yield colorless crystals, which were collected and washed with toluene, m. p. 166–167°C; yield 0.6 g. (78.1%). Two recrystallizations from methanol yielded colorless crystals of N-benzoyl-O-methyl-DL-threo-phenylserine, m. p. 168–169°C.

Anal. Found: N, 4.36. Calcd. for $C_{17}H_{17}O_4N$: N, 4.68%.

**Ethyl O-Methyl-DL-threo-phenylserinate Hydrochloride (III).**—A stream of dry hydrogen chloride was bubbled through a suspension of 4.0 g. of II in 40 cc. of absolute ethanol. After saturation, the mixture was settled at room temperature overnight, and then evaporated under reduced pressure to yield a crude ester hydrochloride; yield 5.2 g. (97.7%). Recrystallization from absolute ethanol-ether yielded colorless crystals of ethyl O-methyl-DL-threo-phenylserinate hydrochloride, m. p. 158–160°C.

Anal. Found: N, 5.22. Calcd. for $C_{12}H_{18}O_3NCl$: N, 5.39%.

**Ethyl O-Methyl-DL-threo-phenylserinate (IV).**—A vigorous stream of dry ammonia was passed through a suspension of 9.5 g. of III in 100 cc. of absolute ether for 20 min.. The ammonium chloride precipitated was removed and washed with absolute ether. The filtrate and washings were evaporated under reduced

pressure to yield a crude, pale-yellow oil of ethyl O-methyl-DL-threo-phenylserinate; yield 5.0 g. (61.2%).

**DL-threo-2-Amino-1-methoxy-1-phenyl-3-propanol (V).**—A solution of 5.0 g. of IV in 50 cc. of absolute ethanol was hydrogenated over 10 g. of Raney nickel catalyst[4] at 50–55°C for 5 hr. under an initial pressure of 120 atm.. The catalyst was removed by filtration, and the filtrate was evaporated under reduced pressure to yield a pale-yellow, oily residue; yield 3.0 g.. The residue was heated with 125 cc. of 0.1 N sodium hydroxide solution for 2 hr. in order to hydrolyze any unchanged ester. The alkaline solution was extracted five times with ethyl acetate under ice cooling. The combined ethyl acetate extract was dried over anhydrous sodium sulfate and concentrated under reduced pressure to yield crude crystals of DL-threo-2-amino-1-methoxy-1-phenyl-3-propanol (V), m. p. 28–32°C; yield 1.7 g. (41.9%).

On bubbling dry hydrogen chloride into the ethereal solution of V, colorless crystals of crude hydrochloride was obtained; m. p. 164–166°C. Two recrystallizations from ethanol-ether gave pure crystals of the hydrochloride of V, m. p. 168–169°C.

Anal. Found: N, 6.21. Calcd. for $C_{10}H_{16}O_2NCl$: N, 6.43%.

**N, O-Dibenzoyl-DL-threo-2-amino-1-methoxy-1-phenyl-3-propanol.**—To a solution of 0.2 g. of V in 2.0 cc. of dry pyridine was added 0.3 cc. of benzoyl chloride and the mixture was allowed to stand in an ice bath for 1 hr. with occasional shaking. Cold water was added to the solution and the crystals formed were collected and washed with 2% sodium carbonate solution, 1% hydrochloric acid and finally with cold water. Recrystallization from methanol gave colorless needles, m. p. 138–139°C; yield 0.4 g. (92.9%). Further recrystallization from methanol gave an analytical pure sample of the N, O-dibenzoyl derivative of V, m. p. 139–140°C.

Anal. Found: N, 3.68. Calcd. for $C_{24}H_{23}O_4N$: N, 3.60%.

**N-Acetyl-DL-threo-2-amino-1-methoxy-1-phenyl-3-propanol (VI).**—To a solution of 0.2 g. of V in 2.0 cc. of ether was added 0.8 cc. of acetic anhydride with stirring at room temperature. Crystals formed were collected and washed with ether to yield colorless crystals, m. p. 178–180°C; yield 0.2 g. (81.0%). Recrystallization from hot water gave colorless needles of N-acetyl derivative of V, m. p. 184–185°C.

Anal. Found: N, 6.12. Calcd. for $C_{12}H_{17}O_3N$: N, 6.27%.

**N, O-Diacetyl-DL-threo-2-amino-1-methoxy-1-phenyl-3-propanol (VII).**—V (0.8 g.) was heated with 6.0 g. of acetic anhydride on a boiling water bath for one hr.. The solution was concentrated under reduce pressure to yield crystals, which were washed with ether, m. p. 119–121°C; yield 1.0 g. (85.5%). Two recrystallizations from acetone gave colorless plates of the N, O-diacetyl derivative of V, m. p. 120–121.5°C.

Anal. Found: N, 5.25. Calcd. for $C_{14}H_{19}O_4N$: N, 5.28%.

**N, O-Diacetyl-DL-threo-2-amino-1-methoxy-1-*p*-nitrophenyl-3-propanol (VIII).**—To 1.3 g. of VII was added 5.0 cc. of a mixture (1 : 1) of concentrated nitric acid (sp. gr. 1.38) and sulfuric acid (sp. gr. 1.84) under ice cooling and shaking. After 15 min. the mixture was kept at room temperature for 20 min. quenched on ice and then immediately neutralized with sodium bicarbonate. The mixture was extracted five times with ethyl acetate and the combined extract was washed with cold water, and dried over anhydrous sodium sulfate. Evaporation under reduced pressure yielded pale-yellow crystals of the nitro derivative of VII, m. p. 80–82°C; yield 1.4 g. (92.2%).

Anal. Found: N, 9.22. Calcd. for $C_{14}H_{18}O_6N_2$: N, 9.03%.

**DL-threo-2-Amino-1-methoxy-1-*p*-nitrophenyl-3-propanol Hydrochloride (IX).**—A portion of 1.4 g. of VIII was hydrolyzed with 10 cc. of 10% hydrochloric acid on a boiling water bath for one hr. The hydrolysate was washed twice with ether and and evaporated to dryness under reduced pressure. The crystalline residue was recrystallized from dilute hydrochloric acid to yield colorless crystals of DL-threo-2-amino-1-methoxy-1-*p*-nitrophenyl-3-propanol hydrochloride, m. p. 235–237°C (dec.); yield 1.1 g. (92.5%). When dried in a "pistol" the compound was unstable and colored.

Anal. Found: N, 9.92. Calcd. for $C_{10}H_{15}O_4N_2Cl$: N, 10.67%.

**DL-threo-2-Amino-1-*p*-nitrophenyl-1, 3-propanediol (X).**—A mixture of 1.1 g. of IX and 12 cc. of 25% hydrochloric acid was placed in a sealed tube and heated at 125–130°C for 4 hr.. The contents were diluted with water, decolorized with active carbon, and then concentrated under reduced pressure to give a crystalline residue; yield 1.0 g. The residue was dissolved in 3.0 cc. of water, cooled with ice, and rendered alkaline with 10% sodium hydroxide solution to pH 10. The free base in the mixture was extracted with ethyl acetate repeatedly and the combined extract was concentrated under reduced pressure to yield 0.7 g. (82.4%) of a crystalline residue, which was recrystallized several times from hot water to give colorless crystals of m. p. 139–140°C; yield 0.3 g. (35.5%). Admixture with DL-threo-2-amino-1-*p*-nitrophenyl-1,3-propanediol synthesized by the route of Controulis et al.[5] caused no depression in the melting point.

X was converted into the N-dichloroacetamide of m. p. 149–150°C by heating with methyl dichloroacetate. The antibacterial activity of the product, viz. DL-chloramphenicol, was 49.7% that of natural chloramphenicol by a cylinder plate assay (test organism E. coli).

**2-Phenylnaphthalene.**—A mixture of 1.0 g. of I and 10 cc. of 20% hydrochloric acid was

4) Organic Syntheses, **21**, 15 (1940).

5) J. Controulis, M. C. Rebstock and H. M. Crooks, Jr., *J. Am. Chem. Soc.*, **71**, 2463 (1949).

placed in a sealed tube and heated at 115-120°C for 4hr.. The contents were extracted with ether. The ether solution was washed with water, dried over anhydrous sodium sulfate, and then concentrated under reduced pressure to yield a yellow crystalline residue; yield 0.4 g. (87.5%). The product was recrystallized from methanol to give pale yellow crystals of m. p. 101-102°C. Admixture with an authentic sample of 2-phenylnaphthalene caused no depression in the melting point.

**N-Formyl-DL-erythro-O-methylphenylserine (XII).**—The other diastereomer (XI) of O-methylphenylserine which melts at 251-253°C (dec.) was prepared by the method of Carter et al[1,2].

One gram of XI was dissolved in 6 cc. of 83% formic acid, warmed to 45°C and then 3.0 cc. of acetic anhydride was added under shaking. The temperature of the reaction mixture was maintained at 70-80°C for 15 min.. Evaporation under reduced pressure gave a crystalline residue, which was recrystallized from 2 cc. of hot water to give crystals of m. p. 143-146°C; yield 0.8 g. (70.0%). Repeated recrystallization from hot water gave the N-formyl derivative of single diastereomer of O-methylphenylserine, m. p. 149-150°C.

Anal. Found: N, 6.32. Calcd. for $C_{11}H_{13}O_4N$: N, 6.28%.

**Ethyl DL-erythro-O-Methylphenylserinate Hydrochloride (XIII).**—A stream of dry hydrogen chloride was bubbled into a suspension of 10 g. of O-methylphenylserine (XI) in 150 cc. of absolute for ethanol for 1.5 hr.. After saturation, the solution was allowed to stand overnight at room temperature and evaporated under reduced pressure to yield a crystalline residue; 13.0 g. (97.7%). Recrystallization from absolute ethanol-ether gave colorless needles of the ester hydrochloride of XI, m. p. 179-181°C (dec.).

Anal. Found: N, 5.44. Calcd. for $C_{12}H_{18}O_3NCl$: N, 5.39%.

**Ethyl DL-erythro-O-Methylphenylserinate (XIV).**—A vigorous stream of dry ammonia was passed through a suspension of 13 g. of the hydrochloride (XIII) in 150 cc. of absolute ether for 20 min.. After-treatment was carried out just as described above in the preparation of IV. The yield of crude, pale-yellow oil was 10.0 g. (89.3%).

**DL-erythro-2-Amino-1-methoxy-1-phenyl-3-propanol (XV).**—A solution of 9.5 g. of XIV in 100 cc. of absolute ethanol was hydrogenated with 10 g. of Raney nickel catalyst[4] at 45-52°C and 120 atm. for 4 hr.. After-treatment was carried out just as described above in the preparation of V to yield a crude product of XV, a pale-yellow oil; yield 2.5 g. (32.4%).

Dry hydrogen chloride was bubbled through the ethereal solution of the crude syrup of XV to yield colorless crystals, which were collected and washed with dry ether and acetone; m. p. 175-177°C. Three recrystallizations from methanol-ether gave an analytical sample of the hydrochloride of XV, m. p. 181-182°C.

Anal. Found: C, 54.83; H, 7.13; N, 6.29. Calcd. for $C_{10}H_{16}O_2NCl$: C, 55.15; H, 7.40; N, 6.43%.

M. p. reported by Tatsuoka et al[6]. is 182-183°C.

**N, O-Dibenzoyl-DL-erythro-2-amino-1-phenyl-3-propanol.**—To a solution of 0.2 g. of the crude syrup of XV in 2.5 cc. of pyridine, was added 0.3 cc. of benzoyl chloride under ice cooling and shaking. The solution was cooled in an ice bath for 1 hr. and then allowed to stand at room temperature for 30 min.. Cold water was added to the solution to yield a crystalline precipitate, which was collected and washed with 2% sodium bicarbonate solution, 1% hydrochloric acid and finally with cold water. Three recrystallizations from methanol gave colorless needles of N, O-dibenzoyl derivative of XV, m. p. 160-161°C; yield 0.3 g. (69.8%).

Anal. Found: N, 3.71. Calcd. for $C_{24}H_{23}O_4N$: N, 3.60%.

M. p. reported by Tatsuoka et al[6]. is 157-158.5°C.

**N-Acetyl-DL-erythro-2-amino-1-methoxy-1-phenyl-3-propanol (XVI).**—To a solution of 2.2 g. of XV in 10 cc. of ether was added 4.0 cc. of acetic anhydride at room temperature. After-treatment was carried out just as described above in the preparation of VI to yield a crude product of XVI, m. p. 115-117°C; yield 2.1 g. (77.5%). Recrystallization from ethyl acetate gave colorless crystals of XVI, m. p. 116-118°C.

Anal. Found: N, 6.05. Calcd. for $C_{12}H_{17}O_3N$: N, 6.27%.

**N, O-Diacetyl-DL-erythro-2-amino-1-methoxy-1-phenyl-3-propanol (XVII).**—A 1.0 g. sample of XVI was heated with 6.0 cc. of acetic anhydride on a boiling water bath for one hr. The solution was concentrated under reduced pressure to yield crude crystals, m. p. 77-80°C; yield 1.2 g. (100.9%).

**N, O-Diacetyl-DL-erythro-2-amino-1-methoxy-1-*p*-nitrophenyl-3-propanol (XVIII).**—To 1.0 g. of XVII was added 5.0 cc. of a mixture (1 : 1) of concentrated nitric acid (sp. gr. 1.38) and sulfuric acid (sp. gr. 1.84) under ice cooling and shaking. After-treatment was carried out just as described above in the preparation of VIII to yield a crude product of XVIII, m. p. 122-140°C; yield 1.2 g. (102.6%). Two recrystallizations from ethanol gave colorless crystals of XVIII, m. p. 150-151°C.

**DL-erythro-2-Amino-1-Nethoxy-1-*p*-nitrophenyl-3-propanol Hydrochloride (XIX).**—A portion of 1.1 g. of XVIII was hydrolyzed with 10 cc. of 10% hydrochloric acid on a boiling water bath for one hr.. The hydrolysate was evaporated to dryness under reduced pressure. The crystalline residue was recrystallized from water to yield colorless crystals of DL-erythro-2-amino-1-methoxy-1-*p*-nitrophenyl-3-propanol hydrochloride, m. p. 233-234°C. (dec.); yield 0.7 g. (75.2%).

6) S. Tatsuoka, M. Miyamoto, T. Kinoshita, R. Nakamori and S. Kimata, *J. Pharm. Soc. Japan*, **71**, 608 (1951).

Anal. Found: N, 10.37. Calcd. for $C_{10}H_{15}O_4N_2Cl$: N, 10.67%.

M. p. reported by Tatsuoka et al[6]. was 232°C.

Admixture with DL-threo-2-amino-1-methoxy-1-*p*-nitrophenyl-3-propanol hydrochloride (IX) caused a depression in the melting point.

**DL-erythro-2-Amino-1-*p*-nitrophenyl-1,3-propanediol Hydrochloride (XX).**—A mixture of 0.7 g. of XIX and 12 cc. of 25% hydrochloric acid was placed in a sealed tube and heated at 125–130°C for 4 hr.. The contents were diluted with water and filtered. Then the filtrate was concentrated under reduced pressure to give a crystalline residue. The residue was recrystallized from methanol to yield colorless crystals, m. p. 207–209°C; yield 0.2 g. (30.3%).

Recrystallization from methanol yielded colorless crystals of DL-erythro-2-amino-1-*p*-nitrophenyl-1,3-propanediol hydrochloride, m. p. 209–210°C..

Anal. Found: C, 43.41; H, 5.04; N, 11.09. Calcd. for $C_9H_{13}O_4N_2Cl$: C, 43.42; H, 5.23; N, 11.26%.

Controulis et al[5]. reported DL-erythro-2-amino-1-*p*-nitrophenyl-1,3-propanediol hydrochloride of m. p. 212–214°C.

## Summary

(1) DL-threo-O-Methylphenylserine has been isolated through its N-formyl derivative from the diastereomeric mixture of O-methylphenylserines which was prepared by the route of Van Loon and Carter[3].

(2) DL-threo-O-Methylphenylserine has been led to DL-threo-2-amino-1-*p*-nitrophenyl-1,3-propanediol and further to DL-chloramphenicol.

(3) The other diastereomer of O-methylphenylserine (m. p. 251–253°C) has been led to DL-erythro-2-amino-1-*p*-nitrophenyl-1,3-propanediol hydrochloride.

(4) Several derivatives of the diastereomers of O-methylphenylserine and O-methylphenylserinol have been described.

The authors are indebted to Mr. S. Nakada of this Laboratory for the microanalytical data.

*Department of Applied Chemistry*
*Engineering Faculty*
*Keio University, Koganei, Tokyo*

# *Dielectric Studies on Colloidal Solutions. IV. The Dielectric Constant of the Solutions of Long-chain Amine Hydrochlorides*

By Micho SHIRAI and Bun-ichi TAMAMUSHI

(Received March 18, 1957)

In the first paper of this series[1], the result of the measurement of high-frequency conductivities of aqueous solutions of colloidal electrolytes has been reported; the measurement of the dielectric constants of their solutions, which is reported in this paper, must also be an important approach to the understanding of the nature of the electrolytes.

## Experimental

**Procedure.**—The measurement of the dielectric constant (D. C.) at 2 Mc./sec. has been carried out by means of the heterodyne beat method. The main part of the apparatus consists of two separate oscillators, one of which is held at a frequency of 2 Mc./sec. by the vibration of a quartz crystal and the other is adjusted by varying its capatity to give a frequency different by a constant amount from that of the former oscillator. A liquid cell is incorporated into the circuit of the latter oscillator. The adjustment of the frequency of the latter oscillator is performed by the addition of a 700 cycles/sec. tuning-fork oscillator to the apparatus, and against that oscillator the beat note is balanced by a cathode-ray oscilloscope. Each electrical component is enclosed in an earthened metal box.

The precision condenser consists of two variable air condensers; the one has a working range of 100 pF traversed in 25 turns and the other that of 11.25 pF traversed in 90 turns. The division of the former condenser is 1/100 turns and that of the latter is 1/50 turns.

The measurement of D. C. at 30 Mc./sec has been carried out by the resonance method used for the measurement of the high-frequency conductivity[1]. The resonance point is obtained by determining the whole resonance curve of the resonant circuit containing the measruring cell, so that the precision of the resonance point is sufficiently accurate.

1) M. Shirai and B. Tamamushi, This Bulletin, **28**, 545 (1955).

The cell used is constructed of parallel plates of platinum enclosed in a glass vessel which is immersed in a constant temperature bath of toluene, and fixed at a definite position. The cell constant is determined by using distilled water as the standard whose D. C. is taken to be 73.02 at 40°C[2].

The electrical conductivity has been measured with the impedance bridge used in the previous work[3].

**Materials.**—Hexadecyl- and octadecylamine hydrochloride were prepared from the corresponding amines (Armour & Co., U. S. A.) by the method given in the previous paper[4].

Ethanol was distilled over calcium oxide: b. p. 78.3°C.

Benzene was purified from a commercial sample by washing with sulfuric acid and then with water, followed by drying over calcium chloride and distillation: b. p. 80°C.

The water used is the conductivity water distilled in an nitrogen atomsphere.

## Results and Discussion

1) **Electrode polarization**—In measuring D. C. of a conductive medium, the electrode polarization often causes a serious error. This error is inversely proportional to the square of the frequency at which the measurement is made[5]. The error in the present investigation is expected to be very small as the frequency employed is high, being 2 Mc./sec. In reality, D. C. of aqueous solutions of potassium chroride at various concentrations obtained has been found nearly constant as shown in Table I. A little increase in D. C. at higher concentrations may be interpreted in terms of Debye-Falkenhagen's effect of potassium chloride. Thus, it is conceivable that the values of D. C. obtained are free from the error due to the electrode polarization at the range of concentration and at the frequency at which the measurement has been carried out.

TABLE I

DIELECTRIC CONSTANT OF AQUEOUS SOLUTION OF POTASSIUM CHLORIDE (temp 40°C)

| conc. (mole/l.) | $\varepsilon$ (2Mc./sec.) |
|---|---|
| 0.0001 | 73.02 |
| 0.0002 | 73.02 |
| 0.0003 | 73.03 |
| 0.0005 | 73.05 |
| 0.0008 | 73.21 |
| 0.001 | 73.45 |

2) J. Wyman, *Phys. Rev.*, **35**, 623 (1930).
3) M. Shirai and B. Tamamushi, This Bulletin, **30**, 411 (1957).
4) M. Shirai and B. Tamamushi. *ibid.*, **29**, 733 (1956).
5) J. F. Johnson and R. H. Cole, *J. Am. Chem. Soc.*, **73**, 4536 (1951).

2) **D. C. of aqueous solutions of salts.**—The result of the measurement of D. C., $\varepsilon$, and the equivalent conductivity (E. C.), $\Lambda$, of aqueous solutions of hexadecyl- and octadecylamine hydrochloride is shown in Table II and in Fig. 1, where the relative increase of D. C. or E. C. is plotted as ordinate against the square root of the concentration of amine salts as abscissa. The relative increase in D. C. is there expressed by

$$100\,\frac{\varepsilon-\varepsilon_0}{\varepsilon_0}$$

in which $\varepsilon$ and $\varepsilon_0$ denote D. C. of the solution and the solvent, respectively. For both salts D. C. remains nearly constant with increasing concentration below the critical micelle concentration, but increases considerably beyond that concentration.

D. C. of aqueous solutions of colloidal electrolytes involves many factors. (1) Sack[6] concluded that in an externally applied, field the electric fields of ions should hinder the orientation of water molecules, thus resulting in lower D. C. (2) According to the predictions of Debye-Falkenhagen's theory[7], the relaxation of ionic atmosphere should increase D. C. (3) If the solute molecules have dipole moments, such as ion-pairs[8], they will act to increase D. C., whereas (4) long hydrocarbon chains contained in the molecules will act to decrease it.

The volume fraction of the hydrocarbon chains is, however, only about 0.2 percent. at the concentration of 0.005 mole/l., assuming that their density is nearly the same as that of pure liquid paraffins, and according to Bruggeman's theory[9], the lowering of D. C. due to the hydrocarbon chains in this case is estimated to 0.3 percent,, so that we can consider this effect to be small at the range of concentration at which the measurement is carried out. Sack's effect should also be very small at the frequency of 2 Mc./sec. employed in this work, taking into account the results obtained with aqueous solutions of various electrolytes[10,11]. The rise of D. C. beyond the critical micelle concentration shown in Fig. 1 may be due to Debye-Falkenhagen's effect or the orientation of dipoles

6) H. Sack, *Physik. Z.*, **27**, 206 (1926); **28**, 199 (1927).
7) P. Debye and H. Falkenhagen, *Physik. Z.*, **29**, 121, 401 (1928); *Z. Elektrochem.*, **34**, 562 (1928).
8) N. Bjerrum, *Erg. exakt. Naturwiss.*, **6**, 125 (1926).
9) D. A. G. Bruggeman. *Ann. d. Phys.*, **24**, 636 (1935).
10) F. H. Drake, G. W. Pierce and M. T. Dow, *Phys. Rev.*, **35**, 613 (1930).
11) R. T. Lattey and W. G. Davies, *Phil. Mag.*, **12**, 1111 (1931); **13**, 444 (1932).

TABLE II

DIELECTRIC CONSTANT AND EQUIVALENT CONDUCTIVITY OF SOLUTIONS OF AMINE SALTS

| substance | concn. (mole/l.) | $\varepsilon$ (2 Mc./sec.) | $\Lambda$ (1000c./sec.) |
|---|---|---|---|
| solvent: water | temp. 40°C | | |
| hexadecylamine hydrochloride | 0.0005 | 73.0 | 126 |
| | 0.0008 | 73.0 | 124 |
| | 0.001 | 73.0 | 123 |
| | 0.0012 | 73.0 | 111 |
| | 0.0015 | 73.0 | 92.0 |
| | 0.002 | 73.4 | 78.5 |
| | 0.003 | 73.9 | 60.6 |
| | 0.005 | 74.6 | 47.8 |
| | 0.01 | 75.2 | 35.4 |
| octadecylamine hydrochloride | 0.0001 | 73.0 | 118 |
| | 0.0002 | 73.0 | 117 |
| | 0.00025 | 73.4 | 112 |
| | 0.0003 | 73.8 | 106 |
| | 0.0005 | 74.8 | 79.8 |
| | 0.0008 | 75.3 | 50.9 |
| | 0.001 | 75.7 | 42.0 |
| | 0.002 | 76.7 | 31.5 |
| | 0.005 | 78.0 | 20.0 |
| solvent: 2 mole/l. aq. ethanol | | temp. 40°C. | |
| hexadecylamine hydrochloride | 0.0005 | 70.5 | 82.2 |
| | 0.0008 | 70.5 | 81.0 |
| | 0.001 | 70.5 | 80.1 |
| | 0.0012 | 70.4 | 79.0 |
| | 0.0015 | 70.5 | 76.0 |
| | 0.002 | 70.7 | 70.3 |
| | 0.003 | 71.0 | 58.3 |
| | 0.005 | 71.2 | 48.0 |
| | 0.01 | 71.5 | 34.4 |
| octadecylamine hydrochloride | 0.0001 | 70.5 | 72.2 |
| | 0.0002 | 70.5 | 72.0 |
| | 0.00025 | 70.5 | 71.5 |
| | 0.0003 | 70.7 | 71.0 |
| | 0.0005 | 71.1 | 67.9 |
| | 0.0008 | 71.5 | 64.0 |
| | 0.001 | 71.7 | 61.0 |
| | 0.002 | 72.3 | 45.0 |
| | 0.005 | 72.9 | 24.0 |
| solvent: 4 mole/l. aq. ethanol | | temp. 40°C. | |
| hexadecylamine hydrochloride | 0.0005 | 67.8 | 56.6 |
| | 0.0008 | 67.8 | 56.6 |
| | 0.001 | 67.8 | 57.2 |
| | 0.0012 | 67.8 | 58.0 |
| | 0.0015 | 67.8 | 59.0 |
| | 0.002 | 67.9 | 59.5 |
| | 0.003 | 67.9 | 59.7 |
| | 0.005 | 68.0 | 55.8 |
| | 0.01 | — | 45.7 |
| octadecylamine hydrochloride | 0.0001 | 67.8 | 47.5 |
| | 0.0002 | 67.8 | 47.5 |
| | 0.00025 | 67.8 | 47.0 |
| | 0.0003 | 67.8 | 47.0 |
| | 0.0005 | 67.8 | 46.6 |
| | 0.0008 | 67.8 | 47.5 |
| | 0.001 | 67.8 | 48.0 |
| | 0.002 | 68.0 | 50.6 |
| | 0.005 | 68.2 | 48.1 |

of ion-pairs, but below the critical micelle concentration the effect of both factors will become insignificant. The orientation of a micelle as a whole need not be considered, provided that the micelle is supposed to be in a liquid state of aggregation[1].

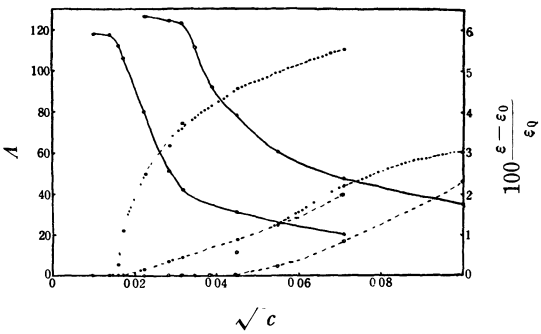



Fig. 1. The relative increase in D. C. and E. C. of amine salts in aqueous solution.
○, hexadecyl-;
●, octadecylamine hydrochloride.
– – equivalent conductivity at 700 c./sec.
----- } the relative increase in D. C. at
-·-·- } { 2 Mc./sec. / 30 Mc./sec.

3) **D. C. of solutions of salts in aqueous ethnol.**—D. C. and E. C. of solutions of hexadecyl- and octadecylamine hydrochloride in aqueous ethanol of 2 mole/l. and 4 mole/l. are shown in Table II as well as in Figs. 2 and 3. The rise of D. C. of these solutions beyond the critical micelle concentration is considerably reduced in the case of aqueous ethanol of 2 mole/l. and almost diminished in the case of aqueous ethanol of 4 mole/l. And, from the conductivity curves in Figs. 2 and 3, it is seen that the micelle formation is inhibited by the increase in alcoholic content of the solution of electrolytes. In aqueous ethanol solutions an anion and a cation of electrolytes tend to associate on account of the lower D. C. of the solvent medium, and therefore, the increase in D. C. due to the orientation of ion-pairs will become significant. On the other hand, in aqueous ethanol solutions the association of counter ions will be promoted and the micelle structure will become loose, and accordingly, Debye Frankenhagen's effect is expected to be reduced considerably.

4) **Effect of solubilization on D. C. of the solution.**—It is well known that water-insoluble substances, such as benzene, are dissolved in the interior of micelles, and

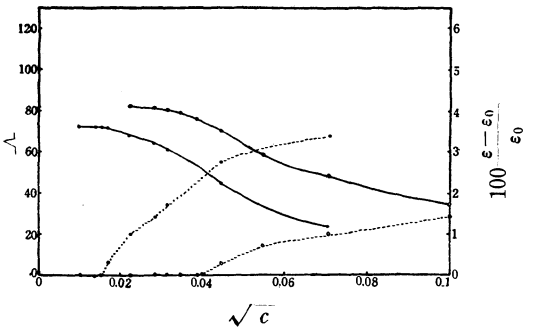



Fig. 2. The relative increase in D. C. and E. C. of hexadecyl- and octadecylamine hydrochloride in 2 mole/l. aq. ethanol.

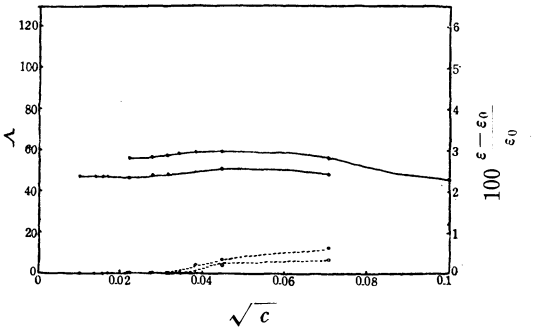



Fig. 3. The relative increase in D. C. and E. C. of hexadecyl- and octadecylamine hydrochloride in 4 mole/l. aq. ethanol.

micelles are enlarged[12]. The larger the radius of the ions, the smaller the Debye-Falkengen's effect. Accordingly, when benzene is solubilized in solutions of colloidal electrolytes, D. C. of the solutions is expected to decrease. In Table III are indicated D. C. of aqueous solutions of octadecylamine hydrochloride containing various amounts of solubilized benzene. The result agrees with the above expectation.

TABLE III

DIELECTRIC CONSTANT OF AQUEOUS SOLUTIONS OF OCTADECYLAMINE HYDROCHLORIDE CONTAING VARIOUS AMOUNTS OF SOLUBILIZED BENZENE temp. 40°C

conc. of octadecylamine hydrochloride 0.003 mole/l.

| moles of benzene per mole of amine salt | ε (2 Mc./sec.) |
|---|---|
| 0 | 77.4 |
| 0.11 | 77.3 |
| 0.34 | 77.2 |
| 0.57 | 76.8 |
| 0.86 | 75.9 |
| 1.1 | 75.8 |

12) cf. A. E. Alexander and P. Johnson, "Colloid Science," Oxford Press (1949), p. 685.

5) **Dependence of D. C. on frequency.** —At the frequency of 2 Mc./sec., the relative increase of D. C. due to Debye-Falkenhagen's effect is significant, but at higher frequencies where the equivalent conductivity increases, the relative increase of D. C. should be diminished according to Debye-Falkenhagen's theory. In Table IV and Fig. 1 is shown the result of the measurement of D. C. of aqueous solutions of hexadecyl- and octadecylamine hydrochlorides at the frequency of 30 Mc./sec. At a certain concentration the relative increase of D. C. at 30 Mc./sec. is smaller than that at 2 Mc./sec., and this experimental fact agrees with our expectation, too. The ratio of D. C. at 30 Mc./sec. to that at 2 Mc./sec. becomes larger with increasing concentration. This is probably due to the shortening of the relaxation time of Debye-Falkenhagen's effect with increasing concentration.

TABLE IV

DIELECTRIC CONSTANT OF AQUEOUS SOLUTIONS OF AMINE SALTS AT 30 Mc./sec. temp. 40°C.

| substance | conc. (mole/l.) | ε (30 Mc./sec.) |
|---|---|---|
| hexadecylamine hydrochloride | 0.0005 | 73.0 |
| | 0.0008 | 73.0 |
| | 0.001 | 73.0 |
| | 0.0012 | 73.0 |
| | 0.0015 | 73.0 |
| | 0.002 | 73.0 |
| | 0.003 | 73.1 |
| | 0.005 | 73.6 |
| | 0.01 | 74.7 |
| octadecylamine hydrochloride | 0.0001 | 73.0 |
| | 0.0002 | 73.0 |
| | 0.00025 | 73.0 |
| | 0.0003 | 37.0 |
| | 0.0005 | 73.1 |
| | 0.0008 | 73.2 |
| | 0.001 | 73.3 |
| | 0.002 | 73.6 |
| | 0.005 | 74.4 |

From these exerimental results, it would be reasonable to conclude that the rise of D. C. observed in the case of aqueous solutions of long alkyl amine hydrochlorides is mainly due to Debye-Falkenhagen's effect. The same effect has been inferred from the result of measurement of high-frequency conductivity[1].

## Summary

The dielectric constant and the equivalent conductivity of solutions of hexadecyl-

and octadecylamine hydrochloride have been measured at the frequencies of 2 Mc./sec. and 30 Mc./sec. The dielectric constant of the solutions shows a considerable increase beyond the concentration for micelle formation.

The dielectric constant and the equivalent conductivity of the solutions of these amine salts in aqueous ethanol of various concentrations have been measured. The rise of the dielectric constant is diminished with increasing concentration of ethanol.

The effect of solubilization of benzene on the dielectric constant of the solutions has been investigated. The relative increase in the dielectric constant is reduced with increasing amount of solubilized benzene.

From these experimental results, it is concluded that the rise of the dielectric constant of the aqueous solutions is mainly due to Debye-Falkenhagen's effect.

*Chemistry Dept., College of General Education and Institute of Science and Technology*
*The University of Tokyo*
*Meguro, Tokyo*

# *Dielectric Investigation on Coals. II. Mixture of Coal Powder and Paraffin Wax.*

By Keniti HIGASI, Isao MIYASITA and Yasutomo OZAWA

(Received March 17, 1957)

## Introduction

Attempts have been described in a previous report[1] to prepare coal disks for examination from a coal block. Difficulties in the preparation of disks suitable for dielectric measurements are generally so great that this method can hardly be considered as practical or as convenient.

In the experiments described in the present article a new method using powdered coal was employed. The coal specimen is reduced to powder form, mixed with melted paraffin wax and cooled in a suitable mould. Test pieces prepared thus from the solidified materials contain usually 56 volume percent of coal. From the dielectric properties of these mixtures the dielectric constants and loss factors of the component coals are to be calculated by using a proper equation for mixtures.

## Experimental

Six specimens of Japanese bituminous coal were examined. Five were chosen among those* studied in a previous paper: I Moziri No. 4, carbon, 85.25%; II Moziri No. 3, carbon, 81.71%; III Moziri No. 9, carbon, 82.98%; IIIa Moziri No.11, carbon, 82.07%; and Vc Mitui-Bibai No. 1-3, carbon, 80.62%. The remaining one is: B Mayazi North-No. 1, for which the proximate analysis is: moisture, 1.01; ash, 8.43; volatile matter, 41.04 and fixed carbon, 49.52 %. Ultimate analysis for B is: ash, 2.47; C, 85.24; H, 5.86; O, 7.06; N, 1.67 and S, 0.16%. Paraffin wax used for preparing mixtures has the following properties at room temperature: dielectric constant, 2.46; loss factor, 0.0000 and specific gravity, 0.904.

Vitrain of coal specimen was pulverized in an agate mortar to a particle size below 100 meshes. The coal powder was dried in a desiccator at 105°C under $10^{-2}$ mmHg for 4-5 days. Then 15 g. of powder which had been thus thoroughly dried was poured into about 10 g. of melted paraffin wax, well mixed and solidified in a mould. A test piece of diameter ca. 40 mm and thickness ca. 5 mm was prepared from the solidified materials. Care was taken to secure uniform distribution of coal particles in the mixture.

The volume fraction of each mixture was controlled to have a constant value 0.56. Deviation from this standard was checked by collating the amounts of ash contained in the mixture and in the original coal specimen. Further examination was made of the range of errors in the final dielectric constant of coal which should arise from inaccuracies of the volume fraction taken (Fig. 1). Curve (b) represents the relation of Böttcher* between the dielectric constant of coal and that of mixture

1) I. Miyasita and K. Higasi, This Bulletin, **30**, 513 (1957).

* Chemical analyses of these samples were given in Ref. 1).

* See later reference.—Ref. 5).

TABLE I

DIELECTRIC CONSTANT ($\varepsilon'$) AND LOSS FACTOR ($\varepsilon''$) OF COAL-POWDER PARAFFIN-WAX MIXTURE (coal powder 56 vol%)

| Sample No. | | 300c | 1kc | 3kc | 10kc | 100kc | 300kc | 1Mc | 3Mc | 10Mc | 20Mc | 50Mc |
|---|---|---|---|---|---|---|---|---|---|---|---|---|
| I | $\varepsilon'$ | 3.48 | 3.46 | 3.42 | 3.40 | 3.32 | 3.30 | 3.28 | 3.26 | 3.26 | 3.26 | 3.27 |
| | $\varepsilon''$ | 0.0570 | 0.0492 | 0.0396 | 0.0365 | 0.0266 | 0.0287 | 0.0301 | 0.0259 | 0.0220 | 0.0213 | 0.0136 |
| II | $\varepsilon'$ | —— | 3.59 | 3.57 | 3.52 | 3.30 | 3.24 | 3.22 | 3.20 | 3.18 | 3.22 | 3.17 |
| | $\varepsilon''$ | | 0.0895 | 0.0805 | 0.0704 | 0.0270 | 0.0205 | 0.0183 | 0.0150 | 0.0147 | 0.0109 | 0.0159 |
| III | $\varepsilon'$ | 3.40 | 3.38 | 3.34 | 3.32 | 3.26 | 3.22 | 3.21 | 3.21 | 3.19 | 3.18 | 3.18 |
| | $\varepsilon''$ | 0.0295 | 0.0294 | 0.0268 | 0.0252 | 0.0212 | 0.0180 | 0.0185 | 0.0152 | 0.0129 | 0.0126 | 0.0114 |
| IIIa | $\varepsilon'$ | —— | 3.38 | 3.36 | 3.33 | 3.30 | 3.28 | 3.27 | 3.25 | 3.23 | 3.18 | —— |
| | $\varepsilon''$ | | 0.0352 | 0.0295 | 0.0267 | 0.0222 | 0.0223 | 0.0206 | 0.0195 | 0.0186 | 0.00868 | |
| Vc | $\varepsilon'$ | 3.61 | 3.57 | —— | 3.51 | 3.46 | —— | 3.42 | —— | 3.37 | —— | —— |
| | $\varepsilon''$ | 0.0600 | 0.0344 | | 0.0327 | 0.0230 | | 0.0247 | | 0.0211 | | |
| B | $\varepsilon'$ | 3.34 | 3.33 | —— | 3.32 | 3.28 | —— | 3.26 | —— | 3.24 | —— | —— |
| | $\varepsilon''$ | 0.0390 | 0.0304 | | 0.0256 | 0.0135 | | 0.0139 | | 0.0112 | | |

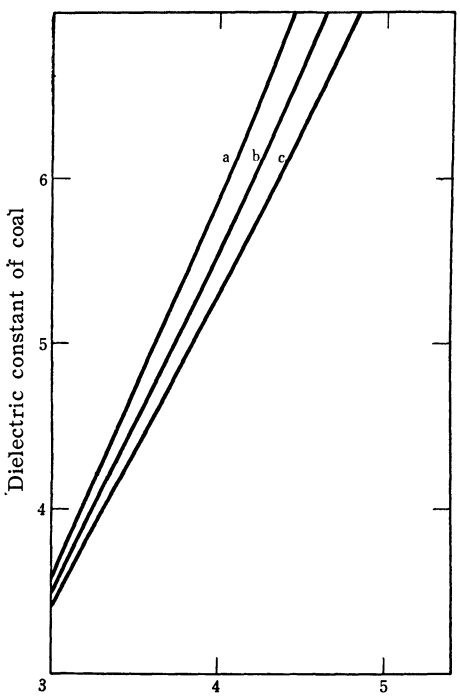



Fig. 1. The relation between the dielectric constant of coal itself and that of the powdered mixture as given by Bottcher equation. Volume fraction of coal in the mixture: curve a, 0.52; curve b, 0.56 and curve c, 0.60.

which has 56 vol% coal. If the volume percentages happen to become 52% or 60%—possibly they correspond to the maximum deviations—the relation between $\varepsilon'_{coal}$ and $\varepsilon'_{mixture}$ will be represented by either curve (a) or (c). A glance at these curves will show that possible maximum error in $\varepsilon'_{coal}$ amounts to several percent, viz., below $\pm 6\%$ for $\varepsilon'_{coal}<5$; below $\pm 6.4\%$ for $\varepsilon'_{coal}<6$.

Three methods of dielectric measurement were used in the frequency range covered. Measurements at frequencies from 300 c/s to 10 kc/s were carried out by means of an impedance bridge. Between 100 kc/s and 50 Mc/s a Q meter was used. A standing-wave method[2] of measuring dielectric properties was used at frequency of 4000 Mc/s.

The accuracy of measurement is considered, in general, to be $\pm$ 3 percent for $\varepsilon'$; but to be $\pm$ 15 percent at the microwave frequency. For $\varepsilon''$ the accuracy is much less, but the order of the values is reliable.

The results of measurements are collected in Tables I and II. They refer to paraffin-wax mixtures, having 56 vol% coal (Table I) and 50 vol% coal (Table II), respectively. All the measurements were carried out at room temperature.

TABLE II

DIELECTRIC CONSTANTS OF 50 VOL% MIXTURES OF MAYAZI COAL B OF VARIOUS DEGREES OF DRYING

| condition | 100 kc | 300 kc | 1Mc | 3Mc | 10 Mc | 4000 Mc |
|---|---|---|---|---|---|---|
| vac. dry (v.d) | 3.17 | —— | 3.14 | —— | 3.11 | 2.8 |
| air dry (a.d) | 3.36 | —— | 3.34 | —— | 3.30 | 2.8 |
| wet (v.d-w) | 3.75 | 3.64 | 3.54 | 3.51 | 3.30 | 3.0 |
| wet (a.d-w) | 4.62 | 4.44 | 4.31 | 4.18 | 4.03 | 2.7 |
| paraffin* | 2.43 | —— | 2.40 | —— | 2.37 | 2.32 |

* Paraffin wax employed in this measurement contained some impurities.

## Discussion

There are available many equations[3,4] concerning the dielectric constants of non-homogeneous mixtures. Suppose that coal particles be nearly spherical in shape and that they be insulated by the medium

2) W. Jackson, *Trans. Faraday Soc.*, **42A**, 91 (1946).
3) W. F. Brown, *J. Chem. Phys.*, **23**, 1514 (1955): R. S. Smith, *J. Appl. Phys.*, **27**, 824 (1956).
4) M. Kubo and S. Nakamura, This Bulletin, **26**, 318 (1953); K. Higasi, *Monogr. Res. Inst. Appl. Elec.*, Hokkaido Univ., **5**, 9 (1955).

TABLE III

DIELECTRIC CONSTANTS OF COALS ESTIMATED BY USING THE FORMULAE OF BÖTTCHER (Bo) AND BRUGGEMAN (Br)

| | | 300c | 1kc | 3kc | 10kc | 100kc | 300kc | 1Mc | 10Mc | 50Mc |
|---|---|---|---|---|---|---|---|---|---|---|
| I | Bo | 4.45 (0.98) | 4.41 (0.97) | 4.33 (0.95) | 4.29 (0.95) | 4.12 (0.92) | 4.08 (0.90) | 4.04 (0.90) | 4.00 (0.91) | 4.02 (0.89) |
| | Br | 4.49 (0.99) | 4.44 (0.98) | 4.35 (0.96) | 4.32 (0.96) | 4.14 (0.92) | 4.10 (0.91) | 4.05 (0.91) | 4.00 (0.91) | 4.02 (0.89) |
| II | Bo | —— | 4.68 (1.07) | 4.64 (1.08) | 4.53 (1.09) | 4.08 (0.98) | 3.96 (1.00) | 3.92 (1.00) | 3.84 (1.01) | 3.81 (1.00) |
| | Br | —— | 4.71 (1.08) | 4.68 (1.09) | 4.56 (1.10) | 4.10 (0.99) | 3.97 (1.00) | 3.94 (1·01) | 3.84 (1.01) | 3.82 (1.01) |
| III | Bo | 4.29 (1.07) | 4.25 (1.06) | 4.17 (1.05) | 4.12 (1.04) | 4.00 (1.02) | 3.92 (1.01) | 3.90 (1.01) | 3.86 (1.00) | 3.84 (1.00) |
| | Br | 4.32 (1.08) | 4.27 (1.07) | 4.18 (1.05) | 4.14 (1.05) | 4.00 (1.02) | 3.94 (1.02) | 3.91 (1.01) | 3.86 (1.00) | 3.84 (1.00) |
| IIIa | Bo | —— | 4.25 (1.01) | 4.21 (1.02) | 4.14 (1.01) | 4.08 (1.02) | 4.04 (1.04) | 4.02 (1.04) | 3.94 (1.04) | —— |
| | Br | —— | 4.27 (1.02) | 4.22 (1.02) | 4.14 (1.01) | 4.10 (1.03) | 4.05 (1.04) | 4.02 (1.04) | 3.95 (1.05) | —— |
| Vc | Bo | 4.73 (1.00) | 4.64 (0.99) | —— | 4.51 (1.01) | —— | —— | —— | —— | —— |
| | Br | 4.77 (1.01) | 4.68 (1.00) | —— | 4.54 (1.01) | —— | —— | —— | —— | —— |

of paraffin wax. The following equation of Böttcher[5] is claimed to have general applicability to such a dispersed system

$$\frac{\varepsilon'-\varepsilon'_1}{3\varepsilon'}=v_2\frac{\varepsilon'_2-\varepsilon'_1}{\varepsilon'_2+2\varepsilon'} \qquad (1)$$

in which $\varepsilon'$, $\varepsilon'_1$ and $\varepsilon'_2$ are the dielectric constants* of the mixture, the paraffin wax and the coal particles, respectively, and $v_2$ is the volume fraction of the coal particle in the mixture.

Bruggeman's equation[6] which has been successfully applied to the analysis of rubber-carbon black mixtures[7] has the following form:

$$\frac{\varepsilon'_2-\varepsilon'}{\varepsilon'_2-\varepsilon'_1}=(1-v_2)\sqrt[3]{\frac{\varepsilon'}{\varepsilon'_1}} \qquad (2)$$

From the values of dielectric constants of mixtures recorded in Table I, the dielectric constants of the coals were calculated by using both Eqs. (1) and (2). The results of the calculation are shown in Table III in which Bo and Br denote Böttcher and Bruggeman, respectively. As the dielectric constants of these coal specimens are known by the direct determination on coal disks[1], a comparison between the estimated and actual values will be of interest. The ratio of $\varepsilon'_{\text{estimated}}/\varepsilon'_{\text{actual}}$ was taken for each sample and for each of the two equations—(See the values in parentheses in Table III). The general agreement may be regarded as satisfactory for most practical purposes.

In the above consideration it is assumed that the coal particles are insulated from each other by the paraffin-wax medium. On the contrary, coal particles are very densely packed in the mixture, so that in some places they must be touching each other. That is, some of them are supposed to be in good contact producing chains or larger aggregates. Considering this situation, two extreme cases will be examined for the sake of illustration. Suppose that neither coal particles nor paraffin wax are mixed but exist in a state of parallel layers. Let it be supposed in one case that the layers are parallel to the electric field; there will be the relation:

$$\varepsilon'=(1-v_2)\varepsilon'_1+v_2\varepsilon'_2 \qquad (3)$$

and in the other case that they are all perpendicular to the field; there will be the relation:

$$\frac{1}{\varepsilon'}=\frac{1-v_2}{\varepsilon'_1}+\frac{v_2}{\varepsilon'_2} \qquad (4)$$

In order to make clear the relations existing among these equations of entirely different appearance, viz., Eqs. (1), (2), (3) and (4), an inspection of Fig. 2 will be useful in which on the basis of these equations $\varepsilon'_2$ is plotted against $\varepsilon'$ using the same assumptions: $v_2=0.56$ and $\varepsilon'_1=2.46$. It is to be noted that curves 4 and 5 which represent Bruggeman and Böttcher equations, respectively, lie in the middle

5) C. J. F. Böttcher, *Rec. trav. chim.*, **64**, 47 (1945); C. J. F. Böttcher, "The Theory of Electric Polarisation," Elsevier, Amsterdam (1952), p. 417.

* Hereafter $\varepsilon'$ and $\varepsilon'_2$ will be used instead of $\varepsilon'_{\text{mixture}}$ and $\varepsilon'_{\text{coal}}$, respectively.

6) D. A. G. Bruggeman, *Ann. Phys.*, **24**, 636 (1935).

7) B. Gross and R. M. Fuoss, *J Phys. Chem.*, **60**, 474 (1956). See references cited there.

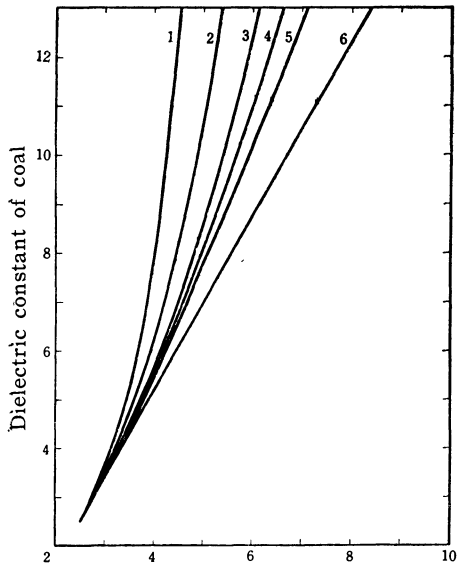



Fig. 2. Relations between the dielectric constant of coal itself and that of the powdered mixture with 56 vol % coal. Curve 1, given by Eq. (4) for a series arrangement; curve 2, Clausius-Mosotti relation; curve 3, Eq. (6) of Lewin; curve 4, Eq. (2) of Bruggeman; curve 5, Eq. (1) of Bottcher; and curve 6, Eq. (3) for a parallel arrangement.

part of the region outlined by curves 1 and 6 which are given by Eqs. (4) and (3).

As the mixture in the present study is not to be considered as a homogeneous phase, the use of the Clausius-Mosotti equation to which Groenewege et al.[8] referred, will be absurd. But as is seen by curve 2 in Fig. 2 this equation does represent some average state between those defined by Eqs. (4) and (1) or Eqs. (4) and (2).

Next, let the case be examined when the coal component has a different volume fraction from 0.56. In Table IV the case of 50 vol % coal is studied. Estimated values from 50 % are in good agreement with those from 56 %. Consequently, it may be concluded that the use of Eqs. (1) and (2) is justified so far.

TABLE IV
ESTIMATED DIELECTRIC CONSTANTS FOR MAYAZI COAL (vac. dry)

| | | 100kc | 1Mc | 10Mc | 4000Mc |
|---|---|---|---|---|---|
| Bo | 56% | 4.04 | 4.00 | 3.96 | —— |
| | 50% | 4.05 | 4.02 | 3.99 | 3.34 |
| Br | 56% | 4.05 | 4.00 | 3.97 | —— |
| | 50% | 4.08 | 4.04 | 4.00 | 3.35 |

8) M. P. Groenewege, J. Schuyer and D. W. van Krevelen, *Fuel*, **34**, 339 (1955).

It is to be noted that the above equations are related only to the dielectric constant and not to the loss factor. A more general equation including the latter has recently been provided by Lewin[9] for the case of perfectly spherical particles* in insulating medium. For the complex dielectric constants as defined by $\varepsilon^*=\varepsilon'-j\varepsilon''$, $\varepsilon_1^*=\varepsilon_1'-j\varepsilon_1''$ and $\varepsilon_2^*=\varepsilon_2'-j\varepsilon_2''$, the following equation holds:

$$\varepsilon^*=\varepsilon_1^*\left(1+\frac{3v_2}{\dfrac{\varepsilon_2^*F(\Theta)+2\varepsilon_1^*}{\varepsilon_2^*F(\Theta)-\varepsilon_1^*}-v_2}\right), \qquad (6)$$

where

$$F(\Theta)=\frac{2(\tan\Theta-\Theta)}{(\Theta^2-1)\tan\Theta+\Theta},$$

and

$$\Theta=\frac{2\pi a}{\chi}\sqrt{\varepsilon_2^*}$$

in which $a$ is the radius of the coal particle and $\lambda$ is the wave length of the electric wave used in the dielectric measurement. The application of Eq. (6) to the present problem was made first for the case when there is no loss factor (see curve 3 in Fig. 2). Then calculation was repeated for the cases when the mixtures have appreciable loss factors. It was ascertained by these calculations that even when $\varepsilon''$ amounts to a considerable magnitude 0.1**, the dielectric constant can be safely estimated within experimental error with the payment of little attention to the presence of the loss factor.

Böttcher and Bruggeman equations have been originally derived only for real dielectric constants, but they may be transformed into more general equations including the imaginary part when a complex dielectric constant is used instead of the real one. It can be proved by numerical calculations using the general equation of Böttcher thus obtained that the existence of appreciable loss factors does not vitiate the results of the estimation shown in Table III.

9) L. Lewin, *J. Inst. Elec. Engrs.*, **94**, 65 (1947); E. Meyer, H. J. Schmidt und H. Severin, *Z. angew. Phys.*, **8**. 257 (1956).

* A comparison of the theoretical curve 3 (Fig. 2) for perfectly spherical particles with the experimental data will suggest that the formation of chains does occur in the mixture.

** The maximum value of $\varepsilon''$ observed in the present study is 0.0895 at 1 kc/s obtained for the coal sample II.

Lastly the results shown in Table II will be again considered. It will be seen that an air-dry sample—coal powder was dried in air for 4–6 days at 105°C—has a slightly higher dielectric contant than that of the vacuum dried sample. This may indicate that some polar substances are produced upon oxidation*. Further, water absorption by dried samples (air-dry as well vac-dry samples) greatly increases the dielectric constant.

It should be noted that all the samples come to have the same dielectric constant of about 2.8 at the frequency of 4000 Mc/s. This fact suggests that all the dipoles in the coal—irrespective of whether they originally belong to the coal, or are produced on oxidation, or are of the water molecules adsorbed by the coal—are completely blocked from rotation**. Further this view is substantiated by the fact that the dielectric constant 3.35 for coal at this frequency of 4000 Mc/s can be regarded as the optical dielectric constant (See Table IV). In fact this magnitude is just equal to the square of the refractive index[10] of the coal having the same carbon content.

* See, in this connection, W. N. Adams and G. J. Pitt, *Fuel*, **34**. 383 (1955).

** The condition of non-rotation of dipoles is not satisfied in the liquid state until the frequency become higher than 30,000 Mc/s (at room temperature). The corresponding frequency in the solid state is expected to be low, since the viscosity or the hindering potential of rotation should be much higher than in the liquid state (C. P. Smyth, "Dielectric Structure and Behavior," (1955)).

10) D. W. van Krevelen, *Brennstoff-Chem.*, **34**, 167 (1953).

## Summary

A new method using powdered coal and paraffin wax was proposed for measuring the dielectric constant of coal concerned. In order to check the validity of this method, experiments were conducted on five coal specimens for which direct determination of dielectric constant had been made by the writers. Special attention was paid to the choice of a mixture formula and also to the influence of the electric conductivity upon the dielectric constant. It was concluded then that the present method could reproduce the dielectric constant of the coal with the fair precision of ± 10%.

The microwave measurement on one specimen reveals that all the dipoles in coal are completely inhibited from rotation at this frequency.

The writers wish to thank Prof. G. Takeya, Faculty of Engineering, for supplying the coal samples examined in this paper.

*Research Institute of Applied Electricity*
*Hokkaido University, Sapporo*

# *Dielectric Investigation on Coals. III. On a Variety of Coals*

By Isao MIYASITA, Keniti HIGASI and Masao KUGO

(Received March 17, 1957)

## Introduction

A preceding paper[1] has shown that by a method using mixture of powdered coal and paraffin wax, the dielectric constant of coal could be estimated with fair precision of ±10 per cent. It has been pointed out that almost the same amount of deviation is to be found when testing different samples of the same specimen.

The present article deals with the dielectric constant data obtained by using the mixture method on a variety of Japanese coals and on five coals from foreign sources.

## Experimental

Coal samples here examined do not include all the types of Japanese coals, but are representative caking coals produced in Japan. Some of the conclusions reached for them will be applicable to all other Japanese coals. Foreign coals are chosen from among those which have been imported to certain iron works in Japan. Chemical analyses of all these coal specimens are recorded in Tables I and II.

The coal samples were reduced to fine powders, thoroughly dried at 105°C in a vacuum, and then mixed with melted paraffin wax[1]. The volume

1) K. Higasi, I. Miyasita and Y Ozawa, This Bulletin, **30**, 546 (1957).

TABLE I

PROXIMATE ANALYSES

| Coal No. | Source of Sample | Moisture | Ash | Volatile matter | Fixed carbon | Total sulfur |
|---|---|---|---|---|---|---|
| A1 | Yubari No. 2—10 | 1.38 | 4.71 | 51.44 | 42.47 | — |
| B1 | Mayazi No. 1a | 0.97 | 1.80 | 43.38 | 53.85 | — |
| B2 | Mayazi No. 2 | 0.72 | 1.61 | 47.37 | 50.30 | — |
| B3 | Mayazi No. 3 | 1.11 | 2.26 | 47.29 | 49.34 | — |
| C1 | Sunagawa No. 2 | 1.02 | 4.35 | 44.63 | 50.00 | — |
| C2 | Sunagawa No. 3 | 0.83 | 6.85 | 38.67 | 53.65 | — |
| C3 | Sunagawa No. 4 | 2.65 | 4.68 | 48.65 | 44.02 | — |
| C4 | Sunagawa No. 8 | 1.20 | 2.54 | 46.26 | 50.00 | — |
| C5 | Sunagawa No. 9 | 2.30 | 3.61 | 57.06 | 37.03 | — |
| C6 | Sunagawa No. 10 | 1.78 | 8.93 | 52.76 | 36.53 | — |
| C7 | Sunagawa No. 11 | 1.13 | 6.36 | 42.83 | 49.68 | — |
| D1 | Yatake | 1.11 | 2.94 | 21.29 | 74.86 | 0.65 |
| E1 | Taihei (lignite) | 12.86 | 5.84 | 45.33 | 35.97 | 0.76 |
| E2 | Tempoku (brown coal) | 12.80 | 1.52 | 35.62 | 50.06 | 0.77 |
| F1 | India | — | 14.96 | 27.65 | 57.39 | — |
| F2 | Pocahontas, Western (U. S. A.) | — | 7.33 | 22.00 | 70.67 | — |
| F3 | Pocahontas (U. S. A.) | — | 5.92 | 18.60 | 75.48 | — |
| F4 | Pocahontas (U. S. A.) | — | 4.85 | 19.30 | 75.85 | — |
| F5 | Durham (England) | 0.85 | 1.70 | 26.14 | 71.31 | — |

TABLE II

ULTIMATE ANALYSES (dry, ash-free basis)

| Coal No. | Source | C% | H% | O% | N% | S% |
|---|---|---|---|---|---|---|
| C3 | Sunagawa No. 4 | 82.09 | 6.21 | 10.26 | 1.36 | 0.09 |
| C7 | Sunagawa No. 11 | 81.84 | 5.50 | 10.75 | 1.59 | 0.32 |
| D1 | Yatake | 89.4 | 4.86 | 3.06 | 1.88 | 0.64 |
| E1 | Taihei | 65.1 | 4.93 | 28.42 | 0.93 | 0.62 |
| E2 | Tempoku | 70.2 | 4.74 | 23.4* | 1.10 | 0.6 |
| F1 | India | 88.03 | 5.28 | 4.69 | 1.66 | 0.34 |
| F4 | Pocahontas | 87.99 | 4.98 | 5.17 | 1.51 | 0.35 |
| F5 | Durham (England) | 89.31 | 4.31 | — | — | — |

* Estimated from (O+S)% 23.96 on the assumption S% 0.6.

fraction of the coal was kept as 0.56 of the whole part.

The dielectric measurements[2] were made at room temperature with a Q meter for the frequency range of 50 Mc/s to 100 kc/s, and with an impedance bridge for the range of 10 kc/s to 300 c/s.

The results of measurements are collected in Tables III and IV. Dielectric constants, $\varepsilon'$ and loss factors, $\varepsilon''$ without parenthesis all refer to the paraffin-wax mixtures of 56 vol % coal. Figures in parentheses show the dielectric constants of the coals themselves which were obtained by the use of the following mixture formula due to Bottcher[3].

$$\frac{\varepsilon'-\varepsilon'_1}{3\varepsilon'} = v_2 \frac{\varepsilon'_2-\varepsilon'_1}{\varepsilon'_2+2\varepsilon'} \qquad (1)$$

in which $\varepsilon'$, $\varepsilon'_1$, and $\varepsilon'_2$ are the dielectric constants of the mixture, the paraffin wax and the coal particles, respectively, and $v_2$ is the volume fraction of the coal particles in the mixture.

When the mixture has an appreciable loss factor, the application of Eq. (1) becomes questionable. For instance, the mixture with the British sample (F5) has $\varepsilon''$ 0.284 at the frequency of 1 kc/s. To check errors arising from this, a general equation for complex dielectric constant $\varepsilon^*=\varepsilon'-j\varepsilon''$ derived from Eq. (1) was employed for comparsion's sake. By putting $\varepsilon^*=4.79-0.284j$ in this modified equation, the following values of the coal were obtained: $\varepsilon_2^*=7.36-0.664j$ in contrast to $\varepsilon_2'=7.37$ obtained from Eq. (1) (See Table IV). This one example will illustrate well the validity of other approximate calculations on Eq. (1).

As the error due to conductivity is very important, a further check was made by the use of an equation presented by Lewin[4]. The results were: $\varepsilon^*=4.79-0.284j$ gives $\varepsilon_2^*=7.96-0.895j$

2) I. Miyasita and K. Higasi, This Bulletin, **30**, 513 (1957).

3) C. J. F. Böttcher, *Rec. trav. chim.*, **64**, 47 (1945); and cf. ref. 1) above.

4) L. Lewin, *J. Inst. Elec. Engrs.*, **94**, 65 (1947).

TABLE III

DIELECTRIC CONSTANTS ($\varepsilon'$) AND LOSS FACTORS ($\varepsilon''$) OF JAPANESE COALS*

(Paraffin-wax mixture, coal 56 vol %)

| Coal No. | | 300 c | 1 kc | 10 kc | 100 kc | 1 Mc | 10 Mc |
|---|---|---|---|---|---|---|---|
| A1 | $\varepsilon'$ | 3.36 (4.21) | 3.32 (4.12) | 3.30 (4.08) | 3.27 (4.02) | 3.24 (3.96) | 3.24 (3.96) |
| | $\varepsilon''$ | 0.0333 | 0.0212 | 0.0144 | 0.0087 | 0.0115 | 0.0083 |
| B1 | $\varepsilon'$ | 3.24 (3.96) | 3.24 (3.96) | 3.24 (3.96) | 3.22 (3.92) | 3.19 (3.86) | 3.16 (3.79) |
| | $\varepsilon''$ | 0.0256 | 0.0193 | 0.0135 | 0.0088 | 0.0080 | 0.0068 |
| B2 | $\varepsilon'$ | 3.29 (4.06) | 3.28 (4.04) | 3.26 (4.00) | 3.25 (3.98) | 3.22 (3.92) | 3.22 (3.92) |
| | $\varepsilon''$ | 0.026 | 0.0198 | 0.0154 | 0.0109 | 0.0082 | 0.0080 |
| B3 | $\varepsilon'$ | 3.28 (4.07) | 3.24 (3.96) | 3.24 (3.96) | 3.22 (3.92) | 3.19 (3.86) | 3.15 (3.77) |
| | $\varepsilon''$ | 0.0242 | 0.0176 | 0.0145 | 0.0113 | 0.0097 | 0.0085 |
| C1 | $\varepsilon'$ | 3.39 (4.27) | 3.36 (4.21) | 3.36 (4.21) | 3.31 (4.10) | 3.30 (4.08) | 3.30 (4.08) |
| | $\varepsilon''$ | 0.0309 | 0.0252 | 0.0170 | 0.0089 | 0.0131 | 0.0112 |
| C2 | $\varepsilon'$ | 3.29 (4.06) | 3.28 (4.04) | 3.24 (3.96) | 3.22 (3.92) | 3.18 (3.84) | 3.17 (3.81) |
| | $\varepsilon''$ | 0.0312 | 0.022 | 0.019 | 0.0135 | 0.0100 | 0.0065 |
| C3 | $\varepsilon'$ | 3.11 (3.69) | 3.08 (3.63) | 3.06 (3.59) | 3.05 (3.58) | 3.04 (3.56) | 3.02 (3.52) |
| | $\varepsilon''$ | 0.0180 | 0.0135 | 0.0103 | 0.0097 | 0.0072 | 0.0059 |
| C4 | $\varepsilon'$ | 3.34 (4.17) | 3.32 (4.12) | 3.28 (4.04) | 3.26 (4.00) | 3.24 (3.96) | 3.24 (3.96) |
| | $\varepsilon''$ | 0.0242 | 0.0161 | 0.0147 | 0.0114 | 0.0096 | 0.0095 |
| C5 | $\varepsilon'$ | 3.42 (4.33) | 3.34 (4.17) | 3.32 (4.12) | 3.21 (3.90) | 3.19 (3.86) | 3.17 (3.82) |
| | $\varepsilon''$ | 0.0570 | 0.0407 | 0.0290 | 0.0153 | 0.0154 | 0.0128 |
| C6 | $\varepsilon'$ | 3.44 (4.37) | 3.40 (4.29) | 3.37 (4.23) | 3.37 (4.23) | 3.32 (4.12) | 3.31 (4.10) |
| | $\varepsilon''$ | 0.0320 | 0.0190 | 0.0132 | 0.0099 | 0.0086 | 0.0099 |
| C7 | $\varepsilon'$ | 3.36 (4.21) | 3.34 (4.17) | 3.29 (4.06) | 3.28 (4.04) | 3.25 (3.98) | 3.22 (3.92) |
| | $\varepsilon''$ | 0.0407 | 0.0272 | 0.0168 | 0.0080 | 0.0097 | 0.0098 |
| D1 | $\varepsilon'$ | 3.08 (3.55) | 3.07 (3·53) | 3.02 (3.43) | 3.01 (3.41) | 3.03 (3.45) | 3.00 (3.40) |
| | $\varepsilon''$ | 0.034 | 0.0248 | 0.0126 | 0.0097 | 0.0053 | 0.00306 |
| E1 | $\varepsilon'$ | 3.76 (4.83) | 3.73 (4.78) | 3.61 (4.56) | 3.59 (4.52) | 3.55 (4.45) | 3.44 (4.24) |
| | $\varepsilon''$ | 0.115 | 0.0904 | 0.0482 | 0.0421 | 0.043 | 0.0428 |
| E2 | $\varepsilon'$ | 3.64 (4.61) | 3.62 (4.58) | 3.57 (4.48) | 3.58 (4.50) | 3.52 (4.38) | 3.46 (4.27) |
| | $\varepsilon''$ | 0.031 | 0.0284 | 0.023 | 0.0248 | 0.0256 | 0.0312 |

* Values in parenthesis refer to $\varepsilon'$ of coals themselves.

while $\varepsilon^*=4.79-0.00j$ gives $\varepsilon_2^*=7.99-0.00j$. Again there is hardly any significant difference between the values of $\varepsilon'_2$, i. e. 7.96 versus 7.99.

A comparison of the values of Tables III and IV would reveal that the coals from foreign sources here examined exhibit entirely different dielectric behavior from the Japanese coals. In all of them strong frequency dependence of dielectric properties is found which is not so pronounced in most of the Japanese specimens.

The $\varepsilon'$ values of Japanese coals generally show slight increases at the lower frequency side. Among them two samples E1 and E2 of higher oxgen contents may be noted, since they have a little higher value in $\varepsilon'$ and show somewhat noteworthy dependence of $\varepsilon''$ upon frequency.

TABLE IV

DIELECTRIC CONSTANTS ($\varepsilon'$) AND LOSS FACTORS ($\varepsilon''$) OF COALS* FROM FOREIGN SOURCES
(Paraffin-wax mixture, coal 56 vol %)

| Ccal No. | | 300 c | 1 kc | 10 kc | 100 kc | 1 Mc | 10 Mc |
|---|---|---|---|---|---|---|---|
| F1 | $\varepsilon'$ | 4.93 (7.69) | 4.62 (6.98) | 4.12 (5.84) | 3.91 (5.37) | 3.74 (5.00) | 3.60 (4.71) |
| | $\varepsilon''$ | 0.53 | 0.419 | 0.285 | 0.149 | 0.097 | 0.0588 |
| F2 | $\varepsilon'$ | 4.62 (6.98) | 4.43 (6.53) | 4.11 (5.81) | 4.04 (5.66) | 3.82 (5.18) | 3.68 (4.87) |
| | $\varepsilon''$ | 0.315 | 0.236 | 0.187 | 0.115 | 0.0867 | 0.0760 |
| F3 | $\varepsilon'$ | 4.66 (7.07) | 4.41 (6.48) | 4.14 (5.88) | 3.96 (5.48) | 3.82 (5.18) | 3.66 (4.83) |
| | $\varepsilon''$ | 0.318 | 0.246 | 0.151 | 0.116 | 0.0902 | 0.0688 |
| F4 | $\varepsilon'$ | 4.66 (7.07) | 4.48 (6.64) | 4.14 (5.88) | 3.97 (5.51) | 3.81 (5.16) | 3.66 (4.83) |
| | $\varepsilon''$ | 0.359 | 0.262 | 0.171 | 0.123 | 0.0948 | 0.0768 |
| F5 | $\varepsilon'$ | 5.01 (7.88) | 4.79 (7.37) | 4.44 (6.55) | 4.22 (6.06) | 3.97 (5.51) | 3.82 (5.18) |
| | $\varepsilon''$ | 0.327 [0.775] | 0.284 [0.664] | 0.196 [0.448] | 0.143 [0.321] | 0.120 [0.264] | 0.0936 [0.203] |

* Values in parenthesis are $\varepsilon'$ of coals and those in square bracket refer to $\varepsilon''$ of the coal concerned.

The behavior of $\varepsilon''$ of E1 and E2 is entirely different from other Japanese coals. Definite increase in $\varepsilon''$ with increasing frequency is found in these samples as was found in Tempoku brown coal[2], indicating the existence of some dispersion which is probably due to the rotation of OH groups.

As a general trend there is observed a slight increase of $\varepsilon''$ at the lower frequency side in most of the Japanese coals. No definite explanation can be offered for this phenomenon. Possibly it may be due to the presence of impurities such as trace of water which forms a conducting phase*.

## Discussion

Having obtained rather ample data of dielectric constants of coals, either directly determined in a previous study[2] or indirectly estimated in the present research, it was thought of interest to make some comparison between the dielectric constant and other properties of coal.

To begin with, the change of the dielectric constant with carbon-content (dry, ash-free) will be examined. As the observed dielectric properties are not independent of the frequency of the measurement**, two graphs of $\varepsilon'$ vs. C % plots are drawn for two representative frequencies, 1 kc/s and 1 Mc/s (Figs. 1 and 2).

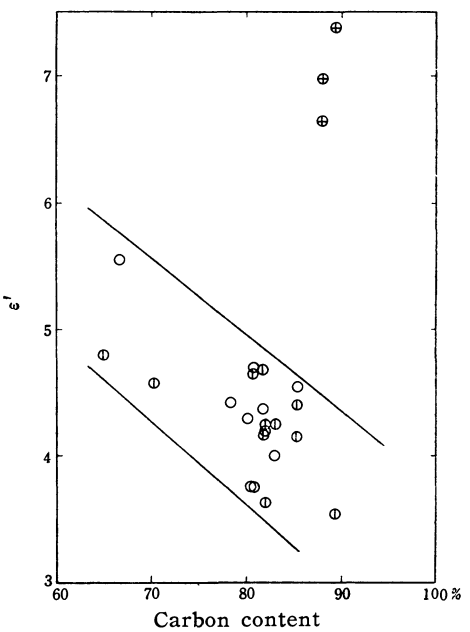



Fig. 1. Dielectric constants measured at frequency of 1 kc/s of coals of various carbon contents. ○, determined directly on Japanese coals; ⓘ, estimated from powdered mixtures on Japanese coals; ⊕, ditto on foreign coals.

Among the widely scattered points there appears to be a general trend of increase in dielectric constant with decrease in carbon-content.

According to the infra-red absorption

* See for instance, C. P. Smyth, "Dielectric Bahavior and Structure," McGraw-Hill Book Co., New York (1955), p. 191.

** The curves in Fig. 3 illustrate different types of dependence of the dielectric constant upon the frequency.

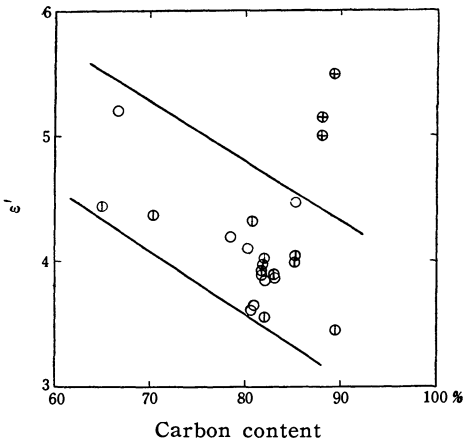



Fig. 2. Dielectric constants measured at frequency of 1 Mc/s of coals of various carbon contents. ○, ⓘ and ⊕, the same with Fig. 1.

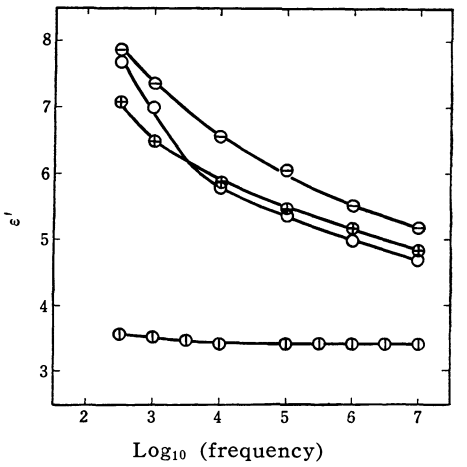



Fig. 3. Dielectric constant-frequency curves of high rank coals. ⓘ, Yatake (Japan); ○, Indian coal; ⊕, Pocahontas (U. S. A.); ⊖, Durham (U. K.).

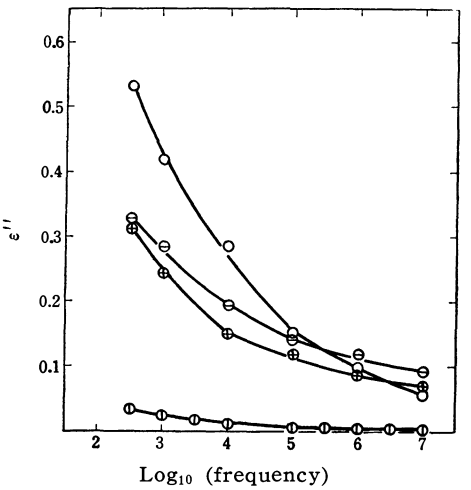



Fig. 4. Loss factor-frequency curves of powdered mixtures of high rank coals. ⓘ, ○, ⊕ and ⊖, the same with Fig. 3.

studies[5,6] the intensities of bands concerning oxygen-containing groups of coal constituents, especially of the bonded OH at near 3.3 $\mu$, appear to decrease as the oxygen-content decreases. These intensities become greater in the low rank coals of which the carbon-contents are in the range from 78 to 84 per cent. They fall in the higher rank coals, especially over 89 per cent carbon coals.

The oxygen-containing groups which appear to be rich in the low rank coals are provided with large electric moments. If the rotation of these polar groups is possible to a certain extent, they would make effective contributions to the dielectric constant.

Consequently it would be reasonable to conclude that the lower rank coals have the higher dielectric constants on account of the higher content of polar groups such as OH or CO.

In the range of carbon 88 to 90 per cent, very remarkable differences are recognized between the dielectric constants of foreign coals and of the Japanese coal here examined (See Fig. 1). The change in $\varepsilon'$ of these coals with frequency is shown in Fig. 3. The value of Yatake coal (C % 89.4) is low and almost independent of frequency, while others (F1, F4 and F5) show pronounced anomalous dispersion: the dielectric constants greatly decrease with increasing frequency.

Regarding the foreign coals it will be of interest to examine the relation between the loss factor and frequency. In Fig. 4 $\varepsilon''$ values of the mixtures of coal and paraffin wax are shown. In each of them a steep rise of $\varepsilon''$ value is found in the lower frequency region. This also makes a remarkable contrast to the almost flat curve of Yatake coal.

Non-dispersive character is not limited to Yatake coal. Most of the Japanese bituminous coals (C % 80–87) may be regarded as lacking in anomalous dispersion*

5) J. K. Brown. *J. Chem. Soc.*, 744 (1955).
6) R. A. Friedel and J. A. Queiser, *Anal. Chem.*, **28**, 22 (1956).

* There is found an increase in $\varepsilon''$ values at the low frequency side, but as compared with values of coals from foreign sources the magnitude of this increase is small so that possibly it may be attributed to the presence of impurities.

(See the results for A1, B1-3, C1-4, C6-7 and D1 in Table III and data of previous reports[1,2]). Their dielectric constants are generally low — their dielectric properties in general resemble those of ordinary electric insulators.

It may be worth while to cite the results of infrared absorption studies on Japanese coals recently reported by Kozima and his co-workers[7]. The ratio of $C_{arom}$—H to $C_{aliph}$—H on the same specimens of Japanese coals, A1 and D1, of the present study was determined by them*. It was pointed out then that the ratio of Yatake coal (C % 89.4) was four times larger than that of Yubari coal (C % ca. 85.5). This remarkable difference, however, is not reflected in the dielectric constant (See Table III).

According to the above facts the following views would be offered. They are not merely of presumptive evidence based only upon the present results.

1) The high $\varepsilon'$ values of foreign coals are due to the condensed aromatic structures with pi-electrons[8]. As described by van Krevelen and his co-workers[9] the influence of electric conductivity is evident. The loss factor-frequency curves in Fig. 4 are of the shape to be expected for a system of semi-conductor particles densely packed in an insulating medium[10,11].

2) Japanese high-rank bituminous coals as represented by Yatake coal appear to have rather different structures from the foreign coals. They are relatively poor in condensed aromatic structures. Possibly they are rich in hydroaromatic rings or in alkyl side chains[12].

## Summary

By using a method of paraffin-wax mixture dielectric constants were determined for a variety of coals including five specimens from foreign sources. It was found that dielectric constants of lower rank coals are generally higher than those of bituminous coals of higher rank. Large difference in dielectric behavior was detected among the coal specimens (C % 87-90) from different sources. The present dielectric measurement supported the view that the nature of Japanese coals is particular as compared with European and American coals.

The writers wish to thank Professor G. Takeya for his kind interest and also for supplying the coal samples examined in this paper. Cordial thanks are also due to Dr. Y. Ozawa and to Mr. Y. Zyomoto for their friendly help in this work.

*Research Institute of Applied Electricity and Faculty of Engineering Hokkaido University, Sapporo*

7) K. Kozima, K. Sakasita and T. Yosino, *J. Chem. Soc. Japan* (Pure Chem.) **77**, 1432 (1956)

* These coal specimens were kindly provided by Dr. H. Honda, Resources Research Institute, Kawaguti-City, both to Prof. Kozima and to one of the present writers.

8) H. Inokuchi, This Bulletin, **24**, 222 (1951); **25**, 28 (1952).

9) M. P. Groenewege, J. Schuyer and D. W. van Krevelen, *Fuel.* **34**, 339 (1955).

10) C. P. Smyth, op. cit. p., 191.

11) B. V. Hamon, *Austra. J. Phys.*, **6**, 304 (1953).

12) A. Baba, "Progress in Coal Science," Vol. 2, Hakuasyobo. Tokyo (1956), p. 86.

# *Dielectric Investigation on Coals. IV. Notes on Dipole Moment*

By Keniti HIGASI, Yosie HIGASI and Isao MIYASITA

(Received March 17, 1957)

## Introduction

Some years ago it was suggested to one of the present writers that a determination of electric dipole moment should be most desirable for coals. Indeed, the usefulness of dipole moments for attacking problems in structural chemistry has long been appreciated[1]. As was true in the cases of simpler molecules, it was then hoped, they migt become the most effective means among the various physical methods applicable for the study of coal structure.

Now, rather ample data[2,3] on the dielectric properties of coals being available, it was thought worth while to make some trials in this direction. One may say that such a trial is destined to be labour lost, since in the solid state the orientation of polar groups is almost completely restricted by lattice forces. However, coals differ from most of the crystalline solids. According to van Krevelen[4] the main constituent such as vitrain is to be regarded as a supercooled liquid. Perhaps coals are sorts of organic glasses or polymers[4]. If this view be correct, one may use equations for liquids in determining a dipole moment[5]. This affords a basis for the trial and speculations to be described in the present paper.

## Equations of Liquids

From among many equations for liquids, the Onsager equation[6] is the only one to have been used extensively in calculating the dipole moment.

$$\mu^2 = \frac{9kT}{4\pi N}\frac{M}{d}\frac{(2\varepsilon+\varepsilon_\infty)(\varepsilon+2)}{3\varepsilon(\varepsilon_\infty+2)} \times\left(\frac{\varepsilon-1}{\varepsilon+2}-\frac{\varepsilon_\infty-1}{\varepsilon_\infty+2}\right) \qquad (1)$$

in which $\mu$ is the molecular dipole moment, $k$ is the Boltzmann constant, $T$ is the absolute temperature, $N$ is the Avogadro number, $M$ is the molecular weight and $d$ is the density. In the above equation $\varepsilon$ is the ordinary dielectric constant*, while $\varepsilon_\infty$ is the optical dielectric constant, or the dielectric constant measured at the frequencies which are so high that the permanent dipoles are unable to exert any influence. In the original form of Eq. (1) the square of refractive index, $n^2$ is used instead of $\varepsilon_\infty$. The above equation is a modification due to Smyth[7] and useful for the present work, where the atom polarization may play a significant role.

The Debye equation is originally an equation for gases and vapours. Its use will be considered on account of the simpler form:

$$\mu^2 = \frac{9kT}{4\pi N}\frac{M}{d}\left(\frac{\varepsilon-1}{\varepsilon+2}-\frac{\varepsilon_\infty-1}{\varepsilon_\infty+2}\right) \qquad (2)$$

The Onsager equation holds mostly for highly polar liquids[8,9]. On the contrary the Debye equation is known to be valid for non-polar liquids and a few groups of polar liquids such as ethers[10], amines[11] and chloroform[12]. There is uncertainty as to the choice of a proper equation for liquids, if other equations excepting the above two are left out of consideration.

The difference in the above equations lies in the factor

$$S = \frac{(2\varepsilon+\varepsilon_\infty)(\varepsilon+2)}{3\varepsilon(\varepsilon_\infty+2)} \qquad (3)$$

1) C. P. Smyth, "Dielectric Behavior and Structure," McGraw-Hill Book Co., New York (1955); J. W. Smith, "Electric Dipole Moments," Butterworths Sci. Publ., London (1955). K. Higasi, "Foundation of Structural Chemistry—Dipole Moments," Kawade Book Co., Tokyo (1952).
2) I. Miyasita and K. Higasi, This Bulletin, **30**, 513 (1957)
3) I. Miyasita, K. Higasi and M. Kugo, This Bulletin, **30**, 550 (1957).
4) D. W. van Krevelen, *Brennstoff-Chem.*, **34**, 167 (1953).
5) C. P. Smyth, *op. cit.*, p. 226; J. W. Smith, *op. cit.*, p. 145; K. Higasi, *op. cit.*, p. 14.
6) L. Onsager, *J. Am. Chem. Soc.*, **58**, 1486 (1936).

* In the present article $\varepsilon$ will be used instead of $\varepsilon'$.
7) C. P. Smyth, *op. cit.*, p. 23.
8) C. J. F. Böttcher, *Physica*, **6**, 59 (1939).
9) H. Fröhlich, *Trans. Faraday soc.*, **42A**, 39 (1946).
10) K. Higasi, *Sci. Pap. Inst. Phys. Chem. Res.*, **24**, 57 (1934).
11) M. Shirai, This Bulletin, **29**, 518 (1956).
12) R. J. W. Le Fèvre et al., *J. Chem. Soc.*, 487, 491, 496 (1936).

If $S=1$*, Eq. (1) will become the same with Eq. (2).

In most bituminous coals both values of $\varepsilon$ and $\varepsilon_\infty$ (as estimated from $n$) do not much vary with the specimen. On putting some average values, $\varepsilon=4$ and $\varepsilon_\infty=3.24$, in Eq. (3), $S$ will be evaluated as 1.07. Consequently the dipole moment calculated from Eq. (1) slightly differs from that estimated by Eq. (2), the difference being only 3-4 per cent. This result is very encouraging, since an error of less than 5% in moment is insignificant in the present case.

Both Eqs. (1) and (2) can be reduced to a very simple equation

$$\mu=A[(\varepsilon-\varepsilon_\infty)M/d]^{1,2} \quad (4)$$

where $A$ has the values

$$A_1^2=0.147/(\varepsilon+2)(\varepsilon_\infty+2) \quad \text{(Debye)} \quad (5)$$

$$A_2^2=0.147(2\varepsilon+\varepsilon_\infty)/3\varepsilon(\varepsilon_\infty+2)^2 \quad \text{(Onsager)} \quad (6)$$

in which dipole moment $\mu$ is expressed in Debye unit ($10^{-18}$e.s.u.cm.) and the temperature is assumed to be 20°C.

Further, in a rough estimation the coefficient $A$ may be regarded as a constant. Usually for coals of C% 65-90 $\varepsilon$ lies between 3.3-5.5 and $\varepsilon_\infty$ between 2.8-4.0 (see Tables I and II). The values of $A$ (Debye) are 0.075-0.057 and $A$ (Onsager) 0.078-0.061, respectively.

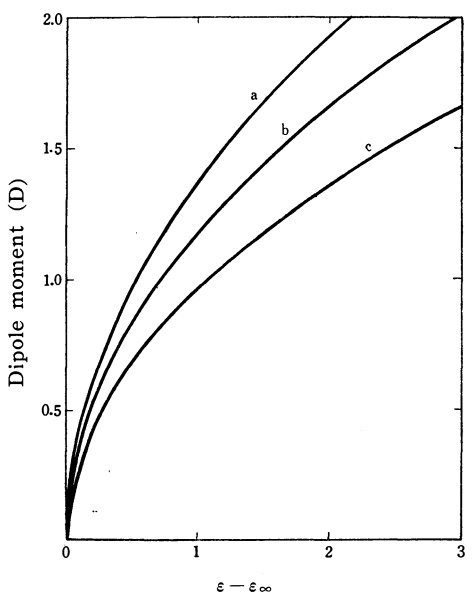



Fig. 1. Dipole moment of coal as a function of the quantity $\varepsilon-\varepsilon_\infty$. Curve a, $M/d=400$; curve b, $M/d=300$; and curve c, $M/d=200$.

For $A=0.068$ ($\varepsilon=4$, $\varepsilon_\infty=3.24$) and $M/d=300$ cc Eq. (4) becomes

$$\mu=1.17\sqrt{\varepsilon-\varepsilon_\infty} \quad (7)$$

The above equation is incorrect but convenient for a quick judgement. Moment values calculated from Eq. (7) are shown by curve b in Fig. 1. In this figure two other curves a and c are drawn for the cases with $M/d=400$ and 200, respectively.

## Dielectric Constant

Both Eqs. (4) and (7) well illustrate the physical significance of the dielectric constant. The dielectric constant $\varepsilon$ of a polar substance has three origins: (a) the orientation effect of the permanent dipole, (b) the displacement effect of the atoms, and (c) the displacement effect of the electrons. As the optical dielectric constant $\varepsilon_\infty$ is contributed only from the latter two effects, the difference $\varepsilon-\varepsilon_\infty$ represents the part of dipole orientation.

As the dielectric constant is a function of frequency, a question arises as to the method of choosing a proper $\varepsilon$ value for the calculation. In the study of liquids, $\varepsilon$ values at frequencies 1-10 Mc/s have been usually employed[13], because the measurement is easiest at these frequencies and also because the obtained values are generally equal to static dielectric constants. As the relaxation time is expected to be different from liquids, a more cautious attitude is demanded in treating coals. Before being able to choose a proper value of $\varepsilon$ one must examine the dependence of the dielectric constant upon frequency.

There are found in coals at least three types of frequency dependences. In one of them (A type) there is apparently little dispersion: that is, both the dielectric constant and loss factor have values almost indepedent of frequency in the range of 300 c/s—50 Mc/s. See curves (A) in Figs. 2 and 3. Examples: most of the Japanese bituminous coals. In the second type (B type), dispersion appears to exist in the high frequency region. Examples: Tempoku brown coal (specimen VI) and probably two other low rank coals (E1 and E2). The third type (C type) is charac-

* If $\varepsilon$ is equal to $\varepsilon_\infty$, $S$ will become unity. See further Böttcher, "The Theory of Electric Polarisation," Elsevier Publ. Co., Amsterdam (1952).

13) C. P. Smyth, *op. cit.*, p. 209; J. W. Smith, *op. cit.*, p. 30; Y. Morino and I. Miyagawa, *Kagaku-no-Ryoiki*, Spec. no., **8**, 1 (1953).

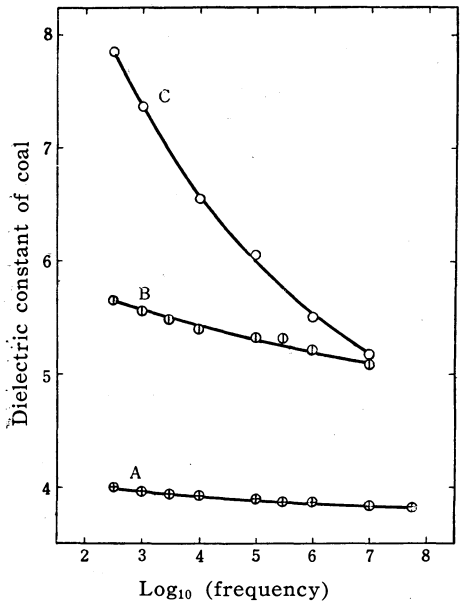



Fig. 2. Frequency dependence of dielectric constant of coal. ⊕, Moziri bituminous coal; ⊙, Tempoku brown coal; and ○, British coal (Durham). Data for the British coal were obtained from powdered mixture.

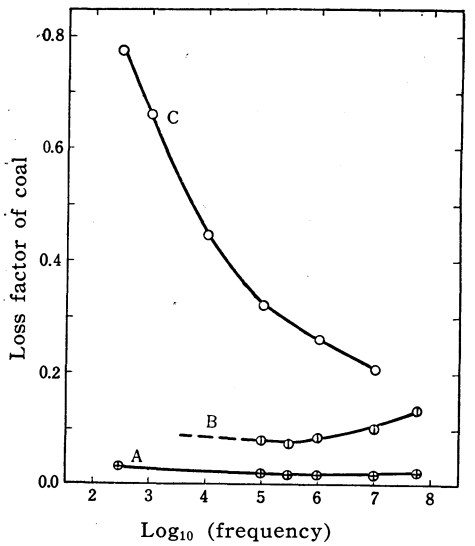



Fig. 3. Frequency dependence of loss factor of coal. ⊕, ⊙, and ○, the same with Fig. 2.

terized by high loss factor and high dielectric constant at the low frequency region. Examples: European and American high rank coals (F1–5).

In view of the above facts the following assumptions will be taken as a basis for some considerations.

1) For A type coals, 1 Mc/s values are preferred. The Q meter gives most reliable values when measured at this frequency.

2) For B type coals, 1 kc/s values are taken. Lower frequency values in general may be preferable. But there is no guarantee that moisture was completely removed. The impedance bridge gives best values at 1 kc/s.

3) For C type coals, 10 Mc/s values are arbitrarily selected. It is questionable whether the dipole rotation at this high frequency is as free as at the static fields. But the high $\varepsilon$ values at low frequencies may not be attributable to the usual dipole effect.

## Opitical Dielectric Constant and Atom Polarization

The optical dielectric constant $\varepsilon_\infty$ is often assumed as equal to the square of refractive index for visible light. But the refraction of visible light is due primarily to the displacement of electrons, while $\varepsilon_\infty$ is due to the displacement of both electrons and atoms in the molecule. The small difference between the two determines the magnitude of the atom polarizations. Regarding the latter quantity there exists no general relationship, but sometimes it was assumed for the sake of convenience that the atom polarization amounts to 5% or 10% of the electron polarization[14].

There is available no literature concerning the refractive index of Japanese coals. The only existing data are those on European coals by van Krevelen[4] who found a relation between the refractive index and carbon content (see curve 3 in Fig. 4).

Dielectric constant of Mayazi coal B (C % 85.24) measured at a micro-wave frequency (4000 Mc/s) is 3.35[15]. This $\varepsilon$ value is just equal to the square of the same carbon content estimated from the curve ($n_D$=1.83). From this astonishing coincidence, one may imagine that $\varepsilon$ at the frequency of 4000 Mc/s is equal to $\varepsilon_\infty$, and further that the contribution from atom polarization is insignificant. Yatake coal (C % 89.4) has $\varepsilon$ 3.45 at 10 Mc/s which is even smaller than $n_D^2$=3.65. Again this may indicate that the contribution from the atom polarization is not important.

14) C. P. Smyth, *op. cit.*, p. 416; J. W. Smith, *op. cit.*, p. 256.

15) K. Higasi, I. Miyasita and Y. Ozawa, This Bulletin, **30**, 546 (1957).

By reason of the above it will be assumed in the next section that the square of refractive index for D-line approximately represents $\varepsilon_\infty$ of the coal of the corresponding carbon content.

There are two points to be considered against this assumption. First, the neglect of atom polarization is not justified by the above argument. To provide an answer for this, two curves 1 and 2 in Fig. 4 are

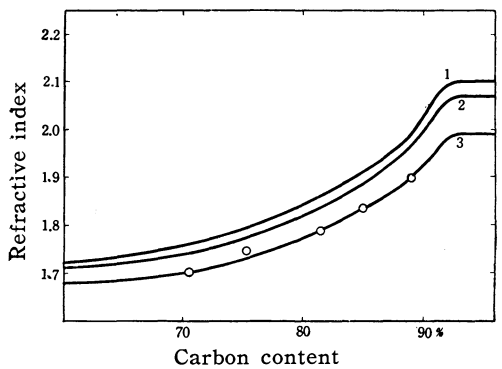



Fig. 4. Variation of refractive index with carbon content. Curve 1, given by the assumption $P_A=7\%\ P_E$; curve 2, given by the assumption $P_A=5\%\ P_E$ and curve 3, observed by van Krevelen[4] on European coals.

plotted. As in usual treatments of atom polarization the following equation is considered.

$$\frac{n'^2-1}{n'^2+2}=(1+\delta)\frac{n^2-1}{n^2+2} \qquad (8)$$

The values of modified refractive indices $n'$ which have been obtained from Eq. (8) are plotted in the graph*. (Curve 2: $n'$ for $\delta=0.05$; curve 1: $n'$ for $\delta=0.07$). By using the values $n'^2$ for $\varepsilon_\infty$, check on the effect of atom polarization will be made.

Second, there is no reason why carbon content should be the determining factor of the refractive index. Further, one is not certain whether or not van Krevelen's relation obtained for European coals is applicable to all the Japanese coals. Under these circumstances any discussion on $\varepsilon_\infty$ has ambiguity to be cleared up in the future.

* The choice of $\delta=0.05$ for the correction of the atom polarization is a practice due to Groves et al. (*J. Chem. Soc.*, 971 (1935); 1779 (1937)). The reason for choosing $\delta=0.07$ is as follows. Suppose that coal is composed of two parts: for the major part (70 %), $P_A$ is taken as 3.4 % $P_E$ from the data of benzene, toluene and ethylene, and for the remaining part (30 %), $P_A=15\%\ P_E$ is assumed from the data for alcohols, ethers and ketones (J. W. Smith, op, cit., Table 39, p. 261). Atom polarization of coal will then have the value of 7 % of $P_E$, viz., $\delta=0.07$.

## Molecular Volume and Dipole moment

Difficulties in measuring the molecular weight of coal are well-known. It is not right to speak of a molecual dipole moment for a substance with unknown molecular weight. But this situation may be saved by considering the fact that a molecular dipole in coal may not rotate as a whole. Actually some rotatable groups in a molecular unit will orient with the direction of an externally applied field. Therefore the "molecular weight" for the present study need not to be a definite quantity.

In the present work a molecular volume 300 cc will be somewhat arbitrarily chosen without regard to the actual weight of coal. Dipole moments of coals are all to be calculated with reference to this volume. If the density of the coal is 1.4, the apparent molecular weight will amount to 420. Dipole moments thus calculated from Eq. (2) are summarized in Tables I and II. Values in Table II are obtained

TABLE I

DIPOLE MOMENTS OF COALS

| | Coal | C % | ε/freq. | $\varepsilon_\infty$ | $\mu$ |
|---|---|---|---|---|---|
| VI | Tempoku (brown coal) | 66.62 | 5.56/1 kc (5.20/1 Mc) | 2.87 | 1.78 (1.69) |
| Vb | Mitui-bibai | 78.40 | 4.19/1 Mc | 3.07 | 1.24 |
| Va | ,, | 80.12 | 4.10/1 Mc | 3.14 | 1.15 |
| V | ,, | 80.47 | 3.61/1 Mc | 3.15 | 0.83 |
| Vc | ,, | 80.62 | (4.70/1 kc) | 3.16 | (1.39) |
| IV | Akabira | 80.76 | 3.66/1 Mc | 3.16 | 0.86 |
| II | Moziri | 81.71 | 3.92/1 Mc (4.37/1 kc) | 3.20 | 1.01 (1.23) |
| IIIa | ,, | 82.07 | 3.69/1 Mc | 3.21 | 0.84 |
| III | ,, | 82.98 | 3.88/1 Mc | 3.26 | 0.93 |
| I | ,, | 85.25 | 4.47/1 Mc | 3.35 | 1.18 |

Values without parentheses are preferred.

TABLE II

DIPOLE MOMENTS OF COALS

(ε is estimated from powdered mixture)

| | Coal | C % | ε/freq. | $\varepsilon_\infty$ | $\mu$ |
|---|---|---|---|---|---|
| E1 | Taihei (lignite) | 65.1 | 4.78/1 kc (4.45/1 Mc) | 2.86 | 1.58 (1.48) |
| E2 | Tempoku (brown coal) | 70.2 | 4.58/1 kc (4.38/1 Mc) | 2.90 | 1.50 (1.43) |
| C7 | Sunagawa | 81.84 | 3.98/1 Mc | 3.20 | 1.04 |
| C3 | ,, | 82.09 | 3.56/1 Mc | 3.21 | 0.72 |
| B | Mayazi | 85.24 | 4.02/1 Mc | 3.35 | 0.95 |
| F4 | Pocahontas (U.S.A.) | 87.99 | 4.83/10 Mc (5.16/1 Mc) | 3.53 | 1.22 (1.33) |
| F1 | India | 88.03 | 4.71/10 Mc (5.00/1 Mc) | 3.54 | 1.17 (1.27) |
| F5 | Durham (England) | 89.31 | 5.18/10 Mc (5.51/1 Mc) | 3.63 | 1.29 (1.39) |
| D1 | Yatake | 89.4 | 3.45/1 Mc | 3.65 | 0 |

from powdered mixtures, so that they are less accurate*.

Groenewege, Schuyer and van Krevelen[16] gave a dipole moment 0.5 D for a certain coal. No particulars were reported except that they employed Eq. (2) and that the molecular weight for the coal was taken as 420.

## Discussion

Polar groups which might exist in coals[17] will be assumed to have the following magnitudes of dipole moments. O-H 1.51; C-O 0.74; C=O 2.3; N-H 1.31 D[18]. Some of these groups must interact upon each other**, and some others must be in a state of complete non-rotation on account of the strong field of lattice forces. Suppose as an extreme case in spite of the above, that all these groups can rotate independently. Then the resultant moment $\mu$ will be given by

$$\mu^2 = 1.51^2 n_{O-H} + 0.74^2 n_{C-O} + 2.3^2 n_{C=O} + 1.31^2 n_{N-H} \quad (9)$$

where $n_{O-H}$, $n_{C-O}$, etc. represent the number of O—H groups, etc. in a molecule —or more exactly in a molecular unit defined by $M/d=300$. In a special case in which none of the others except the O—H group are important so that they can be neglected,

$$n_{OH} = \mu^2/2.28 \quad (10)$$

The numbers of O—H groups will then be calculated. The polarity of brown coals corresponds approximately to one rotatable O—H group, while others to some small fractions in the molecular unit.

For three specimens of Moziri coals a comparison is made between calculated values and the results of chemical analyses.

TABLE III

A COMPARISON WITH CHEMICAL COMPOSITION

| | Coal | C % | O % | $d$ | $M$ | $N_{oxy}$ | $n_{O\text{-}H}$ |
|---|---|---|---|---|---|---|---|
| I | Moziri No. 4 | 85.25 | 6.91 | 1.357 | 407 | 7.00 | 0.61 |
| II | ,, No. 3 | 81.71 | 9.78 | 1.340 | 402 | 8.04 | 0.45 |
| III | ,, No. 9 | 82.98 | 9.07 | 1.304 | 391 | 7.39 | 0.39 |

Table III shows the values of the molecular weights as calculated from specific gravities and $M/d=300$. From $M$ and C%, the number of oxygen atoms, $N_{oxy}$, in this molecular unit is obtained. The ratio $n_{O-H}/N_{oxy}$ is 0.05–0.09. Reliablility of such estimation is certainly low, but it suggests that the rotatable part is only a small fraction of the total oxygen.

It is evident from Table II that Yatake coal (D1) is non-polar. Besides the fact that no moment is detected, there is also no anomalous dispersion in the wide range of frequencies. (See curves in Figs. 3 and 4 in the preceding paper[3].)

For some coals (IIIa, IV and C3) small moments below 0.9D are observed. Regarding these small moments there is uncertainty whether they are real or not. To make this point clearer a little examination on errors will be necessary. First, error in measuring $\varepsilon$ amounts to 5–10 %. If the deviation in $\varepsilon$ is 0.2–0.4, a small moment below 0.5–0.7D will not be distinguishable from zero. See curve b in Fig. 1. Second, there exists an error concerning the estimation of atom polarization, even if van Krevelen's relation be actually valid. An inspection of curves in Fig. 4 will reveal that a small moment less than 0.6 D is unreliable. Under these circumstances it may not be wise to enter into any serious discussion on small moments observed.

Besides the comparatively small polarities found for bituminous coals there is another phenomenon which seems to suggest that these coals are nearly non-polar. That is, there has been observed scarcely any distinct dispersion* in the frequency range of this experiment. See curves A for a Moziri coal in Figs. 2 and 3.

There is one important fact in this connection that Mayazi coal, which has a moment value 0.95 D, shows a remarkable change in $\varepsilon$ between 4000 Mc/s and 10 Mc/s[15]. This strongly suggests that anomalous dispersion due to dipole rotation exists in this region and therefore that the magnitude 0.9 D is real. This is encouraging, but it may not be very convinicing. In view of the fact that the above offers just one example and further that the microwave measurement of the desired accuracy is still lacking, it is premature to speak, with confidence at least, of the polarity of these bituminous coals.

* Maximum errors in $\varepsilon$ are ± 5 % in Table I and ± 10 % in Table II.

16) M. P. Groenewege, J. Schuyer and D. W. van Krevelen, *Fuel*, **34**, 339 (1955).

17) See for instance, R. A. Friedel and J. A. Queiser, *Anal. Chem.*, **28**, 22 (1956).

18) C. P. Smyth, *op. cit.*, p. 244.

** Regarding the interaction between polar groups see for example S. Mizushima, Y. Morino und K. Higasi, *Physik. Z.*, **35**, 905 (1934); S. Mizushima, "Structure of Molecures and Internal Rotation," Academic Press, New York (1954), p. 7.

* Excepting those in the low frequency region which may be due to other causes.

**Summary**

If coal be regarded as a supercooled liquid, a basis will be provided for determining the dipole moment of coals. Further uncertainty as to choosing a proper equation for liquids is dispelled by the fact that the Onsager equation gives for coal almost the same magnitude of dipole moment as obtained by the Debye equation.

After discussion focussed on the values of the ordinary and optical dielectric constants, dipole moments are evaluated for 19 coal specimens including four samples of foreign origin.

Brown coals are found to have a moment near to that of one O—H group. The polarity of bituminous coal is in general too small to be distinguishable from zero. These results are consistent with the observations on the frequency dependence of dielectric constant and loss factor of these coals.

Thanks are expressed to Drs. Y. Ozawa and M. Kugo for valuable discussion.

*Research Institute of Applied Electricity*
*Hokkaido University, Sapporo*

# SHORT COMMUNICATIONS

## *On the Anion-Exchange Behavior of Some Quadrivalent Actinide Elements*

By Nobufusa SAITO and Tatsuya SEKINE

(Received April 5, 1957)

It has been well established that thorium (IV) is not adsorbed on an anion exchange resin from hydrochloric acid solution of any concentration. This fact makes it possible to separate thorium(IV) cleanly from any elements which do form negative ions adsorbable on an anion resin[1]. In 1953, Jenkins and Richardson studied the uptake of thorium(IV) on an anion exchange resin such as Deacidite FF, from solutions containing nitrate and sulfate[2].

The present authors are continuing a systematic study on the adsorbability of quadrivalent actinide elements on anion-exchange resins. It has been observed that thorium(IV) is adsorbed on Dowex 1 both from sulfate and carbonate solutions, while neptunium(IV) is adsorbed from carbonate solutions. The good uptake of uranium(IV) on that resin from a sulfate solution was also observed.

Dowex 1-X8 of 100–200 mesh was employed in this experiment. In column studies, resin columns of 5.0 cm. $\times$ 0.5 $cm^2$ were used. In equilibrium studies, Dowex 1 of sulfate form was first dried for three hours at 70°C and kept in a desiccator over a saturated solution of sodium bromide. The tracer solutions employed were thorium-234 in concentrated nitric acid and neptunium-239 in 6 N hydrochloric acid containing sulfur dioxide. The thorium(IV) solution was almost evaporated to dryness on a water bath and the residue was dissolved in solutions of ammonium sulfate or sodium carbonate of various concentrations. The neptunium (IV) solution was prepared by dissolving the residue in sodium carbonate solution containing a small amount of sulfur dioxide.

The radioactivity of the tracer was measured with a thin end-window Geiger-Müller tube after the tracer was coprecipitated with 5 mg. of ferric iron from acidified sample solutions with ferric hydroxide. In the case of samples containing thorium-234, the radioactive equilibrium between thorium-234 and protactinium-234 was attained at the time of measurement.

a) Experiments on thorium(IV) and uranium(IV) in solutions.

1) E. K. Hyde, Proceedings of the International Conference on the Peaceful Uses of Atomic Energy, Vol, 7, 281 (1956).

2) I. L. Jenkins and R. J. Richardson, A.E.R.E. C/R 1217. (1953).

i) Column studies.

After a resin bed of sulfate form was thoroughly washed with 0.1 M ammonium sulfate solution, 5 ml. of thorium(IV) solution was placed on the top of the column, and allowed to flow down through the column at a rate of 0.3–0.5 ml. per min.. The adsorption of thorium(IV) from 0.1 M ammonium sulfate solution was so complete that no activity of thorium-234 was detected in the effluent. The adsorbed thorium(IV) was easily eluted with 1 N hydrochloric acid solution. The elution curve is shown in Fig. 1.

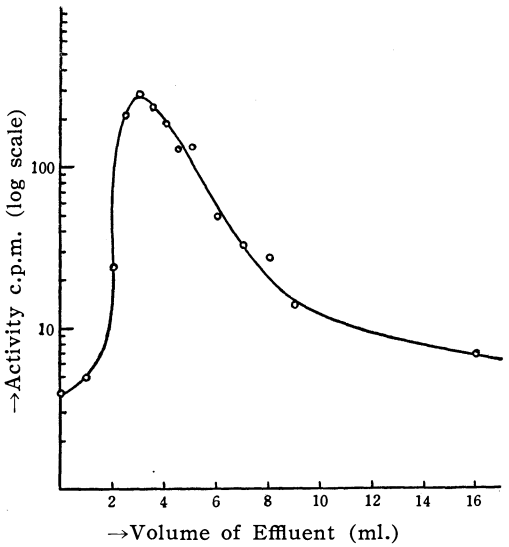



Fig. 1. The elution curve of Th(IV) with 1 N HCl. Column 5cm.×0.5cm² Dowex 1-X8 100-200 mesh.

Quadrivalent uranium, in macro quantities, was adsorbed on a resin bed of sulfate solution containing zinc, which was used for the reduction of uranyl ions. A green adsorption band appeared near the top of the bed. Washing of the column with 10 ml. of 0.01 M ammonium sulfate solution brought about no appreciable shift of the band. The adsorbed uranium (IV) was easily eluted with 6 N hydrochloric acid.

ii) Equilibrium studies.

Some experiments were carried out on thorium(IV). A weighed portion of the resin was allowed to stand overnight in a solution of ammonium sulfate under consideration. After the resin and the solution were placed in a glass-stoppered Erlenmeyer flask, the whole was shaken on a mechanical shaker in a thermostat at 25°C, until the exchange equilibrium was attained. In this case, a certain amount of thorium-232 was added to the tracer solution so that the equililbrium was reached at 0.1–1 % loading of thorium (IV) with respect to the resin capacity. The following values of the equilibrium distribution coefficient, $K_d$ (activity per g. of resin/activity per ml. of solution) were obtained: at 25°C, $K_d$=21 for the adsorption of thorium(IV) from 1 M ammonium sulfate solution, $K_d$=310 from 0.01 M ammonium sulfate solution.

b) Experiments on thorium(IV) and neptunium(IV) in carbonate solutions.

Only column studies were carried out. Thorium(IV) was adsorbed on a resin bed from 0.1 M sodium carbonate solution. No activity of thorium-234 was detected in the effluent. A part of adsorbed thorium (IV) was eluted with 10 ml. of 4 M ammonium chloride. Then most part of thorium(IV) was removed with 20 ml. of 6 N hycrochloric acid solution. A similar adsorption of neptunium(IV) from 0.1 M sodium carbonate solution was observed in preliminary experiments. The nature of adsorption of these elements from carbonate solution is not clear as yet.

Details of the present study will be published elsewhere in the near future.

The authors are indebted to Mr. Kunihiko Mizumachi of this laboratory for his helpful discussion.

*Department of Chemistry, Faculty of Science, The University of Tokyo, Hongo, Tokyo*

# *Anion Exchange Adsorption of Some Metals from Mixed Solvents*[1]

By Yukichi YOSHINO and Yoshimi KURIMURA

(Received January 7, 1957)

Recently K.A. Kraus and his coworkers[2] have carried out an extensive study on anion exchange adsorption of a number of metallic elements from a hydrochloric acid solution and its related media.

In the present paper, anion exchange adsorption data for zinc(II) and copper (II) from organic solvent—hydrochloric acid mixtures are described and the effect of the addition of the organic solvents are discussed.

## Experimental

**Materials.** — The anion exchanger used was polystyrene-divinylbenzene quarternary amine resin Dowex 1-X8, supplied as beads of 50–100 mesh. The resin was cycled twice with 1N sodium hydroxide and then with 1N hydrochloric acid; after complete conversion into the chloride form it was thoroughly washed with deionized water. The chloride resin was dried to constant weight in a desiccator over silica-gel. The resin thus obtained was found to have a capacity of 3.29 milliequiv. per gram. Dowex 1-X4 resin which was conditioned and dried in the same manner had a capacity of 3.15 milliequiv. per gram.

The organic solvents such as methanol, ethanol, *n*-propanol and acetone were all of "JIS"* first class grade and purified by distillation. Concentrated hydrochloric acid of "JIS" special class quality was used without further purification. Dilute hydrochloric acid was prepared from distillate of azeotropic mixture. Other chemicals are all of "JIS" special class grade and purified by distillation or recrystallization when necessary.

The zinc tracer** was $^{65}Zn$ ($T_{1/2}$=250 days). An aliquot of the hydrochloric acid solution was dried up and preserved as 0.1 M perchloric acid solution. The absorption characteristic and cation anion exchange chromatographic behavior showed that the tracer was of satisfactory purity.

**Measurement of Adsorbability.** — The adsorbability of the elements was measured by the equilibrium method and the results were described in terms of distribution coefficient $K_d$ defined as amount of element per gram resin/amount per milliliter solution. In the measurement of $K_d$ of zinc(II), a known weight of dry resin was added to 30 or 40 ml. of mixed solvents and was left overnight until swelling equilibrium was attained. Then 1 ml. of the tracer solution was added and the resulting solution was shaken mechanically in a thermostat at 25±0.1° for three hours. The supernatant solution was pipetted using filter-tubes packed with glass-wool and the radioactivity was measured with a Kobe Kogyo's dipping type G.M. counter of scale-of-64. Factors such as the geometry and the self-absorption were kept as constant as possible. From the resultant decrease in radioactivity of the solution, the values of distribution coefficients were calculated. Preliminary experiments revealed that the constancy of $K_d$ values was attained when the loading of the resin was kept less than ca. 0.5 % of resin capacity.

The distribution coefficient of copper(II) was estimated in the same manner as in the case of zinc(II) except that the decrease in the concentration was measured photometrically using carbamate method[3] (436 mμ). Extinction and spectra were measured by means of a Hitachi's EPU-2 spectrophotometer. The amount of copper was taken so as to be less than 1 % loading with respect to the resin capacity.

The chloride ion concentration was determined by titration with 0.1 or 0.01 N silver nitrate solution using Goodall and Mellor's dead-stop method[4].

## Results and Discussion

**Adsorption of Zinc(II) from Mixed Solvents.**—In Fig. 1, distribution coefficients of zinc(II) in hydrochloric solution containing 30 and 60 % (v/v) methanol were plotted against the molarity of hydrochloric acid (curve 2 and 3). For comparison, the adsorbability in a hydrochloric acid solution was shown by curve 1, which seems to conform very closely to Kraus's[2].

1) Presented at the Symposium on the Complex Compound Chemistry, October 27, 1956, Tokyo.

2) For example, K. A. Kraus and G. E. Moore, *J. Am. Chem. Soc.*, **75**, 1460 (1953); K. A. Kraus, F. Nelson and G W. Smith, *J. Phys. Chem.*, **58**, 11 (1954); K. A. Kraus and F. Nelson, Peaceful Uses of Atomic Energy, Proceedings of the International Conference in Geneva, Vol. VII, 113 (1955) United Nations.

* Japan Industrial Standard.

** Zn-65 (P-1) obtained from U. S. Atomic Energy Commission. The specific activity was 261 mC./g. Zn. on Dec. 23, 1955.

3) E. B. Sandell, "Colorimetric Determination of Traces of Metals" 304 (1950) Interscience Publishers, Inc., New York.

4) R. R. Goodall and N. Mellor, *Anal. Chim. Acta*, **5**, 373 (1952).

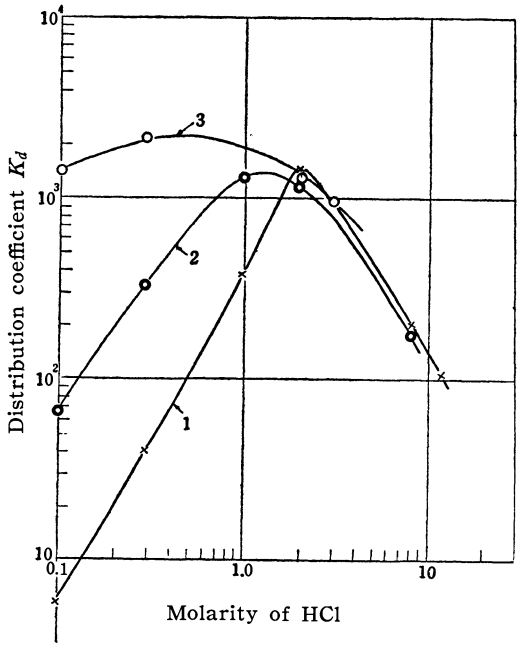



Fig. 1. Anion exchange adsorption of Zn(II).
1. in HCl solution
2. in HCl-30% (v/v) methanol mixture
3. in HCl-60% (v/v) methanol mixture

It is clear that the addition of methanol increases the adsorbability of zinc (II) in the range of lower hydrochloric acid concentrations, i.e. less than 2 M, while in a higher concentration, the effect is not clear. An interesting feature of the results is that the more the concentration of the hydrochloric acid is decreased, the more pronounced the effect and, at the same time, adsorption maxima shift to lower hydrochloric acid concentration.

In order to see the details of the relation between the adsorbability and the concentration of the organic solvent, the distribution coefficient of zinc(II) in various mixed solvents containing methanol, ethanol, *n*-propanol or acetone was examined at constant hydrochloric acid concentration i.e. 0.1 M. The results were summarized in Fig. 2.

The addition of these materials was found to be likewise effective for increasing of the adsorbability of zinc(II). In general the straight line relation between the logarithm of distribution coefficient and the concentration of organic solvents was observed in the range up to at least ca. 60 %. The order of the effect to increase the adsorbability of zinc(II) on the weight bases is:

Acetone≧ethanol>methanol>n-propanol

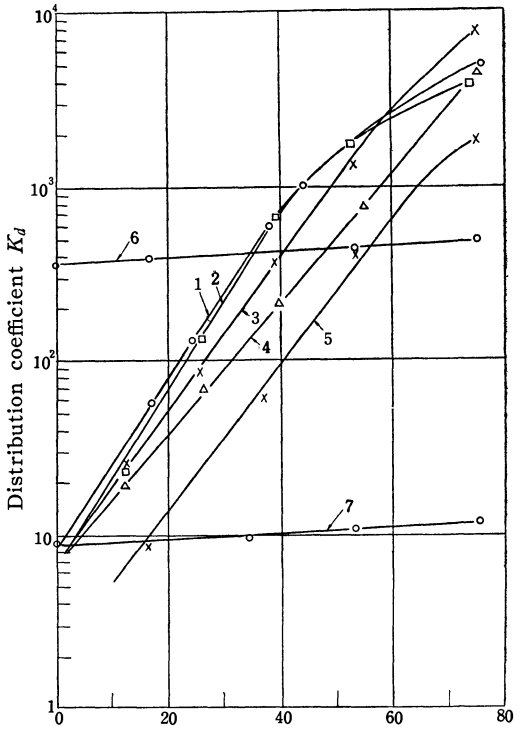



Fig. 2. Effects of various organic solvents on the anion exchange adsorption of Zn(II) in 0.1 M HCl.
1. Acetone
2. Ethanol
3. Methanol
4. *n*-Propanol
5. Methanol(Dowex 1-X4)
6. $RNO_3+Cl^-$, $\mu=0.003$, (NaCl) Methanol
7. $RNO_3+Cl^-$, $\mu=0.1$, ($KNO_3$) Methanol

The experimental data using less cross-linked resin (Dowex 1-X4) in methanol-hydrochloric acid media were also plotted in Fig. 1 (curve 5). The result is very similar to those of 8 % cross-linked resin except that the lower $K_d$ values were obtained.

In the cation exchange equilibria involving alkali and alkaline earth metal ions, Sakaki and Kakihana[5] had previously pointed out that the effect of addition of an alcohol depends, as a first approximation, on the dielectric constants of mixed solvents and is indifferent to the kind of alcohol added, i.e. methanol or ethanol. In the authors' experiments, this relation

5) T. Sakaki and H. Kakihana, *Kagaku (Science)*, **23**, 71 (1953).
T. Sakaki, This Bulletin, **28**, 217, 220 (1955).

was also proved to hold in the media containing methanol and ethanol but the relation no longer holds in cases of other solvents as is seen in Fig. 3.

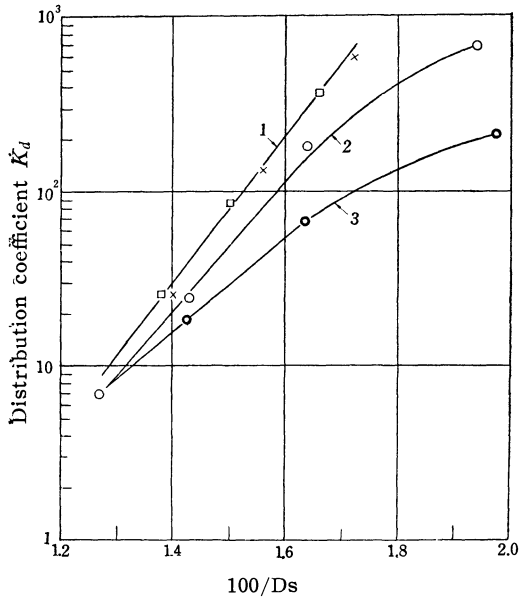



Fig. 3. Relation between $K_d$ of Zn(II) and dielectric constants of solutions in at 0.1 M HCl.
1. Methanol (-×-×-), Ethanol (-□-□-)
2. Acetone
3. *n*-Propanol

Then as a base of comparison, a simple ion, i.e. a chloride ion was equilibrated to the nitrate resin in methanol-water mixtures (curves 6 and 7 in Fig. 2). In this case, the solvent effect was found to be slight as compared with the case described above.

Kraus[2] suggested that in the elements which show adsorption functions with maxima such as zinc(II), cadmium(II) and gallium(III), the portion of increasing absorbability with increasing hydrochloric acid concentrations is due to the formation of the negatively charged complexes and that the maxima occur at approximately those hydrochloric acid concentrations where the negatively charged complexes become predominant. In view of this, all the experimental data described above seem to imply that the addition of organic solvents favors the dehydration of aquated zinc ions and consequently favors the stepwise formation of negatively charged chloro-complexes as may be expressed by the following set of equations,

$$Zn(H_2O)_4^{2+}+Cl^- \longrightarrow ZnCl(H_2O)_3^+ + H_2O$$
$$ZnCl(H_2O)_3^+ + Cl^- \longrightarrow ZnCl_2(H_2O)_2 + H_2O$$
$$ZnCl_2(H_2O)_2 + Cl^- \longrightarrow ZnCl_3(H_2O)^- + H_2O$$
$$ZnCl_3(H_2O)^- + Cl^- \longrightarrow ZnCl_4^{2-} + H_2O$$

**Adsorption of Copper(II) from Mixed Solvents.**—According to Kraus[2], the adsorbability of copper(II) from hydrochloric acid solution is relatively weak, showing a flat maximum in ca. 7 M hydrochloric acid (the elution constant E=ca. 0.1). The results of our measurements up to 8 M hydrochloric acid are shown by curve 1 in Fig. 4, which seems to be in fairly good agreement with Kraus's results. The effect of addition of methanol to this system is summarized in Fig. 4, (curves 2, 3, 4).

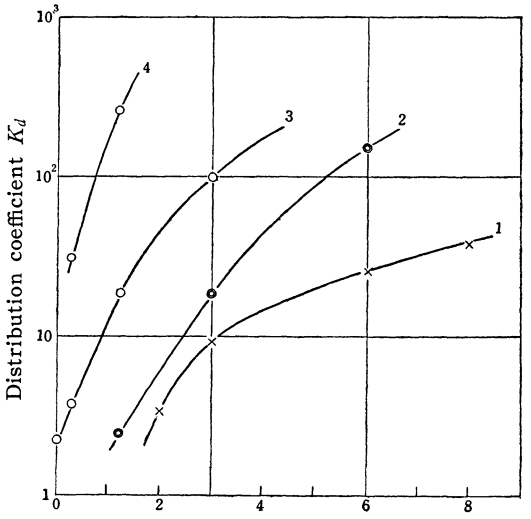
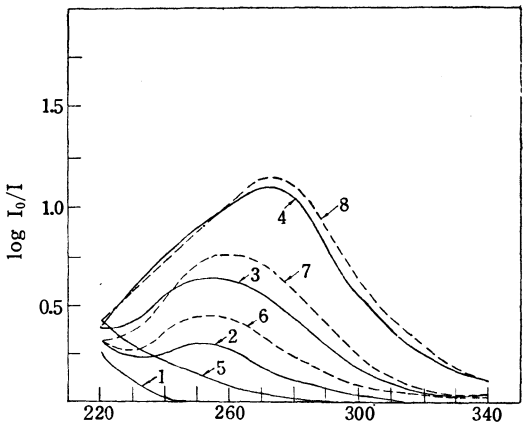



Fig. 4. Effect of methanol addition on the anion exchange adsorbability of Cu(II).
1. HCl only
2. 30% (v/v) methanol
3. 60% (v/v) methanol
4. 80% (v/v) methanol

In comparison to the case of zinc(II), the increase in the adsorbability of copper(II) in the presence of methanol was observed up to higher hydrochloric acid concentrations: This fact seems to suggest that the negatively charged complexes of Cu(II) are not completely formed throughout the range of hydrochloric acid concentration studied.

This may also be understood by the adsorption spectra of the copper(II) solution in the ultraviolet region*. As is seen

* The absorption spectra of chloro-complexes of zinc (II) in the ultraviolet region could be detected only in the range of higher zinc(II) concentration (more than 1 M) where the constancy of $K_d$ can no longer hold and the experimental results are not comparable with each other.




Wave length, mμ

Fig. 5. Absorption spectra of Cu(II) in HCl or HCl-methanol mixtures.
$Cu(ClO_4)_2$, $4\times10^{-4}$ M, Cell, 10 mm
1. in water
2. 1.2 M HCl
3. 3.0 M HCl
4. 5.0 M HCl
5. 80% (v/v) methanol
6. 1.2 M HCl-30% (v/v) methanol
7. 1.2 M HCl-60% (v/v) methanol
8. 1.2 M HCl-80% (v/v) methanol

from the curves 6, 7 and 8 in Fig. 5, the increase of methanol concentration in the 1.17 M hydrochloric acid solution of copper (II) resulted in the increasing formation of chloro-complexes in just the same manner as in increasing the concentration of hydrochloric acid in the absence of methanol (curves 2, 3, 4).

Katzin and Gebert[6] have found the adsorption of various inorganic salts onto anion exchange resin from their solution in acetone and suggested as a possible mechanism that the salts of transition elements might be adsorbed as complex anions. On the other hand, Davies and Owen[7] have postulated the possibility of the passage of the salts from acetone solutions into the resin phase from the standpoint of unequal partition of the solvents between both phases.

However, it was ascertained that tracer scale calcium chloride ($^{45}CaCl_2$*) in 0.1 M hydrochloric acid-methanol solution showed only negligible adsorption in the range less than 80% methanol. Therefore, under the conditions of our experiments, where the content of water is relatively high, the pronounced effect of increase in the adsorbability of zinc(II) and copper(II) might, if not completely, be explained by the dehydration effect of organic solvents added.

The remarkable rise in the adsorbability of the elements in the regions of relatively low hydrochloric acid concentrations may be of great use in the anion exchange separation of the elements which show only slight adsorption in dilute hydrochloric acid solutions and also in their rapid determination using the methods other than radiometry, e.g., complexometric titration[8].

## Summary

1) It was found that the addition of some organic solvents such as methanol, ethanol, *n*-propanol and acetone to the hydrochloric acid solution of zinc(II) and copper(II) increases the anion exchange adsorption of the elements in the range of relatively low hydrochloric acid concentrations (less than 2 M). In the 0.1 M hydrochloric acid solution, the straight line relation between log $K_d$ and concentration of organic solvent was observed up to ca. 60 %.

2) In the case of copper(II), this effect of increasing the adsorbability was observed up to higher hydrochloric acid concentrations i.e., at least 8 M, which seems to reflect that the adsorption maximum occurs at a higher hydrochloric acid concentration than in the case of Zn(II).

3) It was suggested that these solvent effects may be, as a first approximation, explained by the increase in the formation of negatively charged chloride complexes of the metals as a consequence of the decrease in the tendency for solvation of metallic ions in mixed solvents.

The authors wish to express their appreciation to Mr. K. Mizumachi for his suggestion and also to Messrs. M. Kojima and M. Nishikawa for their assistance in part of the experiment. The expense of this study was supplemented by a grant from the Ministry of Education, to which the authors' thanks are also due.

*Department of Chemistry, The College of General Education, The University of Tokyo, Komaba, Meguro-ku, Tokyo*

6) L. I. Katzin and E. Gebert, *J. Am. Chem. Soc.*, **75**, 801 (1953).

* Ca-45 (P-2) ($T_{1/2}$=164 days), obtained from Atomic Energy Commission of U. S. A.. Its specific activity was 14.59 mC./g. solid on Feb. 10, 1955.

7) C. W. Davies and B. D. R. Owen, *J. Chem. Soc.*, **1956**, 1676.

8) For example, G. Schwarzenbach, "Die komplexometrische Titration" 2nd Ed. (1956), Ferdinand Enke Verlag, Stuttgart.

# *Photometric Determination of Thallium with Rhodamine B*

By Hiroshi ONISHI

(Received January 28, 1957)

In an earlier communication[1] a photometric method for the determination of thallium with rhodamine B was briefly described. The purpose of the present paper is to treat the same subject in greater detail. The extraction with dithizone in chloroform was adopted for the separation of thallium from other elements. Although the recoveries of thallium are slightly low, the proposed method may be of general use for the determination of traces of this element.

## Experimental

**Apparatus.** Absorbance measurements were made with Hitachi Models EPB-U and EPV-2 spectrophotometers, using 1-cm. cells. At a later stage of the present investigation, the EPV-2 spectrophotometer was exclusively used.

**Solutions.** *Ammonium citrate*, 20 g. of $(NH_4)_2HC_6H_5O_7$ in 100 ml. of water.

*Potassium cyanide*, 10 g. in 100 ml. of water.

*Hydroxylamine hydrochloride*, 20 g. in 100 ml. of water.

*Dithizone*, 0.50 g. in 500 ml. of redistilled chloroform. Purify it freshly before use by washing the dithizone solution three times with 1 : 100 nitric acid, and then three times with 1 : 1000 ammonium hydroxide.

*Rhodamine B*, 0.20 g. in 100 ml. of water.

*Standard thallium solution.* Dissolve 0.124 g. of pure $Tl_2SO_4$ in 100 ml. of 0.5 N sulfuric acid. From this stock solution (1.00 mg. Tl per ml.) prepare a working standard solution containing 0.010 mg. (10 $\mu$g.) of Tl per ml. by diluting with 0.5 N sulfuric acid. This solution can be kept for at least two weeks.

**Procedure.** Transfer the sample solution (1–10 $\mu$g. Tl in a volume of about 30 ml.), which may conveniently be about 0.1 N in sulfuric acid, to a beaker and add 10 ml. of ammonium citrate solution. Add a few drops of thymol blue indicator solution and 1 : 1 ammonium hydroxide until the color turns blue. If, because of the presence of heavy metals, no color change can be definitely observed, adjust pH of the solution to 10 by the use of a pH meter.

Add 15 ml. of potassium cyanide solution and after a few minutes add 5 ml. of hydroxylamine hydrochloride and 3 ml. of 1 : 1 ammonium hydroxide, mix, and let stand for a few minutes. If the color of the solution fades to a blue color, or nearly so, transfer the solution to a separatory funnel. If the deep red color produced does not fade appreciably upon standing for a few minutes, heat the solution on a water bath for 3–5 minutes, and then cool with water. Transfer the solution to a separatory funnel and wash the beaker with 10 ml. of 1 : 1000 ammonium hydroxide.

*Extraction of thallium.* Shake the solution for one minute with 10 ml. of dithizone solution. When the layers have separated, drain off the chloroform phase into another separatory funnel. Extract further the aqueous phase with two 10 ml. portions of dithizone solution. Combine the extracts and discard the aqueous layer. Wash the extracts with 10–20 ml. of 1 : 1000 ammonium hydroxide followed by 10–20 ml. of water. Drain the chloroform phase into another separatory funnel and shake vigorously for one minute with 10 ml. of 1 : 100 nitric acid to extract thallium. Draw off the chloroform into another separatory funnel and extract with another portion (5–10 ml.) of nitric acid. Drain off and discard the chloroform layer and transfer the aqueous extracts to a 50 ml. beaker containing 0.50 ml. of 1 : 5 sulfuric acid, rinse the separatory funnels with 1–2 ml. of 1 : 100 nitric acid and evaporate to fumes. When the sulfuric acid residue shows a brown color due to the presence of organic matter, add about 20 mg. of ammonium persulfate and allow to fume for a few minutes. Repeat this step until a colorless solution is obtained.

Cool, add 5.0 ml. of 2.0 N hydrochloric acid and 1.0 ml. of saturated bromine water. Heat near the boiling point and stop heating when the color due to bromine has disappeared. Cool to room temperature, transfer the solution to a 10 ml. volumetric flask and dilute to the mark with 2.0 N hydrochloric acid.

*Determination of thallium.* Transfer the solution to a separatory funnel as completely as possible, add 1.0 ml. of rhodamine B solution and mix. Without undue delay add 10.0 ml. of pure benzene and shake for one minute. When the two phases have separated, drain off the aqueous phase, transfer the benzene layer into a centrifuge tube, and centrifuge for about 2 minutes. Measure the absorbance of the clear benzene extract at 560 m$\mu$, using benzene as the reference solution.

Establish the standard curve by taking, for example, 0, 2, 4, 7, and 10 $\mu$g. of thallium into beakers respectively, adding 0.50 ml. of 1 : 5 sulfuric acid, 5.0 ml. of 2.0 N hydrochloric acid, 1.0 ml. of bromine water, and proceeding as described above. Run a blank through the entire procedure.

1) H. Onishi, This Bulletin, **29**, 945 (1956).

As the recoveries of thallium are slightly low, a correction of +10 per cent. is probably advisable. See **Discussion.**

## Results and Discussion

**Photometric Determination of Thallium.** Bromine is a very satisfactory reagent to oxidize univalent thallium to tervalent. Excess of bromine can be easily removed by heating. The use of ammonium persulfate to destroy organic matter in the residue from the evaporation of nitric acid extract gave an opportunity to find another suitable oxidizing agent for thallium (Fig. 1). Oxidation with ammonium persulfate was effected in the following way. A known amount of thallium and 0.50 ml. of 1:5 sulfuric acid in a 50 ml. beaker were heated on a sand bath to fumes, about 20 mg. of ammonium persulfate was added and heated while whirling the beaker. After cooling

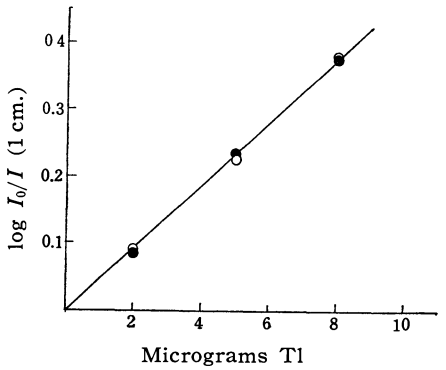



Fig. 1. Oxidation of thallium (I) with ammonium persulfate and bromine.
●: ammonium persulfate
○: bromine
1.6 N HCl, Hitachi EPV-2 spectrophotometer, 560 mμ.

the same amount of persulfate was again added and evaporated to fumes. A few drops of water were added and evaporated to fumes. Ten ml. of 2.0 N hydrochloric acid was added followed by rhodamine B-benzene extraction. When ammonium persulfate is left undecomposed and brought to rhodamine B extraction, rhodamine B is oxidized and erratic results are obtained. The above procedure eliminates this defect. However, that procedure appeared to be slightly more troublesome, so the step of bromine oxidation has been retained in the proposed procedure. Excess of persulfate was decomposed during the treatment with bromine. Tervalent thallium obtained by either oxidation procedure was stable for at least one hour. Several other reagents were tried to oxidize thallium, but it was difficult to remove excess of any reagent without affecting the thallium. An attempt to remove the excess with an excess of rhodamine B was unsuccessful.

The absorptions pectrum (in benzene) of rhodamine B chlorothallate, which is considered to be the compound of thallium (III) with rhodamine B, is shown in Fig. 2. Correction is applied to the reagent blank. The absorption peak is found at

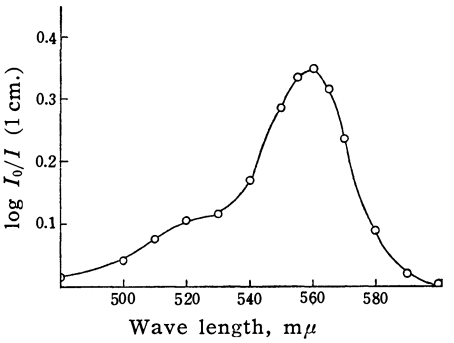



Fig. 2. Absorption spectrum of rhodamine B chlorothallate in benzene (0.8 p.p.m. Tl in benzene). Hitachi EPB-U spectrophotometer.

560 mμ. It is of interest to compare this peak with that of other compounds of the type $(RH)M^{III}Cl_4$ (R=rhodamine B). Rhodamine B chloroantimonate, $(RH)SbCl_6$, shows the maximum at 564 mμ, and rhodamine B chlorogallate at about 565 mμ[2]. The maximum of $RH^+$ in water was found to be at 556 mμ[3]. It does not seem that the absorption spectra of $(RH)FeCl_4$ and $(RH)AuCl_4$ have been described. At any rate, all three known compounds in benzene show the absorption peak at about 560 mμ. Moreover, the shapes of their absorption spectra are quite similar. The molar absorptivities of thallium, gallium, and antimony are 96,000*, 60,000, and 100,000 respectively. The value for $RH^+$ in water is 110,000[3]. It may be concluded that the deep coloration of these compounds is mainly due to $RH^+$ species.

The extractability of rhodamine B

2) H Onishi and E B Sandell, *Anal. Chim. Acta*, **13**, 159 (1955).
3) R. W. Ramette and E. B. Sandell, *J. Am. Chem. Soc.*, **78**, 4872 (1956).
* A value of 87,000 was given in the previous paper. The EPB-U spectrophotometer gave low absorptivities.

chlorothallate as a function of hydrochloric acid concentration is shown in Fig. 3. The concentration was calculated and

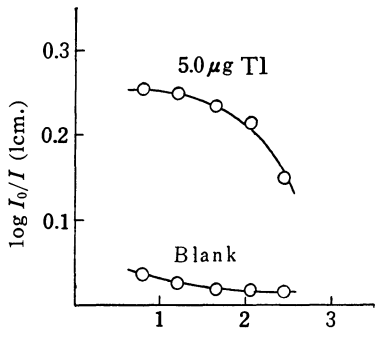



Fig. 3. Extractability of rhodamine B chlorothallate as a function of hydrochloric acid concentration. Hitachi EPV-2 spectrophotometer, 560 mμ.

correction was not made for evaporation loss during the treatment with bromine. A half ml. of 1 : 5 sulfuric acid was present in each case. In the figure 1.6 N corresponds to the concentration of hydrochloric acid in the proposed procedure.

It is seen that the acid concentration must be kept constant to get reproducible results. Consequently heating in bromine treatment must always be done in the same way. At each hydrochloric acid concentration studied, i.e., 0.8, 1.2, 1.6, 2.0, and 2.5 N, the absorbance was proportional to thallium concentration in the range 0.1 to at least 1 p.p.m. (based on the amount of thallium present originally in the aqueous phase).

The effect of the concentration of rhodamine B (reagent grade, Katayama Chemical Works, Osaka) on the absorbance of rhodamine B chlorothallate in benzene is shown in Fig. 4. Corrections for reagent blanks were made. In all cases the hydrochloric acid concentration was maintained at 2.0 N (slightly higher than the acidity recommended for **Procedure**). The absorbance increases very slightly with an increase in the concentration of rhodamine B, and the reagent blank also increases slightly. In the present investigation, about $4\times10^{-4}$ M in rhodamine B (or 1.0 ml. of 0.20 % rhodamine B solution) was adopted. At the concentration the reagent blank was in the range 0.010~0.020 against pure benzene. The extraction coefficient for 1.6 N hydrochloric acid and 0.00038 M rhodamine B in the aqueous phase is

$$\frac{[Tl]_{benzene}}{[Tl]_{H_2O}}=13 \quad \text{(from Table 1)}$$

This constant is independent of the thallium concentration in the range investigated. Consequently the volume of the aqueous phase must be maintained constant for reproducibility.

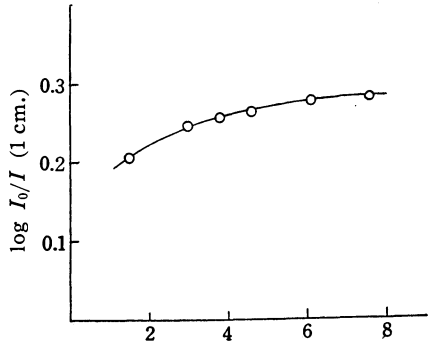



Fig. 4. Effect of rhodamine B concentration on absorbance of rhodamine B chlorothallate. 6.0 μg. Tl taken, 2.0 N HCl, Hitachi EPB-U spectrophotometer.

TABLE I

EXTRACTABILITY OF RHODAMINE B CHLOROTHALLATE WITH BENZENE

[Aqueous phase (11 ml.) 1.6 N in HCl and 0.00038 M in rhodamine B; 10 ml. benzene; temperature 18–20°C]

| Tl present, μg. | 4.0 | 6.0 | 10.0 |
|---|---|---|---|
| Absorbance of first extract (560 mμ) | 0.175 | 0.262 | 0.435 |
| Absorbance of second extract (10 ml.) | 0.013 | 0.022 | 0.033 |
| Extraction coefficient* | 14.5 | 12 | 13.5 |

* Average is 13.

The absorbance of the benzene extract does not change for at least one hour (Table II).

TABLE II

STABILITY OF BENZENE EXTRACT

| Time after extraction, min. | I | II | III |
|---|---|---|---|
| 5 | 0.221 | 0.366 | 0.420 |
| 30 | 0.218 | 0.364 | 0.419 |
| 60 | 0.217 | 0.363 | 0.427 |

Most of the colorimetric methods available at the present time are indirect. The iodine method by Haddock[4] was used for the determination of 10–200 μg. of thallium after extraction with dithizone. Thallium

4) L. A. Haddock, *Analyst*, **60**, 394 (1935).

TABLE III

DETERMINATION OF THALLIUM WITH RHODAMINE B AFTER DITHIZONE-CHLOROFORM EXTRACTION

| Addition | Tl taken, μg. | Tl found, μg.* | | Tl recovered, % | |
|---|---|---|---|---|---|
| | | Single $HNO_3$ extraction | Double $HNO_3$ extraction | Single $HNO_3$ extraction | Double $HNO_3$ extraction |
| none | 2.2 | 1.9**, 2.1** | | 86**, 95** | |
| none | 5.0 | 5.0**, 5.2**, 4.2, 4.5 | 4.5, 4.7 | 100**, 104**, 84, 90 | 90, 94 |
| none | 5.5 | 5.7**, 5.0**, 5.9**, 5.5** | | 104**, 91**, 107**, 100** | |
| none | 8.7 | 7.8**, 7.8** | | 90**, 90** | |
| 10 mg. Cu, 10 mg. Ni | 5.0 | 4.6 | | 92 | |
| 1.0 mg. Ag, 1.1 mg. Pt | 5.0 | 4.2 | | 84 | |
| 1.2 mg. Au(III), 1.0 mg. Sb(III) | 5.0 | 4.9, 4.7 | | 98, 94 | |
| 10 mg. Zn, 10 mg. Hg(II) | 5.0 | | 4.7 | | 94 |
| 40 mg. Al, 1.1 mg. Ga | 5.0 | 4.4 | | 88 | |
| 1.1 mg. In | 5.0 | | 4.7 | | 94 |
| 1.0 mg. Ge(IV), 1.0 mg. Sn(II) | 5.0 | | 4.6 | | 92 |
| 1.0 mg. Pb | 5.0 | | 4.5 | | 90 |
| 10 mg. P(as $KH_2PO_4$), 1.0 mg. As(III) | 5.0 | | 4.6 | | 92 |
| 1.0 mg. Bi | 5.0 | | 4.6 | | 92 |
| 1.0 mg. Mo(VI), 1.0 mg. W(VI) | 5.0 | | 4.4 | | 88 |
| 50 mg. Fe(III) | 5.0 | 4.2, 4.2 | | 84, 84 | |
| 100 mg. Fe(III) | 2.0 | 1.7 | | 85 | |
| 100 mg. Fe(III) | 5.0 | 4.3, 4.1 | 4.6, 4.5 | 86, 82 | 92, 90 |
| 100 mg. Fe(III) | 8.0 | 6.6 | | 83 | |

* Correction applied for blank: 0.0 μg. with no addition, and with Cu+Ni, Ge+Sn, Pb, P+As, Mo+W, and Fe; 0.1 μg. with Au+Sb, Zn+Hg, and Al+Ga; 0.2 μg. with Ag+Pt; 0.3 μg. with In; and 0.4 μg. with Bi.

** $NH_2OH \cdot HCl$ added before KCN, ammonium citrate, and $NH_4OH$.

dithizonate in chloroform was evaporated to dryness followed by oxidation with hydrogen peroxide.

Berg et al.[5] described the determination with thionalide. Among the newer colorimetric methods, the *p*-phenetidine method[6] has a sensitivity of about 0.3 μg. Tl/cm$^2$ corresponding to $\log I_0/I=0.001$, or a molar absorptivity of 6,000. Iron and gold interfere with the determination. Neither the dibenzyldithiocarbamate[7] nor thallium hydroxide[8] methods are sensitive; the molar absorptivity of the former is 1,340 and that of the latter 561. Colorimetric determination of cobalt with nitroso-R salt after precipitation of $[Co(NH_3)_6]TlCl_6$ gave the amount of thallium indirectly[9]. This precipitate was also utilized for the radiometric determination of thallium by means of radioactive cobalt[10,11]. This method and also the radioactivation method[12] appear to be as sensitive as the rhodamine B method described here.

**Separation of Thallium.** Metals that must be separated because of more or less sensitive color reaction with rhodamine B are antimony, gold, iron, and tungsten. As much as 1 mg. of gallium in 2 N hydrochloric acid does not give any appreciable color and does not interfere with the determination of thallium. As a method of separation of thallium, the extraction with dithizone is thought to be superior to the ether extraction of chloride or bromide. By the ether extraction gold will be extracted with thallium and it must be separated by an appropriate method, e.g., reduction to metal and filtration.

5) R. Berg, E. S. Fahrenkamp, and W. Roebling, *Mikrochemie* (Molisch Festschrift), 42 (1936).
6) S. Iijima and Y. Kamemoto, *J. Chem. Soc. Japan, Pure Chem. Sect.*, **75**, 1294 (1954).
7) W. T. Foley and R. F. Pottie, *Anal. Chem.*, **28**, 1101 (1956).
8) V. K. Zolutukhin and A. S. Molotkova, *Zhur. Anal. Khim.*, **11**, 248 (1956).
9) T. Nozaki, *J. Chem. Soc. Japan, Pure Chem. Sect.*, **77**, 493 (1956).
10) T. Ishimori, This Bulletin, **26**, 336 (1953).
11) T. Ishimori and Y. Takashima, *J. Chem. Soc. Japan, Pure Chem. Sect.*, **76**, 858 (1955).
12) C. J. Delbecq, L. E. Glendenin and P. H. Yuster, *Anal. Chem.*, **25**, 350 (1953).

Dithizone extraction of thallium has been investigated by several workers. It is well known that the only metals reacting with dithizone in a slightly basic medium containing cyanide are bismuth, lead, thallium, and tin. Except thallium, none of these reacts with rhodamine B. Recently Ishimori[10,11] determined traces of thallium radiochemically after its separation with dithizone. His results showed that the recoveries of thallium were 46 to 67%, and the loss was found to occur when thallium was extracted with dilute nitric acid from dithizone-chloroform solution. Evaporation of dithizone-chloroform extract followed by oxidative decomposition of organic matter will undoubtedly bring better recoveries. This method is, however, not very convenient. In the present work, Ishimori's procedure was first reexamined. Thallium was reduced with hydroxylamine hydrochloride, and potassium cyanide and ammonium citrate were added. The pH of the solution was adjusted to about 10 by adding ammonium hydroxide. The dithizone extraction was then carried out. In the absence of foreign metals, the recoveries were satisfactory as shown by the results marked by ** in Table III. However, when the procedure was applied in the presence of iron(III), the recoveries of thallium became extremely low and yet the blank became higher. The present investigation has confirmed that the method of Sill and Peterson[13] eliminated this difficulty.

Results obtained in applying the proposed method are collected in Table III. Most of the metals added were in the form of chloride, but some were sulfates or nitrates. It is seen that double nitric acid extraction is preferable to single extraction. In the presence of relatively large amounts of the metals reacting with dithizone, the extraction will have to be carried out more than three times. The recoveries of thallium were slightly low and it is believed that the application of a correction factor of +10% is advisable. If the values in the table are increased by this amount, the recoveries become generally within 5% of the theoretical values.

## Summary

Procedure is given for the spectrophotometric determination of 1–10$\mu$g. of thallium with rhodamine B. Ammonium persulfate was also found to be as effective as bromine in oxidizing thallium preparatory to rhodamine B—benzene extraction. For the separation of thallium from other elements, univalent thallium is extracted with dithizone in chloroform from a basic solution containing cyanide and then transferred to an aqueous solution by shaking the chloroform with dilute nitric acid. The procedure provides for the presence of antimony, gallium, gold, iron and tungsten.

*Government Industrial Research Institute, Nagoya, Kita-ku Nagoya*

13) C. W. Sill and H. E. Peterson, *Anal. Chem.*, **21**, 1268 (1949).

# *Relation between Foaming Properties and the Structure of Surface Active Substances. I. Foaming Properties of Aqueous Soap and Sodium Dodecyl Sulfate*

By Maresuke KASHIWAGI

(Received January 25, 1957)

## Introduction

As was previously reported[1], the foaming power of aqueous sodium dodecyl sulfate (hereafter called SDS) is a function of concentration, and the critical micelle concentration (hereafter called cmc.) can be determined by this method. In a similar fashion, any other surface active substances may be closely correlated to the structure of its solution.

According to the foaming power measurement by Ross-Miles' method, the foaming power of SDS increases with concentration up to cmc. and above the cmc. it becomes nearly constant. In the light of this knowledge, the foaming power measurement of soap, a most typical surface active substance, carbon numbers of which range from ten to sixteen, was undertaken. The mechanism of foaming may be explained partly by Debye's theory[2] and at the same time by surface tension.

Since some inorganic ions are known to lower surface tension, the foaming properties of soap may be expected to be increased by the addition of those ions. In fact, the foaming power increases in the order of lyotropic series.

## Experimental

**Apparatus** — The apparatus used is the same as that of Ross-Miles[3]. The schematic diagram and the dimension were described in the author's previous report[1]. For surface tension measurement DuNouy's tensiometer was used.

**Materials** — The analysis of SDS was described in the previous report[1]. Soap used here is sodium salt of fatty acids which were prepared using fatty acids purchased from Merck and purified. The analysis is shown in Table I.

Inorganic salts, (LiCl, NaCl, KCl and RbCl) were all given by the courtesy of Dr. Y. Murakami, Faculty of Science, University of Tokyo.

**Measurement** — The temperature is kept by the thermostat at 40±0.1°C. All solutions are prepared under the same condition and the measurements are done right after the preparation of the solution, since soaps are very sensitive to temperature and time.

TABLE I
ANALYSIS OF FATTY ACIDS

| Acid | M. P. found | M. P. literature | N. V.* found | N. V.* theoretical |
|---|---|---|---|---|
| Capric | 32.3 | 31.6 | 320.3 | 325.70 |
| Lauric | 45.1 | 44.2 | 278.0 | 280.09 |
| Myristic | 54.0 | 54.4 | 242.9 | 245.67 |
| Palmitic | 60.8 | 63.1 | 213.7 | 218.80 |

* N. V.....Neutralisation Value

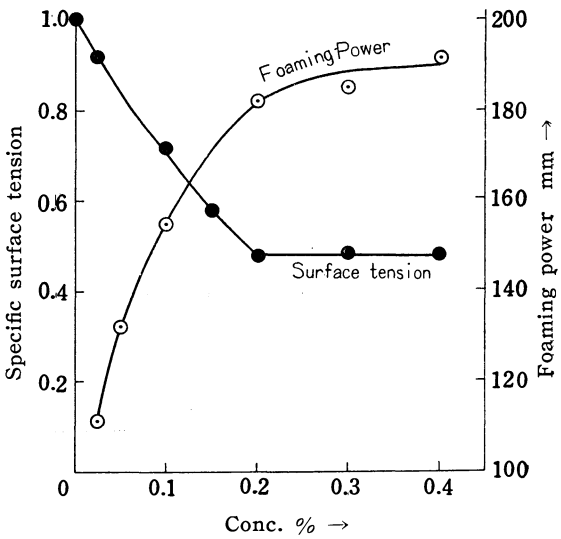



Fig. 1. Surface characteristics of sodium dodecyl sulfate.

## Results

Fig. 1 shows foaming power (i. e. height of the foam part, expressed in mm) and specific surface tension against concentration of SDS. Specific surface tensions are calculated from values measured by DuNouy's tensiometer. By comparing these curves it can be seen that there is a correlation between foaming power and surface tension ; that is, as foaming power

1) M. Kashiwagi, This Bulletin, **29**, 193 (1957).
2) P. Debye, *Ann. N. Y. Acad. Sci.*, **51**, 575-92 (1949).
3) J. Ross and G. D. Miles, *Oil and Soap.*, **18**, 99 (1941).

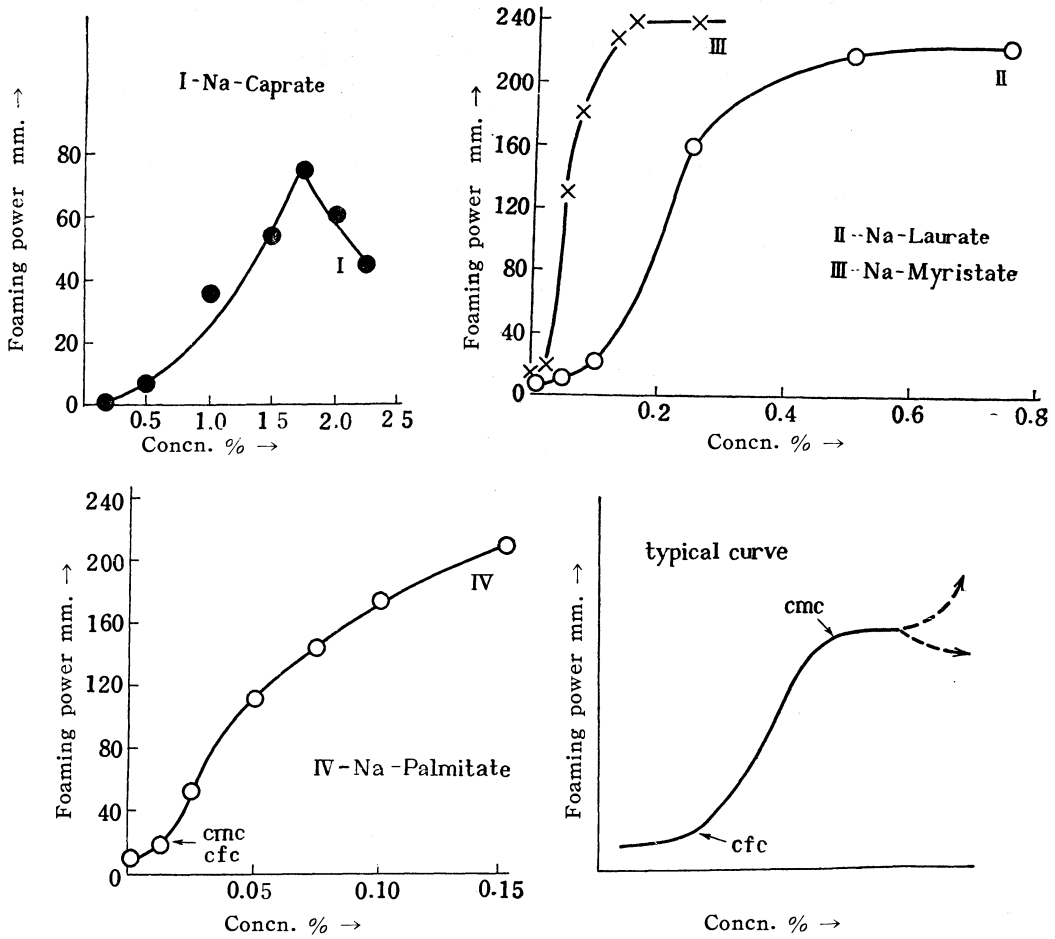



Fig. 2. Foaming power of soap.

increases, surface tension decreases and above the same cmc. both curves become practically constant.

Fig. 2 shows the foaming power of soap. As in the case of SDS already described, the tendency is again the same. The same sort of result was obtained for potassium soap by the other method; however, the method of Ross-Miles seems to be more accurate than this shaking method[4].

From the curves which appeared in Fig. 2, it was found that sodium myristate has more pronounced foaming power than others. Sodium stearate was also studied, but its foaming power was found to be too poor. Since the addition of inorganic ions is known to affect surface tension, it was thought to be interesting to add to soap neutral salts of the series lithium, sodium, potassium and rubidium chloride. Table II shows the influence of the addition of those inorganic salts on 0.1% sodium myristate.

TABLE II
INFLUENCE OF INORGANIC SALTS ON FOAMING POWER
(AVERAGE FOAMING POWER IN mm.)

| Salt | Salt concn. | $10^{-2}$ M | $10^{-1}$ M |
|---|---|---|---|
| LiCl | | 244 | salting out |
| NaCl | | 240 | 245 |
| KCl | | 228 | 230 |
| RbCl | | 228 | 220 |
| None | | 210 | 210 |

It is demonstrated that inorganic ions raise the foaming power of soap in the order $Li^+ > Na^+ > K^+ > Rb^+$.

Nevertheless, the difference between each ion at the concentration of $10^{-2}$ M is only slightly noticeable and ten times increase in concentration of salt did not raise the foaming power noticeably.

4) M. Nakagaki and K. Shinoda, This Bulletin, **27** 367 (1954).

## Discussion

Hobbs[5] derived the following expression by thermodynamic consideration of micelle formation from single molecule.

$$\log \text{cmc.} = -K_0\beta + \text{constant} \qquad (1)$$

Where $\beta$ is the number of carbon atoms in the chain and $K_0$ is constant.

Empirical values of cmc. determined by the foaming power measurement as appeared in Fig. 2 are shown, together with some constants from the measurement, in Table III.

Those measured values of cmc. were found to fit the above equation and the constants are calculated as follows,

$$\log \text{cmc.} = -0.314\,\beta + 1.796 \qquad (2)$$

It might also be added that they are in good agreement with values determined by other methods[6].

Sodium palmitate deviates a little from the above equation, but this should be attributed to the fact that its cmc. can not be distinguished from cfc.

TABLE III
SOME PHYSICAL CONSTANTS OF SOAP

| No. of carbon atoms | cmc. mol/l. | Critical* foam conc. M | Approximate expansion ratio at cmc.** |
|---|---|---|---|
| 10 | 0.0902 | 0.05 | 19 |
| 12 | 0.0228 | 0.009 | 58 |
| 14 | 0.0049 | 0.001 | 58 |
| 16 | 0.0009 | 0.0009 | 28 |

* Critical foam concentration is defined by the author as the concentration at which foaming begins and below which foaming is negligibly small.

** Expansion ratio: $V_f/V_l$ where $V_f$ is the volume of foam converted from liquid state and $V_l$ is the volume of liquid which has been converted into foam.

Although quantitative treatment has not yet been made, decrease in surface tension always seems to result in increase of foaming power as shown in Fig. 1.

For soap the same relationship seems to exist. Comparison of Fig. 2 with surface tension data of Powney and Addison[7] corresponds to this rule.

For foaming properties, the influence of ion seems to be more predominant than that of micelle, since foaming increases with concentration up to cmc. and above it becomes nearly constant. Debye[2] demonstrated through light scattering in soap solutions that, as the number of long chain ions per micelle is of the order of 100, single ionswill predominate below cmc. and above it their concentration will change only slightly. The effect of inorganic ions is in the order of lyotropic series as shown in Table II, but is only slightly noticeable. It is known that cmc. of some surfactants shifts on the addition of inorganic salts; however, change in cmc. is independent of the kind of salt, and depends only on the concentration of cation[8].

## Summary

1) The foaming power measurement by Ross-Miles method was found to be useful for the study of surface active substances.

2) A general rule for the foaming power would be that it increases with concentration up to cmc., and above it, becomes nearly constant or somewhat decreases. The foaming power is also inversely proportional to the surface tension.

3) The cmc. and other physical constants can be determined by the foaming power measurement.

4) Ion rather than micelle is presumed to be predominant with respect to foaming properties.

5) Effect of inorganic ions on foaming is slightly in the order of lyotropic series, namely $Li^+ > Na^+ > K^+ > Rb^+$, just before salting out.

The author expresses deep appreciation to Mr. H. Ezaki for permitting the publication and Dr. Y. Murakami for supplying inorganic salts.

*Mitsuwa Chemical Laboratory*
*Sumidaku, Tokyo*

5) M. E. Hobbs, *J. Phys. and Colloid Chem.*, **55**, 615 (1951).
6) E. K. Goette, *J. Colloid Sci.*, **4**, 459 (1949).
7) J. Powney and C. C. Addison, *Trans. Faraday Soc.*, **34**, 372 (1938).
8) M. L. Corrin and W. P. Harkins, *J. Am. Chem. Soc.*, **69**, 682 (1941).

# *Syntheses of 3-Alkyl-naphtho(1.2-b)furan-2-carboxylic Acids*

By Yuriko TANAKA

(Received January 28, 1957)

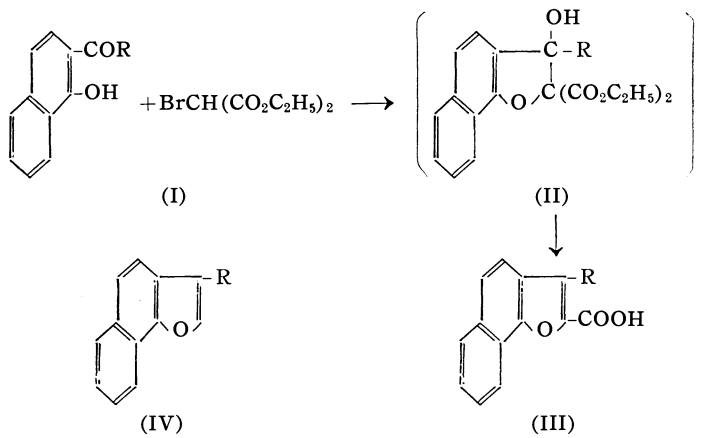
In connection with other synthetical works three 3-alkyl-naphtho(1.2-b)furan-2-carboxylic acids (III R=$CH_3$, $C_2H_5$, $n$-$C_3H_7$) were synthesized.

Search of literature revealed that of these three compounds only 3-methyl-naphtho(1.2-b)furan-2-carboxylic acid had been reported[1], but those synthetical methods are not preferable because of the complexity and the poor yield. Tanaka[2] reported a new general synthetic method for coumarones (benzofurans), and by using this method he synthesized phenanthro(1.2-b)furan derivatives[3]. For the syntheses of the substances mentioned above, his method was applied.

2-Aceto-1-naphthol (I, R=$CH_3$) and ethyl bromomalonate when refluxed in acetone in the presence of anhydrous potassium carbonate gave an oily substance, the structure of which is assumed to be II (R=$CH_3$). The last, without further purification, was hydrolysed with alcoholic potash and the carboxylic acid III(R=$CH_3$) was obtained. An attempt to decarboxylate the acid (III, R=$CH_3$) to 3-methyl-naphtho(1.2-b)furan (IV, R=$CH_3$) by refluxing in quinoline with copper powder[2] ended fruitless; by this procedure an oily substance with a peculiar smell of coumarones was obtained, but neither this oil nor its picrate showed satisfactory analytical value. As for the picrate, its analytical disagreement is likely due to its instability.

Starting from 2-propionyl- (I, R=$C_2H_5$) and 2-butyryl-1-naphthol (I, R=$n$-$C_3H_7$), the corresponding naphtho(1.2-b)furan-2-carboxylic acid (III, R=$C_2H_5$ and R=$n$-$C_3H_7$) were likewise synthesized in rather good yield (about 40%). Attempts to obtain the compounds IV (R=$C_2H_5$; $C_3H_7$) through decarboxylation of the corresponding acids III (R=$C_2H_5$; $C_3H_7$) were again unsuccessful just like the case III (R=$CH_3$) already mentioned.

The synthetic method used in the present paper is far superior to those described in the old literatures[1,*], so far as naphthofuran-2-carboxylic acids are concerned. The facts that the last acids hardly ever undergo decarboxylation are already stated in the literature[1c]. On the other hand benzofuran-2-carboxylic acids are smoothly[2] and phenanthro(1.2-b)furan-2-carboxylic acids are with difficulty decarboxylated[3]. Since the different behavior of decarboxylation of these




1) (a) A. Hantzsch, *Ber.*, **19**, 1303 (1886). (b) R. Stoermer, *Ann.*, **312**, 313 (1900). (c) St. v. Kostanecki and J. Tambor, *Ber.*, **42**, 908 (1909).

2) S. Tanaka, *J. Chem. Soc. Japan, Pure Chem. Sect.*, **72**, 307 (1951); ibid., **73**, 282 (1952); *J. Am. Chem. Soc.*, **73**, 872 (1951).

3) S. Tanaka and S. Kawai, Unpublished work.

* Naphtho(2.3-b)furan derivatives were synthesized by Stoermer (see ref. (1b)) and K. Takeda, T. Schimada and K. Kitanouchi, *J. Pharm. Soc. Japan*, **70**, 268 (1950).

polynuclear benzofuran-2-carboxylic acids attracted the author's interest, the present writer wishes to re-examine the decarboxylation of other sorts of 3-alkyl-naphtho-(1.2-b)furan-2-carboxylic acid in the future.

## Experimental[4]

**3-Methyl-naphtho(1.2-b)furan-2-carboxylic Acid (III, R=$CH_3$)** 2-Aceto-1-naphthol (8 g.), ethyl bromomalonate (10.4 g.), freshly dehydrated potassium carbonate (8 g.) and anhydrous acetone (50 ml.) were mixed together and the whole was gently refluxed in a water bath for ten hr. After distilling off the main part of the solvent, the residue was mixed with water and acidified with dilute mineral acid and then extracted with ether. The ethereal extract was washed with water, dried and the ether was removed, giving a dark brown oily substance. Without purification it was dissolved in alcoholic potash (alcohol 80 ml., potassium hydroxide 8 g., water 4 ml.), and then refluxed on a steam bath for one hr. After removal of the solvent, the residue was dissolved in water, washed with ether, and acidified with mineral acid, yielding grayish white precipitates; yield, about 4 g. (41 %). Recrystallization from glacial acetic acid (with charcoal) gave III (R=$CH_3$) as faint yellow pillars of m.p. 255–256° (dec.)[5]. Its analysis does not show satisfctory coincidence with the theoretical ones, just as in the cases of many sorts of coumarone-2-carboxylic acids[2].

*Anal.* Found: C, 73.21; H, 4.56. Calcd. for $C_{14}H_{10}O_3$: C, 74.33; H, 4.46 %.

**Ethyl 3-Methyl-naphtho(1.2-b)furan-2-carboxylate** The above-mentioned carboxylic acid (1 g.) was dissolved in absolute alcohol (10 ml.) containing 5 % of hydrogen chloride gas and the whole was refluxed in a water bath for five hr. After removal of the solvent, the residue was dissolved in ether, washed successively with aqueous sodium carbonate and water, dried and the ether was removed, leaving crystals (0.5 g.). The crude crystals were recrystallized from alcohol, giving ethyl ester as colorless flat columns of m.p. 107–108°[6].

*Anal.* Found: C, 75.10; H, 5.50. Calcd. for $C_{16}H_{14}O_3$: C, 75.57; H, 5.55 %.

**3-Ethyl-naphtho(1.2-b)furan-2-carboxylic Acid (III, R=$C_2H_5$)** 2-Propionyl-1-naphthol (4.3 g.), ethyl bromomalonate (5 g.), potassium carbonate (3.1 g.) and acetone (60 ml.) were mixed together and the whole was refluxed in a water bath for ten hr. under exclusion of moisture. A similar treatment of the case with methyl derivative gave 2.2 g. (43 %) of crude crystals of carboxylic acid. Recrystallization from benzene gave III (R=$C_2H_5$) as colorless scales of m.p. 218–219°.

*Anal.* Found: C, 75.04; H, 4.94. Calcd. for $C_{15}H_{12}O_3$: C, 74.99; H, 5.03 %.

**3-*n*-Propyl-naphtho(1.2-b)furan-2-carboxylic Acid (III, R=*n*-$C_3H_7$)** 2-Butyryl-1-naphthol (6 g.), ethyl bromomalonate (7.5 g.), potassium carbonate (5 g.) and acetone (65 ml.) were mixed together and the whole was refluxed in a water bath for ten hr. The same treatment as in the case with methyl derivative gave 3 g. (42 %) of the carboxylic acid. Recrystallization from chloroform (with charcoal) gave III (R=*n*-$C_3H_7$) as colorless needles of m.p. 203–204°.

*Anal.* Found: C, 75.35; H, 5.45. Calcd. for $C_{16}H_{14}O_3$: C, 75.57; H, 5.55 %.

**Attempted Decarboxylation of III**— i) 3-Methyl-naphtho(1.2-b)furan-2-carboxylic acid (III, R=$CH_3$) (1 g.) and copper powder (0.1 g.) were refluxed in quinoline (10 ml.) on a wire gauze for 30 min. After cooling, ether (200 ml.) was added and the mixture was filtered from the copper. The ethereal solution was washed successively several times with 2-N-hydrochloric acid, water, aqueous sodium bicarbonate and then with water to remove quinoline and dried. This ethereal extract, when freed from the solvent, gave an oily substance. Distillation in vacuo gave an oil (0.5 g.), b.p. 66–70°/1 mm. A part of the oil solidified[7] on standing, and it has the characteristic smell of coumarones. There is a great difference between the analytical and the theoretical value.

The above-obtained semi crystals (0.2 g.) were dissolved in benzene (5 ml.) and to the solution was added picric acid (0.2 g.). The mixture was gently warmed on a steam bath for about 30 min. After cooling, yellow lustrous pillars were yielded, which showed m.p. 61–62° (dec.). Since the picrate thus obtained decomposed gradually in the recrystallization process, attempts to separate the picrate in pure state were unsuccessful.

ii) 3-Ethyl-, and 3-*n*-propyl-naphtho(1.2-b)-furan-2-carboxylic acids behaved analogously, their decarboxylation being difficult.

This research was supported by a Grant-in-Aid from the Ministry of Education.

*Department of Chemistry, Faculty of Science, Tokyo Metropolitan University, Setagaya-ku Tokyo*

4) All melting points were un-corrected.
5) See ref (1a) Hantzsch gave m. p. 243-245° (dec ).
6) See ref. (1a) Hantzcsh gave m. p. 108°.
7) See ref. (1c). Kostanecki and Tambor gave m. p. 38°, b. p 302-304°/720 mm.

# *Coprecipitation of a Trace Amount of Cesium with Thallous Salts*

By Noboru YAMAGATA, Toshiko YAMAGATA and Sadakata WATANABE

(Received November 15, 1956)

## Introduction

Direct separation of carrier-free radioactive cesium-137 from other fission activities has usually been accomplished, in the first step, by the use of the ammonium or the potassium ion as carrier[1]. The second step, the separation of cecium from the carrier ions is, however, fairly difficult, especially from potassium.

Coprecipitation of a trace amount of cesium with a thallous salt can be employed for this purpose, followed by oxidation to thallic state and precipitation as hydroxide.

The following experiments deal with the coprecipitation of a trace amount of cesium with thallous (1) dipicrylaminate, (2) cobaltinitrite, (3) chloroplatinate, (4) phosphotungstate, (5) silicotungstate, (6) phosphomolybdate, (7) copper ferrocyanide, (8) chloride, (9) bromide, (10) iodide and (11) sulfide.

The other well known precipitation methods, such as iodobismuthate, perchlorate and periodate method, were not tested, because these reagents oxidize thallous ions to thallic.

## Experimental

The conditions of precipitation and filteration were chosen, from the viewpoint of practical convenience, to facilitate rapid precipitation and immediate filtration.

Unless otherwise specified in the following, the precipitating agent is added to the carrier-free cesium solution ($^{137}Cs$ imported from U. S. A. in 1954, Batch No. 14) and then the thallous nitrate solution with constant agitation. The precipitate is filtered off or centrifuged after thirty minutes' agitation and another thirty minutes' digestion without stirring.

The activity was measured by the use of a Geiger-Muller tube of the mica end-window type and a Tracerlab's "1000"-scaler.

**1. Dipicrylaminate Method**[2]. — A proper quantity of carrier-free cesium solution (about $10^4$ cpm. in 0.3 N hydrochloric acid) is taken in a 50 cc. Erlenmeyer flask and neutralized to thymol blue with 0.1 N sodium hydroxide solution. About 100% excess of 3% magnesium dipicrylaminate solution is added and the mixture is made up to 30 cc. After cooling for about half an hour in ice water, 1 cc. of 0.1 N thallous nitrate solution (containing about 20 mg. thallium) is dripped with constant stirring. The product is stirred for thirty minutes and set aside for another thirty minutes in ice water. The precipitate is filtered off and washed first with 2 cc. of ice water, then with two 2 cc. portions of diethyl ether at 0°C.

The filtrate and the washings are united, made up to 50 cc. with water and 5 cc. portions are evaporated up in small dishes, for their activity (A) to be measured. To the same volume of the solution, one tenth quantity of the radioactive cesium first taken is added and the activity (A') is measured after evaporation. The activity of cesium removed by coprecipitation (%) is represented as $100(A'-2A)/(A'-A)$.

**2. Cobaltinitrite Method**[3].—To the carrier-free cesium solution in a flask, the reagent (about 8 cc.), prepared from cobaltous nitrate and sodium nitrite, is added and diluted to 30 cc. Thallous nitrate solution is added dropwise with stirring, at room temperature. The precipitate is filtered off and washed twice with 10% acetic acid solution.

**3. Chloroplatinate Method**[4].—To the carrier-free cesium solution in a flask, about 50% excess of 5% aqueous chloroplatinic acid solution is added and diluted to 30 cc. The thallous nitrate solution is added dropwise with mechanical stirring, at room temperature. The precipitate is filtered off with a glass filter and washed twice with 98% ethyl alcohol. The solubility of thallous chloroplatinate in water is very small and an anhydrous condition as in the case of potassium determination is not necessary. The precipitate is usually colloidal and filtered with difficulty. With vigorous stirring, however, it becomes crystalline and is easily filtered.

**4. Phosphotungstate Method.**—To the carrier-free cesium solution in a flask, 2 cc. of 0.1 M solution of the reagent is added and diluted to 30 cc. with 3 N or 6 N hydrochloric acid. At 0°C or 60°C, with stirring, the thallous nitrate solution is added dropwise. The resulting precipitate

1) T. Shiokawa and M. Yagi, *Japan Analyst*, **5**, 220 (1956.)

2) R. B. Hahn and R. O. Backer, AECU-2903 (1955); E. B. Sandell, "Colorimetric Determination of Traces of Metals" London, (1950) p. 501.

3) R. Overstreet and L. Jacobson, Paper 286 of "Radiochemical Studies: The Fission Products." editted by H. B. Evans, Book 3, New York (1951); F. P. Treadwell and W. T. Hall, "Analytical Chemistry" Vol. 2, 8th ed. John Wiley and Sons, Inc., London (1931) p. 68.

4) "Gmelins Handbuch der Anorganischen Chemie" System Nr. 38, Verlag Chemie, Berlin (1940) p. 164.

is of colloidal nature and must be separated by centrifuging.

**5. Silicotungstate Method**[5].—The procedure is similar to that for the phosphotungstate method; 0.1 M solution of silicotungstic acid was used.

**6. Phosphomolybdate Method**[5].—To the carrier-free cesium solution in a flask are added 18 cc. of 0.15 N nitric acid, 0.15 g. of ammonium molybdate, and 0.3 cc. of conc. phosphoric acid, to be diluted to 30 cc. The thallous nitrate solution is added dropwise with stirring at 40-50°C, for the precipitate to be collected by centrifuging.

**7. Copper Ferrocyanide Method**[6].—To the carrier-free cesium solution in a flask are added 18 cc. of 0.15 N nitric acid, 5 cc. of 1/15M potassium ferrocyanide solution and the thallous nitrate solution. The resulting solution is cooled to 0°C. Five cc. of 1/20 M copper sulfate solution is added with constant stirring, at 0°C. The precipitate is collected by centrifuge. This method, originally described by H. L. Krieger et at.[6] did not use a thallium carrier.

**8. Thallous Chloride Method.**—To the carrier-free cesium solution, 3 N hydrochloric acid and distilled water are added to produce 30 cc. of 1 N acid solution. After being cooled to 0°C with constant stirring, this solution is treated with the thallous nitrate solution. The precipitate is filtered off and washed with 1 N hydrochloric acid at 0°C.

**9. Thallous Bromide Method.**—The cesium solution is submitted to a procedure similar to that mentioned above, by the use of hydrobromic acid.

**10. Thallous Iodide Method**[7].—Free iodine, occasionally found in hydroiodic acid, may oxidize thallous ion to thallic, interfering with the formation of thallous iodide. Potassium iodide was used instead of hydroiodic acid. To the carrier-free cesium solution in a flask, 1 cc. of glacial acetic acid and 5 cc. of 10% potassium iodide solution are added and diluted to 30 cc. The thallous nitrate solution is added with stirring, at 0°C or at room temperature. The precipitate is filtered off and washed first with 1% solution of potassium iodide in 1% acetic acid and then with acetone.

**11. Thallous Sulfide Method.**—The carrier-free cesium solution is evaporated up in a flask to eliminate the free hydrochloric acid and treated with the thallous nitrate solution and 5 cc. of 1 N acetic acid. The product is mixed well and neutralized with concentrated ammonia water with further addition of 1 cc. excess. The resulting solution is made up to 30 cc. and, after being heated to 60°C, bubbled with hydrogen sulfide for thirty minutes or for four hours. The precipitate is immediately filtered off and washed with ammoniacal ammonium sulfide solution.

5) L. E. Glendenin and C. M. Nelson, Paper 283 of "Radiochemical Studies: The Fission Products" ed. by H. B. Evans, Book 3, New York (1951); E. K. Hyde, *J. Am. Chem. Soc.*, **74**, 4181 (1952).

6) H. L. Krieger, B. Kahn and C. P. Straub, ORNL-1966 (1955).

7) "Gmelins Handbuch der Anorganischen Chemie" Syst. Nr. 38, Verlag Chemie, Berlin (1940) p. 160.

## Results and Discussion

The group of methods shown in Table I represents successful coprecipitation; tracer amounts of cesium can be collected almost perfectly by these methods. From the view-point of avoiding contamination with cesium and rubidium which can be introduced from the used reagents containing alkali elements, the cobaltinitrite and the copper ferrocyanide method are not satisfactory. Chloroplatinic acid is rather expensive and is not suitable for practical use. Thus, dipicrylaminate or the phosphotungstate method is recommended, the former being considered to be more suitable. Dipicrylamine is very easily purified from metallic contaminants before use and the thallous salt of dipicrylamine containing cesium activity can be decomposed with a dilute mineral acid to precipitate free dipicrylamine, which is removed by extraction with an organic solvent. The extracted dipicrylamine can be recovered for further use.

The following cautions are, of course, needed for the practical use of this reagent:

1) As the precipitation of thallous dipircylaminate takes place in a slightly alkaline condition, iron, aluminum and other heavy metals must be previously removed.

2) Potassium, ammonium and rubidium ions form a precipitate with dipicrylamine; they must be absent in the solution.

In Table II, the results of unsuccessful coprecipitation are shown. Silicotungstic acid is an effective reagent for coprecipitation of a trace amount of cesium or francium[8], when the cesium ion is used as carrier, but, when the thallous ion is used, it failed to act as a trace-catcher.

Phosphomolybdic acid, which was recommended by H. L. Krieger et al.[6] as an efficient precipitant for cesium, also failed to be so when the thallous ion was used. In those cases, the failure of coprecipitation was supposed to be derived from the difference in crystal structure between cesium and thallous silicotungstate (or phosphomolybdate).

The examination of the separation of cesium activity from thallium and other fission activities is beyond the scope of this article. If any presumption could be possible, however, the results of the methods described in Table II should provide an important suggestion concerning the procedure for separation of thallium

8) E. K. Hyde, *J. Am. Chem. Soc.*, **74**, 4181 (1952).

TABLE I

COPRECIPITATION OF A TRACE AMOUNT OF CESIUM WITH THALLOUS SALTS (1)

| Carrier Tl(I) mg. | Activity of carrier-free Cs, added cpm | Activity of Cs, co-precipitated cpm | Activity of Cs, collected % | Chemical yield of precipitation % | Temp. °C | Remarks |
|---|---|---|---|---|---|---|
| (1) Dipicrylaminate method | | | | | | |
| 20.0 | 1620 | 1480 | 91.4 | 92.0 | 0 | |
| 20.0 | 1544 | 1379 | 89.3 | 91.0 | 0 | |
| 40.0 | 1645 | 1269 | 77.1 | 72.3 | 18 | |
| 40.0 | 1571 | 1174 | 74.7 | 71.8 | 18 | |
| (2) Cobaltinitrite method | | | | | | |
| 20.0 | 826 | 768 | 93.0 | — | 19 | |
| 40.0 | 1158 | 1126 | 97.2 | — | 19 | |
| (3) Chloroplatinate method | | | | | | |
| 20.0 | 1530 | 1387 | 90.7 | 98.9 | 19 | |
| 20.0 | 1615 | 1449 | 95.7 | — | 19 | |
| (4) Phosphotungstate method | | | | | | |
| 20.0 | 1926 | 1889 | 98.1 | — | 60 | 3 N |
| 20.0 | 2041 | 1983 | 97.2 | — | 60 | 6 N |
| 40.0 | 1950 | 1940 | 99.5 | — | 0 | 3 N |
| 40.0 | 2210 | 2161 | 97.8 | — | 0 | 6 N |
| (7) Copper ferrocyanide method | | | | | | |
| 0 | 2891 | 2870 | 99.3 | — | 0 | |
| 20.0 | 1449 | 1433 | 98.9 | — | 0 | |
| 40.0 | 1498 | 1484 | 99.1 | — | 0 | |

TABLE II

COPRECIPITATION OF A TRACE AMOUNT OF CESIUM WITH THALLOUS SALTS (2)

| Carrier Tl(I) mg. | Activity of carrier-free Cs, added cpm | Activity of Cs, co-precipitated cpm | Activity of Cs, collected % | Chemical yield of precipitation % | Temp. °C | Remarks |
|---|---|---|---|---|---|---|
| (5) Silicotungstate method | | | | | | |
| *13.3 | 1620 | 1388 | 85.7 | — | 0 | *Cs- |
| *13.3 | 1716 | 1466 | 85.4 | — | 0 | carrier |
| 20.0 | 1655 | 31 | 1.9 | — | 0 | 3 N |
| 20.0 | 1603 | 23 | 1.4 | — | 0 | 6 N |
| (6) Phosphomolybdate method | | | | | | |
| 20.0 | 1422 | 181 | 12.7 | — | 40–50 | |
| 40.0 | 959 | 57 | 5.9 | — | 40–50 | |
| (8) Chloride method | | | | | | |
| 40.0 | 1700 | 160 | 9.4 | 89.9 | 0 | |
| 60.0 | 1491 | 23 | 1.6 | — | 0 | |
| (9) Bromide method | | | | | | |
| 20.0 | 1457 | 34 | 2.4 | 96.5 | 0 | |
| 40.0 | 1658 | 229 | 14.1 | 98.0 | 0 | |
| (10) Iodide method | | | | | | |
| 20.0 | 1898 | 337 | 12.5 | 99.0 | 18 | |
| 20.0 | 1745 | 144 | 8.4 | 98.5 | 0 | |
| (11) Sulfide method | | | | | | |
| 20.0 | 1610 | 250 | 15.5 | — | 60 | 30 min. |
| 20.0 | 1748 | 33 | 1.9 | — | 60 | 4 hr. |

from a trace amount of cesium. Without being oxidized to the thallic state, the thallous ion can be separated from cesium by precipitation as halide or sulfide with a slight loss in cesium activity. The authors also tested the separation of thallium as thallic hydroxide after oxidation with bromine water. The result also proved promising.

## Summary

The possibility of coprecipitation of a trace amount of cesium with various thallous salts has been studied. The following salts were proved to be efficient: dipicrylaminate, cobaltinitrite, chloroplatinate, phosphotungstate and copper ferrocyanide; of those the dipicrylaminate method was recommended.

Only partial coprecipitation of cesium took place with thallous silicotungstate, phosphomolybdate, chloride, bromide, iodide and sulfide.

*Kiriu College of Technology*
*Gunma University, Kiriu*

# *Carrier-free Separation of Cesium from Fission Products by the Use of Coprecipitation with Thallium(I) Dipicrylaminate*

By Noboru YAMAGATA and Sadakata WATANABE

(Received January 12, 1957)

The authors showed in the previous report[1] an efficient coprecipitation of a trace amount of cesium with thallium (I) dipicrylaminate and suggested several possible ways of its separation from the carrier. The present report deals with its separation from both the carrier ion and other fission activities, including $^{90}Sr$–$^{90}Y$, $^{106}Ru$–$^{106}Rh$, $^{95}Zr$–$^{95}Nb$ and rare earth elements.

## Coprecipitation of Other Fission Activities with Thallium(I) Dipicrylaminate

The radionuclides which coprecipitate with thallium(I) dipicrylaminate were clarified in order to find the later process of separation.

The radionuclides in question were separated from mixed fission products, about one year old, by ion-exchange method[2] and each fraction was converted into nitric acid solution. Their suitable quantities were submitted to direct precipitation with thallium(I) dipicrylaminate after neutralization with sodium hydroxide.

The following percentages of applied activities were found in the directly precipitated thallium(I) dipicrylaminate.

| | |
|---|---|
| Rare earth elements | 0.20 |
| $^{95}Zr$–$^{95}Nb$ | 0.73 |
| $^{90}Sr$–$^{90}Y$ | 0.53 |
| $^{106}Ru$–$^{106}Rh$ | 0.38 |
| U | 56.8[3] |

Those figures indicate that some scavenging pretreament is necessary in the practical separation of cesium from mixed fission products.

## Separation of Cesium Activity from Thallium(I) Dipicrylaminate

For the separation of cesium activity from thallium(I) carrier, three processes were tested: (1) precipitation, (2) ion-exchange and (3) extraction.

(1) Precipitation. Hydrous ferric oxide carries down various kinds of fission activity, but a negligible amount of cesium. Since the thallium(III) ion was expected to behave similarly, the coprecipitation of fission activities with thallium(III) hydroxide was tested.

An acid solution containing 0.1 m mol. of the thallium(I) ion was mixed with a proper quantity of fission products, oxidized with chlorine water, and neutralized to about pH 9. Immediate filtration

1) N. Yamagata, T. Yamagata and S. Watanabe, This Bulletin, **30**, 577 (1957).
2) K. Kimura et al., *Japan Analyst*, **3**, 335 (1954).
3) The value for uranium is so high that, when it is present in fission products, it must be previously removed by solvent extraction.

resulted in about 83.6–85.8 % coprecipitation of overall activities. The loss of a trace amount of cesium under the same condition was only 0.3–0.4 % and about 2 % of thallium entered the filtrate; the latter could be removed, however, by extraction or ion-exchange method as described later.

In practice, the starting material is thallium(I) dipicrylaminate containing a trace amount of cesium; the precipitate is dissolved in hot water and acidified with hydrochloric acid. The precipitate of free dipicrylamine can be easily removed by filtration without loss in cesium activity.

(2) Ion-exchange. Since, the selectivity coefficients of Dowex 50 given by W. C. Bauman and J. Eichhorn[4] are 2.04 for $K_H^{Cs}$ and 8.60 for $K_H^{Tl(I)}$, chromatographic separation of cesium from thallium(I) is expected to be easily accomplished, when both elements are present in appreciable amounts. The present investigation, however, concerns the separation of a trace amount of cesium from a large quantity of thallium.

The selectivity coefficients of the cation exchanger Dowex 50 X-12 for cesium and thallium(I) were determined by the batch method described by one of the authors[5]. The results, shown in Table I, indicate

TABLE I
SELECTIVITY COEFFICIENTS OF THALLIUM(I) AND CESIUM
(Dowex 50, X-12)

| Selectivity coefficients | | Molar fraction in solution $\alpha$ | Molar fraction in resin $\beta$ |
|---|---|---|---|
| $K_H^{Tl(I)}$ | 18.5 | 0.0119 | 0.182 |
| | 19.8 | 0.0084 | 0.143 |
| $K_H^{Cs}$ | 5.8 | 0.078 | 0.33 |
| | 10 | 0.0060 | 0.058 |
| | 12 | $5.8\times10^{-4}$ | 0.0069 |
| | 13 | $1.1\times10^{-8}$ | $1.4\times10^{-7}$ |

that the $K_H^{Cs}$ value for an infinitely dilute solution is greater by twice or more, as compared with the ordinary value. The difficulty, which the simple chromatographic separation involves, was also confirmed by dynamic flow tests.

Another promising method of separation by the use of ion-exchange resin is the utilization of the strong adsorbability of thallium(III) ions upon an anion-exchange resin in hydrochloric acid solution[6]. Selectivity coefficients were determined for three kinds of anion-exchanger by the batch method. Dowex 1 was proved to be the best as shown in Table II, the

TABLE II
SELECTIVITY COEFFICIENTS OF THALLIUM(III) IN HYDROCHLORIC ACID SOLUTION

| Concentration of HCl | Anion exchanger | Selectivity coefficient | Molar fraction in solution $\alpha$ | Molar fraction in solution $\beta$ |
|---|---|---|---|---|
| 1 N | Dowex 1 X-8 | 370 | $5.5\times10^{-4}$ | 0.170 |
| | Dowex 2 X-10 | 250 | $8.1\times10^{-4}$ | 0.169 |
| | Amberlite IRA-410 | 110 | $1.4\times10^{-3}$ | 0.134 |
| 4 N | Dowex 1 X-8 | 3400 | $9.8\times10^{-5}$ | 0.249 |
| | Dowex 2 X-10 | 820 | $3.6\times10^{-4}$ | 0.226 |
| | Amberlite IRA-410 | 360 | $5.9\times10^{-4}$ | 0.174 |

ion-exchange capacity being 2.72 meq. per gram of resin dried at 72°C. Dynamic flow experiments, by use of $^{204}Tl$ as an indicator for breakthrough, also proved this method to be satisfactory

3) Extraction. It is well known that the thallium(III) ion can be extracted from hydrochloric or hydrobromic acid medium with diethyl ether[7]. The authors also determined the efficiency of extraction for the removal of thallium from a trace amount of cesium.

Twenty ml. of the acid solution was shaken with the same volume of diethyl ether, saturated with hydrochloric or hydrobromic acid of corresponding concentration. In the case of 12 N hydrochloric acid and 6 N hydrobromic acid, the procedure was modified so that the acid solution, previously saturated with ether, was shaken with pure ether. When thallium(III) was shaken, several drops of saturated chlorine water were added to avoid possible reduction of thallium.

The results are shown in Table III. The extraction of thallium(III) and the recovery of the cesium activity were satisfactory, when the concentration of acid was kept 1 to 4 N. The results also

4) W. C. Bauman and J. Eichhorn, *J. Am. Chem. Soc.*, **69**, 2830 (1947).
5) N. Yamagata, *J. Chem. Soc. Japan, Pure Chem. Sect.*, **87**, 513 (1957).
6) K. A. Kraus and F. Nelson, A/Conf. 8/P/837 (1955).
7) I. Wada and R. Ishii, *Bull. Inst. Phys. Chem. Research, Tokyo* **13**, 264 (1934).

TABLE III
EXTRACTION OF THALLIUM(III) AND OTHER ELEMENTS FROM HYDROCHLORIC AND HYDROBROMIC ACID SOLUTION WITH DIETHYL ETHER

Percentage of the element remaining in HCl solution after one extraction

| | Concn. of HCl | | | | |
|---|---|---|---|---|---|
| | 1 N | 2 N | 4 N | 6 N | 12 N |
| Carrier-free Tl(III) | 0.79 | 1.6 | 0.83 | 2.8 | 85 |
| 0.1 m mol. Tl(III) | 0.69 | 1.6 | 0.64 | 3.2 | 83 |
| Carrier-free Cs | 98.6 | 99.8 | 98.2 | 99.4 | 99.2 |
| Mixed F.P. | 99.0 | — | 99.0 | 99.0 | 99.0 |
| Tracer U(VI) | 89.3 | — | 91.2 | — | — |

Percentage of the element remaining in HBr solution after one extraction

| | Concn. of HBr | | | |
|---|---|---|---|---|
| | 1 N | 2 N | 4 N | 6 N |
| Carrier-free Tl(III) | 2.5 | 0.59 | 1.3 | 77 |
| 0.1 m mol. Tl(III) | 0.41 | 0.45 | 1.7 | 30 |

indicated that, when 0.1 m mol. of thallium (III) was extracted with ether only once, about 1% or 0.2 mg. of this element entered the cesium solution.

In the practical separation of cesium, the starting material is thallium(I) dipicrylaminate which is insoluble in diethyl ether. An organic solvent, which is immiscible with water and dissolves the precipitate, would be more useful than diethyl ether, because it also removes the free dipicrylamine.

For this purpose, methylisobutyl ketone was found to be the best. It readily dissolves both thallium(I) dipicrylaminate and free dipicrylamine. The extraction of thallium(III) with methylisobutyl ketone was studied from hydrochloric acid solution, and the results are shown in Table IV.

TABLE IV
EXTRACTION OF THALLIUM(III) AND OTHER ELEMENTS FROM HYDROCHLORIC ACID SOLUTION WITH METHYLISOBUTYL KETONE

Persentage of the element remaining in HCl solution after one extraction

| | Concn. of HCl | | | |
|---|---|---|---|---|
| | 1 N | 2 N | 4 N | 6 N |
| 0.1 m mol. Tl(III) | 0.89 | 0.56 | 1.0 | 0.73 |
| Carrier-free Cs | 99.5 | 99.6 | 99.7 | 99.7 |
| Tracer U(VI) | 84.4 | — | 89.2 | — |

## Proposed Procedure

**Step 1.** To the sample of fission material[8], add iron(III) and strontium nitrate solution equivalent to 20 mg. of iron and 5 mg. of strontium. Add sodium hydroxide solution of proper strength until the solution is basic to thymol blue (pH 8–9) and then 1 ml. of 1 M sodium carbonate solution. Filter and wash with a little water.

**Step 2.** After the neutralisation of the filtrate, if necessary, to pH 8–9, add about 100 % excess of sodium dipicrylaminate solution (3 % in water)[9] and cool the resulting solution for about half an hour in ice water. With constant stirring, add 1 ml. of 0.1 N thallium(I) nitrate solution dropwise, and continue the stirring for thirty minutes at 0°C. Filter the precipitate and wash first with 2 ml. of ice water, and then with two 2 ml. portions of diethyl ether at 0°C.

**Step 3.** Take up the precipitate in 5–10 ml. of methylisobutyl ketone into a separatory funnel. Add 1 ml. of saturated chlorine water and 5–10 ml. of 2 N hydrochloric acid. Shake vigorously for one minute and take the aqueous layer in another separatory funnel.

**Step 4.** To the separatory funnel, add the same volume of methylisobutyl ketone and shake for one minute vigorously. Evaporate the aqueous layer to dryness in a small counting dish and mount.

The results of recovery and separation tests are shown in Table V. The gross decontamination factor is greater than

TABLE V
RECOVERY AND SEPARATION TESTS

| Activities taken | cpm | $^{137}$Cs activity found cpm | Recovered Cs % |
|---|---|---|---|
| F.P. | $1.1\times10^5$ | 1142 | — |
| F.P. | $1.1\times10^5$ | | |
| $^{137}$Cs | 1149 | 2148 | 93.8 |
| R.E. | $1.5\times10^5$ | | |
| Sr-Y | $1\times10^4$ | | |
| Ru-Rh | $2\times10^4$ | 1002 | 87.2 |
| Zr-Nb | $2\times10^3$ | | |
| $^{137}$Cs | 1149 | | |

8) The sample must not contain potassium or rubidium, since they will be present in the final product as inert solids and removed with difficulty. If uranium is present in the starting sample, it must be removed previously.

9) E. B. Sandell, "Colorimetric Determination of Traces of Metals" Interscience Pub. Inc., New York(1950) p. 501.

$10^4$, although the proposed procedure is only valid for about one year old fission products; when cesium is to be prepared from or analyzed in a fresher sample, the procedure should be modified.

## Summary

A procedure has been presented for the separation of carrier-free cesium from the fission products. The method makes use of coprecipitation with thallium(I) dipicrylaminate followed by solvent extraction with methylisobutyl ketone in the presence of hydrochloric acid and an oxidizing agent. The recovery of active cesium is about 90% and the gross decontamination factor is more than $10^4$.

*Kiriu College of Technology*
*Gunma University, Kiriu*

# *Rapid Analysis of Gamma-Emitters Using Gamma-Ray Scintillation Spectrometer. I. Quantitative Analysis of* $^{134}$Cs—$^{137}$Cs *Mixture*

By Fumio AOKI*, Toshio KUROSAWA* and Seishi YAJIMA**

(Received January 25, 1957)

## Introduction

Rapid determination of individual species in a mixture of radionuclides will be required in many cases, such as processing of fission products, activation analysis, and chemical, biological or metallurgical experiments with several kinds of radionuclide.

Since the advent of electronic scintillation counting techniques, the application of scintillation spectrometers has been introduced to the study of analysis. Several investigations[1] on the analysis of radionuclide mixtures were reported, and the quantity of each nuclide was obtained from the area under the photopeak resolved by the spectrometer.

The authors have been investigating the possibility of quantitative determination of two nuclides which cannot be resolved by the spectrometer. This report is the result of the study on $^{134}$Cs—$^{137}$Cs mixture.

## Quantitative Measurement of $^{134}$Cs—$^{137}$Cs Mixture

Principal gamma-energies emitted from $^{134}$Cs[2] are 0.57 MeV, 0.60 MeV and 0.79 MeV, others being negligible in intensity. The pulse height scan shows two photopeaks at 0.79 MeV and at 0.57 MeV and 0.60 MeV (unresolved).

The gamma-energy of $^{137}$Cs is 0.66 MeV; the pulse height scan shows one photopeak at 0.66 MeV.

In the presence of both $^{134}$Cs and $^{137}$Cs, two peaks appear as shown in Fig. 1. Let $A$ be the area under 0.6 MeV photopeak (0.57 MeV, 0.60 MeV and 0.66 MeV photopeaks being superposed), then,

$$A=A_4+A_7$$

where $A_4$ and $A_7$ are the areas under the real photopeaks due to $^{134}$Cs and $^{137}$Cs near 0.6 MeV respectively. Or it is approximately obtained from the following expression,

$$A=\sum_a^b \gamma \times E$$

where

$\gamma$: counts per minute per channel width,

$E$: increment of energy equal to the channel width,

$a$ and $b$: minimum points of the pulse height scan (Fig. 1).

So far as the geometry is fixed through out the measurement, and an identical apparatus is used, the pulse height scan normalized to the peak height of the principal gamma-energy is independent of the activity for a gamma-emitter[1]. Hence similar curves will be obtained by the

* Government Chemical Industrial Research Institute, Tokyo, Shibuya, Tokyo.

** Japan Atomic Energy Research Institute.

1) R. E. Connally and M. B. Leboeuf, *Anal. Chem.*, **25**, 1095 (1953); D. H. Peirson, *Atomics*, Sept. 316 (1956); U. L. Upson, R. E. Connally and M. B. Leboeuf, *Nucleonics*, **13**, No. 4, 38 (1955).

2) J. M. Hollander, I. Perlman and G. T. Seaborg, *Rev. Mod. Phys.*, **25**, 552 (1953).

spectrometer scans for the gamma-emitter, and $A_4$ is calculated as follows:

$$A_4 = \gamma_{max} \times C$$

where $\gamma_{max}$ is the height of the 0.79 MeV photopeak, which is not affected by the $^{137}Cs$ pulse height distribution, and $C$ is a constant; the value of the latter is obtained from careful measurements of $^{134}Cs$ standard.

$A$ and $\gamma_{max}$ ($A_4$) are obtained from the pulse height scan; hence $A_7$ is calculated. Through the comparison of $\gamma_{max}$ (or $A_4$) and $A_7$ with those of a mixture of $^{134}Cs$ and $^{137}Cs$ of a known composition, their quantities will be found.

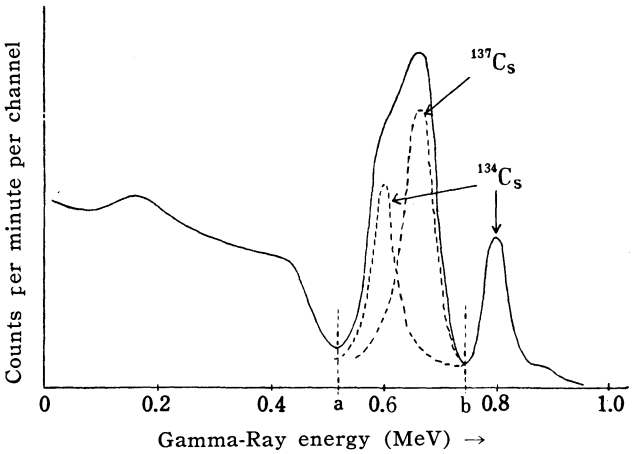



Fig. 1. Gamma-Ray spectrometer scan of $^{134}Cs$—$^{137}Cs$ mixture.

## Experiment

The block diagram of the gamma-ray scintillation spectrometer (Atomic Instrument Co. Model 513) used in the experiment is shown in Fig. 2.

Before the quantitative measurement, the authors had ascertained the counting loss with $^{134}Cs$ and the results are shown in Fig. 3. The linearity of the counts vs. the quantity held up to $1\times10^5$ counts per minute in total counts and $5\times10^3$ counts per minute per channel width (0.02 MeV) in peak counts.

The chemical form of cesium was CsCl in aqueous solution. It was diluted to about 0.1 $\mu$C/ml with demineralized water. Mixed samples of $^{134}Cs$—$^{137}Cs$ were prepared as shown in Table I, taken in glass tubes of equal shape and size, and dried up. All residue remained on the bottom. Each glass tube has 15 mm outside diameter, which fits the geometry of the well of the NaI(Tl) crystal (see Fig. 2); it has 0.2g/cm$^2$ wall thickness. The absorption of the gamma-rays by the glass tube is undoubtedly negligible.

TABLE I
COMPOSITIONS OF SAMPLES

| Nuclides | Quantities (ml) | | | | | | | | | | |
|---|---|---|---|---|---|---|---|---|---|---|---|
| $^{134}Cs$ | 1 | 1 | 1 | 1 | 1 | 1 | 0 | 2 | 3 | 4 | 5 |
| $^{137}Cs$ | 0 | 1 | 2 | 3 | 4 | 5 | 1 | 1 | 1 | 1 | 1 |

One ml. portion each of the $^{134}Cs$ and the $^{137}Cs$ were taken as arbitrary standards, which were carefully measured three times, The measuring system was switched on about three hours before the measurement for stabilization. Every sample was put into the well of the crystal, when its activity was measured.

The results obtained in 0.02 MeV channel width are shown in Table II and III. As their absolute activities were unknown, they were temporarily described by volume (ml.) of the solutions. The area under 0.6 MeV photopeak was calculated by summing up the counts from

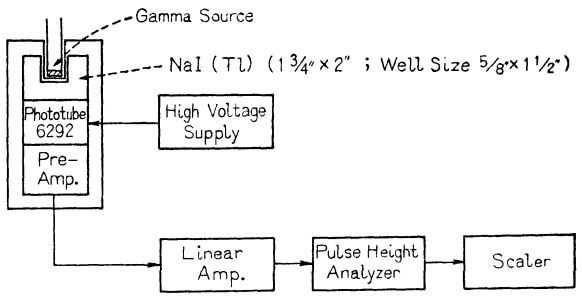



Fig. 2. Block diagram of scintillation spectrometer.

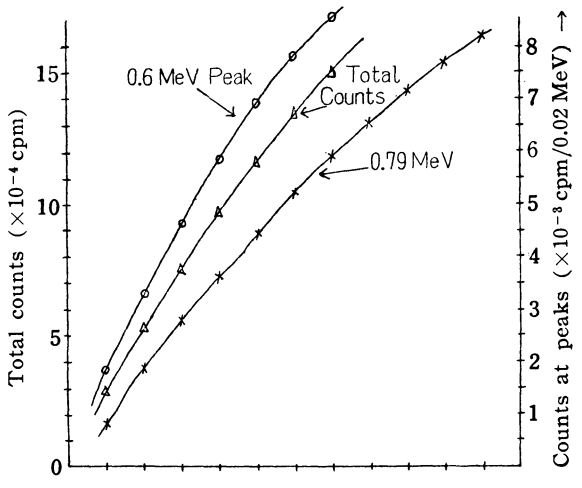



Fig. 3. Counting loss of the spectrometer.

$a$ (0.51 MeV) to $b$ (0.73 MeV) of Fig. 1, both of which were minimum points of the spectra.

## Discussion

Concerning a mixture of $^{134}Cs$ and $^{137}Cs$, the 0.79 MeV photopeak of $^{134}Cs$ is scarcely

TABLE II

ANALYSIS OF THE STANDARDS

| Nuclides | Quantity (ml) | $\gamma$max (0.79 MeV) (cpm/V) | Area under 0.6 MeV peak (cpm) | $C\left(\frac{\text{Area}}{\text{max}}\right)$ |
|---|---|---|---|---|
| $^{134}$Cs | 1 | 572±3.2% | 9.030±0.8% | 17.13±3.3% |
| $^{137}$Cs | 1 | — | 9.766±0.3% | — |

TABLE III

ANALYSIS OF MIXTURES

| Samples $^{134}$Cs/$^{137}$Cs | $\gamma$max 0.79 MeV cpm/ 0.02 MeV | Area 0.6 MeV cpm | $^{134}$Cs | | | $^{137}$Cs | | |
|---|---|---|---|---|---|---|---|---|
| | | | $A_4$ cpm | Quantity ml | Error % | $A_7$ cpm | Quantity ml | Error % |
| 1/1 | 555 | 19,230 | 9,509 | 1.05 | + 5.3 | 9,721 | 0.99 | − 0.5 |
| 1/2 | 532 | 23,126 | 9,080 | 1.00 | + 0.6 | 14,046 | 1.54 | −28.0 |
| 1/3 | 537 | 32,388 | 9,165 | 1.01 | + 1.5 | 23,223 | 2.53 | −20.7 |
| 1/4 | 633 | 44,182 | 10,804 | 1.19 | +19.7 | 33,379 | 3.42 | −14.5 |
| 1/5 | 505 | 48,841 | 8,619 | 0.95 | − 4.5 | 40,222 | 4.14 | −17.6 |
| 2/1 | 1,071 | 28,816 | 18,349 | 2.03 | + 1.6 | 10,467 | 1.07 | + 7.2 |
| 3/1 | 1,621 | 35,552 | 27,775 | 3.07 | + 2.5 | 7,777 | 0.79 | −20.4 |
| 4/1 | 1,984 | 45,857 | 33,998 | 3.76 | − 5.9 | 11,859 | 1.21 | +21.4 |
| 5/1 | 2,694 | 56,713 | 46,160 | 5.11 | + 2.2 | 10,533 | 1.08 | + 8.1 |

affected by the $^{137}$Cs pulse height distribution. It may be considered that this is the reason why the error for $^{134}$Cs quantity is small and apt to come on the positive side. (see Table III).

Beta-rays emitted from $^{134}$Cs (0.65 MeV: 75%, 0.09 MeV: 25%) and $^{137}$Cs (0.51 MeV: 92%, 1.17 MeV: 8%)[2] are almost absorbed by the 0.2 g./cm$^2$ glass tube wall; about 80–90 % of beta-rays incident on the NaI (Tl) crystal are scattered out before being stopped[3]. Therefore the effect of beta rays would be negligible.

If a pulse height scan of a mixture of two nuclides shows two photopeaks and the high energy one involves two peaks of each nuclide, the quantitative determination will be a little more complicated.

The authors wish to thank Dr. Shogo Uchida, Director of the 1st Division, Mr. Kenichi Hashimoto and Dr. Toshio Nakai for encouraging the prosecution of the work.

*Government Chemical, Industrial Research Institute, Shibuya*
*Tokyo*

3) K. Siegbahn, "Beta- and Gamma-Ray Spectroscopy", North-Holland Publishing Co., Amsterdam (1955), p. 134.

# *Determination of Critical Micelle Concentration of Detergent in Non-polar Solvent by Ultraviolet Absorption Spectra**

By Ayao KITAHARA

(Received February 6, 1957)

Micelle formation of detergents in non-polar solvents has been recently ascertained by many authors[1~4]. However, the existence of a concentration for micelle formation (CMC) in non-polar solvents is now questionable. Singleterry et al. have suggested the existence of the CMC of alkyl aryl carboxylate and sulfonate in benzene[3,5]. The present author has pointed out the existence of the apparent CMC in benzene solution of higher alkyl ammonium carboxylate by solubilization of water[6]. Pink et al. have not recognized the CMC in the case of a non-polar solution of a metal soap[4]. It seems, therefore, that the existence of the CMC in a nonpolar solvent is worth investigating by other methods and materials**.

In order to make a further study on the existence of the CMC in a non-polar solvent, the concentration dependence of the ultraviolet absorption spectrum in cyclohexane solution of detergent was studied in the present investigation. The result is compared with that of solubilization of water, and the existence of the CMC is discussed. The determination of the CMC by the change of the ultraviolet spectra was originally made by Harkins et al. with aqueous solution[7]. But the behavior of the change of the spectra are different from that of this paper.

## Experimental

**Material:** Dodecyl ammonium benzoate and octadecyl ammonium benzoate were used as detergents. They were prepared by heating the mixture of higher amine with an equivalent amount of benzoic acid at about 70°C. Boiling points of dodecylamine and octadecylamine used here were 131-133°C/15 mm and 188-190°C/4 mm, respectively. Benzoic acid showed the melting point of 120-121°C. Dodecyl ammonium benzoate was used without further purification, because it was soluble in any solvent. Octadecyl ammonium benzoate was recrystallized from petroleum ether. Both were dried *in vacuo* over anhydrous calcium chloride. The melting point of the former was 40-42°C and that of the latter was 64.0-65.5°C. Cyclohexane was purified until it showed no absorption in the range longer than 230 mμ and then dried and redistilled.

**Method:** Ultraviolet absorption spectra were measured with Shimazu photoelectric spectrophotometer. In order to gain the absorbance of higher accuracy in the concentration range used here, all measurements were carried out with use of a quartz cell of a light path of 1.0 mm, which was obtained by means of the insertion of a quartz block of 9.0 mm thick into a 10.0 mm quartz cell. The absorption spectra of cyclohexane solutions of dodecyl ammonium benzoate and of octadecyl ammonium benzoate were observed in the range from 230 mμ to 300 mμ with varying concentration of detergent from $1\times10^{-3}$ to $4\times10^{-2}$ mole/l. The point-by-point absorbance measurements were carried out at intervals of 0.5 mμ at the neighborhood of the peak. Each solution was made by dilution of a prepared stock solution. Absorption measurement was carried out immediately after every dilution.

The limiting amount of water solubilized into cyclohexane solutions of dodecyl ammonium benzoate and of octadecyl ammonium benzoate was determined at various concentrations of detergent. The method of the measurement was similar to that of the previous paper[6]. The temperature was kept at $20\pm2$ and $30\pm2$°C in both measurements of spectrum and solubilization.

## Results and Discussion

**Existence of CMC:** Absorption peaks appeared at 263, 270 and 276.5-277 mμ on the ultraviolet spectra of dodecyl ammonium benzoate and of octadecyl ammonium benzoate in cyclohexane. These absorption peaks are corresponding to the C-band of benzoic acid in cyclohexane, which has

* This paper was read at the Symposium on Colloid and Surface Chemistry held on November 18, 1956 at Tokyo University under the auspices of the Chemical Society of Japan.

1) L. Arkin and C. R. Singleterry, *J. Am. Chem. Soc.*, **70**, 3965 (1948).
2) M. van der Waarden, *J. Colloid Sci.*, **5**, 448 (1950).
3) S. Kaufman and C. R. Singleterry, *J. Colloid Sci.*, **7**, 453 (1952).
4) S. M. Nelson and R. C. Pink, *J. Chem. Soc.*, **1952**, 1744.
5) S. Kaufman and C. R. Singleterry, *J. Colloid Sci.*, **10**, 139 (1955).
6) A. Kitahara, This Bulletin, **28**, 234 (1955); **29**, 15 (1956).

** C. C. Addison and C. G. L. Furmidge have recently reported a CMC of alkylpyridinium iodides in xylene (*J. Chem. Soc.*, **1956**, 3229).

7) W. D. Harkins, H. Krizek and M. L. Corrin, *J. Colloid Sci.*, **6**, 576 (1951).

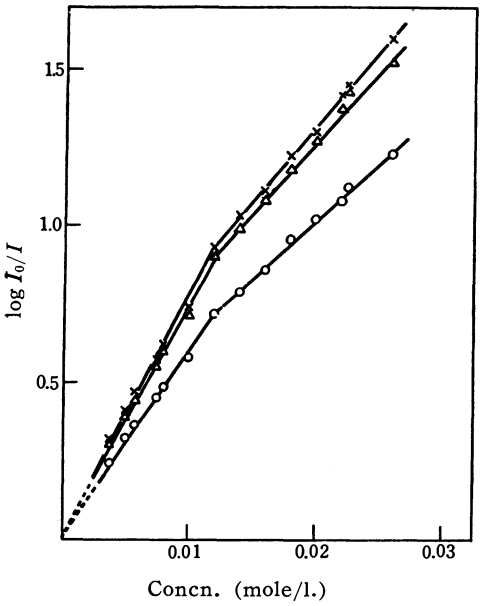



Fig. 1. Plot of absorbance (log $I_0/I$) *vs.* concentration in cyclohexane solution of dodecyl ammonium benzoate at 30±2°C. —△—, for 263 mμ; —×—, 270 mμ; —○—, for 276.5 mμ.

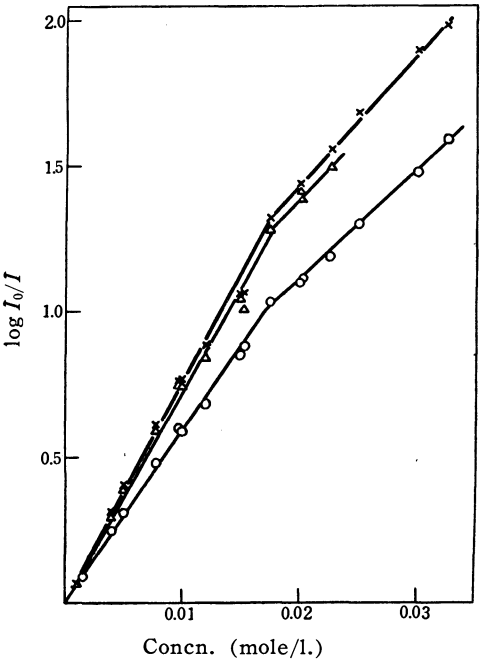



Fig. 2. Plot of absorbance (log $I_0/I$) *vs.* concentration in cyclohexane solution of octadecyl ammonium benzoate at 30±2°C. —△—, for 263 mμ; —×—, 270 mμ; —○—, for 276.5 mμ.

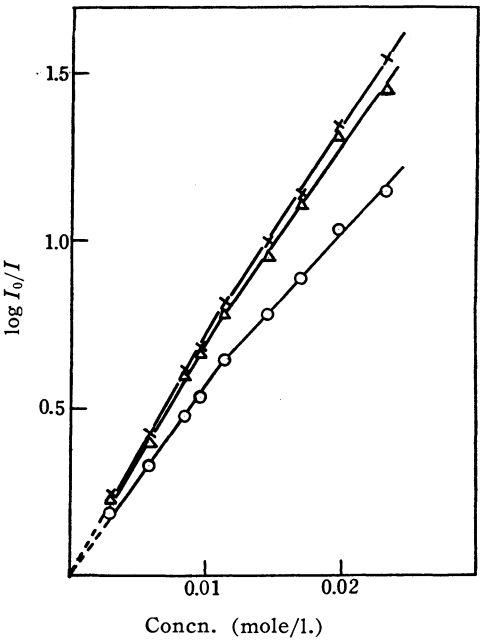



Fig. 3. Plot of absorbance (log $I_0/I$) *vs.* concentration in cyclohexane solution of dodecyl ammonium benzoate at 20±2°C. —△—, for 263 mμ; —×—, 270 mμ; —○—, for 277 mμ.

the peaks of 276 and 284 mμ[8]. No shifts were recognized in each absorption peak with varying concentration. The concentration dependence of the absorbance (log $I_0/I$) of each peak at 30 and 20°C was depicted in Figs. 1, 2 and 3. The concentration was described in terms of the molecular weight of a monomer of alkyl ammonium benzoate. It is readily recognized from the figures that the plots of the absorbance against the concentration consist of two linear parts within the concentration range studied in this experiment. This behavior was not very clear for the peaks of 263 and of 270 mμ of the solution of dodecyl ammonium benzoate at 20°C. The extrapolation of the linear parts of the lower concentration range passes the origin of the coordinates. That is, Beer's law is valid in this concentration range. It is, therefore, thought that the solute exists as monomeric molecule within this range. The break in this linear line at a certain concentration shows us that the state of the solute might be changed above this concentration. In the case of the cyclohexane solution of benzoic acid, no breaks appeared in the

8) H. E. Ungnade and R. W. Lamb, *J. Am. Chem. Soc.*, **74**, 3789 (1952).

TABLE I

CMC OBTAINED FROM SOLUBILIZATION (A) AND CONCENTRATION OF BREAK IN ABSORBANCE LINE (B)

| | | A (mole/l.) | B (mole/l.) |
|---|---|---|---|
| Dodecyl ammonium benzoate | 30°C | 0.012±0.002 | 0.012±0.001 |
| 〃 〃 〃 | 20°C | 0.015±0.002 | 0.012±0.001 |
| Octadecyl ammonium benzoate | 30°C | 0.014±0.002 | 0.018±0.001 |

TABLE II

THE VALUES OF $\varepsilon_s$, $\varepsilon_m$ AND $C_s$ (mole/l.)

| | Dodecyl ammonium benzoate | | | | | | Octadecyl ammonium benzoate | | |
|---|---|---|---|---|---|---|---|---|---|
| Temperature | 30° | | | 20° | | | 30° | | |
| Wave length (mμ) | $\varepsilon_s$ | $\varepsilon_m$ | $C_s$ | $\varepsilon_s$ | $\varepsilon_m$ | $C_s$ | $\varepsilon_s$ | $\varepsilon_m$ | $C_s$ |
| 263 | $73_5$ | 440 | 0.013 | 670 | 610 | 0.014 | 730 | 440 | 0.018 |
| 270 | $77_5$ | 460 | 0.013 | 700 | 630 | 0.013 | 770 | 440 | 0.017 |
| 276.5-277 | 580 | 370 | 0.013 | 560 | 450 | 0.012 | $56_5$ | 370 | 0.018 |

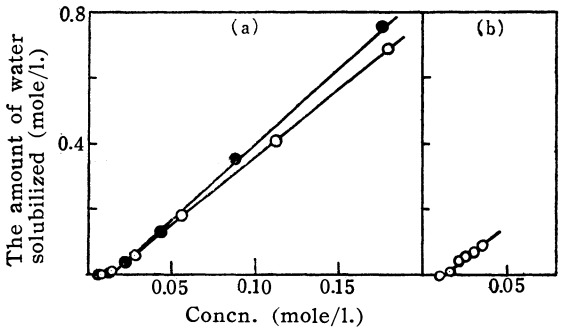



Fig. 4. The amount of water solubilized into the cyclohexane solution.

(a) —○—, for dodecyl ammonium benzoate at 30±2°C.
—●—, for dodecyl ammonium benzoate at 20±2°C.
(b) —○—, for octadecyl ammonium benzoate at 30±2°C.

absorbance lines for any peak of 276 and 284 mμ.

The relation between the limiting amount of water solubilized into detergent solutions and the concentration of detergent is shown in Fig. 4. It is seen in the figure that the relation is linear within the concentration range studied, though the linearity is somewhat ambiguous in the case of octadecyl ammonium benzoate because of its lower solubility. The concentration extrapolated to zero solubilization might be assumed to be the CMC[6]. The values of the CMC (A) obtained thus are listed in Table I. On the other hand, the concentrations corresponding to the break of absorbance lines (B), which are obtained from Figs. 1, 2 and 3 are also shown in the same table. The comparison of the values of B with the corresponding values of A shows us that both are in agreement with each other within the experimental error. Hence it will be reasonable to assume that the break in the absorbance line shows the initiation of micelle formation and that the concentration of the break is the CMC*. It will be, therefore, known that the measurement of the ultraviolet absorption spectrum has also ascertained the existence of the CMC.

**Monomer Concentration:** The equation $\log I_0/I=\varepsilon Cl$ may be used above the CMC. In this case, it is assumed that the overall extinction coefficient ($\varepsilon$) above the CMC can be expressed as follows:

$$\varepsilon=n_s\varepsilon_s+n_m\varepsilon_m, \qquad (1)$$

where $n$ is mole fraction and $\varepsilon$ the extinction coefficient, subscripts $s$ and $m$ representing a monomeric molecule and a molecule participating in micelle formation. If the concentration of a monomeric molecule above the CMC is shown by $C_s$, $n_s=C_s/C$ and $n_m=(C-C_s)/C$, where $C$ is the total concentration described in terms of the molecular weight of a monomer. Then formula (1) may be rewritten as follows:

$$\varepsilon C=\varepsilon_m C+C_s(\varepsilon_s-\varepsilon_m). \qquad (2)$$

As seen in Figs. 1, 2 and 3 the linear relation is obtained between $\log I_0/I$ and $C$ in the range above the CMC. Accordingly, $\varepsilon_m$ can be estimated from the slope of the straight line above the CMC and $C_s(\varepsilon_s-\varepsilon_m)$ from the intercept on the ordinate by extrapolating it. $\varepsilon_s$ is obtained from the slope of the linear part below the CMC. Hence $C_s$ can be calculated. The values of $\varepsilon_s$, $\varepsilon_m$ and $C_s$ obtained for each absorption peak are tabulated in Table II.

* It was presented at the same Symposium by H. Sasaki, H. Okuyama and S. Saito of Osaka University that the extinction coefficient of cetyl pyridinium chloride in the aqueous solution begins to diminish sharply at the CMC.

$\varepsilon_m$ is independent of the concentration as the result of the linearity of the absorbance curve above the CMC. As Harkins et al. pointed[7], the result just mentioned may be taken to indicate that the micelle size is constant in this range or that the transition probability of a molecule participating in micelle formation is not influenced by the micelle size. As the matter of course, the values of $C_s$ are independent of the concentration and equal to the CMC from the assumption of the formula (1). This constancy of $C_s$ corresponds to the case of higher aggregation of the results calculated from the law of mass action by Singleterry et al.[3] It is seen in Table II that the values of $C_s$ obtained for separate peaks are all equal within the experimental error. This suggests that the assumption of the formula (1) might be reasonable. The effect of temperature on the CMC was recognized with difficulty in the case of dodecyl ammonium benzoate.

## Summary

The concentration dependence of the absorbance for the ultraviolet absorption spectra was measured for cyclohexane solutions of dodecyl ammonium benzoate and of octadecyl ammonium benzoate at 20±2 and 30±2°C. The break has been observed in the absorbance-concentration relationship. On the other hand, the relation between the amount of water solubilized into solutions and the concentration of the detergent showed us the values of the CMC. The concordance found between the value corresponding to the break of the absorbance and the assumed CMC obtained from solubilization makes the existence of the CMC more probable. The concentration of the monomeric molecule and the molar extinction coefficient of the molecule participating in micelle formation were calculated with use of a simple assumption.

The author wishes to express his hearty thanks to Mr. H. Tsubomura for the discussion on the results of the ultraviolet spectrum and to Professor H. Akamatsu for his kind encouragement.

The expense of this work has been partly defrayed by aid from the Scientific Research Expenditure of the Ministry of Education, to which the author's thanks are due.

*Department of Chemistry*
*Toho University, Narashino, Chiba*

# *A Phase Transition Study on the Mercerization of Cellulose*

By Yoshizo TSUDA

(Received February 18, 1957)

## Introduction

The mercerization of native cellulose has been investigated by Sisson and Saner[1] with the X-ray method from a phase transitional point of view. The native cellulose contains a crystalline lattice of cellulose I, which is transformed into that of celluose II by the mercerization process. It is well known that the degree of transition depends on both the concentration and the temperature of sodium hydroxide solution used as the mercerizing agent. Furthermore, the concentration range depends also on the origin of the cellulose sample[2].

In a preceding paper[3] the present author has investigated the changes in the lateral order distribution of the native cellulose on the mercerization process and concluded that the lowering of the lateral order is induced with a concentration of sodium hydroxide lower than that required to induce the phase transition. But it is necessary to obtain correct knowledge about the phase transition in order to discuss the transition mechanism.

The main purpose of this investigation is to confirm the concentration range

1) W. A. Sisson and W. R. Saner, *J. Phys, Chem.*, **45**, 717 (1941).

2) B. G. Rånby and H. F. Mark, *Svensk Papperstidning*, **58**, 374 (1955).

3) Y. Tsuda and S. Mukoyama, This Bulletin, **30**, 271 (1957).

necessary to the transition and to obtain more information on the mercerization mechanism.

## Experimental Procedure

**a. Cellulose Samples.**—Cotton linters pulp and sulfate and sulfite wood pulp were used. The analytical data of the samples were as follows:

(A) Cotton linters pulp, viscose grade, α-cellulose 98.3 %, degree of polymerization 610.

(B) Sulfate wood pulp, viscose grade, α-cellulose 94.3 %, degree of polymerization 690.

(C) Sulfite wood pulp, viscose grade, α-cellulose 95.7 %, degree of polymerization 1020.

**b. Treatment with Sodium Hydroxide.**—Before the treatment, the samples were disintegrated with a mixer, and then soaked at 20°C and 45°C in sodium hydroxide solution of various concentrations for two hours. The samples were recovered by suction on a glass filter, regenerated with 0.5 N acetic acid of the same temperature and washed with distilled water. The treated samples were dried with alcohol.

**c. X-ray Diffraction.**—The air dried samples, re-disintegrated with a mixer, were analyzed by Norelco Geiger counter-X-ray diffractometer (Copper $K_\alpha$-radiation with Ni filter) with the specimen mounted by pressing in the specimen holder. The tubes were run at 35 kV. and with 15 mA emission current.

## Measurement and Results

Figs. 1, 2 and 3 show the X-ray diffraction intensity curves of the untreated, completely mercerized and partially mercerized linters pulp respectively. The untreated linters pulp gives the pattern of cellulose I, the completely mercerized one that of cellulose II, and the partially mercerized one a mixed pattern of both. The absolute intensity of X-ray diffraction depends on the density of specimen pressed in the specimen holder, so that fluctuations of the absolute intensity in repeated measurements with the same sample were inevitable. Therefore it was impossible to utilize the absolute intensity itself to estimate the relative amounts of the two phases.

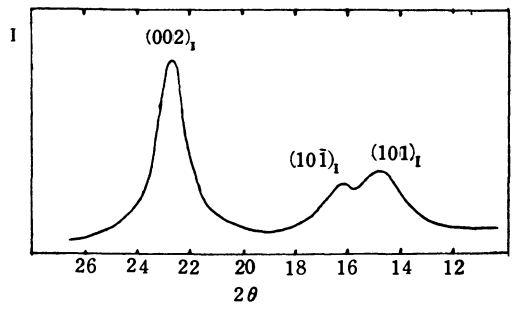



Fig. 1. X-ray diffraction intensity curve of the untreated linters pulp.

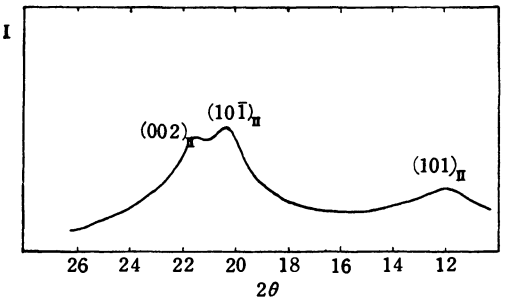



Fig. 2. X-ray diffraction intensity curve of the completely mercerized linters pulp.

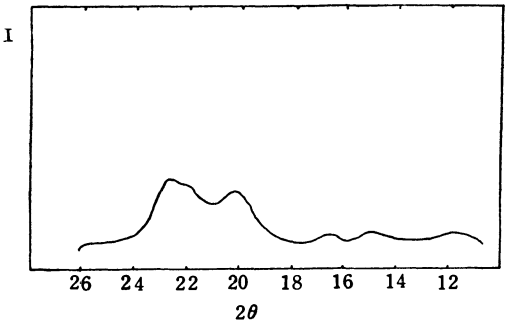



Fig. 3. X-ray diffraction intensity curve of the partially mercerized linters pulp.

In this experiment, to estimate the degree of the transition from cellulose I to cellulose II test experiments were made using samples containing known amounts of untreated and completely mercerized samples. The X-ray diffraction analyses of these samples were made with respect to the three pulp samples and then the degree of transition was followed taking the intensity ratio of (10$\bar{1}$) of cellulose II to (002) of cellulose I. In Figs. 4, 5 and 6 the

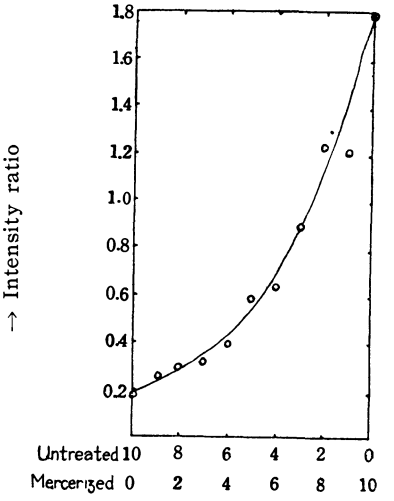



Fig. 4. Calibration curve for the linters pulp.

intensity ratio I $(10\bar{1})_{II}/I(002)_I$ is plotted against the relative amounts of the two phases. These calibration curves show that the gradient of curve increases with the increase in the amounts of cellulose I. Therefore it may be suggested that visual estimation of X-ray diffraction diagrams adopted by Sisson and Saner[1] leads to misunderstanding of the transition range. From the comparison of these figures it may be seen that the intensity ratio of the untreated linters pulp is lower than that for the untreated wood pulps, which is due to the higher lateral order of the native linters pulp.

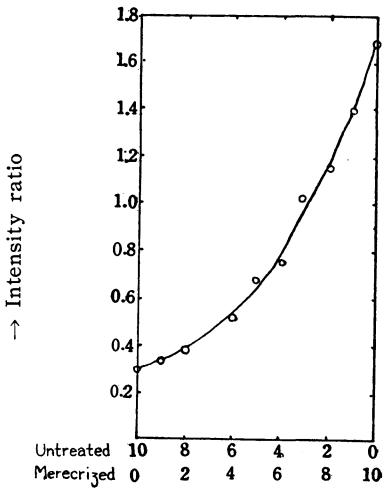



Fig. 5. Calibration curve of the sulfate pulp.

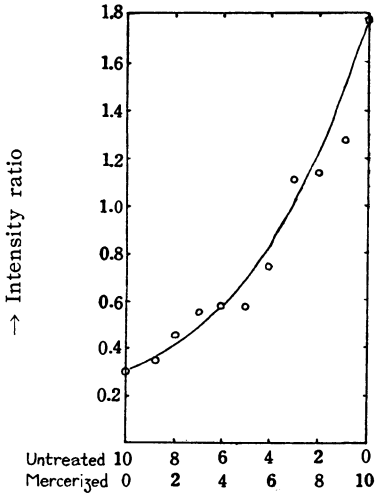



Fig. 6. Calibration curve of the sulfite pulp.

TABLE I

TRANSITION DATA OF SAMPLES TREATED AT 20°C

| Linters Pulp | | | Sulfate Pulp | | | Sulfite Pulp | | |
|---|---|---|---|---|---|---|---|---|
| NaOH[a] wt. % | I.R.[b] | D.T.[c] % | NaOH wt. % | I.R. | D.T. % | NaOH wt. % | I.R. | D.T. % |
| 9.9 | 0.16 | 0 | 8.2 | 0.32 | 5 | 8.0 | 0.32 | 6 |
| 10.7 | 0.20 | 4 | 9.0 | 0.63 | 49 | 9.0 | 0.48 | 28 |
| 11.5 | 0.33 | 28 | 9.9 | 0.72 | 56 | 10.0 | 0.79 | 59 |
| 12.3 | 0.54 | 51 | 10.7 | 1.29 | 87 | 11.0 | 1.60 | 94 |
| 13.1 | 0.83 | 68 | 11.5 | 1.29 | 87 | 12.0 | 1.55 | 93 |
| 13.9 | 1.07 | 77 | 12.3 | 1.68 | 100 | | | |
| 14.6 | 1.23 | 82 | | | | | | |
| 16.8 | 1.51 | 91 | | | | | | |

TABLE II

TRANSITION DATA OF SAMPLES TREATED AT 45°C

| Linters Pulp | | | Sulfate Pulp | | | Sulfite Pulp | | |
|---|---|---|---|---|---|---|---|---|
| NaOH[a] wt. % | I.R.[b] | D.T.[c] % | NaOH wt. % | I.R. | D.T. % | NaOH wt. % | I.R. | D.T. % |
| 10.0 | 0.21 | 8 | 9.0 | 0.28 | 0 | 9.0 | 0.30 | 0 |
| 11.0 | 0.26 | 16 | 10.0 | 0.38 | 18 | 10.0 | 0.36 | 12 |
| 12.0 | 0.31 | 25 | 11.0 | 0.58 | 44 | 11.0 | 0.74 | 54 |
| 13.0 | 0.33 | 28 | 12.0 | 1.07 | 75 | 12.0 | 1.04 | 72 |
| 14.0 | 0.56 | 52 | 13.0 | 1.13 | 78 | 13.0 | 1.40 | 86 |
| 15.0 | 1.18 | 81 | 14.0 | 1.25 | 83 | 14.0 | 1.63 | 96 |
| 16.0 | 1.38 | 87 | 15.0 | 1.56 | 95 | | | |
| 17.0 | 1.48 | 90 | 16.0 | 1.64 | 99 | | | |
| 18.0 | 1.59 | 94 | | | | | | |

a) Concentration of NaOH used as the mercerizing agent.
b) Intensity ratio of I $(10\bar{1})_{II}$ to I $(002)_I$.
c) Degree of transition.

The observed intensity ratio and the corresponding degree of transition estimated from the calibration curves are tabulated in Table I and II.

In Fig. 7 and 8 the obtained degree of transition is plotted against the concentration of alkali. The main transition ranges are tabulated in Table III. As shown in Fig. 7 and Fig. 8, the higher resistance against the mercerization is characteristic of the linters pulp, whereas no difference between the sulfate and the sulfite pulp is observed in the transition behavior. The elevation of the temperature of the alkali treatment induces the increase in the concentration of the main transition range.

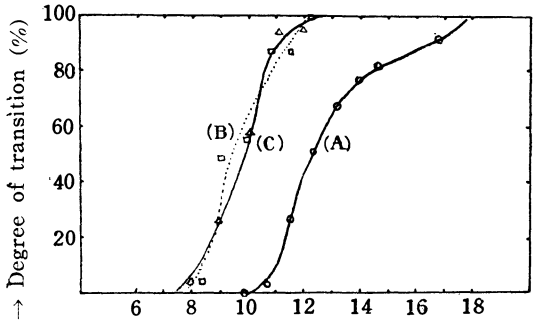



Fig. 7. Phase transition curves (at 20°C).
(A) the linters pulp
(B) the sulfate pulp
(C) the sulfite pulp

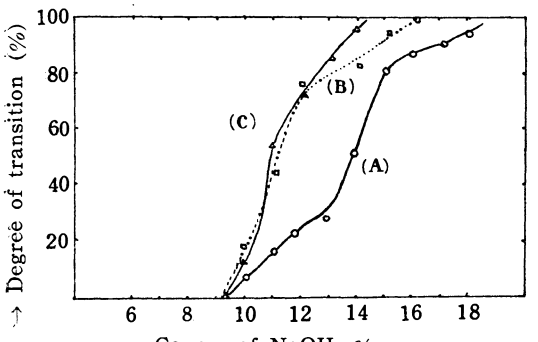



Fig. 8. Phase transition curves (at 45°C).

TABLE III
THE MAIN TRANSITION RANGE (EXPRESSED IN THE CONCENTRATION OF NaOH)

| Pulp Samples | Temperature of Treatment | |
|---|---|---|
| | 20°C | 45°C |
| Linters Pulp | 11-16 | 10-17 |
| Sulfate Pulp | 8-11 | 10-15 |
| Sulfite Pulp | 8-11 | 10-13 |

## Discussion

The results reported here were based on the assumption that the decrystallization, which accompanies the mercerization, proceeds in proportion to the degree of transition. This assumption may contradict the results obtained in the preceding paper[3,4], but it must be mentioned that the pattern of cellulose II appears only for the sample whose cellulose II content is more than 40 per cent., according to the results of the test experiment. Therefore the decrystallization could not be discriminated from the phase transition by such an empirical method.

The transition range of the sulfate pulp is not different from that of the sulfite pulp, which is in good agreement with the lateral order distribution reported in the the preceding paper[4]. On the contrary, Rånby and Mark[2] reported that the sulfate pulp shows a higher resistance against the mercerization than the sulfite pulp. This difference may be due to the difference in the fine structure of both sulfate pulps. According to the results obtained here, it may be concluded that the crystalline structure of the sulfate pulp is not different from that of the sulfite pulp.

As shown in Fig. 8 all pulp samples show at 45°C an increased resistance against the complete mercerization. This tendency is in agreement with the results obtained by Sisson and Saner[1].

The variation in the lateral order distribution on the mercerization process which was reported in the previous paper[3] should be discussed again with the knowledge of transition obtained here. The variation range of lateral order distribution of the linters pulp at 20°C almost corresponds to the transition range obtained here, so that the preceding conclusion must be altered as follows: on the mercerization process the lowering of the lateral order is accompanied simultaneously with the phase transition; in other words, the former does not precede the latter. The misunderstanding of the transition range in the previous paper[4] was due to the visual estimation of the X-ray diffraction diagrams.

One may obtain further information on the mercerization mechanism, comparing the phase transition behavior with the the variation in the lateral order distribution acompanying it.

4) Y. Tsuda and S. Mukoyama, This Bulletin, **29**, 748 (1956).

**Summary**

The phase transition ranges were obtained at 20°C and 45°C for the linters pulp, the sulfate pulp and the sulfite pulp. It was concluded that the resistance of the linters pulp against the mercerization is higher than those of the wood pulp, where as no difference is observed between the sulfate and the sulfite pulp.

It was suggested also that the visual estimation of the X-ray diffraction diagrams may lead to a misunderstanding of the phase transition range.

The author is grateful to Dr. K. Hoshino for permitting this publication.

*Research Department of*
*Toyo Rayon Co., Ltd.*
*Otsu, Shiga*

# *Crystallinity Studies of Polychlorotrifluoroethylene by Infrared Method. I. Measurement of the Degree of Crystallinity*

By Hiroshi MATSUO

(Received February 5, 1957)

## Introduction

The measurement of the degree of crystallinity is becoming of increasing importance in the study of polymer properties. Therefore many methods for its estimation have been devised. The crystallinity of polychlorotrifluoroethylene (PCTFE) was studied by Price[1] by volume method, and by Hoffman[2] by specific heat method. It appears of interest to investigate the subject further by infrared method, which is also available for reliable estimation of crystallinity for a number of common polymers[3].

In the course of examination of infrared spectra of PCTFE, the author believed that they yield some bits information about the crystallinity and the state of the orientation. A survey of the spectrum revealed that some of the bands behaved as if they were given by the crystalline parts of the polymer, while others appeared to be produced by the amorphous parts. These discoveries were utilized in the present study of crystallinity of PCTFE, and the degree of crystallinity was estimated independent of other methods.

## Effect of Crystallization on the Infrared Bands

PCTFE is an extremely intractable material, because there is no proper solvent at room temperature, and furthermore the spectrum of PCTFE shows such strong absorptions at about 1300–900 cm.$^{-1}$ region that thin films of 0.01–0.03 mm. thickness are necessary for infrared method. Thin films were prepared by extruding Daiflon[4] (NST 270) at above its melting point. The orientation of crystallites in the extruded film was estimated from the intensity distribution around the X-ray diffraction ring. It was examined further with a beam of polarized infrared radiation using a polarizer of silverchloride plates placed immediately in front of the entrance slit of the infrared spectrometer. A comparison of the spectra obtained when the electric vector was vibrating parallel and perpendicular to the extruded direction

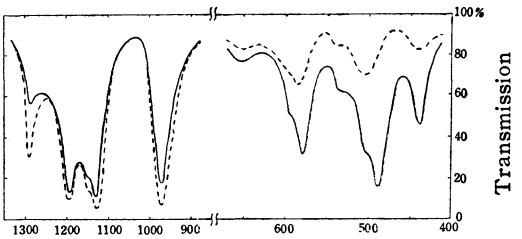



Fig. 1. Infrared spectrum of oriented polychlorotrifluoroethylene, obtained by polarized radiation.
——: electric vector parallel to the extruded direction.
----: electric vector perpendicular to the extruded direction.

1) F. P. Price, *J. Chem. Phys.*, **19**, 973 (1951).
2) J. D. Hoffman, *J. Am. Chem. Soc.*, **74**, 1696 (1952).
3) J. B. Nichols, *J. Appl. Phys.*, **25**, 840 (1954).

4) Trade name of high molecular weight PCTFE produced by Osaka Kinzoku Kogyo Co.

shows significant dichroism on the majority of absorption bands. This is shown in Fig. 1. These absorption bands indicated not only significant dichroism but also intensity changes as the crystallization proceeded[5]. The latter was examined comparing the spectra of annealed, quenched, and molten samples. In order to eliminate the effect of orientation, these samples were heated at above the melting point beforehand and then annealed or quenched to room temperature. Their spectra are shown in Fig. 2. To obtain the infrared spectrum

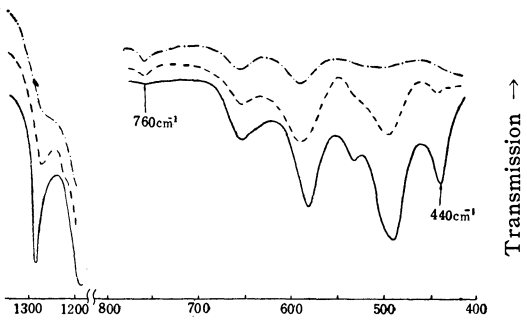



Fig. 2. Infrared spectra of polychlorotrifluoroethylene.
——: annealed sample,
----: quenched sample,
·-·-: molten sample at 230°C.

of molten polymer, a film of the polymer was sealed together with a thermocouple between potassium bromide plates. This was then placed in a heating cell[6] mounted on the spectrometer.

Fig. 2 shows that the absorption bands at 1290, 580, 506, 490 and 440 cm.$^{-1}$ increase markedly in intensity and present small shifts as the crystallization proceeds. This increase in intensity indicates that randomly oriented crystallites have been produced in the polymer by the heat treatment and it agrees with the results obtained by X-ray diffraction. These absorption bands whose intensities increase as the crystallization proceeds can be, therefore, regarded as crystalline bands. On the other hand, the intensity of the absorption band at 760 cm.$^{-1}$ decreases as crystallization proceeds, so that this band can be regarded as an amorphous band[7]. These crystalline and amorphous bands are summarized in Table I, where $\pi$ means that

5) H. Matsuo, *J. Polymer Sci.*, **21**, 331 (1956).
6) R. E. Richards and H. W. Thompson, *Trans. Faraday Soc.*, **41**, 183 (1945).
7) R. G. J. Miller and H. A. Willis, *J. Polymer Sci.*, **19**, 485 (1956).

TABLE I
INTERPRETATION OF THE INFRARED SPECTRUM OF EXTRUDED PCTFE

| Freq. cm.$^{-1}$ | Relative Intensity | Dichroic ratio[a] | Character of band[b] | | Probable assignment[c] |
|---|---|---|---|---|---|
| 438 | s | 3.7 | $\pi$ | c | CClF wagging |
| 490 | s | 5.6 | $\pi$ | c | $CF_2$ rocking |
| 506 | s | | $\sigma$ ? | c | $CF_2$ bending |
| (535) | | | | c | |
| 580 | s | 2.2 | $\pi$ | c | $CF_2$ wagging |
| 658 | m | | $\pi$ | a ? | |
| 723 | w | | $\pi$ | | |
| 755 | w | | $\sigma$ ? | a | |
| 972 | vs | | $\sigma$ | | CCl stretching |
| 1130 | vs | | $\sigma$ | | $CF_2$ stretching |
| (1147) | | | $\sigma$ | | |
| 1194 | vs | | $\sigma$ | | $CF_2$ stretching |
| 1285 | s | 0.3 | $\sigma$ | c | CF stretching |

a) dichroic ratio $=\log(I_0/I)_\pi/\log(I_0/I)_\sigma$.
b) c=crystalline, a=amorphous.
c) These assignments are due to C. Y. Liang and S. Krimm, *J. Chem. Phys.*, **25**, 563 (1956).

the absorption in the case of the electric vector parallel to the extruded direction is greater than in the case of the perpendicular electric vector, and $\sigma$ the reverse case.

## Degree of Crystallinity

The degree of crystallinity was measured by the use of the crystalline band at 440 cm.$^{-1}$ and the amorphous band at 760 cm.$^{-1}$.

The experiments were carried out with a Perkin-Elmer Model 112 Spectrometer equipped with potassium bromide prism. The slit was driven connecting with wavelength drive cam, so as to obtain flat background trace. The resolving powers at 440 cm.$^{-1}$ and 760 cm.$^{-1}$ were approximately 3 cm.$^{-1}$ and 2.5 cm.$^{-1}$, respectively. Stray radiation at 440 cm.$^{-1}$ was less than one percent. of the detected radiation. The starting material was a sheet of melt-extruded, quenched film of 0.03 mm. nominal thickness. Samples with various degrees of crystallinity were obtained from it by quenching to room temperature from 230°C or annealing to various crystallization temperatures between 200° and 130°C. Specific volumes were obtained within the accuracy of ±0.0007 from densities measured by the flotation method at 25°C using a solution of bromoform and xylene. In

this case the optical density $D$ was defined as follows,

$$D=(1/td)\log(I_0/I)$$

where $t$ and $d$ are the thickness and the specific gravity of the sample, $I_0$ is the height of the background trace obtained by the base-line method at the peak of the band, and $I$ the height of the band peak. As the thickness of the sample had to be accurately measured for the optical density measurements, the following method was used. The portion irradiated by the infrared beam was cut out from the film, and weighed by a microbalance. The area of the surface of the film was determined by direct measurement. Density being known, the effective thickness could be calculated. The accuracy was estimated to be $\pm 0.002$ mm.

Since specific volume changes have been used to measure crystallinity, the changes in optical densities at 440 cm.$^{-1}$ and 760 cm.$^{-1}$ were correlated with change in specific volume. Specific volumes were plotted against optical densities for a number of samples. All points lie on a straight line within the accuracy of the experiment, and therefore the following equations were assumed.

$$D_1=K_1^c X+K_1^a(1-X)$$
$$D_2=K_2^a(1-X)$$

and consequently,

$$D_1=K_1^c-[(K_1^c-K_1^a)/K_2^a]D_2 \quad (1)$$
$$R=D_1/D_2=[X/(1-X)](K_1^c/K_2^a)+(K_1^a/K_2^a) \quad (2)$$

where $X$ is the degree of crystallinity; $D_1$ and $D_2$ are optical densities at 440 cm.$^{-1}$ and 760 cm.$^{-1}$, respectively; $K_1^c$ and $K_1^a$ are extinction coefficients of crystalline and amorphous parts at 440 cm.$^{-1}$, respectively, and $K_2^a$ is that of the amorphous part at 760 cm.$^{-1}$ $R$ is the ratio of the observed absorbance at 440 cm.$^{-1}$ to that at 760 cm.$^{-1}$, and is independent of the thickness of the sample since the absorbances are determined for two bands in the same sample.

By plotting $D_1$ against $D_2$, a straight line was observed. Equation (1) means that the value of the inclination of the line corresponds to $(K_1^c-K_1^a)/K_2^a$ and the value of its intersection with the ordinate axis corresponds to $K_1^c$. Furtheremore, Equation (2) indicates that the value of $R$ of the completely amorphous state correspond to $(K_1^a/K_2^a)$. However, since the completly amorphous material could not be obtained by quenching the polymer from the molten state, the value of $R$ of the completely amorphous state was determined by the following method. Daifloil[8] No. 50, which was a product of pyrolysed PCTFE and was a viscous liquid at room temperature, was used as an amorphous standard for the high molecular weight PCTFE. Its spectrum was very similar to that of the molten high molecular weight PCTFE, except for the existence of the absorption band at 1340 cm.$^{-1}$, which would be due to $=CF_2$ group[9]. Thus $R=2.05$ was obtained for completely amorphous polymer at room temperature. The same value of $R$ was measured in the molten state which was obtained by heating Daiflon film to 240°C in the heating cell; it appears, therefore, that little change in the intensity of the absorption bands at elevated temperatures would be expected. Thus $K_1^c=9.02$, $K_1^a=2.12$, and $K_2^a=1.03$ were obtained, and the degree of crystallinity could be calculated from Equation (2):

$$X=(R-2.05)/(R+6.67) \quad (3)$$

The degree of crystallinity of PCTFE as a function of temperature was calculated from the measurement of $R$ at various temperatures by the use of Equation (3). A film of 0.03 mm. thickness of the polymer which was quenched from above its melting point to room temperature, was inserted into the heating cell and degrees of crystallinity at various temperatures were measured. They are shown in Fig. 3. The sample was heated slowly to 100° then

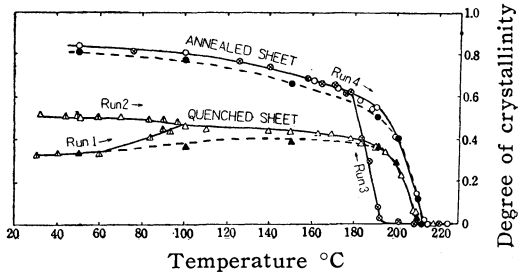



Fig. 3. Degree of crystallinity of polychlorotrifluoroethylene as a function of temperature.
(△) Run 1, (△) Run 2 with quenched sample,
(⊗) Run 3, (○) Run 4 with annealed sample;
(▲, ●) obtained by Hoffman by specific heat method with quenched and annealed samples, respectively.

8) Trade name of low molecular weight PCTFE produced by Osaka Kinzoku Kogyo Co.
9) R. B. Barnes and R. C. Gore, *Anal. Chem.*, **20**, 402 (1948).

cooled down to room temperature (Run 1), and was heated again to 225° (Run 2). These data were listed in Fig. 3 as "quenched". The material was then cooled at a rate of 0.3°C/min. from 225° to room temperature (Run 3), and another run made to 225° (Run 4). These data were listed as "annealed". The degree of crystallinity of the quenched and the annealed sample obtained by the present method and that by Hoffman[2] by specific heat method agree with each other within ca. ±5%; this may be regarded satisfactory. Run 1 shows a definite increase in crystallinity of the quenched sample in the range of 80 to 100° as it is heated. This was confirmed further by the fact that the sample showed higher crystallinity than the original one when it was cooled from 100° to room temperature again. This definite increase must be due to super-cooled amorphous forming crystallites as the viscosity decreases sufficiently to permit recrystallization. On the other hand, the annealed sample apparently contains a few small crystallites which melt as low as 100°, and on further heating, the crystallinity steeply drops from about 196° and reaches zero at 212°. Between 180° and 212°, Run 3 and Run 4 do not coincide, and it may partly owe to non-attainment of equilibrium. The hysteresis shown by the non-coincidence of melting point (212°) and freezing point (195°) in this Figure was also observed in the measurements of specific volume, and dielectric constant and loss of PCTFE[10].

Furthermore, a linear relationship between the degree of crystallinity and the specific volume was obtained within the experimental uncertainty (Fig. 4). It leads to extrapolated values of 0.4901±0.001 and 0.4575±0.001 for specific volumes of completely amorphous and crystalline materials, respectively. Generally the degree of crystallinity can be also determined from specific volume method by the equation

$$X=(V_a-V)/(V_a-V_c)$$

However, so far as PCTFE is concerned, the value of specific volume for completely amorphous material ($V_a$) and that for completely crystalline material ($V_c$) have not as yet been determined with sufficient accuracy for computing absolute values of $X$, even by the extrapolation method of specific volume from the molten state[10,11] and by X-ray diffraction method[12]. Using

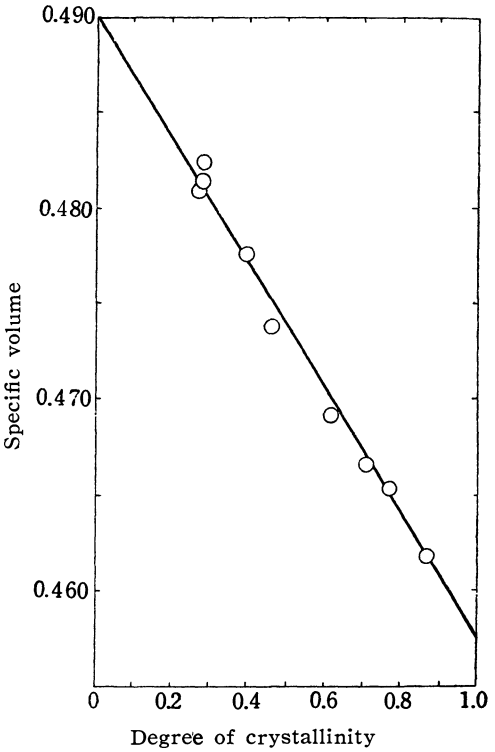



Fig. 4. Correlation of specific volume with degree of crystallinity of polychlorotrifluoroethylene.

$V_a=0.4901$ and $V_c=0.4575$ obtained by the present method, the degree of crystallinity was determined from the measurement of the specific volume $V$ by the following equation,

$$X=(0.4901-V)/0.0326 \qquad (4)$$

In Table II, degrees of crystallinity obtained from infrared method and from specific volume method are shown. From this Table, it is apparent that amorphous material could not be obtained by such a quenching procedure of the molten polymer and the crystallinity of the quenched polymer attains to 27%, and, by annealing at higher crystallization temperature for several hours, the crystallinity of the annealed polymer amounts to 87%.

## Summary

The crystalline-amorphous ratio, and consequently the degree of crystallinity of polychlorotrifluoroethylene was measured by use of the ratio of observed absorbance of crystalline band at 440 cm.$^{-1}$ to that of amorphous band at 760 cm.$^{-1}$. The crystallinity as a function of temperature was measured by this method, and it was in

10) F. P. Price, *J. Am. Chem. Soc.*, **74**, 317 (1952).
11) S. Furuya, *J. Polymer Sci.*, **20**, 587 (1956).
12) H. S. Kaufman, *J. Am. Chem. Soc.*, **75**, 1477 (1953).

TABLE II
PATICULARS OF SAMPLES OF PCTFE

| Specific volume | Thickness mm. | log ($I_0/I$) at 440 cm.$^{-1}$ | log ($I_0/I$) at 760 cm.$^{-1}$ | $R$[a] | Crystallinity, % from I. R.[b] | Crystallinity, % from sp. vol.[c] | Condition of heat treatment |
|---|---|---|---|---|---|---|---|
| — | — | 0.119 | 0.058 | 2.0 | 0 | — | measured at 240° |
| 0.4825 | — | 0.292 | 0.054 | 5.4 | 28 | 23 | quenched from 230° to dry-ice temperature |
| 0.4815 | 0.029 | 0.255 | 0.047 | 5.4 | 28 | 26 | quenched from 230° to room temperature |
| 0.4810 | 0.026 | 0.196 | 0.037 | 5.3 | 27 | 28 | quenched from 230° to room temperature |
| 0.4775 | 0.027 | 0.290 | 0.037 | 7.7 | 39 | 39 | quenched film was heated at 130° |
| 0.4739 | 0.030 | 0.310 | 0.033 | 9.4 | 46 | 50 | quenched film was heated at 130° |
| 0.4691 | 0.024 | 0.301 | 0.019 | 15.8 | 61 | 64 | annealed from 230° to room temperature |
| 0.4666 | 0.032 | 0.522 | 0.023 | 22.7 | 70 | 72 | annealed from 230° to room temperature |
| 0.4654 | 0.030 | 0.487 | 0.016 | 30.4 | 76 | 76 | annealed from 230° to room temperature |
| 0.4618 | — | 0.316 | 0.005 | 63.2 | 87 | 87 | annealed at 190° for 3 hr. |

a) $R = \log(I_0/I)440\,\text{cm.}^{-1} / \log(I_0/I)760\,\text{cm.}^{-1}$.
b) calculated from Equation (3).
c) calculated from Equation (4).

good agreements with that obtained by specific heat methd. Furthermore, a linear relationship between the degree of crystallinity and the specific volume was found, and it leads to extrapolated values of 0.4901 and 0.4575 for the specific volumes of completely amorphous and crystalline materials, respectively.

The author would like to express his appreciation to Mr. S. Owaki of this laboratory for X-ray diffraction work which has assisted in the interpretation of the data, and to Dr. Y. Kubouchi of Osaka Kinzoku Kogyo Co. for supplying Daiflon film and Daifloil No. 50.

*Electrical Communication Laboratory*
*Nippon Telegraph and Telephone*
*Public Corporation*
*Musashino-shi, Tokyo*

# *Microscopic Studies on Fused Catalysts for Ammonia Synthesis. V. Conversion Test with A and B Constituents and Some Studies on "M" Type Crystal*

By Yoshio ŌSUMI and Makoto INOUE

(Received February 21, 1957)

## Introduction

As reported in our previous papers[1-9]. It was shown, by the aid of the optical[1,5], the surface-electron[1,6] and the surface-ion microscopy[2,7], that some fused catalysts promoted with potash with or without some other additions, consisted of two different sorts of grain. Grains of the one sort (B), much less abundant and magnetic than those of the other sort (A), can be singled out magnetically from the finely pulverized catalyst. "B" powder is richer in potash than "A" powder. "A" powder possesses the magnetite lattice, while "B" powder shows a highly complicated "M"-type diffraction[3,8] pattern of lower degree of symmetry, probably owing to a slight modification of the magnetite lattice. "B" powder is less active than "A" powder towards decomposition of ammonia at the atmospheric pressure[4,9].

The present paper deals with the study on some properties of "B" powder and some comparative studies on "A" and "B" powder with respect to their reducibility in hydrogen, their corrodibility in acid, and their conversion activity and BET surface area in the reduced state.

## "M" Type Phase

In ref. 3 it was shown that the content of the water-insoluble potash of A powder attained at most about 0.6 per cent., while that of "M" type "B" powder about five to ten times as much. The chemical analyses were performed after washing out soluble potash with cold distilled water. Recently the amounts of both the soluble and the insoluble potash have been redetermined with new samples. They were washed by boiling in water for one hour. The results are tabulated in Table I (No. II-1, II-4 and II-5) together with the previous ones (No. 3, 4, 10 and 12). The new results confirm the upper limit of potash content in "A" powder at about 0.6 per cent.

The potash content amounting to 0.6 per cent. in "A" powder corresponds to about one atom of potassium for every five unit cells of the magnetite lattice, whereas the potash content in "B" powder about one to two atoms of potassium for each unit cell of the "M" type lattice which is assumed to be equal to that of magnetite.

It is a laborious task to magnetically separate "B" powder from "A" powder. It was attempted to obtain a nearly pure "B" mass by adding as much as 5 per cent. of potash in the usual process of preparing the catalyst. Catalyst II-4 thus prepared gave, however, on magnetic separation, only a small portion of "B" powder comparable in amount with ordinary catalysts. The greater part of potash was found water soluble (Table I).

Of twelve sorts of catalyst previously examined by X-rays, those promoted with potash and alumina always contained "B" powder of the "M" type in which iron is largely in the ferric state. The "B" powder from catalyst II-1 (Table I), however, gives the FeO pattern, instead of the "M" and in fact the iron in it is found mainly in the ferrous state, while the iron in the "A" powder has the usual magnetite composition. The insufficient oxidation of the catalyst in the fusion process seems to affect the oxidation state of iron in the "B" phase rather than in the "A". This fact suggests that the presence of

1) N. Sasaki and Y. Ōsumi, *J. Chem. Soc., Japan (Pure Chem. Sec.)* **73**, 808 (1952).
2) Y. Ōsumi, ibid., **74**, 308 (1953).
3) Y. Ōsumi, This Bulletin, **26**, 519 (1953).
4) Y. Ōsumi, ibid., **28**, 156 (1955). More details of the results are found in 5) etc
5) Y. Ōsumi, *Ammonium Sulfate Engineering* (Japanese), **16**, 13 (1952).
6) Y. Ōsumi, ibid., **17**, 8 (1953).
7) Y. Ōsumi, ibid., **18**, 11 (1953).
8) Y. Ōsumi, ibid., **18**, 14 (1953).
9) Y. Ōsumi, ibid., **23**, 6 (1954).

TABLE I

| Catalyst No. and (promoter in per cent) | species of powder isolated | weight per centage | X-ray diffraction pattern | per centage of oxide found in the powder: $K_2O$ water soluble | $K_2O$ water insoluble | $K_2O$ total | CaO | MgO | $Al_2O_3$ | Fe-oxides* | $T$°C |
|---|---|---|---|---|---|---|---|---|---|---|---|
| II-1 | A | 99.0 | magnetite | 0.4 | 0.5 | 0.9 | 0.5 | | 4.2 | 94.1 | 530 |
| (1 $K_2O$, 1 CaO, 5 $Al_2O_3$ | B | 1.0 | FeO | 0.8 | 0.9 | 1.7 | 1.1 | | 5.6 | 89.0 | 465 |
| II-4 | A | 89.8 | magnetite | 3.0 | 0.6 | 3.6 | | | 5.1 | 90.8 | 550 |
| (5 $K_2O$, 5 $Al_2O_3$) | B | 10.2 | M | 6.8 | 3.1 | 9.9 | | | 6.0 | 82.5 | 550 |
| II-5 | A | 90.5 | magnetite | 0.2 | 0.6 | 0.8 | 0.3 | | 5.3 | 94.1 | 515 |
| (1 $K_2O$, 1 CaO, 5 $Al_2O_3$) | B | 9.5 | M | 0.7 | 5.4 | 6.1 | 1.0 | | 4.4 | 90.4 | 505 |
| 3 | A | 96.1 | magnetite | | 0.58 | | | | | — | — |
| (1 $K_2O$) | B | 3.9 | FeO | | 2.13 | | | | | — | — |
| 4 | A | 96.9 | magnetite | | 0.40 | | | | 4.8 | 92.8 | 510 |
| (1 $K_2O$, 5 $Al_2O_3$) | B | 3.1 | M | | 4.00 | | | | 6.3 | 84.5 | 515 |
| 10 | A | 95.0 | magnetite | | 0.52 | | 0.46 | | 11.3 | 84.4 | 520 |
| (1 $K_2O$, 1 CaO, 10 $Al_2O_3$) | B | 5.0 | M | | 3.49 | | 2.41 | | 25.0 | 71.6 | 515 |
| 12 | A | 92.0 | magnetite | | 0.34 | | | 0.70 | 4.9 | 93.7 | 515 |
| (1 $K_2O$, 1 MgO, 5 $Al_2O_3$) | B | 8.0 | M | | 1.98 | | | 0.61 | 3.4 | 93.1 | 515 |

* These figures are obtained by conveniently assuming all Fe exists as $Fe_3O_4$ in "magnetite", as $Fe_2O_3$ in "M" and as FeO in "FeO". Actually, for example, $Fe^{2+}/Fe^{3+}=36/67$ for Cat II-1, A ("magnetite" type), $Fe^{2+}/Fe^{3+}=9/91$ for Cat II-4, B ("M" type) and $Fe^{2+}/Fe^{3+}=71/29$ for Cat II-1, B ("FeO" type).

alumina is not sufficient for the formation of the "M" type "B" phase and the state of oxidation of iron is rather essential. It may be that alumina is even unnecessary in this connection and the formation of the "FeO" type instead of the "M" type in ctalyst 3 (Table I) is a result of the insufficient oxidation and not of the absence of alumina.

Attempts have been made to synthesize the oxide having the "M" type structure by heating,in an iron boat in nitrogen

TABLE II

THERMOSTABILITY OF B POWDER ("M" type)

| temperature C° | period of heating hr. | X-ray diffraction pattern | $T$°C |
|---|---|---|---|
| 550 | 1 | "M", (Hematite) | |
| 750 | 1 | "M", (Hematite) | 505 |
| 880 | 1 | "M", Hamatite | |
| 960 | 1 | Hematite, "M" | 500 |
| 1000 | 2 | "M", Hematite | |
| 1040 | 1 | "M", Hematite, Magnetite | |
| 1130 | 1 | Magnetite, Hematite, "M" | 520 |
| 1220 | 1 | Magnetite, Hematite | |
| 1340 | 2 | Magnetite, (Hematite) | 540 |

X-ray figures are listed in the order of decreasing intensity and braketed ones are very weak.

TABLE III

POTASH FUSION OF IRON OXIDE

| temperature °C | type of oxide | X-ray diffraction pattern |
|---|---|---|
| 700 | $Fe_3O_4$ | Magnetite, "M" |
| | $Fe_2O_3$ | "M"? |
| 880 | $Fe_3O_4$ | "M", Magnetite |
| | $Fe_2O_3$ | "M"?, (FeO) |
| 930 | $Fe_3O_4$ | "M", Magnetite |
| | $Fe_2O_3$ | Magnetite, FeO |
| 1010 | $Fe_3O_4$ | FeO, Magnetite, FeO |
| | $Fe_2O_3$ | FeO |
| 1200 | $Fe_3O_4$ | Magnetite, FeO |
| | $Fe_2O_3$ | FeO Magnetite |

Each oxide was fused with potassium nitrate of half the weight of the oxide for three hours in a nitrogen stream.

atomosphere, at temperatures given in Table III, a certain quantity of pure magnetite or hematite with half the weight of potassium nitrate and without any addition of alumina. The X-ray examination of specimens after washing with water shows that the "M" type structure can be obtained when the heating temperature was not higher than 1000°C. The conclusion is that for the synthesis of "M" phase the excess of potash alone is necessary, alumina and other additions being unessential. The "M" particles thus synthesized, however, are not at all attracted by the magnet while the "M" type

"B" particles are feebly attracted.

Further attempts were made to synthesize the "M" type crystals containing alumina by potash fusion of mixtures of magnetite and alumina in more or less intimate mixture (Table IV). The structure aimed at was obtained in products fused at about 900°C with a sufficient quantity of potash (the products were also non-magnetic).

The following experiments were performed with "A" and "B" powders prepared from catalyst II-5 (Table-I) with alumina, lime and potash as promoters.

## Thermostability of the "M" type Phase

The thermostability of the "M" type lattice mentioned above was tested as follows. About 0.5 g of B powder placed on a piece of platinum plate was heated in a porcelain tube in the nitrogen stream at temperatures given in Table II and after cooling subjected to the X-ray examination. Table II shows that the "M" type phase becomes unstable at about 1000°C, to change into the magnetite lattice (the powder becomes strongly magnetic). This change is probably caused by the loss of potash and oxygen at high temperatures so that the "M" type phase can survive much higher temperatures when it cools down from the solidifying point as the constituent in the matrics of the "A" phase. It will be noted in this connection that the electron-emission characteristics of "B" grains as revealed by the surface electron microscope[1] may be related to the potash liberated accompanying this lattice transformation.

As to the possible mechanism of the formation of the "M" type phase in fused catalysts, it may be suggested that at higher temperatures fused oxide probably forms a homogeneous phase with potash, which on solidifying yields magnetite crystals with about 0.6 per cent. of potash, the remaining potash being enriched at the crystal boundaries to form "M" type crystals.

## Corrosion in Acid Solutions and Reduction in Hydrogen Gas

The change in appearance of the polished surface of "B" grains, as the optical microscope observations showed[1], was less marked on reduction in hydrogen and more marked on attack in hydrochloric acid than that of "A" grains. But the loss in weight in both cases of "A" powder does not differ much from that of "B" powder.

The action of the acid was observed with 1.5 g of the specimen by dipping in hydrochloric acid at room temperature. In 1 N-acid dissolved 6 per cent. of both "A" and "B" in one day, and in 6 N-acid 17 per cent. of A and 15 per cent. of "B" in three hours.

The weight change during reduction in hydrogen was followed with a quartz fiber torsion balance carrying 0.1 g. of the specimen in powder form (~200 mesh) in a heated tube through which hydrogen gas at atmospheric pressure was passed at the rate of 40 cc. per minute. The temperature was raised at the rate of 100°C per 40 minutes.

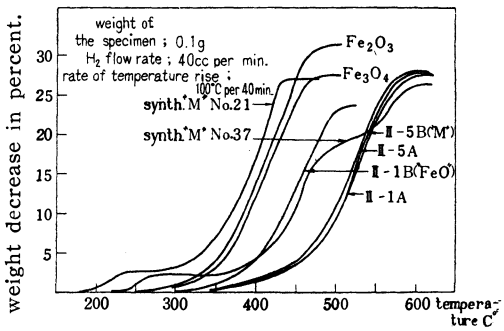



Fig. 1. Rate of weight decrease by hydrogen reduction for A, B powder and some other iron oxides.

The reduction curve of "B" (Fig. 1) is nearly the same in form as that of "A". The temperature $T$ (Table I) at which half the oxide has been reduced to iron is almost the same for "A" and "B" powders from one and the same catalyst. Different values of $T$ were obtained for catalyst II-1, whose "B" powder shows the FeO pattern.

It is a matter of well-established fact[1,5,10] that alumina in magnetite raises the temperature of beginning reduction. It may, therefore, be concluded that the aluminium atoms in the "M" type lattice are situated essentially in the same manner as in the magnetite lattice. But the $T$ values of those "M" type products (No. 37 and 43 in Table IV) prepared by potash fusion of alumina-promoted magnetite are lower than that of the "M" type "B" powder separated from catalysts. This fact may be explained by the assumption that the excessive potash

10) A. Mittash u. E. Kennecke, Z. Elektrochem., **38**, 666 (1932).

TABLE IV

POTASH FUSION OF IRON OXIDE WITH ALUMINA

| No. of specimen | temperature °C | materials and mixing ratio in brackt | | X-ray diffraction pattern | $T$°C |
|---|---|---|---|---|---|
| 21 | 850 | $Fe_3O_4$ (10) $Al_2O_3$ (0.5) | $KNO_3$ (5) | "M" | 395 |
| 22 | | | KOH (5) | "M" | 425 |
| 23 | | | $K_2CO_3$ (5) | FeO | 410 |
| 34 | 520 | catalyst promoted with 5% $Al_2O_3$ (10) | $KNO_3$ (5) | Hematite | 490 |
| 35 | 610 | | | Hematite | 485 |
| 36 | 730 | | | Hematite | 465 |
| 37 | 900 | | | "M" | 465 |
| 79 | 970 | | | FeO | 425 |
| 39 | 900 | catalyst promoted with 5% $Al_2O_3$ (10) | $KNO_3$ (0.5) | Hematite | 490 |
| 42 | | | $KNO_3$ (1) | | 490 |
| 43 | | | $KNO_3$ (2) | "M"? | 490 |
| 41 | | | $KNO_3$ (5) | | 480 |
| 58 | 700 | catalyst promoted with 5% $Al_2O_3$ (10) | $K_2CO_3$ (3) | | 480 |
| 59 | 810 | | | Hem, Mag | 480 |
| 60 | 900 | | | | 485 |
| 77 | 1000 | | | FeO | 470 |
| 73 | 1150 | | | FeO | 465 |
| 52 | 900 | catalyst promoted with 5% $Al_2O_3$ (10) | $K_2CO_3$ (0.2) | | 480 |
| 53 | | | $K_2CO_3$ (0.7) | Mag, Hem | 475 |
| 56 | | | $K_2CO_3$ (2) | | 460 |
| 57 | | | $K_2CO_3$ (5) | Magnetite | 450 |

Specimens were fused for about three hours in air.

during the fusion process has extracted alumina from magnetite to form potassium aluminate.

## Measurements of Conversion Activity and BET Isotherms

Seven g. of "A" (or "B") powder were pressed into small tablets, 3 mm. in diameter and 3 mm. high, and sintered at about 700°C in nitrogen stream. At this temperature the disintegration of the "M" type crystal does not occur. The tablets were placed in a layer, 18 mm. thick and 18 mm. in diameter, in the convertor shown in Fig. 2, and following a fixed schedule (Table V) reduced in hydrogen stream at

TABLE V

REDUCTION SCHEDULE FOR CONVERSION TEST

| temperature °C | reduction period, day | amount of water caught in the trap placed at the outlet of the converter, g A | B |
|---|---|---|---|
| 250 | 1/4 | | |
| 275 | 1/4 | 0.275 | 0.241 |
| 300 | 1/2 | | |
| 325 | 1 | 0.779 | 0.676 |
| 325 | 1 | 0.500 | 0.253 |
| 325 | 1 | 0.260 | 0.277 |
| 350 | 1 | 0.207 | 0.404 |
| 375 | 1 | 0.100 | 0.275 |
| 400 | 1/2 | | |
| 425 | 1/4 | 0.088 | 0.172 |
| 450 | 1/4 | | |
| total | 7 | 2.209 | 2.298 |

The trap was kept at dry-ice temperature.

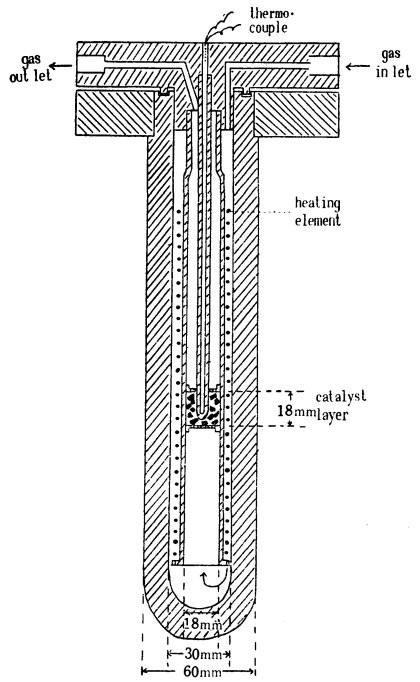



Fig. 2. Experimental convertor.

atmospheric pressure at the space-velocity of about 15000. Hydrogen was purified by being passed through a nickel catalyst, potassium hydroxide and phosphorus pentoxide. The progress of reduction was followed roughly by weighing at intervals the water captured from the issuing hydrogen gas in a trap cooled at −78°C(Table V).

For the conversion tests hydrogen and nitrogen from 150 atm. cylinders were mixed in the ratio of 3 : 1 in a gas holder, and passed over a copper catalyst and compressed into a storage vessel at 100 atm. pressure. For the conversion test at ordinary pressure the raw gas mixture from the storage vessel was reduced to

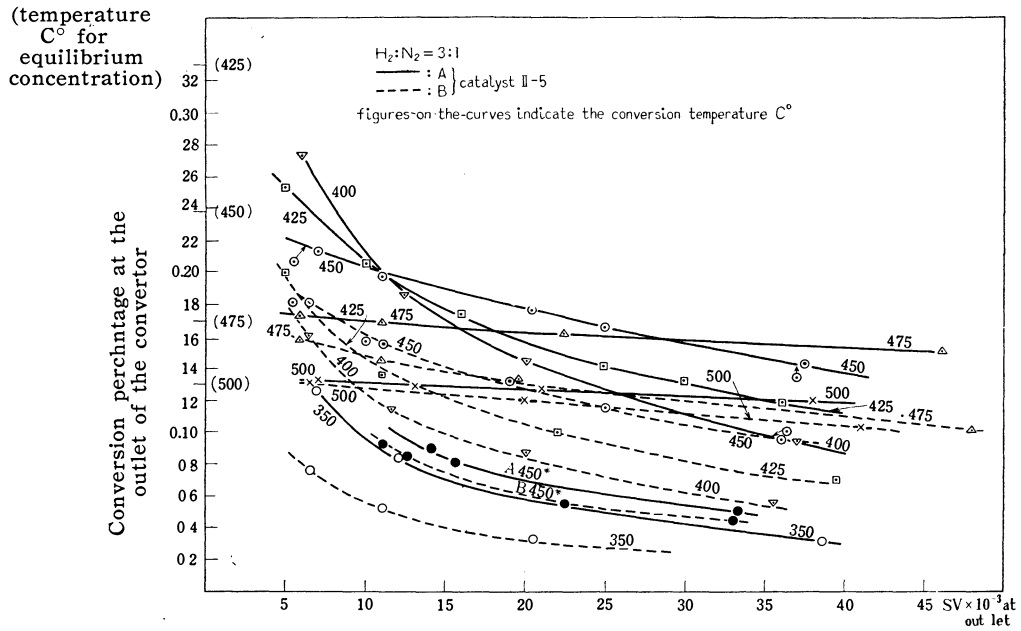



Fig. 3. Conversion activities of A and B powder at atmospheric pressure.

* These curves of low activities were obtained after the experiment of high pressure conversion

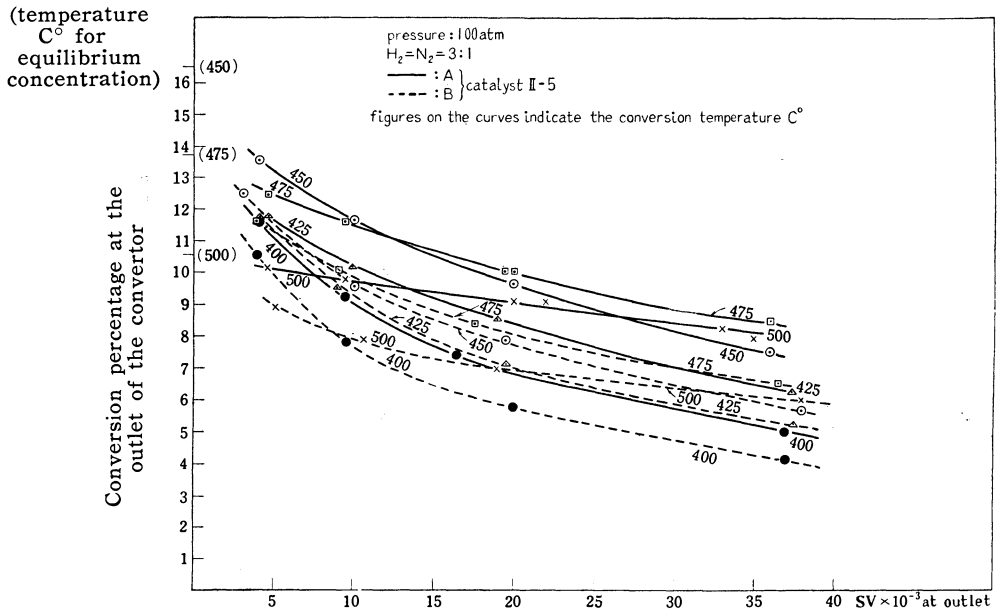



Fig. 4. Conversion activities of A and B powder at a high pressure.

atmospheric pressure and purified in the same way as for the reduction test. For the higher-pressure conversion test, the raw gas at 100 atm. was passed over a nickel catalyst and led through silica-gel and alumina-gel for dehydration.

The results represented in Figs. 3 and 4 clearly show that the conversion activity of "B" powder is lower than that of "A" powder for the whole range of space velocity and particularly at low temperatures.

The influence of water vapor upon the activity was tested by passing the raw gas through a water saturator kept at 0°C. The results (Table VI) show that the water vapor has a similar poisoning effect on the conversion activity as on the decomposition activity at ordinary pressure.

In order to investigate the surface condition of "A" and "B" powders after reduction, BET measurements were carried out by using carbon dioxide and carbon monoxide. Brunauer and Emmett[11,12] state that at the first stage of adsorption at −78°C a rapid chemisorption of carbon dioxide occurs on the surface alkali molecules, followed by the usual physical adsorption on the whole surface (the "total" isotherm).

Seven g. of "A" or "B" powder were reduced in the adsorption bulb made of pyro-glass (about 10 cc.) following the same reduction schedule in the conversion test. Fig. 5 represents adsorption isotherm of carbon dioxide at −78°C on "A" and "B" powders. The isotherm designated as "van der Waals" was obtained at −78°C with the sample outgased for one hour at 0°C after the "total" isotherm measurement. At this temperature all carbon dioxide molecules adsorbed physically are to be removed without the chemisorption being affected, so that from the difference between the two isotherms the amount of chemisorbed carbon dioxide "$V_c$" may be obtained, while from the van der Waals isotherm the amount of the gas forming the monomolecular layer "$V_m$". Since "$V_m$" values for "A" and "B" powders are essentially equal, the total surface of the iron crystallites formed by the reduction seem to be almost the same for the two types of oxides. From "$V_c$" and "$V_m$" values we obtain the coverage by the alkali molecules amounting to about 86 per cent. of the total surface for "B" and 58 per cent. for "A" powder. The difference is apparently not great enough to account for the large difference in the potash content.

After evacuation for about one day at

TABLE VI

EFFECT OF WATER VAPOR ON CONVERSION ACTIVITY AT 450°C, 100 ATOM AND S.V.: 23000

| | percentage of $NH_3$ in the outlet gas | |
|---|---|---|
| | A | B |
| Pure gas | 9.2 | 7.5 |
| Gas containing $H_2O$ | 2.0 | 0.5 |

Gas was bubbled through water saturator kept at 0°C.

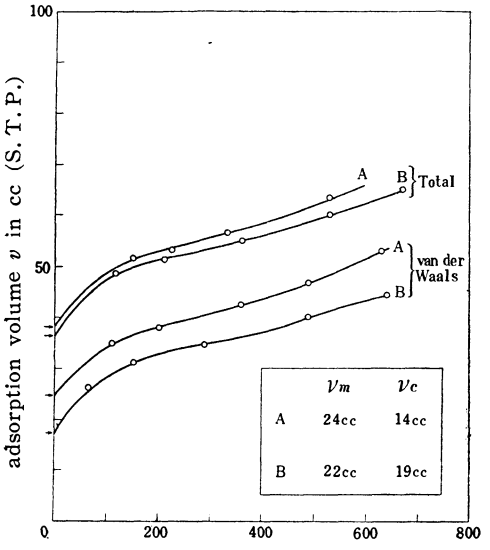



Fig. 5. Adsorption isotherms for carbon dioxide at −78°C on A and B powder.

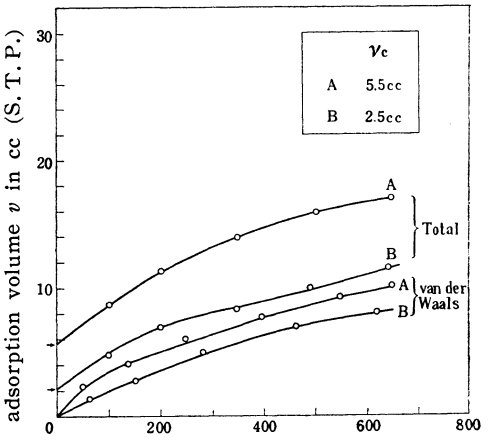



Fig. 6. Adsorption isotherms for carbon monoxide at −78°C on A and B powder.

11) P. H. Emmett and S. Brunauer, *J. Am. Chem. Soc.*, **59**, 310 (1937).
12) Idem., ibid. **59**, 1553 (1937).

400°C, adsorption isotherms were determined with carbon monoxide which is adsorbed on the metallic iron surface only[7,8]. The isotherm may more or less be affected by the carbon dioxide still remaining on the iron surface. Fig. 6 shows that the area of the iron covered surface is smaller for "B" than for "A". The sum of the potash-covered and iron-covered areas is nearly equal to the total area ("$V_m$") for "B" powder, but smaller for "A" powder. This probably is, as Brunauer and Emmett suggested, due to the occupation of the iron surface by alumina.

## Summary

Iron synthetic ammonia catalyst (No. II-4) promoted with aluminium oxide, potassium oxide and calcium oxide was separated magnetically into two different sorts of powder, "A" with magnetite structure and "B" with "M" type structure. As to their catalytic activities for normal and high pressure conversion at temperatures between 400 and 520°C, it was found that "B" was less active than "A" particularly for the low temperature conversion. Some other properties of these powders are as follows:

(1) "B" powder becomes unstable when heated above 1000°C and changes into magnetite. Powder with the lattice structure of "M" type can be synthesized by sintering iron oxide at about 900°C with a sufficient amount of potassium nitrate or hydroxide, but it is completely non-magnetic.

(2) "A" and "B" powder showed almost equal rate of weight decrease when reduced in hydrogen gas or treated with acid solutions.

(3) The BET measurement carried out with "A" and "B" powder reduced in hydrogen revealed that the total specific surface area is almost equal for both "A" and "B" whereas the portion occupied by alkali molecules is larger for "B" powder.

We owe our deep gratitude to Dr. A. Uchida, Tokyo Industrial Research Institute for providing us with Cat. II-5 in this study and also to Mr. Z. Ujino in our Laboratory for his help in chemical analysis.

*Mitsubishi Kasei Laboratory*
*Kawasaki, Kanagawa*

# *Existence of Nitrous Oxide in Gases Produced from Nitrogen Compounds Decomposed by the Strong Phosphoric Acid-Iodic Acid Method*

By Shigeru OHASHI, Yuzi TAKAYAMA*, Hiroshi HIGASHIDANI and Sachiko TAKI

(Received February 16, 1957)

In the previous papers[1] one of the authors presented a new method for the determination of nitrogen in nitrogen compounds. The compounds such as amines and ammonium salts are decomposed by heating with a mixture of strong phosphoric acid and potassium iodate to liberate the nitrogen contained in them. By sending the liberated nitrogen with carbon dioxide into an azotometer filled with a concentrated solution of potassium hydroxide, the nitrogen can be determined gas-volumetrically.

In the first course of this investigation, the gases accumulated in the azotometer by the procedure described above were considered as molecular nitrogen. However, it was found that amounts of liberated iodine[2] by the above reactions always exceeded the theoretical ones which were

* Mitsubishi Rayon Co. Ltd., Tokyo.

1) S. Ohashi, This Bulletin, **28**, 177, 537 (1955); **29**, 700 (1956).

2) For the experimental details, cf S. Ohashi, This Bulletin, **28**, 171 (1955).

TABLE I

IODINE LIBERATED BY THE DECOMPOSITION OF NITROGEN COMPOUNDS WITH STRONG PHOSPHORIC ACID IODIC ACID

| Compound | Sample taken mg. | $I_2$ found mg. | $I_2$ calcd. as $N_2$ mg. | $I_2$ calcd. as $N_2O$ mg. | $N_2O$ % |
|---|---|---|---|---|---|
| Ammonium Sulfate | 102.6 | 136.0 | 118.3 | 157.3 | 44.9 |
| ,, | 102.6 | 134.1 | 118.3 | 157.3 | 39.8 |
| ,, | 102.6 | 138.0 | 118.3 | 157.3 | 49.4 |
| ,, | 205.2 | 263.6 | 236.6 | 316.0 | 33.7 |
| Acetanilide | 15.7 | 116.4 | 115.0 | 117.9 | 75.0 |
| ,, | 17.8 | 132.6 | 130.4 | 133.8 | 80.5 |
| ,, | 24.3 | 179.9 | 178.0 | 182.5 | 74.4 |
| ,, | 29.0 | 212.8 | 212.4 | 218.0 | 57.9 |
| Urea | 22.6 | 69.2 | 57.3 | 76.4 | 61.7 |
| ,, | 39.1 | 118.1 | 99.2 | 132.2 | 57.2 |
| ,, | 51.5 | 155.1 | 129.6 | 172.8 | 56.2 |
| ,, | 71.5 | 228.2 | 181.3 | 242.0 | 77.8 |
| Glycine | 19.5 | 64.7 | 59.3 | 65.8 | 90.4 |
| ,, | 29.9 | 97.8 | 91.0 | 101.1 | 86.0 |
| ,, | 32.5 | 106.8 | 98.9 | 110.0 | 86.1 |

Reaction temp. below 240°C

TABLE II

ANALYSES OF NITROGENOUS GASES BY MASS SPECTROMETER

| Compound | Sample taken | Composition of gases | | | | $N_2O/(N_2+N_2O)$ |
|---|---|---|---|---|---|---|
| | | $CO_2$ | $N_2$ | $N_2O$ | $O_2$ | |
| | mg. | % | % | % | % | % |
| Ammonium sulfate | 15 | 95.6 | $2.8_0$ | $1.6_0$ | 0 | 36 |
| Acetanilide | 33 | 98.4 | $0.5_5$ | $1.0_2$ | 0 | 65 |
| Urea | 25 | 97.1 | $0.4_3$ | $2.2_0$ | | 82 |

Reaction temp. 233°C

calculated on the assumption that the nitrogen in the sample would be changed into molecular nitrogen. The data obtained for several nitrogen compounds are shown in Table I. The discrepancy between the observed and the calculated amount of iodine may be due to the fact that the nitrogen in the samples has not been converted into molecular nitrogen alone, but partly changed into nitrous oxide. For example, if molecular nitrogen is produced from urea by the oxidation with iodic acid, 3 mol. of iodine will be liberated from 5 mol. of urea.

$$5CO(NH_2)_2+6HIO_3 = 5CO_2+13H_2O+5N_2+3I_2$$

And if nitrogen oxide is produced from it, 4 mol. of iodine will be liberated from 5 mol. of urea.

$$5CO(NH_2)_2+8HIO_3 = 5CO_2+14H_2O+5N_2O+4I_2$$

In Table I all the found values of iodine are between those calculated from the two equations mentioned above, respectively. It indicates that the nitrogen in the sample may be converted into both molecular nitrogen and nitrous oxide. The contents of nitrous oxide in the gases calculated from the amounts of liberated iodine are also shown in Table I.

Since the evidence described above is still an indirect one for the existence of nitrous oxide in the gases, then in order to obtain direct evidence, the gases, produced by the decomposition of some nitrogen compounds with the mixture of strong phosphoric acid and potassium iodate, were swept into a gas reservoir with a flow of carbon dioxide and analyzed by a mass spectrometer. Although both nitrous oxide and carbon dioxide indicate the peak of M/e 30 in their mass spectra, the peak height due to carbon dioxide was much less than the observed one. Thus the existence of nitrous oxide was verified and its contents in the gases were determined[3]. The results of the analyses for

3) Cf. Y. Takayama and S. Ohashi, This Bulletin, **30**. 606 (1957).

ammonium sulfate, urea, and acetanilide are shown in Table II. It is clear that the gases from these compounds contain both nitrogen molecule and nitrous oxide and the latter takes about 30 to 80 % of the total nitrogenous gases.

In connection with the above results, the present authors doubted whether gases produced from nitrogen compounds by the Dumas' method are truly nitrogen molecule or not. Therefore isonicotinic acid, 2-methyl-5-vinyl-pyridine polymer, and β-dimethylamino-acetaldehyde-dimethylacetal were decomposed by the normal Dumas' method, in which a flow rate of carbon dioxide was about 6.7 ml./mm., and the gases produced were analyzed by the mass spectrometer. Also in the case of the Dumas' method, the existence of nitrous oxide was pointed out, but its amount was much less than that in the case of the strong phosphoric acid-iodic acid decomposition method.

Full details will be published in the near future.

*Department of Chemistry, Faculty of Science, Kanazawa University*
*Kanazawa*

# *Decomposition of Pyridine Compounds with Strong Phosphoric Acid-Iodic Acid: Some Information Obtained By Mass Spectrometry*

By Yuzi TAKAYAMA and Shigeru OHASHI*

(Received February 16, 1957)

In the previous investigations[1] on the determination of nitrogen in organic compounds by the strong phosphoric acid-iodic acid decomposition method, satisfactory results were obtained for analyses of ammonium salts, amines, azo-compounds, pyrroles, thiazoles, nitro and oxime compounds, etc., but pyridine compounds did not give any good results and the reason for this was uncertain. The present investigation was undertaken to discover the reason and to find out a clue for extending this new analytical method to pyridine compounds. Particularly, for analyses of gases produced by the decomposition of nitrogen compounds, a mass spectrometer was employed effectively.

Several nitrogen compounds were decomposed with a mixture of strong phosphoric acid and potassium iodate at various temperatures, gases produced were swept into a gas reservoir with a flow of carbon dioxide, and then the gases analyzed by the mass spectrometer. On the other hand the sum of volumes of molecular nitrogen and nitrous oxide[2] obtained by the above procedure were compared with the theoretical ones. These results are shown in Table I. An example of analysis of a mass spectrum is illustrated in Table II.

A standard mass spectrum of each gas component anticipated was, of course, previously taken. Since the peak of m/e 22 in a mass spectrum is a characteristic one for carbon dioxide and it does not appear in spectra of the other components, each peak height due to carbon dioxide was calculated from the standard spectrum of pure carbon dioxide and the observed peak height of m/e 22. These are shown in the column 3 of Table II. By deducting the peak heights of carbon dioxide thus calculated from the initially observed peak heights, respectively, peak heights $\Delta_1$ which are due to the other components than carbon dioxide were obtained. As in the peak heights of $\Delta_1$ the peak of m/e 30 is produced only by the presence of nitrous oxide, the peak heights due to nitrous oxide were calculated in a similar way and so on.

* Department of Chemistry, Faculty of Science, Kanazawa University Kanazawa.

1) S. Ohashi, This Bulletin, **28**, 177, 537 (1955); **29**, 700 (1956).

2) Cf. S. Ohashi, Y. Takayama, H. Higashidani and S. Taki, This Bulletin, **30**, 604 (1957).

TABLE I

COMPOSITION OF GASES IN THE GAS RESERVOIR

(mol. %)

10 ml. of strong phosphoric acid and 600 mg. of potassium iodate were used in each analysis. The final reaction temperatures were kept for eight min.

| Compound | Sample taken | Final reaction temp. | Reservoir volume | $CO_2$ | $N_2O$ | $N_2$ | $O_2$ | $(N_2+N_2O)$ found | $(N_2+N_2O)$ calcd. |
|---|---|---|---|---|---|---|---|---|---|
| | mg. | °C | ml. | % | % | % | % | ml. | ml. |
| Isonicotinic acid | 20 | 233 | 125 | ca. 100 | 0 | 0 | 0 | 0 | $1.9_5$ |
| 〃 | 〃 | 253 | 113 | 97.8 | $1.0_1$ | $0.8_5$ | $0.3_8$ | $2.1_0$ | ,, |
| 〃 | 〃 | 275 | 125 | 97.5 | $0.7_8$ | $0.8_0$ | $0.9_7$ | $1.9_8$ | ,, |
| Poly-2-methyl-5-vinyl-pyridine | 〃 | 233 | 113 | ca. 100 | 0 | 0 | 0 | 0 | $2.0_6$ |
| 〃 | 〃 | 260 | 113 | 98.2 | $0.4_4$ | $0.1_7$ | $0.4_1$ | $1.8_2$ | ,, |
| Polyacrylonitrile | 28 | 233 | 125 | 97.4 | $1.5_3$ | $1.2_5$ | 0 | $3.4_8$ | $3.4_7$ |
| Acetanilide | 33 | 233 | 125 | 98.4 | $1.0_2$ | $0.5_5$ | 0 | $1.9_8$ | $1.7_6$ |
| Urea | 25 | 233 | 113 | 97.1 | $2.2_0$ | $0.4_8$ | 0 | $3.0_5$ | $3.2_0$ |
| Ammonium Sulfate | 15 | 233 | 125 | 95.6 | $1.6_0$ | $2.8_0$ | 0 | $5.5_0$ | $5.4_5$ |

TABLE II

ANALYSIS OF MASS SPECTRUM

Sample: Isonicotinic acid 20 mg. Final reaction temp.: 275±2°C
Date: Oct. 25, 1956, No. 4. *n*-Butane m/e 43: 58.99
Magnetic current: 0.25 amp. Ionic current: 12.5 $\mu$ amp.
Scanning voltage: 3550 V. Sample pressure: 44.53 $\mu$ Hg.

| M/e | peak height found | $CO_2$ | $\Delta_1$ | $N_2O$ | $\Delta_2$ | $O_2$ | $\Delta_3$ | $N_2$ | $\Delta_4$ |
|---|---|---|---|---|---|---|---|---|---|
| 14 | 5.4 | $0.9_2$ | $4.4_8$ | $1.9_6$ | $2.5_2$ | | $2.5_2$ | $2.2_4$ | $0.2_8$ |
| 16 | $236.6_7$ | $240.7_1$ | $-0.40_6$ | $0.6_9$ | $-4.7_5$ | $0.3_3$ | $-5.0_8$ | | $-5.0_8$ |
| 18 | 0.8 | | | | | | | | 0.8 |
| 22 | 36.8 | 36.8 | 0 | | | | | | 0 |
| 28 | 260.5 | $242.9_9$ | $17.5_1$ | $1.7_2$ | $15.7_9$ | $0.9_2$ | $14.8_7$ | $14.8_7$ | 0 |
| 30 | 5.0 | $0.5_5$ | $4.4_5$ | $4.4_5$ | 0 | | | | 0 |
| 32 | 15.8 | $0.6_8$ | $15.1_2$ | | $15.1_2$ | $15.1_2$ | 0 | | 0 |
| 44 | 2123.7 | $2117.3_5$ | $6.3_6$ | $11.1_7$ | $-4.8_1$ | | | | $-4.8_1$ |
| 46 | 8.9 | $8.7_9$ | $0.1_7$ | $0.0_2$ | $0.0_9$ | | | | $0.0_9$ |

As indicated in Table I it was disclosed that pyridine compounds such as isonicotinic acid and poly-2-methyl-5-vinyl-pyridine are decomposed almost completely by heating with strong phosphoric acid-iodic acid at the temperature over 253° or 260°C, but at the same time oxygen is liberated by the self-decomposition of iodic acid. On the other hand, it was also found that amine, ammonium salt, and nitrile are completely decomposed at the temperature of 233°C, while pyridine compounds are not attacked at all at the same temperature. From these results it may be suggested that nitrogen in amines, ammonium salts, etc. and nitrogen in pyridine compounds would be separately determined by controlling the decomposition temperature with strong phosphoric acid-iodic acid, if oxygen liberated from iodic acid could be removed by any suitable means in the case of analysis of pyridine compounds.

Full details will be reported elsewhere in the near future.

*Mitsubishi Rayon Co., Ltd.*
*Kyobashi, Tokyo*

# *Cyclopolysiloxanes from Cohydrolysis of Dimethyldichlorosilane with Methyldichlorosilane and Ethyldichlorosilane*

By Rokuro ŌKAWARA, Ukiko TAKAHASHI and Minoru SAKIYAMA

(Received March 4, 1957)

Recently, a series of linear and branched methylhydropolysiloxanes having the formula $\mathbf{M'D'}_n\mathbf{M'}$[a] ($n$=0–6), **MM'**, **M'DM'**, **M'D'DM'**, **M'D$_2$M'**, **M'$_3$**, **T** and **MD'$_n$M** ($n$=1–6) have been reported[1,2]

Now we wish to report on the preparation and properties of methylhydrocyclotetrasiloxanes; **D$_3$D'**, **D$_2$D'$_2$** and **DD'$_3$**, and the similar ethylmethylhydrocyclotetrasiloxanes; **D$_3$D***[b], **D$_2$D*$_2$** and **DD*$_3$**. These compounds were obtained from the cohydrolysis of the mixture of methyldichlorosilane(III') (or ethyldichlorosilane (III*)) and dimethyldichlorosilane(II) in various mole ratios.

Since it has been known that the hydrolysis in an acidic medium is favourable to the formation of the lower membered rings[3] and further, the amount of Si-H split by hydrolysis is not so large even in the case of direct hydrolysis[1], the hydrolysis was carried out by adding chlorosilanes to the mixture of ether and water. Then the product was distilled and thermally rearranged under reduced pressure (10–20 mm.). Almost all the hydrolyzate distilled out as an untreated hydrolyzate and the remaining gel was also thermally rearranged completely without any residue up to the still-pot temperature of 450°C. The amount of the untreated and thermally rearranged hydrolyzates varied with the composition of the starting mixture, but their active hydrogen contents are nearly the same as is shown in Table I. Then both the hydrolyzates were united and the composition of the tetrasiloxanes was determined by fractionation through a high efficient column. About 40–50% of the hydrolyzate was found to be the tetrasiloxanes. For example, the distribution of the tetrasiloxanes **D$_n$D*$_{4-n}$** ($n$=0–4), is shown in Fig. 2 with regard to the composition of the starting mixture.

Formally, **DD'$_3$**, **D$_2$D'$_2$** and **D$_3$D'** are obtained by substituting one unit of **D'** in tetramethylcyclotetrasiloxane successively by **D** unit. Among them, **D$_2$D'$_2$** would consist of at least two isomers: $\lceil$**DDD'D'**$\rfloor$ and $\lceil$**DD'DD'**$\rfloor$. Sauer[4] has already characterized methylhydrocyclopolysiloxanes **D'$_n$** ($n$=4–6), but for comparison, **D'$_n$** ($n$=4–7) was also prepared and characterized in this paper.

Regular changes of the physical constants are read from Table II, referring to the compounds of **D$_n$D'$_{4-n}$** and **D$_n$D*$_{4-n}$** ($n$=0–3). For comparison, the effect of substituting one **D'** unit successively by **D** unit in **D'$_4$** and **M'D'$_2$M'**[c] is summarized in Table III. It may be seen that the effect of substituting one **D'** unit by one **D** unit is the same as the substitution of H(-Si) by one methyl group. In the linear compounds, the effect of introduction of the second methyl group does not cause such a marked increase of refractive index as that of the first methyl group but the density increases by nearly the same amount. However in the series of cyclocompounds **D$_n$D'$_{4-n}$**, successive substitution of a methyl group causes the regular increase of boiling point and refractive index and the regular decrease of density.

Referring to the series of isomeric compounds **D$_n$D*$_{4-n}$** ($n$=0–4), the gradual increase of boiling point, $\Delta d_D^{20}$ and $\Delta n_D^{20}$ are pointed out by substituting **D** unit successively by **D*** unit. Thus the boiling point, the refractive index and the density of **D*$_4$** assumed by this relation were not in accordance with that of the tetramer, but accorded well with the trimer reported

1) R. Ōkawara and M. Sakiyama, This Bulletin, **29**, 236 (1956).

2) R. Ōkawara and M. Sakiyama, ibid., **29**, 547 (1956).

a) The shorthand notations were indicated in the preceding papers 1) and 2).

b) In this paper, in addition to the previous notation, **D*** will be used to indicate $C_2H_5SiHO$ unit.

3) W. I. Patnode and D. F. Wilcock, *J. Am. Chem. Soc.*, **68**, 358 (1946).

4) R. O. Sauer, S. D. Brewer and W. I. Scheiber, ibid., **68**, 962 (1946).

c) Refractive index and density of the linear tetramers **M'D'$_2$M'**, **M'D'DM'** and **M'D$_2$M'** have been reported (*loc. cit.* 1) and 2)) $n_D^{20}$ : 1.3830, 1.3862 and 1.3875, $d_4^{20}$ : 0.8613, 0.8623 and 0.8632, respectively.

in the previous paper[5] in which they were assigned by the determination of the molecular weight in dioxane. Here, again, the first four members of $D^*_n$ were isolated from the hydrolyzate of ethyl dichlorosilane(III*). From the molecular weight determination in benzene and in dioxane, and further from the wave length of the infra-red absorption band associated with the Si-O stretching vibration, the first member of $D^*_n$, though small in amount and unstable, was assigned to be cyclotrimer and the erroneous assignment in the previous paper has been corrected.

## Experimental

**Starting Materials.** — Dimethyldichlorosilane (II) and methyldichlorosilane(III') used in these experiments were supplied from the Shin-etsu Chem. Ind. Co. Ethyldichlorosilane(III*) was prepared by the reaction of industrial ethylchloride with silicon-copper. The two isomeric chlorosilanes, II and III* have been reported to have a close boiling point 70.2°C[6] and 74.9°C[7], respectively. For fear of contamination of a small amount of II, which would be formed in the course of the direct synthesis, the fractions of III* were carefully fractionated by a Stedman column of about 30 theoretical plates. The constant boiling plateau (74°−75°C) having the constant chlorine content was used for the preparation, and especially for the preparation of $D^*_n$ the back part of the plateau was taken to avoid the contamination of II.

*Anal.* Found: Cl, 54.8 %. Calcd. for $C_2H_6SiCl_2$ Cl, 54.9 %.

**Fractionation of the Polysiloxanes.** — Throughout this experiment, the hydrolyzates were fractionated through a Stedman column of about 50 theoretical plates.

**Analysis of Active Hydrogen.**—Active hydrogen content % H(-Si), was measured by decomposing the sample with butanolic sodium hydroxide in a Zerewitinoff's apparatus.

**Hydrolyzates from the Acidic Medium.**— The mixture of chlorosilanes was added to the ice-cooled mixture of ether and water with vigorous stirring. The organic layer was washed with water until it became neutral to methylorange. The oily product from the ether layer was distilled under reduced pressure at 10-20 mm., and the untreated and thermally rearranged products were collected separately in an ice-cooled receiver. The results with regard to the chlorosilane mixture of II and III* are given in Table I.

The untreated and thermally rearranged products which distilled out up to 300°C and 450°C respectively, were collected together and rigorously fractionated. For example, the result of Expt. 2 is shown in Fig. 1.

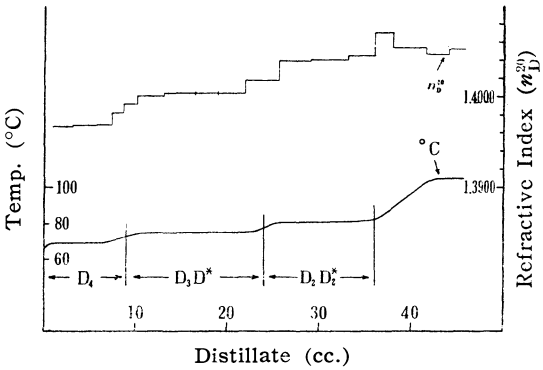



Fig. 1. Distillation curve of the cohydrolyzate (Expt. 2 of Table 1) at 18 mm.

In Fig. 1, the complete plateaus of $D_4$, $D_3D^*$ $D_2D^*_2$ were found and it was easy to calculate the percentage composition of them by cutting on the distillation curve. The plateau of $DD^*_3$ was not found, but from the refractive index, which was higher than the neighboring fractions at the next portion of $D_2D^*_2$, it was supposed to be present in this portion, although small in amount. The distribution of the tetrasiloxanes thus determined is shown in Fig. 2.

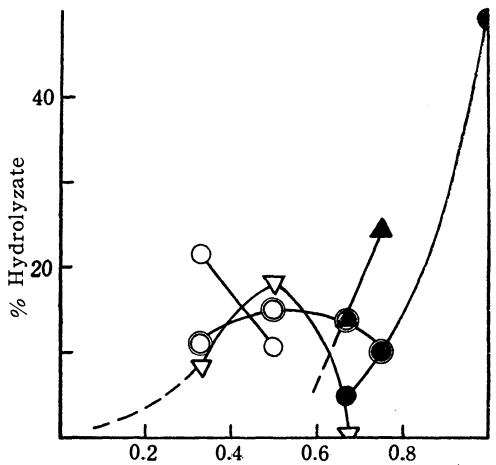



Fig. 2. Distribution of tetrasiloxanes $D_nD^*_{4-n}$ ($n=0-4$) with regard to the mole fraction of ethyldichlorosilane (III*/II+III*).
○ $D_4$ ▽ $D_3D^*$
◎ $D_2D^*_2$ ▲ $DD^*_3$
● $D^*_4$

Fractionation of the hydrolyzate of III* (Expt. 5 of Table I) gave the first plateau at 67°C/20 mm., which amounted to 9 % of the hydrolyzate. The succeeding plateaus amounting to 48, 25 and 6 % of the hydrolyzate, were found to be those of

5) R Ōkawara, E. Asada and T. Watase, This Bulletin, **26**, 141 (1953).
6) W. F. Gilliam, E. M. Hadsell, H. A. Liebhafsky and M. M. Sprung, *J. Am. Chem. Soc.*, **73**. 4252 (1951).
7) R. N. Meals, ibid., **68**, 1880 (1946).

TABLE I

COHYDROLYZATES FROM THE MIXTURE OF DIMETHYLDICHLOROSILANE(II) AND ETHYLDICHLOROSILANE(III*)

In each experiment, the mixture of the starting materials was added to the hydrolyzing medium which consisted of 500 cc. of ether and 1 l. of water.

| Expt. No. | Starting Materials | mol. | Hydrolyzate: Total (T) % theory | Hydrolyzate: Untreated % T | %H(−Si): Untreated | %H(−Si): Thermally Rearranged (Calcd.) |
|---|---|---|---|---|---|---|
| 1 | III* | 0.5 | 84 | 82 | — | — |
| | II | 1.0 | | | | (0.45) |
| 2 | III* | 0.76 | 80 | 73 | — | 0.67 |
| | II | 0.76 | | | | (0.68) |
| 3 | III* | 1.0 | 83 | 63 | 0.90 | 0.80 |
| | II | 0.5 | | | | (0.90) |
| 4 | III* | 1.2 | 83 | 71 | 1.00 | 0.94 |
| | II | 0.4 | | | | (0.98) |
| 5 | III* | 0.83 | 84 | 50 | 1.35 | 1.32 |
| | | | | | | (1.35) |

TABLE II

CYCLIC POLYSILOXANES

| Compound[a] | Boiling point °C/mm. | Refractive index $n_D^{20}$ | Density $n_D^0$ | Molar refraction Found (Calcd.)[c] | Molecular weight Found[d] (Calcd.) | % H(-Si) Found (Calcd.) |
|---|---|---|---|---|---|---|
| **D'**$_4$ | 133/760 ((134.5))[b] | 1.3870 ((1.3870)) | 0.9913 ((0.9912)) | 57.22 (57.08) | — (240.5) | 1.67 (1.68) |
| **D'**$_3$**D** | 143/760 | 1.3900 | 0.9809 | 61.51 (61.45) | — (254.6) | 1.19 (1.19) |
| **D'**$_2$**D**$_2$ | 154/760 | 1.3927 | 0.9709 | 65.96 (65.82) | — (268.6) | 0.75 (0.75) |
| **D'D**$_3$ | 165/760 | 1.3950 | 0.9620 | 70.55 (70.19) | — (282.6) | 0.35 (0.36) |
| **D'**$_5$ | 60/14 ((168.7)) | 1.3918 ((1.3912)) | 0.9986 ((0.9985)) | 71.66 (71.35) | — (300.7) | 1.67 (1.68) |
| **D'**$_6$ | 83/14 ((92.8/21)) | 1.3943 ((1.3944)) | 1.003 ((1.006)) | 86.10 (85.62) | 359 (360.8) | 1.66 (1.68) |
| **D'**$_7$ | 102/14 | 1.3958 | — | — | 411 (420.9) | 1.65 (1.68) |
| **D***$_3$ | 67/20 | 1.4078 | 0.9673 | 56.71 (56.70) | 218 (222.5) | 1.38 (1.36) |
| **D*D**$_3$ | 180/760, 75/18 | 1.4003 | 0.9598 | 74.97 (74.82) | — (296.6) | 0.34 (0.34) |
| **D***$_2$**D**$_2$ | 188/760, 82/19 | 1.4042 | 0.9658 | 75.14 (75.08) | 292 (296.6) | 0.67 (0.68) |
| **D***$_3$**D** | 201/760, 88/16 | 1.4090 | 0.9727 | 75.39 (75.34) | — (296.6) | 1.01 (1.02) |
| **D***$_4$ | 208/760, 105/20 ((106/20)) | 1.4141 ((1.4138)) | 0.9808 ((0.9836)) | 75.39 (75.60) | 294[e] (296.6) | 1.36 (1.36) |
| **D***$_5$ | 80/2 ((135/20)) | 1.4187 ((1.4176)) | 0.9899 ((0.9920)) | 94.53 (94.50) | — (370.8) | 1.37 (1.36) |
| **D***$_6$ | 101/2 ((165/20)) | 1.4215 ((1.4200)) | 0.9942 ((1.0023)) | 113.6 (113.4) | — (445.0) | 1.35 (1.36) |

a) **D'** = $CH_3SiHO$, **D** = $(CH_3)_2SiO$, **D*** = $C_2H_5SiHO$.

b) Reported values are indicated in brackets, (( )). The data of **D'**$_n$ and **D***$_n$ are those reported in 4) and 5) (*loc. cit.*), respectively, but for **D***$_n$, only the polymer size has been corrected.

c) Calculated from bond refractivities by E. L. Warrick, *J. Am. Chem. Soc.*, **68**, 2455 (1946).

d) Cryoscopic measurements in benzene.

e) The values of 293 and 295 were obtained at the concentration of 1.1 g. and 2.3 g. per 100 g. of benzene. Also, from the depression of 0.220° and 0.421°C at the concentration of 1.32 g. and 2.54 g. of the sample in 100g. of dioxane (b. p. 101°C, m. p. 11.67°C, molecular depression 4.95) the molecular weight 298 and 299 were obtained.

succeeding polymers as shown in Table II. The following small plateau at 120°C/2 mm. was also found, but it was too small in amount to be characterized accurately.

Tetrasiloxanes $\mathbf{D}_n\mathbf{D}'_{4-n}$ ($n=0-3$) were prepared as above from the hydrolyzate (yield: 83–87 % theory) of the mixture of II and III′ in various molar ratios. In the case of smaller molar ratios, $x'$ (III′/II), the gel formed above 300°C was completely pyrolyzed until 400°C, but with increasing molar ratios, almost all the hydrolyzate came out below 300°C without any perceptible gelation in a still-pot. In tetrasiloxanes, the elevation of the boilng point at 760 mm. was found to be about 10°C when one unit of **D′** is substituted by one unit of **D**, but it required repeated distillation to obtain satisfactorily pure compounds.

To obtain a series of polymers $\mathbf{D}'_n$, the hydrolyzate(Found: H(-Si), 1.65%. Calcd. for$(CH_3SiHO)_n$: H(-Si), 1.67%) of III′, which distilled out below 300°C at 10–20 mm., was fractionated. A complete plateau was not found at the boiling point of the cyclotrimer (Reported[8]: b. p. 93.7°C) but a knick point. The succeeding plateau amounting to 40, 23, 8, 4 and 3% of the hydrolyzate, were found to be those of $\mathbf{D}'_4$ to $\mathbf{D}'_8$. Since the plateau of $\mathbf{D}'_8$ gradually rose from 114° to 118°C at 15 mm., and its active hydrogen content was somewhat lower (Found: H(-Si), 1.63 %), polymers until $\mathbf{D}'_7$ are shown in Table II. The active hydrogen content of those polymers decreased slowly and regularly with increasing polymer size. The H(-Si) of the residue was 1.48%, from which it may be enough to suppose the contamination of compounds other than $\mathbf{D}'_n$.

TABLE III

CHANGES OF PHYSICAL CONSTANTS DUE TO SUCCESSIVE SUBSTITUTION OF **D′** BY **D** UNIT IN TETRASILOXANES

| Compound | Numbers of **D** unit substituted | Boiling point at 760 mm. Increase of °C | Refractive index Increase of $\Delta n_D^{20}\times10^4$ | Density Increase of $\Delta d_D^{20}\times10^3$ |
|---|---|---|---|---|
| $\mathbf{M}'\mathbf{D}'_2\mathbf{M}'$ | 1 | — | 32 | 1 |
| | 2 | — | 13 | 1 |
| $\mathbf{D}'_4$ | 1 | 10 | 30 | −10 |
| | 2 | 11 | 27 | −10 |
| | 3 | 11 | 23 | − 9 |
| | 4[d] | 10 | 18 | − 6 |

**Infra-red Spectra of $\mathbf{D}^*_n$.**—The contamination of **D** unit in $\mathbf{D}^*_n$ can easily be detected by determining the active hydrogen content and also by the apearance of a sharp band in the infra-red spectra near 1260 $cm^{-1}$, which has been attributed to the methyl grouping in $CH_3$-(Si). In this experiment, the absorption spectra were obtained with a Hilger H-800 infra-red spectrophotometer with a rock salt prism. Samples were observed as solution, 3% in carbon disulfide being used in the range of 650–1300 $cm^{-1}$.

In the region 1200–1300 $cm^{-1}$ two bands were found in the figure of $\mathbf{D}_n\mathbf{D}^*_{4-n}$ ($n=1-3$): the one near 1260 and the other near 1240 $cm^{-1}$, which can be attributable to $CH_3CH_2$-(Si) group[9]. But the figure of $\mathbf{D}^*_n$ showed only the latter band. The band associated with the stretching of Si-O bond was found at 1023, 1085, 1089 and 1086 $cm^{-1}$ for the first four members of $\mathbf{D}^*_n$, respectively. Since the cyclic trisiloxanes[9] have been reported to have the characteristic absorption band at 1010–1020 $cm^{-1}$ and the higher cyclic polysiloxanes near 1080–1090 and 1050–1080 $cm^{-1}$ respectively, it may be natural to suppose that the first member of $\mathbf{D}^*_n$ obtained in this experiment is cyclic trimer. The result accorded well with the molecular weight determination in benzene as shown in Table II.

The measurement of the physical properties of cyclotrimer $\mathbf{D}_3^*$ was carried out immediately after the fractionation and the infra-red spectra were measured after four days. During the measurement, only a slight change of refractive index was observed by the samples which were reserved in an ice box. All the samples which were sealed in glass ampoules became viscous fluid or gel in summer (room temperature of over 30°C) after three months, but there was found no perceptible increase of pressure in the ampoules. Infra-red spectra of the viscous fluid, after four months, gave rise to a strong band at 1094 $cm^{-1}$ and the intensity of the band at 1023 $cm^{-1}$, characteristic to the cyclotrisiloxane ring, decreased. But the other compounds sealed in soft glass ampoules showed no change of refractive index.

## Summary

1) Cyclotetrasiloxanes having **D′** and **D**, and **D*** and **D** units have been prepared and characterized.

2) Methylhydrocyclopolysiloxanes $\mathbf{D}'_n$ ($n=4-7$) and ethylhydrocyclopolysiloxanes $\mathbf{D}^*_n$ ($n=3-6$) have also been prepared and characterized. The erroneous assignment given to the latter compounds have been corrected.

3) Triethylcyclotrisiloxane $\mathbf{D}^*_3$, the first member of $\mathbf{D}^*_n$ was found to be an unstable compound.

*Department of Applied Chemistry Faculty of Engineering, Osaka University, Miyakojima-ku, Osaka*

8) S. D. Brewer, ibid., **70**, 3962 (1948).

d) For $\mathbf{D}_4$, the reported values (*loc. cit.* 3)), $n_D^{20}$ 1.3968 and $d_4^{20}$ 0.9558 were used.

9) C. W. Young, P. C. Servais, C. C. Currie and M. J. Hunter, ibid., **70**, 3758 (1948).

# *Solvent Selectivity of Liquid Ammonia for Pure Hydrocarbons*
## *Tie-Line Data and Comparison of Selectivity with Other Solvents*

By Kiyoharu ISHIDA

(Received February 25, 1957)

### Introduction

Results of extensive studies on the separation of petroleum fractions with liquid ammonia as a solvent, which include the fundamental solubility relationships for various hydrocarbon types and the tests on pilot plant extractions, have recently been published and the utility and the versatility of liquid ammonia as a solvent were stressed[1]. The fact that liquid ammonia has good solvency and selectivity for separating mixtures of naphthenic and aromatic hydrocarbons was clarified through the studies on the system of methylcyclohexane—toluene—liquid ammonia. It has also been demonstrated that it is important to control the dissolving power of the ammonia solvent so that the amount of hydrocarbon in the solvent phase lies between about 10 and 30 weight % either by temperature reduction or water injection or both, in order to prevent the decrease of selectivity accompanied by the increase of solubility. However, from the viewpoint of phase equilibrium, apart what has just been stated above and the relative distribution ratio at 10% solubility, few fundamental equilibrium data are given.

In order to determine the solvency and selectivity of liquid ammonia as a solvent for separating more soluble hydrocarbons such as aromatics and low molecular weight hydrocarbons, systems of cyclohexane—benzene, *n*-hexane—benzene, and ethylbenzene—styrene, the last as an example of two aromatic hydrocarbons, whose separation is a practical problem, were selected, and equilibria of ternary systems of these two components and liquid ammonia were measured. Furthermore, the comparison of selectivity of liquid ammonia with other solvents, which are used or are usable for the separation of various hydrocarbons, was attempted.

1) M. R. Fenske, R. H. McCormick, H. Lawroski and R. G. Geier, *A. I. Ch. E. Journal*, **1**, 335 (1955).

### Experimental Procedure and Materials

The equilibrium data were determined in the same way as described in Part I of this series[2,3]; *n*-hexane and cyclohexane used in the present study are the same materials as described in Part II[3].

Commercial benzene was purified by the usual method and the fraction of b.p. 80.0–80.1°C, m.p. 5.53°C, $d_4^{20}$ 0.8784, $n_D^{20}$ 1.5011, was used.

Ethylbenzene was prepared from bromobenzene and ethyl bromide by the Fittig reaction and was fractionated to obtain one, having constants of b.p. 136.0°C, $d_4^{20}$ 0.8670, $n_D^{20}$ 1.4959.

Styrene was kindly supplied by Nippon Paint Co., Ltd. (purchased from Dow Chemical Co.), and showed $b.p._{24\cdot1}$ 48°C, $d_4^{20}$ 0.9059, $n_D^{20}$ 1.5468, and bromine number[4] of 151.2 (theoretical: 153.3).

The ternary system including styrene was prepared by the use of styrene freshly fractionated under reduced pressure, and after the determination of ammonia, the composition of the binary system of ethylbenzene and styrene was determined by measuring specific gravity, refractive index, and bromine number of the raffinate or the extract. For this system, no correction was made for the slight loss of hydrocarbons due to the volatilization during the determination of ammonia, because their vapor pressures at experimental temperatures are small and nearly of the same order.

### Results

Equilibrium data for the system *n*-hexan-benzene-liquid ammonia (20°C) are shown in Table I, those for cyclohexane-benzene-liquid ammonia (20°C and 0°C) in Table II, and those for ethylbenzene-styrene-liquid ammonia (0°C and −15.5°C) in Table III. The data are presented graphically in Fig. 1–3. Both cyclohexane and benzene are present as crystals at 0°C, but their mixtures with liquid ammonia are liquids at 0°C lowering the melting point.

As will be clear from Fig. 1 and 2, aromatic hydrocarbons are selectively extracted from $C_6$-hydrocarbon mixtures,

2) K. Ishida, *J. Chem. Soc. Japan, Ind. Chem. Sect.*, **56**, 469 (1953).
3) Ibid, **57**, 479 (1954).
4) H. L. Johnson and R. A. Clark, *Anal. Chem.*, **19**, 869 (1947).

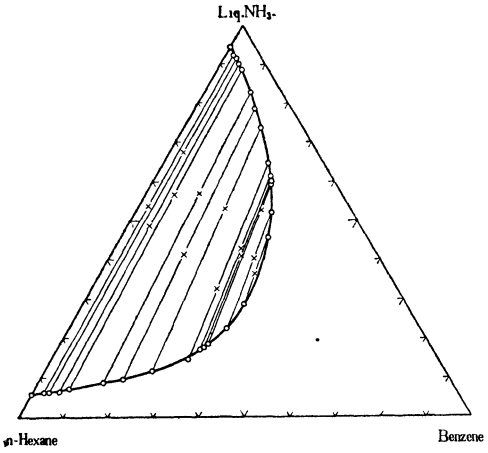



Fig. 1. System *n*-Hexane-Benzene-Liq. $NH_3$ at 20°C, wt. %.

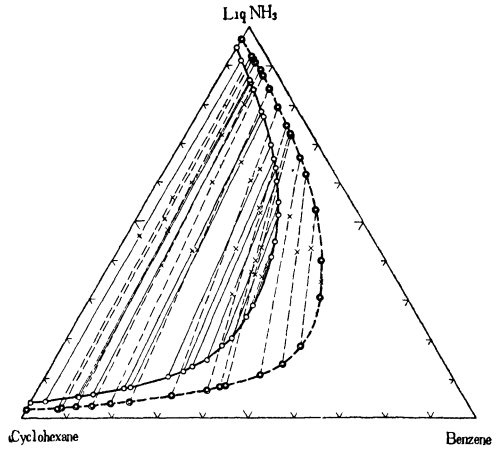



Fig. 2. System Cyclohexane-Benzene-Liq. $NH_3$ at 20°C and 0°C, wt. %.
——○—— 20.0°C
——◎—— 0.0°C

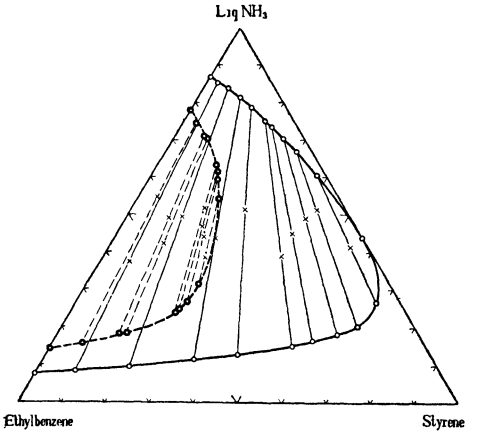



Fig. 3. System Ethylbenzene-Styrene-Liq.$NH_3$ at 0°C and −15.5°C, wt. %.
——◎—— 0.0°C
——○—— −15.5°C.

showing little difference between the paraffinic and naphthenic hydrocarbon present as a diluent. This is in accordance with the expectation from the equilibrium data for the system *n*-hexane-cyclohexane-liquid ammonia[3].

It seems that the separation of aromatic hydrocarbon mixture with the same number of carbon atoms, which contains another compound having more highly unsaturated properties, will be possible by the extraction using liquid ammonia as a solvent, since the increase of unsaturated properties increases the solubility for the solvent. Table III and Fig. 3 indicate that liquid ammonia is also usable for such separation, and that when the extraction is carried out at −15.5°C, the mixture of ethylbenzene and styrene can be separated into the raffinate containing 5 wt. % styrene and the extract containing 98 wt. % styrene under the condition of total reflux with minimum number of theoretical stages of 15.

The composition at plait point in Tables I–III (b) was estimated from Hand plot[5] according to Treybal, et al[6]. The slope of the straight line changes near the plait point for the systems cyclohexane-benzene-liquid ammonia and ethylbenzene-styrene-liquid ammonia at 0.0°C. The method of Othmer and Tobias[7] also gives the same results as by Hand plot. When the author's method[8] is used, in which the ratio of the concentration of the diluent in the diluent phase to the concentration of the solvent in the solvent phase against the former concentration is plotted on double logarithmic coordinates, the data in Table II give two straight lines of different slopes, but all other systems satisfy a linear relationship within the range of experimental error.

## Comparison of Solvent Selectivity

There are various measures[1,9,10,11,12,13]:

5) D. B. Hand, *J. Phys. Chem.*, **34**, 1961 (1930).
6) R. E. Treybal, L. D. Weber and J. F. Daley, *Ind. Eng. Chem*, **38**, 817 (1946).
7) D. F. Othmer and P. E. Tobias, ibid, **34**, 693 (1942).
8) K. Ishida, This Bulletin, **29**, 956 (1956).
9) K. W. Saunders, *Ind Eng. Chem*, **43**, 121 (1951).
10) D. A. Skinner, ibid, **47**, 222 (1955).
11) E. C. Medcalf, A. G. Hill and G. N. Vriens, *Petroleum Refiner*, **30**, No 7, 97 (1951). He used the value at infinite dilution.
12) There are some investigators using the term "separation factor" in the same meaning as the relative distribution ratio, $\beta$. For example; B. Weaver, *Anal. Chem.*, **26**, 474 (1954). Usually, $\beta$ is used for selectivity, e. g, L. F. Crooke, Jr., and M. Van Winkle, *Ind. Eng. Chem*, **46**, 1474 (1954); A. E. Skrzec and N. F. Murphy, ibid., **46**, 2245 (1954), and so on. See also Ref. 14 and 22.
13) L. Alders, "Liquid-Liquid Extraction", Elsevier Pub. Company, London (1955), p. 85.

TABLE I

EQUILIBRIUM DATA FOR THE SYSTEM *n*-HEXANE-BENZENE-LIQUID AMMONIA AT 20.0°C, WT. %

| Total Mixture | | Hydrocarbon Layer | | Solvent Layer | |
|---|---|---|---|---|---|
| Benzene Wt. % (Solvent-free Basis) | $NH_3$ Wt. % | $NH_3$ Wt. % | Benzene Wt. % (Solvent-free Basis) | $NH_3$ Wt. % | Benzene Wt. % (Solvent-free Basis) |
| 0.0 | — | 6.1 | — | 94.4 | — |
| 4.7 | 53.9 | 6.5 | 2.7 | 92.5 | 24.6[a] |
| 9.7 | 67.3 | 6.6 | 4.0 | 91.8 | 34.0 |
| 9.7 | 48.6 | 6.6 | 6.3 | 90.2 | 42.7 |
| 15.1 | 56.6 | 7.1 | 8.3 | 88.7 | 48.6 |
| 27.9 | 56.9 | 8.8 | 16.0 | 82.7 | 60.0 |
| 27.9 | 41.3 | 9.6 | 20.7 | 78.6 | 62.8 |
| 41.3 | 52.8 | 11.7 | 27.1 | 73.7 | 65.0 |
| 41.3 | 32.7 | 14.8 | 35.7 | 64.5 | 65.9 |
| 49.1 | 42.9 | 17.2 | 38.3 | 61.5 | 65.6 |
| 49.1 | 40.8 | 17.8 | 39.4 | 60.2 | 65.5 |
| 58.2 | 52.6 | 18.8 | 40.4 | 59.3 | 65.3 |
| 54.0 | 40.3 | 22.7 | 45.3 | 52.1 | 63.2 |
| 54.0 | 36.6 | 29.0 | 50.3 | 45.7 | 60.0 |
| Plait Point[b] | | 39.7 | 56.7 | 39.7 | 56.7 |

a) This value was calculated from the concentrations of ammonia in both layers and the compositions of the total mixture and raffinate.

b) The plait point was estimated according to Treybal et al.[6]

for the comparison of selectivity, but the useful method for comparing the ability of solvents has not been established. It is inconvenient to compare the selectivity of various solvents from the available data by the relative distribution ratio[1,11,12] or the selective power[13], since they are not always constant in the entire separation zone for all ternary systems. Quantitatively, selectivity may be represented more satisfactorily by the selectivity diagram[14] which expresses the relation between $y$ and $x$, where $y$ is the concentration of the solute in the extract on a solvent-free basis and $x$ is the corresponding concentration in the raffinate. For example, selectivity diagrams for the system cyclohexane-benzene-liquid ammonia at 20°C and 0°C are shown in Fig. 4, a and b, respectively.

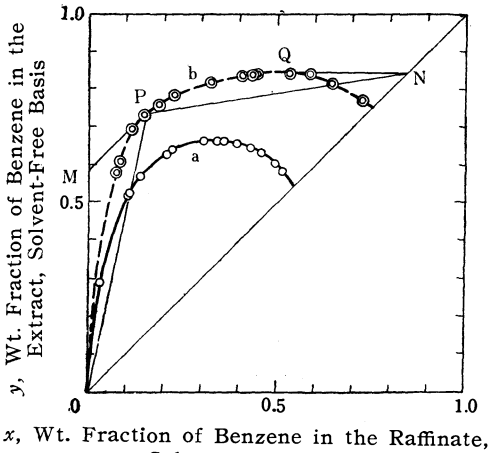



Fig. 4. Selectivity Diagrams for the System Cyclohexane-Benzene-Liq. $NH_3$, Ammonia as solvent.

If the selectivity $I$ is defined as $y$-$x$, then $I$ represents the degree of separation of the solute and the diluent, and is directly related to the selectivity diagram as shown in Fig. 4[15]. The maximum degree of separation of two components in one equilibrium stage is given by $I_{max}$. The greater the value of $I_{max}$, the more effective will be the separation. In addition, among solvents having an equal value of $I_{max}$, the greater the value of $y_{max}$, where $y_{max}$ is the maximum concentration of the solute in the extract, the higher will be the purity of the solute obtained by the extraction using that solvent under the given condition. It would be most practical to cmpare the selectivity of solvents by taking account of $I_{max}$ as well as $y_{max}$ from the viewpoint of separation of the solute and the diluent. In Fig. 4, $I_{max}$ on curve b is represented as MO and $y_{max}$ as the value

14) R. E. Treybal, "Liquid Extraction", McGraw-Hill Book Company, Inc., New York (1951), p. 87.

TABLE II

EQUILIBRIUM DATA FOR THE SYSTEM CYCLOHEXANE—BENZENE—LIQUID AMMONIA AT 20.0°C AND 0.0°C, WT. %

| Total Mixture | | Hydrocarbon Layer | | Solvent Layer | |
|---|---|---|---|---|---|
| Benzene Wt. % (Solvent-free Basis) | $NH_3$ Wt. % | $NH_3$ Wt. % | Benzene Wt. % (Solvent-free Basis) | $NH_3$ Wt. % | Benzene Wt. % (Solvent-free Basis) |
| At 20°C | | | | | |
| 0.0 | — | 4.0 | — | 94.2 | — |
| 5.2 | 46.2 | 4.4 | 3.3 | 91.4 | 29.0 |
| 16.2 | 47.8 | 5.7 | 10.4 | 86.2 | 52.0 |
| 28.4 | 72.3 | 5.5 | 10.8 | 85.7 | 52.4 |
| 44.9 | 80.1 | 6.1 | 13.9 | 84.0 | 57.0 |
| 28.4 | 42.3 | 7.7 | 20.6 | 78.2 | 62.8 |
| 44.9 | 65.4 | 7.9 | 22.1 | 77.1 | 64.0 |
| 56.7 | 63.4 | 10.6 | 30.4 | 70.0 | 66.3 |
| 44.9 | 43.2 | 12.0 | 33.9 | 66.0 | 66.3 |
| 54.9 | 53.6 | 12.8 | 35.9 | 63.8 | 66.2 |
| 44.9 | 31.6 | 14.9 | 39.4 | 60.1 | 65.6 |
| 52.5 | 40.1 | 18.3 | 43.0 | 54.8 | 64.4 |
| 52.5 | 36.9 | 20.3 | 45.7 | 51.4 | 63.2 |
| 54.4 | 35.8 | 25.4 | 49.3 | 44.9 | 60.4 |
| 56.7 | 38.7 | 28.4 | 51.3 | 40.8 | 58.4 |
| Plait Point[b] | | 34.4 | 54.8 | 34.4 | 54.8 |
| At 0.0°C | | | | | |
| 0.0 | — | 2.1 | — | 96.8 | — |
| 12.4 | 56.0 | 2.6 | 7.2 | 92.5 | 58.0 |
| 12.4 | 50.7 | 2.7 | 8.2 | 91.8 | 60.8 |
| 19.0 | 59.5 | 2.8 | 11.3 | 91.1 | 69.3 |
| 19.0 | 38.8 | 3.2 | 14.7 | 88.9 | 73.2 |
| 30.4 | 60.1 | 3.7 | 18.4 | 87.4 | 75.8 |
| 30.4 | 42.7 | 4.1 | 22.9 | 84.2 | 78.2 |
| 51.0 | 60.5 | 5.7 | 32.3 | 79.4 | 81.8 |
| 55.1 | 52.3 | 7.1 | 40.5 | 74.7 | 83.6 |
| 51.0 | 37.2 | 7.9 | 43.5 | 72.9 | 83.8 |
| 55.1 | 43.2 | 8.3 | 44.8 | 72.2 | 84.0 |
| 68.4 | 51.4 | 10.8 | 53.1 | 66.7 | 84.1 |
| 68.4 | 42.5 | 13.5 | 58.9 | 62.2 | 84.0 |
| 74.1 | 43.6 | 18.3 | 64.3 | 53.1 | 81.3 |
| 74.1 | 34.8 | 30.4 | 72.8 | 40.0 | 77.1 |
| Plait Point[b] | | 35.5 | 75.2 | 35.5 | 75.2 |

b) Cf. Table I.

on the ordinate of Q point, and then $I_{max} \cdot y_{max}$ would be twice the area of the triangle PON. Therefore, if the maximum separation factor is defined by the value of $I_{max} \cdot y_{max}$, it will be indicated by the definite value of $I_{max} \cdot y_{max}$ between 1.0 in the most ideal case, and zero with no effectiveness for the separation. This will be used as the convenient measure of comparison for selectivity.

Values of $I_{max} \cdot y_{max}$ calculated from the available data of ternary systems with liquid ammonia as one component are given in Table IV. In order to compare with other solvents, the values of $I_{max} \cdot y_{max}$ of representative solvents, which have been used or may be used as a solvent for the separation of hydrocarbons, are listed in the order of magnitude.

There are many factors other than selectivity which must be considered in choosing a solvent for a liquid extraction process, and it is evident that solvent power is the most important factor among them. In general, the amount of solvent in the raffinate phase is small and the large amount of solvent for recovery is carried in the solvent phase. If the diluent and the solute are to be separated as far as possible, a major amount of

TABLE III
EQUILIBRIUM DATA FOR THE SYSTEM ETHYLBENZENE STYRENE-LIQUID AMMONIA AT 0.0°C AND −15.5°C, WT. %

| Total Mixture | | Hydrocarbon Layer | | Solvent Layer | |
|---|---|---|---|---|---|
| Styrene Wt. % (Solvent-free Basis) | $NH_3$ Wt. % | $NH_3$ Wt. % | Styrene Wt. % (Solvent-free Basis) | $NH_3$ Wt. % | Styrene Wt. % (Solvent-free Basis) |
| At 0.0°C | | | | | |
| 0.0 | — | 14.1 | — | 78.1 | — |
| 9.1 | 54.8 | 15.7 | 8.1 | 74.7 | 11.7 |
| 19.0 | 49.0 | 18.3 | 17.3 | 71.1 | 23.0 |
| 20.7 | 42.3 | 18.4 | 19.2 | 70.5 | 26.2 |
| 34.4 | 51.9 | 24.0 | 31.5 | 63.4 | 36.9 |
| 34.9 | 46.8 | 24.8 | 32.5 | 61.7 | 38.2 |
| 36.1 | 44.0 | 27.0 | 34.5 | 59.5 | 38.5 |
| 38.0 | 38.9 | 31.5 | 37.2 | 54.3 | 40.2 |
| Plait Point[b] | | 47.0 | 41.2 | 47.0 | 41.2 |
| At −15.5°C | | | | | |
| 0.0 | — | 8.0 | — | 87.0 | — |
| 10.5 | 37.3 | 8.5 | 9.9 | 85.2 | 16.5 |
| 25.0 | 49.4 | 9.6 | 23.0 | 83.9 | 34.3 |
| 40.6 | 43.8 | 11.4 | 39.0 | 81.4 | 51.5 |
| 53.3 | 51.4 | 12.7 | 50.2 | 78.8 | 62.4 |
| 66.3 | 39.0 | 15.1 | 64.8 | 75.1 | 73.7 |
| 72.0 | 45.1 | 16.6 | 70.2 | 73.6 | 78.0 |
| 79.8 | 49.0 | 18.2 | 77.4 | 70.3 | 84.0 |
| 86.4 | 51.2 | 20.3 | 84.2 | 66.8 | 89.3 |
| 93.2 | 41.3 | 26.5 | 92.8 | 60.4 | 94.9 |
| 100.0 | — | 43.9[c] | — | 43.9[c] | — |

b) Cf. Table I.
c) Since −15.5°C is the upper critical solution temperature for the binary mixtures of styrene and liquid ammonia, the concentration of ammonia was estimated from the composition at the critical point.

solvent should be recovered at the end of the enriching section of the extraction tower where the extract is obtained. Therefore, the amount of other components dissolved in that solvent, $(1-Sy_{max})$, where $Sy_{max}$ is the concentration of the solvent in the solvent phase at $y_{max}$, will be an index of solvent power of that solvent. This value is given in the column 8 and the product of that value and $I_{max} \cdot y_{max}$ is given in column 9 in Table IV, as a comprehensive index.

As will be clear from Table IV, liquid ammonia is a poor solvent for the separation of paraffins and naphthenes[3,26], but for the separation of $C_6$–$C_7$ saturated hydrocarbons and aromatics or olefins, it is comparable to diethyleneglycol, better than liquid sulfur dioxide with respect to the selectivity and the solvent power. As ammonia has relatively high vapor pressure, it is comparatively easy to separate liquid ammonia from other components. And also, its extensive use as a mixed solvent is possible because of miscibility with water, lower alcohols, amines, and esters[1,27]. Considering the close relationship between the production of ammonia and the petrochemical industry, it is thought that there is a possibility of the use of liquid ammonia as a solvent for the separation of hydrocarbons.

## Summary

Equilibria for the systems *n*-hexane-benzene-liquid ammonia (20°C), cyclohexane-benzene-liquid ammonia (20°C and 0°C), and ethylbenzene-styrene-liquid ammonia (0°C and −15.5°C) were determined. It was shown that the ability of a solvent would be most practically compared by the product of the maximum

26) A. W. Francis, ibid., **36**, 764 (1944).

27) U. S. Pat. 2,721,164 (Oct. 18, 1955), *C. A.*, **50**, 2968c (1956); U. S. Pat. 2,723,940 (Nov. 15, 1955), *C. A.*, **50**, 3748d (1956).

TABLE IV

SELECTIVITIES AND CAPACITIES OF SOLVENTS FROM VARIOUS SYSTEMS

| Components | | | Temp. °C | $I_{max}$ Wt. Fraction | $y_{max}$ Wt. Fraction | $I_{max} \cdot y_{max} \times 10^2$ | 1-$S_{ymax}$ Wt. Fraction | $I_{max} \cdot y_{max} \times (1 - S_{ymax}) \times 10^2$ | Ref. |
|---|---|---|---|---|---|---|---|---|---|
| Diluent | Solute | Solvent | | | | | | | |
| *n*-Hexane | Methylcyclopentane | Aniline | 34.5 | 0.115 | 1.00 | 11.5 | 0.515 | 5.9 | 16 |
| 〃 | Cyclohexane | Liq. $NH_3$ | 20 | 0.055 | 1.00 | 5.5 | 0.058 | 0.3 | 3 |
| *n*-Heptane | 〃 | Furfural | 30 | 0.135 | 1.00 | 13.5 | 0.139 | 1.9 | 17 |
| 〃 | 〃 | Aniline | 25 | 0.097 | 1.00 | 9.7 | 0.262 | 2.5 | 18 |
| *n*-Hexane | Benzene | Ethylenediamine | 20 | 0.615 | 0.848 | 52.1 | 0.225 | 11.7 | 19 |
| 〃 | 〃 | $SO_2$ | −28.9 | 0.61 | 0.68 | 41.5 | 0.15 | 6.2 | 20 |
| 〃 | 〃 | Liq. $NH_3$ | 20 | 0.443 | 0.659 | 29.2 | 0.355 | 10.4 | |
| Cyclohexane | 〃 | $\beta,\beta'$-Thiodipropionitrile | Room temp. | 0.765 | 0.96 | 73.1 | 0.30 | 21.9 | 9 |
| 〃 | 〃 | Liq. $NH_3$ | 0 | 0.585 | 0.842 | 49.3 | 0.333 | 16.4 | |
| 〃 | 〃 | 〃 | 20 | 0.433 | 0.664 | 28.8 | 0.300 | 8.6 | |
| 〃 | 〃 | Nitromethane | 25 | 0.375 | 0.588 | 22.1 | 0.29 | 6.4 | 21 |
| *n*-Heptane | 〃 | Diethyleneglycol | 25 | 0.686 | 1.00 | 68.6 | 0.313 | 21.5 | 22 |
| 〃 | 〃 | 92%-Diethyleneglycol-8% $H_2O$ | 125 | 0.56 | 1.00 | 56.0 | 0.285 | 16.0 | 22 |
| 〃 | 〃 | $SO_2$ | −28.9 | 0.63 | 0.73 | 46.0 | 0.16 | 7.3 | 20 |
| 〃 | 〃 | Furfural | Room temp. | 0.38 | 0.592 | 22.5 | 0.335 | 7.5 | 9 |
| Methylcyclohexane | Toluene | Liq. $NH_3$ | 21.1 | 0.38 | 0.73 | 27.75 | 0.35 | 9.7 | 1 |
| *n*-Heptane | 〃 | $\beta,\beta'$-Thiodipropionitrile | 25 | 0.715 | 1.00 | 71.5 | 0.296 | 21.2 | 10 |
| 〃 | 〃 | Liq. $NH_3$ | −7.5 | 0.595 | 1.00 | 59.5 | 0.575 | 34.2 | 8 |
| 〃 | 〃 | 〃 | 0 | 0.668 | 0.955 | 64.8 | 0.418 | 27.1 | 2,8 |
| 〃 | 〃 | 〃 | −15 | 0.556 | 1.00 | 55.6 | 0.268 | 14.9 | 8 |
| 〃 | 〃 | Diethyleneglycol | 25 | 0.490 | 1.00 | 49.0 | 0.17 | 8.3 | 10 |
| 〃 | 〃 | $SO_2$ | −28.9 | 0.66 | 0.73 | 48.2 | 0.14 | 6.8 | 20 |
| 〃 | 〃 | Liq. $NH_3$ | 20 | 0.468 | 0.808 | 37.8 | 0.306 | 11.6 | 2,8 |
| 〃 | 〃 | Aniline | 25 | 0.290 | 0.470 | 13.6 | 0.266 | 3.6 | 13 |
| 〃 | 〃 | 97%-Acetic acid-3% $H_2O$ | 23 | 0.19 | 0.55 | 10.5 | 0.69 | 7.2 | 23 |
| *n*-Heptane | Octene-1 | Liq. $NH_3$ | 20 | 0.115 | 1.00 | 11.5 | 0.063 | 0.7 | 3 |
| 〃 | 〃 | 〃 | 0 | 0.108 | 1.00 | 10.8 | 0.032 | 0.3 | 3 |
| Decalin | Tetralin | 〃 | 20 | 0.415 | 1.00 | 41.5 | 0.136 | 5.6 | 24 |
| 〃 | 〃 | 〃 | 0 | 0.323 | 1.00 | 32.3 | 0.063 | 2.0 | 24 |
| Ethylbenzene | Styrene | 〃 | −15.5 | 0.126 | 1.00 | 12.6 | 0.561 | 7.1 | |
| 〃 | 〃 | Diethyleneglycol | 25 | 0.103 | 1.00 | 10.3 | 0.271 | 2.8 | 25 |
| 〃 | 〃 | Liq. $NH_3$ | 0 | 0.068 | 0.412 | 2.8 | 0.51 | 1.4 | |

15) K. Ishida, *Science Repts. Research Inst. Tohoku Univ.*, Ser. A, **5**, 377 (1953).
16) B. DeB. Darwent and C A. Winkler, *J. Phys. Chem.*, **47**, 442 (1943).
17) E. N. Pennington and S. J. Marwil, *Ind. Eng. Chem.*, **45**, 1371 (1953).
18) T. G. Hunter and T. Brown, ibid., **39**, 1343 (1947).
19) A. P. C. Cumming and F. Morton, *J. Appl. Chem.*, **3**, 358 (1953).
20) C. N. Satterfield, J. H. Powell, Jr., E. A. Oster, Jr., and J. P. Noyes, *Ind. Eng. Chem.*, **47**, 1458 (1955).
21) H. I. Weck and H. Hunt, ibid., **46**, 2521 (1954).
22) G. C. Johnson and A. W. Francis, ibid., **46**, 1662 (1954).
23) D. F. Othmer and P. E. Tobias, ibid., **34**, 690 (1942).
24) K. Ishida, *J. Chem. Soc. Japan, Ind. Chem. Sect.*, **60**, 864 (1957).
25) M. G. Boobar, P. M. Kerschner, R. T. Struck, S. A. Herbert, N. L. Gruver and C. R. Kinney, *Ind. Eng. Chem.*, **43**, 2922 (1951).

value of selectivity and the maximum concentration of the solute in the extract, i. e. maximum separation factor. Selectivity and solvent power of some solvents were compared by this definition and it was recognized that liquid ammonia is comparable to diethyleneglycol as a solvent for the separation of saturated hydrocarbons and aromatic or olefinic hydrocarbons, rather than liquid sulfur dioxide.

The author wishes to record his thanks to Professor Tokura and his coworkers in this Laboratory for a gift of styrene.

*The Chemical Research Institute of Non-Aqueous Solutions, Tohoku University, Sendai*

# *Organic Semiconductors with High Conductivity II. Structural Aspect of Violanthrene-Iodine Complex*

By Hideo AKAMATU, Yoshio MATSUNAGA and Haruo KURODA

(Received March 25, 1957)

## Introduction

In the preceding paper[1], we have presented that polycyclic aromatic hydrocarbons form solid molecular complexes with bromine or iodine, and these complexes behave as typical semiconductors with high conductivity of $10^{0}$—$10^{-3}$ $ohm^{-1}$. $cm^{-1}$ at room temperature and low activation energy for conduction, the energy gap of 0.1–0.2 eV. It has been suggested that the high conductivity is due to an appropriate electronic structure which arises from the formation of the molecular additive compounds. To throw light upon the mechanism of the electrical conduction in these organic materials, it should be most interesting to make clear the structure of these molecular complexes. In the present paper, the structural aspect of the violanthrene-iodine system is presented.

Violanthrene-iodine complex is the most stable among the complexes between polycyclic aromatic hydrocarbons and halogens so far as is known. The electrical resistivity varies as the composition varies, and has the minimum value at the composition in which the mole ratio of iodine to violanthrene (V) is 2, where the resistivity at room temperature is about 40 ohm. cm with the thermal energy gap of 0.15 eV.

The magnetic susceptibility-composition curve[2] shows a great discrepancy from the additive law, and has also the minimum value (depression of diamagnetism) at the same composition, where the discrepancy exceeds 35 per cent. Both these facts suggest the existence of molecular complex consisting of one molecule of violanthrene and two of iodine. On the other hand, a preliminary examination by X-ray revealed an amorphous pattern, while most of the other complexes showed sharp crystalline patterns.

In this paper, the thermodynamical study on the equilibrium of violanthrene-iodine system as well as the full examinations by X-ray are presented.

## Preparation of the Complex and Isotherm of Violanthrene-Iodine System

The preparation of the complexes has been described in the previous papers. In the present case, however, with the purpose of studying the isothermal equilibrium between violanthrene and iodine, the following method was applied to the preparation of complexes having varied compositions. The crystalline powder of violanthrene of known quantity was treated with carbon tetrachloride solution of iodine for more than three days. After the equilibrium has been reached, the precipitated complex was filtered through glass wool and the concentration of iodine in the filtrate was determined by titration with 0.025 N aqueous solution of sodium thiosulfate. The composition of the complex obtained was estimated from the difference in concentration of iodine between the initial and the final solution.

Two isotherms have been obtained; one is at the room temperature $27\pm1$°C, and the other is at the temperature of refrigerated chamber $-3\pm2$°C. The relation between the equilibrium

1) H. Akamatu, H. Inokuchi and Y. Matsunaga, This Bulletin, **29**, 213 (1956).
2) Y. Matsunaga, ibid, **28**, 475 (1955).

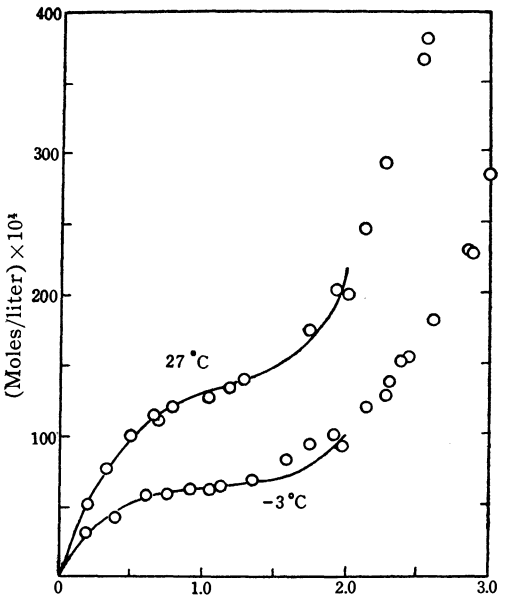



Fig. 1. Equilibrium concentration of iodine in carbon tetrachloride solution plotted against composition of the complex.

concentration of iodine in the carbon tetrachloride solution and in the complex is shown in Fig. 1.

## Equilibrium in Violanthrene-Iodine System

Fig. 1 suggests that the observed isotherms are the ones near a boundary of the univariant and bivariant phases and just above the critical temperature, below which two solid phases should be separated, one has the ideal composition of $V \cdot 2I_2$ and the other is V.

Such an isotherm has been discussed by a few authors. Anderson[3] discussed the conditions of equilibrium of non-stoichiometric chemical compounds. Rees[4] derived the pressure-temperature-composition relations for two-component interstitial solid solutions. His theory is applicable to any non-stoichiometric system in which one component is volatile. Both theories are applicable to the present case. However, referring the results of density measurements described in the later section, Rees' model is more conveniently applicable to our case.

The problem is to derive the pressure-temperature-composition relation in a system composed of molecules A(violanthrene) and B (iodine) up to composition $A_mB_n$ where $m$ and $n$ are small integers, and so delineate a boundary of the univariant and the bivariant phase. The fundamental assumptions are as follows.

The solvent lattice of A molecules is referred to as the parent lattice, and the solute component B is in equilibrium with molecules of B in the vapor phase. B molecules occupy interstitial sites in the parent structure*. Several kinds of site are assumed; they are distinguished from each other by the difference in the amount of energy which is gained by a B molecule against free molecular state when it occupies one kind of site. These energies are denoted as $E^a$, $E^b$ *etc.* for the $a$th, $b$th *etc.* kind of site, respectively.

The interaction energies per pairs of B molecules in each kind of site are considered, and denoted as $E^{aa}$, $E^{bb}$ *etc.* Furthermore, it is assumed that the number of the sites of the $i$th kind accessible for occupation by B molecule depends on the number of sites of the $(i-1)$th kind already occupied by B molecules. Let $N$ stand for the total number of sites of the $a$th kind, $N^a$, $N^b$, $N^c$ *etc.* for the numbers of sites of the $a$th, $b$th, $c$th *etc.* kinds occupied at equilibrium, and $\alpha$, $\beta$ *etc.* for the number of sites of the $b$th, $c$th *etc.* kind created for one of the $a$th, $b$th *etc.* kind occupied by a B molecule respectively. The contribution of the parent lattice of A molecules to the total partition function of the crystal is assumed to be independent of the contents of B molecules, so that it is concerned only with the factor representing the contribution of the added B molecules; then the extra configurational grand partition function is expressed as,

$$\begin{aligned}\Theta(T, \lambda^a, \lambda^b \cdots\cdots N^a, N^b \cdots\cdots) &= \sum_a \sum_b \cdots\cdots [\lambda^a \kappa^a(T)]^{N^a} [\lambda^b \kappa^b(T)]^{N^b} \cdots\cdots \\ &\times \frac{N!}{N^a!\,(N-N^a)!} \frac{(\alpha N^a)!}{N^b!\,(\alpha N^a - N^b)!} \cdots\cdots \\ &\times \exp\left[\left\{N^a E^a + N^b E^b \cdots\cdots + \frac{(N^a)^2}{N} E^{aa} + \frac{(N^b)^2}{\alpha N^a} E^{bb} \cdots\cdots\right\} \Big/ kT\right] \qquad (1)\end{aligned}$$

where $\lambda^a$, $\lambda^b$ ..... are the absolute activities of B molecules in sites of the $a$th, $b$th *etc.*, and $\kappa^a(T)$, $\kappa^b(T)$ *etc.* are the additional factors in the partition function per molecules for the contribution of B molecules

3) J. S. Anderson, *Proc. Roy. Soc.*, **A185**, 69 (1946).
4) A. L. G. Rees, *Trans. Faraday Soc.*, **50**, 335 (1954).

* In the present case, interstitial sites are assumed to arise from violanthrene lattice being made expansion. See the later section.

in the $a$th, $b$th *etc.* sites to the vibrational modes of the crystal. For the equilibrium state where $\partial\Theta/\partial N^a=0$, $\partial\Theta/\partial N^b=0$,

$$\lambda^a=\frac{1}{\kappa^a(T)}\cdot\frac{N^a}{(N-N^a)}\left\{1-\left(\frac{N^b}{\alpha N^a}\right)\right\}^\alpha \times\exp\left[\left\{-E^z-\frac{2N^a}{N}E^{aa}+\frac{1}{\alpha}\left(\frac{N^b}{N^a}\right)^2E^{bb}\right\}\Big/kT\right] \quad (2)$$

$$\lambda^b=\frac{1}{\kappa^b(T)}\cdot\frac{N^b}{(\alpha N^a-N^b)}\left\{1-\left(\frac{N^c}{\beta N^b}\right)\right\}^\beta \times\exp\left[\left\{-E^b-\frac{2N^b}{\alpha N^a}E^{bb}+\frac{1}{\beta}\left(\frac{N^c}{N^b}\right)^2E^{cc}\right\}\Big/kT\right] \quad (3)$$

etc.

In applying the theory to our results, we assume that the composition of $\overline{V\cdot 2I_2}$ (idealized formula) corresponds to that of the interstitial solid solution where the $a$th kind site is saturated and the other sites are completely empty. This means that the violanthrene lattice made of $N_0$ molecules has $2N_0$ sites of the $a$th kind for iodine molecules. In reality, however, $n$ molecules of iodine occupy a part of $2N_0$ sites of the $a$th kind and some numbers of molecules occupy the sites of the $b$th, $c$th *etc.* kind. We have no foundation to assume the numbers of sites of the $b$th, $c$th *etc.* kind. However, in the range of composition where the total mole ratio of iodine to V is not greater than 2, it may not be far from the truth if we presume that the number of iodine molecules occupying the other sites is far less than the number of molecules occupying the $a$th kind sites. This leads to the assumption of $N^b/\alpha N^a\ll 1$ in eq. (2).

Introducing $\theta=n/2N_0$ instead of $N^a/N$ in eq. (2), we obtain

$$\lambda(\theta)=\frac{1}{\kappa^a(T)}\cdot\frac{\theta}{1-\theta}\times\exp[-\{E^a+2\theta E^{aa}\}/kT] \quad (4)$$

for the activity of the iodine molecule in the $a$th site.

In the isotherm of Fig. 1, at the composition of mole ratio being 2, $\theta$ is not equal to unity, but less than unity for the reason mentioned above. Let $\theta$ be $\delta<1$ at the composition where total mole ratio is 2, then the relative activity at any composition can be expressed as

$$\frac{\lambda(\theta)}{\lambda(\delta)}=\frac{\theta}{1-\theta}\cdot\frac{1-\delta}{\delta}\times\exp[4(\delta-\theta)T_c^a/T] \quad (5)$$

where $T_c^a=-E^{aa}/2k$, which is the critical temperature above which two phase region should disappear.

Eq. (5) can be applied to the experimental data to delineate the isotherm. For this purpose, we assume $\lambda(\theta)/\lambda(\delta)\simeq c(\theta)/c(\delta)$, where $c$ is the concentration of iodine in carbon tetrachloride at the equilibrium. We further assumed that $\delta=0.87$, $c(\delta)=0.0105$ at $-3$°C; $\delta=0.84$, $c(\delta)=0.0220$ at 27°C and $T_c^a=260$°K. These values have been estimated to be as good as possible to be fitted to the observed values. The theoretical isotherms are shown by the curves in Fig. 1.

The agreement between the experimetal results and the theoretical calculations is satisfactory when we realize that the theory contains many approximations. This leads to the conclusion that "violanthrene-iodine complex" at room temperature is a solid solution between violanthrene and a non-stoichiometric molecular compound, which has the composition of $\overline{V\cdot 2I_2}$ as the idealized formula and should be separated as a solid phase below the critical temperature of 260°K.

From the isotherms of 27°C and $-3$°C, the heat of dissociation of the complex can be calculated by Clapeyron's relation. This value is 3.8 kcal. per one mole of iodine for the complex having composition of mole ratio being 1 (where assumed $\theta=0.5$). The heat of dissociation depends on the composition in such a manner as expressed as $E^a+2\theta E^{aa}$. Therefore, this value corresponds to the mean heat of dissociation in the composition range from $\theta=0$ to $\theta=1$, where the interstitial sites of the $a$th kind have been completely occupied by iodine molecules. Alternatively one may say that the integral heat of dissociation of the complex having the composition of $\overline{V\cdot 2I_2}$ is 3.8 kcal. per mole of iodine. Then,

$$2I_2(\text{in } CCl_4)+C_{34}H_{18}(\text{solid})=C_{34}H_{18}\cdot 2I_2(\text{solid})+7.6\,\text{kcal.} \quad (6),$$

and, since the heat of dissolution of iodine in carbon tetrachloride is 5.8 kcal. per mole of iodine[5],

$$2I_2(\text{solid})+C_{34}H_{18}(\text{solid})=C_{34}H_{18}\cdot 2I_2(\text{solid})-4.0\,\text{kcal.} \quad (7).$$

## X-Ray Studies on Violanthrene-Iodine Complex

X-Ray studies were made by Norelco

5) K. Hartley and H. A. Skinner, ibid, **46**, 621 (1950).

diffractometer with Ni-filtered Cu-$K_\alpha$ radiation. Typical diffractometer records of complexes having varied compositions are shown in Fig. 2.

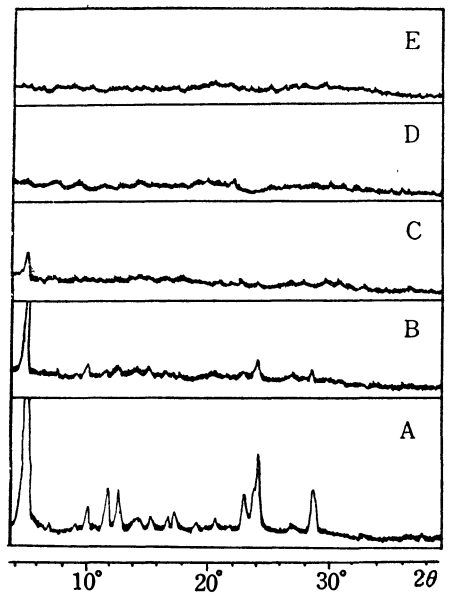



Fig. 2. Diffractometer record of violanthrene-iodine complex.
Mole ratio of iodine to violanthrene: A 0.12, B 0.40, C 1.48, D 2.27, E 4.69.

Sharp crystalline peaks are seen in the diffraction patterns of complexes which have a low content of iodine. These peaks coincide with the diffraction peaks of violanthrene crystal itself, and decrease their intensities as the mole ratio of iodine to V is increased. In this process, no change is found in either positions or the relative intensities of peaks, and no appearence of any other crystalline peaks can be found. These facts show the presence of non-reacted violanthrene crystallites in the specimen, and they also show that the main part which has combined with iodine becomes amorphous. As for the specimens, in which the mole ratio is greater than 2, crystalline peaks disappear completely.

The preliminary examination of violanthrene-bromine complex has also shown an amorphous pattern. However, both these cases seem to belong to the special cases. The complexes between polycyclic aromatic hydrocarbons and halogens are not necessarily amorphous. The complex of perylene or pyranthrene shows a clearly crystalline pattern. For instance, in the case of perylene-iodine complex two kinds of crystalline pattern are found in the same specimen; one is probably due to molecular compound between one molecule of perylene and one of iodine, and the other to one molecule of perylene and two of iodine. This fact makes the analysis of the diffraction pattern of this complex complicated. On the other hand, the violanthrene-iodine system gives a completely amorphous pattern and is suited for the application of the radial-distribution analysis. For this purpose, it is desired that the specimen will have enough iodine content to give a completely amorphous structure, but not such an excess in amount as to separate iodine crystals. An intensity distribution curve of scattered X-rays by the complex is shown in Fig. 3.

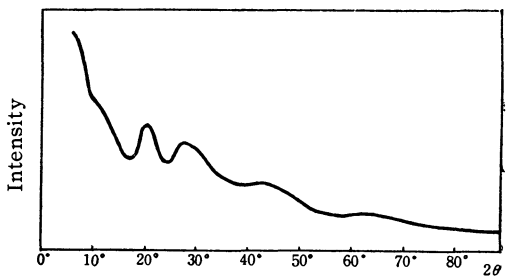



Fig. 3. Intensity distribution curve of violanthrene-iodine complex (1 : 4.9)

## Radial-Distribution Analysis

The intensity, $I$, of scattering in the direction of $2\theta$ (scattering angle) is given by the theory[6] as

$$I=\sum_i f_i^2+\sum_i\sum_j f_i f_j \frac{\sin sr_{ij}}{sr_{ij}},$$
$$s=\frac{4\pi \sin\theta}{\lambda} \qquad (8)$$

where $r_{ij}$ is the distance between the $i$-th and $j$-th atoms, $f$ is the atomic scattering factor, and $\lambda$ the wave length of the X-ray. In the case where the specimen contains more than one kind of atom, the general formula for the intensity of scattering can be written[7] as,

$$I=N\sum_p f_p^2+\sum_m^{m\neq n}\sum_n f_m f_n \cdot \frac{\sin sr_{mn}}{sr_{mn}} \qquad (9)$$

where $m$, $n$,..... denote the kinds of atom constituting an appropriate unit of structure of which the entire specimen is

6) P. Debye, *Ann. Physik*, **46**, 809 (1915).
7) B. E. Warren, H. Krutter and O. Morningstar, *J. Am. Ceram. Soc.*, **19**, 202 (1936); H. P. Klug and L. E. Alexander, "X-Ray Diffraction Procedures" John Wiley and Sons, Inc , 1954, p. 590.

regarded as being composed, and $N$ is the number of such units.

Let the average numbers of atoms lying at $r\sim r+dr$ from the reference atom be $a_m$, $a_n$, *etc.*, and let the atomic density function $\rho_m(r)$ which is defined by eq. (10) be used; then eq. (9) can be expressed as eq. (11),

$$4\pi r^2\rho_m(r)dr=\sum_m a_m f_m \tag{10}$$

$$I=N\left[\sum_m f_m^2+\sum_m f_m\int 4\pi r^2\rho_m(r)\frac{\sin sr}{sr}dr\right] \tag{11}$$

The following approximations are introduced,

$$f_m=K_m f_e \tag{12}$$

$$\rho_m(r)=f_e g_m(r) \tag{13},$$

where $f_e$ is the scattering factor of a single electron, $K_m$ is the effective number of electrons per atom of type $m$, and $g_m(r)$ is the electron-density function. Using those approximations, eq. (11) is expressed as

$$I=N\left[\sum_m f_m^2+4\pi f_e^2\int\sum_m K_m g_m(r)r^2\frac{\sin sr}{sr}dr\right] \tag{14}$$

Finally, introducing $g_0$, the average density of electrons in the specimen, eq. (14) can be transformed to eq. (15) by means of the Fourier integral theorem.

$$4\pi r^2\sum_m K_m\cdot g_m(r)=4\pi r^2\cdot g_0\cdot\sum_m K_m+\frac{2r}{\pi}\int_0^\infty s\cdot i(s)\cdot\sin sr\cdot ds \tag{15}$$

in which

$$i(s)=\left(\frac{I}{N}-\sum_m f_m^2\right)/f_e^2 \tag{16}$$

From the observed intensity curve of scattering, the radial-distribution function, $4\pi r^2\sum_m K_m g_m(r)$, can be obtained by eq, (15).

The approximation of eq. (12) is possible only in the case where the specimen is made of atoms whose atomic numbers are near to each other. In the cases of iodine and carbon, their atomic numbers are far from each other. However, since the atomic number of iodine is much larger than that of carbon, in such a composition as that of one molecule of violanthrene and five of iodine, it has been revealed that the intensity of coherent scattering is determined mainly from the contribution of iodine atoms. In such a case, the above approximation is again allowed.

We assume the structure unit as $I\cdot(C_{34}H_{18})_{0.1}$ for the complex made of one molecule of violanthrene and five molecules of iodine, and the effective numbers of electrons being one for hydrogen, 6 for carbon and 53 for iodine atom. From the observed density, $d=3.03$, $g_0=0.602d\times\sum_m K_m/\sum_m M_m$, where $M_m$ is the atomic weight, is given as 0.809 electrons per Å$^3$.

The integral in eq. (15) is replaced by the equivalent summation,

$$\int_0^\infty s\cdot i(s)\cdot\sin sr\cdot ds=\sum_{s=0}^{s=s\max} s\cdot i(s)\cdot\sin sr\cdot\Delta s \tag{17}$$

and the computation has been made, giving $\Delta S=0.04\pi$, for every interval of 0.2 Å for $r$. The radial-distribution function obtained is shown in Fig. 4.

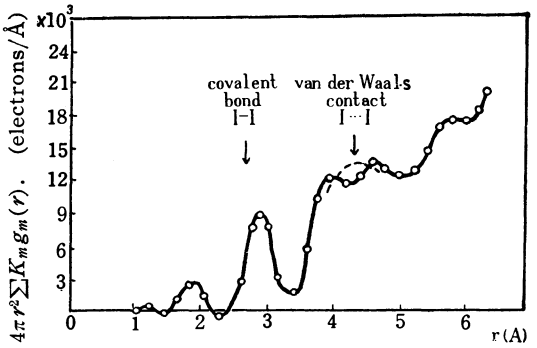



Fig. 4. Radial distribution curve of violanthrene-iodine complex (mole ratio 1 : 4.9).

The radial-distribution curve has a remarkable maximum at $r=2.85$ Å. This peak is clearly resolved and encloses an area of 3500 electrons. If this peak is due to the coherent scattering between carbon atoms in a violanthrene molecule, the area will be $(34/10)\times3\times6^2=368$ electrons, since the statistical average number of carbon atoms surrounding a reference carbon atom at the distance of 2~3 Å is 3. This can not explain the above large area of the peak. On the other hand, I-I distance in an iodine molecule is 2.667 Å from optical data, and 2.70 Å from the analysis of crystal structure. If we assume that the peak is due to the interaction between iodine atoms in an iodine molecule, the area will be $1\times53^2=2800$ electrons. The summation of the effects due to iodine molecule and violanthrene molecule can almost explain the area under the peak. However, it is clear that the

most part of the effect arises from the contribution of the iodine molecule. From this, it is revealed that most iodine molecules do not dissociate into ions, but I-I distance is extended to 2.85 Å.

In the region of $r$=4~5 Å, two maxima are seen. They are rather poorly resolved. In eq. (17), the upper limit, $\infty$, of the integral is replaced by a finite value, $s$. This procedure leads to the result of the so-called termination error[8]. In our case, the termination effect due to the major peak at $r$=2.85 Å will result in the appearance of subsidiary maxima at $r$=1, 1.8, 3.7 and 4.5 Å, and minima at $r$=1.5 and 4.2 Å. In Fig. 4, two small maxima at 1~2 Å may be due to this termination error. Therefore, the similar effect is also presumed in the region of 4~5 Å. The true distribution curve seems to be shown by a dotted line in Fig. 4. The maximum, ranging from 3.5 to 5.5 Å, encloses an area of about 16500 electrons.

In a violanthrene molecule, the average number of carbon atoms surrounding a reference atom at the distance of 3.5~5.5 Å is not more than 5. It is clear that the observed area can not be explained by the interaction between these carbon atoms. The distance of 3.5~5.5 Å corresponds to the distance between iodine atoms which make van der Waals contact with each other. In iodine crystal, from a reference atom there are 2 atoms at 3.6 Å, 8 at 4.4 Å, 2 at 4.8 Å, and 1 at 5.1 Å, i.e., 13 atoms at the distance of this range. If the maximum arises due to the interaction between these iodine atoms, the area should be $13\times53^2=36400$ electrons, which is much larger than the observed area. Therefore, the observed area is not explained by the arrangement of iodine molecules as that in iodine crystal. It appears that an atom should be surrounded by 5~6($=16500/53^2$) atoms. This suggests the presence of small groups of iodine molecules presumably in two dimensional arrangement.

## Density of Violanthrene-Iodine Complex

The density measurement was made with a pycnometer. Carbon tetrachloride solution of iodine which is in equilibrium with complex was used as the liquid medium. The results are shown in Fig. 5, where specific volumes of complexes are plotted against compositions. It has been found that the specific volume of a complex is larger than the sum of the specific volumes of its constituents, in the region up to the mole ratio of 2.5. Beyond this mole ratio, the volume becomes additive. This result suggests that, at an early stage of the complex formation, in the range of low iodine content, violanthrene molecular lattice is expanded and the structure with vacant space is produced. As iodine content increases, the vacancies are gradually occupied by iodine molecules and filled up at the concentration where the total mole ratio becomes 2.5. This is clearly seen in the change of partial molal volume of iodine in this system.

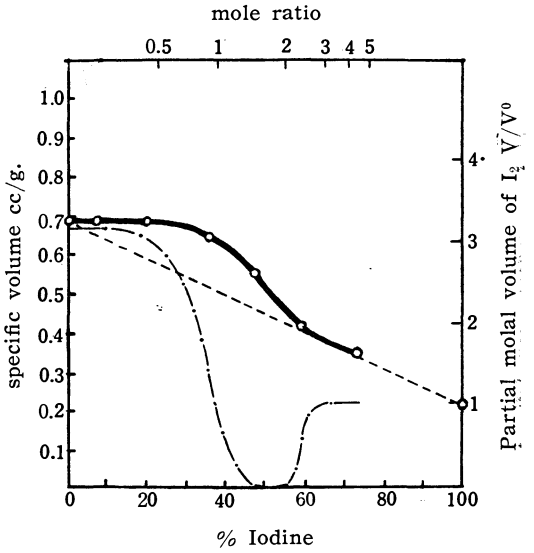



Fig. 5. Specific volume of voilanthrene-iodine system ——, and partial molal volume of iodine in the same system —·—.

The analysis of crystal structure has not yet been made for violanthrene. However, the crystal structures of many kinds of polycyclic aromatic hydrocarbon have been studied by Robertson[9]. The analogy suggests that (001) plane will be the cleavage plane in violanthrene lattice as in other crystals of polycyclic hydrocarbons. If it is so, it will be most facile for iodine molecules to penetrate into interstices between (001) planes. This will lead to the expansion of the crystal in the $c$-axis direction. However, as mentioned in the preceding section, there is no sign of any preferential change of crystal structure in the complex formation, but the whole structure becomes amorphous. Therefore,

8) W. L. Bragg and J. West, *Phil. Mag.*, **10**, 823 (1930).

9) J. M. Robertson, "Organic Crystals and Molecules", Cornell Univ. Press., Ithaca, N. Y., 1953, p. 183.

it may be concluded that iodine molecules do not penetrate into interstices between the preferential crystal plane, but wedge themselves directly between the molecules of violanthrene.

The molecular volume of violanthrene is about five times as large as that of iodine, and the surface of a violanthrene molecule can be occupied by 5~6 iodine molecules. Therefore, as the result of penetration of an iodine molecule between two neighboring violanthrene molecules, a large vacant space is produced. It is noteworthy that the vacancies are filled up by iodine molecules at the composition where the total mole ratio is 2.5, which is a larger value than the composition corresponding to $\overline{V \cdot 2I_2}$. From this it is most plausible to assume that the complex, having the composition of $\overline{V \cdot 2I_2}$, has the structure in which 4 iodine molecules are sandwiched between two neighboring molecules of violanthrene.

Such a model is consistent with the result of the radial-distribution analysis which indicates that an iodine atom is surrounded by statistically 5~6 iodine atoms in van der Waals contact. It is also not inconsistent with the assumption which has been made in the thermodynamical treatment. What we called the *a*th site before can be made to correspond to the site which can be occupied by 4 molecules of iodine between two neighboring violanthrene molecules.

## Summary and Discussion

From the thermodynamical consideration on the isotherm of the violanthrene-iodine system, it was revealed that the system can be seen an interstitial solid solution. Up to the point where the mole ratio is 2, the solid solution is the one between violanthrene and a molecular compound. The latter has no stoichiometric composition, but consists of approximately one violanthrene molecule and two iodine molecules, and can be written as $\overline{V \cdot 2I_2}$ in the idealized formula. Beyond the above mole ratio, the solid solution is the one presumably between $V \cdot 2I_2$ and iodine. The radial distribution analysis of X-ray diffraction also supports the entity of the molecular complex $\overline{V \cdot 2I_2}$.

The heat of formation in eq. (6) or eq. (7) is a roughly estimated value. There is a great deal of information on the heat of formation of the molecular compounds of iodine. For instance, the heat of formation of molecular compound between pyridine and iodine dissolved in pyridine was presumed to be 7.95 kcal[5]. In eq. (6), if we consider the heat of dissolution of violanthrene which is presumably a larger one, the heat of complex formation between iodine and violanthrene molecules should have a much larger value than 7.6 kcal.

The heat of formation, in eq. (7), among the solid phases is endothermic. However, a large amount in entropy change will be expected and it will cover the heat of formation to gain the free energy for complex formation. In reality, when violanthrene crystalline powder is brought into contact with iodine the solid complex is formed spontaneously.

From the radial-distribution analysis, it was revealed that, after the complex formation, the interatomic distance of an iodine molecule is extended to 2.85 Å from 2.67 Å of normal iodine molecule. G. Dallinga[10] reported that in pyridine solution of iodine the I-I distance is increased to 2.90 Å. This value is comparable to our case. If we assume the intermolecular charge-transfer force for the complex formation, an electron will be transferred from violanthrene to iodine molecule, getting into the anti-bonding orbital. This will lead to an increase in the I-I distance according to the degree of contribution of the dative structure $\psi(V^+ - I_2^-)$. However, we can not get any single solution for the ionic character of iodine molecule from its interatomic distance alone.

It was concluded from the density measurement, that the molecular complex of $\overline{V \cdot 2I_2}$ has the structure in which iodine molecules are sandwiched between two neighboring violanthrene molecules. If this is true, such a structure is one of the characteristics of this system, with the facts that the molecular compound is not stoichiometric in its nature and that the system as a whole is amorphous, and is very similar to the molecular compounds of graphite. It is not known in detail how iodine molecules are arranged in relation to hydrocarbon molecules. However, the above structure suggests strongly that each iodine molecule is not localized preferentially to a fixed position of violanthrene molecule, but occupies the sites rather freely with a diffuse interaction force.

10) G. Dallinga, Abstract of paper at the 3rd. Congress of International Union of Crystallography, cf. *Acta Cryst.*, **7**, 665 (1954).

Such a structure like this is frequently seen amongst the intermediate phases of metallic system and among the quasi-metallic compounds. It is most interesting to see such a structure in an organic substance which has a high electrical conductivity.

The cost of this study was defrayed partly from the grant of the Ministry of Education, and partly from the grant in aid for the promotion of scientific research from the Asahi Press, to which the authors' thanks are due.

*Department of Chemistry, Faculty of Science, The University of Tokyo*
*Hongo, Tokyo*

# *On Mangiferin*, the Coloring Matter of Mango (Mangifera indica Linn.). IV*[1]. *Isolation of 1,3,6,7-Tetrahydroxyxanthone and the Skeletal Structure of Mangiferin*[2]

By Syun ISEDA

(Received March 9, 1957)

In Part III[1] of this series, it was shown that mangiferin is a substance agreeing with the composition $C_{19}H_{18}O_{11}$. For the structure of this pigment, Wiechowski[3] proposed a formula having a skeleton of 1,4,5,7-tetrahydroxyxanthone, but failed to offer any evidence supporting such an assumption. The fact that mangiferin changes into euxanthic acid in rabbit body[3] indicates that the pigment molecule possesses a xanthone skeleton or a structure that can easily resume the xanthone skeleton, and Gorter[4] proposed a structural formula favoring the latter. Although structural formulae were proposed, all attempts for the experimental evidence of skeletal structure of the pigment molecule have been unsuccessful.

Mangiferin resists hydrolysis with hydrochloric or sulfuric acid and the "genin" can not be isolated by such a method. Wiechowski[3] tried the application of hydroiodic acid but has not isolated any crystalline product. The writer succeeded in isolating a crystalline product by heating the pigment in phenol with hydriodic or hydrobromic acid.

This product was not found to be purifiable *per se* when it was acetylated, and the acetate was recrystallized from glacial acetic acid to colorless crystals, $C_{21}H_{16}O_{10}$, m.p. 200°C. Hydrolysis of this acetate with an acid afforded a product(I) as pale yellow crystalline powder or microneedle crystals, which colored markedly at 320°C, became brown at around 350°C and decomposed at 370–371°C. The analytical values agreed with $C_{13}H_8O_6$. This compound showed its phenolic property by coloring green with ferric chloride. The crude decomposition product melted with decomposition at 368°C before acetylation and its ultraviolet absorption spectrum agreed practically with that of I, recovered from the purified acetyl derivative; it is therefore certain that no cyclization or other changes in the molecular structure had taken place during acetylation.

Methylation of I with diazomethane gives a derivative (II), $C_{16}H_{14}O_6$, m.p. 218–219°C, which indicates the presence of a free phenolic hydroxyl by the positive ferric chloride reaction. Its acetylation gives crystals of m.p. 216°C, $C_{18}H_{16}O_7$, negative to the ferric chloride test, but its hydrolysis reverts it to II, m.p. 218–219°C. Application of diazomethane to II results in the total recovery of the unchanged II. It follows, therefore, that I contains a phenolic hydroxyl that is not methylated with diazomethane.

The melting points and the analytical

* *Mangiferine*, used to date, is hereafter corrected to *mangiferin* in accordance with international nomenclature.

1) Part III: S. Iseda, *J. Kumamoto Women's Univ.*, **9** (1957), in press. (in Japanese).

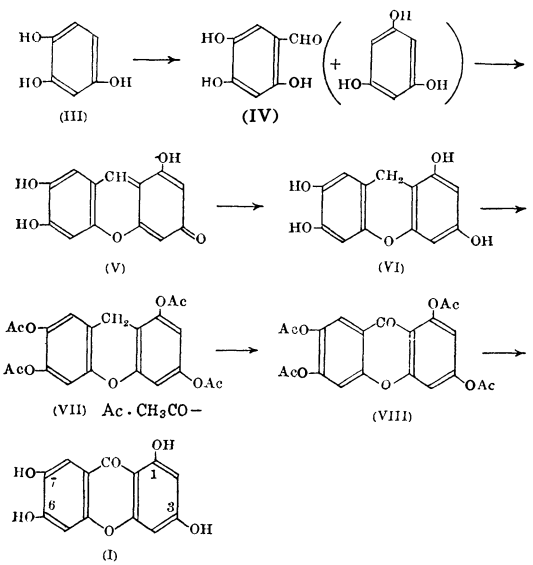
2) Presented at the Kyushu Local Meeting of the Chemical Society of Japan, Kumamoto, December 26, 1956.

3) W. Wiechowski, *Arch. exp. Pathol. Pharmakol.*, **97**, 462 (1923).

4) K. Gorter, *Bull. Jardin Bot. Buitenzorg*, (iii) **4**, 260 (1922).

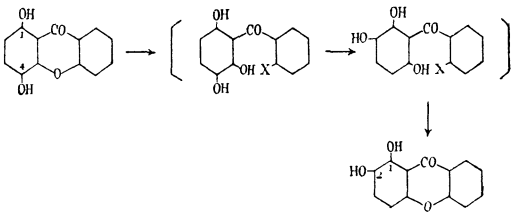
values of the acetyl derivative of I and those of II are respectively identical with the values[5] of 1,3,6,7-tetraacetoxyxanthone, m.p. 198°C, and 1-hydroxy-3,6,7-trimethoxyxanthone, m.p. 216°C. However, the melting point of 1,3,6,7-tetrahydroxyxanthone, thought to be identical with I, is given in the literature[5,6] as decomposing at 320°C. Through the courtesy of Prof. Shoji Shibata of University of Tokyo, a sample synthesized by Tanase[5] was made available. Mixed samples of the acetates and methyl ethers failed to show any depression of the melting point. The phenol also showed the same behavior when the synthetic product alone or in admixture with I was fused.

Since the Tanase sample was about 15 years old, a product was synthesized for comparison. Tanase reported two routes for the preparation of 1,3,6,7-tetrahydroxyxanthone. Hatsuda and Kuyama[6] reported the synthesis of 1,3,6,7-tetrahydroxyxanthone, m.p. 320°C (decomp.), by the preparation of diphenyl ether from 4-bromoveratrole and phloroglucinol dimethyl ether by the Ullmann reaction, according to Tanase's method, and then by deriving it to xanthone derivative by the application of oxalyl chloride. The writer carried out the synthesis by the second method (Scheme 1) and the product thereof was identical with the natural product, decomposing at 370°C. Since Tanase had observed that the products obtained by the two methods of synthesis are identical, the value of m.p. 320°C (decomp.) must indicate the initial browning temperature of the product.




Scheme 1

Heating of some kinds of flavone with hydroxyl group with hydriodic acid often causes rearrangement of the hydroxyl and this phenomenon is called the Wessely-Moser rearrangement[7]. This phenomenon has been observed in xanthones[8] and its mechanism is explained as follows (Scheme 2):



Scheme 2

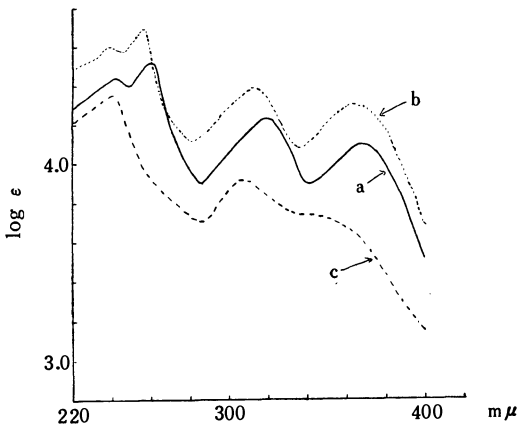
As will be clear from this mechanism, the rearrangement changes the hydroxyls in 1,4-positions to 1,2-positions (the reverse of this has not been observed). Therefore, the hydroxyl in 3-position is independent of this rearrangement and the rearrangement does not occur if there has been no hydroxyl in 1-position from the beginning. Considering such a mechanism, 1,3-dihydroxyxanthone would give a product with the same structure and 2,3-dihydroxyxanthone can not undergo such a rearrangement. Therefor, 1,3,6,7-tetrahydroxyxanthone can not be formed by rearrangement from other isomers. In other words, 1,3,6,7-tetrahydroxyxanthone must have been present in the pigment molecule from the beginning.

Next, considerations will be made on the possibility of a cyclization by the action of hydriodic acid where no xanthone ring was present in the pigment molecule itself. Since there is no possibility of a formation of a new benzene ring by the

5) Y. Tanase, *J. Pharm. Soc. Japan*, **61**, 341 (1941).
6) Y. Hatsuda and S. Kuyama, *J. Agr. Chem. Soc. Japan*, **29**, 14 (1955).
7) F. Wessely and G. H. Moser, *Monatsh.*, **56**, 97 (1930); F. Wessely and F. Kallab, ibid., **60**, 26 (1932); S. Hattori, *Acta Phytochim.*, **5**, 99,117,219 (1930); *J. Chem Soc. Japan*, **50**, 725 (1929); **51**, 570 (1930); Ber., **72**, 1914 (1939); R. C. Shah, C. R. Mehta and T. S. Wheeler, *J Chem. Soc.*, **1938**, 1555.
8) E. M. Philbin, J. Swirski and T. S. Wheeler, *Chem. & Ind.*, **1955**, 445.

action of hydriodic acid**, the point to be considered would be the γ-pyrone ring in the center. In such a case, there will be the diphenyl ether structure with the ketone portion severed and a benzophenone structure with the ether linkage severed. As the latter example, there is sulochrin[9], isolated from the mycelium of *Oospora sulphurea-ochracea*. If mango pigment belongs to the latter group, it must be a hexahydroxybenzophenone compound in order to cyclize into tetrahydroxyxanthone derivative. If such is the case, application of diazomethane must afford a tetramethyl ether, even if two hydroxyls will not be methylated due to a substituent and the chelation to the carbonyl group. However, the pigment only affords a dimethyl ether even when sufficient diazomethane reacted. Since there is no methoxyl group in the pigment itself and the color reaction denies*** the partial structure of *ortho*- and *para*-diphenols, the possibility of a benzophenone derivative for the pigment is excluded.

If the pigment is a diphenyl ether derivative, there must be one carboxyl radical *ortho* to ether linkage, but the infrared spectra*** of the pigment and its methyl derivative do not indicate the presence of a carboxyl or an ester-carbonyl group. It therefore follows that the pigment can not be a diphenyl ether derivative. The fact that the ultraviolet absorption spectrum (Fig. 1) of mangiferin is quite similar to that of 1,3,6,7-tetrahydroxyxanthone supports the presence of such a structure in the pigment molecule.




Wave length

Fig. 1. Ultraviolet absorption spectra of mangiferin (a: ——), 1,3,6,7-tetrahydroxyxanthone (b: ·····), and its tetraacetate (c: - - -).

The known tetrahydroxyxanthone compounds isolated to date from natural substances may be found in the 1,3,5,8-isomer obtained from swertianolin or its aglycone, swertianol, isolated from *Swertia japonica Makino*[10] and *S. tomentosa Makino*[11] of Gentianaceae, and the 1,3,5,6-isomer[12] obtained as the oxidation product of jacareubin, the pigment of the heartwood of *Calophyllum brasiliensis* Camb. of Guttiferae. The skeletal compound of swertinin and decussatin, the pigments of *Swertia decussata*, is said to be the 1,2,6,8-isomer from absorption spectra[13]. The presence of a 1,3,6,7-isomer in natural substances to be the first example and this would be also the first example of a xanthone derivative in plants belonging to Anacardiaceae.

The writer expresses his gratitude to Professor Ryozo Hirohata of the Kyushu University, for his kind guidance and encouragement throughout the course of this work, to Professor Shoji Shibata of the Pharmaceutical Institute, University of Tokyo, for kind supply of a valuable sample, to Professor Yaichiro Tanase of the Pharmaceutical Faculty, Tokushima University, for kind advice and the supply of literature, to Professor Eigai Sebe of the Kumamoto University Medical School for kind help in analysis, and to Dr. Keihei Ueno of the Dojin Pharmaceutical Laboratory for ultraviolet spectral measurements. The writer is also indebted to Mr. Eikichi Aoyagi of the Miike Dye Industries, Oomuta, for elementary analyses.

## Experimental

Unless otherwise noted, all melting and decomposition points are corrected.

**Action of Hydriodic Acid on Mangiferin.**—To 30 g. of phenol, 5.0 g. of finely pulverized mangiferin was added and mixed with warming (remains practically insoluble). While cooling, 50 cc. of hydriodic acid (*d* 1.7) was added

** There is a report [A. Mustafa and M. I. Ali, *J. Org. Chem.*, **21**, 849 (1956)] on the formation of a tetrahydroxanthone by the new formation of a cyclohexene ring in diene synthesis.

9) H. Nishikawa, *Bull. Agr. Chem. Soc. Japan*, **12**, 47 (1936); **13**, 1 (1937). *Acta Phytochim.*, **11**, 167 (1939).

*** See the forthcoming report, Part V.

10) Y. Asahina, J. Asano and Y. Ueno, This Bulletin, **17**, 104 (1942); *J. Pharm. Soc. Japan*, **62**, 22 (1942).

11) T. Nakaoki and Y, Hida, *J. Pharm. Soc. Japan*, **63**, 554 (1943).

12) F. E. King, T. J. King and L. C. Manning, *J. Chem. Soc.*, **1953**, 3932.

13) S. R. Dalal, S. Sethna and R. C. Shah, *J. Indian Chem. Soc.*, **30**, 457, 463 (1953); R. C. Shah, A. B. Kulkarni and S. R. Dalal, *J. Sci. Ind. Research*, **13B**, 175 (1954).

gradually and the mixture was gently refluxed for 6 hours. When cooled, the two-layered mixture was poured into an aqueous solution of sodium bisulfite with agitation and the dark brown, resinous substance that separated was washed thoroughly with water. This resinous substance was boiled with four 500-cc. portions of water, the oily substance insoluble in hot water was collected by filtration, and the cooling of the filtrate afforded a pale brown precipitate. Yield, 2.5 g. of m.p. 368–370°C (decomp.). Ferric chloride reaction: Dusky greenish black.

**Action of Hydrobromic Acid on Mangiferin.**—Application of hydrobromic acid (constant boiling product) under exactly the same conditions as for hydriodic acid, or even without the addition of phenol, 1,3,6,7-tetrahydroxyxanthone was isolated, though in a smaller yield. In the case of an application of the acid alone, without phenol, the pigment dissolved in hydrobromic acid on heating the mixture in an oil bath and a black insoluble matter separated out immediately. After cooling, the insoluble matter was collected, the portion soluble in ethyl acetate was acetylated, and the product was recrystallized from glacial acetic acid to 1,3,6,7-tetra-acetoxyxanthone, m. p. 200°C. Yield, 15–20 % of the original pigment.

**1,3,6,7-Tetra-acetoxyxanthone.**—Two grams of the substance of m.p. 368–370°C, soluble in hot water, obtained by the application of hydriodic acid to the pigment, was acetylated by heating with acetic anhydride and a drop of conc. sulfuric acid for 4 hours. This was decomposed by the addition of water, the precipitate was collected, washed with water, and dried. Five recrystallizations from as small an amount as possible of glacial acetic acid, twice using activated carbon, afforded colorless, long prisms m.p. 199.5–200°C, Yield, 1.6 g. Ferric chloride reaction: Negative. It precipitates out as thick, rhombic plates from hot saturated acetone solution but forms fine needles when the acetone solution is allowed to evaporate or when recrystallized from ethanol, but no difference in the melting point was observed in either case.

*Anal.* Found: C, 58.97, 59.13; H, 4.17, 3.88. Calcd. for $C_{21}H_{16}O_{10}$: C, 58.88; H, 3.77 %.

No depression of the melting point was observed on admixture with the synthesized 1,3,6,7-tetra-acetoxyxanthone, m.p. 198°C. It can be obtained by direct acetylation of the resinous substance obtained on decomposition with hydriodic acid, without extraction with hot water, but the yield is poor.

**1,3,6,7-Tetrahydroxyxanthone.**—A mixture of 350 mg. of the tetra-acetate, m.p. 199.5–200°C, in 20 cc. of ethanol containing 5 cc. of conc. hydrochloric acid was refluxed for 5 hours, the solvent was evaporated under a reduced pressure, and water was added to the bright yellow residue. The pale yellow mass (290 mg.), obtained on washing this residue with water and drying, was dissolved in 4 cc. of ethanol, filtered, and brought to 10 cc. with hot water. On cooling this solution, pale brown needles or a crystalline powder was obtained, which became slightly brownish at around 320°C, became brown colored at around 350°C, and blackened with decomposition at 370–371°C. It is easily soluble in acetone and ethanol and sparingly in ether. Air-dried product gave analytical values almost corresponding to $C_{13}H_8O_6 \cdot H_2O$.

*Anal.* Found: C, 55.72; H, 4.01. Calcd. for $C_{13}H_8O_6 \cdot H_2O$: C, 56.12; H, 3.62 %.

Sample dried for 10 hours in vacuo at room temperature.

*Anal.* Found: C, 59.89; H, 3.20. Calcd. for $C_{13}H_8O_6$: C, 60.01; H, 3.20 %.

The melting point determination of the synthesized 1,3,6,7-tetrahydroxyxanthone[5] alone or in admixture with the foregoing product gave the same results as above.

**1-Hydroxy-3, 6, 7-trimethoxyxanthone.**—Ether solution of diazomethane made from 2.0 g. of nitrosomethylurea was added to a suspension of 0.1 g. of 1,3,6,7-tetrahydroxyxanthone in 20 cc. of ether, by which the phenol gradually disappeared with evolution of bubbles. After 5 hours, the residual diazomethane was decomposed by the addition of a few drops of glacial acetic acid, the solvent was evaporated, and the residue was dissolved in 30 cc. of 5 % potassium hydroxide solution. This solution was continuously extracted with ether for 10 hours, and the colorless ether extract was evaporated, leaving 90 mg. of a pale yellowish brown residue. Recrystallization from dilute ethanol afforded pale yellowish brown microneedles, m.p. 218–219°C. They dissolve in conc. sulfuric acid to form a bright yellow solution with green fluorescence. It colors green gradually with ferric chloride.

*Anal.* Found: C, 63.50; H, 4.72. Calcd. for $C_{16}H_{14}O_6$: C, 63.56; H, 4.67 %.

Mixed m.p. with the synthesized 1-hydroxy-3,6,7-trimethoxyxanthone, m.p. 216°C[5], was 218°C.

**1-Acetoxy-3, 6, 7-trimethoxyxanthone.**—Acetylation of 0.1g. of 1-hydroxy-3,6,7-trimethoxyxanthone with acetic anhydride and a drop of conc. sulfuric acid gave 0.1 g. of a crude product, which was treated with a small amount of acetone to remove a minute amount of soluble pale yellow substance. Recrystallization of the residue from ethanol afforded fine prisms, m.p. 216°C. Ferric chloride reaction, negative.

*Anal.* Found: C, 62.81; H, 4.75. Calcd. for $C_{18}H_{16}O_7$: C, 62.79; H, 4.68 %.

Mixed m.p. with 1-hydroxy-3,6,7-trimethoxyxanthone, m.p. 218–219°C, was 180–195°C. Admixture with mangiferin dimethyl ether acetate, m.p. 216–217°C, melted at 190–205°C. Hydrolysis with ethanolic hydrochloric acid gave 1-hydroxy-3,6,7-trimethoxyxanthone.

**Synthesis of 2,4,5-Trihydroxybenzaldehyde.**—The hydroxyhydroquinone triacetate, obtained by the acetylation of benzoquinone, was hydrolyzed with ethanolic sulfuric acid, concentrated under a reduced pressure, and the residue, to which a small amount of water was added, was extracted with ether, from which hydroxyhydroquinone (III) was obtained. Twenty grams of (III) was dissolved in 200°cc.

14) Ref. 5 and L. Gattermann and M. Köbner, *Ber.*, **32**, 278 (1899).

of ether; 30 g. of freshly prepared zinc cyanide was added, and dry hydrogen chloride gas was bubbled through this solution. Ether was then evaporated, 120 cc. of water was added to the residue, and the mixture was warmed for 5 minutes. After cooling, the mixture was allowed to stand in an ice chest over night and the crystals that precipitated out were removed by filtration. The mother liquor was extracted with ether, ether was evaporated, and the residue crystallized on standing, without recrystallization, to 2,4.5-trihydroxybenzaldehyde IV as pale brown, long prisms, m.p. 229–230°C (decomp.). Yield, 20 g.

*Anal.* Found: C, 54.45; H, 4.28. Calcd. for $C_7H_6O_4$: C, 54.42; H, 4.11 %.

**Synthesis of 1,3,6,7-Tetrahydroxyxanthone.**—A solution of 7.3 g. of IV and 7.5 g. of phloroglucinol dissolved in 50 cc. of glacial acetic acid was mixed with 20 cc. of conc. hydrochloric acid, heated on a sand bath for 30 minutes, allowed to stand over night, and the reddish solid thereby formed was collected by filtration. The solid was washed consecutively with water, sodium bicarbonate solution, and water, and dried, affording 10 g. of 1,6,7-trihydroxyfluorone V. Without purification, this was mixed with 500 cc. of ethanol, mixed with 4 g. of 5 % palladium-charcoal and shaken in a hydrogen stream by which 1 l. of hydrogen was absorbed in 1.5 hours, the solution becoming almost colorless. The catalyst was filtered off and the filtrate was evaporated completely to dryness under a reduced pressure, affording 7.3g. of crude 1,3,6,7-tetrahydroxyxanthene VI. This was directly acetylated and treated by the usual method. Recrystallization of the product from a large amount of ethanol gave 7.5 g. of 1,3,6,7-tetra-acetoxyxanthene (VII), m.p. 177°C.

To a solution of 7.5 g. of VII, dissolved in a mixture of 50 cc. of glacial acetic acid and 30 cc. of acetic anhydride, 2.4 g. of chromium trioxide was added in small portions with shaking. After completion of the addition, the mixture was heated in a water bath for 3 hours, a large amount of water was added to the mixture, and the insoluble matter was recrystallized four times from glacial acetic acid to 5.5 g. of 1,3,6,7-tetra-acetoxyxanthone VIII, as colorless needles, m.p. 200°C, showing no depression on admixture with the product isolated from the natural substance.

*Anal.* Found: C, 58.78; H, 3.85. Calcd. for $C_{21}H_{16}O_{10}$: C, 58.88; H, 3.77 %.

This tetra-acetate VIII was hydrolyzed with an acid and the product was recrystallized from 30 % ethanol. The pale yellowish brown, crystalline powder thereby obtained gradually colored from around 320°C, became markedly brown at around 350°C, and decomposed with blackening at 370–371°C, the behavior being identical with that of 1,3,6,7-tetrahydroxyxanthone from the natural source.

*Anal.* Found: C, 59.88; H, 3.22. Calcd. for $C_{13}H_8O_6$: C, 60.01; H, 3.10 %.

**Ultraviolet Absorption Spectra.**—Measurements were made with the Beckman Model DU spectrophotometer of mangiferin in 70 % ethanol and 1,3,6,7-tetrahydroxyxanthone and its tetra-acetate in methanol.

*Department of Chemistry, Kumamoto Women's University, Kumamoto*

# *On Mangiferin, the Coloring Matter of Mango (Mangifera indica Linn.). V.*[1] *Identification of Sugar Component and the Structure of Mangiferin*[2]

By Syun ISEDA

(Received April 11, 1957)

From the results previously[1,3] reported, it has become clear that mangiferin agrees with the composition of $C_{19}H_{18}O_{11}$ and includes a 1, 3, 6, 7-tetrahydroxyxanthone skeleton ($C_{13}H_8O_6$). The difference in the molecular formula $C_6H_{10}O_5(+H_2O)$ coincides with a hexose group. Wiechowski[4] already proved the formation of levulinic acid by boiling the "mangin" with hydrochloric acid for a long time and indicated the possible presence of a sugar moiety, but failed to isolate the sugar. Gorter[5] proposed a structure containing a glucuronic acid group, but did not isolate it. The present writer also attempted the detection of sugars as described in the first paper of this series[6], but did not obtain any concrete result.

1) Part IV: This Bulletin, **30**, 625 (1957).
2) Paper presented at the Kyushu Local Meeting of the Chemical Society of Japan, in Fukuoka, November 24, 1956.
3) S. Iseda, *J. Kumamoto Women's Univ.*, **9**, 45 (1957).
4) W. Wiechowski, *Arch. exptl. Pathol. Pharmakol.*, **91**, 462 (1923).
5) K. Gorter, *Bull. Jardin Bot. Buitenzorg*, [III], **4**, 260 (1922).
6) S. Iseda and T. Asai, *J. Med. Assoc. Formosa*, **38**, 447 (1939).

Application of periodic acid to the pigment in water results in coloration of the solution to reddish brown, indicating the liberation of iodine, but the consumption of periodic acid varied between 1 and 3 moles and definite values were not obtained. Steam distillation of this aqueous reaction mixture failed to show the presence of formaldehyde in the distillate. Direct distillation of this reaction mixture showed, however, the presence of formaldehyde in the distillate, though in an amount about 1/20 of the calculated. It is known that glucose or glucosides does not form formaldehyde by periodate oxidation[7] and since there is a consumption of periodic acid without the virtual formation of formaldehyde, it seems certain that the $C_6H_{10}O_5$ residue bonded to the xanthone skeleton is not a hexitol ether type.

The sugar is not split off when the pigment is heated with sulfuric or hydrochloric acid under ordinary pressure or with water under high pressure, but when it is heated with 1% or 10% sulfuric acid under high pressure at 140°C, and the aqueous solution of the product is extracted with ether* after deionization, a spot appears on the paper chromatogram of the aqueous solution. This spot was identical with that of glucose. It does not appear, when the heating conditions, such as temperature and duration, are different from those indicated above. This experiment makes it certain that there is a glucose in the mangiferin molecule, but how and why that sugar is not split off by ordinary method is not clear.

Infrared absorption spectrum of mangiferin as a potassium bromide disk is shown in Fig. 1.

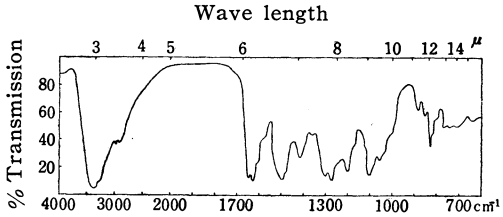



Fig. 1. Infrared spectra of mangiferin (KBr disk method).

The broad absorption around 3338 cm.$^{-1}$ indicates the presence of numerous hydroxyl groups, including those forming intramolecular hydrogen bond. The absorptions at 2932 and 2885 cm.$^{-1}$ indicate the presence of $CH_2$ in the molecule, but the amount seems to be small judging from its intensity. These absorptions, combined with those at 1490 and 1048 cm.$^{-1}$, suggest the presence of a primary alcoholic group in the molecule. Since there are no absorptions corresponding to $CH_3$ near 3000, 1450, and 1375cm.$^{-1}$, it can not be considered that the foregoing primary alcoholic group is due to the residual ethanol used for the purification of the pigment. There is no absorption in the region 1650 to 1750 cm.$^{-1}$ and the ester structure of Gorter[5] or the aldehyde structure of Wiechowski[4] can be excluded. The absorption at 1645 cm.$^{-1}$ is the carbonyl band of xanthone nucleus[8] and the sharp absorption at 828 cm.$^{-1}$ (821 cm.$^{-1}$ in Nujol) must be related to the xanthone structure, since it also appears in the spectrum of 1,3,6,7-tetrahydroxyxanthone (825 cm.$^{-1}$, Fig. 2).

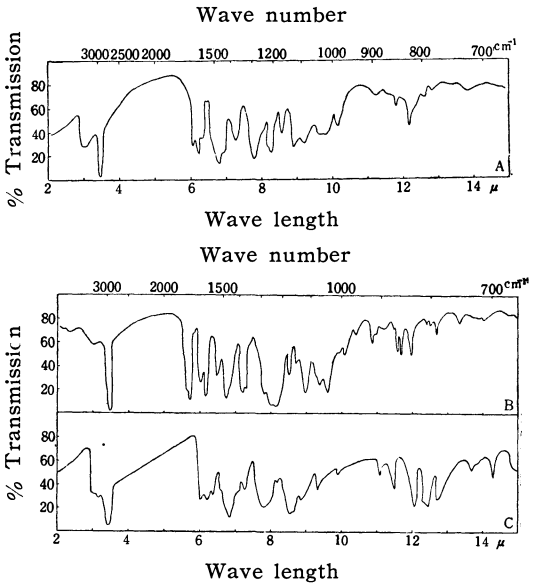



Fig. 2. Infrared spectra (in Nujol) of (A) mangiferin dimethyl ether, (B) mangiferin dimethyl ether acetate, (C) 1,3,6,7-tetrahydroxyxanthone.

According to Barker et al.[9] and Takahashi[10], α-D-glucopyranoside exhibits absorption at 844±8 cm.$^{-1}$ [9] or at 11.6—11.8 μ

7) P. Karrer and M. Pfaehler, *Helv. Chim. Acta*, **17**, 766 (1934).

* When this extraction with ether is omitted, a component that appears above (in ascending paper chromatography) the sugar spot and reduces its $R_f$, cannot be removed.

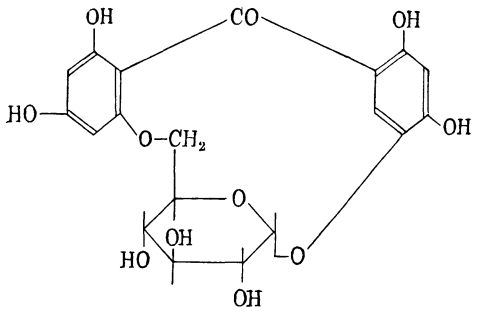
8) S. Kimoto [*J. Pharm. Soc. Japan*, **75**, 763 (1955)] gave 6.07μ (1645cm.$^{-1}$) for xanthone, but E. D. Bergmann and S. Pinchas [*J. chim. phys.*, **49**, 537 (1952); *Chem. Abstr.*, **47**, 3132 (1953)] gave 1658 cm.$^{-1}$. The following values (in Nujol) were obtained: 1,3,6,7-Tetrahydroxyxanthone (1640 cm.$^{-1}$), 1,3,6,7-tetra-acetoxyxanthone (1660 cm.$^{-1}$), 1-hydroxy-3,6,7-trimethoxyxanthone (1665 cm.$^{-1}$).

9) S. A. Barker, E. J. Bourne, M. Stacey and D. H. Whiffen, *J. Chem. Soc.*, **1954**, 171.

10) M. Takahashi, *J. Pharm. Soc. Japan*, **74**, 320 (1954); **75**, 237 (1955).

(862—848 cm.$^{-1}$)[10], irrespective of whether the compound is in the form of glycoside or its derivatives, such as methyl ether. Mangiferin exhibits an absorption at 844 cm.$^{-1}$ and its dimethyl ether and dimethyl ether acetate (Fig. 2) exhibit at 853 cm.$^{-1}$ (in Nujol), but such an absorption is not found in 1,3,6,7-tetrahydroxyxanthone. It follows that the absorption at 844 cm.$^{-1}$ in mangiferin must correspond to that of α-D-glucopyranoside.

The molecular structure shown in (I) may be proposed for mangiferin. Such a structure can be constructed on a molecular model, but this would hardly explain the similarity of the ultraviolet absorption spectrum between mangiferin and 1,3,6,7-tetrahydroxyxanthone, as shown in Part IV. Neither would it explain the formation of only a dimethyl ether with diazomethane. If two hydroxyls are present in the position *peri* to the carbonyl, one could easily be methylated[11].



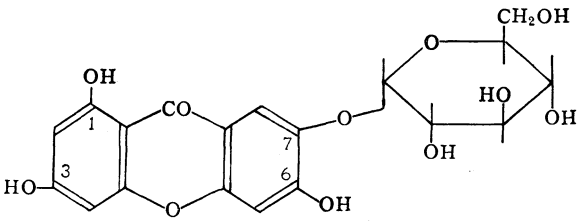
(Formula I)

From the foregoing results, it must be concluded that the sugar is bonded in α-glycosidic type to one of the four hydroxyls in 1,3,6,7-tetrahydroxyxanthone skeleton in mangiferin.

Attempted complete methylation of the pigment with dimethyl sulfate and anhydrous potassium carbonate in dry acetone, turned it into a dark brown syrup, which made it impossible to liberate the sugar portion by acid hydrolysis by the usual method. Assumption of the sugar bonding position was made through coloration reactions.

Mangiferin and its dimethyl ether are both positive to the Gibbs' reaction[12] and Liebermann's nitroso reaction[13], showing the presence of a free hydroxyl without a substituent in the *para*-position (i. e. in 1-position). The presence of a free *meta*-diphenol structure in the mangiferin molecule is known by Brauer's phosphomolybdic acid reaction[14], but this color reaction is negative in mangiferin dimethyl ether. Nagai and Hattori's color reaction[15] with chloropentammincobalt-(III) chloride, $[Co(NH_3)_5Cl]Cl_2$ is negative in both the pigment and its dimethyl ether, indicating the absence of an *ortho*- and *para*-diphenol structures in the molecule. Sevilla and DiMenza[16] have reported a color reaction characteristic of *ortho*-diphenol by ammonium metavanadate, but this was not found applicable in the case of 1,3,6,7-tetrahydroxyxanthone.

From the various experimental results described above, the sugar bonding position may be concluded to be in 6- or 7-position. From the biological fact that euxantic acid(1.7-dihydroxyxanthone 7-glucuronide) is excreted in the urine of rabbits and cattle fed with mangiferin, it may be certain that the sugar is bonded in 7- rather than 6-position. The following formula (II) is proposed as the structural formula for mangiferin.



(Formula II)

If mangiferin were to be represented by the foregoing formula (II), it would be necessary that the hydroxyls in 3- and 6-positions be removed to form euxanthic acid in an animal body. This point still requires further study.

## Experimental

All melting points are corrected.

**Reaction with Periodic Acid** — Mangiferin or its dimethyl ether was suspended in 5% sulfuric acid and powdered potassium periodate was added in small portions to it, by which the solution immediately turned reddish brown. This color faded with sodium thiosulfate and distillation yielded crystals of iodine. The amount of the periodate consumed by titration corresponded to 1.3—3.9 moles, failing to give any definite value. The insoluble portion obtained after the periodate oxidation remained a reddish brown amorphous

11) Y. Tanase, *J. Pharm. Soc. Japan*, **61**, 341 (1941).
12) H. D. Gibbs, *J. Biol. Chem.*, **72**, 649 (1927); M. Tomita and S. Uyeo, *J. Pharm. Soc. Japan*, **61**, 449 (1941).
13) C. Liebermann, *Ber.*, **7**, 247, 1098 (1874).
14) K. Brauer, *Chem. Zeitg.*, **50**, 553 (1926).
15) W. Nagai and S. Hattori, *Acta Phytochim.*, **5**, 1 (1930); *J. Chem. Soc. Japan*, **51**, 162 (1930). Cf. ref. 11).
16) J. Sevilla and A. DiMenza, *Rev. asoc. biochim. argentina*, **14**, 17 (1947); *Chem. Abstr.*, **41**, 6172 (1947).

substance and it could not be induced to crystallize. Beilstein's halogen test: positive.

Aqueous solution of 1 g. of potassium periodate was added dropwise into a suspension of 300mg. of mangiferin in 30 cc. of 5 % sulfuric acid, with shaking, and the mixture was allowed to stand for 36 hours at room temperature (30°C) with occasional shaking. The clear supernatant was decanted and submitted to steam distillation. The addition of 1 cc. of 1 % ethanolic solution of dimedone to 30 cc. of the distillate failed to show the formation of a dimedone adduct. The reaction mixture obtained under the same conditions of oxidation, without separation of the supernatant, was treated with 100 cc. of water, and directly distilled in an oil bath to 50 cc. of the distillate (acid reaction). After removal of iodine crystals, 15 drops of 1 % ethanolic solution of dimedone was added. On standing the mixture over night, 12 mg. of colorless needle crystals were obtained. Recrystallization from ethanol afforded crystals melting at 188°C, undepressed on admixture with authentic sample of formaldimedone, m. p. 188°C.

**High-pressure Hydrolysis** — A mixture of 1.0 g. of mangiferin and 200 cc. of 10 % sulfuric acid was heated for 2 hours at 140°C in an autoclave. The black, insoluble matter that separated out was removed by filtration, the sulfat ion in the filtrate was quantitatively removed with barium hydroxide, and the filtrate concentrated to 50 cc. This solution was passed through the cation and anion exchange resin 'DIA' (product of Mitsubishi Kasei Co.) to effect complete deionization and further concentrated to 1 cc. of a pale yellow liquid.

This liquid was submitted to paper chromatography by the ascending method, using a mixture (4 : 2 : 1) of butanol : acetic acid: water as the developing solvent. A mixed solution of benzidine (1 g.), trichloroacetic acid (20 cc. of 40 %), glacial acetic acid (20 cc.), and 93 % methanol (160 cc.) was used as the coloring reagent.

In this case, the spot of pure glucose appeared at $R_f$ 0.23, while those of the first sample and the sample to which glucose had been added appeared at $R_f$ 0.20, accompanied by a somewhat broad, feathershaped region, above the spot, without any coloration.

This sample was diluted with about 10 volumes of water and extracted with ether for about 30 hours. The ether-soluble portion afforded a minute amount of yellowish green syrupy substance (which reduces the Fehling and ammoniacal silver nitrate solution). The aqueous solution left after ether extraction was again concentrated and submitted to paper chromatography by which the feathery region disappeared and the spots from pure glucose, the first sample, and the sample with added glucose all appeared at the same $R_f$ 0.24. The color of these spots was also of the same tone.

When 1 % sulfuric acid was used instead of 10 % one without alteration in other conditions, a spot also appeared at the same position.

Hydrolyses under the following conditions failed to indicate the presence of a sugar: heating with mere water at 120°C or 140°C for 2 or 4 hours, heating with 1 % or 10 % sulfuric acid at 120°C for 2 or 4 hours, or at 140°C for 4 hours.

**Gibbs' Reaction**[12] — To 1 cc. of saturated solution of mangiferin or its dimethyl ether in 70 % ethanol, a piece of sodium acetate crystal was added, followed by a few drops of freshly prepared ethanolic solution of 2,6-dichloroquinone chlorimide. Both gave bluish green (positive) coloration, while acetylmangiferin showed pale pinkish violet and 1,3,6,7-tetra-acetoxyxanthone a pale yellow color.

**Liebermann's Nitroso Reaction**[13] — A pale brown solution, obtained by dissolving sodium nitrite in well-chilled conc. sulfuric acid, was carefully superimposed on the conc. sulfuric acid solution of mangiferin or its dimethyl ether by which a reddish brown ring appeared at the zone of contact.

**Brauer's Reaction**[14] — To 1 cc. of saturated aqueous solution of the sample, 0.1 cc. of 10 % aqueous solution of phosphomolybdic acid was added (the color here obtained is designated as A). Then 10 % ammonia water was added carefully in drops (color here obtained is designated as B). Mangiferin showed pale yellowish brown in A and blue in B (positive to *meta* diphenol reaction), the blue color disappearing with excess of ammonia. 1,3,6,7-Tetrahydroxyxanthone showed blue color in A and bluish green in B (positive to *ortho*-diphenol reaction), while mangiferin dimethyl ether failed to show any coloration in either A or B.

**Color Reaction to Nagai-Hattori's Cobalt Reagent**[15] — To 2 cc. of saturated solution of the sample in 70 % ethanol, 5 drops of a saturated solution of the cobalt reagent** in ethanol was added. No color change was observed after 5 hours with mangiferin, its dimethyl ether, 1-hydroxy-3,6,7-trimethoxyxanthone, or in 1,3,6,7-tetra-acetoxyxanthone. When powdered mangiferin was floated on the ethanolic solution, the color changed to brown after 15 hours, although no change occured within 5 hours. In the case of 1,3,6,7-tetrahydroxyxanthone, the color changed to brown immediately, with turbidity.

**Sevilla-DiMenza's Reaction** — A few drops of 50 % sulfuric acid containing a small amount of ammonium metavanadate was added to 2 cc. of an aqueous solution containing 1—2 mg. of the sample, or a saturated aqueous solution in the case of mangiferin and xanthone compounds. Only pyrogallol out of the compounds listed below gave a positive reaction (wine red coloration) as described in the literature[16].

| Compound (position of OH) | Coloration |
|---|---|
| Resorcinol (1,3) | Slightly reddish yellow. |
| Hydroquinone (1,4) | ditto. |
| Pyrogallol (1,2,3) | Wine red—pale reddish brown. |
| Phloroglucinol (1,3,5) | Almost colorless. |

** $[Co(NH_3)_5Cl]Cl_2$

| | |
|---|---|
| Orcinol (1—$CH_3$; 3,5) | Dark gray—pale yellow with brown precipitate. |
| Mangiferin | Slightly reddish yellow, gradually turning pale, and finally pale yellowish brown. |
| 1,3,6,7-Tetrahydroxyxanthone | Pale dusky black with brown precipitate, gradually turning pale, with dark brown precipitate; finally the solution became pale yellowish brown. |

**Infrared Absorption Spectra**—Spectra were measured with the Perkin-Elmer Model 21 infrared spectrophotometer, by the potassium bromide disk method by Mr. Yusaku Ikegami of the Research Institute for Chemistry of Non-Aqueous Solution, Tohoku University, and by the Nujol method by Mr. Hirotaka Kozuma of the Technical Department, Shin Nippon Chisso Hiyro Co. Minamata.

The writer expresses his gratitude to those who supplied infrared data, to Assistant Professor Kazuyoshi Yagishita and Mr. Naoshi Toya of this laboratory for cooperation in part of the experiments, and to Mr. Chikashi Adachi, President of the Kumamoto Agricultural High School, for permission to use the autoclave.

*Department of Chemistry*
*Kumamoto Women's*
*University, Kumamoto*

# *Ionization Potentials of Some Organic Molecules. V. Heterocyclic Compounds Containing Nitrogen*

By Itiro OMURA, Hiroaki BABA, Keniti HIGASI and Yuichi KANAOKA

(Received April 10, 1957)

What kind of electron is actually responsible for the first ionization potential of a heterocyclic compound containing a nitrogen atom or nitrogen atoms? There are two contradicting views on the problem. One is to ascribe the most loosely bound electron to one of the non-bonding electrons belonging to the N atom, while the other regards one of the $\pi$-electrons of the conjugated system most easy to be removed[1]. In previous reports[2] dealing with ionization potentials of pyridine and picolines, the present writers tried to interpret the results of their measurement from the former viewpoint.

As a continuation of the study on ionization potentials, measurements were conducted on three isomers of diazines, three isomers of lutidines and *s*-triazine in the hope that they would provide a fresh clue to knowledge on this point. The results of the measurements on these seven heterocyclic compounds will be fully described in the present article with the possible interpretations.

## Experimental Materials

**Pyridazine.**—3,6-Dichloropyridazine prepared by the chlorination of 3,6-pyridazinediol was hydrogenated in ammonia-ethanol solution with palladium-charcoal at atmospheric pressure. The filtered solution was made alkaline with potassium hydroxide, extracted with ether, dried with potassium carbonate, evaporated and distilled. B.p. 84-86°C (at 14 mm) (Mizzori and Spoerri[3] give b.p. 86-87°C/14 mm).

**Pyrimidine.**—3,4-Dichloropyrimidine, obtained by the chlorination of uracil, was hydrogenated as in the case of pyridazine to give pyrimidine. Pyrimidine mercurichloride was precipitated from the filtered solution, and distilled with sodium sulphide (nonahydrate). The aqueous distillate was saturated with potassium hydroxide. The separating pyrimidine layer was extracted with ether, dried with potassium hydroxide, evaporated and fractionated to give pyrimidine. B.p. 123°C (Hilbert and Johnson[4] give b.p. 124°C/758 mm).

**Pyrazine.** — Pyrazine - 2,3 - dicarboxylic acid (kindly provided by Sankyo Pharm. Co., Ltd.) was decarboxylated in acetic acid solution, made alkaline with sodium hydroxide and steam-distilled[5]. Pyrazine was purified through mercurichloride as in the case of pyrimidine. B.p.

1) C. Reid and R. S. Mulliken. *J. Am. Chem. Soc.*, **76**, 3869 (1954)
2) K. Higasi, I. Omura and H. Baba, *J. Chem. Phys.*, **24**, 623 (1956); H. Baba, I. Omura and K. Higasi, This Bulletin, **29**, 521 (1956).
3) R. H. Mizzori and P. E. Spoerri, *J. Am. Chem. Soc.*, **73**, 1873 (1951).
4) G. E. Hilbert and T. B. Johnson, ibid., **52**, 1152 (1930).
5) S. Gabriel und A. Sonn, *Ber.*, **40**, 4852 (1907).

113°C; m.p. 53-54°C (from ether) (Wolff[6] gives m.p. 55°C).

**s-Triazine.**—*s*-Triazine was prepared by Grundmann's method[7] from formamidine[8] and sodium diformamide. M.p. 81-82°C (purified by sublimation). (Grundmann[7] gives m.p. 85°C).

Three isomers of lutidines were obtained from Kwanto Chem. Co., Inc., Tokyo. They were distilled before use. 2,3-*Lutidine*, b.p. 161°C. 2,4-*Lutidine*, 157.5-157.8°C. 2,6-*Lutidine*, b.p. 142.2°C. All the temperatures recorded here were uncalibrated.

## Experimental Method and Result

The measurement of the first appearance potentials was made by the use of the apparatus described in a previous report[9]. Regarding the evaluation of the ionization potentials, a modified critical slope method was employed. The ionization efficiency curves were plotted on a semilog scale. The pressure of the reference gas, argon, was adjusted so that the initial portions of the curves for the sample and reference gases became nearly parallel to each other. The distance between the two curves along the voltage axis was taken to be the difference between the ionization potentials of the sample and the reference gase*.

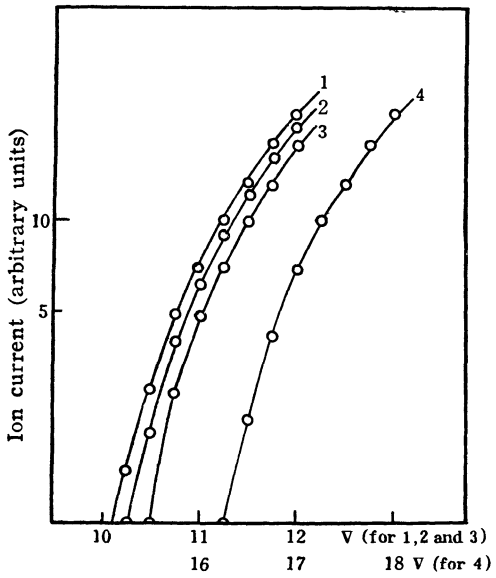



Fig. 1. Relative ionization efficiency curves. 1, pyridazine; 2, pyrimidine; 3, pyrazine; 4, argon.

In Fig. 1 some representative ionization efficiency curves are shown. For *s*-triazine the linear extrapolation method was also used for the sake of comparison.

In a previous report[9] the question was considered as to whether or not the choice of argon as the standard gas is suitable. For the samples treated so far, its use was justified. On account of the following facts the decision then reached is not ultimate nor fully acceptable. The energy spread of emitting electrons is greatly affected by the filament temperature, i.e., about 1800°K in this experiment. Further, the effect of contact potentials contributes to this spread of the energy. As a result the energy difference 0.18 eV between the doublet states, $^2P_{1/2}$ and $^2P_{1/2}$ of argon ion[14] becomes much smaller in comparison with the energy spread of the bombarding electrons used in this sort of experiment*.

In benzene there appears to exist an energy level just under the highest occupied level, the energy separation being only 0.5 eV. It is pointed out by Morrison[15] that the existence of this level becomes a dominant cause of error in the apparent ionization potentials of benzenoid molecules when measured by the ordinary electron impact method. Consequently, if diazines or lutidines are not lacking in respect to such a neighboring level or levels, the measured first potentials of this experiment will correspond to some average values of the first, second and other ionization energies.

The remaining implications come from the space charge effects[16]. With a view to eliminate

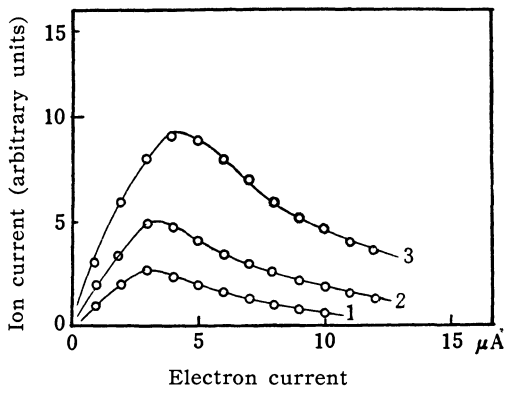



Fig. 2. Dependence of positive ion current (pyridazine) upon electron-beam current. Electron accelerating voltage: 1, 11eV; 2, 12eV; 3, 13eV.

6) L. Wolff, ibid , **26**, 723 (1893).
7) C. Grundmann, H. Schröder und W. Ruske, ibid., **87**, 1866 (1954).
8) D. J. Brown, *J. Appl Chem.*, **2**, 202 (1952).
9) I. Omura, K. Higasi and H. Baba, This Bulletin, **29**, 501 (1956).
* This procedure has actually been adopted in the work of the previous papers[2,9]. It is a modified application of Honig's method[10], and is essentially the same as employed by Dibeler et al.[11], Lossing et al.[12] and others[13].
10) R. E. Honig, *J. Chem Phys* , **16**, 105 (1948).
11) V. H Dibeler, R M Reese and F. L Mohler, *J. Chem. Phys* , **20**, 761 (1952).
12) F. P. Lossing, A W Tickner and W A. Bryce, *J. Chem. Phys.*, **19**, 1254 (1951).
13) A. Jacobson, J. Steigman, R. A Strakna and S. S. Friedland, *J. Chem. Phys.*, **24**, 637 (1956); R W. Law and J. L. Margrave, *J. Chem. Phys.*, **25**, 1086 (1956).
14) T. Mariner and W. Bleakney, *Phys Rev.*, **72**, 807 (1947).
15) J. D. Morrison, *J. Chem. Phys.*, **22**, 1219 (1954).
16) J. Marriott and J. D. Craggs, "Applied Mass Spectrometry", London (1954), p. 173.

these effects as nearly as possible, the variation of ion currents with electron currents was closely examined (See Fig. 2). From the curves shown in Fig. 2 such an intensity of electron currents was chosen as to give a maximum intensity of ion currents.

The results of the measurement are collected in Table I. No data for comparison appear to exist in the literature[17].

TABLE I
IONIZATION POTENTIALS OF THE HETEROCYCLIC COMPOUNDS, eV.

| Substance | Potentials |
|---|---|
| Pyridazine | 9.86±0.05 |
| Pyrimidine | 9.91±0.05 |
| Pyrazine | 10.01±0.02 |
| *s*-Triazine | 10.07±0.05 (10.10±0.02) |
| 2,6-Lutidine | 9.57±0.02 |
| 2,3-Lutidine | 9.68±0.02 |
| 2,4-Lutidine | 9.43±0.02 |

The value in parenthesis was obtained by the linear extrapolation method, while all others refer to a modified critical slope method, argon being used as the standard gas.

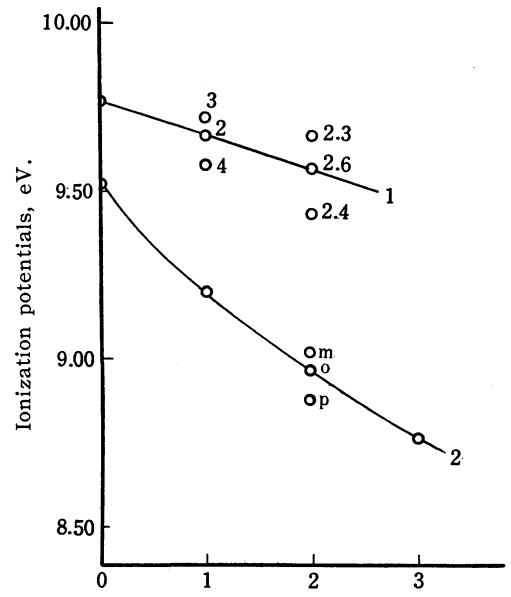



Fig. 3. Ionization potential and methyl substitution. 1, pyridine derivatives; 2, benzene derivatives.

## Discussion

**Lutidines.**—In previous reports[2] dealing with the ionization potentials of xylenes and picolines it was found that the lowering in the potential by methyl substitution was less pronounced in pyridine than in benzene. From this observation it was suggested that the first ionization potentials of pyridine derivatives are largely determined by non-bonding electrons of the N atom, while those of benzene derivatives are determined by $\pi$-electrons.

In lutidines two hydrogen atoms of a pyridine molecule are replaced by methyl groups, while in picolines one hydrogen atom is replaced by a methyl group. In all these molecules methyl substitutions always result in the lowering in the potential, but they are not so large as in benzene derivatives. This trend will be clear upon a comparison of the two curves, 1 and 2, in Fig. 3. The ionization potentials obtained for three isomers of lutidines are thus in good accord with the view of the previous papers[2].

**Diazines and Triazine.**—In previous studies[2] it was found that the replacement of a C–H group of a benzenoid molecule by an N atom always elevates the appearance potential. What would happen, if two or three C–H groups were replaced by the corresponding number of N atoms? The answer will be as follows. If the appearance potential is actually due to non-bonding electrons of the N atom, it will be affected by such a replacement in even the slightest degree. On the contrary, if $\pi$-electrons are responsible for the appearance potential, the magnitude of

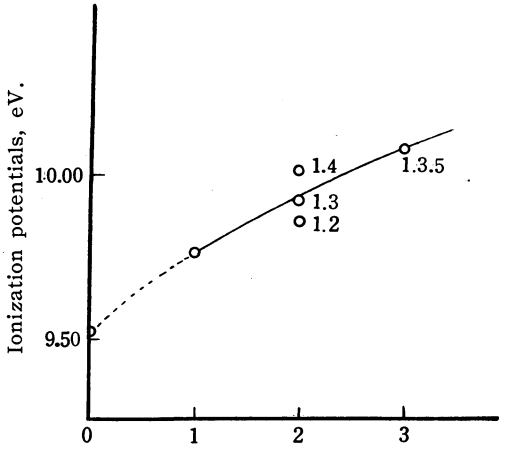



Fig. 4. The effect upon ionization potential of replacement of a C-H group by one or more N atoms.

* The energy spread has not been accurately determined. But refer, for example, to R. H. Vought, *Phys. Rev.*, **71**, 93 (1947).

17) Tables of Ionization Potentials of Molecules and Radicals, *Monogr. Res. Inst. Appl. Elec.*, Hokkaido University, **4**, (1954—7), appendix.

the change will be much greater. Probably its magnitude will be almost the same as in the change when a C–H group in benzene is replaced by one N atom.

With this expectation in mind, the present experiment on diazines and triazine was carried out. The results obtained are shown as a graph in Fig. 4. A smooth curve is obtained when the ionization potentials are plotted against the number of N atoms replaced.

To begin with, it would be better to leave the first view of non-bonding electrons out of consideration, and see if the second view of $\pi$-electrons can satisfactorily account for the data on potentials. Fortunately, there are available calculations on $\pi$-electron energies for pyridine and diazines[18]. In Table II the energy

TABLE II
IONIZATION POTENTIALS ($I$), $\pi$-ELECTRON DENSITY ($q$) AND ENERGY OF THE HIGHEST OCCUPIED LEVEL ($\varepsilon_m$)

| | $I$ (eV) | $\Delta I_{obs}$ (eV) | $\varepsilon_m$ ($\beta$) | $\Delta I_\pi$ (eV) | $q_N$ | $\Delta I_n$ (eV) |
|---|---|---|---|---|---|---|
|  | 9.76 | — | 1.051 | — | 1.29 | — |
|  | 9.86 | 0.10 | 1.305 | 0.70 | 1.24 | 0.14 |
|  | 9.91 | 0.15 | 1.209 | 0.43 | 1.28 | 0.03 |
|  | 10.01 | 0.25 | 1.100 | 0.13 | 1.23 | 0.17 |

of the highest occupied level, $\varepsilon_m$ in $\beta$ unit*, is shown for each of these compounds. By the use of these values and the assumption $\beta=-2.75$ eV**, the differences in ionization potential between diazines and pyridine can be calculated. (See the values denoted by $\Delta I_\pi$ in Table II). It will be seen that the theoretical differences for 1,2- and 1,3-diazines are much greater than those observed. Contrary to this, the theoretical consideration gives the least change for 1,4-diazine, while the actual observation gives the greatest change.

Next, let the problem be considered from the viewpoint of non-bonding electrons. Against the anticipation based upon this view, diazines were found to have larger ionization potentials than pyridine. But this might be a matter of natural consequence, if the N atoms in diazines have much smaller electron densities than the N atom in pyridine.

The interaction between the N atoms in diazines and a triazine may be better understood, when the electron transmission is grouped into those of $\pi$-electrons and $\sigma$-electrons. As is evident from the molecular orbital calculation[18], $\pi$-electron densities on the N atoms of diazines become smaller than that in pyridine. The decrease is marked at 1,2- and 1,4-positions (Compare the values of $q_N$ in Table II). The decrease in density of $\sigma$-electron is also expected in diazines, the order of decrease being 1,2>1,3>1,4. Total electron densities of N atoms in diazines are thus smaller than that of pyridine. Consequently, the effective electronegativities of N atoms increase upon replacement by the N atom.

It will be evident from the above argument that, as far as a qualitative explanation is concerned, the increase in the ionization potentials in diazines and a triazine can be accounted for on the assumption of non-bonding electrons. As the next step, one must make a trial to see whether or not quantitative interpretation is possible on the same basis. In the last column of Table II the results of such a trial are summarized. Indeed, the calculated difference of the ionization potential $\Delta I_n$ is in better accord with the observed values than $\Delta I_\pi$.

The principle of the calculation is as follows. The energy change of the $\pi$-electron system $\delta E$ is expressed by

$$\delta E=\frac{\partial E}{\partial \alpha_r}\delta\alpha_r+\cdots\cdots\simeq q_r\delta\alpha_r, \qquad (1)$$

where $\delta\alpha_r$ is the change of coulomb integral $\alpha_r$ of an atom $r$ and $q_r$ denotes the $\pi$-electron density of the atom $r$[19]. Attention is focussed on the N atom, so that its charge $q_N$ and $\alpha_N$ are considered.

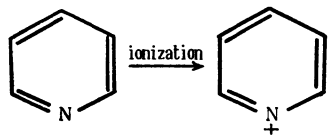
The first ionization may be illustrated as follows.

18) L. E. Orgel, T. L. Cottrell, W. Dick and L. E. Sutton, *Trans. Faraday Soc.*, **47**, 113 (1951).

* The energy $\varepsilon_m$ is measured relative to the coulomb integral for a carbon atom. $\beta$ is defined as the resonance integral of a carbon-carbon bond.

** The value of transition energy to the first excited state for benzene, $-2\beta$, derived from the LCAO MO method (neglecting overlap integral), was put as equal to the observed 5.5 eV (C. C. J. Roothaan and R. S. Mulliken, *J. Chem. Phys.*, **16**, 118 (1948)).

19) C. A. Coulson and H. C. Longuet-Higgins, *Proc. Roy. Soc.*, **A191**, 39 (1947); **A192**, 16 (1947).




When one non-bonding electron is taken from the N atom, it is supposed that the unit positive charge is localized at the N atom: that is, $N^+$ is produced. The total energy change of $\pi$-electrons on ionization will be approximated by

$$\delta E = q_N \delta\alpha_N \tag{2}$$

where

$$\delta\alpha_N = \alpha_{N^+} - \alpha_N \tag{3}$$

and

$$0 > \alpha_N > \alpha_{N^+} \tag{4}$$

As a further approximation[18] one may put $\delta\alpha_N = \beta^*$ and $\beta = -2.75$ eV. The calculation for $\delta E$ can be immediately made**, when use is made of $q_N$ values of diazines of Table II.

The value $\delta E$ thus obtained constitutes only a small fraction of the total energy change in the ionization process. The main part of the ionization energy is of course the energy for removing one electron from a molecule to infinity. But the latter energy is regarded as the same for both pyridine and diazines. By use of this approximation the difference in the ionization potentials between each of the diazines and pyridine may immediately be calculated from the difference in $\delta E$. (See $\Delta I_n$ in Table II).

In view of the assumptions involved, no strong claim will be made for the reliability of the calculated values $\Delta I_n$. But it appears certain that interaction between N atoms can not be neglected safely and that the present results of these experiments and considerations on diazines and triazine do not contradict the writers' view which favors non-bonding electrons.

Lastly a few words must be added on the accuracy of ordinary electron-bombardment values at large. The ionization potential of benzene, 9.52 eV, obtained by electron bombardment[20] is greater by 0.3 eV than 9.24 eV which is given by both spectroscopic[21] and photoionization method[22]. For pyridine there are available two electron-bombardment values, 9.80eV[23] and 9.76eV[2], while photoionization gives a much lower value 9.23 eV[24]. The discrepancy among these values seems to indicate that in pyridine there exists a neighboring level or levels near the highest occupied level.

Under these circumstances one is not absolutely sure as to the accuracy of the values obtained in this sort of measurement. Emphasis in this article has been placed on the general effects of replacement upon the ionization potentials, but not on the fine differences among three isomers. The latter problem is in fact of great importance in chemistry, but at the present stage of research any detailed discussion on this point might be somewhat speculative.

## Summary

First ionization potentials of the following substances were determined by a modified critical slope method. Pyridazine 9.86±0.05, pyrimidine 9.91±0.05, pyrazine 10.01±0.02, *s*-triazine 10.07±0.05, 2,3-lutidine 9.68±0.02, 2,4-lutidine 9.43±0.02, and 2,6-lutidine 9.57±0.02 eV. Interpretations of the results are given from the view-point that the ionization potentials of these compounds are largely determined by the non-bonding electrons at the N atom.

The authors wish to express their gratitude to Dr. S. Nagakura of Tokyo University for valuable suggestion and also to the Ministry of Education for a grant-in-aid.

*Research Institute of Applied Electricity and the Pharmaceutical Institute Hokkaido University, Sapporo*

* $\alpha(-\overset{1}{N}=)=\alpha+\beta$, $\alpha(-\overset{1}{N^+}=)\simeq\alpha(-\overset{1}{N}-)=\alpha+2\beta$. Regarding the latter see H. H. Jaffé, *J. Am. Chem. Soc.*, **76**, 3527 (1954).

** For diazines one may consider that half the unit positive charge appears at each N atom upon the removal of one non-bonding electron. This will not alter the values of $\delta E$, if one assumes that the resulting change in coulomb integral of each N atom is $(1/2)\beta$.

20) J. D. Morrison and A. J. C. Nicholson, *J. Chem. Soc.*, **20**, 1021 (1952).
21) W. C. Price, *J. Chem. Phys.*, **3**, 256, 365, 439 (1954).
22) K. Watanabe, *J. Chem. Phys.*, **24**, 1564 (1954).
23) A. Hustrulid, A. Kusch and J. T. Tate, *Phys. Rev.*, **54**, 1037 (1938).
24) K. Watanabe, Private communication.

# *Relations among Bond Order, Force Constant and Bond Length for the C—C and the C—N Bond in Conjugated Molecules*

By Tosinobu ANNO*, Mitsuo ITO, Ryoichi SHIMADA, Akira SADÔ and Wataru MIZUSHIMA

(Received March 15, 1957)

## Introduction

In a recent communication[1], the present authors derived following relation between bond length $x$ and bond order $p$ calculated by molecular orbital (MO) approximation:

$$p=\frac{2}{1-\frac{D_t a_t}{D_s a_s}\left[\frac{\exp\{-a_t(x-x_t)\}-\exp\{-2a_t(x-x_t)\}}{\exp\{-a_s(x-x_s)\}-\exp\{-2a_s(x-x_s)\}}\right]} \quad (1)$$

where $x_s$ and $x_t$ are the bond length of pure single and triple bonds, respectively. $D$ denotes the bond strength and $a$ is a constant given by

$$a=\sqrt{\frac{k}{2D}}\ , \quad (2)$$

where $k$ is the bond-stretching force constant. It has also been shown briefly for C—C and C—N bonds in the previous communication that the order-length relations calculated from Eq. (1) are in good agreement with the empirical ones. On the other hand, several empirical relations between force constant and bond length have been proposed by many workers[2]. Among these Badger's relation[3] is the best known and has been accepted most widely. However, the theoretical relations between these quantities have not been derived.

In the present paper we shall propose a full account of the previous communication and a theoretical equation correlating the force constant with the bond length will be proposed, confining ourselves to C—C and C—N bonds.

For C—C bonds, there exist many accurate experimental values of bond lengths and the force constants on the one hand and the calculated values of bond orders on the other. Moreover, the empirical values of parameters necessary in the theoretical equations are known for these molecules better than for the other types of conjugated molecules. Thus the test of the theoretical equations are most feasible for C—C bonds.

For C—N bonds the single and the triple bonds are familiar in chemistry and the physical natures of these bonds are fairly well known. However, for the C—N double bond we have only a few experimental data. Therefore it may be interesting to be able to infer the nature of the C—N double bond from reasonably established relations among bond orders, force constant and bond length.

## Derivation of a General Equation Correlating Bond Order and Bond Length

Although Eq. (1) is useful for explaining the relation between bond order and bond length for C—C and C—N bonds, it involves the pure single and triple bonds as references. For C—C bonds, pure single and triple bonds exist in nature as far as the effects of the hyperconjugation or the configuration interaction are neglected. This is also true for C—N single bond, but the pure C—N triple bond does not exist even in the ordinary sense as far as we stand upon the MO viewpoint. Therefore a more general equation which involves Eq. (1) as a special case will be derived first.

Let us take two bonds $A_{ij}$ and $B_{ij}$ whose mobile orders are $p_{Aij}$ and $p_{Bij}$ ($p_{Aij}>p_{Bij}$), respectively, for each bond $i-j$ in a molecule. Other notations used in the following discussion will be easily understood

---

* Chemical Laboratory, General Education Department, Kyushu University, Ootsubo-machi, Fukuoka.

T. Anno is greatly indebted to the Dean of the Faculty of Science of Kyushu University and to Professor S. Imanishi for permitting him to continue his work at that Faculty.

1) T. Anno, M. Ito, R. Shimada, A. Sadô, and W. Mizushima, This Bulletin, **29**, 440 (1956).

2) A brief summary of the empirical equations has been given by (a) C. K. Wu and Chang-Tsing Yang, *J. Phys. Chem.*, **48**, 295 (1944) and (b) G. Herzberg, "Spectra of Diatomic Molecules" (D. van Nostrand Company, Inc., New York, 1950) p. 453f.

3) R. M. Badger, *J. Chem. Phys.*, **2**, 128 (1934); **3**, 710 (1935).

by analogy with those described above. The total bond energy of a molecule can be expressed as follows, taking a suitable energy zero:

$$F=\sum_{i<j} D_{B_{ij}}[1-\exp\{-a_{B_{ij}}(x_{ij}-x_{B_{ij}})\}]^2 +2\sum_{i<j}(p_{ij}-p_{B_{ij}})\beta_{ij} +\sum_{i<j}\left\{\left(\frac{q_i\alpha_i}{n_i}-\frac{q_{B_i}\alpha_{B_i}}{n_{B_i}}\right)+\left(\frac{q_j\alpha_j}{n_j}-\frac{q_{B_j}\alpha_{B_j}}{n_{B_j}}\right)\right\}, \quad (3)$$

where $q$ denotes charge density. Subscripts $i$ and $j$ represent atoms making ends of the bond $i$—$j$, $n_i$ and $n_{B_i}$ being the numbers of bonds[4] which start from atom $i$ in the molecule under consideration and the molecule which contains the reference bond $B_{ij}$, respectively. $\alpha$ and $\beta$ are the usual coulomb and resonance integral, respectively[5]. We assume here that the terms due to the charge density can be distributed equally among various bonds[4] which start from the atom referring to the term. Then, the total energy of a particular bond is

$$F_{ij}=D_{B_{ij}}[1-\exp\{-a_{B_{ij}}(x_{ij}-x_{B_{ij}})\}]^2 +2(p_{ij}-p_{B_{ij}})\beta_{ij} +\left(\frac{q_i\alpha_i}{n_i}-\frac{q_{B_i}\alpha_{B_i}}{n_{B_i}}\right)+\left(\frac{q_j\alpha_j}{n_j}-\frac{q_{B_j}\alpha_{B_j}}{n_{B_j}}\right). \quad (4)$$

The energy difference between two bonds whose mobile orders are $p_A$ and $p_B$ and the internuclear distances are equally $x$ is represented by

$$\left(\frac{q_{A_i}\alpha_{A_i}}{n_{A_i}}-\frac{q_{B_i}\alpha_{B_i}}{n_{B_i}}\right)+\left(\frac{q_{A_j}\alpha_{A_j}}{n_{A_j}}-\frac{q_{B_j}\alpha_{B_j}}{n_{B_j}}\right) +2(p_{A_{ij}}-p_{B_{ij}})\beta_{ij} =\text{const.}+D_{A_{ij}}[1-\exp\{-a_{A_{ij}}(x_{ij}-x_{A_{ij}})\}]^2 -D_{B_{ij}}[1-\exp\{-a_{B_{ij}}(x_{ij}-x_{B_{ij}})\}]^2. \quad (5)$$

From the equilibrium condition that $\frac{\partial F}{\partial x_{ij}}=0$ and from Eqs. (3) and (5) the following equation is obtained:

$$p=\frac{p_A-p_B}{1-\frac{D_A a_A}{D_B a_B}\left[\frac{\exp\{-a_A(x-x_A)\}-\exp\{-2a_A(x-x_A)\}}{\exp\{-a_B(x-x_B)\}-\exp\{-2a_B(x-x_B)\}}\right]}+p_B. \quad (6)$$

It is clear that Eq. (6) reduces to Eq. (1) when the C—C bonds in ethane and acetylene are taken as standards and the effects of hyperconjugation and configuration interaction are neglected. From the meanings of Eqs. (3), (4) and (5) it is clear that $D$'s and $a$'s (equivalently, $D$'s and $k$'s) must refer to hypothetical change where $p$'s and $q$'s do not change from their values in the reference molecules in equilibrium. Let us consider how to derive these constants from those obtained from the "experiment".

When we consider the reference bond $B_{ij}$ at its equilibrium position, Eq. (4) becomes

$$F(x_{B_{ij}})=0. \quad (7)$$

Let the internuclear distance of the reference bond $B_{ij}$ go to infinity leaving $q_i=q_{B_i}$ and $p_{ij}=p_{B_{ij}}$, Eq. (4) becomes

$$F(\infty)_{\text{hypothetical}}=D_{B_{ij}}. \quad (8)$$

Actually, $p_{ij}$ does not necessarily remain equal to $p_{B_{ij}}$ and $q_i\to m_{B_i}$ ($m_{B_i}$ denotes the number of $\pi$-electrons of free atom $i$ in its valence state) when $x_{ij}\to\infty$, so that Eq. (4) becomes

$$F(\infty)_{\text{actual}}=D_{B_{ij}}+\frac{1}{n_{B_i}}(m_{B_i}\alpha^{\infty}_{B_i}-q_{B_i}\alpha_{B_i}) +\frac{1}{n_{B_j}}(m_{B_j}\alpha^{\infty}_{B_j}-q_{B_j}\alpha_{B_j}), \quad (9)$$

considering the fact that $\beta_{ij}\to 0$ when $x_{ij}\to\infty$. $\alpha^{\infty}_{B_i}$ and $\alpha^{\infty}_{B_j}$ denote the limiting values to which $\alpha_{B_i}$ and $\alpha_{B_j}$ approach when $x_{ij}\to\infty$. It is the difference between the left hand sides of Eqs. (7) and (9) that represents the actual $D_{B_{ij}}$ value (denoted by $D'_{B_{ij}}$). Thus,

$$D_{B_{ij}}=D'_{B_{ij}}-\frac{1}{n_{B_i}}(m_{B_i}\alpha^{\infty}_{B_i}-q_{B_i}\alpha_{B_i}) -\frac{1}{n_{B_j}}(m_{B_j}\alpha^{\infty}_{B_j}-q_{B_j}\alpha_{A_j}). \quad (10)$$

Similarly,

$$D_{A_{ij}}=D'_{A_{ij}}-\frac{1}{n_{A_i}}(m_{A_i}\alpha^{\infty}_{A_i}-q_{A_i}\alpha_{A_i}) -\frac{1}{n_{A_j}}(m_{A_j}\alpha^{\infty}_{A_j}-q_{A_j}\alpha_{A_j}). \quad (11)$$

Thus, $D_{A_{ij}}$ and $D_{B_{ij}}$ values corresponding to the hypothetical changes described above may be obtained from actual $D'_{A_{ij}}$ and $D'_{B_{ij}}$ values using Eqs. (10) and (11).

Differentiating twice Eq. (3) with respect to $x_{ij}$ and inserting the expressions for

4) These bonds should be restricted to those which participate in the conjugation.

5) It should be noted that $\beta_{ij}$ is assumed to depend only upon the kinds of atom $i$ and $j$ and the distance between these atoms.

$\frac{\partial\beta_{ij}}{\partial x_{ij}}$ and $\frac{\partial^2\beta_{ij}}{\partial x_{ij}^2}$ obtained from Eq. (5), it follows that[5a]

$$\begin{aligned}\frac{\partial^2 F}{\partial x^2} &= 2a_B D_B[-a_B\exp\{-a_B(x-x_B)\} \\ &\quad +2a_B\exp\{-2a_B(x-x_B)\}] \\ &+\frac{2\pi}{(p_A-p_B)^2}[a_A D_A[\exp\{-a_A(x-x_A)\} \\ &\quad -\exp\{-2a_A(x-x_A)\}] \\ &\quad -a_B D_B[\exp\{-a_B(x-x_B)\} \\ &\quad -\exp\{-2a_B(x-x_B)\}]]^2 \\ &+\left(\frac{p-p_B}{p_A-p_B}\right)[2a_A D_A[-a_A\exp\{-a_A(x-x_A)\} \\ &\quad +2a_A\exp\{-2a_A(x-x_A)\}] \\ &\quad -2a_B D_B[-a_B\exp\{-a_B(x-x_B)\} \\ &\quad +2a_B\exp\{-2a_B(x-x_B)\}]], \qquad (12)\end{aligned}$$

where $\pi$ is the self-polarizability of the bond under consideration. At the equilibrium position of the reference bond B, Eq. (12) becomes

$$\begin{aligned}\left(\frac{\partial^2 F}{\partial x^2}\right)_B &\equiv k'_B = k_B \\ &+\frac{2\pi_B}{(p_A-p_B)^2}(a_A D_A)^2[\exp\{-a_A(x_B-x_A)\} \\ &-\exp\{-2a_A(x_B-x_A)\}]^2, \qquad (13)\end{aligned}$$

and at the equilibrium position of the reference bond A, it becomes

$$\begin{aligned}\left(\frac{\partial^2 F}{\partial x^2}\right)_A &\equiv k'_A = k_A \\ &+\frac{2\pi_A}{(p_A-p_B)^2}(a_B D_B)^2[\exp\{-a_B(x_A-x_B)\} \\ &-\exp\{-2a_B(x_A-x_B)\}]^2, \qquad (14)\end{aligned}$$

using Eq. (2). Since $D_A$ and $D_B$ values can be obtained in the above-described manner and $a$'s are expressible with $D$'s and $k$'s through Eq. (2), Eqs. (13) and (14) give $k_A$ and $k_B$ corresponding to the hypothetical change from the actual force constants $k'_A$ and $k'_B$ through the iterative process.

Similarly, if the Hooke-type potential functions are used the following formula for order-length relation can be obtained:

$$x = x_B - \frac{x_B - x_A}{1+\frac{k_B}{k_A}\left(\frac{1-p'}{p'}\right)}, \qquad (15)$$

where $p' = (p-p_B)/(p_A-p_B)$ and $k_A$ and $k_B$ may be obtained using

$$k'_B = k_B + \frac{\pi_B}{2(p_A-p_B)^2}\{k_A(x_B-x_A)\}^2, \qquad (16)$$

and

$$k'_A = k_A + \frac{\pi_A}{2(p_A-p_B)^2}\{k_B(x_B-x_A)\}^2, \qquad (17)$$

from the actual force constants $k'_A$ and $k'_B$. Equation (15) is the general equation which involves those obtained previously[6-8].

## Numerical Values of Parameters

As can be seen in the derivation of Eq. (6), this equation is based upon the Morse-type bond-stretching potential function which contains $D$'s and $k$'s as parameters. These parameters may be obtained from the actual $D'$ and $k'$ values as described previously. Although in diatomic molecules $D'$'s and $k'$'s can be obtained from experimental data, for polyatomic molecules circumstances are somewhat different.

Let us first seek for the appropriate values of $k'$'s. As is well known, the force constants take different values depending upon the assumed force fields. However, from the derivation of Eq. (6), if the interactions among the non-bonded atoms can be neglected, it is clear that the appropriate value of $k'$ to be used must correspond to the bond stretching, the bond angles and bond lengths, except the bond length in question, having to remain the same as in the equilibrium. This is the bond-stretching force constant in the most general quadratic potential function which contains all cross terms. Normal coordinate treatment has been carried out for ethane and acetylene, which will be taken as reference molecules in the following discussion for C—C bonds, taking all or almost all the cross terms into consideration. Thus, the following values for C—C bond force constants were taken:

$k'_B = 4.57$[9] and $k'_A = 15.79\times10^5$ dynes/cm.[10]

For C—N bonds, the methylamine and

5a) In Eq. (12) subscripts $i$ and $j$ are omitted for brevity.

6) C. A. Coulson, *Proc. Roy. Soc.* (London) **A169**, 413 (1939).
7) T. Anno and A. Sadô, This Bulletin, **28**, 350 (1955).
8) T. Anno and A. Sadô, *J. Chem. Phys.*, **25**, 176 (1956).
9) G. E. Hansen and D. M. Dennison, ibid. **20**, 313 (1952).
10) G. Herzberg, "Infrared and Raman Spectra of Polyatomic Molecules" (D. van Nostrand Co., Inc., New York, 1945), pp. 188—9. This value is the average of the values listed by Herzberg for $C_2H_2$ and $C_2D_2$.

hydrogen cyanide molecules may be taken as the reference molecules. While the normal coordinate treatment including the cross terms for the latter molecule gives $k'_A = 18.58 \times 10^5$ dynes/cm.[11], the C—N force constant of the methylamine is not found in the literature. We took the C—N force constant $4.68 \times 10^5$ dynes/cm. of the trimethylamine molecule[12] instead.

The most serious difficulty in applying Eq. (6) is concerned with the value of $D'$. The necessary value of $D'$ must be the energy needed in the process of the rupture of the bond, leaving the other bond lengths or the bond angles unchanged. Thus, the so-called bond-dissociation energy values are not to be used, since the actual dissociation process involves the reorganization of the dissociation products. The adequate value of $D'$ is the bond energy if the "near-atom-effect", in the sense of Glockler[13], can be neglected. As is mentioned previously this type of effect is also neglected in taking the value of $k'$.

Moreover, in order to calculate the bond energy of the organic compounds from the thermochemical experimental data, it is necessary to know the latent heat of sublimation of carbon ($L(C)$). Unfortunately, however, the precise value of this quantity is still under discussion[14]. Glockler[15] calculated the bond energies in ethane and acetylene for three conflicting values of $L(C)$. In that paper he recommended $L(C) = 169.75$ kcal as the best value for this quantity. The bond-energy values calculated by Glockler based on $L(C) = 169.75$ kcal will be used in the present paper, since $L(C) \approx 170$ kcal seems to be the best[16]. The C—C bond energies taken are

$$D'_B = 85.063 \text{ and } D'_A = 182.948 \text{ kcal/mole.}$$

For C—N bonds in methylamine and hydrogen cyanide the calculation of the bond energy requires the dissociation energy of the nitrogen molecule ($D(N_2)$) as well as $L(C)$. The precise value of $D(N_2)$ has also been under discussion[14]. Gaydon[17] has given discussion which supports $D(N_2) = 9.765$ ev, reviewing the previous literatures. Since later works[18–20] seem to support this value of $D(N_2)$, we used this value of $D(N_2)$ in the calculation of the bond energy. Thus the Glockler-type calculation[15,21] yields 64.3 and 201.4 kcal/mole as the C—N bond energies in methylamine and hydrogen cyanide, respectively. Therefore we took

$$D'_B = 64.3 \text{ and } D'_A = 201.4 \text{ kcal/mole.}$$

The C—C or C—N bond lengths in the reference molecules are known with sufficient accuracy. Bond lengths of C—C bonds in ethane[9] and acetylene[22] have been derived from the analyses of rotation-vibration spectra of these molecules. From these we took

$$x_B = 1.543 \text{ and } x_A = 1.207 \text{ Å.}$$

For C—N bonds in methylamine and hydrogen cyanide, recent spectroscopic investigations have given

$$x_B = 1.474^{23} \text{ and } x_A = 1.157 \text{ Å}^{24,25}.$$

## Calculation of Bond Order

In order to test the theoretical relation derived above, calculated values of bond orders are necessary. Although for C—C bonds there exist many calculated values of bond order in the literature, the calculated values of C—N bond orders are scarce in the literature, so that calculations of the C—N bond orders have been made for several molecules by MO method using the following assumptions:

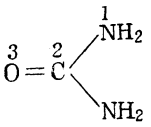
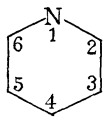
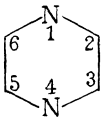
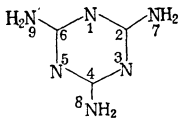
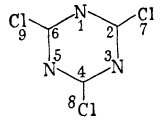
(a) All the resonance integrals between non-adjacent atoms and all the overlap integrals can be neglected.

(b) The ratio of the coulomb integral to the resonance integral in benzene is 4.1; i. e., $\alpha = 4.1\,\beta$[26].

(c) The coulomb integral of each atom, $\alpha_r$, is proportional to its electronegativity.

11) A. E. Douglas and D. Sharma, *J. Chem. Phys.*, **21**, 448 (1953).
12) V. H. Siebert, *Z. anorg. allgem. Chem.*, **273**, 161 (1953).
13) G. Glockler, *J. Phys. Chem.*, **56**, 289 (1952).
14) G. Glockler, *Ann. Rev. Phys. Chem.*, **3**, 151 (1952).
15) G. Glockler, *J. Chem. Phys.*, **21**, 1242 (1953).
16) M. Hock, P. E. Blackburn, D. P. Dingledy and H. L. Johnston, *J. Phys. Chem.*, **59**, 97 (1955); W. A. Chupka and M. G. Inghram, ibid., **59**, 100 (1955).
17) A. G. Gaydon, "Dissociation Energies and Spectra of Diatomic Molecules". (Dover Publications, Inc., New York, 1950) Chapter IX.
18) J. M. Hendrie, *J. Chem. Phys.*, **22**, 1503 (1954).
19) W. Groth, *Z. physik. Chem.* (Frankfurt), **1**, 300 (1954); *Z. Elektrochem.*, **58**, 752 (1954).
20) D. C, Frost and C. A. McDowell, *Proc. Roy. Soc.* (London), **A236**, 278 (1956).
21) G. Glockler, *J. Chem. Phys.*, **19**, 124 (1951).
22) Reference 10, p. 398.
23) T. Nishikawa, T. Itoh and K. Shimoda, ibid. **23**, 1735 (1955).
24) J. W. Simmons, W. E. Anderson and W. Gordy, *Phys. Rev.*, **77**, 77 (1950).
25) I. R. Dagg and H. W. Thompson, *Trans. Faraday Soc.*, **53**, 455 (1956).
26) C. Sandorfy, *Bull. soc. chim. France*, 615 (1949).

TABLE I

| Molecules | $r$ | $\alpha_r$ ($\beta$ unit) | $\beta_{rs}$ ($\beta$ unit) | $\pi$-electron densities | Orbital energies ($\beta$ unit) | |
|---|---|---|---|---|---|---|
| Urea  | 1 | 5.276 | | 1.783 | $B_1$ | 6.335 |
| | | | 0.757 | | $B_1$ | 5.415 |
| | 2 | 4.346 | | 0.654 | $A_2$ | 5.276 |
| | | | 0.861 | | $B_1$ | 3.390 |
| | 3 | 5.518 | | 1.780 | | |
| Pyridine  | 1 | 4.927 | | 1.341 | $B_2$ | 6.178 |
| | | | 0.839 | | $B_2$ | 5.335 |
| | 2 | 4.180 | | 0.888 | $A_2$ | 5.131 |
| | | | 0.984 | | $B_2$ | 3.542 |
| | 3 | 4.113 | | 0.982 | $A_2$ | 3.162 |
| | | | 0.984 | | $B_2$ | 2.322 |
| | 4 | 4.158 | | 0.918 | | |
| Pyrazine  | 1 | 4.987 | | 1.258 | $B_{1u}$ | 6.290 |
| | | | 0.859 | | $B_{3g}$ | 5.607 |
| | 2 | 4.192 | | 0.871 | $B_{2g}$ | 5.158 |
| | | | 0.966 | | $B_{1u}$ | 3.854 |
| | 3 | 4.192 | | 0.871 | $A_u$ | 3.226 |
| | | | | | $B_{3g}$ | 2.606 |
| Melamine  | 1 | 4.862 | | 1.433 | $A''_2$ | 6.557 |
| | | | 0.879 | | $E''$ | 5.914 |
| | 2 | 4.277 | | 0.751 | $A''_2$ | 5.191 |
| | | | 0.767 | | $E''$ | 5.065 |
| | 7 | 5.260 | | 1.816 | $E''$ | 3.421 |
| | | | | | $A''_2$ | 2.652 |
| Cyanuric chloride  | 1 | 4.883 | | 1.404 | $A''_2$ | 6.502 |
| | | | 0.896 | | $E''$ | 5.737 |
| | 2 | 4.270 | | 0.761 | $A''_2$ | 5.000 |
| | | | 0.622 | | $E''$ | 4.965 |
| | 7 | 5.010 | | 1.836 | $E''$ | 3.458 |
| | | | | | $A''_2$ | 2.658 |
| Hydrogen cyanide $HC\equiv N$ (1 2) | 1 | 4.333 | | 1.347 | $\Pi$ | 5.497 |
| | | | 0.876 | | $\Pi$ | 3.644 |
| | 2 | 4.938 | | 2.653 | | |

The values of the electronegativity used were those listed in Kurita and Kubo[27] for B, C, N and O, while for S and Cl Pauling's values[28] were used.

(d) The resonance integral between adjacent atoms, $\beta_{rs}$, is given by $\beta_{rs}=(S_{rs}/S)\beta$[29], where $S_{rs}$ is the overlap integral, which may be evaluated according to Mulliken's Tables[30]. $S$ and $\beta$ are the overlap and resonance integrals in benzene, respectively.

(e) Inductive effects can be neglected.

(f) $\alpha_r$ and $\beta_{rs}$ are to be corrected for the formal charge obtained from the calculated electron density according to the way suggested by Nagakura[31,32].

Under the above assumptions the usual MO calculation is repeated until the final results are self-consistent. In the case of the hydrogen cyanide molecule two $\pi$-bonds exist, nodal planes of which are perpendicular to each other. These $\pi$-bonds will be referred to as $\pi_x$ and $\pi_y$ bonds, $z$ direction being taken along the line connecting

27) Y. Kurita and M. Kubo, This Bulletin, **24**, 13(1951).
28) L. Pauling, "The Nature of the Chemical Bond", Cornell University Press, Ithaca, New York, (1940) p. 64.
29) G. W. Wheland, *J. Am. Chem. Soc.*, **64**, 900 (1942).
30) R. S. Mulliken, C. A. Rieke, D. Orloff and H. Orloff, *J. Chem. Phys.*, **17**, 1248 (1949).
31) S. Nagakura, This Bulletin, **25**, 164 (1952).
32) S. Nagakura and T. Hosoya, ibid. **25**, 179 (1952).

TABLE II

THE CALCULATED VALUES OF BOND ORDER AND THE EXPERIMENTAL VALUES OF BOND LENGTH FOR SOME C—N BONDS

| Molecules | Mobile bond orders | | Bond lengths* (in Å) | |
|---|---|---|---|---|
| | Present calc. | Other methods | | |
| Pyrrole | 0.41[b] | 0.45[d]<br>0.50[e] | 1.385±0.015 | M. W.[h] |
| Urea | 0.540 | | 1.37 | X.[i] |
| Pyridine | 0.620 | 0.534[d],[f]<br>0.64[e]<br>0.652[g] | 1.35 | M. W.[j] |
| Pyrazine | 0.639 | 0.63[e]<br>0.660[g] | 1.35±0.02 | E. D.[k] |
| Melamine<br>C—N (ring)<br>C—N (outer) | <br>0.474<br>0.749 | <br>0.449[a]<br>0.576[a] | <br>1.37±0.03<br>1.34±0.01 | <br>E. D.[a] |
| Cyanuric chloride | 0.584 | 0.622[a] | 1.33±0.02 | E. D.[a] |
| Amide group | 0.660[c] | | 1.32±0.02 | E. D.[l] |
| Hydrogen cyanide | 1.890 | | 1.157 | M. W.[m] |

* E. D.: Electron diffraction. X.: X-ray. M. W.: Microwave.

a) Y. Akimoto, This Bulletin, **28**, 1 (1955).
b) S. Nagakura and T. Hosoya, This Bulletin, **25**, 179 (1952). The method of calculation is the same as that used in the present paper, but slightly different values of electronegativity are used.
c) S. Nagakura, This Bulletin, **25**, 164 (1952). The value of bond order listed in this table is calculated using the final values of $\alpha$'s and $\beta$'s listed in this paper.
d) H. C. Longuet-Higgins and C. A. Coulson, *Trans. Faraday Soc.*, **43**, 87 (1947).
e) L. E. Orgel, T. L. Cottrell, W. Dick and L. E. Sutton, *Trans. Faraday Soc.*, **47**, 113 (1951).
f) C. A. Coulson and H. C. Longuet-Higgins, *Proc. Roy. Soc.* (London), **A193**, 447 (1948).
g) D. W. Davies, *Trans. Faraday Soc.*, **51**, 449 (1955).
h) B. Bak, D. Christensen, L. Hansen and J. Rastrup-Andersen, *J. Chem. Phys.*, **24**, 720 (1956).
i) R. W. G. Wyckoff and R. B. Corey, *Z. Krist.*, **89**, 462 (1934).
j) K. E. McCuloh and G. F. Pollow, *J. Chem. Phys.*, **22**, 681 (1954).
k) V. Schomaker and L. Pauling, *J. Am. Chem. Soc.*, **61**, 1769 (1937).
l) R. B. Corey and J. Donohue, *J. Am. Chem. Soc.*, **72**, 2899 (1950).
m) reference 24.

the nuclei. For this molecule the self-consistent result is not to be obtained if the formal charges resulting from both the $\pi_x$ and $\pi_y$ bonds are taken into account in the next cycle of calculation concerning $\pi_x$ or $\pi_y$ bonds. However, if only the formal charges resulting from the $\pi_x$ bond are taken into account in the next cycle of calculation concerning the same $\pi_x$ bond, the self-consistent results are obtained. The same is true also for $\pi_y$ bond. Therefore calculation of the hydrogen cyanide molecule was made using the additional assumption: only the formal charge resulting from $\pi_x$ (or $\pi_y$) bond should be taken into account for the second cycle of calculation for $\pi_x$ (or $\pi_y$) bond. The final values of $\alpha_r$, $\beta_{rs}$ and orbital energies are listed in Table I. Table II contains the bond orders calculated using these parameters. Bond orders calculated with other methods by several workers are also given in Table II.

## Bond Order-Bond Length Relation: Test of the Theory

**C—C Bonds.** — In applying Eq. (6) to C—C bonds, numerical values of parameter derived directly from experiments which have been discussed in a previous section may be used when we use C—C bonds in the ethane and the acetylene molecules as standards and the effects of the hyperconjugation and the configuration interaction are neglected. Fig. 1 contains the theoretical curve thus obtained. In this figure the calculated values of bond order found in the literature for some C—C bonds are also plotted against the experimental values of bond lengths.

It can be seen that the theoretical curve explains fairly well the empirical trend. Deviation of the empirical points from the theoretical curve may be avoided if we take into account the hybridization of the carbon $\sigma$-atomic orbital in the same manner as that used by Coulson[33].

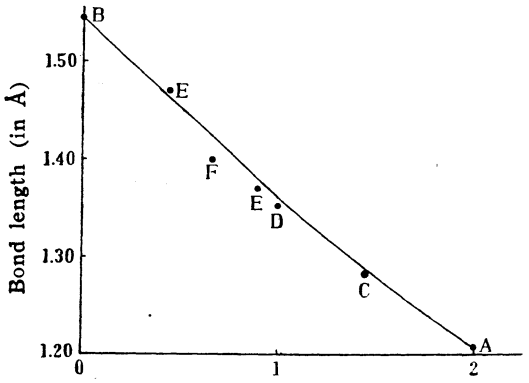



Fig. 1. The relation between bond order and bond length for C—C bonds.
A, Acetylene (a, b)*; B, Ethane (c, b); C, Butatriene (d, e); D, Ethylene (f, b); E, Butadiene (g, b); F, Benzene (g, b).
* (a, b) for example denotes that the bond length and bond order of the acetylene are taken from references a and b, respectively, cited below.
a) reference 22.
b) reference 6.
c) reference 9.
d) B. P. Soicheff, Symposium on Molecular Structure and Spectroscopy, Ohio State University, June 1956.
e) H. C. Longuet-Higgins and F. H. Burkitt, *Trans. Faraday Soc.*, **48**, 1077 (1952).
f) W. S. Gallaway and E. F. Barker, *J. Chem. Phys.*, **10**, 88 (1942).
g) P. W. Allen and L. E. Sutton, *Acta Cryst.*, **3**, 46 (1950).

33) C. A. Coulson, *J. Phys. Chem.*, **56**, 311 (1952).

**C—N Bonds.** — For C—N bonds, bond energies and force constants of the reference molecules obtained in a previous section should be corrected as described above. If we use the C—N bonds in methylamine and hydrogen cyanide as standards and make the usual approximation, the $\pi$-electron densities ($q_C$, $q_N$), $\alpha_C$, $\alpha^{\infty}_C$, $\alpha_N$ and $\alpha^{\infty}_N$, the self-polarizability ($\pi_{CN,CN}$), and the bond order ($p_{CN}$) of the C—N bond in the hydrogen cyanide molecule are sufficient to make this correction.

Using the assumptions described above it follows that

$$\left.\begin{aligned} &q_C=1.3472,\ q_N=2.6528,\\ &\quad \text{in electron unit,}\\ &\pi_{CN,CN}=0.2300/\beta \end{aligned}\right\} \quad (18)$$

and $p_{CN}=1.890$,

where $\beta$ is the resonance integral of the C—C bond in benzene the value of which is determined to be 23,000 cm.$^{-1}$ by Platt[34]. The numerical values in (18) are based on

$$\alpha_C=4.33\beta \quad \text{and} \quad \alpha_N=4.94\beta.$$

On the other hand it may be considered that

$$\alpha^{\infty}_C=4.1\beta \quad \text{and} \quad \alpha^{\infty}_N=5.17\beta,$$

from the assumptions on which the MO calculation is based. Therefore, from Eqs. (10), (11), (13) and (14) and using $D'_A$, $D'_B$, $k'_A$, $k'_B$, $x_A$ and $x_B$, the values of $D_A$, $D_B$, $k_A$ and $k_B$ can be obtained as follows:

$$\left.\begin{aligned} D_A&=175.5\ \text{kcal/mole}\\ D_B&=\ 64.3\ \text{kcal/mole}\\ k_A&=\ 20.01\times10^5\ \text{dynes/cm.}\\ k_B&=\ 4.68\times10^5\ \text{dynes/cm.} \end{aligned}\right\} \quad (19)$$

It is to be noted in the present case that in Eq. (10)

$$m_{Bi}=m_{Bj}=q_{Bi}=q_{Bj}=0,$$

and in Eq. (11)

$$m_{Ai}=m_{Aj}=2, \text{ and } n_{Ai}=n_{Aj}=1.$$

Using the values in (19), Eq. (6) yields a curve shown in Fig. 2.

Plotting the calculated values of bond orders against the experimental data of bond lengths, as is also shown in Fig. 2, it is seen that all the points lie on the theoretical curve within the experimental errors of bond lengths.

Naturally, the numerical value of the bond order is a little affected by the method of calculation as shown in Table

34) J. R. Platt, *J. Chem. Phys.*, **18**, 1168 (1950).

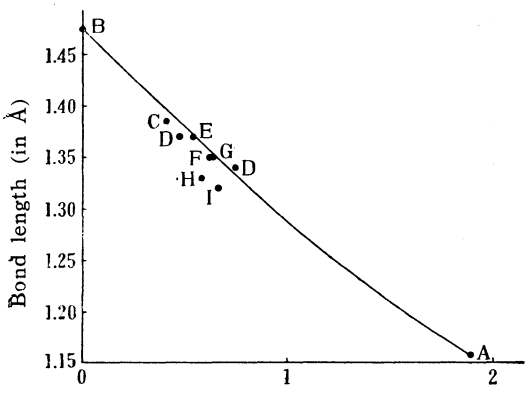



Fig. 2. The relation between bond order and bond length for C—N bonds.
A, Hydrogen cyanide; B, Methylamine; C, Pyrrole; D, Melamine; E, Urea; F, Pyridine; G, Pyrazine; H, Cyanuric chloride; I, Amide group.
In contrast with the corresponding figure in the previous communication (ref. 1) the points for dimeric cyanide are omitted in this figure since the calculation of the bond order of this molecule have been found to be in error.

II. However, the variation is less than 0.10 for most molecules, which may be taken as the measure of reliability of the calculation. According to the theoretical curve, it corresponds to the accuracy of 0.02 Å for bond length, which is nearly the same as the error in the electron-diffraction measurements. We may therefore predict the C—N bond length from the calculated bond order and using the theoretical curve within the experimental errors in the electron diffraction[35].

In concluding this section it is to be noted that the CN "double bond length" can be estimated as follows from the order-length relation obtained above. In the valence bond language the double bond has the "$\pi$-bond order" of one half of that of the triple bond which is realized by the CN bond in the hydrogen cyanide molecule if we neglect the homopolar-ionic resonance. Therefore we may consider the "double bond" as a bond whose mobile bond order is one half of that of the CN bond order of the hydrogen cyanide molecule in the molecular orbital language as well. Thus we obtain as the value of mobile bond order of the "double bond" 0.950. This value yields 1.295 Å as the value of "double bond length" from the order-length curve. This is in good agreement with the value of 1.28 Å evaluated as a sum of the covalent radii given by Pauling[36].

## Relation between Force Constant and Bond Length

Substituting $x$, obtainable from Eq. (6), Eq. (12) would give the bond-stretching force constant as a function of $p$ and $\pi$ and the resulting equation would be analogous to that obtained by Coulson and Longuet-Higgins[37] assuming the Hooke-type potential function. However, since the contribution from the term containing $\pi$ is relatively unimportant in the right hand side of Eq. (12) we can obtain a relation between force constant and bond length for bonds between a particular pair of atoms if the term containing $\pi$ is neglected and $p$ is replaced by the right hand side of Eq. (6). The resulting equation is

$$\frac{\partial^2 F}{\partial x^2} \equiv k = k_B g(2g-1) + \frac{k_A h(2h-1) - k_B(2g-1)}{1 - \dfrac{k_A a_B h(1-h)}{k_B a_A g(1-g)}} \qquad (20)$$

where $g = \exp\{-a_B(x-x_B)\}$

$h = \exp\{-a_A(x-x_A)\}$,

and use has been made of Eq. (2).

Taking the same molecules as those taken in obtaining order-length relationship as references and using the same value of numerical parameters as used there[38], we obtain a curve showing relation between bond length and force constant for bonds of each pair of atoms. They are full lines in Figs. 3 and 4 for C—C and C—N bond, respectively. Available data of force constants are plotted in the same figures against experimental values of bond lengths. For comparison, curves based on Badger's equation[3] are also drawn in the figures (dotted curves)[39].

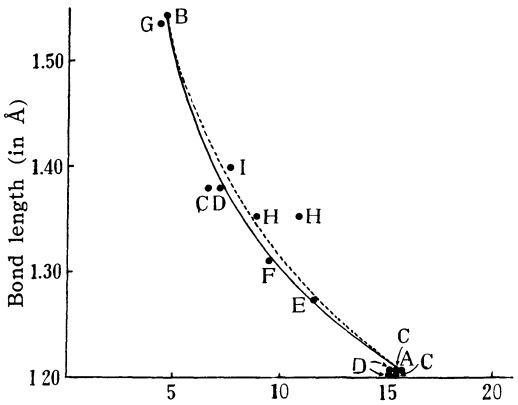
35) Since the CN bond order of the reference HCN molecule and the corrections to $D_A$ and $k_A$ depend upon the assumptions used in the MO calculation, the order-length curve itself depends upon such assumptions. Although this would cause a small additional error in the calculated value of bond length in the region of $p=1\sim2$, it would produce practically no error in the region of $p=0\sim1$ into which the numerical values of the CN bond order of the most interesting molecules fall.

36) Reference 28, p. 164.

37) C. A. Coulson and H. C. Longuet-Higgins, *Proc. Roy. Soc.* (London), **A193**, 456 (1948).

38) For $k_A$ of the CN bonds, the uncorrected value was used in order that the curve may pass through the point for the HCN molecule.

39) In drawing the curve based on the Badger's equation the values of parameters in this equation ($C$ and $d$) were determined from two empirical points for bonds "A" and "B".

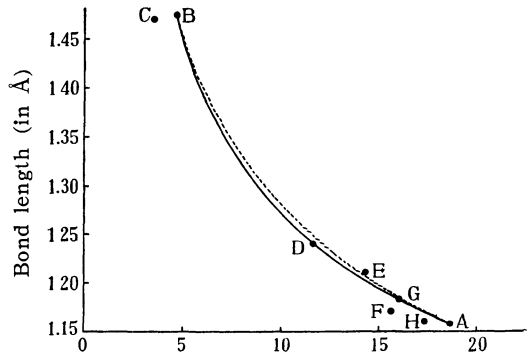



Force constant (in $10^5$ dyne/cm.)

Fig. 3. The relation between force constant and bond length for C—C bonds.
A, Acetylene (a, b)*; B, Ethane (c, c); C, Diacetylene (d, e); D, Diacetylene (d, f); E, $C_2$(c, $^1\Pi_g$) (g, g); F, $C_2$(X, $^3\Pi_u$) (g, g); G, $C_2$(B, $^3\Pi_g$) (g, g); H, Ethylene (h, i); I, Benzene (j, k).
* (a, b) for example denotes that the bond length and force constant of the acetylene are taken from references a and b, respectively, cited below.
a) reference 22.
b) reference 10.
c) reference 9.
d) G. D. Graine and H. W. Thompson, *Trans. Faraday Soc.*, **49**, 1273 (1953).
e) S. M. Ferigle, F. F. Cleveland and A. G. Meister, *J. Chem. Phys.*, **20**, 526 (1952).
f) A. V. Jones, *Proc. Roy. Soc.* (London), **A211**, 285 (1952).
g) reference 2b, p. 513.
h) W. S. Gallaway and E. F. Barker, *J. Chem. Phys.*, **10**, 88 (1942).
i) B. L. Crawford, Jr., J. E. Lancaster and R. G. Inskeep, *J. Chem. Phys.*, **21**, 678 (1953).
j) P. W. Allen and L. E. Sutton, *Acta Cryst.*, **3**, 46 (1950).
k) F. M. Garforth, C. K. Ingold and H. G. Poole, *J. Chem. Soc.*, **1948**, 491.

Comparing our theoretical curve with the curve based on Badger's relation, it is seen that both curves coincide fairly well with each other over the whole region of bond length.

It is mentioned in the preceding section that the bond length of the C—N double bond may be predicted to be 1.295 Å from the theoretical orderlength relation. Combining this value with Eq. (20), we can obtain the force constant of the C—N double bond as $9.1\times10^5$ dynes/cm.




Force constant (in $10^5$ dyne/cm.)

Fig. 4. The relation between force constant and bond length for C—N bonds.
A, Hydrogen cyanide (a, b)*; B, Methylamine (c, d); C, Ethylamine (e, f); D, C=N radical (g, g); E, Thiocyanate ion (h, h); F, C≡N radical (g, g); G, Methyl carbylamine (i, h); H, Ethane nitril (e, h).
* (a, b) for example denotes that the bond length and force constant of the hydrogen cyanide are taken from references a and b, respectively, cited below.
a) reference 24.
b) reference 11.
c) reference 23.
d) reference 12. The precise values of force constants of methylamine are not found in the literature, so we assume that the CN force constant in methylamine is equal to that in trimethylamine.
e) Landolt-Börnstein, "Zahlenwerte und Funktionen" (Springer, Berlin, 1951), Vol. 1, Part 2, Molekeln I, p. 17.
f) ibid., p. 234.
g) ibid., p. 228.
h) ibid., p. 230.
i) ibid., p. 18.

## Summary

A general equation correlating bond orders with bond lengths of bonds between any particular pair of atoms in the conjugated systems are proposed. To test this equation applications have been made for C—C and C—N bonds. Because of the scarcity of the calculated values of bond orders for C—N bonds in the literature, bond orders of several molecules containing C—N bonds have been calculated, It is shown that the order-length relation is in good agreement with experiments. A theoretical, although approximate, equation correlating bond lengths with force constants has also been proposed and applied to C—C and C—N bonds. From these relations the length and the stretching force constant of C—N double bond

are estimated to be 1.295 Å and $9.1\times10^5$ dynes/cm, respectively, the former being in agreement with the value calculated from the covalent radii given by Pauling.

The authors express their hearty thanks to Professor S. Imanishi for his encouragement throughout this work.

*Department of Chemistry*
*Faculty of Science*
*Kyushu University*
*Hakozaki, Fukuoka*

# *Spectrochemical Study of Microscopic Crystals. XIV*[1]. *Absorption Spectra and Structure of Dibenzene-chromium(I) Iodide*

By Shoichiro YAMADA, Hiroji NAKAMURA and Ryutaro TSUCHIDA

(Received March 28, 1957)

In the course of these several years, dicyclopentadienylcompounds of various metallic elements were prepared, and their chemical and physical properties were extensively studied from various sides[2]. Recently Fischer and Hafner[3] succeeded in preparing an interesting compound with a molecular formula of $Cr(C_6H_6)_2$, which was shown through an X-ray examination[4] to consist of sandwich molecules resembling the molecule of dicyclopentadienyliron(II), $Fe(C_5H_5)_2$[5]. Preparations also were reported of several other compounds of similar structure[3,6]. Although reports have appeared concerning the properties of the compounds of this type, their electronic states are still open to question.

In order to study the linkages in the compounds of this type, the present authors have determined absorption spectra of dibenzenechromium(I) iodide, $[Cr(C_6H_6)_2]I$, in water and ethyl alcohol, and also in the crystalline state. Description and discussion of the measurements are given below.

## Experimental

**Material.**—Crystals of dibenzene-chromium(I) iodide were kindly donated by Dr. E. O. Fischer of "Technische Hochschule, München". The yellow crystals of the compound show a well-developed prism face of a rectangular form, on which the measurement of dichroism has been made. It has been found in the course of the measurement that the crystal undergoes photo-decomposition with ultra-violet light. On the contrary, the crystal is comparatively stable in the dark.

**Measurement.**—Visible and ultra-violet spectra of the compound in the crystalline state have been measured on the above-mentioned face using Tsuchida-Kobayashi's microscopic method[7] with polarized light having its electric vector along and perpendicular to the direction of elongation. The *c*- and the *a*-absorption refer to absorption with the electric vector along and perpendicular to the direction of elongation, respectively.

Visible and ultra-violet absorption spectra in solution and an infra-red spectrum in pressed potassium bromide have been determined with a Beckman DU spectrophotometer and a Hilger H 800 infra-red spectrophotometer, respectively. The symbols used here are the same as those in the former reports of this series.

## Results and Discussion

The results of the present measurements are shown in Fig. 1, Table I, Table II and Table III.

Whereas benzene molecules in solution are known to show a characteristic absorption band at about 2600 Å which involves a distinct fine structure, the present measurement indicates that $[Cr(C_6H_6)_2]I$ shows no absorption band of the above sort. It is supposed, therefore, that the electronic state of the benzene rings

1) Part XIII of this series, S. Yamada and R. Tsuchida, This Bulletin, **29**, 894 (1956).
2) See, for example, E. O. Fischer, *Angew. Chem.*, **67**, 475 (1955).
3) E. O. Fischer and W. Hafner, *Z. Naturforsch.*, **10b**, 665 (1955).
4) E. Weiss and E. O. Fischer, *Z. anorg. allgem. Chem.*, **286**, 142 (1956).
5) E. O. Fischer and W. Pfab, *Z. Naturforsch.*, **7b**, 377 (1952); P. F. Eiland and R. Pepinsky, *J. Am. Chem. Soc.*, **74**, 4971 (1952); J. D. Dunitz and L. E. Orgel, *Nature*, **171**, 121 (1953).
6) H. H. Zeiss and W. Herwig, *J. Am. Chem. Soc.*, **78**, 5959 (1956).
7) R. Tsuchida and M. Kobayashi, "The Colour and the Structure of Metallic Compounds," Zoshindo, Osaka, 1944, p. 180 (in Japanese).

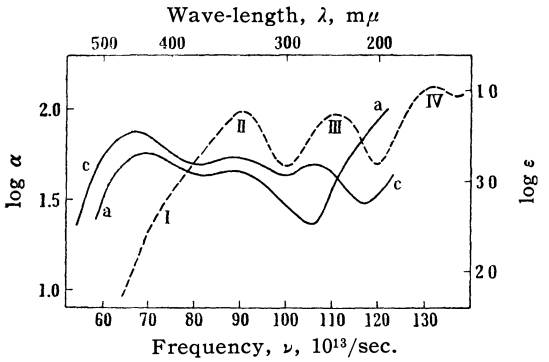



Fig. 1. Absorption spectra of $[Cr(C_6H_6)_2]I$ in the crystalline state (——) and in aqueous solution (·····).

within the chromium(I) compound is quite different from that of a free benzene molecule. Thus it is most likely that the $\pi$-electrons on the benzene rings are considerably attracted toward the central chromium ion to form firm linkages with it.

It is generally known that, when a metal ion having an unfilled *d*-electron shell forms a complex group with ligands, a few absorption bands of moderate intensity, rather characteristic of the metal ion, must appear in the visible or near-ultraviolet regions. To this type of absorption bands may belong the band I of the chromium(I) compound in question. When the solvent is alternated with a more polar one, this band is found to undergo only very slight solvent effect, which seems to be in agreement with the above assignment[8].

TABLE I

VISIBLE AND ULTRA-VIOLET ABSORPTION SPECTRA OF $[Cr(C_6H_6)_2]I$ IN CRYSTALLINE STATE AND IN SOLUTION

| absorption band | I | II | III | IV |
|---|---|---|---|---|
| In crystalline state | | | | |
| $\nu$, $10^{13}$ sec$^{-1}$ | 67.2 | 86–90 | 105.6 | >120 |
| $\Delta$ (log $\alpha$) | 0.12 | 0.1 | 0.4 | marked |
| stronger component | Z | Z | Z | X,Y |
| In $H_2O$ | | | | |
| $\nu$, $10^{13}$ sec$^{-1}$ | ca. 76 | 90 | 110.6 | 133.5 |
| log $\varepsilon$ | ca. 2.75 | 3.76 | 3.75 | 4.14 |
| In $C_2H_5OH$ | | | | |
| $\nu$, $10^{13}$ sec$^{-1}$ | ca. 76 | 89.8 | 110.0 | 139.2 |
| log $\varepsilon$ | ca. 2.75 | 3.80 | 3.78 | 4.28 |
| solvent effect | very slight | slight blue shift | slight blue shift | great red shift |

The fact that the bands II and III have great intensity in solution suggests that they are different from the type I of absorption bands with much lower intensity. We suppose that these bands may be closely related with the benzene molecules. The bands show a slight but definite "blue shift" when the solvent is changed from a less polar to a more polar one. The "blue shift" indicates that the bands in question correspond to transitions of an $n$-$\pi$ type, showing agreement with the above assignment. The bands II and III may not be considered as a band of such a kind that is identical in its origin with the typical absorption bands of free benzene, since the band of free benzene is known to show a "red shift".

The crystal structure of $[Cr(C_6H_6)_2]I$ is not known as yet. Although the exact arrangement of $[Cr(C_6H_6)_2]^+$ ions in the crystal can not be determined, we may be able to estimate the principal features of dichroism for the complex ion itself on a suitable assumption about the arrangement of the complex ions in the crystal. Previous studies on the dichroism of planar metallic complexes[9] indicate that for an absorption band in the longer wave-length of a planar metallic complex, which is closely related with the linkages within the complex, absorption is stronger along the direction in which the linkages exist than along the direction normal to it. Since the band I is assumed to be closely related with the linkage between the chromium ion and the benzene molecules, similar relationships to the above-mentioned should hold for the band I of the chromium(I) compound.

The present dichroism measurement with the crystal indicates that the polarization for the band I is definite, though not very great. Then we may assume that the *c*-absorption in Fig. 1 may represent the main characteristics of the *z*-absorption, the *z*-absorption being absorption with polarized light having its electric vector perpendicular to the benzene rings.

If the linkages between the benzene molecules and a chromium ion were similar to those in aromatic molecular compounds such as the linkage between

8) About the solvent effect upon absorption spectra, see, for example, M. Kasha, *Faraday Soc. Discussion*, No. 9, 14 (1950); H. McConnell, *J. Chem. Phys.*, **20**, 700 (1952); K. Nakamoto, M. Kobayashi and R. Tsuchida, ibid., **22**, 957 (1954).

9) S. Yamada and R. Tsuchida, This Bulletin, **29**, 421 (1956); ibid., **26**, 492 (1953); *J. Am. Chem. Soc.*, **73**, 1182 (1951); *Annual Report of Scient. Works, Fac. Sci. Osaka Univ.*, **4**, 79 (1956), etc.

quinone and hydroquinone molecules in quinhydrone, there should appear on the long wave-length side a new type of absorption band which would be broad and strong, and greatly polarized along the *z*-direction[10]. Since this type of absorption is not observed, the linkage similar to those in aromatic molecular compounds may not be present in the chromium(I) compound.

If aromaticity of the benzene rings in this chromium(I) compound were comparatively marked, the dichroism similar to the benzene rings would be observed, just as in most benzene derivatives. The dichroism of the benzene rings, which was determined with an ordinary type of benzene derivatives, indicates that absorption is more intense along the benzene ring than along the direction normal to it[11]. Since no dichroism of the above sort or a band with a fine structure is observed, the electronic state of the benzene molecules in this chromium(I) compound seems to be far from the state of free benzene molecules. The possibility may still remain that the band with a fine structure would be very weak, being hidden by the bands of much greater intensity. This possibility, however, may be neglected, judging from the general aspect of the absorption curve with the present compound.

The present measurement also indicates that with respect to the band IV absorption is much more intense along the plane of the benzene rings than along the direction normal to the benzene rings. From analogy with the dichroism of the benzene rings[11], it is suggested that the band IV is closely connected with the linkages within the benzene rings.

A marked "red shift" has been observed for the band IV, showing that the band corresponds to a "$\pi$-$\pi$" transition. The band IV does not correspond to the band at 2600 Å of free benzene, since both the magnitude of the red shift and the intensity seem to be too great, as compared with the values for the band at 2600 Å of free benzene.

Infra-red absorption bands of the chromium(I) compound are shown in Table II and Table III together with corresponding values of related compounds. The chromium(I) compound has an absorption band at 1428 cm.$^{-1}$ for a C–C stretching vibration in the benzene plane. It is seen that the C–C vibration in the chromium(I) compound is displaced from the original position of free benzene to a considerably smaller wave-number, being very close to the corresponding values[12] for dicyclopentadienyl-iron. From mutual comparison of the values in Table III, the electronic state of the benzene rings in $[Cr(C_6H_6)_2]I$ may be concluded to be between the states of ordinary aromatic and aliphatic carbon atoms, and to resemble the state of cyclopentadienyl-radicals in dicyclopentadienyl-iron(II). Thus the benzene rings in the chromium (I) compound may have less aromaticity than free benzene, though they still keep some of their unsaturated character.

TABLE II
INFRA-RED ABSORPTION BANDS OF $[Cr(C_6H_6)_2]I$ IN PRESSED POTASSIUM BROMIDE

| freq. cm.$^{-1}$ | intensity | freq. cm.$^{-1}$ | intensity |
|---|---|---|---|
| 795 | v. str. | 1145 | m. |
| 890 | w. | 1385 | w. |
| 974 | str. | 1428 | str. |
| 995, 1005 (double) | m. | 3025 | m. |

TABLE III
SKELETAL C-C VIBRATION

| compound | skeletal vibr. cm$^{-1}$ | ref. |
|---|---|---|
| $Fe(C_5H_5)_2$ | 1410 | 12 |
| $Cr(C_6H_6)_2$ | 1428 | 3 |
| $[Cr(C_6H_6)_2]I$ | 1428 | |
| $C_6H_6$ | 1500 | a) |
| C-C double | 1600-1680 | a) |
| C-C single | 800-1200 | a) |

a) See, for example, J. L. Bellamy, "The Infra-red Spectra of Complex Molecules," Methuen & Co., London, 1954.

Summarizing all the facts as described above, absorption spectra in the infra-red, the visible and the ultra-violet region seems to be understandable on the basis of the following assumption about the electronic state and linkages within the chromium(I) compound in question.

***The benzene rings in $[Cr(C_6H_6)_2]I$ have an electronic state which deviates greatly from the state of the ordinary benzene rings, involving very little aromaticity.***

10) R. Tsuchida, M Kobayashi and K. Nakamoto, *Nature*, **167**, 726 (1951); K. Nakamoto, *J. Am. Chem. Soc.*, **74**, 1739 (1952), *etc.*

11) R. Tsuchida, M. Kobayashi and K. Nakamoto, *J. Chem. Soc. Japan*, **70**, 12 (1949); K. Nakamoto, *J. Am. Chem. Soc.*, **74**, 390 (1952); G. Scheibe, S. Hartwig and H. Müller, *Z. Elektrochem.*, **49**, 372 (1943); D. P. Craig and L. E. Lyons, *Nature*, **169**, 1102 (1952), *etc.*

12) L. Kaplan, W. L. Kester and J. Katz, *J. Am. Chem. Soc.*, **74** 5531 (1952); E. R. Lippincott and R. D. Nelson, *J. Chem. Phys.*, **21**, 1307 (1953).

Thus we are inclined to conclude that $\pi$-electrons of the benzene rings in $[Cr(C_6H_6)_2]I$ may be strongly attracted so that the electronic state of the benzene rings is far from the state of the ordinary benzene rings and somewhat near the state of the cyclopentadienyl-radicals in dicyclopentadienyl-iron(II)[13].

## Summary

Polarized absorption spectra of $[Cr(C_6H_6)_2]I$ in the visible and the ultraviolet region were quantitatively determined by Tsuchida-Kobayashi's microscopic method using a single crystal. Visible and ultraviolet absorption spectra in solution and an infra-red spectrum in potassium bromide disks were also determined.

From the results of the measurements, it was concluded that the electronic state of the benzene rings in $[Cr(C_6H_6)_2]I$ deviates greatly from the state of free benzene and that the $\pi$-electrons of the benzene rings are attracted remarkably toward the chromium ion to form firm linkages.

The present authors wish to express heartiest thanks to Dr. E. O. Fischer for a precious sample of dibenzene-chromium (I) iodide. The work reported here was supported in part by a grant in aid from the Ministry of Education.

*Department of Chemistry, Faculty of Science, Osaka University*
*Kita-ku, Osaka*

13) S. Yamada, A. Nakahara and R. Tsuchida, *J. Chem. Phys.*, **22**. 1620 (1954): This Bulletin, **28**, 465 (1955).

# *Polarography of Bis(nitrophenyl) arsinic Acids**

By Masao MARUYAMA and Toshiko FURUYA

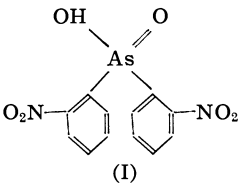
(Received January 17, 1957)

There are numerous reports on the study of polarography of aromatic nitro compounds but those on organic arsenic compounds are comparatively rare, brief reports being made on phenylarsonic acids[1,2], diphenylarsinic oxide, and dephenylarsinic acid[3]. It has been shown that phenylarsonic acids show a reduction wave with a half-wave potential of −1.25 V. vs. N.C.E. in a buffer solution of pH 2.97 but nothing has been given as to its electrolytic reduction mechanism and limiting current value, nor its proportionality with the concentration. As for diphenylarsinic oxide and acid, only brief mention is made of the fact that they show reduction waves and consequently could be utilized for indirect determination of diphenylcyanarsine.

In the present series of experiments, polarographic behavior of bis (nitrophenyl) arsinic acids, including diphenylarsinic acid, was clarified and discussions are made on the results of studies made in order to obtain some fundamental data for its utilization for quantitative determination. Further, a few examples of the determination are described.

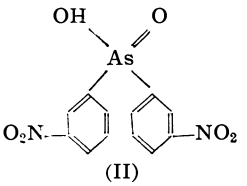
## Experimental

There are six isomers of bis(nitrophenyl)arsinic acid according to the position of the two nitro groups, viz. 2,2'-(I)' 3,3'-(II), 4,4'-(III), 2,3'-(IV), 2,4'-(V), and 3,4'-(VI). These six isomers and a compound without nitro group, diphenylarsinic acid, (VII), were submitted to the experiments. The melting points of these compounds are indicated with their structures.




(I)

m.p. 218°C (decomp.)

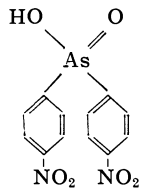



(II)

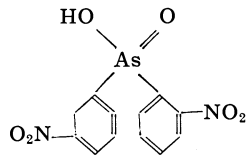
m.p. 244°C (decomp.)

* The Gist of the present report was presented at the 8th Annual Meeting of the Chemical Society of Japan (April, 1955).

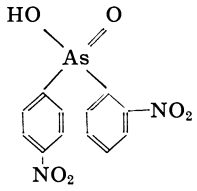
1) B. Breyer, *Ber.*, **71**, 163 (1938).
2) B. Breyer, *Biochem. Z.*, **301**, 65 (1939).
3) M. Suzuki and I. Tachi, *J. Electrochem. Soc. Japan*, **16**. 152 (1948).



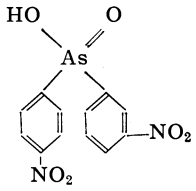

(III)
m.p. 263°C (decomp.)



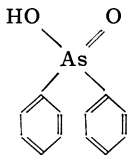

(IV)
m.p. 257°C (decomp.)




(V)
m.p. 248-250°C




(VI)
m.p. 230°C




(VII)
m.p. 167-168°C

The composition of the buffer solutions used is listed below and pH was measured with a glass electrode pH meter (manufactured by the Yamashita Denshiki Kagakukeiki Reserch Laboratory).

pH 1.04 .....0.1 N HCl
pH 2.2-7.0.....McIlvaine
(0.1 M citric acid-0.2 M $Na_2HPO_4$)
pH 8.0-12.38...Sörensen
(0.1 M $KH_2PO_4$-0.05 M $Na_2B_4O_7$)
pH 13.05 .....0.1 N NaOH

All the samples were dissolved in distilled water and mixed with the buffer solution to be used as the electrolytic solution. This solution was bubbled with purified nitrogen gas and washed with chromous chloride solution, for about 15 minutes to remove dissolved oxygen.

The apparatus used was a Heyrovsky-Shikata type photo-recording polarograph (Yanagimoto Model 52). The sensitivity of the galvanometer was $1.47\times10^{-9}$ amp./1 mm./m. and the dropping mercury cathode used had a capillary constant of m=2.35 mg./sec., t=4.26 sec./drop.

The polarographic cell used was an H-type with a ground-glass joint (universal) as shown in Fig. 1, which has long been used in this laboratory.

Microelectrolysis was carried out in accordance with the method of Gilbert and Rideal[4]. A definite amount (0.2-0.3 ml.) of the electrolytic solution was electrolyzed at the dropping mercury electrode and the number of electrons, $n$, was calculated from the decrease in wave height in the polarogram before and after the electrolysis,

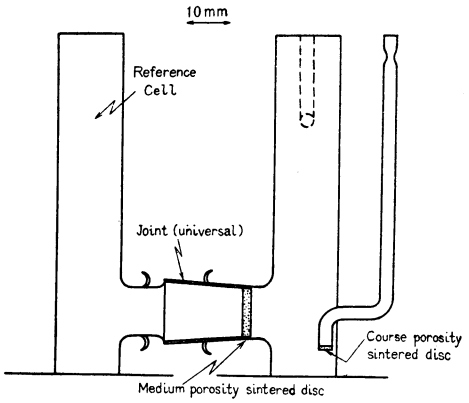



Fig. 1. H-Type-polarographic cell

according to the following equation:

$$\frac{d(\log h)}{dt}=\frac{k_2}{2.30.n.F.v.k_1}$$

All the experiments were carried out in a thermostat maintained at 25°±0.1°C.

## Experimental Results and Discussion

**(I) Reduction in Buffer Solutions of Various pH Values.**—The polarograms of the six isomers of bis(nitrophenyl)arsinic acids in buffer solutions of various pH values show reduction waves of complicated form. Even at the same pH, different isomers show different wave forms, as indicated in Fig. 2, and the wave form changes further with changes in pH.

These complicated reduction waves were classified into two portions, designated as 1st and 2nd waves, and each was examined. The 1st wave that appears initially is composed of one or two steps, the slope is more acute than the 2nd wave, and appears in the whole range of pH 1 to 13. The complicated waves appearing at more negative potentials than the 1st wave are collectively taken as the 2nd wave.

*The 1st Wave.* The half-wave potential of the 1st wave tends to shift to the negative side as the pH value increases but the wave height remains almost constant for all the isomers and through all pH values. The wave form is a one- or two-step wave below pH 7 but becomes a one-step wave above pH 8 for all six isomers (Table I).

Since this 1st wave does not appear in the reduction wave of diphenylarsinic acid, it is certain that the wave is due to

4) G. A. Gilbert and E. K. Rideal, *Trans. Faraday Soc.*, **47**, 396 (1951).

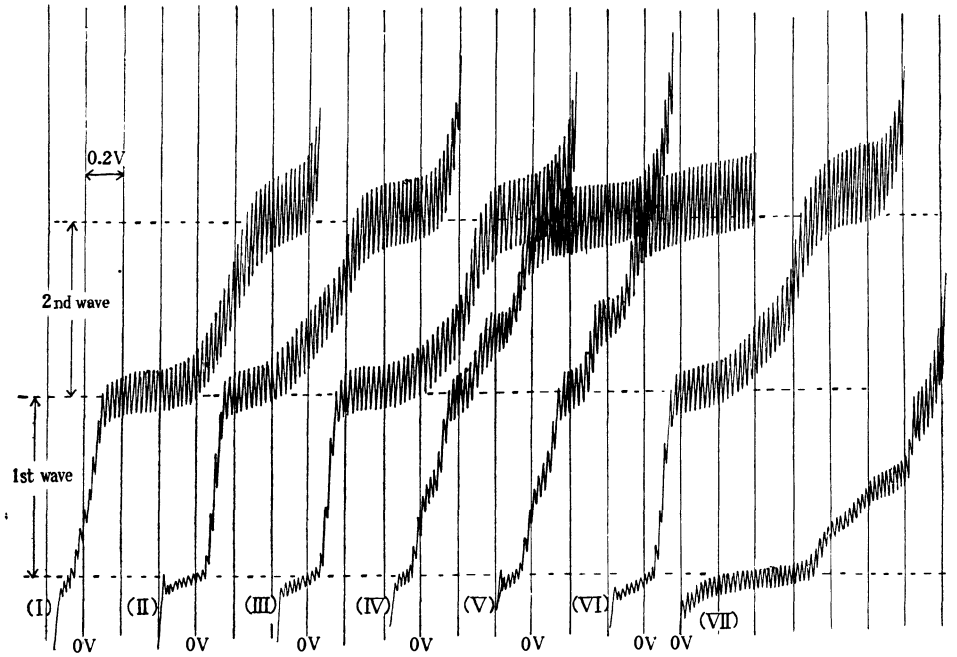



Fig. 2. Typical polarograms of Bis(nitrophenyl)arsinic acids diphenylarsinic acid in buffer solution of pH 2.2.
(I) 2,2′-compound (II) 3,3′-compound (III) 4,4′-compound
(IV) 2,3′-compound (V) 2,4′-compound (VI) 3,4′-compound
(VII) diphenylarsinic acid

TABLE I
HALF-WAVE POTENTIAL OF THE 1ST WAVE OF BIS(NITROPHENYL)ARSINIC ACIDS AT VARIOUS pH VALUES
$\pi_{1/2}$ mV(vs. S. C. E.)

| pH | 2,2′-* | 3,3′- | 4,4′- | 2,3′- | 2,4′- | 3,4′- |
|---|---|---|---|---|---|---|
| 1.04 | −004 | −071 | −056 | +046<br>−076 | +048<br>−064 | −062 |
| 2.2 | −048 | −110 | −111 | +008<br>−128 | +005<br>−120 | −111 |
| 3.0 | −064 | −152 | −146 | −030<br>−171 | −035<br>−160 | −152 |
| 4.0 | −110 | −198 | −196 | −070<br>−215 | −074<br>−220 | −200 |
| 5.0 | −180 | −270 | −272 | −174<br>−284 | −142<br>−265 | −270 |
| 6.0 | −281 | −355 | −340 | −243<br>−352 | −246<br>−348 | −338 |
| 7.0 | −360 | −390 | −388 | −324<br>−392 | −325<br>−378 | −384 |
| 8.0 | −440 | −450 | −450 | −430 | −422 | −440 |
| 9.0 | −500 | −494 | −490 | −490 | −480 | −492 |
| 10.0 | −549 | −550 | −535 | −544 | −534 | −512 |
| 11.0 | −560 | −586 | −552 | −565 | −554 | −528 |
| 12.38 | −630 | −652 | −630 | −650 | −620 | −628 |
| 13.05 | −670 | −660 | −664 | −626 | −650 | −664 |

* It was difficult to measure the half-wave potential on the acid side as a two-step wave and, therefore, it was obtained as a one-step wave.

the reduction of the nitro group, At below pH 7, the nitro group in the 2-position is reduced in a more positive potential than that in the 3- or 4-position, as was evidenced in the case of pH 2.2 shown in Fig. 2, and this results in two-step waves appearing in the 2,3- and 2,4-compounds, the ratio of wave heights being 1 : 1. The wave of the 2,2′-compounds, when well examined, appears to be a two-step wave and its wave height ratio is 1 : 3. This is assumed to be due to the fact that one of the four oxygen atoms of the two nitro groups forms a hydrogen bond with the hydrogen atom of the hydroxyl group in the molecule, so that this oxygen atom is reduced at more positive potentials than the other three oxygen atoms. But it is necessary to study this matter in detail further. A similar phenomenon was assumed to occur with 2,3′- and 2,4′-compounds but such waves could not be observed in the polarogram.

Analysis of the wave form indicated the 1st wave to be irreversible and its limiting current is controlled by a diffusion process, as will be described later. The number of electrons, $n$, taking part in the reduction in buffer solutions of pH 2.2–3.0, by microelectrolysis according to the

method of Gilbert and Rideal[4] was approximately 8, *n* being 7.8 and 7.7 in the 2,2′-compound, 8.1 and 7.7 in the 3,3′-compound, and 8.0 and 7.8 in the 4,4′-compound. From such a fact, it may be assumed that the 1st wave of bis(nitrophenyl)arsinic acids is due to the reduction of the two nitro groups into —NHOH.

$$-NO_2 \xrightarrow[-H_2O]{4e+4H^+} -NHOH$$

*The 2nd Wave.* As shown by the example in Fig. 2, the 2nd wave is composed of complicated wave forms which would be difficult to analyze. The 2nd wave appears only below pH 6 in compounds not possessing $-NO_2$ group in 2-position, the wave disappearing at above pH 7. In the 2,2′-, 2,3′-, and 2,4′-compounds, however, the 2nd wave appears as a complicated wave with a maximum, even at above pH 7 up to pH 10, although the wave height decreases drastically, disappearing at above pH 11. Table II shows the relationship between pH and the 1st and the 2nd wave for all the isomers.

As was mentioned earlier, the half-wave potential of the 2nd wave is difficult to determine, wing to the complicated form of its reduction wave. Moreover, the wave form varies with pH even in one isomer so that it is impossible to compare the half-wave potential of the 2nd wave of each isomer. In each individual isomer,

TABLE II

RELATIONSHIP BETWEEN pH AND 1ST AND 2ND WAVES IN BIS(NITROPHENYL)ARSINIC ACIDS

| Positions of $-NO_2$ | The 1st wave | The 2nd wave |
|---|---|---|
| 2,2′- | pH 1-7: 2-step wave with wave height 1:3<br>pH 8-13: 1-step wave | pH 1-10: 2nd wave observed<br>pH 11-13: not apparent |
| 2,3′- | pH 1-7: 2-step wave with wave height 1:1<br>pH 8-13: 1-step wave | —ditto— |
| 2,4′- | —ditto— | —ditto— |
| 3.3′- | pH 1-13: 1-step wave | pH 1-6: 2nd wave observed<br>pH 7-13: not apparent |
| 3,4′- | —ditto— | —ditto— |
| 4,4′- | —ditto— | —ditto— |

TABLE III

WAVE HEIGHT OF 1ST AND 2ND WAVE AND THEIR RATIO OF BIS(NITROPHENYL)ARSINIC ACIDS

(Sample concentration: $1.14\times10^{-4}$M/l)

| position of $-NO_2$ | | pH 1.04 | pH 2.2 | pH 3.0 | pH 4.0 | pH 5.0 | Mean |
|---|---|---|---|---|---|---|---|
| 2,2′- | 1st wave | 3.63 | 3.60 | 3.71 | 3.62 | ··· | 3.64 |
| | 2nd wave | 3.32 | 3.35 | 3.24 | 2.80 | ··· | 3.18 |
| | ratio | 8 : 7.3 | 8 : 7.5 | 8 : 7.0 | 8 : 6.2 | ··· | 8 : 7.0 |
| 3,3′- | 1st wave | 3.38 | 3.36 | 3.36 | 3.33 | 3.29 | 3.34 |
| | 2nd wave | 3.10 | 3.13 | 3.11 | 2.93 | 2.90 | 3.03 |
| | ratio | 8 : 7.3 | 8 : 7.4 | 8 : 7.4 | 8 : 7.0 | 8 : 7.0 | 8 : 7.3 |
| 4,4′- | 1st wave | 3.54 | 3.35 | 3.34 | 3.33 | 3.32 | 3.38 |
| | 2nd wave | 3.18 | 3.23 | 3.23 | 3.12 | 3.09 | 3.17 |
| | ratio | 8 : 7.2 | 8 : 7.7 | 8 : 7.7 | 8 : 7.5 | 8 : 7.5 | 8 : 7.5 |
| 2,3′- | 1st wave | 3.39 | 3.45 | 3.57 | 3.29 | 3.43 | 3.43 |
| | 2nd wave | 2.94 | 2.96 | 3.08 | 2.90 | 2.87 | 2.95 |
| | ratio | 8 : 6.9 | 8 : 6.9 | 8 : 6.9 | 8 : 7.1 | 8 : 6.9 | 8 : 6.9 |
| 2,4′- | 1st wave | 3.50 | 3.55 | 3.51 | 3.64 | 3.60 | 3.56 |
| | 2nd wave | 3.26 | 3.09 | 3.98 | 3.23 | 3.07 | 3.13 |
| | ratio | 8 : 7.5 | 8 : 7.0 | 8 : 6.8 | 8 : 7.1 | 8 : 6.8 | 8 : 7.4 |
| 3,4′- | 1st wave | 3.64 | 8.64 | 3.72 | 3.37 | 3.33 | 3.54 |
| | 2nd wave | 3.43 | 3.65 | 3.60 | 2.89 | 2.80 | 3.27 |
| | ratio | 8 : 7.5 | 3 : 8.0 | 8 : 7.8 | 8 : 6.9 | 8 : 6.7 | 8 : 7.4 |
| Mean | 1st wave | 3.50 | 3.48 | 3.51 | 3.41 | 3.37 | |
| | 2nd wave | 3.20 | 3.24 | 3.22 | 3.00 | 2.98 | |
| | ratio | 8 : 7.3 | 8 : 7.5 | 8 : 7.3 | 8 : 7.0 | 8 : 7.0 | 8 : 7.2 |

however, the reduction potential tends to shift to the negative side with the increasing pH. As a replacement of comparing the half-wave potential, comparison was made of the potential from the initial portion of the reduction potential to the point of inflexion to the latter stationary phase. As indicated in Fig. 3, the compounds possessing $-NO_2$ group in 2-position give reduction waves in narrower range of potentials than other isomers and the reduction potential shifts to the negative side in the order 2,3′-, 2,4′-, 3,3′-, 3,4′-, 4,4′-, 2,2′-, and diphenylarsinic acid.

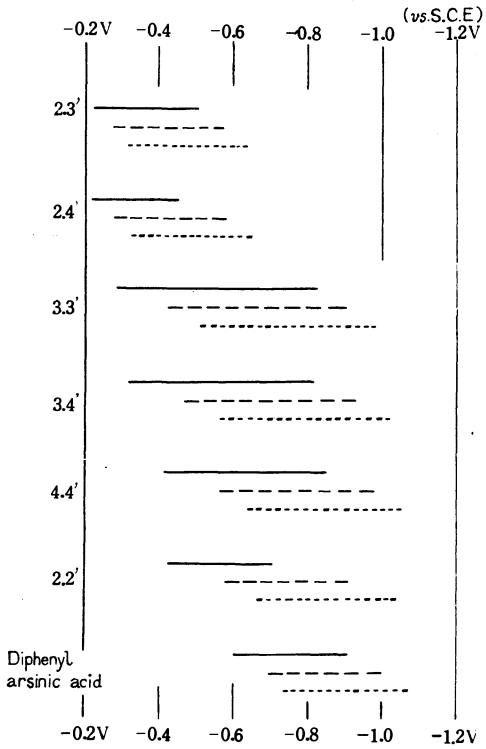
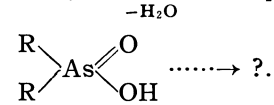



Fig. 3. Relative positions of reduction potential of the 2nd wave in Bis(nitrophenyl)arsinic acids
—— pH 1.04 - - - pH 2.2 ····· pH 3.0

Reduction mechanism of the 2nd wave will next be considered. As will be seen from Table III, the wave height of the 2nd wave is somewhat lower than that of the 1st wave on the acid side and the reduction that could be assumed for the 2nd wave will be in the reduction step of $-NO_2$ group,

$$-NHOH \xrightarrow[-H_2O]{2e+2H^+} -NH_2$$

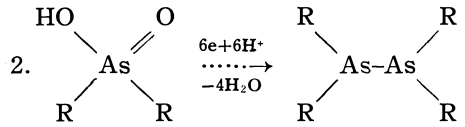
and




$\cdots\cdots\rightarrow$ ?.

Considering the complicated wave form of the 2nd wave, these reactions must occur one after the other and the degree of duplication results in the variation of the breadth of the reduction wave potential, as shown in Fig. 3, and in the variation of wave form.

The number of electrons, $n$, taking part in the reduction was calculated according to the method of Gilbert and Rideal for the 2nd wave and the value of 7.3 for pH 2.2 was obtained in the 2,2′-compound. This result seems to indicate a seven-electron reduction but this is not necessarily conclusive. The value of $n$ calculated for diphenylarsinic acid, without any $-NO_2$ group, was 3.2 and 3.3 at pH 2.2, indicating it to be a three-electron reduction. Since diphenylarsinic acid has the same structure as bis(nitrophenyl)-arsinic acids, with the exception of the absence of $-NO_2$ group, it was assumed that their diffusion coefficients would be approximately equal, and the polarogram of diphenylarsinic acid was taken under identical conditions as those for bis(nitrophenyl)arsinic acids. Subtraction of its wave height from that of the 2nd wave of bis(nitrophenyl)arsinic acids gave a value one-half of that of their 1st waves, i.e. corresponding to a 4-electron reduction from two $-NHOH$ to $NH_2$. Summarizing these facts, it may be assumed that the 2nd wave consists of four-electron reduction of two $-NHOH$ to $-NH_2$ and a three-electron reduction of arsenic. The following type may be considered for the reduction of arsenic:




However, the state of reduction of diphenylarsinic acid may be vastly different and it would be too dangerous to conclude from these results that the foregoing facts indicate a three-electron reduction of arsenic. Further studies on this matter seem to be necessary.

**(2) Effect of Various Factors on the Limiting Current of Bis(nitrophenyl)-arsinic Acids.**

*a) Relationship between Concentration and Limiting Current.*—Polarograms of 2,2′-, 3,3′-, and 4,4′-compounds were taken in a buffer solution of pH 2.2 in various concentrations and the wave height of 1st and 2nd waves were measured. For example, the result of 2,2′-compounds is

presented in Table IV.

It is seen that there is a proportionality between the concentration and the limiting current in both the 1st and the 2nd wave in each of these compounds and $i_d/C$ of the 1st and the 2nd wave in these compounds seem to be approximately equal.

TABLE IV
LIMITING CURRENT VS. CONCENTRATION

2,2'-Bis(nitrophenyl)arsinic acid

| Concentration | 1st wave | | 2nd wave | |
|---|---|---|---|---|
| | $i_d$ | $i_d/C$ | $i_d$ | $i_d/C$ |
| (mM/l) | ($\mu$amp.) | ($\mu$amp./mM) | ($\mu$amp.) | ($\mu$amp./mM) |
| 0.034 | 1.15 | 33.8 | 0.96 | 28.2 |
| 0.046 | 1.50 | 32.6 | 1.23 | 26.7 |
| 0.068 | 2.19 | 32.2 | 1.89 | 27.8 |
| 0.080 | 2.45 | 30.6 | 2.13 | 26.6 |
| 0.091 | 3.10 | 34.1 | 2.77 | 30.4 |
| 0.102 | 3.38 | 33.0 | 2.90 | 28.4 |
| 0.114 | 3.79 | 33.2 | 3.39 | 29.7 |
| 0.123 | 4.13 | 33.0 | 3.84 | 30.7 |
| 0.136 | 4.52 | 33.2 | 3.99 | 29.3 |
| 0.148 | 4.81 | 32.5 | 4.35 | 29.4 |
| 0.159 | 5.10 | 32.1 | 4.61 | 29.0 |
| Mean | | 32.75±0.81 | | 28.74±0.94 |

*b) Relationship between Temperature and Limiting Current.*—Limiting current of the 1st and the 2nd wave was determined from the polarograms of 2,2'-, 3,3'- and 4,4'-compounds in a buffer solution of pH 4.0, sample concentration being $2\times10^{-4}$ M, at 30°, 25°, 20°, 15° and 10°C. The results obtained from the 1st wave indicate that there is a proportionality between the temperature and the limiting current in both 3,3'- and 4,4'-compound in this temperature range. The temperature coefficients of 3,3' and 4,4'-compounds in this case are 1.59% and 1.61%. These coefficients are appoximately equal to that in the case of ordinary diffusion current. The measurement was impossible with the 2,2'-compound since the solubilities decrease below 20°C, at this concentration and pH, and the compound precipitates out.

$$\left\{\left(\frac{i_d(t_1)}{i_d(t_2)}\right)^{1/t_2-t_1}-1\right\}\times100\%$$

*c) Relationship between the Height of Mercury Reservoir and Limiting Current.*—Polarograms of 2,2'-, 3,3'- and 4,4'-compounds in a buffer solution of pH 2.2, in a concentration of $1.14\times10^{-4}$ M, with varying heights of the mercury reservoir and the wave heights of the 1st and the 2nd wave were measured. As indicated in Table V, the results of 2,2'-compound and diphenyl arsinic acid are presented only, a linear relationship was found to hold between the limiting current and the square root of the height of mercury reservoir $h^{1/2}{}_{eff.}$ In other words, these limiting currents do not contain any kinetic current but are controlled by the diffusion process.

**(3) Determination of Bis(nitrophenyl)arsinic Acid Mixture.**—As was

TABLE V
LIMITING CURRENT VS. EFFECTIVE HEIGHT OF THE MERCURY RESERVOIR 2,2'-BIS (NITRO PHENYL) ARSINIC ACID

| $h_{eff.}^{1/2}$ | 1st wave | | 2nd wave | |
|---|---|---|---|---|
| | $i_d$ | $i_d/h_{eff.}^{1/2}$ | $i_d$ | $i_d/h_{eff.}^{1/2}$ |
| ($h$:cm.) | ($\mu$amp.) | | ($\mu$amp.) | |
| 9.19 | 5.66 | 0.63 | 4.98 | 0.54 |
| 8.63 | 5.29 | 0.61 | 4.61 | 0.53 |
| 8.03 | 4.99 | 0.62 | 4.41 | 0.55 |
| 7.38 | 4.58 | 0.62 | 4.04 | 0.55 |
| 6.67 | 4.18 | 0.63 | 3.57 | 0.54 |
| 5.87 | 3.71 | 0.63 | 3.20 | 0.55 |

Diphenyl arsinic acid
(concn.:$2\times10^{-4}$M/l)

| $h_{eff.}^{1/2}$ ($h$:cm.) | $i_d$($\mu$amp.) | $i_d/h_{eff.}^{1/2}$ |
|---|---|---|
| 8.91 | 4.40 | 0.49 |
| 8.03 | 3.94 | 0.49 |
| 7.38 | 3.55 | 0.48 |
| 6.28 | 3.00 | 0.48 |

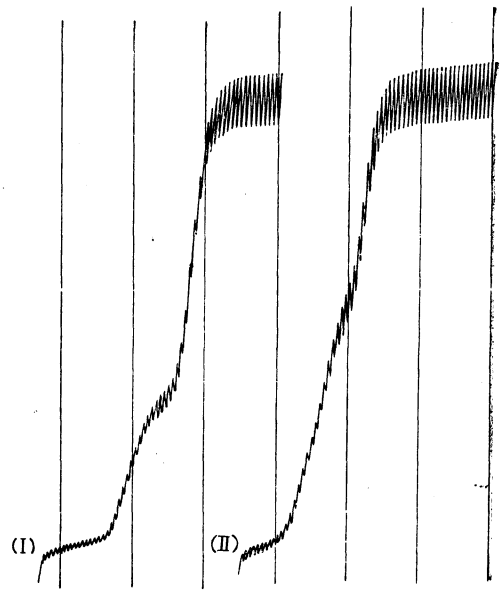



Fig. 4. Typical polarograms of synthetic mixtures of Bis(nitrophenyl)arsinic acids.
(I) 2,2'- : 3,3'-=30 : 70(wt%)
(II) 2,2'- : 4,4'-=50 : 50( ,, )

mentioned earlier, the compounds possessing $-NO_2$ group in 2-position exhibit a reduction wave of the 1st wave in a more positive potential range than those with $-NO_2$ group in other positions and consequently show a divided wave (Fig. 4).

It follows, therefore, that the determination of a mixture of 2,2′- and 3,3′- or 4,4′-bis(nitropenyl)arsinic acid can be made concurrently by determining the 2,2′-compound from the 1st step in the 1st wave and 3,3′- or 4,4′-compound from the 2nd step wave that appears next. Tables VI and VII give results of determination carried out on several mixed samples by the standard addition method.

TABLE VI
DETERMINATION OF A SYNTHETIC MIXTURE OF 2,2′- AND 3,3′-BIS(NITROPHENYL)ARSINIC ACIDS

| No. | Calculated Value (wt. %) | | Observated Value (wt. %) | |
|---|---|---|---|---|
| | 2,2′- | 3,3′- | 2,2′- | 3,3′- |
| 1 | 10.0 | 90.0 | 10.1 | 89.9 |
| 2 | 20.0 | 80.0 | 19.5 | 80.5 |
| 3 | 30.0 | 70.0 | 30.4 | 69.6 |
| 4 | 40.0 | 60.0 | 39.5 | 60.5 |
| 5 | 50.0 | 50.0 | 49.8 | 50.2 |
| 6 | 60.0 | 40.0 | 60.0 | 40.0 |
| 7 | 70.0 | 30.0 | 69.2 | 30.8 |
| 8 | 80.0 | 20.0 | 78.8 | 21.2 |
| 9 | 90.0 | 10.0 | 85.6 | 14.4 |

TABLE VII
DETERMINATION OF A SYNTHETIC MIXTURE OF 2,2′- AND 4,4′-BIS(NITROPHENYL)ARSINIC ACIDS

| No. | Calculated Value (wt. %) | | Observated Value (wt. %) | |
|---|---|---|---|---|
| | 2,2′- | 4,4′- | 2,2′- | 4,4′- |
| 1 | 20.0 | 80.0 | 20.4 | 79.6 |
| 2 | 50.0 | 50.0 | 48.3 | 51.7 |
| 3 | 70.0 | 30.0 | 69.3 | 30.7 |

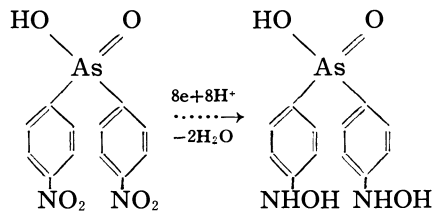
Separatory determination of a mixture of 3,3′- and 4,4′-bis(nitrophenyl)arsinic acids is impossible since such a mixture does not exhibit separate waves but the value of $i_d/C$ is approximately equal in the two compounds so that the approximate value of the content can be obtained.

Mixtures of non-symmetrically substituted 2,3′-, 2,4′-, and 3,4′-compound cannot be determined although the presence of a compound with $-NO_2$ group in the 2-position can be detected from their 1st wave, as is evident from their reduction wave.

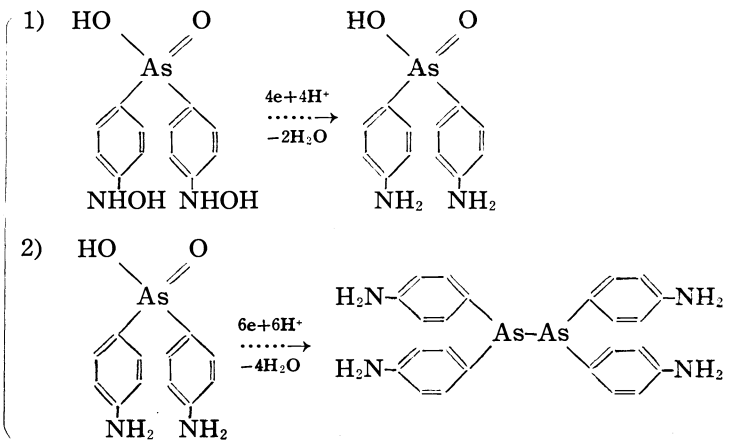
## Summary

1) Polarographic behavior of the six isomers of bis(nitrophenyl)arsinic acid was considered and the waves can roughly be divided into 1st and 2nd waves in acid range at the dropping mercury electrode.

The 1st Wave:




The 2nd Wave:



2) The limiting current is controlled by the diffusion process and the Ilkovič equation is applicable.

3) The electrolytic reduction mechanisms of the 1st and 2nd waves are considered to be in the following manner, taking that of 4,4′-bis(nitropenyl)arsinic acid as an example: (see the figure of the preceding page).

4) By the utilization of the 1st wave, polarography can be used for the determination of bis(nitrophenyl)arsinic acids, especially those with the nitro group in 2-position.

The writers express their deep gratitude to Professor T. Sohmiya for much valuable advice during the course of this work and are grateful to Messrs. M. Ishiwatari and S. Yokouchi for supplying them with samples.

*Engineering Research Institute*
*Faculty of Engineering*
*University of Tokyo*
*Hongo, Tokyo*

# *Polarography of Bis(aminophenyl)arsinic Acids, Phenylarsonic Acid and Arsanilic Acids**

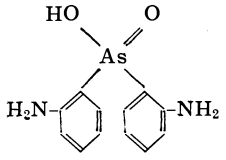
By Masao MARUYAMA and Toshiko FURUYA

(Received January 17, 1957)

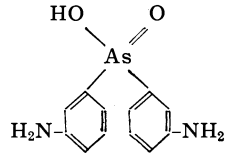
The writers stated in the preceding paper[1] that, on considering the polarographic behavior of bis(nitrophenyl)arsinic acids at the dropping mercury electrode, the 2nd wave that appears in an acid range may contain waves due to a three-electron reduction of arsenic. In order to further clarify this fact and also the polarographic behavior of organic arsenic compounds, reduction waves of bis(aminophenyl)arsinic acids, phenylarsonic acid, and arsanilic acids at the dropping mercury electrode were examined. The present paper also describes the results obtained from experiments on fundamental data for quantitative determinations.

## Experimental

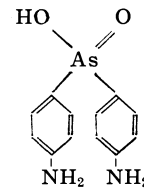
The four isomers of bis(aminophenyl)arsinic acids according to the position of the amino group, 2,2'-(I), 3,3'-(II), 4,4'-(III), and 3,4'-(IV), were used as the sample. Their respective melting points are shown with their structures:



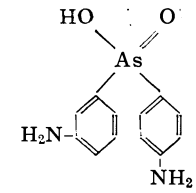

(I)
m.p. 154°C




(II)
m.p. 247°C

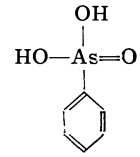



(III)
m.p. 223.5°C (decomp.)

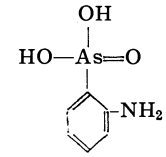



(IV)
m.p. 182°C

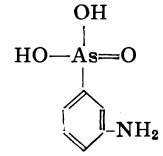
The melting points of phenylarsonic acid and arsanilic acids used for the experiment are as follows:



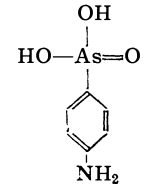

(V)
m.p. 158.5°C




(VI)
m.p. 144°C




(VII)
m.p. 207°C (decomp.)




(VIII)
m.p. 232°C

Experimental conditions and methods used in the present experiments were all the same as those described in the preceding paper[1].

* The gist of this work was presented at the symposium of the Japanese Society of Analytical Chemistry (May; 1955).

1) M. Maruyama and T. Furuya, This Bulletin., **30**, 647 (1957).

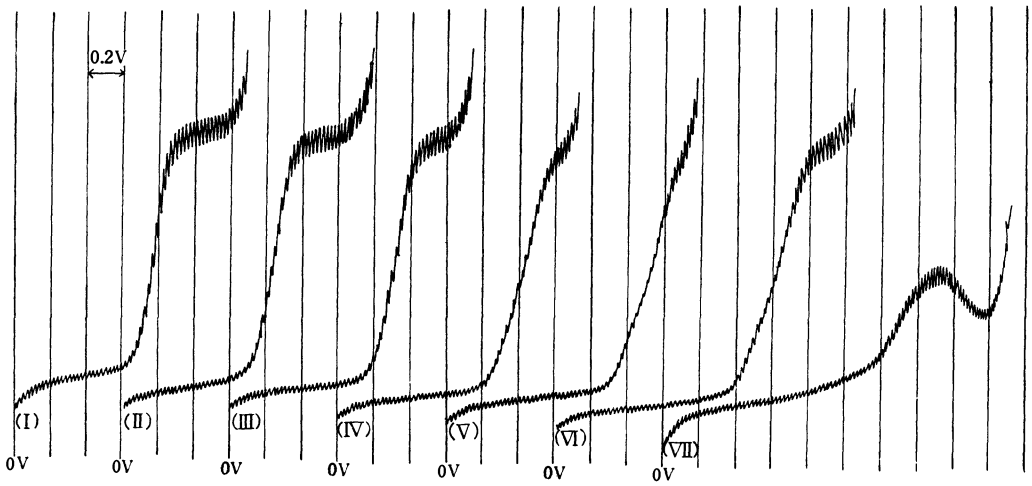



Fig. 1. Typical polarograms of 4,4'-Bis(aminophenyl)arsinic acid in buffer solution at various pH values.
(I) pH 1.04 (II) pH 2.2 (III) pH 3.0 (IV) pH 4.0 (V) pH 5.0
(VI) pH 6.0 (VII) pH 7.0

## Experimental Results and Discussion

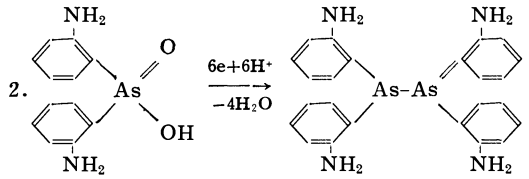
(1) **Reduction of Bis(aminophenyl) arsinic Acids in Buffers Solutions of Various pH.**—2,2'-, 3,3'-, 4,4'-, and 3,4'-Bis (aminophenyl)arsinic acids and diphenylarsinic acid show irreversible reduction wave below pH 7 (polarogram of 4,4'-compound at various pH is shown in Fig. 1 as an example). The wave form is a one-step wave at pH 1 to 3 and a complicated wave form, similar to that of diphenylarsinic acid, appears at pH 4 to 6. As was described in the preceding paper, diphenylarsinic acid shows a very similar, complicated wave form at pH 1 to 5 and an irreversible, three-electron reduction at around pH 2 to 3.

The half-wave potentials in all these compounds shift to the negative side with increasing values of pH, more markedly so in the 2,2-compound than the other isomers, and those of the other three isomers are very close together. The half-wave potentials of these compounds are indicated in Table I.

TABLE I
HALF WAVE POTENTIALS OF BIS(AMINOPHENYL)-ARSINIC ACIDS AT VARIOUS pH VALUES
$\pi_{1/2}$ mV(vs. S.C.E.).

| pH | 4,4'- | 3,4'- | 3,3'- | 2,2'- |
|---|---|---|---|---|
| 1.04 | − 775 | − 782 | − 800 | − 873 |
| 2.2 | − 845 | − 835 | − 872 | − 965 |
| 3.0 | − 905 | − 913 | − 930 | −1078 |
| 4.0 | − 990 | −1010 | −1030 | −1170 |
| 5.0 | −1100 | −1107 | −1140 | −1370 |
| 6.0 | −1212 | −1213 | −1284 | ··· |

The wave height is approximately constant in the acid range, irrespective of pH, except for 2,2'-compound, and decreases suddenly at above pH 6. For the 2,2'-compound, the wave height tends to decrease somewhat with increasing pH values. As will be described later, the limiting current is controlled by the diffusion process and the number of electrons, *n*, taking part in the reduction, obtained by the microelectrolysis, was 3 for all the compounds at pH 2–3. These results suggest the following type as the reduction mechanism:




(2) **Effect of Various Factors on the Limiting Current of Bis(aminophenyl) arsinic Acids.**—

a) *Relationship between Concentration and Limiting Current:* The limiting current of 2,2'-, 3,3'- and 4,4'-bis(aminophenyl) arsinic acid and diphenylarsinic acid was measured in various concentrations in buffer solution of pH 2.2 and the results of 4,4'-compound and diphenylarsinic acid are presented in Table II. Other 2,2'-, 3,3'-compound had the same result.

b) *Relationship between Temperature and Limiting Current:* The results of measurement with various isomers and diphenyl arsinic acid indicate that the limiting

TABLE II
LIMITING CURRENT VS. CONCENTRATION

a) 4,4'-Bis(aminophenyl)arsinic acid

| $C$(mM/l) | $i_d$(μamp.) | $i_d/C$(μamp./mM) |
|---|---|---|
| 0.339 | 4.21 | 12.4 |
| 0.271 | 3.33 | 12.3 |
| 0.203 | 2.48 | 12.2 |
| 0.136 | 1.63 | 12.0 |
| 0.068 | 0.87 | 12.8 |
| | | 12.35±0.41 |

As can be seen from Table II, a proportionality is established between the concentration and the limiting current in all these compounds.

b) Diphenyl arsinic acid

| $C$(mM/l) | $i_d$(μamp.) | $i_d/C$(μamp./mM) |
|---|---|---|
| 0.163 | 2.31 | 14.2 |
| 0.126 | 1.69 | 13.4 |
| 0.082 | 1.11 | 13.6 |
| 0.041 | 0.57 | 13.9 |
| Mean | | 13.78±0.58 |

current increases in proportion to the rise of temperature and the temperature coefficients of 2, 2'-, 3, 3'-, and 4,4'-compound, dephenyl arsinic acid in this case are 1.36%, 1.46%, 1.39% and 1.38%. These coefficients agree approximately with that in the case of diffusion current.

c) *The Relationship between the Height of Mercury Reservoir and Limiting Current:* The results of measurement with various isomers, (shown in Table III; the result of 4,4'-compound is shown as an example), indicate that a linear relationship exists between the limiting current and the square root of the height of the mercury reservoir, $h_{eff.}^{1/2}$, i. e. these limiting currents are controlled by the diffusion process.

TABLE III
LIMITING CURRENT VS. EFFECTIVE HEIGHT OF MERCURY RESERVOIR
4,4'-BIS(AMINOPHENYL)ARSINIC ACID

(Concn.: $3.39\times10^{-4}$M, pH: 2.2)

| | | | | | |
|---|---|---|---|---|---|
| $h_{eff.}^{1/2}$($h$: cm.) | 7.75 | 8.06 | 8.37 | 8.66 | 8.94 |
| $i_d$(μAmp.) | 4.15 | 4.27 | 4.43 | 4.57 | 4.72 |
| $i_d/h_{eff.}^{1/2}$ | 0.54 | 0.53 | 0.53 | 0.53 | 0.53 |

(3) **Reduction of Phenylarsonic Acid and Arsanilic Acids in Buffer Solutions of Various pH.**—The reduction wave of arsanilic acids appear at pH 1 to 3 and 2-, 3- and 4-arsanilic acid and phenylarsonic acid show irreversible waves with similar wave heights and wave forms (Fig. 2).

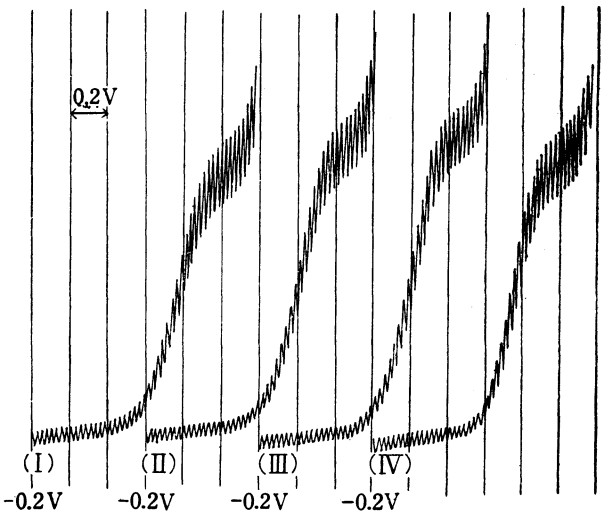


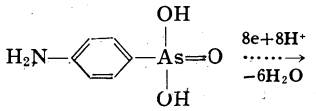

Fig. 2. Typical polarograms of arsanilic acids, phenylarsonic acid in buffer solution at pH 1.04.
(I) 2-Arsanilic acid
(II) 3-Arsanilic acid
(III) 4-Arsanilic acid
(IV) Phenylarsonic acid

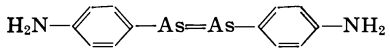
The wave height is approximately constant at pH 1 to 3 but decreases rapidly at above pH 4. The half-wave potentials shift to the negative side with increasing pH values and the values tend to become negative in the order of phenylarsonic acid, and 2-, 3- and 4-arsanilic acid at the same pH, though the difference is very slight (Table IV).

TABLE IV
HALF-WAVE POTENTIALS OF PHENYLARSONIC ACID AND ARSANILIC ACIDS IN BUFFER SOLUTION
$\pi_{1/2}$mV. (vs. S.C.E.)

| pH | Phenylarsonic acid | 2-Arsanilic acid | 3-Arsanilic acid | 4-Arsanilic acid |
|---|---|---|---|---|
| 1.04 | − 955 | − 960 | − 976 | − 985 |
| 2.2 | −1060 | −1072 | −1080 | −1098 |
| 3.0 | −1175 | −1176 | −1175 | −1185 |

The limiting current of these compounds is controlled by the diffusion process and the number of electrons, $n$, taking part in the reduction, obtained by the microelectrolysis, a buffer solution of pH 2.2, was approximately 4, indicating a four-electron reduction. If such is the case, the following type of reduction mechanism may be considered.





**(4) Effect of Various Factors on the Limiting Current of Phenylarsonic Acid and Arsanilic Acids.—**

a) *Relationship between Concentration and Limiting Current:* The results of measurement of limiting current of phenylarsonic acid and various isomers of arsanilic acid in a buffer solution of pH 2.2, at various concentrations, (as shown in Table V, the results of 4-arsanilic acid and phenyl arsinic acid are shown as an example), indicated that a linear relationship exists between concentration and limiting current.

TABLE V
LIMITING CURRENT VS. CONCENTRATION

a) 4-Arsanilic acid

| $C$(mM) | $i_d$(μamp.) | $i_d/C$(μamp./mM) |
|---|---|---|
| 0.538 | 10.67 | 19.8 |
| 0.428 | 8.42 | 19.7 |
| 0.321 | 6.27 | 19.5 |
| 0.214 | 4.17 | 19.5 |
| 0.107 | 2.08 | 19.4 |
| Mean | | 19.59±0.20 |

b) Phenyl arsinic acid

| $C$(mM) | $i_d$(μamp.) | $i_d/C$(μamp./mM) |
|---|---|---|
| 0.520 | 10.30 | 19.8 |
| 0.416 | 8.42 | 20.2 |
| 0.312 | 6.17 | 19.8 |
| 0.208 | 4.07 | 19.6 |
| 0.104 | 1.94 | 18.7 |
| Mean | | 19.61±0.77 |

b) *Relationship between Temperature and Limiting Current:* The results of measurement in a buffer solution of pH 2.2, indicated that the limiting current increases in proportion to the rise of temperature and the temperature coefficients of 4-, 3- and 2- arsanilic acid and phenyl arsinic acid are 1.27%, 1.39%, 1.28% and 1.52%. These coefficient agreed approximately with that in the case of diffusion current.

c) *Relationship between the Height of the Mercury Reservoir and Limiting Current:* The results obtained from the measurement in a buffer solution of pH 2.2, (shown in Table VI) (only 4-arsanilic acid and phenyl arsinic acid), indicate that a linear relationship is established between the square root of the height of the mercury reservoir, $h_{eff.}^{1/2}$ and the limiting current. Therefore, the limiting current does not contain a kinetic current but is controlled by the diffusion process.

TABLE VI
LIMITING CURRENT AND EFFECT HEIGHT OF MERCURY RESERVOIR

a) 4-Arsanilic acid (Conc.: $3.21\times10^{-4}$M)

| $h_{eff.}^{1/2}$($h$: cm.) | 7.75 | 8.06 | 8.37 | 8.66 | 8.94 |
|---|---|---|---|---|---|
| $i_d$(μamp.) | 5.69 | 5.96 | 6.26 | 6.36 | 6.60 |
| $i_d/h_{eff.}^{1/2}$ | 0.74 | 0.74 | 0.75 | 0.73 | 0.74 |

b) Phenyl arsonic acid (Concn.: $3.12\times10^{-4}$M)

| $h_{eff.}^{1/2}$($h$: cm.) | 7.75 | 8.06 | 8.37 | 8.66 | 8.94 |
|---|---|---|---|---|---|
| $i_d$(μamp.) | 5.18 | 5.63 | 5.79 | 5.93 | 6.09 |
| $i_d/h_{eff.}^{1/2}$ | 0.67 | 0.70 | 0.69 | 0.69 | 0.68 |

**(5) Determination of Bis(aminophenyl)arsinic Acids in Arsanilic Acid.** —The foregoing facts indicate that it is possible to determine bis(aminophenyl) arsinic acids and arsanilic acids individually by polarography but separatory determination of their isomers is impossible, considering the wave form and the half-wave potential of the reduction wave.

The problem in industrial process is the determination of bis(aminophenyl)arsinic acids in 4-arsanilic acid, the former being often present as an impurity in the latter during synthetic process. There has been no suitable method of determining this compound and some difficulties have been experienced.

However, the foregoing facts suggest the possibility of the utilization of polarographic method for this purpose. Actually, reduction at the dropping mercury electrode gives a separate wave (occurs first) by bis(aminophenyl)arsinic acids and its determination in 4-arsanilic acid is possible from this wave height.

Analytical results obtained with several kinds of synthetic sample are presented in Table VII.

TABLE VII
DETERMINATION OF BIS(AMINOPHENYL)ARSINIC ACID IN 4-ARSANILIC ACID

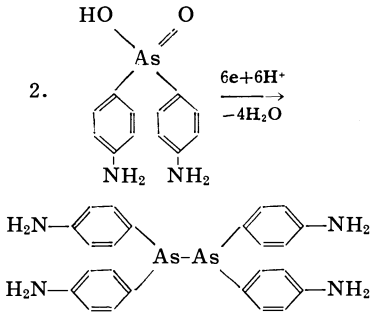
| No. | Calculated Value (%) 4-Arsanilic acid | Calculated Value (%) Bis(aminophenyl) arsinic acid | Observated Value (%) Bis(aminophenyl) arsinic acid |
|---|---|---|---|
| 1 | 85.0 | 15.0 | 14.0 |
| 2 | 70.0 | 30.0 | 30.1 |
| 3 | 60.0 | 40.0 | 41.7 |
| 4 | 40.0 | 60.0 | 56.0 |
| 5 | 20.0 | 80.0 | 76.0 |

## Summary

1) Polarographic behaviors of bis(aminophenyl)arsinic acids, phenylarsonic

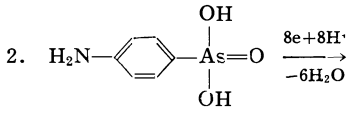
acid and arsanilic acids, were examined with dropping mercury electrode.

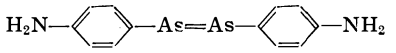
2) The reduction wave of bis(aminophenyl)arsinic acids appearing on the acid side is an irreversible three-electron reduction and this reduction mechanism is considered to be of the following type.



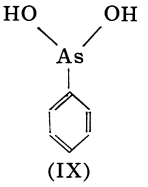
3) An assumption was forwarded in the preceding paper that the 2nd wave shown by bis(nitrophenyl)arsinic acids on the acid side may contain a reduction wave owing to the reduction of arsenic and that it is more likely to be a three-electron rather than a 4-electron reduction. The foregoing results obtained with bis(aminophenyl)arsinic acids suggest that it would be more appropriate to consider an irreversible, three-electron reduction.

4) The reduction waves shown by phenylarsonic acid and arsanilic acids on the acid side are an irreversible, four-electron reduction and the reduction mechanism may be assumed as follows:





5) Compounds like phenylarsinic acid (IX) do not exhibit a reduction wave at the dropping mercury electrode.



(IX)

6) Summarizing the foregoing facts, it may be concluded that these organic arsenic compounds which show a reduction wave at the dropping mercury electrode are quiquevalent arsenic compounds, the reduction wave is that of quinquevalent to tervalent, and that the compounds not possessing As=O are not reduced.

7) The limiting current of these compounds in the acid side is controlled by the diffusion process and is in proportional relationship with the concentration, so that it can be utilized for quantitative analysis.

The writers express their deep gratitude to Professor T. Sohmiya for much valuable advice during the course of this work and are grateful to Messrs. M. Ishiwatari and S. Yokouchi for supplying them with samples.

*Engineering Research Institute*
*Faculty of Engineering*
*University of Tokyo*
*Hongo, Tokyo*

# *Studies on the Mechanism of Eder's Reaction. I. Inducing Photochemical Reaction of Manganese(II)-Oxalate System*

By Shukichi SAKURABA and Shozo IKEYA

(Received August 9, 1956)

## Introduction

Since Eder's paper[1] (1880) the mechanism of the reduction of mercury(II) chloride to mercury(I) chloride with oxalate in a photochemically inducing system[2,3] or in the presence of an inducing catalyst[4,5] has long been studied. Considerable number of literature on the inducing action of $MnO_4^-$—$C_2O_4^{2-}$[6,7] or Mn(III)-$C_2O_4^{2-}$ system[8,9] are found but little has been done on Mn(II)—$C_2O_4^{2-}$ inducing system.

It has been previously reported that in a photochemical sensitive system of Mn (II)—$C_2O_4^{2-}$, mercury(II)chloride is quantitatively reduced to mercury(I) chloride[10]. The present investigation has been undertaken to elucidate the properties of an active intermediate formed by the ultraviolet irradiation on the solution containing the manganese(II) and the oxalate ion. They were persuaded by the estimation of its reducing power towards mercury (II) chloride and by the measurement of the change in absorbance of the reaction mixture.

This active intermediate appears to be correlated with the formation of active oxalic acid on the decomposition of manganese(III)-oxalate complex[11,12], and also with that of hydrogen peroxide on the oxidation of oxalic acid in the presence of the manganese(II) ion[13,14].

1) J R Eder, *Ber.*, **13**, 166 (1880).
2) W. E. Roseveare, *J. Am. Cem. Soc* **51**, 1716 (1929), **52**, 2612 (1930).
3) E. A. Hausman and I. W. Davis, ibid., **76**, 5341 (1954).
4) G. H. Cartledge and T. G. Djang, ibid., **55**, 3214 (1933).
5) G. H. Cartledge, ibid., **63**, 906 (1941).
6) N. Dhar, *J. Chem Soc.*, **111**, 690, 602 (1917).
7) F. Oberhauser and W. Hensinger, *Ber.*, **61**, 521 (1928).
8) K. Weber, *Z. Physik Chem.*, **B25**, 363 (1934), **A172**, 459 (1935).
9) K Weber and A. Rezek. *Ber.*, **70**, 407 (1937).
10) S Sakuraba and S. Ikeya, *J. Chem. Soc. Japan Pure Chem. Sect.*, **77**, 22 (1956)
11) H. Taube, *J. Am Chem. Soc*, **69**, 1418 (1947); **70**, 1216 (1948).
12) F. R. Duke, ibid., **69**, 2885 (1947).
13) P S. MacMahon and B. B. Lal, *J. Indian Chem. Soc*, **20**, 143 (1943).
14) E. Abel, *Monatsh*, **83**, 695 (1952).

## Experimental Results

**Material.**—Sodium oxalate solution (0.100 M) was prepared from Merck's analytical grade chemical.

Manganese(II) sulfate solution (0.0140 M) was prepared from the guaranteed reagent labeled as containing below 0.002% Fe, and standardized by the Volhard method.

Mercury(II) chloride of extra pure grade was further recrystallized three times, and dissolved in water to produce 0.0489 M solution, its 1 ml. containing 0.01353 g. of mercury(II) chloride.

De-ionised water was used for all work.

**Apparatus.**—A low pressure mercury lamp (Kojima Type KY3C, 100V, 3A) was used for ultraviolet irradiation.

A model EPU quartz spectrophotometer (Hitachi, with 1 cm. cells) was used for all absorbance measurements.

**Procedure.**—To avoid an influence of the dissolved oxygen, nitrogen or carbon dioxide gas was passed through the test solution in a quartz flask for 40 min., then the solution was irradiated for various times. To examine the effect of dissolved oxygen, the solution was irradiated directly from the upside of the solution in the air. Experiments were carried out in the dark room.

**1) Photochemical Reduction of Mercury (II) chloride to Mercury(I) chloride.**

*i) Formation of Mercury (I) chloride in the Absence of Oxygen.*—To examine the effect of the manganese(II) ion on the photochemical reaction of mercury(II) chloride and oxalate, two kinds of solution were prepared as under annotation in Table I. A is 0.030 M sodium oxalate solution containing 0.1353 g. mercury(II) chloride per 50 ml. B is 0.030 M sodium oxalate solution containing 0.0001 to 0.002 M manganese(II) sulfate, and 0.1353 g. of mercury(II) chloride per 50 ml. In these solutions, no reaction occured in the dark at room temperature, regardless of the presence of the manganese(II) ion. When the solution was exposed to ultraviolet rays of mercury lamp after removal of dissolved oxygen, reaction took place instantly to form mercury(I) chloride. Experiments were done to analyse the effect of the concentration of the manganese(II) ion and of the hydrogen ion, on the reaction rate; the results are shown in Table I.

The presence of the manganese(II) ion makes the reduction rate about twice as great as in its absence (Table I, group 1). However, change in the manganese(II) ion concentration little affects the reduction rate in the range 0.0001 to

TABLE I
FORMATION OF MERCURY(I) CHLORIDE IN THE ABSENCE OF OXYGEN

| Group of Expt. | | No. of Expt. | $MnSO_4$ M./l. | pH | $Hg_2Cl_2$ found g. | % |
|---|---|---|---|---|---|---|
| Group 1. | A | 1 | 0. | 5.6 | 0.0450 | 38.3 |
| | 〃 | 2 | 0. | 3.2 | 0.0441 | 37.5 |
| | B | 3 | 0.0001 | 5.6 | 0.0890 | 75.7 |
| | 〃 | 4 | 0.0001 | 3.2 | 0.0862 | 73.3 |
| | 〃 | 5 | 0.001 | 5.6 | 0.0813 | 69.1 |
| | 〃 | 6 | 0.002 | 〃 | 0.0862 | 73.3 |
| Group 2. | B | 1 | 0.002 | 5.6 | 0.1147 | 97.5 |
| | 〃 | 2 | 〃 | 4.0 | 0.1164 | 99.0 |
| | 〃 | 3 | 〃 | 3.2 | 0.1170 | 99.5 |
| | 〃 | 4 | 〃 | 1.8 | 0.1142 | 97.1 |

Total volume is 50 ml. Each solution is 0.030 M sodium oxalate, containing 0.1353 g. of mercury(II) chloride (corresponding to 0.1176 g. of mercury(I)chloride).; pH is controlled by sulfuric acid; A: Solution A. B: Solution B. Time of irradiation, 10 min. in Group 1; 30 min., in group 2.;

0.002 M; neither does the pH ragardless of the presence of the manganese(II) ion (Table I, group 1 and 2). Moreover in this reaction system, neither manganese(III) oxalate complex nor hydrogen peroxide is formed in the absence of oxygen. They are formed, however, in its presence in the same system.

*ii) Formation of Mercury(I) chloride in the Presence of Oxygen.*—The same solution in an equilibrium state with atomspheric oxygen was directly irradiated from upside, for an hour at 30°C. Results are given in Table II.

TABLE II
FORMATION OF MERCURY(I) CHLOLIDE IN THE AIR

| Group of Expt. | | No. of Expt. | $MnSO_4$ M./l. | pH | $Hg_2Cl_2$ found, g. | % |
|---|---|---|---|---|---|---|
| Group 3. | A | 1 | 0. | 3.2 | a little | |
| | B | 2 | 0.0001 | 〃 | 0.1169 | 99.4 |
| | 〃 | 3 | 0.001 | 〃 | 0.1168 | 99.3 |
| | 〃 | 4 | 0.002 | 〃 | 0.1175 | 99.9 |
| Group 4. | B | 1 | 0.002 | 5.6 | 0.0790 | 67.2 |
| | 〃 | 2 | 〃 | 4.0 | 0.1145 | 97.4 |
| | 〃 | 3 | 〃 | 3.2 | 0.1178 | 100.2 |
| | 〃 | 4 | 〃 | 1.8 | 0.0359 | 30.5 |

Total volume is 50 ml. Each solution is 0.030 M sodium oxalate, containing 0.1353 g of mercury(II) chloride (corresponding to 0.1176 g. of mercury (1) chloride); pH is controlled by sulfuric acid; Time of irradiation, 60 min. in Group 3 and 4.

It will be seen that in Solution A (without the manganese ion), the reaction is markedly inhibited by dissolved oxygen (Table II, group 3). However, in Solution B (containing the manganese ion) the reaction proceeds significantly, although inhibited by oxygen to some extent at a higher and a lower pH than about 3.2 (compare Table II, group 4 with Table I, group 2). Moreover, the upper part of Solution B assumed faint purpulish red, indicating the presence of manganese(III)-oxalate complex; the formation of hydrogen peroxide is also confirmed by the titanium method. These phenomena will be discussed below.

*iii) Presence of an Active Intermediate.*—In the experiments hither to described, the photochemical action was examined in solutions containing the manganese(II), the oxalate and the mercury(II) ion. The following experiments were carried out to ascertain that an active intermediate is produced in the solution containing neither mercury(II) chloride nor dissolved oxygen, and that it will remain active for a fairly long time and forms the manganese(III) ion and hydrogen peroxide in the atmosphere.

Two kinds of test solution were prepared: Solution C is 0.030 M sodium oxalate and Solution D is 0.030 M sodium oxalate solution, containing 0.002 M manganese sulfate. The pH of the solution was adjusted to 3.2 with surfuric acid. These solutions were irradiated for 30 min. under an atmosphere of carbon dioxide after removal of the dissolved oxygen. Being set aside for various times under an atmosphere of carbon dioxide after irradiation, each solution was treated with 10 ml. of the oxygen-freed mercury(II) chloride solution to make the total volume 50 ml. The resulting Solution C and D are named Mixture C and D, respectively.

The following phenomena were observed. In Mixture C no appreciable reduction took place immediately after irradiation, even if the mixture was exposed to the atmosphere. In Mixture D mercury(I) chloride was formed in the following manner: after 2 min., dense turbidity; after 30 min., apparent; after 3 hours, slight; after 20 hours, no turbidity. When these mixtures were exposed to the air, the precipitate was gradually increased in proportion to the initial quantity. Moreover, hydrogen peroxide was not produced in Mixture C and D in the atmosphere of carbon dioxide; it was formed, however, in Mixture D when this was exposed to the air. When Mixture D was exposed to the air and large quantity of mercury(I) chloride precipitated, the upper part of the solution assumed faint purplish red, indicating the presence of manganese(III) complex. When oxygen was vigorously passed through the irradiated Solution D for a few minutes, the solution losed its reducing power.

The experiments turned out as expected. An active intermediate is formed in the oxalate solution containing the manganese(II) ion by ultraviolet irradiation. The intermediate is able to reduce mercury(II) chloride even after interception of light and survives for several hours at room temperature in the absence of oxygen. When it reacts slowly with dissolved oxygen in the

presence of mercury(II) chloride, it forms a detectable amount of manganese(III) complex and hydrogen peroxide, but when it reacts with bubbling oxygen in the solution, it rapidly loses the activity.

**2) Spectrophotometric Studies.** — Further observation was spectrophotometrically made to ensure the presence of active intermediate. The active intermediate was first formed as an active state of manganese(II)-oxalate complex and at this stage no change in absorption appeared; its presence was indirectly ascertained by increase in the absorbance of manganese(III)-oxalate complex produced by the reaction of the active manganese(II)-oxalate and dissolved oxygen.

Composition of the solution in which the absorbance measurement was made is presented in Table III. Mixture 1 to 8 show the effect of the manganese(II) ion and pH on the absorbance; the absorption curve of some mixtures is shown in Fig. 1, indicating the presence of manganese (II)-oxalate complex and the active intermediate. Mixture 9 to 13 show the effect of varying manganese(II) ion concentration at a constant pH 3.2 (The absorption curve is not shown in Fig. 1).

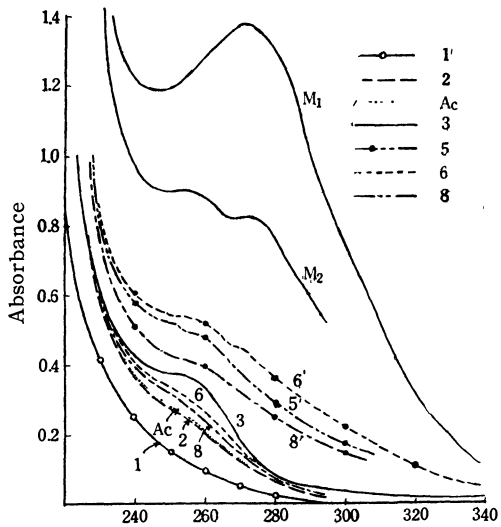



Fig. 1. Absorption curves of solutions containing oxalate and manganese(II) or mangnese(III) ion.
●: after irradiation (5', 6' and 8').

TABLE III
COMPOSITION OF THE SOLUTION USED IN SPECTROPHOTOMETRIC OBSERVATION AND ABSORBANCE AT 260mμ

| Mixture | $MnSO_4$ M./l. | pH | Absorbance at 260 mμ not irradiated | Absorbance at 260 mμ after irradiation |
|---|---|---|---|---|
| 1 | 0 | 5.6* | 0.087 | 0.087 |
| 2 | 〃 | 3.2 | 0.196 | 0.196 |
| Ac | 〃 | 2.3 | 0.203 | 0.203 |
| 3 | 0.005 | 5.6* | 0.327 | 0.330 |
| 4 | 〃 | 4.8 | 0.310 | 0.391 |
| 5 | 〃 | 3.8 | 0.283 | 0.460 |
| 6 | 〃 | 3.2 | 0.265 | 0.515 |
| 7 | 〃 | 2.8 | 0.250 | 0.440 |
| 8 | 〃 | 1.4 | 0.237 | 0.375 |
| 9 | 0.001 | 3.2 | 0.216 | 0.435 |
| 10 | 0.003 | 〃 | 0.250 | 0.468 |
| 11 | 0.005 | 〃 | 0.265 | 0.515 |
| 12 | 0.007 | 〃 | 0.274 | 0.552 |
| 13 | 0.009 | 〃 | 0.282 | 0.539 |

All of the mixtures are 0.005 M/l. of $Na_2C_2O_4$, except Ac is 0.005 M./l. of oxalic acid only. pH is controlled by sulfuric acid.
* Sulfuric acid is not added.

*i) Absorption Spectra of Manganese(II)-oxalate.*——Data of the absorbance (Table III or Fig. 1) of these mixtures which were not irradiated, provide a qualitative information. When the oxalate solution is acidified with sulfuric acid or only contains oxalic acid, the absorbance increases with a little swelling at about 250 to 260 mμ as compared to the pure sodium oxalate solution. (Table III, 1 to Ac, or Fig. 1 curve 1, 2 and Ac). However, mixtures containing the oxalate and the manganese(II) ion have a greater absorption swell at about 250 to 260 mμ than those without the manganese(II) ion (Fig. 1, curve 3, 6 and 8). Mixture 3 which does not contain sulfuric acid, has the largest absorbance over the range of about 250 to 260 mμ. When this solution is set aside overnight at room temperature, manganese(II)-oxalate crystallizes from the solution with a chemical composition of $MnC_2O_4$. The mixtures 4 to 8, the pH values of which were decreased with sulfuric acid, have lower absorbance than mixture 3 of a higher pH, although the absorbance of those mixtures is generally higher than that of free oxalic acid or a mixture of oxalate and sulfuric acid (compare curve 3, 6 and 8 with 1,2 and Ac in Fig. 1). Moreover, manganese(II)-oxalate did not crystallize from Mixture 4 to 8.

These observations suggest the presence of manganese(II)-oxalate complex which was pointed out by Malcolm and Noyes[15]. They showed that a solution containing manganese(II) perchlorate and sodium oxalate has an absorption at about 260 mμ and suggested that a manganese(II)-oxalate complex is formed in the solution, and this complex is regarded as the reactive species in the initial stage of the permanganete-oxalate reaction.

In Mixture 9 to 13 in Table III, the absorption curves are similar to the curve 6 in Fig. 1. The extent, to which the absorbance increases, becomes greater with increase in amount of the manganese(II) ion added, indicating a higher concentration of the manganes(II)-oxalate complex.

*ii) Formation of Manganese(III).* — Mixtures in Table III were irradiated for 30 min. at 20°C. in the atomosphere. In the absence

15) J. M. Malcolm and R. M. Noyes, *J. Am. Chem. Soc.*, **74**, 2769 (1952).

of the manganese(II) ion, the absorbance remained unchanged (Table III. 1, 2 and Ac), whilst in its presence it increases after irradiation (3 to 13 and curve 5', 6' and 8' in Fig. 1). This increase is due to the formation of manganese(III)-oxalate complex having an absorption maximum at 270 mμ*. To confirm this, further experiment was done as follows. When a few milligrams of solid manganese(III)-oxalate complex, $K_3[Mn(C_2O_4)_3]\cdot 3H_2O$**, were dissolved in the oxalate solution of a known pH, the absorption was observed as shown on curve $M_1$ in Fig. 1. The absorption curve gradually changed from $M_1$ to $M_2$ with time, owing to the decomposition of the manganese(III) complex to the manganese (II). It then approached to the curve 6 or 5 (which is omitted in Fig. 1) passing through the curve 6' or 5', according to the initial concentration of the complex salt and the pH of the solution. A quantitative treatment of the decomposition of manganese(III) complex will be discussed in the second report.

The formation of manganese(III) complex is most marked at pH 3.2 to 3.4 (Table III, No. 6 or Fig. 1. curve 6'). This is correlated to the fact that the reduction of Mercury(II) chloride most readily takes place at pH about 3.2 (Table II, pH 3.2 in Group 4). In the reaction mixture of pH 3.2, the quantity of the manganese(III) complex produced by irradiation, also increases with manganese(II) concentration to some extent (Table III. 9 to 13).

The formed manganese (III) complex decomposes gradually to manganese(II)-oxalate in the dark at room temperature, the absorption curve slowly recovering its original shape.

*iii) Activation of Manganese-(II)-oxalate in the Solution.* — The Mixture 6 in Table III was irradiated for 30 min. in the absence of oxygen. The formation of mercury(I) chloride was ascertained by the addition of mercury(II) chloride to a small portion of the mixture. The absorbance was measured with the remaining solution, the results being shown in Fig. 2. The absorbance remained unchanged for a long time in a current of carbon dioxide (Fig. 2. curve a-d). When the solution was exposed to air, however, the absorbance instantly increased (Fig. 2. curve c' and d') to an increasing extent with time (Fig. 2. $c_1'$, $c_2'$ and $c_3'$). However, it gradually decreased with further standing (Fig. 2. $c_3' \rightarrow c_4'$).

These phenomena can be accounted for as follow. The active intermediate formed by irradiation does not affect the absorbance of the solution in the absence of oxygen but changes it by the formation of

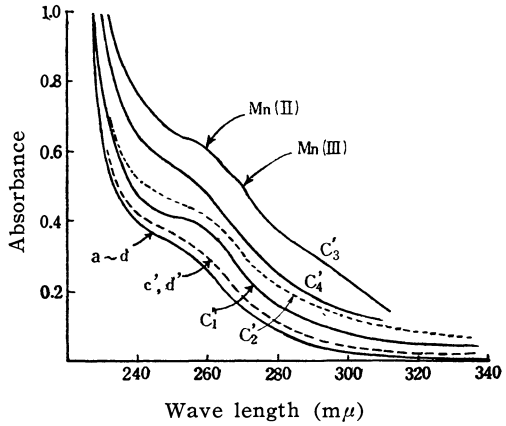



Fig. 2. Formation of manganese(III) by reaction between active intermediate and oxygen in the manganese(II)-oxalate system (at 8-10°C).
a: no treatment; b: irradiated for 30 min. in the absence of oxygen; c and d: b is set aside in the absence of oxygen for 30 min. and 51 hr., respectively; c': c is shaken in the air; d': d is shaken in the air; $c_1'$, $c_2'$, $c_3'$ and $c_4'$: c' is left exposed to air for 16, 20, 74 and 112 hr. respectivery.

manganese(III)-complex in the air even after interception of light. The decrease in absorbance with time is due to the reduction of manganese(III) to manganese(II). A slight swelling of the absorbance at about 270 mμ and 260 mμ in the curve of Fig. 2 may be caused by manganese (III) and manganese(II) oxalate complex, respectively (compare with curve $M_1$ and $M_2$ in Fig. 1).

The fact that, even after fifty hours the irradiated Mixture 6 kept in the atmosphere of carbon dioxide increased its absorbance when exposed to air, suggests that the active intermediate survives for a long time.

## Discussion

Manganese(II)-oxalate is formed in the solution containing the manganese(II) and the oxalate ion, and an equilibrium is established as

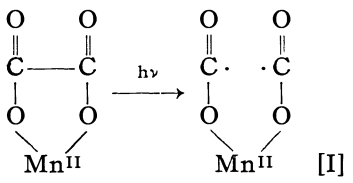
$$Mn^{2+} + C_2O_4^{2-} \rightleftharpoons MnC_2O_4 \quad (1)$$
$$MnC_2O_4 + 2H^+ \rightleftharpoons Mn^{2+} + H_2C_2O_4 \quad (2)$$

When the hydrogen ion concentration is low, manganese(II)-oxalate crystallizes (Table III, mixture 3). The absorption swell at about 250 to 260mμ is presumably due to the light absorption of manganese(II)-oxalate. The active state of manganese

* Part 2 of this series.
** This salt was prepared by the detail of Cartledge and Ericks[16].
16) G. H Cartledge and W. P. Ericks, *J. Am. Chem. Soc.*, **58**, 2061 (1936).

(II)-oxalate by ultraviolet irradiation will result from the absorption of light quantum by manganese(II) oxalate molecules. This aspect is further supported by the fact that manganese(II)-oxalate is activiated even in the solid state by ultraviolet irradiation*. This fact also discloses that hydrogen ion does not take part in the activation of manganese(II)-oxalate molecule (step 2 and see Table III, 3 to 8).

Now, it seems that the C—C bond in the manganese(II)-oxalate molecule may be significantly loosened by steric strain. This effect should be controlled principally by the length of Mn—O bond. If this bond had ionic character, such an effect could be expected. Absorption of one light quantum of 300 mμ by a molecule is equivalent to the absorption of 100 Kcal. per mole, so that the energy of ultraviolet light is sufficient to rupture the bond. A conceivable mechanism could be as follows.




(3)

$$[I] + O_2 \longrightarrow [Mn^{II}-O-\dot{C}=O]^+ \ [II] + O_2^- + CO_2 \quad (4)$$

$$[Mn^{II}-O-\dot{C}=O]^+ + O_2 \longrightarrow Mn^{2+} + O_2^- + H_2O_2 \quad (5)$$

$$Mn(II) + O_2^- + 2H^+ \longrightarrow Mn^{3+} + H_2O_2 \quad (6)$$

$$[Mn^{II}-O-\dot{C}=O]^+ + Mn(III) \longrightarrow 2Mn^{2+} + CO_2 \quad (7)$$

$$[I] + Hg(II) \longrightarrow [II] + Hg(I) + CO_2 \quad (8)$$

$$[II] + Hg(II) \longrightarrow Mn^{2+} + Hg(I) + CO_2 \quad (9)$$

In this mechanism, step (3) is the activation of manganese(II)-oxalate molecule, resulting in the formation of a biradical [I]. When oxygen is present, the biradical [I] reacts rapidly to form the ion radical [II], $O_2^-$ ion and carbon dioxide (step 4). The ion radical [II] further reacts with oxygen through step (5) to form manganese(II) ion, $O_2^-$ ion and carbon dioxide. The $O_2^-$ ion reacts rapidly with both manganese(II) and hydrogen ion, yielding manganese(III) and hydrogen peroxide (step 6)*. Hydrogen ion thus appears to be important in the formation of manganese(III) and hydrogen peroxide. Mixture 3 of pH 5.6 shows only negligible increase in absorbance after irradiation, indicating that the formation of manganese (III) complex is very slight in the deficiency of hydrogen ion. In mixture 8 of a high hydrogen ion concentration, the decrease in absorbance is again observed, presumably because of the decomposition of the manganese(III) complex. This fact is accounted for by step (5), (6) and (7)**. Therefore, optimum pH for the formation of manganese(III) complex is about 3.2.

It is well known that manganese(III) forms either red trisoxalato complex, $[Mn(C_2O_4)_3]^{3-}$, or yellow dioxalato complex, $[Mn(C_2O_4)_2(H_2O)_2]^-$, according to the oxalate ion concentration[17]. However, under the present experimental conditions, the complex in the solution was of so low a concentration, that the absorbance could be only measured in the ultraviolet region.

The photochemical catalytic action of the manganese(II) ion upon the formation of hydrogen peroxide in an oxalic solution is also accounted for by step (3) to (6).

The fact that the absorbance does not change in spite of the activation of manganese(II)-oxalate by irradiation (Fig. 2, b to d), may be possibly accounted for as follows. The concentration of activated manganese(II)-oxalate shoud be very low, and the absorbance swelling at about 250 to 260 mμ is possibly due to the absorption of Mn—O bond in manganese(II)-oxalate molecule and the fission of the C—C bond would not significently affect the absorption.

The reduction of mercury(II) chloride to mercury(I) occurs as steps (8) and (9), and in these steps the manganese(III) is not produced. A chain mechanism should be considered for the succeeding reaction system as in the case of the Hg(II)—Mn (III)—oxalate system[5].

## Summary

Manganese(II)-oxalate is formed in the solution containing the manganese(II) and the oxalate ion and is activated by the ultraviolet absorption. The presence of this active manganese(II)-oxalate was

* This subject will be reported later.

* A kinetic treatment will be discussed in the later report.

** This will be discussed fully in second report of the series.

17) G. H Cartlege and W. P. Ericks, *J. Am. Chem. Soc.*, **58**, 2065 (1936).

supported by the reducing power towards mercury(II) ions and by the spectrophotometric measurement. This active manganese(II)-oxalate reacts with oxygen and hydrogen ion to form hydrogen peroxide and manganese(III) oxalate complex.

The photochemical catalytic action of the manganese(II) ion upon formation of hydrogen peroxide in an oxalic acid solution appears to be due to the activation of manganese(II)-oxalate molecule.

*Department of Chemistry, Faculty of Engineering Shizuoka University*
*Oiwake, Hamamatsu*

# *Neue Synthetische Methode von Tetraphenyl-Phosphoniumhalogeniden*

Von Yôichi HIRUSAWA, Mitsuo OKU und Kazumi YAMAMOTO

(Eingegangen am 21. Januar 1957)

Tetraphenyphosphoniumhalogenide finden jüngst auf dem Gebiete der analytischen Chemie als organisches Reagens Anwendung[1]. Im allgemeinen kann man das quartäre Phosphoniumhalogenid unmittelbar aus tertiärem Phosphin und Alkylhalogenid leicht darstellen:

$$R_3P + RX = R_4PX$$
($R$=Alkylrest, $X$=Halogenatom)

Ist $R$ aber dabei Phenyl, so findet diese Umsetzung überhaupt nicht statt. Mann[2] stellte Tetraphenylphosphoniumhalogenid aus Triphenylphosphin und Phenylhalogenid mit Hilfe von Aluminiumchlorid her.

Dodonow[3] und die anderen Forscher[4] erhielten es aus Phosphortrichlorid unter Anwendung von Grignard-Reagens.

Zwei von den Mitverfassern dieses Berichtes, Yamamoto und Oku, fanden eine rein katalytische, neue Methode zur Herstellung dieser Verbindung. Nach ihrer Methode kann man Tetraphenylphosphoniumhalogenide dadurch leicht herstellen, daß man Triphenylphosphin mit Phenylhalogenid in Methanol in Anwesenheit einer katalytischen Menge von Nickelhalogenid auf 150 bis 250°C erhitzt.

Die Umstzung verläuft leicht in der Reihenfolge von Chlorid, Bromid und Jodid und die Ausbeute beträgt an Chlorid 60%, und an Bromid und Jodid über 80%. Die Schmelzpunkte jeder Halogenide sind in der Tabelle I gegeben.

TABELLE I

| Verbindung | Farbe | Schmelzpunkt °C |
|---|---|---|
| $(C_6H_5)_4PCl\cdot 5H_2O$ | farblos | 265 |
| $(C_6H_5)_4PBr\cdot 2H_2O$ | farblos | 287 |
| $(C_6H_5)_4PJ$ | hellgelb | 333 |

**1. Analytische Methode der Tetraphenylphosphoniumhalogenide.**

Die Verfasser bestimmten Phosphoniumhalogenid durch Argentometrie. Eine Probe wird mit 0,1 N $AgNO_3$ behandelt und dann mit 0,1 N KCNS unter Andwendung von Eisensulfat als Indikator zurücktitriert.

0,1 N $AgNO_3$ 1 ccm=0,03745 g $(C_6H_5)_4PCl$,
0,0419 g $(C_6H_5)_4$ PBr, 0,0466 g $(C_6H_5)_4PJ$.

**2. Beschreibung der Versuche.**

In eine Ampulle von 80 ccm Inhalt werden die nötigen Mengen sowohl von Phenylhalogenid als auch von Triphenylphosphin, Methanol und Nickelhalogenid eingeschlossen und im Ölbad auf die bestimmte Temperatur erhitzt. Nach erfolgter Umsetzung bestimmt man den Phosphoniumgehalt im Reaktionsgemisch nach der Verdünnung mit Methanol (ca. 100 ccm). Alle Experimente wurden der Versuchsordnung gemaß durchgeführt. Zuerst wird über die Ermittelung der Bedingungen zur Darstellung von Tetraphenylphosphoniumbromid als Vertreter angegeben.

*a) Einflüsse von Reaktionstemperatur, Reaktionsdauer, Luft und Verunreinigungen.* — Die Experimente wurden unter folgenden Grundbedingungen gemäß dem Graeco-Latin Quadrat bestehend aus fünf Faktoren (Temperatur, Reaktionsdauer, Dibrombenzol und Wassergehalt von Brombenzol) in vier Gruppen durchgeführt.

1) H. H. Willard, *Ind. Eng. Chem., Anal. Ed*, **11**, 186, 269, 305 (1939); W. T. Smith, *Anal. Chem.*, **20**, 937 (1948); H. A. Portratz, *Anal. Chem*, **21**, 1276 (1919); **23**, 1680 (1951); M Shinagawa, Vortrag bei der 8. Jahresversammlung der japanischen chemischen Gesellschaft (Nr. 14004) (1955).

2) F. G. Mann, *J. Chem. Soc.*, **1942**, 1192; **1942** 666, 1192.

3) J. Dodonow, *Ber*, **61**, 907, (1928).

4) F. F. Bricke, *J. Am. Chem. Soc.*, **55**, 3056 (1933); **61**, 88 (1939); G. M. Kosolapoff, "Organophosphoros Compounds", John Wiley & Sons Inc. (1950), S. 78.

5) K. Yamamoto und M. Oku, J. P. 221,097 (zu Mitsui Chem. Ind. A. G.).

Grundbedingungen:

| | | |
|---|---|---|
| Triphenylphosphin | 6,5 g | (1/40 Mol.) |
| Brombenzol | 3,9 g | (1/40 Mol.) |
| Nickelbromid | 0,11 g | (1/2000 Mol.) |
| Methanol | 4,0 g | (1/8 Mol.) |

Die Ordnungen und Resultate der Versuche sind in der Tabelle 2 zusammengefaßt.
Diese Resultate in die Tabelle der Streuungsanalyse zusammengefaßt erhält man die Tabelle III.

Aus diesen Resultaten ergibt sich:

1) Der Unterschied der Temperatur ist von grosser Bedeutung und die Temperatur von 160°C ist am besten.

2) Auch der Unterschied des Wassergehaltes von Brombenzol ist ebenfalls sehr wichtig und die Wasserfreiheit ist wünschenswert.

3) Der Unterschied von Dibrombenzolgehalt des Brombenzols ist etwas von Bedeutung.

4) Die Reaktion verläuft vorzüglicherweise unter der Atmosphäre von Stickstoff.

5) Die Wechselwirkung zwischen der Atmosphäre und dem Wassergehalt von Brombenzol ist sehr wichtig und zeigt, daß nachteilge Einflüße von Waser unter Atmosphäre von Stickstoff nur geringfügig sind.

6) Die Bedeutung zwischen den Reaktionsdauern in diesem Bereich kann man nicht beobachten.

*b) Einflüsse von Reaktionsdauer, Molverhältnissen von Rohstoffen und geringen Mengen von Wasser in Brombenzol.*—Um die oben erhaltenen Resultate festzustellen, führten die Verfasser die Experimente gemäß dem anderen Latinquadrat bestehend aus vier Faktoren in drei Gruppen durch, wobei die Verfasser weitere Gebiete von Reaktionsdauern, geringere Wassergehalte und verschiedene Molverhältnisse von

TABELLE II

| | Unter Luftatmosphäre | | | | Unter $N_2$-Atmosphäre | | | |
|---|---|---|---|---|---|---|---|---|
| | $T_4$ | $T_2$ | $T_1$ | $T_3$ | $T_4$ | $T_2$ | $T_1$ | $T_3$ |
| $W_4$ | A b | B d | C c | D a | A b | C c | B a | D d |
| | 12,9 | 8,1 | 6,4 | 4,7 | 16,6 | 6,6 | 13,2 | 9.3 |
| $W_3$ | B c | A a | D b | C d | B d | D a | A c | C b |
| | 25,0 | 10,0 | 4,2 | 9,5 | 37,6 | 27,7 | 12,4 | 16,6 |
| $W_2$ | C a | D c | A d | B b | C a | A d | D b | B c |
| | 20,1 | 15,3 | 5,7 | 18,2 | 74,1 | 15,9 | 15,5 | 46,3 |
| $W_1$ | D d | C b | B a | A c | D c | B b | C d | A a |
| | 47,4 | 29,3 | 38,6 | 35,7 | 64,6 | 24,5 | 39,4 | 32,8 |

W ist der Wassergehalt von Brombenzol ($W_1$=0%, $W_2$=3,3%, $W_3$=6,5%, $W_4$=12,1%), T die Temperatur ($T_1$=130°, $T_2$=140°, $T_{33}$=150° $T_4$=160°C), A, B, C und D sind die Reaktionsdauer (A=1, B=2, C=3, D=5 Std.) und a, b, c und d sind der Dibrombenzolgehalt (a=0%, b=7,2%, c=13,3%, d=23,5%). Die Ziffern in der Tabelle II zeigen die Ausbeute von Tetraphenylphosphoniumbromid (% d. Th. an Triphenylphosphin).

TABELLE III

| | Faktoren | Summe der Abweichungsquadrate | Zahl der Freiheitsgrade | Quadrat der mitteleren Abweichungen | $\sigma$-Schätzung |
|---|---|---|---|---|---|
| T | Reaktionstemperatur | 186222 | 3 | 62074 | $9,55^{3+}$ |
| W | Wassergehalt von Brombenzol | 221250 | 3 | 23750 | $11,34^{3+}$ |
| | Reaktionsdauer | 35619 | 3 | 11873 | 1,83 |
| | Dibrombenzolgehalt | 55320 | 3 | 18440 | $2,84^{+}$ |
| N | $N_2$-Atmosphare | 82070 | 1 | 82070 | $12,62^{3+}$ |
| | N×T | 40645 | 3 | 13548 | 2,08 |
| | N×W | 245016 | 3 | 81672 | $12,56^{3+}$ |
| | Fehlerglieder | 78036 | 12 | 6503 | |
| | Insgesammt | 944178 | 31 | | |

| wobei; | Überschreitungswahrscheinlichkeit | $F^1_{12}$ | $F^3_{12}$ |
|---|---|---|---|
| | 1% | 9,33 | 5,95 |
| | 5% | 4,75 | 3,49 |
| | 10% | | 2,61 |

Brombenzol zu Triphenylphosphin gewählt hatten.

Die Grundbedingungen sind wie folgt:

| | |
|---|---|
| Reaktionstemperatur | 160°C |
| Methanol | 0,1 Mol. |
| Triphenylphosphin | 0,02 Mol. |
| Nickelbromid | 1/3640 Mol. |

Die Ordnungen und die Resultate der Experimente werden in der Tabelle IV zusammengefaßt.

TABELLE IV

| Faktoren | Unter Luftatmosphäre | | | Unter $N_2$-Atmosphäre | | |
|---|---|---|---|---|---|---|
| | $t_1$ | $t_2$ | $t_3$ | $t_1$ | $t_2$ | $t_3$ |
| $W_1$ | $M_1$ | $M_2$ | $M_3$ | $M_1$ | $M_2$ | $M_3$ |
| | 77,3 | 75,3 | 81,1 | 78,1 | 87,7 | 81,7 |
| $W_2$ | $M_3$ | $M_1$ | $M_2$ | $M_3$ | $M_1$ | $M_2$ |
| | 72,2 | 77,3 | 77,4 | 79,9 | 83,5 | 82,3 |
| $W_3$ | $M_2$ | $M_3$ | $M_1$ | $M_2$ | $M_3$ | $M_1$ |
| | 73,2 | 78,0 | 78,0 | 77,5 | 88,3 | 81,1 |

Wobei t die Reaktionsdauer ($t_1=3$, $t_2=5$, $t_3=7$ Std.), W der Wassergehalt von Brombenzol ($W_1=0$, $W_2=0,9$, $W_3=1,7\%$) und M das Molverhältnis von Brombenzol zu Triphenylphosphin ($M_1=0,9$, $M_2=1,0$, $M_3=1,1$) ist und die Ziffern in der Tabelle die Ausbeute von Tetraphenylphosphoniumbromid (% d. Th. an Triphenylphosphin) bedeuten. Die Tabelle V zeigt die Resultate der Streuungsanalyse.

Beobachtet man diese Resultate, so kann man folgende Verhältnisse verstehen:

1) Die Vorzüglichkeit der Reaktion unter Atomosphäre von Stickstoff wurde wieder festgestellt.

2) Der Unterschied zwischen diesen Reaktionsdauern ist von großer Bedeutung und die Reaktionsdauer von 7 Stunden ist am besten

3) Man kann die Wechselwirkung zwischen der Laufzeit in $N_2$-Atmosphäre im Bedeutungsniveau von 95% beobachten, d.h. unter $N_2$-Atmosphäre kann man die maximale Ausbeute bei der Reaktionsdauer von 5 Stunden erhalten, dagegen nimmt die Ausbeute unter der Luftatmosphäre mit der Reaktionsdauer geradlinig zu. (Es ist klar, wenn man das Verhältnis zwischen Ausbeute und Reaktionsdauer graphisch darstellt!)

4) Für das Molverhältniss von Dibrombenzol zu Triphenylphosphin und den derart kleinen Wassergehalt von Brombenzol kann man keine Bedeutung erkennen.

*c) Darstellung der Tetraphenylphosphoniumhalogenide.*—Aus den obigen Resultaten ergibt sich die folgende Normalarbeitsweise zur Darstellung von Tetraphenylphosphoniumbromid. Man setzt 26,2 g (0,1 Mol) Triphenylphosphin, 17,3 g (0,1 Mol) Brombenzol, 0,44 g (1/730 Mol) Nickelbromid mit 16 g (0,5 Mol) Methanol in einen Autoklaven (18 : 8 Stahl) von 130 ccm Inhalt ein. Nach dem Belüften mit Stickstoffstrom erhitzt man das Reaktionsgemisch fünf Stunden lang auf 160°C. Wenn man Methanol aus dem Reaktionsgemisch abdestilliert und dem zähen Rückstand ca. 200 ccm Wasser zusetzt, so scheiden sich feine Kristalle von Tetraphenylphosphoniumbromid aus. Nach der Umkristallisation kann man 36,4 g von reinem Bromid erhalten (80% d. Th.).

Auch Tetraphenylphosphoniumjodid kann man auf gleiche Weise unter Anwendung von Jodobenzol anstatt des Brombenzols in einer Ausbeute von über 90% erhalten. Dagegen ist die Synthese des entsprechenden Chlorids ziemlich schwer und bedarf noch höherer Reaktionstemperaturen. Die Ausbeute beträgt 23% bei 180° und 60% bei 230°C. Also ist es zweckmäßiger, nach der Methode von Blicke[6] Chlorid mittelbar aus Bromid herzustellen.

**3. Betrachtung über den Reaktionsmechanismus.** — Die Mitverfasser dieses Berichtes, Yamamoto und Oku[7] teilten früther mit, daß Bistriphenylphosphin-Nickelbromid-Bisphenylbromid, $[(C_6H_5)_3P]_2NiBr_2\cdot 2C_6H_5Br$, das als Katalysator für die Herstellung von Acrylester nach dem Reppe-Verfahren verwendet wird, durch Methanol zu Nickelbromid

TABELLE V

| | Faktoren | Summe der Abweichungsquadrate | Zahl der Freiheitsgrade | Quadrat der mitteleren Abweichungen | $\sigma$-Schätzung |
|---|---|---|---|---|---|
| t | Reaktionsdauer | 9097 | 2 | 4549 | $11,3^{3+}$ |
| W | Wassergehalt | 623 | 2 | 312 | 0,77 |
| M | Molverhältnis | 551 | 2 | 273 | 0,68 |
| N | $N_2$-Atmosphäre | 14056 | 1 | 14056 | $34,9^{3+}$ |
| | $t\times W$ | 3827 | 2 | 1914 | $4.75^{2+}$ |
| | Fehlerglieder | 3220 | 8 | 403 | |
| | Insgesammt | 31274 | 17 | | |
| Wobei: | | Überschreitungswahrscheinlichkeit | $F_8^1$ | $F_8^2$ | |
| | | 1% | 11,26 | 8,65 | |
| | | 5% | 5,32 | 4,46 | |

6) F. F. Blicke. *J. Am. Chem. Soc.*, **70**, 737 (1948).

7) K. Yamamoto und M. Oku, dieses Bulletin, **27**, 511 (1954).

und Tetraphenylphosphoniumbromid zersetzt wird.

Betrachtet man nun den Reaktionmechanismus auf Grund dieser Tatsache, so kann man leicht vermuten, daß diese Reaktion die Zwischenkatalyse von Nickelbromid (unter Bildung der oben genannten Komplexverbindung) verläuft. In der Tat beobachtet man, daß das Reaktionsgemisch während der Destillation des Methanols die charakteristische grüne Farbe von $[(C_6H_5)_3P]_2NiBr_2 \cdot 2C_6H_5Br$ aufweist. Folglich kann der Mechanismus dieser Reaktion mit folgenden Gleichungen gezeigt werden:

$$2(C_6H_5)_3P + NiBr_2 + 2C_6H_5Br = [(C_6H_5)_3P]_2NiBr_2 \cdot 2C_6H_5Br$$

$$[(C_6H_5)_3P]_2NiBr_2 \cdot 2C_6H_5Br = 2(C_6H_5)_4PBr + NiBr_2$$

$$2(C_6H_5)_3P + 2C_6H_5Br = 2(C_6H_5)_4PBr$$

Diese Reaktion geht überhaupt nicht in solchem Lösungsmittel vor sich, wie Aceton oder Cyclohexanon, das die Komplexverbindung stabil auflösen kann. So kann Methanol nicht nur für Lösungsmittel, sondern auch für Katalysator gelten.

TABELLE VI

| | °C | %(Gew.) | °C | %(Gew.) |
|---|---|---|---|---|
| $(C_6H_5)_4PJ$ | 20,8 | 0,15 | 80,0 | 0,72 |
| | 40,2 | 0,18 | 99,8 | 1,55 |
| | 58,5 | 0,36 | | |
| $(C_6H_5)_4PBr$ | 20,8 | 1,72 | 59,8 | 7,68 |
| | 40,0 | 3,13 | 79,3 | 13,07 |
| $(C_6H_5)_4PCl$ | 20,5 | 16,29 | | |
| | 80,0 | 62,80 | | |

**4. Löslichkeit von Tetraphenylphosphoniumhalogeniden.**—Die Resultate von den Bestimmungen der Löslichkeiten der Tetraphenylphosphoniumhalogenide in Wasser sind in der Tabelle VI zusammengefaßt.

## Zusammenfaßung

Die Verfasser fanden eine katalytische Methode zur Herstellung von Tetraphenylphosphoniumhalogeniden heraus. Und die optimalen Reaktionsbedingungen wurden den Versuchsordnungen gemäß festgestellt. Nach dieser Methode kann man Tetraphenylphosphoniumhalogenide dadurch in hoher Ausbeute leicht herstellen, daß man Triphenylphosphin mit Phenylhalogenid in Methanol in Anwesenheit einer katalytischen Menge von Nickelhalogenid 5 bis 7 Stunden lang auf 160° bis 250°C erhitzt. Die Verfasser nehmen an, daß diese Reaktion durch die Zwischenkatalyse von Nickelhalogenid vor sich geht.

Zum Schluß bezeigen die Verfasser ihre Dankbarkeit dem Herrn Dr. K. Yoshikawa für seine eifrige Leitung und der Mitsui Chemischen Industrie A. G., die ihnen die Veröffentlichung dieser Arbeit erlaubte.

(Vorgetragen am 25. 11. 1956 bei der Versammlung der Kyushu-Zweigabteilung der japanischen chemischen Gesellschaft)

*Mitsui Chemische Industrie A. G.*
*Miike Farbestoffwerk*
*Omuta, Fukuoka*

# SHORT COMMUNICATIONS

## *Syntheses of New Phenylfluorone Derivatives and their Reaction with Metal Ions*

By Hirotoshi SANO

(Received April 23, 1957)

Although numerous investigations have been published on the colorimetric determinations of germanium, tin, titanium and zirconium with phenylfluorone (abbr. of 2,3,7-trihydroxy-9-phenylfluorone), researches for phenylfluorone derivatives are insufficient. Only 2,3,7-trihydroxy-9-(4′-dimethylaminophenyl)-fluorone has been synthesized by the author and his coworkers[1]. Subsequently, some derivatives were synthesized by a similar procedure. 2,3,7-Trihydroxy-9-(3′-nitrophenyl)-flurone, 2,3,7-trihydroxy-9-(4′-nitrophenyl)-fluorone and 2,3,7-trihydroxy-9-(2′-sulfophenyl)-fluorone were obtained. These compounds have never been described in the literature of the subject except the 3′-nitro derivative[2].

**Procedure for Synthesis.**—Twenty g. of the benzaldehyde derivative concerned was dissolved in 300 ml. of 20 % ethanol. To the solution were added 100 ml. of ethanolic solutions, containing 70 g. of hydroxyhydroquinone triacetate and 10 ml. of concentrated sulfuric acid or 30 ml. of concentrated hydrochloric acid. The solution was heated on a steam bath for about three hours, and allowed to stand for a week. The yellow or red crystalline precipitate was filtered and suspended in water at pH 4. The hydrolyzed precipitate was filtered, washed and dried in a vacuum desiccator. The yields of 3′-nitro, 4′-nitro, and 2′-sulfo derivative are 21, 30, and 28 %

1) K. Kimura, H. Sano and M. Asada, This Bulletin, **29**, 640(1956).
2) E. Heintschel, *Ber.*, **38**, 2878 (1905).

of the theoretical, respectively.

*Anal. of the 4'-nitro derivative.* Found: C, 60.25; H, 3.27. Calcd. for $C_{19}H_{11}O_7N$: C, 62.47; H, 3.04%.

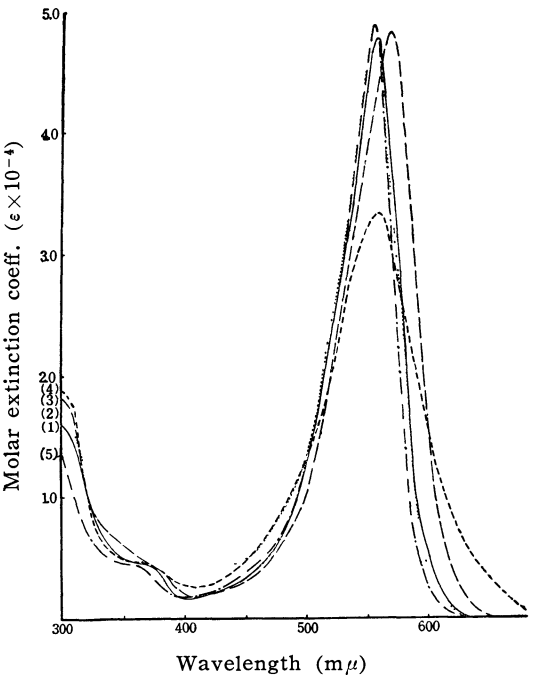



Fig. 1. Absorption spectra of products in alkaline media.
Curve (1) —— Phenylfluorone.
Curve (2) ····· 4'Dimethylaminophenylfluorone.
Curve (3) —— 3'-Nitrophenylfluorone.
Curve (4) ------ 4'-Nitrophenylfluorone.
Curve (5) —·— 2'-Sulfophenylfluorone.

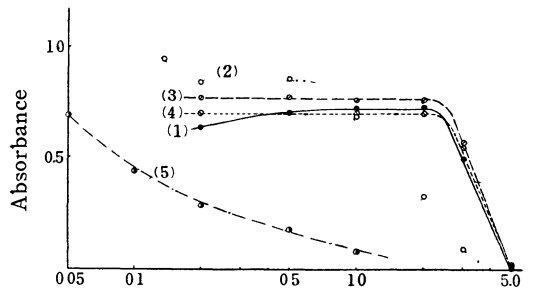



Fig. 2. Effect of acidity on germanium-fluoronates with germanium concentration fixed.
Curve (1) Phenylfluorone (510 mμ).
Curve (2) 4'-Dimethylaminophenylfluorone (510 mμ).
Curve (3) 3'-Nitrophenylfluorone (520 mμ).
Curve (4) 4'-Nitrophenylfluorone (520 mμ).
Curve (5) 2'-Sulfophenylfluorone (500 mμ).

*Anal. of the 2-sulfo derivative.* Found: C, 56.03; H, 3.35. Calcd. for $C_{19}H_{12}O_8S$: C, 57.01; H, 3.02%.

**Properties of the Products.**—The products do not melt below 270°C. The colors of 3'-nitro, 4'-nitro and 2'-sulfo derivative, are red, brownish red, and orange respectively. 3'-Nitro and 4'-nitro derivative are difficultly soluble in water but slightly soluble in ethanol. 2'-Sulfo derivative is slightly soluble both in water and in ethanol. Addition of acid or base to the ethanolic solution increases the solubility. The absorption spectra in strongly alkaline solutions are analogous to that of phenylfluorone or 4'-dimethylaminophenylfluorone as shown in Fig. 1. The absorption maxima shift toward longer wavelength in the cases of 4'- and 3'-nitro derivative, as is expected from the *I*- or *E*- effect of the nitro group. On the other hand the absorption maximum shifts toward shorter side in the case of 2'-sulfo derivative, suggesting that the effect of the phenyl group is reduced by the steric hindrance of the sulfo group. These facts convince the author that the products correspond to the compounds named.

**Reactions with Metal Ions.**—These compounds react with metal ions such as germanium, tin, titanium and zirconium, in adequate conditions. For instance the reactivities of the compounds with germanium at various acidities are illustrated in Fig. 2, including those of the phenylfluorone and the 4'-dimethylaminophenylfluorone for the comparison. The reactivity increases with increasing *I*- or *E*-effect of the substituent. The germanium complexes of 4'- or 3'-nitrophenylfluorone are slightly soluble in ethanolic solution, whereas that of 2'-sulfophenylfluorone is soluble to the same extent as the 4'-dimethylaminophenylfluorone chelate. These suggest that the compounds are useful for the colorimetric determinations of germanium. The complexes with other metals show a similar tendency in the reactions. The other derivatives such as 3',5'-dinitro, 3'-amino, or 4'-sulfophenylfluorone are under investigation. Detailed information on the compounds and their metal chelates will be published before long.

The author is indebted to Mr. Shozo Masuda of this University for the organic analyses of the products.

*Department of Chemistry, Faculty of Science, The University of Tokyo, Hongo, Tokyo*

## *Crystallization of Amorphous Nickel Sulfate*

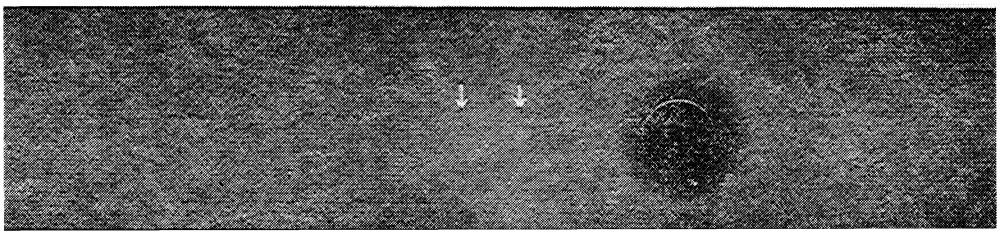
By Hideaki CHIHARA and Syûzô SEKI

(Received May 30, 1957)

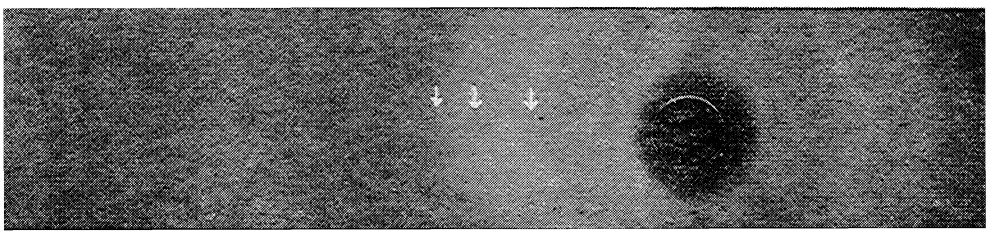
While working with the dehydration of a series of hydrates of nickel sulfate[1], crystallization of amorphous nickel sulfate was observed. Kahlbaum nickel sulfate was used to obtain the hexahydrate from aqueous solution. The hexahydrate structure[2] being identified by the X-ray powder method, the crystals were dehydrated on a quartz helical balance under vacuum less than $10^{-5}$ mm Hg, at temperatures up to 250°C until a constant weight was reached (four hours at 130° and an hour at 250°). The initial formula was calculated to be $NiSO_4 \cdot 5.98H_2O$ on the basis of complete dehydration.

The anhydrous nickel sulfate was brown in color and soluble in water (thus not nickel oxide). The X-ray pattern taken in a closed glass capillary with Cu $K_\alpha$ radiation showed that it was amorphous with two hardly discernible haloes (Fig. 1). Annealing at 100°C made the haloes progressively sharper and an additional halo appeared at a larger diffraction angle. Fig. 2 is the result obtained after four hours annealing at 100°C. Further heating at 110°C for six hours brought about sharp Debye rings as shown in Fig. 3, which remained unchanged on further heating. The observed spacings together with the relative intensities obtained by a recording microphotometer are listed in the accompanying table.

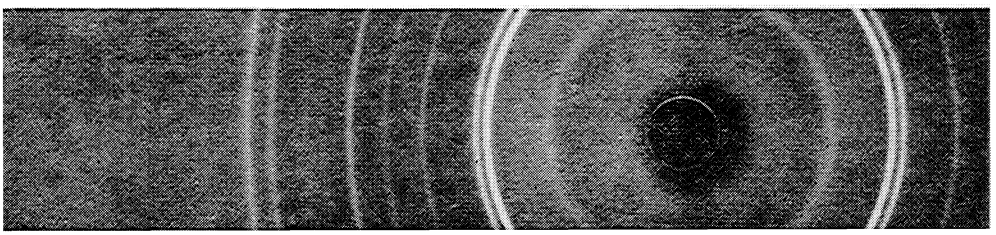
A survey of the literature revealed that F. Hammel reported[3] that the anhydrous nickel sulfate is orthorhombic with the unit cell of dimensions $a=4.6_2$, $b=6.5_1$, and $c=8.4_9$A. The present result is, however, consistent neither with this unit cell nor with the pattern given by Hammel. A



1. Anhydrous $NiSO_4$, amorphous.



2. Anhydrous $NiSO_4$, annealed at 100°C., 4 hours, amorphous.



3. Anhydrous $NiSO_4$ annealed further at 110°C., 6 hours, crystalline.

1) H. Chihara and S. Seki, This Bulletin, **26**, 88 (1953).
2) C. A. Beevers and H. Lipson, *Z. Krist.*, **83**, 123 (1932).
3) F. Hammel, *Compt. rend.*, **202**, 57 (1936).

TABLE

| Spacing in Å. | Intensity | Tentative index based on the tetragonal cell |
|---|---|---|
| 4.72 | 15 | 200 |
| 3.32 | 130 | 111 |
| 3.16 | 95 | 300 |
| 2.55 | 40 | 211 |
| 2.25 | 35 | 301 |
| 2.19 | 5 | 311 |
| 2.16 | 5 | — |
| 2.02 | 75 | 321 |
| 1.88 | 20 | 411 |
| 1.80 | 15 | — |
| 1.78 | 20 | 421 |
| 1.76 | 10 | 520 |
| 1.74 | 5 | |
| 1.66 | 50 | 440 |
| 1.63 | 10 | 550, 002, 551 |
| 1.58 | 70 | 600, 112 |
| 1.57 (shoulder) | 35 | |
| 1.45 | 15 | 222, 531 |
| 1.44 | 10 | 302, 601 |
| 1.27 | 18 | 422 |

comparison of ionic radii of bivalent cations ($Mg^{++}$ 0.65Å, $Ni^{++}$ 0.70Å, and $Zn^{++}$ 0.74Å) suggests that nickel sulfate may well be isomorphous with $MgSO_4$ and/or $ZnSO_4$. The anhydrous nickel sulfate prepared in a different manner from Hammel's may crystallize in a different way. A possibility will be open for finding other modifications of sulfate of metals of the magnesium series.

An attempt was made to assign a unit cell to the new modification which can reasonably account for the observed spacings. There are not fewer than three possibilities. The simplest one is indicated in the third column of the table. This is of simple tetragonal cell with dimensions $a=9.5_4$Å and $c=3.2_5$Å (the volume of the unit cell is 300Å$^3$). An orthorhombic unit cell with dimensions $a=6.9_3$Å, $b=6.3_1$Å, and $c=4.7_1$Å or with dimensions $a=10._0$Å, $b=7.9_3$Å, and $c=4.7_7$Å can equally well or better reproduce the observed spacings, the volume of the unit cell being 200 and 380Å$^3$, respectively. These orthombic cells are considered to be less probable in view of the too small or too great unit cell volume. A trial of finding the crystal class and the unit cell in an unarbitrary way was also made by Ito and Sadanaga's method[4], unsuccessfully, owing to lack of accuracy in the determination of the diffraction angle.

*Department of Chemistry, Faculty of Science, Osaka University, Nakanoshima, Kita-ku, Osaka*

4) T. Ito, X-ray Studies on Polymorphism, Maruzen Co Ltd., Tokyo, (1950).

## *Separation of a Trace Amount of Cesium from Large Amounts of Potassium or Ammonium by Coprecipitation with Thallium (I) Chloroplatinate*

By Noboru YAMAGATA and Eisaku TAJIMA

(Received April 26, 1957)

The carrier-free separation of cesium by the thallium (I) dipicrylaminate method from fission products is successful only when both potassium and ammonium ions are absent[1]. However, it is sometimes

TABLE I
SOLUBILITY OF ALKALI CHLOROPLATINATES IN WATER
(g. anhydrous salt per 100 g. water at 20°C)

| | |
|---|---|
| K | 0.7742 |
| $NH_4$ | 0.5000 |
| Rb | 0.0283 |
| Cs | 0.0086 |
| Tl (I) | 0.0064 (15°C) |

TABLE II
SEPARATION OF CESIUM-137 FROM POTASSIUM AND AMMONIUM
(at room temperature)

| Solution (30ml.) | Thallium (I) added mg. | Chloroplatinic** acid added ml. | Cesium-137 coprecipitated |
|---|---|---|---|
| 0.3 N KCl | 20 | 1 | 54.0 |
| 0.1 N KCl | 20 | 1 | 79.1 |
| 0.1 N KCl | 20 | 1.5 | 81.4 |
| 0.1 N KCl | 40 | 2 | 81.0 |
| 0.03 N KCl | 40 | 2 | 83.1 |
| 0.1 N KCl* | 20 | 1.5 | 77.1 |
| 0.3 N $KNO_3$ | 20 | 1.5 | 57.9 |
| 0.3 N $KNO_3$ | 40 | 1 | 47.0 |
| 0.1 N $KNO_3$ | 20 | 1.5 | 82.0 |
| 0.1 N $KNO_3$ | 20 | 1.5 | 82.0 |
| 0.1 N $KNO_3$ | 10 | 0.75 | 51.3 |
| 0.1 N $KNO_3$ | 5 | 0.38 | 19.0 |
| 0.3 N $NH_4Cl$ | 20 | 1 | 71.0 |
| 0.1 N $NH_4Cl$ | 20 | 1 | 78.9 |

* 5 $\mu$g. of cesium added.
** 5% aqueous solution.

1) This Bulletin, **30**, 580 (1957).

required to separate a trace amount of cesium from a large amount of these ions, especially from potassium.

The solubility of chloroplatinates of alkali metals and thallium (I) in water, as shown in Table I[2], indicates the possibility of the coprecipitation of a small amount of cesium with thallium (I) chloroplatinate in the presence of a large amount of potassium or ammonium ions.

A tracer experiment by the use of cesium-137 was performed to confirm this presumption; the procedure is the same as descrived in the previous report[3]. The results are shown in Table II; carrier-free cesium-137 or a microgram quantity of cesium can be separated from about 0.1 g. potassium in chloride or nitrate solution with a yield of about 80%. As the solubility of thallium (I) chloride is comparatively greater (0.29 g./100 g. water at 15.6°C)[4] than that of thallium (I) chloroplatinate, the formation of the precipitate of the latter is not interfered with by the presence of a large amount of chloride ions.

The precipitated thallium (I) chloroplatinate is dissolved in hot hydrochloric acid containing chlorine. The resulting solution, after being boiled to expel excess of chlorine, is made 2 N hydrochloric acid and passed through an anion-exchanger column (Dowex 1, X-8, $\phi$ 5×50 mm.). The effluent, free from thallium (III) and platinum (IV), contains 100% of the coprecipitated cesium and only a trace of potassium.

*Kiriu College of Technology*
*Gumma University, Kiriu*

2) A. Seidell, "Solubility of inorganic and metal organic compounds", New York, (1940) p. 456, 1086, 1424, 1434.
3) This Bulletin, **30**, 577 (1957).
4) "Gmelin's Handbuch der anorganischen Chemie" Thallium, p. 273.

## *Photometric Determinations of Indicator End Points in Complexometric Titrations*

By Sôichirô MUSHA, Makoto MUNEMORI and Kin'ya OGAWA

(Received July 4, 1957)

In photometric titrations with indicator, the color does not develop linearly with increasing amount of the added titrant. This characteristic has been elucidated by the mathematical treatment of complexometric titrations with a metal indicator[1]. A similar objection which is presented in the neutralization titration could be overcome by Higuchi, Rehm and Barnstein[2], but their method can not be applied directly to the complexometric titration.

In the titration of a metal with such a reagent as Complexon-III (disodium ethylenediamine tetra-acetate) in an aqueous system, there is the following equilibrium:

$$MI+Y^*=MY+I^* \qquad (1)^{**}$$

The equilibrium constant, $K$, is given by

$$K=[MY][I^*]/[MI][Y^*]=K^*_Y/K_I^* \qquad (2)$$

where $[MY]$ = concentration of the metal complex with Complexon-III
$[MI]$ = concentration of the metal complex with the indicator
$[Y^*]$ = sum of the concentration of the metal-free Complexon-III
$[I^*]$ = sum of the concentration of the metal-free indicator
$K_Y^*$ = $[MY]/[M][Y^*]$ = apparent stability constant
$K_I^*$ = $[MI]/[M][I^*]$ = apparent indicator constant

When the total concentrations of the metal and of the titrant in the system are $m_t$ and $c_t$ respectively, the following equation is obtained from eq. (2), so far as $m_t \geqq c_t$:

$$K=\frac{[I^*]}{[MI]}K_Y^*(m_t-c_t+[Y^*]) \qquad (3a)$$

Since in the present case $[Y^*]$ is so small that it can be neglected in the course of titration, eq. (3a) is converted into the following:

$$K=\frac{[I^*]}{[MI]}K_Y^*(m_t-c_t) \qquad (3b)$$

By transposing eq. (3b), comes the following equation:

$$c_t=-\frac{K}{K^*_Y}\frac{[MI]}{[I^*]}+m_t \qquad (4)$$

If the factor of titrant is $n$ and the dilution of the solution by titrant can be neglected, there come the following relationships:

1) J. M. H. Fortuin, P. Karsten and H. L. Kies, *Anal. Chim. Acta*, **10**, 365 (1954).
2) T. Higuchi, C. Rehm and C. Barnstein, *Anal. Chem.*, **28**, 1506 (1956).
** In the following equations, ionic charges were omitted for convenience.

$$m_t = nV_{eq} \text{ and } c_t = nV \qquad (5)$$

where $V_{eq}$ is the volume of titrant equivalent to the total amount of metal, $m_t$, and $V$ is the volume of titrant added.

By substituting eq. (4) with eq. (5), comes the following equation:

$$V = -\frac{K}{nK^*_Y}\frac{[MI]}{[I^*]} + V_{eq} \qquad (6)$$

Values of $[MI]/[I^*]$ can be computed from the absorbancy readings by means of the following equation;

$$[MI]/[I^*] = (A_{S_I} - A_S)/(A_S - A_{S_{MI}}) \qquad (7)$$

where $A_{S_I}$ =absorbancy of the metal free indicator

$A_{S_{MI}}$ =absorbancy of the metal-indicator complex

$A_S$ =absorbancy during the course of titration

If $(A_{S_I} - A_S)/(A_S - A_{S_{MI}})$ is plotted against $V$, will result a straight line whose intercept on the $V$ axis is equal to $V_{eq}$.

This is evident in Fig. 1 where the plot of $(A_{S_I} - A_S)/(A_S - A_{S_{MI}})$ vs. the volume of titrant is shown for the titration of magnesium with Complexon-III using EBT as indicator. About 50 ml. of the solution, which contained the definite amounts of magnesium sulfate, 2 ml. of 1 N ammonium chloride-ammonia buffer solution (pH 10) and 0.3 ml. of 0.5 % solution of EBT in ethanol, was titrated with 0.01 M solution of Complexon-III. Absorbancies 545 mμ were recorded at the beginning of the titration and at every 0.05 ml. of added titrant during the titration, until the minimum absorbancy was obtained. The photometric titration curve of the same titration as in Fig. 1 is shown in Fig. 2. Some of the results, obtained from the intercept as shown in Fig. 1, are given in Table I.

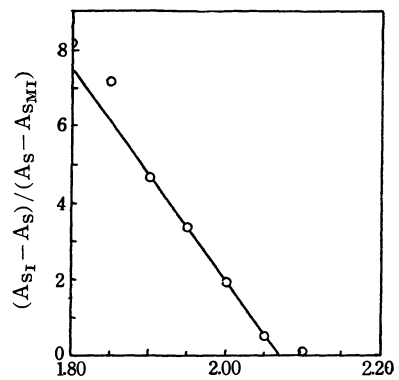



Fig. 1. Plot for titration of $0.504_7$ mg. of Mg with Complexon-III using EBT indicator at pH 10.

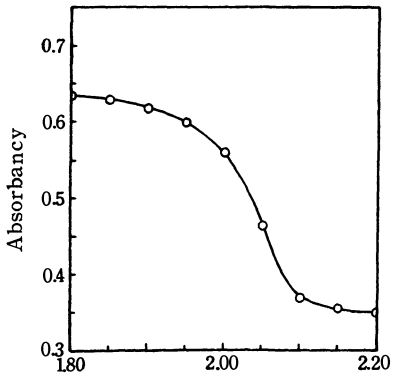



Fig. 2. Titration curve of the same titration as in Fig. 1.

TABLE I

RESULTS OF PHOTOMETRIC TITRATION OF MAGNESIUM WITH COMPLEXON-III USING EBT INDICATOR

| Mg. taken, mg. | Titrimetric end point, ml. | Mg. found mg. | Error % |
|---|---|---|---|
| $0.251_1$ | $1.02_2$ | $0.248_5$ | −1.0 |
| $0.251_1$ | $1.04_5$ | $0.254_1$ | +1.2 |
| $0.504_7$ | $2.07_5$ | $0.504_6$ | 0.0 |
| $0.504_7$ | $2.04_5$ | $0.497_3$ | −1.5 |
| $0.504_7$ | $2.07_0$ | $0.503_4$ | −0.3 |
| $0.504_7$ | $2.08_5$ | $0.507_1$ | +0.5 |

Further studies on the characteristics of this plot and on its other applications will be reported in subsequent publications.

*Department of Applied Chemistry*
*College of Engineering*
*University of Osaka Prefecture*
*Sakai, Osaka*

## *Some Kinds of Reaction Behavior of Lucidusculine*

By Takashi AMIYA

(Received July 18, 1957)

Some reactions concerning lucidusculine[1] (I), an alkaloid from *Aconitum luciduscul um Nakai*, have been investigated in this Laboratory. The methods are here communicated. Oxidation of I by 3% hydrogen peroxide gave lucidusculine N-oxide (II) d. p. 191°C (Found: C, 65.94; H, 8.37; $H_2O$, 3.31. Calcd. for $C_{24}H_{35}O_5N \cdot H_2O$: C, 66.18; H, 8.56; $H_2O$, 4.13%). Also oxidation of I by perbenzoic acid yielded a compound (III), d. p. 200°C, $[\alpha]_D^{15}$ −101° ($CH_3OH$) (Found: C, 65.30; H, 8.53%), identical (analysis, d. p. and methods of formation) with compound II. Reduction of III with zinc and hydrochloric acid regenerated substance I. Compound III afforded anhydrous compound (IV), when reserved in a desiccator, d. p. 205°C(Found; C, 69.32; H, 8.27. Calcd. for $C_{24}H_{35}O_5N$: C, 69.03; H, 8.45). Dehydration of III with 1% potassium chromate gave dehydrolucidusculine (V), m. p. 173—175°C (Found: C, 72.38; H, 8.75. Calcd. for $C_{24}H_{33}O_4N$: C, 72.15; H, 8.33%). Oxidation of I with N-bromosuccinimide gave a compound(VI), m. p. 175—180°C (Found: C, 71.51; H, 8.41%), identical (analysis and mixed m. p.) with compound V. Bromination of I with bromine in methanol gave bromoanhydrolucidusculine (VII), d. p. 210°C (Found: C, 50.02; H, 6.74; Br, 29.70; $H_2O$, 5.5. Calcd. for $C_{24}H_{32}O_3NBr \cdot HBr \cdot 2H_2O$: C, 49.73; H, 6.43; Br, 27.57; $H_2O$, 6.2%). The u. v. absorption of compound VII showed no $\lambda$ max. at wavelengths 210–340 m$\mu$. Oxidation of I with chromic anhydride in pyridine gave monocarboxylic acid (VIII), which showed neither definite m, p. nor definite d. p. (Found: C, 54.22, 54.60; H, 7.88, 7.69; N, 3.05. Calcd. for $C_{24}H_{31}O_5N \cdot 6H_2O$: C, 55.26; H, 8.31; N, 2.68%). In the infrared region the compound VIII showed a strong absorption near 5.85 $\mu$, indicating the presence of the keto group. Methylation of VIII with diazomethan gave methyl ester (IX), which showed neither definite m. p. nor definite d. p. (Found: C, 57.01; H, 7.70. Calcd. for $C_{25}H_{33}O_5N \cdot 5H_2O$: C, 58.00; H, 8.37%). Because of its low yield and difficult purification, the analysis of IX led to only an approximate agreement. Since the presence of the terminal methylene group has already been confirmed[2] in I, the partformula of I may be tentatively summarized as,

$$C_{17}H_{20} \begin{cases} CH_2OH \\ OCOCH_3 \\ >CH(OH) \\ >N-C_2H_5 \\ >C=CH_2 \end{cases}$$

Further work is in progress and will be published later. The author is grateful to Professor Harusada Suginome, President of Hokkaido University, for his unfailing kindness in encouraging this work, and to Professor Shinichiro Fujise, Tohoku University, for his kindness in making the material available.

*Department of Chemistry, Faculty of Science, Hokkaido University*
*Sapporo*

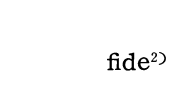
1) R. H. F. Manske and H. L. Holmes, "The Alkaloids", Vol. IV, Academic Press Inc., New York, (1954), p. 287.

2) T. Amiya and T. Shima. read before the 7th Annual Meeting of the Chemical Society of Japan held in Tokyo, April, 1954.

## *On the Near Ultraviolet Absorption Bands of Disulfides*

By Akira KUBOYAMA

(Received May 15, 1957)

The alkyl disulfides whose two sulfur atoms adjoin each other, such as diethyl disulfide[1] ($C_2H_5$—S—S—$C_2H_5$) and cystine[1] show the longest wave length absorption maximum around 250 m$\mu$ ($\log \varepsilon \sim 2.5$) in alcohol or water. But trimethylene disulfide[2] (TMD)  and its derivative, 6,8-thioctic acid[2] ($\alpha$-lipoic acid) have an absorption maximum about 330m$\mu$ ($\log \varepsilon \sim 2.2$) in 95% ethanol. This red-shift observed with cyclic disulfides is remarkable as compared with open chain disulfides (OCD) and will be treated in this communication. R. S. Mulliken[3] regarded the bands under consideration as due to

1) H. Ley and B. Arend, *Z. Phys. Chem., B* **17**, 177 (1932).
2) R. B. Whitney and M. Calvin, *J. Chem. Phys.*, **23**. 1750 (1955).
3) R. S. Mulliken, *J. Chem. Phys.*, **3**, 506 (1953).

the electronic transitions, 3ps(nonbonding)→4ss*[1]. Here, probably 3p non-bonding orbitals are somewhat admixed with 3ss, but, now, as the first approximation this hybridisation is ignored. Briefly expressed by the molecular orbital method, 3ps and 4ss orbitals of disulfides split into $(3ps_1 \pm 3ps_2)$ and $(4ss_1 \pm 4ss_2)$, respectively, by the exchange intraction, and so the transition corresponding to the longest wavelength absorption is $(3ps_1 - 3ps_2) \rightarrow (4ss_1 + 4ss_2)$. According to this Mulliken's assignment, the above problem can be reasonably explained as follows. The S-S bond distances for TMD and OCD are assumed to be nearly equal. The energy of the upper molecular orbital $(4ss_1 + 4ss_2)$ may be considered nearly equal to each other for TMD and OCD, since the overlapping between $4ss_1$ and $4ss_2$ is almost invariant with the rotation around the S-S axis. So, this red-shift which corresponds to the transition energy diminution ($\Delta E_1$), 1.20 eV., may be explained on the basis of the lower orbital $(3ps_1 - 3ps_2)$ energy. It may be thought that the mutual twist angle ($\theta$) of the two C-S bonds around the S-S bond is nearly 90° for OCD, as for N,N-diglycyl-L-cystine dihydrate[4]. The situation is the same for dichlor disulfide[5], and hydrogen peroxide[6]. This is mainly due to the repulsive interaction between $3ps_1$ and $3ps_2$. On the other hand, the two C-S bonds of TMD are forced to take nearly cis-direction to each other around the S-S bond. By a molecular model, the maximum value of $\theta$ for TMD is ca. 40°. If $\theta$ for OCD and TMD are assumed to be 90° and 40°, respectively, the calculated overlap integral values (S) of $3ps_1$ and $3ps_2$ are zero and $(0.136 \times \cos 40° =) 0.103$. This means that in TMD the splitting between two orbital $(3ps_1 \pm 3ps_2)$ levels by the exchange interaction is much greater than that in OCD. Thus, the transition energy diminution can be qualitatively explained.

The fact that the OCD's 250 mμ bands are long-drawn-out absorptions is thought to be due to the change of $\theta$-value caused by the thermal twisting vibration of the two C-S bonds around the S-S bond. In this connection, further comment will be made on the observed absorption specrum of hydrogen peroxide vapor[7]. This band with the continuously increasing intensity from 375 mμ to at least 215 mμ, may also be due to the transition, $(2po_1 - 2po_2) \rightarrow (3so_1 + 3so_2)$[3].

The rotational barrier height ($\Delta E_r$) of the two C-S bonds around the S-S bond in disulfides can be roughly estimated from the above data. As is easily known from the above discussion, the energy ($E_1$) corresponding to the transition $(3ps_1 - 3ps_2) \rightarrow (4ss_1 + 4ss_2)$ and the total energy ($E_2$) of the four electrons of the two non-bonding orbitals $(3ps_1 \pm 3ps_2)$ are changeable with the angle $\theta$. If we take OCD as the standard, the changes in these two quantities with $\theta$ can be represented by the following two formulae[8]:

$$\Delta E_1 = -(\beta - E_S S)/(1 - S),$$

$$\Delta E_2 = 2\{(\beta - E_S S)/(1 + S) - (\beta - E_S S)/(1 - S)\}$$

where, $\beta$, $E_S$ and $S$ denote the resonance integrals, the energy of 3ps orbital and the overlap integrals, respectively. For the derivation of the above formulae, it is assumed that $\theta$ is 90° for OCD. From these two formulae the following simple relation can be derived:

$$\Delta E_2 = \Delta E_1 \times 4S/(1 + S)$$

Under the assumption that the change in the total energy of non-bonding electrons ($E_2$) is the most important factor in determining $\Delta E_r$ and others such as the repulsive interaction between two alkyl groups and electrostatic interaction between C-S bonds can be neglected, $\Delta E_2$ for $\theta = 0°$ roughly equals to $\Delta E_r$. If further reasonable assumption that $\Delta E_1$ is proportional to S which is proportional to $\cos\theta$ is used, $\Delta E_r$ equals $(1.20/\cos\theta_{TMD}) \times 0.544/1.136$ e.v.. Here, $\theta_{TMD}$ denotes $\theta$ in TMD. If $\theta_{TMD}$ is 40°, $\Delta E_r$ is 0.76 eV. This value is in good agreement with the one (0.74 eV.) obtained for dichlor disulfide by K. Hirota and T. Oka[5] from the wave number of the twisting vibration (106 cm.$^{-1}$).

The author wishes to express his sincere thanks to Dr. S. Nagakura of the Institute of Science and Technology, Tokyo University, for his kind guidance.

*Faculty of Agriculture,*
*Miyazaki University.*
*Miyazaki*

*1) In the following, subscription X denotes X atom

*2) Subscription $S_1$, $S_2$ denote the two sulfur atoms of disulfides.

4) H.L. Yakel and E. W. Hughes, *Acta Cryst.*, **7**, 291 (1954).

5) K. Hirota and T Oka, Presented at the Symposium on Structural Chemistry, Nagoya (1956).

6) J. T. Massey and D. R. Bianco, *J. Chem. Phys.*, **22**, 442 (1954).

*3) The overlap intehral values were obtained by Mulliken et al's table, *J. Chem. Phys.*, **17**, 1248 (1949), assuming the atomic distance to be 2.04A; D.P. Stevenson and J. Y. Beach, *J. Am. Chem. Soc.*, **60**, 2872 (1938).

*4) S for $\theta = 0°$ is 0.136.

7) H. C. Urey, L. H. Dawsey and F. O. Rice, *J. Am. Chem. Soc.*, **51**, 1371 (1929).

8) C. A. Coulson, "Valence". Oxford (1952) p. 78.

## *An X-Ray Study on the Crystal Structure of 2-Chloro-2, 3, 3-trimethylbutane**

By Tsutomu KOIDE, Satoshi TAKEUCHI, Tsutomu ODA, Yasusada YAMADA** and Inao TAGUCHI**

(Received May 10, 1957)

Crystals of hexamethylethane undergo phase transition at −125°C.[1] The phase between the transition and the melting point (m. p. 100.6°C) is characterized by the softness and the high volatility. The crystal structure was investigated by West,[2] who vaguely pointed out that the molecules in the crystal are in orientational or rotational disorder. In order to see what will occur in the high temperature modification by replacement of a methyl group by chlorine, we have carried out an X-ray examination of 2-chloro-2, 3, 3-trimethylbutane, which has relatively high melting point, 134–135°C.[3]

Following the method used by Butlerow,[3] we prepared 2-chloro-2, 3, 3-trimethylbutane by adding powder of phosphorus pentachloride to pentamethylethanol hydrate, which had been obtained by the Grignard reaction[4] of pinacolone with methyl magnesium bromide in ether. The final product, $Cl(CH_3)_2C-C(CH_3)_3$ was recrystallized from its ethereal solution and then subjected to sublimation under low pressure.

It was observed that the solid sealed in a thin-walled melting point tube melts at 134–135°C. It recrystallizes readily in a closed vessel to give transparent aggregates. The solid is very soft and plastic. We have found it to be optically isotropic. The vapor has a camphoric odor. These properties are similar to those of cubic hexamethylethane. By the suspension method in the dilute aqueous solution of sodium chloride, the density of the solid was determined as 0.999 g./cc. at 15°C.

As the solid is volatile, we used single crystals sealed in thin-walled glass capillary tubes for X-ray examination. Such a sample was placed on a goniometer-head of an X-ray camera. Using Cu-radiations, we took several Laue photographs and a series of 20° oscillation photographs over a range of 75° about [001] as the axis of rotation. Laue photographs taken with the X-ray beam parallel to [100] and [110] showed holotesseral symmetry, and thus the point group of the crystal should be $T_d-\bar{4}3m$, $O-43$ or $O_h-m3m$. All reflections appearing on the oscillation photographs were indexed satisfactorily by a cubic reciprocal lattice corresponding to $a=7.62$ Å. All spots were extinguished except those for which $h+k+l=2n$. This indicates that the lattice is of the body-centered cubic. Thus the space group should be $T_d^3-I\bar{4}3m$, $O^5-I43$ or $O_h^9-Im3m$. The density indicates two molecules per unit cell, the densities being calculated, 1.01 g./cc.; observed, 0.999 as mentioned above.

Since there are two molecules in the unit cell with the body-centered translation, it is reasonable to place the centers of molecules at the positions 0, 0, 0 and $\frac{1}{2}, \frac{1}{2}, \frac{1}{2}$, of which the symmetry should be $T_d-\bar{4}3m$, $O-43$ or $O_h-m3m$. On the other hand, as the rigid molecule of $(CH_3)_2ClC-C(CH_3)_3$ can have at the highest only one plane of symmetry $C_s-m$, which contains the central C—C bond axis, it becomes necessary to consider some statistical explanation of the structure, as is always so[2,5] in organic plastic crystals. In order that the statistical symmetry of the molecule be as high as $T_d-\bar{4}3m$ at 0, 0, 0 and $\frac{1}{2}, \frac{1}{2}, \frac{1}{2}$, the molecule should orientate its central C—C bond axis parallel to each one of the four body-diagonals statistically equally and at the same time laterally so that the C—C axis acquires a statistical symmetry $3m$ at least. Such a statistical symmetry can also be gained by a model of molecules in rotation about the C—C axis. In the cases of $O^5-I43$ and $O_h^9-Im3m$, it is necessary to add the anti-parallel orientations of the polar C—C axis along the four body-diagonals, these directions having the symmetry of 3 or $3m$. It is also conceivable that the observed feature of the X-ray diffraction can be explained by assuming molecules in free spherical rotation. Which one of

* Part of this paper was read at the 10th Annual Meeting of the Chemical Society of Japan held at Tokyo, April 4, 1957.

** Faculty of Science, Osaka University, Nakanoshima, Osaka.

1) G. S. Parks, H. M. Huffman and B. Thomas, *J. Am. Chem. Soc.*, **52**, 1032 (1930).

2) C. D. West, *Z. Krist.*, **88**, 195 (1934).

3) H. A. Butlerow, *Ann.*, **177**, 183 (1875).

4) L. Henry, *Chem. Zentr.*, II, 748 (1906).

5) I. Nitta and T. Watanabé, This Bulletin, **13**, 28 (1938); T. Oda and T. Watanabé, *J. Chem. Soc. Japan*, **65**, 154 (1944). See also T. Oda, *Memoirs of the Osaka University of the Liberal Arts and Education*, B, No. 2, 1 (1953); R. S. Schwartz, B. Post and I. Fankuchen, *J. Am. Chem. Soc.*, **73**, 4490, 5113 (1951); H. J. Backer and W. G. Perdok, *Rec. trav. chim.*, **62**, 533 (1943).

these possibilities is the case for the actual statistical structure seems indiscernible from the consideration of intensity data, since the observable reflections are few. However, it may be said that the structure found for the present crystal is statistically isomorphous with that of the high temperature modification of $C_2(CH_3)_6$[2].

The rapid decrease in intensity of the X-ray reflections with increasing angle of scattering is evidently due to the disordered orientation of molecules with violent thermal motion. In accordance with these X-ray observations, the crystal is soft, plastic and highly volatile.

With a view that such a "rotational" mode of the molecules in crystals will cease at lower temperatures, we have undertaken a differential thermal analysis, and observed an anomalous heat effect at about −146°C on cooling, and at about −139°C on heating, showing hysteresis phenomenon. We have also taken X-ray oscillation photographs at about −160°C, which give a number of reflections showing that the structure below the thermal transition point is of low symmetry and probably has a more ordered structure.

In conclusion, we desire to express our hearty appreciation to Professor Isamu Nitta, Professor Tokunosuké Watanabé and Dr. Shuzo Seki, Faculty of Science, Osaka University, for their interest during this work. The cost of this research was defrayed from the Scientific Research Grant from the Ministry of Education, to which the thanks of the present authors are due.

*Chemical Laboratory, Osaka University of Liberal Arts and Education*
*Tennoji, Osaka*
*Faculty of Science, Osaka University*
*Nakanoshima, Osaka*

# *The Effect of Organic Vapors on the Stability of Aerosols*

By Yoshiyasu FUJITANI

(Received February 25, 1957)

It is a well-known fact that aerosols are unstable by nature. The particles decrease in number rapidly both by coagulation due to mutual collision and by sedimentation under the gravity. Therefore, it would be difficult to define the stability of an aerosol system by a mathematical expression, since it is affected by many factors which may be co-operative. In evaluating the stability of an aerosol system, the rate of decrease in i) the particle number concentration[1], or ii) the mass concentration[2] is mainly measured and, in some cases, iii) the decrease in optical density or iv) the sedimentation velocity of boundary surface of the system[3] is also observed. The method i) is most essential, but requires skillful techniques and elaborate operation; whilst, the methods ii) to iv) are applicable merely to a routine work.

The coagulation processes of aerosol particles obey Smoluchowski's theory concerning the relationship between the time elapsed and the number of particles of colloidal dispersions. In spite of the theory being based on the many assumptions, the equation has been widely used so it is convenient to adopt his coagulation constant as a measure of the stability of an aerosol system. However, few investigations along these lines are available though numeous reports have been published regarding the stability of aerosols.

It may be expected that, when a substance which exhibits a capillary activity is added to an aerosol, the rate of coagulation of the particles may be influenced both by the nature and the concentration of the admixture. If this is the case, it may offer a most interesting problem on the collision process of aerosol particles, since it has been generally believed that the collision efficiency of aerosol particles is equal to unity under normal circumstances[4].

In a previous paper the stabilizing effect of the vapors of such organic surfactants as lower series of mono-functional alcohols ($C_1$ to $C_5$), acetone and ethyl acetate has been established for the fog of aqueous ammonium chloride solution, but the detailed mechanism of the coagulation process delayed by these vapors has not yet been made clear[5].

In the present paper, to compare the stabilities of aerosols depending on the nature of the added vapors as on well as their concentrations and to inquire into the role of the vapors in stabilizing the aerosols, the rate of coagulation in the presence of such vapors was observed by means of the ultramicroscopic method, using three kinds of aerosol, i.e., the fogs of aqueous ammonium chloride solution, glycerol and dioctyl phthalate (D.O.P.).

## Experimental

The apparatus used for the present work consists of the following parts—an air-driving train, an aerosol generator, a vaporizer for the admixture, a smoke chamber and an ultramicroscope. The functions of these parts are mentioned successively.

The aerosols were prepared by two methods.

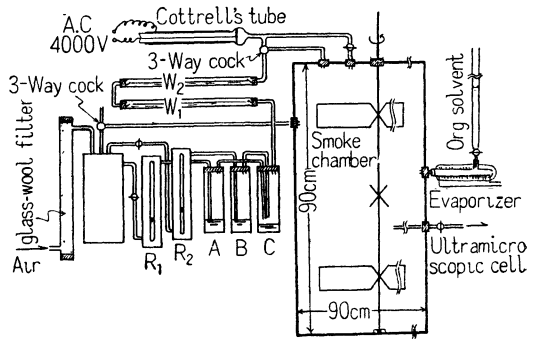



Fig. 1. Preparative system of the fog of aqueous $NH_4Cl$ solution and other constructions.

1) R. Whytlaw-Gray and H. S. Patterson, "Smoke", Edward Arnold and Co., London, 1932, Chapter 5 and 6.
2) Y. Fujitani, *J. Chem. Soc. Japan, Pure Chem. Section*, **74**, 661 (1953).
3) Ibid., **73**, 817 (1952); **75** 89 (1954).
4) Ref. 1., P. 184.; "Handbook on aerosols", The Uuited Stated Atomic Energy Commission, Washington, DC., 1950, p. 65.
5) Y. Fujitani, *J. Chem. Soc. Japan, Pure Chem. Section*, **73**, 817 (1952), **74**, 704 (1953).

a) **The fog of aqueous ammonium chloride solution.**—The fog of aqueous ammonium chloride solution was obtained by almost the same way as used in the previous experiments[5], and its modified generating system is indicated in Fig. 1. In this figure, A and B are 9.6 N hydrochloric acid and 11.2 N aqueous ammonia washing bottles, respectively, each containing 100 c.c. of the reagent, and bubbling velocity of clear air coming from a compressor through a glass wool filter and being regulated by the rota-meters, $R_1$ and $R_2$, is 0.7 l./min. for the former, and 0.3 l./min. for the latter, respectively. The gases of hydrogen chloride and ammonia driven from these bottles were mixed in the reaction chamber, C, where ammonium chloride smoke was produced. During the passage of the ammonium chloride smoke over a water surface in two glass tubes, $W_1$ and $W_2$, (each 2.0 cm. in inside diameter and 60 cm. long), ammonium chloride particles were changed to the fog droplets of aqueous ammonium chloride solution because of a strong tendency of ammonium chloride particle to absorb water vapor[6]. At the same time, the excess gas, chiefly ammonia gas, is absorbed through the water surface. Therefore, water in these two tubes, $W_1$ and $W_2$, was renewed in each run for obtaining a good reproducibility in fog preparation.

The concentration of ammonium chloride in the fog particle was found to be about 20 % by weight as an average which was determined by collecting the droplets of fog through a Cottrell's precipitator and analyzing them chemically by means of Mohr's method, a maximum deviation being less than 3 % by weight. Table I shows the mass

TABLE I

AVERAGE RADII AND MASS-CONCENTRATIONS OF THE FOG OF AQUEOUS $NH_4Cl$ SOLUTION OBSERVED UNDER THE SAME EXPERIMENTAL CONDITIONS

| No. of expt. | Average radii ($\mu$) | No. of expt. | Mass concentration (mg./l.) |
|---|---|---|---|
| 1 | 0.24 | 2 | 17.9 |
| 3 | 0.20 | 4 | 18.1 |
| 5 | 0.24 | 6 | 18.3 |
| 7 | 0.23 | 8 | 17.9 |
| 9 | 0.21 | 10 | 17.4 |
| Mean | 0.22 | Mean | 17.9 |

concentrations and average radii of aqueous ammonium chloride droplets. Average radii shown in the table were determined from the droplet sizedistribution curve obtained by measuring the settling velocity of each fog droplet in an ultramicroscopic cell. The number of fog droplets observed is about 300 for one size-distribution curve. The size-distribution curve is depicted in Fig. 2. It can be seen from Fig. 2 and Table I that the reproducibility is very good.

b) **The fogs of glycerol and D. O. P.**—The fogs of glycerol and D.O.P. were prepared by an all-glassed L-type generator[7], which was the

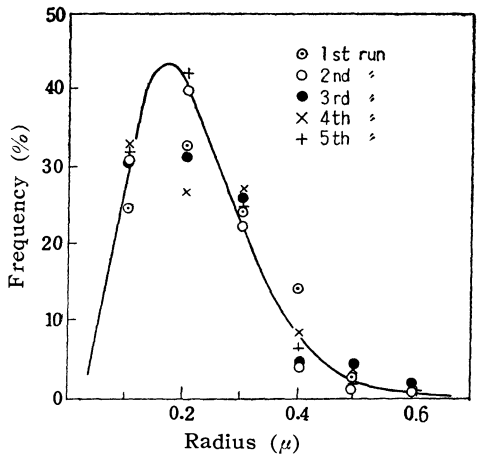



Fig. 2. Size-distribution curve of the fog of aqueous $NH_4Cl$ solution obtained by the measurement of settling velocity of droplets.

modified LaMer-Sinclair's monodisperse aerosol generator[8], consisting of three parts—boiler, reheater and condensation tube. The generator is illustrated in Fig. 3. The boiler (horizontal

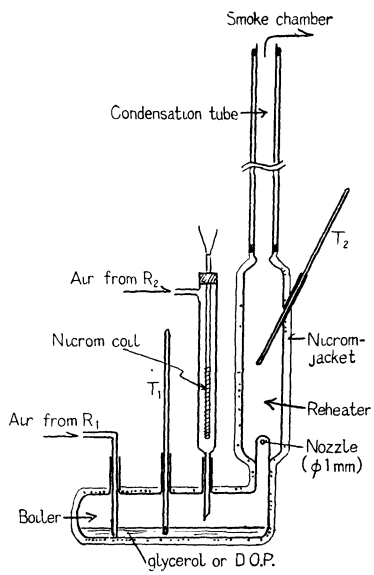



Fig. 3. L-type aerosol generator.

part, 3.5 cm. inside diameter, 20 cm. long) in which liquids or solids to be dispersed were placed, and the reheater (vertical part, 3.5 cm. inside diameter, 18 cm. long) were both electrically heated at the desired temperatures with a nicrom-jacket through variable voltstats. These two temperatures were measured by thermometers, $T_1$ and $T_2$, respectively. The condensation tube was a double-wall glass tube, and its inner tube is 2.0 cm. in inside diameter and 25 cm. long.

6) S. Twomey, *J. Applied Phys.*, **24**, 1099 (1953).
7) To be published for detailed description.
8) V. K. LaMer and D. Sinclair, *Chem. Rev.*, **44**, 245 (1949).

In order to obtain a good monodisperse fog by this generator, the temperatures must be kept properly for each material and the condensation nuclei added in a proper amount. Nuclei were supplied by an electrically heated nicrom-wire which was coiled along a quartz tube 8 cm. long.

The amount of glycerol or D.O.P. put in the boiler is 30 c.c.. The vapor driven from the boiler by bubbling air and the air laden nuclei were completely mixed in the reheater through two nozzles of 1 mm. diameter. The flow velocities of vapor and nuclei are both 0.5 l./min.. The mixture of vapor and nuclei was passed through a condensation tube where slow cooling and subsequent condensation of vapor on nuclei occurred.

The fogs produced were so nearly monodisperse that higher order Tyndall spectra[9] were visible. The temperatures both in the boiler and the reheater under the above mentioned preparative procedure and the average radii obtained under these conditions are as shown in Table II for

TABLE II
TEMPERATURES OF PREPARATIVE CONDITIONS AND AVERAGE RADIUS OF DROPLET

| Substances | Temperature of generator (°C) | | Average radius ($\mu$) |
|---|---|---|---|
| | Boiler | Reheater | |
| Glycerol | 135 | 145 | 0.18 |
| D.O.P. | 160 | 180 | 0.22 |

glycerol and D.O.P.. Average radii were determined from the measurements of settling velocity in the same manner as mentioned above.

The fogs produced by these procedures, a) and b), were re-dispersed homogeneously by stirring for 5 min. in a smoke chamber which is a wooden octagonal box coated with paraffin, 90 cm. in height, its content being 700 l.. The initial particle concentration in the smoke chamber was maintained at 2 to $5\times10^5$ per c.c. through out the whole experiment.

Organic liquid to be tested for its stabilizing action was evaporated into the smoke chamber from a vaporizer which was made of a quartz tube, 2.0 cm. in inside diameter and 20 cm. long, having a side tube connected to a burette. The organic liquid was poured into the vaporizer from the burette. The vaporizer was electrically heated by a nicrom-jacket. The concentration of organic vapor in the smoke chamber, expressed in m. mol./l., was calculated from the burette reading. The mixture of fog and organic vapor was stirred homogeneously for 5 min. as in the case of the fog alone.

The organic liquids used were carefully purified by the usual procedure and their boiling points were found to coincide fairly well with those of the literature[9],

The number of particles per unit volume is counted by an ultramicroscopic technique. The volume of visible field in the ultramicroscopic cell was $1\times10^{-6}$ c.c.. The brilliant points appearing in the dark field were counted and summed up for a fog droplet driven successively into the ultramicroscopic cell. The counting of fog droplets is done every 3 to 5 min. for an interval of 60 to 120 min.. The magnification of ultramicroscope was $\times80$.

All experimentals were carried out at room temperature, 16 to 19°C..

## Results

The decrease in number of fog droplets determined ultramicroscopically is shown in Fig. 4, 5 and 6 as the typical examples.

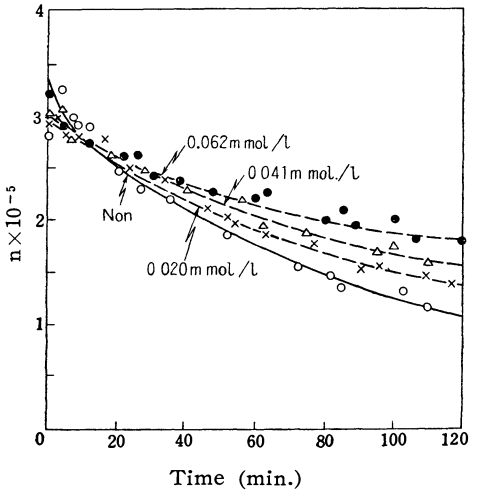



Fig. 4. Variation of droplet number per c.c. as a function of time and concentration of ethyl acetate mixed to the fog of aqueous $NH_4Cl$ solution.

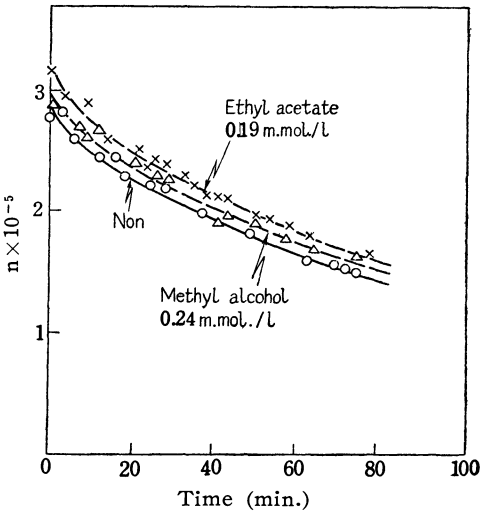



Fig. 5. Variation of droplet number per c.c. as a function of time and some vapors mixed to the fog of glycerol.

9) A. Weissberger et. al., "Organic Solvents···Physical Properties and Methods of Purification", 1955.

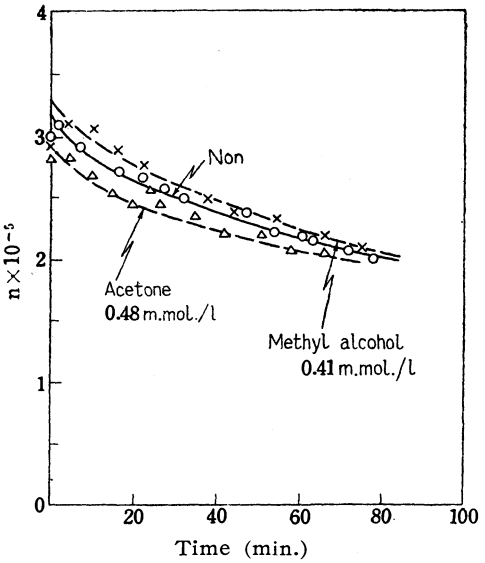



Fig. 6. Variation of droplet number per c. c. as a function of time and some vapors mixed to the fog of D.O.P..

In these figures, solid curves represent a decrease in number of fog droplets for a fog system without organic vapor, and broken curves refer to one with organic vapor. All curves showed a tendency to decrease monotonously in the course of aging.

Converting these droplet number—time graphs into a reciprocal droplet number—time ones, the linear relationships are

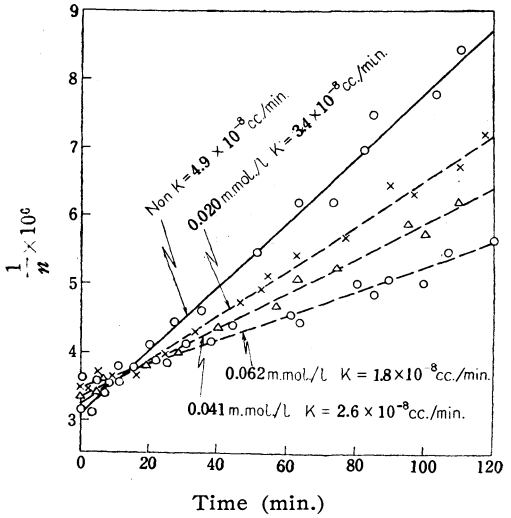



Fig. 7. Linear relationship between reciprocal number of droplet and time obtained as an influence of ethyl acetate concentration mixed to the fog of $NH_4Cl$-aqueous solution. $K$ is a coagulation constant calculated from the slop of observed line.

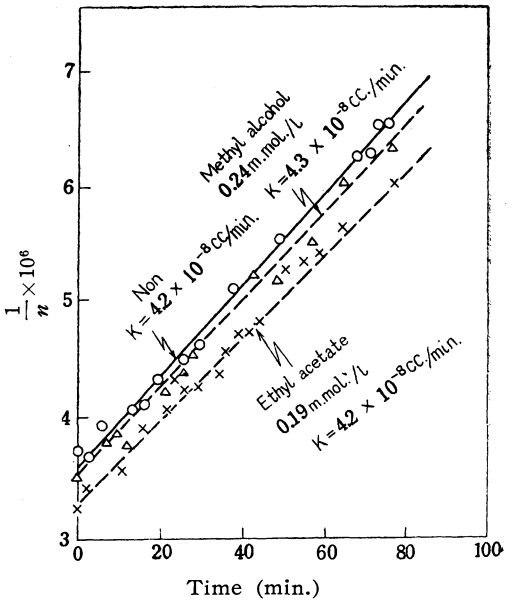



Fig. 8. Linear relationship between reciprocal number of droplet and time obtained as an influence of some vapor mixed to the fog of glycerol.

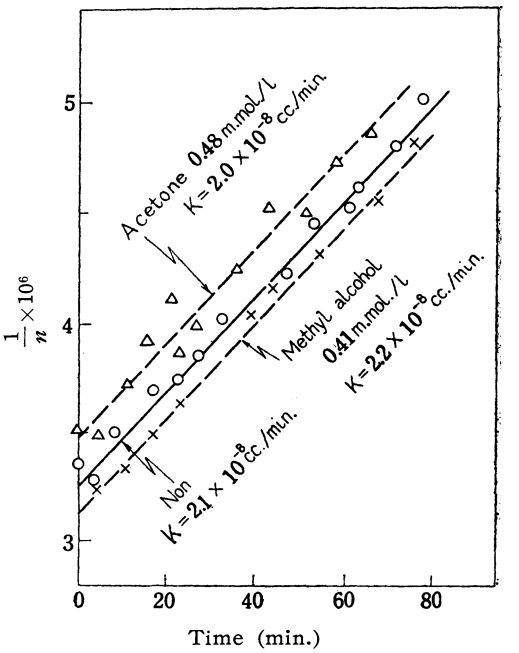



Fig. 9. Linear relationship between reciprocal number of droplet and time obtained as an influence of some vapors mixed to the fog of D.O.P..

obtained for all of them as in Figs. 7, 8 and 9. The linear relationship holds throughout all the runs of experiment. It may be noticed readily that the slope of line varies markedly with the nature

and the concentration of the vapor added to the fog of aqueous ammonium chloride solution, while, in contrast with this, it remains almost unaltered in the case of the fogs of glycerol and D.O.P. even in a greater concentration.

Smoluchowski's equation is expressed as follows,

$$1/n-1/n_0=Kt, \quad (1)$$

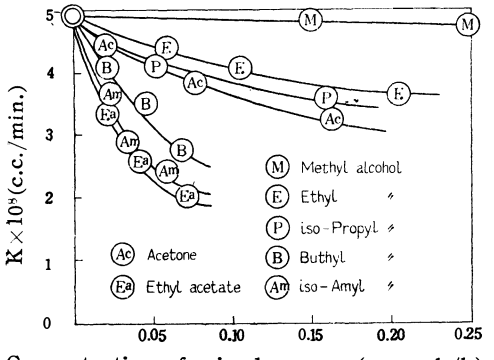
or in a more correct form,

$$1/n-1/n_0=K'(1+A\lambda/r)t \quad (2)$$

where $n_0$ and $n$ are the numbers of droplets per unit volume at the begining, $t=t_0$, and time $t$, respectively, $K$ and $K'$ are the coagulation constants equal to $4kT/3\eta$ ($k$: Boltzman's constant, $\eta$: viscosity of air) numerical value being $1.8\times10^{-8}$ c.c./min. in air at $T=293°K$, $\lambda$ the mean free path of air molecules, $r$ the radius of fog droplet, and $A$ a constant having a value of 0.7 to 1.7. $A\lambda/r$ in equation (2) gives a correction term arising from a slipage between a fog droplet and air molecules during the movement of a fog droplet in still air; therefore, the smaller the value $r$ becomes, the greater becomes the value $A\lambda/r$.

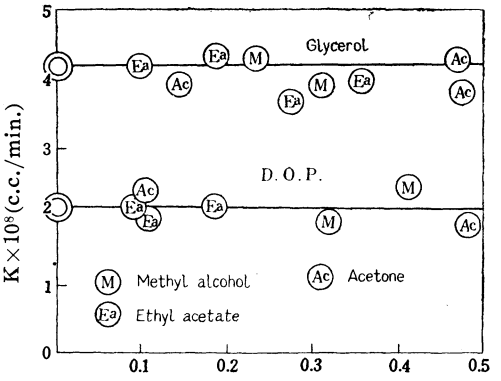
Thus, the slopes obtained experimentally are equal to $K$. However, $K$ might be used instead of $K'$, for the comparison of relative stabilizing effects of organic vapors on the same aerosol since the droplet size-distribution curve was practically unchanged for the fogs used in all runs.

The dependence of coagulation constant, $K$ or $K'$, upon the concentration of various organic vapors mixed are plotted in Figs. 10 and 11 for the fogs of aqueous ammonium chloride solution, glycerol and D.O.P..




Concentration of mixed vapors (m. mol./l.)

Fig. 10. Variation of the coagulation constant, $K$, with the concentration of mixed vapors for the aqueous $NH_4Cl$ solution fog. Symbol ◎ is the average coagulation constant for a pure fog and its value is $4.9\times10^{-8}$ c.c./min..




Concentration of mixed vapors (m. mol./l.)

Fig. 11. Variation of the coagulation constant as a concentration of mixed vapors for the fogs of glycerol and D.O.P.. Symbols ◎ are the coagulation constant for the pure fog of glycerol and D.O.P. and their values are $4.2\times10^{-8}$c.c./min. and $2.1\times10^{-8}$c.c./min., respectively.

From these figures, it is found that for the same vapor the more it is added, the more strongly the fog of aqueous ammonium chloride solution is stabilized, but no effect is observed for the other fogs within the limit of experimental precision. For the former, the coagulation constant falls off to nearly one-third under the most stabilized condition.

## Discussion

Although a number of studies have been made by Russian workers and others since 1930 concerning the effects of admixture[10], the information obtained is not always in agreement with one another, because the experimental conditions and procedures were not unified. Especially, the defect of a criterion for the ability of stabilization must be noticed.

The stability of aerosol should be governed by the internal stability[11], expressed in terms of the particle concentration and the particle size-distribution, both of which are determined a priori by the condition of formation, provided that the collision efficiency has a constant value in all of the collision processes. Therefore if the collision efficiency of aerosol particles may be altered as suggested by Patterson[12] either by the

10) T. Tatibana, *J. Chem Soc. Japan, Pure Chem. Sec.* **68**, 53 (1947); I. S. Artemov, *J. Phys. Chem., (U. S. S. R.)*, **20**, 533 (1946); I. V. Petryanov et al., ibid., **15**, 811 (1941); etc.

11) D. Sinclair, "Air Pollution", Chapter 18, p. 169, McGrow-Hill Book Co., 1952.

12) Ref. 1., Chapter 16.

TABLE

EFFECT OF VAPORS ON THE INCREASE OF CHARGED

| Fog | Sign of elec. charge | Vapor concn. (m.mol./l.) | Percentage of charged droplet for various time in the aging time (min.) | | | | | |
|---|---|---|---|---|---|---|---|---|
| | | | 0 | 10 | 20 | 30 | 40 | 60 |
| Aqueous $NH_4Cl$ solution | + | Non | 9.1 | 9.9 | 14.0 | 14.2 | 15.5 | 19.6 |
| | − | | 8.8 | 11.0 | 11.3 | 16.0 | 14.9 | 19.2 |
| Glycerol | + | Non | 6.5 | 7.9 | 9.5 | 14.5 | 12.8 | 18.8 |
| | − | | 8.1 | 12.2 | 13.2 | 15.4 | 22.1 | 27.0 |
| D.O.P. | + | Non | 14.0 | 17.1 | 19.6 | 27.0 | 28.2 | 37.3 |
| | − | | 13.7 | 14.8 | 17.3 | 20.2 | 23.9 | 27.6 |

physico-chemical structure of surface or by the changes in surface state, we may have a most important problem which has been disregarded up to date. This will be developed from now on. To study this in an orthodox way, it is better to evaluate the coagulation constants experimentally for various fogs to which vapors are added, and to compare them with one another.

From this point of view, the experimental results obtained above are interesting by reason of a large difference among the values of the coagulation constant for the fog of aqueous ammonium chloride solution and the degree of lowering of these values which are parallel with a concentration of mixed vapors. The tendency of a stabilizing effect of mixed vapor agrees with the Traube's rule[13] referring to the surface activity of the homologous series of organic compounds on pure water surface. These facts are considered to be valuable as the fundamental basis in discussing the stabilities of aerosols. It may be inferred that the coalescence of droplets in the collision process is obstructed by a decrease in surface tension somewhat in an analogous manner as the stabilization of emulsion system pointed out by Donnan[14]. Because these organic vapors have not shown capillary activity when mixed with the fogs of glycerol and D.O.P..

In a strict sense of the discussion concerning the effects of admixtures, it appears that many other factors should be taken into account with equal weight. These may be classified chiefly into four factors i.e., i)the changes in density and viscosity of medium, ii) the growth of droplets by the condensation of admixtures[15], iii) the change in distribution in electric charge of fog droplets, iv), particularly, in the case of the aqueous ammonium chloride solution, the disappearance of fog droplets by evaporation of water, etc..

First, the effects of i) and ii) have a relation to the mobility of fog droplets by the Brownian movement and sedimentation under the gravity during standing in a still medium. However, these influences caused by the change of physico-chemical properties of the medium may be small.

Second, the growth of a fog droplet by the condensation of vapor may depend upon its partition ratio between the vapor and the droplet phase, but the concentration of vapor in all experimental conditions is too low to make a droplet grow larger. In fact, no appreciable changes of fog droplet size were ascertained by ultramicroscopic observation.

Third, the change in the proportion of a charged droplet was similar irrespective of the presence of vapor during the aging. The results obtained from the electrophoresis of charged droplets in an electric field of an ultramicroscopic cell are shown in Table III. The contribution of an electric charge on the coalescence process has been also proved to be small[16].

Finally, it is generally accepted that a dissipation of aqueous aerosol by evaporation is very rapid, but, in the present case, the fog droplets consist of an aqueous ammonium chloride solution which is so concentrated that the fog system is very stable.

If the contribution of these factors is not small, it must result in a change in the coagulation constant for the fogs of glycerol and D.O.P.. Therefore, these effects are all negligible in the present work as clearly seen from the afore-said experimental results.

Most of the discussion has gone no

13) I. Traube, *Ann.* **265**, 27 (1891).
14) Donnan, *Z. physik. Chem.*, **31**, 42 (1899).
15) V. K. LaMer and R. Gruen, *Trans. Faraday Soc.*, **48**, 410 (1952); V. K. LaMer and S. Coston, *Science*, **118**, 516 (1953).
16) W. B. Kunkel, *J. Applied Phys.*, **19**, 1053 (1948).

III

DROPLET PERCENTAGE DURING THE AGING

| Increase rate of charged droplet (%/min.) | Vapor concn. (m.mol./l.) | Percentage of charged droplet for various times aging time (min.) | | | | | | Increase rate of charged droplet (%/min.) |
|---|---|---|---|---|---|---|---|---|
| | | 0 | 10 | 20 | 30 | 40 | 60 | |
| 0.17 | 0.24 Acetone | 9.9 | 10.3 | 13.5 | 16.2 | 16.2 | 20.1 | 0.17 |
| 0.17 | | 9.4 | 12.7 | 14.4 | 15.0 | 17.1 | 21.9 | 0.19 |
| 0.22 | 0.42 Acetone | 6.1 | 9.4 | 11.2 | 10.2 | 16.1 | 19.1 | 0.20 |
| 0.31 | | 9.0 | 10.2 | 15.3 | 18.4 | 19.5 | 27.3 | 0.32 |
| 0.37 | 0.39 Ethyl | 15.1 | 20.0 | 23.4 | 25.0 | 28.3 | 39.5 | 0.37 |
| 0.23 | acetate | 11.2 | 14.6 | 18.4 | 17.3 | 23.2 | 27.5 | 0.20 |

further than establishing a few general quantitative remarks, but there is a reason to believe that the mechanism of stabilizing action of the organic vapors on the fog system is largely attributable to a capillarity of admixtures. In order to prove that this conclusion is of general applicability, we need further studies, both theoretical and experimental, to be pursued as the more fundamental problems.

I wish to express my thanks to Prof. Isamu Sano of Nagoya University for his helpful advice.

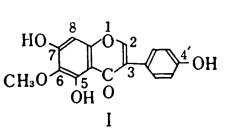
*Department of Chemistry*
*Faculty of Science*
*Nagoya University*
*Chikusa, Nagoya*

# *The Synthesis of 4′, 5, 7-Trihydroxy-8-methoxyisoflavone*

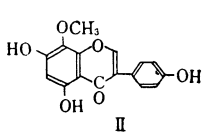
By Yoshiyuki KAWASE, Yuichi FUJINO, Yoshimochi ICHIOKA and Kenji FUKUI

(Received January 8, 1957)

Tectorigenin[1] was isolated from *Iris tectorum Maxim* and the structure[2] of 4′, 5, 7-trihydroxy-6-methoxyisoflavone (I) was assigned to it, but it is not yet synthesized. We have been attempting the syntheses of this isoflavone and related compounds. The present paper describes the synthesis of 4′, 5, 7-trihydroxy-8-methoxyisoflavone (II), an isomer of tectorigenin. Although it was shown by W. Baker et al.[3] that 4′, 5, 7-trihydroxy-8-methoxyisoflavone (II) was obtained from 2, 4, 6-trihydroxy-3-methoxyphenyl 4-hydroxybenzyl ketone (IV) with the ethoxalylation process[4], their communication did not give any detailed description of the procedure or of the melting points of the compounds. It appeared of interest to investigate further W. Baker et al's method in detail for the following reason. If the direction of ring closure of the ketone (IV) was opposite to that observed by them, the possibility of the synthesis of tectorigenin might occur. So it seemed desirable to prepare 4′, 5, 7-trihydroxy-8-methoxy-isoflavone (II) by an unambiguous synthetic method for comparison with the isoflavone prepared with the ethoxalylation process. Specimens of the isoflavone prepared by two alternative methods (see Experimental) proved to be the same compound (II). The experiments described here established, therefore, the fact that 4′, 5, 7-trihydroxy-8-methoxyisoflavone (II) was obtained with the methoxalylation and the ethoxalylation process, the direction of ring closure being the same as that observed by W. Baker et al.[3].



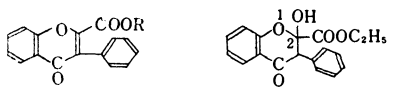
I



II

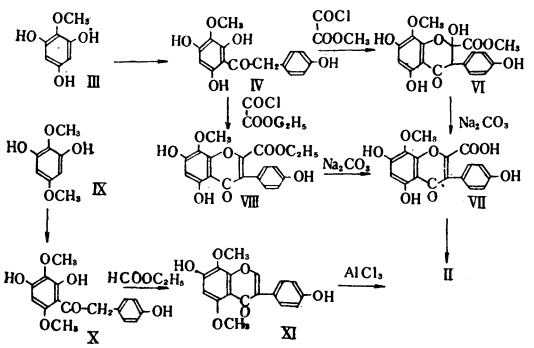
1) B. Shibata, *J. Pharm, Soc. Japan.* **47**, 380 (1927).
2) Y. Asahina, B. Shibata and Z. Ogawa, ibid., **48**, 1087 (1928).
3) W. Baker I. Dunstan, J. B. Harborne, W. D. Ollis and R. Winter, *Chem. and Ind.*, **1953**, 277.
4) W. Baker, J. Chadderton, J. B. Harborne and W. D. Ollis, *J. Chem. Soc.*, **1953**, 1852.

Iretol (III) when condensed with *p*-hydroxyphenylacetonitrile, gave 2, 4, 6-trihydroxy-3-methoxyphenyl 4-hydroxybenzyl ketone (IV), m. p. 220—1.5°. The ketone (IV) was treated at 0° with methoxalyl chloride in pyridine to give yellow crystals, m. p. 215—6.5°, which contained one molecule of water in excess of that required by the corresponding methyl isoflavone-2-carboxylate derivative (Va ; R=$CH_3$). The cyclization of *o*-hydroxyphenyl benzyl ketones to isoflavone-2-carboxylic esters (Va ; R=$C_2H_5$) with the ethoxalylation process was postulated as proceeding through the intermediates of type (Vb) which were isolated in some cases[4]. On the basis of this fact, it seemed reasonable to assume the structure of the yellow crystals to be methyl 2-hydroxyisoflavanone-2-carboxylate derivative (VI). This intermediate was converted into the corresponding isoflavone-2-carboxylic acid, m. p. 288—9° (VII) by mild alkaline hydrolysis and thence the acid was decarboxylated with copper powder in boiling quinoline to the isoflavone (II), m. p. 241—2°, in colorless needles, (its acetate, m. p. 167°). When the cyclization reaction was carried out with ethoxalyl chloride instead of methoxalyl chloride, the usual isoflavone-2-carboxylic ester, m. p. 219—20° (VIII), was obtained and it was converted into the acid (VII) by mild alkaline hydrolysis.



Va R ; $CH_3$, $C_2H_5$ Vb

2, 5-Dimethoxyresorcinol (IX) was condensed with *p*-hydroxyphenylacetonitrile by Hoesch reaction to give 2, 4-dihydroxy-3, 6-dimethoxyphenyl 4-hydroxybenzyl ketone (X), m. p. 98—9.5°. This ketone (X) was converted into 4′, 7-dihydroxy-5, 8-dimethoxyisoflavone (XI) with ethyl formate in the presence of sodium. The action of aluminium chloride on XI in nitrobenzene caused partial demethylation (in the 5-position) without affecting the other methoxy group, and the demethylated product isolated was 4′, 5, 7-trihydroxy-8-methoxyisoflavone, m. p. 238—9° (II). When this was mixed with the isoflavone which had been prepared with the methoxalylation and the ethoxalylation process, no melting point depression occured.



## Experimental*

**2, 4, 6-Trihydroxy-3-methoxyphenyl 4-hydroxybenzyl ketone (IV).**—A solution of iretol (4.1 g.)[5] and *p*-hydroxyphenylacetonitrile (4.5 g.) in absolute ether (100 ml.) containing anhydrous zinc chloride (2 g.) was saturated at 0° with dry hydrogen chloride. After being kept over-night, the viscous oily layer was separated, washed twice with ether and hydrolyzed with water (150 ml.) on a steam-bath for an hour. The solid which was separated on cooling was purified from aqueous methanol to form the ketone (4.8 g.) in colorless needles. m. p. 220—1.5°, having a violet ferric reaction in alcohol.

*Anal.* Found: C, 62.43; H, 4.99. Calcd. for $C_{15}H_{14}O_6$: C, 62.07; H, 4.83%.

**Methyl 2, 4′, 5, 7-tetrahydroxy-8-methoxyisoflavanone-2-carboxylate (VI).**—To a solution of 2, 4, 6-trihydroxy-3-methoxyphenyl 4-hydroxybenzyl ketone (2.4 g.) in pyridine (25 ml.), methoxalyl chloride (5.5 g.) was added drop by drop with stirring at 0°. After standing overnight, the mixture was poured into ice-water and extracted with chloroform. The chloroform solution was washed with dilute hydrochloric acid, dried over anhydrous sodium sulfate and evaporated. A part (0.3 g.) of the residue thus obtained was recrystallized from methanol. Yellow microcrystals, m. p. 215.5-6.5° were obtained.

*Anal.* Found: C, 57.49; H, 4.55. Calcd. for $C_{18}H_{16}O_9$: C, 57.45; H, 4.26%.

Alcoholic ferric chloride showed green color.

**4′, 5, 7-Trihydroxy-8-methoxyisoflavone-2-carboxylic acid (VII).**—To a solution of the remaining crude ester (VI) in acetone (30 ml.), 3% aqueous sodium carbonate solution (30 ml.) was added, and the mixture was refluxed for four hours. Acetone being evaporated on a steam-bath, the solution was cooled by ice-water and filtered. The product was isolated by acidification of the filtrate with dilute hydrochloric acid. Upon purification from aqueous methanol it gave rise to 4′, 5, 7-trihydroxy-8-methoxyisoflavone-2-carboxylic acid (1.1 g.) in orange yellow microcrystals, m. p. 288—9° (dec.), having a green ferric reaction in alcohol.

*Anal.* Found: C, 58.72; H, 3.82. Calcd. for $C_{17}H_{12}O_8$: C, 59.31; H, 3.51%.

* The melting points were uncorrected.

5) This was prepared from trinitroanisole by the analogous method to that used in the preparation of phloroglucinol. (H. T. Clarke and W. W. Hartman, *Organic Syntheses*, John Wiley and Sons, Inc., New York, 1932, Coll. Vol. I, p. 496).

**Ethyl 4',5,7-trihydroxy-8-methoxyisoflavone-2-carboxylate (VIII) and the acid (VII)**—Cyclization of 2,4,6-trihydroxy-3-methoxyphenyl 4-hydroxybenzyl ketone (1.7 g.) with ethoxalyl chloride (4.5 g.) in pyridine (25 ml.) in a similar way to that described before, followed by extraction with chloroform, gave rise to microcrystals of ethyl 4',5,7-trihydroxy-8-methoxyisoflavone-2-carboxylate, m. p. 219—20°.

*Anal.* Found: C, 61.22; H, 4.49. Calcd. for $C_{19}H_{16}O_8$: C, 61.29; H, 4.33%.

Hydrolysis of this ester in boiling acetone containing aqueous sodium carbonate solution gave rise to the free acid (0.8 g.) identical with the above sample.

**2,4-Dihydroxy-3,6-dimethoxyphenyl 4-hydroxybenzyl ketone (X).**—A solution of 2,5-dimethoxyresorcinol[6] (1.5 g.) and *p*-hydroxyphenylacetonitrile (1.2 g.) in absolute ether (50 ml.) containing anhydrous zinc chloride (0.5 g.) was saturated with hydrogen chloride at 0°. Isolation of the product in the usual way gave rise to the ketone (1.3 g.) which was purified from aqueous methanol in colorless needles, m.p. 98—9.5°, having a violet ferric reaction in alcohol.

*Anal.* Found: C, 62.70; H, 5.43. Calcd. for $C_{16}H_{16}O_6$: C, 63.15; H, 5.30%.

**4',7-Dihydroxy-5,8-dimethoxyisoflavone (XI).**—A solution of 2,4-dihydroxy-3,6-dimethoxyphenyl 4-hydroxybenzyl ketone (1 g.) in ethyl formate (20 ml.) was added drop by drop with stirring to a suspension of powdered sodium (1 g.) in ethyl formate (10 ml.) at −4° under nitrogen. The reaction mixture was allowed to stand overnight at 10°, and was decomposed by the addition of ice-water. Ethyl formate being removed in vacuo, the residual aqueous solution was acidified and warmed on a steam-bath. The precipitate was collected and recrystallized from methanol to 4',7-dihydroxy-5,8-dimethoxyisoflavone (0.2 g.) in colorless needles, m. p. 274—5°, having a negative ferric reaction in alcohol.

*Anal.* Found: C, 64.90; H, 4.65. Calcd. for $C_{17}H_{14}O_6$: C, 64.96; H, 4.49%.

**4',5,7-Trihydroxy-8-methoxyisoflavone (II). Method (a).**—A mixture of 4',5,7-trihydroxy-8-methoxyisoflavone-2-carboxylic acid (0.6 g.) and copper powder (0.6 g.) in quinoline (30 ml.) was heated with stirring under nitrogen for ten minutes at 230—40° (bath temperature). After cooling, the mixture was acidified with dilute hydrochloric acid and filtered. The filtrate was extracted with ether and the precipitate was also washed with ether. The combined ether solution was washed with dilute hydrochloric acid, with aqueous sodium carbonate solution, and finally with water. The ether solution being dried over sodium sulfate and evaporated, the residual product was purified from aqueous methanol and then ethyl acetate to 4',5,7-trihydroxy-8-methoxyisoflavone (0.1 g.) in colorles needles, m. p. 241—2°, having a green ferric reaction in alcohol.

*Anal.* Found: C, 63.97; H, 4.11. Calcd. for $C_{16}H_{12}O_6$: C, 64.00; H, 4.03%.

Acetylation of this isoflavone by the acetic anhydride-pyridine method gave rise to its acetate which was purified from aqueous methanol in colorless needles, m. p. 167°, having a negative ferric reaction in alcohol.

*Anal.* Found: C, 62.36; H, 4.29. Calcd. for $C_{22}H_{18}O_9$: C, 61.97; H, 4.26%.

**Method (b).**—A mixture of 4',7-dihydroxy-5,8-dimethoxyisoflavone (0.1 g.) and aluminium chloride (0.2 g.) in nitrobenzene (10 ml.) was heated on a steam-bath for an hour. After cooling, ice-water was added and the nitrobenzene was removed by the steam distillation. The precipitate was filtered, and the unchanged substance (50 mg.) was recovered. By acidification of the filtrate with dilute hydrochloric acid, a crystalline precipitate, was separated. Purification from aqueous methanol gave 4',5,7-trihydroxy-8-methoxyisoflavone (30 mg.), colorless needles m. p. 238—9°. The mixed melting point with the product prepared by method (a) showed no depression.

*Anal.* Found: C, 63.56; H, 4.54. Calcd. for $C_{16}H_{12}O_6$: C, 64.00; H, 4.03%.

We are grateful to the Institute of Agricultural Chemistry, Faculty of Agriculture, Kyoto University for microanalyses.

*Faculty of Literature and Science*
*Toyama University, Toyama*

6) T. A. Geissman and T. G. Halsall, *J. Am. Chem. Soc.*, **73**, 1280 (1951).

# *Crystallization of Quartz at High Temperatures*

By Taneki TOKUDA

(Received March 8, 1957)

It has generally been accepted that amorphous silica[1] and vitreous silica[2] crystallize into cristobalite when they are heated in the absence of a flux. It has also been reported that a mixture of quartz and cristobalite was obtained[3] when amorphous silica was heated at 1200—1300°C with addition of a mineralizer which did not contain alkali or strontium compounds, although at these temperatures quartz is unstable*. Crystallization of quartz as a single phase has been described by Wittels[4], who obtained it by annealing,at 930°C for 16 hours, metamict silica produced by fast neutron bombardment ($2\times10^{20}$neutrons/cm).

It has become evident that the presence of a very small amount of alkali plays an important role in the crystallization of silica, whereas the previous workers do not seem to have paid attention on this point. Therefore, the author has reinvestigated the crystallization of silica at high temperatures using amorphous silica which is free from alkali. It was found that quartz was obtained as a single phase even at 1388±5°C.

## Experimental

"Aerosil", amorphous silica, made by DEGUSSA was used as the starting material. Chemical analysis and physical constants of this material are shown in Table I. No trace of alkali was found by means of a chemical analysis. The specimen was held in a platinum boat, and was heated at a given temperature (±5°C) in an electric tube furnance, and was very rapidly cooled in air. No flux was added. The cooled

TABLE I
CHEMICAL ANALYSIS AND PHYSICAL CONSTANTS OF UNFIRED SILICA SPECIMEN

| | |
|---|---|
| $SiO_2$ | 99.9% |
| $Fe_2O_3$ | 0.004% |
| CaO | None |
| MgO | None |
| Free moisture | 1.72% |
| Ignition loss (= Total $H_2O$) | 4.2% |
| Specific density | 2.2 |
| Bulk density | 0.050 |

TABLE II
FIRED SILICA SPECIMEN

| Heating Temperature (°C) | Heating hours (hr.) | Cristobalite (111) Intensity (Counts/sec) | Cristobalite (111) Diffraction angle (2θ) (°) | Cristobalite (111) Spacing (Å) | Quartz (101) Intensity (Counts/sec) | Quartz (101) Diffraction angle (2θ) (°) |
|---|---|---|---|---|---|---|
| ca. 1600 | 5 | ca. 2000 | 22.06 | 4.029 | 0 | — |
| 1453 | 1/2 | 16 | 22.03 | 4.034 | 0 | — |
| 1413 | 1 | 26 | 21.96 | 4.047 | 0 | — |
| 1399 | 2 | 28 | 21.95 | 4.050 | 0 | — |
| 1392 | 2 | 35 | 21.92 | 4.054 | 0 | — |
| 1388 | 1 | 0 | — | — | 29 | 26.65 |
| 1374 | 1 | 0 | — | — | 16 | 26.65 |
| 1373 | 1 | 0 | — | — | 0 | — |
| 1362 | 1 | 0 | — | — | 0 | — |
| 1352 | 1 | 0 | — | — | 0 | — |

* According to Flörke[7] and Scairer and Yagi[8], quartz is unstable above ca. 1050°C, while according to Fenner[5] it is unstable above 870°C.

1) R. B. Sosman, "The Properties of Silica", The Chemical Catalog Co., Inc., New York, 1927, p. 171.
2) ibid., p. 97.
3) J. H. Schulman, E. W. Claffy and R. J. Ginter, *Am. Mineral.*, **34**, 68 (1949): D. A. Bailey, ibid. **34**, 601(1949); L. S. Birks and J. H. Schulman, ibid. **35**, 1035 (1950); G. D. Rieck and J. M. Stevels, *J. Soc. Glass Technol.*, **35**, 284 (1951).
4) M. Wittels and F. A. Sherrill, *Phys. Rev.*, **93**, 1117 (1954).
5) C. N. Fenner, *Am. J. Sci.*, **36**, 331 (1913).
6) T. Tokuda, *Mem. Inst. Sci. Ind. Res. Osaka Univ.*, **14** (1957) in press.
7) O. W. Flörke, *Naturwiss.*, **43**, 419 (1956).
8) J. F. Scairer and K. Yagi, *Am. J. Sci.*, Bowen Vol., 500 (1952).

specimens were analysed by the "Norelco" X-ray diffractometer. Filtered Cu—$K_\alpha$ was used with an X-ray tube running at 30 kV, 15 mA. Divergence and scatter slits were 1°, and the receiving slit was 0.006" in width respectively.

## Results

The reflection (111) for cristobalite was detected along with the amorphous band with specimens which were heated at 1392, 1399, 1413, or 1453°C for one hour (Fig. 1). The reflection (101) for quartz was detected along with the amorphous band with those which were heated at 1388 or 1374°C for one hour (Fig. 2). These are the highest temperatures at which quartz has

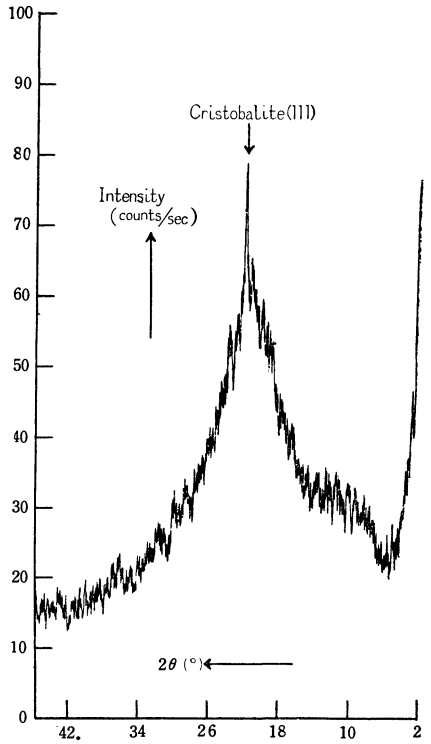



Fig. 1. X-ray diffraction powder pattern of amorphous silica heated at 1413±5°C for one hour in air, showing the appearance of cristobalite.

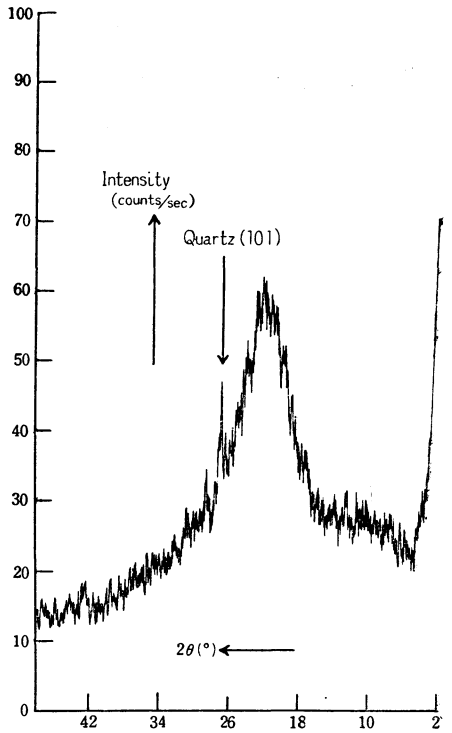



Fig. 2. X-ray diffraction powder pattern of amorphous silica heated at 1388±5°C for one hour in air, showing the appearance of quartz.

been crystallized, reported in the literature. The diffraction angle for (101) of quartz of these products is, as is shown in Table II, equal to that of a large transparent Brazilian quartz within an experimental error (0.01°). On the other hand, it was found that, for crisiobalite, as the temperature of heating is lower, the products show larger spacing. Thus a specimen which was heated at 1392°C±5 for one hour showed a spacing for cristobalite 0.6% larger compared to that of the standard specimen which was obtained by heating amorphous silica at ca. 1600°C for five hours.

*Osaka University, Osaka*

# *On 2-Arylaminotropones. II*[1]. *Bromination of 2-Anilino- and 2-(p-Toluidino)tropones*[2]

By Syun ISEDA

(Received March 22, 1957)

The present paper describes the bromination of 2-anilino- and 2-(*p*-toluidino)-tropone, reported in Part I of this series[1], together with discussions on related matter.

Bromination in glacial acetic acid, in the presence of anhydrous sodium acetate, of 2-anilinotropone affords, irrespective of the amount of bromine added, a tribromo derivative (I) of m.p. 262.8°C*, and the same of 2-(*p*-toluidino)-tropone affords a dibromo derivative (II), m.p. 180–181°C or a tribromo derivative (III), m.p. 190°C, with a given amount of bromine. In the absence of sodium acetate, I is obtained from 2-anilinotropone and III from 2-(*p*-toluidino)tropone.

In order to establish the structure of these compounds, their hydrolysis was attempted by heating with 4N ethanolic potassium hydroxide. I afforded *p*-bromoaniline(N-acetyl derivative, m.p. 163.5°C) as a basic component and 3,5-dibromotropolone, m.p. 154°C(*p*-toluidine salt, m.p. 122.5°C)[3] as an acidic component. II formed *p*-toluidine (N-acetyl derivative, m.p. 153°C) and 3,5-dibromotropolone. III remained inert on refluxing with 2N ethanolic potassium hydroxide for 30 minutes, almost all the starting material being recovered. Its ultraviolet absorption spectrum (Fig. 1)[4] indicated the presence of a tropone ring and that aromatization had not taken place.

When III was refluxed with 6N ethanolic potassium hydroxide for 6—8 hours or with sodium methoxide in methanol for 3 hours, it was separated into a basic component IV (N-acetyl derivative, m.p. 118–119°C) and an acidic component.

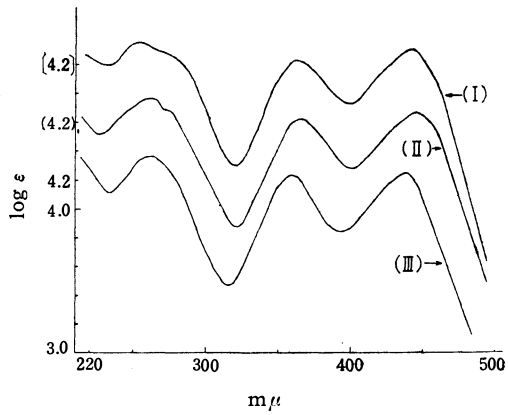



Fig. 1. Ultraviolet absorption spectra of (III), (II) (log ε+0.4), and (I) (log ε +0.8) (in methanol).

Vacuum sublimation of this acidic component yielded a small amount of 3,5-dibromotropolone, indicating that no additional bromine substitution of the tropone ring had taken place and that the substitution occurred in the benzenoid portion. It is therefore assumed that IV is a bromo-*p*-toluidine and that the bromine had entered into the position *meta* to the methyl group in *p*-toluidine, in accordance with the results of bromination of *p*-acetotoluidide[5] and 3-nitrosalicylic acid *p*-toluidide[6]. Comparison with an authentic specimen proved IV to be 4-amino-3-bromotoluene.

It can be concluded from the foregoing results that I is 2-(4′-bromoanilino)-5,7-dibromotropone, and II and III are respectively 2-(*p*-toluidino)- and 2-(2′-bromo-*p*-toluidino)-5,7-dibromotropone. The ultraviolet absorption spectra of I, II, and III are shown in Fig. 1.

Their infrared spectra[7] all indicated the absorption of 1,4-disubstituted benzene

1) Part I: S. Iseda, *Bull. Chem. Soc. Japan*, **28**, 617 (1955).

2) Presented at the Kyushu Local Meeting of the Chemical Society of Japan, Kumamoto, December 4, 1954.

* All melting points corrected.

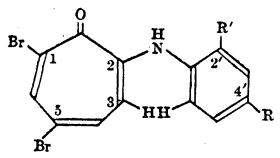
3) T. Nozoe, Y. Kitahara, K. Yamane and A. Yoshikoshi, *Proc. Japan Acad.*, **27**, 18 (1951).

4) Ultraviolet absorption spectra were determined by a Beckman spectrophotometer by members of the Chemistry Department, Faculty of Science, Tohoku University, Sendai.

5) "Organic Syntheses", Coll. Vol. I (Japanese translation), p. 113 (1935).

6) G. V. Jadhav and P. G. Nerlekar, *J. Indian Chem. Soc.*, **29**, 765 (1952); *J. Univ. Bombay*, **20**, part 3, 47 (1951).

7) Infrared spectra were determined by Messrs. H. Kozuma and K. Kawasaki, Technical Department, Shin Nippon Chisso Hiryo K. K., Minamata.



| | R | R′ |
|---|---|---|
| (I) | Br | H |
| (II) | $CH_3$ | H |
| (III) | $CH_3$ | Br |

TABLE I

WAVE LENGTH OF ABSORPTIONS OF 1,4-DISUBSTITUTED BENZENE AT 8–10 $\mu$ region.

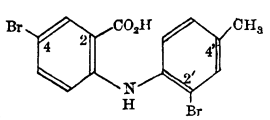
(Unit in microns).

| | | | |
|---|---|---|---|
| I | 8.28 | 9.15 | 9.59 |
| II | 8.29 | 9.16 | 9.62 |
| III | 8.25 | 9.15 | 9.62 |

(Table I), while that of III indicated the additional absorption at 8.74 $\mu$ characteristic of 1,2,4-trisubstituted benzene[8].

The substitution of bromine in the tropone ring of 2-aminotropone itself occurs in the order of $C_7$, $C_5$ and $C_3$[9]. In the present series of experiments, no significant difference was observed between $C_7$ and $C_5$ but the third bromine atom entered the benzene ring, instead of the tropone ring. This indicates that the $C_3$ position of the tropone ring in 2-arylaminotropone suffers the steric hindrance of the arylamino group while such a hindrance does not exist in the 2-aminotropone [see constitution of I].

Application of sodium methoxide to III yielded a small amount of 4-amino-3-bromotoluene and 3,5-dibromotropolone, and most part (73% of the starting material) of the product turned to yellow prisms (V), m.p. 247°C, $C_{14}H_{11}O_2NBr_2$. V is negative to the ferric chloride test and forms a sodium salt of pale yellow needles, sparingly soluble in water. Application of diazomethane to V easily affords its methyl derivative VI, m.p. 93–94°C, $C_{15}H_{13}O_2NBr_2$. The infrared spectra of V and VI (Fig. 2) indicate the presence of a carboxyl(5.93$\mu$) in V and an ester(5.85$\mu$) in VI, and their ultraviolet spectra (Fig. 3) are notable in that the absorption in the wave length region longer than 420 m$\mu$ has disappeared. The probable constitution of



(V)

V, 2-carboxy-2′, 4-dibromo-4′methyldiphenylamine, is now under study by synthesis.

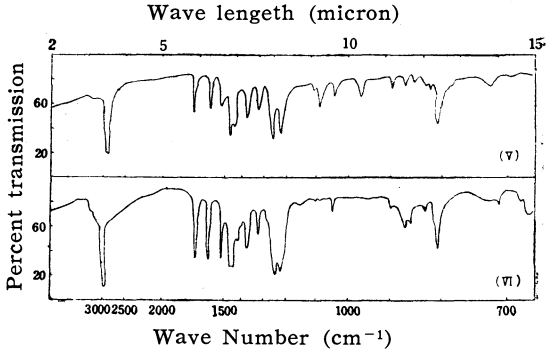



Fig. 2. Infrared absorption spectra of (V) and (VI) (in Nujol).

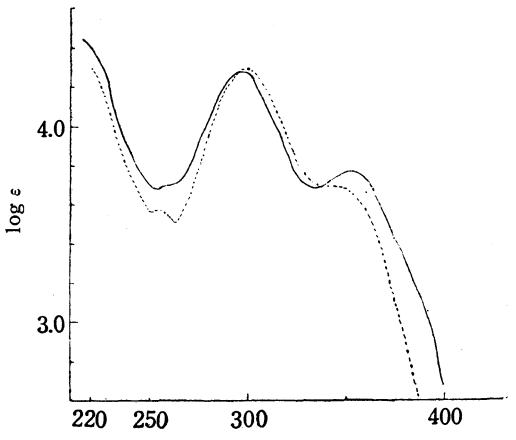



Fig. 3A. Ultraviolet absorption spectra of (V) in neutral (——), and in alkaline medium (……).

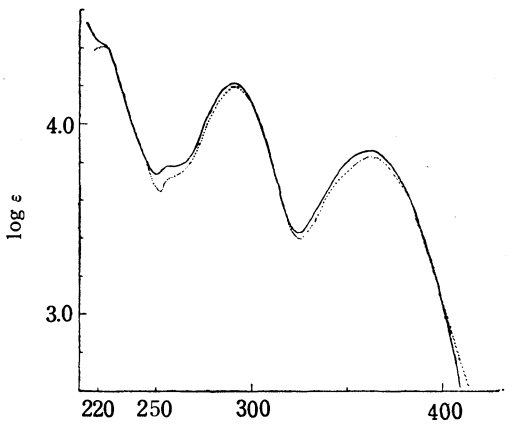


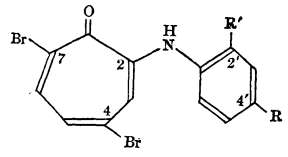

Fig. 3B. Ultraviolet absorption spectra of (VI) in neutral (——), and in alkaline medium (……).

(Note. Neutral: in methanol. Alkaline: in 0.1 N NaOH in methanol).

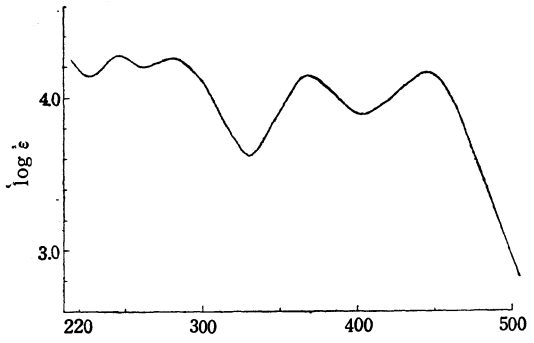
8) L. J. Bellamy, "The Infra-red Spectra of Complex Molecules", p. 70 (1954).

9) T. Nozoe, S. Seto, H. Takeda, S. Morosawa and K. Matsumoto, *Proc. Japan Acad.*, **27**, 556 (1951); **28**, 192 (1952); *Sci. Repts Tohoku Univ.*, Ser., I, **36**, 126 (1952).

Bromination of 2-anilino- and 2-(*p*-toluidino)-4,7-dibromotropone[2] in glacial acetic acid, with or without the addition of sodium acetate, resulted in an introduction of one atom of bromine in both cases and respectively afforded orange yellow prismatic needles, (VII), m.p. 294.5°C, $C_{13}H_8ONBr_3$, and VIII, m.p. 264°C, $C_{14}H_{10}ONBr_3$. Since the newly introduced bromine atom is not in the form of a salt, the following structure in which the substitution has occurred in the benzene ring, can be assumed. This structure is supported by the fact that its ultraviolet spectra are similar to those of I and III. (See Fig. 4.)




| | R | R' |
|---|---|---|
| (VII) | Br | H |
| (VIII) | $CH_3$ | Br |




Wave length in mμ

Fig. 4. Ultraviolet absorption spectra of (VII) (in methanol).

## Experimental

**2-(4'-Bromoanilino)-5,7-dibromotropone (I)**—Bromination of 2-anilinotropone gave the same results whether sodium acetate was added or not, but when it was added, some complications arose in making the product completely free of ash. A solution of 600 mg. (0.003 mole) of 2-anilinotropone dissolved in 5.0 cc. of glacial acetic acid was treated with 1020 mg. (0.0063 mole) of bromine[10] under stirring and the yellow precipitate that began to form a few minutes later was collected by filtration after 3 hours. Yield, 510 mg.

The mother liquor failed to yield any more crystals on further standing for 2 days, but precipitated crystals immediately on the addition of further 510 mg. of bromine. Total yield, 1260 mg. (almost 100% of the calculated amount). The two lots of precipitate were each dried over sodium hydroxide in vacuo, weighed and recrystallized successively from ethyl acetate and benzene. Both formed the same yellow prisms, m.p. 262–262.8°C (sealed tube), and their admixture indicated them to be an identical substance.

***Anal.*** Found: C, 36.15; H, 1.94%. Calcd. for $C_{13}H_8ONBr_3$: C, 35.96; H, 1.86%.

The same product was obtained whether 3.5 molar equivalents of bromine were added at once or 4–5 molar equivalents. In the case of the latter, some red prisms were found to be mixed in the yellow crystals but these turned yellow during suctional filtration. The crystals of m.p. 262–262.8°C remained unchanged on heating in 5% aqueous ammonia or on shaking of its benzene solution with 2% sodium hydroxide. Its infrared spectrum also failed to exhibit the absorption of $>C=N^+<$ at around 5.9 μ.

**Bromination of 2-(*p*-Toluidino)tropone.**—a) *With the addition of sodium acetate*: To a solution of 210 mg. (0.001 mole) of 2-(*p*-toluidino)-tropone dissolved in 4.0 cc. of glacial acetic acid and containing 0.5 g. of anhydrous sodium acetate, 180 mg. (0.0011 mole) of bromine was added while stirring under chilling in ice water, by which crystals began to precipitate out after a few minutes. After allowing the mixture to stand overnight with occasional agitation, the precipitate was collected by filtration, dried over sodium hydroxide in vacuo, and 210 mg. of the product was dissolved in 50 cc. of benzene. The benzene solution was washed consecutively with water, diluted hydrochloric acid, dilute sodium hydroxide solution, and water, dried over anhydrous sodium sulfate, and the solvent was distilled off. The residue was recrystallized three times from ethyl acetate and afforded 2-(*p*-toluidino)-5,7-dibromotropone (II) as lemon-yellow needles, m.p. 180–181°C.

*Anal.* Found: C, 45.57; H, 3.25; N, 3.87%. Calcd. for $C_{14}H_{11}ONBr_2$: C, 45.54; H, 3.01; N, 3.79%.

Crystals did not appear on standing of the mother liquor of II for one week and addition of 320 mg. (0.002 mole) of bromine gradually precipitated crystals. The mixture was allowed to stand at 30°C for 40 hours and the precipitate was purified as for II, affording 180 mg. of 2-(2'-brome-*p*-toluidino)-5,7-dibromotropone (III). Recrystallization from ethyl acetate gave lemon-yellow needles, m.p. 190°C, which melted at 150–153°C on admixture with II.

*Anal.* Found: C, 37.94; H, 2.44; N, 3.23%. Calcd. for $C_{14}H_{10}ONBr_3$: C, 37.52; H, 2.25; N, 3.13%.

Addition of water to the glacial acetic acid mother liquor of III only formed a minute amount of reddish brown resinous matter.

b) *Without the addition of sodium acetate*: To a stirred solution of 210 mg. of 2-(*p*-toluidino)-tropone dissolved in 4.0 cc. of gracial acetic acid, 500 mg. (0.0031 mole) of bromine was added under cooling and crystals began to precipitate out gradually after about one hour. After this

10) All the bromine used in this experiment was a glacial acetic acid solution containing 100 mg. of bromine in 1.0 cc. of the solution.

11) The microanalyses were carried out at the Institute of Polytechnics, Osaka City University, and at the Pharmaceutical Department, Kumamoto University.

mixture being set aside for 5 hours with occasional agitation, the yellow crystals mixed with yellowish brown to reddish brown crystals were collected by suctional filtration by which all the crystals turned yellow. Yield, 400 mg. (88 %). After drying, the crystals were recrystallized twice from ethyl acetate to yellow needles, m.p. 190°C, identical with III.

When 180 mg. (0.0011 mole) of bromine was added under the same conditions, the crystals failed to precipitate out even after a few days. When a further amount of bromine (220 mg.) was added, or 400 mg. (0.0025 mole) of bromine was added at first, 330 mg. of III, m.p. 190°C, was obtained.

**Decomposition of 2-(4'-Bromoanilino)-5,7-dibromotropone (I).**—A mixture of I (500 mg.) and 40 cc. of 4 N ethanolic solution of sodium hydroxide was refluxed for 4 hours, the solvent was distilled off under a slight suction, and the distillate was collected in a receiver containing a small amount of hydrochloric acid. The residue in the distillation flask was mixed with water, and the mixture (A) was extracted with ether. The combined distillate and the ether extract was adjusted to pH 3.0 with hydrochloric acid and evaporated to dryness. A few drops of acetic anhydride was added to the residue, allowed to stand over night, mixed with water and again evaporated to dryness. The residue was recrystallized from aqueous ethanol and 25 mg. of *p*-bromoacetanilide was obtained as colorless needles, m.p. and mixed m.p. 161°C.

The alkaline aqueous solution (A) left after shaking with ether was acidified with hydrochloric acid, extracted with ether, and the ether was evaporated. Vacuum sublimation of the residue resulted in the sublimation of ca. 1/4 of the substance and 55 mg. of pale yellow crystals, giving positive ferric chloride reaction, was obtained. Recrystallization from dilute ethanol with charcoal afforded crystals of m.p. 152°C, which formed a *p*-toluidine salt, m.p. 122°C, by the usual method. No depression of the melting point occurred on admixture with 3,5-dibromotropolone.

**Decomposition of 2-(*p*-Toluidino)-5,7-dibromotropone (II).**—The sample (400 mg.) was refluxed for 6 hours as with I to effect hydrolysis and 20 mg. of *p*-acetotoluidide, m.p. 151°C and 30 mg. of 3,5-dibromotropolone were obtained.

**Reaction of 2-(2'-Bromo-*p*-toluidino)-5,7-dibromotropone (III) and 2N Sodium Hydroxide.**—A mixture of 300 mg. of (III) and 30 cc. of 2N ethanolic sodium hydroxide solution was refluxed for 30 minutes; cooling of the clear reaction mixture precipitated crystals. Recrystallization from ethyl acetate afforded crystals m.p. 186–188°C, undepressed on admixture with III. Rate of recovery, ca. 160 mg.

**Reaction of (III) and Sodium Methoxide.**—A mixture of 300 mg. of III and sodium methoxide solution (2g. of metallic sodium dissolved in 50cc. of absolute methanol) was refluxed for 3 hours. the most part of the solvent was distilled off under a reduced pressure, and the residue was treated as for I, affording 10 mg. of a basic component. Its acetylation and recrystallization of the product from dilute ethanol gave the N-acetate as fine needles, m.p. 119–120°C, undepressed on admixture with the synthesized 4-acetamino-3-bromotoluene, m.p. 119–120°C. This substance melted at 90–93°C when admixed with 4-acetamino-2-bromotoluene, m.p. 112–113°C[12]. 4-Acetamino-2-bromotoluene was obtained through the diazotation of 2-amino-4-nitrotoluene to 2-bromo-4-nitrotoluene, followed by reduction with tin and hydrochloric acid, and application of acetic anhydride to the amine so obtained, at room temperature.

The acidic component obtained from this hydrolysis was warmed with 4 cc. of ethyl acetate and the solution was allowed to stand for a few days, depositing 220 mg. of crystals. The ethyl acetate mother liquor was evaporated to dryness and the residue (30 mg.) was submitted to vacuum sublimation, from which ca. 8 mg. of 3,5-dibromotropolone, m.p. 152°C, was obtained. The sublimation residue was an acidic, amorphous brown mass. Crude crystals (220 mg.) were recrystallized several times from 80 % ethanol, using charcoal a few times, to lustrous yellow needles, m.p. 247°C (V).

*Anal.* Found: C, 44.00; H, 2.91 %. Calcd. for $C_{14}H_{11}O_2NBr_2$: C, 43.66; H, 2.88 %.

This substance gives negative ferric chloride reaction in ethanol and forms a sodium salt of almost colorless needles, somewhat sparingly soluble in water, with sodium bicarbonate solution. This sodium salt melts once at 95°C, solidified again, and does not melt up to 275°C. The sodium salt regenerates the original substance, m.p. 246–247°C, by the action of hydrochloric acid.

An excess of diazomethane in ether was added to 150 mg. of the substance of m.p. 247°C suspended in 30 cc. of ether, by which the crystals gradually disappeared. After 3 hours, the remaining diazomethane was decomposed with acetic acid and recrystallization of the product from 85 % ethanol afforded the methyl ester (VI) as pale yellow needles, m.p. 93–94°C. Maximum absorption in Nujol: 5.85 $\mu$ (ester carbonyl). The analytical values corresponded to those of the monomethyl derivative.

*Anal.* Found: C, 45.35; H, 3.39 %. Calcd. for $C_{15}H_{13}O_2NBr_2$: C, 45.15; H, 3.28 %.

**2-(4'-Bromoanilino)-4,7-dibromotropone (VII).**—A mixture of 0.7 g. of 2-anilino-4,7-dibromotropone and 60 cc. of glacial acetic acid, containing 2 g. of anhydrous sodium acetate, was heated, cooled, and 500 mg. of bromine was added to the crystalline brei. After a little time, yellow crystals began to precipitate out. The mixture was allowed to stand over night and the crystals were recrystallized from benzene or ethyl acetate, affording 0.50 g. of (VII) as reddish yellow prisms, m.p. 294–295°C.

*Anal.* Found: C, 35.90; H, 1.90 %. Calcd. for $C_{13}H_8ONBr_3$: C, 35.96; H, 1.86 %.

12) J. J. Blanksma, *Chem. Weekbl.*, **6**, 899 (1909); *Chem. Zentr.*, **1910**, I, 260.

**2-(2'-Bromo-*p*-toluidino)-4,7-dibromotropone (VIII).**—This was prepared from 1.2 g. of 2-(*p*-toluidino)-4,7-dibromotropone by the method used for that of the aniline analog and recrystallization from benzene afforded 1.2 g. of (VIII) as yellow prisms with a slight reddish tint, m.p. 264°C.

*Anal.* Found: C, 37.47; H, 2.30 %. Calcd. for $C_{14}H_{10}ONBr_3$: C, 37.52; H, 2.25 %.

Concentration of the benzene mother liquor yielded 0.14 g. of yellow fine prisms, m.p. 213–215°C.

A part of the experiment reported herein was carried out at the Chemistry Department Faculty of Science, Tohoku University, Sendai, and the writer takes this opportunity to express his sincere gratitude to Professor Tetsuo Nozoe for his kind guidance and encouragement throughout the course of this work. The writer is also indebted to those who supplied analytical data.

The present series of studies constitute a part of the general research on azulenoid compounds (Representative: Professor T. Nozoe). Part of the expenses for the present work was defrayed by a Grant in Aid for Scientific Research provided by the Ministry of Education, which is gratefully acknowledged.

*Department of Chemistry, Kumamoto Women's University*
*Kumamoto*

# *A Simplified Method for the Preparation of N-Acetylphenylalanines*

By Tôru OKUDA and Yasuo FUJII

(Received March 25, 1957)

Among various synthetic preparations of phenylalanine and its nuclear-substituted derivatives the Erlenmeyer's azlactone method[1,2] seems to be the most accepted one. During the course of the study on the synthesis of aromatic amino acids by this method, a simple and practical procedure has been found in a step of the reductive cleavage of the azlactone ring to yield N-acetylphenylalanines. The application of this method to several azlactones is described in this communication.

It is well-known that benzoyl- or acetylglycine, when heated with aromatic aldehyde in acetic anhydride in the presence of fused sodium acetate as condensing catalyst, yields 2-phenyl- or 2-methyl-4-benzal-5-oxazolone respectively. The route to N-acetylphenylalanines from the azlactones that has ever been utilized is as follows: neutral, alkaline or acidic hydrolysis of azlactones and subsequent hydrogenation of the resulting acetylaminocinnamic acids to acetylphenylalanines. The reducing agents which have been used for this conversion are: 1. Sodium[3,4] or sodium amalgam and water or ethanol. 2. Catalytic hydrogenation (Pt, Pd[5] or Raney nickel[6]).

Since N-acetylphenylalanines were found to be susceptible to optical resolution[7,8] it seemed worthy to study to find a good and simple preparative method for these compounds.

Oxazolones were found to be easily reduced in a dilute aqueous solution of an equivalent amount of sodium hydroxide under pressure using Raney nickel catalyst. The reduction proceeded very smoothly at lower temperature and at the same time the cleavage of the azlactone ring occurred to form sodium salts of N-acetylphenylalanines during the course of hydrogenation. The reduction of the C=C double bond may be facilitated by the presence of alkali which also naturally acts as hydrolyzing agent. By acidification of the reduction mixture with concentrated hydrochloric acid N-acetylphenylalanines were readily obtained.

1) E. Erlenmeyer, *Ann.*, **275**, 1 (1893).
2) H. E. Carter, "Organic Reactions", Vol. **3**, 198, John Wiley & Sons Inc., New York, N. Y., 1946.
3) G. Barger and A. J. Ewins, *Biochem. J.*, **11**, 58 (1917).
4) A. Ellinger and Z. Matsuoka, *Z. Physiol. Chem.*, **91**, 45 (1914).
5) R. M. Herbst and D. Shemin, "Organic Syntheses", Coll. Vol. **2**, 491, John Wiley & Sons Inc., New York, N. Y., 1943.
6) J. Elks, D. F. Eiliott and B. A. Hems, *J. Chem. Soc.*, **1944**, 629.
7) N. F. Albertson, *J. Am. Chem. Soc.*, **73**, 452 (1951).
8) D. G. Doherty and E. A. Pope, *J. Biol. Chem.*, **189**, 447 (1951).

TABLE I

N-ACETYL-β-(SUBSTITUTED PHENYL)-ALANINES

| Substituted Group | Yield[a], % | m.p.[b], °C | Formula | C % Calcd. | C % Found | H % Calcd. | H % Found | N % Calcd. | N % Found |
|---|---|---|---|---|---|---|---|---|---|
| none | 98 | 144 | $C_{11}H_{13}O_3N$ | 63.77 | 63.56 | 6.28 | 5.91 | 6.76 | 6.62 |
| *p*-methyl | 99 | 164 | $C_{12}H_{15}O_3N$ | 65.16 | 65.65 | 6.79 | 6.81 | 6.33 | 6.04 |
| *p*-methoxy | 96 | 150 | $C_{12}H_{15}O_4N$ | 60.76 | 60.71 | 6.33 | 6.29 | 5.91 | 5.69 |
| 3,4-methylenedioxy | 92 | 164—6 | $C_{12}H_{13}O_5N$ | 57.37 | 57.31 | 5.18 | 5.17 | 5.58 | 5.51 |

a) Yields are based upon weight of crude product since in general no purification was required before hydrolysis or resolution.

b) Melting point of the analytical sample.

Four azlactones prepared from acetylglycine, benzaldehyde, tolualdehyde, anisaldehyde and piperonal by usual method were all converted in to the corresponding N-acetylphenylalanines in almost quantitative yield by the procedure described above. The results are summarized in Table I.

It was also found that 2-phenyl-5-oxazolone was very resistant to this hydrogenation unlike 2-methyl-5-oxazolone.

From the standpoint of preparation, the above procedure is characterized by excellent yield and readiness of operation.

## Experimental

**2-Methyl-4-benzal-5-oxazolone.**—This azlactone was prepared according to Herbst's procedure[5].

**2-Methyl-4-(*p*-methylbenzal)-5-oxazolone.**—By analogous procedure given for 2-methyl-4-benzal-5-oxazolone this compound was prepared. The experimental conditions are as follows: a mixture of 165 g. of acetylglycine, 97.5 g. of fused sodium acetate, 250g. of freshly distilled *p*-methylbenzaldehyde, and 380 g. of 90 % acetic anhydride was warmed until the solution was complete. The resulting solution was then heated for one hour under reflux, cooled and placed in a refrigerator overnight. The brown solid mass obtained was digested with cold water. The yellow crystals melting at 133—135°C weighed 188 g. An analytical sample was obtained by recrystallization from chloroform and petroleum ether.

*Anal.* Found: C, 71.54; H, 5.42; N, 6.83%. Calcd. for $C_{12}H_{11}O_2N$: C, 71.64; H, 5.47; N, 6.96%.

**2-Methyl-4-(*p*-methoxybenzal)-5-oxazolone.**—A mixture of 54.4 g. of anisaldehyde, 38.6 g. of acetylglycine and 19.7 g. of anhydrous sodium acetate in 82 ml. of acetic anhydride was treated in the same manner. Thirty grams of yellow crystals with melting point of 114°C was obtained. The azlactone was recrystallized from chloroform-petroleum ether.

*Anal.* Found: C, 66.65; H, 5.26; N, 6.34%. Calcd. for $C_{12}H_{11}O_3N$: C, 66.36; H, 5.07; N, 6.45%.

**2-Methyl-4-(3′, 4′-methylenedioxybenzal)-5-oxazolone.**—With 37.5 g. of piperonal, 23.4 g. of acetylglycine, 12.3 g. of sodium acetate and 52 ml. of acetic anhydride, 46.2 g. of the azlactone was obtained as yellowish crystals melting at 176—180°C. An analytical sample was obtained by recrystallization from acetic acid and petroleum ether.

*Anal.* Found: N, 5.77%. Calcd. for $C_{12}H_9O_4N$: N, 6.06%.

**General Procedure of Preparation of N-Acetylphenylalanines.**—Four azlactones prepared as described above were all converted into the corresponding N-acetylphenylalanines in the following manner: one mole of the crude benzaloxazolone, an about five per cent. aqueous solution of an equivalent amount of sodium hydroxide and Raney nickel catalyst (as alloy, one tenth or one twentieth of the oxazolone used, by weight) were placed in a stainless steel autoclave. An initial hydrogen pressure of 40—70 atm. was applied and the apparatus was shaken at room temperature or, if necessary, at a higher temperature of 30—50°C. Hydrogen was absorbed rapidly in most cases. When, after 0.2—2 hours, one mole of hydrogen had been absorbed, the reaction was stopped and the catalyst was removed by filtration. The pH of the clear orange-yellow filtrate was adjusted to 2—3 with concentrated hydrochloric acid. After being kept overnight in an ice-box, the crystals were collected and washed with water. The crude products thus obtained could be recrystallized from hot water. Table I shows the results of yield, melting point and elementary analysis of four N-acetylphenylalanines.

## Summary

A simple and practical procedure is described of preparing N-acetylphenylalanines by hydrogenation of the corresponding unsaturated azlactones in an aqueous sodium hydroxide solution with Raney nickel under pressure. By this method N-acetyl derivatives of phenylalanine, *p*-methylphenylalanine, *p*-methoxyphenylalanine and 3,4-methylenedioxyphenylalanine were synthesized in good yield.

The authors wish to acknowledge the advice of Professor S. Akabori and Mr. Y.

Izumi and the technical assistance of Mr. M. Tanaka, Morishita Pharmaceutical Co., and of Miss K. Murashima in some phase of the present work.

*Laboratory of Organic Chemistry and Institute for Protein Research*
*University of Osaka*
*Nakanoshima, Kita-ku, Osaka*

# *Synthesis of β- and γ-Thujaplicins*

By Shigeo KATSURA, Tatsuo MOROE and Norio IKEGAMI

(Received March 22, 1957)

Synthesis of α-, β- and γ-thujaplicins were reported by Nozoe[1] in 1950 and by Cook[2] in 1951. These methods were started with the preparation of the three isomers of Isopropylcycloheptanone by cyclization or ring enlargement, followed by oxidation to the dione compounds. Dehydrobromination after bromination afforded isomeric thujaplicins.

The present writers synthesized β-thujaplicins by the following two methods (A) and (B), which are herein described.

In the *A* method, perillaldehyde oxime (I) is used as the starting material and this is converted into tetrahydroperillamine (II) and via 4-isopropylcycloheptanone (IV) to the objective VI. The other *B* method starts with 4-isopropylcyclohexanone (VII) which is submitted to ring enlargement with nitromethane and via 4-isopropylcloheptanone to VI. The route of synthesis in this *A* method is shown in Fig. 1.

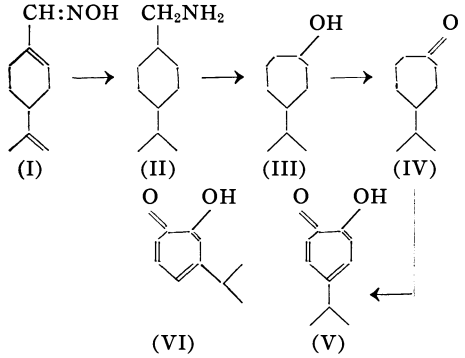



Fig. 1.

In this preparative method, perillartin, the oxime of perillaldehyde, was hydrogenated in ethanolic solution with nickel catalyst at 100°C and 100 atom., for about one hour and tetrahydroperillamine II was obtained in 63% yield. Ring enlargement of II was effected by the method of Ruzicka[3] and of Smith and Baer[4].

We prepared 4-isopropylcycloheptanol (III) in 31% yield by application of nitrous acid to the acetic acid solution of II at 40—50°C and its oxidation by the usual method gave 4-isopropylcycloheptanone (IV) in 50% yield.

Treatment of 4-isopropylcycloheptanone IV by the method of the afore-mentioned Nozoe and Cook, gave a mixture of β- and γ-thujaplicins(V), but the β-isomer was not isolated in pure state and was identified by paper chromatography[5].

The yield by this method of synthesis is 0.4% from the starting material, perillaldoxime, and it cannot be called an advantageous process since in the ring enlargement of perillamine, a fair amount of by-products form besides the objective 4-isopropylcycloheptanol (III), such as tetrahydroperillyl alcohol.

The route of synthesis in the *B* method is shown in Fig. 2.

In this method, the ring enlargement of isopropylcyclohexanone was effected by the nitromethane method of Dauben et al.[6]. The synthesis of thujaplicins from 4-isopropylcyclohexanone VII has not been made by this method as yet. The yield of

1) T. Nozoe, S. Seto and K. Kikuchi, *Proc. Japan Acad.*, **26**, 43 (1950); T. Nozoe, Y. Kitahara and S. Ito, ibid., **26**, 47, (1950); T. Nozoe, S. Seto, K. Kikuchi and H. Takeda, ibid., **27**, 146 (1951).

2) J. W. Cook, R. A. Raphael and A. I. Scott, *J. Chem. Soc.*, **1951** 695.

3) L. Ruzicka and W. Burgger, *Helv. Chim. Acta*, **9**, 399 (1926).

4) P. A. S. Smith and D. R. Baer, *J. Am. Chem. Soc.*, **74**, 6135 (1952).

5) E. Zavarin and A. B. Anderson, *J. Org. Chem.*, **21**, 332 (1956).

6) H. J. Dauben Jr., H. J. Ringold, R. H. Wade and A. G. Anderson, *J. Am. Chem. Soc.*, **73** 2359 (1951).

TABLE I
Rf VALUE OF THUJAPLICINS

| Mobile Phase | Stationary Phase (% $H_3PO_4$) | β-Thujaplicin from Taiwan Hinoki) | γ-Thujaplicin (synthetic) | β- and γ-Thujaplicin mixture | |
|---|---|---|---|---|---|
| Ligroine-toluene (3 : 1) | 17 | 0.45 | 0.32 | 0.44 | 0.32 |

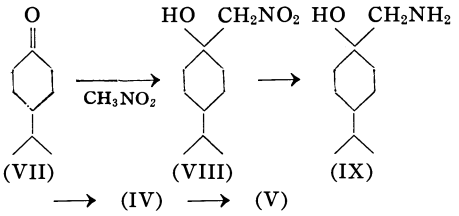


Fig. 2.

IV from VII is about 23.7% and further examination seems required as a synthetic method for thujaplicins. Derivation of IV to thujaplicins followed the same route as in A method. The starting material, 4-isopropylcyclohexanone VII was obtained according to the method described by Frank and Berry[7].

## Experimental

**Tetrahydroperillamine (II).**—A mixture of 33 g. of perillartin (I) in 66 cc. of ethanol was submitted to hydrogenation with Raney nickel as a catalyst, at 100°C and 100 atm.. The catalyst was filtered off, ethanol was distilled off from the filtrate, and the residue was distilled under a reduced pressure, affording 21 g. of II, b. $p._{18}$ 100—115°C $n_D^{21}$ 1.4772

**4-Isopropylcycloheptanol (III).**—A solution of 21 g. of II, 8.5 g. of glacial acetic acid, and 70 cc. of water was warmed to 40—50°C, and a solution of sodium nitrite in 20 cc. of water was added dropwise during thirty minutes. After stirring this mixture for thirty minutes at this temperature, the oily layer was separated and submitted to steam distillation. The oily distillate was distilled under a reduced pressure. B. $p._{12}$ 95—110°C, yield of III 6.5 g. (31%) $n_D^{22}$ 1.4735.

**4-Isopropylcycloheptanone (IV).**—A mixture of 6.5 g. of III, 4.5 g. of potassium dichromate, 11 g. of 50% sulfuric acid and 10 g. of benzene was heated for thirty minutes at 50—60°C to effect oxidation and 3.3 g. (50%) of IV was obtained as an oil of b. $p._{15}$ 105—115°C. $n_D^{22}$ 1.4689.

Semicarbazone: m. p. 153-4°C.

*Anal.* Found: C, 62.59; H, 9.62; N, 19.89%. Calcd. for $C_{11}H_{21}ON_3$: C, 62.6; H, 9.95; N, 19.9%.

**Sodium Salt of Bromo-β- and -γ-thujaplicins.**—To heated solution of 12 g. of IV dissolved in 25 cc. of dehydrated ethanol, a solution of 10.5 g. of selenium dioxide dissolved in 60 cc. of dehydrated ethanol was added dropwise during two hours and the mixture was stirred at the same temperature for five hours. After standing this over night, the precipitated selenium was filtered off, the filtrate was steam distilled, and the oily residue was extracted with benzene. The benzene extract was washed with water, dried, and benzene distilled off. The residue was distilled under a reduced pressure and 9.5 g. (79%) of a mixture of the diones, b. $p._{16}$ 130—140°C, was obtained. $n_D^{25}$ 1.4730.

A solution of 15 g. of the foregoing dione mixture dissolved in 0.5 cc. of acetic anhydride and 4.5 cc. of glacial acetic acid was chilled to 0°C to 10°C and a solution of 29 g. of bromine in 3 cc. of gracial acetic acid was added dropwise during four hours. The mixture was stirred at this temperature for 1.5 hours, allowed to stand over night (during which a vigorous evolution of hydrogen bromide was observed), and further stirred for four hours while gradually raising the temperature of the reaction mixture to 60°C. The mixture was then submitted to steam distillation, the residual oil was extracted with ether, and a solid substance was filtered off. To this ether extract, 100 cc. of 10% sodium hydroxide solution was added, the crystals that separated out were collected by filtration, and dried, affording 13 g. (86%) of a mixture of sodium salts of bromo-β- and -γ-thujaplicins.

**β- and γ-Thujaplicins.**—Catalytic reduction of 13 g. of the sodium salt mixture of bromo-β- and γ-thujaplicins in ethanol, with $Pd(OH)_2$—$CaCO_3$ catalyst, was carried out. After filtration of the catalyst, ethanol was removed by low-pressure distillation and about 10 g. of a solid thus obtained was extracted with toluene. The toluene solution was extracted with phosphoric acid, the acid extract was decomposed with water, and further extracted with toluene. After washing with water and drying, toluene was distilled off and the residue was distilled under a reduced pressure. The oily distillate crystallized and was purified from petroleum ether to 50 mg. of γ-thujaplicin, m. p. 78°C. From this mother liquor, 800 mg. of a mixture of β- and γ-thujaplicin was obtained.

Results of paper chromatography of this mixture was as shown in Table I.

**1-Nitromethyl-4-isopropyl-1-cyclohexanol (VIII).**—A mixture of 150 g. of 4-isopropylcyclohexanone VII (b. $p._{14}$ 90—95°C, $n_D^{21}$ 1.4570. Semicarbazone, m.p. 186—187°C) and 110 g. of nitromethane was added dropwise during 2.5 hours into sodium alkoxide (prepared from 27 g. of metallic sodium and 750 cc. of dehydrated ethanol) while being stirred at 40—43°C and a mixture was stirred for further nine hours at the same temperature. When cooled, the reaction mixture was cooled in

7) R. L. Frank, R. E. Berry and O. L. Shotwell, ibid., **71**, 3889 (1949).

ice, the reaction product was collected by filtration, and dried. About 400 g. of this sodium salt was placed in a three-necked flask, the flask was chilled in ice, and a thoroughly chilled solution of 142 g. of glacial acetic acid in 1200 cc. of water was added under stirring. After stirring this mixture for further thirty minutes (crystals precipitated out during chilling), this was neutralized and an oily layer was separated. The aqueous solution was extracted with ether, the ether extract was combined with the oily layer, dried, and ether distilled off. The residue was distilled off. The residue was distilled under a reduced pressure and 140 g. (93.9%) of VIII, b. $p._{15}$ 145—8°C was obtained. m. p. 56—58°C, $n_D^{20}$ 1.4786.

*Anal.* Found: C, 60.58; H, 9.20; N, 7.04%. Calcd. for $C_{19}H_{19}O_3N$: C, 59.7; H, 9.45; N, 6.97%.

From the mother liquor of the sodium salt, 16 g. of the starting material VII was recovered.

**1-Aminomethyl-4-isopropyl-1-cyclohexanol Acetate.**—Using a stainless steel autoclave of 300-cc. capacity, 41 g. of VIII in 82 cc. of glacial acetic acid was hydrogenated with Raney nickel catalyst, cooling the autoclave at first, gradually warming to the room temperature, and hydrogenated at 30°±2°C for seven hours (absorption of hydrogen, 10.2 l.). After removal of the catalyst by filtration, the solvent was distilled off under a reduced pressure, and the residual oil was cooled with addition of a small amount of ether by which the oil solidified into crystals. The crystals were collected by filtration, the filtrate was diluted with water, and extracted with ether. The aqueous solution was concentrated to a small volume and the foregoing procedure was repeated, isolating a further crop of crystals, m. p. 119—125°C. Total yield of acetate, 38 g. (90%).

About 3 g. of 4-isopropylcyclohexanone VII was obtained from the ether extract, its semicarbazone, m. p. 185—7°C, did not show any melting point depression on admixture with semicarbazone of VII.

**4-Isopropylcycloheptanone (IV).**—A solution of 50 g. of 1-aminomethyl-4-isopropyl-1-cyclohexanol acetate dissolved in 32 g. of glacial acetic acid was diluted with 52 cc. of water, chilled to 0°C, and 60 g. of sodium nitrite solution was added dropwise during two hours (vigorous effervescence). After stirring for one hour at the same temperature, the reaction mixture was allowed to stand over night, neutralized with sodium bicarbonate, and an oily layer was separated. The oil was steam distilled and the oily distillate was distilled under a reduced pressure, affording 20 g. of a fraction of b. $p._{17}$ 90—112°C. This was purified through the semicarbazone and decomposed with oxalic acid, b. $p._{17}$ 108—110°C. Yield 14 g. (28%). $n_D^{26}$ 1.4625. Semicarbazone, m. p. 144—5°C.

*Anal.* Found: C, 62.75; H, 9.95; N, 20.50%. Calcd. for $C_{11}H_{21}ON_3$: C, 62.6; H, 9.95; N, 19.9%).

The infrared spectrum of IV exhibited an absorption of C=0 at 1694 $cm^{-1}$.

## Summary

$\beta$- and $\gamma$-Thujaplicins were synthesized through 4-isopropylcycloheptanone from perillaldehyde and 4-isopropylcyclohexanone.

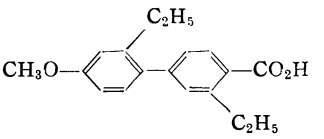
*Research Laboratory Takasago Perfumery Co., Ltd.*
*Kamata, Tokyo*

# *Estrogenic Biphenyls. II. 2',5'-Diethyl-4-methoxybiphenyl-4'-carboxylic Acid*

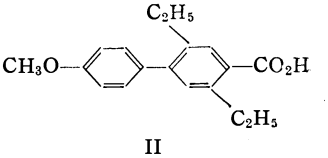
By Michinori ŌKI* and Takeo SATO

(Received April 10, 1957)

In the first paper[1] of the present series it was reported that 2,3'-diethyl-4-methoxybiphenyl-4'-carboxylic acid (I) is estrogenic and the activity can be explained on the basis of the postulation[2] of the suitable distance between the two active hydrogen atoms and the suitable thickness of the molecule for an estrogen.




I

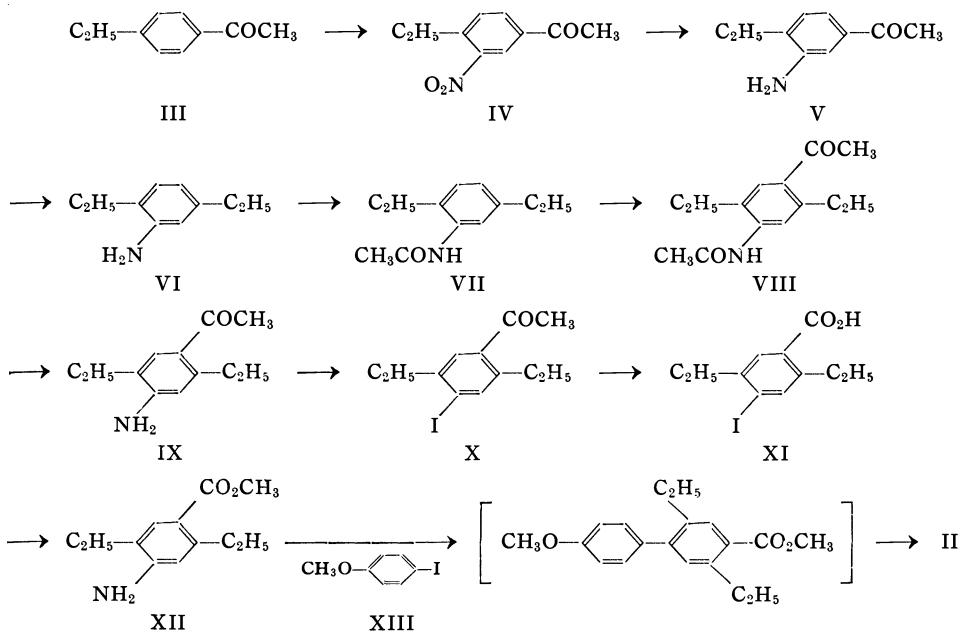



II

* Present address: Department of Chemistry, Faculty of Science, The University of Tokyo.

1) M. Ōki and T. Sato, This Bulletin, **30**, 508 (1957).

2) M. Ōki and Y. Urushibara, ibid., **25**, 109 (1952).



It is considered that the suitable thickness of compound I is obtained through the steric effect of the ethyl group at position 2, which causes a deformation of the coplanar structure, and thus increases the molecular thickness of the biphenyl system. As an ethyl group at position 2′ or 6′ should have the same steric effect as the one at position 2, 2′, 5′-diethyl-4-methoxybiphenyl-4′-carboxylic acid (II) has been prepared and tested on estrogenic activity.

Compound II was sythesized in the following way: nitration of 4-ethylacetophenone (III) gave 4-ethyl-3-nitroacetophenone (IV), which was reduced to the corresponding amine (V) with stannous chloride and hydrochloric acid. Modified Wolff-Kischner reduction of compound V yielded 2, 5-diethylaniline (VI), of which acetylation product VII showed no depression of the melting point on admixture with the authentic specimen of 2, 5-diethylacetanilide[3]. Reduction[3,4] of 2, 5-diethylnitrobenzene to VI gave an unsatisfactory result especially on a larger scale, because of the instability of the nitro-compound to heat. Compound VII was treated with acetyl chloride and aluminium chloride and the product, 4-acetamido-2, 5-diethylacetophenone (VIII), was hydrolyzed to yield 4-amino-2, 5-diethylacetophenone (IX). Compound IX was converted into 2, 5-dietyl-4-iodo-acetophenone (X) through a diazo-reaction and the iodo-ketone (X) was oxidized with sodium hypobromite to produce 2, 5-diethyl-4-iodo-benzoic acid (XI). Methyl 2, 5-diethyl-4-iodo-benzoate (XII) was prepared in the usual way. The ester (XII) and 4-iodoanisole (XIII) were submitted to the Ullmann reaction and the product was hydrolyzed and purified by chromatography through alumina.

TABLE I
ULTRAVIOLET ABSORPTION MAXIMUM

| Compound | $\lambda_{max.}$ (m$\mu$) | log $\varepsilon_{max.}$ |
|---|---|---|
| I | 270 | 4.09 |
| II | 268 | 4.14 |

The ultraviolet absorption data of compounds I and II are shown in Table I. The absorption spectra of the two compounds were similar and suggested that the deformation in the biphenyl skeletons of these compounds is nearly the same.

Compound II in oil was injected subcutaneously to ovariectomized mice. The minimum active dose to produce full estrus in 100% of the animals was found to be 100 $\gamma$ and the same as that of compound I[1].

## Experimental[5]

**4-Ethyl-3-nitroacetophenone (IV).**—4-Ethylacetophenone (III) was prepared from ethylbenzene and acetyl chloride according to the method

3) W. J. Gaudion, W. H. Hook and S. G. P. Plant, *J. Chem. Soc.*, **1947** 1631.
4) A. Voswinkel, *Ber.*, **22**, 315 (1889)

5) All melting and boiling points are uncorrected. The authors are indebted to Dr. Y. Osawa of the University of Tokyo for microanalyses.

described by Mowry et. al.[6]. One mole or 148 g. of compound III was dropped into 300 ml. of concentrated sulfuric acid with good stirring, while the temperature was kept below 5° by adding solid carbon dioxide. A mixed acid consisting of 80 ml. of nitric acid (d : 1.42) and 120 ml. of concentrated sulfuric acid was dropped into the sulfuric acid solution of the ketone (III) in forty-five minutes, the temperature being kept below 0° by adding solid carbon dioxide. The mixture was stirred for further ten minutes and poured into 2.5 l. of ice-water. The supernatant layer was decanted off and the lower one was dissolved in ether. The ethereal solution was washed with aqueous sodium hydroxide and then with water and dried over calcium chloride. Fractional distillation gave a pale yellow oil boiling at 135—136°/1 mm. which solidified at 0° and melted at the room temperature. Yield 164 g. or 85%, of the theoretical.

*Anal.* Found: N, 7.46%. Calcd. for $C_{10}H_{11}O_3N$: N, 7.25%.

**3-Amino-4-ethylacetophenone (V).** — When a mixture of 193 g. (1 mole) of compound IV, 750 g. (3.3 moles) of stannous chloride and 1.2 l. (6.6 moles) of dilute hydrochloric acid (1 : 1) was stirred, a spontaneous reaction set in and the mixture began to boil. The homogenous solution was allowed to cool and was basified with an excess of 33% aqueous sodium hydroxide. The organic material was extracted with ether and the combined extracts were dried over potassium carbonate. After the solvent was evaporated, the product distilled over at 144-145°/2 mm. as a pale yellow oil. Yield 147 g. or 90% of the theoretical.

*Anal.* Found: N, 8.76%. Calcd. for $C_{10}H_{13}ON$: N, 8.58%.

**2, 5-Diethylaniline (VI).**—A solution of 163 g. (1 mole) of the amino-ketone (V), 120 g. (1.6 moles) of 80% hydrazine hydrate and 280 g. of potassium hydroxide in 1 kg. of diethylene glycol was heated under reflux for one hour and the reflux condenser was then replaced by a downward condenser. Distillation was continued until the remainder in the flask attained the temperature of 200°, and it was heated again for thirty minutes. The reaction mixture was cooled and steam-distilled. The oily product was extracted with ether and the extract was dried over potassium hydroxide. Distillation gave a colorless oil boiling at 120—125°/20 mm. Reported boiling points of 2, 5-diethylaniline are 122°/13 mm[3] and 140—142°/20 mm.[4]. Yield 134 g. or 90% of the theoretical. The acetylation product (VII) was recrystallized from aqueous alcohol and melted at 150—151°. Reported melting point of 2, 5-diethylacetanilide (VII) is 154°[3].

**4-Acetamido-2, 4-diethylacetophenone (VIII).**—To a boiling suspension of 95.5 g. (0.5 mole) of compound VII in 56 g. (0.8 mole) of acetyl chloride and 400 ml. of carbon disulfide, was added 160 g. (1.2 moles) of aluminum chloride with stirring at such a rate that the mixture boiled briskly. The reaction mixture was refluxed with stirring for one hour and then allowed to stand for two hours at the room temperature. The supernatant carbon disulfide layer was decanted off and the lower layer was decomposed by pouring into ice-water in which 200 ml. of concentrated hydrochloric acid had been added. The crystals were collected and recrystallized from aqueous alcohol. Colorless prisms, m.p. 149.5—150°. Yield 100 g. or 90% of the theoretical.

*Anal.* Found: N, 6.25%. Calcd. for $C_{14}H_{19}O_2N$: N, 6.00%.

**4-Amino-2, 5-diethylaetophenone (IX).** — A mixture of 111.5 g. (0.5 mole) of the acetyl compound (VIII) and 600 ml. of dilute hydrochloric acid (1 : 1) was heated under reflux for two hours and basified with sodium hydroxide after cooling. The crystals were collected and recrystallized from benzene-petroleum ether. Colorless needles, m. p. 72.5—73°. Yield 71.6 g. or 75% of the theoretical.

*Anal.* Found: N, 7.38%. Calcd. for $C_{12}H_{17}ON$: N, 7.32%.

**2, 5-Diethyl-4-iodoacetophenone (X).** — A diazonium salt solution prepared from 95.5 g. (0.5 mole) of compound IX, 150 g. (1.5 moles) of concentrated sulfuric acid, 300 ml. of water and 35 g. (0.5 mole) of sodium nitrite in a minimum quantity of water was gradually added to a warm solution of 166 g. (1 mole) of potassium iodide in 200 ml. of water. The mixture was warmed at 50° for thirty minutes. The heavy oil was extracted with ether and the ethereal extract was washed with water, with aqueous sodium thiosulfate, and again with water, and dried over calcium chloride. Fractional distillation under nitrogen atmosphere gave a pale yellow oil boiling at 136°/2 mm. Yield 91 g. or 60% of the theoretical.

*Anal.* Found: I, 42.00%. Calcd. For $C_{12}H_{15}OI$: I, 42.29%.

This compound is unstable and quickly discolors on exposure to air. The 2, 4-dinitrophenylhydrazone was recrystallized from alcohol-ethyl acetate. Orange leaflets, m. p. 150—151°.

*Anal.* Found: N, 11.49%. Calcd. for $C_{17}H_{17}O_4N_4I$: N, 11.62%.

**2, 5-Diethyl-4-iodobenzoic Acid (XI).** — A solution of 30.2 g. (0.1 mole) of the iodo-ketone (X) in 150 ml. of dioxane was dropped into a sodium hypobromite solution prepared from 56 g. (1.4 moles) of sodium hydroxide, 72 g. (0.45 mole) of bromine and 300 ml. of water in one hour, at the temperature below 10° and with continuous stirring. The excess of sodium hypobromite was decomposed with sodium bisulfite and bromoform was removed by steam-distillation. After cooling, the solution was acidified with hydrochloric acid, and the crystalline substance was recrystallized from aqueous alcohol. Colorless needles, m. p. 134—135°. Yield 25 g. or 82% of the theoretical.

*Anal.* Found: I, 42.21%. Calcd. for $C_{11}H_{13}O_2I$: I, 41.76%.

**Methyl-2, 5-diethyl-4-iodobenzoate (XII).** — A solution of 30.1 g. of the acid (XI) in 100 ml. of methanol was saturated with dry hydrogen

6) D. T. Mowry, M. Renoll and W. E. Huber, *J. Am. Chem. Soc.*, **68**, 1105 (1946).

chloride at 0° and the mixture was warmed on a water bath for two hours. The reaction mixture was poured into water and extracted with ether. The extracts were washed with aqueous sodium bicarbonate and dried over potassium carbonate. The ester boiled at 137°/1 mm. Yield 27 g. or 87% of the theoretical.

*Anal.* Found: I, 40.20%. Calcd. for $C_{12}H_{15}O_2I$: I,39.89%.

**4-Methoxy-2′, 5′-diethylbiphenyl-4′-carboxylic Acid (II).**—To a well stirred mixture of 10 g. (0.043 mole) of 4-iodoanisole (XIII), prepared by iodination of anisole[7], and 5 g. (0.016 mole) of compound XII, heated at 240—250°, was added 15 g. (0.235 atom) of copper bronze activated by iodine[8] in portions in twenty minutes. The temperature was then raised to 280° and the mixture was stirred for forty minutes at that temperature. After cooling, the reaction mixture was extracted with acetone and the solvent was evaporated. To the residue was added 50 ml. of 10% sodium hydroxide in 50% aqueous alcohol, and the mixture was heated under reflux for two hours, and then diluted with 500 ml. of water. The insoluble material was filtered off with the aid of active charcoal. The filtrate was acidified with hydrochloric acid and the crystalline substance was collected. The crude acid was dissolved in ether and purified by passing the solution through an alumina column and eluting with the same solvent. Colorless needles, m. p. 161—162°. Yield 0.6 g. or 11% of the theoretical amount based on the used iodoester (XII).

*Anal.* Found: C, 76.28: H, 7.36%. Calcd. for $C_{18}H_{20}O_3$: C, 76.03: H, 7.09%.

**Ultraviolet Absorption Spectra.**—The specimens were submitted to measurements in 95% alcohol by the use of Hitachi Photoelectric Spectrophotometer Model EPU-2. 2,3′-Diethyl-4-methoxybiphenyl-4′-carboxylic acid (I) was prepared as described in the previous paper[1].

The authors' hearty thanks are due to Professor Y. Urushibara of the University of Tokyo for his encouragement throughout this work and to the Research Department of Teikoku Hormone Manufacturing Co., Ltd., Kawasaki, for bioassay. The authors are also indebted to the Ministry of Education for the Grant in Aid for Fundamental Scientific Research.

*Department of Chemistry, Faculty of Science, Tokyo Metropolitan University Setagaya, Tokyo*

7) M. P. Brenans, *Bull. chim. soc. France*, [3] **25**, 819 (1901).

8) E. C. Kleiderer and R. Adams, *J. Am. Chem. Soc.*, **55**, 4225 (1933).

# *The Bond Refraction Values for Ti-O in Organic Titanates*

By Tooru TAKATANI

(Received April 6, 1957)

Many liquid organic titanates are known, but little attention has been paid to the calculation of the molecular refraction values of these compounds.

English and Sommer[1] have recently obtained tetrakis-(trimethylsiloxy)-titane, and have measured its molecular refraction, estimating the bond refraction for Ti-O as 4.02 ml./mol. This seems to be the only example which has appeared in the literature published so far.

For the present paper, the establishment of bond refraction for Ti-O and its application for some organic titanates were undertaken.

## Experiment

**Ethyl, iso-propyl, and n-butyl titanate** were prepared by treating titanium tetrachloride with corresponding alcohol in the presence of ammonia[2].

**n-Propyl, sec-butyl, tert-butyl, and tert-pentyl titanate** were prepared by the transesterification reaction (1) between ethyl titanate and the corresponding alcohol[3].

$$(C_2H_5O)_4Ti + 4\ ROH = (RO)_4Ti + 4\ C_2H_5OH \quad (1)$$

The preparation of *n-Heptyl titanate* followed a similar method, n-butyl titanate being used in place of ethyl titanate.

Some of the physical properties and titanium contents of the titanates prepared are shown in Table I and II.

**Ethyl Titanate.**—Ethanol (460 g, 10 mol.) was saturated with ammonia in a flask fitted with a reflux condenser, and all openings were protected against moisture. Titanium tetrachloride (190 g, 1 mol.) was then added drop by drop while

1) W. D. English and L. H. Sommer, *J. Am. Chem. Soc.*, **77**, 170 (1955).

2) J. Nelles, U. S. Patent 2,187,821 (1940), *Chem. Abst.*, **34**, 3764[7] (1940).

3) B. A. Arbuzov and Z. G. Isaeva, *Zhur. Obshchei Khim.* S. S. S. R., **22**, 566 (1952), *Chem. Abst.*, **47**, 2684f (1953).

stirring under cooling by ice during five hours at a temperature below 60°C. After the addition, the mixture was allowed to stand overnight at room temperature. White precipitates of ammonium chloride were removed and the filtrate was heated on a water bath to eliminate the excess of ethanol. The residue was distilled under reduced pressure, to obtain a fraction b.p. 140–145°C/3mmHg (reported, 130–132°C/2mmHg[4]). It was redistilled and used for further experiments.

*Anal.* Found: Ti, 21.1; $C_2H_5O$, 79.3. Calcd. for $(C_2H_5O)_4Ti$: Ti, 21.0; $C_2H_5O$, 79.0 %.

Titanium was determined by the Speer's method[5] and the ethoxy group by Bradley's oxidation method[6].

TABLE I
PROPERTIES AND ANALYSES OF THE PREPARED TITANATES

| Compd. | B.P. °C/mmHg | M.P. °C | Ti Found | Ti Calcd. |
|---|---|---|---|---|
| (*n*-$C_3H_7O)_4Ti$ | 137-40/3a) | | 16.9% | 17.0% |
| (*iso*-$C_3H_7O)_4Ti$ | 97- 8/8 | 15 | 16.8 | 17.0 |
| (*sec*-$C_4H_9O)_4Ti$ | 107- 9/3b) | | 14.2 | 14.1 |
| (*tert*-$C_4H_9O)_4Ti$ | 85- 7/3c) | | 14.2 | 14.1 |
| (*n*-$C_5H_{11}O)_4Ti$ | 182- 3/3d) | | 12.3 | 12.1 |
| (*tert*-$C_5H_{11}O)_4Ti$ | 129-30/2e) | | 12.2 | 12.1 |
| $(C_6H_{11}O)_4Ti$ | 220- 5/3f) | 43 | 10.6 | 10.8 |
| (*n*-$C_7H_{15}O)_4Ti$ | 215-20/1g) | | 9.47 | 9.42 |

a) 170/3[5], 171/14[7], b) 90-2/0.5-1[5], c) 62-3/1[5], 102/1[7], d) 175/0.8[8], 158/0.1[8], 211/11[7], e) 98/0.1[9], f) 1)0.5-2.0/1[10], g) 213/0.4[9], 201/0.1[9]264-5/15[11].

***n*-Propyl Titanate.**—A mixture of ethyl titanate (22.8 g, 0.1 mol.) and *n*-propanol 30.1 g, 0.5 mol.) was heated to remove the ethanol produced during the reaction. After the theoretical quantity of ethanol was recovered, the residue was distilled under reduced pressure. *n*-Propyl titanate was obtained in 75 % yield.

***tert*-Butyl Titanate.**—It was impossible to prepare this compound by reacting titanium tetrachloride with *tert*-butanol or sodium-*tert*-butoxide. The manipulation of the transesterification reaction between ethyl titanate and *tert*-butanol was somewhat complicated, because the separation of ethanol produced and *tert*-butanol by fractional distillation was difficult.

*tert*-Butyl titanate was obtained from ethyl titanate (22.8 g, 0.1 mol.) and *tert*-butanol (37.0 g, 0.5 mol.) following the method as in the case of *n*-propyl titanate. After ethanol and *tert*-butanol were distilled off, the residue was treated with *tert*-butanol (7. 4 g, 0.1 mol.). This procedure was repeated ten times to complete reaction, *tert*-butyl titanate being obtained by distillation under reduced pressure in 52 % yield.

## Results and Discussion

There are eighteen sets of densities and refractive indices of organic titanates and chlorotitanates which were observed at the same temperature as shown in Table III. From these data, molecular refraction of each compound was calculated. The sum of Denbigh's bond refraction[15] for C–C, C–H, C–O was reduced from the molecular refraction of the compound, the remainder being divided by the number of Ti–O bonds in a molecule, and the bond refraction for Ti–O was obtained. As the bond refraction for Ti–Cl has not appeared in the literature, it was calculated, using

TABLE II
MOLECULAR REFRACTIONS OF THE PREPARED TITANATES

| Compd. | Dens. $d_4^t$ | Refr. Ind. $n_D^t$ | Temp. °C | Mol. Refr. (ml./mol.) Obs. | Calcd. | Error |
|---|---|---|---|---|---|---|
| (*n*-$C_3H_7O)_4Ti$ | 1.0358a) | 1.4907a) | 35 | 79.41 | 79.68 | −0.34% |
| (*iso*-$C_3H_7O)_4Ti$ | 0.9711 | 1.4678 | 20 | 81.34 | 79.68 | +2.0 |
| (*sec*-$C_4H_9O)_4Ti$ | 0.9463a) | 1.4587a) | 35 | 98.27 | 98.20 | +0.07 |
| (*tert*-$C_4H_9O)_4Ti$ | 0.8917a) | 1.4368a) | 20 | 99.96 | 98.20 | +1.8 |
| (*n*-$C_5H_{11}O)_4Ti$ | 0.9703 | 1.4813 | 35 | 116.34 | 116.56 | −0.18 |
| (*tert*-$C_5H_{11}O)_4Ti$ | 0.9118 | 1.4543 | 20 | 117.82 | 116.56 | +1.1 |
| $(C_6H_{11}O)_4Ti$ | 1.0589b) | 1.5155b) | 35 | 126.69 | 126.72 | −0.12 |
| (*n*-$C_7H_{15}O)_4Ti$ | 0.9430a) | 1.4830a) | 20 | 154.05 | 153.76 | +0.20 |

a) Literature is shown in Table III.
b) Supercooled Liquid.

4) O. V. Nogina, and A. B. Belyavskii, *Akad. Nauk S. S. S. R., Inst. Org. Khim., Sintezy Org. Soedinenii, Sbornik*, **2**, 164 (1952), *Chem. Abst.*, **48**, 567 c (1954).
5) R. J. Speer, *J. Org. Chem.*, **14**, 655 (1949).
6) D. C. Bradley, F. M. Abd-el Halim and W. Wardlaw, *J. Chem. Soc.*, **1950**, 3450.
7) N. M. Cullinane, S. J, Chard, G. F. Price, B. B. Millward and G. Langlois, *J. Appl. Chem.*, **1**, 400 (1951).
8) D. C. Bradley, R. C. Mehrotra and W. Wardlaw, *J. Chem. Soc.*, **1952**, 2027.
9) D. C. Bradley, R. C. Mehrotra, J. D. Swanick and W. Wardlaw, ibid., **1953**, 2025.
10) O. A. Nogina, R. Kh. Freidlina and A. N. Nesmeyanov, *Izvest. Akad. Nauk S. S. S. R., Otdel. Khim. Nauk*, **1950**, 32, *Chem. Abst.*, **44**, 8854 i (1950).
11) B. A Arbuzov and T. G. Shavsha, *Doklady Akad, Nauk S. S. S. R.*, **68**, 859 (1949), *Chem. Abst.*, **44**, 886 e (1950).

TABLE III

CALCULATED BOND REFRACTIONS FOR Ti-O FROM THE DATA IN LITERATURE

| Compounds | Dens. $d_4^t$ | Refr. Ind. $n_D^t$ | Temp. °C | Bond Refr. for Ti-O ml./mol. | Lit. |
|---|---|---|---|---|---|
| $(C_2H_5O)_4Ti$ | 1.1071 | 1.5051 | 35 | 4.07 | 5) |
| $(n\text{-}C_3H_7O)_4Ti$ | 0.9970 | 1.4803 | 35 | 4.42a) | 5) |
| $(n\text{-}C_4H_9O)_4Ti$ | 1.0051 | 1.4925 | 20 | 4.11 | 12) |
| $(n\text{-}C_4H_9O)_4Ti$ | 0.9927 | 1.4863 | 35 | 4.16 | 5) |
| $(sec\text{-}C_4H_9O)_4Ti$ | 0.9196 | 1.4550 | 35 | 4.63a) | 5) |
| $(tert\text{-}C_4H_9O)_4Ti$ | 0.8893 | 1.4436 | 20 | 4.93a) | 5) |
| $(n\text{-}C_6H_{13}O)_4Ti$ | 0.9573 | 1.4830 | 20 | 4.03 | 12) |
| $(n\text{-}C_7H_{15}O)_4Ti$ | 0.8963 | 1.4810 | 20 | 4.59a) | 11) |
| $(n\text{-}C_8H_{17}O)_4Ti$ | 0.9339 | 1.4810 | 20 | 4.09 | 12) |
| $(n\text{-}C_9H_{19}O)_4Ti$ | 0.9241 | 1.4785 | 20 | 3.97 | 12) |
| $(CH_3OC_2H_4O)_4Ti$ | 1.1910 | 1.5077 | 18 | 4.17 | 13) |
| $(C_2H_5OC_2H_4O)_4Ti$ | 1.1106 | 1.4920 | 21 | 4.17 | 13) |
| $[(CH_3)_3SiO]_4Ti$ | 0.9078 | 1.4278 | 20 | 4.02 | 1) |
| $(n\text{-}C_4H_9O)_3TiCl$ | 1.0985 | 1.5169 | 20 | 4.16 | 14) |
| $(C_2H_5OC_2H_4O)_3TiCl$ | 1.2035 | 1.5178 | 20 | 4.03 | 14) |
| $(iso\text{-}C_4H_9O)_3TiCl$ | 1.1043 | 1.5158 | 20 | 3.97 | 14) |
| $(iso\text{-}C_5H_{11}O)_3TiCl$ | 1.0600 | 1.5092 | 20 | 4.13 | 14) |
| $(n\text{-}C_6H_{13}O)_3TiCl$ | 1.0039 | 1.5050 | 20 | 5.25a) | 14) |
| | | | | Mean 4.08 | |

a) Except for the calculation of the mean value.

the values of titanium tetrachloride, $d_4^{20.1}$ 1.7344 and $n_D^{20.1}$ 1.6085, obtaining 9.46 ml./mol.[16] This value was used throughout the present investigation.

Eighteen bond refraction values for Ti-O were thus obtained, but as five values among them were far apart from the other thirteen values, the mean value was taken for all except these five values. The average bond refraction for Ti-O was obtained as 4.08 ml./mol.

Then, *n*-propyl, *sec*-butyl, *tert*-butyl, *n*-heptyl, *iso*-propyl, *n*-pentyl, *tert*-pentyl and cyclohexyl titanate were prepared, purified, and their densities and refractive indices were measured. In the calculation of the mean value of bond refractions for Ti-O the first four titanates were excepted.

Densities and refractive indices measured at the same temperature of the last four titanates have not been reported in the literature.

Molecular refractions obtained from these data of the titanates prepared were compared with the calculated ones using the bond refraction for Ti-O, 4.08 ml./mol. Both were in good agreement except for *iso*-propyl, *tert*-butyl, and *tert*-pentyl titanate. Thus the value 4.08 ml./mol. for Ti-O, was justified by these considerations.

The errors of molecular refractions of *iso*-propyl, *tert*-butyl, and *tert*-pentyl titanate amount to +2.0, +1.8, +1.1 %, respectively. According to Denbigh, the observed molecular refractions of many compounds agree with the calculated ones in a range of ±0.7 % error.

Considering this fact, the observed molecular refractions of these three titanates seem to be considarably large. The purity of these titanates was sufficient, viewed from their titanium contents. Particularly, *iso*-propyl titanate was obtained in a crystalline form by leaving the liquid standing for a long time. The cause of the observed greater molecular refractions of these titanates may be attributed to their greater hygroscopicity. Actually, refractive indices of these compounds gradually change greater during the measurement using Abbe's refractometer.

In the course of the preparation of *tert*-butyl and *tert*-butyl titanate, an interesting fact was observed. It has been indicated by us[17] that the transesterification reaction between ethyl silicate and *tert*-butanol

12) B. A. Arbuzov and T. G. Lsaeva, *Zhur. Obshchei Khim. S. S. S. R.*, **22**, 566 (1952), *Chem. Abst.*, **47**, 2684 g (1953).

13) A. N. Nesmeyanov, R. Kh. Freidlina and O. V. Nogina, *Izvest. Akad. Nauk S. S. S. R., Otdel. Khim. Nauk*, **1951**, 518, *Chem. Abst.*, **46**, 7038 i (1952).

14) O. V. Nogina, R. Kh. Freidlina and A. N. Nesmeyanov, *Izvest. Akad. Nauk S. S. S. R., Otdel. Khim. Nauk*, **1952**, 74, *Chem. Abst.*, **47**, 1583 f (1953).

15) K. G. Denbigh, *Trans. Farad. Soc.*, **36**, 936 (1940).

16) "Landolt-Börnstein Physiknlisch-Chemischen Tabellen". 5 Aufl. Zweiter Frgänzba. Zweiter Teil. Verlag von, Julius Springer Berlin (1931), S. 815.

17) Presented at the Annual Meeting of the Chem. Soc. of Japan in 1955.

or *tert*-pentanol proceeds incompletely as shown in the following equation (2)

$$(C_2H_5O)_4Si + 2\,tert\text{-}C_4H_9OH = (C_2H_5O)_2(tert\text{-}C_4H_9O)_2Si + 2\,C_2H_5OH. \quad (2)$$

However, when ethyl titanate was used in place of ethyl silicate, the transesterification reaction proceeded almost completely, and the titanates tetrasubstituted by *tert*-alkyl groups were obtained. It seems that titanium, the central metallic atom of the titanate, is large enough to diminish the steric effect of *tert*-alkoxy groups, which caused the incomplete transesterification reaction in the case of silicium.

The author wishes to express his sincere gratitute to Dr. M. Tachimori, Dr. S. Tsuruta and Dr. H. Kitagawa for their interest kindly extended to him throughout the present investigation.

*Hitachi Central Research Laboratory*
*Kokubunji, Tokyo*

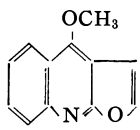
# *Synthetic Studies of Dictamnine, an Alkaloid of Skimmia repens, Nakai. II. The Synthesis of Dictamnine*

By Tadashi SATO and Masaki OHTA

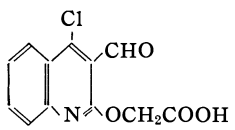
(Received October 20, 1956)

As an approach to the synthesis of dictamnine (I), some experiments were reported in our previous paper[1]. Recently the synthesis of dictamnine was reported by Tuppy et al.[2], but its details have not yet been known. In this communication we describe the synthesis of dictamnine accomplished independently in our laboratory.

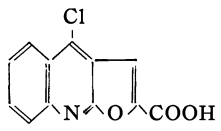
As previously reported, we synthesized the aldehyde II, and tried to cyclize it to the furoquinoline derivative III. Numerous attempts, however, to effect the cyclization of II to III were unsuccessful.




I




II




III

In their study of synthesizing dictamnine, Grundon et al. obtained 2,4-dichloro-3-(2-chloroethyl)-quinoline (IV)[3]. In our previous paper we reported that only the 2-chlorine atom of the 2,4-dichloroquinoline derivatives could selectively be replaced by a hydroxyl group by treatment with glacial acetic acid. On applying the same method to the trichloro derivative IV, a mixture of two substances was obtained, and these were considered as the 2-hydroxyquinoline derivative V and the dihydrofuroquinoline derivative VII, from their ultraviolet spectroscopic characteristics. The spectra of V (Fig. 1) were similar to those of the 2-hydroxyquinoline derivatives in neutral as well as in acid solution. As noted in our previous paper, the absorption

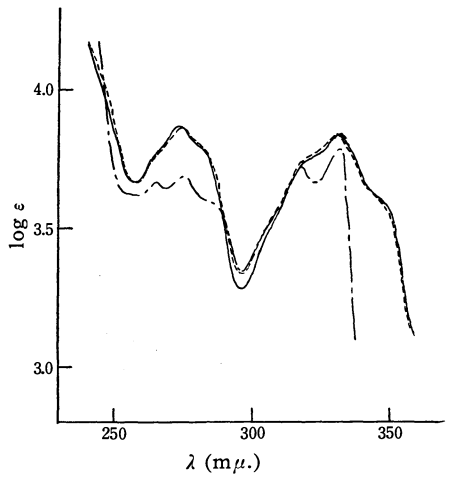
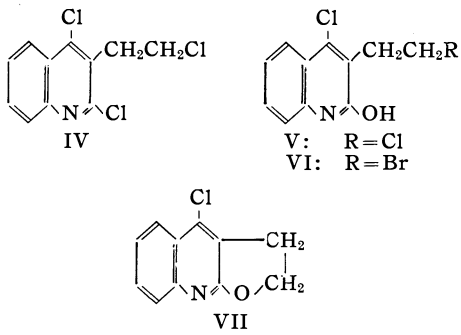



Fig. 1. 2-Hydroxy-3-(2-chloethyl)-4-chloroquinoline (V)
——— neutral ---- acid
— — — alkaline

1) T. Sato and M. Ohta, This Bulletin, **29**, 817 (1956).
2) H. Tuppy, et al., *Angew. Chem.*, **68**, 388 (1956).
3) M. F. Grundon, et al., *J. Chem. Soc.*, **1955**, 4284.




maximum (275 mμ) of 2-hydroxyquinoline derivatives flattens generally in alkaline solution, but the spectrum of V in alkaline solution becomes identical with that of VII (Fig. 2) owing to cyclization, and the

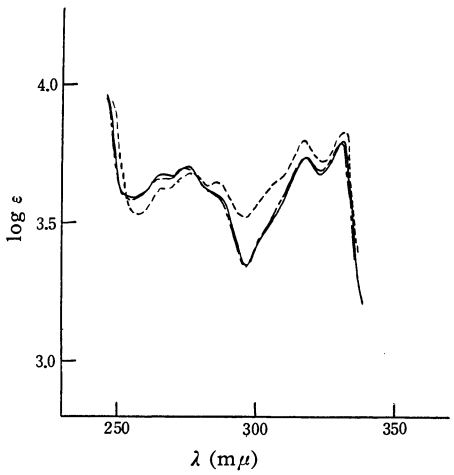
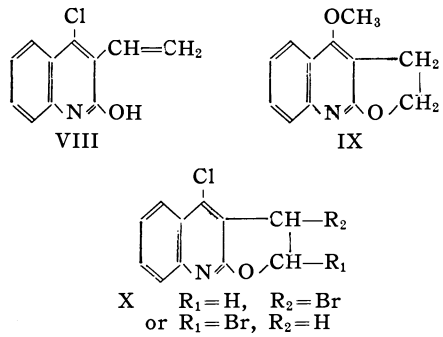



Fig. 2. 4-Chloro-2, 3-dihydrofuro[2, 3-b] quinoline (VII)
——— neutral ---- acid
— — — alkali

characteristics described above could not be observed. The different spectroscopic characteristics of VII from those of the 2-hydroxyquinoline derivatives exclude the possibility that VII might be the vinyl derivative such as VIII. When VII was heated with hydrogen bromide, the bromo derivative VI was obtained, whose spectroscopic characteristics were very similar to those of the chloro derivative V.

Though it was difficult to separate V and VII, VII was obtained readily in pure state when the crude product was treated with methanolic sodium hydroxide. The methoxy derivative IX was obtained from the chloro derivative VII by treatment with sodium methylate at 100°. Our methoxy derivative melted at 92° (sintering at 82–3°), and gave the picrate having a m.p. of 187°, while the m.p's of the specimens from a natural source are 96–7° and 183°, respectively[4].




The dehydrogenation of the dihydrofuroquinoline derivatives VII and IX to the corresponding furoquinoline derivatives was not effected by palladium-charcoal in boiling diphenyl ether.

In order to obtain the bromo derivative X, we treated the chloro derivative VII with bromine, but the substance thus obtained was the perbromide having an empirical formula of $C_{11}H_8NOClBr$.

The desired bromo derivative X was obtained when the chlorodihydrofuroquinoline derivative VII was refluxed with N-bromosuccinimide in carbon tetrachloride in the presence of a small amount of benzoyl peroxide, and the solvent was removed under a reduced pressure though the position of the bromine atom was uncertain. When carbon tetrachloride was not removed, another substance decomposing at 92° was obtained. Although its structure has not yet been determined, it gave the bromo derivative X when treated with pyridine. The methoxydihydrofuroquinoline derivative IX gave no well-defined product with N-bromosuccinimide. The desired dictamnine (I) was obtained by the reaction of the bromo derivative X with sodium methylate in a sealed tube at 100°.

The synthetic dictamnine was shown to be identical with the natural specimen by their melting points, mixed melting points and melting points of their picrates.

## Experimental

**Absorption spectra.**—All spectra were determined in the same way as reported in our previous paper.

**2,4-Dichloro-3-(2-chloroethyl)-quinoline (IV).**—It was prepared by the Grundon's method[3] with slight modifications. Methyl cellosolve was used as a starting material instead of cellosolve;

4) T. Ohta, et al., *J. Pharm. Soc. Japan*, **74**, 708(1954).

p-toluenesulfonyl chloride instead of benzenesulfonyl chloride was used for preparing the malonic acid derivative; and the amount of diphenyl ether in the condensation of aniline with the malonic acid derivative was minimized. Namely, 40 g. of diethyl (2-methoxyethyl)-malonate and 12 g. of aniline were refluxed in 60 g. of diphenyl ether for three hours. Thus, on cooling the reaction mixture, fairly pure 4-hydroxy-2,3-dihydrofuro[3,2-*c*]quinoline, m.p. 275° (decomp.), was obtained. Yield 19 g. The crude product was treated with phosphorus oxychloride and the trichloro derivative IV thus obtained was used without purification in the next step.

**2-Hydroxy-3-(2-chloroethyl)-4-chloroquinoline (V).**—A solution of 17 g. of the trichloro derivative IV in 100 cc. of glacial acetic acid was heated under a reflux for three hours, after which about 200 cc. of water was added. The product was collected, and washed with water, m.p. 130—170°. Yield 15 g. Repeated recrystallization from dilute methanol or dilute acetic acid raised the m.p. to 190°.

*Anal.* Found: C, 54.62; H, 3.94; N, 5.47. Calcd. for $C_{11}H_9NOCl_2$: C, 54.55; H, 3.72; N, 5.78%.

**4-Chloro-2,3-dihydrofuro[2,3-*b*]quinoline (VII).**—In the other recrystallization process of the crude product described above, the cyclized derivative VII, m.p. 113°, was obtained instead of the open-chain derivative V.

*Anal.* Found: C, 63.92; H, 4.09; N, 7.10. Calcd. for $C_{11}H_8NOCl$: C, 64.08; H, 3.88; N, 6.79%.

VII was more conveniently obtained as follows: A mixture of 15 g. of the crude product melting at 130—170°, resulting from the reaction of the trichloro derivative IV with glacial acetic acid, and 100 cc. of methanol solution containing 5 g. of sodium hydroxide was heated under a reflux for two hours, and then about 200 cc. of water was added. The dihydrofuroquinoline derivative VII thus obtained was sufficiently pure for the next step, m.p. 111°. Yield 8 g.

**2-Hydroxy-3-(2-bromoethyl)-4-chloroquinoline (VI).**—To a solution of 0.1 g. of the dihydrofuroquinoline derivative VII in 1.5 cc. of glacial acetic acid was added 1 cc. of 48% aqueous hydrobromic acid solution and heated under a reflux for fifteen minutes. On adding water, white needles were obtained. Recrystallization from dilute acetic acid gave an analytical sample, m.p. 190°.

*Anal.* Found: C, 46.10; H, 3.44; N, 5.26. Calcd. for $C_{11}H_9NOBrCl$: C, 45.99; H, 3.14; N, 4.88%.

**4-Methoxy-2,3-dihydrofuro[2,3-*b*]quinoline (IX).**—To a solution of 0.4 g. of the chloro derivative VII in 3 cc. of methanol, 5 cc. of sodium methylate solution containing 0.15 g. of sodium, was added and heated in a sealed tube at 100° for three hours. After being set aside overnight the sodium chloride was filtered off and the filtrate was concentrated to about 3 cc. under a reduced pressure. On addition of water, white crystals were obtained. Recrystallization from dilute methanol afforded white needles, m.p. 92° (sintering at 82—3°).

*Anal.* Found: C, 70.32; H, 5.67; N, 7.14. Calcd. for $C_{12}H_{11}NO_2$: C, 71.64; H, 5.47; N, 6.96%.

The picrate was prepared in ether and was recrystallized from methanol, m.p. 187°.

*Anal.* Found: N, 13.12. Calcd. for $C_{18}H_{14}N_4O_9$: N, 13.02%.

**4-Chloro-2,3-dihydrofuro[2,3-*b*]quinoline perbromide.**—To a solution of 0.3 g. of VII in 10 cc. of carbon tetrachloride was added 0.23 g. of bromine dissolved in 1 cc. of carbon tetrachloride within twenty minutes with stirring at room temperature. After being stirred for one additional hour, the yellow crystals were collected and reprecipitated from methanol solution with water at room temperature, m.p. 122°(decomp.).

*Anal.* Found: C, 46.69; H, 3.17; N, 5.09. Calcd. for $C_{11}H_8NOClBr$: C, 46.15; H, 2.80; N, 4.89%.

**2- or 3-bromo-4-chloro-2,3-dihydrofuro[2,3-*b*]quinoline (X).**—A mixture of 1 g. of dihydrofuroquinoline derivative VII, 1 g. of N-bromosuccinimide and 0.1 g. of benzoyl peroxide in 50 cc. of carbon tetrachloride was heated under a reflux for forty-five minutes. Afrer the succinimide was filtered off, the solution was concentrated to about 15 cc. On cooling, the bromo derivative X was obtained, m.p. 120°.

*Anal.* Found: C, 46.08; H, 2.78; N, 5.26. Calcd. for $C_{11}H_7NOClBr$: C, 46.31; H, 2.46; N, 4.91%.

When carbon tetrachloride was not removed, a substance decomposing at 92° was obtained. When its pyridine solution was diluted with water, the bromo derivative X crystallized in white needles, but its further recrystallization from pyridine-water was unsuccessful. Recrystallization of the substance decomposing at 92° or of the bromo derivative X from dilute methanol gave a substance with a m.p. of 113°, whose structure could not be determined.

**Dictamnine (I).**—To a solution of 0.15 g. of the bromo derivative X in 2 cc. of methanol was added 2.5 cc. of sodium methylate solution containing 0.075 g. of sodium. The mixture was heated in a sealed tube at 100° for two hours and allowed to stand overnight. After the inorganic salts were filtered off and methanol was partly evaporated, water was added. The dictamnine thus obtained was fairly pure, melting at 130—1°, (natural product; m.p. 132—3°)[5]; a mixed melting point with natural dictamnine was 130—1°.

*Anal.* Found. C, 72.11; H, 4.72; N, 7.14. Calcd. for $C_{12}H_9NO_2$: C, 72.35; H, 4.55; N, 7.03%.

The melting point of its picrate obtained in the same way as described in the literature[5] also coincided with that from natural source (m.p. 163°).

5) Y. Asahina, T. Ohta and M. Inubuse, *Ber.*, **63**, 2045 (1930).

We wish to express our grateful appreciation to Professor T. Ohta of the Tokyo College of Pharmacy who kindly provided us with the natural dictamnine for identification, and to Mr. A. Kondo for microanalyses.

*Laboratory of Organic Chemistry*
*Tokyo Institute of Technology*
*Ookayama, Tokyo*

# *Hydrogen Bonding Effect on the Fluorescence of π-Electron System. III.* Fluorescence Quenching of Some Nitrogen Heterocycles Caused by Hydrogen Bond Formation*

By Noboru MATAGA and Shizuyo TSUNO

(Received April 16, 1957)

In II[1] of this series, we have interpreted the inner quenching of fluorescence of some nitrogen heterocycles as due to the interaction between *n*- and π-electrons, on the basis of the fact that the enhancements of fluorescence yields of these molecules caused by hydrogen bonding is greater, the stronger the donating powers of proton donors used. The fluorescence yields of acridine hydrogen bonded with ethanol, β-phenylethylalcohol and benzylalcohol are almost the same. We can observe, however, no enhancement of fluorescence yield, when acridine is hydrogen bonded with phenol which is capable of making hydrogen bond intimately connected with π-electron system in contrast to molecules such as benzylalcohol and β-phenylethylalcohol. Actually, we have observed a remarkable fluorescence quenching by phenol when 3,6-diaminoacridine (DAA) and 3,6-bisdimethylaminoacridine (BDAA) which are able to fluoresce fairly well even in non-polar solvent, are used as fluorescer and proton acceptor.

These facts indicate that the interaction between π-electron systems via the hydrogen bond may lead to the non-radiative degradation of excited state. To elucidate the problem further, we have used various proton donors such as naphthols, phenol, aniline and pyrrole, the hydrogen bonding by which are intimately related with π-electron system.

For all of these donors, strong or moderate decrease of fluorescence intensity was observed. Moreover, the effect of viscosity on the quenching was studied by changing the hydrocarbon solvents from *n*-hexane to liquid paraffin, and no viscosity dependence of quenching was observed. In the present paper, we will report these facts with some discussions on the mechanism of fluorescence quenching caused by the interaction between π-electron systems of fluorescer and of quencher molecules.

## Experimental

**Apparatus.**—Absorption spectra were measured with Beckman spectrophotometer model DU. Fluorometer was the same as described previously[2]. A high pressure mercury lamp with appropriate filters was used as an exciting light source. Matsuda color filter UV-DI was used for all samples as an exciting light filter.

For the fluorescent light, the light filter used for acridine was the same as before[2], and for DAA and BDAA, Matsuda color filter VY—I was used.

**Reagents.**—Acridine, DAA[3] and BDAA[3] were the same sample as used previously. *n*-Hexane and benzene were the same as reported before[1]. Cyclohexane and decaline were shaken with fuming sulfuric acid diluted with conc. sulfuric acid and distilled carefully. Liquid paraffin was purified through the column of activated alumina for removing the fluorescing impurity. Extra pure grade phenol was distilled carefully before use. Aniline was purified by the method of Keyes and Hildebrand[4], and stored in vacuo. Commercial pyrrole was distilled carefully and stored in vacuo.

## Experimental Results

### A. Change of Absorption Spectrum by

* I and II of this series: N. Mataga, Y. Kaifu and M. Koizumi, This Bulletin, **29**, 115 (1956), and N. Mataga and S. Tsuno, ibid., **30**, 368 (1957).

1) N. Mataga and S. Tsuno, loc. cit.

2) N. Mataga, Y. Kaifu and M. Koizumi, This Bulletin **29**, 373 (1956).

3) N. Mataga, ibid., **30**, 375 (1957).

4) D. B. Keyes and J. H. Hildebrand, *J. Am. Chem. Soc.*, **39**, 2126 (1917).

**Hydrogen Bonding.**—According to Zanker[5], the lowest excited singlet states of DAA and BDAA are $^1L_a$ as it is the case for acridine. When the proton donors are added to the solutions of these nitrogen heterocycles in non-polar solvents, the absorption spectra show characteristic changes due to the hydrogen bonding equilibrium. In all these molecules, hydrogen bonding induces the red shift of $^1L_a$ band. Some examples of these spectral changes caused by hydrogen bonding are shown in Figs. 1 and 2.

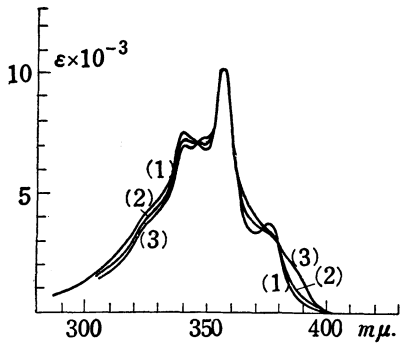



Fig. 1. Change of absorption spectrum of acridine in benzene by added phenol. Concentration of acridine: $5.00\times10^{-5}$ mole/l. Concentration of phenol: (1) 0, (2) $7.12\times10^{-3}$ mole/l., (3) $3.56\times10^{-2}$ mole/l.

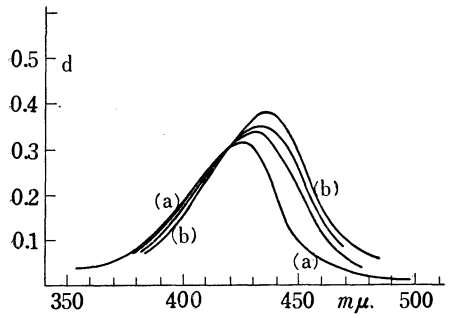



Fig. 2. Change of absorption spectrum of BDAA in benzene by added phenol. Concentration of BDAA: $1.36\times10^{-5}$ mole/l. Cell length: 1 cm. Concentration of added phenol: (a) 0, (b) $9.4\times10^{-3}$ mole/l.

5) V. Zanker, *Z. physikal. Chem.*, N. F., **2**, 52 (1954).

* The concentration ranges of donors used for the calculation of equilibrium constants, are as follows.
phenol and naphthols: $10^{-4}$~$10^{-2}$ mol./l., where nearly 100% monomer exists. [a]
(a) R. Mecke, *Disc. Faraday Soc.*, No. **9**, 161 (1950).
aniline: $10^{-2}$~$10^{-1}$ mol./l., where nearly 100% monomer exists.[b]
pyrrole: $5\times10^{-2}$~$4\times10^{-1}$ mol./l., where 90~70% monomer exists.[b]
(b) N. Fuson, M. L. Josien, R. L. Powell and E. Utterback, *J. Chem. Phys.*, **20**, 145 (1952).

From these spectral changes, we can evaluate the equilibrium constant of hydrogen bond formation in the ground state, using Eq. (1)[1]*.

$$\frac{1-(d_0/d)}{[D]} = -K+\left(\frac{\varepsilon_c}{\varepsilon_a}\right)K(d_0/d) \qquad (1)$$

Some examples of analyses using this formula were given in Figs. 3 and 4.

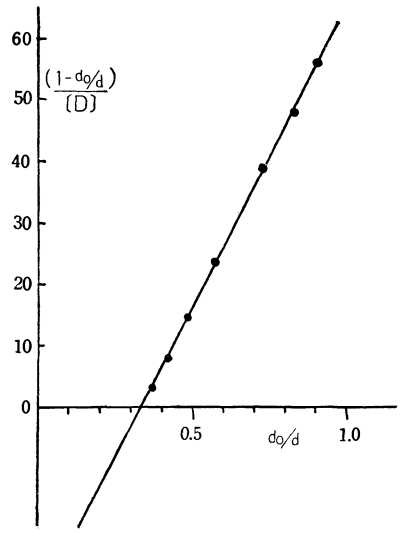



Fig. 3. $(1-d_0/d)/[D]\sim d_0/d$ relation for acridine-phenol-benzene system at 386 mμ.

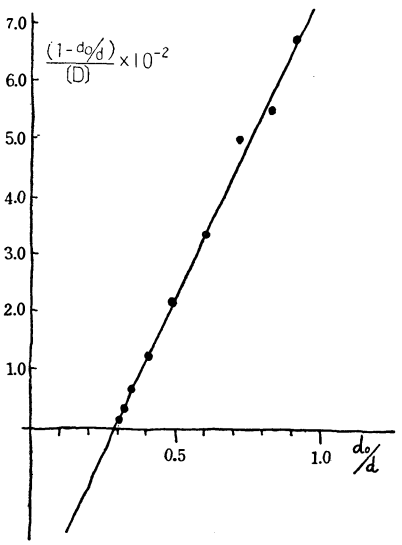



Fig. 4. $(1-d_0/d)/[D]\sim d_0/d$ relation for BDAA-phenol-benzene system at 448 mμ.

**B. Effect of Hydrogen Bonding on the Fluorescence Intensity.**—Acridine is non-fluorscent in non-polar solvent, and no enhancement of fluorescence intensity was

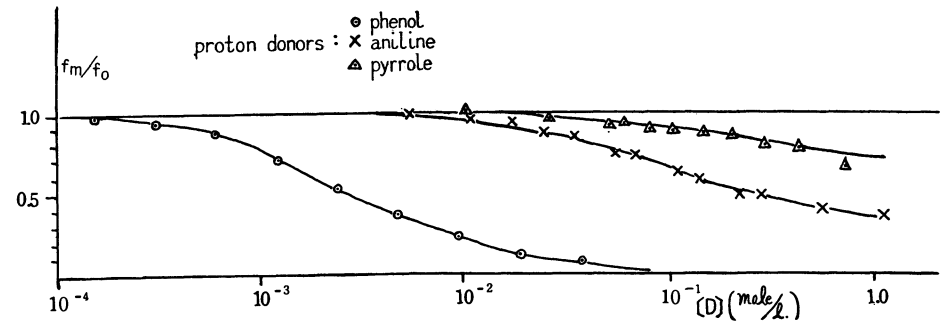



Fig. 5. Changes of relative fluorescence intensity of BDAA in benzene by added various proton donors.

observed when it is hydrogen bonded with phenol.

DAA and BDAA are fluorescent even in a non-polar solvent, and decrease in fluorescence intensity is observed, when various proton donors such as phenol, naphthols, aniline and pyrrole are added in the solution. Some examples of quenching curves for BDAA in benzene are given in Fig. 5.

The observed changes of fluorescence intensity may most probably be attributed to the fact that the free and the hydrogen bonded molecules have different efficiency of fluorescence and that the concentration of these molecular species are determined by association equilibrium. Then, from these changes of fluorescence intensity, we can evaluate the equilibrium constant of hydrogen bond formation and the ratio of the quantum yields of fluorescences of hydrogen bonded and free molecules, using the following formulas, (2) and (3)[1]*.

$$\frac{1-(f_0/f_m)}{[D]} = -K+\alpha\left(\frac{\varepsilon_c}{\varepsilon_a}\right)K(f_0/f_m) \qquad (2)$$

$$\frac{1-(f_0/f_m)(d_m/d_0)}{[D]} = -K'+\alpha\left(\frac{d_m}{d_0}\right)K'(f_0/f_m) \qquad (3)$$

Owing to a very small difference of extinction coefficients of free and hydrogen bonded molecules at the wave length of exciting light, (2) and (3) practically coincide in their forms and it has been established that the experimental results can be reproduced by either Eq. (2) or (3) satisfactorily for all cases studied, the equilibrium constants evaluated by Eqs. (2) and (3) being paractically the same. Some examples of these analysis are given in Figs. 6 and 7. Further, the equilibrium constant obtained in this way from fluorescence intensity measurement agrees with that evaluated from the change in absorption spectrum.

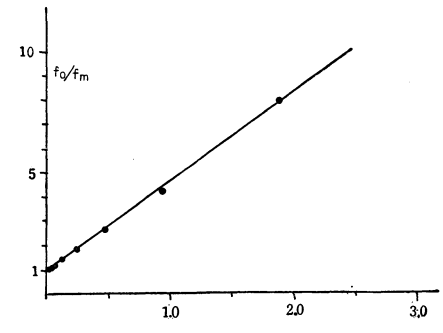



Fig. 6. $f_0/f_m \sim [D]$ relation for BDAA-phenol-benzene system[a]
(a) Conditions, $\alpha=0$ in Eq. (2) or $\alpha=0$, $d_m=d_0$ in Eq. (3), are satisfied in this case.

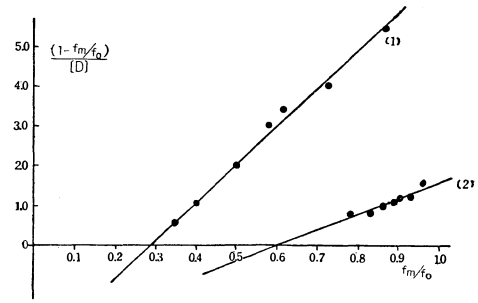



Fig. 7. $\frac{(1-f_m/f_0)}{[D]} \sim f_m/f_0$ relations for BDAA-aniline-benzene (1) and BDAA pyrrole-benzene (2) systems[b].
(b) (Conditions $d_m=d_0$ in Eq. (3) or $\varepsilon_c=\varepsilon_a$ in Eq. (2), are satisfied in these cases.)

Therefore, the association equilibrium in the excited state is practically the same as that in the ground state.

**C. Effect of Solvent Viscosity on the Fluorescence Quenching.**—If the diffusion controlled dynamical processes in the excited state such as the energy dissipation due to dissociation of hydrogen bond or

TABLE I

| acceptor | donor | solvent | $T$ | $K_T$ | $\phi_c/\phi_0$ |
|---|---|---|---|---|---|
| acridine | phenol | benzene | 287 | 32 | |
| BDAA | $\alpha$-naphthol | 〃 | 306 | $5.7\times10^2$ | ~0 |
| | $\beta$-naphthol | 〃 | 304 | $2.9\times10^2$ | ~0 |
| | phenol | 〃 | 300 | $3.7\times10^2$ | ~0 |
| | aniline | 〃 | 300 | 9.6 | 0.29 |
| | pyrrole | 〃 | 300 | 3.8 | 0.59 |
| | phenol | n-hexane | 294 | $1.3\times10^3$ | 0.02 |
| | 〃 | cyclohexane | 298 | $1.4\times10^3$ | 0.01 |
| | 〃 | decalin | 298 | $0.9\times10^3$ | 0.06 |
| | 〃 | liquid paraffin | 297 | $1.4\times10^3$ | ~0 |
| DAA | phenol | benzene | 286 | $6.3\times10^2$ | ~0 |
| | aniline | 〃 | 287 | 20 | 0.29 |

rotation around the hydrogen bond[6] are concerned with the non-radiative degradation of excited state, the ratio of the fluorescence yields of hydrogen bonded and free molecules, $\phi/\phi_0$, may show some dependence on the solvent viscosity. From such a viewpoint, we have examined the effect of solvent viscosity on the fluorescence quenching of BDAA by phenol, changing the solvent from n-hexane to liquid paraffin. The results obtained are shown in Fig. 8 and Table I.

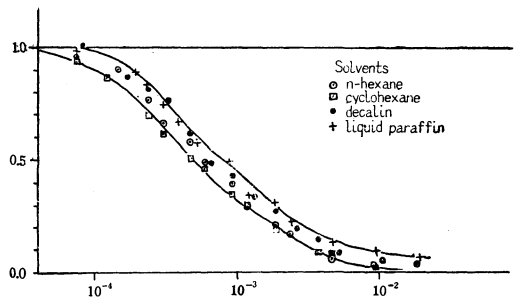



Fig. 8. Changes in relative fluorescence intensity of BDAA in various solvents of different viscosities by added phenol.

No viscosity dependence has been observed and the fluorescence is almost completely quenched by hydrogen bonding with phenol, in all the solvents examined. Therefore, no dynamical mechanism, in which the molecule moves as a whole, may prevail in the quenching of the present type.

## Discussion

The results obtained are collected in the Table I. When hydrogen bond is isolated from $\pi$-electron system of donor molecule by $\sigma$-bond such as the case for benzylalcohol and $\beta$-phenylethylalcohol, the enhancement of fluorescence yield by the mechanism described previously[1], occurs. However, when hydrogen bond is intimately related with $\pi$-electron system, i. e. the conjugation of hydrogen bond with $\pi$-electron system is possible, such as the case for phenol, naphthols, aniline and pyrrole, the decrease in fluorescence yield was observed. Moreover, from the independence of quenching of the viscosity of the solvent, it is clear that any dynamical process in the excited state, in which the quencher molecule moves as a whole, does not concern the degradation of excited state. Therefore, it is most likely that the cause of non-radiative degradation may be ascribed to the interaction between $\pi$-electron systems via the hydrogen bond, i. e. the delocalization of $\pi$-electron through the hydrogen bond, in the excited state. An analogous mechanism in which the charge transfer interaction between excited anthracene and solvent molecule leads to the fluoresecnce quenching, was proposed by Bowen and West[7]. From the stand-point mentioned above, a merely electrostatic model of the hydrogen bond may not be appropriate.

A charge transfer model of hydrogen bond using molecular orbital and perturbation theory, was proposed by Nukasawa, et al.[8] and supported by Tsubomura on the basis of his detailed calculation[9] for the system O—H···O and also from the result of his infrared measurement[10]. From the viewpoint of the quenching phenomenon with which the present paper

6) G. Oster and Y. Nishijima, *J. Am. Chem. Soc.*, **78**, 1581 (1956).

7) E. J. Bowen and K. West, *J. Chem. Soc.*, **1955**, 4394.

8) K. Nukasawa, J. Tanaka and S. Nagakura, *J. Phys. Soc. Japan*, **8**, 792 (1953).

9) H. Tsubomura, This Bulletin, **27**, 445 (1954).

10) H. Tsubomura, *J. Chem. Phys.*, **23**, 2130 (1955); ibid., **24**, 927 (1956).

is concerned, the charge transfer model of hydrogen bond is more favored than the merely electrostatic one, especially in the excited state.

A similar phenomenon was also observed for the fluorescence quenching of naphthols and naphthylamines due to hydrogen bonding with pyridine, and this type of non-radiative degradation of the excited state due to the delocalization of $\pi$-electron through the hydrogen bond, may form a group in the quenching phenomena by complex formation.

## Summary

1. Hydrogen bonding effect on the fluorescence of acridine, 3, 6-diaminoacridine and 3, 6-bisdimethylaminoacridine was studied in non-polar solvent added with proton donors such as phenol, naphthols, aniline and pyrrole.

2. Their fluorescence yields are decreased when hydrogen bonded with these proton donors, in which the hydrogen bond is capable of conjugation with $\pi$-electron system, in contrast to the case of donors such as benzylalcohol and $\beta$-phenylethylalcohol in which the hydrogen bond is isolated by $\sigma$-bond from $\pi$-electron system, and hydrogen bonding with which leads to the enhancement of fluorescence yield.

3. No viscosity dependence of quenching has been observed. From this fact participation of diffussion controlled dynamical process in the non-radiative degradation of excited state is unlikely.

4. The cause of non-radiative degradation of excited state by hydrogen bonding was ascribed to the delocalization of $\pi$-electrons through the hydrogen bond, especially in the excited state.

The authors express their gratitude to Professor M. Koizumi of Tohoku University and Professor R. Fujishiro for their interest in the present work. Their cordial thanks are due to Mr. H. Tsubomura of Tokyo University for his illuminating discussions.

*Institute of Polytechnics, Osaka City University, Kita-ku, Osaka*

# *Spectrochemical Study of Microscopic Crystals. XV*[1]. *Structure and Light Absorption of Bis-(dimethylglyoximato) gold(III) Dichloro-aurate(I)*[2]

By Shoichiro YAMADA and Ryutaro TSUCHIDA

(Received April 17, 1957)

In the former publications[3] the present authors reported on those compounds which display enormously deep colors owing to possible metal-to-metal interaction. A recent study indicated that bis-(dimethylglyoximato)-gold(III) dichloro-aurate(I), $[Au(dgH)_2][AuCl_2]$[4], would be a compound of a similar sort. Rundle[5] examined with X-ray the crystal structure of the compound, showing that in the crystal of the compound the linear dichloro-aurate(I), $[AuCl_2]^-$, and planar bis-(dimethylgyloximato)-gold(III) ions, $[Au(dgH)_2]^+$, are arranged parallel to each other, with the gold(I) and the gold(III) ions disposed at an equal distance along the *c*-axis of the crystal. Sinec the distance between the gold(I) and the gold(III) ions was found to be comparatively short, he assumed the existence of the direct interaction between the gold(I) and the gold(III) ions. As our former reports revealed that those compounds involving direct interaction between metallic ions showed an extra-ordinary type of dichroism, it was thought that it would be significant to examine dichroism of bis-(dimethylglyoximato)-gold(III) dichloro-aurate(I) with reference to the relationships on the dichroism which were formerly derived.

1) Part XIV of this series, S. Yamada, H. Nakamura and R. Tsuchida, This Bulletin, **30**, 647 (1957).

2) R. Tsuchida and S. Yamada, Presented before the Annual Meeting of Japan Chemical Society, Tokyo, April 6th, 1957.

3) S. Yamada and R. Tsuchida, This Bulletin, **27**, 156 (1954); *J. Am. Chem. Soc.*, **73**, 1579 (1951); ibid., **75**, 6351 (1953), etc.

4) The notation, $dgH_2$, represents a molecule of dimethylglyoxime.

In this work we have quantitatively determined the dichroism of the above-mentioned compound in the visible and the ultra-violet. The result has been found to disagree with the hypothesis of the existence of the metal-to-metal interaction in the present compound.

## Experimental

**Material.**—The compound, $[Au(dgH)_2][AuCl_2]$ was prepared in brown needles according to the method reported by Rundle[5]. Crystals having an identical external form were always obtained in all of our experiments. A marked dichroism was observed under the microscope. The crystal is yellow with the electric vector along the *c*-axis and brownish orange with the electric vector normal to the *c*-axis. The dichroism measurement was carried out with polarized light having its electric vector along and normal to the *c*-axis. The *c*- and *a*-absorption represent the absorption with the electric vector along and normal to the *c*-axis, respectively.

**Measurement.**—Quantitative dichroism measurement was done by Tsuchida-Kobayashi's microscopic method using polarized light[6]. The symbols used here are the same as those in our former papers of this series.

## Results and Discussion

The result of the dichroism measurement is shown in Fig. 1 and Table I. According to the crystal structure analysis of $[Au(dgH)_2][AuCl_2]$ reported by Rundle, the planar cations of $[Au(dgH)_2]^+$ and linear anions of $[AuCl_2]^-$ are arranged alternately in the crystal of the present compound such that the planes and the lines of the complex ions are parallel to each other and perpendicular to the *c*-axis, that is, the needle axis. The *c*-absorption is seen

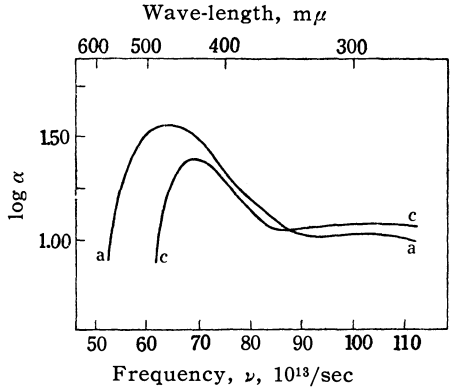



Fig. 1. Absorption spectra of $[Au(dgH)_2][AuCl_2]$ in the crystalline state.

to correspond with the ⊥-absorption, the absorption with the electric vector normal to the direction in which lie the linkages of the ligands with the metallic ion. The *a*-absorption is found to represent the main features of the ∥-absorption of the complex ion; that is, the absorption with the electric vector along the linkage.

The present measurement of dichroism shows that *for the absorption band at the longer wave-length, the ∥-absorption is about four and a half times as intense as the ⊥-absorption.*

From the short Au(I)-Au(III) distance of 3.26 Å, Rundle[5] suggested the existence

TABLE I
ABSORPTION MAXIMA OF $[Au(dgH)_2][AuCl_2]$

| | ν, $10^{13}$/sec. | log α | half width, $10^{13}$/sec. |
|---|---|---|---|
| *a*-abs. | 64 | 1.55 | 18 |
| *c*-abs. | 69 | 1.37 | 6.5 |

of weak linkage between the Au(I) and Au(III) ions in the present compound. The weak metal-to-metal linkage as proposed for the present compound would be somewhat similar to the metal-to-metal linkage for Magnus's green salt, bis-(dimethylglyoximato)-nickel(II), and so forth. Our former researches[3] indicate that for the absorption band at the longer wave-length of those compounds involving the metal-to-metal interaction, absorption is stronger in the direction normal to the complex plane; i. e. in the direction in which the metal-to-metal linkage is expected to exist than along the plane of the complex. This is not the case with the present compound. Thus the present dichroism measurement seems to indicate that *the metal-to-metal interaction may not exist between the Au(I) and the Au(III) ions in the present compound.*

Assuming the absence of the metal-to-metal interaction between the Au(I) and the Au(III) ions, the absorption band at about $60\text{–}70\times10^{13}$/sec. may be due to the planar $[Au(dgH)_2]^+$ ions under slight perturbation from the surrounding ions, since the $[AuCl_2]^-$ ion is not expected to show absorption in this wave-length region. For planar metallic complexes involving no metal-to-metal interaction, previous studies[7] show that with the absorption band at the longer wave-length, electric vector is more strongly absorbed along the plane of the complex than along the direction normal to the complex plane.

5) R. E. Rundle, *J. Am. Chem. Soc.*, **76**, 3101 (1954).
6) R. Tsuchida and M. Kobayashi, "The Colour and the Structure of Metallic Compounds", Zoshindo, Osaka, 1944, p. 180. See also the previous papers of this series.
7) S. Yamada and R. Tsuchida, This Bulletin, **26**, 489 (1953); ibid., **29**, 289 (1956); ibid., **29**, 694 (1956); *Ann. Rep. Scient. Works, Fac. Sci. Osaka Univ.*, **4**, 79 (1956), etc.

A similar relationship may reasonably be expected for the dichroism of the planar $[Au(dgH)_2]^+$ ion. The relationship obtained with $[Au(dgH)_2][AuCl_2]$ is seen to agree with that for typical planar complexes without the metal-to-metal interaction. This fact is also compatible with the conclusion that the metal-to-metal interaction is absent in the present compound.

It is to be noted that the metal-to-metal interaction is absent in the crystal of $[Au(dgH)_2][AuCl_2]$, where the Au(I)-Au(III) distance is comparatively short and almost equal to the Ni-Ni distance in the crystal of $Ni(dgH)_2$, in which the metal-to-metal interaction was concluded to exist.

This difference between $[Au(dgH)_2][AuCl_2]$ and $Ni(dgH)_2$ will be discussed in the following part of the present paper. The ionic radius of Ni(II) in the molecule of $Ni(dgH)_2$ is expected to be larger than that of Au(III) in the ion of $[Au(dgH)_2]^+$, judging from difference in the electronic charge between them. This might be one of the reasons for the absence of the metal-to-metal interaction.

In addition to this, however, there may be another reason for this phenomenon, which we are inclined to regard as more important. The central nickel ion in the $[Ni(dgH)_2]$ molecule is assumed to have non-bonding *d*-electrons spreading in the regions above and below the metallic ion in the direction normal to the plane of the complex. These non-bonding *d*-electrons may be available for some additional bonding, since a very great amount of energy may not be required to promote these electrons for the additional bonding. It was assumed in the former papers[3,8] that the nickel ions lying at an equal distance along the *c*-axis form octahedral $sp^3d^2$ hybridization orbitals, overlapping of the orbitals being responsible for the metal-to-metal interaction. For the overlapping of the orbitals resulting in the metal-to-metal linkage may be used the non-bonding 3*d*-electrons which originally spread in the direction perpendicular to the plane. This seems to be consistent with the idea proposed by Rundle and Sturdivant[9], who pointed out that the existence of a low-lying orbital was necessary for the metal-to-metal linkage. The existence of electrons which can be promoted for the linkage with a comparatively small amount of energy may also be important.

As for $[Au(dgH)_2][AuCl_2]$, the $[Au(dgH)_2]^+$ ion involves similar situation to that of $[Ni(dgH)_2]$, the above condition for the metal-to-metal linkage being satisfied. On the contrary, the Au(I) ion in the $[AuCl_2]^-$ ion forms linear *sp* hydridization orbitals in the outside of the $5d^{10}$ closed shell. For the metal-to-metal linkage, the Au(I) must form square hybridization orbitals and at the same time electrons in the $5d^{10}$ closed shell must be available. We prefer to suppose that the considerably great stability of the $5d^{10}$ closed shell might make the above conditions difficult to be fulfilled. Thus the conclusion that the Au(I)-Au(III) interaction is absent in the present compound may be understood on the basis of these considerations.

In advancing the hypothetical metal-to-metal linkage in the present compound, Rundle[5] assumed $5d6s6p^2$ hybridization orbitals of the Au(I) ion which would result in overlapping with some of the hybridization orbitals of the Au(III) ion. A comparatively great amount of energy may be required for the $5d6s6p^2$ hybridization because of the possibly great stability of the $5d^{10}$ closed shell. In our view on the basis of the present observation, the hybridization of $5d6s6p^2$ can hardly be assumed to occur at such a distance as observed for the crystal of the present compound.

## Summary

Dichroism of $[Au(dgH)_2][AuCl_2]$ has been determined in the visible and the ultraviolet region by the microscopic method. For the absorption band at about $60–70\times10^{13}$/sec., absorption has been found to be about four and a half times as strong along the complex plane as along the direction normal to the plane.

From discussion on the result of the dichroism measurement, it has been concluded that the metal-to-metal interaction does not exist between the Au(I) and Au(III) ions in this crystal.

The present authors wish to thank the Ministry of Education for a grant.

*Department of Chemistry, Faculty of Science, Osaka university*
*Kita-ku, Osaka*

8) L. E. Godycki and R. E. Rundle, *Acta Cryst.*, **6**, 487 (1953).
9) R. E. Rundle and J. H. Sturdivant, *J. Am. Chem. Soc.*, **69**, 1561 (1947).

# *The Formation of Cellulose IV in the Viscose Spinning**

By Yoshizo TSUDA and Sadataka MUKOYAMA

(Received April 17, 1957)

It has been generally acknowledged that the crystal form of the cellulose in viscose rayon may be designated as cellulose II. However, as pointed out by Ingersol[1] and Howsmon[2] a small amount of cellulose IV may also be formed during the spinning of viscose rayon under special conditions, although those conditions have not been elucidated. Thus the mechanism of the cellulose IV formation in the spinning of viscose rayon is still unknown.

One will be able to find the presence of cellulose IV in the X-ray diagram of tire cord rayon, while none can be found in that of textile rayon. This fact suggests that the formation of cellulose IV may be facilitated by the spinning process characteristic of the spinning of tire cord rayon. It has been the purpose of this work to investigate the mechanism of the formation of cellulose IV in the spinning of tire cord rayon.

It has been suggested[2] that cellulcse IV may be formed by the direct decomposition of cellulose xanthates. If this is true, the zinc cellulose xanthate formed temporarily in the viscose spinning process may play an important role in the formation of cellulose IV. According to this suggestion the present work was started with the investigation of the regeneration of zinc cellulose xanthate model filament and it was shown that high temperature of regeneration is the necessary condition to form cellulose IV in this case. The mechanism of the formation of the cellulose IV in the viscose spinning process was investigated with the experimental rayon spun by the stretch spinning method on the basis of the conclusion obtained above.

## The Crystal Structure of Cellulose IV

It has been confirmed by a number of investigations[3] that cellulose I is stable at higher temperatures and can be formed by transforming cellulose IV at higher temperatures by various methods. The unit cell of cellulose is described as rhombic with the dimension $a=8.11$ Å, $b=10.3$ Å, $c=7.9$ Å and the angle $\beta$ approximately 90°. The principal X-ray evidence for the existence of cellulose IV lies in the fact that only one equatorial interference occurs in place of the 101, 101 doublet of cellulose I. As pointed out by Howsmon[2] cellulose IV may be regarded as a disordered form of cellulose I.

## Experimental

(a) **Cellulose Samples.**—Ammonium cellulose xanthate model filament was prepared according to the procedure employed by Hermans[4]. Zinc cellulose xanthate model filament was obtained by immersing ammonium cellulose xanthate model filament in a cold saturated zinc sulfate solution for half an hour,, stretching to twice its original length and then regenerating. Dilute sulfuric acid solutions at various temperatures (40°C, 60°C, 80°C, 100°C) as well as boiling water and glycerine at 150°C were employed for the regeneration.

Experimental rayon was spun in Müller-type baths of various compositions followed by a second bath either at a higher temperature (95°C) or at a lower temperature (60°C). In the following table the compositions of the Müller-type baths employed and the corresponding temperature of the second bath are shown.

TABLE I
SPINNING CONDITIONS OF EXPERIMENTAL RAYON

| No. of Sample | Composition of Müller-type bath wt. % | | | Temp. of second bath °C |
|---|---|---|---|---|
| | $H_2SO_4$ | $Na_2SO_4$ | $ZnSO_4$ | |
| I | 8 | 20 | 1 | 60 |
| II | 8 | 20 | 1 | 95 |
| III | 8 | 20 | 2 | 60 |
| IV | 8 | 20 | 2 | 95 |
| V | 8 | 20 | 3 | 60 |
| VI | 8 | 20 | 3 | 95 |
| VII | 8 | 20 | 4 | 60 |
| VIII | 8 | 20 | 4 | 95 |

* The main part of this paper was presented at the 10th Annual Meeting of the Chemical Society of Japan, April 1957.

1) H. G. Ingersol, *J. Applied Phys.*, **11**, 924 (1946).

2) J. A. Howsmon, W. A. Sisson, "Cellulose and Cellulose Derivatives" (E. Ott) Part 1. pp. 241-244 (1954).

3) K. Hutino and I. Sakurada, *Naturwissenschaften* 577 (1940); T. Kubo, *Z. phisik. Chem.*, A **49**, 297 (1940); K. Hess and H. Kiessig, *Z. phisik. Chem.*, B **49**, 235 (1941).

4) P. H. Hermans, "Physics and Chemistry of Cellulose Fibres", p. 439 (1949).

The temperature of the first bath (Müller-type bath) was kept at 50°C, the spinning speed at 25 m. and the first bath travel at 30 cm.

(b) X-Ray Diffraction.—The Norelco diffractometer of the North American Philips Company, Inc., with auxiliary equipments, consisting of a recording potentiometer and a scaler counting unit, was used in these studies. Nickel-filtered radiation from a copper target operated at 35 kV and 15 mA tube current was used.

In order to obtain pulverous specimens, the cellulose samples were methanolized for a day with one normal hydrochloric acid in absolute methyl alcohol at 40°C. This treatment gave a ninety-five per cent. yield of cellulose.

No change in the crystal form through the methanolysis was confirmed by comparing the X-ray diffraction intensity curve of the methanolized sample with the X-ray diffraction diagram of the fibrous sample.

## Results and Discussion

The X-ray diffraction intensity curves of textile rayon and tire cord rayon are shown in Fig. 1. No peak of cellulose IV appears in the diffraction intensity curve of textile rayon. In contrast, a remarkable peak of cellulose IV is observed in the diffraction intensity curve of tire cord rayon. The difference of this nature will be found between any textile and tire cord rayons.

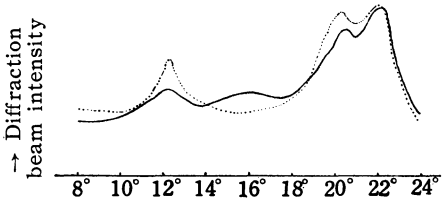



Fig. 1. X-ray diffraction intensity curves of tire cord rayon (full line) and textile rayon (dotted line).

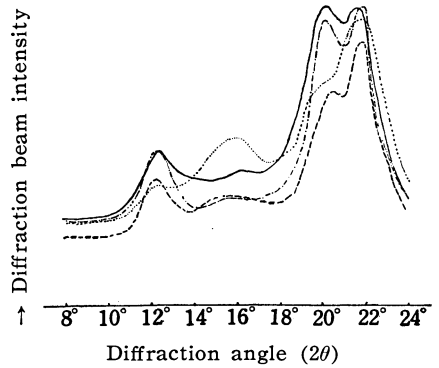



Fig. 2. X-ray diffraction intensity curves of model filaments regenerated at various temperatures: 40°C (full line), 60°C (chain line), 80°C (broken line) and 100°C (dotted line).

The X-ray diffraction intensity curves of the model filaments regenerated with dilute sulfuric acid solutions at various temperatures are shown in Fig. 2. It is seen that the relative intensity of the peak of cellulose IV increases slightly with the increase in the temperature of regeneration from 40°C to 80°C, while a marked increase of cellulose IV is observed with the sample regenerated at 100°C. It should be mentioned that the critical temperature which determines the formation of cellulose IV lies between 80°C and 100°C.

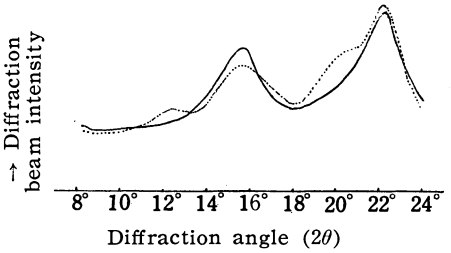



Fig. 3. X-ray diffraction intensity curves of model filaments regenerated with boiling water (dotted line) and regenerated with glycerine at 150°C (full line).

The X-ray diffraction intensity curves of the model filaments regenerated with boiling water and with glycerine at 150°C are shown in Fig. 3. The curve for the sample regenerated with boiling water is identical with that for the sample regenerated with dilute sulfuric acid at 100°C. This fact indicates that the formation of cellulose IV depends solely on the temperature of regeneration.

The curve for the sample regenerated with glycerine at 150°C shows that the crystal form of the sample consists of cellulose IV alone. It may be concluded that the degree of formation of cellulose IV by the decomposition of zinc cellulose xanthate is determined by the temperature and that the regeneration temperature above a critical temperature which is between 80°C and 100°C, is required for the formation of cellulose IV.

The X-ray diffraction intensity curves of the experimental rayon are shown in Fig. 4. It can be seen from those curves that the formation of cellulose IV depends on the temperature of the second bath. Namely the samples which passed through the second bath at 95°C contain the crystal

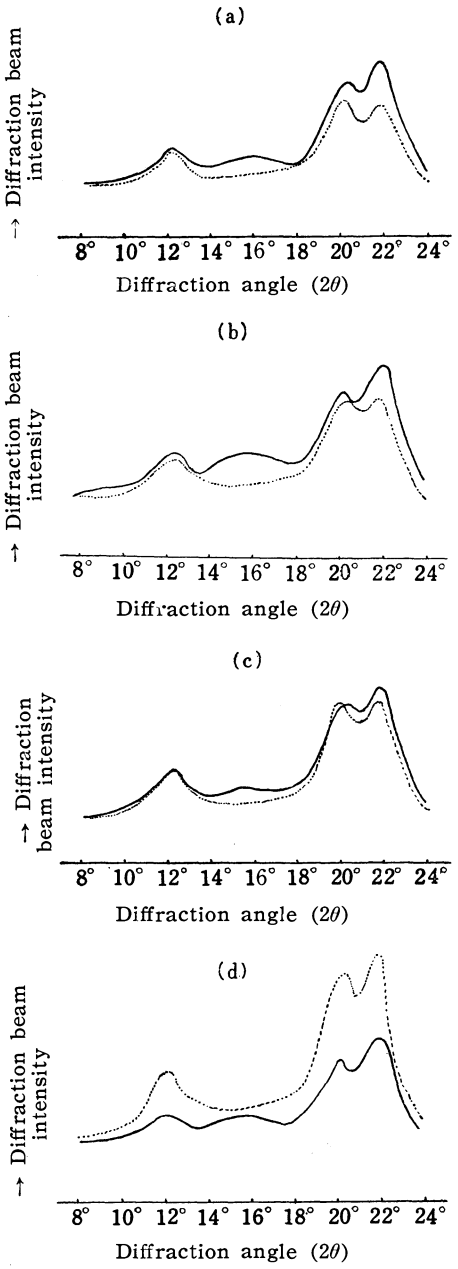



Fig. 4. X-ray diffraction intensity curves of experimental rayon: (a) I, II, (b) III, IV; (c) V, VI; (d) VII, VIII; here I, III, V and VII are drawn in dotted lines and the rests in full lines.

form of cellulose IV, while the samples which passed through the second bath at 60°C contain no crystal form of cellulose IV. In addition, the relative intensity of the peak of cellulose IV as compared of cellulose II increases with that with the increase in the concentration of zinc sulfate in the first bath. These facts will be elucidated as follows. The zinc cellulose xanthate which is formed temporarily in the first bath is brought into the second bath maintained at a higher temperature where it is regenerated. Thus the crystal form of the cellulose IV is included in the sample which passed through the second bath at a sufficiently high temperature. The formation of zinc cellulose xanthate depends on the concentration of zinc sulfate in the first bath. Consequently, the higher the concentration of zinc sulfate, the greater the content of cellulose IV in the regenerated sample.

It may be concluded from the results that the partical formation of cellulose IV in tire cord rayon is due to the higher temperature of the second bath and the higher content of zinc sulfate in the first bath.

## Summary

The formation of cellulose IV in the viscose spinning process was investigated by the X-ray diffraction measurements. Zinc cellulose xanthate model filaments were regenerated at various temperatures and their X-ray diffraction diagrams were examined. It was observed that the formation of cellulose IV is remarkable when zinc cellulose xanthate is regenerated at the temperature above a critical temperature which lies between 80°C and 100°C. The mechanism of partial formation of cellulose IV in the viscose spinning process was elucidated as follows: when zinc cellulose xanthate formed in the first bath is regenerated at a sufficiently high temperature in the second bath, the formation of cellulose IV consequently results. The main factors involved for the formation of cellulose IV are higher temperature of the second bath and higher concentration of zinc sulfate in the first bath.

The authors are grateful to Dr. K. Hoshino for premission of this publication. The authors sincer thanks are also due to Professor K. Maeda of Tokyo Institute of Technology and Mr. T. Yurugi of the Textile Research Institute for their kind discussions.

*Research Center, Toyo Rayon Company Ltd., Otsu, Shiga Prefecture*

# *Studies on Carbon-Chlorine Bonds in Some Aromatic Compounds by Their Pure Quadrupole Spectra*

By Hisao NEGITA, Sumio SATOU, Teijiro YONEZAWA and Kenichi FUKUI

(Received April 25, 1957)

Pure quadrupole spectra of many chlorine compounds have been reported so far and their resonance absorption frequencies or nuclear quadrupole coupling constants have been interpreted from various points of view[1]. Some years ago, Meal[2] found a nearly linear relationship between the frequencies and Hammett's $\sigma$ of various substituents in monosubstituted chlorobenzene. Later, the same result as this has been recognized also in bromobenzene, iodobenzene[3], and dichlorobenzene[4].

In this paper we studied other effects on the frequencies, that is, the frequency shifts which resulted from replacement of one or more carbon atoms in the benzene ring by the corresponding numbers of nitrogen atoms. The compounds used for comparison were chlorobenzene, 2-chloropyridine, 1,3,5-trichlorobenzene, and cyanuric chloride. As the frequencies due to $^{35}Cl$ of the first three compounds were already known[5~7], we measured only those of the last, which were closely spaced and higher than those of trichlorobenzene. This result is evidently contrary to that of chloropyridine, where its frequency is lower than that of chlorobenzene. However, these opposing phenomena due to nitrogen atoms may be correlated with each other by the theoretical consideration, for the decrease of $\pi$-electron density at chlorine atoms, which accompanies that of $\sigma$-electron necessarily, is much more remarkable in the former than in the latter, compared to the increase of bond order of carbon-chlorine bonds.

## Experimental

**Sample.**—To obtain cyanuric chloride $(CNCl)_3$, cyanuric acid $(CNOH)_3$ was prepared from urea and anhydrous zinc chloride, and then it was chlorinated by phosphorus pentachloride in phosphorus oxychloride as the solvent[8,9]. The product was purified by recrystallization from chloroform and then by sublimation in a long test tube. The sample thus obtained melted around 146°C, which was in good agreement with the value already known.

**Apparatus.**—The resonance absorption frequencies due to $^{35}Cl$ were measured by the frequency modulated super-regenerative spectrometer described in the previous paper[4,10] and was ascertained by those due to $^{37}Cl$, which should be found at the lower frequency region[11]. To obtain the data at lower temperature, solid carbon dioxide and toluene were used as the freezing mixture, and the temperature was measured with copper-constantan and a potentiometer.

The experimental error in frequency would be introduced from reading off both frequency and temperature of the sample, and amounts to several kilocycles/sec., which might not be so serious in the following considerations.

## Results and Discussions

The experimental results are shown in Table I. From this table, it is seen that two resonance absorption lines are so closely spaced, especially at a lower temperature, that they are observed without any interferences from side bands.

TABLE I

NUCLEAR QUADRUPOLE RESONANCE FREQUENCIES ($\nu$) DUE TO $^{35}Cl$ OF CYANURIC CHLORIDE

| Temp. | 195°K | 285°K |
|---|---|---|
| $\nu$ (Mc./sec.) | 36.533—Weak<br>36.537—Strong | 36.323—Strong<br>36.338—Weak |

At room temperature, 285°K, the lower line was much stronger than the other, which would tell the fact that the chlorine atoms corresponding to the former are

1) H. Negita, *Chem. and Chem. Ind., Japan*, **8**, 415 (1955).
2) H. C. Meal, *J. Am. Chem. Soc.*, **74**, 6074 (1952).
3) J. Hatton and B. V. Rollin, *Trans. Faraday Soc.*, **50**, 398 (1954).
4) H. Negita, H. Yamamura and H. Shiba, This Bulletin, **28**, 271 (1955).
5) R. Livingston, *Phys. Rev.*, **82**, 289 (1951).
6) S. Segel, R. G. Barnes and P. J. Bray, *J. Chem. Phys.*, **25**, 1286 (1956).
7) P. J. Bray, R. G. Barnes and R. Bersohn, *J. Chem. Phys.*, **25**, 813 (1956).
8) Beilsteins Handbuch der Organischen Chemie, 4 Aufl., Julius Springer, Berlin, (1937), XXVI, p. 35.
9) Z. Yoshida and R. Oda, *J. Chem. Soc., Japan, Ind. Chem. Sec.*, **56**, 92 (1953).
10) H. Negita and S. Satou, This Bulletin, **29**, 426 (1956).
11) R. Livingston, *J. Phys. Chem.*, **57**, 496 (1953).

are more abundant than the others, the ratio presumanbly being 2 : 1. However, the situation is reversed at 185°K. Thus, it may be concluded that the two lines are different from each other in the temperature gradient and they seem to overlap at some intermediate temperature, or else there are some transition points. In spite of this extraordinary behavior, our present interest is in the following fact.

The average value of the frequencies of cyanuric chloride is higher than that of trichlorobenzene, taking account of the temperature effect. To see this more precisely, the two average values in Table I were extrapolated to 77°K and about 36.725 Mc./sec. was obtained as the value at that temperature. It is obviously higher than that of trichlorobenzene[7] and this fact is contrary to the case of 2-chloropyridine[6] and chlorobenzene[5].

For comparison, the frequencies of these compounds are tabulated in Table II. At first sight, the replaced nitrogen atom in the ring will be thought to attract more electrons from the chlorine atom, with the result that the electron density around the latter is decreased, which in turn increases the frequency. However, this is not the case in the first row of Table II. Accordingly, the decrease in the frequency may be attributed to the increase in double bond character induced simultaneously, as pointed out by Segel et al.[6]

TABLE II

NUCLEAR QUADRUPOLE RESONANCE FREQUENCIES ($\nu$) DUE TO $^{35}Cl$ OF SOME AROMATIC COMPOUNDS AT 77°K

| Compd. | $\nu$ (Mc./sec.) | Compd. | $\nu$ (Mc./sec.) |
|---|---|---|---|
| Chlorobenzene | 34.6216 | 2-Chloropyridine | 34.194 |
| 1,3,5-Trichlorobenzene | 35.851 (Average) | Cyanuric chloride | 36.725 (Average) |

On the contrary, the increase in the frequency in the second row is supposed to result from the decrease in electron density, compensating the increase in the double bond character of carbon-chlorine bond. As a rule, circumstances around a molecule in the solid are more complex than in the vapor, owing to the neighboring molecules. However, such compounds as listed in the same row of Table II may be compared with each other by their isolated molecules, since they form molecular crystals alike in size and shape. Thus it will be worth while to examine the data of pure quadrupole spectra with reference to electronic structures computed from molecular orbital theory.

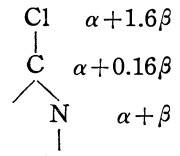
Now the ionic character and double bond character of carbon-chlorine bond may be considered in terms of $\pi$-electron density ($q$) at chlorine atom and mobile bond order ($p$) of the bond, respectively[12]. These two quantities are calculated in Table III for the compounds concerned.

TABLE III

$\pi$-ELECTRON DENSITIES ($q$) AT CHLORINE ATOMS AND MOBILE BOND ORDERS ($p$) OF CARBON CHLORINE BONDS

| Compd. | $q$ & $p$ | Compd. | $q$ & $p$ |
|---|---|---|---|
| Chlorobenzene | $q=1.9225$ $p=0.2728$ | 2-Chloropyridine | $q=1.9084$ $p=0.3391$ |
| 1,3,5-Trichlorobenzene | $q=1.9209$ $p=0.2744$ | Cyanuric chloride | $q=1.8650$ $p=0.4167$ |

Parameters adopted in calculation are as follows. Coulomb integrals are such that




and resonance integral of C—Cl is 0.8 $\beta$, where $\alpha$ and $\beta$ are the Coulomb and the resonance integral in benzene, respectively.

As seen in Table III, the decrease in the $\pi$-electron density at chlorine atom in the second row amounts to about four times as much as that of the first row, whereas the increase in carbon-chlorine bond order in the former is only twice as large as that of the latter. From these figures, the resonance frequency may decrease or increase as illustrated in Fig. 1,

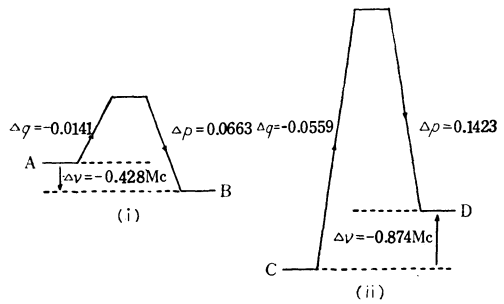



Fig. 1. Correlation of molecular constants and nuclear quadrupole resonance frequencies due to $^{35}Cl$.
(i) A···chlorobenzene,
B···2-chloropyridine.
(ii) C···1,3,5-trichlorobenzene,
D···cyanuric chloride.

12) C. A. Coulson and H. C. Longuet-Higgins, *Proc. Roy. Soc.* (*London*), **A191**, 39 (1937).

where A, B, C and D represent chlorobenzene, 2-chloropyridine, 1,3,5-trichlorobenzene, and cyanuric chloride, respectively.

It may be noted that the decrease in the $\pi$-electron density at a chlorine atom accompanies the decrease in the $\sigma$-electron and results in an increase in the frequency. As seen in Fig. 1, this increase is assumed for convenience to be proportional to the decrease in the former, for there is no straightforward way to compute the latter, but the frequency shifts are not so large in our cases. Thus, from the simplified schemes, it follows that $\Delta\nu/\Delta q \simeq -69$ Mc./sec. and $\Delta\nu/\Delta p \simeq -21$ Mc./sec..

The absolute value of the former is relatively large, though it includes the effect of the $\sigma$-electron. However, it is very difficult to justify the value. Thus it will be fair only to say that there is considerable transfer of the $\sigma$-electron accompanied with the $\pi$-electron. On the other hand, the latter value may be accepted easily, for it is near to the value $-27.4$ Mc./sec., which is computed as follows. From the experimental value of the coupling constant of free chlorine atom[13] and the number of unbalanced $p$-electrons, the frequency is assumed to be 54.8 Mc./sec. for pure —Cl state and $54.8\times\frac{1}{2}=27.4$ Mc./sec. for $=Cl^+$, while the bond order is 0 for the former and 1 for the latter, so that $\Delta\nu/\Delta p = -27.4$ Mc./sec. when $\Delta p=1$. It will be interesting to see whether the above relations might hold also in other cases, or not.

The authors wish to express their sincere thanks to Professor T. Ichikawa and Dr. H. Yamamura for their encouragement throughout this research, and also to Messers F. Okada and Z. Hirano for their able assistance to this work.

*Faculty of Science, Hiroshima University, Hiroshima Faculty, of Education Kagawa University, Takamatsu, and Faculty of Engineering, Kyoto University, Kyoto*

13) V. Jaccarino and J. G. King, *Phys. Rev.*, **83**, 471 (1951).

# *An Account on the Infrared Absorption of Guanidiniums*

By Toshio GOTO, Koji NAKANISHI and Mamoru OHASHI

(Received April 25, 1957)

The infrared spectra of several guanidine hydrochlorides have been examined in connection with the structural elucidation of roseonine[1] and roseothricin[2]. Except for a few scattered data[3] it seems that as yet no systematic study has been undertaken on the infrared absorption of guanidines, and accordingly, though the studies are far from comprehensive, results of diagnostic value are reported herein. The spectra are summarised in Fig. 1. The apparent general tendency is that with unsubstituted and symmetrically trisubstituted guanidine hydrochlorides (Nos. 1, 9 and 10) there is only a single strong absorption around 1650 $cm^{-1}$, whilst with mono- and disubstituted guanidine hydrochlorides (Nos. 2—8) there are two conspicuous bands in the region 1700—1580 $cm^{-1}$. Furthermore the separation between the two bands is generally wider with disubstituted guanidiniums (ca. 90 $cm^{-1}$) than with monosubstituted guanidiniums (ca. 20 $cm^{-1}$). For the sake of convenience we would like to refer to these bands as the guanidinium bands, and in cases when splitting is observed as the guanidinium I (higher frequency) and II (lower frequency) bands. The guanidinium band(s) apparently corresponds to the band around 1660 $cm^{-1}$ of free guanidines which is assigned to the C=N stretching[4]. With guanidine hydrcchlorides it would be due to an antisymmetric stretching of the carbon nitrogen bonds in the guanidinium

1) K. Nakanishi and M. Ohashi, following paper.
2) T. Goto, Y. Hirata, S. Hosoya and N. Komatsu, following paper.
3) H. M. Randall, R. G. Fowler, N. Fuson, J. R. Dangl, "Infrared Determ. of Org. Structures", D. van Nostrand (1949).
4) E. Lieber, D. R. Levering and L. Patterson, *Anal. Chem.*, **23**, 1594 (1951).

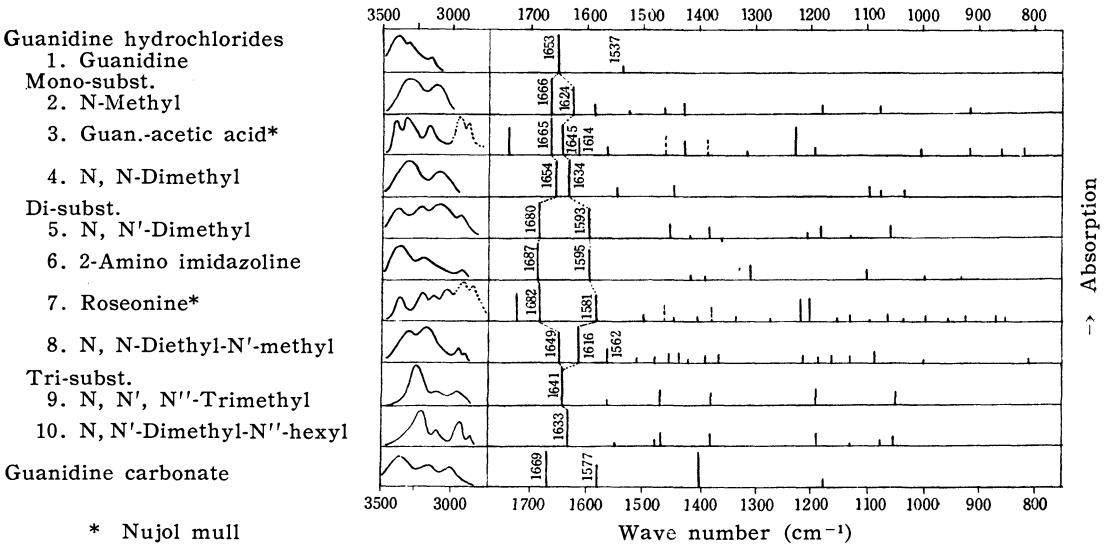
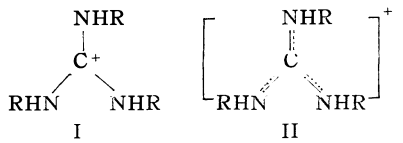



Fig. 1

group, probably coupled to some extent with $NH_2^-$ bending vibrations[5]. A single antisymmetric carbon nitrogen stretching vibration would be expected to be infrared active with unsubstituted and sym. trisubstituted guanidiniums, whilst two such vibrations would be expected with mono- and disubstituted guanidiniums; these expectations are thus in agreement with experimental observations. Since the symmetric carbon nitrogen stretching vibration of guanidiniums reveals itself as a strong absorption around 1000 $cm^{-1}$ in the Raman spectra[6], some of the weak infrared bands around 1000 $cm^{-1}$ could possibly be due to this sort of vibration; however they are of no diagnostic value. The absorption of guanidine carbonate (No. 11) which show bands at 1669 and 1577 $cm^{-1}$ as compared to the single band at 1653 $cm^{-1}$ of guanidine hydrochloride is anomalous. Since the spectra were all recorded in the solid state this is probably due to the influence of the negative ion on the crystal structure, and accordingly the results mentioned in the present paper are valid only for the hydrochlorides.

The relationship between an amino group and a positively charged ammonium group is probably of a continuous nature with no qualitative difference between them. Taking into account the fact that typical ammonium absorptions ($N^+H$ stretching) occur below ca. 3200 $cm^{-1}$ [7], whereas typical amine absorptions (N–H stretching) occur above 3200 $cm^{-1}$, the following generalisations regarding charge distribution within the guanidinium group may be inferred from the absorption of the guanidiniums in the 3000 $cm^{-1}$ region. Namely, the position of the absorptions in this region (Fig. 1.) corresponds to those of free amines rather than to amine salts, and this suggests that the positive charge resides mainly on the central carbon atom (I) rather than being distributed over the entire guanidinium group (II). This is further supported by the




fact that the absorptions of sym-trisubstituted guanidine hydrochlorides (Nos. 9, 10) which, according to structure I, would mainly possess only —NHR groups, reveal themselves as a more or less single major band, whereas those of other guanidiniums (which sould possess —$NH_2$ groups as well) reveal themselves as a broad band with two or more maxima, a behavior similar to that of free secondary and primary amines, respectively.

## Experimental

The guanidines were prepared according to the following methods.

5) A. Yamaguchi, *J. Chem. Soc. Japan, Pure Chem. Sec.* **78**, 140 (1957). The authors are greatly indebted to Ass. Profs. T. Shimanouchi (Tokyo Univ.) and M. Kimura (Nagoya Univ.) for valuable suggestions.

6) J. T. Edsall, *J. Phys. Chem.*, **41**, 133 (1937).

7) K. Nakanishi, T. Goto and M. Ohashi, This Bulletin, **30**, 403 (1957).

N-Methyl guanidine picrate, m. p. 196—198° [8].

N, N-Dimethyl guanidine picrate, m. p. 216—218° [8].

N' N'-Dimethyl guanidine picrate, m. p. 174—175° [9].

2-Aminoimidazoline picrate, m. p. 217°.

N, N-Diethyl-N'-methyl guanidine was prepared by the condensation of methyl isothiocyanate and dimethylamine, followed by treatment with ammonia and mercuric oxide in absolute ethanol solution. This is a new compound. Picrate, yellow plates, m. p. 128—129°.

*Anal.* Found: C, 40.60, 40.55, H, 4.88, 5.12, N, 23.19, 23.38%. Calcd. for $C_{12}H_{13}O_7N_6$: C, 40.22, H, 5.06. N, 23.46.

N, N', N''-Trimethyl guanidine picrate, m. p. 210—212° [10].

N, N'-Methyl-N''-*n*-hexyl guanidine was prepared by the treatment of N-methyl-N'-*n*-hexyl thiourea with methylamine and mercuric oxide in absolute ethanol. This is also a new compound but the picrate could not be obtained crystalline, and the crude hydrochloride was submitted directly to infrared measurements.

The picrates were treated with dilute hydrochloric acid, the liberated picric acid was extracted with ether, and the aqueous layer was evaporated to dryness in vacuo to give the respective hydrochlorides.

Infrared absorption measurements. The spectra were recorded on a Hilger H 800 double beam instrument equipped with a sodium chloride prism. Potassium bromide disks were used, and the die and the handpress were those supplied by Hilger and Watts, Co. Analytical grade potassium bromide was ground to pass a 200 mesh sieve and dried at 150°C for 24 hours; the samples (ca. 0.5 mg.) were ground evenly with 300 mg. of this potassium bromide for 5 minutes.

The authors are indebted to Professor Y. Hirata for his interest in this research.

*Department of Chemistry, Faculty of Science, Nagoya University*
*Chikusa, Nagoya*

8) E. A. Werner and J. Bell, *J. Chem. Soc.*, **1922**, 1790; E. Philippi and K. Morsch, *Ber.*, **60**, 2120. (1927).

9) T. L. Davis and E. N. Rosenquist, *J. Am. Chem. Soc.*, **59**, 2112 (1937).

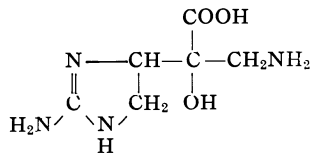
10) T. L. Davis and R. C. Elderfield, *J. Am. Chem. Soc.*, **54**, 1499 (1932).

# *Confirmation of Structure of Roseonine**

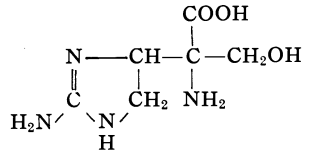
By Koji NAKANISHI and Mamoru OHASHI

(Received April 25, 1957)

Roseonine[1] is one of the two β-amino acids obtained as the hydrolysis products of roseothricin[2,3], and is identical with streptolidine from streptolin[4] and geamine from geomycin[5]; it has also recently been obtained from racemomycin B[6]. On account of the poor crystallizing properties of the reaction products from roseonine, and especially because the starting material was so scarce, the reasoning that led to the previously proposed structure I[1,7] was somewhat indirect. The validity of structure I and the possibilities of three



(I)



(II)

* Reported at 9th Annual Meeting, *Chem. Soc. Japan, Kyoto*, April, 1956.

1) K. Nakanishi, T. Ito, M. Ohashi, I. Morimoto and Y. Hirata, This Bulletin, **27**, 539 (1954).
K. Nakanishi, T. Ito and Y. Hirata, *J. Am. Chem. Soc.*, **76**, 2845 (1954).
K. Nakanishi, *J. of Antibiotics*, Ser. B., VII-7, 228 (1954).

2) S. Hosoya, M. Soeda, N. Komatsu, S. Imamura, M. Iwasaki, Y. Sonoda and K. Okada, *Jap. J. Exp. Med.*, **20**, 121 (1949); *J. of Antibiotics*, Ser. B, III-4, 217 (1950).

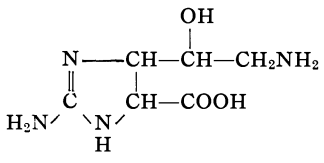
3) T. Goto, Y. Hirata, S. Hosoya and N. Komatsu, following paper.

4) H. E. Carter, W. R. Hearn and W. R. Taylor, "Abstracts of Papers", 120th Meeting, Am. Chem. Soc., New York, N. Y., September, 1951, p. 31.
E. E. Smissmann, R. W. Sharpe and E. E. van Tamelen, "Abstracts of Papers", 121st Meeting, Am. Chem. Soc., Milwaukee, Wisc., April 1952, p. 80.
Identity of roseonine with streptolidine confirmed by direct comparison of infrared spectra (personal communication from Dr. van Tamelen).

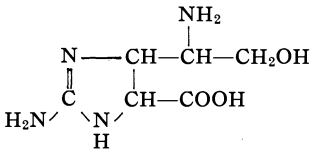
5) H. Brockamnn and H. Musso, *Ber.*, **88** 648 (1955).

6) H. Taniyama and S. Takemura, "Abstracts of Papers", 10th Annual Meeting, Pharm. Soc. Japan, Tokyo, April, 1957, p. 88.

7) For simplicity the structures I-IV are represented in the classical fashion and not in the zwitterionic form in which distribution of the positive charge within the guanidinium moiety should have to be considered. However, see structure I of preceding paper.



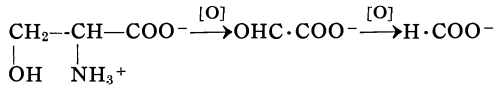
(III)



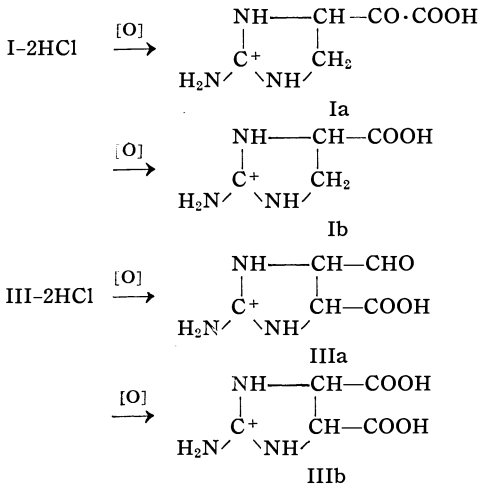
(IV)

other structures, II–IV, have accordingly been re-investigated. In the present paper we wish to furnish additional evidence pointing to structure I, and thus to clarify a few ambiguities[8]. Firstly, potentiometric titration and consideration of the hydrogen ion-binding curve[9] excluded structures III and IV, and secondly, evidence from infrared spectra pointed to the correctness of structure I.

Free D,L-serine was chosen as the model for the first method, and this was subjected to a two-mole periodate oxidation. Potentiometric titration of the aqueous reaction solution gave a $pK'_a$ value of 3.8, and the hydrogen ion-binding curve occurred *below* the zero reference line (i.e., the inflection corresponded to a hydrogen ion-binding group). The dissociation constant corresponded to that of formic acid, and thus the two oxidative steps may be correctly formulated by the following scheme:



Oxidation of roseonine dihydrochloride with one mole periodate yielded one mole each of formaldehyde and ammonia[1] and an unisolated product with a $pK'_a$ of 2.1[10]. Oxidation with a second mole of periodate afforded a product with a $pK'_a$ value of 3.3. Since neither formaldehyde nor 2-amino-2-imidazoline hydrochloride was attacked by periodate to any measurable extent under similar conditions, it is apparent that the inflection at 3.3 is neither due to the transformation of formaldehyde to formic acid, nor to an oxidative decomposition of the 2-imidazoline nucleus. Hence the oxidative steps may be represented as follows for structures I (or II)[11] and III (or IV)[11], respectively:



The oxidation product could not be isolated from the reaction solution owing to poor crystallizing properties and the minute amount of starting material available. Otherwise a simple analysis would have sufficed to differentiate between structures Ib and IIIb. Though no clear differentiation between structures Ia and IIIa, or between Ib and IIIb is possible from the two

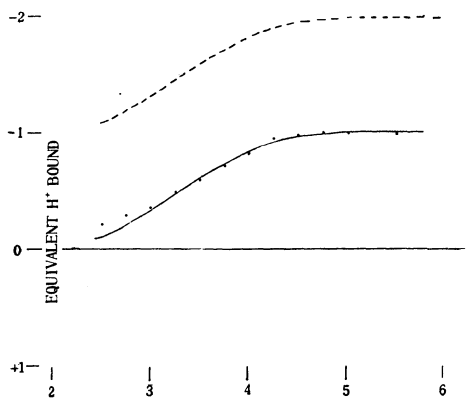



Fig. 1. Hydrogen ion-binding curve for 2 mole periodate oxidation product.
·····: Experimental
——: Theoretical curve for $pK'_a$ 3.3
– – –: Hypothetical curve for structure IIIb.

8) Ref. 5 and H. Musso, *Angew. Chem.*, **68**, 313 (1956).
9) T. V. Parke and W. W. Davis, *Anal. Chem.*, **26**, 642 (1954).
10) The titration was carried out only in the region of pH 2.3 to 6, since the end point was obscured in the other pH regions by the effect of the slightly excess periodic acid ($pK_{a_1}$ at 1.64, $pK_{a_2}$ 6.92 : N. V. Sidgwick, "The Chemical Elements and their Compounds", Vol. II, p. 1237 (1950), Oxford) and the buffering action of the formed ammonium chloride. The inflection at 2.1 was obtained by extrapolation.
11) Inasmuch as the side chain aminoethanol structure is destroyed by the first mole of periodate, it makes no difference whether the structure is I or II. The same applies to III and IV.

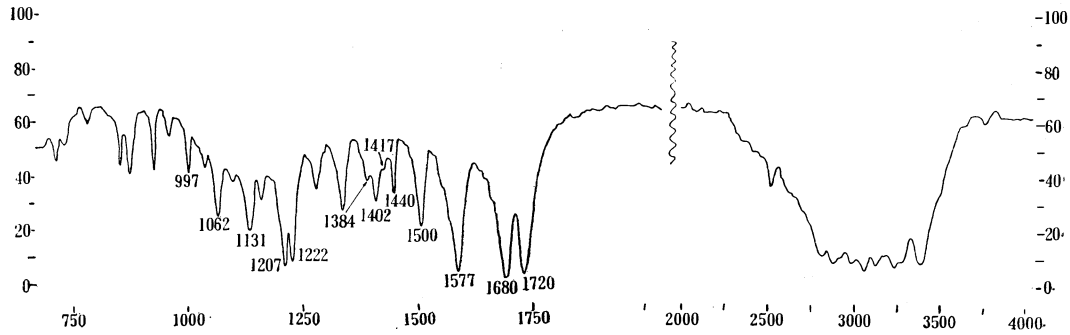



Fig. 2. Roseonine-2HCl (1.1 mg./300 mg. KBr): 1720 (COOH), 1680 (G—I)*, 1577 (G—II, $NH_3^+$)*,**, 1500($NH_3^+$)**

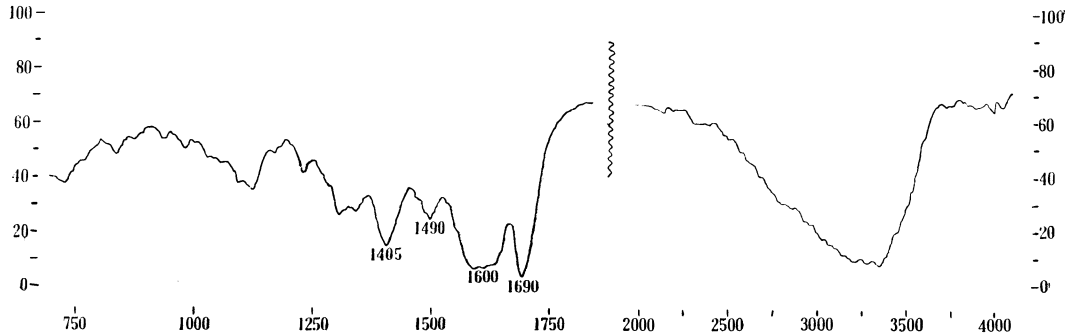



Fig. 3. Free roseonine (crude) (KBr): 1690 (G—I)*, 1600 ($NH_3^+$, G—II, $COO^-$)*,**, 1490($NH_3^+$)**

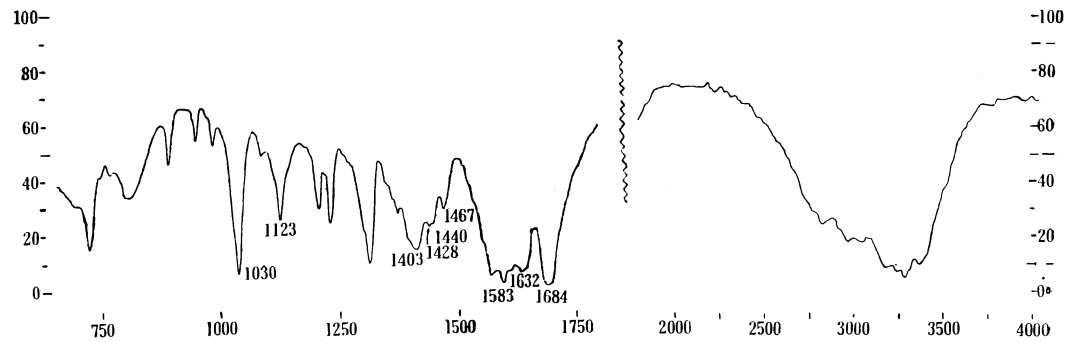



Fig. 4. Roseonine Diol (1.0 mg./300 mg. KBr): 1684 (G—I)*, 1632 ($COO^-$), 1583 (G—II)*

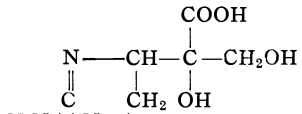
* cf. Guanidinum I and II band, Goto, Nakanishi, Ohashi, preceding paper.
** cf. Nakanishi, Goto, Ohashi, This Bulletin, **30**, 403 (1957).

$pK'_a$ values of 2.1 and 3.3, differentiation may be made by taking into account the hydrogen ionbinding curve for the two-mole oxidation product (Fig. 1). It is to be noted that since the dihydrochloride was used as the starting material, structure Ib possesses one hydrogen ion-releasing carboxyl group, and structure IIIb possesses two such groups; the entire titration curve, in either case, should thus lie *above* the zero line. The incompatibility of structure IIIb with Fig. 1 may be inferred as follows. First, assuming 3.3 to be the first $pK'_a$ value, the second dissociation constant arising from the second carboxyl group must then lie somewhere above 7 since the upper end of the experimental curve ending at about pH 5 as yet shows no sign of a second inflection. The $pK'_{a2}$ values for 1,2-*cis*- and *trans*-cyclopentanedicarboxylic acid are at 6.51 and 5.91, respectively[12], and

12) H. C. Brown, D. H. McDaniel and O. Häfliger in "Determination of Organic Structures by Physical Methods", Academic Press (1955), p. 625.

if the additional acid strengthening effect of the guanidinium group is considered, a $pK'_a2$ value above 7 would be unexplicable. Second, assuming 3.3 to be the second $pK'_a$ value, the first $pK'_a$ should then be below 2 and the experimental curve for the second constant should be that represented by the dotted lines in Fig. 1. Thus it becomes apparent that the observed inflection at 3.3 is due to the carboxylic group of Ib strengthened by the guanidinium group[13], and that roseonine possesses either structure I or II.

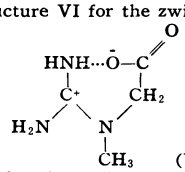
The decision between these two structures, i.e., whether the side chain is an isoserine residue or a serine residue, was further made possible from the infrared spectra. Namely, conversion of roseonine dihydrochloride into the diol V[14] resulted in the appearance of a band at 1467 $cm^{-1}$



(V)

(Fig. 4) which is absent in the spectra of roseonine dihydrochloride (Fig. 2) or free roseonine (Fig. 3, see experimental for preparation of this compound). This new band can only be assigned to a normal methylene bending vibration, and a new methylene group in the diol could, in turn, only be derived from formula I and not from II. The appearance of a conspicuous absorption at 1030 $cm^{-1}$ in the diol (*prim*-hydroxyl; corresponding to a similar strong band in the spectra of L- and D,L-serine at 1017 and 1036 $cm^{-1}$, respectively—D-serine was not examined) is also to be noted.

13) The $pK'_a$ of creatine, which like Ib also has a guanidinium group alpha to the carboxyl group is 3.0 at 20°C (Eadie and Hunter, *J. Biol. Chem.*, **67**, 237, 243 (1926)). This slightly enhanced acidity might be explained by structure VI for the zwitterion.



(VI)

14) Obtained by the action of silver nitrite on the dihydrochloride this was the only relatively easily accessible derivative.

## Experimental

**Potentiometric Titration of Periodate Oxidation Products.**—Roseonine dihydrochloride (9.7 mg., 0.037 m.mol.) was dissolved in 3 ml. of water, and to this there was added 3 ml. of an aqueous 0.03 m.mol./ml. solution of sodium metaperiodate. After being kept in an incubator at 35°C, 2 ml. of this mixed solution was pippetted out after 30 minutes and after 20 hours. These solutions were acidified by addition of 1 ml. of 0.0480 N-hydrochloric acid and were titrated with 0.0480 N-sodium hydroxide using a Beckman type-G pH-meter. The $pK'_a$ values were determined by the method of Parke and Davis[9]. The blank curve was obtained by carrying out an identical procedure on a periodate solution to which 3 ml. of water had been added instead of the roseonine-dihydrochloride solution. A parallel reaction mixture was employed for following the periodate consumption; this was measured by conventional techniques. The periodate consumption after 30 minutes was 1.0 mol., and that after 20 hours was 2.1 mol. The titrations were carried out at 11±2°C and not under thermostatted conditions.

**Free Roseonine.**—This was prepared by dissolving 10 mg. of sodium (0.44 m.mol.) in 1 ml. of absolute ethanol, adding 52 mg. of roseonine-dihydrochloride (0.21 m.mol.), stirring, and leaving overnight. The precipitates of sodium chloride and free roseonine were collected, dried, and pressed into disks. Though the infrared bands were diffuse owing to the presence of sodium chloride, it was sufficient for the purpose of showing the absence of strong absorptions around 1000 $cm^{-1}$ and 1470 $cm^{-1}$ (Fig. 3).

**Infrared Absorption Measurements.**—The spectra were recorded on a Hilger H 800 double beam instrument equipped with a sodium chloride prism; when necessary the region 1300-1750 $cm^{-1}$ was scanned with a calcium fluoride prism. Potassium bromide disks were used, and the die and the handpress were those supplied by Hilger and Watts, Co. Analytical grade potassium bromide was ground to pass a 200 mesh sieve and dried at 150°C for 24 hours; the samples (ca. 1 mg.) were ground evenly with 300 mg. of this potassium bromide for 5 minutes.

The authors wish to express their gratitude to Professor Yoshimasa Hirata for his guidance and interest in this research and to Mr. Toshio Goto for valuable discussion. We are also grateful for a grant from the Ministry of Education.

*Department of Chemistry, Faculty of Science, Nagoya University*
*Chikusa, Nagoya*

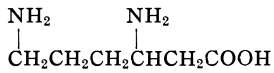
# *Structure of Roseothricin A***

By Toshio GOTO, Yoshimasa HIRATA, the late Seigo HOSOYA* and Nobuhiko KOMATSU*

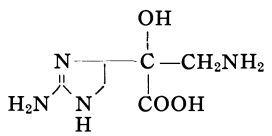
(Received April 25, 1957)

Roseothricin is an antibiotic substance produced by *Streptomyces Roseochromogenus*[1] and has a strong resemblance to streptothricin, streptolin, geomycin etc. Hitherto, two components, β-lysine (I)[2] and roseonine (II)[3], both of which are β-amino acids, have been obtained from the hydrolysate of roseothricin. These two amino acids have also been obtained from the acid hydrolysates of streptothricin[4], streptolin[5], geomycin[6], and racemomycin[7].

Roseothricin is not a simple compound, but consists of three components, roseothricin A, B and C, and these components can be separated by means of paper chromatography, paper electrophoresis or ion exchange chromatography[8]. In order to obtain greater amounts of roseothricin A, the method of ion exchange chromatography was employed: the roseothricin complex was passed through a column packed with Amberlite IRC-50 (Na-form) resin, the column was subsequently eluted with 2% ammonium sulfate solution, and roseothricin A was finally precipitated from the eluate as its phosphotangstate by addition of sodium phosphotangstate solution (cf. experimental part). By this method roseothricin A was obtained in a pure state from the roseothricin complex, and was employed for the following experiments.



(I)



(II)

**Components of Roseothricin A.**—Acid hydrolysis of roseothricin A with 6 N hydrochloric acid at 100° afforded two ninhydrin positive substances, β-lysine and roseonin, but during the hydrolysis considerable amounts of insoluble black resinous substances were produced[3]. Roseothricin A was therefore hydrolysed with 6 N hydrochloric acid at 50° for 11 days in nitrogen atmosphere, the hydrolysate was passed through a column of Dowex 50 (H-form) and the column was eluted with hydrochloric acid. The results are shown in Fig. 1.

Further hydrolysis of compound B afforded compound A and roseonine, and of compound C afforded β-lysine in addition to the two substances. Thus β-lysine, roseonine, compound A, carbon dioxide and ammonia resulted from the hydrolysis of roseothricin A.

Compound A is a new substance, properties of which are as follows: colorless crystals, dec. p. 145—155°, it shows positive ninhydrin, Fehling, Elson-Morgan, triphenyl tetrazolium chloride, and Tollens reaction and is, in these respects, similar to glucosamine. Paper chromatography: buthanol: acetic acid: water (4 : 1 : 1) $R_f$ 0.33 (glucosamine [G] 0.33); collidine 0.44 (G. 0.43); phenol : 1% ammonia (concd.) 0.74 (G. 0.70); ethyl acetate : pyridine : water (2:1:2) 0.86 (G. 0.87); methyl ethyl ketone 0.03 (G.

* Institute for Infections Diseased, Tokyo University, Minato, Tokyo.

** A communication (the part of compound A) has appeared in this Bulletin, **30**, 725 (1957).

1) S. Hosoya, M. Soeda, N. Komatsu, S. Imamura, M. Iwasaki, Y. Sonoda and K. Okada, *Jap. J. Exptl. Med.*, **20**, 121 (1949); *J. Antibiotocs*, **3**, (4), 217 (1950).

2) E. E. van Tamelen and E. E. Smissman, *J. Am. Chem. Soc.*, **75**, 2031 (1953).

3) K. Nakanishi, T. Ito, M. Ohashi, I. Morimoto and Y. Hirata, This Bulletin, **27**, 539 (1954); *J. Am. Chem. Soc.*, **76**, 2843 (1954); This Bulletin **30**, 725 (1957).

4) H. E. Carter, R. K. Clark, Jr., P. Kohn, J. W. Rothrock, W. R. Taylor, C. A. West, G. B. Whitfield and W. G. Jackson, *J. Am. Chem. Soc.*, **76**, 566 (1954).

5) E. E. Smissman, R. W. Sharpe, B. F. Aycock, E. E. van Tamelen and W. H. Peterson, ibid., **75**, 2029 (1953).

6) H. Brockmann and H. Musso, *Chem. Ber.*, **88**, 648 (1955).

7) H. Taniyama and S. Takemura, "Abstracts of Papers", 10th Annual Meeting, Pharm. Soc. Japan, April, 1957.

8) S. Hosoya, M. Soeda, N. Komatsu, N. Hara, Y. Sonoda and R. Arai, *J. Antibiotics*, **4** (5), 314 (1951); *Jap. J. Exptl. Med.*, **20**, 683 (1950); Y. Saburi, *J. Antibiotics*, Ser. B **6** (8), 402 (1953).

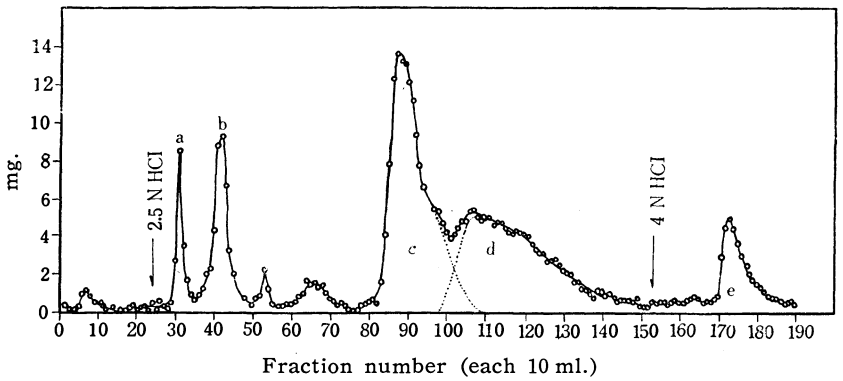



Fig. 1.

Four hundred mg. of roseothricin A HCl salt was hydrolysed to afford 470 mg. of the hydrolysate.

| Tube number | Yield | |
|---|---|---|
| 1—27 | 9 mg. | |
| a. 28—34 | 18 mg. | compound A |
| b. 35—50 | 45 mg. | ammonium chloride |
| 51—80 | 23 mg. | (negative ninhydrin test) |
| c. 81—100 | 153 mg. | 125 mg. β-lysine. 2HCl<br>28 mg. roseonine. 2HCl* |
| d. 101—138 | 129 mg. | compound B |
| 139—169 | 21 mg. | |
| e. 170—190 | 40 mg. | compound C |
| Total | 438 mg. | (recovery 93%) |
| | 25 mg. | $CO_2$ (as 111 mg. $BaCO_3$) |

* It was calculated from the periodate consumption of fraction C.

0.03). Compound A was scarcely distinguishable from glucosamine by means of paper chromatography using several solvent systems, but there was a small difference between their infrared spectra (Fig. 2). Compound A could not be analysed because of its very minute quantity and of the difficulty obtaining it in a crystalline state. However, according to the analysis and the periodate consumption of compound B, it was shown that compound A was neither a pentosamine nor a branched chain hexosamine, but a straight-chain hexosamine. Recently a hexosamine[9] (m. p. 152—162° dec.) has been isolated from streptothricin and streptolin B, and its structure elucidated as 2-amino-2-deoxy-α-D-gulose (α-D-gulosamine), which is a stereoisomer of glucosamine. Therefore, although no direct comparison between the two has as yet been made, it may be safe to regard compound A as being identical with gulosamine (III).

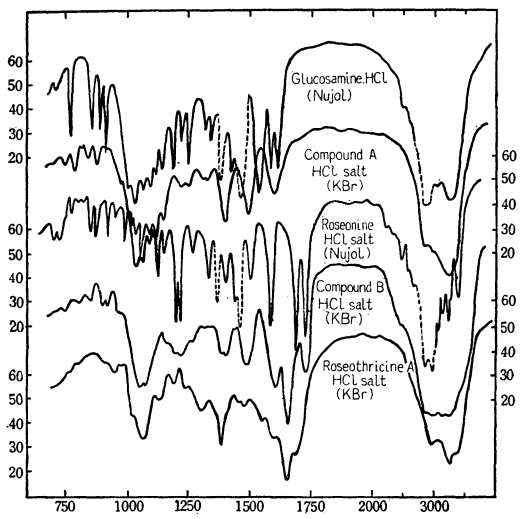
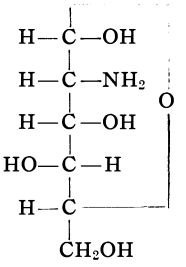



Fig. 2

**Structure of Compound B.**—Compound B was 2,4-dinitrophenylated incompletely by the method described in the experimental part, and the products were separated by means of counter current distribution. The result is shown in Fig. 3. The two peaks at $K=0.16$ and 9.0 suggest that compound B has two amino

9) E. E. van Tamelen, J. R. Dyer, H. E. Carter, J. V. Pierce and E. E. Daniels, *J. Am. Chem. Soc.*, **78**, 4817 (1956).




(III)

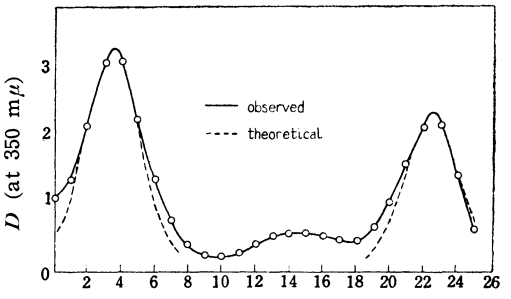



Fig. 3.

groups capable of being 2, 4-dinitrophenylated. The product of complete DNP-ation of compound B has an $E^{1\%}_{1cm}$ value of 306 at 350 mμ, and assuming the presence of two amino groups and taking into account the ε value of 15,900[10] (350 mμ) for a single DNP group, the calculated molecular weight of compound B is ca. 700 for

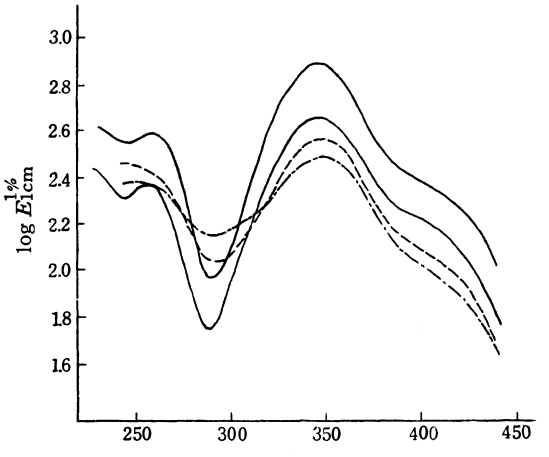



Fig. 4

—— (upper) Di-DNP-β-lysine in tetrahydrofuran $\varepsilon_{350m\mu}=18,000$
—— (lower) DNP-Roseonine in methanol $\varepsilon_{350m\mu}=15,900$
–––– DNP-Roseothricin A in T. H. F.
–·–· DNP-Compound B in T. H. F.

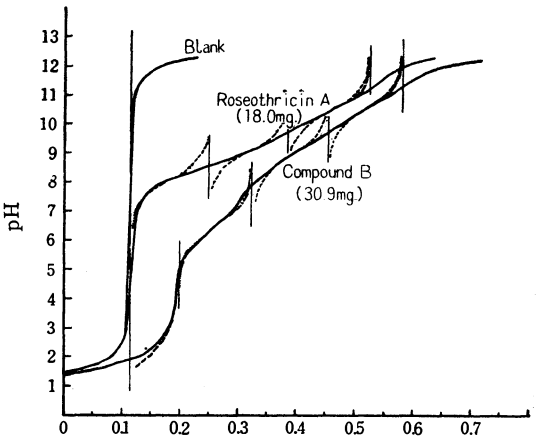



Fig. 5

—— Titration curve
–––– Titration curve minus blank
····· Theoretical curve

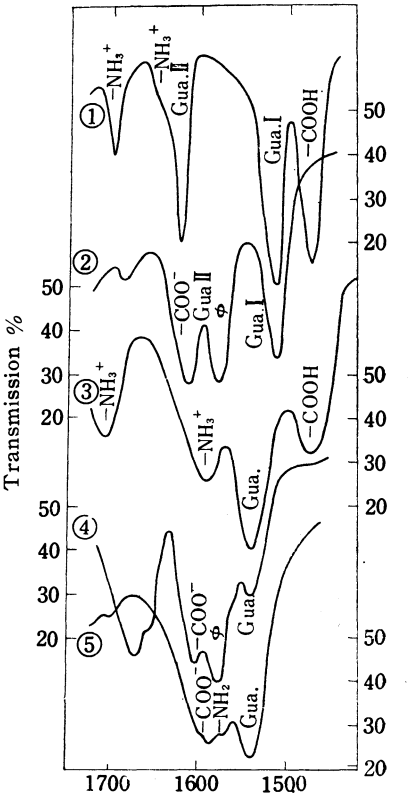



Fig. 6

① Roseonine-2HCl
② DNP- 〃
③ Compound B-HCl
④ DNP-Compound B
⑤ Compound B added $NMe_3$

10) A. R. Batterby and L. C. Craig, ibid., **73**, 1887 (1951). The ε value of 15,900 at 350 mμ is that of DNP-roseonine (roseonine can only be mono DNP-ated).

the free base (Fig. 4). Though compound B itself could not be hydrolysed without decomposition, roseonine and hexosamine were found in a 1 : 0.8 ratio in the hydrolysate of roseothricin A (Fig. 1). Coupled with the molecular weight (ca. 700) it is assumed that compound B is composed of 2 moles each of roseonine and hexosamine. Compound B, therefore, should have the molecular formula of $C_{24}H_{44}O_{13}N_{10}$ (2 moles each of roseonine and hexosamine minus $3H_2O$) and a molecular weight of 681 as the free base.

Compound B has eight $pK_a'$s: two at 2.4, two at 6.5, two at 8.9 and two at 10.4 (Fig. 5). Since the first two $pK_a'$s at 2.4 undoubtedly arise from the carboxyl groups evident in the IR spectrum (vide infra), it follows that compound B forms a hexa-hydrochloride with the remaining six groups.

*Anal.* Found; C, 32.65, H, 6.25, N, 16.12 %. Calcd. for $C_{24}H_{44}O_{13}N_{10}$. 6HCl; C, 32.05, H, 5.60, N, 15.57%.

The IR spectrum of compound B showed a band at 1732 $cm^{-1}$; when trimethylamine was added and the mixture was immediately evaporated to dryness, this band was displaced to ca. 1600, a position corresponding to the absorption of a carboxylate group. Furthermore, this band is present in DNP-compound B, and this is due to the fact that the guanidine portion cannot be DNP-ated and forms an intramolecular salt with this carboxyl group (Fig. 6). The IR of DNP-roseonine led to similar conclusions. This observation coupled with the two $pK_a'$s at ca. 2.4 suggests that the two carboxyl groups of compound B arising from two molecules of roseonine are free, and neither exist in the form of an ester or an amide group. By comparing the $pK_a'$s of compound B with those of roseonine and hexosamine (Table I), it is apparent that the $pK_a'$s at 10.2 originate from the guanidine portion and those at 6.5 and 8.9 originate from amino groups.

Though the IR spectrum of compound B is very similar to the addition spectrum of roseonine and hexosamine (Fig. 2), the spectra of compound B and roseonine differ in the fact that two bands at 1682 and 1581 in the latter are replaced by a single band at 1658 in the former. These two bands of roseonine originate in the N, N′-disubstituted guanidinium group, and if the guanidinium group is N, N′, N″-trisubstituted, its IR spectrum shows only one band around 1650 $cm^{-1}$ [11]. The guanidinium groups in compound B is, therefore, symmetrically trisubstituted. Thus the data so far mentioned point to the presence of the following groups in compound B: two amino groups which can be DNP-ated, two carboxyl groups, and two symmetrically trisubstituted guanidine groups. Since hydrolysis of compound B

TABLE I
$pK_a'$ VALUES

| Compound | −COOH | $-NH_3^+$ | Guanidinium$^+$ |
|---|---|---|---|
| β-Lysine | 3.2 | 9.5, 10.8 | — |
| Roseonine | 2.4 | 9.3 | 11.9 |
| Glucosamine | — | 7.8 | — |
| Compound B | 2.4(2)* | 6.5(2)*, 8.9(2)* | 10.4(2)* |
| Roseothricin A | — | 8.1(2)*, 9.0(2)* | 10.4(2)* |

* There are two $pK_a'$s which have the same values; they may not completely coincide but they cannot be distinguished from each other.

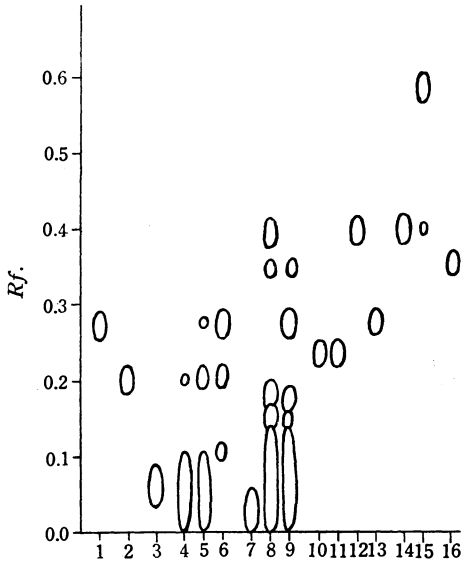
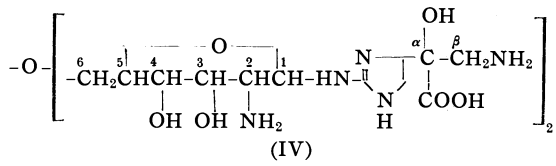



Fig. 7

Solvent system: buthanol : acetic acid : water (4 : 1 : 1). 1. β-lysine. 2. roseonine. hydrolysis of roseothricin A with 0.2 N NaOH at 30°: 3. before hyd. 4. after 1 hour. 5. after 1 day. 6. completely. methanolysis of roseothricin A: 7. with 5% HCl-methanol at 60° for 15 minutes. 8. 20% HCl-methanol, 90°, 3 hrs. 9. hydrolysis of No. 8 with aq. HCl. 10. β-lysine amide 11. treatment of No. 10 with 5% HCl-methanol at 60° for 15 min. 12. treatment of No. 10 with 20% HCl-methanol at 90° for 3 hrs. 13. hydrolysis of No. 12 with aq. HCl. 14. β-lysine methyl ester. 15. treatment of No. 14 with 5% HCl-propanol at 60° for 15 min. 16. compound A.

11) T. Goto, K. Nakanishi and M. Ohashi, This Bulletin, **30**, 723 (1957).

affords roseonine and hexosamine, the only position capable of forming a linkage in the hexosamine moiety is at $C_1$, which in turn is linked to the guanidine group of roseonine to form a trisubstituted guanidine group (N-glucoside linkage). This is consistent with the fact that compound B gives a positive Elson-Morgan test (glucosamine test) but a negative Fehling test, and the fact that it also gives a positive tetrazolium reaction (semiacetal test) after a longer heating period than that of hexosamine. The strong electron attracting influence of the guanidinium ion probably accounts for the $pK_a'$ (6.5) which is lower than that of hexosamine (ca. 8). The fact that the N-glucoside linkage is more stable under acidic condition than alkaline, is also explicable in terms of this effect. Namely, compound B is extremely resistant towards acid hydrolysis, and no appreciable hydrolysis occurred upon heating for 22 days with concentrated hydrochloric acid at 34°C. It was, however, easily hydrolysed by alkali (1 N sodium hydroxide at 34°C), and gave roseonine (Fig. 7). In this case hexosamine could not be isolated; it was probably decomposed by alkali. As above-menitoned, when compound B was DNP-ated, only two among the four amino groups could be DNP-ated. This partial DNP-ation is probably due to the much slower rate of DNP-ation of the hexosamine residue as compared to the roseonine residue; further DNP-ation of the partial DNP-ated product is thus prevented by precipitation of DNP-compound B. Actually the rate of DNP-ation of glucosamine is less than one fourth of that of roseonine (Fig. 8). Furthermore, it is reported that the amino group of glucosaminide, which has a glucoside linkage, does not react with methyl isothiourea in alkaline condition to form guanidine derivative. This negative evidence may suggest that the glucosidic group affords some protection to the amino group[12]. The positive charge of the guanidinium group in compound B could also retard the reaction between this amino group and the reagent. From these evidences, compound B may be represented by structure (IV).



(IV)

The consumption of periodic acid (6 moles to one mole of compound B, Fig. 9)

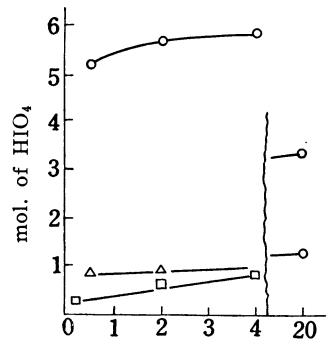



Fig. 9.
○— Compound B
□— Roseonine
△— Roseothricin A

suggests that 2-$NH_2$, 3- and 4-OH, $\alpha$-OH, and $\beta$-$NH_2$ are all free. Though there exists no direct evidence concerning the linkage between the two hexosamines, ester or amide bands are not observable in the region 1750–1500 $cm^{-1}$, and this together with the amount of periodic acid consumption suggests that the primary hydroxyl groups and not the secondary hydroxyl groups participate in an ether linkage.

**Structure of Roseothricin A.**—Roseothricin A was 2,4-dinitrophenylated incompletely, and the products were separated by means of counter current distribution. The result is shown in Fig. 10.

Since there are four peaks (at $K$=0.026, 0.15, 2.0 and 6.9) roseothricin A should have four amino groups capable of being 2,4-DNP-ated. The complete DNP-ated

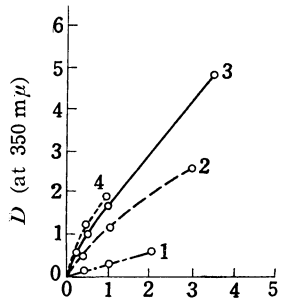



Fig. 8
1 Glucosamine
2 β-Lysine (1/2 eq.)
3 Roseonine
4 Compound B

12) M. Viscontini and J. Meier, *Helv. Chim. Acta*, **35**, 807 (1952).

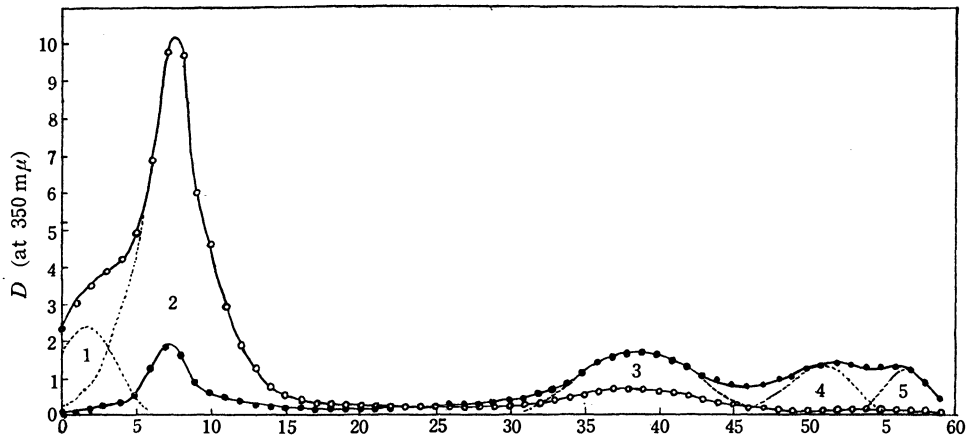


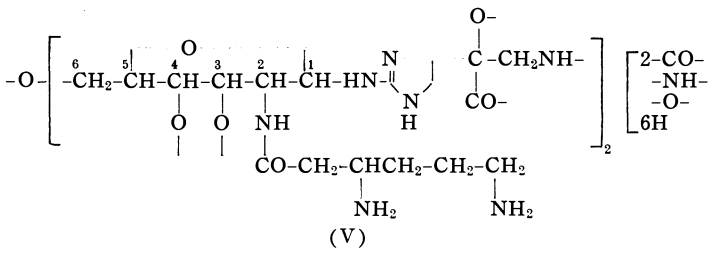

Fig. 10.

—○— upper phase —●— lower phase ····· theoretical

product of roseothricin A has an $E^{1\%}_{1cm}$ value of 357 at 350 mμ (Fig. 4). The E value[10] coupled with the presence of four amino groups leads to a molecular weight of ca. 1100 for roseothricin A free base. Acid hydrolysis of DNP-roseothricin A gave di-DNP-β-lysine as the sole product and no derivatives of roseonine or hexosamine were produced. It is thus inferred that there exists two moles of β-lysine in one mol. of roseothricin A and that the four amino groups are all free. Acid hydrolysis of roseothricin A (Fig. 1) afforded 2 mol. of β-lysine (as standard), 1.6 mol. of roseonine, 1.5 mol. of hexosamine, 1.9 mol. of carbon dioxide and 2.2 mol. of ammonia (compound B was divided between roseonine and hexosamine for convenience of calculation). Roseothricin A is, therefore, composed of two moles each of β-lysine, roseonine, hexosamine, and carbon dioxide and one mole of ammonia (the further mole of ammonia was probably produced from roseonine or hexosamine by decomposition, otherwise analytical data do not agree with calculation), and its molecular weight should be 966 as the free base.

*Anal.* Found: C, 37.97; H, 6.31; N, 16.75%. (no acetyl group). Calcd. for $C_{38}H_{65}O_{16}N_{15}\cdot 6HCl$: C, 37.83; H, 5.93, N, 17.41%.

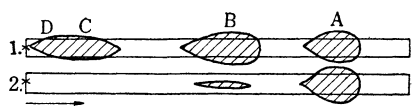
Roseothricin A has six $pK_a'$s: two at 8.1, two at 9.0, two at 10.4 (Fig. 5). This result coupled with the fact that the IR spectrum of roseothricin A is not changed by addition of trimethylamine, suggests that no free carboxyl group is in roseothricin A. Since the amino groups of β-lysine are all free, the four $pK_a'$s at 8.1 and 9.0 must originate from the β- and ε-$NH_2$ of β-lysine, respectively; the $pK_a'$s at 10.4 are caused by the guanidinium groups. The amino groups of roseonine and hexosamine in roseothricin A are therefore linked to some other groups. When potentiometric titration was carried out in the presence of formaldehyde, the six $pK_a'$s were lowered to two at 3.5, two at 6.1, and two at 8.2. The last $pK_a'$ values (8.2) are higher than that of ordinary amino groups, the $pK_a'$ of which is usually below 7. These data are also consistent with the presence of two guanidinium groups in roseothricin A. Since hydrolysis of roseothricin A with 0.2 N sodium hydroxide at 30°C, afforded first roseonine and subsequently β-lysine, the latter could not be linked to roseonine but should be linked to the hexosamine portion. Heating of roseothricin A with 5% hydrochloric acid-methanol at 60°C afforded neither β-lysine nor its methyl ester, but boiling with 20% hydrochloric acid-methanol afforded β-lysine methyl ester. This behavior was similar to that of synthetic β-lysine amide and not to β-lysine methyl ester (Fig. 7). β-Lysine in roseothricin A, therefore, must be linked to hexosamine through the amino group of the latter. Since roseothricin A did not consume periodate (Fig. 9), at least either the $C_3$—or $C_4$—OH in hexosamine is engaged in a linking (IR spectrum of roseothricin A shows a band at ca. 1717 $cm^{-1}$, which may be caused by an ester or urethane linkage). We wish to present partial structure (V) for roseothricin A.



(V)

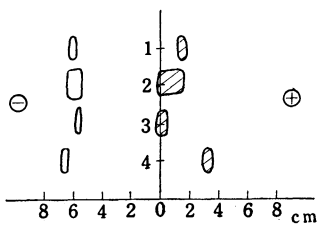
## Experimental

**Purification of Roseothricin A.**—Roseothricin complex (6 g.) was dissolved in 50 ml. of water, and passed through a column of Amberlite IRC-50 (2.5×100 cm tube, 300 c.c. of the resin), after which the column was washed well with water, and eluted with 2% ammonium sulfate solution. The first 10 l. of the eluate did not show any activity on *Bacillus subtilis*, and was discarded. Since the next 20 l. showed strong activity, this fraction was treated with 100 g. of active charcoal. The active charcoal was filtered, washed with water, and added to 250 ml. of 20% acetone-water and an appropriate amount of 1 N hydrochloric acid to adjust the pH to 2, and then filtered. After repetition of this elution procedure for four times, the filtrates were combined, and neutralized to pH 7 by addition of 10% sodium hydroxide solution, and then there was added sodium phosphotangstate solution. The precipitate was centrifuged, washed with water thrice, and dried in a desiccator. This phosphotangstate (ca. 5 g.) was dissolved in 60 ml. acetone and 30 ml. of 2 N hydrochloric acid, filtered from any undissolved substance, and added to 200 ml. of acetone. After being hept overnight in a refrigerator, the precipitate was obtained by decantation, and again dissolved in 10 ml. of water and reprecipitated with 300 ml. of acetone. Finally, the precipitate was dissolved in a small amount of water and freeze dried. Yield ca. 1 g., dec. p. 208–215°. The results of paper chromatography and paper electrophoresis are shown in Fig. 11. The spots were determined by the methods using ninhydrin or *B. subtilis*. The results of electrophoresis suggested that roseothricin had strong basic groups and no acidic groups.




1. Roseothricin complex. 2. Roseothricin A. descending method: solvent; ethanol and 0.5% ammonium sulfate (1 : 1).

Paper electrophoresis




1. Roseonine. 2. Roseothricin complex. 3. Roseothricin A. 4. β-Lysine.
White spot: buffer; 80 ml. of 0.5 M veronal sodium, 2.0 ml. of 2.0N HCl, 72 ml. of 5 M NaCl are diluted to 4 l. (pH 9). 20 mA. 2 hr. Black spot: buffer; 4 ml. of 10% NaOH, 6 ml. of 5 MNaCl are diluted to 500 ml. (pH ca. 12). 20 mA. 4 hr.

Fig. 11.

**Hydrolysis of Roseothricin A.**—Four hundred mg. of roseothricin A was dissolved in 40 ml. of 6 N hydrochloric acid, and heated at about 50°C under an atmosphere of nitrogen gas which was introduced through two traps containing saturated barium hydroxide solution. After 11 days, the hydrolysate was evaporated to dryness in vacuo, redissolved in a small amount of water and evaporated in a vacuum desiccator containing sulfuric acid and sodium hydroxide. Yield 470mg. The solution of the hydrolysate in 6 ml. water was poured on a column of Dowex 50 (H-form) resin (2×60 cm. tube, ca. 150 c.c. of resin). The column was eluted with water (250 ml.), 2.5 N hydrochloric acid (1300 ml.), and 4 N hydrochloric acid (400 ml.), successively, and the eluates were collected in 10 ml. aliquots by means of a fraction collector. The result is shown in Fig. 1. Each fraction was evaporated to dryness in vacuo below 50°C and weighed. The precipitated barium carbonate in the traps was filtered and weighed.

**Partial 2,4-Dinitrophenylations of Compound B and Roseothricin A.**—Roseothricin A (83 mg.) and sodium bicarbonate (100 mg.) were dissolved in 10 ml. of 50% ethanol, treated with 5 ml. of 2,4-dinitrofluorobenzene (DNFB 25 mg.) in ethanol (5 ml.), and the solution was allowed to stand overnight at room temperature. A small quantity of yellow precipitate was produced. The solution was acidified with acetic acid, evaporated in vacuo, and then placed in a counter current distributing machine using the solvent system of buthanol: methanol: acetic acid: water (18 : 2: 1 : 19). The result is shown in Fig. 10. The peak No. 5 is 2,4-dinitrophenol. The peak No. 2 was evaporated to dryness, and again 2,4-dinitrophenylated by the same procedure. The result of CCD showed the peaks 2, 3, 4, and 5, except No. 1. The peak No. 2 is much sharper than the theoretical curve; the cause is not elucidated yet.

Partial DNP-ation of compound B was also carried out by the same procedure (9 mg. compound B, 15 mg. sodium bicarbonate 10 mg. DNFB). This result is shown in Fig. 3.

**Complete 2,4-Dinitrophenylation of Compound B and Roseothricin A.**—Compound B (18 mg.) and sodium bicarbonate (50 mg.) were dissolved in 6 ml. of 50% ethanol, treated with 0.6 ml. of 5% DNFB in ethanol, and incubated at 34°C for two days. The solution was acidified with hydrochloric acid, and the precipitate was

filtered and washed with water, ethanol, and ether, successively. It was dissolved in tetrahydrofuran, and reprecipitated by adding water. Yield 10 mg., m.p. 192–196° (dec.).

In the case of roseothricin A, the same procedure was also employed (117 mg. roseothricin A, 300 mg. sodium bicarbonate, 6 ml. 5% DNFB in ethanol). The precipitate was dissolved in tetrahydrofuran and reprecipitated with ether. Yield 158 mg., m.p. 210°C (dec. sintered at ca. 200°C).

**Hydrolysis of DNP-Roseothricin A.**—DNP-Roseothricin A (50 mg.) was dissolved in 5 ml. conc. hydrochloric acid, and incubated in a sealed tube at 37° for 14 days. A yellow precipitate separated gradually after two days. Water was added to the mixture and the precipitates were filtered. The filtrate was almost colorless and contained about 10 mg. of roseonine and no β-lysine (by semi-quantitative paper chromatography). The precipitate (23 mg.) was extracted with ethyl acetate. The ethyl acetate soluble portion was 14 mg.; IR spectra and paper chromatography showed this to be identical with di-DNP-β-lysine. The ethyl acetate insoluble portion (9 mg.) was identical with unchanged DNP-roseothricin A (IR spectra).

**Synthesis of Di-DNP-β-lysine and DNP-Roseonine.**—β-Lysine dihydrochloride (22 mg.) and sodium bicarbonate (60 mg.) were dissolved in 4 ml. of 50% ethanol, treated with 1 ml. of 5% DNFB in ethanol and allowed to stand overnight. The solution was acidified with hydrochloric acid extracted with ethyl acetate, and the ethyl acetate layer was washed with water, and then extracted with 5% potassium carbonate solution. The aqueous layer was separated and acidified with hydrochloric acid. The precipitate was filtered, washed with water, and recrystallized from a mixture of methanol and acetone. Yellow crystals, m.p. 195–196°C.

Roseonine dihydrochloride (39 mg.) and sodium bicarbonate (90 mg.) were dissolved in 5 ml. of 50% ethanol, treated with 1.5 ml. of 5% DNFB in ethanol and allowed to stand overnight. The reaction mixture was added to 10 ml. of water, acidified with hydrochloric acid, and extracted thrice with ethyl acetate. The aqueous layer was evaporated to 3 ml. and the pH was adjusted to ca. 5 with sodium acetate. DNP-roseonine gradually crystallized from the solution as yellow needles, m.p. 226–229°C (dec.).

**Measurements of DNP-ation Rates.**—*Reagents*: 0.1% aq. sodium bicarbonate solution, 0.4% DNFB ethanol solution (freshly prepared), 1% hydrochloric acid.

Each sample (10 μ mol.) was dissolved in a mixture of 20 ml. of sodium bicarbonate, 2 ml. of DNFB, and 18 ml. of ethanol at 15°C. At suitable intervals, 5 ml. of the solution was poured into 5 ml. of hydrochloric acid, stop the reaction. The absorption intensity of this solution was measured at 320 mμ and 350 mμ. Calculation was based on the density at 350 mμ and the ratio of the density at 320 to that at 350 mμ. The reaction mixture contained the DNP derivative of the sample used, 2,4-dinitrophenol and unchanged DNFB. 2,4-Dinitrophenol and DNFB had about equal values for the density ratio at 320 mμ/350 mμ, i.e., 2.27 and 2.07, respectively, and 2,4-dinitrophenylamino groups also had equal values (0.50). The absorption density originating from 2,4-dinitrophenol and DNFB could thus be subtracted from that of the reaction mixture. The results are shown in Fig. 8.

**Measurements of Periodic Acid Consumption.**—*Reagents*: 0.01 M sodium periodate, 0.005 M arsenous oxide, 0.01 M iodine, saturated aq. sodium bicarbonate solution, 10% potassium iodide, and starch solution.

One ml. of compound B solution (9.5 mg. in 10 ml. water) and 2 ml. of 0.01 M sodium periodate were mixed and allowed to stand at 30°C. At suitable intervals the solution was treated with 1 ml. saturate sodium bicarbonate, 2 ml. 0.005 M arsenous oxide, and 1 ml. 10% potassium iodide solution in the order mentioned. After 2 minutes the mixture was titrated with 0.01M iodine using starch solution as indicator. From the difference between the volumes of this titration and blank, the amount of periodate consumption was calculated. By the same procedure, periodate consumptions of the following compounds were measured: roseothricin A (24.6 mg. in 10 ml. water); roseonine dihydrochloride (9.0 mg. in 10 ml.). The results are shown in Fig. 9. The reason that the periodate consumption of roseothricin A increases slowly but linearly and exceeds 3 moles after 20 hours, may be that roseothricin A is gradually hydrolysed during the incubation and consumes periodate.

**$pK_a'$ Measurements.**—The $pK_a'$s were measured by potentiometric titration in water using Beckmann Model G pH meter.

For example, compound B (18 mg. of its hydrochloride) was dissolved in 1 ml. water (carbon dioxide free), treated with 0.10 ml. 0.40 N hydrochloric acid and titrated with 0.334 N sodium hydroxide. The results are shown in Fig. 5 and Table I.

$pK_a'$ *measurements in the presence of formaldehyde*: As is well known in the formol titration of amino acids, addition of formalin to the solution of primary amino acids causes the $pK_a'$ to drop from a value above 7 to that below 7. For example, β-lysine dihydrochloride (12 mg.) was dissolved in 1 ml. water, treated with 0.3ml. of formalin and 1.0 ml. 0.017 N hydrochloric acid and titrated with 0.268 N sodium hydroxide the results are summarised in the following table;

| Compound | $pK_a'_1$ | $pK_a'_2$ | $pK_a'_3$ |
|---|---|---|---|
| β-Lysine | 3.2* | 4.8 | 6.9 |
| Roseonine | 2.4* | 4.9 | 10.6** |
| Glucosamine | 5.8 | | |
| Roseothricin A | 3.5(2)+ | 6.1(2)+ | 8.2(2)+** |

* $pK_a'$ of COOH. ** $pK_a'$ of guanidinium.
+ Cf. footnote of Table I.

**Infrared Spectra.**—Infrared spectra were measured with a Hilger H 800 spectrophotometer, sodium chloride prism, by the potassium bromide method.

**β-Lysine Ester and Amide.**—β-Lysine dihydrochloride (3 mg.) was dissolved in 1 ml. of 5% hydrochloric acid-methanol, heated on a water bath for twenty minutes, and then evaporated to dryness. The residue was shown to be β-lysine methyl ester by means of paper chromatography. This ester was dissolved in conc. aq. ammonia and evaporated to dryness to produce β-lysine amide. When β-lysine methyl ester was heated with 5% hydrochloric acid-propanol at 60°C for 15 minutes, β-lysine propyl ester was produced. β-Lysine amide, however, did not produce β-lysine methyl ester by heating with 5% hydrochloric acid-methanol at 60°C for 15 minutes; the ester was first produced by boiling with 20% hydrochloric acid-methanol. The same procedures were applied to roseorthricin A. Roseothricin A produced β-lysine methyl ester by boiling with 20% hydrochloric acid-methanol, but did not produce the ester by heating with 5% hydrochloric acid-methanol at 60°C for 15 minutes. The ester further hydrolysed to β-lysine by boiling in aq. hydrochloric acid. All procedures were protected from moisture.

We wish to acknowledge the helpful advice of Dr. K. Nakanishi in this research, and to thank the Sanyo Pharmaceutical Co. for preparing a portion of roseothricin.

*Chemistry Department, Faculty of Science, Nagoya University*
*Chikusa, Nagoya*

# *A Study on the Molecular Structure of Acrylyl Chloride by Electron Diffraction*[1]

By Takeshi UKAJI

(Received May 21, 1957)

Mackle and Sutton[2] proposed a planar structure of acrolein molecule along with other related molecular dimensions, and there is Coulson's discussion[3] regarding the relation between the bond length and the bond order of the compound. Here, the molecular structure of acrylyl chloride was treated by means of electron diffraction method.

## Experimental

The preparation of acrylyl chloride was as follows[4]. β-Chloropropionic acid was prepared by passing dry hydrogen chloride through acrylic acid which had been made by hydrolysis of methyl acrylate of commercial grade. It was treated with thionyl chloride at about 80°C to be converted into β-chloropropionic acid chloride. Then the β-chloropropionic acid chloride was gradually dropped onto a catalyser heated to about 200°C which was composed of alumina containing a few per cent. of aluminium chloride and barium chloride. By careful distillation of the chloride, a fraction boiling at 73±1°C was collected.

The electron diffraction photographs were taken in the usual manner using a camera reported in the previous paper[5] (camera distance, ca. 9 cm.; electron wave length, 0.056-0.063 Å, determined by calibration with gold foil). Ten satisfactory photographs were obtained. The diffraction patterns were visually measured up to ca. 90 of $q$-values.

## Analysis

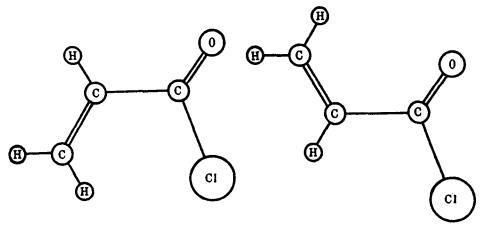
The diffraction photographs were measured by the usual visual method, and the results were shown in Fig. 2 and Table II. The well known formulae for the calculation of the theoretical intensity curves are

$$I_{(q)}=\sum_i\sum_j \frac{Z_iZ_j}{r_{ij}}\exp(-a_{ij}q^2)\sin\frac{\pi}{10}qr_{ij} \quad (1)$$

$$q=(40/\lambda)\sin(\theta/2) \quad a_{ij}=(\pi^2/200)<\Delta r_{ij}^2>$$

where $r_{ij}$ is the distance between the $i$-th and $j$-th atom, $\lambda$ the electron wave length, $\theta$ the scattering angle, $Z_i$ the atomic number of the $i$-th atom, and $<\Delta r_{ij}^2>$ the mean square amplitude of $r_{ij}$. The thermal vibration term was neglected for the first approximation, i.e. $<\Delta r_{ij}^2>=0$. It was assumed that all the atoms in this molecule were coplanar, and that the distance of C—H and the angle of CCH were 1.08 Å and 120°, respectively. The parameters

1) Presented partly at the Symposium on the structral chemistry held on October 16, 1956, at Nagoya.
2) H. Mackle and L. E. Sutton, *Trans. Faraday Soc.*, **47**, 691 (1951).
3) C. A. Coulson, ibid., **42**, 106 (1946).
4) H. Ueda, T. Sugita and Y. Tanaka, *The Report of the Institute of Synthetic Fiber*, **1**, 635 (1943).
5) T. Yuzawa and M. Yamaha, This Bulletin, **26**, 414 (1953).



*trans*-form *cis*-form

Fig. 1. Schematic models showing the *trans*- and *cis*-form acrylyl chloride.

C=C and C—C, used in the calculation of theoretical intensity curves, were varied from 1.32 to 1.40 Å and from 1.40 to 1.54 Å in steps of 0.02 or 0.03 Å, and C=O and C—Cl were varied from 1.18 to 1.24 Å and from 1.68 to 1.77 Å with the same increments, while the angles of CCC, CCO, and OCCl were varied from 110° to 130°, from 120° to 130° and from 110° to 130° in steps of 2° or 3°, respectively.

The effect of thermal vibration on the theoretical curves was examined, using the vibration factors $a_j$ listed in Table I, and the curves including thermal terms are shown in the dotted lines in Fig. 2.

A careful comparison was made between the visual intensity curve and the theoretical ones. The curves $C_t$ and $C_1$ are in the best agreement with the visual one. The curves of several other models also resemble the visual, but they differ from it in the features of the fourth and the fifth maximum and the seventh shelf.

TABLE I

VALUES FOR $a_{ij}$ USED FOR ACRYLYL CHLORIDE MODELS*

| Atom Pairs | $a_{ij}\times10^5$ |
|---|---|
| C—H | 15.0 |
| C=O | 0 |
| C=C | 0 |
| C—C | 0 |
| C—Cl | 12.0 |
| C'···H | 20.5 |
| C'···O | 5.0 |
| C'···C | 8.0 |
| C'···Cl | 15.0 |
| C'···Cl | 13.0 |
| C''···O (*cis*-form) | 20.5 |
| C''···O (*trans*-form) | 30.0 |
| C''···Cl (*cis*-form) | 28.0 |
| C''···Cl (*trans*-form) | 23.5 |

* All the values are assumed.

The theoretical intensity curves of the *trans*- and the *cis*-form (Fig. 2) remain almost unchanged throughout the features of intensity relation, except the discrepancies of the features of the fourth and the fifth maximum and the seventh shelf. Curves $C_1$, $C_2$, and $C_3$ are the curves of mixtures composed of three parts of the *trans*-form and one part of the *cis*-form, equal parts of the *trans*- and the *cis*-, and one part of the *trans*- and three parts of the *cis*-, respectively.

The fourth and the fifth maximum of the curves A and B are both shifted inward and the seventh shelf has a different shape, while in curve D the fourth maximum changes to a shelf and the sixth minimum shifts outward. Curve E shows that the intensity of the fourth and the eighth maximum is too great in comparison with the fifth and the ninth maximum, and the seventh shelf changes to a peak. Curve F was taken as the typical one for the models which had a greater angle of CCO, the fourth and the eleventh maximum shifting inward and the seventh shelf changing to a small peak. In curves G and H, the features of the fourth maximum and the seventh shelf disagree with the visual ones; in curves I and J the third, the fourth, and the fifth maximum are shifted inward. Curves K and L were made for the purpose of ascertaining the limit of acceptability for C=O distance, both curves being in good agreement with the visual ones in all respects, except the seventh shelf. Likewise, curves O and P were used to show the limit for angle CCC. These curves are rejected because of the disagreement with the visual ones, in the range $q>50$. In curve M, the fourthand the eighth maximum shifted outward, and the tenth maximum changed its position and turned out to be a shelf of the ninth maximum. In curve N, each of the fifth, the sixth, and the eighth minimum, and each of the fifth and the ninth maximum shifted inward; the tenth maximum almost disappeared.

From the above consideration, the models $C_t$ and $C_1$ are regarded as the most acceptable fits, while the others are all accepted as borderline fits. Nine models are selected from them, and their $q_c/q_o$ values are summarized in Table II.

The radial distribution function for this molecule (Fig. 3) was calculated using the following equation,

$$rD_{(r)}=\sum_{q=1}^{q_{max}} I_{(q)}\exp(-bq^2)\sin\frac{\pi}{10}qr \qquad (2)$$

where $I_{(q)}$ is the intensity read from the visual curve. The value of $b$ was determined by setting $\exp(-bq^2)=0.1$ at $q=90$.

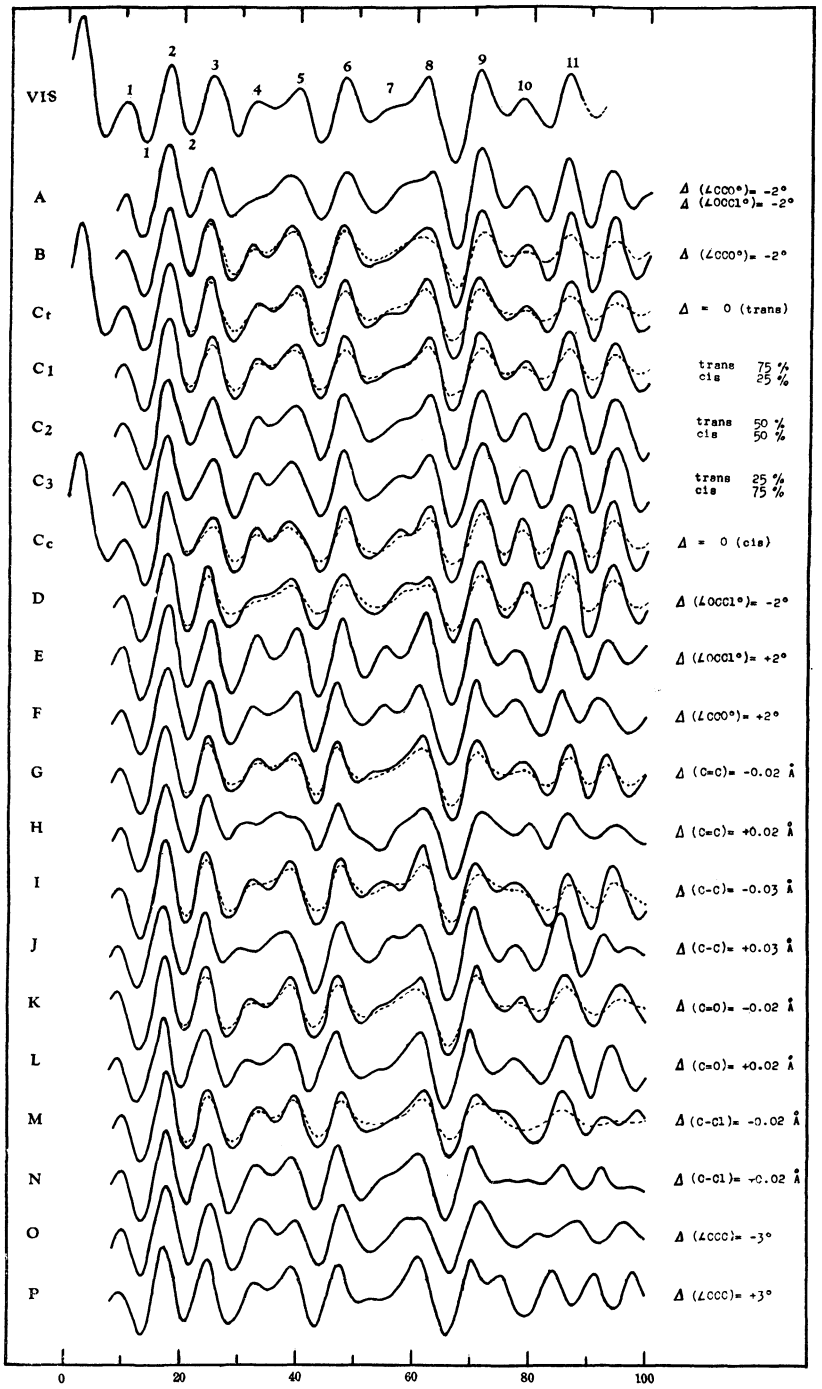



Fig. 2. Visual (VIS) and theoretical intensity curves for acrylyl chloride. The notations on the right hand side of this figure show that the models are deviated from the most probable model, for example, $\Delta=0$ is the most probable model which C—H=1.08, C=C=1.36, C=O=1.20, C—C=1.44, C—Cl=1.74 Å, $\angle$CCH=120°, $\angle$CCC =120° and $\angle$CCO=$\angle$OCCl=125°.

TABLE II
$q_c/q_o$ VALUES FOR ACRYLYL CHLORIDE

| Feature | | $q_0$ | Model | | | | | | | | Wt. |
|---|---|---|---|---|---|---|---|---|---|---|---|
| Max. | Min. | | B | $C_t$ | $C_1$ | $C_c$ | D | G | I | K | M | |
| 1 | | 10.36 | 0.923 | 0.912 | 0.922 | 0.965 | 0.941 | 0.927 | 0.946 | 0.913 | 0.951 | 0 |
| | 1 | 13.53 | 0.957 | 0.968 | 0.982 | 1.009 | 0.950 | 0.976 | 0.979 | 0.994 | 0.979 | 1 |
| 2 | | 16.88 | 1.030 | 1.031 | 1.021 | 1.007 | 1.028 | 1.016 | 1.011 | 1.036 | 1.037 | 1 |
| | 2 | 21.17 | 0.990 | 1.000 | 0.997 | 0.987 | 0.992 | 0.999 | 0.994 | 0.999 | 1.027 | 1 |
| 3 | | 25.07 | 0.997 | 0.983 | 0.987 | 1.015 | 0.977 | 0.981 | 0.983 | 0.989 | 0.997 | 2 |
| | 3 | 29.15 | 0.961 | 0.983 | 0.995 | 1.003 | 0.971 | 0.983 | 0.973 | 0.978 | 0.997 | 1 |
| 4 | | 32.61 | 0.986 | 1.012 | 1.000 | 1.000 | 1.027 | 1.035 | 1.004 | 1.004 | 1.012 | 1 |
| | 4 | 36.86 | 0.922 | 0.975 | 0.974 | 0.943 | 0.958 | 0.970 | 0.963 | 0.950 | 0.996 | 1 |
| 5 | | 39.89 | 0.969 | 0.991 | 0.989 | 0.963 | 0.974 | 0.992 | 0.985 | 0.985 | 1.002 | 2 |
| | 5 | 43.44 | 0.994 | 1.014 | 0.997 | 1.012 | 0.997 | 0.995 | 1.001 | 1.000 | 1.009 | 2 |
| 6 | | 47.58 | 0.996 | 0.999 | 1.000 | 1.005 | 1.001 | 0.984 | 1.008 | 1.000 | 1.010 | 4 |
| | 6 | 51.14 | 1.008 | 1.008 | 1.007 | 1.009 | 1.028 | 0.987 | 0.997 | 1.005 | 1.026 | 1 |
| 7 | | (55.15) | — | 1.015 | 0.997 | 1.042 | 1.056 | 0.988 | 1.015 | 0.993 | — | 0 |
| 8 | | 61.82 | 1.000 | 1.000 | 1.003 | 1.009 | 1.009 | 1.000 | 1.003 | 0.995 | 1.011 | 1 |
| | 8 | 66.26 | 1.003 | 1.006 | 1.001 | 0.996 | 1.004 | 1.006 | 1.004 | 1.002 | 1.003 | 2 |
| 9 | | 70.50 | 1.007 | 1.000 | 1.002 | 1.012 | 1.001 | 1.004 | 1.004 | 1.009 | 1.006 | 4 |
| | 9 | 75.00 | 1.003 | 1.003 | 1.003 | 1.003 | 1.010 | 0.995 | 0.998 | 1.009 | 0.984 | 1 |
| 10 | | 78.38 | 1.007 | 1.002 | 1.002 | 0.998 | 1.008 | 1.010 | 0.998 | 1.010 | 0.963 | 1 |
| 11 | | 86.29 | 0.998 | 0.996 | 0.998 | 1.001 | 1.001 | 1.007 | 1.008 | 1.004 | 0.994 | 1 |
| Wt. mean | | | 0.993 | 0.999 | 0.999 | 1.002 | 0.996 | 0.995 | 0.997 | 0.997 | 1.004 | |
| Wt. mean sq. dev. | | | 0.004 | 0.003 | 0.002 | 0.003 | 0.004 | 0.003 | 0.002 | 0.003 | 0.003 | |

The curve shows that the first and the second peaks correspond to the C—H, C=O, C=C and C—C distances, the third to the C—Cl, the fourth and fifth to the C′···H, C′···O and C′···C, the sixth to the C′···Cl, O′···Cl, C″···Cl (in the *trans*-form) and C″···O (in the *cis*-form), the seventh to the C″···O (in the *trans*-form) and the eighth to the C″···Cl (in the *cis*-form), respectively. Owing to the complex nature of the peaks, no attempt was made to resolve the distances. It may be noted, however, that the positions determined from the most acceptable model fairly well agree with the peaks observed in this radial distribution curve.

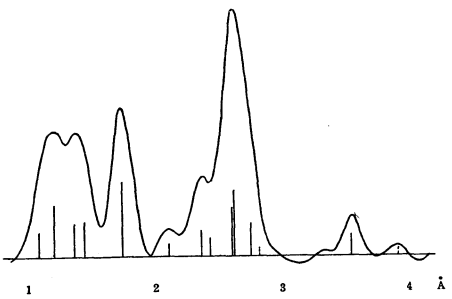



Fig. 3. Radial distribution curve for acrylyl chloride. The most probable interatomic distances are shown by the vertical lines.

In conclusion, the bond distances and bond angles obtained for acrylyl chloride of coplanar configuration are: C=C=1.36 ±0.02 Å, C—C=1.44±0.03 Å, C=O=1.20 ±0.02 Å, C—Cl=1.74±0.02 Å, ∠CCC=120 ±3°, ∠CCO=∠OCCl=125±2°. The *trans*-form is predominant in this molecule.

## Discussion of the Results

An electron diffraction investigation of butadiene[6] gave values of 1.35±0.02 Å and 1.46±0.03 Å for the distances of C=C and C—C bond respectivery, and coplanar structure which predominantly had the *trans*-form; these results are in good agreement with the values of 1.36 Å and 1.46 Å in acrolein, respectively. These values agreed with those obtained by C. A. Coulson's theoretical calculation[3] on the C=C, C—C and C=O distances of butadiene, acrolein, and glyoxal. Bond shortening and bond elongation of C—C and C=C bonds in conjugated molecules were plausibly explained by the delocalization of $\pi$-electrons. Within the limits of accuracy of this investigation, the circumstances regarding the C=C, C=O distances and the predominance of the *trans* configuration are the same in the case of acrolein.

One of structural studies on acetyl

6) A survey of electron diffraction results through 1949 is found in the tabulation by P. W. Allen and L. E. Sutton, *Acta, Cryst.*, 3, 46 (1950).

chloride[7] shows that the carbon-carbon single bond distance is 1.50 Å and shorter than the normal distance 1.54 Å. Further, the single bond distance between chlorine atom and aromatic nucleus is shorter than the bond length of C—Cl 1.77 Å. From the results of this investigation, it may be considered that the corresponding C—C distance is shorter than that of acrolein, and the C—Cl distance is shorter than that of acetyl chloride.

The values for the C=O bond distance and the angles of CCO and OCCl (1.20 ±0.02 Å and 125±2°, respectively) obtained here are reasonablly compared with those of related compounds shown in reference to the view of the limit of accuracy of the present experiment.

The author wishes to express his sincere thanks to Professor A. Kotera and Mr. M. Igarashi of Tokyo University of Education for their kind advice and encouragement and for the use of the apparatus of this work. The author also wishes to thank to Dr. T. Takeshima of this University for his helpful advice.

*Department of Chemistry, Faculty of Science, Ibaraki University, Mito*

7) Y. Morino et al., *J. Chem. Soc. Japan Pure Chem. Sec.*, **75**, 647 (1954).

# *The Electronic Structure of the Hydrogen Fluoride Ion*

By Hidekazu HAMANO

(Received August 16, 1956)

In order to throw light upon the hydrogen bond, the author has taken up the $[FHF]^-$ ion that is the simplest one in a theoretical treatment, and has carried out quantum-mechanical calculations for this ion.

As is well known, the hydrogen fluoride ion exists in such ionic crystals as sodium, potassium, and ammonium hydrogen fluorides and consists of the F-H-F hydrogen bond. An X-ray study[1] of potassium hydrogen fluoride has given the F···F distance of 2.26 Å. It has hitherto been a question whether the proton is at the center of two fluorine atoms or not. Peterson and Levy[2] have recently found by the neutron diffraction study that the proton occupies the central position in the linear F-H-F ion.

Based on this fact, the "LCAO SCF MO method" developed by Roothan[3] was applied to the ground state of the $[FHF]^-$ ion and the nature of the F-H-F hydrogen bond was discussed.

## Outline of Calculations

The calculation was carried out by taking the eleven atomic orbitals $f$, $f'$, $s$, $s'$, $\sigma$, $\sigma'$, $\pi_+$, $\pi_+'$, $\pi_-$, $\pi_-'$ and $h$ into consideration, which stand for $1s$, $2s$, $2p\sigma$*, $2p\pi_+$ and $2p\pi_-$ orbitals of two fluorine atoms and $1s$ orbital of the hydrogen atom, respectively. All the electrons were assigned to MO's extending throughout the ion and the interactions between them were explicitely included, while the $1s$ electrons of two fluorine atoms were treated as the inner-shell of the ion, because of the very small mixing with the valence electrons.

The AO's used were the analytical SCF AO's[4] for neutral fluorine, fluorine anion and hydrogen. The one-center integrals of fluorine atoms were evaluated as the arithmetic mean values of those for neutral fluorine and fluorine anion, using these SCF AO's. This procedure is based on the fact that each fluorine atom in this ion is considered as $F^{-1/2}$. The evaluations of the two-center and the three-center integral using the SCF AO's are, however, very cumbersome and it was, therefore, assumed that the use of Slater-type AO's**

1) L. Helmholz and M. Rogers, *J. Am. Chem. Soc.*, **61**, 2590 (1939).
2) S. W. Peterson and H. A. Levy, *J. Chem. Phys.*, **20**, 704 (1952).
3) C. C. J. Roothan, *Rev. Modern Phy.*, **23**, 69 (1951).

* The $2p\sigma$ and $2p\sigma'$ orbitals are pointed towards the central atom along the molecular axis, respectively.

4) F. W. Brown, *Phys. Rew.* **44**. 214 (1933); Hamano, *Bull. Tokyo Gakugei University* **6**, 9, (1955).

** $h=(1/\pi)^{1/2}\exp(-r)$,
$f=(z_1^3/\pi)^{1/2}\exp(-z_1 r)$,
$s=(z_2^5/3\pi)^{1/2}\exp(-z_2 r)$,
$\sigma=(z_2^5/\pi)^{1/2}\exp(-z_2 r)\, r\cos\theta$,
$\pi_\pm=(z_2^5/\pi)^{1/2}\exp(-z_2 r)\, r\sin\theta\exp(\pm\phi_i)$
where $z_1=8.75$, $z_2=2.47$.

TABLE I
SYMMETRY ORBITALS

| Symmetry species | $\sigma_g$ | $\sigma_u$ | $\pi_u$ | $\pi_g$ |
|---|---|---|---|---|
| Symmetry orbitals | $\sigma_1=f+f'$ | $\sigma_5=f-f'$ | $\sigma_8=\pi_\pm-\pi_\pm'$ | $\sigma_9=\pi_\pm+\pi_\pm'$ |
| | $\sigma_2=s+s'$ | $\sigma_6=s-s'$ | | |
| | $\sigma_3=\sigma+\sigma'$ | $\sigma_7=\sigma-\sigma'$ | | |
| | $\sigma_4=h$ | | | |

TABLE II
LCAO MO

| | | |
|---|---|---|
| $K(\sigma_g)=2^{-1/2}\sigma_1$ | $K(\sigma_u)=2^{-1/2}\sigma_5$ | $1\pi_u=a_{66}\sigma_8$ |
| $1\sigma_g=a_{11}\sigma_2+a_{12}\sigma_3+a_{13}\sigma_4$ | $1\sigma_u=a_{44}\sigma_6+a_{45}\sigma_7$ | $1\pi_g=a_{77}\sigma_9$ |
| $2\sigma_g=a_{21}\sigma_2+a_{22}\sigma_3+a_{23}\sigma_4$ | $2\sigma_u=a_{54}\sigma_6+a_{55}\sigma_7$ | |
| $3\sigma_g=a_{31}\sigma_2+a_{32}\sigma_3+a_{33}\sigma_4$ | | |

instead of the SCF AO's gives satisfactory approximations to these integral values. The greater part of the two-center integrals and a few one-electron three-center integrals*** were exactly calculated. The other two-center and three-center integrals were obtained by Mulliken's approximation[6]. The numerical values of these integrals are given in the appendix.

The $[FHF]^-$ ion is a linear ion belonging to the symmetry group $D_{\infty h}$. The LCAO MO's were chosen so that they belong in sets to irreducible representations of the group $D_{\infty h}$. It is convenient to introduce symmetry orbitals. These were given in Table I with the irreducible representations of the group $D_{\infty h}$.

The LCAO MO's were made up by taking linear combinations of symmetry orbitals, as shown in Table II.

Here the order of increasing number for the MO's within each symmetry species is the order of increasing energy. $K$ refers to MO's made up of inner shell electrons only.

The ground state of this ion is to be $^1\Sigma^+_g$, resulting from configuration $(K(\sigma_g))^2$, $(K(\sigma_u))^2$, $(1\sigma_g)^2$, $(1\sigma_u)^2$, $(2\sigma_g)^2$, $(2\sigma_u)^2$, $(1\pi_u)^4$, $(1\pi_g)^4$.

The total normalized wave function is then built up as an anti-symmetrized product of these LCAO MO's. The requirement that the electronic energy should be an absolute minimum leads to the following matrix equations:

$$(\boldsymbol{H}+\boldsymbol{G})\boldsymbol{a}_i=\varepsilon_i\boldsymbol{S}\boldsymbol{a}_i \qquad (1)$$

As the definitions of these notations are given in detail by Roothan[3] and Mulligan[7], they will not be repeated here. The problem of finding the best LCAO MO's for the ground state thus reduces to the solution of the secular equation (1). This is attained by repeating a self-consistent field procedure.

## Results and Discussion

The LCAO SCF MO's of the lowest energy state obtained by the SCF procedure are given in Table III.

TABLE III
LCAO SCF MO

| LCAO SCF MO | Orbital energies (eV) |
|---|---|
| $K(\sigma_g)=2^{-1/2}(f+f')$ | — |
| $1\sigma_g=0.768(s+s')+0.039(\sigma+\sigma')-0.199\,h$ | −41.22 |
| $2\sigma_g=-0.133(s+s/)+0.533(\sigma+\sigma')+0.464\,h$ | −19.20 |
| $3\sigma_g=0.476(s+s')+0.777(\sigma+\sigma')-1.669\,h$ | — |
| $K(\sigma_u)=2^{-1/2}(f-f')$ | — |
| $1\sigma_u=0.708(s-s')+0.082(\sigma-\sigma')$ | −41.07 |
| $2\sigma_u=-0.069(s-s')+0.711(\sigma-\sigma')$ | −18.46 |
| $1\pi_u=0.502(\pi_\pm-\pi_\pm')$ | −16.22 |
| $1\pi_g=0.498(\pi_\pm+\pi_\pm')$ | −15.99 |

Except $3\sigma_g$ orbital, they are filled by two electrons with paired spins in the ground state.

The "LCAO orbital energies" obtained for these LCAO SCF MO's are also shown in Table III. These orbital energies represent good approximations to the ionization energies of the corresponding electron shells. Unfortunately, the experimental values of the ionization energies of the $[FHF]^-$ ion have not yet been obtained. The calculated minimum ionization energy in the present work is 15.99 eV. This value is somewhat lower than that of a fluorine atom (17.42 eV)[8] and that of a hydrogen

*** These integral values were calculated by Oohata's method[5].

5) K. Oohata, *Busseiron Kenkyu*, **50**, 38 (1952).
6) R. S. Mulliken, *J. Chim. Phys.*, **46**, 500, 521 (1949).
7) J. F. Mulligan, *J. Chem. Phys.*, **19**, 347 (1951).
8) C. E. Moore, "Atomic Energy Levels", Vol. 1, Nat. Bur. Standards, Circ. 467, U. S. Department of Commerce, Washington (1949).

fluoride (19.38 eV)****. But this value seems to be too high considering that this ion is an anion. This is considered to be caused by the increasing inter-electronic repulsion compared to fluorine atom and hydrogen fluoride, because this ion is an anion.

It is convenient to adopt an equivalent orbital representation to indicate localized features of the electronic distribution in molecules or ions. The localized equivalent orbitals can be obtained by a unitary transformation of the above MO's. In the case of this ion, the localized equivalent orbitals for the $\sigma$-direction can be derived from the four occupied MO's $1\sigma_g$, $2\sigma_g$, $1\sigma_u$, and $2\sigma_u$ as linear sums of these MO's: the two $(b\sigma)$, $(b\sigma)'$ which have a bonding character, the other two $(l\sigma)$, $(l\sigma)'$ which have a lone pair character. These orbitals obtained are given in Table IV.

TABLE IV

EQUIVALENT LOCALIZED ORBITALS

$(l\sigma)=0.943s+0.353\sigma$

$(l\sigma)'=0.943s'+0.353\sigma'$

$(b\sigma)=-0.468s-0.132s'+0.809\sigma-0.139\sigma'+0.359\,h$

$(b\sigma)'=-0.468s'-0.132s+0.809\sigma'-0.139\sigma+0.359\,h$

As is seen from this result, the lone-pair orbitals have mainly $s$-character. On the other hand, in the bonding orbitals, only the $\sigma$-electron has a bonding property with the 1$s$ orbital of hydrogen. This indicates that the fluorine orbitals of the F-H bonds have the almost pure $p$-character.

As a rough estimation of the electron distribution throughout this ion, the polarity of the $[FHF]^-$ ion has been examined. The result from the present calculation indicates that the charge densities of the $[FHF]^-$ ion may be formulated as $F^{-0.78}H^{+0.56}F^{-0.78}$. It would be expected that the polarity of the bond in this ion may be very great, because of the large difference of electronegativity between the fluorine and the hydrogen atom. The above result agrees with this expectations and it indicates that this hydrogen bond is also electrostatic. The special strength of this hydrogen bond is, therefore, considered to be based on the contributions of strong ionic character as well as covalency.

The conclusion obtained may be qualitatively correct, but should not be taken as final. The reasons are as follows: (1) The approximate atomic orbitals were used. (2) Most of the values of energy integrals were approximately evaluated. (3) A configuration interaction was neglected. (4) The MO method was applied to the large distance such as was the case for this ion. For example, the $S_{\sigma h}$ value in this work was 0.2671, while the $S_{\sigma h}$ value using the SCF AO's for fluorine and fluorine anion are 0.3525 and 0.4287, respectively.

In view of these factors, the quantum-mechanical treatment of the hydrogen bonds seems to be more troublesome than that of normal chemical bonds. It is desirable that the improvement of these points should be done in future.

The author wishes to thank Professor K. Kozima and Mr. H. Tsubomura for their kind criticism and Mr. J. Higuchi and Mr. S. Maeda for their helpful advice and discussion.

## Appendix

**Numerical Tables of Energy Integrals:** Values for all but the overlap integrals are given in atomic units (1 atomic unit = 27.204 eV). In the Tables, the energy integrals marked by an asterisk are the approximate values. We shall list the following notations for the many types of energy integrals.

Overlap integrals:

$$S_{pq}=\int\phi_p(1)\phi_q(1)d\tau^1.$$

Kinetic energy integrals:

$$(\phi_p|-1/2\Delta|\phi_q')=\int\phi_p(1)(-1/2\Delta)\phi_q(1)d\tau^1.$$

Nuclear attraction integrals:

$$(A:\phi_p\phi_q')=\int\phi_p(1)(1/r_{a_1})\phi_q'(1)d\tau^1.$$

Coulomb integrals:

$$(pq:r't')=\int\phi_p(1)\phi_r'(2)(1/r_{12})\phi_q(1)\phi_t'(2)d\tau^{1,2}.$$

Exchange integrals:

$$(pr':qt')=\int\phi_p(1)\phi_q(2)(1/r_{12})\phi_r(1)\phi_t'(2)d\tau^{1,2}.$$

Hybrid coulomb-exchange integrals:

$$(pq:rt')=\int\phi_p(1)\phi_r(2)(1/r_{12})\phi_q(1)\phi_t'(2)d\tau^{1,2}.$$

TABLE V

ONE-CENTER INTEGRALS

| | | | |
|---|---|---|---|
| $(F:ff)$ | 8.7500 | $(ff:pp)$ | 1.1349 |
| $(F:ss)$ | 1.3125 | $(ss:ss)$ | 0.7755 |
| $(F:pp)$ | 1.1456 | $(pp:pp)$ | 0.8061 |
| $\left(f\left\|-\frac{1}{2}\Delta\right\|f\right)$ | 38.2813 | $(ss:pp)$ | 0.7612 |
| $\left(s\left\|-\frac{1}{2}\Delta\right\|s\right)$ | 3.5945 | $(p_xp_x:p_zp_z)$ | 0.7284 |
| $\left(p\left\|-\frac{1}{2}\Delta\right\|p\right)$ | 2.7875 | $(fs:fs)$ | 0.0955 |
| $(ff:ff)$ | 5.4688 | $(fp:fp)$ | 0.0413 |
| $(ff:ss)$ | 1.1759 | $(p_xp_z:p_xp_z)$ | 0.0388 |

**** This value[9] was obtained by the same method as this work. The experimental value for this molecule has not yet been obtained.

9) H. Hamano, *J. Chem. Soc. Japan, Pure Chem. Sec.*, **77**, 985 (1956).

10) R. S. Mulliken, *J. Chem. Phys.*, **46**, 497, 675 (1949).

TABLE VI

TWO-CENTER INTEGRALS

| | | | |
|---|---|---|---|
| $S_{sh}$ | 0.3772 | $(sh : hh)$ | 0.1976 |
| $S_{\sigma h}$ | 0.2671 | $(\sigma h : \sigma h)$ | 0.0767 |
| $(F : hh)$ | 0.4478 | $(\sigma h : hh)$ | 0.1851 |
| $(F : sh)$ | 0.3311 | $(\pi h : \pi h)$ | 0.0157 |
| $(F : \sigma h)$ | 0.1920 | $(ss : sh)$ | 0.2722 |
| $(H : sh)$ | 0.2506 | $(ss : \sigma h)$ | 0.1725 |
| $(H : \sigma h)$ | 0.2671 | $(s\sigma : sh)$ | 0.0349 |
| $(ff : hh)$ | 0.4474 | $(s\sigma : \sigma h)$ | 0.0711 |
| $(ss : hh)$ | 0.4338 | $(s\pi : \pi h)$ | 0.0499 |
| $(\sigma\sigma : hh)$ | 0.4574 | $(\sigma\sigma : sh)$ | 0.2781 |
| $(s\sigma : hh)$ | 0.0898 | $(\sigma\sigma : \sigma h)$ | 0.1878 |
| $(\pi\pi : hh)$ | 0.4220 | $(\sigma\pi : \pi h)$ | 0.0068 |
| * $(fh : fh)$ | 0.0023 | $(\pi\pi : sh)$ | 0.2692 |
| $(sh : sh)$ | 0.1061 | $(\pi\pi : \sigma h)$ | 0.1648 |
| $(sh : \sigma h)$ | 0.0773 | | |
| | | | |
| $S_{ss'}$ | 0.0122 | $(s\sigma : \pi'\pi')$ | 0.0307 |
| $S_{s\sigma'}$ | 0.0176 | $(s\pi : s'\pi')$ | 0.0044 |
| $S_{\sigma\sigma'}$ | 0.0249 | $(s\pi : \sigma'\pi')$ | 0.0013 |
| $S_{\pi\pi'}$ | 0.0035 | $(\sigma\sigma : \sigma'\sigma')$ | 0.2478 |
| $(F : ss')$ | 0.0062 | $(\sigma\sigma : \pi'\pi')$ | 0.2368 |
| $(F : s\sigma')$ | 0.0096 | $(\sigma\pi : \sigma'\pi')$ | 0.0005 |
| $(F : \sigma\sigma')$ | 0.0123 | $(\pi_+\pi_+ : \pi_+'\pi_+')$ | 0.2281 |
| $(F : \pi\pi')$ | 0.0016 | $(\pi_+\pi_- : \pi_-'\pi_+')$ | 0.0003 |
| $(F : s'\sigma)$ | 0.0081 | * $(fs' : fs')$ | 0.0000 |
| $(F : s's')$ | 0.2342 | * $(f\sigma' : f\sigma')$ | 0.0000 |
| $(F : s'\sigma')$ | 0.0320 | * $(fs' : f\sigma')$ | 0.0000 |
| $(F : \sigma'\sigma')$ | 0.2405 | * $(f\pi' : f\pi')$ | 0.0000 |
| $(F : \pi'\pi')$ | 0.2310 | * $(ss' : ss')$ | 0.0001 |
| $(H : ss)$ | 0.4673 | * $(ss' : \sigma s')$ | 0.0002 |
| $(H : s\sigma)$ | 0.1263 | * $(ss' : \sigma\sigma')$ | 0.0002 |
| $(H : \sigma\sigma)$ | 0.5155 | * $(ss' : \pi\pi')$ | 0.0000 |
| $(H : \pi\pi)$ | 0.4431 | * $(s\sigma' : \sigma s')$ | 0.0002 |
| * $(ff : f'f')$ | 0.2342 | * $(s\sigma' : \sigma\sigma')$ | 0.0003 |
| * $(ff : s's')$ | 0.2342 | * $(s\sigma' : \pi\pi')$ | 0.0000 |
| * $(ff : \sigma'\sigma')$ | 0.2405 | * $(s\pi' : \pi s')$ | 0.0000 |
| * $(ff : \pi'\pi')$ | 0.2310 | * $(s\pi' : \pi\sigma')$ | 0.0000 |
| $(ss : s's')$ | 0.2342 | * $(\sigma s' : \sigma s')$ | 0.0002 |
| $(ss : \sigma'\sigma')$ | 0.2405 | * $(\sigma\sigma' : \sigma\sigma')$ | 0.0004 |
| $(ss : s'\sigma')$ | 0.0320 | * $(\sigma\sigma' : \pi\pi')$ | 0.0000 |
| $(ss : \pi'\pi')$ | 0.2310 | * $(\sigma\pi' : \pi\sigma')$ | 0.0000 |
| $(s\sigma : s'\sigma')$ | 0.0088 | * $(\pi s' : \pi s')$ | 0.0000 |
| $(s\sigma : \sigma'\sigma')$ | 0.0346 | * $(\pi s' : \pi\sigma')$ | 0.0000 |
| * $(\pi\sigma' : \pi\sigma')$ | 0.0000 | * $(s\sigma : ss')$ | 0.0002 |
| * $(\pi_+\pi_+' : \pi_+\pi_+')$ | 0.0000 | * $(s\sigma : \sigma s')$ | 0.0003 |
| * $(s\sigma : s\sigma')$ | 0.0003 | * $(s\sigma : \pi\pi')$ | 0.0001 |
| * $(s\sigma : \sigma\sigma')$ | 0.0004 | * $(s\pi : \pi\sigma')$ | 0.0000 |
| * $(\pi_+\pi_-' : \pi_+\pi_-')$ | 0.0000 | * $(s\pi : \sigma\pi')$ | 0.0000 |
| * $(ff : ss')$ | 0.0089 | * $(\sigma\sigma : ss')$ | 0.0070 |
| * $(ff : s\sigma')$ | 0.0129 | * $(\sigma\sigma : s\sigma')$ | 0.0101 |
| * $(ff : \sigma s')$ | 0.0128 | * $(\sigma\sigma : \sigma s')$ | 0.0106 |
| * $(ff : \sigma\sigma')$ | 0.0183 | * $(\sigma\sigma : \sigma\sigma')$ | 0.0151 |
| * $(ff : \pi\pi')$ | 0.0026 | * $(\sigma\sigma : \pi\pi')$ | 0.0019 |
| * $(fs : fs')$ | 0.0001 | * $(\sigma\pi : \pi s')$ | 0.0000 |
| * $(fs : f\sigma')$ | 0.0000 | * $(\sigma\pi : s\pi')$ | 0.0000 |
| * $(f\sigma : fs')$ | 0.0000 | * $(\sigma\pi : \pi\sigma')$ | 0.0000 |
| * $(f\sigma : f\sigma')$ | 0.0000 | * $(\sigma\pi : \sigma\pi')$ | 0.0000 |
| * $(f\pi : f\pi')$ | 0.0000 | * $(\pi\pi : s\sigma')$ | 0.0100 |
| * $(ss : ss')$ | 0.0069 | * $(\pi\pi : \sigma s')$ | 0.0096 |
| * $(ss : s\sigma')$ | 0.0100 | * $(\pi\pi : \sigma\sigma')$ | 0.0137 |
| * $(ss : \sigma s')$ | 0.0100 | * $(\pi_+\pi_+ : \pi_+\pi_+')$ | 0.0002 |
| * $(ss : \sigma\sigma')$ | 0.0142 | * $(\pi_+\pi_- : \pi_-\pi_+')$ | 0.0000 |
| * $(ss : \pi\pi')$ | 0.0020 | | |

TABLE VII

THREE CENTER INTEGRALS

| | | | |
|---|---|---|---|
| $(F' : hs)$ | 0.1066 | * $(sh : s\sigma')$ | 0.0023 |
| $(F' : h\sigma)$ | 0.0954 | * $(sh : \sigma s')$ | 0.0034 |
| * $(H : ss')$ | 0.0057 | * $(sh : \sigma\sigma')$ | 0.0048 |
| * $(H : s\sigma')$ | 0.0022 | * $(sh : \pi\pi')$ | 0.0007 |
| * $(H : \sigma\sigma')$ | 0.0128 | * $(sh : s'h)$ | 0.0614 |
| * $(H : \pi\pi')$ | 0.0016 | * $(sh : \sigma'h)$ | 0.0442 |
| * $(f'f' : sh)$ | 0.1285 | * $(\sigma h : ss')$ | 0.0016 |
| * $(f'f' : \sigma h)$ | 0.0919 | * $(\sigma h : s\sigma')$ | 0.0024 |
| * $(f's : f'h)$ | 0.0000 | * $(\sigma h : \sigma s')$ | 0.0025 |
| * $(f'\sigma : f'h)$ | 0.0000 | * $(\sigma h : \sigma\sigma')$ | 0.0354 |
| * $(ss : s'h)$ | 0.1260 | * $(\sigma h : \pi\pi')$ | 0.0005 |
| * $(ss : \sigma'h)$ | 0.0900 | * $(\sigma h : \sigma'h)$ | 0.0319 |
| * $(s\sigma : s'h)$ | 0.0230 | * $(\pi h : \pi s')$ | 0.0000 |
| * $(s\sigma : \sigma'h)$ | 0.0166 | * $(\pi h : \pi\sigma')$ | 0.0000 |
| * $(s\pi : \pi h')$ | 0.0000 | * $(\pi h : s\pi')$ | 0.0000 |
| * $(\sigma\sigma : s'h)$ | 0.1316 | * $(\pi h : \sigma\pi')$ | 0.0000 |
| * $(\sigma\sigma : \sigma'h)$ | 0.0942 | * $(\pi h : \pi'h)$ | 0.0000 |
| * $(\sigma\pi : \pi'h)$ | 0.0000 | * $(hh : ss')$ | 0.0053 |
| * $(\pi\pi : s'h)$ | 0.1231 | * $(hh : s\sigma')$ | 0.0078 |
| * $(\pi\pi : \sigma'h)$ | 0.0880 | * $(hh : \sigma\sigma')$ | 0.0114 |
| * $(sh : ss')$ | 0.0023 | * $(hh : \pi\pi')$ | 0.0015 |

*Chemical Laboratory Tokyo Gakugei University, Koishikawa, Tokyo.*

# *Measurements of the Amounts of Bound Water by Ultrasonic Interferometer. III. Application to Organic Electrolyte*

By Koin ITO and Hazime SHIIO

(Received March 22, 1957)

Recently many studies have been reported in order to estimate the amount of bound water of solute by measuring the ultrasonic velocity in the aqueous solution. In our laboratory, a general theory was suggested which seemed to give proper result in every kind of solution, and has been applied to solutions of saccharides[1], polyvinylalcohol and its derivatives[2]. In the present paper, an attempt is made to test the theory in the cases of the solutions of several organic electrolytes, and the results are discussed in comparison with those obtained by other methods. Authors chose aminoacids and gelatin as examples of low and high molecular electrolytes, respectively.

As introduced in a previous paper,

$$K=(\beta/\beta_0-V_0)/c\cdot\beta_0/\beta_w=\beta_1/\beta_w\cdot 1/d_1 -(\beta_0/\beta_w\cdot v_0/c-\beta_2/\beta_w\cdot v_2/c) \quad (1)$$

where the notations are as follows:

$V_0$=apparent specific volume fraction of total solvent,
i. e., $V_0=(d-c)/d_0$
$v_0$=apparent specific vol. fraction of the bound water, the density being assumed normal
$v_2$=specific vol. fraction of the bound water
$d$=density of solution
$d_1$=density of solute in solution, i. e., $(1-V_0)/c=1/d_1$
$c$=concentration of solute in g./cc. of solution
$\beta$=adiabatic compressibility of solution
$\beta_0$=adiabatic compressibility of solvent
$\beta_1$=adiabatic compressibility of solute molecule
$\beta_2$=adiabatic compressibility of bound water
$\beta_w$=adiabatic compressibility of water.

In the solutions of electolytes, it has been supposed that the bound water might be attached so strongly by the electrostatic force of the ionic radicals of the solute molecule that its compressibility becomes negligibly small. Then, Eq. (1) may be rewritten as

$$K=\beta_1/\beta_w\cdot 1/d_1-\beta_0/\beta_w\cdot v_0/c \quad (2)$$

Here again, the following procedure previously reported is used to estimate the amount of bound water. When any other bad solvent, though miscible with water, is added to the aqueous solution, the amount of bound water decreases. Therefore, using a bad solvent-water mixture containing a high fraction of the bad solvent, $v_0/c$ has to become small and accordingly Eq. (1) reduces to

$$K=\beta_1/\beta_w\cdot 1/d_1 \quad (3)$$

Thus, $K$ in such solutions depends on $\beta_1$ only. In present cases, ethanol was used as the bad solvent.

## Experimental

Commercial chemicals of glycine and α-DL-alanine were purified by recrystallization. Gelatin was dissolved in water and purified by electrodialysis until its electroconductivity decreased to the value of water. Its isoelectric point was pH 4.9.

The adiabatic compressibilities of solution and solvent were calculated by Laplace's relation, $\beta=1/d\mu^2$, from the ultrasonic velocity, $\mu$, which was measured by the ultrasonic interferometer. pH of solution was determined by a glass electrode and pH test paper. The measurements were carried out at 30°C for aminoacids and at 35°C for gelatin.

## Results and Discussion

In Table I is shown an example of the

TABLE I
EXAMPLES OF THE MEASUREMENTS (GLYCINE)

| Ethanol concn. % | $c$ | $d$ | $\beta/\beta_0$ | $V_0$ | $K$ |
|---|---|---|---|---|---|
| 0.0 | 0.0819 | 1.0322 | 0.8958 | 0.9520 | −0.69 |
| 21.1 | 0.0521 | 0.9893 | 0.9539 | 0.9689 | −0.25 |
| 33.9 | 0.0105 | 0.9517 | 0.9932 | 0.9937 | −0.05 |
| 35.3 | 0.0105 | 0.9488 | 0.9941 | 0.9935 | +0.06 |
| 44.2 | 0.0102 | 0.9307 | 0.9938 | 0.9935 | +0.07 |
| 48.2 | 0.0102 | 0.9229 | 0.9938 | 0.9941 | −0.03 |

1) H. Shiio, T. Ogawa and H. Yoshihashi, *J. Am. Chem. Soc.*, **77**, 4980 (1955).
2) H. Shiio and H. Yoshihashi, *J. Phys. Chem.*, **60**, 1049 (1956).

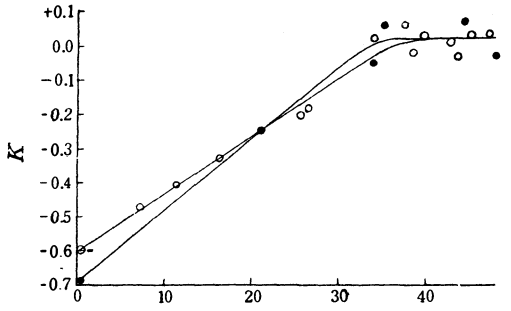



Fig. 1. ●, Glycine; ○, α-DL-alanine

measurements. The results of aminoacids are given in Fig. 1, in which are illustrated the plots of $K$ against ethanol concentration in solvent. The situations are exactly the same as in the cases of glucose and maltose in the previous paper. As the ethanol concentration in solvent increases to some magnitude, $K$ becomes nearly zero. However, in the solutions containing more than about 35 per cent. of ethanol, the solubility of both aminoacids becomes so small that the measurements give inaccurate results. Therefore, the line to which the $K$ curve approaches is not determined exactly, but $K$ may be assumed to be nearly zero in these region. Thus, by extrapolation of this part of the curve to pure aqueous solution, $\beta_1$ in aqueous solution is calculated by means of Eq. (3), giving the value approximately zero. Consequently, in such cases of the electrolytic solutions as well as non-electrolytic solutions, the term containing $\beta_1$ in Eqs. (1) and (2) can be assumed to be always zero, and so Eq. (1) becomes

$$K=-(\beta_0/\beta_w\cdot v_0/c-\beta_2/\beta_w\cdot v_2/c)$$

which is similar to the equations proposed by others[3]. This agrees with the fact that when the amount of bound water of the solute of low molecular weight has been calculated from the compressibility difference between solvent and solution, the compressibility of the solute molecule has been ignored by many investigators. Thus, the values obtained by the present procedure are clearly about the same magnitude as those of others[4].

Results of gelatin solution are collected in Fig. 2. As the solvents for gelatin, various ethanol-water mixtures were made by

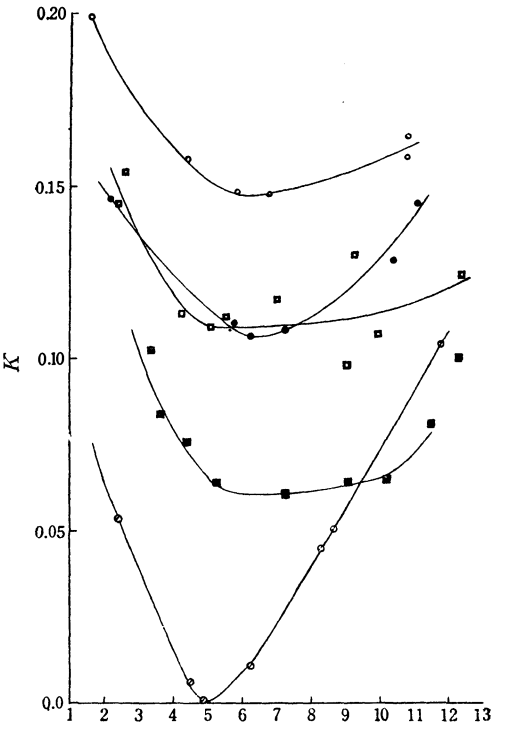



Fig. 2. Ethanol Concn: ⓥ, 0%; ●, 12.9%; ○, 25.0%; □, 34.9%; ■, 42.4%.

adding various small amounts of hydrochloric acid or sodium hydroxide to vary their pH. The fluidity of gelatin solution decreases with the increase in ethanol concentration in the solution. When the ethanol concentration exceeds 45 per cent., gelation takes place in a solution containing several per cent. gelatin even at 35°C. It is shown in Fig. 2 that in each ethanol concentration $K$ has the minimum value at a certain pH which is regarded as the isoelectric point of gelatin in each solution. This may be due to the fact that at the isoelectric point, gelatin holds the highest value of the amount of bound water, or, as Miyahara and Shiio have supposed[5], the compressibility of the gelatin molecule acquires a minimum value as a results of the contraction of the molecule by the intramolecular electric field due to its ionic radicals. The plots of $K$ at some definite pH values against ethanol concentration are shown in Fig. 3 by rearranging Fig. 2. The froms of the curves at each pH are similar to each other

3) T. Yasunaga and T. Sasaki, *J. Chem. Soc. Japan Pure Chem. Sec.*, **72**, 87 (1951); Y. Miyahara, This Bulletin, **25**, 326 (1952).

4) Y. Miyahara, This Bulletin, **26**, 390 (1953).

5) Y. Miyahara and H. Shiio, *J. Chem. Soc. Japan Pure Chem. Sec.*, **73**, 265 (1952).

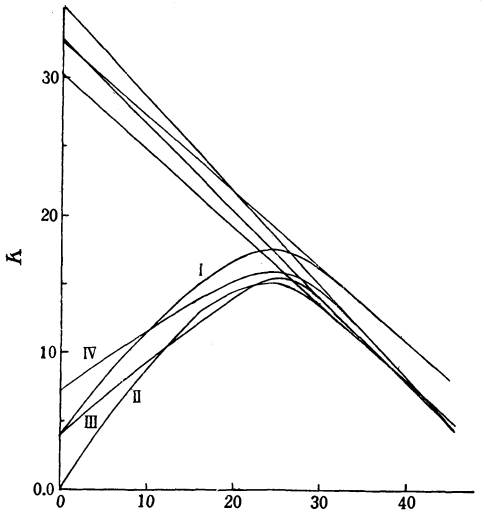



Fig. 3. I, pH 3; II, pH 5; III, pH 8; IV, pH 10

and to those of dextrine and polyvinylalcohol in a previous paper. Accordingly, it may be expected also in the present case that at the left part of curves, their relatively steep slopes are mainly contributed by the decrease in $v_0/c$ and that at the right part of curves their decreases results from the change in $\beta_1$ only. On the basis of these assumptions, the values of $v_0/c$ and $\beta_1$ in aqueous solution at various pH are evaluated by means of Eqs. (3) and (1), and given in Table II.

TABLE II
THE RESULTS FOR GELATIN IN AQUEOUS SOLUTION

| pH | $K$ | $\beta_1/\beta_w \cdot 1/d_1$ | $\beta_1 \times 10^{12}$ | $v_0/c$ |
|---|---|---|---|---|
| 3 | 0.04 | 0.33 | 21. | 0.29 |
| 5 | 0.00 | 0.30 | 19. | 0.30 |
| 8 | 0.04 | 0.33 | 21. | 0.29 |
| 10 | 0.07 | 0.35 | 22. | 0.28 |

From these values it may be seen that $\beta_1$ increases gradually with the deviation of pH from the isoelectric point, while $v_0/c$ changes very little. Consequently, the variation in $K$ in aqueous solution caused by pH change is mainly due to the change of the compressibility of the gelatin particle. The above values of $v_0/c$ agree with the generally assumed values of proteins, and the behavior of $v_0/c$ with pH change agrees with the fact reported by Weber et al.[6].

The hydration of gelatin has been evaluated by Passynski[7]. He proposed an approximate equation to calculate the amount of hydration from the compressibility difference between solvent and solution, which was similar to the present ones, and applied it to many solutions. He derived his equation, however, by assuming that when the concentration of solute approached zero, the effect of compressibility of solute could be ignored. But, according to the present procedure, it is shown that $K$ must be also correlated by the compressibility of solute itself, perticularly in high polymer solutions. Consequently, the effect of the compressibility of solute cannot be neglected at the evaluation of the amount of bound water in these procedures. Further more, when the compressibility of solute molecule changes with the variation of composition of solution, the compressibility of solute should be taken into consideration, as the authors have done.

Miyahara has evaluated the compressibility of egg albumin in aqueous solution, giving $13\times10^{-12}$ c.g.s. unit at its isoelectric point by analogical calculation using the date of aminoacids[8]. Jacobson has computed also the compressibilities of natural proteins, the magnitude of which is in the order of $10\times10^{-12}$ c.g.s. unit by his own procedure[9]. In comparison with these values, the present values of gelatin are appreciably larger. This difference may be due to the difference of properties of molecules, that is to say, natural proteins have the rigid three-dimensionally definite structure, but gelatin is a degradation product of some proteins and has not any definite structure, freely extending, somewhat similar to synthetic polymers such as polyvinylalcohol.

To calculate the values of $v_0/c$ and $\beta_1$ of gelatin strictly, however, the facts that there are several interactions between the components of solution must be taken into account. The change of pH of the solution caused by the buffer action of gelatin might also be well considered.

It may be concluded that the present procedure holds not only for the solutions of non-electrolytes but also for those of electrolytes and that the values of the amount of bound water and the compressibility of solute are always separately obtained.

6) H. H. Weber and D. Nachmannsohn, *Chem. Abst.*, **23**, 1917 (1929).

7) A. Passynski, *Acta Physicochim. U. R. S. S.*, **3**, 779 (1935); **22**, 137 (1947).

8) Y. Miyahara, This Bulletin, **29**, 742 (1956).

9) B. Jacobson, *Arkiv För Kemi*, **2**, 177 (1950).

## Summary

1. The previously introduced theory on the amount of bound water and the compressibility of solute has been tested with the solutions of organic electrolytes.

2. The proposed procedure was found to be satisfactory and gave separately the values of the amount of bound water and the compressibility of solute in each case. These results appear to be proper compared with others.

3. The compressibility of the solute could be neglected in aminoacid solutions by the same reason as in the case of glucose where the solute is of low molecular weight.

4. It is shown that the amount of bound water of gelatin varies very little as pH of solution goes apart from the isoelectric point where the compressibility of gelatin molecule has a minimum value, as had been expected.


The authors wish to express their sincere thanks to Professor I. Sano and Assist. Professor Y. Miyahara for their kind encouragement and discussion throughout this work.

*Department of Chemistry, Faculty of Science, Nagoya University, Chikusa-ku, Nagoya*

# *Studies on the Mechanism of Eder's Reaction. II. On the Properties of the Active Oxalic Acid in Manganese (III and VII)-Oxalate Reaction Systems*

By Shukichi SAKURABA and Syozo IKEYA

(Received August 15, 1956)

## Introduction

The reduction of mercury(II) chloride by oxalate according to so-called Eder's reaction,

$$2HgCl_2+C_2O_4^{2-}=Hg_2Cl_2+2Cl^-+2CO_2$$

can be induced by addition of very small amount of strong oxidizing agents such as potassium permanganate, manganese dioxide, and the manganese(III)-oxalate complexes.

In these induced reactions, an active oxalic acid, which appears to be formed by the decomposition* of manganese(III)-oxalate complex, is usually regarded as one of the chain propagating intermediates[1,2]. The active oxalic acid is very reactive and is able to reduce mercury(II) chloride; for its formula, $CO_2^{-}$[3], $C_2O_4^{-2}$,[4] or $Mn\begin{matrix}O-C=O\\ \vdots\\ O-C=O\end{matrix}$[5] has been conveniently used to account for the reaction mechanism. Although the chemical formula of the active oxalic acid is not known as yet, its presence was futher confirmed by the fact that when the manganese(III)-oxalate complex was decomposed in the air, hydrogen peroxide was formed in the solution.

Weiss[2] and Abel[6] explained the formation of hydrogen peroxide as follows: the $O_2^-$ ion is produced by the reaction between the active oxalic acid, $CO_2^-$ or $C_2O_4^-$, and the dissolved oxygen. Launer[3] showed that the net rate in the decomposition of manganese(III)-oxalate complex is decreased by oxygen, and he proposed the following mechanism:

$$CO_2^-+O_2=O_2CO_2^-$$
$$O_2CO_2^-+Mn^{2+}+2H^+=Mn^{3+}+CO_2+H_2O_2$$

In these mechanisms, the regeneration of the manganese(III) ion and the formation of hydrogen peroxide are involved.

* In its nature, this is an auto-reduction of manganese(III) complex to manganese(II) salt; those reactions that follow are the same.

1) C. H. Cartledge, *J. Am. Chem. Soc.*, **63**, 906 (1941).
2) J. Weiss, *Discussions Faraday Soc.*, No. 2, 188 (1947).
3) H. F. Launer, *J. Am. Chem. Soc.*, **55**, 865 (1933); H. F. Launer and D. M. Yost, ibid., **56**, 2571 (1934).
4) H. Taube, ibid., **69**, 1418 (1947); ibid., **70**, 1216 (1948).
5) F. R. Duke, ibid., **69**, 2885 (1947).
6) E. Abel, *Monatsh*, **83**, 695 (1952).

TABLE I
COMPOSITION AND pH OF MIXTURES USED IN THE EXPERIMENT

| Mixture | $K_3Mn(C_2O_4)_3$ | $KMnO_4$ | $MnSO_4$ | $Na_2C_2O_4$ | $H_2SO_4$ | pH |
|---|---|---|---|---|---|---|
| A | 0.0025 | | | | 0.005 | 2.8* |
| B | | | 0.0025 | 0.005 | 0.003 | 3.2 |
| C | | 0.005 | | 0.0175 | 0.024 | 3.2* |
| D | | | 0.005 | 0.005 | 0.003 | 3.2 |

Numerical values are concentration in mol./l.
* Value after the reaction was completed

As to the inhibitory action of oxygen, however, it has been hardly discussed since Launer's report*.

In our previous report[7], it was described that the photochemical reaction between the manganese(II) ion and oxalate induces Eder's reaction, i. e., the reaction proceeds through an active intermadiate produced by the ultraviolet absorption of manganese(II) oxalate in the solution. This active intermadiate seems to be a long-life radical, $Mn\begin{matrix}O-C=O\\ \cdot\\ O-\dot{C}=O\end{matrix}$ or $[Mn^{II}-O-\dot{C}=O]^+$, which will be able to reduce mercury(II) chloride, and react on dissolved oxygen and hydrogen ion to form hydrogen peroxide and manganese(III) complex.

From similarity of the properties, it will be expected that the active oxalic acid formed by the decomposition of manganese (III)-oxalate complex is the same as the above-mentioned active intermadiate. In the study reported here, the properties of the active oxalic acid were examined from a new angle, by means of the spectrophotometric measurement, and the mechanism of the reaction system of manganese (III and VII)-oxalate was presumed.

## Experimental

**Materials.**—All chemicals used in the investigation were the same as described in the first report. Potassium trioxalato-manganese(III) trihydrate, $K_3[Mn(C_2O_4)_3]\cdot 3H_2O$, was prepared by Cartledge and Ericks' method[8].

The solutions used in the absorption measurement were prepared to give the composition shown in Table I, by mixing the known stock solutions.

Mixture A was used to examine the change in the absorption spectra on the decomposition of manganese(III)-oxalate complex, and Mixture C was used on the reaction system of permanganate and oxalate. Mixture B and D are comparative solutions of A and C, respectively, that is, in the final state of reaction, the manganese (II) and the oxalate ion concentrations of A and C are the same as those of B and D, respectively.

**Procedure.**—The decomposition of potassium trioxalato-manganese(III) in acidic solution (Mixture A) and the reaction between permaganate and sodium oxalate (Mixture C) were carried out in an Erlenmeyer flask which was kept at 8° to 10°C and 20°C with a thermostat, respectively, in the dark room. To avoid the influence of dissolved oxygen in the latter reaction, carbon dioxide or nitrogen gas was passed through the solution in the flask containing sodium oxalate and sulfuric acid for 40 minutes, then the solution was mixed with permanganate solution through which nitrogen gas was previously passed at 20°C. At intervals of appropriate times, a few milliliters of the reaction solution was taken out from the flask, and its absorption spectra were measured by Hitachi model EPU quartz spectrophotometer with 1 cm. cells.

## Results

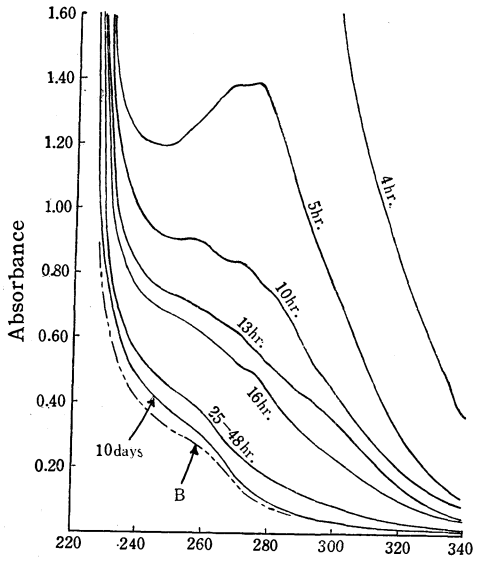
**1) The Decomposition of Potassium Trioxalato-Manganese(III) in the Air.**—Potassium trioxalato-manganese(III) complex assumes a reddish brown color in water or a neutral solution, and yellow color in an acidic solution, the colors gradually fading away with standing until colorless. It was said that the yellowish color in acidic solution results from the formation of dioxalato-diaquo-manganese(III), $[Mn(C_2O_4)_2(H_2O)_2]^-$ [8].

In the reaction mixture A, it was initially yellow, and its absorption spectra at appropriate times were shown in Fig. 1. After five hours, the solution was pale yellow, and an absorption maximum appeared at about 270 mμ; after ten hours, it became almost colorless, and two absorbance swelling appeared about at 255 and 270 mμ; after thirteen hours, it was colorless, and the absorption swell at 270 mμ almost disappeared. However, the absorbance decreased still more untill it showed slight declining even after ten days. The settled absorption curve had an absorbance swell at about 250 to 260 mμ, and approached to that of the mixture B with a very slow rate. This absorbance swell is due to the absorption of manganese(II)-oxalate complex[7], and that at about 270 mμ, presumably to the absorption of dioxalato-diaquo manganese(III).

* The inhibitory action of oxygen upon the reduction of mercury(II) chloride to mercury(I) chloride has been discussed in numerous reports[1].

7) S. Sakuraba and S. Ikeya, This Bulletin, **30**, 662 (1957).

8) G. H. Cartledge and W. P. Ericks, *J. Am. Chem. Soc.*, **58**, 2061, 2065 (1936).



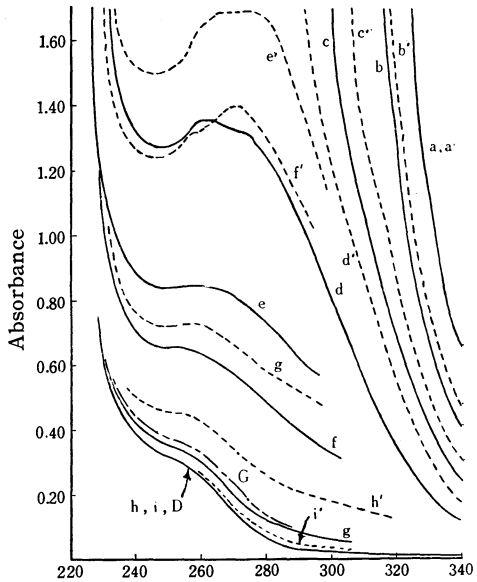

B: Mixture

Fig. 1. Decomposition of potassium trioxalato manganese (III) in the air. (Mixture A)

From these results, it is evident that the declination of absorbance in mixture A signifies the reduction of manganese(III) complex to manganese(II) which is present as manganese(II)-oxalate complex[7] in the solution. After the reaction completed, a large quantity of hydrogen peroxide was detected in the solution*.

**2) The Reaction between Permanganate and an Excess of Oxalate.**—The reaction between permanganate and oxalate in the composition of mixture C was investigated both in the absence and the presence of dissolved oxygen (in the air).

A start was appointed at the time of addition of the potassium permanganate solution to the oxalate solution. The absorption spectra of the reaction mixture were measured at intervals of an appropriate time, as shown in Fig. 2. The full line is the absorption curve in the absence of oxygen, and the dotted line is that in air. After 50 minutes, the color of the solution changed from violet to purplish red regardless of the presence of dissolved oxygen ; after 70 minutes, it became deep yellow ; after 78 minutes, the color remained unchanged and the absorption curve in the absence of oxygen coincided with that in its presence (curve a, a' in Fig. 2). After 90 minutes, the color is golden yellow, and the absorption curve in the absence of oxygen became lower than that in its presence (b and b' or c and c', etc.). The solutions in the absence and the presence of dissolved oxygen became colorless in curve e (after 130 min.) and curve g' (after 3 hr.), respectively ; and after about 130 minutes,




—— in nitrogen atomosphere, - - - in air. a, a': 78 min. b, b': 90 min. c, c': 100 min. d, d': 117 min. e, e': 130 min f, f': 142 min. g, g': 3 hrs. h, h': 5hrs. i, i': 24 hrs. D: Mixture D; G: When g was exposed to air.

Fig. 2. Reaction between $KMnO_4$ and $Na_2C_2O_4$. (Mixture C)

the curves in air showd an absorption maximum at about 270 mμ (curve e' and f') and the declining of its curve was much slower than that in the absence of oxygen. The declination of these curves was almost the same as that of manganese(III)-oxalate complex shown in Fig. 1, although the rate for the former was greater than that for the latter*. The pH of the final solution was 3.2, regardless of the presence of the dissolved oxygen, and its absorption curve coincided with that of the mixture D.

These facts suggest that the reaction of permanganate-oxalate proceeds with the formation of manganese(III) on the way to the final state of manganese(II) and carbon dioxide, and that the reduction of manganese(III) complex is retarded by the dissolved oxygen.

When the solution corresponding to the absorption curve g in the absence of oxygen in Fig. 2 was exposed to air and shaken for a few minutes, the curve changed itself to G in Fig. 2**. The same effect was clearly seen, although to a smaller extent, when the solution corresponing to the curve h (after 5 hrs.) and the curve i (after 24 hr.) were exposed to air, but was not seen at all in the mixture D solution. These facts suggest that the manganese(III) complex is produced by an action of the dissolved oxygen. In order to make this suggestion clearer, the absorbance at 270 mμ was plotted against time

* Under this condition of the investigation, the absorption spectrum of hydrogen peroxide was not observed.

* The difference in rate is due to the difference of manganese(II) ion concentration and reaction temperature.

** No effect was exhibited by a violent passing of oxygen gas.

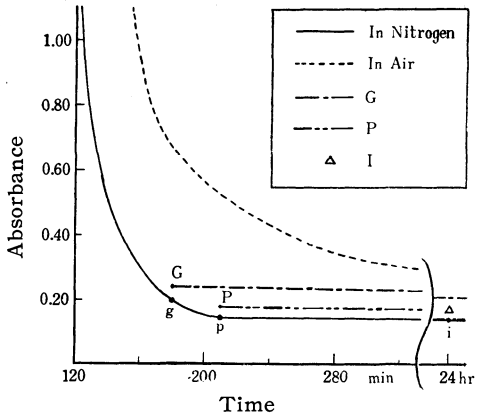



Fig. 3. Regeneration of manganese(III) ion by oxygen; Absorbances 270 mμ in Fig. 2 vis. times.

and shown in Fig. 3. The full line is the curve in the absence of oxygen, the dotted line is that in its presence. When the solutions in the state of g (corresponding curve g in Fig. 2) and p (omitted in Fig. 2) absorbed oxygen in the air, the absorbance increased to G and P in Fig. 3, respectively. On further standing, the slow declination occured along the one and the two dotted lines, respectively. Twenty four hours after standing in the air, the absorbance of solution P almost settled down to that of solution p, but the absorbance of solution G did not entirely to that of solution g. The solution i in Fig. 3 (corresponding the curve i in Fig. 2), which was spectrophotometrically confirmed to be in the final state of the reaction, does not contain manganese (III) salt any more; nevertheless, when the solution was exposed to air, its absorbance increased up to a state of point I, and the solution of i was able to reduce mercury(II) chloride, although the power was weak. Mixture D has the same absorbance with the solution in the state of i (D and i in Fig. 2), however, it does not change the absorbance regardless of the presence of oxygen and has no reducing power towards mercury(II) chloride in the dark at room temperature. Of course, the solutions in which the presence of manganese(III) complex was shown spectrophotometrically (i', g, G, h', etc. in Fig. 2) had also the reducing power towards mercury (II) chloride.

## Discussion

From the experimental results above mentioned, the following facts could be stated. The manganese(III)-oxalate complex was formed in the course of the reaction between permanganate and an excess of oxalate, and gradually decomposed to form manganese(II)-oxalate, producing active oxalic acid. The active oxalic acid gives manganese (III) complex and hydrogen peroxide by the action of the hydrogen ion and dissolved oxygen. Hence the reduction of manganese(III) complex will be retarded by the dissolved oxygen. When the manganese(III) complex was completly reduced to manganese(II) in a carbon dioxide or a nitrogen atmosphere and then the solution exposed to air, manganese(III) complex and hydrogen peroxide were reproduced in the solution, therefore, the active oxalic acid appears to survive for a long time.

On the other hand, when the permanganate or the manganese(III) complex was reduced in a solution containing an excess of oxalate ion, its solution possessed reducing power towards mercury(II) chloride, its power was the strongest at pH about 3.2[10].

In the previous report[7], it was stated that an active intermediate was formed by the irradiation of ultraviolet rays on the manganese(II)-oxalate solution, and reacted with the hydrogen ion and dissolved oxygen, forming hydrogen peroxide and manganese(III) complex, and that this formation and the reducing power of the irradiated manganese(II)-oxalate solution towards mercury(II) chloride were most marked at pH about 3.2*.

The active oxalic acid seemingly has the same properties as the active intermediate formed by the irradiation of ultraviolet rays on the manganese(II)-oxalate solution; it seems that the former is to be the same structure as the latter. A possible mechanism can be

$$[Mn(C_2O_4)_2(H_2O)_2]^- \longrightarrow \underset{[I]}{\left[\begin{array}{c} O \quad O \\ \| \quad \| \\ C\cdot \quad C \\ | \quad \| \\ O \quad O^+ \\ \diagdown \quad \diagup \\ Mn^{II} \end{array}\right]} + C_2O_4^{2-} + 2H_2O \qquad (1)$$

(or $[Mn(C_2O_4)_3]^{3-} \longrightarrow [I] + 2C_2O_4^{2-}$)

$$[I] \longrightarrow \underset{[II]}{[Mn^{II}-O-\dot{C}=O]^+} + CO_2 \qquad (2)$$

$$[II] + O_2 \longrightarrow Mn^{2+} + O_2^- + CO_2 \qquad (3)$$

$$Mn^{2+} + O_2^- + 2H^+ \longrightarrow Mn^{3+} + H_2O_2 \qquad (4)$$

$$Mn^{3+} + nC_2O_4^{2-} \longrightarrow Mn(III) \qquad (5)$$

10) S. Sakuraba, *J. Chem. Soc. Japan Pure Chem. Sec.*, **77**, 18, 22 (1956). Experiment was done with the solution in 0.030 mol./l. of $Na_2C_2O_4$, 0.002 mol./l. of manganese(III or VII) and 0.010 mol./l. of $HgCl_2$.

* Experiments were done with the solution in 0.030 mol./l. of $Na_2C_2O_4$, 0.002 mol./l. of $MnSO_4$ and 0.010 mol./l. of $HgCl_2$.

$$[II] + Mn^{3+} \longrightarrow 2Mn^{2+} + CO_2 \quad (6)$$

$$[II] + Hg(II) \longrightarrow Mn^{2+} + Hg(I) + CO_2 \quad (7)$$

The manganese(III)-oxalate complex will be present as trioxalato manganese(III) ion, $[Mn(C_2O_4)_3]^{3-}$, in the solution containing oxalate ions in excess, and as dioxalato-diaquo manganese(III) ion, $[Mn(C_2O_4)_2(H_2O)_2]^-$, in lower oxalate ion concentration. When these ions are subject to auto-oxidation reduction, the active oxalic acid will be produced, and its form was described as $CO^-$, $C_2O_4^-$ or $CO_2+CO_2^-$, etc., by many investigators. Duke[5] proposed that the electron attractivity of tervalent manganese in a molecule of manganese(III)-oxalate complex is so strong that an electron is donated to the metal ion with simultanious breaking of C—C bond in $C_2O_4^{2-}$ radical, resulting in active complex, to which he gave the formula $(H_2O)_2Mn(O-C=O)(O-\dot{C}=O)C_2O_4^{2-}$. From the facts that manganese(II)-oxalate, in the solution as well as in the solid state, is activiated by the light absorption*, and that the properties of this activiated substance are similar to those of active oxalic acid, a formula of the active oxalic acid can be given by [I] as Duke's formula. However, the active intermediate [I] will decompose instantly to form an ionic radical [II] and carbon dioxide. It seems that this ionic radical must have the same formula as the active intermediate formed photochemically from manganese(II) oxalate.

The formation of hydrogen peroxide and the reproduction of manganese(III) complex will be interpreted by steps (3), (4), and (5).

When a sufficient amount of the manganese(III) ion is present in the acidic solution, the active intermediate might be consumed according to step (6), hence, in an acidic solution containing dissolved oxygen, the active intermediate will become extinct by step (3), (4) and (6), and the formation of mercury(I) chloride by step (7) will be also inhibited. On the other hand, in a weak acidic solution containing dissolved oxygen and an excess of the oxalate ion step (1) and (4) will be retarded; consequently, step (6) and (7) will be also inhibited**.

The decomposition of manganese(III) complex in the absence of oxygen will proceed through an equilibrium reaction, $[Mn(C_2O_4)_3]^{3-}+6H^+ \rightleftarrows Mn^{3+}+3H_2C_2O_4$, step (1), (2) and (6), so it will occur more rapidly in an acidic solution. In a weak acidic solution, the concentration of $Mn^{3+}$ is low, and so is that of active radical [I] or [II]; in a strong acid solution, step (6) proceeds more rapidly, because the concentration of $Mn^{3+}$ and [I] or [II] are high, Therefore, contents of the active radical in the solution will scarcely increase more than a limitted extent**.

Through the above consideration, it causes that the decomposition of manganese(III) complex in air is the slowest at pH about 3.2, and the formation of mercury(I) chloride takes place in large quantities at this pH. If the reaction indicated by step (7) is a chain reaction, another intermediate must be considered***.

## Summary

1) The active oxalic acid produced in the manganese(III or VII)-oxalate reaction system has the same properties with the activiated manganese oxalate formed by ultraviolet irradiation. These active intermediates are able to reduce mercury (II) chloride and, if oxygen is dissolved in the solution, react with oxygen to form hydrogen peroxide and the manganese(III) ion. These will probably be an ionic radical with a long life that has the same formula.

2) The inhibitory action of oxygen on the decomposition of the manganese(III) oxalate complex can be interpreted by the reproduction of the manganese (III) ion, and it is most remarkable at pH about 3.2.

*Department of Appled Chemistry, Faculty of Engineering, Shizuoka University Oiwake, Hamamatsu*

* The activiation occurs also by X-ray or γ-ray radiation.

** A kinetic treatment will discussed in the following report.

*** According to Cartledge, the active oxalic acid was regarded as the first necessary chain carrier and the other intermediate was $Hg^+$ ion[1].

# *Studies on the Molecular Structure of Bisacetylacetone-Nickel(II) by Electron Diffraction**,[1]

By Shuzo SHIBATA

(Received May 7, 1957)

Recently, the structures and the properties of metal chelate compounds have attracted considerable attention of many investigators. Acetylacetone chelate is a repesentative of such metal chelate compounds. The author has already investigated the structure of bisacetylacetone-copper(II)[2]. The present paper deals with the structure of bisacetylacetone-nickel(II).

It is interesting to decide whether the arrangement of four oxygen atoms of bisacetylacetone-nickel(II) about the bivalent nickel atom is planar or tetrahedral. The structure of this chelate has already been investigated by magnetic measurements[3] and by absorption spectra[4]. On the basis of the paramagnetic property of bisacetylacetone-nickel(II), Pauling[5] presumed that the chelate has a tetrahedral configuration. However, this evidence has not yet been clarified by other more powerful methods, e.g., the preparation of isomers and the X-ray investigation. In particular, the latter is the most direct method to determine the molecular structure. Recently, the X-ray analysis has been taken by Bullen[6], who showed that there are three nickel atoms in an asymmetric unit, the three atoms being very nearly collinear. Unfortunately he could not definitely clarify the molecular structure of the chelate. The acetylacetone chelate can readily be vaporized without suffering decomposition at a high temperature. Therefore the author has undertaken to apply the electron diffraction method to determine the molecular structure of the nickel chelate in the same way as in a previous study on the copper chelate.

## Experimental

Bisacetylacetone-nickel(II) recrystallized several times from ethanol was furnished by Dr. K. Sone. The anhydrous compound was prepared by sublimation in vacuo. The apparatus[7] used was that already reported by the present author and his collaborators. The sample was vaporized at about 170°C and led through a high temperature nozzle into a vacuum chamber to interfere with an electron beam of about 0.06 Å in wavelength. Non-sector photographs (The camera length was about 11 cm.) were taken in the usual way. Further examination was carried out by $r^2$ sector photographs (The camera length was about 12 or 28 cm.)

## Visual Curve and Radial Distribution Curve

Visual measurements were made of the $q$ values and the intensities of maxima

TABLE I
THE OBSERVED AND THE CALCULATED $q$ VALUES OF THE MAXIMA AND THE MINIMA.

| max. | min. | $q_{obs.}$ | $q_{calc.}$(model F) | $q_{calc.}/q_{obs.}$[a] |
|---|---|---|---|---|
| | 2 | 7.66 | 7.7 | (1.005) |
| 2 | | 10.20 | 10.2 | 1.000 |
| 3 | | 14.92 | 15.0 | 1.005 |
| 4 | | 17.85 | 17.5 | 0.980 |
| 5 | | 21.26 | 21.2 | 0.997 |
| 6 | | 24.10 | 23.7 | 0.992 |
| 7 | | 28.73 | 29.2 | 1.016 |
| 8 | | 34.40 | 34.3 | 0.997* |
| | 10 | 40.78 | 40.4 | 0.991 |
| 10 | | 44.07 | 43.9 | 0.996* |
| | 11 | 48.28 | 48.3 | 1.000 |
| 11 | | 51.44 | 52.4 | 1.019 |
| 12 | | 58.22 | 57.6 | 0.990 |
| 13 | | 65.62 | 65.6 | 1.000 |
| average of $q_{calc.}/q_{obs.}$ | | | | 0.998 |
| average deviation | | | | 0.007 |

a) The value of $q_{calc.}/q_{obs.}$ in parentheses was omitted in calculating the average. Those marked with an asterisk were given double weight.

* Presented at Symposium on the Metal Complex Compounds held in November 11, 1952.

1) S. Shibata, M. Kishita and M. Kubo, *Nature*, **179**, 320 (1957).
2) S. Shibata and K. Sone, This Bulletin, **29**, 852 (1956).
3) L. Cambi and L. Szego, *Ber.*, **64**, 2951 (1931).
4) A. E. Martell and M. Calvin, "Chemistry of the Metal Chelate Compounds", Prentice-Hall, New York, (1952), p. 220.
5) L. Pauling, "Nature of the Chemical Bond", Cornell Univ. Press, Ithaca, (1948), p. 119.
6) G. J. Bullen, *Nature* **177**, 537, (1956).
7) M. Kimura, *Chem, Researches*, **9**, 53(1951); S. Shibata and M. Kimura, This Bulletin, **27**, 485 (1954); M. Kimura, K. Kimura and S. Shibata, *J. Chem. Phys.*, **24**, 622 (1956).

and the minima below $q=70$ in the photographs. The measured $q$ values of maxima and minima are given in Table I. The positions of some minima were not measured, because the period of the halos was very short. The visual intensity curve depicted in Fig. 3 was drawn from the measurement of the features of the halos and their positions so as to be represented by the following simplified intensity expression:

$$I(q)=\sum_{i\neq j}(Z_iZ_j/r_{ij})\sin(\pi qr_{ij}/10)$$

Here notations have their usual significances. On the non-sector photographs, the measurements of intensities were considerably difficult in the region of small $q$ (2nd maximum and 2nd and 3rd minima) on account of the intense background of the photographs. Thus the error of this intensity measurement may affect the radial distribution curve. The use of $r^2$-sector photographs could probably eliminate such a difficulty. The portion of the intensity curve below $q=7$, which could not be observed, was necessary for the calculation of a correct radial distribution curve. Therefore from the observed curve, to which the unobservable part below $q=7$ was properly added, the radial distribution (R.D.) curve was calculated by use of the following formula:

$$rD(r)=\sum_i I(q_i)\exp(-aq_i^2)\sin(\pi q_i r/10)$$

Here the constant $a$ was chosen to be 0.000545 and the summation was carried out up to $q_i=70$. Using the values of some interatomic distances obtained from the resulting curve, the theoretical intensity curves of several models were computed by the above formula. In this case, the ligands were assumed to be planar and to possess a symmetry $C_{2v}$. This assumption was made throughout in order to simplify this analysis. This assumption would be quite adequate if the contribution of the possible resonance structures of the ligand molecule were taken into account. The calculated $I(q)$ curves indicated that the intensity in the region of small $q$ values (below about 13) was almost invariable, irrespective of whether the configuration of the calculated model was planar or tetrahedral. Accordingly, the observed part was continued with a dotted curve shown in Fig. 3 (upper curve) for the unobservable part of the intensity curve with reference to the calculated curve. The R.D. curve shown in Fig. 1 was calculated from this intensity curve in the same way as before. This curve is almost non-negative. The negative portions in the neighborhood of 3.5 Å and 5.3 Å are attributable to low frequency loops superimposed on this curve, and they seem to be due to the inaccuracy of the intensities for small $q$ values (particularly to the 2nd maximum which was estimated much too high). However, no attempts were made to revise the visual curve because the positions of peaks presumably remain unchanged by this revision. The peaks of this curve could be assigned to the atomic pairs as given in Table II: thus peaks at 1.90, 2.84, 3.20 and

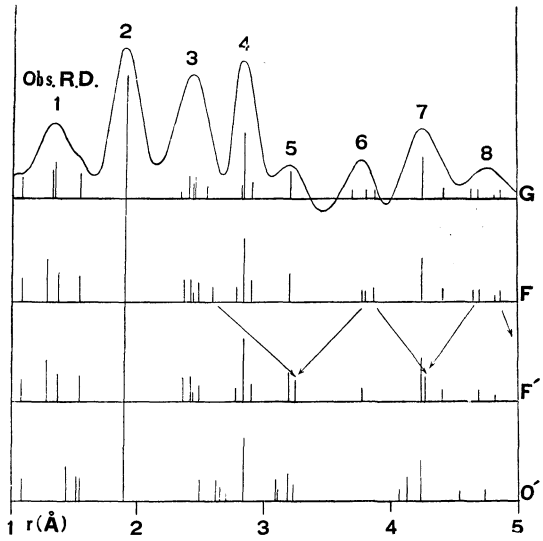



Fig. 1. The R. D. curves of bisacetylacetone-nickel(II). All the atomic pairs of each model are shown by the vertical bars in the computed R.D.

TABLE II

THE POSITIONS AND THE ASSIGNMENTS OF THE PEAKS IN THE R.D. CURVE

| peak | distance (Å) | assignment[a] |
|---|---|---|
| 1 | 1.33 | $C_1O_1(3)$ $C_1C_2(2)$ $C_1C_4(2)$ $CH(2)$ |
| 2 | 1.90 | $NiO_1(10)$ |
| 3 | 2.42 | $C_2O_1(2)$ $C_4O_1(2)$ $C_2C_4(1)$ $C_1C_3(1)$ $O_1O_2'(1)$ |
| 4 | 2.84 | $NiC_1(5)$ $C_3O_1(1)$ $O_1O_2(1)$ |
| 5 | 3.20 | $NiC_2(2)$ |
| 6 | 3.74 | $O_1O_1'(1)$ $O_1C_3'(1)$ $C_1C_5(1)$ |
| 7 | 4.25 | $NiC_4(3)$ $C_5O_1(1)$ |
| 8 | 4.75 | $O_1C_2'(1)$ $O_1C_1'(1)$ $O_1C_5'(1)$ $C_4C_5(0)$ |

a) These assignments correspond to the best models, G and F. Numbers in parentheses show approximately the relative magnitudes of $Z_iZ_j/r_{ij}$. The italicized atomic distances vary with the configuration of the chelate.

4.25 Å correspond to Ni–$O_1$*, Ni–$C_1$, Ni–$C_2$ and Ni–$C_4$, respectively. These four peaks are single or nearly single peaks because in these peaks one atomic pair has a predominant scattering power. Hence, it

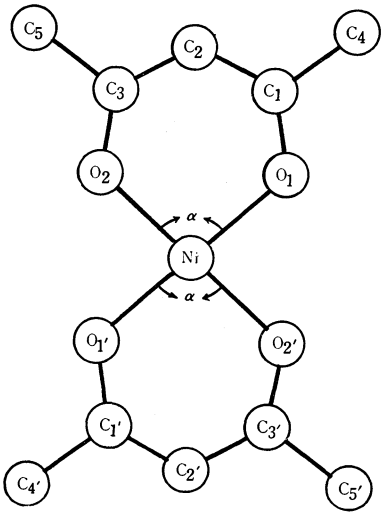



Fig. 2. The shape of the best model and the numbering of atoms.

appears most likely that the values of these interatomic distances are reliable. Furthermore, from the R. D. thus obtained, the reasonable model of the ligand molecule was estimated as follows. When the structure of the ligand is assumed to be as mentioned above, the geometric consideration of the $C_2$–$C_4$ and the $C_4$–$O_1$ (the 3rd perk at 2.42 Å) and the $C_1$–$C_5$ (the 6th peak at 3.74 Å) with the above four distances leads to the model having the following parameters: $\angle O_1NiO_2=92°$, $C_1$–$C_2=1.37$ Å, $C_1$–$O_1=1.26$ Å and $C_1$–$C_4=1.51$ Å. Then the structure of the molecule is determined by the configuration depending on the angle between two ligand planes. Thus the calculation of the theoretical intensity curves for planar and rectangular twisted models showed that the planar model could well reproduce the observed curve but the rectangular model could not. Details will be described below. However it is to be noted for the above assignment that if the molecule takes a rectangular form, the 5th peak can also be assigned to the $O_1$–$O_1'$ as well as to the Ni–$C_2$ (this assignment leads to $\angle O_1NiO_2=99°$). Also the height of the 5th peak is fairly low. Therefore the assignment of this peak and the value of the Ni–$C_2$ distance were carefully taken into consideration.

## Theoretical Intensity Curves

A calculation was made of the theoretical intensity curves for a number of models in order to determine the molecular structure in more detail and to check the accuracy of the interatomic distances obtained from the radial distribution method. However, in a complex molecule such as acetylacetone chelate, a complete determination of the molecular structure by the trial and error method would be very difficult on account of a large number of parameters. Therefore, in order to simplify this task, the present analysis was undertaken by the following assumption on the model. First, the interatomic distances of the Ni–$O_1$, Ni–$C_1$ and Ni–$C_4$, were taken to be equal to the most probable values obtained by R.D. method, i.e., 1.90, 2.84 and 4.25 Å, respectively. (The contribution of these atomic pairs to the total scattering power was about 40 %.) Secondly, the structure of the ligands was assumed to be the same as before ($C_{2v}$ symmetry). Then, it follows from the assumptions that molecular models can be determined by four independent parameters for the ligand, i.e., $\angle O_1NiO_2$ (denoted by $\angle\alpha$), $C_1$–$C_2$, $C_1$–$C_4$ and Ni–$C_2$ and the angle between the planes of the two ligands. As regards the configuration of the molecule, two cases of a planar form and a rectangular twisted form (including the tetrahedral form) were taken into account. Thus, the theoretical intensity curves were calculated of a large number of carefully selected models (about eighty) with various values for the above parameters. The values of the parameter $\angle\alpha$ was taken over the range from 84° to 110°, that of the $C_1$–$C_2$ from 1.32 Å to 1.57 Å. The value of the Ni–$C_4$ was taken to be 3.20 Å (the value obtained from the R.D.) and 3.10 Å (This smaller value makes the internuclear strain of the ligand smaller in the case of $\angle\alpha$=tetrahedral angle.) The length of $C_1$–$C_4$ was taken to be 1.54 Å and 1.51 Å, (because these values are quite reasonable and also because this bond nearly bisects $\angle O_1C_1C_2$ when $C_1$–$C_4$ is assumed to take these definite values.) These calculated intensity curves contain the contributions from all the atomic pairs, the pairs pertaining to hydrogen being

* The notation "Ni-$O_1$" also means Ni-$O_1'$, Ni-$O_2$ and Ni-$O_2'$ by the assumed symmetry of ligand. The situation is the same in the case of other atomic pairs.

ignored except for H–C bondings which were assumed to be 1.08 Å.

The calculation of the intensity curves was performed with the aid of Remington Rand punch cards. When these intensity curves are compared with each other with respect to the variation in the positions and the relative intensities of maxima and minima with the change of parameters, the following facts can be found. In general, the theoretical curves are particularly sensitive to the parameters, $\angle\alpha$ and $C_1$–$C_2$. The maxima and these minima sensitive to the parameters are the 8th, 9th, 11th and 12th maxima, and the 10th and 11th minima. The parameter $C_1$–$C_4$ does not seriously affect the intensity curve even when this distance differs from 1.54 and 1.51 Å so long as the Ni–$C_4$ distance does not change. It was also found that the long interatomic distances (greater than 5 Å such as $O_1$–$C_{4'}$, $C_1$–$C_{1'}$, $C_1$–$C_{2'}$, $C_1$–$C_{4'}$, $C_1$–$C_{5'}$, $C_2$–$C_{4'}$, etc.) contribute to the appearance of the 4th and 6th minima. (This contribution is about 7 %.) Some of the intensity curves are shown in Fig. 3.

TABLE III
MODELS FOR THE THEORETICAL INTENSITY CURVES

| model | $\angle\alpha$ | $C_1$–$C_2$ (Å) | $C_1$–$O_1$ (Å) | $C_1$–$C_4$ (Å) | Ni–$C_4$ (Å) | configuration |
|---|---|---|---|---|---|---|
| A | 88° | 1.32 | 1.23 | 1.54 | 3.20 | planar |
| B | 90° | 〃 | 1.26 | 〃 | 〃 | 〃 |
| C | 〃 | 1.42 | 1.20 | 〃 | 〃 | 〃 |
| D | 92° | 1.37 | 1.26 | 〃 | 〃 | 〃 |
| E | 〃 | 1.47 | 1.21 | 〃 | 〃 | 〃 |
| F | 94° | 1.37 | 1.28 | 1.54 | 〃 | 〃 |
| F′ | 〃 | 1.37 | 1.28 | 〃 | 〃 | rectangular |
| G | 96° | 1.32 | 1.34 | 〃 | 〃 | planar |
| $G_t$ | 〃 | 〃 | 〃 | 〃 | 〃 | 〃 |
| $G_{1.51}$ | 〃 | 〃 | 〃 | 1.51 | 〃 | 〃 |
| H | 〃 | 1.42 | 1.28 | 1.54 | 〃 | 〃 |
| I | 〃 | 1.52 | 1.23 | 〃 | 〃 | 〃 |
| J | 98° | 1.32 | 1.37 | 〃 | 〃 | 〃 |
| K | 〃 | 1.37 | 1.34 | 〃 | 〃 | 〃 |
| K′ | 〃 | 〃 | 〃 | 〃 | 〃 | rectangular |
| L | 〃 | 1.47 | 1.28 | 〃 | 〃 | planar |
| M | 100° | 1.37 | 1.37 | 〃 | 〃 | 〃 |
| M′ | 〃 | 〃 | 〃 | 〃 | 〃 | rectangular |
| N | 108° | 1.52 | 1.40 | 〃 | 〃 | planar |
| O | 110° | 1.52 | 1.43 | 〃 | 〃 | 〃 |
| O′ | 〃 | 1.52 | 〃 | 〃 | 3.10 | rectangular (nearly tetrahedral) |
| P | 96° | 1.32 | 1.31 | 〃 | 〃 | planar |
| Q | 100° | 1.37 | 1.34 | 〃 | 〃 | 〃 |
| Q′ | 〃 | 1.37 | 〃 | 〃 | 〃 | rectangular |
| R′ | 110° | 1.52 | 1.40 | 1.54 | 〃 | rectangular (nearly tetrahedral) |

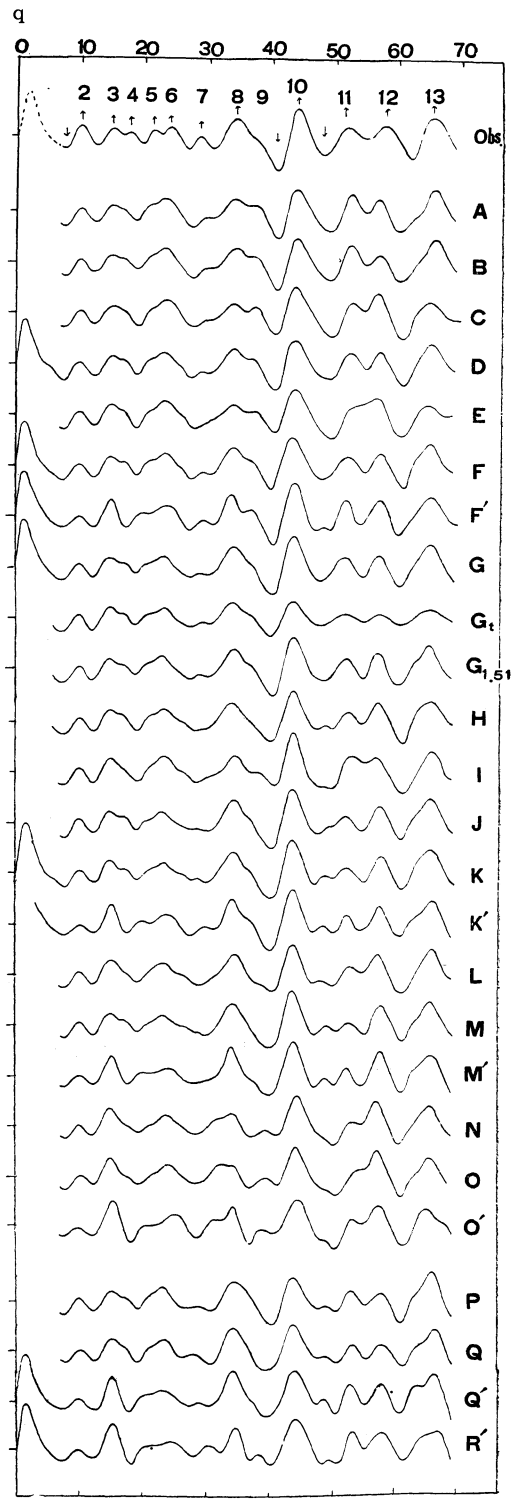



Fig. 3. The observed and the theoretical intensity curves.

The parameters of the corresponding models are listed in Table III. The curve A is unsatisfactory since the 8th maximum is too low and the 9th maximum is too high. Curve B is somewhat unsatisfactory in the same points as for the curve A as well as in the relative intensities of the 11th and 12th maxima. This model gives the lower limit of $\angle\alpha$. The curve C is unsatisfactory, because the 8th and 9th maxima (The observed 9th shelf was so faint that its position could not be measured definitely.) and the 10th minimum (too shallow) are not well reproduced. The curve D is acceptable. This model corresponds to the most probable one estimated from the R.D. curve. The curve E is unacceptable because of the features of the 7th, 8th and 9th maxima, the relative depths of the 10th and 11th minima and the features of the 11th and 12th maxima. The curve F is satisfactory. The curve G is also satisfactory and an agreement with the observed is better than the curve D in regard to the feature of the 9th shelf and the positions of the 11th and 12th maxima and the 11th minimum. The comparison of the curve G with the curve $G_{1.51}$ shows that the parameter $C_1$–$C_4$ is sensitive only to the relative heights of the 11th and 12th maxima. The curve H is somewhat unsatisfactory and provides the upper limit of $C_1$–$C_2$ since the 7th and 9th maxima are too faint. The curve I with $C_1$-$C_2$=1.52 Å is also unsatisfactory because of the feature of the 7th, 8th and 9th maxima and the relative depths of the 10th and 11th minima. The curve J is somewhat unsatisfactory because the relative heights of the 11th and 12th maxima deviate from observations and it provides the upper limit of $\angle\alpha$. The curve K is unacceptable because of the feature of the 11th maximum. The curve L is unacceptable. Model M having $\angle\alpha$ larger than 98° is unacceptable. Model N and O having $\angle\alpha$ almost equal to the tetrahedral angle are definitely unacceptable since they require the intensity curve which is discrepant from the observed curve particularly in regard to the range of $q$ from 30 to 60. In models having large $\angle\alpha$, $C_1$–$C_2$ cannot be taken smaller than the above value because $C_1$–$O_1$ becomes unreasonably longer than 1.42 Å. The above models are indicated in a parameter chart, Fig. 4. Although a number of intensity curves were also calculated for the corresponding

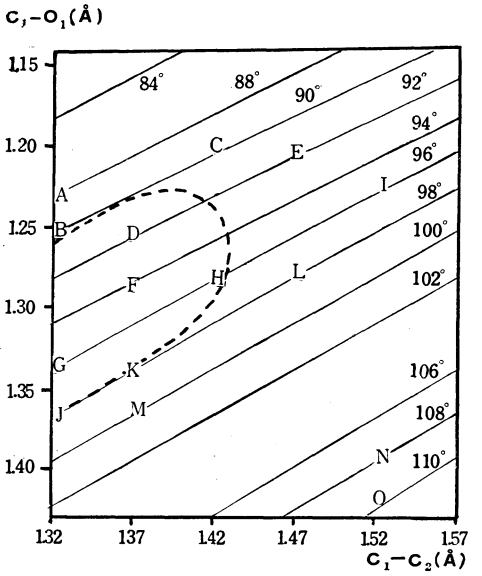



Fig. 4. Parameter chart. This chart shows the case of the parameter Ni–$C_2$ =3.20 Å. The positions of letters indicate the parameters of the models for which intensity curves are shown in Fig. 3.

models mentioned above with Ni–$C_2$=3.10Å, these curves did not agree with the observed one. Some of them are shown in Fig. 3. (see curve P and Q.) For example, if the curve P is compared with the corresponding curve G, it is found that the shortening of Ni–$C_2$ makes the 9th maximum lower and shifts the 11th maximum to a larger $q$ value. In the present analysis the value of Ni–$C_4$ was also varied, but better agreement could not be obtained. The calculations show that the parameter Ni–$C_4$ is sensitive only to the relative heights of 5th and 6th maxima. If the molecule takes a configuration with one ligand plane at right angles to the other ligand plane, such as in models F′, K′, M′ and O′ (The last is a tetrahedral model.), in general, the features of the 3rd and 4th (disappearing) maxima and the position of the 5th maximum disagree remarkably with those of the observed curve. It is to be noted that these changes occur in the range below $q$=30, because in regard to other acetylacetone chelates the configurations of these chelates can easily be determined by only the intensities in this part. Quite similar kinds of behavior are seen in the case of the models having Ni–$C_2$=3.10 Å such as models Q′ and R′. Therefore, all the rectangular models including the

tetrahedral models are ruled out*.

This conclusion was also confirmed by the computed R.D. shown by the vertical bars below the observed R.D. in Fig. 1. The positions of the bars show the interatomic distances; the heights of the bars are drawn proportional to $Z_iZ_j/r_{ij}$ of the respective atomic pairs. The upper computed R.D. corresponds to the model G which is in good agreement with the observed R.D. as regards the positions and the areas of the peaks. The R.D. F also agrees well with the observed R. D., whereas the computed R.D. F′ is in poor agreement with the observed R.D. with respect to the 5th, 6th and 8th peaks because the ratio of the area of each of these peaks to the sum of the heights of the corresponding bars extremely deviates from the ratio on other peaks. Here oblique arrows connect corresponding atomic pairs. Accordingly the planar model is superior to the rectangular twisted models. The lower R.D. corresponds to the tetrahedral model O′ and the disagreement with the observed R.D. is much enhanced. If the molecule takes the tetrahedral form, the 5th peak in the observed R.D. would rise and the 6th peak would disappear.

It must be mentioned also that the effect of molecular vibration was not taken into account in the above description because it did not seriously affect the features of the intensity curve below $q=70$. This effect was included in the calculation with the following values for root mean square amplitude, $<l_{ij}^2>_{Av}^{1/2}$, 0.07**Å for Ni–O, 0.06 Å for C–C, 0.05 Å for C–O, and 0.08 Å for C–H, by use of the formula:

$$I(q)=\sum_{i\neq j}(Z_iZ_j/r_{ij})\exp(-bq^2)\sin(\pi qr_{ij}/10),$$

where $b=(\pi^2/200)<l_{ij}^2>_{Av}$

As an example, curve $G_t$ is shown in Fig. 3. From the comparison of curve $G_t$ with curve G, it was found that this effect did not affect the positions and the relative intensities of the maxima and the minima except the introduction of simple intensity damping but that this effect produced a slight change in the relative intensities only for the 10th and 11th minima and the 11th and 12th maxima.

* The intensity curves were also calculated for the mixture of the planar and the rectangular models at the ratio of 25~75%, but these curves did not agree with the observed one.

** This value was obtained from a preliminary study on cobalt(II) acetylacetone chelate by the sector-microphotometer method. Also the values for non-bonding atomic pairs were estimated using the data and the calculated values on other compounds.

## Results

The computation of intensity curves showed that the general appearance of the the photographs was well reproduced by planar model. In the parameter chart, Fig. 4, the dashed line separates satisfactory models from unsatisfactory ones with due regard to atomic vibrations. The $q$ values of the maxima and the minima for best model are listed in Table I for comparison with those of the observed maxima and minima. From the analysis described above, the molecule of bisacetylacetone-nickel(II) was found to have the planar configuration, with the following parameters: Ni–$O_1$=1.90 Å, Ni–$C_1$=2.84 Å, Ni–$C_2$=3.20 Å, Ni–$C_4$=4.25 Å (These values were obtained from the R.D. and the correctness of these values were checked by the calculations of the theoretical intensity curves.), $\angle\alpha=94\pm4°$, $C_1$–$C_2$=1.37 ±0.05 Å, $C_1$–$O_1$=1.30±0.06 Å, and $C_1$–$C_4$ =1.51 Å~1.54 Å. Although it is impossible to determine accurately C–C and C–O distances on account of the complexity of the molecule, it is an important conclusion that the chelate has a planar configuration with Ni–O distance equal to 1.90 Å.

## Discussion

It is convenient to discuss the results under two headings: (i) bond lengths and bond types, and (ii) stereochemical configuration.

(i) *Bond lengths and bond types.* It must, at first, be mentioned that the observed Ni–O distance of 1.90 Å leads to the radius 1.24 Å for Ni(II) in square configuration with coordination number 4, in contrast with the known radius, 1.39 Å in octahedral configuration, although Pauling[8] estimated the square radius of Ni(II) to be 1.21 Å from the octahedral radius.

The observed Ni–O distance is slightly greater than the sum of the covalent radius of oxygen (0.66 Å) and the metallic radius[9] of nickel with a coordination number 8 (1.22 Å), but is in good agreement with the sum of the covalent radius of oxygen and the metallic radius[9] of nickel with a coordination number 12 (1.25 Å) or the neutral atomic radius[10] (1.24 Å). This may afford an evidence for the Ni–O bond is fairly covalent. On the

8) Ref., 5, chapt. 5.
9) Ref., 5, chapt. 11.
10) N. V. Sidgwick, "The Chemical Elements and their Compounds" Vol. II, Oxford Univ. Press, (1950), p. 1317.

other hand, if Ni–O bond were purely ionic, the distance would be predicted from a simple calculation* to be about 2.2 Å. Such examples are NiO, $NiSO_4 \cdot 6H_2O$, and $NiSO_4 \cdot 7H_2O$[11], in which Ni–O distances have actually been found to be equal to 2.0~2.2 Å. Because no structure of chelates containing an Ni–O bond has yet been studied in detail, the Ni–O bond length observed for bisacetylacetone-nickel (II) cannot directly be compared with other data. The recent data on Ni $(CH_3COO)_2 \cdot 4H_2O$[12] gave about 2.1 Å for Ni–O, but this bond may be considered to be essentially ionic.

Bisacetylacetone-nickel(II) chelate possesses non-ionic properties and a considerable stability. The non-ionic properties of the chelate, i.e., the volatility and the solubility in organic solvents, may naturally be explained by the covalent character of the Ni–O bonds described above. It is noticed that the Ni–O bond length is almost equal to the covalent bond length although the electronegativity difference between Ni and O atoms leads to an ionic character of about 50 per cent. for the Ni–O bond. This is presumably due to the formation of double bond by use of some of the $d\pi$-type orbitals of the nickel atom. On the other hand, the stability of the chelate is attributable to the great strength of $dsp^2$ hybrid orbitals of nickel atom. This seems to be also due to the contributions of many resonance structures of the ligand molecule which are due to the conjugation among $2p\pi$ orbitals of ligand atoms and $3d\pi$ or $4p\pi$ orbitals of the nickel atom. Further, the fact that the chelate forms the planar rather than the tetrahedral configuration makes more possible the conjugation over the whole molecule consisting of eleven members, resulting in the enhanced stability of the chelate.

(ii) *Stereochemical configuration.* In general, it is well known[13] that the quadricovalent complexes of copper(II) are invariably planar, whereas those of nickel(II) and cobalt(II) may be either planar or tetrahedral depending on the ligand. It is generally found further that with nickel(II) complexes the choice of these configurations is particularly sensitive to the electronegativity of the donor atoms. In other words, Ni(II) complexes with the donor atoms, N or S take a planar configuration and those with O take the tetrahedral one. No planar configuration of the Ni(II) complexes having the donor atoms of O has been found experimentally until the present study was made on bisacetylacetone-nickel(II) chelate.

According to magnetic measurement[1,3], bisacetylacetone-nickel(II) chelate is paramagnetic. From this result, Pauling presumed that Ni(II) has the tetrahedral orbitals which are constructed from $sp^3$ hybridization. The present result is contradictory to his presumption, although it seems likely that magnetic data do not necessarily exclude the planar form because the promotion of a $3d$ electron to a $4p$ orbit makes the chelate paramagnetic even in $3d4s4p^2$ planar configuration and also the use of $4d$ orbit makes it likewise paramagnetic in $4s4p^24d$ planar configuration as suggested by Huggins[14].

However, the present result that the chelate takes the planar rather than tetrahedral configuration seems to be not surprising because $dsp^2$ bonds are stronger than $sp^3$ bonds and moreover the conjugation over the whole molecule in favor of the planar form probably makes the chelate more stable. Some energy may be, of course, required when the Ni(II) takes the electron configuration of $3d4s4p^2$ with paired electrons promoted in one of the $3d$ orbitals or an unpaired electron promoted in one of the $4p$ orbitals. However, such promotion energy will probably be compensated by the stabilization energy acquired by taking this configuration.

It is interesting to note for the above contradiction that the present experiment deals with free molecules at a high temperature, while magnetic measurement and other experiments deal with the chelate in the solid state at room temperature. If the presumption of Pauling is true, it is possible that the configuration of the chelate would vary with the phase change (or temperature**), taking planar in gaseous state and tetrahedral in solid state, because the energy difference between

* Pauling's univalent ionic radii were used after the correction for the ionic valence and coordination number.

11) R. W. G. Wyckoff, "Crystal Structure", Interscience Publishers, New York, Vol. I (1948), Vol. II (1951).

12) J. N. van Niekerk and F. R. L. Schoening, *Acta Cryst.*, **6**, 609 (1953).

13) Ref., 4, p. 278.

14) M. L. Huggins, *J. Chem. Phys.*, **5**, 527 (1937).

** In genaral, the configuration of the chelate is distinguishable by the color of the chelate. Although it is doubtful whether the following is related to the above or not, it is actually observed in experiment that the green color of the chelate was slightly tinged with yellow on heating. (Ref., 5, p. 122).

the planar and the tetrahedral structures is very small. Recently it is found that, for example, bis-N-methylsalicylaldimine-nickel(II)[15] behaves in a similar manner although all such chelates hitherto reported have both N and O atoms as donors. In order to clarify the above suggestion and the discrepancy between the conclusions from the magnetic data and the electron diffraction data on bis-acetylacetone-nickel(II), the following two investigations are very desirable; the complete determination of the structure of the chelate on single crystals by X-ray method*** and the measurement of the magnetic moment of the chelate in gaseous state. The latter will also give the information on the electronic state of Ni(II) atom which has the planar orbitals.

The author wishes to thank Professor M. Kubo for his valuable advice and encouragement, and Professor Y. Morino for his kindness in providing facilities for the numerical computations by punch cards. The author also expresses his deep appreciation to the Ministry of Education for supporting this research.

*Department of Chemistry, Faculty of Science, Nagoya University*
*Chikusa, Nagoya*

15) S. Fujii and M. Sumitani, *Science Repts. Tôhoku Univ., First Series*, **37**, 49 (1953); J. B. Willis and D. P. Mellor, *J. Amer. Chem. Soc.*, **69**, 1237 (1947).

*** Our preliminary investigation by powder method showed that the chelate has probably the tetrahedral configuration.

# *A New Analytical Method of Electroconductivity Data of Surfactant Solutions. I**

By Kenjiro MEGURO, Tamotsu KONDO, Noriaki OHBA, Takashi INO and Osamu YODA

(Received December 15, 1956)

In the estimation of *C. M. C.* value by the electroconductivity method, the equivalent conductivity ($\Lambda$) *vs.* square root of concentration ($\sqrt{c}$) diagram or the specific conductivity ($\kappa$) *vs.* concentration ($c$) diagram plays an important role. In the former diagram the *C. M. C.* has been defined as an intersecting point of two curves; one is a straight line below *C. M. C.* and the other is a concave curve above it.

In many cases, however, the precise examination of experimental data shows that the plots of conductivity in highly diluted regions are not a straight line[1], but a slight maximum appears[2]. The deviation from a straight line is especially conspicuous when surfactant molecules contain a double long chain alkyl group[3] or highly hydrated counter ions[4]. The similar effects upon the conductivity result from the addition of a solvent[5], such as dioxane or alcohol, to surfactant solutions.

On the other hand, it is well known that the Kohlrausch's equation is not applicable exactly to the conductivity of a simple electrolyte. Therefore, it may be unsuitable to treat the plots of electroconductivity data below *C. M. C.* as a straight line, as if they obeyed the Kohlrausch's equation.

In a simple electrolyte solution, the electroconductivity usually obeys a corrected formula such as Onsager's[6] or Shedlovsky's[7] approximate equation:

Onsager's approx. eq.

$$\Lambda=\Lambda_0-A\sqrt{C}+BC, \qquad (1)$$

Shedlovsky's approx. eq.

* Presented at the 9th Annual Meeting of the Chemical Society of Japan held in Kyoto, April, 1956.

1) P. F. Grieger and C. A. Kraus, *J. Am. Chem. Soc.*, **70**, 3803 (1948).

2) M. E. L. McBain, W. B. Dye and S. A. Johnston, ibid., **61**, 3210 (1939).

3) A. W. Ralston, D.N. Eggenberger and P.L. DuBrow, ibid., **70**, 977 (1948).

4) G. L. Brown, P. F. Grieger and C. A. Kraus, ibid., **71**, 95 (1949).

5) E. C. Evers and C. A. Kraus, ibid., **70**, 3049 (1948).

6) L. Onsager, *Physik. Z.*, **27**, 388 (1926).

7) T. Shedlovsky, *J. Am. Chem. Soc.*, **54**, 1405 (1932).

TABLE I

COMPARISON OF THE CONDUCTIVITY AT THE MINIMUM OR THE MAXIMUM POINT WITH THE *C. M. C.* ESTIMATED BY THE USUAL METHODS

| Subst. | $C_{min}$ | $C_{max}$ | *C. M. C.* (in mM./l.) estimated by: Elect. conductivity | Dye | Surface tension | Viscosity | Solubilization | Light scatt. | Trans port number | Osmotic coeff. | Vapor press. |
|---|---|---|---|---|---|---|---|---|---|---|---|
| $C_{10}SO_3Na$ | 40° 40 | 40° 91.5 | 40° 40 | 38.7 | 40° 36.4 | | | | | | |
| $C_{10}SO_4Na$ | | | | room 26.2 | | | | | | | |
| $C_{10}$ K soap | | | | 25° 99.8 | | | 71.4 | | | | |
| $C_{10}N^+(CH_3)_3Br^-$ | 40° 51.0 | 40° 103.7 | 40° 70 | 63.6 | | | | 70 | | | |
| $C_{12}SO_3Na$ | 40° 10.5 | 40° 27.2 | 40° 11.0 | 23.5° 9.8 | 40° 10.0 | 40° 12 | 10 | | | | |
| $C_{12}SO_4Na$ | 30° 6.08 | 30° 20.2 | 40° 8.9 | room 5.8 | 40～75° 6～9.6 | | | | | | 30° 7.0 |
| $C_{12}$ K soap | | | | 25.8° 23.5 | | | 21.4 | | | 11.1 | 20.5 |
| $C_{12}$ Na soap | 40° 22.5 | 40° 59 | 40° 28 | | | 96 | 50° 26 | | | | 27 |
| $C_{12}N^+(CH_3)_3Br^-$ | 40° 12.1 | 40° 34.2 | 40° 17.5 | | | | | 15 | | | |
| $C_{12}N^+$⬡$Br^-$ | | | 30° 12.0 | room 11.5 | | | | | | | 30° 20.6 |
| $C_{12}NH_3Cl$ | 60° 12.1 | 60° 44.1 | 60° 13 | | | 15 | 14 | | 30° 15 | | 30° 16.5 |
| $C_{14}SO_3Na$ | 40° 2.71 | 40° 8.51 | 40° 2.5 | | 40° 2.6 | | | | | | |
| $C_{14}NH_3Cl$ | 60° 2.91 | 60° 16.1 | 60° 4.0 | | | | | | 30° 4.0 | | |

$$\Lambda_0 = \frac{\Lambda - \beta\sqrt{C}}{1-\alpha\sqrt{C}} - BC, \qquad (2)$$

in which $A$, $B$, $\alpha$ and $\beta$ are constants, and $BC$ is a corrected term for the higher order interaction between ions.

The fact of micelle formation of surfactant ions suggests that the interaction of those ions can not be neglected even in an appreciably dilute region below *C. M. C.* Accordingly, it is more reasonable to adopt the Onsager's equation (1) etc. than the Kohlrausch's equation, because we must consider the contribution of the interaction between surfactant ions to the conductivity in solution of the concentration below *C. M. C.* The deviation from the Onsager's equation (1) must be considered as "real deviation from the simple electrolyte".

The order of approximation of Shedlovsky's equation is higher than that of Onsager's equation, but we use the Onsager's equation (1) in this report to simplify the calculation and the analysis.

Now we defined the quantity;

$$(\Lambda_0 - \Lambda)/\sqrt{C}, \qquad (3)$$

which is denoted by $H$ and can be expressed as follows;

$$H = (\Lambda_0 - \Lambda)/\sqrt{C} = A - B\sqrt{C}. \qquad (4)$$

If the quantity $H$ is plotted against $\sqrt{C}$, the $H$ *vs.* $\sqrt{C}$ diagram becomes a straight line in the case of the simple electrolyte, and the intercept on the axis of $H$ is equal to $A$, while the slope of the plots gives $B$, the coefficient of corrected term.

In the case of surfactant solution, the deviation, from the linearity is observed in diluted region, that is, the remarkable minimum or kink and maximum are found in the diagram. Therefore, we use merely the value $B$ as a parameter to appraise the slope of curve and not to show the corrected term exactly.

This deviation can be considered as "real deviation from the simple electrolyte", and will be due to the micelle formation. In Fig. 1 the relation between the

usual *C. M. C.* and the concentration at the minimum or the maximum point is shown by the arrow line.

It is noticed here that the value $\Lambda_0$ which is necessary to draw the above diagram was obtained by the extrapolation of the plots to infinite dilution in usual $\Lambda$ *vs.* $\sqrt{C}$ diagram, because the data in very diluted concentration—more diluted than the concentration where the slight maximum appears—can be treated as being in accordance with the Kohlrausch's equation.

The concentration of minimum does not always coincide with the usual *C. M. C.*; rather it is situated in the lower concentration than the latter. The numerical values of the concentration corresponding to the minimum or the maximum in contrast with the usual *C. M. C.* determined by various methods are listed in Table I. From this table it is found that the usual *C. M. C.* values determined by various methods fall into the region between the minimum and the maximum. We adopt this minimum and this maximum as parameters to show the critical phenomenon in surfactant solution, instead of the *usual C. M. C.*, and will show by the actual example that this method is more reasonable than the usual one.

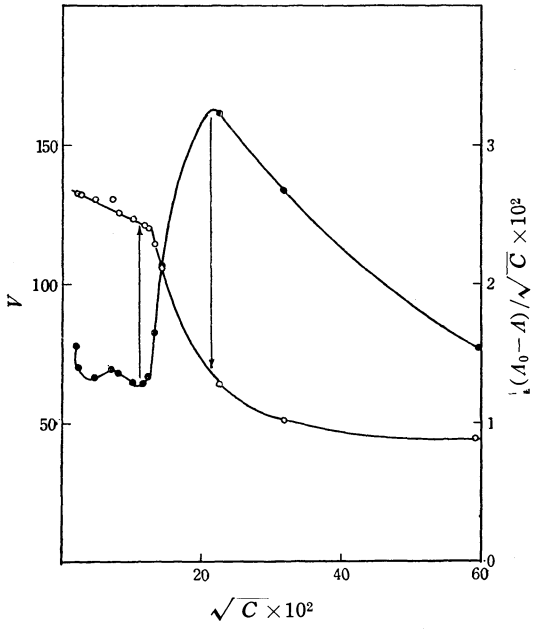



Fig. 1. Comparison of $(\Lambda_0-\Lambda)/\sqrt{C}$ *vs.* $\sqrt{C}$ diagram with the $\Lambda$ *vs.* $\sqrt{C}$ diagram for dodecyl trimethyl ammonium bromide;
○ $\Lambda$ *vs.* $\sqrt{C}$, ● $(\Lambda_0-\Lambda)/\sqrt{C}$ *vs.* $\sqrt{C}$.

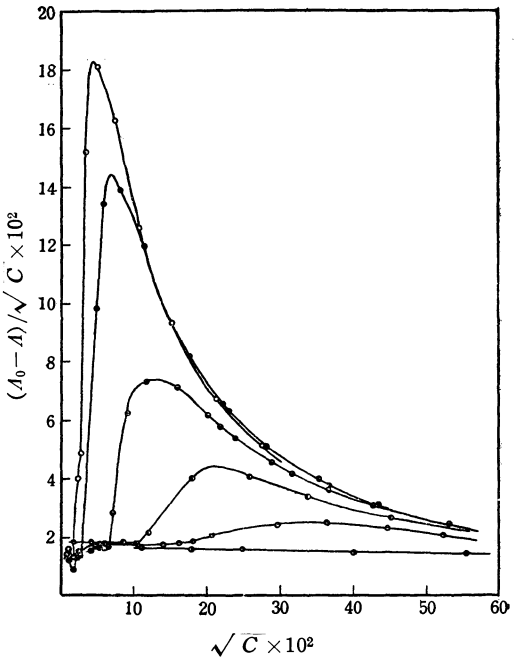



Fig. 2. $(\Lambda_0-\Lambda)\sqrt{C}$ *vs.* $\sqrt{C}$ curves for the aqueous solution of ○ octadecyl-, ● hexadecyl-, ◒ tetradecyl-, ◐ dodecyl-, ◓ decyl-, and ◑ octyl ammonium chlorides at 60°C.

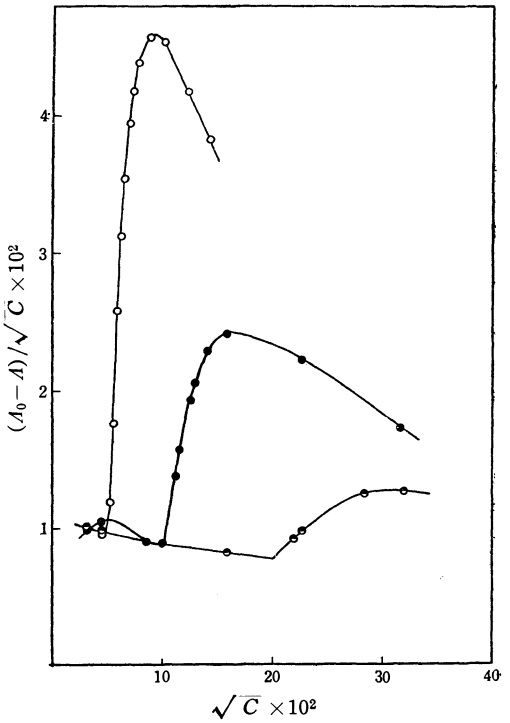



Fig. 3. $(\Lambda_0-\Lambda)/\sqrt{C}$ *vs.* $\sqrt{C}$ curves for the aqueous solution of ○ sodium tetradecyl-, ● sodium dodecyl- and ◓ sodium decyl-sulfonate at 40°C.

### Effect of Alkyl Chain Length

The effect of alkyl chain length on the *C. M. C.* has been investigated by some authors and they have concluded that the longer the chain length, the lower the *C. M. C.*

Applying our method to the data of alkyl ammonium chlorides[8,9] and sodium alkyl sulfonates[10], we obtained the following results as shown in Figs. 2 and 3.

(a) Each curve shows a remarkable minimum and a maximum.

(b) The position of the minimum or the maximum shifts toward lower concentration with increasing alkyl chain length.

(c) The value of $H$ at the maximum position increases with the length of alkyl chain.

(d) The slope between the minimum and the maxium becomes steep with the increase in the length of alkyl chain.

Harkins[11] found the following relation between the *C. M. C.* and alkyl chain length.

$$\log C.M.C. = a + bN, \qquad (5)$$

in which $a$ and $b$ are constants and $N$ is the number of carbon atoms in an alkyl radical. A similar relation can be obtained by plotting the logarithm of the position of the minimum or the maximum against the number of carbon atoms in an alkyl radical. Fig. 4 shows the relation between $\log C_{min}$ or $\log C_{max}$ and $N$.

As the concentration at the minimum is nearly equal to the *C. M. C.* determined by Harkins. it is natural to obtain such a linear relation between the position of minimum and the number of carbon atoms. However, no attention has been paid to the concentration of the maximum position, the magnitude of which is several times that of the usual *C. M. C.* We found that a similar relation also exists between the position of the maximum and the number of carbon atoms. This fact is very interesting and could not be found at all by any of the earlier methods.

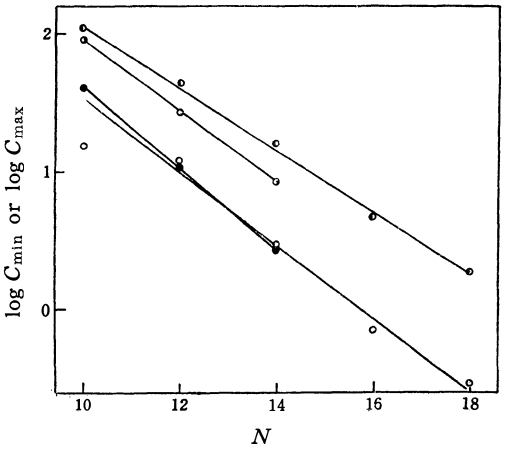



Fig. 4. The relation between logarithm of $C_{min}$ or $C_{max}$ and the number of carbon atoms, $N$, in an alkyl radical : for alkyl ammonium chlorides, ○ $C_{min}$ and ◐ $C_{max}$; for sodium sulfonates, ● $C_{min}$ and ◑ $C_{max}$.

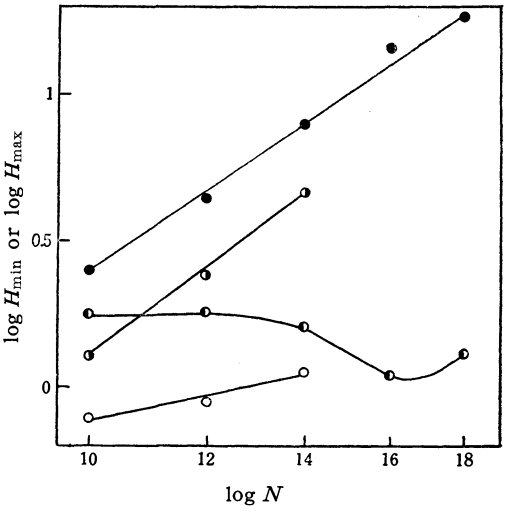



Fig. 5. log $H$ *vs.* log $N$ diagram for alkyl ammonium chlorides, ◐ $H_{min}$, ● $H_{max}$; for sodium alkyl sulfonates, ○ $H_{min}$ and ◑ $H_{max}$.

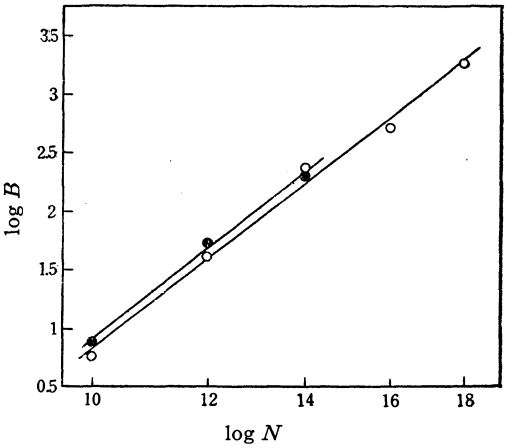



Fig. 6. log $B$ *vs.* log $N$ diagrams, ○ alkyl ammonium chlorides and ● sodium alkyl sulfonates.

8) A. W. Ralston, C. W. Hoerr and K. J. Hoffman, *J. Am. Chem. Soc.*, **64**, 97 (1942).
9) A. W. Ralston and C. W. Hoerr, ibid., **64**, 773 (1942).
10) K. A. Wright, A. D. Abott, V. Sivertz and H. V. Tartar, ibid., **61**, 549 (1939).
11) M. L. Corrin and W. D. Harkins, ibid., **65**, 692 (1943).

On the other hand, when we plot both logarithms of $H$ and $B$ against the logarithm of $N$, we can also find a linear relation between them. These results are shown in Figs. 5 and 6.

The values of $B$ are almost the same in the case of the samples containing the equal number of carbon atoms. For reference the $B$ values obtained for many examples are shown in Table II. This fact may be used to estimate the alkyl chain length of an unknown surfactant.

TABLE II
$B$ VALUES FOR OBTAINED VARIOUS SURFACTANTS

| Substance | | $B$ |
|---|---|---|
| $C_{18}H_{37}NH_3Cl$ | 60° | 1800 |
| $N^+$⟨⟩$Cl^-$ | 25° | 1530 |
| $N^+(CH_3)_3Br^-$ | 25° | 1200 |
| $C_{16}H_{33}NH_3Cl$ | 60° | 517 |
| $N^+$⟨⟩$Cl^-$ | | 1080 |
| $N^+(CH_3)_3Br^-$ | 60° | 375 |
| $C_{14}H_{29}NH_3Cl$ | 60° | 238 |
| $SO_3Na$ | 40° | 201 |
| $C_{12}H_{25}NH_3Cl$ | 60° | 41 |
| $SO_3Na$ | 40° | 56 |
| $OSO_3Na$ | 25° | 59 |
| $N^+(CH_3)_3Br^-$ | 60° | 35 |
| $C_{10}H_{21}NH_3Cl$ | 60° | 6 |
| $SO_3Na$ | 40° | 8 |
| $N^+(CH_3)_3Br^-$ | 60° | 6 |

## Effect of the Number of Alkyl Chains

Ralston[12] found an anomalously high $\Lambda$ value in a low concentration region of the surfactant containing two long alkyl chains, such as dialkyl ammonium salts, and he reported that it was difficult to determine the *C. M. C.* exactly owing to this anomalous maximum.

According to our method, however, it is easy to determine the minimum and the maximum values even in such a case. The result obtained is shown in Fig. 7. The anomality does not appear in our analysis as in the case of compounds with a single long chain, except the fact that the minimum merely becomes more pronounced in this case.

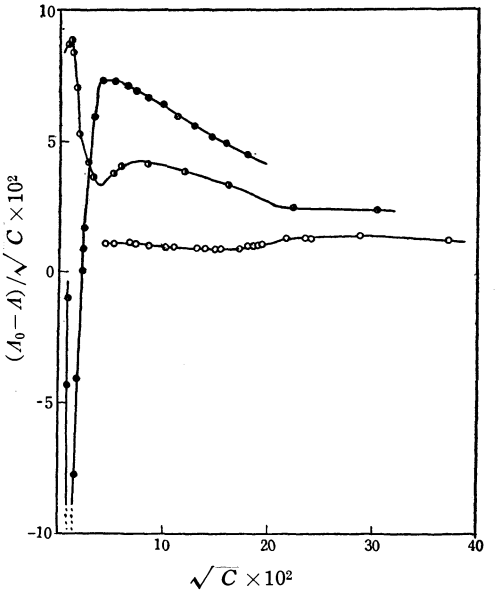



Fig. 7. $(\Lambda_0-\Lambda)/\sqrt{C}$ *vs.* $\sqrt{C}$ diagram, for the aqueous solutions of ○ dioctyl-, ◑ didecyl- and ● didodecyl- dimethylammonium chlorides.

## Effect of Ionic Head Group

Now we extend our analysis to the compounds with an alkyl chain of the same length but a different ionic head group.

TABLE III
VALUE OF $C_{min}$, $C_{max}$, $H_{min}$, $H_{max}$, $B$ AND THE USUAL *C. M. C.*, SHOWING THE EFFECT OF IONIC HEAD GROUP

| Substance | | $C_{min}$ | $C_{max}$ | $H_{min}$ | $H_{max}$ | $B$ | *C. M. C* |
|---|---|---|---|---|---|---|---|
| $C_{12}H_{25}SO_3Na$ | 40° | 10.5 | 27.2 | 0.89 | 2.42 | 56 | 11.0 |
| $C_{12}H_{25}OSO_3Na$ | 20° | 6.08 | 20.2 | 0.50 | 2.20 | 58.8 | 8.6 |
| $C_{11}H_{23}COONa$ | 40° | 22.5 | 59.0 | 1.18 | 1.78 | 129 | 28 |
| $C_{18}H_{37}NH_3Cl$ | 60° | 0.78 | 1.85 | 4.50 | 18.3 | 1800 | 0.53 |
| $C_{18}H_{37}N^+(CH_3)_3Cl^-$ | 25° | 0.29 | 0.99 | 3.65 | 13.3 | 1200 | 0.34 |
| $C_{18}H_{37}N^+$⟨⟩$Cl^-$ | 25° | 0.24 | 1.09 | 0.30 | 11.0 | 1530 | 0.25 |

12) A. W. Ralston, D.N. Eggenberger and P.L. DuBrow, *J. Am. Chem. Soc.*, **70**, 977 (1948).

For this purpose the data for sodium dodecyl sulfate[13,14], sodium dodecyl sulfonate[15] and sodium dodecanoate[16] as anionic surfactants, and those for octadecyl ammonium chlorides[8], octadecyl pyridonium chloride[5] and octadecyl trimethyl ammonium chloride[1] as cationic surfactants, were analysed, in which sodium dodecanoate and octadecyl ammonium chloride were chosen especially as hydrolysable surfactants.

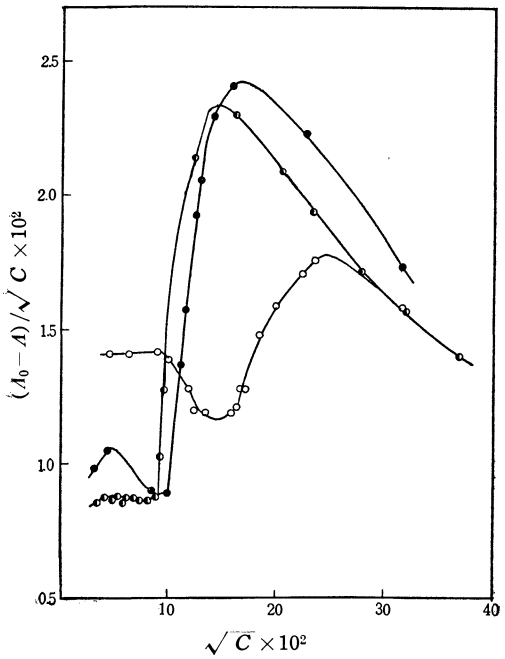



Fig. 8. $(\Lambda_0-\Lambda)/\sqrt{C}$ *vs.* $\sqrt{C}$ diagram for the aqueous solutions of ◐ sodium dodecyl sulfate, ● sodium dodecyl sulfonate and ○ sodium dodecanoate at 40°C.

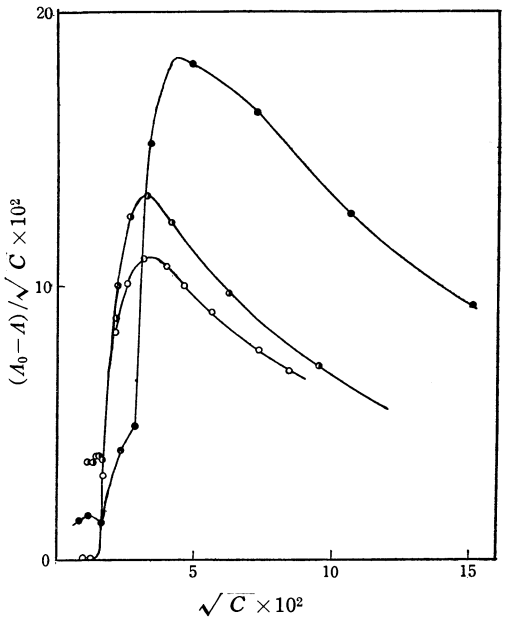



Fig. 9. $(\Lambda_0-\Lambda)/\sqrt{C}$ *vs.* $\sqrt{C}$ diagrams for the aqueous solutions of ● octadecyl ammonium chlorides at 60°C, ◑ octadecyl trimethyl ammonium chloride at 25°C and ○ octadecyl pyridonium chloride at 25°C.

The results are shown in Figs. 8 and 9. The obtained value of $C_{min}$, $C_{max}$, $H_{min}$, $H_{max}$ and $B$ are tabullated in Table III, in which the values of *C. M. C.* estimated by the usual method are given in the last column for reference.

The authors wish to thank Professor B. Tamamushi, Tokyo University, for his encouragement and advice in this work.

*Nedzu Chemical Laboratory*
*Musashi University*
*Nerima, Tokyo*

13) A. F. Ward, *Proc. Roy. Soc.*, **A176**, 412 (1940).
14) A. F. Ward, *J. Chem. Soc.*, **1939**, 522.
15) K. A. Wright, A. D. Abott, V. Sivertz and H. V. Tartar, *J. Am. Chem. Soc.*, **61**, 599 (1948).
16) P. Eckwall, *Kolloid Z.*, **101**, 135 (1942).

# *Oxidimetric and Reductometric Titrations in Neutral Solutions. (Application of Sodium Triphosphate as Masking Agent to Volumetric Analysis.)*

By Susumu SUZUKI, Kenji HARIMAYA, Morio UENO, Nobuo TSUJI and Noriko YAMAOKA

(Received December 12, 1956)

In the estimation of metallic ions in neutral media by means of oxidimetric or reductometric titrations, most of them produce insoluble hydroxides or carbonates. In the case of iron (II), its hydroxide is oxidized by the air. So the determination is incomplete. The same is the case with titanium (III). With a view to avoid these effects, the present authors have been trying to apply masking reactions to such cases. In the present paper, they show the use of polyphosphates as the masking agent and as complexing agent, and the extention of the new method will be described. The stability of the reducing standard solutions is also studied.

## Oxidimetric Titration

**Reagent.**—The same oxidizing standard solutions given below were used as in the case of acidic media: one tenth normal solution of ceric sulfate, sodium vanadate, potassium-dichromate, -bromate, -permanganate and -triiodide. Two tenth % solutions of redox indicators were used, namely amarance for bromometry, cacoterin for chromometry, and crystal violet for permanganimetry. Sodium bicarbonate was used for neutralization and sodium triphosphate for masking.

**Materials.** — One tenth N solutions of iron (II)-, titanium(III)- and chromium(II)- sulfate, sodium -vanadate and -molybdate, thallium(I) nitrate, tin(II)- and antimony(III)- chloride, sodium arsenite and selenium dioxide were prepared (if necessary in an acid medium) and standardized by the usual methods.

**Procedure.**—Take an aliquot sample solution, add 3 g. of solid sodium triphosphate hexahydrate, stir gently, and add solid sodium bicarbonate in small portions until some pieces remain undissolved. Add a few drops of indicator and titrate with the standard solution. The solution should be moderately and constantly stirred in the course of titration. When too much triphosphate is added, a precipitate may appear. If necessary, add more sodium bicarbonate to keep the solution neutral.

## Result and Discussion

(*A*) *Permanganimetry.* ($Fe^{2+}$, $Ti^{3+}$, $VO^{2+}$, $Cr^{2+}$, $Mo^{5+}$, $Tl^{+}$.) : As the masking force of triphosphate for manganese chloride is incomplete, chlorides should not be present in the sample. In the titration of iron (II), it is completely masked with triphosphate in a neutral medium and the results are satisfactory (Table I). When a fairly

TABLE I
PERMANGANATE METHOD

| Element | Sample formula | Element mg. Content | Element mg. Found |
|---|---|---|---|
| Fe | $FeSO_4$ | 54.6<br>163.8 | 54.5<br>163.5 |
| Cr | $CrSO_4$ | 42.4<br>127.4 | 42.3<br>127.4 |
| Mo | $Mo_2(SO_4)_5$ | 55.4<br>166.2 | 55.4<br>166.7 |
| Ti | $Ti_2(SO_4)_3$ | 52.1<br>156.3 | 52.6<br>154.9 |
| Tl | $Tl_2SO_4$ | 50.2<br>150.6 | 50.1<br>149.6 |
| V | $VO(SO_4)$ | 36.7<br>110.1 | 36.3<br>109.4 |

large amont of titanium(III) is titrated, a gelatinous substance is precipitated. The end point is given by the color change from gray to pink. Vanadium(IV) prepared by means of liquid amalgam method, is yellowish green in a neutral solution, and the end point is given by the pink color of permanganate. Chromium(II) is also green in a neutral solution, and it is not difficult to find the end point in permanganimetry. Molybdenum(V) has a pale brown color in a solution containing triphosphate; no precipitate is perceived in solutions of quinquevalent as well as hexavalent molybdenum on addition of triphosphate. Thallium(I) is oxidized to thallium(III), which gives no precipitate (Table I).

(*B*) *Bromometry* ($Sn^{2+}$, $Fe^{2+}$, $Ti^{3+}$, $As^{3+}$, $Sb^{3+}$, $Se^{4+}$.): As methyl orange has a yellow color itself in a neutral medium, it is difficult to determine the end point by its decoloration. Amarans is a good redox indicator in a neutral solution which has a red color and is decomposed by oxidizing agents after the element to be oxidised has been quantitatively oxidized. Tin(II) and others are thus completely estimated bromometrically (Table II). The blank for 2 drops of the 0.2% indicator solution is about 0.01 ml. of each 0.1 N oxidizing standard solution.

TABLE II
SODIUM HYPOBROMITE METHOD

| Element | Sample formula | Element mg. | |
|---|---|---|---|
| | | Content | Found |
| As | $Na_3AsO_3$ | 34.6 | 34.7 |
| | | 103.8 | 104.1 |
| Fe | $FeSO_4$ | 30.9 | 31.1 |
| | | 92.7 | 92.5 |
| Sb | $SbCl_3$ | 41.1 | 41.2 |
| | | 123.3 | 123.5 |
| Se | $SeO_2$ | 33.8 | 33.9 |
| | | 101.4 | 102.0 |
| Sn | $SnCl_2$ | 35.2 | 35.2 |
| | | 105.6 | 104.9 |
| Ti | $Ti_2(SO_4)_3$ | 43.2 | 43.0 |
| | | 129.6 | 128.6 |

(*C*) *Chromometry* ($Fe^{2+}$, $Ti^{3+}$, $Sn^{2+}$, $Sb^{3+}$.): The leuco compound is formed when methylene blue is added to iron(II) sample solution; at the end point, the former is oxidizied to the colored state. In the case of titanium(III) or tin(II), cacoterin is added which combines with these metals forming colored compounds that are decomposed and decolored at the end point. In the estimation of antimony(III), the end point is determined when the yellow color of chromate is perceived in the green color of the solution (Table III).

TABLE III
POTASSIUM DICHROMATE METHOD

| Element | Sample formula | Element mg. | |
|---|---|---|---|
| | | Content | Found |
| Fe | $FeSO_4$ | 45.3 | 45.2 |
| | | 135.9 | 136.4 |
| Sb | $SbCl_3$ | 37.6 | 37.2 |
| | | 112.8 | 111.4 |
| Sn | $SnCl_2$ | 30.9 | 29.9 |
| | | 92.7 | 91.5 |
| Ti | $Ti_2(SO_4)_3$ | 43.2 | 43.6 |
| | | 129.6 | 127.8 |

(*D*) *Vanadometry* ($Fe^{2+}$, $Ti^{3+}$, $Sn^{2+}$, $Sb^{3+}$): The metal ions are estimated using methylene blue for iron(II), titanium(III) and molybdenum(V), and cacoterin for tin(II) (Table IV).

In the above-mentioned oxidation titrations, the effect of the following elements was studied:

Li, Na, Ca, K, Sr, Ba, Mg, Cu, Zn, Cd, B, Al, Pb, Nb, As, Mn, Sb, Cr, Ni, Co, Bi, F, Si, Zr, Th, Ce, Tl, Be, W, Ag, Hf, U, Mo, Sn, Fe, Pt, Os, Rh, Pd, and Au.

TABLE IV
SODIUM VANADATE METHOD

| Element | Sample formula | Element mg. | |
|---|---|---|---|
| | | Content | Found |
| Fe | $FeSO_4$ | 45.2 | 44.8 |
| | | 136.5 | 135.1 |
| Mo | $Mo_2(SO_4)_5$ | 55.4 | 55.0 |
| | | 166.2 | 165.4 |
| Sn | $SnCl_2$ | 30.9 | 29.9 |
| | | 92.7 | 91.3 |
| Ti | $Ti_2(SO_4)_3$ | 37.6 | 37.1 |
| | | 112.8 | 110.9 |

Of these, Ag, Au, Hg, Cu, Sn, Sb, As, and Pd interfere with the determination of iron(II) and titanium(III), Ag, Sn, Sb, Pd and U with that of arsenic(III), and Ag, Hg, Au, Sn, As, Pd and Mo with that of antimony(III).

(*E*) *Mixture of iron(II) and titanium (III)*: Total concentration of these metals is estimated by direct titration with permanganate solution (Second column in Table V). On the other hand, titanium (III) can be masked with ammonium bifluoride in the permanganate method; iron(II) can thereby be estimated after its addition, methylene blue being used as indicator (First and fourth column in Table V). Titanium(III) is estimated from the difference between these two titres (First and second column).

(*F*) *Mixture of iron(II) and vanadium (IV)*: Total concentration can be determined by direct titration with permanganate solution without indicator. As the leuco compound of methylene blue is oxidized before vanadyl ion is oxidised, iron (II) can be estimated. From the difference between these two titres, vanadium(IV) can be estimated (Table VI).

(*G*) *Mixture of titanium(III) and vanadium(IV)*: Total concentration can be determined by direct titration with permanganate solution without indicator, and titanium(III) can be estimated by the use of methylene blue (Table VII).

TABLE V

MIXTURE OF IRON(II) AND TITANIUM(III)

| 0.1229 N $KMnO_4$ used ml. | | Fe mg. | | Ti mg. | |
|---|---|---|---|---|---|
| $NH_4HF_2$ & $Na_5P_3O_{10}$ as masking agent & methylene blue as indicator | $Na_5P_3O_{10}$ as masking agent without indicator | Content | Found | Content | Found |
| 3.78 | 8.08 | 26.2 | 25.9 | 25.6 | 25.4 |
| 3.78 | 16.64 | 26.2 | 25.9 | 76.1 | 75.7 |
| 7.59 | 20.46 | 52.3 | 52.1 | 76.1 | 74.8 |
| 11.38 | 15.66 | 78.5 | 78.1 | 25.4 | 25.2 |
| 11.35 | 19.97 | 78.5 | 77.9 | 50.7 | 50.6 |

TABLE VI

MIXTURE OF IRON(II) AND VANADIUM(IV)

| 0.1229 N $KMnO_4$ used ml. | | Fe mg. | | V mg. | |
|---|---|---|---|---|---|
| $Na_5P_3O_{10}$ as masking agent & methylene blue as indicator | $Na_5P_3O_{10}$ only | Content | Found | Content | Found |
| 3.77 | 6.94 | 25.8 | 25.8 | 19.9 | 19.9 |
| 3.75 | 13.24 | 25.8 | 25.7 | 59.5 | 59.3 |
| 7.49 | 16.98 | 51.7 | 51.4 | 59.5 | 59.5 |
| 11.27 | 14.42 | 77.5 | 77.4 | 19.9 | 19.6 |
| 11.24 | 17.56 | 77.5 | 77.3 | 39.7 | 39.6 |

TABLE VII

MIXTURE OF TITANIUM(III) AND VANADIUM(IV)

| 0.1229 N $KMnO_4$ used ml. | | Ti mg. | | V mg. | |
|---|---|---|---|---|---|
| $Na_5P_3O_{10}$ as masking agent & methylene blue as indicator | $Na_5P_3O_{10}$ only | Content | Found | Content | Found |
| 4.61 | 7.83 | 27.0 | 27.0 | 20.2 | 20.1 |
| 4.57 | 14.18 | 27.0 | 27.0 | 60.5 | 60.2 |
| 9.16 | 18.75 | 53.9 | 53.9 | 60.5 | 60.1 |
| 13.73 | 17.07 | 80.9 | 80.8 | 20.2 | 20.1 |
| 13.71 | 20.22 | 80.9 | 80.7 | 40.3 | 40.1 |

TABLE VIII

MIXTURE OF CHROMIUM(II) AND TITANIUM(III)

| 0.0898 N $KMnO_4$ used ml. | | Cr mg. | | Ti mg. | |
|---|---|---|---|---|---|
| $NH_4HF_2$ & $Na_5P_3O_{10}$ as masking agent & methylene blue as indicator | $Na_5P_3O_{10}$ only | Content | Found | Content | Found |
| 2.71 | 8.89 | 12.7 | 12.6 | 26.6 | 26.6 |
| 2.69 | 21.22 | 12.7 | 12.6 | 79.8 | 79.6 |
| 5.41 | 23.93 | 25.4 | 25.3 | 78.9 | 79.8 |
| 8.12 | 14.24 | 38.1 | 37.9 | 26.6 | 26.3 |
| 8.11 | 20.49 | 38.1 | 37.9 | 53.2 | 53.1 |

(*H*) *Mixture of chromium(II) and titanium(III)*: Total concentration is estimated by direct titration with permanganate solution without indicator; after masking titanium(III) with ammonium bifluoride, chromium(II) is determined similarly. Titanium(III) can be estimated from the difference between these titres (Table VIII).

(*I*) *Mixture of iron(II), titanium(III) and vanadium(IV)*: Total concentration can be determined by means of direct titration with permanganate solution without indicator (Third column in Table IX). The sum of the concentrations of iron(II) and titanium(III) can be determined by direct titration in the presence of methylene blue (Second column in Table IX).

TABLE IX
MIXTURE OF IRON(II), TITANIUM(III) AND VANADIUM(IV)

| 0.0998 N $KMnO_4$ used ml. | | | Fe mg. | | Ti mg. | | V mg. | |
|---|---|---|---|---|---|---|---|---|
| $NH_4HF_2$ & $Na_5P_3O_{10}$ as masking agents & methylene blue as indicator | $Na_5P_3O_{10}$ only as masking agent & methylene blue as indicator | $Na_5P_3O_{10}$ without indicator | Content | Found | Content | Found | Content | Found |
| 5.09 | 11.28 | 15.59 | 25.7 | 25.5 | 26.7 | 26.6 | 20.1 | 20.1 |
| 10.21 | 28.78 | 33.01 | 51.3 | 51.2 | 80.0 | 78.9 | 20·1 | 19.8 |
| 15.38 | 21.56 | 25.79 | 77.0 | 77.1 | 26.7 | 26.5 | 20.1 | 19.8 |
| 15.35 | 27.74 | 40.42 | 77.0 | 76.9 | 53.3 | 53.3 | 60.4 | 59.2 |
| 15.36 | 33.88 | 38.12 | 77.0 | 77.0 | 80.0 | 79.6 | 20.1 | 18.9 |
| 5.09 | 23.76 | 36.52 | 25.7 | 25.5 | 80.0 | 79.8 | 60.4 | 59.7 |

Iron(II) is estimated by means of masking titration, in the presence of ammonium bifluoride and methylene blue (First column in Table IX). From these three titrations, titanium(III) and vanadium(IV) are estimated.

## Reductometric Titration

**Reagent.**—Add 20 g. of sodium triphosphate to one liter of 0.1 N acidic standard solution, cautiously neutralized with solid sodium bicarbonate until no more carbone dioxide is evolved. Stock the solution in a dark box. Iron(II)-, titanium (III)-, vanadium(IV)-, and chromium(II)- triphosphate solution are fairly stable. Indigo carmine, methylene blue, methyl violet, crystal violet, and amarance are used as indicators.

**Material.**—As the sample, solution of potassium -permanganate, -bichromate, cerium(IV)-, and iron(III)- sulfate were used, their titres being determined beforehand in acidic solutions.

**Procedure.**—Add 3 g. of sodium triphosphate hexahydrate to an aliquot sample solution, and neutralize it with sodium bicarbonate, avoiding an excess. Titrate the mixture with a standard solution.

## Result and Discussion

(*J*) *Ferrousmetry* ($MnO_4^-$, $IO_4^-$, $Ce^{4+}$, $CrO_4^{2-}$, $VO_3^-$, $BrO^-$, $Br_2$, $H_2O_2$). Potassium -permanganate and -iodate are titrated with a reducing standard solution directly: the color of the sample solution disappears at the end point. In the cases of cerium(IV) sulfate, potassium chromate, sodium vanadate and hydrogen peroxide, cacoterin is used as indicator which imparts a violet coloration to the medium containing an excess of iron(III) solution. In the determination of hypobromite (or bromine), the indicator is decomposed before the end point, so that it is necessary to reduce $BrO^-$ with an excess of iron(II) solution (Table X).

(*K*) *Chromometry* ($IO_3^-$, $I_3^-$, $MnO_4^-$, $CrO_4^{2-}$, $VO_3^-$, $Ce^{4+}$, $Fe^{3+}$, $BrO^-$). The solution of potassium triiodide is decolorized at the end point. In the cases of potassium -permanganate and -chromate, sodium vanadate and cerium(IV) sulfate, indigocarmine is used; neutral red may be used for chromate and neutral red as well as crystal violet for iron(III). Hypobromite is determined by back titration as in ferrousmetry (Table XI).

TABLE X
FERROUSMETRY

| Element | Sample formula | Element mg. Content | Found |
|---|---|---|---|
| Br | NaBrO | 40.7<br>125.8 | 40.6<br>125.7 |
| Ce | $Ce(SO_4)_2$ | 56.2<br>170.8 | 56.0<br>170.6 |
| Cr | $K_2CrO_4$ | 29.3<br>87.7 | 29.2<br>87.6 |
| $H_2O_2$ | | 22.9<br>68.2 | 22.8<br>68.2 |
| $I_2$ | $KI_3$ | 67.8<br>202.4 | 67.5<br>201.6 |
| Mn | $KMnO_4$ | 33.8<br>101.7 | 33.7<br>101.7 |
| V | $NaVO_3$ | 23.5<br>71.7 | 23.5<br>71.5 |

TABLE XI
CHROMOMETRY

| Element | Sample formula | Element mg. Content | Found |
|---|---|---|---|
| Br | NaBrO | 37.6<br>112.7 | 37.2<br>112.2 |
| Ce | $Ce(SO_4)_2$ | 56.2<br>170.8 | 55.9<br>170.5 |
| Cr | $K_2CrO_4$ | 26.2<br>78.6 | 26.2<br>78.5 |
| Fe | $Fe_2(SO_4)_3$ | 10.6<br>59.1 | 10.3<br>58.8 |
| I | $KI_3$ | 67.8<br>202.4 | 67.5<br>201.6 |
| Mn | $KMnO_4$ | 33.8<br>101.7 | 33.7<br>101.7 |
| V | $NaVO_3$ | 16.1<br>49.1 | 15.8<br>48.7 |

(*L*) *Vanadyl sulfate method* ($MnO_4^-$, $CrO_4^{2-}$, $Ce^{4+}$). Permanganate is the only ion determinable by direct titration. For chromate and cerium(IV) sulfate, an excess of vanadyl sulfate is added and back-titrated with standard iron(III) sulfate solution (Table XII).

TABLE XII
VANADYL SULFATE METHOD

| Element | Sample formula | Element mg. | |
|---|---|---|---|
| | | Content | Found |
| Ce | $Ce(SO_4)_2$ | 56.2 | 56.9 |
| | | 170.8 | 170.6 |
| Cr | $K_2CrO_4$ | 26.2 | 26.0 |
| | | 78.6 | 78.0 |
| Mn | $KMnO_4$ | 37.3 | 37.2 |
| | | 110.9 | 110.7 |

(*M*) *Mixture of chromate and iron(III)*. Chromate is reduced with chromium(II) solution; indigo carmine is decolorized at the end point and used as indicator. Total concentration of chromate and iron (III) is determined by the titration using crystal violet as indicator which is reduced by the standard solution with more difficulty than iron(III); iron is estimated from the difference between these two titrations (Table XIII).

TABLE XIII
MIXTURE OF IRON(III) AND CHROMATE

| 0.0921 N $CrSO_4$ required ml. $Na_5P_3O_{10}$ as masking agent | | Cr mg. | | Fe mg. | |
|---|---|---|---|---|---|
| Indigo carmine | Crystal violet | Content | Found | Content | Found |
| 5.47 | 8.94 | 26.2 | 26.1 | 19.6 | 19.5 |
| 5.45 | 15.96 | 26.2 | 26.0 | 59.2 | 58.9 |
| 10.93 | 17.86 | 52.6 | 52.2 | 59.1 | 58.9 |
| 16.39 | 19.01 | 78.6 | 78.2 | 19.6 | 19.0 |
| 16.42 | 23.35 | 78.6 | 78.4 | 39.4 | 39.0 |

(*N*) *Mixture of vanadate and iron(III)*. Indigo carmine is used as indicator in the chromometric titration of vanadate; the total concentration of these two components is determined by the use of neutral red as indicator. (Table XIV).

TABLE XIV
MIXTURE OF IRON(III) AND VANADATE

| 0.0921 N $CrSO_4$ solution required $Na_5P_3O_{10}$ as masking agent | | V mg. | | Fe mg. | |
|---|---|---|---|---|---|
| Indigo carmine | Neutral red | Content | Found | Content | Found |
| 2.42 | 5.21 | 15.6 | 15.1 | 19.6 | 19.1 |
| 2.43 | 11.04 | 15.6 | 15.1 | 59.1 | 58.8 |
| 4.99 | 13.59 | 31.2 | 31.1 | 59.1 | 58.8 |
| 7.46 | 10.25 | | | | |
| 7.44 | 13.14 | 46.9 | 46.5 | 39.4 | 39.0 |

## Summary

Antimony(III), arsenic(III), chromium (II), iron(II), molybdenum(V), selenium (IV), thallium(I), titanium(III) and vanadium(IV) are titrated in neutral solutions with oxidizing standard solutions, chromate, bromate, hypobromite, permanganate, and vanadate solution, in the presence of triphosphate. A few of these elements, chromium(II), iron(II), titanium(III) and vanadium(IV) in their mixture are also determined.

On the other hand, cerium(IV), hypobromite, chromate, triiodide, permanganate, vanadate and hydrogen peroxide, are titrated with reducing standard solutions, chromium(II), iron(II), titanium(III), and vanadyl solution containing triphosphate. Some of them in mixtures are also determined.

The authors wish to express their hearty thanks to Professor Matsusuke Kobayashi for his valuable advice and encouragement throughout this study.

*Institute of Chemistry, Faculty of Science, Kinki Uuiversity*
*Fuse, Osaka*

# *Determination of Sulfate by Means of Metal-Polyphosphate Reduction Method*

By Susumu SUZUKI, Kenji HARIMAYA, Nobuo TSUJI, and Noriko YAMAOKA

(Received December 12, 1956)

Various methods for the estimation of sulfate by reduction to hydrogen sulfide have been known, and recently Madsen[1], Johnson[2], Kiba[3], and Ohashi[4] have given procedures for volumetric determination of sulfate. Madsen used a mixture of tin (II) chloride and phosphoric acid as reductant. But his method is applicable only to the determination of sodium sulfate. Johnson and Nishita[2] have shown methods for micro determination of sulfur, sulfate and organic sulfur compounds using a reducing mixture of hydroiodic acid and red phosphorus at 115°C. Kiba gives a new procedure involving the use of tin(II)-strong phosphoric acid mixture. By his method, sulfur in barium, magnesium, sodium and zinc sulfate as well as aluminium and chromium alum, are estimated. Ohashi reported also on the rapid determination of sulfur in organic compounds by means of the tin(II)-strong phosphoric acid method. According to his method, nitro compounds are determined within 0.5% accuracy. On the other hand, a few applications of triphosphate have been reported by the present authors. In the present paper, will be described the determination of soluble and insoluble sulfate by means of new reducing agents, metal-polyphosphate systems: titanium(III), chromium(II), molybdenum(IV), tungsten (V), and vanadium(IV), pyrophosphate, triphosphate and mixed polyphosphate systems.

## Equipment and Material

**Equipment.**—The apparatus for reduction of sulfate consists of two parts, (A) reduction- and (B) absorption- vessel. For the former a 50 ml. pear-shaped flask is used in a reaction below 120°C or a 10 ml. porcelain boat between 700°C and 900°C. The flask is provided with one glass tube for introduction of carbon dioxide and another one, through which the resultant gas mixture can be drawn to the absorption vessels. The boat is inserted into a silica tube, (length, ca. 40 cm. diameter, ca. 2 cm.) which is provided also with gas inlet- and delivery- tube as mentioned above. For the latter three 150 ml. flasks connected to each other with ruber tubings are used; the first is a gaurd flask and the remaining two are for absorption. A porcelain crucible No.5 is used for fusion of the mixture of polyphosphate and powdered metal.

**Material.**—Sodium sulfite, and barium, lead, and sodium sulfate were used as samples. The purity of lead and sodium sulfate was determined gravimetrically, while sodium sulfite was estimated iodimetrically. Barium sulfate was prepared from barium chloride and potassium sulfate.

**Standard Solution.**—One tenth normal potassium triiodide solution was used as absorbent, and sodium thiosulfate solution of the same normality as a reference standard solution. No indicator was used in the titration.

**Titanium Polyphosphate Systems.** — (a) Five g. of metallic titaninm is added to 200 g. of orthophosphoric acid (sp. gr. 1.86), which is boiled to dissolve the metals. Titanium is oxidized to tervalent state; even if colorless quadrivalent ion should be formed here, it would be reduced to tervalent state by the elementary one. Tervalent titanium in polyphosphate is very stable in the cold and has a vigorous reducing force at high temperatures. In separate experiments, 0.3 g. portions of titanium are dissolved in mixtures containing each 5 g. of orthophosphoric acid, (sp. gr. 1.83) along with (b) 2.5 g. of pyrophosphate, (c) 2.5 g. of triphosphate, (d) 2.5 g. of hexametaphosphate, and (e) 5g. of a mixture of the hexameta- and tri- phosphate in equal proportion respectively; (a) and (b) are used at 200°C, while (c), (d) and (e) at 700°—900°C.

**Chromium-, Manganese-, Molybdenum-, and Tungsten- Polyphosphate Systems.**—Metallic chromium is dissolved in phosphoric acid; the solution which exerts a reducing force at a high temperature, contains the metal in bivalent and tervalent state and is of green color. Chromium-polyphosphate reducing systems as well as those containing manganese, molybdenum and tungsten are prepared as in the case of titanium.

**Vitreous Polyphosphates.** — Mixtures prepared from phosphoric acid and pyro-, tri- and hexa- phosphate without the additon of metals are used as diluents.

1) E. R. Madsen, *Acta. Chim. Scand.*, **3**, 773 (1949); **6**, 305 (1952).
2) C. M. Johnson and H. Nishita, *Anal. Chem.*, **24**, 736 (1952).
3) T. Kiba, This Bulletin, **28**, 641 (1955).
4) S. Ohashi, This Bulletin, **28**, 645 (1955).

### Procedure

Place a sample of approximately 0.01 g. of air dry sulfate in the reduction flask or in the ignition boat. Add ca. 7 g. of reducing metal-polyphosphate mixture. To each absorber for hydrogen sulfide, add 25 ml. of one tenth normal potassium triiodide solution and 20 ml. of water. Pass a current of carbone dioxide for at least 2 minutes through the reduction flask or the silica tube into which the ignition boat is inserted, in order to remove atmospheric oxygen. Allow the reaction to proceed gradually at a boiling temperature of the mixture in the current of carbon dioxide for about 20 minutes. After heating, the potassium triiodide solution, in which hydrogen sulfide gas is absorbed, is titrated with standard sodium thiosulfate solution. One ml. of one tenth normal solution of sodium thiosulfate corresponds to 7.103 mg. of sodium sulfate, 6.9043 mg. of sodium sulfite, 14.377 mg. of zinc sulfate monohydrate, 15.164 mg. of lead sulfate and 11.671 mg. of barium sulfate.

### Result and Discussion

**Titanium Polyphosphate Systems.**—(1) When barium, lead, or sodium sulfate is treated with $H_3PO_4$–Ti reducing system at about 200°C for 15–20 minutes, it is reduced to sulfide; the evolved hydrogen sulfide is absorped in standard potassium triiodide solution and the excess of triiodide is titrated with standard sodium thiosulfate solution. The results are satisfactory as shown in Table I. Sodium sulfite can not be reduced, however, to sulfide by this reducing system, presumably because the sulfide is easily decomposed by the heat treatment, and the resultant sulfur volatilizes at a high temperature. The results are shown in Table I.

TABLE I
$H_3PO_4$–Ti SYSTEM

| Sample form | Heating time (min.) | Sample mg. Content | Found |
|---|---|---|---|
| $K_2SO_4$ | 20 | blanck | 0.0 |
| | 15 | 12.2 | 11.8 |
| | 〃 | 30.4 | 29.9 |
| | 〃 | 61.9 | 61.1 |
| | 25 | 123.6 | 101.1 |
| $PbSO_4$ | 15 | 33.4 | 33.9 |
| $BaSO_4$ | 15 | 28.6 | 28.0 |
| | 〃 | 32.3 | 31.9 |
| | 20 | 61.7 | 62.3 |
| | 30 | 97.4 | 81.8 |
| | 〃 | 122.3 | 95.5 |
| $Na_2SO_3$ | 20 | 29.5 | 29.4 |
| | 30 | 67.9 | 62.8 |

(2) Solid samples of sulfates are reduced also by means of $H_3PO_4$–$(HPO_3)_6$–Ti system. In this case, the samples are heated at a higher temperature, about 200°C. for 15 minutes. The results are shown in Table II. A small quantity of sodium sulfite is reduced completely, but such is not the case with its large amount.

TABLE II
$H_3PO_4$–$(HPO_3)_6$–Ti SYSTEM

| Sample form | Heating time (min.) | Sample mg. Content | Found |
|---|---|---|---|
| $K_2SO_4$ | 15 | 46.8 | 46.4 |
| | 〃 | 83.7 | 83.9 |
| $PbSO_4$ | 〃 | 40.1 | 40.4 |
| $BaSO_4$ | 〃 | 27.0 | 26.9 |
| $Na_2SO_3$ | 〃 | 18.1 | 17.8 |

(3) When $H_3PO_4$–$Na_5P_3O_{10}$–Ti system is used as a reducing agent, sulfates are determined satisfactorily as shown in Table III. Nevertheless it must be recognized that their large amounts can not be completely reduced by this method. This owes to the fact that the reaction temperature is higher than in other cases.

TABLE III
$H_3PO_4$–$Na_5P_3O_{10}$–Ti SYSTEM

| Sample form | Heating time (min.) | Sample mg. Content | Found |
|---|---|---|---|
| $K_2SO_4$ | 10 | 27.4 | 27.2 |
| | 15 | 57.9 | 57.5 |
| | 〃 | 91.3 | 82.1 |
| $PbSO_4$ | 〃 | 60.9 | 61.1 |
| | 〃 | 102.4 | 94.3 |
| $BaSO_4$ | 〃 | 68.5 | 68.3 |
| | 〃 | 102.0 | 100.4 |
| $Na_2SO_3$ | 10 | 32.8 | 32.6 |
| | 15 | 31.0 | 30.9 |
| | 〃 | 63.0 | 53.9 |

TABLE IV
$H_3PO_4$–$NaPO_3$–Ti SYSTEM

| Sample form | Heating time (min.) | Sample mg. Content | Found |
|---|---|---|---|
| $H_2SO_4$ | 25 | 21.1 | 21.6 |
| $K_2SO_4$ | 15 | 22.0 | 21.8 |
| $PbSO_4$ | 〃 | 24.6 | 24.4 |
| $BaSO_4$ | 〃 | 23.0 | 23.2 |
| $Na_2SO_3$ | 〃 | 9.5 | 9.6 |

(4) The same fact is also observed in $H_3PO_4$–$NaPO_3$–Ti reducing system. About 20 mg. of sulfate are treated with the reductant in a pear-shaped flask for about

15 minutes, and found to be reduced completely, but a sample weighing more than 20 mg. can not be determined satisfactorily. The results are shown in Table IV.

(5) A reducing agent prepared from $H_3PO_4$, $HPO_3$, $Na_5P_3O_{10}$ and metallic titanium is used at about 700°C. The reaction velocity being still small, the result after 20 minutes' heating is unsatisfactory; one hour is necessary for complete reduction. The results are shown in Table V.

TABLE V

$H_3PO_4$-$(HPO_3)_6$-$Na_5P_3O_{10}$-Ti SYSTEM

| Sample form | Heating time (min.) | Sample mg. | |
|---|---|---|---|
| | | Content | Found |
| $K_2SO_4$ | 20 | 32.3 | 29.3 |
| | 60 | 36.5 | 36.7 |
| $PbSO_4$ | 20 | 35.8 | 30.4 |
| | 60 | 57.8 | 57.8 |
| $BaSO_4$ | 20 | 34.1 | 29.7 |
| | 60 | 45.9 | 45.7 |
| $Na_2SO_3$ | 20 | 34.5 | 25.1 |
| | 40 | 30.0 | 25.1 |
| | 60 | 38.4 | 33.0 |

(6) Table VI shows the results obtained from reactions between $H_3PO_4$-$Na_4P_2O_7$-Ti reducing agent and sulfates. The reacting mixture is heated in the boat at 800°C; one hour's heating is necessary.

TABLE VI

$H_3PO_4$-$Na_4P_2O_7$-Ti SYSTEM

| Sample form | Heating time (min.) | Sample mg. | |
|---|---|---|---|
| | | Content | Found |
| $K_2SO_4$ | 30 | 22.0 | 16.4 |
| | 60 | 29.0 | 28.7 |
| $PbSO_4$ | 30 | 32.1 | 32.6 |
| | 60 | 37.4 | 37.6 |
| $BaSO_4$ | 30 | 42.1 | 37.6 |
| | 60 | 41.9 | 41.7 |
| $Na_2SO_3$ | 30 | 21.3 | 16.4 |
| | 60 | 20.4 | 17.8 |

TABLE VII

$H_3PO_4$-$(HPO_3)_6$-$KNaCO_3$-Ti SYSTEM

| Sample form | Heating time (min.) | Sample mg. | |
|---|---|---|---|
| | | Content | Found |
| $K_2SO_4$ | 30 | 16.6 | 11.1 |
| | 60 | 12.3 | 12.2 |
| $PbSO_4$ | 30 | 17.9 | 12.2 |
| | 60 | 13.5 | 13.6 |

(7) When potassium-sodium carbonate is added to the reducing system, its melting point rises, which makes the treatment of reducing reaction more difficult. When heated for 60 minutes however, sulfates are satisfactorily determined as shown in Table VII.

**Other Metal-Polyphosphate Systems.**— (8) $H_3PO_4$-$Na_5P_3O_{10}$-metal systems. Metallic chromium, manganese, molybdenum or tungsten are dissolved by heating in a mixture of phosphoric acid and sodium triphosphate, and used as reducing agent. But the results of the estimation are satisfactory only in the case of the chromium system as shown in Table VIII.

TABLE VIII

$H_3PO_4$-$Na_4P_2O_7$-Cr SYSTEM

| Sample form | Heating time (min.) | Sample mg. | |
|---|---|---|---|
| | | Content | Found |
| $K_2SO_4$ | 15 | 34.2 | 34.2 |
| $PbSO_4$ | 〃 | 35.7 | 35.4 |
| $BaSO_4$ | 〃 | 30.7 | 30.7 |

(9) In order to increase acidic properties and rise the melting point, metaphosphate is added to this system; the sulfate is completely reduced by the reductant as shown in Table IX. These estimations required a heating period of 1 hour.

TABLE IX

$H_3PO_4$-$(HPO_3)_6$-$Na_3PO_4$-METAL SYSTEMS

| Metal | Sample form | Heating time (min.) | Sample mg. | |
|---|---|---|---|---|
| | | | Content | Found |
| Cr | $K_2SO_4$ | 30 | 11.7 | 10.1 |
| | | 60 | 10.8 | 10.9 |
| | $PbSO_4$ | 30 | 10.7 | 10.2 |
| | | 60 | 11.9 | 11.8 |
| | $BaSO_4$ | 30 | 10.0 | 7.8 |
| | | 60 | 10.4 | 10.4 |
| Mn | $K_2SO_4$ | 30 | 12.3 | 11.3 |
| | | 60 | 13.4 | 13.5 |
| | $PbSO_4$ | 30 | 17.0 | 16.2 |
| | | 60 | 23.4 | 23.3 |
| | $BaSO_4$ | 30 | 10.7 | 9.7 |
| | | 60 | 16.5 | 16.5 |
| Mo | $K_2SO_4$ | 30 | 15.6 | 13.1 |
| | | 60 | 20.1 | 20.1 |
| | $PbSO_4$ | 30 | 20.2 | 19.8 |
| | | 60 | 19.2 | 19.2 |
| | $BaSO_4$ | 30 | 15.8 | 13.3 |
| | | 60 | 17.8 | 18.0 |
| W | $K_2SO_4$ | 30 | 11.6 | 11.0 |
| | | 60 | 11.7 | 11.8 |
| | $PbSO_4$ | 30 | 20.0 | 16.5 |
| | | 60 | 10.0 | 10.0 |
| | $BaSO_4$ | 30 | 10.0 | 7.7 |
| | | 60 | 10.0 | 10.0 |

(10) Prolonged heating is also required in the $HPO_3$–$H_3PO_4$–$KNaCO_3$–metal system. Sulfates are completely reduced to sulfide by heating for 1 hour with these reducing agents, and the results are shown in Table X.

TABLE X

$H_3PO_4$-$(HPO_3)_6$-$KNaCO_3$-METALS SYSTEMS

| Metal | Sample form | Heating time (min.) | Sample mg. Content | Found |
|---|---|---|---|---|
| Cr | $K_2SO_4$ | 30 | 12.4 | 11.5 |
| | | 60 | 11.0 | 11.0 |
| | $PbSO_4$ | 30 | 13.7 | 11.3 |
| | | 60 | 10.7 | 10.7 |
| | $BaSO_4$ | 30 | 13.5 | 12.6 |
| | | 60 | 14.3 | 14.3 |
| Mn | $K_2SO_4$ | 30 | 23.9 | 21.1 |
| | | 60 | 18.8 | 18.4 |
| | $PbSO_4$ | 30 | 21.2 | 18.8 |
| | | 60 | 20.7 | 20.7 |
| | $BaSO_4$ | 30 | 21.7 | 14.0 |
| | | 60 | 15.7 | 15.7 |
| Mo | $K_2SO_4$ | 30 | 10.6 | 9.1 |
| | | 60 | 10.0 | 9.9 |
| | $PbSO_4$ | 30 | 10.7 | 9.0 |
| | | 60 | 13.8 | 13.8 |
| | $BaSO_4$ | 30 | 13.0 | 12.5 |
| | | 60 | 11.3 | 11.3 |
| W | $K_2SO_4$ | 30 | 13.2 | 9.9 |
| | | 60 | 10.0 | 9.9 |
| | $PbSO_4$ | 30 | 13.2 | 12.4 |
| | | 60 | 12.2 | 12.1 |
| | $BaSO_4$ | 30 | 10.0 | 7.5 |
| | | 60 | 11.7 | 11.6 |

(11) $H_3PO_4$–$Na_5P_3O_{10}$–metal systems are also used as reducing agents for sulfates, as shown in Table XI. In these systems, chromium is assumed to be present mainly as bivalent, molybdenum as tervalent, manganese as bivalent, and tungsten as quadrivalent compounds respectively, to which the reducing property of the systems is due.

TABLE XI

$H_3PO_4$-$Na_5P_3O_{10}$-METALS SYSTEMS

| Metal | Sample form | Heating time (min.) | Sample mg. Content | Found |
|---|---|---|---|---|
| Cr | $K_2SO_4$ | 30 | 14.3 | 12.7 |
| | | 60 | 10.4 | 10.4 |
| | $PbSO_4$ | 30 | 9.8 | 8.3 |
| | | 60 | 10.1 | 10.2 |
| | $BaSO_4$ | 30 | 10.4 | 8.9 |
| | | 60 | 10.0 | 10.0 |
| Mo | $K_2SO_4$ | 30 | 15.9 | 14.0 |
| | | 60 | 16.0 | 16.0 |
| | $PbSO_4$ | 30 | 14.6 | 13.6 |
| | | 60 | 10.6 | 10.6 |
| | $BaSO_4$ | 30 | 10.8 | 9.1 |
| | | 60 | 15.8 | 15.8 |
| W | $K_2SO_4$ | 30 | 10.0 | 8.3 |
| | | 60 | 11.8 | 11.8 |
| | $PbSO_4$ | 30 | 15.9 | 13.3 |
| | | 60 | 11.0 | 10.9 |
| | $BaSO_4$ | 30 | 9.6 | 8.1 |
| | | 60 | 11.0 | 10.9 |

The authours wish to express their hearty thanks to Professor Matsusuke Kobayashi for his valuable advice and encouragement throughout this study.

*Institute of Chemistry, Faculty of Science, Kinki University*
*Fuse, Osaka*

# *Determination of Nitro Compounds with Titanium(III)-Polyphosphate Solution. (Application of Polyphosphate to Masking Volumetric Analysis)*

By Susumu SUZUKI, Yoshihiro MURAMOTO, Morio UENO and Teruzo SUGANO

(Received December 12, 1956)

The quantitative reduction of nitro compounds by means of standard titanium(III) chloride solution was proposed by Knecht and Hibbert[1] and applied to many compounds by Duin[2], English[3] and Callen[4]. According to their methods, the sample is dissolved in water or alcohol and excess titanium(III) chloride is added. After the reaction mixture has been boiled, the excess of titanium(III) chloride is titrated with standard iron(III) chloride solution, ammonium thiocyanate being used as indicator. Six equivalents of titanium(III) chloride are required for each nitro group; the nitro nitrogen present in the compound is thereby estimated. On the other hand, new quantitative reduction of sulfate by means of metal-polyphosphate system was reported by S. Suzuki[5]. In the present paper we shall describe the determination of mono-, di-, and tri- nitro compounds by reduction with an excess of standard titanium(III)-polyphosphate solution and back-titration with potassium dichromate, cerium(IV) sulfate, or sodium vanadate solution; indicators which were used are methylene blue, diphenylamine and indigocarmine.

## Experimental

**Equipment.**—A sample of nitro compound is dissolved in water or ethanol in a 200-ml. flask, which is warmed under reflux in a current of carbon dioxide after addition of the standard titanium(III) triphosphate solution.

**Material.**—Mononitro compounds in Table I, dinitro compounds in Table II, and trinitro compounds in Table III, are used as samples for nitro compounds. These nitro compounds are prepared in the authors' laboratory.

**Reagents.**—Titanium phosphate solution: 5 g. of metallic titanium is dissolved in 100 ml. of concentrated phosphoric acid (sp. gr. 1.82) by heating at 110—150°C. for about 1 hour. In this case, metallic titanium is gradually added within 10 minutes to the hot phosphoric acid, and stirred carefully not to cause overflow through foaming. This titanium(III) phosphate solution is added to 1 liter of about one tenth normal sodium triphosphate solution. The concentration of tervalent titanium is determined by titration with standard potassium permanganate solution.

**Reference Standard Solution.** — Potassium dichromate: A tenth normal potassium dichlomate solution is prepared.

Cerium(IV) sulfate: Sixty g. of cerium(IV) sulfate is dissolved in 1 liter of 2 N sulfuric acid, and this solution is used after filtration and standardization.

Sodium vanadate: About one tenth normal solution of sodium vanadate is prepared, and standardized by means of liquid amalgam method.

TABLE I
MONONITRO COMPOUND

α-nitronaphthalene
*o*-nitrophenol
*p*-nitrotoluene
*o*-nitroaniline
*o*-chloronitrobenzene
*p*-chloronitrobenzene
*p*-bromonitrobenzene
*o*-nitrobenzenesulfoamide
4-nitrosalisylic acid
2-nitro-*p*-toluidine
4-nitro-*o*-toluidine
*m*-nitro-*p*-toluidine
2-acetoamino-4-nitro-toluene
2-nitro-4-acetoamino-toluene

TABLE II
DINITRO COMPOUND

*m*-dinitrobenzene
2,4-dinitrotoluene
2,4-dinitrochlorobenzene
2,6-dinitro-4-toluidine
di-*o*-nitrophenyldisulfide

TABLE III
TRINITRO COMPOUND

2,4,6-trinitrophenol (picric acid)
2,4,6-trinitrotoluene

1) E. Knecht and E. Hibbert, *Ber.*, **36**, 1549 (1903); **38**, 3318 (1905); **40**, 3819 (1907).
2) C. F. van Durin, *Chem. Weekblad*, **16**, 1111 (1919); *Chem. Abst.*, **13**, 3113 (1919).
3) F. L. English, *Anal. Chem.*, **20**, 745 (1948).
4) T. Callan et al., *J. Soc. Chem. Ind.*, **39**, 86 (1920); **41**, 157 (1922).
5) S. Suzuki, This Bulletin, **30**, 766 (1957).

Indicator: 0.1% methylene blue, 0.1% indigo carmine and 0.2% diphenylamine solutions are used as indicators.

### Recommended Procedure

Place each sample of accurately measured 0.0300 g. of air dry nitro compounds in a 200-ml. three necksed flask, add 5 ml. of ethanol to dissolve it, and then 25 ml. of a standard titanium polyphosphate solution. Connect a reflux condenser with the flask and a tube into which carbon dioxide has been introduced. Boil the solution well for 5 minutes on a hot plate. Cool the flask in ice water and titrate the solution with a standard oxidizing solution, in a current of carbon dioxide. The indicator is added near the end point, where methylene blue changes color from colorless to blue, indigo carmine also from colorless to blue, while diphenylamine from chocolate violet to pink.

## Results and Discussion

**Mononitro Compounds:** *α-Nitronaphthalene* prepared within 80% yield by means of nitration of naphthalene and recrystallization from ethyl alcohol is estimated with titanium(III) polyphosphate as shown in Table IV. When the sample solution is titrated using methylene blue as indicator, the end point is given a little earlier than the theoretical end point. This is due to the fact that colorless leuco compound of methylene blue produced by reduction of the indicator with titanium (III) salt, is oxidized by standard oxidizing solution before complete oxidation of titanium(III) in solution, which should be oxidized in advance, is achieved. Accordingly it appears as if excess of titanium is consumed by the sample solution and the result shows a higher value. In order to avoid this effect of indicator, iron(II) sulfate is added to the sample solution, in the presence of which methylene blue is not affected till all titanium remaining there has been completely oxidized with the standard solution; then the results show real values as given in the iron(II) sulfate column of Table IV. These facts will also be described hereafter. The result of the estimation of nitronaphthalene by this method is unsatisfactory, the experimental value being 75% of the theoretical one. When indigo carmine is used as indicator, it is oxidized simultaneously with titanium, because of its lower oxidation potential than methylene blue. The end point is determined at the point of decoloration of indigo carmine which is oxidized to colorless leuco compound. In the titration of the solution to which the standard iron(II) sulfate is added, excess of titanium(III) and iron(II) as well as the indicator are all oxidized at the end point. Here lies the difference between methylene blue and indigo carmine. In the presence of triphosphate, in nearly neutral solution, the dichromate ion is changed to the chlomate, whose oxidizing force becomes so weak that it can not oxidize diphenylamine indicator completely; consequently the end point is indistinct. *o-Nitrophenol* is prepared by means of nitration of phenol and separation from *p*-nitrophenol by steam distillation. This nitro compound is determined satisfactorily as shown in Table IV. After nitration of toluene in sulfuric acid medium, *p-nitrotoluene* is separated by means of vacuum distillation and recrystallized from ethyl alcohol; it melts at 56°C. The result of the estimation of *p*-nitrotoluene by the present reduction method corresponds to 72% of nitro group present in the sample. Addition of iron solution to the sample is unsuitable for this compound, except in the case of methylene blue indicator. *o-Nitroaniline* is obtained by nitration of acetanilide in acetic acid anhydride. When methylene blue is used as indicator and iron(II) sulfate is added to the sample solution of *o*-nitroaniline, the titre of cerium(IV) sulfate or sodium vanadate enormously increases, and the estimated value of nitro group correspondingly falls away. A similar fact is also recognized in the determination of 2-nitro-*p*-toluidine described below; it appears as if the resultant diamine compound comes to interfere with the titration. *p-Chloronitrobenzene* is prepared by means of nitration of chlorobenzene in sulfuric acid and recrystallization from ethyl alcohol. The result of determination of this compound is accurate when a sample solution is titrated in the presence of iron(II) sulfate and methylene blue indicator. In the determination of *p-bromonitrobenzene*, diphenylamine shows a pseduo-end point giving rise to a higher result. This compound is prepared by means of nitration of bromobenzene in sulfuric acid, and recrystallization from ethyl alcohol. *o*-Nitrobenzenesulfonylchloride is obtained by oxidation of di-*o*-nitrodiphenylsulfide with chlorine in a mixture of nitric and hydrochloric acid. By means of ammoniation of sulfochloride radical to sulfoamid radical, *o-nitrobenzenesulfoamide* is prepared from *o*-nitrobenzenesulfonylchloride. The determination of this

TABLE IV
DETERMINATION OF MONONITRO COMPOUNDS

| Sample | Indicator | Oxidizing agent | Estimated % $H_3PO_4$—$Na_5P_3O_{10}$ | Estimated % $FeSO_4$ added |
|---|---|---|---|---|
| α-nitronaphthalene | M. B. | Cr | 83.01 | 74.40 |
| | | Ce | 86.58 | 65.01 |
| | | V | 84.34 | 77.01 |
| | I. C. | Cr | 82.34 | 88.42 |
| | | Ce | 83.46 | 78.42 |
| | D. A. | Cr | 94.32 | excess |
| | | Ce | 85.56 | 76.34 |
| o-nitrophenol | M. B. | Cr | 105.82 | 103.21 |
| | | Ce | 107.23 | 101.34 |
| | | V | 99.68 | 99.25 |
| | D. A. | Cr | 106.35 | 102.54 |
| | | Ce | 106.46 | 97.34 |
| | | V | 105.99 | 98.87 |
| p-nitrotoluene | M. B. | Cr | 67.44 | 71.70 |
| | | Ce | 84.69 | 67.31 |
| | | V | 88.64 | 72.45 |
| | I. C. | Cr | 71.32 | excess |
| | | Ce | 72.32 | 72.48 |
| | | V | 72.85 | 71.63 |
| | D. A. | Cr | 70.11 | excess |
| | | Ce | 73.93 | 73.34 |
| | | V | 83.58 | 73.34 |
| o-nitroaniline | M. B. | Cr | 102.23 | 99.54 |
| | | Ce | 103.56 | trace |
| | | V | 101.36 | 〃 |
| | D. A. | Cr | 101.73 | excess |
| | | Ce | 100.53 | 99.32 |
| | | V | 89.79 | 97.35 |
| p-chloronitrobenzene | M. B. | Cr | 100.96 | 97.35 |
| | | Ce | 102.35 | 99.23 |
| | | V | 102.52 | 98.32 |
| | I. C. | Ce | 97.38 | 99.01 |
| | D. A. | Ce | excess | 101.56 |
| p-bromonitrobenzene | M. B. | Cr | 113.34 | 105.31 |
| | | Ce | 111.86 | 102.33 |
| | | V | 112.81 | 104.01 |
| | D. A. | Cr | excess | excess |
| | | V | 〃 | 〃 |
| o-nitrobenzenesulfoamide | M. B. | Cr | 109.56 | 104.61 |
| | | Ce | 105.15 | 107.07 |
| | | V | excess | 105.34 |
| | I. C. | Ce | 106.36 | 105.84 |
| | D. A. | Cr | 105.41 | excess |
| 4-nitrosalisylic acid | M. B. | Cr | 114.16 | 〃 |
| | | Ce | 100.21 | trace |
| | | V | 103.56 | 〃 |
| | I. C. | Ce | 101.43 | 101.32 |
| | D. A. | Ce | 101.02 | 98.72 |
| 2-nitro-p-toluidine | M. B. | Ce | 93.21 | trace |
| | | V | 94.62 | 95.55 |
| | I. C. | Ce | 96.30 | excess |
| | D. A. | Cr | excess | 〃 |
| | | Ce | 97.89 | 95.64 |
| 2-acetoamino-4-nitrotoluene | M. B. | Ce | 100.85 | 96.28 |
| | | V | 102.13 | 96.51 |
| | I. C. | Ce | 113.54 | 95.86 |
| | D. A. | Ce | 96.46 | 97.37 |
| 4-acetoamino-2-nitrotoluene | M. B. | Cr | 112.45 | 98.43 |
| | | Ce | 108.23 | 96.58 |
| | | V | 90.57 | 96.65 |
| | D. A. | V | 90.57 | 97.78 |
| o-chloronitrobenzene | M. B. | Cr | 98.66 | trace |
| | | Ce | 112.45 | 〃 |
| | | V | 98.21 | 〃 |
| | I. C. | Ce | 97.89 | 97.60 |
| | D. A. | Ce | 98.44 | 97.53 |
| | | V | 83.05 | 99.32 |

TABLE V
DETERMINATION OF DINITRO COMPOUNDS

| Sample | Indicator | Oxidizing agent | Estimated % $H_3PO_4$—$Na_5P_3O_{10}$ | Estimated % $FeSO_4$ added |
|---|---|---|---|---|
| di-o-nitrophenyldisulfide | M. B. | Cr | 32.56 | 28.41 |
| | | Ce | 54.29 | 36.78 |
| | | V | 48.62 | 30.41 |
| | D. A. | Ce | 46.31 | trace |
| 2,4-dinitrochlorobenzene | M. B. | Cr | 102.56 | 100.76 |
| | | Ce | 114.63 | trace |
| | I. C. | Ce | 103.52 | 102.43 |
| | D. A. | Ce | 101.01 | 102.08 |
| | | V | 103.73 | 99.60 |
| 2,6-dinitro-4-toluidine | M. B. | Cr | excess | 98.31 |
| | | Ce | 97.46 | 96.53 |
| | | V | 97.34 | 95.53 |
| | I. C. | Ce | excess | 96.58 |
| | D. A. | Ce | 98.13 | excess |
| m-dinitrobenzene | M. B. | Cr | 115.38 | 98.73 |
| | | Ce | 104.59 | 98.82 |
| | | V | 101.10 | 97.30 |
| | D. A. | Cr | 104.12 | excess |
| | | Ce | 98.02 | 96.13 |
| | | V | 99.02 | 98.34 |
| 2,4-dinitrotoluene | M. B. | Cr | 101.34 | 99.47 |
| | | Ce | 111.22 | trace |
| | | V | 114.32 | 〃 |
| | I. C. | Ce | 106.35 | 103.83 |
| | | V | 99.05 | 99.43 |
| | D. A. | Ce | 100.87 | 100.51 |

nitroamide gives a higher result in the similar titration. *4-Nitro-2-aminobenzoic acid* is diazoated at a low temperature, and hydrolyzed by heating the solution to 4-nitrosalisylic acid; the nitrosalisylic acid is recrystallized from the mixture of equal parts of ethyl alcohol and acetic acid. The determination of this compound, using methylene blue as indicator in the presence of iron(II) sulfate, gives a lower result. *p*-Toluidine is nitrated to *2-nitro-p-toluidine* in an excess of sulfuric acid. On the other hand, 2-nitro-*p*-toluidine is also prepared through reduction of dinitrotoluene. The titration of the solution using methylene blue and iron(II) sulfate also gives a lower result. 2-Nitro-4-aminotoluene is acetylated to *2-nitro-4-acetoamino-toluene* and 4-nitro-*o*-toluidine to 2-acetoamino-4-nitrotoluene in acetic acid anhydride, and these acetoaminoes are estimated satisfactorily with iron(II) sulfate-titanium(III)-polyphosphate system.

**Dinitro Compounds.**—*m-Dinitrobenzene* is prepared by nitration of nitrobenzene and determined as shown in Table V. Although English pointed out that the estimation of dinitro compound gave a higher result, no such discrepancy is observed in the present investigation. *p*-Nitrotoluene is oxidized to *2,4-dinitrotoluene* by nitration in a large amount of sulfuric acid, and it is purified by recrystallization from ethanolic solution. The dinitro compound is determined by the above-mentioned procedure, but methylene blue-iron(II) sulfate system gives lower results for it. *2,4-Dinitrochlorobenzene* prepared by nitration of *p*-nitrochlorobenzene, is estimated as in Table V and gives a slightly higher value. When treated with ammonium sulfide in an ethanolic solution, trinitrotoluene, TNT, is subject to partial reduction in *p*-nitro position and changes to *2,6-dinitro-4-toluidine*. This amino compound is satisfactorily determined as shown in Table V. When *o*-chloronitrobenzene is boiled with sodium sulfide in an ethanolic solution, it begins to change into *di-o-nitrophenyldisulfide*. The derivatives can not be estimated by means of the metal-polyphosphate reduction systems.

**Trinitro Compound.**—*Commercial picric acid* can not be determined in this way, because its solution containing titanium (III) polyphosphate is of a greenish brown color, and so it is impossible to observed the end point. *Trinitro toluene*, TNT, prepared through nitration of dinitrotoluene is determined; the obtained values, though in good agreement with one another, are somewhat lower corresponding to only 96% of theory (Table VI).

TABLE VI
DETERMINATION OF TRINITRO COMPOUNDS

| Sample | Indicator | Oxidizing agent | Estimated % | |
|---|---|---|---|---|
| | | | $H_3PO_4$—$Na_5P_3O_{10}$ | $FeSO_4$ added |
| picric acid | M. B. | Cr | 96.34 | 86.42 |
| | I. C. | Ce | 107.48 | 102.45 |
| | D. A. | V | 101.35 | 98.54 |
| 2,4,6-trinitro-toluene | M. B. | Cr | excess | 98.31 |
| | | Ce | 97.46 | 96.53 |
| | | V | 97.34 | 95.23 |
| | I. C. | Cr | excess | 96.58 |
| | D. A. | Cr | 98.13 | excess |
| | | V | excess | 〃 |

*Institute of Chemistry, Faculty of Science, Kinki University*
*Fuse, Osaka*

# *Proton Resonance in Oil Paraffin*

By Shizuo FUJIWARA and Ichiro YAMAGUCHI

(Received May 17, 1957)

## Introduction

Wilson and Pake[1] proposed a nuclear magnetic resonance method to determine the degree of crystallinity of linear polymers and made an extensive study of the resonance line shape and the spin lattice-relaxation time of polytetrafluoroethylene, 'Teflon.'[2] Though their method is quite straightforward and seems useful for the structural study of linear polymers, further investigations of this method seem necessary, and the present authors have planned to make proton resonance study of oil paraffin which is one of the most typical linear polymers with simple molecular structure and structurally well studied[3].

## Experimental

**Samples.** — Samples investigated are commercial oil paraffins and microcrystalline paraffin waxes. The samples of the former are seven species, from No. 1 to No. 7, differing in their melting points by about 5°F from one another in the range from 115°F (47.7°C) to 145°F (62.8°C); samples from No. 1 to No. 4 are 1 : 1 mixtures of two kinds of crude oil paraffin produced in Ceria and Southern Sumatra, and those from No. 5 to No. 7 are the ones produced in Southern Sumatra.

**Apparatus.** — The apparatus used for the proton resonance measurement is one of the auto-dyne—detector type with a narrow band amplifier and phase sensitive detector. The schematic diagram and some descriptions of the apparatus were given elsewhere.[4] The magnetic field applied is of about 4,000 gauss produced by an electromagnet which is charged by storage batteries. The inhomogeneity of the magnetic field over the specimen is about 50 milligauss. Derivative curves are recoreded automatically by the field modulation, whose amplitude is about 0.3 gauss.

**Measurement.**—For the measurements at room temperature, the oil paraffin specimens are made into rods of 5 mm$\phi$×15 mm and mounted in a *rf* coil whose axis is perpendicular to the magnetic field. The microcrystalline waxes are sealed in glass tubes with diameters of 5 mm. For the measurements of temperature dependence of the resonance, samples sealed in glass tubes of 3 mm. diameter are mounted in *rf* coil, inserted in a Dewar vessel, and warmed up by a heater. To get the temperature equilibrium in the vessel, about half an hour was taken before the onset of the measurement at each temperature. The temperature range investigated is from room temperature to just below the melting point of the sample. Temperature measurements were made by a copper—constantan thermocouple with one junction 5 mm. apart from the sample.

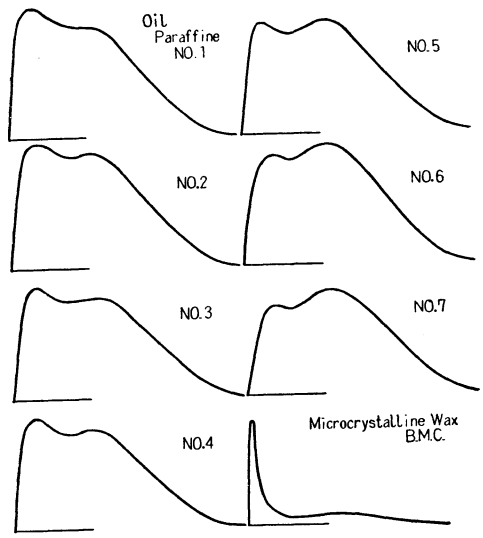



Fig. 1. Experimental derivative curves (at room temperature).

## Results and Discussion

Fig. 1 shows the derivative curves of the proton resonance absorption lines at room temperature. According to Wilson and Pake, a resonance curve with the line shape as shown in Fig. 1 may be assumed as a superposition of two lines;[1] a very narrow and a broad one. With the results of their investigations of line shape and relaxation time, they concluded that such a structure of the resonance line was due to coexistence of two components in the sample;[2] one is motional and amorphous and the other rigid and crystalline. According to their proposal, our results may

1) C. W. Wilson III and G. E. Pake, *J. Polymer Sci.*, **10**, 503 (1953).
2) C. W. Wilson III and G. E. Pake, *J. Chem. Phys.* **27**, 115 (1957).
3) A. Müller, *Proc. Roy. Soc.*, **A 120**, 437 (1928); **A 127**, 417 (1930).
4) S. Fujiwara, S. Hayashi and G. Hattori, *J. Chem. Soc. Japan, Ind. Chem. Sec.*, **59**, 803 (1956).

be treated as shown in Fig. 2, where the derivative curve is decomposed into two parts with the assumption that the line

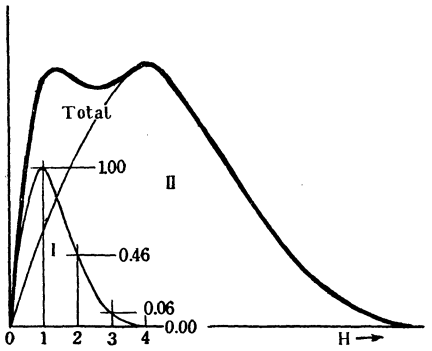



Fig. 2. Decomposition of experimental derivative curve. Experimental curve is decomposed with the assumption that the Part I of the absorption curve is of *Gaussian* type.
—— Experimental curve
—— Decomposing curve

shape of the narrow part is of Gaussian type. In Fig. 2, two components with narrow line-width and with broad one are referred to I and II, respectively. The line-width, $\Delta H$, defined as the separation between the maxima of the derivative curve, and the second moment, $\langle \Delta H^2 \rangle$, are measured for component II (see Figs. 3 and 4).

The weight percent. of the component II, $X_{II}$, is also calculated from the area occupied by II in the integrated absorption line (Fig. 5), which is referred to the degree of crystallinity as defined by Wilson and Pake.[1] The correlation time, $\tau_c$ or $(1/\nu_c)$, characteristic time scale for the molecular motion which causes the motional narrowing of the line-width, is calculated from the line-width (Fig. 6). In practice, we made a calculation of the correlation time with the assumption that the $\Delta H$ value for normal paraffin in rigid state was 15 gauss, being equal to the value for rigid polyethylene.[5]

Since the correlation time, $(1/\nu_c)$, may be related with temperature as $(1/\nu_c)=(1/\nu_0)\exp(V/kT)$,[6] where $(1/\nu_0)$ is a time constant characteristic of the sample, the activation energy $V$ for the molecular motion in the sample to cause the narrowing of the line-width may be calculated by the measurements of the temperature dependence of the line-width.

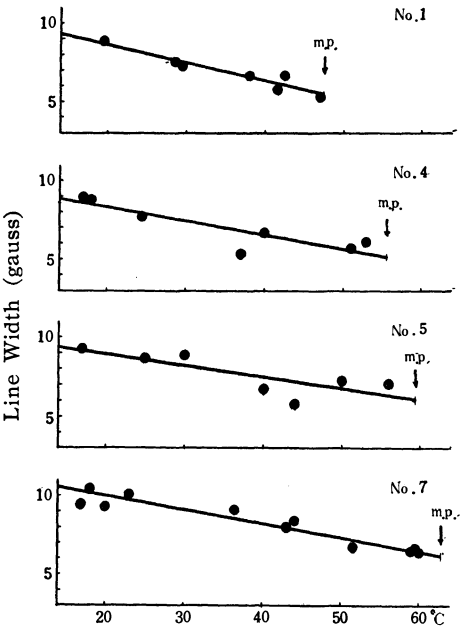



Fig. 3. Temperature dependence of the line widths. $(\Delta H)_{II}$

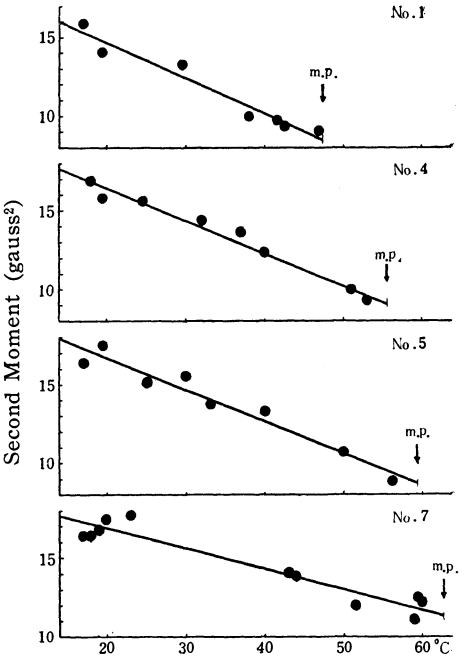



Fig. 4. Temperature dependence of the second moments. $\langle \Delta H^2 \rangle_{II}$

The experimental results of $(\Delta H)_{II}$, $X_{II}$, and $\langle \Delta H^2 \rangle_{II}$ at 19°C and $V_{II}$ are listed in Table I, and the data of temperature dependence depicted in Figs. 3, 4, 5 and 6, where the straight lines are obtained from about ten adequate points for each sample

5) A. Nishioka, private communication.
6) H. S. Gutowsky and L. H. Meyer, *J. Chem. Phys.*, **21**, 2122 (1953).

TABLE I

| Samples | m. p. °C | $(\Delta H)_{II}$* gauss | $\langle\Delta H^2\rangle_{II}$* gauss$^2$ | $X_{II}$* % | $V_{II}$ kcal./mol. |
|---|---|---|---|---|---|
| No. 1 | 47.7 | 8.8 | 14.1 | 92.9 | 3.6 |
| 2 | 50.4 | 9.7 | 15.7 | 96.7 | — |
| 3 | 52.9 | 9.6 | 16.0 | 96.7 | — |
| 4 | 55.6 | 9.8 | 15.8 | 96.3 | 2.8 |
| 5 | 59.4 | 10.2 | 17.1 | 98.0 | 2.4 |
| 6 | 60.8 | 10.2 | 17.0 | 97.6 | — |
| 7 | 62.8 | 10.5 | 16.6 | 97.0 | 2.5 |

* at 19°C

by the method of least squares, and the suffix II refers to the data for the component II.

Findings in Table I and Figs. 3, 4, 5 and 6 may be summarized as follows: first, there seems to be intimate correlation between the nuclear magnetic resonance data, such as $(\Delta H)_{II}$ and $\langle\Delta H^2\rangle_{II}$, and the composition of the samples; second, $(\Delta H)_{II}$ values are reduced gradually with temperature and become about 6 gauss just below the melting point; third, $X_{II}$ values are not much reduced with temperature; lastly, the magnitudes of the activation energies $V_{II}$ are almost equal to one another among the samples with the value of 2—3 kcal./mol.

According to the first finding, $(\Delta H)_{II}$ and $\langle\Delta H^2\rangle_{II}$ values for the samples with higher melting point are larger than those with lower melting point. This may suggest that the component II in the samples with higher melting point is less motional than that in those with lower melting point. In another words, line-width data of the component II may be useful for the qualitative analysis of the melting point.

The second finding on the temperature dependece of the line-width of component II seems valuable to answer the question, "What kind of molecular motion would occur prior to melting of linear polymers?" Information we have had so far for this problem by any method such as dielectric measurements is rather insufficient.[7] According to the present results, as seen in Fig. 3, the molecular motion in component II increases with temperature, but the magnitude of this motion, of vibrational or diffusional nature, appears to be small* and the molecular state to be relatively close to the rigid lattice state up to melting.

7) R. F. Boyer, *J. Appl. Phys.*, **25**, 825, (1954).

* Magnetic dipolar broadening of the line-width value is easily reduced to one half or one third of the rigid lattice value by any molecular rotation[8]. In the present results, the $(\Delta H)_{II}$ values are ranged around 6 to 10 gauss, which are compared with the rigid value of 15 gauss.

As shown by one of the present authors,[9] the difference in the line-width, and consequently in the correlation time, among the samples with the same magnitude of $V$ is attributed to the difference in the degree of polymerization among the samples. Thus the difference in line-width or correlation time among the samples No. 1, 4, 5 and 7 seems to be attributed to the difference in their molecular dimensions.

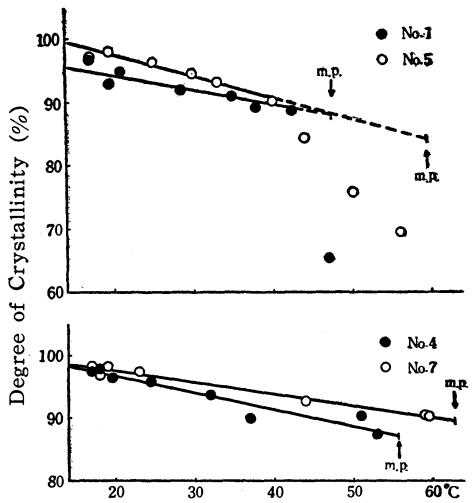



Fig. 5. Temperature dependence of the degree of crystallinity. $X_{II}$%.

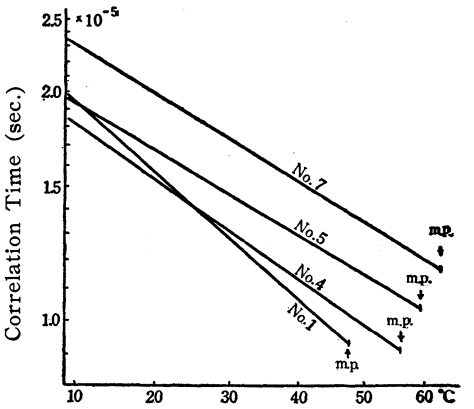



Fig. 6. Temperature dependence of the correlation time. $1/\nu_c$.

It is noted, especially, that the degree of crystallinity, $X_{II}$, is not much reduced prior to melting. This will suggest that the molecules maintain relatively rigid configurations between the nuclear nearest neighbors up to melting.

8) E. R. Andrew, *J. Chem. Phys.*, **18**, 607 (1950).

9) S. Fujiwara, to be published in this Bulletin.

Throughout the cases of the experiments, it was also found that both line-width and second moment values kept sizable magnitudes up to just below the melting point. These findings are very prominent and in contrast to the result on cyclohexane, where rapid decrease of the second moment occurs 130°C prior to melting.[10]

Namely, in the latter case, the molecular reorientation with fixed center of mass occurs 130°C prior to melting, whereas in the former, the molecules are relatively static up to just below the melting point.

The degree of crystallinity of microcrystalline paraffin waxes is much smaller than that of oil paraffins, and is about 90% at room temperature. This result perhaps shows the segments in microcrystalline waxes are much smaller and easier to diffuse in the sample than that in oil paraffins.

Many thanks are due to Mr. Kenzo Fusegawa of Dai Nippon Seiro Co., who gave us the samples used in the present experiments.

*University of Electro-communications*
*Chofu, Tokyo*

10) E. R. Andrew and R. G. Eades, *Proc. Roy, Soc.*, **A 216**, 398 (1953).

# *Stoichiometric Investigations of the Liquid State IV*[*1]. Viscosity of Associated Liquid*

By Kiyoshi TYUZYO[*2]

(Received May 9, 1957)

It is well known that viscosity of pure liquid is generally expressed by eq. (1), according to Eyring's absolute reaction rate theory.

$$\eta=\frac{hN}{V}e^{\Delta F^{\ddagger}/RT} \tag{1}$$

where $h$ is Planck's constant, $N$, Avogadro's number, $\Delta F^{\ddagger}$, standard free energy of activation per mole, and

$$\Delta F^{\ddagger}=\Delta H^{\ddagger}-T\Delta S^{\ddagger} \tag{2}$$

Ep. (1) can be rewritten as eq. (3)

$$\eta=\left[\left(\frac{hN}{V}\right)e^{-\Delta S^{\ddagger}/R}\right]e^{\Delta H^{\ddagger}/RT} \tag{3}$$

where $\Delta H^{\ddagger}$, standard energy of activation per mole and $\Delta S^{\ddagger}$ standard entropy of activation per mole.

In general, the temperature variance of the frequency factor of eq. (3) is very little compared with that of the exponential energy factor. Therefore, eq. (1) can be rewritten as eq. (4).

$$\eta=Ae^{E_{vis}/RT} \tag{4}$$

where $E_{vis}$ is activation energy per mole for viscous flow.

In the case of associated liquid, Eyring and others[1] thought that $E_{vis}$ depends upon temperature because of the destruction of hydrogen bond with increase in temperature. They showed that $E_{vis}$ decreases with the increase of temperature in the case of water, ethylene glycole and glycerin, but said nothing about typical associated liquid such as saturated alcohol and fatty acid. Thereafter, investigations concerning the viscosity of associated liquid[2-4] are unexpectedly few. The present author discussed the reasonableness of classifying associated liquid into two kinds from analysis of sound velocity in liquid in the previous paper[5]. In the other paper[6], an empirical method for calculating the degree of association of associated liquid of the first kind was proposed. In this paper, detailed analysis of viscosity of associated liquid is presented.

## Method and Result

$E_{vis}$ can be calculated by eq. (5) from eq. (4).

*1 The third paper of this series, *Bull. Chem. Soc. Japan*, **27**, 306 (1954).

*2 Present address: Research Laboratory, Dai-Nippon Celluloid Co., Sakai, Osaka.

1) S. Glasstone, K. J. Laidler and H. Eyring, "The Theory of Rate Processes" p. 477 (1941).
2) O. Kimura, *J. Chem. Soc. Japan*, **63**, 1068 (1942).
3) Y. Wada, *J. Phys. Soc. Japan*, **4**, 136 (1949).
4) L. Grunberg, and A. H. Nissan, *Trans. Faraday Soc*,, **45**, 125 (1949).
5) K. Tyuzyo, This Bulletin **27**, 306 (1954).
6) K. Tyuzyo, *Kolloid-Z*, **131**, 40 (1953).

TABLE I

$E_{vis}$, $A$ AND DIELECTRIC CONSTANT OF ASSOCIATED LIQUID

| Substance | $E_{vis}$ (Kcal/mole) | $A$ | Range (°C) | Dielectric constant | {temp. / freq.} |
|---|---|---|---|---|---|
| | saturated fatty acid | | | | |
| formic acid | 3.35 | $5.63\times10^{-5}$ | 8～100[a] | 58.5 | {16 / 0} |
| acetic acid | 2.66 | $1.29\times10^{-4}$ | 31～119 | 6.17 | {20 / 0} |
| propionic acid | 2.47 | 1.63 〃 | 17～137 | 3.1 | {room. temp. / $\lambda$=83 cm} |
| n-butylic acid | 2.81 | 1.25 〃 | 18～156 | 3.0 | {room. temp. / 0} |
| *n*-valeric acid | 3.27 | $8.24\times10^{-5}$ | 16～90[a] | | |
| *n*-caproic acid | 3.57 | 7.06 〃 | 〃 | | |
| *n*-heptylic acid | 3.84 | 6.05 〃 | 20～90 | | |
| *n*-caprylic acid | 4.18 | 4.07 〃 | 50～90 | | |
| *n*-pelargonic acid | 4.58 | 3.11 〃 | 20～90 | | |
| *n*-capric acid | 4.76 | 2.71 〃 | 50～70 | | |
| *n*-lauric acid | 5.10 | 2.69 〃 | 50～160 | | |
| *n*-myristic acid | 5.34 | 2.46 〃 | 60～90 | | |
| *n*-palmitic acid | 5.54 | 2.40 〃 | 70～95 | | |
| *n*-stearic acid | 5.74 | 2.26 〃 | 70～98 | | |
| | saturated aliphatic alcohol | | | | |
| methyl alcohol | 2.61 | $6.92\times10^{-5}$ | 0～60 | 31.8 | {19 / 0} |
| ethyl alcohol | 3.57 | 2.74 〃 | 10～90 | 25.8 | {20 / 0} |
| propyl alcohol | 4.39 | 1.24 〃 | 10～96 | 21.3 | {19 / 0} |
| *n*-butyl alcohol | 4.64 | 1.07 〃 | 10～114 | 19.1 | {19 / 0} |
| *n*-amyl alcohol | 5.20 | $7.30\times10^{-6}$ | 12～80 | 16.0 | {room temp. / 0} |
| *n*-hexyl alcohol | 5.40 | 4.97 〃 | 25～50 | | |
| *n*-heptyl alcohol | 5.76 | 3.63 〃 | 25～90 | | |
| *n*-octyl alcohol | 5.99 | 3.13 〃 | 15～90 | | |
| *n*-cetyl alcohol | 6.86 | 2.74 〃 | | | |
| | others | | | | |
| hydrogen cyanide | 1.64 | $1.15\times10^{-4}$ | 0～20 | ca. 95 | {21 / $\lambda$=84cm.} |
| hydrogen fluoride | 1.69 | 1.19 〃 | −90～20 | 83.6 | {0 / 0} |
| formamide | 4.10 | $3.07\times10^{-5}$ | 0～120 | 111.5 | {20 / 0} |
| water | varies with temperature | varies with temp. | | 81 | {19 / 0} |
| ethylene glycole | | | | 38.7 | |
| glycerine | | | | 63 | {−50 / 0} |
| aniline | | | | 7.21 | {20 / 0～$4\times10^{8}$} |
| ammonia | | | | 25 | {−77.7 / 0} |

a) $\log\eta$ vs. $1/T$ somewhat curves.

$$E_{.i}=\frac{\mathrm{d}\ln\eta}{\mathrm{d}(1/T)}\times R \qquad (5)$$

When $\ln\eta$ vs. $1/T$ is linear, $E_{vis}$ it constant, independent of the temperature. In Table I, $E_{vis}$ and $A$ of several kinds of associated liquid are shown. In the table, dielectric constant is also shown, to be used aftewards*.

* Viscosity and dielectric constant are adopted from the following literatures.
*International Critical Tables*; *Landolt-Börnstein, Phys.-Chem Tabellen*; D'Ans-Lax, *Taschenbuch für Chemiker und Physiker.*

## Discussion

**(1) Classification of associated liquid.**—It is clear from Tab. I, that associated liquid can be distinguished clearly into two classes. $E_{vis}$ of one class is constant, independent of the temperature, that of the other class decreases with increase in temperature. Several examples are shown in Fig. 1. In the figure, formic acid and methyl alcohol belong to the former, whereas water and aniline to the latter. Therefore, the author proposes to classify associated liquid into two groups, as shown below. This method of classification is almost consistent with that based on sound velocity discussed in the previous paper[5]. This method is also almost completely consistent with that of Ewell and others[7].

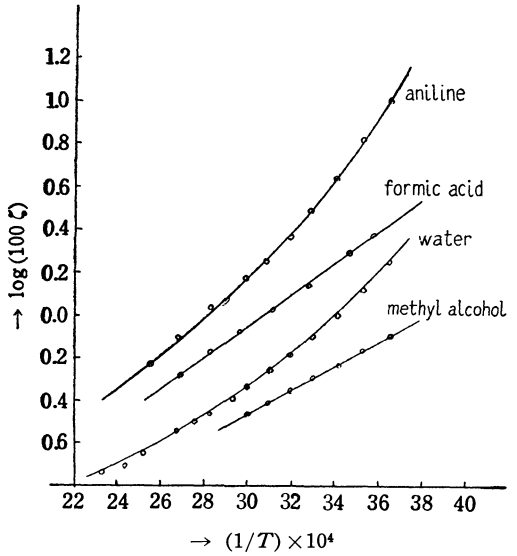



Fig. 1. Viscosity vs. temperature of several associated liquids.

a) *Associated liquid of the first kind*

$E_{vis}$ is constant, independent of the temperature as high as the boiling point. In this class of associated liquid, associated bodies can be distinguished clearly from one another, owing to the strong hydrogen bond. Each associated body flows as a unit without destroying hydrogen bond on viscous flow.

Example: saturated fatty acid, saturated alcohol*, hydrogen cyanide, hydrogen flouoride, formamide.

b) *Associated liquid of the second kind*

$E_{vis}$ decreases with increase in temperature. In this class of associated liquid, there are no distinguishable associated bodies owing to the weak hydrogen bond. The whole liquid makes a three-dimensional network structure and hydrogen bond is destroyed on viscous flow. This flow mechanism is consistent with that of Eyring and others[1].

Examples: water, ethylene glycole, glycerin, ammonia, aniline.

In Table II, values of hydrogen bond energy are shown[10]. In general, hydrogen bond energy of the associated liquid of the first kind is somewhat larger than that of the associated liquid of the second kind except hydrogen cyanide. However, the idea that this small difference in hydrogen bond energy causes the above-mentioned fundamental difference of the behavior of viscous flow is quite questionable. Details of hydrogen bond energy may be discussed in the next paper of this series.

TABLE II
ENERGY OF HYDROGEN BOND

| Substance | State | Method | Energy (Kcal./mole) |
|---|---|---|---|
| HF | gas | vapor density | 6～10 |
| Fatty acid | gas | vapor density | 7～9 |
| Alcohol | liquid | heat of vapor | 6～7 |
| | gas | heat conduct. | 7～8 |
| HCN | gas | vapor density | 3～4 |
| Water | s, l, g | heat of vapor | 4～5 |
| | | second virial | |
| | gas | second virial | 3～4 |
| Ammonia | liquid | dielectric const. | 6 |
| | solid | heat of sublim. | 1.3 |
| Acetamide | solid | heat of sublim. | 3.5 |
| Aniline | | partition coeff. ($CCl_4$—$H_2O$) | 1.93 |

**(2) $E_{vis}$ of unassociated liquid.**—In this paragraph, $E_{vis}$ of unassociated liquid is treated in outline, in order to clarify the structure and the degree of association of associated liquid of the first kind.

a) *$E_{vis}$ of n-paraffin*

Relation between $E_{vis}$ and molar volume ($V$)* at room temperature of $n$-paraffin is shown in Fig. 2. In this figure, $E_{vis}$ is

7) R. H. Ewell, J. M. Harrison and L. Berg, *Ind. Eng. Chem.*, **36**, 871 (1944).

* In some papers[8,9], it is said that $E_{vis}$ of fatty acid and alcohol varies with temperature but this variance is little. Moreover, $E_{vis}$ is dependent upon temperature with some degree even in $n$-paraffin. Therefore, it is reasonable to regard $E_{vis}$ of fatty acid and alcohol as being independent of temperature at this time.

8) A. Bondi, *J. Chem. Phys.*, **14**, 591 (1946).

9) T. A. Litovitz, *J. Chem. Phys.*, **20**, 1088 (1952).

10) L. N. Fergusson, "Electron Structures of Organic Molecules", p. 57 (1952); S. Seki, *Chem. and Chem. Ind., Japan*, **6**, 217 (1953).

* Molar volume at 50°C is adopted in the case of higher members.

calculated from recent data[11]. From this figure, eq. (6) is obtained.

$$E_{vis}(\text{Kcal/mole}) = 5.18 \log V(\text{cc/mole}) - 9.07 \quad (6)$$

Eq. (6) is applicable at least to the range of $V$ from 80 to 570. It is natural that eq. (6) is not applicable when viscous flow becomes segmental because of independence of $E_{vis}$ upon $V$ in such a region.

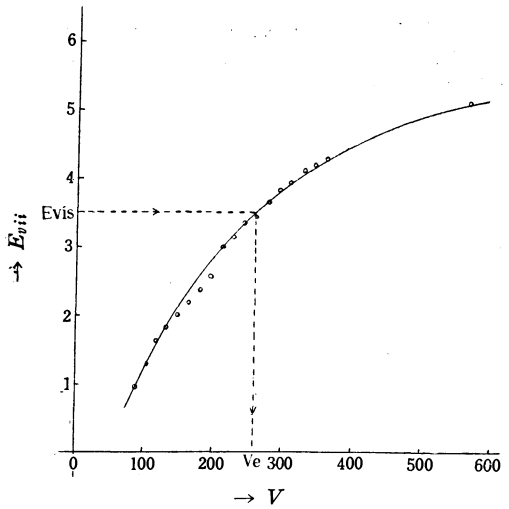



Fig. 2. $E_{vis}$ vs. $V$ of $n$-paraffins.

b) *$E_{vis}$ of unassociated liquid except n-paraffin*

$E_{vis}$ of unassociated liquid is compared with that of $n$-paraffin. Results are summarized as follows.

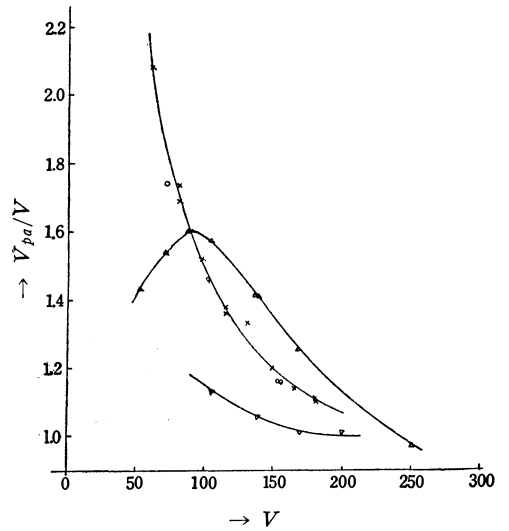



Fig. 3. $V_{pa}/V$ vs. $V$ of polar liquids.
×: ester ○: ketone
△: alkyl-chloride ▽: ether

11) "Selected Values of Properties of Hydrocarbons", (National Bureau of Standards), 1947.

i) Compared with the same value of $V$, $E_{vis}$ of branched aliphatic compounds is almost the same as that of linear aliphatic compound within ±10%. This means that the influence of branching upon $E_{vis}$ is very small.

ii) Compared with the same value of $V$, $E_{vis}$ of polar compounds is greater than that of $n$-paraffin, but this difference decreases rapidly with higher homologous members and is almost zero in the region of $V$ greater than 200. Fig. 3 shows this relation. In the figure, abscissa is $V$ and ordinate is the ratio of $V$ of $n$-paraffin having the same value as $E_{vis}$ of the polar compound (hereafter, $V_{pa}$) to $V$ of the polar compound.

iii) Compared with the same value of $V$, $E_{vis}$ of cyclic compounds having no substituted group is much greater than that of $n$-paraffin. Namely, $V_{pa}/V \fallingdotseq 2.0$, independent of polarity. This is shown in Table III. It is clear from this fact that rigidity of structure has great influence upon viscous flow.

TABLE III
$V_{pa}/V$ OF CYCLIC COMPOUND WITH NO SUBSTITUTED GROUP

| Substance | $V$ | $E_{vis}$ | $V_{pa}/V$ |
|---|---|---|---|
| Benzene | 89 | 2.52 | 2.0 |
| Cyclohexane | 108 | 2.90 | 1.9 |
| Dioxane | 85.4 | 2.88 | 2.4 |
| Thiophene | 78.7 | 2.17 | 1.9 |
| Pyridine | 80.8 | 2.48 | 2.2 |
| Cycopentane | 94 | 1.88 | 1.4 |
| Biphenyl | 155 | 3.61 | 1.8 |

iv) $V_{pa}/V$ decreases rapidly with increase of the number of substituted group of cyclic compound. Some examples are shown in Table 4.

TABLE IV
INFULENCE OF SUBSTITUTED GROUP OF CYCLIC COMPOUND UPON $V_{pa}/V$

| Substance | $V$ | $E_{vis}$ | $V_{pa}/V$ |
|---|---|---|---|
| Benzene | 89 | 2.52 | 2.0 |
| Toluene | 106 | 2.90 | 1.9 |
| Ethyl benzene | 122 | 2.17 | 1.3 |
| $n$-Butyl benzene | 156 | 2.03 | 0.9 |
| Cyclohexane | 108 | 2.90 | 1.9 |
| Methyl cyclohexane | 128 | 2.50 | 1.4 |
| 1,2-Dimethyl cyclohexane | 144 | 2.35 | 1.2 |

(3) **Entropy of activation, $\Delta S^{\neq}$ of viscous flow of unassociated liquid**—$\Delta S^{\neq}$ is calculated as follows.

In eq. (4),

TABLE V
ENTROPY OF ACTIVATION OF VISCOUS FLOW OF UNASSOCIATED LIQUID

| Substance | $A$ | $\Delta S^{\ddagger}$ (E.U./mole) |
|---|---|---|
| Methane | $1.09\times10^{-4}$ | −0.93 |
| Carbon tetrachloride | 1.23 〃 | −2,21 |
| Benzene | $8.71\times10^{-5}$ | −1.32 |
| Cyclohexane | 6.76 〃 | −1.21 |
| Dioxane | 9.16 〃 | −1.40 |
| Carbon disulfide | $4.25\times10^{-4}$ | −3.71 |
| Toluene | 1.55 〃 | −2.83 |
| Acetone | 1.95 〃 | −2.56 |
| Methyl ethyl ketone | 1.55 〃 | −2.76 |
| Ether | 1.55 〃 | −2.71 |
| *n*-Ethyl valeriate | 1.32 〃 | −3.20 |
| *n*-Butyl valeriate | 1.12 〃 | −3.23 |
| *n*-Butyl butylate | 1.32 〃 | −3.37 |
| *n*-Amyl n-butylate | 1.20 〃 | −3.38 |
| Ethyl chloride | 2.29 〃 | −2.80 |
| Ethylene chloride | 2.95 〃 | −3.10 |
| Chloroform | 2.82 〃 | −3.46 |
| *n*-Propyl chloride | 1.32 〃 | −2.14 |
| Ethyl bromide | 1.55 〃 | −2.13 |
| Thiophene | 1.62 〃 | −2.40 |
| Pyridine | 1.41 〃 | −2.20 |
| Ethane | 2.49 〃 | −3.06 |
| Propane | 2.69 〃 | −3.57 |
| *n*-Butane | 1.94 〃 | −3.19 |
| *n*-Pentane | 1.36 〃 | −2.76 |
| *n*-Hexane | 1.34 〃 | −2.99 |
| *n*-Heptane | 1.33 〃 | −3.20 |
| *n*-Octane | 1.29 〃 | −3.34 |
| *n*-Nonane | 1.23 〃 | −3.44 |
| *n*-Decane | 1.15 〃 | −3.45 |
| *n*-Undecane | $7.13\times10^{-5}$ | −2.68 |
| *n*-Dodecane | 6.70 〃 | −2.69 |
| *n*-Tridecane | 6.11 〃 | −2.64 |
| *n*-Tetradecane | 6.40 〃 | −2.87 |
| *n*-Pentadecane | 5.53 〃 | −2.69 |
| *n*-Hexadecane | 4.92 〃 | −2.57 |
| *n*-Heptadecane | 4.72 〃 | −2.59 |
| *n*-Octadecane | 4.13 〃 | −2.44 |
| *n*-Nonadecane | 4.34 〃 | −2.65 |
| *n*-Eicosane | 3.65 〃 | −2.40 |
| | Average | −2.9 |

$$A=\frac{hN}{V}e^{-\Delta S^{\ddagger}/R} \tag{7}$$

Inserting numerical values of $R$, $h$, $N$ into eq. (7),

$$\Delta S^{\ddagger}=-11.1-4.6\log(VA) \tag{8}$$

$\Delta S^{\ddagger}$ is easily calculated from eq. (8). Results are shown in Table V. It is clear from the table that

a) $\Delta S^{\ddagger}$ is almost constant and approximately equal to −2.9 E.U./mole, irrespective of polar and non-polar liquid except spherical molecules.

b) $\Delta S^{\ddagger}$ of spherical molecules is abnormal and approximately equal to −1.0∼−2.0 E.U./mole. Abnormality of $E_{vis}$ of spherical molecules is already shown by Eyring and others[12]. It is very interesting that $\Delta S^{\ddagger}$ of spherical molecules is also abnormal as is shown above.

(4) **Method for calculating degree of association of associated liquid of the first kind.**—As is shown in (1), hydrogen bond is not destroyed on viscous flow of associated liquid of the first kind. Then, it is probable that viscous flow of this kind of associated liquid is quite analogous to that of unassociated liquid. Therefore, degree of association is calculated by the following method, on trial[6].

a) *Method based on $E_{vis}$*

It is already shown that relation between $E_{vis}$ and $V$ at room temperature for *n*-paraffin is as Fig. 2 and expressed by eq. (6). $V$ of *n*-paraffin, corresponding to $E_{vis}$ of associated liquid of the first kind, can be obtained from Fig. 2 or eq. (6). This is termed $V_e$. Then, degree of association is calculated by eq. (9). Degree of association calculated by eq. (9) is termed as $n_e$.

$$n_e=V_e/V \tag{9}$$

where $V$ is normal molar volume.

$n_e$ is shown in Table VI. $n_s$ in the table is referred to in the next paragraph. Degree of association from literature is also shown in the table. The following points are clear from the table.

i) $n_e$ is surprisingly consistent with value from literature.

ii) It is possible to calculate easily the degree of association which has not been known until now.

iii) The $n_e$ values for formic and acetic acid are much greater than 2 on the contrary to propionic acid and higher members of saturated fatty acid. This means that the state of association is different from each other. Investigation of the state of association in the pure liquid state is very rare. But according to the investigation of infra-red spectra by Batuev[14], formic and acetic acid make linear chain association and propionic acid and higher members make ring-like dimer association,

12) H. Eyring, *J. Chem. Phys.*, **4**, 283 (1936); R. H. Ewell and H. Eyring, *J. Chem. Phys.*, **5**, 726 (1937).

13) W. Kauzmann and H. Eyring, *J. Am. Chem. Soc.*, **62**, 3113 (1640).

14) M. I. Batuev, *Chem. Abst.*, 1936, 2994, 2995, 6154(1947).

TABLE VI

DEGREE OF ASSOCIATION OF THE ASSOCIATED LIQUID OF THE FIRST KIND

| Substance | $V$ | $V_e$ | $n_e$ | $V_s$ | $n_s$ | $n$ | Lit. of $n$ |
|---|---|---|---|---|---|---|---|
| | saturated fatty acid | | | | | | |
| formic acid | 37.7 | 251 | 6.7 | 303 | 8.0 | Polymer | Batuev[14] |
| acetic acid | 57.2 | 194 | 3.4 | 132 | 2.3 | 〃 | 〃 |
| propionic acid | 74.6 | 179 | 2.4 | 105 | 1.4 | 2 | Batuev[14] & |
| *n*-butylic acid | 91.9 | 206 | 2.2 | 136 | 1.5 | 〃 | Gibling[15] |
| *n*-valeric acid | 108.9 | 245 | 2.2 | 201 | 1.9 | 〃 | 〃 |
| *n*-caproic acid | 125.0 | 268 | 2.1 | 249 | 2.0 | 〃 | 〃 |
| *n*-heptylic acid | 141.9 | 298 | 2.1 | 315 | 2.2 | 〃 | 〃 |
| *n*-caprylic acid | 158.6 | 337 | 2.1 | 426 | 2.7 | 〃 | 〃 |
| *n*-pelargonic acid | 174.5 | 400 | 2.3 | 541 | 3.1 | 〃 | 〃 |
| *n*-capric acid | 196.2 (50°C) | 433 | 2.2 | 608 | 3.1 | 〃 | 〃 |
| *n*-lauric acid | 229.8 (50°C) | 516 | 2.2 | 655 | 2.8 | 〃 | 〃 |
| *n*-myristic acid | 270.4 (50°C) | 603 | 2.2 | 695 | 2.6 | 〃 | 〃 |
| *n*-palmitic acid | 304.6 (50°C) | 668 | 2.2 | 725 | 2.4 | 〃 | 〃 |
| *n*-stearic acid | 338.9 (50°C) | 724 | 2.1 | 758 | 2.2 | 〃 | 〃 |
| | saturated aliphatic alcohol | | | | | | |
| methyl alcohol | 40.5 | 191 | 4.7 | 245 | 6.0 | 5.0 | Eucken[16] |
| ethyl alcohol | 58.3 | 268 | 4.6 | 605 | 10.0 | 4.7 | 〃 |
| propyl alcohol | 75.0 | 367 | 4.9 | 1170 | 15.6 | 4.7 | 〃 |
| *n*-butyl alcohol | 92.0 | 411 | 4.5 | 1690 | 18.4 | — | — |
| *n*-amyl alcohol | 107.7 | 575 | 5.3 | 2610 | 24.3 | — | — |
| *n*-hexyl alcohol | 125.2 | 617 | 4.9 | 3390 | 27.0 | — | — |
| *n*-heptyl alcohol | 140.7 | 741 | 5.3 | 4240 | 29.8 | — | — |
| *n*-octyl alcohol | 156.7 | 813 | 5.2 | 5660 | 35.6 | — | — |
| *n*-cetyl alcohol | (285) | 1202 | 4.3 | 6780 | 23.0 | — | — |
| | others | | | | | | |
| hydrogen cyanide | 38.5 | 119 | 3.1 | 148 | 3.8 | 3 | Pauling[17] |
| hydrogen fluoride | 20.4 | 112 | 6.0 | 143 | 7.1 | 6～10 | Bauer et al[18] |
| formamide | 39.9 | 331 | 8.3 | 553 | 13.8 | — | — |

as is generally recognised. This is quite consistent with the above result. The following paragraph (5) may be refered to about this fact.

iv) $n_e$ of saturated aliphatic alcohol is 5, independent of the carbon number. This result is consistent with Eucken's[16].

v) $V_e$ and $n_e$ of stearic acid are 724 and 2 respectively. $V_e$ and $n_e$ of octyl alcohol are 813 and 5.2 respectively. These are quite reasonable values. But $n_e$ of cetyl alcohol is 4.3 and is slightly smaller than 5. From these facts, it can be supposed that the limit of eq. (6) exists between 810 and 1200 of $V$. Namely, it can be supposed that segmental flow occurs at least in the range of carbon numbers of greater than 50 for *n*-paraffin. This result is different from Kauzmann and Eyring's[13].

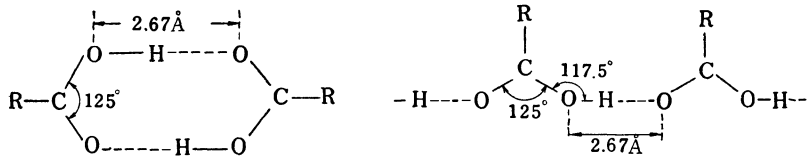
vi) No conclusive method has been so far found for determining degree of association in the pure liquid state. Moreover, accessible methods are all roundabout and complex. Although the above method is quite empirical, it is very effective under such a circum-stance.

b) *Method based on* $\Delta S^*$

It is shown in Paragraph (3) that $\Delta S^*$ of unassociated liquid is about $-2.9$ EU./mole except in the case of spherical molecules. Inserting $\Delta S^* = -2.9$ in eq. (8), eq. (10) is obtained. $V$ from this is expressed as $V_s$.

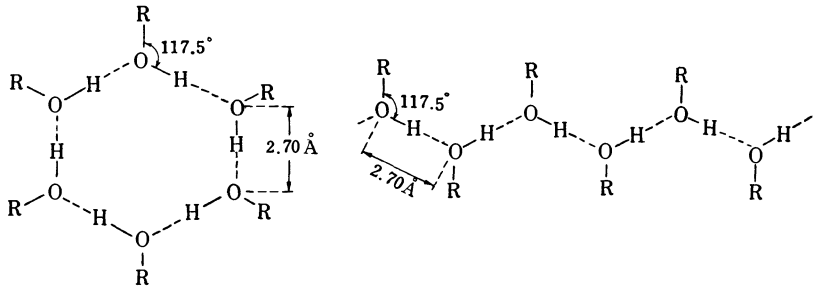
$$V_s = 1.70 \times 10^{-2}/A \qquad (10)$$

15) T. W. Gibling *J. Chem. Soc.*, 665 (1942).
16) A. Fucken, *Z. Elektrochem.*. **52**, 255 (1948).
17) L. Pauling, *Nature of Chemical Bond*, p. 275 (1939).
18) S. H. Bauer, J. Y. Beach and J. H. Simons, *J. Am. Chem. Soc.*, **67**, 757 (1945).




(a) (b)

Fig. 4. Associated state of saturated fatty acids.




(a) (c)

Fig. 5. Associated state of saturated aliphatic alcohols[20].

In eq. (10), $A$ is obtained from temperature variance of viscosity by eq. (4). Degree of association, $n_s$ may be calculated by eq. (11).

$$n_s = V_s/V \qquad (11)$$

where $V$ is normal molar volume. The $n_s$ values are shown in Table VI.

It is clear from the table that $n_s$ is fairly consistent with values from literature, although the agreement is not so good as for $n_e$. However, $n_s$ of saturated alcohol is quite different from the observed value. The reason for this is not clear, but it may be supposed that polydispersity of association of saturated alcohol[19] in the liquid state may have some influence upon this point.

(5) **Associated state of associated liquid of the first kind.**—In this paragraph, association state of associated liquid of the first kind is discussed in detail.

(a) *formic acid*

According to (4), degree of association of formic acid is 7 to 8. If association state is a ring-like dimer as is shown in Fig. 4-(a), $V_{pa}/V \fallingdotseq 2.0$ from (2)-(b), because this state is non-branched ring. But as

$$E_{vis}=3.35,\ V_{pa}/V=251/2\times 37.7=3.3\neq 2.0$$

This is unreasonable. Moreover, the dielectric constant is very great (58.5 as is shown Table I), and liquid viscosity is almost the same as that of valeric acid, which is higher than acetic and propionic acid. Considering these facts, it is reasonable that association is chain association as is shown in Fig. 4-(b).

(b) *acetic acid*

According to (4), $n$ is about 3. If association state is ring-like dimer as is shown in Fig. 4-(a), $V_{pa}/V=194/2\times 57.2=1.7$. But $V_{pa}/V$ of such a slightly branched ring compound is 1.2 to 1.5 from (2)-(b). Moreover, dielectric constant is comparatively small (6.17 as is shown in Table I) and viscosity is higher than that of propionic acid. Considering these facts, it is reasonable that association state is the mixture of dimer association and chain association as is shown in Fig. 4-(a), (b).

(c) *saturated fatty acid higher than propionic acid.*

According to (4), $n=2$. If association state is a perfect ring-like dimer as is shown in Fig. 4-(a), $V_{pa}/V=1.0$. $V_{pa}/V$ of such a branched ring compound is 1 from (2)-(b). Both these are quite consistent. Moreover, dielectric constant is small (2 to 3 as is shown in Table I). Considering these facts, it is reasonable to assume that association state is dimer association as is shown in Fig. 4-(a).

(d) *saturated alcohol*

According to (4), $n=5$. If association state is ring-like association of $n=6$, $V_{pa}/V=1.0$ from (2)-(b). However, $V_{pa}/V = \frac{5}{6} \neq 1$. Moreover, the dielectric constant

19) K. L. Wolf and R. Wolff, *Angew. Chem.*, **61**, 191 (1949).

20) L. Pauling, "Nature of Chemical Bond", p. 285 (1939).

is the greatest for methyl alcohol (31.8) and becomes smaller with increasing number of carbon atom. However, dielectric constants of all these compounds are much greater than those of fatty acid higher than propionic acid. Therefore, it is reasonable that association state is chain association as is shown in Fig. 5-(b). Eucken concluded chain association of $n=5$ for lower alcohols[16]. This conclusion is quite consistent with the above.

(e) *hydrogen fluoride*

According to (4), $n=6\sim7$ and is consistent with the value from literature[18]. If association state is unbranched ring-like association, $V_{pa}/V=2.0$ from (2)-(b). Then from observed $E_{vis}$, $V_{ag}=V_{pa}/2.0=122/2.0=61$. Therefore. $n=61/20.4\fallingdotseq3$. This value is unreasonable, on the basis of the ring-like structure and is not consistent with the observed value. Moreover, dielectric constant is very great (83.6 as is shown in Table I). When these facts are considered, it is reasonable that association state is chain association of $n=6\sim7$ as is shown in Fig. 6.

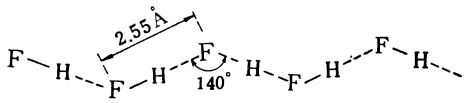



Fig. 6. Association state of hydrogen fluoride[21].

(f) *Hydrogen cyanide*

According to (4), $n=3$ and is consistent with the value from literature[17]. If association state is unbranched ring-like association, $V_{pa}/V=2.0$ from (2)-(b). Then from observed $E_{vis}$, $V_{ag}=V_{pa}/2.0=59.5$. Therefore, $n=59.5/38.5=1.6$. This value is unreasonable, on the basis of the ring-like structure and is not consistent with the observed value. Moreover, dielectric constant is very great (ca. 95 as is shown in Table I). When these facts are considered, it is reasonable that association state is chain association of $n=3$.

(g) *Formamide*

According to (4), $n=8\sim14$. If association state is unbranched ring-like association, $V_{pa}/V=2.0$ from (2)-(b). Then from observed $E_{vis}$, $V_{pa}/V=V_{pa}/2=165.5$. Therefore, $n=165.5/39.9\fallingdotseq4$. A decisive conclusion cannot be made because of the lack of the observed value. The dielectric constant is very great (111.5 as is shown in Table I). Considering these, it is probable that association state is chain association of $n=8\sim14$.

(6) Association degree of alcohols, hydrogen fluoride and hydrogen cyanide from (4) is quite consistent with the observed degree. On the other hand, these liquids are chain association and their dielectric constants are great as is discussed in (5). If the non-polar part is extremely great compared with the polar part of polar liquid, $V_{pa}/V=1.0$ according to (2). But, in the case of the above compounds, polar part is not always extremely small compared with non-polar part. In spite of this, $V_{pa}/V_{ag}=1$ as is shown in (5). A complete explanation of this fact can not be given at present.

## Summary

(1) It is concluded from analysis of viscous flow that associated liquid can be classified as follows.

*The first kind:* Associated bodies can be distinguished clearly from one another, owing to the strong hydrogen bond. Each associated body flows as a unit in the case of viscous flow.

Examples: saturated fatty acid, saturated aliphatic alcohol, hydrogen fluoride, hydrogen cyanide.

*The second kind:* There are no associated bodies which are distinguished clearly from one another, owing to the weak hydrogen bond. The liquid makes overall three-dimensional network structure. Hydrogen bond is destroyed in the case of viscous flow.

Examples: water, ethylene glycole, glycerin, ammonia.

(2) Influence of branching, polar group and ring upon activation energy of viscous flow of unassociated liquid is discussed.

(3) It is found that entropy of activation of viscous flow of unassociated liquid is constant and equal to ca. −2.9 E.U./mole with some exceptions.

(4) The method for calculating degree of association of associated liquid of the first kind from energy and entropy of activation of viscous flow is presented.

(5) Association state of the first kind liquid is discussed in detail.

The author expresses his sincere thanks to Professor Dr. N. Sata and Mr. M. Okuyama of Osaka University for their kind instruction.

*Department of Chemistry, Faculty of Science, Osaka University, Nakanoshima, Kita-ku, Osaka*

21) L. Pauling, "Nature of Chemical Bond", p. 276 (1939),

# *Studies on Organic Reagents for Inorganic Analysis. II*[1]. *Spectrophotometric Study on Phenylfluorone Chelates of the Fourth Group Metal Elements**

By Hirotoshi SANO

(Received March 26, 1957)

## Introduction

The study on the nature of the reaction of metals with organic reagents is very important for the purpose of selecting or sythesizing an organic reagent useful for the colorimetric determination of a metal. There are two groups of organic reagents used for this purpose; (1) For the first group, e. g. ethylene diamine or EDTA, the light absorption is attributed to the electronic transition from nonbonding orbital to antibonding orbital in a central metal atom as is usual with simple inorganic complexes[2]. (2) Most organic dyes used as the reagents for the colorimetric determination of metals belong to the second group, and their color changes are, as is stated in the following, ascribable to the shift of the $\pi \rightarrow \pi^*$ absorption spectra of the organic system caused by the bond formation between the metal and the donor atom of the reagent. For the investigation of such a color change, it is necessary to understand the general theory of light absorption of organic dyes. As is well known, there are essentially three methods, valency bond method, molecular orbital method, and free electron gas model method. Among them, the last method is much simpler than the others, and moreover its utility is almost comparable to that of the molecular orbital (L. C. A. O.) method which needs the cumbersome procedure of solving secular equations[3].

Recently, the free electron gas model method has been used extensively for calculating the wavelength of the absorption maximum in the spectrum of conjugated organic compound[4-11]. In particular, H. Kuhn has applied this method successfully to various organic dyes[7-11]. According to him, the electron gas in the cases of polyenes, unsymmetrical cyanines, oxanoles etc. suffers a disturbance, and the $\pi$-electrons are considered to be placed in a one-dimensional potential having a sine curve periodicity[8]. The wavelength of absorption maximum is expressed by the following equation.

$$\frac{1}{\lambda_{max}} = \frac{V_0}{h \cdot c}\left(1 - \frac{1}{N}\right) + \frac{h}{8mc} \cdot \frac{N+1}{L^2} \qquad (1)$$

where, $L$ is the length of the path of the free $\pi$-electron measured along the conjugated chain, $N$, the number of $\pi$-electrons, $m$, the mass of the electron, $c$, the velocity of light, $h$, Planck's universal constant, and $V_0$ the amplitude of the sine-shaped potential along the chain. In the present study, this model was adopted to examine the relation between the nature of the chelating bond and the color change of reagent. 2,3,7-Trihydroxy-9-phenyl-fluorone was chosen as a suitable organic reagent, and is an excellent compound for such a purpose because of its symmetric structure and of the high stability of its chelates with fourth group metals.

## Experimental and Results

**Reagents and Apparatus.** — The ethanolic solution of phenylfluorone (1 ml. contains 0.6 mg. of phenylfluorone*) was prepared by dissolving 0.120 g. of phenylfluorone in 150 ml. of ethyl alcohol containing 1 m. of 5.0 N hydrochloric acid, and the resulting solution was diluted to 200 ml. with ethyl alcohol.

* This study was presented at the Meeting of the Chemical Society of Japan on Oct. 28, 1956 (Symposium on Chemistry of Complex Compounds).

1) K. Kimura and H. Sano, This Bulletin, **30**, 80 (1957).
2) H. Yamatera, *J. Inst, Polytechnics Osaka City Univ.*, **5**, 163 (1956).
3) H. H. Jaffé, *J. Chem. Phys.*, **20**, 1646 (1952); ibid, **21**, 1287 (1953).
4) N. S. Bayliss, *J. Chem. Phys.*, **16**, 287 (1948).
5) J. R. Platt, ibid., **17**, 484 (1949).
6) W. T. Simpson, ibid, **17**, 1218 (1949).
7) H. Kuhn, *Helv. Chim. Acta*, **31**, 1441 (1948); *J. Chem. Phys.*, **16**, 840 (1948).
8) H. Kuhn, *Z. Elektrochem.*, **53**, 165 (1949); *J. Chem. Phys.*, **17**, 1198 (1949).
9) H. Kuhn, *Helv. Chim. Acta*, **34**, 2371 (1951); *Z. Elecktrochem.*, **55**, 220 (1951).
10) W. Huber, H. Kuhn and W. Huber, *Helv. Chim. Acta*, **36**, 1957 (1953).
11) H. Kuhn, *Z. Naturforsch*, **9a**, 989 (1954); *Z. Elektrochem.*, **58**, 219 (1954).

* Abbreviation of 2, 3, 7-trihydroxy-9-phenylfluorone.

*Metal solutions* were prepared from their oxides (germanium, titanium), chloride (tin), or oxychloride (zirconium), and then standardized gravimetrically. These stock solutions contain enough hydrochloric acid to prevent the hydrolysis of metals, being free from foreign metal ions. The working solution was prepared by diluting an aliquot of each stock solution with water or diluted hydrochloric acid.

*Gum arabic solution* was prepared by dissolving 0.5 g. of gum arabic in 200 ml. of water by warming. The solution was filtered when necessary.

*Cyclohexanol.* — Analytical grade reagent was used without further purification.

Absorbance values of the sample and the blank solution were measured with a Beckman spectrophotometer Model DU, using 1-cm. glass cells and distilled water as a reference solution. From the difference the absorption spectrum of the dye or the chelate was obtained.

**Absorption spectra of dyes.**—The solution whose absorption spectrum is shown in Fig. 1, contains 20 ml. of ethanol, and 0.6 or 1.2 mg. of phenylfluorone. The desirable acidity or basicity in the final solution was maintained by adding the appropriate volume of hydrochloric acid or aqueous potassium hydroxide solution. The solution was diluted to 50 ml. with water.

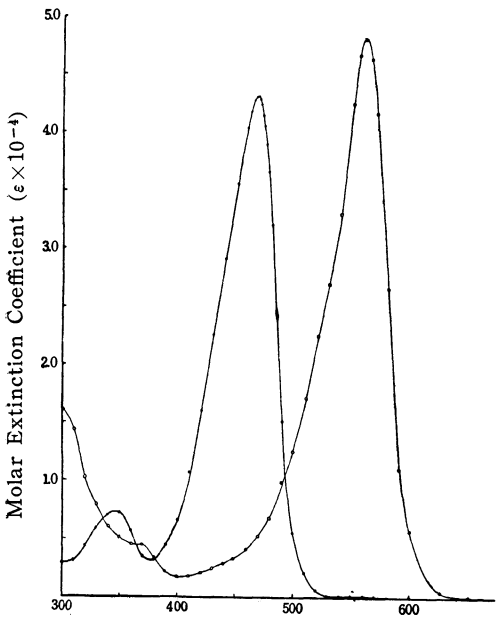



Fig. 1. Absorption Spectra of Phenyfluorone.
—●— in 0.5 N HCl solution
—○— in 1.0 N KOH solution

The absorption maximum of this dye is found at 468 mμ in an acidic solution, whereas it lies at 560 mμ in an alkaline solution. The value of molar extinction coefficient in alkaline solution might be slightly underestimated, because of the rapid fading of color due to the oxidation of the dye. With respect to the absorption maxima, the same results were obtained in the presence of either 5 ml. of cyclohexanol or gum arabic in the solution, although there was a slight difference in the detailed shape of their absorption curves. The solutions cause the precipitation of phenylfluorone in hydrochloric acic concentration below 0.04 N or in potassium hydroxide concentration below 0.01 N.

**Reaction with Metals.**—Phenylfluorone is one of the ortho-diphenol derivatives having the mesomeric group at its para position, which reacts remarkably with several metals, particularly titanium, germanium, zirconium, tin and thorium, giving striking color change[1,12].

Because the resulting complexes are insoluble in many solvents, the absorbance values were measured in the presence of a suitable stabilizer such as gum arabic or cyclohexanol*. The position and the intensity of absorption maximum is almost independent of the kind of the stabilizer used. On the other hand, the absorbance decreases with increasing acidity of solution. The effect of acidity is shown in Fig. 2. Beyond a certain value of acidity, the absorbance of chelate increases rapidly with the decrease in acidity. This specific value should be dependent on the stability of the chelate[13]. Then, the absorbance becomes nearly constant at lower acidity. In this range the molar extinction coefficients of the metal chelates are calculated, except for the case of titanium and tin chelate in which this range was not observed.

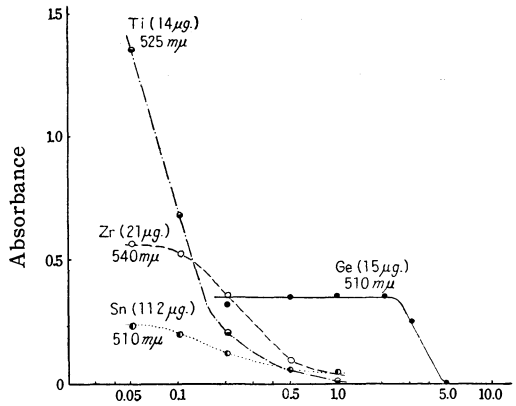



Fig. 2. Effect of Acidity. The solution contains 6 mg. of phenylfluorone, 20 ml. of ethanol, and 5 ml. of cyclohexanol or gum arabic solution in a final volume 50 ml.

* The light scattering effect of the colloidal particle on the absorption spectra is negligible for several hours after the preparation of the solution.

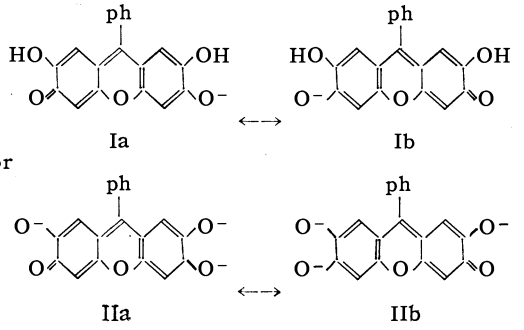
12) F. Ihmura, H. Sano and M. Asada; Unpublished report.

13) A. E. Martell and M. Calvin, "Chemistry of the Metal Chelate Compounds", New York Prentice-Hall, Inc. N. Y. (1952) p. 119.

The absorption sepectra of metal chelates with phenylfluorone were measured at various acidities, but the position of the absorption maximum was constant. The ratio of reagent to metal was obtained by the gravimetric analysis of the chelate precipitate. Their results are shown in Table I, together with the several properties of the metal. These results show that the value of $\varepsilon_{max}$ is roughly proportional to the ratio of the reagent to the metal in each chelate complex. This fact suggests that the absorption spectra in this wavelength range depend on the $\pi \rightarrow \pi'$ transition of the conjugated $\pi$-electron in the ligand.

## Discussion

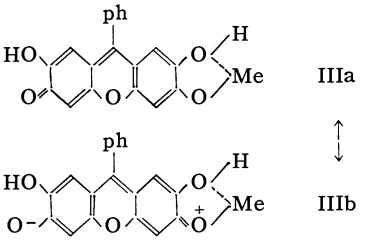
The anionic phenylfluorone, which is responsible for the red-pink color observed in an alkaline solution, is considered to be resonating between two limiting structures, Ia and Ib, or IIa and IIb, each of which makes the same contribution to the normal state of the anion, because of its symmetrical structure. One form results from the other when the single and double




bonds of the conjugated chain change over. This shows that each conjugated C—C bond has an equal bond length and bond order as a rough approximation. The value of $V_0$ is, therefore, considered to be zero. Then, the equation (1) is expressed as follows.

$$\lambda_{max} = \frac{8mc}{h} \cdot \frac{L^2}{N+1} \qquad (2)$$

In the equation (2), $N$, $m$, $c$ and $h$ are constants. But $L$, the length of the conjugated chain, has a somewhat arbitrary character. In the present study, $L$ was calculated from the observed wavelength of absorption maximum of the phenylfluorone anion, and this value was used in the following calculation and discussion*. For the phenylfluorone metal chelates the two limiting structures, IIIa and IIIb, are not equal in energy and they will not have equal contributions to the normal state, unlike the case of the symmetrical phenylfluorone anion. $V_0$ has, therefore, a difinite value.




On the other hand, if we conventionally apply the ionic-covalent resonance to the chelating bond, it can be assumed as the first approximation that with increasing ionic character in the metal-oxygen bond, the value of parameter, $V_0$, decreases and the absorption maximum shifts toward a longer wavelngth. The ionicity is dependent upon the difference of electronegativity between the metal and the oxygen atom. When the chelating bond has a pure covalency, the conjugated system is considered to be similar to that of polyene which has the same number of conjugated double bond, whereas it becomes equal to that of symmetrical polymethine when the chelating bond is pure ionic. The values of $V_0$ calculated from the experimentally

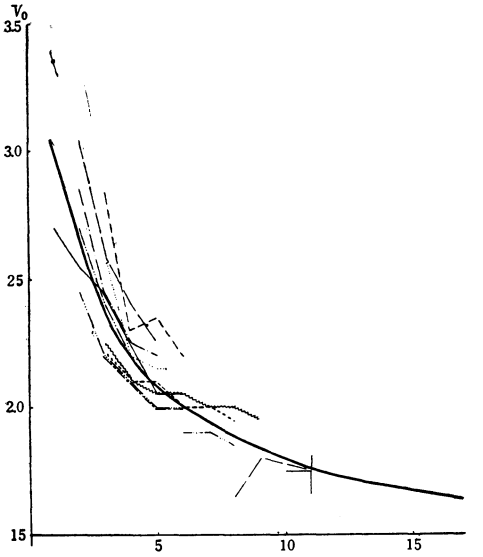



Fig. 3. Correlation between $V_0$ and Number of Conjugated Double Bond in Polyenes.

* The value of $L$, 14.6$_5$ Å, is reasonable, because this value is comparable to that obtained in the same manner[9] for many cyanine dyes possessing the same number ot conjugated double bond. See also the references 8, 9 and 11 with respect to the propriety to apply the one dimensional free electron gas model method to the branched double bond system.

TABLE I

| Metal | H | Ge | Sn | Ti* | Zr | ionic |
|---|---|---|---|---|---|---|
| $\lambda_{max}$ (m$\mu$) | 468 | 510 | 510 | 525 | 540 | 560 |
| $\varepsilon_{max}$ | $4.3\times10^4$ | $8.5\times10^4$ | $1.2\times10^4$ | $4.7\times10^4$ | $15\times10^4$ | $4.8\times10^4$ |
| Ratio, Reagent: Metal. | (1 : 1) | 2 : 1** | — | 2 : 1 | 4 : 1 | — |
| Ionic Radius[13] (Å) | — | 0.53 | 0.71 | 0.68 | 0.80 | — |
| Electronegativity[14] | 2.1 | 1.8—1.9 | 1.8—1.9 | 1.6 | 1.5 | — |
| $V_0$(eV.) | $0.49_0$ | $0.23_6$ | $0.23_6$ | $0.16_2$ | $0.094_5$ | 0 |

* Ti is soluble as a true solution in 0.1 N or more concentrated hydrochloric acid.
** This value was gven by Dr. K. Saito.

determined absorption maxima of a number of polynes* have been collected in Fig. 3, showing the relationship between $V_0$ and number of conjugated double bond.

By the aid of the Pauling's[14] or Hannay-Smyth's empirical equation[15] or Dailey-Townes' empirical diagram[16], the ionic character of the chelating bond between the metal and the oxygen atom was estimated from the electronegativity of the atoms concerned**. The relationship between $V_0$ and ionic character $I$ (or covalent character, $C$) will be expressed by the following equation,

$$V_0=F(1-I), \text{ or } V_0=F(C). \quad (3)$$

In this equation, the function $F$ should have the property that $V_0$ increases up to the value of corresponding polyene with decreasing $I$ or increasing $C$, whereas it becomes zero when $I$ reaches unity or $C$ comes to zero. The following $n$'th power function, one of the functions expected, is applied to examine the experimental results;

$$V_0=k(1-I)^n \text{ or } V_0=k\cdot C^n \quad (4)$$

where $k$ and $n$ are parameters to be determined by the experiment. The values of $V_0$ calculated from the experiments for the metal-phenylfluorone chelates are listed in Table I, together with other characters of the metal concerned. The value of $n$ was determined from the relationship between the value of $V_0$ and the covalent character of the bond. The value of $k$ is equal to that of $V_0$ obtained for the polyene which has the same number of conjugated double bond as phenylfluorone. These results were shown in Fig. 4a, b and c, in which all data met a straight line relation.

These results show that the shift of the wavelength of absorption maximum in the metal chelate depends on the ionic character of the bond between the metal and the functional atom of reagent. Conversely this fact makes it possible to estimate qualitatively the ionic character of the bond or the electronegativity of the metal concerned.

For many oragnic dyes used for the colorimetric determination of various metals, it is generally known that when the dye reacts with metal the absorption maximum shifts toward a longer wavelength. These phenomena will be explained as follows.

From equation (1), the following equation is derived,

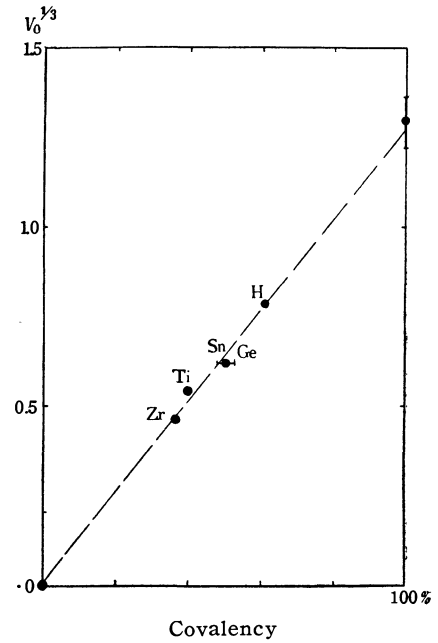



Fig. 4, a. Based on Pauling's equation.

* The absorption maxima were taken from the following: A. E. Gillam and E. S. Stern "An Introduction to Electronic Absorption Spectroscopy in Organic Chemistry", Edward Arnold Ltd. London, (1954); Y. Urushibara, "Organic Chemistry II", Kyoritsu Shuppan, Tokyo, (1955).

** The value of electronegativity was taken from the Table presented recently by H. O. Pritchard and H. A. Skinner, *Chem. Rev.*, **55**, 745 (1955).

14) L. Pauling, "The Nature of the Chemical Bond", Cornell Univ. Press, Ithaca, 1939.

15) N. B. Hannay and C. P. Smyth, *J. Am. Chem. Soc.*, **68**, 171 (1946).

16) B. P. Dailey and C. H. Townes, *J. Chem. Phys.*, **23**, 118 (1955).

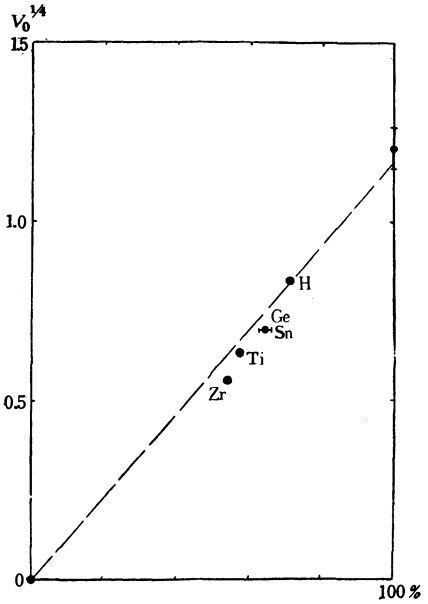



Fig. 4, b. Based on Smyth-Hanney's equation.

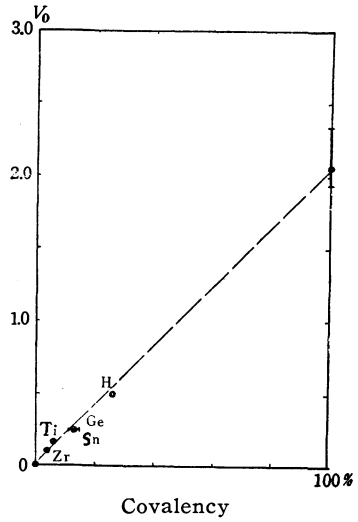



Fig. 4, c. Based on Dailey-Towne's diagram.

$$V_0=N\cdot h(\nu-\nu_i)/(N-1)=N\cdot h\{(\nu_H-\nu_i)-(\nu_H-\nu)\}/(N-1)=N\cdot h(\nu_0-\Delta\nu)/(N-1) \quad (5)$$

where $\nu$ is the frequency of absorption maximum observed with the metal chelate, $\nu_H$ and $\nu_i$, the frequency of absorption maximum of the reagent in the acidic and the alkaline solution, respectively, and $\Delta\nu$, the shift ("red shift") of the frequency, which is equal to $(\nu_H-\nu)$. From the equation (4) and (5), $\Delta\nu$ can be derived as follows,

$$\Delta\nu=\nu_0-k(N-1)(1-I)^n/N\cdot h=\nu_0-k(N-1)\cdot C^nN\cdot h \quad (6)$$

where $\nu_0(=\nu_H-\nu_i)$ is constant for the reagent used. From equation (6), it is seen, that $\Delta\nu$ is affected with the covalent character of the bond, where $k$ and $n$ are chracteristic of the reagent used. In general, however, this relation will not always be satisfied because of their unsymmetrical structure, branched conjugated system, or uncertainty of the ionicity of the bond which is estimated empirically from the difference of electronegativity.

## Summary

The absorption spectra of phenylfluorone and its chelates with the fourth group metal elements, titanium, germanium, zirconium and tin were studied. It was found that in acidic solutions the absorption maxima of these metal chelates shift towards a longer wavelength with increasing ionicity of the bond between the metal and the terminal oxygen atom of the ligand phenylfluorone. These absorption spectra were examined by the aid of free electron gas model method. Kuhn's theory was applied to the calculation of the value $V_0$ from the absorption maximum observed in each metal chelate. It was shown that there was a certain relationship between the value of $V_0$ obtained and the ionicity of the chelating bond which is estimated from the difference of electronegativity between the metal and the terminal oxygen atom. The relation can be expressed as follows:

$$V_0=k(1-I)^n \quad (4')$$

where, $n$ is a parameter depending on the method used for the estimation of the ionicity, $k$ a parameter characteristic of the chelating dye used and equal to the value of $V_0$ for the polyene having the same number of the conjugated double bond. These results were applied to explain the "red shift" observed in acidic solutions of organic dyes in the colorimetric determinations of metals. A more detailed investigation concerning the nature of the chelating bond will be reported later.

The author indebted to Dr. Kenjiro Kimura, former Professor and Dr. Nobufusa Saito, Professor in this laboratory, for their benevolent encouragement to carry out this study.

*Department of Chemistry, Faculty of Science, The University of Tokyo*
*Hongo, Tokyo*

# *Studies on Crystals of Metallic Tris-ethylenediamine Complexes. III. The Determination of the Absolute Configuration of Optically Active Complex Ion, [Co en$_3$]$^{3+}$, by Means of X-rays*

By Yoshihiko SAITO, Kazumi NAKATSU, Motoo SHIRO* and Hisao KUROYA

(Received May 23, 1957)

## Introduction

In 1951, Bijvoet, Peerdeman and van Bommel[1] first succeeded in determining the absolute configuration of *d*-tartaric acid by means of X-rays, using absorption edge technique.

However, no attempt has ever been made to determine the absolute configuration of optically active tris-ethylenediamine-cobaltic complex ion, [Co en$_3$]$^{3+}$ (en: ethylenediamine), one of the most familiar complex ions in the chemistry of complex compounds. The present paper deals with this problem, including a brief description of the principle of the method and the experimental procedure. A brief account of this work has been published already[2].

## Principle of the Method

As is well known, Friedel's law states that it is not possible, by ordinary methods in X-ray diffraction study, to detect the presence or the absence of centrosymmetry in a crystal, from which it follows immediately that in the case of non-centrosymmetry one can not conclude whether a model or its inversion actually corresponds with a given optically active crystal, say—dextro compound. However, it is not true when use is made of X-rays whose wave length is a little shorter than the absorption edge of a particular atom in the crystal. If this condition is fulfilled, a difference in intensity between the reflections from $(hkl)$ and $(\bar{h}\bar{k}\bar{l})$ can be observed for non-centrosymmetrical crystal.

This is due to the scattering of X-rays by the particular atom with anomalous phase and amplitude. From the difference between $I(hkl)$ and $I(\bar{h}\bar{k}\bar{l})$, one can determine the absolute configuration of a structure which belongs to one of the pairs of enantiomorphous space groups, provided that the crystal structure is fully known in all respects except that of "hand". The actual intensities $I(hkl)$ and $I(\bar{h}\bar{k}\bar{l})$ can be calculated on the basis of a final set of atomic coordinates determined in the usual way, taking the anomalous dispersion into account. If the observed inequality relations are the reverse of those calculated, the real atomic parameters must be the inversion of the initial set.

Besides these inequality relations, the following equality exists:

$$I_d(hkl)=I_l(\bar{h}\bar{k}\bar{l}) \qquad (1)$$

where the subscript $d$ and $l$ are used to distinguish the two enantiomorphous crystals. It follows immediately:

$$\text{if } I_d(hkl)\gtrless I_d(\bar{h}\bar{k}\bar{l}), \text{ then } I_l(hkl)\gtrless I_l(\bar{h}\bar{k}\bar{l}), \qquad (2)$$

that is, the inequality relations must be reversed in the case of *d*-compound and *l*-compound.

Since the wave length of Cu $K\alpha$ radiation ($\lambda=1.5418$ Å) is a little shorter than the *K*-absorption edge of the cobalt atom ($\lambda_k=1.6081$ Å), anomalous dispersion is expected to take place. The crystal structures of D- and L-2[Co en$_3$]Cl$_3$·NaCl·6H$_2$O are fully known except that of "hand" as reported previously[3]. Therefore, the absolute configuration of these compounds can be determined without ambiguity, if the difference between $I(hkil)$ and $I(\bar{h}\bar{k}\bar{i}\bar{l})$ can be observed when Cu $K\alpha$ radiation is used.

The phase change on scattering may be included in the usual expression for the structure factor without changing its form, if we consider the atomic scattering factor to be complex numbers[4]:

$$f=f^0+\Delta f'+i\Delta f'' \qquad (3)$$

* Present adress; Momotani Juntenkan Co. Ltd., Osaka.

1) J. M. Bijvoet, A. F. Peerdeman and A. J. van Bommel, *Nature*, **168**, 271 (1951).

2) Y. Saito, K. Nakatsu, M. Shiro and H. Kuroya, *Acta Cryst.*, **8**, 729 (1955).

3) K. Nakatsu, M. Shiro, Y. Saito and H. Kuroya, This Bulletin, **30**, 158 (1957).

4) R. W. James, "The Optical Principles of the Diffraction of X-rays", G. Bell and Sons, Ltd., London (1948), Chap. IV.

where $f^0$ is the scattering factor for wave lengths far from any one of the absorption edges of electrons and $\Delta f'$ and $\Delta f''$ represent the corrections to be applied to the real and the imaginary part of the scattering factor because of dispersion.

When Cu $K\alpha$ radiation is used to take diffraction photographs of the complex compound above mentioned, the $K$-level electrons of the cobalt atom are excited. Therefore, we have for the scattering factor of the cobalt atom:

$$f_{Co}=f^0_{Co}+\Delta f'_{Co}+i\Delta f''_{Co} \qquad (4)$$

The structure factor $F(hkil)$ for $l=2n$ can be written as follows, if we assume regular structure postulated in the previous paper:

$$F(hkil)=A(hkil)+iB(hkil), \qquad (5)$$

where

$$A(hkil)=\sum_j m_j f_j \cos 2\pi l z_j \{\cos 2\pi(hx_j+ky_j)+\cos 2\pi(kx_j+iy_j)+\cos 2\pi(ix_j+hy_j)\}$$

$$B(hkil)=\sum_j m_j f_j \sin 2\pi l z_j \{\cos 2\pi(hx_j+ky_j)+\cos 2\pi(kx_j+iy_j)+\cos 2\pi(ix_j+hy_j)\}$$

and

$f_j$: atomic scattering factor for the $j$-th atom

$m_j$: a suitable factor to allow for the reduced multiplicity for atoms on the special positions

$x_j$, $y_j$, $z_j$: atomic coordinates for the $j$-th atom.

It can easily be shown from the above expression that $F(hki\bar{l})$ is equivalent to $F(\bar{h}\bar{k}\bar{i}l)$ and is a complex conjugate of $F(hkil)$. Because of eq. (4), $|F(hkil)|$ is no more equal to $|F(hki\bar{l})|$, hence, the intensity $I(hkil)$ is unequal to $I(hki\bar{l})$. Accordingly, to observe the effect of anomalous dispersion, it is more convenient to compare the reflections from $(hkil)$ and $(hki\bar{l})$ instead of those from $(hkil)$ and $(\bar{h}\bar{k}il)$. These reflections can be observed on the same oscillation photograph taken around the $c$-axis and moreover, various correction factors come out exactly the same for these two reflections.

## Experimental Procedure and the Determination of the Absolute Configuration

i) *Observation of Inequality Relations by Oscillation Photographs.*

Thin needle-like crystals of about 0.2 mm. in diameter were selected. First, a few oscillation photographs were taken using Fe $K\alpha$ radiation, in order to confirm that the crystal setting is perfect and $(hkil)$ and $(hkil)$ intensities are practically equal. Photographs were then taken with Cu $K\alpha$ radiation, which is scattered by the cobalt atoms anomalously. In Fig. 1, the effect of anomalous dispersion is shown, where reflections of Fe $K\alpha$ and Cu $K\alpha$ from the plane $(32\bar{5}2)$ and $(3\bar{2}\bar{5}\bar{2})$ are recorded on one film, the latter being equivalent to $(\bar{3}2\bar{5}\bar{2})$ because of symmetry. For D-compound the intensity of reflection of Cu $K\alpha$ from the plane $(3\bar{2}\bar{5}\bar{2})$ is clearly stronger than that from the plane $(32\bar{5}2)$, while they are equal in intensity in case of Fe $K\alpha$ radiation. The inequality relation is reversed for L-compound.

There are many such pairs of reflections for which slight but discernible differences in intensities were observed, whereas no such differences could be found when Fe $K\alpha$ radiation was used.

It was also found that the intensity relations observed for the one crystal are the reverse of those found for its enantiomorph. This observation strongly suggests that these differences are due to the anomalous dispersion of cobalt atoms in the crystal. In Table I observed and calculated relations between $I(hkil)$ and $I(hki\bar{l})$ are compared for all the observed pairs. The visual estimates of the last two columns are the results of observations by a few persons independently. In Table I the inequality sign $>$ or $<$ shows that the observed intensity for $(hkil)$ is greater or smaller than that for $(hki\bar{l})$. The sign $?>$ or $?<$ means that the inequality is not so definite as that without the symbol ?. The symbol ? shows that the inequality could not be observed or was different according to different observers. In the calculation of intensities of reflections, $\Delta f'$ and $\Delta f''$ were calculated according to the formula derived by Hönl[5]. They amount to $\Delta f'=-3.0$ and $\Delta f''=3.4$, respectively. The calculated values shown in the first column are based on the regular model. Those shown in the second column were calculated on the basis of a model having disorder due to submicroscopic twinning. In this case, $F(hki2n)$ is not exactly equal but very near to the complex conjugate of $F(hki\overline{2n})$ even when no anomalous dispersion occurs. Thus the difference between $I_c(hkil)$ and $I_c(hki\bar{l})$ calculated for Fe $K\alpha$ radiation is

5) H. Hönl, *Zeit. f. Physik*, **84**, 1 (1933); *Ann. Physik*, **18**, 625 (1933).

TABLE I

OBSERVED AND CALCULATED INTENSITIES

| | Calculated on the Basis of | | | | Observed for | |
|---|---|---|---|---|---|---|
| | Regular Model | | Twinned Model | | | |
| *hkil* | $I(hkil)$ | $I(hki\bar{l})$ | $I(hkil)$ | $I(hki\bar{l})$ | D-Cryst. | L-Cryst. |
| 1012 | 1985 | 1810 | 2300 | 2140 | ? | < |
| 1122 | 2.9 | 159 | 17 | 100 | < | > |
| 1232 | 86 | 173 | 196 | 381 | < | > |
| 1342 | 965 | 910 | 921 | 865 | ? > | ? < |
| 1452 | 781 | 705 | 824 | 738 | ? > | ? < |
| 1562 | 312 | 296 | 300 | 292 | > | < |
| 1892 | 51 | 47 | 50 | 47 | ? > | < |
| 1, 9, 10, 2 | 33 | 34 | 33 | 37 | — | ? > |
| 2022 | 148 | 269 | 334 | 423 | < | > |
| 2132 | 3710 | 3460 | 3310 | 3200 | > | < |
| 2242 | 38 | 159 | 30 | 102 | < | > |
| 2352 | 418 | 448 | 444 | 485 | ? < | ? > |
| 2462 | 112 | 99 | 124 | 112 | ? | ? |
| 2572 | 15 | 17 | 17 | 14 | ? | ? |
| 2682 | 6.4 | 7.1 | 6.8 | 11.5 | — | > |
| 2792 | 71 | 65 | 67 | 62 | ? > | ? |
| 2, 8, 10, 2 | 84 | 75 | 101 | 89 | ? > | ? |
| 2, 9, 11, 2 | 47 | 41 | 45 | 41 | ? < | — |
| 3032 | 72 | 167 | 146 | 171 | < | > |
| 3142 | 315 | 434 | 514 | 557 | < | > |
| 3252 | 141 | 82 | 120 | 82 | > | < |
| 3362 | 165 | 194 | 212 | 241 | ? < | ? > |
| 3472 | 34 | 46 | 25 | 35 | ? < | ? |
| 3582 | 146 | 141 | 149 | 146 | ? > | ? < |
| 3, 7, 10, 2 | 58 | 61 | 59 | 68 | ? < | ? |
| 3, 8, 11, 2 | 39 | 32 | 35 | 29 | ? > | ? |
| 4042 | 1252 | 1160 | 1106 | 1083 | ? > | ? < |
| 4152 | 21 | 27 | 45 | 25 | < | > |
| 4262 | 291 | 310 | 310 | 329 | ? | ? |
| 4482 | 3.3 | 28 | 2.2 | 24 | < | > |
| 4, 7, 11, 2 | 0.4 | 6.9 | 2.1 | 4.1 | < | > |
| 5052 | 412 | 394 | 371 | 363 | ? | ? |
| 5272 | 0.7 | 11 | 3.3 | 6.7 | < | > |
| 5382 | 86 | 76 | 84 | 77 | ? > | < |
| 5492 | 99 | 104 | 105 | 115 | ? < | ? > |
| 6172 | 43 | 37 | 41.3 | 41.1 | > | < |
| 6282 | 88 | 86 | 84 | 86 | ? < | > |
| 6392 | 187 | 169 | 207 | 178 | ? > | ? |
| 6, 4, 10, 2 | 125 | 112 | 112 | 106 | ? > | < |
| 7072 | 233 | 213 | 219 | 196 | ? | ? |
| 7292 | 164 | 131 | 123 | 120 | > | < |
| 7, 3, 10, 2 | 93 | 94 | 92 | 94 | ? | ? < |
| 7, 4, 11, 2 | 0.1 | 6.2 | 2.7 | 4.8 | ? > | ? |
| 8192 | 5.1 | 7.9 | 6.0 | 10.4 | — | > |
| 8, 2, 10, 2 | 9.4 | 4.9 | 13.4 | 5.2 | > | < |
| 8, 3, 11, 2 | 5.2 | 5.4 | 5.2 | 6.9 | ? | — |
| 9, 1, 10, 2 | 37 | 40 | 40 | 44 | ? | ? |
| 10, 0, 10, 2 | 14 | 12 | 12 | 9.8 | ? > | — |

small and within the errors of experiments for most cases, and the calculated intensities based on the latter model for Cu $K\alpha$ radiation lead to the same inqeuality relations with only a few exceptions. Therefore, the same conclusion was drawn from both models.

Namely, the concordance, in general, of intensity signs in the observed and the calculated intensities seen in the Table I indicates that the drawing of a complex ion $[Co\ en_3]^{3+}$ shown in Fig. 2 corresponds to the dextrorotatory form with respect to Na D line. This result has been indeed verified by computing the $P_s(\mathbf{u})$ function of Okaya, Saito and Pepinsky[6,7].

ii) *Observation of Inequality Relations by Laue Photographs.*

Grenville-Wells and Lonsdale[8] showed that the effect of anomalous dispersion could also be observed by means of Laue photographs. This method has certainly some advantages over the one using oscillation photographs. However, when applied to the present case, the observation could not be carried out without experimental difficulties. Since the crystals disintegrated by losing their water of crystallization when exposed in the X-ray beam for several hours, it was difficult to set the crystal perfectly and obtain appropriate Laue photographs before decomposition. Moreover, no suitable pairs of reflections could be found which were of high order and strong enough in intensity to reduce the influence of the setting error of the crystal.

Though not satisfactorily, the inequality relations were observed about a few pairs of (*hki*2) reflections in accord with the results obtained by using oscillation photographs.

## Some Remarks on Experimental Procedure

It is to be noted here that the same coordinate system must be used in the indexing of the oscillation photographs and calculation of the structure factors. The right handed system was used throughout this investigation. As pointed out by Bijvoet and his coworkers, the calculation of the differences between ($hkl$) and ($\bar{h}\bar{k}\bar{l}$) intensities does not need very accurate $F$-values. Theoretically, observation of a single pair of reflections is enough to decide the diffraction model and its mirror image. However, it is advisable to observe the difference of as many corresponding spots as possible. From this point, the Laue photographic method might be laborious.

When anomalous dispersion occurs in the crystal, incident beam is in general heavily absorbed and fluorescent radiation is copiously excited, so that the photograph shows weak diffraction spots on a rather heavily blackened background. Usually its takes a pretty long time to take a diffraction photograph. To avoid the blackening as much as possible and to obtain a picture with clear background in a relatively short time, it is necessary to make the range of oscillation of the crystal small.

Practically it is a rather difficult task to compare the intensities from a front ($hkl$) and a rear face ($\bar{h}\bar{k}\bar{l}$) of a crystal, since it is not easy to obtain a crystal whose front and rear surface are exactly at the same condition with regard to their perfection etc. However, in most cases it is possible to avoid this difficulty. If, for instance, $F(hkl)$ is equivalent to $F(hk\bar{l})$ because of the symmetry of the space group, it is more convenient to use the reflection ($hk\bar{l}$) instead of ($\bar{h}\bar{k}\bar{l}$), as pointed out in the previous section.

The best method to measure the difference of $I(hkl)$ and $I(\bar{h}\bar{k}\bar{l})$ would be to use two Geiger counters arranged in such a way that the two reflections are received at the same time and to use a circuit by which the difference can be read off directly.

## Summary

The absolute configuration of an optically active complex ion $[Co\ en_3]^{3+}$ has been determined by means of X-ray absorption edge technique. Cu $K\alpha$ radiation was used to excite the cobalt atoms in the crystals of D- and L-2$[Co\ en_3]Cl_3 \cdot NaCl \cdot 6H_2O$. The effects of the anomalous dispersion were observed by single crystal oscillation photographs as well as Laue photographs. A brief description of the principle of the method and the experimental procedure is included.

The authors express their sincere thanks to Professors I. Nitta and T. Watanabé of the Osaka University for their encouragement and invaluable advice. Part of the cost of this study was defrayed from a Grant of the Ministry of Education.

*Institute of Polytechnics, Osaka City University Kita-ku, Osaka*

6) Y. Okaya, Y. Saito and R. Pepinsky, *Phys. Rev.*, **98**, 1857 (1955).
7) Y. Saito, Y. Okaya and R. Pepinsky, In press; cf. also, Phys. Rev., **100**, 970 (1955).
8) H. J. Grenville-Wells and K. Lonsdale, *Nature*, **173**, 1145 (1954).

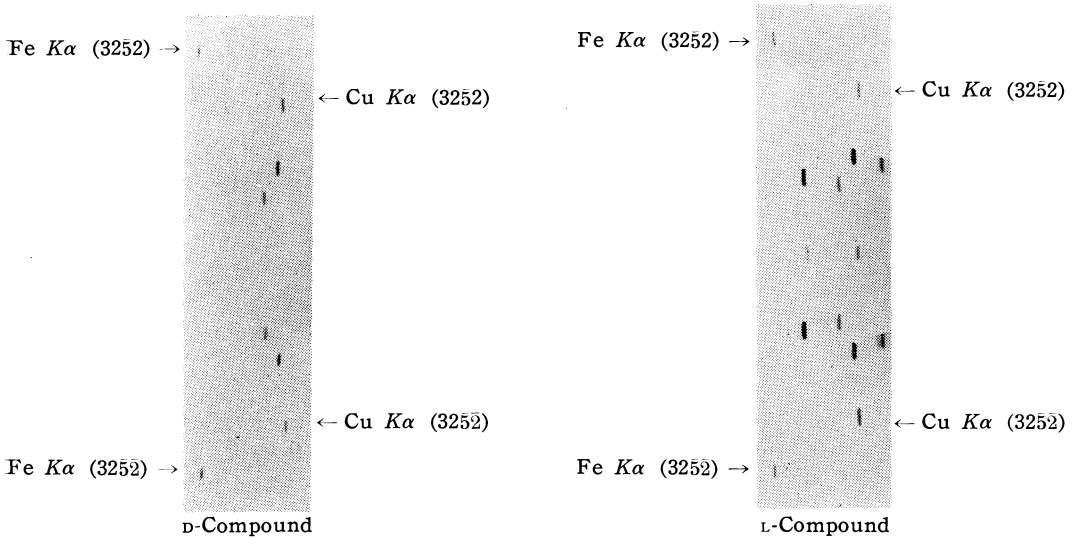



Fig. 1. Parts of oscillation photographs of D- and L-2[Co $en_3$]$Cl_3 \cdot NaCl \cdot 6H_2O$, showing the effect of anomalous dispersion.

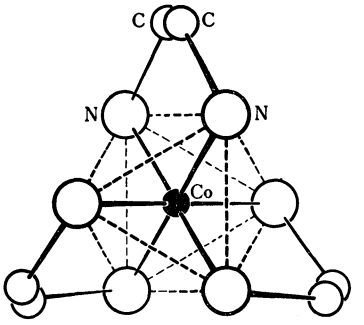



Fig. 2. Drawing of the D(+)-[Co $en_3$]$^{3+}$ complex ion.

# *A Rapid Spectrophotometric Method for Determination of a Minute Amount of Vanadium in Natural Waters*

By the late Hideo NAITÔ and Ken SUGAWARA

(Received April 15, 1957)

In a previous paper[1] the writers reported with M. Tanaka a method for determining a minute quantity of vanadium in natural waters, consisting of the following three steps: 1) co-precipitation of vanadium with ferric hydroxide, 2) separation of the vanadium from the co-precipitant and from the accompanying elements, and 3) the final colorimetry of vanadium oxinate in pentanol.

The new method which we will detail below is an improvement on this previous method. The essential improvement is in simplifying the processes for vanadium separation from co-precipitant. The simplification is based upon the findings that so long as the solution is sufficiently cool below room temperature, tartrate can keep iron from hydroxide formation even in a strongly alkaline medium and that when the solution is warmed in this condition, iron and aluminium can easily be precipitated leaving vanadium completely in solution.

## Experimental

**Reagents.**—*Mixed solution of sodium hydroxide and tartaric acid.*—Dissolve 30 g. of tartaric acid and 200 g. of sodium hydroxide in distilled water and dilute to 1000 ml.

*Ferric chloride solution.*—Dissolve 24.2 g. of ferric chloride crystal (the special grade for analytical purposes) in distilled water. Add 5 ml. of 6 N hydrochloric acid and dilute to 500 ml.

*Sodium acetate buffer solution.*—Dissolve 136 g. of sodium acetate in about 200 ml. of distilled water. Heat the solution on a water bath, then filter through a filterpaper. To the filtrate add 3 ml. of glacial acetic acid and dilute to 250 ml.

*Oxine solution.*—To 100 ml. of distilled water, dissolve 2 g. of oxine (special grade for analytical purposes) and 5 g. of malonic acid crystal.

**Procedure.**—Take a sample of 5—20 liters depending upon the probable content of vanadium. Acidify with hydrochloric acid. Then add a solution of ferric chloride, ferric nitrate or iron alum so that the solution contains 10 mg. iron per liter. While warming in a water bath, the solution is neutralized with 4 N aqueous ammonia to bromcresolpurple and the precipitate is collected by an automatic filter.

Gently burn to ashes the filterpaper with its contents in a platinum dish. To the ash add 5 ml. of 6 N hydrochloric acid. Then heat the dish with a cover on a steam bath. Loss of hydrochloric acid causes no essential trouble. The final volume of the hydrochloric acid must not exceed 5 ml. After complete dissolution, transfer the contents to a 100 ml. beaker. Wash the dish with 50 ml. of distilled water. With constant stirring, add 15 ml. of the tartrate-sodium hydroxide solution. The solution turns dark brown without precipitation.

Heat the solution on a steam bath until ferric hydroxide completely precipitates and the supernatant solution is left clear and colorless. The process usually takes 30 minutes and sometimes longer. After it has cooled to room temperature, dilute the solution exactly 100 ml. and put to centrifugation for 10 minutes at 3000 r.p.m.

Transfer 80 ml. of the supernatant solution to a 100 ml. beaker, neuturalize to *p*-nitrophenol with 4 N sulfuric acid. Then add 3 ml. of the same solution in excess. Heat in a water bath. To the hot solution add 2 ml. of the oxine solution, neutralize with 4 N ammonia and then add 4 ml. of the same reagent in excess, whereby a trace of iron which escaped from the previous precipitation process is fixed in the form of oxinate, partly precipitated and partly in solution. When the precipitate is appreciably great, it can be separated by centrifugation. Otherwise go directly on to the next process.

The next process is the extraction of the formed oxinate by an organic solvent. Transfer the solution into a separatory funnel and add about 20 ml. of benzene. Shake vigorously for one minute. Two benzene extractions are sufficient for complete removal of the iron oxinate.

Neutralize the remaining solution with 4 N sulfuric acid and add 3.0 ml. of the same acid in excess. Adjust the pH to nearly 4 by the addition of 4 ml. of a sodium acetate solution. Then add 1.0 ml. of an oxine solution and extract the formed vanadium oxinate by pentanol. The extraction is repeated until the final extract bears no perceptible coloration. Transfer the united extracts into a 10 ml. measuring flask and make up with pentanol to the mark. Then the optical density of the solution is determined by using a spectrophotometer at wave length of 475 mμ.

1) K. Sugawara, M. Tanaka, and H. Naitô, This Bulletin **26**, 417 (1953).

## Discussion

Whether the vanadium co-precipitation with ferric hydroxide is complete or not depends upon the pH of the milieu. As shown in Table I[2], it is complete only within the pH range up to 9.6. Therefore, in the first step of the precedure the precipitation was arranged so that it occurs at that pH whereby a trace of vanadium can be completely collected in the coagulum.

TABLE I
VANADIUM CO-PRECIPITATION BY IRON AT VARIOUS pH VALUES

| pH of the solution | Fe added mg. | V added μg. | V found in the ppt. μg. |
|---|---|---|---|
| 7.9 | 2 | 33.0 | 33.2 |
| 8.8 | 2 | 33.0 | 32.2 |
| 9.6 | 2 | 33.0 | 33.2 |
| 10.8 | 2 | 33.0 | $<1$ |
| 12.3 | 2 | 33.0 | $<1$ |

The situation is quite contrary for the second step of the procedure where vanadium must remain in solution to its trace when hydroxides are precipitated. The requirement is that:

1) In the alkalinization process, iron and aluminium must be kept in solution until the pH of the solution becomes sufficiently high for these elements to precipitate free from a trace of vanadium.

2) Finding a process which causes a homogeneous precipitation at this pH of the iron and aluminium, which have been kept in solution up to the pH.

The addition of tartrate satisfies this requirement. At the stated pH, iron and aluminium can be masked by this substance at low temperatures and easily demasked with precipitation when warmed. Recovery of vanadium was the final question which was solved by the following experiment:

To a series of solutions containing various amounts of vanadium, 100 ml. of iron and 500 ml. of a tartaric acid solution were added. Each solution was made alkaline by the addition of 15 ml. of 5 N sodium hydroxide solution which had previously been cooled below room temperature. Then the solution was warmed in a boiling water bath whereby iron hydroxide was precipitated. The supernatant solution thus obtained was processed as given in the procedure. As shown in Table II, the recovery of vanadium is perfect.

TABLE II
RECOVERY OF VANADIUM FROM IRON PRECIPITATE

| Fe added mg. | V added μg. | V found μg. | % |
|---|---|---|---|
| 100 | 20 | 19.5 | 98 |
| 100 | 20 | 19.6 | 98 |
| 100 | 20 | 20.4 | 102 |
| 100 | 20 | 20.8 | 104 |
| 100 | 20 | 19.6 | 98 |
| 100 | 20 | 19.7 | 99 |
| 100 | 20 | 19.9 | 100 |
| 100 | 8 | 8.1 | 101 |
| 100 | 8 | 8.5 | 106 |

As to the amount of iron added, when it is less than 5 mg., separation is complete without the addition of tartrate, and when it exceeds 20 mg., hydrogen peroxide treatment is not sufficient for a complete separation, which can be first realized by the addition of tartrate.

**Interferences by other elements.**

Some other elements remaining in the solution from which ferric hydroxide had been separated, interfere with the final colorimetry of vanadium by forming oxinates. By the addition of malonic acid, aluminium can be prevented from forming oxinate in a neutral or a slightly acidic solution. No harmful effect is caused by the presence of 50 mg. of aluminium, 10 mg. of manganese or zinc, and 1 mg. of cadmium, bismuth, copper, silver, mercury, tin, selenium, tungsten, molybdenum or titanium.

The present study was accomplished by using a Coleman Model 14 Universal Spectrophotometer supplied by the Elizabeth Thompson Science Fund. The writers express their appreciation to the Trustees of that Fund.

The senior writer is sorry to report the tragic death on October 11, 1956, of his co-worker, H. Naitô, when during his surveying work on Lake Kizaki-ko, rough water suddenly capsized the boat and was drowned.

*Chemistry Department Faculty of Science, Nagoya University, Chikusa Nagoya*

2) M. Tanaka, unpublished.

# *Sedimentation and Diffusion Studies of Calf Thymus Histone**

By Nobuo Ui

(Received April 30, 1957)

In a previous paper[1], it was reported that calf thymus histone consists of two fractions, histones I and II, which were different in respect to chemical as well as physico-chemical properties. The present paper deals with the molecular-kinetic properties of these two fractions. In spite of their heterogeneity as revealed by electrophoresis, they behaved like a single protein in sedimentation and diffusion, and the molecular weights have been calculated.

As there have been few data about the molecular weight of histone, especially of mono-disperse preparation, it seems of value to present the results in some detail. A preliminary report of this investigation has already been published[2].

## Experimental

**Materials.**—The preparations of histone used in this study were extracted from isolated calf thymus nuclei using sulfuric acid, purified by an ethanol-precipitation method at a temperature below 0°C, and finally lyophilized as histone chlorides. Histone I is the main fraction of histone precipitated with 20 per cent. ethanol, and histone II is the fraction precipitated by 45 per cent. Details of the procedure for the preparation and fractionation have been described[1].

As it was found that histone I had a tendency to aggregate, especially at higher temperature, care was taken to avoid the aggregation; i. e., each preparation was dissolved in a cold buffer solution and kept at about 0°C until measurements were performed (less than one day). In most of this study an acetate buffer of pH 5.0 at ionic strength of 0.2 was used as a solvent. In this the aggregation did not take place appreciably even if the solution was kept at 20°C for 24 hours.

Protein concentrations were usually determined by the micro-Kjeldahl method. The author is indebted to Miss T. Kitamura for this analysis.

**Methods.**—Ultracentrifugal characteristics of these materials have been studied using a Spinco model E ultracentrifuge. In the case of histone II, a synthetic boundary cell[3] was used in order to measure its low sedimentation coefficient. Runs were made always at 59,780 r. p. m. The temperature of each run was taken as the mean of the rotor temperature at the beginning and the end of the run without correction for a change in rotor temperature during acceleration and deceleration[4]. The observed sedimentation coefficient was corrected to the value in water at 20°C ($s_{20,w}$) by a conventional manner[5].

Diffusion measurements were made at 20.0°C in a Neurath-type diffusion cell[6] equipped with a Philpot-Svensson's schlieren optical system[7]. Diffusion coefficients were computed from the second moments of the diffusion curves[8] and corrected to the value in water at 20°C ($D_{20,w}$).

Partial specific volume of histone I was determined at 20.0°C, using a pycnometer of 5-cc. capacity.

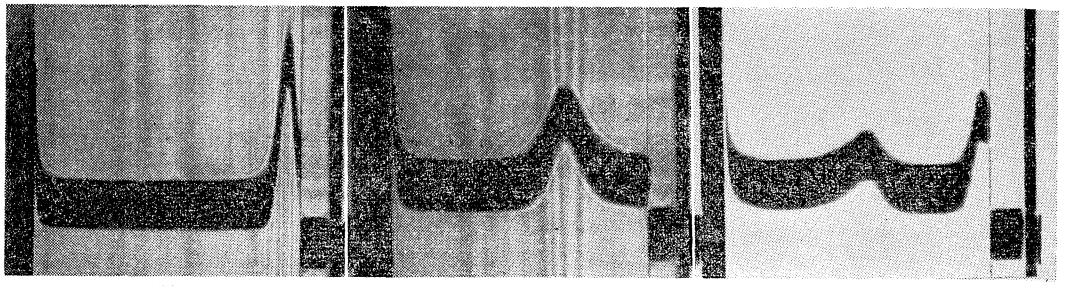
## Results

**A. Sedimentation Characteristics of Histone I.**—The preparation of histone I, the main fraction of calf thymus histone, was examined in the ultracentrifuge in a pH range of between 4.0 and 9.9. Only a single homogeneous boundary was observed below pH 7, as is shown in Fig. 1 (1A and 1B). These photographs were taken using an acetate buffer of pH 5.0 and ionic strength of 0.2.

At pH values higher than 7, except in tris(hydroxymethyl)aminomethane buffer of pH 8.0, a faster component was observed (see Fig. 1C) even when the solution had not been exposed to a high temperature. The amount of the fast component varied with the pH and the composition of the buffer. It was also found that the faster boundary disappeared when the solution was quickly brought to pH 5.0 by dialysis in a cold room and examined by the ultracentrifuge. The presence of the fast component at a higher pH than 7 would not be due to the inhomogeneity of this preparation, but would

* A part of this work was read before the 8th Annual Meeting of the Chemical Society of Japan held in Tokyo, April 1, 1955.

1) N. Ui, *Biochim. Biophys. Acta*, in press.
2) N. Ui, *Biochim. Biophys. Acta*, **22**, 205 (1956).
3) H. K. Schachman, *Proc. Natl. Acad. Sci. U. S. A.*, **38**, 943 (1952).
4) D. F. Waugh and D. A. Yphantis, *Rev. Sci. Instruments*, **23**, 609 (1952).
5) T. Svedberg and K. O. Pedersen, "Ultracentrifuge," Oxford (1940).
6) H. Neurath, *Chem. Revs.*, **30**, 357 (1942).
7) J. St. L. Philpot, *Nature*, **141**, 283 (1938); H. Svensson. *Kolloid-Z.*, **87**, 181 (1939).
8) O. Lamm, *Nova Acta Regiae Soc. Sci. Upsaliensis*, Ser. IV, **10**, No. 6 (1937).



(A) (B) (C)

Fig. 1. Sedimentation patterns of calf thymus histone I.
(A): In acetate buffer of pH 5.0 at ionic strength of 0.2 after 23 min. at 59,780 r. p. m.
(B): The same as (A), but after 190 min.
(C): In veronal-NaCl buffer of pH 9.0 at ionic strength of 0.2, after 16 min. at 59,780 r. p. m.

be accounted for if a (reversible) formation of aggregate took place in an alkaline solution.

In Fig. 2 (curve I) is shown the concentration dependency of the sedimentation coefficient of histone I in the acetate buffer of pH 5.0 at ionic strength of 0.2. The sedimentation coefficient slightly increased with decrease in concentration. A value of $2.0_3$ S (Svedberg unit) was obtained when extrapolated to infinite dilution by the least square method.

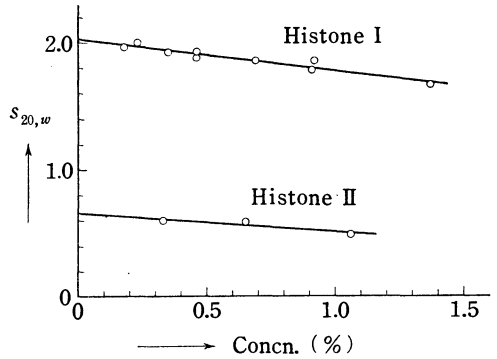



Fig. 2. Concentration dependency of sedimentation coefficients of histones I and II in an acetate buffer of pH 5.0 at ionic strength of 0.2.

The sedimentation coefficients obtained at other pH values are given in Table I. In all cases, the concentration was nearly 1.0 per cent. Amounts of the faster component, if present, are also recorded in the last column. It was noticed that a little higher sedimentation coefficient was obtained at a higher pH.

**B. Diffusion of Histone I.**—The measurements of free diffusion of histone I were made at 20.0°C in the acetate buffer of pH 5.0 at ionic strength of 0.2. Runs lasted less than 20 hours. Therefore, the effect of aggregation would be small.

TABLE I
SEDIMENTATION COEFFICIENT OF HISTONE I IN BUFFER SOLUTIONS OF IONIC STRENGTH 0.2 (Concn. = ca. 1%)

| Buffer | pH | Sedimentation coefficient | | Amount of fast comp. |
|---|---|---|---|---|
| | | Slow comp. (S) | Fast comp. (S) | (%) |
| Acetate | 4.0 | $1.5_9$ | — | 0 |
| 〃 | $4.2_5$ | $1.3_6$ | — | 0 |
| 〃 | 5.0 | $1.7_8$ | — | 0 |
| Acetate-$Na_2SO_4$ | 〃 | $1.5_5$ | — | trace |
| Cacodylate-NaCl | 6.0 | $1.7_6$ | — | 0 |
| NaCl (unbuffered) | 6.3 | $1.8_3$ | — | trace |
| Cacodylate | 6.8 | $1.8_9$ | — | 0 |
| Phosphate | 7.7 | $2.2_8$ | 19.1 | 8 |
| Tris* | 8.0 | $2.1_0$ | — | 0 |
| $NH_4Cl$-$NH_3$-NaCl | 8.6 | $2.0_5$ | 26.3 | 32 |
| Veronal-NaCl | 9.0 | $2.1_9$ | 30.2 | 60 |
| $NH_4Cl$-$NH_3$ | 9.9 | $2.4_2$ | 22.0 | 70 |

* tris(hydroxymethyl)aminomethane buffer.

Diffusion curves obtained were always symmetrical and showed nearly Gaussian curves. The homogeneity of this preparation was thus confirmed. The diffusion coefficients calculated from the second moments of the refractive-index gradient

TABLE II
DIFFUSION DATA ON HISTONE I

| Concn. (%) | $D_{20,w} \times 10^7$ ($cm^2$/sec.) | $Y_{max}$ | $X_{max}$ |
|---|---|---|---|
| 0.93 | $4.9_3$ | 2.11 | 0.02 |
| 0.47 | $4.9_4$ | 2.01 | 0.00 |
| 0.41 | $4.8_3$ | 2.00 | 0.00 |
| 0.34 | $5.3_9$ | 2.03 | 0.00 |
| 0.30 | $5.5_3$ | 2.03 | 0.00 |
| 0.28 | $5.1_5$ | 2.13 | 0.00 |
| Mean | $5.1_3$ | 2.05 | 0.00 |

curves were almost independent of concentration and the averaged value was taken as the diffusion constant. The results of the experiments are shown in Table II together with the values of $Y_{max}$ and $X_{max}$, which show the degree of homogeneity and of concentration dependency of diffusion coefficient, respectively*.

**C. Partial Specific Volume of Histone I.**—The partial specific volume ($\bar{V}$) of histone I was calculated using the equation,

$$\bar{V}=\frac{m_0-(m-h)}{\rho_0 h} \quad (1)$$

where $m$ is the weight of the pycnometer filled with the solution in which $h$ gram of protein is dissolved, and $m_0$ is the weight of the pycnometer filled with a solvent with density $\rho_0$.

The calculated values at the concentrations of $0.96_0$, $0.64_0$ and $0.42_7$ per cent. were $0.73_7$, $0.73_7$ and $0.73_4$, respectively. A value of 0.74 was taken as the mean value.

**D. The Molecular Weight and Shape of Histone I.**—From these results, the molecular weight ($M$) of histone I was calculated using the formula deduced by Svedberg and Pedersen[5], viz.,

$$M=\frac{RTs}{D(1-\bar{V}\rho)} \quad (2)$$

where $R$ is the gas constant and $T$ is the absolute temperature. The value (*unhydrated* molecular weight), 37,000, was obtained (see Table IV).

When sedimentation and diffusion constants are known, it is possible to calculate the frictional ratio, $f/f_0$, i.e., the ratio of the frictional coefficient of the protein to that for a compact spherical and unhydrated molecule of the same volume[5]. In the case of histone I, $f/f_0$ was calculated to be 1.88.

The fairly large value of $f/f_0$ raised a question concerning the molecular configuration of histone I. If it could be assumed that molecule is a rigid ellipsoid of revolution and the density of the hydrated water has the same value as that of free solvent, its axial ratio could be calculated using Perrin's equation[9]. Since the extent of hydration is not known, the plausible range of values usually accepted, i.e., 0—0.5 gram water per gram protein, was taken. Then the value of axial ratio, 17—11, was obtained for a prolate ellipsoid. However, in view of the assumption involved in this calculation, it is not convincing that histone I is really such an asymmetric molecule. Recently, Scheraga and Mandelkern[10] attempted to interpret observed physical properties of the protein in terms of a rigid "equivalent ellipsoid of revolution" characterized by its effective volume $V_e$ and its axial ratio without any assumption concerning hydration. They showed that the function, $\beta$, defined as $Ns[\eta]^{1/3}\eta/M^{2/3}(1-\bar{V}\rho)$, is dependent only upon the shape of the hydrodynamic particle. For histone I, $\beta$ was calculated using the above-mentioned values of sedimentation constant and molecular weight as well as its limiting viscosity number, $[\eta]$, measured in the same buffer, 0.111 (cc./g.). A value of $2.05\times10^6$ was obtained, which fell outside the range for a rigid ellipsoid ($\beta=2.12\times10^6$ for spheres and $\beta>2.12\times10^6$ for ellipsoids). As the validity of Scheraga and Mandelkern's treatment has not been established, no definite conclusion would be deduced from this consideration*. However, taking the extreme sensitivity of $\beta$ to errors in experimental data into consideration, the fact that $\beta$ was not far from $2.12\times10^6$ might show that histone I is not highly elongated, but is much swollen by imbibition of a solvent**. Recently, Noda[13] has proposed an experimental equation relating the volume fraction concentration and sedimentation coefficient in a suspension of spheres, and, taking advantage of this equation, he explained the large value of frictional ratio in histone I by the increase of apparent volume by solvation. Our finding that the limiting viscosity number of histone I was very sensitive to the change in ionic strength or pH of the solution[14] might support this view.

* For a homogeneous preparation with a single diffusion coefficient independent of concentration, $Y_{max}=2.00$ and $X_{max}=0^{8)}$. Slightly higher values of $Y_{max}$ than 2.00 in some of the present experiments may be due to the presence of a small amount of aggregate.

9) F. Perrin, *J. phys. radium*, (7) **7**, 1 (1936).

10) H. A. Scheraga and L. Mandelkern, *J. Am. Chem. Soc.*, **75**, 179 (1953).

* Tanford and Buzzell[11] have shown that the value of $\beta$ for bovine serum albumin calculated by using accurate molecular-kinetic data was definitely lower than the permissible range for rigid ellipsoids.

11) C. Tanford and J. G. Buzzell, *J. Am. Chem. Soc.*, **76**, 3356 (1954).

** Ogston[12] has also considered several methods for making an estimate of dimensions of solute particles from dynamic properties of their solution. According to one of his most reliable methods, IIb, the axial ratio of the spheroidal hydrodynamic model, $J$, the effective hydrodynamic volume per gram of unhydrated mass, $V'$, and the molecular weight were calculated for histone I from $s_0$, $d(1/s)/dc$, and $[\eta]$; the values, $J=5$, $V'=1.9$, $M=35{,}000$, were obtained. It was again suggested that histone I is only moderatly elongated, and it carries a fairly large amount of solvent with it.

12) A. G. Ogston, *Trans. Faraday Soc.*, **49**, 1481 (1953).

13) H. Noda, This Bulletin, **30**, 495 (1957).

14) N. Ui, unpublished.

**E. Results on Histone II.**—Similar measurements were made on histone II, the other fraction of calf thymus histone. Ultracentrifugal patterns of histone II (see Fig. 3) showed only one boundary

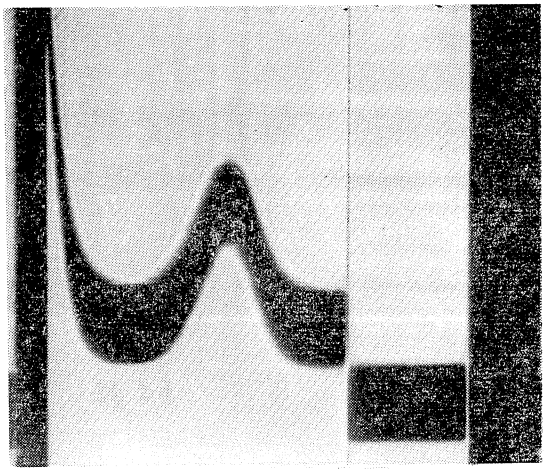


Fig. 3. Sedimentation pattern of calf thymus histone II in acetate buffer of pH 5.0 at ionic strength of 0.2.
After 110 min. at 59,780 r. p. m. in a synthetic boundary cell.

indicating the homogeneity of this preparation. The sedimentation coefficient of this protein was definitely lower than that of histone I in the acetate buffer of pH 5.0 at ionic strength of 0.2. Unlike histone I, histone II did not aggregate even if the solution was kept at 30°C for several days. The sedimentation coefficient vs. concentration curve is given in Fig. 2 (curve II). The sedimentation constant at infinite dilution was obtained by extrapolation as $0.6_6$ S.

Diffusion study also confirmed the homogeneity of this preparation. The diffusion coefficients together with the values of $Y_{max}$ and $X_{max}$ calculated from the diffusion curves in the acetate buffer are tabulated in Table III. The mean value was taken as the diffusion constant.

TABLE III
DIFFUSION DATA ON HISTONE II

| Concn. (%) | $D_{20,w}\times10^7$ (cm²/sec.) | $Y_{max}$ | $X_{max}$ |
|---|---|---|---|
| 0.85 | $7.1_6$ | 2.00 | 0.00 |
| 0.36 | $7.5_9$ | 2.02 | 0.00 |
| 0.29 | $7.1_5$ | 2.02 | 0.01 |
| Mean | $7.3_0$ | 2.01 | 0.00 |

Assuming the same value of partial specific volume as histone I, the molecular weight of histone II was calculated using equation (2). The value, 8,400, was nearly a quarter of that of histone I. A value of 2.16 was obtained for the frictional ratio, which was even higher than that for histone I.

Several data obtained for histone I and II are listed and compared in Table IV.

TABLE IV
MOLECULAR-KINETIC DATA ON HISTONES I AND II

| | Histone I | Histone II |
|---|---|---|
| Sedimentation constant, $s_{20,w}$ (S) | $2.0_3$ | $0.6_6$ |
| Diffusion constant, $D_{20,w}\times10^7$ (cm²/sec.) | $5.1_3$ | $7.3_0$ |
| Partial specific volume | 0.74 | (0.74)* |
| Molecular weight | 37,000 | 8,400 |
| Frictional ratio, $f/f_0$ | 1.88 | 2.16 |
| Axial ratio, assuming a rigid ellipsoid without hydration | 17 | 25 |

* Assumed value.

## Discussion

As shown in Table IV, a difference in molecular-kinetic properties is clear between the two fractions of histone, histone I and histone II. The view that histone II is due to the disaggregation of histone I seems unlikely, since histone I could not be converted into a smaller molecule under several conditions examined and the difference of these two fractions was definitely shown by chemical analyses[1]. Therefore, it might be reasonable to assume that calf thymus histone consists of two fractions with different molecular weights; the main fraction (80—90 per cent. of total histone) has a molecular weight of 37,000, and a lower molecular-weight fraction (molecular weight=8,400) is also contained as a minor fraction.

In this connection, it is of interest to compare the results of the present investigation with those reported by other workers. Numerous values of sedimentation constant have been recorded on the preparations of calf thymus histone prepared by various methods, although most other workers used ultracentrifugally inhomogeneous preparations. The presence of a faster component with much higher sedimentation coefficient than 2 S was often reported[15—20], but it is likely that

15) L. Ahlström, *Arki. Kemi, Mineral. Geol.*, **24A**, No. 31 (1947).
16) D. Hamer, *Brit. J. Cancer*, **5**, 130 (1951).

such a component is due to the aggregation that occurred during the isolation or in the solution in which sedimentation was performed. The view was supported by the fact that a similar boundary was also observed in our experiments on histone I at pH values higher than 7 or on using a solution (pH<7) which had been kept at room temperature for a while. The component with a sedimentation coefficient of approximately 2 S was also observed by most investigators[16-20]; the somewhat lower value recorded would be due either to the fact that the values were not extrapolated to infinite dilution or to insufficient separation of a slower component. Although it was reported by some workers that the amount of 2 S component was less than that of the component with a higher sedimentation coefficient[19,20], our conclusion that 2 S component (histone I) is the main fraction of histone would be reasonable, if we consider the great tendency of this component to aggregate. The results of Butler and coworkers aggreed to a fair extent with our results. However, their "slow component" purified as a homogeneous fraction showed higher value of sedimentation constant, 1.06 S[18], than histone II. As the properties and the amino acid composition of these two preparations are similar, further study would be necessary to explain the discrepancy.

The diffusion constant of histone has been measured by Cruft et al.[21], and Butler et al.[17,18] The former authors found that the diffusion coefficient of their preparation ($\beta$-histone) depended markedly upon pH and accounted for this phenomenon by aggregation. The highest value reported by them, $4.2\times10^{-7}$ cm$^2$/sec., which was obtained at pH 1.7, nearly coincided with our values for histone I at pH 5.0. The value obtained by Butler et al. markedly varied with preparations, and it was noticed that even an ultracentrifugally inhomogeneous preparation showed nearly a Gaussian curve[17]. The diffusion constant of a homogeneous fraction with a low molecular weight[18] was $5.3\times10^{-7}$ cm$^2$/sec., definitely lower than our value for histone II. Luck et al.[20] noted that the diffusion curves of their two fractions were not Gaussian.

Molecular weight of calf thymus histone has been calculated by Butler et al. by combining the values of sedimentation and diffusion constants[17,18]. For the homogeneous fraction with a low sedimentation constant (the slow component) a value of 18,000 was obtained, which was approximately twice as great as that of our histone II. The molecular weights of unfractionated preparations were also calculated by them, but, owing to the scattered values obtained, no definite conclusion are to be expected. Other recorded values of molecular weight calculated from sedimentation constant (or sedimentation coefficient) by assuming that the molecule is spherical would not be worth mentioning, as it was found by the present study as well as by Butler et al. that the frictional ratio of histones always showed a high value of about 2. Of interest is the view of Luck et al.[20] that the monomeric molecular weight of any fraction of histones is as low as about 10,000. They came to this conclusion by measurements of osmotic pressure and sedimentation in the presence of guanidinium chloride or urea and by end-group analysis. However, the results of our N-terminal analysis[22] have failed to support their view, although more work is necessary to see if the dissociation of our preparation does occur.

As the preparation used in this study had been obtained under milder conditions, and measurements were made under a suitable condition using ultracentrifugally homogeneous samples, it is more likely that the values of molecular weight obtained in this investigation would be reliable. It might be noted that, although rather high values of frictional ratio were obtained with both fractions, it does not necessarily mean that they are asymmetric molecules. The results in favor of this view have been obtained as described in the previous section, and further research is now in progress.

## Summary

Two fractions of calf thymus histone, histone I and histone II, were examined by sedimentation and diffusion.

Histone I was ultracentrifugally homogeneous in the buffer solutions below pH

17) J. A. V. Butler, P. F. Davison, D. W. F. James and K. V. Shooter, *Biochim. Biophys. Acta*, **13**, 224 (1954).
18) P. F. Davison, D. W. F. James, K. V. Shooter and J. A. V. Butler, ibid., **15**, 415 (1954).
19) B. Bakay, J. J. Kolb and B. Toennies. *Arch. Biochem. Biophys.*, **58**, 144 (1955).
20) J. M. Luck, H. A. Cook, N. T. Eldredge, M. I. Haley, D. W. Kupke and P. S. Rasmussen, ibid., **65**, 449 (1956).
21) H. J. Cruft, C. M. Mauritzen and E. Stedman, *Nature*, **174**, 580 (1954).
22) M. Yamasaki, N. Ui, S. Ishii, H. Fujioka, K. Iwai and T. Ando, The 29th General Meeting of the Japanese Biochemical Society, Fukuoka, Nov. 1, 1956.

7, but showed the presence of an aggregate above pH 7. The sedimentation constant (at infinite dilution) of histone I was calculated to be $2.0_3$ S in an acetate buffer of pH 5.0 at ionic strength of 0.2. The homogeneity of this sample was also confirmed by diffusion experiments in the same buffer, and $5.1_3 \times 10^{-7}$ cm$^2$/sec. was obtained as the diffusion constant. Combining the values of sedimentation and diffusion constants as well as the value of partial specific volume, 0.74, the molecular weight was calculated to be 37,000.

Histone II was also found to be homogeneous by sedimentation and diffusion measurements in the acetate buffer of pH 5.0. Its sedimentation constant, diffusion constant, and molecular weight were calculated as $0.6_6$ S, $7.3_0 \times 10^{-7}$ cm$^2$/sec., and 8,400, respectively.

The author wishes to express his sincere thanks to Professor Itaru Watanabe for his valuable suggestion and encouragement. His thanks are also due to the Research Laboratory of Precision Machinery and Electronics, Tokyo Institute of Technology, for the kind permission to use their Spinco ultracentrifuge. The expense of this research was partly defrayed by a Grant in Aid of Scientific Research from the Ministry of Education, to which the author's thanks are due.

*Institute of Science and Technology*
*The University of Tokyo*
*Meguro, Tokyo*

# *On the Aggregation of Calf Thymus Histone**

By Nobuo Ui

(Received April 30, 1957)

In recent years, increasing attention has been directed toward protein interactions[1]. Indeed, it has been recognized that many reactions of biological importance, such as enzyme reactions, antigen-antibody reactions, etc., involve interaction of proteins with other proteins or other molecules. By studying the nature of these interactions, not only is it possible to interpret biological phenomena on a molecular basis, but it is also possible to obtain an information about protein structure in an aqueous environment.

It has been found that some proteins associate (aggregate) or dissociate with suitable change in their environment[2]. As these interactions which occur between protein molecules of the same kind are the most simple cases of protein-protein interactions, it would be of value to examine their nature from the physico-chemical point of view.

In the course of studies on purification and characterization of calf thymus histone, it was found that its main fraction, histone I, had a great tendency to aggregate[3]. The protein, when purified cautiously, showed a single homogeneous boundary in an ultracentrifuge at pH values below 7[4,5], but a heavier component appeared when the solution was kept at room temperature, and its amount varied markedly with change in the conditions of pretreatment and measurements. The present author was interested in this finding and studied the aggregation reaction systematically, the results of which are reported in this paper.

## Experimental

**Material.**—The sample used in this study was histone I, i. e., the main fraction of calf thymus histone. The method used for its preparation has already been described[4].

**Methods.**—Sedimentation and diffusion studies were carried out in the same apparatus described in the preceding paper[5]. Sedimentation measurements were made at room temperature (15—30°C), while those of diffusion were made at 20.0°C. The observed sedimentation and diffusion coefficients were always corrected for the values in water at 20.0°C.

* A part of this work was read before the Symposium on Protein Structure held in Tokyo on November 5, 1955.

1) I. M. Klotz, in H. Neurath and K. Bailey, "The Proteins," New York, Vol. I, p. 727 (1953).

2) D. F. Waugh, *Advances in Protein Chem.*, **9**, 325 (1954).

3) N. Ui, *Biochim. Biophys. Acta.*, **22**, 205 (1956).

4) N. Ui, ibid. in press.

5) N. Ui, This Bulletin, **30**, 801 (1957).

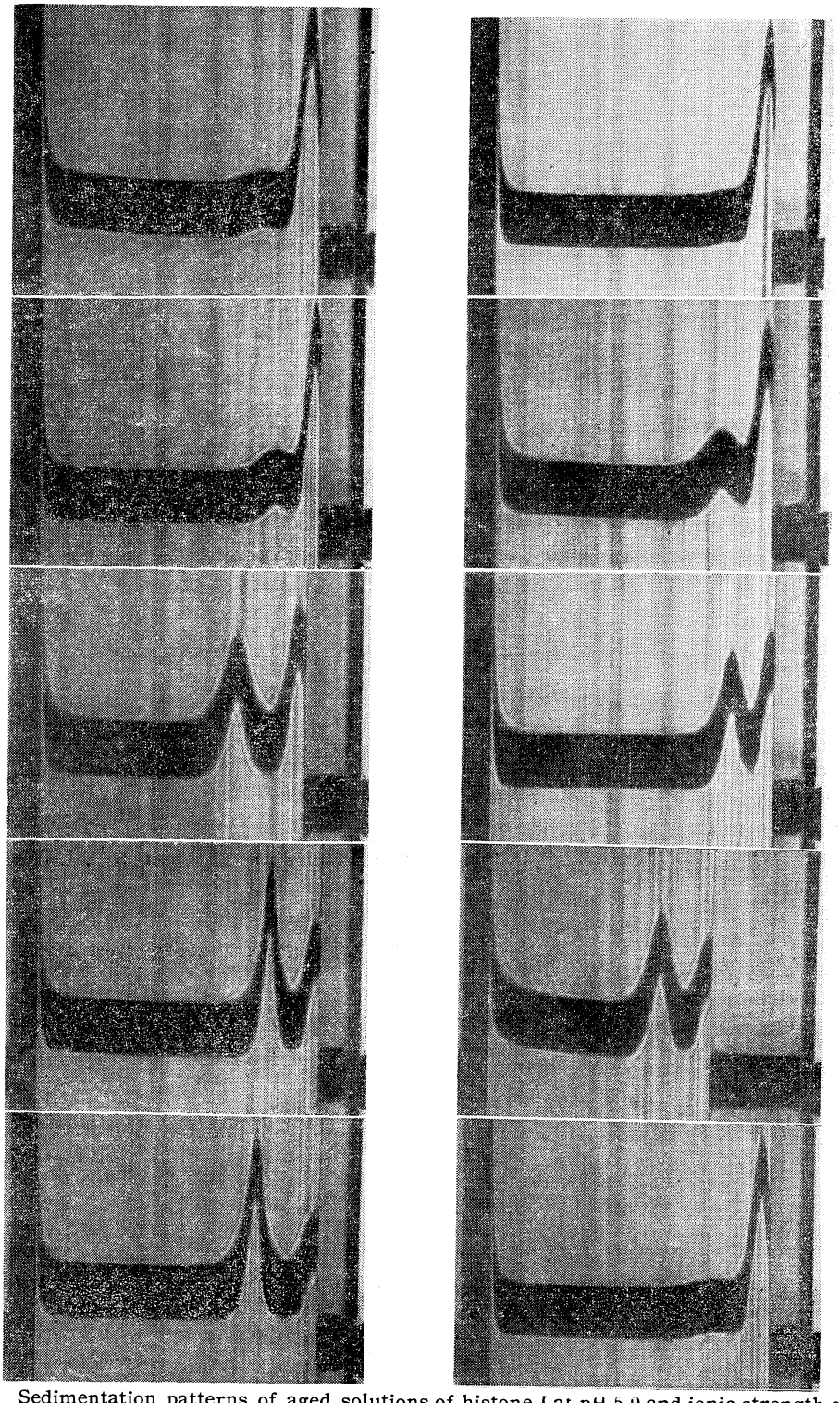


Fig. 1. Sedimentation patterns of aged solutions of histone I at pH 5.0 and ionic strength of 0.1.
Left : Solutions were kept at 30°C in the presence of sodium sulfate (2/300 M) for periods of 30 min., 3, 24, 48 and 168 hr. from top to bottom.
Right : Upper 4 patterns were obtained after aging at 30°C in the absence of sulfate ions for 30 min., 28, 76 and 168 hr. Extreme bottom pattern was obtained after 7 days' keeping at 0°C in the presence of sulfate ions.
Sedimentation proceeds from right to left.

Electrophoretic measurements were made in a Tiselius-type apparatus[6] equipped with a Philpot-Svensson's schlieren optical system[7], and a medium cell with a tall center section[8] was used.

Viscosity was measured at 30.0°C in an Ostwald viscosimeter.

## Results

**A. Aggregation at 30°C at pH 5.0 and Ionic Strength 0.1.**—When a 1 per cent. solution of histone I in an acetate buffer of pH 5.0 at ionic strength of 0.1 was allowed to stand at 30°C and examined in an ultracentrifuge, a faster component with a sedimentation coefficient of 8—10 S was observed besides the original component of this preparation (about 2 S) as is shown in Fig. 1. The amount of the faster component increased slowly with time of aging at 30°C, and reached 55 per cent. of the total protein (see Fig. 2, curve II).

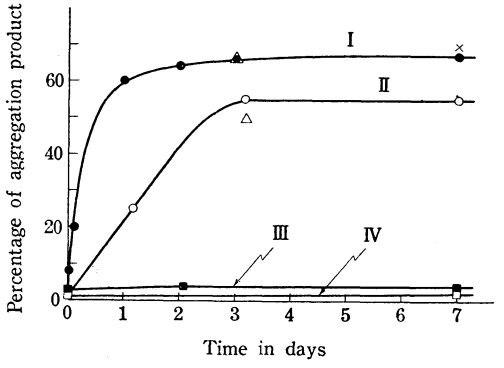



Fig. 2. Increase of the aggregation product with time at pH 5.0 and ionic strength of 0.1.
Curve I : 30°C, in the presence of sulfate ions.
Curve II : 30°C, in the absence of sulfate ions.
Curve III : 0°C, in the presence of sulfate ions.
Curve IV : 0°C, in the absence of sulfate ions.

Sulfate ion was found to be an effective aggregating agent; if an acetate buffer of the same pH and total ionic strength as before but containing sodium sulfate (2/300 M) was used as a solvent, the faster component appeared more rapidly and the amount reached 67 per cent. after one or two days (see Fig. 2, curve I). Some of the sedimentation patterns are shown in Fig. 1.

In contrast with the observation at 30°C, the aggregation did not proceed appreciably at 0°C (see curves III and IV in Fig. 2). Although a small amount (2—3 per cent.) of aggregation was observed in this experiment, it would be due to the high temperature (nearly 30°C) at which the sedimentation was performed. In fact, no faster boundary was found when another solution of histone I was kept for 25 days at 0°C and examined at a lower temperature.

In Fig. 3 is shown the sedimentation coefficient of the faster component as a function of its amount. It was found that the more the aggregation proceeded, the higher was the sedimentation coefficient obtained.

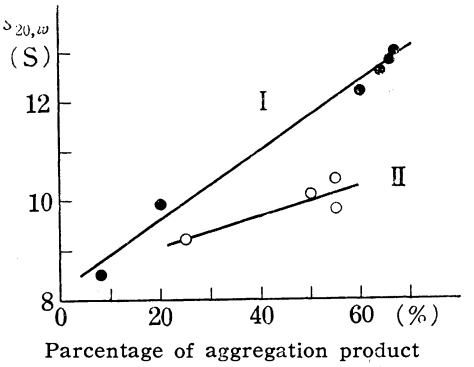



Fig. 3. Relation of sedimentation coefficient of the aggregate with its amount.
Curve I : Aged at 30°C in acetate-$Na_2SO_4$ buffer of pH 5.0 at ionic strength of 0.1.
Curve II : Aged at 30°C in acetate buffer (sulfate-ion free) of pH 5.0 at ionic strength of 0.1.

The aggregation was not reversed by lowering the temperature. Therefore, when solutions of aggregated histone were examined before and after keeping them at 0°C for 4 days, the amount of aggregate was found to be nearly the same (see marks △ in Fig. 2)*. It was also found that the aggregate, which had been produced in the solution containing sodium sulfate, did not dissociate when sulfate ions were removed by addition of barium chloride (see mark × in Fig. 2).

**B. Effect of Variation in Temperature.**—Fig. 4 shows the amounts of aggregate formed when a 1 per cent. solution

6) A. Tiselius, *Trans. Faraday Soc.*, **33**, 524 (1937).
7) J. St. L. Philpot, *Nature*, **141**, 283 (1938); H. Svensson, *Kolloid-Z.*, **87**, 181 (1939).
8) L. G. Longsworth, *Chem. Revs.*, **30**, 323 (1942).

* In Fig. 2, the amounts of aggregate are plotted against the time kept at 30°C. As the aggregation was not reversed by cooling, it was not necessary to perform sedimentation experiments at the same temperature as in the case of the aging. A lower temperature was rather desirable to prevent progress of aggregation during the measurements.

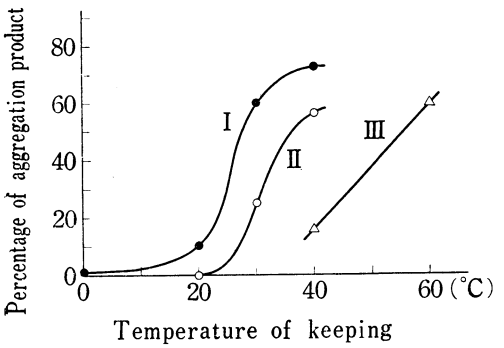



Fig. 4. Effect of temperature upon aggregation.
Curves I and II: Aged for 24 hrs. at pH 5.0 and ionic strength of 0.1, in the presence and absence of sulfate ions.
Curve III: Aged for an hour at pH 5.0 and ionic strength of 0.1, in the absence of sulfate ions.

of histone I in acetate buffers (pH=5.0, ionic strength=0.1) with and without sodium sulfate (2/300 M) were kept at various temperatures. Curves I and II were obtained by keeping the solutions for 24 hours, while curve III was obtained after one hour's keeping.

It was clear that the higher the temperature, the higher the extent of aggregation. At 20°C, histone I did not aggregate during 24 hour's keeping in the absence of sulfate ion, but the aggregation occurred by aging for a longer time (8 per cent. after 4 days' keeping). A lower temperature than 20°C was necessary to keep the solution free from the aggregate for long time.

At higher temperatures, it was found that, not only was the extent of aggregation increased, but also the reaction rate was accelerated. For instance, the initial slope of the amount of aggregate vs. aging time curve was steeper at 40°C than at 30°C. At 40°C, the amounts of aggregate reached 82 per cent. in the presence of sulfate ions and 62 per cent. in its absence, which were higher than those obtained at 30°C.

**C. Effect of Variation in Protein Concentration.**—A series of histone I solutions in the same solvents as before at various protein concentrations were examined after keeping at 30°C for 24 hours.

As shown in Fig. 5, a higher concentration favored the aggregation. In the presence of sulfate ions, the extent of aggregation in 2 per cent. solution was lower than that in 1 per cent. solution, but it might be due to the decrease in

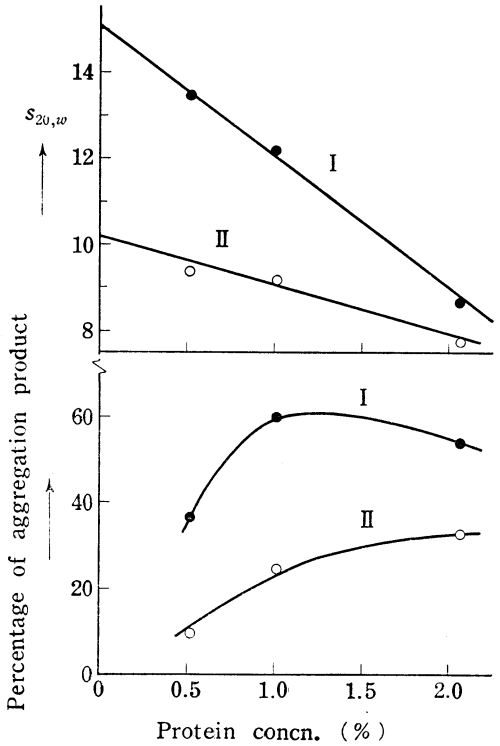



Fig. 5. Effect of protein concentration upon aggregation.
Aged at 30°C for 24 hrs. at pH 5.0 and ionic strength of 0.1, in the presence (curve I) or absence (curve II) of sulfate ions.

the molar ratio of sulfate to the protein with increase in protein cencentration, since the concentration of sodium sulfate was always kept constant (2/300 M) in this experiment.

**D. Effect of Variation in Ionic Strength of the Solution.**—Effect of ionic strength was studied at pH 5.0 with 1 per cent. solutions of histone I. The concentration of sodium sulfate, if present, was kept always constant at 2/300 M.

The amounts of aggregate produced during 24 hours' aging at 30°C are plotted against ionic strength of the solution in Fig. 6. It was shown that high ionic strength favored aggregation. In the absence of sulfate ions aggregation hardly occurred below ionic strength of 0.05. It was also indicated that the effect of sulfate ion on aggregation was accentuated at lower ionic strengths.

The temperature dependency of this aggregation was again noted; at 0°C the aggregate was not produced appreciably even if the ionic strength was higher and sulfate ions were present (see Fig. 6, curve III).

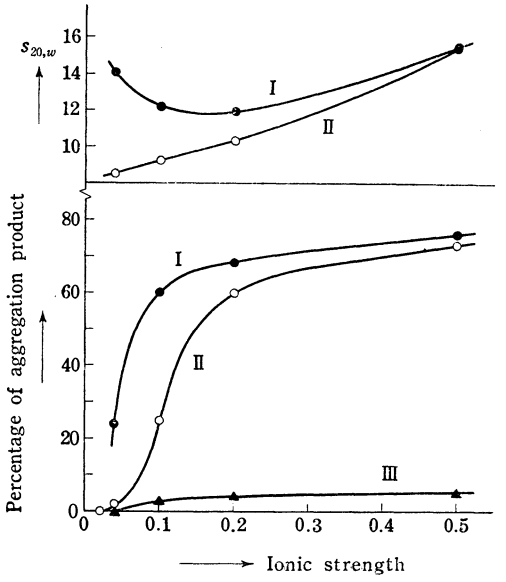



Fig. 6. Effect of ionic strength upon aggregation.
Aged at 30°C for 24 hr. at pH 5.0 in the presence (curve I) or absence (curve II) of sulfate ions. Curve III is that of aged solutions at 0°C.

The sedimentation coefficient of the aggregate also depended upon the ionic strength of the solution (see upper figure in Fig. 6), and a higher value was obtained at a higher ionic strength. In the case of solutions containing sulfate ions, however, sedimentation coefficient vs. ionic strength curve showed a minimum, suggesting the complicated effect of sulfate ion upon aggregation.

**E. Effect of Adding Sodium Sulfate.**—In view of the finding that the aggregation of histone was greatly accelerated by the presence of sulfate ions, a different amount of sodium sulfate was added to the solution of histone I (pH 5.0) and the effects were compared.

When sodium sulfate was added to a concentration higher than 2/300 M, no appreciable change was observed in the amount of the aggregate formed after 48 hours' aging at 30°C, but the sedimentation coefficient of the aggregate was definitely higher at higher concentration of sulfate ions; for instance, 17.0 S was obtained for 5/300 M sodium sulfate instead of 11.8 S for 2/300 M (total ionic strength was equal to 0.1).

Even a slight addition of sulfate ions was effective for the aggregation. Therefore, histone I sulfate aggregates more easily than its chloride. However, it might be noted that the aggregation of histone I chloride in the acetate buffer (without sodium sulfate) was not due to a slight contamination of sulfate ions in the solution; a curve similar to curve II in Fig. 2 was obtained when the acetate buffer containing barium chloride was used and aged at 30°C.

**F. Effect of Variation in pH.**—Dependence of the aggregation of histone I upon pH was studied by using buffer solutions of constant ionic strength of 0.1*. Protein concentration was always kept at 1 per cent. and the concentration of sodium sulfate, if present, was 2/300 M.

The amount of the aggregate formed after

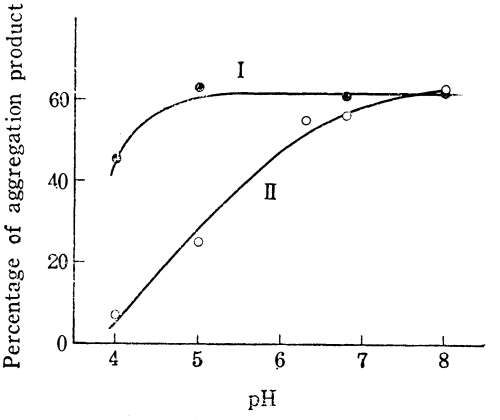



Fig. 7. Effect of pH upon aggregation.
Aged at 30°C for 24 hr. at ionic strength of 0.1 in the presence (curve I) or absence (curve II) of sulfate ions.

24 hours' aging at 30°C is plotted in Fig. 7 as a function of pH. It was noted that higher pH favored aggregation in absence of sulfate ions, but the amount of aggregate found was almost independent of pH values when sodium sulfate was added.

It was also found that some electrolytes caused marked influence upon the aggregation; a gel-like precipitate formed after keeping histone I at 30°C in a phosphate buffer of pH 7.7 or in a veronal buffer of pH 9.0.

As described in the preceding paper[6], histone I showed the presence of a faster component when sedimentation experiment was performed in an alkaline solution above pH 7 except in tris(hydroxymethyl)aminomethane buffer, even if the solutions had not been exposed to a higher temperature. In some cases, especially when pH was 9—10, a precipitate was

* The Following buffers were used in this study: pH 4.0 and pH 5.0, acetate buffer; pH 6.3, NaCl solution (unbuffered); pH 6.8, cacodylate buffer; pH 8.0, tris-(hydroxymethyl)aminomethane buffer.

formed by several days' keeping at 0°C. It was also found that the aggregate disappeared when the solution was soon brought to pH 5.0, so the reversibility of aggregation was suggested.

**G. Reversibility of the Aggregation Reaction.**—As stated before (see section **A**), the aggrgation was not reversed by lowering the temperature. However, a disaggregation occurred when an aggregated solution was brought to a lower ionic strength by dialysis. Results are shown in Table I.

TABLE I
DISAGGREGATION OF AGGREGATE BY DIALYSIS
pH : 5.0 (acetate buffer) ;
Protein concn. : ca. 1%

| Aging | | | Amount of aggregate after dialysis against buffer with ionic strength of | | |
|---|---|---|---|---|---|
| Ionic strength | Time at 30°C | Aggregate formed | 0.02 | 0.04 | 0.1 |
| 1.0 | 72 hr. | 73% | — | — | 30% |
| 0.1 | 72 | 50 | — | 24% | — |
| 0.1 | 96 | 55 | 15% | — | (15%)* |
| 0.1 | 24 | 20 | — | — | 20%** |

* This value was obtained on the solution which had been re-adjusted to ionic strength of 0.1 after being brought to ionic strength of 0.02 by dialysis.

** The solution was once brought to pH 2 by addition of hydrochloric acid and then dialyzed against the acetate buffer of ionic strength 0.1.

**H. Molecular-kinetic Properties of the Aggregates.**—In order to obtain some information on the size and the shape of the aggregates, sedimentation and diffusion experiments were made with 1 per cent. solution of histone I in an acetate buffer of pH 5.0 at ionic strength of 0.2. The solution had been kept for 4 days at 30°C in the presence and the absence of sodium sulfate (2/300 M). The amount of aggregate formed did not decrease with dilution.

In Fig. 8 is plotted the sedimentation coefficient of the aggregate against concentration, and the sedimentation constant at infinite dilution was calculated by extrapolation.

Diffusion curves markedly deviated from Gaussian curves, as the solution also contained the unaggregated protein. However, since the diffusion coefficient of the unaggregated histone I is known[5], the diffusion coefficients of the aggregates could be calculated, although not accurately, making use of the weight-averaged diffusion coefficients (obtained by the second-moment method) as well as the composition of the solutions determined by sedimentation analysis. The results are shown in Table II. As the diffusion patterns did not show concentration dependency of the

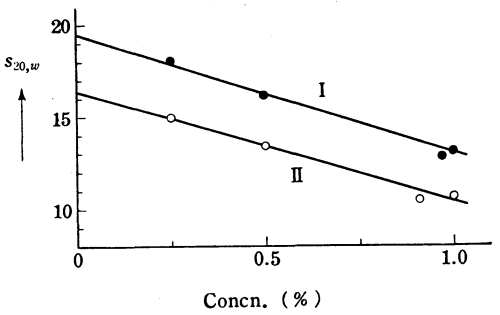



Fig. 8. Concentration dependency of sedimentation coefficient of aggregate at pH 5.0 and ionic strength of 0.2.
Curve I : The aggregate was prepared by aging at 30°C for 4 days in the presence of sodium sulfate (2/300 M).
Curve II : The aggregate was prepared in the same way but in a sulfate ion-free buffer.

TABLE II
DIFFUSION DATA ON AGED SOLUTION OF HISTONE I

| Buffer | Aggregate formed (%) | Weight-averaged diffusion coefficient ($D_{20,w}\times10^7$ cm²/sec.) | Diffusion coefficient of aggregate ($D_{20,w}\times10^7$ cm²/sec.) |
|---|---|---|---|
| Acetate | 66 | $1.3_3$ | $1.4_7$ |
| Acetate-$Na_2SO_4$ | 83 | $1.6_1$ | $1.7_5$ |

diffusion coefficients of the constituents, the values were taken as diffusion constants.

The molecular weight of the aggregate formed either in the presence or the absence of sulfate ions was thus calculated by combining the values of sedimentation and diffusion constants and by assuming that the partial specific volume of the aggregate was the same as unaggregated histone I. In both cases, a value of $1.1\times10^6$ was obtained (see Table III) and it was found that the aggregate formed in these solutions consisted of about 30 molecules of histone I.

The frictional ratio of the aggregate nearly agreed with that of unaggregated histone. A similar result was obtained when the change in viscosity with time was measured at 30°C. In the absence of sulfate ions (pH=5.0, ionic strength=0.1), $\eta_r$

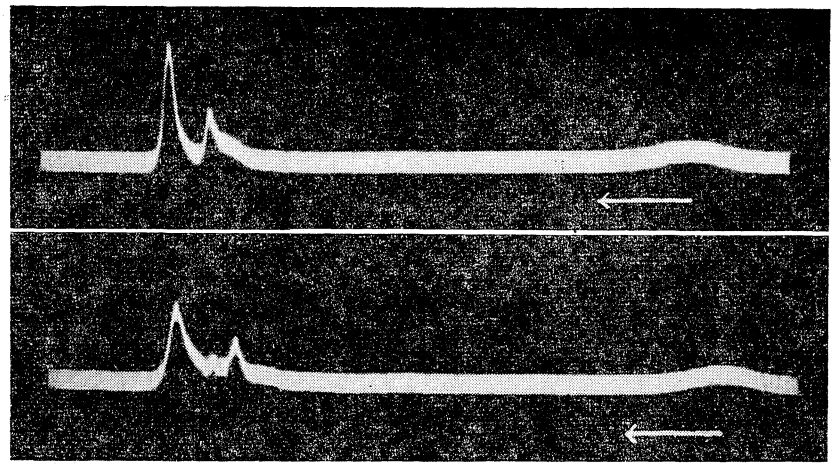



Fig. 9. Electrophoretic patterns of unaggregated (A) and aggregated (B) solutions of histone I in the acetate buffer of pH 5.0 at ionic strength of 0.1. Only ascending patterns are shown.

TABLE III
MOLECULAR-KINETIC DATA ON AGGREGATED HISTONE I

| Buffer | $s_{20,w}$ (S) | $D_{20,w} \times 10^7$ ($cm^2$/sec.) | $M$ | $f/f_0$ |
|---|---|---|---|---|
| Acetate | 16.4 | $1.3_3$ | 1,150,000 | 2.30 |
| Acetate-$Na_2SO_4$ | 19.7 | $1.6_1$ | 1,140,000 | 1.91 |

(viscosity ratio) of 1.18 per cent. solution increased slightly, i. e., from 1.20 to 1.35 after 120 hours. Similarly, when sulfate ions were present, $\eta_r$ of 1.16 per cent. solution changed from 1.18 to 1.25 after 32 hours' keeping.

**I. Electrophoretic Behavior of the Aggregate.**—When the aggregation of histone I took place, some change in electrophoretic patterns were observed. An example is shown in Fig. 9.

Although even unaggregated histone I did not show a single boundary (see Fig. 9 A), the electrophoretic patterns became more complex when aggregation occurred (Fig. 9 B); the patterns shown in Fig. 9 were obtained in the acetate buffer of pH 5.0 at ionic strength of 0.1 using the solution which had not been exposed to a high temperature and the solution which had been kept at 30°C for 2 days (the latter solution contained the aggregate about 24 per cent.). It was found that the fastest boundary in the case of the aggregated solution moved to the cathode faster than the fastest component of unaggregated histone I*. A similar variation in electrophoretic pattern with aggregation was observed at other ionic strengths, at a different temperature (25°C), or in the presence of sulfate ions. Therefore, it was concluded that the aggregate had an electrophoretic mobility higher than unaggregated histone at pH 5.0.

* The electrophoretic mobility (descending) of the fastest component was calculated as $8.0 \times 10^{-5}$ $cm^2$/sec. volt in the absence of the aggregate, while $8.6 \times 10^{-5}$ in the case of the aggregated solution.

## Discussion

It is indicated by the results of ultracentrifugal studies described above that histone I produces a rapidly sedimenting component with aging at a temperature higher than about 20°C at the expense of the original component of this protein (2 S), provided that the ionic strength of the solution is not too low. As the molecular-kinetic studies had shown that the size of the faster component was definitely larger than the original protein, the reaction occurring would be due to an aggregation.

The sedimentation coefficient of the newly formed component increased continuously as the reaction proceeded and varied with aging conditions. In view of this finding, the term "aggregation" was used throughout this paper in preference to "association" (for the definition of "aggregation" and "association", see the reference[2]). However, the fairly regular nature of the reaction was suggested, as the aggregate always showed a single boundary with moderate sharpness in an ultracentrifuge; its sedimentation coefficient and the amount were constant so far as the aging conditions were the same.

The aggregation proceeded at a rate sufficiently small to permit the estimation

of the degree of aggregation at desired levels by sedimentation analysis, and this slowness was one of the main features of this reaction. High temperature or high ionic strength was highly effective in promoting the aggregation and an equilibrium was thereby rapidly established. However, the aggregation could not be reversed by the lowering of the temperature. Disaggregation only occurred when the electrolyte concentration of the solution was reduced by dialysis*. Therefore, it seems that the process involves an equilibrium dependent on ionic strength between the monomer and the aggregate. As the rate of aggregation was slow, it might also be suggested that some modification of the protein precedes aggregation. The experimental results presented here would be accounted for if this conversion is favored by high temperature, and no significant change in the size and the shape of the molecule is assumed to occur by this process. However, as a temperature-dependent modification of calf thymus histone has not been proved, further study is needed to check this conclusion.

Of interest are the forces involved in forming the aggregate. Histone I has an isoelectric point definitely higher than pH 10.3 as revealed by electrophoresis[9]. When amino acid composition of this preparation is assumed to be the same as that of "arginine-rich histone" of Daly and Mirsky[10], it follows that histone I has about 78 positively charged and 21 negatively charged groups per molecule at pH 5.0 (net charge=+57). Therefore, strong repulsion between molecules is expected to exist at this pH, and it must be overcome by specific attractive forces in oder that an appropriate interaction may occur. The contribution of van der Waals' forces or hydrogen bonds to the formation of aggregate might be considerable, although electrostatic attraction between oppositely charged groups, which are disposed appropriately, would also be responsible. In this connection, it might be pertinent to describe our finding that the aggregation was prevented by the presence of urea, which is a well-known hydrogen bond breaking agent; when a solution of histone I was kept at 30°C for 4 days in the presence of 5 M urea (pH=5.0, ionic strength 0.1), no faster sedimenting boundary was observed and only a single sedimentation boundary with the normal sedimentation coefficient of about 2 S was found after the aged solution was dialyzed against the acetate buffer of pH 5.0 and ionic strength 0.1.

It is also to be noted that the suitable configuration of the protein molecule would be required in order that the aggregate might be stabilized by forming a number of bondings due to short range attractive forces (such as hydrogen bonds or van der Waals' forces). Since an electrostatic, repulsive force between charged groups is less prominent at a high ionic strength or a high pH, the aggregated form must become favorable when ionic strength or pH is elevated.

The specific effect of sulfate ions on promoting the aggregation should be emphasized. As the electrophoretic mobility of histone I (unaggregated) at pH 5.0 was found to be markedly diminished by the addition of sodium sulfate[9], it is clear that a large number of sulfate ions are bound with one molecule of histone I. Accordingly, the electrostatic repulsive force between molecules would not be strong enough when sulfate ions are present. It might be also probable that sulfate ions in some manner stabilize the modified form of histone I, which was assumed in the above discussion to be an intermediate in the aggregation reaction. Another bivalent anion, dibasic phosphate ion, was also found to be an effective aggregating agent.

The aggregation product was found to consist of fairly a large number of histone I molecules; i.e., the number of units was about 30 when calculated for the preparation aged at 30°C for 4 days in the presence or the absence of sulfate ions (pH=5.0 and total ionic strength=0.2). Although exact shape of the aggregate is not known, the frictional ratio, which depends upon both shape and hydration, was found to be similar to that of the unaggregated histone I. Electrophoretic mobillty at pH 5.0 only slightly increased with the aggregation. Thus, no significant change except size was found to occur with aggregation. However, it was noticed that histone I solution solubilized sparingly water-soluble materials, such as dimethylaminoazobenzene, especially under conditions in which the aggregation is favorable (unpublished

* The aggregate formed at pH's higher than at low temperature disaggregated when the solution was brought to lower pH's. However, the aggregation in an alkaline solution became more or less irreversible after keeping the solution for a longer time.

9) N. Ui, This Bulletin, in press.

10) M. M. Daly and A. E. Mirsky, *J. Gen. Physiol.*, **38**, 405 (1955).

data). A similar phenomenon has often been reported in an aqueous solution of soap or detergent[11], and is thought to be due to the formation of micelles through the mutual association of hydrophobic and hydrophilic groups in which a sparingly water-soluble material is taken in. On the analogy of this interpretation, it might be possible that the molecules of histone I are specifically arranged in the structure of the aggregate to take in these materials. However, as the interpretation is a matter of speculation, more work is necessary as to the structure of the aggregate.

Since the aggregation of histone I proceeds even at room temperature, especially when the ionic strength of the solution is high, the temperature should be kept as low as possible during the preparation of histone. At pH's higher than 7, the aggregation occurs even if the solution is kept cold and becomes more or less irreversible with time. Therefore, the method for the preparation of histone which takes advantage of its precipitability in an alkaline solution is not recommended. A faster sedimenting component of histone with a sedimentation coefficient much higher than 2 S, which has often been reported by other investigators (see D scussions in the preceding paper[5]) seems to be due to the aggregation that occurred during the isolation of the protein or in the solution in which measurement was performed.

In agreement with the present study, the aggregation of histone has also been pointed out by Cruft, Mauritzen and Stedman[12] and by Davison, James, Shooter and Butler[13]. The former workers came to this conclusion by diffusion measurements which were performed at various pH's. Davison et al. took advantages of sedimentation and other methods, but no detailed data have been reported. They also interpreted the complicated electrophoretic patterns, which were obtained with unfractionated histone at various pH values, by assuming a complex formation between different fractions of histone, and suggested that the greater part of the aggregation reaction involves both 2 S and 1 S component. However, as the electrophoretic patterns were highly complicated[9], more extensive work seems necessary to confirm Davison et al's view.

It is of interest to compare the results of the present study with those of similar studies on other proteins. While association or aggregation occurs with several proteins, it has been known that, only in a few cases of these interactions, an equilibrium is attained at such a slow rate as described in this paper. Johnson et al.[14] have shown that an association-dissociation equilibrium exists in the solution of arachin, a seed globulin in peanut, and that the rate of association or dissociation was slow. It was also shown that pH and ionic strength as well as sulfate ion strongly changed the state of equilibrium and reaction rate[15]. As to the aggregation of conalbumin with acid, Cann et al.[16] showed that the ability of positively charged conalbumin molecules to aggregate resulted from structural modification when the protein was exposed to acidic media. The remarkable effect of sulfate ion upon this aggregation was also stressed. Specific effects of some electrolytes upon a more rapidly attained association-dissociation equilibrium have been reported with hemocyanin[17], insulin[18] and salmine[19].

## Summary

The aggregation reaction of histone I, i. e., the main fraction of calf thymus histone, was studied by means of sedimentation, diffusion, viscosity measurement and electrophoresis.

The aggregation was found to proceed usually at a temperature higher than 20°C, although it occurred at pH's above 7 even at 0°C. High temperature, pH, ionic strength or protein concentration promoted the reaction. It was also found that sulfate ion was an effective aggregating agent.

The aggregation was not reversed by lowering the temperature, but disaggregation occurred when the ionic strength of the solution containing the aggregate was reduced by dialysis.

The aggregate was rather large in size.

11) H. B Klevens, *Chem. Revs.*, **47**, 1 (1950).
12) H. J. Cruft, C. M. Mauritzen and E. Stedman, *Nature*, **174**, 580 (1954).
13) P. F. Davison, D. W. F. James, K. V. Shooter and J. A. V. Butler, *Biochim. Biophys.* Acta, **15**, 415 (1954).
14) P. Johnson and E. M. Shooter, ibid., **5**, 361 (1950); P. Johnson, E. M. Shooter and E. K. Rideal, ibid., **5**, 376 (1950),
15) P. Johnson and F. J. Joubert, *J. Polymer Sci.*, **7**, 605 (1951).
16) J. R. Cann and R. A. Phelps, *Arch. Biochem. Biophys.*, **52**, 48 (1954); R. A. Phelps and J. R. Cann, ibid., **61**, 51 (1956).
17) S. Brohult, *J. Phys. & Colloid Chem.*, **51**, 206 (1947).
18) E. Fredericq and H. Neurath, *J. Am. Chem. Soc.*, **72**, 2684 (1950).
19) N. Ui, *Repts. Institute Science and Technol., Univ. of Tokyo*, **8**, 255 (1954).

It consisted of about 30 molecules of histone I under certain aging conditions (pH 5.0) and had nearly the same frictional ratio as that of the monomer. Electrophoretic mobility slightly increased with aggregation at pH 5.0.

On the basis of the data presented, a possible mechanism in forming the aggregate was discussed.

The author wishes to express his sincere thanks Professor Itaru Watanabe for his valuable suggestions and encouragement. His thanks are also due to the Research Laboratory of Precision Machinery and Electronics, Tokyo Institute of Technology, for the kind permission to use their Spinco ultracentrifuge. The expense of this research was partly defrayed by a Grant in Aid for Scientific Research from the Ministry of Education, to which the author's thanks are due.

*Institute of Science and Technology*
*The University of Tokyo*
*Meguro, Tokyo*

# *Electrophoretic Studies of Calf Thymus Histone*

By Nobuo Ui

(Received May 7, 1957)

As was reported in the previous papers[1,2], calf thymus histone consists of two fractions (histones I and II). It was also shown that both were ultracentrifugally homogeneous. However, electrophoretic investigation on these fractions revealed that neither of them was homogeneous.

The present paper deals with the electrophoretic properties of histone I, the main component. A few experiments with histone II are also reported and the results are compared with those of histone I. Although electrophoretic heterogeneity of calf thymus histone has also been proved by other workers[3-7] the present experiments showed the presence of more components than had ever been reported before.

## Experimental

**Materials.**—Two fractions of calf thymus histone used in this investigation, i.e., histones I and II, were prepared by the method described in a previous paper[1]. The preparation of histone I mainly used was obtained from the extract of isolated nuclei with 0.2 N sulfuric acid after removing histone II by extraction with 0.1 N sulfuric acid.

**Methods.**—Electrophorsis was carried out in a Tiselius-type apparatus[8] equipped with a Philpot-Svensson's shlieren optical system[9]. Prior to electrophoresis, each preparation was dissolved in a desired buffer and dialyzed against a large quantity of the buffer in a cold room which was maintained approximately at 0°C, although, in some experiments, the dialysis was omitted or performed at 25°C.

The pH value of some buffers, such as ammonium chloride ammonia buffers, markedly varied with temperature. Accordingly, pH measurements were made at a temperature nearly the same as that of electrophoresis. Acetate buffers used in most of the experiments did not show any change in pH with temperature.

In most cases, runs were made at a constant temperature of approximately 0°C (at 0.2°C or slightly higher), but some experiments were made at 25.0°C to see the effect of temperature.

A medium electrophoretic cell with a tall center section was used throughout this investigation, and electrophoresis was continued usually until the distance of migration of the fastest boundary reached 6 cm. or more, as it was found that separation of boundaries was poor when the migration distance was shorter.

Specific electric conductivity of the solution was measured in a bath maintained at 0.0°C (or 25.0°C when electrophoresis was carried out at 25.0°C). Therefore, the electrophoretic mobility

1) N. Ui, *Biochim. Biophys. Acta*, in press.
2) N. Ui, This Bulletin, **30**, 801 (1957).
3) J. Grégoire and M. Limozin, *Bull. Soc. Chim. Biol.*, **36**, 15 (1954).
4) J. A. V. Butler, P. F. Davison, D. W. F. James and K. V. Shooter, *Biochim. Biophys. Acta*, **13**, 224 (1954).
5) P. F. Davison, D. W. F. James, K. V. Shooter and J. A. V. Butler, ibid., **15**, 415 (1954).
6) H. J. Gruft, C. M. Mauritzen and E. Stedman, *Nature*, **174**, 580 (1954).
7) J. M. Luck, H. A. Cook, N. T. Eldredge, M. I. Haley, D. W. Kupke and P. S. Rasmussen, *Arch. Biochem. Biophys.*, **65**, 449 (1956).
8) A. Tiselius, *Trans. Faraday Soc.*, **33**, 524 (1937).
9) J. St., L. Philpot, *Nature*, **141**, 283 (1938); H. Svensson, *Kolloid-Z.*, **87**, 181 (1939).

($u$) obtained was thought to be the value at 0.0°C (or 25.0°C).

The greatest difficulty encountered in this investigation was due to the fact that solutions of histone solubilized some kinds of water-insoluble material. Thus, when ground surfaces of flanged plates at each end of cell segments were greased as usual with vaseline or silicone grease (Dow Corning's high vacuum silicone grease), there occurred serious disturbance in initial boundaries formed between the protein solution and buffer at the beginning of the experiments. The difficulty was overcome by using silicone oil with high viscosity (Shin-Etsu Silicone Oil KF 96, 100,000 cs.). The author is indebted to Dr. K. Hayashi, Shin-etsu Chemical Co., for his kind supply of various preparations of silicone oil.

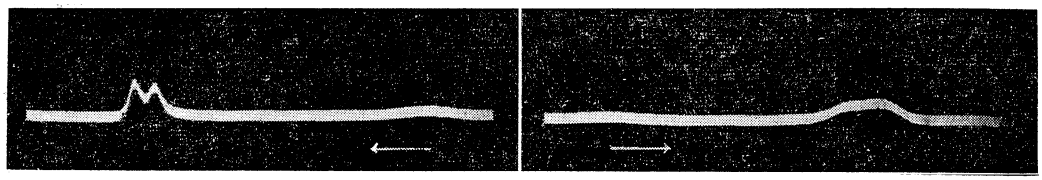
## Results and Discussion

**A. Electrophoretic Behavior of Histone I at pH 5.0.**—The preparation of histone I was examined by electrophoresis in acetate buffers of pH 5.0 at various ionic strengths. The protein concentration was almost at one per cent. It was found that at least three components with similar electrophoretic mobilities migrated towards the cathodes, although separation was poor at higher ionic strength. Some electrophoretic patterns are shown in Fig. 1 (A—C).

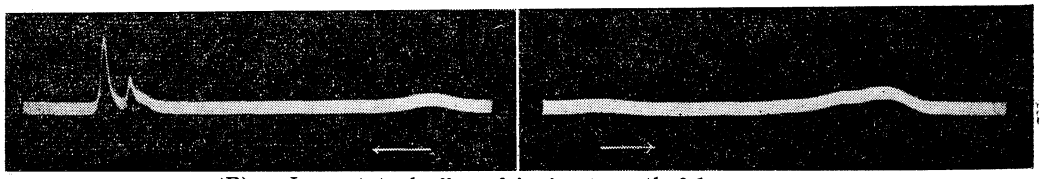
It was also noticed that the electrophoretic composition varied markedly with change in ionic strength. The apparent relative concentrations of the fastest migrating component computed from the ascending pattern was 48 per cent. at ionic strength of 0.2, while at ionic strength of 0.05 a much higher value, 73 per cent., was obtained. Slightly lower, but essentially the same relative concentration was obtained from the corresponding descending pattern, although the value was not accurate owing to the broadness and overlapping of the boundaries.

A similar change in apparent relative concentrations was also observed when the protein concentration was lowered from one to 0.5 or 0.3 per cent. at constant ionic strength of 0.1.

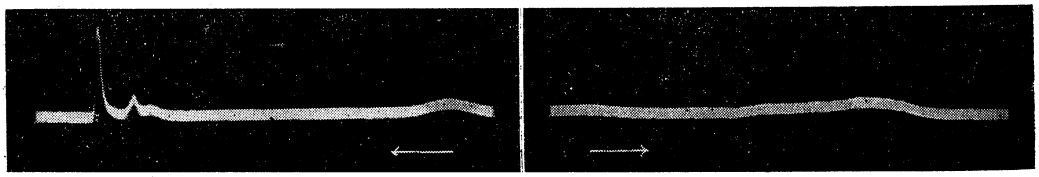
As the change in electrophoretic patterns with change in ionic strength or protein concentration was astonishingly great, it was felt, at first, that more than



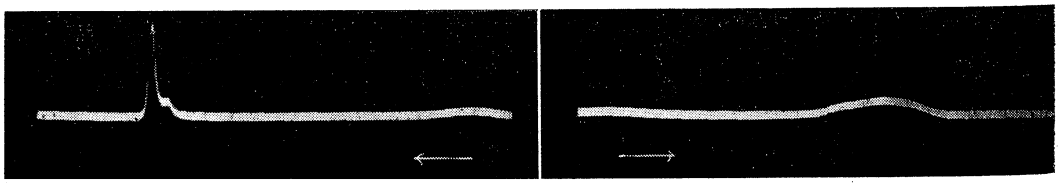
(A) : In acetate buffer of ionic strength 0.2.



(B) : In acetate buffer of ionic strength 0.1.



(C) : In acetate buffer of ionic strength 0.05.



(D) : In acetate—$Na_2SO_4$ (5/300 M) buffer ionic strength 0.1.

Fig. 1. Electrophoretic patterns of histone I at pH 5.0 (0°C). Ascending patterns on the left and descending patterns on the right.

one form of the protein existed in solutions and the state of equilibrium was sensitive to ionic strength or protein concentration. However, this view was soon found to be incorrect. When the deviation of apparent composition from the true composition was estimated with the aid of the moving-boundary theory developed by Dole[10], it was found that the apparently abnormal phenomenon could be accounted for on the basis of the so-called boundary anomalies[11], which were greatly exaggerated in the case of histone I solution; large errors in the apparent analysis would be made in the case of a mixture with nearly the same mobilities[12] as encountered in the present experiments, since the contribution of superimposed gradients of buffer ions and foreign proteins becomes great in such a system.

With the aid of the Dole's equation[10], change in the theoretical, apparent composition with change in ratio of protein concentration to ionic strength ($c/\mu$)* was calculated for hypothetical mixtures of two components with the relative mobilities ($r$) of 0.28 and 0.26 which corresponded to the estimated mobility values of the two main components (faster components) of histone I. The net positive charge on each component was assumed to be 27 or 25 per molecule with a molecular weight of 37,000**. In addition, it was assumed, for the sake of simplicity, that the solution contained only sodium ($r=1.00$) and acetate ($r=-0.79$) ions besides the proteins. In so far as it is permissible to neglect the minor, third component in histone I observed in the case of lower ionic strength, such a solution would be a simplified system representing a histone I solution at pH 5.0. The refractive-index increment of each constituent in the solution was appropriately assumed.

The results of calculations for mixtures containing 30 and 40 per cent. of the fastest component are shown in Fig. 2. It is clear that the dependency of the apparent concentration upon the ratio of protein concentration to ionic strength is very great. In spite of many assumptions

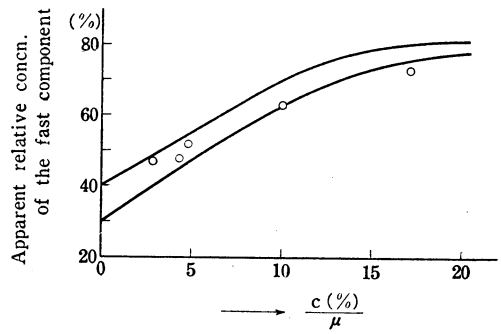



Fig. 2. Variation of apparent relative concentration of the fastest component of histone I with the ratio of protein concentration to ionic strength.

involved in theory and calculation, the theoretical curve for the solution containing 30 or 40 per cent. of the faster component fitted fairly well with the experimental points, which are represented as circles in this figure. Thus, the heterogeneity of histone I was confirmed and the true percentage of the fastest component was estimated to be 30—40 per cent. of the total proteins.

As might be expected from the results described above, it was shown that exposure of the solution to high ionic strength had no effect; when a 2 per cent. solution in the acetate buffer of ionic strength 0.2 (pH 5.0) was kept at 0°C for one day and subjected to electrophoresis without dialysis after being diluted with the same volume of distilled water, the electrophoretic pattern was found to be nearly the same as that obtained at ionic strength of 0.1.

A small variation in the electrophoretic composition of components was found with different preparations of histone I. It was thought that different procedures for extraction had caused this variation.

In Table I are shown the electrophoretic mobility data of histone I at pH 5.0. It should be noticed that the values, except those of the fastest component calculated from descending patterns, are only apparent ones, since the specific conductivity of

10) V. P. Dole, *J. Am. Chem. Soc.*, **67**, 1119 (1945).
11) L. G. Longsworth, *J. Phys. & Colloid Chem.*, **51**, 171 (1947).
12) C. Hoch-Ligeti and H. Hoch, *Biochem. J.*, **43**, 556 (1948).

* An apparent composition will agree with a true composition when the ratio of protein concentration to ionic strength becomes equal to zero.

** The net charge on either of two main components of histone I was calculated from its electrophoretic mobility by using Gorin's equation[13] for a long cylinder. Taking the results of sedimentation and diffusion studies[2] into consideration, a cylinder of 7.1 Å in diameter and 290 Å in length was assumed for both of the components. However, as it seems unlikely that the molecules are so elongated (see discussion in a previous paper[2]), the values of charges thus obtained would be only tentative. Calculated from amino acid composition using the data of Daly and Mirsky[14] on their arginine-rich histone, the valency was 57 at pH 5.0 and was almost twice as high as that adopted in the present study.

13) H. A. Abramson, L. S. Moyer and M. H. Gorin, "Electrophoresis of Proteins," New York (1942).
14) M. M. Daly and A. E. Mirsky, *J. Gen. Physiol.*, **38**, 405 (1955).

TABLE I
ELECTROPHORETIC MOBILITY DATA ON HISTONE I AT 0°C IN ACETATE BUFFERS OF pH 5.0

| Ionic strength | Concn. (%) | | $u \times 10^5$ cm²/sec. volt | | |
|---|---|---|---|---|---|
| | | | Comp. 1 | Comp. 2 | Comp .3 |
| 0.2 | 0.90 | Des. | 6.4 | 5.8 | — |
| | | As. | 7.0 | 6.6 | — |
| 0.1 | 1.00 | Des. | 8.0 | 6.9 | — |
| | | As. | 9.1 | 8.4 | 5.6 |
| 0.1 | 0.51 | Des. | 8.3 | 7.5 | 6.0 |
| | | As. | 9.0 | 8.1 | 7.7 |
| 0.1 | 0.29 | Des. | 8.5 | 7.7 | 6.1 |
| | | As. | 8.9 | 7.9 | 7.3 |
| 0.05 | 0.85 | Des. | 9.4 | 7.6 | 5.9 |
| | | As. | 11.5 | 10.4 | 9.9 |

protein solutions was used for these calculations.

**B. Effect of Sulfate Ion on the Electrophoretic Behavior of Histone I.**—It has been found[15] that the aggregation of histone I was greatly accelerated when histone I sulfate was used or when the sulfate ion was added to the solution. Therefore, the effect of the sulfate ion upon electrophoretic behavior of histone I was studied, using acetate buffers of pH 5.0 containing sodium sulfate.

As shown in Table II, it was found that electrophoretic mobility markedly decreased when the sulfate ion was present. When sodium sulfate was added to one-half of the total ionic strength of 0.1, the mobility was about two-thirds of the value

TABLE II
ELECTROPHORETIC MOBILITY DATA ON HISTONE I AT 0°C IN ACETATE BUFFERS CONTAINING SODIUM SULFATE

| Ionic strength | Concn. of sodium sulfate | | $u \times 10^5$ cm²/sec. volt | |
|---|---|---|---|---|
| | | | Comp. 1 | Comp. 2 |
| 0.2 | 1/30 M | Des. | 4.3 | 3.9 |
| | | As. | 4.9 | 4.6 |
| 0.1 | 5/300 M | Des. | 5.6 | 4.7 |
| | | As. | 6.5 | 6.2 |

in the absence of the sulfate ion. Perhaps, it would be due to the fact that a fairly large number of sulfate ions is bound to the proteins. Positively charged groups, such as guanidinium and ε-amino groups would be responsible for this interaction.

The effect of the sulfate ion on the electrophoretic composition was also observed. In accordance with the observations described in section **A**, the apparent concentration of the fastest component increased with the decrease in ionic strength, but, when compared at the same ionic strength, the value was higher than that obtained in the sulfate ion-free buffer (see Fig. 1D). The fact was again accounted for on the basis of boundary anomalies, since it was shown by the moving-boundary equation that the presence of bivalent sulfate ions accentuates the anomaly.

**C. Effect of Aggregation Reaction on the Electrophoretic Behavior of Histone I.**—As was shown in a previous paper[15], a component with a slightly higher mobility appeared when a solution of histone I formed an aggregate (see Fig. 9 in a previous paper[15]). Although the amount of the newly formed component could not be estimated owing to its poor separation from the fastest component in the original solution, this component was thought to correspond to the aggregation product as seen in sedimentation patterns. Although Davison, James, Shooter and Butler[5] reported that calf thymus histone contained two electrophoretically distinguishable components and that the third component appeared when the aggregation took place, it seemed that none of the boundaries described in **A** or **B** (see Fig. 1) was due to aggregation.

**D. Electrophoretic Behavior of Histone I at 25°C.**—To see the effect of temperature on the electrophoretic behavior of histone I, a series of experiments were carried out at 25°C using solutions of histone I which had been dialyzed at 0°C. The solvents used were acetate buffers of pH 5.0 at ionic strength of 0.2, 0.1 and 0.05, and acetate-sodium sulfate buffer of the same pH and ionic strength of 0.1.

Since the solutions used in these experiments had not been exposed to a high temperature before the initiation of electrophoresis except that they were kept at 25°C for a short period in the cell to establish a temperature equilibrium, no appreciable aggregation occurred. Only a small amount of aggregate was found in the case of solution at ionic strength of 0.2 (4 per cent.) or containing sodium sulfate (5 per cent.).

The electrophoretic patterns obtained are shown in Fig. 3. When they are compared with those obtained at 0°C (see Fig. 1), it is clear that they differ definitely at a higher ionic strength or in the presence of sulfate ions, while the difference was not large at a lower ionic strength. As these temperature dependencies could not entirely be interpreted by the spreading of boundaries due to diffusion, it was thought more likely that some changes in

15) N. Ui, This Bulletin, **30**, 806 (1957).

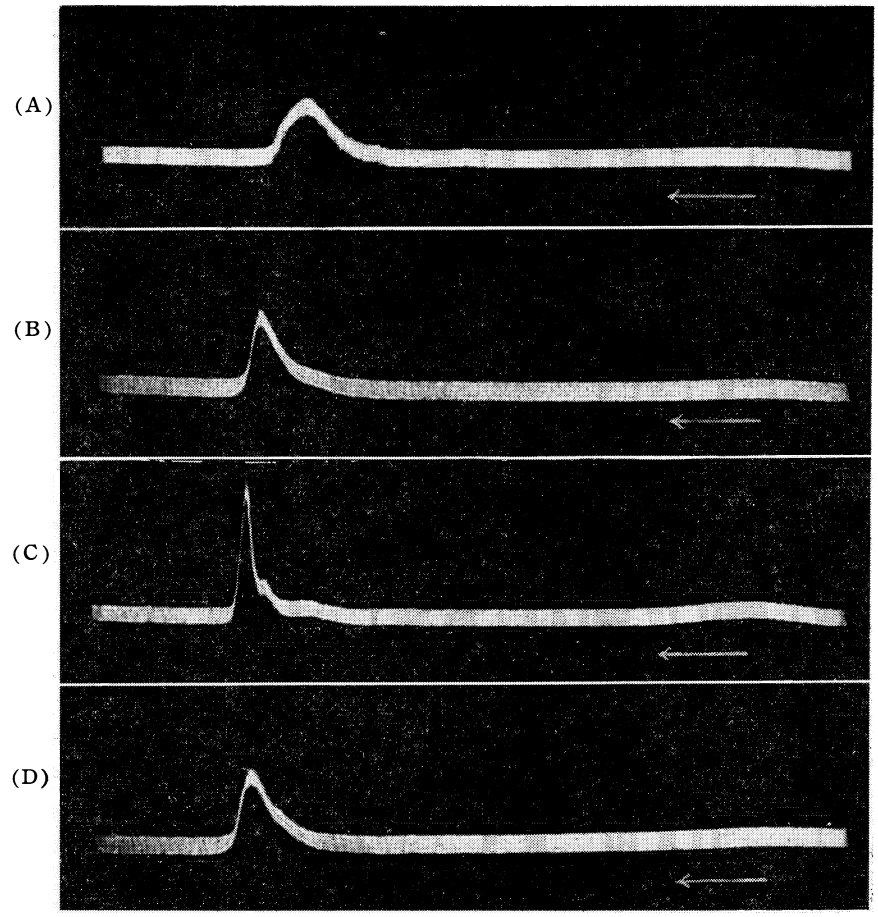



Fig. 3. Electrophoretic patterns of histone I at 25°C.
(A)—(C) : In acetate buffers of pH 5.0 at ionic strengths of 0.2, 0.1 and 0.05.
(D) : In acetate-$Na_2SO_4$(2/300 M) buffer of pH 5.0 at ionic strength of 0.1.
Only ascending patterns are shown.

the proteins occurred with change in temperature. However, it must also be considered that the aggregation might proceed, if not considerably, during the electrophoresis. Therefore, other interpretations might also be possible.

In other experiments, solutions of histone I aged and dialyzed at 25°C were subjected to electrophoresis. With these solutions which contained aggregate, appearance of a new component with higher mobility than that of any original component of histone I was always observed. The results agreed with the observation at 0°C described in C.

**E. Electrophoretic Behavior of Histone I at pH's other than 5.0.**—Effect of pH on the electrophoretic behavior of histone I was studied at 0°C using buffers* of various pH's at a constant ionic strength of 0.1. Although the solutions used had not been exposed to a high temperature, the aggregation product was present in the cases of alkaline solutions.

By this study, it was found that at least two components were present and they always moved toward the cathode in a range of pH's from 4.0 to 10.3. Some of the patterns are shown in Fig. 4.

Electrophoretic mobilities of the two main components (the fastest and the second fastest components) of this preparation calculated from descending patterns are plotted against pH in Fig. 5. The values decreased slowly with increase in pH below pH 9 and decreased rapidly at a higher pH region. Even at pH 10.3, however, each boundary migrated toward the cathode fairly rapidly. Although the

* The following buffers were used in this study : pH 4.0 and 5.0, acetate buffer ; pH 6.5, phosphate buffer ; pH 6 8, cacodylate or cacodylate-NaCl buffer ; pH 8.7, tris (hydroxymethyl)aminomethane buffer ; pH 9.3, veronal or veronal-NaCl buffer ; pH 10.0 and 10.3, $NH_4Cl$-$NH_3$ buffer.

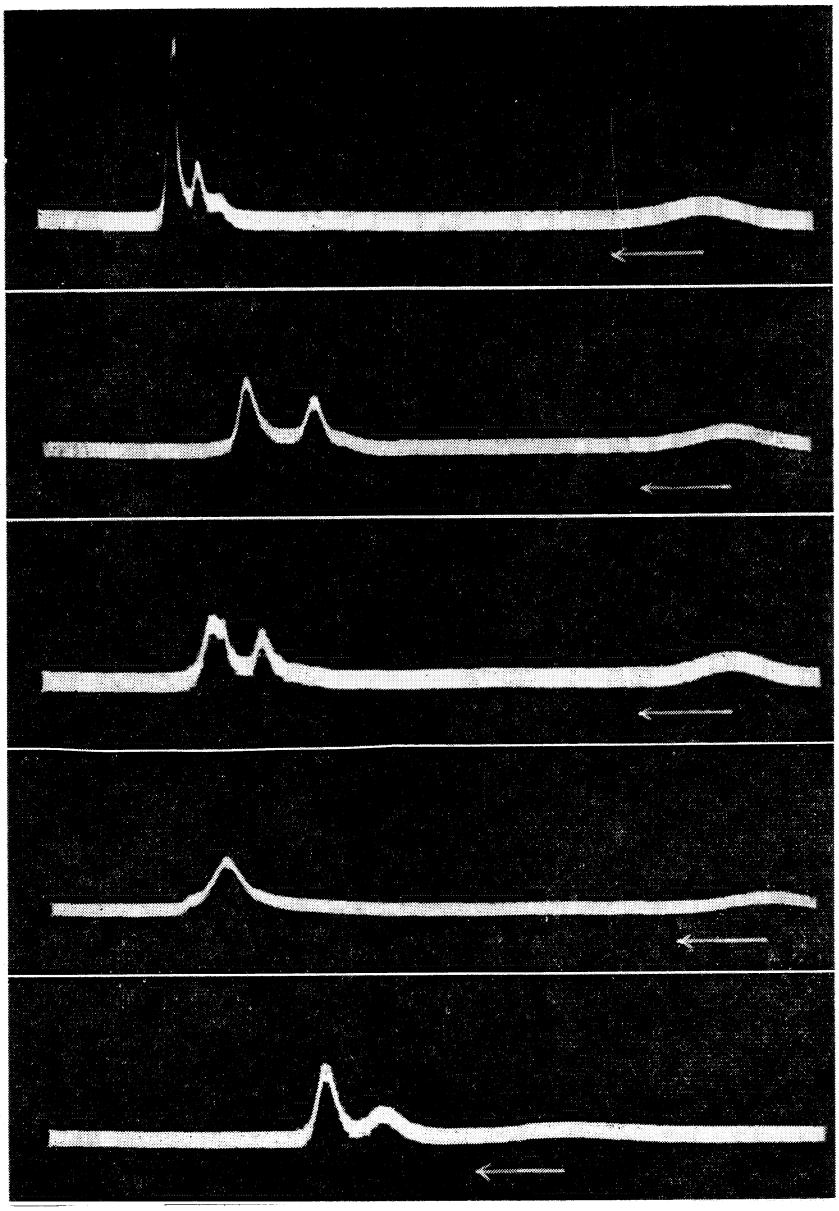


Fig. 4. Electrophoretic patterns of histone I at various pH's (0°C). The pH's are from top to bottom 4.0, 6.5, 6.8, 8.0 and 10.3, respectively. Ionic strength=0.1. Protein concn.=1%. Only ascending patterns are shown.

isoelectric point of each component could not be determined owing to the insolubility of this preparation in more alkaline solution, it was thought from the shape of the pH-mobility curve that the value was higher than pH 10.5.

At ionic strength of 0.2, similar patterns were obtained, but separation of boundaries was poorer in agreement with the results at pH 5.0.

**F. Electrophoretic Behavior of Histone II.**—The other fraction of calf thymus histone, histone II, was subjected to electrophoresis in acetate buffers of pH 5.0 at 0°C. As shown in Fig. 6 (A and B), one main and three minor components migrated toward the cathode. Unlike histone I, the apparent concentration of the fastest component did not vary appreciably with change in ionic strength; the values of relative concentration calculated from descending and ascending patterns were 63 and 62 per cent. at ionic strength of 0.2, and 62 and 65 per cent. at ionic strength

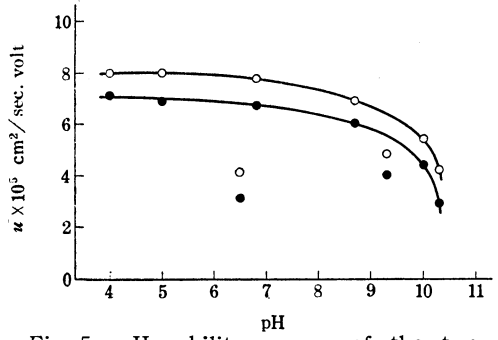



Fig. 5. pH-mobility curves of the two main components of histone I at ionic strength of 0.1 (0°C).

of 0.1. The independency of apparent concentration upon ionic strength would be due to the fact that a large mobility difference exists among the components of histone II.

The electrophoretic mobility data of histone II are shown in Table III. The mobility of the main component was even much higher than that of the fastest component in histone I. It was also found that the preparation of histone II was not contaminated with any component of histone I, since the electrophoretic mobility of none of the components of histone II agreed with the values obtained with histone I. The fact was also confirmed by an electrophoretic experiment on a mixture of histones I and II.

The isoelectric point of any of the components of histone II was found to be higher than pH 10.0, since none of the boundaries migrated toward the anode at this pH (see Fig. 6 and Table III).

## Summary

Electrophoretic studies were made on histone I, the main fraction of calf thymus histone, at various ionic strengths, pH's and temperatures. It was found that at least three components are present in this fraction.

Histone II, the other fraction, was electrophoretically not homogeneous either. One main and three minor components were found to exist, and their mobilities differed from that of any component of histone I.

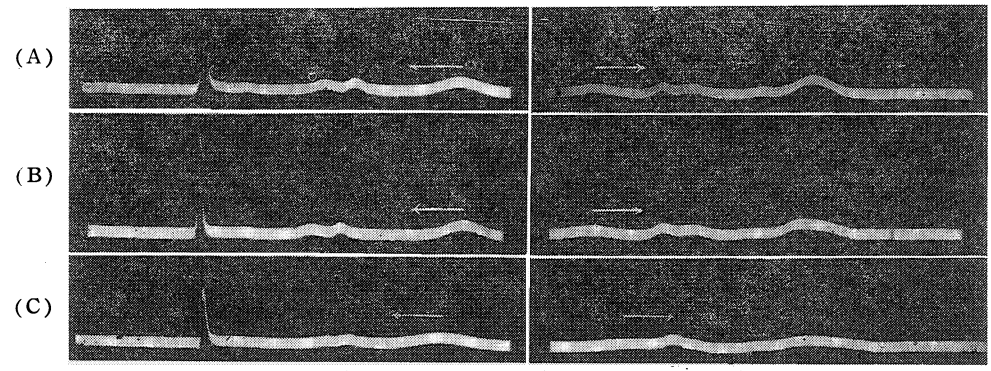



Fig. 6. Electrophoretic patterns of histone II at 0°C.
(A): In acetate buffer of pH 5.0 at ionic strength of 0.2.
(B): In acetate buffer of pH 5.0 at ionic strength of 0.1.
(C): In $NH_4Cl$-$NH_3$ buffer of pH 10.0 at ionic strength of 0.1.

TABLE III
ELECTROPHORETIC MOBILITY DATA ON HISTONE II AT 0°C*

| Buffer | pH | Ionic strength | | $u \times 10^5$ cm²/sec. volt | | | |
|---|---|---|---|---|---|---|---|
| | | | | Comp. 1 | Comp. 2 | Comp. 3 | Comp. 4 |
| Acetate | 5.0 | 0.2 | Des. | **8.3** | 6.5 | 3.9 | 2.7 |
| | | | As. | **9.3** | 7.9 | 4.9 | 3.9 |
| Acetate | 5.0 | 0.1 | Des. | **10.1** | 7.7 | 4.7 | 3.3 |
| | | | As. | **12.2** | 10.3 | 6.9 | 5.5 |
| $NH_4Cl$-$NH_3$ | 10.0 | 0.1 | Des. | **9.0** | 6.5 | 3.7 | 2.0 |
| | | | As. | **10.3** | 9.1 | 4.9 | 3.9 |

* The values of the main component are shown in bold type.

The author wishes to express his sincere thanks to Professor Itaru Watanabe for his interest in this work. The expence of this research was partly defrayed by a Grant in Aid for Scientific Research from the Ministry of Education, to which the author's thanks are due.

*Institute of Science and Technology*
*The University of Tokyo*
*Meguro, Tokyo*

# *Further Studies on the Preparation of Calf Thymus Histone*

By Nobuo UI

(Received May 31, 1957)

In a previous paper[1], it was reported that calf thymus histone, which had been extracted with sulfuric acid from the isolated nuclei and precipited by addition of ethanol at a low temperature, showed the presence of two fractions (histones I and II). In spite of their ultracentrifugal homogeneity, their electrophoretic patterns were complex and it was concluded that calf thymus histone consists of several components. However, as acids often caused irreversible modifications of many proteins, it was thought necessary to prove that no changes had occurred during the course of the extraction of histone with an acid.

In this investigation, histone was prepared by three methods without using acid, and their properties were compared with those of two preparations obtained by the acid and ethanol method[1].

## Experimental and Results

**(1) Preparation of Histone by Ultracentrifugation.**—Calf thymus nucleohistone (TNH) is generally believed to dissociate into histone and desoxyribonucleic acid (DNA) in a concentrated saline solution[2]. In fact, when TNH was subjected to a prolonged high-speed centrifugation in concentrated saline, histone was left separate in the upper layer of the supernatant[3].

In this study, TNH* solutions both in 1 M and 2 M sodium chloride were used and different preparations of histone were obtained from the supernatants. Typical examples are as follows.

i) TNH was dissolved in 1 M sodium chloride in a concentration of about 0.4 per cent. and centrifuged at 42,040 r. p. m. in a Spinco model E ultracentrifuge using a preparative rotor B. After centrifugation for 6 hours at about 10°C, centrifuge tubes were removed as gently as possible. A sharp boundary was observed at the middle of the tube. The upper layer was withdrawn with a syringe without disturbing the boundary. It was dialyzed against distilled water and lyophilized after removing a small amount of insoluble material formed during the dialysis with a centrifuge. About 40 mg. of histone was obtained from 400 mg. of TNH.

ii) TNH solution in 2 M sodium chloride at a concentration of about 0.2 per cent. was centrifuged in the same apparatus, but a preparative rotor A was used this time and centrifuged at 50,740 r. p. m. for 5 hours. The temperature was nearly 15°C. Although no boundary was observed in this case, the upper half of the supernatant was found from the ultraviolet absorption curve to be free from nucleic acid. It was with-drawn with a syringe, dialyzed against cold distilled water and lyophilized. Twenty three mg. of histone was obtained from 160 mg. of TNH.

The preparations of histone thus obtained were essentially free from DNA and usually showed only one boundary in an ultracentrifuge. In an acetate buffer of pH 5.0 at ionic strength of 0.2, the sedimentation coefficient of the preparation obtained from the supernatant of 1 M

1) N. Ui, *Biochim. Biophys. Acta*, in press.

2) E. Chargaff, in E. Chargaff and J N. Davidson, "The Nucleic Acids," New York, Vol. 1, p. 307 (1955).

3) A. E Mirsky and A. W. Pollister, *J. Gen. Physiol.*, **30**, 117 (1946).

* TNH was prepared by the following method. Fresh calf thymus glands, freed from fat and extraneous tissues, were frozen over solid carbon dioxide, minced, and homogenized in an electric mixer with 0 14 M NaCl (pH 7) at a temperature below 5°C. The homogenate was then centrifuged for about ten minutes at 4,000 r. p. m. The sediment was resuspended in 0.14 M NaCl, placed in the mixer for a few minutes and centrifuged as before. The same washing was repeated three times more.

Cold 1 M NaCl was added to the sediment and the mixture was stirred overnight in a cold room. The solution was then clarified by centrifugation for 2 hours at 20,000 r. p m. The clean but slightly opalescent supernatant was poured into six volumes of cold distilled water and a fibrous precipitate of TNH was obtained. The precipitate was washed twice with 0.14 M NaCl, and as much water as possible was pressed out of it. It was then briefly washed in water and lyophilized.

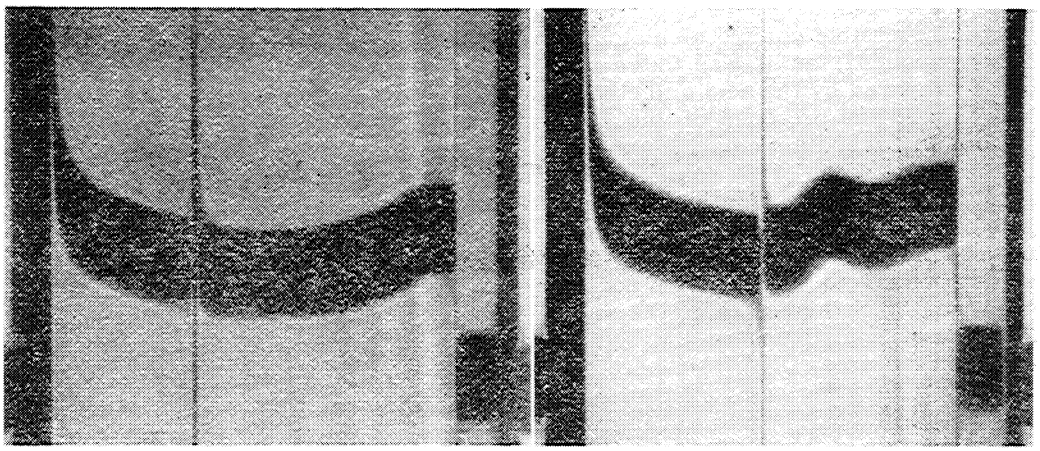
TABLE I

SEDIMENTATION COEFFICIENTS OF NUCLEOHISTONE AND SOME PREPARATIONS OF HISTONE

| Sample | Solvent | Concn. (%) | $s_{20,w}$ (S) Fast | Middle | Slow |
|---|---|---|---|---|---|
| TNH | 1 M NaCl | 0.6 | 10.6 | — | <1 |
| 〃 | 〃 | 0.5 | 11.2 | — | <1 |
| 〃 | 2 M NaCl | 0.8 | 4.9 | 3.4 | <1 |
| 〃 | 〃 | 0.7 | 5.3 | 3.4 | <1 |
| Histone obtained by ultracentrifugation in 1 M NaCl | Acetate buffer pH 5.0, $\mu$=0.2 | 0.7 | — | — | 0.7 |
| Histone obtained by ultracentrifugation in 2 M NaCl | 〃 | 1.0 | — | 1.4 | ? |
| Histone obtained by means of adsorption on Hyflo Super-Cel | 〃 | 0.6 | — | 2.2 | — |
| Histone obtained by using La salt | 〃 | 0.7 | — | 1.8 | ? |
| Histone I* | 〃 | —** | — | $2.0_3$ | — |
| Histone I* | 2 M NaCl | 1.0 | — | 3.5, 1.7 | — |
| Histone I* once exposed to 2 M NaCl | Acetate buffer pH 5.0, $\mu$=0.2 | 1.0 | — | 1.7 | — |
| Histone II* | 〃 | —** | — | — | 0.6$_6$ |

* These samples were prepared by the method described in a previous paper[1].

** The values were extrapolated to infinite dilution[1,4],



(A) (B)

Fig. 1. Sedimentation patterns of TNH.

(A) In 1 M NaCl after 66 min. at 59,780 r. p. m. ($c$=0.6%).

(B) In 1 M NaCl after 109 min. at 59,780 r. p. m. ($c$=0.8%).

sodium chloride solution was found to be 0.7 S and agreed with the value of histone II in previous papers[1,4] while the preparation from 2 M sodium chloride solution gave a value of 1.4 S, which was slightly lower than that of histone I (see Table I). In the case of latter preparations, the presence of a slower component was suspected from the shape of sedimentation pattern. The difference between these two kinds of preparation was also found in their solubility behavior; although the preparation from 2 M sodium chloride almost precipitated by the addition of ammonia or the same volume of 10% trichloroacetic acid, the solutions of the preparation obtained from 1 M sodium chloride remained clear on these additions. Judged from these results, the preparation from 2 M sodium chloride was thought to correspond

4) N. Ui, This Bulletin, **30**, 801 (1957).

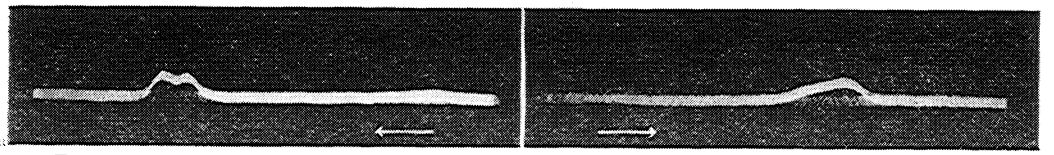


Fig. 2. Electrophoretic pattern of a histone preparation obtained by means of adsorption on Hyflo Super-Cel. Solvent: an acetate buffer of pH 5.0 at ionic strength of 0.2. Ascending pattern on left and descending pattern on right.

to a mixture of histones I and II, while the preparation from 1 M sodium chloride corresponded to histone II.

The fact that the proteins left in the upper layer of the fluid differed with the change in saline concentration, was also and more directly shown by sedimentation study of TNH. The sedimentation patterns of TNH in 1 M and 2 M sodium chloride (pH 6.3) are shown in Fig. 1. It is clear that, besides a sharp, faster boundary, one slower boundary exists in 1 M sodium chloride, and two in 2 M sodium chloride. The sedimentation coefficient of the slowest components in each case was below 1 S. A 3.4-S component was found only in the case of 2 M sodium chloride (see Table I). This component would be due to the reversible change of histone I, the 2-S component, as it was found that histone I prepared by the acid and ethanol method showed the presence of the 3.4-S component in 2 M sodium chloride and that it disappeared when the solution was brought to an ionic strength of 0.2 by dialysis.

The sedimentation coefficient of the faster component of TNH in 1 M sodium chloride was much higher than the value of the fastest component in 2 M sodium chloride or of free DNA[5]. Therefore, the faster sedimenting component of TNH in 1 M sodium chloride would not be free nucleic acid but a partially dissociated nucleohistone.

**(2) Preparation of Histone by Means of Adsorption.**—As histone is adsorbed on Hyflo Super-Cel from TNH solution in concentrated saline[6], an attempt was made to isolate histone by elution of the adsorbent.

TNH was extracted from the cell nucei with 1 M sodium chloride. To the clarified extract, solid sodium chloride was added to saturation. The solution became milky and a small amount of precipitate was formed. After being kept in the cold, it was filtered with suction using Hyflo Super-Cel on a Buchner funnel. The filter cake containing histone was thus obtained*.

After being washed several times with saturated saline, the filter cake was mixed with a large volume of distilled water. Then the suspension was centrifuged and the supernatant was dialyzed against distilled water. After clarification by a centrifuge, it was lyophilized. About 400 mg. of histone was obtained from 200 g. of the glands.

The preparation of histone thus obtained contained less than 0.1 per cent. of phosphorus, so the contamination of DNA in this preparation was thought to be negligible. In an acetate buffer of pH 5.0 at ionic strength of 0.2, it showed only one sedimentation boundary and the sedimentation coefficient at a concentration of 0.6 per cent. was found to be 2.2 S. The electrophoretic pattern of this preparation in the same buffer is shown in Fig. 2. It closely resembled the pattern of histone I reported previously[1,7]. It could be precipitated by addition of ammonia or trichloroacetic acid (5 per cent.). Therefore, according to our designation, it corresponds to histone I.

Thus, only one fraction of histones, histone I, was obtained by this method and the other fraction, histone II, was not. It might be due to the failure of this histone II fraction to be retained on the filter cake under the condition mentioned above.

**(3) Preparation of Histone Using Lanthanum Salt.**—Lanthanum salt is known as a powerful precipitant of DNA[2]. Therefore, an attempt was made to isolate histone from TNH using lanthanum acetate.

To 100 mg. of purified TNH described before (see method (1)), 400 ml. of 2 M sodium chloride containing 3% lanthanum acetate was added and the mixture was kept in a cold room with occasional stirring. TNH swelled slowly and histone was released from it. After two days this suspension was centrifuged. The same extraction was repeated once more. The two extracts were

5) Y. Kawade, *Biochem. Biophys. Acta*, in press.
6) N. Schwander and R. Singer, *Helv. Chim. Acta*, **33**, 1521 (1950).

* This filter cake was kindly supplied by Dr. Y. Kawade
7) N. Ui, This Bulletin, **30**, 815 (1957).

combined and, after clarification, dialyzed against distilled water and lyophilyzed. Yield, 30 mg.

When the preparation of histone obtained was subjected to ultracentrifugation in an acetate buffer of pH 5.0 at ionic strength of 0.2, only one boundary appeared. The sedimentation coefficient varied a little with the preparations i. e., 1.5—1.8 S. As the sedimentation pattern did not give a symmetrical peak, it was thought that this preparation also contained a slower component. When ammonia or the same volume of 10 per cent. trichloroacetic acid was added to its solution, a precipitate was formed, but part of the proteins remained in the solution. Therefore, this preparation was considered to be a mixture of histone I and histone II.

When TNH was extracted with the solutions of lower ionic strengths, a smaller amount of histone was extracted, presumably owing to the insufficient dissociation of TNH. In the case of 1 M sodium chloride—3% lanthanum acetate a fairly large amount of histone remained in the residue and could be extracted with 0.5 N sulfuric acid. An extract with 0.5 M sodium chloride—1.5% lanthanum did not give a precipitate in 5 per cent. trichloroacetic acid, and contained only a fraction corresponding to histone II.

Copper sulfate could be substituted for lanthanum acetate and a similar preparation was obtained.

## Discussion

The three methods for the preparation of histone described above are milder than those usually adopted; neither acid, alkali nor organic solvent was used in these methods. Therefore, these preparations would be least likely to be modified during the purification. Although degradation of histone by the action of proteolytic enzyme at neutral pH was suggested by Butler et al.[8], the experiments presented here have failed to reveal it.

It was shown by the examination of these preparations that histone contained two fractions with different molecular weights. The lower molecular-weight fraction was isolated by the high-speed centrifugation experiments on TNH in 1 M sodium chloride, while the higher molecular-weight fraction was obtained by the other methods including the centrifugation in 2 M sodium chloride. Sedimentation as well as solubility studies indicated that the former corresponded to histone II described in a previous paper[1] and the latter to histone I. It was also found that the higher molecular-weight fraction was electrophoretically not homogeous.

From these results it was confirmed that the preparations of histone obtained by the standard method adopted by us[1] were not altered with acid or ethanol. The view that calf thymus histone consists of several components was also ascertained. In view of these findings, the previously reported method using acid and ethanol will be recommended, since it is easy to operate and gives a good yield.

Recently, evidences[5,9,10] were accumulated indicating that the progressive dissociation of TNH into components is induced by increasing concentrations of sodium chloride. It was also shown that dissociation was not complete in 1 M sodium chloride[5,9-11]. Failue of histone I, the higher molecular-weight fraction of histone, to be obtained by the centrifugation experiments in 1 M sodium chloride would be due to the binding of this fraction with DNA under this condition; lower molecular-weight fraction, histone II, was the only fraction present as the free protein in 1 M sodium chloride. In fact, it was shown[5] by the measurements of viscosity and sedimentation that histone I interacted with DNA in 1 M sodium chloride, while histone II did not.

## Summary

Calf thymus histone was prepared as gently as possible without using acids, alkalis or organic solvents. It was clearly shown that two components with sedimentation coefficients of 2 S and 0.7 S are present.

Sedimentation, electrophoresis and solubility behaviors of these preparations were similar to those of the preparations obtained by the previously reported method using acid and ethanol, and it was confirmed that histone consists of two fractions, histones I and II. It was also ascertained that acid as well as ethanol causes no alteration of the proteins.

8) J. A. V. Butler, P. F. Davison, D. W. F. Jamse and K. V. Shooter, *Biochim. Biophys. Acta*, **13**, 224 (1954).

9) C. F. Crampton, R. Lipshitz and E. Chargaff, *J. Biol. Chem.*, **206**, 499 (1954).

10) L. B. Smillie, A. M. Marko and G. C. Butler, *Can. J. Biochem Physiol.*, **33**, 263 (1955).

11) M. Fleming anb D. O. Jordan, *Discussions Faraday Soc.*, **No. 13**, 580 (1953).

The author wishes to express his sincere thanks to Professor Itaru Watanabe for his valuable suggestion and encouragement. His thanks are also due to Professors S. Sasaki and O. Taniguchi of Tokyo Institute of Technology for their kind permission to use their ultracentrifuge. The expense of this research was partly defrayed from a Grant in Aid for Scientific Research from the Ministry of Education.

*Institute of Science and Technology*
*The University of Tokyo*
*Meguro, Tokyo*

# *Fluorometric Determination of Thallium with Rhodamine B*

By Hiroshi ONISHI

(Received May 24, 1957)

After a study of a photometric (absorptiometric) determination of traces of thallium with rhodamine B[1,2], it was thought worthwhile to attempt a fluorometric determination of the element by making use of the same rhodamine B-benzene extraction technique. The orange-yellow fluorescence of the benzene extract of rhodamine B chlorothallate was already used by Feigl, Gentil, and Goldstein[3] for the detection of thallium.

## Experimental

**Apparatus.** — A Hitachi EPV-2 spectrophotometer with a fluorescence attachment, type L-2, was used. It was equipped with a Toshiba SHL-100 UV lamp and a filter to transmit the 365 m$\mu$ mercury line. One-centimeter glass cells of which four sides are transparent, were used.

**Solutions.** — *Rhodamine B*, 0.0020% (W/V). This was chosen as a reference standard to adjust the instrument to a given sensitivity. Other solutions used were the same as described before[2].

**Procedure.**—The separation of thallium and the rhodamine B-benzene extraction were made essentially according to the directions previously described[2]. In establishing the standard curve, however, evaporation of standard thallium solution and 0.50 ml. of 1 : 5 sulfuric acid to fumes followed by the treatment with 5.0 ml. of 2.0 N hydrochloric acid and 1.0 ml. of saturated bromine water is recommended.

*Measurement of the fluorescence intensity.* Set the wave length scale at 580 m$\mu$. For determining 1 to 10 $\mu$g. of thallium, set the sensitivity of the instrument at 10 (the highest sensitivity), and adjust the scale reading with 0.0020% rhodamine B solution to 100%. Measure the fluorescence intensity of the sample solution immediately.

## Results and Discussion

The fluorescence spectra of aqueous rhodamine B solution[4] and rhodamine B chlorothallate in benzene are given in Figures 1 and 2. The fluorescence peaks of rhodamine B and rhodamine B chlorothallate are found at about 575 and 580 m$\mu$ respectively. As the slit widths used were large, these figures are somewhat approximate. However, the two curves are so similar that rhodamine B solution has been adopted as a reference standard to adjust the fluorometer scale. If total fluorescence measurements were made, other reference standards such as quinine sulfate could be used.

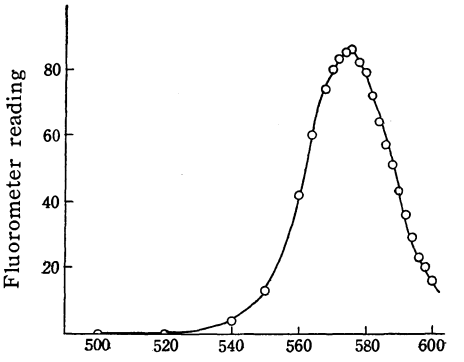



Fig. 1. Fluorescence spectrum of rhodamine B solution. 0.0020%, 1-cm. cell, slit width = 0.28 mm.

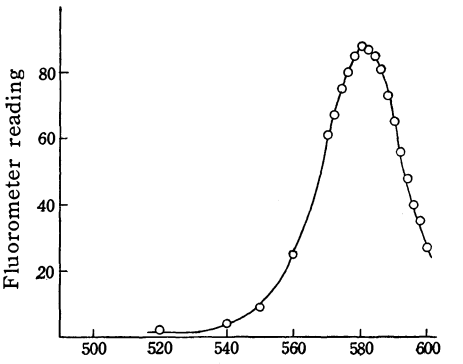



Fig. 2. Fluorescence spectrum of rhodamine B chlorothallate in benzene. 10 $\mu$g. Tl taken, 1-cm. cell, slit width = 0.36 mm.

In the present work, effects of variables such as the concentration of hydrochloric acid and rhodamine B were not particularly studied, and the conditions developed for the absorptiometry were accepted. A working curve is shown in Fig. 3. Curve

1) H. Onishi, This Bulletin, **29**, 945 (1956).
2) H. Onishi, This Bulletin, **30**, 567 (1957).
3) F. Feigl, V. Gentil, and D. Goldstein, *Anal. Chim. Acta*, **9**, 393 (1953).
4) For a more concentrated rhodamine B solution, see A. Murata and F. Yamauchi, *J. Chem. Soc. Japan, Pure Chem. Sect.*, **77**, 1259 (1956).

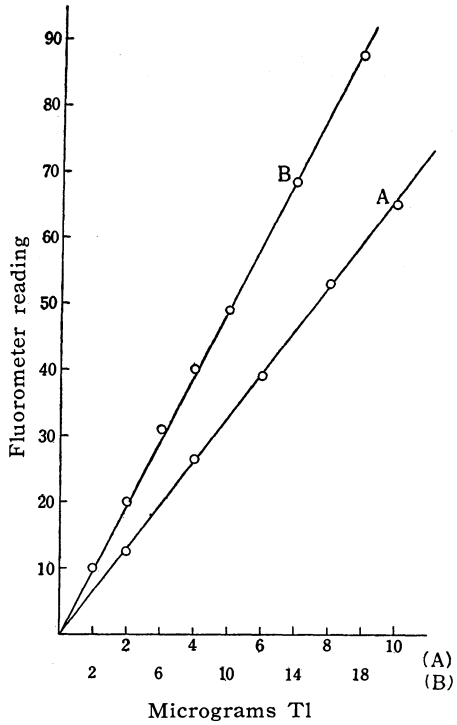



Fig. 3. Fluorescence intensity-concentration curve of thallium. Reference standard set at 100 for curve A, and at 70 for B, temperature 14—17°C.

A was obtained in setting the reference standard (0.0020% rhodamine B solution) at 100, whereas curve B was obtained at 70. It was observed that the fluorescence intensity of both rhodamine B solution and the benzene extract of rhodamine B chlorothallate decreased as the temperature was raised*. Consequently, working solutions as well as the sample should be at the same temperature. With the fluorometer used, the measurement of fluorescence intensity was made immediately after transferring the reference standard and the sample to the cell compartment. Fig. 3 shows that a satisfactory standard curve can be obtained by a careful and quick measurement. By decreasing the sensitivity and slit width of the instrument, larger amounts of thallium may be determinable. This point has not, however, been tested.

Effect of other elements on the photometric determination of thallium was previously described[2]. No serious interference was found by the elements studied. In fluorometry, it is not very uncommon that the presence of foreign substances sometimes interferes with the determination in a peculiar way, e. g., quenching. By carrying out the dithizone-chloroform extraction from basic solution containing cyanide, only lead, bismuth, and tin(II) are extracted with thallium (I). However, these elements in small quantities do not interfere with the fluorometric determination of thallium (Table I).

* With the instrument used (Hitachi EPV-2 with fluorescence attachment), the cell compartment was not well insulated from the heat of the light source.

TABLE I
DETERMINATION OF THALLIUM IN SYNTHETIC MAFIC ROCK*

| Addition | Tl added, p.p.m. | Tl found, p.p.m. |
|---|---|---|
| none | none | 0.15, 0.1 |
| none | 3.0 | 3.1, 2.6 |
| 0.1 mg. each Pb, Bi, Sn | none | 0.1, 0.1 |
| 0.1 mg. each Pb, Bi, Sn | 3.0 | 3.0, 2.8 |

* Percentage composition: 48 $SiO_2$, 12 $Al_2O_3$, 15 $Fe_2O_3$, 10 MgO, 10 CaO, 3 ($Na_2O+K_2O$), 1.5 $TiO_2$, 0.3 $P_2O_5$, 0.25 MnO.

A 1.0 g. sample simulating a mafic rock (10 per cent Fe) was decomposed with sulfuric- hydrofluoric acid, and the excess of sulfuric acid was driven off. The residue was taken up in water and the procedure for the dithizone extraction[2] was followed. Rhodamine B chlorothallate was extracted with 10 ml. of benzene after addition of 1 ml. of 0.20% (W/V) rhodamine B solution. In the table, +10% correction suggested previously, is not applied.

Although the present work has demonstrated the feasibility of a fluorometric determination of thallium, it does not appear that the method has any distinct advantages over the absorptiometric method. In sensitivity, the absorptiometric method is probably superior to the fluorometric. In accuracy, there may not be much difference between the two. The fluorometry is more susceptible to temperature.

## Summary

A method is presented for the fluorometric determination of traces of thallium. Except for the step of fluorometry, the procedure is essentially the same as previously described for the absorptiometry. A synthetic mafic rock was analyzed for thallium by the method which involves hydrofluoric acid decomposition of the sample, dithizone extraction, rhodamine B-benzene extraction, and the measurement of fluorescence intensity on the benzene extract.

*Government Industrial Research Institute, Nagoya, Kita-ku, Nagoya*

# *The Leakage Method and the Sandwich Type Zisman Method for Measurements of Contact Potential Differences between two Metals Immersed in Poorly Conductive Dielectric Liquids*

By Akira TANAKA

(Received March 12, 1957)

The first measurement of contact potentials for metals immersed in a dielectric liquid was reported by H. J. Plumley[1], using a modified Kelvin method, in connection with the problem of the origin of the electrical conductivity of non-polar dielectric liquids. Since then no report has appeared on this subject except those by J. T. Davies[2] who measured the contact potentials at the oil-water interface by applying the Zisman method. Still there remain some important problems to be solved in their measurements. Quite independently of them our efforts have been devoted for several years to extend the Zisman's vibrating electrode method[3] to liquid phase; our intention has been to apply the measurement of contact potential difference (abbreviated to C.P.D.) or surface potential difference as a powerful tool to the research of surface chemical phenomena occurring at metal surfaces immersed in dielectric liquids. The reports on the technique of the measurement[4] and on the distinction between "true C. P. D." and "apparent C. P. D."[5-7] were published previously. The measured values of the C. P. D. between platinum and silver in various dielectric liquids were also reported[8].

Although various methods were reported for the measurement of C. P. D. in vacuo and in gaseous media, the Zisman method has been most widely used because of its convenience especially in gas phase. At an early stage of this research "immersion type Zisman method" was used for the purpose of measuring the C. P. D. between two metals immersed in a dielectric liquid. During the course of this study, it was found that the decrease in the C. P. D. was often caused by the passage of leakage current in the case of conductive dielectric liquids. Therefore, at the present time "sandwich type Zisman method" is recommended as the most suitable one in poorly conductive dielectric liquids. The immersion type Zisman method should be applied only in the dielectric liquids having a very high leakage resistance such as benzene.

The Zisman method, however, is accompanied by a disadvantage, which is that we have to compel one of the two electrodes to vibrate. Vibration of the electrode often brings about troublesome problems in the construction of the apparatus in vacuo or in dielectric liquids. In our laboratory, another new method without electrode vibration for measuring the C. P. D. in dielectric liquids having electrical conductivity was established by employing an electrometer and was named "leakage method". In order to measure C. P. D. without vibrating the electrode, generally, the medium between the two electrodes must have a certain degree of electrical conductivity. In this new method, a small conductivity which is inherent in the liquid was utilized without any additional ionization. Provided that the charge carriers of leakage current do not obey Faraday's laws of electrolysis, the C. P. D. in the liquid can be measured easily by this new method which resembles, in its operation, the ionization method. The ionization method in gas phase has been well known, and that in liquid phase for measuring the interfacial potentials of oil-water was already described by J. T. Davies[9]. But this leakage method utilizing the small electrical conductivity in herent in the liquid is not only entirely new but also interesting. By the analysis of the

1) H. J. Plumley, *Phys. Rev.*, **52**, 140 (1937).
2) J. T. Davies, *Nature*, **167**, 193 (1951); J. T. Davies, *Z. Elektrochem.*, **55**, 559 (1951).
3) W. A. Zisman, *Rev. Sci. Instr.*, **3**, 367 (1932).
4) A. Kanamori, *Bull. Nagoya Inst. Tech.*, **6**, 261 (1954).
5) Y. Yashiro and A. Kanamori, *J. Appl. Phys., Japan*, **23**, 129 (1954); Y. Yashiro, *Bull. Nagoya Inst. Tech.*, **6**, 281 (1954).
6) Y. Yashiro, ibid. **50th** Anniversary, 343 (1955).
7) A. Tanaka, ibid., **8**, 293 (1956).
8) Y. Yashiro, *J. Appl. Phys., Japan*, **24**, 144 (1955).
9) J. T. Davies, *Trans. Faraday Soc.*, **49**, 683 (1953)

experimental conditions of the two measurement methods, it became clear that, in order to compare directly the values of the C. P. D. obtained by this leakage method with those by the Zisman's, electrical resistance of the liquid between the two electrodes must be approximately $10^7$—$10^{12}\,\Omega$. Some of the experimental evidences were also described.

## Principles of the Measurement

For the first place, a case of the leakage method is illustrated. A liquid having suitable value of leakage resistance is sandwiched between the metal electrodes A and B as seen in Fig. 1. Under the condition that there exists a C. P. D. between the electrodes, leakage current $i$ will flow through the liquid owing to the electrical field arising from the C. P. D. It is desirable that this current flow through the liquid is kept as small as possible throughout the measurement, because there is a possibility that so much of leakage current flow may cause the change in the C. P. D. In Fig. 1, as an excellent null indicator, a dynamic condenser electrometer is employed together with a cathode ray oscilloscope. The $C_c$ is a coupling condenser whose insulation resistance is infinite. Assuming that each of the two electrodes is in a uniform surface state, the dynamic condenser of the electrometer $C_e$ will be charged up by the C. P. D. until the voltage between the points E and F, $V_{EF}$, just balances the C. P. D. as shown in the round brackets. Then there is no potential difference between A and B, and no current flows*.

For the purpose of measuring this voltage, $V_{EF}$, this d. c. voltage is converted into an a. c. signal by means of the vibration of $C_e$, then this a. c. signal is amplified and finally connected to an indicator, e. g. a cathode ray oscilloscope. Under the condition that the voltage between the points E and F, $V_{EF}$, caused by the C. P. D. is just compensated through the liquid and the input resistor $R_i$ with the aid of the potentiometer P. M. as shown in the square brackets, the input signal to the amplifier must become zero and so the oscilloscope exhibits no signal. Consequently we can determine the C. P. D. between the electrodes A and B from the difference of the potentiometer readings obtained by the change-over of the switch $S_1$ as in the usual case. The C. P. D. has the same magnitude as the difference of the potentiometer, but with the opposite sign.

At this stage of explanation, we call our attention to the fact that, if we suppose that these two electrodes A and B are the electrodes of an ordinary chemical cell, A is the cathode and B is the anode in the present instance (Fig. 1). On the other hand, when we consider that this voltage is exclusively caused by the C. P. D. between A and B, A is positive with respect to B. However, at the present stage of this research the distinction between electrochemical electromotive forces[10] and C. P. D. which is supposed by the author, is not yet well known in these fields and will become clearer with the progress of this research.

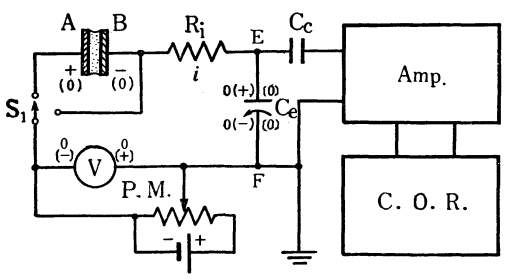



Fig. 1. Schematic diagram of the leakage method.
A, B=the metal electrodes. $R_i$=input resistor. $i$=leakage current. $C_c$=coupling condenser. $C_e$=dynamic condenser of the electrometer. $S_1$=switch. V=voltmeter. P. M.=potentiometer. Amp.=amplifier. C. O. R.=cathode ray oscilloscope.

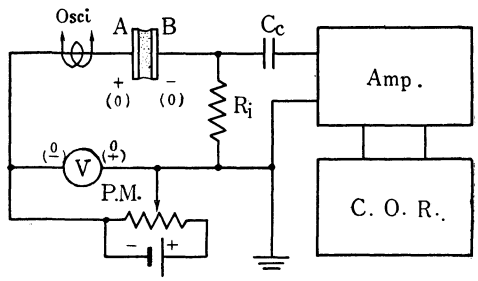



Fig. 2. Schematic diagram of the sandwich type Zisman method.

For the second place, in order to measure the C. P. D. by applying the Zisman method, we connect the circuit as shown in Fig. 2. When one of the two electrodes, A or B,

* The condition of surface uniformity will be important to measure accurately the C. P. D. or the surface potential difference by the ionization method. Otherwise, errors will probably be introduced.

10) A. Gemant, *Trans. Electrochem. Soc.*, **78**, 49 (1940); A. von Hippel, "Dielectric Materials and Applications", The Technology Press of M. I. T. and John Wiley & Sons, Inc., New York (1954), p. 165.

is vibrated by means of an audio frequency oscillator, an a. c. signal will be generated across input resistor $R_i$ and amplified as in the ordinary case. Under the condition that the C. P. D. is just compensated by the potentiometer as shown in the parentheses, the input to the amplifier will vanish. The C. P. D. must be equal to the reading of the potentiometer, but with the opposite sign in this case again.

Moreover, when the surface state of each electrode is uniform, when the liquid is held between the electrodes A and B like a sandwich, and when the C. P. D. is cancelled by adjusting the voltage of the potentiometer, then the potential difference between the electrodes A and B will disappear and no leakage current flows even though the liquid has electrical conductivity. As shown in our experiments[5], in which the apparent C. P. D. is distinguished from the true C. P. D., the spurious increase in the C. P. D. will not arise in this case. Therefore, the measured values of the C. P. D. using this sandwich type Zisman method must be equal to the true C. P. D. This conclusion was also confirmed experimentally even in nitrobenzene with such a small leakage resistance as that of the order $10^7\Omega$*. But, in this sandwich type Zisman method too, it is advisable to check this fact occasionally following the method reported previously[5].

### Electrical Equipment and Apparatus

In this experiment to check directly the data of C. P. D. measured by this leakage method compared with those obtained by the sandwich type Zisman method, the electrical circuit was connected as seen in Fig. 3. With slight improvements, a dynamic condenser pH-meter (electrometer) was employed as the parts of dynamic condenser $C_e$ and amplifier. A cathode ray oscilloscope was employed as an indicator and the potentiometer was the same as reported previously[6,11]. The operation to measure C. P. D. was illustrated above. Careful attention should always be paid to the shielding of the input circuit to amplifier. All the measurement was carried out by manual null method and the sensitivity of this equipment was within $\pm 2$ mV.

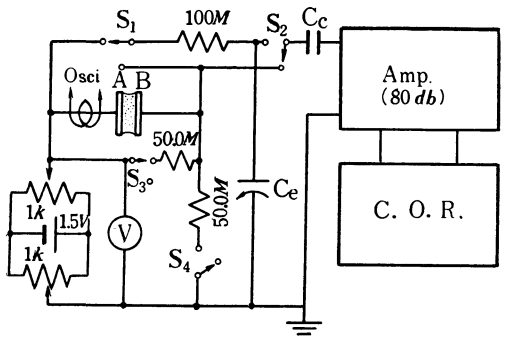



Fig. 3. Practical circuit used in the measurements.
$S_1$=switch, same as in Fig. 1. $S_2$, $S_3$= linked switch for the change-over of circuit from the sandwich type Zisman method to the leakage method, and vice versa. $S_4$=switch for measuring the true and the apparent C. P. D. Osci.= CR oscillator, operated at 150—160 c/s. $C_c$=500 pF polystyrene condenser.

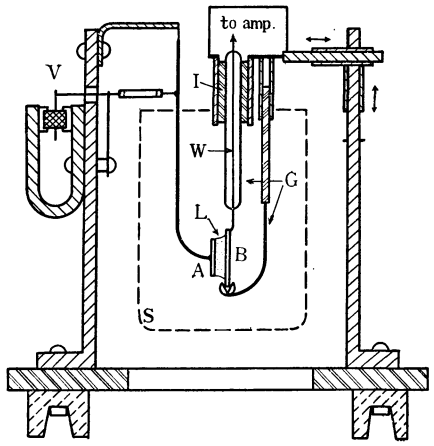



Fig. 4. Apparatus for mounting the electrodes.
V=vibrating reed of magnetic speaker. I=insulator. W=lead wire. G=glass supporter. A=Pt reference electrode. B=sample of metal. L=dielectric liquid. S=shielding.

The part of the electrodes was sketched in Fig. 4, which was designed for another experiment[4] and was used in this measurement too. A dielectric liquid was sandwiched between the two electrodes with a syringe. The distance between the electrodes was so small (0.5—1.0 mm) that the liquid neither dropped down nor evaporated within a short time except when the liquid had very high vapor pressure at room temperature.

### Examples of the Measurement

Although electrical potential differences at metal-liquid interfaces will result from various origins, yet the electrical potential difference between two metal electrodes immersed in the dielectric liquids which satisfy the following conditions, should be called "contact potential

* Details of this experiment will be published in near future.

11) Y. Yashiro, *Kōbunshi*, 5, 392 (1956).

difference" of the metals in the liquid according to the author's view. These requirements are as follows;—

1) The decomposition voltage of the liquid, if it exists, must be much higher than the C.P.D. between the two metals immersed in the liquid.

2) In case of the presence of electrical conductivity, the charge carriers of leakage current do not cause chemical reactions with the electrodes by its passage through the liquid. Nevertheless, there may be a case that these carriers cause the change in the C. P. D. by the space-charge polarization arising from the selective accumulation of the carriers at metal-liquid interfaces, when the current is flowing through the liquid under the influence of external electrical field; but this is not involved in the present requirement. Therefore, the term "chemical reaction" should be accepted in its narrower sense and the C. P. D., in its broader sense[1] in this statement.

In addition, in order to compare the data obtained by the leakage method with those by the sandwich type Zisman method, it is desirable to choose a liquid having a leakage resistance ranging $10^7$—$10^{12}\Omega$ as a sample of measurement for the reasons discussed below. In the present measurement, nitrobenzene and *o*-dichlorbenzene were used.

TABLE I
COMPARISONS OF THE DATA OBTAINED BY THE TWO METHODS

| Dielectric liquid | Sample of metal | The leakage method | The sandwich type Zisman method |
|---|---|---|---|
| Nitrobenzene | Al | +500 (mV) | +505 (mV) |
| | Cu | +220 | +220 |
| | Ni | +330 | +340 |
| *o*-Dichlorbenzene | Al | +470 | +470 |
| | Cu | +120 | +130 |
| | Ni | +415 | +410 |

Nitrobenzene and *o*-dichlorobenzene of chemical pure grade were used after two redistillations. The leakage resistance of the former was $10^7\Omega$ and that of the latter was $10^8\Omega$ under the condition of this measurement. All the metals used were of commercial quality and in the form of a plate (2 cm×2 cm×0.5 mm). These plates were polished in the air with clean gauze and purified carborundum powder. The polished-up platinum plate was used as a reference electrode. Within some time from the beginning of the measurement, the C. P. D. values settled into a constant value, then both values of the C. P. D. were obtained by the two methods respectively following the operations described above.

In this measurement, individual values of the C. P. D. were not of great concern, but the degree of agreement of the results by the two methods, was important. As seen in Table I, both data agreed well within the error ±10 mV. Usually the error of this extent will be inevitable at the present stage of this experiment. These samples were all positive with respect to the platinum reference and the data were obtained at room temperature.

## Discussion on the Limit of Measurement

The limit that the C. P. D. can be measured by the leakage method is determined mainly by the magnitude of the time constant of the input circuit. Fig. 5 shows

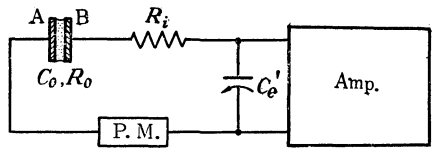



Fig. 5. Equivalent circuit of the leakage method.
$C_0$=capacitance between A and B. $R_0$ =leakage resistance of the liquid. $R_i$ input resistor, usually $10^8$—$10^{10}\Omega$. $C_e'$= average capacitance of the dynamic condenser plus stray capacitances. Amp.= ideal amplifier, i. e., one whose input impedance is infinite. P. M.=potentiometer, whose internal resistance $R_{P.M.} \ll R_0$ or $R_i$.

an equivalent circuit of the leakage method, and this belongs to a *CR* circuit. Representing the sum of $R_0$ and $R_i$ by $R_s$, and that of $C_0$ and $C_e'$ by $C_s$, the time constant of this *CR* circuit should be $\tau_s = C_s \times R_s$. If this time constant becomes too large, it is practically impossible to measure C. P. D. because too long a time is taken for charging up the dynamic condenser Ce. Considering that the minimum value of $C_s$ experimentally chosen will be, at the best, roughly ten *pF* and that the maximum value of $\tau_s$ permitted by practical operations will be several seconds, $R_s$ or $R_0$ should be smaller than the order of $10^{12}\Omega$ where $R_0 \gg R_i$. In this method, however, no limitation is required on the lower range of $R_0$.

In the sandwich type Zisman method (Fig. 2), however, the lower limit does exist but the upper limit does not. As the leakage resistance of the liquid becomes smaller, the a. c. voltage generated by the electrode vibration decreases correspondingly and, at last, becomes comparable to the intrinsic noise of the amplifier; in other words, the lower limit of $R_0$ will be determined mainly by the amplifier sensitivity. Full analysis of this problem is so complicated that it is beyond our scope in this experiment. Perhaps it will be sufficient for the present purpose

to determine this lower limit experimentally on the simplest condition. When all the electric circuit constants remain unchanged except $R_o$, the lower limit of $R_o$ is roughly $10^7\Omega$ in the equipment shown in Fig. 3.

Therefore, only in the liquid having leakage resistance of $10^7$—$10^{12}\Omega$ or specific resistance of $10^8$—$10^{13}\Omega\cdot$cm, can the measured values of the C. P. D. by the leakage method and by the sandwich type Zisman method, be compared with each other.

## Summary and Conclusion

For the purpose of measuring the C. P. D. between two metals immersed in poorly conductive dielectric liquids, two methods were presented in this report. One is the leakage method, which appears to resemble the ionization method but is different in one point; because in this leakage method we make use of the small electrical conductivity inherent in the liquid. It is another merit of this method that the measurement can be carried out without vibrating the electrode. When the liquid and the electrodes are properly chosen, this leakage method may be applied to various purposes. The other is the sandwich type Zisman method, which is an excellent device of improvement of the vibrating electrode method in dielectric liquids. On the comparison of the measured values by the two methods, satisfactory agreements were obtained.

Of course, there is only limited knowledge at the present time on the nature of the electrical potentials observed in these dielectric liquids, yet the author ventures to say that the use of the term, "contact potential difference", is most suitable in the case of these experiments.

The author wishes to express his hearty thanks to Assist. Professor Y. Yashiro of this Institute for his many valuable suggestions and his constant interest throughout the present work.

*Department of Chemistry, Nagoya Institute of Technology, Showa-ku, Nagoya*

# *Studies on Inorganic Constituents in Biological Materials.—On the Inorganic Constituents in Human Stones*

By Naoichi OHTA

(Received April 11, 1957)

Human stones, or calculi, are mainly formed in the liver, gall-bladder, biliary duct, pancreas, kidney, urethra, bladder, etc. in consequence of the isolation and coagulation of their respective humours caused by various reasons. Although many studies on calculi have been undertaken hitherto, most of them are dealing with etiological or clinical problems, and with all those studies no perfect explanation in the field has yet been made. Concerning the chemical composition of calculi, a long time has passed since their major constituents were made known, but there are only a few studies that deal with the inorganic constituents of calculi systematically. Recently, owing to developments in the instrumental method of analysis, many elements have been detected in calculi, and discussions on the significance of those elements have become active. However, all the analyses whcih have ever been made are limited almost entirely to qualitative research, or even if quantitative, to only a few constituents.

Regarding the formation of calculi as a special chemical phenomenon, the author considers that on the one hand it is important to determine etiologically the contents of inorganic constituents in calculi which are formed in various organs and their respective humours of a human body and to reveal the status of distribution of those constituents in those materials, and that on the other hand it is a matter of interest to clarify the cycle and function of elements in biological materials. The author[1] has reported his studies on each of the constituents of human stones several times up to this time. In this paper, he will report (1) the results of

1) N. Ohta, *J. Chem. Soc. Japan, Pure Chem. Sec.*, **74**, 506 (1953); **76**, 590, 1235 (1955); **78**, 7, 13, 1033, 1038, 1043 (1957).

quantitative analyses of various human stones and of the humours in which the stones were formed, determining calcium, magnesium, phosphorus, sodium and potassium as major inorganic constituents and iron, copper, zinc, lead and manganese as heavy metal constituents, (2) the distribution of those constituents in various human stones and in their respective humours, and, (3) the mutual relation existing among those constituents.

## Experimental

**Materials.**—The human stones used for this study were 25 gallstones (since three of them were divided into the internal and the external portions, the total number of analyses was 28), 10 urinary calculi and two pancreatic calculi, all of them being (kindly) providedly by the First National Hospital of Tokyo. The characters of these materials have been described in the author's earlier reports[1]. The samples of related humours provided for the analyses were 10 of gall-bladder biles which had been collected at the time of the autopsies at Tokyo Medical Examiner Office, 12 of normal human blood and 12 of normal human urine.

**Methods.**—Samples were analysed after conversion of their organic matters into ashes with redistilled fuming nitric acid and 60 % perchloric acid.

Calcium and magnesium were determined by the complexometric titration method[2]. The sum of calcium and magnesium was titrated with disodium salt ethylendiamintetra-acetic acid solution using Eriochrom Black T as an indicator, while the calcium was determined indirectly by determining magnesium after precipitation of calcium as oxalate. On the analysis of samples rich in phosphate like urinary calculi, the cation exchanger, Dowex 50, was used for preliminary separation of the phosphoric acid radical. This method was also applied to the determination of lead and zinc in the samples rich in phosphate.

Sodium and potassium were determined by the flamephotometric method[3], using Perkin-Elmer Model-52C flamephotometer, acetylene being used as fuel.

Phosphorus was determined by molybdenum blue method modified by Ikeda[4].

Iron was determined by nitroso-R salt method modified by Dean and Lady[5].

Copper, zinc and lead were determined according to Sandell's dithizone method[6].

Manganese was determined by permanganate method[7].

Of the elements described above, last five were determined by Beckmann Model D. U. Quartz Spectrophotometer.

## Results

Analytical results for gallstone, normal gallbladder bile, normal human blood, urinary calculus, normal human urine and pancreatic calculus were shown in Table I, II, III, IV, V and VI, respectively. In these tables, the values of the major and the heavy metal constituents were shown in the mg. per g. (ml.) and p. p. m. unit, respectively, of undried samples. "*m*" is an average value calculated statistically at the 95 % confidence interval.

## Discussion

**1. Major Constituents.**—(*1*) *Gallstone.*—The chemical composition of a gallstone varies in accordance with the difference among human races and regions. The greater part of a gallstone consists of organic materials[8,9], such as cholesterin, bilirubin and fatty acid, and the content of inorganic constituents is very small, as shown in the ash content in Table I.

Although various gallstones have been classified clinically according to the content of above-mentioned organic constituents in them, most stones are either a mixture or a layer of several kinds (this shows the change of the circumstance in which the sedimentations were made), so that it is difficult to analyse a slight quantity of inorganic constituents after separating these components individually. Accordingly, the materials used in this study were divided into three groups, such as mineral stone, cholesterinpigment-calcium stone and cholesterin stone, and each sample of the gallstone was analysed as it was.

A cholesterin stone consists mainly of cholesterin (soluble in ether), and contains a slight amount of ash and bilirubin. A cholesterinpigment-calcium stone contains a considerable amount of bilirubin (soluble in chloroform) and calcium besides cholesterin. A mineral stone is scarcely soluble in chloroform and ether. It is either hard and contains a considerable amount of ash, or it has a black vitreous appearance.

The content of major constituents in various gallstones varies considerably according to these three kinds of stone

2) G. Schwarzenbach and H. Ackermann, Helv. Chim. Acta, **30**, 1798 (1947).
3) C. E. Bills, F. G. McDonald, W. Niedermier and M. C. Schwartz, *Anal. Chem.*, **21**, 1076 (1949).
4) N. Ikeda, *J. Chem. Soc. Japan, Pure Chem. sec.*, **72**, 23 (1951).
5) J. A. Dean and J. H. Lady, *Anal. Chem.*, **25**, 947 (1953).
6) E. B. Snandell, "Colorimetric Determination of Traces of Metals", Interscience Publisher, Inc., New York, (1950), pp. 295, 616, 388.
7) E. B. Sandell, ibid., p.433.
8) M. Nishimura, *J. Biochem.*, **28**, 265 (1938).
9) K. Kodama, "Clinical Biochemistry", Nanzando, Tokyo, (1951), p. 117.

TABLE I

INORGANIC CONSTITUENTS IN HUMAN GALLSTONES

| Species | Sample | Ash, % | Ca mg./g. | Mg mg./g. | Na mg./g. | K mg./g. | P mg./g. | Fe p.p.m. | Cu p.p.m. | Zn p.p.m. | Pb p.p.m. | Mn p.p.m. |
|---|---|---|---|---|---|---|---|---|---|---|---|---|
| Mineral stone | G-4004 | 6.83 | 28.70 | 3.05 | 1.02 | 0.26 | 6.52 | 860 | 1,794 | 43 | 134 | 53 |
| | G-4011 | 7.48 | 36.00 | 3.11 | 0.86 | 0.20 | 5.00 | 1,170 | 1,435 | 146 | 81 | 157 |
| | G-4011 B | 12.57 | 31.82 | 4.37 | — | — | 21.30 | 2,290 | 10,400 | 385 | 84 | 277 |
| | G-4012 | 9.12 | 29.24 | 4.52 | 1.10 | 0.19 | 10.60 | 598 | 8,705 | 1,043 | 97 | 140 |
| | G-4017 | 15.56 | 70.40 | 21.00 | 0.77 | 0.17 | 4.20 | 250 | 1,665 | 108 | 47 | 98 |
| | G-5007 | 8.45 | 39.20 | 9.41 | 0.93 | 0.21 | 4.01 | — | 2,107 | 168 | 33 | — |
| | G-5012 | 8.75 | 34.00 | 10.70 | 1.34 | 0.21 | 5.65 | 411 | 1,355 | 423 | 45 | 66 |
| | G-5017 | 32.96 | 132. | 16.10 | 1.69 | 0.51 | 48.50 | 629 | 420 | 550 | 173 | 654 |
| | G-5019 | 10.01 | 46.44 | 4.95 | 2.30 | 0.49 | 7.25 | — | 3,585 | 238 | — | 124 |
| | G-5019 A | 8.26 | 35.31 | 3.71 | — | — | 9.32 | 68 | 1,382 | 279 | 43 | 83 |
| | G-5019 B | 9.08 | 45.84 | 3.90 | — | — | 5.28 | 373 | 2,440 | 574 | 95 | 118 |
| | G-5021 | 54.79 | 285. | 35.52 | 0.31 | 0.09 | 28.10 | 287 | 548 | 159 | 51 | 540 |
| | G-5022 | 36.89 | 173. | 18.15 | 4.37 | 0.76 | 23.30 | 1,520 | 7,345 | 329 | 296 | 3,850 |
| | G-8002 | 5.73 | 21.87 | 4.32 | — | — | 4.82 | 282 | 2,660 | 216 | 192 | 107 |
| | Average | 16.18 | 72.06 | 10.20 | 1.47 | 0.31 | 13.13 | 728 | 3,274 | 333 | 105 | 482 |
| Cholesterin-pigment-calcium stone | G-1003 | 10.24 | 53.94 | 3.62 | 1.21 | 0.18 | 7.86 | 102 | 598 | 172 | 21 | 32 |
| | G-1005 | 5.37 | 28.54 | 2.60 | 0.10 | 0.04 | 3.37 | 30 | 70 | 40 | 18 | 6 |
| | G-4011 A | 6.95 | 34.92 | 3.27 | — | — | 4.77 | 61 | 281 | 116 | 46 | 33 |
| | G-5009 | 8.59 | 43.58 | 4.65 | 1.55 | 0.27 | 4.92 | 85 | 253 | 243 | 55 | 248 |
| | G-5010 | 1.84 | 9.06 | 0.89 | 0.18 | 0.04 | 1.42 | 93 | 87 | 9 | 55 | 48 |
| | G-5013 | 9.30 | 48.34 | 4.15 | 0.91 | 0.18 | 6.86 | 163 | 1,052 | 140 | 83 | 153 |
| | G-5014 | 7.32 | 39.20 | 3.38 | 0.65 | 0.15 | 4.42 | 278 | 185 | 50 | 168 | 186 |
| | G-5018 | 2.97 | 12.25 | 1.18 | 0.40 | 0.16 | 2.45 | 79 | 229 | 50 | 29 | 49 |
| | G-8004 A | 1.33 | 5.37 | 0.42 | — | — | 1.82 | 71 | 255 | 149 | 51 | 55 |
| | G-8004 B | 2.95 | 14.90 | 0.87 | — | — | 1.78 | 277 | 858 | 451 | 148 | 94 |
| | Average | 5.68 | 29.01 | 2.50 | 0.71 | 0.15 | 3.97 | 124 | 387 | 142 | 67 | 90 |
| Cholesterin stone | G-4015 | 0.06 | (0.03) | — | 0.07 | 0.02 | 0.12 | 15 | 65 | 17 | 24 | 11 |
| | G-4016 | 0.04 | (0.02) | — | 0.07 | 0.02 | 0.04 | 31 | 35 | 58 | 28 | 6 |
| | G-5001 | 0.08 | (0.03) | — | 0.15 | 0.08 | 0.14 | 13 | 35 | 67 | 24 | 11 |
| | G-5015 | 0.04 | (0.02) | — | 0.06 | 0.02 | 0.06 | 29 | 17 | 79 | — | 10 |
| | G-8001 | 0.03 | — | — | — | — | — | 16 | 27 | 12 | 23 | 10 |
| | G-8003 | 0.44 | 0.94 | 0.13 | — | — | 0.94 | 133 | 80 | 105 | 79 | 27 |
| | Average | 0.12 | 0.21 | 0.13 | 0.09 | 0.04 | 0.26 | 40 | 43 | 56 | 36 | 13 |
| *m.* | | 6.25 ±1.74 | 31.18 ±12.04 | 5.52 ±2.36 | 0.78 ±0.30 | 0.17 ±0.06 | 6.30 ±2.71 | 293 ±147 | 871 ±383 | 185 ± 61 | 71 ±20 | 121 ± 59 |

TABLE II

INORGANIC CONSTITUENTS IN POST-MORTEM GALLBLADDER BILE

| Samples | Collected volume, ml. | Ca mg./ml. | Mg mg./ml. | Na mg./ml. | K mg./ml. | P mg./ml. | Fe p.p.m. | Cu p.p.m. | Zn p.p.m. | Pb p.p.m. | Mn p.p.m. |
|---|---|---|---|---|---|---|---|---|---|---|---|
| No. 1 | 10.0 | 1.55 | 0.24 | 4.3 | 1.4 | 2.52 | 20.3 | 26.8 | 15.0 | 0.15 | 1.11 |
| 2 | 22.0 | 0.36 | 0.06 | 3.2 | 1.0 | 0.50 | 9.1 | 3.2 | 5.6 | 0.30 | 0.53 |
| 3 | 5.0 | 0.68 | 0.12 | 6.5 | 2.4 | 1.03 | 97.4 | 3.5 | 38.2 | 0.60 | 3.10 |
| 4 | 7.5 | 0.70 | 0.12 | 4.9 | 1.7 | 1.19 | 25.8 | 9.2 | 10.0 | 0.40 | 4.20 |
| 5 | 7.0 | 0.98 | 0.15 | 6.4 | 2.0 | 1.66 | 45.0 | 20.5 | 4.3 | 0.32 | 1.46 |
| 6 | 14.5 | 0.27 | 0.04 | 4.3 | 1.4 | 0.42 | 33.3 | 7.3 | 10.2 | 0.15 | 0.96 |
| 7 | 16.5 | 0.30 | 0.05 | 4.1 | 1.3 | 0.58 | 10.8 | 2.6 | 4.6 | 0.10 | 0.83 |
| 8 | 8.0 | 1.02 | 0.18 | 6.6 | 1.5 | 1.56 | 22.0 | 12.0 | 9.4 | 0.62 | 0.27 |
| 9 | 7.0 | 1.05 | 0.14 | 6.3 | 1.6 | 1.33 | 34.4 | 12.3 | 13.3 | 0.36 | 0.90 |
| 10 | 12.0 | 0.44 | 0.06 | 4.5 | 1.7 | 0.67 | 30.1 | 11.2 | 12.5 | 0.51 | 0.18 |
| *m.* | 11.0 | 0.74 ±0.30 | 0.12 ±0.05 | 5.1 ±0.9 | 1.6 ±0.3 | 1.15 ±0.47 | 25.6 ± 8.8 | 10.9 ± 5.5 | 9.4 ± 3.0 | 0.35 ±0.13 | 1.35 ±0.93 |

TABLE III

INORGANIC CONSTITUENTS IN NORMAL HUMAN BLOOD

| Sample | Ca mg./ml. | Mg mg./ml. | Na mg./ml. | K mg./ml. | P mg./ml. | Fe p.p.m. | Cu p.p.m. | Zn p.p.m. | Pb p.p.m. | Mn p.p.m. |
|---|---|---|---|---|---|---|---|---|---|---|
| No. 1 | 0.127 | 0.053 | 2.18 | 2.26 | 0.20 | 530 | 1.31 | 10.9 | 0.28 | 0.45 |
| 2 | 0.133 | 0.055 | 2.50 | 2.20 | 0.20 | 482 | 1.26 | 8.44 | 0.25 | 0.36 |
| 3 | 0.114 | 0.038 | 2.09 | 1.62 | 0.16 | 480 | 1.15 | 7.79 | 0.29 | 0.37 |
| 4 | 0.083 | 0.032 | 1.81 | 1.43 | 0.10 | 390 | 0.89 | 5.50 | 0.22 | 0.28 |
| 5 | 0.105 | 0.043 | 2.36 | 1.96 | 0.18 | 488 | 1.10 | 6.50 | 0.30 | 0.25 |
| 6 | 0.130 | 0.053 | 2.40 | 2.08 | 0.23 | 542 | 1.28 | 7.82 | 0.36 | 0.46 |
| 7 | 0.111 | 0.045 | 2.47 | 1.81 | 0.18 | 474 | 1.13 | 8.60 | 0.27 | 0.27 |
| 8 | 0.103 | 0.045 | 2.33 | 1.90 | 0.16 | 469 | 1.17 | 7.97 | 0.25 | 0.30 |
| 9 | 0.087 | 0.037 | 2.00 | 1.99 | 0.16 | 498 | 1.24 | 8.06 | 0.34 | 0.32 |
| 10 | 0.094 | 0.040 | 2.34 | 2.05 | 0.22 | 522 | 1.22 | 8.25 | 0.33 | 0.48 |
| 11 | 0.090 | 0.037 | 2.34 | 2.01 | 0.16 | 477 | 1.19 | 7.21 | 0.30 | 0.45 |
| 12 | 0.082 | 0.036 | 2.15 | 2.09 | 0.15 | 470 | 1.15 | 7.11 | 0.32 | 0.39 |
| *m.* | 0.105 | 0.043 | 2.25 | 1.95 | 0.18 | 494 | 1.20 | 7.57 | 0.29 | 0.37 |
| | ±0.012 | ±0.005 | ±0.13 | ±0.15 | ±0.02 | ± 17 | ±0.04 | ±0.62 | ±0.03 | ±0.05 |

TABLE IV

INORGANIC CONSTITUENTS IN HUMAN URINARY CALCULI

| Species | Sample | Ash, % | Ca mg./g. | Mg mg./g. | Na mg./g. | K mg./g. | P mg./g. | Fe p.p.m. | Cu p.p.m. | Zn p.p.m. | Pb p.p.m. | Mn p.p.m. |
|---|---|---|---|---|---|---|---|---|---|---|---|---|
| Bladder | U-1001 | 17.09 | 52 | 7.0 | 4.30 | 8.14 | 30.5 | 270 | 4.8 | 345 | 36 | 1.0 |
| calculus | U-5009 | 24.12 | 137 | 7.2 | 2.55 | 5.41 | 9.9 | 144 | 26.8 | 239 | 20 | 4.5 |
| Renal | U-5002 | 58.16 | 286 | 12.7 | 4.57 | 0.52 | 63.3 | 256 | 17.8 | 913 | 43 | 4.1 |
| calculus | U-5005 | 57.02 | 271 | 12.0 | 4.76 | 2.00 | 69.2 | 198 | 7.8 | 577 | 26 | 1.3 |
| | U-5006 | 63.29 | 264 | 9.7 | 3.66 | 1.90 | 94.3 | 340 | 14.7 | 578 | 37 | 4.1 |
| | U-5007 | 38.58 | 150 | 8.3 | 7.65 | 4.90 | 61.3 | 118 | 26.5 | 673 | 31 | 3.0 |
| Urethral | U-5001 | 78.28 | 450 | 18.2 | 7.19 | 0.92 | 45.8 | 199 | 6.3 | 705 | 58 | 0.7 |
| calculus | U-5003 | 51.67 | 233 | 3.8 | 4.59 | 1.41 | 70.5 | 286 | 8.7 | 343 | 19 | 1.0 |
| | U-5004 | 37.37 | 254 | 1.5 | 1.69 | 0.98 | 3.3 | 172 | 16.9 | 561 | 22 | 1.7 |
| | U-5008 | 62.61 | 184 | 31.4 | 4.70 | 2.71 | 120. | 166 | 6.7 | 615 | 43 | 1.8 |
| *m.* | | 48.82 | 228 | 11.2 | 4.57 | 2.89 | 56.8 | 215 | 13.7 | 555 | 34 | 2.3 |
| | | ±13.66 | ± 77 | ± 6.1 | ±1.30 | ±1.77 | ±25.8 | ± 50 | ± 6.3 | ±142 | ± 9 | ±1.0 |

TABLE V

INORGANIC CONSTITUENTS IN NORMAL HUMAN URINE

| Sample No. | Vol. ml./day | Average concentration mg./ml. Ca | Mg | Na | K | P | Sample No. | Vol. ml./day | Average concentration p.p.m. Fe | Cu | Zn | Pb | Mn |
|---|---|---|---|---|---|---|---|---|---|---|---|---|---|
| 1 | 1480 | 0.116 | 0.052 | 3.84 | 1.14 | 0.64 | 7 | 1050 | 1.83 | 0.15 | 1.40 | 0.045 | <0.01 |
| 2 | 2010 | 0.098 | 0.051 | 4.79 | 1.10 | 0.70 | 8 | 900 | 2.08 | 0.25 | 1.54 | 0.120 | <0.01 |
| 3 | 1600 | 0.099 | 0.034 | 4.19 | 0.92 | 0.53 | 9 | 1000 | 2.40 | 0.22 | 1.45 | 0.080 | <0.01 |
| 4 | 2000 | 0.077 | 0.035 | 3.20 | 0.76 | 0.55 | 10 | 1750 | 1.07 | 0.08 | 1.22 | 0.020 | <0.01 |
| 5 | 1550 | 0.152 | 0.057 | 4.93 | 1.00 | 0.67 | 11 | 1200 | 1.66 | 0.14 | 1.82 | 0.052 | <0.01 |
| 6 | 1630 | 0.127 | 0.049 | 1.74 | 0.51 | 0.73 | 12 | 1000 | 2.25 | 0.23 | 1.69 | 0.088 | <0.01 |
| Average | | 0.112 | 0.046 | 3.78 | 0.91 | 0.64 | Average | | 1.88 | 0.18 | 1.52 | 0.068 | <0.01 |

TABLE VI

INORGANIC CONSTITUENTS IN HUMAN PANCREATIC CALCULI

| Sample | Ash, % | Ca mg./g. | Mg mg./g. | Na mg./g. | K mg./g. | P mg./g. | Fe p.p.m. | Cu p.p.m. | Zn p.p.m. | Pb p.p.m. | Mn p.p.m. |
|---|---|---|---|---|---|---|---|---|---|---|---|
| P-1001 | 55.06 | 382 | 1.8 | 0.22 | 0.09 | 0.74 | 75.0 | 11. | 282 | 136 | 0.3 |
| P-4002 | 64.45 | 440 | 3.7 | 1.49 | 0.68 | 2.30 | 52.4 | 19. | 345 | 112 | 0.5 |
| Average | 59.76 | 411 | 2.8 | 0.86 | 0.39 | 1.52 | 63.7 | 15. | 314 | 124 | 0.4 |

as shown in Table I. The ratios of average content of ash between mineral, cholesterinpigment-calcium and cholesterin stones are 135 : 47 : 1, while the mutual ratios between each of the major constituents do not vary so much as those in ash content. As for the value (weight proportion) of Ca/Mg, that of a cholesterinpigment-calcium stone (12.0) is greater than that of a mineral stone (7.7) or of a cholesterin stone (7.2). As for the value of (Ca+Mg)/P, there is no significant difference between that of a mineral stone (7.5) and that of a cholesterinpigment-calcium stone (7.6), but the value of a cholesterin stone (0.5) is far smaller than the values of the other two. If calcium and magnesium that present (in the stones) as phosphates, the values of Ca/P and Mg/P would be 1.94 and 1.18, respectively. Accordingly, the value of (Ca+Mg)/P may be regarded as a standard for measuring the state of alkaline-earth metals. Epprecht et al.[10] reported in their experiment using X-ray that calcium in a gallstone was present as a bilirubinate, while Cameron et al.[11] reported the presence of calcium carbonate in a gallstone. As for the value of Na/K, there is no significant difference between that of a mineral stone (4.7) and that of a cholesterinpigment-calcium stone (4.5), while that of a cholesterin stone (3.0) shows that the proportion of potassium is greater than in the other two.

According to the result of an examination of relations existing among major constituents of a gallstone (as a whole), there are positive correlations between calcium and magnesium, sodium and potassium, phosphorus and sodium, and phosphorus and potassium, respectively, with 5% degree of significance.

(*2*) *Bile and Blood.*—Bile is a complexed colloidal solution containing bilirubine which is a decomposition product of hemoglobin. There are two kinds of bile, hepatic and gallbladder bile, the latter being concentrated 7 to 10 times as densely as the former[12]. A gallstone is nothing but the product of condensed bile constituents. Therefore, it is not only interesting to research the relation between inorganic constituents of bile and blood and those of gallstones in order to understand the cycle of elements in biological materials, but also it is important to clarify the mechanism of the formation of a gallstone.

The relationship between the formation of a gallstone and inorganic constituents mainly in regard to alkali and alkaline-earth metals has been studied previously, and there are several reports on the metabolism of those materials in humours obtained from experiments on animals[13–17].

When the content of potassium is taken as a standard, the ratio of existence of each of the constituents in blood, bile and gallstones are given in Table VII.

TABLE VII

| | Ca | Mg | P | Na | K |
|---|---|---|---|---|---|
| Blood ..... | 0.054 | 0.022 | 0.092 | 1.2 | 1.0 |
| Bile..... | 0.46 | 0.075 | 0.72 | 3.2 | 1.0 |
| Gallstone ... | 183. | 31. | 37. | 4.6 | 1.0 |

That is to say, gallstones are rich in alkaline-earth metals, especially in calcium and phosphorus, while blood and bile are rich in alkali metals.

When the content of each element in blood is taken as a standard, the ratios of the average content of each of the constituents in blood, bile and a gallstone are given in Table VIII (the figures shown in brackets indicate that the content of each of those constituents in bile is regarded as a standard).

TABLE VIII

| Blood | Bile | Gallstone |
|---|---|---|
| Ca .....1. | 7.0 (1.) | 297. (42. ) |
| Mg.....1. | 2.8 (1.) | 128. (46. ) |
| P .....1. | 6.4 (1.) | 35. ( 5.5 ) |
| Na.....1. | 2.3 (1.) | 0.35 ( 0.15) |
| K .....1. | 0.82(1.) | 0.087( 0.11) |

We see then that calcium, magnesium and phosphorus increase according to the process of blood—bile—gallstone, while potassium decreases in the same process. Sodium increases in the process of turning from blood to bile, but the content of the element in a gallstone is less than that in blood. When the differences among solubilities of various salts composed of these metals, $PO_4^{3-}$ and organic matters in a gallstone, and the relation between

10) W. Epprecht, H. Rosenmund and H. R. Schinz, *Fortshr. Gebiete Röntogenstrahlen*, **79**, 1 (1953) ; *C. A.*, **47**, 11458 (1953).
11) A. T. Cameron, F. D. White and S. Meltzer, *Can. Med. Assoc. J.*, **39**, 441 (1938) : *C. A.*, **33**, 1811 (1939).
12) K. Kodama, "Clinical Biochemistry", Nanzando, Tokyo, (1951), p. 114.
13) R. Ohta, *J. Gastroenterology*, **2**, 1201 (1927).
14) T. Maruno, ibid., **6**, 642 (1931).
15) Y. Tachikawa, ibid., **10**, 1349, 1361, 1375 (1935).
16) T. Hukuda and Y. Tachikawa, ibid., **11**, 763 (1936).
17) R. Kono, *Jap. Arch. Internal Med.*, **1**, No. 2, 44, 49 (1954).

these metal ions and the stability[18] of the colloidal state of bile are considered, it is obvious that the abnormality of the metabolism of these major constituents has a strict connection with the formation of a gallstone.

All the values of Ca/Mg, (Ca+Mg)/P and Na/K increase according to the order of blood (2.4±0.1, 0.88±0.10 and 1.2±0.1), bile (6.4±0.5, 0.75±0.06 and 3.4±0.4) and gallstone (9.0±1.3, 5.8±1.3 and 4.3±0.6), because both the rate of increase of calcium and the rate of decrease of potassium are high.

(*3*) *Urinary Calculus and Urine.*—The history of research of a urinary calculus is long. Much literature on this subjects has been published since the end of the eighteenth century. According to the results of all the crystallographic studies using X-rays[19-23] and polarized microscope[24-29], chemical analysis[30-32] and infrared spectroscopic studies[33] ever made, it has been clarified that the urinary calculus contains one or more of the following compounds:

$Ca_3(PO_4)_2$, $CaHPO_4 \cdot 2H_2O$, $Ca_{10}(PO_4)_6(OH)_2$, $Ca_{10}(PO_4CO_3OH)_6(OH)_2$, $CaC_2O_4 \cdot H_2O$, $CaC_2O_4 \cdot 2H_2O$, $Mg_3(PO_4)_2$, $MgNH_4PO_4 \cdot 6H_2O$, carbonate, uric acid, $NH_4$ or Na acid urate, cystine, and xanthine.

Table IV gives the calculi assorted according to the parts where they had been formed, but the samples were so few that it was difficult to compare one with another. According to the result of analysis, it was ascertained that all of these calculi consisted of a large quantity of phosphate and oxalate of calcium and of a small quantity of magnesium compounds. According to Epprecht et al.[22], the genesis of $MgNH_4PO_4 \cdot 6H_2O$ in Europeans is more frequent than in Orientals.

As a whole, the ash content of urinary calculi is greater than that of gallstones, but there is no significant difference between them, so far as the mutual ratio of major constituents is concerned, except that the magnesium content is less. Therefore, regarding the values of (Ca+Mg)/P and Na/K, there is no significant difference between urinary calculi (5.1±3.4 and 3.0±2.1) and gallstones with the exception that Ca/Mg in urinary calculi (23.2±12.3) is greater than that in gallstones.

Urine is usually in a persaturate state against its solute, which may be crystallized to a urinary calculus owing to various reasons. Therefore, the relation between the formation of a urinary calculus and the colloidal character of urine has been observed for a long time[34-38].

The concentrations of calcium, magnesium, sodium, potassium and phosphorus in urinary calculus are 2036, 265, 1.2, 3.2 and 89 times, respectively, as much as those in urine. When the content of potassium is taken as a standard, the ratio of existence of each of the constituents in urinary calculus and urine are given in Table IX.

TABLE IX

| | Ca | Mg | Na | K | P |
|---|---|---|---|---|---|
| Urinary calculus... | 78.8 | 3.9 | 1.6 | 1.0 | 19.7 |
| Urine ..... | 0.12 | 0.05 | 4.2 | 1.0 | 0.7 |

Thus urinary calculi are rich in alkaline-earth metals and phosphorus, while urine is rich in alkali metals.

The Values of Ca/Mg and (Ca+Mg)/P increase according to the process of urine (2.4 and 0.25)—urinary calculus (there are, however, a great differences between urinary calculi and gallstones in regard to the enrichment of calcium and magnesium), but there is no significant difference between them in regard to the value of Na/K (urine is 4.1).

(*4*) *Pancreatic Calculus.*—Both of the two examples have a greater amount of

18) T. Yuta, *Acta Medica* (IGAKU KENKYU), **23**, 1434 (1953).
19) J. A. Barclay, W. T. Cooke, M. Stacey, A. D. Booth and P. W. Kent, *J. Physiol.*, **103**, 249 (1944); *C. A.*, **39**, 978 (1945).
20) E. Brandenberger, H. R. Schinz and Fr. de Quervain, *Experimentta*, 3, 106 (1947); *C. A.*, **41**, 4560 (1947).
21) S. Fukushima, *Fukuoka Acta Medica*, **40**, 95 (1949).
22) W. Epprecht and H. R. Schinz, *Schweiz. med. Woch.*, **80**, 792 (1950): *C. A.*, **45**, 751 (1951).
23) J. Barraud, *Bull. Soc. Franç. Mineral.*, **75**, 166 (1952); *C. A.*, **46**, 6725 (1952).
24) A. Randell, IV., *J. Urol.*, **48**, 642 (1942); *C. A.*, **37**, 1455 (1943).
25) E. L. Prien and C. Frondel, *J. Urol.*, **57**, 949 (1947).
26) E. L. Prien, ibid., **61**, 821 (1949).
27) T. Sekimura, *Jap. J. Urol.*, **40**, 113, 116 (1949).
28) M. Ishibashi, *J. Kurume Med. Assoc.*, **13**, 48 (1950).
29) J. Boissier, *Ann. Biol. Clin.*, **10**, 523, 572 (1952); *C. A.*, **47**, 5474, 5529 (1953).
30) L. W. La Towsky, *J. Urol.*, **49**, 720 (1943); *C. A.*, **37**, 5094 (1943).
31) T. Sekimura, *Jap. J. Urol.*, **36**, 319 (1944).
32) E. D. Carpenter, *Can. J. Med. Technol.*, **16**, 53 (1954); *C. A.*, 10894 (1954).
33) D. E. Beischer, *J. Urol.*, **73**, 653 (1955).
34) I. Yoshikawa, *Acta Medica* (IGAKU KENKYU), **19**, 269 (1949).
35) L. Aschoff, *Kolloid Z.*, **89**, 107 (1939).
36) I. Palôcz, *Orvosok Lapja Népegészségügy*, **2**, 1473 (1946): *C.A.*, **42**, 8926 (1948).
37) K. Kodama, "Clinical Biochemistry", Nanzando, Tokyo, (1951), p. 350.
38) E. A. Hauser and D. S. Le Beau, *Kolloid Z.*, **132**, 78 (1953).

ashes than in other sorts of human stone, and they are almost entirely composed of calcium carbonate. They contain only a small quantity of phosphates. Butturini and Meduri[39] reported similar results.

For this reason, the ratios of existence among those major constituents are (as K=1); Ca : Mg : Na : K : P=1054 : 7.2 : 2.2 : 1 : 3.9 and the mutual ratios are : Ca/Mg=166. (Ca+Mg)/P=35.6.

These values differ considerably from those of urinary calculi and gallstones.

**2. Heavy Metal Constituents.**—(*1*) *Gallstone, Bile and Blood.*—Heavy metal constituents, such as copper, iron, zinc and manganese are contained in gallstones, especially in mineral stones, much greater in quantity than in any other biological materials. Therefore, in several examples the amount of these metals even exceeds that of alkali metals which are regarded as major constituents.

Although the presence of a large quantity of the heavy metals in gallstones was pointed out long ago[40], most of the successive researches[18,41-45] have been limited merely to the detection of trace elements. The quantitative analysis of the heavy metals has not been made, what with the scantiness of samples and what with the incompleteness of the micro analytical method. Accordingly, reports on the quantitative analysis of heavy metals are very rare (copper was determined quantitatively by Newell[46] and Telfer[47], and lead, by Anderson[48]).

A gallstone was reported to be formed experimentally as a result of continuous feeding of heavy metals, such as copper[49,50], iron[51] and manganese[51], to animals, though physiological hindrances were caused by doing so. Yuta[18] reported that he ascertained the establishment of Hardy-Schulz's law on addition of various electrolytes to dialyzed bile, and also that, in this case, heavy metal ions, even if very small in quantity, took part in accerelating the coagulation of bile constituents by alkaline-earth metals. On the one hand these facts indicate the significance of heavy metals in the formation of gallstones. On the other hand Telfer[47] denies the importance of copper in chololithiasis. However, the significance of heavy metals in a gallstone will be ascertained from their behavior in the process of the formation of a gallstone. Table I shows that the contents of these heavy metals decrease in order of mineral stone, cholesterinpigment-calcium stone and cholesterin stone. The average values of heavy metals of all samples of gallstones are arranged as follows:

Cu>Fe>Zn>Mn>Pb

However, there are some differences among the values of various groups of stones as follows:

Mineral stone.....
Cu>Fe>Mn>Zn>Pb

Cholesterinpigment-calcium stone.....
Cu>Zn>Fe>Mn>Pb

Cholesterin stone.....
Zn>Cu>Fe>Pb>Mn

When the content of each constituent in blood is taken as a standard, the ratios of the average contents in blood, bile and a gallstone are given in Table X (the figures shown in brackets indicate that the content of each of those constituents in bile is regarded as a standard).

TABLE X

| | Blood | Bile | Gallstone |
|---|---|---|---|
| Fe | .....1. | 0.052(1) | 0.59( 11) |
| Cu | .....1. | 9.1 (1) | 726. ( 80) |
| Zn | .....1. | 1.2 (1) | 24. ( 20) |
| Pb | .....1. | 1.2 (1) | 245. (203) |
| Mn | .....1. | 3.6 (1) | 327. ( 90) |

That is, copper, zinc, lead and manganese are concentrated according to the process of the formation of a gallstone. A large quantity of iron is contained in blood as a constituent of hemoglobin, but its large proportion would be lost when hemoglobin decomposes to bilirubine and moves into bile.

The results of this study are insufficient to explain how these heavy metals take part in the formation of a gallstone, and for this purpose further studies should be made to reveal the content of these metals in the bile of chololithiasic patients, and the status of presence of these metals in

39) U. Butturini and G. Meduri, *Giorn. Clin. Med.*, **31**, 693 (1950) : *C.A.*, **44**, 10304 (1950).
40) R. Schönheimer and W. Herkel, *Klinische Woch.*, **1931**, 345.
41) W. Gerlach, *Verhand, Deut. Pathol. Gesel.*, Tag. **27**, 277 (1934).
42) E. Müller, *Bioch. Z.*, **286**, 182 (1936).
43) E. Takino, *Trans. Soc. Pathol. Jap.*, **33**, 262 (1944).
44) E. Schairer, *Arch. Path. Anat. Physiol.*, **312**, 534 (1944) ; *C. A.*, **41**, 5953 (1947).
45) M. Mukai, *Medicine and Biology* (IGAKU-to-SEIBUTSUGAKU), **10**, 327 (1947).
46) W. E. Newell, *Brit. Med. J*, **1**, 262 (1936) ; *C. A.*, **32**, 2602 (1938).
47) S. V. Telfer, *Glasgow Med. J.*, **27**, 181 (1946) : *C. A.*, **40**, 5825 (1946).
48) A. B. Anderson, *Biochem. J.*, **39**, 58 (1945).
49) T. Yokoyama, *J. Gastroenterology*, **10**, 708 (1935).
50) K. Fujita and T. Fukuda, ibid., **10**, 709 (1935).
51) K. Seki, ibid., **14**, 878, 921 (1939).

blood, bile and a gallstone (Epprecht et al.[22]) ascertained the presence of copper calcium-bilirubinate in gallstone by means of X-ray analysis). But their significance can not be overlooked when the above result is considered together with those of pathological and colloidal studies. There is a positive correlation among the heavy metals at the 95% confidence interval, except the combination of iron and zinc.

(2) *Urinary Calculus and Urine.*—Studies of heavy metals in a urinary calculus have been undertaken mainly by means of qualitative spectrographic analyses[34,41,44,52-54]. Yokoyama[55] reported on the renal calculi alimentarily formed in animals by the use of copper and calcium. According to Ishibashi's report[56], zinc, lead, iron and tin in the crystallization of uric and oxalic acid were promoters. Yoshikawa[34] reported that greater quantities of copper, lead, tin, manganese and iron were contained in diseased urine than in normal urine.

The order of average values of heavy metal contents in urinary calculus and urine are arranged as follows:

Urinary calculus...Zn>Fe>Pb>Cu>Mn
Urine.....Fe>Zn>Cu>Pb>Mn

The concentrations of iron, copper, zinc, lead and manganese in urinary calculus are 114, 76, 365, 500 and 230 times, respectively, as much as those in urine. Zinc is the most abundant in urinary calculus just as copper is in a gallstone, and is considerably concentrated. These facts suggest the similar function of copper and zinc in the formation of gallstone and urinary calculus, respectively. Parsons[57] reported that $Zn_3(PO_4)_2 \cdot 4H_2O$ was found in urinary calculus by means of X-ray analysis. Although the content of lead in a urinary calculus or a gallstone is not always abundant compared with the other constituents, the rate of its concentration is the highest both in cases of urinary calculus (from urine) and gallstone (from bile). In a living body, lead is usually accumulated in the bone in which calcium salts are more abundant than in any other parts of the body. These results indicate the strict connection between lead and the formation of calculi which mainly consist of calcium salt, as suggested by Gerlach[41].

There are positive correlations between manganese and copper and between lead and zinc in a urinary calculus at the 95% confidence interval.

(3) *Pancreatic Calculus.*—Two reports were made by Schairer[44] and by Kobayashi et al.[58] in regard to the spectrographic analysis of the pancreatic calculus, but the determination of heavy metal constituents in them has not been made as yet.

Table VI indicates that a relatively greater quantity of contents of zinc and lead exists and that iron, copper and manganese are contained but in a very small quantity. Especially, zinc is the most abundant of all, and it is a matter of interest that this relates to the fact that *Insulin*[59]—which is well known as an organic compound that contains zinc in it—exists in the pancreas.

Both of the samples were composed mainly of calcium carbonate, while zinc is contained in *Carbonic anhydrase*[60] as a constituent, and these facts suggest the existence of some relation between zinc and the formation of a pancreatic calculus.

**3. Distribution of Inorganic Constituents between the Internal and the External Portion of a Gallstone.**—From the standpoint of mechanical structure, gallstones are classified into three types, radial, layer and a combination of the two.

Table XI shows the distribution of inorganic constituents in the internal and the external portions of three samples of gallstones which are typical ones having layer structures. The sample G-4011 consists of mineral stone (internal portion) and cholesterinpigment-calcium stone (external portion). Both the internal and the external portion of samples G-5019 and G-8004 consist of mineral stone and cholesterinpigment-calcium stone respectively. These results indicate, with a few exceptions in the case of calcium and phosphorus, that the internal portion is richer in inorganic constituents, especially heavy metals, than the external portion.

These layer structures demonstrate that the sedimentation circumstance is changed

52) C. P. Mathe and R. C. Archambeault, *Pacific Coast Med.*, **7**, 13 (1940); *C. A.*, **36**, 5538 (1942).
53) T. Sekimura, *Jap. J. Urol.*, **36**, 252 (1944).
54) M. M. Kovalev, *Klin. Med.*, **33**, No. 11, 54 (1955): *C. A.*, **50**, 7290 (1956).
55) T. Yokoyama, *J. Jap. Surg. Soc.*, **38**, 722 (1937).
56) M. Ishibashi, *J. Kurume Med. Assoc.*, **13**, 39 (1950).
57) J. Persons, *Science*, **118**, 217 (1953).
58) H. Kobayashi and Y. Yasumoto, *Medicine and Biology* (IGAKU-to-SEIBUTSUGAKU), **13**, 283 (1948).
59) A. M. Fischer and D. A. Scott, *Biochem. J.*, **29**, 1048 (1935).
60) D. Keilin and T. Mann, ibid., **34**, 1163 (1940).

TABLE XI

DISTRIBUTION OF INORGANIC CONSTITUENTS BETWEEN THE INTERNAL AND THE EXTERNAL PORTION OF HUMAN GALLSTONES

| Sample | | Ash, % | Ca mg./g. | Mg mg./g. | P mg./g. | Fe p.p.m. | Cu p.p.m. | Zn p.p.m. | Pb p.p.m. | Mn p.p.m. |
|---|---|---|---|---|---|---|---|---|---|---|
| G-4011 | Internal portion | 12.57 | 31.82 | 4.37 | 21.30 | 2,290 | 10,400 | 385 | 84 | 277 |
| | External portion | 6.95 | 34.92 | 3.27 | 4.77 | 61 | 281 | 116 | 46 | 33 |
| G-5019 | Internal portion | 9.08 | 45.84 | 3.90 | 5.28 | 373 | 2,440 | 574 | 95 | 118 |
| | External portion | 8.26 | 35.31 | 3.71 | 9.32 | 68 | 1,382 | 279 | 43 | 83 |
| G-8004 | Internal portion | 2.95 | 14.90 | 0.87 | 1.78 | 277 | 858 | 451 | 148 | 94 |
| | External portion | 1.33 | 5.37 | 0.42 | 1.82 | 71 | 255 | 149 | 51 | 55 |

at the time of the formation of a gallstone, and especially that the character of the internal portion has a direct connection with the reason why a calculus is formed. Although it is not easy to draw out a conclusion from the results of only three examples, from the above mentioned standpoint, it is interesting that the inorganic constituents, especially heavy metals, are abundant in the internal portion of a gallstone.

## Summary

Quantitative analyses of major constituents (calcium, magnesium, phosphorus, sodium and potassium) and heavy metal constituents (iron, copper, zinc, lead and manganese) were made on human stones (gallstone, urinary and pancreatic calculus) and their respective humours (blood, bile and urine). Then the distribution of these elements and the mutual relations present among them were discussed.

(1) According to the process of formation of gallstone (blood→bile→gallstone), the concentration of calcium, magnesium and phosphorus increases, while that of sodium and potassium decreases in case of major constituents, On the other hand, the concentration of heavy metal constituents, copper, zinc, lead and manganese increases. The concentration of iron decreases in the process of blood→bile and then increases again in the process of bile →a gallstone, whilst copper is extremely concentrated throughout these processes.

(2) In the process of urine→urinary calculus, each of major constituents increases; calcium, magnesium and phosphorus are extraordinarily concentrated, and heavy metal constituents also increase zinc is especially the most abundant of all. The correlation between lead and the calcification phenomenon in biological materials is observed, for lead indicates the highest concentration ratio in every case of gallstones (203 times that of bile) and urinary calculi (500 times that of urine).

(3) Pancreatic calculi differ greatly from the other stones, as their major constituents are calcium carbonate and they contain but little of the other constituents. Among heavy metals, zinc and lead are contained in a relatively high quantity; it seems that special connections exist between zinc and *Insulin* and between zinc and *Carbonic anhydrase*.

(4) The internal portion of a gallstone that is of layer structure contains a greater quantity of heavy metals than the external portion.

The author gratefully acknowledges the instruction of Dr. H. Hamaguchi, Professor of Tokyo University of Education, and also wishes to express his appreciation to Drs. E. Hamaguchi, Y. Iwai, I. Nakano, G. Taneda, Y. Tomita and T. Ueno for their assistance in obtaining some of the materials and instruments.

*Department of Chemistry, Faculty of Science, Tokyo Metropolitan University, Setagaya-ku Tokyo*

# *Studies on the Structure of Bisacetylacetone-Nickel(II) by the X-ray Powder Method*

By Shuzo SHIBATA

(Received May 30, 1957)

Pauling[1] proposed the tetrahedral configuration of bisacetylacetone-nickel(II) on the basis of the paramagnetic property of the complex with the aid of his theory. On the other hand, experiments[2,3] by electron diffraction of gas gave the result that the molecule assumes a planar configuration. If it is noted for this contradiction that the electron diffraction study dealt with free molecules at high temperature (about 170°), whereas the magnetic measurement was made on the solid at room temperature, it seems likely that the configuration of the molecule depends on the environment of a molecule*1.

According to the recent theoretical consideration[4], however, the magnetic data (paramagnetic) are not necessarily conclusive for the choice to be made between the tetrahedral and the planar arrangement. Therefore the X-ray method has been undertaken to afford a more direct evidence for the configuration of a bisacetylacetone-nickel(II) molecule in the solid state at room and high temperatures. Although X-ray analysis on single crystals is desirable for the complete determination of the structure of the molecule, it was difficult to prepare single crystals of an appropriate size of an anhydrous nickel complex. Therefore, investigations were carried out by the powder method. The powder patterns of nickel complex were compared with those of copper and zinc complexes.

## Experiments and Results

The powder photographs*2 of copper, nickel and zinc complexes were prepared by the use of Cu-K$\alpha$ radiation from the samples enclosed in a capillary tube made of glass. Samples recrystallized from ethanol were furnished by Dr. Sone. Anhydrous compounds were prepared by sublimation in vacuo; hydrates*3 were obtained by leaving them to stand in moist air. The patterns thus obtained are shown in Fig. 1.

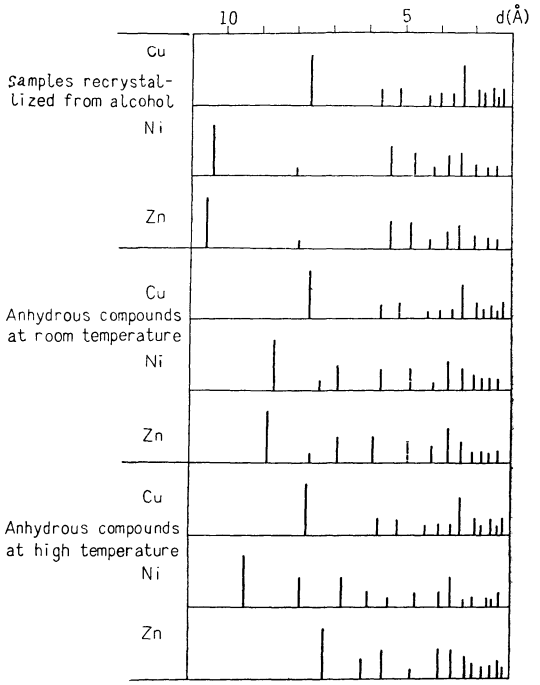



Fig. 1. The powder patterns of Cu, Ni and Zn acetylacetones.

1) Bisacetylacetone-copper(II). The sample recrystallized from ethanol and that sublimed in vacuo, both of which were dark blue in color, gave identical powder patterns. The sample heated up to about 200° also gave the same powder patterns.

2) Bisacetylacetone-nickel(II). The sample recrystallized from ethanol and the hydrate

1) L. Pauling, "Nature of the Chemical Bond", Cornell Univ. Press, Ithaca, (1948), p. 119.
2) S. Shibata, M. Kishita and M. Kubo, *Nature*, **179**, 320 (1957).
3) S. Shibata, This Bulletin, to be published shortly.
*1 From this point, magnetic measurements have been made on the solid at high temperature, but the results showed no indication of the change in magnetic moment with temperature. (Ref. 2).
4) D. P. Craig, A. Maccoll, R. S. Nyholm, L. E. Orgel and L. E. Sutton, *J. Chem. Soc.*, **1954**, 332; Y. Kuroda and K. Ito, *J. Chem. Soc. Japan, Pure Chem Sect.*, **76**, 762 (1954).

*2 The patterns of cobalt(II) complexes were also taken by the use of Fe-K$\alpha$ radiation. The results showed that pink hydrate and red-violet anhydrate were isomorphous with the corresponding nickel(II) complexes, respectively.
*3 Only the copper(II) complex was not hydrated and did not contain alcohol when it was recrystallized from an alcoholic solution.

thereof*4, both of which were blue in color, gave the identical patterns. On heating at about 130° the green color of the anhydrous compound changed into yellow-green, which color persisted up to about 170°. These two samples showed different powder patterns as shown in Fig. 1, suggesting that a change was taking place in the crystal structure. They are designated as the room and the high temperature modification, respectively. The green anhydrous compound (the room temperature modification) was readily hydrated in moist air, but the yellow-green anhydrous compound (the high temperature modification) was fairly stable even in moist air. The blue hydrate*5 was reversely converted into a green anhydrous compound at about 80°.

TABLE I
INTERPLANAR SPACINGS FROM POWDER PATTERNS*

| $Cu(C_5H_7O_2)_2$ | | $Ni(C_5H_7O_2)_2$ | | $Zn(C_5H_7O_2)_2$ | |
|---|---|---|---|---|---|
| $d$(Å) | I | $d$(Å) | I | $d$(Å) | I |
| 7.61 | vs | 8.66 | vs | 8.82 | vs |
| 5.66 | w | 7.41 | vw | 7.60 | vw |
| 5.14 | w | 6.82 | mw | 6.85 | m |
| 4.35 | vw | 5.67 | mw | 5.86 | mw |
| 3.99 | w | 4.80 | mw | 4.88 | mw |
| 3.60 | w | 4.18 | vw | 4.22 | w |
| 3.37 | ms | 3.78 | m | 3.73 | m |
| 2.94 | w | 3.39 | mw | 3.40 | mw |
| 2.78 | vw | 3.07 | w | 3.09 | w |
| 2.50 | w | 2.83 | w | 2.82 | w |
| 2.34 | vw | 2.61 | w | 2.63 | vw |
| 2.22 | w | 2.38 | w | 2.35 | w |
| 2.00 | w | | | | |

* The lines which may be due to an impurity such as a hydrate were not listed.

3) Bisacetylacetone-zinc(II). White bisacetylacetone-zinc(II) gave three different patterns i. e., one for the hydrate, which was found to be isomorphous with the hydrate of nickel complex, and two for the anhydrous compound. This behavior with changing temperature was quite similar to the case of bisacetylacetone-nickel(II).

## Discussion

The crystal structure of bisacetylacetone-copper(II) has already been determined by Koyama et al.[5] by X-ray analysis on a single crystal. The result showed that the complex takes a planar (square) configuration*6; a copper atom completes a distorted octahedron. On the other hand, the tetrahedral nature of four-covalent zinc(II) complexes is established from theoretical and experimental[6] basis. When the powder patterns of anhydrous copper, nickel and zinc complexes are compared with one another, the patterns of the room temperature modification of the nickel complex are clearly distinguishable from those of the copper complex, while it is essentially identical with those of the zinc complex. The interplanar spacings are listed in Table 1. Accordingly, it seems to be sure that the bisacetylacetone-nickel(II) has a tetrahedral configuration rather than a planar one, in agreement with the deduction by Pauling.

In order to investigate a possible change in the structure of bisacetylacetone-nickel (II) with temperature, the powder patterns of anhydrous copper, nickel and zinc complexes were taken at high temperature, but these patterns were different from one another. The pattern of high temperature modification of the anhydrous nickel complex seems to show a possibility of the change in the molecular structure of this complex, but does not simply permit a choice between a tetrahedral and planar coordination.

Recently Bullen[7] investigated the crystal structure of anhydrous bisacetylacetone-nickel(II) by X-ray analysis on a single crystal, determined the lattice constants, and reported the presence of trinuclear molecules in the crystal. Although he did not definitely elucidate the molecular structure of the complex, the short distance between nickel atoms would favor the planar configuration of the complex. On the other hand, it was found that the interplanar spacings calculated by the use of his lattice constants are more consistent with those of the high temperature modification than with those of room temperature modification of this complex. Therefore, it is possible that the nickel complex of the high temperature modification may have the planar configuration, although the determination is not complete. If this

*4 Experiments showed that the hydrate contains two molecules of water per one molecule of the complex.

*5 It seems likely that, in the hydrate, water molecules are loosely coordinated to metal atoms and presumably from an octahedral configuration about the central metal atom with other ligand atoms and are easily removed on drying at high temperature.

5) H. Koyama, Y. Saito and H. Kuroya, *Journal of the Institute of Polytechnics, Osaka City University*, **4**, Series C, 43, (1953).

*6 The square planar configuration of a free molecule of bisacetylacetone-copper(II) has been indicated also by electron diffraction investigation. (S. Shibata and K. Sone, This Bulletin, **29**, 852 (1956)).

6) A. E. Martell and M. Calvin, "Chemistry of the Metal Chelate Compounds", Prentice-Hall, New York, (1952), p. 245. J. C. I. Liu and J. C. Bailar, *J. Am. Chem. Soc.*, **73**, 5432 (1951); H. Koyama and Y. Saito, This Bulletin, **27**, 113 (1954).

7) G. J. Bullen, *Nature*, **117**, 537 (1956).

is the case, this fact indicates that the configuration of bisacetylacetone-nickel(II) varies with temperature.

## Conclusion

X-ray powder pattern method led to the result that four-covalent bisacetylacetone-nickel(II) takes a tetrahedral configuration in agreement with the presumption of Pauling. On the other hand, a previous experiment by electron diffraction showed that the free molecule of this complex has a planar configuration. Thus, these experimental evidences lead to the following interesting inference: the configuration of anhydrous bisacetylacetone-nickel(II) varies with the change of the phase from gas to solid (or with temperature). This is evidently due to the fact that the energy difference between the tetrahedral and planar configuration is quite small.

The author wishes to thank Professor M. Kubo for his helpful advice. The author's thanks are also due to Dr. M. Yokoi and Dr. Y. Kainuma for their help in carrying out the experiments and for valuable suggestions throughout the present investigation and also to Dr. K. Sone for providing the materials.

*Department of Chemistry*
*Faculty of Science*
*Nagoya University*
*Chikusa, Nagoya*

# *Hydrolysis of Carbohydrates in the Presence of Hydrochloric Acid or Acidic Ion-exchange Resins*

By Shōzō KAICHI

(Received May 7, 1957)

There have been several reports concerning the effect of the size of ion-exchange resin catalyst on the rate of organic reactions; e. g., esterification of oleic acid[1], hydrolyses of sucrose[2] and lower esters[3], and iodine-acetone reaction[4]. None of these investigators, however, has given any general quantitative conclusion theoretically supported. The present study is concerned with the development of this subject. First, the result of the hydrolysis of potato amylose and sucrose is shown in this paper. The amylose was chosen because of its high molecular weight and sucrose because of its low molecular weight.

## Experimental

**Preparation of Amylose.**—A modified procedure[5] of K. H. Meyer's method was employed. That is, the amylose in potato starch was extracted into hot water (70°C), precipitated with *n*-butanol, dissolved once more into hot water (60°C), reprecipitated with ethanol and then dried at 70°C to a constant weight. The yield from 250 g. starch was 15 g.

**Molecular Weight and Purity of Amylose.**—The number average degree of polymerization of the amylose was measured by K. H. Meyer's method[6] (3, 5-dinitrosalicylic acid method) and found to be $175 \pm 10$. Hence the number average molecular weight was $(3.2 \pm 0.2) \times 10^4$. The absorption maximum of the amylose-iodine complex, prepared according to R. M. Mc Cready's method[7], was 625 m$\mu$, which agreed well with R. E. Rundle's[8] result (626 m$\mu$, for potato amylose). Hence the purity of the amylose was high enough to carry out this work.

**Sucrose.**—Twenty % aqueous solution of commercial crystalline sugar, demineralized by means of ion-exchanger, was used.

**Ion-Exchange Resins.**—Strongly acidic ion-exchange resin Amberlite IR-120, conditioned and washed, was fractionated into ten portions according to the grain size. The six larger fractions were prepared by a combined process of sieving and sedimentation of the original spherical resins. The four smaller fractions were

1) C. L. Levesque and A. M. Craig, *Ind. Eng. Chem.*, **40**, 96 (1948).
2) G. Bodamer and R. Kunin, ibid., **43**, 1082 (1951).
3) L. P. Hammett, et al., *J. Am. Chem. Soc.*, **71**, 1284 (1949), ibid., **75**, 1788, 5834 (1953).
4) S. L. Bafna, *J. Phys. Chem.*, **59**, 1199 (1955).
5) E. Husemann und R. Resz, *J. Polymer Sci.*, **19**, 397 (1956).
6) K. H. Meyer, *J. Phys. Colloid Chem.*, **53**, 319 (1949); J. Nikuni, *Starch Chemistry (in Japanese)*, Asakura-shoten Ltd., Tokyo, Japan (1951), p. 359.
7) R. M. McCready and W. Z. Hassid, *J. Am. Chem. Soc.*, **65**, 1154 (1943).
8) R. E. Rundle, ibid., **66**, 111 (1944).

prepared by sedimentation of pulverized resins. The average radius ($R$) of each fraction was determined microscopically according to the formula (1),

$$R=\bar{d}/2=\sum nd^3/2\sum nd^2 \quad (1)$$

where $d$ is the horizontal diameter of each particle, $n$ is the number of particles, and $\bar{d}$ is the average diameter. The values of $R$ were found to be 482, 418, 332, 300, 219, 191, 56.9, 37.2, 26.8 and 17.5 $\mu$ respectively.

**Hydrolysis of Amylose** (hydrochloric acid catalyst). — Two % amylose solution in N-sodium hydroxide was acidified with hydrochloric acid and stirred in a sealed vessel at 65±0.1°C. After every five minutes, a portion of the reaction mixture was taken out and neutralized with alkali to stop the reaction. This neutral solution was used for both preparation of the starch-iodine complex and determination of the number average degree of polymerization ($P_n$). The starch-iodine complex was prepared by the Mc Cready's method[7]. $P_n$ was determined according to the Meyer's method[6], using glucose as a standard.

**Hydrolysis of Amylose** (pulverized resin catalyst) — Two % amylose solution in N-sodium hydroxide was demineralized with ion-exchange resins, added to a known volume of resin suspension containing a known weight of pulverized resin, and then stirred at 65±0.1°C. After a given period, the reaction mixture was quickly filtered to remove the resin. The filtrate was used for both preparation of starch-iodine complex and determination of $P_n$.

**Hydrolysis of Sucrose.**—The demineralized 20% sucrose solution was mixed with catalyst (conc. hydrochloric acid, pulverized resin suspension, or swollen spherical resin filtered to remove the extra water) and stirred in a sealed vessel at 50±0.1°C. The stirring velocity was kept within a range of 500—550 r. p. m. and did not affect the reaction rate. After a given period, a portion of the reaction mixture was taken out to measure the optical rotation ($\alpha$) by a saccharimeter. The $\alpha$ value at complete hydrolysis was also measured ($\alpha_\infty$). When $\ln(\alpha-\alpha_\infty)$ were plotted against $t$ (reaction time), straight lines were obtained, the slopes indicating the rate constants $k$ according to the formula (2).

$$kt=\ln(\alpha-\alpha_\infty)+const. \quad (2)$$

## Results and Discussions

### Hydrolysis of Amylose

*i. N-Hydrochloric acid catalyst*—Amylose was easily hydrolysed at 65°C. Both $P_n$ of the hydrolyzate (Table I) and the absorption spectrum of the hydrolyzate-iodine complex (Fig. 1) changed with time. The relation between the wave length of the absorption maximum and $P_n$ was nearly in harmony with that in the case of synthetic dextrins worked by Swanson[9] (Table II), showing that the mechanism of hydrolysis was just the inverse of synthesis. The mean rate constants through time $0\sim t$ ($k$ in Table II) were computed, applying Ekenstam's[10] equation (3) of random degradation.

$$\ln[1-P_n(t)^{-1}]=\ln[1-P_n(0)^{-1}]-kt \quad (3)$$

$k$ increased as the reaction proceeded, resembling Freudenberg's[11] result of hydrolysis of soluble starch in 50% sulfuric acid.

TABLE I

HYDROLYSIS OF AMYLOSE (HCl CAT.)

| Time (min.) | $-\log T$ [a] | $P_n$ | $k\times10^4$ (min.$^{-1}$) |
|---|---|---|---|
| 0 | 0.010 | 175±10 | — |
| 5 | 0.062 | 95± 3 | 4.3±0.5 |
| 10 | 0.144 | 55± 1 | 5.5±0.3 |
| 15 | 0.170 | 49± 1 | 4.3±0.2 |
| 20 | 0.303 | 31.2±0.3 | 5.9±0.2 |
| 25 | 0.355 | 27.0±0.2 | 6.0±0.1 |
| 30 | 0.450 | 21.9±0.1 | 6.0±0.1 |
| 35 | 0.575 | 17.5±0.1 | 6.6±0.1 |

a) $T$ is the transmission coeff. of sample soln. treated with 3,5-dinitrosalicylic acid, at the wave length of 525 m$\mu$. Sugar concentration was 1.67 % concerning the original amylose.

TABLE II

ABSORPTION MAXIMA OF STARCH-IODINE COMPLEXES

| $P_n$ | Wave length (m$\mu$) D[a] | A[a] |
|---|---|---|
| 7.4 | 500 | |
| 12.9 | 520 | |
| 17.5±0.1 | | 550 |
| 18.3 | 540 | |
| 20.2 | 560 | |
| 27.0±0.2 | | 560 |
| 29.3 | 580 | |
| 34.7 | 580 | |
| 49±1 | | 585 |
| 55.6 | 600 | |
| 95±3 | | 600 |
| 97.4 | 600 | |
| 146.5 | 600 | |
| 175±10 | | 625 |

a) D: Synthetic dextrins by Swanson[9].
A: Hydrolyzed amyloses by the author.

9) M. A. Swanson, *J. Biol. Chem.*, **172**, 825 (1948); J. Nikuni, *Starch Cecmistry*, Asakura-shoten Ltd., Tokyo, Japan (1951), p. 57.
10) A. af Ekenstam, *Ber.*, **69**, 540, 553 (1936).
11) K. Freudenberg, et al., *Ber.*, **63**, 1519 (1930).

TABLE III
HYDROLYSIS OF AMYLOSE (RESIN CAT.)

| Resin | Time (min.) | Ppt.[c] | $-\log T$ |
|---|---|---|---|
| $R=17.5\mu$[a] | 0 | − | 0.002 |
| | 30 | − | 0.004 |
| | 60 | − | 0.003 |
| | 94 | − | 0.005 |
| | 124 | + | — |
| original[b], unfractionated | 0 | − | 0.004 |
| | 10 | − | 0.004 |
| | 30 | − | 0.004 |
| | 40 | + | — |

a), b): Sugar concentrations of the sample solutions were 1.33% and 2.00%, respectively.
c) Ppt. of retrograded amylose.

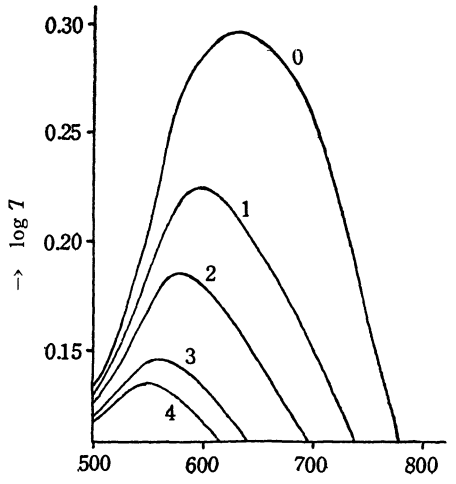



Fig. 1. Absorption spectra of iodine-hydrolyzed amylose complexes.

| No. | 0 | 1 | 2 | 3 | 4 |
|---|---|---|---|---|---|
| Reaction time (min.) | 0 | 5 | 15 | 25 | 35 |

*ii. resin catalyst.* — The resin of the smallest size ($R=17.5\,\mu$) was used at a concentration of nearly 0.02 equivalent per liter and caused no significant change in either the transmission coefficient of solution for measurement of $P_n$ (Table III) or the absorption maximum of tho iodine complex. There seemed to be, therefore, no significant hydrolysis even at the end of 94 min. at 65°C. Several other experiments, using resins of a larger size at concentrations up to one equivalent per liter, also showed no proof of hydrolysis. One of these data is also shown in Table III.

*iii. Comparison of hydrochloric acid and resin catalyst.*—These experimental results show that the efficiency of resin catalyst is negligibly small as compared with hydrochloric acid in the case of hydrolysis of amylose. It is more desirable to compare their efficiencies numerically. But unfortunately it is impossible in this study.

**Hydrolysis of Sucrose.** — Sucrose was easily hydrolyzed by means of resin catalysts at 50°C and the first order rate constants ($k$) were obtained. The second order rate constants ($k'$) were computed according to the formula (4),

$$k'=k/\rho H=kV/A \qquad (4)$$

where $\rho$ is the volume ratio of swollen resin and the outer solution, $H$ the exchange capacity per unit volume of the resin, $V$ the total volume of the solution, and $A$ the total exchange capacity of the resin catalyst.

The relationships $k'\sim R$ and $k'\sim 1/R$ are shown in Fig. 2. If the rate were proportional to the surface area of the catalyst, $k'\sim 1/R$ curve would be a straight line passing through the original point. Though the curve in Fig. 2 does not agree with this, it is inclined to approach a linear figure near the original point ($R\to\infty$). On the other hand, if the rate were proportional to the volume of resin phase, $k'\sim 1/R$ curve would be a straight line parallel to the $1/R$ axis. The curve in Fig. 2 does not agree with this, either. But it seems probable that the curve approaches a linear horizontal line as $R$ approaches zero.

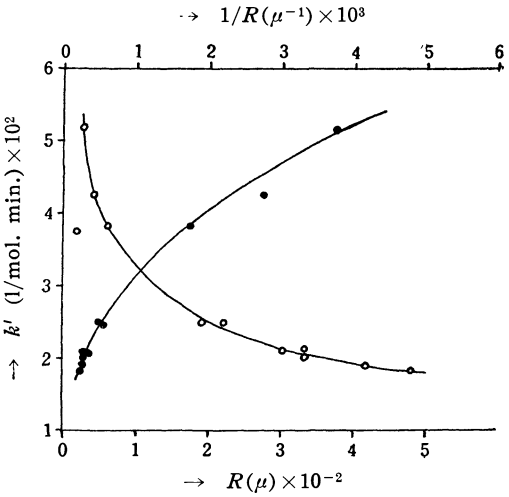



Fig. 2. $k'\sim R$, $k'\sim 1/R$ Curves.

At any rate, $R$ and $k'$ are related in a mediate way between the afore-mentioned two extremes. It is concluded that neither the surface only nor the whole resin phase uniformly acts as catalyst, but the real is

a compromise. This is a proof that the overall rate is largely affected by the diffusion rate of sucrose in the resin. This knowledge will be valuable in studying the theoretical expression of the overall rate.

In the case of hydrochloric acid catalyst, $k$ was directly proportional to the concentration of the acid. The proportionality constant (equals $k'$, because $\rho=1$) was found to be 0.104 l/mol. min. at 50°C, which was greater than $k'$ of any resin catalyst.

## Summary

Potato amylose and sucrose were hydrolyzed in the presence of hydrochloric acid or acidic ion-exchange resin catalyst. In hydrolysis of amylose at 65°C, the efficiency of resin catalysts was negligibly small as compared with that of hydrochloric acid. In hydrolysis of sucrose at 50°C, the efficiency of resin catalysts was less than that of hydrochloric acid and different according to their sizes. The relation between the average radius and the rate constant was obtained in a broader range than ever.

This work was supported by a grant-in-aid for Development of Scientific Research (1956) from the Ministry of Education. The author would like to thank Professor I. Kagawa for his encouragement. Thanks are also due Mr. T. Kainuma for his aid in carrying out the experiment.

*Department of Industrial Chemistry*
*Faculty of Engineering*
*Shizuoka University, Oiwake, Hamamatsu*

# *Spectrophotometric Method for the Determination of Small Amounts of Sulfate Ions*

By Iwaji IWASAKI, Satori UTSUMI, Ken HAGINO, Toshikazu TARUTANI and Takejiro OZAWA

(Received February 28, 1957)

A more rapid and accurate method for determining sulfate of low concentration in natural waters is desirable. An indirect colorimetric determination of sulfate, using solid barium chromate and diphenylcarbazide was previously reported by us[1]. However, this method can only be applied to the determination in the range 0.2 to 10 p. p. m. Recently, T. Kato, Y. Nomizo and K. Shinra[2] studied a photometric method of determination of 2 to 120 p. p. m. of sulfate using a perchloric acid solution of barium chromate and ammonia. The authors have devised an improved method for the determination of sulfate over the range 0.3 to 100 p. p. m., using barium chromate suspended in an acid solution.

## Experimental Results and Discussion

### Reagents

(1) *Standard solution of sulfate* (1,000 p. p. m. $SO_4^{2-}$): — Recrystallized potassium sulfate (guaranteed reagent) 1.815 g. is dissolved and diluted to 1 l. with distilled water. Solutions of various concentrations can be prepared by diluting this stock solution. All solutions are stored in polyethylene bottles.

(2) *Barium chromate suspension.*—One hundred cc. of a hot solution of barium chloride containing 10 g. of $BaCl_2$-$2H_2O$ is added slowly to 800 cc. of a hot solution of potassium chromate containing 8 g. of $K_2CrO_4$ to obtain a yellow precipitate of barium chromate. This precipitate is washed three times by decantation with about 500 cc. portions of hot water, dissolved in 100 cc. of hot 2 M hydrochloric acid, and diluted to 700 cc. with hot water. A 105~110 cc. portion of 2 M ammonia water is added slowly in order to reprecipitate the barium chromate. The precipitate thus obtained is washed again in the same way as mentioned above, and after drying at 105°C for about one hour, it is pulverized in an agate motar. Barium chromate suspension is prepared by adding 2.5 g. of the barium chromate in 200 cc. of the aqueous solution consisting of 0.5 M acetic acid and 0.01 M hydrochloric acid. The pH of this suspension is about 2.4. The reagent is stored in a polyethylene bottle.

(3) *Ammonia water containing calcium ions.*—

1) I. Iwasaki, S. Utsumi and T. Tarutani, *J. Chem. Soc. Japan, Pure Chem. Sec.*, **74**, 400 (1953).
2) T. Kato, Y. Nomizo and K. Shinra, ibib., **76**, 373 (1955).

The reagent is prepared by dissolving 1.85 g. of $CaCl_2 \cdot 2H_2O$ in 500 cc. of purified 6 M ammonia water (1 mg. $Ca^{2+}$/cc.). The solution is stored in a container shown in Fig. 1.

(4) *Diphenylcarbazide reagent.*—The reagent is prepared by dissolving 1 g. of diphenylcarbazide in a mixture of 100 cc. of ethanol and 1 cc. of 1 M hydrochloric acid. This reagent is stable for 2~3 weeks in a brown bottle.

(5) Ethanol (guaranteed reagent) is used after being purified by distillation.

(6) Hydrochloric acid (6 M).

**Apparatus**

(1) Measurements were carried out with the Hitachi Type E. P. U. 2 spectrophotometer and with 5 mm. absorption cells.

(2) Centrifuge (about 4,000 r. p. m.).

(3) Glass filter (15 cc., No. 4),

(4) Centrifuge tube (15 cc.) with a glass stopper[3].

(5) Apparatus for storing ammonia water. To keep ammonia water free from carbon dioxide in the air, a polyethylene bottle attached with a buret and two soda-lime tubes as shown in Fig. 1 was used.

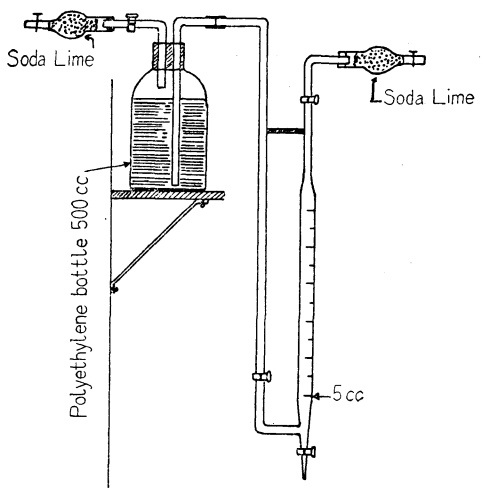



Fig. 1. Apparatus for storing ammonia water.

**Procedure**

Pipet 5 cc. of a sample solution into a centrifuge tube, add 2 cc. of a uniformly suspended solution of barium chromate and mix. After standing for 2~3 minutes, add 0.5 cc. of ammonia water containing calcium ions and mix. Add 5 cc. of ethanol and shake for about one minute (pH of the solution is about 9.8). Let the mixture stand for about ten minutes.

When the sulfate concentration of a sample solution is higher than 20 p. p. m., measure the absorbance of the supernatant solution at 370 mμ directly after the centrifugation (Procedure A).

For the cases of concentration lower than 20 p. p. m., filter the supernatant solution of the centrifugate gradually through a glass filter, add 1 cc. of diphenylcarbazide reagent and 0.7 cc. of 6 N hydrochloric acid to the filtrate and mix well. After five minutes, measure the absorbance of this violet colored solution at 545 mμ (Procedure B).

**Absorption Spectral Curves**

The absorption of the yellow color due to the chromate ion replaced in the solution was measured over the wave length range 230 to 450 mμ. The absorption spectral curve is shown in Fig. 2, in which there are two absorption maxima at about 275 mμ and 370 mμ.

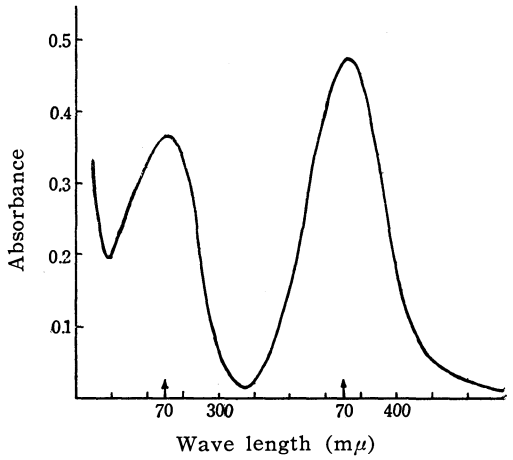



Fig. 2. Absorption spectral curve of chromate.

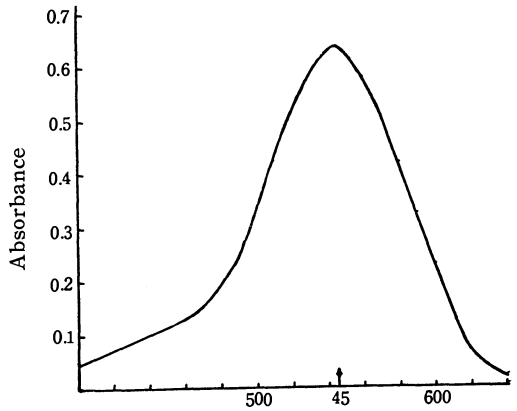



Fig. 3. Absorption spectral curve of Cr(VI)-Diphenylcarbazide.

The chromate ion reacted with diphenylcarbazide in an acidified solution to give a violet coloration. The absorption of the violet color was measured over the range 400 to 640 mμ, as shown in Fig. 3, in which there is one absorption maximum at about 545 mμ.

3) S. Utsumi, *J. Chem. Soc. Japan, Pure Chem. Sect.*, **74**, 35 (1953).

The maximum color development of the solution(chromium(VI)-diphenylcarbazide) was obtained after letting it stand for five minutes at room temperature. The violet color was stable for a long time.

**Calibration Curves**

(1) *For concentrations lower than 20 p. p. m. of sulfate.* — The calibration curve(I) shown in Fig. 4 was obtained by Procedure B with standard sulfate solutions of known concentration. The absorbance and the concentration were in a good linear relationship for the range 2 to 20 p. p. m. $SO_4^{2-}$, but were not good for concentrations lower than 2 p. p. m.

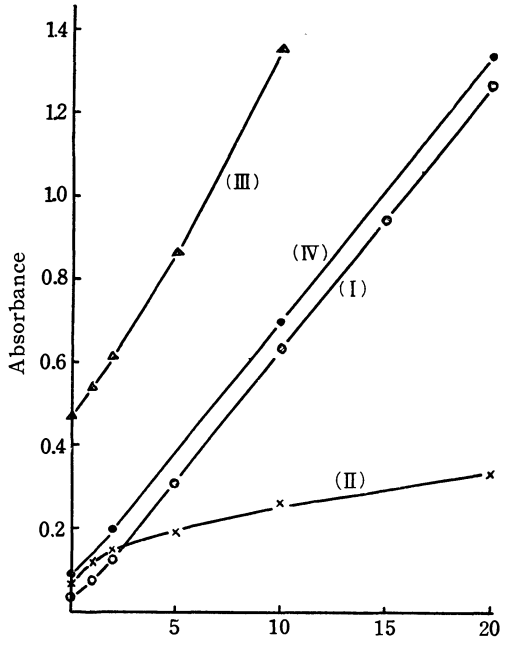



Fig. 4. Calibration curves at 545 mμ, 5 mm cells.

The calibration curve had to be renewed whenever solid barium chromate was newly prepared. In order to obtain reproducible results, it was necessary to use barium chromate suspension which had been stored for a few days after preparation.

When a blank test was made with redistilled water, a faint coloration appeared. The absorbance of the blank test solution was small and constant. The lowest concentration of sulfate, whose coloration could be distinguished from that of the blank test was 0.3 p. p. m. $SO_4^{2-}$ ($3.1 \times 10^{-6}$ $M/l$).

The calibration curve(I) shown in Fig. 4 was reproducible within the error of ±0.2 p. p. m. $SO_4^{2-}$. Thus, the method may be available for determining sulfate over the range from 0.3 to 20 p. p. m.

(2) *For concentrations higher than 20 p. p. m.* $SO_4^{2-}$.—The calibration curve shown in Fig. 5 was obtained by Procedure A using standard sulfate solutions.

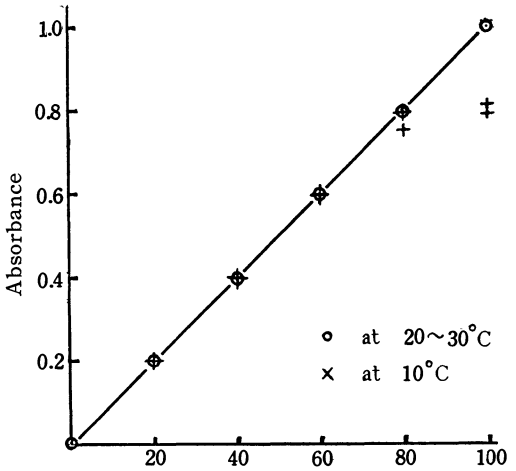



Fig. 5. Calibration curve at 370 mμ, 5 mm cells.

As can be seen in Fig. 5, Beer's law was conformable up to 100 p. p. m. and 70—80 p. p. m. of sulfate respectively at 20—30°C and 10°C. Since barium chromate was more soluble at higher temperatures and hence a sufficient amount of barium ion was available for the precipitation of barium sulfate, it seemed that sulfate of higher concentrations could be determined at higher temperatures.

The absorbance of the blank solution was negligible. The calibration curve was reproducible within 1%.

**Conditions for the Analysis**

(1) *Reasons for the use of barium chromate suspension.*—When a dilute solution of barium chromate in acidic medium was used instead of its suspension, there was a tendency to form a colloidal solution after the addition of ammonia water. Moreover, the calibration curve was not reproducible. For an accurate determination of a small amount of sulfate, the use of barium chromate suspension was better than that of its solution, because particles of barium chromate in the suspension carried colloidal precipitates of barium

chromate, formed by the addition of ammonia water.

(2) *Influence of acids in barium chromate suspension on the determination of sulfate.* —When a barium chromate suspended in distilled water was used in Procedure B, instead of the suspension mentioned above, the calibration curve(II) as shown in Fig. 4 was obtained, which was not linear with respect to the concentration. When a barium chromate suspended in 0.5 M acetic acid was used, sulfate ions could be determined only up to the concentration of 40—50 p. p. m. at 20—30°C (Procedure A).

On the other hand, when a barium chromate suspended in 0.01 M hydrochloric acid was used, the clear solution, once obtained after the addition of ammonia water containing calcium ion followed by centrifugation, gradually became turbid owing to the formation of calcium carbonate with carbon dioxide in the air.

(3) *Effect of the amounts of barium chromate.*—It was found that the coincident results were obtained by the use of between 2 to 3 g. of reprecipitated barium chromate in 200 cc. of the acid solution (0.5 M acetic and 0.01 M hydrochloric acid). Therefore, the authors would like to recommend the use of 2.5 g. of barium chromate.

(4) *Effect of alcohol.* — Since barium chromate was much less soluble in ethyl alcohol than in water, the influence of ethanol upon the determination of sulfate was examined. The experiment was carried out under the following conditions: 10 cc. of a sample solution was pipetted into a centrifuge tube, then 2 cc. of barium chromate suspension was added and mixed. After being set aside for 2—3 minutes, 0.5 cc. of ammonia water containing calcium ions was added and shaken for about one minute without ethanol. The subsequent treatment was done in the same way as procedure B, by which the calibration curve(III) in Fig. 4 was obtained. Not only was the absorbance of the blank solution larger owing to the greater solubility of barium chromate, but the calibration curve did not give a linear relationship, bending upward though slightly.

In order to decrease the solubility of barium chromate, 5 cc. of ethanol was used for 5 cc. of the sample solution.

(5) *Effect of the calcium ion in ammonia water.*—Since barium carbonate was also difficultly soluble, the absorbance would be considerably affected by the presence of carbonate in ammonia water. Without calcium ions, calibration curve(IV) shown in Fig. 4 was obtained. The curve was influenced by the concentration of carbonate in ammonia water. In order to remove the dissolved carbonate, the authors recommend the addition of some calcium ions into the ammonia water.

(6) *Effect of temperature.* — Since the concentration range of determination was affected by temperature, as shown in Fig. 5, it was desirable to carry out Procedure A at 20—30°C in order to determine the sulfate up to 100 p. p. m. satisfactorily. On the other hand, in the case of Procedure B the effect of temperature was negligible.

**Influence of Various Ions.**

The effect of different kinds of ion on this method was examined in the presence of 10 p. p. m. $SO_4^{2-}$ and in its absence. The experimental results were summarized as follows.

(1) Neither sodium nor chloride ions interfere even when present in the amount of 5,000 p. p. m.

(2) One thousand p. p. m. of potassium or ammonium ions do not interfere, but 5,000 p. p. m. of each ion gives lower results.

(3) One thousand p. p. m. of perchlorate and 50 p. p. m. of silicate ions have no effect.

(4) The presence of nitrate ions gives somewhat higher results at 50 p. p. m. and considerably higher results at 1,000 p.p.m.

(5) The presence of carbonate or bicarbonate does not interfere at 50 p.p.m. but at 100 p. p. m. slightly higher results are obtained. When larger amounts of these substances are present, it is necessary to remove them beforehand. Carbonate (or bicarbonate) can easily be expelled by boiling a sample solution for a short time after neutralization with dilute hydrochloric acid. The necessary amount of hydrochloric acid may be determined by neutralizing an aliquot portion of the same sample, using methyl orange as indicator.

(6) Neither 100 p. p. m. of magnesium or calcium ions, nor 10 p. p. m. of strontium ion interfere.

(7) Each 10 p. p. m. of $Ag^+$, $Zn^{2+}$, $Hg^{2+}$, $Fe^{3+}$, $Al^{3+}$ or $Mn^{2+}$ ions does not interfere.

(8) Since lead chromate is difficultly soluble, lead ions interfere even in small amounts.

(9) As the copper ion also reacts with diphenylcarbazide, the presence of copper is undesirable. When the copper ion is present in a sample solution, 0.1 cc. of E·

D. T. A. (0.2 M) should be added before the addition of diphenylcarbazide.

(10) Phosphate, vanadate and selenate give remarkably higher results even in small amounts, because barium salts of these anions are also insoluble in water.

(11) Also arsenate, molybdate, selenite and thiosulfate give some interference even at 10 p. p. m.

However, the undesirable substances described above are not usually contained in common natural waters (rain water, river water etc.) in such concentrations as would give a serious error, therefore this rapid analytical method of sulfate may be applicable to the ordinary water analysis with satisfactory results.

**Summary**

The authors have devised a new method for the determination of small amounts of sulfate. Sulfate is precipitated as barium sulfate using barium chromate suspension in an acid solution (0.5 M acetic, 0.01 M hydrochloric acid), and the excess of barium is almost completely precipitated as barium chromate by adding ammonia water (containing calcium ion) and ethanol. Finally the amount of chromate which is exchanged with sulfate is estimated.

The proposed method may be applicable to the determination of 0.3—100 p. p. m. sulfate with satisfactory results.

*Laboratory of Analytical Chemistry and Geochemistry, Tokyo Institute of Technology, Ookayama Meguro-ku, Tokyo*

# *Stoichiometric Investigations of the Liquid State. V*[*1]. *Vaporization Phenomenon of Associated Liquids*

By Kiyoshi TYUZYO[*2]

(Received May 9, 1957)

Reasonablesness of classifying associated liquids in two kinds was discussed in the previous paper[1]. In that paper, a method for determining the degree of association of associated liquid of the first kind from viscous flow was proposed and the association state was discussed in detail.

In this paper, a method for determining the degree of association from energy of vaporization and a method for calculating energy of hydrogen bond are proposed.

## Energy of vaporization of *n*-paraffin

Relation between energy of vaporization at boiling point of *n*-paraffin ($E_{vap,b}$ in Kcal./mole) and molar volume at room temperature ($V$ in cc./mole) is shown in Fig. 1. The following equation is established approximately in the range of $V$ larger than 250.

$$E_{vap,b}=16\log V-28.4 \qquad (1)$$

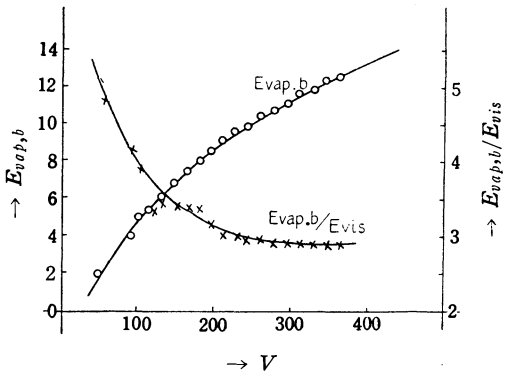



Fig. 1. $E_{vap,b}$ and $E_{vap,b}/E_{vis}$ vs. $V$ of *n*-paraffins.

Relation between $E_{vap,b}/E_{vis}$ and $V$ is shown in Fig. 1. This ratio decreases with increase in $V$ and converges to about 2.8. $\log(E_{vap,b}/E_{vis}-2.80)$ vs. $\log V$ is approximately linear as is shown in Fig. 2. Eq. 2 is established from this.

$$E_{vap,b}/E_{vis}=2.80+(100/V)^2 \qquad (2)$$

This equation is applicable at least in the range of $V$ from 60 to 370. According

*1) The fourth paper of this series, This Bulletin, **30**, 782 (1957).

*2) Present address, Research Laboratory, Dai-Nippon Celluloid Co., Sakai, Osaka

1) K. Tyuzyo, This Bulltein, **30**, 782 (1957).

to Eyring et al.[2], $E_{vap,b}/E_{vis}$ is about 3.5 for unassociated liquid, but this relation is not established rigorously as is shown in Fig. 1.

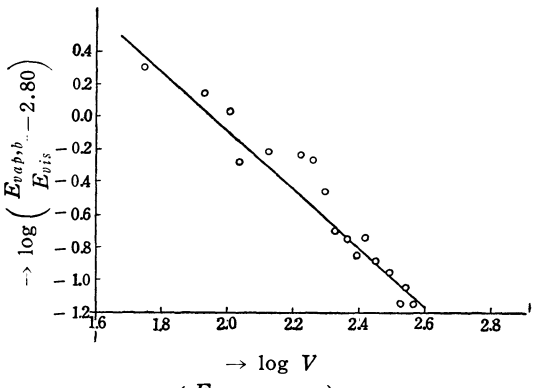



Fig. 2. $\log\left(\frac{E_{vap,b}}{E_{vis}}-2.80\right)$ vs. $\log V$ of $n$-paraffins.

## Method for calculating degree of association of associated liquids of the first kind from energy of vaporization

Viscous flow of associated liquids of the first kind is closely analogous to that of $n$-paraffin as is shown in the previous paper. Therefore, if an associated body transfers from liquid to vapor phase without dissociation during vaporization, eq. 1 may be established between molar volume of associated body and energy of vaporization of this process. At the same time, eq. 2 may be established among this energy of vaporization, molar volume of associated body and energy of activation of viscous flow. Namely, when the molar volume of an associated body and the energy of vaporization of this process are respectively termed as $V_a$ (cc/mole) and $E_{vap,a}$ (Kcal./mole), then

$$E_{vap,a}=f(V_a)$$
$$=16\log V_a-28.4 \quad \text{for } V_a>250 \qquad (3)$$
$$E_{vap,a}=E_{vis}\cdot[2.80+(100/V_a)^2] \qquad (4)$$
$$V_a=n\times V \qquad (5)$$

where $n$ is degree of association and $V$ is normal molar volume.

$V_a$ satisfying both eq. 3 and 4 can be obtained as is shown in Fig. 3. In the figure, curve-(a) is common for all associated liquids of the first kind and is expressed by eq. 3. Curve-(b) is characteristic for each associated liquid and is expressed by eq. 4. $V_a$ is obtained from intersecting point of curve-(a) and (b). Then $n$ is calculated from eq. 5.

Degree of association obtained from this method is termed as $n_v$ and given in Table I. In the Table, $n$ values from literature are also shown. It is clear from

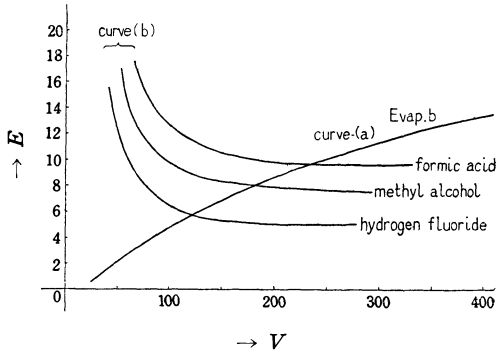



Fig. 3. Calculation of degree of association of formic acid, methanol and hydrogen fluoride.

TABLE I
DEGREE OF ASSOCIATION CALCULATED FROM EQ. 3 AND 4

| Substance | $V$ | $V_v$ | $n_v$ | $n$ |
|---|---|---|---|---|
| saturated fatty acids | | | | |
| formic acid | 37.7 | 246 | 6.5 | polymer |
| acetic acid | 57.2 | 186 | 3.3 | polymer |
| propionic acid | 74.6 | 173 | 2.3 | 2 |
| $n$-butylic acid | 91.9 | 198 | 2.2 | 〃 |
| $n$-valeric acid | 108.7 | 238 | 2.2 | 〃 |
| $n$-caproic acid | 125.0 | 270 | 2.2 | 〃 |
| $n$-heptylic acid | 141.9 | 296 | 2.1 | 〃 |
| $n$-caprylic acid | 158.6 | 336 | 2.1 | 〃 |
| $n$-pelargonic acid | 174.5 | 394 | 2.2 | 〃 |
| $n$-capric acid | 196.2 | 423 | 2.2 | 〃 |
| $n$-lauric acid | 229.8 | 482 | 2.1 | 〃 |
| $n$-myristic acid | 270.4 | 523 | 1.9 | 〃 |
| $n$-palmitic acid | 304.6 | 564 | 1.9 | 〃 |
| $n$-stearic acid | 338.9 | 603 | 1.8 | 〃 |
| saturated aliphatic alcohols | | | | |
| methanol | 40.5 | 182 | 4.5 | 5.0 |
| ethanol | 58.3 | 270 | 4.6 | 4.7 |
| propanol | 75.0 | 367 | 4.9 | 4.7 |
| $n$-butanol | 92.0 | 403 | 4.4 | — |
| $n$-pentanol | 107.7 | 500 | 4.6 | — |
| $n$-hexanol | 125.2 | 534 | 4.3 | — |
| $n$-heptanol | 140.7 | 606 | 4.3 | — |
| $n$-octanol | 156.7 | 673 | 4.3 | — |
| $n$-cetanol | 285 | (955) | 3.4 | — |
| others | | | | |
| hydrogen cyanide | 38.5 | 118 | 3.1 | 3 |
| hydrogen fluoride | 20.4 | 122 | 6.0 | 6～10 |
| formamide | 39.9 | 328 | 8.2 | — |

2) H. Eyring, *J. Chem. Phys.*, **4**, 283 (1936); R. H. Ewell and H. Eyring, ibid., **5**, 726 (1937).

the table that $n_v$ is quite consistent with $n$. Literature of the $n$ value is referred to in the previous paper. It may be understood from these facts that viscous flow of associated liquid of the first kind is closely analogous to that of $n$-paraffin.

## A new method for calculating energy of hydrogen bonds

Vaporization process of associated liquid of the first kind is schematically shown in Fig. 4. In the figure,

State A: liquid system composed of 1 mole of associated body of $n$-mer just before vaporization

State B: hypothetical gas system composed of 1 mole of associated body of $n$-mer just after vaporization

State C: hypothetical liquid system composed of $n/n'$ mole of associated body of $n'$-mer just before vaporization

State D: gas system composed of $n/n'$ mole of associated body of $n'$-mer just after vaporization

$E_1$: dissociation energy of 1 mole of associated body of $n$-mer of liquid into $n/n'$ mole of associated body of $n'$-mer of the liquid

$E_2$: Energy of vaporization of $n/n'$ mole of associated body of $n'$-mer of the liquid

$E_3$: dissociation energy of 1 mole of associated body of $n$-mer of the gas into $n/n'$ mole of associated body of $n'$-mer of the gas

$E_4$: energy of vaporization of 1 mole of associated body of $n$-mer of the liquid. This value is different from $E_{vap,a}$ in the preceding paragraph. Namely, $E_4$ is energy of vaporization at observed boiling point, compared with $E_{vap,a}$ which is energy of vaporization at the boiling point of $n$-paraffin corresponding to $V_a$.

$E_5$: energy required to produce $n/n'$ mole of associated body of $n'$-mer of gas from 1 mole of associated body of $n$-mer of the liquid

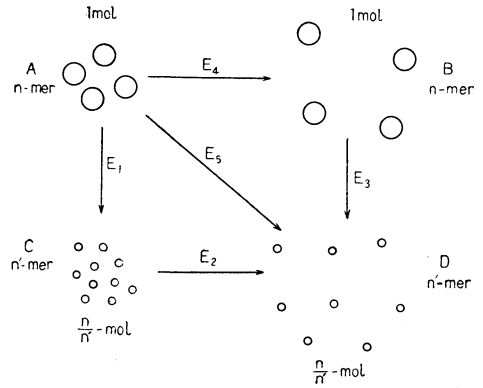



Fig. 4. Schematic representation of the vaporization process of the associated liquid of the first kind.

It is clear that the following equations are established.

$$E_4+E_3=E_1+E_2=E_5 \tag{6}$$

$$E_5=n\cdot\Delta E_{vap} \tag{7}$$

where $\Delta E_{vap}$ is observed energy of vaporization at an observed boiling point in Kcal./mole.

If the associated state is linear chain association,

$$E_3=N_A\cdot\left[(n-1)-\frac{n}{n'}(n'-1)\right]\cdot\varepsilon_{hb} \tag{8}$$

where $\varepsilon_{hb}$ is energy of hydrogen bond per bond and $N_A$ Avogadro's number. Namely,

$$E_3=\left(\frac{n}{n'}-1\right)\cdot E_{hb} \tag{9}$$

where $E_{hb}$ is energy of hydrogen bond per mole in Kcal.

If the associated state is ring-like dimer association and $n=2$, $n'=1$,

$$E_3=2\cdot E_{hb} \tag{10}$$

$E_4$ can be calculated as follows. This is the energy of vaporization per mole of asociated body of $n$-mer at observed boiling point. It is widely known that the following equation is established between heat of vaporization and temperature for unassociated liquid[3].

$$\frac{\Delta H}{\Delta H_b}=\left(\frac{1-T/T_c}{1-T_b/T_c}\right)^{0.38} \tag{11}$$

where $\Delta H$ and $\Delta H_b$ are the heat of vaporization at $T$ and $T_b$ in °K respectively and $T_c$ is critical temperature in °K. Therefore, energy of vaporization at $T$ can be given by eq. 12.

$$\Delta E=(\Delta E_b+RT_b)\left(\frac{1-T/T_c}{1-T_b/T_c}\right)^{0.38}-RT \tag{12}$$

On the other hand, the following equations are established between $T_b$, $T_c$ and $V$ for $n$-paraffin.

$$T_c=664\log V-906 \tag{13}$$

$$T_b=620\log V-975 \tag{14}$$

It is clear from the previous paper and the preceding paragraph that an associated

3) K. M. Watson, *Ind. Eng. Chem.*, **35**, 398 (1943); K. Sato, *Kagaku Kogaku* (*Chemical Engineering*), **18**, 266 (1954) (in Japanese).

body of the first kind shows an analogous behavior to that of *n*-paraffin of equal molar volume. Therefore, critical temperature and boiling point of the associated body may be calculated by eq. 13 and 14. These are termed as $T_{c,a}$ and $T_{b,a}$. Then, $E_4$ can be calculated by inserting $T_{c,a}$ and $T_{b,a}$ in eq. 12 and adopting observed boiling point as $T$. Namely,

$$E_4=(\Delta E_{b,a}+RT_{b,a})\left(\frac{1-T_b/T_{c,a}}{1-T_{b,a}/T_{c,a}}\right)^{0.38}-RT_b \tag{15}$$

where,

$$\Delta E_{b,a}=[2.80+(100/nV)^2]\cdot E_{vis} \tag{16}$$

$$T_{b,a}=620\log(nV)-975 \tag{17}$$

$$T_{c,a}=664\log(nV)-906 \tag{18}$$

TABLE II
CALCULATION OF ENERGY OF HYDROGEN BOND

| Substance | $E_{vis}$ | $\Delta E_{vap}$ | $V$ | $T_b$ | $T_{b,a}$ | $T_{c,a}$ | $n$ | $n'$ | $E_{hb}$ | lit. for $n'$ |
|---|---|---|---|---|---|---|---|---|---|---|
| saturated aliphatic alcohols | | | | | | | | | | |
| methanol | 2.61 | 7.73 | 40.5 | 338 | 440 | 631 | 5 | 1 | 7230 | (4) |
| ethanol | 3.57 | 8.75 | 58.3 | 351 | 532 | 732 | 〃 | 〃 | 7440 | 〃 |
| propanol | 4.39 | 9.08 | 75.0 | 370 | 615 | 804 | 〃 | 〃 | 6800 | 〃 |
| *n*-butanol | 4.64 | 9.60 | 92.0 | 391 | 637 | 864 | 〃 | 〃 | 7420 | 〃 |
| *n*-pentanol | 5.20 | 10.25 | 107.7 | 411 | 698 | 907 | 〃 | 〃 | 7420 | 〃 |
| *n*-hexanol | 5.40 | 10.75 | 125.2 | 429 | 715 | 951 | 〃 | 〃 | 8030 | 〃 |
| *n*-heptanol | 5.76 | 11.30 | 140.7 | 449 | 749 | 985 | 〃 | 〃 | 8270 | 〃 |
| *n*-octanol | 5.99 | 11.70 | 156.7 | 468 | 778 | 1017 | 〃 | 〃 | 8520 | 〃 |
| saturated fatty acids | | | | | | | | | | |
| formic acid | 3.35 | 4.77 | 37.7 | 374 | 508 | 728 | 7 | 2 | 8430<br>3610 | (5) |
| acetic acid | 2.66 | 5.03 | 57.2 | 391 | 432 | 586 | 3 | 1.8 | 8580<br>360 | (6) |
| propionic acid | 2.47 | 6.48 | 74.6 | 414 | 412 | 586 | 2.3 | (1.4) | 11150<br>2600 | |
| *n*-butylic acid | 2.81 | 9.16 | 91.9 | 437 | 449 | 605 | 2 | 1.1 | 11300<br>5650 | (7) |
| *n*-valeric acid | 3.27 | 9.60 | 108.7 | 460 | 500 | 651 | 〃 | (1) | 8200<br>4100 | |
| *n*-caproic acid | 3.57 | (9.96) | 125.0 | 478 | 532 | 690 | 〃 | (1) | 7850<br>3930 | |
| *n*-heptylic acid | 3.84 | (10.40) | 141.9 | 496 | 558 | 725 | 〃 | 1 | 7860<br>3930 | (7) |
| *n*-caprylic acid | 4.18 | (10.85) | 158.6 | 512 | 594 | 756 | 〃 | (1) | 7120<br>3560 | |
| *n*-pelargonic acid | 4.58 | (11.28) | 174.5 | 527 | 633 | 784 | 〃 | (1) | 5990<br>3000 | |
| *n*-capric acid | 4.76 | (11.86) | 196.2 | 541 | 653 | 816 | 〃 | (1) | 6530<br>3270 | |
| *n*-lauric acid | 5.10 | 12.58 | 229.8 | 574 | 688 | 864 | 〃 | (1) | 7030<br>3520 | |
| *n*-myristic acid | 5.34 | 13.50 | 270.4 | 601 | 709 | 911 | 〃 | (1) | 8700<br>4350 | |
| *n*-palmitic acid | 5.54 | (14.01) | 304.6 | 628 | 731 | 944 | 〃 | (1) | 9380<br>4690 | |
| *n*-stearic acid | 5.74 | 14.56 | 338.9 | 658 | 747 | 974 | 〃 | (1) | 10480<br>5240 | |
| others | | | | | | | | | | |
| hydrogen cyanide | 1.64 | 6.05 | 38.5 | 299 | 306 | 462 | 3 | 1.1 | 7070 | (8) |
| hydrogen fluoride | 1.69 | 6.46 | 20.4 | 293 | 315 | 481 | 6 | 1.8 | 14000 | (9) |

4) L. Grunberg and A. H. Nissan, *Trans. Faraday Soc.*, **45**, 125 (1949).
5) R. Wolff, *Angew. Chem.*, **67**, 89 (1955).
6) M. Toda, Structure of Liquid, p. 51 (1949) (in Japanese); Ref, (6).
7) R. E. Lundin, F. E. Harres and L. K. Nash, *J. Am. Chem. Soc.*, **74**, 743 (1952).
8) W. F. Giauque and R. O. Ruehervin, ibid., **61**. 2626 (1939).
9) J. Simon and J. H. Hildebrand, ibid., **46**, 2183 (1924); R. W. Long, J. H. Hildebrand and W.E. Morrell, ibid., **65**, 182 (1943).
10) S. Seki, *Chemistry and Chemical Industry*, **6**, 182 (1953) (in Japanese); L. N. Fergusson, Electron "Structures of Organic Molecules," p. 57 (1952).

TABLE III
ENERGY OF HYDROGEN BOND

| Substance | State | Method | Energy (Kcal./mole) |
|---|---|---|---|
| Hydrogen fluoride | gas | vapor density | 6~10 |
| Fatty acid | gas | vapor density | 7~ 9 |
| Alcohol | liquid | heat of vapor. | 6~ 7 |
| | gas | heat conduct. | 7~ 8 |
| Hydrogen cyanide | gas | vapor density | 3~ 4 |
| Water | s, l, g | heat of vapor. | 4~ 5 |
| | | second virial | |
| Ammonia | gas | second virial | 3~ 4 |
| | liquid | dielectric constant | 6 |
| | solid | heat of sublim. | 1.3 |
| Acetamide | solid | heat of sublim. | 3.5 |
| Aniline | | partition coeff. ($CCl_4$—$H_2O$) | 1.93 |

Following equations may be deduced from equation 6, 7, 9, 10 and 15.

(i) linear chain association

$$(\Delta E_{b,a}+RT_{b,a})\left(\frac{1-T_b/T_{c,a}}{1-T_{b,a}/T_{c,a}}\right)^{0.38}-RT_b+\left(\frac{n}{n'}-1\right)\cdot E_{hb}=n\Delta E_{vap} \quad (19)$$

(ii) ring-like dimer association

$$(\Delta E_{b,a}+RT_{b,a})\left(\frac{1-T_b/T_{c,a}}{1-T_{b,a}/T_{c,a}}\right)^{0.38}-RT_b+2E_{hb}=2\Delta E_{vap} \quad (20)$$

Using eq. 19 and 20, one of the values, $n$, $n'$ and $E_{hb}$ can be calculated from the remaining two, when $V$, $E_{vis}$, $T_b$ and $\Delta E_{vap}$ are known.

In Table II are shown $T_b$, $T_{b,a}$ and $T_{c,a}$ from eq. 17 and 18, $n$, $n'$ and $E_{hb}$ from eq. 19 and 20 and literature for $n'$. Moreover, energy of hydrogen bond from literature is shown in Table III.

The following is clear from the tables.

1) Calculated values of energy of hydrogen bond of alcohols are quite consistent with those from literatures and are independent of the length of carbon chain.

2) Calculated values of energy of hydrogen bond of formic- and acetic acid are quite consistent with those from the literature of the subject if the associated state is linear chain association, but are quite inconsistent if the associated state is ring-like dimer association. This fact suggests linear chain association of these compounds in the liquid state.

3) In propionic- and *n*-butylic acid, $E_{hb}$ values based on linear chain association are too great and those based on ring-like dimer association are too small. This fact suggests mixture of linear chain and ring-like association in the liquid state. These results are quite consistent with those in the previous paper.

4) In higher fatty acids, calculated values of $E_{hb}$ are fairly consistent with those from literature, which assumes linear chain association. However, a decisive answer cannot be given because of the lack of accurate data of degree of association in the gaseous state, $n'$. $E_{hb}$ based upon ring-like dimer association may be more consistent with the observed value even if $n'$ is slightly greater than unity.

5) Calculated value of $E_{hb}$ of hydrogen cyanide is about two times as great as that from literature. However, accurate data of $E_{hb}$ of this compound are very rare. Moreover, $E_{hb}$ of water is greater than that of hydrogen cyanide from literature, though water belongs to the associated liquid of the second kind and its hydrogen bond is easily destroyed with increase in temperature according to the previous paper. Considering these facts, the $E_{hb}$ value of hydrogen cyanide from literature seems to be too small. A detailed investigation may be required.

6) Calculated value of $E_{hb}$ of hydrogen fluoride is some what greater than that from literature, but the cause is not clear at present. However, the value from literature is not quite accurate.

The starting equation is $E_4+E_3=E_5$ in the above treatment, but it is of course possible to start from the equation, $E_1+E_2=E_5$. However, $E_1$ does not consist of the energy required to destroy hydrogen bond, because this process is a dissociation reaction in the liquid state. Moreover, eq. 2 which is established in the case of *n*-paraffin is not always applicable to $E_2$, because $E_2$ is the energy of vaporization

of a polar liquid. Therefore, the method based on $E_1$ and $E_2$ is more difficult than that based on $E_4$ and $E_3$. At any rate, it is very remarkable that energy of hydrogen bond can be calculated as shown above, on the assumption that the associated body of the first kind is analogous to *n*-paraffin.

## Summary

1) Energy of vaporization of *n*-paraffin is discussed. It is shown that relation between $\Delta E_{vap}$ at the boiling point and $E_{vis}$ is different from that of Eyring et al..

2) A new method for calculating the degree of association of the first kind from energy of vaporization is proposed. The degree of association calculated by this method is quite consistent with the result of the previous paper and the value from literature.

3) A new method for calculating the energy of hydrogen bond is proposed. Energy of hydrogen bond obtained by this method is fairly consistent with the value from literature.

4) Considering all results, it can be concluded that the associated body of the first kind shows analogous behavior to *n*-paraffin.

The author wishes to express his sincere thanks to Professor N. Sata of Osaka University for his kind instruction.

*Department of Chemistry Faculty of Science Osaka University*
*Kita-ku, Osaka*

# *Dye-sensitized Photopolymerization of Acrylonitrile-Vinyl Acetate Copolymers*

By Masakazu TANIYAMA and Gerald OSTER

(Received June 3, 1957)

It has been discovered that vinyl polymerization may be initiated by irradiating with visible light a solution containing certain dyes and a mild reducing agent[1]. Oxygen is necessary for the process. The dye is photoreduced to its leuco form and, on reacting with ambient oxygen free, radicals are produced which initiate the polymerization.

In all the studies carried out with such an initiator, very high molecular weight polymer is obtained. For example, the use of riboflavin (a naturally occurring dye-reducing agent combination) as the photosensitizer results in the polymerization of acrylamide to give a polymer having a molecular weight exceeding ten millions[2]. Copolymers of acrylonitrile and allyl alcohol have been produced by dye-sensitized photopolymerization having molecular weights far in excess of those produced by conventional catalysts[3].

It is the purpose of the present work to study the copolymerization of acrylonitrile and vinyl acetate by dye sensitization under conditions which resemble those carried out using conventional catalysts (e. g., organic peroxides)[4] in order to compare reactivity ratios obtained by the two different methods. A practical consequence of the present work may be to suggest a convenient method of producing these polymers which may be controlled simply by suitably adjusting the light intensity.

## Experimental

**Materials.** — Acrylonitrile (American Cyanamid) and vinyl acetate (Eastman Kodak) having boiling points of 77° and 72°C, respectively, were distilled under helium to remove inhibitor. The dye used was acriflavine (National Aniline) and the reducing agent was allyl thiourea (Eastman Kodak). Dimethylformamide (Matheson) was used as the solvent.

1) G. Oster, *Nature*, **173**, 300 (1954).
2) G. K. Oster, G. Oster and G. Prati, *J. Am. Chem. Soc.*, **79**, 595 (1957).
3) G. Oster and Y. Mizutani, *J. Polymer Sci.*, **22**, 173 (1956).
4) C. G. Swain and P. D. Bartlett, *J. Am. Chem. Soc.*, **68**, 2381 (1946); G. M. Burnett and H. W. Melville, *Proc. Roy. Soc.* (London), **A189**, 456 (1947); G. Dixon-Lewis, ibid., **A198**, 510 (1949); M. S. Matheson, E. E. Auer, E. Bevilacqua and E. J. Hart, *J. Am. Chem. Soc.*, **71** 2610 (1949); H. Kwart, H. S. Broadbent and P. D. Bartlett, ibid., **72**, 1060 (1950); F. R. Mayo, F. M. Lewis, C. Walling, and W. F. Hulse, ibid., **70**, 1523 (1948).

TABLE I

SOME PROPERTIES OF THE COMONOMER AND COPOLYMER SYSTEMS

| Exp. No. | 1 | 2 | 3 | 4 | 5 | 6 | 7 | 8 | 9 | 10 |
|---|---|---|---|---|---|---|---|---|---|---|
| Acrylonitrile molar ratio in initial mixture | 1.000 | 0.936 | 0.867 | 0.792 | 0.708 | 0.618 | 0.519 | 0.410 | 0.289 | 0.153 |
| Acrylonitrile molar ratio in copolymer | 1.000 | 0.959 | 0.978 | 0.954 | 0.912 | 0.850 | 0.816 | 0.767 | 0.704 | 0.618 |
| Relative rate of conversion | 8.14 | 9.78 | 12.25 | 14.68 | 14.78 | 12.07 | 5.90 | 3.48 | 2.61 | 1.61 |
| Intrinsic viscosity of copolymer (dl./gm.) | 1.239 | 0.907 | 0.810 | 0.690 | 0.752 | 0.733 | 0.879 | 0.672 | 0.474 | 0.364 |
| 4.46 $\mu$/5.75 $\mu$ infra red absorbance | — | — | 1.352 | 0.865 | 0.739 | 0.662 | 0.602 | 0.530 | 0.495 | 0.467 |

**Procedure and Results.**—A total of 10 g. of mixtures in various proportions of acrylonitrile and vinyl acetate was added to 15 ml. of dimethylformamide. To the solution were added the dye and the reducing agent to give a final concentration of 0.00625% and 0.04%, respectively. The final solution was placed in a 50 ml. test tube at a distance 45 cm. from a 500 watt projection lamp. At various times during the irradiation samples were withdrawn and added to a 50—50 mixture of methanol and water. The precipitate was washed with the methanol-water mixture and dried in a vacuum oven at 55°C. The amount of monomer converted as a function of time of irradiation for the various initial mixtures are illustrated in Fig. 1 and the relative rates are given in Table I.

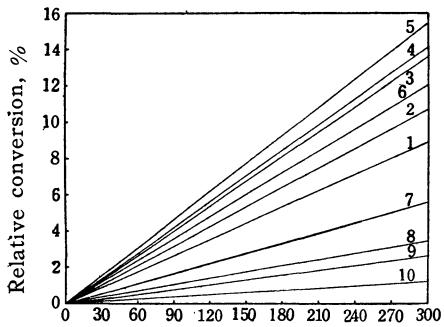



Fig. 1. Conversion as a function of time of irradiation for various initial monomer mixtures.

| Curve No. | 1 | 2 | 3 | 4 | 5 |
|---|---|---|---|---|---|
| acrylonitrile molar ratio | 1.000 | 0.936 | 0.867 | 0.792 | 0.708 |
| Curve No. | 6 | 7 | 8 | 9 | 10 |
| acrylonitrile molar ratio | 0.618 | 0.519 | 0.410 | 0.289 | 0.153 |

When the molar ratio of acrylonitrile in the original mixture exceeds 0.792, the system becomes turbid during irradiation. In such cases the suspensions were agitated prior to the withdrawal of samples.

For other studies (see below) the samples were purified by first dissolution in dimethylformamide, precipitation and repeated washing with the alcohol-water mixture.

Nitrogen analyses were carried out by the Kjeldahl method and the results obtained were corrected according to the procedure of Nozaki[5]. The nitrile content of the polymer, as determined from the nitrogen analyses, are given in Fig. 2 as a function of acrylonitrile concentration in the starting mixture.

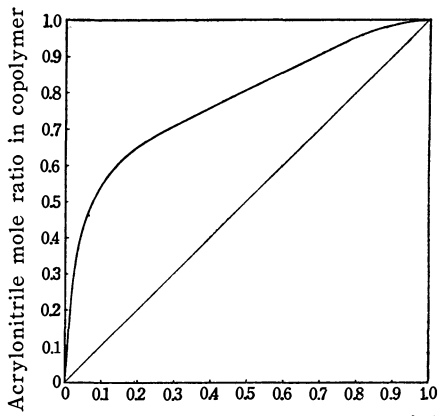



Fig. 2. Copolymerization curve. The straight line represents that expected for an "ideal" copolymerization system.

All the copolymers studied were soluble in dimethylformamide. The copolymers, obtained when the initial molar ratio was 0.519 or greater in acrylonitrile, exhibited only slight swelling in acetone. On the other hand, for a ratio of 0.410, the copolymer was swollen by acetone and for a ratio of 0.289, the copolymer was completely soluble in acetone. The viscosities of solutions of the copolymers in dimethylformamide at 30°C. were determined at 30°C. were determined in a Ubbelohde viscometer with a flow time of 300 sec. The intrinsic viscosities, calculated in the usual manner, are given in Table I.

Samples of the polymers were prepared for infrared analysis by mixing 5 mg. of the polymers with 500 mg. of dried potassium bromide and made into a disc tablet by means of a hydraulic press. In Fig. 3 are illustrated the infrared spectra as obtained on a Perkin-Elmer Model 21 Infra Red spectrometer.

5) K. Nozaki, *J. Polymer Sci.*, **1**, 455 (1946).

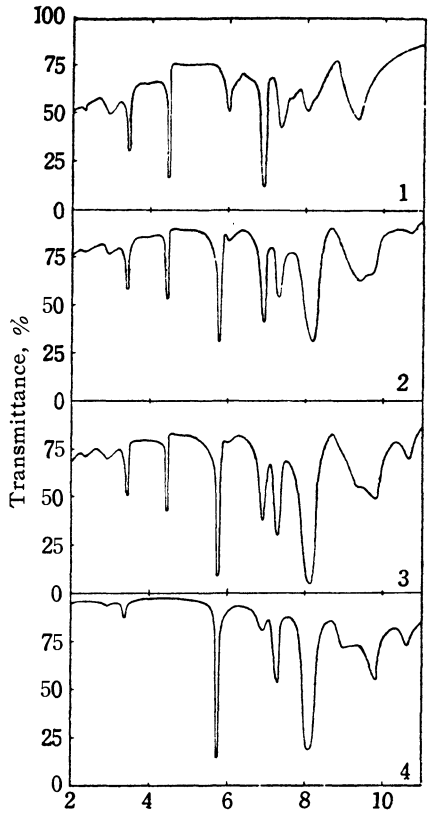



Fig. 3. Infra red spectra of the polymers having the molar ratios of acrylonitrile in the polymers of (1) 1.000, (2) 0.954, (3) 0.767, and (4) 0, respectively.

## Discussion

It is instructive to represent the data of Fig. 1 in terms of conversion as a function of acrylonitrile content in the initial mixture (Fig. 4). A maximum rate is obtained when the molar ratio of acrylonitrile is about 0.70. If the intrinsic viscosity-molecular weight relation is the same for all the polymers, (which it probably is not) then the molecular weight is the greatest for the pure acrylonitrile system. In any case, the molecular weights probably do not exceed 20,000. On the other hand, dye sensitized photopolymerization of acrylonitrile in saturated zinc chloride solutions yields polymer with molecular weights exceeding one million[6].

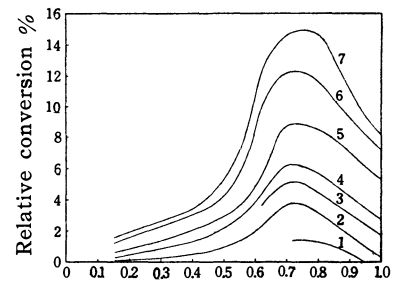



Fig. 4. Conversion of monomer as a function of acrylonitrile in original mixture.

| Curve No. | 1 | 2 | 3 | 4 | 5 | 6 | 7 |
|---|---|---|---|---|---|---|---|
| Time of irradiation (min.) | 30 | 60 | 90 | 120 | 180 | 240 | 300 |

The infra red spectra of the polymers shown in Fig. 3 are consistent with the nitrogen analysis. With decreasing nitrile content in the copolymer, the absorption band characteristic of that group at 4.46 $\mu$ is suppressed as the absorption band characteristic of the carbonyl group of acetate at 5.75 $\mu$ increases. Hence the ratio of these two absorption peaks decreases as the nitrogen content decreases (see Table I). Other significant changes in the infra red spectra take place in the 9—10 $\mu$ region.

From the data in Fig. 2 we calculate the reactivity ratios $r_1$ and $r_2$ (for acrylonitrile and vinyl acetate, respectively) using the well known expression[7],

$$F_1 = \frac{r_1 f_1^2 + f_1 f_2}{r_1 f_1^2 + 2 f_1 f_2 + r_2 f_2^2}$$

where $F_1$ is the acrylonitrile molar ratio in the copolymer, and $f_1$ and $f_2$ are the molar ratios of acrylonitrile and vinyl acetate, respectively, in the original mixture. By curve fitting methods, we obtain the values $r_1=3.88$ and $r_2=0.009$. These results differ somewhat from those of Mayo et al.[4] who obtain values of $r_1=4.05$ and $r_2=0.016$ for bulk polymerization of acrylonitrile-vinyl acetate mixtures using peroxide catalysts.

The copolymer having a molar ratio of acrylonitrile of 0.704 (initial mixture ratio of 0.289) is soluble in acetone and hence could be dry spun from this inexpensive solvent. It is interesting that although this polymer is rich in nitrile groups it is, nevertheless, soluble in acetone. Apparently the polymer has random alternation of nitrile and acetate groups since the product $r_1 r_2$ is small.

## Summary

Copolymers of acrylonitrile and vinyl acetate have been produced using a dye-

6) G. Oster and H. Lieberman, to be published.
7) I. Skeist, *J. Am. Chem. Soc.*, **68**, 1781 (1946).

reducing agent combination as the photosensitizer. Visible light was employed as the radiation source. Nitrogen analyses and infra red analyses were performed on the polymers obtained. The copolymerization ratios were 3.88 and 0.009 for acrylonitrile and vinyl acetate, respectively. Below an initial monomer molar ratio of acrylonitrile of 0.3, the resultant copolymer dissolves in acetone.

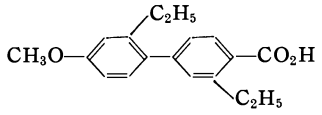
*Institute of Polymer Research*
*Polytechnic Institute of Brooklyn*
*Brooklyn 1, New York, U. S. A.*

# *Estrogenic Biphenyls. III. 2-Alkyl-4-methoxybiphenyl-4'-carboxylic Acids*

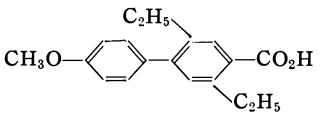
By Takeo SATO and Michinori ŌKI*

(Received June 3, 1957)

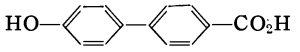
In the previous papers[1,2] of this series, it was reported that 2, 3'-diethyl-4-methoxybiphenyl-4'-carboxylic acid(I) and 2', 5'-diethyl-4-methoxybiphenyl-4'-carboxylic acid(II) were fully estrogenic at the doses of 100 $\gamma$ when administered to ovariectomized mice. Enhancement of the estrogenic activity of compounds I and II, compared with that of 4-hydroxybiphenyl-4'-carboxylic acid(III), by the presence of the two ethyl groups was attributed to the steric effect causing the two benzene rings to rotate out of the otherwise coplanar structure and the increasing thickness of the molecules, which was shown by the hypsochromic effect in the ultraviolet absorption spectra.



I



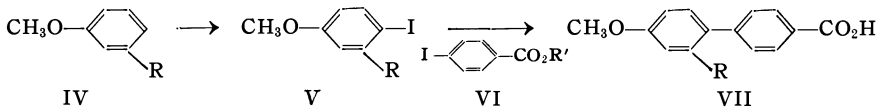
II



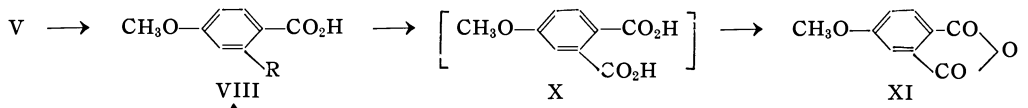
III

It is unknown, however, whether the introduction of ethyl groups into 4-hydroxy- or 4-methoxy-biphenyl-4'-carboxylic acid at positions 2 and 3' or 2' and 5' is the optimum substitution for developement of the estrogenic activity. Therefore, the authors hoped to find out first the most suitable alkyl group substituted at position 2 only of 4-methoxybiphenyl-4'-carboxylic acid.

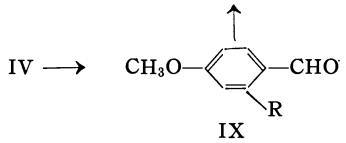
2-Alkyl-4-methoxybiphenyl-4'-carboxylic acids(VII) were synthesized in the following way. 3-Alkylanisoles(IV) were iodinated with iodine in the presence of yellow



IV V VI VII



VIII X XI



IX

R
a H
b $CH_3$
c $CH_3CH_2$
d $CH_3CH_2CH_2$

* Present address : Department of Chemistry, Faculty of Science, The University of Tokyo, Hongo, Tokyo.

1) M. Ōki and T. Sato, This Bulletin, **30**, 508 (1957).
2) M. Ōki and T. Sato, ibid., 702.

mercuric oxide[3]. The structures of 3-alkyl-4-iodoanisoles(V), compounds Va[3] and Vc[1] being known, were proved as follows:

The reaction of Grignard compound from 4-iodo-3-methylanisole (Vb) with solid carbon dioxide produced a carboxylic acid. It was identified with 4-methoxy-2-methylbenzoic acid (VIIIb) which was prepared by permanganate oxidation of 4-methoxy-2-methylbenzaldehyde (IXb), obtained from 3-methylanisole(IVb), zinc cyanide, hydrogen chloride and aluminium chloride[4]. The acid (VIIId) obtained from 4-iodo-3-propylanisole (Vd) in the same way was oxidized with potassium permanganate. The product was sublimed in vacuo to produce an anhydride, which was identical with 4-methoxyphthalic anhydride (XI) prepared from 4-methoxy-2-methylbenzoic acid (VIIIb). 3-Alkyl-4-iodoanisoles (V) and 4-iodobenzoic esters (VI) were submitted to the Ullmann reaction. Any unchanged materials were removed in vacuo when necessary, and hydrolysis of the condensation products gave the desired biphenyls (VII).

TABLE I

ULTRAVIOLET ABSORPTION MAXIMA AND ESTROGENIC ACTIVITY OF 2-ALKYL-4-METHOXYBIPHENYL-4'-CARBOXYLIC ACID (VII)

| Compound | $\lambda_{max.}$ (mμ) | log $\varepsilon_{max.}$ | Minimum active dose in mice (γ) |
|---|---|---|---|
| VIIa[5] | 289 | 4.36 | 1000* |
| VIIb | 224<br>280 | 4.27<br>4.17 | 200 |
| VIIc | 222<br>278 | 4.28<br>4.10 | 500 |
| VIId | 224<br>278 | 4.28<br>4.13 | 250 |

* Active in 50% animals.

The ultraviolet absorption data and the estroganic activity of compounds VIIa, VIIb, VIIc, and VIId are given in Table I. 4-Methoxybiphenyl-4'-carboxylic acid (VIIa) showed a strong absorption at 289 mμ, while its homologs (VIIb, c, d) possessed absorption at about 278 mμ. It can be deduced from the spectral study that the introduction of an alkyl group into position 2 modifies the coplanar conformation of the biphenyl skeleton, because the observed hypsochromic shift and decrease in K-band intensity in the present series (VII) can be attributed to the non-planar conformation of the system, if the wave length of the maximum absorption depends on the extent of conjugation. Further, it may be inferred that the deterioration in conjugation in the series (VII) is similar regardless of the length of the alkyl chains, and then, it may be assumed that the first methylene group only interferes with the benzene rings. The present observation is in good agreement with others[6]. Namely, it is known that by a single substitution at position 2 of biphenyl a little change occurs in the ultraviolet absorption and the K-band appears, though the maximum shifts to a shorter wave length and the intensity diminishes, and that 2-methylbiphenyl absorbs at 237 mμ and 2-ethylbiphenyl at 233 mμ while biphenyl itself does at 249 mμ.

The minimum active doses of the members of the series VII to produce full estrus were determined by the vaginal smear test with ovari-ectomized mice. The substances in oil solution were injected subcutaneously. 4-Hydroxybiphenyl-4'-carboxylic acid (III) produced estrus in 60% of the test animals at the dose of 500 γ but the assay could not be carried out at 1 mg. dose because of its small solubility in oil[1]. On the other hand, compound VIIa was found to be active to 40% and 50% of the animals at the doses of 500 γ and 1 mg., respectively. Natural estrogens, hexestrol, and stilbestrol, lose potency markedly when they are converted into methyl ethers[7], while there is no remarkable difference in estrogenic activity between a free phenol and its methyl ether of the type of doisynolic acid[8] or allenolic acid[9]. 4-Hydroxybiphenyl-4'-carboxylic acid, and presumably its 2-alkylhomologs, fall in the latter category both in the two functional groups and in the effect of the methylation of the hydroxyl group. It is striking, however, that the kind of the alkyl group gives almost no difference in the estrogenic activity in contrast to the case of dialkylstilbestrol dimethyl ethers[10]. This may be understood on the basis of the molecular thickness being similar irrespective of the kind

3) M. P. Brenans, *Bull. Soc. chim. France*, [3] **25**, 819 (1901).
4) R. Adams and E. Montgomery, *J. Am. Chem. Soc.*, **46**, 1518 (1924).
5) Prepared according to the method given by L. F. Fieser and C. K. Bradsher, ibid., **58**, 1738 (1936).
6) E. A. Braude, F. Sondheimer and W. F. Forbes, *Nature*, **173**, 117 (1954): R. A. Friedel, M. Orchin and L. Reggel, *J. Am. Chem. Soc.*, **70**, 199 (1948): C. D. Freedman, ibid., **77**, 6223 (1955).
7) U. V. Solmssen, *Chem. Rev.*, **37** 481 (1945).
8) K. Miescher, ibid., **43**. 367 (1948),
9) See A. Horeau and Jacque, *Bull. Soc. chim. France*, **1945**, 1001 and the following papers.
10) M. Ōki and Y. Urushibara, This Bulletin, **25**, 109 (1952).

of the alkyl group as judged from the ultraviolet absorption, provided that the molecular thickness is mainly given by the rotated benzene rings.

## Experimental[11]

**3-Propylaniline.** A mixture of 130 g. (0.87 mole) of 3-aminopropiophenone, prepared from 3-nitropropiophenone according to Kenford and Simpson[12], 120 g. (1.8 moles) of 72% hydrazine hydrate, 280 g. of potassium hydroxide and 700 ml. of diethylene glycol, was heated under reflux for one hour. The reflux condenser was replaced by a downward condenser. Distillation was continued until the pot temperature rose to 190° and the mixture was maintained at this temperature for three hours. Then the mixture was steam-distilled. The combined distillate was extracted with ether and the extract was dried over potassium carbonate. Distillation gave a colorless oil boiling at 102—107°/8 mm. Yield 113 g. or 96% of the theoretical. The reported boiling point is 118—119°/12—13 mm.[13]

The picrate, prepared in the usual way, melted at 155—156°. The reported melting point is 155°[13].

*Anal.* Found: N, 15.83. Calcd. for $C_{15}H_{16}N_4O_6$: N, 16.09%.

**3-Alkyl-4-iodoanisole (V).** The general procedure is described by an example of the preparation of 4-iodo-2-methylanisole. To a solution of 28 g. (0.23 mole) of 3-methylanisole (IVb)[14] in 46 ml. of ethanol were alternatively added 58 g. (0.23 mole) of iodine and 60 g. (0.28 mole) of yellow mercuric oxide in small portions during ten to fifteen minutes, while the reaction mixture was kept at the temperature below 25° and the flask was well swirled. Then the mixture was heated under reflux for ten minutes, cooled, and filtered with suction. The filtrate was diluted with water and the oil was extracted with ether. The ethereal extract was washed with aqueous potassium iodide, dried over calcium chloride, and fractionally distilled. 4-Iodo-2-methylanisole (Vb) boiled at 123—125°/7 mm. and solidified on cooling. The analytical sample was obtained by recrystallization from ethanol. Colorless needles, m. p. 43—45°. Yield 31 g. or 54% of the theoretical.

*Anal.* Found: I, 51.26. Calcd. for $C_8H_9OI$: I, 51.18%.

**3-Ethyl-4-iodoanisole (Vc)** was prepared as described elsewhere[1].

**4-Iodo-2-propylanisole (Vd)** was obtained from 2-propylanisole (IVd)[15]. Colorless oil, b. p. 120—121°/4 mm. Yield 62%.

*Anal.* Found: C, 43.77; 4.85. Calcd. for $C_{10}H_{13}IO$: C, 43.50; H, 4.75%.

**4-Methoxy-2-methylbenzoic Acid (VIIIb).** *A. From 4-Methoxy-2-methylbenzaldehyde (IXb).* The benzaldehyde, prepared according to Adams and Montgomery[4], was oxidized with aqueous potassium permanganate to give colorless plates melting at 173°. The reported melting point is 176°[16].

*Anal.* Found: C, 65.23; H, 6.11. Calcd. for $C_9H_{10}O_3$: C, 65.05; H, 6.07%.

*B. From 4-Iodo-2-methylanisole (Vb).* 4-Methoxy-2-methylphenylmagnesium iodide was prepared in the usual way from 5 g. of compound Vb, 0.6 g. (0.029 atom) of magnesium turnings and 50 ml. of ether. Solid carbon dioxide was added to this solution and the product was decomposed with dilute hydrochloric acid. The acid in the ethereal layer was taken up in aqueous sodium bicarbonate and the aqueous solution was acidified with hydrochloric acid. The acid was recrystallized from aqueous ethanol. Colorless plates, m. p. 176—177°. Yield 2 g. or 60% of the theoretical. The melting point did not depress when this compound was mixed with 4-methoxy-2-methylbenzoic acid.

**4-Methoxy-2-propylbenzoic Acid (VIIId).** 4-Methoxy-2-propylphenylmagnesium iodide, prepared from 7 g. (0.025 mole) of compound Vd and 0.8 g. (0.033 atom) of magnesium in 50 ml. of ether was treated with solid carbon dioxide and the reaction mixture was worked up as in the preparation of compound VIIIb. Colorless plates, m. p. 106—107°, were obtained on recrystallization of the product from aqueous ethanol. Yield 2 g. or 41% of the theoretical.

*Anal.* Found: C, 68.03; H, 7.46. Calcd. for $C_{11}H_{14}O_3$; C, 68.02; H, 7.27%.

**4-Methoxyphthalic anhydride (XI).** *A. From 4-Methoxy-2-methylbenzoic Acid (VIIIb).* The acid VIIIb was oxidized according to Shall[16] and the dicarboxylic acid (X) was sublimed in vacuo. Colorless needles, m. p. 88—90°. The reported melting point is 93°.

*B. From 2-Ethyl-4-methoxybenzoic Acid (VIIIc)*[1]. A solution of 500 mg. of compound VIIIc, 3 g. of potassium permanganate and 1 ml. of 10% sodium hydroxide in 60 ml. of water, was heated under reflux for three hours. Sulfur dioxide was bubbled into the mixture and the resulting solution was extracted with ether for five hours. After concentration of the ethereal extract, the residue was heated in vacuo and the crystalline material was collected. The compound melted at 90—90.5° and showed no depression of the melting point on admixture with the authentic specimen of 4-methoxyphthalic anhydride obtained from 4-methoxy-2-methylbenzoic acid as described above.

C. *From 4-Methoxy-2-propylbenzoic Acid (VIIId).* The acid VIIId was treated in the same way as described above. The ahnydride obtained melted at 85—86° and showed no depression of the melting point when mixed with the authentic 4-methoxyphthalic anhydride.

**2-Alkyl-4-methoxybiphenyl-4'-carboxylic Acid (VII).** 4-Iodobenzoic esters (VI) were

11) All melting and boiling points are uncorrected.
12) J. R. Kenford and J. E. Simpson, *J. Chem. Soc.*, **1948**, 354.
13) R. Long and K. Schofield, ibid., **1953**, 2066.
14) c. f. G. S. Hiers and F. D. Hager, *Org. Synth.*, Coll. Vol. **1**, 58 (1940).
15) 3-Propylanisole was prepared from the corresponding phenol which was obtained by the diazo-reaction of 3-propylaniline.
16) C. Shall, *Ber.*, **12**, 816 (1879).

obtained from 4-iodobenzoic acid in the usual way. Methyl ester, m. p. 113—114° [17] and ethyl ester, b. p. 154°/16 mm.[15] were prepared.

For the general procedure of the preparation, 4-methoxy-2-methylbiphenyl-4'-carboxylic acid (VIIb) is described as follows. To a well stirred mixture of 10 g. (0.040 mole) of 4-iodo-3-methylanisole (Vb) and 5 g. (0.019 mole) of methyl 4-iodobenzoate, 15 g. of activated copper bronze[19] was added in twenty-five minutes, the temperature being kept at 240—250°. The reaction mixture was then heated at 280—290° for twenty-five minutes and extracted with acetone after cooling. The solvent was removed by distillation and the residue was hydrolyzed by refluxing with a mixture of 50 ml. of 10% aqueous sodium hydroxide and 100 ml. of ethanol for two hours. Ethanol was evaporated and the residue was diluted with 500 ml. of water. The oily insoluble material was removed by filtration with the aid of active charcoal and the filtrate was acidified with hydrochloric acid. The precipitate was collected and boiled with acetic acid, and any insoluble material was removed by filtration. The extract was concentrated and the residue was again treated with boiling benzene. The filtrate gave brown crystals, which yielded colorless plates, m. p. 211—212°, on recrystallization from benzene. Yield 0.4 g. or 9% of the theoretical.

*Anal.* Found: C, 74.05; H, 5.76. Calcd. for $C_{15}H_{14}O_3$: C, 74.36; H, 5.83%.

**2-Ethyl-4-methoxybiphenyl-4'-carboxylic Acid (VIIc).** It was obtained from compounds Vc and VI ($R'=C_2H_5$). It was necessary to remove any unchanged ester in vacuo before hydrolysis for easier purification of the desired material. The acid was finally recrystallized from aqueous ethanol. M. p. 173.5—174.5°. Yield about 7% of the theoretical.

*Anal.* Found: C, 74.56; H, 6.21. Calcd. for $C_{16}H_{16}O_3$: C, 74.98; H, 6.29%.

**4-Methoxy-2-propylbiphenyl-4'-carboxylic Acid (VIId).** It was prepared in the same way as described for compound VIIc, starting from 4-iodo-2-propylanisole (Vd) and ethyl 4-iodobenzoate. M. p. 175.5—176°. Yield about 8% of the theoretical.

*Anal.* Found: C, 75.52; H, 7.03. Calcd. for $C_{17}H_{18}O_3$: C, 75.53; H, 6.71%

**Ultraviolet Absorption Spectra.** They were measured by using Hitachi Photo-electric Spectrophotometer Model EPU-2. Substances were dissolved in 95% ethanol.

The authors wish to express their hearty thanks to Professor Y. Urushibara of the University of Tokyo for his encourgement throughout this work and to Research Department of Teikoku Hormone Manufacturing Co., Kawasaki, for bio-assay. The authors' thanks are also due to the Ministry of Education for the Grant in Aid for Fundamental Research.

*Department of Chemistry*
*Faculty of Science*
*Tokyo Metropolitan University*
*Setagaya, Tokyo*

17) P. P. T. Sah and Chang-lin Hsü, *Rec. Trav. Chim.*, **59**, 349 (1940).
18) K. Kindler, *Ann.*, **450**, 1 (1926).
19) E. C. Kleiderer and R. Adams, *J. Am. Chem. Soc.*, **55**, 4219 (1933).

# *Über den Zucker des Narcissins**

Von Munio KOTAKE und Hisao ARAKAWA

(Eingegangen am 17 März 1957)

Es wurde das Narcissin von Kubota und Hase[1] als Isorhamnetin-3-rutinosid vermutet und in dem vorgehenden Berichte hat einer von uns[2] mit Hilfe der Papierchromatographie zeigen können, dass der Zucker des Narcissins mit der Biose des Rutins identisch ist, aber eine Gewinnung seines kristallinischen Derivates als Biose ist noch nicht gelungen. Es ist das Ziel dieser Untersuchung, ein kristallinisches Derivat der Biose des Narcissins zu isolieren und mit demselben der Rutinose zu vergleichen.

Zur Vorprobe der Spaltung unterwarfen wir das Rutin einer Ozonisierung nach Zemplén et al[3], da seine Ozonspaltung in der Literatur noch nicht beschrieben worden ist, und so wurden Oxalsäure und Zucker gewonnen; letzterer wurde nach Acetylierung mit dem synthetischen Präparat als Rutinose-heptaacetat identifiziert.

* III. Mitteilung über die Flavonolglykoside aus den Pollen von *Lilium auratum* RINDLF.

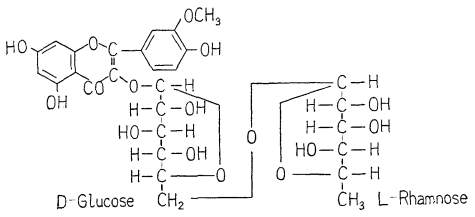
1) T. Kubota und T. Hase, *J. Chem. Soc. Japan, Pure Chem. Sec.*, **77**, 1059 (1956).

2) H. Arakawa, ibid., **77**, 1314 (1956).

3) G. Zemplén et al, *Ber.*, **75**, 489 (1942).

Auf die gleiche Weise ozonisierten wir das Narcissin aus den Pollen[4] und bei der Papierchromatographie ergab sich nur ein Fleck, dessen $R_f$ Wert mit demselben des Entacetylierungsproduktes vom Rutinose-heptaacetat übereinstimmte; nach Acetylierung konnte der Zucker des Narcissins als Rutinose charakterisiert werden.

Nun ist es nachgewiesen worden, dass Narcissin Isorhamnetin-3-rutinosid ist.




Narcissin

## Beschreibung der Versuche

**Rutinose-Heptaacetat (Hepta-*O*-acetyl-6-β-L-Rhamnopyranosyl-β-D-Glukopyranose) und seine Entacetylierung:** Die nach Zemplén et al.[5] dargestellte Rutinose-heptaacetat schmolz bei 169,7°C; $[\alpha]_D^{21} = -28,8°$ ($c = 3,27$ in Chloroform). (Lit. Schmp. 168—169°C; $[\alpha]_D^{20} = -28,84°$[6]) Das IR-Spektrum zeigte keine α-Bindung, wohl aber die β-Glykosidbindung bei 11,19 μ, den β-Anomer des Glukose-Acetates** bei 9,64 μ (in Nujol).

Acetat (200 mg) wurde in 13 cc., 0,02 N Natriummethylat gelöst und 6 Std. bei Zimmertemperatur stehen gelassen; danach wurden Amberite IR 4B und IR 120 und dann Wasser unter Rühren durch Einleitung von Kohlendioxyd versetzt, abfiltriert und im Vak.-Exsiccator getrocknet. Das erhaltene Produkt wurde in 0,5 ccm Wasser gelöst und mit 10 ccm absol. Alkohol und 10 ccm absol. Äther versetzt; dabei fiel ein farbloser Niederschlag aus, der mit absol. Äther und absol. Chloroform gewaschen und getrocknet wurde. Er schmeckte etwas süss und ergab bei Papierchromatographie den einzigen Fleck der Rutinose[2], zeigte sich aber sehr hygroskopisch und noch nicht analysierein.

**Ozonspaltung des Rutins:** (Rutin[7] 1,5 g) wurde in 80 ccm 90 proz. Essigsäure 15 Std. ozonisiert. Die Lösung wurde dann im Vak. eingeengt. Der erhaltene Rückstand wurde mit Alkohol verdünnt und wiederum verdampft, mit etwas Wasser versetzt und über Nacht stehen gelassen, wobei ausgeschiedene Kristalle abfiltriert wurden. Man erhielt 65 mg Oxalsäure, die nach Umkristallisieren aus Wasser bei 99,5—100,5°C schmolzen. Mischschmp. mit dem authentischen Präparat 100.5°C.

*Anal.* Gef.: C, 19,36; H, 5,04. Ber. für $C_2H_2O_4 \cdot 2H_2O$: C, 19,05; H, 4,80%.

Aus dem Filtrat wurden nach Behandeln mit basischem Bleiacetat und dann Acetylierung 63 mg Kristalle von Acetat erhalten. Nach 2-maligem Umkristallisieren aus heissem Alkohol ergaben sich farblose Kristalle vom Schmp. 167,5—168°C. Ein Mischschmp. mit dem synth. Präparat zeigte 169—169,5°C. Die IR-Spektren der zwei Präparate erwiesen sich als identisch.

*Anal.* Gef.: C, 50,07; H, 6,17. Ber. für $C_{25}H_{36}O_{17}$: C, 50,32; H, 5,85%.

**Ozonspaltung des Narcissins:** Eine Lösung von 200 mg Narcissin in 10 ccm 90 proz. Essigsäure wurde 80 Min. lang ozonisiert. Sie wurde dann im Vak. verdampft. Der Rückstand wurde wie oben beschrieben behandelt und der fast farblose Zucker betrug 60 mg nach dem Trocknen. Papierchromatographie wurde mit drei Lösungsmitteln (Pyridin, Butanol, Wasser 1:6:1; Eisessig, Butanol, Wasser 1:4:5; Essigester, Pyridin, Wasser 2:1:2)[2] durchgeführt. Nach Acetylierung wurden 39 mg rohe Kristalle erhalten. Dreimaliges Umkristallisieren gab farblose Kristalle vom Schmp. 167—168°C. Ein Mischschmp. mit dem synthetishen Produkt zeigte 168,5—169°C. Die IR-Spektren der beiden Präparate übereinstimmten. Zur Analyse wurde das Acetat nochmals umkristallisiert; Schmp. 169—169,5°C.

*Anal.* Gef.: C, 50,44; H, 6,15. Ber. für $C_{25}H_{36}O_{17}$: C, 50,32; H, 5,85%.

Bei der Ausführung der Synthese arbeitete Herr Toshiaki Miyajima mit.

*Organisch-chemisches Laboratorium*
*im Polytechnishen Institut*
*der Städtischen Universität zu Osaka*
*Kita-ku, Osaka*

4) M. Kotake und H. Arakawa, *Naturwiss.*, **43**, 327 (1956); H. Arakawa, *J. Chem. Soc. Japan*, **77**, 1057 (1956). Nochmals sammelten wir den Pollen.
5) G. Zemplén und A. Gerces, *Ber.*, **67**, 2049 (1934).
6) G. Zemplén und A. Gerces, *Ber.*, **68**, 1318 (1935).
7) Herrn Prof. T. Kubota sei für die freundliche Überlassung des Präparates gedankt.
** Vgl. F. A. H. Rice und L. C. Browning, *Science*, **125**, 496 (1957).

# *The Composition of Strong Phosphoric Acids*

By Shigeru OHASHI and Hiroko SUGATANI

(Received June 6, 1957)

Since several years ago new analytical methods[1] for the determination of carbon, nitrogen, sulfur and so on by the use of strong phosphoric acids as reaction media have been investigated in the authors' laboratory and a preliminary study on the composition of strong phosphoric acids was already reported[2].

The composition of strong phosphoric acids having 72 to 89 wt. % phosphorus(V) oxide was studied by Bell[3] who employed the so-called zinc titration method for the analysis of pyro- and tripolyphosphate. Thereafter many analytical methods were developed for the determination of various types of condensed phosphate; filterpaper chromatography[4], anion-exchange chromatography[5], pH-titration method[6], X-ray diffractometry[7], isotope dilution method[8], cobaltcomplex method[9], and infrared absorption spectrometry[10].

Higgins and Baldwin[11] used the anion-exchange chromatography, which was presented by Beukenkamp, Rieman III, and Lindenbaum[5], for their study on the composition of strong phosphoric acids which were prepared by dehydration of 85 wt. % orthophosphoric acid at the constant temperatures, 100° and 176°C. During the course of the present work Huhti and Gartaganis[12] published their report on the composition of strong phosphoric acids having 68.8 to 86.3 wt. % phosphorus (V) oxide, which were analyzed by the method of filterpaper chromatography.

In the present paper the composition of strong phosphoric acids containing about 67 to 80 wt. % phosphorus (V) oxide, which were prepared from 85 wt. % orthophosphoric acid under various conditions, was investigated in detail by the use of the anion-exchange chromatography[5] combined with the usual molybdenum-blue colorimetric analysis for orthophosphate.

## Experimental

*Preparation of Strong Phosphoric Acids.*— About 30 g. of 85 wt. % orthophosphoric acid was heated on an electric heater as shown in Fig. 1 until a thermometer immersed in the acid indicated a definite temperature, 161°, 183°, 203°, 220°, 244°, 260°, 280°, 301°, 340°, or 380°C, respectively (sample Nos. 1 to 10 in Table I). The

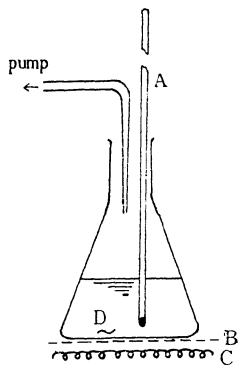



Fig. 1. Dehydration of orthophosphoric acid.
A: Thermometer C: Electric Heater
B: Wire Gauze D: Platinum Wire

time required for the dehydration was eight, sixteen, twenty five, thirty one, and sixty minutes for the temperatures, 183°, 220°, 301°, 340°, and 380°C, respectively. In a similar way about 30g. and 300 g. of 85 wt. % orthophosphoric acid were

1) T. Kiba, S. Ohashi, T. Takagi and Y. Hirose, *Japan Analyst*, **2**, 446 (1953); S. Ohashi, This Bulletin, **28**, 171, 177, 537, 585 and 645 (1955); T. Kiba, T. Takagi, Y. Yoshimura and I. Kishi, ibid., **28**, 641 (1955); T. Takagi, *Japan Analyst*, **4**, 624 (1955); S. Ohashi and H. Makishima, This Bulletin, **29**, 700 (1956); T. Kiba and I. Kishi, ibid., **30**, 44 (1957); S. Takagi and N. Hayashi, *J. Chem. Soc. Japan, Pure Chem. Sec.*, **78**, 445 (1957).

2) S. Ohashi, This Bulletin, **28**, 537 (1955).

3) R. N. Bell, *Ind. Eng. Chem.*, **40**, 1464 (1948); cf. R. N. Bell, A. R. Wreath and W. T. Curless, *Anal. Chem.*, **24**, 1997 (1952).

4) J. P. Ebel et al., *Compt. rend.*, **233**, 415 (1951), **242**, 647 (1956) and *Bull. Soc. Chim. France*, **1953**, 991, 998, 1089 and 1096; J. P. Crowther, *Anal. Chem.*, **26**, 1383 (1954); E. Karl-Kroupa, ibid., **28**, 1091 (1956).

5) J. Beukenkamp, W. Rieman III and S. Lindenbaum, ibid., **26**, 505 (1954); S. Lindenbaum, T. V. Peters, Jr., and W. Rieman III, *Anal. Chim. Acta*, **11**, 530 (1954).

6) J. R. Van Wazer, E. J. Griffith and J. F. McCullough, *Anal. Chem.*, **26**, 1755 (1954).

7) A. J. Mabis and O. T. Quimby, ibid., **25**, 1814 (1953).

8) O. T. Quimby, A. J. Mabis and H. W. Lampe, ibid., **26**, 661 (1954).

9) H. W. McCune and G. J. Arquette, ibid., **27**, 401 (1955).

10) D. E. C. Corbridge and E. J. Lowe, ibid., **27**, 1383 (1955).

11) C. E. Higgins and W. H. Baldwin, ibid., **27**, 1780 (1955).

12) A. L. Huhti and P. A. Gartaganis, *Can. J. Chem.*, **34**, 785 (1956).

TABLE I
COMPOSITION OF STRONG PHOSPHORIC ACIDS

| Sample No. | Initial Weight g. | Temp. °C | Specific Gravity at 15°C | Total $P_2O_5$ wt. % | Ortho $H_3PO_4$ wt. % | Pyro $H_4P_2O_7$ wt. % | Tripoly $H_5P_3O_{10}$ wt. % | Tetrapoly $H_6P_4O_{13}$ wt. % | Water $H_2O$ wt. % |
|---|---|---|---|---|---|---|---|---|---|
| 1 | 25.68 | 161 | 1.77 | 62.5 | 86.3 | — | — | — | 13.7 |
| 2 | 26.37 | 183 | 1.81 | 66.7 | 90.9 | 1.1 | — | — | 8.0 |
| 3 | 28.63 | 203 | 1.84 | 68.5 | 89.9 | 4.4 | — | — | 5.8 |
| 4 | 29.28 | 220 | 1.87 | 68.9 | 90.5 | 4.2 | — | — | 5.3 |
| 5 | 28.14 | 244 | 1.89 | 69.2 | 90.0 | 5.0 | — | — | 5.0 |
| 6 | 28.92 | 260 | 1.90 | 71.8 | 89.8 | 8.1 | 0.3 | — | 1.8 |
| 7 | 28.79 | 280 | 1.92 | 75.1 | 66.1 | 29.3 | 4.6 | — | — |
| 8 | 29.24 | 301 | 1.95 | 76.2 | 53.8 | 39.5 | 6.8 | — | — |
| 9 | 33.52 | 340 | 2.03 | 78.3 | 29.4 | 47.4 | 22.7 | 0.5 | — |
| 10 | 32.06 | 380 | 2.08 | 80.1 | 16.7 | 38.6 | 24.8 | 19.9 | — |
| 11 | 30 | 300 | 1.99 | 78.4 | 29.8 | 45.4 | 20.4 | 4.4 | — |
| 12 | 300 | 301 | 2.07 | 77.2 | 44.4 | 39.8 | 12.3 | 3.6 | — |
| 13 | 10.70 | 140[a)] | 1.92 | 74.5 | 74.1 | 23.5 | 2.5 | — | — |
| 14 | 10 | 140[a)] | 1.93 | 74.7 | 69.4 | 28.2 | 2.1 | 0.3 | — |

a) at the constant temperature, 140°±2°C.

dehydrated by raising the temperature of the liquid up to 300°C for sixty minutes (samples Nos. 11 and 12 in Table I). The latter is the so-called "300°C-strong phosphoric acid", which has been used for many analytical purposes in the authors' laboratory. There was no apparent attack on the glass in the preparation described above.

On the other hand about 10 g. of 85 wt. % orthophosphoric acid was taken in a platinum crucible and dehydrated by heating in a constant temperature oven at 140°±2°C for twenty one and thirty one hours, respectively (sample Nos. 13 and 14 in Table 1).

*Specific Gravities of the Strong Phosphoric Acids* were measured using a 1-ml. or 2.5-ml. specific gravity bottle at 15°C.

*Analysis of the Strong Phosphoric Acids.*—A 0.2 to 0.8 g. portion of the strong phosphoric acid was weighed in a weighing tube, dissolved in 30 ml. of distilled water in 100-ml. volumetric flask, immediately neutralized to phenolphthalein with 1 N sodium hydroxide and the volume adjusted to the mark with distilled water. An aliquot of this solution, 2 ml. was poured into a column filled with resin. Anion exchanger, Dowex 1 was used under the following conditions: 120 to 200 mesh, 8% cross-linked, a column of 0.79 sq. cm. ×20 cm., exchange capacity of 2.28 meq./g., 2.62 g. in the dry state, chloride form. Elutions of individual phosphates were made by the method of Higgins and Baldwin[11]. Using a flow rate of 0.5 to 0.7 ml./min., orthophosphate was removed with 0.05 M hydrochloric acid, pyrophosphate with 0.20 M potassium chloride, tripolyphosphate with 0.27 to 0.35 M potassium chloride, and tetrapolyphosphate with 0.35 to 0.50 M potassium chloride.

By the first run the phosphate contained in each fraction of 5 ml. of eluate solution was determined colorimetrically by means of Nakamura's molybdenum-blue method[13]. Although

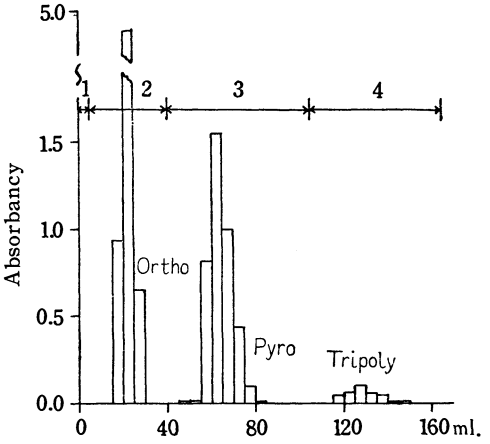



Fig. 2. Elution curve of sample No. 8.
1: Sample soln. and water
2: 0.05 M HCl
3: 0.20 M KCl
4: 0.35 M KCl

orthophosphate was directly determined by the colorimetry, polyphosphates were hydrolyzed by heating with diluted sulfuric acid to orthophosphate before the colorimetric determination. A typical elution curve is shown in Fig. 2. In the second run, after the resin was again loaded with the same sample solution, the quantity of each eluant solution, required to separate the phosphate mixture, was let flow through the column, collected in a volumetric flask, and diluted to the mark with distilled water. An appropriate aliquot of the solution, after being hydrolyzed and concentrated, if necessary, was subjected to determination of phosphorus as previously described.

13) M. Nakamura, *J. Agr. Chem. Soc. Japan*, **24**, 1 (1950).

## Results and Discussion

The results of the analyses of the strong phosphoric acids are shown in Table I. This indicates that the formation of pyro-, tripoly- and tetrapolyphosphoric acid starts at the concentration of phosphorus (V) oxide, around 67, 72 and 75 wt. %, respectively. The so-called "300°C-strong phosphoric acid" in the authors' laboratory, the sample No. 12, is composed of 44.4 wt. % orthophosphoric acid, 39.8 wt. % pyrophosphoric acid, 12.3 wt. % tripolyphosphoric acid, and 3.6 wt. % tetrapolyphosphoric acid. However, even the strong phosphoric acids which were prepared by heating orthophosphoric acid up to the same temperature, 300°C, have quite different compositions depending upon the weight of orthophosphoric acid taken and the elevation rate of the temperature. These facts may be clarified by comparing the results of the sample Nos. 8, 11 and 12.

Higgins and Baldwin[11] heated orthophosphoric acid at the constant temperature, 176°C for sixteen hours and obtained a mixture of 51 wt. % orthophosphoric acid, 38 wt. % pyrophosphoric acid, 9 wt. % tripolyphosphoric acid, 2 wt. % tetrapolyphosphoric acid, and 0.2 wt. % pentapolyphosphoric acid. No change in the composition was noted on prolonged heating up to 32.5 hours at 176°C. Therefore, the difference between the composition of the sample Nos. 13 and 14 in Table I, which were prepared by heating at 140°±2°C, may be due to the fluctuation of the temperature.

In Fig. 3 the relation between the composition of the strong phosphoric acids and their contents of phosphorus (V) oxide are illustrated. Generally they coincide with the data obtained by Bell[3], Higgins and Baldwin[11], and Huhti and Gartaganis[12], even if the strong phosphoric acids were prepared under different conditions. As indicated by Bell[3] and Huhti and Gartaganis[12], this means that a dynamic equilibrium between the component acids is set up, when the strong phosphoric acids are prepared by heating. However, Bell's data in higher phosphorus (V) oxide content may not be correct, because he did not determine separately the polyacid components higher than tripolyphosphoric acid. In the study by Huhti and Gartaganis small quantities of penta-, hexa- and heptapolyphosphoric acid were determined in the range from 78 to 80 wt. %

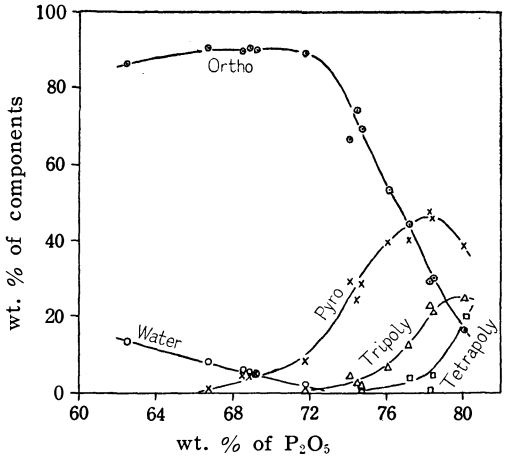



Fig. 3. Relation between the composition of the strong phosphoric acids and the contents of phosphorus (V) oxide.

phosphorus (V) oxide, but the present authors were not able to find them. In this respect the method of anion-exchange chromatography should be furthermore examined for the determination of higher polyphosphates.

During the course of the present investigation Parks and Van Wazer[14] published their treatise, in which a reorganization theory for the condensed phosphates as well as the strong phosphoric acids was developed. According to their theory for the strong phosphoric acids, in the general case, all five of the structural units, i. e. branching $PO_4$ units, middle $PO_4$ units, end $PO_4$ units, orthophosphoric acid units, and unreacted water molecule units may be present, with mole fractions $b$, $m$, $e$, $o$ and $u$. All of the combinations whereby these units can interchange roles with each other are given by the following equations with the equilibrium constants.

$$2m=b+e \qquad K_1=b\cdot e/m^2 \qquad (1)$$

$$2e=m+o \qquad K_2=m\cdot o/e^2 \qquad (2)$$

$$2o=2e+u \qquad K_3'=(2e)\cdot u/o^2 \qquad (3)[15]$$

In addition to the equations (1), (2) and (3), there are two other equations (4) and (5).

$$R=H_2O/P_2O_5=H/P$$
$$=(3o+2e+m+2u)/(b+m+e+o) \qquad (4)$$

$$b+m+e+o+u=1 \qquad (5)$$

14) J. R. Parks and J. R. Van Wazer, *J. Am. Chem. Soc.*, in press.

15) For this equilibrium another equilibrium constant $K_3=e^2\cdot u/o^2$ may be supposed, but the values of $K_3$ calculated from the experimental data were not constant in Parks and Van Wazer's study.

From the experimental data obtained by Huhti and Gartaganis[12] it was assumed that $K_1=1.0\times10^{-3}$, $K_2=8\times10^{-2}$, and $K_3'=2.0\times10^{-2}$ on a mole fraction basis. The theoretical curves of mole fractions of *b*, *m*, *e*, *o* and *u* were plotted as a function of $R$ on the assumption mentioned above. These curves are shown in Fig. 4. The

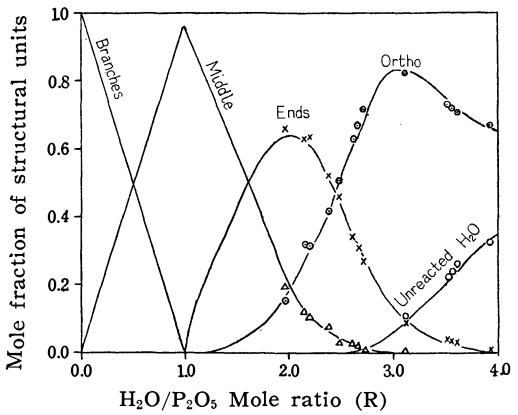



Fig. 4. Mole fractions of structural units as a function of $H_2O/P_2O_5$ mole ratio.

experimental data obtained by Huhti and Gartaganis agreed with the theoretically derived curves, although the data covered only the range from $R=1.2$ to $R=3.6$. The experimental data of the present study are shown as individual points in Fig. 4 and they also agree very well with the theory at least in the range from $R=2.0$ to $R=4.0$. This may prove the correctness of Parks and Van Wazer's theory.

## Summary

The strong phosphoric acids in the range from 67 to 80 wt. % phosphorus(V) oxide were analyzed by the anion-exchange chromatography combined with the usual molybdenum-blue colorimetry. The so-called "300°C-strong phosphoric acid" which has been used for many analytical purposes in the authors' laboratory is composed of 44.4 wt. % orthophosphoric acid, 39.8 wt. % pyrophosphoric acid, 12.3 wt. % tripolyphosphoric acid, and 3.6 wt. % tetrapolyphosphoric acid. It was found that the relation of mole fractions of middle $PO_4$ units, end $PO_4$ units, orthophosphoric acid units, and unreacted water molecule units versus the mole ratio $H_2O/P_2O_5$ agrees with the reorganization theory for the strong phosphoric acids, presented by Parks and Van Wazer.

The authors wish to thank Professor T. Kiba for many helpful suggestions and criticism. They also thank the Ministry of Education for the financial support of this research.

*Department of Chemistry*
*Faculty of Science*
*Kanazawa University*
*Kanazawa*

# *Oxidation of Chromia Supported on Alumina*

By Yoshio MATSUNAGA

(Received May 25, 1957)

Since 1946 Selwood and his coworkers[1] have carried out a detailed study of the magnetic properties of certain catalysts. By determining susceptibility-composition isotherms for a variety of supported oxides of transition elements, they deduced the oxidation state, the interaction covalence, and the dispersion of the paramagnetic ions. In the case of chromia on alumina[2], they concluded that, while the moment is nearly constant over the whole composition range, the change in susceptibility of chromium is almost entirely brought about by a change in the Weiss constant, namely the degree of dispersion. Selwood stated that the plus-three oxidation state of chromium is probably stabilized by the inductive action of the alumina support.

On the other hand, chromia has been known as a p-type semiconductor in an ordinary atmosphere and contains an excess of oxygen. The surface oxidation of chromia and chromia-alumina catalysts has been studied by many workers. Weller and Voltz[3] showed that the amount of excess of oxygen after treatment with oxygen at 500°C corresponds to the coverage of about one third of the total surface of the chromia. However, their study was concerned with only one commercial chromia-alumina catalyst, so it seems of interest to examine the correlation between the degree of dispersion and the stability of chromia towards oxidation at various temperatures.

## Experimental

**Preparation of Catalysts**—The alumina and the chromia-alumina catalyst used in this study were prepared by a method similar to that described by Eischens and Selwood. Aluminum was dissolved in a ten per cent. solution of potassium hydroxide, then precipitated by acidification with a stream of carbon dioxide. The washed precipitate was dried and calcined at 600 °C for twelve hours. The product was identified as gamma-alumina by X-ray diffraction. Alpha-alumina was prepared by further heat-treatment at about 1100°C for two weeks. The magnetic susceptibilities were found to be $-0.37\times10^{-6}$ for gamma-alumina and $-0.33\times10^{-6}$ for alpha-alumina. These values were independent of the field strength.

Catalyst samples were prepared by the impregnation method with chromic acid solution. By modifying the concentration of the chromic acid solution, catalysts with chromium concentration from about 1 to 33 per cent. were obtained. Samples were dried for eight hours at 350°C and reduced in a stream of hydrogen for five hours at 360°C. Analysis of each catalyst sample was carried out as follows. The samples were dissolved in hot concentrated sulfuric acid and diluted. The chromic ion was oxidized with potassium persulfate using silver nitrate as catalyst and the excess of the oxidant was decomposed by boiling the solution. After cooling, an excess of ferrous ammonium sulfate was added and the solution was titrated with standard dichromate solution, using diphenylamine in concentrated sulfuric acid as indicator.

**Oxygen Treatment**—The reduced catalysts were cooled in a stream of hydrogen and oxidized with air at room temperature. Further oxidations were carried out in a stream of oxygen for five hours at 250, 350 and 450°C.

**Determination of Oxidation Number of Chromium**—An iodometric method was employed for this purpose as described by Weller and Voltz[3]. A weighed amount from 100 to 300 milligrams of the sample was placed in about 30 cc. of distilled water and to it were added about two grams of potassium iodide and 10 cc. of distilled hydrochloric acid. The mixture was allowed to stand for about thirty minutes and the suspension was titrated with standard sodium thiosulfate solution (0.02N) with the use of starch solution as indicator. The mean oxidation number of chromium was calculated on the assumption that chromic ions equivalent to the active oxygen are present in a valent state higher than three.

**Magnetic Measurement**—The susceptibilities were measured at room temperature using a Gouy balance as previously described[4]. The field was calibrated at two constant current strengths with distilled water. When samples exhibited field strength dependence of susceptibility,

1) P. W. Selwood, "Catalysis" vol. 1 ed. by P. H. Emmett, Reinhold Pub. Corp., New York, 1954, p. 353.
2) R. P. Eischens and P. W. Selwood, *J. Am. Chem. Soc.*, **69**, 1590, 2698 (1947).
3) S. W. Weller and S. E. Voltz, ibid., **76**, 4695, 4701 (1954) and references cited there.
4) H. Akamatu and Y. Matsunaga, This Bulletin, **26**, 364 (1953).

the ferromagnetic effect was calibrated by the formula[5],

$$\chi_H = \chi + 2\sigma c/H$$

where $\chi_H$ is the apparent susceptibility observed at the field strength $H$, $\sigma$ the saturation magnetization of the ferromagnetic impurity, $c$ its concentration, and $\chi$ the susceptibility free from ferromagnetism.

The gram susceptibility of chromium was evaluated on the assumption that the susceptibility contributions of chromium, aluminium, and oxygen ions are additive, and those of the last two are independent of concentration.

## Results

The first series to be considered is that in which gamma-alumina is used as a carrier. Fig. 1 shows the apparent oxidation number of chromium, determined by the chemical analysis, plotted against the concentration of chromium. The specific susceptibilities of chromium derived by direct application of the Wiedemann additivity law from the values per gram of catalyst samples are conveniently shown graphically in Fig. 2. Eischens and Selwood chose to call such curves "susceptibility-composition isotherms". Similar data for the second series, in which chromic acid is impregnated on alpha-alumina, are shown in Figs. 5 and 6.

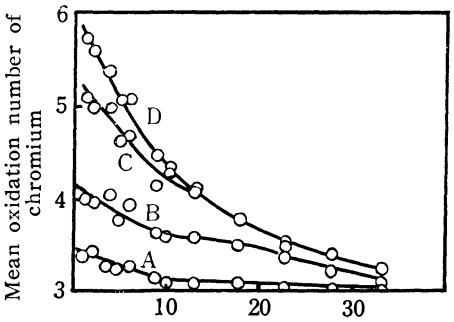



Fig. 1. Relation of oxidation number of chromium supported on gamma-alumina to its concentration: A, oxidized at room temperature; B, at 250°C; C, at 350°C; D at 450°C.

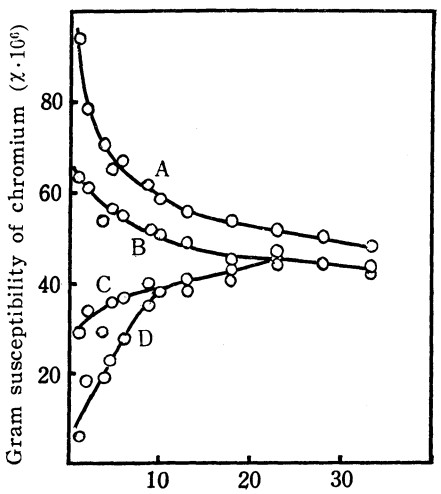



Fig. 2. Susceptibility-composition isotherms for chromia impregnated on gamma-alumina: A, oxidized at room temperature; B, at 250°C; C, at 350°C; D, at 450°C.

## Discussion

The reduced catalyst samples are green or bluish white in a stream of hydrogen, but those of low concentration of chromium change their color to grayish white or grayish green in a short time after contact with air. These color changes suggest that the oxidation proceeds perceptibly at room temperature and, as the concentration of chromium decreases, air reacts with the chromic ion more rapidly. By direct chemical analysis, chromium in an oxidation state higher than three was detected over the whole concentration range. As shown in Fig. 1 curve A, the mean oxidation number is appreciably higher than three in the catalyst samples which contain less than ten per cent. of chromium and the limiting value at infinite dilution seems to be about 3.5.

When the temperature of oxygen treatment is raised above 250°C, the catalyst samples in the concentration range of less than eight per cent. change their color to yellowish white and those in the range from eight to twenty per cent. show grayish brown color. These remarkable color changes indicate that a drastic increase in oxidation number of chromium is likely to occur during oxygen treatment at such high temperatures and the results of chemical analysis confirm this view. In the limiting case, infinite dilution of chromium, the oxidation number increases until it finally reaches six, namely chromia is oxidized completely to chromic anhydride. The oxidation of chromia found here is in sharp contrast to our knowledge of the thermal decomposition of chromic anhydride. Glemser and his coworkers[6] showed that chromic

5) L. F. Bates, "Modern Magnetism" Cambridge Univ. Press, 1951, p. 135.

6) O. Glemser, U. Hauschild and F. Trüpel, *Z. anorg. allgem. Chem.*, **277**, 113 (1954).

anhydride begins to decompose in a stream of oxygen at about 250°C, the products being $CrO_{2.6}$ at temperature range from 283 to 314°C, $CrO_{2.4-5}$ from 334 to 388°C, and $CrO_{1.6}$ above 400°C. Therefore, the remarkable oxidation of supported chromia can not be attributed to a gross change in crystal nuclei, but the large surface area due to their dispersed structure may be responsible. It appears that the stabilization of the plus-three state of chromium by the inductive action of the alumina support is not effective enough for surface oxidation of chromia to be appreciably prevented.

To elucidate the shapes of the curves in Fig. 1, we must refer to the susceptibility isotherm method developed by Eischens and Selwood; this method revealed the dispersed structure of supported chromia from the magnetic data. Eischens and Selwood established that the susceptibility of chromium in supported chromia follows the Curie-Weiss law, $\chi=C/(T+\Delta)$, and noticed that the Curie constant $C$ which relates to the oxidation state of chromium is almost constant but that the Weiss constant $\Delta$ is markedly dependent on the chromium concentration. According to Heisenberg's theory, the Weiss constant may be related to the exchange effect between neighboring paramagnetic chromium ions by the formula,

$$\Delta=-2JzS(S+1)/3k,$$

where $J$ is the exchange integral, $z$ the number of equidistant paramagnetic neighboring ions, $S$ the vector sum of spin moments, and $k$ the Boltzmann constant. Eischens and Selwood calculated the relationship between $z$ and the number of layers of chromia on the assumptions that the variation in the exchange integral can be ignored and also that supported chromia has the corundum structure consisting of a hexagonal close-packed oxide-ion lattice with chromic ions in two thirds of the octahedral holes. Their calculations are reproduced graphically in Fig. 3. They pointed out that the graph of $z$ against the number of layers changes its direction fairly sharply at about three layers and concluded that at the point where the susceptibility-composition isotherm changes its direction, the crystal nuclei of chromia spread on gamma-alumina are, on the average, three layers thick. In our results shown in Fig. 2 curve A, such a characteristic point which was called "point 1" is found at about ten per cent. of chromium. In the higher concentration range of chromium, these crystal nuclei tend to grow and to thicken. On the other hand, as the concentration of chromium decreases, the crystal nuclei shrink and, at the limit, chromium ions may be in two-dimensional atomic dispersion.

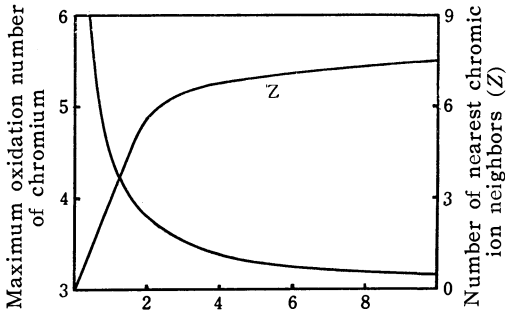



Fig. 3. Relation of maximum oxidation number of chromium and number of nearest chromic ion neighbors to number of layers of chromia.

It must be noted that the oxidation of chromia is especially marked in the concentration range of chromium less than that corresponding to point 1. The decrease in gram susceptibility of chromium means an increase of chromium in a valence state higher than three. Chromium ions in the plus-four and five states are less paramagnetic than those in the plus-three state and susceptibility of chromic acid may be nearly zero; therefore, the shapes of the susceptibility isotherms for the catalyst samples oxidized at higher temperatures (curves B, C and D in Fig. 2) are not only consistent with the above-mentioned view, but also show such a tendency more clearly. A chromium ion in the interior of crystalline chromia is completely surrounded by oxide ions and can not be oxidized directly with oxygen unless it migrates to the surface. But a chromic ion situated on the surface has not a sufficient number of oxide ions to enclose it and there is a possibility of suffering oxidation. The relationship between $z$ and the number of chromia

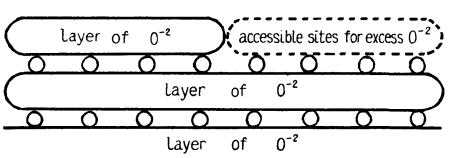



Fig. 4. Schematic representation of two layers of chromia, ○ $Cr^{+3}$.

layers is determined by the relative importance of the surface layer, hence, we can conclude easily that the degree of possible oxidation stands in close relation with $z$.

We shall examine the expected relation more quantitatively. Fig. 4 is a very schematic representation of supported chromia which is just two layers thick. Electroneutrality can be achieved in a chromia nucleus when the number of chromic ions situated in the outermost layer is the same as that in the layer just below, and half of them are not covered with oxide ions as shown in the model. The vacant sites on the surface can accommodate excess oxygen atoms until half of the chromic ions in the outermost layer are oxidized completely to the sexavalent state. Therefore, if sufficient oxide ions are supplied into such a space in the outermost oxide layer, the increase in the mean oxidation number of chromium must be $(6-3)/2\times2$ as shown in Fig. 4. Similar examination of a crystal model shows that the maximum value of the mean oxidation number of chromium has the following values; for one layer, +4.50; for three layers, +3.50; for five layers, +3.30; and for ten layers, +3.15. The possible oxidation numbers thus calculated are shown graphically in Fig. 3 for the purpose of comparing with the relation between $z$ and the number of layers of chromia. The magnitude of the calculated values seems to be rather small. The disaccordance may be due to the existence of defects in the interior of the crystal which we ignored in the above examination. Some of them may contribute to oxidation directly and others may promote the migration of ions to the surface and create a further possibility of oxidation. Therefore, it is not too much to say that the possibility of surface oxidation explains satisfactorily the remarkable observed oxidation of supported chromia.

In the second series, the position of point 1 in the susceptibility isotherm for the catalyst samples oxidized at room temperature (Fig. 6 curve A) is not clear. However, by analogy to the first series, we can easily locate it in the isotherms for the catalysts oxidized at higher temperatures (Fig. 6 curves C and D) and also in the relations between the mean oxidation number and the concentration of chromium shown in Fig. 5. Point 1 is found at about two or three per cent. of chromium and its shift to a lower concentration of

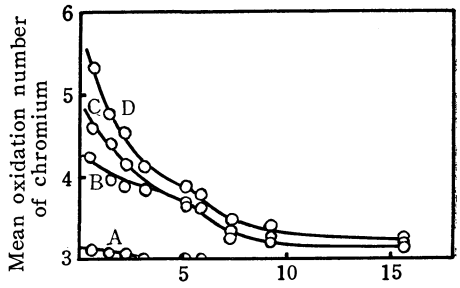



Fig. 5. Relation of oxidation number of chromium supported on alpha-alumina to its concentration: A, oxidized at room temperature; B, at 250°C; C, at 350°C; D, at 450°C.

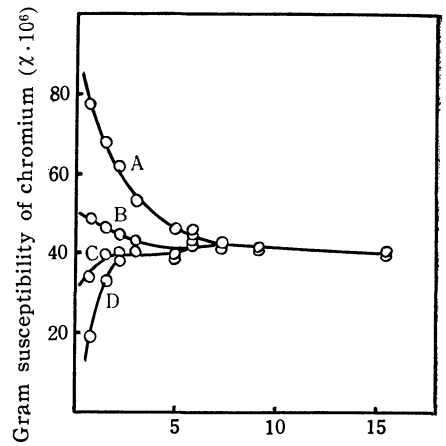



Fig. 6. Susceptibility-composition isotherms for chromia impregnated on alpha-alumina: A, oxidized at room temperature; B, at 250°C; C, at 350°C; D, at 450°C.

chromium may be due to a decrease in surface area of the carrier.

The susceptibility isotherms C and D in both the first and the second series show the existence of a characteristic point where the concentration of chromium is about twice that at point 1. The magnetic susceptibility of chromium in the catalyst samples oxidized at 350 and 450°C is nearly constant between these two points. At present the author can not give any explanation to this new point.

Although point 1 was shown at first in the susceptibility isotherm by Eischens and Selwood and its meaning was given on the basis of the magnitude of Weiss constant as clarified in the preceeding paragraphs, its position in the chromia-alumina catalyst system can be easily pointed out in the relation between the

mean oxidation number and the concentration of chromium in the samples oxidized at the temperature higher than 350°C. The latter method may be more convenient than the magnetic method as it needs only the apparatus for the usual chemical analysis. Besides, at least in this catalyst system our chemical method has the possibility of giving a measure of the surface area of promoter. It is not yet clear whether or not the application of the method described here is limited to this case.

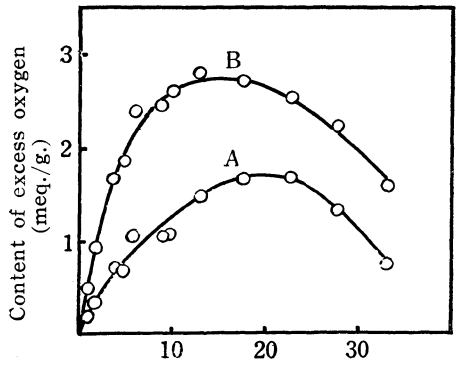



Fig. 7. Relation of content of excess oxygen in chromia-gamma-alumina catalysts to chromium concentration: A, oxidized at 250°C; B, at 450°C.

As the oxidation of supported chromia can be closely related to its high surface area, if we plot the content of excessive oxygen in one gram of the oxidized catalyst sample against the concentration of chromium, the composition at which the surface area of chromia per gram of catalyst reaches its maximum value will be indicated. As shown in Fig. 7, the catalysts which contain from 15 to 20 per cent. of chromium have the greatest values of excessive oxygen. Therefore, when we need to prepare the chromia-alumina catalyst in which the surface area of chromia is as high as possible, we must impregnate chromic acid solution on gamma-alumina, as the final concentration of chromium will be from 1.5 to 2 times that corresponding to point 1.

A similar study on the chromia-zinc oxide catalyst system was also made. The results will be presented in a later paper.

## Summary

Oxidation of chromia supported on gamma- and alpha-alumina at room temperature, 250, 350 and 450°C was examined by chemical and magnetic method. The mean oxidation number of chromium in the oxidized catalyst samples was determined as a function of the concentration of chromium. In the extreme case, infinite two-dimensional dilution of chromium, it was shown that chromia is oxidized completely to chromic anhydride. This chemical change is in sharp contrast to our knowledge of the thermal decomposition of chromic anhydride. The remarkable property of supported chromia to suffer oxidation was attributed to the relative importance of surface oxidation and explained nearly quantitatively by comparing it with the conclusion deduced from the susceptibility-composition isotherm method developed by Selwood and his coworkers. Therefore, the study of oxidation of the chromia-alumina catalyst system by chemical analysis seems to be useful to the same degree as the magnetic method proposed by Selwood and more convenient for deducing the dispersed structure of supported chromia. Finally the condition of preparing the catalyst sample which has the greatest surface area of chromia per gram of catalyst was examined in reference to the above-mentioned conclusion.

The author wishes to express his hearty thanks to Professor H. Akamatu for his kind direction.

*Department of Chemistry*
*Faculty of Science*
*The University of Tokyo*
*Hongo, Tokyo*

# *Reaction Rate and Electron Transfer Mechanism in Disproportionation Reaction of Uranium (V)**

By Hideo IMAI

(Received May 8, 1957)

In acid solution, sexavalent uranium ($UO_2^{++}$) is reduced to unstable quinqulvalent uranium at the dropping mercury electrode, and is regenerated by the disproportionation reaction of the reductant (U(V)) as is schematically shown in the following equations:

$$U(VI)+e=U(V): \text{ Electrode Reaction (1)}$$

$$U(V)+U(V)=U(VI)+U(IV): \text{ Disproportionation Reaction (2)}$$

Since both the sexavalent uranium diffused from the bulk solution and the one regenerated by the disproportionation reaction reach the electrode and are reduced, the limiting current has a reaction-controlled as well as a diffusion-controlled component[1]. The increase in the current beyond that corresponding to a one-electron diffusion-controlled reduction is a function of the rate of the disproportionation, and one can estimate the rate constant from the measurement of the limiting current.

Hitherto, it has been found that the rate linearly increases with the hydrogen ion concentration[2] and it increases in the presence of chloride[3]. With regard to this effect of chloride it was assumed that the increment in the rate may be assigned to the $\zeta$-potential of the electrode surface.

In this connection, the increase in the rate of some isotopic electron exchange reactions such as Fe(II)—Fe(III)[4], Hg(I)—Hg(II)[5], Ce(III)—Ce(IV)[6], Eu(II)—Eu(III)[7] and Cr(II)—Cr(III)[8] has been observed in homogeneous solutions containing chloride. The present author has also found that the electron transfer of some electrode processes such as the electrolytic reduction of thallous, cadmium and zinc ions under the continuously changing potential is facilitated in solutions containing sulfate, chloride, bromide and iodide in the order given[9]. In this paper a similar effect of various anions on the disproportionation rate process of uranium (V) is investigated, and a tentative reaction mechanism presented.

## Experimental

**Apparatus.**—The current-voltage curves were recorded with a SHIMADZU Model SH-2 photographically recording polarograph, whose maximum current-sensitivity was $2.85\times10^{-9}$ amp./mm./m. The cell used was an H type with triple sintered glass partitions. In two compartments between the test solution and the saturated calomel electrode, the saturated solution of sodium perchlorate and that of sodium chloride were instilled in order to avoid the formation of insoluble potassium perchlorate and also to avoid the contamination of the test solution by chloride. The construction was as follows:

(S.C.E.(Anode))—(Sat. NaCl)—(Sat. $NaClO_4$)—(Test solution-D. M. E. (Cathode)).

The temperature was kept constant within the error of $\pm0.1$°C by a thermostat. With a head of 30 cm. of mercury the mean life-time of the dropping mercury electrode in 2 f sodium perchlorate solution was $5.5_8$ sec. at the applied voltage of $-0.4$ volts vs. S. C. E.

**Reagent.**—All the reagents were of analytical grade. To prepare the stock solution of uranyl perchlorate, uranyl acetate ($UO_2(C_2H_3O_2)_2\cdot2H_2O$) was evaporated three times with perchloric acid and dissolved in 2 f perchloric acid solution. The test solutions were prepared by diluting this with supporting electrolyte solutions.

The concentration of uranyl ions was determined as follows. Ammonium hydroxide was added to 10 ml. test solution and, after digestion

* Presented at the Discussion on Polarography held by the Electrochemical Society of Japan in November, 1956, and the 10th Annual Meeting of the Chemical Society of Japan held in April, 1957.

1) I. M. Kolthoff and W. E. Harris, *J. Am. Chem. Soc.*, **67**, 1484 (1945); **68**, 1175 (1946).
2) E. F. Orlemann and D. M. Kern, ibid., **75**, 3059 (1953).
3) J. Koryta and J. Koutecky, *Collection Czechoslov. Chem. Communs.*, **20**, 423 (1955).
4) J. Silverman and R. W. Dodson, *J. Phys. Chem.*, **56**, 846 (1952).
5) R, L. Wolfgang and R. W. Dodson, ibid., **56**, 872 (1952).
6) H. C. Hornig and W. F. Libby, ibid., **56**, 869 (1952).
7) D. J. Meier and C. S. Garner, ibid., **56**, 853 (1952).
8) H. Taube and H. Myers, *J. Am. Chem. Soc.*, **76**, 2103 (1954).
9) H. Imai and S. Chaki, This Bulletin, **29**, 498 (1955).

for thirty minutes on a water bath, the precipitate was filtered on a No. 7 Tōyō filter paper. Then, the precipitate was washed with water containing ammonium hydroxide and ignited to red heat. The residue was weighed as $U_3O_8$.

The concentration of perchloric acid in the test solution was determined by titration with the standard solution of sodium hydroxide. Since the basic salt of uranyl perchlorate begins to precipitate at pH greater than 4, methyl orange is qualified for the indicator. The ionic strength was kept at a constant value of 2.1 f by adding sodium perchlorate. In all cases no surface active reagent was used, since it reduced the reaction rate. Nitrogen gas purified by van C. Brunt's method was used to remove the dissolved oxygen in the test solution prior to submission to polarography.

**Current-Voltage Curve.**—The current-voltage curves of uranyl in various supporting electrolytes are shown in Fig. 1. Uranyl developed well-defined polarographic waves in 2 f sodium perchorate solution, there being no polarographic maxima. The half-wave potential of the first wave was $-0.17_0$ volts vs. S. C. E., and that of the second $-0.92_5$ volts vs. S. C. E. The apparent

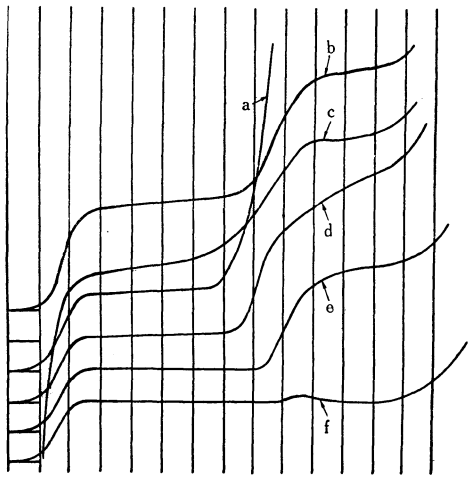



Fig. 1. Current-voltage curves of uranyl in various supporting electrolytes: Each curve starts at 0V vs. S. C. E. and each voltage interval corresponds to 0.1 V. A short horizontal line represents a galvanometer zero line. ($UO_2^{2+}$), 4.22 mf. Temp., 25°C. Ionic strength, 2.1 f.

a ($1\times10^{-1}$ f $H^+$, 2 f $NO_3^-$) b ($1\times10^{-1}$ f $H^+$, 2 f $Cl^-$)
c ($1\times10^{-1}$ f $H^+$, 2 f $Br^-$) d ($1\times10^{-1}$ f' $H^+$, 2 f $ClO_4^-$)
e ($5\times10^{-3}$ f $H^+$, 2 f $ClO_4^-$) f ($2\times10^{-3}$ f $H^+$, 2 f $ClO_4^-$)

number of electrons transferred per ion was one in the case of the first reduction, and two in the case of the second reduction. When the hydrogen-ion concentration was less than $10^{-3}$ f, the second wave disappeared, while the first wave decreased to a definite height, giving a pure diffusion-controlled current. The first reduction gives quinquevalent uranium, which is unstable in acid solution and disproportionates into sexavalent uranium and quadrivalent uranium. The quinquevalent uranium is reduced to tervalent uranium in the second reduction. It is assumed that in a slightly acidic solution the basic salt of quinquevalent uranium precipitates, and accordingly, the second wave disappears.

**Estimation of the Rate Constant.**—The disproportionation reaction (equation 2) is of the second order with respect to quinquevalent uranium. Accordingly, the rate of the regeneration of uranium (VI) is given as follows;

$$dU(VI)/dt = 1/2 \cdot kU(V)^2 \qquad (3)$$

where $k$ is the rate constant.

This flux of the sexavalent uranium contributes to the first reduction as well as the flux of the pure diffusion. Hence, one arrives at the equations

$$\partial U(VI)/\partial t = D\partial^2 U(VI)/\partial x^2 + (2x/3t)\partial U(VI)/\partial x + 1/2 \cdot kU(V)^2 \qquad (4)$$

$$\partial U(V)/\partial t = D\partial^2 U(V)/\partial x^2 + (2x/3t)\partial U(V)/\partial x - kU(V)^2 \qquad (5)$$

the boundary condition being the same as in the case of a pure diffusion, i. e.,

$$\left.\begin{aligned} &t=0,\ x>0;\ U(VI)=a^*,\ U(V)=0 \\ &t>0,\ x=0;\ U(VI)=0,\ \partial U(VI)/\partial x = -\partial U(V)/\partial x \end{aligned}\right\} \qquad (6)$$

where $a^*$ is the concentration of uranyl in the bulk solution, and the diffusion constant ($D$) of the oxidant is assumed to be equal to that of the reductant.

The solution of equations 3 and 4 was given by Orlemann and Kern[2] by means of the concept of a reaction volume and was followed by Koutecky-Koryta's approximate solution[10] as is illustrated in the following;

$$\left.\begin{aligned} &\bar{i}_l/\bar{i}_d = 1 + \sum_{i=1}^{\infty} D_i \xi_1^i \\ &\xi_1 = 2a^* kt \end{aligned}\right\} \qquad (7)$$

where $\bar{i}_l$ is the mean limiting current, $\bar{i}_d$ is the mean diffusion-controlled current, $D_i$ is a numerical constant ($D_1=4.716\times10^{-2}$, $D_2=-4.679\times10^{-3}$, $D_3=5.350\times10^{-4}$, $D_4=-6.771\times10^{-5}$, ……) and $t$ is the reaction time.

The pure diffusion-controlled current ($\bar{i}_d$) can be estimated in the solution containing about $10^{-3}$ f hydrogen ion, since in this solution the disproportionation reaction is virtually negligible. In this experiment $\bar{i}_l$ and $\bar{i}_d$ were measured at the applied voltage of $-0.4$ volts vs. S. C. E., where a plateau was given in the current-voltage curve, and $t$ was the mean of the life-time of ten drops of the D. M. E. Thus, the rate constant was calculated and it was confirmed that, as far as the value of $\bar{i}_l/\bar{i}_d$ did not exceed 1.18, equation 7 gave sufficiently accurate values in comparison

10) J. Koutecky and J. Koryta, *Collection Czechoslov. Chem. Communs.*, **19**, 845 (1954).

TABLE I

EFFECT OF THE HYDROGEN ION ON THE DISPROPORTIONATION RATE CONSTANT

| No. | $(H^+)$ f | $t$ sec. | $E_{1/2}$, $V_{vs.}$ S. C. E. | $\bar{i}_l$ $\mu$A | $\bar{i}_l/\bar{i}_d$ | $\xi$ | $k$ $f^{-1}\cdot sec.^{-1}$ | $k_0$ $f^{-2}\cdot sec.^{-1}$ |
|---|---|---|---|---|---|---|---|---|
| 1 | 0.002 | $5.5_8$ | $-0.17_0$ | 14.2 | 1 | 0 | 0 | 0 |
| 2 | 0.005 | $5.5_8$ | $-0.17_0$ | 14.2 | 1 | 0 | 0 | 0 |
| 3 | 0.03 | $5.5_8$ | $-0.17_0$ | 14.5 | $1.02_1$ | 0.48 | 10 | 340 |
| 4 | 0.06 | $5.5_8$ | $-0.17_0$ | 14.9 | $1.04_9$ | 1.16 | 25 | 410 |
| 5 | 0.09 | $5.5_8$ | $-0.17_0$ | 15.3 | $1.07_7$ | 1.93 | 41 | 456 |
| 6 | $0.101_5$ | $5.5_8$ | $-0.17_0$ | 15.4 | $1.08_5$ | 2.19 | 47 | 458 |
| 7 | 0.12 | $5.5_8$ | $-0.17_0$ | 15.5 | $1.09_2$ | 2.40 | 51 | 425 |
| 8 | 0.15 | $5.5_8$ | $-0.17_0$ | 15.7 | $1.10_6$ | 2.86 | 61 | 405 |
| 9 | 0.18 | $5.5_8$ | $-0.17_1$ | 16.0 | $1.12_7$ | 3.62 | 77 | 427 |
| 10 | 0.21 | $5.5_8$ | $-0.17_1$ | 16.3 | $1.14_8$ | 4.43 | 94 | 448 |
| 11 | 0.24 | $5.5_8$ | $-0.17_1$ | 16.5 | $1.16_2$ | 5.08 | 108 | 450 |
| 12 | 0.27 | $5.5_8$ | $-0.17_2$ | 16.8 | $1.18_3$ | — | — | — |
| 13 | 0.30 | $5.5_8$ | $-0.17_2$ | 17.1 | $1.20_4$ | — | — | — |
| | | | | | | | | (436) mean |

($a^*=4.22\times10^{-3}$ f, $\mu=2.1$ f ($NaClO_4$))

with those measured in homogeneous solutions[11]. The error for the estimation of the rate constant amounts to ±10%.

## Results and Discussion

**Effect of Hydrogen Ion.** — Uranyl developed no well-defined wave in buffered media, so the acidity of the solution was controlled by perchloric acid. Strictly speaking the hydrogen ion concentration was not equal to the concentration at the electrode surface where the disproportionation reaction occurred. When there was a trace of the dissolved oxygen, the hydrogen ion concentration appreciably decreased at the electrode surface, owing to the formation of the hydroxide ion as the electrolytic reductant. Accordingly, the experiment was carried out after careful removal of the dissolved oxygen.

The hydrogen ion concentration, the limiting current and the rate constant are illustrated in Table I, and the rate constant is plotted against the hydrogen ion concentration in Fig. 2. The experimental conditions are appended to Table I.

From Table I and Fig. 2 one can conclude that the disproportionation reaction of equation 2 is of the first order with respect to the hydrogen ion; the rate constant ($k_0$) reduced to unit hydrogen ion concentration is given by

$$k_0=k/(H^+). \qquad (8)$$

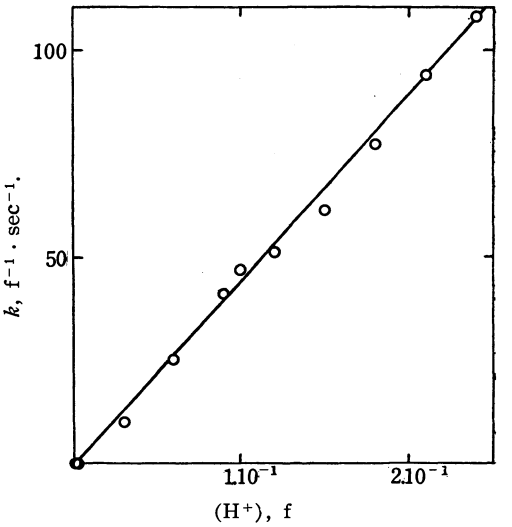



Fig. 2. Effect of the hydrogen ion on the disproportionation rate constant. Supporting electrolyte, 2.1 f $NaClO_4$; Temp., 25°C.

For convenience sake, the comparison of the rate constant will be referred to as $k_0$ in the following description.

**Effect of Chloride.**—The experimental conditions were as follows: the hydrogen ion concentration, $(H^+)=0.04_0$ f; the uranyl concentration, $a^*=1.95_4\times10^{-3}$ f; the reaction time $t=5.5_4$ sec.; the ionic strength, $\mu=2.04$ f; temperature, $T=298.2$°K.

Since the effect of chloride was multiplied by that of the hydrogen ion to yield too great an effect to bear on equation 7, a low concentration of the hydrogen ion was preferable to measure the effect in

11) D. M. Kern and E. F. Orlemann, *J. Am. Chem. Soc.*, **71**, 2102 (1949); K. A. Kraus et al., ibid., **71**, 2510 (1949); H. G. Heal and J. Thomas, *Trans. Faraday Soc.*, **45**, 11 (1949).

TABLE II
EFFECT OF CHLORIDE ON THE DISPROPORTIONATION RATE CONSTANT

| No. | $(Cl^-)$ f | $t$ sec. | $E_{1/2}$, V vs. S. C. E. | $\bar{i}_l$ $\mu$A | $\bar{i}_l/\bar{i}_d$ | $\xi$ | $k$ $f^{-1}\cdot sec.^{-1}$ | $k_0$ $f^{-2}\cdot sec.^{-1}$ |
|---|---|---|---|---|---|---|---|---|
| 1 | 0 | $5.5_4$ | $-0.17_0$ | $7.8_2$ | $1.01_9$ | 0.42 | 19 | 475 |
| 2 | 0.2 | $5.5_4$ | $-0.17_2$ | $7.9_4$ | $1.03_5$ | 0.81 | 37 | 925 |
| 3 | 0.4 | $5.5_4$ | $-0.17_4$ | $8.0_1$ | $1.04_3$ | 1.01 | 48 | 1200 |
| 4 | 0.6 | $5.5_4$ | $-0.17_5$ | $8.0_8$ | $1.05_2$ | 1.12 | 52 | 1300 |
| 5 | 0.8 | $5.5_3$ | $-0.17_8$ | $8.1_1$ | $1.05_6$ | 1.34 | 62 | 1550 |
| 6 | 1.0 | $5.5_3$ | $-0.18_0$ | $8.1_3$ | $1.05_9$ | 1.42 | 66 | 1650 |
| 7 | 1.2 | $5.5_3$ | $-0.18_4$ | $8.2_1$ | $1.06_9$ | 1.70 | 79 | 1975 |
| 8 | 1.4 | $5.5_3$ | $-0.18_7$ | $8.2_8$ | $1.07_8$ | 1.96 | 91 | 2275 |
| 9 | 1.6 | $5.5_2$ | $-0.19_1$ | $8.4_4$ | $1.09_9$ | 2.62 | 121 | 3025 |
| 10 | 1.8 | $5.5_1$ | $-0.19_3$ | $8.4_7$ | $1.10_3$ | 2.76 | 128 | 3200 |
| 11 | 2.0 | $5.4_8$ | $-0.19_5$ | $8.5_4$ | $1.11_2$ | 3.08 | 149 | 3725 |

the wide range of the chloride concentration.

Under the above mentioned conditions, the pure diffusion-controlled current was $7.6_8$ microamp., when the hydrogen ion concentration was $5.6\times10^{-3}$ f.

The change in supporting electrolyte may result in the variation in the diffusion constant of a reducible species. Especially, this effect will increase, when a supporting electrolyte acts as a complexing agent. However, in this case the net variation of the diffusion constant is not noticeable; and furthermore, the diffusion-controlled current is proportional to the square root of the diffusion constant. Therefore, the diffusion rate will not play a leading role in the variation of the limiting current, while, it will be a cause of the error in the estimation of the rate constant. On the other hand, the increment of the $\zeta$-potential of the electrode surface in the concentration region above 1 f is less than that in the concentration region below 1 f. Accordingly, the steady increase of the limiting current in the chloride concentration ranging from 0.2 to 2 f is mainly attributable to the increase in the rate constant.

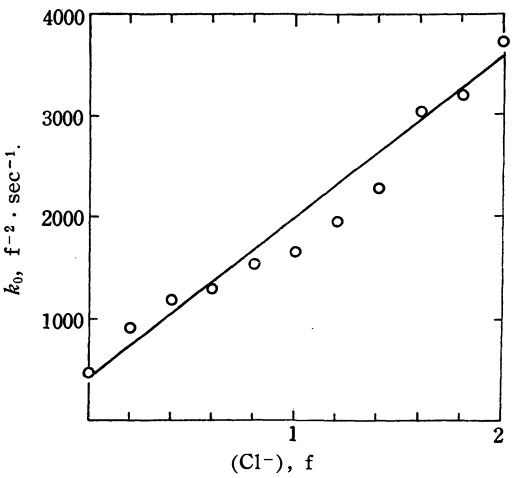



Fig. 3. Effect of chloride on the reduced rate constant, $k_0$. Temp., 25°C; Ionic strength, 2.1 f.

The results of this experiment are illustrated in Table II, and the rate constant is plotted against the chloride concentration in Fig. 3.

From these results it can be seen that the rate of the disproportionation reaction is of the first order with respect to chloride.

The variation of the half-wave potential with the chloride concentration indicates tacitly the existence of the uranyl chloride complex. In this case the kinetic current slightly affects the measurement of the half-wave potential and the mean discrepancy between the 1/4-wave potential and the 3/4-wave potential was about 62 millivolts, which was sufficiently close to the theoretically expected value of a reversible electrode process (59 millivolts)[12]. Hence, assuming that the stability constant of the complex does not vary in the high concentration region of the complexing agent, one can estimate the variation of the coordination number by the equation[13].

$$\bar{p}-\bar{q}=(\mathrm{d}(E_{1/2})_c/\mathrm{d}\log(X^-))\cdot(2.303RT/nF) \qquad (9)$$

where $\bar{p}$ and $\bar{q}$ are the mean coordination number of the higher oxidation state and that of the lower oxidation state, respectively. The plot of the logarithm of the

12) T. Thomas, *Collection Czechoslov. Chem. Communs.*, **9**, 12, 81, 150 (1937).
13) J. J. Lingane, *Chem. Revs.*, **29**, 1 (1941).

chloride concentration against the half-wave potential gives a straight line in the concentration region ranging from 1 f to 2 f as is illustrated in Fig. 4. The value of $\bar{p}-\bar{q}$ calculated from the tangent of the straight line was about unity.

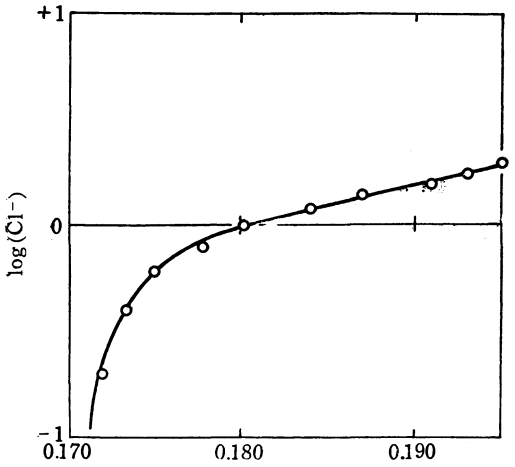



Fig. 4. Shift of the half-wave potential of the first reduction of uranyl by chloride. Temp., 25°C; Ionic strength, 2.1 f.

**Effect of Various Anions.** — By the author's datum the rate constant, $k_0$, was 436 $f^{-2} \cdot sec^{-1}$. in 2 f sodium perchlorate solution. By Koryta and Koutecky[3] it was 143 $f^{-2} \cdot sec^{-1}$. in 0.4 f sodium perchlorate, and was 700 $f^{-2} \cdot sec^{-1}$. in 3.8 f sodium perchlorate. From these data it can be seen that perchlorate appreciably affects the rate constant, while the effect of perchlorate was smallest in comparison with nitrate and bromide, and in particular, it was negligibly small in comparison with chloride and iodide. Accordingly, sodium perchlorate was qualified for keeping the ionic strength constant.

The experimental conditions were as follows: $(H^+)=0.101_5$ f; $a^*=4.22_5\times10^{-3}$ f; $\mu=2.1$ f; $T=298.2$°K.

The results are illustrated in Table III in which the life-time ($t$) of the D. M. E. appreciably changes with the bromide or the iodide concentration. Since the diffusion-controlled current is proportional to $t^{1/6}$ according to Ilkovic's equation, the variation in the life-time which amounts to 5% does not require any significant calibration for the pure diffusion-controlled current estimated in 2 f sodium perchlorate solution. The value of $\xi$, however, is a linear function of $t$, hence, the variation of the reaction time was taken into account.

In Figs. 5 and 6 is plotted the anion concentration against the limiting current and the rate constant, respectively. In all cases the rate constant is a linear function of the anion concentration. This leads to the following equation;

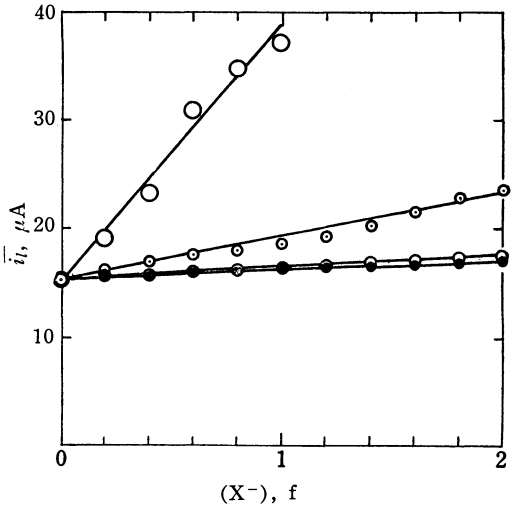



Fig. 5. Variation of the limiting current with the concentration of various anions. Temp., 25°C. Ionic strength, 2.1 f. $(H^+)$, $0.101_5$ f. ●···$NO_3^-$, ○···$Br^-$, ⊙···$Cl^-$, ○···$I^-$.

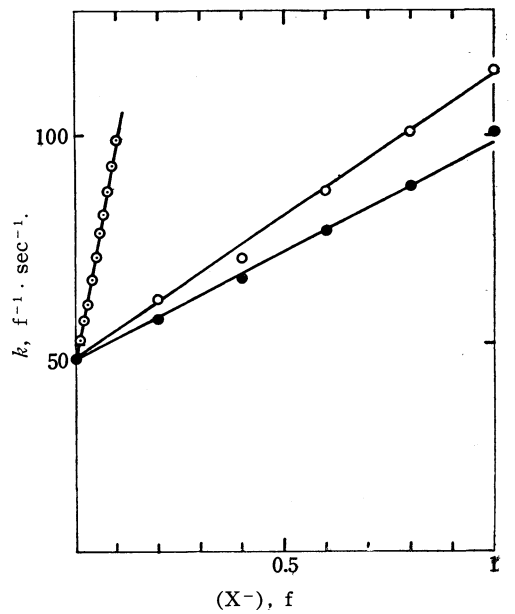



Fig. 6. Effect of various anions on the disproportionation rate constant. Temp., 25°C. Ionic strength, 2.1 f. ●···$NO_3^-$, ○···$Br^-$, ⊙···$Cl^-$.

TABLE III

COMPARISON OF THE EFFECT OF NITRATE, BROMIDE, CHLORIDE AND IODIDE ON THE DISPROPORTIONATION RATE CONSTANT

| | No. | $(X^-)$ f | $t$ sec. | $\bar{i}_l$ $\mu$A | $\bar{i}_l/\bar{i}_d$ | $\xi$ | $k$ $f^{-1}\cdot sec.^{-1}$ | $k_0$ $f^{-2}\cdot sec.^{-1}$ |
|---|---|---|---|---|---|---|---|---|
| $NO_3^-$ | 1 | 0 | $5.5_6$ | 15.4 | $1.08_5$ | 2.19 | 47 | 458 |
| | 2 | 0.2 | $5.5_6$ | 15.6 | $1.09_9$ | 2.63 | 56 | 550 |
| | 3 | 0.4 | $5.5_6$ | 15.8 | $1.11_3$ | 3.11 | 66 | 650 |
| | 4 | 0.6 | $5.5_6$ | 16.0 | $1.12_7$ | 3.62 | 77 | 758 |
| | 5 | 0.8 | $5.5_6$ | 16.2 | $1.14_1$ | 4.14 | 88 | 866 |
| | 6 | 1.0 | $5.5_5$ | 16.4 | $1.15_5$ | 4.75 | 101 | 995 |
| | 7 | 1.2 | $5.5_5$ | 16.6 | $1.16_9$ | 5.45 | 116 | 1143 |
| | 8 | 1.4 | $5.5_4$ | 16.8 | $1.18_8$ | 6.18 | 131 | 1291 |
| | 9 | 1.6 | $5.5_4$ | 17.0 | $1.19_7$ | — | — | — |
| $Br^-$ | 1 | 0 | $5.5_8$ | 15.4 | $1.08_5$ | 2.19 | 47 | 458 |
| | 2 | 0.2 | $5.5_4$ | 15.7 | $1.10_6$ | 2.86 | 61 | 598 |
| | 3 | 0.4 | $5.5_0$ | 15.9 | $1.12_0$ | 3.35 | 71 | 700 |
| | 4 | 0.6 | $5.4_5$ | 16.0 | $1.12_7$ | 3.62 | 77 | 758 |
| | 5 | 0.8 | $5.4_1$ | 16.4 | $1.15_5$ | 4.75 | 101 | 995 |
| | 6 | 1.0 | $5.3_9$ | 16.7 | $1.17_6$ | 5.82 | 124 | 1222 |
| | 7 | 1.2 | $5.3_7$ | 16.9 | $1.19_0$ | — | — | — |
| $Cl^-$ | 1 | 0 | $5.6_0$ | 15.6 | $1.09_1$ | 2.37 | 47 | 461 |
| | 2 | 0.04 | $5.6_0$ | 15.8 | $1.10_5$ | 2.83 | 56 | 551 |
| | 3 | 0.08 | $5.6_0$ | 16.0 | $1.11_9$ | 3.32 | 66 | 646 |
| | 4 | 0.12 | $5.6_0$ | 16.3 | $1.13_6$ | 3.96 | 78 | 770 |
| | 5 | 0.16 | $5.6_0$ | 16.4 | $1.14_7$ | 4.38 | 87 | 852 |
| | 6 | 0.20 | $5.6_0$ | 16.6 | $1.16_1$ | 5.04 | 99 | 973 |
| | 7 | 0.40 | $5.5_8$ | 17.4 | $1.22_5$ | — | — | — |
| $I^-$ | 1 | 0 | $5.5_8$ | 15.4 | $1.08_5$ | 2.19 | 47 | 458 |
| | 2 | 0.2 | $4.7_5$ | 19.1 | $1.34_5$ | — | — | — |

TABLE IV

TEMPERATURE DEPENDENCE OF THE LIMITING CURRENT AND THE DISPROPORTIONATION RATE CONSTANT

| | $T$°K | 281 | 285 | 289 | 293 | 297 | 301 | 305 | 309 |
|---|---|---|---|---|---|---|---|---|---|
| $\bar{i}_d$ | $t$, sec. | $5.8_0$ | $5.7_4$ | $5.6_8$ | $5.6_4$ | $5.6_0$ | $5.5_6$ | $5.5_2$ | $5.4_9$ |
| | $\bar{i}_d$, $\mu$A | 10.6 | 11.4 | 12.1 | 12.9 | 13.7 | 14.4 | 15.2 | 15.9 |
| $(H^+)$ | $t$, sec. | $5.8_0$ | $5.7_4$ | $5.6_8$ | $5.6_4$ | $5.6_0$ | $5.5_6$ | $5.5_2$ | $5.4_9$ |
| | $\bar{i}_l$, $\mu$A. | 10.9 | 11.8 | 12.7 | 13.6 | 14.6 | 15.6 | 16.6 | 17.6 |
| | $\bar{i}_l/\bar{i}_d$ | $1.02_8$ | $1.03_5$ | $1.05_0$ | $1.05_4$ | $1.06_6$ | $1.08_3$ | $1.09_2$ | $1.10_7$ |
| | $\xi$ | 0.65 | 0.82 | 1.19 | 1.29 | 1.61 | 2.12 | 2.40 | 2.90 |
| | $k$, $f^{-1}\cdot sec.^{-1}$ | 13 | 17 | 25 | 27 | 34 | 45 | 52 | 63 |
| $(H^+, Cl^-)$ | $t$, sec. | $5.8_0$ | $5.7_4$ | $5.6_8$ | $5.6_4$ | $5.6_0$ | $5.5_6$ | $5.5_2$ | $5.4_9$ |
| | $\bar{i}_l$, $\mu$A. | 11.0 | 12.0 | 13.0 | 14.1 | 15.2 | 16.5 | 17.9 | 19.3 |
| | $\bar{i}_l/\bar{i}_d$ | $1.03_8$ | $1.05_3$ | $1.07_4$ | $1.09_3$ | $1.10_9$ | $1.14_6$ | $1.17_8$ | $1.21_4$ |
| | $\xi$ | 0.89 | 1.26 | 1.84 | 2.44 | 2.96 | 4.34 | (5.92) | — |
| | $k$, $f^{-1}\cdot sec.^{-1}$ | 19 | 26 | 38 | 51 | 63 | 93 | (127) | — |
| $(H^+, Br^-)$ | $t$, sec. | $5.5_9$ | $5.5_4$ | $5.5_0$ | $5.4_6$ | $5.4_3$ | $5.4_0$ | $5.3_7$ | $5.3_5$ |
| | $\bar{i}_l$, $\mu$A. | 11.1 | 12.1 | 13.2 | 14.4 | 15.7 | 17.1 | 18.6 | 20.3 |
| | $\bar{i}_l/\bar{i}_d$ | $1.04_7$ | $1.06_1$ | $1.09_1$ | $1.11_6$ | $1.14_6$ | $1.18_8$ | $1.22_4$ | $1.27_7$ |
| | $\xi$ | 1.11 | 1.47 | 2.37 | 3.21 | 4.34 | (6.48) | — | — |
| | $k$, $f^{-1}\cdot sec.^{-1}$ | 24 | 31 | 51 | 70 | 95 | (142) | — | — |

($a^* = 4.22\times10^{-3}$ f)

$$dU(V)/dt = k_0^0 \cdot (X^-) \cdot U(V)^2 \qquad (10)$$

where $(X^-)$ is the anion concentration. Thus, it can be concluded that the disproportionation reaction of uranium (V) is of the third order in this case. In view of the fact that the diffusion-controlled current of the cadmium ion increases in the presence of bromide and iodide, the increase in the limiting current of Table III can not be solely assigned to the increase in the disproportionation rate, but it may presumably include the effect of the $\zeta$-potential. In this connection, it is noteworthy that a polarographic maximum appears in the test solution containing 1 f iodide. Furthermore, iodide was oxidized to iodine by perchloric acid in the test solution. Hence, the data in Table III are ill-defined in the cases of bromide and iodide.

The apparent half-wave potential was ill-defined in the solution containing iodide on account of the anodic current flowing at more negative potentials than the reduction potential of uranyl. Also, this effect exists in the case of bromide (cf. Fig. 1). However, it could be confirmed from the measurement in the solution containing low concentration bromide that the half-wave potential was slightly shifted by the presence of bromide. Similarly, the effect of nitrate was too small to deserve any attention**. However, the half-wave potential was appreciably shifted by chloride. It is noteworthy that a parallelism lies between the shift of the half-wave potential and the rate constant, except for the case of the hydrogen ion which does not affect the half-wave potential but increases the rate constant (cf. Table I).

From these results one can conclude that uranyl complex, whose change of the complexity is predominant in the course of the uranyl reduction, is liable to increase the rate of the disproportionation.

**Temperature Dependence of the Rate Constant.** — Test solutions containing $0.101_5$ f hydrogen ion, $0.101_5$ f hydrogen ion and 0.1 f chloride, and $0.101_5$ f hydrogen ion and 1 f bromide were prepared, and each solution was represented by $(H^+)$, $(H^+, Cl^-)$ and $(H^+, Br^-)$, respectively, in the following description. The ionic strength of each solution was maintained at 2.1 f. The other experimental conditions are appended to Table IV. The experiment was carried out at the temperature ranging from 280°K to 310°K, and the results are illustrated in Table IV.

The temperature dependence of the pure diffusion-controlled current and of the limiting current is illustrated in Fig. 7. In Fig. 7 the variation of the pure diffusion-controlled current is about 1.9%/deg., which corresponds to the theoretically expected value. On the other hand, the

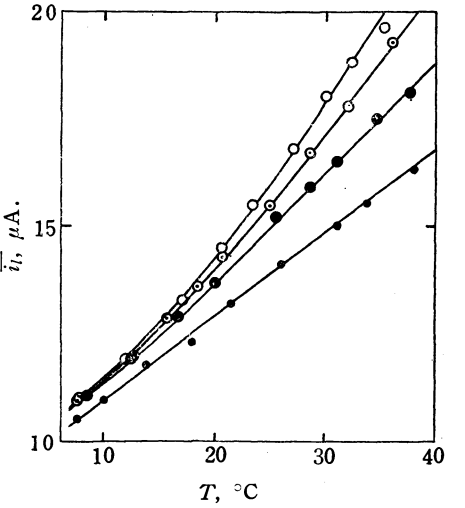



Fig. 7. Temperature dependence of the limiting current. Ionic strength, 2.1 f. $(UO_2^{2+})$, 4.22 mf. •···pure diffusion-controlled current, ●···0.1 f $H^+$, ⊙···0.1 f $H^+$+0.1 f $Cl^-$, ○···0.1 f $H^+$+1 f $Br^-$.

variation in the limiting current is greater than the pure diffusion-controlled current, and it becomes greater in the solution of $(H^+)$, $(H^+, Cl^-)$, $(H^+, Br^-)$ in the order given. As was previously described, the variation in the life-time of the D. M. E. did not appreciably affect the pure diffusion-controlled current. The variation of the reaction time, however, was taken into account and the rate constant was calculated.

In Fig. 8 the logarithm of the rate constant is plotted against the reciprocal of the temperature, and the plot gives a good linear relation in every case. From the tangent of the plot the heat of activation ($\Delta H^*$) was calculated by Arrhenius's

** In this connection the existence of the uranyl nitrate complex can be observed in the catalytic reduction of nitrate at the reduction potential of quinquevalent uranium. For instance, this phenomenon can be observed in Fig. 1 as a drastic increase of the second wave of uranyl in 2 f sodium nitrate solution. Recently, a detailed investigation of this catalytic current was reported by Koryta[14].

14) J. Koryta, *Collection Czechoslov. Chem. Communs.*, **20**, 667 (1955).

equation. The heat of activation ($\Delta H^{\ddagger}$) was calculated by equation 11 in order to apply the absolute rate expression.

$$\Delta H^{*}=\Delta H^{\ddagger}+RT \tag{11}$$

and the entropy of activation ($\Delta S^{\ddagger}$) was calculated from the equation

$$k=(eKT/h)\cdot e^{-\Delta H^{\ddagger}/RT}\cdot e^{\Delta S^{\ddagger}/R} \tag{12}$$

where $K$ is the Boltzmann constant and the other symbols have their usual significance. The free energy of activation ($\Delta F^{\ddagger}$) was calculated by the equation

$$\Delta F^{\ddagger}=\Delta H^{\ddagger}-T\Delta S^{\ddagger} \tag{13}$$

All these data are illustrated in Table V.

TABLE V
THE HEAT OF ACTIVATION, $\Delta H^{*,\ddagger}$, THE ENTROPY OF ACTIVATION, $\Delta S^{\ddagger}$, AND THE FREE ENERGY OF ACTIVATION, $\Delta F^{\ddagger}$, OF THE DISPROPORTIONATION REACTION OF U(V)

| Medium | $\Delta H^{*}$ kcal./mole | $\Delta H^{\ddagger}$ kcal./mole | $\Delta S^{\ddagger}$ e. u. | $\Delta F^{\ddagger}$ kcal. |
|---|---|---|---|---|
| 2 f $NaClO_4$ +0.1 f $H^+$ | 10.8 | 10.2 | −17.1 | 15.2 |
| 1.9 f $NaClO_4$ +0.1f $H^+$ +0.1f NaCl | 13.3 | 12.7 | −2.7 | 14.1 |
| 1f f $NaClO_4$ +0.1f $H^+$ +1f NaBr | 15.4 | 14.8 | +0.4 | 14.7 |

(Ionic strength was kept at 2.1 f with $NaClO_4$.)

It seems from the entropy of activation that the specific function is performed by the hydrogen ion in the actual mechanism involving a different character from those of chloride and bromide.

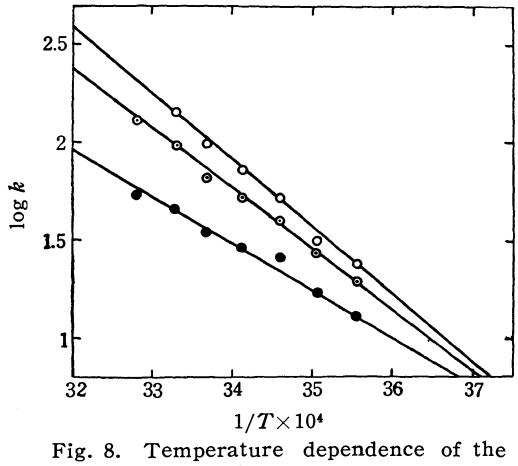



Fig. 8. Temperature dependence of the disproportionation rate constant. Ionic strength, 2.1 f. ●···0.1 f $H^+$, ⊙···0.1 f $H^+$+0.1 f $Cl^-$, ○···0.1 f $H^+$+1 f $Br^-$.

With regard to the function of the hydrogen ion, F. R. Duke and M. C. Pinkerton[15] have proposed a tentative mechanism, that is, the hydrogen ion increases the concentration of $UOOH^{2+}$ (cf. eq. 15) pertaining to the disproportionation and the charge transfer is not performed by the proton transfer but by the hydroxyl-radical transfer. This postulation is supported by the author's result giving a good agreement with an isotopic electron exchange reaction of $Fe^{2+}$—$FeOH^{2+}$ [4], in which the entropy of activation is −18 e. u., the free energy of activation is 12.2 kcal. and the mechanism of the charge transfer is assumed to be a typical case of the bridge transfer of the hydroxyl-radical. Accordingly, the following mechanism can be confirmed:

$$UO_2^{2+}+e=UO_2^{+}:$$
Electrode Reaction (14)

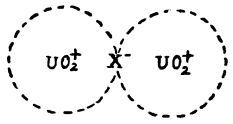
$$UO_2^{+}+H^{+}\rightleftarrows UOOH^{2+} \tag{15}$$

$$UO_2^{+}+UOOH^{2+}=HOUO_2^{+}+OU^{2+}:$$
Disproportionation Reaction (16)

Since we may consider $UOOH^{2+}$ to be a strong acid, the equilibrium in equation 15 shifts toward the right-hand side and results in the increase in the concentration of $UOOH^{2+}$ with the increase in the hydrogen ion concentration. This effect will result in the increase in the disproportionation rate in an acid solution.

On the contrary, an alternate mechanism can be proposed to the cases of chloride and bromide. In Table V it can be seen that the most rapid reaction path has a less negative entropy of activation. Furthermore, in the cases of ($H^+$, $Cl^-$) and ($H^+$, $Br^-$) the entropies of activation are virtually equal to zero. Since it has been reasoned that the entropy of activation is approximately zero for a unimolecular reaction, the disproportionation is likely to proceed as a unimolecular reaction in these cases. The rate of the disproportionation is of the first order with respect to the anion concentration, and the existence of the uranyl nitrate- or chloride-complex is confirmed, as is previously described. These results lead to the ease of the formation of uranyl complex involving a sharing of the coordination sphere by two center atoms as is formulated in the following:

15) F. R. Duke and M. C. Pinkerton, *J. Am. Chem. Soc.*, **73**, 2361 (1951).




In this state the structure of the two complexes is symmetrical with respect to the shared anion, hence, one can predict that the exchange rate will increase as is clearly enunciated by Libby[16] by applying a quantum mechanical expression of the exchange frequency of the hydrogen molecular ion. It is assumed that the difference in the rate constant among various anions will depend upon the firmness of the coordination, and upon the interatomic distance.

The author wishes to express his hearty gratitude to Professor Teiji Ichikawa, Professor Takeshi Taketa, Professor Mutsuaki Shinagawa and Dr. Hitoshi Yamamura for their advice and encouragement throughout this study.

*Chemical Laboratory, Minami College*
*Hiroshima University*
*Minamimati, Hiroshima*

16) W. F. Libby, *J. Phys. Chem.*, **56**, 863 (1952).

# *Analytical Studies of Boron. VI. Determination of Boron Using Ion Exchange Resin*

By Satoru MUTO*

(Received March 24, 1956)

## Introduction

When boric acid was treated with a cation exchange resin, it could be separated quantitatively from cations which coexisted with boric acid. Such a separation procedure was reported by the author[1] and applied to the determination of boron in steels[2], silicon[3] and silicate rocks[4]. For the determination of boron, a sample solution was passed through a cation exchange resin column and the effluent was titrated with an alkaline solution. However, weak acids such as phosphoric and silicic interfere with the titration.

After a solution containing a small amount of boron was treated with an ion exchange resin column, a colorimetric procedure was applied to the effluent. The results were satisfactory.

## Treatment of Boric Acid Solution with an Ion Exchange Resin Column

**Reagents and Chemicals**: *Resins*; Cation exchange resins, Amberlite IR-120 and Diaion K in Na- or H-form.

Anion exchange resins, Amberlite IRA-400 and Diaion A in Cl- or OH-form.

*Washing solution*; Three normal aqueous solution of chemically pure grade sodium hydroxide, hydrochloric acid and sodium chloride.

*Sodium carbonate*; Guaranteed grade sodium carbonate.

*pH regulating solution*; One normal guaranteed grade sodium hydroxide. One normal guaranteed grade hydrochloric acid.

*Standard boric acid solution*; Guaranteed grade boric acid was recystallized and a solution containing 1.1mg. B/cc. was prepared. This solution was diluted to the given concentration before use.

**Preliminary Experiment**: Standard boric acid solutions containing 1 $\gamma$—20 mg. B were taken, and made up to 20 cc. with distilled water. These solutions were divided into 3 groups. The first group, (a), contained 1—20 mg. B, the second, (b), 10—500 $\gamma$B, and the third, (c), 1—9 $\gamma$B.

One normal hydrochloric acid and 1 N sodium hydroxide solution were added to 20 cc. of the boric acid solution and its pH was adjusted to various values. The resulting solution was passed through a cation exchange resin column. The column was washed with distilled water, and a titration method was applied to the (a) group. To the (b) group containing 10—500 $\gamma$B was applied the colorimetric procedure using acetone-curcumin. The effluent and the washing solution were combined together and diluted to 100 cc. The resulting solution was made alkaline with solid sodium carbonate, evaporated on a water bath,

* Present address: Textbook Sect., Elementary and Secondary Education Bureau, Ministry of Education, Kasumigaseki, Tokyo.

1) S. Muto, *J. Chem. Soc. Japan, Pur. Chem. Sec.*, **72**, 976 (1951).
2) J. R. Martin and J. R. Hays, *Anal. Chem.*, **24**, 182 (1952).
3) C. L. Luke, ibid., **27**, 1150 (1955).
4) H. Kramer, ibid., **27**, 144 (1955).

and then the colorimetric procedure was applied. The same procedure was applied to the (c) group. The results are shown in Table I, II and III.

TABLE I
DETERMINATION OF BORON IN (a) GROUP. (mg. B)

| | | | | | |
|---|---|---|---|---|---|
| Taken | 0.0 | 1.1 | 5.5 | 11. | 22. |
| | 0.01 | 1.14 | 5.50 | 10.9 | 22.1 |
| Found | −0.02 | 1.14 | 5.47 | 10.9 | 22.2 |
| | 0.02 | 1.08 | 5.51 | 11.0 | 21.7 |
| Mean | 0.00 | 1.12 | 5.49 | 10.9 | 22.1 |
| | ±0.01 | ±0.01 | ±0.01 | ±0.0 | ±0.3 |

TABLE II
DETERMINATION OF BORON IN (b) GROUP. (γB)

| | | | | | |
|---|---|---|---|---|---|
| Taken | 11. | 55. | 110. | 220. | 550. |
| | 11.3 | 54.6 | 110. | 215. | 554. |
| Found | 10.1 | 54.6 | 107. | 281. | 546. |
| | 11.4 | 55.2 | 105. | 221. | 546. |
| Mean | 10.9 | 54.8 | 107. | 218. | 548. |
| | ±0.3 | ±0.2 | ±1. | ±1. | ±2. |

TABLE III
DETERMINATION OF BORON IN (c) GROUP. (γB)

| | | | | | |
|---|---|---|---|---|---|
| Taken | 0.0 | 1.1 | 2.2 | 5.5 | 9.9 |
| | 0.04 | 1.07 | 2.24 | 5.45 | 9.90 |
| Found | −0.02 | 1.05 | 2.15 | 5.50 | 9.84 |
| | −0.02 | 1.14 | 2.15 | 5.48 | 9.92 |
| Mean | 0.00 | 1.09 | 2.18 | 5.48 | 9.89 |
| | ±0.01 | ±0.02 | ±0.02 | ±0.01 | ±0.02 |

These results indicate that boron is not adsorbed on the cation exchange resin and separated from cations quantitatively. For the second place, the pH of the boric acid solution, whose volume was diluted to 20 cc., was adjusted by adding hydrochloric acid and sodium hydroxide solutions, for the resulting solution to be passed through an anion exchange resin column of Cl- or OH- form. The direct titration method was applied to the effluent. The content of boron in the effluent is shown in Fig. 1.

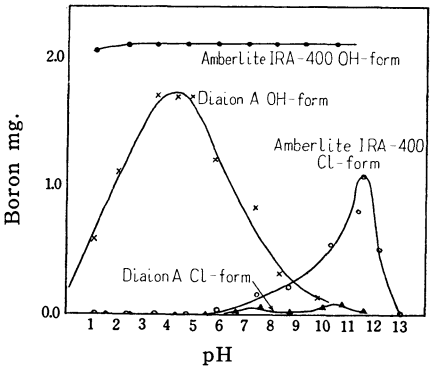



Fig. 1. Boron adsorbed by various forms of anion exchange resins. (The original solution contained 2.12 mg. B.)

Boron was adsorbed to some extent on a weak-base resin, like Diaion A. The adsorption on the resin of OH-form was most marked at pH 3 to 4. The resin of Cl-form did not adsorb boron from acidic solution. When the pH was higher than 5, however, the resin adsorbed boron slightly. A strong-base resin, Amberlite IRA-400, of Cl-form showed the highest adsorption value at pH 11 to 12. When the pH value is higher than 12, the adsorption decreased. Boron was not adsorbed on the resin and separated quatitatively when the pH of solution was lower than 4. This fact makes it possible to separate boron from other anions. When the pH value was higher than 2, Amberlite IRA-400 of OH-form adsorbed boron quantitatively.

A solution containing 5γ boron was prepared from the standard boric acid solution. The solution was treated with the resin column, and the boron in the effluent was determined colorimetrically by the acetone-curcumin method. The results are shown in Fig. 2. The curve has a similar tendency to that in Fig. 1. Boron can be adsorbed to some extent by the Amberlite IRA-400 of Cl-form in the pH range of 11 to 12. It flows down quantitatively when the pH is lower than 5.

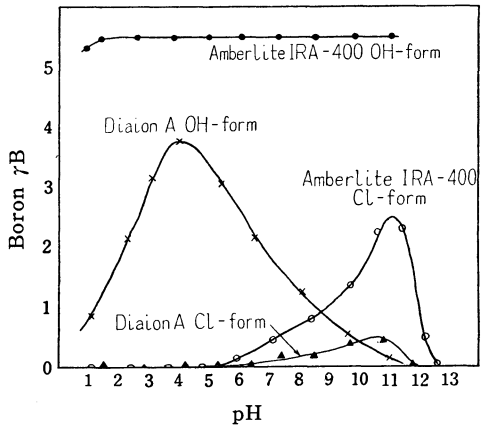



Fig. 2. Boron adsorbed by various forms of anion exchange resins. (The original solution contained 5.5 γB.)

## Experimental

**Decomposition of Samples:** Since the samples are treated with resin column, acid decomposition is better than alkaline fusion. When the samples are decomposed with acid and heated, however, a considerable amount of boric acid volatilizes with water vapor. For this reason, the author placed the sample in a 100 cc. round flask, a slight excess of 6 N hydrochloric acid was added, and the sample was decomposed on

a water bath with a reflux condenser. Samples which could not be decomposed by acids were fused with sodium carbonate of guaranteed grade. The melts were dissolved in a slight excess of 6 N hydrochloric acid.

In order to examine this decomposition method, the guaranteed grade sodium carbonate was added to the standard boric acid solution to make the

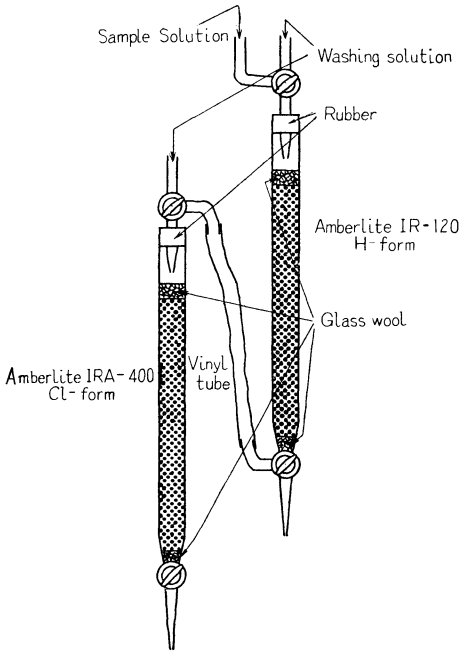



Fig. 3. Resin columns.

solution alkaline, and evaporated on a water bath. The residue was dissolved with a small amount of water and the solution was poured into a 100 cc. round flask. This solution was neutralized with 6 N hydrochloric acid and 1 cc. excess of the acid added. The flask was connected to a reflux condenser and heated on a water bath for 1 hour. The solution was diluted with 50—100 cc. of water and passed through the cation and the anion exchange resin column using the apparatus as shown in Fig. 3. The effluent was analyzed by either titrimetric or colorimetric procedure.

**Titrimetric Procedure:**

*Reagents and Chemicals*: Standard sodium hydroxide solution (N/20); Guaranteed grade sodium hydroxide was dissolved in carbonate-free distilled water. The factor of the solution was 1.165.

Sodium hydroxide solution (1 N); Guaranteed grade sodium hydroxide was dissolved in carbonate-free distilled water.

Hydrochloric acid (1 N); Distilled hydrochloric acid was diluted to 1 N.

*p*-Nitrophenol indicator; 0.1% ethanolic solution.

Phenolphthalein indicator; 0.1% ethanolic solution.

Mannitol; Analytical grade reagent in solid.

*Procedure*: After a sample solution was treated with a resin column, 1—5 mg. B was pipetted out and poured into a 300 cc. conical flask and the volume of the solution was adjusted to 100 cc. To this solution was applied an improved Foote's titrimetric procedure[5]. One drop of *p*-nitrophenol solution was added as indicator and the solution was neutralized with 1 N sodium hydroxide solution until yellow color of the indicator just appeared. One drop of 1 N hydrochloric acid was added to this solution to make the yellow color vanish, then the flask was connected to an aspirator. The solution was heated and boiled at a low pressure. Carbon dioxide gas being bubbled out, the pH of the solution became higher. When the yellow color of the indicator appeared again, one drop of 1 N hydrochloric acid was added and then the boiling was continued. After 2 to 3 minutes of boiling, the aspirator was removed and the solution was cooled by cold water. One twentieth normal sodium hydroxide solution was added to the solution until the yellow color of *p*-nitrophenol was just visible. This is the starting point of the titration. Two grams of mannitol and 5 drops of phenolphthalein were added to the solution, which was titrated with N/20 sodium hydroxide solution. At the end point, the color of the solution was yellowish brown. The color of phenolphthalein appears at pH 8.0, and the neutralization point of mannitol-boric acid complex lies at pH 7.6. Therefore, the end point of the titration is shown by the appearance of yellowish brown color in the solution.

Table IV

Determination of boron by titrimetric procedure. (mg. B)

| | | | | | |
|---|---|---|---|---|---|
| Taken | 0.0 | 1.1 | 5.5 | 11. | 22. |
| | −0.04 | 1.05 | 5.50 | 10.7 | 21.6 |
| Found | 0.03 | 1.09 | 5.45 | 11.3 | 22.0 |
| | −0.03 | 1.13 | 5.54 | 10.9 | 22.4 |
| Mean | −0.01 | 1.09 | 5.50 | 11.0 | 22.0 |
| | ±0.01 | ±0.02 | ±0.02 | ±0.04 | ±0.02 |

When the yellowish brown color changes to yellow or sometimes disappears on the addition of 2 grams of mannitol, the titration should be continued. The results on the experiment with known amounts of boron is shown in Table IV.

**Colorimetric Procedure:**

*Reagents and Chemicals*: Sodium carbonate; Guaranteed grade sodium carbonate (solid).

Hydrochloric acid-oxalic acid solution; Mix one volume of distilled 6 N hydrochloric acid with four volumes of saturated solution of guaranteed grade oxalic acid.

Acetone-curcumin solution; Dissolve 0.0625 g. of curcumin in 5 cc. of carbitol (monomethyl ether of diethyl glycol), then dilute to 500 cc. with acetone. The solution is stable for 2 to 3 months.

Acetone; Distilled with calcium oxide.

5) F. J. Foote, *Ind. Eng. Chem., Anal. Ed.*, **4**, 39 (1932).

*Procedure*: The Naftel's[6] and the Silverman's[7] method were modified and the following procedure was applied to the sample. After the sample solution was treated with resin, a portion containing 1 to 5 $\gamma$B was pipetted out and poured into a 50 cc. porclain dish, to which 0.2 g. of sodium carbonate was added. The resulting solution was evaporated on a water bath and acidified with 2 cc. of the hydrochloric acid-oxalic acid solution. The product was evaporated on a water bath at 55±2°C. The heating was continued for 30 min. after the solution was dried. The red color of rosocyanine appeared in the presence of boron. After the colored residue was cooled, it was treated with acetone. The colored acetone solution was centrifuged for 20 minutes at 3000 r. p. m. The clear solution was poured into a 10 mm cell of Hitachi APO-I photocolorimeter equipped with No. G (520 m$\mu$) filter. This method was applied to solutions containing a known amount of boric acid, which were not treated with the resin columns. A known amount of the standard boric acid solution was treated by the above mentioned procedure and the scale of photocolorimeter was plotted in Fig. 4. The results are shown in Table V.

TABLE V
DETERMINATION OF BORON BY COLORIMETRIC PROCEDURE. ($\gamma$B)

| | | | | | |
|---|---|---|---|---|---|
| Taken | 0.0 | 1.1 | 2.2 | 5.5 | 11. |
| | 0.04 | 1.10 | 2.18 | 5.43 | 10.8 |
| Found | 0.02 | 1.08 | 2.18 | 5.51 | 10.6 |
| | 0.00 | 1.06 | 2.18 | 5.49 | 11.3 |
| Mean | 0.02 | 1.08 | 2.18 | 5.48 | 10.9 |
| | ±0.01 | ±0.01 | ±0.00 | ±0.02 | ±0.1 |

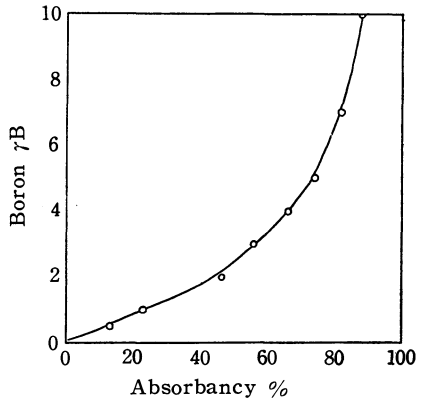



Fig. 4. Standard curve of boron-absorbancy.

This procedure could be applied to a sample containing a small quantity of boron within the error of ±5%.

As shown in Table VI and VII, iron and aluminium interfered with this colorimetric procedure.

6) J. A. Naftel, *Ind. Eng. Chem., Anal. Ed.*, **11**, 407 (1939).
7) L. Silverman and K. Trego, *Anal. Chem.*, **25**, 1264 (1953).

TABLE VI
INTERFERENCE OF IRON. ($\gamma$)

| B (taken) | $Fe^{3+}$ | B (found) | Error $\gamma$B |
|---|---|---|---|
| 0.0 | 0 | 0.02 | 0.02 |
| 0.0 | 9 | 0.02 | 0.02 |
| 0.0 | 45 | 0.05 | 0.05 |
| 0.0 | 90 | 0.05 | 0.05 |
| 0.0 | 900 | 0.14 | 0.14 |
| 0.0 | 9000 | 0.00 | 0.00 |
| 3.3 | 0 | 3.33 | 0.03 |
| 3.3 | 9 | 3.40 | 0.07 |
| 3.3 | 45 | 3.40 | 0.07 |
| 3.3 | 90 | 3.65 | 0.35 |
| 3.3 | 900 | 3.85 | 0.55 |
| 3.3 | 9000 | 0.08 | −2.22 |
| 5.5 | 0 | 5.45 | 0.05 |
| 5.5 | 9 | 5.54 | 0.04 |
| 5.5 | 45 | 5.55 | 0.05 |
| 5.5 | 90 | 5.63 | 0.13 |
| 5.5 | 900 | 6.00 | 0.45 |
| 5.5 | 9000 | 0.11 | −4.39 |

TABLE VII
INTERFERENCE OF ALUMINIUM. ($\gamma$)

| B (taken) | Al | B (found) | Error $\gamma$B |
|---|---|---|---|
| 0.0 | 0 | −0.01 | −0.01 |
| 0.0 | 0.5 | 0.00 | 0.00 |
| 0.0 | 1 | −0.02 | −0.02 |
| 0.0 | 10 | 0.04 | 0.04 |
| 0.0 | 100 | −0.01 | −0.01 |
| 0.0 | 1000 | −0.02 | −0.02 |
| 3.3 | 0 | 3.32 | 0.02 |
| 3.3 | 0.5 | 3.29 | −0.01 |
| 3.3 | 1 | 3.18 | −0.12 |
| 3.3 | 10 | 3.10 | −0.20 |
| 3.3 | 100 | 3.09 | −0.21 |
| 3.3 | 1000 | 3.05 | −0.25 |
| 5.5 | 0 | 5.48 | −0.02 |
| 5.5 | 0.5 | 5.50 | 0.00 |
| 5.5 | 1 | 5.36 | −0.14 |
| 5.5 | 10 | 5.24 | −0.26 |
| 5.5 | 100 | 5.24 | −0.26 |
| 5.5 | 1000 | 5.08 | −0.42 |

When the ferric ion exists in small quantities, the error tends to become larger. The presence of the aluminium ion gives negative error. Sodium chloride does not interfere with this method.

## Application

Kotoite, paigeite and tourmaline were sampled. Kotoite and paigeite were decomposed with hydrochloric acid in a flask connected with a reflux condenser. Tourmaline was fused with sodium carbonate and the melt was dissolved in hydrochloric acid. When the samples were rich in

TABLE VIII
BORON IN BORON MINERALS
(Determined on the regulated volume of the effluent as explained before)

| | Determined | | Added | | Determined (total) | | Recovered | |
|---|---|---|---|---|---|---|---|---|
| | Tit.(i) mg. B | Colo.(ii) γB | Tit. mg. B | Colo. γB | Tit.(iii) mg. B | Colo.(iv) γB | (iii)-(i) mg. B | (iv)-(ii) γB |
| Kotoite | 1.77 | 1.75 | 1.1 | 0.11 | 2.90 | 1.82 | 1.3 | 0.07 |
| (Miyako, Iwate.) | 1.72 | 1.82 | 5.5 | 1.1 | 7.21 | 2.89 | 5.4 | 1.1 |
| 5.38±0.06% $B_2O_3$ | 1.80 | 1.73 | 11. | 5.5 | 12.85 | 7.17 | 11. | 5.4 |
| Paigeite | 5.67 | 5.55 | 1.1 | 0.11 | 6.82 | 5.61 | 1.2 | 0.06 |
| (Kamaishi, Iwate.) | 5.65 | 5.80 | 5.5 | 1.1 | 11.05 | 6.86 | 5.4 | 1.1 |
| 16.00±0.12% $B_2O_3$ | 5.67 | 5.65 | 11. | 5.5 | 16.80 | 11.25 | 11. | 5.6 |
| Tourmaline | 5.13 | 5.20 | 1.1 | 0.11 | 6.17 | 5.28 | 1.0 | 0.08 |
| (Shima, Gunma.) | 5.22 | 5.16 | 5.5 | 1.1 | 10.62 | 6.30 | 5.4 | 1.1 |
| 7.93±0.04% $B_2O_3$ | 5.19 | 5.14 | 11. | 5.5 | 16.20 | 10.57 | 11. | 5.4 |

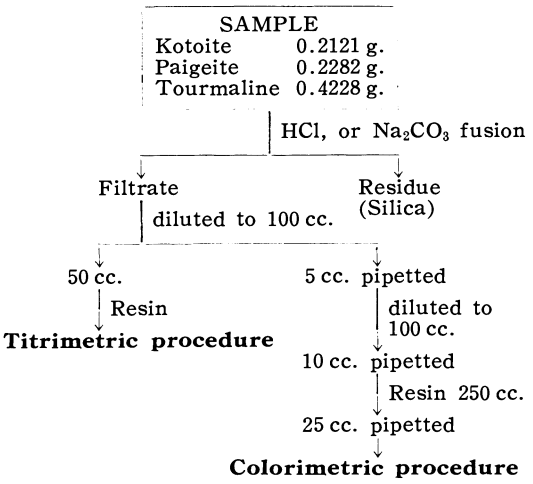



Fig. 5. Decomposition of samples

silica, the acidic solution had to be filtered. The solutions were treated with resin columns, as shown in the Fig. 5. The results in Table VIII were obtained when boron in the effluent was determined by the titrimetric and the colorimetric procedure. The errors of the colorimetric procedure were greater than those of the titrimetric procedure, but less than ±5%. The accuracy of the procedures was examined by adding a known amount of the standard boric acid solution to the minerals. The results were satisfactory as shown in Table VIII. The boron could be determined by the titrimetric procedure, but the colorimetric procedure gave more satisfactory results for micro amounts of boron.

The author wishes to express his sincere thanks to Dr. N. Yamagata and Dr. T. Watanabe for their helpful suggestions and aids during the course of the present investigation.

*Kiriu College of Technology*
*Gunma University, Kiriu*

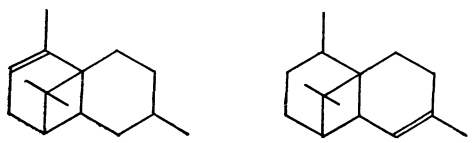
# *Polyterpenes I. Permanganate Oxidation of Thujopsene, Part 1**

By Saburo AKIYOSHI and Shizuo NAGAHAMA

(Received June 18, 1957)

Hiba, *Thujopsis dolabrata Sieb. et Zucc.* is an arbor native to Japan, abounding especially in the northern parts of Honshū island, namely Ōu, Hokuriku, and Tōhoku district. In view of the strong resisting power of Hiba wood against saprophytes, the wood oil has long been a target of much attention, and both Yano[1] and Uchida[2] proved in their early investigation that its main constituent is a tricyclic sesquiterpene, which was subsequently named thujopsene by Kawamura[3]. It may be noted that the anti-saprophytic property is due to the minor acidic parts of the oil, the components of which were elucidated by Nozoe, Yasue and Yamane[4].

By the permanganate oxidation of thujopsene, Kawamura[3] obtained a glycol $C_{15}H_{26}O_2$, m.p. 92—3°, a keto-aldehyde $C_{15}H_{24}O_2$, b. p. 170—7°/11 mm, disemicarbazone m. p. 221° (decomp.), and a keto-carboxylic acid $C_{15}H_{24}O_3$, b. p. 180—5°/4 mm, semicarbazone m. p. 219° (decomp.). The ketonic acid was further degradated with hypobromite to a dicarboxylic acid $C_{14}H_{22}O_4$, m. p. 208—9°. On the basis of these degradations and several other observations, he suggested the structure A or B for thujopsene. Unfortunately little has been known about this paper in foreign countries, as it was written only in Japanese and was not introduced in abstracting journals.



A B

Structures A and B suggested by Kawamura.

Later Obata and Fukushi[5] stated that they could not find thujopsene in Hiba wood oil and that its main constituent has the constants between the dicyclic and the tricyclic. To make clear of this discrepancy, Fujita[6] collected ten samples of Hiba wood from various districts where it grows, and confirmed the fact that the main constituent of the oil obtained from them was a tricyclic sesquiterpene. Recently Tanaka and Aikawa[7] reported that thujopsene is a mixture of endo- and semicyclic double bond isomer.

As it is regrettable that the study on the structure of this interesting substance has been interrupted for long years, the authors have decided to take it up at this time. The present paper deals with some of the degradation products by the oxidation of thujopsene with potassium permanganate in acetone solution. Unlike the procedure followed by Kawamura, the authors did not add water to the reaction mixture.

The main product was a crystalline keto-carboxylic acid $C_{15}H_{24}O_3$ (I), m. p. 164—5°, which was oxidized with hypobromite to a dicarboxylic acid $C_{14}H_{22}O_4$, m. p. 210°. This dicarboxylic acid was easily converted into an anhydride m. p. 109—110° by the treatment with acetic anhydride, which shows infrared absorption at 1799 and 1752 $cm^{-1}$ (in carbon tetrachloride), agreeing with glutaric anhydride derivatives[8]. The ring containing double bond, therefore, becomes five membered and Kawamura's formulae are rejected. Since the dicarboxylic acid can be esterified into monomethyl ester m. p. 60°, for the most part, with methanol and sulfuric acid, one of the carboxyl groups may be considered to be attached to the tertiary carbon atom. The ketonic acid I was

* Presented before the 10th Annual Meeting of the Chemical Society of Japan held in Tokyo, April, 1957. Simultaneously two other reports on the same subject were presented independently by Tanaka et al. and Nozoe et al. at this meeting.

1) M. Yano, *J. Soc. Chem. Ind. Japan*, **16**, 443 (1913).
2) S. Uchida, ibid., **31**, 501 (1928).
3) J. Kawamura, *Bull. Govt. Forest Expt. Station*, **30**, 59 (1930).
4) T. Nozoe, A. Yasue and K. Yamane, *Proc. Japan Acad.*, **27**, 15 (1951).
5) Y. Obata and S. Fukushi, *J. Agr. Chem. Soc. Japan*, **26**, 113 (1952).
6) N. Fujita, *Bull. Govt. Forest Expt. Station*, **76**, 175 (1954).
7) J. Tanaka and T. Aikawa, 9th Annual Meeting of the Chemical Society of Japan, Kyoto, April 1956.
8) H. H. Wasserman and H. E. Zimmerman, *J. Am. Chem. Soc.*, **72**, 5787 (1950); G. Stork and R. Breslow, ibid., **75**, 3291 (1953); G. Büchi and R. E. Erickson, ibid., **78**, 1262 (1956).

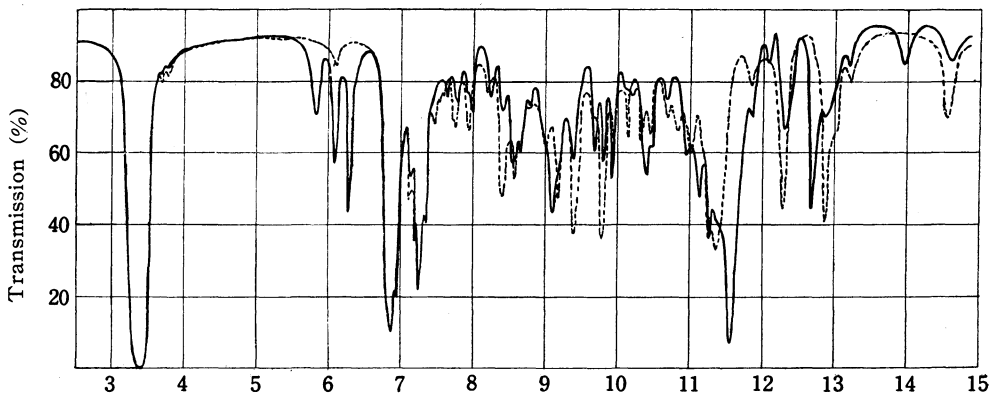



Fig. 1. Infrared spectra of thujopsene and isomerized hydrocarbon.
····· Thujopsene —— Isomerized hydrocarbon

soluble gradually into concentrated hydrobromic acid or sulfuric acid and a ketonic $\gamma$-lactone m. p. 56° was obtained from the solution. Curiously, attempted esterification of the acid I with methanol and sulfuric acid gave the same lactone.

Besides this ketonic acid, the authors separated, from the acidic portion of the oxidation product, three crystalline substances, namely an oxylactone $C_{15}H_{22}O_4$ (II), m. p. 123.5°; a hydroxyketonic acid $C_{15}H_{22}O_4$ (III), m. p. 193° (decomp.); and a hydroxylic acid $C_{12}H_{14}O_3$ (IV), m. p. 153°. The acid III was converted into a dehydrated ketonic acid, m. p. 206—7°, by heating it to the decomposing point.

The neutral portion of the oxidation product was fractionated into unchanged thujopsene, isomerized hydrocarbon, and an oxygen-containing high boiling fraction, from which an unsaturated ketone $C_{14}H_{20}O$ (V), m. p. 70° was separated by alumina chromatography.

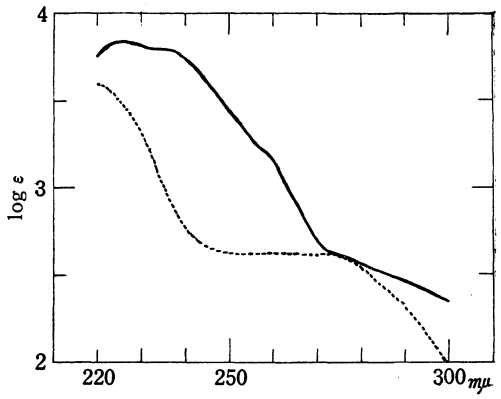



Fig. 2. Ultraviolet spectra of thujopsene (·····) and isomerized hydrocarbon (——) in hexane.

## Experimental*

**Thujopsene.**—Hiba wood oil was purchased from the Soda Aromatic Co. and the Takasago Perfumery Co. The former was transparent, free from acidic portion, $d_4^{25}$ 0.9341, $n_D^{21}$ 1.5035 and the latter raw oil of dark red color, $d_4^{15}$ 0.9518. The thujopsene fraction with following constants was obtained from both oils with an yield of 50—60%. B. p. 121—2°/12 mm, $d_4^{25}$ 0.9311, $n_D^{25}$ 1.5015, $[\alpha]_D^{20}$ −79.7° MR 64.71 infrared and ultraviolet spectra are shown in Figs. 1 and 2.

**Permanganate Oxidation.**—To a mixture of 100 g. thujopsene and 400 cc. acetone, 120 g. of powdered potassium permanganate was added in portions in the course of 7 hours. The temperature was kept under 30° during the reaction. With the consumption of permanganate, manganese dioxide was filtered off, washed with acetone and the filtrate was concentrated. Manganese dioxide was further extracted several times with hot water, the extract was combined with acetone solution, acidified and extracted with benzene. Then the benzene solution was extracted with 7% sodium bicarbonate solution and 10% sodium hydroxide solution successively, washed with water and dried with sodium sulfate. The semi-solid substance, which was separated from the sodium bicarbonate extract by acidification with hydrochloric acid, was crystallized from benzene. The keto-acid I was obtained at first; removal of the keto-acid I by condensing the mother liquor several times, gave oxylactone (II). Acidifying the sodium hydroxide extract in the presence of benzen precipitate of III was separated between benzene and water layer. From the benzene extract, acid I and acid IV were separated by fractional crystallization. Analytical data of these substances were shown in Table I. Semicarbazone of I, prisms. m. p. 219° (decomp.), 2, 4-Dinitrophenylhydrazone of I, yellow, m. p. 187—9°; III, red, m. p. 250—252° (decomp.).

* All melting points are corrected.

TABLE I

OXIDATION PRODUCTS OF THUJOPSENE

| | m. p. | Formula | Analysis Found C | Found H | Calcd. C | Calcd. H | Yield* (g.) |
|---|---|---|---|---|---|---|---|
| I | 164—5° | $C_{15}H_{24}O_3$ | 71.15 | 9.36 | 71.39 | 9.59 | 4.4 |
| II | 122.5—3.5° | $C_{15}H_{22}O_4$ | 67.47 | 8.44 | 67.64 | 8.33 | 0.2 |
| III | 193° (decomp.) | $C_{15}H_{22}O_4$ | 67.24<br>67.89 | 8.35<br>8.49 | 67.64 | 8.33 | 0.7 |
| IV | 152.5—3.5° | $C_{12}H_{14}O_3$ | 69.95 | 7.16 | 69.88 | 6.84 | 0.3 |
| V | 68—70° | $C_{14}H_{20}O$ | 82.09<br>82.13 | 9.92<br>9.89 | 82.30 | 9.87 | 0.2 |

* In another run, using 200 g. of permanganate, there was obtained 7.0 g of I and 1.4 g. of III.

The neutral portion was about 60 g. and was fractionated into the following three fractions with a concentric column 20 cm high: (1) recollected thujopsene about 30 g.; (2) isomerized hydrocarbon about 10 g. $n_D^{25}$ 1.5111, $d_4^{25}$ 0.9297, MR 65.74: infrared and ultraviolet spectrum Figs. 1 and 2; (3) oxygen-containing high boiling fraction 9 g.

Fraction 3 was chromatographed with alumina column, 5 cm. in diameter and 8 cm. high, developed successively with petroleum ether, benzene, ethyl acetate and methanol. From the benzene eluate a ketone $C_{14}H_{20}O$ (V) was crystallized. It has infrared absorption at 1653 and 1618 $cm^{-1}$ (in Nujol) and is probably an $\alpha,\beta$-unsaturated ketone. Semicarbazone m. p. 239° (decomp.).

**Dicarboxylic Acid.**—The keto-carboxylic acid (I) (2.0 g.) in 10 cc. of 10% sodium hydroxide solution, was added to the hypobromite solution prepared from 8.0 g. sodium hydroxide, 125 cc. water and 3.5 cc. bromine, under ice cooling. After being set aside for 1 hour, the solution was acidified with hydrochloric acid and the needles of dicarboxylic acid were separated. m. p. 205—6° (from dil. ethanol), yield 1.47 g. (73%). The melting point rose to 209.5—210.5° by further recrystallization.

*Anal.* Found: C, 66.12; H, 8.62; N.E. 127. Calcd. for $C_{14}H_{22}O_4$: C, 66.11; H, 8.72%, N.E. 127.

**Dicarboxylic Acid Anhydride.**—The dicarboxylic acid (75 mg.) was dissolved in 3 cc. of acetic anhydride and refluxed for 3 hrs. Acetic anhydride was removed under reduced pressure and the residue was crystallized by rubbing. M. p. 109—110° (from acetic anhydride). The anhydride (20 mg.) was added to 0.4 cc. of 10% sodium hydroxide solution, allowed to stand overnight, warmed for few min., and then acidified. The crystals obtained were recrystallized from dil. ethanol, m. p. 210.5—211°. This was mixed with dicarboxylic acid (m. p. 208°) and melted at 208—210°. The infrared spectra of the two coincided.

**Esters of Dicarboxylic Acid.**—A mixture of the dicarboxylic acid (494 mg.), methanol (20 cc.), and conc. sulfuric acid (8 drops) was refluxed for 5 hr., poured into ice-water and extracted with ether. The ether solution was extracted twice with 7% sodium bicarbonate solution, washed with water and dried. Evaporation of the ether gave 70 mg. of dimethyl ester m. p. 71—3°. By acidifying the sodium bicarbonate extract with hydrochloric acid, monomethyl ester was obtained in needles, (300 mg.) m. p. 59—60° (from methanol-water). Infrared absorption max. 3490, 1705 $cm^{-1}$ (in Nujol) N. E. 308, calcd. for $C_{15}H_{24}O_4 \cdot 2H_2O$ N. E. 304. The sample was kept in a desiccator for 2 weeks and analysed (infrared max. of 3490 $cm^{-1}$ disappeared, and an ester band appeared at 1736 $cm^{-1}$).

*Anal.* Found: C, 67.16; H, 9.27. Calcd. for $C_{15}H_{24}O_4$: C, 67.13; H, 9.02%.

Saponification of the monomethyl ester gave the dicarboxylic acid m. p. 209—210°.

**Isomerization of the Keto-acid (I) to the Keto-lactone.**— (a) To 10 cc. of conc. hydrobromic acid was added 810 mg. of I, which gradually dissolved to yield pink color. After being set aside overnight, the solution was poured onto crushed ice, the needle crystals were collected (470 mg.) and recrystallized twice from ether-petroleum ether mixture and finally with petroleum ether, m. p. 55—56°, yield 200 mg. The ether extract of the aqueous solution produced 100 mg. of the same crystals m. p. 56°. When 50% sulfuric acid was used instead of hydrobromic acid, the same substance was obtained. (b) A mixture of I (100 mg.), methanol (3 cc.) and conc. sulfuric acid (3 drops) was refluxed for 1 hr., poured into water and extracted with ether. The ether was evaporated, and the residue was crystallized by rubbing, yield 75 mg., recrystallized from petroleum ether m. p. 54.5—55.5°. Infrared max. 1774 and 1723 $cm^{-1}$ (in carbon tetrachloride). Semicarbazone, leaflets m. p. 205° (decomp.), 2, 4-dinitrophenylhydrazone, yellow orange leaflets m. p. 162°.

*Anal.* Found: C, 71.42; H, 9.83. Calcd. for $C_{15}H_{24}O_3$: C, 71.39; H, 9.59%.

**Thermal Dehydration of Hydroxyketonic Acid (III)** — The acid (210 mg.) was heated to 210° in an oil bath. The crystals melted with bubbles, and dehydration was completed within 2 min. When the reaction tube was pulled up from the bath, the product crystallized immediately, m. p. 206—7° (from benzene), yield

130 mg. 2, 4-Dinitrophenylhydrazone, red prisms m. p. 251—3°.

*Anal.* Found: C, 72.36; H, 8.01. Calcd. for $C_{15}H_{20}O_3$: C, 72.55; H, 8.12%.

The authors wish to express their gratitude to Professor H. Saikachi and Mr. H. Hoshida of the Pharmaceutical Department of this University for rendering help in the measurements of rotation and the elemental analysis. Thanks are due to Mr. M. Shido of the Service Centre of Elementary Analysis of Organic Compounds of this University for undertaking most of the analysis.

*Department of Applied Chemistry*
*Faculty of Engineering*
*Kyushu University*
*Hakozaki, Fukuoka*

# *The Structure of Kainic Acid, the Most Active Component of Digenea simplex Ag*. I. The Molecular and Crystal Structure of Zinc Kainate Dihydrate*

By Hideo WATASE and Isamu NITTA

(Received May 21, 1957)

*Digenea simplex Agardh*, distributed over a wide area from the Mediterranean Sea, through the Red Sea and Indian Ocean, to the South Chinese Sea and the southern sea near Japan, is an important seaweed which has been well-known as an anthelmintic since more than one thousand years ago. From the beginning of this century, numerous senior workers of this country endeavoured to find out the active components of this substance. In 1953, Murakami, Takemoto and their collaborators[1] succeeded in isolating the most active component, an acidic and optically active** compound of a comparatively small molecule $C_{10}H_{15}O_4N$, m.p. 251° (decomp.), with an intense anthelmintic effect equivalent to about ten times that of santonin without by-effects. They named it kainic acid (digenic acid) after "*Kaininso*", the Japanese name of the mother alga.

Many studies based on organic chemistry were attempted to determine the chemical structure of this interesting compound. In connection with these we have carried out the structure determination by a more direct method, X-ray crystal analysis.

As an orthodox X-ray procedure applied to a chemically unknown structure, the research was commenced with the zinc salt containing a heavy atom such as zinc. From its electron-density projections along the two principal crystal axes, the three-dimensional structure of the molecule in the zinc salt was determined thoroughly and quantitatively except for the absolute configuration. This X-ray result coincided with the conclusions[2] deduced from the chemical behavior.

This paper deals with the structure determination of the zinc salt in detail.

## Experimental

By adding zinc acetate to an aqueous kainic acid solution, two hydrogens of kainic acid are replaced by a zinc atom, and the crystal of the zinc salt with two waters of crystallization is obtained[3]. Crystalline zinc kainate dihydrate ($C_{10}H_{13}O_4NZn\cdot 2H_2O$) is of a colorless prism elongated along a crystal axis chosen as the *c* axis, having a plane of cleavage perpendicular to another principal axis (*a* axis), and insoluble in water and usual organic solvents. It melts with decomposition at higher than 300°C, but one of

* This paper was presented at the Antumnal Joint Meeting of Chemical Societies of Japan, Tokyo, 1956.

1) S. Murakami, T. Takemoto and Z. Shimizu, *J. Pharm. Soc. Japan*, **73**, 1026 (1953); ibid., **74**, 560 (1954).

** $[\alpha]_D^{29}$: −14.8° (*c*=1, $H_2O$).

2) M. Miyasaki, ibid., **75**, 695 (1955); Y. Ueno, H. Nawa, J. Ueyanagi, H. Morimoto, R. Nakamori and T. Matsuoka, ibid., **75**, 840 (1955); S. Murakami, T. Takemoto, Z. Tei and K. Daigo, ibid., **75**, 869 (1955); H. Morimoto and R. Nakamori, ibid., **76**, 294 (1956); *Proc. Japan Acad.*, **32**, 41 (1956); T. Takemoto, Z. Tei and K. Daigo, *J. Pharm. Soc. Japan*, **76**, 298 (1956).

3) Y. Ueno, H. Nawa, J. Ueyanagi, H. Morimoto, R. Nakamori and T. Matsuoka, ibid., **75**, 807 (1955).

the two waters of crystallization is easily desiccated in a desiccator or by warming it about 40°C, the crystal being broken in pieces to become white powder.

Resulting from the preliminary X-ray examinations, the crystal belonged to the orthorhombic system, and the dimensions of the unit cell were as follows;

$$a = 25.50 \pm 0.07 \text{Å}$$
$$b = 6.93 \pm 0.03 \text{Å}$$
$$c = 7.60 \pm 0.03 \text{Å}$$

Systematic absences of reflexions were recognized only in ($h$ 0 0), (0 $k$ 0) and (0 0 $l$) when $h$, $k$ and $l$ were odd respectively, thus leading to the space group of $D_2^4$–$P2_12_12_1$. Since the unit cell with this crystal symmetry has four crystallographic equivalent general positions[4], it must contain four molecules or integral multiple of four. Judging from the volume of the unit cell, in the present case, four chemical formula units were contained in the unit cell, namely an asymmetric unit was one formula unit.

The axial periods of the $b$ and $c$ axes seemed to be short enough to permit a good resolution of many of the atoms, although the $a$ axis was too long for a projection to provide any useful picture of the structure, and so the investigation was directed to determination of the projections along the $b$ and $c$ axes.

Two specimens of the single crystal were prepared to take the photographs around the $b$ and $c$ axes. The one used for ($h$ 0 $l$) zone was obtained by cutting the crystal at right angle to the elongated $c$ axis, and the cross-section perpendicular to the $b$ axis was 0.08×0.3 mm. The other used for ($h$ $k$ 0) zone had a rhombic cross-section with the following diagonals at right angles to the axis of rotation; 0.15 mm. along the $a$ axis and 0.08 mm. along the $b$ axis.

Then, integrated Weissenberg photographs were taken with filtered Cu $K_\alpha$ radiation, rotating each crystal around each axis in limited angular range, and the reflexions from 221 planes of ($h$ 0 $l$) and 199 of ($h$ $k$ 0) were observed out of 249 and 227 possible ones respectively. By comparing with a calibrated scale, the intensities of the reflexions were estimated visually, multiple-film technique being used for accurate measurements of the strong and the weak reflexions, of which the relative intensities ranged from 10.000 to 1 for ($h$ 0 $l$) zone and from 60.000 to 1 for ($h$ $k$ 0) zone. The corrections for absorption were made for ($h$ 0 $l$) in the usual way and were neglected for ($h$ $k$ 0), the linear absorption coefficient for Cu $K_\alpha$ radiation being $\mu = 27.2\ \text{cm}^{-1}$. Relative structure factors were then deduced from these intensity data by the ordinary process.

## Heavy-Atom and Trial Methods

The space group involved is $D_2^4$–$P2_12_12_1$, and there is no center of symmetry in the crystal. For the sake of convenience in practice, each two-dimensional projection was treated separately with the origin lying on the two-fold screw axis so that the origin was a center of symmetry in the projection. Therefore, the origins used in this analysis are not identical in the two different projections. The relation between the coordinates of the two projections along the $b$ and $c$ axes are clearly shown in Fig. 1. In this account, however, the atomic parameters (Table I) and the final electron-density projections (Figs. 2 and 3) are described reducing to the usual cell.

From the general feature of the reflexions of ($h$ 0 $l$) and ($h$ $k$ 0), the position of the zinc atom was easily determined without ambiguity, and the contributions of this atom to the structure factors were then calculated from its parameters, assuming a value of $B = 2.0\ \text{Å}^2$ as the temperature factor. By considering the values of the contributions of zinc, the observed structure factors could be nearly reduced from the relative values to those in the absolute scale.

Using the structure factors whose signs appeared to be reliable from the contributions of the zinc atom, the first Fourier summations of the electron-density projections along the $b$ and $c$ axes were calculated, and the maps (I) and (II) of Fig. 1 were derived. As listed in Tables II and III, 100 terms of $F(h\ 0\ l)$ were used for the map (I) projected on (0 1 0) and 79 terms of $F(h\ k\ 0)$ for the map (II) projected on (0 0 1).

In each projection, the peak of the zinc atom was of course distinct in the expected position, having a reasonable height. However, since the signs for a number of the structure factors could not be given from the position of the zinc atom alone, these maps were sufficient neither for giving any useful information about the structure of the molecule nor for a perfectly straightforward analysis. In spite of such difficulties, it still seemed that the projection along the $b$ axis at the final stage would reveal the molecular structure better than the other, and the further analysis was tried with this projection.

Thus, at first, the $b$ axis projection was attacked by the Fourier method, based on the trial-and-error, in reference to the various peaks of the map (I). However, immediately it was judged to be scarcely possible to come to the correct result in

4) "Internationale Tabellen zur Bestimmung von Kristallstrukturen", Bornträger, Berlin (1935); "International Tables for X-ray Crystallography", Kynoch Press, Birmingham (1952).

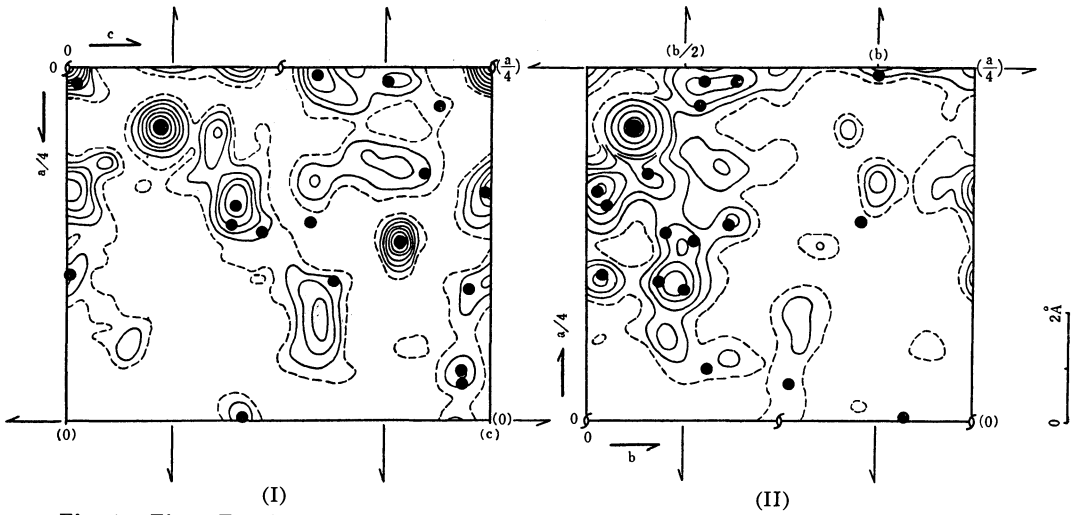



Fig. 1. First Fourier summations of electron-density projections, (I) projected on (0 1 0), (II) projected on (0 0 1). The signs of the structure factors used in the calculations were determined only by zinc. Contours are drawn at equal intervals on an arbitrary scale, but those on the zinc are reduced by a factor of five. Black circles indicate the final atomic positions, that of the zinc being large. The coordinates are taken among those used for the analysis, showing the relation between the two projections, and those to the usual cell are given in brackets.

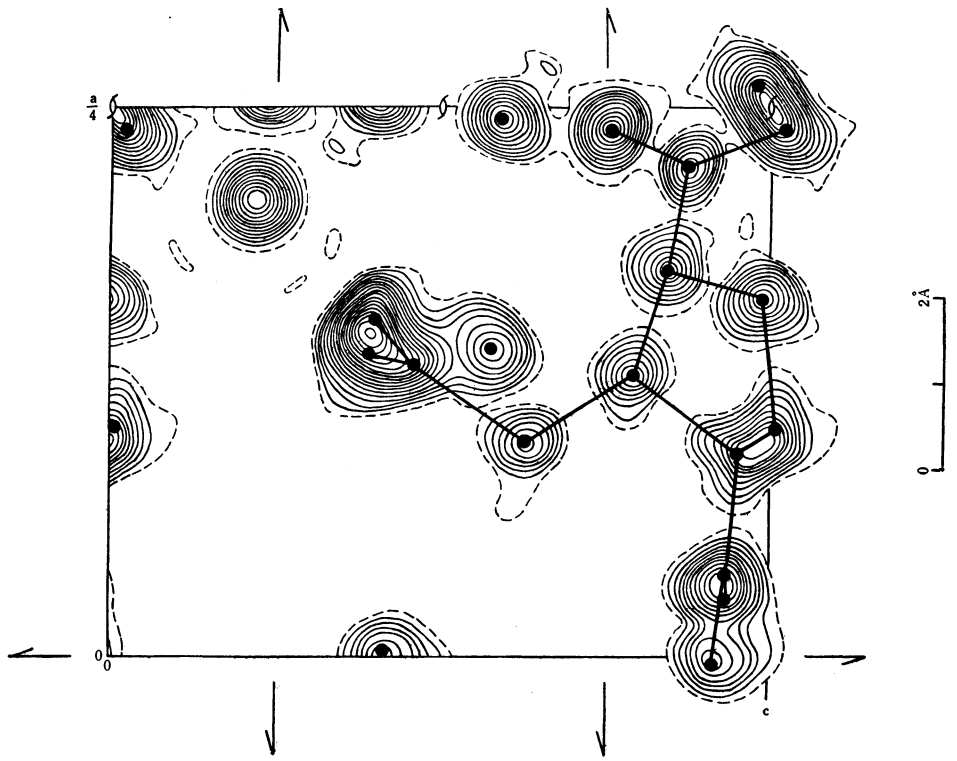



Fig. 2. Electron-density projection along the *b* axis. Contour lines at unit electron intervals, except for those on the zinc at five electrons intervals, the lowest line, broken line, being 3 electrons per Å$^2$. Black circles show the atomic positions, but the position of the zinc is omitted.

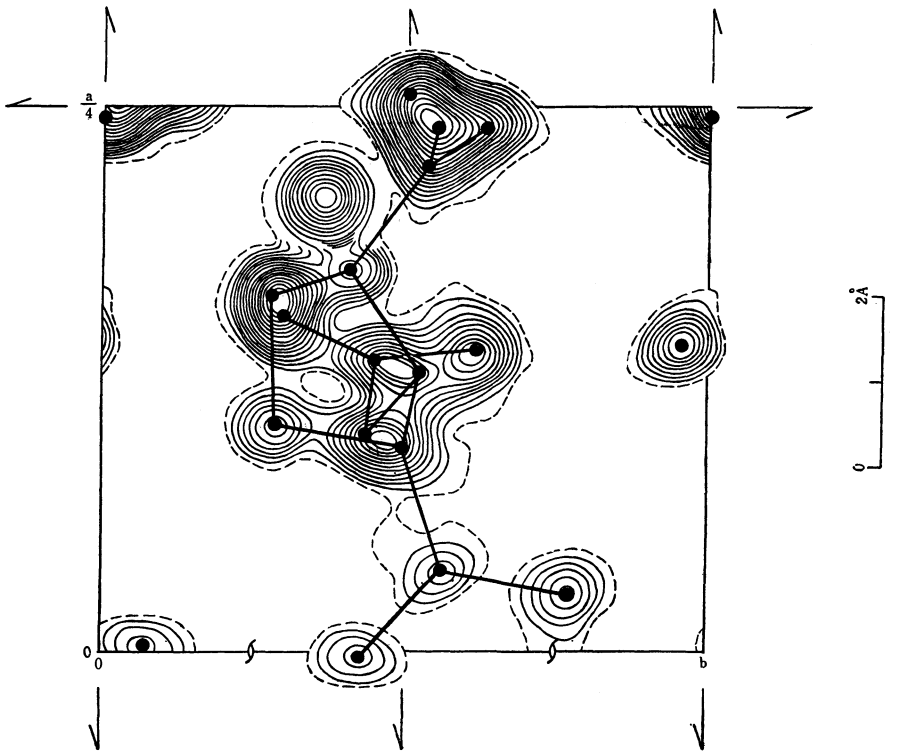



Fig. 3. Electron-density projection along the $c$ axis. Contours and symbols are the same as those of Fig. 2.

such a way, although some of the peaks of this map seemed likely to be real, for example, the peak at the origin, because, in the cases of $h+l$ even, the structure factors with the positive contribution of the zinc were generally greater than its own contribution and those with the negative smaller. In addition to the already fixed zinc atom, these seemingly reliable peaks were made use of as the starting-point, and the structure factors of the lower order were tried without exception quantitatively. Thus an approximate distribution of the atoms in this projection being made reliable for the lower orders, the trial was carried on step by step from the lower to the higher orders, until all the atoms were located satisfactorily to permit the Fourier refinements. In this trial, the structure factors with small resultant value but with great contribution of the zinc atom could be used most effectively, and the change in the sign of (8 0 0) was a key to the further analysis. The electron-density projection of Fig. 2 was the final one thus obtained, and the atomic positions were further refined from this map.

In the same way, the two-dimensional analysis along the $c$ axis was examined on the basis of the $x$ parameters determined above. The electron-density projection was derived as shown in Fig. 3 and the atomic parameters of this projection were obtained. The $x$ parameters for the two projections were in complete

TABLE I
ATOMIC PARAMETERS

| Atom | $x/a$ | $y/b$ | $z/c$ |
|---|---|---|---|
| Zn | 0.2081 | 0.3643 | 0.220 |
| N | $0.162_5$ | 0.273 | 0.987 |
| $C_1$ | $0.222_3$ | 0.533 | 0.873 |
| $C_2$ | $0.175_0$ | 0.407 | 0.840 |
| $C_3$ | $0.127_5$ | 0.523 | 0.790 |
| $C_4$ | $0.093_4$ | 0.497 | 0.950 |
| $C_5$ | $0.104_1$ | 0.287 | 0.007 |
| $C_6$ | $0.099_2$ | 0.433 | 0.627 |
| $C_7$ | $0.133_3$ | 0.450 | 0.460 |
| $C_8$ | $0.036_7$ | 0.560 | 0.933 |
| $C_9$ | $0.025_8$ | 0.773 | 0.933 |
| $C_{10}$ | $0.002_5$ | 0.073 | 0.413 |
| $O_1$ | $0.240_0$ | 0.550 | 0.020 |
| $O_2$ | $0.240_0$ | 0.630 | 0.757 |
| $O_3$ | $0.152_5$ | 0.300 | 0.400 |
| $O_4$ | $0.138_3$ | 0.617 | 0.390 |
| $O_5(H_2O)$ | $0.245_0$ | 0.000 | 0.590 |
| $O_6(H_2O)$ | $0.140_8$ | 0.957 | 0.573 |

agreement. All the parameters are listed in Table I (to the usual cell).

At this stage, the discrepancy indices ($R=\sum||F_o|-|F_c||/\sum|F_o|$) are 0.156 for ($h$ 0 $l$) and 0.146 for ($h$ $k$ 0), employing the data up to sin $\theta/\lambda=0.640$, assuming the values of the unobserved structure factors to be precisely zero, and neglecting the contribution of the hydrogen atoms. In the structure-factor calculations, the values $B=2.0$ Å$^2$ for ($h$ 0 $l$), with the exception of ($h$ 0 0), and 3.0 Å$^2$ for ($h$ $k$ 0) and ($h$ 0 0) were used as the temperature factors common to all the atoms. The atomic scattering factors were taken for zinc from the Internationale Tabellen[4] modifying as $Zn^{++}$ and for the other three from McWeeny's paper[5]; for oxygen $f_o=1/3(f_{\parallel}+2f_{\perp})$ and for carbon the value for 'valence states'.

The observed and the calculated structure factors together with the contributions of the zinc atom are listed in Tables II and III.

TABLE II

OBSERVED AND CALCULATED STRUCTURE FACTORS $F(h\ 0\ l)$, TOGETHER WITH THE CONTRIBUTIONS OF THE ZINC ATOM

The values for ($h$ 0 0) are listed in Table III.

* These structure factors were employed on the first Fourier summations (Fig. 1), using the signs of $F_{Zn}$.

| $h$ $k$ $l$ | $1/4F_o$ | $1/4F_c$ | $1/4F_{Zn}$ |
|---|---|---|---|
| 1 0 1 | 6.6 | 6.7 | 4.8 |
| 2 0 1 | 1.2 | − 0.8 | −12.5 |
| 3 0 1 | 5.8 | 6.3 | 3.4 |
| 4 0 1 | 22.8* | −22.0 | −21.7 |
| 5 0 1 | 21.5 | 24.6 | 1.2 |
| 6 0 1 | 15.0* | −15.2 | −23.3 |
| 7 0 1 | 8.1 | − 8.2 | − 1.1 |
| 8 0 1 | 10.9* | − 8.9 | −18.3 |
| 9 0 1 | 15.0 | −15.3 | − 2.9 |
| 10 0 1 | 4.6 | − 4.8 | − 9.5 |
| 11 0 1 | 11.1 | −10.7 | − 3.4 |
| 12 0 1 | 2.7 | − 2.6 | 0.0 |
| 13 0 1 | 12.0 | 13.1 | − 3.1 |
| 14 0 1 | 12.3* | 12.9 | 7.7 |
| 15 0 1 | 2.4 | 1.9 | − 2.0 |
| 16 0 1 | 19.6* | 19.8 | 12.6 |
| 17 0 1 | 10.5 | −10.8 | − 0.7 |
| 18 0 1 | 16.6* | 16.7 | 12.7 |
| 19 0 1 | 3.3 | − 5.1 | 0.7 |
| 20 0 1 | 13.3* | 13.0 | 9.6 |
| 21 0 1 | — | − 0.5 | 1.5 |
| 22 0 1 | 3.2* | 3.9 | 4.8 |
| 23 0 1 | 3.2 | 5.8 | 1.7 |
| 24 0 1 | — | − 0.7 | − 0.5 |
| 25 0 1 | — | 0.2 | 1.5 |
| 26 0 1 | 2.7* | − 3.4 | − 4.3 |
| 27 0 1 | — | − 0.5 | 1.0 |
| 28 0 1 | 2.5* | − 3.2 | − 6.2 |
| 29 0 1 | — | − 2.5 | 0.3 |
| 30 0 1 | 4.6* | − 6.0 | − 6.1 |
| 31 0 1 | — | 0.3 | − 0.3 |
| 32 0 1 | 2.2* | − 3.9 | − 4.5 |
| 0 0 2 | 8.5 | 9.3 | −22.1 |
| 1 0 2 | 15.2 | 17.9 | − 2.1 |
| 2 0 2 | 25.6* | −23.9 | −19.1 |
| 3 0 2 | 3.0 | − 0.1 | − 6.3 |
| 4 0 2 | 16.6* | −16.7 | −10.2 |
| 5 0 2 | 3.5 | 3.6 | − 8.0 |
| 6 0 2 | 4.0 | − 3.8 | 0.0 |
| 7 0 2 | 22.2* | −20.7 | − 7.5 |
| 8 0 2 | 18.0* | 18.9 | 10.2 |
| 9 0 2 | 9.7 | − 8.4 | − 4.9 |
| 10 0 2 | 19.5* | 20.8 | 15.2 |
| 11 0 2 | 2.2 | 2.3 | − 1.6 |
| 12 0 2 | 22.2* | 19.9 | 15.8 |
| 13 0 2 | 2.5 | 4.3 | 1.4 |
| 14 0 2 | 12.7* | 12.7 | 12.3 |
| 15 0 2 | 2.7 | 2.6 | 3.9 |
| 16 0 2 | — | 0.6 | 6.2 |
| 17 0 2 | 2.8 | 2.3 | 4.7 |
| 18 0 2 | — | 2.5 | 0.0 |
| 19 0 2 | 4.5 | 4.1 | 4.1 |
| 20 0 2 | — | − 1.3 | − 5.6 |
| 21 0 2 | — | 0.2 | 2.6 |
| 22 0 2 | 7.4* | − 7.9 | − 7.9 |
| 23 0 2 | 3.2 | − 3.7 | 0.8 |
| 24 0 2 | 6.7* | − 8.8 | − 8.1 |
| 25 0 2 | — | − 1.4 | − 0.9 |
| 26 0 2 | 4.6* | − 5.5 | − 6.1 |
| 27 0 2 | 3.7 | − 4.2 | − 2.0 |
| 28 0 2 | 1.8 | − 1.7 | − 3.1 |
| 29 0 2 | 3.0 | − 3.3 | − 2.3 |
| 30 0 2 | 1.6 | − 1.6 | 0.4 |
| 31 0 2 | 2.8 | − 4.2 | − 1.9 |
| 32 0 2 | 2.3 | 3.1 | 2.6 |
| 1 0 3 | 3.1 | − 2.3 | −10.7 |
| 2 0 3 | 5.8 | 7.6 | 8.4 |
| 3 0 3 | 12.6 | −13.0 | − 7.5 |
| 4 0 3 | 5.0 | 5.1 | 14.6 |
| 5 0 3 | 1.3 | 1.8 | − 2.5 |
| 6 0 3 | 26.2* | 26.0 | 16.0 |
| 7 0 3 | 10.4 | 8.1 | 2.4 |
| 8 0 3 | 17.8* | 15.2 | 12.6 |
| 9 0 3 | 8.4* | 9.7 | 6.7 |
| 10 0 3 | 4.1 | 5.1 | 6.8 |
| 11 0 3 | 13.4* | 11.7 | 8.2 |
| 12 0 3 | 7.8 | − 8.1 | 0.0 |
| 13 0 3 | 17.2* | 15.7 | 7.5 |
| 14 0 3 | 3.1 | − 2.6 | − 5.7 |
| 15 0 3 | 3.5 | 3.5 | 4.8 |
| 16 0 3 | 9.2* | − 7.8 | − 9.3 |

5) R. McWeeny, *Acta Cryst.*, **4**, 513 (1951).

| | | | | | | | |
|---|---|---|---|---|---|---|---|
| 17 0 3 | 3.0 | − 2.2 | 1.5 | 15 0 5 | 3.9* | − 4.9 | − 5.6 |
| 18 0 3 | 15.3* | −13.9 | − 9.5 | 16 0 5 | 3.6* | 3.2 | 5.0 |
| 19 0 3 | 3.4 | 3.0 | − 1.8 | 17 0 5 | — | − 0.1 | − 1.9 |
| 20 0 3 | 7.5* | − 7.0 | − 7.2 | 18 0 5 | 3.2* | 3.9 | 5.2 |
| 21 0 3 | — | 1.5 | − 3.7 | 19 0 5 | 3.8 | 5.4 | 2.1 |
| 22 0 3 | 5.1* | − 6.0 | − 3.7 | 20 0 5 | 5.1* | 7.1 | 4.1 |
| 23 0 3 | 3.5* | − 4.1 | − 4.5 | 21 0 5 | 7.7* | 8.4 | 4.6 |
| 24 0 3 | 3.1 | − 0.6 | 0.4 | 22 0 5 | 2.7 | 2.7 | 2.1 |
| 25 0 3 | 3.8* | − 5.5 | − 3.9 | 23 0 5 | 5.3* | 4.7 | 5.5 |
| 26 0 3 | 1.8 | 0.2 | 3.3 | 24 0 5 | 2.6 | 2.2 | − 0.3 |
| 27 0 3 | 2.6 | − 2.4 | − 2.5 | 25 0 5 | 6.9* | 6.2 | 4.8 |
| 28 0 3 | 3.9* | 5.5 | 4.7 | 26 0 5 | 1.1 | − 1.1 | − 1.9 |
| 29 0 3 | 1.7 | − 2.0 | − 0.8 | 27 0 5 | 3.1* | 4.1 | 3.0 |
| 30 0 3 | 2.2* | 3.7 | 4.7 | 28 0 5 | 1.8 | − 1.7 | − 2.7 |
| 31 0 3 | 1.0 | 0.2 | 0.9 | 0 0 6 | 10.4* | −12.4 | − 5.0 |
| 0 0 4 | 10.3* | 10.0 | 12.6 | 1 0 6 | — | 0.1 | − 2.7 |
| 1 0 4 | 9.9 | 10.8 | 2.9 | 2 0 6 | 4.2 | − 3.2 | − 4.3 |
| 2 0 4 | 13.6* | 14.2 | 10.9 | 3 0 6 | 10.3* | − 9.9 | − 7.6 |
| 3 0 4 | 2.5 | 1.2 | 8.5 | 4 0 6 | 6.3 | − 5.7 | − 2.4 |
| 4 0 4 | 8.8 | 10.1 | 5.8 | 5 0 6 | 16.1* | −13.2 | − 9.9 |
| 5 0 4 | 13.8* | 12.1 | 10.9 | 6 0 6 | — | 0.7 | 0.0 |
| 6 0 4 | 4.4 | 7.9 | 0.0 | 7 0 6 | 12.0* | − 9.4 | − 9.6 |
| 7 0 4 | 9.1* | 6.9 | 10.4 | 8 0 6 | 3.2 | − 4.1 | 2.4 |
| 8 0 4 | 3.6 | − 4.9 | − 5.9 | 9 0 6 | 7.1* | − 5.6 | − 6.5 |
| 9 0 4 | 5.8* | 5.7 | 7.0 | 10 0 6 | — | − 1.2 | 3.7 |
| 10 0 4 | 9.6* | − 8.4 | − 9.2 | 11 0 6 | 6.6 | − 5.1 | − 2.3 |
| 11 0 4 | — | − 0.6 | 2.3 | 12 0 6 | 4.3 | 4.7 | 4.1 |
| 12 0 4 | 7.3* | − 7.9 | − 9.7 | 13 0 6 | — | − 1.8 | 2.1 |
| 13 0 4 | 2.8 | − 3.2 | − 2.2 | 14 0 6 | 4.9* | 6.1 | 3.3 |
| 14 0 4 | 3.1* | − 1.8 | − 7.9 | 15 0 6 | 5.9* | 7.3 | 5.7 |
| 15 0 4 | 4.8* | − 4.8 | − 5.8 | 16 0 6 | 3.1 | 0.8 | 1.7 |
| 16 0 4 | 2.2 | − 1.6 | − 3.9 | 17 0 6 | 6.8* | 5.9 | 7.0 |
| 17 0 4 | 12.6* | −12.7 | − 7.0 | 18 0 6 | 4.2 | − 5.2 | 0.0 |
| 18 0 4 | — | − 0.4 | 0.0 | 19 0 6 | 7.2* | 7.3 | 6.3 |
| 19 0 4 | 8.9* | − 9.0 | − 6.2 | 20 0 6 | 3.1 | − 4.2 | − 1.6 |
| 20 0 4 | 3.1* | 2.6 | 3.6 | 21 0 6 | 5.1* | 3.4 | 4.1 |
| 21 0 4 | 3.7* | − 4.8 | − 4.1 | 22 0 6 | 2.6 | − 1.4 | − 2.3 |
| 22 0 4 | 6.1* | 8.1 | 5.2 | 23 0 6 | — | 0.2 | 1.4 |
| 23 0 4 | 2.8 | − 2.6 | − 1.3 | 24 0 6 | 2.4 | − 2.5 | − 2.4 |
| 24 0 4 | 6.7* | 7.3 | 5.5 | 25 0 6 | 1.3 | − 0.7 | − 1.5 |
| 25 0 4 | 2.7 | 1.8 | 1.5 | 1 0 7 | 7.0* | − 4.6 | − 8.9 |
| 26 0 4 | 3.7* | 3.5 | 4.0 | 2 0 7 | 2.1 | 3.7 | 1.1 |
| 27 0 4 | 1.8 | 1.6 | 3.1 | 3 0 7 | 4.2* | − 2.4 | − 6.2 |
| 28 0 4 | 1.6 | − 1.0 | 2.0 | 4 0 7 | 3.0 | 2.8 | 2.0 |
| 29 0 4 | 2.3* | 2.7 | 3.6 | 5 0 7 | 4.7 | − 4.8 | − 2.2 |
| 1 0 5 | 26.6* | 26.8 | 11.1 | 6 0 7 | — | 0.2 | 2.2 |
| 2 0 5 | 2.3 | − 1.7 | − 4.0 | 7 0 7 | 2.1 | 3.1 | 2.1 |
| 3 0 5 | 6.0* | 5.9 | 7.4 | 8 0 7 | 3.6 | − 3.6 | 1.8 |
| 4 0 5 | 10.2* | −10.2 | − 7.2 | 9 0 7 | 5.5* | 7.2 | 6.1 |
| 5 0 5 | 3.8 | − 4.5 | 2.8 | 10 0 7 | 4.6 | − 2.1 | 1.0 |
| 6 0 5 | 9.4* | − 7.7 | − 8.0 | 11 0 7 | 12.2* | 12.3 | 7.7 |
| 7 0 5 | 1.8 | 3.9 | − 2.6 | 12 0 7 | 2.0 | − 1.2 | 0.0 |
| 8 0 5 | 9.8* | −10.5 | − 6.5 | 13 0 7 | 8.5* | 7.5 | 7.2 |
| 9 0 5 | 1.9 | 1.1 | − 7.4 | 14 0 7 | 1.9 | − 1.1 | − 0.9 |
| 10 0 5 | 1.9 | − 0.7 | − 3.4 | 15 0 7 | 3.8* | 4.6 | 4.8 |
| 11 0 5 | 3.4* | − 2.1 | − 9.2 | 16 0 7 | 3.3 | − 4.4 | − 1.5 |
| 12 0 5 | 2.0 | 1.1 | 0.0 | 17 0 7 | 1.9 | 1.1 | 1.6 |
| 13 0 5 | 5.1* | − 6.1 | − 8.6 | 18 0 7 | 4.2 | − 4.3 | − 1.6 |
| 14 0 5 | 3.1 | 4.6 | 2.9 | 19 0 7 | 3.7 | − 3.0 | − 1.8 |

| | | | |
|---|---|---|---|
| 20 0 7 | 2.7 | − 2.8 | − 1.2 |
| 21 0 7 | 2.4 | − 1.9 | − 3.9 |
| 22 0 7 | 2.2 | − 2.3 | − 0.6 |
| 0 0 8 | 3.4 | 2.0 | 0.5 |
| 1 0 8 | 2.8 | 1.1 | 2.0 |
| 2 0 8 | 3.4 | 4.9 | 0.5 |
| 3 0 8 | 7.0* | 6.9 | 5.6 |
| 4 0 8 | — | 0.0 | 0.2 |
| 5 0 8 | 7.9* | 6.9 | 7.3 |
| 6 0 8 | 2.7 | 2.8 | 0.0 |
| 7 0 8 | 9.0* | 8.6 | 7.2 |
| 8 0 8 | 2.7 | 0.8 | − 0.2 |
| 9 0 8 | 3.3* | 2.9 | 4.8 |
| 10 0 8 | — | − 0.1 | − 0.4 |
| 11 0 8 | — | 0.3 | 1.7 |
| 12 0 8 | 2.7 | 2.0 | − 0.4 |
| 13 0 8 | 2.7 | − 2.5 | − 1.6 |
| 14 0 8 | — | 0.0 | − 0.4 |
| 15 0 8 | 4.2* | − 3.3 | − 4.3 |
| 16 0 8 | 2.3 | − 0.8 | − 0.2 |
| 17 0 8 | 5.3* | − 5.6 | − 5.3 |
| 18 0 8 | 1.8 | − 2.8 | 0.0 |
| 1 0 9 | 5.5* | 6.1 | 6.0 |
| 2 0 9 | — | 0.2 | 0.3 |
| 3 0 9 | 4.8* | 5.7 | 4.1 |
| 4 0 9 | 1.8 | 1.9 | 0.7 |
| 5 0 9 | — | 1.2 | 1.5 |
| 6 0 9 | 2.4 | 1.5 | 0.8 |
| 7 0 9 | 1.7 | 0.7 | − 1.5 |
| 8 0 9 | 2.3 | 1.8 | 0.6 |
| 9 0 9 | 3.1* | − 3.8 | − 4.0 |
| 10 0 9 | 2.1 | − 2.0 | 0.3 |
| 11 0 9 | 7.3* | − 5.1 | − 5.2 |
| 12 0 9 | — | − 0.4 | 0.0 |

TABLE III

OBSERVED AND CALCULATED STRUCTURE FACTORS $F(h\ k\ 0)$, TOGETHER WITH THE CONTRIBUTIONS OF THE ZINC ATOM.

* These structure factors were employed on the first Fourier summations (Fig. 1), using the signs of $F_{Zn}$.

| $h\ k\ l$ | $1/4F_o$ | $1/4F_c$ | $1/4F_{2n}$ |
|---|---|---|---|
| 0 0 0 | | 162 | 28 |
| 2 0 0 | 42.3* | −43.2 | −24.2 |
| 4 0 0 | 2.8 | 2.6 | 12.6 |
| 6 0 0 | 0.3 | − 0.6 | 0.0 |
| 8 0 0 | 24.3* | 26.8 | −12.0 |
| 10 0 0 | 2.3 | − 5.0 | 17.6 |
| 12 0 0 | 6.7 | − 6.4 | −17.7 |
| 14 0 0 | 8.8 | 10.0 | 13.0 |
| 16 0 0 | 9.0 | − 8.0 | − 6.4 |
| 18 0 0 | 6.2 | − 6.6 | 0.0 |
| 20 0 0 | 11.0* | 9.9 | 5.5 |
| 22 0 0 | 5.0* | − 4.6 | − 7.6 |
| 24 0 0 | 10.3* | 7.5 | 7.4 |
| 26 0 0 | 9.2* | − 8.1 | − 5.2 |
| 28 0 0 | 4.8* | 4.5 | 2.6 |
| 30 0 0 | 3.1 | 3.3 | 0.3 |
| 32 0 0 | 0.9 | − 1.0 | − 2.0 |
| 1 1 0 | 9.5 | 10.5 | 5.0 |
| 2 1 0 | 39.1* | −38.8 | − 8.2 |
| 3 1 0 | 27.6* | −29.2 | −14.3 |
| 4 1 0 | 13.9* | 15.3 | 14.0 |
| 5 1 0 | 13.6* | 12.7 | 18.1 |
| 6 1 0 | 12.2* | −11.9 | −14.9 |
| 7 1 0 | 12.5* | −10.1 | −16.7 |
| 8 1 0 | 21.5* | 19.6 | 11.5 |
| 9 1 0 | 4.5 | 3.3 | 10.8 |
| 10 1 0 | 13.7* | −15.5 | − 6.0 |
| 11 1 0 | 12.5 | 10.6 | − 3.4 |
| 12 1 0 | — | 1.6 | 0.0 |
| 13 1 0 | — | − 0.1 | − 3.0 |
| 14 1 0 | — | 0.4 | 5.1 |
| 15 1 0 | 4.8 | 5.0 | 7.7 |
| 16 1 0 | 2.3 | − 1.5 | − 7.4 |
| 17 1 0 | 9.9* | − 9.0 | − 9.2 |
| 18 1 0 | 7.0* | 6.6 | 7.3 |
| 19 1 0 | 18.4* | 17.0 | 7.8 |
| 20 1 0 | 1.2 | − 1.0 | − 5.3 |
| 21 1 0 | 6.5* | − 6.2 | − 4.9 |
| 22 1 0 | 4.3 | 3.8 | 2.6 |
| 23 1 0 | 1.9 | 1.7 | 1.5 |
| 24 1 0 | 1.2 | − 1.2 | 0.3 |
| 25 1 0 | — | 1.9 | 1.6 |
| 26 1 0 | 2.9 | − 2.8 | − 2.1 |
| 27 1 0 | 2.8* | − 2.2 | − 3.2 |
| 28 1 0 | 6.2* | 5.2 | 3.0 |
| 29 1 0 | 3.5* | 2.8 | 3.6 |
| 30 1 0 | — | − 1.9 | − 2.8 |
| 31 1 0 | 1.7 | − 1.8 | − 2.9 |
| 32 1 0 | 1.0 | 0.8 | 2.0 |
| 0 2 0 | 19.2 | −23.1 | 2.9 |
| 1 2 0 | 18.3* | −19.2 | −21.8 |
| 2 2 0 | 8.4 | 8.1 | − 2.5 |
| 3 2 0 | 2.0 | 0.5 | 15.1 |
| 4 2 0 | 3.9 | − 5.3 | 1.1 |
| 5 2 0 | 11.2 | 13.4 | − 5.3 |
| 6 2 0 | 17.5 | 17.1 | 0.0 |
| 7 2 0 | 16.5 | −14.5 | − 5.0 |
| 8 2 0 | 17.2 | −19.2 | − 1.3 |
| 9 2 0 | 22.8* | 23.6 | 13.0 |
| 10 2 0 | 6.3 | 5.6 | 1.9 |
| 11 2 0 | 17.4* | −16.9 | −15.5 |
| 12 2 0 | 0.6 | − 0.9 | − 2.0 |
| 13 2 0 | 12.2* | 12.0 | 14.1 |
| 14 2 0 | 2.1 | 1.1 | 1.4 |
| 15 2 0 | 11.9* | −11.5 | − 8.7 |
| 16 2 0 | 8.5 | − 7.7 | − 0.6 |
| 17 2 0 | 8.5 | 6.9 | 2.8 |
| 18 2 0 | 5.7 | 4.9 | 0.0 |
| 19 2 0 | 2.6 | 2.1 | 3.1 |
| 20 2 0 | 1.9 | 0.2 | 0.7 |
| 21 2 0 | 7.2* | − 7.6 | − 6.1 |
| 22 2 0 | 7.2 | − 7.1 | − 0.9 |
| 23 2 0 | 6.6* | 6.3 | 7.0 |

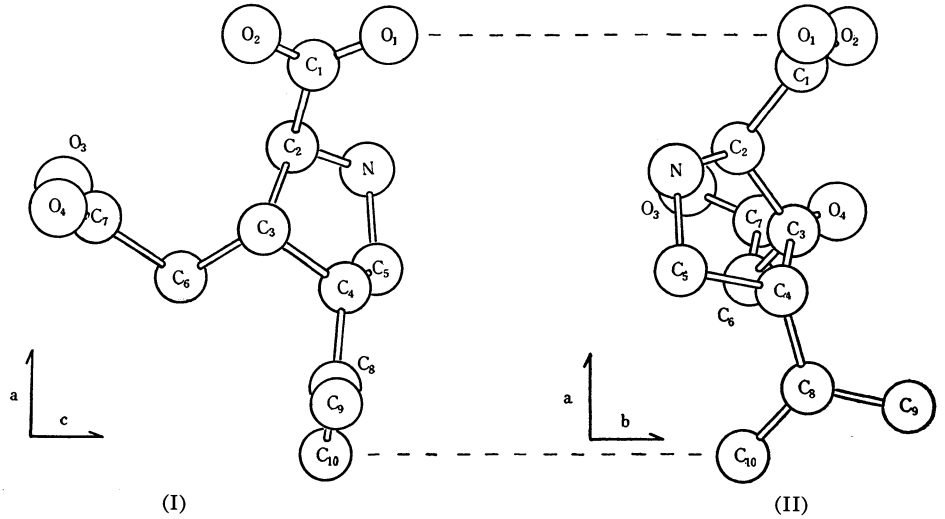
| | | | | | | | |
|---|---|---|---|---|---|---|---|
| 24 2 0 | 1.9 | − 1.4 | 0.9 | 21 4 0 | 3.0 | − 2.6 | − 1.2 |
| 25 2 0 | 7.4* | − 5.7 | − 5.9 | 22 4 0 | 3.2* | 3.5 | 5.1 |
| 26 2 0 | 1.4 | 2.0 | − 0.6 | 23 4 0 | 3.9 | 3.6 | 1.4 |
| 27 2 0 | 5.6* | 5.1 | 3.6 | 24 4 0 | 4.1* | − 4.8 | − 5.2 |
| 28 2 0 | 1.0 | − 1.2 | 0.2 | 25 4 0 | 0.7 | 0.7 | − 1.2 |
| 29 2 0 | — | − 0.6 | − 0.9 | 26 4 0 | 2.9* | 3.1 | 3.7 |
| 30 2 0 | — | − 0.9 | 0.1 | 27 4 0 | — | − 1.2 | 0.7 |
| 31 2 0 | 1.1 | − 0.5 | − 1.2 | 28 4 0 | 3.2* | − 2.8 | − 1.8 |
| 1 3 0 | 1.7 | 1.3 | − 2.6 | 29 4 0 | — | − 0.4 | − 0.2 |
| 2 3 0 | 11.7 | −12.2 | − 7.6 | 1 5 0 | 2.4 | − 1.9 | − 2.6 |
| 3 3 0 | 6.9 | − 8.0 | 7.1 | 2 5 0 | 1.7 | 0.2 | 2.4 |
| 4 3 0 | 22.9* | 22.5 | 13.4 | 3 5 0 | 6.3* | 5.5 | 7.4 |
| 5 3 0 | 12.8* | −11.4 | − 9.2 | 4 5 0 | 4.3* | − 4.3 | − 4.1 |
| 6 3 0 | 10.7* | − 9.1 | −14.3 | 5 5 0 | 14.9* | −12.1 | − 9.7 |
| 7 3 0 | 11.7* | 11.5 | 8.7 | 6 5 0 | 7.8* | 7.5 | 4.6 |
| 8 3 0 | 3.7 | 3.4 | 11.3 | 7 5 0 | 12.1* | 10.6 | 9.2 |
| 9 3 0 | 6.0 | − 7.4 | − 5.6 | 8 5 0 | 2.9 | − 2.4 | − 3.7 |
| 10 3 0 | 2.7 | − 4.1 | − 6.0 | 9 5 0 | 6.4* | − 5.8 | − 6.1 |
| 11 3 0 | 9.2 | −11.0 | 1.8 | 10 5 0 | 1.9 | 4.1 | 2.0 |
| 12 3 0 | 4.6 | 6.1 | 0.0 | 11 5 0 | 6.0 | 7.0 | 2.1 |
| 13 3 0 | 7.2 | 7.1 | 1.6 | 12 5 0 | — | − 0.3 | 0.0 |
| 14 3 0 | 2.6 | 3.0 | 5.3 | 13 5 0 | 1.9 | 3.0 | 1.9 |
| 15 3 0 | 7.6* | − 7.2 | − 4.4 | 14 5 0 | 3.0 | − 2.7 | − 1.8 |
| 16 3 0 | 8.8* | − 8.0 | − 7.8 | 15 5 0 | 5.5* | − 4.4 | − 4.9 |
| 17 3 0 | 4.1* | 3.8 | 5.1 | 16 5 0 | 1.2 | 2.3 | 2.6 |
| 18 3 0 | 9.2* | 8.3 | 7.7 | 17 5 0 | 7.3* | 7.5 | 6.0 |
| 19 3 0 | 5.1* | − 5.4 | − 4.4 | 18 5 0 | — | 0.2 | − 2.7 |
| 20 3 0 | 7.7* | − 5.9 | − 5.7 | 19 5 0 | 2.9* | − 2.6 | − 5.2 |
| 21 3 0 | 4.3* | 4.9 | 2.7 | 20 5 0 | 1.1 | − 1.0 | 2.0 |
| 22 3 0 | — | − 0.8 | 2.9 | 21 5 0 | 4.4* | 4.6 | 3.4 |
| 23 3 0 | 3.8 | − 3.4 | − 0.9 | 22 5 0 | 1.0 | − 0.9 | − 1.0 |
| 24 3 0 | 2.6 | 2.6 | 0.3 | 23 5 0 | — | − 0.9 | − 1.1 |
| 25 3 0 | 1.7 | 0.9 | − 1.0 | 24 5 0 | — | − 0.3 | − 0.2 |
| 26 3 0 | 1.6 | − 2.2 | − 2.4 | 25 5 0 | 0.8 | − 1.0 | − 1.1 |
| 27 3 0 | 2.5 | 2.1 | 1.9 | 26 5 0 | — | 0.4 | 0.9 |
| 28 3 0 | 2.8* | 2.9 | 3.2 | 27 5 0 | — | 1.4 | 2.3 |
| 29 3 0 | 2.2 | − 1.8 | − 2.2 | 0 6 0 | 3.8 | − 1.1 | − 3.2 |
| 30 3 0 | 5.4* | − 5.5 | − 3.1 | 1 6 0 | 3.8 | 3.6 | 7.8 |
| 0 4 0 | 4.6 | − 5.2 | −14.4 | 2 6 0 | 4.3 | 5.4 | 2.7 |
| 1 4 0 | 9.9 | − 8.5 | − 3.6 | 3 6 0 | 11.6* | − 9.7 | − 5.5 |
| 2 4 0 | 12.9* | 11.6 | 12.4 | 4 6 0 | 1.9 | − 2.0 | − 1.5 |
| 3 4 0 | 6.8 | 5.4 | 2.5 | 5 6 0 | 8.4 | 7.7 | 1.9 |
| 4 4 0 | 7.8* | − 8.1 | − 6.7 | 6 6 0 | 2.7 | 4.3 | 0.0 |
| 5 4 0 | 5.6 | − 5.8 | − 0.8 | 7 6 0 | 1.9 | 2.4 | 1.8 |
| 6 4 0 | 3.3 | − 2.0 | 0.0 | 8 6 0 | — | 0.5 | 1.5 |
| 7 4 0 | 2.4 | − 2.3 | − 0.8 | 9 6 0 | 6.4* | − 8.3 | − 5.0 |
| 8 4 0 | 11.0* | 9.4 | 6.7 | 10 6 0 | 1.0 | − 1.4 | − 2.3 |
| 9 4 0 | 1.5 | − 2.7 | 2.2 | 11 6 0 | 6.9* | 7.7 | 6.3 |
| 10 4 0 | 11.6* | −11.1 | −10.3 | 12 6 0 | 3.0 | 2.4 | 2.5 |
| 11 4 0 | 1.1 | − 2.0 | − 2.7 | 13 6 0 | 5.0* | − 5.9 | − 5.8 |
| 12 4 0 | 12.7* | 11.4 | 10.6 | 14 6 0 | 2.6 | − 2.3 | − 1.9 |
| 13 4 0 | 1.0 | 0.3 | 2.5 | 15 6 0 | 1.8 | 1.5 | 3.8 |
| 14 4 0 | 11.7* | − 9.6 | − 8.0 | 16 6 0 | — | 0.5 | 1.1 |
| 15 4 0 | 2.7 | − 2.5 | − 1.6 | 17 6 0 | — | − 1.6 | − 1.3 |
| 16 4 0 | 1.2 | 1.1 | 4.1 | 18 6 0 | 1.0 | 1.3 | 0.0 |
| 17 4 0 | 3.8 | 3.0 | 0.5 | 19 6 0 | 1.5 | 0.9 | − 1.4 |
| 18 4 0 | — | − 0.4 | 0.0 | 20 6 0 | 1.5 | − 1.5 | − 0.9 |
| 19 4 0 | — | 0.0 | 0.6 | 21 6 0 | 1.0 | 1.3 | 2.9 |
| 20 4 0 | 3.0* | − 3.2 | − 3.6 | 22 6 0 | 1.9 | 2.0 | 1.3 |

| | | | |
|---|---|---|---|
| 23 6 0 | 3.3* | − 4.7 | − 3.4 |
| 24 6 0 | 1.2 | − 1.4 | − 1.3 |
| 1 7 0 | — | 0.7 | 0.5 |
| 2 7 0 | 1.9 | 1.1 | 2.9 |
| 3 7 0 | 1.2 | − 2.4 | − 1.5 |
| 4 7 0 | 3.7* | − 4.1 | − 5.1 |
| 5 7 0 | 2.6 | 3.2 | 1.8 |
| 6 7 0 | 5.2* | 6.2 | 5.7 |
| 7 7 0 | 1.4 | − 2.6 | − 1.7 |
| 8 7 0 | 5.0* | − 5.3 | − 4.7 |
| 9 7 0 | 1.4 | 1.2 | 1.2 |
| 10 7 0 | 3.8* | 3.8 | 2.6 |
| 11 7 0 | — | − 0.7 | − 0.4 |
| 12 7 0 | 1.0 | 0.0 | 0.0 |
| 13 7 0 | 1.0 | − 0.1 | − 0.4 |
| 14 7 0 | 3.4* | − 3.2 | − 2.4 |
| 15 7 0 | — | 0.1 | 1.0 |
| 16 7 0 | 4.1* | 5.7 | 3.5 |
| 17 7 0 | 0.8 | 0.0 | − 1.2 |
| 18 7 0 | 2.0* | − 2.4 | − 3.6 |
| 19 7 0 | 0.6 | 1.0 | 1.1 |
| 20 7 0 | 0.6 | 2.1 | 2.7 |
| 0 8 0 | 3.7* | 3.4 | 4.0 |
| 1 8 0 | — | 0.0 | 2.4 |
| 2 8 0 | 3.4* | − 5.1 | − 3.5 |
| 3 8 0 | — | − 1.2 | − 1.7 |
| 4 8 0 | 2.1 | 2.5 | 1.8 |
| 5 8 0 | — | 0.0 | 0.6 |
| 6 8 0 | 0.9 | − 1.4 | 0.0 |
| 7 8 0 | — | 0.2 | 0.6 |
| 8 8 0 | 0.9 | − 1.8 | − 1.9 |
| 9 8 0 | 1.8 | − 1.8 | − 1.6 |
| 10 8 0 | 2.1 | 2.5 | 3.0 |
| 11 8 0 | 2.3 | 2.0 | 2.0 |
| 12 8 0 | 1.7 | − 2.4 | − 3.1 |
| 13 8 0 | 3.1 | − 3.8 | − 1.9 |
| 14 8 0 | 1.2 | 1.8 | 2.5 |

## Determination of the Molecular Structure

From the agreement between the corresponding peaks in the two projections, the $x, y$ and $z$ parameters of all the atoms could be easily determined without requiring the three-dimensional analysis. The two water oxygens ($O_5$, $O_6$) were recognized by the fact that they are isolated from the other atoms in reasonable distances, and from the knowledge about bond lengths and bond angles the atoms of the molecule could be linked to each other in a reasonable way as indicated in the electron-density maps (Figs. 2 and 3). The four oxygen, one nitrogen and ten carbon atoms of the molecule were recognized to be as illustrated in Fig. 4, and these assignments will be discussed below. The bond lengths and the bond angles, calculated by the atomic parameters of Table I, are shown in Fig. 5, and it may be said these lengths will be correct at least to ±0.04Å.

In the upper, the middle and the lower part of the electron-density maps, there are seen three planar trigonal groupings formed by every four atoms in the molecule. The two of these, the upper and the middle grouping, are considered to be carboxyl groups, judging from the heights of their peaks and the short distances from these to the zinc atom (Figs. 6 and 7), and the bond lengths and the bond angles within these grouping; they are $C_2$—($C_1$—$O_1$, $O_2$) and $C_6$—($C_7$—$O_3$, $O_4$). The $C_3$—$C_6$ distance of 1.56 Å being of carbon-carbon




(I) (II)

Fig. 4. The structure of kainic acid, (I) viewed along the $b$ axis, (II) viewed along the $c$ axis.

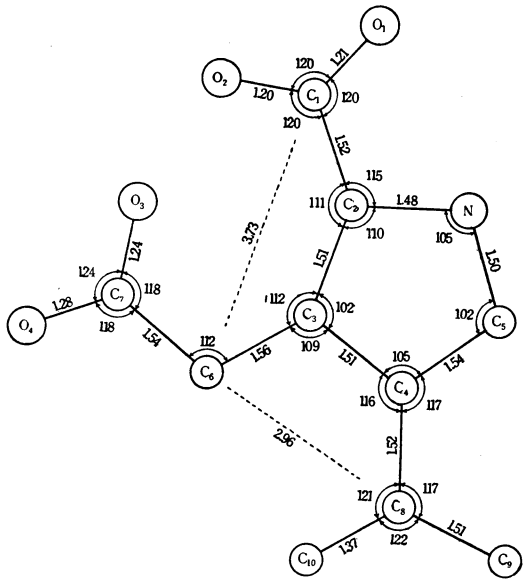


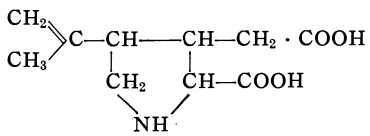

Fig. 5. Bond lengths (Å) and bond angles (°).

single bond, $C_3$—($C_6$—$C_7$—$O_3$, $O_4$) is an acetic acid group.

That of the lower part, having low peaks, is attributable to an isopropenyl group, $C_4$—($C_8$—$C_9$, $C_{10}$), since their bond lengths and bond angles are conformable to the characterics of this group, the $C_8$—$C_{10}$ bond of 1.37 Å being its double bond.

The nitrogen atom is distinguished from the carbon atoms by the short distance from the zinc atom and by the height of its peak higher than the surrounding carbon atoms. The five-membered ring, N, $C_2$, $C_3$, $C_4$, $C_5$, is of pyrrolidine as identified by the values in Fig. 5.

Thus the structure of kainic acid is concluded to be 2-carboxy-3-carboxymethyl-4-isopropenylpyrrolidine.




As for the stereochemical configuration of the molecule, the carboxyl group of $C_2$ and the acetic acid group of $C_3$ take the *trans*-configuration relative to the ring, and the latter group and the isopropenyl group of $C_4$ are in the *cis*-configuration. In the isopropenyl group, the double bond $C_8$—$C_{10}$ is so located as to be nearer to the ring than the single bond $C_8$—$C_9$. These stereochemical configurations are well shown in Fig. 4.

The five-membered pyrrolidine ring is in the present case considerably more distorted from the planar form than that of hydroxyproline[6], and this may owe mainly to the two side-chains attached to the neighboring $C_3$ and $C_4$, the side-chains closely approaching each other because of the *cis*-configuration. The distance between $C_6$ and $C_8$ is found to be about 3.0 Å, much larger but more adequate than the value of 2.6 Å calculated tentatively using the standard bond distances and bond angles.

## Description of the Crystal Structure

The views of the crystal structure along the *b* and *c* axes are illustrated in Figs. 6 and 7, giving the intermolecular distances. The unit cell contains four zinc cations, eight water molecules and four kainate anions, the molecular structure having already given in the last section. As a whole, the crystal structure is a layered one as can be supposed from the plane of cleavage.

The nitrogen, the four oxygens of the two carboxyl groups and the oxygen $O_5$ of the water surround the zinc, and these six atoms form an octahedron around it. The distances from the zinc to these oxygens, except for Zn...$O_4$ of 2.81 Å, vary from 2.02 to 2.15 Å, as generally found in the zinc salts of oxygen acids, and the distance between the zinc and the nitrogen is 2.21 Å, again the usual value for Zn...N. While the one water ($O_5$) is the coordinated water, the other ($O_6$) does not coordinate to the zinc. It is conceivable that the water $O_6$ is easily desiccated in a desiccator or by heating.

All the hydrogens of the two waters form the O—H...O hydrogen bonds between the two waters or the waters and oxygens of the carboxyl groups. These hydrogen bond distances are 2.68 Å of $O_5$—H...$O_6$, 2.81 Å of $O_5$—H...$O_2$, 2.73 Å of $O_6$—H...$O_3$ and 2.74 Å of $O_6$—H...$O_4$. The hydrogen attached to the nitrogen may be considered also to form the intermolecular hydrogen-bridge between the nitrogen of one molecule and a carboxyl group of another, its N—H...$O_1$ distance being 2.93 Å.

By all the above-mentioned interactions, the zinc cations, the waters and the kainate anions are linked to each other

6) J. Zussman, *Acta Cryst.*, **4**, 493 (1951); J. Donohue, ibid., **5**, 419 (1952).

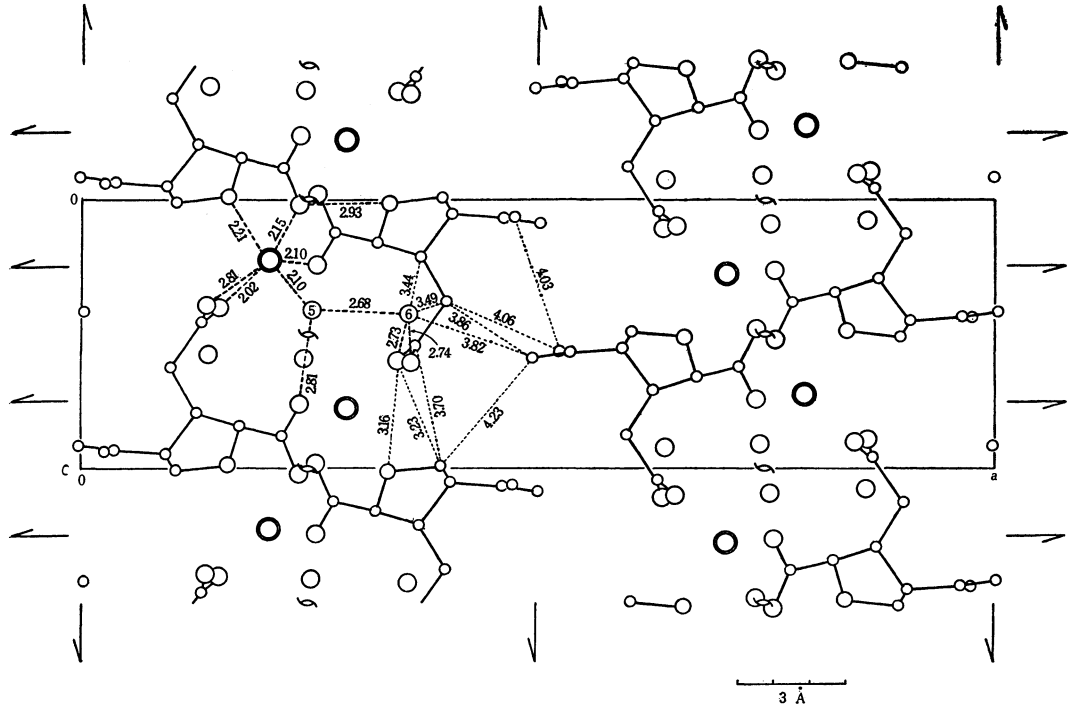



Fig. 6. View of the crystal structure along the *b* axis. The intermolecular distances are shown in Å. Double circles represent zinc, and single circles other atoms, being large, middle and small circles for oxygen, nitrogen and carbon, respectively.

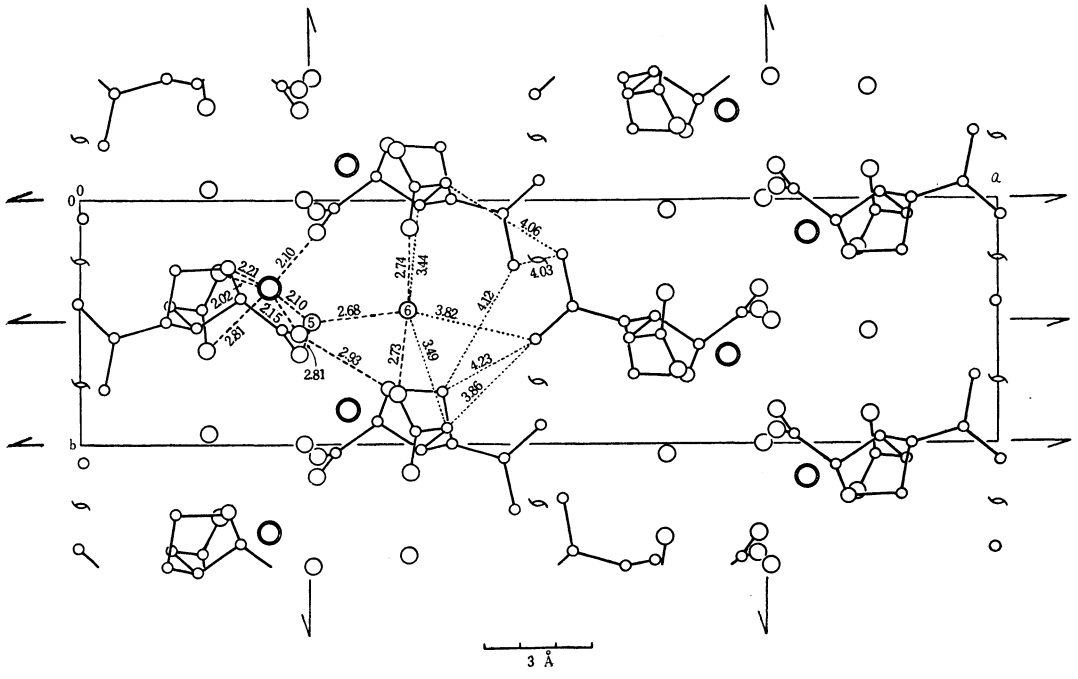



Fig. 7. View of the crystal structure along the *c* axis. The intermolecular distances are shown in Å. Symbols are the same as those of Fig. 6.

forming a layered structure perpendicular to the *a* axis, and between the layers only weak van der Waals attractive forces of the non-polar groups or atoms are operative. The distances of the closest approach between the layers are 3.86 Å of $C_{10}...C_6$, 4.03 Å of $C_9...C_9$ and 4.06 Å of $C_9...C_6$. It is obvious that the cleavage of (1 0 0) plane takes place here.

We wish to express our thanks to Professor-Emeritus S. Murakami, Dr. T. Takemoto and their collaborators of this University, and Drs. S. Kuwada, S. Tatsuoka, Y. Ueno and their collaborators of the Research Laboratories of Takeda Pharmaciutical Industries, Ltd., for supplying the specimens, kind discussions and micro-analyses. Thanks are also due to Drs. Y. Tomiie and H. Tani of this University for helpful advice and continued interest. Appreciations are also expressed to Messrs T. Siba, S. Sakakibara and M. Okumiya and Miss K. Koike of this University for their help in microanalysis.

*Department of Chemistry*
*Faculty of Science*
*Osaka University*
*Kita-ku, Osaka*

# *Fundamental Studies on the Biogeochemical Prospecting for Manganese*

By Noboru YAMAGATA and Toshiko YAMAGATA

(Received February 4, 1957)

Most of the manganese ores of economic importance in Japan form very small ore bodies near the surface, and the mining industries are generally of very small scale. Systematic prospecting has not yet been performed but only groping has been carried on. Geochemical prospecting for manganese ore by the analyses of soil and surface water has been studied by M. Shima[1] in this country and he suggested such possibilities in several mines. Surface water is not always available; when a representative soil sample is required, the sampling method may become rather complicated. These considerations led the authors to make an attempt of a geochemical prospecting for manganese by use of plant leaves as an aid.

## Principle

Several problems are underlying in the application of plant material in practice as an indicator for manganese level in soil. Those problems could be briefly described as follows:

(1) Correlation of manganese level between soil and plants.

Numerous investigators performed experiments on some culture plants by use of water and sand culture method and positive correlation of manganese level between the medium and the plant has been confirmed. This relationship is likely to be applied to natural plants, herbs and trees, although the direct evidence has not been submitted.

Above mentioned correlation is only appropriate for manganese in solution. In our case, the matter in question is the correlation between mineral content of manganese in soil and manganese level in plants. Fortunately, several problems on the soil manganese conditions were solved by G. D. Sherman and P. M. Harmer in 1942[2], and we can use their results as the basis for further research.

(2) In practice, to obtain the plant samples which are as representative as possible, a tree is preferred to small herbaceous plants, because the latter are sensitive to small local variations in soil. Only two grams or less in dry weight is required for the analysis of manganese in plant leaves; two problems arise about the sampling method to avoid variations.

1) M. Shima, "Geochemical Prospecting" (in Japanese) Maruzen Co., Ltd., Tokyo (1955) p. 180.

2) G. D. Sherman and P. M. Harmer, *Soil Sci. Soc. Amer. Proc.*, **7**, 398 (1942).

One of the variations of manganese content is due to the difference in age and position of leaves of a tree, and the other is due to the age of the tree. The dimensions of those variations must be confirmed at the beginning of the experiment.

## Experimental

In the chemical analysis of manganese and iron in plant leaves, the air-dried (100°C for 6 hours) samples were first ashed in a porcelain dish over an open flame. The ash was moistened with water, decomposed with 5 ml. of nitric acid (1 : 1) and 2 ml. of sulfuric acid, evaporated to dryness, and then heated to fumes. When the resultant liquid was dark colored, one ml. of hydrogen peroxide solution and 2 ml. of concentrated nitric acid were added and again heated to fumes. To the colorless or pale-yellow liquid was added hot water and insoluble matter was filtered. The filtrate was made up to 50 ml., and a 40 ml. aliquot was used for colorimetric determination of manganese as described in A. O. A. C. official methods of analysis[3], and 10 ml. aliquot for iron determination by use of thiocyanate colorimetric method as usual[4].

Soil extractions were made on freshly taken soil samples, and a separate portion was taken for moisture determination. Further procedure was the same as that of Sherman and Harmer[5].

The manganese mineral content in soil was determined as follows. One to ten grams of soil sample was taken in a beaker and 5 to 30 ml. of concentrated sulfuric acid and 20 to 100 ml. of concentrated nitric acid were added. This was heated gently until brown fumes diminished, and boiled until white fumes appeared. Phosphoric acid was added, boiled for a few minutes and after cooling made to 100 ml. or one litre. A suitable quantity of the clear supernatant solution was taken and the manganese determined as described before. The manganese extraction methods for the various states in soil are schematically shown in Fig. 1.

| State of Mn in soil | | Extractant |
|---|---|---|
| Active-Mn | Water-soluble | $H_2O$ |
| | Exchangeable | 1 N-$NH_4$-acetate |
| | Easily-reducible | 1 N-$NH_4$-acetate and hydroquinone |
| | Acid-soluble | $HNO_3+H_2SO_4$ |

Fig. 1. State of manganese in soil and extractants.

3) "Official Methods of Analysis of the A. O. A. C." 7th ed. Association of Official Agricultural Chemists, Washington (1950).

4) E. B. Sandell, "Colorimetric Determination of Traces of Metals" 2nd Ed., Interscience Publ., Inc., New York (1950).

5) Care must be taken for hydroquinone in use, because commercial hydroquinone frequently contains a considerable amount of manganese.

Errors in the colorimetric analyses of manganese and iron were calculated from the quadruplicate determinations on a powdered and well-mixed plant sample (*Chamaecyparis obtusa* Endlicher, "Hinoki"). The results are shown in Table I. The relative error was 0.4% for manganese and 1.3% for iron.

TABLE I
ERRORS IN THE COLORIMETRIC ANALYSES OF MANGANESE AND IRON IN PLANT MATTER
(On fresh basis)

| *Chamaecyparis* | Mn(p.p.m.) | Fe(p.p.m.) | Mn/Fe |
|---|---|---|---|
| *obtusa* | 78.9 | 222 | 0.355 |
| | 77.3 | 216 | 0.358 |
| | 76.9 | 209 | 0.368 |
| | 77.4 | 225 | 0.344 |
| Mean | 77.6 | 218 | 0.356 |
| Average deviation | 0.31 | 2.8 | 0.0034 |

## Results and Discussion

**Culture Experiments.**—At first, a water-culture experiment was carried out with about thirty-days seedlings of tomato plants. The plants had been cultured for two weeks in glazed clay pots with a perfect universal culture solution[6] when the solution was replaced by those of six levels of manganese concentrations. After twenty days culturing with occasional renewal of the solution, the plants were harvested and the leaves were analyzed for manganese.

The result shown in Table II indicates a fair correlation between the manganese content in plants and the manganese level

TABLE II
WATER CULTURE EXPERIMENT WITH *Solanum Lycopersicum* L

| Pot No. | Mn level in culture sol. p.p.m. | Mn content in cultured plant p.p.m. (dry basis) | Conc. ratio |
|---|---|---|---|
| 1 | 0.03 | 74.5 | 2500 |
| 2 | 0.1 | 126 | 1260 |
| 3 | 0.3 | 196 | 650 |
| 4 | 1 | 302 | 300 |
| 5 | 3 | 323 | 100 |
| 6 | 10 | 1029 | 100 |

in culture solution which ranged from 0.03 to 10 p. p. m. But, the concentration ratio of manganese by a plant grows small when the manganese level in solution is raised. In other words, the magnitude of

6) Devised by the authors grounded on the distribution of chemical elements in natural plants; *Japan Analyst*, **6**, 75 (1957).

TABLE III
CULTURE EXPERIMENT ON THE SOIL MIXED WITH RHODONITE
(p. p. m. on dry basis)

| Pot No. | pH of soil | Acid soluble Mn | Active Mn | | | Plants Mn | |
|---|---|---|---|---|---|---|---|
| | | | Water soluble Mn | Exchangeable Mn | Easily reducible Mn | Aster sp. | Carex sp. |
| Contrast | 7.1 | 700 | 0 | 7.1 | 92 | 95 | 6.2 |
| 1 | 7.1 | 710 | 0 | 2.4 | 138 | 109 | 13 |
| 2 | 7.0 | 1400 | 1.0 | 11 | 163 | 118 | 17 |
| 3 | 7.0 | 2350 | 3.2 | 23 | 504 | 168 | 33 |
| 4 | 7.0 | 5440 | 9.3 | 52 | 958 | 379 | 71 |
| 5 | 7.0 | 7000 | 10 | 116 | 1940 | 622 | 113 |
| 6 | 7.0 | 18500 | — | — | — | — | 3090* |

* died in two weeks

TABLE IV
CULTURE EXPERIMENT ON THE SOIL MIXED WITH HAUSMANNITE
(p. p. m. on dry basis)

| Pot No. | pH of soil | Acid soluble Mn | Active Mn | | | Tomato plant | |
|---|---|---|---|---|---|---|---|
| | | | Water soluble Mn | Exchangeable Mn | Easily reducible Mn | Mn | Mn/Fe |
| Contrast | 7.2 | 700 | 0 | 7.1 | 92 | 174 | 1.58 |
| 1 | 7.0 | 1480 | 2.9 | 0 | 239 | 219 | 0.90 |
| 2 | 7.2 | 2130 | 2.0 | 1.0 | 495 | 203 | 2.42 |
| 3 | 7.3 | 4810 | 3.7 | 2.1 | 1700 | 256 | 4.57 |
| 4 | 7.3 | 12900 | 23 | 6.5 | 4520 | 419 | 5.66 |
| 5 | 7.3 | 22800 | 34 | 11.5 | 5740 | 393 | 9.82 |

fluctuations in the manganese content of a plant is smaller than that of manganese in the medium. The former is only 1/24 of the latter in this experiment, and the relationship is also valid in the soil experiments as described later.

Soil culture experiments were carried out with two kinds of manganese mineral mixed with a normal soil. The soil was mixed with various quantities of rhodonite[7] and hausmannite[8] minerals separately and plants were cultured on them for about one month in pots. At the same time when the cultured plants were harvested, fresh soil samples were collected from the pots and extraction of manganese in various states was performed, and then a separate portion of the sample was used for soil reaction test with 100 ml. distilled water by use of glass electrode pH meter. The results are shown in Tables III and IV.

Addition of rhodonite to the soil slightly increased acidity of the soil and vice versa in the case of hausmannite, but the extent of increase or decrease was not remarkable.

When the two soils mixed with almost the same quantity (in acid soluble-manganese) of rhodonite and hausmannite, were compared with respect to their manganese status, the levels of water-soluble and the easily reducible manganese are of comparable order in both soils, but the level of exchangeable manganese in the soil mixed with rhodonite (Table III) is much higher, about twenty times or more, than that in the other soil.

In accordance with the variation of acid-soluble manganese in soil, the manganese content of *Aster* sp. and *Carex* sp. varied from 95 to 622 p. p. m. and from 6.2 to 113 p. p. m. respectively. The magnitude of fluctuation is about 6.5 in the former, and 18 in the latter; in this sense, *Carex* sp. can more sensitively indicate the manganese level in soil than *Aster* sp. but its response for manganese is lower.

In the case of the culture experiment with hausmannite, a tomato plant was used and the magnitude of fluctuation was only about 2 when acid soluble manganese varied from 700 to 22800 p. p. m. In this case iron content of the plant was also determined and Mn/Fe ratio calculated. As shown in Table IV, the fluctuation of Mn/Fe is much greater than that of

7) Contained a small amount of hausmannite and braunite.
8) Contained a small amount of braunite.

manganese content itself. Thus, under certain circumstances, we can employ the ratio of manganese to iron in a plant as the more sensitive indicator for the manganese level in soil.

**Variation of Manganese and Iron Content due to the Sampling Position of a Tree.**—A "Hinoki" tree (*Chamaecyparis obtusa* ENDLICHER), about thirty years of age, was chosen in the campus of our college. Four samples of leaves, about 200 grams each were pulled off from the south, the east, the north and the west side of the tree, and young leaves were collected from the top of the tree. Those samples were separately analyzed in the same way as described before. The result shown in Table V indicates that the variation due to the sampling position of a tree is great enough to be beyond the errors in determination. Thus, it can be concluded that to obtain leaves which are as representative as possible, a composite sample must be taken from around the tree.

TABLE V
VARIATION DUE TO THE SAMPLING POSITION OF A TREE
(*Chamaecyparis obtusa* leaves, on fresh basis)

| Sampling position | Mn p.p.m. | Fe p.p.m. | Mn/Fe |
|---|---|---|---|
| East side leaves | 25.1 | 125 | 0.201 |
| West side leaves | 23.2 | 131 | 0.177 |
| South side leaves | 20.0 | 121 | 0.165 |
| North side leaves | 29.8 | 130 | 0.229 |
| Top young leaves | 23.4 | 82.4 | 0.284 |

**Variation due to the Age of the Tree.**—Five "Hinoki" trees of different ages were chosen in the campus and composite samples were taken for analyses. The result shown in Table VI indicates the increasing manganese content and Mn/Fe ratio of plant in consequence of the growing age. So, it can be concluded that to guess manganese levels in soil we must take foliar samples from the trees of an age as similar as possible, e.g. from twenty to thirty years.

TABLE VI
VARIATION DUE TO THE AGE OF A TREE
(*Chamaecyparis obtusa* leaves, on fresh basis)

| Proximate age Years | Mn p.p.m. | Fe p.p.m. | Mn/Fe |
|---|---|---|---|
| 3 | 25.6 | 265 | 0.097 |
| 10 | 20.8 | 155 | 0.13 |
| 20 | 49.8 | 169 | 0.29 |
| 30 | 34.8 | 133 | 0.26 |
| 40 | 77.1 | 212 | 0.36 |

**Possibility of the Practical Application.**—In order to find out whether this method of manganese analysis was applicable to the practical soil investigation and the prospecting of ores and to examine how much the manganese content of a plant varied with circumstances, the authors collected, in September 1956, a number of samples in the mine district near the river Kiriu, about four kilometers from the city of Kiriu.

The bed rock consists of paleozoic chert and slate, and the principal manganese ore consists of rhodochrosite, rhodonite, tephroite, penwithite and various oxide minerals.

Five samples of "Hinoki" (20—30 years) leaves were collected in a non-mineralized district near the river Kiriu about one kilometer away from the mineralized district where eight samples were collected. As shown in Table VII, even in the non-mineralized district, the trees contained much larger quantities, about three times

TABLE VII
VARIATION OF MANGANESE CONTENT OF "HINOKI" IN MINERALIZED AND NON-MINERALIZED DISTRICTS

| In mineralized district | | | In non-mineralized district | | |
|---|---|---|---|---|---|
| Location No. | Mn p. p. m. dry basis | Mn/Fe | Location No. | Mn p. p. m. dry basis | Mn/Fe |
| 6 | 569 | 19.4 | 1 | 246 | 4.6 |
| 7 | 629 | 13.4 | 2 | 169 | 2.6 |
| 8 | 1228 | 26.8 | 3 | 109 | 2.1 |
| 9 | 832 | 29.1 | 4 | 196 | 3.6 |
| 10 | 505 | 10.1 | 5 | 215 | 4.6 |
| 11 | 817 | 21.7 | Av. | 187 | 3.5 |
| 12 | 485 | 9.1 | | | |
| 13 | 656 | 17.8 | | | |
| Av. | 715 | 18.4 | | | |

TABLE VIII

CORRELATION OF MANGANESE LEVELS BETWEEN SOIL AND PLANT IN THE MINERALIZED DISTRICT

| Location No. | pH of soil | Acid soluble Mn p.p.m. | Active Mn | | | *Quercus acutissima* | | *Chamaecyparis obtusa* | |
|---|---|---|---|---|---|---|---|---|---|
| | | | Water soluble Mn p.p.m. | Exchangeable Mn p.p.m. | Easily red.-Mn p.p.m. | Mn p.p.m. | Mn/Fe | Mn p.p.m. | Mn/Fe |
| 1 | 7.3 | 350 | 0 | 1.2 | 16.8 | 265 | 4.2 | 337 | 5.7 |
| 2 | 7.4 | 300 | 0 | 0.2 | 19.7 | 244 | 3.4 | 414 | 9.6 |
| 3 | 7.0 | 425 | 0 | 1.8 | 71.1 | 1020 | 16.4 | 924 | 16.4 |
| 4* | 7.0 | 1737 | 0 | 1.2 | 424 | 875 | 11.6 | 917 | 16.8 |
| 5* | 7.1 | 5565 | 0 | 0.9 | 720 | 1050 | 21.3 | 671 | 12.5 |

* near the deposits.

as much manganese and less iron than those trees in the campus (Table VI).

The Mn/Fe ratio indicates more sensitively those relationships: the ratio in the non-mineralized district is 3.5 on average and this value is more than ten times as great as those in the campus. The ratio grows as big as 29.1 in the mineralized district. The antagonistic behavior of manganese and iron in relation to plant uptake is a very interesting object of physiological research, although it is beyond the scope of this article.

Each of five samples of "Hinoki" and also *Quercus acutissima*, a latifoliate tree which showed as vast distribution as "Hinoki" was collected at five locations in the mineralized district. Soil samples were also taken at those locations and analyzed. The results are shown in Table VIII. Acid-soluble and easily reducible manganese contents in the soils at the locations No. 4 and 5 which stand on or near the deposits are considerably high and the foliar analyses also seem to indicate the deposits. Both *Quercus* and "Hinoki" are applicable to the prospecting but the latter is better, because its leaves are available all the year round.

## Summary

The possibility of practical application of foliar analyses for geochemical prospecting for manganese were examined. A positive correlation of manganese level between soil and plants was revealed by the experiments using water and soil culture.

For the practical application, a tree, *Chamaecyparis obtusa* was chosen to avoid small local variations, and the sampling variations due to age and position were determined.

The Mn/Fe ratio was found to be a more sensitive indicator than the manganese content itself and its average value in the mineralized district was 18.4; on the other hand, it was only 3.5 in non-mineralized district.

*Kiriu College of Technology*
*Gunma University, Kiriu*

# *A New Analytical Method of Electroconductivity Data of Surfactant Solutions. II**

By Kenjiro MEGURO, Tamotsu KONDO and Noriaki OHBA

(Received December 15, 1956)

In the previous paper[1], a new analytical method for the electroconductivity data of aqueous solution of surfactant was reported. In this paper we apply this method to arrange and analyse the effect of temperature and of the addition of organic solvents and inorganic salts on the properties of surfactant solution.

## The Effect of Temperature

It has been reported that the dependence of critical micelle concentration (C. M. C.) of surfactant solution on temperature is not evident; but it will be expected that some parameter which is related to the critical phenomena of surfactant solution will change with temperature.

According to our analysis of the electroconductivity data for dodecyl ammonium chloride at various temperatures, taken from Ralston[2], it is pointed out that the concentration of the minimum and the maximum in $(\Lambda_0-\Lambda)/\sqrt{c}$ vs. $\sqrt{c}$ curve and the slope between them do not vary considerably, but $H_{min}$ and $H_{max}$,—the magnitude of $\Lambda_0-\Lambda/\sqrt{c}$ at the minimum and the maximum—, vary conspicuously with temperature. The results are shown in Fig. 1.

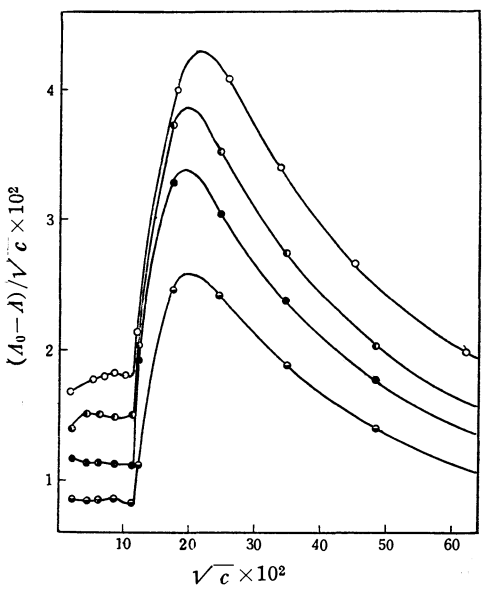



Fig. 1. $(\Lambda_0-\Lambda)/\sqrt{c}$ vs. $\sqrt{c}$ curves for the aqueous solution of dodecyl ammonium chloride at 20° ◒, 30° ●, 40° ◐ and 60°C ○.

The usual C. M. C. being remarkably invariant with temperature, $H$ values might be of greater importance for the analysis of the effect of temperature on the critical phenomena of surfactant solution.

## The Effect of Organic Solvent

From earlier data, it is noticed that the effects of addition of organic solvent upon the C. M. C. can be classified into those of lower fatty alcohols and of higher alcohols or hydrocarbons.

On the addition of a lower fatty alcohol, such as methyl or ethyl, the C. M. C. of surfactant shifts toward higher concentration with increasing alcohol content[3-5]. On the other hand, by the addition of a higher alcohol or a hydrocarbon, the C. M. C. is lowered[6-8], probably owing to solubilization. Such being the case, it is convenient to apply our analysis to each of two effects.

**a) The Effect of Lower Fatty Alcohol:** —Ward[3,4] and Kraus and his collaborators[5] measured the electroconductivity of sodium dodecyl sulfate and hexadecyl

* Presented at the 9th Annual Meeting of the Chemical Society of Japan held in Kyoto, April, 1956.

1) K. Meguro, T. Kondo, N. Ohba, et al., This Bulletin, **30**, 760 (1957).

2) A. W. Ralston, C. W. Hoerr and E. J. Hoffman, *J. Am. Chem. Soc.*, **64**, 97 (1942).

3) A. F. Ward, *Proc. Roy. Soc.*, **A176**, 412 (1940).

4) A. F. Ward, *J. Chem. Soc.*, **1939**, 552.

5) E. C. Evers and C. A. Kraus, *J. Am. Chem. Soc.*, **70**, 3049 (1948).

6) G. L. Brown, R. F. Grieger and C. A. Kraus, ibid., **71**, 95 (1949).

7) S. H. Herzfeld, M. L. Corrin and W. D. Harkins, *J. Phys. Coll. Chem.*, **54**, 971 (1950).

8) A. W. Ralston and D. N. Eggenberger, *J. Am. Chem. Soc.*, **70**, 983 (1948).

pyridonium bromide in water alcohol mixtures.

Our results by a new method are shown in Figs. 2 and 3. With increasing alcohol content of the solvent, the minimum and

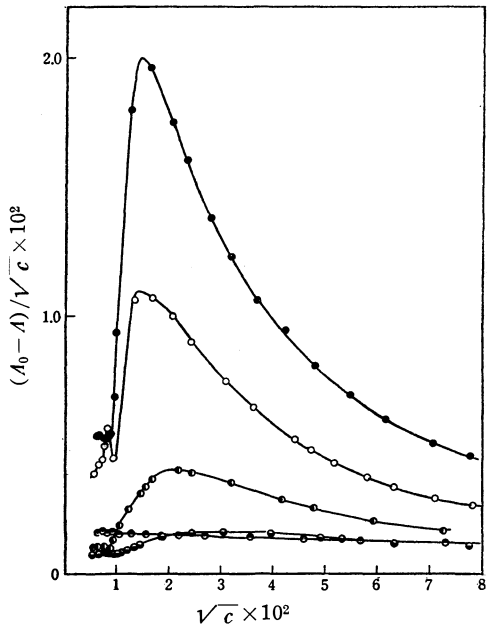



Fig. 2. $(\Lambda_0-\Lambda)/\sqrt{c}$ vs. $\sqrt{c}$ diagrams for sodium dodecyl sulfate in water-ethanol mixture: ● 0.0%, ○ 9.91%, ◐ 20.02%, ◒ 29.78%, and ◓ 39.60% of ethanol.

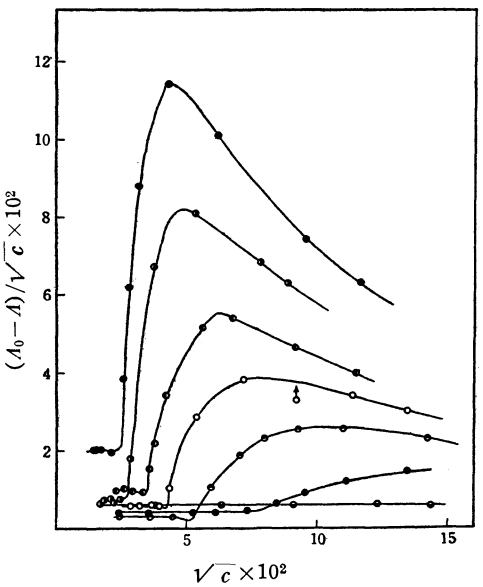



Fig. 3. $(\Lambda_0-\Lambda)/\sqrt{c}$ vs. $\sqrt{c}$ diagrams for hexadecyl pyridonium bromide in water-methanol mixture: ● 0.0%, ◑ 6.36%, ◐ 14.70%, ○ 19.91%, ◓ 26.02%, ● 35.20% and ◒ 54.14% of methanol.

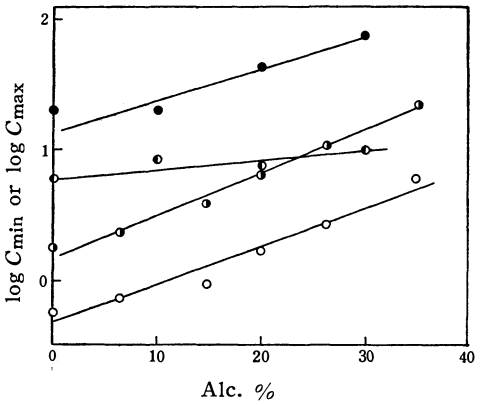



Fig. 4. The relations between alcohol content and $C_{min}$ or $C_{max}$ : for sodium dodecyl sulfate, ◐ $C_{min}$ and ● $C_{max}$ : for hexadecyl pyridonium bromide, ○ $C_{min}$ and ◑ $C_{max}$.

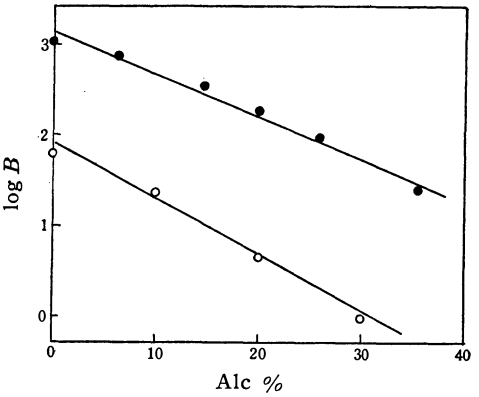



Fig. 5. The relations between alcohol content and log $B$; ○ sodium dodecyl sulfate and ● hexadecyl pyridonium bromide.

the maximum point shift toward higher concentrations, and the value of $H_{max}$ decreases and at last the maximum disappears, while the slope between the minimum and the maximum becomes gradually gentle. From these data, we can find linear relations between log $C_{min}$ or log $C_{max}$ and alcohol content, between log $H_{max}$ and alcohol content, and between log $B$ and alcohol content as shown in Figs. 4 and 5 and Table I. (The meaning of the notations, $C_{min}$, $C_{max}$ and $B$ is the same as in the previous paper.)

**b) The Effect of Solubilization:—** Previously it was noted that the effect of the addition of higher alcohols or hydrocarbons on the C. M. C. was due to the solubilization of these substances in the micelle of surfactant. It is well known that there are two types in solubilization phenomena. One is of "palisade type",

TABLE I

THE CHANGE OF $C_{min}$, $C_{max}$, $H_{min}$, $H_{max}$ AND $B$ VALUES WITH ALCOHOL CONTENT

| Substance | Alc. content % | $C_{min}$ | $C_{max}$ | $H_{min}$ | $H_{max}$ | $B$ |
|---|---|---|---|---|---|---|
| $C_{12}H_{25}OSO_3Na$—EtOH | 0.00 | 6.08 | 20.2 | 0.50 | 2.34 | 58.8 |
| | 9.91 | 8.50 | 20.2 | 0.45 | 1.10 | 23.6 |
| | 20.02 | 7.35 | 44.1 | 0.10 | 0.40 | 4.63 |
| | 29.78 | 9.90 | 75.8 | 0.08 | 0.16 | 0.98 |
| $C_{16}H_{33}N^+$(C$_6$H$_5$)$Br^-$—MeOH | 0.00 | 0.45 | 1.76 | 1.93 | 11.4 | 1080 |
| | 6.36 | 0.50 | 2.30 | 0.66 | 8.2 | 650 |
| | 14.70 | 1.16 | 3.85 | 0.95 | 5.5 | 350 |
| $C_{18}H_{37}N^+$(C$_6$H$_5$)$Cl^-$—MeOH | 0.00 | 0.24 | 1.06 | 0.30 | 11.0 | 1530 |
| | 9.90 | 0.56 | 2.03 | 0.83 | 6.80 | 700 |
| | 14.86 | 0.39 | 3.70 | −0.73 | 4.52 | 333 |

TABLE II

| Type of Solubilization | Effect | $H_{min}$ | $H_{max}$ | $C_{min}$ | $C_{max}$ |
|---|---|---|---|---|---|
| Palisade type | Increase in the amount of solubilizate | 0 | + | − | − |
| | Increase in the alkyl chain length of solubilizate | 0 | + | − | − |
| Sandwich type | Increase in the alkyl chain length of solubilizate | ? | − | 0 | 0 |

0: no remarkable change; +, increase; −, decrease

and the other of "sandwich type". The solubilization of higher alcohols belongs to the former type, and the solubilizates are situated in the micelle like palisades. On the other hand, the solubilization of nonpolar hydrocarbons, such as alkane and benzene, belongs to the latter type, and the solubilizates are situated, like contents of a sandwich, between surfactant molecules which construct a micelle.

If the difference between these types of solubilization could be observed by a suitable plotting of electroconductivity data, it would be very interesting, but it is impossible to do so by the usual plotting such as $\Lambda$ vs. $\sqrt{c}$. According to our method, however, we can clearly distinguish them. In Fig. 6 and 7 is shown our analysis of palisade type solubilization, and in Fig. 8 that of sandwich type.

Comparing the effect of increase in the amount and in the alkyl chain length in the palisade layer on $H_{min}$, $H_{max}$, $C_{min}$ and $C_{max}$, with the effect of increase in the alkyl chain length of solubilizates in the sandwich layer on the same values, we can obtain the results shown in Table II. The effects on these values, especially on $H_{max}$ and $C_{max}$, form a good contrast between the palisade and the sandwich type. The fact that the effects of increase in the amount and in the alkyl chain length of solubilizates in the palisade layer correspond to those of increase in alkyl chain length of a surfactant molecule is suggestive of the existence of an intimate relation between them.

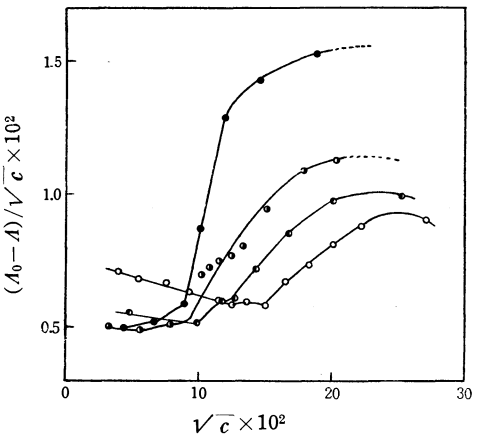



Fig. 6. $(\Lambda_0-\Lambda)/\sqrt{c}$ vs. $\sqrt{c}$ curves for dodecyl ammonium chloride in 24.65% methanol on addition of moles dodecanol per mole salt: ○ 0.0%, ◐ 0.110%, ◑ 0.261% and ● 0.651%.

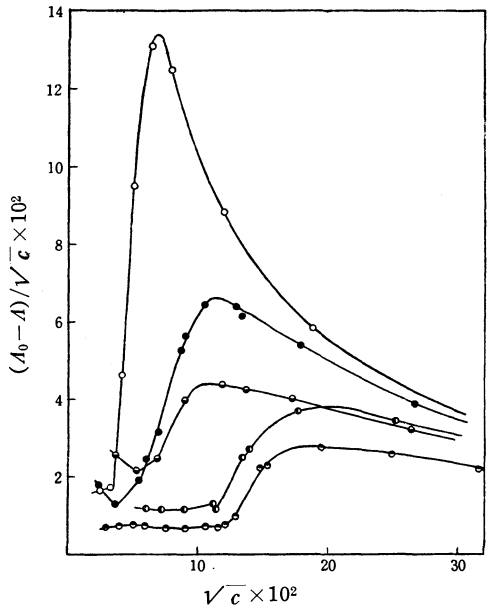



Fig. 7. $(\Lambda_0-\Lambda)/\sqrt{c}$ vs. $\sqrt{c}$ curves for dodecyl ammonium chloride solutions at 30°C in the presence of following substances; ◓ in water, ◒ hexanol, ● octanol, ○ dodecanol and ◐ octadecanol. (Adopted from Ref. 8)

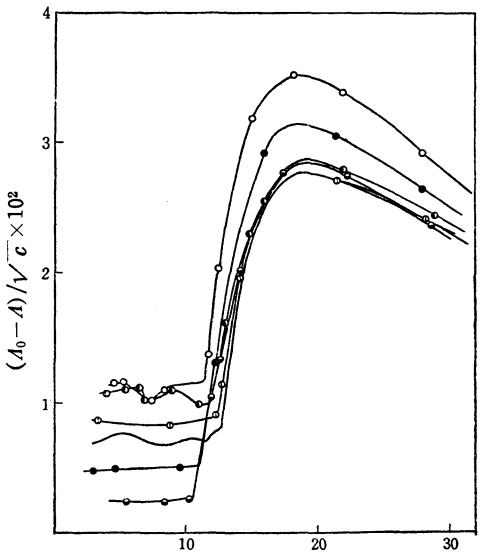



Fig. 8. $(\Lambda_0-\Lambda)/\sqrt{c}$ vs. $\sqrt{c}$ curves for dodecyl ammonium chloride solutions at 30°C in the presence of the following substances: (—) in water, ○ hexane, ● octane, ◒ dodecane, ⦶ heptadecane and ◑ octadecane. (Adopted from Ref. 8)

## The Effect of Added Salt

It is well known that the presence of an electrolyte affects considerably the behavior of aqueous solution of surfactants[9,10]. In general, the added salt promotes the micelle formation of surfactants. In order to apply our method to this case, Ralston's data[9] on the electroconductivity of aqueous solution of dodecyl ammonium chloride in 0.005 N and 0.015 N sodium chloride were used. The results obtained are shown in Fig. 9.

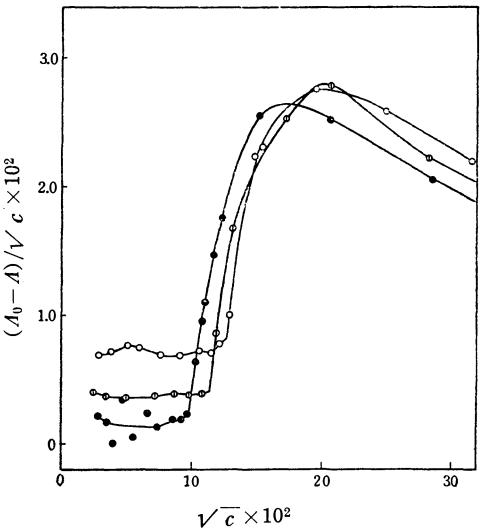



Fig. 9. $(\Lambda_0-\Lambda)/\sqrt{c}$ vs. $\sqrt{c}$ curves for dodecyl ammonium chloride in sodium chloride solutions: ○ 0.0 N, ⦶ 0.005 N and ● 0.015 N.

The most remarkable thing is the occurring of influence upon $H_{min}$ and no remarkable effect on $H_{max}$ by the addition of salt, while $C_{min}$ and $C_{max}$ shift toward lower concentration with increasing concentration of the salt.

The authors wish to thank Professor B. Tamamushi, Tokyo University for his encouragement and advice in this work.

*Nedzu Chemical Laboratory*
*Musashi University*
*Nerima, Tokyo*

9) A. W. Ralston and D. N. Eggenberger, ibid., **70**, 980 (1948).
10) M. L. Corrin and W. D. Harkins, ibid., **69**, 683 (1947).

# *Polarographic Studies of Metallic Complexes. I. Oxalato-ammine, Glycinato-ammine and Ethylenediamine-ammine Series of Cobalt(III) Complexes*[1]

By Nobufumi MAKI, Yoichi SHIMURA and Ryutaro TSUCHIDA

(Received May 23, 1957)

There have been reported some polarographic researches concerning the relation between the structures of cobalt(III) complexes and the half-wave potentials of their $Co^{III} \rightarrow Co^{II}$ reduction. For instance, Willis, Friend and Mellor[2] studied nitro-ammine series of cobalt(III) complexes and found the following order of the half-wave potentials:

$[Co(NO_2)_6]^{3-}$, $[Co(NH_3)_3(NO_2)_3]$, *cis*-$[Co(NH_3)_4(NO_2)_2]^+$, $[Co(NH_3)_2(NO_2)_4]^-$, *trans*-$[Co(NH_3)_4(NO_2)_2]^+$, $[Co(NH_3)_5NO_2]^{2+}$, $[Co(NH_3)_6]^{3+}$ (from positive to negative).

It was also reported by Brigando[3] that the polarographic stability of luteo-type cobalt(III) complexes increased as unidentate ligands were replaced by polydentate ligands. Thus the half-wave potentials of the luteo-type cobalt(III) complexes were in the order of

$[Co(NH_3)_4(NH_2CH_3)_2]^{3+}$, $[Co(NH_3)_6]^{3+}$, $[Co\ en_3]^{3+}$, $[Co\ dien_2{*}]^{3+}$.

Recently, Holtzclaw et al.[4-6] reported that the *cis* isomer exhibited a less negative half-wave potential than the corresponding *trans* isomer for the cobalt(III) complexes containing negative ligands on two of the coordination positions and neutral ligands on the other four. The complexes which contain only one or no negative ligands scarcely ever show such a trend.

The present paper deals with the polarography of oxalato-ammine, glycinato-ammine and ethylenediamine-ammine series of cobalt(III) complexes. The main purpose of this study is to examine the relation between the polarographic stabilities of these complexes and their structures.

## Experimental

*Apparatus.*—A Heyrovsky-Shikata type polarograph was employed with the circuit for extendable and adjustable e.m.f. An H-cell with a saturated calomel electrode was used. The capillary used had an m-value of 5.828 mg./sec. and a drop time of 4.00 sec./drop in distilled water at the mercury height of 96 cm. with an open circuit. All measurements were carried out in a thermostat of 18.0±0.1°C.

The half-wave potentials were determined from the enlarged polarograms by "plotting method". The potential values were calibrated for iR drop, using the minimum value of the cell resistance.

*Materials.*—The complex compounds studied were prepared by the method described in the literature[7-17] (the references are given in Tables I-III). The concentration of the solution was 0.001 gram complex ion per liter.

The supporting electrolytes used were potassium chloride, potassium sulfate or ammonium oxalate. The concentration of each supporting electrolyte was 0.1 F.

Oxygen was removed from the solutions for electrolysis by bubbling nitrogen gas through them for about half an hour, preventing the evaporation. Polarographic measurements were made as soon as possible after the removal of oxygen.

No maximum suppressor was used because it was feared that the presence of it might cause

1) Presented at the Tenth Annual Meeting of the Chemical Society of Japan, Tokyo, April 6, 1957.
2) J. B. Willis, J. A. Friend and D. P. Mellor, *J. Am. Chem. Soc.*, **67**, 1680 (1945).
3) J. Brigando, *Compt. rend.*, **236**, 708 (1953).
* dien=$NH_2CH_2CH_2NHCH_2CH_2NH_2$
4) H. F. Holtzclaw, Jr., *J. Am. Chem. Soc.*, **73**, 1821 (1951).
5) H. F. Holtzclaw, Jr., and D. P. Sheetz, ibid. **75**, 3053 (1953).
6) H. F. Holtzclaw, Jr., *J. Phy. Chem.*, **59**, 300 (1955).
7) "*Inorganic Syntheses*", **1**, 37 (1939).
8) E. H. Riesenfeld and R. Klement, *Z. anorg. Chem.*, **124**, 11 (1922).
* Polyoxyethylene sorbitan monooleate.
9) W. Schramm, ibid., **180**, 167 (1929).
10) T. Klobb, *Bull. soc. chim. France*, (3), **25**, 1025 (1901).
11) A. Werner and A. Vilmos, *Z. anorg. Chem.*, **21**, 145 (1899).
12) H. Ley and H. Winkler, *Ber.*, **42**, 3894 (1909).
13) Y. Shimura, to be reported later.
14) M. Linhard, *Z. Elektrochem.*, **50**, 224 (1944).
15) J. Meisenheimer, L. Angerman and H. Holsten, *Ann.*, **438**, 261 (1924).
16) Y. Shimura and R. Tsuchida, This Bulletin, **29**, 311 (1956).
17) A. Werner, *Ann.*, **386**, 1 (1912); A. Werner, F. Bräunlich, E. Rogowina and C. Kreutzer, ibid., **351**, 65 (1907).

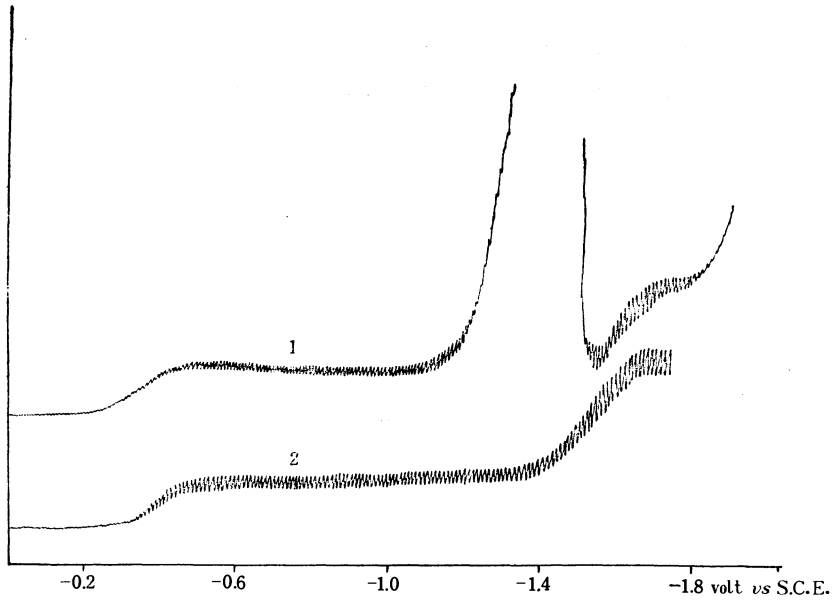



Fig. 1. (1) Polarogram of [Co $en_2$ gly]$Cl_2 \cdot H_2O$ in the absence of suppressor.
(2) Polarogram of [Co $en_2$ gly]$Cl_2 \cdot H_2O$ in the presence of 0.02% Tween-80.
Supporting electrolyte is 0.1 F KCl.

TABLE I
HALF-WAVE POTENTIALS OF OXALATO-AMMINE SERIES OF Co(III) COMPLEXES
(Supporting electrolyte: 0.1 F $(NH_4)_2C_2O_4$ or 0.1 F KCl).

| Compound | First wave (volt *vs.* S. C. E.) | | Second wave (volt *vs.* S. C. E.) | |
|---|---|---|---|---|
| | in $(NH_4)_2C_2O_4$ | in KCl | in $(NH_4)_2C_2O_4$ | in KCl |
| $K_3[Co\ ox_3]$[7] | + | | No reduction | |
| $NH_4[Co(NH_3)_2ox_2] \cdot H_2O$[8] | −0.03 | −0.03 | −1.58 | −1.23 |
| $[Co(NH_3)_4ox]NO_3$[9] | −0.21 | −0.21 | −1.46 | −1.25 |
| $[Co(NH_3)_6]SO_4 \cdot Cl \cdot 3H_2O$[10] | — | −0.24 | — | −1.23 |
| [Co $en_2$ ox]Cl[11] | −0.32 | — | −1.35 | — |

TABLE II
HALF-WAVE POTENTIALS OF GLYCINATO-AMMINE SERIES OF Co(III) COMPLEXES
(Supporting electolyte: 0.1 F KCl or 0.1 F $K_2SO_4$)

| Compound | First wave (volt *vs.* S. C. E.) | | Second wave (volt *vs.* S. C. E.) | |
|---|---|---|---|---|
| | in KCl | in $K_2SO_4$ | in KCl | in $K_2SO_4$ |
| $\alpha$-[Co $gly_3$][12] | −0.14 | −0.07 | * | * |
| $[Co(NH_3)_2\ gly_2]Cl$[13] | $-0.23_0$ | −0.28 | −1.24 | −1.31 |
| $[Co(NH_3)_4\ gly]SO_4$[13] | $-0.23_4$ | −0.36 | −1.26 | * |
| $[Co(NH_3)_6](ClO_4)_3$[14] | −0.24** | −0.43 | −1.25** | −1.26 |
| [Co $en_2$ gly]$Cl_2 \cdot H_2O$[15] | −0.36 | −0.41 | * | * |

* Maximum wave
** The data of the chloride sulfate, $[Co(NH_3)_6]Cl \cdot SO_4 \cdot 3H_2O$.

the lowering of the limiting current and the shift of the half-wave potential to negative direction. For example, 0.02% Tween-80* shifted the half-wave potential of the first wave of glycinato-diethylenediamine cobalt(III) complex to the negative direction by −0.03 V (Fig. 1).

## Results and Discussion

The half-wave potentials of the oxalato-ammine, glycinato-ammine and ethylenediamine-ammine series of cobalt(III)

complexes measured are given in Tables I-III.

TABLE III
HALF-WAVE POTENTIALS OF ETHYLENEDIAMINE-AMMINE SERIES OF Co(III) COMPLEXES
(Supporting electrolyte: 0.1 F KCl)

| Compound | First wave (volt *vs.* S.C.E.) | Second wave (volt *vs.* S.C.E.) |
|---|---|---|
| $[Co\ en_3](ClO_4)_3$[14] | −0.43 | * |
| *cis*-$[Co\ en_2(NH_3)_2](ClO_4)_3$[16] | −0.31 | * |
| *trans*-$[Co\ en_2(NH_3)_2]Cl_3\cdot H_2O$[17] | −0.31 | * |
| $[Co\ en\ (NH_3)_4]_2(SO_4)_3\cdot 4H_2O$[13] | −0.27 | * |
| $[Co(NH_3)_6](ClO_4)_3$ | −0.24 | −1.23 |

* Maximum wave

All the compounds examined are reduced polarographically in two steps except in the case of the trioxalato complex, $[Co\ ox_3]^{3-}$, in the presence of an excess of $C_2O_4^{2-}$. On plotting $\log i/(i_d-i)$ against $E_{d.e.}$ for these three series of cobalt(III) complexes, straight lines were usually obtained. Only in a few cases, lines, having slight inflection were obtained. The reciprocal slopes of such lines for all the complexes showed that every reduction was irreversible.

The ratio of the height of first wave to that of the second is approximately 1 : 2. Consequently, it is concluded that the first wave, corresponding to a gain of one electron, apparently represents the reduction to cobalt(II) state, and the second, corresponding to two electrons, represents the reduction to the metal. The half-wave potential of the latter is always very near to that of hexaaquo cobalt(II) $[Co(OH_2)_6]^{2+}$ ion (−1.428 V *vs.* S.C.E. in 1 F $K_2SO_4$ solution[2]).

As regards the process of the reduction of hexammine cobalt(III) $[Co(NH_3)_6]^{3+}$, Laitinen et al.[18] offered the following mechanism:

$$[Co(NH_3)_6]^{3+}+e^- \longrightarrow [Co(NH_3)_6]^{2+}$$

$$[Co(NH_3)_6]^{2+}+6H_2O \xrightarrow{\text{very rapid}} [Co(OH_2)_6]^{2+}+6NH_3$$

$$[Co(OH_2)_6]^{2+}+2e^- \longrightarrow Co+6H_2O.$$

The similar mechanism of reduction is probably true for the oxalato-ammine and glycinato-ammine series of cobalt(III) complexes. In the case of the trisoxalato complex, $[Co\ ox_3]^{3-}$, no reduction wave is observed below the final current rise in solutions containing an excess of oxalate ion. This fact has already been reported by Watters and Kolthoff[19]. This is probably an indication of the presence of a stable cobalt(II) oxalato-complex in the solution such as dioxalatodiaquo cobaltate (II) $[Co\ ox_2(OH_2)_2]^{2-}$ or a similar one.

All the second waves of the ethylenediamine-ammine complexes have maxima, which can be easily suppressed by a capillary active substance. According to Kivalo[20], the product of the first reduction of trisethylenediamine cobalt(III) $[Co\ en_3]^{3+}$ is an equilibrium mixture of aquo-ethylenediamine cobalt(II) complexes. The second waves of the ethylenediamine-ammine cobalt(III) complexes are, therefore, due to the similar aquo-ethylenediamine cobalt(II) complexes.

As to the relation between the half-wave potential of the first wave of these complexes and their structure, the authors are led to the following conclusion. As the ammonia molecules in hexa-ammine cobalt(III) $[Co(NH_3)_6]^{3+}$ are replaced with ethylenediamine, the half-wave potential of the first wave shifts to the negative direction. If the ammonia molecules in $[Co(NH_3)_6]^{3+}$ are replaced by glycinate the first wave shifts to the positive direction. similarly, by successive replacements of the ammonia molecules in $[Co(NH_3)_6]^{3+}$ with oxalate, the first wave shifts to further more positive. Since the half-wave potential of the first wave of trisoxalato cobaltate(III) $[Co\ ox_3]^{3-}$, a chelate produced by exhaustive replacement with oxalate, is in the positive region of applied potential *vs.* S.C.E., it is hardly possible to measure its value at

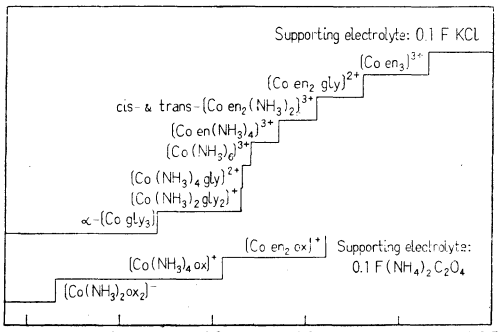



Fig. 2. Half-wave potentials of the first wave of oxalato-ammine, glycinato-ammine and ethylenediamine-ammine series of Co(III) complexes.

18) H. A. Laitinen, J. C. Bailar, Jr., H. F. Holtzclaw and J. V. Quagliano, *J. Am. Chem. Soc.*, **70**, 2999 (1948).

19) J. I. Watters and I. M. Kolthoff, *Anal. Chem.*, **21**, 1466 (1949).

20) P. Kivalo, *J. Am. Chem. Soc.*, **77**, 2678 (1955).

the dropping mercury electrode.

Eventually, the polarographic stability of cobalt(III) complexes increases in the following order of the ligands (see Fig. 2): $ox^{2-}$, $gly^{-}$, $NH_3$, en. The half-wave potential of $[Co\ en_2\ gly]^{2+}$ is more negative than that of $[Co\ en_2\ (NH_3)_2]^{3+}$. This is an exception of the order above mentioned. As is also seen from the work of Willis et al.[2] on the nitro-ammine cobalt(III) complexes, it is suggested that many factors affect the position of the first wave of cobalt(III) complexes.

In agreement with the observation of Holtzclaw et al.[5], *cis*- and *trans*-forms of $[Co\ en_2(NH_3)_2]^{3+}$ have identical values of the half-wave potential of the first wave.

## Summary

The ions $[Co\ ox_n(NH_3)_{6-n}]^{(2n-3)-}$, $[Co\ gly_n(NH_3)_{6-n}]^{(3-n)+}$, $[Co\ en_n(NH_3)_{6-n}]^{3+}$, $[Co\ en_2\ gly]^{2+}$ and $[Co\ en_2\ ox]^{+}$ were all reduced irreversibly in two steps at the dropping mercury electrode.

The first diffusion current corresponds to the reduction, $Co^{III} \rightarrow Co^{II}$ and the second to the reduction, $Co^{II} \rightarrow Co^{0}$. The diffusion current and the concentration were linearly related.

The half wave potential of the first wave of the cobalt(III) complexes shifts to negative direction in the following order of the ligands: $ox^{2-}$, $gly^{-}$, $NH_3$, en.

The authors wish to thank Professor Y. Otsuka and Mr. Y. Yamamoto of Kobe University of Merchantile Marine for their kindness in permitting them to use the apparatus. They also acknowledge the grant from the Ministry of Education.

*Department of Chemistry, Faculty of Science, Osaka University*
*Kita-ku, Osaka*

# *Further Studies on the Degradation of Yeast Ribonucleic Acid by Lanthanum Hydroxide*

By Masazumi MIYAZAKI

(Received May 13, 1957)

By applying lanthanum hydroxide, which E. Bamann[1] introduced as a phosphatase model, to ribonucleic acid (RNA), F. Egami and M. Shimomura[2,3] found that RNA was almost completely hydrolysed to nucleosides and inorganic phosphate. This finding was confirmed and extended by E. Bamann[4,5], K. Dimroth[6], F. W. Allen[7] and their coworkers. The present paper deals with further studies on the degradation of yeast ribonucleic acid by lanthanum hydroxide gel with special reference to the nature of the products and the order of their formation.

## Experimental

**Materials and Solvent Systems.**—*Yeast ribonucleic acid.*—A commercial RNA (Schwarz Laboratories) was used as such or after purification by the chloroform gel method[8]. The phosphorus content of the purified preparation was 8.5% and that of the original RNA about 8.0%.

*LaRF.*—M. Shimomura[9] found that a part of RNAwas resistant to lanthanum hydroxide. He named this fraction "lanthanum hydroxide resistant fraction (LaRF)". It was prepared according to Shimomura[9].

*Solvent Systems for Paper Chromatography.*—Solvent system 1[10], 70% (vol.) isopropanol in concentrated aqueous ammonia in the bottom of the chamber (0.35 ml for each liter of gas space); descending for 17 to 18 hr.; suitable for fractionation of various oligo- and mononucleotides.

1) E. Bamann, *Angew. Chem.*, **52**, 186 (1939).
2) F. Egami and M. Shimomura, *Science (Japan)*, **18**, 472 (1948).
3) M. Shimomura and F. Egami, This Bulletin, **26**, 263 (1953).
4) E. Bamann, F. Fischler and H. Trapmann, *Biochem. Z.*, **325**, 413 (1954).
5) E. Bamann, H. Trapmann and F. Fischler, *Biochem., Z.*, **326**, 89 (1954).
6) K. Dimroth, L. Jaenicke and D. Heinzel, *Ann. Chem.*, **566**, 206 (1950). K. Dimroth, L. Jaenicke and D. Heinzel, *Z. Physiol. Chem.*, **289**, 71 (1952).
7) J. E. Backer and F. W. Allen, *J. Biol. Chem.*, **188**, 59 (1951).
8) M. G. Sevag, D. B. Lackman and J. Smolens, *J. Biol. Chem.*, **124**, 425 (1938).
9) M. Shimomura, This Bulletin, **27**, 29 (1954).
10) R. Markham and J. D. Smith, ibid., **52**, 552, 558, 565 (1952).

Solvent system 2, 5 ml. of concentrated aqueous ammonia added to 100 ml. of 86% (vol./vol.) aqueous *n*-butanol; descending for 17 to 18 hr.; useful for separation of the four nucleosides.

Solvent system 3[11], a mixture of saturated ammonium sulfate in water (79 ml.), water (19 ml.) and isopropanol (2 ml.); ascending for 7 hr.; used for separation of 2'- and 3'-purine nucleotides.

Solvent system 4[12], a mixture of isopropanol (170 ml.), concentrated hydrochloric acid (41 ml.) and water (total 250 ml.); ascending for 36 hr.; used for separation of adenine, guanine, cytidylic and uridylic acid.

**Process of Degradation of RNA by Lanthanum Hydroxide.**—The lanthanum hydroxide suspension was made by dissolving lanthanum carbonate with hydrochloric acid and then by bringing the pH of the solution to the alkaline side. When the RNA solution was mixed with the lanthanum hydroxide suspension, RNA was bound completely to lanthanum hydroxide in the presence of an excess of the latter as shown in Figs. 1, 2, 3, and in Tables II and III, where 2 g. of lanthanum carbonate was used per gram of RNA. When 0.35 g. of the carbonate was used per gram of RNA, this being the condition in experiments for Fig. 4 and Table I, some amount of RNA was left unbound. Nucleosides, which were liberated during the reaction, were not adsorbed on lanthanum hydroxide, whereas liberated inorganic phosphate was bound to lanthanum hydroxide.

*Fractionation of Oligo- and Mononucleotides formed from RNA by Lanthanum Hydroxide.*—At intervals, the precipitates containing nucleotides and phosphate were separated from the reaction mixture by centrifuge and washed with hot water. They were extracted with 5% sodium bicarbonate solution and fractionated by paper chromatogram using solvent system 1. Thus a chromatogram shown in Fig. 1. was obtained. The reaction was carried out under the following conditions: pH 8.5 and 60°C, 500 mg. RNA and 1g. lanthanum carbonate.

By analysing the base constituents and comparing the spots with those of mononucleotides, it was suggested that fraction A contained pyrimidine nucleotides and adenylic acid, fraction B guanylic acid and oligonucleotides and fractions C, D and E polynucleotides. Under more drastic conditions, at 80°, a few hours were sufficient to degrade RNA to fractions A and B. When 10—20% of the original RNA was dephosphorylated, most of products were composed of fractions A and B.

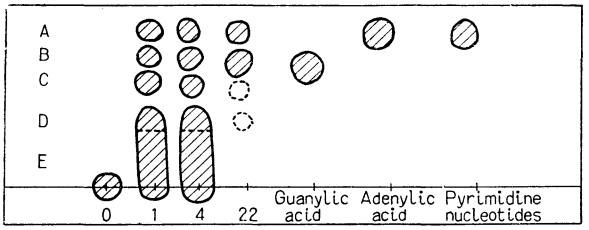



Fig. 1. Fractionation of lanthanum hydroxide hydrolysates by paper chromatography.

On the other hand, degradation of RNA by a less amount of lanthanum hydroxide (lanthanum carbonate 70 mg. to RNA 200 mg., that is, the atomic ratio of lanthanum to RNA phosphorus was 1/4), proceeded as shown in Table I.

Although the supernatant contained RNA, dephosphorylation did not occur in this fraction, but only in the precipitate fraction. On the other hand, paper chromatography with solvent system 1 showed that RNA in both the supernatant and the precipitate was similarly degraded to fractions A and B within 12 hr.

TABLE I

DEPHOSPHORYLATION OF RNA BY A LESS AMOUNT OF LANTHANUM HYDROXIDE. THE REACTION WAS CARRIED OUT AT 60° FOR 9 HR. AND CONTINUED AT 80°. THE WHOLE REPRESENTS THE ENTIRE REACTION MIXTURE AND, AT INTERVALS, WAS DIVIDED INTO THE SUPERNATANT CONTAINING UNBOUND RNA AND THE PRECIPITATE

| Fraction | Time (hr.) | | | |
|---|---|---|---|---|
| | 5 | 12 | 27 | 51 |
| Supernatant | 0% | 0% | 0% | 0% |
| Whole | ca. 0 | 3.3 | 18 | 31 |
| Precipitate | ca. 0 | 12 | 49 | 74 |

*Production of 2'- and 3'-Purine Nucleotides.*—The precipitates, which were separated from the reaction mixture by centrifuge and washing, were extracted with 5% sodium carbonate solution. By two dimensional paper chromatography with solvent system 1 and 3, 2'- and 3'-adenylic, and 2'- and 3'-guanylic acid were detected in the extracts.

According to this chromatogram, 2'-purine nucleotides were produced less than the corresponding 3'-nucleotides, and

11) R. Markahm and J. D. Smith, ibid., **49**, 401 (1951).
12) G. R. Wyatt, ibid., **48**, 584 (1951).

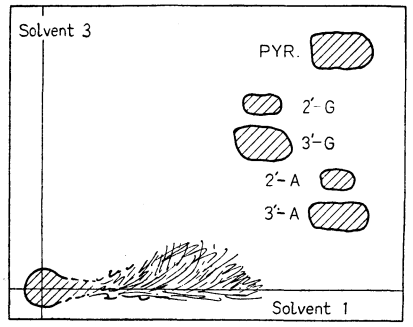



Fig. 2. Two dimensional paper chromatogram

A proviso: RNA 500 mg. lanthanum carbonate 1 g. at pH 8.5 and 80, after 1 hr.

Spots: PYR., 2'-G, 3'-G, 2'-A, 3'-A, are abbreviations for pyrimidine nucleotides, 2'- and 3'-guanylic, 2'- and 3'-adenylic acid, respectively.

this tendency was still more markedly observed in the precipitate fraction under the same conditions as in Table I. Besides we were not successful in detecting 5'-mononucleotides by the Boeseken reaction and the periodate oxidation method[13].

*Liberation of Nucleosides.*—Purine-bound ribose was measured by the orcinol reaction on the assumption that the color intensity was given quantitatively and only by purine-bound ribose. The molar ratio of purine-bound ribose/RNA-phosphorus of the original RNA preparation was taken as 0.5, assuming that equimolar proportions of purine and pyrimidine nucleotides were present.

As shown in Fig. 3, the ratio increased with reaction time. It seems to indicate that there is an increase in the amount of purine-bound phosphorus in the undephosphorylated RNA; it is evident that pyrimidine nucleosides were liberated faster than purine nucleosides on the whole (Fig. 3).

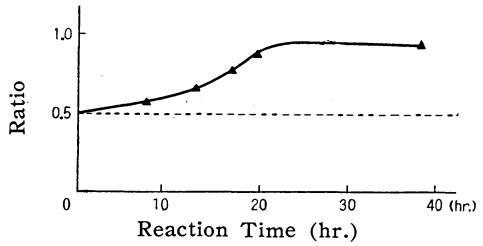



Fig. 3. Change in the purine-bound ribose/RNA-phosphorus ratio of the undephosphorylated RNA with time under the same conditions as used in Fig. 2.

Interrelation between purine nucleosides and also between pyrimidine nucleosides was observed as in the following Tables IIa and IIb. Adenosine was liberated faster than guanosine, and cytidine faster than uridine as expected from the dephosphorylation of mononucleotides[5] (Table III). However unexpected liberation of nucleosides was observed at the initial stage of reaction. Namely, at the initial stage liberation of adenosine was extraordinarily more than that of guanosine, and that of uridine was faster than that of cytidine, and increased later again during the reaction.

TABLE IIa

LIBERATION OF PURINE NUCLEOSIDES AT VARIOUS INTERVALS, THE MOLAR RATIO TAKING GUANOSINE AS UNITY

| Nucleosides | Time (hr.) 0 to 0.5 | 0.5 to 6 | 6 to 20 | 20 to 40 |
|---|---|---|---|---|
| Guanosine | 1 | 1 | 1 | 1 |
| Adenosine | 2.5 | 1.7 | 0.5 | 0.3 |

TABLE IIb

LIBERATION OF PYRIMIDINE NUCLEOSIDES AT VARIOUS INTERVALS, THE MOLAR RATIO TAKING URIDINE AS UNITY

| Nucleosides | Time (hr.) 0 to 0.5 | 0.5 to 6 | 6 to 20 | 20 to 40 |
|---|---|---|---|---|
| Uridine | 1 | 1 | 1 | 1 |
| Cytidine | 0.6 | 1.3 | 0.9 | 0.6 |

TABLE III

DEPHOSPHORYLATION OF MONONUCLEOTIDES UNDER THE FOLLOWING CONDITIONS: pH 8.5 AND 80°, EMPLOYING MONONUCLEOTIDES 30 mg. EACH AND LANTHANUM CARBONATE 200 mg.

| Nucleotide | Time (hr.) 5 | 20 | 40 |
|---|---|---|---|
| Guanylic acid | 39% | 90% | 100% |
| Adenylic acid | 55 | 94 | 100 |
| Uridylic acid | 40 | 93 | 100 |
| Cytidilic acid | 70 | 97 | 100 |
| 5'-Adenylic acid | 12 | 54 | 100 |

The preferential liberation of uridine in the beginning was clearly observed on the chromatogram of the nucleosides in the supernatant of the reaction mixture under the same conditions as in Table I. In this experiment, the atomic ratio of lanthanum to RNA phosphorus was about 1/4 (Fig. 4). For the first 5 hr., uridine was detected as the only nucleoside on

13) K. Makino, *J. Japan. Biochem. Soc.*, **27**, 489 (1955).

the chromatogram; it was observed that, at this time, little of RNA was dephosphorylated and only a small amount of pyrimidine nucleotides was detected on the chromatogram with solvent system 3.

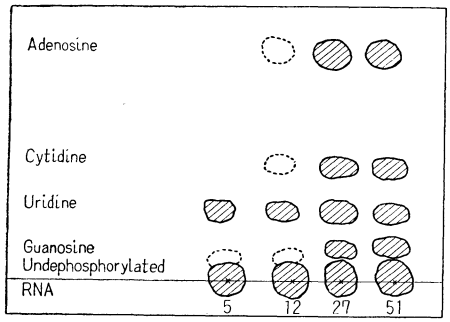



Fig. 4. Nucleosides chromatogram with solvent system 2

**On the Nature of LaRF.**—After dialysis of LaRF against distilled water through a cellophane bag for 2 days, the dialysed fraction showed the following broad absorption curve with maximum about 260 mμ; however the nondialysable fraction had no absorption maximum at 260 mμ (Fig. 5). The latter fraction did not give the orcinol reaction either.

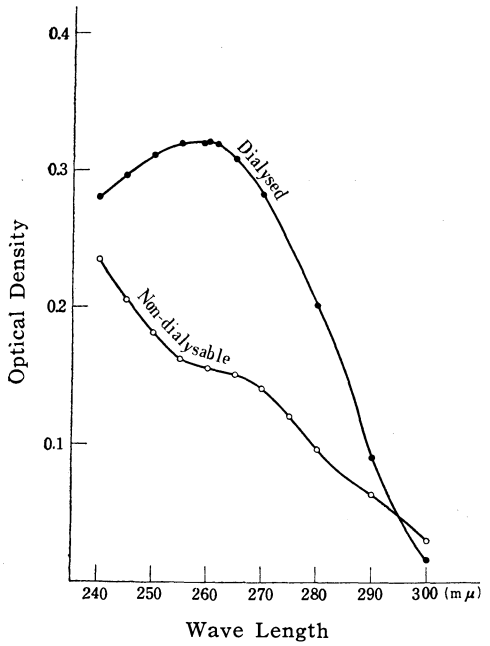



Fig. 5. Absorption curve after dialysis

LaRF at the concentration of 4 to 5 mg./cc. was not precipitated with uranium reagent (0.25% uranyl acetate in 2.5% aqueous trichloroacetic acid solution; this is a powerful precipitant of oligo- and polynucleotides) and by lowering pH to 1 by hydrochloric acid, either.

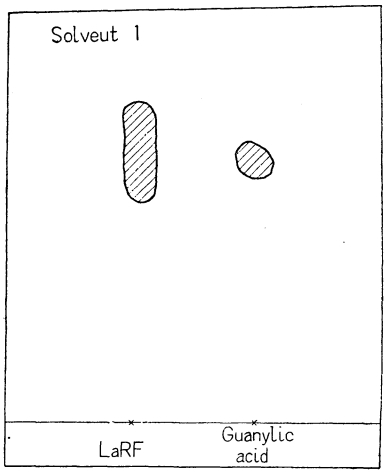



Fig. 6. Paper chromatogram of LaRF

*Paper Chromatography of LaRF.*—Fig. 6 shows the paper chromatogram of LaRF with solvent system 1. The $R_f$ value of LaRF was close to that of guanylic acid and no spots were detected near the origin. So LaRF seems to contain no large polynucleotides. The spot of LaRF on this chromatogram showed fluorescence by hydrogen chloride fume. Molar ratios of bases in LaRF:

TABLE IV
MOLAR RATIOS OF BASES IN LaRF WHERE GUANINE IS UNITY

| Guanine | Adenine | Uracile | Cytosine |
|---|---|---|---|
| 1 | 0.8 | ca. 0.2 | ca. 0.3 |

According to this analysis of the base constituents, LaRF contained predominantly guanine, and adenine and a much smaller amount of uracil and cytosine as already suggested by Shimomura[9].

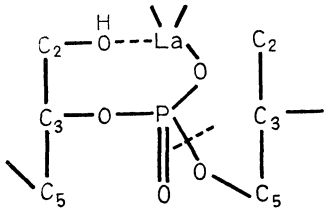
## Discussion

The formation of four mononucleotides at the early stage of reaction (10~20% dephosphorylation) and the parallelism between the liberation of nucleosides and the dephosphorylation velocity of mononucleotides seem to indicate that most of the RNA was degraded to mononucleotides, and the latter were in turn dephosphorylated.

However it should be noted that the liberation of uridine and adenosine was unexpectedly fast at the beginning and

that the liberation of uridine increased later again. These findings seem to suggest that lanthanum hydroxide binds more easily with certain specific positions of RNA, and uridine exists in two different positions.

As intermediate reaction products, 2′- and 3′-purine nucleotides were detected. 2′-Nucleotides were less in amount than corresponding 3′-nucleotides, especially in the experiments with a small quantity of lanthanum hydroxide. These facts may be explained by Bamanns inner complex hypothesis[5].




Concerning LaRF, its chemical nature could not be finally elucidated. However it was concluded that it is a low molecular weight compound with high guanylic and adenylic acid content. It is not yet resolved, on what its resistance to lanthanum hydroxide depends.

## Summary

The degradation of yeast ribonucleic acid by lanthanum hydroxide was reinvestigated. The results may be summarized as follows:

1) Most of the RNA seems to be degraded through mononucleotides to nucleosides and inorganic phosphate.

2) 2′- and 3′-purine nucleotides were detected as intermediate products. 2′-Nucleotides were produced in less amounts than the corresponding 3′-nucleotides.

3) On the whole, pyrimidine nucleosides were liberated faster than purine nucleosides.

4) Liberation of uridine was characteristic. It was preferencially liberated at the beginning and its liberation predominated again at the last stage of reaction.

5) "Lanthanum hydroxide resistant fraction (LaRF)" was dialysable, not precipitated with uranium reagent and had $R_f$ value close to that of guanylic acid.

The author wishes to thank Professor Fujio Egami and Dr. Michio Shimomura for their useful discussion as well as their constant encouragement in the course of the work. The expense of this study was defrayed in part by a grant from the Ministry of Education.

*Chemical Institute, Facutly of Science*
*Nagoya University, Chikusa-ku*
*Nagoya*

# *Molecular Rotations of Glucides in Relation to their Structures. III. Optical Superposition in Pentoses*

By Shukichi YAMANA

(Received May 14, 1957)

In 1874, vant't Hoff suggested that the partial rotation contributed by a given asymmetric carbon atom to the total rotation of a molecule containing several such atoms, is independent of the configuration of these other atoms*1. He predicted also that the rotation of arabinose should be equal to the sum of those of xylose, ribose and the expected fourth type of pentose at that time (lyxose), from the standpoint of the orientations of OH groups in their open chain structure[1]. His prediction, however, was proved to be invalid by many experiments. Hudson found some interesting facts, suitable for proving van't Hoff's principle of optical superposition*1 in glucides, and he put forward two

*1 Guye and Gautier (Ph. A. Guye and M. Gautier, *Compt. rend.*, **119**, 740 (1894)) named this idea "principe de la superposition algébrique des effets optiques des carbones asymétriques". This is called generally "vant't Hoff's principle of optical superposition".

1) Van't Hoff, *Bull. Soc. Chim.*, **23**, 298 (1875).
2) C. S. Hudson, *J. Am. Chem. Soc.*, **31**, 66 (1909).

TABLE I

| Name | Unit Groups | $[M]_D^{20}(W)$ | Lit. |
|---|---|---|---|
| $\beta$-L-arabinose | $[(OH)^{1\alpha}, (OH)^{2\alpha}, (OH)^{3\beta}, (OH)^{4\beta}, Ring]$ | 303.3° | (a) |
| $\alpha$-L-arabinose | $[(OH)^{1\beta}, (OH)^{2\alpha}, (OH)^{3\beta}, (OH)^{4\beta}, Ring]$ | 133.6° | (a) |
| $\alpha$-D-xylose | $[(OH)^{1\alpha}, (OH)^{2\alpha}, (OH)^{3\beta}, (OH)^{4\alpha}, Ring]$ | 138.1° | (b) |
| $\beta$-D-xylose | $[(OH)^{1\beta}, (OH)^{2\alpha}, (OH)^{3\beta}, (OH)^{4\alpha}, Ring]$ | | |
| $\alpha$-D-ribose | $[(OH)^{1\alpha}, (OH)^{2\alpha}, (OH)^{3\alpha}, (OH)^{4\alpha}, Ring]$ | | |
| $\beta$-D-ribose | $[(OH)^{1\beta}, (OH)^{2\alpha}, (OH)^{3\alpha}, (OH)^{4\alpha}, Ring]$ | | |

isorotation rules as set out below[2];

Rule 1—"The rotation of $C^1$- atom in the case of many substances of the sugar group is affected in only a minor degree by changes in the structure of the remainder of the molecule".

Rule 2—"Changes in the structure of $C^1$- atom in the case of many substances of sugar group affect in only a minor degree the rotation of the remainder of the molecule".

But mannose deviates from the first empirical rule. Then, in order to explain this anormality, Hudson assigned to $\alpha$-D-mannose a five-membered (furanose) ring, whilst admitting the presence of the six-membered (pyranose) ring in glucose and galactose, as well as in $\beta$-D-mannose[3]. Nevertheless, his idea was not supported by any independent chemical evidence. In 1929, under the hypothesis that the van't Hoff's principle exists in glucide, that is to say, every one of the asymmetric carbon atoms in the aldopyranose-ring possesses its own definite partial molecular rotation, Isbell calculated the values of these partial molecular rotations by simple algebraic summation and subtraction of $[M]_D^{20}(W)$*2 of several glucides. By using these calculated values, he presumed $[M]_D^{20}(W)$ of sixteen glucides, then unknown[4]. However, many independent experiments have proved most of them to be inaccurate. Haworth and Hirst attributed these irregularities of rotatory power to the influence of dissimilarities of configuration[5], in accordance with the view of Rosanoff[6] who held that the optical rotatory power of an asymmetric carbon atom depends not only upon the composition and constitution, but also upon the configuration of the glucides. Rosanoff's view was very splendid. But it had no ground of physical theory and was not quantitative. In 1951, the author proposed the application of the calculation-method based on quantum mechanics, to illustrate $[M]_D^{20}(W)$ of glucides[7]. Lately, the author succeeded in explaining Hudson's first isorotation rule and the deviation of mannose from this[8], on the basis of Kirkwood's polarizability theory of optical rotatory power[9], which adopted the idea that the partial rotation is caused by the dynamical coupling effect between any two unit groups in a molecule.

By using the method which is similar to that used in the previous paper[8], the author tried here to elucidate the relation between the structure of pentoses*3 and the value of their molecular rotations; this attempt had been continued since the time of van't Hoff without success, and it was found that there exists the principle of optical superposition of Kirkwood's idea in the pentose group.

## Molecular Model and Data Used*4

The names of pentoses, to which the calculations were applied, unit groups in their molecules, and their corresponding molecular rotations are tabulated in Table I*5.

In order to simplify the calculations, the molecular model of an aldopyranose-ring of Reeves' C 1 conformation (the bond length of C–O is 1.42 Å) which was used in the previous paper[8], was also adopted here. (Fig. 1)

The optical data for OH group and H

3) C. S. Hudson, *J. Am. Chem. Soc.*, **52**, 1680 (1930).

*2 $[M]_D^{20}(W)$ is a notation which represents the optical molecular rotation of the plane polarized light of wave-length of D line at 20°C by an aqueous solution.

4) H. S. Isbell, *Bureau of Standards. J. Res.*, **3**, 1041 (1929).

5) W. N. Haworth and E. L. Hirst, *J. Chem. Soc.*, **1930**, 2615.

6) M. A. Rosanoff, *J. Am. Chem. Soc.*, **28**, 525 (1906); **29**, 536 (1907).

7) S. Yamana, Presentation and Discussion at the XIIth International Congress of Pure and Applied Chemistry. September (1951), New York.

8) S. Yamana, This Bulletin, **30**, 207 (1957).

9) J. G. Kirkwood, *J. Chem. Phys.*, **5**, 479 (1937).

*3 In the cases of hexose and methyl pentose, there are $CH_2OH$ and $CH_3$ groups which combine with $C^5$-atom of the aldopyranose-ring, respectively. Then, the calculations become very complicated. In order to avoid this intricacy, only the pentose group is treated in this article. (Concerning the problem of hexose and methyl pentose, refer to Part IV of this study.

*4 Abbreviated symbols and notations, used in this paper, are the same as those in the previous paper (8).

*5 According to Reeves' continued investigations of cuprammonium-glycoside complexes (R. E. Reeves, *J. Am. Chem. Soc.*, **72**, 1499 (1950)), all of the following pentoses are of the C1 conformation of ring structure in their aqueous solutions, but the one remaining pentose (lyxose) is of both C1 and 1C conformations in its aqueous solution. Reeves, however, did not speak of the value of the quantitative ratio between these two types of conformation. Accordingly, it is impossible to try to make the calculation on lyxose in this paper.

a) E. Montogomery and C. S. Hudson, *J. Am. Chem. Soc.*, **56**, 2074 (1934).

b) J. K. Wolfe, R. M. Hann and C. S. Hudson, ibid., **64** 1493 (1942).

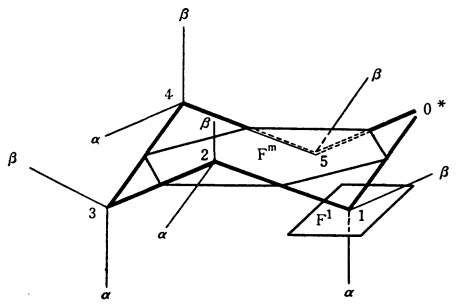



Fig. 1. Perspective drawing of the molecular model of an aldopyranose-ring of Reeves' C 1 conformation.
$F^m$.....(Flar)$^m$-plane
$F^1$.....(Flar)$^1$-plane

atom, used in the previous paper[10], were employed again without any correction. The refractive indices of the aqueous solutions of pentoses under question are presumed to be nearly equal (1.34)*6.

## Method Proposed

The principle of the method of calculation is similar to that used in the previous paper[8]. The outline of this method is as follows;

(i)—The molecular model of pentose was divided into unit groups*7.

(ii)—$[\mu]^{20}_{D\text{calcd}}(3/n^2+2)$, caused by the dynamical coupling effect between any two members of these unit groups were calculated according to Kirkwood's polarizability theory*8.

(iii)—$[\mu]^{20}_{D\text{obs}}$ was calculated from $[\mu]^{20}_{D\text{calcd}}(3/n^2+2)$, above obtained*9.

(iv)—In order to avoid the difficulty, caused by the impossibility of calculation of the terms with which the aldopyranose-ring is concerned, quasi-empirical methods were devised by using the experimental data of $[M]^{20}_{D}(W)$ of β-L-arabinose, α-L-arabinose and α-D-xylose.

(v)—By algebraic summation of $[\mu]^{20}_{D\text{obs}}$s, above obtained, $[M]^{20}_{D}(W)$s of β-D-xylose, α-D-ribose and β-D-ribose were calculated.

(vi)—These calculated values were compared with the molecular rotations which have been observed under such conditions as close to $[M]^{20}_{D}(W)$ as possible.

TABLE II

$[\mu]^{20}_{D\text{obs}}$, CAUSED BY THE DYNAMICAL COUPLING EFFECT BETWEEN ANY TWO MEMBERS OF UNIT GROUPS (EXCEPT RING)

| | 4β | 4α | 3β | 3α | 2β | 2α |
|---|---|---|---|---|---|---|
| 1α | 0 | 0 | 6.8 | 0 | 0 | 26.8 |
| 1β | 0 | 0 | 0 | − 6.8 | 26.8 | −26.8 |
| 2α | 6.8 | 0 | 26.8 | −26.8 | | |
| 2β | 0 | − 6.8 | −26.8 | 0 | | |
| 3α | 0 | 26.8 | | | | |
| 3β | 26.8 | −26.8 | | | | |

This method of calculation is illustrated by an example. The $[\mu]^{20}_{D\text{obs}}$, caused by dynamical coupling effect between any two members of unit groups in α-D-xylose molecule, are*7 (1α)Λ(2α)*10, (1α)Λ(3β), (1α)Λ(4α), (1α)ΛR*11, (2α)Λ(3β), (2α)Λ(4α), (2α)ΛR, (3β)Λ(4α), (3β)ΛR and (4α)ΛR. Then, $[M]^{20}_{D}(W)$ of α-D-xylose, 138.1[b], should be equal to the sum of these $[\mu]^{20}_{D\text{obs}}$s*12. This relation is given by the following equation. (ref. Table II)

$$\begin{aligned}138.1 \equiv \sum[\mu]^{20}_{D\text{obs}} &= 26.8+6.8+0 \\ &+(1\alpha)\Lambda R+26.8+0+(2\alpha)\Lambda R \\ &-26.8+(3\beta)\Lambda R+(4\alpha)\Lambda R \\ &=33.6+(1\alpha)\Lambda R+(2\alpha)\Lambda R \\ &+(3\beta)\Lambda R+(4\alpha)\Lambda R \qquad (1)\end{aligned}$$

Owing to the symmetry of the aldopyranose-ring,

$$(3\beta)\Lambda R \equiv 0 \qquad (2)$$

10) S. Yamana, This Bulletin, **30**, 203 (1957).

*6 Ref. *8 in the previous paper (8).

*7 Ref. Table 1 in this article.

*8 Concerning the method of calculation, refer to the previous paper (10).

*9 According to the previous paper(8), $[\mu]^{20}_{D\text{calcd}}$, caused by the dynamical coupling effect between two OH groups in an aldopyranose molecule of C1 conformation in aqueous solution, becomes equal to $[\mu]^{20}_{D\text{obs}}$, when multiplied by $\kappa=12.37/n^2+2$. Then, in order to obtain $[\mu]^{20}_{D\text{obs}}$ from $[\mu]^{20}_{D\text{calcd}}(3/n^2+2)$, the latter must be multiplied by $(n^2+2/3)\ (12.37/n^2+2)=12.37/3=4.123$. Consequently, the table of $[\mu]^{20}_{D\text{obs}}$, caused by the dynamical coupling effect between any two OH groups in this case, can be made by multiplying the values of $[\mu]^{20}_{D\text{calcd}}(3/n^2+2)$ in Table I of the previous paper (8) with this coefficient, 4.123. But, in order to obtain the first significant decimal figures of $[\mu]^{20}_{D\text{obs}}$ more precisely, the absolute values, 1.66 and 6.50, should be used instead of 1.7 and 6.5 of the previous paper, respectively. It is important that the coefficient 4.123 was obtained by using the data of $[M]^{20}_{D}(W)$ of four hexoses(α-D-glucose, β-D-glucose, α-D-mannose and β-D-mannose), indifferent to those of pentoses.

*10 The notation X was used in the previous papers (10) (8) to represent $[\mu]^{20}_{D\text{calcd}}(3/n^2+2)$, caused by the dynamical coupling effect between two unit groups. But, in this paper, $[\mu]^{20}_{D\text{obs}}$ is used instead of $[\mu]^{20}_{D\text{calcd}}(3/n^2+2)$ for the algebraic summation course. Then, the other notation becomes necessary. The symbol, Λ, was devised for this reason. This is inverted Y [wai] and is called "iaw [iɔ:]". $(1\alpha)\overset{20}{\underset{D}{\Lambda}}(2\alpha)$ means $[\mu]^{20}_{D\text{obs}}$, caused by the dynamical coupling effect between $(OH)^{1\alpha}$ and $(OH)^{2\alpha}$. But 20 and D in $\overset{20}{\underset{D}{\Lambda}}$ were omitted generally for convenience.

*11 R is an abbreviated symbol of Ring.

*12 Ref. Eq. (3) in the previous paper (10).

and $(2\alpha)\lambda R+(4\alpha)\lambda R\equiv 0$ (3)

Combining these two conditional equations with Eq. (1),

$$(1\alpha)\lambda R=104.5 \quad (4)$$

A similar treatment was applied also to the cases of $\beta$-L- and $\alpha$-L-arabinose, and the following two equations were obtained. From $\beta$-L-arabinose,

$$(1\alpha)\lambda R+(2\alpha)\lambda R+(4\beta)\lambda R=209.3 \quad (5)$$

and from $\alpha$-L-arabinose,

$$(1\beta)\lambda R+(2\alpha)\lambda R+(4\beta)\lambda R=100.0 \quad (6)$$

By subtracting Eq. (4) from (5),

$$(2\alpha)\lambda R+(4\beta)\lambda R=104.8 \quad (7)$$

and by subtacting Eq. (7) from (6),

$$(1\beta)\lambda R=-4.8 \quad (8)$$

Thus, the values of two $[\mu]^{20}_{D\text{obs}}$s, $\{(1\alpha)\lambda R$ and $(1\beta)\lambda R\}$, and one $\sum[\mu]^{20}_{D\text{obs}}$, $\{(2\alpha)\lambda R+(4\beta)\lambda R\}$ were shown by Eqs. (4), (8) and (7). These values which were obtained quasi-empirically, seem to be reasonable, from the viewpoint of the geometry of the molecule, as described below :

[1]—The orientation of $1\alpha$ is essentially perpendicular to the hypothetical flat plane which is symbolized by $(Flar)^m$-plane*13 in Fig. 1 (axial bond), while that of $1\beta$ is almost in parallel with this flat plane (equatorial bond)[11]. (ref. Fig. 1). Accurately speaking, the direction of $1\beta$ projects out, greatly inclined toward the $(Flar)^1$-plane*14 on the opposite side of $1\alpha$. Then, $(1\alpha)\lambda R$ and $(1\beta)\lambda R$ should be opposite in sign, and the absolute value of the former must be far greater than that of the latter*15. These conditions, which are required from the standpoint of the geometry of the molecule, are all satisfied by Eqs. (4) and (8). This indicates that Eqs. (4) and (8) are reasonable in their sign and magnitudes.

[2]—$4\beta$ and $2\alpha$ are axial and equatorial orientations respectively. (ref. Fig. 1). Then, the absolute value of $(4\beta)\lambda R$ must be far greater than that of $(2\alpha)\lambda R$. In other words, the sign of $(2\alpha)\lambda R+(4\beta)\lambda R$ should be the same as that of $(4\beta)\lambda R$..... (Condition A)

On the other hand, the positions of $C^1$- and $C^4$- atoms are on the opposite half of the aldopyranose-ring together, in relation to the symmetrical plane of this ring in which the centers of the ring-O-atom (represented by O*) and $C^3$- atom lie. Of course, the orientations of $\alpha$ and $\beta$ project out to the opposite sides of $(Flar)^m$-plane together; then the second condition is obtained.

$(1\alpha)\lambda R$ and $(4\beta)\lambda R$ must be equal to each other in their sign*15.....(Condition B) Referring to Conditions A and B, it is concluded as below; $\{(2\alpha)\lambda R+(4\beta)\lambda R\}$ and $(1\alpha)\lambda R$ should have the same sign..... (Condition C)

This condition is satisfied by Eqs. (4) and (7). As Eq. (4) has already been proved to be reasonable, above, Eq. (7) is concluded also to be probable.

In spite of the difficulties of calculating them by the purely theoretical procedure, the values of the terms containing R could be thus obtained quasi-empirically.

Now, $[M]^{20}_D(W)$ of three pentoses, can be calculated by using the values $[\mu]^{20}_{D\text{obs}}$s, above obtained. The $[\mu]^{20}_{D\text{obs}}$ in the case of $\beta$-D-xylose are $(1\beta)\lambda(2\alpha)$, $(1\beta)\lambda(3\beta)$, $(1\beta)\lambda(4\alpha)$, $(1\beta)\lambda R$, $(2\alpha)\lambda(3\beta)$, $(2\alpha)\lambda(4\alpha)$, $(2\alpha)\lambda R$, $(3\beta)\lambda(4\alpha)$, $(3\beta)\lambda R$ and $(4\alpha)\lambda R$*16. Then the calculated value of $[M]^{20}_D(W)$ of $\beta$-D-xylose is to be given by the following equation. (ref. Table II and Eqs. (2), (3), (8)).

$$[M]^{20}_D(W)=\sum[\mu]^{20}_{D\text{obs}}=-26.8+0+0+(1\beta)\lambda R+26.8+0+(2\alpha)\lambda R-26.8+(3\beta)\lambda R+(4\alpha)\lambda R=-31.6^{*17}$$

The corresponding observed value of $[M]^{20}_D(W)$ of $\beta$-D-xylose has not been found in any referential literatures, but Hudson reported that $[M]^{20}_D$ of this pentose in 80% alcoholic solution is $-30°$c), which is almost equal to the above calculated value. Next, this calculation-method was

*13 The molecular model of the aldopyranose-ring, used in this article, is one of Sachse strainless ring conformations and is not perfectly flat. (ref. the previous paper (8)). Then it is improper to use this aldopyranose-ring itself as a standard for comparing the orientations of hydroxyl O atom in the molecule. $(Flar)^m$-plane was devised for this reason. It is a perfectly flat plane in which the middle points of $C^1$—$C^2$, $C^2$—$C^3$, $C^3$—$C^4$, $C^4$—$C^5$, $C^5$—O* and O*—$C^1$ bonds lie. (ref. Fig. 1). "Flar" is an abbreviated symbol of "Flat Aldose Ring".

11) D. H. R. Barton, O. Hassel, K. S. Pitzer and V. Prelog, *Nature*, **172**, 1096 (1953).

*14 $(Flar)^1$-plane, on which the centre of $C^1$ atom lies, is parallel with $(Flar)^m$-plane. (ref. Fig. 1).

*15 Concerning the reason for these deductions from the relative geometry of unit groups, refer to Eq. (1) of the previous paper (10).

*16 Ref. Table 1 in this article.

*17 $[\mu]^{20}_{D\text{obs}}$s for the anomeric differences (*19) of D-xylose and D-ribose, calculated by using McDonald and Beevers' molecular model, are 168.7 and 171.3, respectively. (Concerning this new molecular model, refer to the next paper, This Bulletin, **30**, 920 (1957). In this case, the presumed value of $[M]^{20}_D(W)$ of $\beta$-D-xylose becomes −30.6.

c) C. S. Hudson and E. Yanovsky, *J. Am. Chem. Soc.*, **39**, 1013 (1917).

applied to the cases of α-D- and β-D-riboses*18. 131.3 and −38.4 were obtained as the calculated values of $[M]_D^{20}$(W) of α-D- and β-D-riboses, respectively. The value observed for β-D-ribose is −34.7[d]. The datum of $[M]_D$(W) of α-D-ribose has not been found in any referential literatures, but the calculated value (131.3) is greater than that of β-D-ribose (−38.4) by 169.7. The magnitude of this difference is equal to the observed value of the anomeric difference*19 of L-arabinose. This fact is to be expected by Hudson's first isorotation rule*20. Thus, the calculated values of $[M]_D^{20}$(W)s of β-D-xylose, α-D-ribose and β-D-ribose seem to be all probable. This fact means that the principle of optical superposition of Kirkwood's idea exists in the pentose group.

*18 In this case, the conditional equation $(3\alpha)\Delta R \equiv O$ was used in calculation. This was obtained from the symmetry of the Ring.

d) F. P. Phelps, H. S. Isbell and W. W. Pigman, *J. Am. Chem. Soc.*, 56, 747 (1934).

*19 This is the difference in optical rotation of α and β aldoses. (ref. (8)).

*20 Ref. "Introduction" in this article.

## Summary

The method of calculation of optical rotatory power, devised by Kirkwood and improved by the author was applied to the pentose group, and it was concluded that the principle of optical superposition of Kirkwood's idea exists in this group.

The author wishes to express his sincere gratitude to Professor S. Tanaka (Kyoto University) for his valuable advice and kind encouragement throughout the course of this study.

*Department of Chemistry*
*Kyoto Gakugei University*
*Fushimi-ku, Kyoto*

# *Molecular Rotations of Glucides in Relation to their Structures. IV. The Internal Conformation of $C^6$—O Bond in D-Mannopyranose and D-Glucopyranose in their Aqueous Solutions*

By Shukichi YAMANA

(Received May 14, 1957)

From the results of X-ray analysis on crystalline methyl-D-mannopyranoside, Cox and Goodwin proposed a presumption on the internal conformation of $C^6$—O bond in D-mannopyranose in crystalline state[1],*1. Mc Donald and Beevers also determined the same conformation in crystalline D-glucopyranose by X-ray analysis about the crystal of this substance[2]. But, for lack of any suitable method, the internal conformation in the molecules in aqueous solutions has been yet undetermind. In aqueous solution, OH group which combines with $C^6$ atom is considered to be free to rotate about the axis of $C^5$—$C^6$ bond and the position which has minimal potential and makes that OH group rest, will be decided principally by steric repulsions and secondarily by electrostatic

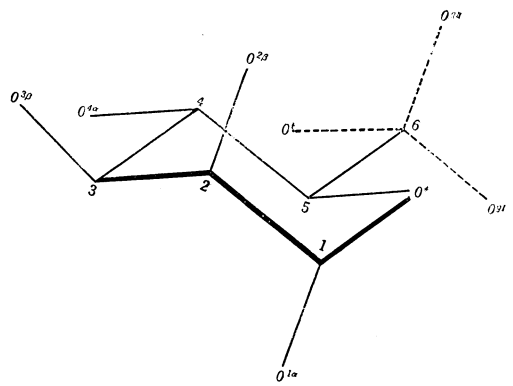



Fig. 1. Perspective drawing of the molecular model of α-D-mannopyranose *g*I—*gauche* I (Φ=120°), *g*II—*gauche* II (Φ=240°), *t*—*trans* (Φ=0°)

1) E. G. Cox and T. H. Goodwin, *J. Chem. Soc.*, **1932**, 1844.

*1 Cox and Goodwin presumed that the aldopyranose-ring is flat, but their presumption was proved to be improper by McDonald and Beevers. (ref. (2)).

2) T. R. R. McDonald and C. A. Beevers, *Acta Cryst.*, **5**, 654 (1952).

Table I

| Name | Unit Groups | $[M]_D^{20}(W)$ | Lit. |
|---|---|---|---|
| α-D-mannose | [$(OH)^{1\alpha}$, $(OH)^{2\beta}$, $(OH)^{3\beta}$, $(OH)^{4\alpha}$, $(CH_2OH)^{5\beta}$, Ring] | 53.8° | (a) |
| β-D-mannose | [$(OH)^{1\beta}$, $(OH)^{2\beta}$, $(OH)^{3\beta}$, $(OH)^{4\alpha}$, $(CH_2OH)^{5\beta}$, Ring] | −29.3° | (a) |
| α-D-rhamnose | [$(OH)^{1\alpha}$, $(OH)^{2\beta}$, $(OH)^{3\beta}$, $(OH)^{4\alpha}$, $(CH_3)^{5\beta}$, Ring] | 14.0° | (b) |
| β-D-rhamnose | [$(OH)^{1\beta}$, $(OH)^{2\beta}$, $(OH)^{3\beta}$, $(OH)^{4\alpha}$, $(CH_3)^{5\beta}$, Ring] | −63.0° | (b) |

forces and hydrogen bonding forces between the atoms in the molecule[3]. (Fig. 1).

According to the idea that the optical rotatory power should be a function of the angle which defines the internal conformation of $CH_2Cl$ group in that molecule, Wood, Fickett and Kirkwood calculated the value of the optical rotatory power of 1,2-dichloropropane, and checked these values comparing them with the observed values. By this method, they could determine the absolute configuration of 1,2-dichloropropane[4]. The author wants to offer a new method of presuming the internal conformation of a bond. The principle of this method is the calculation in reversing order of Kirkwood's method, described above. By using this method, the author was able to presume the internal conformations of $C^6$—O bond in D-mannopyranose and D-glucopyranose in aqueous solutions.

## Molecular Model and Data Used*2

Unit groups in hexose molecules under question and their corresponding molecular rotations, are shown in Table I. (Fig. 1).

In this paper, the hypothetically ideal model of Reeves' C 1 conformation*3 and Mc Donald and Beevers' model*4 which was determined by X-ray analysis of crystalline α-D-glucose, were used as the molecular model. The optical data for OH group and H atom, used in the previous paper[7], were also employed without any correction. The refractive indices of the aqueous solutions of glucides under question are presumed to be nearly equal (1.34)*5.

## Method Proposed

The geometry of D-mannopyranose, except that of $C^6$—O bond, has been determined in the previous paper[6]. At first, the author intended to calculate the optical rotatory power of D-mannopyranose as a function of the angle Φ which defines the internal conformation of $C^6$—O bond*6 according to Kirkwood's polarizability theory. But, in order to avoid the complexity of calculation, the author used the anomeric difference*7 instead of the molecular rotation itself, and compared the calculated values with the observed one to presume the internal conformation of $C^6$—O bond. In the molecule of α-D-mannopyranose, $\sum[\mu]^{20}_{D\text{obs}}$, caused by the dynamical coupling effect of $(OH)^1$ is $(1\alpha)\lambda(2\beta)$*2$+(1\alpha)\lambda(3\beta)+(1\alpha)\lambda(4\alpha)+(1\alpha)\lambda(CH_2OH)^{5\beta}+(1\alpha)\lambda R$, and the value in the molecule of β-D-mannopyranose is also calculated as

$$(1\beta)\lambda(2\beta)+(1\beta)\lambda(3\beta)+(1\beta)\lambda(4\alpha)+(1\beta)\lambda(CH_2OH)^{5\beta}+(1\beta)\lambda R^{5,7)}$$

Therefore, $[\mu]^{20}_{D\text{obs}}$ for the anomeric difference*7 of D-mannopyranose should be equal to the difference between the above two $\sum[\mu]^{20}_{D\text{obs}}$s. That is

$$\{(1\alpha)\lambda(2\beta)-(1\beta)\lambda(2\beta)\}+\{(1\alpha)\lambda(3\beta)-(1\beta)\lambda(3\beta)\}+\{(1\alpha)\lambda(4\alpha)-(1\beta)\lambda(4\alpha)\}+\{(1\alpha)\lambda(CH_2OH)^{5\beta}-(1\beta)\lambda(CH_2OH)^{5\beta}\}+\{(1\alpha)\lambda R-(1\beta)\lambda R\}\equiv P$$

By the similar treatment, $[\mu]^{20}_{D\text{obs}}$ for the

3) S. Mizushima, Y. Morino and T. Shimanouchi, *J. Chem. Soc. Japan, Pure Chem. Sec.* **73**, 621 (1952); I. Miyagawa, ibid. **75**, 1169 (1954).

4) W. W. Wood, W. Fickett and J. G. Kirkwood, *J. Chem. Phys.*, **20**, 561 (1952).

*2 Abbreviated symbols, used in this paper, are the same as those in the preceding article (5).

5) S. Yamana, This Bulletin, **30**, 916 (1957).

a) C. N. Rüber and J. Minsaas, *Ber.*, **60**, 2402 (1927).

b) C. S. Hudson and E. L. Jackson, *J. Am. Chem. Soc.*, **59**, 1076 (1937).

*3 See the previous paper (6).

6) S. Yamana, This Bulletin, **30**, 207 (1957).

*4 The shape of McDonald and Beevers' model is almost the same as that of the ideal model of Reeves' C 1 conformation, above mentioned. Mc Donald and Beevers decided the following values for the bond lengths and the valency angles in crystalline α-D-glucose molecule[2]; $C^1$—$C^2$ 1.54 Å; $C^2$—$C^3$ 1.56 Å; $C^3$—$C^4$ 1.53 Å; $C^4$—$C^5$ 1.54 Å; $C^5$—O* 1.40 Å; O*—$C^1$ 1.42 Å; $C^1$—$O^1$ 1.32 Å; $C^2$—$O^2$ 1.41 Å; $C^3$—$O^3$ 1.44 Å; $C^4$—$O^4$ 1.40 Å; $C^5$—$C^6$ 1.53 Å; $C^6$—$O^6$ 1.32 Å; O*—$C^1$—$C^2$ 110°; $C^1$—$C^2$—$C^3$ 104°; $C^2$—$C^3$—$C^4$ 110°; $C^3$—$C^4$—$C^5$ 108°; $C^4$—$C^5$—O* 109 1/2°; $C^5$—O*—$C^1$ 111°; O*—$C^1$—$O^1$ 112°; $C^2$—$C^1$—$O^1$ 115°; $C^1$—$C^2$—$O^2$ 109°; $C^3$—$C^2$—$O^2$ 109°; $C^2$—$C^3$—$O^3$ 102°; $C^4$—$C^3$—$O^3$ 108°; $C^3$—$C^4$—$O^4$ 110 1/2°; $C^5$—$C^4$—$O^4$ 112°; $C^4$—$C^5$—$C^6$ 112°; O*—$C^5$—$C^6$ 110°; $C^5$—$C^6$—$O^6$ 113°.

7) S. Yamana, This Bulletin, **30**, 203 (1957).

*5 ref. *8 in the previous paper (6).

*6 The author defined an angle φ specifying the internal conformation as follows; (i) φ is zero at the situation which the O atom in $C^6$—O bond and the ring-O-atom (represented by O*) are in *trans* position each other. (ii) Its positive direction of rotation from zero increases the distance between $C^4$-atom and the O atom in $C^6$—O bond.

*7 This is the difference in optical rotation of α and β aldoses. (ref. (6)).

anomeric difference of D-rhamnopyranose*8 is obtained as

$$\{(1\alpha)\chi(2\beta)-(1\beta)\chi(2\beta)\}+\{(1\alpha)\chi(3\beta)-(1\beta)\chi(3\beta)\}+\{(1\alpha)\chi(4\alpha)-(1\beta)\chi(4\alpha)\}+\{(1\alpha)\chi(CH_3)^{5\beta}-(1\beta)\chi(CH_3)^{5\beta}\}+\{(1\alpha)\chi R-(1\beta)\chi R\}\equiv Q$$

Both of the above obtained two $[\mu]^{20}_{D\text{obs}}$s (P and Q) contain the terms concerning the aldopyranose-ring R. It is impossible to calculate these terms at present. Then, in order to avoid this difficulty, Q was subtracted from P and the terms concerning R disappear as below:

Difference between the anomeric difference of D-mannopyranose (P) and that of D-rhamnopyranose (Q) is as follows,

$$\text{P minus Q}=[(1\alpha)\chi(CH_2OH)^{5\beta}-(1\beta)\chi(CH_2OH)^{5\beta}]-[(1\alpha)\chi(CH_3)^{5\beta}-(1\beta)\chi(CH_3)^{5\beta}]$$

The terms of this difference can be simplified by the following procedure. $(CH_2OH)^{5\beta}$ may be considered to occur by replacing an H atom in $(CH_3)^{5\beta}$ by an OH group. Becauses of its small polarizability, $[\mu]^{20}_{D\text{obs}}$, caused by the dynamical coupling effect of H atom, may be neglected[8],*9. Then (P minus Q) becomes as below*10;

$$[(1\alpha)\chi\{(CH_2)^{5\beta}+(OH)^6\}-(1\beta)\chi\{(CH_2)^{5\beta}+(OH)^6\}]-[(1\alpha)\chi\{(CH_2)^{5\beta}+(H)^6\}-(1\beta)\chi\{(CH_2)^{5\beta}+(H)^6\}]=(1\alpha)\chi(OH)^6-(1\beta)\chi(OH)^6$$

Referring to the previous papers[5-7], the value for $\{(1\alpha)\chi(OH)^6-(1\beta)\chi(OH)^6\}$ was calculated as a function of $\Phi$*11. The results of calculation are given in Table II.

$(53.8+29.3)-(14.0+63.0)=6.1$*12 is gained as the corresponding observed value. This value coincides with the calculated values in Table II when $\Phi$ is 0° and 240°*13. Therefore, the internal conformation of $C^6$—O bond should correspond to one

TABLE II

$\sum[\mu]^{20}_{D\text{obs}}$ FOR THE DIFFERENCE BETWEEN THE ANOMERIC DIFFERENCE OF D-MANNOPYRANOSE (P) AND THAT OF D-RHAMNOPYRANOSE (Q), AS A FUNCTION OF $\Phi$

| $\Phi$ | Ideal Model | McDonald and Beevers' Model |
|---|---|---|
| 0 | 7.2 | 7.3 |
| 20 | 2.8 | 2.8 |
| 40 | − 3.0 | − 3.1 |
| 60 | −10.4 | −10.1 |
| 80 | −15.6 | −16.8 |
| 100 | −18.9 | −21.2 |
| 120 | −18.2 | −21.5 |
| 140 | −13.8 | −17.5 |
| 160 | − 8.1 | −11.0 |
| 180 | − 2.6 | − 4.3 |
| 200 | 1.7 | 1.3 |
| 220 | 4.7 | 5.4 |
| 240 | 7.2 | 8.3 |
| 260 | 9.2 | 10.3 |
| 280 | 10.8 | 11.8 |
| 300 | 11.6 | 12.3 |
| 320 | 11.4 | 11.9 |
| 340 | 9.9 | 10.3 |

or both of these two angles. According to Mizushima, Morino and Shimanouchi's empirical rule*14, the molecule of $XH_2C$—$CH_2Y$ type can exist in several forms of rotational isomer in liquid or gaseous state. Then, there may exist an equilibrium between these two types of internal conformations of $C^6$—O bond in aqueous solutions. These two types happen in the two of the three structures of potentially minimal 1,2-dichloropropane[9] (*trans* form and *gauche* II form). (Fig. 2)*15

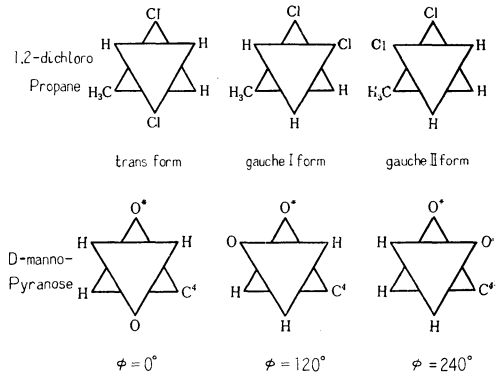



Fig. 2. Internal conformation along the $C^6$—$C^5$ axis.

8* D-rhamnopyranose has been confirmed to have Reeves' C 1 conformation by the experiments of cupram-monium-glycoside complexes. (R. E. Reeves, *J. Am Chem. Soc.*, **72**, 1499 (1950).

8) J. G. Kirkwood, *J. Chem. Phys.*, **5**, 479 (1937).

*9 Consequently. $(1\alpha)\chi(H)^6=1\beta\chi(H)^6=0$

*10 $(OH)^6$ and $(H)^6$ mean OH group and H atom which combine with the C atoms in $(CH_2OH)^{5\beta}$ and $(CH_3)^{5\beta}$, respectively.

*11 When using McDonald and Beevers' model, $\kappa$ is $241.2/19.68(n^2+2)$. Then, in order to obtain $[\mu]^{20}_{D\text{obs}}$ from $[\mu]^{20}_{D\text{calcd}}(3/n^2+2)$, the latter must be multiplied by $80.4/19.68=4.085$.

*12 Ref. Table 1 in this paper.

*13 When using the value of C—O bond length of 1.48 Å (M. Kimura, *J. Chem. Soc. Japan, Pure Chem. Sec.* **71**, 18 (1950)), $\kappa$ is $13.2/n^2+2$ and both of the calculated values of the difference between two anomeric differences, corresponding to $\Phi=0°$ and 240°, become 7.5.

*14 Ref. "Discussion on the Results" in this article.

9) I. Miyagawa, *J. Chem. Soc. Japan, Pure Chem. Sec.* **75**, 1165 (1954).

*15 But the O atom in D-mannopyranose molecule corresponds to the Cl atom in 1,2-dichloropropane molecule.

The above obtained two types of internal conformation of $C^6$—O bond in D-mannopyranose in aqueous solution are presumed to happen also in D-glucopyranose. The reason for this is as follows; If the orientation of $(OH)^{2}$*16 of D-mannopyranose changes from $\beta$ to $\alpha$, D-glucopyranose-molecule can be obtained. But the distance between the O atom in $(OH)^2$ and that in $C^6$—O bond is too large*17 to give rise to any influence of the orientation-change of $(OH)^2$ on the internal conformation of $C^6$—O bond*18.

## Discussion on the Results

According to Mc Donald and Beevers' experiment[2], the internal conformation of $C^6$—O bond in $\alpha$-D-glucopyranose, in crystalline state, is almost consistent with the conformation corresponding to *gauche* 1 form*19. Then, it may be concluded that, when $\alpha$-D-glucopyranose is dissolved in water, the internal conformation of $C^6$—O bond changes from *gauche* 1 to *trans* and *gauche* II types. On the other hand, Mizushima, Morino and Shimanouchi[3] found an empirical rule that the molecule of $XH_2C$—$CH_2Y$ type, may be able to exist in several forms of rotational isomer in liquid or gaseous state, and one of these forms is identical with the form in the solid state. The author's conclusion*20 on the conformation of $C^6$—O bond in $\alpha$-D-glucose somewhat seems to deviate from this empirical rule. This disharmony may be explained as follows. As Mc Donald and Beevers observed[2] that $O^6$- atom of a molecule of crystalline $\alpha$-D-glucopyranose is combined, by hydrogen bonding forces, with both $O^2$- and $O^3$- atoms of the neighboring molecule*21, the internal conformation of $C^6$—O bond in crystalline $\alpha$-D-glucopyranose is greatly influenced by the atoms of the other molecules in the crystal. These forces contribute to make $O^6$- atom rest at such a position that $C^6$—O bond takes *gauche* I conformation. But when $\alpha$-D-glucose is dissolved in water, each molecule is separated from other molecules and the influences of the neighboring molecule decrease. Therefore, the internal conformation of $C^6$—O bond in that molecule is influenced principally by the atoms in its own molecule. Moreover, as the distance between $O^{4\alpha}$ and $O^6$ is almost equal to that between $O^6$- and $C^4$- or O*-atoms (ref. Table III), the influence of $O^{4\alpha}$ on $O^6$ may be unable to neglect. (Fig. 1)

TABLE III
THE DISTANCES BETWEEN $O^6$- ATOM AND ITS NEIGHBORING ATOMS IN MCDONALD AND EEVERS' MODEL AND THE IDEAL MODEL*22

| | *trans* | *gauche* I | *gauche* II |
|---|---|---|---|
| $O^6$ and $O^{4\alpha}$ | 2.69Å(2.51) | 4.18Å(4.19) | 3.45Å(3.42) |
| $O^6$ and $C^4$ | 2.96Å(2.89) | 3.73Å(3.76) | 2.96Å(2.89) |
| $O^6$ and O* | 3.57Å(3.76) | 2.81Å(2.89) | 2.81Å(2.89) |

In Table III, the distance between $O^6$ and $O^{4\alpha}$ in *trans* form is the shortest (this is 2.69 Å) and is just equal to the length of a hydrogen bond*23. Therefore, $O^6$- atom which is only one movable atom in Table III, may be attracted by $O^{4\alpha}$- atom most strongly and is forced to rest at the *trans* position*24 by making a hydrogen bond between $(OH)^6$ and $(OH)^{4\alpha}$ group. In order to find a reason for non-existence of *gauche* I form in aqueous solutions against its expectation of appearance by the empirical rule, the affinity of $O^6$- atom to *gauche* I and *gauche* II positions should be compared. By using Table III, it is noticed that the distances between $O^6$ and any one of these neighboring atoms ($O^{4\alpha}$, $C^4$ and O*) in *gauche* I form is always larger than (or at least equal to) that in *gauche* II form, respectively. Then the total of the attractive forces of the neighboring atoms on $C^6$-atom in *gauche* II form should be greater than that in *gauche* I form. This fact causes the affinity of $O^6$- atom to *gauche* II rather than to *gauche* I position. These may be the reason for non-existence of *gauche* I form of rotational isomer of D-glucopyranose and D-mannopyranose in aqueous solutions.

*16 $(OH)^2$ means OH group which combines with the $C^2$- atom of the aldopyranose-ring.

*17 The distances between the O atom in $(OH)^2$ and that in $C^6$—O bond are as below;

| | longest | shortest |
|---|---|---|
| $(OH)^{2\alpha}$ | 6.49 Å (at $\phi$=40°) | 6.03 Å (at $\phi$=220°) |
| $(OH)^{2\beta}$ | 5.82 Å (at $\phi$=60°) | 4.56 Å (at $\phi$=240°) |

*18 It must be remembered here, that the coefficient 4.123 (in the previous paper (5)) and 4.085 (in *11 of this article), used in calculating $[\mu]^{20}_{D\text{obs}}$ from $[\mu]^{20}_{D\text{calcd}}$ $(3/n^2+2)$ were obtained under this hypothesis.

*19 The observed internal conformation of $C^6$—O bond corresponds to $\phi=111^1/_2°$ in Mc Donald and Beevers' model.

*20 The possible internal conformation of $C^6$—O bond are *trans* and *gauche* II in aqueous solution but *gauche* 1 only, in crystalline state.

*21 $O^2$—$O^6$ 2.74 Å; $O^3$—$O^6$ 2.70 Å

*22 The values in the ideal model are given in parentheses.

*23 cf. *21 in this paper.

*24 This is the position of $O^6$- atom which corresponds to *trans*-type conformation of $C^6$—O bond.

**Summary**

The internal conformation of $C^6$—O bond in the molecules of D-mannopyranose and D-glucopyranose in aqueous solutions were presumed by a new method, and was concluded to take *trans* (mostly) and *gauche* II (only sometimes) forms.

The author wishes to express his sincere gratitude to Professor S. Tanaka (Kyoto University) for his valuable advice and cordial encouragement throughout the course of this study. Also the author wants to express his great thanks to Assistant Professor Y. Saito (Osaka City University) for his kind teaching of the fundamental knowledge in X-ray analysis.

*Department of Chemistry*
*Kyoto Gakugei University*
*Fushimi-ku, Kyoto*

# *Absorption Spectra and Chemical Behavior of the Hexahydroxylamine Cobalt (III) Complex*[1]

By Hayami YONEDA

(Received May 17, 1957)

In general, complexes of a transition metal ion having an unsaturated *d*-shell have several absorption bands in the region ranging from the near infrared to the ultraviolet. These bands can be considered, to a good approximation, as arising from the energy transitions between the *d*-levels which are split by the electrical field set up by the ligands[2]. The energy transitions between such split *d*-levels correspond to the frequencies of the absorption maxima of the complex. As the energy intervals of such split *d*-levels increase with the increase of the electrical field by the ligands, the strength of the electrical field produced by various ligands can be estimated by comparing the maximum position of the absorption band of various complexes. Such a comparison must have a special significance in the case of complexes of the same type having a series of ligands which have the same donor atom. Because, by such an investigation, we can look for the main factors governing the stability of the coordination bond. With this purpose, the absorption spectra of a series of hexammine nickel(II) and tetrammine platinum (II) complexes were investigated in the previous study[3]. As a result, it was found that the weaker the basic strength of an amine, the shorter the wavelength at which the characteristic absorption bands of the complex appear. This fact indicates that the interaction between the metal ion and the ligands increases with the decreasing order of the basic strengths of co-ordinating amines. A similar rule must be observed more clearly in the case of cobalt(III) ammine complex which is regarded as having more covalent character. With this in mind, the absorption spectrum of hexahydroxylamine cobalt(III) complex was measured and compared with the hitherto measured data of other hexammine cobalt(III) complexes. The result indicated that both the first and the second absorption band of the hydroxylamine complex lay in a much shorter wavelength than those of other hexammine complexes. As the basic strength of hydroxylamine is much weaker than that of ammonia, methylamine or ethylenediamine, this result indicates that the same rule as found in nickel(II) and platinum(II) ammine complexes holds also in the cobalt(III) complex.

In the course of this study it was found that hexahydroxylamine cobalt(III) complex was very unstable in a solution and decomposed gradually to the cobalt(II) salt. This fact seemed to be apparently inconsistent with the above mentioned spectrochemical result. To clarify the cause of this inconsistency, a detailed study of the decomposition of the complex was carried out by measuring the rate of

1) This paper is Part II of "Stabilities of Metal Ammine Complexes".
2) For examle, L. E. Orgel, *J. Chem. Phys.*, **23**, 1004 (1955).
3) Yoneda, This Bulletin, **30**, 132 (1957).

decomposition under various conditions. It was revealed that a very strong binding between the central cobalt(III) ion and the nitrogen atom of the co-ordinating hydroxylamine caused the instability of the complex as a whole. Accordingly, this proved that the instability of hexahydroxylamine cobalt(III) complex supported the validity of the above mentioned rule.

## Experimental

**Preparation of Hexahydroxylamine cobalt (III) Complex.**—Hexahydroxylamine cobalt(III) chloride $[Co(NH_2OH)_6]Cl_3$ was prepared by the following modification of Werner's method[4]. Three g. of *trans*-dichloro-diethylenediamine-cobalt(III) chloride $[Co\ en_2\ Cl_2]Cl$ and 4 g. hydroxylamine hydrochloride $NH_2OH \cdot HCl$ were dissolved in a small amount of water. The solution was cooled below 0°C. To this solution, a concentrated solution containing 2 g. sodium hydroxide was added, and the mixed solution was vigorously stirred. After a while, a light brown precipitate appeared. Then a large excess of concentrated hydrochloric acid was added until the color of the solution became dark green. Within a few minutes, the desired complex began to appear in the form of glittering golden leaflets. After kept standing for an hour, the crystals were filtered and redissolved in slightly acid warm water (near above 50°C in temperature) and reprecipitated by the addition of concentrated hydrochloric acid. The corresponding bromide and perchlorate of the complex* were obtained by the addition of the concentrated corresponding acid to the concentrated solution of the chloride.

**Measurement of the Absorption Spectra.**—When hexahydroxylamine cobalt(III) complex is dissolved in distilled water, it decomposes fairly rapidly. This decomposition can be stopped by the addition of strong acids. Therfore, the absorption spectrum of the complex was measured in 0.1 N perchloric acid solution. In order to know how the absorption spectrum changes with the variation of pH, the absorption spectrum was measured in a buffer solution of pH 4.8. The absorption measurement was carried out using Beckman DU spectrophotometer.

**Determination of the Rate of Decomposition.**—The rate of decomposition of hexahydroxylamine cobalt(III) complex was measured in the following buffer solutions;

Mixture of 0.5 N acetic acid and 0.5 N sodium acetate pH 4.8

Mixture of 0.05 N acetic acid and 0.5 N sodium acetate pH 5.8

The buffer solution was heated to the desired temperature, and in this solution the complex was dissolved quickly, to let the decomposition start. Five cc. of the reacting solution was taken out with a pipette and pourd into 2 cc. of 2 N perchloric acid, to stop the decomposition. At appropriate time-intervals, this procedure was repeated. Thus, we obtained a series of solutions which contained the complex in various concentrations. Therefore, if we can determine the concentration of the complex in these solutions, we can trace the decomposition of the complex. For this purpose, the optical densities of these solutions were measured at several wavelengths near the maximum position of the first absorption band of the complex. The ratios of the optical densities of these solutions to that of the innitial solution give the relative concentrations of the complex. From these values we can trace the decrease in the concentration of the complex in the decomposition process.

4) A. Werner und E. Berl, Ber., **38**, 893 (1905).

* The crystals of bromide and chloride cannot be preserved for a long time, because they change gradually into the cobaltous salt even in a closed vessel. On the contrary, perchlorate does not change even in summer or in the sunlight, in the absence of moisture.

## Results

The results of the absorption measurement are shown in Fig. 1 and Table I. In the Table are listed also the maximum positions of the first and the second absorption band of other hexammine cobalt (III) complexes hitherto measured.

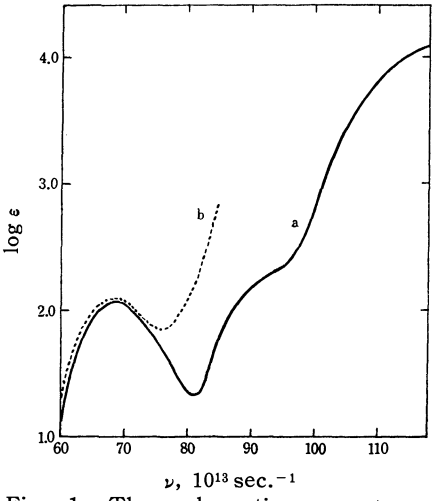



Fig. 1. The absorption spectra of $[Co(NH_2OH)_6](ClO_4)_3$.
a) in 0.1 N $HClO_4$.
b) in the buffer solution of pH 4.8.

The results of the measurement of the rate of decomposition of the complex are represented in Figs. 2 and 3. Each curve in these figures can be transformed into a straight line, when the logarithmic value of the concentration is taken as an ordinate and the time as an abscissa. This indicates that the decomposition of the complex proceeds apparently in the form of the first order reaction. The rate constants of the reaction are as follows: in the solution of pH 4.8 at 50°C 0.0990min.

TABLE I

MAXIMUM POSITIONS OF THE FIRST AND THE SECOND ABSORPTION BAND OF COBALT(III) HEXAMINE COMPLEXES (in $10^{13}$ sec.$^{-1}$ unit)

| Complex | pK of the co-ordinating amine | 1st Band | 2nd Band |
|---|---|---|---|
| $[Co(NH_2OH)_6]^{3+}$ | 6.03[5] | 68.5 (log ε 2.07) | ca. 94 (log ε ca. 2.3) |
| $[Co\ en_3]^{3+}$ | 8.55*[6] | 63.9 | 88.4 |
| $[Co(NH_3)_6]^{3+}$ | 9.25[7] | 62.9 | 88.3 |
| $[Co(NH_3)_4(CH_3NH_2)_2]^{3+}$ | 10.63**[7] | 61.9 | 86.3 |

* mean value of $pK_1$ 7.19 and $pK_2$ 9.92

** $pK_a$ of $CH_3NH_2$

liter mole., 45°C 0.0462 and 40°C 0.0198; in the solution of pH 5.8 at 35°C 0.0815 min. liter mole., 30°C 0.0347 and 25°C 0.0139.

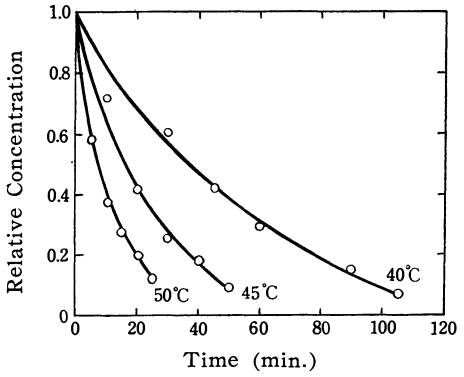



Fig. 2. Decomposition of $[Co(NH_2OH)_6](ClO_4)_3$ in the buffer solution of pH 4.8.

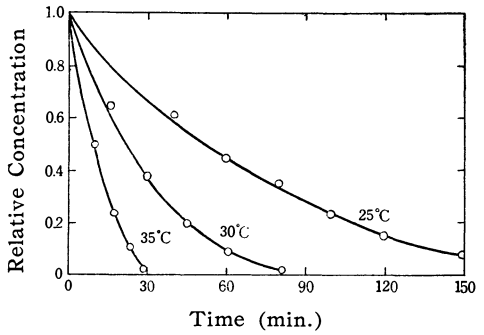



Fig. 3. Decomposition of $[Co(NH_2OH)_6](ClO_4)_3$ in the buffer solution of pH 5.8.

Taking the logarithmic values of these rate constants as an ordinate, and the reciprocals of the absolute temperatures as an abscissa, a straight line is obtained. From its slope, the activation energy is calculated to be 32.5 kcal mole$^{-1}$. As the two straight lines in Fig. 4 are parallel it is concluded that the activation energy is independent of the variation of pH. Besides, as the ordinate-interval between the two lines is unity, it is concluded that the reaction rate is proportional to the concentration of the hydroxyl ion.

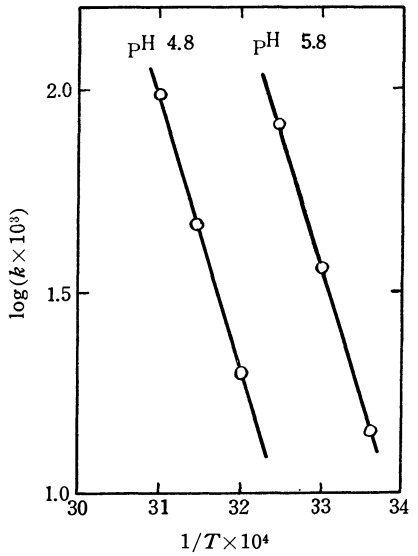



Fig. 4. Determination of the activation energy for the decomposition of $[Co(NH_2OH)_6](ClO_4)_3$ from plots of log $k$ against $1/T°$.
a) log $k$ for pH 4.8.
b) log $k$ for pH 5.8.

## Discussion

As expected, the first and the second absorption bands of hydroxylamine cobalt (III) complex lie much farther in the shorter wavelength than those of other hexammine cobalt(III) complexes hitherto measured. In addition, as is easily seen in Table I, both the first and the second absorption band of hexammine cobalt(III) complexes show the blue shift with the increase in the acid dissociation constants

5) H. Hagisawa, Bull. Inst. Phys. Chem. Research, Tokyo, **20**, 251 (1954).
6) G. A. Carlson, J. P. McReynolds and F. H. Verhoek, *J. Am. Chem. Soc.*, **67**, 1334 (1945).
7) H. S. Harned and B. B. Owen, ibid. **52**, 5079 (1930).
8) Y. Shimura and R. Tsuchida, This Bulletin, **29**, 311 (1956).
9) J. Brigando, *Compt. rend.*, **236**, 708 (1953).

of the co-ordinating amine. This fact indicates that the weaker the basic strength the co-ordinating amine has, the more strongly it combines with the central cobalt(III) ion. This tendency can be concluded also from the marked red shift of the charge transfer band of hexahydroxylamine cobalt(III) complex compared with that of hexa-ammonia cobalt(III) complex. In the free state, both hydroxylamine and ammonia have the absorption band in the shorter wavelength region near 2000 Å. This absorption band of hydroxylamine shows a marked red shift when it is co-ordianted to the cobalt(III) ion and this band is superposed partly upon the second absorption band of the complex. In contrast to this, the absorption band of ammonia shows only a slight red shift in the co-ordinated state. Here, it is noteworthy that in the case of the hydroxylamine complex the red shift of such a charge transfer band becomes much more marked as the pH of the solution increases, and conceals completely the second absorption band. This indicates that the interaction between the central cobalt(III) ion and the co-ordinating hydroxylamine increases when the pH of the solution increases. Such a marked change of the charge transfer band was not observed in the case of the ammonia complex, so far as the perchlorate of the complex was concerned. Such a strong interaction between hydroxylamine and the cobalt(III) ion was presumed from the method of preparation of hexahydroxylamine cobalt(III) chloride. As described in the experimental part, hydroxylamine can expel even ethylenediamine from its co-ordination sphere, which is very firmly linked to the central cobalt(III) ion.

When the electronic cloud of the nitrogen atom of hydroxylamine penetrates so deeply into the central cobalt(III) ion, we can expect the relaxation of the N–H bond, which facilitates the proton dissociation in an aqueous solution. Therefore, the following equilibrium may be formed;

$$[Co(NH_2OH)_6]^{3+} + H_2O \rightleftarrows [Co(NH_2OH)_5NHOH]^{2+} + H_3O^+$$

$[Co(NH_2OH)_5NHOH]^{2+}$ thus produced is regarded as the intermediate toward the reduction of the complex. The main reason why hydroxylamine having a strong reducing power does not reduce the cobalt (III) ion and can coexist with the cobalt (III) ion within the hexahydroxylamine cobalt(III) ion, can be attributable to the fact that six co-ordinating hydroxylamine molecules contend with each other and cancel the polarizing power of the cobalt (III) ion. When this balance is lost by the proton dissociation from one co-ordinating hydroxylamine, other hydroxylamine molecules are subjected to the increased polarizing power of the central cobalt(III) ion, so that an electron is easily snatched up by the central cobalt (III) ion, resulting in complete reduction. This is based upon the following empirical rule: the electronic cloud of the ligand, which has lost a proton, must penetrate into the central cobalt(III) ion much more weakly than that of the ligand which keeps a proton. This means that the $NHOH^-$ group is linked to the cobalt(III) ion less covalently and less firmly than the hydroxylamine molecule. As is seen from its position in the spectrochemical series, water is linked to the cobalt(III) ion much more strongly than the hydroxyl ion. A similar relation may be expected in the case of hydroxylamine and $NHOH^-$ too. In fact, the first absorption band of hexahydroxylamine cobalt(III) complex ion makes a slight red shift, when the pH of the solution increases. As the percentage of the complex which has lost a proton must increase more in a weakly acid solution than in a strongly acid solution, and as the red shift means that the field set up by the ligands decreases, the above mentioned red shift suggests that the $NHOH^-$ group is linked to the cobalt (III) ion less firmly than the hydroxylamine molecule. Thus, when one co-ordinating hydroxylamine becomes a less polarizable $NHOH^-$, the degree of the charge neutralization of the central cobalt (III) ion by the co-ordinating electrons of the donor atoms decreases, and consequently, the remaining hydroxylamine molecules in the complex radical is polarized more strongly by the central cobalt (III) ion. Such an increase in polarization induces the reduction. Therfore, if we could depress the proton dissociation by some means, the decomposition of the complex would not take place. Indeed, in a strongly acid solution the decomposition of the complex does not occur. This is the present author's interpretation. With this view, we can understand the cause why penta-, tetra-, and tri-hydroxylamine cobalt(III) complexes such as $[Co(NH_2OH)_5Cl]^{2+}$, $[Co(NH_2OH)_4CO_3]^+$, and

$[Co(NH_2OH)_3(H_2O)_3]^{3+}$ can not be obtained. Even if such complxes could be prepared, the large polarizing power of the central cobalt(III) ion would polarize hydroxylamine over its limit, and the reduction of cobalt(III) to cobalt(II) would take place. Accordingly, if we chose the ligand which decreases the polarizing power of the central cobalt(III) ion very much, we could obtain the cobalt(III) complex containing hydroxylamine. As one of such ligands we know the dimethylglyoximato group*.

The above mentioned view was confirmed further by the investigation of the decomposition of the hexahydroxylamine cobalt (III) complex in an aqueous solution. The result shows that rate of decomposition of the complex is proportional to the concentration of the hydroxyl ion as well as to the concentration of the complex ion. This fact indicates that although the decomposition of the complex is apparently a reaction of the first order in the complex ion, in fact, the rate-determining step of the decomposition is second order in the hydroxyl ion as well as in the complex ion. As such a reaction of the second order in the hydroxyl ion and the complex ion, we can assume the substitution reaction as well as the proton dissociation, such as

*substitution*

$$[Co(NH_2OH)_6]^{3+}+OH^- \rightarrow [Co(NH_2OH)_5OH]^{2+}+NH_2OH$$

*proton dissociation*

$$[Co(NH_2OH)_6]^{3+}+OH^- \rightarrow [Co(NH_2OH)_5NHOH]^{2+}+H_2O$$

But as is already stated, the spectrochemical consideration reveals that hydroxylamine is linked to the cobalt(III) ion more firmly than ammonia and that the hydroxyl ion is linked to the cobalt(III) ion less firmly than ammonia. Accordingly, the possibility of substituting the hydroxylamine can be excluded, and the proton dissociation can be regarded as the only possible rate-determining step of the decomposition.

* According to Nakahara's report, the dimethylglyoximato group is situated ahead of ethylenediamine in the spectrochemical series, and forms a strongly covalent bond with the central cobalt(III) ion. A. Nakahara, This Bulletin, **27**, 260 (1954).

## Summary

The absorption spectrum of hexahydroxylamine cobalt(III) complex was measured and compared with the hitherto obtained data of the other hexammine cobalt(III) complexes. The frequencies of the first and second absorption bands of this complex were $68.5\times10^{13}$ and ca. $94\times10^{13}$ sec.$^{-1}$ respectively. These values are much greater than those found in other hexammine cobalt(III) complexes, and this fact may indicate the strong interaction between the central cobalt(III) ion and nitrogen atoms of the co-ordinating hydroxylamine. In addition to the study of absorption spectra, the rate of decomposition of this complex was measured. The rate of decomposition was proportional to the concentration of the hydroxyl ion, and the activation energy was 32.5 kcal. mole$^{-1}$. In order to explain the above results, the following equilibrium, assuming the proton dissociation, was proposed;

$$[Co(NH_2OH)_6]^{3+}+H_2O \rightleftarrows [Co(NH_2OH)_5NHOH]^{2+}+H^3O^+$$

The author wishes to express his sincere thanks to Professor R. Tsuchida of Osaka University for his kind advice and encouragement during this work. The author's appreciation is also expressed to Professor O. Nagai of Wakayama Medical College, who gave the author a chance to use a Beckman DU spectrophotometer, to Mr. S. Kida for his valuable discussion, and to Mr. Y. Morimoto for his experimental help.

*Department of Chemistry,*
*Wakayama University,*
*Wakayama*

# *Crystalline Cypridina Luciferin*

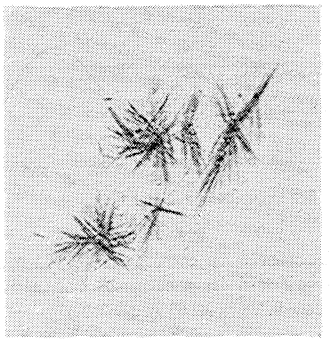
By Osamu SHIMOMURA, Toshio GOTO and Yoshimasa HIRATA

(Received June 3, 1957)

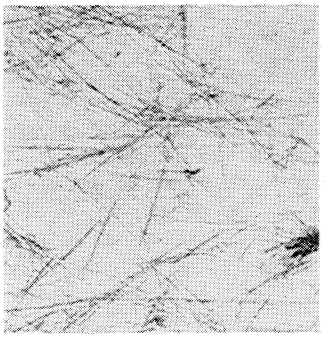
The luminescence of *Cypridina hilgendorfii* has been investigated so far by many workers[1], including Anderson, Kanda and Harvey, and it has been found that firefly luminescence requires ATP and magnesium ion as well as luciferin, luciferase and oxygen for its functioning, whereas *Cypridina* requires only the last three. *Cypridina* luciferin is therefore the simplest system and is most suited for investigating the phenomenon of biological luminescence. For the study of the chemical constitution of *Cypridina* luciferin, it is necessary to obtain pure luciferin. Among several studies concerning the purification of luciferin, the most valuable one is Anderson's benzoylation method[2] reported about twenty years ago. Recently various purification methods have been attempted by Mason[3] and by Tsuji[4]; however, luciferin has as yet not been obtained crystalline. Nevertheless many views relating to the constitution of luciferin have been submitted, including proteose, phospholipid, polyhydroxy benzene, hydroquinones, flavoprotein and chromopeptide[5]. Recently, Mason[7] and Tsuji[5] found that the acid hydrolysis of luciferin afforded many kinds of amino acids.

We have carried out the purification of luciferin and have succeeded in obtaining it crystalline. Investigations on the constitution of luciferin using the crystalline luciferin has also been carried out and preliminary results are reported herewith.

**Isolation and crystallization of luciferin.** — Pulverized dry *Cypridina hilgendorfii* was de-fatted with benzene and extracted with methanol in hydrogen atmosphere. The extract was purified according to a modified Anderson's benzoylation method[2] and by means of partition chromatography on cellulose powder to obtain "purified" luciferin. Acidification of the purified luciferin solution with hydrochloric acid afforded crystalline luciferin as orange-red needles (Fig. 1).



(×370)
Crystalline Luciferin



(×280)
Oxyluciferin A
Fig. 1

Crystalline luciferin melted at 182—195° (darkened at 175°) it is easily soluble in methanol and ethanol, soluble with difficulty in water and acetone, and insoluble in ether and benzene. The luminescent activity induced by luciferase is 37,000 times as intense as that of the starting material, dry *Cypridina hilgendorfii*. Ninhydrin- and *p*-dimethylaminobenzaldehyde-test were negative. When heated with lime, it decomposed with a skatole-like odor, and the molybdenum blue reaction of its residue was negative. Accordingly, phosphoric acid is probably

1) E. N. Harvey: "Bioluminescence", Academic Press Inc. Publishers, New York, 299 (1952).
2) R. S. Anderson; *J. Gen. Physiol.*, **19**, 301 (1935).
3) H. S. Mason and E. F. Davis; *J. Biol. Chem.*, **197**, 41 (1952).
4) F. 1. Tsuji; *Arch. Biochem. and Biophys.*, **59**, 452 (1955).
5) F. I. Tsuji, A. M. Chase, E. N. Harvey; F. H. Johnson: "The Luminescence of Biological Systems", American Association for the Advancement of Science, p. 127—156 (1955).

absent in luciferin. Ultra-violet and visible spectra of crystalline luciferin were nearly identical with those measured by Chase[6] and Tsuji[5] but the absorption at 435 mμ of the present sample was much stronger (Fig. 2).

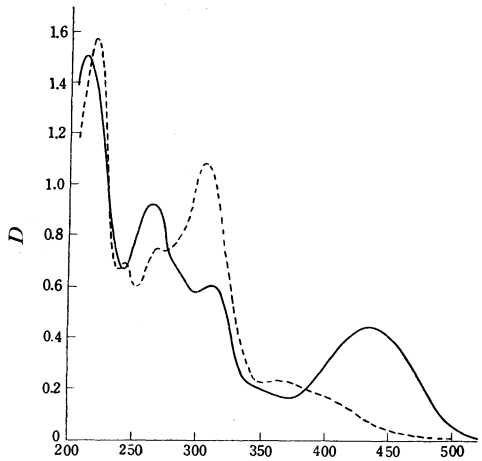



Fig. 2

—— Luciferin in methanol (0.161 mg/5 cc.)
---- Luciferin in methanol containing HCl (ca. 0.1 N) (0.161 mg/5 cc.)

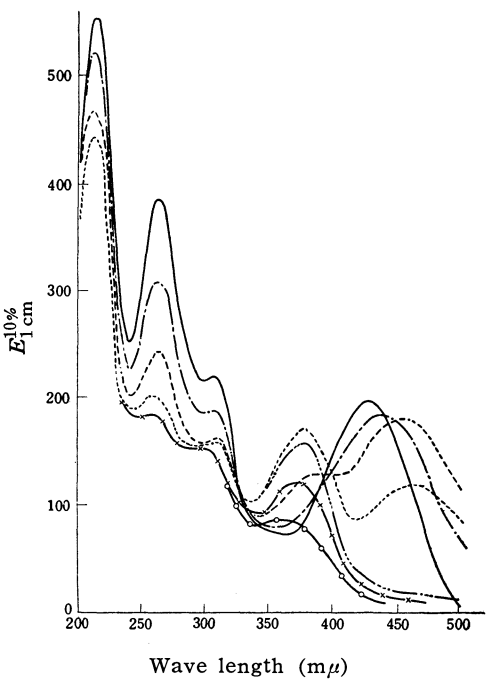



Fig. 3. Aq. luciferin solution (pH 5.6 phosphate buffer).

——— freshly dissolved
— — — after 7 hrs.
------ after 1 day
--------- after 3 days
—·—·— after 7 days
—×— after 12 days
—○— after 52 days

**Oxidation of luciferin.**—When an aqueous solution of luciferin was allowed to stand in the air, its color changed gradually from yellow to red, and finally became almost colorless. The change of its UV absorption spectra is shown in Fig. 3. After being allowed to stand for 2 days, an ethanolic solution of luciferin afforded three spots as revealed by means of paper chromatography, i. e., one spot was a red colored substance and the other two were colorless blue-fluorescent substances (they were named oxyluciferin A and B) (solvent: ethyl acetate : ethanol : water, 5 : 2 : 3, Rf 0.97, 0.9 and 0.7, respectively). These substances were separated by the method of cellulose powder partition chromatography. The aqueous solutions of these substances were allowed to stand for a few days. Though the solutions of A and B were almost unchanged, the solution of the red substance was decolorized and afforded oxyluciferin A and B. These experiments and the UV absorption spectra suggest that luciferin is oxidized by at least three steps in the air; i. e., luciferin is first oxidized to the red substance ($\lambda_{max.}$ ca. 465 mμ), subsequently to oxyluciferin A and B ($\lambda_{max.}$ ca. 380 mμ in Fig. 2), and finally decomposed to unknown substances which show no fluorescence and no definite ultraviolet absorption except a maximum at 210 mμ.

The red substance has no luminescence activity, and is decolorized by addition of sodium borohydride. Its color is changed to a bluish violet by addition of concentrated sodium hydroxide solution. The red substance can be obtained easily by oxidation of luciferin with potassium ferricyanide (Fig. 4), though other oxidants oxidize luciferin to colorless substances directly.

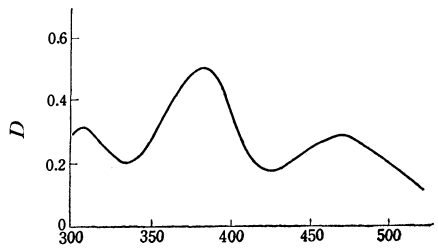



Fig. 4.

6) A. M. Chase and E. H. Brigham, *J. Biol. Chem.*, **190**, 529 (1951).
7) H. S. Mason, *J. Am. Chem. Soc.*, **74**, 4727 (1952).

Oxyluciferin A and B can be obtained in a good yield by addition of ammonia to the luciferin solution. Oxyluciferin A is obtained as yellow needles and melts at 140—148° (darkens at 135°) (Fig. 1).

Oxyluciferin B could not be obtained crystalline and became dark red upon addition of concentrated hydrochloric acid. Oxyluciferin A and B may be very similar substances, because their UV absorption spectra (Fig. 5) and their hydrolysis products (mentioned below) are very similar.

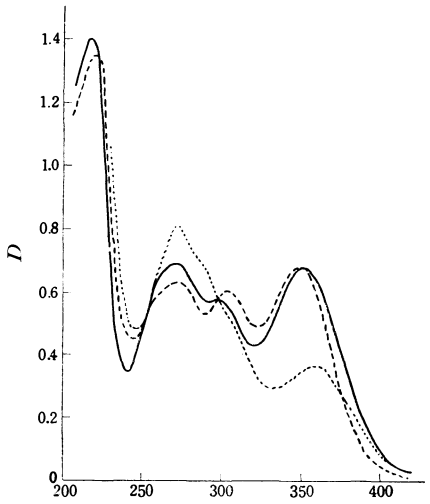



Fig. 5

—— A in phosphate buffer (pH 5.6) 0.084 mg/3 cc.
---- A in MeOH 0.123 mg./3 cc.
------ B in MeOH concn. unknown.

The oxidative decomposition of an aqueous solution of luciferin by air is also influenced by the pH of the solution. Generally, in an acidic medium the oxidation rate is slow and the red substance is stable for a long time, but in an alkaline medium the rate is very great and a yellowish green fluorescent substance is produced as well as A and B. When luciferin was decomposed by luciferase, luminescence occurred and the reaction mixture consisted mainly of oxyluciferin A and a small amount of B.

**Hydrogenation of luciferin.**—Hydrogenation of luciferin in methanol with Adams' platinum oxide catalyst afforded a colorless substance, the ultraviolet absorption spectrum of which was very similar to that of tryptophan or tryptamine (Fig. 6). The difference in the log $D$ values at 220 and 280 mμ is 0.755, and this value is almost equal to that of tryptophan (0.79) or tryptamine (0.70). It is, therefore, apparent that these two absorption maxima originate in an indole type chromophore and are not caused by overlapping absorptions. Moreover the absorption intensity of hydroluciferin at 220 mμ is stronger than that of luciferin before hydrogenation. These observations suggest that the indole

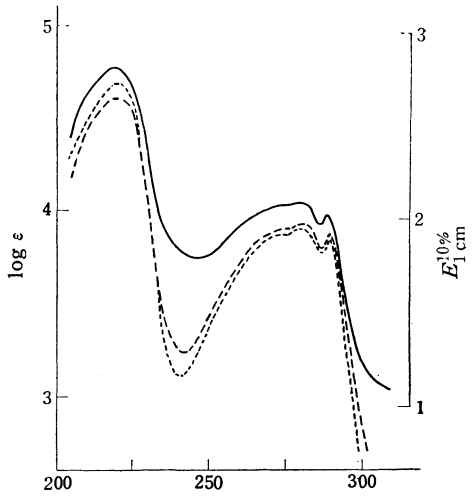



Fig. 6.

—— Hydroluciferin (right scale)
---- Tryptamine } (left scale)
------ Tryptophan }
in methanol

structure in hydroluciferin does not exist in luciferin, but is produced during hydrogenation. Hydrogenation of oxyluciferin A did not afford a substance which has an indole type absorption. The portion which is responsible for the indole type absorption after hydrogenation may be destroyed during oxidation of luciferin to oxyluciferin A. This observation is consistent with the fact that luciferin, and oxyluciferin A and B do not give positive reactions with p-dimethylaminobenzaldehyde (indole test), whereas hydroluciferin affords a positive reaction.

**Hydrolysis of luciferin.**—Acid hydrolysis of luciferin afforded glycine, isoleucine and a fluorescent substance. Hydrolysis of luciferin with barium hydroxide afforded glycine, isoleucine, a strong ninhydrin positive substance, a fairly large amount of anthranilic acid, and a small amount of indole or indole acetic acid, but no tryptophan. Since tryptophan is readily subject to oxidation, it was considered that tryptophan was decomposed during hydrolysis. Accordingly, the alkali hydrolysis was carried out in the presence

of small amounts of cystein as an antioxidant. Though tryptophan was not obtained either a new ninhydrin positive spot was obtained and identified to be tryptamine; in this case the amount of anthranilic acid was decreased.

## Discussion

Acid hydrolysis of crystalline luciferin afforded only two amino acids, glycine and isoleucine; this reult is very different from that of Mason[7] and Tsuji[5], who obtained the following amino acids from the acid hydrolysate of "purified" luciferin: (Tsuji) arginine, leucine, isoleucine, glutamic acid, alanine, valine, sarcosine, lysine, taurine and methionine, and either aspartic acid, threonine, or serine; (Mason) taurine, aspartic acid, threonine, serine, sarcosine, glutamic acid, proline glysine, alanine, valine, methionine, isoleucine, leucine, tyrosine, phenylalanine, lysine, histidine and arginine. Acid hydrolysis of the "purified" luciferin obtained by the present authors also afforded at least eight amino acids and a fluorescent substance. Since crystalline luciferin and "purified" luciferin have the same $R_f$ values on paper chromatography in hydrogen atmosphere, it is assumed that the extra amino acids in the hydrolysate of "purified" luciferin are impurities, which may be contained in luciferin as polypeptides. Since glycine is often produced from other substances by decomposition, care should be taken in order to identify it as one of the constituents, but by means of semi-quantitative paper chromatography it was shown that the amount of glycine was almost the sams as that of isoleucine. Thus glycine is regarded to be a component of luciferin.

The comparison of th UV absorption spectra and of the alkali hydrolysates of various indole derivatives (2-methyl indole, 3-methyl indole, 2,3-dimethyl indole, tetrahydrocarbazole, tryptophan, tryptamine, indole acetic acid, indole, etc.) suggest that anthranilic acid and indole derivatives resulting from hydrolysis of luciferin with barium hydroxide were produced from a $\beta$-substituted indole type moiety in luciferin.

The facts that hydrogenation of luciferin afforded indole type absorption and that hydrogenation of oxyluciferin A did not, suggest that the indole-type structure may be connected with the luminescent activity of luciferin. Comparison of $\varepsilon$ values at 280 m$\mu$ of hydroluciferin and tryptophan or tryptamine leads to the result that the mole equivalent of luciferin for one indole group is ca. 500—800.

## Experimental

Collected *Cypridina* was dried by being exposed to sunlight and then stored in a vacuum desiccator. Five hundred grams of completely dried *Cypridina* was pulverised and packed in the extraction apparatus (Fig. 7). It was defatted by

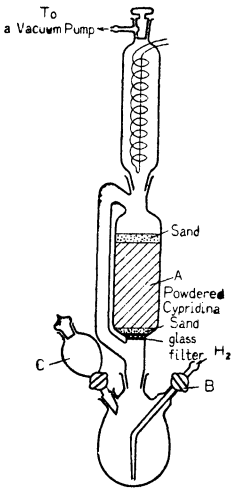



Fig. 7.

refluxing with 1.2 l. of well-dried benzene under reduced pressure (ca. 80 mm.Hg.) for 50 hr. The benzene extract was discarded, wet *Cypridina* was dried in vacuo (about 12 hr.), and then the apparatus was filled with purified hydrogen. The purified hydrogen was obtained by passing hydrogen through a soda-lime tube, red-heated metallic copper packed in a silica tube, and a washing bottle containing concentrated sulfuric acid. Absolute methanol (1.2 l.) was introduced into flask A through funnel C, and the extraction was started under reduced pressure (ca. 80 mm.Hg of hydrogen). After 50 hr. methanol was evaporated in vacuo to give a reddish brown foamy paste. The extraction apparatus was filled again with hydrogen, and 0.5 N hydrochloric acid (850 ml.) was added to the residual paste through funnel C. After being heated at 100°C on a water bath for 10 min. in hydrogen atmosphere, the yellow solution was cooled to about 0° and extracted with ether, at first with 200 ml. and subsequently thrice with 100 ml. The ether extract was discarded. Then the acid solution was extracted several times with *n*-butanol (total ca. 350 ml.), and the butanol extract was purified by a modified Anderson's benzoylation method as follows.

The butanol extract was benzoylated with benzoyl chloride (3 ml. of benzoyl chloride per 100 ml. of butanol soln.) at 0°C. After ten min. the reaction mixture was washed thrice with equal volumes of distilled water within about forty

min. and added to 8 to 10 volumes of water. The aqueous solution was extracted thrice with ether (care was taken to avoid formation of a stable emulsion; total volume ca. 400 ml.). After evaporation of the combined ether extracts to 70 ml. in vacuo, the apparatus was filled with hydrogen and 0.5 N hydrochloric acid (700 ml.) was added to the residual solution. Then benzoyl luciferin was hydrolysed by being heated on a water bath at 100° for half an hour in hydrogen atmosphere. After cooling, the acid solution was extracted with ether to remove impurities, and then with butanol (several times, total volume ca. 200 ml.) to extract luciferin.

The modified Anderson's benzoylation method (above mentioned) was repeated again on the butanol extract. The resulting butanol solution of prified luciferin was neutralized with a saturated sodium bicarbonate solution, and evaporated in vacuo to a red residue.

In the meantime, there was prepared an apparatus for partition chromatography, which was made from a cellulose powder column (2.5×20 cm.), a hydrogen inlet tube, a funnel for addition of solvent to the upper end of the column, and three flasks at the lower end to fractionate eluates. The apparatus was first completely filled with hydrogen, and the cellulose powder column was washed with a developing solvent (ethyl acetate-ethanol-water, 5 : 2 : 3). The red residue was dissolved in a small amount of methanol (2 to 3 ml.), adsorbed on the column and then developed with the developing solvent. The developing band were as follows: 1. blue-fluorescent band, 2. faintly yellow band with bluish green fluorescence, 3. yellow band with yellow fluorescence, 4. blue-fluorescent band, 5. yellow band. The eluate of band 3 contained luciferin and was evaporated to drynes in vacuo. The residue was extracted with a small amount of methanol and evaporated again, when "purified" luciferin was obtained as an orange-colored powder.

The "purified" luciferin was dissolved in dilute methanol and centrifuged from any insoluble materials. The supernatant was acidified with hydrochloric acid and allowed to stand overnight in a desiccator in which hydrogen was substituted and somewhat depressured, upon which orange-red crystals of luciferin precipitated. Yield ca. 3 mg.

**Quantitative estimation of luminescent activity of luciferin.** — Determination of the luminescent activity was carried out by a modified Anderson's apparatus, which will be reported in a separate paper.

**Preparation of luciferase solution for luminescent test of luciferin.**—The dry residue of methanol extract of *Cypridina* (20 g.) was added to 200 ml. of water, the mixture was allowed to stand overnight and filterd. The filtrate was dialysed using cellophan for 24 hr, the dialysate was once frozen, remelted and filtered. The filtrate was diluted with water to 200 ml.

**Oxidation of luciferin with ferricyanide.**—To the methanol solution of luciferin was added saturated potassium ferricyanide solution, and the reaction mixture was centrifuged. The supernatant was evaporated to dryness in vacuo and the residue extracted with a small quantity of methanol to measure the ultraviolet absorption spectrum (Fig. 4).

**Preparation of Oxyluciferin A and B.**—One drop aqueous ammonia was added to the luciferin solution and allowed to stand overnight. The reaction mixture was evaporated to dryness and chromatographed on a cellulose powder column (solvent system; ethylacetate-ethanol-water, 5 : 2:3). Oxyluciferin A and B were eluted in separate fractions. Crystalline oxyluciferin A was obtained by evaporating fraction A, dissolving the residue in water and acidifying with hydrochloric acid; the crystals were re-crystallized from a mixture of methanol and diluted hydrochloric acid. Oxyluciferin B was not obtained crystalline. The ultraviolet absorption spectra are shown in Fig. 5. Oxyluciferin A and B are easily soluble in methanol and ethanol, but insoluble in benzene and ether.

**Hydrogenation of luciferin.**—After measurement of the UV absorption spectrum, the methanol solution of crystalline luciferin (ca. 50 $\gamma$ in 2 ml.) was hydrogenated with ca. 0.1 mg. of Adams' platinum oxide catalyst. When the solution became almost colorless (ca. 24 hr.), the catalyst was removed by filtration and the UV absorption spectrum of the filtrate measured (Fig. 6). The amount of absorbed hydrogen could not be measured because of its minute quantity.

**General procedure for hydrolysis.** — *Acid hydrolysis.* — The subtsance to be hydrolysed (100—200 $\gamma$) as heated with 0.5 ml. of 4 N hydrochloric acid at 100—105° for 12 hr. in a sealed glass tube, and the hydrolysate evaporated to dryness in vacuo.

*Alkali hydolysis.*—The substances (100—200 $\gamma$) was heated with 0.5 ml. of 10% barium hydroxide at 100—105° for 12 hr., the hydrolysate was diluted with equal volumes of water and slightly acidified with diluted sulfuric acid. After being heated on a water bath for a few minutes, the precipitated barium sulfate was contrifuged, and the supernatant was evaporated in vacuo. The hydrolysates were analysed by means of paper chromatography.

**Paper chromatography of the hydrolysates.**—Toyo filter paper No. 51 was used for this purpose (ascending method). Solvent butanol-acetic acid-water (4 : 1 : 1) or 2,6-lutidine-water (3 : 2).

The authors express their gratitude to Dr. Y. Haneda, the Curator of Yokosuka Museum, and Professor N. Nakamura, Tokyo University, for collection of *Cypridina*, and to Professor T. Sato, Nagoya University, for taking the photographs of the crystals.

*Chemical Department, Nagoya University, Chikusa-ku, Nagoya*

# SHORT COMMUNICATIONS

## *Tryptic Cleavage of Synthetic Poly-ε-aminocaproyl-α-amino Acids*

By Mituo EBATA

(Received August 15, 1957)

The syntheses of several linear poly-ε-aminocaproyl-α-amino acids such as poly-ε-aminocaproyl-D, L-alanine (M. W. 21,800)[1], poly-ε-aminocaproyl-L-alanine (M. W. 7,000)[2], poly-ε-aminocaproyl-L-phenylalanine (M. W. 51,200)[3], poly-ε-aminocaproyl-α-aminoisobutyric acid (M. W. 35,000)[4], poly-ε-aminocaproyl-L-leucine (M. W. 22.300)[4] and poly-ε-aminocaproylglycine (M. W. 19,300)[4] have recently been achieved by Noguchi and his coworkers, with the aid of their "N-carbothiophenylamino acid method"[5]. Among these synthetic polymers, the alanine and the α-aminoisobutyric acid derivatives, like the Bence Jones protein, possess an unusual property; they are reversibly coagulated by heat in acidic or neutral aqueous solutions[6]. In the present communication, we wish to report that crystalline trypsin of relatively high concentrations can partly hydrolyse these polymers.

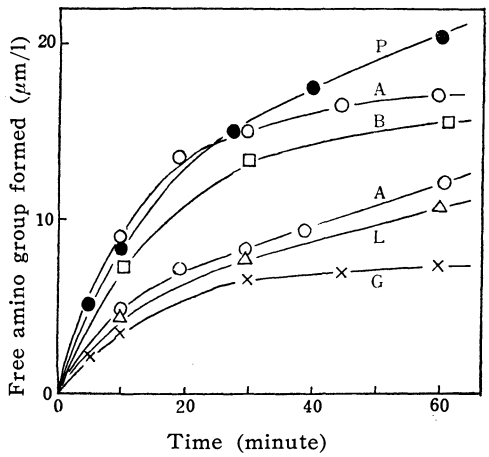



Fig. 1. Hydrolyses of poly-ε-aminocaproyl-α-amino acids by trypsin.
P, poly-ε-aminocaproyl-L-phenylalanine; A, poly-ε-aminocaproyl-D, L-alanine (above); A, poly-ε-aminocaproyl-L-alanine (bellow); B, poly-ε-aminocaproyl-α-aminoisobutyric acid; L, poly-ε-aminocaproyl-L-leucine; G, poly-ε-aminocaproylglycine.
Each reaction mixture contained 0.2 per cent of polymer, 185 μg. of twice recrystallized trypsin, and 0.013 M phosphate buffer (pH 7.1) in a final volume of 5.0 ml. Incubation was carried out at 25°.

As can be seen from Fig. 1, a considerable hydrolysis of several poly-ε-aminocaproyl-α-amino acids has occurred with 37 μg. per ml. of twice recrystallized trypsin, as evidenced in Fig. 1 by the appearance of free amino groups. The free amino groups were determined by the ninhydrin method according to Moore and Stein[7]. The viscosity of the reaction mixture decreased as the hydrolysis proceeded. No detectable hydrolysis was observed when the concentration of trypsin was reduced to 7 μg. per ml., a concentration of the enzyme suitable for its usual substrates. The polymers were resistant against the action of crystalline α-chymotrypsin and carboxypeptidase of high concentrations under the same conditions.

A search for the cleavage products of poly-ε-aminocaproyl-D, L-alanine by quantitative paper chromatography revealed that about a half mole of ε-aminocaproic acid and alanine, together with a large amount of dialysable fragments, were released from one molecule of the polymer. This suggests that the ε-aminocaproic acid and the alanine were derived from the N-terminal and the next amino acid residues of the polymer, respectively, assuming that the D-linkages were not split by the action of trypsin. The dialysable fragments yielded ε-aminocaproic acid and alanine on hydolysis with hydrochloric

1) J. Noguchi, T. Hayakawa, J. Suzuki and M. Ebata, *J. Chem. Soc. Japan, Pure Chem. Sec.* **76**, 648 (1955).
2) M. Ebata, J. Biochem. (Japan), will be published.
3) J. Noguchi, T. Hayakawa and T. Motoi, *J. Chem. Soc. Japan, Pure Chem. Sec.* **76**, 645 (1955).
4) J. Noguchi, M. Ebata and T. Saito, ibid., **77**, 469 (1956).
5) J. Noguchi and T. Hayakawa *J. Am. Chem. Soc.*, **76**, 2846 (1954).
6) J. Noguchi, T. Hayakawa and M. Ebata, *J. Polymer Sci.*, **23**, 843 (1957).
7) S. Moore and W. H. Stein, *J. Biol. Chem.*, **176**, 367 (1948).

acid, and their mean degree of polymerization was estimated to be 6.

Information available up to date show that only lysyl and arginyl peptide or ester linkages are susceptible to the tryptic attack[8,9]. The results reported here, however, clearly indicate that poly-ε-aminocaproyl-α-amino acids can also be hydrolysed by the action of the proteolytic enzyme when relatively high concentrations of the enzyme are employed. It is interesting, in this connection, to note that ε-aminocaproic acid possesses a structure corresponding to α-deaminolysine. In the polymers of ε-aminocaproyl-α-amino acids, the ε-amino group, except for that of the N-terminal residue, is not in a free state. This is remarkable since the free amino groups of lysyl and arginyl residues have been believed to be required for the tryptic hydrolysis of the susceptible compounds.

Thus, the finding described above has an important bearing on the substrate specificity of trypsin and calls for a more extensive study on this point, using a number of synthetic substrates. An investigation along this line is now being carried out in our laboratory.

The author wishes to express his thanks to Professor J. Noguchi of this university, Dr. R. Sato, Osaka University and to Dr. N. Sakota, Dainippon Zoki Laboratory, for their kind encouragements throughout the course of this study.

*Department of Chemistry, Faculty of Science, Kanazawa University, Kanazawa*

8) M. Bergmann and J. S. Fruton, "*Advances in Enzymol.*" vol. I, 63 (1941).
9) G. W. Schwert., H. Neurath, S. Kaufman and J. E. Snoke, *J. Biol. Chem.*, **172** 221 (1948).

## *The Degree of Polarization of Dichroic Polarizer of Polyvinyl Alcohol-Iodine in the Region of 240–1000 mμ*

By Yoshié Tanizaki

(Received July 24, 1957)

Descriptions were given of the nature and the optical properties of several kinds of sheet polarizer[1], and of the quantitative expressions of partial dichroic polarizers[2]. But most attention was merely confined to the visible light. The present communication shows the degree of polarization, extending from 240 mμ to 1000 mμ, of a dichroic polarizer which is made by stretching the sheet of polyvinyl alcohol-iodine colored in a deep blue.

PVA (abbreviation for polyvinyl alcohol) of which the degree of polymerization was about 1500 was served to make sheet. The preparation of the sheet was described in another place[3]. The iodine solution in which the PVA sheet was soaked was prepared as the aqueous solution in the following percentages: iodine (0.1–1 g. %), ammonium iodide (2.5 times as much as iodine), sodium iodide (the same as ammonium iodide) and boric acid (5 g. %). The PVA sheet soaked in the above solution was colored in a deep blue within ten or twenty seconds. The colored sheet was stretched about five times its length in the aqueous solution of 5 % boric acid keeping about 40°C. Thus the sheet polarizer was prepared. Such a sheet looks almost neutral in color when viewed in unpolarized light, but it looks a remarkably deep blue when viewed in linerly polarized light with the electric vector parallel with the stretch direction.

Now, the degree of polarization $V$ of the light transmitted by a single polarizer is expressed in terms of the principal transmissions $k_y$ and $k_z$ as follows:

$$V=\frac{k_y-k_z}{k_y+k_z} \tag{1}$$

where $k_y$ is the transmission for the incident light completely and linerly polarized when the electric vector is at right angles to the stretch direction, and similarly $k_z$ is the corresponding transmission when the electric vector is parallel with the stretch direction. On the other hand, for the incident unpolarized light, each of the transmissions $H_{\parallel}$ and $H_{\perp}$ of two identical partial polarizers, whose corresponding directions are respectively parallel and crossed, can be associated with $k_y$ and $k_z$ as follows[2];

$$\begin{aligned} H_{\parallel}&=\frac{1}{2}(k_y^2+k_z^2) \\ H_{\perp}&=k_yk_z \end{aligned} \tag{2}$$

1) E. H. Land *J. Opt. Soc. Am.* **41**, 957 (1951).
2) C. D. West and R. Clark Jones, *J. Opt. Soc. Am.* **41**, 976 (1951).
3) Y. Tanizaki and N. Ando, *J. Chem. Soc. Japan, Pure Chem. Sec.* **78**, 542 (1957).

Then, in this case, the degree of polarization $V(\%)$ of the light transmitted by a single partial polarizer is also given by

$$V=\left(\frac{H_{\parallel}-H_{\perp}}{H_{\parallel}+H_{\perp}}\right)^{\frac{1}{2}}\times 100(\%) \qquad (3)$$

The Beckman DU spectrophotometer was used to measure the transmissions $H_{\parallel}$ and $H_{\perp}$ according to the procedure repotred previously[3]. One of the experimental results is shown, as a typical example, by the solid lines in Fig. 1. In

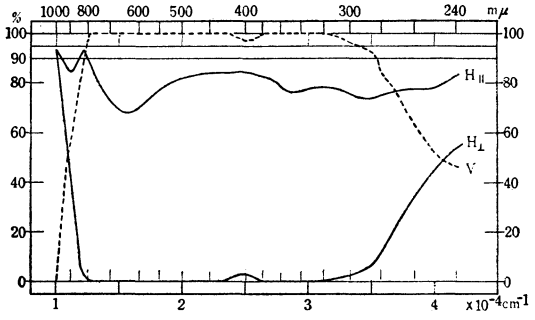



Fig. 1.

the same figure the dotted line indicates the degree of polarization, calculated from equation (3), of the light transmitted by the single sheet. The curve $V$ shows that the degree of polarization is higher than 95 % in 295–800 mμ and is almost 100% in 320–380mμ and 420–790mμ. In case of this measurement the partially polarized incident light of the spectrophotometer (e. g., about 5 % at 500 mμ) was disregarded for the degree of polarization, and the correction for reflection at (four) surfaces of sheet polarizers had not been carried out. If these neglected values are taken into account, the $V$ values all over the region will certainly become higher. It is interesting to notice that the pair of sheet polarizers, piled so as to cross their stretch directions, cuts off sharply the light in 250–800 mμ, as shown by the $H_{\perp}$ curve in Fig. 1.

This kind of sheet polarizer prepared under some conditions is not only of practical use[1] but also useful for some investigation[3], because this sheet has a high degree of polarization in the considerably broad region in wavelength and the sheet polarizer itself is comparatively stable. In our laboratory, more than two years have passed since the sheet polarizer was made and set in the filter hole of the spectrophotometer, but it has been kept in the same optical property as described above.

The author wishes to express his gratitude to Mr. T. Kobayashi, who assisted the author in the experiment, and also to Mr. T. Yoda for helpful advice regarding the preparation of the iodine solution.

*Laboratory of Physical Chemistry,*
*Tokyo Institute of Technology,*
*Ookayama, Meguro-ku, Tokyo*

# *A New Synthesis of Threonine*

By Mikio SATO, Kenji OKAWA and Shiro AKABORI

(Received July 6, 1957)

Despite a little information available concerning the conversion of glycyl residue to threonyl or seryl residue[1-3], there is as yet no satisfactory method for the synthesis of threonine from glycine or glycyl peptides.

In this paper the authors present a new method for the synthesis of threonine from copper glycinate and acetaldehyde. The possibility for such a method has been suggested from the considerations that the methylene group in copper glycinate may be more active than that in free glycine and that the amino group in the copper salt may be protected from unfavorable side reactions. In the established method, the copper salt of glycine is subjected to the reaction with acetaldehyde in a weakly alkaline aqueous solution at 50–70° for 1–2 hours. After removal of copper and other inorganic salts, a mixture of threonine and allothreonine is obtained in a high yield. It seems likely that the reaction proceeds as shown in Fig. 1. The initial reaction of copper glycinate (I) with acetaldehyde appears to give rise to a coordination state (II) of copper threoninate, which is then transformed into a second coordination state (III). The overall reaction equilibrium is shifted in favor of the formation of threonine, since compound III seems to be more stable than compound II especially in alkaline media. These inferences have been drawn from the following observations: (1) while copper threoninate exhibits low pH values in aqueous solution (below 5), copper glycinate is neutral (pH 7.4), (2) the former is adsorbed on an anion exchange resin of OH-form, while the latter is not, and (3) the light absorption of the former is shifted considerably towards shorter wave-lengths as compared with that of the latter (see

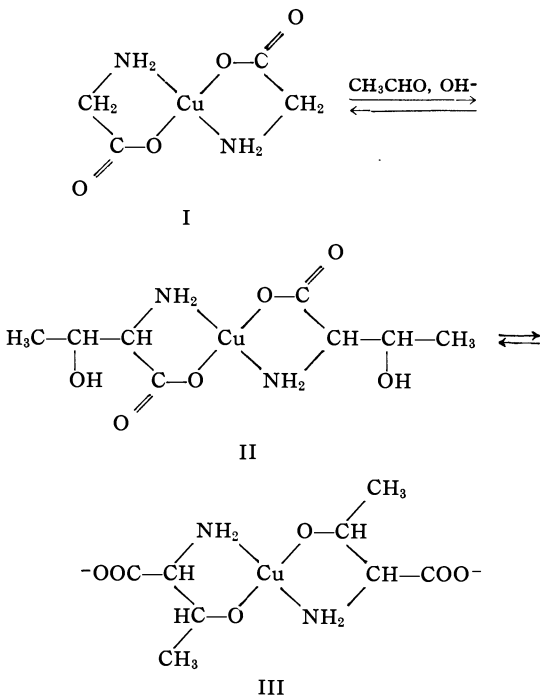



Fig. 1. Mechanism of the threonine synthesis from copper-glycinate and acetaldehyde.

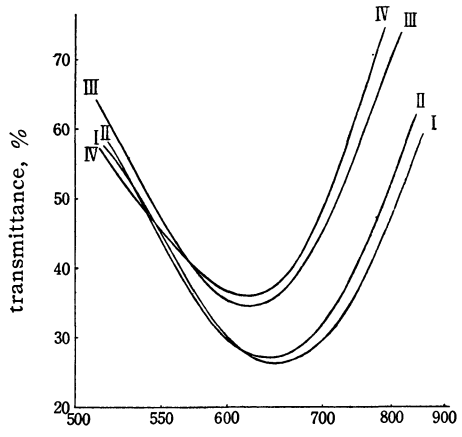



Fig. 2. Absorption spectra of various copper salts (10 μM/ml. of 8% $Na_2CO_3$ solution). (I), copper glycinate; (II), (I)+$CH_3CHO$ at the beginning of the reaction; (III), (I)+$CH_3CHO$ after the reaction; (IV) copper threoninate.

1) E. Snell, D. Metzler and J. Longenecker, *J. Am. Chem. Soc.*, **75**, 2786 (1953); ibid., **76**, 639 (1954).
2) Th. Wieland and K. Dose, *Angew. Chem.*, **66**, 781 (1954).
3) S. Akabori, K. Okawa and M. Sato, This Bulletin, **29**, 608 (1956).

Fig. 2). Copper threoninate is in fact bluish purple in color and resembles "biuret" or complexes of amino-alcohols in this respect.

It is expected from the structural formula of compound III that the threo-form of the copper salt may be stereochemically more stable than the allo-form. In fact it has been shown that the former is always produced predominantly over the latter (the ratio of threo/allo being more than 1.6), although the ratio may vary according to the conditions of the reaction. The results presented in this paper may suggest a possible mechanism of the biosynthesis of threonine*. Further experiments are now in progress to find out more favorable conditions for the selective preparation of the threo-form.

## Experimental

*Copper glycinate* $(NH_2CH_2CO_2)_2Cu \cdot H_2O$.—This was prepared by the two following methods. (a) An aqueous solution of glycine was heated with basic cupric carbonate, the excess of the latter was filtered off from the hot solution, the filtrate concentrated in vacuo and cooled. Crystals of copper glycinate thus formed were collected, washed and dried. (b) Glycine (2 moles) was converted into sodium glycinate in aqueous solution and a saturated solution of cupric sulfate (1 mole) was added with stirring. Crystals of copper glycinate deposited were filtered off, washed three times with water and dried.

*Copper threoninate.*—This was prepared according to the method (a) described for copper glycinate.

*Threonine.*—A mixture of 115 g. of well-ground copper glycinate, 30 g. of anhydrous sodium carbonate, 370 ml. of water and 160 ml. of freshly distilled acetaldehyde was stirred under reflux on a water bath at 50° for 1 hour. After cooling, excess of acetaldehyde was removed by distillation. One liter of water and 700 ml. of concentrated aqueous ammonia (ca. 15 N) were then added and the solution was filtered. The filtrate was passed through a column of Dowex 50X 12 (H-form, 200-400 mesh, 10 cm×20 cm) which had previously been percolated with 5 N aqueous ammonia. The effluent was concentrated in vacuo and treated with charcoal. The solution was again concentrated in vacuo until the crystallization of threonine began, and then about four volumes of methanol were added. After being kept in a refrigerator for 24 hours, the crystals consisting of both threonine and allo-threonine were collected, washed three times with methanol, and dried in vacuo. The yield was 70 g. From the mother liquor, 6 g of almost the same product was obtained. The total yield was 76 g., or 64 %.

The crystals thus obtained gave, on paper chromatograms, only two spots corresponding to threonine and allo-threonine, except for an insignificant spot due to glycine. Chromatographic analysis of the dinitrophenylated crystals using a column of Amberlite-IRC 50[4] showed that the ratio of threonine to allo-threonine was 1.8.

*Anal.* Found: C, 40.34; H, 7.14; N, 11.52. Calcd. for $C_4H_9O_3N$: C, 40.34; H, 7.56; N, 11.76%.

In another experiment, a mixture of 115 g. of copper glycinate, 29 g. of potassium carbonate, 230 ml. of water, and 116 ml. of freshly distilled acetaldehyde, was brought to react by heating at 70° for 2 hours. After acidification with hydrochloric acid, the reaction mixture was treated with hydrogen sulfide and filtered. The filtrate was treated with 400 g. of wet Dowex 50 (H-form), and after being freed from water the substanse was dissolved in absolute alcohol. After removal of the precipitated inorganic salts, the free amino acids were precipitated by the addition of aniline. By repeated recrystallization, 27 g. (22.7 %) of crystals (threo/allo=2.4) was obtained. Further 5.5 g. (4.6 %) of crystals (threo/allo=9) was recovered from the mother liquor. The total yield was 32.5 g. (27.3 %).

## Summary

A new method is described for the synthesis of threonine from acetaldehyde and copper glycinate. This method gives a mixture of allo-threonine and threonine in a high yield (64 %).

*Laboratory of Biochemistry, Faculty of Science, Osaka University*
*Kita-ku, Osaka*

* After we completed this manuscript, we have become aware of a recent report by J. B. Gilbert (*J. Am. Chem. Soc.*, **79**, 2242 (1957)) which shows that a mixture of allo-threonine and threonine can be formed from acetaldehyde and glycine in the presence of an enzyme preparation from rat liver.

4) T. Seki, to be published.

# *A New Balancing Drop Method for the Determination of the Density of Heavy Water*

By Yoshihide NAITO

(Received June 28, 1957)

The usual falling drop method[1] for the determination of the density or the deuterium-concentration of heavy water is based upon Stokes' law; the falling velocity of a drop of sample water through a suitable organic liquid is compared with that of standard water. Consequently in this method the size of the drop must be kept strictly constant and the falling velocity must be measured very accurately. Furthermore, the temperature of the working room must be kept as constant as possible in order to secure the equilibration of temperature between the falling drop and the surrounding organic liquid medium. To avoid such troubles we have tried a new method, in which the drop of the sample water is brought to balance in the liquid medium by changing the temperature of the latter as in the case of the float method[2]. Then the density of the sample can easily be known from the temperature dependence of the density of the medium liquid.

The main part of the apparatus is shown in the appended diagram. It consists of an ordinary glass tube about 30 cm. long and 13 mm. wide, the lower end of which is hermetically closed. The tube is provided with a glass stopper S at the upper end and the lower part of the tube is surrounded with a glass jacket J, through which cooling water can be circulated. A suitable organic liquid or a liquid mixture, the density of which is almost equal to that of the sample water, is placed in the tube up to marking M and the whole is immersed in the water of the thermostat down to the level W, while cooling water is circulated through the water jacket J. But as the temperature of the cooling water is kept somewhat lower than that of the thermostat, the density of the liquid column in the tube between H and K is always greater than that of the same

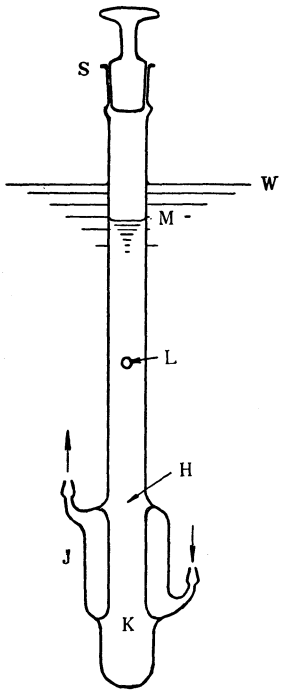



Fig. 1. Apparatus

liquid between M and H. In other words there is a discontinuity in the density of the liquid column at the point H. It is not difficult to choose the temperature of the thermostat in such a way that the density of the liquid column above the point H is less, while that below the point H is greater than that of the sample water, so that the drop of sample water, which has been dropped into the tube, remains at the point H in the liquid column. In this way the drop of water is prevented from falling and adhering to the bottom of the tube.

Now the temperature of the thermostat is carefully lowered and in this way the density of the liquid column in the tube between M and H is gradually increased. Then the drop of the water, which has been allowed to remain at first at the point H, gradually floats up and finally under some adjustment of the temperature it

1) H. G. Barbour and W. F. Hamilton, *Am. J. Physiol.*, **69**, 654 (1924).

2) Such a control of the temperature can be made, because the thermal expansion coefficient of organic liquids is generally greater than that of water.

stops at a certain point (L) in the liquid column between M and H. When this balancing temperature is read off from Beckmann's thermometer immersed in the thermostat, the density of the sample water can easily be known from the temperature dependence of the organic liquid in the tube.

TABLE
EXAMPLES OF THE MEASUREMENTS
Deuterium-concentration atom %

| By the pycnometric method | By the present method |
|---|---|
| 0.015* | 0.02±0.01** |
| 0.25 | 0.25±0.01 |
| 0.49 | 0.48±0.01 |
| 0.70 | 0.70±0.02 |
| 0.94 | 0.96±0.01 |
| 1.17 | 1.16±0.01 |
| 1.40 | 1.40±0.01 |
| 1.67 | 1.66±0.01 |
| 1.87 | 1.89±0.02 |
| 2.31 | 2.31±0.00** |

* Natural water.
** These samples were used as standards.

Some examples of the determinations are given in the appended table, where the deuterium-concentration of various dilute heavy waters is determined by the present method and the results are compared with those obtained by the ordinary pycnometric method. As an organic liquid, a mixture of 100 parts of chlorobenzene and about 60 parts of xylene was used and the balancing temperature lay at about 35°C.

As will be seen from the table, deuterium-concentration of water between 0—3 atom per cent. can easily be measured by the present method with a relative error of 1 %. One of the advantages of the present method over the usual falling drop method is that an accurate micropipette for the making of the drop is unnecessary. An ordinary pipette or a syringe is enough for the making of a drop of water of an arbitrary size for the present method. Furthermore, at the end of an experiment, the water in the liquid column can easily be sucked off by means of a pipette after bringing the drop on the surface of the liquid column by slightly lowering the temperature of the thermostat.

The author wishes to express his gratitude to Professor T. Titani for much help and encouragement in this work.

*Department of Chemistry, Faculty of Science, Tokyo Metropolitan University, Setagaya, Tokyo*

# *Heat of Mixing of Mono- and Di-propylene Glycol with Water*

By Kazuo AMAYA and Ryoichi FUJISHIRO*

(Received June 24, 1957)

It will be important to investigate what changes of physical properties of the solutions occur according to the size of the solute molecules. As an attempt we measured the heat of mixing of propylene glycol and di-propylene glycol with water. The di-propylene glycol molecule is thought to be about twice as large as that of propylene glycol; both molecules have the same number of hydroxyl group, but are different in that the former has the ether group.

Measurements of heats of mixing of these solutions, therefore, will give some interesting bits of information about the effect of the molecular size and the interaction power of the ether and the hydroxyl groups with water.

## Experimental

The apparatus used was already described in the previous paper[1]. Propylene glycol and di-propylene glycol were distilled with a long column under reduced pressure.

* Present address: Institute of Polytechnics, Osaka City University, Kita-ku, Osaka.

1) K. Amaya and R. Fujishiro, This Bulletin, 29, 270 (1956).

## Results and Discussion

The heat which was evolved when propylene glycol (or di-propylene glycol) and water were mixed and then when the solution was diluted successively with propylene glycol (or di-propylene glycol) or water, was measured at 25°C. By integrating these heats evolved by mixing and dilution, the heat of mixing at various concentrations was obtained as shown in Tables I and II. For reference, the heat of mixing and dilution of tri-propylene glycol with water was also measured. But tri-propylene glycol was not distilled because of its high boiling point and so the data may not be reliable enough. Using these data, the heat of mixing per mole of solution was calculated and plotted in Fig. 1.

It will be found that the di-propylene glycol solution shows different and characteristic behavior compared with the propylene glycol solution. One of these behaviors is the shift of the maximum position of the curve to the lower concentration of di-propylene glycol and the other is the increase in the maximum height in the heat of mixing.

TABLE I
HEAT OF MIXING OF PROPYLENE GLYCOL AND WATER AT 25°C

| W. of P.G. g. | W. of water g. | Mole fraction of PG | Heat evolved cal. |
|---|---|---|---|
| 1.670 | 15.649 | 0.0247 | $45.9_7$ |
| 1.670 | 10.131 | 0.0376 | $43.7_1$ |
| 1.670 | 6.082 | 0.0611 | $39.5_2$ |
| 1.670 | 4.018 | 0.0896 | $34.7_2$ |
| 1.670 | 2.079 | 0.1598 | $24.5_2$ |
| 1.996 | 2.055 | 0.1870 | $27.5_1$ |
| 4.027 | 2.055 | 0.3170 | $31.8_7$ |
| 7.958 | 2.055 | 0.4784 | $34.8_3$ |
| 15.010 | 2.055 | 0.6336 | $37.4_5$ |

TABLE II
HEATS OF MIXING OF DI-PROPYLENE GLYCOL AND WATER AT 25°C

| W. of di-PG g. | W. of water g. | Mole fraction of di-PG | Heat evolved cal. |
|---|---|---|---|
| 1.991 | 16.496 | 0.0160 | $52.6_2$ |
| 1.991 | 8.277 | 0.0313 | $46.8_8$ |
| 1.991 | 4.178 | 0.0602 | $36.0_0$ |
| 2.058 | 2.002 | 0.1213 | $28.2_0$ |
| 4.146 | 2.002 | 0.2176 | $30.6_0$ |
| 8.073 | 2.002 | 0.3513 | $30.7_1$ |
| 14.813 | 2.002 | 0.4984 | $30.7_4$ |

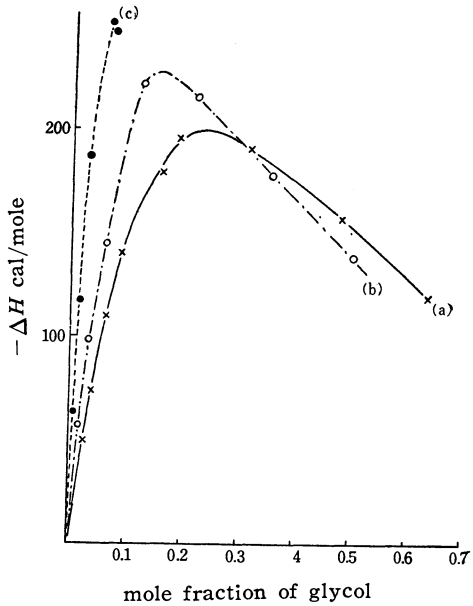



Fig. 1.
(a) Propylene glycol-water
(b) Di-propylene glycol-water
(c) Tri-propylene glycol-water

Usually the heat of mixing per unit volume of the solution of two kinds of normal liquid which have no specially interacting group, may be represented by the following van Laar equation:

$$\Delta H_m/cc = \alpha v(1-v) \quad (1)$$

where $\alpha$ is the interaction parameter between the solute and the solvent molecules and $v$ is the volume fraction of the solute. According to this equation the position of the maximum of $|\Delta H_m/cc|$ will be at the equi-volume concentration. Assuming that the ratio of molecular volume of the solute to the solvent be $n$, the heat of mixing per mole of solution will be rewritten as the function of mole fraction $x$ by

$$\Delta H_m/\text{mole} = V_0\alpha x(1-x)/\{1-(n-1)x\}$$

where $V_0$ is the molar volume of the solvent. Accordingly, the maximum of $\Delta H_m$/mole may be easily calculated to be at $x_{max}=(\sqrt{n}-1)/(n-1)$, which shows that $x_{max}$ decreases as the molecular size of the solute increases.

When one or both liquids have specific groups of interaction, the value of $x_{max}$ will deviate more or less from these normal ones with the degree of interaction, because in such cases the van Laar equation can not be applied owing to the deviation from random mixing.

The propylene glycol-water and the di-propylene glycol-water system which have the effective hydroxyl groups, may be such cases, and the deviation from the normal behavior in both cases is supposed to be considerable.

The ratio $n$ of the molecular volume of propylene glycol or di-propylene glycol to water being 4.1 or 7.2, $x_{max}$ is expected to be 0.33 or 0.27 respectively, which should be compared with the observed value 0.24 or 0.15.

It will not be surprising that both the observed values deviate in similar order from the normal ones and that the observed value of $x_{max}$ for the di-propylene glycol-water system is lower than that for the propylene glycol-water system. It seems strange that the height of the maximum for the di-propylene glycol-water system is higher than that for the propylene glycol-water system, as di-propylene glycol and propylene glycol have the same number of hydroxyl groups which are supposed to show the main interaction with water. But the di-propylene glycol molecule has the oxygen atom making the ether bonding in its center, while the propylene glycol molecule has not. This oxygen atom in the di-propylene glycol molecule may be supposed to play an important role as an acceptor of hydrogen bonding with water, and to make a considerable contribution to the heat of mixing.

This remarkable power of the oxygen atom may be seen in the tri-propylene glycol-water system shown in Fig. 1, in which the former molecule has two such oxygen atoms making the ether bonding.

In order to make a further study of this fact, the heat of mixing per mole of propylene glycol or di-propylene glycol was calculated from the experimental data and plotted against the concentration of propylene glycol or di-propylene glycol in Fig. 2. In the low concentration range, the plots prove to be nearly linear. Extrapolation to the infinite dilution of propylene glycol or di-propylene glycol gives 2.3 kcal. and 4.1 kcal. for the propylene glycol-water solution and the di-propylene glycol solution respectively. This great difference of 1.8 kcal. may be attributed to the existence of the oxygen atom making the ether bonding in the di-propylene glycol molecule.

By considering di-propylene glycol as two unit molecules of propylene glycol, the heat of mixing per unit mole of solution (number of water molecules plus two times number of the di-propylene glycol molecules equal to a mole) was calculated from the experimental data and shown in Fig. 3 with that of the propylene glycol system. It will be seen that the curves for both systems nearly

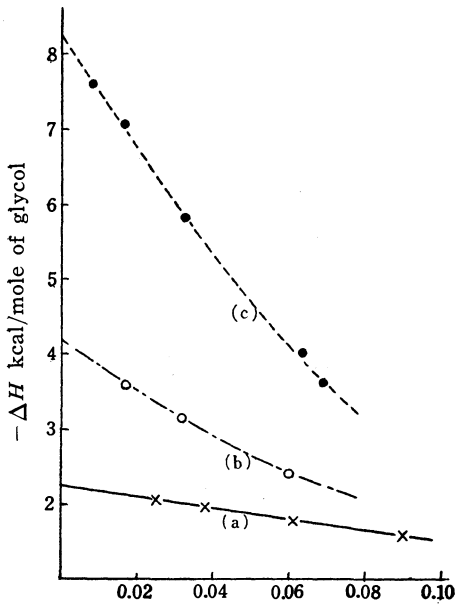



Fig. 2.
(a) Propylene glycol-water
(b) Di-propylene glycol-water
(c) Tri-propylene glycol-water

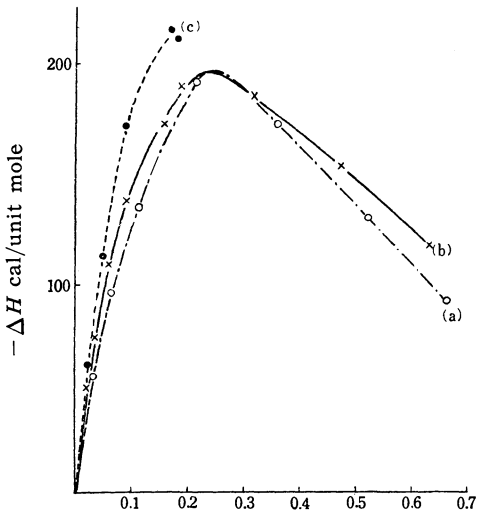



Fig. 3.
(a) Propylene glycol-water
(b) Di-propylene glycol-water
(c) Tri-propylene glycol-water

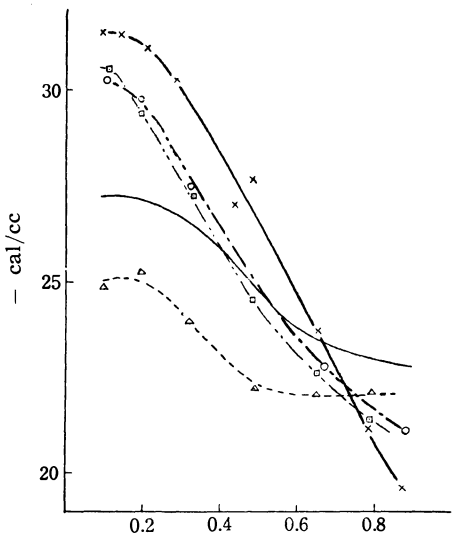



Fig. 4.
—×— Propylenglycol-water
-○- - Di-propylene glycol-water
-⊡-·· 1.3-Butanediol-water
—— Ethylene glycol-water
- -△- - 1.4-Butandiol-water

coincide in the height and in the position of the maximum. It may be reasonable to suppose that the di-propylene glycol molecule shows the same behavior as that of two units of a propylene glycol molecule and hence the oxygen atom in the ether bonding has the same power of interaction for water as that of two hydroxyl groups.

Finally, we shall compare the interaction parameter $\alpha$ of our two systems with those of the solutions containing such molecules as ethylene glycol[2] and butanediol[3] which have two hydroxyl groups. Using Eq. (1) the values of $\alpha$ for several systems were calculated and illustrated in Fig. 4. The similar behaviors in cases where the values of $\alpha$ are fairly great in magnitude and decrease considerably as the concentration of diol increases, will be found for all systems shown in Fig. 4 and hence may be characteristic of these solutions in which hydroxyl groups play an important role.

## Summary

The heat of mixing of propylene glycol and di-propylene glycol with water was measured. The results obtained for these systems were compared with each other and it was found that the oxygen atom in the ether bond of di-propylene glycol plays an important role for the acceptor of hydrogen bonding and makes a great contribution to the heat of mixing.

We would like to express our gratitude to Professor Y. Morino of Tokyo University for his encouragment and discussion.

*Department of Chemistry, Faculty of Science, Kobe University*
*Higashinada-ku, Kobe*

2) Schwers, *Rec. trav. chim.*, **28**, 44 (1909).
3) K. Amaya and R. Fujishiro, This Bulletin, **29**, 830 (1956).

# *The Static Electrode Potential Behavior of Tantalum and its Behavior on Anodic Polarisation*

By E. M. Khairy and M. Kamal Hussein

(Received October 10, 1956)

As is well known, tantalum shows remarkable resistivity towards chemical action and behaves frequently as a passive metal. A study of its static electrode potential behavior and of its anodic polarization would be of importance for obtaining insight into its mode of oxidation leading to the observed resistivity. For this purpose, the electrode potential of tantalum was measured in buffer solutions covering the pH range 1—12 and initially free from its ions. The repetitive oscillographic method was also applied to study its anodic behavior in various media.

## Experimental

The electrodes used in this investigation were pure tantalum wires each 1 cm. long and 1 mm. in diameter. The static electrode potential measurements were performed at 30°C in the Clark and Lub's-Ringer series of buffers covering the pH range 1—12. Before use the electrodes were polished with different grades of emery paper, thoroughly washed with redistilled water and finally rinsed with the solution to be used. Cells and devices were essentially the same as those used in previous papers[1]. A saturated calomel electrode was used as the reference half cell.

The anodic polarization experiments were carried out at 30°C by the repetitive oscillographic method, using the same circuit as that applied by us in a previous publication[2]. The trip voltage of the thyratron valve was always adjusted at 65 V. The electrolytes used were buffer solutions chosen in the acid, the neutral and the alkaline range, together with buffered potassium fluoride of concentrations ranging from $10^{-2}$ to 5 N. Polarization curves were also taken in several unbuffered electrolytes including hydrofluoric, hydrochloric, sulfuric and nitric acid and their neutral salts. All these electrolytes were prepared from the purest Analar products.

## Results and Discussion

### The Electrode Potential Behavior of Tantalum in Solutions Initially Free from its Ions.

—The electrode potential of tantalum in buffer solutions varies with time in such a way that the first steady state values are generally characterised in acid media by considerable drifts towards more negative overnight values. Alternatively, the potentials obtained in neutral and slightly alkaline media show pronounced drifts towards more positive values when the electrodes were left overnight in contact with the electrolytes.

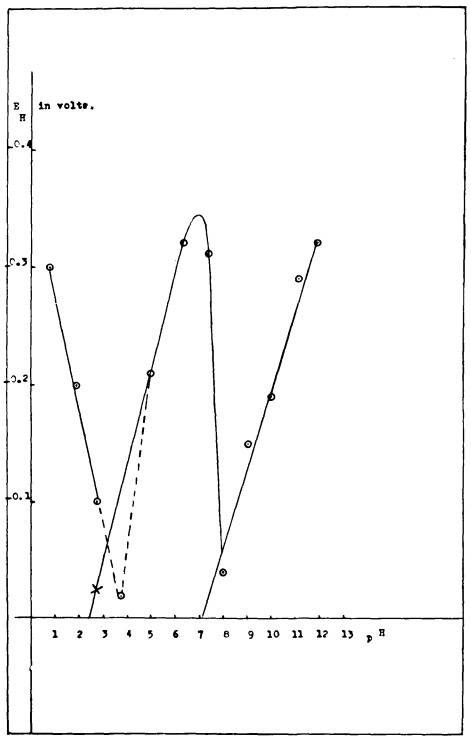



Fig. 1. (×: overnight value)

By plotting the first steady state potentials against pH, a "W"-shaped curve as shown in Fig. 1 is obtained. It consisits of a more or less linear but rather rapid fall of potential within the pH range 1 to 3. The curve then passes through a sharp peak whereupon the potential varies linearly up to pH 7, yielding a coefficient

1) A. Riad Tourky and S. E. S. El Wakkad, *J. Chem. Soc.*, **1948**, 740.
2) W. Machu, E. M. Khairy and M. K. Hussein, *Corrosion*, U. S. A., **11**, 3751 (1955).

of 81 mV per unit pH. Another straight line can be traced along the pH range 8—12, the slope of which amounts to 66 mV per unit pH. By extrapolating the lines running across the pH ranges 3—7 and 8—12, $E'_0$ values are obtained amounting to +0.192 and +0.473 V, respectively.

In order to interpret the phenomena manifested by the tantalum electrode, the thermodynamic potentials of the systems $Ta/Ta_2O_5$ and $Ta/Ta_2O_5/TaO_2^+$ have been computed. According to the calculations reported by Latimer (3), the $E_0'$ value of the former system amounts to −0.8114 V. In order to evaluate the thermodynamic potential of the latter system, the following equilibrium reactions have been considered:

$$Ta_2O_5+H_2O \rightleftarrows 2\,TaO_2^+ +2OH^- \quad (1)$$

By applying the relation

$$\log K=-(2\mu^0_{TaO_2^+}+2\mu^0_{OH^-} -\mu^0_{Ta_2O_5}-\mu^0_{H_2O})/1{,}363 \quad (2)$$

and using Latimer values for $\mu^0$ potentials of $Ta_2O_5$, $OH^-$ and $H_2O$ which amount to −470.6, −37.596 and −56.690 kcal., respectively it follows that:

$$\mu^0_{TaO_2^+}=-226.050-0.682\log K \quad (3)$$

Using this value, the $E_0'$ value of the reaction:

$$Ta+2H_2O=TaO_2^+ +4H^+ +5e^- \quad (4)$$

amounts to:

$$E_0'=-0.9763-0.0059\log K \quad (5)$$

Assuming that the electrode potential of tantalum is determined by the activity of the tantalyl ion in solution, it follows that:

$$E_H=E_{0(Ta/TaO_2^+)}+\frac{RT}{F}\log a_{(TaO_2^+)} \quad (6)$$

Substituting for $a_{(TaO_2^+)}$ from the relation:

$$a_{(TaO_2^+)}=\frac{K^{1/2}}{a_{(OH^-)}}$$

where $K$ denotes the equilibrium constant of reaction (1), equation (6) transforms into:

$$E_H=-0.9763-0.0059\log K+\frac{RT}{F}\log\frac{K^{1/2}}{a_{OH^-}}$$

$$=-0.9763+0.0236\log K-0.059\log\frac{K_w}{a_{H^+}}$$

$$=-0.1503+0.0236\log K-\frac{RT}{F}pH \quad (7)$$

or

$$E_H=E_0'-\frac{RT}{F}pH \quad (8)$$

where

$$E_0'=-0.1503+0.0236\log K \quad (9)$$

The results obtained with the tantalum electrode in buffer solutions initially free from its ions may be explained in view of its decided tendency to acquire the passive state (4). This state is most probably attained when the electrode is covered with an inhibitive film of the pentoxide overlayered with adsorbed oxygen doublets (5). The presence of such a layer together with the passive nature of the surface oxide, accounts for the observed surplus in potential. In the light of the above discussion, one may interpret the $E_H$/pH plot as follows: from pH 1 to 3, the electrode which has been rendered passive by exposure to atmospheric oxygen is subjected to the dissolving action of the electrolyte. This type of attack which takes place through the pores of the pre-immersion film, proceeds with subsequent depolarisation of some of the oxygen doublets, an effect which becomes less pronounced with increase in pH. This makes up for the shift of potential towards more positive values within that range. The electrodic behavior may be conceived under such conditions as that of a metal/metal pentoxide electrode superimposed by varying contributions of overvoltage brought about by the adsorbed oxygen doublets. At pH 3 upwards, the attack is materially diminished and the passive state seems to predominate, the electrode behaving thus as a $Ta/Ta_2O_5/O_2^-$ at a more or less constant overvoltage effect. On comparing the $E_0'$ value obtained within the pH range 3—7 (0.192 V) with the thermodynamic potential of the $Ta/Ta_2O_5$ couple (−0.8114 V), it appears that the overvoltage contributed by the adsorbed gas layer and/or the polarisation brought about the passive nature of the surface film, amounts to as high a value as one volt.

Owing to the complexity of the quinquivalent tantalum ion, it is legitimate to assume that the metal as well as the oxide dissolve in alkaline media in the form of tantalyl ions ($TaO_2^+$), according to the reaction:

$$Ta+2H_2O=TaO_2^+ +4H^+ +5e^- \quad (i)$$

3) W. M. Latimer, "Oxidation Potentials", 265 (1953).
4) R. Audubert and M. L. Roulleau, *J. Chim. Phys.*, **37**, 101 (1940).
5) G. Gesterheld, *Z. Electrochem.*, **11**, 47, 503 (1905).

and the equilibrium reaction:

$$Ta_2O_5+H_2O \rightleftarrows 2\,TaO_2^+ +2\,OH^- \qquad (ii)$$

Supposing that the behavior along the pH range 8—12 is given by the system $Ta/Ta_2O_5/TaO_2^+$ and assuming that the overvoltage contributed by the adsorbed doublets acquires but little variation with pH, the equilibrium constant $K$ of the reaction (ii) may be evaluated. Thus by substituting for $E_0'$ in equation (9) by the value computed from the slope of the respective straight line from which one volt (the difference between the experimental and the theoretical potential) is subtracted, it follows that:

$$0.473-1.0=-0.150+0.024\log K.$$

Therefore,

$$\log K=15.7,$$

from which $K=5\times10^{-16}$.

**The Anodic Behavior Investigated by the Repetitive Oscillographic Method.** —The study of the anodic behavior of tantalum by the aid of the cathode ray oscillograph reveals generally the presence of three domains. The first domain comprises two main stages, one of which occurs at a more or less constant negative potential corresponding to the desorption of hydrogen supposedly formed through the cathodic action of the repetitive current. The second stage in this domain consists of a gradual potential rise varying regularly with the applied quantity of electricity, a stage to be described to the building up of the double layer potential. The second domain in these curves includes the stages corresponding to the different states of oxidation of the metal, whereas the third domain covers the regions of attainment of passivity and gas evolution. The results of these polarisation experiments may be outlined as follows:

a) *Experiments in Buffer Solutions*:—The anodic behavior of tantalum was investigated in different buffer solutions within the pH range 1—14. The oscillograms obtained were essentially of the same general form, showing that the electrode maintains its passive nature all over the pH range. Figs. 2—5 contain representative curves taken, successively, in solutions of pH 1, 7, 12 and 14 at the polarising current densities 8.2, 6.2, 13.8 and 7 $mA/cm^2$. The appropriate amounts of electricity were supplied by means of a 0.2, 0.4, 1 and 1 $\mu F/cm^2$ condensers, respectively.

On comparing the first domains of these curves, it may be noted that the curve obtained at pH 14, in contradistinction from the other three curves, is characterised by a rather extended stage corresponding to the desorption of hydrogen. This may be explained by assuming that the natural oxide is partially attacked during the initial stages of the anodic process owing to the tendency of tantalum pentoxide to form tantalate in the strong alkaline media. The process takes place with the formation of hydrogen which is sorbed by the metal, together with the

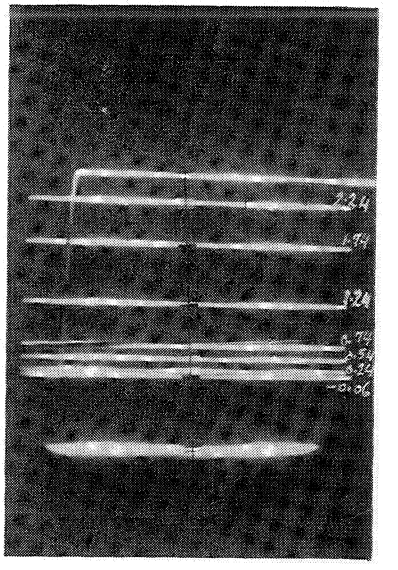


Fig. 2

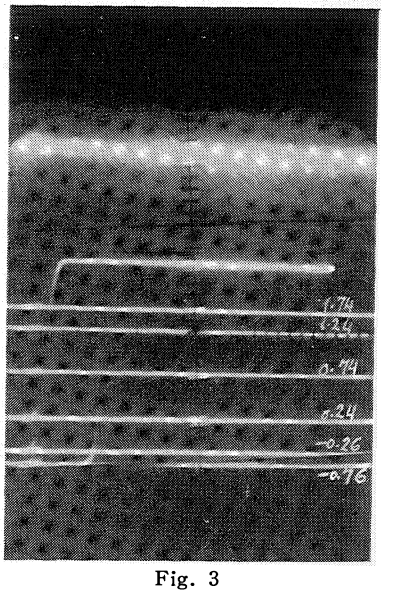


Fig. 3

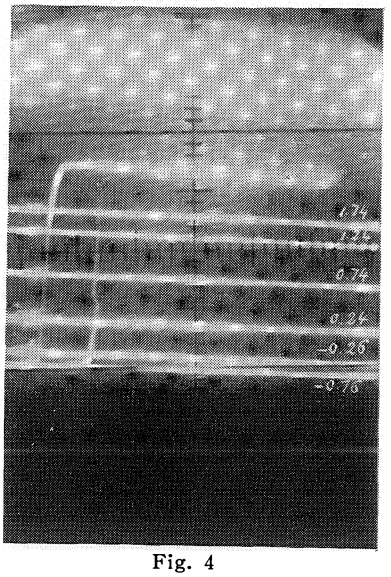


Fig. 4

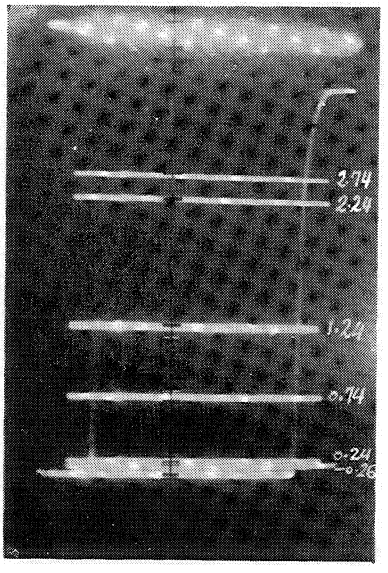


Fig. 5

gas evolved during the cathodic passage of the repetitive current. The removal of the sorbed gas consumes comparatively greater amounts of electricity.

After the process of desorption of hydrogen, the potential jumps abruptly towards appreciably more positive values, attaining a value ranging from 2.5 to 3.5V at which oxygen evolution takes place. This indicates that the electrode surface is passivated by the time the double layer has been fully charged. The capacity of the double layer may be calculated for each curve from the slope of the respective linear potential rise, the horizontal shift of the cathode ray track being proportional to the quantity of electricity and the vertical shift to the acquired potential. The total amount of electricity used up in the overall process is equal to the product of the trip voltage of the thyratron valve (65 V) and the capacity of the applied condenser. The values thus obtained are almost the same averaging around 1 $\mu$F/cm$^2$ of the apparent surface area. The ease with which oxygen is evolved together with the exceedingly low double layer capacities substantiates the passive nature of the electrode surface. This behavior corroborates the results of the static potential measurements regarding the persistence of a naturally present protective oxide film on the electrode surface.

b) *Experiments in Solutions Containing Fluoride Ions*:—Anodic polarization experiments have been carried out in potassium fluoride solutions buffered within the pH range 2—12 with the object of investigating the corroding effect of the fluoride ion when present at lower and higher concentrations ($10^{-2}$—5 M). The oscillograms thus obtained are essentially of the same shape inasmuch as pronounced passivity is achieved in both dilute and concentrated solutions. A representative curve is shown in Fig. 6. It contains two curves "A" and "B" being taken in $10^{-2}$ and 5 M potassium fluoride solutions buffered at pH 7, both at a current density of 9.2 mA/cm$^2$ together with a 0.3 $\mu$F condenser. The potential jumps abruptly after the double layer has been fully charged and oxygen is readily evolved at 3.5 V, consuming the

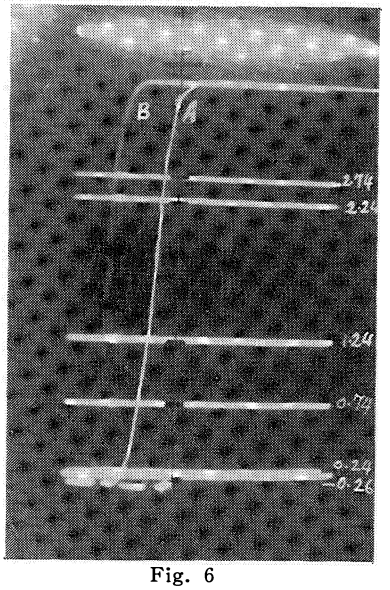


Fig. 6

most part of the applied quantity of electricity. This shows that the fluoride ion introduces no appreciable effect on the attainment of anodic passivity even at the higher concentration. Therefore, it appears legitimate to extend the study to a still higher fluoride ion concentration. For this purpose the electrode was anodically polarized in 10 N hydrofluoric acid, whereupon two oscillograms "C" and "D" were obtained (Fig. 7), taken at 10.5 and 9.4mA/cm$^2$ together with a 0.3, respectively a 1 $\mu$F condenser. Consideration of these curves reveals that when the applied quantity of electricity is relatively small (curve C), the electrode acquires a rather active potential of ~0.2 V after the double layer has been built up, indicating that

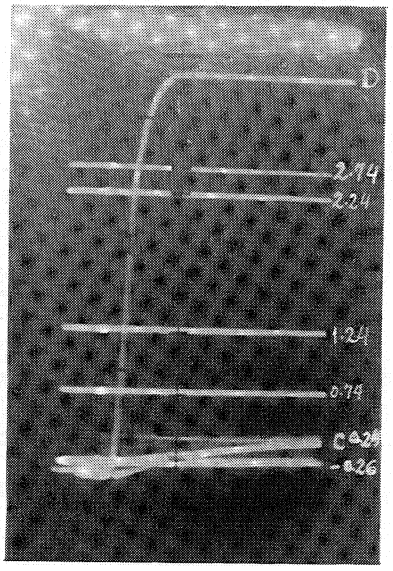



Fig. 7

the corroding effect exerted by the fluoride ion hampers the achievement of passivity. The capacity of the double layer amounts to 30 $\mu$F/cm$^2$ as compared with 1 $\mu$F/cm$^2$ in buffered potassium fluoride solutions, revealing the relative activity of the surface. The electrode behavior may be conceived under such conditions as to be governed by a tantalum/tantalum pentoxide system subject to some overvoltage effect, a picture which conforms to the static electrode potential behavior. Alternatively, prominent passivity is readily achieved on passing higher quantities of electricity. The capacity of the double layer amounts to a value of 3 $\mu$F/cm$^2$ and oxygen is evolved at 3.5 V.

c) *Experiments in Chloride, Sulfate and Nitrate Media*:—The oscillograms shown in Figs. 8 and 9 were taken in 6 N hydrochloric acid and 1 N sodium chloride solutions. The applied quantities of electricity were 9.7 and 6.5 mA/cm$^2$, using a 0.3 and 1 $\mu$F condenser, respectively. These curves show also that the electrode surface acquires the passive state simultaneously as the double layer has been fully charged, oxygen being evolved at ~4 V. The double layer capacity amounts to 1.5 and 1.1 $\mu$F/cm$^2$ for the acid and the neutral solutions, respectively.

The electrode shows a remarkably

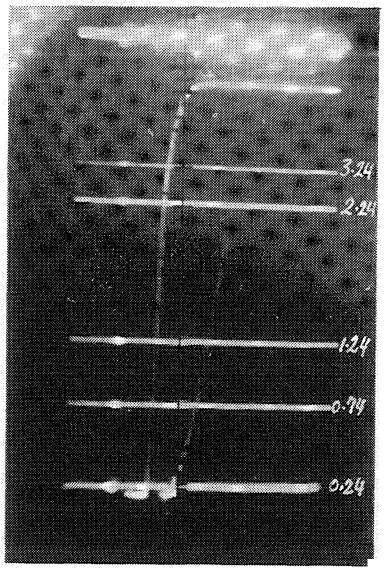



Fig. 8

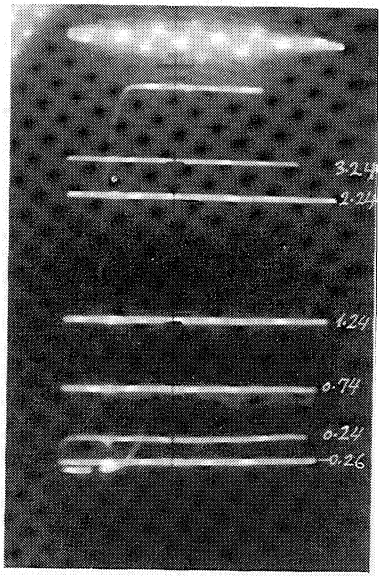



Fig. 9

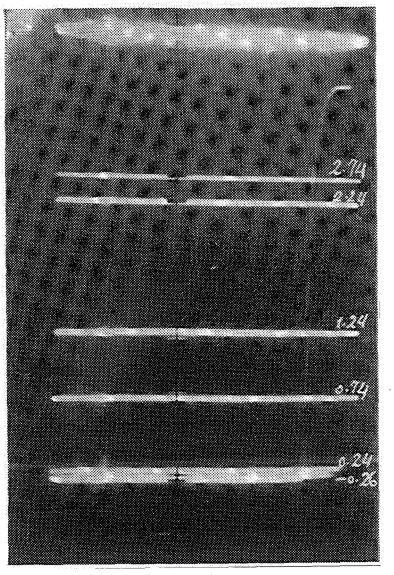



Fig. 10

similar behavior in 1 N sulfuric and nitric acid solutions. A representative curve is shown in Fig. 10 which was taken in 1 N sulfuric acid at 4 mA/cm$^2$ together with a 0.5 $\mu$F condenser. It is apparent that although passivity is rapidly attained, as was the case in chloride media, yet the first domain in this representative curve manifests a rather extended stage which corresponds to the desorption of hydrogen. This indicates that the activation encountered by the repetitive nature of the current is much more effective in sulfuric and nitric rather than in hydrochloric acid. It has to be inferred, however, that on carrying out experiments in sodium sulfate and sodium nitrate solutions, the curves obtained are essentially the same as those given in the sodium chloride solutions (Fig. 9), owing to the diminished dissolving action of these neutral electrolytes.

## Summary

The electrode potential behavior of tantalum is investigated in buffer solutions initially free from the metal ions covering the pH range 1—12. A "W"-shaped $E_H$/pH plot is obtained and the results reveal the existence of a natural passive pentoxide film overlayered with oxygen doublets. The electrode behaves within the pH range 3—7 as a metal-metal oxide electrode subject to an overvoltage of about one volt. From pH 7 to 12 the behavior is given by the system: $Ta/TaO_2^+$ yielding an equilibrium constant $K=5.10^{-16}$.

Anodic polarization experiments by the repetitive oscillographic method have been also utilised in buffer solutions and in other different media. The oscillograms are mostly characterised by sharp potential jumps associating the charging of the double layer, showing the decided resistivity of the surface film. The capacity of the double layer scarcely exceeds 1 $\mu$F/cm$^2$, except in hydrofluoric acid solutions where it attains a maximum value of 30 $\mu$F/cm$^2$.

The authors wish to express their full gratitude to Professor Dr. A. Riad Tourky, Head of the Chemistry Department for his valuable criticism and cordial facilities in carrying out this work.

*Chemistry Department*
*Faculty of Science*
*University of Cairo*
*Cairo, Egypt*

# *The Photochemical Degradation of 6 Nylon*. I*

By Takeshi HASHIMOTO

(Received July 10, 1957)

The photochemical degradation of nylon has been the subject of several recent publications[1-3]. This topic has been under investigation in this laboratory for some time, and the author has found that the photochemical degradation of 6 nylon is accompanied with considerable decrease in molecular weight and increase in water soluble material. The water soluble material of nylon consists of monomers and oligomers. In this paper it is attempted to elucidate the mechanism of the photochemical degradation of 6 nylon from the relationship between molecular weight and the amount of monomer produced.

## Various Possible Modes of Linear Polymer Degradation

Grassie and Melville[4] made a consideration of various possible modes of molecular weight change the starting point in their study of the reaction. Before appreciable amounts of monomer appear in a random scission process in large molecules, the number-average molecular weight of the residue is reduced to a small fraction of its initial value. This behavior is represented by AD in Fig. 1. Another suggestion was that the bonds joining the end units to the rest of the chain might be particularly vulnerable and thus exclusively broken. Such a process has been called stepwise depolymerization and would result in decrease in molecular weight, directly proportional to the amount of monomer produced. This behavior is represented by AC in Fig. 1.

A third possible depolymerization mechanism is the exact reverse of polymerization. Initiation would consist of chain scission resulting in the production of radicals. These would then rapidly lose

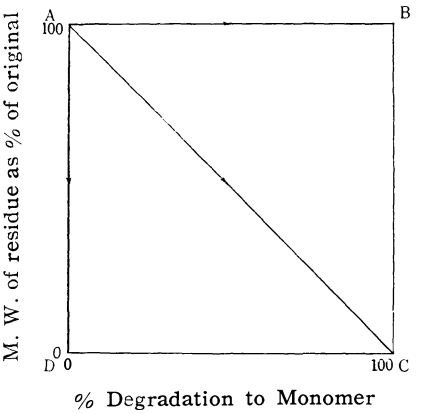



Fig. 1. Theoretical reaction curves for possible depolymerization mechanisms (Grassie and Melville).

monomer until they had completely disintegrated. If these degrading radicals had a lifetime of the order of those of the growing radicals in polymerizing systems (approximately $10^{-3}$ —10 sec.), virtually all the monomer units would exist at any instant as free monomer or unchanged polymer. No great change in the molecular weight of the residue would therefore be expected throughout the whole course of the reaction. This mechanism is represented by AB in Fig. 1.

## Experimental

Scoured and heat-set nylon taffeta of $70^{D}$ $34^{fil.}$ 6 nylon yarn (Amilan) was used in these experiments. Samples of the fabric were irradiated in a Fade-Ometer for various periods of time and then the amount of water-soluble material and the degree of polymerization of the sample were measured.

1) *The measurement of the amount of water soluble material.* — Half a gram, of irradiated nylon taffeta was dried in vacuo over phosphorous pentoxide for 24 hr. and weighed. After 4 hr. extraction with water in a Soxhlet extractor, decrease in the weight of the sample was referred to as the amount of water soluble material.

2) *The measurement of the degree of polymerization.*—Number-average degree of polymerization $\bar{P}_n$ is calculated from intrinsic viscosity

* This paper was read before the 10th Annual Meeting of the Chemical Society of Japan held in Tokyo, April, 1957.

1) B. G. Achhammer et al., *J. Appl. Chem.*, **1**, 301 (1951).
2) R. A. Ford, *Nature*, **176**, 1023 (1955).
3) M. Schwemmer, *Textil-Rundschau*, **11**, 1, 70, 131 (1956).
4) N. Grassie and H. W. Melville, *Proc. Roy. Soc.* **A 199**, 1, 14, 24 (1949).

TABLE I

WATER-SOLUBLE MATERIAL AND NUMBER AVERAGE DEGREE OF POLYMERIZATION OF IRRADIATED NYLON

| Exposure time (hr.) | | 0 | 10 | 20 | 40 | 60 | 80 | 120 |
|---|---|---|---|---|---|---|---|---|
| Sample weight (mg.) | | 490 | 458 | 487 | 487 | 487 | 484 | 488 |
| Water-soluble (%) | | 0.7 | 0.8 | 1.1 | 1.9 | 2.9 | 3.6 | 5.6 |
| Material | | | | | | | | |
| $[\eta]$ | Before extraction | 1.02 | 0.70 | 0.50 | 0.33 | 0.17 | 0.30 | 0.19 |
| | After extraction | | 0.73 | 0.65 | 0.42 | 0.31 | 0.34 | 0.23 |
| $\bar{P}_n$ | Before extraction | 131 | 76 | 47 | 26 | 10 | 22 | 12 |
| | After extraction | | 81 | 68 | 36 | 23 | 27 | 15 |

$[\eta]$ which is measured in *m*-cresol at 25.00°C. Thus $\bar{P}_n = 127.4\,[\eta]^{1.435}$ [5].

## Results

All the results are summarized in Table I.

Fig. 2 shows the increase in amount of water-soluble material and the decrease in intrinsic viscosity during irradiation. The increase in amount of water-soluble material is approximately proportional to the exposure time, while the decrease in intrinsic viscosity is rapid at the beginning of exposure. It might be due to the presence of water-soluble material that the intrinsic viscosity after extraction always shows a little higher value than that before extraction.

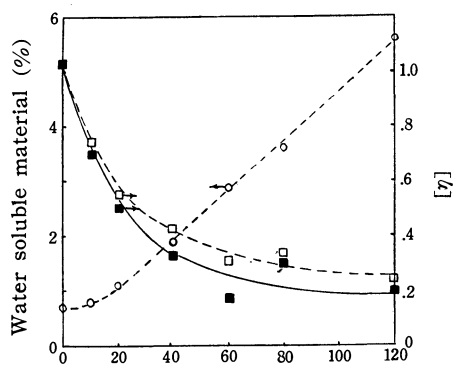



Fig. 2. Variation with time of the amount of water-soluble material and intrinsic viscosity (○ water soluble material, ■ intrinsic viscosity before extraction, □ intrinsic viscosity after extraction).

The relationship between the amount of water soluble material and the number-average degree of polymerization after extraction is shown in Fig. 3. Monomer is not the only water-soluble material produced. From the analogy of Fig. 1, however, it is deduced that the molecular chain of nylon is randomly split off by light.

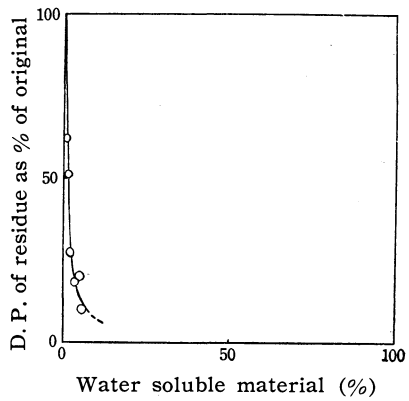



Fig. 3. Relationships between the amount of water-soluble material and the number-average degree of polymerization of residue.

## Discussion

A theory regarding the random breaking of polymer chain has been elaborated by a number of workers. The theory makes it possible to obtain mathematical expressions for the various size distributions at definite stages of the degradation process. Here is cited Hoshino and Watanabe's[6] theory from which the relationship between the amount of monomer or oligomer produced and the number-average degree of polymerization is derived in the following way.

Supposing the molecular size distribution at initial stage follows Flory's distribution. That is

$$N = N_p^{x-1}(1-p) \qquad (1)$$

where $N_x$ is the number of molecules

5) O. Fukumoto, *J. Polymer Sci.*, **22**, 263 (1956).

6) K. Hoshino and M. Watanabe *J. Chem. Soc. Japan, Pure Chem. Sec.*, **70**, 170 (1949); *J. Am. Chem. Soc.*, **73**, 4816 (1951).

TABLE II
WEIGHT FRACTION OF OLIGOMERS DURING RANDOM DEGRADATION

| Number-average degree of polymerization | Degree of degradation | Weight fraction of (%) | | | |
|---|---|---|---|---|---|
| | | Monomer | Dimer | Trimer | Total |
| 130 | | | | | |
| 65 | 0.0078 | 0.023 | 0.046 | 0.068 | 0.137 |
| 130/3 | 0.0155 | 0.054 | 0.105 | 0.154 | 0.313 |
| 26 | 0.0310 | 0.148 | 0.285 | 0.410 | 0.843 |
| 130/9 | 0.0620 | 0.479 | 0.892 | 1.245 | 2.616 |
| | $p=0.9923$ | Initial degree of polymerization 130 | | | |

composed of $x$ monomer units, $N$ is the total number of molecules and $p$ is the extent of reaction. In a case where the bonds of all chains in the mixture at any given time are equally accessible to reaction independent of both their position in a chain and the length of their parent chains, the molecular weight distribution after degradation is given by

$$N_y(\alpha)=N[1-p(1-\alpha)]^2[p(1-\alpha)]^{y-1}(1-p)^{-1} \quad (2)$$

where $N_y(\alpha)$ is the number of molecules composed of $y$ monomer units at the degree of degradation $\alpha$. Substituting 1, 2, 3 etc. for $y$ in equation (2), one can calculate the fraction of monomer, dimer, trimer etc. respectively at any degree of degradation. The results are summarized in Table II.

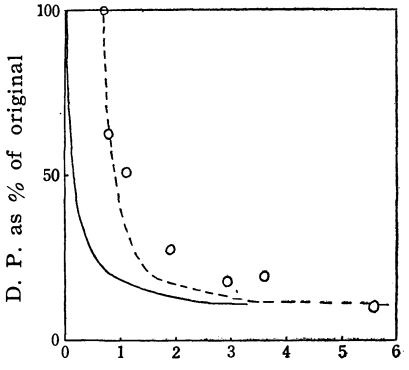



Fig. 4. Theoretical curve and observed relationship between the amount of water-soluble material and the number average degree of polymerization.
—— theoretical
- - - corrected
○ experimental

When the total weight fraction of monomer, dimer and trimer is plotted against number-average degree of polymerization, one can obtain the full line in Fig. 4. Observed values are represented by points. Taking it into account that a sample before degradation already has water-soluble material of 0.7%, one can reasonably say that the corrected value (dotted line) shows good agreement with the observed value.

## Summary

1) The photochemical degradation of 6 nylon was investigated through the measurement of intrinsic viscosity and the amount of water-soluble material of 6 nylon taffeta irradiated for various periods of time in Fade-Ometer.

2) The intrinsic viscosity or the number-average degree of polymerization decreases rapidly at the initial stage, while the amount of water-soluble material increases approximately in proportion to the exposure time.

3) It is deduced from the relationship between the number-average degree of polymerization and the amount of water-soluble material that the molecular chain of 6 nylon is randomly split off by light. The relationship is well explained by the theory of random breaking of the polymer chain.

The author wishes to express his sincere thanks to Dr. K. Hoshino and Mr. M. Yoshida for their kind encouragement and permission to publish this paper.

*Research Department Toyo Rayon Co., Ltd., Otsu, Shiga Prefecture*

# *Spectrochemical Study of Microscopic Crystals. XVI*[1]. *Structure of Cupric Formate, Acetate and Propionate*[2]

By Shoichiro YAMADA, Hiroji NAKAMURA and Ryutaro TSUCHIDA

(Received July 5, 1957)

On the basis of magnetic measurements, Bleaney and Bowers[3] supposed that in the crystal of cupric acetate monohydrate there were isolated pairs of copper ions coupled by exchange forces, with each copper ion bonded by four oxygen atoms in a plane. Van Niekerk and Schoening[4] examined the crystal structure of cupric acetate monohydrate and found that the compound in the crystalline state consists of dimeric molecules having a molecular formula of $Cu_2(CH_3COO)_4 \cdot 2H_2O$, in which a sort of direct interaction might exist between the copper ions, judging from the comparatively short copper-to-copper distance. The nature of the possible copper-to-copper interaction, however, was not completely clarified by those studies. It seems significant to examine this point on the basis of other properties. In order to study the above problem in more detail and to find, if possible, some correlation between the light absorption and the possible metal-to-metal interaction, we have determined dichroism of cupric formate tetrahydrate, cupric acetate monohydrate, anhydrous cupric propionate and its monohydrate.

## Experimental

**Materials.**—Cupric formate tetrahydrate was prepared from cupric carbonate and formic acid. Blue crystals belonging to the monoclinic system are usually obtained in rectangular plates with a well developed (001)-plane. The compound is soluble in water, but insoluble in organic solvents. The measurement of dichroism was made on the (001)-plane with polarized light having its electric vector along the *b*- and the *a*-axis[5]. The *b*- and the *a*-absorption represent the absorption with the electric vector along the *b*- and the *a*-axis, respectively.

Cupric acetate monohydrate of reagent grade was recrystallized from 50% ethanol. Bluish green crystals were usually obtained in monoclinic plates with the (001)- or the $(20\bar{1})$-plane well-developed[5]. The compound is soluble in water and ethanol, but insoluble in chloroform. The measurement of dichroism was made on the $(20\bar{1})$-plane with polarized light having its electric vector along and perpendicular to the *b*-axis. The *b*- and the *a*-absorption represent the absorption with the electric vector along and perpendicular to the *b*-axis.

Cupric propionate monohydrate was prepared from cupric hydroxide and propionic acid. Recrystallization from ethanol-water mixture yielded bluish green crystals having an empirical formula of $Cu(C_2H_5COO)_2 \cdot H_2O$. The measurement of dichroism was made on one of the well-developed planes[6].

Anhydrous cupric propionate was obtained in bluish green crystals by repeated recrystallization of the cupric propionate monohydrate from chloroform. The color of the anhydrous compound is similar to that of the monohydrate. The absence of water of crystallization was readily confirmed by its infra-red spectrum. The measurement of dichroism was carried out on a well-developed plane. Anhydrous cupric propionate is almost insoluble in water, but is soluble in organic solvents such as ethanol and chloroform.

**Measurement.** — Quantitative dichroism measurement in the visible and the ultra-violet region was made by Tsuchida-Kobayashi's microscopic method[7].

Absorption spectra of the compounds in ethanol or chloroform were determined with a Beckman DU spectrophotometer. When a solution is too dilute, Beer's law is not obeyed. Even in such a dilute solution, however, Beer's law holds in the presence of an excess of the free aliphatic carboxylic acid. When ethanol was used as a solvent, it was apt to form some amount of ethyl carboxylate with the free ligand which was added in excess. The measurement, therefore, was made as quickly as possible after the solution was prepared. In any case, the obedience of the solution to Beer's law was always confirmed in the presence of free ligand.

1) Part XV of this series, S. Yamada and R. Tsuchida, This Bulletin, **30**, 715 (1957).

2) A brief summary of the present article was published as a letter to the editor: R. Tsuchida and S. Yamada, *Nature*, **176**, 1171 (1955).

3) B. Bleaney and K. D. Bowers, *Proc. Roy. Soc.*, **A214**, 451 (1952).

4) J. N. van Niekerk and F. R. L. Schoening, *Acta Cryst.*, **6**, 227 (1953).

5) We are indebted to Dr. R. Kiriyama of the Chemistry Department for the identification of the planes.

6) P. Groth, "*Chemische Kristallographie*", part 3, Engelmann, Leipzig, 1910 p. 205.

7) R. Tsuchida and M. Kobayashi, "*The Colour and the Structure of Metallic Compounds*", Zoshindo, Osaka, 1944, p. 180. See also previous papers of the present series.

Absorption spectra of cupric formate and acetate in aqueous solution were found to be essentially similar to that of the aquated cupric ion and, therefore, are not reported here.

The notations in the present paper are the same as those used in the former papers of this series. Extinction coefficients, $\varepsilon$, are calculated on the basis of the empirical formula instead of the molecular formula.

## Results and Discussion

**Cupric Formate Tetrahydrate.** — The results of the dichroism measurements are shown in Fig. 1. According to the

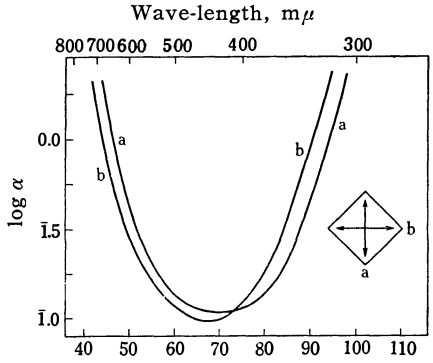



Fig. 1. Absorption spectra of cupric formate tetrahydrate.

crystal structure analysis[8], a copper ion is co-ordinated to four oxygen atoms in a plane of four formate ions, with two oxygen atoms of water molecules at a greater distance in the direction normal to the above plane. The crystal is found to show a band at about 38 to $39\times10^{13}$/sec. and a strong absorption band in the further ultra-violet region.

Typical compounds of copper(II) are usually known to show only one absorption band of moderate intensity in the near infrared to the near ultra-violet and another absorption band of much greater intensity in the further ultra-violet region. This is found to be the case with the cupric formate. Hence, it is suggested that no extraordinary linkage may be involved in the crystal of cupric formate tetrahydrate.

Although we could not determine the maximum of the band, the slope in the long wave-length region suggests the following relationship. For the band of the cupric formate at the longer wave-length, which is supposed to be closely related with the linkage between a copper ion and ligands, absorption is much stronger along the complex plane than along the direction normal to the plane. This is in good agreement with the relationship on the dichroism of planar cupric complexes of an ordinary type[9,10].

**Cupric Acetate Monohydrate.**—The results of the measurements are shown in Fig. 2 and Table I. The crystal structure

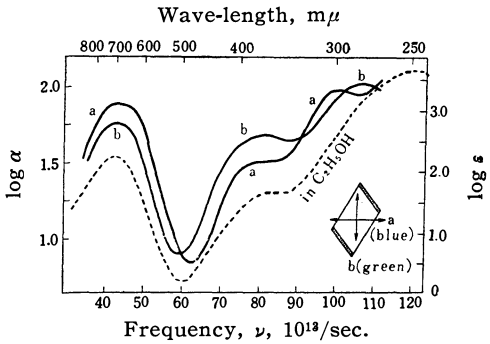



Fig. 2. Absorption spectra of cupric acetate monohydrate in the crystalline state (——), and in ethanol (----).

TABLE I

ABSORPTION MAXIMA OF CUPRIC ACETATE MONOHYDRATE IN THE CRYSTALLINE STATE

| | band I | | band II | | band III | |
|---|---|---|---|---|---|---|
| | ν | log α | ν | log α | ν | log α |
| *a*-abs. | 43 | 1.89 | 81 | 1.51 | 101 | 1.99 |
| *b*-abs. | | 1.76 | | 1.69 | 107 | 2.09 |

ν: $10^{13}$/sec.

analysis of cupric acetate monohydrate was reported by van Niekerk and Schoening[4]. According to the structure analysis, the line joining the two copper ions within the dimeric molecule in the crystal makes an angle of 34.6° with the *ac*-plane and its projection onto the *ac*-plane an angle of 32.5° with the *c*-axis. Although the absorption spectra, which have been determined with the crystal, may represent the absorption spectra of the dimeric molecules under the crystalline field, we may approximately assume that the absorption spectra with the crystal represent the principal characteristics of the molecule itself. The intensity ratio of the Z-absorption to the X-absorption has been estimated from the present dichroism measurement and on the basis of the

8) R. Kiriyama, H. Ibamoto and K. Matsuo, *Acta Cryst.*, **7**, 482 (1954).

9) S. Yamada and R. Tsuchida, This Bulletin, **29**, 694, 289 (1956).

10) Idem, *Annual Rep. Scient. Works, Fac. Sci. Osaka Univ.*, **4**, 79 (1956).

structure analysis. For both the bands at 43 and $80\times10^{13}$/sec., the ratio has been found to be marked; *the ratio of $K_z$ to $K_x$ is nearly one tenth for the band at $43\times10^{13}$/sec., and about ten for the band at $80\times10^{13}$/sec.* The Z-absorption means the absorption with the electric vector along the line joining the two copper ions within a molecule, and the X-absorption, the absorption, with the electric vector along the plane which is normal to the *b*-axis (Fig. 3). It is assumed in the estimation that all the linkages between the copper and oxygen atoms are equivalent to one another.

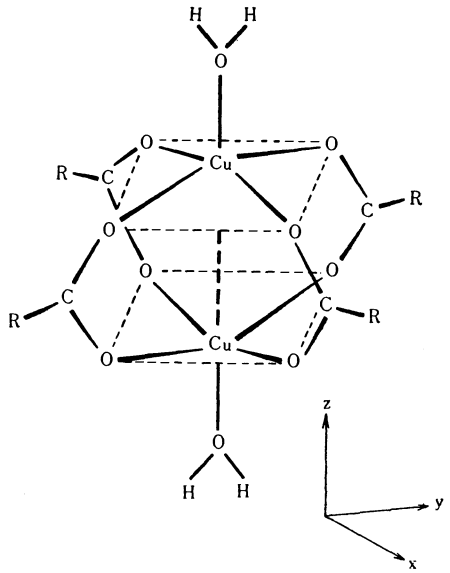



Fig. 3. Molecular structure of $Cu_2(R\cdot COO)_4\cdot 2H_2O$.

As was described in the preceding section, most cupric complexes of an ordinary type show only one band of moderate intensity in the region from the near infra red to the near ultra-violet. On the contrary, the present measurement indicates that cupric acetate monohydrate in the crystalline state shows two absorption bands at about 43 and $80\times10^{13}$/sec. (Fig. 2). The band at $43\times10^{13}$/sec. may apparently correspond to the so-called "copper band" which is characteristic of typical cupric complexes and which is supposed to be closely related with the linkages between the copper and the oxygen atoms. The band is usually considered as originating from the copper ion under the effect of the ligands. *For the band at $43\times10^{13}$/sec. absorption is found to be about ten times as strong with the electric vector along the complex plane as with the electric vector along the line joining the two copper ions within a molecule.* This is the same as the relationship found for the "copper band" of ordinary planar complexes of copper(II). These facts seem to support the above assignment of the absorption bands at about $43\times10^{13}$/sec. to the "copper band".

The absorption band at $80\times10^{13}$/sec. may be considered as an absorption band of a new kind for cupric complexes, judging from the wave-length and the intensity of the band. Therefore, the appearance of this band seems to suggest an extraordinary structure for this compound. This may be consistent with the hypothesis of the dimeric molecule with a formula of $Cu_2(CH_3COO)_4\cdot 2H_2O$.

Moreover, the polarization property with this new band at about $80\times10^{13}$/sec. is seen to be the reverse of the polarization with the band at $43\times10^{13}$/sec. *Thus for the band at about $80\times10^{13}$/sec. electric vector is absorbed much more strongly in the direction normal to the complex plane than along the plane.* The polarization with the band at $80\times10^{13}$/sec. may be understandable on the assumption of the copper-to-copper interaction, since the interaction may be expected in the direction normal to the complex plane. The band at about $80\times10^{13}$/sec. may be closely related with the copper-to-copper interaction.

The compound in the crystalline state shows an absorption band at about $100\times10^{13}$/sec. in addition to the two absorption bands. Although the origin of this band is not clear, we might assume the band to be due to the acetate groups in co-ordination. The band may well be called a kind of "specific absorption band" originating from the acetate ions in co-ordination. This band in solution is supposed to be hidden under a larger absorption band.

It is seen from Fig. 2 that cupric acetate in ethanol shows absorption bands at 43 and $80\times10^{13}$/sec., both with moderate intensity. French and Lowry[11] also reported absorption spectrum of cupric acetate in ethanol. The absorption curve, which they reported, agrees with ours in the longer wave-length, but differs from ours in the shorter wave-length. Thus they failed to find a band at about $80\times10^{13}$/sec. which has been clearly seen in our measurement. The appearance of the band at about $80\times10^{13}$/sec.,

11) H. S. French and T. M. Lowry, *Proc. Roy. Soc.*, **A 106**, 489 (1924).

as has been shown in the present measurement, may indicate that cupric acetate in ethanol involves similar components to those in the crystalline cupric acetate. It is supposed, therefore, that cupric acetate in alcohol consists of the dimeric molecules having a formula of $Cu_2(CH_3COO)_4 \cdot X_2$, X being the solvent molecule.

Summarizing the above discussion, we may conclude that *cupric acetate in organic solvents as well as in the crystalline state consists of dimeric molecules, in which a direct type of interaction may exist between the two copper(II) ions.*

**Cupric Propionate Monohydrate.**—The results of the measurements are shown in Fig. 4 and Table II. It is seen that

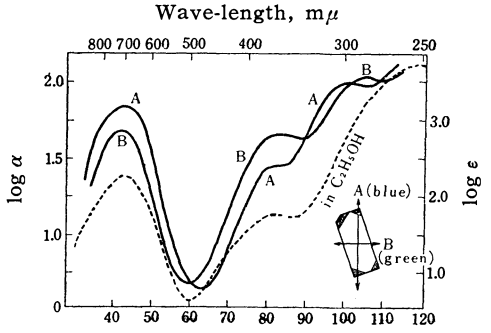



Fig. 4. Absorption spectra of cupric propionate monohydrate in the crystalline state (——), and in ethanol (----).

TABLE II
ABSORPTION MAXIMA OF CUPRIC PROPIONATE MONOHYDRATE IN THE CRYSTALLINE STATE

| | band I | | band II | | band III | |
|---|---|---|---|---|---|---|
| | ν | log α | ν | log α | ν | log α |
| A-abs. | 43 | 1.84 | 83 | 1.44 | 101 | 1.99 |
| B-abs. | | 1.68 | | 1.66 | 106 | 2.03 |

ν: $10^{13}$/sec.

the absorption spectrum bears a close resemblance to the spectrum of cupric acetate. Thus cupric propionate in ethanol and chloroform and in the crystalline state exhibits two absorption bands at 43 and $80\times10^{13}$/sec. having almost the same intensity as the corresponding value of cupric acetate. As described in the above section, the appearance of the new absorption band at about $80\times10^{13}$/sec. may be regarded as showing the existence of the dimeric molecules.

Analysis of the crystal structure has not been done as yet. The present dichroism measurement, however, indicates that the polarization property with the band at about $80\times10^{13}$/sec. is the reverse of the polarization property with the band at about $43\times10^{13}$/sec. The reversal of the polarization property may readily be understood on the assumption of the presence of the dimeric molecule.

All the above facts seem to lead us to the conclusion that *cupric propionate monohydrate in organic solvents such as chloroform and ethanol and in the crystalline state may consist of the dimeric molecules with a formula of* $Cu_2(C_2H_5COO)_4 \cdot X_2$, *where X represents* $OH_2$ *or a molecule of the organic solvent.* This conclusion seems to be in agreement with the anomalous paramagnetic resonance absorption of cupric propionate monohydrate[12].

**Anhydrous Cupric Propionate.** — The dichroism of the anhydrous cupric propionate is shown in Fig. 5 and in the data given in Table III. The crystal structure

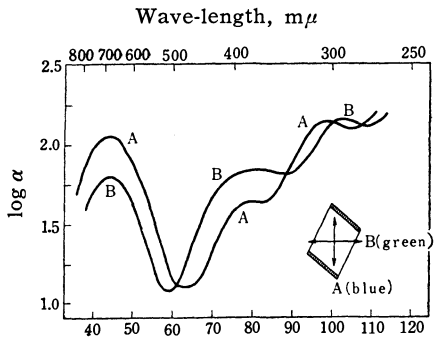



Fig. 5. Absorption spectra of anhydrous cupric propionate in the crystalline state.

TABLE III
ABSORPTION MAXIMA OF ANHYDROUS CUPRIC PROPIONATE IN THE CRYSTALLINE STATE

| | band I | | band II | | band III | |
|---|---|---|---|---|---|---|
| | ν | log α | ν | log α | ν | log α |
| A-abs. | 44 | 2.05 | 80 | 1.63 | 98 | 2.13 |
| B-abs. | | 1.79 | | 1.84 | 102 | 2.15 |

ν: $10^{13}$/sec.

analysis of the anhydrous compound has not been reported as yet. But comparison of the dichroism of the anhydrous propionate with that of the monohydrate clearly indicates that the dichroisms for both compounds are essentially of an identical type, suggesting the existence of similar components in both the compounds. *Thus anhydrous cupric propionate in the crystalline*

12) H. Abe, *Phys. Rev.*, **92**, 1572 (1953).

*state is supposed to consist of the dimeric molecules, in which a direct type of interaction may exist between the two copper ions.*

It may also be concluded that *the water of crystallization has very little effect upon the dichroism,* and that *the linkage, if any, of the water molecules to the copper ion is not very strong in the crystal of cupric acetate monohydrate nor in cupric propionate monohydrate either.*

**Direct Type of Interaction between the Copper Ions within a Molecule.**—We have concluded in the preceding part of the present paper that cupric acetate and propionate in organic solvents and in the crystalline state consist of the dimeric molecules which involve a direct type of interaction between the two copper ions within the molecule. The absorption band at about $80\times10^{13}$/sec. may be related very closely with the direct interaction between the copper ions, although the nature of this band is not completely clear.

In previous papers we reported some examples in which a direct type of interaction might be expected between metallic ions[10,13]. In these compounds, there appeared, in the longer wave-length than the original absorption of their components, to exist a new type of absorption band polarized along the direction in which the metal-to-metal interaction was concluded. From this type of absorption bands the band at about $80\times10^{13}$/sec. of cupric acetate may differ, since the latter lies in the far shorter wave-length than the "copper band" which lies at $43\times10^{13}$/sec. We are inclined to suppose that the copper-to-copper interaction in cupric acetate may be akin to a kind of ordinary linkage. This seems to be compatible with the significantly shorter distance of 2.64Å between the metallic ions in the molecule of cupric acetate than the corresponding distance in Magnus's green salt or bis-(dimethylglyoximato)-nickel(II), in which the metal-to-metal interaction may be assumed to be weaker. The metal-to-metal distances in the latter two compounds were found to be 3.16 and 3.25 Å, respectively[14,15].

It would be worth noting that the intensity of the absorption band at about $43\times10^{13}$/sec. of cupric acetate and propionate in solution is considerably great, as compared with the intensity of the ordinary "copper band" for typical complexes of copper (II). This fact might have some relation with the unusual structure of the present cupric compounds.

13) S. Yamada, *J. Am. Chem. Soc.*, **73**, 1579 (1951); This Bulletin, **24**, 125 (1951); S. Yamada and R. Tsuchida, ibid., **27**, 156 (1954).
14) E. G. Cox, *J. Chem. Soc.*, **1932**, 1905.
15) L. E. Godycki and R. E. Rundle, *Acta Cryst.*, **6**, 487 (1953).

## Summary

Dichroisms in the visible and the ultraviolet region have been determined by the microscopic method with cupric formate tetrahydrate, cupric acetate monohydrate, anhydrous cupric propionate and its monohydrate.

The cupric formate shows an absorption band at about $38—39\times10^{13}$/sec. which is considered to be due to the copper ion in combination with the ligands. For this band, electric vector is much more strongly absorbed along the plane of the complex than in the direction normal to the plane. The dichroism and the absorption spectrum of the cupric formate are of the same type as those of most cupric complexes involving no special effect upon the complexes.

Cupric acetate monohydrate, anhydrous cupric propionate and its monohydrate show an absorption band of a new kind at about $80\times10^{13}$/sec., in addition to a band at about $43\times10^{13}$/sec. which corresponds to the band at about $40\times10^{13}$/sec. of the cupric formate. The polarization for the band at $80\times10^{13}$/sec. is the reverse of the polarization for the band at $43\times10^{13}$/sec. From the appearance of the new band at $80\times10^{13}$/sec. and the reversal of the polarization property with this band, it has been concluded that the cupric compounds examined in this work, except the formate, consist of dimeric molecules having a structure similar to that of cupric acetate monohydrate.

It has also been shown that the water of crystallization has very little effect upon the linkages within the complex molecules. The cupric compounds, except the formate, show in organic solvents a band at $80\times10^{13}$/sec., involving the dimeric molecules in solution.

The present authors wish to thank Dr. R. Kiriyama and Dr. H. Abe for their interest in the present work. The work reported here was supported in part by a grant-in-aid from the Ministry of Education.

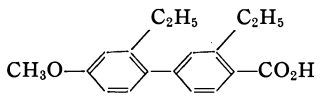
*Department of Chemistry, Faculty of Science, Osaka Uuiversity*
*Nakanoshima, Osaka*

# *Estrogenic Biphenyls. IV. 3'-Alkyl-4-methoxybiphenyl-4'-carboxylic Acids*

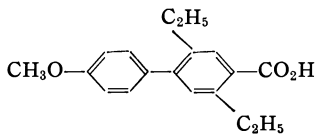
By Takeo SATO and Michinori ŌKI*

(Received July 22, 1957)

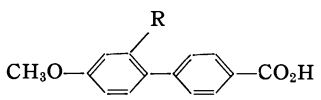
It has been found that 2,3'-diethyl-4-methoxybiphenyl-4'-carboxylic acid[1] (I) and 2',5'-diethyl-4-methoxybiphenyl-4'-carboxylic acid[2] (II) are fully estrogenic to ovariectomized mice at the doses of 100 $\gamma$ and that the enhanced estrogenic potency has been attributed to the presence of the two ethyl groups. In the previous paper[3], the role of the alkyl group of 2-alkyl-4-methoxybiphenyl-4'-carboxylic acids (III) in the estrogenic activity was studied and no significant difference was found in the activity of the members of this series.



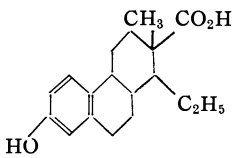
I



II



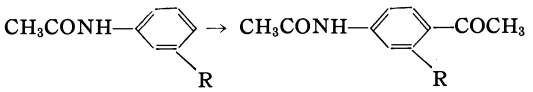
III



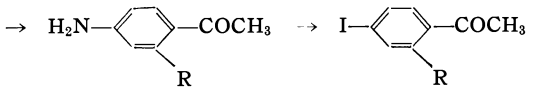
IV

Since these compounds are related structurally to doisynolic acid (IV), the effect of the alkyl group at position 3' on the estrogenic activity is expected to be great[4]. Therefore the authors wished to find out the optimum alkyl group at position 3' of 4-methoxybiphenyl-4'-carboxylic acid (III, R=H).

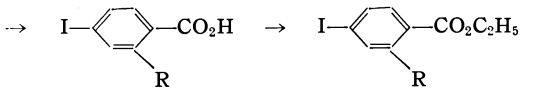
3'-Alkyl-4-methoxybiphenyl-4'-carboxylic acids (XII) were synthesized in the same way as compound I. All the compounds up to X where R is ethyl are known[1].



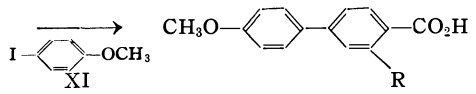
V VI



VII VIII



IX X



XII

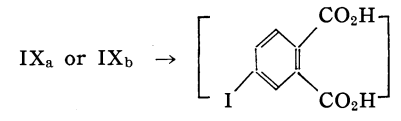
a: $CH_3$ b: $C_2H_5$ c: $n$-$C_3H_7$

*m*-Alkylacetanilide (V) was treated with acetyl chloride and aluminium chloride to give 4-acetamido-2-alkylacetophenone (VI), which was hydrolyzed to 2-alkyl-4-aminoacetophenone (VII). Diazotization of compound VII and treatment of the diazonium salt with potassium iodide yielded 2-alkyl-4-iodoacetophenone (VIII), which was oxidized with sodium hypobromite to produce 2-alkyl-4-iodobenzoic acid (IX). The ethyl ester (X) was prepared in the usual way. Compound X and *p*-iodoanisole (XI) were submitted to the Ullmann reaction and the product was hydrolyzed to produce the desired compound (XII).

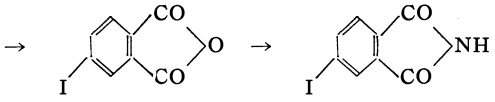
The structure of 2-alkyl-4-iodobenzoic acid ($IX_a$ and $IX_b$) was proved in the following way. Compound IX gave a dibasic acid (XIII) on oxidation with potassium permanganate and the acid (XIII) gave known 4-iodophthalic anhydride (XIV) on sublimation and then 4-iodophthalimide (XV)[5] when the compound XIV was treated with ammonia.

* Present address: Department of Chemistry, Faculty of Science, The University of Tokyo, Hongo, Tokyo.

1) M. Ōki and T. Sato, This Bulletin, **30**, 508 (1957).
2) M. Ōki and T. Sato, ibid., **30**, 702 (1957).
3) T. Sato and M. Ōki, ibid., in press.
4) See K. Miescher, *Chem. Rev.*, **43**, 367 (1948).
5) A. Edinger, *J. prakt. Chem.*, (2), **53**, 375 (1896).



XIII



XIV XV

TABLE I

ULTRAVIOLET ABSORPTION MAXIMA AND ESTROGENIC ACTIVITY OF 3'-ALKYL-4-METHOXYBIPHENYL-4'-CARBOXYLIC ACID (XII)

| Compound | $\lambda_{max.}$ (mμ) | log $\varepsilon_{max.}$ | Minimum active dose in mice (γ) |
|---|---|---|---|
| XIIa | 287 | 4.39 | 500 |
| XIIb | 286 | 4.36 | 250 |
| XIIc | 286 | 4.38 | 500 |

The ultraviolet absorption data and the estrogenic activity of compounds XIIa, XIIb and XIIc are given in Table I. All the members of the present series showed a strong absorption at about 286 mμ (log ε =4.36), while 4-methoxybiphenyl-4'-carboxylic acid (III, R=H) at 289 mμ, as previously reported[3]. The spectra of compounds XII and III (R=H) were expected to resemble, since substitution at position 3' was regarded to have little effect on the conformation of the biphenyl skeleton. However, it may be noted that a hypsochromic shift of the absorption maxima has been observed rather than a bathochromic shift which is common when an alkyl group is introduced into the benzene ring. Similar results have been noted by other workers, when alkyl substitution takes place at the ortho position to the carboxyl group of the benzoic acid[6-8] and have been explained on the basis of the steric effect of the alkyl group which enforces the carbonyl group to rotate and to lose resonance with the benzene ring.

The minimum active doses of the members of the series XII to produce full estrus were determined by the vaginal smear test with ovariectomized mice. The alkyl substitution at position 3' enhances the estrogenic activity of 4-methoxybiphenyl-4'-carboxylic acid, probably because of the increasing width of the molecule. It is noted, however, that the kinds of alkyl group show no remarkable difference in the estrogenic activity. This may be attributed to the similar molecular thickness, as is shown by the ultraviolet absorption.

6) S. D. Ross, *J. Am. Chem. Soc.*, **70**, 4039 (1948).
7) E. A. Fehner, ibid., **72**, 1404 (1950).
8) C. M. Moser and A. J. Kohlenberg, *J. Chem. Soc.*, **1951**, 804.

## Experimental[9]

***m*-Propylacetanilide** (Vc). — *m*-Propylaniline[3] was treated with acetic anhydride in the usual way. The oily product distilled at 165—169°/3 mm. and solidified on cooling. Recrystallization from aqueous ethanol gave colorless needles, m. p. 51—52°. Yield 96% of the theoretical.

*Anal.* Found: N, 7.79. Calcd. for $C_{11}H_{15}ON$: N, 7.90%.

**4-Acetamido-2-methylacetophenone** (VIa). —To a well-stirred mixture of 45 g. (0.30 mole) of *m*-methylacetanilide (Va)[10], 43 g. (0.55 mole) of acetyl chloride, and 240 ml. of carbon disulfide, 142 g. (1.1 moles) of aluminium chloride was added in small portions in one hour. The mixture was then heated under reflux for one hour and allowed to stand at room temperature for another hour. The supernatant carbon disulfide layer was decanted off and the lower layer was poured into a mixture of cracked ice and hydrochloric acid. The precipitate was collected and used for the subsequent reaction without purification. The analytical sample was obtained by recrystallization from aqueous ethanol. Colorless needles, m. p. 135—136°.

*Anal.* Found: N, 7.40. Calcd. for $C_{11}H_{13}O_2N$: N, 7.33%.

**4-Amino-2-methylacetophenone** (VIIa). —A mixture of the crude VIa and 300 ml. of dilute hydrochloric acid (1 : 1) was heated under reflux for two hours, and, after cooling, basified with aqueous sodium hydroxide. The organic material was extracted with ether and the ethereal extract was dried over potassium carbonate and concentrated to give crystals, which were recrystallized from benzene-petroleum ether. Pale yellow plates, m. p. 94—95°. Yield 29 g. or 64% of the theoretical based on the *m*-methylacetanilide.

*Anal.* Found: N, 9.18. Calcd. for $C_9H_{11}ON$: N, 9.15%.

**4-Amino-2-propylacetophenone** (VIIc). — Treatment of 140 g. (0.79 mole) of compound Vc with 70 g. (0.89 mole) of acetyl chloride and 300 g. (2.26 moles) of aluminium chloride in 700 ml. of carbon disulfide yielded a viscous oil. The mixture was extracted with benzene and the extract was heated under reflux with 500 ml. of hydrochloric acid (1 : 1) for two hours. The aqueous layer was separated and basified with sodium hydroxide. The base was extracted with ether and the extract was fractionated. Repeated fractionation gave an oil boiling at 155°/2 mm. which solidified on standing. The analytical sample was obtained by recrystallization from benzene-petroleum ether. Colorless needles, m.

9) All melting and boiling points are uncorrected.
10) F. Beilstein and Al Kuhlberg, *Ann.*, **156**, 66 (1870).

p. 77.5—79°. Yield 53 g. or 38% of the theoretical.

*Anal.* Found: N, 7.88. Calcd. for $C_{11}H_{15}ON$: N, 7.90%.

The acetyl compound ($VII_c$) was obtained in the usual way. Colorless plates, m. p. 95.5—96°, were obtained on recrystallization from aqueous ethanol.

*Anal.* Found: N, 6.74. Calcd. for $C_{13}H_{17}O_2N$: N, 6.39%.

**2-Alkyl-4-iodoacetophenones (VIII).** — The general procedure is described by an example of the preparation of 4-iodo-2-methylacetophenone. The diazonium salt solution prepared from 30 g. (0.2 mole) of compound $VII_a$, dilute sulfuric acid (42 g. or 0.42 mole of sulfuric acid and 100 ml. of water) and 14 g. (0.2 mole) of sodium nitrite in 30 ml. of water, was slowly added to a solution of 50 g. (0.3 mole) of potassium iodide in 70 ml. of water. Stirring was continued for thirty minutes at a low temperature and then at 50—60° for two hours. The mixture was extracted with ether and the ethereal extract was washed with aqueous sodium hydroxide, aqueous sodium thiosulfate, and water. 4-Iodo-2-methylacetophenone boiled at 134—138°/4 mm. and solidified on long standing. The analytical sample was obtained by recrystallization from petroleum ether. Colorless prisms, m. p. 23—24°. Yield 27 g. or 52% of the theoretical.

*Anal.* Found: C, 41.40; H, 3.13. Calcd. for $C_9H_9OI$: C, 41.56; H, 3.49%.

4-Iodo-2-propylacetophenone ($VIII_c$) was obtained in 51% yield from the corresponding amine ($VII_c$). Brown oil, b. p. 158—159°/8 mm. Since the purification of this compound was a tedious process, the crude product was used for the subsequent reaction without purification.

**2,4-Dinitrophenylhydrazone of 4-Iodo-2-methylacetophenone ($VIII_a$).** — Recrystallized from ethanol-ethyl acetate. Orange plates, m. p. 167—168°.

*Anal.* Found: N, 12.50. Calcd. for $C_{15}H_{13}O_4N_4I$: N, 12.73%.

**2,4-Dinitrophenylhydrazone of 4-Iodo-2-propylacetophenone ($VIII_c$).** — Recrystallized from ethanol-ethyl acetate. Deep-orange plates, m. p. 160—161°.

*Anal.* Found: N, 11.86. Calcd. for $C_{17}H_{17}O_4N_4I$: N, 11.97%.

**2-Alkyl-4-iodobenzoic Acids (IX).** — The general procedure is given by an example of the preparation of 4-iodo-2-methylbenzoic acid ($IX_a$) as follows. To a well stirred sodium hypobromite solution, prepared from 65 g. (0.36 mole) of bromine, 50 g. (1.25 moles) of sodium hydroxide and 250 ml. of water, a solution of 25 g. (0.096 mole) of compound $VIII_a$ in 130 ml. of dioxan was added in one hour. The temperature was kept below 10° during the addition and then at 50—60° for one hour. The excess of hypobromite was decomposed with sodium sulfite and the mixture was steam-distilled to remove bromoform. The remaining solution was acidified with hydrochloric acid and the product was recrystallized from aqueous ethanol. Colorless needles, m. p. 169—170.5°. Yield 20 g. or 79% of the theoretical.

*Anal.* Found: C, 36.74; H, 2.53. Calcd. for $C_8H_7O_2I$: C, 36.66; H, 2.69%.

4-Iodo-2-propylbenzoic acid ($IX_c$) was obtained in 80% yield. Colorless needles, m. p. 127—128°.

*Anal.* Found: C, 41.60; H, 3.50. Calcd. for $C_{10}H_{11}O_2I$: C, 41.41; H, 3.82%.

**4-Iodophthalimide (XV). (A). From 4-Iodo-2-propylbenzoic Acid ($IX_d$).**—A mixture of 1 g. of compound $IX_d$, 5 g. of potassium permanganate, and 80 ml. of water, was heated under reflux for eighteen hours. Sulfur dioxide was bubbled into the mixture and the resulting solution was extracted with ether for five hours. The ethereal extract was dried over anhydrous magnesium sulfate and evaporated. The residue was distilled and 800 mg. of pale yellow prisms, m. p. 111—112°, were obtained. A purer sample of 4-iodophthalic anhydride (XIV) was obtained by sublimation in vacuo. Colorless prisms, m. p. 114—116°. The reported melting point is 123°[5].

A mixture of the crude 4-iodophthalic anhydride (500 mg.) and 1 ml. of 28% aqueous ammonia was heated over a free flame to remove excess of ammonia and water and the residue was sublimed in vacuo. 4-Iodophthalimide was obtained in pale yellow plates melting at 226—228°. Yield 400 mg. or 80% of the theoretical. Reported melting point is 222—224°[5].

*Anal.* Found: N, 5.08. Calcd. for $C_8H_4O_2NI$: N, 5.13%.

**(B) From 4-Iodo-2-methylbenzoic Acid ($IX_a$).**—Compound $IX_a$ was treated in the same way as described above. Pale yellow plates melting at 224—226° were obtained and showed no depression of the melting point when mixed with another specimen of 4-iodophthalimide described above.

**Ethyl 2-Alkyl-4-iodobenzoates (X).**—The general procedure is exemplified by the preparation of ethyl 4-iodo-2-methylbenzoate ($X_a$) as follows. A solution of 20 g. of compound $IX_a$ in 200 ml. of ethanol was saturated with hydrogen chloride and the mixture was heated under reflux for six hours. The solution was concentrated and diluted with water. Extraction with ether followed by fractionation gave the pure ester boiling at 141—144°/4 mm. Yield 17 g. or 78% of the theoretical.

*Anal.* Found: C, 41.87; H, 4.07. Calcd. for $C_{10}H_{11}O_2I$: C, 41.40; H, 3,82%.

Ethyl 2-ethyl-4-iodobenzoate ($X_b$) was prepared as described elsewhere[1]. Ethyl 4-iodo-2-propylbenzoate ($X_c$) was obtained in 77% yield. B. p. 179—182°/16 mm.

*Anal.* Found: C, 45.72; H, 4.74. Calcd. for $C_{12}H_{15}O_2I$: C, 45.30; H, 4.75%.

**3'-Alkyl-4-methoxybiphenyl-4'-carboxylic Acids (XII).**—The general procedure of synthesis was illustrated by the following example. A mixture of 18.6 g. (0.079 mole) of *p*-iodoanisole (XI)[11] and 10.0 g. (0.035 mole) of compound $X_a$, was heated at 220—228° with stirring and 30 g. (0.47 atom) of activated copper bronze[12] was

11) M. P. Brenans, *Bull. soc. chim. France*, (3), **25**, 819 (1901).

12) E. C. Kleiderer and R. Adams, *J. Am. Chem. Soc.*, **55**, 4291 (1933).

added over a period of twenty-five minutes. The temperature was kept at 220—230° for ten minutes and then at 280° for forty minutes. The reaction mixture was extracted with acetone and the solvent was evaporated. The residue was refluxed with a mixture of 100 ml. of 10% aqueous sodium hydroxide and 200 ml. of ethanol for six hours. The mixture was concentrated and the residue diluted with water. Insoluble material was removed by filtration and the filtrate was acidified with hydrochloric acid. The crystalline material was collected and boiled with benzene. Removal of the insoluble material followed by concentration gave the desired product. 4-Methoxy-3'-methylbiphenyl-4'-carboxylic acid ($XII_a$) was obtained in colorless needles, m.p. 199.5—200°, on recrystallization from aqueous ethanol. Yield 1.0 g. or 12% of the theoretical.

*Anal.* Found: C, 74.35; H, 5.55. Calcd. for $C_{15}H_{14}O_3$: C, 74.36; H, 5.83%.

3'-Ethyl-4-methoxybiphenyl-4'-carboxylic acid ($XII_b$) was obtained in 15% yield. Colorless needles, m. p. 182—183°.

*Anal.* Found: C, 74.82; H, 6.57. Calcd. for $C_{16}H_{16}O_3$: C, 74.98; H, 6.29%.

4-Methoxy-3'-propylbiphenyl-4'-carboxylic acid ($XII_c$) was obtained in 16% yield. Colorless needles, m. p. 170.5—171°.

*Anal.* Found: C, 75.85; H, 6.63. Calcd. for $C_{17}H_{18}O_3$: C, 75.53; H, 6.71%.

**Ultraviolet Absorption Spectra.** — These were measured by using Hitachi Photo-electric Spectrophotometer Model EPU-2. Substances were dissolved in 95% ethanol.

The authors wish to express their hearty thanks to Professor Y. Urushibara of the University of Tokyo for encouragement throughout this work and to the Research Department of Teikoku Hormone Manufacturing Co., Kawasaki, for bio-assay. The authors' thanks are also due to the Ministry of Education for the Grant in Aid for Fundamental Research.

*Department of Chemistry, Faculty of Science, Tokyo Metropolitan University, Setagaya, Tokyo*

# *Studies on Polyelectrolytes XXXVIII. Polyion in Simple Salt Solution*

By Mitsuru NAGASAWA and Ikumi KAGAWA

(Received July 9, 1957)

The study of electrical potential and counter ion distributions around a polyion in simple salt solution is one of the most important for clarifying the abnormal behavior of polyion. In this field, several interesting theories have so far been reported, including, Hermans and Overbeek's (H. O. theory)[1], Kimball, Cutler and Samelson's (K. C. S.)[2], Oosawa, Imai and Kagawa's (O. I. K.)[3], and Wall and Berkowitz's (W. B.)[4]. Although almost the same model of polyion was used in these theories, different potential distribution curves and free energies of the system were obtained because of the difference in procedure. Calculated from their expressions of the potential distribution and the free energy, therefore, the volume of polyion differs considerably, and, moreover, all volumes thus calculated as well as that calculated from assuming the balance between osmotic pressure and Kuhn entropy force by Flory[5] are much larger than the volume experimentally estimated[6-8]. The disagreement between observed and calculated volumes has sometimes been explained by presuming an association of counter ion with polyion and sometimes by pointing out the failure of the Debye-Hückel approximation for the exponentials in Poisson-Boltzmann equation.

The present paper is offered for the purpose of making a contribution toward the comprehension of the relationship among the theories so far published and an understanding of the cause of disagreement between theories and experiments. Taking into account the differences

1) J. J. Hermans and Th. G. Overbeek, *Rec. trav. chim.*, **67**, 761 (1948).
2) G. E. Kimball, M. Cutler and H. Samelson, *J. Phys. Chem.*, **56**, 57 (1952).
3) F. Oosawa, N. Imai and I. Kagawa, *J. Polymer Sci.*, **13**, 93 (1954).
4) F. T. Wall and J. Berkowitz, *J. Chem. Phys.*, **26**, 114 (1957).
5) P. F. Flory and I. E. Osterheld, ibid., **58**, 653 (1954).
6) N. S. Schneider and P. Doty, ibid., **58**, 762 (1954).
7) H. J. L. Trap and J. J. Hermans, ibid., **58**, 757 (1954).
8) H. Fujita, M. Mitsuhashi and T. Homma, *J. Colloid Sci.*, **9**, 466 (1954).

observed in several divisions of their theories, the authors' discussion is centered around the following three points: First, the relationship among the theories of H.O., K.C.S. and O.I.K. is compared and, based on the comparison, the authors introduce an analytical equation of potential distribution which is thought to be more reasonable in this category of polyelectrolyte theory. The characteristic features of the potential curve thus obtained are described in detail in relation to the Donnan membrane potential. Second, it is shown that when this potential distribution curve is used, the electrical free energy of the system can be easily calculated by simultaneously charging all ions in the solution from the non-charged state to the real state. The free energy thus obtained is compared with those of other theories[1,3,9]. Third, the polyion volume is calculated on the usual assumption that the electrical repulsive force is equal to the Kuhn entropy force. The volume obtained is still much larger than the volume estimated from the viscosity data, despite the fact that it must be the smallest of all theoretical volumes. Some comments are made on the cause of this.

The model of polyion employed here is a sphere having a uniform charge density throughout. It is assumed that the polyion is in an infinitely large volume of uni-uni valent simple electrolyte solution, and also that it has negatively charged groups and that the counter ion is the same univalent ion as the positive ion of the added electrolyte.

## Potential and Ionic Distribution Around Polyion

Let us consider that $R$ denotes the radius of polyion sphere and $Ze$ the fixed charge of the polyion, then the density of fixed charge in the polyion $\rho_0$ is given by

$$\rho_0 = Ze/\frac{4}{3}\pi R^3 \tag{1}$$

If it is assumed that we can express the relationship among this charge density ($\rho_0$), the concentration of the simple electrolyte in the solvent phase ($n_c$) and the concentration in the polyion sphere phase ($n_c^P$) by Donnan equilibrium, it follows that

$$n_c^P(\rho_0/e+n_c^P)=n_c^2 \tag{2}$$

and also that the potential difference between the polyion phase and the solvent phase ($E_D$) can be given by the following Donnan membrane potential equation:

$$E_D=-\frac{kT}{e}\ln\frac{\rho_0/e+n_c^P}{n_c}=-\frac{kT}{e}\ln\frac{n_c}{n_c^P} \tag{3}$$

Substitution of $n_c^P$ calculated from Eq. (1) into Eq. (2) yields

$$E_D=-\frac{kT}{e}\ln\frac{1+\sqrt{1+\left(\frac{8\pi}{3}\frac{1}{Z}R^3n_c\right)^2}}{\left(\frac{8\pi}{3}\frac{1}{Z}R^3n_c\right)} \tag{4}$$

from which it follows that

$$E_D^\circ=-\frac{kT}{e}\frac{1}{\left(\frac{8\pi}{3}\frac{1}{Z}R^3n_c\right)}=\frac{kT}{e}\frac{\rho_0/e}{2n_c} \tag{5}$$

when $n_c \gg 2\rho_0/e$, i. e., $\frac{8\pi}{3}\frac{1}{Z}R^3n_c \gg 1$.

When $E_D$ or $E_D^\circ$ is used, the potential distribution curves for a polyion at infinite dilution in H.O., K.C.S. and O.I.K. theory are simplified as follows:

H.O.,

$$\psi_1=E_D^\circ\left\{1-e^{-\kappa R}(1+\kappa R)\frac{\sinh(\kappa r)}{\kappa r}\right\} \qquad (r<R) \tag{6}$$

$$\psi_2=\frac{1}{2}E_D^\circ\{(1+\kappa R)e^{-\kappa R}-(1-\kappa R)e^{\kappa R}\}\frac{e^{-\kappa r}}{\kappa r} \qquad (r>R) \tag{7}$$

K.C.S., (1) When Donnan approximation is applied:

$$\psi_1=\frac{kT}{e}\sinh^{-1}\frac{e}{kT}E_D^\circ=E_D \tag{8}$$

$$\psi_2=0 \tag{9}$$

(2) When $e\psi/kT \ll 1$:

Both $\psi_1$ and $\psi_2$ are the same as Eqs. (6) and (7).

O.I.K.,

$$\psi_1=E_D\left\{1-\frac{2}{e^{\kappa R}+e^{-\kappa R}}\frac{\sinh(\kappa r)}{\kappa r}\right\} \tag{10}$$

Here, in the theory of K.C.S. the equations for uniform distribution of fixed charge only are considered and in the theory of O.I.K. the equation at infinite dilution of polyion only is considered, $\kappa$ being the reciprocal thickness of ionic atmosphere, i.e.,

$$\kappa^2=\frac{8\pi e^2}{DkT}n_c \tag{11}$$

9) S. Lifson and A. Katchalsky, *J. Polymer Sci.*, **13**, 43 (1954).

In all three theories it can be easily observed that the potential $\psi_1$ becomes $E_D$ or $E_D^\circ$ and $\psi_2$ becomes zero when $R$ is very large, that is

H.O., $\psi_1=E_D^\circ$

K.C.S.,

(1) for Donnan approximation $\psi_1=E_D$

(2) for $e\psi/kT\ll1$ $\psi_1=E_D^\circ$

O.I.K., $\psi_1=E_D$ (12)

This fact suggests a very close relationship among these three theories and the simple Donnan theory of ionic distribution, which is later discussed in more detail. (see p. 966)

The theory of Oosawa, Imai and Kagawa distingushes itself from the other theories in the feature that no Debye-Hückel approximation is used in its solution to the Poisson-Boltzmann equation. The fact that $E_D$, instead of $E_D^\circ$, appears in the potential equation, Eq. (10) of this theory manifests this feature. Another difference observed between these three theories is the difference between the factors of the second term in the $\psi_1$ equations. This difference comes from the fact that in the O.I.K. theory the effect of the ionic distribution outside the polymer sphere upon the potential distribution inside is entirely neglected, while in the H.O. and the K.C.S. theory that effect is taken into account.

An inspection of the two differences among H.O., K.C.S. and O.I.K. theory may lead us to expect the following equations to be a better approximation in this category of the polyelectrolyte theory:

$$\psi_1=E_D\left\{1-e^{-\kappa R}(1+\kappa R)\frac{\sinh(\kappa r)}{\kappa r}\right\} \quad (r<R) \quad (13)$$

$$\psi_2=\frac{1}{2}E_D\{(1+\kappa R)e^{-\kappa R}-(1-\kappa R)e^{\kappa R}\}\frac{e^{-\kappa R}}{\kappa r} \quad (r>R) \quad (14)$$

This result can be easily verified through the following calculation: eqs. (13) and (14) can be easily calculated from the same fundamental equations as used by Hermans and Overbeek if the assumption $e(E_D-\psi_1)\ll1$ instead of $e\psi_1/kT\ll1$ is used. That is,

$$\Delta\psi_1=-\frac{4\pi}{D}[-\rho_0+n_c e\exp(-e\psi_1/kT)-n_c e\exp(e\psi_1/kT)] \quad (15)$$

$$\Delta\psi_2=-\frac{4\pi}{D}[n_c e\exp(-e\psi_2/kT)-n_c e\exp(e\psi_2/kT)] \quad (16)$$

As $\psi_2$ is in general smaller than $kT/e$, the Debye and Hückel approximation can be used for the exponentials in Eq. (16) and hence from that equation it follows that

$$\psi_2=A_2\frac{e^{-\kappa r}}{r}+A'_2\frac{e^{\kappa r}}{r} \quad (17)$$

where $A_2$ and $A_2'$ are integral constants. However, $\psi_1$ may sometimes become considerably great, but even in such a case the difference between $E_D$ and $\psi_1$, i.e., $\psi_1'=E_D-\psi_1$, may be so small that the linear approximation of the exponentials of $e\psi_1'/kT$ can be applied (see Fig. 1).

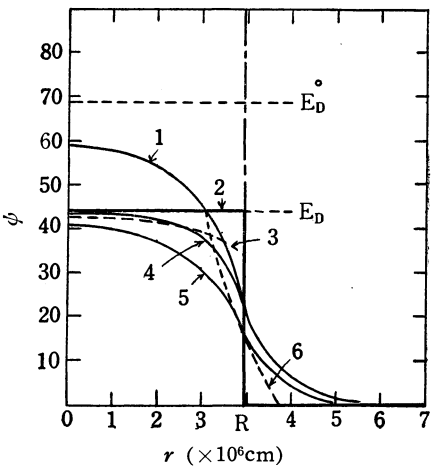



Fig. 1. Comparison of theoretical equations.
Sodium polyvinyl sulfate
$Z=1070$, $R=3.94\times10^{-6}$ cm
NaCl concn. $=1.31\times10^{-3}$ N
1. H.O.; 2. K.C.S.; 3. O.I.K.
4. Eqs. (13') and (14')
5. Eqs. (13) and (14)
6. Donnan-Helmholtz model

(Experimentally, $\psi_1$ is often greater than $kT/e=25.7$ mV at 25°C, but it is seldom greater than 2 $kT/e$ even in considerably diluted solutions of simple salt. The assumption $e\psi_1'/kT<1$, therefore, may be true for a very wide range of simple salt solution.) When $\psi_1=E_D-\psi_1'$ is inserted in Eq. (15), the series expansion of exponentials of $e\psi_1'/kT$ are applied and higher terms are neglected, the equation becomes

$$\Delta\psi_1'=\kappa^2\cosh(eE_D/kT)\psi_1'=\kappa'^2\psi_1' \quad (18)$$

from which it follows that

$$\psi_1=E_D-\psi_1'=E_D-A_1\frac{e^{-\kappa' r}}{r}-A_1'\frac{e^{\kappa' R}}{r} \quad (19)$$

where $A_1$ and $A_1'$ are integral constants and $\kappa'^2=\kappa^2\cosh(eE_D/kT)$.

Based on the boundary conditions that $\psi$ is everywhere finite, is zero at infinity and is continuous on the surface of the sphere, all constants in Eqs. (17) and (19) can be determined. The final equations thus obtained are as follows:

$$\psi_1=E_D\left[1-\frac{1+\kappa R}{\kappa'\cosh(\kappa' R)+\kappa\sinh(\kappa R)}\cdot\frac{\sinh(\kappa' r)}{\kappa' r}\right] \quad (13')^*$$

$$\psi_2=E_D\left[\frac{(1+\kappa' R)e^{-\kappa' R}-(1-\kappa' R)e^{\kappa' R}}{\kappa'(e^{-\kappa' R}+e^{\kappa' R})-\kappa(e^{-\kappa' R}-e^{\kappa' R})}\cdot e^{\kappa R}\right]\frac{e^{-\kappa r}}{r} \quad (14')^*$$

If we assume $\kappa'=\kappa$ in Eqs. (13') and (14'), we obtain Eqs. (13) and (14). As shown by Wall and Berkowitz in their numerical solution of Eqs. (15) and (16), the term $E_D$ has a strong effect on ionic distribution, but the factor of the second term is less important. Therefore, to assume $\kappa'=\kappa$ in this stage, i.e., the assumption that $E_D$ is not *very* large, scarecely lessens the applicability of the theoretical equations.

We have made a comparison between the results calculated from these theoretical equations for an experimental example in Fig. 1. It is observed that the values calculated from Eqs. (13) and (14) are the smallest of all calculated values. The difference between the values calculated from these equations and others grows smaller as the concentration of the simple salt solution increases.

The charge distribution around polyion can be calculated as follows. As the charge density $\rho$ is given by the following equation,

$$4\pi r^2\cdot\rho=-\Delta\psi\cdot r^2 D \quad (20)$$

from this equation and Eqs. (13) and (14) it follows that

$$4\pi r^2\rho_1=D\cdot E_D e^{-\kappa R}(1+\kappa R)\kappa r\cdot\sinh(\kappa r) \quad (r<R) \quad (21)$$

$$4\pi r^2\rho_2=-\frac{DE_D}{2}\{(1+\kappa R)e^{-\kappa R}-(1-\kappa R)e^{\kappa R}\}(\kappa r)e^{-\kappa r} \quad (r>R) \quad (22)$$

The total amount of the free charge inside and outside the polyion sphere ($[q]_1$ and $[q]_2$) can be calculated from the following integrations:

$$[q]_1=\int_0^R 4\pi r^2\rho_1 dr \quad (23)$$

$$[q]_2=\int_R^\infty 4\pi r^2\rho_2 dr \quad (24)$$

Hence, carrying out these integrations by using Eqs. (21) and (22), we have

$$[q]_1=-[q]_2=D\cdot\frac{E_D}{2\kappa}(1+\kappa R)e^{-\kappa R}[(1+\kappa R)e^{-\kappa R}-(1-\kappa R)e^{\kappa R}] \quad (25)$$

In Fig. 2, the result calculated from Eqs. (21) and (22) for the same example as in Fig. 1 is shown.

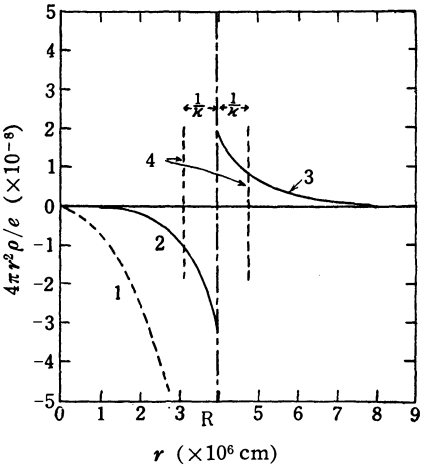



Fig. 2. Charge distribution calculated by Eqs. (21) and (22).
1. $4\pi r^2\rho_0$
2. $4\pi r^2\rho_1$
3. $4\pi r^2\rho_2$
4. Donnan-Helmholtz model

## Calculation of the Electrical Free Energy

The electrical free energy discussed here means the difference between the free energy of systems at the real state and at the imaginary non-charged state, which causes the electrical repulsion of polyion sphere. That is, the electrical free energy is equal to the work which must be done when all ions in the solution are charged simultaneously from the imaginary non-charged state to the real state, keeping the interior and the exterior

* These equations agree entirely with those independently derived by Lifson[16]. He pointed out that these equations are very close to the numerical solution of Wall and Berkowitz. Eqs. (13') and (14') have a little wider applicability to experiments than Eqs. (13) and (14), but to calculate the free energy using them is very difficult. The order of applicability of various theoretical equations is as follows:

H. O.<Eqs. (13), (14)<Eqs. (13'), (14')<W. B.

In real experiments, however, experiments are rarely carried out in such a dilute simple salt solution as that in which the Hermans and Overbeek's theory does not hold, although Wall and Berkowitz have reported that H. O. theory gives far too high potential values.

16) S. Lifson, private communication.

of the polyion sphere at equilibrium. (This electrical free energy is not necessarily equal to that defined in the well-known theory of Debye and Hückel, where the work done while each ion is being charged against the electrical potential caused by the self-charge, must be subtracted from the electrical free energy defined here.)

The electrical free energy ($F_e$) of the system is given by the following integration:

$$F_e=\int_0^{\infty}\int_0^1\psi(\xi)\rho(\xi)/\xi 4\pi r^2\cdot dr\cdot d\xi$$
$$=\int_0^{R}\int_0^1\psi_1(\xi)\rho_1(\xi)/\xi\cdot 4\pi r^2\cdot dr\cdot d\xi$$
$$+\int_R^{\infty}\int_0^1\psi_2(\xi)\rho_2(\xi)/\xi\cdot 4\pi r^2\cdot dr\cdot d\xi \quad (26)$$

where $\xi$ denotes the fraction of final charges which the ions have at any stage of the integration. After some simple calculations using Eqs. (13), (14), (21) and (22), $F_e$ becomes

$$F_e=\frac{1}{2}D\frac{(\kappa R)^2}{2\kappa}E_D^2\int_0^{\kappa R}f(x)dx$$
$$=\frac{1}{2}D\frac{(\kappa R)^2}{2\kappa}E_D^2\sigma(\kappa R) \quad (27)$$

where

$$f(x)=\frac{(3+6x+5x^2+2x^3)e^{-2x}+(x^2-3)}{x^3} \quad (28)$$

$$\sigma(\kappa R)=\int_0^{\kappa R}f(x)dx \quad (29)$$

and the values of $\sigma(\kappa R)$ can be easily obtained by graphical integration.

## Calculated Dimension of Polyion Sphere and a Comparison of Calculated and Experimental Dimensions

The dimension of polyion sphere may be calculated from the condition that the total free energy of the system, that is, the sum of the electrical free energy and the Kuhn entropy, must have the minimum value. That is,

$$\frac{d}{dR}[F_e+TS_K]=0 \quad (30)$$

Therefore,

$$dF_e/dR=-TdS_K/dR \quad (31)$$

The value of $dF_e/dR$ is given by differentiating Eq. (27) as follows:

$$\frac{dF_e}{dR}=\frac{1}{2}D(\kappa R)E_D\left[E_D\left\{\sigma(\kappa R)+\frac{1}{2}(\kappa R)\frac{d\sigma(\kappa R)}{d(\kappa R)}\right\}+R\frac{dE_D}{dR}\sigma(\kappa R)\right] \quad (32)$$

Numerical values of $\sigma(\kappa R)$ and $d\sigma(\kappa R)/dR$ can be easily calculated by graphical method. In calculating the Kuhn entropy, we must express it as a function of $R$. Since such a calculation has already been performed by Hermans and Overbeek[10], we use their calculated result although it is a little different from the original Kuhn entropy; that is,

$$-T\frac{dS_K}{dR}=kT\left[\frac{3}{R^2-\frac{5}{36}NA^2}-\frac{108}{5}\frac{1}{NA^2}\right]\cdot R \quad (33)$$

where $A$ is the dimension of statistical segment and $N$ the number of segments in a polyion.

Thus, when we know the polymerization degree and the charge density, we can graphically calculate the value of $R$ from Eqs. (30)–(33) by assuming a value of $A$.

The experimental value of $R$ can be calculated from the data of intrinsic viscosity; that is, the end-to-end distance of polymer is first calculated based on Flory's theory[11], and next is transformed into the radius of polyion sphere. According to Flory, the intrinsic viscosity of a polymer is expressed as follows:

$$[\eta]=\frac{\Phi(\sqrt{\bar{h}^2})^3}{M} \quad (34)$$

where $M$ is the molecular weight of polymer and $\Phi$ is $2.1\times10^{21}$ when $[\eta]$ is expressed by 100 c.c./g. The $\bar{h}$ is related to $R$ by Hermans and Overbeek as follows:

$$R^2=\frac{5}{36}NA^2\left(1+\frac{\bar{h}^2}{NA^2}\right) \quad (35)$$

The calculated and the experimental values of $R$ thus obtained for polyvinyl alcohol sulfate are shown as an example in Table I. In this Table, in addition, the values of $-T(dS_K/dR)$ and $(dF_e/dR)$ calculated by using the experimental values of $R$ are shown. The value of $A$ used for the calculation is 20–40 Å, which is thought to be reasonable for vinyl polymer[8].

It is observed that there is considerable disagreement between observed and calculated radii of polyion; values of the

10) D. T. F. Pals and J. J. Hermans, *Rec. trav. chim.*, **71**, 434 (1954).
11) P. F. Flory, "The Principles of Polymer Chemistry", Cornell University Press. p. 616 (1953).

TABLE
SODIUM POLYVINYL
Deg. of polym.=1470,

| NaCl concn. in solvent (N) | $A=20$ Å | | | |
|---|---|---|---|---|
| | $R_\eta$ | $R_{calcd.}$ | $\left(-T\frac{dS_K}{dR}\right)_{R,obs.}$ | $\left(\frac{dF_e}{dR}\right)_{R,obs.}$ |
| 1.00 | $1.73\times10^{-6}$ | $1.75\times10^{-6}$ | $1.3\times10^{-7}$ | $1.6\times10^{-7}$ |
| $5.00\times10^{-1}$ | 1.89 | 2.07 | 1.7 | 2.8 |
| 1.00 | 2.25 | 2.83 | 2·3 | 9.6 |
| $5.02\times10^{-2}$ | 2.41 | 3.34 | 2.5 | $1.7\times10^{-6}$ |
| 2.01 | 2.76 | 4.14 | 3.0 | 2.3 |
| 1.00 | 2.99 | 4.65 | 3.3 | 2.9 |
| $5.04\times10^{-3}$ | 3.31 | 5.60 | 3.7 | 2.7 |
| 2.02 | 3.69 | 6.75 | 4.2 | 1.2 |
| 1.31 | 3.81 | 8.25 | 4.4 | $(2.0\times10^{-7})$ |
| $8.09\times10^{-4}$ | 3.92 | — | 4.5 | $(-1.1\times10^{-6})$ |
| 4.00 | 4.50 | — | 5.2 | (−1,3 ) |

former are much lower than those of the latter, that is to say, $(dF_e/dR)_{R,obs.}$ is much larger than $-T(dS_K/dR)_{R,obs.}$. If we arbitarily choose the dimension $A$, we can find better agreement, but here the value of $A$ becomes so great that it can not be recognized as reasonable. These facts agree with those reported by Fujita[8] based on the theory of Hermans and Overbeek[1]. The results calculated using another sample of lower polymerisation degree are the same as those mentioned above.

TABLE II
SODIUM CARBOXYMETHYL CELLULOSE
(by Pals and Hermans[10])
Deg. of Polym.=725, $Z=405$, $A=180$ Å

| NaCl concn. in solvent (N) | $R_\eta$ | $\left(-T\frac{dS_K}{dR}\right)_{R,obs.}$ | $\left(\frac{dF_e}{dR}\right)_{R,obs.}$ |
|---|---|---|---|
| ∞ | $4.25\times10^{-6}$ | 0 | 0 |
| 0.192 | 4.31 | $1.3\times10^{-9}$ | $2.9\times10^{-9}$ |
| 0.096 | 4.39 | 6.1 | 9.0 |
| 0.048 | 4.53 | $1.3\times10^{-8}$ | $1.5\times10^{-8}$ |
| 0.024 | 4.66 | 1.7 | 4.5 |
| 0.012 | 4.83 | 2.4 | 6.5 |
| 0.006 | 5.07 | 3.1 | $2.0\times10^{-7}$ |
| 0.003 | 5.29 | 3.7 | 2.1 |
| 0.0015 | 5.57 | 4.5 | 3.5 |
| 0.00075 | 5.80 | 5.0 | 4.9 |
| 0.000375 | 6.11 | 5.6 | 4.5 |

In Table II, results calculated from data on carboxymethyl cellulose by Pals and Hermans[10] are given for reference. The value of $A$ used for C.M.C. is 183 Å which is the same as used by Pals and Hermans. In this case also the calculated values are larger than the observed values. In section 2 it has been pointed out that the electrical potential $\psi$ calculated from Eq. (13) is the smallest of all the calculated potentials. As shown later, not only the electrical potential $\psi$, but also the free energy equation used in this paper seem to give the smallest calculated values, and hence the values of $R$ calculated from the present theory can be expected to be lower than those calculated from H.O. theory and others. Nevertheless, they are still much larger than the experimental values. Therefore, it is concluded that the improvement of Debye-Hückel linearization approximation is not sufficient to account for the discrepancy between calculated and experimental volumes of the polyion. The cause of the disagreement is discussed in the following section.

## Discussion

a) **The relationship between the present theory and the Donnan approximation.**—From the discussion in section 2, it has been pointed out that theories based on the uniform sphere model have very close relationship with the Donnan theory. Here let us look over the details of the relationship. The survey may help us to understand the character of the theories.

At the Donnan membrane equilibrium, the potential difference between polyion sphere and outer solution $E_D$ is expressed by Eq. (3). The existence of the potential difference means the existence of free charges at the boundary of two phases. In considering the charge distribution to be expressed by Helmholtz double layer model (see Fig. 3) and expressing the free charge by $[q]$ and the capacity of the double layer by $K$, there must be a relationship between $[q]$, $K$ and $E_D$, as follows:

I
SULFATE
$Z=1070$

$A=40$ Å

| $R_\eta$ | $R_{\text{calcd.}}$ | $\left(-T\frac{dS_K}{dR}\right)_{R,\text{obs.}}$ | $\left(\frac{dF_e}{dR}\right)_{R,\text{obs.}}$ |
|---|---|---|---|
| $2.00\times10^{-6}$ | $2.15\times10^{-6}$ | $3.7\times10^{-8}$ | $8.0\times10^{-8}$ |
| 2.60 | 2.50 | 5.6 | $1.5\times10^{-7}$ |
| 2.46 | 3.40 | 9.3 | 5·6 |
| 2.61 | 3.85 | $1.1\times10^{-7}$ | $1.2\times10^{-6}$ |
| 2.94 | 4.75 | 1.4 | 1.9 |
| 3.17 | 5.30 | 1.6 | 2.5 |
| 3.46 | 6.35 | 1.8 | 2.7 |
| 3.81 | 7.65 | 2.1 | 1.4 |
| 3.94 | — | 2.2 | $4.6\times10^{-7}$ |
| 4.07 | — | 2.2 | $(-8.1\times10^{-7})$ |
| 4.60 | — | 2.6 | $(-1.3\times10^{-6})$ |

$$-[q]=KE_D \tag{36}$$

As these free charges constitute a sphere condenser, the electrical capacity $K$ is expressed by

$$K=D\frac{R^2-\frac{\delta^2}{4}}{\delta}\fallingdotseq D\cdot\frac{R^2}{\delta} \tag{37}$$

where $\delta$ is the thickness of the double layer. When $R$ is sufficiently great, $\delta$ can be assumed to be equal to $2/\kappa$. From Eqs. (36) and (37), it follows that

$$[q]\fallingdotseq -D\frac{(\kappa R)^2}{2\kappa}E_D \tag{38}$$

which agrees with Eq. (25) when $\kappa R$ is greater than unity, (If the effect of free charges in the solution phase be neglected that is, if it is assumed that $K=D\cdot R$, the surface charge of Oosawa, Imai and Kagawa can be obtained.)

From these considerations it is concluded that the Donnan model corresponds to the ion distribution which would have been obtained if the free ions distributed inside and outside the polymer according, respectively, to Eqs. (21) and (22) were rearranged to concentrate at the center of gravity of their respective distribution curves, as shown schematically in Fig. 2. The potential distribution corresponding to the model is shown in Fig. 1. When $\kappa$ is sufficiently great, we can find no difference between the H. O. or the present theory and the Donnan theory. If not however, $E_D$ does not equal $E_D^0$, but even in that case the potential and the charge distribution of the present paper can completely agree with that by the Donnan theory when $R$ is very great (see Fig. 1).

b) **Comparison between the electrical free energies described in the present paper and in others.**—If we assume the model shown in Fig. 3, we can easily

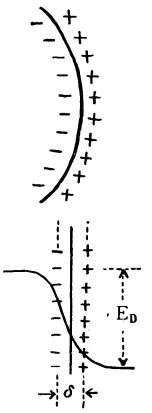



Fig. 3. Helmholtz double layer model.

calculate the electrical free energy of the system by the well-known theory of electrocapillarity[12]. That is,

$$\frac{dF_e}{dE}=-[q]=D\frac{(\kappa R)^2}{2\kappa}E_D \tag{39}$$

By integrating this equation at $R=$const., we have

$$F_e=\frac{1}{2}\cdot\frac{(\kappa R)^2}{2\kappa}E_D \tag{40}$$

By comparing this equation with Eq. (27), we can know that the charge distribution through the sphere results in the appearance of $\sigma(\kappa R)$.

In addition to these calculations, there are several others published on the electrical free energy: Hermans and Overbeek[1], Lifson and Katchalsky[9], and

12) J. Frenkel, "Kinetic Theory of Liquids", Oxford University press. p. 361 (1946).

Oosawa, Imai and Kagawa[3]. Hermans and Overbeek have given the following equation:

$$F_e(\text{H.O.}) = \frac{1}{2}\int_0^\infty \rho_0\psi \cdot 4\pi r^2 \mathrm{d}r \qquad (41)$$

where

$$\rho_0 = Ze/\frac{4}{3}\pi R^3 \qquad (42)$$

As can be understood from the physical meaning of this equation given by Hermans and Overbeek, their electrical free energy may equal the work done during the time when all charged groups of polyion are placed one-by-one on a non-charged skeleton of the polyion in simple salt solution, not taking into account the presence of counter ions. That is,

$$F_e(\text{H.O.}) = \int_0^R \int_0^Z \frac{e\psi}{\frac{3}{4}\pi R^3} 4\pi r^2 \cdot \mathrm{d}Z \cdot \mathrm{d}r \qquad (43)$$

It can be proved that this integration give the same result as Eq. (41). Considering the features of Eqs. (26) and (43), therefore, we can see that

$$F_e(\text{H.O.}) > F_e(\text{Eq.(27)})$$

According to Lifson and Katchalsky, the electrical free energy is given by the following equation:

$$F_e(\text{L.K.}) = \int_0^1 \frac{U(\xi)}{\xi}\,\mathrm{d}\xi \qquad (44)$$

where

$$U = \frac{D}{8\pi}\int_V (\text{grad}\ \psi)^2 \cdot \mathrm{d}V$$

Although it is too difficult to calculate this $F_e$ using Eqs. (13) and (14), if the charge distribution be assumed to be expressed by the Donnan approximation, $F_e$ can easily be calculated as follows:

$$F_e(\text{L.K.}) = \int_0^1 \frac{D}{8\pi}\frac{\kappa^2 \cdot E_D^2}{4} 4\pi R^2 \frac{2}{\xi\kappa}\frac{1}{\xi}\mathrm{d}\xi$$

$$= \frac{1}{2}D\frac{(\kappa R)^2}{2\kappa}E_D^2\int_0^1 \frac{1}{\xi^2}\mathrm{d}\xi \qquad (45)$$

because

$$\text{grad.}\ \psi(\xi) \fallingdotseq \frac{E_D(\xi)}{\frac{2}{\kappa(\xi)}} = \frac{E_D \cdot \kappa}{2} \qquad (46)$$

Except for the difference between integral terms of Eqs. (45) and (40), both show the same result. (That the integral term of Eq. (45) becomes infinity at $\xi=0$ is because of the failure of the Donnan model.) We way now conclude that the electrical free energy of Eq. (26) may agree, at least qualitatively, with that of Lifson and Katchalsky.

The calculation of $F_e$ used in the theory of Oosawa, Imai and Kagawa is not applicable to our system, in as much as the free volume is assumed in their theory. From numerical comparison, however, we can see that $F_e$ of Eq. (27) may not have values higher than their free energy. As presumed by Flory[13], the osmotic pressure calculated from the number of simple ions gives almost the same value as our electrical repulsive force, but, strictly speaking, the former is a little higher than the latter. Thus, the electrical free energy calculated from Eq. (27) may be expected to be the smallest of all the calculated values.

c) **On the cause of discrepancy observed between calculated and observed values.**—When we consider the reason for the disagreement, we must first remember that the Donnan potential difference observed for macroscopic polyelectrolyte solution is usually much lower than the ideal value, Eq. (3)[14]. If the character of term $E_D$ in Eqs. (13) and (14) be similar to that of the Donnan potential observed for macroscopic polyelectrolyte solution, the potential expressed by Eq. (13) may be much higher than the real potential, and hence the electrostatic repulsive force may have been overestimated in this paper. It is true that there is no reason why we should consider the ionic distribution around a polyion to be the same as that observed for the macroscopic system. Considering, however, the fact that the concentration of the counter ion within the polymer phase is almost the same as the concentration usually used for experiments of macroscopic Donnan equilibrium (for example, $8.19\times10^{-2}$—$4.35\times10^{-3}$N for sodium polyvinylsulfate in Table I), it seems to be also true that there is no reason why we should not consider the term $E_D$ in Eqs. (13) and (14) to be of the same character as the macroscopic Donnan potential. (The result that the calculated values are comparatively close to the observed ones in concentrated solutions of sodium chloride, agrees with the behavior of macroscopic Donnan membrane equilibrium.) Although for a complete elucidation of this phenomenon there must be

13) P. F. Flory, ibid., p. 631.
14) M. Nagasawa, H. Nakoji and I. Kagawa, *J. Chem. Soc. Japan, Ind. Chem. Soc.*, **57**, 9 (1954).

more intensive work, it seems certain that there are some important electrostatic effects other than those considered here. On further speculation we can name one of these effects which may be expressed in the following several ways:

(1) The association of the counter ion with polyion must be taken into account; this was pointed out by Flory and Osterheld[5].

(2) The "P" binding must occur in the polyion sphere, as reported by Oosawa, Imai and Kagawa[3].

(3) The activity coefficients of ions gathering within polyion sphere are very low compared with unity owing to their strong electrostatic interaction. In other words, the effect of the local ionic atmosphere around a simple ion must be taken into account.

(4) Schematically speaking, the fact that the polyion thread is enveloped by a double layer of cylindrical symmetry must be taken into account, as pointed out by Overbeek and Stigter (see Fig. 4)[15].

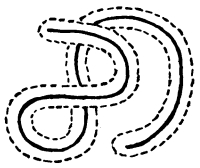


Fig. 4. Schematic picture of coiled polyelectrolyte chain.

It is to be noted that these expressions have the same meaning and give the same results of decrease in the value of the term $E_D$ of potential distribution.

*Department of Applied Chemistry*
*Faculty of Engineering*
*Nagoya University*
*Chikusa-ku, Nagoya*

15) J. Th. G. Overbeek and D. Stigter, *Rec. trav. chim.*, **75**, 543 (1956).

# *The Vapor Pressure of Germanium Dioxide*

Eiichi SHIMAZAKI, Noboru MATSUMOTO and Kichizo NIWA

(Received July 25, 1957)

Though germanium dioxide is expected to be more or less volatile at higher temperatures, the exact magnitude of its vapor pressure is not known. Moreover, the thermodynamic properties of the dioxide have been but little studied. To make a contribution to the chemistry of germanium, we have determined the vapor pressure of solid germanium dioxide; the measurements were made by Knudsen's effusion method over the temperature range from 1,040°C up to its melting point.

There is no evidence for the existence of gaseous germanium dioxide. The most important gas species over the solid dioxide around these temperatures is considered to be monoxide vapor[1]; so the vaporization can be regarded as the dissociation reaction,

$$GeO_2\,(c)^*=GeO\,(g.)+1/2\;O_2\,(g.). \qquad (1)$$

The possibility of other reactions, for instance the dissociation into constituent elements, is excluded from the free energy consideration; and, as the non existence of solid monoxide has been discussed by so many investigators, there may be no room for it as a dissociation product.

## Experimental

**Apparatus and Procedure.**—The apparatus was the same as that used in the previous investigations carried out in this laboratory; the measuring technique was slihgtly modified as described elsewhere[2]. The weight of vapor effusing through an orifice out from the quartz Knudsen cell is measured by means of a microthermobalance enclosed in the vacuum system. The vapor pressure is then calculated from the relation

$$p=\sqrt{\frac{2\pi RT}{M}}\cdot\frac{1}{A}\cdot\frac{G}{\tau} \qquad (2)$$

where $G$ is the weight loss of the sample in duration of $\tau$ seconds, $A$ the orifice area and $M$ the molecular weight of the gas molecule.

1) L. Brewer *Chem. Rev.*, **52**, 62 (1953).
2) E. Shimazaki and T. Wada, This Bulletin, **29**, 294 (1956).
* In this paper, $GeO_2$(c) means crystalline germanium dioxide of hexagonal $\alpha$-quartz structure.

In this investigation, the mean molecular weight of two gaseous components was taken as $M$, the germanium monoxide vapor being assumed to be unimolecular. Inserting the values of constants and of the mean molecular weight, together with $A=4.19\times10^{-3}$ cm$^2$, we obtain from equation (2)

$$p\ (\text{mmHg}) = 489.99\frac{G}{\tau}\sqrt{T}. \qquad (3)$$

**The Sample.**—The sample of germanium dioxide, stated 99.99% pure, was of the make of Deutsche Otavi Eisenbahngesellschaft, and was used without any further purification. Prior to the measurements, it was heated in the air above 1,000° for several hours to remove any absorbed gases or moisture. This microcrystalline white powder, as well as the residue remaining in the cell after the experiment, showed nothing but the pattern of germanium dioxide of hexagonal quartz structure in the X-ray diffraction studies.

The coincidence of the cell temperature with the thermometer reading was ensured by the fact that the sample held at the temperature just above its melting point (1,116°C) was in glassy appearance in the quartz cell, indicating that it had melted.

## Results and Discussion

The results of the experiment are summarized in Table I and plotted in Fig. 1. By means of the method of least squares, the results are expressed by equation (4), corresponding to the straight line in the $\log p$ vs. $1/T$ plot in Fig. 1.

$$\log p_{\text{mm.}} = -\frac{25,517}{T} + 16.245 \qquad (4)$$

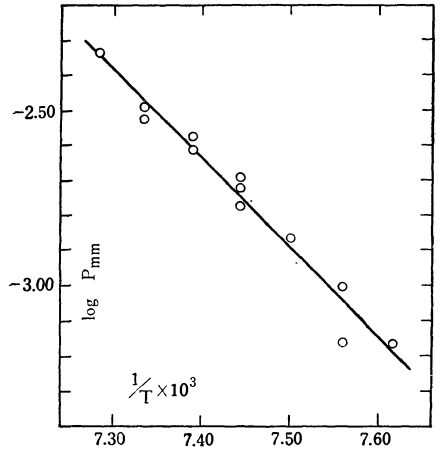



Fig. 1.

By differentitation of equation (4) with respect to $1/T$, or from the inclination of the straight line in Fig. 1, the heat of reaction (1) is obtained as

$$\Delta H_T = 116.7 \pm 0.2 \text{ kcal./mol.}$$

TABLE I

| Tem. $T$°K | Loss in Weight $G\times10^3$ g. | Duration $\tau$ sec. | Vapor Pressure $p\times10^3$ mmHg. | $\log p+4$. |
|---|---|---|---|---|
| 1,313 | 0.827 | 21,600 | 0.680 | 0.832 |
| 1,323 | 0.808 | 18,000 | 0.689 | 0.838 |
| 〃 | 1.000 | 〃 | 0.990 | 0.996 |
| 1,333 | 1.365 | 18,000 | 1.356 | 1.132 |
| 1,343 | 1.173 | 12,600 | 1.672 | 1.223 |
| 〃 | 2.038 | 18,000 | 2.033 | 1.308 |
| 〃 | 1.500 | 14,400 | 1.870 | 1.272 |
| 1,353 | 1.327 | 9,000 | 2.657 | 1.424 |
| 〃 | 1.923 | 14,400 | 2.407 | 1.381 |
| 1,363 | 2.384 | 14,400 | 2.995 | 1.476 |
| 〃 | 2.557 | 〃 | 3.212 | 1.506 |
| 1,373 | 2.769 | 10,800 | 4.655 | 1.668 |

The orifice area $A=4.19\times10^{-3}$ cm$^2$.

The free energy and the entropy change are also calculated,

$$\Delta G_T = 34.0 \text{ kcal./mol.}$$

$$\Delta S_T = 61.1 \text{ kcal./mol./deg.}$$

where underscript $T$ denotes the mean temperature in the experiment. To construct the free energy equation, the following heat capacity equations were used:

$\text{GeO}_2$(c) [3] $\quad C_p = 11.2 + 7.17\times10^{-3}T$

$\text{O}_2$(g) [3] $\quad C_p = 7.16 + 1.00\times10^{-3}T - 0.40\times10^5 T^{-2}$

GeO(g) $\quad C_p = \frac{7}{2}R + C_{vib}$

where $C_{vib}$ is the heat capacity resulting from the atomic vibration in the gaseous GeO molecule and is equal to the Einstein heat capacity function $E(\theta/T)$.

Hence

$$\Delta C_p = -0.67 - 6.67\times10^{-3}T - 0.20\times10^5 T^{-2} + E(\theta/T)$$

On integration we botain

$$\Delta H = \int_0^T \Delta C_p dT = \Delta H_0 - 0.67T - 3.335\times10^{-3}T^2 + 0.20\times10^5 T^{-1} + \int_0^T E\left(\frac{\theta}{T}\right)dT \qquad (5)$$

where $\Delta H_0$ is the constant of integration. Then the free energy equation is obtained as

$$\Delta G = \Delta H_0 + 0.67T\ln T + 3.335\times10^{-3}T^2 + 0.10\times10^5 T^{-1} - T\int_0^T \frac{dT}{T^2}\int_0^T E\left(\frac{\theta}{T}\right)dT + JT \qquad (6)$$

3) K. K. Kelley, *Bur. Mines Bulletin*, No. 476 (1949).

where $J$ is another constant of integration.

These two constants were evaluated in the usual manner. With the relation

$$\Delta G = -RT \ln p_{atm} = -4.575T \log p_{atm}$$

equation (6) is changed to

$$\sum = -4.575 \log p - 0.67 \times 2.303 \log T - 3.335 \times 10^{-3} T - 1 \times 10^{4} T^{-2} + \int_0^T \frac{dT}{T^2} \int_0^T E\left(\frac{\theta}{T}\right) dT = \frac{\Delta H_0}{T} + J$$

$E(\theta/T)$ was evaluated for each temperature from the table[4] as $E(\theta/T) = 1/3\, C_v$ with the characteristic temperature $\theta = 1{,}411$ which in turn was calculated from Barrow's spectroscopic data[5]. Integration and double integration of $E(\theta/T)$-function were carried out graphically. By means of the method of least squares using twelve $\sum$ functions, $\Delta H_0$ and $I$ were obtained:

$$\Delta H_0 = 122{,}122 \pm 285$$

and

$$J = -73.583$$

With these values, the heat of reaction, the free energy and the entropy change at 298°K were calculated from equations (5) and (6) as follows:

$$\Delta H_{298} = 121.7 \pm 0.3 \text{ kcal./mol.}$$

$$\Delta G_{298} = 101.7 \text{ kcal./mol.}$$

$$\Delta S_{298} = 67.3 \text{ cal./mol./deg.}$$

The heat of reaction can also be obtained by combining the thermal data from the literature (Table II).

TABLE II

| Reaction | $\Delta H_{298}$, kcal. |
|---|---|
| $GeO_2(s) = Ge(s) + O_2(g)$ | $128.3 \pm 1.0$[6] |
| $Ge(s) = Ge(g)$ | $91.5 \pm 3.0$[7] |
| $1/2\ O_2(g) = O(g)$ | 59.2 |
| $Ge(g) + O(g) = GeO(g)$ | $-159.0$[8] |
| $GeO_2(s) = GeO(g) + 1/2\ O_2(g)$ | $120.0 \pm 4$ kcal |

It must be remembered that the heat of formation of solid germanium dioxide, 128.3 kcal., is referred to its amorphous state. The heat of transition $GeO_2$ (amorph.) $= GeO_2$(cryst.) is unknown, but considering the case of silicon dioxide, it may not be bold to take it as high as 2 kcal. Adding this, the heat of reaction is obtained as 122.0 kcal., which is in good accord with our experimental value of 121.7 kcal.

The heat of dissociation of gaseous germanium monoxide cited above, 159 kcal., was calculated by Herzberg from the spectroscopic evidence by Birge-Sponer linear extrapolation. Though the applicability of the linear extrapolation to all oxides of group-4 elements was discussed by Brewer[1,9], our experimental result also suggests that Herzberg's value is preferable to Gaydon's, $127 \pm 27$ kcal.

From $\Delta S_{298} = 67.3$ e. u., together with the entropy values from the literature[10] $S_{298} = 49.01 \pm 0.1$ e. u. for oxygen and $S_{298} = 53.55 \pm 0.1$ e. u. for gaseous germanium monoxide, the entropy of solid germanium dioxde is obtained as $S_{298} = 10.8 \pm 1.0$ e. u. This is in fair agreement with the estimated value 11.5 which was evaluated by Bues and von Wartenberg, by interpolation from normal entropies of dioxides of silicon and tin[11].

## Summary

The apparent vapor pressure of solid germanium dioxide, or the dissociation pressure for the reaction $GeO_2(c) = GeO(g) + 1/2\, O_2(g)$, was measured over the temperature range 1,040—1,100°C by the Knudsen's effusion method; the results are expressed by equation (4).

From the free energy equation, the heat of reaction, the free energy and the entropy change of the reaction were calculated as $\Delta H_{298} = 121.7 \pm 0.3$kcal./mol., $\Delta G_{298} = 101.7$ kcal./mol. and $\Delta S_{298} = 67.3$ e. u., respectively. The heat of reaction is in good agreement with the value calculated from accessible thermal data. The normal entropy of solid germanium dioxide was calculated as $S_{298} = 10.8 \pm 1.0$ e. u., which is in agreement with the computed value obtained by Bues and von Wartenberg.

We are indebted to Professor Saburo Yanagizawa of Keio University, for his interest in this research to furnish us with the sample of pure germanium dioxide.

*Department of Chemistry, Faculty of Science, University of Hokkaido*
*Sapporo*

4) Landolt-Börnstein, Tabellen, Erg. I., p. 702.
5) R. F. Barrow, *Proc. Phys. Soc.*, **56**, 204 (1944).
6) J. P. Coughlin, *Bur. Mines Bulletin*, No. 542 (1954).
7) A. W. Searcy and R. D. Freeman, *J. Chem. Phys.*, **23**, 88 (1955).
8) G. Herzberg, "Molekülspektren und Molekülstruktur." Th. Steinkopf, Dresden und Leipzig, 1939, 336.
9) L. Brewer and D. F. Mastick, *J. Chem.* Phys., **19**, 834 (1951).
10) K. K. Kelley, *Bur. Mines Bulletin*, No. 477 (1951).
11) W. Bues and H. von Wartenberg, *Z. anorg. allg. Chem.*, **266**, 281 (1951).

# *Rapid Determination of Inorganic Sulfur in Various Forms, Particularly in Sulfide Ores, by the Tin(II)-Strong Phosphoric Acid Reduction Method*

By Toshiyasu KIBA, Ikuko AKAZA and Nobuyuki SUGISHITA

(Received August 12, 1957)

Previously it was shown that both soluble and insoluble sulfates could be easily reduced to hydrogen sulfide by heating with tin(II)-strong phosphoric acid, a new powerful and stable reducing agent first described by the authors[1]. The discovery of this reagent led the authors to the development of a new rapid and simple method for the determination of sulfate sulfur, in which hydrogen sulfide evolved by the reaction was absorved by zinc acetate solution and titrated iodimetrically or estimated colorimetrically as usual. Both the volumetric procedure for semimicro scale and the colorimetric method for micro quantities of sulfate were already established by the authors and have been widely accepted in this country for investigative and industrial purposes[1,2]. Extension of this method to rapid determination of organic sulfur was also accomplished in this laboratory[3]. The organic sulfur was oxidized to sulfate by means of chromium(VI)-strong phosphoric acid and then estimated in the same way as inorganic sulfates, the volumetric or the colorimetric method being used in the final stage according to the sulfur content of the sample[4].

The present paper describes a later investigation in which the above method was extended to the determination of inorganic sulfur in other forms, e. g., thiosulfates, sulfites, thiocyanates and sulfides, in particular to rapid estimation of sulfur in sulfide ores such as pyrite, galena and zinc blende. The rapidity and the simplicity of the original method are retained in this procedure, in which all the sulfur in the samples is converted into hydrogen sulfide and determined iodimetrically.

## Experimental

**Apparatus**:—The apparatus used in this study is shown in Fig. 1. It is composed of two parts,

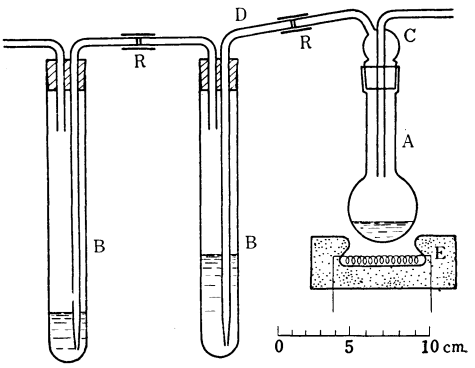



Fig. 1. Apparatus for reduction and absorption.
A: Reaction vessel, a round bottom flask
B: Absorbing vessels
C: Glass cap fitted to the reaction vessel
D: Gas-delivery tube
R: Short pieces of rubber tubing
E: Electric heater

a reaction vessel (A) and an absorption part (B). The reaction vessel (A) is a round bottomed flask of hard glass having a glass cap fitted to its top and provided with inlet and outlet tubes. The absorption part (B) is composed of two test-tubes 3 cm. in diameter. A gas delivery tube (D) is connected with a piece of rubber tubing to the outlet arm of the reaction vessel (A) and inserted into the absorbing solution. A Kipp's apparatus is employed for the production of carbon dioxide, which is purified by six gas-washing bottles (not shown Fig. 1.) and introduced into the reaction vessel through the inlet arm. The solutions used for the purification of carbon dioxide are described below.

**Reagents**:—*Storong Phosphoric Acid.*—Four hundred grams of commercial ortho phosphoric acid of extra pure grade ($d$=1.7) is placed in a 300-ml. flask or a 350 ml. conical beaker, and dehydrated by heating on a hot plate until a thermometer dipped in the liquid indicates 300°C. If the heating takes too long a time the liquid will become extremely turbid and viscous, and useless for the purpose in view. During the heating, the water vapor and the mist of phosphoric acid evolved should be rapidly removed from the neighborhood of the liquid surface through a glass tube, an end of which is hung down near the liquid surface, the other end being connected to a suction pump. It saves much time in heating.

1) T. Kiba et al., This Bulletin **28**, 641 (1955).
2) T. Kiba and I. Kishi, (present surname Akaza), ibid., **30**, 44 (1957).
3) S. Ohashi, ibid., **28**, 645 (1955).
4) T. Kiba, I. Akaza and S. Taki, ibid., **30**, 482 (1957).

*Tin(II)-Strong Phosphoric Acid.*—Fifty grams of tin(II)-chloride dihydrate of extra pure grade is placed in a 300-ml. conical beaker and on it, is poured 250 g. of the strong phosphoric acid prepared above. The content is heated within about one hour to 300°C after the manner of the preparation of the strong phosphoric acid. After cooling the tin(II)-strong phosphoric acid thus obtained, a very viscous and occasionally turbid liquid, may be stored in a closed vessel.

*Zinc Acetate Solution, 4% or 8%.*—Forty or 80 g. of zinc acetate dihydrate of pure grade is dissolved in 1 l. of distilled water. If necessary, two or three drops of glacial acetic acid are added to clarify the solution, but the pH of the solution should not fall below 5. A solution of suitable concentration is used depending upon the amount of sulfur to be analyzed.

*Iodine, 0.02 N or 0.05 N.*—These are standardized accurately by the ordinary procedure. Either of them is used depending on the amount of sulfur to be analyzed.

*Sodium Thiosulfate, 0.02 N or 0.05 N.*—These are standardized accurately by the ordinary procedure.

*Carbon Dioxide.*—Carbon dioxide produced in the Kipp's apparatus is purified by passing it through five gas-washing bottles containing, respectively, water, 1% potassium permanganate in 10% sodium carbonate solution, 2% vanadium(II) sulfate in 6N sulfuric acid solution[3], 5% barium chroride, and a zinc acetate absorbing solution. A sixth empty bottle is placed to intercept the droplets coming from the washing liquids.

*Barium Hydroxide Solution.*—Barium hydroxide dihydrate crystals of pure grade are saturated in distilled water and stored away from atomospheric carbon dioxide.

*Bromine Water.*—Bromine of pure grade is saturated in distilled water.

*Various Samples Containing Sulfur.* — Pure grade reagents of sodium thiosulfate, barium thiosulfate, sodium sulfite, potassium thiocyanate, and sodium sulfide were employed for the evaluation of the method. The salts were dissolved in water to prepare solutions of known concentration. The sulfur content of a definite volume of each solution was estimated by the conventional gravimetric or volumetric method. The sulfide ores used were natural pyrite, zinc blende and galena, from Ogoya Mine near Kanazawa city, and their sulfur contents were estimated by the gravimetric analysis according to the procedure described in ordinary text-books.

**Procedure:** — *Procedure A.* — Take an accurately measured sample — pipet a solution; weigh a solid—containing less than 20 mg. of sulfur and put it into the reaction vessel (A, Fig. 1). Add 0.5 ml. of the barium hydroxide solution, and evaporate the content to dryness at the bottom of the vessel. Pour 10 ml. of tin(II)-strong phosphoric acid over the dried residue with a pipet. Put 40 ml. of the zinc acetate solution into the first absorbing vessel and 20 ml. of the same solution into the second. Connect all the apparatus as shown in Fig. 1. Pass carbon dioxide very rapidly through the apparatus for five minutes to expel the air from the apparatus. Then reduce the flow of the gas to a rate of one bubble per second. Heat the bottom of the reaction vessel on a small electric heater which is regulated by a variable transformer, until white fumes of the strong phosphoric acid appear. It is unnecessary to keep the reaction temperature constant, but it should be high enough to ensure that the content of the vessel exhibits a white turbidity near the end of the reaction. Stop the heating and continue the passage of carbon dioxide for five minutes.

Disconnect the absorbing vessels from the gas-outlet arm of the reaction vessel and quickly pour into them 20 ml. of 0.02 N iodine solution—the bulk into the first vessel and only a bit into the second. A part of the zinc sulfide precipitate may cling to the glass tubes; it is allowed to remain in the absorbing vessels. Swirl the vessel to mix the content thoroughly, transfer it to a beaker and back titrate the excess of the iodine with 0.02 N sodium thiosulfate solution using starch as indicator.

The whole determination can be carried out in thirty or forty minutes. A blank test should be run without a sample. One ml. of 0.02 N iodine corresponds to 0.3206 mg. of sulfur.

*Procedure B.*—Take the sample into the reaction vessel. Add two or three drops of the bromine water to oxidize the sulfur to sulfate form and then fix it as barium sulfate by adding 0.5 ml. of the barium hydroxide solution. Evaporate the content on a water-bath, and carry out the reduction of the sulfate according to Procedure A as shown above.

Thiosulfates, thiocyanates and sulfites should be treated by procedure B before the reduction with tin(II)-strong phosphoric acid.

## Results and Discussion

**Sulfide Ores.**—Zinc blende, galena and pyrite were analyzed using procedure A. In Table I the results obtained by the gravimetric method are tabulated together. As all the sulfur in these sulfide ores could be generated as hydrogen sulfide by the simple treatment with the tin(II)-strong phosphoric acid, all troublesome treatments such as dissolving of the ores in acids and evaporation of the solution were dispensed with, in the course of the analysis. The determination of the sulfur could be accomplished very quickly — within twenty or thirty minutes. Because of the relatively small amount of the sample employed in this method care should be taken to grind the ore into fine powder and to mix it thoroughly, so that the sample may correctly represent the whole. The standard deviation ($\sigma$) and the average deviation ($\delta$) of the results obtained by this method were comparable to those

TABLE I

DETERMINATION OF SULFUR IN SULFIDE ORES

A: Zinc Blende

| Sample Taken[a] mg. | S Found mg. | S Content[b] % |
|---|---|---|
| 37.46 | 11.84 | 31.60 |
| 37.47 | 11.63 | 31.03 |
| 40.33 | 12.64 | 31.34 |
| 42.65 | 13.18 | 30.90 |
| 47.69 | 15.03 | 31.49 |

($\sigma=0.246\%$, $\delta=0.298\%$)

a) The sample ore was ground into 200-mesh and weighed by a micro-balance.

b) The mean value of sulfur content obtained by gravimetric method was 30.12%.

B: Galena

| By Procedure A | | | By Gravimetric Method | |
|---|---|---|---|---|
| Sample Taken[c] mg. | S Found mg. | S % | Sample Taken g. | S Found % |
| 73.52 | 9.38 | 12.75 | 0.2626 | 12.32 |
| 76.56 | 9.85 | 12.86 | 0.2900 | 12.79 |
| 82.53 | 10.48 | 12.69 | 0.2820 | 13.02 |
| 83.92 | 10.72 | 12.77 | 0.2685 | 12.09 |
| 96.19 | 12.13 | 12.61 | 0.3477 | 12.47 |

($\sigma=0.068\%$, $\delta=0.093\%$) ($\sigma=0.294\%$, $\delta=0.370\%$)

c) The sample ore was ground into 200-mesh and weighed by a micro-balance.

C: Pyrite

| By Procedure A | | | By Gravimetric Method (According to Lunge) | |
|---|---|---|---|---|
| Sample Taken[d] mg. | S Found mg. | S % | Sample Taken g. | S Found % |
| 16.50 | 8.61 | 52.18 | 0.0838 | 51.88 |
| 17.82 | 9.12 | 51.17 | 0.1107 | 51.04 |
| 26.63 | 13.90 | 52.19 | 0.1490 | 52.10 |
| 27.43 | 14.13 | 51.51 | 0.1252 | 52.14 |
| 28.51 | 14.61 | 51.24 | 0.1402 | 50.98 |

($\sigma=0.422\%$, $\delta=0.497\%$) ($\sigma=0.488\%$, $\delta=0.572\%$)

d) The sample ore was ground into 200-mesh and weighed by a micro-balance.

by the gravimetric analysis. In both cases the ores were ground to about 200 meshes (per inch). Slightly higher values of sulfur content were obtained by this than by the gravimetric method. Probably because no sulfur in the sample was lost during the couse of this method, while with the gravimetric method, a small amount of the sulfur might escape as sulfur dioxide or hydrogen sulfide during the process of dissolution in acid and evaporation of the solution. The results obtained by this method may thus be regarded as more reliable.

**Sulfide.**—An aliquot of freshly prepared sodium sulfide solution was employed for the analysis, the sulfur content having been estimated by iodimetry. Two methods were employed here. In one of them procedure B was employed, and in the other a few drops of the zinc acetate solution were added to the sample and the sulfur was analysed by procedure A. The results obtained by the above two methods are shown in Table II, from which it is revealed that whether the oxidation of sulfide ion takes place or not, all of the sulfur in the sample is ultimately converted in to hydrogen sulfide by this reduction method.

TABLE II

DETERMINATION OF SULFUR IN SODIUM SULFIDE

| S Contained in an Aliquot[a] mg. | S Found By This Method mg. | Note |
|---|---|---|
| 2.99 | 2.98 | Zinc acetate was added. |
| 〃 | 2.99 | 〃 |
| 〃 | 2.94 | 〃 |
| 〃 | 2.93 | 〃 |
| 〃 | 2.99 | By procedure B. |
| 〃 | 3.01 | 〃 |
| 〃 | 3.00 | 〃 |

a) The amount of the sulfide ion in an aliquot was determined by iodimetry.

TABLE III

DETERMINATION OF SULFUR IN THIOSULFATES

A: Barium thiosulfate $BaS_2O_3\cdot H_2O$ (Purity of the sample: 99.95%) S content: 23.96%, analysis was carried out by procedure A.

| Sample Taken mg. ($A$) | S Content (Calcd.) ($A\times0.2396$) mg. | S Found mg. | S Found % |
|---|---|---|---|
| 10.06 | 2.41 | 2.40 | 23.85 |
| 22.63 | 5.42 | 4.88 | 21.56 |
| 24.35 | 5.83 | 5.42 | 22.25 |
| 10.06 | 2.41 | 2.41 | 23.95 |
| 〃 | 〃 | 2.41 | 23.95 |
| 〃 | 〃 | 2.39 | 23.75 |
| 〃 | 〃 | 2.42 | 24.05 |
| 〃 | 〃 | 2.40 | 23.85 |
| 17.24 | 4.13 | 4.15 | 24.07 |
| 17.25 | 4.13 | 4.16 | 24.11 |
| 19.46 | 4.66 | 4.65 | 23.89 |

B: Sodium Thiosulfate $Na_2S_2O_3\cdot5H_2O$ (S content: 25.84%)

| Sample Taken mg. ($A$) | S Content (Calcd.) ($A\times0.2584$) mg. | S Found mg. | S Found % |
|---|---|---|---|
| 17.16 | 4.43 | 4.44 | 25.87 |
| 〃 | 〃 | 4.42 | 25.75 |
| 〃 | 〃 | 4.43 | 25.81 |
| 8.58 | 2.21 | 2.22 | 25.87 |
| 〃 | 〃 | 2.22 | 25.87 |

**Thiosulfate.**—Sodium thiosulfate solution and barium thiosulfate solid were analyzed by procedure B. The thiosulfate ion could not be reduced quantitatively to hydrogen sulfide merely by heating with the tin(II)-stong phosphoric acid. It had to be oxidized to sulfate before the reduction. Assay of the sulfur in the sample was carried out by iodimetry. The results obtained are shown in Table III.

**Sulfite.**—An aliquot of sodium sulfite solution was employed for the analysis. The solution usually contains both sulfite and sulfate ions, for the former is easily oxidized to the latter during the preparation and storage of the solution; the content of the total sulfur, however, remains unaffected. The analysis was carried out according to procedure A and B, but the results coincide closely with each other as shown in Table IV.

TABLE IV

DETERMINATION OF SULFUR IN SODIUM SULFITE

| Sample Taken mg. (*A*) | S Content (Calcd.) (*A*×0.2059) mg. | S Found mg. | S Found % | Procedure |
|---|---|---|---|---|
| 20.14 | 4.15 | 4.14 | 20.55 | A. |
| 〃 | 〃 | 4.16 | 20.65 | 〃 |
| 〃 | 〃 | 4.14 | 20.55 | 〃 |
| 〃 | 〃 | 4.21 | 20.90 | B. |
| 〃 | 〃 | 4.13 | 20.50 | 〃 |
| 〃 | 〃 | 4.21 | 20.90 | 〃 |

a) Purity of the reagent as a solid: $Na_2SO_3$ 60.225%

b) Total sulfur content of an aliquot taken was gravimetrically determined as barium sulfate; sulfur content: 20.59%.

TABLE V

DETERMINATION OF SULFUR IN POTASSIUM THIOCYANATE

| Sample Taken ml. (*A*) | S Content (Calcd.) (*A*×3.84 mg.) | S Found mg. | S Found % | Procedure |
|---|---|---|---|---|
| 2.0 | 7.68 | 2.56 | 11.04 | A. |
| 5.0 | 19.20 | 4.19 | 0.72 | 〃 |
| 2.0 | 7.68 | 7.64 | 32.83 | B. |
| 〃 | 〃 | 7.65 | 32.87 | 〃 |
| 〃 | 〃 | 7.74 | 33.26 | 〃 |
| 〃 | 〃 | 7.69 | 33.04 | 〃 |
| 3.0 | 11.52 | 11.38 | 32.60 | 〃 |
| 〃 | 〃 | 11.58 | 33.18 | 〃 |
| 〃 | 〃 | 11.50 | 32.95 | 〃 |

a) Sulfur content of potassium thiocyanate was calculated from the results obtained by argentiometry. One milliliter of the solution used here contained 3.84 mg. of sulfur.

**Thiocyanate.**—A solution of potassium thiocyanate was used for the analysis. As sulfur in a thiocyanate can not be reduced to hydrogen sulfide merely by treatment with the tin(II)-strong phosphoric acid, procedure B was adopted for this compound. Results obtained by procedures A and B are listed together in Table V.

The determination of inorganic sulfur in various forms can be done by procedure A or by procedure B within thirty minutes. With reference to rapidity of analysis this method is greatly superior to all the conventional ones. In accuracy this method is comparable to gravimetric methods, but the amount of sample to be taken for analysis is far smaller than that needed for other routine methods, as shown in Table I in the case of sulfide ores.

## Summary

The procedure for the determination of sulfate sulfur using a new reagent, tin (II)-strong phosphoric acid, previously devised by the authors, has been extended to the determination of sulfur in other forms of inorganic compounds, e.g., sulfide ores (zinc blende, galena and pyrite), sulfides, thiosulfates, sulfites and thiocyanates. Two procedures of the analysis have been proposed by the authors: one, suitable for sulfide ores, sulfides, and sulfites, in which samples are treated directly with tin(II)-strong phosphoric acid to reduce the sulfur to hydrogen sulfide, and the other, suitable for sulfites, thiosulfates, and thiocyanates, in which samples are previously treated with bromine water to oxidize the sulfur to sulfate, and the sulfate is reduced to hydrogen sulfide. The hydrogen sulfide evolved from the sample is absorbed in zinc acetate solution and titrated iodimetrically as usual. The rapidity and the simplicity of the original method are still retained in this case, by which less than 30 milligrams of sulfur in the sample can be estimated within thirty minutes with good reproducibility.

The expense of the present research was met in part by a Grant for Scientific Research from the Ministry of Education to which the authors' thanks are due.

*Department of Chemistry, Faculty of Science, Kanazawa University*
*Kanazawa*

# *Studies on Serine Peptides. III. Synthesis of L-Seryl-L-Histidine, L-Seryl-L-Histidyl-L-Leucine and Carbobenzyloxy-Glycyl-O-Benzyl-DL-Serine Ethyl Ester*

By Kenji OKAWA

(Received August 12, 1957)

Seryl-histidyl peptide was found in insulin by Sanger, who suggested that the peptide plays an important role in the biological action[1]. It was reported that the same peptide groups might also be contained in ribonuclease[2] and chymotrypsin[3].

With regard to synthetic studies of seryl peptides, the author reported in the previous paper[4] that the *O*-Bz*-L-serine was a useful starting material for the synthesis of seryl peptides, and *N*-Cbzo**-*O*-Bz-L-seryl-L-histidine methyl ester was synthesized in a good yield. Although the synthetic studies on histidyl peptides have been reported by Holley and Fischer[5,6] only a few simple peptides were obtained by the azide method in an unsatisfactory yield. Fischer and Whetston reported that Cbzo-glycyl-L-histidine azide was coupled with L-serine methyl ester or L-tyrosin methyl ester in the yields of 25 and 43% of theory, respectively.

In the present work, *N*-Cbzo-*O*-Bz-L-seryl-L-histidine was coupled with leucine methyl ester in dioxane by the use of Sheehan's dicyclohexylcarbodiimide[7] to give *N*-Cbzo-*O*-Bz-L-seryl-L-histidyl-L-leucine methyl ester in 68% yield. The free peptides, L-seryl-L-histidine and L-seryl-L-histidyl-L-leucine, were prepared from their Cbzo-*O*-benzyl derivatives by treatment with hydrogen bromide in dioxane. The esterification of *O*-Bz-L- and DL-serine was carried out in the ethanol-dry hydrogen chloride solution at low temperature. *N*-Cbzo-glycyl-*O*-Bz-DL-serine ethyl ester was obtained in 88% yield by Sheehan's method.

**Acknowledgement:** Low yields in the synthesis of histidyl peptides by means of azide method are possibly caused by the condensation of imidazole and acyl azide group.

This difficulty was overcome by the use of dicyclohexylcarbodiimide method. *N*(α)-Cbzo-histidine still has a zwitter ion character owing to the presence of imidazole ring, nevertheless the amino group is carbobenzoxylated, and it is difficultly soluble in usual organic solvents. On the contrary, *N*-Cbzo-*O*-Bz-L-seryl-L-histidine is not soluble in hot water but soluble in dioxane and chloroform. This fact favors the homogeneous reaction giving high yields of the reaction product.

The author tried to remove the protecting groups of the *N*-Cbzo-*O*-Bz-L-serine by using dry hydrogen bromide in glacial acetic acid according to the Ben-Ishai's method[8], but hereby *O*-acetyl-serine was obtained in place of free L-serine. In dioxane, the elimination of protective groups from peptide derivatives proceeded smoothly and free peptides were obtained in desirable yields. It is interesting that the benzyl residue in *O*-Bz-serine is not attacked in the esterification procedure but is readily cleft by the use of hydrogen bromide in dioxane. The results provide further evidences that the free hydroxy group of serine must be protected by a suitable group to obtain good results in peptide synthesis.

## Experimental

***N*-Cbzo-*O*-Bz-L-seryl-L-histidine.**—*N*-Cbzo-*O*-Bz-L-seryl-L-histidine methyl ester[9] was prepared from *N*-Cbzo-*O*-$B_2$-L-serine and L-histidine methyl ester by Sheehan's method. Into the solution of 25 g. of the carbobenzoxy-peptide ester in 52 cc. of dioxane was added 52 cc. of aqueous solution of

* Bz-; Benzyl-

** Cbzo-; Carbobenzyloxy-

1) *Symposium on Peptide Chemistry*, 1955 (London), p. 24.

2) C. H. W. Hirs, *Fed. Proc.*, **16**, 196 (1957), R. R. Redfield and C. B. Anfinsen, *J. Biol. Chem.*, **221**, 385 (1956). C. H. W. Hirs, W. H. Stein and S. Moore, ibid., **221**, 151 (1956).

3) J. R. Whitaker and B. J. Jandorf, *J. Biol. Chem.*, **223**, 751 (1956).

4) K. Okawa, This Bulletin, **29**, 486 (1956).

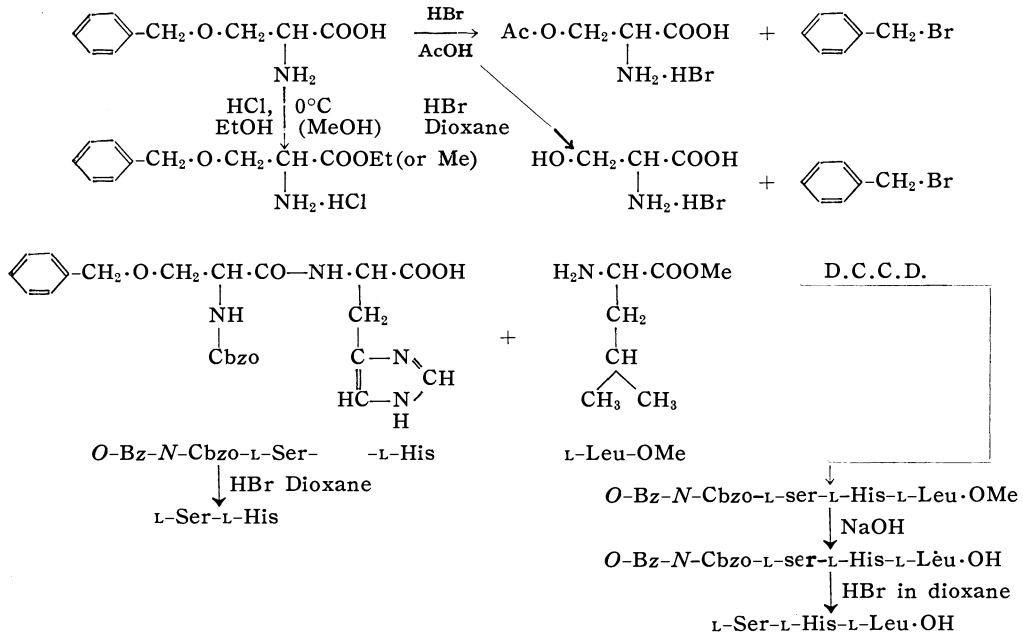
5) R. W. Holley and E. Sondheimer, *J. Am. Chem. Soc.*, **76**, 1326 (1954).

6) R. F. Fischer and R. R. Whetstone, ibid., **76**, 5076 (1954).

7) J. C. Sheehan and G. P. Hess, ibid., **77**, 1067 (1955).

8) Ben-Ishai and A. Berger, *J. Org. Chem.*, **17**, 1564 (1952).

9) K. Okawa, This Bulletin, **29**, 489 (1956).




1 N-sodium hydroxide portion-wise in 20 minutes under stirring. After kept standing for 30 minutes, the reaction mixture was brought to pH 2.0 with hydrochloric acid, and washed with ethylacetate. The aqueous layer was brought to pH 4.4, and 18.0 g. of Cbzo-peptide was precipitated, m.p. 156°C. Recrystallization from methanol-ether gave 16.0 g. of pure material, m.p. 164°C. in 66.8 % yield. $[\alpha]_D^{13} = +20.7$ (10 mg/cc. AcOH)

*Anal.* Found: C, 60.40; H, 5.39; N, 12.04. Calcd. for $C_{24}H_{26}O_6N_4$: C, 61.80; H, 5.58 N, 12.02 %.

***N*-Cbzo-*O*-Bz-L-seryl-L-histidyl-L-leucine Methyl Ester.**—Two grams of *N*-Cbzo-*O*-Bz-L-seryl-L-histidine in 80 cc. of dioxane was coupled with 1 g. of dicyclohexylcarbodiimide in 20 cc. of tetrahydrofurane and L-leucine methyl ester in 10 cc. of tetrahydrofurane (prepared from 1.0 g. of its hydrochloride by the use of ammonia-chloroform solution[10]). After the solution was left at room temperature overnight, 0.3 cc. of acetic acid was added to remove the unchanged dicyclohexylcarbodiimide, and the urea derivative produced was filtered off. The filtrate was concentrated in vacuo, the residue dissolved in ethylacetate, the solution washed with dilute acid, alkali and water and then dried over anhydrous sodium sulfate. The solvent was removed in vacuo and the residual precipitate was collected and washed with petroleum ether. The yield was about 2.0 g. Recrystallization from ethylacetate-petroleum ether gave 1.5 g. of carbobenzoxypeptide ester. From the mother liquor, 0.1 g. of the crystals were obtained. The total yield was 1.6 g. (64 %), m.p. 152-153°C. $[\alpha]_D^{13} = -20.14$ (10 mg./cc. EtOH)

10) G. Hillmann, *Z. Naturforsch*, **1**, 682 (1946).

*Anal.* Found: C, 62.60; H, 6.60; N, 11.61. Calcd. for $C_{31}H_{39}O_7N_5$: C, 62.73; H, 6.57; N, 11.79 %.

***N*-Cbzo-*O*-Bz-L-seryl-L-histidyl-L-leucine.**—By the usual method, 1.2 g. of the peptide ester was dissolved in 2cc. of dioxane and 2 cc. of an aqueous solution of 1 N sodium hydroxide was added portion-wise into dioxane solution and the reaction mixture was allowed to stand for 50 minutes at room temperature. When the hydrolysis was over, 1 cc. of 2 N hydrochloric acid was added into the solution, and the fine precipitate produced was filtered (1.1 g.). Recrystallization from methanol gave 0.7 g. of the carbobenzoxypeptide in 68.7 % yield, m. p. 172-173°C.

*Anal.* Found: C, 61.00; H, 6.17; N, 11.99. Calcd. for $C_{30}H_{37}O_7N_5$: C, 62.17; H, 6.38; N, 12.08 %.

***O*-Ac-L-serine.**—Dry hydrogen bromide was passed into the solution of *N*-Cbzo-*O*-$B_2$-L-serine (1.1 g.) in 7 cc. of acetic acid for twenty minutes. After the solution was left at room temperature for 30 minutes, 70 cc. of absolute ether was added into the reaction mixture. The white precipitate produced was washed twice with dry ether. The products (0.65 g., 94.2 %) were dried in a vaccum desiccator over sodium hydroxide.

By treating this product with triethylamine in absolute ethanol, *O*-Ac-L-serine was obtained.

*Anal.* Found: C, 40.35; H, 5.87; N, 9.56. Calcd. for $C_5H_9O_4N$: C, 40.81; H, 6.09; N, 9.52 %.

Dioxane was used in place of acetic acid in the above procedure. The crystals of L-serine monohydrogen bromide could be obtained in 90 % yield.

**L-Seryl-L-histidine Mono Hydrogen bromide.**—Dry hydrogen bromide was passed into the suspension of 1 g. of *N*-Cbzo-*O*-Bz-L-seryl-L-histidine in 7 g. of dioxane at room temperature

until the concentration of hydrogen bromide reached 25% and then the mixture was allowed to stand for an hour. In this reaction period, the carbobenzoxy-peptide was dissolved perfectly into the dioxane solution. To the reaction mixture was added dry ether and the precipitate was collected and washed with ether three times. The precipitate was likely to be slightly hygroscopic. The yield was about 1.2 g. The precipitate was dissolved in 5 cc. of ethanol and dry pyridine was added until the solution became slightly turbid (pH 6.5). After a few minutes, the colloidal precipitate was removed and the filtrate was allowed to stand for an hour in an ice-box. Fine powdery crystals (300 mg.) were obtained, m.p. 205–207°C with decomposition. (in 57% yield) $[\alpha]_D^{13}=+26.43$ (30 mg./cc. water)

*Anal.* Found: C, 33.17; H, 4.48; N, 16.88. Calcd. for $C_9H_{15}O_4N_4Br$: C, 33.43; H, 4.33; N, 17.33%.

**L-Seryl-L-histidyl-L-leucine.** — *N*-Cbzo-*O*-Bz-L-seryl-L-histidyl-L-leucine (0.5 g.) was dissolved in 5 cc. of dioxane and dry hydrogen bromide was passed to produce about 25% solution. After standing for an hour at room temperature, dihydrobromide of free peptide (0.4 g.) was precipitated on addition of dry ether. The precipitated dihydrobromide was dissolved in 3 cc. of absolute ethanol, followed by addition of 0.2 cc. of triethylamine and the mixture was allowed to stand overnight in an ice-box. The free peptide (300 mg., m. p. 215–216°C with decomposition) was obtained. Recrystallization from ethanol containing a small amount of water gave 200 mg. of the pure peptide in 70% yield, m. p. 230°C with decomposition. $[\alpha]_D^{13}=-25.3$ (10 mg./cc. water)

*Anal.* Found: C, 49.03; H, 6.90; N, 18.84. Calcd. for $C_{15}H_{25}O_5N_5\cdot H_2O$: C, 48.22; H, 7.20; N, 18.80%.

***O*-Bz-DL-serine Ethylester Hydrochloride.**— Ten grams of *O*-Bz-DL-serine was suspended in 100 cc. of absolute ethanol and the solution was saturated with dry hydrogen chloride at 0°C. After kept standing overnight at 5°C the mixture was evaporated in vacuo and this procedure was repeated. The residual crystals were recrystallized twice from ethanol-ether. The yield (11 g.) was about 80%, m.p. 118°C.

*Anal.* Found: C, 54.90; H, 6.79; N, 5.59. Calcd. for $C_{12}H_{18}O_3NCl$: C, 55.49; H, 6.98; N, 5.40%.

**Cbzo-glycyl-*O*-Bz-DL-serine Ethylester.** — *O*-Bz-DL-serine ethylester was prepared from 5.2 g. of its hydrochloride by the use of ammonia-chloroform solution. This free ester in 30 cc. of chloroform was coupled with 2.9 g. of Cbzo-glycine in 20 cc. of chloroform and 3.1 g. of dicyclohexycarbodiimide in 10 cc. of chloroform. The reaction mixture was allowed to stand overnight, and shaken with 5 cc. of 0.5 N hydrochloric acid to remove the unchanged dicyclohexylcarbodiimide. After filtration of the dicyclohexyl urea produced, the filtrate was washed with dilute acid, alkali and water, and then dried over anhydrous sodium sulfate. The solvent was removed in vacuo. By adding petroleum ether to the residual, 5.1 g. of Cbzo-glycyl-*O*-Bz-DL-serine ester was obtained in 88% yield, m.p. 80–83°C. Recrystallization from ethylacetate-petroleum ether gave the pure material, m. p. 84°C.

*Anal.* Found: C, 63.81; H, 6.58; N, 6.84. Calcd. for $C_{22}H_{26}O_6N_2$: C, 63.74; H, 6.32; N, 6.76%.

**Cbzo-glycyl-*O*-Bz-DL-serine Hydrazide.** — Into the solution of 2.1 g. of Cbzo-glycyl-*O*-Bz-DL-serine ethyl ester in 40 cc. of ethanol was added 0.3 g. of hydrazine hydrate and the mixture was allowed to stand overnight at room temperature. The crystals produced were collected and washed with ethanol. Recrystallization from hot ethanol gave 1.8 g. of hydrazide in 90% of theory, m.p. 188–189°C.

*Anal.* Found: C, 60.22; H, 5.50; N, 14.08. Calcd. for $C_{20}H_{24}O_5N_4$: C, 59.99; H, 6.04; N, 13.99%.

***O*-Bz-L-serine Methylester Hydrochloride.** —From 5.7 g. of *O*-Bz-L-serine, 7.2 g. of its methyl ester was obtained by the same method as in the case of O-Bz-L-serine ethyl ester. Recrystallization from methanol-ether gave 6.5 g. of pure crystals in 90% yield, m.p. 169°C. $[\alpha]_D^{13}=-2.7$ (30 mg./cc. water)

*Anal.* Found: C, 53.76; H, 6.20; N, 5.52. Calcd. for $C_{11}H_{16}O_3NCl$: C, 53.77; H, 6.54; N, 5.70%.

## Summary

L-Seryl-L-histidine and L-seryl-L-histidyl-L-leucine have been synthesized in good yields by Sheehan's dicyclohexylcarbodiimide method. In the removal of protecting groups of *O*-Bz-serine derivatives by Ben-Ishai's method, dioxane must be used as the solvent in place of glacial acetic acid. *O*-Bz-L- and DL-serine ester was synthesized the mild esterification condition.

The author wishes to express his appreciation to Professer S. Akabori for his kind guidance during the course of this work and also to Mr. T. Yamakawa and Mr. F. Sakiyama for their assistance.

*Chemistry Department, Faculty of Science, Osaka University*
*Kita-ku, Osaka*

# *Chemical Constitution of Renieratene*

By Masaru YAMAGUCHI

(Received August 7, 1957)

Renieratene is the main consistuent of carotenoids of a sponge "*Reniera japonica*"[1,2]. The most conspicuous characteristic of the pigment is that it has the most unsaturated composition of all the carotenoids hitherto reported. The light absorption maxima of the pigment, however, are located at nearly the same position as those of γ-carotene, which has only twelve double bonds in the molecule.

It has been reported in the previous paper[2] that renieratene has the molecular formula $C_{40}H_{48}$ or $C_{40}H_{50}$ (the former is more probable). Further confirmation of its molecular weight has been given by means of isothermal distillation. On catalytic hydrogenation, renieratene absorbs 15 moles of hydrogen. It is therefore considered to be a cyclic compound with one or two rings.

The quasi-equilibrium mixture of *cis-trans* isomerization of the pigment with iodine, shows the absorption maxima at a shorter wavelength region than those of the original solution, and a marked *cis*-peak also appears (Fig. 1). It can therefore, be concluded that renieratene is not a *cis*-isomer of a carotenoid with the absorption maxima of longer wavelength but has an all-*trans* form as to the configuration of conjugated double bonds. High melting point and low solubility of the pigment also support the conclusion.

The infrared spectrum (Fig. II) indicates the absence of vinyl group, which is further supported by the fact that renieratene is a rather stable carotenoid and has little tendency to polymerize. When a $C_{40}$—carotenoid with two 2,2,6-trimethylcyclohexyl-skeletons has no vinyl group, the maximum number of double bonds which are allowed to exist is fourteen, as in the case of anhydroeschscholtzxantin[3], I. If the carotenoid had throughout an open chain structure it might of course be possible to contain fifteen double

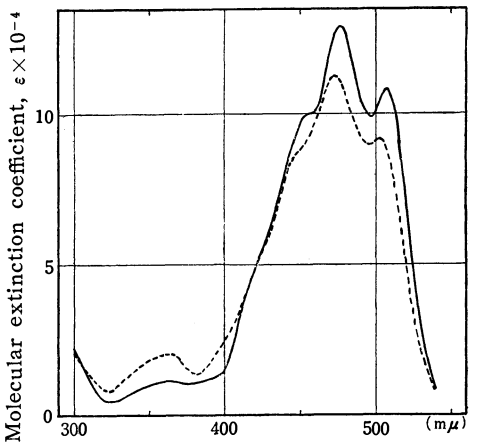



Fig. 1. Absorption curves of renieratene
—— fresh solution (benzene)
---- isomerized solution with iodine.

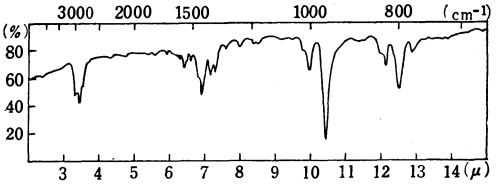



Fig. 2. Infra-red spectrum of renieratene.

bonds in the molecule. However even if it were so, all these double bonds would be in conjugation as in the case of dehydrolycopene[4], II ; therefore the absorption maxima should be situated at much longer wavelength regions. These considerations lead to a presumption that a highly unsaturated group with a slight bathochromic effect must exist in the molecule of renieratene. There are two presumable cases which satisfy this requirement, i. e. the presence of triple bonds or the presence of benzene rings in the molecule of renieratene, although the former is less likely because of the reasons described below.

In the infra-red spectrum (Fig. II), no bands are observed which are characteristic of triple or allenic bond. On the other hand, a sharp absorption at 800 $cm^{-1}$, which seems to be characteristic of renieratene

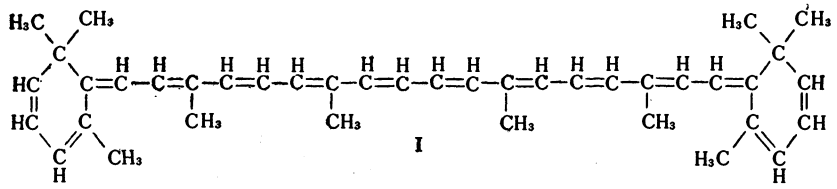
* Pigments of Marine Animals, IV.; III of this series; This Bulletin, **30**, 111 (1957).

1) T. Tsumaki, M. Yamaguchi and T. Tsumaki, *J. Chem. Soc. Japan, Pure Chem. Sec.*, **75**, 297 (1954).

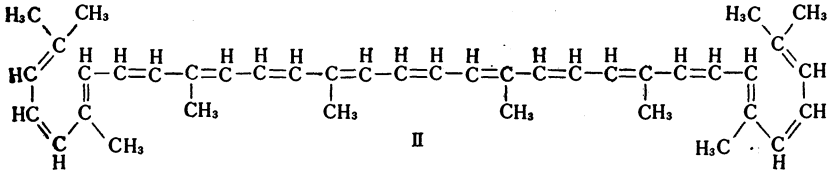
2) M. Yamaguchi, This Bulletin, **30**, 111 (1957).

3) P. Karrer and E. Leumann, ibid., **34**, 445 (1951).

4) P. Karrer and J. Rutschmann, *Helv. chim. Acta* **28**, 793 (1945).



I



II

because of the general lack of this absorption in common carotenoids, is considered to give an indication of the presence of the benzene ring with two or three adjacent free hydrogen atoms. However this interpretation is not decisive, for the absorption in 3030 $cm^{-1}$, 1500—1600 $cm^{-1}$ and other regions which are useful for the identification of aromatic structures, are not distinctive, because of the simultaneous presence of the absorption due to the polyene structure in the same regions.

Renieratene gives only a very small amount of acetone (0.03—0.05 mole) on ozonolysis. It has been reported that one isopropylidene group gives 0.8—0.9 mole of acetone[5], one isopropyl group 0.3 mole[5] and an $\alpha$- or a $\beta$-ionone group 0.15 mole[6]. Therefore it seems that renieratene has neither isopropylidene group nor ionone ring. This result seems to be in favor of the presumption of the presence of the benzene ring.

Renieratene has no provitamin A activity in the rat when applied in daily doses of 60 $\gamma$. This is in agreement with the results of the ozonolysis.

By the mild oxidation of reniertene in benzene-acetic acid soultion with chromic acid corresponding to two atoms of oxygen per mole of the pigment, followed by chromatographic separation, two pigments are obtained in small yield. One of them forms purple crystals of m. p. 199°, and the other forms brown crystals of m. p. 127°. Both the pigments have the formula of $C_{30}H_{36}O$ and are considered to be polyene aldehydes. Therefore these two pigments seem to be in an isomeric relation. The term *renieral* is tentatively proposed for the pigment of m. p. 199°, and *isorenieral* for the pigment of m. p. 127°. On catalytic hydrogenation, both the pigments absorb 12 moles of hydrogen. This

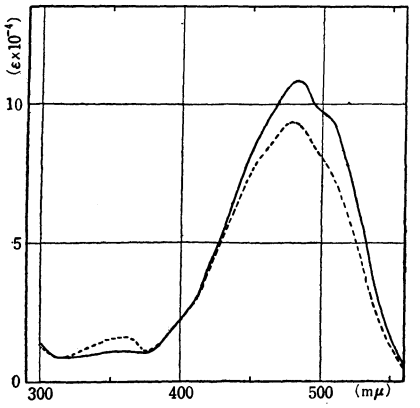



Fig. 3. Absorption curves of renieral.
—— fresh solution (benzene).
---- isomerized solution with iodine

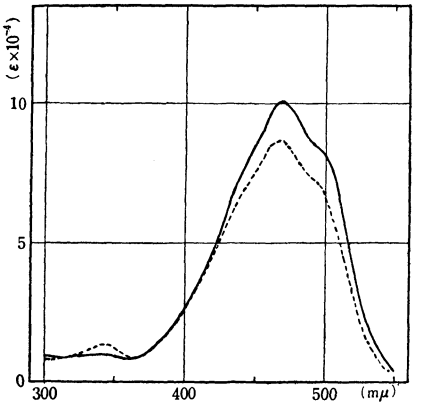



Fig. 4. Absorption curves of isorenieral.
—— fresh solution (benzene)
---- isomerized solution with iodine.

5) R. Kuhn and H. Roth, *Ber.*, **65**, 1285 (1932).
6) L. Zechmeister and W. A. Schroeder, *Arch. Biochem.*, **1**, 231 (1942).

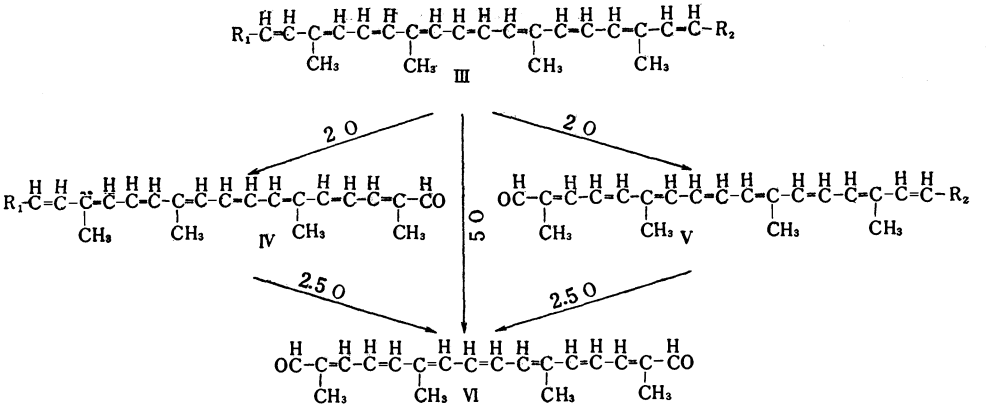



Fig. 6. Mild oxidation of renieratene.

fact indicates that they have 11 carbon-carbon double bonds in their molecules. Renieral exhibits the absorption maxima at 540 and 501 mμ in (carbon disulfide). Isorenieral exhibits absorption maxima at 526 and 489 mμ (in carbon disulfide) and gives phenylhydazone of m. p. 207°. Absorption curves in benzene with and without iodine are given by Fig. 3 and Fig. 4.

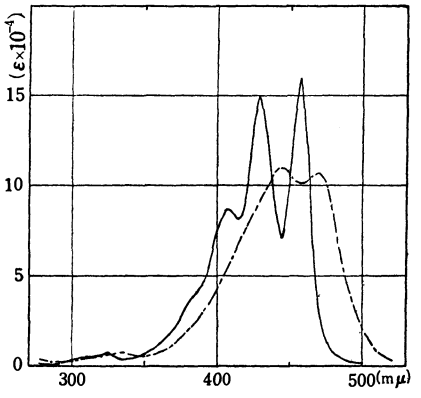



Fig. 5. Absorption curves of the pigment of m. p. 190°.
—— in petroleum ether,
-·-· in ethanol

When renieratene is oxidized with chromic acid corresponding to five atoms of oxygen, the principal product is the pigment of m. p. 190°, which forms orange red plates with purple reflex. The molecular formula of the pigment is $C_{20}H_{24}O_2$, and the absorption maxima are at 457, 430 and 407 mμ (in petroleum ether). The absorption curves are given in Fig. 5. As the pigment gives a bisphenylhydrazone of m. p. 239—242°, it seems to be a dialdehyde. These facts and the other properties of the pigment indicate that it is identical with crocetin dialdehyde, VI, (violet red plates, m. p. 190—191°, $C_{20}H_{24}O_2$, absorption maxima in petroleum ether, 458, 430 and 408 mμ; bisphenylhydrazone, m. p. 243°), which has been synthesized by Isler and coworkers[7]. It is for the first time that crocetin dialdehyde is obtained by the degradation of a carotenoid. Both renieral and isorenieral give crocetin dialdehyde by the oxydation with chromic acid corresponding to 2.5 atoms of oxygen. However, renieral does not give isorenieral on oxidation and neither does the reverse occur. These relationships are illustrated in Fig, 6, and the facts described above lead to the conclusion that renieratene, renieral and isorenieral are expressed by the partial formulae III, IV and V in Fig. 6, respectively. Both $R_1$- and $R_2$ groups seem to correspond to $C_9H_{11}$- which probably contain one ring and three double bonds.

From the positions of the absorption maxima of renieral and isorenieral, it is indicated that at least nine double bonds in these pigments should be in conjugation[8]. Therefore at least one double bond in $R_1$- and one double bond in $R_2$- group should be in conjugation with principal chromophore of renieratene. Numerous instances[9] of the mild oxidation of carotenoids have shown that the oxidative fission of double bond generally occurs at the outer end of the conjugated double bond system. However, in the case of renieratene, none of the pigments which have the absorption maxima at a longer

7) O. Isler, H. Gutmann, H. Lindlar, M. Montavon, R. Rüegg, G. Ryser and P. Zeller, *Helv. chim. Acta*, **39**, 463 (1956).
8) Calculated according to K. Hirayama's method, *J. Chem. Soc. Japan, Pure Chem. Sec.*, **75**, 674 (1954).
9) For example, R. Kuhn and C. Grundmann, *Ber.*, **65**, 900 (1932); R. Kuhn and H. Brockmann, ibid., **65**, 894 (1934); *Ann.*, **516**, 123 (1935).

wavelength region are obtained i. e. those which have a longer conjugated double bond system, than the above-mentioned aldehydes have. Therefore, in renieratene, the oxidation of double bond does not occur at the outer end of the conjugated system but at the inner position of the system. This indicates that the partial double bond systems contained in $R_1$- or $R_2$- group may be highly sablet towards oxidation, which also suggests the presence of benzene rings.

However, it seems to be contradictory to the view of the presence of benzene ring, that renieratene gives 7 moles of acetic acid on determination of side chain methyl groups. If renieratene had benzene rings in the molecule, non-volatile benzene polycarboxylic acid would be formed by such a serious oxidation as is employed in the determination; because the benzene ring in renieratene might be replaced by several methyl groups, as would be expected from the formula. In such a case, the amount of volatile acid should be no more than 4 moles when estimated as acetic acid. The account of this result can not be given in the present stage of the study.

## Experimental

Renieratene prepared in the way described in the preceding papers[1,2] was employed. It formed fine purple red needles of m. p. 185° and was chromatographically homogeneous. Absorption maxima, 532, 496, 463 mμ (in carbon disulfide).

*Anal.* Found: C, 90.95; H, 9.26. Calcd. for $C_{40}H_{48}$; C, 90.85; H, 9.15%.

**Infrared spectrum.**—It was taken in a potassium bromide pellet, with a Perkin-Elmer 21 double beamins trument equipped with a potassium bromide prism (Fig. 2).

**Molecular weight.**—Signer's method[10] (method of isothermal distillation) was slightly modified. The solutions (128.1 $mm^3$ and 194.1 $mm^3$) of renieratene (5.913 mg. and 6.270 mg.) in benzene exhibited the same vapor pressures as those of the solutions (133.6 $mm^3$ and 193.8 $mm^3$) of benzil (2.531 mg. and 2.501 mg.) in benzene respectively. Found; 526.8, 536.7. Calcd. for $C_{40}H_{48}$, 528.8. In a parallel experiment on lycopene, 539.2 was obtained (Calcd. 536.9).

**Catalytic hydrogenation** (Kuhn and Möller's method[11]).—Pure sorbic acid was employed for the test substance. Catalyst, platinum oxide. Solvent, decalin-acetic acid (1:1). Found: 15.23, 15.17, 14.98 moles hydrogen. In parallel experiments, lycopene absorbed 13.03 moles hydrogen and β- carotene 10.94 moles hydrogen.

**Isopropylidene group** (Kuhn and Roth's method[5]).—On ozonolysis, renieratene (15.116 mg. and 8.912 mg.) gave acetone (0.077 mg. and 0.031 mg.) after subtraction of the blank value. These corresponded to 0.05 and 0.03 mole of acetone per mole of renieratene. In parallel experiments, lycopene and β-carotene gave 1.5 and 0.35 mole of acetone, respectively.

**Side-chain methyl group** (Kuhn and Roth's method[12]).—Renieratene (4.603 mg. and 4.196 mg.) gave volatile acid corresponding to 6.07 cc. and 5.73 cc. of 0.01 N sodium hydroxide solution. These corresponded to 6.97 and 7.22 moles of acetic acid. A parallel determination on lycopene gave 5.61 moles of acetic acid.

**Vitamin A activity.**—Renieratene was examined in experiments on four groups of rats in daily doses of 7, 15, 30 and 60 γ respectively. The rats of these four groups lost 26 g., 28 g., 27 g. and 26 g. (average on the rats of each group) in bodyweight, and finally died. The rats of the group for the positive control, which 7 γ of β-carotene were applied in daily doses, gained 33 g. on the average in body-weight in 30 days.

**Cis-trans isomerization**[13].—The solution (25 cc.) of renieratene (1.175 mg.) in benzene was prepared in a dark room, and 10 cc. of the solution was exposed to scattered light after the addition of iodine (ca. 6 γ) in benzene (0.8 cc.). The remainder was kept in the dark after the addition of benzene (1.2 cc.). After 30 minutes, 1 cc. of each solution was diluted to 25 cc. with benzene and the absorption curves were determined. They are given in Fig. 1. A remarkable *cis*-peak was ovserved at 362 mμ in the isomerized solution.

**Chromic acid oxidation.**—*a*) *Renieral and isorenieral.* Renieratene (133 mg.) was dissolved in a mixture of benzene (130 cc.) and acetic acid (130 cc.). To 10 cc. of this solution (containing ca. 5 mg. of the pigment), was added the mixture of the aqueous chromic acid (0.1 N, 0.2 cc.) and acetic acid (2 cc.) in one portion with vigorous stirring. The color changed into deep red. After 4—5 seconds the mixture was poured into water (20 cc.) covered with petroleum benzine (10 cc.), and washed with water several times. The procedure was repeated with other 10 cc. portions. All oxidized portions were combined together and dried with anhydrous sodium sulfate. The concentrated solution (30 cc.) was chromatographed on alumina (Merck) (column, 2.5 cm×20 cm; developer, benzene) and gave the following zones in the sequence of decreasing adsorbability. 1) A thin yellow zone. It gave a small quantity of oily brown residue having absorption maxima at 454 and 425 mμ in petroleum benzine. 2) A thin yellow zone. It gave a small quantity of oily yellowish brown residue with absorption maxima at 455 and 425 mμ in petroleum benzine. 3) A thin orange zone. On treatment with petroleum benzine the residue afforded a minute quantity of red crystals having absorption maxima

10) R. Signer, ibid., **478**, 246 (1930).
11) R. Kuhn and E. E. Möller, *Angew. Chem.*, 145 (1934),
12) R. Kuhn and H. Roth, *Ber.*, **66**, 1274 (1933).
13) L. Zechmeister and A. Polgár, *J. Am. Chem. Soc.*, **65**, 1522 (1943).

at 456 and 429 mμ in petroleum benzine. It was crocetin dialdehyde. 4) A deep purple zone. After rechromatography on alumina, the residue of the eluate gave 8.5 mg. of renieral when recrystallized once from benzene-methanol. 5) A purplish red zone. After rechromatography on alumina and recrystallization of the residue of the eluate from petroleum benzine, 17.5 mg. of isorenieral was obtained. 6) A red zone. A small quantity of renieratene was recovered. Another experiment with 60 mg. of renieratene afforded 3.3 mg. of renieral and 7 mg. of isorenieral.

Renieral (further purified by recrystallization twice from benzene-methanol and twice from benzene-petroleum benzine) forms purplish brown needles, m. p. 198—199° (total 8.1 mg). It is soluble in benzene and difficultly soluble in petroleum benzine and methanol. Absorption maxima; 540, 501 mμ (in carbon disulfide); 499, 468 mμ (in hexane). Absorption curves (in benzene) with and without iodine (ca. 1.5% of the pigment) are given in Fig. III. On catalytic hydrogenation, 12.2 moles of hydrogen were absorbed.

Isorenieral (further purified by recrystallization thrice from petroleum benzine) forms brown crystals, m. p. 125—127° (12.5 mg.). It is soluble in benzene, petroleum benzine and hot ethanol, but is less soluble in methanol. Absorption maxima: 526, 489 mμ (in carbon disulfide); 486, 455 mμ (in hexane). Absorption curves (in benzene) with and without iodine are given in Fig. 4.

*Anal.* Found: C, 87.19; H, 8.88. Calcd. for $C_{30}H_{36}O$: C, 87.33; H, 8.80%.

On catalytic hydrogenation, 12.1 moles of hydrogen were absorbed. Phenylhydrazone, prepared by mixing the pigment (2 mg.) with phenylhydrazine in acetic acid and recrystallized once from benzene-methanol, formed purplish red needles, m. p. 207° (in an evacuated tube). It melted at 185° in an open capillary tube.

*Anal.* Found; N, 5.56. Calcd. for $C_{36}H_{42}N_2$; N, 5.57%.

*b) Crocetin dialdehyde.* Renieratene (120 mg.) was dissolved in a mixture of benzene (120 cc.) and acetic acid (120 cc.), and the solution was divided into 24 portions. Each portion (10 cc.) was oxidized with the mixture of the chromic acid solution (0.1 N, 0.5 cc.) and acetic acid (2 cc.), under vigorous stirring for one minute. The color of the solution changed into deep red and then gradually into orange yellow. The products were treated as in the case of a), and chromatographed on alumina. The main zone was orange red (it corresponded to the zone 3 of the chromatogram described in a)), while the zones of renieral and isorenieral were fairly faint. The residue of the eluate was recrystallized thrice from benzene-methanol and gave crocetin dialdehyde in purple red plates m. p. 190° (7.7 mg.). All the mother liquors of crystallizations of reneiral and isorenieral were combined together and oxidized as above with sufficient chromic acid to change the deep red color of the solution into orange yellow; 4.7 mg. of crocetin dialdehyde was further obtained. Absorption curve is given in Fig. 5.

*Anal.* Found: C, 81.46; H, 8.12%. Calcd. for $C_{20}H_{24}O_2$; C, 81.04; H, 8.16%.

Bisphenylhydrazone. Purple crystals, m. p. 256° (in an evacuated tube). In an open capillary tube, it melted at 239—242°.

*Anal.* Found; N, 11.79% Calcd. for $C_{32}H_{36}N_4$ 11.76%.

*c) Oxidation of renieral.* Renieral (0.8 mg.) was oxidized as above with chromic acid solution (0.1 N, 0.03 cc.), and the product was chromatographed. The principal zone gave a minute quantity of crocetin dialdehyde (m. p. 189°, mixed m. p. 189—190°).

*d) Oxidation of isorenieral.* Isorenieral (1.4 mg.) was oxidized with chromic acid solution (0.04 cc.). Crocetin dialdehyde was obtained as the main product (m. p. 189°, mixed m. p. 189—190°).

The author wishes to express his thanks to Professor Tokuichi Tsumaki for his exceedingly kind direction throughout this work. The author also thanks Mr. Kiyoshi Nakamura of Dainippon Pharmaceutical Co. Ltd. for the infra-red determination, Mr. Toshihiko Mukai and Mr. Yoichi Demura for their help in the collection of materials, and Mr. Michio Shido and Miss Sachiko Indo for microanalysis. The cost of this work has been partially covered by the Scientific Research Grant of Ministry of Education.

*Department of Chemistry Faculty of Science, Kyushu University*
*Hakozaki, Fukuoka*

# SHORT COMMUNICATIONS

## *Decomposition of Aqueous Hydrogen Peroxide by Oxidized Chromia-Alumina Catalysts*

By Yoshio MATSUNAGA

(Received August 7, 1957)

Our previous work[1] has established the fact that chromia-alumina catalysts contain an excess of surface oxygen after contact with air even at room temperature. In the extreme case, it has been shown that chromic ion can be oxidized completely to the plus-six state in sharp contrast with our knowledge of the thermal decomposition of chromic anhydride. Voltz and Weller[2] examined the catalytic decomposition of aqueous hydrogen peroxide by chromic oxide catalysts treated with oxygen at 500°C and suggested that the activities of the oxidized catalysts can be largely attributed to the chromic anhydride or its equivalent formed on the surface of these catalysts. However, their prediction was supported by measurements on three samples only, chromina gel, 20% chromia-alumina (Houdry Type R), and co-precipitated chromia-alumina. As we had many samples of various concentrations of chromium and also various degrees of oxidation, a more detailed examination of the relation between catalytic activity for the decomposition of aqueous hydrogen peroxide and the content of excess oxygen, has been undertaken.

The catalyst samples used in this study are those of the first series in our previous paper and the temperatures of oxygen treatments are 250°, 350° and 450°C. The content of excess oxygen, determined by an iodometric titration, ranges from 0.34 to 2.83 mg. eq./g. of catalyst and these amounts of excess oxygen cover the range of the mean oxidation number of chromium from 3.12 to 5.65. The volume of oxygen liberated by the reaction between 100 mg. of catalyst and 5.0 cc. of 30 % hydrogen peroxide (Edogawa Kagaku, Analytical Reagent) at 25°C was followed as a function of time for about ten minutes. The curves were found to be nearly straight. The catalytic activity represented by the volume of liberated oxygen per minute per g. of chromium is plotted against the concentration of chromium in Fig. 1. The curves bear a striking resemblance to those of the mean oxidation number as a function of chromium concentration shown in Fig. 1 of the previous paper. The above-mentioned activity is divided by the mean oxidation number of chromium and plotted against the concentration of chromium in Fig. 2.

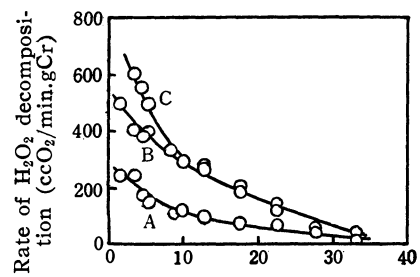



Fig. 1. Catalytic activity of oxidized chromia-alumina as a function of chromium concentration.
A; oxidized at 250°C, B; at 350°C, C; at 450°C.

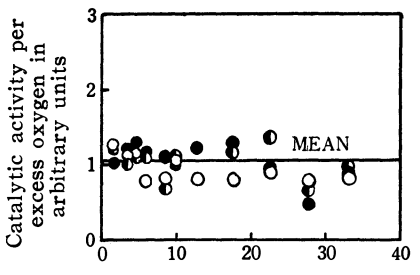



Fig. 2. Catalytic activity per excess oxygen in oxidized chromia-alumina as a function of chromium concentration.
○; oxidized at 250°C, ◑; at 350°C, ●; at 450°C.

It appears that the catalytic activity for a given amount of excess oxygen is nearly

1) Y. Matsunaga, This Bulletin, **30**, 868 (1957).
2) S. E. Voltz and S. W. Weller, *J. Am. Chem. Soc.*, **76**, 1586 (1954).

constant regardless of the mean oxidation number of chromium over the whole concentration range of chromium. In some of our catalyst samples the mean oxidation number of chromium exceeds plus five; therefore, we can conclude that the activity is largely due to the chromic anhydride formed on the surface of these catalysts. This conclusion is not only consistent with the suggestion given by Voltz and Weller, but also clarifies more definitely the nature of the surface of these catalysts.

The author wishes to express his hearty thanks to Professor H. Akamatu for his kind direction.

*Department of Chemistry, Faculty of Science, The University of Tokyo*
*Hongo, Tokyo*